CHEMICAL PROCESS EQUIPMENT

Selection and Design

SECOND EDITION

James R. Couper

W. Roy Penney

James R. Fair

Stanley M. Walas
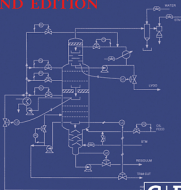
Chemical Process Equipment

Chemical Process Equipment

Selection and Design

Second Edition

James R. Couper
W. Roy Penney
James R. Fair
Stanley M. Walas

♾ Recognizing the importance of preserving what has been written,
Elsevier prints its books on acid-free paper whenever possible.

Contents

v

Preface to the Second Edition

The editors of the revised edition are in agreement with the philosophy and the approach that Professor Stanley Walas presented in the original edition. In general, the subject headings and format of each chapter have been retained but the revised edition has been corrected to eliminate errors and insofar as possible update the contents of each chapter. Material that we consider superfluous or beyond the scope and intent of the revised edition has been eliminated. Most of the original text has been retained, since the methods have stood the test of time and we felt that any revision had to be a definite improvement.

Chapter 3, Process Control, and Chapter 10, Mixing and Agitation, have been completely revised to bring the content of these chapters up to date. Chapter 18, Process Vessels, has been expanded to include the design of bins and hoppers. Chapter 19, Membrane Separations, is an entirely new chapter. We felt that this topic has gained considerable attention in recent years in chemical processing and deserved to be a chapter devoted to this important material. Chapter 20, Gas-Solid Separation and Other Topics, consists of material on gas-solid handling as well as the remainder of the topics in Chapter 19 of the original edition. Chapter 21, Costs of Individual Equipment, is a revision of Chapter 20 in the original edition and the algorithms have been updated to late 2002. Costs calculated from these algorithms have been spot-checked with equipment suppliers and industrial sources. They have been found to be within 20 to 25% accurate.

We have removed almost all the Fortran computer program listings, since every engineer has his or her own methods for solving such problems. There is one exception and that is the fired heater design Fortran listing in Chapter 8, Heat Transfer and Heat Exchangers. Our experience is that the program provides insight into a tedious and involved calculation procedure.

Although the editors of this text have had considerable industrial and academic experience in process design and equipment selection, there are certain areas in which we have limited or no experience. It was our decision to ask experts to serve as collaborators. We wish to express our profound appreciation to those colleagues and they are mentioned in the List of Contributors.

We particularly wish to acknowledge the patience and understanding of our wives, Mary Couper, Merle Fair, and Annette Penney, during the preparation of this manuscript.

James R. Couper
James R. Fair
W. Roy Penney

Preface to the First Edition

This book is intended as a guide to the selection or design of the principal kinds of chemical process equipment by engineers in school and industry. The level of treatment assumes an elementary knowledge of unit operations and transport phenomena. Access to the many design and reference books listed in Chapter 1 is desirable. For coherence, brief reviews of pertinent theory are provided. Emphasis is placed on shortcuts, rules of thumb, and data for design by analogy, often as primary design processes but also for quick evaluations of detailed work.

All answers to process design questions cannot be put into a book. Even at this late date in the development of the chemical industry, it is common to hear authorities on most kinds of equipment say that their equipment can be properly fitted to a particular task only on the basis of some direct laboratory and pilot plant work. Nevertheless, much guidance and reassurance are obtainable from general experience and specific examples of successful applications, which this book attempts to provide. Much of the information is supplied in numerous tables and figures, which often deserve careful study quite apart from the text.

The general background of process design, flowsheets, and process control is reviewed in the introductory chapters. The major kinds of operations and equipment are treated in individual chapters. Information about peripheral and less widely employed equipment in chemical plants is concentrated in Chapter 19 with references to key works of as much practical value as possible. Because decisions often must be based on economic grounds, Chapter 20, on costs of equipment, rounds out the book. Appendixes provide examples of equipment rating forms and manufacturers' questionnaires.

Chemical process equipment is of two kinds: custom designed and built, or proprietary "off the shelf." For example, the sizes and performance of custom equipment such as distillation towers, drums, and heat exchangers are derived by the process engineer on the basis of established principles and data, although some mechanical details remain in accordance with safe practice codes and individual fabrication practices.

Much proprietary equipment (such as filters, mixers, conveyors, and so on) has been developed largely without benefit of much theory and is fitted to job requirements also without benefit of much theory. From the point of view of the process engineer, such equipment is predesigned and fabricated and made available by manufacturers in limited numbers of types, sizes, and capacities. The process design of proprietary equipment, as considered in this book, establishes its required performance and is a process of selection from the manufacturers' offerings, often with their recommendations or on the basis of individual experience. Complete information is provided in manufacturers' catalogs. Several classified lists of manufacturers of chemical process equipment are readily accessible, so no listings are given here.

Because more than one kind of equipment often is suitable for particular applications and may be available from several manufacturers, comparisons of equipment and typical applications are cited liberally. Some features of industrial equipment are largely arbitrary and may be standardized for convenience in particular industries or individual plants. Such aspects of equipment design are noted when feasible.

Shortcut methods of design provide solutions to problems in a short time and at small expense. They must be used when data are limited or when the greater expense of a thorough method is not justifiable. In particular cases they may be employed to obtain information such as:

1. an order of magnitude check of the reasonableness of a result found by another lengthier and presumably accurate computation or computer run,
2. a quick check to find if existing equipment possibly can be adapted to a new situation,
3. a comparison of alternate processes,
4. a basis for a rough cost estimate of a process.

Shortcut methods occupy a prominent place in such a broad survey and limited space as this book. References to sources of more accurate design procedures are cited when available.

Another approach to engineering work is with rules of thumb, which are statements of equipment performance that may obviate all need for further calculations. Typical examples, for instance, are that optimum reflux ratio is 20% greater than minimum, that a suitable cold oil velocity in a fired heater is 6 ft/sec, or that the efficiency of a mixer-settler extraction stage is 70%. The trust that can be placed in a rule of thumb depends on the authority of the propounder, the risk associated with its possible inaccuracy, and the economic balance between the cost of a more accurate evaluation and suitable safety factor placed on the approximation. All experienced engineers have acquired such knowledge. When applied with discrimination, rules of thumb are a valuable asset to the process design and operating engineer, and are scattered throughout this book.

Design by analogy, which is based on knowledge of what has been found to work in similar areas, even though not necessarily optimally, is another valuable technique. Accordingly, specific applications often are described in this book, and many examples of specific equipment sizes and performance are cited.

For much of my insight into chemical process design, I am indebted to many years' association and friendship with the late Charles W. Nofsinger who was a prime practitioner by analogy, rule of thumb, and basic principles. Like Dr. Dolittle of Puddleby-on-the-Marsh, "he was a proper doctor and knew a whole lot."

Stanley M. Walas

Contributors

James R. Couper, D.Sc. *(Editor)*, Professor Emeritus, Department of Chemical Engineering, University of Arkansas, Fayetteville, AR; Fellow, A.I.Ch.E., Registered Professional Engineer (Arkansas and Missouri)

James R. Fair, Ph.D. *(Distillation and Absorption, Extraction and Leaching) (Co-editor)*, McKetta Chair Emeritus Professor, Department of Chemical Engineering, The University of Texas, Austin, TX; Fellow, A.I.Ch.E., Registered Professional Engineer (Missouri and Texas)

E. J. Hoffman, Ph.D. *(Membrane Separations)*, Professor Emeritus, Department of Chemical Engineering, University of Wyoming, Laramie, WY

W. Roy Penney, Ph.D. *(Flow of Fluids, Fluid Transport Equipment, Drivers for Moving Equipment, Heat Transfer and Heat Exchangers,* *Mixing and Agitation) (Co-editor)*, Professor of Chemical Engineering, University of Arkansas, Fayetteville, AR; Registered Professional Engineer (Arkansas and Missouri)

A. Frank Seibert, Ph.D. *(Extraction and Leaching)*, Professor, Department of Chemical Engineering, University of Texas, Austin, TX, Registered Professional Engineer (Texas)

Terry L. Tolliver, Ph.D. *(Process Control)*, Retired, Solutia, St. Louis, Fellow, A.I.Ch.E. and ISA, Registered Professional Engineer (Missouri)

John H. Wolf, B.S. *(Crystallization)*, Retired President, Swenson Process Equipment, Inc., A.I.Ch.E., over 35 years' experience in crystallization.

RULES OF THUMB: SUMMARY

Although experienced engineers know where to find information and how to make accurate computations, they also keep a minimum body of information readily available, made largely of short-cuts and rules of thumb. This compilation is such a body of information from the material in this book and is, in a sense, a digest of the book.

Rules of thumb, also known as *heuristics*, are statements of known facts. The word *heuristics* is derived from Greek, to discover or to invent, so these rules are known or discovered through use and practice but may not be able to be theoretically proven. In practice, they work and are most safely applied by engineers who are familiar with the topics. Such rules are of value for approximate design and preliminary cost estimation, and should provide even the inexperienced engineer with perspective and whereby the reasonableness of detailed and computer-aided design can be appraised quickly, especially on short notice, such as a conference.

Everyday activities are frequently governed by rules of thumb. They serve us when we wish to take a course of action but we may not be in a position to find the best course of action.

Much more can be stated in adequate fashion about some topics than others, which accounts, in part, for the spottiness of the present coverage. Also, the spottiness is due to the ignorance and oversights on the part of the authors. Therefore, every engineer undoubtedly will supplement or modify this material (Walas, 1988).

COMPRESSORS AND VACUUM PUMPS

1. *Fans* are used to raise the pressure about 3% (12 in. water), *blowers* raise to less than 40 psig, and *compressors* to higher pressures, although the blower range commonly is included in the compressor range.
2. Vacuum pumps: reciprocating piston type decrease the pressure to 1 Torr; rotary piston down to 0.001 Torr, two-lobe rotary down to 0.0001 Torr; steam jet ejectors, one stage down to 100 Torr, three stage down to 1 Torr, five stage down to 0.05 Torr.
3. A three-stage ejector needs 100 lb steam/lb air to maintain a pressure of 1 Torr.
4. In-leakage of air to evacuated equipment depends on the absolute pressure, Torr, and the volume of the equipment, V cuft, according to $w = kV^{2/3}$ lb/hr, with $k = 0.2$ when P is more than 90 Torr, 0.08 between 3 and 20 Torr, and 0.025 at less than 1 Torr.
5. Theoretical adiabatic horsepower (THP) = $[(SCFM)T_1/8130a]$ $[(P_2/P_1)^a - 1]$, where T_1 is inlet temperature in $°F + 460$ and $a = (k-1)/k, k = C_p/C_v$.
6. Outlet temperature $T_2 = T_1(P_2/P_1)^a$.
7. To compress air from $100°F$, $k = 1.4$, compression ratio = 3, theoretical power required = 62 HP/million cuft/day, outlet temperature $306°F$.
8. Exit temperature should not exceed $350-400°F$; for diatomic gases ($C_p/C_v = 1.4$) this corresponds to a compression ratio of about 4.
9. Compression ratio should be about the same in each stage of a multistage unit, ratio = $(P_n/P_1)^{1/n}$, with n stages.
10. Efficiencies of reciprocating compressors: 65% at compression ratio of 1.5, 75% at 2.0, and 80–85% at 3–6.
11. Efficiencies of large centrifugal compressors, 6000–100,000 ACFM at suction, are 76–78%.
12. Rotary compressors have efficiencies of 70%, except liquid liner type which have 50%.

CONVEYORS FOR PARTICULATE SOLIDS

1. *Screw conveyors* are suited to transport of even sticky and abrasive solids up inclines of $20°$ or so. They are limited to distances of 150 ft or so because of shaft torque strength. A 12 in. dia conveyor can handle 1000–3000 cuft/hr, at speeds ranging from 40 to 60 rpm.
2. *Belt conveyors* are for high capacity and long distances (a mile or more, but only several hundred feet in a plant), up inclines of $30°$ maximum. A 24 in. wide belt can carry 3000 cuft/hr at a speed of 100 ft/min, but speeds up to 600 ft/min are suited to some materials. Power consumption is relatively low.
3. *Bucket elevators* are suited to vertical transport of sticky and abrasive materials. With buckets 20×20 in. capacity can reach 1000 cuft/hr at a speed of 100 ft/min, but speeds to 300 ft/min are used.
4. *Drag-type conveyors* (Redler) are suited to short distances in any direction and are completely enclosed. Units range in size from 3 in. square to 19 in. square and may travel from 30 ft/min (fly ash) to 250 ft/min (grains). Power requirements are high.
5. *Pneumatic conveyors* are for high capacity, short distance (400 ft) transport simultaneously from several sources to several destinations. Either vacuum or low pressure (6–12 psig) is employed with a range of air velocities from 35 to 120 ft/sec depending on the material and pressure, air requirements from 1 to 7 cuft/cuft of solid transferred.

COOLING TOWERS

1. Water in contact with air under adiabatic conditions eventually cools to the wet bulb temperature.
2. In commercial units, 90% of saturation of the air is feasible.
3. Relative cooling tower size is sensitive to the difference between the exit and wet bulb temperatures:

$\Delta T(°F)$	5	15	25
Relative volume	2.4	1.0	0.55

4. Tower fill is of a highly open structure so as to minimize pressure drop, which is in standard practice a maximum of 2 in. of water.
5. Water circulation rate is 1–4 gpm/sqft and air rates are 1300–1800 lb/(hr)(sqft) or 300–400 ft/min.
6. Chimney-assisted natural draft towers are of hyperboloidal shapes because they have greater strength for a given thickness; a tower 250 ft high has concrete walls 5–6 in. thick. The enlarged cross section at the top aids in dispersion of exit humid air into the atmosphere.
7. Countercurrent induced draft towers are the most common in process industries. They are able to cool water within $2°F$ of the wet bulb.
8. Evaporation losses are 1% of the circulation for every $10°F$ of cooling range. Windage or drift losses of mechanical draft towers are 0.1–0.3%. Blowdown of 2.5–3.0% of the circulation is necessary to prevent excessive salt buildup.

CRYSTALLIZATION FROM SOLUTION

1. Complete recovery of dissolved solids is obtainable by evaporation, but only to the eutectic composition by chilling. Recovery by melt crystallization also is limited by the eutectic composition.
2. Growth rates and ultimate sizes of crystals are controlled by limiting the extent of supersaturation at any time.
3. The ratio $S = C/C_{sat}$ of prevailing concentration to saturation concentration is kept near the range of 1.02–1.05.
4. In crystallization by chilling, the temperature of the solution is kept at most 1–2°F below the saturation temperature at the prevailing concentration.
5. Growth rates of crystals under satisfactory conditions are in the range of 0.1–0.8 mm/hr. The growth rates are approximately the same in all directions.
6. Growth rates are influenced greatly by the presence of impurities and of certain specific additives that vary from case to case.

DISINTEGRATION

1. Percentages of material greater than 50% of the maximum size are about 50% from rolls, 15% from tumbling mills, and 5% from closed circuit ball mills.
2. Closed circuit grinding employs external size classification and return of oversize for regrinding. The rules of pneumatic conveying are applied to design of air classifiers. Closed circuit is most common with ball and roller mills.
3. Jaw crushers take lumps of several feet in diameter down to 4 in. Stroke rates are 100–300/min. The average feed is subjected to 8–10 strokes before it becomes small enough to escape. Gyratory crushers are suited to slabby feeds and make a more rounded product.
4. Roll crushers are made either smooth or with teeth. A 24 in. toothed roll can accept lumps 14 in. dia. Smooth rolls effect reduction ratios up to about 4. Speeds are 50–900 rpm. Capacity is about 25% of the maximum corresponding to a continuous ribbon of material passing through the rolls.
5. Hammer mills beat the material until it is small enough to pass through the screen at the bottom of the casing. Reduction ratios of 40 are feasible. Large units operate at 900 rpm, smaller ones up to 16,000 rpm. For fibrous materials the screen is provided with cutting edges.
6. Rod mills are capable of taking feed as large as 50 mm and reducing it to 300 mesh, but normally the product range is 8–65 mesh. Rods are 25–150 mm dia. Ratio of rod length to mill diameter is about 1.5. About 45% of the mill volume is occupied by rods. Rotation is at 50–65% of critical.
7. Ball mills are better suited than rod mills to fine grinding. The charge is of equal weights of 1.5, 2, and 3 in. balls for the finest grinding. Volume occupied by the balls is 50% of the mill volume. Rotation speed is 70–80% of critical. Ball mills have a length to diameter ratio in the range 1–1.5. Tube mills have a ratio of 4–5 and are capable of very fine grinding. Pebble mills have ceramic grinding elements, used when contamination with metal is to be avoided.
8. Roller mills employ cylindrical or tapered surfaces that roll along flatter surfaces and crush nipped particles. Products of 20–200 mesh are made.

DISTILLATION AND GAS ABSORPTION

1. Distillation usually is the most economical method of separating liquids, superior to extraction, adsorption, crystallization, or others.
2. For ideal mixtures, relative volatility is the ratio of vapor pressures $\alpha_{12} = P_2/P_1$.
3. Tower operating pressure is determined most often by the temperature of the available condensing medium, 100–120°F if cooling water; or by the maximum allowable reboiler temperature, 150 psig steam, 366°F.
4. Sequencing of columns for separating multicomponent mixtures: (a) perform the easiest separation first, that is, the one least demanding of trays and reflux, and leave the most difficult to the last; (b) when neither relative volatility nor feed concentration vary widely, remove the components one by one as overhead products; (c) when the adjacent ordered components in the feed vary widely in relative volatility, sequence the splits in the order of decreasing volatility; (d) when the concentrations in the feed vary widely but the relative volatilities do not, remove the components in the order of decreasing concentration in the feed.
5. Economically optimum reflux ratio is about 1.2 times the minimum reflux ratio R_m.
6. The economically optimum number of trays is near twice the minimum value N_m.
7. The minimum number of trays is found with the Fenske–Underwood equation

$$N_m = \log \{[x/(1-x)]_{ovhd}/[x/(1-x)]_{btms}\}/\log \alpha.$$

8. Minimum reflux for binary or pseudobinary mixtures is given by the following when separation is essentially complete ($x_D \simeq 1$) and D/F is the ratio of overhead product and feed rates:

$$R_m D/F = 1/(\alpha - 1), \quad \text{when feed is at the bubblepoint,}$$
$$(R_m + 1)D/F = \alpha/(\alpha - 1), \quad \text{when feed is at the dewpoint.}$$

9. A safety factor of 10% of the number of trays calculated by the best means is advisable.
10. Reflux pumps are made at least 25% oversize.
11. For reasons of accessibility, tray spacings are made 20–24 in.
12. Peak efficiency of trays is at values of the vapor factor $F_s = u\sqrt{\rho_v}$ in the range 1.0–1.2 (ft/sec) $\sqrt{\text{lb/cuft}}$. This range of F_s establishes the diameter of the tower. Roughly, linear velocities are 2 ft/sec at moderate pressures and 6 ft/sec in vacuum.
13. The optimum value of the Kremser–Brown absorption factor $A = K(V/L)$ is in the range 1.25–2.0.
14. Pressure drop per tray is of the order of 3 in. of water or 0.1 psi.
15. Tray efficiencies for distillation of light hydrocarbons and aqueous solutions are 60–90%; for gas absorption and stripping, 10–20%.
16. Sieve trays have holes 0.25–0.50 in. dia, hole area being 10% of the active cross section.
17. Valve trays have holes 1.5 in. dia each provided with a liftable cap, 12–14 caps/sqft of active cross section. Valve trays usually are cheaper than sieve trays.
18. Bubblecap trays are used only when a liquid level must be maintained at low turndown ratio; they can be designed for lower pressure drop than either sieve or valve trays.
19. Weir heights are 2 in., weir lengths about 75% of tray diameter, liquid rate a maximum of about 8 gpm/in. of weir; multipass arrangements are used at high liquid rates.
20. Packings of random and structured character are suited especially to towers under 3 ft dia and where low pressure drop is desirable. With proper initial distribution and periodic redistribution, volumetric efficiencies can be made greater than those

of tray towers. Packed internals are used as replacements for achieving greater throughput or separation in existing tower shells.

21. For gas rates of 500 cfm, use 1 in. packing; for gas rates of 2000 cfm or more, use 2 in.

22. The ratio of diameters of tower and packing should be at least 15.

23. Because of deformability, plastic packing is limited to a 10–15 ft depth unsupported, metal to 20–25 ft.

24. Liquid redistributors are needed every 5–10 tower diameters with pall rings but at least every 20 ft. The number of liquid streams should be 3–5/sqft in towers larger than 3 ft dia (some experts say 9–12/sqft), and more numerous in smaller towers.

25. Height equivalent to a theoretical plate (HETP) for vapor–liquid contacting is 1.3–1.8 ft for 1 in. pall rings, 2.5–3.0 ft for 2 in. pall rings.

26. Packed towers should operate near 70% of the flooding rate given by the correlation of Sherwood, Lobo, et al.

27. Reflux drums usually are horizontal, with a liquid holdup of 5 min half full. A takeoff pot for a second liquid phase, such as water in hydrocarbon systems, is sized for a linear velocity of that phase of 0.5 ft/sec, minimum diameter of 16 in.

28. For towers about 3 ft dia, add 4 ft at the top for vapor disengagement and 6 ft at the bottom for liquid level and reboiler return.

29. Limit the tower height to about 175 ft max because of wind load and foundation considerations. An additional criterion is that L/D be less than 30.

DRIVERS AND POWER RECOVERY EQUIPMENT

1. Efficiency is greater for larger machines. Motors are 85–95%; steam turbines are 42–78%; gas engines and turbines are 28–38%.

2. For under 100 HP, electric motors are used almost exclusively. They are made for up to 20,000 HP.

3. Induction motors are most popular. Synchronous motors are made for speeds as low as 150 rpm and are thus suited for example for low speed reciprocating compressors, but are not made smaller than 50 HP. A variety of enclosures is available, from weather-proof to explosion-proof.

4. Steam turbines are competitive above 100 HP. They are speed controllable. Frequently they are employed as spares in case of power failure.

5. Combustion engines and turbines are restricted to mobile and remote locations.

6. Gas expanders for power recovery may be justified at capacities of several hundred HP; otherwise any needed pressure reduction in process is effected with throttling valves.

DRYING OF SOLIDS

1. Drying times range from a few seconds in spray dryers to 1 hr or less in rotary dryers and up to several hours or even several days in tunnel shelf or belt dryers.

2. Continuous tray and belt dryers for granular material of natural size or pelleted to 3–15 mm have drying times in the range of 10–200 min.

3. Rotary cylindrical dryers operate with superficial air velocities of 5–10 ft/sec, sometimes up to 35 ft/sec when the material is coarse. Residence times are 5–90 min. Holdup of solid is 7–8%. An 85% free cross section is taken for design purposes. In countercurrent flow, the exit gas is 10–20°C above the solid; in parallel flow, the temperature of the exit solid is 100°C.

Rotation speeds of about 4 rpm are used, but the product of rpm and diameter in feet is typically between 15 and 25.

4. Drum dryers for pastes and slurries operate with contact times of 3–12 sec, produce flakes 1–3 mm thick with evaporation rates of 15–30 kg/m² hr. Diameters are 1.5–5.0 ft; the rotation rate is 2–10 rpm. The greatest evaporative capacity is of the order of 3000 lb/hr in commercial units.

5. Pneumatic conveying dryers normally take particles 1–3 mm dia but up to 10 mm when the moisture is mostly on the surface. Air velocities are 10–30 m/sec. Single pass residence times are 0.5–3.0 sec but with normal recycling the average residence time is brought up to 60 sec. Units in use range from 0.2 m dia by 1 m high to 0.3 m dia by 38 m long. Air requirement is several SCFM/lb of dry product/hr.

6. Fluidized bed dryers work best on particles of a few tenths of a mm dia, but up to 4 mm dia have been processed. Gas velocities of twice the minimum fluidization velocity are a safe prescription. In continuous operation, drying times of 1–2 min are enough, but batch drying of some pharmaceutical products employs drying times of 2–3 hr.

7. Spray dryers: Surface moisture is removed in about 5 sec, and most drying is completed in less than 60 sec. Parallel flow of air and stock is most common. Atomizing nozzles have openings 0.012–0.15 in. and operate at pressures of 300–4000 psi. Atomizing spray wheels rotate at speeds to 20,000 rpm with peripheral speeds of 250–600 ft/sec. With nozzles, the length to diameter ratio of the dryer is 4–5; with spray wheels, the ratio is 0.5–1.0. For the final design, the experts say, pilot tests in a unit of 2 m dia should be made.

EVAPORATORS

1. Long tube vertical evaporators with either natural or forced circulation are most popular. Tubes are 19–63 mm dia and 12–30 ft long.

2. In forced circulation, linear velocities in the tubes are 15–20 ft/sec.

3. Elevation of boiling point by dissolved solids results in differences of 3–10°F between solution and saturated vapor.

4. When the boiling point rise is appreciable, the economic number of effects in series with forward feed is 4–6.

5. When the boiling point rise is small, minimum cost is obtained with 8–10 effects in series.

6. In backward feed the more concentrated solution is heated with the highest temperature steam so that heating surface is lessened, but the solution must be pumped between stages.

7. The steam economy of an N-stage battery is approximately $0.8N$ lb evaporation/lb of outside steam.

8. Interstage steam pressures can be boosted with steam jet compressors of 20–30% efficiency or with mechanical compressors of 70–75% efficiency.

EXTRACTION, LIQUID–LIQUID

1. The dispersed phase should be the one that has the higher volumetric rate except in equipment subject to backmixing where it should be the one with the smaller volumetric rate. It should be the phase that wets the material of construction less well. Since the holdup of continuous phase usually is greater, that phase should be made up of the less expensive or less hazardous material.

2. There are no known commercial applications of reflux to extraction processes, although the theory is favorable (Treybal).

3. Mixer–settler arrangements are limited to at most five stages. Mixing is accomplished with rotating impellers or circulating

pumps. Settlers are designed on the assumption that droplet sizes are about 150 μm dia. In open vessels, residence times of 30–60 min or superficial velocities of 0.5–1.5 ft/min are provided in settlers. Extraction stage efficiencies commonly are taken as 80%.

4. Spray towers even 20–40 ft high cannot be depended on to function as more than a single stage.

5. Packed towers are employed when 5–10 stages suffice. Pall rings of 1–1.5 in. size are best. Dispersed phase loadings should not exceed 25 gal/(min) (sqft). HETS of 5–10 ft may be realizable. The dispersed phase must be redistributed every 5–7 ft. Packed towers are not satisfactory when the surface tension is more than 10 dyn/cm.

6. Sieve tray towers have holes of only 3–8 mm dia. Velocities through the holes are kept below 0.8 ft/sec to avoid formation of small drops. Redispersion of either phase at each tray can be designed for. Tray spacings are 6–24 in. Tray efficiencies are in the range of 20–30%.

7. Pulsed packed and sieve tray towers may operate at frequencies of 90 cycles/min and amplitudes of 6–25 mm. In large diameter towers, HETS of about 1 m has been observed. Surface tensions as high as 30–40 dyn/cm have no adverse effect.

8. Reciprocating tray towers can have holes 9/16 in. dia, 50–60% open area, stroke length 0.75 in. , 100–150 strokes/min, plate spacing normally 2 in. but in the range 1–6 in. In a 30 in. dia tower, HETS is 20–25 in. and throughput is 2000 gal/(hr)(sqft). Power requirements are much less than of pulsed towers.

9. Rotating disk contactors or other rotary agitated towers realize HETS in the range 0.1–0.5 m. The especially efficient Kuhni with perforated disks of 40% free cross section has HETS 0.2 m and a capacity of 50 m³/m² hr.

FILTRATION

1. Processes are classified by their rate of cake buildup in a laboratory vacuum leaf filter: rapid, 0.1–10.0 cm/sec; medium, 0.1–10.0 cm/min; slow, 0.1–10.0 cm/hr.

2. Continuous filtration should not be attempted if 1/8 in. cake thickness cannot be formed in less than 5 min.

3. Rapid filtering is accomplished with belts, top feed drums, or pusher-type centrifuges.

4. Medium rate filtering is accomplished with vacuum drums or disks or peeler-type centrifuges.

5. Slow filtering slurries are handled in pressure filters or sedimenting centrifuges.

6. Clarification with negligible cake buildup is accomplished with cartridges, precoat drums, or sand filters.

7. Laboratory tests are advisable when the filtering surface is expected to be more than a few square meters, when cake washing is critical, when cake drying may be a problem, or when precoating may be needed.

8. For finely ground ores and minerals, rotary drum filtration rates may be 1500 lb/(day)(sqft), at 20 rev/hr and 18–25 in. Hg vacuum.

9. Coarse solids and crystals may be filtered at rates of 6000 lb/(day)(sqft) at 20 rev/hr, 2–6 in. Hg vacuum.

FLUIDIZATION OF PARTICLES WITH GASES

1. Properties of particles that are conducive to smooth fluidization include: rounded or smooth shape, enough toughness to resist attrition, sizes in the range 50–500 μm dia, a spectrum of sizes with ratio of largest to smallest in the range of 10–25.

2. Cracking catalysts are members of a broad class characterized by diameters of 30–150 μm, density of 1.5 g/mL or so, appre-

ciable expansion of the bed before fluidization sets in, minimum bubbling velocity greater than minimum fluidizing velocity, and rapid disengagement of bubbles.

3. The other extreme of smoothly fluidizing particles is typified by coarse sand and glass beads both of which have been the subject of much laboratory investigation. Their sizes are in the range 150–500 μm, densities 1.5–4.0 g/mL, small bed expansion, about the same magnitudes of minimum bubbling and minimum fluidizing velocities, and also have rapidly disengaging bubbles.

4. Cohesive particles and large particles of 1 mm or more do not fluidize well and usually are processed in other ways.

5. Rough correlations have been made of minimum fluidization velocity, minimum bubbling velocity, bed expansion, bed level fluctuation, and disengaging height. Experts recommend, however, that any real design be based on pilot plant work.

6. Practical operations are conducted at two or more multiples of the minimum fluidizing velocity. In reactors, the entrained material is recovered with cyclones and returned to process. In dryers, the fine particles dry most quickly so the entrained material need not be recycled.

HEAT EXCHANGERS

1. Take true countercurrent flow in a shell-and-tube exchanger as a basis.

2. Standard tubes are 3/4 in. OD, 1 in. triangular spacing, 16 ft long; a shell 1 ft dia accommodates 100 sqft; 2 ft dia, 400 sqft, 3 ft dia, 1100 sqft.

3. Tube side is for corrosive, fouling, scaling, and high pressure fluids.

4. Shell side is for viscous and condensing fluids.

5. Pressure drops are 1.5 psi for boiling and 3–9 psi for other services.

6. Minimum temperature approach is 20°F with normal coolants, 10°F or less with refrigerants.

7. Water inlet temperature is 90°F, maximum outlet 120°F.

8. Heat transfer coefficients for estimating purposes, Btu/(hr)(sqft)(°F): water to liquid, 150; condensers, 150; liquid to liquid, 50; liquid to gas, 5; gas to gas, 5; reboiler, 200. Max flux in reboilers, 10,000 Btu/(hr)(sqft).

9. Double-pipe exchanger is competitive at duties requiring 100–200 sqft.

10. Compact (plate and fin) exchangers have 350 sqft/cuft, and about 4 times the heat transfer per cuft of shell-and-tube units.

11. Plate and frame exchangers are suited to high sanitation services, and are 25–50% cheaper in stainless construction than shell-and-tube units.

12. Air coolers: Tubes are 0.75–1.00 in. OD, total finned surface 15–20 sqft/sqft bare surface, $U = 80$–100 Btu/(hr)(sqft bare surface)(°F), fan power input 2–5 HP/(MBtu/hr), approach 50°F or more.

13. Fired heaters: radiant rate, 12,000 Btu/(hr)(sqft); convection rate, 4000; cold oil tube velocity, 6 ft/sec; approx equal transfers of heat in the two sections; thermal efficiency 70–75%; flue gas temperature 250–350°F above feed inlet; stack gas temperature 650–950°F.

INSULATION

1. Up to 650°F, 85% magnesia is most used.

2. Up to 1600–1900°F, a mixture of asbestos and diatomaceous earth is used.

3. Ceramic refractories at higher temperatures.

4. Cryogenic equipment (−200°F) employs insulants with fine pores in which air is trapped.

5. Optimum thickness varies with temperature: 0.5 in. at 200°F, 1.0 in. at 400°F, 1.25 in. at 600°F.

6. Under windy conditions (7.5 miles/hr), 10–20% greater thickness of insulation is justified.

MIXING AND AGITATION

1. Mild agitation is obtained by circulating the liquid with an impeller at superficial velocities of 0.1–0.2 ft/sec, and intense agitation at 0.7–1.0 ft/sec.

2. Intensities of agitation with impellers in baffled tanks are measured by power input, HP/1000 gal, and impeller tip speeds:

Operation	HP/1000 gal	Tip speed (ft/min)
Blending	0.2–0.5	
Homogeneous reaction	0.5–1.5	7.5–10
Reaction with heat transfer	1.5–5.0	10–15
Liquid–liquid mixtures	5	15–20
Liquid–gas mixtures	5–10	15–20
Slurries	10	

3. Proportions of a stirred tank relative to the diameter D: liquid level $= D$; turbine impeller diameter $= D/3$; impeller level above bottom $= D/3$; impeller blade width $= D/15$; four vertical baffles with width $= D/10$.

4. Propellers are made a maximum of 18 in., turbine impellers to 9 ft.

5. Gas bubbles sparged at the bottom of the vessel will result in mild agitation at a superficial gas velocity of 1 ft/min, severe agitation at 4 ft/min.

6. Suspension of solids with a settling velocity of 0.03 ft/sec is accomplished with either turbine or propeller impellers, but when the settling velocity is above 0.15 ft/sec intense agitation with a propeller is needed.

7. Power to drive a mixture of a gas and a liquid can be 25–50% less than the power to drive the liquid alone.

8. In-line blenders are adequate when a second or two contact time is sufficient, with power inputs of 0.1–0.2 HP/gal.

PARTICLE SIZE ENLARGEMENT

1. The chief methods of particle size enlargement are: compression into a mold, extrusion through a die followed by cutting or breaking to size, globulation of molten material followed by solidification, agglomeration under tumbling or otherwise agitated conditions with or without binding agents.

2. Rotating drum granulators have length to diameter ratios of 2–3, speeds of 10–20 rpm, pitch as much as 10°. Size is controlled by speed, residence time, and amount of binder; 2–5 mm dia is common.

3. Rotary disk granulators produce a more nearly uniform product than drum granulators. Fertilizer is made 1.5–3.5 mm; iron ore 10–25 mm dia.

4. Roll compacting and briquetting is done with rolls ranging from 130 mm dia by 50 mm wide to 910 mm dia by 550 mm wide. Extrudates are made 1–10 mm thick and are broken down to size for any needed processing such as feed to tabletting machines or to dryers.

5. Tablets are made in rotary compression machines that convert powders and granules into uniform sizes. Usual maximum diameter is about 1.5 in., but special sizes up to 4 in. dia are possible. Machines operate at 100 rpm or so and make up to 10,000 tablets/min.

6. Extruders make pellets by forcing powders, pastes, and melts through a die followed by cutting. An 8 in. screw has a capacity of 2000 lb/hr of molten plastic and is able to extrude tubing at 150–300 ft/min and to cut it into sizes as small as washers at 8000/min. Ring pellet extrusion mills have hole diameters of 1.6–32 mm. Production rates cover a range of 30–200 lb/(hr)(HP).

7. Prilling towers convert molten materials into droplets and allow them to solidify in contact with an air stream. Towers as high as 60 m are used. Economically the process becomes competitive with other granulation processes when a capacity of 200–400 tons/day is reached. Ammonium nitrate prills, for example, are 1.6–3.5 mm dia in the 5–95% range.

8. Fluidized bed granulation is conducted in shallow beds 12–24 in. deep at air velocities of 0.1–2.5 m/s or 3–10 times the minimum fluidizing velocity, with evaporation rates of 0.005–1.0 kg/m^{2}sec. One product has a size range 0.7–2.4 mm dia.

PIPING

1. Line velocities and pressure drops, with line diameter D in inches: liquid pump discharge, $(5 + D/3)$ ft/sec, 2.0 psi/100 ft; liquid pump suction, $(1.3 + D/6)$ ft/sec, 0.4 psi/100 ft; steam or gas, $20D$ ft/sec, 0.5 psi/100 ft.

2. Control valves require at least 10 psi drop for good control.

3. Globe valves are used for gases, for control and wherever tight shutoff is required. Gate valves are for most other services.

4. Screwed fittings are used only on sizes 1.5 in. and smaller, flanges or welding otherwise.

5. Flanges and fittings are rated for 150, 300, 600, 900, 1500, or 2500 psig.

6. Pipe schedule number $= 1000P/S$, approximately, where P is the internal pressure psig and S is the allowable working stress (about 10,000 psi for A120 carbon steel at 500°F). Schedule 40 is most common.

PUMPS

1. Power for pumping liquids: HP = (gpm)(psi difference)/(1714) (fractional efficiency).

2. Normal pump suction head (NPSH) of a pump must be in excess of a certain number, depending on the kind of pumps and the conditions, if damage is to be avoided. NPSH = (pressure at the eye of the impeller – vapor pressure)/(density). Common range is 4–20 ft.

3. Specific speed $N_s = $ (rpm)(gpm)$^{0.5}$/(head in ft)$^{0.75}$. Pump may be damaged if certain limits of N_s are exceeded, and efficiency is best in some ranges.

4. Centrifugal pumps: Single stage for 15–5000 gpm, 500 ft max head; multistage for 20–11,000 gpm, 5500 ft max head. Efficiency 45% at 100 gpm, 70% at 500 gpm, 80% at 10,000 gpm.

5. Axial pumps for 20–100,000 gpm, 40 ft head, 65–85% efficiency.

6. Rotary pumps for 1–5000 gpm, 50,000 ft head, 50–80% efficiency.

7. Reciprocating pumps for 10–10,000 gpm, 1,000,000 ft head max. Efficiency 70% at 10 HP, 85% at 50 HP, 90% at 500 HP.

REACTORS

1. The rate of reaction in every instance must be established in the laboratory, and the residence time or space velocity and product distribution eventually must be found in a pilot plant.

2. Dimensions of catalyst particles are 0.1 mm in fluidized beds, 1 mm in slurry beds, and 2–5 mm in fixed beds.

3. The optimum proportions of stirred tank reactors are with liquid level equal to the tank diameter, but at high pressures slimmer proportions are economical.
4. Power input to a homogeneous reaction stirred tank is 0.5–1.5 HP/1000 gal, but three times this amount when heat is to be transferred.
5. Ideal CSTR (continuous stirred tank reactor) behavior is approached when the mean residence time is 5–10 times the length of time needed to achieve homogeneity, which is accomplished with 500–2000 revolutions of a properly designed stirrer.
6. Batch reactions are conducted in stirred tanks for small daily production rates or when the reaction times are long or when some condition such as feed rate or temperature must be programmed in some way.
7. Relatively slow reactions of liquids and slurries are conducted in continuous stirred tanks. A battery of four or five in series is most economical.
8. Tubular flow reactors are suited to high production rates at short residence times (sec or min) and when substantial heat transfer is needed. Embedded tubes or shell-and-tube construction then are used.
9. In granular catalyst packed reactors, the residence time distribution often is no better than that of a five-stage CSTR battery.
10. For conversions under about 95% of equilibrium, the performance of a five-stage CSTR battery approaches plug flow.

REFRIGERATION

1. A ton of refrigeration is the removal of 12,000 Btu/hr of heat.
2. At various temperature levels: 0–50°F, chilled brine and glycol solutions; −50–40°F, ammonia, freons, butane; −150–−50°F, ethane or propane.
3. Compression refrigeration with 100°F condenser requires these HP/ton at various temperature levels: 1.24 at 20°F; 1.75 at 0°F; 3.1 at −40°F; 5.2 at −80°F.
4. Below −80°F, cascades of two or three refrigerants are used.
5. In single stage compression, the compression ratio is limited to about 4.
6. In multistage compression, economy is improved with interstage flashing and recycling, so-called economizer operation.
7. Absorption refrigeration (ammonia to −30°F, lithium bromide to +45°F) is economical when waste steam is available at 12 psig or so.

SIZE SEPARATION OF PARTICLES

1. Grizzlies that are constructed of parallel bars at appropriate spacings are used to remove products larger than 5 cm dia.
2. Revolving cylindrical screens rotate at 15–20 rpm and below the critical velocity; they are suitable for wet or dry screening in the range of 10–60 mm.
3. Flat screens are vibrated or shaken or impacted with bouncing balls. Inclined screens vibrate at 600–7000 strokes/min and are used for down to 38 μm although capacity drops off sharply below 200 μm. Reciprocating screens operate in the range 30–1000 strokes/min and handle sizes down to 0.25 mm at the higher speeds.
4. Rotary sifters operate at 500–600 rpm and are suited to a range of 12 mm to 50 μm.
5. Air classification is preferred for fine sizes because screens of 150 mesh and finer are fragile and slow.
6. Wet classifiers mostly are used to make two product size ranges, oversize and undersize, with a break commonly in the range between 28 and 200 mesh. A rake classifier operates at about 9 strokes/min when making separation at 200 mesh, and 32 strokes/min at 28 mesh. Solids content is not critical, and that of the overflow may be 2–20% or more.
7. Hydrocyclones handle up to 600 cuft/min and can remove particles in the range of 300–5 μm from dilute suspensions. In one case, a 20 in. dia unit had a capacity of 1000 gpm with a pressure drop of 5 psi and a cutoff between 50 and 150 μm.

UTILITIES: COMMON SPECIFICATIONS

1. Steam: 15–30 psig, 250–275°F; 150 psig, 366°F; 400 psig, 448°F; 600 psig, 488°F or with 100–150°F superheat.
2. Cooling water: Supply at 80–90°F from cooling tower, return at 115–125°F; return seawater at 110°F, return tempered water or steam condensate above 125°F.
3. Cooling air supply at 85–95°F; temperature approach to process, 40°F.
4. Compressed air at 45, 150, 300, or 450 psig levels.
5. Instrument air at 45 psig, 0°F dewpoint.
6. Fuels: gas of 1000 Btu/SCF at 5–10 psig, or up to 25 psig for some types of burners; liquid at 6 million Btu/barrel.
7. Heat transfer fluids: petroleum oils below 600°F, Dowtherms below 750°F, fused salts below 1100°F, direct fire or electricity above 450°F.
8. Electricity: 1–100 Hp, 220–550 V; 200–2500 Hp, 2300–4000 V.

VESSELS (DRUMS)

1. Drums are relatively small vessels to provide surge capacity or separation of entrained phases.
2. Liquid drums usually are horizontal.
3. Gas/liquid separators are vertical.
4. Optimum length/diameter = 3, but a range of 2.5–5.0 is common.
5. Holdup time is 5 min half full for reflux drums, 5–10 min for a product feeding another tower.
6. In drums feeding a furnace, 30 min half full is allowed.
7. Knockout drums ahead of compressors should hold no less than 10 times the liquid volume passing through per minute.
8. Liquid/liquid separators are designed for settling velocity of 2–3 in./min.
9. Gas velocity in gas/liquid separators, $V = k\sqrt{\rho_L/\rho_v - 1}$ ft/sec, with $k = 0.35$ with mesh deentrainer, $k = 0.1$ without mesh deentrainer.
10. Entrainment removal of 99% is attained with mesh pads of 4–12 in. thicknesses; 6 in. thickness is popular.
11. For vertical pads, the value of the coefficient in Step 9 is reduced by a factor of 2/3.
12. Good performance can be expected at velocities of 30–100% of those calculated with the given k; 75% is popular.
13. Disengaging spaces of 6–18 in. ahead of the pad and 12 in. above the pad are suitable.
14. Cyclone separators can be designed for 95% collection of 5 μm particles, but usually only droplets greater than 50 μm need be removed.

VESSELS (PRESSURE)

1. Design temperature between −20°F and 650°F is 50°F above operating temperature; higher safety margins are used outside the given temperature range.
2. The design pressure is 10% or 10–25 psi over the maximum operating pressure, whichever is greater. The maximum operating pressure, in turn, is taken as 25 psi above the normal operation.

3. Design pressures of vessels operating at 0–10 psig and 600–1000°F are 40 psig.
4. For vacuum operation, design pressures are 15 psig and full vacuum.
5. Minimum wall thicknesses for rigidity: 0.25 in. for 42 in. dia and under, 0.32 in. for 42–60 in. dia, and 0.38 in. for over 60 in. dia.
6. Corrosion allowance 0.35 in. for known corrosive conditions, 0.15 in. for non-corrosive streams, and 0.06 in. for steam drums and air receivers.
7. Allowable working stresses are one-fourth of the ultimate strength of the material.
8. Maximum allowable stress depends sharply on temperature.

Temperature (°F)	−20–650	750	850	1000
Low alloy steel SA203 (psi)	18,750	15,650	9550	2500
Type 302 stainless (psi)	18,750	18,750	15,900	6250

VESSELS (STORAGE TANKS)

1. For less than 1000 gal, use vertical tanks on legs.
2. Between 1000 and 10,000 gal, use horizontal tanks on concrete supports.
3. Beyond 10,000 gal, use vertical tanks on concrete foundations.
4. Liquids subject to breathing losses may be stored in tanks with floating or expansion roofs for conservation.
5. Freeboard is 15% below 500 gal and 10% above 500 gal capacity.

6. Thirty days capacity often is specified for raw materials and products, but depends on connecting transportation equipment schedules.
7. Capacities of storage tanks are at least 1.5 times the size of connecting transportation equipment; for instance, 7500 gal tank trucks, 34,500 gal tank cars, and virtually unlimited barge and tanker capacities.

REFERENCE

S.M. Walas, *Chemical Process Equipment: Selection and Design*, Butterworth-Heinemann, Woburn, MA, 1988.

BIBLIOGRAPHY

The following are additional sources for rules of thumb:

C.R. Branan, *Rules of Thumb for Chemical Engineers*, 3rd ed., Elsevier Science, St. Louis, MO, 2002.
W.J. Korchinski and L.E. Turpin, *Hydrocarbon Processing*, 129–133 (January 1966).
G.D. Ulrich, *A Guide to Chemical Engineering Process Design and Economics*, Wiley, New York, 1984.
D.R. Woods, *Process Design and Engineering Practice*, PTR Prentice-Hall, Englewood Cliffs, NJ, 1995.

1

INTRODUCTION

*A*lthough this book is devoted to the selection and design of individual equipment, some mention should be made of integration of a number of units into a process. Each piece of equipment interacts with several others in a plant, and the range of its required performance is dependent on the others in terms of material and energy balances and rate processes. This chapter will discuss general background material relating to complete process design, and Chapter 2 will treat briefly the basic topic of flowsheets.

1.1. PROCESS DESIGN

Process design establishes the sequence of chemical and physical operations; operating conditions; the duties, major specifications, and materials of construction (where critical) of all process equipment (as distinguished from utilities and building auxiliaries); the general arrangement of equipment needed to ensure proper functioning of the plant; line sizes; and principal instrumentation. The process design is summarized by a process flowsheet, a material and energy balance, and a set of individual equipment specifications. Varying degrees of thoroughness of a process design may be required for different purposes. Sometimes only a preliminary design and cost estimate are needed to evaluate the advisability of further research on a new process or a proposed plant expansion or detailed design work; or a preliminary design may be needed to establish the approximate funding for a complete design and construction. A particularly valuable function of preliminary design is that it may reveal lack of certain data needed for final design. Data of costs of individual equipment are supplied in this book, but the complete economics of process design is beyond its scope.

1.2. EQUIPMENT

Two main categories of process equipment are proprietary and custom-designed. Proprietary equipment is designed by the manufacturer to meet performance specifications made by the user; these specifications may be regarded as the process design of the equipment. This category includes equipment with moving parts such as pumps, compressors, and drivers as well as cooling towers, dryers, filters, mixers, agitators, piping equipment, and valves, and even the structural aspects of heat exchangers, furnaces, and other equipment. Custom design is needed for many aspects of chemical reactors, most vessels, multistage separators such as fractionators, and other special equipment not amenable to complete standardization.

Only those characteristics of equipment are specified by process design that are significant from the process point of view. On a pump, for instance, process design will specify the operating conditions, capacity, pressure differential, NPSH, materials of construction in contact with process liquid, and a few other items, but not such details as the wall thickness of the casing or the type of stuffing box or the nozzle sizes and the foundation dimensions—although most of these omitted items eventually must be known before a plant is ready for construction. Standard specification forms are available for most proprietary kinds of equipment and for summarizing the details of all kinds of equipment. By providing suitable checklists, they simplify the work by ensuring that all needed data have been provided. A collection of such forms is in Appendix B.

Proprietary equipment is provided "off the shelf" in limited sizes and capacities. Special sizes that would fit particular applications more closely often are more expensive than a larger standard size that incidentally may provide a worthwhile safety factor. Even largely custom-designed equipment, such as vessels, is subject to standardization such as discrete ranges of head diameters, pressure ratings of nozzles, sizes of manways, and kinds of trays and packings. Many codes and standards are established by government agencies, insurance companies, and organizations sponsored by engineering societies. Some standardizations within individual plants are arbitrary choices made to simplify construction, maintenance, and repair, and to reduce inventory of spare parts: for example, limiting the sizes of heat exchanger tubing and pipe sizes, standardization of centrifugal pumps, and restriction of process control equipment to a particular manufacturer. There are instances when restrictions must be relaxed for the engineer to accommodate a design.

VENDORS' QUESTIONNAIRES

A manufacturer's or vendor's inquiry form is a questionnaire whose completion will give him the information on which to base a specific recommendation of equipment and a price. General information about the process in which the proposed equipment is expected to function, amounts and appropriate properties of the streams involved, and the required performance are basic. The nature of additional information varies from case to case; for instance, being different for filters than for pneumatic conveyors. Individual suppliers have specific inquiry forms. A representative selection is in Appendix C.

SPECIFICATION FORMS

When completed, a specification form is a record of the salient features of the equipment, the conditions under which it is to operate, and its guaranteed performance. Usually it is the basis for a firm price quotation. Some of these forms are made up by organizations such as TEMA or API, but all large engineering contractors and many large operating companies have other forms for their own needs. A selection of specification forms is in Appendix B.

1.3. CATEGORIES OF ENGINEERING PRACTICE

Although the design of a chemical process plant is initiated by chemical engineers, its complete design and construction requires the inputs of other specialists: mechanical, structural, electrical, and instrumentation engineers; vessel and piping designers; and purchasing agents who know what may be available at attractive prices. On large projects all these activities are correlated by a project manager; on individual items of equipment or small projects, the process engineer naturally assumes this function. A key activity is the writing of specifications for soliciting bids and ultimately purchasing equipment. Specifications must be written so explicitly that the bidders are held to a uniform standard and a clear-cut choice can be made on the basis of their offerings alone.

For a typical project, Figures 1.1 and 1.2 are generally the shape of the curves. Note that in Figure 1.1, engineering begins early so that critical material (e.g., special alloys) can be committed for the project. Figure 1.2 shows that, in terms of total engineering effort, process engineering is a small part.

In terms of total project cost, the cost of engineering is a small part, ranging from 5 to 20% of the total plant cost. The lower figure is for large plants that are essentially copies of ones built before, while the higher figure is for small plants or those employing new technology, unusual processing conditions, and specifications.

1.4. SOURCES OF INFORMATION FOR PROCESS DESIGN

A selection of books relating to process design methods and data is listed in the references at the end of this chapter. Items that are especially desirable in a personal library or readily accessible are identified. Specialized references are given throughout the book in connection with specific topics.

The extensive chemical literature is served by the items cited in References. The book by Leesley (References, Section B) has much information about proprietary data banks and design methods. In its current and earlier editions, the book by Peters and Timmerhaus has many useful bibliographies on various topics.

For general information about chemical manufacturing processes, the major encyclopedic references are Kirk-Othmer (1978–1984) (1999), McKetta (1992), McKetta and Cunningham (1976), and Ullman (1994) in Reference Section 1.2, Part A, as well as Kent (1992) in Reference Section 1.2, Part B.

Extensive physical property and thermodynamic data are available throughout the literature. Two such compilations are found in the DECHEMA publications (1977) and the Design Institute for Physical Property Research (DIPPR) (1985). DECHEMA is an extensive series (11 volumes) of physical property and thermodynamic data. Some of the earlier volumes were published in the 1980s but there are numerous supplements to update the data. The main purpose of the DECHEMA publication is to provide chemists and chemical engineers with data for process design and development. DIPPR, published by AIChE, is a series of volumes on physical properties. The references to these publications are found in References, Section 1.2, Part C. The American Petroleum Institute (API) published data and methods for estimating properties of hydrocarbons and their mixtures, called the API Data Book. Earlier compilations include Landolt-Bornstein work, started in 1950 but has been updated. The later editions are in English. There are many compilations of special property data, such as solubilities, vapor pressures, phase equilibria, transport, and thermal properties. A few of these are listed in References, Section 1.2, Parts B and C. Still other references of interest may be found in References, Section C.

Information about equipment sizes, configurations, and sometimes performance is best found in manufacturers' catalogs and manufacturers' web sites, and from advertisements in the journal literature, such as *Chemical Engineering* and *Hydrocarbon Processing*. In References, Section 1.1, Part D also contains information that may be of value. Thomas Register covers all manufacturers and so is less convenient for an initial search. Item 2 of References, Section 1.1, Part D, is of value in the listing of manufacturers by the kind of equipment. Manufacturers' catalogs and web site information often have illustrations and descriptions of chemical process equipment.
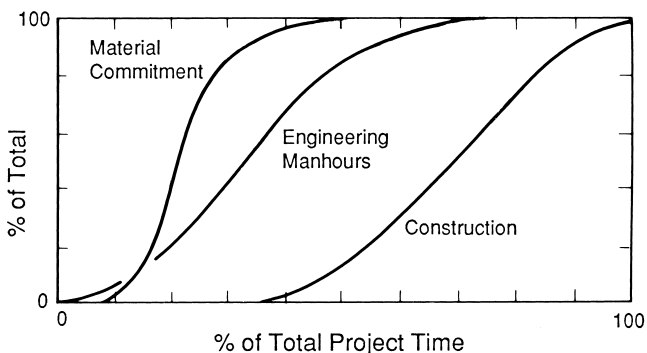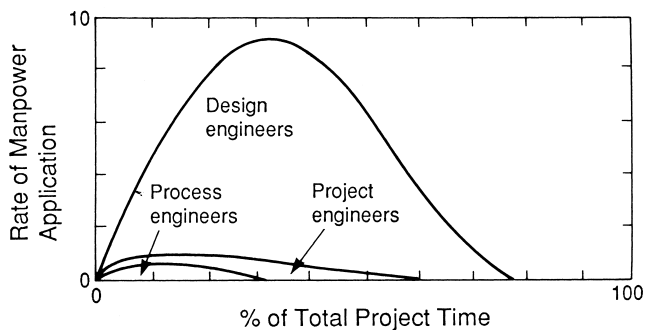
1.5. CODES, STANDARDS, AND RECOMMENDED PRACTICES

A large body of rules has been developed over the years to ensure the safe and economical design, fabrication and testing of equipment, structures, and materials. Codification of these rules has been done by associations organized for just such purposes, by professional societies, trade groups, insurance underwriting companies, and government agencies. Engineering contractors and large manufacturing companies usually maintain individual sets of standards so as to maintain continuity of design and to simplify maintenance of plant. In the first edition, Walas (1984) presented a table of approximately 500 distinct internal engineering standards that a large petroleum refinery found useful.

Typical of the many thousands of items that are standardized in the field of engineering are limitations on the sizes and wall thicknesses of piping, specifications of the compositions of alloys, stipulation of the safety factors applied to strengths of construction materials, testing procedures for many kinds of materials, and so on.

Although the safe design practices recommended by professional and trade associations have no legal standing where they have not actually been incorporated in a body of law, many of them have the respect and confidence of the engineering profession as a whole and have been accepted by insurance underwriters so they are widely observed. Even when they are only voluntary, standards constitute a digest of experience that represents a minimum requirement of good practice.

There are several publications devoted to standards of importance to the chemical industry. See Burklin (1982), References, Section 1.1, Part B. The National Bureau of Standards published an extensive list of U.S. standards through the NBS-SIS service (see Table 1.1). Information about foreign standards is available from the American National Standards Institute (ANSI) (see Table 1.1).

Figure 1.1. Typical timing of material, engineering manhours, and construction.

Figure 1.2. Rate of application of engineering manhours by engineering function: process engineering, project engineering, and design engineering.

A list of codes pertinent to the chemical industry is found in Table 1.1 and supplementary codes and standards in Table 1.2.

TABLE 1.1. Codes and Standards of Direct Bearing on Chemical Process Design (a Selection)

A. American Institute of Chemical Engineers, 345 E. 47th St., New York, NY 10017
  1. Standard testing procedures; 21 have been published, for example on centrifuges, filters, mixers, firer heaters
B. American Petroleum Institute, 2001 L St. NW, Washington, DC 20037
  2. Recommended practices for refinery inspections
  3. Guide for inspection of refinery equipment
  4. Manual on disposal of refinery wastes
  5. Recommended practice for design and construction of large, low pressure storage tanks
  6. Recommended practice for design and construction of pressure relieving devices
  7. Recommended practices for safety and fire protection
C. American Society of Mechanical Engineers, 345 W. 47th St., New York, NY 10017
  8. ASME Boiler and Pressure Vessel Code. Sec. VIII, Unfired Pressure Vessels
  9. Code for pressure piping
  10. Scheme for identification of piping systems
D. American Society for Testing Materials, 1916 Race St., Philadelphia, PA 19103
  11. ASTM Standards, 66 volumes in 16 sections, annual, with about 30% revision each year
E. American National Standards Institute (ANSI), 1430 Broadway, New York, NY 10018
  12. Abbreviations, letter symbols, graphical symbols, drawing and drafting room practice
F. Chemical Manufacturers' Association, 2501 M St. NW, Washington, DC 20037
  13. Manual of standard and recommended practices for containers, tank cars, pollution of air and water
  14. Chemical safety data sheets of individual chemicals
G. Cooling Tower Institute, 19627 Highway 45 N, Spring, TX 77388
  15. Acceptance test procedure for water cooling towers of mechanical draft industrial type
H. Hydraulic Institute, 712 Lakewood Center N, 14600 Detroit Ave., Cleveland, OH 44107
  16. Standards for centrifugal, reciprocating, and rotary pumps
  17. Pipe friction manual
I. Instrument Society of America (ISA), 67 Alexander Dr., Research Triangle Park, NC 27709
  18. Instrumentation flow plan symbols
  19. Specification forms for instruments
  20. Dynamic response testing of process control instrumentation
J. Tubular Exchangers Manufacturers' Association, 25 N Broadway, Tarrytown, NY 10591
  21. TEMA standards
K. International Standards Organization (ISO), 1430 Broadway, New York, NY 10018
  22. Many standards

TABLE 1.2. Codes and Standards Supplementary to Process Design (a Selection)

A. American Concrete Institute, 22400 W. 7 Mile Rd., Detroit, MI 48219
  1. Reinforced concrete design handbook
  2. Manual of standard practice for detailing reinforced concrete structures
B. American Institute of Steel Construction, 400 N. Michigan Ave., Chicago, IL 60611
  3. Manual of steel construction
  4. Standard practice for steel buildings and bridges
C. American Iron and Steel Institute, 1000 16th St. NW, Washington, DC 20036
  5. AISI standard steel compositions
D. American Society of Heating, Refrigerating and Air Conditioning Engineers (ASHRE), 1791 Tullie Circle NE, Atlanta, GA 30329
  6. Refrigerating data book
E. Institute of Electrical and Electronics Engineers, 345 E. 47th St., New York, NY 10017
  7. Many standards
F. National Bureau of Standards, Washington, DC
  8. American standard building code
  9. National electrical code
G. National Electrical Manufacturers Association, 2101 L St. NW, Washington, DC 20037
  10. NEMA standards

a bounded region called a system. Input and output quantities of an entity cross the boundaries. A source is an increase in the amount of the entity that occurs without crossing a boundary; for example, an increase in the sensible enthalpy or in the amount of a substance as a consequence of chemical reaction. Analogously, sinks are decreases without a boundary crossing, as the disappearance of water from a fluid stream by adsorption onto a solid phase within the boundary.

Accumulations are time rates of change of the amount of the entities within the boundary. For example, in the absence of sources and sinks, an accumulation occurs when the input and output rates are different. In the steady state, the accumulation is zero.

Although the principle of balancing is simple, its application requires knowledge of the performance of all the kinds of equipment comprising the system as well as the phase relations and physical properties of all mixtures that participate in the process. As a consequence of trying to cover a variety of equipment and processes, the books devoted to the subject of material and energy balances always run to several hundred pages. Throughout this book, material and energy balances are utilized in connection with the design of individual kinds of equipment and some processes. Cases involving individual items of equipment usually are relatively easy to balance, for example, the overall balance of a distillation column in Section 13.4 and of nonisothermal reactors of Tables 17.4–17.7. When a process is maintained isothermal, only a material balance is needed to describe the process, unless it is also required to know the net heat transfer for maintaining a constant temperature.

In most plant design situations of practical interest, however, the several items of equipment interact with each other, the output of one unit being the input to another that in turn may recycle part of its output to the input equipment. Common examples are an absorber-stripper combination in which the performance of the absorber depends on the quality of the absorbent being returned from the stripper, or a catalytic cracker–catalyst regenerator system whose two parts interact closely.

Because the performance of a particular item of equipment depends on its input, recycling of streams in a process introduces

1.6. MATERIAL AND ENERGY BALANCES

Material and energy balances are based on a conservation law which is stated generally in the form

input + source = output + sink + accumulation.

The individual terms can be plural and can be rates as well as absolute quantities. Balances of particular entities are made around

temporarily unknown, intermediate streams whose amounts, compositions, and properties must be found by calculation. For a plant with dozens or hundreds of streams the resulting mathematical problem is formidable and has led to the development of many computer algorithms for its solution, some of them making quite rough approximations, others more nearly exact. Usually the problem is solved more easily if the performance of the equipment is specified in advance and its size is found after the balances are completed. If the equipment is existing or must be limited in size, the balancing process will require simultaneous evaluation of its performance and consequently is a much more involved operation, but one which can be handled by computer when necessary.

The literature of this subject naturally is extensive. An early book (for this subject), Nagiev's *Theory of Recycle Processes in Chemical Engineering* (Macmillan, New York, 1964, Russian edition, 1958) treats many practical cases by reducing them to systems of linear algebraic equations that are readily solvable. The book by Westerberg et al., *Process Flowsheeting* (Cambridge Univ. Press, Cambridge, 1977) describes some aspects of the subject and has an extensive bibliography. Benedek in *Steady State Flowsheeting of Chemical Plants* (Elsevier, New York, 1980) provides a detailed description of one simulation system. Leesley in *Computer-Aided Process Design* (Gulf, Houston, 1982) describes the capabilities of some commercially available flowsheet simulation programs. Some of these incorporate economic balance with material and energy balances.

Process simulators are used as an aid in the formulation and solution of material and energy balances. The larger simulators can handle up to 40 components and 50 or more processing units when their outputs are specified. ASPEN, PROSYS, DESIGN II, and HYSIM are examples of such process simulators.

A key factor in the effective formulation of material and energy balances is a proper notation for equipment and streams. Figure 1.3, representing a reactor and a separator, utilizes a simple type. When the pieces of equipment are numbered i and j, the notation $A_{ij}^{(k)}$ signifies the flow rate of substance A in stream k proceeding from unit i to unit j. The total stream is designated
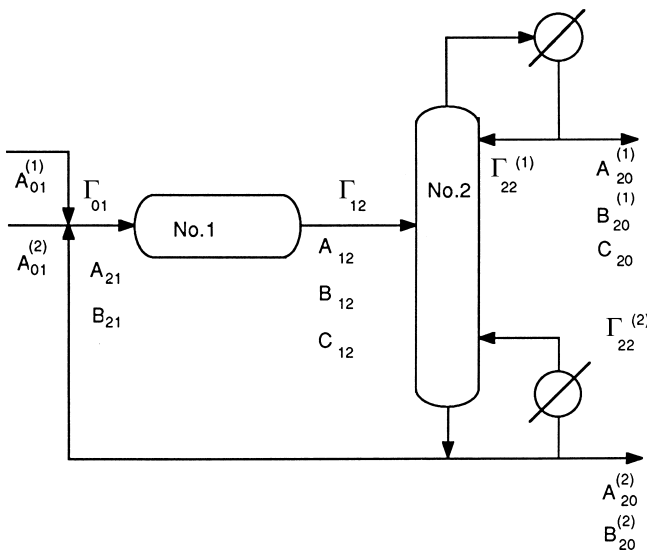
$\Gamma_{ij}^{(k)}$. Subscript t designates a total stream and subscript 0 designates sources or sinks outside the system. Example 1.1 adopts this notation for balancing a reactor–separator process in which the performances are specified in advance.

Since this book is concerned primarily with one kind of equipment at a time, all that need be done here is to call attention to the existence of the abundant literature on these topics of recycle calculations and flowsheet simulation.

1.7. ECONOMIC BALANCE

Engineering enterprises are subject to monetary considerations, and the objective is to achieve a balance between fixed and variable costs so that optimum operating conditions are met. In simple terms, the main components of fixed expenses are depreciation and plant indirect expenses. The latter consist of fire and safety protection, plant security, insurance premiums on plant and equipment, cafeteria and office building expenses, roads and docks, and the like. Variable operating expenses include utilities, labor, maintenance, supplies, and so on. Raw materials are also an operating expense. General overhead expenses beyond the plant gate are sales, administrative, research, and engineering overhead expenses not attributable to a specific project. Generally, as the capital cost of a processing unit increases, the operating expenses will decline. For example, an increase in the amount of automatic control equipment results in higher capital cost, which is offset by a decline in variable operating expenses. Somewhere in the summation of the fixed and variable operating expenses there is an economic balance where the total operating expenses are a minimum. In the absence of intangible factors, such as unusual local conditions or building for the future, this optimum should be the design point.

Costs of individual equipment items are summarized in Chapter 21 as of the end of the second quarter 2002. The analysis of costs for complete plants is beyond the scope of this book. References are made to several economic analyses that appear in the following publications:

1. AIChE Student Contest Problems (annual) (AIChE, New York).
2. Bodman, *Industrial Practice of Chemical Process Engineering* (MIT Press, Cambridge, MA, 1968).
3. Rase, *Chemical Reactor Design for Process Plants, Vol. II, Case Studies* (Wiley, New York, 1977).
4. Washington University, St. Louis, *Case Studies in Chemical Engineering Design* (22 cases to 1984).

Somewhat broader in scope are:

5. Couper et al., *The Chemical Process Industries Infrastructure: Function and Economics* (Dekker, New York, 2001).
6. Skinner et al., *Manufacturing Policy in the Oil Industry* (Irwin, Homewood, IL., 1970).
7. Skinner et al., *Manufacturing Policy in the Plastics Industry* (Irwin, Homewood, IL., 1968).

Many briefer studies of individual equipment appear in some books, of which a selection is as follows:

- Happel and Jordan (1975):
  1. Absorption of ethanol from a gas containing CO_2 (p. 403).
  2. A reactor-separator for simultaneous chemical reactions (p. 419).
  3. Distillation of a binary mixture (p. 385).
  4. A heat exchanger and cooler system (p. 370).

Figure 1.3. Notation of flow quantities in a reactor (1) and distillation column (2). $A_{ij}^{(k)}$ designates the amount of component A in stream k proceeding from unit i to unit j. Subscripts 0 designates a source or sink beyond the boundary limits. Γ designates a total flow quantity.

EXAMPLE 1.1
Material Balance of a Chlorination Process with Recycle
A plant for the chlorination has the flowsheet shown. From pilot plant work, with a chlorine/benzene charge weight ratio of 0.82, the composition of the reactor effluent is

A.	C_6H_6	0.247
B.	Cl_2	0.100
C.	C_6H_5Cl	0.3174
D.	$C_6H_4Cl_2$	0.1559
E.	HCl	0.1797

Separator no. 2 returns 80% of the unreacted chlorine to the reactor and separator no. 3 returns 90% of the benzene. Both recycle streams are pure. Fresh chlorine is charged at such a rate that the weight ratio of chlorine to benzene in the total charge remains 0.82. The amounts of other streams are found by material balances and are shown in parentheses on the sketch per 100 lbs of fresh benzene to the system.

---
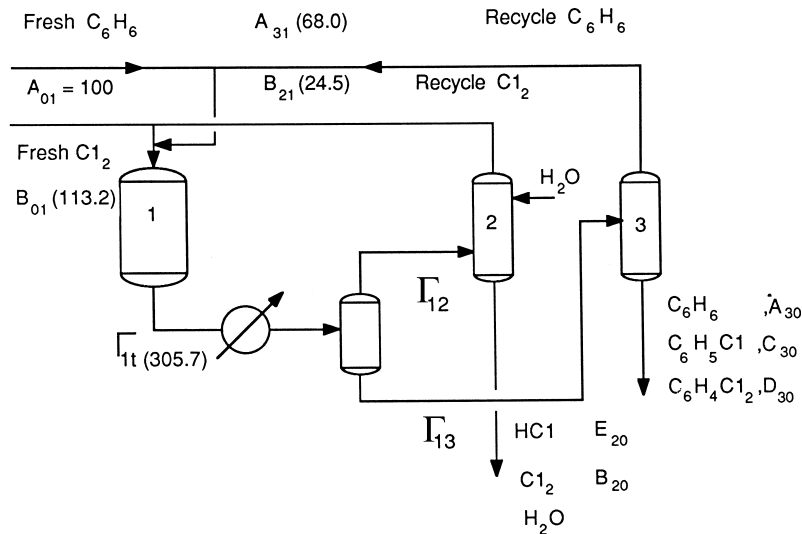
5. Piping of water (p. 353).
6. Rotary dryer (p. 414).

- Humphreys, *Jelen's Cost and Optimization Engineering*, 3rd. ed., McGraw-Hill, New York, 1991).
  7. Drill bit life and replacement policy (p. 257).
  8. Homogeneous flow reactor (p. 265).
  9. Batch reactor with negligible downtime (p. 272).

- Peters and Timmerhaus, 4th ed. (1991)
  10. Shell and tube cooling of air with water (p. 635).

- Rudd and Watson (1968):
  11. Optimization of a three stage refrigeration system (p. 172).

- Sherwood (1963):
  12. Gas transmission line (p. 84).
  13. Fresh water from sea water by evaporation (p. 138).

- Ulrich, (1984).
  14. Multiple effect evaporator for concentrating Kraft liquor (p. 347).

- Walas, (1959):
  15. Optimum number of vessels in a CSTR battery (p. 98).

Capital, labor, and energy costs have not escalated at the same rate over the years since these studies were prepared, so the conclusions must be revisited. However, the methodologies employed and the patterns of study used should be informative.

Since energy costs have escalated, appraisals of energy utilization are necessary from the standpoints of the first and second laws of thermodynamics. Such analyses will reveal where the greatest generation of entropy occurs and where the most improvement in energy saved might be made by appropriate changes of process and equipment.

Analyses of cryogenic processes, such as air separation or the separation of helium from natural gas, have found that a combination of pressure drops involving heat exchangers and compressors was most economical from the standpoint of capital invested and operating expenses.

Details of the thermodynamic basis of availability analysis are dealt with by Moran (*Availability Analysis,* Prentice-Hall, Englewood Cliffs, NJ, 1982). He applies the method to a cooling tower, heat pump, a cryogenic process, coal gasification, and particularly to the efficient use of fuels.

An interesting conclusion reached by Linnhoff [in Seider and Mah (Eds.), (1981) is that "chemical processes which are properly designed for energy versus capital cost tend to operate at approximately 60% efficiency." A major aspect of his analysis is recognition of practical constraints and inevitable losses. These may include material of construction limits, plant layout, operability, the need for simplicity such as limits on the number of compressor stages or refrigeration levels, and above all the recognition that, for low grade heat, heat recovery is preferable to work recovery, the latter being justifiable only in huge installations. Unfortunately, the edge is taken off the dramatic 60% conclusion by Linnhoff's

admission that efficiency cannot be easily defined for some complexes of interrelated equipment.

1.8. DESIGN SAFETY FACTORS

A number of factors influence the performance of equipment and plant there are elements of uncertainty and the possibility of error, including inaccuracy of physical data, basic correlations of behavior such as pipe friction or column tray efficiency or gas–liquid distribution. Further, it is often necessary to use approximations of design methods and calculations, unknown behavior of materials of construction, uncertainty of future market demands, and changes in operating performance with time. The solvency of the project, the safety of the operators and the public, and the reputation and career of the design engineer are at stake. Accordingly, the experienced engineer will apply safety factors throughout the design of a plant. Just how much of a factor should be applied in a particular case cannot be stated in general terms because circumstances vary widely. The inadequate performance of a particular piece of equipment may be compensated for by the superior performance of associated equipment, as insufficient trays in a fractionator may be compensated for by increases in reflux and reboiling, if that equipment can take the extra load.

The safety factor practices of some 250 engineers were ascertained by a questionnaire and summarized in Table 1.3; additional figures are given by Peters and Timmerhaus (1991). Relatively inexpensive equipment that can conceivably serve as a bottleneck, such as pumps, always is liberally sized; perhaps as much as 50% extra for a reflux pump.

In an expanding industry, it may be the policy to deliberately oversize critical equipment that cannot be modified for increased capacity. The safety factors in Table 1.3 account for future trends; however, considerable judgment must be exercised to provide reasonable chances of equipment operating without unreasonably increasing capital investment.

Safety factors must be judiciously applied and should not be used to mask inadequate or careless design work. The design should be the best that can be made in the time economically justifiable, and the safety factors should be estimated from a careful consideration of all factors entering into the design and the possible future deviations from the design conditions.

Sometimes it is possible to evaluate the range of validity of measurements and correlations of physical properties, phase equilibrium behavior, mass and heat transfer efficiencies and similar factors, as well as the fluctuations in temperature, pressure, flow, etc., associated with practical control systems. Then the effects of

such data on the uncertainty of sizing equipment can be estimated. For example, the mass of a distillation column that is related directly to its cost depends on at least these factors:

1. The vapor–liquid equilibrium data.
2. The method of calculating the reflux and number of trays.
3. The tray efficiency.
4. Allowable vapor rate and consequently the tower diameter at a given tray spacing and estimated operating surface tension and fluid densities.
5. Corrosion allowances.

Also such factors as allowable tensile strengths, weld efficiencies, and possible inaccuracies of formulas used to calculate shell and head thicknesses may be pertinent—that is, the relative uncertainty or error in the function is related linearly to the fractional uncertainties of the independent variables. For example, take the case of a steam-heated thermosyphon reboiler on a distillation column for which the heat transfer equation is

$$q = UA\Delta T.$$

The problem is to find how the heat transfer rate can vary when the other quantities change. U is an experimental value that is known only to a certain accuracy. ΔT may be uncertain because of possible fluctuations in regulated steam and tower pressures. A, the effective area, may be uncertain because the submergence is affected by the liquid level controller at the bottom of the column. Accordingly,

$$\frac{dq}{q} = \frac{dU}{U} + \frac{dA}{A} + \frac{d(\Delta T)}{\Delta T},$$

that is, the fractional uncertainty of q is the sum of the fractional uncertainties of the quantities on which it is dependent. In practical cases, of course, some uncertainties may be positive and others negative, so that they may cancel out in part; but the only safe viewpoint is to take the sum of the absolute values.

It is not often that proper estimates can be made of uncertainties of all the parameters that influence the performance or required size of particular equipment, but sometimes one particular parameter is dominant. All experimental data scatter to some extent, for example, heat transfer coefficients; and various correlations of particular phenomena disagree, for example, equations of state of liquids and gases. The sensitivity of equipment sizing to uncertainties in such data has been the subject of some published

TABLE 1.3. Safety Factors in Equipment Design: Results of a Questionnaire

Equipment	Design Variable	Range of Safety Factor (%)
Compressors, reciprocating	piston displacement	11–21
Conveyors, screw	diameter	8–21
Hammer mills	power input	15–21[a]
Filters, plate-and-frame	area	11–21[a]
Filters, rotary	area	14–20[a]
Heat exchangers, shell and tube for liquids	area	11–18
Pumps, centrifugal	impeller diameter	7–14
Separators, cyclone	diameter	7–11
Towers, packed	diameter	11–18
Towers, tray	diameter	10–16
Water cooling towers	volume	12–20

[a]Based on pilot plant tests (Walas, 1984).

information, of which a review article is by [Zudkevich, 1982]; some of the cases cited are:

1. Sizing of isopentane/pentane and propylene/propane splitters.
2. Effect of volumetric properties on sizing of an ethylene compressor.
3. Effect of liquid density on metering of LNG.
4. Effect of vaporization equilibrium ratios, K, and enthalpies on cryogenic separations.
5. Effects of VLE and enthalpy data on design of plants for coal-derived liquids.

Examination of such studies may lead to the conclusion that some of the safety factors of Table 1.3 may be optimistic. But long experience in certain areas does suggest to what extent various uncertainties do cancel out, and overall uncertainties often do fall in the range of 10–20% as stated there. Still, in major cases the uncertainty analysis should be made whenever possible.

1.9. SAFETY OF PLANT AND ENVIRONMENT

The safe practices described in the previous section are primarily for assurance that the equipment have adequate performance over anticipated ranges of operating conditions. In addition, the design of equipment and plant must minimize potential harm to personnel and the public in case of accidents, of which the main causes are

a. human failure,
b. failure of equipment or control instruments,
c. failure of supply of utilities or key process streams,
d. environmental events (wind, water, and so on).

A more nearly complete list of potential hazards is in Table 1.4, and a checklist referring particularly to chemical reactions is in Table 1.5.

Examples of common safe practices are pressure relief valves, vent systems, flare stacks, snuffing steam and fire water, escape hatches in explosive areas, dikes around tanks storing hazardous materials, turbine drives as spares for electrical motors in case of power failure, and others. Safety considerations are paramount in the layout of the plant, particularly isolation of especially hazardous operations and accessibility for corrective action when necessary.

Continual monitoring of equipment and plant is standard practice in chemical process plants. Equipment deteriorates and operating conditions may change. Repairs are sometimes made with materials or equipment whose ultimate effects on operations may not have been taken into account. During start-up and shutdown, stream compositions and operating conditions are much different from those under normal operation, and their possible effect on safety must be considered. Sample checklists of safety questions for these periods are in Table 1.6.

Because of the importance of safety and its complexity, safety engineering is a speciality in itself. In chemical processing plants of any significant size, loss prevention reviews are held periodically by groups that always include a representative of the safety department. Other personnel, as needed by the particular situation, are from manufacturing, maintenance, technical service, and possibly research, engineering, and medical groups. The review considers any changes made since the last review in equipment, repairs, feedstocks and products, and operating conditions.

Detailed safety checklists appear in books by Fawcett and Wood (1982) and Wells (1980). These books and the volume by Lees (1996) also provide entry into the vast literature of chemical

TABLE 1.4. Some Potential Hazards

Energy Source
Process chemicals, fuels, nuclear reactors, generators, batteries
Source of ignition, radio frequency energy sources, activators, radiation sources
Rotating machinery, prime movers, pulverisers, grinders, conveyors, belts, cranes
Pressure containers, moving objects, falling objects

Release of Material
Spillage, leakage, vented material
Exposure effects, toxicity, burns, bruises, biological effects
Flammability, reactivity, explosiveness, corrosivity and fire-promoting properties of chemicals
Wetted surfaces, reduced visibility, falls, noise, damage
Dust formation, mist formation, spray

Fire Hazard
Fire, fire spread, fireballs, radiation
Explosion, secondary explosion, domino effects
Noise, smoke, toxic fumes, exposure effects
Collapse, falling objects, fragmentation

Process State
High/low/changing temperature and pressure
Stress concentrations, stress reversals, vibration, noise
Structural damage or failure, falling objects, collapse
Electrical shock and thermal effects, inadvertent activation, power source failure
Radiation, internal fire, overheated vessel
Failure of equipment/utility supply/flame/instrument/component
Start-up and shutdown condition
Maintenance, construction and inspection condition

Environmental Effects
Effect of plant on surroundings, drainage, pollution, transport, wind and light change, source of ignition/vibration/noise/radio interference/fire spread/explosion
Effect of surroundings on plant (as above)
Climate, sun, wind, rain, snow, ice, grit, contaminants, humidity, ambient conditions
Acts of God, earthquake, arson, flood, typhoon, *force majeure*
Site layout factors, groups of people, transport features, space limitations, geology, geography

Processes
Processes subject to explosive reaction or detonation
Processes which react energetically with water or common contaminants
Processes subject to spontaneous polymerisation or heating
Processes which are exothermic
Processes containing flammables and operated at high pressure or high temperature or both
Processes containing flammables and operated under refrigeration
Processes in which intrinsically unstable compounds are present
Processes operating in or near the explosive range of materials
Processes involving highly toxic materials
Processes subject to a dust or mist explosion hazard
Processes with a large inventory of stored pressure energy

Operations
The vaporisation and diffusion of flammable or toxic liquids or gases
The dusting and dispersion of combustible or toxic solids
The spraying, misting or fogging of flammable combustible materials or strong oxidising agents and their mixing
The separation of hazardous chemicals from inerts or diluents
The temperature and pressure increase of unstable liquids

(Wells, 1980)

TABLE 1.5. Safety Checklist of Questions About Chemical Reactions

1. Define potentially hazardous reactions. How are they isolated? Prevented? (See Chaps. 4, 5, and 16)
2. Define process variables which could, or do, approach limiting conditions for hazard. What safeguards are provided against such variables?
3. What unwanted hazardous reactions can be developed through unlikely flow or process conditions or through contamination?
4. What combustible mixtures can occur within equipment?
5. What precautions are taken for processes operating near or within the flammable limits? (Reference: S&PP Design Guide No. 8.) (See Chap. 19)
6. What are process margins of safety for all reactants and intermediates in the process?
7. List known reaction rate data on the normal and possible abnormal reactions
8. How much heat must be removed for normal, or abnormally possible, exothermic reactions? (see Chaps. 7, 17, and 18)
9. How thoroughly is the chemistry of the process including desired and undesired reactions known? (See NFPA 491 M, *Manual of Hazardous Chemical Reactions*)
10. What provision is made for rapid disposal of reactants if required by emergency?
11. What provisions are made for handling impending runaways and for short-stopping an existing runaway?
12. Discuss the hazardous reactions which could develop as a result of mechanical equipment (pump, agitator, etc.) failure
13. Describe the hazardous process conditions that can result from gradual or sudden blockage in equipment including lines
14. Review provisions for blockage removal or prevention
15. What raw materials or process materials or process conditions can be adversely affected by extreme weather conditions? Protect against such conditions
16. Describe the process changes including plant operation that have been made since the previous process safety review

(Fawcett and Wood, 1982, pp. 725–726. Chapter references refer to this book.)

TABLE 1.6. Safety Checklist of Questions About Start-up and Shut-down

Start-up Mode (§4.1)
D1 Can the start-up of plant be expedited safely? Check the following:
  (a) Abnormal concentrations, phases, temperatures, pressures, levels, flows, densities
  (b) Abnormal quantities of raw materials, intermediates and utilities (supply, handling and availability)
  (c) Abnormal quantities and types of effluents and emissions (§1.6.10)
  (d) Different states of catalyst, regeneration, activation
  (e) Instruments out of range, not in service or de-activated, incorrect readings, spurious trips
  (f) Manual control, wrong routeing, sequencing errors, poor identification of valves and lines in occasional use, lock-outs, human error, improper start-up of equipment (particularly prime movers)
  (g) Isolation, purging
  (h) Removal of air, undesired process material, chemicals used for cleaning, inerts, water, oils, construction debris and ingress of same
  (i) Recycle or disposal of off-specification process materials
  (j) Means for ensuring construction/maintenance completed
  (k) Any plant item failure on initial demand and during operation in this mode
  (l) Lighting of flames, introduction of material, limitation of heating rate

TABLE 1.6.—(continued**)**

  (m) Different modes of the start-up of plant:
    Initial start-up of plant
    Start-up of plant section when rest of plant down
    Start-up of plant section when other plant on-stream
    Start-up of plant after maintenance
    Preparation of plant for its start-up on demand

Shut-down Mode (§§4.1,4.2)
D2 Are the limits of operating parameters, outside which remedial action must be taken, known and measured?
D3 To what extent should plant be shut down for any deviation beyond the operating limits? Does this require the installation of alarm and/or trip? Should the plant be partitioned differently? How is plant restarted? (§9.6)
D4 In an emergency, can the plant pressure and/or the inventory of process materials be reduced effectively, correctly, safely? What is the fire resistance of plant (§§9.5,9.6)
D5 Can the plant be shut down safely? Check the following:
(a) See the relevant features mentioned under start-up mode
(b) Fail-danger faults of protective equipment
(c) Ingress of air, other process materials, nitrogen, steam, water, lube oil (§4.3.5)
(d) Disposal or inactivation of residues, regeneration of catalyst, decoking, concentration of reactants, drainage, venting
(e) Chemical, catalyst, or packing replacement, blockage removal, delivery of materials prior to start-up of plant
(f) Different modes of shutdown of plant:
  Normal shutdown of plant
  Partial shutdown of plant
  Placing of plant on hot standby
  Emergency shutdown of plant

(Wells, 1980).

process plant safety. Lees has particularly complete bibliographies. Standard references on the properties of dangerous materials are the books by Lewis (1993, 2000).

1.10. STEAM AND POWER SUPPLY

For smaller plants or for supplementary purposes, steam and power can be supplied by package plants which are shippable and ready to hook up to the process. Units with capacities in the range of sizes up to about 350,000 lb/hr steam at 750° F and 850 psi are on the market and are obtainable on a rental/purchase basis for energy needs.

Modern steam plants are quite elaborate structures that can recover 80% or more of the heat of combustion of the fuel. The simplified sketch of Example 1.2 identifies several zones of heat transfer in the equipment. Residual heat in the flue gas is recovered as preheat of the water in an economizer and in an air preheater. The combustion chamber is lined with tubes along the floor and walls to keep the refractory cool and usually to recover more than half the heat of combustion. The tabulations of this example are of the distribution of heat transfer surfaces and the amount of heat transfer in each zone.

More realistic sketches of the cross section of a steam generator are in Figure 1.4. Part (a) of this figure illustrates the process of natural circulation of water between an upper steam drum and a lower drum provided for the accumulation and eventual blowdown of sediment. In some installations, pumped circulation of the water is advantageous.

Both process steam and supplemental power are recoverable from high pressure steam which is readily generated. Example 1.3 is of such a case. The high pressure steam is charged to a turbine-

EXAMPLE 1.2
Data of a Steam Generator for Making 250,000 lb/hr at 450 psia and 650°F from Water Entering at 220°F
Fuel oil of 18,500 Btu/lb is fired with 13% excess air at 80°F. Flue gas leaves at 410°F. A simplified cross section of the boiler is shown. Heat and material balances are summarized. Tube selections and arrangements for the five heat transfer zones also are summarized. The term A_g is the total internal cross section of the tubes in parallel. Assure 85% recovery (*Steam: Its Generation and Use*, 14.2, Babcock and Wilcox, Barberton, OH, 1972). (a) Cross section of the generator: (b) Heat balance:

Fuel input	335.5 MBtu/hr
To furnace tubes	162.0
To boiler tubes	68.5
To screen tubes	8.1
To superheater	31.3
To economizer	15.5
Total to water and steam	285.4 Mbtu/hr
In air heater	18.0 MBtu/hr

(c) Tube quantity, size, and grouping:

Screen
2 rows of $2\frac{1}{2}$-in. OD tubes, approx 18 ft long
Rows in line and spaced on 6-in. centers
23 tubes per row spaced on 6-in. centers
$S = 542$ sqft
$A = 129$ sqft
Superheater
12 rows of $2\frac{1}{2}$-in. OD tubes (0.165-in. thick), 17.44 ft long
Rows in line and spaced on $3\frac{1}{4}$-in. centers
23 tubes per row spaced on 6-in. centers
$S = 3150$ sqft
$A_g = 133$ sqft
Boiler
25 rows of $2\frac{1}{2}$-in. OD tubes, approx 18 ft long
Rows in line and spaced on $3\frac{1}{4}$-in. centers
35 tubes per row spaced on 4-in. centers
$S = 10,300$ sqft
$A_g = 85.0$ sqft
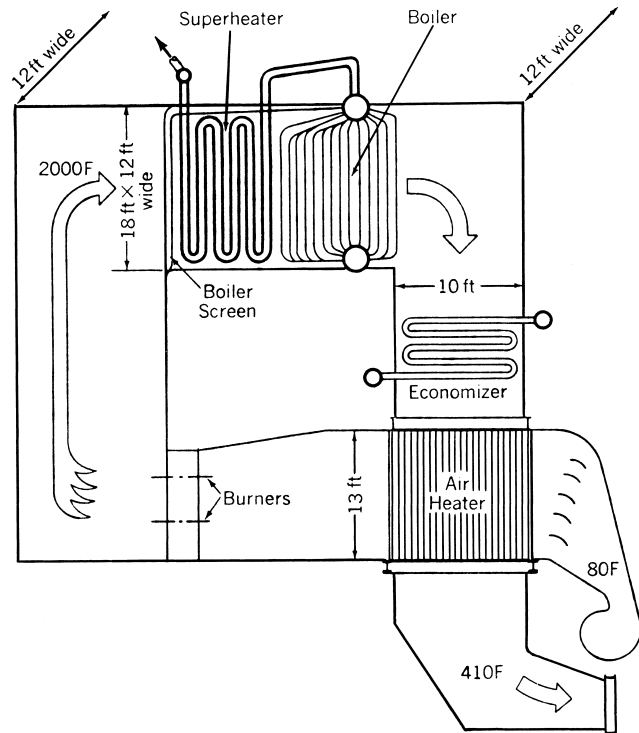
Economizer
10 rows of 2-in. OD tubes (0.148-in. thick), approx 10 ft long
Rows in line and spaced on 3-in. centers
47 tubes per row spaced on 3-in. centers
$S = 2460$ sqft
$A_g = 42$ sqft
Air heater
53 rows of 2-in. OD tubes (0.083-in. thick), approx 13 ft long
Rows in line and spaced on $2\frac{1}{2}$-in. centers
47 tubes per row spaced on $3\frac{1}{2}$-in. centers
$S = 14,800$ sqft
A_g (total internal cross section area of 2173 tubes) $= 39.3$ sqft
A_a (clear area between tubes for crossflow of air) $= 70$ sqft
Air temperature entering air heater $= 80°$F

generator set, process steam is extracted at the desired process pressure at an intermediate point in the turbine, and the rest of the steam expands further and is condensed.

In plants such as oil refineries that have many streams at high temperatures or high pressures, their energy can be utilized to generate steam and/or to recover power. The two cases of Example 1.4 are of steam generation in a kettle reboiler with heat from a fractionator sidestream and of steam superheating in the convection tubes of a furnace that provides heat to fractionators.

Recovery of power from the thermal energy of a high temperature stream is the subject of Example 1.5. A closed circuit of propane is the indirect means whereby the power is recovered with an expansion turbine. Recovery of power from a high pressure gas is a fairly common operation. A classic example of power recovery from a high pressure liquid is in a plant for the absorption of CO_2 by water at a pressure of about 4000 psig. After the absorp-

tion, the CO_2 is released and power is recovered by releasing the rich liquor through a turbine.

1.11. DESIGN BASIS

Before a chemical process design can be properly started, a certain body of information must be agreed upon by all participants in the proposed plant design (engineering, research, plant supervision, safety and health personnel, environmental personnel, and plant management). The design basis states what is to be made, where it is to be made, and what are the raw materials. Distinctions must also be clear between grass-roots facilities, battery-limits facilities, plant expansions, and plant retrofits. The required data may be classified into basic design and specific design data. These data form the basis for the project scope that is essential for any design and the scope includes the following:

(a)

(b)

(c)
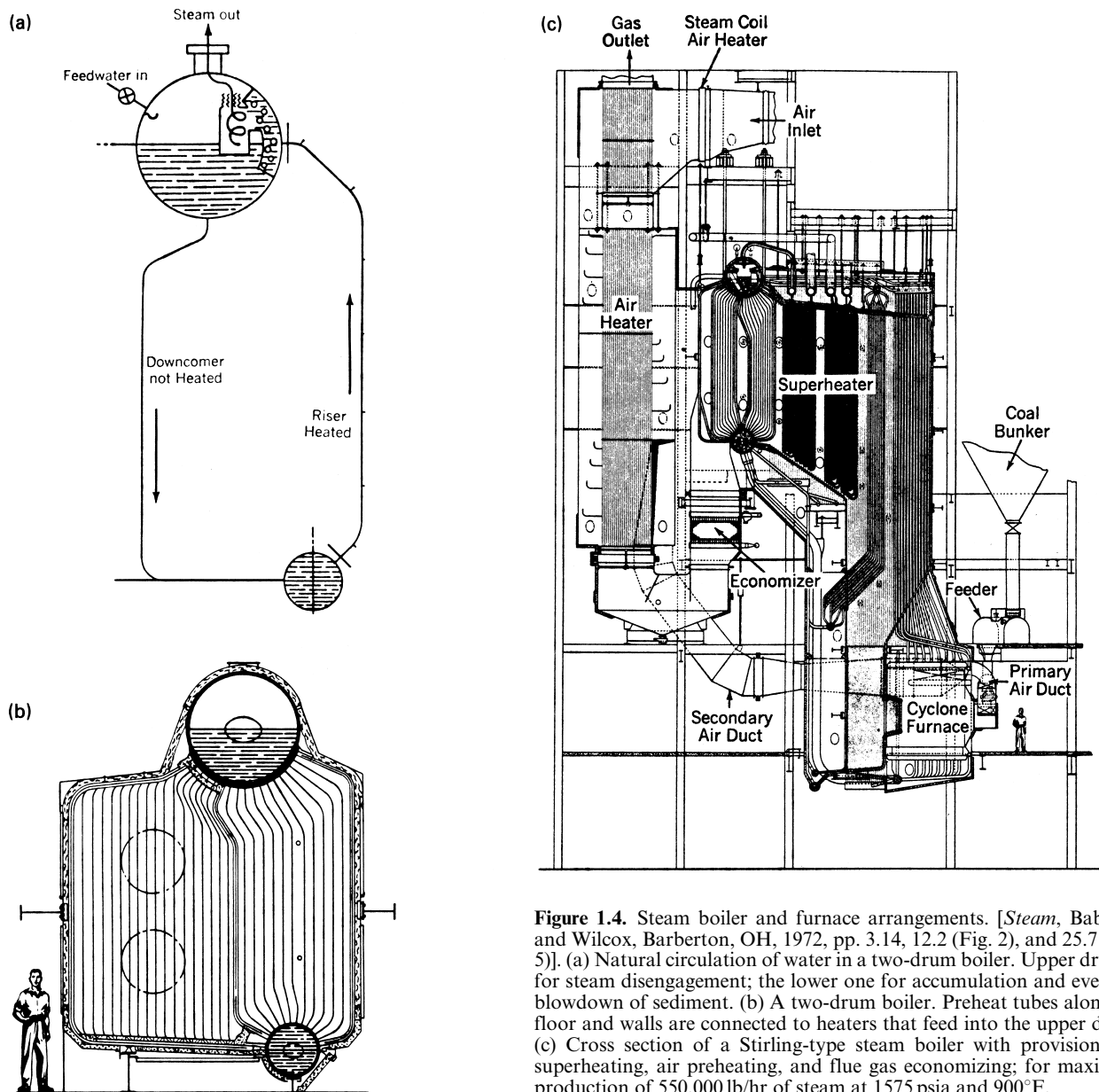
Figure 1.4. Steam boiler and furnace arrangements. [*Steam*, Babcock and Wilcox, Barberton, OH, 1972, pp. 3.14, 12.2 (Fig. 2), and 25.7 (Fig. 5)]. (a) Natural circulation of water in a two-drum boiler. Upper drum is for steam disengagement; the lower one for accumulation and eventual blowdown of sediment. (b) A two-drum boiler. Preheat tubes along the floor and walls are connected to heaters that feed into the upper drum. (c) Cross section of a Stirling-type steam boiler with provisions for superheating, air preheating, and flue gas economizing; for maximum production of 550,000 lb/hr of steam at 1575 psia and 900°F.

1. Required products: their compositions, amounts, purities, toxicities, temperatures, pressures, and monetary values.
2. Available raw materials: their compositions, amounts, toxicities, temperatures, pressures, monetary values, and all pertinent physical properties unless they are standard and can be established from correlations. This information about properties applies also to products of item 1.
3. Daily and seasonal variations of any data of items 1 and 2 and subsequent items of these lists.
4. All available laboratory and pilot plant data on reaction and phase equilibria, catalyst degradation, and life and corrosion of equipment.
5. Any available existing plant data of similar processes.
6. Local restrictions on means of disposal of wastes.

Basic engineering data include:

7. Characteristics and values of gaseous and liquid fuels that are to be used and their unit costs.
8. Characteristics of raw makeup and cooling tower waters, temperatures, maximum allowable temperature, flow rates available, and unit costs.
9. Steam and condensate: mean pressures and temperatures and their fluctuations at each level, amount available, extent of recovery of condensate, and unit costs.
10. Electrical power: Voltages allowed for instruments, lighting and various driver sizes, transformer capacities, need for emergency generator, unit costs.
11. Compressed air: capacities and pressures of plant and instrument air, instrument air dryer.

EXAMPLE 1.3
Steam Plant Cycle for Generation of Power and Low Pressure Process Steam
The flow diagram is for the production of 5000 kW gross and 20,000 lb/hr of saturated process steam at 20 psia. The feed and hot well pumps make the net power production 4700 kW.
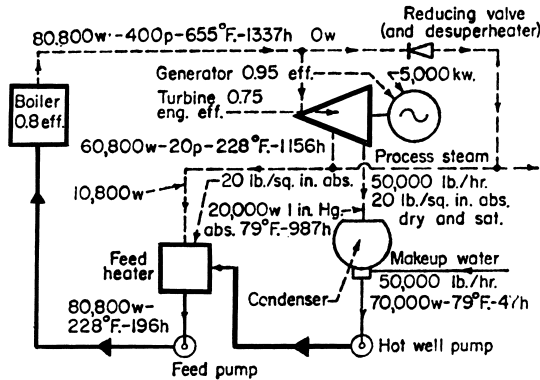
Conditions at key points are indicated on the enthalpy–entropy diagram. The process steam is extracted from the turbine at an intermediate point, while the rest of the stream expands to 1 in. Hg and is condensed (example is corrected from Perry, 6th ed., 9.43, 1984).
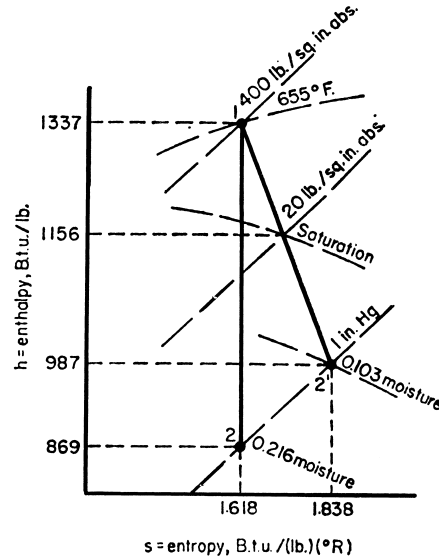
EXAMPLE 1.4
Pickup of Waste Heat by Generating and Superheating Steam in a Petroleum Refinery
The two examples are generation of steam with heat from a sidestream of a fractionator in a 9000 Bbl/day fluid cracking plant, and superheating steam with heat from flue gases of a furnace whose main function is to supply heat to crude topping and vacuum service in a 20,000 Bbl/day plant. (a) Recovery of heat from a

sidestream of a fractionator in a 9000 Bbl/day fluid catalytic cracker by generating steam, $Q = 15,950,000$ Btu/hr. (b) Heat recovery by superheating steam with flue gases of a 20,000 Bbl/day crude topping and vacuum furnace.
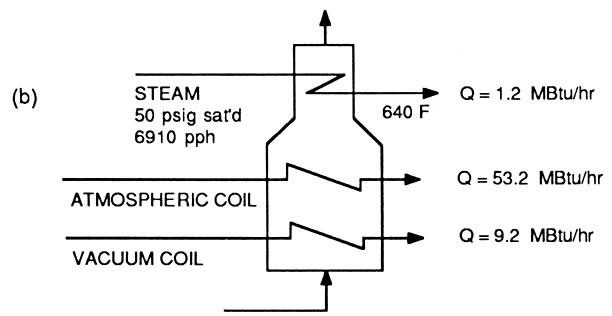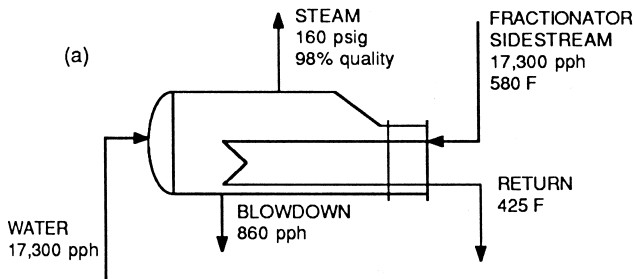
12. Plant site elevation.
13. Soil bearing value, frost depth, ground water depth, piling requirements, available soil test data.
14. Climatic data. Winter and summer temperature extremes, cooling tower drybulb temperature, air cooler design temperature, strength and direction of prevailing winds, rain and snow-fall maxima in 1 hr and in 12 hr, earthquake and hurricane provision.
15. Blowdown and flare: What may or may not be vented to the atmosphere or to ponds or to natural waters, nature of required liquid, and vapor relief systems.
16. Drainage and sewers: rainwater, oil, sanitary.

EXAMPLE **1.5**
Recovery of Power from a Hot Gas Stream

A closed circuit of propane is employed for indirect recovery of power from the thermal energy of the hot pyrolyzate of an ethylene plant. The propane is evaporated at 500 psig, and then expanded to 100°F and 190 psig in a turbine where the power is recovered. Then the propane is condensed and pumped back to the evaporator to complete the cycle. Since expansion turbines are expensive machines even in small sizes, the process is not economical on the scale of this example, but may be on a much larger scale.
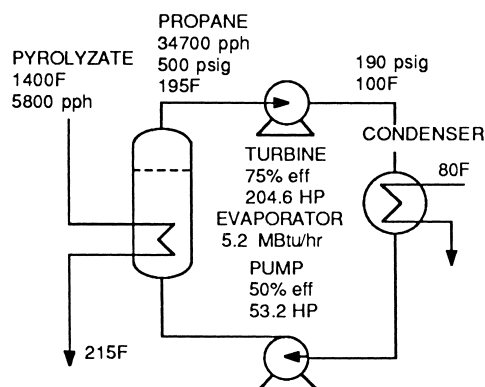
17. Buildings: process, pump, control instruments, special equipment.
18. Paving types required in different areas.
19. Pipe racks: elevations, grouping, coding.
20. Battery limit pressures and temperatures of individual feed stocks and products.
21. Codes: those governing pressure vessels, other equipment, buildings, electrical, safety, sanitation, and others.
22. Miscellaneous: includes heater stacks, winterizing, insulation, steam or electrical tracing of lines, heat exchanger tubing size standardization, instrument locations.
23. Environmental regulations.
24. Safety and health requirements.

A convenient tabular questionnaire is presented in Table 1.7 and it may become part of the scope. For anything not specified, for instance, sparing of equipment, engineering standards of the designer or constructor will be used. A proper design basis at the very beginning of a project is essential to getting a project completed and on stream expeditiously.

UTILITIES

These provide motive power as well as heating and cooling of process streams, and include electricity, steam, fuels, and various fluids whose changes in sensible and latent heats provide the necessary energy transfers. In every plant, the conditions of the utilities are maintained at only a few specific levels, for instance, steam at certain pressures, cooling water over certain temperature ranges, and electricity at certain voltages. If a company generates its own power, provision for standby electric power from a public or private utility should be made in the event of plant utility failure. At some stages of some design work, the specifications of the utilities may not have been established. Then, suitable data may be selected from the commonly used values itemized in Table 1.8.

1.12. LABORATORY AND PILOT PLANT WORK

Basic physical and thermodynamic property data are essential for the design and selection of equipment. Further, the state-of-the-art design of many kinds of equipment may require more or less extensive laboratory or pilot plant studies. Equipment manufacturers who are asked to provide performance guarantees require such information. As indicated in Appendix C, typical equipment suppliers' questionnaires may require the potential purchaser to have performed such tests.

Some of the more obvious areas definitely requiring test work are filtration, sedimentation, spray, or fluidized bed or any other kind of solids drying, extrusion pelleting, pneumatic and slurry conveying, adsorption, and others. Even in such thoroughly researched areas as vapor-liquid and liquid-liquid separations, rates, equilibria, and efficiencies may need to be tested, particularly of complex mixtures. A great deal can be found out, for instance, by a batch distillation of a complex mixture.

In some areas, suppliers may make available small-scale equipment, such as leaf filters, that can be used to determine suitable operating conditions, or they may do the work themselves at suppliers' facilities (e.g., use of drying equipment).

Pilot plant experimentation is expensive and can be time consuming, delaying the introduction of the product in the marketplace. There have been trends and reports of recent successes whereby extensive pilot plant research has been bypassed. One such study involved the manufacture of bisphenol A in which laboratory work bypassed the pilot plant stage and a full-scale production unit was designed and operated successfully. This is not recommended, but using some laboratory research and simulation, may make it possible to reduce or eliminate expensive pilot plant work. However, confidence must be developed in using simulation to replace pilot plant work and this is obtained only through experience.

TABLE 1.7. Typical Design Basis Questionnaire

1.101 Plant Location _____

1.102 Plant Capacity, lb or tons/yr. _____

1.103 Operating Factor or Yearly Operating Hours
(For most modern chemical plants, this figure is generally 8,000 hours per year).

1.104 Provisions for Expansion _____
_____

1.105 Raw Material Feed (Typical of the analyses required for a liquid)

Assay, wt per cent min _____
Impurities, wt per cent max_____
Characteristic specifications
Specific gravity _____
Distillation range °F _____
Initial boiling point °F _____
Dry end point °F _____
Viscosity, centipoises _____
Color APHA _____
Heat stability color _____
Reaction rate with established reagent _____
Acid number _____
Freezing point or set point °F _____
Corrosion test _____
End-use test _____

For a solid material chemical assay, level of impurities and its physical characteristics, such as specific density, bulk density, particle size distribution and the like are included. This physical shape information is required to assure that adequate processing and material handling operations will be provided.

1.1051 Source

Supply conditions at process	Max	Min	Normal
plant battery limits	_____	_____	_____
Storage capacity (volume or day's inventory)	_____	_____	_____

Required delivery conditions at battery limits
Pressure _____
Temperature _____
Method of transfer _____

1.106 Product Specifications

Here again specifications would be similar to that of the raw material in equivalent or sometimes greater detail as often trace impurities affect the marketability of the final product.

Storage requirements (volume or days of inventory) _____

Type of product storage _____

For solid products, type of container or method of shipment and loading facilities should be outlined. _____

1.107 Miscellaneous Chemicals and Catalyst Supply

In this section the operating group should outline how various miscellaneous chemicals and catalysts are to be stored and handled for consumption within the plant.

1.108 Atmospheric Conditions

Barometric pressure range _____
Temperature
Design dry bulb temperature (°F)_____
% of summer season, this temperature is exceeded. _____
Design wet bulb temperature _____
% of summer season, this temperature is exceeded. _____
Minimum design dry bulb temperature winter condition (°F) _____
Level of applicable pollutants that could affect the process.
Examples of these are sulfur compounds, dust and solids, chlorides and salt water mist when the plant is at a coastal location. _____

2.100 Utilities

2.101 Electricity

Characteristics of primary supply _____
Voltage, phases, cycles_____
Preferred voltage for motors

Over 200 hp _____
Under 200 hp_____
Value, c/kWh _____

(If available and if desired, detailed electricity pricing schedule can be included for base load and incremental additional consumption.)

2.102 Supply Water_____
Cleanliness_____
Corrosiveness _____
Solids content analysis_____
_____
Other details _____
_____
_____

Pressure (at grade)	Maximum	Minimum
Supply	_____	_____
Return	_____	_____

2.103 Cooling Water

Well, river, sea, cooling tower, other._____
Quality_____
Value _____
Use for heat exchanger design
Fouling properties _____
Design fouling factor_____
Preferred tube material_____

TABLE 1.7. —(*continued*)

2.104 Steam	Max	Normal	Min
High pressure, psig	_____	_____	_____
Temperature, °F	_____	_____	_____
Moisture, %	_____	_____	_____
Value per thousand lb	_____	_____	_____
Medium pressure, psig	_____	_____	_____
Temperature, °F	_____	_____	_____
Moisture, %	_____	_____	_____
Value per thousand lb	_____	_____	_____
Low pressure, psig	_____	_____	_____
Temperature, °F	_____	_____	_____
Moisture, %	_____	_____	_____
Value per thousand lb	_____	_____	_____

2.105 Steam Condensate

Disposition _____

Required pressure at battery limits _____

Value per thousand lb or gal _____

2.106 Boiler Feed Water

Quality

    Hardness, ppm _____

    Silica content _____

Hardness

    Total solids, ppm _____

    Other details _____

Chemical additives _____

	Max	Min
Supply pressure	_____	_____
Temperature, °F	_____	_____
Value per thousand gal	_____	_____

2.107 Process Water

(If the quality of the process water is different from the make-up water or boiler feed water, separate information should be provided.)

Quality	Max	Min
Supply pressure	_____	_____
Temperature, °F	_____	_____
Value per thousand gal	_____	_____

2.108 Inert Gas	Max	Min
Pressure, psig	_____	_____
Dew point, °F	_____	_____

Composition

    Per cent CO_2 _____

    Per cent oxygen _____

    Per cent CO _____

    Other trace impurities _____

Quantity available _____

Value per thousand cu ft _____

2.109 Plant Air

Supply Source

    Offsite battery limits (OSBL) _____

    Portable compressor _____

    Process air system _____

    Special compressor _____

Supply pressure, psig

2.110 Instrument Air

Supply source (OSBL) _____

Special compressor _____

Supply pressure, psig _____

Dew point, °F _____

Oil, dirt and moisture removal requirements _____

In general a value of plant and instrument air is usually not given as the yearly over-all cost is insignificant in relation to the other utilities required.

3.101 Waste Disposal Requirements

In general, there are three types of waste to be considered: liquid, solid and gaseous. The destination and disposal of each of these effluents is usually different. Typical items are as follows:

Destination of liquid effluents _____

Cooling water blowdown _____

Chemical sewer _____

Storm sewer _____

Method of chemical treating for liquid effluents _____

Preferred materials of construction for

    Cooling water blowdown _____

    Chemical sewer _____

    Storm sewer _____

    Facilities for chemical treating for liquid effluents _____

    Facilities for treatment of gaseous effluents _____

    Solids disposal _____

14

(Landau, 1966).

TABLE 1.8. Typical Utility Characteristics

Steam

Pressure (psig)	Saturation (°F)	Superheat (°F)
15–30	250–275	
150	366	
400	448	
600	488	100–150

Heat Transfer Fluids

°F	Fluid
Below 600	petroleum oils
Below 750	Dowtherm, Therminol and others
Below 1100	fused salts
Above 450	direct firing and electrical heating

Refrigerants

°F	Fluid
40–80	chilled water
0–50	chilled brine and glycol solutions
−50–40	ammonia, freons or suitable substitutes, butane
−150–−50	ethane or propane
−350–−150	methane, air, nitrogen
−400–−300	hydrogen
Below −400	helium

Cooling Water

Supply at 80–90°F
Return at 115°F, with 125°F maximum
Return at 110°F (salt water)
Return above 125°F (tempered water or steam condensate)

Cooling Air

Supply at 85–95°F
Temperature approach to process, 40°F
Power input, 20 HP/1000 sqft of bare heat transfer surface

Fuel

Gas: 5–10 psig, up to 25 psig for some types of burners,
   pipeline gas at 1000 Btu/SCF
Liquid: at 6 million Btu/barrel

Compressed Air

Pressure levels of 45, 150, 300, 450 psig

Instrument Air

45 psig, 0°F dewpoint

Electricity

Driver HP	Voltage
1–100	220, 440, 550
75–250	440
200–2500	2300, 4000
Above 2500	4000, 13,200

REFERENCES

Some of the following items were referenced in this chapter; the rest form a bibliography. Although some of the references and bibliography entries are old, many are classics and provide insight to data, methods, and so on.

1.1 Process Design

A. Books Essential to a Private Library

D.M. Himmelblau, *Basic Principles and Calculations in Chemical Engineering*, 6th ed., PTR Prentice Hall, Englewood Cliffs, NJ, 1996.

E.E. Ludwig, *Applied Process Design for Chemical and Petrochemical Plants*, 3rd. ed., Gulf, Houston, 1995–2000, 3 vols.

W.L. McCabe, J. C. Smith, and P. Harriott, *Unit Operations of Chemical Engineering*, 6th ed., McGraw-Hill, New York, 2002.

R.H. Perry, and D.W. Green, *Perry's Chemical Engineers Handbook*, 6th ed., McGraw-Hill, New York, 1984; 7th ed., 1999. Earlier editions also contain valuable information.

J.M. Smith, H.C. Van Ness, and M.M. Abbott, *Introduction to Chemical Engineering Thermodynamics*, 6th ed., McGraw-Hill, New York, 2001.

S.M. Walas, *Reaction Kinetics for Chemical Engineers*, McGraw-Hill, New York, 1959.

B. Other Books

F. Aerstin, and G. Street, *Applied Chemical Process Design,* Plenum, New York, 1978.

W.D. Baasel, *Preliminary Chemical Engineering Plant Design*, 2nd ed., Van Nostrand Reinhold, New York, 1990.

P. Benedek (Ed.), *Steady-State Flowsheeting of Chemical Plants*, Elsevier, New York, 1980.

G.R. Branan, *Process Engineers Pocket Book*, Gulf, Houston, 1976, 1983, 2 vols.

C.R. Burklin, *Encycl. Chem. Process Des.* **14,** 416–431, Dekker, New York, 1982.

D.R. Coughanowr, *Process Systems Analysis and Control*, 2nd ed., McGraw-Hill, New York, 1991.

J.R. Couper, *Process Engineering Economics*, Dekker, New York, 2003.

Crowe et al., *Chemical Plant Simulation*, Prentice-Hall, Englewood Cliffs, NJ, 1971.

J.M. Douglas, *Conceptual Design of Chemical Processes*, McGraw-Hill, New York, 1991.

T.F. Edgar, and D.M. Himmelblau, *Optimization of Chemical Processes*, McGraw-Hill, New York, 1988.

F.L. Evans, *Equipment Design Handbook for Refineries and Chemical Plants*, Gulf, Houston, 1979, 2 vols.

R.G.E. Franks, *Modelling and Simulation in Chemical Engineering*, Wiley, New York, 1972.

J. Happel, and D.G. Jordan, *Chemical Process Economics*, 2nd ed., Dekker, New York, 1975.

K.E. Humphries, *Jelen's Cost and Optimization Engineering*, 3rd ed., McGraw-Hill, New York, 1991.

D.Q. Kern, *Process Heat Transfer*, McGraw-Hill, New York, 1950.

H.Z. Kister, *Distillation Design*, McGraw-Hill, New York, 1992.

R. Landau (Ed.), *The Chemical Plant*, Reinhold, New York, 1966.

M.E. Leesley, (Ed.), *Computer-Aided Process Design*, Gulf, Houston, 1982.

O. Levenspiel, *Chemical Reaction Engineering*, 3rd ed., Wiley, New York, 1999.

N.P. Lieberman, *Process Design for Reliable Operations*, Gulf, Houston, 1983.

R.S.H. Mah, and W.D. Seider, *Foundations of Computer-Aided Chemical Process Design*, Engineering Foundation, New York, 1981, 2 vols.

M.J. Moran, *Availability Analysis*, Prentice-Hall, Englewood Cliffs, NJ, 1982.

F. Nagiev, *Theory of Recycle Processes in Chemical Engineering*, Macmillan, New York, 1964.

M.S. Peters, and K.D. Timmerhaus, *Process Design and Economics for Chemical Engineers*, 4th ed., McGraw-Hill, New York, 1991, and 5th

ed. McGraw-Hill, New York, 2003. (The units in the fourth edition are in the English System and in the SI System in the fifth edition.)

H.F. Rase, and M.H. Barrows, *Project Engineering for Process Plants*, Wiley, New York, 1957.

W. Resnick, *Process Analysis and Design for Chemical Engineers*, McGraw-Hill, New York, 1981.

R.W. Rousseau, (Ed.), *Handbook of Separation Process Technology*, Wiley, New York, 1987.

D.F. Rudd, and C.C. Watson, *Strategy of Process Engineering*, Wiley, New York, 1968.

T.K. Sherwood, *A Course in Process Design*, MIT Press, Cambridge, MA, 1963.

G.D. Ulrich, *A Guide to Chemical Engineering Process Design and Economics*, Wiley, New York, 1984.

J.F. Valle-Riestra, *Project Evaluation on the Chemical Process Industries*, McGraw-Hill, New York, 1983.

A.W. Westerberg, et al., *Process Flowsheeting*, Cambridge University Press, Cambridge, England, 1977

D.R. Woods, *Process Design and Engineering Practice*, PTR Prentice Hall, Englewood Cliffs, NJ, 1995.

D. Zudkevich, *Encycl. Chem. Process Des*. **14,** 401–483 (1982).

C. Estimation of Properties

AIChE Manual for Predicting Chemical Process Data, AIChE, New York, 1984–date.

W.J. Lyman, W.F. Reehl, and D.H. Rosenblatt, *Handbook of Chemical Property Estimation Methods: Environmental Behavior of Organic Compounds*, McGraw-Hill, New York, 1982.

R.C. Reid, J.M. Prausnitz, and B.E. Poling, *The Properties of Gases and Liquids*, 4th ed., McGraw-Hill, New York, 1987.

Z. Sterbacek, B. Biskup, and P. Tausk, *Calculation of Properties Using Corresponding States Methods*, Elsevier, New York, 1979.

S.M. Walas, *Phase Equilibria in Chemical Engineering*, Butterworths, Stoneham, MA, 1984.

D. Equipment

Chemical Engineering Catalog, Penton/Reinhold, New York, annual.

Chemical Engineering Equipment Buyers' Guide, Chemical Week, New York, annual.

Thomas Register of American Manufacturers, Thomas, Springfield, IL, annual.

(Manufacturers' equipment brochures are the most reliable source of information.)

E. Safety Aspects

H.H. Fawcett and W.J. Wood (Eds.), *Safety and Accident Prevention in Chemical Operations*, Wiley and Sons, New York, 1982.

M. Kutz (Ed.), *Mechanical Engineers' Handbook*, 2nd ed., Wiley, New York, 1998.

F.P. Lees, *Loss Prevention in the Process Industries*, 2nd ed., Butterworth-Heinemann, Woburn, MA, 1996, 3 vols.

R.J. Lewis, *Hazardous Chemicals Desk Reference*, 3rd ed., Van Nostrand Reinhold, New York, 1993.

R.J. Lewis, *Sax's Dangerous Properties of Industrial Materials*, 8th ed., Van Nostrand Reinhold, New York, 2000.

N.P. Lieberman, *Troubleshooting Refinery Processes*, PennWell, Tulsa, OK, 1981. *Process Safety Guidelines*, Center for Chemical Process Safety, American Institute of Chemical Engineers, New York, 1992–date, 22 guidelines.

R.C. Rosaler (Ed.), *Standard Handbook of Plant Engineering*, McGraw-Hill, New York, 1983.

G.L. Wells, *Safety in Process Plant Design*, Wiley, New York, 1980.

1.2 Process Equipment

A. Encyclopedias

Kirk-Othmer Concise Encyclopedia of Chemical Technology, 4th ed., Wiley, New York, 1999.

Kirk-Othmer Encyclopedia of Chemical Technology, Wiley, New York, 1978–1984, 26 vols.

McGraw-Hill Encyclopedia of Science and Technology, 5th ed., McGraw-Hill, New York, 1982.

J.J. McKetta, *Chemical Processing Handbook*, Dekker, New York, 1992.

J.J. McKetta, and W. Cunningham (Eds.), *Encyclopedia of Chemical Processing and Design*, Dekker, New York, 1976–date.

D.G. Ullman, *Encyclopedia of Chemical Technology*, Verlag Chemie, Weinheim, FRG, English edition, 1994.

B. General Data Collections

American Petroleum Institute, *Technical Data Book-Petroleum Refining*, American Petroleum Institute, Washington, DC, 1971–date.

CRC Handbook of Chemistry and Physics, CRC Press, Washington, DC., annual.

Gas Processors Suppliers Association, *Engineering Data Book*, 11th ed., Tulsa., OK, 1998.

J.A. Kent, *Riegel's Handbook of Industrial Chemistry*, 9th ed., Van Nostrand Reinhold, 1992.

L.M. Landolt-Bornstein, *Numerical Data and Functional Relationships in Science and Technology*, Springer, New York, 1950–date.

Lange's Handbook of Chemistry, 13th ed., McGraw-Hill, 1984.

J.C. Maxwell, *Data Book on Hydrocarbons*, Van Nostrand Reinhold, New York, 1950.

C.L. Yaws, et al., *Physical and Thermodynamic Properties*, McGraw-Hill, New York, 1976.

C. Special Data Collections

Azeotropic Data, American Chemical Society, Washington, DC.

Beilstein Handbook, Beilstein Information Systems, Frankfurt, Germany.

Design Institute of Physical Properties and Data (DIPPR), American Institute of Chemical Engineers, New York, 1985–9 databases.

Dortmund Data Bank, University of Oldenburg, Germany, 1996–date.

Gmelin Handbook, Gmelin Institute, Germany.

J. Gmehling et al., *Chemistry and Chemical Engineering Data Series*, DECHEMA, Frankfurt/Main, FRG., 1977–date, 11 vols.

J.H. Keenan et al., *Thermodynamic Properties of Steam*, Wiley, New York, English Units, 1969, SI Units, 1978.

Larkin, *Selected Data on Mixtures, International Data Series B, Thermodynamic Properties of Organic Aqueous Systems*, Engineering Science Data Unit Ltd., London, 1978–date.

Thermodynamic Properties of Organic Substances, Thermodynamic Research Center, Texas A & M University, Bryan, TX, 1977–date.

D.D. Wagman, *The NBS Tables of Chemical Thermodynamic Properties*, American Chemical Society, Washington, DC., 1982.

D.R. Woods, *Data for Process Design and Engineering Practice*, PTR Prentice Hall, Englewood Cliffs, NJ, 1995.

2

FLOWSHEETS

A plant design consists of words, numbers, and pictures. An engineer thinks in terms of sketches and drawings that are his or her "pictures." To solve a material balance problem, the engineer will start with a block to represent the equipment and then will show the entering and leaving streams with their amounts and properties. When asked to describe a process, an engineer will begin to sketch equipment, show how it is interconnected, and show the process flows and operating conditions.

Such sketches develop into flow sheets, which are more elaborate diagrammatic representations of the equipment, the sequence of operations, and the expected performance of a proposed plant or the actual performance of an already operating one. For clarity and to meet the needs of the various persons engaged in design, cost estimating, purchasing, fabrication, operation, maintenance, and management, several different kinds of flowsheets are necessary. Four of the main kinds will be described and illustrated.

2.1. BLOCK FLOWSHEETS

At an early stage or to provide an overview of a complex process or plant, a drawing is made with rectangular blocks to represent individual processes or groups of operations, together with quantities and other pertinent properties of key streams between the blocks and into and from the process as a whole. Such block flowsheets are made at the beginning of a process design for orientation purposes or later as a summary of the material balance of the process. For example, the coal carbonization process of Figure 2.1 starts with 100,000 lb/hr of coal and process air, involves six main process units, and makes the indicated quantities of ten different products. When it is of particular interest, amounts of utilities also may be shown; in this example the use of steam is indicated at one point. The block diagram of Figure 2.2 was prepared in connection

with a study of the modification of an existing petroleum refinery. The three feed stocks are separated into more than 20 products. Another representative petroleum refinery block diagram, in Figure 13.20 identifies the various streams but not their amounts or conditions.

2.2. PROCESS FLOWSHEETS

Process flowsheets embody the material and energy balances and include the sizes of major equipment of the plant. They include all vessels, such as reactors, separators, and drums; special processing equipment; heat exchangers; pumps; and so on. Numerical data include flow quantities, compositions, pressures, and temperatures. Major instrumentation essential for process control and the complete understanding of the flowsheet without reference to other
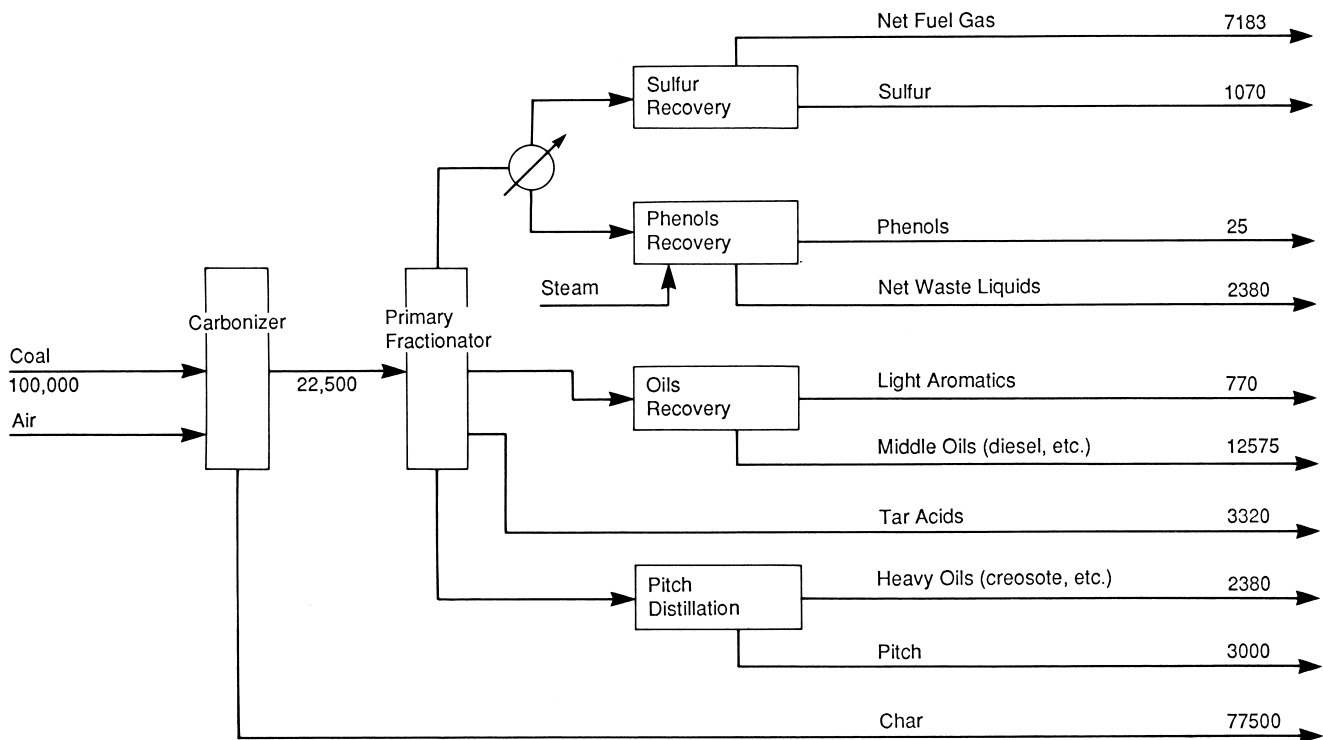
Figure 2.1. Coal carbonization block flowsheet. Quantities are in lb/hr.

Figure 2.2. Block flowsheet of the revamp of a 30,000 Bbl/day refinery with supplementary light stocks. (*The C. W. Nofsinger Co.*)

information is required, particularly in the early stages of a design, since the process flowsheet is drawn first and is the only diagram available that represents the process. As the design develops and a mechanical flowsheet is prepared, instrumentation may be removed to minimize clutter. A checklist of information usually included on a process flowsheet is found in Table 2.1.

Working flowsheets are necessarily elaborate and difficult to represent on the page of a book. Figure 2.3 originally was 30 in. wide. In this process, ammonia is made from available hydrogen supplemented by hydrogen from the air oxidation of natural gas in a two-stage reactor F-3 and V-5. A large part of the plant is devoted to the purification of the feed gases—namely, the removal of carbon dioxide and unconverted methane before they enter the converter CV-1. Both commercial and refrigeration grade ammonia are made in this plant. Compositions of 13 key streams are summarized in the tabulation. Characteristics of streams, such as temperature, pressure, enthalpy, volumetric flow rates, and so on, sometimes are conveniently included in the tabulation, as in Figure 2.3. In the interest of clarity, it may be preferable to have a separate sheet if the material balance and related stream information is voluminous.

A process flowsheet of the dealkylation of toluene to benzene is in Figure 2.4; the material and enthalpy flows and temperature and pressures are tabulated conveniently, and basic instrumentation is represented.

2.3. PROCESS AND INSTRUMENTATION DIAGRAMS (P&ID)

Piping and instrument (P&ID) diagrams emphasize two major characteristics. They do not show operating conditions or compositions or flow quantities, but they do show all major as well as minor equipment more realistically than on the process flowsheet.

TABLE 2.1. Checklist of Data Normally Included on a Process Flowsheet

1. Process lines, but including only those bypasses essential to an understanding of the process
2. All process equipment. Spares are indicated by letter symbols or notes
3. Major instrumentation essential to process control and to understanding of the flowsheet
4. Valves essential to an understanding of the flowsheet
5. Design basis, including stream factor
6. Temperatures, pressures, flow quantities
7. Weight and/or mol balance, showing compositions, amounts, and other properties of the principal streams
8. Utilities requirements summary
9. Data included for particular equipment
   a. Compressors: SCFM (60°F, 14.7 psia); ΔP psi; HHP; number of stages; details of stages if important
   b. Drives: type; connected HP; utilities such as kW, lb steam/hr, or Btu/hr
   c. Drums and tanks: ID or OD, seam to seam length, important internals
   d. Exchangers: Sqft, kBtu/hr, temperatures, and flow quantities in and out; shell side and tube side indicated
   e. Furnaces: kBtu/hr, temperatures in and out, fuel
   f. Pumps: GPM (60°F), ΔP psi, HHP, type, drive
   g. Towers: Number and type of plates or height and type of packing identification of all plates at which streams enter or leave; ID or OD; seam to seam length; skirt height
   h. Other equipment: Sufficient data for identification of duty and size

Included are sizes and specification classes of all pipe lines, all valves, and all instruments. In fact, every mechanical aspect of the plant regarding the process equipment and their interconnections is represented except for supporting structures and foundations. The equipment is shown in greater detail than on the process flowsheet, notably with respect to external piping connections, internal details, and resemblance to the actual appearance.

Many chemical and petroleum companies are now using Process Industry Practices (PIP) criteria for the development of P&IDs. These criteria include symbols and nomenclature for typical equipment, instrumentation, and piping. They are compatible with industry codes of the American National Standards Institute (ANSI), American Society of Mechanical Engineers (ASME), Instrument Society of America (ISA), and Tubular Exchanger Manufacturers Association (TEMA). The PIP criteria can be applied irrespective of whatever Computer Assisted Design (CAD) system is used to develop P&IDs. Process Industries Practice (1998) may be obtained from the Construction Industry Institute mentioned in the References.

Catena et al. (1992) showed how "intelligently" created P&IDs that are prepared on a CAD system can be electronically linked to a relational database that is helpful in meeting OSHA regulations for accurate piping and instrumentation diagrams.

Since every detail of a plant design is recorded on electronic media and paper, many other kinds of flowsheets are also required: for example, electrical flow, piping isometrics, and piping tie-ins to existing facilities, instrument lines, plans, and elevations, and individual equipment drawings in detail. Models and three-dimensional representations by computer software are standard practice in design offices.

The P&ID flowsheet of the reaction section of a toluene dealkylation unit in Figure 2.5 shows all instrumentation, including indicators and transmitters. The clutter on the diagram is minimized by tabulating the design and operating conditions of the major equipment below the diagram.

The P&I diagram of Figure 2.6 represents a gas treating plant that consists of an amine absorber and a regenerator and their immediate auxiliaries. Internals of the towers are shown with exact locations of inlet and outlet connections. The amount of instrumentation for such a comparatively simple process may be surprising. On a completely finished diagram, every line will carry a code designation identifying the size, the kind of fluid handled, the pressure rating, and material specification. Complete information about each line—its length, size, elevation, pressure drop, fittings, etc.—is recorded in a separate line summary. On Figure 2.6, which is of an early stage of construction, only the sizes of the lines are shown. Although instrumentation symbols are fairly well standardized, they are often tabulated on the P&I diagram as in this example.

2.4. UTILITY FLOWSHEETS

There are P&I diagrams for individual utilities such as steam, steam condensate, cooling water, heat transfer media in general, compressed air, fuel, refrigerants, and inert blanketing gases, and how they are piped up to the process equipment. Connections for utility streams are shown on the mechanical flowsheet, and their conditions and flow quantities usually appear on the process flowsheet.

2.5. DRAWING OF FLOWSHEETS
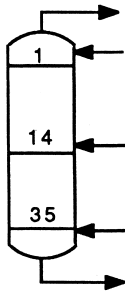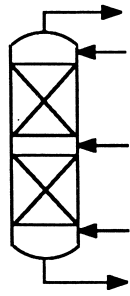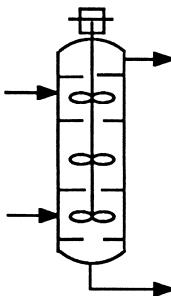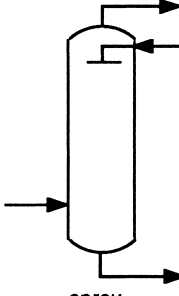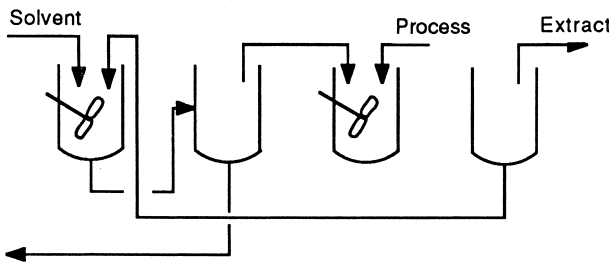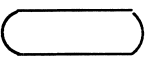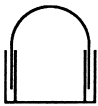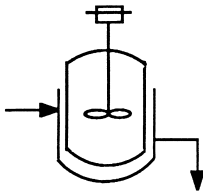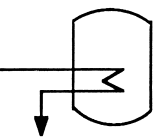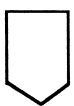
Flowsheets may be drawn by hand at preliminary stages of a project, but with process simulators and CAD software packages, it is a simple matter to develop flowsheets with a consistent set of

Figure 2.3. Process flowsheet of a plant making 47 tons/day of ammonia from available hydrogen and hydrogen made from natural gas. (*The C. W. Nofsinger Co.*).

TABLE 2.2 Flowsheet Equipment Symbols

Fluid Handling	Heat Transfer

FLUID HANDLING

HEAT TRANSFER

Centrifugal pump or blower, motor driven		Shell-and-tube heat exchanger	Tubeside / Shellside
Centrifugal pump or blower, turbine driven		Condenser	Process
Rotary pump or blower		Reboiler	Process
Reciprocating pump or compressor		Vertical thermosiphon reboiler	Process / Shellside
Centrifugal compressor		Kettle reboiler	Process
Centrifugal compressor, alternate symbol		Air cooler with finned tubes	
Steam ejector	Stm / Process	Fired heater	Process / Fuel
Coil in tank		Fired heater with radiant and convective coils	
Evaporator		Rotary dryer or kiln	Process / Heat source
Cooling tower, forced draft	Air / Water	Tray dryer	
		Spray condenser with steam ejector	Stm water

(continued)

TABLE 2.2.—(*continued***)**
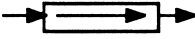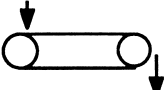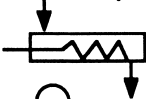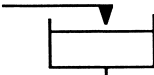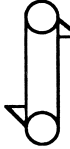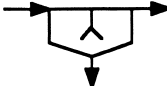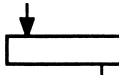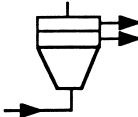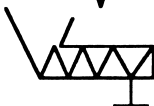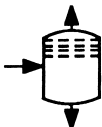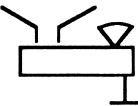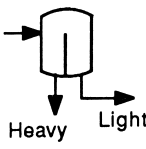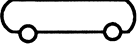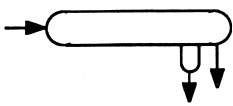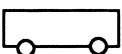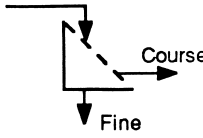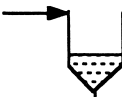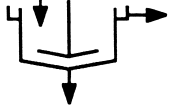
Mass Transfer	Vessels

symbols for equipment, piping, and operating conditions contained in the software packages. There is no generally accepted set of standards, although attempts have been made with little success. Every large engineering office has its own internal standards. Some information appears in the ANSI (American National Standards Institute) and British Standards publications with respect to flowsheets and piping. Useful compilations of symbols appear in books by Austin (1979), Sinnott et al. (1983) and Ulrich (1984). Many

flowsheets that appear in journals such as *Chemical Engineering* and *Hydrocarbon Processing* use a fairly consistent set of symbols. As mentioned earlier, PIP (1998) is being used for flowsheets and P&IDs by many companies.

Equipment symbols are a compromise between a schematic representation of the equipment and simplicity and ease of drawing. A selection for the more common kinds of equipment appears in Table 2.2. Less common equipment or any with especially

TABLE 2.2.—(*continued***)**

Conveyors and Feeders	Separators

CONVEYORS & FEEDERS

SEPARATORS

Conveyor

Belt conveyor

Screw conveyor

Elevator

Feeder

Star feeder

Screw feeder

Weighing feeder

Tank car

Freight car

Conical settling tank

Raked thickener

Plate-and-frame filter

Rotary vacuum filter

Sand filter

Dust collector

Cyclone separator

Centrifuge

Mesh entrainment separator

Liquid-liquid separator

Heavy   Light

Drum with water settling pot

Screen

Course

Fine

(continued)

intricate configuration often is represented simply by a circle or rectangle. Since a symbol does not usually speak entirely for itself but also may carry a name and a letter-number identification, the flowsheet can be made clear even with the roughest of equipment symbols. The letter-number designation consists of a letter or com-

bination to designate the class of the equipment and a number to distinguish it from others of the same class, as two heat exchangers by E-112 and E-215. Table 2.3 is a typical set of letter designations. Operating conditions such as flow rate, temperature, pressure, enthalpy, heat transfer rate, and also stream numbers are identified

TABLE 2.2.—(*continued***)**

Mixing and Comminution	Drivers

MIXING & COMMINUTION

Liquid mixing impellers: basic, propeller, turbine, anchor

Ribbon blender

Double cone blender

Crusher

Roll crusher

Pebble or rod mill

DRIVERS

Motor

DC motor

AC motor, 3-phase

Turbine

Turbines: steam, hydraulic, gas

with symbols called flags, of which Table 2.4 is a commonly used set. Particular units are identified on each flowsheet, as in Figure 2.3.

Letter designations and symbols for instrumentation have been thoroughly standardized by the Instrument Society of America (ISA). An abbreviated set that may be adequate for the usual flowsketch appears on Figure 2.7. The P&I diagram of Figure 2.6 affords many examples.

For clarity as well as aesthetic purposes, equipment should be represented with some indication of relative sizes. True scale is not always feasible because a tower may be 150 feet high while a process drum may be only 3 feet high and this would not be possible to represent on a drawing.

An engineer or draftperson will arrange the flowsheet as artistically as possible consistent with clarity, logic, and economy of space on a drawing. A fundamental rule is that there should be no large gaps. Flow is predominantly from the left to the right.

On a process flowsheet, distillation towers, furnaces, reactors, and large vertical vessels often are arranged at one level, condenser and accumulator drums on another level, reboilers on

still another level, and pumps more or less on one level but sometimes near the equipment they serve in order to minimize excessive crossing of lines. Streams enter the flowsheet from the left edge and leave at the right edge. Stream numbers are assigned to key process lines. Stream compositions and other desired properties are gathered into a table that may be on a separate sheet if it is especially elaborate. A listing of flags with the units is desirable on the flowsheet.

Rather less freedom is allowed in the construction of mechanical flowsheets. The relative elevations and sizes of equipment are preserved as much as possible, but all pumps usually are shown at the same level near the bottom of the drawing. Tabulations of instrumentation symbols or of control valve sizes or of relief valve sizes also often appear on P&I diagrams. Engineering offices have elaborate checklists of information that should be included on the flowsheet, but such information is beyond the scope here.

Appendix 2.1 provides the reader with material for the construction of flowsheets with the symbols of this chapter and possibly with some reference to Chapter 3.

TABLE 2.3. Letter Designations of Equipment

Equipment	Letters	Equipment	Letters
Agitator	M	Grinder	SR
Air filter	FG	Heat exchanger	E
Bin	TT	Homogenizer	M
Blender	M	Kettle	R
Blower	JB	Kiln (rotary)	DD
Centrifuge	FF	Materials handling equipment	G
Classifying equipment	S	Miscellaneous[a]	L
Colloid mill	SR	Mixer	M
Compressor	JC	Motor	PM
Condenser	E	Oven	B
Conveyor	C	Packaging machinery	L
Cooling tower	TE	Precipitator (dust or mist)	FG
Crusher	SR	Prime mover	PM
Crystallizer	K	Pulverizer	SR
Cyclone separator (gas)	FG	Pump (liquid)	J
Cyclone separator (liquid)	F	Reboiler	E
Decanter	FL	Reactor	R
Disperser	M	Refrigeration system	G
Drum	D	Rotameter	RM
Dryer (thermal)	DE	Screen	S
Dust collector	FG	Separator (entrainment)	FG
Elevator	C	Shaker	M
Electrostatic separator	FG	Spray disk	SR
Engine	PM	Spray nozzle	SR
Evaporator	FE	Tank	TT
Fan	JJ	Thickener	F
Feeder	C	Tower	T
Filter (liquid)	P	Vacuum equipment	VE
Furnace	B	Weigh scale	L

[a]Note: The letter L is used for unclassified equipment when only a few items are of this type; otherwise, individual letter designations are assigned.

TABLE 2.4. Flowsheet Flags of Operating Conditions in Typical Units
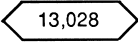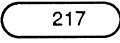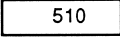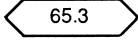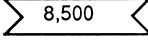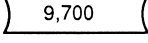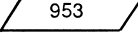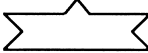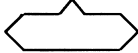
Mass flow rate, lbs/hr	13,028
Molal flow rate, lbmols/hr	217
Temperature, °F	510
Pressure, psig (or indicate if psia or Torr or bar)	155 psia
Volumetric liquid flow rate, gal/min.	65.3
Volumetric liquid flow rate, bbls/day	8,500
Kilo Btu/hr, at heat transfer equipment	9,700
Enthalpy, Btu/lb	953
Others	

Figure 2.4. Process flowsheet of the manufacture of benzene by dealkylation of toluene. (*Wells, 1980*).

Equipment list:

| E-107 RECYCLE COOLER 0.19 GCAL/H | TK-101 TOLUENE STORAGE 7.6M I.D. X 8.0M HT. | P-101 A/B TOLUENE FEED PUMPS 18M³/HR 312 M.L.H. | E-101 FEED PREHEATER 5.26 GCAL/H. | H-101 HEATER 4.96 GCAL/H | R-101 REACTOR 2.4M I.D. X 5.5M T/T | C-101 RECYCLE GAS COMPRESSOR 1070 AM3/H ΔP 3.6 BAR | D-102 RECYCLE GAS KNOCKOUT POT 0.6M I.D. X 1.8M T/T |

LEGEND

○ PRESSURE BAR
◇ TEMPERATURE °C
▢ STREAM NUMBER

							MATERIAL BALANCE			
STREAM NUMBER		**1**	**2**	**3**	**4**	**5**	**6**	**7**	**8**	**9**	**10**
HYDROGEN	KMOL/H	0.0	0.0	470.80	285.00	730.80	730.80	730.80	25.00	647.30	647.30
METHANE	KMOL/H	0.0	0.0	329.40	15.00	326.90	326.90	326.90	17.50	452.90	452.90
BENZENE	KMOL/H	0.0	0.40	6.10	0.00	5.80	6.20	6.20	0.30	115.00	115.00
TOLUENE	KMOL/H	108.70	143.90	0.43	0.00	0.41	144.31	144.31	0.02	35.83	35.83
TOTAL MOLAR FLOW	KMOL/H	108.70	144.30	806.73	300.00	1063.91	1208.21	1208.21	42.82	1251.03	1251.03
TOTAL MASS FLOW	KG H	10.000	13.270	6727	810	7.132	20452	20452	355	20807	20807
TEMPERATURE	°C	15	18	38	38	38	320	600	58	649	531
PRESSURE	BAR	14	1.1	20.4	24.0	24.0	23.7	230	240	220	212
TOTAL HEAT FLOW	GCALS/H	1.33	1.77	-3.36	0.40	-257	4.46	942	-017	913	7.24

Figure 2.5. Engineering (P&I) flowsheet of the reaction section of plant for dealkylation of benzene. (*Wells, 1980*).

ITEM NO		R-101	D-102	TX-101	ITEM NO	E-101A/B
TITLE		REACTOR	RECYCLE GAS KNOCKOUT POT	TOLUENE STORAGE	TITLE	FEED PREHEATER
I.D. = T/T M		2.4 x 5.5	0.6 x 1.8	7.6 x 8.0 HT	DUTY G CAL/H	5.26
OP TEMP °C		649	38	18	SHELL SIDE ΔP BAR	0.3
OP PRESS BARS G		230	20.6	ATMOS	TUBE SIDE ΔP BAR	0.3
DESIGN TEMP °C		700	66	46		
DES. PRESS BARS G		260	230	FULL LIQUID		

11 COOLING WATER SUPPLY 14 FUEL GAS
12 COOLING WATER RETURN 15 OXYGEN
13 M.P STEAM 16 NITROGEN

26

Equipment list (top)

| E-102 REACTOR EFFLUENT CONDENSER 3·74 GCAL/H | D-101 HIGH PRESSURE KNOCKOUT POT 2.3 MID X 6.7M T/T | E-103 BENZENE COLUMN PREHEATER 0.18G CAL/H | T-101 BENZENE COLUMN 1.5 MID X 200M T/T | E-104 OVERHEAD CONDENSER 1·83 GCAL/H | D-103 REFLUX ACCUMULATOR 1.0 MID X 2.5M T/T | P-102 A/B REFLUX PUMPS 27M3/H 35 M.L.H. | E-105 PRODUCT COOLER 0.25 GCAL/H | E-106 BENZENE REBOILER 2.07 GCAL/M |

C.W.

T-101

E-104

C.W.

D-103

L.C

C.W.

E-105

BENZENE TO STORAGE

D-102

E-102

E-103

D-101

LC

PC

M

P.102 A/B

LC

FUEL GAS RING MAIN

F.C

Stream data table
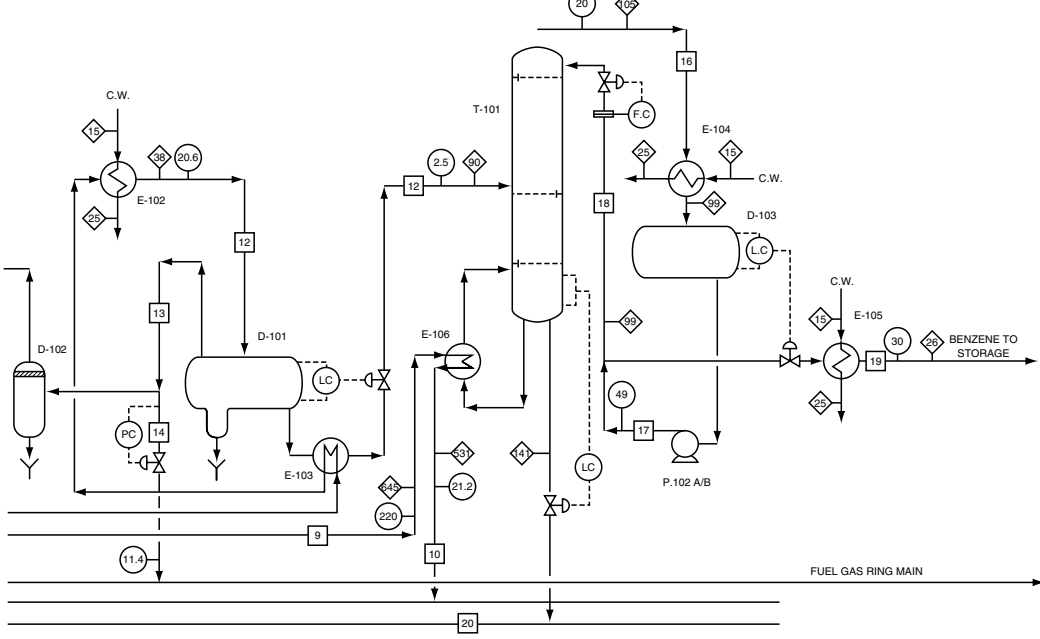
	11	12	13	14	15	16	17	18	19	20
	647.30	647.30	647.30	176.50	0.00	0.00	0.00	0.00	0.00	0.00
	452.90	452.90	452.90	123.50	0.00	0.00	0.00	0.00	0.00	0.00
	115.00	115.00	8.40	2.30	106.60	245.70	245.70	139.50	106.20	0.40
	35.83	35.83	0.59	0.16	3524	0.09	0.09	0.05	0.04	35.00
	1251.03	1251.03	1109.19	302.46	14184	245.79	245.79	139.55	106.24	35.60
	20.807	20.807	9.250	2523	11.557	19173	19173	10.836	8.287	3270
	278	38	38	38	90	105	99	99	30	1.11
	21.0	20.6	20.6	20.6	2.5	2.0	2.9	2.9	26	0.3
	198	-194	-462	-126	286	718	539	3.06	206	0.63

XYZ ENGINEERING LTD.

TITLE:

PROCESS FLOW DIAGRAM

BENZENE PLANT

Drawn By F.T. | Date | DRG. No **A-1001** | Rs

Lower diagram (Engineering Line Diagram)

RELIFE TO ATMOSPHERE AT SAFE LOCATION

RELIEF TO ATMOSPHERE AT SAFE LOCATION

OXYGEN

SNUFFING STEAM

NO POCKETS

E-101B

E-101A

MIXING ELBOW

PILOT

M-101

FLAME FAILURE

R-101

NORMALLY LEAVE SPOOL OUT

EL MIN

SHUTDOWN BY FLAME FAILURE LOW RECYCLE FLOW

SET AT 26 BARS G

D-102

EL MIN

RECYCLE GAS FREE DRAINING TO D-102

MANUAL UNLOADING VENT

SHUT DOWN SYSTEM OPERATES ON HIGH LEVEL, LOW LUBE OIL PRESSURE

C-101

SET AT 26 BARS G

REACTOR EFFLUENT

TO E-103

FROM E-106

RECYCLE TOLUENE

10" D1L2 (600°C-HG)

10" D1L1 (649°C-HC)

3" B1A1 (278°C-HC)

3" B1A1 (531°C-HC)

1½" A1A1 (141°C-PP)

6" B1A1 (58°C-NI)

6" B1A1 (38°C-N1)

6" B1A1 (38°C-N1)

12" A1A1 (58°C-N1)

(N.B. LINE & INSTRUMENT Nos OMITTED FOR CLARITY)

F/S 2 (repeated)

Lower table

R-107	H-101	ITEM NO	P-101A	P-101B	ITEM NO	C-101		**XYZ ENGINEERING LTD.**
RECYCLE COOLER	HEATER	TITLE	TOLUENE FEED PUMP	SPARE FOR P-101A	TITLE	RECYCLE GAS COMPRESSOR		TITLE
0.19	4.96	CAPACITY M³/H	18	18	CAPACITY AM³/H	1070		ENGINEERING LINE DIAGRAM
0.35	-	HEAD M L C	312	312	Δ PRESS BAR	3.6		(Sheet 1 of 2)
0.7	0.7	PUMPING TEMP °C	18	18				REACTION STAGE
		SG. AT. P.T	0.87	0.87				BENZENE PLANT

REV | | Drawn By FTT | Date 25.9.78 | DRG No **B-1001** |

Figure 2.6. Engineering flowsheet of a gas treating plant. Note the tabulation of instrumentation flags at upper right. (*Fluor Engineers, by way of Rase and Barrow, 1957*).
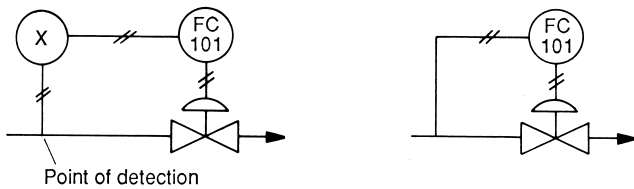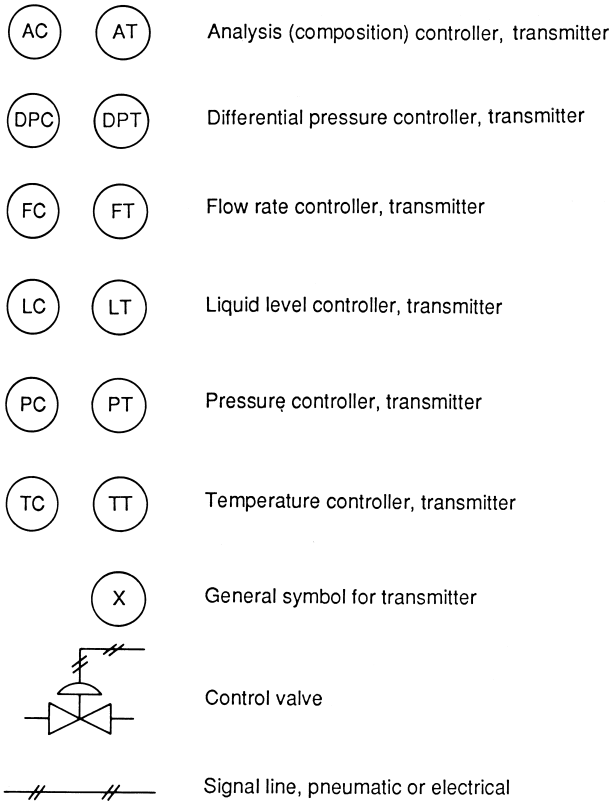
Figure 2.7. Symbols for control elements to be used on flowsheets. Instrument Society of America (ISA) publication no. S51.5 is devoted to process instrumentation terminology.

REFERENCES

D.G. Austin, *Chemical Engineering Drawing Symbols,* George Godwin, London, 1979.

D. Catena, et al., Creating Intelligent P&IDs, *Hydrocarbon Processing*, 65–68, (November 1992).

Graphic Symbols for Piping Systems and Plant, British Standard 1553, Part 1: 1977.

Graphic Symbols for Process Flow Diagrams, ASA Y32.11.1961, American Society of Mechanical Engineers, New York.

E.E. Ludwig, *Applied Process Design for Chemical and Petrochemical Plants,* Gulf, Houston, Vol. 1, 1995.

Process Industry Practices, Construction Industry Institute, University of Texas, Austin, 1998.

H.F. Rase, and M.H. Barrow, *Project Engineering of Process Plants,* Wiley, New York, 1957.

R.K. Sinnott, J.M. Coulson, and J.F. Richardson, *Chemical Engineering, Vol. 6, Design,* Pergamon, New York, 1983.

G.D. Ulrich, *A Guide to Chemical Engineering Process Design and Economics,* Wiley, New York, 1984.

G.L. Wells, *Safety in Process Design,* George Godwin, London, 1980.

Descriptions of Example Process Flowsheets

The following are examples of process descriptions from which flowsheets may be prepared for practice. Necessary auxiliaries such as drums and pumps are to be included even when they are not mentioned. Essential control instrumentation also is to be provided. Chapter 3 has examples. The processes are as follows:

1. visbreaker operation,
2. cracking of gas oil,
3. olefin production from naptha and gas oil,
4. propylene oxide synthesis,
5. manufacture of butadiene sulfone,
6. detergent manufacture,
7. natural gas absorption,
8. tall oil distillation,
9. recovery of isoprene,
10. vacuum distillation.

1. VISBREAKER OPERATION

Visbreaking is a mild thermal pyrolysis of heavy petroleum fractions whose object is to reduce fuel production in a refinery and to make some gasoline.

The oil of 7.2 API and 700°F is supplied from beyond the battery limits to a surge drum F-1. From there it is pumped with J-1A&B to parallel furnaces B-1A&B from which it comes out at 890°F and 200 psig. Each of the split streams enters at the bottom of its own evaporator T-1A&B that has five trays. Overheads from the evaporators combine and enter at the bottom of a 30-tray fractionator T-2. A portion of the bottoms from the fractionator is fed to the top trays of T-1A&B; the remainder goes through exchanger E-5 and is pumped with J-2A&B back to the furnaces B-1A&B. The bottoms of the evaporators are pumped with J-4A&B through exchangers E-5, E-3A (on crude), and E-3B (on cooling water) before proceeding to storage as the fuel product.

A side stream is withdrawn at the tenth tray from the top of T-2 and proceeds to steam stripper T-3 equipped with five trays. Steam is fed below the bottom tray. The combined steam and oil vapors return to T-2 at the eight tray. Stripper bottoms are pumped with J-6 through E-2A (on crude) and E-2B (on cooling water) and to storage as "heavy gasoline."

Overhead of the fractionator T-2 is partially condensed in E-1A (on crude) and E-1B (on cooling water). A gas product is withdrawn overhead of the reflux drum which operates at 15 psig. The "light gasoline" is pumped with J-5 to storage and as reflux.

Oil feed is 122,480 pph, gas is 3370, light gasoline 5470, heavy gasoline is 9940, and fuel oil is 103,700 pph.

Include suitable control equipment for the main fractionator T-2.

2. CRACKING OF GAS OIL

A gas oil cracking plant consists of two cracking furnaces, a soaker, a main fractionator, and auxiliary strippers, exchangers, pumps, and drums. The main fractionator (150 psig) consists of four zones, the bottom zone being no. 1.

A light vacuum gas oil (LVGO) is charged to the top plate of zone 3, removed from the bottom tray of this zone and pumped to furnace no. 1 that operates at 1000 psig and 1000°F. A heavy vacuum gas oil (HVGO) is charged to the top plate of zone 2, removed at the bottom tray and charged to furnace no. 2 that operates at 500 psig and 925°F.

Effluents from both furnaces are combined and enter the soaker; this is a large vertical drum designed to provide additional residence time for conversion under adiabatic conditions. Effluent at 500 psig and 915°F enters the bottom zone of the main fractionator.

Bottoms from zone 1 goes to a stripping column (5 psig). Overhead from that tower is condensed, returned partly as reflux and partly to zone 3 after being cooled in the first condenser of the stripping column. This condensing train consists of the preheater for the stream being returned to the main fractionator and an air cooler. The cracked residuum from the bottom of the stripper is cooled to 170°F in a steam generator and an air cooler in series. Live steam is introduced below the bottom tray for stripping.

All of the oil from the bottom of zone 3 (at 700°F), other than the portion that serves as feed to furnace no. 1, is withdrawn through a cooler (500°F) and pumped partly to the top tray of zone 2 and partly as spray quench to zone 1. Some of the bottoms of zone 1 likewise is pumped through a filter and an exchanger and to the same spray nozzle.

Part of the liquid from the bottom tray of zone 4 (at 590°F) is pumped to a hydrogenation unit beyond the battery limits. Some light material is returned at 400°F from the hydrogenation unit to the middle of zone 4, together with some steam.

Overhead from the top of the column (zone 4) goes to a partial condenser at 400°F. Part of the condensate is returned to the top tray as reflux; the rest of it is product naphtha and proceeds beyond the battery limits. The uncondensed gas also goes beyond the battery limits. Condensed water is sewered.

3. OLEFIN PRODUCTION

A gaseous product rich in ethylene and propylene is made by pyrolysis of crude oil fractions according to the following description. Construct a flowsheet for the process. Use standard symbols for equipment and operating conditions. Space the symbols and proportion them in such a way that the sketch will have a pleasing appearance.

Crude oil is pumped from storage through a steam heated exchanger and into an electric desalter. Dilute caustic is injected into the line just before the desalting drum. The aqueous phase collects at the bottom of this vessel and is drained away to the sewer. The oil leaves the desalter at 190°F, and goes through heat exchanger E-2 and into a furnace coil. From the furnace, which it leaves at 600°F, the oil proceeds to a distillation tower.

After serving to preheat the feed in exchanger E-2, the bottoms proceeds to storage; no bottoms pump is necessary because the tower operates with 65 psig at the top. A gas oil is taken off as a sidestream some distance above the feed plate, and naphtha is taken off overhead. Part of the overhead is returned as reflux to the tower, and the remainder proceeds to a cracking furnace. The gas oil also is charged to the same cracking furnace but into a separate coil. Superheated steam at 800°F is injected into both cracking coils at their inlets.

Effluents from the naphtha and gas oil cracking coils are at 1300°F and 1200°F, respectively. They are combined in the line just before discharge into a quench tower that operates at 5 psig and

235°F at the top. Water is sprayed into the top of this tower. The bottoms is pumped to storage. The overhead is cooled in a water exchanger and proceeds to a separating drum. Condensed water and an aromatic oil separate out there. The water is sewered whereas the oil is sent to another part of the plant for further treating.

The uncondensed gas from the separator is compressed to 300 psig in a reciprocating unit of three stages and then cooled to 100°F. Condensed water and more aromatic distillate separate out. Then the gas is dried in a system of two desiccant-filled vessels that are used alternately for drying and regeneration.

Subsequently the gas is precooled in exchanger E-6 and charged to a low temperature fractionator. This tower has a reboiler and a top refluxing system. At the top the conditions are 280 psig and −75°F. Freon refrigerant at −90°F is used in the condenser. The bottoms is recycled to the pyrolysis coil. The uncondensed vapor leaving the reflux accumulator constitutes the product of this plant. It is used to precool the feed to the fractionator in E-6 and then leaves this part of the plant for further purification.

4. PROPYLENE OXIDE SYNTHESIS

Draw a process flowsheet for the manufacture of propylene oxide according to the following description.

Propylene oxide in the amount of 5000 tons/yr will be made by the chlorohydrin process. The basic feed material is a hydrocarbon mixture containing 90% propylene and the balance propane which does not react. This material is diluted with spent gas from the process to provide a net feed to chlorination which contains 40 mol % propylene. Chlorine gas contains 3% each of air and carbon dioxide as contaminants.

Chlorination is accomplished in a packed tower in which the hydrocarbon steam is contacted with a saturated aqueous solution of chlorine. The chlorine solution is made in another packed tower. Because of the limited solubility of chlorine, chlorohydrin solution from the chlorinator is recirculated through the solution tower at a rate high enough to supplement the fresh water needed for the process. Solubility of chlorine in the chlorohydrin solution is approximately the same as in fresh water.

Concentration of the effluent from the chlorinator is 8 lb organics/100 lb of water. The organics have the composition

Propylene chlorohydrin	75 mol **%**
Propylene dichloride	19
Propionaldehyde	6

Operating pressure of the chlorinator is 30 psig, and the temperature is 125°F. Water and the fresh gas stream are at 80°F. Heat of reaction is 2000 Btu/lb chlorine reacted. Percentage conversion of total propylene fed to the chlorinator is 95% (including the recycled material).

Overhead from the chlorinator is scrubbed to remove excess chlorine in two vessels in succession which employ water and 5% caustic solution, respectively. The water from the first scrubber is used in the chlorine solution tower. The caustic is recirculated in order to provide adequate wetting of the packing in the caustic scrubber; fresh material is charged in at the same rate as spent material is purged. Following the second scrubber, propylene dichloride is recovered from the gas by chilling it. The spent gas is recycled to the chlorinator in the required amount, and the excess is flared.

Chlorohydrin solution is pumped from the chlorinator to the saponifier. It is mixed in the feed line with a 10% lime slurry and preheated by injection of live 25 psig steam to a temperature of 200°F. Stripping steam is injected at the bottom of the saponifier, which has six perforated trays without downcomers. Propylene oxide and other organic materials go overhead; the bottoms contain unreacted lime, water, and some other reaction products, all of which can be dumped. Operating pressure is substantially atmospheric. Bubblepoint of the overhead is 60°F.

Separation of the oxide and the organic byproducts is accomplished by distillation in two towers. Feed from the saponifier contains oxide, aldehyde, dichloride, and water. In the first tower, oxide and aldehyde go overhead together with only small amounts of the other substances; the dichloride and water go to the bottom and also contain small amounts of contaminants. Two phases will form in the lower section of this tower; this is taken off as a partial side stream and separated into a dichloride phase which is sent to storage and a water phase which is sent to the saponifier as recycle near the top of that vessel. The bottoms are a waste product. Tower pressure is 20 psig. Live steam provides heat at the bottom of this column.

Overhead from the first fractionator is condensed and charged to the second tower. There substantially pure propylene oxide is taken overhead. The bottoms is dumped. Tower pressure is 15 psig, and the overhead bubblepoint is 100°F. Reactions are

$$Cl_2 + H_2O \rightarrow ClOH + HCL$$
$$C_3H_6 + Cl_2 + H_2O \rightarrow C_3H_6ClOH + HCl \;\big|\; 2C_3H_6ClOH + Ca(OH)_2$$
$$C_3H_6 + Cl_2 \quad \rightarrow \qquad\qquad C_3H_6Cl_2 \;\big|\rightarrow 2C_3H_6O + CaCl_2 + 2H_2O$$
$$C_3H_6ClOH \quad \rightarrow \; C_2H_5CHO + HCl \;\big|$$
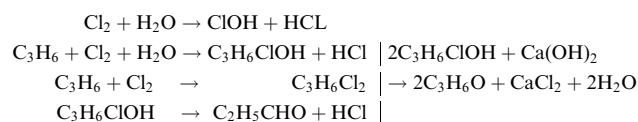
Show all necessary major equipment, pumps, compressors, refrigerant lines. Show the major instrumentation required to make this process continuous and automatic.

5. MANUFACTURE OF BUTADIENE SULFONE

A plant is to manufacture butadiene sulfone at the rate of 1250 lb/hr from liquid sulfur dioxide and butadiene to be recovered from a crude C_4 mixture as starting materials. Construct a flowsheet for the process according to the following description.

The crude C_4 mixture is charged to a 70 tray extractive distillation column T-1 that employs acetonitrile as solvent. Trays are numbered from the bottom. Feed enters on tray 20, solvent enters on tray 60, and reflux is returned to the top tray. Net overhead product goes beyond the battery limits. Butadiene dissolved in acetonitrile leaves at the bottom. This stream is pumped to a 25-tray solvent recovery column T-2 which it enters on tray 20. Butadiene is recovered overhead as liquid and proceeds to the BDS reactor. Acetonitrile is the bottom product which is cooled to 100°F and returned to T-1. Both columns have the usual condensing and reboiling provisions.

Butadiene from the recovery plant, liquid sulfur dioxide from storage, and a recycle stream (also liquified) are pumped through a preheater to a high temperature reactor R-1 which is of shell-and-tube construction with cooling water on the shell side. Operating conditions are 100°C and 300 psig. The combined feed contains equimolal proportions of the reactants, and 80% conversion is attained in this vessel. The effluent is cooled to 70°C, then enters a low temperature reactor R-2 (maintained at 70°C and 50 psig with cooling water) where the conversion becomes 92%. The effluent is flashed at 70°C and atmospheric pressure in D-1. Vapor product is compressed, condensed and recycled to the reactor R-1. The liquid is pumped to a storage tank where 24 hr holdup at 70°C is provided to ensure chemical equilibrium between sulfur dioxide, butadiene, and butadiene sulfone. Cooling water is available at 32°C.

6. DETERGENT MANUFACTURE

The process of making synthetic detergents consists of several operations that will be described consecutively.

ALKYLATION

Toluene and olefinic stock from storage are pumped (at 80°F) separately through individual driers and filters into the alkylation reactor. The streams combine just before they enter the reactor. The reactor is batch operated 4 hr/cycle; it is equipped with a single impeller agitator and a feed hopper for solid aluminum chloride which is charged manually from small drums. The alkylation mixture is pumped during the course of the reaction through an external heat exchanger (entering at −10°F and leaving at −15°F) which is cooled with ammonia refrigerant (at −25°F) from an absorption refrigeration system (this may be represented by a block on the FS); the exchanger is of the kettle type. HCl gas is injected into the recirculating stream just beyond the exit from the heat exchanger; it is supplied from a cylinder mounted in a weigh scale. The aluminum chloride forms an alkylation complex with the toluene. When the reaction is complete, this complex is pumped away from the reactor into a storage tank with a complex transfer pump. To a certain extent, this complex is reused; it is injected with its pump into the reactor recirculation line before the suction to the recirculation pump. There is a steam heater in the complex line, between the reactor and the complex pump.

The reaction mixture is pumped away from the reactor with an alkymer transfer pump, through a steam heater and an orifice mixer into the alkymer wash and surge tank. Dilute caustic solution is recirculated from the a.w.s. tank through the orifice mixer. Makeup of caustic is from a dilute caustic storage tank. Spent caustic is intermittently drained off to the sewer. The a.w.s. tank has an internal weir. The caustic solution settles and is removed at the left of the weir; the alkymer overflows the weir and is stored in the right-hand portion of the tank until amount sufficient for charging the still has accumulated.

DISTILLATION

Separation of the reactor product is effected in a ten-plate batch distillation column equipped with a water-cooled condenser and a Dowtherm-heated (650°F, 53 psig) still. During a portion of the distillation cycle, operation is under vacuum, which is produced by a two-stage steam jet ejector equipped with barometric condensers. The Dowtherm heating system may be represented by a block. Product receiver drums are supplied individually for a slop cut, for toluene, light alkymer, heart alkymer, and a heavy alkymer distillate. Tar is drained from the still at the end of the operation through a water cooler into a bottoms receiver drum which is supplied with a steam coil. From this receiver, the tar is loaded at intervals into 50 gal drums, which are trucked away. In addition to the drums which serve to receive the distillation products during the operation of the column, storage tanks are provided for all except the slop cut which is returned to the still by means of the still feed pump; this pump transfers the mixture from the alkymer wash and surge tank into the still. The recycle toluene is not stored with the fresh toluene but has its own storage tank. The heavy alkymer distillate tank connects to the olefinic stock feed pump and is recycled to the reactor.

SULFONATION

Heart alkymer from storage and 100% sulfuric acid from the sulfuric acid system (which can be represented by a block) are pumped by the reactor feed pump through the sulfonation reactor. The feed pump is a positive displacement proportioning device with a single driver but with separate heads for the two fluids. The reactor is operated continuously; it has a single shell with three stages which are partially separated from each other with horizontal doughnut shaped plates. Each zone is agitated with its individual impeller; all three impellers are mounted on a single shaft. On leaving the reactor, the sulfonation mixture goes by gravity through a water cooler (leaving at 130°F) into a centrifuge. Spent acid from the centrifuge goes to storage (in the sulfuric acid system block); the sulfonic acids go to a small surge drum or can bypass this drum and go directly to a large surge tank which is equipped with an agitator and a steam jacket. From the surge drum, the material is sent by an extraction feed pump through a water cooler, then a "flomix," then another water cooler, then another "flomix" (leaving at 150°F), and then through a centrifuge and into the sulfonic acid surge tank. Fresh water is also fed to each of the "flomixers." Wash acid is rejected by the centrifuge and is sent to the sulfuric acid system. The "flomix" is a small vertical vessel which has two compartments and an agitator with a separate impeller for each compartment.

NEUTRALIZATION

Neutralization of the sulfonic acid and building up with sodium sulfate and tetrasodium pyrophosphate (TSPP) is accomplished in two batch reactors (5 hr cycle) operated alternately. The sodium sulfate is pumped in solution with its transfer pump from the sodium sulfate system (which can be represented by a block). The TSPP is supplied as a solid and is fed by means of a Redler conveyor which discharges into a weigh hopper running on a track above the two reactors. Each reactor is agitated with a propeller and a turbine blade in a single shaft.

Sodium hydroxide of 50% and 1% concentrations is used for neutralization. The 50% solution discharges by gravity into the reactor; the 1% solution is injected gradually into the suction side of the reactor slurry circulating pump. As the caustic is added to the reactor, the contents are recirculated through a water-cooled external heat exchanger (exit at 160°F), which is common to both reactors. When the reaction is completed in one vessel, the product is fed gradually by means of a slurry transfer pump to two double drum dryers which are steam-heated and are supplied with individual vapor hoods. The dry material is carried away from the dryers on a belt conveyor and is taken to a flaker equipped with an air classifier. The fines are returned to the trough between the dryer drums. From the classifier, the material is taken with another belt conveyor to four storage bins. These storage bins in turn discharge onto a belt feeder which discharges into drums which are weighed automatically on a live portion of a roller conveyor. The roller conveyor takes the drums to storage and shipping.

Notes: All water cooled exchangers operate with water in at 75°F and out at 100°F. All pumps are centrifugal except the complex transfer, and the sulfonation reactor feed, which are both piston type; the neutralization reactor recirculation pump and the transfer pumps are gear pumps.

Show all storage tanks mentioned in the text.

7. NATURAL GAS ABSORPTION

A gas mixture has the composition by volume:

Component	N_2	CH_4	C_2H_6	C_3H_8
Mol fraction	0.05	0.65	0.20	0.10

It is fed to an absorber where 75% of the propane is recovered. The total amount absorbed is 50 mol/hr. The absorber has four theoretical plates and operates at 135 psig and 100°F. All of the absorbed material is recovered in a steam stripper that has a large number of plates and operates at 25 psig and 230°F.

Water is condensed out of the stripped gas at 100°F. After compression to 50 psig, that gas is combined with a recycle stream. The mixture is diluted with an equal volume of steam and charged to a reactor where pyrolysis of the propane occurs at a temperature of 1300°F. For present purposes the reaction may be assumed to be simply $C_3H_8 \rightarrow C_2H_4 + CH_4$ with a specific rate $k = 0.28/sec$. Conversion of propane is 60%. Pressure drop in the reactor is 20 psi.

Reactor effluent is cooled to remove the steam, compressed to 285 psig, passed through an activated alumina drying system to remove further amounts of water, and then fed to the first fractionator. In that vessel, 95% of the unconverted propane is recovered as a bottoms product. This stream also contains 3% ethane as an impurity. It is throttled to 50 psig and recycled to the reactor. In two subsequent towers, ethylene is separated from light and heavy impurities. Those separations may be taken as complete.

Construct a flow diagram of this plant. Show such auxiliary equipment as drums, heat exchangers, pumps, and compressors. Show operating conditions and flow quantities where calculable with the given data.

8. TALL OIL DISTILLATION

Tall oil is a byproduct obtained from the manufacture of paper pulp from pine trees. It is separated by vacuum distillation (50 mm Hg) in the presence of steam into four primary products. In the order of decreasing volatility these are unsaponifiables (US), fatty acid (FA), rosin acids (RA), and pitch (P). Heat exchangers and reboilers are heated with Dowtherm condensing vapors. Some coolers operate with water and others generate steam. Live steam is charged to the inlet of every reboiler along with the process material. Trays are numbered from the bottom of each tower.

Tall oil is pumped from storage through a preheater onto tray 10 of the pitch stripper T-1. Liquid is withdrawn from tray 7 and pumped through a reboiler where partial vaporization occurs in the presence of steam. The bottom 6 trays are smaller in diameter and serve as stripping trays. Steam is fed below tray 1. Pitch is pumped from the bottom through steam generator and to storage. Overhead vapors are condensed in two units E-1 and E-2. From the accumulator, condensate is pumped partly as reflux to tray 15 and partly through condenser E-1 where it is preheated on its way as feed to the next tower T-2. Steam is not condensed in E-2. It flows from the accumulator to a barometric condenser that is connected to a steam jet ejector.

Feed enters T-2 at tray 5. There is a pump-through reboiler. Another pump withdraws material from the bottom and sends it to tower T-3. Liquid is pumped from tray 18 through a cooler and returned in part to the top tray 20 for temperature and reflux control. A portion of this pumparound is withdrawn after cooling as unsaps product. Steam leaves the top of the tower and is condensed in the barometric.

Tray 5 of T-3 is the feed position. This tower has two reboilers. One of them is a pumparound from the bottom, and the other is gravity feed from the bottom tray. Another pump withdraws material from the bottom, and then sends it through a steam generator and to storage as rosin acid product. A slop cut is withdrawn from tray 20 and pumped through a cooler to storage. Fatty acid product is pumped from tray 40 through a cooler to storage. Another stream is pumped around from tray 48 to the top tray 50 through

a cooler. A portion of the cooled pumparound is sent to storage as another unsaps product. A portion of the overhead steam proceeds to the barometric condenser. The rest of it is boosted in pressure with high pressure steam in a jet compressor. The boosted steam is fed to the inlets of the two reboilers associated with T-3 and also directly into the column below the bottom tray.

The vapors leaving the primary barometric condenser proceed to a steam ejector that is followed by another barometric. Pressures at the tops of the towers are maintained at 50 mm Hg absolute. Pressure drop is 2 mm Hg per tray. Bottom temperatures of the three towers are 450, 500, and 540°F, respectively. Tower overhead temperatures are 200°F. Pitch and rosin go to storage at 350°F and the other products at 125°F. The steam generated in the pitch and rosin coolers is at 20 psig. Process steam is at 150 psig.

9. RECOVERY OF ISOPRENE

Draw carefully a flowsheet for the recovery of isoprene from a mixture of C_5 hydrocarbons by extractive distillation with aqueous acetonitrile according to the following description.

A hydrocarbon stream containing 60 mol % isoprene is charged at the rate of 10,000 pph to the main fractionator D-1 at tray 40 from the top. The solvent is acetonitrile with 10 wt % water; it is charged at the rate of 70,000 pph on tray 11 of D-1. This column has a total of 70 trays, operates at 10 psig and 100°F at the top and about 220°F at the bottom. It has the usual provisions for reboiling and top reflux.

The extract is pumped from the bottom of D-1 to a stripper D-2 with 35 trays. The stripped solvent is cooled with water and returned to D-1. An isoprene-acetonitrile azeotrope goes overhead, condenses, and is partly returned as top tray reflux. The net overhead proceeds to an extract wash column D-3 with 20 trays where the solvent is recovered by countercurrent washing with water. The overhead from D-3 is the finished product isoprene. The bottoms is combined with the bottoms from the raffinate wash column D-4 (20 trays) and sent to the solvent recovery column D-5 with 15 trays.

Overhead from D-1 is called the raffinate. It is washed countercurrently with water in D-4 for the recovery of the solvent, and then proceeds beyond the battery limits for further conversion to isoprene. Both wash columns operate at substantially atmospheric pressure and 100°F. The product streams are delivered to the battery limits at 100 psig.

Solvent recovery column D-5 is operated at 50 mm Hg absolute, so as to avoid the formation of an azeotrope overhead. The required overhead condensing temperature of about 55°F is provided with a propane compression refrigeration system; suction condition is 40°F and 80 psig, and discharge condition is 200 psig. Vacuum is maintained on the reflux accumulator with a two-stage steam ejector, with a surface interstage condenser and a direct water spray after-condenser. The stripped bottoms of D-5 is cooled to 100°F and returned to the wash columns. Some water makeup is necessary because of leakages and losses to process streams. The solvent recovered overhead in D-5 is returned to the main column D-1. Solvent makeup of about 20 pph is needed because of losses in the system.

Steam is adequate for all reboiling needs in this plant.

10. VACUUM DISTILLATION

This plant is for the distillation of a heavy petroleum oil. The principal equipment is a vacuum tower with 12 trays. The top tray is numbered 1. Trays 1, 2, 10, 11, and 12 are one-half the diameter of the other trays. The tower operates at 50 mm Hg.

Oil is charged with pump J-1 through an exchanger E-1, through a fired heater from which it proceeds at 800°F onto tray 10 of the tower. Live steam is fed below the bottom tray.

Bottoms product is removed with pump J-3 through a steam generator and a water cooled exchanger E-3 beyond the battery limits. A side stream is taken off tray 6, pumped with J-2 through E-1, and returned onto tray 3 of the tower. Another stream is removed from tray 2 with pump J-4 and cooled in water exchanger E-2; part of this stream is returned to tray 1, and the rest of it leaves the plant as product gas oil.

Uncondensed vapors are removed at the top of the column with a one-stage steam jet ejector equipped with a barometric condenser.

Show the principal controls required to make this plant operate automatically.

3

PROCESS CONTROL

*O*n typical grass-roots, chemical processing facilities, as much as 10% of the total capital investment is allocated to process control equipment, design, implementation, and commissioning. Process control is a very broad topic with many distinct aspects. The following possible sub-topics give some idea of the full breadth of this topic:

In the field, the topic of process control includes the selection and installation of sensors, transmitters, transducers, actuators, valve positioners, valves, variable-speed drives, switches and relays, as well as their air supply, wiring, power, grounding, calibration, signal conditioning, bus architecture, communications protocol, area classification, intrinsic safety, wired interlocks, maintenance, troubleshooting, and asset management.

In the control room, process control encompasses the selection and installation of panel-mounted alarms, switches, recorders, and controllers, as well as Program Logic Controllers (PLC) and Distributed Control Systems (DCS). These include analog and digital input/output hardware, software to implement control strategies,

interlocks, sequencing and batch recipes, as well as display interfaces, alarm management, and Ethernet communication to networked computers, which are used to provide supervisory control, inferential measures, data historians, performance monitoring, and process optimization.

Also, the design practice includes P&ID documentation, database specification and verification of purchased equipment, control design and performance analysis, software configuration, real-time simulation for DCS system checkout and operator training, reliability studies, interlock classification and risk assessment of safety instrumented systems (SIS), and hazard and operability (HAZOP) studies.

Books have been written about each of these sub-topics and many standards exist to specify best practices or provide guidance. The Instrumentation, Systems and Automation Society (ISA) is the primary professional society that addresses many of these different aspects of process control. The focus of this chapter will be on control loop principles, loop tuning, and basic control strategies for continuous processes.

3.1. FEEDBACK CONTROL LOOP

Feedback control utilizes a loop structure with negative feedback to bring a measurement to a desired value, or setpoint. A block diagram of a typical process control loop is shown in Figure 3.1, with key elements of the loop being the controller, valve, process, and measurement. Note that in addition to the setpoint entering the loop, there is also a load shown. Changes in setpoint move the process to a new value for the controlled variable, whereas changes in load affect the process, resulting in a disturbance to the con-trolled variable.

The control loop must respond to either a change in setpoint or a change in the load, by manipulating the valve in a manner that affects the process and restores the controlled variable to its setpoint. Reacting to setpoint changes is called *servo operation*, and reacting to load changes is called *regulator operation*. A flow

control loop is a simple process example where both servo and regulator operation is often required. The flow setpoint may be changed to establish a new production rate; however, once set, it must be maintained during load changes, which disturb the flow through the valve by altering upstream or downstream pressures.

Control loop performance is determined by the response characteristics of the block elements in the loop: the controller, valve, process, and measurement. Design choices can be made for the valve, process, and measurement, which can improve the achievable performance of the loop. The controller may then be tuned for the best performance of the resulting control loop, but must also provide an operating margin from control instability. The controller tuning always establishes a trade-off between resulting loop performance and robustness due to this operating margin.
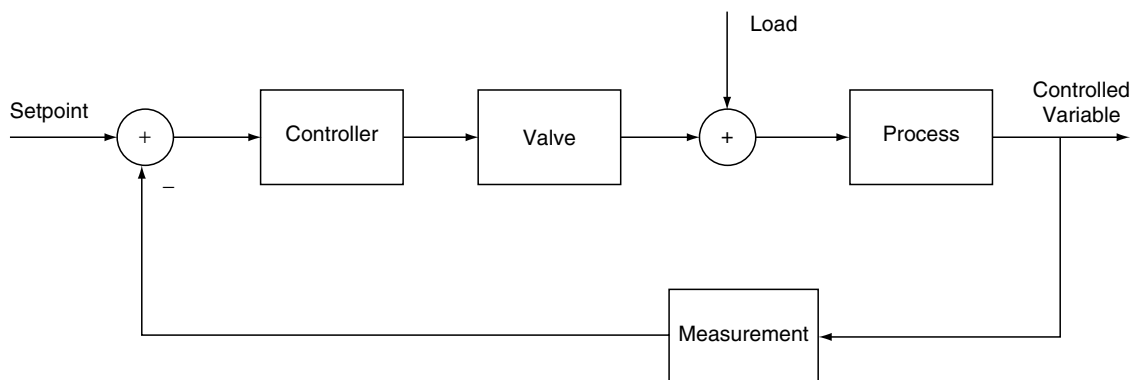
Figure 3.1. Block diagram of a control loop.

OVERALL RESPONSE CHARACTERISTICS

Both steady-state and dynamic response characteristics affect loop performance. Steady-state gain is the most basic and important of these response characteristics. Gain for a block element can be simply defined as the ratio of change in output to a change in input. For several blocks in series, the resulting overall gain is the product of the individual block gains.

Dynamic responses can be divided into the categories of self-regulating and non-self-regulating. A self-regulating response has inherent negative feedback and will always reach a new steady-state in response to an input change. Self-regulating response dynamics can be approximated with a combination of a deadtime and a first-order lag with an appropriate time constant.

Non-self-regulating responses may be either integrating or run-away. An integrating response continues to change due to a lack of inherent feedback. Since the output of an integrating response continues to change, its steady-state gain must be determined as the ratio of rate of change of the output to a change in the input. Its response dynamics can be approximated with a combination of a deadtime, a first-order lag, and a ramp. Self-regulating responses with a very large time constant, or a very large gain, can also be approximated as a pseudo-integrator during the first portion of their response.

A run-away response continues to change at an increasing rate due to inherent positive feedback. The response is exponential and may be thought of as a first-order lag with a negative time constant. Run-away response dynamics may be approximated with a combination of deadtime, a first-order lag, and a second, longer lag with a negative time constant.

VALVE CHARACTERISTICS

Control valves have unique characteristics that can significantly affect the performance of a loop. The steady-state gain of the valve relates controller output to a process flow. How this flow affects the controlled variable of the process defines the range of control. For servo control, the range of control would be defined as the range of setpoints achievable at a given load. For regulator control, it would be defined as the range of loads for which the given setpoint could be maintained. Attempting to operate outside the range of control will always result in the valve being either fully open or closed and the controlled variable offset from setpoint.

The steady-state gain of a control valve is determined at its operating point, since its gain may vary somewhat throughout its stroke. Valves have internal trim that provides a specified gain as a function of position, such as Linear, Equal Percentage, or Quick Opening inherent characteristics. Typically, the trim is chosen such that the installed characteristics provide an approximately linear flow response. Thus, for a valve operating with critical gas flow, Linear trim would provide an approximately linear flow response. An Equal Percentage trim may be used to provide a more linear response for gas or liquid flow where line pressure drop is equal or greater than the valve pressure drop. The Quick Opening trim is usually not chosen for linear response in continuous control applications; however, it provides a high gain near the closed position, which is useful for fast-responding, pressure-relief applications.

One common nonlinear characteristic of control valves is hysteresis, which results in two possible flows at a given valve position, depending on whether the valve is opening or closing. In the steady-state, hysteresis limits resolution in achieving a specific flow with its desired effect on the process. Dynamically, hysteresis also creates pre-stoke deadtime, which contributes to total loop deadtime, thus degrading the performance of the loop. Pre-stroke deadtime is the time that elapses as the controller output slowly traverses across the dead band before achieving any change in actual valve position or flow.

The use of a valve positioner can significantly reduce both hysteresis and pre-stroke deadtime. *A valve positioner is recommended for all control loops requiring good performance.* Typical hysteresis may be 2–5% for a valve without a positioner, 0.5–2% for a valve with an analog positioner, and 0.2–0.5% for a valve with a digital positioner.

On some control loops, a variable-speed drive on a pump, fan, or blower may be used as the final element connecting the controller output to the process. Variable-speed drives provide fast and linear response with little or no hysteresis and are therefore an excellent choice with respect to control performance. As the initial cost of variable-speed drives continues to decrease, their use should become a more widespread practice.

PROCESS CHARACTERISTICS

An agitated tank is often used as an example of a first-order lag process. However, mixing in real tanks falls far short of the ideal well-mixed tank. Real tanks have composition responses that are a combination of a first-order lag and deadtime. If the pumping rate of the agitator (F_a) is known, the deadtime (T_d) of the real tank may be estimated by the following equation: $T_d = V/(F + F_a)$, where V is the volume of the tank and F is the flow through it.

Process responses often consist of multiple lags in series. When these lags are noninteracting, the resulting response is predominantly deadtime, varying linearly with the number of lags in series. However, when these lags are interacting, such as the trays on a distillation column, the resulting response remains predominantly a first-order lag with a time constant proportional to the number of lags squared.

Other process characteristics that affect control performance are both steady-state and dynamic nonlinear behavior. Steady-state nonlinear behavior refers to the steady-state gain varying, dependent on operating point or time. For example, the pH of a process stream is highly nonlinear, dependent on the operating point on the titration curve. Further, depending on the stream component composition, the titration curve itself may vary over time.

Nonlinear dynamic behavior can occur due to operating point, direction, or magnitude of process changes. For example, the time constant of the composition response for a tank will depend on the operating point of liquid level in the tank. Some processes will respond in one direction faster than in the other direction, particularly as the control valve closes. For example, liquid in a tank may drain quite rapidly, but once the drain valve closes, the level can rise only as fast as the inlet stream flow allows. The magnitude of a change may cause different dynamic response whenever inherent response limits are reached. Process examples may include a transition to critical flow, or a transition from a heat transfer to a mass transfer limiting mechanism in a drying processes.

These nonlinearities are the main reason an operating margin must be considered when tuning the controller. If the loop is to be robust and operate in a stable manner over a wide range of conditions, conservative values of the tuning parameters must be chosen. Unfortunately, this results in poorer performance under most conditions. One technique to handle known nonlinearities is to provide tuning parameters that vary based on measured process conditions.

MEASUREMENT CHARACTERISTICS

Sensor type and location, as well transmitter characteristics, noise, and sampled data issues, also can affect loop performance. Most continuous measurement sensors and transmitters have relatively fast dynamics and a noise filter, which can be approximated by a

first-order lag with a one- or two-second time constant. Temperature sensors are somewhat slower, as the sensor is in a thermowell, and these measurements have a larger, 15- to 30-second time constant.

Noise is often a problem in flow, pressure, and level measurements. Because flow is a very fast loop, controller tuning can be set to ignore noise by using low gain and rely on a large amount of reset to take significant action only on sustained deviations. On slower, non-self-regulating loops, noise in the measurement can degrade potential control performance by preventing the use of higher gains and/or derivative action in the controller.

Excessive filtering of a signal to reduce noise would add effective deadtime to the loop, thus degrading the loop performance. One technique for reducing high-amplitude, high-frequency noise, without introducing an excessive lag, is to limit the rate of change of the signal to a rate comparable to the largest physically realizable upset. This approach chops off peak noise and allows a smaller time constant filter to effectively reduce the remaining lower-amplitude, high-frequency noise.

Noncontinuous measurements, such as those produced by the sample-and-hold circuitry of a chromatograph, can introduce significant deadtime into a loop. Also, the nature of the periodic step change in value prevents the use of derivative action in the controller.

Distributed Control Systems often sample the transmitted signal at a one-second interval, sometimes faster or slower depending on the characteristics of the process response. One concern related to sample data measurement is aliasing of the signal, which can shift the observed frequency. However, at a one-second sample interval, this has seldom been a problem for all but the fastest process responses. A general rule for good performance is to make the period between scans less than one-tenth of the deadtime, or one-twentieth of the lag in the process response.

CONTROLLER CHARACTERISTICS

The design of the valve, process, and measurement should be made such as to minimize deadtime in the loop while providing a reliable, more linear response, then the controller can be tuned to provide the best performance, with an acceptable operating margin for robustness. The PID controller is the most widespread and applicable control algorithm, which can be tuned to provide near optimal responses to load disturbances. PID is an acronym for Proportional, Integral, and Derivative modes of control.

The Proportional mode establishes an algebraic relationship between input and output. The proportionality is set by a tunable gain parameter. This unitless parameter, controller gain (K_c), specifies percent change in output divided by percent change in input. On earlier versions of PID controllers, an alternate parameter, Proportional Band (PB), was defined as the percent change in input required to cause a 100 percent change in output. Thus, by combining definitions, these two terms are related as follows: $K_c = 100/PB$.

The Integral mode is sometimes referred to as "reset" because it continues to take action over time until the error between measurement and setpoint is eliminated. The parameter to specify this action is Integral time, which can be thought of as the length of time for the controller to repeat the initial proportional response if the error remained constant. Note that as this parameter is made smaller, the reset increases as the control action is repeated in a shorter period of time. Some controllers use an alternate parameter, Reset, that is the reciprocal of Integral time and is referred to as repeats/unit time. This latter approach is perhaps more intuitive in that as the Reset parameter is increased, there is more reset action being applied.

The Derivative mode is sometimes referred to as "rate" because it applies control action proportional to the rate of change of its input. Most controllers use the process measurement, rather than the error, for this input in order to prevent an exaggerated response to step changes in the setpoint. Also, noise in the process measurement is attenuated by an inherent filter on the Derivative term, which has a time constant 1/8 to 1/10 of the Derivative time. Even with these considerations, process noise is a major deterrent to the use of Derivative mode.

Another, perhaps the most important, controller parameter is the control action, which is set as either "direct" or "reverse." By convention, if the valve position is to increase as the measurement increases, then the controller is considered direct acting. The actual output signal from the controller will further depend on the specified failure mode of the valve. For example, a fail-closed valve will require an increase-to-open signal, whereas a fail-open valve will require an increase-to-close signal. In order to minimize confusion, rather than displaying actual output, most controllers display an "implied valve position," which indicates the desired position of the valve.

The response characteristics of a direct acting PID controller are shown in Figure 3.2. For illustrative purpose, a step change to the measurement is made and held constant without feedback. In response to this disturbance, the independent contributions of each controller mode are provided in Figure 3.2(A, B, and C), and the combined PID response is presented in Figure 3.2(D). Note that the Proportional mode has an immediate effect on the output, as defined by its algebraic relationship. The Integral mode keeps changing the output at a constant rate as long as the constant error persists. The Derivative mode provides an initial exaggerated response, which decays rapidly since the measurement stops changing after the initial step disturbance.

Although there are many ways to implement PID modes into a controller, the ISA standard algorithm is an ideal, noninteracting combination of the modes. This algorithm is a relatively new standard, made feasible by digital implementation. Note that many previously published tuning guidelines have been developed based on various analog implementations of an interacting, series combination of these modes.

3.2. CONTROL LOOP PERFORMANCE AND TUNING PROCEDURES

Any systematic tuning procedure must strive to provide optimal performance against some objective function. The first decision to be made is whether this objective function is for setpoint response or load response. Optimizing setpoint response will result in sluggish load response, so if the primary objective of the loop is regulation, then the objective function should be a measure of load response performance.

A variety of criteria have been proposed for this objective function, such as the integral of square error (ISE), the integral of absolute error (IAE), or the integral of the time weighted absolute error (ITAE). The ISE criterion provides the greatest emphasis on peak error, but is more oscillatory and less robust than the other criteria. Although for any given loop, "the beauty of the response is in the eye of the beholder," in general the IAE criterion has become the more widely accepted objective function to provide both responsive and robust tuning.

Numerous empirical correlations have been developed to determine PID tuning parameters for load responses of processes. These correlations are based either on closed-loop procedures, which directly identify the ultimate gain and ultimate period of the loop, or on open-loop procedures, which identify the time
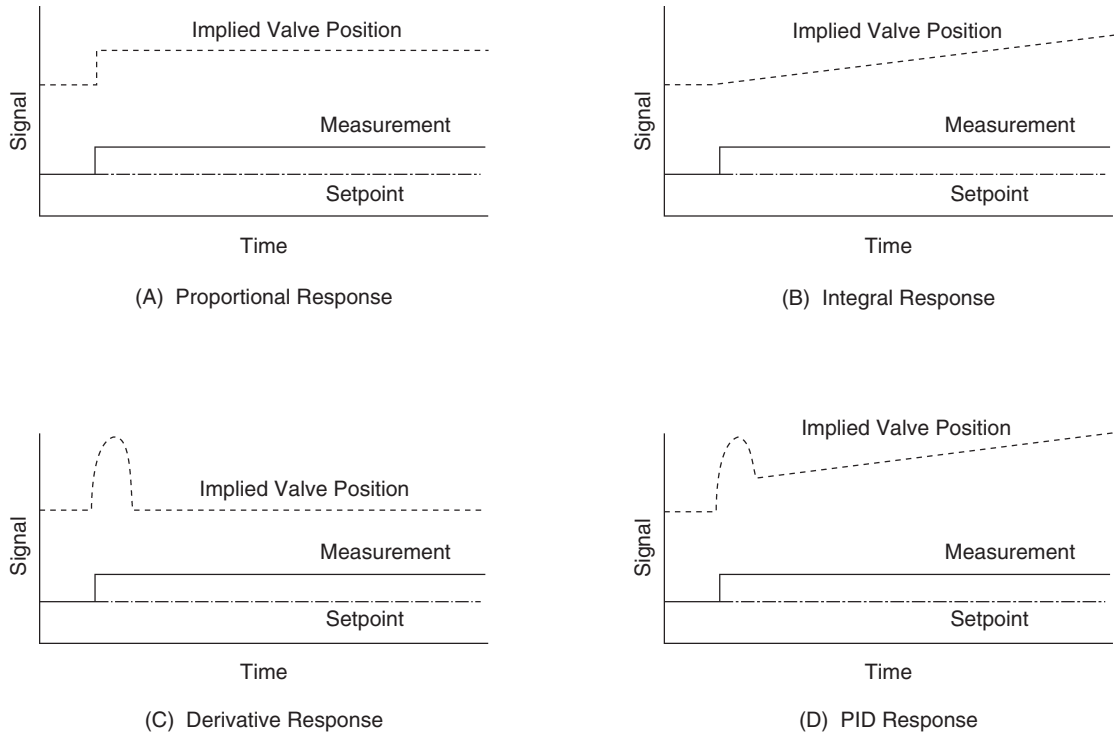
Figure 3.2. Response characteristics of a direct acting PID controller.

constant and deadtime of a first-order plus deadtime approximation of the process response.

CLOSED-LOOP PROCEDURE

The closed-loop procedure requires tuning a controller with only gain and increasing that parameter until sustained oscillations are observed. When this occurs, the gain is called the ultimate gain (K_u) and the time between successive cycles is called the ultimate period (T_u).

An alternative closed-loop approach called the "relay method" uses temporary narrow limits on the controller output and toggles between output limits each time the controller error changes sign. The ultimate period is determined as before and the ultimate gain is computed as $K_u = 4d/(3.14a)$, where d is the range of the output limits and a is the range of the process measurement, both in percent.

Correlations such as those provided in Table 3.1 may then be used to determine the values of tuning parameters based on the closed-loop response (Edgar, 1999).

OPEN-LOOP PROCEDURE

The open-loop procedure requires that the loop be placed in manual mode and a step change in the controller output is made.

The process response is recorded such that a time constant (T_c) and deadtime (T_d) may be determined from the data. For non-self-regulating processes, a pseudo time constant may be determined from the total time it takes the process to move an amount equivalent to the controller output minus the deadtime before the process begins to respond.

Correlations such as those presented in Table 3.2 may then be used to determine the values of tuning parameters based upon the open-loop response (Edgar, 1999).

DEFAULT TUNING

It is useful to have a set of robust, if not optimal, tuning parameters for loops at startup. The values provided in Table 3.3 may be used for that purpose. Loops with tuning outside the suggested range of values indicate either an unusual process or fundamental problems with the valve, process, or measurement responses.

3.3. SINGLE STREAM CONTROL

Flow, level, and pressure are process variables that can be controlled by manipulating their own process stream. Flow control is typically used to establish throughput, whereas level and pressure are measures of liquid and gas inventory, which must be main-

TABLE 3.1. Tuning Parameter Values from Closed-Loop Response

Controller Type	Gain	Integral Time	Derivative Time
Proportional only, P	$0.50K_u$	-	-
Proportional-Integral, PI	$0.58K_u$	$0.81T_u$	-
Proportional-Integral-Derivative, PID$_n$	$0.76K_u$	$0.48T_u$	$0.11T_u$
Proportional-Integral-Derivative, PID$_i$	$0.55K_u$	$0.39T_u$	$0.14T_u$

Where: PID$_n$ = noninteracting ISA algorithm; PID$_i$ = interacting, series algorithm.

TABLE 3.2. Tuning Parameter Values from Open-Loop Response

Controller Type	Gain	Integral Time	Derivative Time
Proportional only, P	$0.56T_c/T_d$	–	–
Proportional-Integral, PI	$0.65T_c/T_d$	$3.5T_d$	–
Proportional-Integral-Derivative, PID_n	$1.30T_c/T_d$	$2.1T_d$	$0.63T_d$
Proportional-Integral-Derivative, PID_i	$0.88T_c/T_d$	$1.8T_d$	$0.70T_d$

Where: PID_n = noninteracting ISA algorithm; PID_i = interacting, series algorithm.

TABLE 3.3. Default and Range of Typical Tuning Parameter Values

Process	Gain	Integral Time (seconds)	Derivative Time (seconds)	Scan Period (seconds)
Liquid Flow/Pressure	0.3 (0.1–0.8)	6 (1–12)	0 (0–2)	1 (0.2–2)
Liquid Level	5.0 (0.5–20)	600 (120–6000)	0 (0–60)	2 (1–30)
Gas Pressure	5.0 (0.5–20)	300 (60–600)	0 (0–30)	1 (0.1–1)
Inline Blending	1.0 (0.1–10)	30 (10–60)	0 (0–30)	1 (0.5–2)
Exchanger Temperature	0.5 (0.1–10)	120 (30–300)	12 (6–120)	2 (0.5–5)
Column Temperature	0.5 (0.1–10)	300 (120–3000)	30 (6–600)	2 (1–30)
Reactor Temperature	2.0 (0.1–10)	600 (300–6000)	60 (6–600)	2 (1–10)
Inline pH	0.2 (0.1–0.3)	30 (12–60)	0 (0–6)	1 (0.2–2)
Neutralizer pH	0.2 (0.001–10)	300 (60–600)	60 (6–120)	2 (1–5)
Reactor pH	1.0 (0.001–50)	120 (60–600)	30 (6–60)	2 (1–5)

tained to establish the overall process material balance. The process material balance is typically controlled in the forward direction, as shown in Figure 3.3(A), where the feed flow rate to the process is set, establishing the throughput and ultimate product rate after allowing for yield losses.

For the reaction area of a process, the large tank shown first in these figures may be thought of as a shift or day tank, with its inventory maintained by the periodic transfer of raw material into it from outside the boundary limits of the process. For the refining area of a process, it may be thought of as a large crude tank used to isolate the crude and refining areas of the process. In either case, the tank is sized large enough to provide continued operation of the downstream equipment during short periods of interrupted supply. When such a tank is used as a transition between a batch and continuous process, it is desirable for the tank to hold at least three batches of material.

By contrast, in Figure 3.3(B), a less common material balance approach is taken, where the product flow rate is set directly and each process unit must then adjust its inlet flow to maintain inventories. No yield assumptions are required by this approach. Alternatively, an intermediate flow could be set, as shown in Figure 3.3(C), in which case the units ahead would have to adjust their inlet flow and the units following would adjust their outlet flow. Although these latter strategies are less common, they can offer the advantage of fixing the feed to a specific unit that may be difficult to operate.

FLOW CONTROL

Flow control is probably the most common control loop in most processes. Typically, a liquid or gas flow rate is maintained in a pipe by a throttling valve downstream of the measurement, as shown in Figure 3.4(A). Locating the valve upstream of the measurement is not recommended because many measurement problems can arise.

Another method of controlling liquid flow is to adjust the speed of a variable-speed drive on a pump, as shown in Figure 3.4(B). This approach is applicable to either centrifugal or positive displacement pumps and can provide significant energy savings at lower rates because the power required is proportional to the speed cubed. This approach also provides good control performance; however, a separate block valve is required to prevent leakage when the pump is stopped. Variable-speed drives have become much more practical in recent years due to advanced electronics and microprocessor developments, which allow variable frequency "vector" drives for standard AC induction motors. In addition to providing precise control and energy savings, these drives provide a soft start/stop and do not require separate starting circuits.

Gas flow rate may also be controlled with variable-speed drives on compressors, blowers, or fans. The adjustment of louvers

Figure 3.3. Material balance control.

or variable pitch fan blades, as shown in Figure 3.4(C), are additional methods for gas flow control. However, these latter devices have mechanical linkages that require high maintenance and introduce significant hysteresis, which will degrade control loop performance.

Solids may have their flow controlled by adjusting a motor speed and inferring flow from the rate of displacement. Figure 3.4(D) shows granular solids being flow controlled by a rotary vane feed valve at the bottom of a supply hopper. Figure 3.4(E) shows the linear line speed of a belt feeder with a manually adjustable underflow weir height at the hopper. Figure 3.4(F) shows a rotary feed plate, which controls solids flow by variable rotation speed with a manually adjustable collar height and plow position. Figure 3.4(G) shows a horizontal screw feeder or extruder, which controls flow by adjusting the shaft speed. The flow of solids in the form of strings or sheets may be controlled by adjusting the line speed of rollers, as shown in Figure 3.4(H).

LEVEL CONTROL

Level control can be designed into the process with gravity, pressure, and elevation determining outlet flow. For example, the use of inlet and outlet weirs on the trays of a distillation column maintain both downcomer and tray levels, as shown in Figure 3.5(A). For operation at a pressure similar to downstream equipment, a sump level may be maintained by elevating external piping to provide a seal, with a vent line to prevent siphoning, as shown in Figure 3.5(B). If downstream pressure is greater, then a barometric leg may be used to maintain a seal, as shown in Figure 3.5(C). The overflow line shown must be adequately sized to self-vent; otherwise, it may begin to siphon.

For pumped systems, such as shown in Figure 3.6, the tank level may be controlled by manipulating either the outlet or inlet flow. Direct control action is used when the outlet flow is adjusted. Reverse action is required when the inlet flow is adjusted. Tank level is an integrating process, usually with negligible deadtime, therefore high gain and long integral time are recommended tuning when tight level control is desired. Tight level control is often required for reactor and heat transfer vessels, but loose level control is preferred for surge tanks.

The purpose of a surge tank is to reduce variations in the manipulated flow by absorbing the effect of temporary disturbances. Ideally, the tuning would be gain only, allowing the level to vary about a midlevel setpoint with offset. However, in most processes, a setpoint at midlevel and permanent offset are not acceptable. More typical is a setpoint either at the low end to allow upstream equipment to keep running if the outlet flow stops, or at the high end to provide feed for downstream equipment if the inlet flow stops. For these latter cases, some integral action is required to return the level to the setpoint. An error-squared PI algorithm has proven effective for surge level control, providing low gain near setpoint and proportionally higher gain at larger deviations. In addition, logic that turns off the integral action when the level is near setpoint, can be helpful in eliminating slow continuous cycling.

Figure 3.4. Flow control.

(A) Weirs

(B) Elevated Piping

(C) Barometric Leg
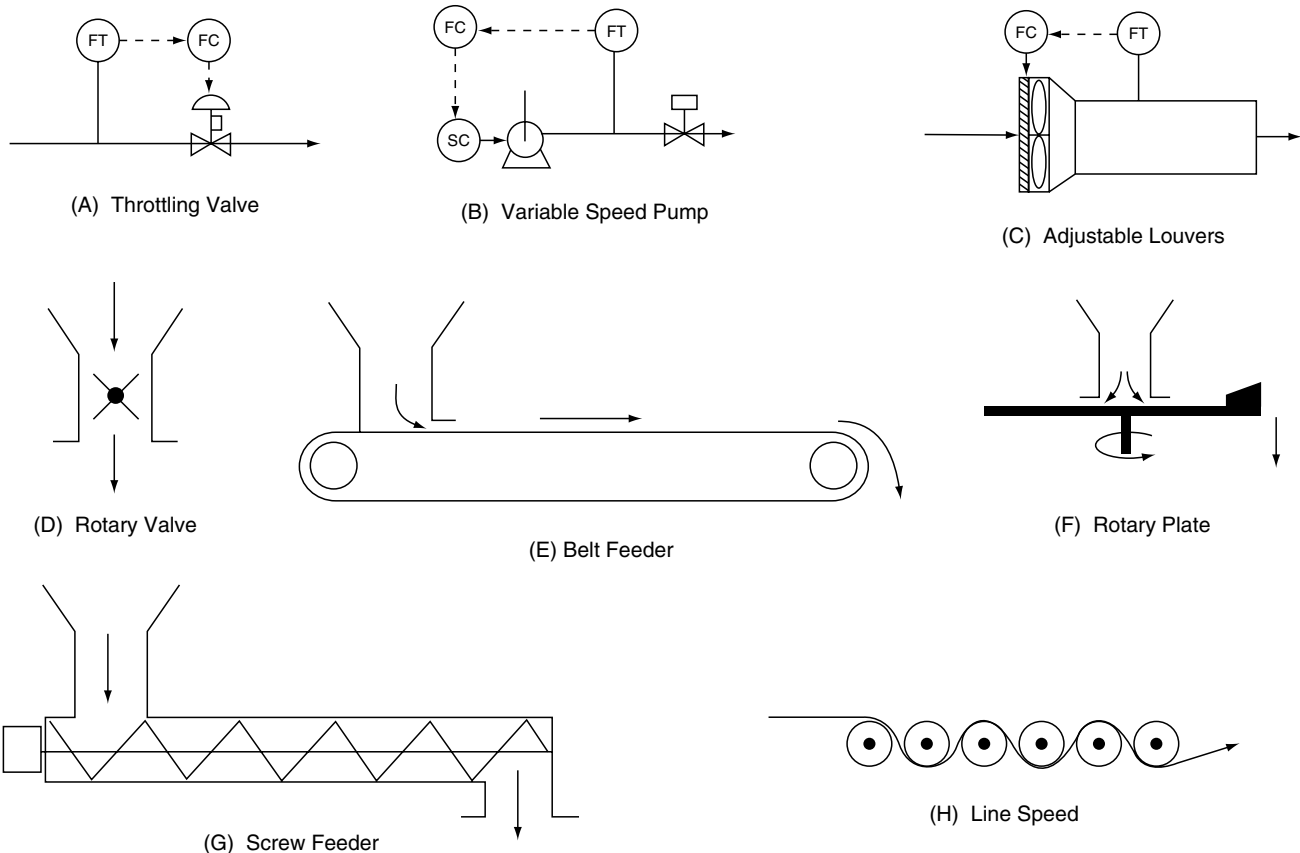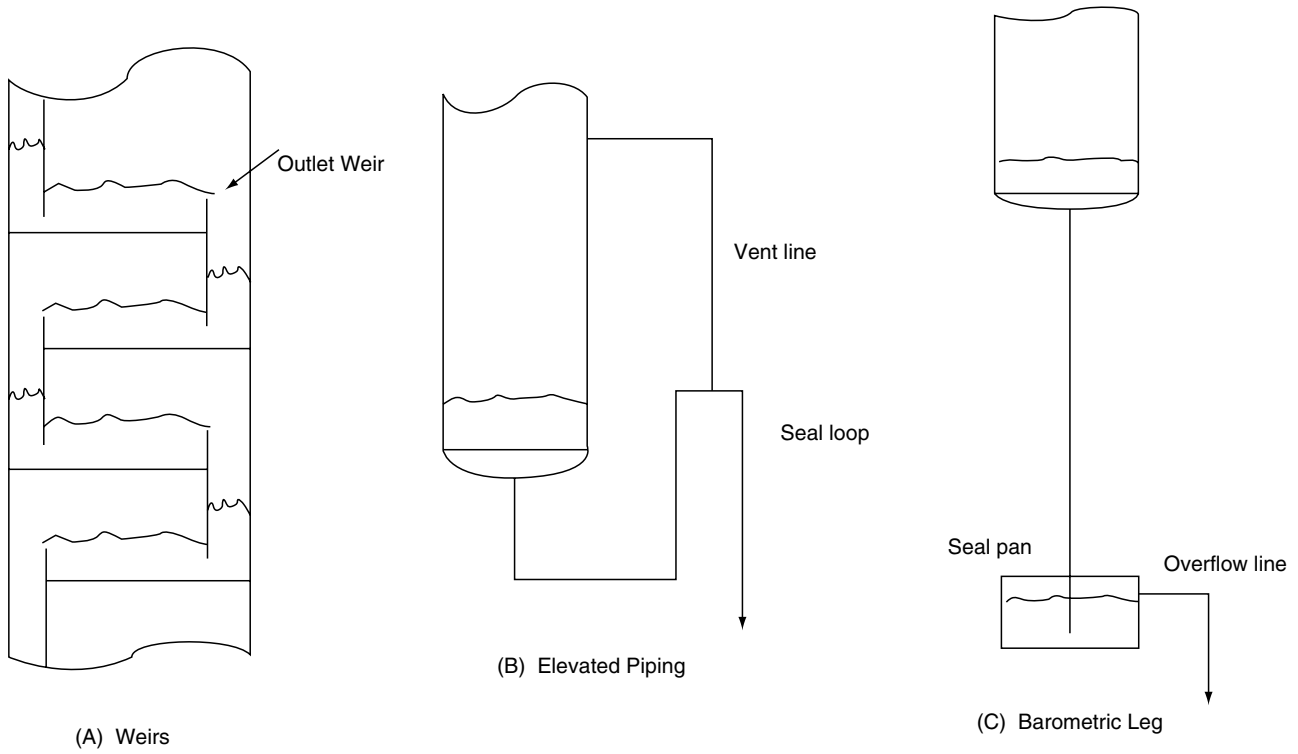
Figure 3.5. Inherent level control.

(A) Forward

(B) Reverse
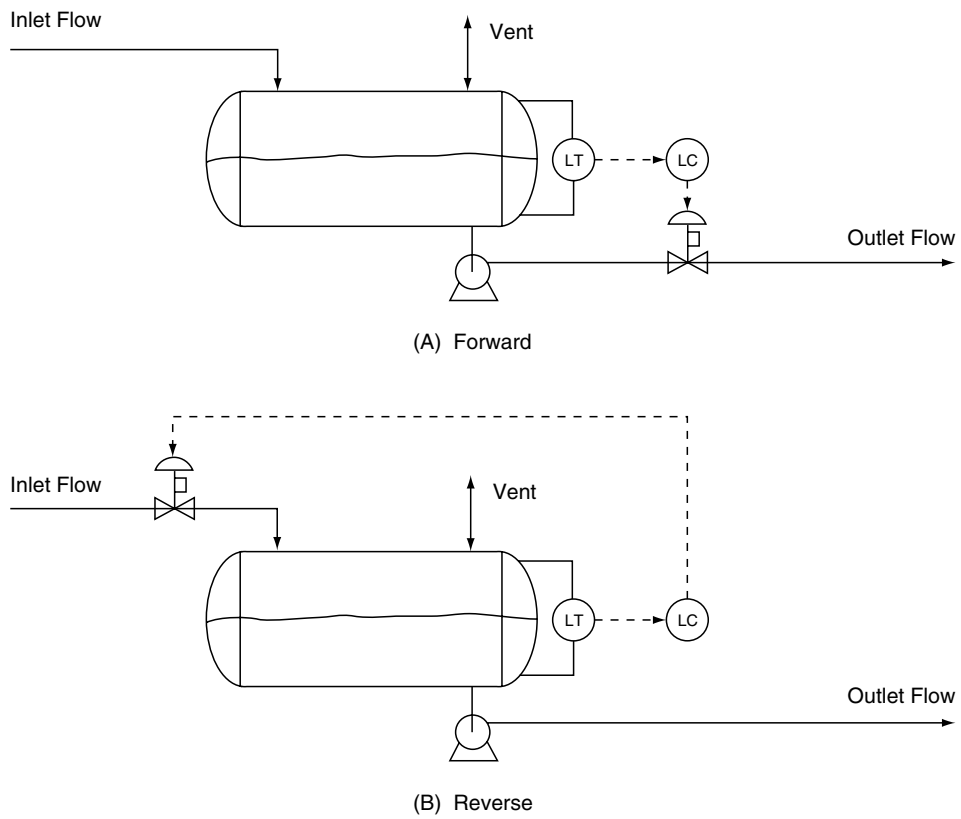
Figure 3.6. Level control.

PRESSURE CONTROL

Pressure in a pipe line may be controlled by manipulating either the inlet or outlet flow, as shown in Figure 3.7(A). Pressure is an integrating process, usually with negligible deadtime, therefore high gain and long integral time are recommended tuning. A pressure regulator is a self-contained valve and field controller with high gain about a preset setpoint. Pressure regulators are often used on plant utility streams, such as instrument air or inert gas, the latter being shown to lower the pressure on the nitrogen supply in Figure 3.7(B).

Pressure control of a tank at atmospheric conditions can be achieved with a simple vent. However, often air cannot be allowed to come into contact with the process, or volatile material cannot be allowed to escape to the atmosphere. In these cases, an inert gas is used to ''blanket'' the material in the tank at a pressure slightly above atmospheric. Pressure control is achieved with split range control valves, as shown in Figure 3.7(C). If liquid is withdrawn from the tank, the pressure will decrease and the controller will open valve PV-1, allowing nitrogen to restore the pressure to setpoint. If the tank fills with liquid, the pressure will increase and the controller will close valve PV-1, and then open PV-2 to let excess nitrogen out of the tank.

The graph in Figure 3.7(D) shows the relationship between controller output and the valve positions. Sometimes a gap in the controller output about the point where both valves are closed will be used to assure no overlap that would have both valves open at the same time. However, any gap should be minimized because the pressure control performance will suffer, as deadtime is introduced into the loop when the controller output must pass through the gap.

3.4. UNIT OPERATION CONTROL

Successful control loop implementation also requires a functional design strategy. A functional design strategy provides an equip-ment layout and control loop interaction that best achieves the functional task required. The control strategy may apply a single control loop or multiple control loops as required to achieve this functional objective of a unit operation.

HEAT EXCHANGERS WITHOUT PHASE CHANGE

Heat exchangers that exchange only sensible heat between the hot and cold streams may have one process stream and one utility stream, such as hot oil, cooling tower water, chilled water, or air. The flow rate of the utility stream is often adjusted to control the outlet temperature of the process stream, as shown in Figure 3.8(A). The temperature response will be nonlinear with deadtime and multiple lags. The control performance will benefit from tuning with Derivative action. The valve on the utility stream may be either on the inlet or the return. Cooling tower water is best throttled at the inlet as the cooler water is less likely to cavitate in the valve. Cooling tower water should not be throttled to the extent that its return temperature exceeds 120°F, at which point fouling becomes a problem.

Figure 3.8(B) shows an alternative control scheme, including a bypass of the process stream around the exchanger. This arrangement can offer much better temperature control, as now the temperature response is linear and fast, because the dynamics of the exchanger are no longer within the control loop. Note that the process now being controlled is simply the linear, thermal blending of a hot and cold stream.

The two valves being adjusted by the temperature controller are implemented such that their stroking fully overlaps, with one valve closing as the other valve opens, as shown in Figure 3.8(C). With smaller pipe sizes, these two valves could economically be replaced with a three-way valve located at the start of the bypass line. It should not be located at the end of the bypass line where thermal stresses would exist from the two different temperature streams. The three-way valve has flow characteristics similar to

(A) Forward

(B) Reverse

(C) "Inert Blanket"

(D) Split Range Valves
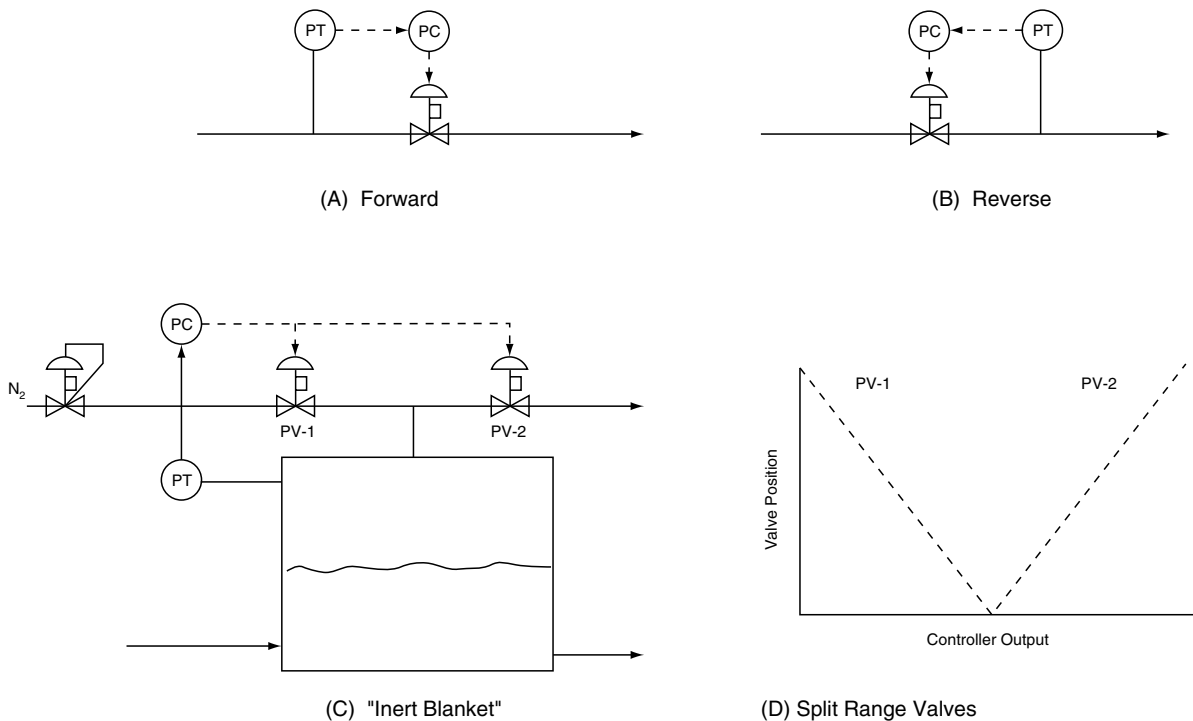
Figure 3.7. Pressure control.
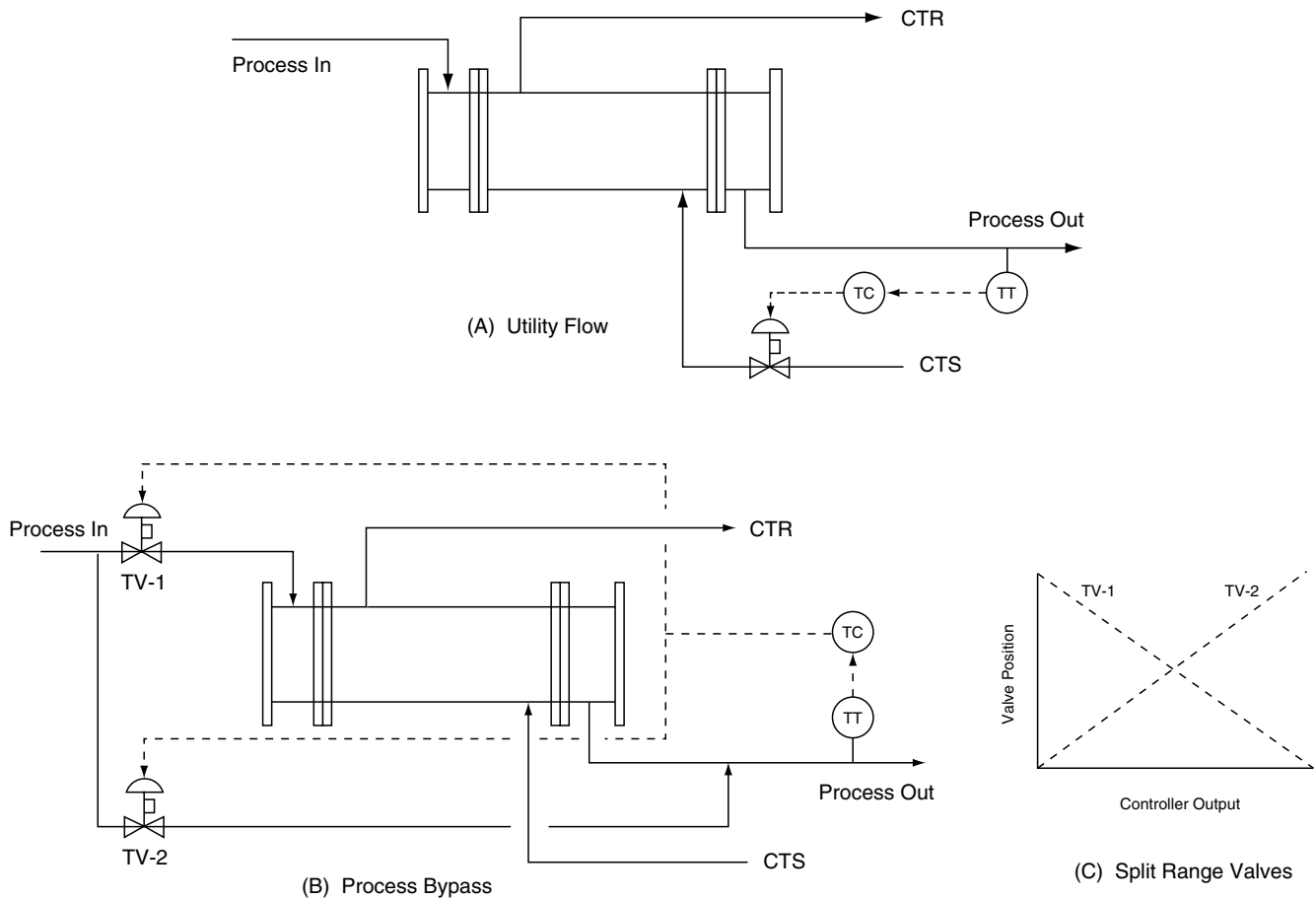
Figure 3.8. Temperature control of heat exchangers without phase change.

the fully overlapped two valves, which achieve an approximately constant resistance to total flow.

An interchanger would exchange heat between two process streams, such as a pre-heater on a distillation column recovering heat from the bottom stream to the feed stream, or a pre-heater on a boiler recovering heat from the stack gas to the combustion air. In these cases, the flow rates of the two process streams are set by other control objectives and they are not available as manipulated variables. Only one process stream temperature can be controlled, and this should be achieved with a bypass of that stream, as previously discussed.
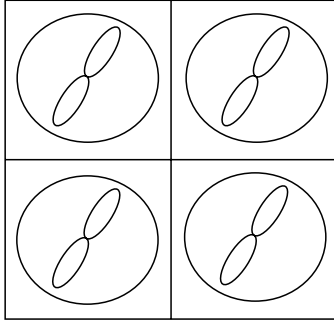
AIR COOLERS AND COOLING TOWERS

Air coolers and cooling towers often use multiple two-speed fans and discrete control logic that steps the fan speeds progressively to adjust air flow in order to maintain a stream temperature. For example, consider a cooling tower shown in Figure 3.9(A) using four 50-Hp fans, each capable of being set to off, half-speed, or full-speed operation. Air flow is proportional to the fan speed, while power consumed is proportional to speed cubed. There would be 9 distinct air flows available for cooling, with a resolution of 12.5%, providing rather coarse temperature control. With PID control, the fan speeds will cycle continually as the temperature oscillates above and below setpoint. Tight tuning will cycle the fan speeds more frequently. Cycling a fan speed more than 4 times an hour may be considered severe service for its motor, likely to incur greater maintenance costs.

An equivalent area cooling tower could be designed using two 100 Hp-fans with variable-speed drives, as shown in Figure 3.9(B). Turndown operation would first decrease both fan speeds down to their minimum speed, at approximately 12% of full speed. Then one fan would shut off as the other fan doubled its speed, in order to maintain the air flow. The running fan would then decrease again to its minimum speed before being shut off. On increasing operation, first one fan would start at 18% output and increase up to 36%, at which point the second fan would start and the controller output would reduce back to 18% for both fans to maintain air flow. Both fans would then be increased up to full speed if required. Note there is a gap between shutting off a fan at 12% and starting it back up at 18%, which prevents cycling. The cost of the variable-speed drives would be offset by the simpler construction and no need for two speed fans and their start/stop circuitry. In addition, the variable-speed drives would provide improved temperature control and less power usage. For example, at 75% air flow, the two variable-speed drives would use $(100 + 100)(.75)^{\wedge}3 = 84.4\,\text{Hp}$; whereas the four two-speed motors with two at high speed and two at low speed would use $(50 + 50)(1.0)^{\wedge}3 + (50 + 50)\,(.50)^{\wedge}3 = 112.5\,\text{Hp}$.

Make-up water must be added because the cooling tower has direct contact, evaporative cooling between the water and the air. Although not shown, a continuous purge of water is required, because impurities will build up as water evaporates. Also not shown are chemical additives, which treat the water to retard bacterial and fungal activity. A level control loop is shown adjusting make-up water flow as required by the resulting water balance.

Fan-1	Fan-2	Fan-3	Fan-4	%Air
Off	Off	Off	Off	0
Lo	Off	Off	Off	12.5
Lo	Lo	Off	Off	25.0
Lo	Lo	Lo	Off	37.5
Lo	Lo	Lo	Lo	50.0
Hi	Lo	Lo	Lo	62.5
Hi	Hi	Lo	Lo	75.0
Hi	Hi	Hi	Lo	87.5
Hi	Hi	Hi	Hi	100

(A) Multiple 2-Speed Fans
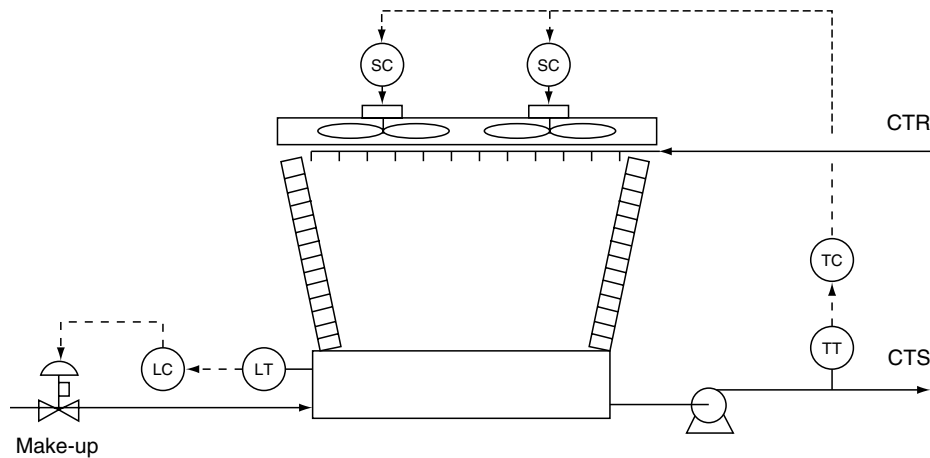
(B) Variable Speed Fans

Figure 3.9. Temperature control of air-cooled exchangers and cooling towers.

HEAT EXCHANGERS WITH PHASE CHANGE

A steam heater, as shown in Figure 3.10(A), can provide responsive temperature control because the entire steam side is at the condensing temperature and has a high heat transfer coefficient. The pressure on the steam side is determined by the temperature that provides heat transfer equal to the heat released by the condensing steam. The steam trap provides condensate level control within the trap in order to provide a seal for the condensing steam.

A refrigerant cooler likewise provides responsive temperature control because the entire refrigerant side is at the boiling temperature and has a high heat transfer coefficient. The pressure on the refrigerant side is determined by the temperature that provides heat transfer equal to the heat absorbed by the boiling refrigerant. A level controller is shown in Figure 3.10(B), maintaining the liquid level above the tubes of the exchanger.

Measurement of the steam or refrigerant flow can provide a good indication of heat duty. If there are multiple users, which cause disturbances to the utility, then a temperature to flow cascade control arrangement should be considered. In such a cascade arrangement, the temperature controller output provides the setpoint for the flow controller. The flow controller minimizes the effect of utility stream disturbances and linearizes the temperature control loop.

PROCESS CONDENSERS

Condensing process vapor usually requires adjustment of the heat removal such that the amount of vapor condensed matches the vapor supply—in other words, pressure control. The most effective manner of adjusting the heat removal is to vary the area available for condensing. This may be accomplished by blocking a portion of the total area with condensate or noncondensable gas (inerts). In Figure 3.11(A), a condenser is shown with inerts blanking the lower portion of its tubes. Vapor, as it is being condensed, pushes the inerts to the far end of the condenser. When pressure rises due to more vapor arriving at the condenser, the inerts are pushed out, exposing more tube area for condensing. When pressure drops due to less vapor arriving, inerts flow back into the condenser, blanking off more tube area.

For a condenser operating at atmospheric pressure, an adequate vent is all that is necessary. However, air is often not suitable for contact with the process due to concern about contamination or flammability. In these cases, the vent may be connected to a source of low pressure nitrogen, or other inert gas. For vacuum operation, the vent must also be connected to a vacuum pump or steam jet (eductor), as shown in Figure 3.11(B). The pressure controller adjusts the split range control valves such that as its output decreases, first PV-2 closes then PV-1 opens. Normal operation would

(A) Steam Heater

(B) Refrigerant Cooler
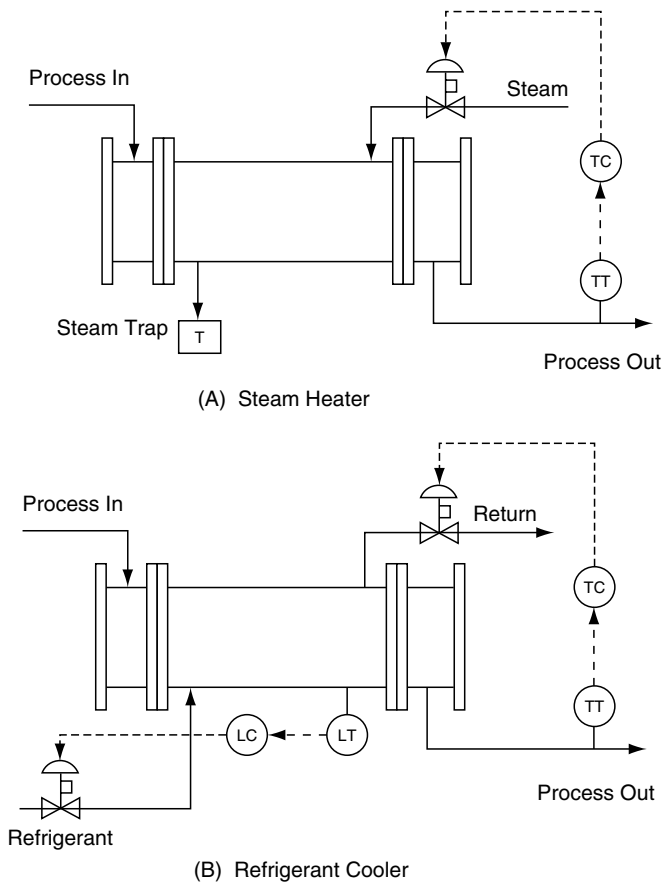
Figure 3.10. Temperature control of exchangers with phase change.

have PV-1 closed and PV-2 open; therefore, the inert gas is used only sparingly.

Coolant flow is generally not throttled for pressure control, but it is occasionally adjusted for temperature control of the sub-cooled condensate. Unless there is significant sub-cooling, this latter temperature loop is often ineffectual. At best, it will require loose tuning, or often it will be placed into manual for seasonal adjustment only.

As mentioned previously, condensate may also be used to blank off tube area for pressure control. The two methods shown in Figure 3.12 may be used when inerts are not present in significant amounts.

The first method, shown in Figure 3.12(A), places a valve in the condensate line and directly backs up the liquid into the condenser as needed. The second method places a control valve in a vapor line, added to bypass the condenser and go directly into the accumulation tank (see Figure 3.12(B)). Although somewhat counterintuitive, the vapor bypass valve must open as pressure drops, in order to raise the pressure at the accumulation tank and force liquid condensate back into the condenser to restore the energy balance. Care must be taken that the surface of the liquid in the tank is not disturbed, as undesirable pressure transients can develop with the hot vapor in contact with the sub-cooled liquid. Another concern with both of these condensate methods is the venting of process inerts as they build up over time. Valve position is the best indication of this pending problem.

PROCESS VAPORIZERS

A vaporizer is typically used in a process to provide a vapor feed to downstream equipment. In that case, it may be desirable to set the flow of vapor directly with the setpoint of a flow control loop. Then the heat input is adjusted for pressure control and the liquid level is maintained by adjusting the inlet flow, in a reverse material balance manner, as shown in Figure 3.13(A). If heat transfer limits throughput, then both the vapor valve and the steam valve will operate fully open and the pressure will droop to an equilibrium point, where heat transfer equals the flow through the downstream equipment.

For a direct material balance, the inlet liquid is flow controlled, the level is maintained by adjusting the steam flow and the pressure is then controlled by adjusting the vapor flow, as shown in Figure 3.13(B). If the feed pump limits capacity, the pressure should be allowed to droop by putting the controller into manual with a fully open valve. Then the feed flow controller will run with its valve fully open and the pressure will droop to an equilibrium point, where inlet flow equals the flow through the downstream equipment.

Because of impurities in the liquid feed, it may be necessary to purge or blowdown the vaporizer periodically, as indicated by a rising boiling point temperature or the steam valve approaching a full open position. Although not shown, vaporizers often have a separate, temperature-controlled superheater to ensure the vaporization of any entrained droplets and to prevent condensation.

Smaller, low-cost, vendor-packaged vaporizers often employ self-regulation of the level. These units typically have blade heaters, which allow the level to vary until the area available for heat transfer to the liquid provides vaporization to match the feed rate. This design requires excess blade heater area, which also serves to provide superheat to the vapor.

EVAPORATORS

An evaporator provides one stage of separation based on relative volatility. It is typically used with systems having a large relative volatility, such as salts and solvents. When water is being removed as an overhead vapor, multieffect operation may be used to provide improved energy efficiency. Figure 3.14 shows two alternative direct material balance evaporator control schemes.

In both of these schemes, the feed is flow controlled and the overhead vapor flow is adjusted for pressure control. The arrangement shown in Figure 3.14(A) is more common, with the level controller adjusting the bottom flow and the temperature controller adjusting the steam flow. Note that the temperature is an inferred measure of composition. This inferred composition control is achieved by adjusting the steam flow such that the material balance has more or less vapor removed overhead.

If the bottom flow is a small fraction of the feed, then it will not provide satisfactory level control. A better arrangement for that situation is the alternative shown in Figure 3.14(B), with the level controller adjusting the steam flow and the temperature controller adjusting the bottom flow. As before, the temperature is an inferred measure of composition, which is controlled by adjusting the material balance split. When the temperature is above setpoint, implying that the high boiler composition is too high, the bottom flow must be increased to remove more of the high boiler.

DISTILLATION COLUMNS

In simple distillation, a feed is separated into a distillate and bottoms product with multiple stages of separation based on relative volatility. Both distillate and bottom composition may be

(A) Condenser Detail

(B) Condenser with Steam Jet
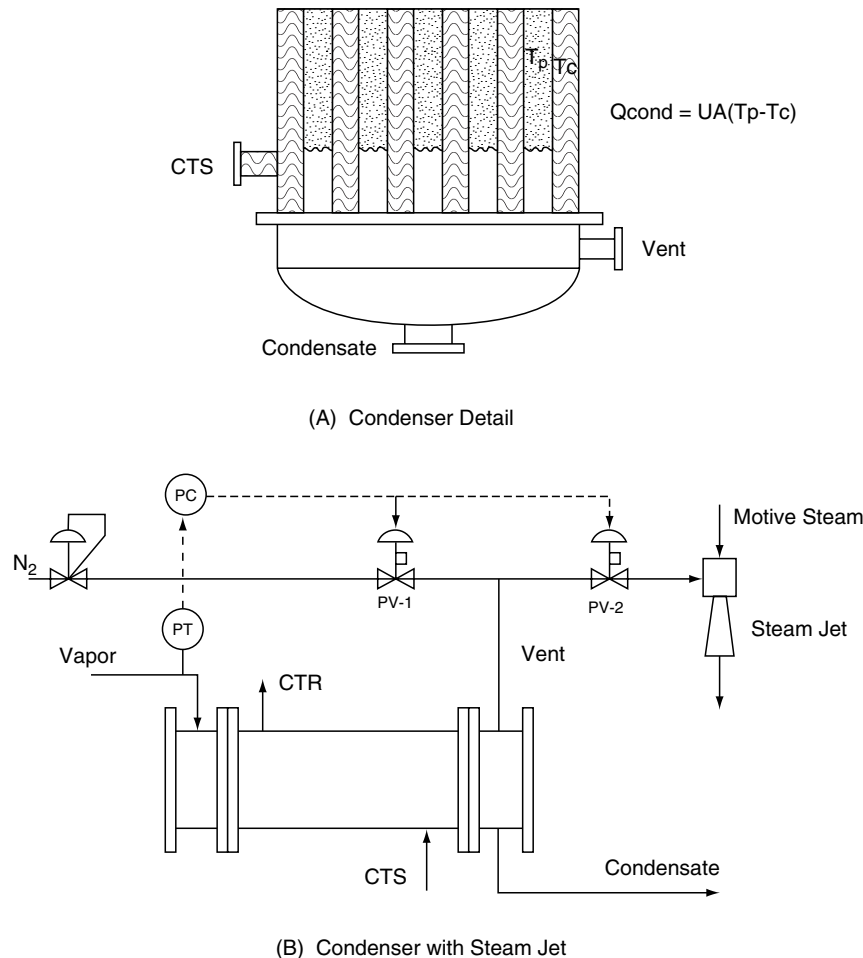
Figure 3.11. Condenser pressure control with inert gas.

controlled by adjusting the material balance split and the separation. However, basic column control schemes attempt to control only one composition within the column by adjusting the material balance, and simply fix the separation at an optimal value.

Four alternative control schemes are commonly used for distillation column control, as shown in Figure 3.15 through Figure 3.18, respectively. Scheme 1 directly adjusts the material balance by manipulation of the distillate flow. If the distillate flow is increased, then the reflux accumulator level controller decreases the reflux flow. As less liquid proceeds to flow down to the sump, the sump level controller decreases the bottoms flow a like amount. The separation is held constant by manually setting the reboiler steam flow to maintain a constant energy per unit feed.

This scheme is recommended when the distillate flow is one of the smaller flows in the column, particularly when the reflux ratio is large ($R/D > 3$). Also, it is important that the reflux accumulator level control can be tightly tuned and that the liquid holdup is not too large (< 5 min). This scheme has the least interaction with the energy balance, as it provides a good range of control with only small changes in the distillate flow, and it also provides a form of automatic internal reflux control. If the reflux becomes more subcooled, initially additional vapors will be condensed inside the column. However, the overhead vapors will be reduced by exactly the same amount, and with tight level control, the reflux will then be reduced accordingly.

Another advantage of this scheme is that it lends itself readily to the application of feedforward control in order to maintain the D/F ratio for measured changes in feed flow. This feedforward signal would be trimmed by the addition of a feedback signal from the column temperature controller.

Scheme 2 (Figure 3.16) indirectly adjusts the material balance through the two level control loops. If the reflux flow is increased, then the reflux accumulator level controller decreases the distillate flow. As the additional liquid proceeds to flow down to the sump, the sump level controller increases the bottoms flow a like amount. The separation is held constant by manually setting the reboiler steam flow to maintain a constant energy per unit feed. This scheme is recommended for columns with a small reflux ratio ($R/D < 1$). This scheme also offers improved dynamics, which may be required, particularly if the column has a large horizontal reflux accumulator.

Scheme 3 (Figure 3.17) indirectly adjusts the material balance through the two level loops. If the steam flow is increased, then the sump level controller decreases the bottom flow. As the additional vapors go overhead and condense, the reflux accumulator level control increases the distillate flow a like amount. The separation is held constant by manually setting the reflux flow to maintain a relatively constant energy per unit feed. This scheme is recommended for columns with a small energy per unit feed ($V/F < 2$). This scheme also offers the fastest dynamics.

(A) Valve in Condensate Line

(B) Valve in Vapor Bypass
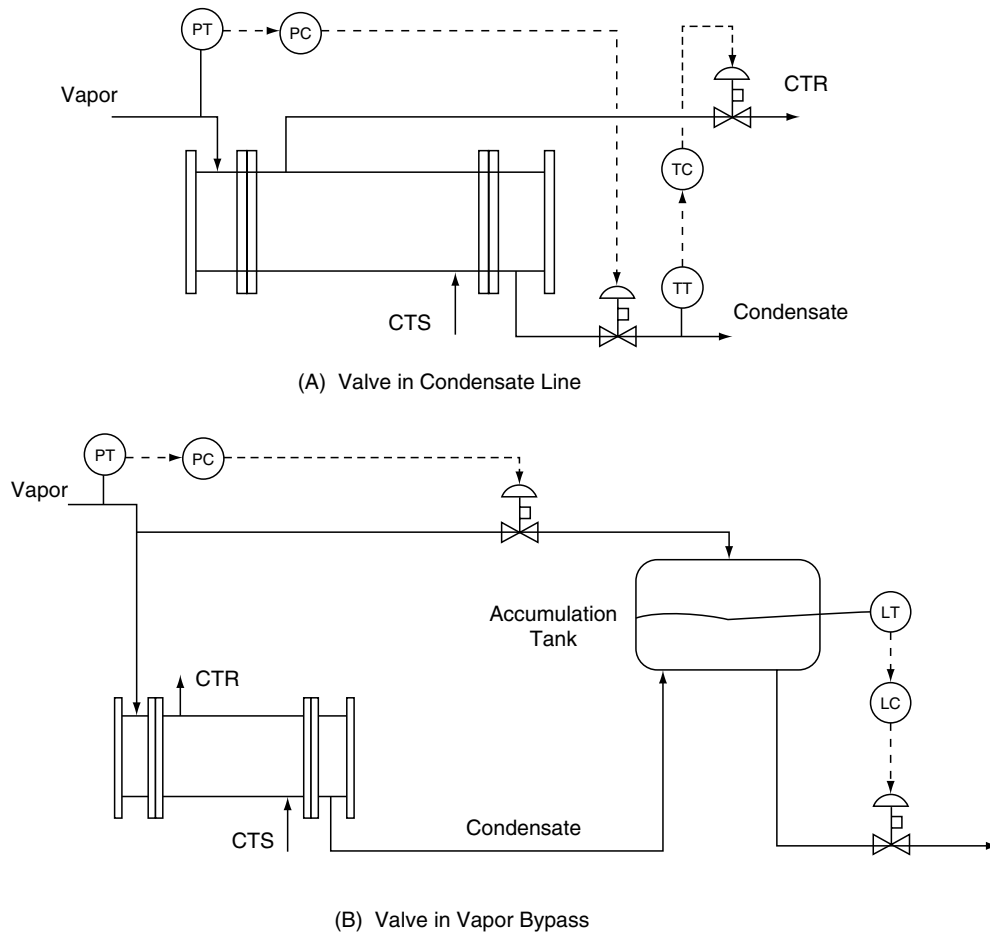
Figure 3.12. Condenser pressure control with condensate.

Scheme 4 (Figure 3.18) directly adjusts the material balance by manipulation of the bottom flow. If the bottom flow is decreased, then the sump level controller increases the reboiler steam flow. As the additional vapors go overhead and condense, the reflux accumulator level control increases the distillate flow a like amount. The separation is held constant by manually setting the reflux flow to maintain a relatively constant energy per unit feed.

This scheme is recommended when the bottom flow is one of the smaller flows in the column, particularly when the bottom flow is less than 20% of the vapor boilup. This scheme has little inter-action with the energy balance, as it provides a good range of control with only small changes in the bottom flow. However, the tuning of the sump level loop usually makes this scheme slower than the others. An inverse response is also possible with this sump level control loop. This type of response occurs when an increase in steam flow temporarily causes the sump level to increase before it begins to decrease. If this occurs, the level loop must be detuned even more.

An advantage of scheme 4 is that it lends itself readily to the application of feedforward control in order to maintain the *B*/*F* ratio for measured changes in feed flow. This feedforward signal would be trimmed by the feedback signal from the temperature controller.

Once a basic column control scheme is chosen, simulation of parametric steady-state cases can be used to determine the best temperature control stage location. These cases should hold the separation variable constant and adjust the material balance in the manner of the chosen control scheme. Temperature profiles from these parametric cases can then be plotted together as shown in Figure 3.19. The best control stage location is where the largest, most symmetrical temperature deviation from the base case occurs. On new columns, it is recommended that additional thermowells be installed one stage above and below this location because of uncer-tainty in tray efficiencies and VLE data.

Product compositions from these same parametric cases can be plotted against the temperature occurring on the uncontrolled control stage, as shown in Figure 3.20. The steady-state effect on product composition due to temperature measurement errors can be determined in this manner.

LIQUID-LIQUID EXTRACTION

Liquid-liquid extraction can take place in a column with various internals to foster contact between the dispersed and continuous liquid phases. Internals can include sieve trays, baffle trays and packing, as well as mechanical agitation and pulsing of the liquid.

The solvent flow is often maintained in proportion to the feed flow. When the dispersed phase is the heavy phase, an interface will form toward the bottom of the column and is controlled, as shown in Figure 3.21. When the dispersed phase is the light phase, an interface will then form toward the top of the column; however, the bottom flow is still manipulated to maintain the interface level.

One or more mixer/settlers in series can also be used to perform liquid-liquid extraction. Often a series of mixer/settlers will be

(A) Reverse Material Balance

(B) Direct Material Balance
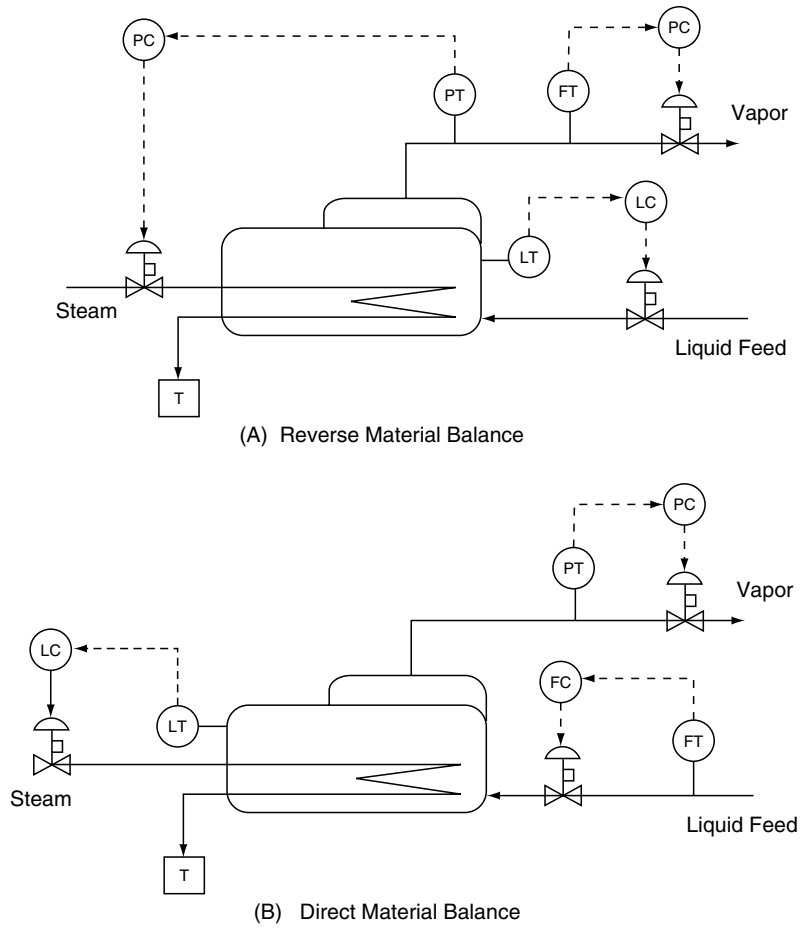
Figure 3.13. Vaporizer control.

(A) Level Control by Adjusting Liquid

(B) Level Control by Adjusting Steam
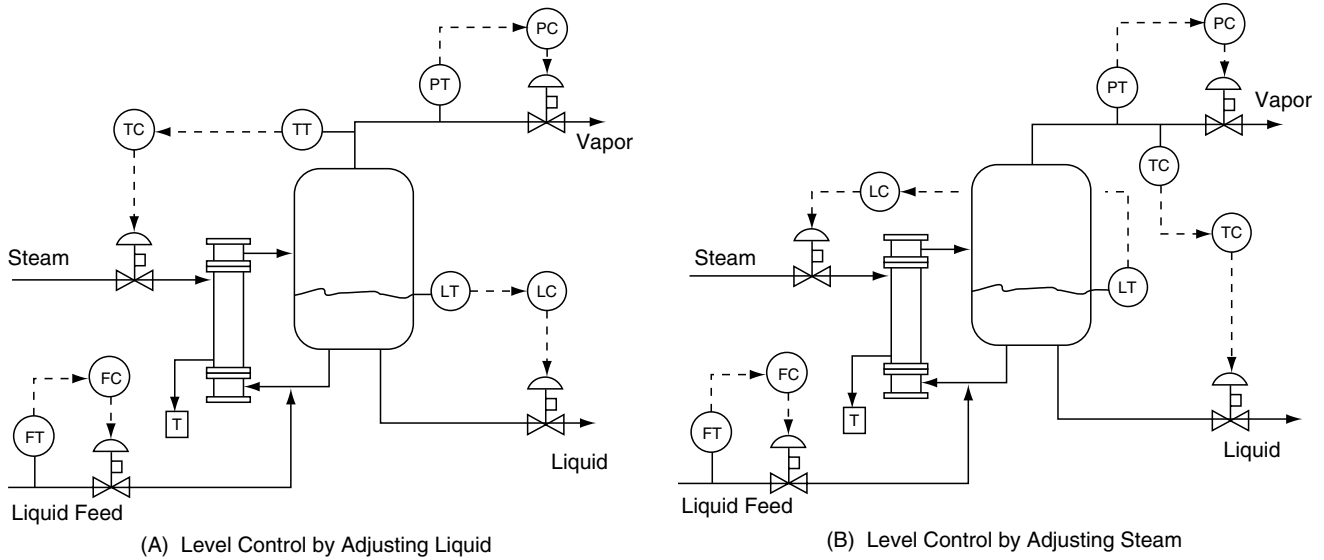
Figure 3.14. Evaporator control.
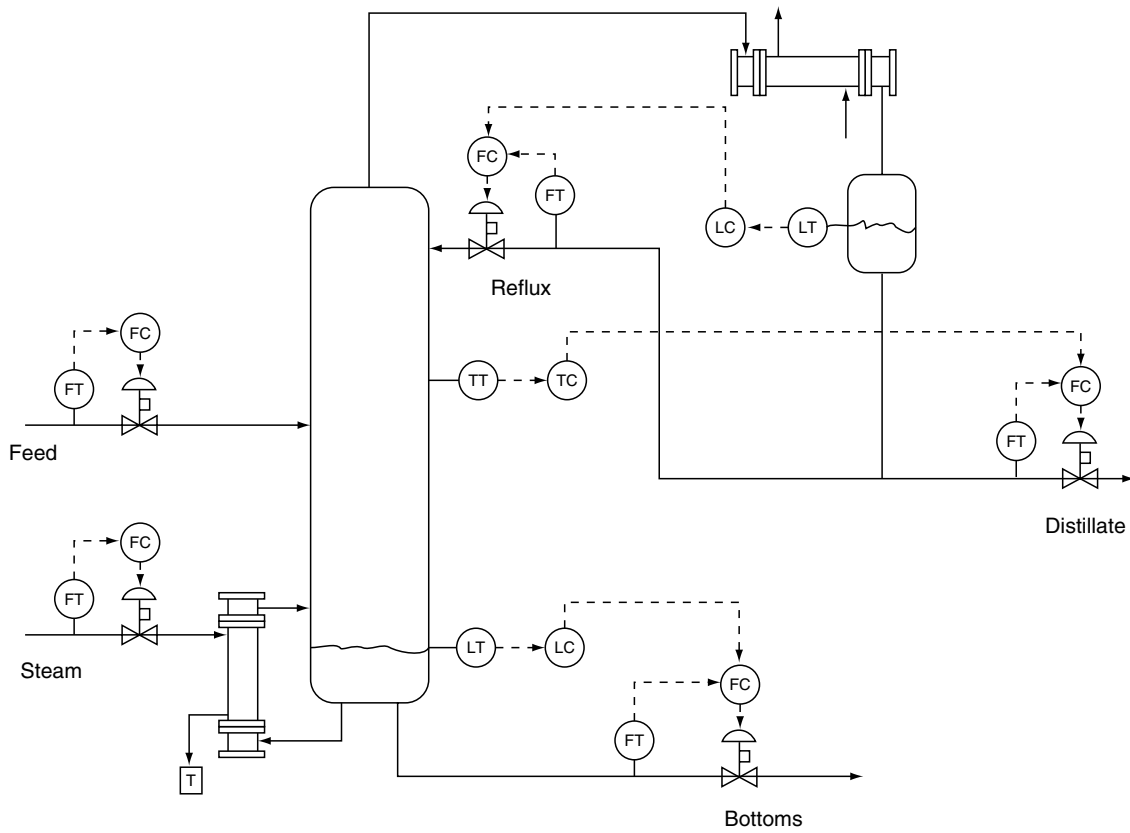
Figure 3.15. Distillation column control—Scheme 1.
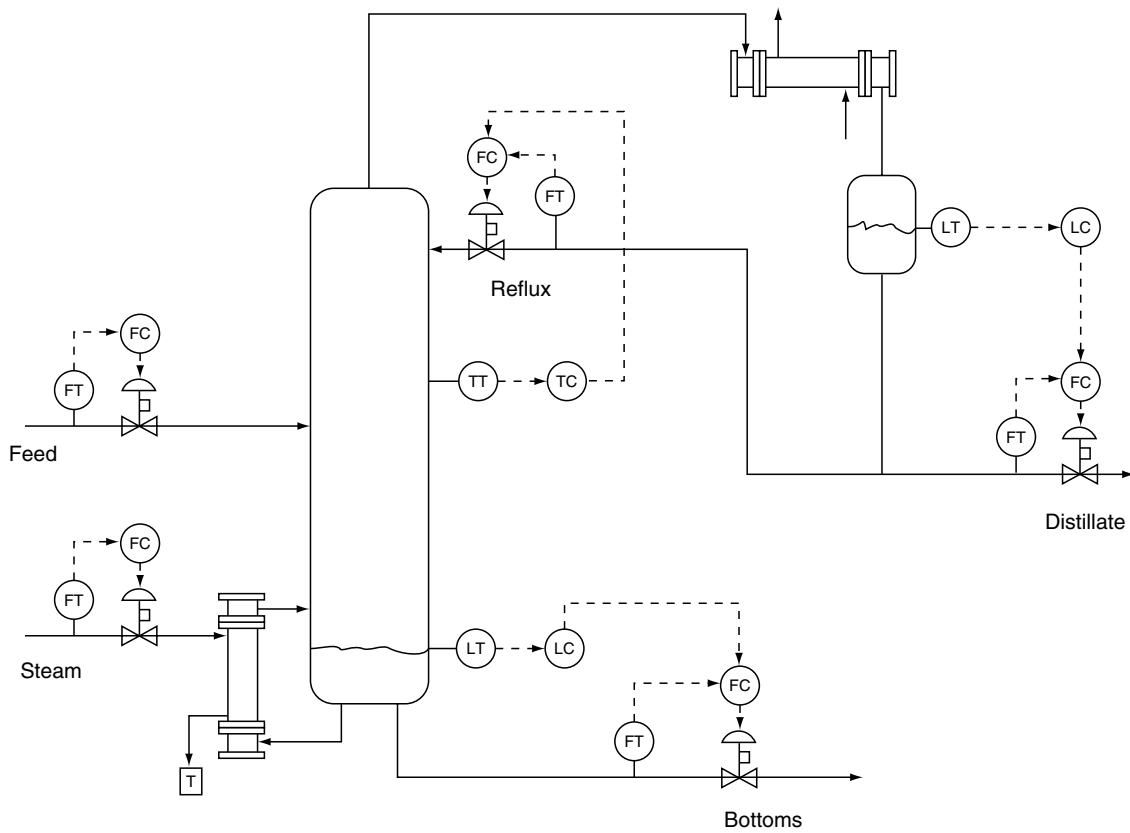
Figure 3.16. Distillation column control—Scheme 2.
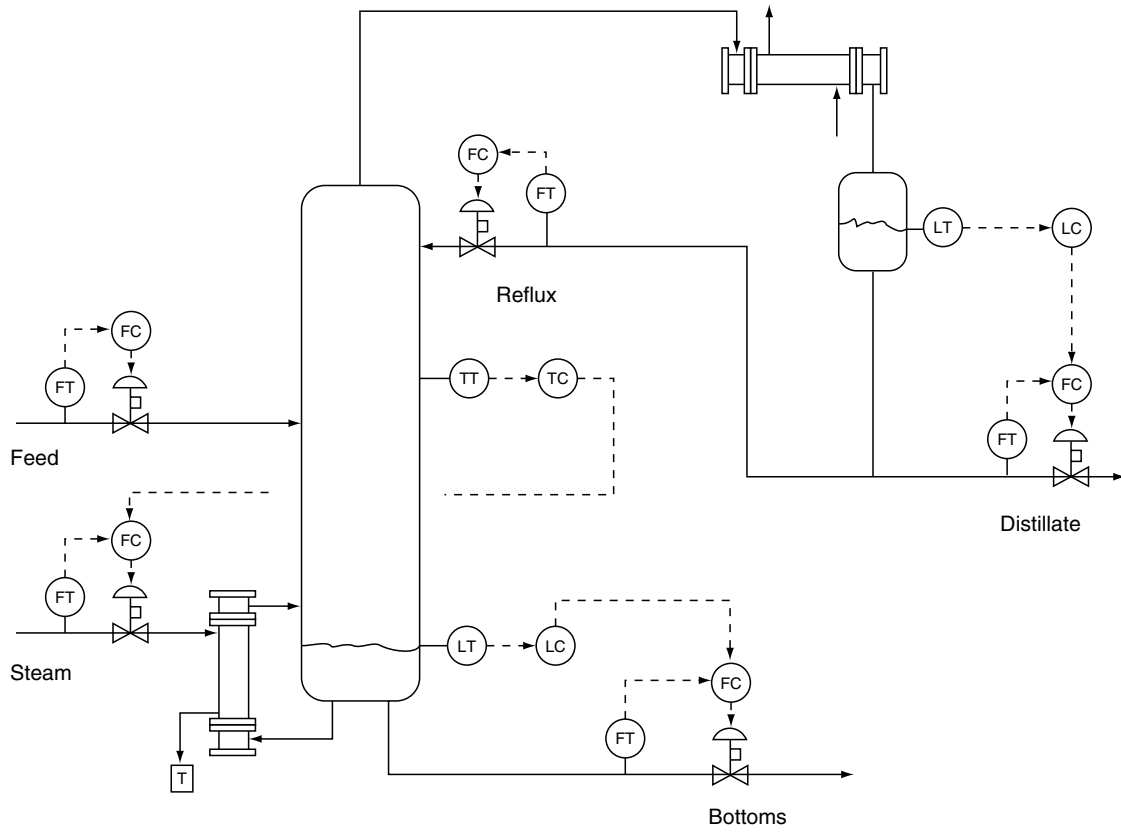
Figure 3.17. Distillation column control—Scheme 3.
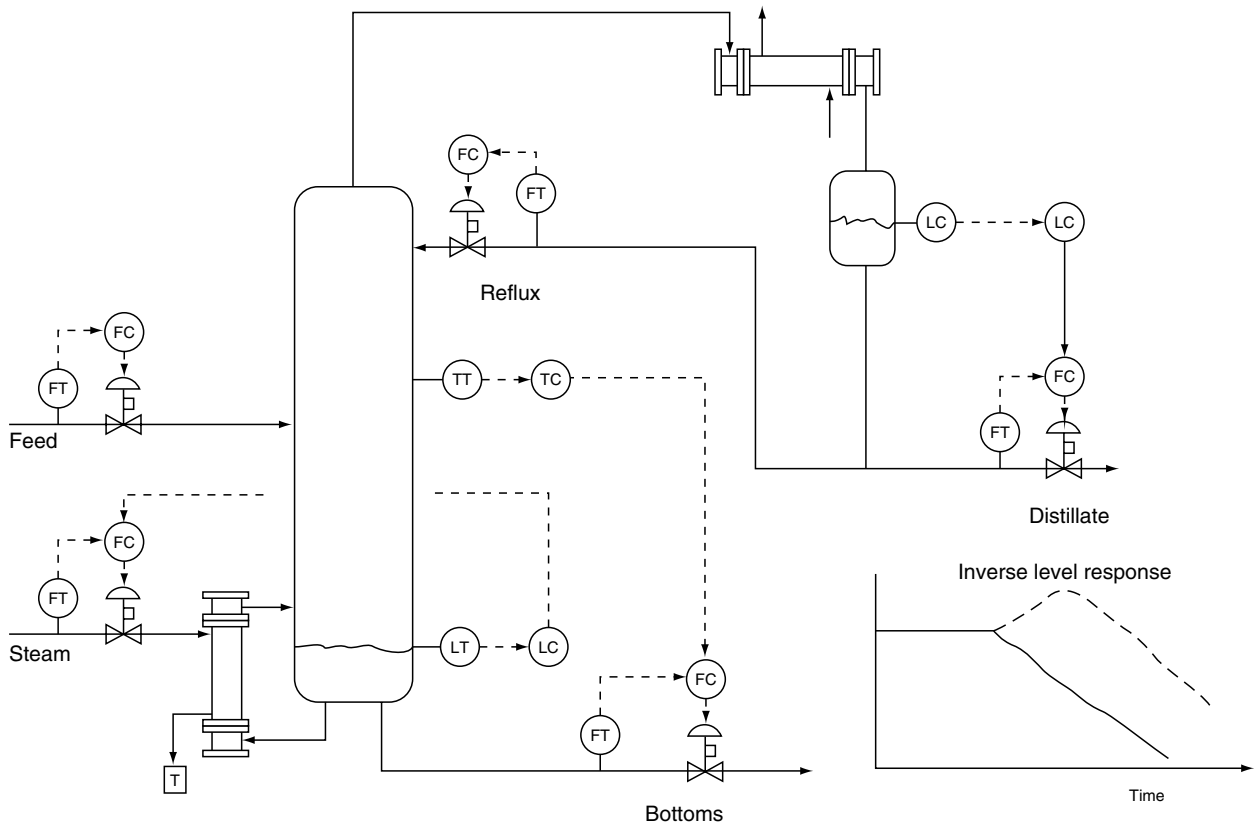
Figure 3.18. Distillation column control—Scheme 4.
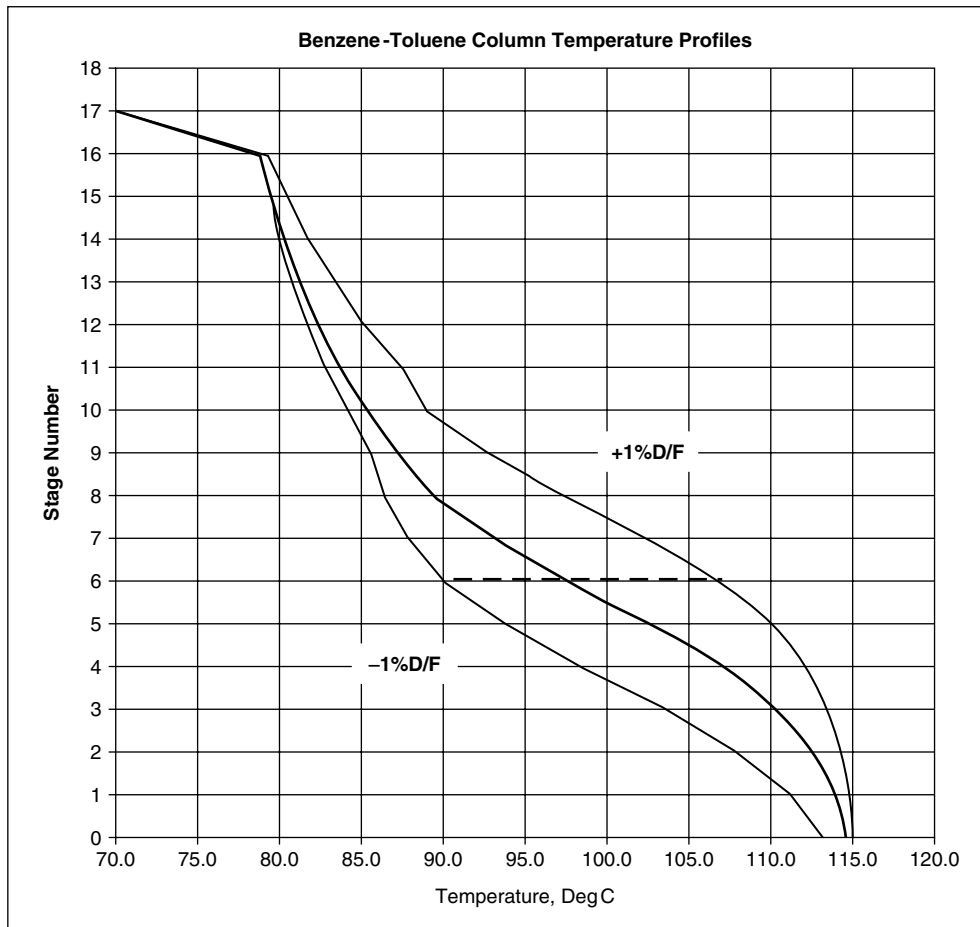
Figure 3.19. Distillation column control—Control plate location.
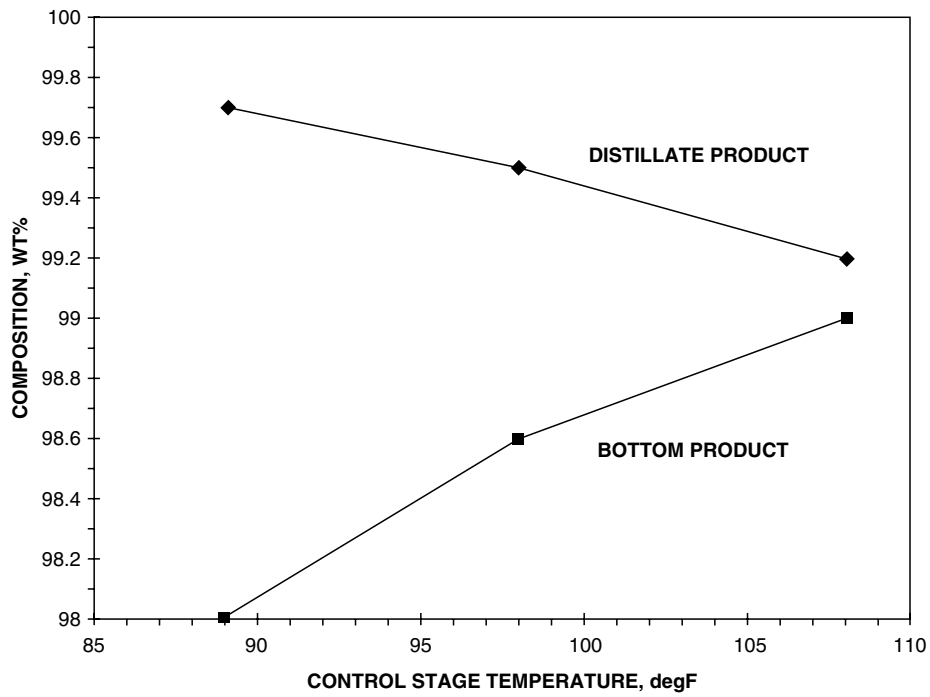
Figure 3.20. Distillation column control—Temperature sensitivity.
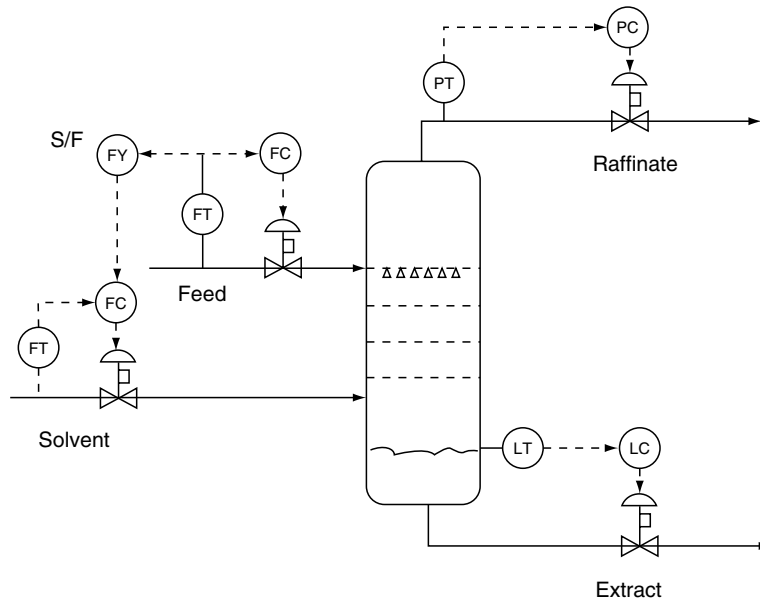
Figure 3.21. Liquid-liquid extraction tower.

installed on a gradient to allow gravity flows between vessels, as shown in Figure 3.22. Adjustable piping and sight glasses allow the system to be set up to be self-regulating over a narrow range of feed rates. Often the solvent is added in ratio to the feed. Different ratios and sometimes different solvents are used in subsequent stages.

REACTORS

Reactor control is largely about maintaining stoichiometric ratios of feeds and temperature control. Often composition measurement is not available for feedback correction of flow, therefore precise flow measurements are required. Mass flow corriolis meters are
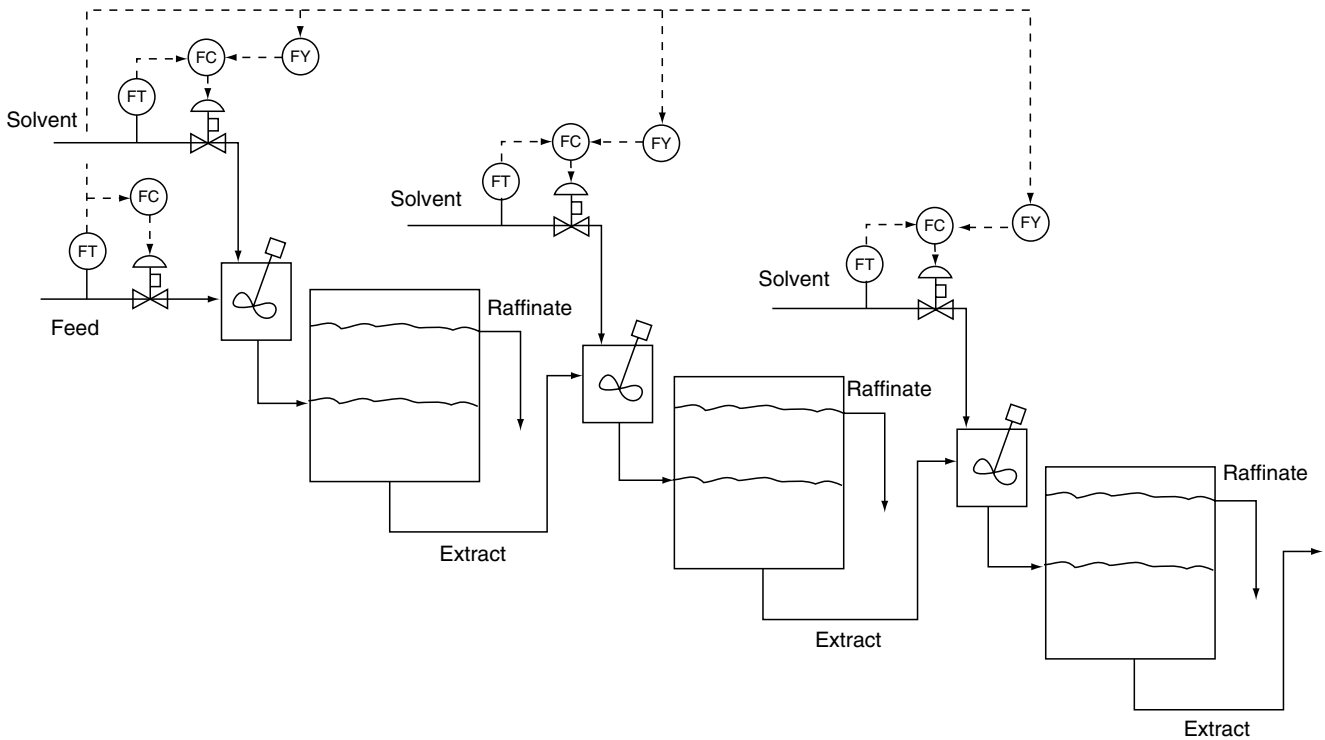
Figure 3.22. Liquid-liquid extraction with mixer/settlers.
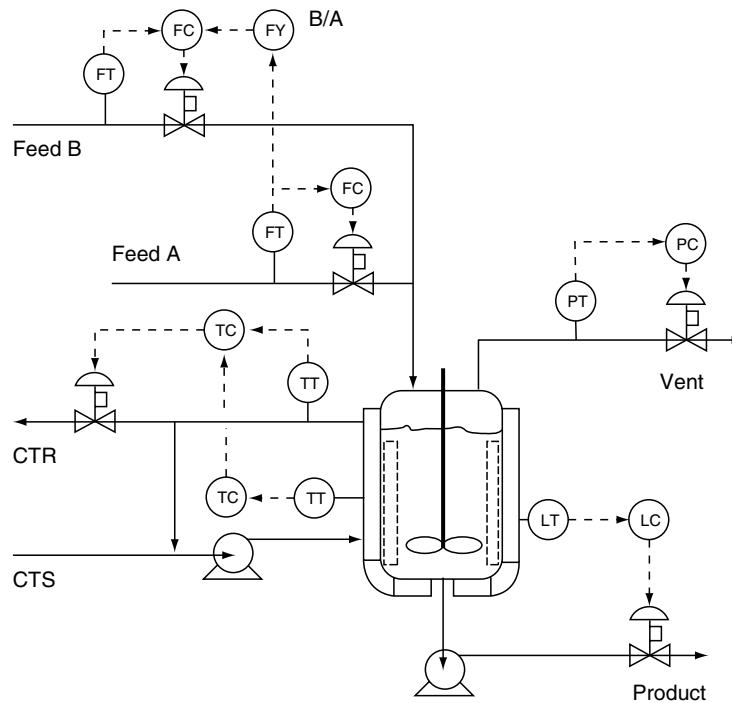
Figure 3.23. Jacketed reactor control.

ideal for feed line sizes below 6 inches. Multiple feeds should be ratioed off of one primary feed flow.

A jacketed vessel, as shown in Figure 3.23, is often used for maintaining temperature; however, it has limited surface area and low heat transfer coefficients. Sometimes internal reactor cooling coils are also used to provide additional heat transfer area. In order to manipulate the heat transfer, maximum flow is maintained in a circulation loop, while the jacket temperature is adjusted by bringing in and letting out coolant. The reactor temperature controller provides a setpoint to the jacket temperature controller. Heat transfer is linear and proportional to the temperature difference.

Another approach for removing heat is a circulation loop through an external heat exchanger, as shown in Figure 3.24. The circulation rate is maximized for good heat transfer on the process side, while the heat transfer medium is throttled by the reactor temperature controller. If the reactor is small and well mixed, the cascade temperature control arrangement as shown may not be necessary, and the reactor temperature controller may be connected directly to the valve.

When the reaction temperature is high enough to vaporize the reactants, an external condenser is an effective way to remove heat, as shown in Figure 3.25. The reactor pressure is adjusted to maintain the corresponding boiling temperature.

For fast reaction kinetics, the feed flow may also be adjusted to maintain temperature. In this case, the rate of heat removal sets the production rate. For the fluid bed reactor, shown in Figure 3.26, a series of separate cooling coils may be manually put into service to establish incremental production rate.

pH

Measuring pH is difficult and often unreliable. When a high degree of reliability is required, a three-probe system with an automatic mid-selector is recommended as shown in Figure 3.27(C). Most titration curves are highly nonlinear with respect to pH but

can be linearized somewhat by converting the signal to reagent demand.

If the reagents react rapidly, then in-line control of pH is practical, with a signal filter to reduce the noise. A pump or in-line static mixer should be used to provide thorough mixing of the process and reagent as shown in Figure 3.27 (A) and (B).

Often existing agitated tanks merely provide enough circulation to keep solids from settling; however, for pH control the
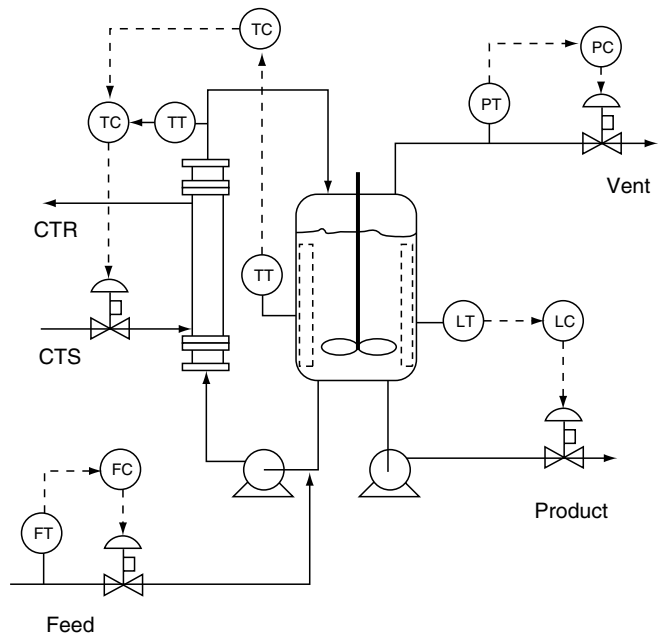
Figure 3.24. External heat exchange reactor control.
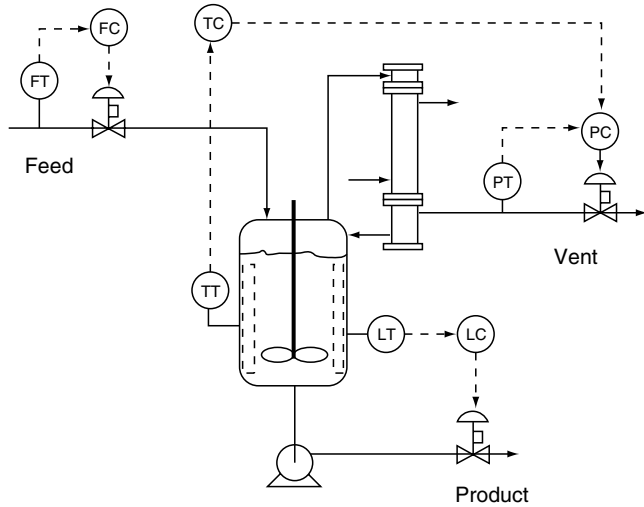
Figure 3.25. External condenser reactor control.

agitator must circulate liquid at a rate of 20 times the throughput to be considered well mixed. For tanks that are not well mixed, it is better to provide in-line pH on the feed to the tank.

TURBINES AND COMPRESSORS

Steam turbines are most often used in processes to provide power to compressors or electric generators as shown in Figure 3.28. Multi-stage turbines may also admit or extract steam between stages. Turbine speed is a fast loop, controlled by manipulating the supply steam valve or valves, as often there will be a rack of parallel steam valves supplied as part of the turbine system.

Steam turbines with electrical generators are used to recover the power from high pressure steam when the plant steam balance requires additional low pressure steam. As such, they provide more energy-efficient pressure regulation than a simple pressure control valve. Admission or extraction of steam to a header between stages, and/or condensation of exhaust steam fulfill additional steam balance and energy recovery needs.

For electrical generators, at start-up, the turbine speed must be ramped up until the generator is providing electrical cycles that are synchronized with the power grid. Once connected to the grid, the speed becomes essentially self-regulating, and the electrical power generated varies directly with steam supplied. Steam header pressures may then be controlled by adjusting the inlet steam, extraction/admittance steam, and exhaust condenser.

Steam turbines with compressors are used for providing process gas flow at a required pressure in high throughput processes. The process demand is determined by a pressure controller, which adjusts the setpoint on the turbine speed controller. In smaller processes, fixed speed compressors may be used by adjusting either an inlet or discharge valve to achieve pressure control. It is more energy efficient to adjust an inlet valve, or better yet to adjust inlet vanes which provide a pre-rotation to the gas. However, adjustment of speed is the most energy-efficient method control.

Both axial and centrifugal compressors are subject to an unstable region of low flow operation called surge. This region is defined by the pressure-flow relationship which has a peak determined by the operating speed. For various compressor speeds, these peaks may be connected to determine a surge line, which defines a region of unstable operation at lower flows.

Flow control by recycle of process gas is used to maintain the minimum flow requirements of the anti-surge control system. Inputs from the pressure and speed transmitters are used to compute the required minimum flow setpoint, based on an anti-surge control line relationship, as shown in Figure 3.29. The anti-surge
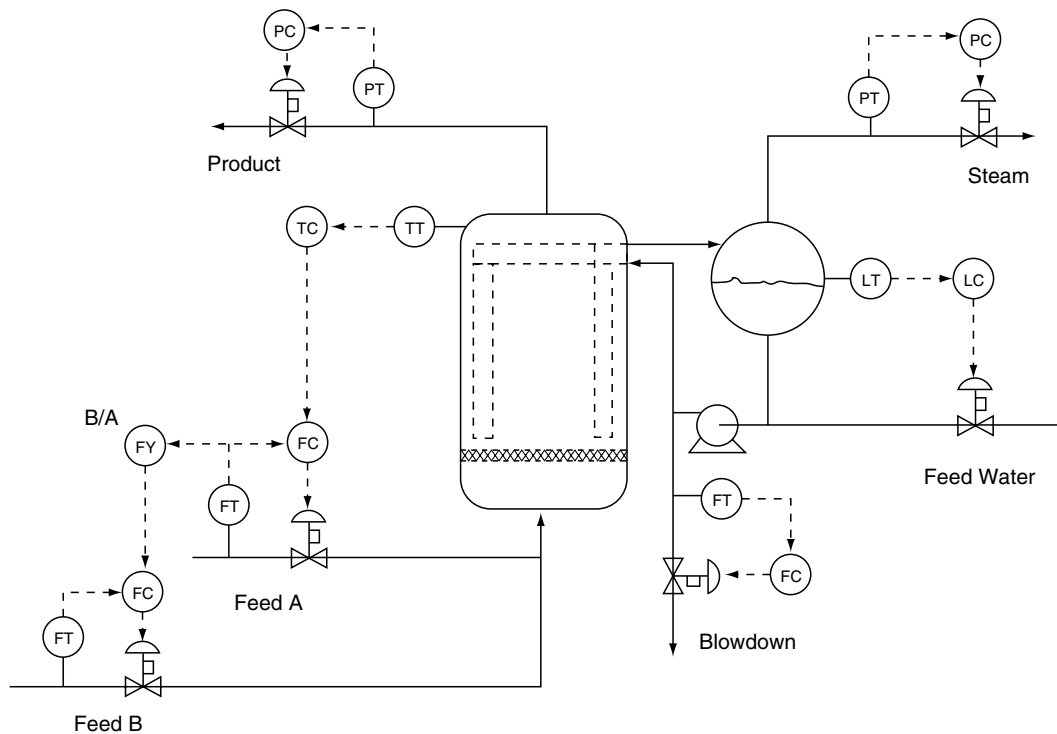
Figure 3.26. Feed rate reactor control.

(A) Static Mixing

(B) Pump Mixing

(C) Agitated Tank
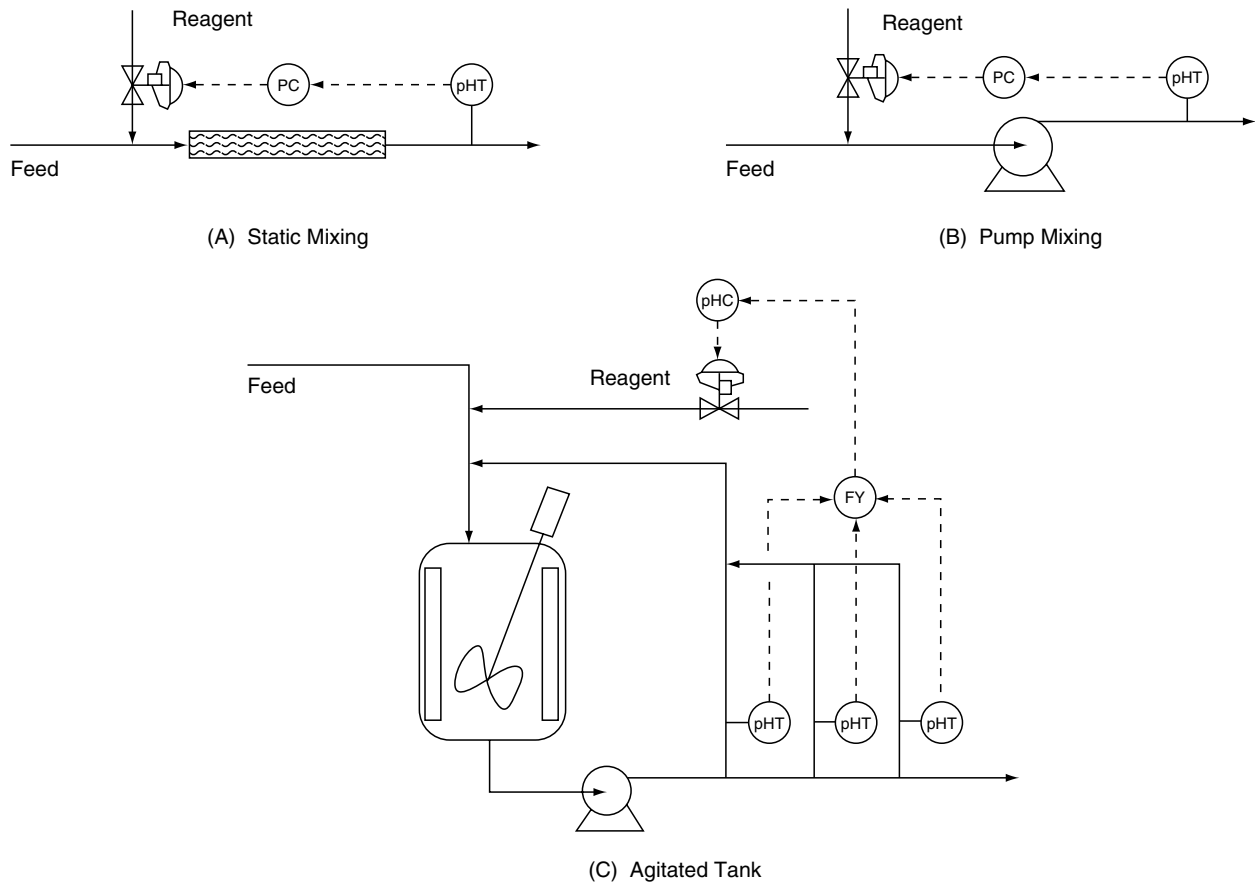
Figure 3.27. pH Control
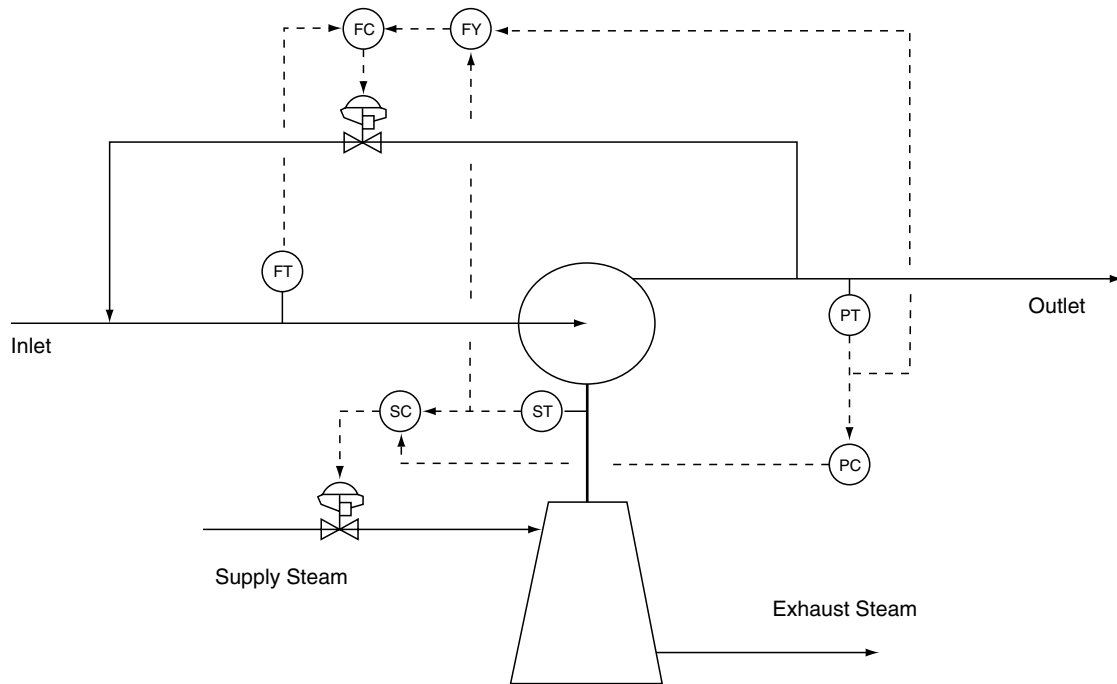
Figure 3.28. Compressor/Turbine Control
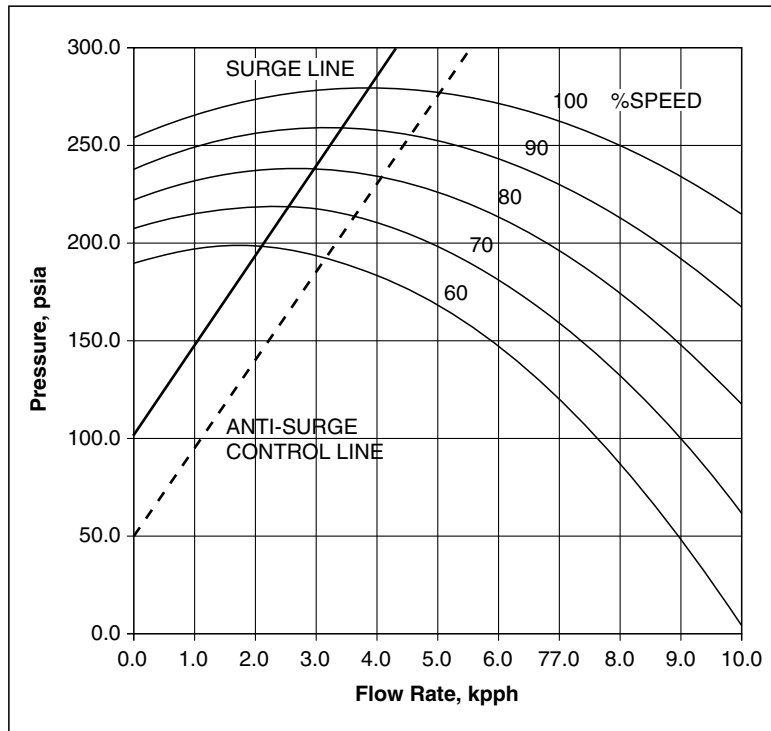
Figure 3.29. Compressor Surge Curve

control line is determined by applying an operating margin to the actual surge line. This operating margin is required because if the compressor crosses over into unstable surging, it cannot be returned to stable operation by the closed-loop control system. A vibration interlock system is often used to throw open the flow valve in order to move the compressor out of its surge condition.

REFERENCES

T.L. Blevins et al., *Advanced Control Unleashed*. Research Triangle Park: ISA—The Instrumentation, Systems, and Automation Society, 2003.

T.F. Edgar et al., *Perry's Chemical Engineering Handbook*, 6th ed., McGraw-Hill, New York, 1999, Chapter 8.

W.L. Luyben, *Practical Distillation Control*, Van Nostrand Reinhold, New York, 1992.

G.K. McMillan, *Process/Industrial Instruments and Controls Handbook*, 5th ed., McGraw-Hill, New York, 1999.

G.K. McMillan, *Tuning and Control Loop Performance*, 3rd ed., Research Triangle Park: ISA—The Instrument Society of America, 1994.

F.G. Shinskey, *Feedback Controllers for the Process Industries Systems*. McGraw-Hill, New York, 1994.

F.G. Shinskey, *Process Control Systems*, 3rd ed., McGraw-Hill, New York, 1988.

C.A. Smith and A.B. Corripio, *Principles and Practice of Automatic Process Control Systems*. Wiley, New York, 1985.

4

DRIVERS FOR MOVING EQUIPMENT

*P*owered chemical processing equipment includes pumps, compressors, agitators and mixers, crushers and grinders, and conveyors. Drivers are electric motors, steam or gas turbines, and internal combustion engines. For loads under 150 HP or so electric motors are almost invariably the choice. Several criteria are applicable. For example, when a pump and a spare are provided, for flexibility one of them may be driven by motor and the other by turbine. Centrifugal and axial blowers and compressors are advantageously driven by turbines because the high operating speeds of 4000–10,000 rpm are readily attainable whereas electric motors must operate through a speed increasing gear at extra expense. When fuel is relatively cheap or accessible, as in the field, gas turbines and internal combustion engines are preferred drivers. Turbines, internal combustion engines, and direct current

motors are capable of continuous speed adjustment over a wide range. Energy efficiencies vary widely with the size and type of driver as shown in this table.

	Efficiency (%)			
Driver	*10 kW*	*100 kW*	*1000 kW*	*10,000 kW*
Gas turbine and internal combustion engine		28	34	38
Steam turbine		42	63	78
Motor	85	92	96	97

Since the unit energy costs are correspondingly different, the economics of the several drive modes often are more nearly comparable.

4.1. MOTORS

Although each has several subclasses, the three main classes of motors are induction, synchronous, and direct current. Higher voltages are more efficient, but only in the larger sizes is the housing ample enough to accomodate the extra insulation that is necessary. The voltages commonly used are

Horsepower	Voltage
1–100	220, 440, 550
75–250	440
200–2500	2300, 4000
Above 2500	4000, 13,200

Direct current voltages are 115, 230, and 600.

The torque-speed characteristic of the motor must be matched against that of the equipment, for instance, a pump. As the pump comes up to speed, the torque exerted by the driver always should remain 5% or so above that demanded by the pump.

The main characteristics of the three types of motors that bear on their process applicability are summarized following.

INDUCTION

Induction motors are the most frequent in use because of their simple and rugged construction, and simple installation and control. They are constant speed devices available as 3600 (two-pole), 1800, 1200, and 900 rpm (eight-pole). Two speed models with special windings with 2:1 speed ratios are sometimes used with agitators, centrifugal pumps and compressors and fans for air coolers and cooling towers. Capacities up to 20,000 HP are made. With speed

increasing gears, the basic 1800 rpm model is the economical choice as drivers, for centrifugal compressors at high speeds.

SYNCHRONOUS

Synchronous motors are made in speeds from 1800 (two-pole) to 150 rpm (48-pole). They operate at constant speed without slip, an important characteristic in some applications. Their efficiencies are 1–2.5% higher than that of induction motors, the higher value at the lower speeds. They are the obvious choice to drive large low speed reciprocating compressors requiring speeds below 600 rpm. They are not suitable when severe fluctuations in torque are encountered. Direct current excitation must be provided, and the costs of control equipment are higher than for the induction types. Consequently, synchronous motors are not used under 50 HP or so.

DIRECT CURRENT

Direct current motors are used for continuous operation at constant load when fine speed adjustment and high starting torque are needed. A wide range of speed control is possible. They have some process applications with centrifugal and plunger pumps, conveyors, hoists, etc.

Enclosures. In chemical plants and refineries, motors may need to be resistant to the weather or to corrosive and hazardous locations. The kind of housing that must be provided in particular situations is laid out in detail in the National Electrical Code, Article 500. Some of the classes of protection recognized there are in this table of differential costs.

Type	% Cost above Drip Proof	Protection Against
Drip proof		Dripping liquids and falling particles
Weather protected, I and II	10–50	Rain, dirt, snow
Totally enclosed fan cooled, TEFC, below 250 HP	25–100	Explosive and nonexplosive atmospheres
Totally enclosed, water, cooled, above 500 HP	25–100	Same as TEFC
Explosion proof, below 3000 HP	110–140	Flammable and volatile liquids

Clearly the cost increments beyond the basic drip-proof motor enclosures are severe, and may need to be balanced in large sizes against the cost of isolating the equipment in pressurized buildings away from the hazardous locations.

Applications. The kinds of motors that are being used successfully with particular kinds of chemical process equipment are identified in Table 4.1. As many as five kinds of AC motors are shown in some instances. The choice may be influenced by economic considerations or local experience or personal preference. In this area, the process engineer is well advised to enlist help from electrical experts. A checklist of basic data that a supplier of a motor must know is in Table 4.2. The kind of enclosure may be specified on the last line, operating conditions.

TABLE 4.1. Selection of Motors for Process Equipment

	Motor Type[a]	
Application	**A.C.**	**D.C.**
Agitator	1a, 1b, 2b	5a
Ball mill	1c, 2b, 3a	5b
Blower	1a, 1b, 2b, 3a, 4	5a
Compressor	1a, 1b, 1c, 3a, 4	5b, 7
Conveyor	1a, 1c, 2b, 3a	5b, 7
Crusher	1a, 1c, 1d	5a, 5b
Dough mixer	1a, 1b, 1c, 2b	5a, 5b
Fan, centrifugal and propeller	1a, 1b, 2c, 3a, 4	5a, 7
Hammer mill	1c	5a
Hoist	1d, 2a, 3b	6
Pulverizer	1c	5b
Pump, centrifugal	1a, 1b, 2b, 3a, 4	5b
Pump, positive displacement	1c, 2b, 3a	5b
Rock crusher	3a	5b, 6

[a]Code:
1. Squirrel-cage, constant speed
   a. normal torque, normal starting current
   b. normal torque, low starting current
   c. high torque, low starting current
   d. high torque, high slip
2. Squirrel-cage, multispeed
   a. constant horsepower
   b. constant torque
   c. variable torque
3. Wound rotor
   a. general purpose
   b. crane and hoist
4. Synchronous
5. Direct current, constant speed
   a. shunt wound
   b. compound wound
6. Direct current, variable speed series wound
7. Direct current, adjustable speed
(After Allis-Chalmers Mfg. Co., Motor and Generator Reference Book, Colorado Springs, CO).
Standard NEMA ratings for induction motors:
General purpose: $\frac{1}{2}$, $\frac{3}{4}$, 1, $1\frac{1}{2}$, 2, 3, 5, $7\frac{1}{2}$, 10, 15, 20, 25, 30, 40, 50, 60, 75, 100, 125, 150, 200, 250, 300, 350, 400, 450, 500.
Large motors: 250, 300, 350, 400, 450, 500, 600, 700, 800, 900, 1000, 1250, 1500, 1750, 2000, 2250, 2500, 3000, 3500, 4000, 4500, 5000 and up to 30,000.

4.2. STEAM TURBINES AND GAS EXPANDERS

Turbines utilize the expansion of steam or a gas to deliver power to a rotating shaft. Salient features of such equipment are

TABLE 4.2. Checklist for Selection of Motors

Motor Data

General
Type of motor (cage, wound-rotor, synchronous, or dc) . . . .
Quantity . . . . Hp . . . . Rpm . . . . Phase . . . .
Cycles . . . . Voltage . . . .
Time rating (continuous, short-time, intermittent) . . . .
Overload (if any) . . . . % for . . . . Service factor . . . . %
Ambient temperature . . . . C Temperature rise C
Class of insulation: Armature . . . . Field . . . . Rotor of w-r motor . . . .
Horizontal or vertical . . . . Plugging duty . . . .
Full- or reduced-voltage or part-winding starting (ac) . . . .
    If reduced voltage—by autotransformer or reactor . . . .
Locked-rotor starting current limitations . . . .
Special characteristics . . . .

Induction Motors
Locked-rotor torque . . . . . % Breakdown torque . . . % or for general-purpose cage motor: NEMA Design (A, B, C, D) . . . .

Synchronous Motors
Power factor . . . . . . Torques: Locked-rotor . . . . . % Pull-in . . . . . %
Pull-out . . . . . . % Excitation . . . . . . volts dc. Type of exciter . . . . . .
    If m-g exciter set, what are motor characteristics? . . . .
Motor field rheostat . . . . Motor field discharge resistor . . . .

Direct-current Motors
Shunt, stabilized shunt, compound, or series wound . . . .
Speed range . . . . Non-reversing or reversing . . . .
Continuous or tapered-rated . . . .

Mechanical Features
Protection or enclosure . . . . Stator shift . . . .
Number of bearings . . . . Type of bearings . . . .
Shaft extension: Flanged . . . . Standard or special length
Press on half-coupling . . . . Terminal box
NEMA C or D flange . . . . Round-frame or with feet
Vertical: External thrust load . . . . . lbs. Type of thrust bearing . . . . .
    Base ring type . . . . Sole plates . . . .
Accessories . . . .

Load Data
Type of load . . . .
If compressor drive, give NEMA application number . . . .
Direct-connected, geared, chain, V-belt, or flat-belt drive . . . .
Wk^2 (inertia) for high inertia drives . . . . lb-ft^2
Starting with full load, or unloaded . . . .
    If unloaded, by what means? . . . .
For variable-speed or multi-speed drives, is load variable torque, constant torque, or constant horsepower? . . . .
Operating conditions . . . .

(By permission, *Allis Chalmers Motor and Generator Reference Book*, Bul. 51R7933, and E.S. Lincoln (Ed.), *Electrical Reference Book*, Electrical Modernization Bureau, Colorado Springs, CO.).

1. high speed rotation,
2. adjustable speed operation,
3. nonsparking and consequently nonhazardous operation,
4. simple controls,
5. low first cost and maintenance, and
6. flexibility with regard to inlet and outlet pressures.

Single stage units are most commonly used as drivers, but above 500 HP or so multistage units become preferable. Inlet steam pressures may be any value up to the critical and with several hundred
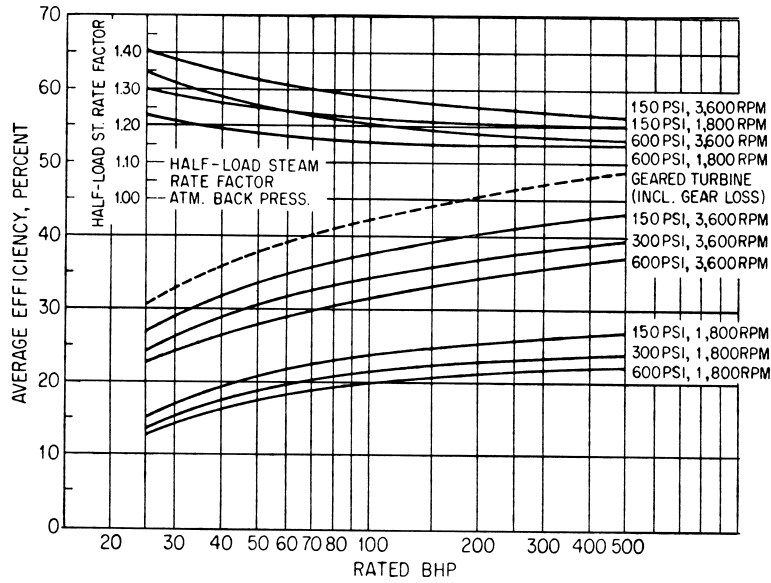
Average efficiency of single-stage turbines (noncondensing, dry, and saturated steam).

(a)
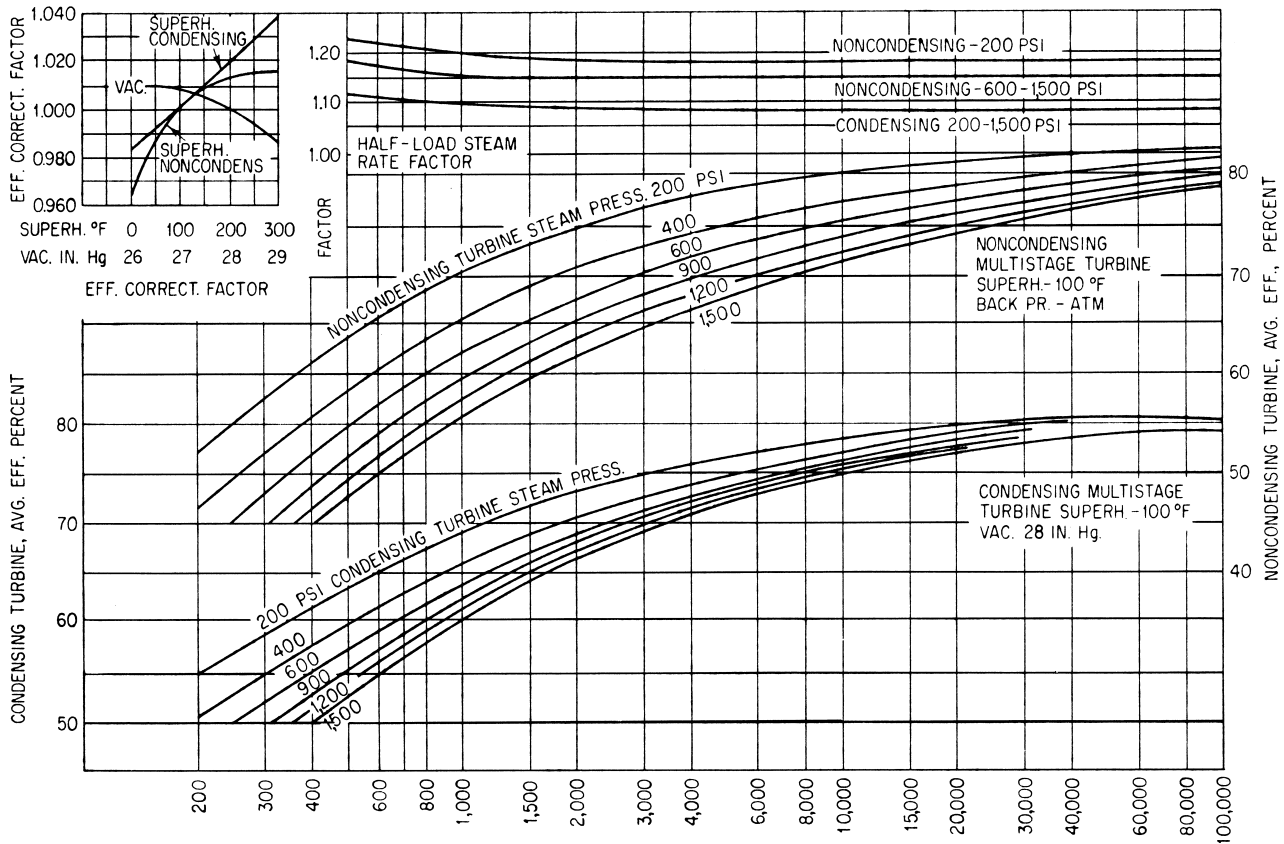
Average efficiency of multistage turbines (gear loss not included).

(b)

Figure 4.1. Efficiencies of (a) single-stage and (b) multistage turbines. (*Gartmann, 1970, pp. 5.8-5.9, Figs. 5.2 and 5.3.*)

degrees of superheat. In larger sizes turbines may be convenient sources of low pressure exhaust steam in the plant. From multistage units, steam may be bled at several reduced pressures. When the expansion is to subatmospheric conditions, the operation is called condensing because the exhaust steam must be condensed before removal from the equipment. Although the efficiency of condensing turbines is less, there is an overall reduction of energy consumption because of the wider expansion range.

Several parameters affect the efficiency of steam turbines, as shown partially on Figure 4.1. Closer examination will need to take into account specific mechanical details which usually are left to the manufacturer. Geared turbines [the dashed line of Fig. 4.1(a)] have higher efficiencies, even with reduction gear losses, because they operate with especially high bucket speeds. For example, for a service of 500 HP with 300 psig steam, a geared turbine has an efficiency of 49.5% and one with a direct drive at 1800 rpm has an efficiency of 24%.

The flow rate of steam per unit of power produced is represented by

$$\dot{m} = -\frac{2545}{\eta(H_2 - H_1)}\,\text{lb/HP hr}$$
$$= -\frac{3412}{\eta(H_2 - H_1)}\,\text{lb/kWh}$$

with the enthalpies in Btu/lb. The efficiency is η, off Figure 4.1, for example. The enthalpy change is that of an isentropic process. It may be calculated with the aid of the steam tables or a Mollier diagram for steam. For convenience, however, special tables have been derived which give the theoretical steam rates for typical combinations of inlet and outlet conditions. Table 4.3 is an abbreviated version.

Example 4.1 illustrates this kind of calculation and compares the result with that obtained by taking the steam to behave as an ideal gas. For nonideal gases with known PVT equations of state and low pressure heat capacities, the method of calculation is the same as for compressors which is described in that section of the book.

On a Mollier diagram like that with Example 4.1, it is clear that expansion to a low pressure may lead to partial condensation if insufficient preheat is supplied to the inlet steam. The final condition after application of the efficiency correction is the pertinent one, even though the isentropic point may be in the two-phase region. Condensation on the blades is harmful to them and must be avoided. Similarly, when carbon dioxide is expanded, possible formation of solid must be guarded against.

When gases other than steam are employed as motive fluids, the equipment is called a gas expander. The name gas turbine usually is restricted to equipment that recovers power from hot combustion gases. The name turboexpander is applied to machines

TABLE 4.3. Theoretical Steam Rates for Typical Steam Conditions (lb/kWh)[a]

Initial Pressure, lb/in² gage															
150	250	400	600	600	850	850	900	900	1,200	1,250	1,250	1,450	1,450	1,800	2,400
Initial Temp, °F															
365.9	500	650	750	825	825	900	825	900	825	900	950	825	950	1000	1000
Initial Superheat, °l															
0	94.0	201.9	261.2	336.2	297.8	372.8	291.1	366.1	256.3	326.1	376.1	232.0	357.0	377.9	337.0
Initial Enthalpy, Btu/lb															

Exhaust Pressure	1,195.5	1,261.8	1,334.9	1,379.6	1,421.4	1,410.6	1,453.5	1,408.4	1,451.6	1,394.7	1,438.4	1,468.1	1,382.7	1,461.2	1,480.1	1,460.4
inHg abs																
2.0	10.52	9.070	7.831	7.083	6.761	6.580	6.282	6.555	6.256	6.451	6.133	5.944	6.408	5.900	5.668	5.633
2.5	10.88	9.343	8.037	7.251	6.916	6.723	6.415	6.696	6.388	6.584	6.256	6.061	6.536	6.014	5.773	5.733
3.0	11.20	9.582	8.217	7.396	7.052	6.847	6.530	6.819	6.502	6.699	6.362	6.162	6.648	6.112	5.862	5.819
4.0	11.76	9.996	8.524	7.644	7.282	7.058	6.726	7.026	6.694	6.894	6.541	6.332	6.835	6.277	6.013	5.963
lb/in² gage																
5	21.69	16.57	13.01	11.05	10.42	9.838	9.288	9.755	9.209	9.397	8.820	8.491	9.218	8.351	7.874	7.713
10	23.97	17.90	13.83	11.64	10.95	10.30	9.705	10.202	9.617	9.797	9.180	8.830	9.593	8.673	8.158	7.975
20	28.63	20.44	15.33	12.68	11.90	11.10	10.43	10.982	10.327	10.490	9.801	9.415	10.240	9.227	8.642	8.421
30	33.69	22.95	16.73	13.63	12.75	11.80	11.08	11.67	10.952	11.095	10.341	9.922	10.801	9.704	9.057	8.799
40	39.39	25.52	18.08	14.51	13.54	12.46	11.66	12.304	11.52	11.646	10.831	10.380	11.309	10.134	9.427	9.136
50	46.00	28.21	19.42	15.36	14.30	13.07	12.22	12.90	12.06	12.16	11.284	10.804	11.779	10.531	9.767	9.442
60	53.90	31.07	20.76	16.18	15.05	13.66	12.74	13.47	12.57	12.64	11.71	11.20	12.22	10.90	10.08	9.727
75	69.4	35.77	22.81	17.40	16.16	14.50	13.51	14.28	13.30	13.34	12.32	11.77	12.85	11.43	10.53	10.12
80	75.9	37.47	23.51	17.80	16.54	14.78	13.77	14.55	13.55	13.56	12.52	11.95	13.05	11.60	10.67	10.25
100		45.21	26.46	19.43	18.05	15.86	14.77	15.59	14.50	14.42	13.27	12.65	13.83	12.24	11.21	10.73
125		57.88	30.59	21.56	20.03	17.22	16.04	16.87	15.70	15.46	14.17	13.51	14.76	13.01	11.84	11.28
150		76.5	35.40	23.83	22.14	18.61	17.33	18.18	16.91	16.47	15.06	14.35	15.65	13.75	12.44	11.80
160		86.8	37.57	24.79	23.03	19.17	17.85	18.71	17.41	16.88	15.41	14.69	16.00	14.05	12.68	12.00
175			41.16	26.29	24.43	20.04	18.66	19.52	18.16	17.48	15.94	15.20	16.52	14.49	13.03	12.29
200			48.24	29.00	26.95	21.53	20.05	20.91	19.45	18.48	16.84	16.05	17.39	15.23	13.62	12.77
250			69.1	35.40	32.89	24.78	23.08	23.90	22.24	20.57	18.68	17.81	19.11	16.73	14.78	13.69
300				43.72	40.62	28.50	26.53	27.27	25.37	22.79	20.62	19.66	20.89	18.28	15.95	14.59
400				72.2	67.0	38.05	35.43	35.71	33.22	27.82	24.99	23.82	24.74	21.64	18.39	16.41
425				84.2	78.3	41.08	38.26	38.33	35.65	29.24	26.21	24.98	25.78	22.55	19.03	16.87
600						78.5	73.1	68.11	63.4	42.10	37.03	35.30	34.50	30.16	24.06	20.29

[a]From Theoretical Steam Rate Tables—Compatible with the 1967 ASME Steam Tables, ASME, 1969.

EXAMPLE 4.1
Steam Requirement of a Turbine Operation
Steam is fed to a turbine at 614.7 psia and 825°F and is discharged at 64.7 psia. (a) Find the theoretical steam rate, lb/kWh, by using the steam tables. (b) If the isentropic efficiency is 70%, find the outlet temperature. (c) Find the theoretical steam rate if the behavior is ideal, with $C_p/C_v = 1.33$.

(a) The expansion is isentropic. The initial and terminal conditions are identified in the following table and on the graph. The data are read off a large Mollier diagram (Keenan et al., 1969).

Point	P	T^0F	H	S
1	614.7	825	1421.4	1.642
2	64.7	315	1183.0	1.642
3	64.7	445	1254.5	1.730

$$\Delta H_s = H_2 - H_1 = -238.4 \text{ Btu/lb}$$

Theoretical steam rate $= 3412/238.4 = 14.31$ lb/kWh. This value is checked exactly with the data of Table 4.3.

(b) $H_3 - H_1 = 0.7(H_2 - H_1) = -166.9$ Btu/lb

$H_3 = 1421.4 - 166.9 = 1254.5$ Btu/lb

The corresponding values of T_3 and S_3 are read off the Mollier diagram, as tabulated.

(c) The isentropic relation for ideal gases is

$$\Delta H = \frac{k}{k-1} RT_1[(P_2/P_1)^{(k-1)/k} - 1]$$
$$= \frac{1.987(1285)}{0.25}[(64.7/614.7)^{0.25} - 1]$$
$$= -4396 \text{ Btu/lbmol}, -244 \text{ Btu/lb}.$$
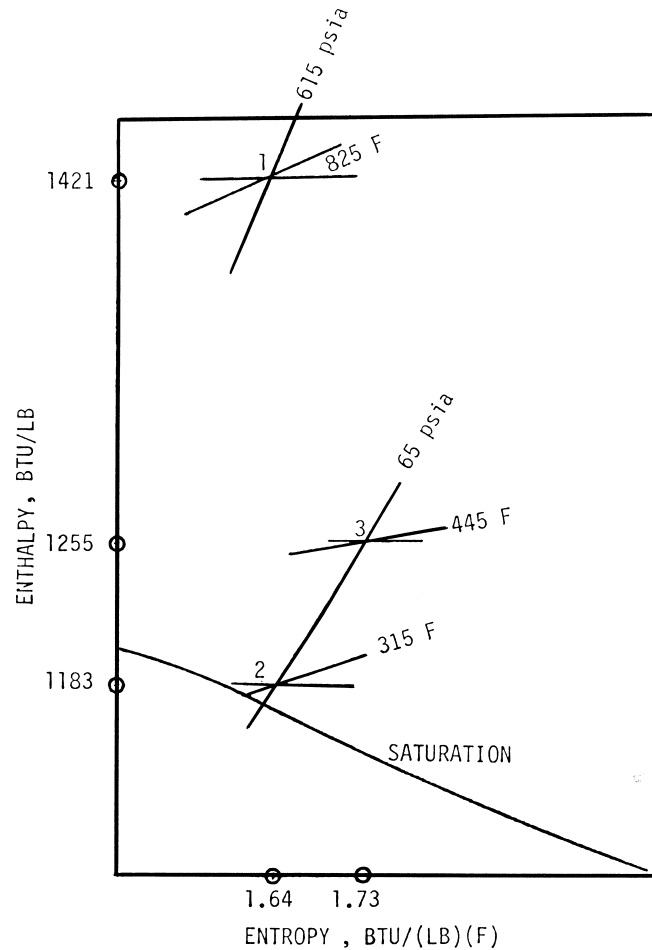
whose objective is to reduce the energy content (and temperature) of the stream, as for cryogenic purposes.

Gas expanders are used to recover energy from high pressure process gas streams in a plant when the lower pressure is adequate for further processing. Power calculations are made in the same way as those for compressors. Usually several hundred horsepower must be involved for economic justification of an expander. In smaller plants, pressures are simply let down with throttling valves (Joule–Thomson) without attempt at recovery of energy.

The specification sheet of Table 4.4 has room for the process conditions and some of the many mechanical details of steam turbines.

4.3. COMBUSTION GAS TURBINES AND ENGINES

When a low cost fuel is available, internal combustion drivers surpass all others in compactness and low cost of installation and operation. For example, gas compression on a large scale has long been done with integral engine compressors. Reciprocating engines also are widely used with centrifugal compressors in low pressure applications, but speed increasing gears are needed to up the 300–600 rpm of the engines to the 3000–10,000 rpm or so of the compressor.

Process applications of combustion gas turbines are chiefly to driving pumps and compressors, particularly on gas and oil trans-

mission lines where the low thermal efficiency is counter-balanced by the convenience and economy of having the fuel on hand. Offshore drilling rigs also employ gas turbines. Any hot process gas at elevated pressure is a candidate for work recovery in a turbine. Offgases of catalytic cracker regenerators, commonly at 45 psig and as high as 1250°F, are often charged to turbines for partial recovery of their energy contents. Plants for the manufacture of nitric acid by oxidation of ammonia at pressures of 100 psig or so utilize expanders on the offgases from the absorption towers, and the recovered energy is used to compress the process air to the reactors.

Combustion gas turbine processes are diagrammed on Figure 4.2 and in Example 4.2. In the basic process, a mixture of air and fuel (or air alone) is compressed to 5–10 atm, and then ignited and burned and finally expanded through a turbine from which power is recovered. The process follows essentially a Brayton cycle which is shown in Figure 4.2 in idealized forms on TS and PV diagrams. The ideal process consists of an isentropic compression, then heating at constant pressure followed by an isentropic expansion and finally cooling at the starting pressure. In practice, efficiencies of the individual steps are high:

Compressor isentropic efficiency, 85%
Expander isentropic efficiency, 85–90%
Combustion efficiency, 98%

TABLE 4.4. Data Sheet for General Purpose Steam Turbines, Sheet 1 of 2[a]

GENERAL-PURPOSE STEAM TURBINE
DATA SHEET
CUSTOMARY UNITS

CONTRACT NO. _____
ITEM NO. _____
REV. NO. _____ DATE _____
BY _____ REVIEWED _____
SHEET ___1___ OF ___2___
P.O. NO. _____

Applicable to:	○ Proposal	○ Purchase	○ As – Built
For		Unit	
Site		No. Required	
Service		Driven Equipment	
Manufacturer		Model	Serial No.

NOTE: ○ Indicates Information Completed By Purchaser   ☐ By Manufacturer

○ OPERATING CONDITIONS			☐ PERFORMANCE		
Operating Point	Power, BHP	Speed, RPM	Operating Point/ Steam Condition	No. Hand Valves Open (3.4.1 4)	Steam Rate, Lbs/HP · Hr.
Normal			Normal/Normal		
Rated			Rated/Normal		
Other			Rated/Min. Inlet, Max. Exhaust		
			Indicate Guarantee Point By *		

○ STEAM CONDITIONS	MAX.	NORMAL	MIN.	☐ CONSTRUCTION		
Inlet Press, PSIG				Turbine Type ○ Horiz. ○ Vertical		
Inlet Temp, °F				No. Stages Wheel Dia., In.		
Exhaust Press (PSIG) (In. Hg)				Rotor: ☐ Built Up ☐ Solid		
Unusual Conditions (2.12.2.6)				Blading ☐ 2 Row ☐ 3 Row ☐ Re Entry		
Duty ○ Continuous ○ Standby ○ Auto Start				Casing Split ☐ Axial ☐ Radial		
Eval. Steam Cost, $/1000 Lbs				Casing Support ☐ Centerline ☐ Foot		
Payout Period, Years Hrs/Yr				☐ NEMA "P" Base		
TURBINE DATA				Trip Valve ☐ Integral ☐ Separate		
☐ Minimum Allowable Speed, RPM				Interstage Seals ☐ Labyrinth ☐ Carbon		
☐ Maximum Continuous Speed, RPM				End Seals ☐ Carbon Ring, No/Box		
☐ Trip Speed, RPM				☐ Labyrinth		
☐ First Critical Speed, RPM				Type Radial Bearings		
○ Turbine Construction Safe For Runaway Speed (2.11.1)				Type Thrust Bearing (2.9.2)		
☐ Exh. Temp. °F Normal No Load				Thrust Collar (2.9.8) ☐ Replaceable ☐ Integral ☐ None		
☐ Potential Max. Power, BHP				Lube Oil Viscosity (2.10.2) SUS @ 100°F SUS @ 210°F		
☐ Max. Nozzle Steam Flow, Lbs/Hr				Lubrication ○ Ring Oiled ○ Pressure		
☐ Max. Allowable Speed, RPM				○ Purge Oil Mist ○ Pure Oil Mist		
○ Rotation Facing Gov. End ○ CCW ○ CW				○ Shaft Areas Suitable For Observing By Non-Contacting Type		
○ Driven Equipment Thrust, Lbs. (2.9.3) Up				Vibration Probes (2.6.2.2)		

○ Driven Equipment Thrust (Vertical Turbine) Down	CASING DESIGN	INLET	EXHAUST
○ Mount Turbine on Baseplate Furnished by Driven Equipment Vendor	Max. Allow. Press, PSIG		
○ Water Piping Furn. by ○ Vendor ○ Others	Max. Allow. Temp, °F		
○ Oil Piping Furn. by ○ Vendor ○ Others	Hydro Test Pressure, PSIG		
	MATERIALS		
	High Pressure Casing		
	Exhaust Casing		
○ SITE AND UTILITY DATA	Nozzles		
Location (2.1.13) ○ Indoor ○ Heated ○ Unheated	Blading		
○ Outdoor ○ Roof ○ Without Roof	Wheels		
Ambient Temp. °F Min. Max.	Shaft		
Unusual Conditions ○ Dust ○ Salt Atmosphere	Under Packing Application Method		
○ Winterization Required	Gov. Valve Trim		
Elect. Area (2.1.12) Class Group Div	Inlet Strainer Mesh Size		
○ Non-hazardous	Governor Type ○ Mech. ○ Hydr. ○ Oil Relay		
Control Power V Ph. Hz	NEMA Class Adj. Speed Range +% −%		
Aux. Motors V Ph. Hz	Speed Changer ○ Manual ○ Pneum. ○ Elect.		
Cooling Water: Press, PSIG ΔP, PSI	Mfr. Model		
Flow, GPM ΔT, °F			
Allowable Sound Level (2.1.11) dBA @ ft.	Turbine Weight, Lbs		

[a]Also available in SI units (API Standard 611, January 1982). (Reprinted courtesy of the American Petroleum Institute).
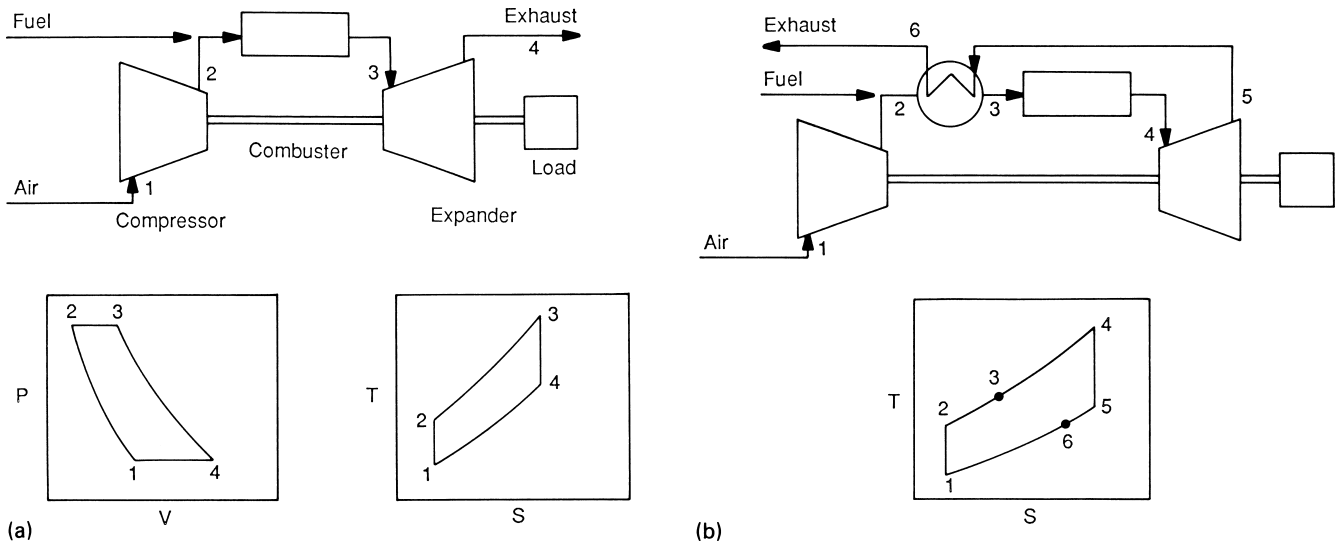
Figure 4.2. Combustion gas turbine arrangements and their thermodynamic diagrams. (a) Basic unit with PV and TS diagrams. (b) Unit with an air preheater and TS diagram.

EXAMPLE 4.2
Performance of a Combustion Gas Turbine
Atmospheric air at 80°F (305K) is compressed to 5 atm, combined with fuel at the rate of 1 kg/s, then expanded to 1 atm in a power
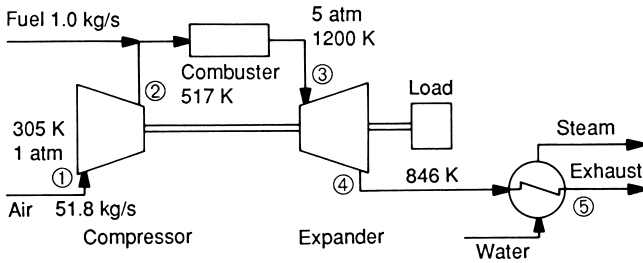
turbine. Metallurgical considerations limit the temperature to 1700°F (1200K). The heat capacities of air and combustion products are

$$C_p = 0.95 + 0.00021T \text{ (K) kJ/kg},$$

the heat of combustion is 42,000 kJ/kg, the furnace efficiency is 0.975, the isentropic efficiency of the compressor is 0.84, and that of the expander is 0.89. Find

a. the required air rate,
b. the power loads of the compressor and expander, and
c. the overall efficiency as a function of the temperature of the exhaust leaving a steam generator.

Point	P	T_s	T
1	1		305
2	5	483	517
3	5		1200
4	1	802	846
5	1		400

Compression:

$$k = 1.4, \ k/(k-1) = 3.5,$$

$$T_{2s} = T_1(P_2/P_1)^{1/3.5} = 305(5)^{1/3.5} = 483K,$$

$$T_2 = 305 + \frac{483 - 305}{0.84} = 517K.$$

Combustion:

m'_a = flow rate of air, kg/kg fuel

$$0.975(42000) = \int_{305}^{1200} C_p \, dT + m'_a \int_{517}^{1200} C_p \, dT$$
$$= 991682 + 771985m'_a$$

$$m'_a = 51.8$$

Expansion:

$$k = 1.33, \ k/(k-1) = 4.0$$

$$T_{4s} = T_3(P_4/P_1)^{0.25} = 1200(0.2)^{0.25} = 802°K$$

$$T_4 = 1200 - 0.89(1200 - 802) = 846°K$$

Power calculations:

$$\text{Compressor}: w'_c = -m'_a \Delta H = -51.8 \int_{305}^{517} C_p \, dT$$
$$= -51.8(216.98) = -11.240 \text{ kJ/s}$$

$$\text{Expander}: w'_e = -52.8 \int_{1200}^{517} C_p \, dT = 52.8(412.35) = 21,772 \text{ kJ/s}$$

$$\text{Steam generator}: Q' = 52.8 \int_T^{846} C_p \, dT$$

$$\eta_t = \text{overall efficiency} = \frac{21772 - 11380 + Q'}{42000}$$

The tabulation shows efficiency with three different values of the exhaust temperature.

T	Q'	η_t
846	0	0.247
600	14311	0.588
500	19937	0.722

Other inefficiencies are due to pressure drops of 2–5%, loss of 1–3% of the enthalpy in the expander, and 1% or so loss of the air for cooling the turbine blades. The greatest loss of energy is due to the necessarily high temperature of the exhaust gas from the turbine, so that the overall efficiency becomes for the order of 20% or so. Some improvements are effected with air preheating as on Figure 4.2(b) and with waste heat steam generators as in Example 4.2. In many instances, however, boilers on 1000°F waste gas are economically marginal. Efficiencies are improved at higher pressure and temperature but at greater equipment cost.

Inlet temperature to the expander is controlled by the amount of excess air. The air/fuel ratio to make 1700°F is in the range of 50 lb/lb. Metallurgical considerations usually limit the temperature to this value. Special materials are available for temperature up to 2200°F but may be too expensive for process applications.

REFERENCES

M.P. Boyce, *Gas Turbine Engineering Handbook*, Gulf, Houston, 1982.

F.L. Evans, *Equipment Design Handbook for Refineries and Chemical Plants*, Gulf, Houston, 1979, vol. 1.

H. Gartmann, *De Laval Engineering Handbook*, McGraw-Hill, New York, 1970.

R.T.C. Harman, *Gas Turbine Engineering*, Macmillan, New York, 1981.

J.H. Keenan et al. *Steam Tables*, Wiley, New York, 1969.

E.E. Ludwig, *Applied Process Design for Chemical and Process Plants*, Gulf, Houston, 1983, vol. 3.

Marks' Standard Handbook for Mechanical Engineers, 16th ed. McGraw-Hill, New York, 1996.

5

TRANSFER OF SOLIDS

*I*n contrast to fluids which are transferred almost exclusively through pipelines with pumps or blowers, a greater variety of equipment is employed for moving solids to and from storage and between

process equipment. Most commonly, solids are carried on or pushed along by some kind of conveyor. Solids in granular form also are transported in pipelines as slurries in inert liquids or as suspensions in air or other gases.

5.1. SLURRY TRANSPORT

In short process lines slurries are readily handled by centrifugal pumps with open impellers and large clearances. When there is a distribution of sizes, the fine particles effectively form a homogeneous mixture of high density in which the settling velocities of larger particles are less than in clear liquid. Turbulence in the line also helps to keep particles in suspension. It is essential, however, to avoid dead spaces in which solids could accumulate and also to make provisions for periodic cleaning of the line. A coal–oil slurry used as fuel and acid waste neutralization with lime slurry are two examples of process applications.

Many of the studies of slurry transfer have been made in connection with long distance movement of coal, limestone, ores, and others. A few dozen such installations have been made, in length from several miles to several hundred miles.

Coal–water slurry transport has been most thoroughly investigated and implemented. One of the earliest lines was 108 miles long, 10 in. dia, 50–60 wt % solids up to 14 mesh, at velocities of 4.5–5.25 ft/sec, with positive displacement pumps at 30-mile intervals. The longest line in the United States is 273 miles, 18 in. dia and handles 4.8–6.0 million tons/yr of coal; it is described in detail by Jacques and Montfort (1977). Other slurry pipeline literature is by Wasp, Thompson, and Snoek (1971), Bain and Bonnington (1970), Ewing (1978), and Zandi (1971).

Principally, investigations have been conducted of suitable linear velocities and power requirements. Slurries of 40–50 vol % solids can be handled satisfactorily, with particle sizes less than 24–48 mesh or so (0.7–0.3 mm). At low line velocities, particles settle out and impede the flow of the slurry, and at high velocities the frictional drag likewise increases. An intermediate condition exists at which the pressure drop per unit distance is a minimum. The velocity at this condition is called a critical velocity of which one correlation is

$$u_c^2 = 34.6 C_v D u_t \sqrt{g(s-1)/d}, \quad \text{consistent units,} \qquad (5.1)$$

where

u_c = critical flow velocity,
u_t = terminal settling velocity of the particle, given by Figure 5.1,
C_v = volume fraction of solids,
D = pipe diameter,
d = particle diameter,
s = ratio of densities of solid and liquid,
g = acceleration of gravity, 32.2 ft/sec^2, or consistent units.

The numerical coefficient is due to Hayden and Stelson (1971).

Another criterion for selection of a flow rate is based on considerations of the extent of sedimentation of particles of various sizes under flow conditions. This relation is developed by Wasp, Aude, Seiter, and Thompson (1971),

$$\frac{C}{C_0} = \exp(-2.55 u_t / k u \sqrt{f}), \qquad (5.2)$$

where

C = concentration of a particular size at a level 92% of the vertical diameter,
C_0 = concentration at the center of the pipe, assumed to be the same as the average in the pipe,
f = Fanning friction factor for pipe flow

$$= 0.25 \frac{\Delta P}{\rho} \frac{L}{D} \frac{u^2}{2 g_c} \qquad (5.3)$$

At high Reynolds numbers, for example, Blasius' equation is

$$f = 0.0791 / N_{\text{Re}}^{0.25}, \quad N_{\text{Re}} \geq 10^5 \qquad (5.4)$$

k in Eq. (5.2) is a constant whose value is given in the referenced paper as 0.35, but the value 0.85 is shown in a computer output in a paper by Wasp, Thompson, and Snoek (1971, Fig. 9). With the latter value, Eq. (5.2) becomes

$$C/C_0 = \exp(-3.00 u_t / u \sqrt{f}). \qquad (5.5)$$

The latter paper also states that satisfactory flow conditions prevail when $C/C_0 \geq 0.7$ for the largest particle size. On this basis, the minimum line velocity becomes

$$u = \frac{3 u_t}{\sqrt{f} \ln(C_0/C)} = 8.41 u_t / \sqrt{f}, \qquad (5.6)$$

where u_t is the settling velocity of the largest particle present.

As Example 5.1 shows, the velocities predicted by Eqs. (5.1) and (5.6) do not agree closely. Possibly an argument in favor of Eq. (5.6) is that it is proposed by the organization that designed the successful 18 in., 273 mi Black Mesa coal slurry line.

Pressure drop in flow of aqueous suspensions sometimes has been approximated by multiplying the pressure drop of clear liquid at the same velocity by the specific gravity of the slurry. This is not borne out by experiment, however, and the multiplier has been correlated by other relations of which Eq. (5.7) is typical:

$$\Delta P_s / \Delta P_L = 1 + 69 C_v \left[\frac{g D(s-1)}{u^2 \sqrt{C_D}} \right]^{1.3}. \qquad (5.7)$$
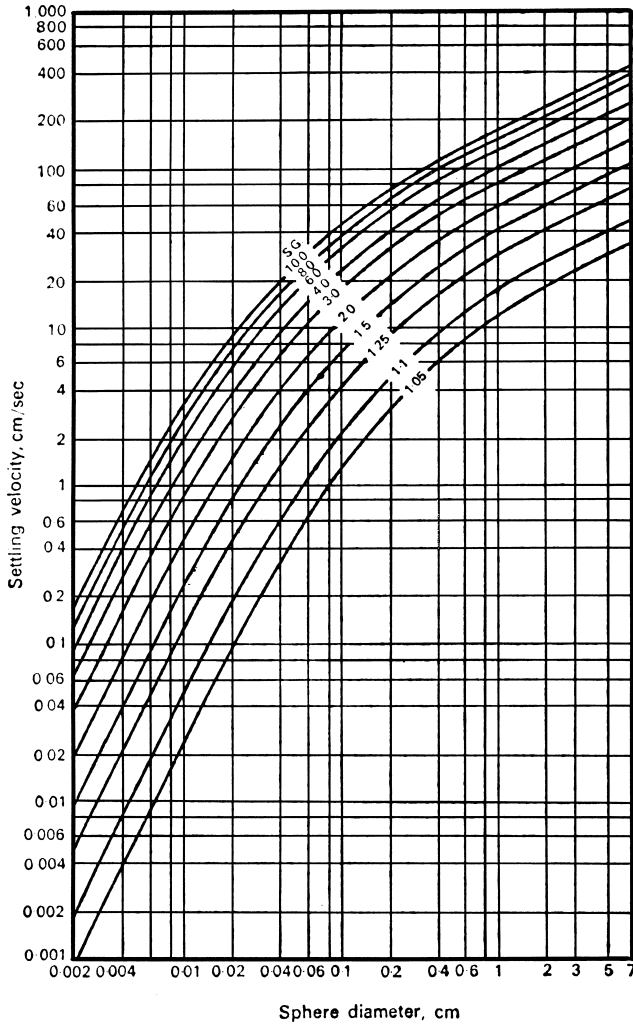
Figure 5.1. Settling velocities of spheres as a function of the ratio of densities of the two phases. Stokes law applies at diameters below approximately 0.01 cm. (*Based on a chart of Lapple, et al., 1984, p. 5.67*).

This equation is a modification by Hayden and Stelson (1971) of a series of earlier ones. The meanings of the symbols are

C_v = volume fraction occupied by the solids in the slurry,
d = particle diameter,
D = pipe diameter,
s = ratio of specific gravities of solid and liquid.

The drag coefficient is

$$C_D = 1.333gd(s-1)/u_t^2. \tag{5.8}$$

For mixtures, a number of rules has been proposed for evaluating the drag coefficient, of which a weighted average seems to be favored,

$$\sqrt{C_D} = \sum w_i \sqrt{C_{Di}}, \tag{5.9}$$

where the w_i are the weight fractions of particles with diameters d_i.

For particles of one size, Eqs. (5.7) and (5.8) combine to

$$\Delta P_s/\Delta P_L = 1 + 100C_v[(u_t D/u^2)\sqrt{g(s-1)/d}]^{1.3},$$
$$\text{consistent units.} \tag{5.10}$$

EXAMPLE 5.1
Conditions of a Coal Slurry Pipeline
Data of a pulverized coal slurry are

$C_v = 0.4$,
$D = 0.333$ ft,
$f = 0.0045$ (Blasius' eq. at $N_{re} = 10^5$),

Mesh size	24	48	100	Mixture
d(mm)	0.707	0.297	0.125	0.321
Weight fraction	0.1	0.8	0.1	1
u_t (ft/sec)	0.164	0.050	0.010	0.0574

The terminal velocities are read off Figure 5.1, and the values of the mixture are weight averages.

The following results are found with the indicated equations:

Item	Eq.	24	48	100	Mixture
u_c	5.1	7.94	5.45	3.02	
u	5.6	20.6	6.27	1.25	
$\sqrt{c_D}$	5.8	1.36	2.89	9.38	2.62
$\Delta P_s/\Delta P_L$	5.11				1.539
$\Delta P_s/\Delta P_L$	5.13				1.296

Eq.(5.1):
$$u_c^2 = 34.6(0.4)(0.333)\sqrt{32.2(0.5)}\frac{u_t}{\sqrt{d_{mm}/304.8}}$$
$$= 323\frac{u_t}{\sqrt{d_{mm}}},$$

Eq.(5.6):
$$u = \frac{8.41u_t}{\sqrt{0.0045}} = 125u_t,$$

Eq.(5.8):
$$c_D = \frac{4}{3}\frac{32.2(1.5-1)}{u_t^2}\frac{d_{mm}}{304.8} = \frac{0.0704d_{mm}}{u_t^2},$$

Eq.(5.11):
$$\frac{\Delta P_s}{\Delta P_L} = 1 + \frac{0.69}{0.4^{0.3}}\left[\frac{1}{0.0574}\sqrt{\frac{32.2(0.5)0.321}{304.8(3.39)^2}}\right]^{1.3}$$
$$= 1.5391,$$

Eq.(5.13):
$$\frac{\Delta P_s}{\Delta P_L} = 1 + 0.272(0.4)\left[\frac{0.0045(0.333)32.2(0.5)}{(0.0574)^2(3.39)}\right]^{1.3}$$
$$= 1.296.$$

With coal of sp gr = 1.5, a slurry of 40 vol % has a sp gr = 1.2. Accordingly the rule, $\Delta P_s/\Delta P_L$ = sp gr, is not confirmed accurately by these results.

The pressure drop relation at the critical velocity given by Eq. (5.1) is found by substitution into Eq. (5.7) with the result

$$\Delta P_s/\Delta P_L = 1 + \frac{0.69}{C_v^{0.3}}[(1/u_t)\sqrt{gd(s-1)/C_D}]^{1.3}. \tag{5.11}$$

With Eq. (5.10) the result is

$$\Delta P_s/\Delta P_L = 1 + 1/C_v^{0.3}. \tag{5.12}$$

With the velocity from Eq. (5.6), Eq. (5.7) becomes

$$\Delta P_s/\Delta P_L = 1 + 0.272C_v[fgD(s-1)/u_t^2\sqrt{C_D}]^{1.3} \tag{5.13}$$

and, for one-sized particles,

$$\Delta P_s / \Delta P_L = 1 + 0.394 C_v [(fD/u_t)\sqrt{g(s-1)/d}]^{1.3}. \qquad (5.14)$$

These several pressure drop relations hardly appear consistent, and the numerical results of Example 5.1 based on them are only roughly in agreement.

Darby (1996) wrote a review article updating the methods for determining settling rates of particles in non-Newtonian fluids.

From statements in the literature, it appears that existing slurry lines were designed on the basis of some direct pilot plant studies.

Nonsettling slurries are formed with fine particles, plastics, or fibers. Although their essentially homogeneous nature would appear to make their flow behavior simpler than that of settling slurries, they often possess non-Newtonian characteristics which complicate their flow patterns. In Newtonian flow, the shear stress is proportional to the shear strain,

$$stress = \mu(strain),$$

but in other cases the relation between these two quantities is more complex. Several classes of non-Newtonian behavior are recognized for suspensions. Pseudoplastic or power-law behavior is represented by

$$stress = k(strain)^n, \quad n < 1,$$

where k is called the consistency index. Plastic or Bingham behavior is represented by

$$stress = k_1 + \eta(strain),$$

where η is called the plastic viscosity. Data for some suspensions are given on Figure 5.2.

The constants of such equations must be found experimentally over a range of conditions for each particular case, and related to the friction factor with which pressure drops and power requirements can be evaluated. The topic of nonsettling slurries is treated by Bain and Bonnington (1970) and Clift (1980). Friction factors of power-law systems are treated by Dodge and Metzner (1959) and of fiber suspensions by Bobkowicz and Gauvin (1967).

5.2. PNEUMATIC CONVEYING

Granular solids of free-flowing natures may be conveyed through ducts in any direction with high velocity air streams. In the normal plant, such lines may be several hundred feet long, but dusty materials such as fly ash and cement have been moved over a mile in this way. Materials that are being air-veyed include chemicals, plastic pellets, grains, and powders of all kinds. The transfer of catalysts between regenerator and reactor under fluidized conditions is a common operation. Stoess (1983) has a list of recommendations for about 150 different materials, of which Table 5.1 is a selection. Basic equipment arrangements are represented in Figure 5.3.

The performance of pneumatic conveyors is sensitive to several characteristics of the solids, of which the most pertinent ones are

1. bulk density, as poured and as aerated,
2. true density,
3. coefficient of sliding friction (= tangent of the angle of repose),
4. particle size distribution,
5. particle roughness and shape,
6. moisture content and hygroscopicity, and
7. characteristics such as friability, abrasiveness, flammability, etc.

The capacity of pneumatic-conveying systems depends on several factors besides the characteristics of the solids, such as the diameter of the conveyor line, the length of the line, and the energy of the conveying air. In fact, some materials (e.g., sulfur) build up an electrostatic charge and may cause explosion risks.

In comparison with mechanical conveyors, pneumatic types must be designed with greater care. They demand more power input per unit weight transferred, but their cost may be less for complicated paths, when exposure to the atmosphere is undesirable and when operator safety is a problem. Although in the final analysis the design and operation of pneumatic conveyors demands the attention of experienced engineers, a preliminary design can be
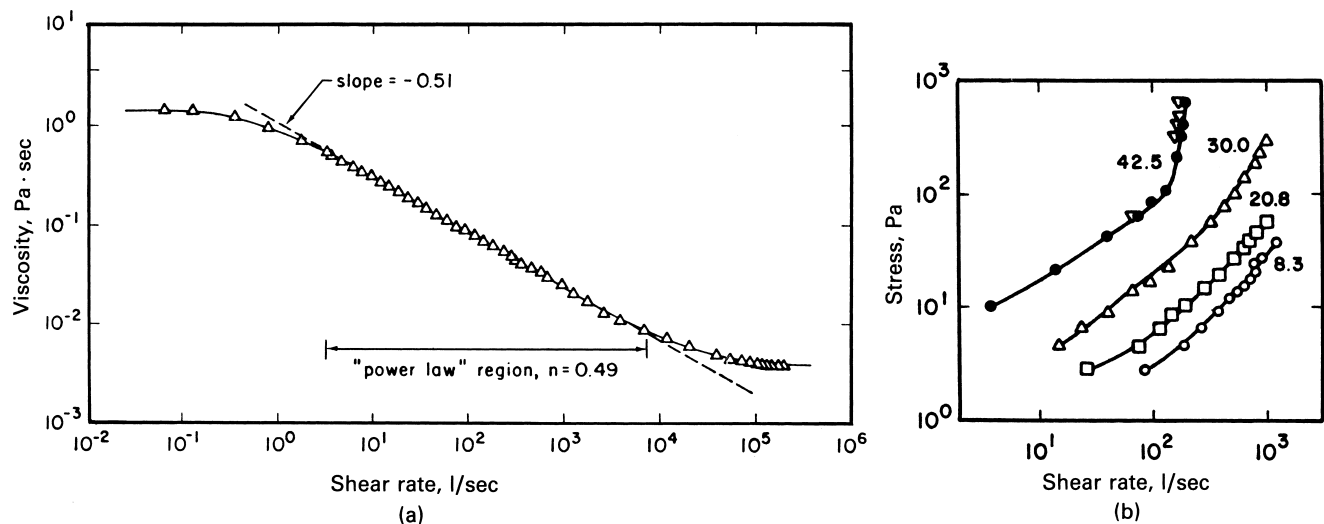
Figure 5.2. Non-Newtonian behavior of suspensions: (a) viscosity as a function of shear rate, 0.4 wt % polyacrylamide in water at room temperature; (b) shear stress as a function of shear rate for suspensions of TiO_2 at the indicated vol % in a 47.1 wt % sucrose solution whose viscosity is 0.017 Pa sec. (*Denn, 1980*).

TABLE 5.1. Flow Rates and Power Requirements of Vacuum and Low Pressure Pneumatic Conveying Systems[a]

Material	Wt per cu ft	Vacuum System (8–9 psia)												Low Pressure System (6–12 psig)							
		Conveying Distance										Velocity ft/sec	Pressure Factor	Conveying Distance						Velocity (ft/sec)
		100 ft		150 ft		250 ft		400 ft					100 ft		250 ft		400 ft		
		Sat.	hp/T	Sat.	hp/T	Sat.	hp/T	Sat.	hp/T				Sat.	hp/T	Sat.	hp/T	Sat.	hp/T	
Alum	50	3.6	4.5	3.9	5.0	4.3	5.7	4.7	6.3	110	4.0		1.6	2.7	2.0	3.4	2.2	3.8	65
Alumina	60	2.4	4.0	2.8	4.7	3.4	5.7	4.0	6.4	105	5.0		1.1	2.4	1.6	3.4	1.9	3.9	60
Carbonate, calcium	25–30	3.1	4.2	3.0	5.0	3.9	5.5	4.2	6.0	110	3.5		1.4	2.5	1.8	3.3	2.0	3.6	65
Cellulose acetate	22	3.2	4.7	3.5	5.1	3.8	5.7	4.1	6.0	100	3.0		1.4	2.8	1.7	3.4	1.9	3.6	55
Clay, air floated	30	3.3	4.5	3.5	5.0	3.9	5.5	4.2	6.0	105	4.0		1.5	2.7	1.8	3.3	1.9	3.6	50
Clay, water washed	40–50	3.5	5.0	3.8	5.6	4.2	6.5	4.5	7.2	115	4.5		1.6	3.0	1.9	3.9	2.1	4.4	60
Clay, spray dried	60	3.4	4.7	3.6	5.2	4.0	6.2	4.4	7.1	110	4.3		1.5	2.8	1.8	3.7	2.0	4.3	55
Coffee beans	42	1.2	2.0	1.6	3.0	2.1	3.5	2.4	4.2	75	5.0		0.6	1.2	0.9	2.1	1.1	2.5	45
Corn, shelled	45	1.9	2.5	2.1	2.9	2.4	3.6	2.8	4.3	105	5.0		0.9	1.5	1.1	2.2	1.3	2.6	55
Flour, wheat	40	1.5	3.0	1.7	3.3	2.0	3.7	2.5	4.4	90	2.5		0.7	1.8	0.9	2.2	1.1	2.7	35
Grits, corn	33	1.7	2.5	2.2	3.0	2.9	4.0	3.5	4.8	100	3.5		0.8	1.5	1.3	2.4	1.6	2.9	70
Lime, pebble	56	2.8	3.8	3.0	4.0	3.4	4.7	3.9	5.4	105	5.0		1.3	2.3	1.6	2.8	1.8	3.3	70
Lime, hydrated	30	2.1	3.3	2.4	3.9	2.8	4.7	3.4	6.0	90	4.0		0.6	1.8	0.8	2.2	0.9	2.6	40
Malt	28	1.8	2.5	2.0	2.8	2.3	3.4	2.8	4.2	100	5.0		0.8	1.5	1.1	2.0	1.3	2.5	55
Oats	25	2.3	3.0	2.6	3.5	3.0	4.4	3.4	5.2	100	5.0		1.0	1.8	1.4	2.6	1.6	3.1	55
Phosphate, trisodium	65	3.1	4.2	3.6	5.0	3.9	5.5	4.2	6.0	110	4.5		1.4	2.5	1.8	3.3	1.9	3.6	75
Polyethylene pellets	30	1.2	2.0	1.6	3.0	2.1	3.5	2.4	4.2	80	5.0		0.55	1.2	0.9	2.1	1.1	2.5	70
Rubber pellets	40	2.9	4.2	3.5	5.0	4.0	6.0	4.5	7.2	110									
Salt cake	90	4.0	6.5	4.2	6.8	4.6	7.5	5.0	8.5	120	5.0		2.9	3.9	3.5	4.5	4.0	5.1	83
Soda ash, light	35	3.1	4.2	3.6	5.0	3.9	5.5	4.2	6.0	110	5.0		1.4	2.5	1.8	3.3	1.9	3.6	65
Soft feeds	20–40	3.0	4.2	3.4	4.5	3.7	5.0	4.2	5.5	110	3.8		1.3	2.5	1.7	3.1	1.9	3.7	70
Starch, pulverized	40	1.7	3.0	2.0	3.4	2.6	4.0	3.4	5.0	90	3.0		0.8	1.7	1.1	2.4	1.5	3.0	55
Sugar, granulated	50	3.0	3.7	3.2	4.0	3.4	5.2	3.9	6.0	110	5.0		1.4	2.2	1.6	3.1	1.7	3.6	60
Wheat	48	1.9	2.5	2.1	2.9	2.4	3.6	2.8	4.3	105	5.0		0.9	1.5	1.1	2.1	1.3	2.6	55
Wood flour	12–20	2.5	3.5	2.8	4.0	3.4	4.9	4.4	6.5	100									

[a] HP/ton = (pressure factor)(hp/T)(sat.). The units of sat. $= \left(\frac{\text{cu.ft.air}}{\text{min.}}\right) / \left(\frac{\text{lb solid transferred}}{\text{min.}}\right) = \frac{\text{cu.ft.air}}{\text{lb. solid transferred}}$ and those of hp/T are horsepower/(tons/hr of solid transferred). (Stoess, 1983).

prepared on the basis of general knowledge, data in manufacturers' catalogs or web sites, and rules of thumb that appear in the literature. Articles by Solt (1980, 2002), Kimbel (1998), as well as Dhodapkar and Jacob (2002) are devoted to preventive trouble-shooting.

Some basic design features are the avoidance of sharp bends, a minimum of line fittings, provision for cleanout, and electrical grounding. In many cases equipment suppliers may wish to do pilot plant work before making final recommendations. Figure 5.4 shows a typical pilot plant arrangement. A preliminary design procedure is given by Raymus (1984). Many details of design and operation are given in books by Stoess (1983) and Kraus (1980) and in articles by Gerchow (1980), and Perkins and Wood (1974). More recent information on the design, operation, and troubleshooting of pneumatic conveying systems are found in Mills (1999, 2001, 2002), Kimbel (1998), Dhodapar and Jacob (2002), and Solt (2002). Raymus (1999) presented five nomographs for preliminary design of pneumatic conveying systems. Some of the information from these sources will be restated in this section. Pressure drop and power requirements can be figured largely on the basis of general knowledge.

EQUIPMENT

The basic equipment consists of a solids feeding device, the transfer line proper, a receiver, a solid-air separator, and either a blower at the inlet or a vacuum pump at the receiver. There are four types of pneumatic systems: pressure, vacuum, combination, and fluidized

systems. In the pressure system, material enters the air stream by a rotary air-lock feeder and the velocity of the air stream suspends the bulk material until it reaches its destination. In vacuum systems, the material is moved by an air stream under a pressure less than atmospheric. The material is drawn into the system without the need of a rotary valve. In the combination system, a fan is used to suck the solids from the source to a separator. Air then passes to the suction side of a blower and material is then fed by a rotary valve into the positive pressure air stream that comes from the blower discharge. In fluidizing systems, air passes through a membrane that forms the bottom of the conveyor. The material to be fluidized comes from a hopper so that the discharge from the hopper is over the membrane. The air then fluidizes the material. At the terminal end of all these systems is a receiving vessel where the material is separated from the air by means of a cyclone separator and/or a filter. Vacuum systems are favored for shorter distances and when conveying from several sources to one destination. Appropriate switching valves make it possible to service several sources and destinations with either a vacuum or pressure system. Normally the vacuum system is favored for single destinations and the pressure for several destinations or over long distances. Figure 5.3(b) shows a rotary valve feeder and Figure 5.3(c) a Venturi feeder which has a particularly gentle action suitable for friable materials. Figure 5.3(d) utilizes a fan to suck the solids from a source and to deliver them under positive pressure. Friable materials also may be handled effectively by the equipment of Figure 5.5 in which alternate pulses of granular material and air are transported.

The advantages of a pneumatic conveying system are that there are few mechanical parts, there is a clean controlled environ-
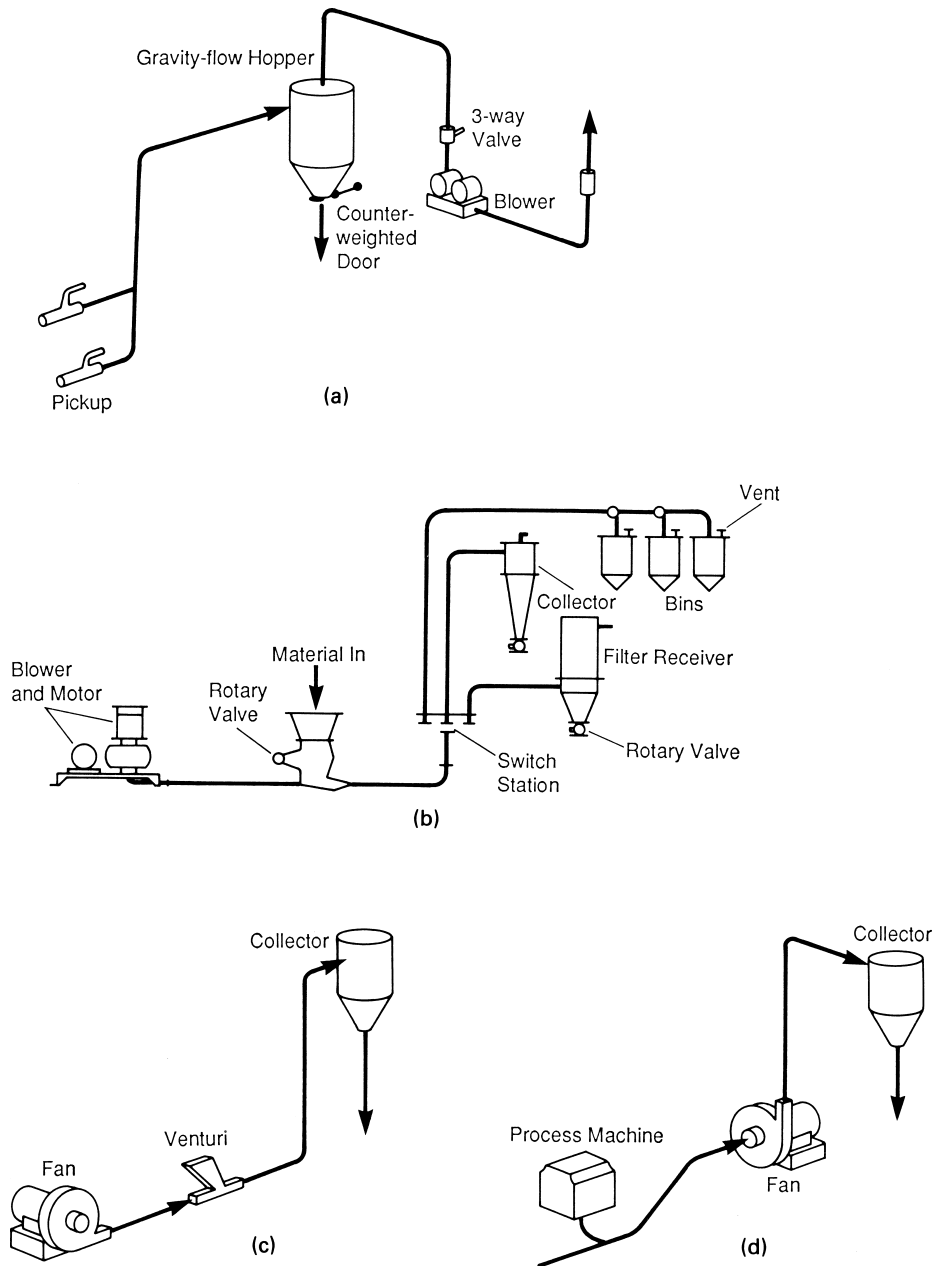
Figure 5.3. Basic equipment arrangements of pneumatic conveying systems. (a) Vacuum system with several sources and one destination, multiple pickup; (b) pressure system with rotary valve feeder, one source and several destinations, multiple discharge; (c) pressure system with Venturi feed for friable materials; (d) pull–push system in which the fan both picks up the solids and delivers them. [*After Gerchow, 1975, p. 88*, Raymus, 1999].

ment, and the ductwork or piping can be modified to fit the space available such that vertical and horizontal distances can be easy to achieve. The disadvantage is that the solids must be removed from the air or carrier gas stream, so pollution control equipment may be needed (Woods, 1995).

Typical auxiliary equipment is shown on Figure 5.6. The most used blower in pneumatic conveying is the rotary positive displacement type; they can achieve vacua 6–8 psi below atmospheric or positive pressures up to 15 psig at efficiencies of about 65%. Axial positive displacement blowers also are used, as well as centrifugals for large capacities. Rotary feeders of many proprietary designs are

available; Stoess (1983) and Kraus (1980) illustrate several types. Receivers may be equipped with fabric filters to prevent escape of fine particles; a dacron fabric suitable for up to 275°F is popular. The receivers may consist of a cyclone separator and a hopper with a filter downstream of this equipment to minimize dusting. A two-stage design is shown in Figure 5.6(d). Typical dimensions are cited by Stoess (1983), for example:

line diameter (in.)	3	5	8
primary diameter (ft)	3.5	4.5	6.75
secondary diameter (ft)	2.75	3.5	5.0
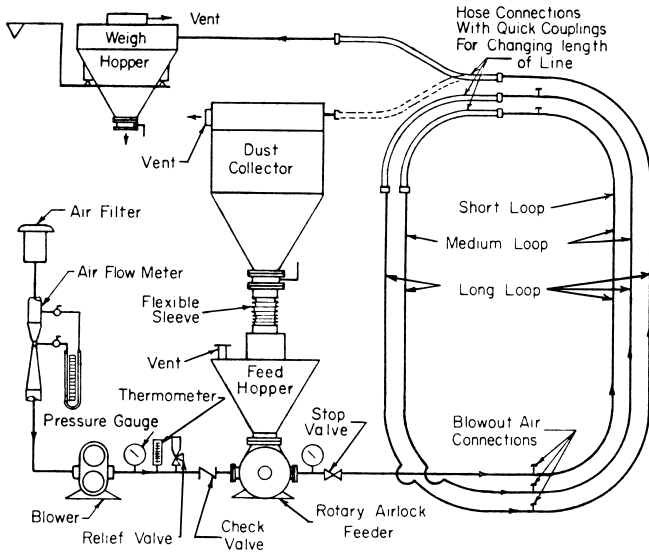
Figure 5.4. Sketch of pilot plant arrangement for testing pneumatic conveying under positive pressure. (*Kraus, 1980*).

Piping usually is standard steel, Schedule 40 for 3–8 in. IPS and Schedule 30 for 8–12 in. IPS. In order to minimize pressure loss and abrasion, bends are made long radius, usually with radii equal to 12 times the nominal pipe size, with a maximum of 8 ft. Special reinforcing may be needed for abrasive conditions.

OPERATING CONDITIONS

Vacuum systems usually operate with at most a 6 psi differential; at lower pressures the carrying power suffers. With rotary air lock
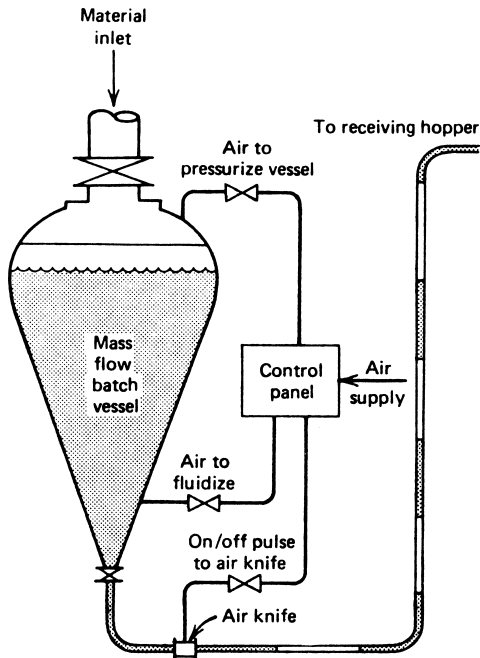
Figure 5.5. Concept of dense phase transfer of friable materials, by intermittent injection of material and air pulses, air pressures normally 10–30 psig and up to 90 psig. (*Sturtevant*).

feeders, positive pressure systems are limited to about 12 psig. Other feeding arrangements may be made for long distance transfer with 90–125 psig air. The dense phase pulse system of Figure 5.4 may operate at 10–30 psig.

Linear velocities, carrying capacity as cuft of free air per lb of solid (Sat.) and power input as HP/tons per hour (tph) are listed in Table 5.1 as a general guide for a number of substances. These data are for 4-, 5-, and 6-in. lines; for 8-in. lines, both Sat. and HP/tph are reduced by 15%, and for 10-in. by 25%. Roughly, air velocities in low positive pressure systems are 2000 ft/min for light materials, 3000–4000 ft/min for medium densities such as those of grains, and 5000 ft/min and above for dense materials such as fly ash and cement; all of these velocities are of free air, at atmospheric pressure.

Another set of rules for air velocity as a function of line length and bulk density is attributed to Gerchow (1980) and is

| Line length | ft/min | | |
(ft)	55 lb/cuft	55–85	85–115
200	4000	5000	6000
500	5000	6000	7000
1000	6000	7000	8000

Conveying capacity expressed as vol % of solids in the stream usually is well under 5 vol %. From Table 5.1, for example, it is about 1.5% for alumina and 6.0% for polyethylene pellets, figured at atmospheric pressure; at 12 psig these percentages will be roughly doubled, and at subatmospheric pressures they will be lower.

POWER CONSUMPTION AND PRESSURE DROP

The power consumption is made up of the work of compression of the air and the frictional losses due to the flows of air and solid through the line. The work of compression of air at a flow rate m'_a and $C_P/C_v = 1.4$ is given by

$$w_c = 3.5(53.3)(T + 460)m'_a[(P_2/P_1)^{0.2857} - 1] \text{ (ft lbf/sec)}$$

$$(5.15)$$

with the flow rate in lb/sec.

Frictional losses are evaluated separately for the air and the solid. To each of these, contributions are made by the line itself, the elbows and other fittings, as well as the receiving equipment. It is conservative to assume that the linear velocities of the air and solid are the same. Since the air flow normally is at a high Reynolds number, the friction factor may be taken constant at $f_a = 0.015$. Accordingly the frictional power loss of the air is given by

$$w_1 = \Delta P_1 m'_a/\rho_a = (u^2/2g)\left[1 + 2n_c + 4n_f + (0.015/D)\left(L + \sum L_i\right)\right]m'_a$$

$$\text{(ft lbf/sec). } (5.16)$$

The unity in the bracket accounts for the entrance loss, n_c is the number of cyclones, n_f is the number of filters, L is the line length, and L_i is the equivalent length of an elbow or fitting. For long radius bends one rule is that the equivalent length is 1.6 times the actual length of the bend. Another rule is that the long bend radius is 12 times the nominal size of the pipe. Accordingly,

$$L_i = 1.6(\pi R_i/2) = 2.5R_i = 2.5D''_i \text{ ft, with } D''_i \text{ in inches.} \quad (5.17)$$
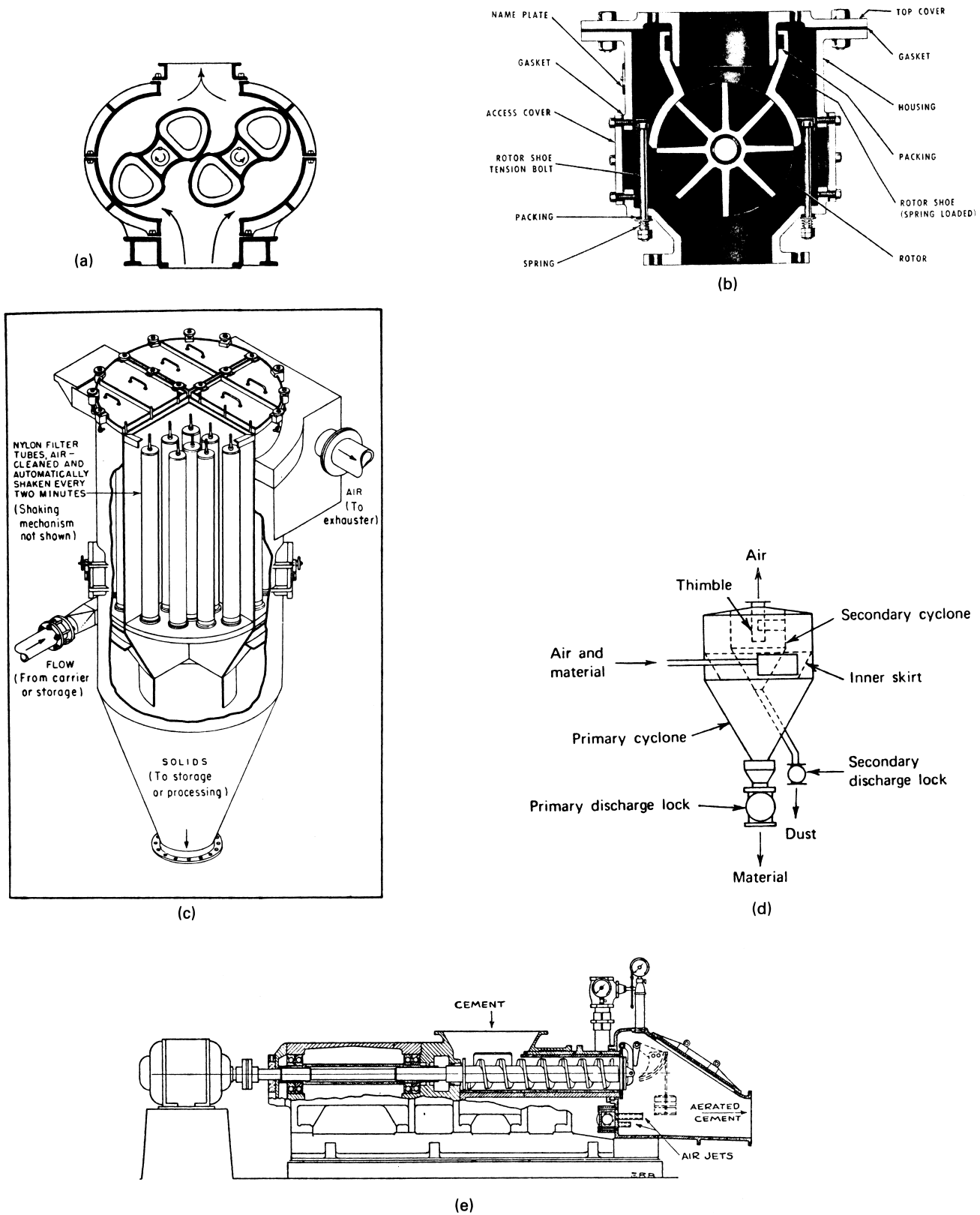
Figure 5.6. Components of pneumatic conveying systems. (a) Rotary positive displacement blower for pressure or vacuum. (b) A rotary airlock feeder for fine materials. (c) A four-compartment receiver-filter. (*Fuller*). (d) A two-stage cyclone receiver. (e) The Fuller–Kinyon pump for cement and other fine powders. Powder is fed into the aeration chamber with a screw and is fluidized with compressed air. (*Fuller*).

The value of g is 32.2 ft lb m/(lbf sec^2).

The work being done on the solid at the rate of m'_s lb/sec is made up of the kinetic gain at the entrance (w_2), the lift (w_3) through an elevation Δz, friction in the line (w_4), and friction in the elbow (w_5). Accordingly,

$$w_2 = \frac{u^2}{2g} m'_s \text{ (ft lbf/sec)}. \tag{5.18}$$

The lift work is

$$w_3 = \Delta z \frac{g}{g_c} m'_s = \Delta z m'_s \text{ (ft lbf/sec)}. \tag{5.19}$$

The coefficient of sliding friction f_s of the solid equals the tangent of the angle of repose. For most substances this angle is 30–45° and the value of f_s is 0.58–1.00. The sliding friction in the line is

$$w_4 = f_s L m'_s \text{ (ft lbf/sec)}, \tag{5.20}$$

where L is the line length.

Friction in the curved elbows is enhanced because of centrifugal force so that

$$w_5 = f_s \frac{u^2}{gR} \left(\frac{2\pi R}{4}\right) m'_s = 0.0488 f_s u^2 m'_s \text{ (ft lbf/sec)}. \tag{5.21}$$

The total frictional power is

$$w_f = w_1 + w_2 + w_3 + w_4 + w_5, \tag{5.22}$$

and the total power consumption is

$$w = \frac{(w_c + w_f)}{550\eta(1.8 m'_s)} \text{ [HP/(ton/hr)]}, \tag{5.23}$$

where η is the blower efficiency. Pressure drop in the line is obtained from the frictional power, the total flow rate, and the density of the mixture:

$$\Delta P = \frac{w_f}{144(m'_a + m'_s)} \rho_m \quad \text{(psi)}. \tag{5.24}$$

The specific air rate, or saturation, is

$$\text{saturation} = 0.7854(60)D^2$$
$$\text{(cuft/min of air)/(lb/min of solid)]}, \tag{5.25}$$

where the velocity of the air is evaluated at atmospheric pressure.

Example 5.2 illustrates the calculations described here for power and pressure drop, and compares the result with the guidelines of Table 5.1.

5.3. MECHANICAL CONVEYORS AND ELEVATORS

Granular solids are transported mechanically by being pushed along, dragged along, or carried. Movement may be horizontal or vertical or both. In the process plant distances may be under a hundred feet or several hundred feet. Distances of several miles may be covered by belts servicing construction sites or mines or power plants. Capacities range up to several hundred tons/hr. The principal kinds of mechanical conveyors are illustrated in Figures 5.7–5.13 and will be described. Many construction features of these machines are arbitrary. Thus manufacturers' catalogs or internet webpages are the ultimate sources of information about suitability for particular services, sizes, capacities, power requirements and auxiliaries. Much of the equipment has been made in essentially the present form for about 100 years by a number of manufacturers so that a body of standard practice has developed.

PROPERTIES OF MATERIALS HANDLED

The physical properties of granular materials that bear particularly on their conveying characteristics include size distribution, true and bulk densities, and angle of repose or coefficient of sliding friction, but other less precisely measured or described properties are also of concern. A list of pertinent characteristics of granular materials appears in Table 5.2. The elaborate classification given there is applied to about 500 materials in the FMC Corporation Catalog 100 (1983, pp. B.27–B.35) but is too extensive for reproduction here. For each material the table also identifies the most suitable design of screw conveyor of this company's manufacture and a factor for determining the power requirement. An abbreviated table of about 150 substances appears in the *Chemical Engineers Handbook* (6th ed. 1984, p. 7.5 and 7th ed. p21–6, 1999). Hudson (1954, pp. 6–9), describes the characteristics of about 100 substances in relation to their behavior in conveyors. Table 5.3 lists bulk densities, angles of respose at rest, and allowable angles of inclination which are angles of repose when a conveyor is in motion; references to more extensive listings of such data are given in this table.

The angle of repose is a measure of the incline at which conveyors such as screws or belts can carry the material. The tangent of the angle of repose is the coefficient of sliding friction. This property is a factor in the power needed to transfer the material by pushing or dragging as in pneumatic, screw, flight, and Redler equipment.

Special provisions need to be made for materials that tend to form bridges; Figure 5.13(a) is an example of a method of breaking up bridges in a storage bin so as to ensure smooth flow out. Materials that tend to pack need to be fluffed up as they are pushed along by a screw; adjustable paddles as in Figure 5.7(d) may be sufficient.

SCREW CONVEYORS

These were invented by Archimedes and assumed essentially their present commercial form a hundred years or so ago. Although the equipment is simple in concept and relatively inexpensive, a body of experience has accumulated whereby the loading, speed, diameter, and length can be tailored to the characteristics of the materials to be handled. Table 5.4(b), for example, recognizes four classes of materials, ranging from light, freeflowing, and nonabrasive materials such as grains, to those that are abrasive and have poor flowability such as bauxite, cinders, and sand. Only a portion of the available data are reproduced in this table.

Lengths of screw conveyors usually are limited to less than about 150 ft; when the conveying distance is greater than this, a belt or some other kind of machine should be chosen. The limitation of length is due to structural strength of the shaft and coupling. It is expressed in terms of the maximum torque that is allowable. Data for torque and power of screw conveyors are given in Table 5.4 and are applied to selection of a conveyor in Example 5.3.

Several designs of screws are shown in Figure 5.7. The basic design is one in which the pitch equals the diameter. Closer spacing is needed for carrying up steep inclines, and in fact very fine pitch screws operating at the relatively high speeds of 350 rpm are used to convey vertically. The capacity of a standard pitch screws drops off sharply with the inclination, for example:

EXAMPLE 5.2
Size and Power Requirement of a Pneumatic Transfer Line
A pneumatic transfer line has 300 ft of straight pipe, two long radius elbows, and a lift of 50 ft. A two-stage cyclone is at the receiving end. Solid with a density of 125 lb/cuft is transferred at the rate of 10 tons/hr and the free air is at 5000 ft/min. Inlet condition is 27 psia and 100°F. Investigate the relation between line diameter and power requirement.

On a first pass, the effect of pressure loss on the density of the air will be neglected.

Mass flow rate of solid:

$$m'_s = 20,000/3600 = 5.56\,\text{lb/sec.}$$

Mass flow rate of air:

$$m'_a = \frac{5000}{60}\frac{\pi}{4}(0.075)D^2 = 4.91D^2\,\text{lb/sec.}$$

Density of air:

$$\rho_a = 0.075\left(\frac{27}{14.7}\right) = 0.138\,\text{lb/cuft.}$$

Density of mixture:

$$\rho_m = \frac{(m'_a + m'_s)}{m'_a/\rho_a + m'_s/\rho_s}$$
$$= \frac{(m'_a + 5.56)}{m'_a/0.138 + 5.56/125}$$

Linear velocity of air at inlet:

$$u = \frac{5000}{60}\left(\frac{14.7}{27}\right) = 45.37\,\text{fps.}$$

Assume air and solid velocities equal. Elbow radius $= 12D$. Elbow equivalent length,

$$L_e = 1.6(\pi/2)(12D) = 30.2D$$

Power for compression from 14.7 psia and 560 R to 27 psia,

$$k/(k-1) = 3.5,$$
$$w_c = 3.5RT_1[(P_2/P_1)^{0.2857} - 1]m'_a$$
$$= 3.5(53.3)(560)[(27/14.7)^{0.2857} - 1]4.91D^2$$
$$= 97305D^2\,\text{ft lbf/sec.}$$

Frictional contribution of air

$$w_1 = \frac{u^2}{2g}[5 + (0.015/D)(300 + 2(30.2)D]m'_a$$

$$= [(45.4)^2/64.4][5.9 + (4.5/D)](4.91D^2)$$
$$= 157.1D^2(5.9 + 4.5/D)$$

For the solid, take the coefficient of sliding friction to be $f_s = 1$. Power loss is made up of four contributions. Assume no slip velocity;

$$w_s = w_2 + w_3 + w_4 + w_5$$
$$= [u^2/2g + \Delta Z + f_sL + 2(0.0488)f_su^2]m'_s$$
$$= 5.56[45.4^2/64.4 + 50 + 300 + 2(0.0488)45.4^2]$$
$$= 3242.5\,\text{ft lbf/sec.}$$

Total friction power:

$$w_f = 3242.5 + 157.1D^2(5.9 + 4.5/D).$$

Pressure drop:

$$\Delta P = \frac{w_f}{144(m'_a + m'_s)}\rho_m\,\text{psi.}$$

Fan power at $\eta = 0.5$:

$$\dot{P} = \frac{w_c + w_f}{550(0.5)(10)} = \frac{w_c + w_f}{2750}\text{HP/tph,}$$

$$\text{saturation} = \frac{5000(\pi/4)D^2}{20,000/60} = 11.78D^2\text{SCFM/(lb/min).}$$

IPS (in.)	D (ft)	m'_a	ρ_m	W_c	W_f
3	0.2557	0.3210	2.4808	6362	3484
4	0.3356	0.5530	1.5087	10,959	3584
5	0.4206	0.8686	1.0142	17,214	3704
6	0.5054	1.2542	0.7461	24,855	3837

IPS (in.)	ΔP (psi)	HP/TPH	SCFM/lb/min
3	10.2	3.58	0.77
4	6.1	5.29	1.33
5	4.1	7.60	2.08
6	2.9	10.44	3.00

From Table 5.1, data for pebble lime are

sat $= 1.7$ SCFM/(lb/min)
power $= 3.0$ HP/TPH

and for soda ash:

sat $= 1.9$ SCFM/(lb / min)
power $= 3.4$ HP/TPH.

The calculated values for a 4 in. line are closest to the recommendations of the table.

TABLE 5.2. Codes for Characteristics of Granular Materials[a]

Major Class	Material Characteristics Included	Code Designation
Density	Bulk Density, Loose	Actual lbs/ft^3
Size	Very Fine {No. 200 Sieve (.0029″) And Under / No. 100 Sieve (.0059″) And Under / No. 40 Sieve (.016″) And Under}	A_{200} / A_{100} / A_{40}
	Fine No. 6 Sieve (.132″) And Under	B_0
	Granular 1/2″ And Under	$C_{1/2}$
	Granular 3″ And Under	D_3
	(′) Lumpy Over 3″ To Be Special X=Actual Maximum Size	D_x
	Irregular Stringy, Fibrous, Cylindrical, Slabs, etc.	F
Flowability	Very Free Flowing–Flow Function > 10	1
	Free Flowing–Flow Function > 4 But < 10	2
	Average Flowability–Flow Function > 2 But < 4	3
	Sluggish–Flow Function < 2	4
Abrasiveness	Mildly Abrasive – Index 1–17	5
	Moderately Abrasive – Index 18–67	6
	Extremely Abrasive – Index 68–416	7
Miscellaneous Properties Or Hazards	Builds Up and Hardens	F
	Generates Static Electricity	G
	Decomposes–Deteriorates in Storage	H
	Flammability	J
	Becomes Plastic or Tends to Soften	K
	Very Dusty	L
	Aerates and Becomes Fluid	M
	Explosiveness	N
	Stickiness-Adhesion	O
	Contaminable, Affecting Use	P
	Degradable, Affecting Use	Q
	Gives Off Harmful or Toxic Gas or Fumes	R
	Highly Corrosive	S
	Mildly Corrosive	T
	Hygroscopic	U
	Interlocks, Mats or Agglomerates	V
	Oils Present	W
	Packs Under Pressure	X
	Very Light and Fluffy–May Be Windswept	Y
	Elevated Temperature	Z

[a]Example: A fine 100 mesh material with an average density of 50 lb/cuft that has average flowability and is moderately abrasive would have a code designation $50A_{100}36$; if it were dusty and mildly corrosive, it would be $50A_{100}$ 36LT.
(FMC Corp., 1983).

Angle (degrees)	<8	20	30	45
Percent of capacity	100	55	30	0

Allowable loadings as a percentage of the vertical cross section depend on the kind of material being processed as shown in Table 5.4.

BELT CONVEYORS

These are high capacity, relatively low power units for primarily horizontal travel and small inclines. The maximum allowable inclination usually is 5–15° less than the angle of repose; it is shown as "recommended maximum inclination" in Table 5.3 for some substances, and is the effective angle of repose under moving conditions.

The majority of conveyor belts are constructed of fabric, rubber, and wire beads similarly to automobile tires, but they are made also of wire screen or even sheet metal for high temperature

TABLE 5.3. Bulk Densities, Angles of Repose, and Allowable Angles of Inclination

Material	Average Weight (lb/cuft)	Angle of Repose (degrees)	Recommended Maximum Inclination
Alum, fine	45–50	30–45	
Alumina	50–65	22	10–12
Aluminum sulfate	54	32	17
Ammonium chloride	45–52		
Ammonium nitrate	45		
Ammonium sulfate	45–58		
Asbestos shred	20–25		
Ashes, coal, dry, $\frac{1}{2}$ in. max	35–40	40	20–25
Ashes, coal, wet, $\frac{1}{2}$ in. max	45–50	50	23–27
Ashes, fly	40–45	42	20–25
Asphalt, $\frac{1}{2}$ in. max	45		
Baking powder	40–55		18
Barium carbonate	72		
Bauxite, ground	68	35	20
Bentonite, 100 mesh max	50–60		
Bicarbonate of soda	40–50		
Borax, $\frac{1}{2}$ in.	55–60		
Borax, fine	45–55		20–22
Boric acid, fine	55		
Calcium acetate	125		
Carbon, activated, dry, fine	8–20		
Carbon black, pelleted	20–25		
Casein	36		
Cement, Portland	94	39	20–23
Cement, Portland, aerated	60–75		
Cement clinker	75–95	30–40	18–20
Charcoal	18–25	35	20–25
Chips, paper mill	20–25		
Clay, calcined	80–100		
Clay, dry, fine	100–120	35	20–22
Clay, dry, lumpy	60–75	35	18–20
Coal, anthracite, $\frac{1}{2}$ in. max	60	35	18
Coal, bituminous, 50 mesh max	50–54	45	24
Coal, bituminous, $\frac{1}{2}$ in. max	43–50	40	22
Coal, lignite	40–45	38	22
Coke breeze, $\frac{1}{4}$ in. max	25–35	30–45	20–22
Copper sulfate	75–85	31	17
Cottonseed, dry, delinted	35	29	16
Cottonseed, dry, not delinted	18–25	35	19
Cottonseed meal	35–40	35	22
Cryolite dust	75–90		
Diatomaceous earth	11–14		
Dicalcium phosphate	40–50		
Disodium phosphate	25–31		
Earth, as excavated, dry	70–80	35	20
Earth, wet, containing clay	100–110	45	23
Epsom salts	40–50		
Feldspar, $\frac{1}{2}$ in. screenings	70–85	38	18
Ferrous sulfate	60–75		
Fleur, wheat	35–40		
Fullers earth, dry	30–35	23	
Fullers earth, oily	60–65		
Grain, distillery, spen, dry	30		
Graphite, flake	40		
Grass seed	10–12		
Gravel, bank run	90–100	38	20
Gravel, dry, sharp	90–100		15–17
Gravel, pebbles	90–100	30	12
Gypsum dust, aerated	60–70	42	23
Gypsum, $\frac{1}{2}$ in. screenings	70–80	40	21
Iron oxide pigment	25	40	25
Kaolin talc, 100 mesh	42–56	45	23
Lactose	32		
Lead arsenate	72		
Lead oxides	60–150		
Lime, $\frac{1}{4}$ in. max	60–65	43	23
Lime, hydrated, $\frac{1}{4}$ in. max	40	40	21
Lime, hydrated, pulverized	32–40	42	22
Limestone, crushed	85–90	38	18
Limestone dust	80–85		20
Lithopone	45–50		
Magnesium chloride	33		
Magnesium sulfate	70		

TABLE 5.3.—(*continued*)

Milk, dry powder	36		
Phosphate, triple super, fertilizer	50–55	45	30
Phosphate rock, pulverized	60	40	25
Polystyrene beads	40		
Potassium nitrate	76		
Rubber, pelletized	50–55	35	22
Salt, common, coarse	40–55		
Salt, dry, fine	70–80	25	11
Salt cake, dry, coarse	85	36	21
Salt cake, dry, pulverized	60–85		
Saltpeter	80		
Sand, bank, damp	100–130	45	20–22
Sand, bank, dry	90–110	35	16–18
Sawdust	10–13	36	22
Shale, crushed	85–90	39	22
Soap chips	15–25	30	18
Soap powder	20–25		
Soda ash briquetts	50	22	7
Soda ash, heavy	55–65	32	19
Soda ash, light	20–35	37	22
Sodium bicarbonate	41	42	23
Sodium nitrate	70–80	24	11
Starch	25–50	24	12
Sugar, granulated	50–55		
Sugar, powdered	50–60		
Trisodium phosphate, pulverized	50	40	25
Wood chips	10–30		27
Zinc oxide, heavy	30–35		
Zinc oxide, light	10–15		

Other tables of these properties appear in these publications:
1. Conveyor Equipment Manufacturers Association, 1966, pp. 25–33.
2. Stephens–Adamson Mfg. Co., 1954, pp. 634–636.
3. FMC Corporation 1983, pp. B.27–B.35.
4. *Perry's* 6th ed, 1984, p. 7.5, and 7th ed., 1989.

TABLE 5.4. Sizing Data for Screw Conveyors[a]

(a) Diameter (rpm and cuft/hr)

Diam. of Con- veyor, Inches	△ Max. Lump Size, Inches	Maximum Recommended Speed R.P.M.	Capacities, Cubic Feet Per Hour		Maximum Recommended Speed R.P.M.	Capacities, Cubic Feet Per Hour	
			At Maximum Recommend- ed Speed	At One R.P.M.		At Maximum Recommend- ed Speed	At One R.P.M.
		Loading of Materials in Trough Class I—45% Full			Loading of Materials in Trough Class II—30% Full		
6	¾	165	375	2.27	120	180	1.5
9	1½	150	1200	8.0	100	560	5.6
12	2	140	2700	19.3	90	1200	13.3
14	2½	130	4000	30.8	85	1790	21.1
16	3	120	5600	46.6	80	2510	31.4
18	3	115	7600	66.1	75	3400	45.4
20	3½	105	9975	95.0	70	4340	62.1

Diam. of Con- veyor, Inches	△ Max. Lump Size, Inches	Maximum Recommended Speed R.P.M.	Capacities, Cubic Feet Per Hour		Maximum Recommended Speed R.P.M.	Capacities, Cubic Feet Per Hour	
			At Maximum Recommend- ed Speed	At One R.P.M.		At Maximum Recommend- ed Speed	At One R.P.M.
		Loading of Materials in Trough Class II X—30% Full			Loading of Materials in Trough Class III—15% Full		
6	¾	60	90	1.5	60	45	.75
9	1½	50	280	5.6	50	140	2.8
12	2	50	665	13.3	50	335	6.7
14	2½	45	950	21.1	45	470	10.5
16	3	45	1410	31.4	45	705	15.7
18	3	40	1850	45.4	40	910	22.7
20	3½	40	2485	62.1	40	1240	31.1

[a]Example 5.3 utilizes these data.
(Stephens–Adamson Mfg. Co., 1954, p. 69).

(b) Characteristics of Some Materials (A Selection From the Original Table)

Materials	Approx. Weight per Cubic Foot	Capacity Classifi- cation	‡Type of Conveyor to Use	Horse- power Factor "F"
Alfalfa meal	17	II	A,B,C	.4
Alum, lumpy	50–60	II	G,H,J	1.5
Alum, pulverized	45–50	II	A,B,C	.8
•Alumina	60	III	K	2.0
Aluminum, hydrate	15–20	II	A,B,C	.8
Ammonium sulphate	52	...	...	....
Asbestos, shredded	20–25	II	G,H,J	1.0
•Ashes, dry	35–40	IIX	D	2.0
Asphalt, crushed	45	II	A,B,C	.5
Bakelite, powdered	30–40	II	A,B,C	1.4
Baking powder	41	II	A,B,C	.6
Barley	38	I	A,B,C	.4
†Bauxite, crushed	75–85	III	E	1.8
Beans, castor	36	I	A,B,C	.5
Beans, navy, dry	48	I	A,B,C	.4
Bentonite	51	IIX	D	1.0
*Bones, crushed	35–40	IIX	D	2.0
*Bones, granulated or ground	50	IIX	D	1.7
*Bone black	20–25	IIX	D	1.7
Bonechar	40	IIX	D	1.7
*Bone meal	55–60	IIX	D	1.7
Borax, powdered	53	II	A,B,C	.7
Boric acid powder	30–40	II	A,B,C	.8
Bran	16	II	A,B,C	.4

(c) Factor *S* in the Formula for Power *P*

Diameter of Conveyor, Inches	Type of Hanger Bearing			
	SEALMASTER Ball Bearing	Babbitt, Bronze or Oil-Impreg- nated Wood	Self- Lubricating Bronze	Hard Iron
4	12	21	33	50
6	18	33	54	80
9	32	54	96	130
10	38	66	114	160
12	55	96	171	250
14	78	135	255	350
16	106	186	336	480
18	140	240	414	600
20	165	285	510	700
24	230	390	690	950

(d) Limits of Horsepower and Torque

Diameter of Conveyor, Inches	Diameter of Coupling, Inches	Maximum Horsepower at 100 R.P.M.	Maximum Torque Capacity in Inch Pounds
4	1	1.5	950
6,9,10	1½	5.0	3200
9,10,12	2	10.0	6300
12,14	2⁷⁄₁₆	15.0	9500
12,14,16,18	3	25.0	16000
20	3⁷⁄₁₆	40.0	25000

services. A related design is the apron conveyor with overlapping pans of various shapes and sizes (Fig. 5.8), used primarily for short travel at elevated temperatures. With pivoted deep pans they are also effective elevators.

Flat belts are used chiefly for moving large objects and cartons. For bulk materials, belts are troughed at angles of 20–45°. Loading of a belt may be accomplished by shovelling or directly from

Sizing a Screw Conveyor

Dense soda ash with bulk density 60 lb/cuft is to be conveyed a distance of 100 ft and elevated 12 ft. The material is class II-X with a factor $F = 0.7$. The bearings are self-lubricated bronze and the drive is V-belt with $\eta = 0.93$. The size, speed, and power will be selected for a rate of 15 tons/hr.

$$Q = 15(2000)/60 = 500 \text{cuft/hr}.$$

According to Table 5.4(a) the capacity for conveying of Class II-X material can be accommodated by a 12 in. conveyor operating at

$$\omega = (500/665)(50) = 37.6 \text{ rpm}, \quad \text{say } 40 \text{ rpm}$$

From Table 5.4(c) the bearing factor for a 12 in. diameter conveyor is

$$s = 171.$$
$$G = 1.25$$

Accordingly,

$$\dot{P} = [171(40) + 0.7(500)(60)]100 + 0.51(12)(30,000)/10^6$$
$$= 2.78 \text{HP}$$

$$\text{motor HP} = G\dot{P}/\eta = 1.25(2.97)/0.93 = 3.74$$

$$\text{torque} = 63,000(2.97)/40 = 4379 \text{ in.lb}.$$

From Table 5.4(d) the limits for a 12 in. conveyor are 10.0 HP and 6300 in. lb so that the selection is adequate for the required service.

A conveyor 137 ft long would have a shaft power of 4.00 HP and a torque of 6300 in. lbs, which is the limit with a 2 in. coupling; a sturdier construction would be needed at greater lengths.

For comparison, data of Table 5.5 show that a 14 in. troughed belt has an allowable speed of 267 fpm at allowable inclination of 19° (from Table 5.3), and the capacity is

$$2.67(0.6)(38.4) = 61.5 \text{tons/hr},$$

[38.4 is from Table 5.5 for a 20° inclination] far more than that of the screw conveyor.
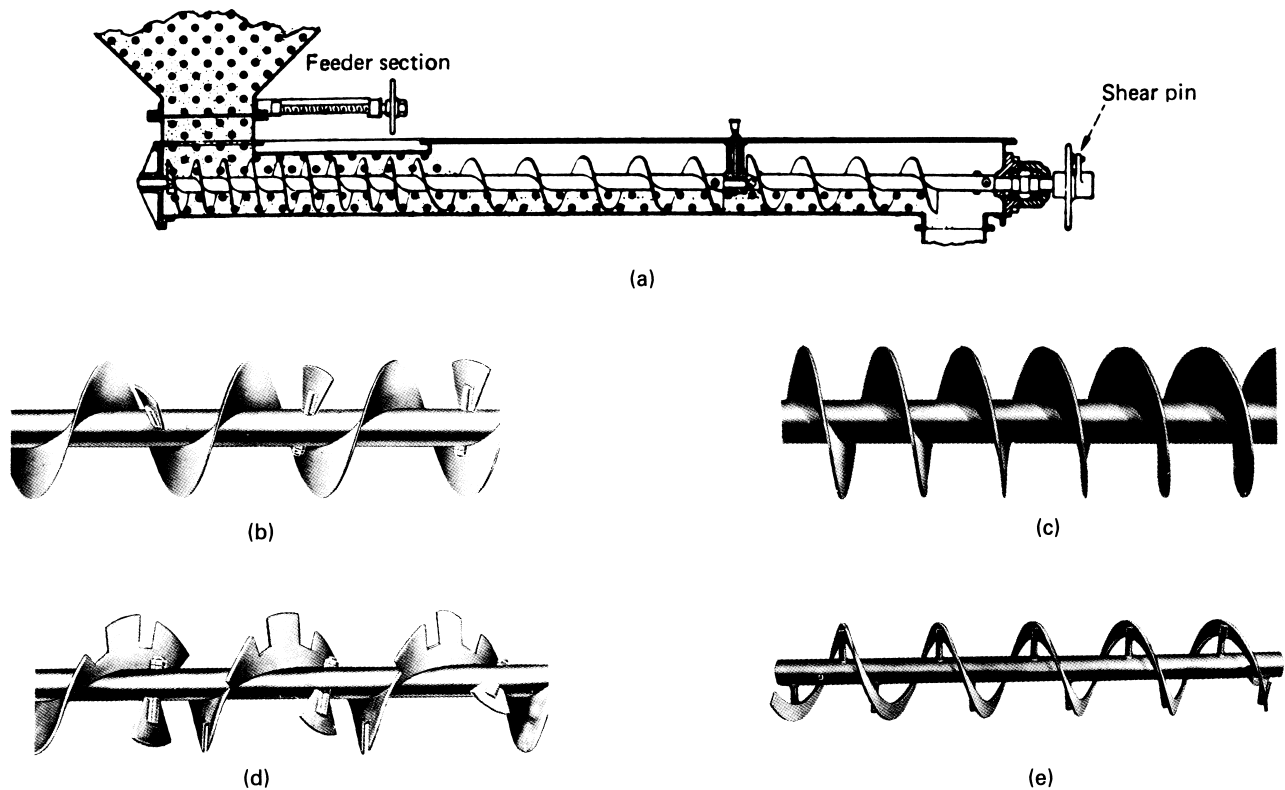
Figure 5.7. A screw conveyor assembly and some of the many kinds of screws in use. (a) Screw conveyor assembly with feed hopper and discharge chute. (b) Standard shape with pitch equal to the diameter, the paddles retard the forward movement and promote mixing. (c) Short pitch suited to transfer of material up inclines of as much as 20°. (d) Cut flight screws combine a moderate mixing action with forward movement, used for light, fine, granular or flaky materials. (e) Ribbon flights are suited to sticky, gummy or viscous substances.

(a)

(b)   (c)

(d)

(e)

Figure 5.8. Flight conveyors in which the material is scraped along, and apron conveyors in which the material is carried along in a closed path of interconnected pans. (a) Flight conveyor, in which the material is scraped along a trough with flights attached to a continuous chain. (b) Scraper-type of flight. (c) Roller flights. (d) Apron conveyor, in which the material is carried along in moving, overlapping pans. (e) Shallow and deep types of overlapping pans.

TABLE 5.5. Belt Conveyor Data[a]

(a) Capacity (tons/hr) at 100 ft/min, 100 lb/cuft, and Indicated Slope Angle

45° Troughed Belt

Belt Width (inch)	$0°$	$10°$	$20°$	$30°$
14	27.99	33.00	38.40	43.80
16	38.70	45.60	52.50	60.00
18	51.00	60.00	69.00	78.60
20	65.10	76.20	87.90	100.0
24	98.10	114.9	132.0	149.7
30	160.8	187.5	214.8	243.6
36	238.5	277.8	318.0	360.3
42	331.8	385.8	441.3	499.5
48	440.1	511.5	584.4	661.2
54	563.1	654.6	747.9	845.7
60	702.0	815.4	931.2	1053.0
66	856.5	994.2	1134.9	1282.8
72	1026.0	1190.1	1358.4	1535.4

Flat Belt

Belt width (inches)	$5°$	$10°$	$20°$	$30°$
14	2.85	6.69	14.01	21.42
16	3.87	9.18	19.05	29.16
18	5.07	11.88	24.90	38.10
20	6.39	15.06	31.50	48.24
24	9.57	22.47	47.10	72.06
30	13.51	36.45	76.32	116.8
36	22.86	53.73	112.6	172.3
42	31.65	74.37	155.9	238.5
48	39.84	90.15	196.2	300.0
54	53.49	125.7	263.4	403.2
60	66.60	156.5	327.9	501.9
66	81.12	190.5	399.6	611.1
72	96.99	238.0	477.9	731.1

[a]Example 5.4 utilizes these data. Power $= P_{horizontal} + P_{vertical} + P_{empty}$ (HP), where $P_{horizontal} = (0.4 + L/300)(W/100)$, $P_{vertical} = 0.001\,HW$, and P_{empty} obtained from part (c), with $H =$ lift (ft), $L =$ horizontal travel (ft), and $W =$ tons/hr.
(a) From Conveyor Equipment Manufacturers Association, 1979; (b) from Stephens–Adamson Mfg. Co., 1954; (c) (Hudson, 1954).

(b) Maximum Recommended Belt Speeds for Nondusting Service

Belt Width, Inches	Belt Speed in Feet per Minute						
	Lump Stone or Ore	Gravel	Lump Coal	Crushed Ore and Stone †	Slack Coal †	Sand	Wood Chips Grain
12	250	300	250	350	350	350	400
18	300	350	300	400	400	400	500
24	350	400	350	450	450	450	600
30	400	450	400	500	500	500	700
36	450	500	450	550	550	550	800
42	500	550	500	550	600	600	800
48	550	600	550	550	650	600	800
54	550	600	600	550	700	600	800
60	550	600	650	550	700	600	800
66	550	600	700	550	700	600	800
72	550	600	700	550	700	600	800

TABLE 5.5.—(*continued***)**

(c) Power to Drive Empty Conveyor
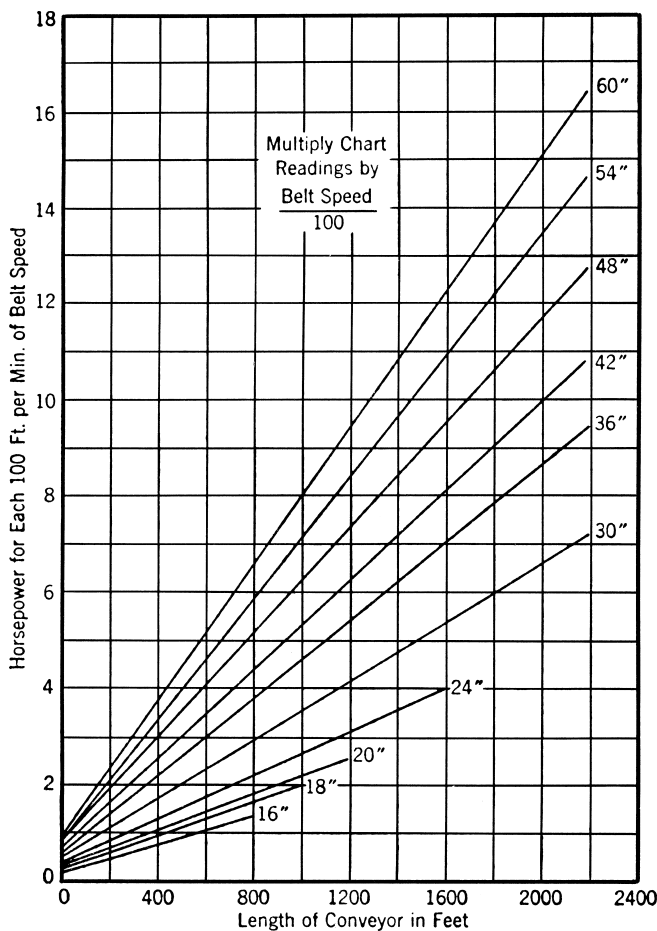
overhead storage or by one of the methods shown on Figure 5.9. Discharge is by throwing over the end of the run or at intermediate points with plows.

Power is required to run the empty conveyor and to carry the load horizontally and vertically. Table 5.5 gives data and equations, and they are applied in Example 5.4. Squirrel-cage ac induction motors are commonly used as drives. Two-and four-speed motors are available. Mechanical efficiencies of speed reducing couplings between motor and conveyor range from 95 to 50%. Details of idlers, belt trippers, cleaners, tension maintaining devices, structures, etc. must be consulted in manufacturers' catalogs or on manufacturers websites. The selection of belt for strength and resistance to abrasion, temperature, and the weather also is a topic for specialists.

BUCKET ELEVATORS AND CARRIERS

Bucket elevators and carriers are endless chains to which are attached buckets for transporting granular materials along vertical, inclined or horizontal paths. Figure 5.10 shows two basic types: spaced buckets that are far apart and continuous which overlap. Spaced buckets self-load by digging the material out of the boot and are operated at speeds of 200–300 fpm; they are discharged centrifugally. Continuous buckets operate at lower speeds, and are used for friable materials and those that would be difficult to pick up in the boot; they are fed directly from a loading chute and are discharged by gravity. Bucket carriers are essentially forms of pan conveyors; they may be used instead of belt conveyors for shorter distances and when they can be made of materials that are particularly suited to a process. Capacity and power data for bucket machines are given in Table 5.6. Flight and apron conveyors are illustrated in Figure 5.11.

CONTINUOUS FLOW CONVEYOR ELEVATORS

One design of a drag-type of machine is the Redler shown on Figure 5.8. There are various designs for the flights as illustrated in Figure 5.8. One type of drag conveyor, the Hapman conveyor, consists of circular disks mounted on a chain inside a pipe. As the conveyor is operated, the disks entrap material from the inlet to the outlet of the conveyor. The clearance between the disk and the
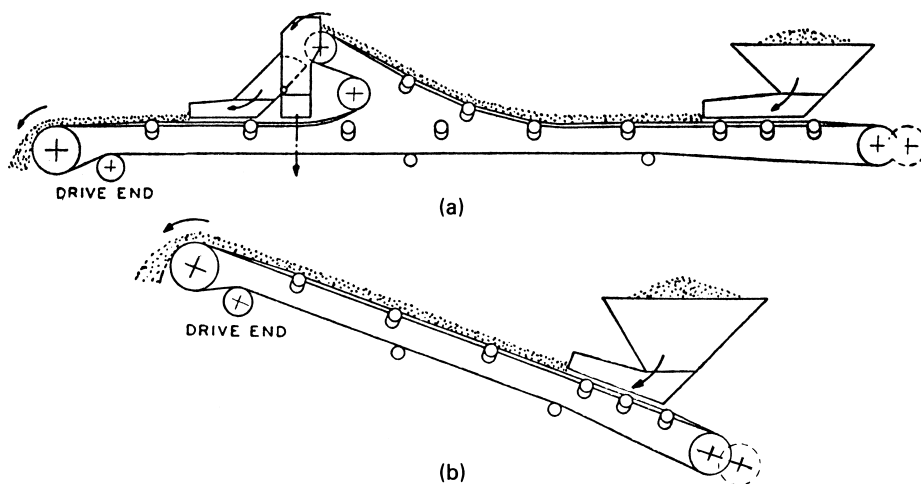
Figure 5.9. Some arrangements of belt conveyors (*Stephens-Adamson Mfg. Co.*, 1954) and types of idlers (*FMC Corp*, 1983). (a) Horizontal conveyor with discharge at an intermediate point as well as at the end. (b) Inclined conveyor, satisfactory up to 20° with some materials. (c) Inclined or retarding conveyor for lowering materials gently down slopes. (d) A flat belt idler, rubber cushion type. (e) Troughed belt idler for high loadings; usually available in 20°, 35°, and 45° side inclinations.

(c)

(d)

(e)
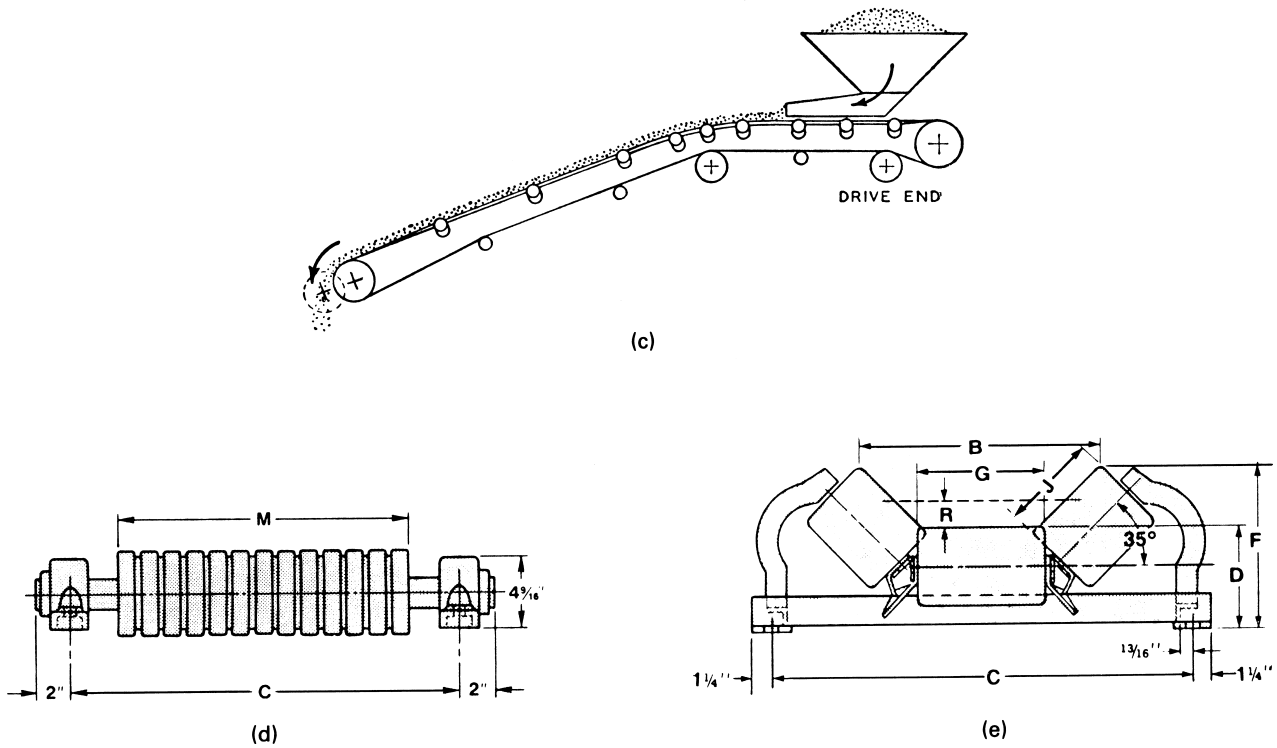
Figure 5.9.—(*continued*)

inside of the pipe is small. It is an enclosed system and is often used to transport fine chemicals and pharmaceuticals, minimizing contamination. They function because the friction against the flight is greater than that against the wall. Clearly they are versatile in being able to transfer material in any direction and have the often important merit of being entirely covered. Circular cross sections like the Hapman conveyor are available but usually they are square, from 3 to 30 in. on a side, and operate at speeds of 30–250 ft/min, depending on the material handled and the construction. Some data are shown in Table 5.7. Most dry granular materials such as wood chips, sugar, salt, and soda ash are handled very well in this kind of conveyor. More difficult to handle are very fine materials such as cement or those that tend to pack such as hot grains or abrasive materials such as sand or crushed stone. Power requirement is dependent on the coefficient of sliding friction. Factors for power calculations of a few substances are shown in Table 5.7.

The closed-belt (zipper) conveyor of Figure 5.12 is a carrier that is not limited by fineness or packing properties or abrasiveness. Of course, it goes in any direction. It is made in a nominal 4-in. size, with a capacity rating by the manufacturer of 0.07 cuft/ft of travel. The power requirement compares favorably with that of open belt conveyors, so that it is appreciably less than that of other types. The formula is

$$HP = 0.001[(L_1/30 + 5)u + (L_2/16 + 2L_3)T], \tag{5.26}$$

where

u = ft/min,
T = tons/hr,
L_1 = total belt length (ft),
L_2 = length of loaded horizontal section (ft),
L_3 = length of loaded vertical section (ft).

EXAMPLE 5.4
Sizing a Belt Conveyor
Soda ash of bulk density 60 lb/cuft is to be transported at 400 tons/hr a horizontal distance of 1200 ft up an incline of 5°. The running angle of repose of this material is 19°. The conveyor will be sized with the data of Table 5.5.

Consider a 24 in. belt. From Table 5.5(a) the required speed is

$$u = (400/132)100 = 303 \text{ ft/min}.$$

Since the recommended maximum speed in Table 5.5(b) is 350 fpm, this size is acceptable:

conveyor length = $1200/\cos 5° = 1205$ ft,
rise = $1200 \tan 5° = 105$ ft.

With the formulas and graph (c) of Table 5.5, the power requirement becomes

$$Power = P_{horizontal} + P_{vertical} + P_{empty}$$
$$= (0.4 + 1200/300)(400/100)$$
$$+ 0.001(105)(400) + 303(3.1)/100$$
$$= 69.0 \text{ HP}.$$

Perhaps 10 to 20% more should be added to compensate for losses in the drive gear and motor.
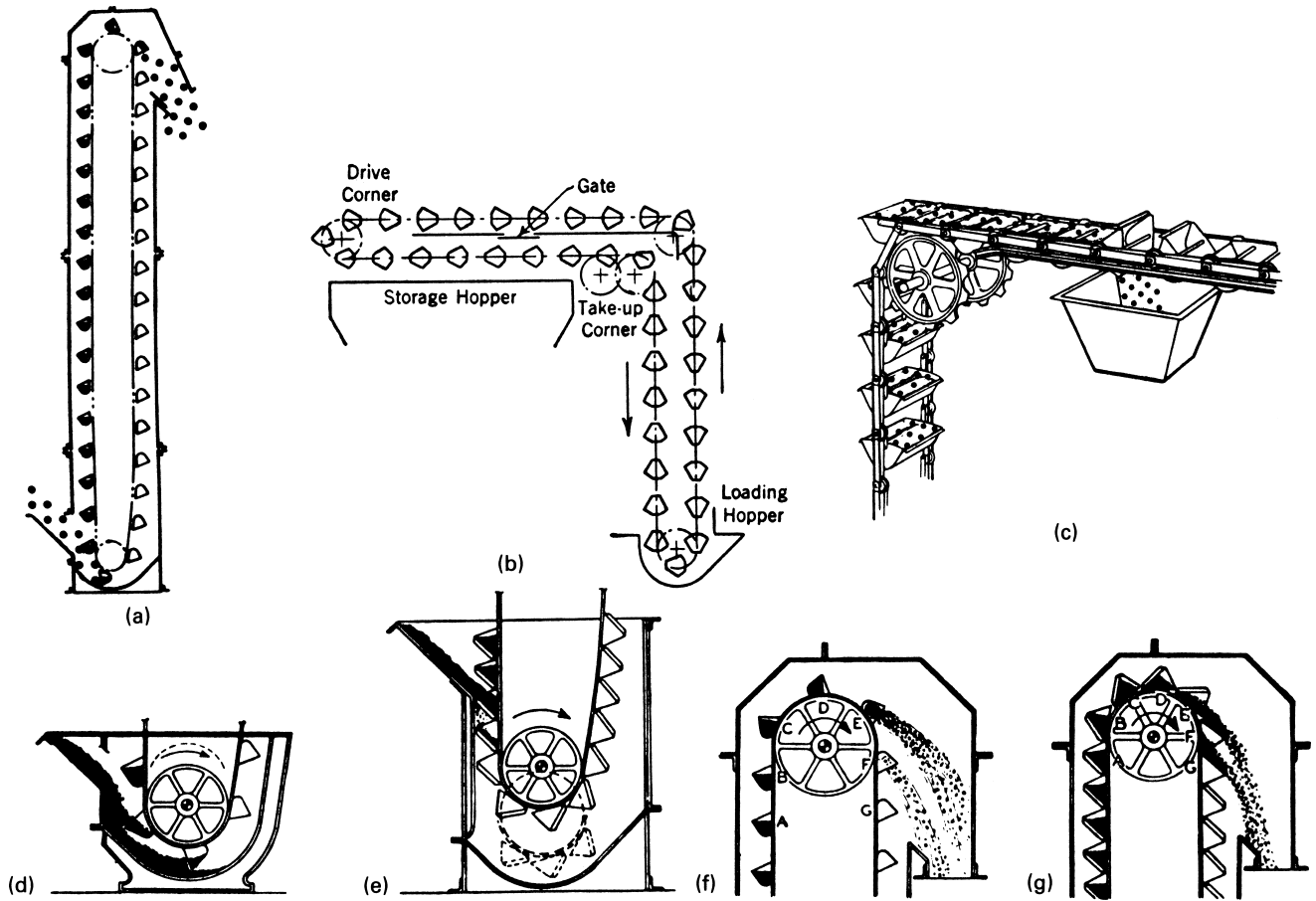
Figure 5.10. Bucket elevators and conveyors. (a) Spaced bucket elevator. (b) Bucket conveyor for vertical and horizontal travel. (c) Discharge of pivoted buckets on horizontal path. (d) Spaced buckets receive part of their load directly and part by scooping the bottom. (e) Continuous buckets are filled as they pass through the loading leg with a feed spout above the tail wheel. (f) Centrifugal discharge of spaced buckets. (g) Discharge mode of continuous buckets.

TABLE 5.6. Capacities and Power Requirements of Bucket Elevator Conveyors

(a) Gravity Discharge Elevators Used Primarily For Coal[a,c]

Size of bucket, in. $L \times W$	Capacity, tons/hr. at 100 ft./min. Bucket spacing, in.			Hp.† with material at 50 lb./cu. ft. Per 10-ft. vertical lift			Per 100-ft. horizontal run		
				Spacing of buckets, in.					
	18	24	36	18	24	36	18	24	36
16 × 15	46	35	23	0.59	0.44	0.30	5.32	4.24	3.04
20 × 15	58	44	29	.74	.56	.37	6.32	4.97	3.54
24 × 15	70	52	35	.90	.67	.45	7.34	5.74	4.04
20 × 20	104	..	52	1.30	....	.66	9.20	....	4.85
24 × 20	125	..	63	1.60	....	.80	10.92	....	5.74
30 × 20	159	..	79	2.00	....	1.00	13.70	....	7.08
36 × 20	191	..	95	2.42	....	1.21	16.30	....	8.40

(b) Capacities and Maximum Size of Lumps of Centrifugal Discharge Elevators[b,c]

Bucket spacing, in.	Size, length by width, in.	Speed, ft./min.	Max. lumps All lumps	10% lumps	Capacity, tons/hr. 35-lb. material	50-lb. material	100-lb. material
13	6 × 4	225	½	2½	5	7	14
16	8 × 5	230	¾	3	9	13	27
16	10 × 6	230	1	3½	16	23	47
18	12 × 7	268	1¼	4	27	38	77
18	14 × 7	268	1¼	4	32	46	92
19	16 × 8	262	1½	4½	44	63	127

TABLE 5.6.—(continued)

(c) Centrifugal Discharge of Continuous Belt and Bucket Elevators[c]

Bucket spacing, in.	Size, length by width	Speed, ft./min.	Max. lumps All lumps	10% lumps	Capacity, tons/hr. 35 lb. material	50 lb. material	100 lb. material
13	6 × 4	225	½	2½	5	7	14
16	8 × 5	258	⅔	3	11	15	30
16	10 × 6	258	1	3½	18	26	52
18	12 × 7	298	1¼	4	30	42	85
18	14 × 7	298	1¼	4	36	52	103
18	16 × 8	298	1½	4½	53	114	152

[a]Buckets 80% full.
[b]Buckets 75% full.
[c]Horsepower = 0.002 (tons/hr)(lift in feet).
(Link Belt Co.)

Speeds of 200 ft/min or more are attainable. Example 5.5 shows that the power requirement is much less than that of the Redler conveyor.

Closing Comments. Most kinds of conveyors and elevators are obtainable from several manufacturers, each of whom builds equipment to individual standards of sturdiness, materials of construction, mechanical details, performance, and price. These differences may be decisive in individual cases. Accordingly, a selection usually must be made from a manufacturer's catalog, and ultimately with the advice of the manufacturer.

TABLE 5.7. Speed and Horsepower of Drag-Type Conveyors of Redler Design[a]

(a) Typical Speeds (ft/min)[b]

Material Handled	1000 Conv.	1000 Elev.	2000 Conv.	3000 Conv.
Coal	125	125	80	150
Coke	40	40	40	40
Flyash	30	30	30	30
Grain (Whole)	125	125	80	250
(Processed)	125	100	80	150
Salt	125	100	80	150
Wood (Chips)	100	80	80	150
(Sawdust)	100	100	80	150

[a]HP = 0.001(FL + GH + K) (tons/hr), where H = rise (ft), L = horizontal run (ft), F, G, and K are factors from Table (b); factor E is not used in this formula.

[b]Series 1000, 2000, and 3000 differ in the shapes and sturdiness of the flights. (Stephens–Adamson Mfg. Co., 1954).

(b) Factors F, G, and K for Use in the Power Equation for Three Sizes of Units

Material	Weight per Cubic Foot, pounds	K	3″ Units			11″ Units			19″ Units		
			E	F	G	E	F	G	E	F	G
Beans, dry navy	54	100	1.5	2.9	4.4	1.2	2.3	3.1	1.1	2.0	2.6
Bicarbonate of soda, dry, pulverized	55	0	3.0	6.9	8.1	2.4	5.2	5.4	2.2	4.6	4.3
Bran	26	0	4.1	8.3	3.8	3.0	5.9	2.8	2.6	5.0	2.4
Cellulose acetate dry, coarse granular	10	80	8.0	15.9	4.4	5.3	10.0	3.1	4.4	8.5	2.6
Cement, dry Portland	60–90	0	2.9	7.4	6.0	2.3	5.4	4.1	2.1	4.8	3.4
Clay, dry lumpy	40–100	80	3.1	5.9	4.6	2.4	4.5	3.3	2.1	4.0	2.8
Clay, pulverized	25–80	0	6.0	17.7	6.8	4.3	11.9	4.6	3.8	9.9	3.7
Coal, minus ¼″ slack dry with l'ge proportion fines	40–50	40	2.4	4.6	4.4	1.9	3.5	3.1	1.7	3.1	2.6
Coal, minus ¼″ slack moderately wet	45–55	40	3.3	6.1	5.4	2.6	4.7	3.8	2.3	4.2	3.1
Coal, minus ¼″ slack very wet	50–60	20	2.5	5.4	5.7	2.0	4.1	4.0	1.8	3.6	3.2
Coal, minus 1½″ slack dry or damp	40–50	40				2.0	3.7	3.1	1.8	3.3	2.6
Coal, sized wet or dry	40–50	80	2.2	4.1	3.8	1.7	3.1	2.8	1.5	2.8	2.4
Coconut, shredded	25	20	3.0	6.1	3.2	2.2	4.3	2.4	1.9	3.7	2.1
Coffee, ground	28	20	2.4	4.8	3.2	1.8	3.5	2.4	1.5	3.0	2.1
Corn flakes	12	0	3.8	7.9	2.3	2.6	5.2	1.9	2.1	4.3	1.7
Flour, wheat	30–40	0	3.2	7.1	3.5	2.4	5.0	2.6	2.1	4.3	2.3
Fuller's earth, dry granular	42	80	3.1	6.9	7.3	2.3	5.0	4.9	2.1	4.4	4.0
Lime, burned or " quick " lump or " pebble "	50	200	2.7	5.0	7.0	2.2	3.9	4.8	2.0	3.5	3.8
Lime, dry burned small lumps and dust	50	120	3.5	6.9	6.5	2.8	5.5	4.4	2.5	4.9	3.6
Lime, fine with tendency to pack	40–60	300	4.4	8.8	7.5	3.4	6.6	5.1	3.0	5.8	4.1
Lime, hydrated	10–25	0	11.1	35.5	7.0	7.3	22.5	4.8	6.0	18.1	3.8
Salt, dry granulated	80	80	1.9	3.8	5.7	1.6	3.1	4.0	1.5	2.8	3.2
Salt rock	75	100	1.9	3.5	6.5	1.6	2.9	4.4	1.5	2.6	3.6
Sand, silica coarse dry	90–100	160	2.1	4.2	7.0	1.8	3.4	4.8	1.7	3.2	3.8
Sand very fine, dry	90–100	120	2.4	5.2	7.3	2.0	4.1	4.9	1.9	3.8	4.0
Sawdust, dry	10–30	0	6.2	14.5	4.1	4.1	9.4	3.0	3.4	7.6	2.5
Soda ash, light	25–35	20	4.5	11.4	6.5	3.3	7.8	4.4	2.8	6.6	3.6
Soybean meal	40	20	2.2	4.8	4.6	1.7	3.5	3.3	1.5	3.1	2.8
Starch, lump	30	80	2.1	3.9	3.8	1.6	2.9	2.8	1.4	2.5	2.4
Starch, pulverized	25–45	0	5.4	15.9	6.0	3.9	10.7	4.1	3.4	8.9	3.4
Sugar, dry granulated	50	160	2.7	5.8	9.1	2.2	4.4	6.1	2.0	3.9	4.8
Sugar, brown	40–50	40	4.4	8.5	7.5	3.4	6.4	5.1	3.0	5.6	4.1
Wheat, dry fairly clean	48	40	1.7	3.3	5.2	1.3	2.5	3.6	1.2	2.2	3.0
Wood chips, dry	15–30	40	3.5	6.6	2.8	2.4	4.5	2.2	2.0	3.7	1.9
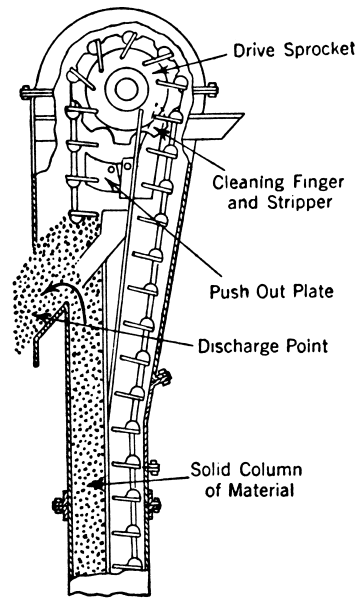
(a)
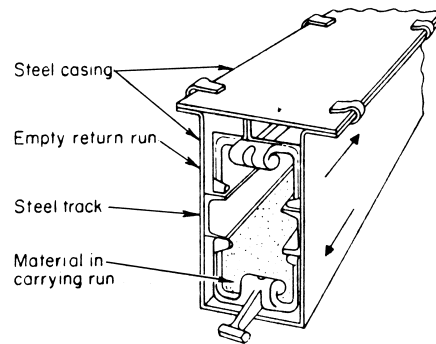
(b)
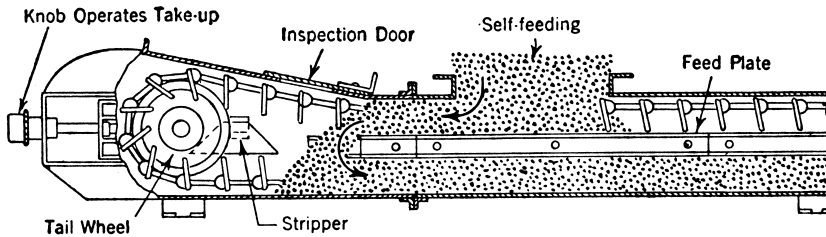
(c)
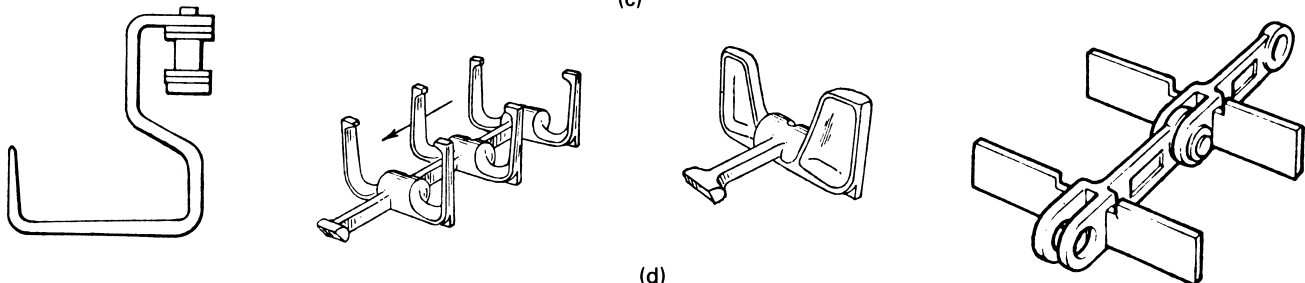
(d)

Figure 5.11. Drag-type enclosed conveyor-elevator (Redler Design) for transfer in any direction (Stephens-Adamson Mfg. Co., 1954). (a) Head and discharge end of elevator. (b) Carrying and return runs. (c) Loading end. (d) Some shapes of flights; some are made close-fitting and edged with rubber or plastics to serve as cleanouts.
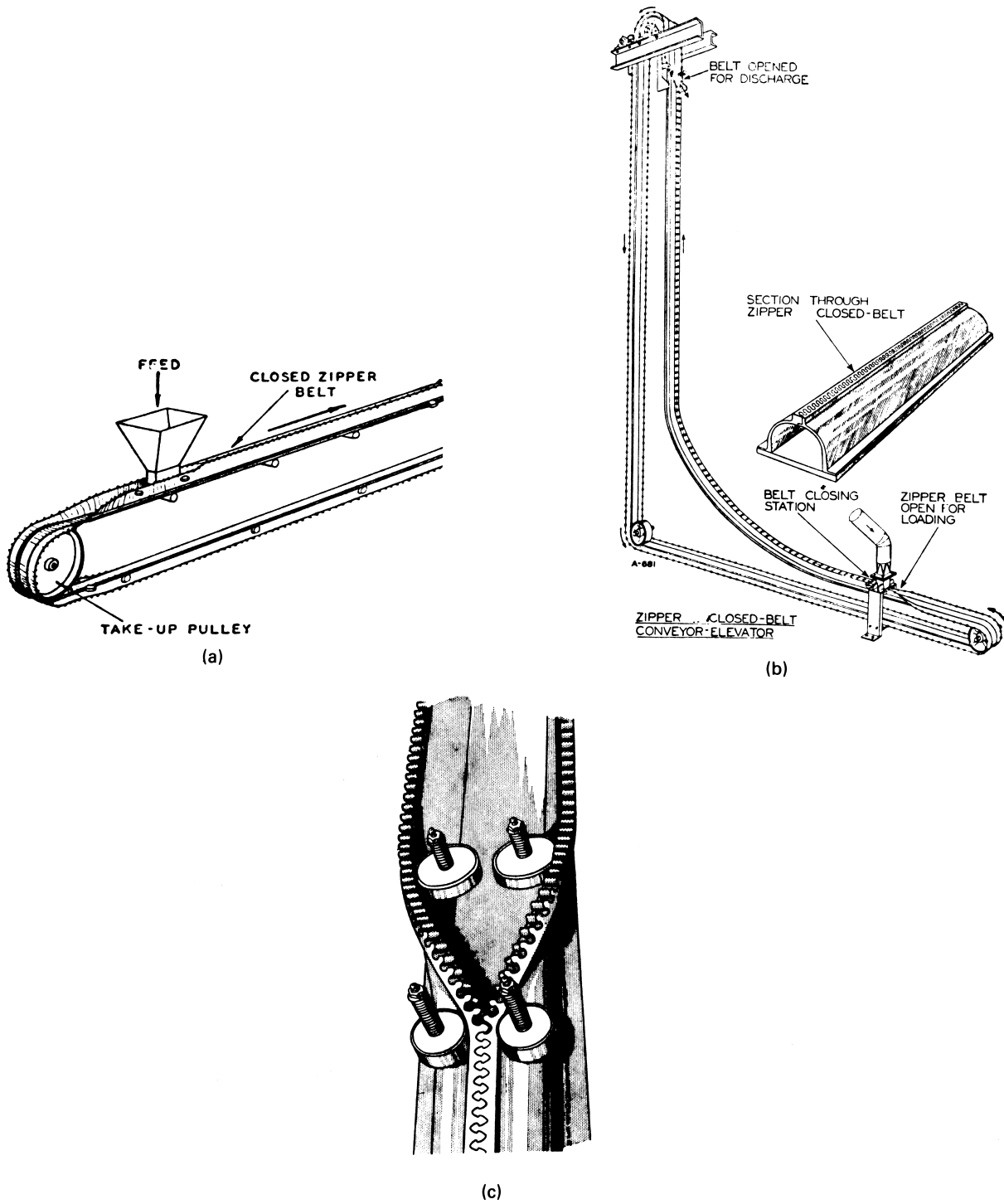
Figure 5.12. Closed belt (zipper) for conveying in any direction (*Stephens-Adamson* Mfg. Co., 1954). (a) Arrangement of pulley, feed hopper and open and closed belt regions. (b) The tubular belt conveyor for horizontal and vertical transport; a section of the zippered closed belt is shown. (c) Showing how the zipper closes (on downward movement of the belt in this sketch) or opens (on upward movement of the belt).
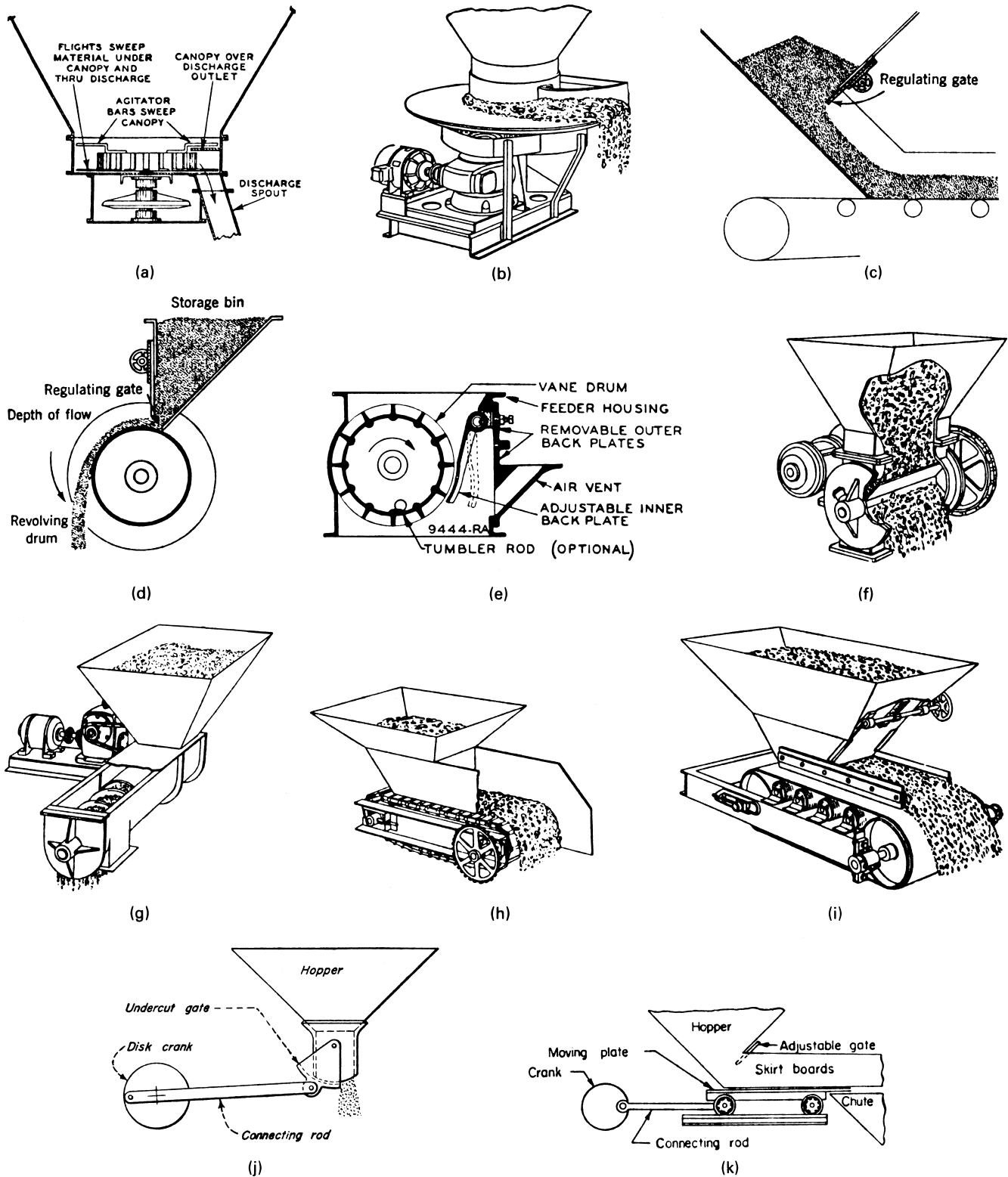
Figure 5.13. Types of feeders for granular solids; also suitable are conveyors such as closed belt, Redler, and bucket types. (a) Bin discharge feeder. (b) Rotary plate feeder with adjustable collar and speed. (c) Flow controlled by an adjustable gate. (d) Rotary drum feeder, regulated by gate and speed. (e) Rotary vane feeder, can be equipped with air lock for fine powders. (f) Vane or pocket feeder. (g) Screw feeder. (h) Apron conveyor feeder. (i) Belt conveyor feeder. (j) Undercut gate feeder. (k) Reciprocating plate feeder. (l) Vibrating feeder, can transfer uphill, downhill, or on the level. (m) "Air-slide" feeder for powders that can be aerated. (n) Weighing belt feeder; unbalance of the weigh beam causes the material flow rate onto the belt to change in the direction of restoring balance.

(l)

(m)

(n)
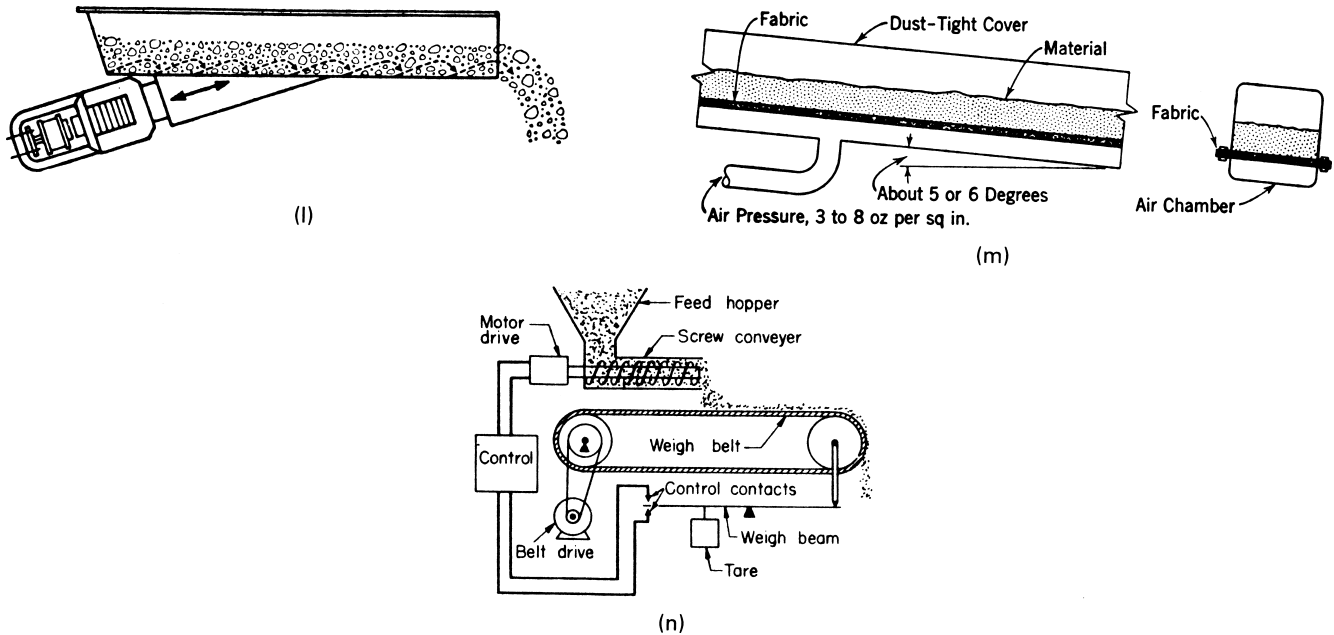
Figure 5.13.—(*continued*)

EXAMPLE 5.5
Comparison of Redler and Zippered Belt Conveyors

Soda ash of bulk density 30 lb/cuft is to be moved 120 ft horizontally and 30 ft vertically at the rate of 350 cuft/hr. Compare power requirements of Redler and zippered belt conveyors for this service.

A 3-in Redler is adequate:

$$u = \frac{350}{60(\pi/4)(3/12)^2} = 118.8 \text{ fpm},$$

which is within the range of Table 5.7(a),

$$\text{tons/hr} = 350(30)/2000 = 5.25$$

Take constants from Table 5.7(b) for a Redler.

$$\text{HP} = \frac{5.25}{1000}[11.4(120) + 6.5(30) + 20] = 8.31.$$

For a closed belt,

$$u = \frac{350}{0.07(60)} = 83.3 \text{ fpm},$$

0.07 capacity rating by manufacturer
which is well under the 200 fpm that could be used,

$$L_1 = 300, \ L_2 = 120, \ L_3 = 30.$$

Use Eq. (5.26):

$$\text{HP} = 0.001\{(300/30 + 5)83.3 + [120/16 + 2(30)]5.25\} = 1.29$$

5.4. SOLIDS FEEDERS

Several types are illustrated in Figure 5.13. Rates are controlled by adjusting gates or rotation speeds or translation speeds. All of these methods require free flow from a storage bin which may be inhibited by bridging or arching. The device of Figure 5.13a provides motion to break up such tendencies.

For the most part the devices shown provide only rough feed rate control. More precise control is achieved by continuous weighing. This equipment employs measurements of belt speed and the weight impressed on one or several of the belt idlers to compute and control the weight rate of feed; precision better than 0.5% is achievable. For some batch processes, the feeder discharges into an overhead weighing hopper for accurate measurement of the charge. Similar systems are used to batch feed liquids when integrating flow meters are not sufficiently accurate.

REFERENCES

T.H. Allegri, *Materials Handling Principles and Practice,* Van Nostrand Reinhold, New York, 1984.
A.G. Bain and S.T. Bonnington, *The Hydraulic Transport of Solids by Pipeline,* Pergamon, New York, 1970.
M.V. Bhatic, and P.N. Cheremisinoff, *Solid and Liquid Conveying Systems,* Technomic, Lancaster, PA, 1982.
A.J. Bobkowicz and W.G. Gauvin, The effects of turbulence in the flow characteristics of model fiber suspensions, *Chem. Eng. Sci.*, **22**, 229–247 (1967).
R. Clift, Conveyors, hydraulic, *Encycl. Chem. Process Des.*, **11**, 262–278 (1980).
H. Colijn, *Mechanical Conveyors for Bulk Solids,* Elsevier, New York, 1985.
Conveyor Equipment Manufacturers Association, *Belt Conveyors for Bulk Materials,* Van Nostrand Reinhold, New York, 1996, 1979, pp. 25–33.
R. Darby, Determining settling rates of particles, *Chem. Eng.*, 109–112 (December 1996).

M.M. Denn, *Process Fluid Mechanics,* PTR Prentice Hall, Englewood Cliffs, NJ, 1980.

S. Dhodapkar and K. Jacob, Smart ways to troubleshoot pneumatic conveyors, *Chem. Eng.* 95–98 (March 2002).

D.W. Dodge and A.B. Metzner, Turbulent flow of non-newtonian systems, *AIChE J.*, **5,** 189 (1959).

G.H. Ewing, Pipeline transmission in *Marks' Mechanical Engineers' Handbook,* McGraw-Hill, New York, 1978, pp. 11.134–11.135.

FMC Corp. Material Handling Equipment Division, Catalog 100, pp. B.27–B.35, Homer City, PA, 1983.

Fuller Co., Bethlehem, PA.

F.J. Gerchow, Conveyors, pneumatic, in *Encycl. Chem. Process. Des.* **11,** 278–319, (1980); *Chem. Eng.*, (17 February 1975; 31 March 1975).

H.V. Hawkins, Pneumatic conveyors, in *Marks' Mechanical Engineers Handbook,* McGraw-Hill, New York, 1978, pp. 10.50–10.63.

J.W. Hayden and T.E. Stelson, Hydraulic conveyance of solids in pipes in Zandi, 1971, pp. 149–163.

W.G. Hudson, *Conveyors and Related Equipment,* Wiley, New York, 1954.

E. Jacques and J.G. Montfort, Coal transportation by slurry pipeline, in Considine (Ed.), *Energy Technology Handbook,* McGraw-Hill, New York, 1977, pp. 1.178–1.187.

K.W. Kimbel, Trouble free pneumatic conveying, *Chem. Eng.*, 78–82 (April 1998).

M. Kraus, *Pneumatic Conveying of Bulk Materials,* McGraw-Hill, New York, 1980.

R.A. Kulwiec (Ed.), *Material Handling Handbook,* Wiley, New York, 1985.

C.E. Lapple et al., in *Perry's Chemical Engineers Handbook,* 6th ed., McGraw-Hill, New York, 1984, p. 5.67.

D. Mills, Safety aspects of pneumatic conveying, *Chem. Eng.*, 84–91 (April 1999).

D. Mills, Optimizing pneumatic conveying systems; air movers, *Chem. Eng.*, 83–88 (February 2001).

D. Mills, Material flow rates in pneumatic conveying, *Chem. Eng.*, 74–78 (April 2002).

D.E. Perkins and J.E. Wood, Design and select pneumatic conveying systems, *Hydrocarbon Processing,* 75–78 (March 1974).

Perry's Chemical Engineers' Handbook, 6th ed., McGraw-Hill, New York, 1984.

G.J. Raymus, Pneumatic conveyors in *Perry's Chemical Engineers Handbook, McGraw-Hill, New York,* 6th ed., McGraw-Hill, New York, 1984, pp. 7.17–7.25; 7th ed., 1999, pp 21.19–21.27.

J. Rentz and C. Churchman, Streamline predictions for pneumatic conveyors, *Chem. Eng. Progr.*, 47–54 (1998).

P.E. Solt, Conveying, pneumatic troubleshooting, *Encycl. Chem. Process. Des.*, **11**, 214–226 (1980).

P.E. Solt, Solve the five most common pneumatic conveying problems, *Chem. Eng. Progr.*, 52–55 (January 2002).

Stephens-Adamson Mfg. Co., General Catalog 66, pp. 634–636, Aurora, IL, 1954 and updated sections.

H.A. Stoess, *Pneumatic Conveying,* Wiley, New York, 1983.

Sturtevant, Inc., Hanover, MA.

E.J. Wasp, T.C. Aude, R.H. Seiter, and T.L. Thompson, in Zandi, 1971, pp. 199–210.

E.J. Wasp, J.P. Kenny, and R.L. Gandhi, *Solid-Liquid Flow in Slurry Pipeline Transportation,* Trtans. Tech. Publ., 1977, Gulf, Houston, 1979.

E.L. Wasp, T.L. Thompson, and P.E. Snoek, The era of slurry pipelines, *Chem. Technol.*, 552–562 (September 1971).

O.A. Williams, *Pneumatic and Hydraulic Conveying of Solids,* Dekker, New York, 1983.

D.R. Woods, *Process Design and Engineering Practice,* PTR Prentice Hall, Englewood Cliffs, NJ, 1995.

I. Zandi (Ed.), *Advances in Solid-Liquid Flow in Pipes and its Applications,* Pergamon, New York, 1971.

6

FLOW OF FLUIDS

*T*he transfer of fluids through piping and equipment is accompanied by friction and may result in changes in pressure, velocity, and elevation. These effects require input of energy to maintain flow at desired rates. In this chapter, the concepts and theory of fluid mechanics bearing on these topics will be reviewed briefly and practical and empirical methods of sizing lines and auxiliary equipment will be emphasized.

6.1. PROPERTIES AND UNITS

The basis of flow relations is Newton's relation between force, mass, and acceleration, which is

$$F = (m/g_c)a. \tag{6.1}$$

When F and m are in lb units, the numerical value of the coefficient is $g_c = 32.174 \, \text{lb ft/lbf sec}^2$. In some other units,

$$g_c = 1\frac{\text{kg m/sec}^2}{\text{N}} = 1 \, \frac{\text{g cm/sec}^2}{\text{dyn}} = 9.806 \frac{\text{kg m/sec}^2}{\text{kg}_\text{f}}.$$

Since the common engineering units for both mass and force are 1 lb, it is essential to retain g_c in all force–mass relations. The interconversions may be illustrated with the example of viscosity whose basic definition is force/(velocity)(distance). Accordingly the viscosity in various units relative to that in SI units is

$$1\text{Ns/m}^2 = \frac{1}{9.806}\text{kg}_\text{f} \, \text{s/m}^2 = 10 \, \text{g/(cm)(s)}$$
$$= 10 \, \text{P} = 0.0672 \, \text{lb/(ft)(sec)}$$
$$= \frac{0.0672}{32.174}\text{lbf sec/ft}^2 = 0.002089 \, \text{lbf sec/ft}^2.$$

In data books, viscosity is given either in force or mass units. The particular merit of SI units (kg, m, s, N) is that $g_c = 1$ and much confusion can be avoided by consistent use of that system. Some numbers of frequent use in fluid flow problems are

Viscosity: $1\text{cPoise} = 0.001 \, \text{N s/m}^2 = 0.4134 \, \text{lb/(ft)(hr)}$.
Density: $1 \, \text{g m/cm}^3 = 1000 \, \text{kg/m}^3 = 62.43 \, \text{lb/ft}^3$.
Specific weight: $62.43 \, \text{lbf/cuft} = 1000 \, \text{kg}_\text{f}/\text{m}^3$.
Pressure: $1 \, \text{atm} = 0.10125 \, \text{MPa} = 0.10125(10^6) \, \text{N/m}^2 = 1.0125 \, \text{bar}$.

Data of densities of liquids are empirical in nature, but the effects of temperature, pressure, and composition can be estimated; suitable methods are described by Reid et al. (*Properties of Gases and Liquids*, McGraw Hill, New York, 1977), the *API Refining Data Book* (American Petroleum Institute, Washington, DC, 1983), the *AIChE Data Prediction Manual* (1984–date) and *Perry's Chemical Engineers' Handbook*, 7th ed. (1999, pp. 2-365 to 2-367). The densities of gases are represented by equations of state of which the simplest is that of ideal gases; from this the density is given by:

$$\rho = 1/V = MP/RT, \text{ mass/volume} \tag{6.2}$$

where M is the molecular weight. For air, for example, with P in atm and T in $^\circ R$,

$$\rho = \frac{29P}{0.73T'} \, \text{lb/cuft.} \tag{6.3}$$

For nonideal gases a general relation is

$$\rho = MP/zRT, \tag{6.4}$$

where the compressibility factor z is correlated empirically in terms of reduced properties T/T_c and P/P_c and the acentric factor. This subject is treated for example by Reid et al. (1977, p. 26), Walas (1985, pp. 17, 70), and *Perry's Chemical Engineers' Handbook*, 7th ed. (1999), pp. 2-355 to 2-361). Many PVT equations of state are available. That of Redlich and Kwong may be written in the form

$$V = b + RT/(P + a/\sqrt{T}V^2), \tag{6.5}$$

which is suitable for solution by direct iteration as used in Example 6.1.

Flow rates are expressible as linear velocities or in volumetric, mass, or weight units. Symbols for and relations between the several modes are summarized in Table 6.1.

The several variables on which fluid flow depends may be gathered into a smaller number of dimensionless groups, of which the Reynolds number and friction factor are of particular importance. They are defined and written in the common kinds of units also in Table 6.1. Other dimensionless groups occur less frequently and will be mentioned as they occur in this chapter; a long list is given in *Perry's Chemical Engineers' Handbook*, p. 6–49).

EXAMPLE 6.1
Density of a Nonideal Gas from Its Equation of State
The Redlich–Kwong equation of carbon dioxide is

$$(P + 63.72(10^6)/\sqrt{T}V^2)(V - 29.664) = 82.05T$$

with P in atm, V in mL/g mol and T in K. The density will be found at $P = 20$ and $T = 400$. Rearrange the equation to

$$V = 29.664 + (82.05)(400)/(20 + 63.72(10^6)/\sqrt{400}V^2).$$

Substitute the ideal gas volume on the right, $V = 1641$; then find V on the left; substitute that value on the right, and continue. The successive values of V are

$$V = 1641, 1579, 1572.1, 1571.3, 1571.2, \ldots \text{ mL/g mol}$$

and converge at 1571.2. Therefore, the density is

$$\rho = 1/V = 1/1571.2, \text{ or } 0.6365 \, \text{g mol/L or } 28.00 \, \text{g/L}.$$

TABLE 6.1. Flow Quantities, Reynolds Number, and Friction Factor

Flow Quantity	Symbol and Equivalent	Typical Units	
		Common	SI
Linear	u	ft/sec	m/sec
Volumetric	$Q = uA = \pi D^2 u/4$	cuft/sec	m³/sec
Mass	$\dot{m} = \rho Q = \rho A u$	lb/sec	kg/sec
Weight	$\dot{w} = \gamma Q = \gamma A u$	lbf/sec	N/sec
Mass/area	$G = \rho u$	lb/(sqft)(sec)	kg/m² sec
Weight/area	$G_\gamma = \gamma u$	lbf/(sqft)(sec)	N/m² sec

Reynolds Number (with $A = \pi D^2/4$)

$$\text{Re} = \frac{Du\rho}{\mu} = \frac{Du}{v} = \frac{DG}{\mu} = \frac{4Q\rho}{\pi D\mu} = \frac{4\dot{m}}{\pi D\mu} \tag{1}$$

Friction Factor

$$f = \frac{\Delta P}{\rho} / \left(\frac{L}{D}\frac{u^2}{2g_c}\right) = 2g_c D\Delta P/L\rho u^2 = 1.6364 / \left[\ln\left(\frac{0.135\varepsilon}{D} + \frac{6.5}{\text{Re}}\right)\right]^2 \tag{2}$$

(Round's equation)

$$\frac{\Delta P}{\rho} = \frac{L}{D}\frac{u^2}{2g_c}f = \frac{8LQ^2}{g_c\pi^2 D^5}f = \frac{8L\dot{m}^2}{g_c\pi^2\rho^2 D^5}f = \frac{LG^2}{2g_c D\rho^2}f \tag{3}$$

In the units

$D = $ in., $\dot{m} = $ lb/hr

$Q = $ cuft/sec, $\mu = $ cP

$\rho = $ specific gravity

$$\text{Re} = \frac{6.314\dot{m}}{D\mu} = \frac{1.418(10^6)\rho Q}{D\mu} \tag{4}$$

$$\frac{\Delta P}{L} = \frac{3.663(10^{-9})\dot{m}^2}{\rho D^5}f, \text{ atm/ft} \tag{5}$$

$$= \frac{5.385(10^{-8})\dot{m}^2}{\rho D^5}f, \text{ psi/ft} \tag{6}$$

$$= \frac{0.6979\rho Q^2}{D^5}f, \text{ psi/ft} \tag{7}$$

Laminar Flow

$\text{Re} < 2300$

$$f = 64/\text{Re} \tag{2a}$$

$$\Delta P/L = 32\mu u/D^2$$

$$= \frac{1.841(10^{-7})\mu\dot{m}}{\rho D^4}, \text{ atm/ft} \tag{5a}$$

$$= \frac{2.707(10^{-6})\mu\dot{m}}{\rho D^4}, \text{ psi/ft} \tag{6a}$$

$$= \frac{35.083\mu Q}{D^4}, \text{ psi/ft} \tag{7a}$$

Gravitation Constant

$g_c = 1 \text{ kg m/N sec}^2$

$= 1 \text{ g cm/dyn sec}^2$

$= 9.806 \text{ kg m/kgf sec}^2$

$= 32.174 \text{ lbm ft/lbf sec}^2$

$= 1 \text{ slug ft/lbf sec}^2$

$= 1 \text{ lbm ft/poundal sec}^2$

6.2. ENERGY BALANCE OF A FLOWING FLUID

The energy terms associated with the flow of a fluid are

1. Elevation potential $(g/g_c)z$,
2. Kinetic energy, $u^2/2g_c$,
3. Internal energy, U,
4. Work done in crossing the boundary, PV,
5. Work transfer across the boundary, W_s,
6. Heat transfer across the boundary, Q.

Figure 6.1 represents the two limiting kinds of regions over which energy balances are of interest: one with uniform conditions throughout (completely mixed), or one in plug flow in which gradients are present. With single inlet and outlet streams of a uniform region, the change in internal energy within the boundary is

$$d(mU) = m\,dU + U\,dm = m\,dU + U(dm_1 - dm_2)$$
$$= dQ - dW_s + [H_1 + u_1^2/2g_c + (g/g_c)z_1]dm_1 \tag{6.6}$$
$$-[H_2 + u_2^2/2g_c + (g/g_c)z_2]dm_2.$$

One kind of application of this equation is to the filling and emptying of vessels, of which Example 6.2 is an instance.

Under steady state conditions, $d(mU) = 0$ and $dm_1 = dm_2 = dm$, so that Eq. (6.6) becomes

$$\Delta H + \Delta u^2/2g_c + (g/g_c)\Delta z = (Q - W_s)/m, \tag{6.7}$$

or

$$\Delta U + \Delta(PV) + \Delta u^2/2g_c + (g/g_c)\Delta z = (Q - W_s)/m, \tag{6.8}$$

or

$$\Delta U + \Delta(P/\rho) + \Delta u^2/2g_c + (g/g_c)\Delta z = (Q - W_s)/m. \tag{6.9}$$

For the plug flow condition of Figure 6.1(b), the balance is made in terms of the differential changes across a differential length dL of the vessel, which is

$$dH + (1/g_c)u\,du + (g/g_c)\,dz = dQ - dW_s, \tag{6.10}$$

where all terms are per unit mass.
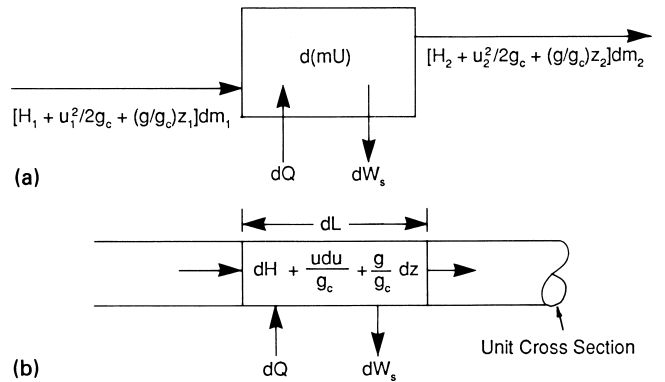
Figure 6.1. Energy balances on fluids in completely mixed and plug flow vessels. (a) Energy balance on a bounded space with uniform conditions throughout, with differential flow quantities dm_1 and dm_2. (b) Differential energy balance on a fluid in plug flow in a tube of unit cross section.

EXAMPLE 6.2
Unsteady Flow of an Ideal Gas through a Vessel
An ideal gas at 350 K is pumped into a 1000 L vessel at the rate of 6 g mol/min and leaves it at the rate of 4 g mol/min. Initially the vessel is at 310 K and 1 atm. Changes in velocity and elevation are negligible. The contents of the vessel are uniform. There is no work transfer.

Thermodynamic data:

$$U = C_v T = 5T,$$
$$H = C_p T = 7T.$$

Heat transfer:

$$dQ = h(300 - T) \, d\theta$$
$$= 15(300 - T) \, d\theta.$$

The temperature will be found as a function of time θ with both $h = 15$ and $h = 0$.

$$dn_1 = 6 \, d\theta,$$
$$dn_2 = 4 \, d\theta,$$
$$dn = dn_1 - dn_2 = 2 \, d\theta,$$
$$n_0 = P_0 V / RT_0 = 1000/(0.08205)(310) = 39.32 \, \text{g mol},$$
$$n = n_0 + 2\theta,$$
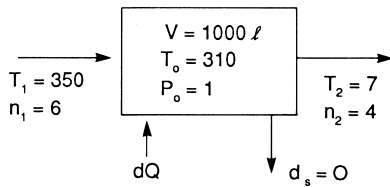
Energy balance

$$d(nU) = n \, dU + U \, dn = nC_v \, dT + C_v \, T(2d\theta)$$

$$= H_1 \, dn_1 - H_2 \, dn_2 + dQ - dw_s$$
$$= C_p(6T_1 - 4T) \, d\theta + h(300 - T) \, d\theta.$$

This rearranges into

$$\int_0^\theta \frac{d\theta}{n_0 + 2\theta} = \int_{310}^{T_2} \frac{dT}{(1/C_v)[6C_p T_1 + 300h - (4C_p + 2C_v + h)T}$$

$$= \begin{cases} \displaystyle\int_{310}^{T_2} \frac{dT}{3840 - 10.6T}, & h = 15, \\[3mm] \displaystyle\int_{310}^{T_2} \frac{dT}{2940 - 7.6T}, & h = 0. \end{cases}$$

The integrals are rearranged to find T,

$$T_2 = \begin{cases} 362.26 - 52.26\left(\dfrac{1}{1 + 0.0509\theta}\right)^{5.3}, & h = 15, \\[4mm] 386.84 - 76.84\left(\dfrac{1}{1 + 0.0509\theta}\right)^{3.8}, & h - 0. \end{cases}$$

Some numerical values are

	T_2		P	
θ	$h = 15$	$h = 0$	$h = 15$	$h = 0$
0	310	310	1	1
0.2	312.7	312.9	1.02	1.02
0.5	316.5	317.0		
1	322.1	323.2		
5	346.5	354.4		
10	356.4	370.8	1.73	1.80
∞	362.26	386.84	∞	∞

The pressures are calculated from

$$P = \frac{nRT}{V} = \frac{(39.32 + 2\theta)(0.08205)T}{1000}.$$

Friction is introduced into the energy balance by noting that it is a mechanical process, dW_f, whose effect is the same as that of an equivalent amount of heat transfer dQ_f. Moreover, the total effective heat transfer results in a change in entropy of the flowing liquid given by

$$T \, dS = dQ + dW_f. \tag{6.11}$$

When the thermodynamic equivalent

$$dH = V \, dP + T \, dS = dP/\rho + T \, dS \tag{6.12}$$

and Eq. (6.11) are substituted into Eq. (6.10), the net result is

$$V \, dP + (1/g_c)u \, du + (g/g_c) \, dz = -(dW_s + dW_f), \tag{6.13}$$

which is known as the mechanical energy balance. With the expression for friction of Eq. (6.18) cited in the next section, the mechanical energy balance becomes

$$V \, dP + (1/g_c)u \, du + (g/g_c)dz + \frac{fu^2}{2g_c D}dL = -dW_s. \tag{6.13'}$$

For an incompressible fluid, integration may be performed term by term with the result

$$\Delta P/\rho + \Delta u^2/2g_c + (g/g_c)\Delta z = -(W_s + W_f). \tag{6.14}$$

The apparent number of variables in Eq. (6.13) is reduced by the substitution $u = V/A$ for unit flow rate of mass, where A is the cross-sectional area, so that

$$V \, dP + (1/g_c A^2)V \, dV + (g/g_c) \, dz = -(dW_s + dW_f). \tag{6.15}$$

Integration of these energy balances for compressible fluids under several conditions is covered in Section 6.7.

The frictional work loss W_f depends on the geometry of the system and the flow conditions and is an empirical function that will be explained later. When it is known, Eq. (6.13) may be used to find a net work effect W_s for otherwise specified conditions.

The first three terms on the left of Eq. (6.14) may be grouped into a single stored energy terms as

$$\Delta E = \Delta P/\rho + \Delta u^2/2g_c + (g/g_c)\Delta z, \tag{6.16}$$

and the simpler form of the energy balance becomes

$$\Delta E + W_f = -W_s. \tag{6.17}$$

The units of every term in these energy balances are alternately:

ft lb$_f$/lb with $g_c = 32.174$ and g in ft/sec^2 (32.174 at sea level).
N m/kg = J/kg with $g_c = 1$ and g in m/sec^2 (1.000 at sea level).
kg$_f$ m/kg with $g_c = 9.806$ and g in m/sec^2 (9.806 at sea level).

Example 6.3 is an exercise in conversion of units of the energy balances.

The sign convention is that *work input is a negative quantity* and consequently results in an increase of the terms on the left of Eq. (6.17). Similarly, work is produced by the flowing fluid only if the stored energy ΔE is reduced.

6.3. LIQUIDS

Velocities in pipe lines are limited in practice because of

1. the occurrence of erosion.
2. economic balance between cost of piping and equipment and the cost of power loss because of friction which increases sharply with velocity.

Although erosion is not serious in some cases at velocities as high as 10–15 ft/sec, conservative practice in the absence of specific knowledge limits velocities to 5–6 ft/sec.

Economic optimum design of piping will be touched on later, but the rules of Table 6.2 of typical linear velocities and pressure drops provide a rough guide for many situations.

The correlations of friction in lines that will be presented are for new and clean pipes. Usually a factor of safety of 20–40% is advisable because pitting or deposits may develop over the years. There are no recommended fouling factors for friction as there are for heat transfer, but instances are known of pressure drops to double in water lines over a period of 10 years or so.

In lines of circular cross section, the pressure drop is represented by

$$\Delta P = f \rho \frac{L}{D} \frac{u^2}{2g_c}. \tag{6.18}$$

For other shapes and annular spaces, D is replaced by the hydraulic diameter

$$D_h = 4(\text{cross section})/\text{wetted perimeter}.$$

For an annular space, $D_h = D_2 - D_1$.

In laminar flow the friction is given by the theoretical Poiseuille equation

$$f = 64/N_{re}, \quad N_{Re} < 2100, \text{ approximately}. \tag{6.19}$$

At higher Reynolds numbers, the friction factor is affected by the roughness of the surface, measured as the ratio ε/D of projections on the surface to the diameter of the pipe. Values of ε are as follows; glass and plastic pipe essentially have $\varepsilon = 0$.

	ε (ft)	ε (mm)
Riveted steel	0.003–0.03	0.9–9.0
Concrete	0.001–0.01	0.3–3.0
Wood stave	0.0006–0.003	0.18–0.9
Cast iron	0.00085	0.25
Galvanized iron	0.0005	0.15
Asphalted cast iron	0.0004	0.12
Commercial steel or wrought iron	0.00015	0.046
Drawn tubing	0.000005	0.0015

The equation of Colebrook [*J. Inst. Civ. Eng.* London, **11**, pp. 133–156 (1938–1939)] is based on experimental data of Nikuradze [*Ver. Dtsch. Ing. Forschungsh. 356* (1932)].

$$\frac{1}{\sqrt{f}} = 1.14 - 0.869 \ln\left(\frac{\varepsilon}{D} + \frac{9.38}{N_{Re}\sqrt{f}}\right), \quad N_{Re} > 2100. \tag{6.20}$$

Other equations equivalent to this one but explicit in f have been devised. A literature review and comparison with more recent experimental data are made by Olujic [*Chem. Eng.*, 91–94, (14 Dec. 1981)]. Two of the simpler but adequate equations are

$$f = 1.6364\left[\ln\left(\frac{0.135\varepsilon}{D} + \frac{6.5}{N_{Re}}\right)\right]^{-2} \tag{6.21}$$

[Round, *Can. J. Chem. Eng.* **58**, 122 (1980)],

$$f = \left\{-0.8686 \ln\left[\frac{\varepsilon}{3.7D} - 2.1802 \ln\left(\frac{\varepsilon}{3.7D} + \frac{14.5}{N_{Re}}\right)\right]\right\}^{-2} \tag{6.22}$$

EXAMPLE 6.3
Units of the Energy Balance
In a certain process the changes in stored energy and the friction are

$$\Delta E = -135 \text{ ft lbf/lb}$$
$$w_f = 13 \text{ft lbf/lb}.$$

The net work will be found in several kinds of units:

$$w_s = -(\Delta E + w_f) = 122 \text{ ft lbf/lb},$$
$$w_s = 122 \frac{\text{ft lbf}}{\text{lb}} \frac{4.448N}{\text{lbf}} \frac{2.204 \text{ lb}}{\text{kg}} \frac{m}{3.28\text{ft}}$$

$$= 364.6 \frac{\text{Nm}}{\text{kg}}, \ 364.6 \frac{\text{J}}{\text{kg}},$$
$$w_s = 364.6 \frac{\text{N m}}{\text{kg}} \frac{\text{kgf}}{9.806 \text{ N}} = 37.19 \frac{\text{m kgf}}{\text{kg}}.$$

At sea level, numerically lbf = lb and kgf = kg. Accordingly,

$$w_s = 122 \frac{\text{ft lbf}}{\text{lb}} \frac{\text{lb}}{\text{lbf}} \frac{\text{kgf}}{\text{kg}} \frac{m}{3.28 \text{ ft}} = 37.19 \frac{\text{kgf m}}{\text{kg}},$$

as before.

TABLE 6.2. Typical Velocities and Pressure Drops in Pipelines

	Liquids (psi/100 ft)		
	Liquids within 50°F of Bubble Point	Light Oils and Water	Viscous Oils
Pump suction	0.15	0.25	0.25
Pump discharge	2.0	2.0	2.0
	(or 5–7 fps)	(or 5–7 fps)	(or 3–4 fps)
Gravity flow to or from tankage, maximum	0.05	0.05	0.05
Thermosyphon reboiler inlet and outlet	0.2		

	Gases (psi/100 ft)	
Pressure (psig)	0–300 ft Equivalent Length	300–600 ft Equivalent Length
−13.7 (28 in. Vac)	0.06	0.03
−12.2 (25 in. Vac)	0.10	0.05
−7.5 (15 in. Vac)	0.15	0.08
0	0.25	0.13
50	0.35	0.18
100	0.50	0.25
150	0.60	0.30
200	0.70	0.35
500	2.00	1.00

Steam	psi/100 ft	Maximum ft/min
Under 50 psig	0.4	10,000
Over 50 psig	1.0	7000

Steam Condensate

To traps, 0.2 psi/100 ft. *From bucket traps*, size on the basis of 2–3 times normal flow, according to pressure drop available. *From continuous drainers*, size on basis of design flow for 2.0 psi/100 ft

Control Valves

Require a pressure drop of at least 10 psi for good control, but values as low as 5 psi may be used with some loss in control quality

Particular Equipment Lines (ft/sec)

Reboiler, downcomer (liquid)	3–7
Reboiler, riser (liquid and vapor)	35–45
Overhead condenser	25–100
Two-phase flow	35–75
Compressor, suction	75–200
Compressor, discharge	100–250
Inlet, steam turbine	120–320
Inlet, gas turbine	150–350
Relief valve, discharge	$0.5v_c$[a]
Relief valve, entry point at silencer	v_c[a]

[a]v_c is sonic velocity.

[Schacham, *Ind. Eng. Chem. Fundam.* **19**(5), 228 (1980)]. These three equations agree with each other within 1% or so. The Colebrook equation predicts values 1–3% higher than some more recent measurements of Murin (1948), cited by Olujic (*Chemical Engineering*, 91–93, Dec. 14, 1981).

Another useful equation was developed by [Wood, *Civil Eng.*, pp. 60–61, Dec. 1966] and given by Streeter [*Fluid Mechanics*, 5th ed., McGraw-Hill, p. 292, 1971].

$$f = a + b(N_{Re})^{-c}, \qquad N_{Re} > 2100 \tag{6.23}$$

where
$$a = 0.094(\varepsilon/D)^{0.225} + 0.53(\varepsilon/D)$$
$$b = 88(\varepsilon/D)^{0.44}$$
$$c = 1.62(\varepsilon/D)^{0.134}$$

Under some conditions it is necessary to employ Eq. (6.18) in differential form. In terms of mass flow rate,

$$dP = \frac{8\dot{m}^2 f}{g_c \pi^2 \rho D^5} dL. \tag{6.24}$$

Example 6.4 is of a case in which the density and viscosity vary along the length of the line, and consequently the Reynolds number and the friction factor also vary.

FITTINGS AND VALVES

Friction due to fittings, valves and other disturbances of flow in pipe lines is accounted for by the concepts of either their equivalent lengths of pipe or multiples of the velocity head. Accordingly, the pressure drop equation assumes either of the forms

$$\Delta P = f(L + \sum L_i)\rho u^2 / 2g_c D, \tag{6.25}$$

$$\Delta P = [f(L/D) + \sum K_i]\rho u^2 / 2g_c. \tag{6.26}$$

Values of equivalent lengths L_i and coefficients K_i are given in Tables 6.3 and 6.4. Another well-documented table of K_i is in the *Perry's Chemical Engineers' Handbook*, 7th ed. (1999), p. 6-18, Table 6-4.

Comparing the two kinds of parameters,

$$K_i = fL_i/D \tag{6.27}$$

so that one or the other or both of these factors depend on the friction factor and consequently on the Reynolds number and possibly ε. Such a dependence was developed by Hooper [*Chem. Eng.*, 96–100, (24 Aug. 1981)] in the equation

$$K = K_1/N_{Re} + K_2(1 + 1/D), \tag{6.28}$$

where D is in inches and values of K_1 and K_2 are in Table 6.5. Hooper states that the results are applicable to both laminar and turbulent regions and for a wide range of pipe diameters. Example 6.5 compares the several systems of pipe fittings resistances. The K_i method usually is regarded as more accurate.

ORIFICES

In pipe lines, orifices are used primarily for measuring flow rates but sometimes as mixing devices. The volumetric flow rate through a thin plate orifice is

$$Q = C_d A_0 \left(\frac{2\Delta P/\rho}{1 - \beta^4}\right)^{1/2}, \tag{6.29}$$

A_0 = cross sectional area of the orifice,
$\beta = d/D$, ratio of the diameters of orifice and pipe.

EXAMPLE 6.4
Pressure Drop in Nonisothermal Liquid Flow
Oil is pumped at the rate of 6000 lb/hr through a reactor made of commercial steel pipe 1.278 in. ID and 2000 ft long. The inlet condition is 400°F and 750 psia. The temperature of the outlet is 930°F and the pressure is to be found. The temperature varies with the distance, L ft, along the reactor according to the equation

$$T = 1500 - 1100 \exp(-0.0003287L) \; (°F)$$

The viscosity and density vary with temperature according to the equations

$$\mu = \exp\left(\frac{7445.3}{T + 459.6} - 6.1076\right), \; \text{cP},$$

$$\rho = 0.936 - 0.00036T, \; \text{g/mL}.$$

Round's equation applies for the friction factor:

$$N_{\text{Re}} = \frac{4\dot{m}}{\pi D \mu} = \frac{4(6000)}{\pi(1.278/12)2.42\mu} = \frac{29,641}{\mu},$$

$$\varepsilon/D = \frac{0.00015(12)}{1.278} = 0.00141,$$

$$f = \frac{1.6364}{\left[\ln\left[0.135(0.00141) + 6.5/N_{\text{Re}}\right]\right]^2}.$$

The differential pressure is given by

$$-dP = \frac{8\dot{m}^2}{g_c \pi^2 \rho D^5} f \, dL = \frac{8(6000/3600)^2}{32.2\pi^2 62.4\rho(1.278/12)^5(144)} f \, dL$$

$$= \frac{0.568f}{\rho} dL, \; \text{psi},$$

$$P = 750 - \int_0^L \frac{0.586f}{L} dL = 750 - \int_0^L I \, dL.$$

The pressure profile is found by integration with the trapezoidal rule over 200 ft increments. The results from a computer program computer program are given below. The outlet pressure is 700 psi. For comparison, taking an average temperature of 665°F,

$$\mu = 1.670, \; \rho = 0.697$$

$$N_{\text{Re}} = 17,700, \; f = 0.00291,$$

$$P_{\text{out}} = 702.5.$$

L	T	$\frac{N_{\text{Re}}}{1000}$	100 f	P
0	400.0	2.3	4.85	750.0
200	470.0	4.4	3.99	743.6
400	535.5	7.5	3.49	737.9
600	596.9	11.6	3.16	732.8
800	654.4	16.7	2.95	727.9
1000	708.2	22.7	2.80	723.2
1200	758.5	29.5	2.69	718.5
1400	805.7	37.1	2.61	713.9
1600	849.9	45.2	2.55	709.3
1800	891.3	53.8	2.51	704.7
2000	930.0	62.7	2.47	700.1

TABLE 6.3. Equivalent Lengths of Pipe Fittings[a]

Pipe size, in.	Standard ell	Medium radius ell	Long-radius ell	45-deg ell	Tee	Gate valve, open	Globe valve, open	Swing check, open
1	2.7	2.3	1.7	1.3	5.8	0.6	27	6.7
2	5.5	4.6	3.5	2.5	11.0	1.2	57	13
3	8.1	6.8	5.1	3.8	17.0	1.7	85	20
4	11.0	9.1	7.0	5.0	22	2.3	110	27
5	14.0	12.0	8.9	6.1	27	2.9	140	33
6	16.0	14.0	11.0	7.7	33	3.5	160	40
8	21	18.0	14.0	10.0	43	4.5	220	53
10	26	22	17.0	13.0	56	5.7	290	67
12	32	26	20.0	15.0	66	6.7	340	80
14	36	31	23	17.0	76	8.0	390	93
16	42	35	27	19.0	87	9.0	430	107
18	46	40	30	21	100	10.2	500	120
20	52	43	34	23	110	12.0	560	134
24	63	53	40	28	140	14.0	680	160
36	94	79	60	43	200	20.0	1,000	240

[a]Length of straight pipe (ft) giving equivalent resistance.
(Hicks and Edwards, *Pump Application Engineering*, McGraw-Hill, New York, 1971).

TABLE 6.4 Velocity Head Factors of Pipe Fittings[a]
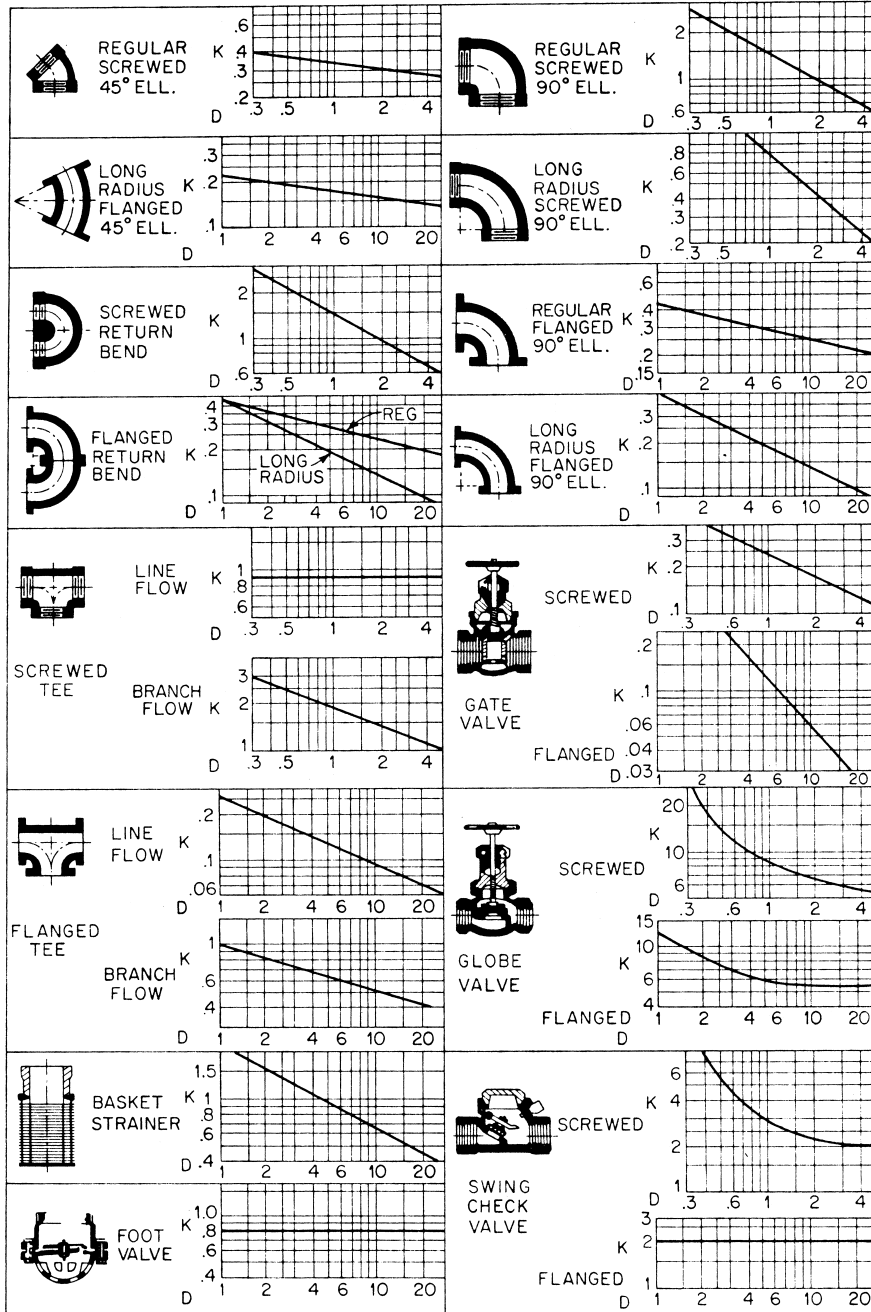
TABLE 6.5. Velocity Head Factors of Pipe Fittings[a]

	Fitting Type		K_1	K_∞
Elbows	90°	Standard ($R/D = 1$), screwed	800	0.40
		Standard ($R/D = 1$), flanged/welded	800	0.25
		Long-radius ($R/D = 1.5$), all types	800	0.20
	Mitered elbows ($R/D = 1.5$)	1 Weld (90° angle)	1,000	1.15
		2 Weld (45° angles)	800	0.35
		3 Weld (30° angles)	800	0.30
		4 Weld (22 1/2° angles)	800	0.27
		5 Weld (18° angles)	800	0.25
	45°	Standard ($R/D = 1$), all types	500	0.20
		Long-radius ($R/D = 1.5$), all types	500	0.15
		Mitered, 1 weld, 45° angle	500	0.25
		Mitered, 2 weld, 22 1/2° angles	500	0.15
	180°	Standard ($R/D = 1$), screwed	1,000	0.60
		Standard ($R/D = 1$), flanged/welded	1,000	0.35
		Long radius ($R/D = 1.5$), all types	1,000	0.30
Tees	Used as elbow	Standard, screwed	500	0.70
		Long-radius, screwed	800	0.40
		Standard, flanged or welded	800	0.80
		Stub-in-type branch	1,000	1.00
	Run-through tee	Screwed	200	0.10
		Flanged or welded	150	0.50
		Stub-in-type branch	100	0.00
Valves	Gate, ball, plug	Full line size, $\beta = 1.0$	300	0.10
		Reduced trim, $\beta = 0.9$	500	0.15
		Reduced trim, $\beta = 0.8$	1,000	0.25
	Globe, standard		1,500	4.00
	Globe, angle or Y-type		1,000	2.00
	Diaphragm, dam type		1,000	2.00
	Butterfly		800	0.25
	Check	Lift	2,000	10.00
		Swing	1,500	1.50
		Tilting-disk	1,000	0.50

Note: Use $R/D = 1.5$ values for $R/D = 5$ pipe bends, 45° to 180°. Use appropriate tee values for flow through crosses.

[a] Inlet, flush, $K = 160/N_{Re} + 0.5$. Inlet, intruding, $K = 160/N_{Re} = 1.0$. Exit, $K = 1.0$. $K = K_1/N_{Re} + K_2(1 + 1/D)$, with D in inches. [Hooper, *Chem. Eng.*, 96–100 (24 Aug. 1981)].

For corner taps the coefficient is given by

$$C_d \approx 0.5959 + 0.0312\beta^{2.1} - 0.184\beta^8$$
$$+ (0.0029\beta^{2.5})(10^6/Re_D)^{0.75} \tag{6.30}$$

(International Organization for Standards Report DIS 5167, Geneva, 1976). Similar equations are given for other kinds of orifice taps and for nozzles and Venturi meters.

POWER REQUIREMENTS

A convenient formula in common engineering units for power consumption in the transfer of liquids is

$$\dot{P} = \frac{(\text{volumetric flow rate})(\text{pressure difference})}{(\text{equipment efficiency})}$$

$$= \frac{(\text{gals/min})(\text{lb/sq in.})}{1714(\text{fractional pump eff})(\text{fractional driver eff})} \text{ horsepower.} \tag{6.30a}$$

Efficiency data of drivers are in Chapter 4 and of pumps in Chapter 7. For example, with 500 gpm, a pressure difference of 75 psi, pump efficiency of 0.7, and driver efficiency of 0.9, the power requirement is 32.9 HP or 24.5 kw.

6.4. PIPELINE NETWORKS

A system for distribution of fluids such as cooling water in a process plant consists of many interconnecting pipes in series, parallel, or branches. For purposes of analysis, a point at which several lines meet is called a node and each is assigned a number as on the figure of Example 6.6. A flow rate from node i to node j is designated as Q_{ij}; the same subscript notation is used for other characteristics of the line such as f, L, D, and N_{Re}.

Three principles are applicable to establishing flow rates, pressures, and dimensions throughout the network:

1. Each node i is characterized by a unique pressure P_i.
2. A material balance is preserved at each node: total flow in equals total flow out, or net flow equals zero.
3. The friction equation $P_i - P_j = (8\rho/g_c\pi^2)f_{ij}L_{ij}Q_{ij}^2/D_{ij}^5$ applies to the line connecting node i with j.

In the usual network problem, the terminal pressures, line lengths, and line diameters are specified and the flow rates throughout are required to be found. The solution can be generalized, however, to determine other unknown quantities equal in number to the number of independent friction equations that describe the network. The procedure is illustrated with the network of Example 6.6.

The three lines in parallel between nodes 2 and 5 have the same pressure drop $P_2 - P_5$. In series lines such as 37 and 76 the flow rate is the same and a single equation represents friction in the series:

$$P_3 - P_6 = kQ_{36}^2(f_{37}L_{37}/D_{37}^5 + f_{76}L_{76}/D_{76}^5).$$

The number of flow rates involved is the same as the number of lines in the network, which is 9, plus the number of supply and destination lines, which is 5, for a total of 14. The number of material balances equals the number of nodes plus one for the overall balance, making a total of 7.

The solution of the problem requires $14 - 7 = 7$ more relations to be established. These are any set of 7 friction equations that involve the pressures at all the nodes. The material balances and pressure drop equations for this example are tabulated.

From Eqs. (4)–(10) of Example 6.6, any combination of seven quantities Q_{ij} and/or L_{ij} and/or D_{ij} can be found. Assuming that the Q_{ij} are to be found, estimates of all seven are made to start, and the corresponding Reynolds numbers and friction factors are found from Eqs. (2) and (3). Improved values of the Q_{ij} then are found from Eqs. (4)–(10) with the aid of the Newton–Raphson method for simultaneous nonlinear equations.

Some simplification is permissible for water distribution systems in metallic pipes. Then the Hazen–Williams formula is adequate, namely

$$\Delta h = \Delta P/\rho = 4.727L(Q/130)^{1.852}/D^{4.8704} \tag{6.31}$$

with linear dimensions in ft and Q in cuft/sec. The iterative solution method for flowrate distribution of Hardy Cross is popular. Examples of that procedure are presented in many books on fluid mechanics, for example, those of Bober and Kenyon (*Fluid Mechanics*, Wiley, New York, 1980) and Streeter and Wylie (*Fluid Mechanics*, McGraw-Hill, New York, 1979).

With particularly simple networks, some rearrangement of equations sometimes can be made to simplify the solution. Example 6.7 is of such a case.

EXAMPLE 6.5
Comparison of Pressure Drops in a Line with Several Sets of Fittings Resistances

The flow considered is in a 12-inch steel line at a Reynolds number of 6000. With $\varepsilon = 0.00015$, Round's equation gives $f = 0.0353$. The line composition and values of fittings resistances are:

	Table 6.4	Table 6.5	Table 6.6		
	L	K	K_1	K_2	K
Line	1000	—	—	—	—
6 LR ells	20	0.25	500	0.15	0.246
4 tees, branched	66	0.5	150	0.15	0.567
2 gate valves, open	7	0.05	300	0.10	0.158
1 globe valve	340	5.4	1500	4.00	4.58
	1738	9.00			8.64

Table 6.4, $\dfrac{\Delta P}{(\rho u^2/2g_c)} = \dfrac{f}{D}(1738) = 61.3,$

Table 6.5, $\dfrac{\Delta P}{(\rho u^2/2g_c)} = f\dfrac{L}{D} + \sum K_i$

$= \dfrac{0.0353(1000)}{1} + 9.00 = 44.3,$

Table 6.6, $\dfrac{\Delta P}{(\rho u^2/2g_c)} = 35.3 + 8.64 = 43.9.$

The value $K = 0.05$ for gate valve from Table 6.4 appears to below: *Chemical Engineering Handbook*, for example, gives 0.17, more nearly in line with that from Table 6.5. The equivalent length method of Table 6.3 gives high pressure drops; although convenient, it is not widely used.

EXAMPLE 6.6
A Network of Pipelines in Series, Parallel, and Branches: the Sketch, Material Balances, and Pressure Drop Equations

Pressure drop:

$$\Delta P_{ij} = (8\rho/g_c\pi^2)f_{ij}L_{ij}Q_{ij}^2/D_{ij}^5 = kf_{ij}L_{ij}Q_{ij}^2/D_{ij}^5. \quad (1)$$
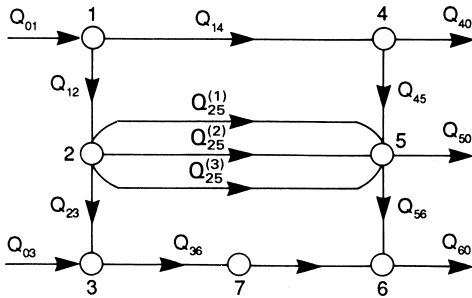
Reynolds number:

$$(N_{Re})_{ij} = 4Q_{ij}\rho/\pi D_{ij}\mu. \quad (2)$$

Friction factor:

$$f_{ij} = 1.6364/[\ln(\varepsilon/D_{ij} + 6.5/(N_{Re})_{ij})]^2. \quad (3)$$

Pressure drops in key lines:

$$\Delta p_{12} = P_1 - P_2 - kf_{12}L_{12}Q_{12}^2/D_{12}^5 = 0, \quad (4)$$
$$\Delta p_{23} = P_2 - P_3 - kf_{23}L_{23}Q_{23}^5/D_{23}^2 = 0, \quad (5)$$
$$\Delta p_{25} = P_2 - P_5 = kf_{25}^{(1)}L_{25}^{(1)}(Q_{25}^{(1)})^2/(D_{25}^{(1)})^5 \quad (6)$$
$$= kf_{25}^{(2)}L_{25}^{(2)}(Q_{25}^{(2)})^2/(D_{25}^{(2)})^5 \quad (7)$$
$$= kf_{25}^{(3)}L_{25}^{(3)}(Q_{25}^{(3)})^2/(D_{25}^{(3)})^5, \quad (8)$$
$$\Delta p_{45} = P_4 - P_5 - kf_{45}L_{45}Q_{45}^2/D_{45}^5 = 0, \quad (9)$$
$$\Delta p_{56} = P_5 - P_6 - kf_{56}L_{56}Q_{56}^2/D_{56}^5 = 0 \quad (10)$$

Node	Material Balance at Node:	
1	$Q_{01} - Q_{12} - Q_{14} = 0$	(11)
2	$Q_{12} - Q_{23} - Q_{25}^{(1)} - Q_{25}^{(2)} - Q_{25}^{(3)} = 0$	(12)
3	$Q_{03} + Q_{23} - Q_{36} = 0$	(13)
4	$Q_{14} - Q_{40} - Q_{45} = 0$	(14)
5	$Q_{45} + Q_{25}^{(1)} + Q_{25}^{(2)} + Q_{25}^{(3)} - Q_{50} - Q_{56} = 0$	(15)
6	$Q_{36} + Q_{56} - Q_{60} = 0$	(16)
Overall	$Q_{01} + Q_{03} - Q_{40} - Q_{50} - Q_{60} = 0$	(17)

EXAMPLE 6.7
Flow of Oil in a Branched Pipeline

The pipeline handles an oil with sp gr $= 0.92$ and kinematic viscosity of 5 centistokes(cS) at a total rate of 12,000 cuft/hr. All three pumps have the same output pressure. At point 5 the elevation is 100 ft and the pressure is 2 atm gage. Elevations at the other points are zero. Line dimensions are tabulated following. The flow rates in each of the lines and the total power requirement will be found.

Line	L (ft)	D (ft)
14	1000	0.4
24	2000	0.5
34	1500	0.3
45	4000	0.75
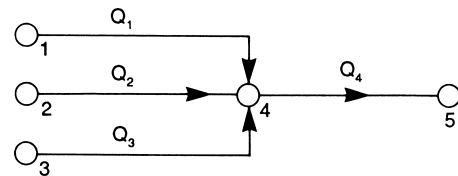
$$Q_1 + Q_2 + Q_3 = Q_4 = 12,000/3600 = 3.333 \text{ cfs} \quad (1)$$

$$N_{Re} = \frac{4Q}{\pi DV} = \frac{4Q}{\pi D(5/92,900)} = \frac{23,657Q}{D}$$

$$= \begin{cases} 59,142Q_1 \\ 47,313Q_2, \\ 78,556Q_3, \\ 31,542Q_4, \end{cases} \quad (2)$$

EXAMPLE 6.7—(*continued*)

$\varepsilon = 0.00015$ ft,

$$h_f = \frac{8fLQ^2}{g_c\pi^2 D^5} = 0.0251fLQ^2/D^5 \text{ ft}, \tag{3}$$

$$h_{f1} = h_{f2} = h_{f3}, \tag{4}$$

$$\frac{f_1 L_1 Q_1^2}{D_1^5} = \frac{f_2 L_2 Q_2^2}{D_2^5} = \frac{f_3 L_3 Q_3^2}{D_3^5} \tag{5}$$

$$Q_2 = Q_1\left[\frac{f_1 L_1}{f_2 L_2}\left(\frac{D_2}{D_1}\right)^5\right]^{1/2} = 1.2352\left(\frac{f_1}{f_2}\right)^{1/2}Q_1, \tag{6}$$

$$Q_3 = Q_1\left[\frac{f_1 L_1}{f_3 L_3}\left(\frac{D_3}{D_1}\right)^5\right]^{1/2} = 0.3977\left(\frac{f_1}{f_3}\right)^{1/2}Q_1, \tag{7}$$

$$Q_1\left[1 + 1.2352\left(\frac{f_1}{f_2}\right)^{1/2} + 0.3977\left(\frac{f_1}{f_3}\right)^{1/2}\right] = Q_4 = 3.333, \tag{8}$$

$$f = \frac{1.6364}{[\ln(2.03(10^{-5})/D + 6.5/N_{Re}]^2}.$$

For line 45,

$$(N_{Re})_4 = 31542\,(3.333) = 105{,}140,$$

$$f_4 = 0.01881,$$

$$(h_f)_{45} = \frac{0.02517(0.01881)(4000)(3.333)^2}{(0.75)^5} = 88.65 \text{ ft}.$$

Procedure:

1. As a first trial assume $f_1 = f_2 = f_3$, and find $Q_1 = 1.266$ from Eq. (8).
2. Find Q_2 and Q_3 from Eqs. (6) and (7).
3. With these values of the Q_i, find improved values of the f_i and hence improved values of Q_2 and Q_3 from Eqs. (6) and (7).

4. Check how closely $Q_1 + Q_2 + Q_3 - 3.333 = 0$.
5. If check is not close enough, adjust the value of Q_1 and repeat the calculations.

The two trials shown following prove to be adequate.

Q_1	Q_2	Q_3	Q_4	$10/3 - Q_4$	f_1
1.2660	1.5757	0.4739	3.3156	0.0023	0.02069
1.2707	1.5554	0.5073	3.3334	0.0001	0.02068

Summary:

Line	N_{Re}	f	Q	h_f
14	75,152	0.02068	1.2707	82.08
24	60,121	0.02106	1.5554	82.08
34	99,821	0.02053	0.5073	82.08
45	105,140	0.01881	3.3333	88.65

$$h_{f14} = h_{f24} = h_{f34} = \frac{0.02517(0.02068)(1000)(1.2707)^2}{(0.4)^5} = 82.08 \text{ ft}.$$

Velocity head at discharge:

$$\frac{u_5^2}{2g_c} = \frac{1}{2g_c}\left(\frac{Q_4}{(\pi/4)D^2}\right)^2 = 0.88 \text{ ft}.$$

Total head at pumps:

$$h_p = \frac{2(2117)}{0.92(62.4)} + 100 + 0.88 + 82.08 + 88.65$$

$$= 345.36 \text{ ft}.$$

Power

$$= \gamma Q_4 h_p$$

$$(62.4)(10/3)345.36$$

$$= 66{,}088 \text{ ft lb/sec}$$

HP, 89.6 kW.

6.5. OPTIMUM PIPE DIAMETER

In a chemical plant the capital investment in process piping is in the range of 25–40% of the total plant investment, and the power consumption for pumping, which depends on the line size, is a substantial fraction of the total cost of utilities. Accordingly, economic optimization of pipe size is a necessary aspect of plant design. As the diameter of a line increases, its cost goes up but is accompanied by decreases in consumption of utilities and costs of pumps and drivers because of reduced friction. Somewhere there is an optimum balance between operating cost and annual capital cost.

For small capacities and short lines, near optimum line sizes may be obtained on the basis of typical velocities or pressure drops such as those of Table 6.2. When large capacities are involved and lines are long and expensive materials of construction are needed, the selection of line diameters may need to be subjected to complete economic analysis. Still another kind of factor may need to be taken into account with highly viscous materials: the possibility that heating the fluid may pay off by reducing the viscosity and consequently the power requirement.

Adequate information must be available for installed costs of piping and pumping equipment. Although suppliers quotations are desirable, published correlations may be adequate. Some data and references to other published sources are given in Chapter 20. A simplification in locating the optimum usually is permissible by ignoring the costs of pumps and drivers since they are essentially insensitive to pipe diameter near the optimum value. This fact is clear in Example 6.8 for instance and in the examples worked out by Happel and Jordan (*Chemical Process Economics*, Dekker, New York, 1975).

Two shortcut rules have been derived by Peters et al. [*Plant Design and Economics for Chemical Engineers*, McGraw-Hill, New York, 2003, p. 403], for laminar (eq. 6.33) and turbulent flow conditions (eq. 6.32):

$$D = Q^{0.448}\rho^{0.132}\mu_c^{0.025}\frac{[1.63 \times 10^{-6}K(1+J)H_y]^{0.158}}{[(1+F)(X)(E)(K_F)]^{0.158}}$$

$$\text{for } D > 0.0254 \text{ m} \tag{6.32a}$$

EXAMPLE 6.8
Economic Optimum Pipe Size for Pumping Hot Oil with a Motor or Turbine Drive

A centrifugal pump and its spare handle 1000 gpm of an oil at 500°F. Its specific gravity is 0.81 and its viscosity is 3.0 cP. The length of the line is 600 ft and its equivalent length with valves and other fittings is 900 ft. There are 12 gate valves, two check valves, and one control valve.

Suction pressure at the pumps is atmospheric; the pump head exclusive of line friction is 120 psi. Pump efficiency is 71%. Material of construction of line and pumps is 316 SS. Operation is 8000 hr/yr. Characteristics of the alternate pump drives are:

a. Turbines are 3600 rpm, exhaust pressure is 0.75 bar, inlet pressure is 20 bar, turbine efficiency is 45%. Value of the high pressure steam is $5.25/1000 lbs; that of the exhaust is $0.75/1000 lbs.
b. Motors have efficiency of 90%, cost of electricity is $0.065/kWh.

Cost data are:

1. Installed cost of pipe is $7.5D$ $/ft and that of valves is $600D^{0.7}$ $ each, where D is the nominal pipe size in inches.
2. Purchase costs of pumps, motors and drives are taken from *Manual of Economic Analysis of Chemical Processes, Institut Francais du Petrole* (McGraw-Hill, New York, 1976).
3. All prices are as of mid-1975. Escalation to the end of 1984 requires a factor of 1.8. However, the location of the optimum will be approximately independent of the escalation if it is assumed that equipment and utility prices escalate approximately uniformly; so the analysis is made in terms of the 1975 prices. Annual capital cost is 50% of the installed price/year.

The summary shows that a 6-in. line is optimum with motor drive, and an 8-in. line with turbine drive. Both optima are insensitive to line sizes in the range of 6–10 in.

$$Q = 1000/(7.48)(60) = 2.2282\,\text{cfs}, \ 227.2\,\text{m}^3/\text{hr},$$

$$N_{\text{Re}} = \frac{4Q\rho}{\pi D\mu} = \frac{4(2.2282)(0.81)(62.4)}{\pi(0.000672)(3)D} = \frac{71{,}128}{D},$$

$$f = 1.6364\left[\ln\frac{0.135(0.00015)}{D} + \frac{6.5D}{71{,}128}\right]^2.$$

Pump head:

$$h_p = \frac{120(144)}{0.81(62.4)} + \frac{8fLQ^2}{g\pi^2 D^5}$$
$$= 341.88 + 124.98f/D^5 \ \text{ft}.$$

Motor power:

$$P_m = \frac{Q\rho}{\eta_p\eta_m}h_p = \frac{2.2282(50.54)}{550(0.71)(0.90)}h_p$$
$$= 0.3204h_p, \ \text{HP}$$

Turbine power:

$$P_t = \frac{2.2282(50.54)}{550(0.71)}h_p = 0.2883h_p, \ \text{HP}.$$

Steam

$$= 10.14\,\text{kg/HP(from the ``manual'')}$$
$$= 10.14(0.2883)(2.204)h_p/1000 = 0.006443h_p, \ 1000\,\text{lb/hr}.$$

Power cost:

$$0.065(8000)(\text{kw}), \ \$/\,\text{yr},$$

Steam cost:

$$4.5(8000)(1000\,\text{lb/hr}), \ \$/\text{yr}.$$

Installed pump cost factors for alloy, temperature, etc (data in the "manual")

$$= 2[2.5(1.8)(1.3)(0.71)] = 8.2.$$

Summary:

IPS	4	6	8	10
D (ft)	0.3355	0.5054	0.6651	0.8350
100 f	1.89	1.87	1.89	1.93
h_p (ft)	898	413	360	348
Pump efficiency	0.71	0.71	0.71	0.71
motor (kW)	214.6	98.7	86.0	83.2
Steam, 1000 lb/hr	5.97	2.66	2.32	2.25
Pump cost, 2 installed	50,000	28,000	28,000	28,000
Motor cost, 2 installed	36,000	16,000	14,000	14,000
Turbine cost, 2 installed	56,000	32,000	28,000	28,000
Pipe cost	18,000	27,000	36,000	45,000
Valve cost	23,750	31,546	38,584	45,107
Equip cost, motor drive	127,750	93,546	107,584	123,107
Equip cost, turbine drive	147,750	109,546	121,584	137,107
Power cost ($/yr)	111,592	51,324	44,720	43,264
Steam cost ($/yr)	208,440	95,760	83,520	80,834
Annual cost, motor drive	175,467	98,097	98,512	104,817
Annual cost, turbine drive	282,315	150,533	144,312	149,387

$$D = Q^{0.487}\rho^{0.144}\mu_c^{0.027}\frac{[1.53\times10^{-5}K(1+J)H_y]^{0.171}}{[n(1+F)(X)(E)(K_F)]^{0.171}}$$

for $D < 0.0254\,\text{m}$ \hfill (6.32b)

and for laminar flow (i.e., $N_{Re} < 2,100$)

$$D = Q^{0.364}\mu_c^{0.20}\frac{[4.39\times10^{-4}K(1+J)H_y]^{0.182}}{[(1+F)(X)(E)(K_F)]^{0.182}}$$

for $D > 0.0254\,\text{m}$ \hfill (6.33a)

$$D = Q^{0.40}\mu_c^{0.20}\frac{[4.39\times10^{-4}K(1+J)H_y]^{0.182}}{[(1+F)(X)(E)(K_F)]^{0.182}}$$

for $D < 0.0254\,\text{m}$ \hfill (6.33b)

where D is pipe diameter (m), Q is volumetric flow rate (m^3/s), ρ is fluid density (kg/m^3) and μ_c is fluid viscosity (Pa·s) and

$K = \$/kWh$, typically $0.05/kWh

$J = $ Fractional frictional loss through fittings, typically 0.35.

$H_y = $ Operational hours/year, 8,760 for a full year.

$E = $ Fractional efficiency of motor and pump, typically 0.5.

$F =$ Ratio, fittings and installation cost to pipe purchase cost, typically 1.4.

$K_F =$ Ratio, annual fixed charges to initial pipe installed cost, typically 0.2.

$X =$ \$/m for new 0.0254 m ID pipe, typically \$2.43/m for carbon steel.

Example 6.8 takes into account pump costs, alternate kinds of drivers, and alloy construction.

6.6. NON-NEWTONIAN LIQUIDS

Not all classes of fluids conform to the frictional behavior described in Section 6.3. This section will describe the commonly recognized types of liquids, from the point of view of flow behavior, and will summarize the data and techniques that are used for analyzing friction in such lines.

VISCOSITY BEHAVIOR

The distinction in question between different fluids is in their viscosity behavior, or relation between shear stress τ (force per unit area) and the rate of deformation expressed as a lateral velocity gradient, $\dot{\gamma} = du/dx$. The concept is represented on Figure 6.2(a): one of the planes is subjected to a shear stress and is translated parallel to a fixed plane at a constant velocity but a velocity gradient is developed between the planes. The relation between the variables may be written

$$\tau = F/A = \mu(du/dx) = \mu\dot{\gamma}, \tag{6.34}$$

where, by definition, μ is the viscosity. In the simplest case, the viscosity is constant, and the fluid is called Newtonian. In the other cases, more complex relations between τ and $\dot{\gamma}$ involving more than one constant are needed, and dependence on time also may present. Classifications of non-Newtonian fluids are made according to the relation between τ and $\dot{\gamma}$ by formula or shape of plot, or according to the mechanism of the resistance of the fluid to deformation.

The concept of an apparent viscosity

$$\mu_a = \tau/\dot{\gamma} \tag{6.35}$$

is useful. In the Newtonian case it is constant, but in general it can be a function of τ, $\dot{\gamma}$, and time θ.

Non-Newtonian behavior occurs in solutions or melts of polymers and in suspensions of solids in liquids. Some $\tau - \dot{\gamma}$ plots are shown in Figure 6.2, and the main classes are described following.

1. *Pseudoplastic liquids* have a $\tau - \dot{\gamma}$ plot that is concave downward. The simplest mathematical representation of such relations is a power law

$$\tau = K\dot{\gamma}^n, \ n < 1 \tag{6.36}$$

with $n < 1$. This equation has two constants; others with many more than two constants also have been proposed. The apparent viscosity is

$$\mu_a = \tau/\dot{\gamma} = K/\dot{\gamma}^{1-n}. \tag{6.37}$$

Since n is less than unity, the apparent viscosity decreases with the deformation rate. Examples of such materials are some polymeric solutions or melts such as rubbers, cellulose acetate and napalm; suspensions such as paints, mayonnaise, paper pulp, or detergent slurries; and dilute suspensions of inert solids. Pseudoplastic properties of wallpaper paste account for good spreading and adhesion,

and those of printing inks prevent their running at low speeds yet allow them to spread easily in high speed machines.

2. *Dilatant liquids* have rheological behavior essentially opposite those of pseudoplastics insofar as viscosity behavior is concerned. The $\tau - \dot{\gamma}$ plots are concave upward and the power law applies

$$\tau = K\dot{\gamma}^n, \ n > 1, \tag{6.38}$$

but with n greater than unity; other mathematical relations also have been proposed. The apparent viscosity, $\mu_a = K\dot{\gamma}^{n-1}$, increases with deformation rate. Examples of dilatant materials are pigment-vehicle suspensions such as paints and printing inks of high concentrations; starch, potassium silicate, and gum arabic in water; quicksand or beach sand in water. Dilatant properties of wet cement aggregates permit tamping operations in which small impulses produce more complete settling. Vinyl resin plastisols exhibit pseudoplastic behavior at low deformation rates and dilatant behavior at higher ones.

3. *Bingham plastics* require a finite amount of shear stress before deformation begins, then the deformation rate is linear. Mathematically,

$$\tau = \tau_0 + \mu_B(du/dx) = \tau_0 + \mu_B\dot{\gamma}, \tag{6.39}$$

where μ_B is called the coefficient of plastic viscosity. Examples of materials that approximate Bingham behavior are drilling muds; suspensions of chalk, grains, and thoria; and sewage sludge. Bingham characteristics allow toothpaste to stay on the brush.

4. *Generalized Bingham or yield-power law* fluids are represented by the equation

$$\tau = \tau_0 + K\dot{\gamma}^n. \tag{6.40}$$

Yield-dilatant ($n > 1$) materials are rare but several cases of yield-pseudoplastics exist. For instance, data from the literature of a 20% clay in water suspension are represented by the numbers $\tau_0 = 7.3\,\mathrm{dyn/cm^2}$, $K = 1.296\,\mathrm{dyn(sec)^n/cm^2}$ and $n = 0.483$ (Govier and Aziz, 1972, p. 40). Solutions of 0.5–5.0% carboxypolymethylene also exhibit this kind of behavior, but at lower concentrations the yield stress is zero.

5. *Rheopectic fluids* have apparent viscosities that increase with time, particularly at high rates of shear as shown on Figure 6.3. Figure 6.2(f) indicates typical hysteresis effects for such materials. Some examples are suspensions of gypsum in water, bentonite sols, vanadium pentoxide sols, and the polyester of Figure 6.3.

6. *Thixotropic fluids* have a time-dependent rheological behavior in which the shear stress diminishes with time at a constant deformation rate, and exhibits hysteresis [Fig. 6.2(f)]. Among the substances that behave this way are some paints, ketchup, gelatine solutions, mayonnaise, margarine, mustard, honey, and shaving cream. Nondrip paints, for example, are thick in the can but thin on the brush. The time-effect in the case of the thixotropic crude of Figure 6.4(a) diminishes at high rates of deformation. For the same crude, Figure 6.4(b) represents the variation of pressure gradient in a pipe line with time and axial position; the gradient varies fivefold over a distance of about 2 miles after 200 min. A relatively simple relation involving five constants to represent thixotropic behavior is cited by Govier and Aziz (1972, p. 43):

$$\tau = (\mu_0 + c\lambda)\dot{\gamma}, \tag{6.41}$$

$$d\lambda/d\theta = a - (a + b\dot{\gamma})\lambda. \tag{6.42}$$
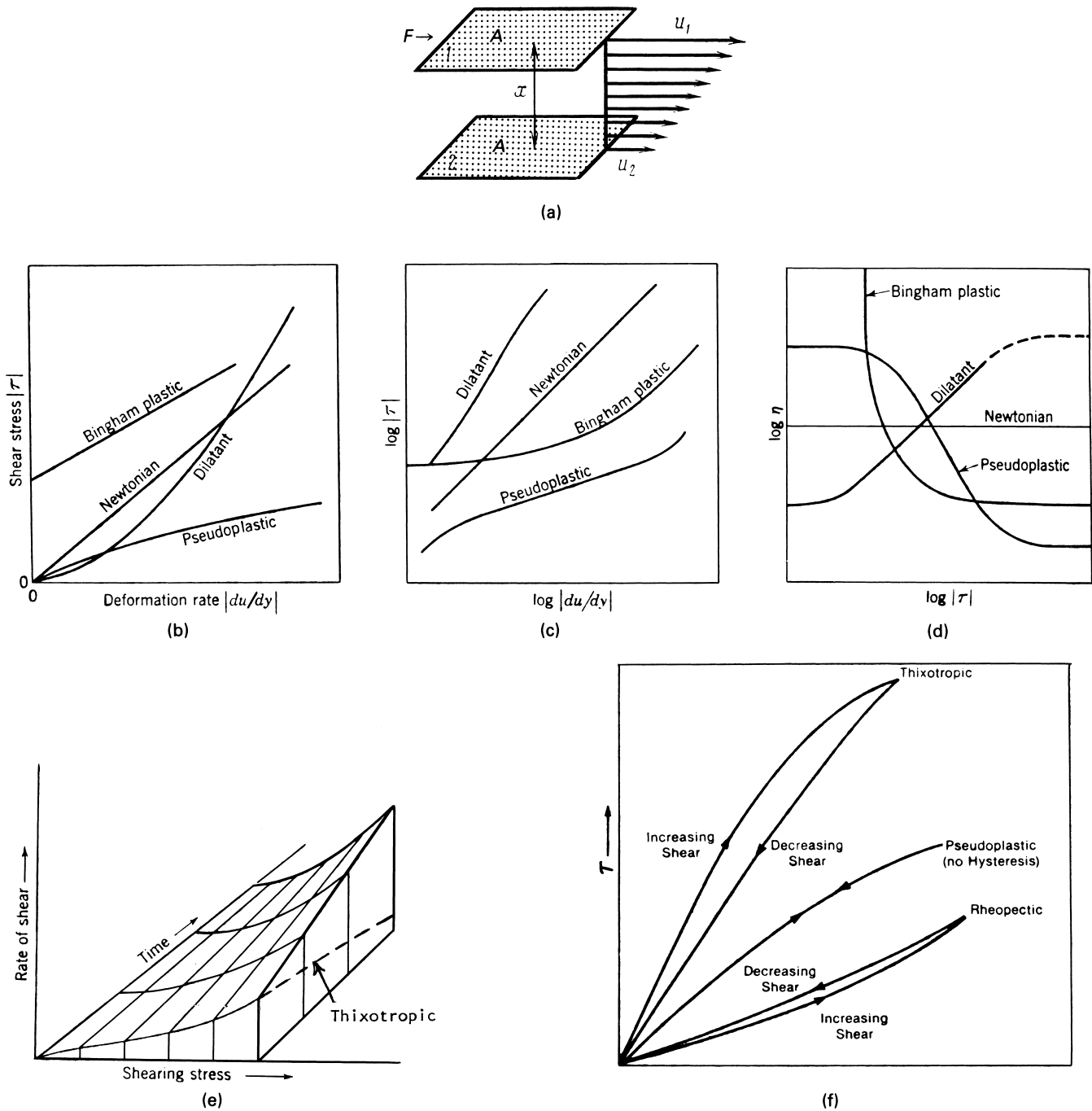
Figure 6.2. Relations between shear stress, deformation rate, and viscosity of several classes of fluids. (a) Distribution of velocities of a fluid between two layers of areas A which are moving relatively to each other at a distance x under influence of a force F. In the simplest case, $F/A = \mu(du/dx)$ with μ constant. (b) Linear plot of shear stress against deformation. (c) Logarithmic plot of shear stress against deformation rate. (d) Viscosity as a function of shear stress. (e) Time-dependent viscosity behavior of a rheopectic fluid (thixotropic behavior is shown by the dashed line). (f) Hysteresis loops of time-dependent fluids (arrows show the chronology of imposed shear stress).

The constants, μ_0, a, b, and c and the structural parameter λ are obtained from rheological measurements in a straightforward manner.

7. *Viscoelastic fluids* have the ability of partially recovering their original states after stress is removed. Essentially all molten polymers are viscoelastic as are solutions of long chain molecules such as polyethylene oxide, polyacrylamides, sodium carboxymethylcellulose, and others. More homely examples are egg whites, dough, jello, and puddings, as well as bitumen and napalm. This property enables eggwhites to entrap air, molten polymers to form threads, and such fluids to climb up rotating shafts whereas purely viscous materials are depressed by the centrifugal force.
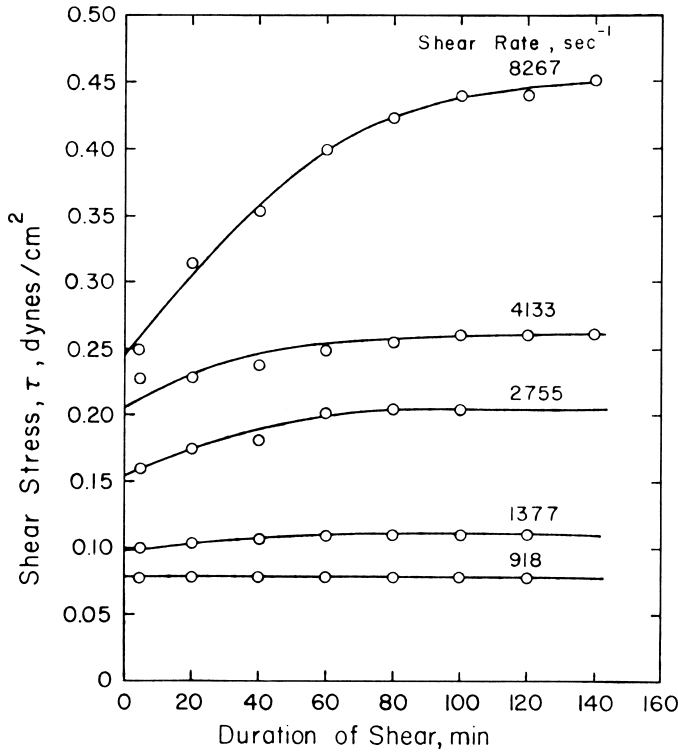
Figure 6.3. Time-dependent rheological behavior of a rheopectic fluid, a 2000 molecular weight polyester. [*After Steg and Katz, J. Appl. Polym. Sci.* **9,** *3177 (1965)*].

Two concepts of deformability that normally are applied only to solids, but appear to have examples of gradation between solids and liquids, are those of shear modulus E, which is

$$E = \text{shear stress/deformation}, \tag{6.43}$$

and relaxation time θ^*, which is defined in the relation between the residual stress and the time after release of an imposed shear stress, namely,

$$\tau = \tau_0 \exp(-\theta/\theta^*). \tag{6.44}$$

A range of values of the shear modulus (in kgf/cm^2) is

Gelatine	
0.5% solution	4×10^{-10}
10% solution (jelly)	5×10^{-2}
Raw rubber	1.7×10^2
Lead	4.8×10^4
Wood (oak)	8×10^4
Steel	8×10^5

and that of relaxation time (sec) is

Water	3×10^{-6}
Castor oil	2×10^{-3}
Copal varnish	2×10
Colophony (at 55°C)	5×10
Gelatine, 0.5% solution	8×10^2
Colophony (at 12°C)	4×10^6
Ideal solids	∞
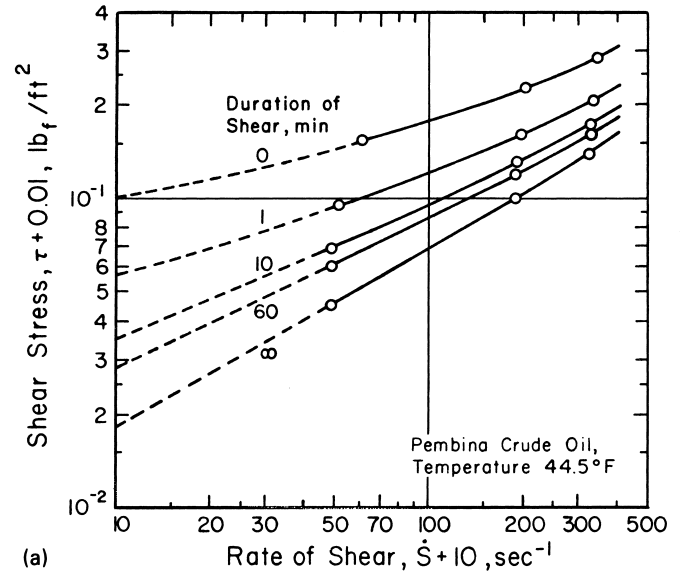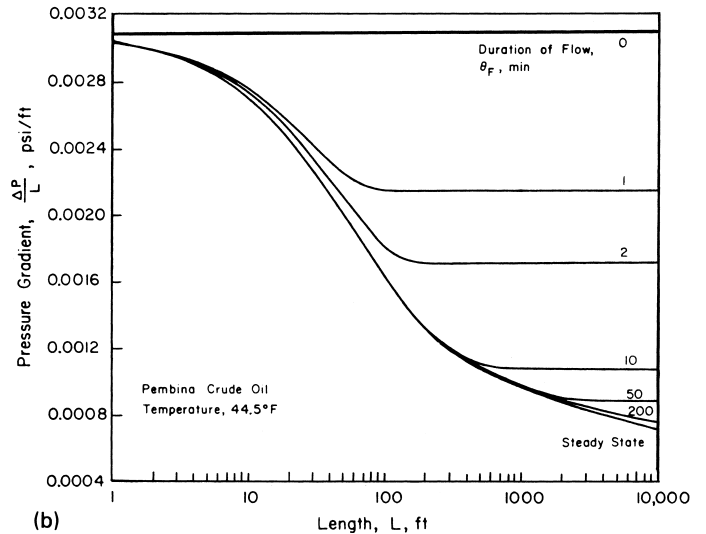
Figure 6.4. Shear and pipeline flow data of a thixotropic Pembina crude oil at 44.5°F. (a) Rheograms relating shear stress and rate of shear at several constant durations of shear. (*Ritter and Govier, Can. J. Chem. Eng.* **48,** *505 (1970)*]. (b) Decay of pressure gradient of the fluid flowing from a condition of rest at 15,000 barrels/day in a 12 in. line. [*Ritter and Batycky, SPE Journal* **7,** *369 (1967)*].

Examples thus appear to exist of gradations between the properties of normally recognized true liquids (water) and true solids.

Elastic properties usually have a negligible effect on resistance to flow in straight pipes, but examples have been noted that the resistances of fittings may be as much as 10 times as great for viscoelastic liquids as for Newtonian ones.

PIPELINE DESIGN

The sizing of pipelines for non-Newtonian liquids may be based on scaleup of tests made under the conditions at which the proposed line is to operate, without prior determination and correlation of rheological properties. A body of theory and some correlations are available for design with four mathematical models:

$$\tau_w = K\dot{\gamma}^n, \qquad \text{powerlaw}, \tag{6.45}$$

$$\tau_w = \tau_y + \mu_B\dot{\gamma}, \qquad \text{Bingham plastic}, \tag{6.46}$$

$$\tau_w = \tau_y + K\dot{\gamma}^n, \qquad \begin{array}{l}\text{Generalized Bingham or}\\ \text{yield-power law},\end{array} \tag{6.47}$$

$$\tau_w = K'(8\bar{V}/D)^n \quad \begin{array}{l}\text{Generalized power law}\\ \text{(Metzner--Reed)}(\textit{AIChE J.}\mathbf{1},\ 434,\ 1955).\end{array} \tag{6.48}$$

In the last model, the parameters may be somewhat dependent on the shear stress and deformation rate, and should be determined at magnitudes of those quantities near those to be applied in the plant.

The shear stress τ_w at the wall is independent of the model and is derived from pressure drop measurements as

$$\tau_w = D\Delta P/4L. \tag{6.49}$$

Friction Factor. In rheological literature the friction factor is defined as

$$f = \frac{D\Delta P}{4L\rho V^2/2g_c} \tag{6.50}$$

$$= \frac{\tau_w}{\rho V^2/2g_c}. \tag{6.51}$$

This value is one-fourth of the friction factor used in Section 6.3. For the sake of consistency with the literature, the definition of Eq. (6.50) will be used with non-Newtonian fluids in the present section.

Table 6.2 lists theoretical equations for friction factors in laminar flows. In terms of the generalized power law, Eq. (6.48),

$$f = \frac{\tau_w}{\rho V^2/2g_c} = \frac{K'(8V/D)^{n'}}{\rho V^2/2g_c}$$

$$= \frac{16}{D^{n'}V^{2-n'}\rho/g_c K'8^{n'-1}}. \tag{6.52}$$

By analogy with the Newtonian relation, $f = 16/\text{Re}$, the denominator of Eq. (6.52) is designated as a modified Reynolds number,

$$\text{Re}_{\text{MR}} = D^{n'}V^{2-n'}\rho/g_c K'8^{n'-1}. \tag{6.53}$$

The subscript MR designates Metzner–Reed, who introduced this form.

Scale Up. The design of pipelines and other equipment for handling non-Newtonian fluids may be based on model equations with parameters obtained on the basis of measurements with viscometers or with pipelines of substantial diameter. The shapes of plots of τ_w against $\dot{\gamma}$ or $8V/D$ may reveal the appropriate model. Examples 6.9 and 6.10 are such analyses.

In critical cases of substantial economic importance, it may be advisable to perform flow tests—Q against ΔP—in lines of moderate size and to scale up the results to plant size, without necessarily trying to fit one of the accepted models. Among the effects that may not be accounted for by such models are time dependence, pipe roughness, pipe fitting resistance, wall slippage, and viscoelastic behavior. Although some effort has been devoted to them, none of these particular effects has been well correlated. Viscoelasticity has been found to have little effect on friction in straight lines but does have a substantial effect on the resistance of pipe fittings. Pipe roughness often is accounted for by assuming that the relative effects of different roughness ratios ε/D are represented by the Colebrook equation (Eq. 6.20) for Newtonian fluids. Wall slippage due to trace amounts of some polymers in solution is an active field of research (Hoyt, 1972) and is not well predictable.

The scant literature on pipeline scaleup is reviewed by Heywood (1980). Some investigators have assumed a relation of the form

$$\tau_w = D\Delta P/4L = kV^a/D^b$$

and determined the three constants K, a, and b from measurements on several diameters of pipe. The exponent a on the velocity appears to be independent of the diameter if the roughness ratio

---

EXAMPLE 6.9
Analysis of Data Obtained in a Capillary Tube Viscometer
Data were obtained on a paper pulp with specific gravity 1.3, and are given as the first four columns of the table. Shear stress τ_w and deformation rate $\dot{\gamma}$ are derived by the equations applying to this kind of viscometer (Skelland, 1967, p. 31; Van Wazer et al., 1963, p. 197):

$$\tau_w = D\Delta P/4L,$$

$$\dot{\gamma} = \frac{3n'+1}{4n'}\left(\frac{8V}{D}\right)$$

$$n' = \frac{d\ln(\tau_w)}{d\ln(8V/D)}$$

The plot of log τ_w against log $(8V/D)$ shows some scatter but is approximated by a straight line with equation

$$\tau_w = 1.329(8V/D)^{0.51}.$$

Since

$$\dot{\gamma} = (2.53/2.08)(8V/D),$$

the relation between shear stress and deformation is given by the equation

$$\tau_w = 1.203\dot{\gamma}^{0.51}$$

D (cm)	L (cm)	$\dot{m}$ (g/sec)	P (Pa)	$8V/D$ (1/sec)	τ_w (Pa)
0.15	14	0.20	3200	464	8.57
0.15	14	0.02	1200	46.4	3.21
0.30	28	0.46	1950	133.5	5.22
0.30	28	0.10	860	29.0	2.30
0.40	28	1.20	1410	146.9	5.04
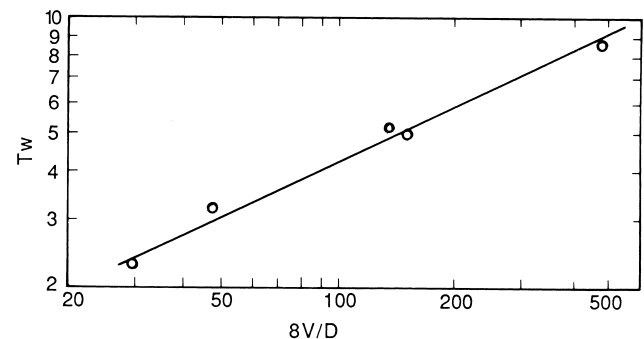
EXAMPLE 6.10
Parameters of the Bingham Model from Measurements of Pressure Drops in a Line

Data of pressure drop in the flow of a 60% limestone slurry of density 1.607 g/ml were taken by Thomas [*Ind. Eng. Chem.* **55,** 18–29 (1963)]. They were converted into data of wall shear stress $\tau_w = D\Delta P/4L$ against the shear rate $8V/D$ and are plotted on the figure for three line sizes.

The Buckingham equation for Bingham flow in the laminar region is

$$\frac{8V}{D} = \frac{\tau_w}{\mu_B}\left[1 - \frac{4}{3}\left(\frac{\tau_0}{\tau_w}\right) + \frac{1}{3}\left(\frac{\tau_0}{\tau_w}\right)^4\right]$$
$$\simeq \frac{1}{\mu_B}\left(\tau_w - \frac{4}{3}\tau_0\right)$$

The second expression is obtained by neglecting the fourth-power term. The Bingham viscosity μ_B is the slope of the plot in the laminar region and is found from the terminal points as

$$\mu_B = (73-50)/(347-0) = 0.067 \text{ dyn sec/cm}^2.$$

From the reduced Buckingham equation,

$$\tau_0 = 0.75\tau_w \text{ (at } 8V/D = 0)$$
$$= 37.5.$$

Accordingly, the Bingham model is represented by

$$\tau_w = 37.5 + 0.067(8V/D), \text{ dyn/cm}^2$$

with time in seconds.

Transitions from laminar to turbulent flow may be identified off the plots:

$$D = 2.06 \text{ cm}, 8V/D = 465, V = 120 \text{ cm/sec}$$
$$\quad 4.04 \qquad\qquad 215, \qquad 109$$
$$\quad 7.75 \text{ (critical not reached).}$$

The transition points also can be estimated from Hanks' correlation [*AIChE J.* **9,** 45, 306 (1963)] which involves these expressions:

$$x_c = (\tau_0/\tau_w)_c,$$
$$\text{He} = D^2\tau_0\rho/\mu_B^2,$$
$$x_c/(1 - x_c)^3 = \text{He}/16,800,$$
$$\text{Re}_{Bc} = (1 - \frac{4}{3}x_c + \frac{1}{3}x_c^4)\text{He}/8x_c.$$

The critical linear velocity finally is evaluated from the critical Reynolds number of the last equation with the following results;

D (cm)	10^{-4} He	x_c	Re$_{BC}$	V_c
2.06	5.7	0.479	5635	114(120)
4.04	22.0	0.635	8945	93(109)
7.75	81.0	0.750	14,272	77

The numbers in parentheses correspond to the break points on the figure and agree roughly with the calculated values.

The solution of this problem is based on that of Wasp et al. (1977).
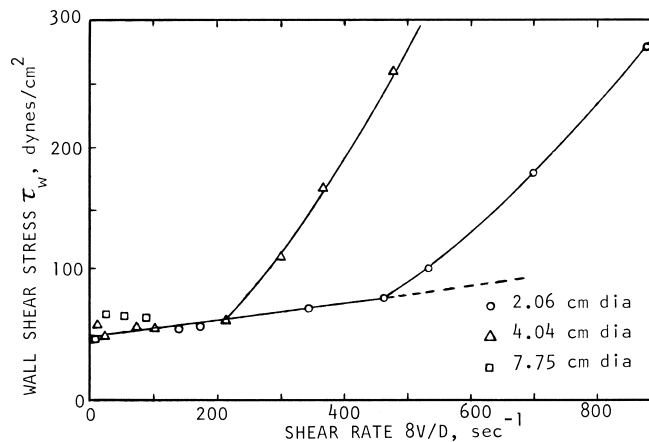
ε/D is held constant. The exponent b on the diameter has been found to range from 0.2 to 0.25. How much better this kind of analysis is than assuming that $a = b$, as in Eq. (6.48), has not been established. If it can be assumed that the effect of differences in ε/D is small for the data of Examples 6.9 and 6.10, the measurements should plot as separate lines for each diameter, but such a distinction is not obvious on those plots in the laminar region, although it definitely is in the turbulent region of the limestone slurry data.

Observations of the performance of existing large lines, as in the case of Figure 6.4, clearly yields information of value in analyzing the effects of some changes in operating conditions or for the design of new lines for the same system.

Laminar Flow. Theoretically derived equations for volumetric flow rate and friction factor are included for several models in Table 6.7. Each model employs a specially defined Reynolds number, and the Bingham models also involve the Hedstrom number,

$$\text{He} = \tau_0\rho D^2/\mu_B^2. \tag{6.54}$$

These dimensionless groups also appear in empirical correlations of the turbulent flow region. Although even in the approximate Eq. (9) of Table 6.6, group He appears to affect the friction factor, empirical correlations such as Figure 6.5(b) and the data analysis of

TABLE 6.6 Laminar Flow: Volumetric Flow Rate, Friction Factor, Reynolds Number, and Hedstrom Number

Newtonian

$$f = 16/\text{Re}, \quad \text{Re} = DV\rho/\mu \tag{1}$$

Power Law [Eq. (6.45)]

$$Q = \frac{\pi D^3}{32}\left(\frac{4n}{3n+1}\right)\left(\frac{\tau_w}{K}\right)^{1/n} \tag{2}$$

$$f = 16/\text{Re}' \tag{3}$$

$$\text{Re}' = \frac{\rho VD}{K}\left(\frac{4n}{1+3n}\right)^n \cdot \left(\frac{D}{8V}\right)^{n-1} \tag{4}$$

Bingham Plastic [Eq. (6.46)]

$$Q = \frac{\pi D^3 \tau_w}{32\mu_B}\left[1 - \frac{4}{3}\frac{\tau_0}{\tau_w} + \frac{1}{3}\left(\frac{\tau_0}{\tau_w}\right)^4\right] \tag{5}$$

$$\text{Re}_B = DV_\rho/\mu_B \tag{6}$$

$$\text{He} = \tau_0 D^2 \rho/\mu_B^2 \tag{7}$$

$$\frac{1}{\text{Re}_B} = \frac{f}{16} - \frac{\text{He}}{6\text{Re}_B^2} + \frac{\text{He}^4}{3f^3\text{Re}_B^8} \quad (\textit{solve for } f) \tag{8}$$

$$f \simeq \frac{96\text{Re}_B^2}{6\text{Re}_B + \text{He}}[\text{neglecting}(\tau_0/\tau_w)^4\text{in Eq.(5)}] \tag{9}$$

Generalized Bingham (Yield-Power Law) [Eq. (6.47)]

$$Q = \frac{\pi D^3}{32}\frac{4n}{3n+1}\left(\frac{\tau_w}{K}\right)^{1/n}\left(1 - \frac{\tau_\gamma}{\tau_w}\right)$$
$$\times \left\{1\frac{\tau_\gamma/\tau_w}{2n+1}\left[1 + \frac{2n}{n+1}\left(\frac{\tau_\gamma}{\tau_w}\right)\left(1 + n\frac{\tau_\gamma}{\tau_w}\right)\right]\right\} \tag{10}$$

$$f = \frac{16}{\text{Re}'}\left(1 - \frac{2\text{He}}{f\text{Re}'^2}\right)$$
$$\times \left\{1 - \frac{1}{(2n-1)}\frac{2\text{He}}{f\text{Re}'^2}\left[1 + \frac{2n}{(n+1)}\frac{2\text{He}}{f\text{Re}'^2}\left(1 + n\cdot\frac{2\text{He}}{f\text{Re}'^2}\right)\right]\right\} \tag{11}$$

[Re′ by Eq. (4) and He by Eq. (7)]

Example 6.10 indicate that the friction factor is determined by the Reynolds number alone, in every case by an equation of the form, $f = 16/\text{Re}$, but with Re defined differently for each model. Table 6.6 collects several relations for laminar flows of fluids.

Transitional Flow. Reynolds numbers and friction factors at which the flow changes from laminar to turbulent are indicated by the breaks in the plots of Figures 6.4(a) and (b). For Bingham models, data are shown directly on Figure 6.6. For power-law liquids an equation for the critical Reynolds number is due to Mishra and Triparthi [*Trans. IChE* **51**, T141 (1973)],

$$\text{Re}_c' = \frac{1400(2n+1)(5n+3)}{(3n+1)^2}. \tag{6.55}$$

The Bingham data of Figure 6.6 are represented by the equations of Hanks [*AIChE J.* **9**, 306 (1963)],

$$(\text{Re}_B)_c = \frac{\text{HE}}{8x_c}\left(1 - \frac{4}{3}x_c + \frac{1}{3}x_c^4\right), \tag{6.56}$$

$$\frac{x_c}{(1-x_c)^3} = \frac{\text{He}}{16,800}. \tag{6.57}$$

They are employed in Example 6.10.

Turbulent Flow. Correlations have been achieved for all four models, Eqs. (6.45)–(6.48). For power-law flow the correlation of Dodge and Metzner (1959) is shown in Figure 6.5(a) and is represented by the equation

$$\frac{1}{\sqrt{f}} = \frac{4.0}{(n')^{0.75}}\log_{10}\left[\text{Re}_{n'}f^{(1-n'/2)}\right] - \frac{0.40}{(n')^{1.2}}. \tag{6.58}$$

These authors and others have demonstrated that these results can represent liquids with a variety of behavior over limited ranges by evaluating K' and n' in the range of shear stress $\tau_w = D\Delta P/4L$ that will prevail in the required situation.

Bingham flow is represented by Figure 6.5(b) in terms of Reynolds and Hedstrom numbers.

Theoretical relations for generalized Bingham flow [Eq. (6.47)] have been devised by Torrance [*S. Afr. Mech. Eng.* **13**, 89 (1963)]. They are
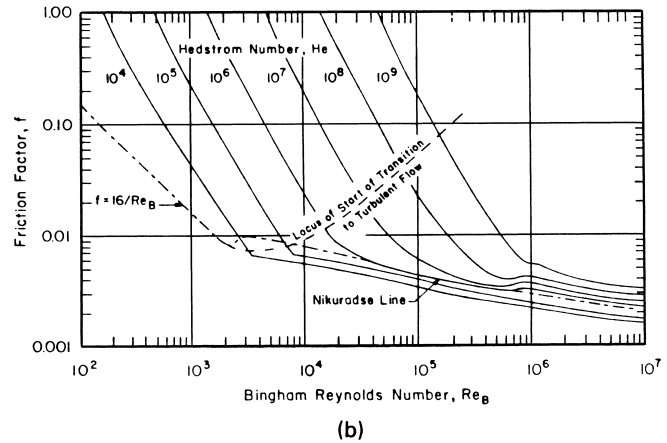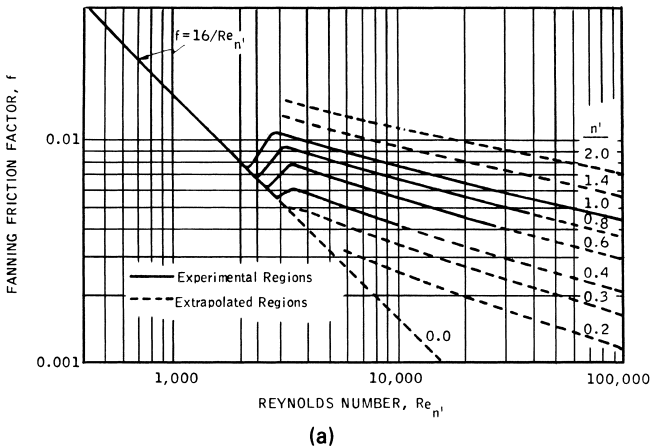
Figure 6.5. Friction factors in laminar and turbulent flows of power-law and Bingham liquids. (a) For pseudoplastic liquids represented by $\tau_w = K'(8V/D)^{n'}$, with K' and n' constant or dependent on τ_w: $1/\sqrt{f} = [4.0/(n')^{0.75}]\log_{10}[\text{Re}_{n'}f^{(1-n'2)}] - 0.40/(n')^{1.2}$. [*Dodge and Metzner*, AIChE J. **5**, *189 (1959)*]. (b) For Bingham plastics, $\text{Re}_B = DV\rho/\mu_B$, $\text{He} = \tau_0 D^2 \rho/\mu_B^2$. [*Hanks and Dadia*, AIChE J. **17**, *554 (1971)*].
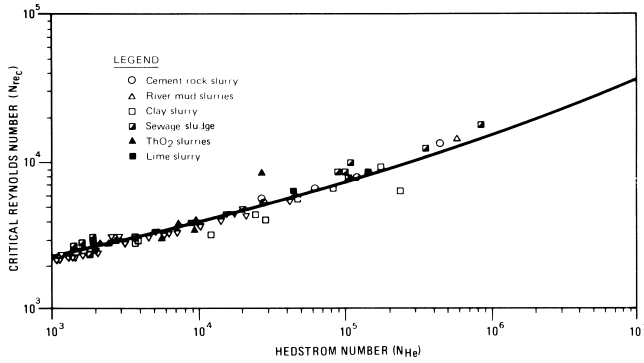
Figure 6.6. Critical Reynolds number for transition from laminar to turbulent flow of Bingham fluids. The data also are represented by Eqs. (6.56) and (6.57): ($\bigcirc$) cement rock slurry; ($\triangle$) river mud slurries; ($\square$) clay slurry; ($\blacksquare$) sewage sludge; ($\blacktriangle$) ThO_2 slurries; ($\blacksquare$) lime slurry. [*Hanks and Pratt*, SPE Journal, *342–346* (*Dec. 1967*)].

$$\frac{1}{\sqrt{f}} = \left(\frac{2.69}{n} - 2.95\right) + \frac{1.97}{n}\ln(1 - x)$$
$$+ \frac{1.97}{n}\ln(\mathrm{Re}'_T f^{1-n/2}) + \frac{0.68}{n}(5n - 8) \tag{6.59}$$

with the Reynolds number

$$\mathrm{Re}_T = D^n V^{2-n}\rho/8^{n-1}K \tag{6.60}$$

and where

$$x = \tau_0/\tau_w. \tag{6.61}$$

In some ranges of operation, materials may be represented approximately equally well by several models, as in Example 6.11 where the power-law and Bingham models are applied.

6.7. GASES

The differential energy balances of Eqs. (6.10) and (6.15) with the friction term of Eq. (6.18) can be integrated for compressible fluid flow under certain restrictions. Three cases of particular importance are of isentropic or isothermal or adiabatic flows. Equations will be developed for them for ideal gases, and the procedure for nonideal gases also will be indicated.

ISENTROPIC FLOW

In short lines, nozzles, and orifices, friction and heat transfer may be neglected, which makes the flow essentially isentropic. Work transfer also is negligible in such equipment. The resulting theory is a basis of design of nozzles that will generate high velocity gases for power production with turbines. With the assumptions indicated, Eq. (6.10) becomes simply

$$dH + (1/g_c)u\,du = 0, \tag{6.62}$$

which integrates into

$$H_2 - H_1 + \frac{1}{2g_c}(u_2^2 - u_1^2) \approx 0. \tag{6.63}$$

One of these velocities may be eliminated with the mass balance,

$$\dot{m} = u_2 A_2/V_2 = u_1 A_1/V_1 \tag{6.64}$$

so that

$$u_2^2 - u_1^2 = (\dot{m}V_2/A_2)^2[1 - (A_2 V_1/A_1 V_2)^2]. \tag{6.65}$$

For ideal gases substitutions may be made from

$$H_2 - H_1 = C_p(T_2 - T_1) \tag{6.66}$$

and

$$T_2/T_1 = (P_2/P_1)^{(k-1)/k} = (V_1/V_2)^k. \tag{6.67}$$

After these substitutions are made into Eq. (6.63), the results may be solved for the mass rate of flow as

$$\dot{m}/A_2 = \frac{\left(\frac{2g_c P_1}{V_1}\right)^{1/2}\left\{\frac{k}{k-1}\left[\left(\frac{P_2}{P_1}\right)^{2/k} - \left(\frac{P_2}{P_1}\right)^{(k+1)/k}\right]\right\}^{1/2}}{\left[1 - \left(\frac{A_2}{A_1}\right)^2\left(\frac{P_2}{P_1}\right)^{2/k}\right]^{1/2}}. \tag{6.68}$$

EXAMPLE 6.11
Pressure Drop in Power-Law and Bingham Flow
A limestone slurry of density 1.693 g/mL is pumped through a 4-in. (152 mm) line at the rate of 4 ft/sec (1.22 m/sec). The pressure drop (psi/mile) will be calculated. The slurry behavior is represented by

a. The power-law with $n = 0.165$ and $K = 34.3$ dyn $\sec^{0.165}/cm^2$ (3.43 *Pa* $sec^{0.165}$).
b. Bingham model with $\tau_0 = 53$ dyn/cm^2(5.3 Pa) and $\mu_B = 22$ cP (0.022 Pa sec).

Power law:

$$\mathrm{Re}' = D^n V^{2-n}\rho/8^{n-1}K$$
$$= (0.152)^{0.165}(1.22)^{1.835}(1693)(8)^{0.835}/3.43$$
$$= 2957,$$
$$f = 0.0058 \text{ [Fig.6.6(a)]}$$

$$\frac{\Delta P}{L} = \frac{4f\rho V^2}{2g_c D} = \frac{4(0.0058)(1693)(1.22)^2}{2(0.152)}$$
$$= 192.3\,N/(m^2)(m)\ [g_c = \mathrm{kgm/sec}^2/N],$$
$$\rightarrow 192.3(14.7/101,250)1610 = 45.0\,\mathrm{psi/mile}.$$

Bingham:

$$\mathrm{Re}_B = \frac{DV\rho}{\mu_B} = \frac{0.152(1.22)(1693)}{0.022} = 14,270,$$
$$\mathrm{He} = \tau_0 D^2\rho/\mu_B^2 = 5.3(0.152)^2(1693)/(0.022)^2$$
$$= 428,000,$$

critical $\mathrm{Re}_B = 12,000$ (Fig.6.5),

$$f = 0.007 \text{ [Fig.6.6(b)]},$$
$$\frac{\Delta P}{L} = \frac{0.007}{0.0058}45.0 = 54.3\,\mathrm{psi/mile}.$$

At specified mass flow rate and inlet conditions P_1 and V_1, Eq. (6.68) predicts a relation between the area ratio A_2/A_1 and the pressure ratio P_2/P_1 when isentropic flow prevails. It turns out that, as the pressure falls, the cross section at first narrows, reaches a minimum at which the velocity becomes sonic; then the cross section increases and the velocity becomes supersonic. In a duct of constant cross section, the velocity remains sonic at and below a critical pressure ratio given by

$$\frac{P_s}{P_1} = \left(\frac{2}{k+1}\right)^{k/(k+1)}. \tag{6.69}$$

The sonic velocity is given by

$$u_s = \sqrt{g_c(\partial P/\partial \rho)_s} \rightarrow \sqrt{g_c k R T/M_w}, \tag{6.70}$$

where the last result applies to ideal gases and M_w is the molecular weight.

ISOTHERMAL FLOW IN UNIFORM DUCTS

When elevation head and work transfer are neglected, the mechanical energy balance equation (6.13) with the friction term of Eq. (6.18) become

$$V\,dP + (1/g_c)u\,du + \frac{fu^2}{2g_c D}dL = 0. \tag{6.71}$$

Make the substitutions

$$u = G/\rho = GV \tag{6.72}$$

and the ideal gas relation

$$V = P_1 V_1/P \text{ and } dV/V = -dP/P \tag{6.73}$$

so that Eq. (6.71) becomes

$$\frac{P\,dP}{P_1 V_1} - \frac{G^2}{g_c}\ln\left(\frac{P_1}{P_2}\right) + \frac{fG^2}{2g_c D}\,dL = 0. \tag{6.74}$$

This is integrated term-by-term between the inlet and outlet conditions,

$$\frac{P_2^2 - P_1^2}{2P_1 V_1} + \frac{G^2}{g_c}\ln\left(\frac{P_1}{P_2}\right) + \frac{fG^2 L}{2g_c D} = 0 \tag{6.75}$$

and may be rearranged into

$$P_2^2 = P_1^2 - \frac{2P_1 V_1 G^2}{g_c}\left[\frac{fL}{2D} + \ln\left(\frac{P_1}{P_2}\right)\right]. \tag{6.76}$$

In terms of a density, ρ_m, at the average pressure in the line,

$$P_2 = P_1 - \frac{fG^2 L}{2g_c D\rho_m}. \tag{6.77}$$

The average density may be found with the aid of an approximate evaluation of P_2 based on the inlet density; a second trial is never justified. Eqs. (6.76) and (6.77) and the approximation of Eq. (6.76) obtained by neglecting the logarithmic term are compared in Example 6.12. The restriction to ideal gases is removed in Section 6.7.

ADIABATIC FLOW

The starting point for development of the integrated adiabatic flow energy balance is Eq. (6.71), and again ideal gas behavior will be assumed. The equation of condition of a static adiabatic process, $PV^k = \text{const}$, is not applicable to the flow process; the appropriate one is obtained as follows. Begin with

$$dH = -d\left(\frac{u^2}{2g_c}\right) = \frac{G^2 V dV}{g_c} \tag{6.78}$$

$$= C_p\,dT = \frac{Rk}{k-1}dT = \frac{k}{k-1}d(PV), \tag{6.79}$$

from which

$$d(PV) = \left(\frac{k-1}{k}\right)\frac{G^2}{g_c}V\,dV, \tag{6.80}$$

and the integral is

$$PV = P_1 V_1 - \left(\frac{k-1}{k}\right)\frac{G^2}{2g_c}(V^2 - V_1^2). \tag{6.81}$$

Also

$$V\,dP = d(PV) - (PV)\frac{dV}{V} \tag{6.82}$$

Substitutions into Eq. (6.71) result in

$$d(PV) - PV\frac{dV}{V} + \frac{G^2}{g_c}V\,dV + \frac{fG^2}{2g_c D}\,dL = 0. \tag{6.83}$$

Further substitutions from Eqs. (6.80) and (6.81) and multiplying through by $2kg_c/G^2 V^2$ result in

$$2\frac{dV}{V} - \left[\frac{2kg_c P_1 V_1}{G^2} + (k-1)V_1^2\right]\frac{dV}{V^3} + (k-1)\frac{dV}{V} + \frac{kf}{D}dL = 0. \tag{6.84}$$

Integrating from V_1 to V_2 and $L = 0$ to L gives

$$(k+1)\ln\frac{V_2}{V_1} + \frac{1}{2}\left[\frac{2kg_c P_1 V_1}{G^2} + (k-1)V_1^2\right]\left(\frac{1}{V_2^2} - \frac{1}{V_1^2}\right) + \frac{kfL}{D} = 0 \tag{6.85}$$

or

$$\frac{fL}{D} = \frac{1}{2k}\left[\frac{2kg_c P_1 V_1}{G^2 V_1^2} + (k-1)\right]\left[1 - \left(\frac{V_1}{V_2}\right)^2\right] + \frac{k+1}{2k}\ln\left(\frac{V_1}{V_2}\right)^2. \tag{6.86}$$

In terms of the inlet Mach number,

$$M_1 = u_1/\sqrt{g_c k R T/M_w} = GV_1/\sqrt{g_c k R T/M_w}, \tag{6.87}$$

the result becomes

$$\frac{fL}{D} = \frac{1}{2k}\left(k - 1 + \frac{2}{M_1^2}\right)\left[1 - \left(\frac{V_1}{V_2}\right)^2\right] + \frac{k+1}{2k}\ln\left(\frac{V_1}{V_2}\right)^2. \tag{6.88}$$

EXAMPLE 6.12
Adiabatic and Isothermal Flow of a Gas in a Pipeline
Steam at the rate of 7000 kg/hr with an inlet pressure of 23.2 barabs and temperature of 220°C flows in a line that is 77.7 mm dia and 305 m long. Viscosity is $28.5(10^{-6})$ Nsec/m^2 and specific heat ratio is $k = 1.31$. For the pipe, $\varepsilon/D = 0.0006$. The pressure drop will be found in (a) isothermal flow; (b) adiabatic flow. Also, (c) the line diameter for sonic flow will be found.

$$V_1 = 0.0862 \, \text{m}^3/\text{kg},$$

$$G = 7000/(3600)(\pi/4)(0.0777)^2 = 410.07 \, \text{kg/m}^2\text{sec},$$

$$\text{Re}_1 = \frac{DG}{\mu} = \frac{0.0777(410.07)}{28.5(10^{-6})} = 1.12(10^6),$$

$$f = 1.6364/[\ln(0.135)(0.0006) + 6.5/1.2(10^6)]^2 = 0.0187.$$

Inlet sonic velocity:

$$u_{s1} = \sqrt{g_c k R T_1/M_w} = \sqrt{1(1.31)(8314)493.2/18.02} = 546 \, \text{m/sec}$$

$$M_1 = u_1/u_{s1} = GV_1/u_{s1} = 410.07(0.0862)/546 = 0.0647.$$

As a preliminary calculation, the pressure drop will be found by neglecting any changes in density:

$$\Delta P = \frac{fG^2 L}{2g_c D\rho} = \frac{0.0187(410.07)^2(305)}{2(1)(0.0777)(1/0.0862)} = 5.32(10^5)\text{N/m}^2,$$

$$\therefore P_2 = 23.2 - 5.32 = 17.88 \, \text{bar}.$$

(a) Isothermal flow. Use Eq. (6.76):

$$\frac{2P_1 V_1 G^2}{g_c} = 2(23.2)(10^5)(0.0862)(410.07)^2 = 6.726(10^{10}),$$

$$P_2 = \left[P_1^2 - \frac{2P_1 V_1^2 G}{g_c}\left(\frac{fL}{2D} + \ln\frac{P_1}{P_2}\right) \right]^{1/2}$$

$$= 10^5 \sqrt{538.24 - 6.726\left(0.0187(305)/2(0.0777) + \ln\frac{23.2(10^5)}{P_2}\right)}$$

$$= 17.13(10^5)\text{N/m}^2,$$

and

$$\Delta P = 23.2 - 17.13 = 5.07 \, \text{bar}.$$

When the logarithmic term is neglected,

$$P_2 = 17.07(10^5)\text{N/m}^2.$$

(b) Adiabatic flow. Use Eq. (6.88):

$$\frac{fL}{D} = \frac{1}{2k}\left(k - 1 + \frac{2}{M_1^2}\right)\left[1 - \left(\frac{V_1}{V_2}\right)^2\right] + \frac{k+1}{2k}\ln\left(\frac{V_1}{V_2}\right)^2, \quad (1)$$

$$\frac{0.0187(305)}{0.0777} = \frac{1}{2.62}\left(0.31 + \frac{2}{0.0647^2}\right)$$

$$\times \left[1 - \left(\frac{V_1}{V_2}\right)^2\right] + \frac{2.31}{2.62}\ln\left(\frac{V_1}{V_2}\right)^2,$$

$$73.4 = 182.47\left[1 - \left(\frac{V_1}{V_2}\right)^2\right] + 0.8817\ln\left(\frac{V_1}{V_2}\right)^2,$$

$$\therefore \frac{V_1}{V_2} = 0.7715.$$

Equation (6.89) for the pressure:

$$\frac{P_2 V_2}{P_1 V_1} = \frac{T_2}{T_1} = \left[1 + \frac{(k-1)}{2k}M_1^2\right]\left[1 - \left(\frac{V_2}{V_1}\right)^2\right]$$

$$= 1 + \frac{0.31(0.0647)^2}{2.62}[1 - (1.2962)^2]$$

$$= 0.9997,$$

$$P_2 = 0.9997 P_1\left(\frac{V_1}{V_2}\right) = 0.9997(23.2)(10^5)(0.7715)$$

$$= 17.89(10^5)\text{N/m}^2,$$

$$\Delta P = 23.2 - 17.89 = 5.31 \, \text{bar}.$$

(c) Line diameter for sonic flow. The critical pressure ratio is

$$\frac{P_2}{P_1} = \left(\frac{2}{k+1}\right)^{k/(k-1)} = 0.5439, \text{ with } k = 1.31,$$

$$G = \frac{7000/3600}{(\pi/4)D^2} = \frac{2.4757}{D^2}, \quad (2)$$

$$M_1 = \frac{GV_1}{U_{si}} = \frac{2.4757(0.0862)}{546D^2} = \frac{3.909(10^{-4})}{D^2}.$$

Equation (6.89) becomes

$$0.5439(V_2/V_1) = 1 + 0.1183 M_1^2[1 - (V_2/V_1)^2], \quad (3)$$

$$fL/D = 0.0187(305)/D = 5.7035/D \quad (4)$$
$$= \text{rhs of Eq. (6.88)}.$$

Procedure

1. Assume D.
2. Find M_1 [Eq. (2)].
3. Find V_2/V_1 from Eq. (6.89) [Eq. (3)].
4. Find rhs of Eq. (6.88) [Eq. (1)].
5. Find $D = 5.7035/[\text{rhs of Eq. (6.88)}]$ [Eq. (4)].
6. Continue until steps 1 and 5 agree.

Some trials are:

D	M₁	Eq. (6.89) V₁/V₂	Eq. (6.88) rhs	D
0.06	0.1086	0.5457	44.482	0.1282
0.07	0.0798	0.5449	83.344	0.06843
0.0697	0.08046	0.5449	81.908	0.06963

$$\therefore D = 0.0697 \, \text{m}.$$

When everything else is specified, Eqs. (6.86) or (6.88) may be solved for the exit specific volume V_2. Then P_2 may be found from Eq. (6.81) or in the rearrangement

$$\frac{P_2 V_2}{P_1 V_1} = \frac{T_2}{T_1} = 1 + \left(\frac{k-1}{2k} M_1^2\right)\left[1 - \left(\frac{V_2}{V_1}\right)^2\right], \qquad (6.89)$$

from which the outlet temperature likewise may be found.

Although the key equations are transcendental, they are readily solvable with hand calculators, particularly those with root-solving provisions. Several charts to ease the solutions before the age of calculators have been devised: M.B. Powley, *Can. J. Chem. Eng.*, 241–245 (Dec. 1958); C.E. Lapple, reproduced in *Perry's Chemical Engineers' Handbook*, McGraw-Hill, New York, 1973, p. 5.27; O. Levenspiel, reproduced in *Perry's Chemical Engineers' Handbook*, 7th ed., p. 6-24; Hougen, Watson, and Ragatz, *Thermodynamics*, Wiley, New York, 1959, pp. 710–711.

In all compressible fluid pressure drop calculations it is usually justifiable to evaluate the friction factor at the inlet conditions and to assume it constant. The variation because of the effect of temperature change on the viscosity and hence on the Reynolds number, at the usual high Reynolds numbers, is rarely appreciable.

NONIDEAL GASES

Without the assumption of gas ideality, Eq. (6.71) is

$$\frac{dP}{V} + \frac{G^2}{g_c}\frac{dV}{V} + \frac{fG^2}{2g_c D}dL = 0. \qquad (6.90)$$

In the isothermal case, any appropriate PVT equation of state may be used to eliminate either P or V from this equation and thus permit integration. Since most of the useful equations of state are pressure-explicit, it is simpler to eliminate P. Take the example of one of the simplest of the non-ideal equations, that of van der Waals

$$P = \frac{RT}{V - b} - \frac{a}{V^2}, \qquad (6.91)$$

of which the differential is

$$dP = \left(-\frac{RT}{(V-b)^2} + \frac{2a}{V^3}\right)dV. \qquad (6.92)$$

Substituting into Eq. (6.90),

$$\left(-\frac{RT}{(V-b)^2} + \frac{2a}{V^3} + \frac{G^2}{g_c}\right)\frac{dV}{V} + \frac{fG^2}{2g_c D}dL = 0. \qquad (6.93)$$

Although integration is possible in closed form, it may be more convenient to perform the integration numerically. With more accurate and necessarily more complicated equations of state, numerical integration will be mandatory. Example 6.13 employs the van der Waals equation of steam, although this is not a particularly suitable one; the results show a substantial difference between the ideal and the nonideal pressure drops. At the inlet condition, the compressibility factor of steam is $z = PV/RT = 0.88$, a substantial deviation from ideality.

6.8. LIQUID–GAS FLOW IN PIPELINES

The hydrodynamics of liquid-gas flow in pipelines is complex and the literature is voluminous, as indicated by the 83-page coverage by N.P. Cheremisinoff and R. Gupta, *Handbook of Fluids in Motion*, Butterworth, pp. 369–452, Chapters 14–16, 1983. The most useful predictive methods have been summarized and presented in *Perry's Chemical Engineers' Handbook*, 7th ed., pp. 6-26–6-29. The coverage here parallels that in *Perry's*. In flow of mixtures of the two phases in pipelines, the liquid tends to wet the wall and the gas to concentrate in the center of the channel, but various degrees of dispersion of each phase in the other may exist, depending on operating conditions, particularly the individual flow rates. The main patterns of flow that have been recognized are indicated on Figures 6.7(a) and (b). The ranges of conditions over which individual patterns exist are represented on maps like those of Figures 6.7(c) and (d). through horizontal pipelines. A flow regime map for cocurrent upward liquid-gas flow in vertical pipelines is given in *Perry's Chemical Engineers' Handbook*, 7th ed., p. 6-28, Fig. 6-29. Since the concept of a particular flow pattern is subjective and all the pertinent variables apparently have not yet been correlated, boundaries between regions are fuzzy, as in (d).

It is to be expected that the kind of phase distribution will affect such phenomena as heat transfer and friction in pipelines. For the most part, however, these operations have not been correlated yet with flow patterns, and the majority of calculations of two-phase flow are made without reference to them. A partial exception is annular flow which tends to exist at high gas flow rates and has been studied in some detail from the point of view of friction and heat transfer.

The usual procedure for evaluating two-phase pressure drop is to combine pressure drops of individual phases in some way. To this end, multipliers ϕ_i are defined by

$$(\Delta P/L)_{\text{two-phase}} = \phi_i^2 (\Delta P/L)_i. \qquad (6.94)$$

In the following table, subscript L refers to the liquid phase, G to the gas phase, and $L0$ to the total flow but with properties of the liquid phase; x is the weight fraction of the vapor phase.

Subscript	Re	$\Delta P/L$	ϕ^2
G	DGx/μ_G	$f_G G^2 x^2/2g_c D\rho_G$	$(\Delta P/L)/(\Delta P/L)_G$
L	$DG(1-x)/\mu_L$	$f_L G^2 (1-x)^2/2g_c D\rho_L$	$(\Delta P/L)/(\Delta P/L)_L$
$L0$	DG/μ_L	$f_{L0} G^2/2g_c D\rho_L$	$(\Delta P/L)/(\Delta P/L)_{L0}$

In view of the many other uncertainties of two phase flow correlations, the friction factors are adequately represented by

$$f = \begin{cases} 64/\text{Re}, \ \text{Re} < 2000, \ \text{Poiseuille equation}, & (6.95) \\ 0.32/\text{Re}^{0.25}, \ \text{Re} > 2000, \ \text{Blasius equation}. & (6.96) \end{cases}$$

HOMOGENEOUS MODEL

The simplest way to compute line friction in two-phase flow is to adopt some kinds of mean properties of the mixtures and to employ the single phase friction equation. The main problem is the assignment of a two-phase viscosity. Of the number of definitions that have been proposed, that of McAdams et al. [*Trans.* ASME **64,** 193–200 (1942)] is popular:

EXAMPLE 6.13
Isothermal Flow of a Nonideal Gas

The case of Example 6.12 will be solved with a van der Waals equation of steam. From the *CRC Handbook of Chemistry and Physics* (CRC Press, Boca Raton, FL, 1979),

$$a = 5.464 \, \text{atm}(\text{m}^3/\text{kg mol})^2 = 1703.7 \, \text{Pa}(\text{m}^3/\text{kg})^2,$$

$$b = 0.03049 \, \text{m}^3/\text{kg mol} = 0.001692 \, \text{m}^3/\text{kg},$$

$$RT = 8314(493.2)/18.02 = 2.276(10^5) \, \text{Nm/kg}.$$

Equation (6.93) becomes

$$\int_{0.0862}^{V_2} \left[\frac{-2.276(10^5)}{(V - 0.00169)^2} + \frac{3407.4}{V^3} + (410.07)^2 \right] \frac{dV}{V}$$
$$+ \frac{0.0187(410.07)^2(305)}{2(0.0777)} = 0,$$

$$\phi = \int_{0.0862}^{V_2} \left[\frac{-0.0369}{(V - 0.00169)^2} + \frac{5.52(10^{-4})}{V^3} + 0.0272 \right] \frac{dV}{V} + 1 = 0$$

The integration is performed with Simpson's rule with 20 intervals. Values of V_2 are assumed until one is found that makes $\phi = 0$. Then the pressure is found from the v dW equation:

$$P_2 = \frac{2.276(10^5)}{(V_2 - 0.00169)} - \frac{1703.7}{V_2^2}$$

Two trials and, a linear interpolation are shown. The value $P_2 = 18.44$ bar compares with the ideal gas 17.13.

V_2	ϕ	P_2
0.120	−0.0540	
0.117	+0.0054	
0.1173	0	18.44 bar

$$1/\mu_{\text{two-phase}} = x/\mu_G + (1 - x)/\mu_L. \tag{6.97}$$

The specific volumes are weight fraction additive,

$$V_{\text{two-phase}} = xV_G + (1 - x)V_L \tag{6.98}$$

so that

$$1/\rho_{\text{two-phase}} = x/\rho_G + (1 - x)/\rho_L, \tag{6.99}$$

where x is the weight fraction of the gas. Pressure drops by this method tend to be underestimated, but are more nearly accurate at higher pressures and higher flow rates.

With the Blasius equation (6.96), the friction factor and the pressure gradient become, with this model,

$$f = \frac{0.32}{(DG)^{0.25}} \left(\frac{x}{\mu_g} + \frac{1 - x}{\mu_L} \right)^{0.25}, \tag{6.100}$$

$$\frac{\Delta P}{L} = \frac{fG^2}{2g_c D[x/\rho_G + (1 - x)/\rho_L]}. \tag{6.101}$$

A particularly simple expression is obtained for the multiplier in terms of the Blasius equation:

$$\phi_{L0}^2 = \frac{\Delta P/L}{(\Delta P/L)_{L0}} = \frac{1 - x + x\rho_L/\rho_G}{(1 - x + x\mu_L/\mu_G)^{0.25}}. \tag{6.102}$$

Some values of ϕ_{L0}^2 from this equation for steam are

x	$P = 0.689$ bar	$P = 10.3$ bar
0.01	3.40	1.10
0.10	12.18	1.95
0.50	80.2	4.36

High values of multipliers are not uncommon.

SEPARATED FLOW MODELS

Pressure drop in two-phase flow is found in terms of pressure drops of the individual phases with empirical multipliers. The basic relation is

$$(\Delta P/L)_{\text{two-phase}} = \phi_G^2(\Delta P/L)_G = \phi_L^2(\Delta P/L)_L = \phi_{L0}^2(\Delta P/L)_{L0}. \tag{6.103}$$

The last term is the pressure drop calculated on the assumption that the total mass flow has the properties of the liquid phase.

Some correlations of multipliers are listed in Table 6.7. Lockhart and Martinelli distinguish between the various combinations of turbulent and laminar (viscous) flows of the individual phases; in this work the transition Reynolds number is taken as 1000 instead of the usual 2000 or so because the phases are recognized to disturb each other. Item 1 of Table 6.7 is a guide to the applicability of the Lockhart–Martinelli method, which is the oldest, and two more recent methods. An indication of the attention that has been devoted to experimentation with two phase flow is the fact that Friedel (1979) based his correlation on some 25,000 data points.

Example 6.14 compares the homogeneous and Lockhart–Martinelli models for the flow of a mixture of oil and hydrogen.

OTHER ASPECTS

The pattern of annular flow tends to form at higher gas velocities; the substantial amount of work done on this topic is reviewed by Hewitt (1982). A procedure for stratified flow is given by Cheremisinoff and Davis [*AIChE J.* **25,** 1 (1979)].

Voidage of the holdup in the line is different from that given by the proportions of the incoming volumetric flows of the two phases, but is of course related to it. Lockhart and Martinelli's work indicates that the fractional gas volume is

$$\varepsilon = 1 - 1/\phi_L, \tag{6.104}$$
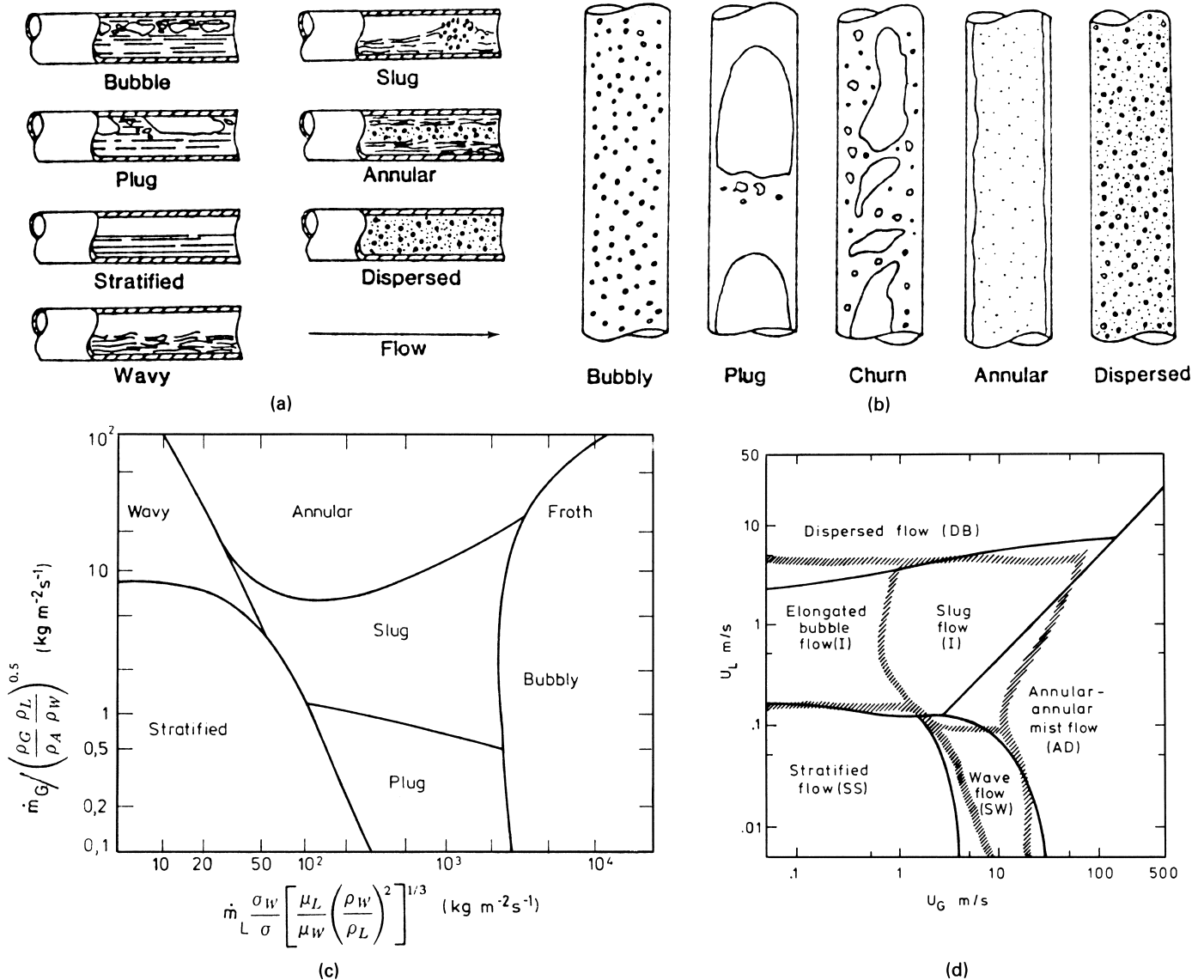
Figure 6.7. Flow patterns and correlations of flow regimes of liquid–gas mixtures in pipelines. (a) Patterns in horizontal liquid–gas flow. (b) Patterns in vertical liquid–gas flow. (c) Correlations of ranges of flow patterns according to Baker [*Oil Gas J.* **53**(*12*), *185* (*1954*)], as replotted by Bell et al. [Chem. Eng. Prog. Symp. Ser. **66**, *159* (*1969*)]; σ is surface tension of the liquid, and σ_w that of water. (d) Flow regimes of water/air at 25°C and 1 atm. [*Taitel and Dukler*, AIChE J. **22**, *47* (*1976*)]; the fuzzy boundaries are due to Mandhane et al. [Int. J. Two-Phase Flow **1**, *537* (*1974*)].

where ϕ_L is defined in Table 6.8. This relation has been found to give high values. A correlation of Premoli et al. [*Termotecnica* **25**, 17–26 (1971); cited by Hewitt, 1982] gives the void fraction in terms of the incoming volumetric flow rates by the equation

$$\varepsilon_G = Q_G/(Q_G + SQ_L), \tag{6.105}$$

where S is given by the series of equations

$$S = 1 + E_1[y/(1 + yE_2) - yE_2]^{1/2},$$
$$E_1 = 1.578 \text{Re}^{-0.19}(\rho_L/\rho_G)^{0.22}, \tag{6.105'}$$

$$E_2 = 0.0273 \text{We Re}^{-0.51}(\rho_L/\rho_G)^{-0.08},$$
$$y = Q_G/Q_L, \quad \text{Re} = DG/\mu_L, \quad \text{We} = DG^2/\sigma\rho_L.$$

Direct application of these equations in Example 6.14 is not successful, but if E_2 is taken as the reciprocal of the given expression, a plausible result is obtained.

6.9. GRANULAR AND PACKED BEDS

Flow through granular and packed beds occurs in reactors with solid catalysts, adsorbers, ion exchangers, filters, and mass transfer equipment. The particles may be more or less rounded or may be shaped into rings, saddles, or other structures that provide a desirable ratio of surface and void volume.

Natural porous media may be consolidated (solids with holes in them), or they may consist of unconsolidated, discrete particles. Passages through the beds may be characterized by the properties of porosity, permeability, tortuosity, and

TABLE 6.7. Two-Phase Flow Correlations of Pressure Drop

1. Recommendations

μ_L/μ_G	G(kg/m^{2}sec)	Correlation
< 1000	all	Friedel
> 1000	>100	Chisholm–Baroczy
> 1000	<100	Lockhart–Martinelli

2. Lockhart-Martinelli Correlation

PARAMETER X
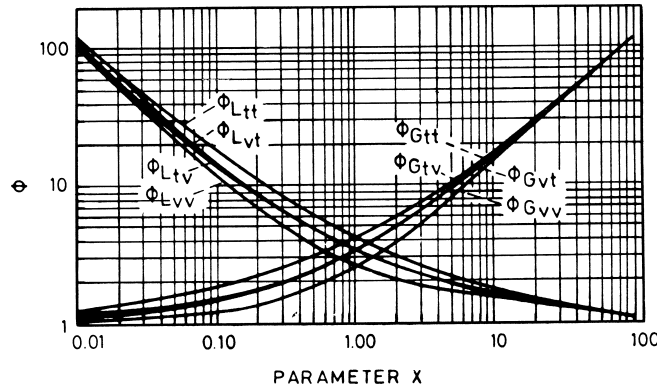
$\phi_L^2 = 1 + C/X + 1/X^2$

$\phi_G^2 = 1 + CX + X^2$

$X^2 = (\Delta P/L)_L/(\Delta P/L)_G$

Liquid	Gas	Subscript	C
Turbulent	Turbulent	tt	20
Viscous	Turbulent	vt	12
Turbulent	Viscous	tv	10
Viscous	Viscous	vv	5

3. Chisholm-Baroczy Correlation

$\phi_{L0}^2 = 1 + (Y^2 - 1)(Bx^{(2-n)/2}(1-x)^{(2-n)/2} + x^{2-n}] = (\Delta P/L)/(\Delta P/L)_{L0}$

$n = 0.25$

$Y^2 = (\Delta P/L)_{G0}/(\Delta P/L)_{L0}$

$B = 55/G^{0.5}$, $0 < Y < 9.5$

$\quad = 520/YG^{0.5}$, $9.5 < Y < 28$

$\quad = 15,000/Y^2 G^{0.5}$, $Y > 28$

x = weight fraction gas

4. Friedel Correlation

$\phi_{L0}^2 = E + \dfrac{3.24FH}{Fr^{0.045}We^{0.035}}$, $Fr = G^2/g_c D\rho_{TP}^2$

$E = (1-x)^2 + x^2 \dfrac{\rho_L f_{G0}}{\rho_G f_{L0}}$, $We = G^2 D/\rho_{TP}\sigma$

$F = x^{0.78}(1-x)^{0.24}$, $\rho_{TP} = \left(\dfrac{x}{\rho_G} + \dfrac{1-x}{\rho_L}\right)^{-1}$

$H = \left(\dfrac{\rho_L}{\rho_G}\right)^{0.91}\left(\dfrac{\mu_G}{\mu_L}\right)^{0.19}\left(1 - \dfrac{\mu_G}{\mu_L}\right)^{0.7}$, x = weight fraction gas

1. (P.B. Whalley, cited by G.F. Hewitt, 1982). 2. [Lockhart and Martinelli, *Chem. Eng. Prog.* 45, 39–48 (1949); Chisholm, *Int. J. Heat Mass Transfer* 10, 1767–1778 (1967)]. 3. [Chisholm, *Int. J. Heat Mass Transfer* 16, 347–348 (1973); Baroczy, *Chem. Eng. Prog. Symp. Ser.* 62, 217–225 (1965)]. 4. (Friedel, European Two Phase Flow Group Meeting, Ispra, Italy, Paper E2, 1979, cited by G.F. Hewitt, 1982).

connectivity. The flow of underground water and the production of natural gas and crude oil, for example, are affected by these characteristics. The theory and properties of such structures is described, for instance, in the book of Dullien (*Porous Media, Fluid Transport and Pore Structure*, Academic, New York, 1979). A few examples of porosity and permeability are in Table 6.8. Permeabil-

ity is the proportionality constant k in the flow equation $u = (k/\mu)\, dP/dL$.

Although consolidated porous media are of importance in chemical engineering, only unconsolidated porous media are incorporated in process equipment, so that further attention will be restricted to them.

<EXAMPLE 6.14>

EXAMPLE 6.14
Pressure Drop and Void Fraction in Liquid–Gas Flow
A mixture of an oil and hydrogen at 500 psia and 200°F enters a 3 in. Schedule 40 steel line. Data are:

Oil: 140,000 lb/hr, 51.85 lb/cuft, 2700 cfh, viscosity 15 cP.
Hydrogen: 800 lb/hr, 0.142 lb/cuft, 5619 cfh, viscosity 2.5 (10^{-7}) lbf sec/sqft.

The pressure drop in 100 ft of line will be found, and also the voidage at the inlet condition.

$$\text{Re}_L = \frac{4\dot{m}}{\pi D g_c \mu} = \frac{4(140,000/3600)}{\pi(0.2557)(32.2)0.15},$$

$$\text{Re}_G = \frac{4(800/3600)}{\pi(0.2557)(32.2)(2.5)(10^{-7})} = 137,500,$$

$$\frac{\varepsilon}{D} = 0.00059.$$

Round equations:

$$f = \frac{1.6434}{[\ln(0.135\varepsilon/D + 6.5/\text{Re}]^2} = \begin{cases} 0.0272, & \text{liquid}, \\ 0.0204, & \text{gas}, \end{cases}$$

$$(\Delta P/L)_L = \frac{8f\dot{m}^2}{\pi^2 g_c \rho D^5} = \frac{8(0.0272)(38.89)^2}{\pi^2(32.2)(51.85)(0.2557)^5}$$
$$= 18.27 \text{ psf/ft},$$

$$(\Delta P/L)_G = \frac{8(0.0204)(0.222)^2}{\pi^2(32.2)(0.142)(0.2557)^5} = 0.1663 \text{ psf/ft},$$

$$X^2 = 18.27/0.1633 = 111.8.$$

Lockhart–Martinelli–Chisholm:
$c = 20$ for TT regime (Table 6.8),

$$\phi_L^2 = 1 + \frac{C}{X} + \frac{1}{X^2} = 2.90,$$

$$\therefore (\Delta P/L) \text{ two phase} = \phi_L^2(\Delta P/L)_L = 2.90(18.27)$$
$$= 53.0 \text{ psf/ft}, \ 36.8 \text{ psi/100ft}.$$

Check with the *homogeneous model:*

$$x = \frac{800}{140,000 + 800} = 0.0057 \text{wt fraction gas},$$

$$\mu = \left[\frac{0.0057}{2.5(10^{-7})} + \frac{0.9943}{3.13(10^{-4})}\right]^{-1} = 3.85(10^{-5}) \frac{\text{lbf sec}}{\text{sqft}},$$

$$\rho = \left[\frac{0.0057}{0.142} + \frac{0.9943}{51.85}\right]^{-1} = 16.86 \text{lb/cuft},$$

$$\text{Re} = \frac{4(39.11)}{\pi(32.2)(0.2557)3.85(10^{-5})} = 157,100$$

$$f = 0.0202,$$

$$\frac{\Delta P}{L} = \frac{8(0.0202)(39.11)^2}{\pi^2(32.2)(16.86)(0.2557)^5} = 42.2 \text{ psf/ft},$$

compared with 53.0 by the LMC method.
Void fraction by Eq. (6.104):

$$\varepsilon_G = 1 - 1/\phi_L = 1 - 1/\sqrt{2.90} = 0.413,$$

compared with input flow condition of

$$\varepsilon = \frac{Q_G}{Q_G + Q_L} = \frac{5619}{5619 + 2700} = 0.675.$$

Method of Premoli [Eqs. (6.105) and (6.106)]: Surface tension $\sigma = 20 \text{ dyn/cm}$, 0.00137 lbf/ft,

$$\text{We} = \frac{DG^2}{g_c \rho_L \sigma} = \frac{16\dot{m}^2}{\pi^2 g_c D^3 \rho_L \sigma}$$
$$= \frac{16(38.89)^2}{\pi^2(32.2)(0.2557)^3(51.85)(0.00137)} = 64,118,$$

$$\text{Re} = 19,196,$$

$$E_1 = 1.578(19196)^{-0.19}(51.85/0.142)^{0.22} = 0.8872,$$

$$E_2 = 0.0273(6411.8)(19196)^{-0.51}(51.85/0.142)^{-0.08} = 7.140,$$

$$y = 5619/2700 = 2.081,$$

$$yE_2 = 2.081(7.140) = 14.86.$$

Clearly, this term must be less than unity if Eq. (6.105a) for S is to be valid, so that equation is not applicable to this problem as it stands. If yE_2 is replaced by $y/E_2 = 0.2914$, *then*

$$S = 1 + 0.8872\left(\frac{2.081}{1.2914} - 0.2914\right)^{0.5} = 2.02,$$

and the voidage is

$$\varepsilon = \frac{5619}{5619 + 2.02(2700)} = 0.51,$$

which is a plausible result. However, Eqs. (6.105) and (6.105a) are quoted correctly from the original paper; no numerical examples are given there.

Granular beds may consist of mixtures of particles of several sizes. In flow problems, the mean surface diameter is the appropriate mean, given in terms of the weight fraction distribution, x_i, by

$$D_p = 1/(\sum x_i/D_i). \tag{6.106}$$

When a particle is not spherical, its characteristic diameter is taken as that of a sphere with the same volume, so that

$$D_p = (6V_p/\pi)^{1/3}. \tag{6.107}$$

SINGLE PHASE FLUIDS

Extensive measurements of flow in and other properties of beds of particles of various shapes, sizes and compositions are reported by Leva et al. (1951). Differences in voidage are pronounced as Figure 6.8(b) shows.

A long-established correlation of the friction factor is that of Ergun (*Chem. Eng. Prog.* **48**, 89–94, 1952). The average deviation from his line is said to be ±20%. The friction factor is

$$f_p = \frac{g_c D_p \varepsilon^3}{u^2(1 - \varepsilon)}\left(\frac{\Delta P}{L}\right) \tag{6.108}$$

TABLE 6.8. Porosity and Permeability of Several Unconsolidated and Consolidated Porous Media

Media	Porosity (%)	Permeability (cm^2)
Berl saddles	68–83	$1.3 \times 10^{-3} - 3.9 \times 10^{-3}$
Wire crimps	68–76	$3.8 \times 10^{-5} - 1.0 \times 10^{-4}$
Black slate powder	57–66	$4.9 \times 10^{-10} - 1.2 \times 10^{-9}$
Silica powder	37–49	$1.3 \times 10^{-10} - 5.1 \times 10^{-10}$
Sand (loose beds)	37–50	$2.0 \times 10^{-7} - 1.8 \times 10^{-6}$
Soil	43–54	$2.9 \times 10^{-9} - 1.4 \times 10^{-7}$
Sandstone (oil sand)	8–38	$5.0 \times 10^{-12} - 3.0 \times 10^{-8}$
Limestone, dolomite	4–10	$2.0 \times 10^{-11} - 4.5 \times 10^{-10}$
Brick	12–34	$4.8 \times 10^{-11} - 2.2 \times 10^{-9}$
Concrete	2–7	$1.0 \times 10^{-9} - 2.3 \times 10^{-7}$
Leather	56–59	$9.5 \times 10^{-10} - 1.2 \times 10^{-9}$
Cork board	—	$3.3 \times 10^{-6} - 1.5 \times 10^{-5}$
Hair felt	—	$8.3 \times 10^{-6} - 1.2 \times 10^{-5}$
Fiberglass	88–93	$2.4 \times 10^{-7} - 5.1 \times 10^{-7}$
Cigarette filters	17–49	1.1×10^{-5}
Agar-agar	—	$2.0 \times 10^{-10} - 4.4 \times 10^{-9}$

(A.E. Scheidegger, *Physics of Flow through Porous Media*, University of Toronto Press, Toronto, Canada, 1974).

$$= 150/\text{Re}_p + 1.75 \tag{6.109}$$

with

$$\text{Re}_p = D_p G / \mu (1 - \varepsilon). \tag{6.110}$$

The pressure gradient accordingly is given by

$$\frac{\Delta P}{L} = \frac{G^2(1-\varepsilon)}{\rho g_c D_p \varepsilon^3} \left[\frac{150(1-\varepsilon)\mu}{D_p G} + 1.75 \right]. \tag{6.111}$$

For example, when $D_p = 0.005\,\text{m}$, $G = 50\,\text{kg/m}^2\text{sec}$, $g_c = 1$ kgm/Nsec^2, $\rho = 800\,\text{kg/m}^3$, $\mu = 0.010\,\text{Nsec/m}^2$, and $\varepsilon = 0.4$, the gradient is $\Delta P / L = 0.31(10^5)\text{Pa/m}$.

An improved correlation is that of Sato (1973) and Tallmadge (*AIChE J.* **16,** 1092 (1970)] shown on Figure 6.8(a). The friction factor is

$$f_p = 150/\text{Re}_p + 4.2/\text{Re}_p^{1/6} \tag{6.112}$$

with the definitions of Eqs. (6.108) and (6.110). A comparison of Eqs. (6.109) and (6.112) is

Re$_P$	5	50	500	5000
f_p (Ergun)	31.8	4.80	2.05	1.78
f_p (Sato)	33.2	5.19	1.79	1.05

In the highly turbulent range the disagreement is substantial.

TWO-PHASE FLOW

Operation of packed trickle-bed catalytic reactors is with liquid and gas flow downward together, and of packed mass transfer equipment with gas flow upward and liquid flow down.

Concurrent flow of liquid and gas can be simulated by the homogeneous model of Section 6.8.1 and Eqs. 6.109 or 6.112, but several adequate correlations of separated flows in terms of Lockhart–Martinelli parameters of pipeline flow type are available. A number of them is cited by Shah (*Gas-Liquid-Solid Reactor Design*, McGraw-Hill, New York, 1979, p. 184). The correlation of Sato (1973) is shown on Figure 6.9 and is represented by either

(a)

(b)
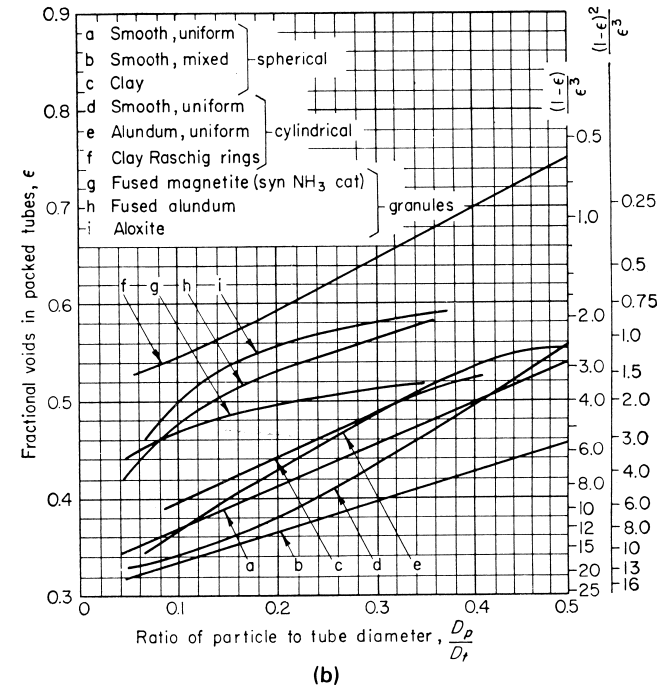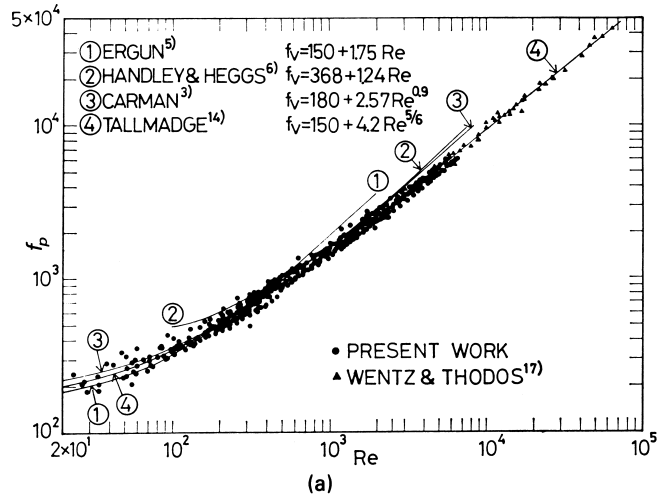
Figure 6.8. Friction factors and void fractions in flow of single phase fluids in granular beds. (a) Correlation of the two-phase friction factor, $\text{Re} = D_p G / (1 - \varepsilon)\mu$ and $f_p = [g_c D_p \varepsilon^3 / \rho u^2 (1 - \varepsilon)]$ $(\Delta P / L) = 150/\text{Re} + 4.2/(\text{Re})^{1/6}$. [*Sato et al.*, J. Chem. Eng. Jpn. **6,** *147–152 (1973)*]. (b) Void fraction in granular beds as a function of the ratio of particle and tube diameters. [*Leva, Weintraub, Grummer, Pollchik, and Storch*, U.S. Bur. Mines Bull. *504 (1951)*].

$$\phi = (\Delta P_{LG} / \Delta P_L)^{0.5} = 1.30 + 1.85(X)^{-0.85}, \; 0.1 < X < 20, \tag{6.113}$$

or

$$\log_{10}\left(\frac{\Delta P_{LG}}{\Delta P_L + \Delta P_G} \right) = \frac{0.70}{\left[\log_{10}(X/1.2) \right]^2 + 1.00}, \tag{6.114}$$

where

$$X = \sqrt{(\Delta P/L)_L / (\Delta P/L)_G}. \tag{6.115}$$
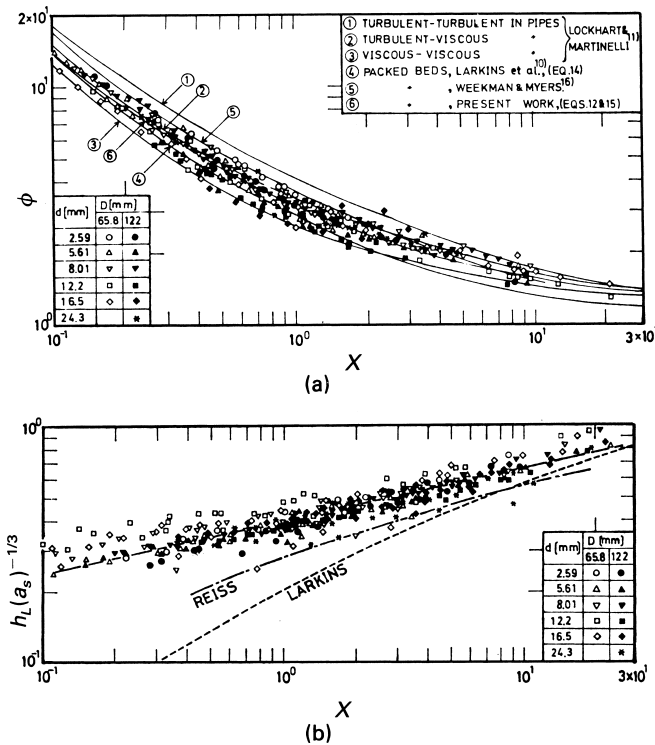
Figure 6.9. Pressure drop gradient and liquid holdup in liquid–gas concurrent flow in granular beds. [*Sato, Hirose, Takahashi, and Toda*, J. Chem. Eng. Jpn. **6**, *147–152 (1973)*]. (a) Correlation of the two phase pressure drop gradient $\Delta P/L$, $\phi = 1.30 + 1.85X^{-0.85}$. (b) Correlation of frictional holdup h_L of liquid in the bed; a_s is the specific surface, 1/mm, d is particle diameter, and D is tube diameter. $h_L = 0.4a_s^{1/3}X^{0.22}$.

The pressure gradients for the liquid and vapor phases are calculated on the assumption of their individual flows through the bed, with the correlations of Eqs. (6.108)–(6.112).

The fraction h_L of the void space occupied by liquid also is of interest. In Sato's work this is given by

$$h_L = 0.40(a_s)^{1/3}X^{0.22}, \tag{6.116}$$

where the specific surface is

$$a_s = 6(1 - \varepsilon)/D_p. \tag{6.117}$$

Additional data are included in the friction correlation of Specchia and Baldi [*Chem. Eng. Sci.* **32**, 515–523 (1977)], which is represented by

$$f_{LG} = \frac{g_c D_p \varepsilon}{3\rho_G u_G^2 (1 - \varepsilon)}\left(\frac{\Delta P}{L}\right), \tag{6.118}$$

$$\ln f_{LG} = 7.82 - 1.30\ln(Z/\psi^{1.1}) - 0.0573[\ln(Z/\psi^{1.1})]^2. \tag{6.119}$$

The parameters in Eq. (6.119) are

$$Z = (\mathrm{Re}_G)^{1.167}/(\mathrm{Re}_L)^{0.767}, \tag{6.120}$$

$$\psi = \frac{\sigma_w}{\sigma_L}\left[\frac{\mu_L}{\mu_w}\left(\frac{\rho_w}{\rho_L}\right)^2\right]^{1/3}. \tag{6.121}$$

Liquid holdup was correlated in this work for both nonfoaming and foaming liquids.

Nonfoaming, $h_L = 0.125(Z/\psi^{1.1})^{-0.312}(a_s D_p/\varepsilon)^{0.65}$, (6.122)

Foaming, $h_L = 0.06(Z/\psi^{1.1})^{-0.172}(a_s D_p/\varepsilon)^{0.65}$. (6.123)

The subscript w in Eq. (6.121) refers to water.

Countercurrent flow data in towers with shaped packings are represented by Figure 6.9. The pressure drop depends on the viscosity of the liquid and on the flow rates and densities of the liquid and gas, as well as on characteristics of the packing which are represented here by the packing factor F. Nominally, the packing factor is a function of the specific surface a_s and the voidage ε, as

$$F = a_s/\varepsilon^3, \tag{6.124}$$

but calculated values are lower than the experimental values shown in the table by factors of 2–5 or so. Clearly the liquid holdup reduces the effective voidage to different extents with different packings. The voidages of the packings in the table range from 70 to 95%, whereas voidages obtained with small spherical or cylindrical packings normally used as catalysts are less than 40% or so, which makes them impractical for countercurrent operation. However, catalysts are made in the forms of rings or saddles when very low pressure drop or countercurrent operation is desirable.

Even when they are nominally the same type and size, packings made by different manufacturers may differ substantially in their pressure drop and mass transfer behavior, so that manufacturers data should be obtained for final design.

Many data on individual packings are given by Billet (*Distillation Engineering*, Chemical Pub. Co., New York), in *Chemical Engineers Handbook* (McGraw-Hill, New York, 1984, p. 18.23), and with Figure 6.9.

The uppermost line of Figure 13.37(a) marks the onset of flooding which is the point at which sharp increase of pressure drop obtains on a plot against liquid rate. Flooding limits also are represented on Figure 13.36; in practice, it is customary to operate at a gas rate that is 70% of that given by the line, although there are many data points below this limit in this correlation.

Mesh or other open structures as vessel packing have attractive pressure drop and other characteristics, but each type has quite individual behavior so that it is best to consult their manufacturer's data.

6.10. GAS–SOLID TRANSFER

The hydrodynamics of gas-solid transfer is complex and the literature is voluminous, as indicated by the 224-page coverage by N.P. Cheremisinoff and R. Gupta, *Handbook of Fluids in Motion*, Butterworth, pp. 623–847, Chapters 23–31, 1883. Equipment for pneumatic conveying is described in Section 5.2 along with some rules for calculating power requirements. Here the latter topic will be supplemented from a more fundamental point of view.

CHOKING VELOCITY

Although the phenomena are not clearcut, partial settling out of solids from the gas stream and other instabilities may develop below certain linear velocities of the gas called choking velocities. Normal pneumatic transport of solids accordingly is conducted above such a calculated rate by a factor of 2 or more because the best correlations are not more accurate. Above choking velocities

the process is called dilute phase transport and, below, dense phase transport.

What appears to be the best correlation of choking velocities is due to Yang [*AIChE J.* **21**, 1013–1015 (1975)], supplemented by Punwani et al. and Yang (cited by Teo and Leung, 1984, pp. 520–521). The choking velocity U_{gc} and voidage ε_c are found by simultaneous solution of the equations

$$G_s/\rho_s = (U_{gc} - U_t)(1 - \varepsilon_c) \tag{6.125}$$

or

$$\varepsilon_c = 1 - G_s/\rho_s(U_{gc} - U_t) \tag{6.126}$$

and

$$gD(\varepsilon_c^{-4.7} - 1) = 3.41(10^5)(\rho_g/\rho_s)^{2.2}(U_{gc} - U_t)^2, \tag{6.127}$$

where G_s is the mass rate of flow of solid per unit cross section and the other terms are defined in Table 6.9. When ε_c from Eq. (6.126) is substituted into Eq. (6.127), the single unknown in that equation is readily found with a root solving routine. For the case of Example 6.15, $G_s = 29.6\,\text{kg/m}^2\text{sec}$, $U_t = 0.45\,\text{m/sec}$, $\rho_s = 1282\,\text{kg/m}^3$, and $\rho_g = 1.14\,\text{kg/m}^3$. Accordingly, $U_{gc} = 1.215\,\text{m/sec}$ and $\varepsilon_c = 0.9698$.

PRESSURE DROP

The relatively sparse data on dense phase transport is described by Klinzing (1981) and Teo and Leung (1984). Here only the more important category of dilute phase transport will be treated.

The pressure drop in simultaneous flow of gas and solid particles is made up of contributions from each of the phases. When the particles do not interact significantly, as in dilute transport, the overall pressure drop is represented by

$$\Delta P = \rho_p(1 - \varepsilon)Lg + \rho_f \varepsilon Lg + \frac{2f_g \rho_f U_f^2 L}{D} + \frac{2f_s \rho_p(1 - \varepsilon)U_p^2 L}{D} \tag{6.128}$$

for vertical transport; in horizontal transport only the two frictional terms will be present. The friction factor f_g for gas flow is the normal one for pipe flow; except for a factor of 4, it is given by Eq. (6.19) for laminar flow and by the Round equation (6.21) for turbulent flow. For the solid friction factor f_s, many equations of varying complexity have been proposed, of which some important ones are listed in Table 6.9.

These equations involve the free settling velocity U_t, for which separate equations also are shown in the table. At lower velocities Stokes' law applies, but corrections must be made at higher ones. The particle velocity U_p is related to other quantities by Eqs. (12)–(14) of the table, and the voidage in turn is represented by Eq. (15). In a review of about 20 correlations, Modi et al. (*Proceedings, Powder and Bulk Solids Handling and Processing Conference*, Powder Advisory Center, Chicago, 1978, cited by Klinzing, 1981) concluded that the correlations of Konno and Saito (1969) and of Yang (1976, 1978) gave adequate representation of pneumatic conveying of coal. They are applied in Example 6.15 and give similar results there.

6.11. FLUIDIZATION OF BEDS OF PARTICLES WITH GASES

As the flow of fluid through a bed of solid particles increases, it eventually reaches a condition at which the particles are lifted out of permanent contact with each other. The onset of that condition

TABLE 6.9. Equations for the Calculation of Pressure Drop in Gas–Solid Transport

Solid Friction Factor f_s According to Various Investigators

Investigator	f_s	
Stemerding (1962)	0.003	(1)
Reddy and Pei (1969)	$0.046 U_p^{-1}$	(2)
Van Swaaij, Buurman, and van Breugel (1970)	$0.080 U_p^{-1}$	(3)
Capes and Nakamura (1973)	$0.048 U_p^{-1.22}$	(4)
Konno and Saito (1969)	$0.0285\sqrt{gD}\,U_p^{-1}$	(5)
Yang (1978), vertical	$0.00315 \frac{1-\varepsilon}{\varepsilon^3}\left[\frac{(1-\varepsilon)U_t}{U_t - U_p}\right]^{-0.979}$	(6)
Yang (1976), horizontal	$0.0293 \frac{1-\varepsilon}{\varepsilon^3}\left[\frac{(1-\varepsilon)U_t}{\sqrt{gD}}\right]^{-1.15}$	(7)

Free Setting Velocity

$= D_p\left[\frac{g\rho_f(\rho_p - \rho_f)}{\mu_f^2}\right]^{1/3}$		(8)
$U_{t(\text{Stokes})} = \frac{gD_p^2(\rho_p - \rho_f)}{18\mu_f}$, $K < 3.3$	$K < 3.3$	(9)
$U_{t(\text{intermediate})} = \frac{0.153 g^{0.71} D_p^{1.14}(\rho_p - \rho_f)^{0.71}}{\rho_f^{0.29} \mu_f^{0.43}}$,	$3.3 < K < 43.6$	(10)
$U_{t(\text{Newton})} = 1.75\left(\frac{gD_p(\rho_p - \rho_f)}{\rho_f}\right)^{1/2}$,	$43.6 < K < 2360$	(11)

Particle Velocity

Investigator	U_p	
Hinkle (1953)	$U_g - U_t$	(12)
IGT (1978)	$U_g(1 - 0.68 D_p^{0.92}\rho_p^{0.5}\rho_f^{-0.2}D^{-0.54})$	(13)
Yang (1976)	$U_g - U_t\left[\left(1 + \frac{f_s U_p^2}{2gD}\right)^{\varepsilon 4.7}\right]^{1/2}$	(14)

Voidage

$\varepsilon = 1 - 4\dot{m}_p/\pi D^2(\rho_p - \rho_f)U_p$	(15)

Notation: U_f is a fluid velocity, U_p is particle velocity, U_t is particle free settling velocity, $\dot{m}_s$ is mass rate of flow of solid, D = pipe diameter, D_p is particle diameter, $g = 9.806\,\text{m/sec}^2$ at sea level. (Klinzing, 1981).

is called minimum fluidization. Beyond this point the solid–fluid mass exhibits flow characteristics of ordinary fluids such as definite viscosity and flow through lines under the influence of hydrostatic head difference. The rapid movement of particles at immersed surfaces results in improved rates of heat transfer. Moreover, although heat transfer rate between particles and fluid is only moderate, 1–4 Btu/(hr)(sqft)(°F), the amount of surface is so great, 10,000–150,000 sqft/cuft, that temperature equilibration between phases is attained within a distance of a few particle diameters. Uniformity of temperature, rapid mass transfer, and rapid mixing of solids account for the great utility of fluidized beds in process applications.

As the gas flow rate increases beyond that at minimum fluidization, the bed may continue to expand and remain homogeneous for a time. At a fairly definite velocity, however, bubbles begin to form. Further increases in flow rate distribute themselves between the dense and bubble phases in some ways that are not well correlated. Extensive bubbling is undesirable when intimate contacting between phases is desired, as in drying processes or solid catalytic reactions. In order to permit bubble formation, the particles appear to interlock to form a skin around the bubble and thus prevent free particles from raining through those spaces. Bubble sizes become large at high rates of flow and may

EXAMPLE 6.15
Pressure Drop in Flow of Nitrogen and Powdered Coal
Powdered coal of $100\,\mu m$ dia and 1.28 specific gravity is transported vertically through a 1-in. smooth line at the rate of 15 g/sec. The carrying gas in nitrogen at 1 atm and 25°C at a linear velocity of 6.1 m/sec. The density of the gas is $1.14\,kg/m^3$ and its viscosity is $1.7(10^{-5})N\ sec/m^2$. The equations of Table 6.10 will be used for the various parameters and ultimately the pressure gradient $\Delta P/L$ will be found:

Eq.(8), $\quad K = 10^{-4}\left\{\dfrac{9.806(1.14)(1282-1.14)}{[1.7(10^{-5})]^2}\right\}^{1/3} = 3.67,$

Eq.(10), $\quad U_t = \dfrac{0.153(9.806)^{0.71}(0.0001)^{1.14}(1282-1.14)^{0.71}}{1.14^{0.29}[1.7(10^{-5})]^{0.43}}$

$\qquad\qquad = 0.37\,m/sec(0.41\,m/sec\ by\ Stokes\ law),$

Eq.(15), $\quad \varepsilon = 1 - \dfrac{0.015}{(\pi/4)(0.0254)^2(1282-1.14)U_p} = 1 - \dfrac{0.0231}{U_p},$

$\hfill \text{(I)}$

Eq.(14), $\quad U_p = 6.1 - 0.45\sqrt{1 + f_s U_p^2/2(9.806)(0.0254)}$

$\qquad\qquad = 6.1 - 0.45\sqrt{1 + 2.007 f_s U_p^2} \hfill \text{(II)}$

Eq.(7), $\quad f_s = \dfrac{0.00315(1-\varepsilon)}{\varepsilon^3}\left[\dfrac{(1-E)0.45}{6.1-U_p}\right]^{-0.979}$

$\hfill \text{(III)}$

Equations (I), (II), and (III) are solved simultaneously with the results:

$\quad \varepsilon = 0.9959$ and $U_p = 5.608,$

For the calculation of the pressure drop,

$\quad f_s = 0.0031(\text{Yang equation}),$

$$\mathrm{Re}_f = \frac{DU_f\rho_f}{\mu_f} = \frac{0.0254(6.1)(1.14)}{1.7(10^{-5})} = 10,390.$$

Therefore, Round's Eq. (6.21) applies:

$$f_f = \frac{1}{4}f_{\text{Round}} = 0.0076,$$

Eq. (6.128),

$$\Delta P/L = 9.806[1282(1-0.9959) + 1.14(0.9959)]$$
$$+ (2/0.0254)[0.0076(1.14)(6.1)^2$$
$$+ 0.0031(1282)(0.0041)(5.608)^2]$$
$$= 51.54 + 11.13 + 25.38 + 40.35 = 128.4\,\text{Pa/m}.$$

With Eqs. (5) and (13), no trial calculations are needed.

Eq.(13), $\qquad U_p = 6.1[1 - 0.68(0.0001)^{0.92}(1282)^{0.5}$
$\qquad\qquad\qquad \times(1.14)^{-0.2}(0.0254)^{-0.54}]$
$\qquad\qquad\quad = 5.88\,\text{m/sec},$

Eq.(15), $\qquad\qquad \varepsilon = 1 - 0.0231/5.78 = 0.9960,$

Eq.(5), $\qquad f_s = 0.0285\sqrt{9.806(0.0254)}/5.88 = 0.00242.$

Therefore, the solid frictional gradient is obtained from the calculated value 40.35 in the ratio of the friction factors.

$$(\Delta P/L)_{\text{solid friction}} = 40.35(0.00242/0.0031) = 31.5\,\text{Pa/m}.$$

---

eventually reach the diameter of the vessel, at which time slugging and severe entrainment will occur.

Onset of fluidization commonly is detected by noting a break in the plot of flow against pressure drop. For a range beyond the minimum fluidizing velocity, the pressure drop remains constant and equal to the weight of the bed but the bed level rises gradually and bubbles are generated at an increasing rate. Not in all cases, however, is the fluidization behavior entirely smooth. Figure 6.10(a) compares "normal" with a case of 'abnormal' behavior. Among the reasons for abnormality are aggregation of particles because of stickiness or attractive forces between small particles and interlocking of rough surfaces. It is even possible for bubbling to occur before the onset of fluidization by formation of channels in the bed.

CHARACTERISTICS OF FLUIDIZATION

Six different regimes of fluidization are identified in Figure 6.11 and its legend. Particulate fluidization, class (b) of the figure, is desirable for most processing since it affords intimate contacting of phases. Fluidization depends primarily on the sizes and densities of the particles, but also on their roughness and the temperature, pressure, and humidity of the gas. Especially small particles are subject to electrostatic and interparticle forces.

Four main classes characterized by diameters and differences in densities of the phases are identified in Figure 6.12 and its legend. Groups A and B are most frequently encountered; the boundary between them is defined by the equation given in the legend. Group A particles are relatively small, $30\text{--}150\,\mu m$ dia, with densities below 1.5 g/cc. Their bed behavior is "abnormal" in that the bed expands appreciably before bubbling sets in, and the minimum bubbling velocity always is greater than the minimum fluidization velocity. The bubbles disengage quickly. Cracking catalysts that have been studied extensively for their fluidization behavior are in this class. Group B materials have $d_p = 150\text{--}500\,\mu m$ and are 1.5–4.0 g/mL. The bed expansion is small, and minimum bubbling and fluidization velocities are nearly the same. The bubbles also disengage rapidly. Coarse sand and glass beads that have been favorite study materials fall in this group. Group C comprises small cohesive particles whose behavior is influenced by electrostatic and van der Waals forces. Their beds are difficult to fluidize and subject to channelling. Group D particles are large, 1 mm or more, such as lead shot and grains. They do not fluidize well and are usually handled in spouted beds, such as Figure 9.13(f).

Among the properties of particles most conducive to smooth fluidization are the following:

1. rounded and smooth shape,
2. in the range of 50–500 μm diameter,

(a)

(b)

(c)

(d)
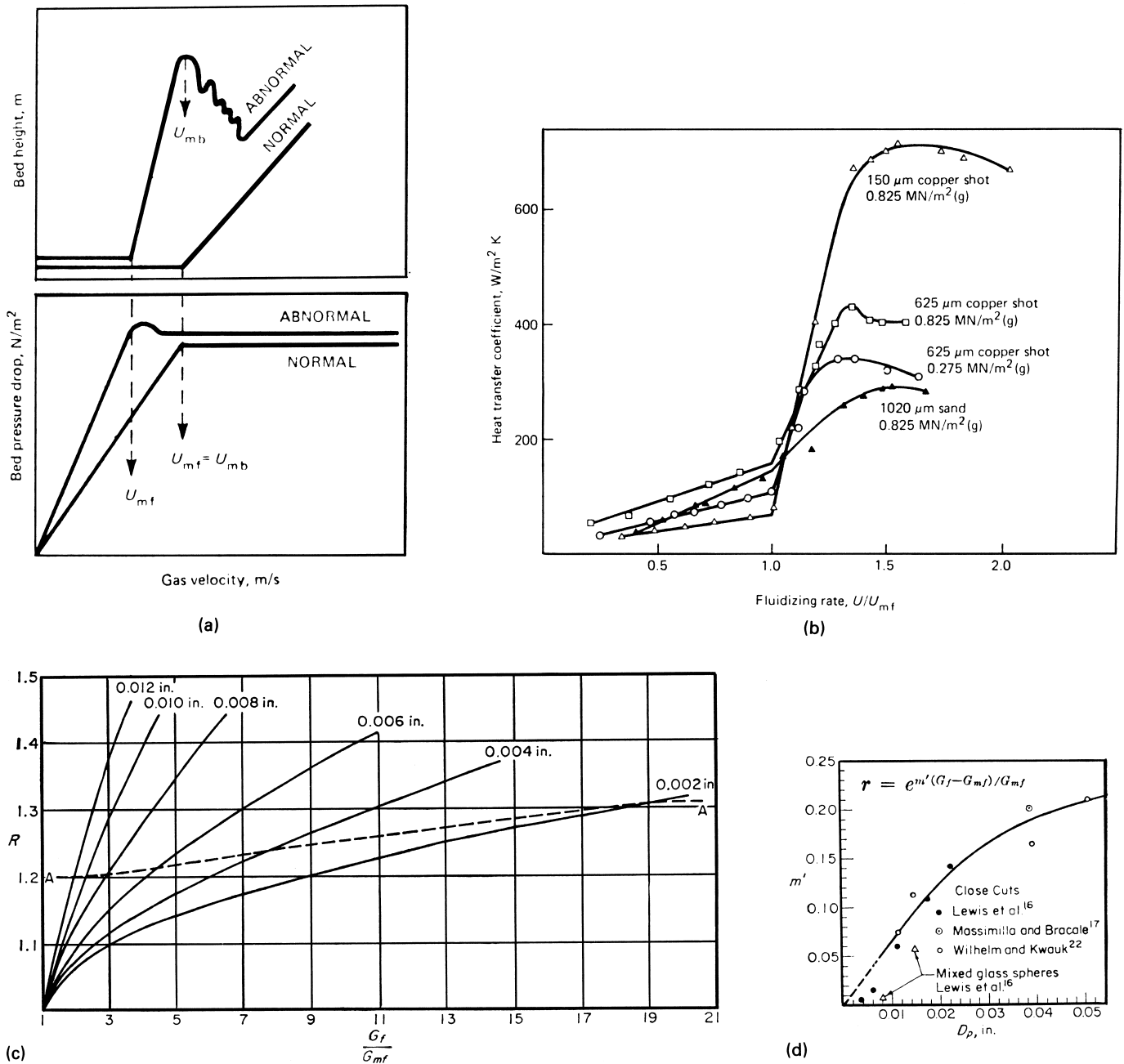
Figure 6.10. Characteristics of gas–solid fluidization. (a) Schematic of the progress of pressure drop and bed height with increasing velocity, for "normal" and "abnormal" behavior. For normal systems, the rates at minimum fluidization and minimum bubbling are the same. (b) Behavior of heat transfer coefficient with gas flow rate analogous to part (a). The peak depends on the density and diameter of the particles. (*Botteril*, Fluid Bed Heat Transfer, *Academic, New York, 1975*). (c) Bed expansion ratio as a function of reduced flow rate and particle size. The dashed line is recommended for narrow size range mixtures. (*Leva, 1959, p. 102*). (d) Correlation of fluctuations in level, the ratio of the maximum level of disturbed surface to average level. (*Leva, 1959, p. 105*). (e) Bed voidage at minimum fluidization. (*Leva, 1959*). Agarwal and Storrow: (*a*) soft brick; (*b*) absorption carbon; (*c*) broken Raschig rings; (*d*) coal and glass powder; (*e*) carborundum; (*f*) sand. U.S. Bureau of Mines: (*g*) round sand, $\phi_S = 0.86$; (*h*) sharp sand, $\phi_S = 0.67$; (*i*) Fischer–Tropsch catalyst, $\phi_S = 0.58$; (*j*) anthracite coal, $\phi_S = 0.63$; (*k*) mixed round sand, $\phi_S = 0.86$. Van Heerden et al.: (*l*) coke; (*m*) carborundum. (*f*) Coefficient C in the equation for mass flow rate at minimum fluidization. (*Leva, 1959*): $G_{mf} = CD_p^2 g_c \rho_F (\rho_S - \rho_F)/\mu$ and $C = 0.0007\ \mathrm{Re}^{-0.063}$. (g) Minimum bubbling and fluidization velocities of cracking catalysts. (*Harriott and Simone, in* Cheremisinoff and Gupta, Eds., Handbook of Fluids in Motion, *Ann Arbor Science, Ann Arbor, MI, 1983*, p. *656*). (h) Minimum fluidization and bubbling velocities with air as functions of particle diameter and density. [*Geldart*, Powder Technol. **7**, *285* (*1973*)]. (i) Transport disengagement height, TDH, as a function of vessel diameter and superficial linear velocity. [*Zenz and Weil*, AIChE J. **4**, *472* (*1958*)]. (j) Good fluidization conditions. (*W.V. Battcock and K.K. Pillai, "Particle size in Pressurised Combustors,"* Proc. Fifth International Conference on Fluidised Bed Combustion, Mitre Corp., Washington D.C., *1977*).
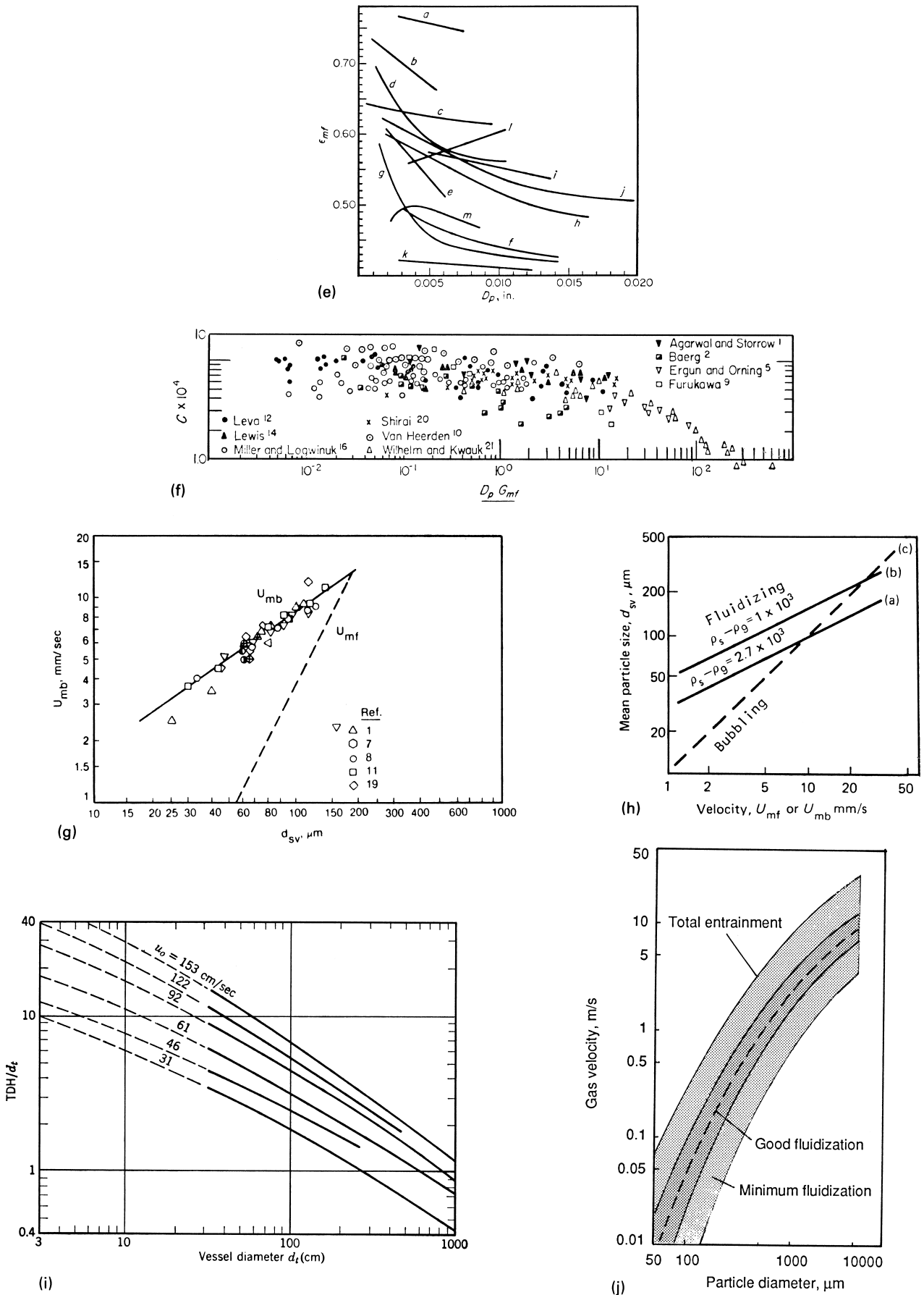
Figure 6.10.—(*continued*)
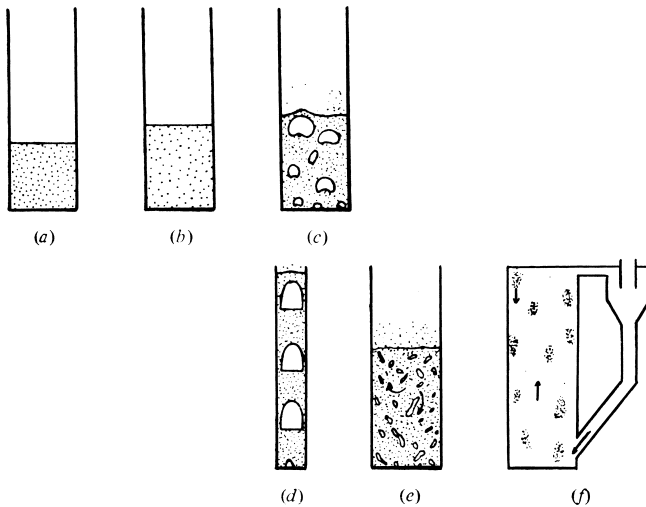
Figure 6.11. Six regimes of fluidization identified with increasing gas superficial velocity. (*Grace, 1982*).

Velocity Range	Regime	Appearance and Principal Features
(a) $0 \leq u < u_{mf}$	fixed bed	particles are quiescent; gas flows through interstices
(b) $u_{mf} \leq u < u_{mb}$	particulate fluidization	bed expands smoothly in a homogeneous manner; top surface is well defined; some small-scale particle motion; little tendency for particles to aggregate; very little fluctuation
(c) $u_{mb} \leq u < u_{ms}$	bubbling fluidization	void regions form near the distributor, grow mostly by coalescence, and rise to the surface; top surface is well defined with bubbles breaking through periodically; irregular pressure fluctuations of appreciable amplitude
(d) $u_{ms} \leq u < u_k$	slugging regime	voids fill most of the column cross section; top surface rises and collapses with reasonably regular frequency; large and regular pressure fluctuations
(e) $u_k \leq u < u_{tr}$	turbulent regime	small voids and particle clusters dart to and fro; top surface difficult to distinguish; small-amplitude pressure fluctuations only
(f) $u_{tr} \leq u$	fast fluidization	no upper surface to bed; particles are transported out the top and must be replaced by adding solids at or near the bottom; clusters or strands of particles move downward, mostly near the wall, while gas, containing widely dispersed particles, moves upward; at fixed solid feed rate, increasingly dilute as u is increased

3. a broad spectrum of particle sizes, with ratios of largest to smallest sizes in the range of 10 to 25,
4. enough toughness to resist attrition.

Such tailoring of properties is feasible for many catalyst-carrier formulations, but drying processes, for instance, may be restricted by other considerations. Fluidization of difficult materials can be maintained by mechanical or ultrasonic vibration of the vessel, or

pulsation of the supply of the fluid, or mechanical agitation of the contents of the vessel, or by addition of fluidization aids such as fine foreign solids.

SIZING EQUIPMENT

Various aspects of the hydrodynamics of gas–solid fluidization have been studied extensively with conclusions that afford guidance to the interpretation and extension of pilot plant data. Some of the leading results bearing on the sizing of vessels will be discussed here. Heat transfer performance is covered in Chapter 17. Example 6.16 applies to some of the cited data.

Solids of practical interest often are mixtures of a range of particle diameters, but, for convenience, correlations are expressed in terms of a single size which is almost invariably taken as the surface average diameter given by

$$d_P = 1/\sum x_i d_i, \tag{6.129}$$

where x_i is the weight fraction of the material having a diameter d_i measured by screen analysis. Particles that deviate substantially from a spherical shape are characterized as having the diameter of a sphere with the same volume as the particle. The sphericity is defined as the ratio

$$\phi = \text{(surface of a sphere)}/\text{(surface of the particle with the same volume)} \tag{6.130}$$

and is always less than unity. Accordingly, the relation between the effective particle size d_p and that found by screen analysis is

$$d_p = \phi d_{\text{screen}}. \tag{6.131}$$

Minimum Fluidization. The fundamental nature of this phenomenon has led to many correlations for its prediction. That of Leva (1959) applies to Reynolds numbers $\text{Re}_{mf} = d_p G_{mf}/\mu < 5$, and is

$$G_{mf} = 688 D_P^{1.82} \frac{[\rho_F(\rho_s - \rho_F)]^{0.94}}{\mu^{0.88}} \tag{6.132}$$

in the English units G_{mf} in lb/(hr)(sqft), D_p in inches, densities in lb/cuft, and viscosity in cP. In SI units it is

$$U_{mf} = \frac{0.0093 d_p^{1.82} (\rho_p - \rho_f)^{0.94}}{\mu^{0.88} \rho_f^{0.06}}. \tag{6.133}$$

The degree of confidence that can be placed in the correlation is indicated by the plot of data on which it is based in Figure 6.10(f). An equation more recently recommended by Grace (1982) covers Reynolds numbers up to 1000:

$$\text{Re}_{mf} = d_p u_{mf} \rho/\mu = \sqrt{(27.2)^2 + 0.0408(\text{Ar})} = 27.2, \tag{6.134}$$

where

$$\text{Ar} = \rho(\rho_p - \rho)g d_p^3/\mu^2. \tag{6.135}$$

Here also the data show much scatter, so that pilot plant determinations of minimum fluidization rates usually are advisable.
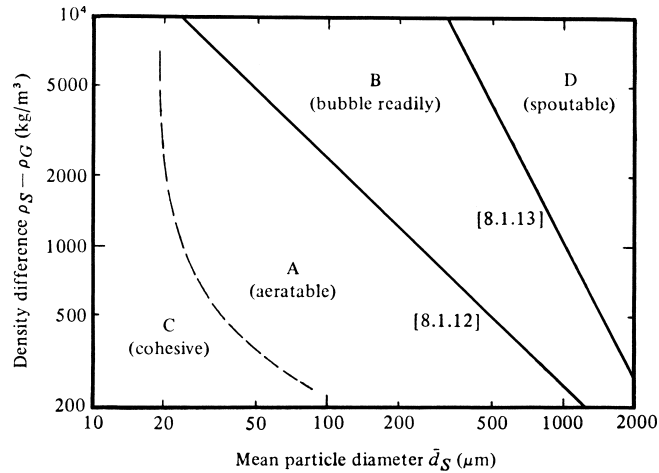
Figure 6.12. Characteristics of four kinds of groups of particles classified by Geldart. [Powder Technol. **6**, *201–205 (1972)*; **7**, *285–292 (1973)*]. The boundary between *A* and *B* is represented by the equation $\bar{d}_S = 44{,}000\rho_F^{0.1}\mu_F^{0.9}/g(\rho_S - \rho_F)$ and that between *B* and *D* by $(\rho_S - \rho_F)\bar{d}_S^2 = 10^{-3}\text{kg/m}$.

Feature	Group C	Group A	Group B	Group D
Distinguishing word or phrase	Cohesive	aeratable	bubble readily	spoutable
Example	Flour	fluid cracking catalyst	sand	wheat
Particle size for $\rho_S = 2.5\,\text{g/cm}^3$	$\leq 20\,\mu m$	$20 < \bar{d}_S \leq 90\,\mu m$	$90 < \bar{d}_S \leq 650\,\mu m$	$> 650\,\mu m$
Channeling	Severe	little	negligible	negligible
Spouting	None	none	shallow beds only	readily
Collapse rate	—	slow	rapid	rapid
Expansion	Low because of channeling	high; initially bubble-free	medium	medium
Bubble shape	channels, no bubbles	flat base, spherical cap	rounded with small indentation	rounded
Rheological character of dense phase	high yield stress	apparent viscosity of order 1 poise	apparent viscosity of order 5 poise	apparent viscosity of order 10 poise
Solids mixing	very low	high	medium	low
Gas back mixing	very low	high	medium	low
Slugging mode	flat raining plugs	axisymmetric	mostly axisymmetric	mostly wall slugs
Effect of $\bar{d}_S$ (within group) on hydrodynamics	unknown	appreciable	minor	unknown
Effect of particle size distribution	unknown	appreciable	negligible	can cause segregation

Minimum Bubbling Conditions. Minimum bubbling velocities for Group B substances are about the same as the minimum fluidization velocities, but those of Group A substances are substantially greater. For Group A materials the correlation of Geldart and Abrahamsen [*Powder Technol* **19**, 133 (1978)] for minimum bubbling velocity is

$$u_{mb} = 33d_p(\mu/\rho)^{-0.1}. \tag{6.136}$$

For air at STP this reduces to

$$u_{mb} = 100d_p. \tag{6.137}$$

For cracking catalysts represented on Figure 6.10(g), Harriott and Simone (1983) present an equation for the ratio of the two kinds of velocities as

$$\frac{u_{mb}}{u_{mf}} = \frac{82\mu^{0.6}\rho^{0.06}}{gd_p^{1.3}(\rho_p - \rho)}. \tag{6.138}$$

The units of this equation are SI; the coefficient given by Cheremisinoff and Cheremisinoff (1984, p. 161) is incorrect. Figures 6.10(g) and (h) compare the two kinds of velocities over a range of particle diameters. Voidage at minimum bubbling is correlated by an equation of Cheremisinoff and Cheremisinoff (1984, p. 163):

$$\varepsilon_{mb}^3/(1 - \varepsilon_{mb}) = 47.4(gd_p^3\rho_p^2/\mu^2)^{-0.5}. \tag{6.139}$$

Bed Expansion and Fluctuation. The change of bed level with increasing gas rate is represented schematically in Figure 6.10(a). The height remains constant until the condition of minimum fluidization is reached, and the pressure drop tends to level off. Then the

EXAMPLE 6.16
Dimensions of a Fluidized Bed Vessel

A fluidized bed is to hold 10,000 kg of a mixture of particles whose true density is 1700 kg/m³. The fluidizing gas is at 0.3 m³/sec, has a viscosity of 0.017 cP or $1.7(E-5)$ Nsec/m² and a density of 1.2 kg/m³. The size distribution of the particles is

d (μm)	252	178	126	89	70	50	30	10
x (wt fraction)	0.088	0.178	0.293	0.194	0.113	0.078	0.042	0.014
u_t (m/sec)	3.45	1.72	0.86	0.43	0.27	0.14	0.049	0.0054

The terminal velocities are found with Stokes' equation

$$u_t = \frac{g(\rho_P - \rho)}{18\,\mu}d_p^2 = \frac{9.81(1700-1.2)(E-12)}{18[1.7(E-5)]}[d_p(\mu m)]^2.$$

(a) The average particle size is

$$d_p = 1/\sum(x_i/d_i) = 84.5\,\mu m.$$

(b) With $d_p = 84.5$ and density difference of 1699 kg/m³, the material appears to be in Group A of Figure 6.12.

(c) Minimum fluidization velocity with Eq. (6.133)

$$u_{mf} = \frac{0.0093[84.5(E-6)]^{1.82}(1700-1.2)^{0.94}}{[1.7(E-5)]^{0.88}(1.2)^{0.06}}$$

$$= 0.0061\,m/sec,$$

and with Eqs. (6.134) and (6.135),

$$Ar = \frac{1.2(1700-1.2)(9.81)[84.5(E-6)]^3}{[1.7(E-5)]^2} = 41.75,$$

$$Re_{mf} = \sqrt{(27.2)^2 + 0.0408(41.75)} - 27.2 = 0.0313,$$

$$u_{mb} = \frac{\mu Re_{mf}}{d_p\rho} = \frac{1.7(E-5)(0.0313)}{84.5(E-6)(1.2)} = 0.0052\,m/sec.$$

Use the larger value, $u_{mf} = 0.0061$, as the conservative one.

(d) Minimum bubbling velocity, with Eq. (6.136),

$$u_{mb} = 33(84.5)(E-6)[1.2/1.7(E-5)]^{0.1} = 0.0085\,m/sec,$$

$$\therefore u_{mb}/u_{mf} = 0.0085/0.0061 = 1.39.$$

From Eq. (6.139),

$$\frac{u_{mb}}{u_{mf}} = \frac{82[1.7(E-5)]^{0.6}(1.2)^{0.06}}{9.81[84.5(E-6)]^{1.3}(1700-1.2)} = 1.35,$$

which is in rough agreement.

(e) Voidage at minimum bubbling from Eq. (6.138):

$$\frac{\varepsilon_{mb}^3}{1-\varepsilon_{mb}} = 47.4\left\{\frac{[1.7(E-5)]^2}{9.81[84.5(E-6)]^3(1700)^2}\right\}^{0.5} = 0.1948,$$

$$\therefore \varepsilon_{mb} = 0.469.$$

It is not certain how nearly consistent this value is with those at minimum fluidization read off Figure 6.10(e). Only a limited number of characteristics of the solids are accounted for in Eq. (6.138).

(f) Operating gas velocity. The ratios of entraining and minimum fluidizing velocities for the two smallest particle sizes present are

$$0.049/0.0061 = 8.03,\ for\ 30\,\mu m,$$

$$0.0054/0.0061 = 0.89,\ for\ 10\,\mu m.$$

Entrainment of the smallest particles cannot be avoided, but an appreciable multiple of the minimum fluidizing velocity can be used for operation; say the ratio is 5, so that

$$u_f = 5u_{mf} = 5(0.0061) = 0.0305\,m/sec.$$

(g) Bed expansion ratio. From Figure 6.10(c) with $d_p = 84.5\,\mu m$ or 0.0033 in. and $G_f/G_{mf} = 5$,

$$R = \begin{cases} 1.16,\ by\ interpolation\ between\ the\ full\ lines, \\ 1.22,\ off\ the\ dashed\ line. \end{cases}$$

Take $R = 1.22$ as more conservative. From Eq. (6.140) the ratio of voidages is

$$\varepsilon_{mb}/\varepsilon_{mf} = 5^{0.22} = 1.42.$$

From part (e), $\varepsilon_{mb} = 0.469$ so that $\varepsilon_{mf} = 0.469/1.42 = 0.330$. Accordingly, the ratio of bed levels is

$$L_{mb}/L_{mf} = (1-\varepsilon_{mf})/(1-\varepsilon_{mb}) = 0.67/0.531 = 1.262.$$

Although the value of ε_{mf} appears somewhat low, the value of R checks roughly the one from Figure 6.10(c).

(h) Fluctuations in level. From Figure 6.10(d), with $d_p = 0.0033$ in., the value of $m' = 0.02$, so that

$$r = \exp[0.02(5-1)] = 1.083.$$

(i) TDH from Figure 6.10(i). At $u_f = u_{mf} - 4(0.0061) = 0.0244\,m/sec$, the abscissa is off the plot, but a rough extrapolation and interpolation indicates about 1.5 m for TDH.

(j) Dimensions of the bed and vessel. With a volumetric flow rate of 0.3 m³/sec, the required diameter is

$$D = \sqrt{0.3/(0.305)(\pi/4)} = 3.54\,m.$$

With a charge of 10,000 kg of solids and a voidage at minimum bubbling of 0.469, the height of the minimum bubbling bed is

$$L = \frac{10000}{1700(1-0.469)(\pi/4)D^2} = 1.13\,m.$$

This value includes the expansion factor which was calculated separately in item (g) but not the fluctuation parameter; with this correction the bed height is

$$L_b = 1.13(1.083) = 1.22\,m.$$

The vessel height is made up of this number plus the TDH of 1.5 m or

$$vessel\ height = 1.22 + 1.5 = 2.72\,m.$$

bed continues to expand smoothly until some of the gas begins to disengage from the homogeneous dense phase and forms bubbles. The point of onset of bubbling corresponds to a local maximum in level which then collapses and attains a minimum. With increasing gas rate, the bed again continues to expand until entrainment develops and no distinct bed level exists. Beyond the minimum bubbling point, some fraction of the excess gas continues through the dense phase but that behavior cannot be predicted with any accuracy.

Some smoothed data of expansion ratio appear in Figure 6.10(c) as a function of particle size and ratio of flow rates at minimum bubbling and fluidization. The rather arbitrarily drawn dashed line appears to be a conservative estimate for particles in the range of 100 μm.

Ordinarily under practical conditions the flow rate is at most a few multiples of the minimum fluidizing velocity so the local maximum bed level at the minimum bubbling velocity is the one that determines the required vessel size. The simplest adequate equation that has been proposed for the ratio of voidages at minimum bubbling and fluidization is

$$\varepsilon_{mb}/\varepsilon_{mf} = (G_{mb}/G_{mf})^{0.22} \tag{6.140}$$

$$= 2.64\mu^{0.89}\rho^{0.54}/g^{0.22}d_p^{1.06}(\rho_p - \rho)^{0.22} \tag{6.141}$$

The last equation results from substitution of Eq. (6.138) into (6.140). Then the relative bed level is found from

$$L_{mb}/L_{mf} = (1 - \varepsilon_{mf})/(1 - \varepsilon_{mb}). \tag{6.142}$$

Either ε_{mb} or ε_{mf} must be known independently before Eq. (6.141) can be applied, either by application of Eq. (6.139) for ε_{mb} or by reading off a value of ε_{mf} from Figure 6.8(c) or Figure 6.10(e). These values are not necessarily consistent.

At high gas velocities the bed level fluctuates. The ratio of maximum disturbed level to the average level is correlated in terms of G_f/G_{mf} and the particle diameter by the equation

$$r = \exp[m'(G_f - G_{mf})/G_{mf}], \tag{6.143}$$

where the coefficient m' is given in Figure 6.10(d) as a function of particle diameter.

Freeboard. Under normal operating conditions gas rates somewhat in excess of those for minimum fluidization are employed. As a result particles are thrown into the space above the bed. Many of them fall back, but beyond a certain height called the transport disengaging height (TDH), the entrainment remains essentially constant. Recovery of that entrainment must be accomplished in auxiliary equipment. The TDH is shown as a function of excess velocity and the diameter of the vessel in Figure 6.10(i). This correlation was developed for cracking catalyst particles up to 400 μm dia but tends to be somewhat conservative at the larger sizes and for other materials.

Viscosity. Dense phase solid–gas mixtures may be required to flow in transfer line catalytic crackers, between reactors and regenerators and to circulate in dryers such as Figures 9.13(e), (f). In dilute phase pneumatic transport the effective viscosity is nearly that of the fluid, but that of dense phase mixtures is very much greater. Some data are given by Schügerl (in Davidson and Harrison, 1971, p. 261) and by Yates (1983). Apparent viscosities with particles of 50–550 μm range from 700 to 1300 cP, compared with air viscosity of 0.017 cP at room temperature. Such high values of the viscosity place the flow definitely in the laminar flow range. However, information about friction in flow of fluidized mixtures through pipelines is not easy to find in the open literature. Someone must know since many successful transfer lines are in operation.

REFERENCES

General

M.M. Denn, *Process Fluid Mechanics*, Prentice-Hall, Englewood Cliffs, NJ, 1980.
O. Levenspiel, *Engineering Flow and Heat Exchange*, Plenum, New York, 1984.
M. Modell and R.C. Reid, *Thermodynamics and Its Applications*, Prentice-Hall, Englewood Cliffs, NJ, 1983.
R.H. Perry, D.W. Green, and J.O. Maloney, *Perry's Chemical Engineers' Handbook*, 7th ed., McGraw-Hill, New York, 1999.
V.L. Streeter and E.B. Wylie, *Fluid Mechanics*, McGraw-Hill, New York, 1979.

Non-Newtonian Fluids

G.W. Govier and K. Aziz, *Flow of Complex Mixtures in Pipes*, Van Nostrand Reinhold, New York, 1972.
N.I. Heywood, Pipeline design for non-Newtonian fluids, *Inst. Chem. Eng. Symp. Ser. No.* 60, 33–52 (1980).
J.W. Hoyt, The effect of additives on fluid friction, *Trans. ASME J. Basic Eng.*, 258 (June 1972).
P.A. Longwell, *Mechanics of Fluid Flow*, McGraw-Hill, New York, 1966.
R.D. Patel, Non-Newtonian flow, in *Handbook of Fluids in Motion*, (Cheremisinoff and Gupta, Eds.), Ann Arbor Science, Ann Arbor, MI, 1983, pp. 135–177.
A.H.P. Skelland, *Non-Newtonian Flow and Heat Transfer*, Wiley, New York, 1967.
J.R. Van Wazer, J.W. Lyons, K.Y. Kim, and R.E. Colwell, *Viscosity and Flow Measurement*, Wiley-Interscience, New York, 1963.
E.J. Wasp, J.P. Kenny, and R.L. Gandhi, *Solid Liquid Flow Slurry Pipeline Transportation*, Trans. Tech. Publications, Clausthal, Germany, 1977.

Two-Phase Flow

D. Chisholm, Gas–liquid flow in pipeline systems, in *Handbook of Fluids in Motion*, (Cheremisinoff and Gupta, Eds.) Ann Arbor Science, Ann Arbor, MI, 1983, pp. 483–513.
D. Chisholm, *Two-Phase Flow in Pipelines and Heat Exchangers*, George Godwin, London, 1983.
G.W. Govier and K. Aziz, *The Flow of Complex Mixtures in Pipes*, Van Nostrand Reinhold, New York, 1972.
G.F. Hewitt, Liquid–gas systems, in *Handbook of Multiphase Systems*, (G. Hetsroni, Ed.), Hemisphere, New York, 1982, pp. 2.1–2.94.

Gas–Solid (Pneumatic) Transport

G. Klinzing, *Gas–Solid Transport*, McGraw-Hill, New York, 1981.
N.P. Cheremisinoff, and R. Gupta (Eds.), Gas–solid flows, in *Handbook of Fluids in Motion*, Ann Arbor Science, Ann Arbor, MI, 1983, pp. 623–860.
C.S. Teo and L.S. Leung, Vertical flow of particulate solids in standpipes and risers, in *Hydrodynamics of Gas–Solids Fluidization*, (N.P. Cheremisinoff and P.N. Cheremisinoff, Eds.), Gulf, Houston, 1984, pp. 471–542.

Fluidization

J.S.M. Botteril, *Fluid-Bed Heat Transfer*, Academic, New York, 1975.

N.P. Cheremisinoff and P.N. Cheremisinoff, *Hydrodynamics of Gas–Solid Fluidization*, Gulf, Houston, 1984.

J.F. Davidson and D. Harrison (Eds.), *Fluidization*, Academic, New York, 1971.

J.R. Grace, Fluidization, Section 8 of G. Hetsroni, 1982.

G. Hetsroni (Ed.), *Handbook of Multiphase Systems*, McGraw-Hill, New York, 1982.

M. Leva, *Fluidization*, McGraw-Hill, New York, 1959.

J.C. Yates, *Fundamentals of Fluidized-Bed Chemical Processes*, Butterworths, London, 1983.

7

FLUID TRANSPORT EQUIPMENT

*A*lthough liquids particularly can be transported by operators carrying buckets, the usual mode of transport of fluids is through pipelines with pumps, blowers, compressors, or ejectors. Those categories of equipment will be considered in this chapter. A few statements will be made at the start about piping, fittings, and valves, although for the most part this is information best gleaned from manufacturers' catalogs. Special problems such as mechanical flexibility of piping at elevated temperatures are beyond the scope here, and special problems associated with sizing of piping for thermosyphon reboilers and the suction side of pumps for handling volatile liquids are deferred to elsewhere in this book.

7.1. PIPING

Standard pipe is made in a discrete number of sizes that are designated by nominal diameters in inches, as "inches IPS (iron pipe size)." Table A5 in Appendix A lists some of these sizes with dimensions in inches. Depending on the size, up to 14 different wall thicknesses are made with the same outside diameter. They are identified by schedule numbers, of which the most common is Schedule 40. Approximately,

Schedule number = 1000 P/S,

where

P = internal pressure, psig
S = allowable working stress in psi.

Tubing for heat exchangers, refrigeration, and general service is made with outside diameters measured in increments of 1/16 or 1/8 in. Standard size pipe is made of various metals, ceramics, glass, and plastics.

Dimensional standards, materials of construction, and pressure ratings of piping for chemical plants and petroleum refineries are covered by ANSI Piping Code B31.3 which is published by the ASME, latest issue 1980. Many details also are given in such sources as Crocker and King, *Piping Handbook* (McGraw-Hill, New York, 1967) *and Perry's Chemical Engineers' Handbook* (1999) and *Marks' Standard Handbook for Mechanical Engineers* (1996).

In sizes 2 in. and less screwed fittings may be used. Larger joints commonly are welded. Connections to equipment and in lines whenever need for disassembly is anticipated utilize flanges. Steel flanges, flanged fittings, and valves are made in pressure ratings of 150, 300, 600, 900, 1500, and 2500 psig. Valves also are made in 125 and 250 psig cast iron. Pressure and temperature ratings of this equipment in various materials of construction are specified in the piping code, and are shown in *Perry's Chemical Engineers' Handbook*, 7th ed. (1999, pp. 10–104 to 106, Table 10–45).

VALVES

Control of flow in lines and provision for isolation of equipment when needed are accomplished with valves. The basic types are relatively few, some of which are illustrated in Figure 7.1. In gate valves the flow is straight through and is regulated by raising or lowering the gate. The majority of valves in the plant are of this type. In the wide open position they cause little pressure drop. In globe valves the flow changes direction and results in appreciable friction even in the wide open position.

This kind of valve is essential when tight shutoff is needed, particularly of gas flow. Multipass plug cocks, butterfly valves, slide valves, check valves, various quick-opening arrangements, etc. have limited and often indispensable applications, but will not be described here.

The spring in the relief valve of Figure 7.1(c) is adjusted to open when the pressure in the line exceeds a certain value, at which time the plug is raised and overpressure is relieved; the design shown is suitable for pressures of several hundred psig.

More than 100 manufacturers in the United States make valves that may differ substantially from each other even for the same line size and pressure rating. There are, however, independent publications that list essentially equivalent valves of the several manufacturers, for example the books of Zappe (1981) and Lyons (1975).

CONTROL VALVES

Control valves have orifices that can be adjusted to regulate the flow of fluids through them. Four features important to their use are capacity, characteristic, rangeability and recovery.

Capacity is represented by a coefficient

$$C_d = C_v/d^2,$$

where d is the diameter of the valve and C_v is the orifice coefficient in equations such as the following

$$Q = C_v\sqrt{(P_1 - P_2)/\rho_w}, \text{ gal/min of liquid},$$
$$Q = 22.7C_v\sqrt{(P_1 - P_2)P_2/\rho_a T}, \text{ SCFM of gas when}$$
$$P_2/P_1 > 0.5,$$
$$Q = 11.3C_vP_1/\sqrt{\rho_a T}, \text{ SCFM of gas when } P_2/P_1 < 0.5,$$

where P_i is pressure in psi, ρ_w is specific gravity relative to water, ρ_a is specific gravity relative to air, and T is temperature °R. Values of C_d of commercial valves range from 12 for double-seated globe valves to 32 for open butterflies, and vary somewhat from manufacturer to manufacturer. Chalfin (1980) has a list.

Characteristic is the relation between the valve opening and the flow rate. Figure 7.1(h) represents the three most common forms. The shapes of plugs and ports can be designed to obtain any desired mathematical relation between the pressure on the diaphragm, the travel of the valve stem, and the rate of flow through the port. *Linear* behavior is represented mathematically by $Q = kx$ and *equal percentage* by $Q = k_1 \exp(k_2 x)$, where x is the valve opening. *Quick-opening* is a characteristic of a bevel-seated or flat disk type of plug; over a limited range of 10–25% of the maximum stem travel is approximately linear.

Over a threefold load change, the performances of linear and equal percentage valves are almost identical. When the pressure drop across the valve is less than 25% of the system drop, the equal percentage type is preferred. In fact, a majority of characterized valves currently are equal percentage.

Rangeability is the ratio of maximum to minimum flows over which the valve can give good control. This concept is difficult to quantify and is not used much for valve selection. A valve generally can be designed properly for a suitably wide flow range.

Recovery is a measure of the degree of pressure recovery at the valve outlet from the low pressure at the vena contracta. When flashing occurs at the vena contracta and the pressure recovery is high, the bubbles collapse with resulting cavitation and noise. The more streamlined the valve, the more complete the pressure recov-

ery; thus, from this point of view streamlining seems to be an undesirable quality. A table of recovery factors of a number of valve types is given by Chalfin (1980); such data usually are provided by manufacturers.

These characteristics and other properties of 15 kinds of valves are described by Chalfin (1980).

Pressure drop. Good control requires a substantial pressure drop through the valve. For pumped systems, the drop through the valve should be at least 1/3 of the pressure drop in the system, with a minimum of 15 psi. When the expected variation in flow is small, this rule can be relaxed. In long liquid transportation lines, for instance, a fully open control valve may absorb less than 1% of the system pressure drop. In systems with centrifugal pumps, the variation of head with capacity must be taken into account when
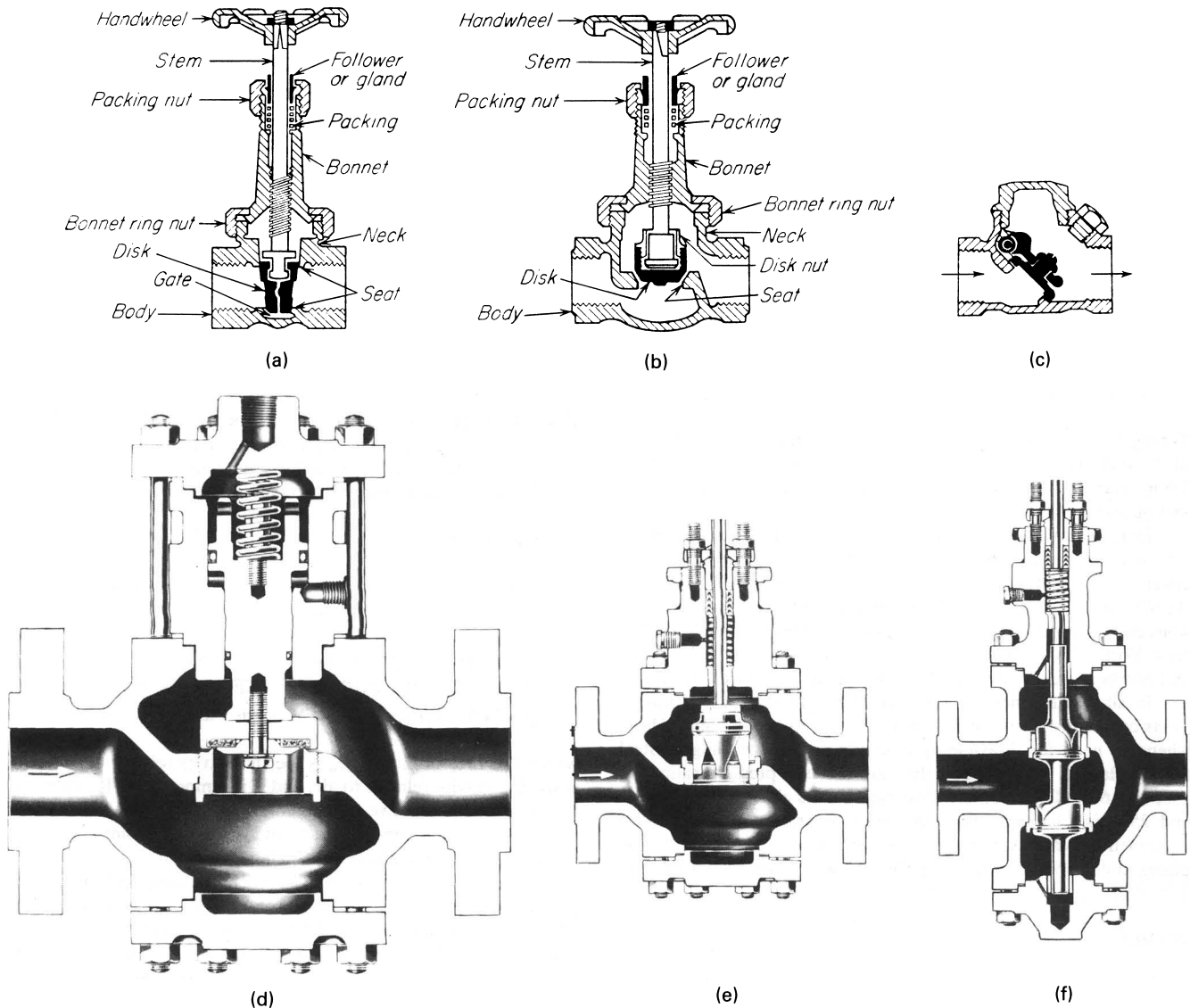
Figure 7.1. Some kinds of manual and automatically controlled valves. (a) Gate valve, for the majority of applications. (b) Globe valve, when tight shutoff is needed. (c) Swing check valve to ensure flow in one direction only. (d) A pressure relief valve, in which the plug is raised on overpressure. (e) A control valve with a single port. (f) A double-port, reverse-acting control valve. (g) A control valve with a double port, in which the correct opening is maintained by air pressure above the diaphragm. (*A*) valve body; (*B*) removable seat; (*C*) discs; (*D*) valve-stem guide; (*E*) guide bushing; (*F*) valve bonnet; (*G*) supporting ring; (*H*) supporting arms; (*J*) diaphragm; (*K*) coupling between diaphragm and valve stem; (*L*) spring-retaining rod; (*M*) spring; (*N*) spring seat; (*O*) pressure connection. (*Fischer*.) (h) Relation between fractional opening and fractional flow of three modes of valve openings.

(g)

(h)
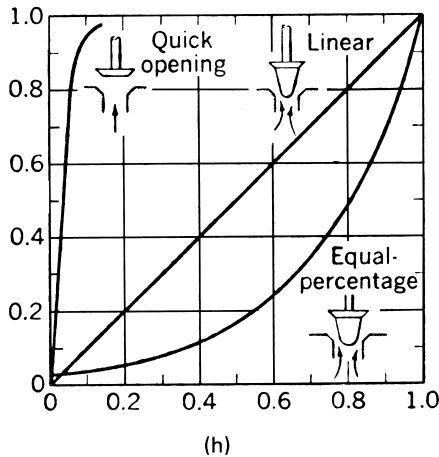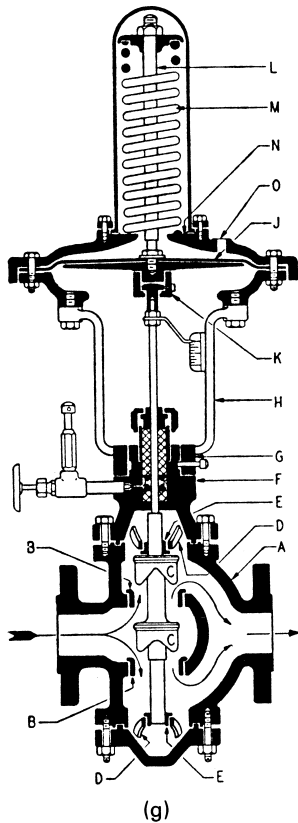
Figure 7.1—(*continued*)

sizing the valve. Example 7.2, for instance, illustrates how the valve drop may vary with flow in such a system.

Types of valves. Most flow control valves are operated with adjustable air pressure on a diaphragm, as in Figure 7.1(d), since this arrangement is more rapid, more sensitive and cheaper than electrical motor control. Double-ported valve (d) gives better control at large flow rates; the pressures on the upper and lower plugs are balanced so that less force is needed to move the stem. The single port (e) is less expensive but gives a tighter shutoff and is generally satisfactory for noncritical service. The reverse acting valve (f) closes on air failure and is desirable for reasons of safety in some circumstances.

7.2. PUMP THEORY

Pumps are of two main classes: centrifugal and the others. These others mostly have positive displacement action in which the discharge rate is largely independent of the pressure against which they work. Centrifugal pumps have rotating elements that impart high velocity initially and high pressure head ultimately to the liquid. Elements of their theory will be discussed here. A glossary of pump terms and terms relating primarily to centrifugal pumps are defined in the Glossary at the end of this chapter. The chief variables involved in pump theory are listed here with typical units:

D, diameter of impeller (ft or m),
H, output head (ft or m),
n, rotational speed (1/sec),
$\dot{P}$, output power (HP or kW),
Q, volumetric discharge rate (cfs or m^3/sec),
μ, viscosity (lb/ft sec or N sec/m^2),
ρ, density (lb/cuft or kg/m^3),
ε, surface roughness (ft or m).

BASIC RELATIONS

A dimensional analysis with these variables reveals that the functional relations of Eqs. (7.1) and (7.2) must exist:

$$gH/n^2D^2 = \phi_1(Q/nD^3, D^2n\rho/\mu, \varepsilon/D), \tag{7.1}$$

$$\dot{P}/\rho n^3 D^5 = \phi_2(Q/nD^3, D^2n\rho/\mu, \varepsilon/D). \tag{7.2}$$

The group $D^2n\rho/\mu$ is the Reynolds number and ε/D is the roughness ratio. Three new groups also have arisen which are named

capacity coefficient, $C_Q = Q/nD^3,$ (7.3)

head coefficient, $C_H = gH/n^2D^2,$ (7.4)

power coefficient, $C\dot{P} = \dot{P}/\rho n^3 D^5.$ (7.5)

The hydraulic efficiency is expressed by these coefficients as

$$\eta = gH\rho Q/\dot{P} = C_H C_Q/C_P. \tag{7.6}$$

Although this equation states that the efficiency is independent of the diameter, in practice this is not quite true. An empirical relation is due to Moody [*ASCE Trans.* **89**, 628 (1926)]:

$$\eta_2 = 1 - (1 - \eta_1)(D_1/D_2)^{0.25}. \tag{7.7}$$

Geometrically similar pumps are those that have all the dimensionless groups numerically the same. In such cases, two different sets of operations are related as follows:

$$Q_2/Q_1 = (n_2/n_1)(D_2/D_1)^3, \tag{7.8}$$

$$H_2/H_1 = (n_2D_2/n_1D_1)^2, \tag{7.9}$$

$$\dot{P}_2/\dot{P}_1 = (\rho_2/\rho_1)(n_2/n_1)^3(D_2/D_1)^5. \tag{7.10}$$

The performances of geometrically similar pumps also can be represented in terms of the coefficients C_Q, C_H, C_P, and η. For instance, the data of the pump of Figure 7.2(a) are transformed into the plots of Figure 7.2(b). An application of such generalized curves is made in Example 7.1.
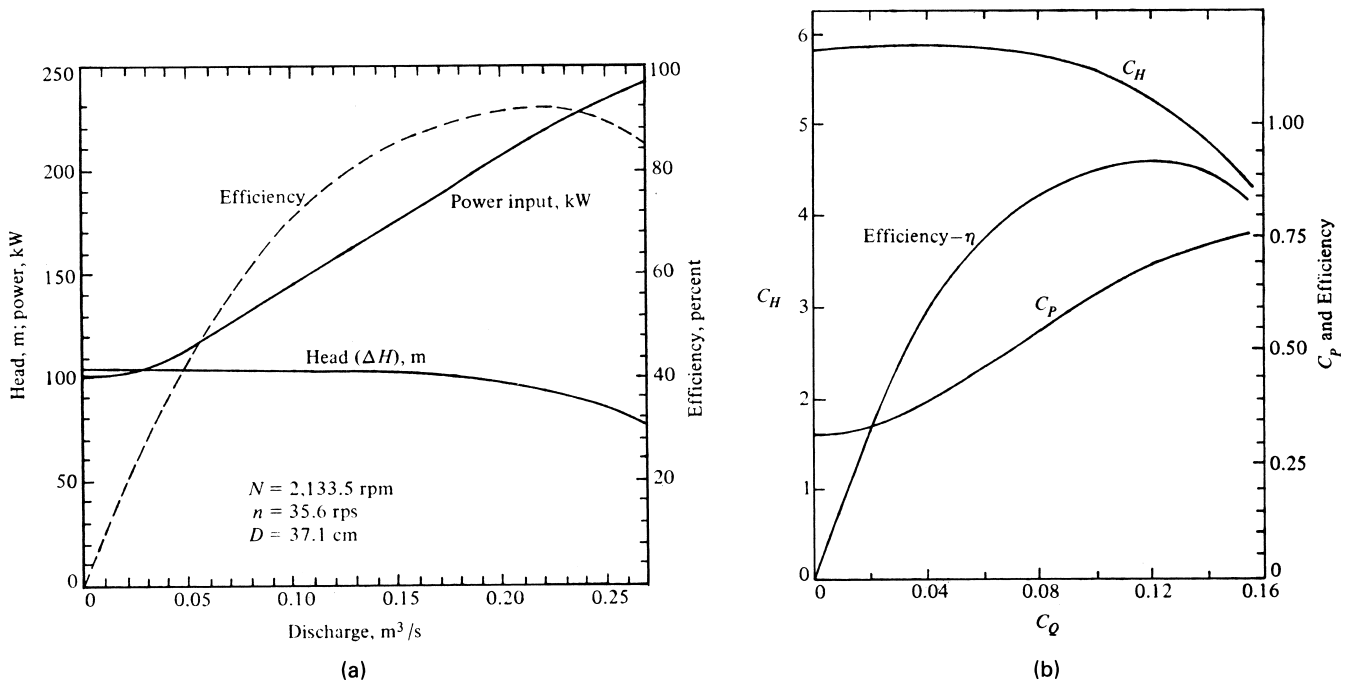
Figure 7.2. Performance curves in dimensional and dimensionless forms: (a) Data of a pump with a specific diameter and rotation speed. (b) Dimensionless performance curves of all pumps geometrically similar to (a). The dashed lines identify the condition of peak efficiency. (*After Daugherty and Franzini*, Fluid Mechanics with Engineering Applications, *McGraw-Hill, New York, 1957*).

EXAMPLE 7.1
Application of Dimensionless Performance Curves
Model and prototypes are represented by the performance curves of Figure 7.2. Comparisons are to be made at the peak efficiency, assumed to be the same for each. Data off Figure 7.2(b) are:

$$\eta = 0.93,$$
$$C_H = gH/n^2D^2 = 5.2,$$
$$C_P = \dot{P}/\rho n^3 D^5 = 0.69,$$
$$C_Q = Q/nD^3 = 0.12.$$

(a) The prototype is to develop a head of 76 m:

$$n = \left(\frac{gH}{C_H D^2}\right)^{0.5} = \left(\frac{9.81(76)}{5.2(0.371)^2}\right)^{0.5} = 32.27 \text{ rps},$$
$$Q = nD^3 C_Q = 32.27(0.371)^3(0.12) = 0.198 \text{ m}^3/\text{sec},$$
$$\dot{P} = \rho n^3 D^5 C_P = 1000(32.27)^3(0.371)^5(0.69)$$
$$= 0.163(10^6)\text{W, } 163 \text{ kW}.$$

(b) The prototype is to have a diameter of 2 m and to rotate at 400 rpm:

$$Q = nD^3 C_Q = (400/60)(2)^3(0.12) = 6.4 \text{ m}^3/\text{sec},$$
$$H = n^2 D^2 C_H/g = (400/60)^2(2)^2(5.2)/9.81 = 94.2 \text{ m},$$

$$\dot{P} = \rho n^3 D^5 C_p = 1000(400/60)^3(2)^5(0.69)$$
$$= 6.54(10^6) \text{ kgm}^2/\text{sec}^3,$$
$$6.54(10^6)\text{N m/sec,6540 kW}.$$

(c) Moody's formula for the effect of diameter on efficiency gives

$$\eta_2 = 1 - (1 - \eta_1)(D_1/D_2)^{0.25} = 1 - 0.07(0.371/2)^{0.25}$$
$$= 0.954 \text{ at 2 m},$$

compared with 0.93 at 0.371 m.

(d) The results of **(a)** and **(b)** also are obtainable directly from Figure 7.2(a) with the aid of Eqs. (7.7), (7.8), and (7.9). Off the figure at maximum efficiency,

$$\eta = 0.93, \ Q = 0.22, \ H = 97, \text{ and} P = 218.$$

When the new value of H is to be 76 m and the diameter is to remain the same,

$$n_2 = 35.6(H_2/H_1)^{0.5} = 35.6(76/97)^{0.5} = 31.5 \text{ rps},$$
$$Q_2 = Q_1(n_2/n_1) = 0.22(H_2/H_1)^{0.5} = 0.195 \text{ m}^3/\text{sec},$$
$$\dot{P}_2 = \dot{P}_1(\rho_2/\rho_1)(n_2/n_1)^3(D_2/D_1)^5 = 218(H_2/H_1)^{1.5} = 151.2 \text{ kW}.$$

These values agree with the results of **(a)** within the accuracy of reading the graphs.

EXAMPLE **7.2**
Operating Points of Single and Double Pumps in Parallel and Series
The head loss in a piping system is represented by the equation

$$H_s = 50 + 6.0(Q/100)^2 + H_v,$$

where H_v is the head loss in the control valve. The pump to be used has the characteristic curve of the pump of Figure 7.7(b) with an 8 in. impeller; that curve is represented closely by the equation

$$H_p = 68 - 0.5(Q/100) - 4.5(Q/100)^2.$$

The following will be found (see Figure 7.17):

(a) The values of H_v corresponding to various flow rates Q gpm.
(b) The flow rate and head on the pumps when two pumps are connected in parallel and the valve is wide open ($H_v = 0$).
(c) The same as (b) but with the pumps in series.
(d) The required speed of the pump at 80 gpm when no control valve is used in the line.

(a) The operating point is found by equating H_s and H_p from which

$$H_v = 68 - 0.5(Q/100) - 4.5(Q/100)^2 - [50 + 6.0(Q/100)^2].$$

Some values are

Q/100	0.8	1.0	1.2	1.286
H_v	10.88	7.00	2.28	0
H_s				59.92

(b) In parallel each pump has half the total flow and the same head H_s:

$$50 + 6.0(Q/100)^2 = 68 - (0.5/2)(Q/100) - (4.5/4)(Q/100)^2,$$
$$\therefore Q = 157.2 \text{ gpm}, \; H_s = 64.83 \text{ ft}.$$

(c) In series each pump has the same flow and one-half the total head loss:

$$\tfrac{1}{2}[50 + 6.0(Q/100)^2] = 68 - 0.5(Q/100) - 4.5(Q/100)^2,$$
$$\therefore Q = 236.1 \text{ gpm}, \; H_s = 83.44 \text{ ft}.$$

Series flow allows 50% greater gpm than parallel.

$$\text{(d)} H_s = 50 + 4.8 = 54.8,$$
$$H_p = (68 - 0.4 - 2.88)(n/1750)^2,$$
$$\therefore n = 1750\sqrt{54.8/64.72} = 1610 \text{ rpm}.$$

Another dimensionless parameter that is independent of diameter is obtained by eliminating D between C_Q and C_H with the result,

$$N_s = nQ^{0.5}/(gH)^{0.75}. \tag{7.11}$$

This concept is called the specific speed. It is commonly used in the mixed units

$$N_s = (\text{rpm})(\text{gpm})^{0.5}/(\text{ft})^{0.75}. \tag{7.12}$$

For double suction pumps, Q is one half the pump output.
The net head at the suction of the pump impeller must exceed a certain value in order to prevent formation of vapor and resulting cavitation of the metal. This minimum head is called the net positive suction head and is evaluated as

$$
\begin{aligned}
\text{NPSH} = \;& (\text{pressure head at the source}) \\
& + (\text{static suction head}) \\
& - (\text{friction head in the suction line}) \\
& - (\text{vapor pressure of the liquid}).
\end{aligned}
\tag{7.13}
$$

Usually each manufacturer supplies this value for his equipment. (Some data are in Figure 7.7.) A suction specific speed is defined as

$$S = (\text{rpm})(\text{gpm})^{0.5}/(NPSH)^{0.75}. \tag{7.14}$$

Standards for upper limits of specific speeds have been established, like those shown in Figure 7.6 for four kinds of pumps. When these values are exceeded, cavitation and resultant damage to the pump may occur. Characteristic curves corresponding to widely different values of N_s are shown in Figure 7.3 for several kinds of pumps handling clear water. The concept of specific speed is utilized in Example 7.3. Further data are in Figure 7.6.

Recommendations also are made by the Hydraulic Institute of suction specific speeds for multistage boiler feed pumps, with $S = 7900$ for single suction and $S = 6660$ for double suction. Thus the required NPSH can be found by rearrangement of Eq. (7.14) as

$$\text{NPSH} = [(\text{rpm})(\text{gpm})^{0.5}/S]^{4/3}. \tag{7.15}$$

For example, at 3500 rpm, 1000 gpm, and $S = 7900$, the required NPSH is 34 ft.
For common fluids other than water, the required NPSH usually is lower than for cold water; some data are shown in Figure 7.16.

PUMPING SYSTEMS

The relation between the flow rate and the head developed by a centrifugal pump is a result of its mechanical design. Typical curves are shown in Figure 7.7. When a pump is connected to a piping system, its head must match the head loss in the piping system at the prevailing flow rate. The plot of the flow rate against the head loss in a line is called the system curve. The head loss is given by the mechanical energy balance,

$$H_s = \frac{\Delta P}{\rho} + \frac{\Delta u^2}{2g_c} + \Delta z + \frac{fLu^2}{2gD} + H_v, \tag{7.16}$$

where H_v is the head loss of a control valve in the line.
The operating point may be found as the intersection of plots of the pump and system heads as functions of the flow rate. Or an equation may be fitted to the pump characteristic and then solved simultaneously with Eq. (7.16). Figure 7.17 has such plots, and Example 7.2 employs the algebraic method.
In the normal situation, the flow rate is the specified quantity. With a particular pump curve, the head loss of the system may need
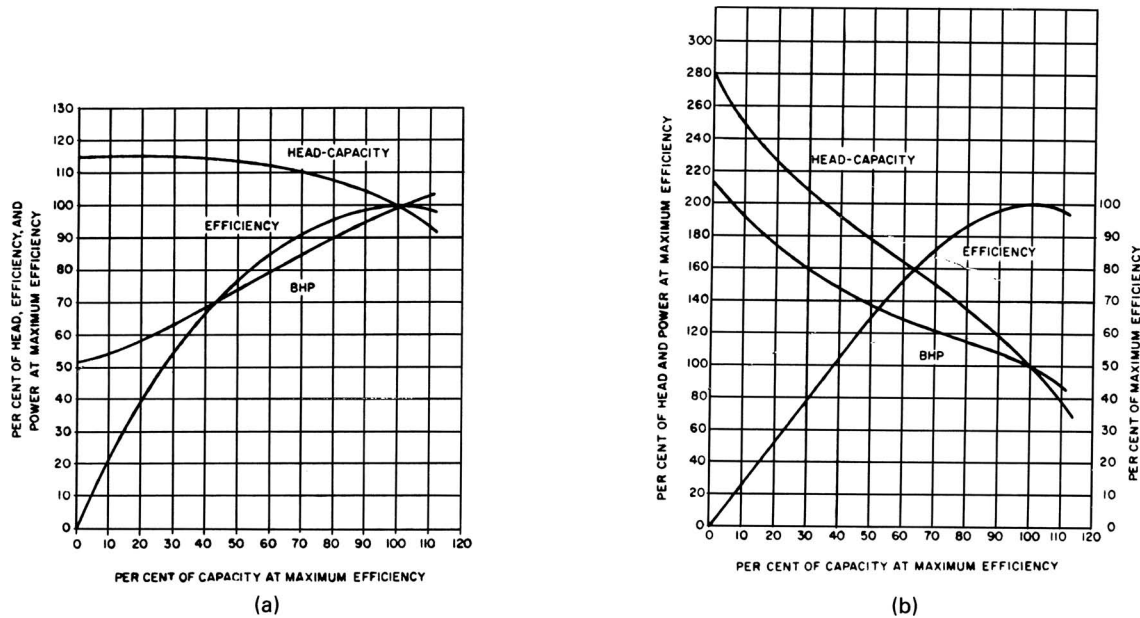
Figure 7.3. Performance curves of single-suction impellers corresponding to two values of the specific speed. (a) $N_s = 1550$, centrifugal pump. (b) $N_s = 10,000$, mixed and axial flow pumps.

to be adjusted with a control valve in the line to make the system and pump heads the same. Alternately, the speed of the pump can be adjusted to make the pump head equal to that of the system. From Eq. (7.9) the relation between speeds and pump heads at two conditions is

$$n_2 = n_1(H_2/H_1)^{0.5}. \tag{7.17}$$

Example 7.2 is of cases with control valve throttling and pump speed control. In large systems, the value of power saved can easily overbalance the extra cost of variable speed drives, either motor or steam turbine.

When needed, greater head or greater capacity may be obtained by operating several pumps in series or parallel. In parallel operation, each pump develops the same head (equal to the system head), and the flow is the sum of the flows that each pump delivers at the common head. In series operation, each pump has the same flow rate and the total head is the sum of the heads developed by the individual pumps at the prevailing flow rate, and equal to the

system head. Example 7.1 deals with a pair of identical pumps, and corresponding system and head curves are shown in Figure 7.17.

7.3. PUMP CHARACTERISTICS

A centrifugal pump is defined in the glossary at the end of this chapter as a machine in which a rotor in a casing acts on a liquid to give it a high velocity head that is in turn converted to pressure head by the time the liquid leaves the pump. Other common nomenclature relating to the construction and performance of centrifugal and related kinds of pumps also is in that table.

The basic types of centrifugals are illustrated in Figure 7.9. A volute is a gradually expanding passage in which velocity is partially converted to pressure head at the outlet. The diffuser vanes of Figures 7.9(b) and 7.10(d) direct the flow smoothly to the periphery. The volute design is less expensive, more amenable to use with impellers of different sizes in the same case, and, as a consequence, by far the most popular construction. Diffuser con-

---

EXAMPLE 7.3
Check of Some Performance Curves with the Concept of Specific Speed

(a) The performance of the pump of Figure 7.7(b) with an 8 in. impeller will be checked by finding its specific speed and comparing with the recommended upper limit from Figure 7.6(b). Use Eq. (7.12) for N_s

Q (gpm)	100	200	300
H (ft)	268	255	225
N_s (calcd)	528	776	1044
N_s [Fig. 7.10(a)]	2050	2150	2500
NPSH	5	7	13

Clearly the performance curves are well within the recommended upper limits of specific speed.

(b) The manufacturer's recommended NPSH of the pump of Figure 7.7(c) with an 8 in. impeller will be checked against values from Eq. (7.15) with $S = 7900$:

Q (gpm)	100	150	200
H (ft)	490	440	300
NPSH (mfgr)	10	18	35
NPSH [Eq. (7.15)]	7.4	9.7	11.8

The manufacturer's recommended NPSHs are conservative.
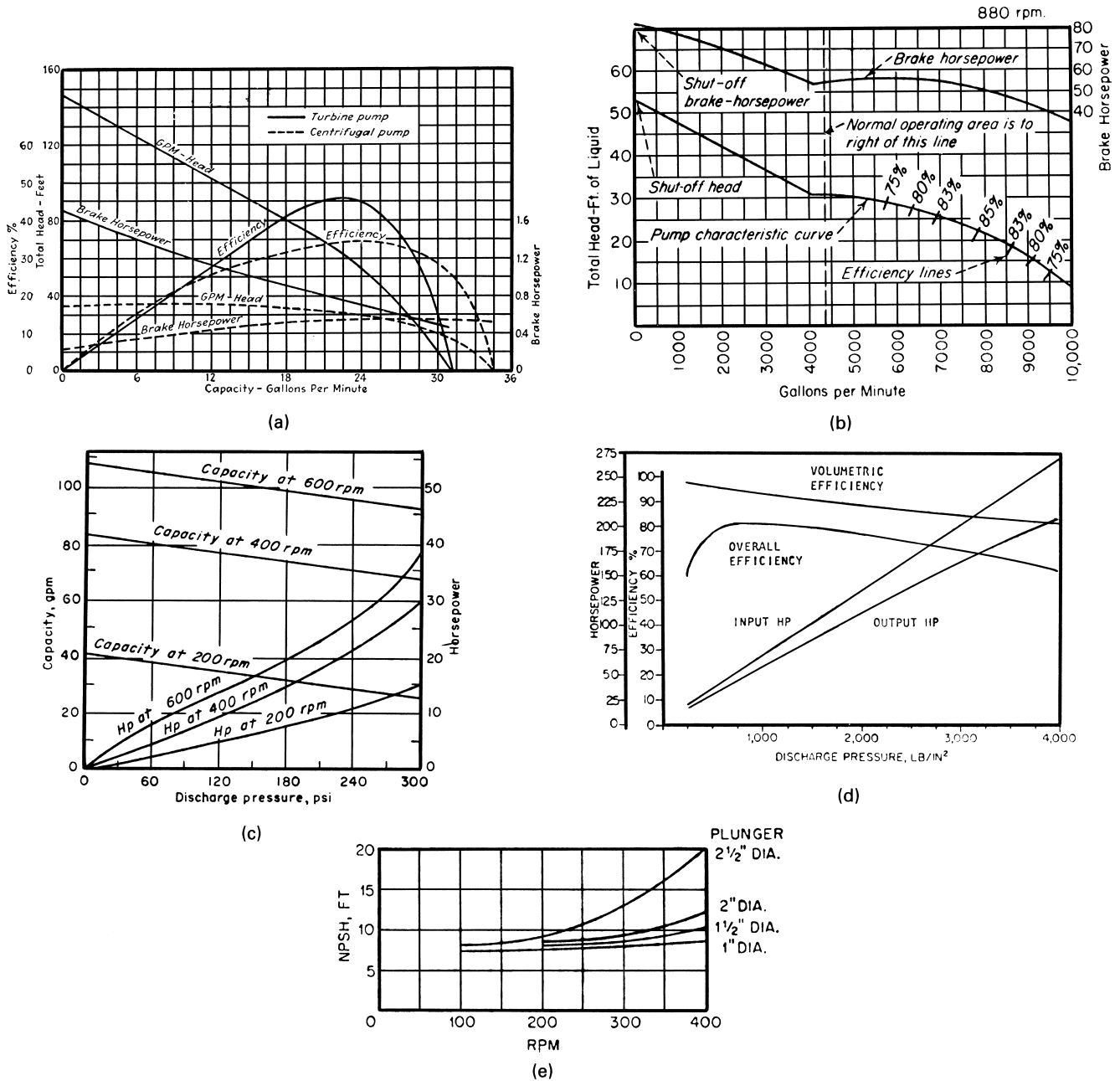
Figure 7.4. Performance of several kinds of pumps. (a) Comparison of small centrifugal and turbine pumps. (*Kristal and Annett, 1940*). (b) An axial flow pump operating at 880 rpm. (Chem. Eng. Handbook, *1973*). (c) An external gear pump like that of Figure 7.12(e). (*Viking Pump Co.*). (d) A screw-type positive displacement pump. (e) NPSH of reciprocating positive displacement pumps.

struction is used to a limited extent in some high pressure, multi-stage machines. The double suction arrangement of Figure 7.9(d) has balanced axial thrust and is favored particularly for severe duty and where the lowered NPSH is an advantage. Multistage pumps, however, are exclusively single suction.

Some of the many kinds of impellers are shown in Figure 7.10. For clear liquids, some form of closed impeller [Figure 7.10(c)] is favored. They may differ in width and number and curvature of the vanes, and of course in the primary dimension, the diameter. Various extents of openness of impellers, [Figs. 7.10(a) and (b)] are desirable when there is a possibility of clogging as with slurries

or pulps. The impeller of Figure 7.10(e) has both axial propeller and centrifugal vane action; the propeller confers high rates of flow but the developed pressure is low. Figure 7.3(b) represents a typical axial pump performance.

The turbine impeller of Figure 7.10(h) rotates in a case of uniform diameter, as in Figure 7.12(j). As Figure 7.4(a) demonstrates, turbine pump performance resembles that of positive displacement types. Like them, turbines are essentially self-priming, that is, they will not vapor bind.

All rotating devices handling fluids require seals to prevent leakage. Figure 7.13 shows the two common methods that are used:

(a) Efficiencies as % of those with direct piston drive:

Stroke, in	5	8	10	20	30	40	50
Crank-and-flywheel pump				87	88	90	92
Piston pump	60	70	74	84	86	88	90
High-pressure pump	55	64	67	76	78	80	81

(b) Efficiencies of crankshaft-driven pumps of various sizes:

Water HP	3	5	10	20	30	50	75	100	200
Efficiency (%)	55	65	72	77	80	83	85	86	88

(c) % of flow above and below the mean; curve is shown for triplex double-acting:

Type	Number of Plungers	% above Mean	% below Mean	Plunger Phase
Duplex (double)	2	24	22	180°
Triplex	3	6	17	120°
Quaduplex	4	11	22	90°
Quintaplex	5	2	5	72°
Sextuplex	6	5	9	60°

(d) Efficiency as a function of % reduced pressure or % reduced speed:

% Full-Load Developed Pressure	Mechanical Efficiency	% Speed	Mechanical Efficiency
20	82	44	93.3
40	88	50	92.5
60	90.5	73	92.5
80	92	100	92.5
100	92.5		

(e) Approximate steam consumption of reciprocating pumps (*Hydraulic Institute, Cleveland, OH, 1957*). *Example:* A pump with a 10 × 10 cylinder and developing 33 HP at 90 ft/min needs 73 lb steam/water HP. The 50 fpm line is a reference line.

Figure 7.5. Data relating to the performance of piston and plunger pumps.

stuffing boxes or mechanical seals. Stuffing boxes employ a soft packing that is compressed and may be lubricated with the pump liquid or with an independent source. In mechanical seals, smooth metal surfaces slide on each other, and are lubricated with a very small leakage rate of the pump liquid or with an independent liquid.

Performance capability of a pump is represented on diagrams like those of Figure 7.7. A single point characterization often is made by stating the performance at the peak efficiency. For example, the pump of Figure 7.7(c) with a 9 in. impeller is called a 175 gpm and 560 ft head pump at a peak efficiency of 57%; it requires a 15 ft suction lift, an 18 ft NPSH and 43 BHP. Operating ranges and costs of commercial pumps are given in Figure 7.8. General operating data are in Figure 7.4.

Although centrifugal pumps are the major kinds in use, a great variety of other kinds exist and have limited and sometimes unique applications. Several kinds of positive displacement types are sketched in Figure 7.12. They are essentially self-priming and have a high tolerance for entrained gases but not usually for solids unless they may be crushed. Their characteristics and applications are discussed in the next section.

7.4. CRITERIA FOR SELECTION OF PUMPS

The kind of information needed for the specification of centrifugal, reciprocating and rotary pumps is shown on forms in Appendix B.

General characteristics of classes of pumps are listed in Table 7.1 and their ranges of performance in Table 7.2. Figure 7.14 shows recommended kinds of pumps in various ranges of pressure and flow rate. Suitable sizes of particular styles of a manufacturer's pumps are commonly represented on diagrams like those of Figure 7.8. Here pumps are identified partly by the sizes of suction and discharge nozzles in inches and the rpm; the key number also identifies impeller and case size and other details which are stated in a catalog. Each combination of head and capacity will have an efficiency near the maximum of that style. Although centrifugal pumps function over a wide range of pressure and flow rates, as represented by characteristic curves like those of Figures 7.2 and 7.7, they are often characterized by their performance at the peak efficiency, as stated in the previous section. Approximate efficiencies of centrifugal pumps as functions of head and capacity are on Figure 7.11 and elsewhere here.

Centrifugal pumps have a number of good qualities:

1. They are simple in construction, are inexpensive, are available in a large variety of materials, and have low maintenance cost.
2. They operate at high speed so that they can be driven directly by electrical motors.
3. They give steady delivery, can handle slurries and take up little floor space.

Some of their drawbacks are
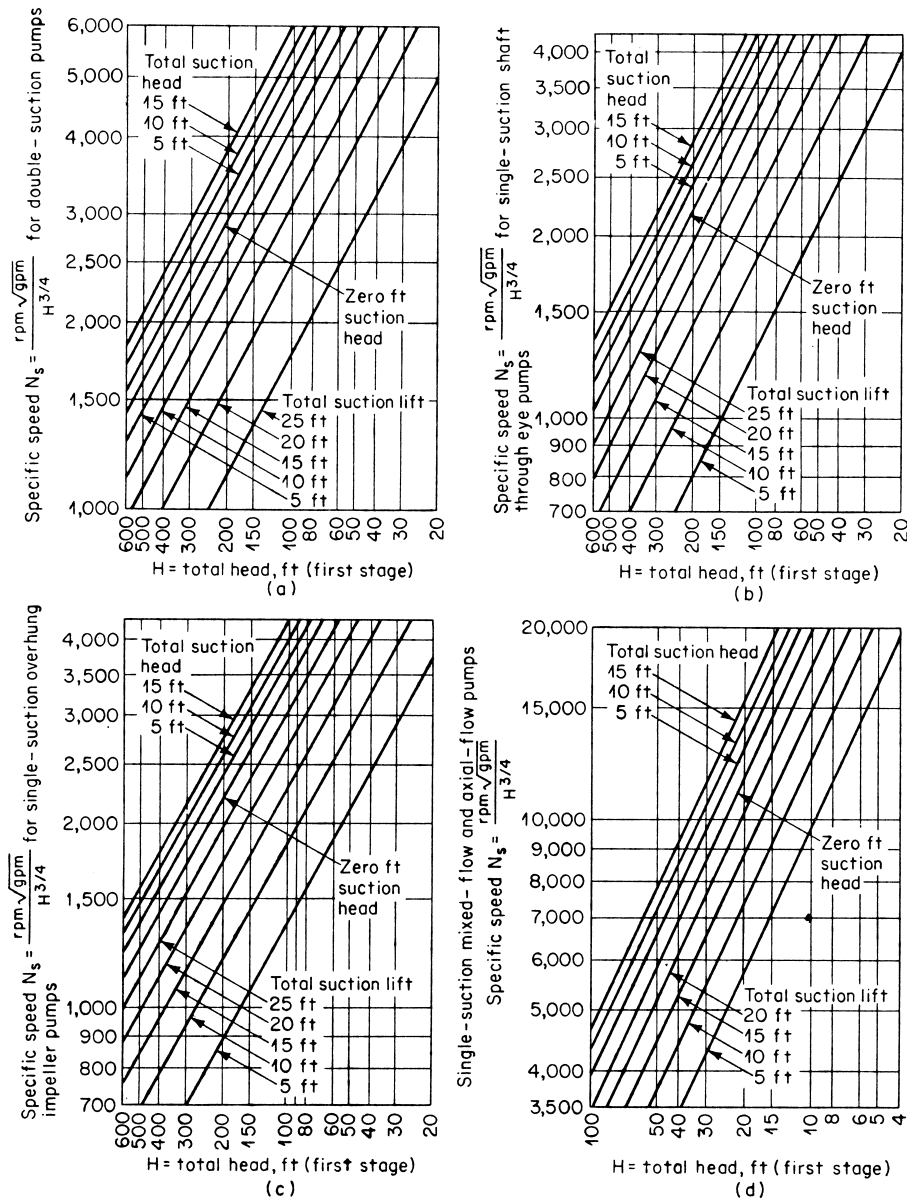
Figure 7.6. Upper specific-speed limits for (a) double-suction pumps (shaft through impeller eye) handling clear water at 85°F at sea level, (b) single-suction pumps (shaft through impeller eye) handling clear water at 85°F at sea level, (c) single-suction pumps (overhung-impeller type) handling clear water at 85°F at sea level, (d) single-suction mixed- and axial-flow pumps (overhung-impeller type) handling clear water at 85°F at sea level. (*Hydraulic Institute, Cleveland, OH, 1957*).

4. Single stage pumps cannot develop high pressures except at very high speeds (10,000 rpm for instance). Multistage pumps for high pressures are expensive, particularly in corrosion-resistant materials.

5. Efficiencies drop off rapidly at flow rates much different from those at peak efficiency.

6. They are not self-priming and their performance drops off rapidly with increasing viscosity. Figure 7.15 illustrates this effect.

On balance, centrifugal pumps always should be considered first in comparison with reciprocating or rotary positive displacement types, but those do have their places. Range of applications of various kinds of pumps are identified by Figure 7.14.

Pumps with reciprocating pistons or plungers are operated with steam, motor or gas engine drives, directly or through gears or belts. Their mode of action is indicated on Figure 7.12(a). They are always used with several cylinders in parallel with staggered action to smooth out fluctuations in flow and pressure. Figure 7.5(c) shows that with five cylinders in parallel the fluctuation is reduced to a maximum of 7%. External fluctuation dampers also are used. Although they are self-priming, they do deteriorate as a result of cavitation caused by release of vapors in the cylinders. Figure 7.4(e) shows the NPSH needed to repress cavitation. Application of reciprocating pumps usually is to low capacities and high pressures of 50–1000 atm or more. Some performance data are shown in Figure 7.5.

(a)

(b)

(c)
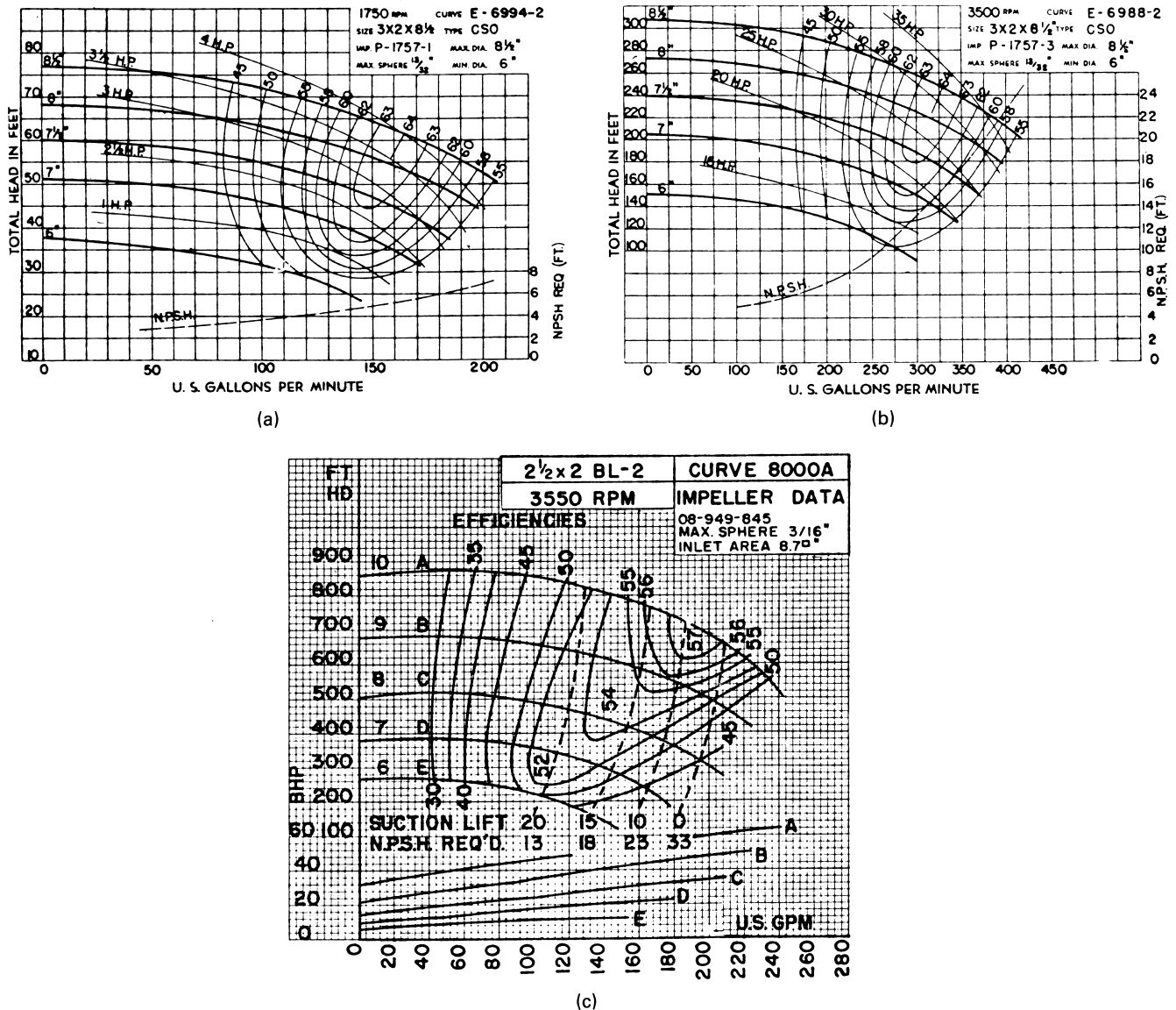
Figure 7.7. Characteristic curves of centrifugal pumps when operating on water at 85°F (*Allis Chalmers Co.*). (a) Single suction, 1750 rpm. (b) The pump of (a) operated at 3500 rpm. (c) Multistage, single suction, 3550 rpm.

Diaphragm pumps [Fig. 7.12(i)] also produce pulsating flow. They are applied for small flow rates, less than 100 gpm or so, often for metering service. Their utility in such applications overbalances the drawback of their intrinsic low efficiencies, of the order of 20%.

Screw pumps [Fig. 7.12(g)] are suited for example to high viscosity polymers and dirty liquids at capacities up to 2000 gpm and pressures of 200 atm at speeds up to 3000 rpm. They are compact, quiet, and efficient. Figure 7.4(d) shows typical performance data.

Gear pumps [Figs. 7.12(e) and (f)] are best suited to handling clear liquids at a maximum of about 1000 gpm at 150 atm. Typical performance curves are shown in Figure 7.4(c).

Peristaltic pumps [Fig. 7.12(h)] move the liquid by squeezing a tube behind it with a rotor. Primarily they are used as metering pumps at low capacities and pressures in corrosive and sanitary services when resistant flexible tubes such as those of teflon can be used, and in laboratories.

Turbine pumps [Figs. 7.9(f), 7.12(i), and 7.4(a)] also are called regenerative or peripheral. They are primarily for small capacity and high pressure service. In some ranges they are more efficient than centrifugals. Because of their high suction lifts they are suited to handling volatile liquids. They are not suited to viscous liquids or abrasive slurries.

7.5. EQUIPMENT FOR GAS TRANSPORT

Gas handling equipment is used to transfer materials through pipe lines, during which just enough pressure or head is generated to overcome line friction, or to raise or lower the pressure to some required operating level in connected process equipment. The main classes of this kind of equipment are illustrated in Figures 7.18 and 7.19 and are described as follows.

(a) Single-suction, 1800 rpm standard pumps:
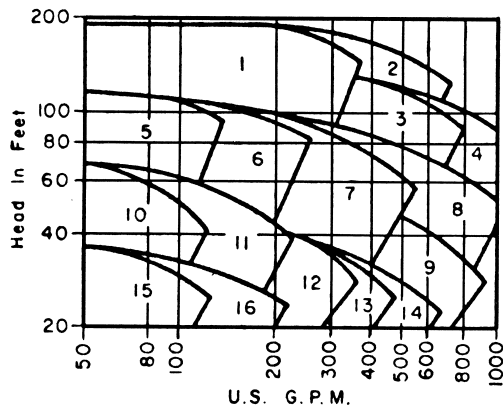
Key No.	Suction and Discharge	Approximate Cost	Horsepower Range at 1.0 Sp Gr
1	4×3	$1200	$7\frac{1}{2}$–25
2	6×4	1350	20–30
3	4×3	1200	15–25
4	5×4	1500	15–30
5	$2 \times 1\frac{1}{2}$	750	2–$7\frac{1}{2}$
6	$2\frac{1}{2} \times 2$	1050	3–10
7	4×3	1200	5–15
8	5×4	1350	$7\frac{1}{2}$–20
9	5×4 (1200 rpm)	1500	3–$7\frac{1}{2}$
10	$1\frac{1}{2} \times 1\frac{1}{2}$	700	1–2
11	2×2	750	$1\frac{1}{2}$–3
12	$3 \times 2\frac{1}{2}$ (1200 rpm)	1050	$1\frac{1}{2}$–3
13	4×3 (1200 rpm)	1200	2–5
14	5×4 (1200 rpm)	1350	2–5
15	$2\frac{1}{2} \times 2\frac{1}{2}$	500	$\frac{3}{4}$–$1\frac{1}{2}$
16	3×3	600	1–2

(b) Single-suction, 3600 rpm standard pumps:
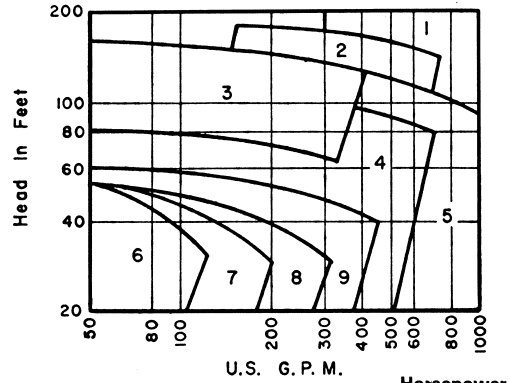
Key No.	Suction and Discharge	Approximate Cost	Horsepower Range at 1.0 Sp. Gr.
1	5×4	$2250	40–60
2	4×3	1950	20–40
3	$3 \times 2\frac{1}{2}$	1650	$7\frac{1}{2}$–20
4	4×4	1800	3–20
5	5×5	1950	5–30
6	$2 \times 1\frac{1}{2}$	1200	$\frac{3}{4}$–2
7	$2\frac{1}{2} \times 2$	1350	1–3
8	$3 \times 2\frac{1}{2}$	1500	2–$7\frac{1}{2}$
9	4×3	1650	2–$7\frac{1}{2}$

(c) Single-suction 1800 and 3600 rpm refinery pumps for elevated temperatures and pressures:
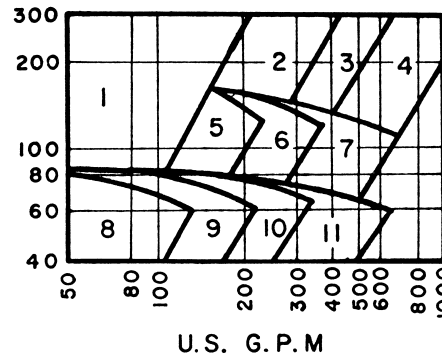
Key No.	Suction and Discharge	Approximate Cost	Horsepower Range at 1.0 Sp Gr
1	$2 \times 1\frac{1}{2}$	$3400	$7\frac{1}{2}$–30
2	3×2 (3600 rpm)	3700	15–50
3	4×3	4300	20–75
4	6×4	4800	40–125
5	3×2	4200	5–15
6	4×3 (1800 rpm)	4500	$7\frac{1}{2}$–20
7	6×4	5400	15–40
8	$2 \times 1\frac{1}{2}$	3400	1–5
9	3×2 (1800 rpm)	3700	2–$7\frac{1}{2}$
10	4×3	4300	3–10
11	6×4	4800	5–15

Figure 7.8. Typical capacity-head ranges of some centrifugal pumps, their 1978 costs and power requirements. Suction and discharge are in inches. (*Evans, 1979*).

(a)

(b)

(c)

(d)

(e)

(f)
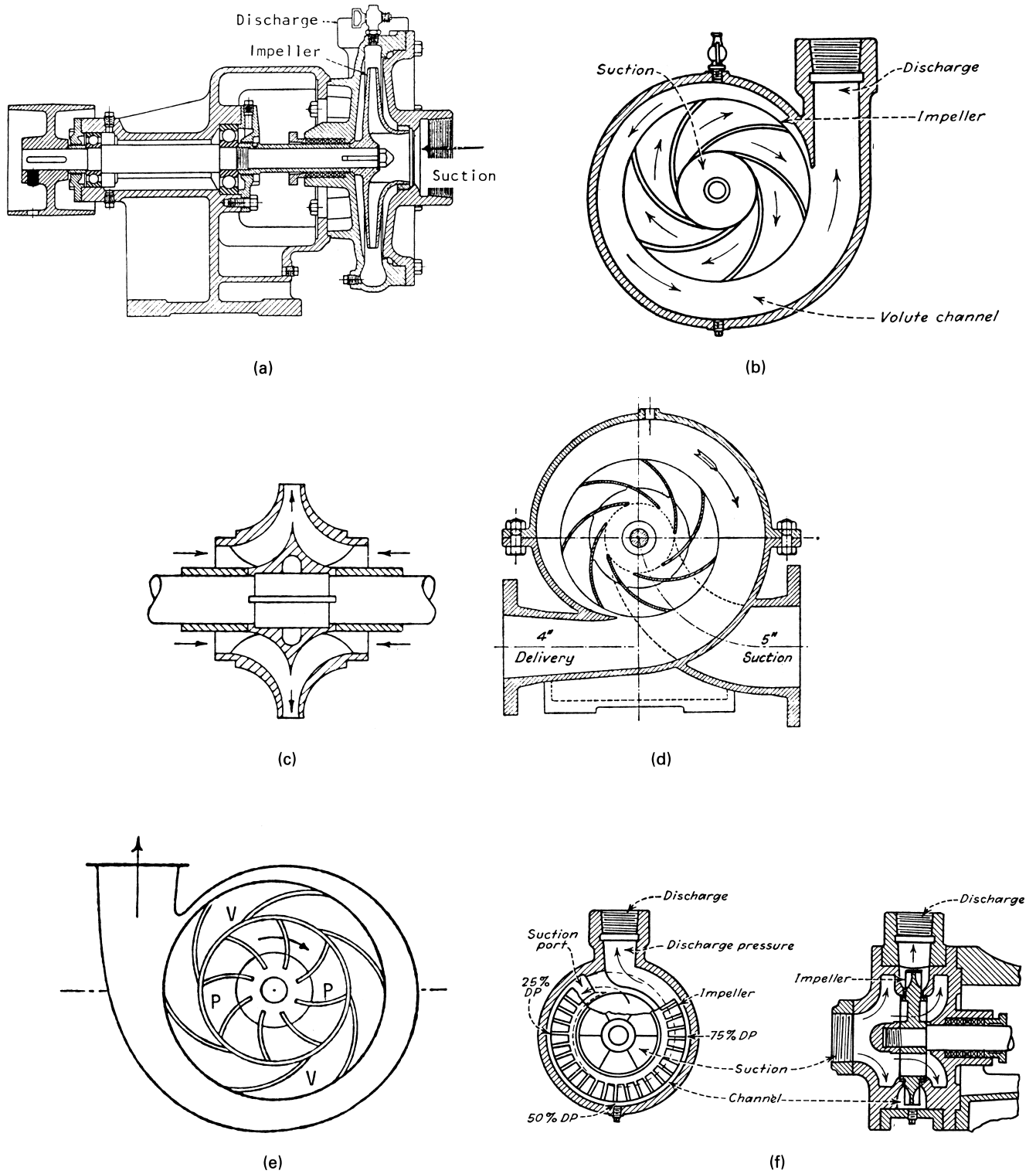
Figure 7.9. Some types of centrifugal pumps. (a) Single-stage, single suction volute pump. (b) Flow path in a volute pump. (c) Double suction for minimizing axial thrust. (d) Horizontally split casing for ease of maintenance. (e) Diffuser pump: vanes V are fixed, impellers **P** rotate. (f) A related type, the turbine pump.
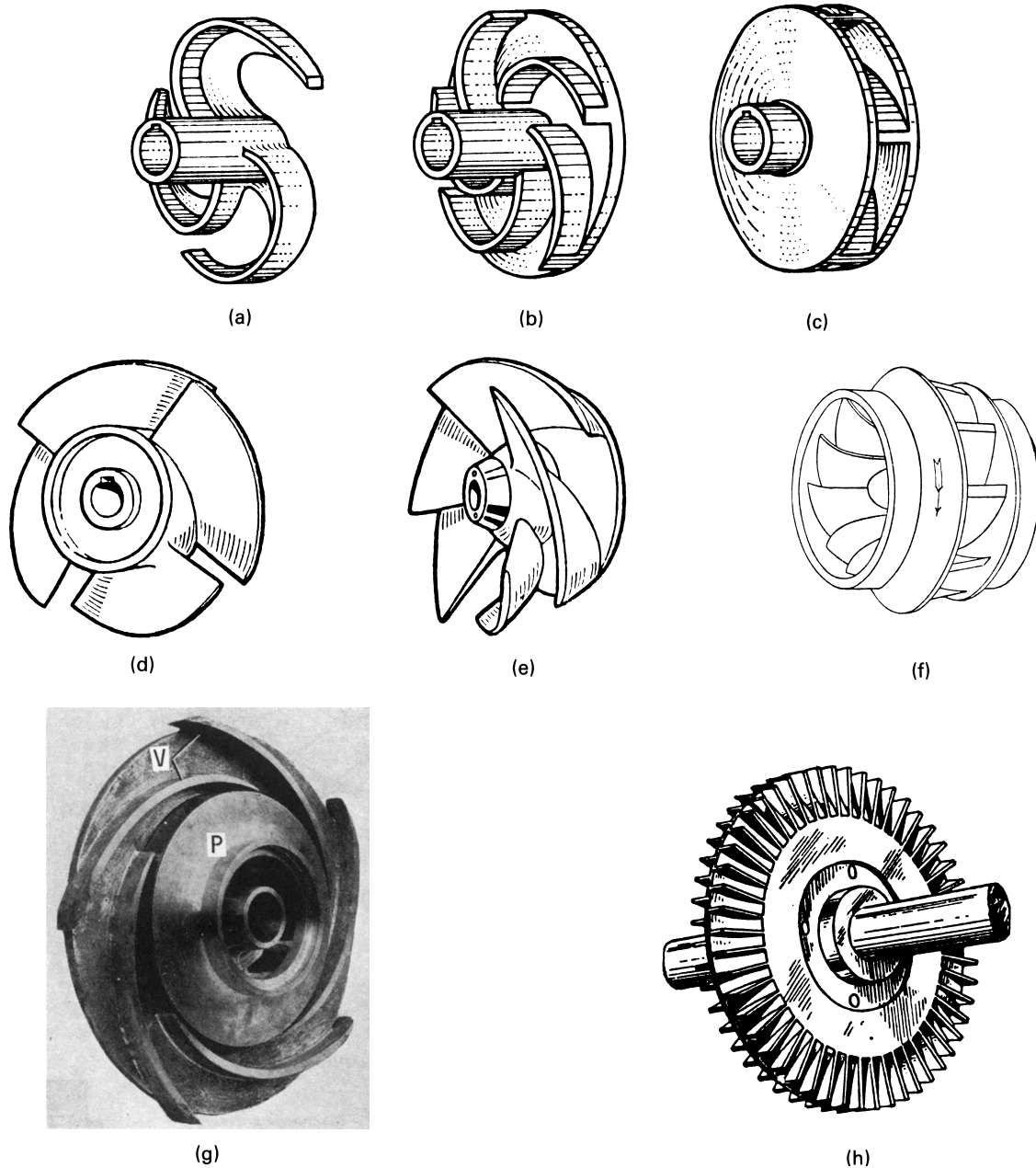
Figure 7.10. Some types of impellers for centrifugal pumps. (a) Open impeller. (b) Semiopen impeller. (c) Shrouded impeller. (d) Axial flow (propeller) type. (e) Combined axial and radial flow, open type. (f) Shrouded mixed-flow impeller. (g) Shrouded impeller (P) in a case with diffuser vanes (V). (h) Turbine impeller.

1. *Fans* accept gases at near atmospheric pressure and raise the pressure by approximately 3% (12 in. of water), usually on air for ventilating or circulating purposes.
2. *Blowers* is a term applied to machines that raise the pressure to an intermediate level, usually to less than 40 psig, but more than accomplished by fans.
3. *Compressors* are any machines that raise the pressure above the levels for which fans are used. Thus, in modern terminology they include blowers.
4. *Jet compressors* utilize a high pressure gas to raise other gases at low pressure to some intermediate value by mixing with them.

5. *Vacuum pumps* produce subatmospheric pressures in process equipment. Often they are compressors operating in reverse but other devices also are employed. Operating ranges of some commercial equipment are stated in Table 7.3.
6. *Steam jet ejectors* are used primarily to evacuate equipment but also as pumps or compressors. They are discussed in Section 7.7.

Application ranges of fans and compressors are indicated on Figures 7.20 and 7.21. Some of these categories of equipment now will be discussed in some detail.
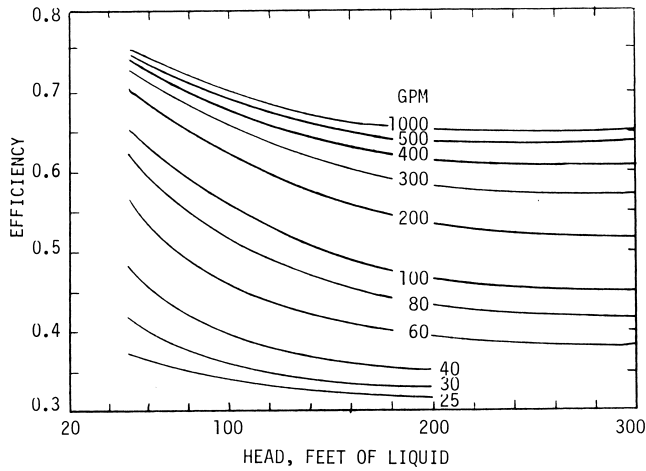
Figure 7.11. Approximate efficiencies of centrifugal pumps in terms of GPM and head in feet of liquid.

FANS

Fans are made either with axial propellers or with a variety of radial vanes. The merits of different directions of curvature of the vanes are stated in Figure 7.24 where the effect of flow rate of pressure, power, and efficiency also are illustrated. Backward curved vanes are preferable in most respects. The kinds of controls used have a marked effect on fan performance as Figure 7.23 shows. Table 7.4 shows capacity ranges and other characteristics of various kinds of fans. Figure 7.24 allows exploration of the effects of changes in specific speed or diameter on the efficiencies and other characteristics of fans. The mutual effects of changes in flow rate, pressure, speed, impeller diameter, and density are related by the "fan laws" of Table 7.5, which apply to all rotating propelling equipment.

COMPRESSORS

The several kinds of commercial compressors are identified in this classification:

1. Rotodynamic
   a. Centrifugal (radial flow)
   b. Axial flow
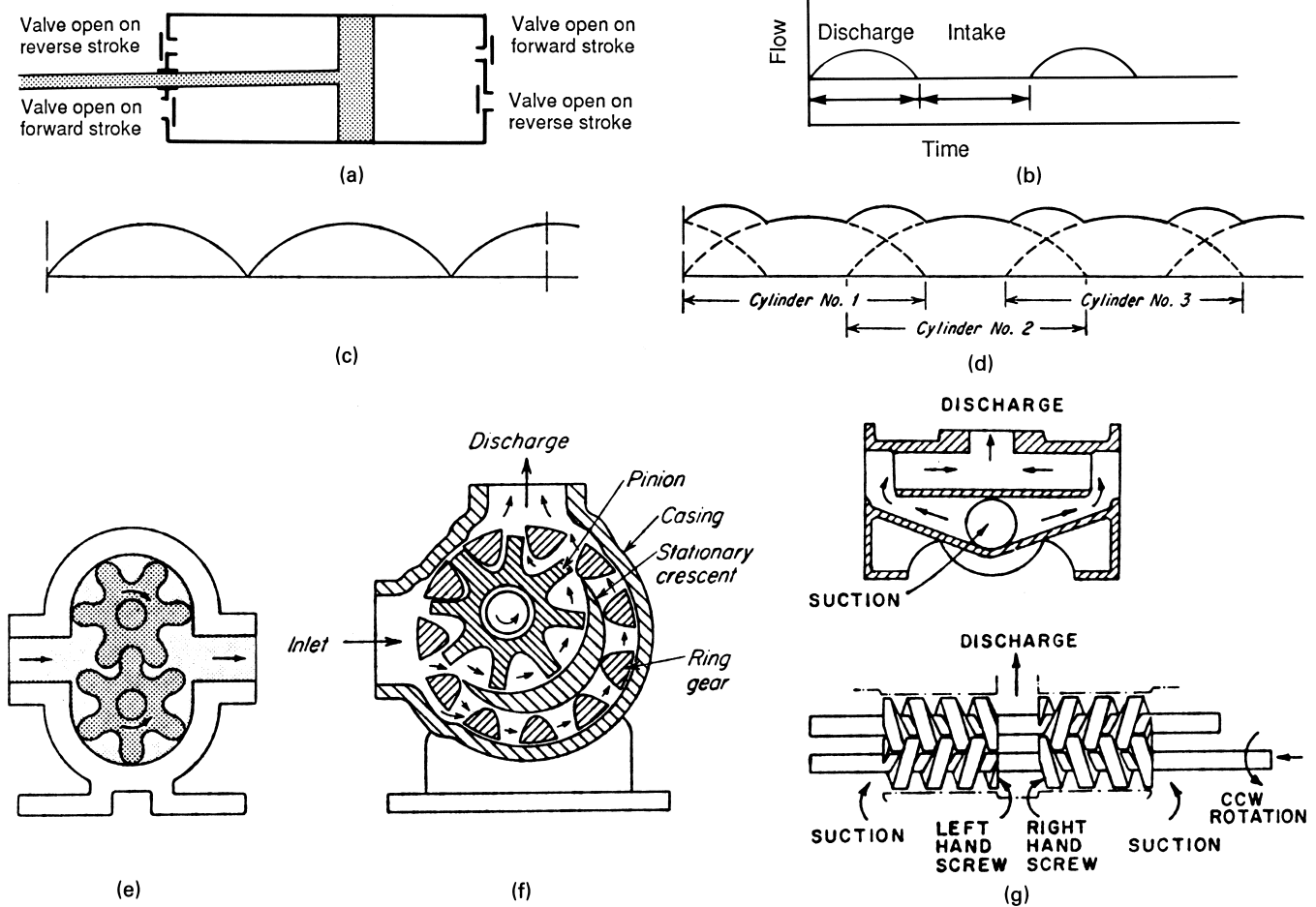
Figure 7.12. Some types of positive displacement pumps. (a) Valve action of a double acting reciprocating piston pump. (b) Discharge curve of a single acting piston pump operated by a crank; half-sine wave. (c) Discharge curve of a simplex double acting pump as in (a). (d) Discharge curve of a duplex, double acting pump. (e) An external gear pump; characteristics are in Figure 7.8(c). (f) Internal gear pump; the outer gear is driven, the inner one follows. (g) A double screw pump. (h) Peristaltic pump in which fluid is squeezed through a flexible tube by the follower. (i) Double diaphragm pump shown in discharge position (BIF unit of General Signal). (j) A turbine pump with essentially positive displacement characteristics. [*Data on Fig. 7.4(a)*].

(h)   (i)   (j)
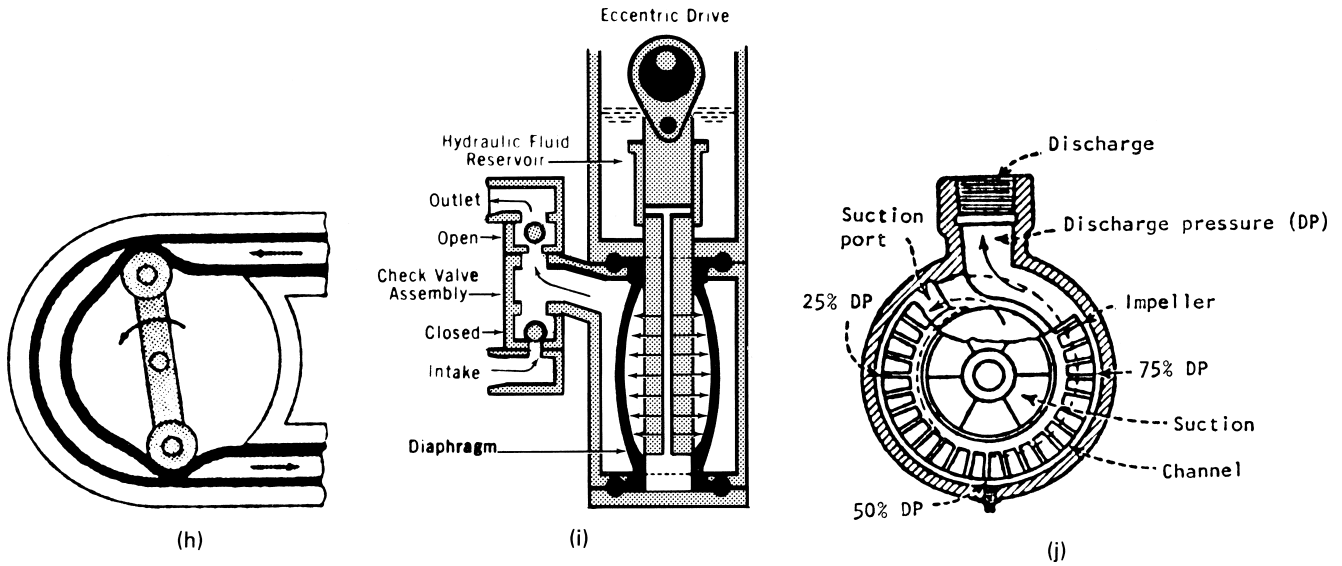
Figure 7.12—(*continued*)

(a)   (b)

(c)   (d)
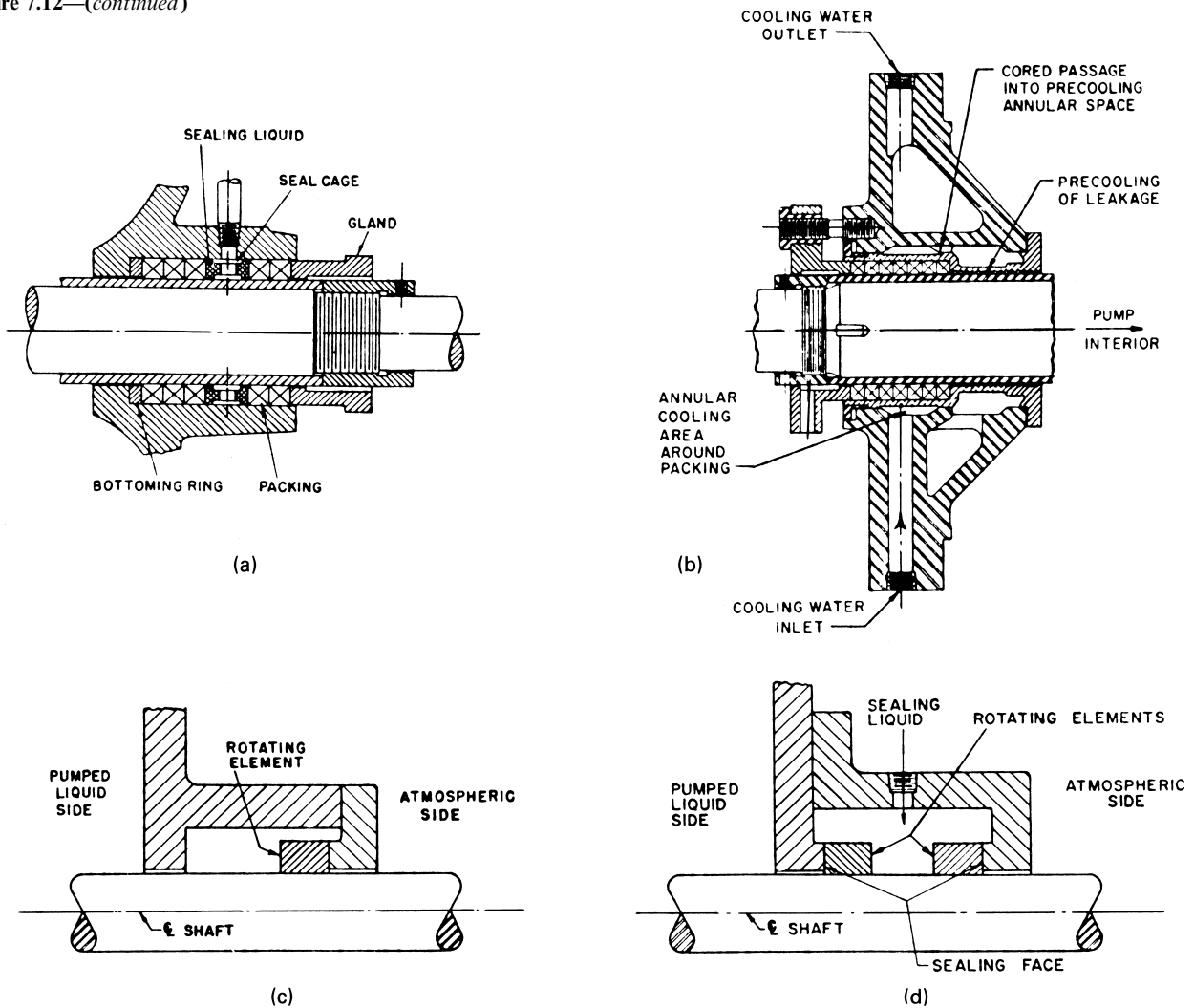
Figure 7.13. Types of seals for pump shafts. (a) Packed stuffing box; the sealing liquid may be from the pump discharge or from an independent source. (b) Water cooled stuffing box. (c) Internal assembly mechanical seal; the rotating and fixed surfaces are held together by the pressure of the pump liquid which also serves as lubricant; a slight leakage occurs. (d) Double mechanical seal with independent sealing liquid for handling toxic or inflammable liquids.

TABLE 7.1. Characteristics of Various Kinds of Pumps

Pump Type	Construction Style	Construction Characteristics	Notes
Centrifugal (horizontal)	single-stage overhung, process type	impeller cantilevered beyond bearings	capacity varies with head
	two-stage overhung	two impellers cantilevered beyond bearings	used for heads above single-stage capability
	single-stage impeller between bearings	impeller between bearings; casing radially or axially split	used for high flows to 1083 ft (330 m) head
	chemical	casting patterns designed with thin sections for high-cost alloys	have low pressure and temperature ratings
	slurry	designed with large flow passages	low speed and adjustable axial clearance; has erosion control features
	canned	no stuffing box; pump and motor enclosed in a pressure shell	low head capacity limits when used in chemical services
	multistage, horizontally split casing	nozzles located in bottom half of casing	have moderate temperature-pressure ranges
	multistage, barrel type	outer casing contains inner stack of diaphragms	used for high temperature-pressure ratings
Centrifugal (vertical)	single-stage, process type	vertical orientation	used to exploit low net positive section head (NPSH) requirements
	multistage	many stages with low head per stage	low-cost installation
	inline	inline installation, similar to a valve	low-cost installation
	high speed	speeds to 380 rps, heads to 5800 ft (1770 m)	high head/low flow; moderate costs
	slump	casing immersed in sump for easy priming and installation	low cost
	multistage, deep well	long shafts	used for water well service
Axial	propeller	propeller-shaped impeller	vertical orientation
Turbine	regenerative	fluted impeller. Flow path resembles screw around periphery	capacity independent of head; low flow/high head performance
Reciprocating	piston, plunger	slow speeds	driven by steam engine cylinders or motors through crankcases
	metering	consists of small units with precision flow control system	diaphragm and packed plunger types
	diaphragm	no stuffing box	used for chemical slurries; can be pneumatically or hydraulically actuated
Rotary	screw	1, 2, or 3 screw rotors	for high-viscosity, high-flow high-pressure services
	gear	intermeshing gear wheels	for high-viscosity, moderate-pressure/moderate-flow services

(Cheremisinoff, 1981).

TABLE 7.2. Typical Performances of Various Kinds of Pumps[a]

Type	Style	Capacity (gpm)	Max Head (ft)	Max P (psi)	NPSH (ft)	Max T (°F)	Efficiency (%)
Centrifugal (horizontal)	single-stage overhung	15–5,000	492	600	6.56–19.7	851	20–80
	two-stage overhung	15–1,200	1394	600	6.56–22.0	851	20–75
	single-stage impeller between bearings	15–40,000	1099	980	6.56–24.9	401–851	30–90
	chemical	1000	239	200	3.94–19.7	401	20–75
	slurry	1000	394	600	4.92–24.9	851	20–80
	canned	1–20,000	4921	10,000	6.56–19.7	1004	20–70
	multistage horizontal split	20–11,000	5495	3000	6.56–19.7	401–500	65–90
	multistage, barrel type	20–9,000	5495	6000	6.56–19.7	851	40–75
Centrifugal (vertical)	single stage	20–10,000	804	600	0.98–19.7	653	20–85
	multistage	20–80,000	6004	700	0.98–19.7	500	25–90
	inline	20–12,000	705	500	6.56–19.7	500	20–80
	high speed	5–400	5807	2000	7.87–39.4	500	10–50
	sump	10–700	197	200	0.98–22.0		45–75
	multistage deep well	5–400	6004	2000	0.98–19.7	401	30–75
Axial	propeller	20–100,000	39	150	6.56	149	65–85
Turbine	regenerative	1–2000	2493	1500	6.56–8.20	248	55–85
Reciprocating	piston, plunger	10–10,000	1.13×10^6	>50,000	12.1	554	65–85
	metering	0–10	1.70×10^5	50,000	15.1	572	20
	diaphragm	4–100	1.13×10^5	3500	12.1	500	20
Rotary	screw	1–2000	6.79×10^4	3000	9.84	500	50–80
	gear	1–5000	11,155	500	9.84	653	50–80

[a]1 m^3/min = 264 gpm, 1 m = 3.28 ft, 1bar = 14.5 psi, °C = (°F − 32)/1.8.
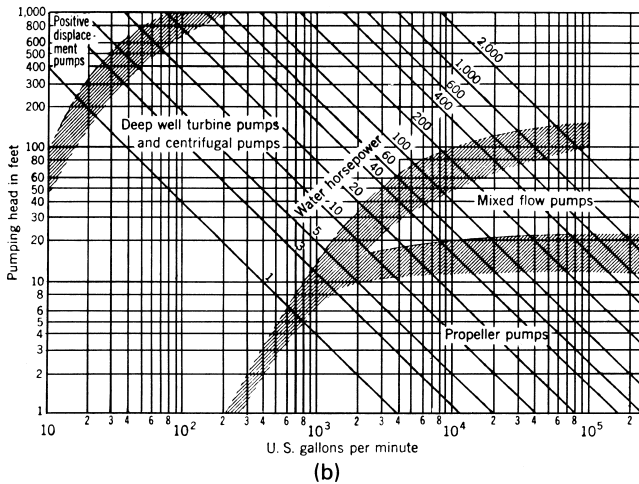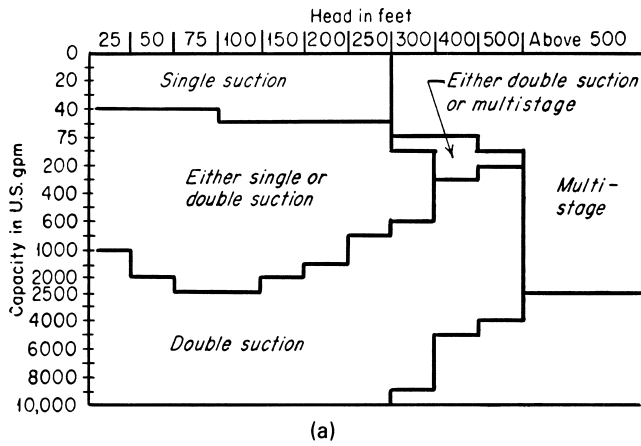
Figure 7.14. Range of applications of various kinds of pumps. (a) Range of applications of single and double suction pumps. (*Allis-Chalmers Co.*). (b) Recommended kinds of pumps for various kinds of head and flow rate. (*Fairbanks, Morse, and Co.*).

2. Positive displacement
   a. Reciprocating piston
   b. Rotary (screws, blades, lobes, etc.).

Sketches of these several types are shown in Figures 7.19 and 7.20 and their application ranges in Figures 7.20 and 7.21.

CENTRIFUGALS

The head-flow rate curve of a centrifugal compressor often has a maximum as shown on Figure 3.21, similar to the pump curve of Figure 7.7(c). To the left the developed head increases with flow, but to the right the head decreases with increasing flow rate. At the peak the flow pulsates and the machine vibrates. This operating point is called the *surge limit* and is always identified by the manufacturer of the equipment, as shown on Figure 7.25 for those centrifugal and axial machines. Stable operation exists anywhere right of the surge limit. Another kind of flow limitation occurs when the velocity of the gas somewhere in the compressor approaches sonic velocity. The resulting shock waves restrict the flow; a slight increase in flow then causes a sharp decline in the developed pressure.

Table 7.6 shows as many as 12 stages in a single case. These machines are rated at either 10K or 12K ft/stage. The higher value

corresponds to about 850 ft/sec impeller tip speed which is near the limit for structural reasons. The limitation of head/stage depends on the nature of the gas and the temperature, as indicated on Figure 7.26. Maximum compression ratios of 3–4.5 per stage with a maximum of 8–12 per machine are commonly used. Discharge pressures as high as 3000–5000 psia can be developed by centrifugal compressors.

A specification form is included in Appendix B and as Table 4.4. Efficiency data are discussed in Section 7.6, Theory and Calculations of Gas Compression: Efficiency.

AXIAL FLOW COMPRESSORS

Figure 7.18(b) shows the axial flow compressor to possess a large number of blades attached to a rotating drum with stationary but adjustable blades mounted on the case. Typical operating characteristics are shown on Figure 7.22(a). These machines are suited particularly to large gas flow rates at maximum discharge pressures of 80–130 psia. Compression ratios commonly are 1.2–1.5 per stage and 5–6.5 per machine. Other details of range of applications are stated on Figure 7.20. According to Figure 7.21, specific speeds of axial compressors are in the range of 1000–3000 or so.

Efficiencies are 8–10% higher than those of comparable centrifugal compressors.

TABLE 7.3. Operating Ranges of Some Commercial Vacuum Producing Equipment

Type of Pump	Operating Range (mm Hg)
Reciprocating piston	
1-stage	760–10
2-stage	760–1
Rotary piston oil-sealed	
1-stage	$760–10^{-2}$
2-stage	$760–10^{-3}$
Centrifugal multistage (dry) liquid jet	760–200
Mercury Sprengel	$760–10^{-3}$
Water aspirator (18°C)	760–15
Two-lobe rotary blower (Roots type)	$20–10^{-4}$
Turbomolecular	$10^{-1}–10^{-10}$
Zeolite sorption (liquid nitrogen cooled)	$760–10^{-3}$
Vapor jet pumps	
Steam ejector	
1-stage	760–100
2-stage	760–10
3-stage	760–1
4-stage	$760–3 \times 10^{-1}$
5-stage	$760–5 \times 10^{-2}$
Oil ejector (1-stage)	$2–10^{-2}$
Diffusion-ejector	$2–10^{-4}$
Mercury diffusion with trap	
1-stage	$10^{-1}– < 10^{-6}$
2-stage	$1– < 10^{-6}$
3-stage	$10– < 10^{-6}$
Oil diffusion	
1-stage	$10^{-1}–5 \times 10^{-6}$
4-stage fractionating (untrapped)	$5 \times 10^{-1}–10^{-9}$
4-stage fractionating (trapped)	$5 \times 10^{-1}–10^{-12}$
Getter-ion (sputter-ion)	$10^{-3}–10^{-11}$
Sublimation (titanium)	$10^{-4}–10^{-11}$
Cryopumps (20 K)	$10^{-2}–10^{-10}$
Cryosorption (15 K)	$10^{-2}–10^{-12}$

(*Encyclopedia of Chemical Technology,* Wiley-Interscience, New York, 1978–1984).
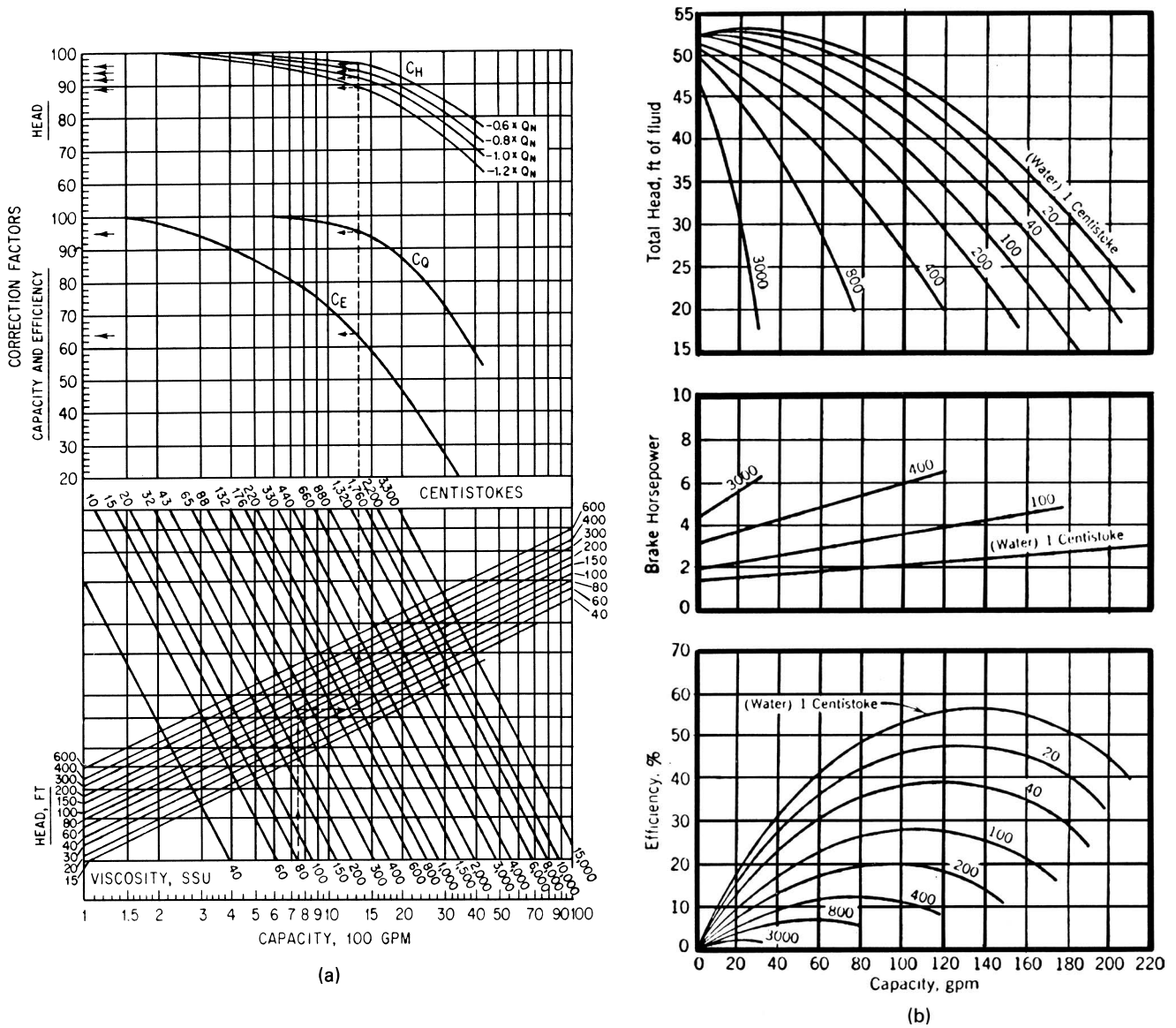
Figure 7.15. Effects of viscosity on performance of centrifugal pumps: (a) Hydraulic Institute correction chart for pumping liquids. (b) Typical performances of pumps when handling viscous liquids. The dashed lines on the chart on the left refer to a water pump that has a peak efficiency at 750 gpm and 100 ft head; on a liquid with viscosity 1000 SSU (220 CS) the factors relative to water are efficiency 64%, capacity 95% and head 89% that of water at 120% normal capacity ($1.2Q_H$).

RECIPROCATING COMPRESSORS

Reciprocating compressors are relatively low flow rate, high pressure machines. Pressures as high as 35,000–50,000 psi are developed with maximum compression ratios of 10/stage and any desired number of stages provided with intercoolers. Other data of application ranges are in Figure 7.20. The limitation on compression ratio sometimes is due to the limitations on discharge temperature which normally is kept below 300°F to prevent ignition of machine lubrications when oxidizing gases are being compressed, and to the fact that power requirements are proportional to the absolute temperature of the suction gas.

A two-stage double-acting compressor with water cooled cylinder jackets and intercooler is shown in Figure 7.18(c). Selected dimensional and performance data are in Table 7.7. Drives may be with steam cylinders, turbines, gas engines or electrical motors.

A specification form is included in Appendix B. Efficiency data are discussed in Section 7.6, Theory and Calculations of Gas Compression: Temperature Rise, Compression Ratio, Volumetric Efficiency.

ROTARY COMPRESSORS

Four of the many varieties of these units are illustrated in Figure 7.19. Performances and comparisons of five types are given in Tables 7.8–7.9. All of these types also are commonly used as vacuum pumps when suction and discharge are interchanged.

Lobe type units operate at compression ratios up to 2 with efficiencies in the range of 80–95%. Typical relations between volumetric rate, power, speed, and pressure boost are shown in Figure 7.19(b).
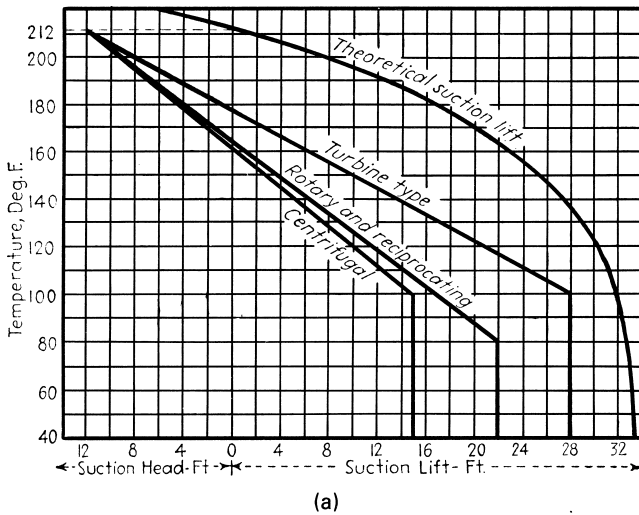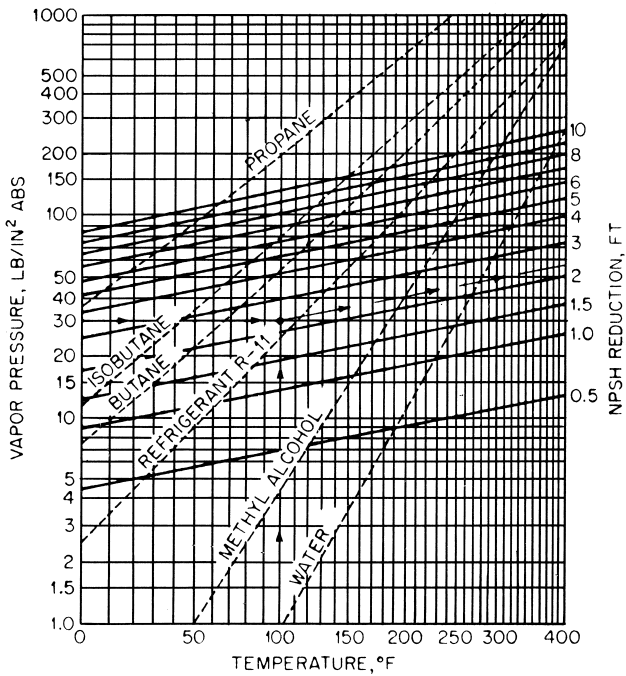
Figure 7.16. Recommended values of net positive suction head (NPSH) at various temperatures or vapor pressures: (a) NPSH of several types of pumps for handling water at various temperatures. (b) Correction of the cold water NPSH for vapor pressure. The maximum recommended correction is one-half of the cold water value. The line with arrows shows that for a liquid with 30 psia vapor pressure at 100°F, the reduction in NPSH is 2.3 ft (*data of Worthington International Inc.*).

Spiral screws usually run at 1800–3600 rpm. Their capacity ranges up to 12,000 CFM or more. Normal pressure boost is 3–20 psi, but special units can boost pressures by 60–100 psi. In vacuum service they can produce pressures as low as 2 psia. Some other performance data are shown with Figure 7.19(d).

The sliding vane compressor can deliver pressures of 50 psig or pull a vacuum of 28 in. of mercury. A two-stage unit can deliver 250 psig. A generous supply of lubricant is needed for the sliding vanes. Table 7.9 shows that power requirements are favorable in comparison with other rotaries.

Liquid-liner compressors produce an oil-free discharge of up to 125 psig. The efficiency is relatively low, 50% or so, but high enough to make them superior to steam jet ejectors for vacuum service. The liquid absorbs the considerable heat of compression and must be circulated and cooled; a 200 HP compressor requires 100 gpm of cooling water with a 10°F rise. When water vapor is objectionable in the compressed gas, other sealing liquids are used; for example, sulfuric acid for the compression of chlorine. Figure 7.19(e) shows the principle and Table 7.10 gives specifications of some commercial units.

7.6. THEORY AND CALCULATIONS OF GAS COMPRESSION

The main concern of this section is how to determine the work requirement and the effluent conditions of a compressor for which the inlet conditions and the outlet pressure are specified. Theoretical methods allow making such calculations for ideal and real gases and gas mixtures under isothermal and frictionless adiabatic (isentropic) conditions. In order that results for actual operation can be found it is neecessary to know the efficiency of the equipment. That depends on the construction of the machine, the mode of operation, and the nature of the gas being processed. In the last analysis such information comes from test work and its correlation by manufacturers and other authorities. Some data are cited in this section.

DIMENSIONLESS GROUPS

The theory of dimensionless groups of Section 7.2, Basic Relations, also applies to fans and compressors with rotating elements, for example, Eqs. (7.8)–(7.10) which relate flow rate, head, power, speed, density, and diameter. Equivalent information is embodied in Table 7.5. The concept of specific speed, Eqs. (7.11) and (7.12), also is pertinent. In Figures 7.21 and 7.25 it is the basis for identifying suitable operating ranges of various types of compressors.

IDEAL GASES

The ideal gas or a gas with an equation of state

$$PV = zRT \tag{7.18}$$

is a convenient basis of comparison of work requirements for real gases and sometimes yields an adequate approximation of these work requirements. Two limiting processes are isothermal and isentropic (frictionless adiabatic) flows. Changes in elevation and velocity heads are considered negligible here. With constant compressibility z the isothermal work is

$$W = \int_{P_1}^{P_2} V \, dP = zRT \ln (P_2/P_1). \tag{7.19}$$

Under isentropic conditions and with constant heat capacities, the pressure–volume relation is

$$PV^k = P_1 V_1^k = \text{const}, \tag{7.20}$$

where

$$k = C_p/C_v \tag{7.21}$$

is the ratio of heat capacities at constant pressure and constant volume and

$$C_v = R - C_p. \tag{7.22}$$
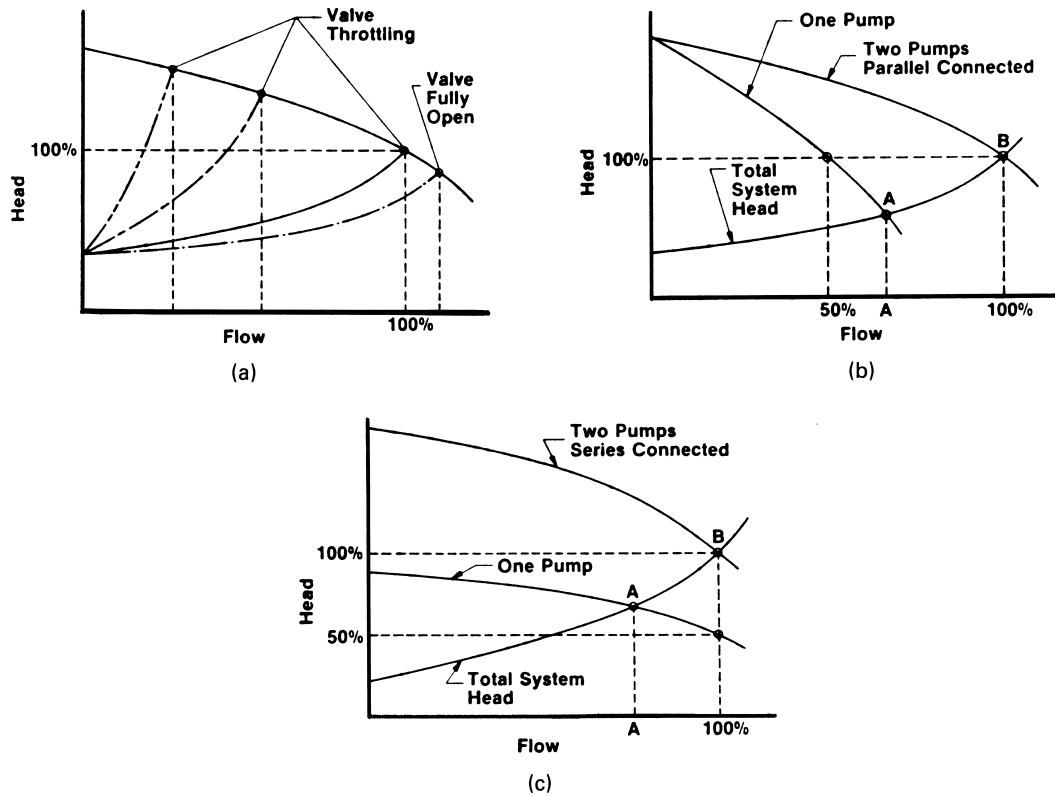
Figure 7.17. Operating points of centrifugal pumps under a variety of conditions. (a) Operating points with a particular pump characteristic and system curves corresponding to various amounts of flow throttling with a control valve. (b) Operating point with two identical pumps in parallel; each pump delivers one-half the flow and each has the same head. (c) Operating point with two identical pumps in series; each pump delivers one-half the head and each has the same flow.
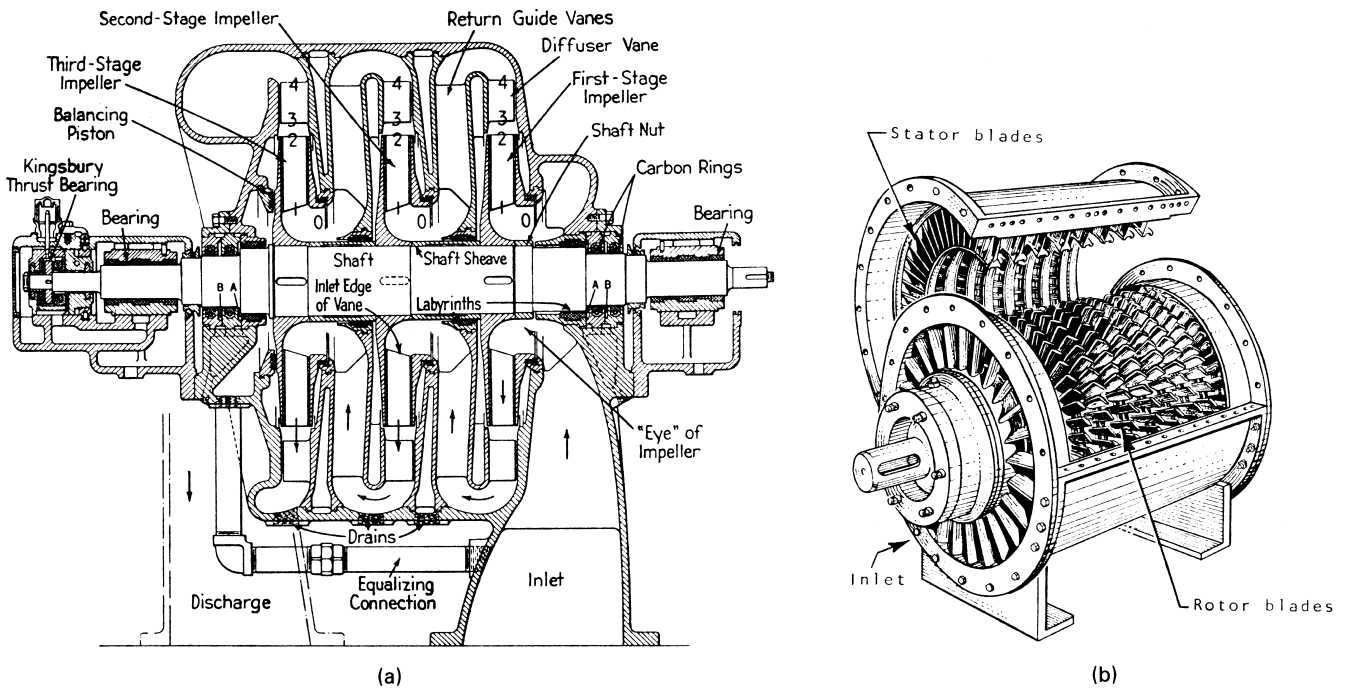
Figure 7.18. Heavy-duty centrifugal, axial, and reciprocating compressors. (a) Section of a three-stage compressor provided with steam-sealed packing boxes. (*DeLaval Steam Turbine Co.*). (b) An axial compressor. (*Clark Brothers Co.*). (c) Double-acting, two-stage reciprocating compressor with water-cooled jacket and intercooler. (*Ingersoll-Rand Co.*).
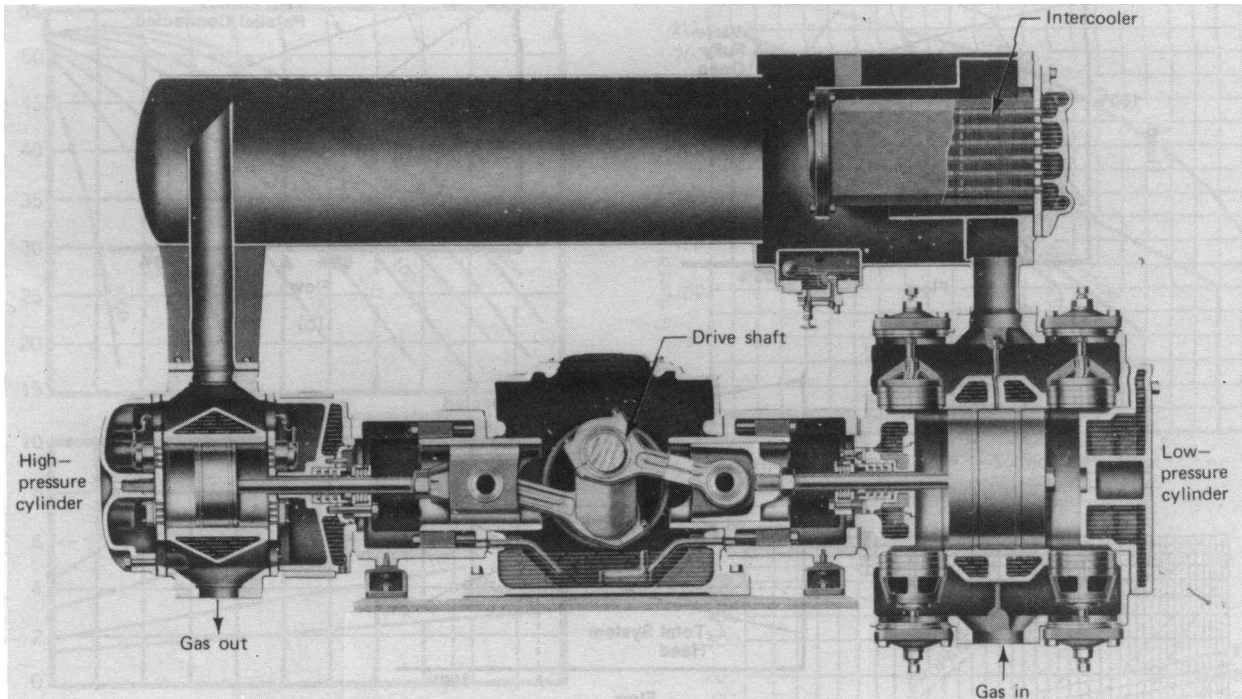
(c)

Figure 7.18—(*continued*)
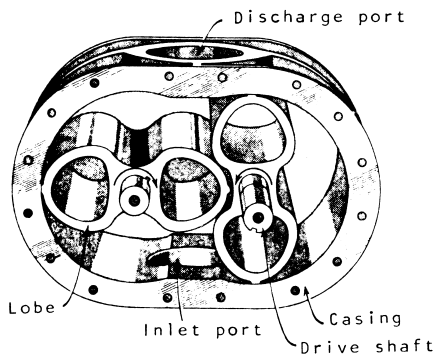
(a)
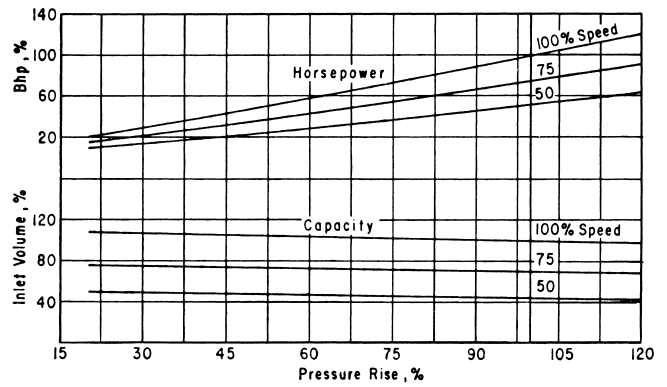
(b)
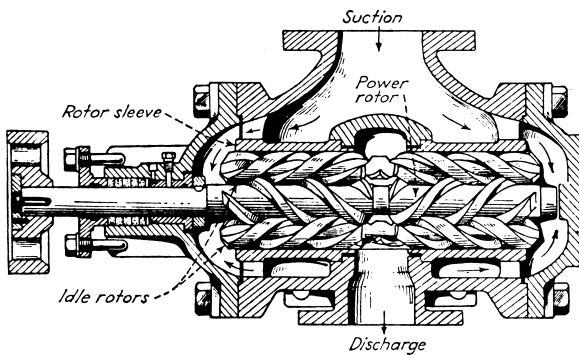
(c)
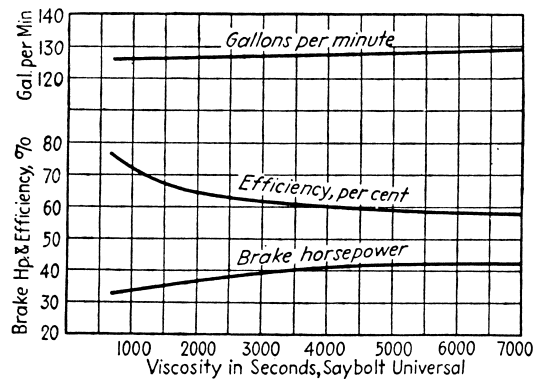
(d)

Figure 7.19. Some rotary positive displacement compressors. (a) A two-lobe blower. (b) Performance of a two-lobe blower. (*Roots-Connersville Co.*). (c) A screw pump with one power and two idle rotors. (*Kristal and Annett, 1940*). (d) Performance of 3.5″ screw pump handling oils at 1150 rpm against 325 psig. (*Kristal and Annett, 1940*). (e) Principle of the liquid ring seal compressor. (*Nash Engineering Co.*). (f) A sliding vane blower. (*Beach-Russ Co.*).

(e)
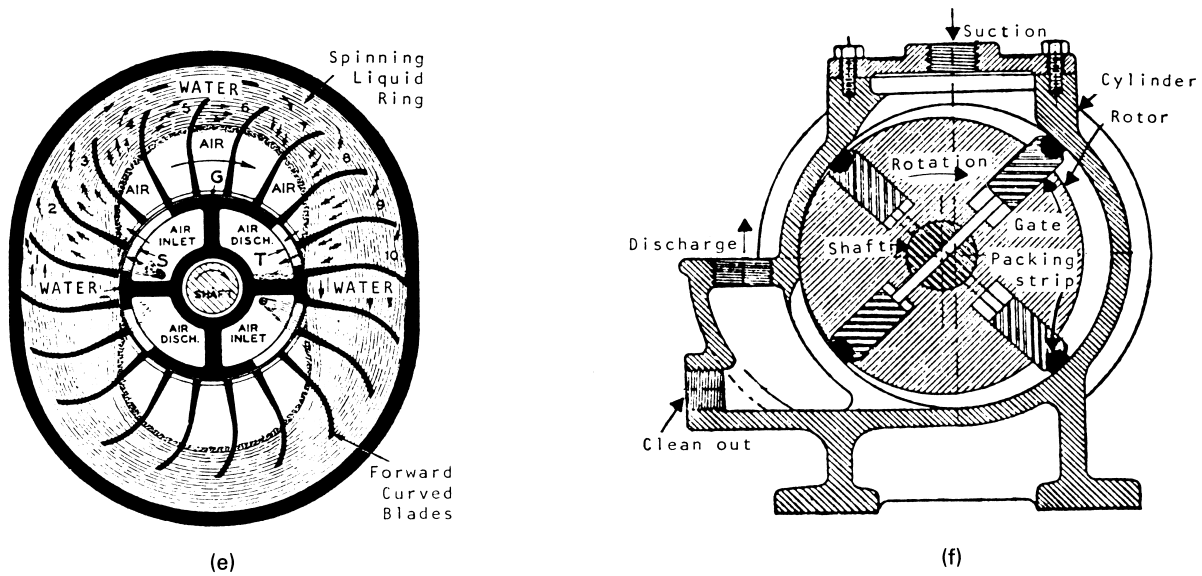
Figure 7.19.—(*continued*)

(f)

(a)

(b)
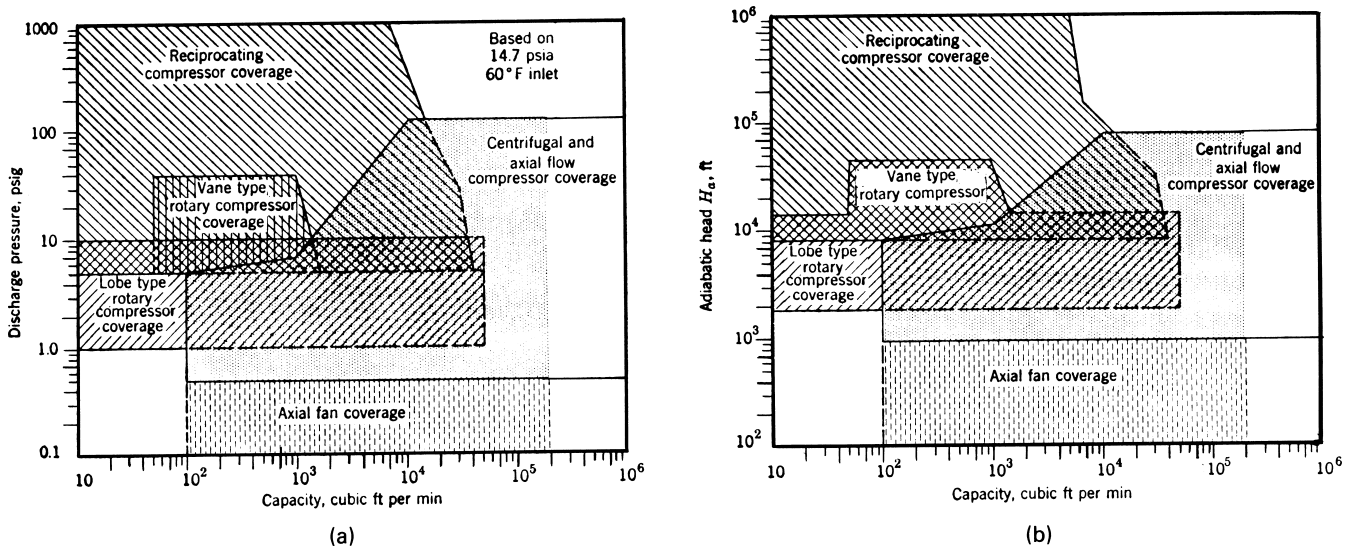
Figure 7.20. Applications ranges of compressors and fans (*Worthington*): (a) Pressure-capacity ranges for air at 1 atm, 60°F, 0.075 lb/cuft. (b) Head-capacity ranges for all gases. Similar charts are given by Ludwig (*1983, Vol. 1, p. 251*) *and Perry's Chemical Engineers' Handbook*, 7th ed. (1999, p. 10–24, Figure 10–26).

A related expression of some utility is

$$T_2/T_1 = (P_2/P_1)^{(k-1)/k}. \tag{7.23}$$

Since k ordinarily is a fairly strong function of the temperature, a suitable average value must be used in Eq. (7.20) and related ones.

Under adiabatic conditions the flow work may be written as

$$W = H_2 - H_1 = \int_{P_1}^{P_2} V dP. \tag{7.24}$$

Upon substitution of Eq. (7.20) into Eq. (7.24) and integration, the isentropic work becomes

$$W_s = H_2 - H_1 = P_1^{1/k} V_1 \int_{P_1}^{P_2} dP/P^{1/k}$$

$$= \left(\frac{k}{k-1}\right) z_1 R T_1 \left[\left(\frac{P_2}{P_1}\right)^{(k-1)/k} - 1\right]. \tag{7.25}$$

In multistage centrifugal compression it is justifiable to take the average of the inlet and outlet compressibilities so that the work becomes

$$W_s = H_2 - H_1 = \left(\frac{k}{k-1}\right) \left(\frac{z_1 + z_2}{2}\right) R T_1 \left[\left(\frac{P_2}{P_1}\right)^{(k-1)/k} - 1\right]. \tag{7.26}$$
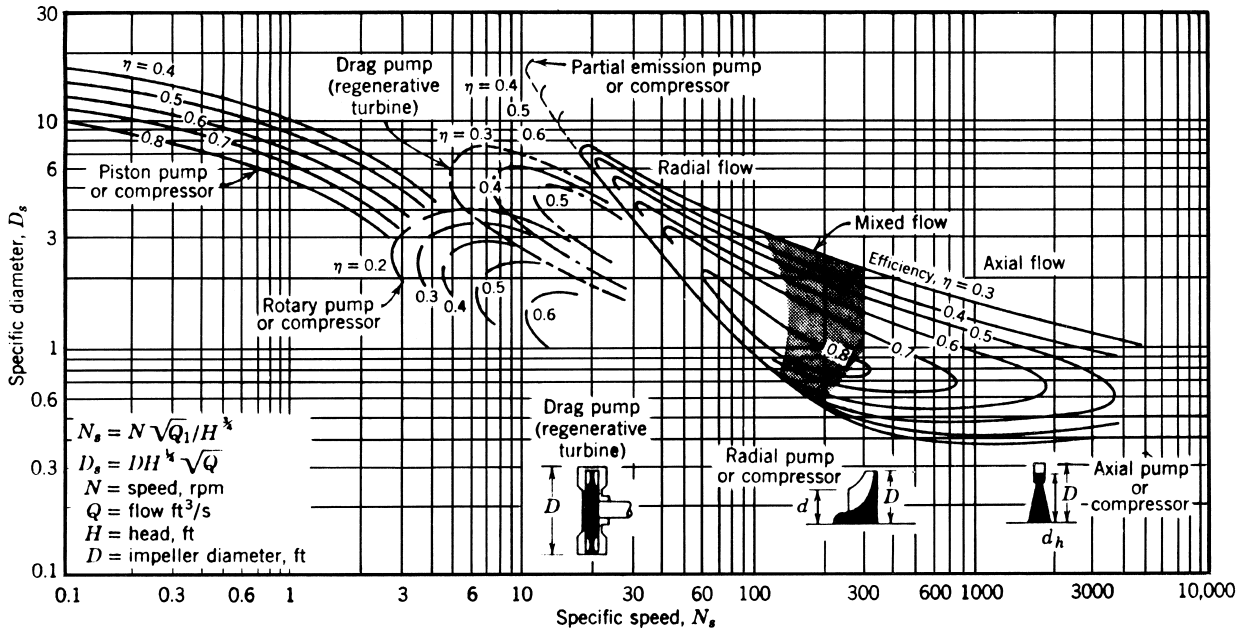
Figure 7.21. Operating ranges of single-stage pumps and compressors [*Balje,* Trans. ASME, J. Eng. Power. **84,** *103* (*1962*)]. *Example:* atmospheric air at the rate of 100,000 SCFM is compressed to 80,000 ft lbf/ft (41.7 psig) at 12,000 rpm; calculated $N_s = 103$; in the radial flow region with about 80% efficiency, $D_s = 1.2$–1.6, so that $D = 2.9$–3.9 ft.

(a)

(b)
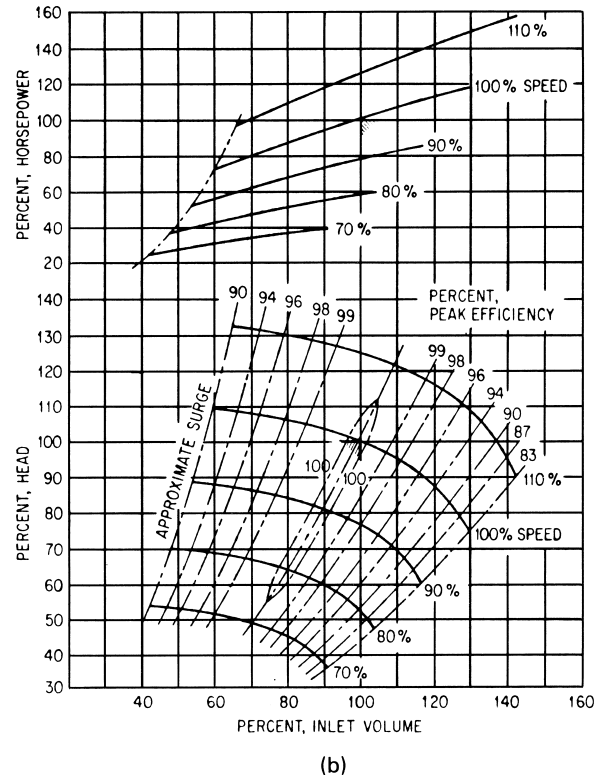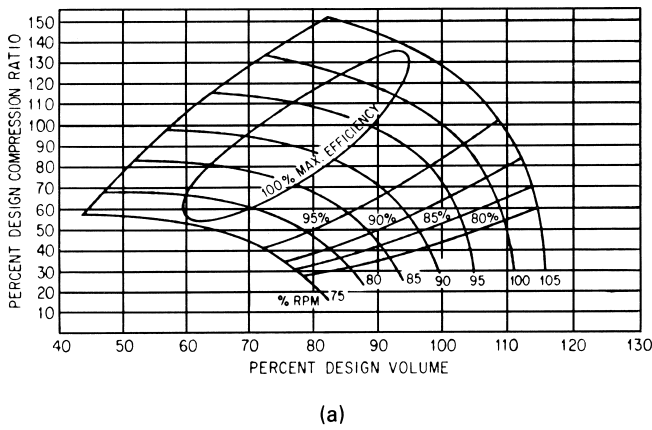
Figure 7.22. Performances of dynamic compressors: (a) Axial compressor. (b) Centrifugal compressor. All quantities are expressed as percentages of those at the design condition which also is the condition of maximum efficiency. (De Laval Engineering Handbook, *McGraw-Hill, New York, 1970*).

TABLE 7.4. Performance Characteristics of Fans[a]

Description	Quantity (1000 acfm) Min	Max	Head Inches Water	Opt. V (fps)	Max q_{ad}	Diameter (in.) Min	Max	N_s	D_s	Peak Eff.
Axial propeller	8	20	10	410	0.13	23	27	470	0.63	77
Axial propeller	20	90	8	360	0.12	27	72	500	0.60	80
Axial propeller	6	120	2.5	315	0.10	27	84	560	0.50	84
Radial air foil	6	100	22	250	0.45	18	90	190	0.85	88
Radial BC	3	35	18	260	0.63	18	90	100	1.35	78
Radial open MH	2	27	18	275	0.55	18	66	97	1.45	56
Radial MH	2	27	18	250	0.55	18	66	86	1.53	71
Radial IS	2	27	18	250	0.55	18	66	86	1.53	66
Vane Bl flat	1	10	12	250	0.43	10	30	210	0.81	70
Vane FC	1	10	2	65	1.15	10	30	166	0.65	66

[a] $q_{ad} = 32.2\,H/V^2$, $N_s = NQ^{0.5}/V^{0.75}$ (specific speed), $D_s = DV^{0.25}/Q^{0.5}$ (specific diameter), where D = diameter (ft), H = head (ft), Q = suction flow rate (cfs), V = impeller tip speed (fps), and N = rotation speed (rpm). (Evans, 1979).
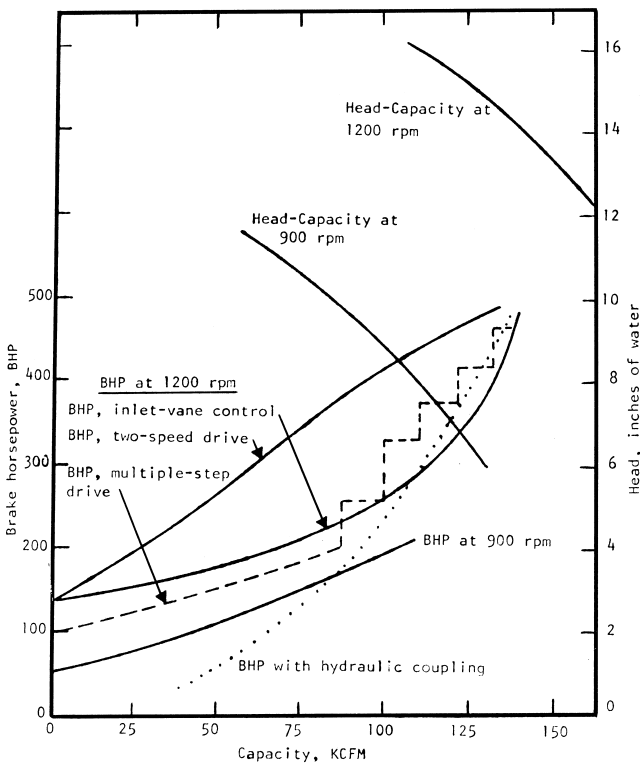
Control Type	Control Cost	Required Power Input	Advantages (A), and Disadvantages (D)
a	low	high	(A) simplicity; (D) high power input
b	moderate	moderate	(A) lower input power; (D) higher cost
c	low	moderate	(A) simplicity; (D) fan erosion
d	moderate	moderate	(D) complex; also needs dampers
e	high	low	(A) simple; no dampers needed

Figure 7.23. Performances of fans with several kinds of controls (*American Standard Co. Inc.*). (a) A damper in the duct with constant-speed fan drive, (b) two-speed fan driver, (c) inlet vanes or inlet louvers with a constant-speed fan drive, (d) multiple-step variable-speed fan drive, and (e) hydraulic or electric coupling with constant-speed driver giving wide control over fan speed.

When friction is present, the problem is handled with *empirical* efficiency factors. The isentropic compression efficiency is defined as

$$\eta_s = \frac{\text{isentropic work or enthalpy change}}{\text{actually required work or enthalpy change}}. \tag{7.27}$$

TABLE 7.5. Fan Laws[a]

Fan Law Number		Ratio of	−	Ratio	×	Ratio	×	Ratio
1	a	cfm		size^3	×	rpm		1
	b	press	−	size^2	×	rpm^2	×	δ
	c	HP		size^5	×	rpm^3		δ
2	a	cfm		size^2	×	press$^{1/2}$		$1/\delta^{1/2}$
	b	rpm	−	1/size	×	press$^{1/2}$	×	$1/\delta^{1/2}$
	c	HP		size^2	×	press$^{3/2}$		$1/\delta^{1/2}$
3	a	rpm		1/size^3	×	cfm		1
	b	press	−	1/size^4	×	cfm^2	×	δ
	c	HP		1/size^4	×	cfm^3		δ
4	a	cfm		size$^{4/3}$	×	HP$^{1/3}$		$1/\delta^{1/3}$
	b	press	−	1/size$^{4/3}$	×	HP$^{2/3}$	×	$\delta^{1/3}$
	c	rpm		1/size$^{5/3}$	×	HP$^{1/3}$		$1/\delta^{1/3}$
5	a	size		cfm$^{1/2}$	×	1/press$^{1/4}$		$\delta^{1/4}$
	b	rpm	−	1/cfm$^{1/2}$	×	press$^{3/4}$	×	$1/\delta^{3/4}$
	c	HP		cfm	×	press		1
6	a	size		cfm$^{1/3}$	×	1/rpm$^{1/3}$		1
	b	press	−	cfm$^{2/3}$	×	rpm$^{4/3}$	×	δ
	c	HP		cfm$^{5/3}$	×	rpm$^{4/3}$		δ
7	a	size		press$^{1/2}$	×	1/rpm		$1/\delta^{1/2}$
	b	cfm	−	press$^{3/2}$	×	1/rpm^2	×	$1/\delta^{3/2}$
	c	HP		press$^{5/2}$	×	1/rpm^2		$1/\delta^{3/2}$
8	a	size		1/HP$^{1/4}$	×	cfm$^{3/4}$		$\delta^{1/4}$
	b	rpm	−	HP$^{3/4}$	×	1/cfm$^{5/4}$	×	$1/\delta^{3/4}$
	c	press		HP	×	1/cfm		1
9	a	size		HP$^{1/2}$	×	1/press$^{3/4}$		$\delta^{1/4}$
	b	rpm	−	1/HP$^{1/2}$	×	press$^{5/4}$	×	$1/\delta^{3/4}$
	c	cfm		HP	×	1/press		1
10	a	size		HP$^{1/5}$	×	1/rpm$^{3/5}$		$1/\delta^{1/5}$
	b	cfm	−	HP$^{3/5}$	×	1/rpm$^{4/3}$	×	$1/\delta^{3/5}$
	c	press		HP$^{2/5}$	×	rpm$^{4/5}$		$\delta^{3/5}$

[a] $\delta = \rho/g_c$.
For example, the pressure P varies as $D^2 N^2 \rho/g_c$ line 1(b), $Q^2(\rho/g_c)/D^4$ line 3(b), $\dot{P}^{2/3}(\rho/g_c)^{1/3}/D^{4/3}$ line 4(b), $Q^{2/3}N^{4/3}\rho/g_c$ line 6(b), $\dot{P}/Q$ line 8(c), and $\dot{P}^{2/5}N^{4/5}(\rho/g_c)^{3/5}$ line 10(c). (Madison, 1949).

(a)

(b)

(c)

	Backwardly Curved	Radial Blade	Forwardly Curved
First Cost *...........	High	Medium	Low
Efficiency..............	High	Medium	Low
Stability of Operation...	Good	Good	Poor
Space Required........	Medium	Medium	Small
Tip Speed.............	High	Medium	Low
Resistance to Abrasion..	Medium	Good	Poor
Ability to Handle Sticky Materials.....	Medium	Good	Poor

(d)
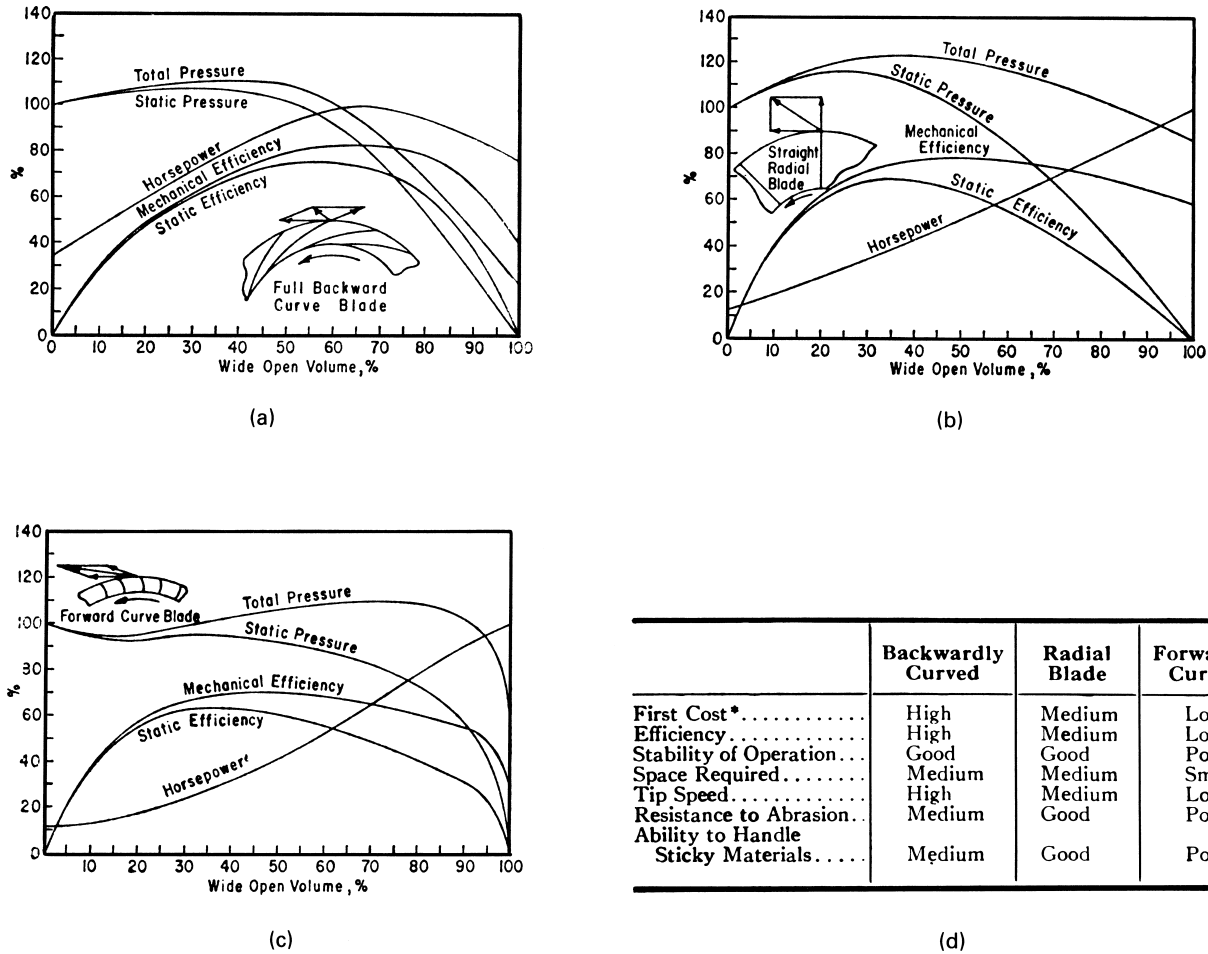
Figure 7.24. Performances of fans with various-shaped blades. (*Green Fuel Economizer Co*.): (a) Backward curved blades. (b) Straight radial blades. (c) Forward curved blades. (d) Comparison of characteristics of the several blade types. (*Sturtevant*).

TABLE 7.6. Specifications of Centrifugal Compressors

Frame	Normal Inlet Flow Range[a] (ft³/min)	Nominal Polytropic Head per Stage[b] (H_p)	Nominal Polytropic Efficiency (η_p)	Nominal Maximum No. of Stages[c]	Speed at Nominal Polytropic Head/Stage
29M	500–8000	10,000	0.76	10	11500
38M	6000–23,000	10,000/12,000	0.77	9	8100
46M	20,000–35,000	10,000/12,000	0.77	9	6400
60M	30,000–58,000	10,000/12,000	0.77	8	5000
70M	50,000–85,000	10,000/12,000	0.78	8	4100
88M	75,000–130,000	10,000/12,000	0.78	8	3300
103M	110,000–160,000	10,000	0.78	7	2800
110M	140,000–190,000	10,000	0.78	7	2600
25MB (H) (HH)	500–5000	12,000	0.76	12	11500
32MB (H) (HH)	5000–10,000	12,000	0.78	10	10200
38MB (H)	8000–23,000	10,000/12,000	0.78	9	8100
46MB	20,000–35,000	10,000/12,000	0.78	9	6400
60MB	30,000–58,000	10,000/12,000	0.78	8	5000
70MB	50,000–85,000	10,000/12,000	0.78	8	4100
88MB	75,000–130,000	10,000/12,000	0.78	8	3300

[a] Maximum flow capacity is reduced in direct proportion to speed reduction.
[b] Use either 10,000 or 12,000 ft for each impeller where this option is mentioned.
[c] At reduced speed, impellers can be added.
(Elliott Co.).
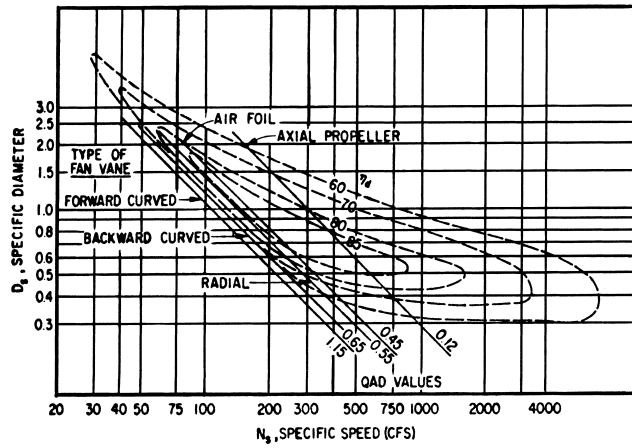
Figure 7.25. Efficiency and head coefficient q_{ad} as functions of specific speeds and specific diameters of various kinds of impellers (*Evans, 1979*). *Example:* An axial propeller has an efficiency of 70% at $N_s = 200$ and $D_s = 1.5$; and 85% at $N_s = 400$ and $D_s = 0.8$. See Table 7.4 for definitions of q_{ad}, N_s, and D_s.

Accordingly,

$$W = \Delta H = W_s/\eta_s = (\Delta H)_s/\eta_s. \tag{7.28}$$

When no other information is available about the process gas, it is justifiable to find the temperature rise from

$$\Delta T = (\Delta T)_s/\eta_s \tag{7.29}$$

so that

$$T_2 = T_1(1 + (1/\eta_s)[(P_2/P_1)^{(k-1)/k} - 1]. \tag{7.30}$$

Example 7.4 calculates the temperature rise using Equations 7.24 and 7.30.

A case with variable heat capacity is worked out in Example 7.5.

For mixtures, the heat capacity to use is the sum of the mol fraction weighted heat capacities of the pure components,

$$C_p = \sum x_i C_{pi}. \tag{7.31}$$

REAL PROCESSES AND GASES

Compression in reciprocating and centrifugal compressors is essentially adiabatic but it is not frictionless. The pressure–volume behavior in such equipment often conforms closely to the equation

$$PV^n = P_1 V_1^n = \text{const.} \tag{7.32}$$

Such a process is called polytropic. The equation is analogous to the isentropic equation (7.20) but the polytropic exponent n is different from the heat capacity ratio k.

Polytropic exponents are deduced from PV measurements on the machine in question. With reciprocating machines, the PV data are recorded directly with engine indicators. With rotary machines other kinds of instruments are used. Such test measurements usually are made with air.

Work in polytropic compression of a gas with equation of state $PV = zRT$ is entirely analogous to Eq. (7.26). The hydrodynamic work or the work absorbed by the gas during the compression is

$$W_{hd} = \int_{P_1}^{P_2} V \, dP = \left(\frac{n}{n-1}\right) z_1 R T_1 \left[\left(\frac{P_2}{P_1}\right)^{(n-1)/n} - 1\right]. \tag{7.33}$$

Manufacturers usually characterize their compressors by their polytropic efficiencies which are defined by

$$\eta_p = \left(\frac{n}{n-1}\right) \bigg/ \left(\frac{k}{k-1}\right) = \frac{n(k-1)}{k(n-1)}. \tag{7.34}$$

The polytropic work done on the gas is the ratio of Eqs. (7.33) and (7.34) and comprises the actual mechanical work done on the gas:

$$W_p = W_{hd}/\eta_p = \left(\frac{k}{k-1}\right) z_1 R T_1 \left[\left(\frac{P_2}{P_1}\right)^{(n-1)/n} - 1\right] \tag{7.35}$$

Losses in seals and bearings of the compressor are in addition to W_p; they may amount to 1–3% of the polytropic work, depending on the machine.

The value of the polytropic exponent is deduced from Eq. (7.34) as

$$n = \frac{k\eta_p}{1 - k(1 - \eta_p)}. \tag{7.36}$$

TABLE 7.7. Some Sizes of One- and Two-Stage Reciprocating Compressors

(a) Horizontal, One-Stage, Belt-Driven

Diameter Cylinder (in.)	Stroke (in.)	Displacement (cuft/min.)	rpm	Air Pressure (lb/sq in.)	Brake HP at Rated Pressure	Openings (in.)	
						Inlet	Outlet
$7\frac{1}{2}$	6	106	310	80–100–125	15.9–17–18	$2\frac{1}{2}$	$2\frac{1}{2}$
$8\frac{1}{2}$	9	170	300	80–100–125	25–27–29	3	3
10	10	250	285	80–100–125	36–38.5–41	$3\frac{1}{2}$	$3\frac{1}{2}$
11	12	350	270	80–100–125	51–57–60	—	4
$8\frac{1}{2}$	6	136	350	40–60	15–18.5	—	3
10	9	245	300	40–75	27–34	$3\frac{1}{2}$	$3\frac{1}{2}$
11	10	312	285	40–75	34–43	4	4
13	12	495	270	40–75	54–70	5	5
12	9	350	300	20–45	30–42	4	4
13	10	435	285	30–45	42–52	6	6
15	12	660	270	30–50	59–74	7	7

(Worthington Corp.).

TABLE 7.7.—(*continued***)**

(b) Horizontal, One-Stage, Steam-Driven[a]

Diameter, Steam Cylinder (in.)	Diameter, Air Cylinder, (in.)	Stroke (in.)	Displacement, (cuft/min)	rpm	Air Pressure, (lb/sq in.)
7	$7\frac{1}{2}$	6	106	350	80–100–125
8	$8\frac{1}{2}$	9	170	300	80–100–125
9	10	10	250	285	80–100–125
10	11	12	350	270	80–100–125
7	$8\frac{1}{2}$	6	136	350	40–60
8	10	9	245	300	40–75[b]
9	11	10	312	285	40–75[b]
10	13	12	495	270	40–75[b]
8	12	9	350	300	20–45[c]
9	13	10	435	285	20–45[c]
10	15	12	660	270	20–50[c]

[a]All machines have piston-type steam valves.
[b]110-lb steam necessary for maximum air pressure.
[c]125-lb steam necessary for maximum air pressure.
(Worthington Corp.).

(c) Horizontal, Two-Stage, Belt-Driven

Diameter Cylinder (in.)		Stroke (in.)	rpm	Piston Displacement (cuft free air/min)
Low Pressure	High Pressure			
4	$2\frac{1}{8}$	4	500	28
6	$2\frac{7}{8}$	6	350	65
8	$3\frac{8}{4}$	8	300	133
10	$4\frac{7}{8}$	10	275	241

(Ingersoll–Rand Co.).

TABLE 7.8. Summary of Rotary Compressor Performance Data

	Type				
	Helical Screw	Spiral Axial	Straight Lobes	Sliding Vanes	Liquid Liner
Configuration, features (male × female)	4 × 6	2 × 4	2 × 2	8 Blades	16 Sprockets
Max displacement (cfm)	20,000	13,000	30,000	6,000	13,000
Max diameter (in.)	25	16	18	33	48
Min diameter (in.)	4	6	10	5	12
Limiting tip speed (Mach)	0.30	0.12	0.05	0.05	0.06
Normal tip speed (Mach)	0.24	0.09	0.04	0.04	0.05
Max L/d, low pressure	1.62	2.50	2.50	3.00	1.1
Normal L/d, high pressure	1.00	1.50	1.50	2.00	1.00
V factor for volumetric efficiency	7	3	5	3	3
X factor for displacement	0.0612	0.133	0.27	0.046	0.071
Normal overall efficiency	75	70	68	72	50
Normal mech. eff. at ±100 HP (%)	90	93	95	94	90
Normal compression ratio R_c	2/3/4	3	1.7	2/3/4	5
Normal blank-off R_c	6	5	5	7	9
Displacement form factor A_e	0.462	1.00	2.00	0.345	0.535

(Evans, 1979).

TABLE 7.9. Five Rotary Compressors for a Common Service

	Type				
	Helical Screw	Spiral Axial	Straight Lobes	Sliding Vanes	Liquid Liner
Suction loss θ_i	9.35	1.32	0.89	0.90	1.40
Discharge loss θ_e	7.35	1.04	0.70	0.70	1.10
Intrinsic corr. B	1.185	1.023	1.016	1.016	1.025
Adiabatic eff. η_{ad}	85.6	97.7	98.5	98.5	97.9
Slippage W_s (%)	28.5	16.6	11.8	11.8	3.0
Slip eff. η_s (%)	71.5	83.4	88.2	88.2	97.0
Thermal eff. η_t (%)	89.2	93.7	95.8	95.5	42.5
Volumetric eff. E_{vr}	68.0	85.7	89.1	89.9	96.6
Displacement (cfm)	14,700	11,650	11,220	11,120	10,370
Rotor dia. (in.)	26.6	26.2	27.0	65.0	45.5
Commercial size, $d \times L$	25 × 25	22 × 33	22 × 33	46 × 92[a]	43 × 48[b]
Speed (rpm)	3,500	1,250	593	284	378
Motor (HP)	1,100	800	750	750	1,400
Service factor	1.09	1.11	1.10	1.12	1.10
Discharge temp °F	309	270	262	263	120

[a]Twin 32.5 × 65 or triplet 26.5 × 33 (667 rpm) are more realistic.
[b]Twin 32 × 32 (613 rpm) alternate where $L = d$.
(Evans, 1979).

The isentropic efficiency is

$$\eta_s = \frac{\text{isentropic work [Eq.(7.25)]}}{\text{actual work [Eq.(7.35)]}} \tag{7.37}$$

$$= \frac{(P_2/P_1)^{(k-1)/k} - 1}{(P_2/P_1)^{(n-1)/n} - 1} \tag{7.38}$$

$$= \frac{(P_2/P_1)^{(k-1)/k} - 1}{(P_2/P_1)^{(k-1)/k\eta_p} - 1} \tag{7.39}$$

The last version is obtained with the aid of Eq. (7.34) and relates the isentropic and polytropic efficiencies directly. Figure 7.27(b) is a plot of Eq. (7.39). Example 7.6 is an exercise in the relations between the two kinds of efficiencies.

WORK ON NONIDEAL GASES

The methods discussed thus far neglect the effect of pressure on enthalpy, entropy, and heat capacity. Although efficiencies often are not known well enough to justify highly refined calculations,

TABLE 7.10. Specifications of Liquid Liner Compressors

Compressor (size)	Pressure (psi)	Capacity (cuft/min)	Motor (HP)	Speed (rpm)
K-6	5	1020	40	570
	10	990	60	
	15	870	75	
	20	650	100	
621		26	7½	3500
1251	35	120	40	1750
1256		440	100	1750
621		23	10	3500
1251	80	110	50	1750
1256		410	150	1750

(Nash Engineering Co.).

they may be worth doing in order to isolate the uncertainties of a design. Compressibility factors are given for example by Figure 7.29. Efficiencies must be known or estimated.

Thermodynamic Diagram Method. When a thermodynamic diagram is available for the substance or mixture in question, the flow work can be found from the enthalpy change,

$$W = \Delta H. \tag{7.40}$$

The procedure is illustrated in Example 7.7 and consists of these steps:

1. Proceed along the line of constant entropy from the initial condition to the final pressure P_2 and enthalpy $(H_2)_s$.
2. Evaluate the isentropic enthalpy change $(\Delta H)_s = (H_2)_s - H_1$.
3. Find the actual enthalpy change as

$$\Delta H = (\Delta H)_s/\eta_s \tag{7.41}$$

and the final enthalpy as

$$H_2 = H_1 + (\Delta H)_s/\eta_s. \tag{7.42}$$

4. At the final condition (P_2, H_2) read off any other desired properties such as temperature, entropy or specific volume.

Thermodynamic diagrams are known for light hydrocarbons, refrigerants, natural gas mixtures, air, and a few other common substances. Unless a substance or mixture has very many applications, it is not worthwhile to construct a thermodynamic diagram for compression calculations but to use other equivalent methods.

EXAMPLE 7.4
Gas Compression, Isentropic and True Final Temperatures
With $k = 1.4$, $P_2/P_1 = 3$ and $\eta_s = 0.71$; the final temperatures are $(T_2)_s = 1.369T_1$ and $T_2 = 1.519T_1$ with Eqs. (7.24) and (7.31).
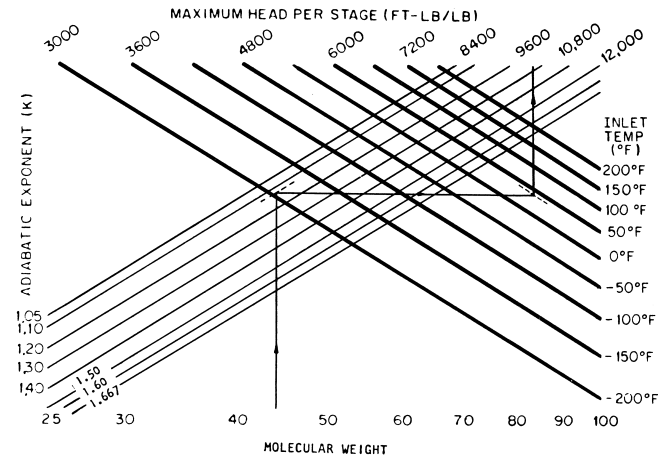
(a)
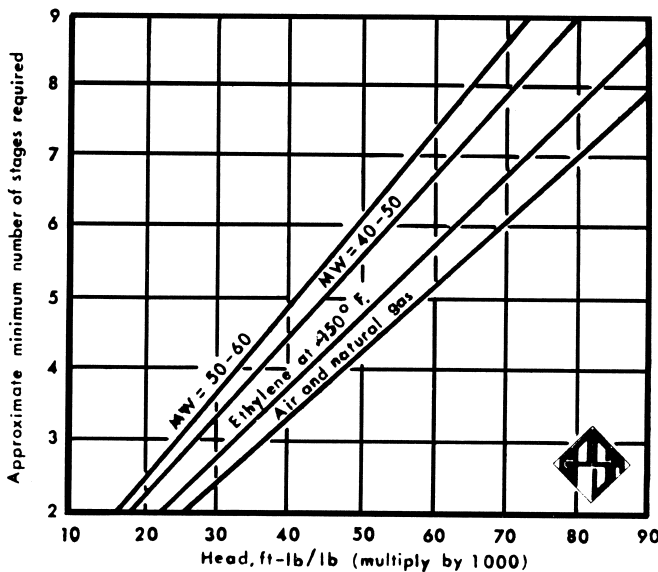
(b)

$$H = \frac{Ku^2}{32.2} \text{ ft / stage}$$

K = 0.50–0.65, empirical coefficient

u = 600–900 ft / sec, impeller peripheral speed

H = 10,000 with average values K = 0.55 and u = 765 ft / sec

(c)

Figure 7.26. Several ways of estimating allowable polytropic head per stage of a multistage centrifugal compressor. (a) Single-stage head as a function of k, molecular weight, and temperature (*Elliott Co.*). (b) Single-stage head as a function of the nature of the gas (NGPSA Handbook, *Gas Processors Assn, Tulsa, OK, 1972*), obtained by dividing the total head of the compressor by number of stages. $H = Ku^2/32.2$ ft/stage, $K = 0.50$–0.65, empirical coefficient, $u = 600$–900 ft/sec, impeller peripheral speed, and $H = 10,000$ with average values $K = 0.55$ and $u = 765$ ft/sec. (c) An equation and parameters for estimation of head.

General Method. The effects of composition of mixtures and of pressure on key properties such as enthalpy and entropy are deduced from *PVT* equations of state. This process is described in books on thermodynamics, for example, Reid, Prausnitz, and Sherwood (*Properties of Liquids and Gases*, McGraw-Hill, New York, 1977) and Walas (*Phase Equilibria in Chemical Engineering*, Butterworths, Stoneham, MA, 1985). Only the simplest correlations of these effects will be utilized here for illustration.

For ideal gases with heat capacities dependent on temperature, the procedure requires the isentropic final temperature to be found by trial from

$$\Delta S = \int_{T_1}^{T_{2s}} (C_p/T)dT - R\ln(P_2/P_1) \to 0, \qquad (7.43)$$

and then the isentropic enthalpy change from

$$\Delta H = \int_{T_1}^{T_{2s}} C_p\, dT. \qquad (7.44)$$

The final temperature T_2 is found by trial after applying a known isentropic efficiency,

$$(\Delta H)_s/\eta_s = \int_{T_1}^{T_2} C_p\, dT. \qquad (7.45)$$

The fact that heat capacities usually are represented by empirical polynomials of the third or fourth degree in temperature accounts for the necessity of solutions of equations by trial.

Example 7.5 applies this method and checks roughly the calculations of Example 7.7 with the thermodynamic diagram of this substance. The pressures are relatively low and are not expected to generate any appreciable nonideality.

This method of calculation is applied to mixtures by taking a mol fraction weighted heat capacity of the mixture,

$$C_p = \sum x_i C_{pi}. \qquad (7.46)$$

When the pressure range is high or the behavior of the gas is nonideal for any other reason, the isentropic condition becomes

$$\Delta S = \int_{T_1}^{T_{2s}} (C_p'/T)\, dT - R\ln(P_2/P_1) + \Delta S_1' - \Delta S_2' \to 0. \qquad (7.47)$$

After the final isentropic temperature T_{2s} has been found by trial, the isentropic enthalpy change is obtained from

$$(\Delta H)_s = \int_{T_1}^{T_{2s}} C_p'\, dT + \Delta H_1' - \Delta H_{2s}'. \qquad (7.48)$$

In terms of a known isentropic efficiency the final temperature T_2 then is found by trial from

$$(\Delta H)_s/\eta_s = \int_{T_1}^{T_2} C_p'\, dT + \Delta H_1' - \Delta H_2'. \qquad (7.49)$$

In these equations the heat capacity C_p' is that of the ideal gas state or that of the real gas near zero or atmospheric pressure. The residual properties $\Delta S_1'$ and $\Delta H_1'$ are evaluated at (P_1, T_1) and $\Delta S_2'$ and $\Delta H_2'$ at (P_2, T_2). Figure 7.28 gives them as functions of reduced

EXAMPLE 7.5
Compression Work with Variable Heat Capacity
Hydrogen sulfide heat capacity is given by

$$C_p = 7.629 + 3.431(E-4)T + 5.809(E-6)T^2$$
$$-2.81(E-9)T^3, \text{ cal/g mol,}$$

with T in K. The gas is to be compressed from $100°F$ (310.9 K) and 14.7 psia to 64.7 psia.

Assuming the heat capacity to be independent of pressure in this low range, the isentropic condition is

$$\Delta S = \int_{T_1}^{T_2} (C_p/T)\, dT - R\ln(P_2/P_1)$$
$$= \int_{310.9}^{T_2} (C_p/T)\, dT - 1.987\ln(64.7/14.7) = 0.$$

By trial, with a root-solving program,

$T_2 = 441.1$ K, $334.4°F$ (compared with $345°F$ from Example 7.7).

The isentropic enthalpy change becomes

$$\Delta H_s = \int_{310.1}^{441.1} C_p\, dT = 1098.1\,\text{cal/g mol}$$
$$\rightarrow 1098.1(1.8)/34.08 = 58.0\,\text{Btu/lb,}$$

compared with 59.0 from Example 7.7. The integration is performed with Simpson's rule on a calculator.

The actual final temperature will vary with the isentropic efficiency. It is found by trial from the equation

$$1098.1/\eta_s = \int_{1098.1}^{T_2} C_p\, dT.$$

Some values are

η_s	1.0	0.75	0.50	0.25
T_2	441.1	482.93	564.29	791.72

---

temperature T/T_c and reduced pressure P/P_c. More accurate methods and charts for finding residual properties from appropriate equations of state are presented in the cited books of Reid et al. (1977) and Walas (1985).

For mixtures, pseudocritical properties are used for the evaluation of the reduced properties. For use with Figure 7.28, Kay's rules are applicable, namely,

$$(P_c)_{\text{mix}} = \sum x_i P_{ci}, \tag{7.50}$$

$$(T_c)_{\text{mix}} = \sum x_i T_{ci}, \tag{7.51}$$

but many equations of state employ particular combining rules.

Example 7.8 compares a solution by this method with the assumption of ideal behavior.

EFFICIENCY

The efficiencies of fluid handling equipment such as fans and compressors are empirically derived quantities. Each manufacturer will supply either an efficiency or a statement of power requirement for a specified performance. Some general rules have been devised for ranges in which efficiencies of some classes equipment usually fall. Figure 7.27 gives such estimates for reciprocating compressors. Fan efficiencies can be deduced from the power-head curves of Figure 7.24. Power consumption or efficiencies of rotary and reciprocating machines are shown in Tables 7.7, 7.8, and 7.9.

Polytropic efficiencies are obtained from measurements of power consumption of test equipment. They are essentially independent of the nature of the gas. As the data of Figure 7.27 indicate, however, they are somewhat dependent on the suction volumetric rate, particularly at low values, and on the compression ratio. Polytropic efficiencies of some large centrifugal compressors are listed in Table 7.6. These data are used in Example 7.9 in the selection of a machine for a specified duty.

The most nearly correct methods of Section 7.6.4 require knowledge of isentropic efficiencies which are obtainable from the polytropic values. For a given polytropic efficiency, which is independent of the nature of the gas, the isentropic value is obtained with Eq. (7.39) or Figure 7.27(b). Since the heat capacity is involved

in this transformation, the isentropic efficiency depends on the nature of the substance and to some extent on the temperature also.

TEMPERATURE RISE, COMPRESSION RATIO, VOLUMETRIC EFFICIENCY

The isentropic temperature in terms of compression ratio is given for ideal gases by

$$(T_2)_s = T_1(P_2/P_1)^{(k-1)/k}. \tag{7.52}$$

For polytropic compression the final temperature is given directly by

$$T_2 = T_1(P_2/P_1)^{(n-1)/n} \tag{7.53}$$

or alternately in terms of the isentropic efficiency by

$$(\Delta T)_{\text{actual}} = T_2 - T_1 = (\Delta T)_{\text{isentropic}}/\eta_s \tag{7.54}$$

so that

$$T_2 = T_1 + (\Delta T)_s/\eta_s = T_1\{1 + (1/\eta_s)[(P_2/P_1)^{(k-1)/k} - 1]\}. \tag{7.55}$$

The final temperature is read off directly from a thermodynamic diagram when that method is used for the compression calculation, as in Example 7.7. A temperature calculation is made in Example 7.10. Such determinations also are made by the general method for nonideal gases and mixtures as in Example 7.8 and for ideal gases in Example 7.4.

Compression Ratio. In order to save on equipment cost, it is desirable to use as few stages of compression as possible. As a rule, the compression ratio is limited by a practical desirability to keep outlet temperatures below $300°F$ or so to minimize the possibility of ignition of machine lubricants, as well as the effect that power requirement goes up as outlet temperature goes up. Typical compression ratios of reciprocating equipment are:
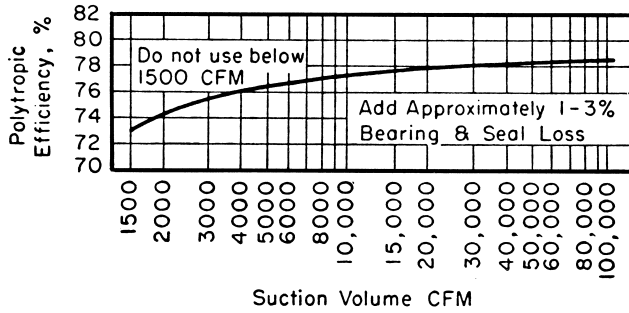
TABLE OF CORRECTION FACTORS DUE TO COMPRESSION RATIO

Compression Ratio	1500	2000	3000	Inlet Volume in CFM 4000	5000	7500	15,000	30,000	60,000 & over
1.35	1.0	1.0	1.0	1.0	1.0	1.0	1.0	1.0	1.0
1.75	.983	.990	.990	.994	.996	.996	.996	.996	1.0
2.25	.976	.977	.986	.985	.991	.995	.995	.995	1.0
2.80	—	.969	.980	.980	.989	.992	.993	.994	1.0
5.00	—	—	.965	.970	.972	.985	.991	.996	.997
10.00	—	—	—	.944*	.955*	.960*	.985*	.989*	.995
15.00	—	—	—	—	.935*	.957*	.971*	.986*	.993

Notes: Asterisk indicates figures applying only to high molecular weight hydrocarbons.
Factors apply on one compressor body with six or less impellers.

(a)
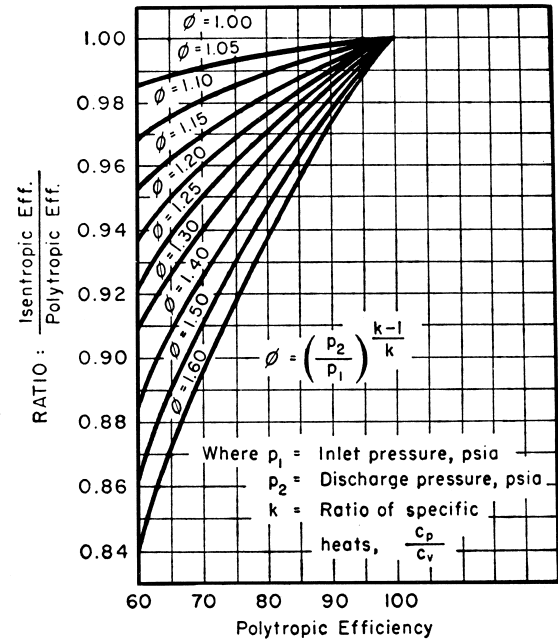
(b)
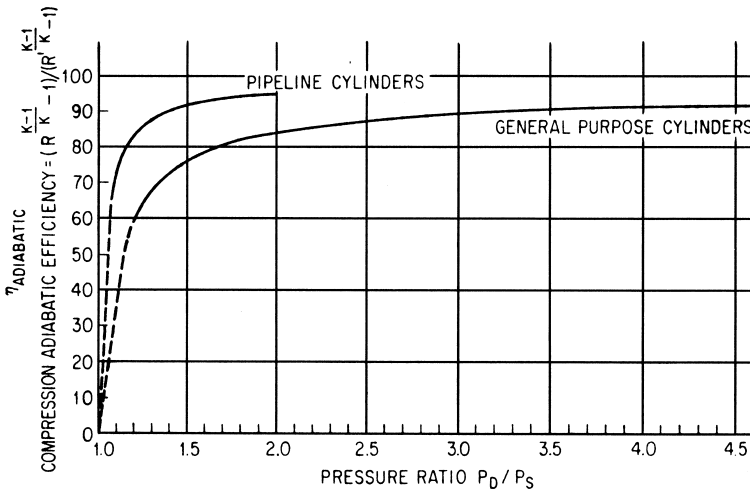
(c)

Compression Ratio	Efficiencies (Engine-driven*)
1.1	50–60
1.2	60–70
1.3	65–80
1.5	70–85
2.0	75–88
2.5	80–89
3.0	82–90
4.0	85–90

*Multiply by 0.95 for motor-driven compressors.

Figure 7.27. Efficiencies of centrifugal and reciprocating compressors. (a) Polytropic efficiencies of centrifugal compressors as a function of suction volume and compression ratio. (*Clark Brothers Co.*). (b) Relation between isentropic and polytropic efficiencies, Eqs. (7.22) (7.23). (c) Isentropic efficiencies of reciprocating compressors. (De Laval Handbook, *McGraw-Hill, New York, 1970*). Multiply by 0.95 for motor drive. Gas engines require 7000–8000 Btu/HP.

Large pipeline compressors	1.2–2.0
Process compressors	1.5–4.0
Small units	up to 6.0

EXAMPLE 7.6
Polytropic and Isentropic Efficiencies

Take $\eta_p = 0.75$, $k = 1.4$, and $P_2/P_1 = 3$. From Eq. (7.39), $n = 1.6154$ and $\eta_s = 0.7095$. With Figure 7.27(b), $\phi = 3^{0.2857} = 1.3687$, $\eta_s = 0.945\eta_p = 0.709$. The agreement is close.

For minimum equipment cost, the work requirement should be the same for each stage. For ideal gases with no friction losses between stages, this implies equal compression ratios. With n stages, accordingly, the compression ratio of each stage is

$$P_{j+1}/P_j = (P_n/P_1)^{1/n}.$$ (7.56)
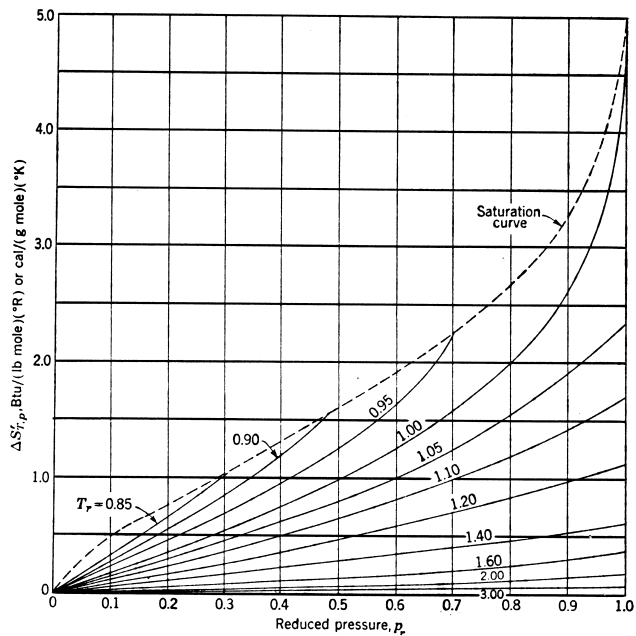
(a)
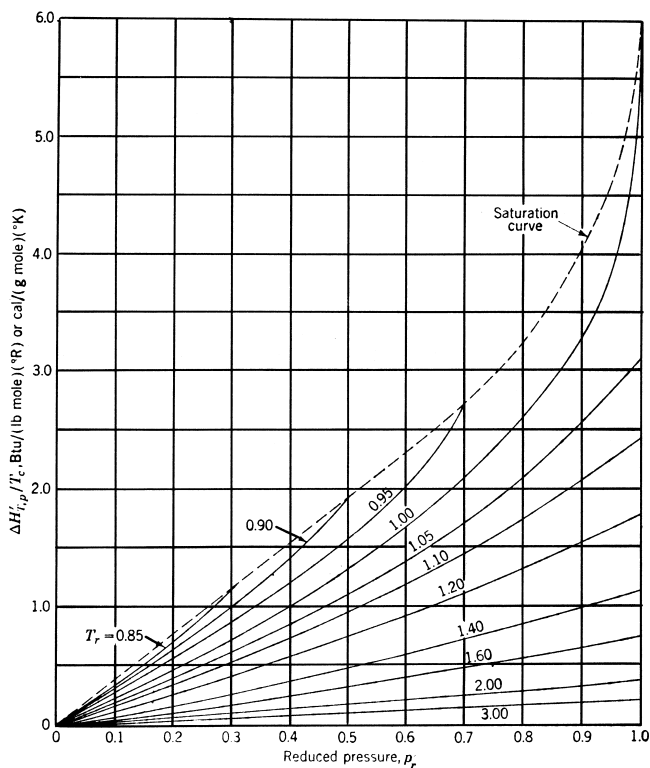
(b)

Figure 7.28. Residual entropy and enthalpy as functions of reduced properties. (a) Residual entropy. (b) Residual enthalpy. *Drawn by Smith and Van Ness* (Introduction to Chemical Engineering Thermodynamics, *McGraw-Hill, New York, 1959*) *from data of Lydersen et al. For illustrative purposes primarily; see text for other sources.*]

Example 7.11 works out a case involving a nonideal gas and interstage pressure losses.

In centrifugal compressors with all stages in the same shell, the allowable head rise per stage is stated in Table 7.6 or correlated in Figure 7.26. Example 7.9 utilizes these data.

Volumetric Efficiency. For practical reasons, the gas is not completely discharged from a cylinder at each stroke of a reciprocating machine. The clearance of a cylinder is filled with compressed gas which reexpands isentropically on the return stroke. Accordingly, the gas handling capacity of the cylinder is less than the product of the cross section by the length of the stroke. The volumetric efficiency is

$$n_v = \frac{\text{suction gas volume}}{\text{cylinder displacement}} \tag{7.57}$$
$$= 1 - f_c[(P_2/P_1)^{1/k} - 1],$$

where

$$f_c = \frac{\text{clearance volume}}{\text{cylinder displacement volume}}.$$

For a required volumetric suction rate Q (cfm), the required product of cross section A_s (sqft), stroke length L_s (ft), and speed N (rpm) is given by

$$A_s L_s N = Q/\eta_v. \tag{7.58}$$

7.7. EJECTOR AND VACUUM SYSTEMS

Application ranges of the various kinds of devices for maintenance of subatmospheric pressures in process equipment are shown in Table 7.3. The use of mechanical pumps—compressors in reverse—for such purposes is mentioned earlier in this chapter. Pressures also can be reduced by the action of flowing fluids. For instance, water jets at 40 psig will sustain pressures of 0.5–2.0 psia. For intermediate pressure ranges, down to 0.1 Torr or so, steam jet ejectors are widely favored. They have no moving parts, are quiet, easily installed, simple, and moderately economical to operate, and readily adaptable to handling corrosive vapor mixtures. A specification form is in Appendix B.

EJECTOR ARRANGEMENTS

Several ejectors are used in parallel when the load is variable or because the process system gradually loses tightness between maintenance shutdowns—then some of the units in parallel are cut in or out as needed.

Multistage units in series are needed for low pressures. Sketches are shown in Figure 7.30 of several series arrangements. In Figure 7.30(a), the first stage drives the process vapors, and the second stage drives the mixture of those vapors with the motive steam of the first stage. The other two arrangements employ interstage condensers for the sake of steam economy in subsequent stages. In contact (barometric) condensers the steam and other condensables are removed with a cold water spray. The tail pipes of the condensers are sealed with a 34 ft leg into a sump, or with a condensate pump operating under vacuum. Surface condensers permit recovery of valuable or contaminating condensates or steam condensate for return as boiler feed. They are more expensive than barometrics, and their design is more complex than that of
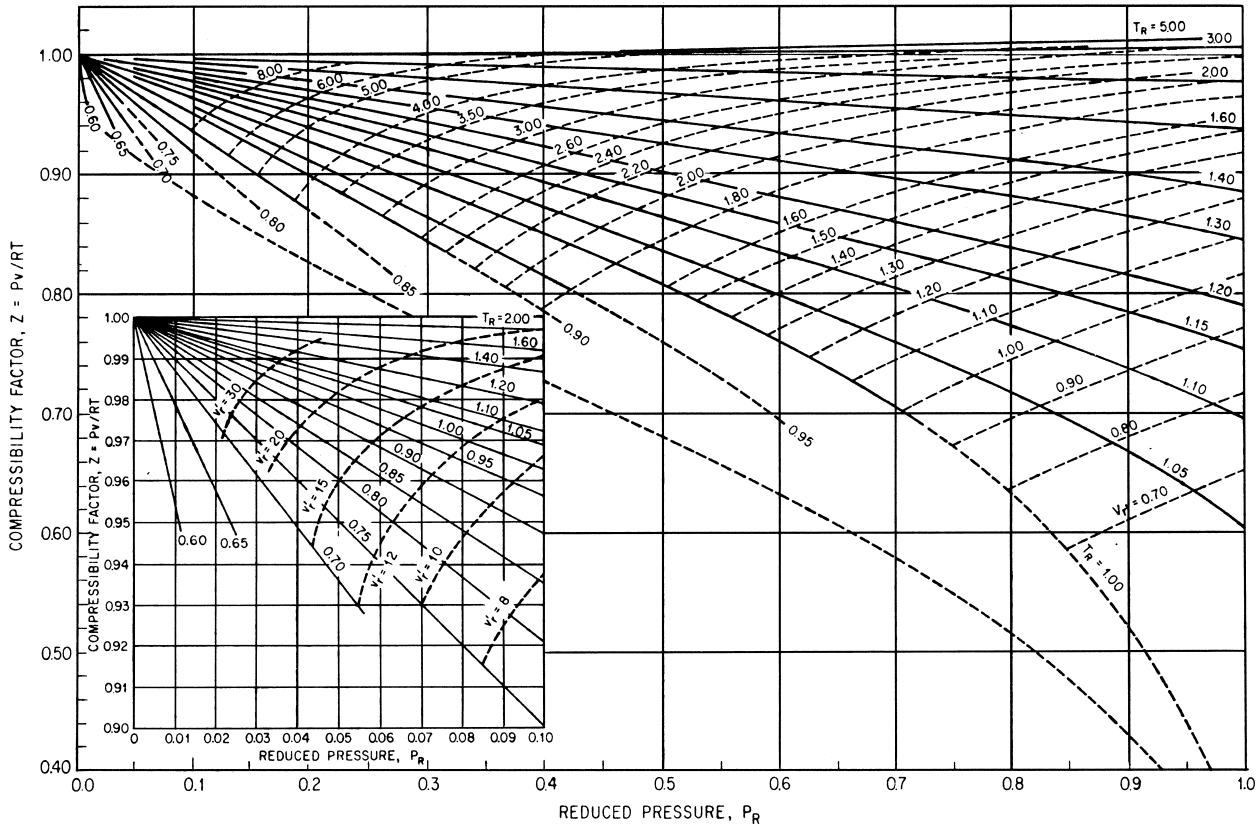
Figure 7.29. Compressibility factors, $z = PV/RT$, of gases. Used for the solution of Example 7.11. $P_R = P/P_c$, $T_R = T/T_c$, and $V_{r'} = P_c V/RT_c$.

EXAMPLE 7.7
Finding Work of Compression with a Thermodynamic Chart

Hydrogen sulfide is to be compressed from 100°F and atmospheric pressure to 50 psig. The isentropic efficiency is 0.70. A pressure-enthalpy chart is taken from Starling (*Fluid Thermodynamic Properties for Light Petroleum Systems*, Gulf, Houston, TX, 1973). The work and the complete thermodynamic conditions for the process will be found.

The path followed by the calculation is 1–2–3 on the sketch. The initial enthalpy is −86 Btu/lb. Proceed along the isentrop $S = 1.453$ to the final pressure, 64.7 psia, and enthalpy $H_2 = -27$. The isentropic enthalpy change is

$$\Delta H_s = -27 - (-86) = 59 \text{Btu/lb}.$$

The true enthalpy change is

$$\Delta H = 59/0.70 = 84.3.$$

The final enthalpy is

$$H_3 = -86 + 84.3 = -1.7.$$

Other conditions at points 2 and 3 are shown on the sketch. The work is

$$\dot{W} = \Delta H = 84.3 \text{Btu/lb}$$
$$\rightarrow 84.3/2.545 = 33.1 \, \text{HP hr}/(1000 \, \text{lb}).$$
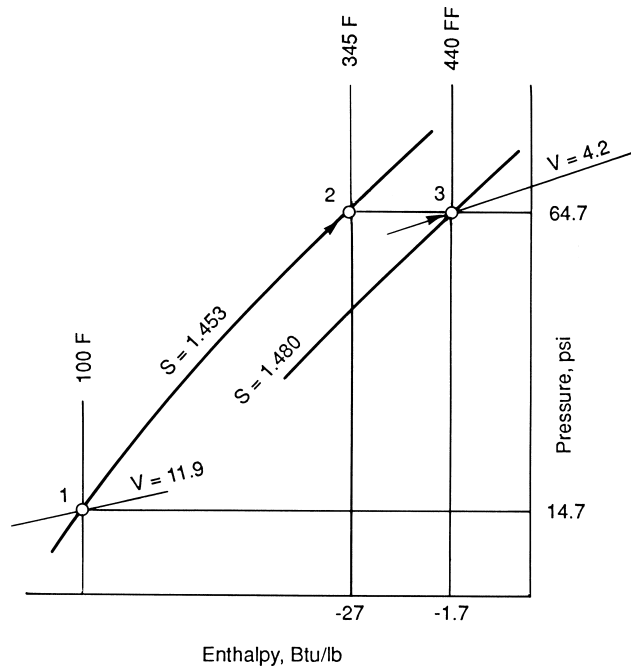
EXAMPLE 7.8
Compression Work on a Nonideal Gas
Hydrogen sulfide at 450 K and 15 atm is to be compressed to 66 atm. The isentropic final temperature and the isentropic enthalpy change will be found with the aid of Figure 7.28 for the residual properties.

The critical properties are $T_c = 373.2$ K and $P_c = 88.2$ atm. The heat capacity is stated in Example 7.5:

$$T_{r1} = 450/373.2 = 1.21,$$
$$P_{r1} = 15/88.2 = 0.17,$$
$$P_{r2} = 66/88.2 = 0.75,$$
$$\therefore \Delta S_1' = 0.15, \tag{1}$$
$$\Delta H_1' = 0.2(373.2) = 75.0,$$
$$\Delta S = \int_{450}^{T_2} \frac{Cp}{T} dT - 1.987 \ln \frac{66}{15} + 0.15 - \Delta S_2' \overset{?}{=} 0,$$
$$\Delta H_s = \int_{450}^{T_2} Cp \, dT + 75.0 - \Delta H_2'. \tag{2}$$

1. Assume a value of T_2.
2. Evaluate T_{r2} and $\Delta S_2'$.
3. Integrate Eq. (1) numerically and note the righthand side.
4. Continue with trial values of T_2 until $\Delta S = 0$.
5. Find $\Delta H_2'$ and finally evaluate ΔH_s.

Two trials are shown.

T_2	Tr_2	$\Delta S'_2$	ΔS	$\Delta H'_2$	ΔH_s
600	1.61	0.2	−0.047		
626.6	1.68	0.2	+0.00009	187	1487.7

When the residual properties are neglected,

$T_2 = 623.33$ K (compared with 626.6 real),
$\Delta H_s = 1569.5$ (compared with 1487.7 real).

Real temperature rise:

With $\eta_s = 0.75$, the enthalpy change is 1487.7/0.75 and the enthalpy balance is rearranged to

$$\Delta = -\frac{1487.7}{0.75} + \int_{450}^{T_2} Cp^* \, dT + 75 - \Delta H_2' \overset{?}{=} 0$$

Trial T_2	T_r	$\Delta H'_2$	rhs
680	1.82	109	+91.7
670.79	1.80	112	−0.021
670.80	1.80		+0.075

$\therefore T_2 = 670.79$ K.
For ideal gas

$$\Delta = -\frac{1569.5}{0.75} + \int_{450}^{T_2} Cp^* \, dT \overset{?}{\rightarrow} 0$$

By trial:

$$T_2 = 670.49 \text{ K}$$

Nonideality is slight in this example.

EXAMPLE 7.9
Selection of a Centrifugal Compressor
A hydrocarbon mixture with molecular weight 44.23 is raised from 41°F and 20.1 psia to 100.5 psia at the rate of 2400 lb mol/hr. Its specific heat ratio is $k = 1.135$ and its inlet and outlet compressibilities are estimated as $z_1 = 0.97$ and $z_2 = 0.93$. A size of compressor will be selected from Table 7.6 and its expected performance will be calculated:

$$2400 \text{ lb mol/hr} = 1769 \text{ lb/min},$$
$$10,260 \text{ cfm}$$

From Table 7.6, the smallest compressor for this gas rate is # 38M. Its characteristics are

$$\dot{N} = 8100 \text{ rpm at } 10\text{–}12 \text{ K ft/stage}$$
$$\eta_p = 0.77$$
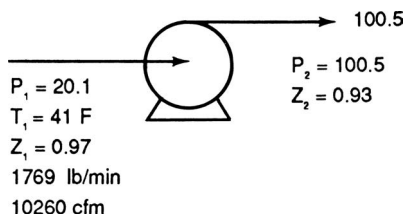
Accordingly,

$$\frac{n-1}{n} = \frac{k-1}{k\eta_p} = \frac{0.135}{1.135(0.77)} = 0.1545.$$

Using Eq. (7.35) for the polytropic head,

$$H_p = \left(\frac{Z_1 + Z_2}{2}\right)\left(\frac{k}{k-1}\right) RT_1 \left[\left(\frac{P_2}{P_1}\right)^{(n-1)/n} - 1\right]$$
$$= 0.95 \left(\frac{1.135}{0.135}\right)\left(\frac{1544}{44.23}\right)(501)[5^{0.1545} - 1]$$
$$= 39430 \text{ ft.}$$

From Figure 7.26(a), the max head per stage is 9700, and from Figure 7.26(b) the min number of stages is about 4.5. Accordingly, use five stages with standard 10,000 ft/stage impellers. The required speed with the data of Table 7.6 is

$$\text{speed} = 8100\sqrt{39430/10,000(5)} = 7190 \text{ rpm.}$$

Power absorbed by the gas is

$$\dot{P}_{\text{gas}} = \frac{\dot{m}H_p}{33,000\eta_p} = \frac{1769(39,430)}{33,000(0.77)} = 2745 \text{ HP.}$$

Friction losses $\cong 3\%$ max;

$$\therefore \text{total power input} = 2745/0.97 = 2830 \text{ HP max.}$$

EXAMPLE 7.10
Polytropic and Isentropic Temperatures
Take $k = 1.4$, $(P_2/P_1) = 3$, and $\eta_p = 0.75$. From Eq. (7.34),

$$(n-1)/n = (k-1)/k\eta_p = 0.3810$$

and from Eq. (7.39)

$$n_s = \frac{3^{0.2857} - 1}{3^{0.3810} - 1} = 0.7094$$

so that from Eq. (7.53),

$$T_2/T_1 = 3^{0.3810} = 1.5198, \text{ isentropic,}$$

and from Eq. (7.54),

$$T_2/T_1 = 1 + (1/0.7094)(3^{0.2857} - 1) = 1.5197, \text{ polytropic.}$$

---

other kinds of condensers because of the large amounts of non-condensables that are present.

As many as six stages are represented on Figure 7.30, combined with interstage condensers in several ways. Barometric condensers are feasible only if the temperature of the water is below its bubblepoint at the prevailing pressure in a particular stage. Common practice requires the temperature to be about 5°F below the bubblepoint. Example 7.13 examines the feasibility of installing intercondensers in that process.

AIR LEAKAGE

The size of ejector and its steam consumption depend on the rate at which gases must be removed from the process. A basic portion of such gases is the air leakage from the atmosphere into the system.

Theoretically, the leakage rate of air through small openings, if they can be regarded as orifices or short nozzles, is constant at vessel pressures below about 53% of atmospheric pressure. However, the openings appear to behave more nearly as conduits with relatively large ratios of lengths to diameters. Accordingly sonic flow is approached only at the low pressure end, and the air mass inleakage rate is determined by that linear velocity and the low density prevailing at the vessel pressure. The content of other gases in the evacuated vessel is determined by each individual process. The content of condensables can be reduced by interposing a refrigerated condenser between process and vacuum pump.

Standards have been developed by the Heat Exchange Institute for rates of air leakage into commercially tight systems. Their chart is represented by the equation

$$m = kV^{2/3}, \tag{7.59}$$

where m is in lb/hr, V is the volume of the system in cuft, and the coefficient is a function of the process pressure as follows:

Pressure (Torr)	>90	20–90	3–20	1–3	<1
k	0.194	0.146	0.0825	0.0508	0.0254

For each agitator with a standard stuffing box, 5 lb/hr of air leakage is added. Use of special vacuum mechanical seals can reduce this allowance to 1–2 lb/hr.

For a conservative design, the rate from Eq. (7.59) may be supplemented with values based on Table 7.11. Common practice is to provide oversize ejectors, capable of handling perhaps twice the standard rates of the Heat Exchange Institute.

Other Gases. The gas leakage rate correlations cited are based on air at 70°F. For other conditions, corrections are applied to evaluate an effective air rate. The factor for molecular weight M is

$$f_M = 0.375 \ln(M/2) \tag{7.60}$$

and those for temperature T in °F of predominantly air or predominantly steam are

$$f_A = 1 - 0.00024(T - 70), \text{ for air,} \tag{7.61}$$

$$f_S = 1 - 0.00033(T - 70), \text{ for steam.} \tag{7.62}$$

An effective or equivalent air rate is found in Example 7.12.

STEAM CONSUMPTION

The most commonly used steam is 100 psig with 10–15° superheat, the latter characteristic in order to avoid the erosive effect of liquids on the throats of the ejectors. In Figure 7.31 the steam consumptions are given as lb of motive steam per lb of equivalent air to the first stage. Corrections are shown for steam pressures other than 100 psig. When some portion of the initial suction gas is condensable, downward corrections to these rates are to be made for those ejector assemblies that have intercondensers. Such corrections and also the distribution of motive steam to the individual stages are problems best passed on to ejector manufacturers who have experience and a body of test data.

When barometric condensers are used, the effluent water temperature should be at least 5°F below the bubblepoint at the prevailing pressure. A few bubblepoint temperatures at low pressures are:

Absolute (in. Hg)	0.2	0.5	1.0	2.0
Bubblepoint °F	34.6	58.8	79.0	101.1

Interstage pressures can be estimated on the assumption that compression ratios will be the same in each stage, with the suction to the first stage at the system pressure and the discharge of the last stage at atmospheric pressure. Example 7.13 examines at what stages it is feasible to employ condensers so as to minimize steam usage in subsequent stages.

EJECTOR THEORY

The progress of pressure, velocity, and energy along an ejector is illustrated in Figure 7.32. The initial expansion of the steam to point C and recompression of the mixture beyond point E proceed adiabatically with isentropic efficiencies of the order of 0.8. Mixing in the region from C to E proceeds with approximate conservation of momenta of the two streams, with an efficiency of the order of 0.65. In an example worked out by Dodge (1944, pp. 289–293), the compounding of these three efficiencies leads to a steam rate five times theoretical. Other studies of single-stage ejectors have been made by Work and Headrich (1939) and DeFrate and Hoerl (1959), where other references to theory and data are made.
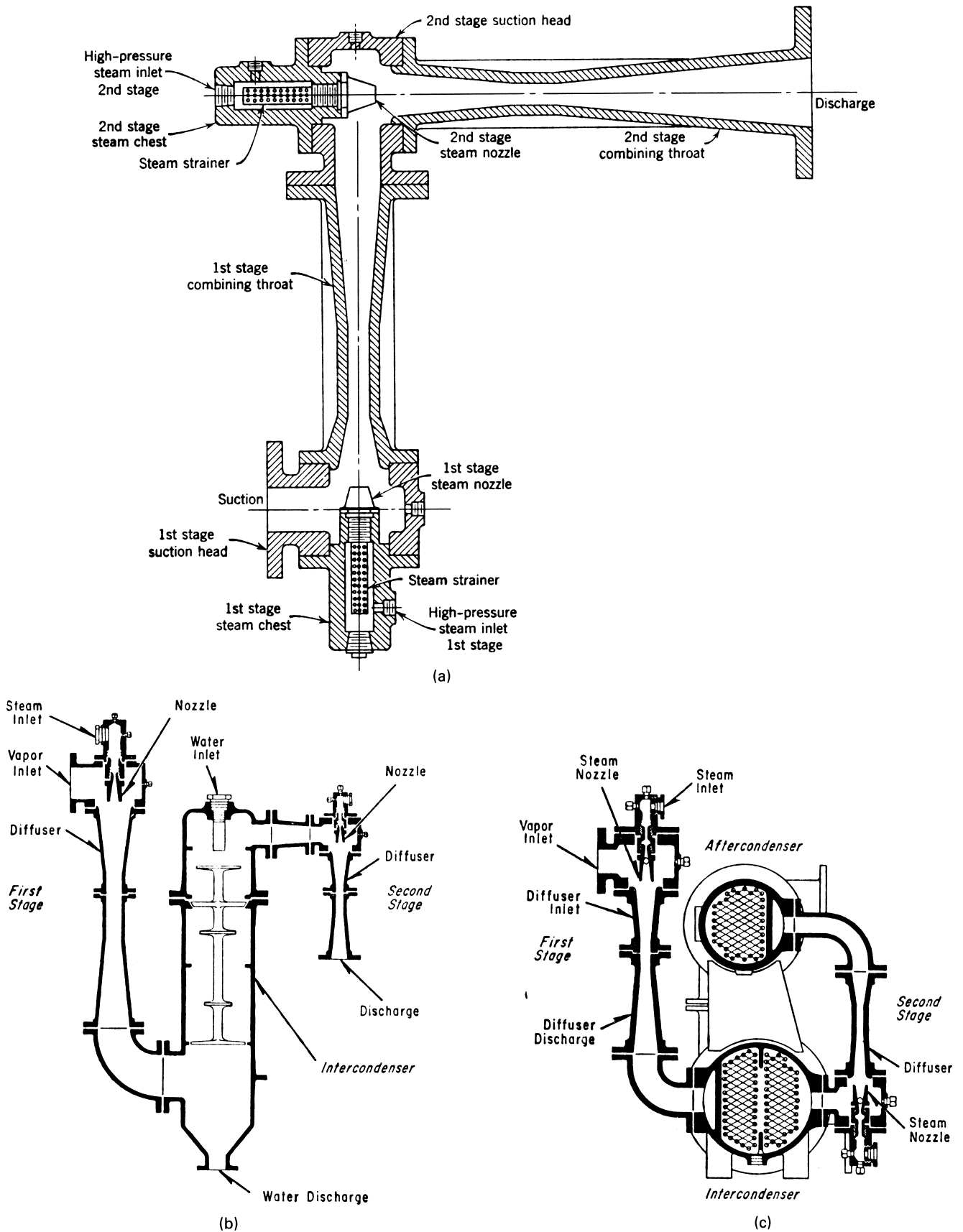
Figure 7.30. Arrangements of two-stage ejectors with condensers. (a) Identification of the parts of a two-stage ejector. (*Croll-Reynolds Co.*). (b) A two-stage ejector with interstage barometric condenser. (*Elliot Co.*). (c) A two-stage ejector with surface condensers interstage and terminal. (*Elliot Co.*).

EXAMPLE **7.11**
Three-Stage Compression with Intercooling and Pressure Loss between Stages
Ethylene is to be compressed from 5 to 75 atm in three stages. Temperature to the first stage is 60°F, those to the other stages are 100°F. Pressure loss between stages is 0.34 atm (5 psi). Isentropic efficiency of each stage is 0.87. Compressibilities at the inlets

to the stages are estimated from Figure 7.29 under the assumption of equal compression ratios as $z_0 = 0.98$, $z_1 = 0.93$, and $z_2 = 0.83$. The interstage pressures will be determined on the basis of equal power load in each stage. The estimated compressibilities can be corrected after the pressures have been found, but usually this is not found necessary. $k = C_p/C_v = 1.228$ and $(k-1)/k = 0.1857$.
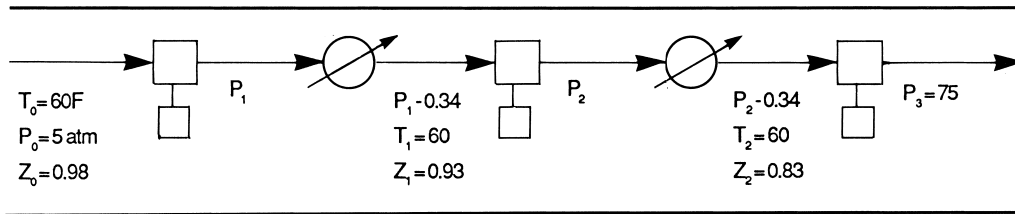
With equal power in each stage

$$\dot{P}_i = \frac{z_i R T_i k}{(k-1)\eta_s}\left[\left(\frac{P}{P_i}\right)^{0.1857} - 1\right]$$

$$= 0.98(520)[(P_1/5)^{0.1857} - 1]$$

$$= 0.93(560)\left\{\left(\frac{P_2}{(P_1 - 0.34)}\right)^{0.1857} - 1\right\}$$

$$= 0.83(560)\{[75/(P_2 - 0.34)]^{0.1857} - 1\}$$

Values of P_1 will be assumed until the value of P_2 calculated by equating the first two terms equals that calculated from the last two terms. The last entries in the table are the interpolated values.

$$\text{Total power} = \frac{3(0.98)(1.987)(520)}{0.1857(2545)0.87}\left[\left(\frac{12.25}{5}\right)^{0.1857} - 1\right]$$

$$= 1.34 \text{ HP/(lb mol/hr)}.$$

	P_2	
P_1	**1 + 2**	**2 + 3**
12	27.50	28.31
12.5	29.85	28.94
13.0	32.29	29.56
12.25		—28.60—
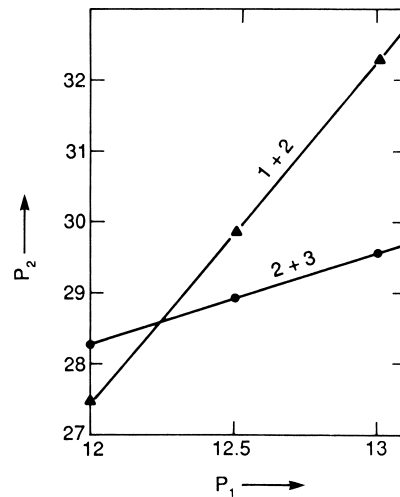
The theory is in principle amenable to the prediction of steam distribution to individual stages of a series, but no detailed procedures are readily available. Manufacturers charts such as Figure 7.31 state only the consumption of all the stages together.

GLOSSARY FOR CHAPTER 7

PUMP TERMS

Head has the dimensions $[F][L]/[M]$; for example, ft lbf/lb or ft; or N m/kg or m:

a. pressure head $= \Delta P/\rho$;
b. velocity head $= \Delta u^2/2g_c$;
c. elevation head $= \Delta z(g/g_c)$, or commonly Δz;
d. friction head in line, $H_f = f(L/D)u^2/2g_c$;
e. system head H_s is made up of the preceding four items;

f. pump head equals system head, $H_p = H_s$, under operating conditions;
g. static suction head equals the difference in levels of suction liquid and the centerline of the pump;
h. static suction lift is the static suction head when the suction level is below the centerline of the pump; numerically a negative number.

NPSH (net positive suction head) = (pressure head of source) + (static suction head) − (friction head of the suction line) − (vapor pressure of the flowing liquid).
Hydraulic horsepower is obtained by multiplying the weight rate of flow by the head difference across the pump and converting to horsepower. For example, HHP = (gpm)(psi)/1714 = (gpm)(sp gr)(ft)/3960.
Brake horsepower is the driver power output needed to operate the pump. BHP = HHP/(pump efficiency).

TABLE 7.11. Estimated Air Leakages Through Connections, Valves, Stuffing Boxes Etc. of Process Equipment[a]

Type Fitting	Estimated Average Air Leakage (lb/hr)
Screwed connections in sizes up to 2 in.	0.1
Screwed connections in sizes above 2 in.	0.2
Flanged connections in sizes up to 6 in.	0.5
Flanged connections in sizes 6 in. to 24 in. including manholes	0.8
Flanged connections in sizes 24 in. to 6 ft	1.1
Flanged connections in sizes above 6 ft	2.0
Packed valves up to $\frac{1}{2}$ in. stem diameter	0.5
Packed valves above $\frac{1}{2}$ in. stem diameter	1.0
Lubricated plug valves	0.1
Petcocks	0.2
Sight glasses	1.0
Gage glasses including gage cocks	2.0
Liquid sealed stuffing box for shaft of agitators, pumps, etc. (per in. shaft diameter)	0.3
Ordinary stuffing box (per in. of diameter)	1.5
Safety valves and vacuum breakers (per in. of nominal size)	1.0

[a]For conservative practice, these leakages may be taken as supplementary to those from Eq. (7.59). Other practices allow 5 lb/hr for each agitator stuffing box of standard design; special high vacuum mechanical seals with good maintenance can reduce this rate to 1–2 lb/hr.
[From C.D. Jackson, *Chem. Eng. Prog.* **44**, 347 (1948)].

Driver horsepower, HP = BHP/(driver efficiency) = HHP/(pump efficiency)(driver efficiency).

TERMS CONCERNING CENTRIFUGAL AND RELATED PUMPS

Axial flow is flow developed by axial thrust of a propeller blade, practically limited to heads under 50 ft or so.

Centrifugal pump consists of a rotor (impeller) in a casing in which a liquid is given a high velocity head that is largely converted to pressure head by the time the liquid reaches the outlet.

Characteristic curves are plots or equations relating the volumetric flow rate through a pump to the developed head or efficiency or power or NPSH.

Diffuser type: the impeller is surrounded by gradually expanding passages formed by stationary guide vanes [Figs. 7.2(b) and 7.3(d)].

EXAMPLE 7.12
Equivalent Air Rate

Suction gases are at the rate of 120 lb/hr at 300°F and have a molecular weight of 90. The temperature factor is not known as a function of molecular weight so the value for air will be used. Using Eqs. (7.60) and (7.61),

$$m = 120(0.375)\ln(90/2)[1 - 0.00024(300 - 70)]$$
$$= 161.8 \text{ lb/hr equivalent air.}$$
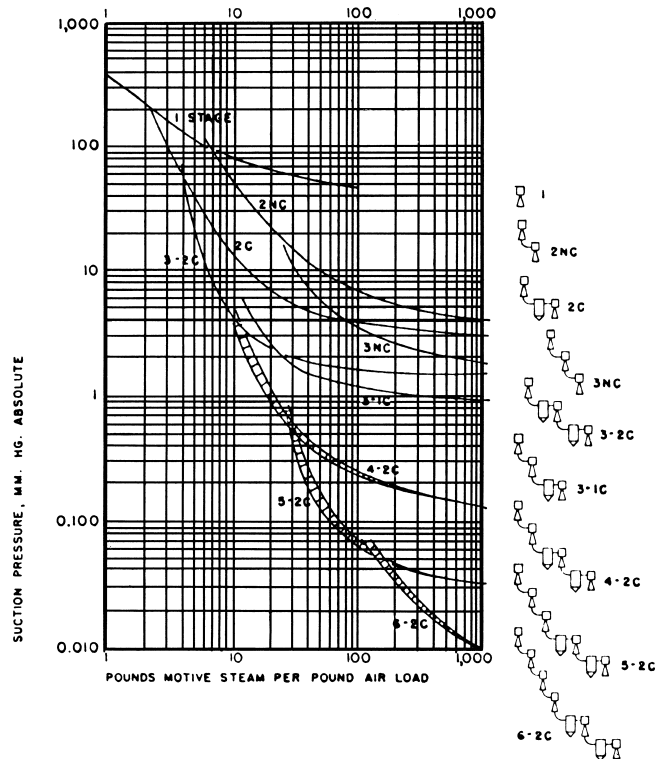
Figure 7.31. Steam requirements of ejectors at various pressure levels with appropriate numbers of stages and contact intercondensers. Steam pressure 100 psig, water temperature 85°F. Factor for 65 psig steam is 1.2 and for 200 psig steam it is 0.80. (*Worthington Corp*).

EXAMPLE 7.13
Interstage Condensers

A four-stage ejector is to evacuate a system to 0.3 Torr. The compression ratio in each stage will be

$$(P_4/P_0)^{1/4} = (760/0.3)^{1/4} = 7.09.$$

The individual stage pressures and corresponding water bubblepoint temperatures from the steam tables are

Discharge of stage	0	1	2	3	4
Torr	0.3	2.1	15.1	107	760
°F		14	63.7	127.4	

The bubblepoint temperature in the second stage is marginal with normal cooling tower water, particularly with the practical restriction to 5°F below the bubblepoint. At the discharge of the third stage, however, either a surface or barometric condenser is quite feasible. At somewhat higher process pressure, two interstage condensers may be practical with a four-stage ejector, as indicated on Figure 7.31.
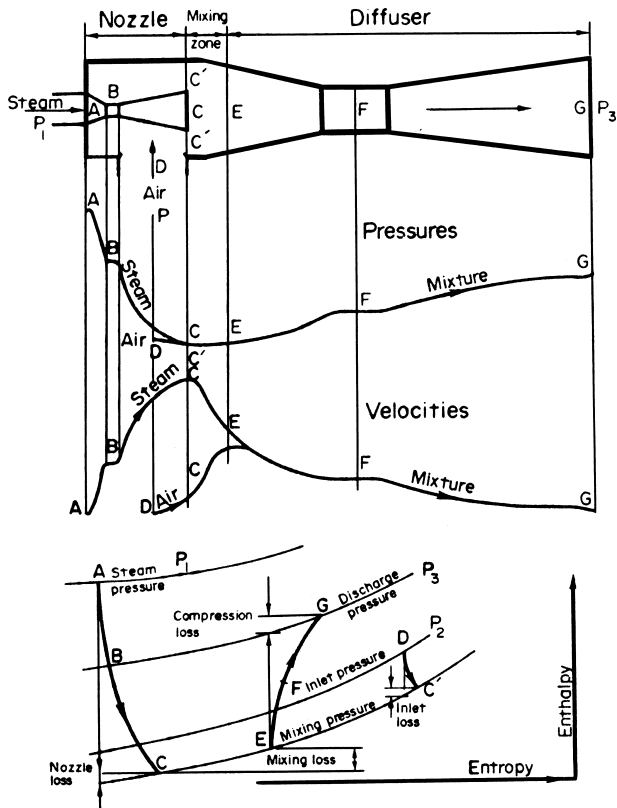
Figure 7.32. Progress of pressures, velocities, enthalpies and entropies in an ejector. (*Coulson and Richardson*, Chemical Engineering, *Pergamon, 1977, New York, Vol. 1*).

Double suction: two incoming streams enter at the eye of the impeller on opposite sides, minimizing axial thrust and worthwhile for large, high head pumps [Fig. 7.2(b)].

Double volute: the liquid leaving the impeller is collected in two similar volutes displaced 180° with a common outlet; radial thrust is counterbalanced and shaft deflection is minimized, resulting in lower maintenance and repair, used in high speed pumps producing above 500 ft per stage.

Impeller: the rotor that accelerates the liquid.

a. Open impellers consist of vanes attached to a shaft without any form of supporting sidewall and are suited to handling slurries without clogging [Fig. 7.2(a)].

b. Semienclosed impellers have a complete shroud on one side [Fig. 7.3(c)]; they are essentially nonclogging, used primarily in small size pumps; clearance of the open face to the wall is typically 0.02 in. for 10 in. diameters.

c. Closed impellers have shrouds on both sides of the vanes from the eye to the periphery, used for clear liquids [Fig. 7.3(b)].

Mechanical seals prevent leakage at the rotating shaft by sliding metal on metal lubricated by a slight flow of pump liquid or an independent liquid [Figs. 7.4(c) and (d)].

Mixed flow: develops head by combined centrifugal action and propeller action in the axial direction, suited to high flow rates at moderate heads [Fig. 7.3(e)].

Multistage: several pumps in series in a single casing with the objective of developing high heads. Figure 7.6(c) is of characteristic curves.

Performance curves (see characteristic curves).

Single suction: the liquid enters on one side at the eye of the impeller; most pumps are of this lower cost style [Fig. 7.2(c)].

Split case: constructed so that the internals can be accessed without disconnecting the piping [Fig. 7.2(a)].

Stuffing box: prevent leakage at the rotating shaft with compressed soft packing that may be wetted with the pump liquid or from an independent source [Figs. 7.4(a) and (b)].

Volute type: the impeller discharges the liquid into a progressively expanding spiral [Fig. 7.2(a)].

REFERENCES

Compressors

1. Compressors in *Encyclopedia of Chemical Processing and Design*, Dekker, New York, 1979, Vol. 10, pp. 157–409.
2. F.L. Evans, Compressors and fans, in *Equipment Design Handbook for Refineries and Chemical Plants*, Gulf, Houston, 1979, Vol. 1, pp. 54–104.
3. H. Gartmann, *DeLaval Engineering Handbook*, McGraw-Hill, New York, 1970, pp. 6.61–6.93.
4. R. James, Compressor calculation procedures, in *Encyclopedia of Chemical Processing and Design*, Dekker, New York, Vol. 10, pp. 264–313.
5. E.E. Ludwig, Compressors, in *Applied Process Design for Chemical and Petrochemical Plants*, Gulf, Houston, 1983, Vol. 3, pp. 251–396.
6. R.D. Madison, *Fan Engineering*, Buffalo Forge Co., Buffalo, NY, 1949.
7. H.F. Rase and M.H. Barrow, *Project Engineering of Process Plants*, Wiley, New York, pp. 297–347.
8. R.C. Reid, J.M. Prausnitz and T.K. Sherwood, *The Properties of Gases and Liquids*, 3rd Ed., McGraw-Hill, New York, 1977.
9. S.M. Walas, *Phase Equilibria in Chemical Engineering*; Butterworths, Stoneham, MA 1985.

Ejectors

1. L.A. DeFrate and V.W. Headrich, *Chem. Eng. Prog. Symp. Ser.* **21**, 43–51 (1959).
2. B.F. Dodge, *Chemical Engineering Thermodynamics*, McGraw-Hill, New York, 1944, pp. 289–293.
3. F.I. Evans, *Equipment Design Handbook for Refineries and Chemical Plants*, Gulf, Houston, 1979, Vol. 1, pp. 105–117.
4. E.E. Ludwig, *loc. cit.*, Vol. 1, pp. 206–239.
5. R.E. Richenberg and J.J. Bawden, Ejectors, steam jet, in *Encyclopedia of Chemical Processing and Design*, Dekker, New York, Vol. 17, pp. 167–194.
6. L.T. Work and V.W. Headrich, *Ind. Eng. Chem.* **31**, 464–477 (1939).

Piping

1. ANSI Piping Code, ASME, New York, 1980.
2. S. Chalfin, Control valves, *Encyclopedia of Chemical Processing and Design*, Dekker, New York, 1980, Vol. 11, pp. 187–213.
3. F.L. Evans, *Equipment Design Handbook for Refineries and Chemical Plants*, Gulf, Houston, 1979, Vol. 2; piping, pp. 188–304; valves, pp. 315–332.
4. J.W. Hutchinson, *ISA Handbook of Control Valves*, Inst. Soc. America, Research Triangle Park, NC, 1976.
5. R.C. King, *Piping Handbook*, McGraw-Hill, New York, 1967.
6. J.L. Lyons, *Encyclopedia of Valves*, Van Nostrand Reinhold, New York, 1975.
7. *Marks' Standard Handbook for Mechanical Engineers*, McGraw-Hill, New York, 1987.

8. *Perry's Chemical Engineers' Handbook*, 7th ed., McGraw-Hill, New York, 1999.
9. R. Weaver, *Process Piping Design*, Gulf, Houston, 1973, 2 Vols.
10. P. Wing, Control valves, in *Process Instruments and Controls Handbook*, (D.M. Considine, Ed.), McGraw-Hill, New York, 1974.
11. R.W. Zappe, *Valve Selection Handbook*, Gulf, Houston, pp. 19.1–19.60, 1981.

Pumps

1. D. Azbel and N.P. Cheremisinoff, *Fluid Mechanics and Fluid Operations*, Ann Arbor Science, Ann Arbor, MI, 1983.

2. N.P. Cheremisinoff, *Fluid Flow: Pumps, Pipes and Channels*, Ann Arbor Science, Ann Arbor, MI, 1981.
3. F.L. Evans, *loc. cit.*, Vol. 1, pp. 118–171.
4. H. Gartmann, *DeLaval Engineering Handbook*, McGraw-Hill, New York, 1970, pp. 6.1–6.60.
5. I.J. Karassik and R. Carter, *Centrifugal Pump Selection Operation and Maintenance*, F.W. Dodge Corp., New York, 1960.
6. I.J. Karassik, W.C. Krutsch, W.H. Fraser, and Y.J.P. Messina, *Pump Handbook*, McGraw-Hill, New York, 1976.
7. F.A. Kristal and F.A. Annett, *Pumps*, McGraw-Hill, New York, 1940.
8. E.E. Ludwig, *loc. cit.*, Vol. 1, pp. 104–143.
9. S. Yedidiah, *Centrifugal Pump Problems*, Petroleum Publishing, Tulsa, OK, 1980.

8

HEAT TRANSFER AND HEAT EXCHANGERS

Basic concepts of heat transfer are reviewed in this chapter and applied primarily to heat exchangers, which are equipment for the transfer of heat between two fluids through a separating wall. Heat transfer also is a key process in other specialized equipment, some of which are treated in the next and other chapters. The three recognized modes of heat transfer are by conduction, convection, and radiation, and may occur simultaneously in some equipment.

8.1. CONDUCTION OF HEAT

In a solid wall such as Figure 8.1(a), the variation of temperature with time and position is represented by the one-dimensional Fourier equation

$$\frac{\partial T}{\partial \theta} = kA \frac{\partial^2 T}{\partial x^2} \tag{8.1}$$

For the most part, only the steady state condition will be of concern here, in which the case the partial integral of Eq. (8.1) becomes

$$Q = -kA \frac{dT}{dx}, \tag{8.2}$$

assuming the thermal conductivity k to be independent of temperature. Furthermore, when both k and A are independent of position,

$$Q = -kA \frac{\Delta T}{\Delta x} = \frac{kA}{L}(T_0 - T_L), \tag{8.3}$$

in the notation of Figure 8.1(a).

Equation (8.3) is the basic form into which more complex situations often are cast. For example,

$$Q = kA_{\text{mean}} \frac{\Delta T}{L} \tag{8.4}$$

when the area is variable and

$$Q = UA(\Delta T)_{\text{mean}} \tag{8.5}$$

in certain kinds of heat exchangers with variable temperature difference.

THERMAL CONDUCTIVITY

Thermal conductivity is a fundamental property of substances that basically is obtained experimentally although some estimation methods also are available. It varies somewhat with temperature. In many heat transfer situations an average value over the prevailing temperature range often is adequate. When the variation is linear with temperature.

$$k = k_0(1 + \alpha T), \tag{8.6}$$

the integral of Eq. (8.2) becomes

$$Q(L/A) = k_0[T_1 - T_2 + 0.5\alpha(T_1^2 - T_2^2)] = k_0(T_1 - T_2)[1 + 0.5\alpha(T_1 + T_2)], \tag{8.7}$$

which demonstrates that use of a value at the average temperature gives an exact result. Thermal conductivity data at several temperatures of some metals used in heat exchangers are in Table 8.1. The order of magnitude of the temperature effect on k is illustrated in Example 8.1.
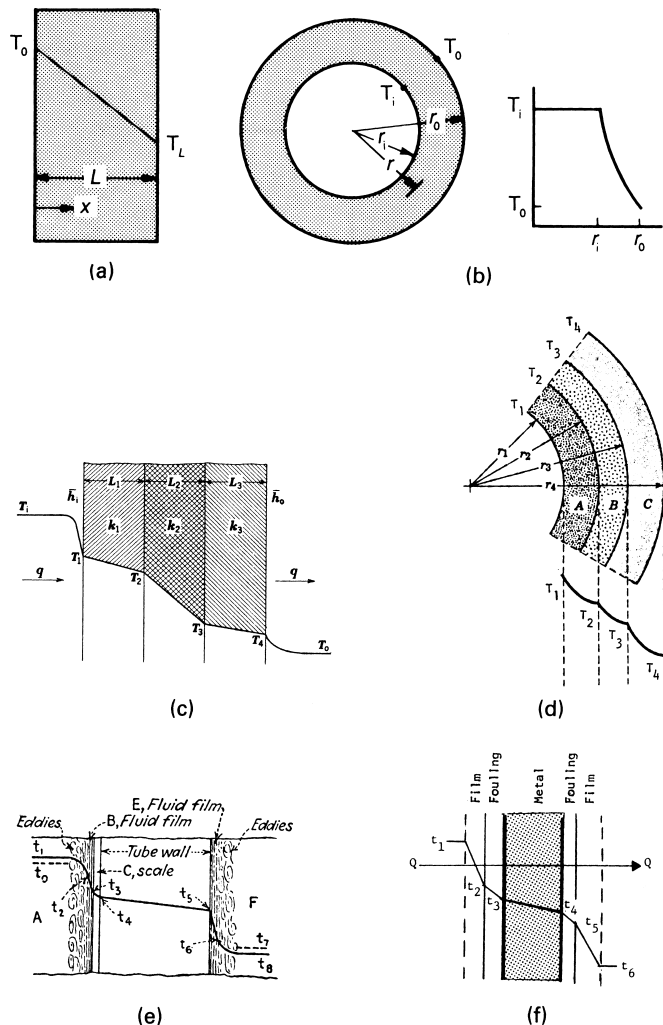
Figure 8.1. Temperature profiles in one-dimensional conduction of heat. (a) Constant cross section. (b) Hollow cylinder. (c) Composite flat wall. (d) Composite hollow cylindrical wall. (e) From fluid A to fluid F through a wall and fouling resistance in the presence of eddies. (f) Through equivalent fluid films, fouling resistances, and metal wall.

165

TABLE 8.1. Thermal Conductivities of Some Metals Commonly Used in Heat Exchangers [kBtu/(hr)(sqft)(°F/ft)]

Metal or Alloy	Temperature (°F)			
	−100	70	200	1000
Steels				
Carbon	—	30.0	27.6	22.2
1 Cr $\frac{1}{4}$ Mo	—	19.2	19.1	18.0
410	—	13.0	14.4	—
304	—	9.4	10.0	13.7
316	8.1	9.4	—	13.0
Monel 400	11.6	12.6	13.8	22.0
Nickel 200	—	32.5	31.9	30.6
Inconel 600	—	8.6	9.1	14.3
Hastelloy C	—	7.3	5.6	10.2
Aluminum	—	131	133	—
Titanium	11.8	11.5	10.9	12.1
Tantalum	—	31.8	—	—
Copper	225	225	222	209
Yellow brass	56	69	—	—
Admiralty	55	64	—	—

HOLLOW CYLINDER

As it appears on Figure 8.1(b), as the heat flows from the inside to the outside the area changes constantly. Accordingly the equivalent of Eq. (8.2) becomes, for a cylinder of length N,

$$Q = -kN(2\pi r)\frac{dT}{dr},\tag{8.8}$$

of which the integral is

$$Q = \frac{2\pi kN(T_1 - T_2)}{\ln(r_2/r_1)}\tag{8.9}$$

This may be written in the standard form of Eq. (8.4) by taking

$$A_m = 2\pi LN r_{\text{lm}}\tag{8.10}$$

and

$$L = r_2 - r_1,\tag{8.11}$$

where

$$r_{\text{lm}} = (r_2 - r_1)/\ln(r_2/r_1)\tag{8.12}$$

EXAMPLE 8.1
Conduction through a Furnace Wall
A furnace wall made of fire clay has an inside temperature of 1500°F and an outside one of 300°F. The equation of the thermal conductivity is $k = 0.48[1 + 5.15(E-4)T]$Btu/(hr)(sqft)(°F/ft). Accordingly,

$$Q(L/A) = 0.48(1500 - 300)[1 + 5.15(E-4)(900)] = 0.703.$$

If the conductivity at 300°F had been used, $Q(L/A) = 0.554$.

---

noting that, for thin-walled tubes, for which $(r_2 - r_1) \to 0$ and $(r_2/r_1) \to 1$, then $(r_2 - r_1)/\ln(r_2/r_1) \to 1$ and $Q = k(\pi[(r_2 + r_1)/2]N)(T_1 - T_2)/(r_2 - r_2) = kA_{\text{mean}}\Delta T/L$.

COMPOSITE WALLS

The flow rate of heat is the same through each wall of Figure 8.1(c). In terms of the overall temperature difference,

$$Q = UA(T_1 - T_4),\tag{8.13}$$

where U is the overall heat transfer coefficient and is given by

$$\frac{1}{U} = \frac{1}{k_a/L_a} + \frac{1}{k_b/L_b} + \frac{1}{k_c/L_c}.\tag{8.14}$$

The reciprocals in Eq. (8.14) may be interpreted as resistances to heat transfer, and, thus, thermal resistances in series are additive.

For the composite hollow cylinder of Figure 8.1(d), with length N,

$$Q = \frac{2\pi N(T_1 - T_4)}{\ln(r_2/r_1)/k_a + \ln(r_3/r_2)/k_b + \ln(r_4/r_3)/k_c}.\tag{8.15}$$

With an overall coefficient U_i based on the inside area, for example,

$$Q = 2\pi N r_i U_i (T_1 - T_4) = \frac{2\pi N(T_1 - T_4)}{1/U_i r_i}.\tag{8.16}$$

On comparison of Eqs. (8.15) and (8.16), an expression for the inside overall is

$$\frac{1}{U_i} = r_i \left[\frac{\ln(r_2/r_1)}{k_a} + \frac{\ln(r_3/r_2)}{k_b} + \frac{\ln(r_4/r_3)}{k_c}\right].\tag{8.17}$$

In terms of the logarithmic mean radii of the individual cylinders,

$$\frac{1}{U_i} = r_i \left[\frac{1}{k_a r_{ma}/(r_2 - r_1)} + \frac{1}{k_b r_{mb}/(r_3 - r_2)} + \frac{1}{k_c r_{mc}/(r_4 - r_3)}\right],$$

which is similar to Eq. (8.14) for flat walls, but includes a ratio of radii as a correction for each cylinder.

FLUID FILMS

Heat transfer between a fluid and a solid wall can be represented by conduction equations. It is assumed that the difference in temperature between fluid and wall is due entirely to a stagnant film of liquid adhering to the wall and in which the temperature profile is linear. Figure 8.1(e) is a somewhat realistic representation of a temperature profile in the transfer of heat from one fluid to another through a wall and fouling scale, whereas the more nearly ideal Figure 8.1(f) concentrates the temperature drops in stagnant fluid and fouling films.

Since the film thicknesses are not definite quantities, they are best combined with the conductivities into single coefficients

$$h = k/L\tag{8.18}$$

so that the rate of heat transfer through the film becomes

$$Q = hA\Delta T.\tag{8.19}$$

Through the five resistances of Figure 8.1(f), the overall heat

transfer coefficient is given by

$$\frac{1}{U} = \frac{1}{h_1} + \frac{1}{h_2} + \frac{1}{k_3/L_3} + \frac{1}{h_4} + \frac{1}{h_5}, \tag{8.20}$$

where L_3 is the thickness of the metal.

If the wall is that of hollow cylinder with radii r_i and $\mathbf{r}_o$, the overall heat transfer coefficient based on the outside surface is

$$\frac{1}{U_o} = \frac{1}{h_1(r_i/r_o)} + \frac{1}{h_2(r_i/r_o)} + \frac{1}{(k_3/L_3)(r_m/r_o)} + \frac{1}{h_4} + \frac{1}{h_5}, \tag{8.21}$$

where r_m is the mean radius of the cylinder, given by Eq. (8.12).

Since wall thicknesses of heat exchangers are relatively small and the accuracy of heat transfer coefficients may not be great, the ratio of radii in Eq. (8.21) often is ignored, so that the equation for the overall coefficient becomes simply

$$\frac{1}{U} = \frac{1}{h_1} + \frac{1}{h_2} + \frac{1}{k_3/L_3} + \frac{1}{h_4} + \frac{1}{h_5}. \tag{8.22}$$

The results of the typical case of Example 8.2, however, indicate that the correction may be significant. A case with two films and two solid cylindrical walls is examined in Example 8.3.

Heat transfer coefficients are empirical data and derived correlations. They are in the form of overall coefficients U for frequently occurring operations, or as individual film coefficients and fouling factors.

8.2. MEAN TEMPERATURE DIFFERENCE

In a heat exchanger, heat is transferred between hot and cold fluids through a solid wall. The fluids may be process streams or independent sources of heat such as the fluids of Table 8.2 or sources of refrigeration. Figure 8.2 shows such a process with inlet and outlet streams, but with the internal flow pattern unidentified because it varies from case to case. At any cross section, the differential rate of heat transfer is

$$dQ = U(T - T')\,dA = -mc\,dT = m'c'\,dT'. \tag{8.23}$$

The overall heat transfer rate is represented formally by

$$Q = UA(\Delta T)_m. \tag{8.24}$$

Figure 8.2. Terminal temperatures and temperature differences of a heat exchanger, with unidentified internal flow pattern.

The mean temperature difference $(\Delta T)_m$ depends on the terminal temperatures, the thermal properties of the two fluids and on the flow pattern through the exchanger.

SINGLE PASS EXCHANGER

The simplest flow patterns are single pass of each fluid, in either the same or opposite directions. Temperature profiles of the main kinds of thermal behavior are indicated on Figure 8.3(a). When there is sensible heat transfer (i.e., no phase change), with constant specific heats on both sides, the mean temperature is expressed in terms of the terminal differences by

$$(\Delta T)_m = (\Delta T)_{\text{log mean}} = \frac{(\Delta T)_2 - (\Delta T)_1}{\ln\left[(\Delta T)_2/(\Delta T)_1\right]}. \tag{8.25}$$

This is called the logarithmic mean temperature difference.

When the profiles consist of linear sections, as in cases (f) and (g), the exchanger can be treated as a three-section assembly, each characterized by its own log mean temperature difference, for which intermediate temperatures may be found by direct calculation or by trial. Heat transfer for a case such as (h) with continuously curved profile must be evaluated by integration of Eq. (8.23).

MULTIPASS EXCHANGERS

For reasons of compactness of equipment, the paths of both fluids may require several reversals of direction. Two of the simpler cases of Figure 8.3 are (b) one pass on the shell side and two passes on the tube side and (c) two passes on the shell side and four on the tube side. On a baffled shell side, as on Figure 8.4(c), the dominant flow is in the axial direction, so this pattern still is regarded as single pass on the shell side. In the cross flow pattern of Figure 8.5(c), each stream flows without lateral mixing, for instance in equipment like Figure 8.6(h). In Figure 8.6(i) considerable lateral mixing would occur on the gas side. Lateral mixing could occur on both sides of the plate exchanger of Figure 8.6(h) if the fins were absent.

EXAMPLE 8.2
Effect of Ignoring the Radius Correction of the Overall Heat Transfer Coefficient

The two film coefficients are 100 each, the two fouling coefficients are 2000 each, the tube outside diameter is 0.1 ft, wall thickness is 0.01 ft, and thermal conductivity of the metal is 30:

$$r_i/r_o = 0.04/0.05 = 0.8,$$
$$r_m = (0.05 - 0.04)/\ln 1.25 = 0.0448,$$
$$r_m/r_o = 0.8963,$$
$$U_o = [1/100(0.8) + 1/2000(0.8) + 1/(30/0.01)(0.8963)$$
$$\quad + 1/100 + 1/2000]^{-1} = 41.6721.$$

Basing on the inside area,

$$U_i = [1/100 + 1/2000 + [(30/0.01)(0.0448/0.04)]^{-1}$$
$$\quad + 0.8/100 + 0.8/2000]^{-1} = 52.0898.$$

Ignoring the corrections,

$$U = (2/100 + 2/2000 + 1/30/0.01)^{-1} = 46.8750.$$

The last value is very nearly the average of the other two.

EXAMPLE 8.3
A Case of a Composite Wall: Optimum Insulation Thickness for a Steam Line

A 3 in. IPS Sched 40 steel line carries steam at 500°F. Ambient air is at 70°F. Steam side coefficient is 1000 and air side is 3 Btu/(hr)(sqft)(°F). Conductivity of the metal is 30 and that of insulation is 0.05 Btu/(hr)(sqft)(°F/ft). Value of the steam is $5.00/MBtu. cost of the insulation is $1.5/(yr)(cuft). Operation is 8760 hr/yr. The optimum diameter d of insulation thickness will be found.

Pipe:

$$d_o = 0.2917 \,\text{ft},$$
$$d_i = 0.2557 \,\text{ft},$$
$$\ln(d_o/d_i) = 0.1317.$$

Insulation:

$$\ln(d_o/d_i) = \ln(d/0.2917). \tag{1}$$

Heat transfer coefficient based on inside area:

$$U_i = d_i \left[\frac{1}{1000 d_i} + \frac{0.1317}{30} + \frac{\ln(d/0.2917)}{0.05} + \frac{1}{3d} \right]^{-1}, \tag{2}$$

$$Q/A_i = U_i \Delta T = 430 U_i.$$

Steam cost:

$$C_1 = 5(10^{-6})(8760)Q/A_i$$
$$= 0.0438 Q/A_i, \quad \$(yr)(sqft\ inside). \tag{3}$$

The yearly costs of steam, insulation and total are tabulated below for 5 valves of the outside diameter of the insulation.

D	U	C_1	C_2	$C_1 + C_2$
.490	.354	6.66	3.56	10.2147
.494	.349	6.57	3.65	10.2118
.495	.347	6.54	3.67	10.2117*
.496	.346	6.52	3.69	10.2118
.500	.341	6.43	3.78	10.2148

Insulation cost:

$$C_2 = 1.5 V_{\text{ins}}/A_i$$
$$= \frac{1.5(d^2 - \overline{0.2917}^2)}{(0.2557)^2}, \quad \$/(yr)(sqft\ inside). \tag{4}$$

Total cost:

$$C = C_1 + C_2 \rightarrow \text{minimum}. \tag{5}$$

Substitute Eqs. (2)–(4) into Eq. (5). The outside diameter is the key unknown.

The cost curve is fairly flat, with a minimum at $d = 0.50$ ft, corresponding to 1.25 in. thickness of insulation. Some trials are shown with the computer program. A more detailed analysis of insulation optima is made by Happel and Jordan [*Chem. Process Econ*., 380 (1975)], although their prices are dated. Section 8.12 also discusses insulation.

Mean temperature differences in such flow patterns are obtained by solving the differential equation. Analytical solutions have been found for the simpler cases, and numerical ones for many important complex patterns, whose results sometimes are available in generalized graphical form.

F-METHOD

When all of the terminal temperatures are known, the mean temperature difference is found directly from

$$(\Delta T)_m = F(\Delta T)_{\text{log mean}}, \tag{8.26}$$

where the correction factor F depends on the flow pattern and is expressed in terms of these functions of the terminal temperatures:

$$P = \frac{T_o - T_i}{T_i' - T_i} = \frac{\text{actual heat transfer}}{\text{maximum possible heat transfer}}, \tag{8.27}$$

$$R = \frac{T_i - T_o}{T_o' - T_i'} = \frac{mc}{m'c'}. \tag{8.28}$$

Some analytical expressions for F are shown in Table 8.3, and more graphical solutions are given in Figure 8.5.

This method is especially easy to apply when the terminal temperatures are all known, because then F and $(\Delta T)_{\text{log mean}}$ are immediately determinable for a particular flow pattern. Then in the heat transfer equation

$$Q = UAF(\Delta T)_{lm} \tag{8.29}$$

any one of the quantities Q, U, or A may be found in terms of the others. A solution by trial is needed when one of the terminal

TABLE 8.2. Properties of Heat Transfer Media

Medium	Trade Name	Phase	°F	atm, gage	Remarks
Electricity	—		100–4500	—	—
Water	—	vapor	200–1100	0–300	—
Water	—	liquid	300–400	6–15	—
Flue gas	—	gas	100–2000	0–7	—
Diphenyl–diphenyl oxide eutectic	Dowtherm A	liquid or vapor	450–750	0–9	nontoxic, carbonizes at high temp
Di + triaryl cpds	Dowtherm G	liquid	20–700	0–3	sensitive to oxygen
Ethylene glycol, inhibited	Dow SR-1	liquid	−40–250	0	acceptable in food industry
Dimethyl silicones	Dow Syltherm 800	liquid	−40–750	0	low toxicity
Mixed silanes	Hydrotherm	liquid	−50–675	0	react with oxygen and moisture
Aromatic mineral oil	Mobiltherm, Mobil	liquid	100–600	0	not used with copper based materials
Chlorinated biphenyls	Therminol, Monsanto	liquid	50–600	0	toxic decomposition products
Molten nitrites and nitrates of K and Na	Hi-Tec, DuPont	liquid	300–1100	0	resistant alloys needed above 850°F
Sodium–potassium eutectic		liquid	100–1400	0	stainless steel needed above 1000°F
Mercury		vapor	600–1000	0–12	low pressure vapor, toxic, and expensive

temperatures is unknown, as shown in Example 8.4. The next method to be described, however, may be more convenient in such a case.

θ-METHOD

One measure of the size of heat transfer equipment is the number of transfer units N defined by

$$N = UA/C_{min}, \qquad (8.30)$$

where C_{min} is the smaller of the two products of mass flow rate and heat capacity, mc or $m'c'$. N is so named because of a loose analogy with the corresponding measure of the size of mass transfer equipment.

A useful combination of P and N is their ratio

$$\theta = \frac{P}{N} = \frac{C_{min}(T_o - T_i)}{UA(T_i' - T_i)} = \frac{Q}{UA(T_i' - T_i)} = \frac{(\Delta T)_m}{(T_i' - T_i)}, \qquad (8.31)$$

where $(T_o - T_i)$ is the temperature change of the stream with the smaller value of mc. Thus θ is a factor for obtaining the mean temperature difference by the formula:

$$(\Delta T)_m = \theta(T_i' - T_i) \qquad (8.32)$$

when the two inlet temperatures are known.

The term P often is called the exchanger effectiveness. Equations and graphs are in Table 8.3 and Figure 8.5. Many graphs for θ, like those of Figure 8.7, may be found in the *Heat Exchanger Design Handbook* (HEDH, 1983). When sufficient other data are known about a heat exchange process, an unknown outlet temperature can be found by this method directly without requiring trial calculations as with the F-method. Example 8.5 solves such a problem.

SELECTION OF SHELL-AND-TUBE NUMBERS OF PASSES

A low value of F means, of course, a large surface requirement for a given heat load. Performance is improved in such cases by using several shells in series, or by increasing the numbers of passes in the same shell. Thus, two 1–2 exchangers in series are equivalent to one large 2–4 exchanger, with two passes on the shell side and four

passes on the tube side. Usually the single shell arrangement is more economical, even with the more complex internals. For economy, F usually should be greater than 0.7.

EXAMPLE

A shell side fluid is required to go from 200 to 140°F and the tube side from 80 to 158°F. The charts of Figure 8.5 will be used:

$$P = (200 - 140)/(200 - 80) = 0.5,$$
$$R = (158 - 80)/(200 - 140) = 1.30.$$

For a 1–2 exchanger, $F = 0.485$:
2–4	0.92
4–8	0.98

The 1–2 exchanger is not acceptable, but the 2–4 is acceptable. If the tube side outlet were at 160 instead of 158, F would be zero for the 1–2 exchanger but substantially unchanged for the others.

8.3. HEAT TRANSFER COEFFICIENTS

Data are available as overall coefficients, individual film coefficients, fouling factors, and correlations of film coefficients in terms of physical properties and operating conditions. The reliabilities of these classes of data increase in the order of this listing, but also the ease of use of the data diminishes in the same sequence.

OVERALL COEFFICIENTS

The range of overall heat transfer coefficients is approximately 10–200 Btu/(hr)(sqft)(°F). Several compilations of data are available, notably in the *Chemical Engineers Handbook* (McGraw-Hill, New York, 1984, pp. 10.41–10.46) and in Ludwig (1983, pp. 70–73). Table 8.4 qualifies each listing to some extent, with respect to the kind of heat transfer, the kind of equipment, kind of process stream, and temperature range. Even so, the range of values of U usually is two-to three-fold, and consequently only a rough measure of equipment size can be obtained in many cases with such data. Ranges of the coefficients in various kinds of equipment are compared in Table 8.5.
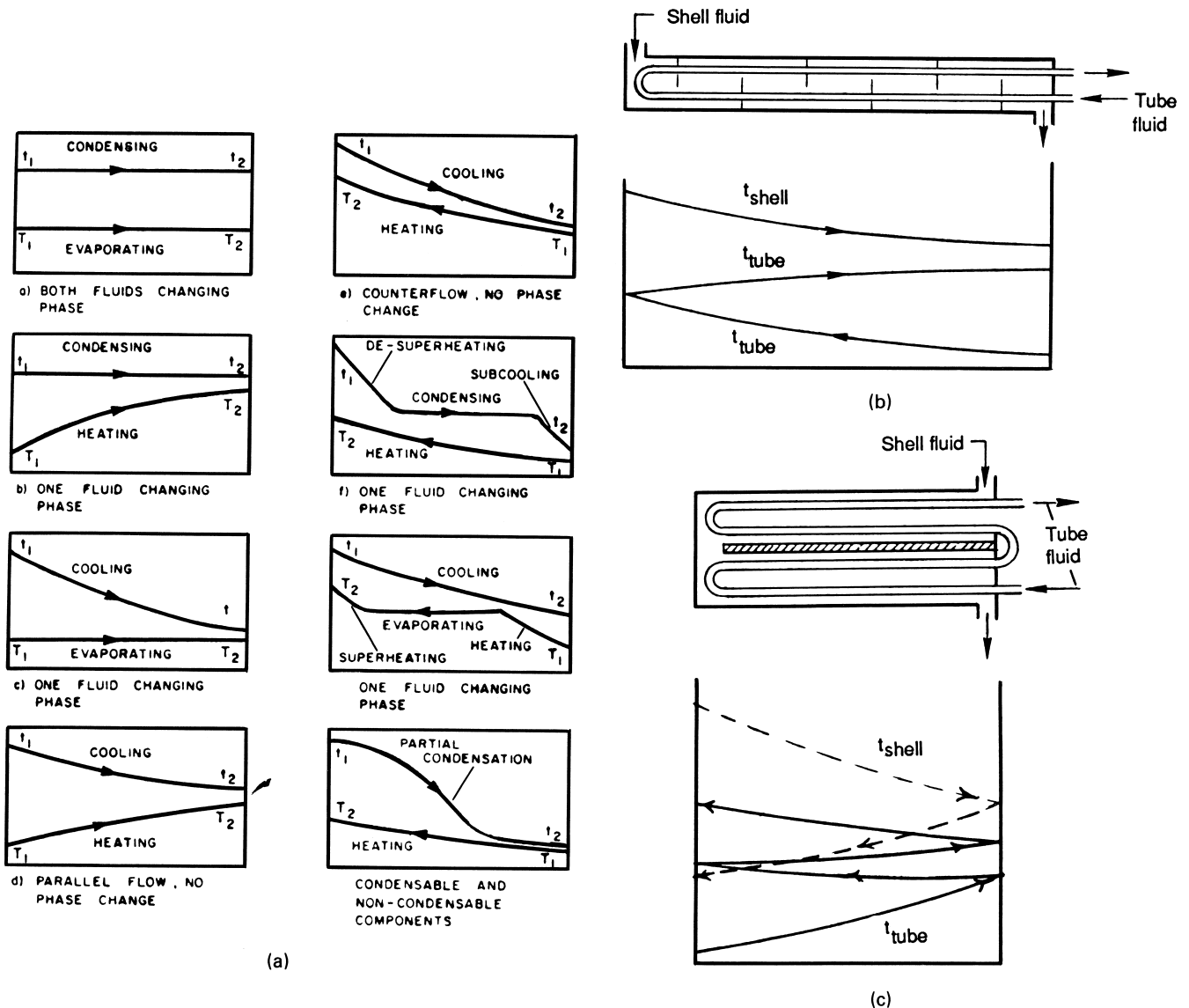
Figure 8.3. Temperature profiles in heat exchangers. (a) In parallel or countercurrent flow, with one or two phases. (b) One shell pass, two tube passes. (c) Two shell passes, four tube passes.

FOULING FACTORS

Heat transfer may be degraded in time by corrosion, deposits of reaction products, organic growths, etc. These effects are accounted for quantitatively by fouling resistances, $1/h_f$. They are listed separately in Tables 8.4 and 8.6, but the listed values of coefficients include these resistances. For instance, with a clean surface the first listed value of U in Table 8.4 would correspond to a clean value of $U = 1/(1/12 - 0.04) = 23.1$. How long a clean value could be maintained in a particular plant is not certain. Sometimes fouling develops slowly; in other cases it develops quickly as a result of process upset and may level off. A high coefficient often is desirable, but sometimes is harmful in that excessive subcooling may occur or film boiling may develop. The most complete list of fouling factors with some degree of general acceptance is in the TEMA (1978) standards. The applicability of these data to any particular situation, however, is questionable and the values probably not better than $\pm$ 50%. Moreover, the magni-

tudes and uncertainties of arbitrary fouling factors may take the edge off the importance of precise calculations of heat transfer coefficients. A brief discussion of fouling is by Walker (1982). A symposium on this important topic is edited by Somerscales and Knudsen (1981).

INDIVIDUAL FILM COEFFICIENTS

Combining individual film coefficients into an overall coefficient of heat transfer allows taking into account a greater variety and range of conditions, and should provide a better estimate. Such individual coefficients are listed in Tables 8.6 and 8.7. The first of these is a very cautious compilation with a value range of 1.5- to 2-fold. Values of the fouling factors are included in the coefficient listings of both tables but are not identified in Table 8.7. For clean service, for example, involving sensible heat transfer from a medium organic to heating a heavy organic,
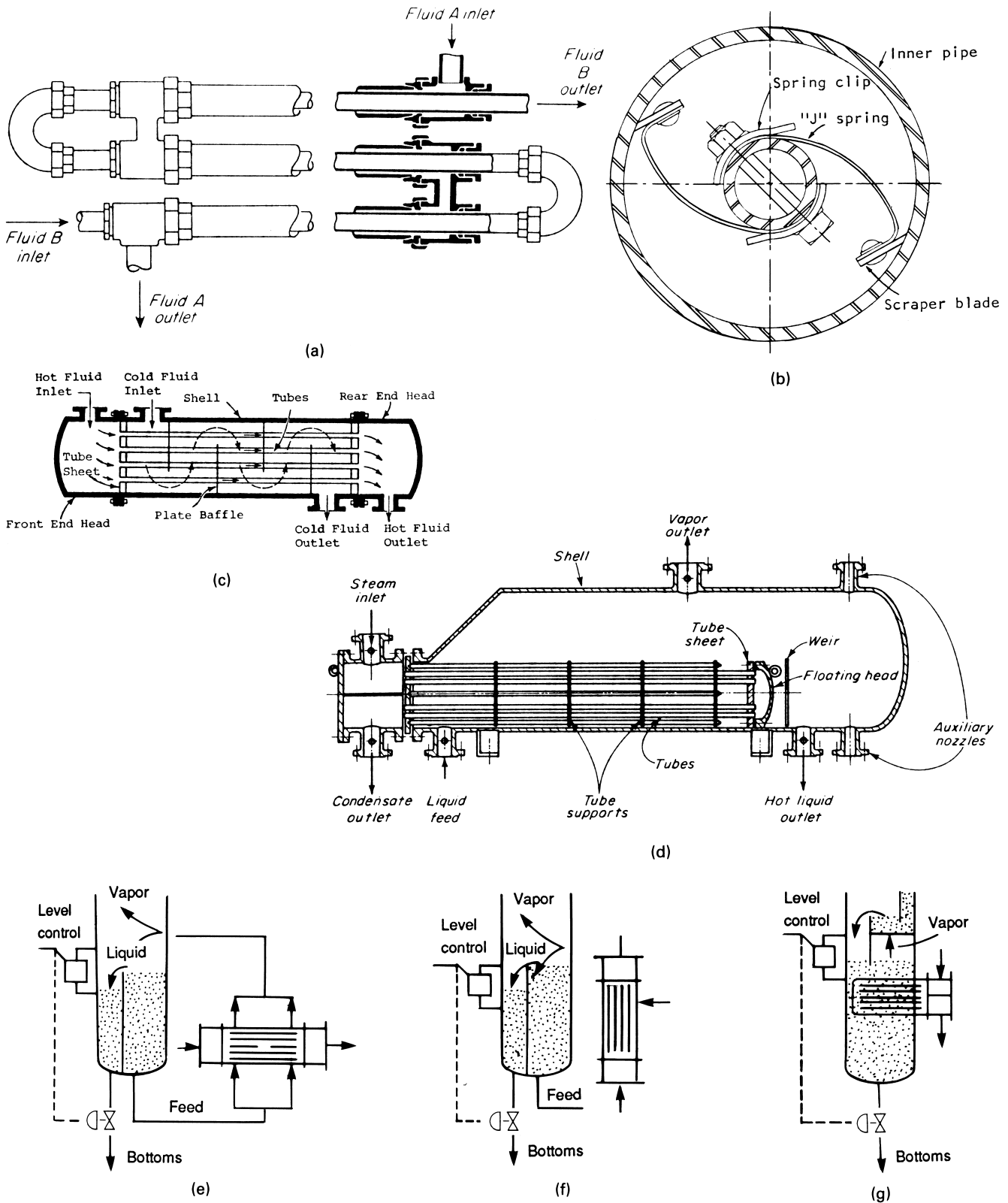
Figure 8.4. Example of tubular heat exchangers (see also Fig. 8.14). (a) Double-pipe exchanger. (b) Scraped inner surface of a double-pipe exchanger. (c) Shell-and-tube exchanger with fixed tube sheets. (d) Kettle-type reboiler. (e) Horizontal shell side thermosiphon reboiler. (f) Vertical tube side thermosiphon reboiler. (g) Internal reboiler in a tower. (h) Air cooler with induced draft fan above the tube bank. (i) Air cooler with forced draft fan below the tube bank.

(h)

(i)
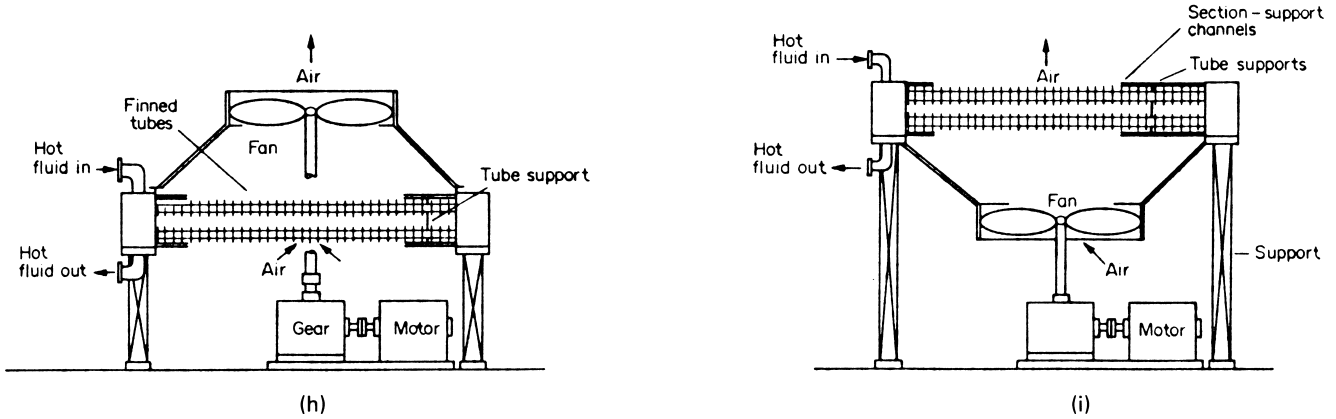
Figure 8.4.—(*continued*)

(a)
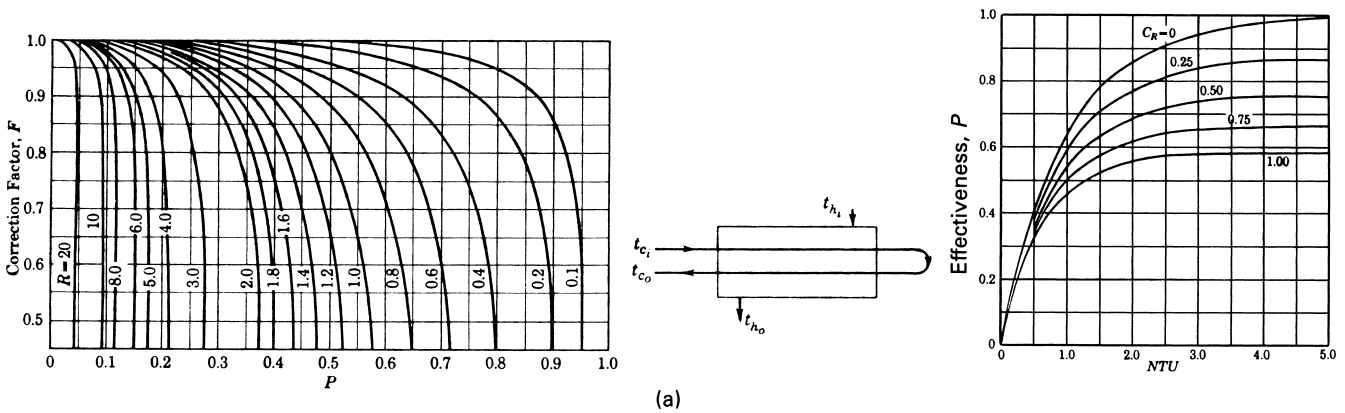
Figure 8.5. Correction factor *F*, effectiveness and number of transfer units in multipass and cross flow heat exchangers (*Bowman et al.*, Trans ASME **283**, *1940; Kays and London, 1984*):

$$P = \frac{T_i - T_o}{T_i - T_i'}, \; R = \frac{T_i' - T_o'}{T_i - T_o},$$

T on the tubeside, *T'* on the shellside. *i* = input, *o* = output. (a) One pass on shellside, any multiple of two passes on tubeside. (b) Two passes on shell side, any multiple of four on tubeside. (c) Cross flow, both streams unmixed laterally. (d) Cross flow, one stream mixed laterally. (e) Cross flow, both streams mixed laterally. (f) Effectiveness and number of transfer units in parallel and countercurrent flows. (g) Three shell passes, multiples of six on tubeside. (h) Four shell passes, multiples of eight on tubeside. (i) Five shell passes, multiples of ten on tubeside. (j) Six shell passes, multiples of 12 on tubeside.

$$U = 10{,}000/(\{[38 + 76]/2 - [9 + 23]/2\} + \{[23 + 76]/2$$
$$-[11 + 57]/2\}) = 175$$

Note that the fouling resistances have been subtracted from the fouled individual heat transfer coefficients to obtain the overall clean coefficient, compared with a normal value of

$$U = 10{,}000/(57 + 50) = 93,$$

where the averages of the listed numbers in Table 8.6 are taken in each case.

METAL WALL RESISTANCE

With the usual materials of construction of heat transfer surfaces, the magnitudes of their thermal resistances may be comparable with the other prevailing resistances. For example, heat exchanger tubing of 1/16 in. wall thickness has these values of $1/h_w = L/k$ for several common materials:

Carbon steel	$1/h_w =$	1.76×10^{-4}
Stainless steel		5.54×10^{-4}
Aluminum		0.40×10^{-4}
Glass		79.0×10^{-4}

which are in the range of the given film and fouling resistances, and should not be neglected in evaluating the overall coefficient. For example, with the data of this list a coefficient of 93 with carbon steel tubing is reduced to 88.9 when stainless steel tubing is substituted.

DIMENSIONLESS GROUPS

The effects of the many variables that bear on the magnitudes of individual heat transfer coefficients are represented most logically
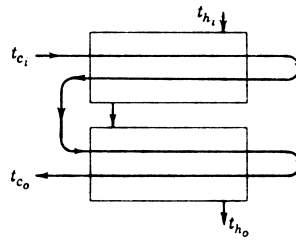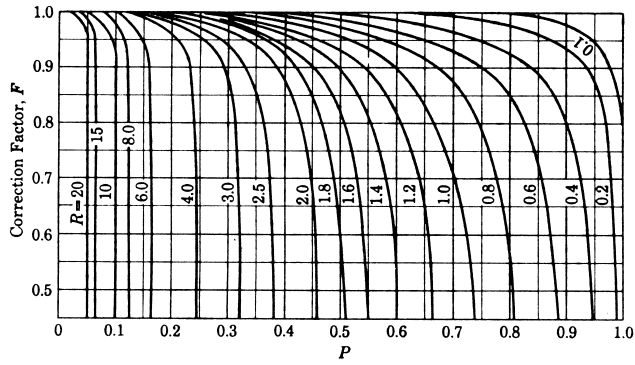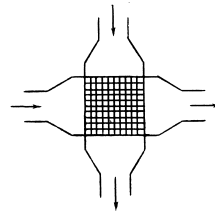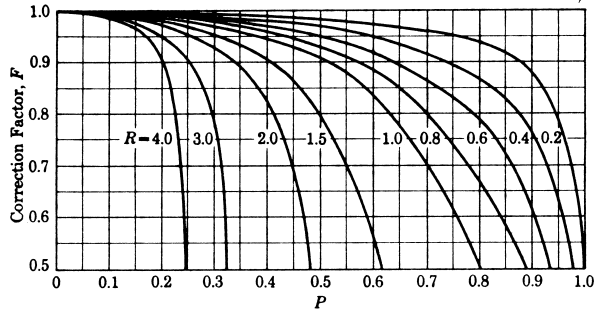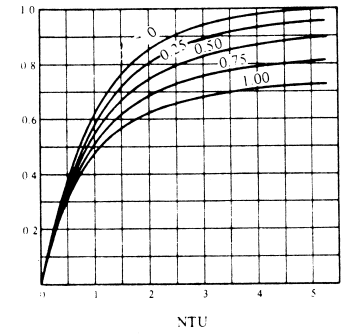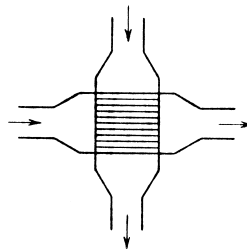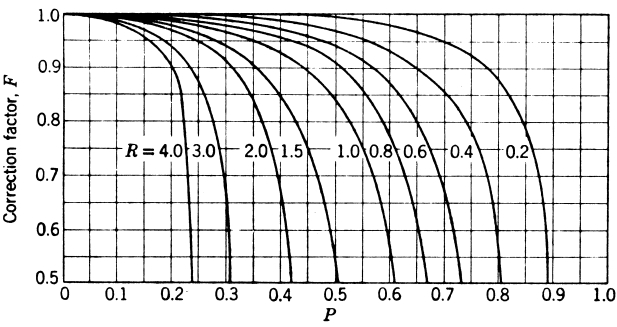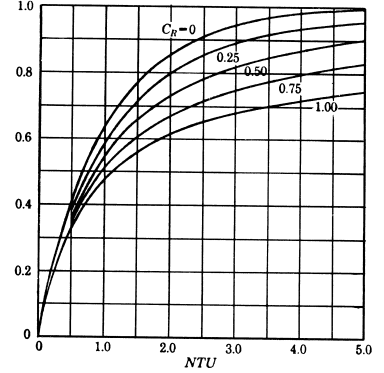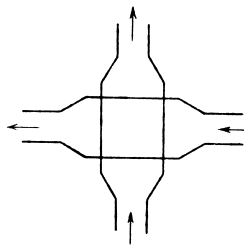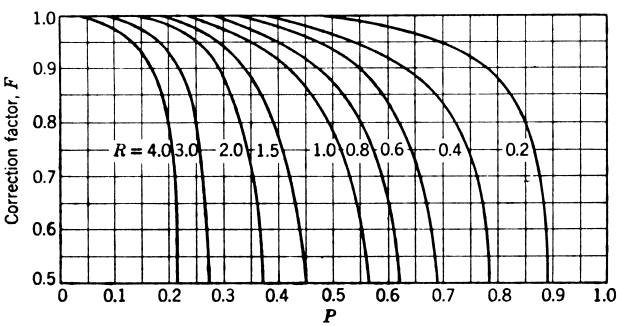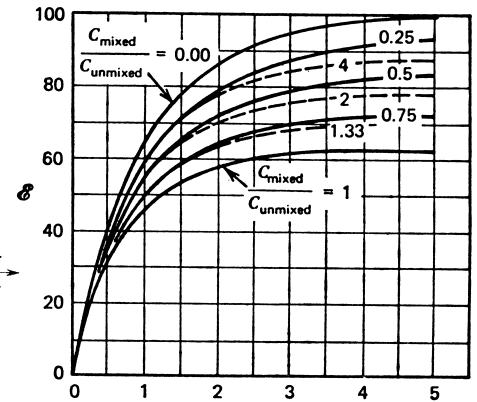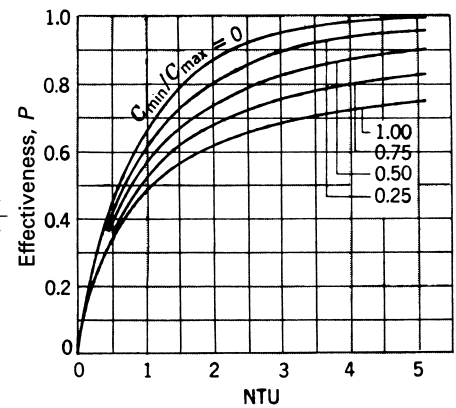
Figure 8.5.—(*continued*)

(f)

(g)

(h)

(i)

(j)
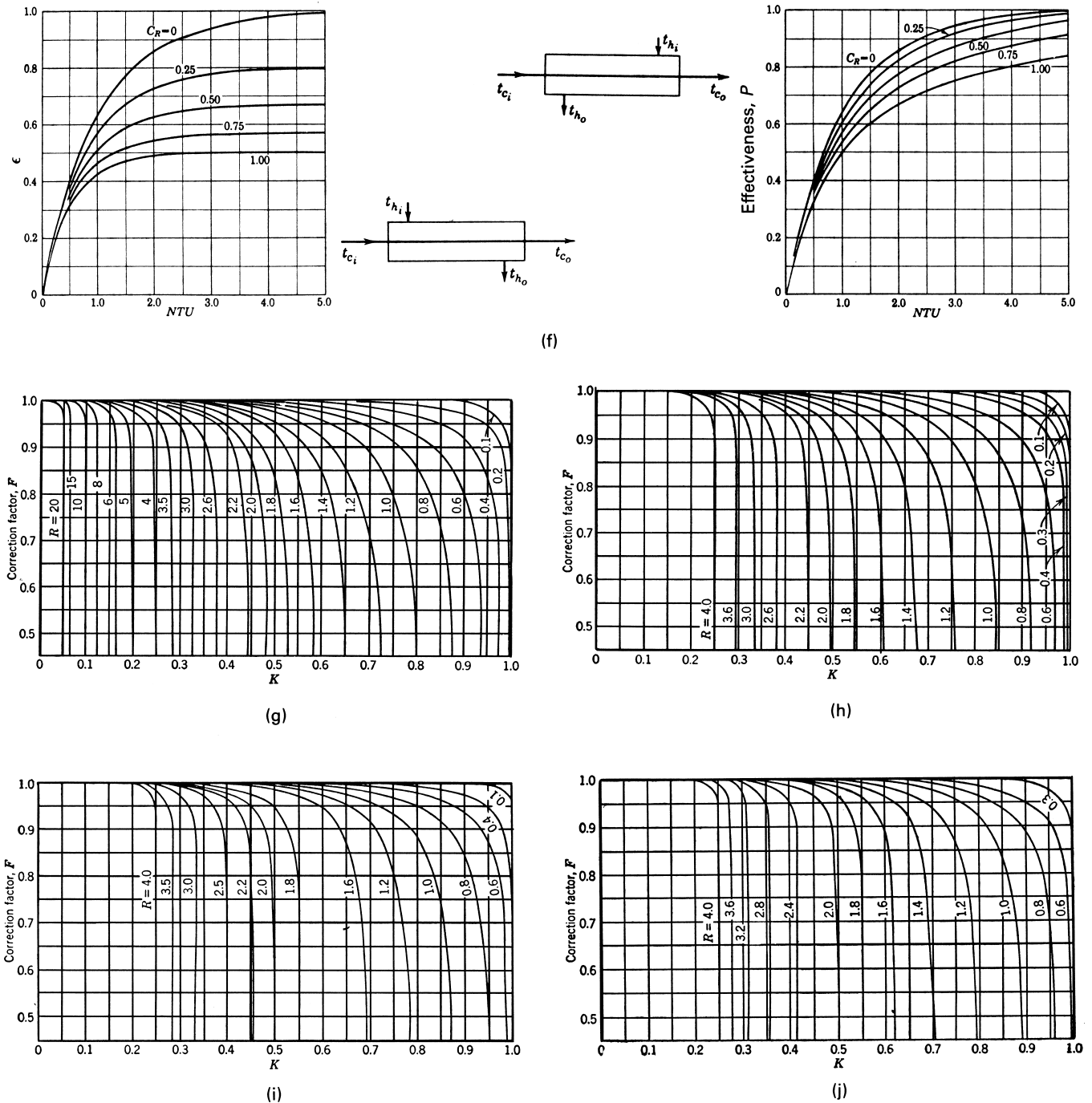
Figure 8.5.—(*continued*)

and compactly in terms of dimensionless groups. The ones most pertinent to heat transfer are listed in Table 8.8. Some groups have ready physical interpretations that may assist in selecting the ones appropriate to particular heat transfer processes. Such interpretations are discussed for example by Gröber et al. (1961, pp. 193–198). A few are given here.

The Reynolds number, $Du\rho/\mu = \rho u^2/(\mu u/D)$, is a measure of the ratio of inertial to viscous forces.

The Nusselt number, $hL/k = h/(k/L)$ is the ratio of effective heat transfer to that which would take place by conduction through a film of thickness L.

The Peclet number, $DGC/k = GC/(k/D)$ and its modification, the Graetz number wC/kL, are ratios of sensible heat change of the flowing fluid to the rate of heat conduction through a film of thickness D or L.

The Prandtl number, $C\mu/k = (\mu/\rho)/(k/\rho C)$, compares the rate of momentum transfer through friction to the thermal diffusivity or the transport of heat by conduction.
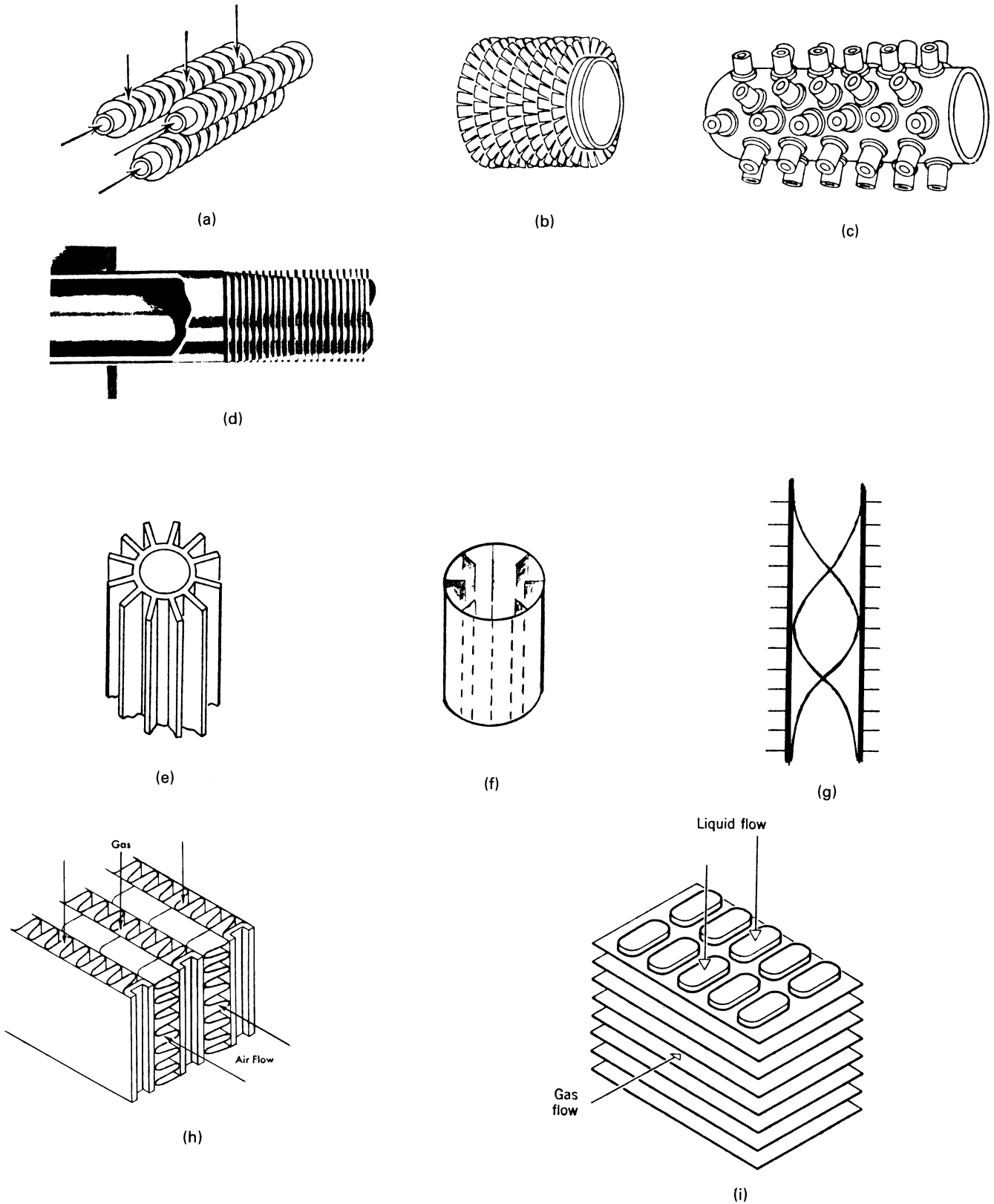
Figure 8.6. Examples of extended surfaces on one or both sides. (a) Radial fins. (b) Serrated radial fins. (c) Studded surface. (d) Joint between tubesheet and low fin tube with three times bare surface. (e) External axial fins. (f) Internal axial fins. (g) Finned surface with internal spiral to promote turbulence. (h) Plate fins on both sides. (i) Tubes and plate fins.

TABLE 8.3. Formulas for Mean Temperature Difference and Effectiveness in Heat Exchangers
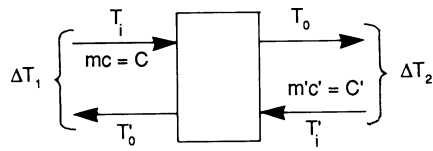
1. Parallel or countercurrent flow,

$$(\Delta T)_m = (\Delta T)_{\text{logmean}} = (\Delta T_1 - \Delta T_2)/\ln(\Delta T_1/\Delta T_2).$$

2. In general,

$$(\Delta T)_m = F(\Delta T)_{\text{logmean}}$$

or

$$(\Delta T)_m = \theta(T_i - T'_i),$$

   where F and θ depend on the actual flow paths on the shell and tube sides and are expressed in terms of these quantities:

$$C = C_{\min}/C_{\max},$$
$$P = (T_o - T_i)/(T'_i - T_i) = \text{actual heat transfer/}$$
$$\text{(maximum possible heat transfer)},$$
$$R = (T_i - T_o)/(T'_o - T'_i) = m'c'/mc.$$

3. Number of transfer units, N or NTU, is

$$N = UA/C_{\min} = P/\theta,$$

   where $C_{\min}$ is the smaller of the two values mc or $m'c'$ of the products of mass rate of flow times the heat capacity.
4. In parallel flow, $P = N\theta = \{1 - \exp[-N(1 + C)]\}/(1 + C)$.
5. In countercurrent flow, $P = N\theta = \{1 - \exp[-N(1 - C)]\}/\{1 - C\exp[-N(1 - C)]\}$.
6. One shell pass and any multiple of two tube passes,

$$F = \frac{\sqrt{R^2 + 1}}{R - 1} \cdot \ln\left(\frac{1 - P}{1 - PR}\right)\Big/\ln\left[\frac{2 - P(R + 1 - \sqrt{R^2 + 1})}{2 - P(R + 1 + \sqrt{R^2 + 1})}\right], \quad R \neq 1,$$

$$F = \frac{P}{1 - P} \cdot \sqrt{2}\Big/\ln\left[\frac{2 - P(2 - \sqrt{2})}{2 - P(2 + \sqrt{2})}\right], \quad R = 1,$$

$$P = 2\left\{1 + C + (1 + C^2)^{1/2}\frac{1 + \exp[-N(1 + C^2)^{1/2}]}{1 - \exp\{-N(1 + C^2)^{1/2}\}}\right\}^{-1}.$$

7. Two shell passes and any multiple of four tube passes,

$$F = \left[\frac{\sqrt{R^2 + 1}}{2(R - 1)}\ln\frac{1 - P}{1 - PR}\right]\Big/$$

$$\ln\left[\frac{2/P - 1 - R + (2/P)\sqrt{(1 - P)(1 - PR)} + \sqrt{R^2 + 1}}{2/P - 1 - R + (2/P)\sqrt{(1 - P)(1 - PR)} - \sqrt{R^2 + 1}}\right].$$

8. Cross flow,
   (a) Both streams laterally unmixed,
   $P = 1 - \exp\{[\exp(-NCn) - 1]/Cn\}$, where $n = N^{-0.22}$.
   (b) Both streams mixed,
   $P = \{1/[1 - \exp(-N)] + C/[1 - \exp(-NC)] - 1/N\}^{-1}$.
   (c) $C_{\max}$ mixed, $C_{\min}$ unmixed,
   $P = (1/C)\{1 - \exp[-C(1 - e^{-N})]\}$.
   (d) $C_{\min}$ mixed, $C_{\max}$ unmixed,
   $P = 1 - \exp\{-(1/C)[1 - \exp(-NC)]\}$.
9. For more complicated patterns only numerical solutions have been made. Graphs of these appear in sources such as Heat Exchanger Design Handbook (HEDH, 1983) and Kays and London (1984).

The Grashof number is interpreted as the ratio of the product of the buoyancy and inertial forces to the square of the viscous forces.

The Stanton number is a ratio of the temperature change of a fluid to the temperature drop between fluid and wall. Also, $St = (Nu)/(Re)(Pr)$.

An analogy exists between the transfers of heat and mass in moving fluids, such that correlations of heat transfer involving the Prandtl number are valid for mass transfer when the Prandtl number $C\mu/k$ is replaced by the Schmidt number $\mu/\rho k_d$. This is of particular value in correlating heat transfer from small particles to fluids where particle temperatures are hard to measure but measurement of mass transfer may be feasible, for example, in vaporization of naphthalene.

8.4. DATA OF HEAT TRANSFER COEFFICIENTS

Specific correlations of individual film coefficients necessarily are restricted in scope. Among the distinctions that are made are those of geometry, whether inside or outside of tubes for instance, or the shapes of the heat transfer surfaces; free or forced convection; laminar or turbulent flow; liquids, gases, liquid metals, non-Newtonian fluids; pure substances or mixtures; completely or partially condensable; air, water, refrigerants, or other specific substances; fluidized or fixed particles; combined convection and radiation; and others. In spite of such qualifications, it should be borne in mind that very few proposed correlations are more accurate than $\pm 20\%$ or so.

Along with rate of heat transfer, the economics of practical exchanger design requires that pumping costs for overcoming friction be taken into account.

DIRECT CONTACT OF HOT AND COLD STREAMS

Transfer of heat by direct contact is accomplished in spray towers, in towers with a multiplicity of segmented baffles or plates (called shower decks), and in a variety of packed towers. In some processes heat and mass transfer occur simultaneously between phases; for example, in water cooling towers, in gas quenching with water, and in spray or rotary dryers. Quenching of pyrolysis gases in transfer lines or towers and contacting on some trays in fractionators may involve primarily heat transfer. One or the other, heat or mass transfer, may be the dominant process in particular cases.

Data of direct contact heat transfer are not abundant. The literature has been reviewed by Fair (1972) from whom specific data will be cited.

One rational measure of a heat exchange process is the number of transfer units. In terms of gas temperatures this is defined by

$$N_g = \frac{T_{g,\text{in}} - T_{g,\text{out}}}{(T_g - T_L)_{\text{mean}}}. \tag{8.33}$$

The logarithmic mean temperature difference usually is applicable. For example, if the gas goes from 1200 to $150°$F and the liquid countercurrently from 120 to $400°$F, the mean temperature difference is 234.5 and $N_g = 4.48$. The height of a contact zone then is obtained as the product of the number of transfer units and the height H_g of a transfer unit. Several correlations have been made of the latter quantity, for example, by Cornell, Knapp, and Fair (1960), as modified in the *Chemical Engineers' Handbook* (1973, pp. 18–33, 18.37) and in *Perry's Chemical Engineers' Handbook* (1999, Table 5-28, pp. 5-74 to 5-77). These correlations for H_g

EXAMPLE **8.4**
Performance of a Heat Exchanger with the F-Method
Operation of an exchanger is represented by the sketch and the equation

$$Q/UA = 50 = F(\Delta T)_{lm}$$
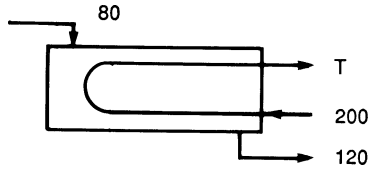
The outlet temperature of the hot fluid is unknown and designated by T. These quantities are formulated as follows:

$$P = \frac{200 - T}{200 - 80},$$
$$R = \frac{200 - T}{120 - 80},$$

$$(\Delta T)_{lm} = \frac{T - 80 - (200 - 120)}{\ln\left[(T - 80)/(200 - 120)\right]}$$

F is represented by the equation of Item 6 of Table 8.3, or by Figure 8.4(a). Values of T are tried until one is found that satisfies $G \equiv 50 - F(\Delta T)_{lm} \cong 0$. The printout shows that

$$T = 145.197.$$

The sensitivity of the calculation is shown in the following tabulation:

T	P	R	$(\Delta T)_{lm}$	F	G
145.0	0.458	1.375	72.24	0.679	0.94
145.197	0.457	1.370	72.35	0.691	0.00061
145.5	0.454	1.363	72.51	0.708	−1.34

were developed from mass transfer data and, thus, they include the Schmidt number; for heat transfer, where the gas phase resistance is controlling, the Prandtl number must be substituted for the Schmidt number. A table by McAdams (1954, p. 361) shows that in spray towers the range of H_g may be 2.5–10 ft and in various kinds of packed towers, 0.4–4 ft or so.

Heat transfer coefficients also have been measured on a volumetric or cross section basis. In heavy hydrocarbon fractionators, Neeld and O'Bara (1970) found overall coefficients of 1360–3480 Btu/(hr)(°F)(sqft of tower cross section). Much higher values have been found in less viscous systems.

Data on small packed columns were correlated by Fair (1972) in the form

$$Ua = CG^m L^n, \text{ Btu/(hr)(cuft)(°F)}, \tag{8.34}$$

where the constants depend on the kind of packing and the natures of the fluids. For example, with air–oil, 1 in. Raschig rings, in an 8 in. column

$$Ua = 0.083G^{0.94} L^{0.25}. \tag{8.35}$$

When G and L are both 5000 lb/(hr)(sqft), for instance, this formula gives $U_a = 2093$ Btu/(hr)(cuft)(°F).

In spray towers, one correlation by Fair (1972) is

$$h_g a = 0.043G^{0.8} L^{0.4}/Z^{0.5} \text{ Btu/(hr)(cuft)(°F)}. \tag{8.36}$$

In a tower with height $Z = 30$ ft and with both G and L at 5000 lb/(hr)(cuft), for example, this formula gives $h_g a = 215$.

In liquid–liquid contacting towers, data cited by Fair (1972) range from 100–12,000 Btu/(hr)(cuft)(°F) and heights of transfer units in the range of 5 ft or so. In pipeline contactors, transfer rates of 6000–60,000 Btu/(hr)(cuft)(°F) have been found, in some cases as high as 200,000.

In some kinds of equipment, data only on mass transfer rates may be known. From these, on the basis of the Chilton–Colburn analogy, corresponding values of heat transfer rates can be estimated.

NATURAL CONVECTION

Coefficients of heat transfer by natural convection from bodies of various shapes, chiefly plates and cylinders, are correlated in terms of Grashof, Prandtl, and Nusselt numbers. Table 8.9 covers the most usual situations, of which heat losses to ambient air are the most common process. Simplified equations are shown for air. Transfer of heat by radiation is appreciable even at modest temperatures; such data are presented in combination with convective coefficients in item 16 of this table.

FORCED CONVECTION

Since the rate of heat transfer is enhanced by rapid movement of fluid past the surface, heat transfer processes are conducted under such conditions whenever possible. A selection from the many available correlations of forced convective heat transfer involving single phase fluids, including flow inside and outside bare and extended surfaces, is presented in Table 8.10. Heat transfer resulting in phase change, as in condensation and vaporization, also is covered in this table. Some special problems that arise in interpreting phase change behavior will be mentioned following.

CONDENSATION

Depending largely on the nature of the surface, condensate may form either a continuous film or droplets. Since a fluid film is a partial insulator, dropwise condensation results in higher rates of condensation. Promoters are substances that make surfaces nonwetting, and may be effective as additives in trace amounts to the vapor. Special shapes of condensing surfaces also are effective in developing dropwise condensation. None of these effects has been generally correlated, but many examples are cited in HEDH and elsewhere. Condensation rates of mixtures are influenced by both heat and mass transfer rates; techniques for making such calculations have been developed and are a favorite problem for implementation on computers. Condensation rates of mixtures that form immiscible liquids also are reported on in HEDH. Generally, mixtures have lower heat transfer coefficients in condensation than do pure substances.
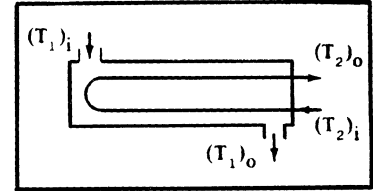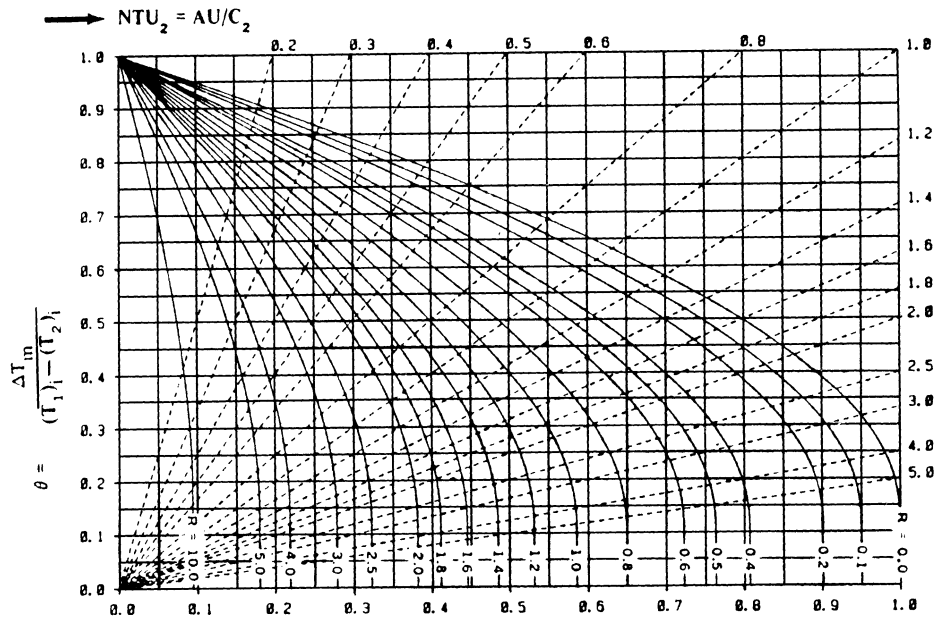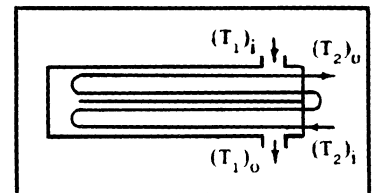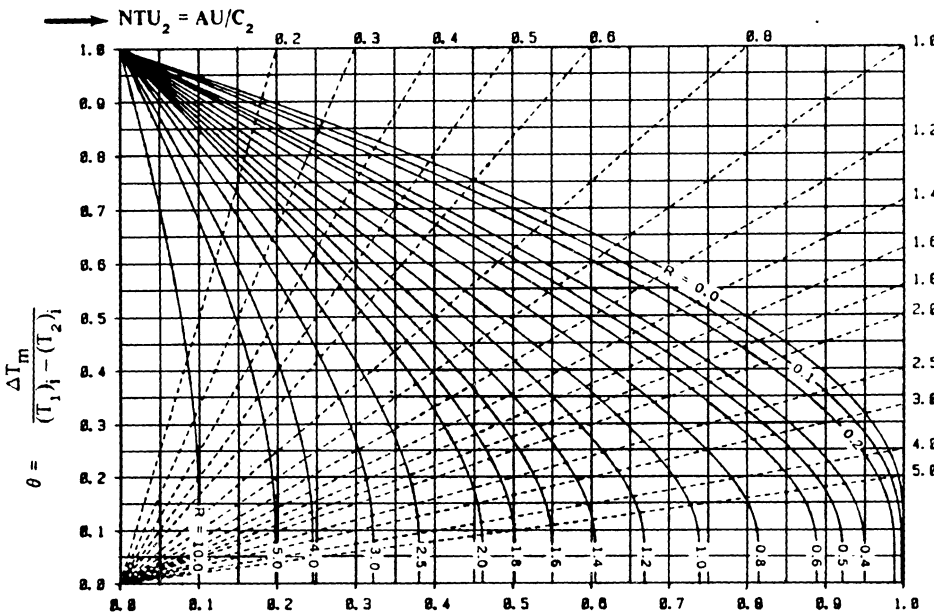
Figure 8.7. θ correction charts for mean temperature difference: (a) One shell pass and any multiple of two tube passes. (b) Two shell passes and any multiple of four tube passes. [(*HEDH, 1983*); *after Mueller in Rohsenow and Hartnett*, Handbook of Heat Transfer, *Section 18, McGraw-Hill, New York, 1973. Other cases also are covered in these references.*]

BOILING

This process can be nuclear or film type. In nuclear boiling, bubbles detach themselves quickly from the heat transfer surface. In film boiling the rate of heat transfer is retarded by an adherent vapor film through which heat supply must be by conduction. Either mode can exist in any particular case. Transition between modes corresponds to a maximum heat flux and the associated critical temperature difference. A table of such data by McAdams (*Heat Transmission*, McGraw-Hill, New York, 1954, p. 386) shows the critical temperature differences to range from 42–90°F and the maximum fluxes from 42–126 KBtu/(hr)(sqft) for organic substances and up to 410 KBtu/(hr)(sqft) for water; the nature of the surface and any promoters are identified. Equations (40) and (41) of Table 8.10 are for critical heat fluxes in kettle and thermosyphon

EXAMPLE 8.5
Application of the Effectiveness and the θ Method
Operating data of an exchanger are shown on the sketch. These data include

$$UA = 2000,$$
$$m'c' = 1000, \quad mc = 800,$$
$$C = C_{min}/C_{max} = 0.8.$$
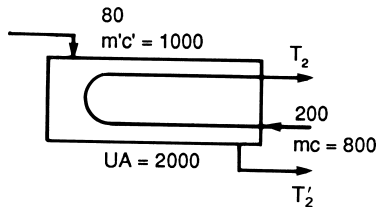
The equation for effectiveness P is given by item 6 of Table 8.3 or it can be read off Figure 8.5(a). Both P and θ also can be read off Figure 8.4(a) at known N and $R = C_2/C_1 = 0.8$. The number of transfer units is

$$N = UA/C_{min} = 2000/800 = 2.5,$$
$$C = C_{min}/C_{max} = 0.8,$$
$$D = \sqrt{1 + C^2} = 1.2806,$$
$$P = \frac{2}{1 + C + D[1 + \exp(-ND)]/1 - \exp(-ND)} = 0.6271,$$
$$\theta = P/N = 0.2508,$$
$$\Delta T_m = \theta(200 - 80) = 30.1,$$
$$Q = UA(\Delta T)_m = 2000(30.1) = 60,200,$$
$$= 800(200 - T_2) = 1000(T_2' - 80),$$
$$\therefore T_2 = 124.75,$$
$$T_2' = 140.2.$$

T^2 also may be found from the definition of P:

$$P = \frac{\text{actual}\Delta T}{\text{max possible}\Delta T} = \frac{200 - T_2}{200 - 80} = 0.6271,$$
$$\therefore T_2 = 124.78.$$

With this method, unknown terminal temperatures are found without trial calculations.

---

reboilers. Beyond the maximum rate, film boiling develops and the rate of heat transfer drops off very sharply.

Evaluation of the boiling heat transfer coefficient in vertical tubes, as in thermosyphon reboilers, is based on a group of equations, (42)–(48), of Table 8.10. A suitable procedure is listed following these equations in that table.

EXTENDED SURFACES

When a film coefficient is low as in the cases of low pressure gases and viscous liquids, heat transfer can be improved economically by employing extended surfaces. Figure 8.6 illustrates a variety of extended surfaces. Since the temperature of a fin necessarily averages less than that of the bare surface, the effectiveness likewise is less than that of bare surface. For many designs, the extended surface may be taken to be 60% as effective as bare surface, but this factor depends on the heat transfer coefficient and thermal conductivity of the fin as well as its geometry. Equations and corresponding charts have been developed for the common geometries and are shown, for example, in HEDH (1983, Sec. 2.5.3) and elsewhere. One chart is given with Example 8.6. The efficiency η of the extended surface is defined as the ratio of a realized heat transfer to the heat transfer that would be obtained if the fin were at the bare tube temperature throughout. The total heat transfer is the sum of the heat transfers through the bare and the extended surfaces:

$$Q = Q_b + Q_e = U_b A_b (1 + \eta A_e/A_b)(T_b - T_{\text{fluid}}).$$

A_b is the tube surface that is not occupied by fins. Example 8.6 performs an analysis of this kind of problem.

8.5. PRESSURE DROP IN HEAT EXCHANGERS

Although the rate of heat transfer to or from fluids is improved by increase of linear velocity, such improvements are limited by the economic balance between value of equipment saving and cost of pumping. A practical rule is that pressure drop in vacuum condensers be limited to 0.5–1.0 psi (25–50 Torr) or less, depending on the required upstream process pressure. In liquid service, pressure drops of 5–10 psi are employed as a minimum, and up to 15% or so of the upstream pressure.

Calculation of tube-side pressure drop is straightforward, even of vapor–liquid mixtures when their proportions can be estimated. Example 8.7 employs the methods of Chapter 6 for pressure drop in a thermosiphon reboiler.

The shell side with a number of segmental baffles presents more of a problem. It may be treated as a series of ideal tube banks connected by window zones, but also accompanied by some bypassing of the tube bundles and leakage through the baffles. A hand calculation based on this mechanism (ascribed to K.J. Bell) is illustrated by Ganapathy (1982, pp. 292–302), but the calculation usually is made with proprietary computer programs, that of HTRI for instance.

A simpler method due to Kern (1950, pp. 147–152) nominally considers only the drop across the tube banks, but actually takes account of the added pressure drop through baffle windows by employing a higher than normal friction factor to evaluate pressure drop across the tube banks. Example 8.8 employs this procedure. According to Taborek (HEDH, 1983, 3.3.2), the Kern predictions usually are high, and therefore considered safe, by a factor as high as 2, except in laminar flow where the results are uncertain. In the case worked out by Ganapathy (1982, pp. 292–302), however, the Bell and Kern results are essentially the same.

8.6. TYPES OF HEAT EXCHANGERS

Heat exchangers are equipment primarily for transferring heat between hot and cold streams. They have separate passages for the two streams and operate continuously. They also are called recuperators to distinguish them from regenerators, in which hot and cold streams pass alternately through the same passages and exchange heat with the mass of the equipment, which is intentionally

TABLE 8.4. Overall Heat Transfer Coefficients in Some Petrochemical Applications, U Btu/(hr)(sqft)(°F)[a]

In Tubes	Outside Tubes	Type Equipment	Velocities (ft/sec)		Overall Coefficient	Temp. Range (°F)	Estimated Fouling		
			Tube	Shell			Tube	Shell	Overall
A. Heating-cooling									
Butadiene mix. (Super-heating)	steam	H	25–35	—	12	400–100	—	—	0.04
Solvent	solvent	H	—	1.0–1.8	35–40	110–30	—	—	0.0065
Solvent	propylene (vaporization)	K	1–2	—	30–40	40–0	—	—	0.006
C$_4$ unsaturates	propylene (vaporization)	K	20–40	—	13–18	100–35	—	—	0.005
Solvent	chilled water	H	—	—	35–75	115–40	0.003	0.001	—
Oil	oil	H	—	—	60–85	150–100	0.0015	0.0015	—
Ethylene-vapor	condensate and vapor	K	—	—	90–125	600–200	0.002	0.001	—
Ethylene vapor	chilled water	H	—	—	50–80	270–100	0.001	0.001	—
Condensate	propylene (refrigerant)	K-U	—	—	60–135	60–30	0.001	0.001	—
Chilled water	transformer oil	H	—	—	40–75	75–50	0.001	0.001	—
Calcium brine-25%	chlorinated C$_1$	H	1–2	0.5–1.0	40–60	−20−+10	0.002	0.005	—
Ethylene liquid	ethylene vapor	K-U	—	—	10–20	−170–(−100)	—	—	0.002
Propane vapor	propane liquid	H	—	—	6–15	−25–100	—	—	0.002
Lights and chlor. HC	steam	U	—	—	12–30	−30–260	0.001	0.001	—
Unsat. light HC, CO, CO$_2$, H$_2$	steam	H	—	—	10–2	400–100	—	—	0.3
Ethonolamine	steam	H	—	—	15–25	400–40	0.001	0.001	—
Steam	air mixture	U	—	—	10–20	−30–220	0.0005	0.0015	—
Steam	styrene and tars	U (in tank)	—	—	50–60	190–230	0.001	0.002	—
Chilled water	freon-12	H	4–7	—	100–130	90–25	0.001	0.001	—
Water[b]	lean copper solvent	H	4–5	—	100–120	180–90	—	—	0.004
Water	treated water	H	3–5	1–2	100–125	90–110	—	—	0.005
Water	C$_2$-chlor. HC, lights	H	2–3	—	6–10	360–100	0.002	0.001	—
Water	hydrogen chloride	H	—	—	7–15	230–90	0.002	0.001	—
Water	heavy C$_2$-chlor.	H	—	—	45–30	300–90	0.001	0.001	—
Water	perchlorethylene	H	—	—	55–35	150–90	0.001	0.001	—
Water	air and water vapor	H	—	—	20–35	370–90	0.0015	0.0015	—
Water	engine jacket water	H	—	—	230–160	175–90	0.0015	0.001	—
Water	absorption oil	H	—	—	80–115	130–90	0.0015	0.001	—
Water	air-chlorine	U	4–7	—	8–18	250–90	—	—	0.005
Water	treated water	H	5–7	—	170–225	200–90	0.001	0.001	—
B. Condensing									
C$_4$ unsat.	propylene refrig.	K	v	—	58–68	60–35	—	—	0.005
HC unsat. lights	propylene refrig.	K	v	—	50–60	45–3	—	—	0.0055
Butadiene	propylene refrig.	K	v	—	65–80	20–35	—	—	0.004
Hydrogen chloride	propylene refrig.	H	—	—	110–60	0–15	0.012	0.001	—

(*continued*)

TABLE 8.4. —(*continued***)**

In Tubes	Outside Tubes	Type Equipment	Velocities (ft/sec)		Overall Coefficient	Temp. Range (°F)	Estimated Fouling		
			Tube	Shell			Tube	Shell	Overall
Lights and chloro-ethanes	propylene refrig.	KU	—	—	15–25	130–(−20)	0.002	0.001	—
Ethylene	propylene refrig.	KU	—	—	60–90	120–(−10)	0.001	0.001	—
Unsat. chloro HC	water	H	7–8	—	90–120	145–90	0.002	0.001	—
Unsat. chloro HC	water	H	3–8	—	180–140	110–90	0.001	0.001	—
Unsat. chloro HC	water	H	6	—	15–25	130–(−20)	0.002	0.001	—
Chloro-HC	water	KU	—	—	20–30	110–(−10)	0.001	0.001	—
Solvent and non cond.	water	H	—	—	25–15	260–90	0.0015	0.004	—
Water	propylene vapor	H	2–3	—	130–150	200–90	—	—	0.003
Water	propylene	H	—	—	60–100	130–90	0.0015	0.001	—
Water	steam	H	—	—	225–110	300–90	0.002	0.0001	—
Water	steam	H	—	—	190–235	230–130	0.0015	0.001	—
Treated water	steam (exhaust)	H	—	—	20–30	220–130	0.0001	0.0001	—
Oil	steam	H	—	—	70–110	375–130	0.003	0.001	—
Water	propylene cooling and cond.	H	—	—	{ 25–50 / 110–150	30–45 (C) } / 15–20 (Co) }	0.0015	0.001	—
Chilled water	air-chlorine (part and cond.)	U	—	—	{ 8–15 / 20–30	8–15 (C) } / 10–15 (Co) }	0.0015	0.005	—
									—
Water	light HC, cool and cond.	H	—	—	35–90	270–90	0.0015	0.003	—
Water	ammonia	H	—	—	140–165	120–90	0.001	0.001	—
Water	ammonia	U	—	—	280–300	110–90	0.001	0.001	—
Air-water vapor	freon	KU	—	—	{10–50} / {10–20}	60–10	—	—	0.01
C. Reboiling									
Solvent, Copper-NH$_3$	steam	H	7–8	—	130–150	180–160	—	—	0.005
C$_4$ unsat.	steam	H	—	—	95–115	95–150	—	—	0.0065
Chloro. HC	steam	VT	—	—	35–25	300–350	0.001	0.001	—
Chloro. unsat. HC	steam	VT	—	—	100–140	230–130	0.001	0.001	—
Chloro. ethane	steam	VT	—	—	90–135	300–350	0.001	0.001	—
Chloro. ethane	steam	U	—	—	50–70	30–190	0.002	0.001	—
Solvent (heavy)	steam	H	—	—	70–115	375–300	0.004	0.0005	—
Mono-di-ethanolamines	steam	VT	—	—	210–155	450–350	0.002	0.001	—
Organics, acid, water	steam	VT	—	—	60–100	450–300	0.003	0.0005	—
Amines and water	steam	VT	—	—	120–140	360–250	0.002	0.0015	—
Steam	naphtha frac.	Annulus Long. F.N.	—	—	15–20	270–220	0.0035	0.0005	—
Propylene	C$_2$, C$_2^-$	KU	—	—	120–140	150–40	0.001	0.001	—
Propylene-butadiene	butadiene, unsat.	H	—	25–35	15–18	400–100	—	—	0.02

[a]Fouling resistances are included in the listed values of *U*.
[b]Unless specified, all water is untreated, brackish, bay or sea. Notes: H = horizontal, fixed or floating tube sheet, U = U—tube horizontal bundle, K = kettle type, V = vertical, R = reboiler, T = thermosiphon, v = variable, HC = hydrocarbon, (C) = cooling range Δ*t*, (Co) = condensing range Δ*t*.
(Ludwig, 1983).

TABLE 8.5. Ranges of Overall Heat Transfer Coefficients in Various Types of Exchangers [U Btu/ (hr)(sqft)(°F)][a]

Equipment	Process	U
Shell- and-tube exchanger [Fig. 8.4(c)]	gas (1 atm)–gas (1 atm)	1–6
	gas (250 atm)–gas (250 atm)	25–50
	liquid–gas (1 atm)	2–12
	liquid–gas (250 atm)	35–70
	liquid–liquid	25–200
	liquid–condensing vapor	50–200
Double-pipe exchanger [Fig. 8.4(a)]	gas (1 atm)–gas (1 atm)	2–6
	gas (250 atm)–gas (250 atm)	25–90
	liquid–gas (250 atm)	35–100
	liquid–liquid	50–250
Irrigated tube bank	water–gas (1 atm)	3–10
	water–gas (250 atm)	25–60
	water–liquid	50–160
	water–condensing vapor	50–200
Plate exchanger [Fig. 8.8(a)]	water–gas (1 atm)	3–10
	water–liquid	60–200
Spiral exchanger [Fig. 8.8(c)]	liquid–liquid	120–440
	liquid–condensing steam	160–600
Compact [Fig. 8.6(h)]	gas (1 atm)–gas (1 atm)	2–6
	gas (1 atm)–liquid	3–10
Stirred tank, jacketed	liquid–condensing steam	90–260
	boiling liquid–condensing steam	120–300
	water–liquid	25–60
Stirred tank, coil inside	liquid–condensing steam	120–440
	water–liquid	90–210

[a]1 Btu/ (hr)(sqft)(˚F) = 5.6745 W/ m^2 K.
Data from (HEDH, 1983).

made with large heat capacity. Recuperators are used mostly in cryogenic services, and at the other extreme of temperature, as high temperature air preheaters. They will not be discussed here; a detailed treatment of their theory is by Hausen (1983).

Being the most widely used kind of process equipment is a claim that is made easily for heat exchangers. A classified directory of manufacturers of heat exchangers by Walker (1982) has several hundred items, including about 200 manufacturers of shell-and-tube equipment. The most versatile and widely used exchangers are the shell-and-tube types, but various plate and other types are valuable and economically competitive or superior in some applications. These other types will be discussed briefly, but most of the space following will be devoted to the shell-and-tube types, primarily because of their importance, but also because they are most completely documented in the literature. Thus they can be designed with a degree of confidence to fit into a process. The other types are largely proprietary and for the most part must be process designed by their manufacturers.

PLATE-AND-FRAME EXCHANGERS

Plate-and-frame exchangers are assemblies of pressed corrugated plates on a frame, as shown on Figure 8.8(a). Gaskets in grooves around the periphery contain the fluids and direct the flows into and out of the spaces between the plates. Hot and cold flows are on opposite sides of the plates. Figure 8.8(b) shows a few of the many combinations of parallel and countercurrent flows that can be maintained. Close spacing and the presence of the corrugations result in high coefficients on both sides—several times those of shell-and-tube equipment—and fouling factors are low, of the order of $1–5 \times 10^{-5}$ Btu/(hr)(sqft)(°F). The accessibility of the heat exchange surface for cleaning makes them particularly suitable for fouling services and where a high degree of sanitation is required, as in food and pharmaceutical processing. Operating pres-

sures and temperatures are limited by the natures of the available gasketing materials, with usual maxima of 300 psig and 400°F.

Since plate-and-frame exchangers are made by comparatively few concerns, most process design information about them is proprietary but may be made available to serious enquirers. Friction factors and heat transfer coefficients vary with the plate spacing and the kinds of corrugations; a few data are cited in HEDH (1983, 3.7.4–3.7.5). Pumping costs per unit of heat transfer are said to be lower than for shell-and-tube equipment. In stainless steel construction, the plate-and-frame construction cost is 50–70% that of shell-and-tube, according to Marriott (*Chem. Eng.*, April 5, 1971).

A process design of a plate-and-frame exchanger is worked out by Ganapathy (1982, p. 368).

SPIRAL HEAT EXCHANGERS

As appears on Figure 8.8(c), the hot fluid enters at the center of the spiral element and flows to the periphery; flow of the cold fluid is countercurrent, entering at the periphery and leaving at the center. Heat transfer coefficients are high on both sides, and there is no correction to the log mean temperature difference because of the true countercurrent action. These factors may lead to surface requirements 20% or so less than those of shell-and-tube exchangers. Spiral types generally may be superior with highly viscous fluids at moderate pressures. Design procedures for spiral plate and the related spiral tube exchangers are presented by Minton (1970). Walker (1982) lists 24 manufacturers of this kind of equipment.

COMPACT (PLATE-FIN) EXCHANGERS

Units like Figure 8.6(h), with similar kinds of passages for the hot and cold fluids, are used primarily for gas service. Typically they have surfaces of the order of 1200 m^2/m^3 (353 sqft/cuft), corrugation height 3.8–11.8 mm, corrugation thickness 0.2–0.6 mm, and fin

TABLE 8.6. Typical Ranges of Individual Film and Fouling Coefficients [h Btu/ (hr)(sqft)(°F)]

Fluid and Process	Conditions	P (atm)	$(\Delta T)_{max}$(°F)	$10^4\ h$	$10^4\ h_f$
Sensible					
Water	liquid			7.6–11.4	6–14
Ammonia	liquid			7.1–9.5	0–6
Light organics	liquid			28–38	6–11
Medium organics	liquid			38–76	9–23
Heavy organics	liquid heating			23–76	11–57
Heavy organics	liquid cooling			142–378	11–57
Very heavy organics	liquid heating			189–568	23–170
Very heavy organics	liquid cooling			378–946	23–170
Gas		1–2		450–700	0–6
Gas		10		140–230	0–6
Gas		100		57–113	0–6
Condensing transfer					
Steam ammonia	all condensable	0.1		4.7–7.1	0–6
Steam ammonia	1% noncondensable	0.1		9.5–14.2	0–6
Steam ammonia	4% noncondensable	0.1		19–28	0–6
Steam ammonia	all condensable	1		3.8–5.7	0–6
Steam ammonia	all condensable	10		2.3–3.8	0–6
Light organics	pure	0.1		28–38	0–6
Light organics	4% noncondensable	0.1		57–76	0–6
Light organics	pure	10		8–19	0–6
Medium organics	narrow range	1		14–38	6–30
Heavy organics	narrow range	1		28–95	11–28
Light condensable mixes	narrow range	1		23–57	0–11
Medium condensable mixes	narrow range	1		38–95	6–23
Heavy condensable mixes	medium range	1		95–190	11–45
Vaporizing transfer					
Water		< 5	45	5.7–19	6–12
Water		< 100	36	3.8–14	6–12
Ammonia		< 30	36	11–19	6–12
Light organics	pure	20	36	14–57	6–12
Light organics	narrow range	20	27	19–76	6–17
Medium organics	pure	20	36	16–57	6–17
Medium organics	narrow range	20	27	23–95	6–17
Heavy organics	pure	20	36	23–95	11–28
Heavy organics	narrow range	20	27	38–142	11–45
Very heavy organics	narrow range	20	27	57–189	11–57

Light organics have viscosity < 1 cP, typically similar to octane and lighter hydrocarbons.
Medium organics have viscosities in the range 1–5 cP, like kerosene, hot gas oil, light crudes, etc.
Heavy organics have viscosities in the range 5–100 cP, cold gas oil, lube oils, heavy and reduced crudes, etc.
Very heavy organics have viscosities above 100 cP, asphalts, molten polymers, greases, etc.
Gases are all noncondensables except hydrogen and helium which have higher coefficients.
Conversion factor: 1 Btu/ (hr)(sqft)(˚F) = 5.6745 W/ m² K. (After HEDH, 1983, 3.1.4-4).

density 230–700 fins/m. The large extended surface permits about four times the heat transfer rate per unit volume that can be achieved with shell-and-tube construction. Units have been designed for pressures up to 80 atm or so. The close spacings militate against fouling service. Commercially, compact exchangers are used in cryogenic services, and also for heat recovery at high temperatures in connection with gas turbines. For mobile units, as in motor vehicles, the designs of Figures 8.6(h) and (i) have the great merits of compactness and light weight. Any kind of arrangement of cross and countercurrent flows is feasible, and three or more different streams can be accommodated in the same equipment. Pressure drop, heat transfer relations, and other aspects of design are well documented, particularly by Kays and London (1984) and in HEDH (1983, Sec. 3.9).

AIR COOLERS

In such equipment the process fluid flows through finned tubes and cooling air is blown across them with fans. Figures 8.4(h) and (i)

show the two possible arrangements. The economics of application of air coolers favors services that allow 25–40°F temperature difference between ambient air and process outlet. In the range above 10 MBtu/(hr), air coolers can be economically competitive with water coolers when water of adequate quality is available in sufficient amount.

Tubes are 0.75–1.00 in. OD, with 7–11 fins/in. and 0.5–0.625 in. high, with a total surface 15–20 times bare surface of the tube. Fans are 4–12 ft/dia, develop pressures of 0.5–1.5 in. water, and require power inputs of 2–5 HP/MBtu/hr or about 7.5 HP/100 sqft of exchanger cross section. Spacings of fans along the length of the equipment do not exceed 1.8 times the width of the cooler. Face velocities are about 10 ft/sec at a depth of three rows and 8 ft/sec at a depth of six rows.

Standard air coolers come in widths of 8, 10, 12, 16, or 20 ft, lengths of 4–40 ft, and stacks of 3–6 rows of tubes. Example 8.8 employs typical spacings.

Two modes of control of air flow are shown in Figure 3.9. Precautions may need to be taken against subcooling to the freezing point in winter.

TABLE 8.7. Individual Film Resistances (1/ _h_) Including Fouling Effects, with _h_ in Btu/ (hr)(sqft)(°F)

| | Kind of Heat Transfer | | |
Fluid	Sensible	Boiling	Condensing
Aromatic liquids			
Benzene, toluene, ethylbenzene, styrene	0.007	0.011	0.007
Dowtherm	0.007	—	—
Inorganic solutions			
$CaCl_2$ Brine (25%)	0.004	—	—
Heavy acids	0.013	—	—
NaCl Brine (20%)	0.0035	—	—
Misc. dilute solutions	0.005	—	—
Light hydrocarbon liquids			
C_3, C_4, C_5	0.004	0.007	0.004
Chlorinated hydrocarbons	0.004	0.009	0.007
Miscellaneous organic liquids			
Acetone	0.007	—	—
Amine solutions			
Saturated diethanolamine and mono	0.007	—	—
ethanolamine (CO_2 and H_2S)			
Lean amine solutions	0.005	—	—
Oils			
Crude oil	0.015	—	—
Diesel oil	0.011	—	—
Fuel oil (bunker C)	0.018	—	—
Gas oil			
Light	0.0125	—	0.015
Heavy (typical of cat. cracker feed)	0.014	—	0.018
Gasoline (400° EP)	0.008	0.010	0.008
Heating oil (domestic 30° API)	0.010	—	—
Hydroformate	0.006	—	—
Kerosine	0.009	—	0.013
Lube oil stock	0.018	—	—
Naphthas			
Absorption	0.008	0.010	0.006
Light virgin	0.007	0.010	0.007
Light catalytic	0.006	0.010	0.007
Heavy	0.008	0.011	0.0085
Polymer (C_8's)	0.008	0.010	0.008
Reduced crude	0.018	—	—
Slurry oil (fluid cat. cracker)	0.015	—	—
Steam (no noncondensables)			0.001
Water			
Boiler water	0.003	—	—
Cooling tower (untreated)	0.007	—	—
Condensate (flashed)	0.002	—	—
River and well	0.007	—	—
Sea water (clean and below 125°F)	0.004	—	—
Gases in turbulent flow			
Air, CO, CO_2, and N_2	0.045		
Hydrocarbons (light through naphthas)	0.035		

(Fair and Rase, Pet Refiner _33_(7), 121, 1854; Rase and Barrow, 1957).

Forced draft arrangement, from below the tubes, Figure 8.4(h), develops high turbulence and consequently high heat transfer coefficients. Escape velocities, however, are low, 3 m/sec or so, and as a result poor distribution, backmixing and sensitivity to cross currents can occur. With induced draft from above the tubes, Figure 8.4(h), escape velocities may be of the order of 10 m/sec and better flow distribution results. This kind of installation is more expensive, the pressure drops are higher, and the equipment is bathed in hot air which can be deteriorating. The less solid mounting also can result in noisier operation.

Correlations for friction factors and heat transfer coefficients are cited in HEDH. Some overall coefficients based on external bare tube surfaces are in Tables 8.11 and 8.12. For single passes in cross flow, temperature correction factors are represented by Figure 8.5(c) for example; charts for multipass flow on the tube side are given in HEDH and by Kays and London (1984), for example. Preliminary estimates of air cooler surface requirements can be made with the aid of Figures 8.9 and 8.10, which are applied in Example 8.9.

DOUBLE-PIPES

This kind of exchanger consists of a central pipe supported within a larger one by packing glands [Fig. 8.4(a)]. The straight length is limited to a maximum of about 20 ft; otherwise the center pipe will sag and cause poor distribution in the annulus. It is customary to operate with the high pressure, high temperature, high density, and corrosive fluid in the inner pipe and the less demanding one in the

TABLE 8.8 Dimensionless Groups and Units of Quantities Pertaining to Heat Transfer

Symbol	Number	Group
Bi	Biot	hL/k
Fo	Fourier	$k\theta/\rho CL^2$
Gz	Graetz	wC/kL
Gr	Grashof	$D^3\rho^2 g\beta\Delta T/\mu^2$
Nu	Nusselt	hD/k
Pe	Peclet	$DGC/k = (Re)(Pr)$
Pr	Prandtl	$C\mu/k$
Re	Reynolds	DG/μ, $Du\rho/\mu$
Sc	Schmidt	$\mu/\rho k_d$
St	Stanton	$hC/G = (Nu)/(Re)(Pr)$

Notation	Name and Typical Units
C	heat capacity [Btu/(lb)(°F), cal/(g)(°C)]
D	diameter (ft, m)
g	acceleration of gravity [ft/(hr)^2, m/sec^2]
G	mass velocity [lb/(hr)(ft)^2, kg/sec)(m)^2]
h	heat transfer coefficient [Btu/(hr)(sqft)(°F), W/(m)^2(sec)]
k	thermal conductivity [Btu/(hr)(sqft)(°F/ft), cal/(sec)(cm)^2(C/cm)]
k_d	diffusivity (volumetric) [ft^2/hr, cm^2/sec]
L	length (ft, cm)
$T, \Delta T$	temperature, temperature difference (°F or °R, °C or K)
u	linear velocity (ft/hr, cm/sec)
U	overall heat coefficient (same as units of h)
w	mass rate of flow (lb/hr, g/sec)
β	Thermal expansion coefficient (1/°F, 1/°C)
θ	time (hr, sec)
μ	viscosity [lb/(ft)(hr), g/(cm)(sec)]
ρ	density [lb/(ft)^3, g/(cm)^3]

annulus. The inner surface can be provided with scrapers [Fig. 8.4(b)] as in dewaxing of oils or crystallization from solutions. External longitudinal fins in the annular space can be used to improve heat transfer with gases or viscous fluids. When greater heat transfer surfaces are needed, several double-pipes can be stacked in any combination of series or parallel.

Double-pipe exchangers have largely lost out to shell-and-tube units in recent years, although Walker (1982) lists 70 manufacturers of them. They may be worth considering in these situations:

1. When the shell-side coefficient is less than half that of the tube side; the annular side coefficient can be made comparable to the tube side.
2. Temperature crosses that require multishell shell-and-tube units can be avoided by the inherent true countercurrent flow in double pipes.
3. High pressures can be accommodated more economically in the annulus than they can in a larger diameter shell.
4. At duties requiring only 100–200 sqft of surface the double-pipe may be more economical, even in comparison with off-the-shelf units.

The process design of double-pipe exchangers is practically the simplest heat exchanger problem. Pressure drop calculation is straightforward. Heat transfer coefficients in annular spaces have been investigated and equations are cited in Table 8.10. A chapter is devoted to this equipment by Kern (1950).

8.7. SHELL-AND-TUBE HEAT EXCHANGERS

Such exchangers are made up of a number of tubes in parallel and series through which one fluid travels and enclosed in a shell through which the other fluid is conducted.

CONSTRUCTION

The shell side is provided with a number of baffles to promote high velocities and largely more efficient cross flow on the outsides of the tubes. Figure 8.4(c) shows a typical construction and flow paths. The versatility and widespread use of this equipment has given rise to the development of industrywide standards of which the most widely observed are the TEMA standards. Classifications of equipment and terminology of these standards are summarized on Figure 8.11.

Baffle pitch, or distance between baffles, normally is 0.2–1.0 times the inside diameter of the shell. Both the heat transfer coefficient and the pressure drop depend on the baffle pitch, so that its selection is part of the optimization of the heat exchanger. The window of segmental baffles commonly is about 25%, but it also is a parameter in the thermal-hydraulic design of the equipment.

In order to simplify external piping, exchangers mostly are built with even numbers of tube passes. Figure 8.12(c) shows some possible arrangements, where the full lines represent partitions in one head of the exchanger and the dashed lines partitions in the opposite head. Partitioning reduces the number of tubes that can be accommodated in a shell of a given size. Table 8.13 is of such data. Square tube pitch in comparison with triangular pitch accommodates fewer tubes but is preferable when the shell side must be cleaned by brushing.

Two shell passes are obtained with a longitudinal baffle, type F in Figures 8.11(a) or 8.3(c). More than two shell passes normally are not provided in a single shell, but a 4–8 arrangement is thermally equivalent to two 2–4 shells in series, and higher combinations are obtained with more shells in series.

ADVANTAGES

A wide range of design alternates and operating conditions is obtainable with shell-and-tube exchangers, in particular:

- Single phases, condensation or boiling can be accommodated in either the tubes or the shell, in vertical or horizontal positions.
- Pressure range and pressure drop are virtually unlimited, and can be adjusted independently for the two fluids.
- Thermal stresses can be accommodated inexpensively.
- A great variety of materials of construction can be used and may be different for the shell and tubes.
- Extended surfaces for improved heat transfer can be used on either side.
- A great range of thermal capacities is obtainable.
- The equipment is readily dismantled for cleaning or repair.

TUBE SIDE OR SHELL SIDE

Several considerations may influence which fluid goes on the tube side or the shell side.

The tube side is preferable for the fluid that has the higher pressure, or the higher temperature or is more corrosive. The tube side is less likely to leak expensive or hazardous fluids and is more easily cleaned. Both pressure drop and laminar heat transfer can be predicted more accurately for the tube side. Accordingly, when these factors are critical, the tube side should be selected for that fluid.

TABLE 8.9. Equations for Heat Transfer Coefficients of Natural Convection

Vertical plates and cylinders, length L

$$X_L = (Gr)(Pr) = \left(\frac{L^3 \rho_f^2 g \beta_f \Delta t}{\mu_f^2}\right)\left(\frac{c_p \mu}{k}\right)_f \tag{1}$$

$hL/k = 0.13 X_L^{1/3}$, turbulent, $10^9 < X_L < 10^{12}$ (2)

$h = 0.19(\Delta t)^{1/3}$, for air, Δt in °F, h in Btu/(hr)(sqft)(°F) (3)

$hL/k = 0.59 X_L^{1/4}$, laminar, $10^4 < X_L < 10^9$ (4)

$h = 0.29(\Delta t/L)^{1/4}$, for air, L in ft (5)

Single horizontal cylinder, diameter D_0

$$X_D = \frac{D_0^3 \rho_s^2 g \beta_s \Delta t}{\mu_s^2}\left(\frac{c_p \mu}{k}\right) \tag{6}$$

$hD_0/k = 0.53 X_D^{1/4}$, $10^3 < X_D < 10^9$ (7)

$h = 0.18(\Delta t)^{1/3}$, for air, $10^9 < X_D < 10^{12}$ (8)

$h = 0.27(\Delta t/D_0)^{1/4}$, $10^4 < X_D < 10^9$ (9)

Horizontal plates, rectangular, L the smaller dimension

$$X_L = \frac{L^3 \rho_f^2 g \beta_f \Delta t}{\mu_f^2}\left(\frac{c_p \mu}{k}\right)_f \tag{10}$$

Heated plates facing up or cooled facing down

$hL/k = 0.14 X_L^{1/3}$, $2(10^7) < X_L < 3(10^{10})$, turbulent (11)

$h = 0.22(\Delta t)^{1/3}$, for air (—)

$hL/k = 0.54 X_L^{1/4}$, $10^5 < X_L < 2(10^7)$, laminar (12)

$h = 0.27(\Delta t/L)^{1/4}$ (13)

Heated plates facing down, or cooled facing up

$hL/k = 0.27 X_L^{1/4}$, $3(10^5) < X_L < 3(10^{10})$, laminar (14)

$h = 0.12(\Delta t/L)^{1/4}$, for air (15)

Combined convection and radiation coefficients, $h_c + h_r$, for horizontal steel or insulated pipes in a room at 80°F (16)

Nominal Pipe Dia (in.)	$(\Delta t)_s$, Temperature Difference (°F) from Surface to Room														
	50	100	150	200	250	300	400	500	600	700	800	900	1000	1100	1200
$\frac{1}{2}$	2.12	2.48	2.76	3.10	3.41	3.75	4.47	5.30	6.21	7.25	8.40	9.73	11.20	12.81	14.65
1	2.03	2.38	2.65	2.98	3.29	3.62	4.33	5.16	6.07	7.11	8.25	9.57	11.04	12.65	14.48
2	1.93	2.27	2.52	2.85	3.14	3.47	4.18	4.99	5.89	6.92	8.07	9.38	10.85	12.46	14.28
4	1.84	2.16	2.41	2.72	3.01	3.33	4.02	4.83	5.72	6.75	7.89	9.21	10.66	12.27	14.09
8	1.76	2.06	2.29	2.60	2.89	3.20	3.88	4.68	5.57	6.60	7.73	9.05	10.50	12.10	13.93
12	1.71	2.01	2.24	2.54	2.82	3.13	3.83	4.61	5.50	6.52	7.65	8.96	10.42	12.03	13.84
24	1.64	1.93	2.15	2.45	2.72	3.03	3.70	4.48	5.37	6.39	7.52	8.83	10.28	11.90	13.70

(McAdams, *Heat Transmission*, McGraw-Hill, New York, 1954).

Turbulent flow is obtained at lower Reynolds numbers on the shell side, so that the fluid with the lower mass flow preferably goes on that side. High Reynolds numbers are obtained by multipassing the tube side, but at a price.

DESIGN OF A HEAT EXCHANGER

A substantial number of parameters is involved in the design of a shell-and-tube heat exchanger for specified thermal and hydraulic conditions and desired economics, including: tube diameter, thickness, length, number of passes, pitch, square or triangular; size of shell, number of shell baffles, baffle type, baffle windows, baffle spacing, and so on. For even a modest sized design program, Bell (in HEDH, 1983, 3.1.3) estimates that 40 separate logical designs

may need to be made which lead to $2^{40} = 1.10 \times 10^{12}$ different paths through the logic. Since such a number is entirely too large for normal computer processing, the problem must be simplified with some arbitrary decisions based on as much current practice as possible.

A logic diagram of a heat exchanger design procedure appears in Figure 8.13. The key elements are:

1. Selection of a tentative set of design parameters, Box 3 of Figure 8.13(a).
2. Rating of the tentative design, Figure 8.13(b), which means evaluating the performance with the best correlations and calculation methods that are feasible.

TABLE 8.10. Recommended Individual Heat Transfer Coefficient Correlations[a]

A. Single Phase Streams

a. Laminar Flow, Re < 2300

Inside tubes

$$\text{Nu}_T = 3.66 + \frac{0.0668(D/L)\text{Pe}}{(1 + 0.04[(D/L)\text{Pe}]^{2/3})} \text{ (for constant wall temperature)} \tag{1}$$

Between parallel plates of length L and separation distance s

$$\text{Nu}_T = 3.78 + \frac{0.0156[\text{Pe}(s/L)]^{1.14}}{1 + 0.058[\text{Pe}(s/L)]^{0.64} \text{Pr}^{0.17}}, \ 0.1 < \text{Pe}(s/L) < 10^3 \tag{2}$$

In concentric annuli with d_i inside, d_o outside, and hydraulic diameter $d_h = d_o - d_i$. I, heat transfer at inside wall; II, at outside wall; III, at both walls at equal temperatures

$$\text{Nu}_T = \text{Nu}_\infty + f\left(\frac{d_i}{d_o}\right)\frac{0.19[\text{Pe}(d_h/L)]^{0.8}}{1 + 0.117[\text{Pe}(d_h/L)]^{0.467}} \tag{3}$$

Case I: $\quad \text{Nu}_{i\infty} = 3.66 + 1.2\left(\frac{d_i}{d_o}\right)^{-0.8}$ \tag{4}

Case II: $\quad \text{Nu}_{o\infty} = 3.66 + 1.2\left(\frac{d_i}{d_o}\right)^{0.5}$ \tag{5}

Case III: $\quad \text{Nu}_b = 3.66 + \left[4 - \frac{0.102}{(d_i/d_o) + 0.2}\right]\left(\frac{d_i}{d_o}\right)^{0.04}$ \tag{6}

Case I: $\quad f\left(\frac{d_i}{d_o}\right) = 1 + 0.14\left(\frac{d_i}{d_o}\right)^{-0.5}$ \tag{7}

Case II: $\quad f\left(\frac{d_i}{d_o}\right) = 1 + 0.14\left(\frac{d_i}{d_o}\right)^{1/3}$ \tag{8}

Case III: $\quad f\left(\frac{d_i}{d_o}\right) = 1 + 0.14\left(\frac{d_i}{d_o}\right)^{0.1}$ \tag{9}

b. Turbulent Flow, Re > 2300

Inside tubes

$$\text{Nu} = 0.0214(\text{Re}^{0.8} - 100)\text{Pr}^{0.4}\left[1 + \left(\frac{d}{L}\right)^{2/3}\right], \ 0.5 < \text{Pr} < 1.5 \tag{10}$$

$$\text{Nu} = 0.012(\text{Re}0.87 - 280)\text{Pr}^{0.4}\left[1 + \left(\frac{d}{L}\right)^{2/3}\right], \ 1.5 < \text{Pr} < 500 \tag{11}$$

Concentric annuli: Use d_h for both Re and Nu. Nu_{tube} from Eqs. (10) or (11)

Case I: $\quad \dfrac{\text{Nu}_i}{\text{Nu}_{tube}} = 0.86\left(\dfrac{d_i}{d_o}\right)^{-0.16}$

Case II: $\quad \dfrac{\text{Nu}_o}{\text{Nu}_{tube}} = 1 - 0.14\left(\dfrac{d_i}{d_o}\right)^{0.6}$ \tag{13}

Case III: $\quad \dfrac{\text{Nu}_b}{\text{Nu}_{tube}} = \dfrac{0.86(d_i/d_o)^{0.84} + [1 - 0.14(d_i/d_o)^{0.6}]}{1 + d_i/d_o}$ \tag{14}

Across one row of long tubes: $d = $ diameter, $s = $ center-to-center distance, $a = s/d$, $\psi = 1 - \pi/4a$, $L = \pi d/2$

$$\text{Re}_{\psi,L} = wL/\psi v \tag{15}$$

$$\text{Nu}_{o,\text{row}} = 0.3 + \sqrt{\text{Nu}_{L,\text{lam}}^2 + \text{Nu}_{L,\text{turb}}^2} \tag{16}$$

$$\text{Nu}_{L,\text{lam}} = 0.664\sqrt{\text{Re}_{\psi,L}}\,\text{Pr}^{1/3} \tag{17}$$

$$\text{Nu}_{L,\text{turb}} = 0.037\text{Re}_{\psi,L}^{0.8}\text{Pr}/[1 + 2.443\,\text{Re}_{\psi,L}^{-0.1}(\text{Pr}^{2/3} - 1)] \tag{18}$$

$$\text{Nu}_{L,\text{row}} = \alpha L/\lambda \tag{19}$$

TABLE 8.10.—(_continued_**)**

Across a bank of n tubes deep:
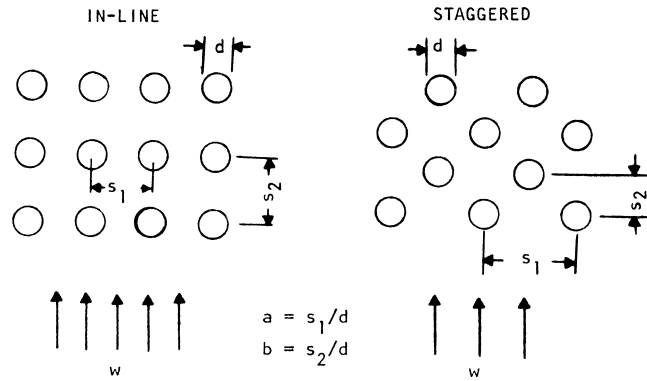
$$\psi = 1 - \pi/4a \quad \text{if} \, b \geq 1 \tag{20}$$

$$\psi = 1 - \pi/4ab \quad \text{if} \, b < 1 \tag{21}$$

$$\mathrm{Nu}_{o, \text{bank}} = \alpha L/\lambda = f_A \mathrm{Nu}_{o, \text{row}}/K, \quad n \geq 10 \tag{22}$$

$$\mathrm{Nu}_{o, \text{bank}} = [1 + (n-1)f_A]\mathrm{Nu}_{o, \text{row}}/Kn, \quad n < 10 \tag{23}$$

[$\mathrm{Nu}_{o, \text{row}}$ from Eq. (16)]

$$f_{A, \text{in-line}} = 1 + (0.7/\psi^{1.5})[(b/a - 0.3)/(b/a + 0.7)^2] \tag{24}$$

$$f_{A, \text{stag}} = 1 + 2/3b \tag{25}$$

$$K = (\mathrm{Pr}/\mathrm{Pr}_w)^{0.25}, \text{ for liquid heating} \tag{26}$$

$$K = (\mathrm{Pr}/\mathrm{Pr}_w)^{0.11}, \text{ for liquid cooling} \tag{27}$$

$$K = (T/T_w)^{0.12}, \text{ for gases} \tag{28}$$

Subscript _w_ designates wall condition

Banks of radial high-fin tubes: $\varepsilon =$ (bare tube surface) / (total surface of finned tube)

In line:

$$\mathrm{Nu} = 0.30\mathrm{Re}^{0.625}\varepsilon^{-0.375}\mathrm{Pr}^{0.333}, \, 5 < \varepsilon < 12, 5000 < \mathrm{Re} < 10^5 \tag{29}$$

Staggered: $a = s_1/d, \, b = s_2/d, \, s =$ spacing of fins

$$\mathrm{Nu} = 0.19(a/b)^{0.2}(s/d)^{0.18}(h/d)^{-0.14}\mathrm{Re}^{0.65}\mathrm{Pr}^{0.33}, \, 100 < \mathrm{Re} < 20,000 \tag{30}$$

Banks of radial low-fin tubes: $D =$ diameter of finned tube, $s =$ distance between fins, $h =$ height of fin; following correlation for $D = 22.2 \, \text{mm}, \, s = 1.25 \, \text{mm},$ and $h = 1.4 \, \text{mm}$

$$\mathrm{Nu} = 0.0729\mathrm{Re}^{0.74}\mathrm{Pr}^{0.36}, \, 5000 < \mathrm{Re} < 35,000 \tag{31}$$

$$\mathrm{Nu} = 0.137\mathrm{Re}^{0.68}\mathrm{Pr}^{0.36}, \, 35,000 < \mathrm{Re} < 235,000 \tag{32}$$

$$\mathrm{Nu} = 0.0511\mathrm{Re}^{0.76}\mathrm{Pr}^{0.36}, \, 235,000 < \mathrm{Re} < 10^6 \tag{33}$$

B. Condensation of Pure Vapors

On vertical tubes and other surfaces; $\dot{\Gamma} =$ condensation rate per unit of periphery

$$\frac{\bar{\alpha}}{\lambda_l}\left[\frac{\eta_l^2}{\rho_l(\rho_l - \rho_g)g_n}\right]^{1/3} = 1.47\left(\frac{4\dot{\Gamma}}{\eta_l}\right)^{-1/3} \tag{34}$$

On a single horizontal tube: $\Gamma =$ condensation rate per unit length of tube

$$\frac{\alpha}{\lambda_l}\left[\frac{\eta_l^2}{\rho_l(\rho_l - \rho_g)g_n}\right]^{1/3} = 1.51\left(\frac{4\dot{\Gamma}}{\eta_l}\right)^{-1/3} \tag{35}$$

(_continued_)

TABLE 8.10.—(continued**)**

On a bank of N horizontal tubes: Γ = condensation rate per unit length from the bottom tube

$$\frac{\alpha}{\lambda_l}\left[\frac{\eta_l^2}{\rho_l(\rho_l - \rho_g)g_n}\right]^{1/3} = 1.51\left(\frac{4\dot{\Gamma}}{\eta_l}\right)^{-1/3}N^{-1/6} \tag{36}$$

<div align="center">

C. Boiling

</div>

Single immersed tube: $\dot{q}$ heat flux (W/m^2), p_c = critical pressure, bars, $p_r = p/p_c$

$$\alpha = 0.1000\dot{q}^{0.7}p^{0.69}[1.8p_r^{0.17} + 4p_r^{1.2} + 10p_r^{10}], \text{ W/m}^2\text{ K} \tag{37}$$

Kettle and horizontal thermosiphon reboilers

$$\alpha = 0.27\exp(-0.027BR)\dot{q}^{0.7}p_c^{0.69}p_r^{0.17} + \alpha_{nc} \tag{38}$$

BR = difference between dew and bubblepoints (°K); if more than 85, use 85

$$\alpha_{nc} = \begin{cases} 250\text{ W/m}^2\text{ K, for hydrocarbons} \\ 1000\text{ W/m K, for water} \end{cases} \tag{39}$$

Critical heat flux in kettle and horizontal thermosiphon reboilers

$$\dot{q}_{\max} = 80,700p_cp_r^{0.35}(1 - p_r)^{0.9}\psi_b, \text{ W/m}^2 \tag{40}$$

$$\psi_b = \text{(external peripheral surface of tube bundle)/}$$
$$\text{(total tube area); if} > 0.45, \text{ use 0.45}$$

Boiling in vertical tubes: thermosiphon reboilers
Critical heat flux: p_c critical pressure, bars; D_i tube ID, m; L tube length, m

$$\dot{q} = 393,000(D_i^2/L)^{0.35}p_c^{0.61}p_r^{0.25}(1 - p_r), \text{ W/m}^2 \tag{41}$$

Heat transfer coefficient with Eqs. (42)–(48) and following procedure

$$\alpha_{tp} = \alpha_{nb} + \alpha_c \tag{42}$$

$$\alpha_c = 0.023\left(\frac{\dot{m}(1 - x)D}{\eta_l}\right)^{0.8}\left(\frac{\eta c_p}{\lambda}\right)_l^{0.4}\frac{\lambda_l}{D}F \tag{43}$$

$$\alpha_{nb} = 0.00122\left(\frac{\lambda_l^{0.79}C_{pl}^{0.45}\rho_l^{0.49}}{\sigma^{0.5}\eta_l^{0.29}\Delta h_v^{0.24}\rho_g^{0.24}}\right)\Delta T_{\text{sat}}^{0.24}\Delta p_{\text{sat}}^{0.75}S \tag{44}$$

$$F = 1 \text{ for } 1/X_{tt} \leq 0.1 \tag{45}$$
$$F = 2.35(1/X_{tt} + 0.213)^{0.736} \text{ for } 1/X_{tt} > 0.1 \tag{46}$$
$$S = 1/(1 + 2.53 \times 10^{-6}\text{Re}_{tp}^{1.17}) \tag{47}$$
$$X_{tt} \cong [(1 - x)/x]^{0.9}(\rho_g/\rho_l)^{0.5}(\eta_l/\eta_g)^{0.1} \tag{48}$$

Procedure for finding the heat transfer coefficient and required temperature difference when the heat flux $\dot{q}$, mass rate of flow $\dot{m}$ and fraction vapor x are specified

1. Find X_{tt}, Eq. (48)
2. Evaluate F from Eqs. (45), (46)
3. Calculate α_c, Eq. (43)
4. Calculate $\text{Re}_{tp} = \dot{m}F^{1.25}(1 - x)D/\eta_l$
5. Evaluate S from Eq. (47)
6. Calculate α_{nb} for a range of values of ΔT_{sat}
7. Calculate α_{tp} from Eq. (42) for this range of ΔT_{sat} values
8. On a plot of calculated $\dot{q} = \alpha_{tp}\Delta T_{\text{sat}}$ against α_{tp}, find the values of α_{tp} and ΔT_{sat} corresponding to the specified $\dot{q}$

---

[a] Special notation used in this table: α = heat transfer coefficient (W/m^{2}K) (instead of h), η = viscosity (instead of μ), and α = thermal conductivity (instead of k).
(Based on HEDH, 1983).

EXAMPLE 8.6
Sizing an Exchanger with Radial Finned Tubes
A liquid is heated from 150 to 190°F with a gas that goes from 250 to 200°F. The duty is 1.25 MBtu/hr. The inside film coefficient is 200, the bare tube outside coefficient is $h_b = 20$ Btu/(hr)(sqft)(°F). The tubes are 1 in. OD, the fins are $\frac{5}{8}$ in. high, 0.038 in. thick, and number 72/ft. The total tube length will be found with fins of steel, brass, or aluminum:

$$\text{LMTD} = (60 - 50)/\ln(60/50) = 54.8,$$
$$U_b = (1/20 + 1/200)^{-1} = 18.18.$$

Fin surface:

$$A_e = 72(2)(\pi/4)[(2.25^2 - 1)/144] = 3.191 \text{ sqft/ft}.$$

Uncovered tube surface:

$$A_b = (\pi/12)[1 - 72(0.038/12)] = 0.2021 \text{ sqft/ft},$$
$$A_e/A_b = 3.191/0.2021 = 15.79,$$
$$y_b = \text{half-fin thickness} = 0.038/2(12) = 0.00158 \text{ ft}.$$

Abscissa of the chart:

$$x = (r_e - r_b)\sqrt{h_b/y_b k} = [(2.25 - 1)/24]\sqrt{20/0.00158k}$$
$$= 5.86/\sqrt{k},$$
$$r_e/r_b = 2.25,$$
$$A_b = Q/U_b\Delta T(1 + \eta A_e/A_b)$$
$$= 1.25(10^6)/18.18(54.8)(1 + 15.79\eta)\text{sq ft}.$$

Find η from the chart. Tube length, $L = A_b/0.2021$ ft.

	k	x	η	A_b	L
Steel	26	1.149	0.59	121.6	602
Brass	60	0.756	0.76	96.5	477
Al	120	0.535	0.86	86.1	426
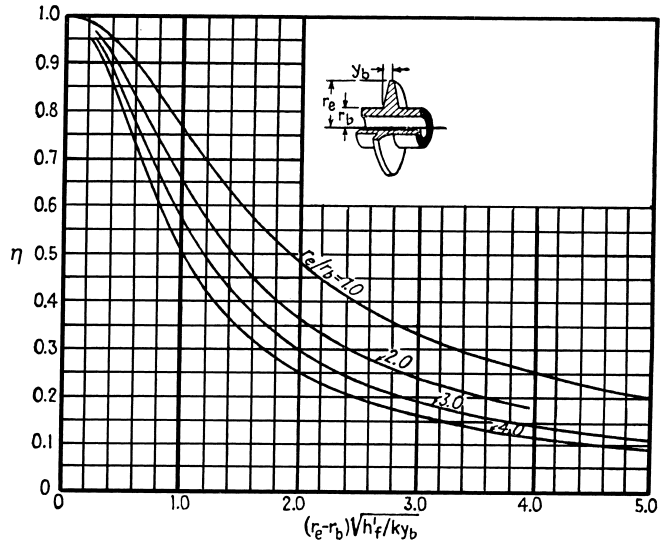
EXAMPLE 8.7
Pressure Drop on the Tube Side of a Vertical Thermosiphon Reboiler
Liquid with the properties of water at 5 atm and 307°F is reboiled at a feed rate of 2800 lb/(hr)(tube) with 30 wt % vaporization. The tubes are 0.1 ft ID and 12 ft long. The pressure drop will be figured at an average vaporization of 15%. The Lockhart–Martinelli, method will be used, following Example 6.14, and the formulas of Tables 6.1 and 6.8:

	Liquid	Vapor
$\dot{m}$ (lb/hr)	2380	420
μ (lb/ft hr)	0.45	0.036
p (lb/cuft)	57.0	0.172
Re	67340	148544
f	0.0220	0.0203
$\Delta P/L$ (psi/ft)	0.00295	0.0281

$$X^2 = 0.00295/0.0281 = 0.1051,$$
$$C = 20,$$
$$\phi_L^2 = 1 + 20/X + 1/X^2 = 72.21,$$
$$(\Delta P/L)\text{two phase} = 72.21(0.00295) = 0.2130,$$
$$\Delta P = 0.2130(12) = 2.56 \text{ psi, } 5.90 \text{ ft water}.$$
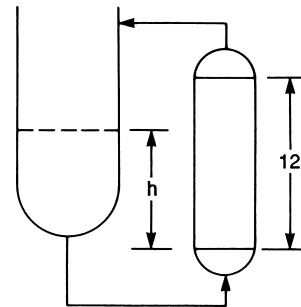
Average density in reboiler tubes is

$$\rho_m = \frac{2800}{2380/57 + 420/0.172} = 1.13 \text{ lb/cuft}.$$

Required height of liquid in tower above bottom of tube sheet

$$\rho_L h = 2.56(144) + 1.13(12),$$
$$h = 382.2/57 = 6.7 \text{ ft}.$$

EXAMPLE 8.8
Pressure Drop on the Shell Side with 25% Open Segmental Baffles, by Kern's Method (1950, p. 147)
Nomenclature and formulas:

hydraulic diameter $D_h = \begin{cases} 1.1028 P_t^2/D_t - D_t, & \text{triangular pitch,} \\ 1.2732 P_t^2/D_t - D_t, & \text{square pitch,} \end{cases}$
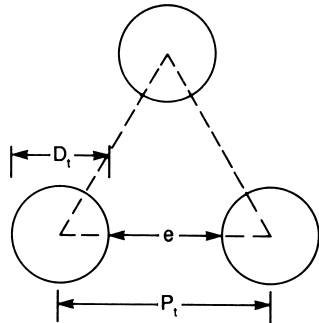
$D_s =$ **s**hell diameter,
$B =$ **d**istance between baffles,
$N =$ **n**umber of baffles,
$A_s =$ **fl**ow area $= D_s B C/P_t$,
$G_s = \dot{m}/A_s$, lb/(hr)(sqft),

$\mathrm{Re} = D_h G_s/\mu$,

$f = 0.0121 \mathrm{Re}^{-0.19}$, $300 < \mathrm{Re} < 10^6$, 25% segmental baffles,

$\Delta P = \dfrac{fG_s^2 D_s(N+1)}{2g\rho D_h} = \dfrac{fG_s^2 D_s(N+1)}{5.22(10^{10})_s D_h}$, psi,

$s =$ specific gravity.

Numerical example:

$\dot{m} = 43,800\,\text{lb/hr}$,
$s = 0.73\,\text{sp gr}$,
$\mu = 0.097\,\text{lb/ft hr}$,
$D_t = 1\,\text{in.}$,
$P_t = 1.25\,\text{in., triangular pitch,}$
$C = 1.25 - 1.00 = 0.25\,\text{in.}$,
$D_s = 21.25\,\text{in., 1.77 ft.}$,
$D_h = 0.723\,\text{in., 0.0603 ft.}$,
$B = 5\,\text{in.}$,
$N = 38\,\text{baffles}$,
$A_s = 21.25(0.25)(5)/1.25(144) = 0.1476\,\text{sqft}$,
$G_s = 43,800/0.1476 = 296,810\,\text{lb/(hr)(sqft)}$,
$\mathrm{Re} = 0.0603(296,810)/0.97 = 18,450$,
$f = 0.0121(18,450)^{-0.19} = 0.00187$,
$\Delta P = \dfrac{0.00187(296,810)^2(1.77)(39)}{5.22(10^{10})(0.73)(0.0603)} = 4.95\,\text{psi}.$

---

3. Modification of some design parameters, Figure 8.13(c), then rerating the design to meet thermal and hydraulic specifications and economic requirements.

A procedure for a tentative selection of exchanger will be described following. With the exercise of some judgement, it is feasible to perform simpler exchanger ratings by hand, but the present state of the art utilizes computer rating, with in-house programs, or those of HTRI or HTFS, or those of commercial services. More than 50 detailed numerical by hand rating examples are in the book of Kern (1950) and several comprehensive ones in the book of Ganapathy (1982).

TENTATIVE DESIGN

The stepwise procedure includes statements of some rules based on common practice.

1. Specify the flow rates, terminal temperatures and physical properties.
2. Calculate the LMTD and the temperature correction factor F from Table 8.3 or Figure 8.5.
3. Choose the simplest combination of shell and tube passes or number of shells in series that will have a value of F above 0.8 or so. The basic shell is 1–2, one shell pass and two tube passes.
4. Make an estimate of the overall heat transfer coefficient from Tables 8.4–8.7.
5. Choose a tube length, normally 8, 12, 16, or 20 ft. The 8 ft long exchanger costs about 1.4 times as much as the 20 ft one per unit of surface.

6. Standard exchanger tube diameters are 0.75 or 1 in. OD, with pitches shown in Table 8.13.
7. Find a shell diameter from Table 8.13 corresponding to the selections of tube diameter, length, pitch, and number of passes made thus far for the required surface. As a guide, many heat exchangers have length to shell diameter ratios between 6 and 8.
8. Select the kinds and number of baffles on the shell side.

The tentative exchanger design now is ready for detailed evaluation with the best feasible heat transfer and pressure drop data. The results of such a rating will suggest what changes may be needed to satisfy the thermal, hydraulic, and economic requirements for the equipment. Example 8.10 goes through the main part of such a design.

8.8. CONDENSERS

Condensation may be performed inside or outside tubes, in horizontal or vertical positions. In addition to the statements made in the previous section about the merits of tube side or shell side: When freezing can occur, shell side is preferable because it is less likely to clog. When condensing mixtures whose lighter components are soluble in the condensate, tube side should be adopted since drainage is less complete and allows condensation (and dissolution) to occur at higher temperatures. Venting of noncondensables is more positive from tube side.

CONDENSER CONFIGURATIONS

The several possible condenser configurations will be described. They are shown on Figure 8.14.

(a)

(i) Parallel and counter flows

(ii) Countercurrent flows

(iii) Parallel flows throughout

(b)

(c)
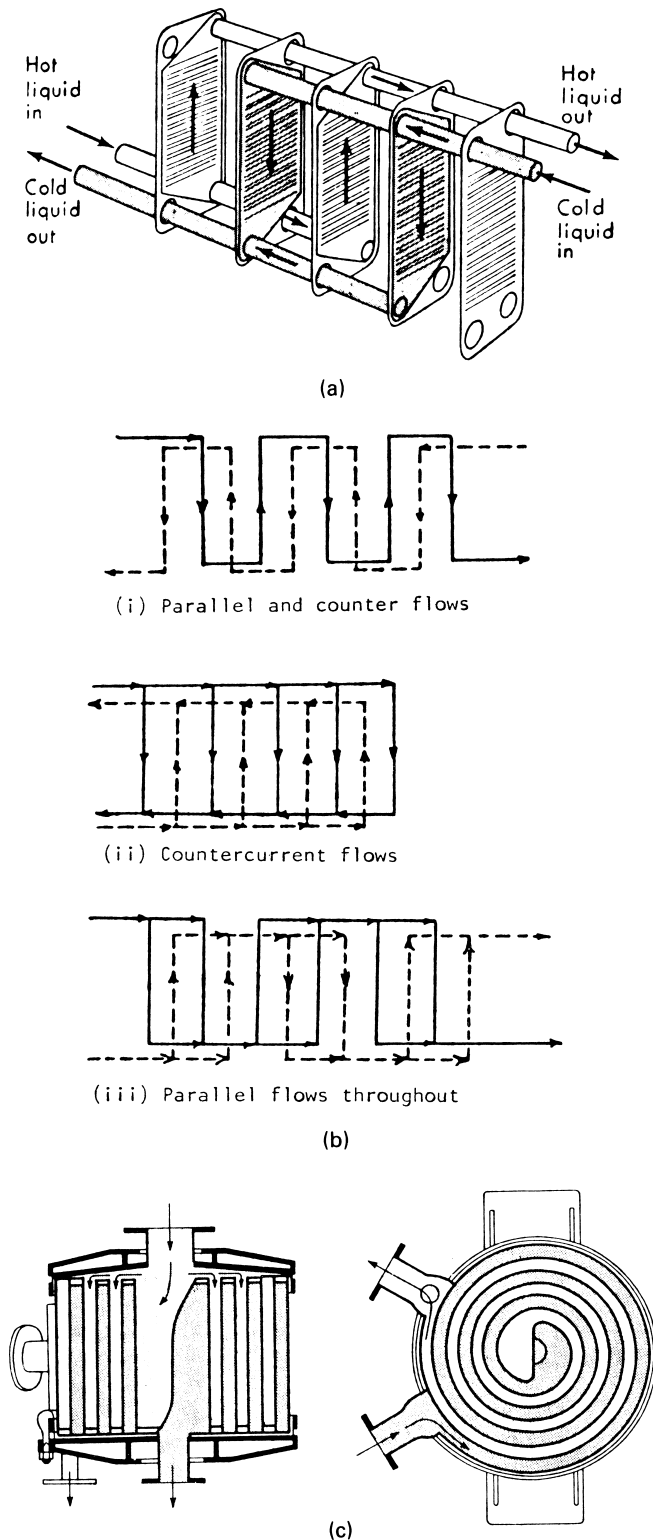
Figure 8.8. Plate and spiral compact exchangers. (a) Plate heat exchanger with corrugated plates, gaskets, frame, and corner portals to control flow paths. (b) Flow patterns in plate exchangers, (i) parallel-counter flows; (ii) countercurrent flows; (iii) parallel flows throughout. (c) Spiral exchanger, vertical, and horizontal cross sections.

Condensation Inside Tubes: Vertical Downflow. Tube diameters normally are 19–25 mm, and up to 50 mm to minimize critical pressure drops. The tubes remain wetted with condensate which assists in retaining light soluble components of the vapor. Venting of noncondensables is positive. At low operating pressures, larger tubes may be required to minimize pressure drop; this may have the effect of substantially increasing the required heat transfer surface. A disadvantage exists with this configuration when the coolant is fouling since the shell side is more difficult to clean.

Condensation Inside Tubes: Vertical Upflow. This mode is used primarily for refluxing purposes when return of a hot condensate is required. Such units usually function as partial condensers, with the lighter components passing on through. Reflux condensers usually are no more than 6–10 ft long with tube diameters of 25 mm or more. A possible disadvantage is the likelihood of flooding with condensate at the lower ends of the tubes.

Condensation Outside Vertical Tubes. This arrangement requires careful distribution of coolant to each tube, and requires a sump and a pump for return to a cooling tower or other source of coolant. Advantages are the high coolant side heat transfer coefficient and the ease of cleaning. The free draining of condensate is a disadvantage with wide range mixtures.

Condensation Inside Horizontal Tubes. This mode is employed chiefly in air coolers where it is the only feasible mode. As condensation proceeds, liquid tends to build up in the tubes, then slugging and oscillating flow can occur.

Condensation Outside Horizontal Tubes. Figure 8.14(d) shows a condenser with two tube passes and a shell side provided with vertically cut baffles that promote side to side flow of vapor. The tubes may be controlled partially flooded to ensure desired subcooling of the condensate or for control of upstream pressure by regulating the rate of condensation. Low-fin tubes often are advantageous, except when the surface tension of the condensates exceeds about 40 dyn/cm in which event the fins fill up with stagnant liquid. The free draining characteristic of the outsides of the tubes is a disadvantage with wide condensing range mixtures, as mentioned. Other disadvantages are those generally associated with shell side fluids, namely at high pressures or high temperatures or corrosiveness. To counteract such factors, there is ease of cleaning if the coolant is corrosive or fouling. Many cooling waters are scale forming; thus they are preferably placed on the tube side. On balance, the advantages often outweigh the disadvantages and this type of condenser is the most widely used.

DESIGN CALCULATION METHOD

Data for condensation are described in Section 8.4 and given in Tables 8.4–8.7, and a few additional overall coefficients are in Table 8.12. The calculation of condensation of pure vapors is straightforward. That of mixtures occurs over a range of temperatures and involves mass transfer resistance through a gas film as well as heat transfer resistance by liquid and fouling films. A model due to Colburn and Hougen (1934) is represented by Figure 8.15. The overall rate of heat transfer is regarded as the sum of the sensible heat transfer through a gas film and the heat of condensation of the material transferred by diffusion from the gas phase to the interface. The equation of this heat balance is, in terms of the notation of Figure 8.15,

$$U(T_i - T_L) = h_g(T_g - T_i) + \lambda k_g(p_g - p_i). \tag{8.37}$$

TABLE 8.11. Overall Heat Transfer Coefficients in Air Coolers [U Btu/(hr)(°F)(sqft of outside bare tube surface)]

Liquid Coolers				Condensers	
Material	Heat-Transfer Coefficient, [Btu/(hr) (ft^2)(°F)]	Material	Heat-Transfer Coefficient, [Btu/(hr)(ft^2)(°F)]	Material	Heat-Transfer Coefficient, [Btu/(hr)(ft^2)(°F)]
Oils, 20° API	10–16	Heavy oils, 8–14° API		Steam	140–150
200°F avg. temp	10–16	300°F avg. temp	6–10	Steam	
300°F avg. temp	13–22	400°F avg. temp	10–16	10% noncondensibles	100–110
400°F avg. temp	30–40	Diesel oil	45–55	20% noncondensibles	95–100
		Kerosene	55–60	40% noncondensibles	70–75
Oils, 30° API		Heavy naphtha	60–65	Pure light hydrocarbons	80–85
150°F avg. temp	12–23	Light naphtha	65–70	Mixed light hydrocarbons	65–75
200°F avg. temp	25–35	Gasoline	70–75	Gasoline	60–75
300°F avg. temp	45–55	Light hydrocarbons	75–80	Gasoline-steam mixtures	70–75
400°F avg. temp	50–60	Alcohols and most organic solvents		Medium hydrocarbons	45–50
			70–75	Medium hydrocarbons w/steam	
Oils, 40° API					55–60
150°F avg. temp	25–35	Ammonia	100–120	Pure organic solvents	75–80
200°F avg. temp	50–60	Brine, 75% water	90–110	Ammonia	100–110
300°F avg. temp	55–65	Water	120–140		
400°F avg. temp	60–70	50% ethylene glycol and water	100–120		

	Vapor Coolers				
	Heat-Transfer Coefficient [Btu/(hr)(ft^2)(°F)]				
Material	10 psig	50 psig	100 psig	300 psig	500 psig
Light hydrocarbons	15–20	30–35	45–50	65–70	70–75
Medium hydrocarbons and organic solvents	15–20	35–40	45–50	65–70	70–75
Light inorganic vapors	10–15	15–20	30–35	45–50	50–55
Air	8–10	15–20	25–30	40–45	45–50
Ammonia	10–15	15–20	30–35	45–50	50–55
Steam	10–15	15–20	25–30	45–50	55–60
Hydrogen					
100%	20–30	45–50	65–70	85–95	95–100
75% vol	17–28	40–45	60–65	80–85	85–90
50% vol	15–25	35–40	55–60	75–80	85–90
25% vol	12–23	30–35	45–50	65–70	80–85

[Brown, *Chem. Eng.* (27 Mar. 1978)].

TABLE 8.12. Overall Heat Transfer Coefficients in Condensers, Btu/(hr)(sqft)(°F)[a]

Liquid Coolants				Air Coolers	
Vapor	Coolant	Btu/(hr)(sqft)(°F)		Vapor	Btu/(hr)(bare sqft)(°F)
Alcohol	water	100–200		Ammonia	100–120
Dowtherm	tall oil	60–80		Freons	60–80
Dowtherm	Dowtherm	80–120		Hydrocarbons, light	80–100
Hydrocarbons				Naphtha, heavy	60–70
high boiling under vacuum	water	18–50		Naphtha, light	70–80
low boiling	water	80–200		Steam	130–140
intermediate	oil	25–40			
kerosene	water	30–65			
kerosene	oil	20–30			
naphtha	water	50–75			
naphtha	oil	20–40			
Organic solvents	water	100–200			
Steam	water	400–1000			
Steam-organic azeotrope	water	40–80			
Vegetable oils	water	20–50			

[a] Air cooler data are based on 50 mm tubes with aluminum fins 16–18 mm high spaced 2.5–3 mm apart; coefficients based on bare tube surface. (Excerpted from HEDH, 1983).
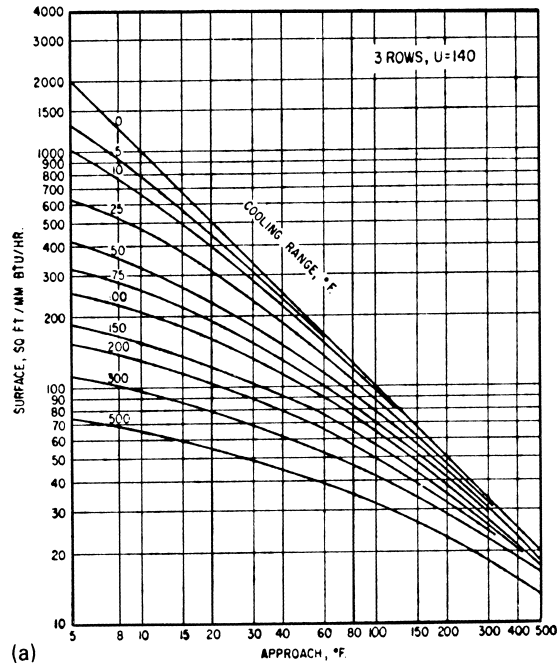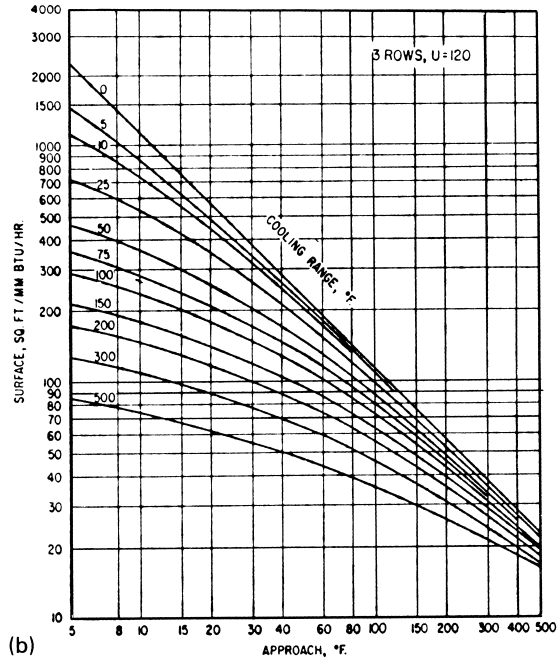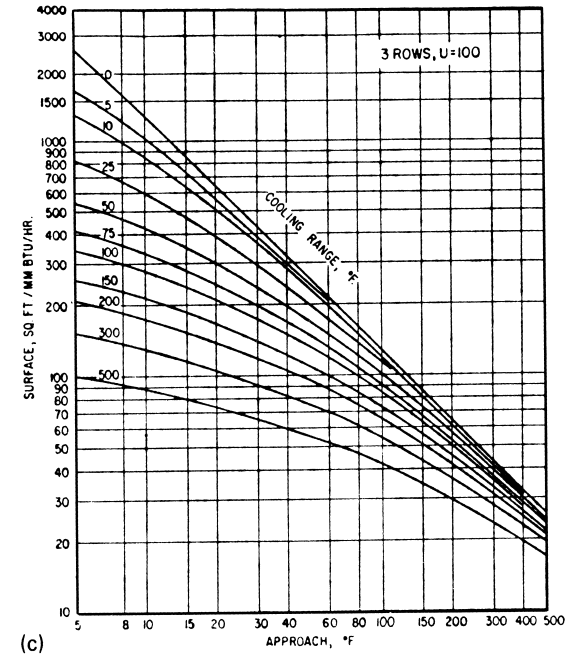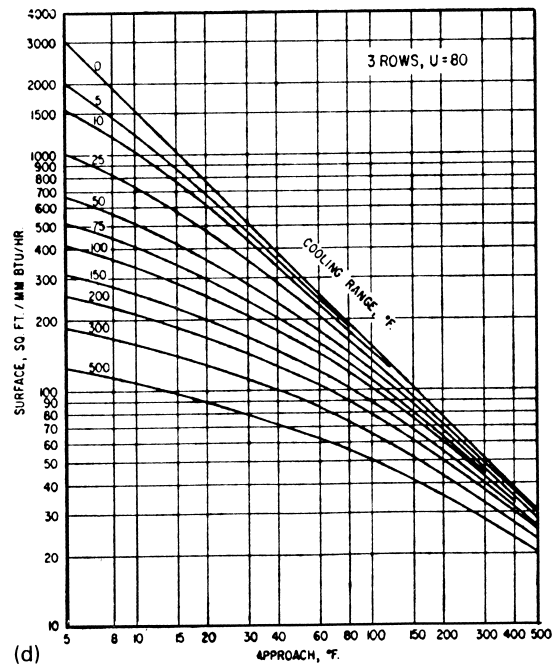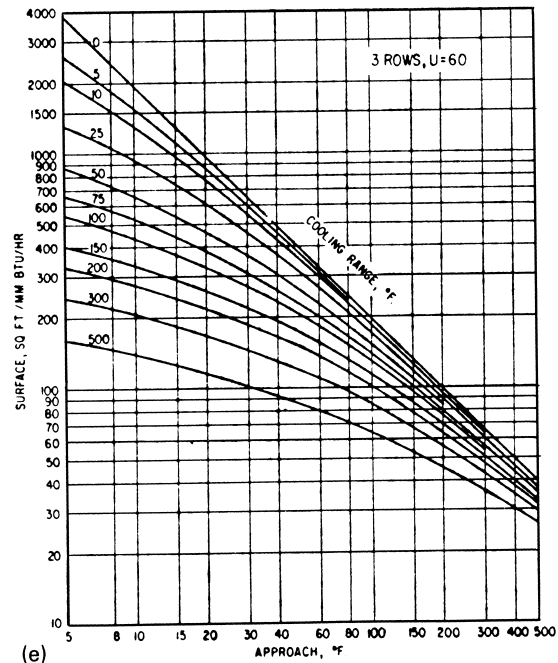
Figure 8.9. Required surfaces of air coolers with three rows of tubes. (a) $U = 140$. (b) $U = 120$. (c) $U = 100$. (d) $U = 80$. (e) $U = 60$. [*Lerner,* Hyd. Proc., *93–100 (Fed. 1972)*].
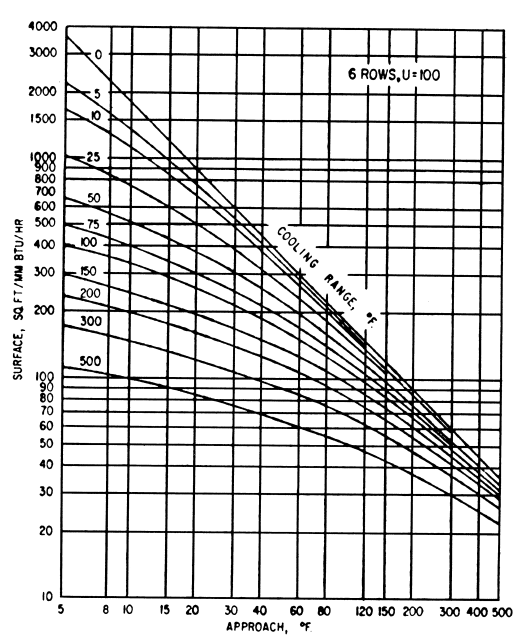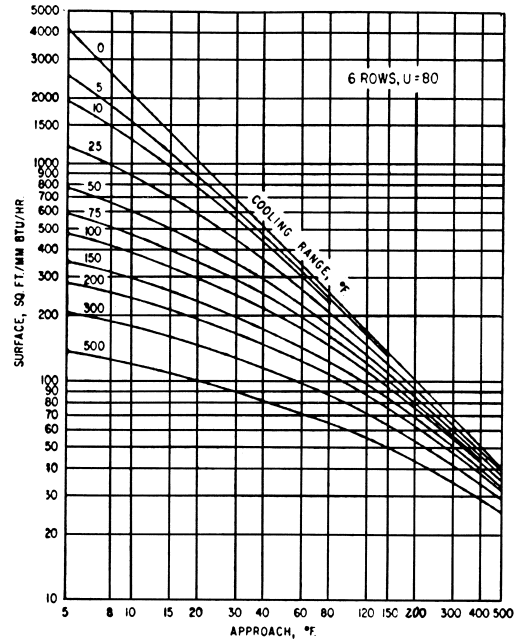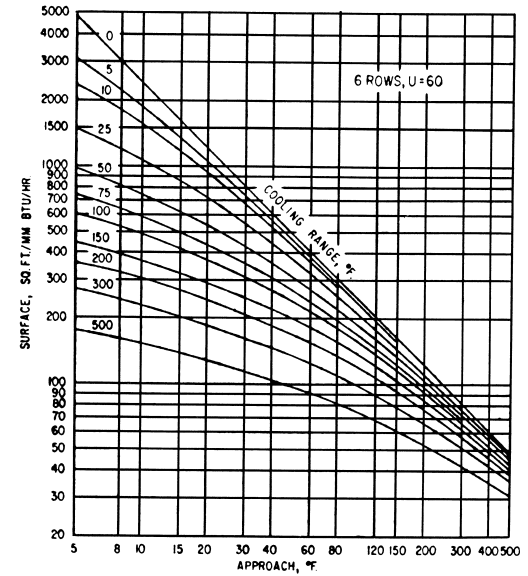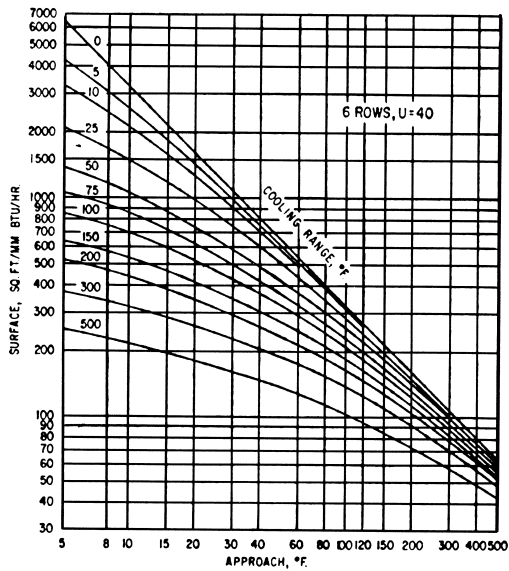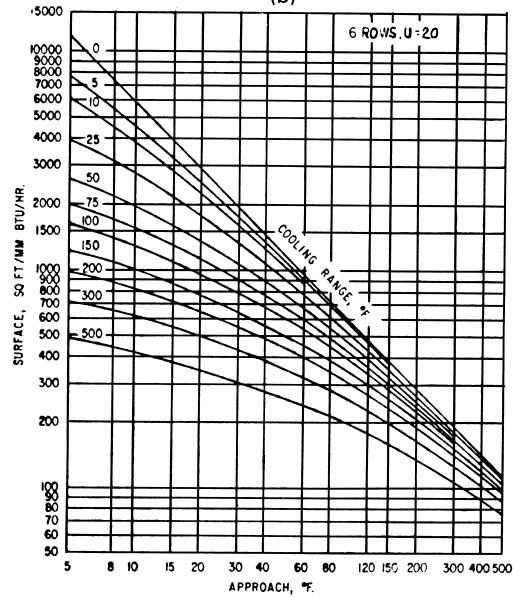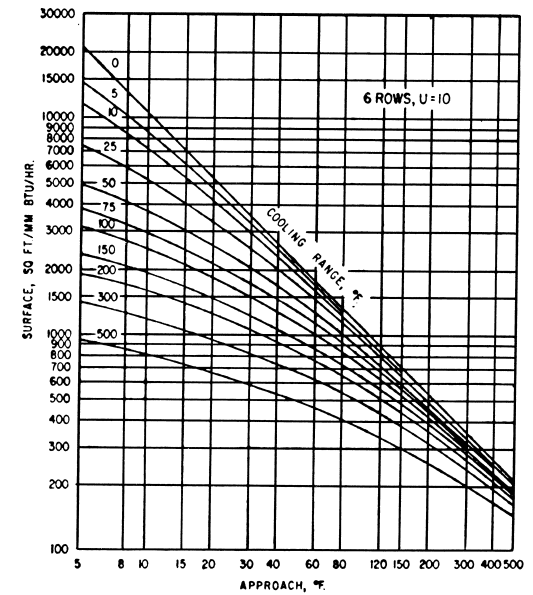
Figure 8.10. Required surfaces of air coolers with six rows of tubes. (a) $U = 100$ Btu/(hr)(sqft)(°F). (b) $U = 80$. (c) $U = 60$. (d) $U = 40$. (e) $U = 20$. (f) $U = 10$. *[Lerner,* Hyd. Proc., *93–100 (Feb. 1972)]*.

EXAMPLE 8.9
Estimation of the Surface Requirements of an Air Cooler
An oil is to be cooled from 300 to 150°F with ambient air at 90°F, with a total duty of 20 MBtu/hr. The tubes have 5/8 in. fins on 1 in. OD and 2–5/16 in. triangular spacing. The tube surface is given by

$A = 1.33NWL$, sqft of bare tube surface,
N = number of rows of tubes, from 3 to 6,
W = width of tube bank, ft,
L = length of tubes, ft.

According to the data of Table 8.12, the overall coefficient may be taken as $U = 60$ Btu/(hr)(°F)(sqft of bare tube surface). Exchangers with 3 rows and with 6 rows will be examined.

Approach $= 150 - 90 = 60$°F,

Cooling range $= 300 - 150 = 150$°F,

From Figure 8.9(f), 3 rows,

$A = 160$ sqft/MBtu/hr)
$\rightarrow 160(20) = 3200$ sqft
$= 1.33(3)WL$.

When $W = 16$ ft, $L = 50$ ft.
  Two fans will make the ratio of section length to width, 25 / 16 $= 1.56$ which is less than the max allowable of 1.8. At 7.5 HP/100 sqft,

$$\text{Power} = \frac{16(50)}{100}7.5 = 60 \text{ HP}.$$

From Figure 8.10(c), 6 rows,

$A = 185$ sqft/(MBtu/hr)
$\rightarrow 185(20) = 3700$ sqft.
$= 1.33(6)WL$.

When $W = 16$ ft, $L = 29$ ft.
Since $L/W = 1.81$, one fan is marginal and two should be used:

$$\text{Power} = [16(29)/100]7.5 = 34.8 \text{ HP}.$$

The 6-row construction has more tube surface but takes less power and less space.

The temperature T_L of the coolant is related to the heat transfer Q by

$$dQ = \dot{m}_L C_L dT_L$$

or the integrated form

$$T_L = T_{L0} + \Delta Q/\dot{m}_L C_L. \tag{8.38}$$

A procedure will be described for taking the vapor from its initial dewpoint T_{g^0} to its final dewpoint corresponding to the required amount of condensation. Gas temperatures are specified at intermediate points and the heat balance is applied over one interval at a time.

1. Prepare the condensing curve, a plot of the vapor temperature T_g against the amount of heat removed Q, by a series of isothermal flashes and enthalpy balances.
2. Starting at the inlet temperature T_{g^0}, specify a temperature T_g a few degrees less, and note the heat transfer ΔQ corresponding to this temperature difference from the condensing curve.
3. Find the temperature T_L of the coolant with Eq. (8.38).
4. Assume an interfacial temperature T_i, then find the corresponding vapor pressure p_i and latent heat λ.
5. From available correlations, find values of the coefficients h_g, k_g, and U which are temperature- and composition-dependent, although they sometimes may be taken as constant over some ranges.
6. Check if these values satisfy the heat balance of Eq. (8.37). If not, repeat the process with other estimates of T_i until one is found that does satisfy the heat balance.
7. Continue with other specifications of the vapor temperature T_g, one interval at a time, until the required outlet temperature is reached.
8. The heat transfer area will be found by numerical integration of

$$A = \int_0^Q \frac{dQ}{U(T_i - T_L)}. \tag{8.39}$$

Examples of numerical applications of this method are in the original paper of Colburn and Hougen (1934), in the book of Kern (1950, p. 346) and in the book of Ludwig (1983, Vol. 3, p. 116).

THE SILVER–BELL–GHALY METHOD

This method takes advantage of the rough proportionality between heat and mass transfer coefficients according to the Chilton–Colburn analogy, and employs only heat transfer coefficients for the process of condensation from a mixture. The sensible heat Q_{sv} of the vapor is transferred through the gas film

$$dQ_{sv} = h_g(T_g - T_i)\, dA. \tag{8.40}$$

In terms of an overall heat transfer coefficient U that does not include the gas film, the total heat transfer Q_T that is made up of the latent heat and the sensible heats of both vapor and liquid is represented by

$$dQ_T = U(T_i - T_L)\, dA. \tag{8.41}$$

When the unknown interfacial temperature T_i is eliminated and the ratio Z of sensible and total heat transfers

$$Z = dQ_{sv}/dQ_T \tag{8.42}$$

is introduced, the result is

$$dQ_T = \frac{U(T_g - T_L)}{1 + ZU/h_g}dA, \tag{8.43}$$

which is solved for the heat transfer area as

$$A = \int_0^{Q_T} \frac{1 + ZU/h_g}{U(T_g - T_L)} dQ_T. \qquad (8.44)$$

Since the heat ratio Z, the temperatures and the heat transfer coefficients vary with the amount of heat transfer Q_T up to a position in the condenser, integration must be done numerically. The coolant temperature is evaluated from Eq. (8.38). Bell and Ghaly (1973) examine cases with multiple tube passes.

The basis of the method was stated by Silver (1947). A numerical solution of a condenser for mixed hydrocarbons was carried out by Webb and McNaught (in Chisholm, 1980, p. 98); comparison of the Silver–Bell–Ghaly result with a Colburn–Hougen calculation showed close agreement in this case. Bell and Ghaly (1973) claim only that their method predicts values from 0 to 100% over the correct values, always conservative. A solution with constant heat transfer coefficients is made in Example 8.11: A review of the subject has been presented by McNaught (in Taborek et al., 1983, p. 35).

8.9. REBOILERS

Reboilers are heat exchangers that are used primarily to provide boilup for distillation and similar towers. All types perform partial vaporization of a stream flowing under natural or forced circulation conditions. Sketches of a kettle and two types of thermosiphon reboilers are in Figure 8.4. Internal reboilers, with a tube bundle built into the tower bottom, also have some application. Flow through a vertical unit like that of Figure 8.4(f) may be forced with a pump in order to improve heat transfer of viscous or fouling materials, or when the vaporization is too low to provide enough static head difference, or when the tower skirt height is too low. A summary guide to the several types of reboilers is in Table 8.14.

KETTLE REBOILERS

Kettle reboilers consist of a bundle of tubes in an oversize shell. Submergence of the tubes is assured by an overflow weir, typically 5–15 cm higher than the topmost tubes. An open tube bundle is preferred, with pitch to diameter ratios in the range of 1.5–2. Temperature in the kettle is substantially uniform. Residence time is high so that kettles are not favored for thermally sensitive materials. The large shell diameters make kettles uneconomic for high pressure operation. Deentraining mesh pads often are incorporated. Tube bundles installed directly in the tower bottom are inexpensive but the amount of surface that can be installed is limited.

HORIZONTAL SHELL SIDE THERMOSIPHONS

The fraction vaporized in thermosiphon reboilers usually can be made less than in kettles, and the holdup is much less. Less static head difference is needed as driving force for recirculation in comparison with vertical units. Circulation rate can be controlled by throttling the inlet line. Because of the forced flow, there is a temperature gradient, from the inlet bubblepoint to the exit bubblepoint, whereas in a kettle the boiling temperature is more nearly uniform, at the exit bubblepoint. Consequently, for the same percentage vaporization, the mean temperature difference between shell and tube sides will be greater for thermosiphons than for kettles. Or for the same mean temperature difference, the percentage vaporization can be made less. Large surface requirements favor horizontal over vertical thermosiphons. Horizontal tube bundles are easier to maintain. The usual arguments for tube side versus shell side also are applicable.

(a)

1.	SHELL	8.	FLOATING HEAD FLANGE	15.	TRANSVERSE BAFFLES OR SUPPORT PLATES
2.	SHELL COVER	9.	CHANNEL PARTITION	16.	IMPINGEMENT BAFFLE
3.	SHELL CHANNEL	10.	STATIONARY TUBESHEET	17.	VENT CONNECTION
4.	SHELL COVER END FLANGE	11.	CHANNEL	18.	DRAIN CONNECTION
5.	SHELL NOZZLE	12.	CHANNEL COVER	19.	TEST CONNECTION
6.	FLOATING TUBESHEET	13.	CHANNEL NOZZLE	20.	SUPPORT SADDLES
7.	FLOATING HEAD	14.	TIE RODS AND SPACERS	21.	LIFTING RING

(b)

Figure 8.11. Tubular Exchanger Manufacturers Association classification and terminology for heat exchangers. (a) TEMA terminology for shells and heads of heat exchangers. (b) Terminology for parts of a TEMA type AES heat exchanger. The three letters A, E, and S come from part (a).

Figure 8.12. Arrangements of cross baffles and tube-side passes. (a) Types of cross baffles. (b) Rod baffles for minimizing tube vibrations; each tube is supported by four rods. (c) Tube-side multipass arrangements.
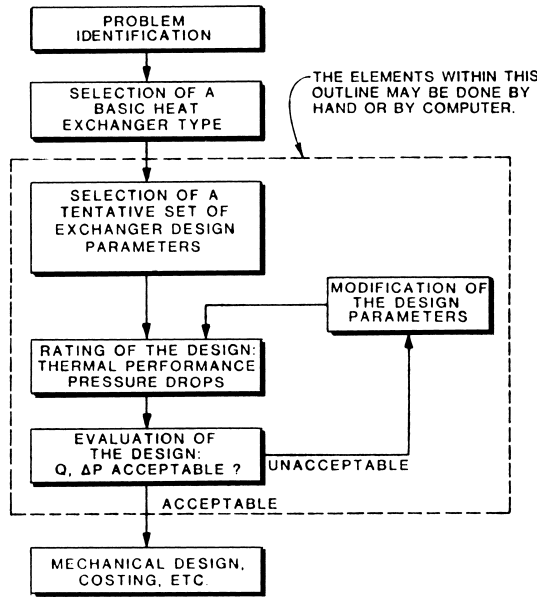
(a)
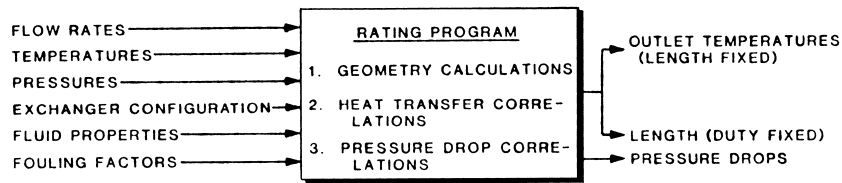
(b)
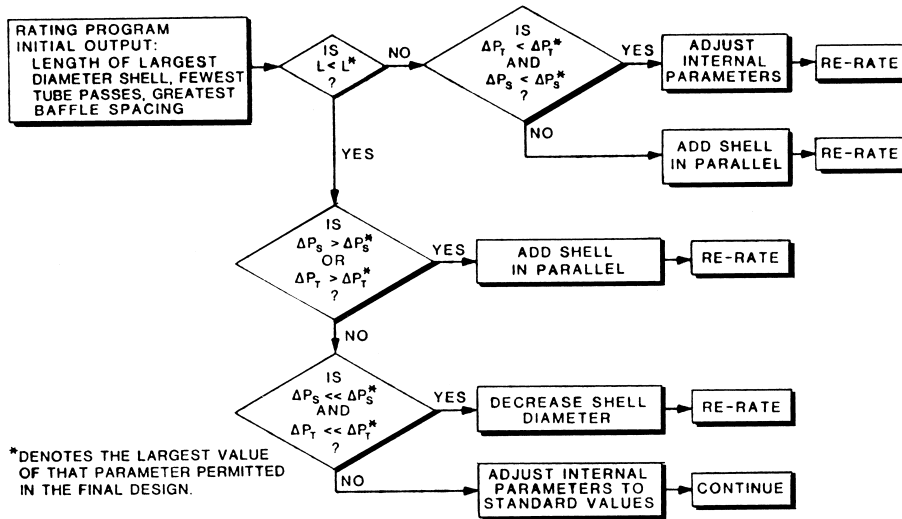
(c)

Figure 8.13. A procedure for the design of a heat exchanger, comprising a tentative selection of design parameters, rating of the performance, modification of this design if necessary, and re-rating to meet specifications. (*See also Bell, in* Heat Exchanger Design Handbook, *Section 3.1.3, Hemisphere Publishing Company, 1983*).

TABLE 8.13. Tube Counts of Shell-and-Tube Heat Exchangers[a]

Heat Exchanger Tube Sheet Layout Count Table

37	35	33	31	29	27	25	23¼	21¼	19¼	17¼	15¼	13¼	12	10	8	I.D. of Shell (In.)	Tubes	Pass
1269	1143	1019	881	763	663	553	481	391	307	247	193	135	105	69	33	¾" on 15/16" △	Fixed Tubes	One-Pass
1127	1007	889	765	667	577	493	423	343	277	217	157	117	91	57	33	¾" on 1" △		
965	865	765	665	587	495	419	355	287	235	183	139	101	85	53	33	¾" on 1" □		
699	633	551	481	427	361	307	247	205	163	133	103	73	57	33	15	1" on 1¼" △		
595	545	477	413	359	303	255	215	179	139	111	83	65	45	33	17	1" on 1¼" □		
1242	1088	964	846	734	626	528	452	370	300	228	166	124	94	58	32	¾" on 15/16" △	Fixed Tubes	Two-Pass
1088	972	858	746	646	556	468	398	326	264	208	154	110	90	56	28	¾" on 1" △		
946	840	746	644	560	486	408	346	280	222	172	126	94	78	48	26	¾" on 1" □		
688	608	530	462	410	346	292	244	204	162	126	92	62	52	32	16	1" on 1¼" △		
584	522	460	402	348	298	248	218	172	136	106	76	56	40	26	12	1" on 1¼" □		
1126	1008	882	768	648	558	460	398	304	234	180	134	94	64	34	8	¾" on 15/16" △	U Tubes[2]	
1000	882	772	674	566	484	406	336	270	212	158	108	72	60	26	8	¾" on 1" △		
884	778	688	586	506	436	362	304	242	188	142	100	72	52	30	12	¾" on 1" □		
610	532	466	396	340	284	234	192	154	120	84	58	42	26	8	XX	1" on 1¼" △		
526	464	406	356	304	256	214	180	134	100	76	58	38	22	12	XX	1" on 1¼" □		
1172	1024	904	788	680	576	484	412	332	266	196	154	108	84	48	XX	¾" on 15/16" △	Fixed Tubes	Four-Pass
1024	912	802	692	596	508	424	360	292	232	180	134	96	72	44	XX	¾" on 1" △		
880	778	688	590	510	440	366	308	242	192	142	126	88	72	48	XX	¾" on 1" □		
638	560	486	422	368	308	258	212	176	138	104	78	60	44	24	XX	1" on 1¼" △		
534	476	414	360	310	260	214	188	142	110	84	74	48	40	24	XX	1" on 1¼" □		
1092	976	852	740	622	534	438	378	286	218	166	122	84	56	28	XX	¾" on 15/16" △	U Tubes[2]	
968	852	744	648	542	462	386	318	254	198	146	98	64	52	20	XX	¾" on 1" △		
852	748	660	560	482	414	342	286	226	174	130	90	64	44	24	XX	¾" on 1" □		
584	508	444	376	322	266	218	178	142	110	74	50	36	20	XX	XX	1" on 1¼" △		
500	440	384	336	286	238	198	166	122	90	66	50	32	16	XX	XX	1" on 1¼" □		
1106	964	844	732	632	532	440	372	294	230	174	116	80	XX	XX	XX	¾" on 15/16" △	Fixed Tubes	Six-Pass
964	852	744	640	548	464	388	322	258	202	156	104	66	XX	XX	XX	¾" on 1" △		
818	224	634	536	460	394	324	266	212	158	116	82	56	XX	XX	XX	¾" on 1" □		
586	514	442	382	338	274	226	182	150	112	82	56	34	XX	XX	XX	1" on 1¼" △		
484	430	368	318	268	226	184	154	116	88	66	44	XX	XX	XX	XX	1" on 1¼" □		
1058	944	826	716	596	510	416	358	272	206	156	110	74	XX	XX	XX	¾" on 15/16" △	U Tubes[2]	
940	826	720	626	518	440	366	300	238	184	134	88	56	XX	XX	XX	¾" on 1" △		
820	718	632	534	458	392	322	268	210	160	118	80	56	XX	XX	XX	¾" on 1" □		
562	488	426	356	304	252	206	168	130	100	68	42	30	XX	XX	XX	1" on 1¼" △		
478	420	362	316	268	224	182	152	110	80	60	42	XX	XX	XX	XX	1" on 1¼" □		
1040	902	790	682	576	484	398	332	258	198	140	94	XX	XX	XX	XX	¾" on 15/16" △	Fixed Tubes	Eight-Pass
902	798	694	588	496	422	344	286	224	170	124	82	XX	XX	XX	XX	¾" on 1" △		
760	662	576	490	414	352	286	228	174	132	94	XX	XX	XX	XX	XX	¾" on 1" □		
542	466	400	342	298	240	190	154	120	90	66	XX	XX	XX	XX	XX	1" on 1¼" △		
438	388	334	280	230	192	150	128	94	74	XX	XX	XX	XX	XX	XX	1" on 1¼" □		
1032	916	796	688	578	490	398	342	254	190	142	102	68	XX	XX	XX	¾" on 15/16" △	U Tubes[2]	
908	796	692	600	498	422	350	286	226	170	122	82	52	XX	XX	XX	¾" on 1" △		
792	692	608	512	438	374	306	254	194	146	106	70	48	XX	XX	XX	¾" on 1" □		
540	464	404	340	290	238	190	154	118	90	58	38	24	XX	XX	XX	1" on 1¼" △		
456	396	344	300	254	206	170	142	98	70	50	34	XX	XX	XX	XX	1" on 1¼" □		
37	**35**	**33**	**31**	**29**	**27**	**25**	**23¼**	**21¼**	**19¼**	**17¼**	**15¼**	**13¼**	**12**	**10**	**8**	**I.D. of Shell (in.)**		

[1] Allowance made for Tie Rods.
[2] R.O.B. = 2½ × Tube Dia. Actual Number of "U" Tubes is one-half the above figures.
[a] A 3/4 in. tube has 0.1963 sqft/ft, a 1 in. OD has 0.2618 sqft/ft. Allowance made for tie rods.
[b] R.O.B. = 2½ × tube dia. Actual number of "U" tubes is one-half the above figures.

EXAMPLE 8.10
Process Design of a Shell-and-Tube Heat Exchanger
An oil at the rate of 490,000 lb/hr is to be heated from 100 to 170°F
with 145,000 lb/hr of kerosene initially at 390°F. Physical properties
are

Oil   0.85 sp gr, 3.5 cP at 135°F, 0.49 sp ht
Kerosene 0.82 sp gr, 0.4 cP at 200°F, 0.61 sp ht

oil, 100 F → → 170 F
490000 pph

← kerosene ← 390 F
200 F
145000 pph
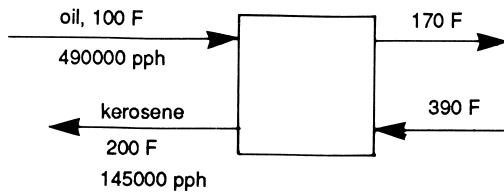
Kerosene outlet:

$$T = 390 - (490,000/145,000)(0.49/0.61)(170 - 100)$$
$$= 200°F,$$
$$\text{LMTD} = (220 - 100)/\ln 2.2 = 152.2,$$
$$P = (170 - 100)/(390 - 100) = 0.241,$$
$$R = (390 - 200)/(170 - 100) = 2.71.$$

From Figure 8.5(a), $F = 0.88$, so a 1–2 exchanger is satisfactory:

$$\Delta T = 152.2(0.88) = 133.9.$$

From Table 8.6, with average values for medium and heavy
organics,

$$U = 10^4/(57 + 16 + 50 + 34) = 63.7,$$
$$Q = 490,000(0.49)(170 - 100) = 1.681(10^7)\text{Btu 1 hr},$$
$$A = Q/U\Delta T = 1.681(10^7)/63.7(133.9) = 1970 \text{ sqft},$$
$$1970/0.2618 = 7524.8 \text{ ft of 1 in. OD tubing.}$$

Use $1\frac{1}{4}$ in. pitch, two tube pass. From Table 8.13,

L (ft)	Required No. Tubes	D_shell (number of tubes)	
		Triangular	Square
8	940	—	—
12	627	35 (608)	37 (584)
16	470	31 (462)	33 (460)
20	376	29 (410)	31 (402)

Use 16 ft tubes on $1\frac{1}{4}$ in. square pitch, two pass, 33 in. shell

$$L/D = 16/(33/12) = 5.82,$$

which is near standard practice. The 20 ft length also is acceptable
but will not be taken.

The pressure drops on the tube and shell sides are to be
calculated.

Tube side: 0.875 in. ID, 230 tubes, 32 ft long: Take one velocity
head per inlet or outlet, for a total of 4, in addition to friction in the
tubes. The oil is the larger flow so it will be placed in the tubes.

$$\dot{m} = 490,000/230 = 2130.4 \text{ lb/(hr)(tube)}.$$

Use formulas from Table 6.1

$$\text{Re} = 6.314(2130.4)/0.875(3.5) = 4392,$$
$$f = 1.6364/[\ln(5(10^{-7})/0.875 + 6.5/4392)]^2 = 0.0385,$$
$$\Delta P_f = 5.385(10^{-8})(2130)^2(32)(0.0385)/0.85(0.875)^5$$
$$= 0.691 \text{ psi.}$$

Expansion and contraction:

$$\Delta P_e = 4\rho(u^2/2g_e) = 4(53.04)(3.26)^2/(64.4)(144) = 0.243 \text{ psi,}$$
$$\therefore \Delta P_{\text{tube}} = 0.691 + 0.243 = 0.934 \text{ psi.}$$

Shellside. Follow Example 8.8:

$$D_h = 1.2732(1.25/12)^2/(1/12) - 1/12 = 0.0824 \text{ ft,}$$
$$B = 1.25 \text{ ft between baffles,}$$
$$E = 0.25/12 \text{ ft between tubes,}$$
$$D_s = 33/12 = 2.75 \text{ ft shell diameter,}$$
$$A_s = 2.75(1.25)(0.25/12)/(1.25/12) = 0.6875 \text{ sqft,}$$
$$G_s = 145,000/0.6875 = 210,909 \text{ lb/(hr)(sqft),}$$
$$\text{Re} = 0.0824(210,909)/0.4(2.42) = 17,952,$$
$$f = 0.0121(17,952)^{-0.19} = 0.00188,$$
$$\Delta P_{\text{shell}} = 0.00188(210,909)^2(2.75)(13)/5.22(10^{10})(0.82)(0.0824)$$
$$= 0.85 \text{ psi.}$$

The pressure drops on each side are acceptable. Now it
remains to check the heat transfer with the equations of Table
8.10 and the fouling factors of Table 8.6.

VERTICAL THERMOSIPHONS

Circulation is promoted by the difference in static heads of supply
liquid and the column of partially vaporized material. The exit
weight fraction vaporized should be in the range of 0.1–0.35 for
hydrocarbons and 0.02–0.10 for aqueous solutions. Circulation
may be controlled with a valve in the supply line. The top tube sheet
often is placed at the level of the liquid in the tower. The flow area of
the outlet piping commonly is made the same as that of all the tubes.
Tube diameters of 19–25 mm diameter are used, lengths up to 12 ft or
so, but some 20 ft tubes are used. Greater tube lengths make for less
ground space but necessitate taller tower skirts.

Maximum heat fluxes are lower than in kettle reboilers. Be-
cause of boiling point elevations imposed by static head, vertical

thermosiphons are not suitable for low temperature difference
services.

Shell side vertical thermosiphons sometimes are applied when
the heating medium cannot be placed on the shell side.

FORCED CIRCULATION REBOILERS

Forced circulation reboilers may be either horizontal or vertical.
Since the feed liquid is at its bubblepoint, adequate NPSH must be
assured for the pump if it is a centrifugal type. Linear velocities in
the tubes of 15–20 ft/sec usually are adequate. The main disadvan-
tages are the costs of pump and power, and possibly severe main-
tenance. This mode of operation is a last resort with viscous or
fouling materials, or when the fraction vaporized must be kept low.
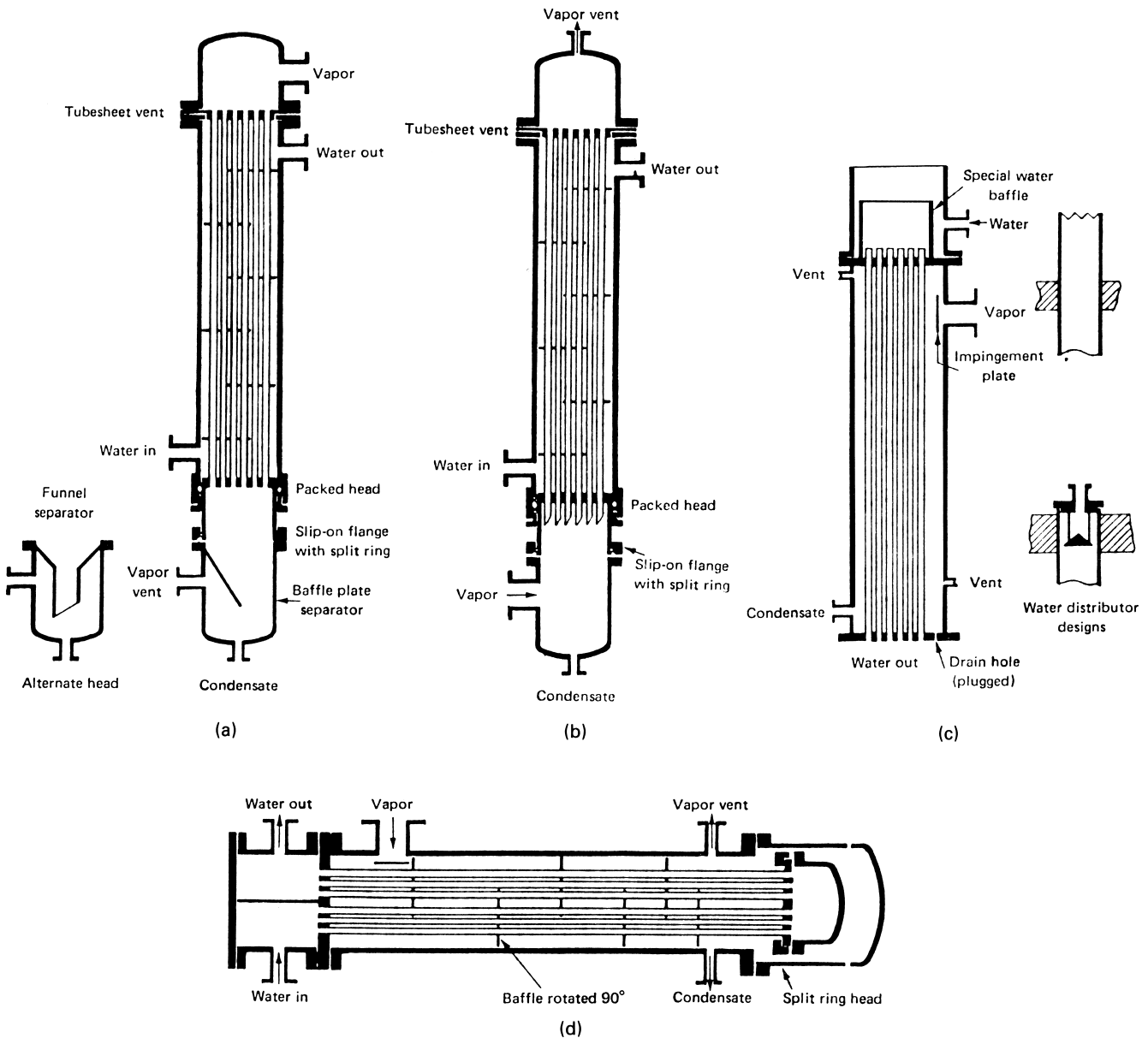
Figure 8.14. Some arrangements of shell-and-tube condensers. (a) Condensate inside tubes, vertical upflow. (b) Inside tubes, vertical downflow. (c) Outside tubes, vertical downflow. (d) Condensate outside horizontal tubes. (HEDH, *1983, 3.4.3*).

CALCULATION PROCEDURES

Equations for boiling heat transfer coefficients and maximum heat fluxes are Eqs. (37) through (44) of Table 8.10. Estimating values are in Tables 8.4–8.7. Roughly, boiling coefficients for organics are 300 Btu/(hr)(sqft)(°F), or 1700 W/m² K; and for aqueous solutions, 1000 Btu/(hr)(sqft)(°F), or 5700 W/m² K. Similarly, maximum fluxes are of the order of 20,000 Btu/(hr)(sqft), or 63,000 W/m², for organics; and 35,000 Btu/(hr)(sqft) or 110,000 W/m², for aqueous systems.

The design procedure must start with a specific geometry and heat transfer surface and a specific percentage vaporization. Then the heat transfer coefficient is found, and finally the required area is calculated. When the agreement between the assumed and calculated surfaces is not close enough, the procedure is repeated with another assumed design. The calculations are long and tedious and nowadays are done by computer.

Example 8.12 summarizes the results of such calculations made on the basis of data in *Heat Exchanger Design Handbook* (1983). Procedures for the design of kettle, thermosiphon and forced circulation reboilers also are outlined by Polley (in Chisholm, 1980, Chap. 3).

8.10. EVAPORATORS

Evaporators employ heat to concentrate solutions or to recover dissolved solids by precipitating them from saturated solutions. They are reboilers with special provisions for separating liquid and vapor phases and for removal of solids when they are precipi-
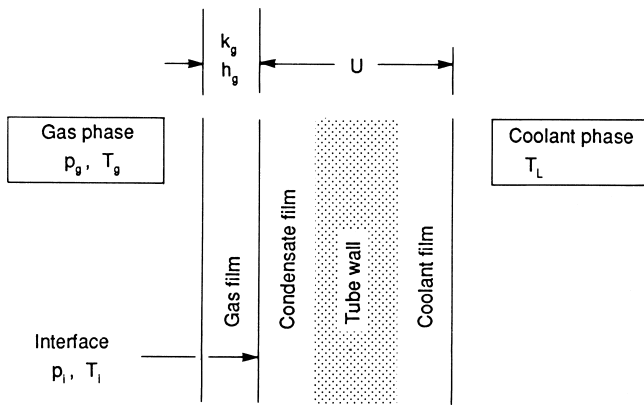
Figure 8.15. Model for partial condensation in the presence of uncondensed material: $U(T_i - T_L) = h_g(T_g - T_i) + \lambda k_g(p_g - p_i)$. [*A.P. Colburn and O.A. Hougen*, Ind. Eng. Chem. **26**, *1178–1182 (1934)*].

tated or crystallized out. Simple kettle-type reboilers [Fig. 8.4(d)] may be adequate in some applications, especially if enough free-board is provided. Some of the many specialized types of evaporators that are in use are represented on Figure 8.16. The tubes may be horizontal or vertical, long or short; the liquid may be outside or inside the tubes, circulation may be natural or forced with pumps or propellers.

Natural circulation evaporators [Figs. 18.16(a)–(e)] are the most popular. The forced circulation type of Figure 18.16(f) is most versatile, for viscous and fouling services especially, but also the most expensive to buy and maintain. In the long tube vertical design, Figure 8.16(d), because of vaporization the liquid is in annular or film flow for a substantial portion of the tube length, and accordingly is called a rising film evaporator. In falling film evaporators, liquid is distributed to the tops of the individual tubes and flows down as a film. The hydrostatic head is eliminated, the pressure drop is little more than the friction of the vapor flow, and heat transfer is excellent. Since the contact time is short and separation of liquid and vapor is virtually complete, falling film evaporation is suitable for thermally sensitive materials.

Long tube vertical evaporators, with either natural or forced circulation are the most widely used. Tubes range from 19 to 63 mm diameter, and 12–30 ft in length. The calandria of Figure 8.16(b) has tubes 3–5 ft long, and the central downtake has an area about equal to the cross section of the tubes. Sometimes circulation in calandrias is forced with built in propellors. In some types of evaporators, the solids are recirculated until they reach a desired size. In Figure 8.16(f), fresh feed is mixed with the circulating slurry. In Figure 8.16(g) only the clear liquid is recirculated, and small more nearly uniform crystals are formed.

THERMAL ECONOMY

Thermal economy is a major consideration in the design and operation of evaporators. This is improved by operating several vessels in series at successively lower pressures and utilizing vapors from upstream units to reboil the contents of downstream units. Figure 8.17 shows such arrangements. Thermal economy is expressed as a ratio of the amount of water evaporated in the complete unit to the amount of external steam that is supplied. For a single effect, the thermal economy is about 0.8, for two effects it is 1.6, for three effects it is 2.4, and so on. Minimum cost usually is obtained with eight or more effects. When high pressure steam is available, the

pressure of the vapor can be boosted with a steam jet compressor [Fig. 8.16(c)] to a usable value; in this way savings of one-half to two-thirds in the amount of external steam can be achieved. Jet compressor thermal efficiencies are 20–30%. A possible drawback is the contamination of condensate with entrainment from the evaporator. When electricity is affordable, the pressure of the vapor can be boosted mechanically, in compressors with efficiencies of 70–75%.

Because of the elevation of boiling point by dissolved solids, the difference in temperatures of saturated vapor and boiling solution may be 3–10°F which reduces the driving force available for heat transfer. In backward feed [Fig. 8.17(b)] the more concentrated solution is heated with steam at higher pressure which makes for lesser heating surface requirements. Forward feed under the influence of pressure differences in the several vessels requires more surface but avoids the complications of operating pumps under severe conditions.

Several comprehensive examples of heat balances and surface requirements of multiple effect evaporation are worked out by Kern (1950).

SURFACE REQUIREMENTS

The data of Tables 8.4–8.7 and particularly Table 8.10 for boiling liquids are applicable to evaporators when due regard is given the more severe fouling that can occur. For example, cases have been cited in which fouling presents fully half the resistance to heat transfer in evaporators. Some heat transfer data specifically for evaporators are in Figure 8.18. Forced circulation and falling film evaporators have the higher coefficients, and the popular long tube vertical, somewhat poorer performance.

With such data, an estimate can be made of a possible evaporator configuration for a required duty, that is, the diameter, length, and number of tubes can be specified. Then heat transfer correlations can be applied for this geometry and the surface recalculated. Comparison of the estimated and calculated surfaces will establish if another geometry must be estimated and checked. This procedure is described in Example 8.12.

8.11. FIRED HEATERS

High process temperatures are obtained by direct transfer of heat from the products of combustion of fuels. Maximum flame temperatures of hydrocarbons burned with stoichiometric air are about 3500°F. Specific data are cited by Hougen, Watson, and Ragatz (*Chemical Process Principles*, Vol. I, Wiley, New York, 1954, p. 409) and in.... *Marks' Standard Handbook for Mechanical Engineers* (1996, p. 4-29, Table 4:1:9). With excess air to ensure complete combustion the temperatures are lower, but still adequate for the attainment of process temperatures above 2000°F when necessary. Lower temperatures are obtained with heat transfer media such as those of Table 8.2 which are in turn serviced in direct-fired heaters.

DESCRIPTION OF EQUIPMENT

In fired heaters and furnaces, heat is released by combustion of fuels into an open space and transferred to fluids inside tubes which are ranged along the walls and roof of the combustion chamber.

The heat is transferred by direct radiation and convection and also by reflection from refractory walls lining the chamber.

Three zones are identified in a typical heater such as that of Figure 8.19(a). In the *radiant zone*, heat transfer is predominantly (about 90%) by radiation. The *convection zone* is "out of sight" of the burners; although some transfer occurs by radiation because the temperature still is high enough, most of the transfer here is by

EXAMPLE 8.11
Sizing a Condenser for a Mixture by the Silver–Bell–Ghatly Method
A mixture with initial dewpoint 139.9°C and final bubblepoint 48.4°C is to be condensed with coolant at a constant temperature of 27°C. The gas film heat transfer coefficient is 40 W/m²K and the overall coefficient is 450. Results of the calculation of the condensing curve are

T (°C)	139.9	121.6	103.3	85.0	66.7	48.4
Q(W)	0	2154	3403	4325	5153	5995

In the following tabulation, over each temperature interval are shown the average gas temperature, the value of Z, and the value of the integrand of Eq. (8.44). The integrand is plotted following.

Interval	1	2	3	4	5
$(T_g)_m$	130.75	112.45	94.15	75.85	57.4
Z	0.1708	0.1613	0.1303	0.0814	0.0261
Integrand $\times (10^5)$	6.26	7.32	8.31	8.71	9.41

The heat transfer surface is the area under the stepped curve, which is $a = 0.454$ m². A solution that takes into account the substantial variation of the heat transfer coefficients along the condenser gives the result $A = 0.385$ m² (Webb and McNaught, in Chisholm, 1980, p. 98).
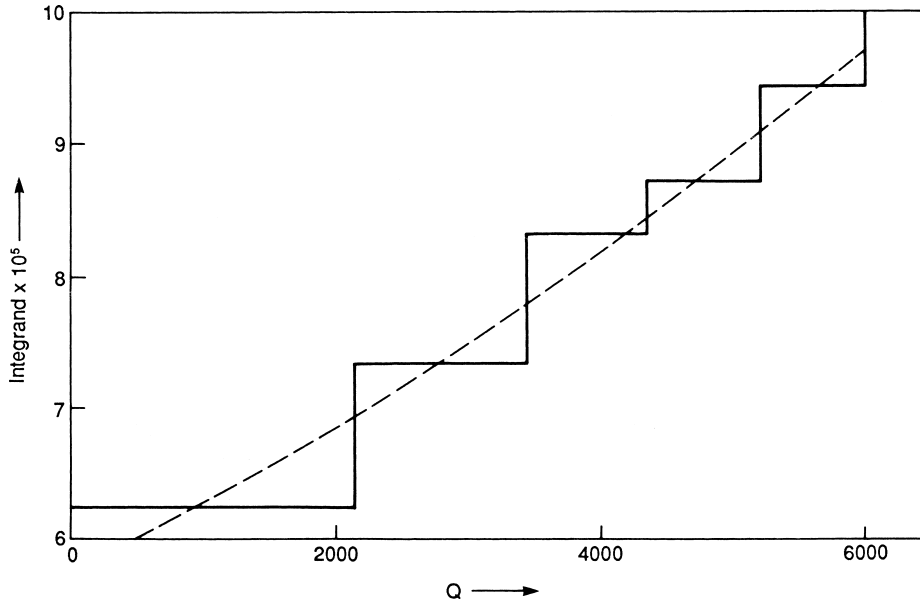
TABLE 8.14. A Guide to the Selection of Reboilers

	Reboiler Type			
Process Conditions	**Kettle or Internal**	**Horizontal Shell-Side Thermosiphon**	**Vertical Tube-Side Thermosiphon**	**Forced Flow**
Operating pressure				
Moderate	E	G	B	E
Near critical	B-E	R	Rd	E
Deep vacuum	B	R	Rd	E
Design ΔT				
Moderate	E	G	B	E
Large	B	R	G-Rd	E
Small (mixture)	F	F	Rd	P
Very small (pure component)	B	F	P	P
Fouling				
Clean	G	G	G	E
Moderate	Rd	G	B	E
Heavy	P	Rd	B	G
Very heavy	P	P	Rd	B
Mixture boiling range				
Pure component	G	G	G	E
Narrow	G	G	B	E
Wide	F	G	B	E
Very wide, with viscous liquid	F-P	G-Rd	P	B

[a]Category abbreviations: B, best; G, good operation; F, fair operation, but better choice is possible; Rd, risky unless carefully designed, but could be best choice in some cases; R, risky because of insufficient data; P, poor operation; E, operable but unnecessarily expensive.
(HEDH, 1983, 3.6.1).

convection. The application of extended surfaces permits attainment of heat fluxes per unit of bare surface comparable to those in the radiant zone. *Shield section* is the name given to the first two rows or so leading into the convection section. On balance these tubes receive approximately the same heat flux as the radiant tubes because the higher convection transfer counteracts the lesser radiation due to lack of refractory wall backing. Accordingly, shield tubes are never finned.

The usual temperature of flue gas entering the shield section is 1300–1650°F and should be 200–300°F above the process temperature at this point. The proportions of heat transferred in the radiant and convection zones can be regulated by recirculation of hot flue gases into the radiant zone, as sketched on Figure 8.19(b). Such an operation is desirable in the thermal cracking of hydrocarbons, for instance, to maintain a proper temperature profile; a negative gradient may cause condensation of polymeric products that make coke on the tubes. Multiple chambers as in Figure 8.19(d) also provide some flexibility. In many operations, about 75% of the heat is absorbed in the radiant zone of a fired heater.

Horizontal tube supports are made of refractory steel to withstand the high temperatures. Hangers for vertical tubes make for a less expensive construction per unit of tube surface. Furnaces are lined with shaped light weight refractory brick 5–8 in. thick. A 1 in. layer of insulating brick is placed between the lining and the metal shell.

Differences of opinion exist among designers with respect to housing shapes and tube arrangements. Nelson (*Petroleum Refinery Engineering*, McGraw-Hill, New York, 1958, p. 587), for example, describes a dozen types. The most common are cylindrical shells with vertical tubes and cabin or box types with horizontal tubes. Figures 8.19 and 17.16 are of typical constructions. Convection zones are most commonly at the top. Process fluid goes first through the convection section and usually leaves the radiant tubes

at the top, particularly when vaporization occurs in them. In the more complex flow pattern of Figure 8.19(b), some of the convection tubes are used for preheat and the remainder to maintain the process fluid at a suitable reaction temperature that was attained in the radiant tubes. Some of the convection zone also may be used for steam generation or superheating or for other heat recovery services in the plant.

Capacities of 10–200 MBtu/hr can be accommodated in heaters with single radiant chambers, and three to four chambers with a common convection section are feasible. Stoichiometric combustion air requirements of typical fuels are tabulated:

Fuel	LHV (Btu/lb)	Combustion Air lb/lb	Combustion Air lb/1000 Btu
Methane	21,500	17.2	0.800
Propane	19,920	15.2	0.763
Light fuel oil	17,680	14.0	0.792
Heavy fuel oil	17,420	13.8	0.792
Anthracite	12,500	4.5	0.360

Burners may be located in the floor or on the ends of the heaters. Liquid fuels are atomized with steam or air or mechanically. A particularly effective heater design is equipped with radiant panel (surface combustion) burners, illustrated in Figure 17.16(a), (b). The incandescent walls are located 2–3 ft from the tubes. The furnace side of the panel may reach 2200°F whereas the outer side remains at 120°F because of continual cooling by the air–gas mixture. Radiant panel burners require only 2–5% excess air compared with 10–20% for conventional burners. Heaters equipped with radiant panels cost more but provide better control of temperatures of reactions such as pyrolysis of hydrocarbons to ethylene for instance.

Distances between tube banks are of the order of 20 ft or so. A rough guide to box size is about 4 cuft/sqft of radiant

---

Comparison of Three Kinds of Reboilers for the Same Service
The service is reboiling a medium boiling range hydrocarbon mixture at 10 atm with a duty of 14,600 kW. The designs are calculated in HEDH (1983, 3.6.5) and are summarized here.

In each case a specific geometry and surface are assumed; then the heat transfer coefficients are evaluated, and the area is checked. When agreement between assumed and calculated areas is not close, another design is assumed and checked.

Of the three sets of calculations summarized here, only that for the kettle need not be repeated. Both the others should be repeated since the assumed designs are too conservative to be economical.

Quantity	Kettle	Horizontal TS	Vertical TS
Rated area (m^2)	930	930	480
Tube length (m)	6.1	6.1	4.9
Tube OD (mm)	19	19	—
Tube ID (mm)	—	—	21.2
Vaporization (%)	30	25	25
U (W/m^2 K)	674	674	928
$(\Delta T)_m$	25	44.8	44.8
Calculated area (m^2)	866	483	350
Calculated $\dot{q}$ (W/m^2)	16,859	30,227	41,174
$\dot{q}_{max}$ (W/m^2)	—	—	67,760

Kettle reboiler

Horizontal thermosiphon

Vertical thermosiphon

(a)

(b)

(c)

(d)

(e)

(f)

(g)
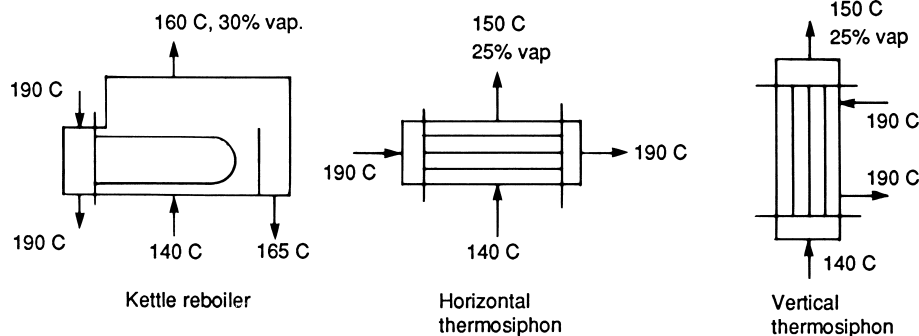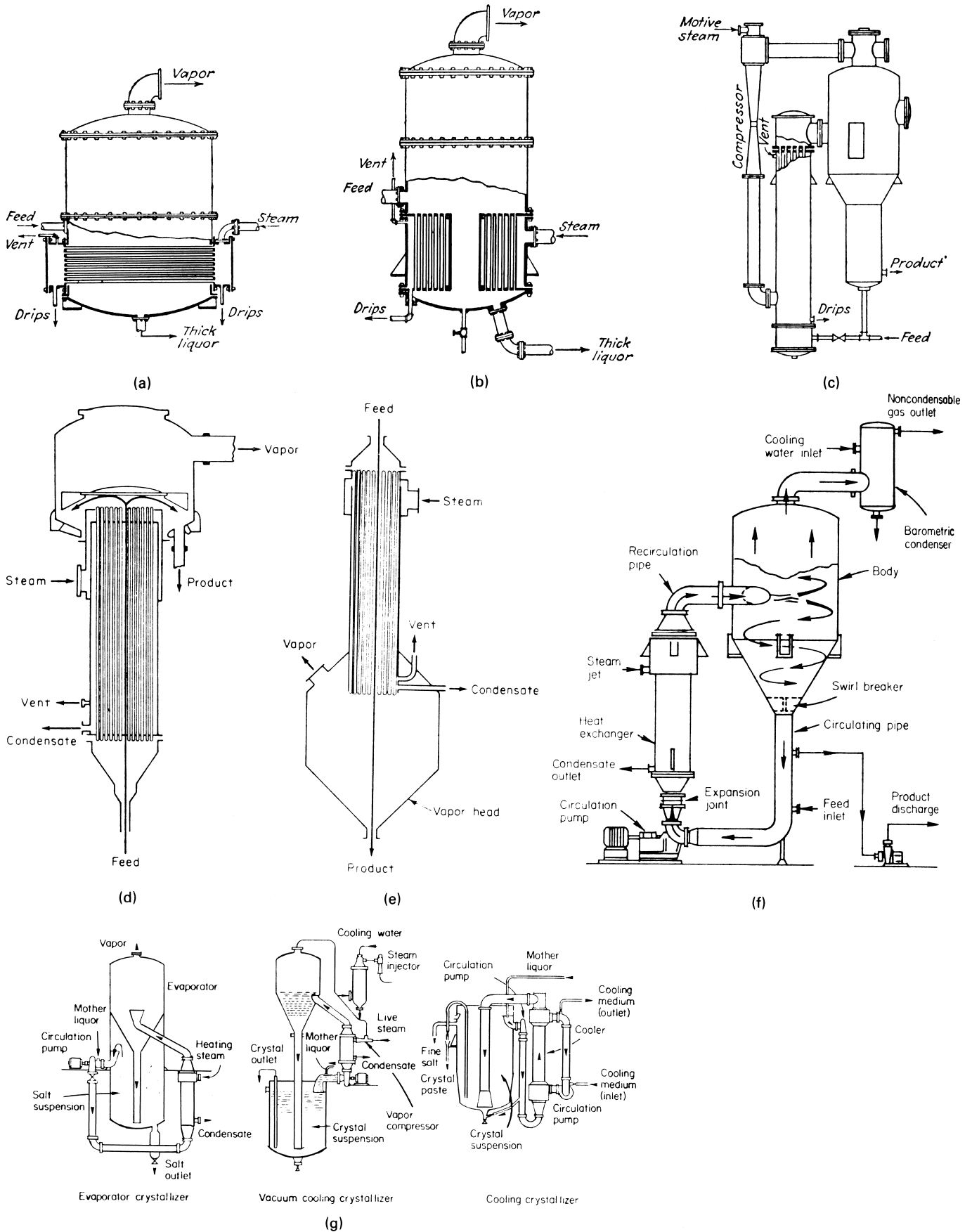
Figure 8.16. Some types of evaporators. (a) Horizontal tube. (b) Calandria type. (c) Thermocompressor evaporator. (d) Long tube vertical. (e) Falling film. (f) Forced circulation evaporator-crystallizer. (g) Three types of "Oslo/Krystal" circulating liquid evaporator-crystallizers.

transfer surface, but the ultimate criterion is sufficient space to avoid impingement of flames on the tubes. Some additional notes on dimensions are stated with the design procedure of Tables 8.16, 8.17, and 8.18.

Tubes are mounted approximately one tube diameter from the refractory walls. Usual center-to-center spacing is twice the outside tube diameter. Wider spacings may be employed to lower the ratio of peak flux at the front of the tube to the average flux. For single rows of tubes, some values of these ratios are

Center-to-center/diameter	1	1.5	2	2.5	3
Max flux/avg flux	3.1	2.2	1.8	1.5	1.2

Less is gained by extending the ratio beyond 2.0. Excessive fluxes may damage the metal or result in skin temperatures that are harmful to the process fluid.

A second row of tubes on triangular spacing contributes only about 25% of the heat transfer of the front row. Accordingly, new furnaces employ only the more economical one-row construction. Second rows sometimes are justifiable on revamp of existing equipment to marginally greater duty.

HEAT TRANSFER

Performance of a heater is characterized by the average heat flux in the radiant zone and the overall thermal efficiency. Heat fluxes of representative processes are listed in Table 8.15. Higher fluxes make for a less expensive heater but can generate high skin

(a)

(b)

Figure 8.17. Forward and backward of liquid flow with respect to steam flow in triple-effect evaporators. (a) Forward flow of liquid by action of pressure differences in the vessels. (b) Backward-pumped flow of liquid through the vessels.

(a)

(b)

Figure 8.18. Overall heat transfer coefficients in some types of evaporators. (a) Water and sugar juice evaporators; (b) Sea water evaporators. [*F.C. Standiford*, Chem. Eng., *157–176 (9 Dec. 1963)*].

temperatures inside and out. Thermal sensitivity of the process fluid, the strength of the metal and its resistance to corrosion at elevated temperatures are factors to be taken into account in limiting the peak flux. Because of the refractory nature of water, however, allowable fluxes in steam boilers may reach 130,000 Btu/(hr)(sqft), in comparison with a maximum of about 20,000 in hydrocarbon service. Example 8.13 is a study of the effect of tube spacing on inside film peak temperatures.

A certain amount of excess air is needed to ensure complete combustion. Typical minimum excess requirements are 10% for gaseous fuels and 15–20% for liquids. Radiant panel burners may get by with 2–5% excess air.

Efficiency is the ratio of total heat absorbed in radiant, convection, and heat recovery sections of the heater to the heat released by combustion. The released heat is based on the lower heating
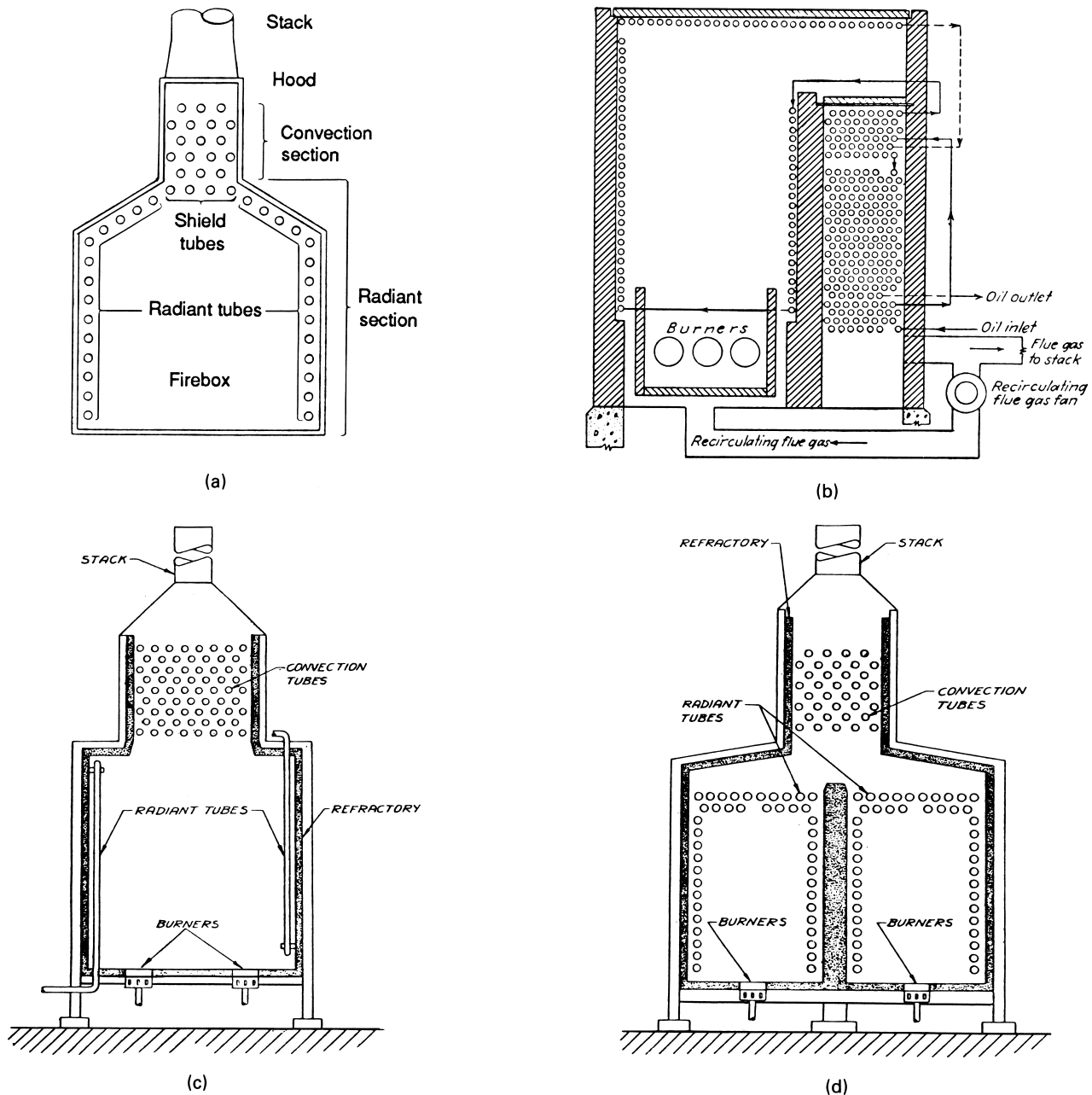
Figure 8.19. Some types of process fired heaters (See also Fig. 17.16 for a radiation panel heater). (a) Radiant, shield, and convection sections of a box-type heater. (b) Heater with a split convection section for preheating before and soaking after the radiant section (*Lobo and Evans, 1939*). (c) Vertical radiant tubes in a cylindrical shell. (d) Two radiant chambers with a common convection section.

value of the fuel and ambient temperature. With standard burners, efficiencies may be in the range 60–80%; with radiant panels, 80–82%. Within broad limits, any specified efficiency can be attained by controlling excess air and the extent of recovery of waste heat.

An economical apportionment of heat absorption between the radiant and convection zones is about 75% in the radiant zone. This can be controlled in part by recirculation of flue gases into the radiant chamber, as shown in Figure 8.19(b).

Because of practical limitations on numbers and possible locations of burners and because of variations in process temperatures, the distribution of radiant flux in a combustion chamber is not uniform. In many cases, the effect of such nonuniformity is not important, but for sensitive and chemically reacting systems it may need to be taken into account. A method of estimating quickly a flux distribution in a heater of known configuration is illustrated by Nelson (1958, p. 610). A desired pattern can be achieved best in a long narrow heater with a multiplicity of burners, as on Figure 17.16 for instance, or with a multiplicity of chambers. A procedure for design of a plug flow heater is outlined in the *Heat Exchanger Design Handbook* (1983, 3.11.5). For most practical purposes, however, it is adequate to assume that the gas temperature and the heat flux are constant throughout the radiant chamber. Since the heat transfer is predominantly radiative and varies with the fourth power of the absolute temperature, the effect of even sub-

TABLE 8.15. Typical Radiant Fluxes and Process Temperatures

Service	Average Radiant Rate (Btu/hr/ft²) (Based on OD)	Temperature (°F)
Atmospheric crude heaters	10,000–14,000	400–700
Reboilers	10,000–12,000	400–550
Circulating oil heaters	8000–11,000	600
Catalytic reformer change and reheat	7500–12,000	800–1000
Delayed coking heater	10,000–11,000	925
Visbreaker heaters—heating section	9000–10,000	700–950
Soaking section	6000–7000	950
Lube vacuum heaters	7500–8500	850
Hydrotreater and hydrocracker charge heaters	10,000	700–850
Catalytic-cracker feed heaters	10,000–11,000	900–1050
Steam superheaters	9000–13,000	700–1500
Natural gasoline plant heaters	10,000–12,000	—
Ethylene and propylene synthesis	10,000–15,000	1300–1650

EXAMPLE 8.13
Peak Temperatures
An average flux rate is 12,000 Btu/(hr)(sqft) and the inside film coefficient is 200 Btu/(hr)(sqft)(°F). At the position where the average process temperature is 850°F, the peak inside film temperature is given by $T = 850 + 12,000 R/200$. At the several tube spacings the peak temperatures are:

Center-to-center/diameter	1	1.5	2	2.5	3
Peak (°F)	1036	982	958	948	9.22

For heavy liquid hydrocarbons the upper limit of 950°F often is adopted.

stantial variation in stock temperature on flux distribution is not significant. Example 8.14 studies this problem.

DESIGN OF FIRED HEATERS

The design and rating of a fired heater is a moderately complex operation. Here only the completely mixed model will be treated. For this reason and because of other generalizations, the method to be described affords only an approximation of equipment size and performance. Just what the accuracy is, it is hard to say. Even the relatively elaborate method of Lobo and Evans (1939) is able to predict actual performance only within a maximum deviation of 16%.

Pertinent equations and other relations are summarized in Table 8.16, and a detailed stepwise procedure is listed in Table 8.17. A specific case is worked out in detail in Example 8.15. Basically, a heater configuration and size and some aspects of the performance are assumed in advance. Then calculations are made of the heat transfer that can be realized in such equipment. Adjustments to the design are made as needed and the process calculations repeated. Details are given in the introduction to Example 8.16. Figures 8.20, 8.21, and 8.22 pertain to this example. Some of the approximations used here were developed by Wimpress (1963); his graphs were converted to equation form for convenience. Background and more accurate methods are treated notably by Lobo and Evans (1939) and more briefly by Kern (1950) and Ganapathy (1982). Charts of gas emissivity more elaborate than Figure 8.23 appear in these references.

An early relation between the heat absorption Q in a radiant zone of a heater, the heat release Q_f, the effective surface A_{cp} and the air/fuel ratio R lb/lb is due to Wilson, Lobo, and Hottel [*Ind. Eng. Chem.* **24**, 486, (1932)]:

$$Q_f/Q = 1 + (R/4200)\sqrt{Q_f/A_{cp}}. \tag{8.45}$$

Although it is a great simplification, this equation has some utility in appraising directional effects of changes in the variables. Example 8.16 considers changes in performance with changes in excess air.

Heat transfer in the radiant zone of a fired heater occurs largely by radiation from the flue gas (90% or so) but also significantly by convection. The combined effect is represented by

$$Q/A = h_r(T_g^4 - T_s^4) + h_c(T_g - T_s), \tag{8.46}$$

where T_g and T_s are absolute temperatures of the gas and the receiving surface. The radiative properties of a gas depend on its chemical nature, its concentration, and the temperature. In the thermal range, radiation of flue gas is significant only from the triatomic molecules H_2O, CO_2, and SO_2, although the amount of the last is small and usually neglected. With fuels having the composition C_xH_{2x}, the ratio of partial pressures is $p_{H_2O}/p_{CO_2} = 1$. In Figure 8.23, the emissivity of such a gas is represented as a function of temperature and the product PL of the partial pressures of water and carbon dioxide and the path of travel defined by the mean beam length. Item 8 of Table 8.16 is a curve fit of such data.

EXAMPLE 8.14
Effect of Stock Temperature Variation
A combustion chamber is at 2260°R, a stock enters at 1060°R and leaves at 1360°R. Accordingly, the heat fluxes at the inlet and outlet are approximately in the ratio $(2.26^4 - 1.06^4)/(2.26^4 - 1.36^4) = 1.095$. The small effect of even greater variation in flux on a mild cracking operation is illustrated in Figure 8.22.

TABLE 8.16. Equations and Other Relations for Fired Heater Design

1. Radiant zone heat transfer

$$\frac{Q_R}{\alpha A_R F} = 1730\left[\left(\frac{T_g + 460}{1000}\right)^4 - \left(\frac{T_t + 460}{100}\right)^4\right] + 7(T_g - T_t)$$

2. Radiant zone heat balance

$$\frac{Q_R}{\alpha A_R F} = \frac{Q_n}{\alpha A_R F}\left(1 + \frac{Q_a}{Q_n} + \frac{Q_f}{Q_n} - \frac{Q_L}{Q_n} - \frac{Q_g}{Q_n}\right)$$

Q_R is the enthalpy absorbed in the radiant zone, Q_a is the enthalpy of the entering air, Q_f that of the entering fuel, Q_L is the enthalpy loss to the surroundings, Q_g is the enthalpy of the gas leaving the radiant zone; Q_a and Q_f are neglected if there is no preheat, and Q_L/Q_n is about 0.02–0.03; Q_n is the total enthalpy released in the furnace

3. Enthalpy Q_s, of the stack gas, given by the overall heat balance

$$Q_s/Q_n = 1 + (1/Q_n)(Q_a + Q_f - Q_L - Q_R - Q_{\text{convection}})$$

4. Enthalpy Q_g, of the flue gas as a function of temperature, °F

$$Q_g/Q_n = [a + b(T/1000 - 0.1)](T/1000 - 0.1)$$

    $z = $ fraction excess air

    $a = 0.22048 - 0.35027z + 0.92344z^2$

    $b = 0.016086 + 0.29393z - 0.48139z^2$

5. Absorptivity, α, of the tube surface with a single row of tubes

    $\alpha = 1 - [0.0277 + 0.0927(x - 1)](x - 1)$

    $x = $ (center-to-center spacing)/(outside tube diameter)

6. Partial pressure of $CO_2 + H_2O$

    $P = 0.288 - 0.229x + 0.090x^2$

    $x = $ fraction excess air

7. Mean beam lengths L of radiant chambers

Dimensional Ratio[a]	Mean Length L (ft)
Rectangular Furnaces	
1. 1-1-1 to 1-1-3	$2/3\sqrt[3]{\text{furnace volume, (ft}^3)}$
1-2-1 to 1-2-4	
2. 1-1-4 to 1-1-∞	1.0 × smallest dimension
3. 1-2-5 to 1-2-8	1.3 × smallest dimension
4. 1-3-3 to 1-∞-∞	1.8 × smallest dimension
Cylindrical Furnaces	
5. $d \times d$	2/3 diameter
6. $d \times 2d$ to $d \times \infty d$	1 × diameter

    [a] Length, width, height in any order.

8. Emissivity ϕ of the gas (see also Fig. 8.20).

    $\phi = a + b(PL) + c(PL)^2$

    $PL = $ product of the partial pressure (6) and the mean beam length (7)

    $z = (T_g + 460)/1000$

    $a = 0.47916 - 0.19847z + 0.022569z^2$

    $b = 0.047029 + 0.0699z - 0.01528z^2$

    $c = 0.000803 - 0.00726z + 0.001597z^2$

9. Exchange factor F

    $F = a + b\phi + c\phi^2$

    $\phi = $ gas emissivity,(8)

    $z = A_w/\alpha A_R$

    $a = 0.00064 + 0.0591z + 0.00101z^2$

    $b = 1.0256 + 0.4908z - 0.058z^2$

    $c = -0.144 - 0.552z + 0.040z^2$

TABLE 8.16.—(continued**)**

10. Overall heat transfer coefficient U_c in the convection zone

$U_c = (a + bG + cG^2)(4.5/d)^{0.25}$
G = flue gas flow rate, lb/(sec)(sqft open cross section)
d = tube outside diameter, (in.)
$z = T_f/1000$, average outside film temperature
$a = 2.461 - 0.759z + 1.625z^2$
$b = 0.7655 + 21.373z - 9.6625z^2$
$c = 9.7938 - 30.809z + 14.333z^2$

11. Flue gas mass rate G_f

$$\frac{10^6 G_f}{Q_n} = \begin{bmatrix} 840 + 8.0x, & \text{with fuel oil} \\ 822 + 7.78x, & \text{with fuel gas} \end{bmatrix} \text{lb/MBtu heat release}$$

x = fraction excess air

TABLE 8.17. Procedure for the Rating of a Fired Heater, Utilizing the Equations of Table 8.16

1. Choose a tube diameter corresponding to a cold oil velocity of 5–6 ft/sec
2. Find the ratio of center-to-center spacing to the outside tube diameter. Usually this is determined by the dimensions of available return bends, either short or long radius
3. Specify the desired thermal efficiency. This number may need modification after the corresponding numbers of tubes have been found
4. Specify the excess combustion air
5. Calculate the total heat absorbed, given the enthalpies of the inlet and outlet process streams and the heat of reaction
6. Calculate the corresponding heat release, (heat absorbed)/efficiency
7. Assume that 75% of the heat absorption occurs in the radiant zone. This may need to be modified later if the design is not entirely satisfactory
8. Specify the average radiant heat flux, which may be in the range of 8000–20,000 Btu/(hr)(sqft). This value may need modification after the calculation of Step 28 has been made
9. Find the needed tube surface area from the heat absorbed and the radiant flux. When a process-side calculation has been made, the required number of tubes will be known and will not be recalculated as stated here
10. Take a distance of about 20 ft between tube banks. A rough guide to furnace dimensions is a requirement of about 4 cuft/sqft of radiant transfer surface, but the ultimate criterion is sufficient space to avoid flame impingement
11. Choose a tube length between 30 and 60 ft so as to make the box dimensions roughly comparable. The exposed length of the tube, and the inside length of the furnace shell, is 1.5 ft shorter than the actual length
12. Select the number of shield tubes between the radiant and convection zones so that the mass velocity of the flue gas will be about 0.3–0.4 lb/(sec)(sqft free cross section). Usually this will be also the number of convection tubes per row
13. The convection tubes usually are finned
14. The cold plane area is

    A_{cp} = (exposed tube length)(center-to-center spacing)(number of tubes exclusive of the shield tubes)

15. The refractory area A_w is the inside surface of the shell minus the cold plane area A_{cp} of Step 14

    $A_w = 2[W(H + L) + H \times L)] - A_{cp}$

    where W, H, and L are the inside dimensions of the shell
16. The absorptivity α is obtained from Eq. (5) when only single rows of tubes are used. For the shield tubes, $\alpha = 1$
17. The sum of the products of the areas and the absorptivities in the radiant zone is

    $\alpha A_R = A_{\text{shield}} + \alpha A_{cp}$

18. For the box-shaped shell, the mean beam length L is approximated by

    $L = \frac{2}{3}(\text{furnace volume})^{1/3}$

19. The partial pressure P of $CO_2 + H_2O$ is given in terms of the excess air by Eq. (6)
20. The product PL is found with the results of Steps 18 and 19
21. The mean tube wall temperature T_t in the radiant zone is given in terms of the inlet and outlet process stream temperatures by
    $T_t = 100 + 0.5(T_1 + T_2)$

22. The temperature T_g of the gas leaving the radiant zone is found by combining the equations of the radiant zone heat transfer [Eq. (1)] and the radiant zone heat balance [Eq. (2)]. With the approximation usually satisfactory, the equality is

    $$\frac{Q_n}{\alpha A_R F}\left(1 - 0.02 - \frac{Q_g}{Q_n}\right) = 1730\left[\left(\frac{T_g + 460}{1000}\right)^4 - \left(\frac{T_t + 460}{1000}\right)^4\right] + 7(T_g - T_t)$$

TABLE 8.17.—(*continued***)**

The solution of this equation involves other functions of T_g, namely, the emissivity ϕ by Eq. (8), the exchange factor F by Eq. (9) and the exit enthalpy ratio Q_g/Q_n by Eq. (4)

23. The four relations cited in Step 22 are solved simultaneously by trial to find the temperature of the gas. Usually it is in the range 1500–1800°F. The Newton–Raphson method is used in the program of Table 8.18. Alternately, the result can be obtained by interpolation of a series of hand calculations

24. After T_g has been found, calculate the heat absorbed Q_R by Eq. (1)

25. Find the heat flux

$$Q/A = Q_R/A_{\text{radiant}}$$

and compare with value specified in Step 8. If there is too much disagreement, repeat the calculations with an adjusted radiant surface area

26. By heat balance over the convection zone, find the inlet and outlet temperatures of the process stream

27. The enthalpy of the flue gas is given as a function of temperature by Eq. (4). The temperature of the inlet to the convection zone was found in Step 23. The enthalpy of the stack gas is given by the heat balance [Eq. (3)], where all the terms on the right-hand side are known. Q_s/Q_n is given as a function of stack temperature T_s by Eq. (4). That temperature is found from this equation by trial

28. The average temperature of the gas film in the convection zone is given in terms of the inlet and outlet temperatures of the process stream and the flue gas approximately by

$$T_f = 0.5\left[T_{L1} + T_{L0} + \frac{(T_{g1} - T_{L1}) - (T_s - T_{L0})}{\ln\left[(T_{g1} - T_{L1})/(T_s - T_{L0})\right]}\right]$$

The flow is countercurrent

29. Choose the spacing of the convection tubes so that the mass velocity is $G = 0.3$–0.4 lb/(sec)(sqft free cross section). Usually this spacing is the same as that of the shield tubes, but the value of G will not be the same if the tubes are finned

30. The overall heat transfer coefficient is found with Eq. (10)

31. The convection tube surface area is found by

$$A_c = Q_c/U_c(\text{LMTD})$$

and the total length of bare of finned tubes, as desired, by dividing A_c by the effective area per foot

32. Procedures for finding the pressure drop on the flue gas side, the draft requirements and other aspects of stack design are presented briefly by Wimpress.

(Based partly on the graphs of Wimpress, 1963).

EXAMPLE 8.15
Design of a Fired Heater

The fuel side of a heater used for mild pyrolysis of a fuel oil will be analyzed. The flowsketch of the process is shown in Figure 8.20, and the tube arrangement finally decided upon is in Figure 8.21. Only the temperatures and enthalpies of the process fluid are pertinent to this aspect of the design, but the effect of variation of heat flux along the length of the tubes on the process temperature and conversion is shown in Figure 8.22. In this case, the substantial differences in heat flux have only a minor effect on the process performance.

Basic specifications on the process are the total heat release (102.86 MBtu/hr), overall thermal efficiency (75%), excess air (25%), the fraction of the heat release that is absorbed in the radiant section (75%), and the heat flux (10,000 Btu/(hr)(sqft)).

In the present example, the estimated split of 75% and a radiant rate of 10,000 lead to an initial specification of 87 tubes, but 90 were taken. The final results are quite close to the estimates, being 77.1% to the radiant zone and 9900 Btu/(hr)(sqft) with 90 tubes. If the radiant rate comes out much different from the desired value, the number of tubes is changed accordingly.

Because of the changing temperature of the process stream, the heat flux also deviates from the average value. This variation is estimated roughly from the variation of the quantity

$$\beta = 1730(T_g^4 - T_L^4) + 7.0(T_g - T_L),$$

where the gas temperature T_g, in the radiant zone is constant and T_L is the temperature of the process stream, both in °R. In comparison with the average flux, the effect is a slightly increased

preheat rate and a reduced flux in the reaction zone. The inside skin temperature also can be estimated on the reasonable assumptions of heat transfer film coefficients of more than 100 before cracking starts and more than 200 at the outlet. For the conditions of this example, with $Q/A = 9900$ and $T_g = 2011$°R, these results are obtained:

T_L (°F)	β/β_{724}	h	T_{skin}(°F)
547	1.093	>100	<655
724	1	>100	<823
900	1.878	>200	<943

The equation numbers cited following are from Table 8.16. The step numbers used following are the same as those in Table 8.17:

1. Flow rate $= 195{,}394/3600(0.9455)(62.4) = 0.9200$ cfs, velocity $= 5.08$ fps in 6–5/8 in. OD Schedule 80 pipe.
2. Short radius return bends have 12 in. center-to-center.
3. $\eta = 0.75$.
4. Fraction excess air $= 0.25$.
5. From the API data book and a heat of cracking of 332 Btu/(lb gas + gasoline):

$$H_{900} = 0.9(590) + 0.08(770) + 0.02(855) = 609.6 \text{ Btu/lb,}$$
$$Q_{\text{total}} = 195{,}394(609.6 - 248) + 19{,}539(332) = 77.14(E6).$$

6. Heat released:

$$Q_n = 77.14/0.75 = 102.86(E6) \text{ Btu/lb.}$$

EXAMPLE 8.15—(*continued*)

7. Radiant heat absorption:

$$Q_R = 0.75(77.14)(E6) = 57.86(E6).$$

8. (Q/A) rad = 10,000 Btu/(hr)(sqft), average.

9. Radiant surface:

$$A = 57.86(E6)/10,000 = 5786\,\text{sqft}.$$

11. Tube length = $5786/1.7344 = 3336\,\text{ft}$; 40 foot tubes have an exposed length of 38.5 ft; $N = 3336/38.5 = 86.6$, say 92 radiant tubes.

12. From Eq. (11) the flue gas rate is

$$G_f = 102.85(1020) = 104,907\,\text{lb/hr}.$$

With four shield tubes, equilateral spacing and 3 in. distance to walls,

$$G = \frac{104,907(12)}{3600(38.5)(27.98)} = 0.325\,\text{lb/sec sqft}.$$

13. The 90 radiant tubes are arranged as shown on Figure 8.22: 4 shields, 14 at the ceiling, and 36 on each wall. Dimensions of the shell are shown.

14. $A_{cp} = (38.5)(1)(90 - 4) = 3311\,\text{sqft}.$

15. Inside surface of the shell is

$$A_s = 2[20(37 + 38.5) + 37(38.5)] = 5869\,\text{sqft}.$$

Refractory surface,

$$A_w = 5869 - 3311 = 2558\,\text{sqft}.$$

16. (Center-to-center)/OD = $12/6.625 = 1.81$,

$$\alpha = 0.917, \text{single rows of tubes[Eq.(5)]}.$$

17. Effective absorptivity:

$$\alpha A_R = 4(38.5)(1) + 0.917(3311) = 3190\,\text{sqft},$$
$$A_w/\alpha A_r = 2558/3190 = 0.8018.$$

18. Mean beam length:

$$L = (2/3)(20 \times 37 \times 38.5)^{1/3} = 20.36.$$

19. From Eq. (6), with 25% excess air,

$$P = 0.23.$$

20. $PL = 0.23(20.36) = 4.68\,\text{atm ft}.$

21. Mean tube wall temp: The stream entering the radiant section has absorbed 25% of the total heat.

$$H_1 = 248 + 0.25(77.14)(E6)/195,394 = 346.7,$$
$$T_1 = 565°\,\text{F},$$
$$T_t = 100 + (565 + 900)/2 = 832.5.$$

22–24. Input data are summarized as:

$$PL = 4.68,$$
$$D_1 = 0.8018,$$
$$D_2 = 0.25,$$
$$T_1 = 832.5,$$
$$Q_1 = Q_n/\alpha A_R = 102.86(E6)/3190 = 32,245.$$

From the computer program listed in Table 8.18,

$$T_g = 1553.7,$$
$$F = 0.6496\,\text{[Eq.(9)]},$$

$$Q_R = \alpha A_R F\left\{1730\left[\left(\frac{T_g + 460}{1000}\right)^4 - \left(\frac{T_t + 460}{1000}\right)^4\right] + 7(T_g - T_t)\right\}$$
$$= 3190(0.6496)(28,679) = 59.43(E6).$$

Compared with estimated 57.86(E6) at 75% heat absorption in the radiant section. Repeat the calculation with an estimate of 60(E6)

$$H_1 = 248 + (77.14 - 60)(E6)/195,394 = 335.7,$$
$$T_1 = 542,$$
$$T_t = 100 + 0.5(542 + 900) = 821,$$
$$T_g = 1550.5,$$
$$F = 0.6498,$$
$$Q_R = 3190(0.6498)(28,727) = 59.55(E6).$$

Interpolating,

$Q_{assumed}$	T_1	T_t	T_g	Q_{calcd}	Q/A
57.86	565	832.5	1553.7	59.43	
60.00	542	821	1550.5	59.55	
Interpolation	[547		1551.2	59.50	9900]

26–27.

$$Q_{conv} = (77.14 - 59.50)(E6)$$
$$= 17.64(E6).$$

Fraction lost in stack gas

$$Q_s/Q_n = 1 - 0.02 - 0.75 = 0.23.$$

From (Eq. (4),

$$T_s = 920°\text{F}.$$

28–31.

$$\text{LMTD} = 735.6$$

mean gas film temp is

$$T_f = 0.5(400 + 547 + 735.6) = 841.3.$$

Since $G = 0.325\,\text{lb/(sec)(sqft)}$,

$$V_c = 5.6\,\text{Btu/(hr)(sqft)(°F)[(Eq.(10)]},$$
$$A_{conv} = \frac{17.64(E6)}{735.6(5.6)} = 4282\,\text{sqft},$$
$$\frac{4282}{1.7344(38.5)} = 64.1\text{bare tubes}$$

or 16 rows of 4 tubes each. Spacing the same as of the shield tubes. Beyond the first two rows, extended surfaces can be installed.

$$\text{Total rows} = 2 + 14/2 = 9.$$

EXAMPLE 8.16
Application of the Wilson–Lobo–Hottel Equation
In the case of Example 8.15, 25% excess air was employed, corresponding to 19.0 lb/air/lb fuel, the heat release was $Q_f = 102.86$ (10^6) Btu/hr, and $\alpha A_{cp} = 3036$. The effect will be found of changing the excess air to 10% (16.72 lb air/lb fuel) on the amount of fuel to be fired while maintaining the same heat absorption.

Ratioing Eq. (8.45) to yield the ratio of the releases at the two conditions,

$$\frac{Q_{f2}}{102.86(106)} = \frac{1 + (16.72/4200)\sqrt{Q_{f2}/3036}}{1 + (19.0/4200)\sqrt{102.86(10^6)/3036}}$$

$$= \frac{1 + 0.0722\sqrt{Q_{f2}(10^{-6})}}{1.8327}$$

$$\therefore Q_{f2} = 95.82(10^6)\text{Btu/hr},$$

which is the heat release with 10% excess air.

With 25% excess air, $Q/Q_f = 1/1.8327 = 0.5456,$
With 10% excess air, $Q/Q_f = 0.5456(102.86/95.82) = 0.5857,$

which shows that approximately 7% more of the released heat is absorbed when the excess air is cut from 25% down to 10%.

When other pertinent factors are included and an approximation is introduced for the relatively minor convection term, the heat transfer equation may be written

$$Q/\alpha A_{cp}F = 1730[(T_g/1000)^4 - (T_s/1000)^4] + 7(T_g - T_s).$$
(8.47)

Here the absorptivity depends on the spacing of the tubes and is given by item 5 of Table 8.16. The cold plane area A_{cp} is the product of the number of tubes by their lengths and by the center-to-center spacing. The combination αA_{cp} is equal to the area of an ideal black plane that has the same absorptivity as the tube bank, and is called the equivalent cold plane area. Evaluation of the exchange factor F is explained in item 9 of Table 8.16. It depends on the emissivity of the gas and the ratio of refractory area A_w to the equivalent cold plane area αA_{cp}. In turn, $A_w = A - A_{cp}$, where A is the area of the inside walls, roof, and floor that are covered by refractory.

In the convection zone of the heater, some heat also is transferred by direct radiation and reflection. The several contributions to overall heat transfer specifically in the convection zone of fired heaters were correlated by Monrad [*Ind. Eng. Chem.* **24**, 505

(1932)]. The combined effects are approximated by item 10 of Table 8.16, which is adequate for estimating purposes. The relation depends on the temperature of the gas film which is taken to be the sum of the average process temperature and one-half of the log mean temperature difference between process and flue gas over the entire tube bank. The temperature of the gas entering the convection zone is found with the trial calculation described in Steps 22–23 of Table 8.17 and may utilize the computer program of Table 8.18.

Figure 8.21. Tube and box configuration of the fired heater of Example 8.16.

Figure 8.20. Flowsketch of process of Example 8.16.
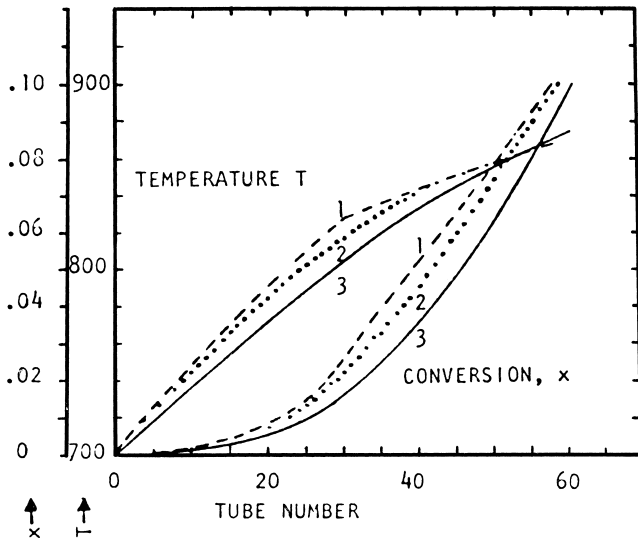
Figure 8.22. Effects of three modes of heat flux distribution on temperature and conversion in pyrolysis of a fuel oil: (1) two levels, 12,500 and 7500; (2) linear variation between the same limits; (3) constant at 10,000 Btu/(hr)(sqft). Obtained by method of Example 8.16.

8.12. INSULATION OF EQUIPMENT

Equipment at high or low temperatures is insulated to conserve energy, to keep process conditions from fluctuating with ambient conditions, and to protect personnel who have occasion to approach the equipment. A measure of protection of the equipment metal against atmospheric corrosion also may be a benefit. Application of insulation is a skilled trade. Its cost runs to 8–9% of purchased equipment cost.

In figuring heat transfer between equipment and surroundings, it is adequate to take account of the resistances of only the insulation and the outside film. Coefficients of natural convection are in Table 8.9 and properties of insulating materials at several temperature levels are in Tables 8.19–8.21. Outdoors under windy conditions, heat losses are somewhat greater than indoors at natural convections.... *Perry's Chemical Engineers' Handbook* (McGraw-Hill, 1997, pp. 11–71 to 73) suggests 10–20% greater thickness of insulation is justified at wind velocities of 7.4 miles/hr; temperature

AQ1
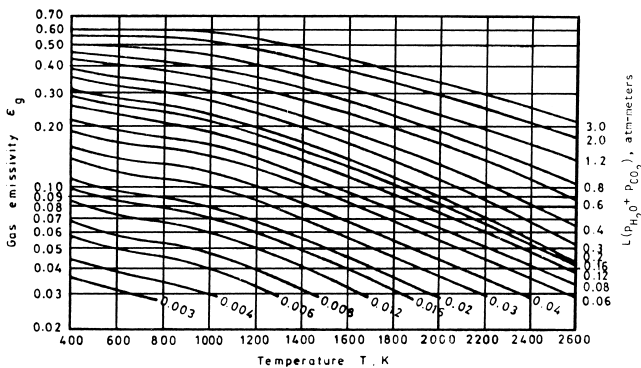
Figure 8.23. Total emissivity of carbon dioxide and water with $P_{H_2O}/P_{CO_2} = 1$ and a total pressure of 1 atm. *[Hadvig*, J. Inst. Fuel **43**, *129* (1970)].

ranges of 150–1200°F, and energy costs of 1–8 dollars/million Btu are also considered.

The optimum thickness of insulation can be established by economic analysis when all of the cost data are available, but in practice a rather limited range of thicknesses is employed. Table 8.22 of piping insulation practice in one instance is an example.

The procedure for optimum selection of insulation thicknesses is exemplified by Happel and Jordan [*Chem. Process Economics*, 380 (1975)]. They take into account the costs of insulation and fuel, payout time, and some minor factors. Although their costs of fuel are off by a factor of 10 or more, their conclusions have some validity if it is recognized that material costs likewise have gone up by roughly the same factor. They conclude that with energy cost of $2.5/million Btu (adjusted by a factor of 10), a payout time of 2 years, for pipe sizes of 2–8 in., the optimum thicknesses in insulation depend on the process temperature according to:

T(°F)	200	400	600
Thickness (in.)	0.5	1.0	1.25

TABLE 8.18. Program for Finding the Radiant Gas Temperature by Steps 22 and 23 of Table 8.17

```
 10 ! Example 8.16. Design of a fired heater. Radiant gas temp by
      step 22. Program "FRN – 1", tape 2
 20 ! P=PL, product of partial pressures of CO₂ + H₂O and mean
      beam length
 30 ! D1 = Aw/αAr
 40 ! D2 = fraction excess air
 50 ! T1 = tube surface temperature
 60 ! Q1 = Qn/αAr
 70 ! Q2 = Qa/Qn, Eq. 8
 80 ! F1 = emissivity, Eq. 6
 90 ! F = exchange factor, Eq. 7
100 ! J = RHS–LHS of step 22
110 SHORT T
120 READ P, D1, D2, T1, Q1
130 DATA 4. 1, 9605, .25,672, 42828
140 INPUT T
150 GOSUB 270
160 J1 = J
170 T = 1 .0001*T
180 GOSUB 270
190 J2 = J
200 DISP T
210 H = .0001 ∗ T ∗ J1/(J2–J1)
220 T = T/1.0001–H
230 IF ABS(H/T) <= .0001 THEN 250
240 GOTO 150
250 PRINT "RADIANT GAS TEMP ="; T
260 END
270 Z1 = (T + 460)/1000
280 A1 = .47916 − .19847 ∗ Z1 + .022569 ∗ Z1 ∧ 2
290 B1 = .047029 + .0699 ∗ Z1 − .01528 ∗ Z1 ∧ 2
300 C1 = −.000803 − .00726 ∗ Z1 + .001597 ∗ Z1 ∧ 2
310 F1 = A1 + B1 ∗ P + C1 ∗ P ∧ 2
320 Z2 = D1
330 A2 = .00064 + .0591 ∗ Z2 + .00101 ∗ Z2 ∧ 2
340 B2 = 1.0256 + .4908 ∗ Z2 − .058 ∗ Z2 ∧ 2
350 C2 = −.144 − .552 ∗ Z2 + .04 ∗ Z2 ∧ 2
360 F = A2 + B2 ∗ F1 + C2 ∗ F1 ∧ 2
370 Z3 = D2
380 A3 = .22048 − .35057 ∗ Z3 + .92344 ∗ Z3 ∧ 2
390 B3 = .016086 + .29393 ∗ Z3 − .48139 ∗ Z3 ∧ 2
400 Q2 = (A3 + B3 ∗ (T/1000 − .1)) ∗ (T/1000 − .1)
410 J = −(Q1/F ∗ (.98 − Q2)) + 1730 ∗ (((T + 460)/1000) ∧ 4−
      ((T1 + 460)/1000) ∧ 4) + 7 ∗ (T − T1)
420 RETURN
```

TABLE 8.19. Thermal Conductivities of Insulating Materials for Low Temperatures [k Btu/(hr)(sqft)(°F/ft)]

Material	Bulk/Density, (lb/cuft)	Temp (°F)	h	Material	Bulk Density, (lb/cuft)	Temp (°F)	h
Corkboard	6.9	100	0.022	Rubber board, expanded, "Rubatex"			
		−100	0.018				
		−300	0.010		4.9	100	0.018
Fibreglas with asphalt coating (board)	11.0	100	0.023	Silica aerogel, powder "Santocel"	5.3	100	0.013
		−100	0.014			0	0.012
		−300	0.007			−100	0.010
Glass blocks, expanded, "Foamglas"	10.6	100	0.036	Vegetable fiber-board, asphalt coating			
		−100	0.033				
		−300	0.018				
					14.4	100	0.028
						−100	0.021
						−300	0.013
						−100	0.015
Mineral wool board, "Rockcork"	14.3	100	0.024	Foams: Polystyrene[a] Polyurethane[b]	2.9 5.0	−100	0.019
		−100	0.017				
		−300	0.008				

[a]Test space pressure, 1.0 atm; $k = 0.0047$ at 10^{-3} mm Hg.
[b]Test space pressure, 1.0 atm; $k = 0.007$ at 10^{-3} mm Hg.
(*Marks Mechanical Engineers Handbook*, 1978, p. 4.64).

The data of Table 8.22 are roughly in agreement with these calculations. Optimum thicknesses of pipe insulation also are given in *Perry's Chemical Engineers' Handbook* (1997, pp. 11–70 to 73, Tables 11–21 & 22)

For very large tanks storing volatile liquids and subject to pressure buildup and breathing losses, it is advisable to find economic thickness of insulation by economic analysis. The influence of solar radiation should be taken into account; a brief treatment of this topic is in the book of Threlkeld (*Thermal Environmental Engineering,* Prentice-Hall, Englewood Cliffs, NJ, 1970). In at least one application, rigid urethane foam sprayed onto storage tanks in 2 in. thickness and covered with a 4 mil thickness of neoprene rubber for weather proofing was economically attractive.

Although resistance to heat transfer goes up as the thickness of pipe insulation is increased, the external surface also increases; a thickness may be reached at which the heat transfer becomes a minimum and then becomes larger. In accordance with this

kind of behavior, heat pickup by insulated refrigerated lines of small diameters can be greater than that of bare lines. In another instance, electrical transmission lines often are lagged to increase the rate of heat loss. An example worked out by Kreith (*Principles of Heat Transfer,* Intext, New York, 1973, p. 44) reveals that an insulated 0.5 in. OD cable has a 45% greater heat loss than a bare one.

LOW TEMPERATURES

Insulation suited to cryogenic equipment are characterized by multiple small spaces or pores that occlude more or less stagnant air of comparatively low thermal conductivity. Table 8.19 lists the most common of these materials. In application, vapor barriers are provided in the insulating structure to prevent inward diffusion of atmospheric moisture and freezing on the cold surface with resulting increase in thermal conductivity and deterioration of the

TABLE 8.20. Thermal Conductivities of Insulating Materials for High Temperatures [k Btu/(hr)(sqft)°F/ft)]

Material	Bulk Density, lb/cuft	Max Temp (°F)	100°F	300°F	500°F	1000°F	1500°F	2000°F
Asbestos paper, laminated	22	400	0.038	0.042				
Asbestos paper, corrugated	16	300	0.031	0.042				
Diatomaceous earth, silica, powder	18.7	1500	0.037	0.045	0.053	0.074		
Diatomaceous earth, asbestos and bonding material	18	1600	0.045	0.049	0.053	0.065		
Fiberglas block, PF612	2.5	500	0.023	0.039				
Fiberglas block, PF614	4.25	500	0.021	0.033				
Fiberglas block, PF617	9	500	0.020	0.033				
Fiberglas, metal mesh blanket, #900	—	1000	0.020	0.030	0.040			
Glass blocks, average values	14–24	1600	—	0.046	0.053	0.074		
Hydrous calcium silicate, "Kaylo"	11	1200	0.032	0.038	0.045			
85% magnesia	12	600	0.029	0.035				
Micro-quartz fiber, blanket	3	3000	0.021	0.028	0.042	0.075	0.108	0.142
Potassium titanate, fibers	71.5	—	—	0.022	0.024	0.030		
Rock wool, loose	8–12	—	0.027	0.038	0.049	0.078		
Zirconia grain	113	3000	—	—	0.108	0.129	0.163	0.217

(*Marks' Standard Handbook for Mechanical Engineers*, 1996, p. 4–84, Table 4.4.6).

TABLE 8.21. Properties of Refractories and Insulating Ceramics[a]
(a) Chemical Composition of Typical Refractories

No.	Refractory Type	SiO_2	Al_2O_3	Fe_2O_3	TiO_2	CaO	MgO	Cr_2O_3	SiC	Alkalies	Resistance to Siliceous Steel-Slag	High-lime Steel-Slag	Fused Mill-Scale	Coal-Ash Slag
1	Alumina (fused)	8–10	85–90	1–1.5	1.5–2.2	—	—	—	—	0.8–1.3[a]	E	G	F	G
2	Chrome	6	23	15[b]	—	—	17	38	—	—	G	E	E	G
3	Chrome (unburned)	5	18	12[b]	—	—	32	30	—	—	G	E	E	G
4	Fire clay (high-heat duty)	50–57	36–42	1.5–2.5	1.5–2.5	—	—	—	—	1–3.5[c]	F	P	P	F
5	Fire clay (super-duty)	52	43	1	2	—	—	—	—	2[c]	F	P	F	F
6	Forsterite	34.6	0.9	7.0	—	1.3	55.4							
7	High-alumina	22–26	68–72	1–1.5	3.5	—	—	—	—	1–1.5[c]	G	F	F	F
8	Kaolin	52	45.4	0.6	1.7	0.1	0.2	—	—	—	F	P	G[d]	F
9	Magnesite	3	2	6	—	3	86	—	—	—	P	E	E	E
10	Magnesite (unburned)	5	7.5	8.5	—	2	64	10	—	—	P	E	E	E
11	Magnesite (fused)	—	—	—	—	—	—	—	—	—	F	E	E	E
12	Refractory porcelain	25–70	25–60	—	—	—	—	—	—	1–5	G	F	F	F
13	Silica	96	1	1	—	2	—	—	—	—	E	P	F	P
14	Silicon carbide (clay bonded)	7–9	2–4	0.3–1	1	—	—	—	85–90	—	E	G	F	E
15	Sillimanite (mullite)	35	62	0.5	1.5	—	—	—	—	0.5[c]	G	F	F	F
16	Insulating fire-brick (2600°F)	57.7	36.8	2.4	1.5	0.6	0.5	—	—	—	P	P	G[e]	P

(b) Physical Properties of Typical Refractories[g]

Refractory No.	Fusion Point °F	Pyrometric Cone	Deformation under Load (% at °F and lb/in.)	Spalling Resistance[f]	Repeat Shrinkage after 5 hr (% °F)	Wt. of Straight 9 in. Brick (lb)
1	3390+	39+	1 at 2730 and 50	G	+0.5 (2910)	9–10.6
2	3580+	41+	shears 2740 and 28	P	−0.5–1.0 (3000)	11.0
3	3580+	41+	shears 2955 and 28	F	−0.5–1.0 (3000)	11.3
4	3060–3170	31–33	2.5–10 at 2460 and 25	G	±0–1.5 (2550)	7.5
5	3170–3200	33–34	2–4 at 2640 and 25	E	±0–1.5 (2910)	8.5
6	3430	40	10 at 2950	F	—	9.0
7	3290	36	1–4 at 2640 and 25	E	−2–4 (2910)	7.5
8	3200	34	0.5 at 2640 and 25	E	−0.7–1.0 (2910)	7.7
9	3580+	41+	shears 2765 and 28	P	−1–2 (3000)	10.0
10	3580+	41+	shear 2940 and 28	F	−0.5–1.5 (3000)	10.7
11	3580+	41+		F	—	10.5
12	2640–3000	16 + 30		G		
13	3060–3090	31–32	shears 2900 and 25	P	+0.5–0.8 (2640)	6.5
14	3390	39	0–1 at 2730 and 50	E	+2 (2910)	8–9.3
15	3310–3340	37–38	0–0.5 at 2640 and 25	E	−0–0.8 (2910)	8.5
16	2980–3000	29–30	0.3 at 2200 and 10	G	−0.2 (2600)	2.25

[a]Divide by 12 to obtain the units k Btu/(hr)(sqft)(°F/ft).
[b]As FeO.
[c]Includes lime and magnesia.
[d]Excellent if left above 1200°F.
[e]Oxidizing atmosphere.
[f]E = Excellent. G = Good. F = Fair. P = Poor.
[g][Some data from Trostel, *Chem. Met. Eng.* (Nov. 1938)].
(Marks' Standard Handbook for Mechanical Engineers, 1996, p. 6–152 & 153; Tables 6.8.13 & 14.)

insulation. Sealing compounds of an asphalt base are applied to the surface of the insulation which then is covered with a weatherproof jacket or cement coating. For truly cryogenic operations such as air liquefaction and rectification in which temperatures as low as $-300°F$ are encountered, all of the equipment is enclosed in a box, and then the interstices are filled with ground cork.

MEDIUM TO HIGH TEMPERATURES

Up to about $600°F$, 85% magnesia has been the most popular material. It is a mixture of magnesia and asbestos fibers so constructed that about 90% of the total volume is dead air space. Equivalents are available for situations where asbestos is undesirable. Such insulants are applied to the equipment in the form of slabs or blankets which are held in place with supports and clips spotwelded to the equipment. They are covered with cement to seal gaps and finished off with a canvas cover that is treated for resistance to the weather. A galvanized metal outer cover may be preferred because of its resistance to mechanical damage of the insulation.

Table 8.20 lists several materials which can be used above 500 °F. A mixture of diatomaceous earth and an asbestos binder is suitable for temperatures up to the range of 1600–1900°F. Johns-Manville "Superex" is one brand. Since this material is more expensive than 85% magnesia, a composite may be used to save money: sufficient thickness of the high temperature resistant material to bring its external surface to below 600°F, finished off with 85% magnesia in appropriate thickness. Table 8.22(c) is one standard specification of this type.

Table 8.22 give thickness specifications for 85% magnesia and mobled diatomecous earth piping insulation.

REFRACTORIES

Equipment made of metal and subject to high temperatures or abrasive or corrosive conditions often is lined with ceramic material.

When the pressure is moderate and no condensation is likely, brick construction is satisfactory. Some of the materials suited to this purpose are listed in Table 8.21. Bricks are available to withstand 3000°F. Composites of insulating brick next to the wall and stronger brick inside are practical. Continuous coats of insulants are formed by plastering the walls with a several inch thickness of concretes of various compositions. "Gunite" for instance is a mixture of 1 part cement and 3 parts sand that is sprayed onto walls and even irregular surfaces. Castable refractories of lower density and greater insulating powers also are common. With both brickwork and castables, an inner shell of thin metal may be provided to guard against leakage through cracks that can develop in the refractory lining. For instance, a catalytic reformer 4 ft OD designed for 650 psig and 1100°F has a shell 1.5 in. thick, a light weight castable lining 4–5/8 in. thick and an inner shell of metal 1/8 in. thick. A catalytic cracker 10 ft dia designed for 75 psig and 1100°F has a 3 in. monolithic concrete liner and 3 in. of blanket insulation on the outside. Ammonia synthesis reactors that operate at 250 atm and 1000°F are insulated on the inside to keep the wall below about 700°F, the temperature at which steels begin to decline in strength, and also to prevent access of hydrogen to the shell since that causes embrittlement. An air gap of about 0.75 in. between the outer shell and the insulating liner contributes significantly to the overall insulating quality.

8.13. REFRIGERATION

Process temperatures below those attainable with cooling water or air are attained through refrigerants whose low temperatures are obtained by several means:

TABLE 8.22. Specifications of Thicknesses of Pipe Insulation for Moderate and High Temperatures, in Single or Double Strength as May Be Needed

(a) Insulation of 85% Magnesia or Equivalent up to 600°F

Pipe Size (in.)	Standard Thick (in.)	Double Standard Thick (in.)
1–1/2 or less	7/8	1–15/16
2	1–1/32	2–5/32
2–1/2	1–1/32	2–5/32
3	1–1/32	2–5/32
4	1–1/8	2–1/4
5	1–1/8	2–5/16
6	1–1/8	2–5/16
8	1–1/4	2–1/2
10	1–1/4	2–1/2
12–33	1–1/2	3

(b) Molded Diatomaceous Earth Base Insulation, to 1900°F, Single or Double Thickness as Needed

Pipe Size (in.)	Thickness (in.)	
1–1/2	2	2
2	1–1/4	2–1/8
2–1/2	1–5/16	1–13/16
3	1–9/16	2–1/16
4	1–9/16	2–1/16
5	1–1/2	2
6	1–1/2	2–1/16
8	1–1/2	2
10	1–9/16	2–1/8
12	1–9/16	2–1/8
14–33	1–1/2	2

(c) Combination Insulation, Inner Layer of Diatomaceous Earth Base, and Outer of 85% Magnesia or Equivalent, for High Level Insulation to 1900°F

Inner Layer		Outer Layer	
Pipe Size (in.)	Thickness (in.)	Nominal Pipe Size (in.)	Thickness (in.)
1–1/2 or less	2	no outer layer	–
2	1–1/4	4–1/2	1–1/2
2–1/2	1–5/16	5	1–1/2
3	1–9/16	6	1–1/2
4	1–9/16	7	1–1/2
5	1–1/2	8	2
6	1–1/2	9	2
8	1–1/2	11	2
10	1–9/16	14	2
12	1–9/16	16	2
14–33	1–1/2	17–36	2

(Data of an engineering contractor).

1. Vapor compression refrigeration in which a vapor is compressed, then condensed with water or air, and expanded to a low pressure and correspondingly low temperature through a valve or an engine with power takeoff.
2. Absorption refrigeration in which condensation is effected by absorption of vapor in a liquid at high pressure, then cooling and expanding to a low pressure at which the solution becomes cold and flashed.

3. Steam jet action in which water is chilled by evaporation in a chamber maintained at low pressure by means of a steam jet ejector. A temperature is 55°F or so is commonly attained, but down to 40°F may be feasible. Brines also can be chilled by evaporation to below 32°F.

The unit of refrigeration is the ton which is approximately the removal of the heat of fusion of a ton of ice in one day, or 288,000 Btu/day, 12,000 Btu/hr, 200 Btu/min. The reciprocal of the efficiency, called the coefficient of performance (COP) is the term employed to characterize the performances of refrigerating processes:

$$COP = \frac{\text{energy absorbed by the refrigerant at the low temperature}}{\text{energy input to the refrigerant}}$$

A commonly used unit of COP is (tons of refrigeration)/(horse-power input). Some of the refrigerants suited to particular temperature ranges are listed in Tables 8.23, and 8.24.

COMPRESSION REFRIGERATION

A basic circuit of vapor compression refrigeration is in Figure 8.24(a). After compression, vapor is condensed with water cooling and then expanded to a low temperature through a valve in which the process is essentially at constant enthalpy. In large scale installations or when the objective is liquefaction of the "permanent" gases, expansion to lower temperatures is achieved in turbo-expanders from which power is recovered; such expansions are approximately isentropic. The process with expansion through a valve is represented on a pressure–enthalpy diagram in Figure 8.24(b).

A process employing a circulating brine is illustrated in Figure 8.24(c); it is employed when cooling is required at several points distant from the refrigeration unit because of the lower cost of circulation of the brine, and when leakage between refrigerant and process fluids is harmful.

For an overall compression ratio much in excess of four or so, multistage compression is more economic. Figure 8.24(d) shows two stages with intercooling to improve the capacity and efficiency of the process.

Many variations of the simple circuits are employed in the interest of better performance. The case of Example 8.17 has two stages of compression but also two stages of expansion, a scheme due originally to Windhausen (in 1901). The flashed vapor of the intermediate stage is recycled to the high pressure compressor. The numerical example shows that an improved COP is attained with the modified circuit. In the circuit with a centrifugal compressor of Figure 8.25, the functions of several intermediate expansion valves and flash drums are combined in a single vessel with appropriate internals called an economizer. This refrigeration unit is used with a fractionating unit for recovering ethane and ethylene from a mixture with lighter substances.

Low temperatures with the possibility of still using water for final condensation are attained with cascade systems employing coupled circuits with different refrigerants. Refrigerants with higher vapor pressures effect condensation of those with lower vapor pressures. Figure 8.26 employs ethylene and propylene in a cascade for servicing the condenser of a demethanizer which must be cooled to −145°F. A similar process is represented on a flow-sketch in the book of Ludwig (1983, Vol. 1, p. 249). A three element

cascade with methane, ethylene and propylene refrigerants is calculated by Bogart (1981, pp. 44–47); it attains −240°F with a maximum pressure of 527 psia.

REFRIGERANTS

Several refrigerants commonly used above −80°F or so are compared in Table 8.23. Ethylene and butane also are in use, particularly in refineries where they are recoverable from the process streams. Properties of the freons (also known by the trade name genetrons) are listed in Table 8.24. Freon 12 is listed in both tables so some comparisons of all of these refrigerants is possible. The refrigerants of Table 8.23 have similar performance. When ammonia or some hydrocarbons are made in the plant, their election as refrigerants is logical. Usually it is preferred to operate at suction pressures above atmospheric to avoid inleakage of air. The nonflammability and nontoxicity of the freons is an attractive quality. Relatively dense vapors such as Ref-12, -22, and -500 are preferred with reciprocating compressors which then may have smaller cylinders. For most equipment sizes, Ref-12 or -114 can be adopted for greater capacity with the same equipment. Ref-22 and -500 are used with specially built centrifugals to obtain highest capacities. The physical properties and performance characteristics of Freon 134a can be found in the 2001 *ASHRAE Hand book, Fundamentals*, pp. 19.8 and 19.9.

Ammonia absorption refrigeration is particularly applicable when low level heat is available for operation of the stripper reboiler and power costs are high. Steam jet refrigeration is the large scale system of choice when chilled water is cold enough, that is, above 40°F or so. The physical properties and performance characteristics of Freon 134a can be found in the *2001 ASHRAE Handbook, Fundamentals*, pp. 19.8 and 19.9.

ABSORPTION REFRIGERATION

The most widely used is ammonia absorption in water. A flow-sketch of the process is in Figure 8.27. Liquid ammonia at a high pressure is obtained overhead in a stripper, and then is expanded through a valve and becomes the low temperature vapor–liquid mixture that functions as the refrigerant. The low pressure vapor is absorbed in weak liquor from the bottom of the stripper. Energy input to the refrigeration system is primarily that of the steam to the stripper reboiler and a minor amount of power to the pump and the cooling water circulation.

This kind of system has a useful range down to the atmospheric boiling point of ammonia, −28°F or −33°C, or even lower. Two or three stage units are proposed for down to −94°F. Sizing of equipment is treated by Bogart (1981).

Another kind of absorption refrigerant system employs aqueous lithium bromide as absorbent and circulating water as the refrigerant. It is used widely for air conditioning systems, in units of 600–700 tons producing water at 45°F.

CRYOGENICS

This term is applied to the production and utilization of temperatures in the range of liquid air, −200°F and lower. A great deal of information is available on this subject of special interest, for instance in *Chemical Engineers Handbook* (1984, 12.47–12.58) and in the book of Arkhanov et al. (1981).
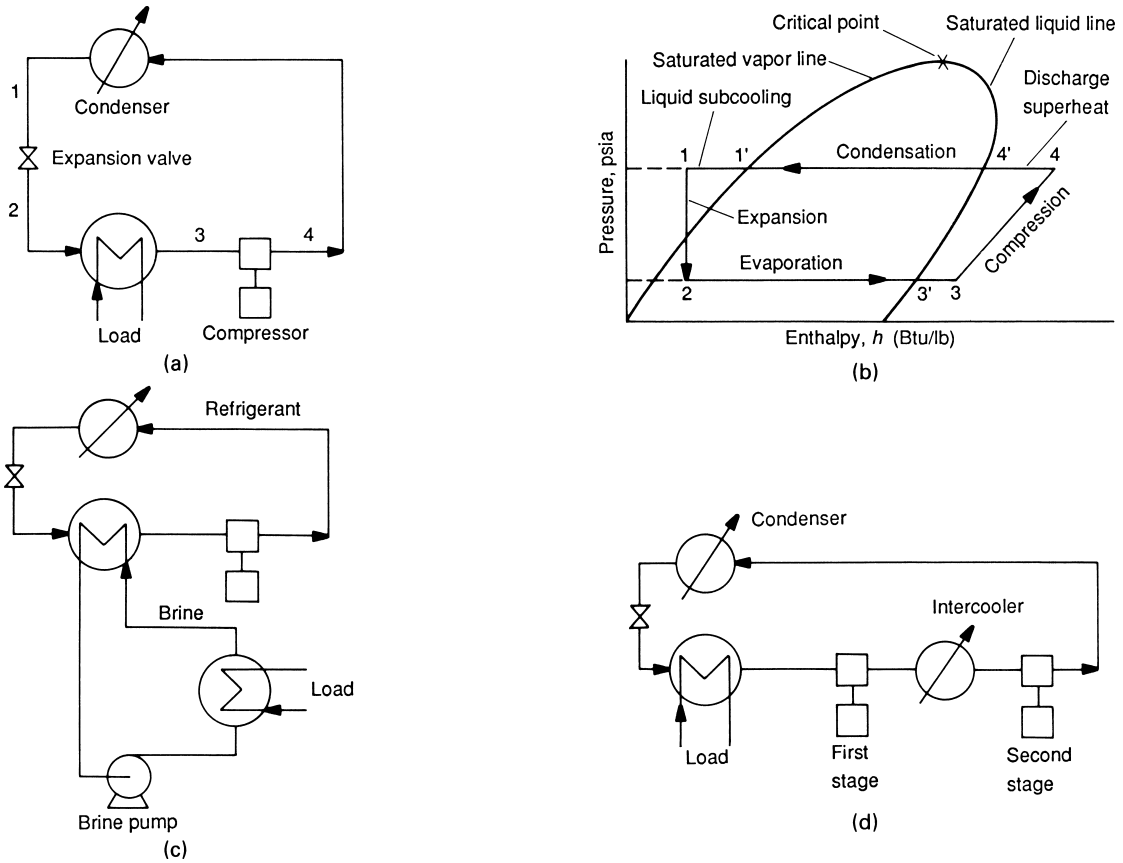
Figure 8.24. Simpler circuits of compression refrigeration (see also Example 8.17). (a) Basic circuit consisting of a compressor, condenser, expansion valve and evaporator (load). (b) Conditions of the basic circuit as they appear on a pressure–enthalpy diagram; the primed points are on the vapor–liquid boundary curve. (c) Circuit with circulation of refrigerated brine to process loads. (d) Circuit with two-stage compression and intercooling.

EXAMPLE **8.17**
Two-Stage Propylene Compression Refrigeration with Inter-stage Recycle
A propylene refrigeration cycle operates with pressures of 256, 64, and 16 psia. Upon expansion to 64 psia, the flashed vapor is re-cycled to the suction of the high pressure stage while the liquid is expanded to 16 psia to provide the needed refrigeration at $-9°F$. The ratios of refrigeration to power input will be compared without and with interstage recycle.

Basis: 1 lb of propylene to the high pressure stage. Conditions are shown on the pressure–enthalpy and flow diagrams. Isentropic
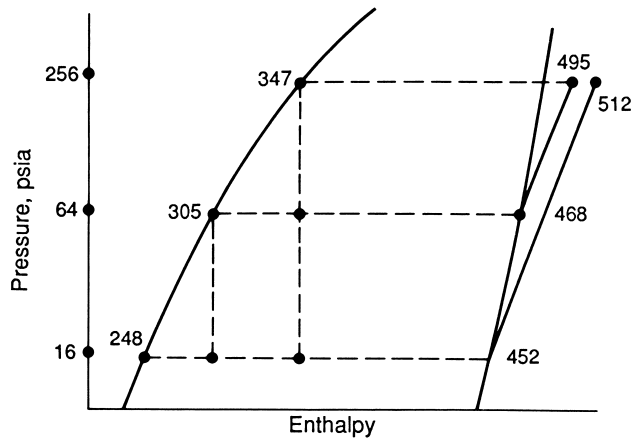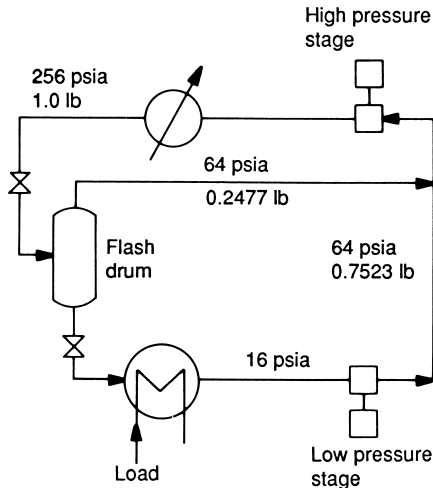
EXAMPLE 8.17—(*contiuned*)
compression and isenthalpic expansion are taken. Without recycle,

refrigeration = 452 − 347 = 105 Btu/lb,
work = 512 − 452 = 60 Btu/lb,
COP = 105/60 = 1.75.

With recycle,

interstage vapor = (347 − 305)/(468 − 305) = 0.2577 lb/lb,
refrigeration = (452 − 305)0.7423 = 109.1 Btu/lb,
work = (495 − 468)0.2577 + (512 − 452)0.7423 = 51.5 Btu/lb,
COP = 109.1/51.5 = 2.12,

which points out the improvement in coefficient of performance by the interstage recycle.
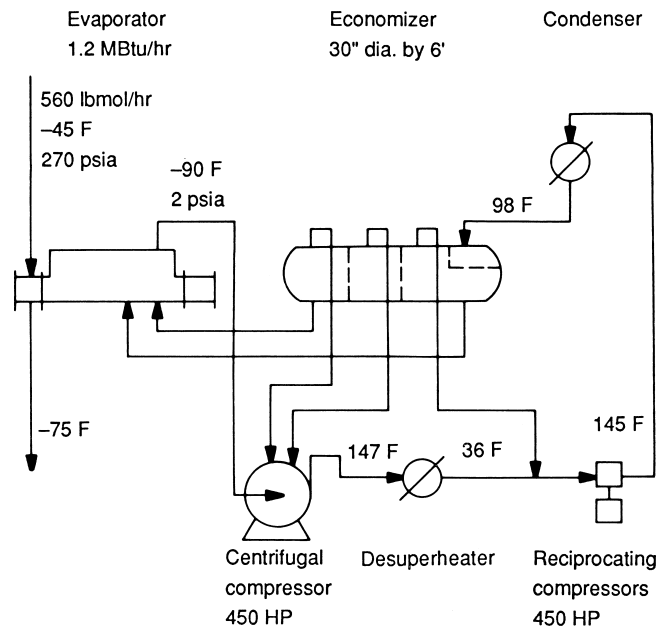
Figure 8.25. A refrigeration system for the overhead condenser of a fractionator for recovering ethane and ethylene. Freon-12 is the refrigerant. The economizer combines the functions of several expansion valves and flash drums for intermediate recycle of flashed vapors.
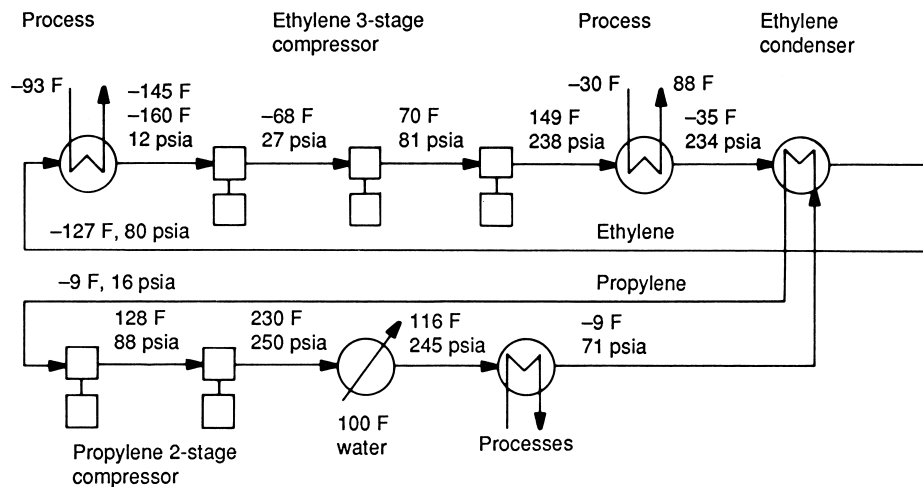
Figure 8.26. A cascade refrigeration system employing ethylene and propylene for condensing the overhead of a demethanizer at −145°F. The diagram is somewhat simplified.

TABLE 8.23. Comparative Refrigerant Performance per Kilowatt at Various Evaporating and Condensing Temperatures

No.	Refrigerant Chemical Name or Composition (% by mass)	Suction Temp., K	Evaporator Pressure, MPa	Condenser Pressure, MPa	Compression Ratio	Net Refrigerating Effect, kJ/kg	Refrigerant Circulated, g/s	Specific Volume of Suction Gas, m³/kg	Compressor Displace-ment, L/s	Power Consump-tion, kW
	183 K Saturated Evaporating, 0 K Suction Superheat, 233 K Saturated Condensing									
1150	Ethylene	183	0.211	1.446	6.84	330.40	3.03	0.2422	0.733	0.373
170	Ethane	183	0.093	0.774	8.31	364.21	2.75	0.5257	1.443	0.347
13	Chlorotrifluoromethane	183	0.062	0.607	9.72	106.49	9.39	0.2263	2.125	0.358
23	Trifluoromethane	183	0.062	0.706	11.41	184.56	5.42	0.3438	1.863	0.372
508A	R-23/116 (39/61)	183	0.087	0.843	9.69	102.63	9.74	0.167	1.635	0.369
508B	R-23/116 (46/54)	183	0.086	0.847	9.85	110.49	9.05	0.179	1.620	0.368
	213 K Saturated Evaporating, 0 K Suction Superheat, 258 K Saturated Condensing									
1150	Ethylene	213	0.755	2.859	3.79	272.31	3.67	0.0729	0.268	0.314
170	Ethane	213	0.377	1.623	4.31	322.65	3.10	0.1430	0.443	0.279
23	Trifluoromethane	213	0.311	1.628	5.23	162.02	6.17	0.0756	0.467	0.296
13	Chlorotrifluoromethane	213	0.282	1.325	4.70	91.63	10.91	0.0549	0.600	0.293
125	Pentafluoroethane	213	0.056	0.404	7.20	117.76	8.49	0.2561	2.175	0.271
290	Propane	213	0.042	0.291	6.91	342.79	2.92	0.9343	2.726	0.254
22	Chlorodifluoromethane	213	0.037	0.296	7.90	195.80	5.11	0.5364	2.740	0.253
717	Ammonia	213	0.022	0.234	10.83	1242.9	0.81	4.7738	3.822	0.265
12	Dichlorodifluoromethane	213	0.023	0.183	8.09	138.57	7.22	0.6396	4.615	0.248
134a	Tetrafluoroethane	213	0.016	0.163	10.36	181.3	5.52	1.0904	6.012	0.251
410A	R-32/125 (50/50)	213	0.065	0.481	7.40	215.99	4.63	0.364	1.691	0.255
407C	R-32/125/134a (23/25/52)	213	0.034	0.300	8.82	202.07	4.95	0.608	3.017	0.255
	277 K Saturated Evaporating, 0 K Suction Superheat, 310 K Saturated Condensing									
T25	Pentafluoroethane	277	0.756	1.858	2.46	84.51	11.83	0.0210	0.249	0.165
290	Propane	277	0.533	1.272	2.39	279.91	3.57	0.0863	0.308	0.145
22	Chlorodifluoromethane	277	0.566	1.390	2.46	160.57	6.23	0.0415	0.258	0.142
717	Ammonia	277	0.494	1.423	2.88	1120.41	3.13	0.2606	0.817	0.137
500	R-12/152a (73.8/26.2)	277	0.413	1.053	2.55	141.50	7.07	0.0501	0.354	0.145
12	Dichlorodifluoromethane	277	0.352	0.891	2.53	117.99	8.48	0.0493	0.417	0.145
134a	Tetrafluoroethane	277	0.336	0.934	2.78	149.15	23.57	0.0608	1.433	0.144
124	Chlorotetrafluoroethane	277	0.188	0.543	2.89	126.55	7.90	0.0840	0.663	0.141
600a	Isobutane	277	0.181	0.493	2.73	270.81	3.69	0.2072	0.765	0.145
600	Butane	277	0.119	0.347	2.91	301.82	3.31	0.3170	1.050	0.141
11	Trichlorofluoromethane	277	0.047	0.156	3.33	158.67	22.15	0.3484	7.717	0.133
123	Dichlorotrifluoroethane	277	0.039	0.139	3.57	146.61	23.97	0.3790	9.083	0.135
113	Trichlorotrifluoroethane	277	0.018	0.070	3.87	127.46	7.85	0.6720	5.274	0.134
10A	R-32/125 (50/50)	277	0.916	2.286	2.5	160.67	6.22	0.0284	0.177	0.153
407C	R-32/125/134a (23/25/52)	277	0.581	1.551	2.67	159.54	6.27	0.0404	0.254	0.148

*The book by Walker (Appeadix D, 1982) has a guide to the literature of heat transfer in book form and deacribes the proprietary services HTFS (Heat Transfer and Fluid Services) and HTRI (Heat Transfer Research Inc.).
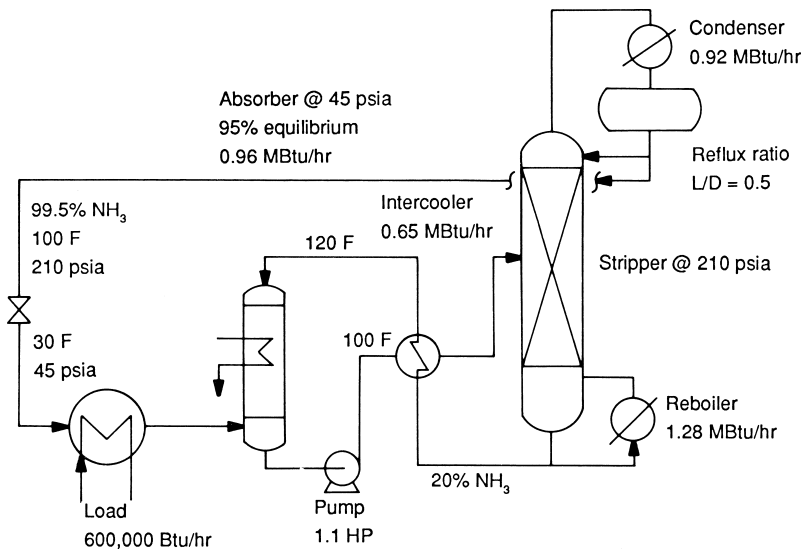
Figure 8.27. An ammonia absorption refrigeration process for a load of 50 tons at 30°F. The conditions were established by Hougen, Watson, and Ragatz. (Thermodynamics, *Wiley, New York, 1959, pp. 835–842*).

TABLE 8.24. Comparative Refrigerant Performance per Kilowatt of Refrigeration

No.	Refrigerant Chemical Name or Composition (% by mass)	Evaporator Pressure, MPa	Condenser Pressure, MPa	Compression Ratio	Net Refrigerating Effect, kJ/kg	Refrigerant Circulated, g/s	Liquid Circulated, L/s	Specific Volume of Suction Gas, m^3/kg	Compressor Displacement, L/s	Power Consumption, kW	Coefficient of Performance	Comp. Discharge Temp., K
170	Ethane	1.623	4.637	2.86	162.44	6.16	0.0232	0.0335	0.206	0.364	2.74	324
744	Carbon dioxide	2.291	7.208	3.15	134.24	7.45	0.0123	0.0087	0.065	0.338	2.96	343
13B1	Bromotrifluoromethane	0.536	1.821	3.39	66.14	15.12	0.0101	0.0237	0.358	0.274	3.65	313
1270	Propylene	0.362	1.304	3.60	286.48	3.49	0.0070	0.1285	0.449	0.221	4.54	375
290	Propane	0.291	1.077	3.71	279.88	3.57	0.0074	0.1542	0.551	0.211	4.74	320
502	R-22/115 (48.8/51.2)	0.349	1.319	3.78	104.39	9.58	0.0080	0.0500	0.479	0.226	4.43	310
507A	R-125/143a (50/50)	0.381	1.465	3.84	109.98	9.09	0.0089	0.0506	0.461	0.239	4.18	308
404A	R-125/143a/134a (44/52/4)	0.367	1.426	3.88	113.93	8.78	0.0086	0.0534	0.470	0.237	4.21	309
410A	R-32/125 (50/50)	0.481	1.88	3.91	167.68	5.96	0.0058	0.0542	0.318	0.227	4.41	324
125	Pentafluoroethane	0.400	1.570	3.93	87.76	11.39	0.0098	0.0394	0.449	0.272	3.68	315
22	Chlorodifluoromethane	0.296	1.190	4.02	163.79	6.09	0.0052	0.0785	0.478	0.215	4.65	327
12	Dichlorodifluoromethane	0.183	0.745	4.07	116.58	8.58	0.0066	0.0914	0.784	0.213	4.69	311
500	R-12/152a (73.8/26.2)	0.214	0.879	4.11	140.95	7.09	0.0062	0.0938	0.665	0.213	4.69	314
407C	R-32/125/134a (23/25/52)	0.290	1.264	4.36	162.28	6.16	0.0055	0.0796	0.492	0.222	4.51	320
600a	Isobutane	0.089	0.407	4.60	262.84	3.80	0.0070	0.4029	1.533	0.220	4.55	318
134a	Tetrafluoroethane	0.164	0.770	4.69	149.95	6.66	0.0056	0.1223	0.814	0.217	4.60	309
124	Chlorotetrafluoroethane	0.090	0.440	4.89	118.49	8.44	0.0063	0.1705	1.439	0.224	4.47	305
717	Ammonia	0.236	1.164	4.94	1102.23	0.91	0.0015	0.5106	0.463	0.207	4.84	371
600	Butane	0.056	0.283	5.05	292.01	3.42	0.0060	0.6641	2.274	0.214	4.68	318
114	Dichlorotetrafluoroethane[a]	0.047	0.252	5.41	99.19	10.08	0.0070	0.2700	2.722	0.225	4.44	303
11	Trichlorofluoromethane	0.020	0.126	6.24	156.22	6.40	0.0044	0.7641	4.891	0.196	5.09	313
123	Dichlorotrifluoroethane	0.016	0.110	7.06	142.76	7.00	0.0048	0.8953	6.259	0.205	4.86	305
113	Trichlorotrifluoroethane[a]	0.007	0.054	7.84	127.34	7.85	0.0051	1.6793	13.187	0.205	4.88	303

Notes: Data based on 258 K evaporation, 303 K condensation, 0 K subcool, and 0 K superheat.
[a]Saturated suction except R-113 and R-114. Enough superheat was added to give saturated discharge.
(2001 ASHRAE Handbook, Fundamentals, p. 19.8, Table 7).

REFERENCES

K.J. Bell and M.A. Ghaly, An approximate generalized design method for multicomponent partial condensers, *Chem. Eng. Prog. Symp. Ser.* **131,** 72–79 (1973).

V. Cavaseno et al. (Eds.), *Process Heat Exchange*, McGraw-Hill, New York, 1979.

D. Chisholm (Ed.), *Developments in Heat Exchange Technology I*, Applied Science, London, 1980.

J.R. Fair, Process heat transfer by direct fluid-phase contact, *Chem. Eng. Prog. Symp. Ser.* **118,** 1–11 (1972); *Chem. Eng.*, (12 June 1972).

V. Ganapathy, *Applied Heat Transfer*, PennWell Books, Tulsa, OK, 1982.

H. Gröber, S. Erk, and U. Grigull, *Fundamentals of Heat Transfer*, McGraw-Hill, New York, 1961.

H. Hausen, *Heat Transfer in Counterflow, Parallel Flow and Cross Flow*, McGraw-Hill, New York, 1983.

HEDH, *Heat Exchanger Design Handbook* (E.U. Schlünder et al., Eds.), Hemisphere, New York, 1983–date, 5 vols.

M. Jakob, *Heat Transfer*, Wiley, New York, 1957, Vol. 2.

S. Kakac, A.E. Bergles, and F. Mayinger (Eds.), *Heat Exchangers: Thermal-Hydraulic Fundamentals and Design*, Hemisphere, New York, 1981.

W.M. Kays and A.L. London, *Compact Heat Exchangers*, McGraw-Hill, New York, 1984.

D.Q. Kern, *Process Heat Transfer*, McGraw-Hill, New York, 1950.

S.K. Kutateladze and V.M. Borishanskii, *Concise Encyclopedia of Heat Transfer*, Pergamon, New York, 1966.

E.E. Ludwig, *Applied Process Design for Chemical and Petrochemical Plants*, Gulf, Houston, 1983, Vol. 3, pp. 1–200.

P.E. Minton, Designing spiral plate and spiral tube exchangers, *Chem. Eng.*, (4 May 1970); (18 May 1970).

R.K. Neeld and J.T. O'Bara, Jet trays in heat transfer service, *Chem. Eng. Prog.* **66**(7), 53 1970.

P.A. Schweitzer (Ed.), *Handbook of Separation Techniques for Chemical Engineers*, McGraw-Hill, New York, 1979, Sec. 2.3, Evaporators, Sec. 2.4, Crystallizers.

L. Silver, Gas cooling with aqueous condensation, *Trans. Inst. Chem. Eng.* **25,** 30–42 (1947).

E.F.C. Somerscales and J.G. Knudsen (Eds.), *Fouling of Heat Transfer Equipment*, Hemisphere, New York, 1981.

J. Taborek, G.F. Hewitt, and N. Afgan (Eds.), *Heat Exchangers Theory and Practice*, Hemisphere, New York, 1983.

TEMA Standards, Tubular Exchanger Manufacturers Association, Tarrytown, NY, 1978.

G. Walker, *Industrial Heat Exchangers*, Hemisphere, New York, 1982.[*]

R.H. Perry and D.W. Green, Perry's Chemical Engineers' Handbook, 7th ed., McGraw-Hill, 1997.

O. Cornell, W.G. Knapp and J.R. Fair, "Mass Transfer Efficiency–Packed columns–Part 1, CEP, Vol. 56, No. 7, July 1960, P. 68–74."

Fired Heaters (see also Ganapathy, HEDH, and Kern above)

F.A. Holland, R.M. Moores, F.A. Watson, and J.K. Wilkinson, *Heat Transfer*, Heinemann, London, 1970.

H.C. Hottel, in *McAdams Heat Transmission*, McGraw-Hill, New York, 1954.

W.E. Lobo and J.E. Evans, Heat transfer in the radiant section of petroleum heaters, *Trans. AIChE* **35,** 743 (1939).

C.C. Monrad, Heat transmission in the convection section of pipe stills, *Ind. Eng. Chem.* **24,** 505 (1932).

D.W. Wilson, W.E. Lobo, and H.C. Hottel, Heat transmission in the radiant section of tube stills, *Ind. Eng. Chem.* **24,** 486 (1932).

R.N. Wimpress, Rating fired heaters, *Hydrocarbon Process.* **42**(10), 115–126 (1963); Generalized method predicts fired-heater performance, *Chem. Eng.*, 95–102 (22 May 1978).

Selected American Petroleum Institute Standards (API, Washington, D.C.)

Std. 660, Shell-and-Tube Heat Exchangers for General Refinery Services, 1982.

Std. 661, Air-Cooled Heat Exchangers for General Refinery Services, 1978.

Std. 665, API Fired Heater Data Sheet, 1966, 1973.

Insulation

Marks' Standard Handbook for Mechanical Engineers, McGraw-Hill, New York, 1996.

H.F. Rase and M.H. Barrow, *Project Engineering of Process Plants*, Wiley, New York, 1957, Chap. 19.

G.B. Wilkes, *Heat Insulation*, Wiley, New York, 1950.

Refrigeration

A. Arkhanov, I. Marfenina, Ye. Mikulin, *Theory and Design of Cryogenic Systems*, Mir Publishers, Moscow, 1981.

2001 ASHRAE HANDBOOK, American Society of Heating, Refrigeration and Air-Conditioning Engineers, 2001.

M. Bogart, *Ammonia Absorption Refrigeration in Industrial Processes*, Gulf, Houston, 1981.

Carrier System Design Manual, Carrier Air Conditioning Co., Syracuse, NY, 1964, Part 4, Refrigerants, brines and oils.

F.L. Evans, *Equipment Design Handbook for Refineries and Chemical Plants*, Gulf, Houston, 1979, Vol. 1, pp. 172–196.

T.M. Flynn and K.D. Timmerhaus, Cryogenic processes, in *Chemical Engineers Handbook*, 1984, pp. 12.46–12.58.

W.B. Gosney, *Principles of Refrigeration*, Cambridge University Press, Cambridge, 1982.

E.E. Ludwig, *Applied Process Design for Chemical and Petroleum Plants*, Gulf, Houston, 1983, Vol. 1, pp. 201–250.

Y.R. Mehra, Refrigerating properties of ethylene, ethane, propylene and propane, *Chem. Eng.*, 97 (18 Dec. 1978); 131 (15 Jan. 1979); 95 (12 Feb. 1979); 165 (26 Mar. 1979).

9

DRYERS AND COOLING TOWERS

he processes of the drying of solids and the evaporative cooling of process water with air have a common foundation in that both deal with interaction of water and air and involve simultaneous heat and mass transfer. Water cooling is accomplished primarily in packed towers and also in spray ponds or in vacuum spray chambers, the latter for exceptionally low temperatures. Although such equipment is comparatively simple in concept, it is usually large and expensive, so that efficiencies and other aspects are considered proprietary by the small number of manufacturers in this field.

In contrast, a great variety of equipment is used for the drying of solids. Thomas Register and Chemical Engineering Buyers' Guide (2003) list many manufacturers of drying equipment, classified according to the type of equipment or the nature of the material being dried. An indication of the difficulty of any process is the vast amount of equipment available, and drying is a good example. Dryers may perform additional tasks besides the handling and transporting of the product being dried. For example, perforated belt conveyors and pneumatic conveyors through which hot air is blown transport material, while other models have the ability to cool, react, heat treat, calcinate, humidify, agglomerate, sublime, or roast. These processes can be done separately

or, if required, combined with each other. Solids being dried cover a range of sizes from micron-sized particles to large slabs and may have varied and distinctive drying behaviors. As in some other long-established industries, drying practices of necessity have outpaced drying theory. In the present state of the art, it is not possible to design a dryer by theory without experience, but a reasonably satisfactory design is possible from experience plus a little theory.

Performances of dryers with simple flow patterns can be described with the aid of laboratory drying rate data. In other cases, theoretical principles and correlations of rate data are of value largely for appraisal of the effects of changes in some operating conditions when a basic operation is known. The essential required information is the residence time in the particular kind of dryer under consideration. Along with application of available rules for vessel proportions and internals to ensure adequate contact between solids and air, material and energy balances complete a process design of a dryer.

In order to aid in the design of dryers by analogy, examples of dimensions and performances of the most common types of dryers are cited in this chapter. Theory and correlation of heat and mass transfer are treated in detail elsewhere in this book, but their use in the description of drying behavior will be indicated here.

9.1. INTERACTION OF AIR AND WATER

Besides the obvious processes of humidification and dehumidification of air for control of environment, interaction of air and water is a major aspect of the drying of wet solids and the cooling of water for process needs. Heat and mass transfer then occur simultaneously. For equilibrium under adiabatic conditions, the energy balance is

$$k_g \lambda = (p_s - p) = h (T - T_w), \tag{9.1}$$

where k_g = mass transfer coefficient
λ = latent heat of vaporization
h = heat transfer coefficient
p_s = partial pressure of water at saturation
p = partial pressure of water at operating conditions
T = absolute temperature
T_w = wet bulb temperature

All the symbols must be in consistent set of units, be they English or SI.

The moisture ratio, H lb water/lb dry air, is related to the partial pressure of the water in the air by

$$H = \frac{18}{29}\frac{p}{P - p} \simeq \frac{18}{29}\frac{p}{P}, \tag{9.2}$$

where p = partial pressure of water
P = total pressure on system

the approximation being valid for relatively small partial pressures. Accordingly, the equation of the adiabatic saturation line may be written

$$H_s - H = (h/\lambda k)(T - T_w) \tag{9.3}$$
$$= (C/\lambda)(T - T_s). \tag{9.4}$$

where H_s = humidity at adiabatic saturation conditions
T_s = adiabatic saturation temperature

For water, numerically $C \simeq h/k$, so that the wet bulb and adiabatic saturation temperatures are identical. For other vapors, this conclusion is not correct and C must be determined.

For practical purposes, the properties of humid air are recorded on psychrometric (or humidity) charts such as those of Figures 9.1 and 9.2, but tabulated data and equations also are available for greater accuracy. A computer version is available (Wiley Professional Software, Wiley, New York). The terminal properties of a particular adiabatic humification of air are located on the same saturation line, one of those sloping upwards to the left on the charts. For example, all of these points are on the same saturation line: $(T, H) = (250, 0.008), (170, 0.026)$ and $(100, 0.043)$; the saturation enthalpy is 72 Btu/lb dry, but the individual enthalpies are less by the amounts 2.5, 1.2, and 0, respectively.

Properties such as moisture content, specific volume, and enthalpy are referred to unit mass of dry air. Figures 9.1 and 9.2 are psychometric charts in English units of lb, cuft, F, and Btu. The data are for standard atmospheric pressure. How to correct them for minor deviations from standard pressure is explained for example in *Chemical Engineers' Handbook* (1999). An example of
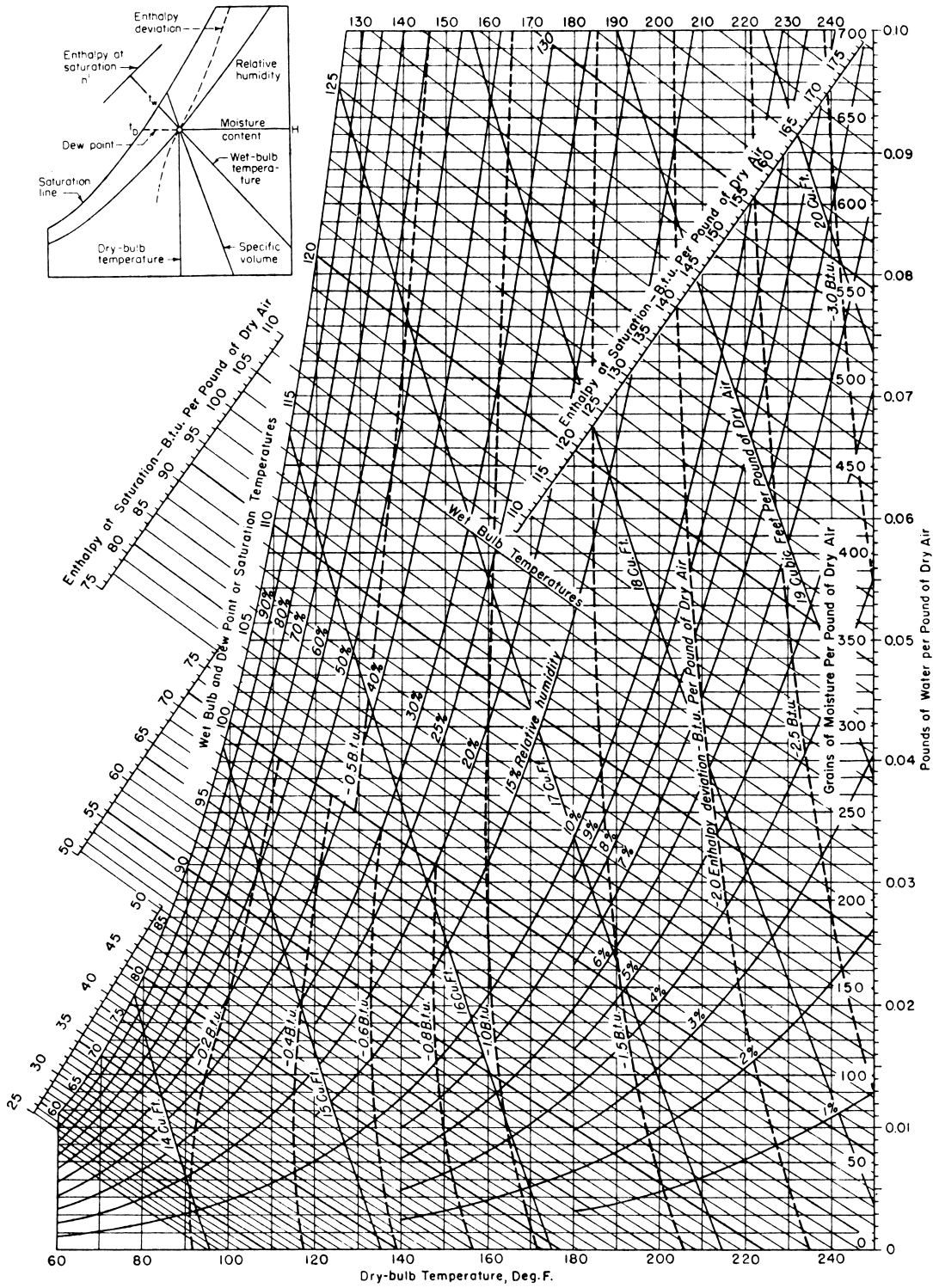
Figure 9.1. Psychrometric chart in English units (*Carrier Corp. Syracuse, NY*). Example: For air at 200°F with $H = 0.03$ lb/lb: $T_s = 106.5°F$, $V_h = 17.4$ cuft/lb dry, $100H/H_s = 5.9°$, $h = h_s + D = 84 - 1.7 = 82.3$ Btu/lb dry. (Walas, 1988).
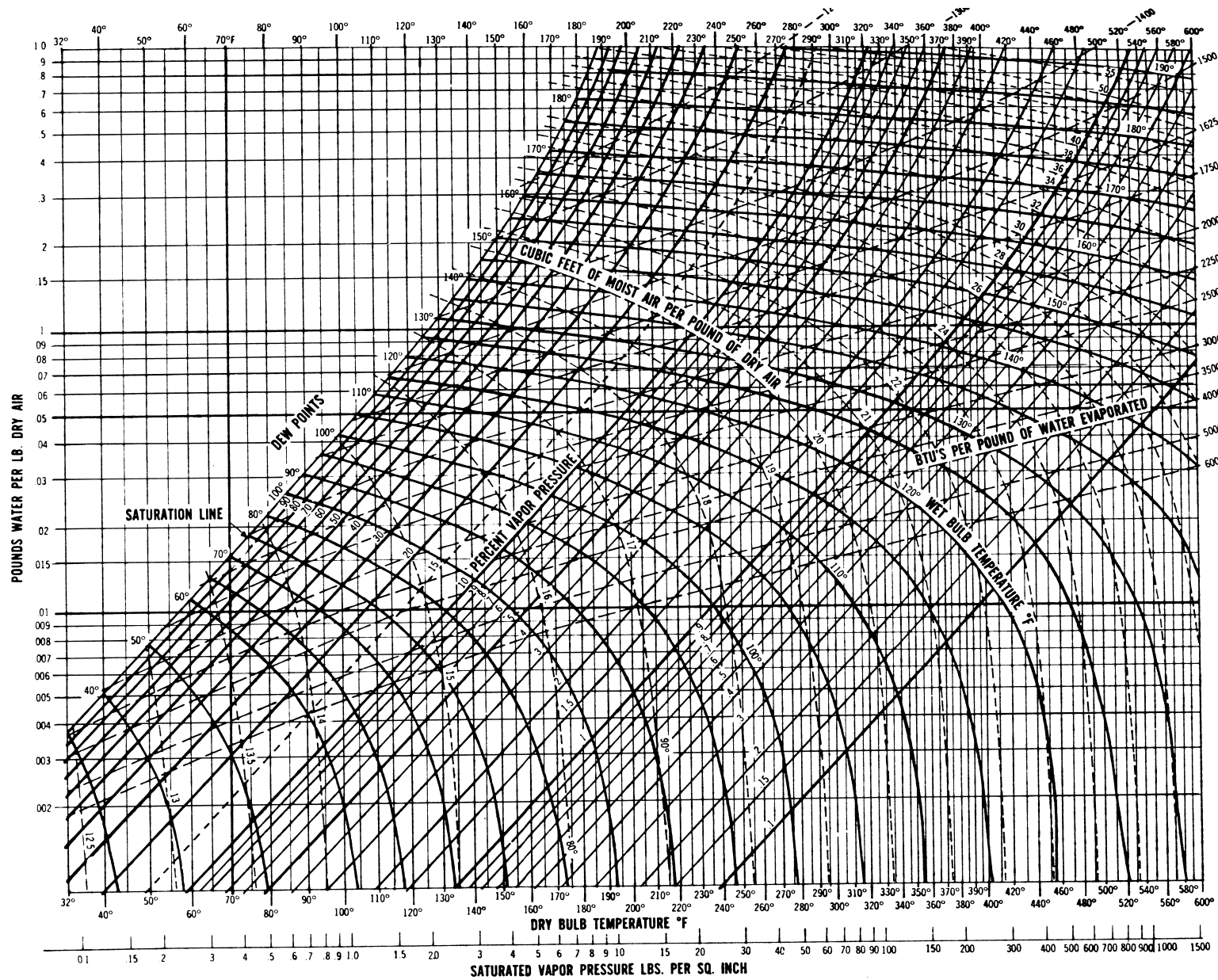
Figure 9.2. Psychometric chart for a wide temperature range, 32–600°F (*Proctor and Schwartz, Inc., Horsham, PA*; Walas, 1988).

227

reading the charts is with the legend of Figure 9.1. Definitions of common humidity terms and their units are given following.

1. Humidity is the ratio of mass of water to the mass of dry air,

$$H = W_w/W_a. \tag{9.5}$$

where W_w = mass of water
W_a = mass of air

2. Relative humidity or relative saturation is the ratio of the prevailing humidity to the saturation humidity at the same temperature, or the ratio of the partial pressure to the vapor pressure expressed as a percentage,

$$\%RH = 100H/H_s = 100p/p_s. \tag{9.6}$$

3. The relative absolute humidity is

$$(H/H_s)_{absolute} = (\frac{p}{P-p})/(\frac{p_s}{P-p_s}) \tag{9.7}$$

4. Vapor pressure of water is given as a function of temperature by

$$p_s = \exp(11.9176 - 7173.9/(T + 389.5)), \text{atm}, °F. \tag{9.8}$$

5. The humid volume is the volume of 1 lb of dry air plus the volume of its associated water vapor,

$$V_h = 0.73(1/29 + h/18)(T + 459.6)/P,$$
$$\text{cuft/(lb dry air).} \tag{9.9}$$

where V_h = humid volume

6. Humid specific heat is

$$C_h = C_a + C_w H = 0.24 + 0.45H,$$
$$\text{Btu/(F)(lb dry air).} \tag{9.10}$$

where C_h = humid specific heat
C_a = specific heat of air
C_w = specific heat of water

7. The wet bulb temperature T_w is attained by measurement under standardized conditions. For water, T_w is numerically nearly the same as the adiabatic saturation temperature T_s.

8. The adiabatic saturation temperature T_s is the temperature attained if the gas were saturated by an adiabatic process.

9. With heat capacity given by item 6, the enthalpy of humid air is

$$h = 0.24T + (0.45T + 1100)H. \tag{9.11}$$

where h = enthalpy of humid air.

On the psychrometric chart of Figure 9.1, values of the saturation enthalpy h_s and a correction factor D are plotted. In these terms the enthalpy is

$$h = h_s + D. \tag{9.12}$$

In Figure 9.2, the enthalpy may be found by interpolation between the lines for saturated and dry air.

In some periods of drying certain kinds of solids, water is brought to the surface quickly so that the drying process is essentially evaporation of water from the free surface. In the absence of intentional heat exchange with the surrounding or substantial heat losses, the condition of the air will vary along the adiabatic saturation line. Such a process is analyzed in Example 9.1.

For economic reasons, equilibrium conditions cannot be approached closely. In a cooling tower, for instance, the effluent air is not quite saturated, and the water temperature is not quite at the wet bulb temperature. Percent saturation in the vicinity of 90% often is feasible. Approach is the difference between the temperatures of the water and the wet bulb. It is a significant determinant of cooling tower size as these selected data indicate:

Approach (°F)	5	10	15	20	25
Relative tower volume	2.4	1.6	1.0	0.7	0.55

Other criteria for dryers and cooling towers will be cited later.

9.2. RATE OF DRYING

In a typical drying experiment, the moisture content and possibly the temperature of the material are measured as functions of the time. The inlet and outlet rates and compositions of the gas also are noted. From such data, the variation of the rate of drying with either the moisture content or the time is obtained by mathematical differentiation. Figure 9.3(d) is an example. The advantage of expressing drying data in the form of rates is that their dependence on thermal and mass transfer driving forces is more simply correlated. Thus, the general drying equation may be written

---

EXAMPLE 9.1
Conditions in an Adiabatic Dryer
The air to a dryer has a temperature of 250°F and a wet bulb temperature of 101.5°F and leaves the process at 110°F. Water is

T₁ = 250 F
T_{wb} = 101.5 F
H = 0.010 lb/lb dry
V_h = 18.2 cuft/lb dry
Water 1500 lb/hr
Air In
Air Out
T₂ = 100 F
H = 0.043
$100H/H_s$ = 73%
V_h = 15.3 cuft/lb dry
Product
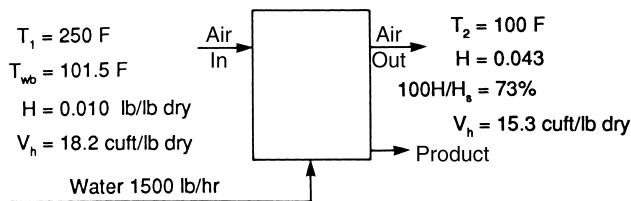
evaporated off the surface of the solid at the rate of 1500 lb/hr. Linear velocity of the gas is limited to a maximum of 15 ft/sec. The diameter of the vessel will be found.
Terminal conditions of the air are read off the adiabatic saturation line and appear on the sketch:

$$\text{Dry air} = \frac{1500}{0.043 - 0.010} = 45,455\text{lb/hr}$$

$$\rightarrow \frac{45,455(18.2)}{3600} = 229.8\text{cfs,}$$

$$D = \sqrt{229.8/15(\pi/4)} = 4.4\text{ft.}$$
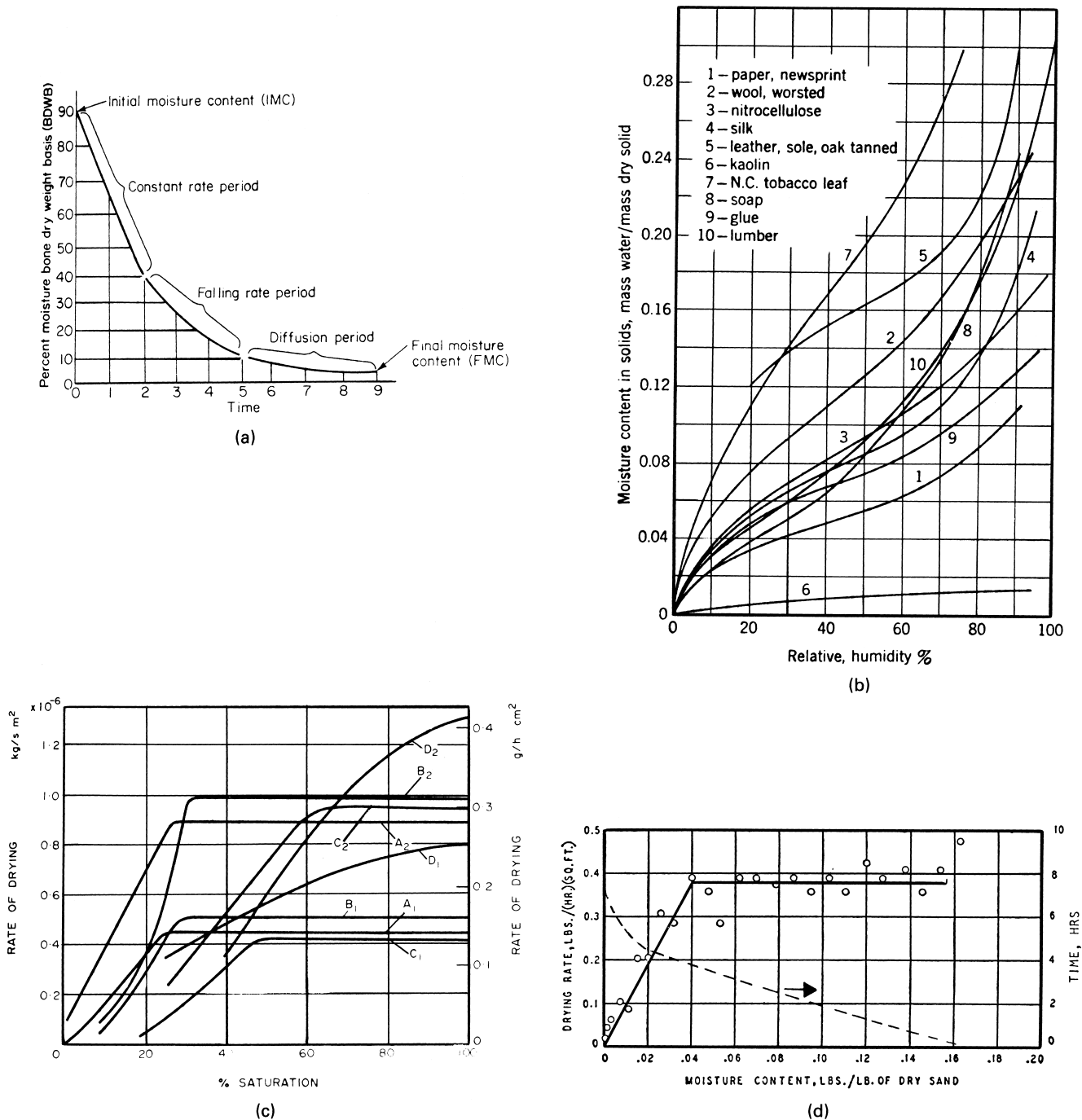
Figure 9.3. (a) Classic drying curve of moisture content against time; a heat-up period in which no drying occurs also is usually present (*Proctor and Schwartz, Inc.; Schweitzer, p. 4.144*). (b) Equilibrium moisture content as a function of relative humidity; many other data are tabulated in Chemical Engineers Handbook (*McGraw-Hill, New York, 1984, 20.12*). (*These data are from National Academy of Science, copyright 1926.*) (c) Rate of drying as a function of % saturation at low (subscript 1) and high (subscript 2) drying rates: (A) glass spheres, 60 μm, bed 51 mm deep; (B) silica flour, 23.5 μm, 51 mm deep; (C) silica flour, 7.5 μm, 51 mm bed; (D) silica flour, 2.5 μ, 65 mm deep (*data of Newitt et al.*, Trans. Inst. Chem. Eng. **27,** *1 (1949)*. (d) Moisture content, time and drying rates in the drying of a tray of sand with superheated steam; surface 2.35 sqft, weight 27.125 lb. The scatter in the rate data is due to the rough numerical differentiation (*Wenzel, Ph.D. thesis, University of Michigan, 1949*). (e) Temperature and drying rate in the drying of sand in a tray by blowing air across it. Dry bulb 76.1°C, wet bulb 36.0°C (*Ceaglske and Hougen*, Trans. AIChE **33,** *283 (1937)*. (f) Drying rates of slabs of paper pulp of several thicknesses *[after McCready and McCabe,* Trans. AIChE **29,** *131 (1933)].* (g) Drying of asbestos pulp with air of various humidities *[McCready and McCabe,* Trans. AIChE **29,** *131 (1933)].* (h) Effect of temperature difference on the coefficient K of the falling rate equation $-dW/d\theta = KW$ *[Sherwood and Comings,* Trans. AIChE **27,** *118 (1932)].* (i) Effect of air velocity on drying of clay slabs. The data are represented by $R = 2.0u^{0.74}(H_w - H)$. The dashed line is for evaporation in a wetted wall tower (*Walker, Lewis, McAdams, and Gilliland,* Principles of Chemical Engineering, *McGraw-Hill, New York, 1937*). (Walas, 1988).

(e)

(f)

(g)

(h)

(i)
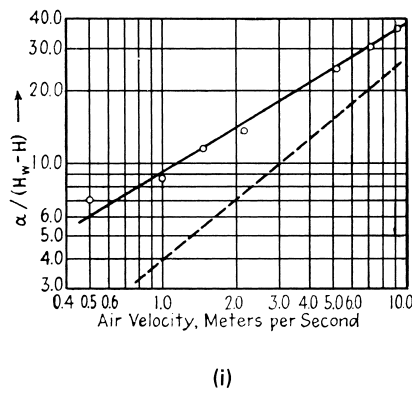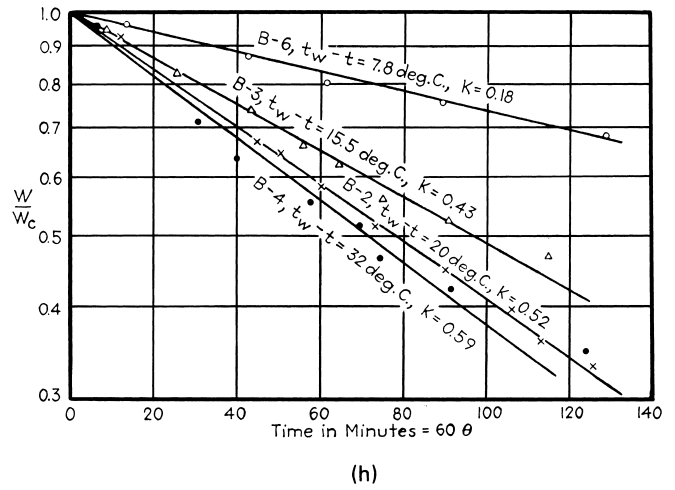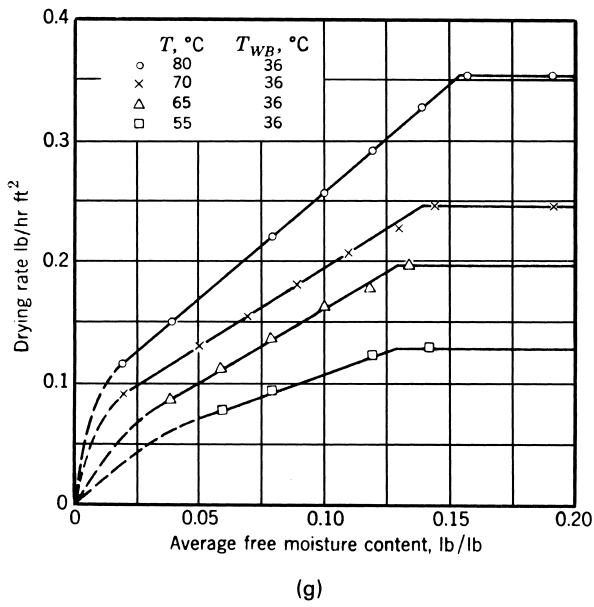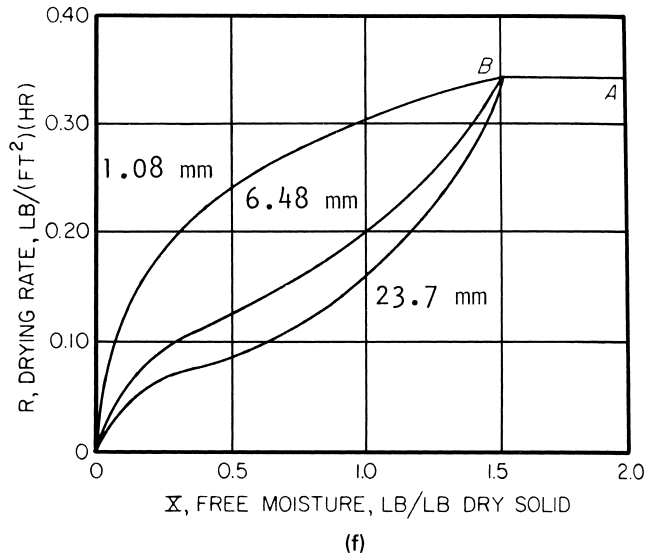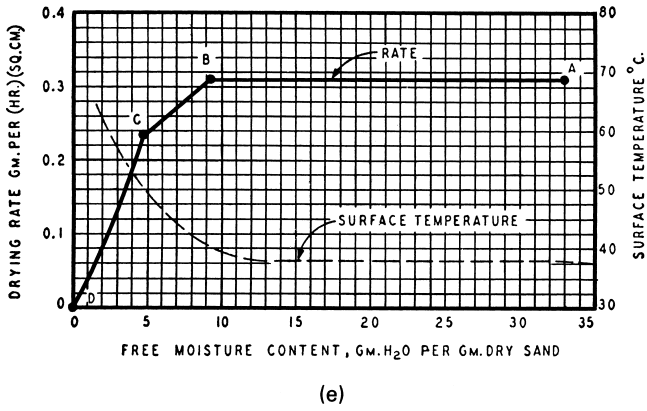
Figure 9.3.—(*continued*)

$$-\frac{1}{A}\frac{dW}{d\theta} = h(T_g - T) = k_p(P - P_g) = k_H(H - H_g), \qquad (9.13)$$

where subscript g refers to the gas phase and H is the moisture content, (kg/kg dry material), corresponding to a partial or vapor pressure P. Since many correlations of heat and mass transfer coefficients are known, the effects of many changes in operating conditions on drying rates may be ascertainable. Figures 9.3(g) and (h) are experimental evidence of the effect of humidity of the air and (i) of the effect of air velocity on drying rates.

Other factors, however, often complicate drying behavior. Although in some ranges of moisture contents the drying process may be simply evaporation from a surface, the surface may not dry uniformly and consequently the effective amount of surface may change as time goes on. Also, resistance to diffusion and capillary flow of moisture may develop for which there are no adequate correlations to describe these phenomena. Furthermore, shrinkage may occur on drying, particularly near the surface, which hinders further movement of moisture outwards. In other instances, agglomerates of particles may disintegrate on partial drying.

Some examples of drying data appear in Figure 9.3. Commonly recognized zones of drying behavior are represented in Figure 9.3(a). Equilibrium moisture contents assumed by various materials in contact with air of particular humidities is represented by (b). The shapes of drying rate curves vary widely with operating conditions and the physical state of the solid; (b) and others are some examples. No correlations have been developed or appear possible whereby such data can be predicted. In higher ranges of moisture content of some materials, the process of drying is essentially evaporation of moisture off the surface, and its rate remains constant until the surface moisture is depleted as long as the condition of the air remains the same. During this period, the rate is independent of the nature of the solid. The temperature of the evaporate assumes the wet bulb temperature of the air. Constant rate zones are shown in (d) and (e), and (e) indicates that temperatures are truly constant in such a zone.

The moisture content at which the drying rate begins to decline is called critical moisture content. Some of the variables on which the transition point depends are indicated in Figures 9.3(c) and (g)—for example, the nature of the material, the average free moisture content, and so on. The shape of the falling rate curve sometimes may be approximated by a straight line, with equation

$$-\frac{dW}{d\theta} = k(W - W_e), \qquad (9.14)$$

where W_e is the equilibrium moisture content. When W_e is zero as it often is of nonporous granular materials, the straight line goes through the origin. (d) and (h) illustrate this kind of behavior. The drying time, θ_1 is found by integration of the rate plots or equations. The process is illustrated in Example 9.2 for straight line behavior. Other cases require numerical integration. Each of the examples of Figure 9.3 corresponds to a particular substantially constant gas condition. This is true of shallow bed drying without recirculation of humid gas, but in other kinds of drying equipment the variation of the rate with time and position in the equipment, as well as with the moisture content, must be taken into account.

An approximation that may be justifiable is that the critical moisture content is roughly independent of the drying conditions and that the falling rate curve is linear. Then the rate equations may be written

$$-\frac{1}{A}\frac{dW}{d\theta} = \begin{cases} k(H_s - H_g), & W_c < W < W_o, \\ \frac{k(H_s - H_g)(W - W_e)}{W_c - W_e}, & W_e < W < W_e \end{cases} \qquad (9.15)$$

Examples 9.3 and 9.4 apply these relations to a countercurrent dryer in which the humidity driving force and the equilibrium moisture content vary throughout the equipment.

LABORATORY AND PILOT PLANT TESTING

The techniques of measuring drying of stationary products, as on trays, are relatively straightforward. Details may be found in the references made with the data of Figure 9.3. Mass transfer resistances were eliminated by Wenzel (1951) through use of superheated steam as the drying medium.

In some practical kinds of dryers, the flow patterns of gas and solid are so complex that the kind of rate equation discussed in this section cannot be applied readily. The sizing of such equipment is essentially a scale-up of pilot plant tests in similar equipment. Some manufacturers make such test equipment available. The tests may establish the residence time and the terminal conditions of the gas and solid.

In an effort to reduce exhaust to the atmosphere, save heat, minimize pollutant discharges, and keep costs at a minimum, partial recycle is used (Cook, 1996).

Walas (1988) presented minimum sizes of laboratory and pilot plant drying equipment for full-size plant equipment. Scale-up factors as small as 2 may be required in critical cases; however, factors of 5 or more often are practicable, particularly when

---

EXAMPLE 9.2
Drying Time over Constant and Falling Rate Periods with Constant Gas Conditions

The data of Figure 9.3(d) were obtained on a sample that contained 27.125 lb dry sand and had an exposed drying surface of 2.35 sqft. Take the case of a sample that initially contained 0.168 lb moisture/lb dry material and is to be dried to $W = 0.005$ lb/lb. In these units, the constant rate shown on the graph is transformed to $-(1/2.35)(dW/d\Theta) = $ [(constant drying rate, lb/hr sqft) / (lb dry solid)]

$$-\frac{1}{2.35}\frac{dW}{d\theta} = \frac{0.38}{27.125} \text{ (lb/lb)/(hr)(sqft)},$$

which applies down to the critical moisture content $W_c = 0.04$ lb/lb. The rate behavior over the whole moisture range is

$$-\frac{dW}{d\theta} = \begin{cases} 0.03292, & 0.04 < W < 0.168, \\ 0.823W, & W < 0.04 \end{cases}.$$

Accordingly, the drying time is

$$\begin{aligned} \theta &= \frac{W - W_c}{0.03292} + \frac{1}{0.823}\ln\left(\frac{W_c}{W}\right) \\ &= \frac{0.168 - 0.04}{0.03292} + \frac{1}{0.823}\ln\left(\frac{0.04}{0.005}\right) \\ &= 6.42 \text{ hr}. \end{aligned}$$

This checks the drying time from the plot of the original data on Figure 9.3(d).

EXAMPLE 9.3
Drying with Changing Humidity of Air in a Tunnel Dryer
A granular material deposited on trays or a belt is moved through a tunnel dryer countercurrently to air that is maintained at 170°F with steam-heated tubes. The stock enters at 1400 lb dry/hr with $W = 1.16$ lb/lb and leaves with 0.1 lb/lb. The air enters at 5% relative humidity ($H_g = 0.0125$ lb/lb) and leaves at 60% relative humidity at 170°F ($H_g = 0.203$ lb/lb). The air rate found by moisture balance is 7790 lb dry/hr:
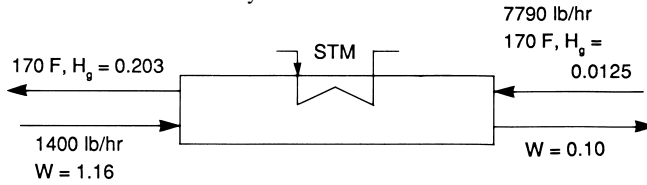
Drying tests reported by Walker, Lewis, McAdams, and Gilliland, *Principles of Chemical Engineering*, McGraw-Hill, New York, (1937, p. 671) may be represented by the rate equation

$$-100\frac{dW}{d\theta} = \begin{cases} 0.28((\text{lb/lb})/\text{hr}, & W_c < W < W_0 \quad 0.58 < W <,1.16, \\ 0.28(W - W_e)/(0.58 - W_e), & W_e < W < W_c \\ W_e < W < 0.58. \end{cases}$$

(1)

The air was at 95°F and 7% relative humidity, corresponding to a humidity driving force of $H_s - H_g = 0.0082$. Equilibrium moisture content as a function of the fraction relative humidity (RH), and assumed independent of temperature, is represented by

$$W_e = 0.0036 + 0.1539(\text{RH}) - 0.097(\text{RH})^2.$$

(2)

The critical moisture content is assumed indpendent of the drying rate. Accordingly, under the proposed operating conditions, the rate of drying will be

$$-100\frac{dW}{d\theta} = \begin{cases} \dfrac{0.28(H_s - H_g)}{0.0082}, & 0.58 < W < 1.16, \\ \dfrac{0.28(H_s - H_g)(W - W_e)}{0.0082(0.58 - 0.014)}, & W_e < W < 0.58. \end{cases}$$

(3)

With moisture content of the stock as a parameter, the humidity of the air is calculated by moisture balance from

$$H_g = 0.0125 + (1400/7790)(W - 0.1).$$

(4)

The corresponding relative humidities and wet bulb temperatures and corresponding humidities H_s are read off a psychrometric chart. The equilibrium moisture is found from the relative humidity by Eq. (2). The various corrections to the rate are applied in Eq. (3). The results are tabulated, and the time is found by integration of the rate data over the range $0.1 < W < 1.16$.

W	H_g	H_s	RH	W_e	Rate	1/Rate
1.16	0.203	0.210			0.239	4.184
1.00	0.174	0.182			0.273	3.663
0.9	0.156	0.165			0.303	3.257
0.8	0.138	0.148			0.341	2.933
0.7	0.120	0.130			0.341	2.933
0.58	0.099	0.110	0.335	0.044	0.356	2.809
0.50	0.084	0.096	0.29	0.040	0.333	3.003
0.4	0.066	0.080	0.24	0.035	0.308	3.247
0.3	0.048	0.061	0.18	0.028	0.213	4.695
0.2	0.030	0.045	0.119	0.021	0.162	6.173
0.1	0.0125	0.0315	0.050	0.011	0.102	9.804

The drying time is

$$\theta = \int_{1.16}^{0.10} \frac{dw}{\text{rate}} = 4.21 \text{hr, by trapezoidal rule.}$$

The length of tunnel needed depends on the space needed to ensure proper circulation of air through the granular bed. If the bed moves through the dryer at 10 ft/hr, the length of the dryer must be at least 42 ft.

Length of dryer $= (4.21\,\text{hr})\,(10\,\text{ft/hr}) = 42.1$ ft
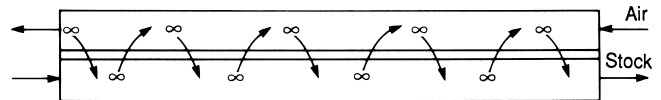
analyzed by experienced persons. Moyers (1992) presented information on the testing of small quantities of solids and the reliability of scale up from these tests. Tray, plate, and fluid-bed units can be tested using small quantities of material and the scale up is reliable; however, rotary, flash, and spray dryers do not provide for reliable scale up from small quantities of solids.

9.3. CLASSIFICATION AND GENERAL CHARACTERISTICS OF DRYERS

Removal of water from solids is most often accomplished by contacting them with air of low humidity and elevated temperature. Less common, although locally important, drying processes apply heat radiatively or dielectrically; in these operations as in freeze drying, the role of any gas supply is that of entrainer of the humidity.

The nature, size, and shape of the solids, the scale of the operation, the method of transporting the stock and contacting it with gas, the heating mode, etc. are some of the many factors

that have led to the development of a considerable variety of equipment.

Elaborate classification of dryers has been presented by Kroll (1978) and Keey (1972) but less comprehensive (but perhaps more practical) classifications are shown in Table 9.1. In this table, the method of operation, physical form of the stock, scale of production, special features, and drying time are presented. Two other classifications of dryers may be found in Perry (1999). One classifies the equipment on the basis of heat transfer (Figure 12-45) and the other on the basis of the material handled (Table 12-9) in Perry.

In a later section, the characteristics and performances of the most widely used equipment will be described in some detail. Many types are shown in Figure 9.4. Here some comparisons are made. Evaporation rates and thermal efficiencies are compared in Table 9.2, while similar and other data appear in Table 9.3. The wide spreads of these numbers reflect the diversity of individual designs of the same general kind of equipment, differences in moisture contents, and differences in drying properties of various materials. Fluidized bed dryers, for example, are operated as batch or

EXAMPLE 9.4
Effects of Moist Air Recycle and Increase of Fresh Air Rate in Belt Conveyor Drying

The conditions of Example 9.3 are taken except that recycle of moist air is employed and the equilibrium moisture content is assumed constant at $W_e = 0.014$. The material balance in terms of the recycle ratio R appears on the sketch:

A = 7790 R
W = 1581.4 R

A = 7790
W = 1581.4

A = 7790
W = 97.4

170° F

S = 1400
W = 140

S = 1400
W = 1624

A = air, W = water, S = dry solid
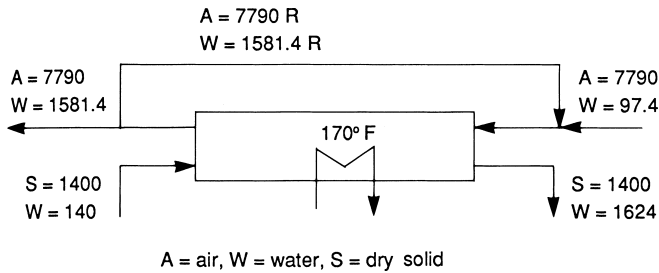
Humidity of the air at any point is obtained from the water balance

$$H_g = \frac{1581.4R + 97.4 + 1400(W - 0.1)}{7790(R + 1)}. \tag{1}$$

$$[97.4(R + 1) + 1400(W - 0.1)] / [7790(R + 1)] \tag{1a}$$

The vapor pressure is

$$p_s = \exp\left[11.9176 - 7173.9/(T_s + 389.5)\right] \text{atm}. \tag{2}$$

The saturation humidity is

$$H_s = (18/29)p_s/(1 - p_s). \tag{3}$$

The heat capacity is

$$C = 0.24 + 0.45H_g. \tag{4}$$

With constant air temperature of 170°F, the equation of the adiabatic saturation line is

$$170 - T_s = \frac{\lambda}{C}(H_s - H_g) \simeq \frac{900}{C}(H_s - H_g). \tag{5}$$

The drying rate equations above and below the critical moisture content of 0.58 are

$$-100\frac{dW}{d\theta}$$
$$= \begin{cases} 34.15(R + 1)^{0.8}(H_s - H_g), & 0.58 < W < 1.16, \tag{6} \\ 60.33(R + 1)^{0.8}(H_s - H_g)(W - 0.014), & W < 0.58. \tag{7} \end{cases}$$

When fresh air supply is simply increased by a factor $R + 1$ and no recycle is employed, Eq. (1) is replaced by

$$H_g = \frac{97.4(R + 1) + 1400(W - 0.1)}{7790(R + 1)} \tag{8}$$

The solution procedure is:

1. Specify the recycle ratio R (lbs recycle/lb fresh air, dry air basis).
2. Take a number of discrete values of W between 1.16 and 0.1. For each of these find the saturation temperature T_s and the drying rates by the following steps.
3. Assume a value of T_s.
4. Find H_g, p_s, H_s, and C from Eqs. (1)–(4).
5. Find the value of T_s from Eq. (5) and compare with the assumed value. Apply the Newton–Raphson method with numerical derivatives to ultimately find the correct value of T_s and the corresponding value of H_s.
6. Find the rate of drying from Eqs. (6), (7).
7. Find the drying time by integration of the reciprocal rate as in Example 9.3, with the trapezoidal rule.

A computer program may be written to solve this problem for residence times as a function of the recycle ratio, R. The above outline of the solution procedure may be programmed using MATHCAD, TK SOLVER, FORTRAN, or any other method. The printouts below show the saturation temperature, T_s, and reciprocal rates, 1/Rate, for recycle ratios of $R = 0$, 1, and 5, and for $R = 1$ with only the fresh air rate increased, using Eq. 8. When there is no recycle, use Eq. (1a) instead of Eq. (1). The residence times for the four cases are:

$R = 0$, moist air,	$\theta = 3.667$ hrs
$= 1$, moist air,	$= 2.841$
$= 5$, moist air,	$= 1.442$
$= 1$, fresh air,	$= 1.699$.

Although recycling of moist air does reduce the drying time because of the increased linear velocity, an equivalent amount of fresh air is much more effective because of its lower humidity. The points in favor of moist air recycle, however, are saving in fuel when the fresh air is much colder than 170°F and possible avoidance of case hardening or other undesirable phenomena resulting from contact with very dry air.

R = 0

W	T_s	1/Rate
1.16	150.21	3.9627
1.00	145.92	3.4018
.90	142.86	3.1043
.80	139.45	2.8365
.70	135.62	2.5918
.60	131.24	2.3680
.50	126.19	2.5187
.40	120.25	2.8795
.30	113.08	3.5079
.20	104.15	4.8223
.10	92.45	9.2092

R = 1, fresh air

W	T_s	1/Rate
1.16	132.62	1.3978
1.00	128.81	1.2989
.90	126.19	1.2395
.80	123.35	1.1815
.70	120.25	1.1248
.60	116.85	1.0693
.58	116.12	1.0582
.50	113.08	1.1839
.40	108.89	1.4112
.30	104.15	1.7979
.20	98.74	2.6014
.10	92.45	5.2893

(*continued*)

R = 1, moist air

W	T$_s$	1/Rate
1.16	150.21	2.2760
1.00	148.15	2.1043
.90	146.77	2.0088
.80	145.33	1.9181
.70	143.81	1.8323
.60	142.21	1.7509
.58	141.88	1.7351
.50	140.52	1.9534
.40	138.72	2.3526
.30	136.82	3.0385
.20	134.79	4.4741
.10	132.62	9.3083

R = 5, moist air

W	T$_s$	1/Rate
1.16	150.21	.9451
1.00	149.54	.9208
.90	149.11	.9060
.80	148.68	.8916
.70	148.24	.8776
.60	147.79	.8630
.58	147.70	.8604
.50	147.33	.9918
.40	146.87	1.2302
.30	146.40	1.6364
.20	145.92	2.4824
.10	145.43	5.3205

continuous, for pharmaceuticals or asphalt, at rates of hundreds or many thousands of pounds per hour.

An important characteristic of a dryer is the residence time distribution of solids in it. Dryers in which the particles do not move relatively to each other provide uniform time distribution. In spray, pneumatic conveying, fluidized bed, and other equipment in which the particles tumble about, a substantial variation in residence time develops. Accordingly, some particles may overdry and some remain wet. Figure 9.5 shows some data. Spray and pneumatic conveyors have wide time distributions; rotary and fluidized bed units have narrower but far from uniform ones. Differences in particle size also lead to nonuniform drying. In pneumatic conveying dryers particularly, it is common practice to recycle a portion of the product continuously to ensure adequate overall drying. In other cases recycling may be performed to improve the handling characteristics when the feed materials is very wet.

PRODUCTS

More than one kind of dryer may be applicable to a particular product, or the shape and size may be altered to facilitate handling in a preferred kind of machine. Thus, application of through-circulation drying on tray or belt conveyors may require prior extrusion, pelleting, or briquetting. Equipment manufacturers know the capabilities of their equipment, but they are not always reliable guides to comparison with competitive kinds since they tend to favor what they know best. Industry practices occasionally change over a period of time. For example, at one time rotary kilns were used to dry and prepare fertilizer granules of a desired size range by accretion from concentrated solutions onto the mass of drying particles. Now this operation is performed almost exclusively in fluidized bed units because of economy and controlability of dust problems.

Typical examples of products that have been handled successfully in particular kinds of dryers are listed in Table 9.4. The performance data of later tables list other examples.

COSTS

Differences in thermal economies are stated in the comparisons of Table 9.2 and other tables. Some equipment cost data are in Chapter 21. When the capacity is large enough, continuous dryers are less expensive than batch units. Those operating at atmospheric pressure cost about 1/3 as much as those at vacuum. Once-through

air dryers are one-half as expensive as recirculating gas equipment. Dielectric and freeze driers are the most expensive and are justifiable only for sensitive and specialty products. In the range of 1–50 Mtons/yr, rotary, fluidized bed and pneumatic conveying dryers cost about the same, although there are few instances where they are equally applicable.

SPECIFICATION FORMS

A listing of key information relating to dryer selection and design is in Table 9.5. Sample questionnaires of manufacturers of several kinds of dryers are in Appendix C.

9.4. BATCH DRYERS

Materials that require more than a few minutes drying time or are in small quantity are treated on a batch basis. If it is granular, the material is loaded on trays to a depth of 1–2 in. with spaces of approximately 3 in. between the trays. Perforated metal bottoms allow drying from both sides with improved heat transfer. Hot air is blown across or through the trays. Cross velocities of 1000 ft/min are feasible if dusting is not a problem. Since the rate of evaporation increases roughly with the 0.8 power of the linear velocity, high velocities are desirable and are usually achieved by internal recirculation with fans. In order to maintain humidity at operable levels, venting and fresh air makeup are provided at rates of 5–50% of the internal circulation rate. Rates of evaporation of 0.05–0.4 lb/(hr)(sqft tray area) and steam requirements of 1.5–2.3 lbs/lb evaporation are realized.

Drying under vacuum is commonly practiced for sensitive materials. Figure 9.6 shows cross and through circulation tray arrangements. The typical operating data of Table 9.6 cover a wide range of drying times, from a fraction of an hour to many hours. Charging, unloading, and cleaning are labor-intensive and time-consuming, as much as 5–6 hr for a 200-tray dryer, with trays about 5 sqft and 1–1.5 in. deep, a size that is readily handled manually. They are used primarily for small productions of valuable and thermally sensitive materials. Performance data are in Tables 9.6(b) and (c). Standard sizes of vacuum shelf dryers may be found in *Perry's* (1997, p.12.46).

Through circulation dryers employ perforated or open screen bottom tray construction and have baffles that force the air through the bed. Superficial velocities of 150 ft/min are usual,

TABLE 9.1. Classification of Dryers by Several Criteria[a]

(a) Classification of dryers based on method of operation

Dryer
- **Batch**
  - **Conduction**
    - **Vacuum**
      - Tray: Paste, Preform, Hard, Granular, Fibrous, Sheet
      - Agitated: Liquid, Slurry, Paste, Granular
    - **Atmos.**
      - Tray: Paste, Preform, Hard, Granular, Fibrous, Sheet
  - **Convection**
    - Through-circulation: Preform, Granular, Fibrous
    - Fluid bed: Preform, Granular, Fibrous
- **Continuous**
  - **Conduction**
    - **Vacuum**
      - Band: Slurry, Paste
    - **Atmos.**
      - Drum: Liquid, Slurry, Paste, Sheet
      - Indirect rotary: Hard, Granular, Fibrous
  - **Convection**
    - Spray: Liquid, Slurry, Paste
    - Pneumatic: Paste, Preform, Granular, Fibrous
    - Fluid bed: Paste, Preform, Granular, Fibrous
    - Direct rotary: Granular, Fibrous
    - Band: Paste, Preform, Hard, Sheet
    - Tray: Paste, Preform, Hard, Granular, Fibrous, Sheet
    - Through-circulation: Preform, Granular, Fibrous

(b) Classification of dryers based on physical form of feed

Wet feed:
- Liquid — (Evaporate →)
- Pumpable slurry or suspension — (Evaporate or back-mix →)
- Soft paste or sludge — (Preform → Preformed paste)
- Hard paste or matrix — (Press →) (Preform → Preformed paste)
- Free-flowing granular or crystalline solid — (Grind →)
- Fibrous solid — (Grind or preform →)
- Sheet

Liquid	Slurry	Paste	Preform	Hard	Granular	Fibrous	Sheet
Agitated batch	Agitated batch	Vacuum tray	Vacuum tray	Vacuum tray	Vacuum tray	Vacuum tray	Vacuum tray
Drum	Vacuum band	Agitated batch	Convection tray	Convection tray	Agitated batch	Convection tray	Convection tray
Spray	Drum	Convection tray	Batch through-circulation	Indirect rotary	Convection tray	Batch through-circulation	Drum
	Spray	Fluid bed	Fluid bed	Cont. tray	Batch through-circulation	Fluid bed	Cont. tray
		Vacuum band	Pneumatic		Fluid bed	Indirect rotary	
		Drum	Convection band		Indirect rotary	Pneumatic	
		Spray	Cont. tray		Pneumatic	Direct rotary	
		Pneumatic	Cont. through-circulation		Direct rotary	Convection band	
		Convection band			Cont. tray	Cont. tray	
		Cont. tray			Cont. through-circulation	Cont. through-circulation	

(continued)

with pressure drops of 1 in. or so of water. If it is not naturally granular, the material may be preformed by extrusion, pelleting, or briquetting so that it can be dried in this way. Drying rates are greater than in cross flow. Rates of 0.2–2 lb/(hr)(sqft tray area) and thermal efficiencies of 50% are realized. Table 9.6(d) has performance data.

Several types of devices that are used primarily for mixing of granular materials have been adapted to batch drying. Examples appear in Figure 9.8. They are suited to materials that do not stick to the walls and do not agglomerate during drying. They may be jacketed or provided with heating surfaces in the form of tubes or platecoils, and are readily arranged for operation under vacuum when handling sensitive materials. The double-cone tumbler has been long established. Some operating data are shown in Table 9.7. It and V-shaped dryers have a gentle action that is kind to fragile materials, and are discharged more easily than stationary cylinders or agitated pans. The fill proportion is 50–70%. When heated with 2 atm steam and operating at 10 Torr or so, the evaporation rate is 0.8–1.0 lb/(hr)(sqft of heating surface).

TABLE 9.1.—(*continued*)

(c)

Classification of dryers by scale of production

Process

Small scale to 20/50 kg/h	Medium scale 50 to 1000 kg/h		Large scale tonnes/h
Batch	**Batch**	**Continuous**	**Continuous**
Vacuum tray	Agitated	Fluid bed	Indirect rotary
Agitated	Through-circulation	Vacuum band	Spray
Convection tray	Fluid bed	Indirect rotary	Pneumatic
Through-circulation		Spray	Direct rotary
Fluid bed		Pneumatic	Fluid bed
		Band	
		Tray	
		Through-circulation	

(d)

Classification of dryers by suitability for special features

Process

Hazards			Sensitive product			Special form of product	Low capital cost per unit of output
Dust	Toxic	Flame	Temperature	Mechanical	Oxidation		
Agitated batch	Agitated batch	Agitated batch	Agitated batch	Through-circulation	Vacuum tray	Through-circulation	Fluid bed
Vacuum band	Vacuum band	Vacuum band	Through-circulation	Vacuum band	Vacuum band	Vacuum band	Direct rotary
Indirect rotary			Fluid bed	Cont. band	Spray	Spray	
			Vacuum band	Cont. tray		Drum	
			Pneumatic				

^aSee Figure 9.4 for sketches of dryer types.
(Items (a)–(d) by Nonhebel and Moss, 1971, pp. 45, 48–50).
(Walas, 1988).

Fixed cylinders with rotating ribbons or paddles for agitation and pans with vertical agitators are used to a limited extent in batch operation. Pans are used primarily for materials that become sticky during drying. Table 9.7 and Figure 9.7 are concerned with this kind of equipment.

A detailed example of capital and operating costs of a jacketed vacuum dryer for a paste on which they have laboratory drying data is worked out by Nonhebel and Moss (1971, p. 110).

Fluidized bed dryers are used in the batch mode on a small scale. Table 9.14(a) has some such performance data.

Papagiannes (1992) presented tips on how best to choose among rotary, spray, flash, and fluid-bed dryers.

9.5. CONTINUOUS TRAY AND CONVEYOR BELT DRYERS

Trays of wet material loaded on trucks may be moved slowly through a drying tunnel: When a truck is dry, it is removed at one end of the tunnel, and a fresh one is introduced at the other end. Figure 9.6(c) represents such equipment. Fresh air inlets and humid air outlets are spaced along the length of the tunnel to suit the rate

of evaporation over the drying curve. This mode of operation is suited particularly to long drying times, from 20 to 96 hr for the materials of Table 9.6(e).

In the rotating tray assembly of Figure 9.8(a), material enters at the top and is scraped onto successive lower trays after complete revolutions. A leveler on each tray, shown in Figure 9.8(b), ensures uniform drying. Although the air flow is largely across the surface of the bed, the turnover of the material as it progresses downward makes the operation more nearly through-circulation. A cooling zone is readily incorporated in the equipment. The contacting process is complex enough that laboratory tray drying tests are of little value. A pilot plant size unit was cited in Section 9.2 of Walas 1998. Some industrial data on rotary tray drying are in Table 9.8, and some other substances that have been handled successfully in this equipment are listed in Table 9.4.

Krauss Maffei Corporation manufactures an indirectly heated plate dryer with arms and plows that transfer the material to be dried from the top of the unit to the discharge at the bottom, being conveyed downward in a spiral fashion by a rotating shaft to which stationary plates are attached. An illustration of this dryer is found
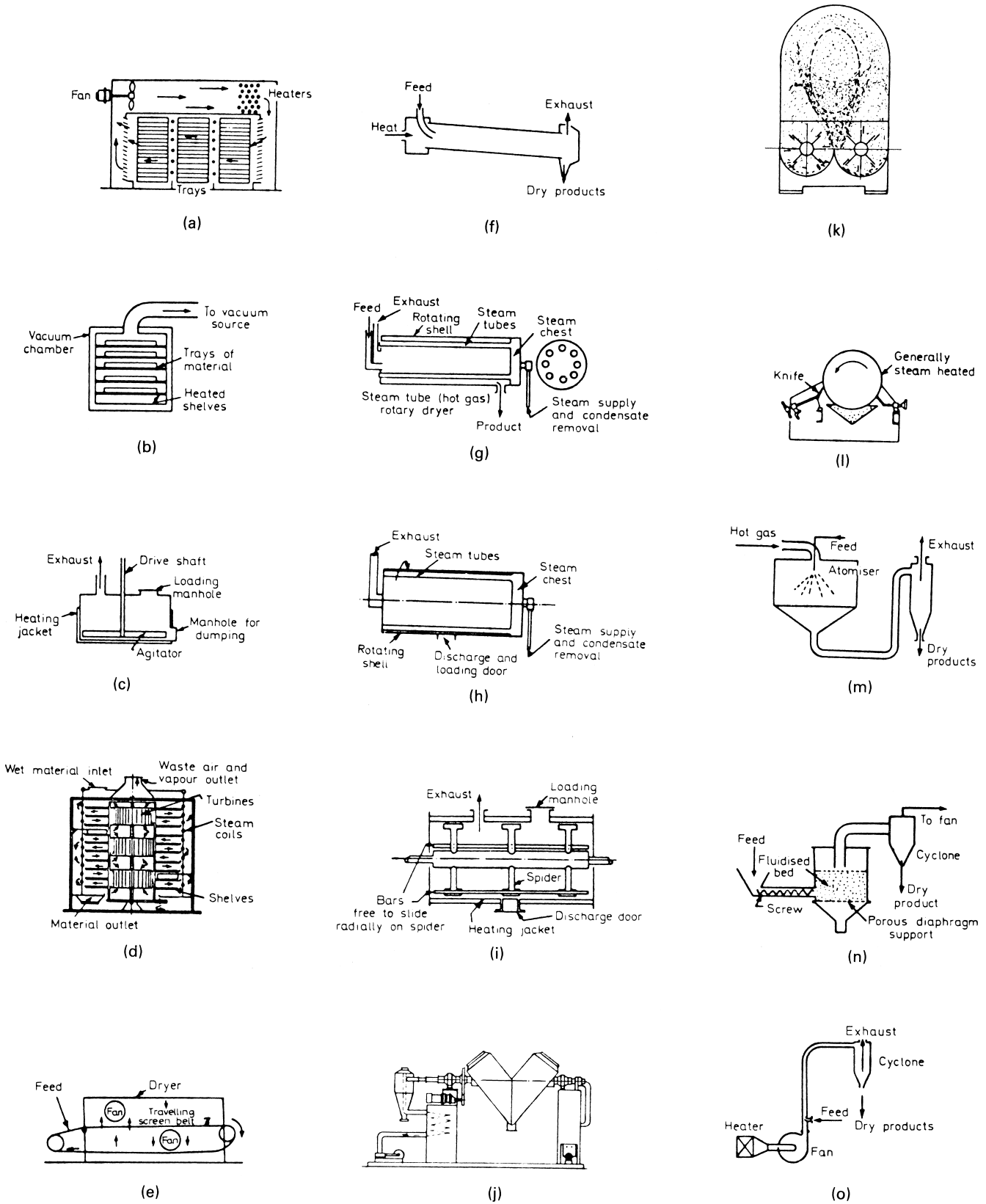
Figure 9.4. Types of dryers cited in Tables 9.1 and 9.2. (a) Tray or compartment. (b) Vacuum tray. (c) Vertical agitated batch vacuum drier. (d) Continuous agitated tray vertical turbo. (e) Continuous through circulation. (f) Direct rotary. (g) Indirect rotary. (h) Agitated batch rotary (atmos or vacuum). (i) Horizontal agitated batch vacuum drier. (j) Tumble batch dryer. (k) Splash dryer. (l) Single drum. (m) Spray. (n) Fluidized bed dryer. (o) Pneumatic conveying. *(Mostly after Nonhebel and Moss, 1971)*. (Walas, 1988).

TABLE 9.2. Evaporation Rates and Thermal Efficiencies of Dryers

Equipment	Figure 9.4	(lb/hr)/sqft	(lb/ hr)/cuft	Efficiency[a] (%)
Belt conveyor	e			46–58
Shelf				
Flow through	a	0.02–2.5		18–41
Flow past	a	0.02–3.1		18–41
Rotary				
Roto-louvre		7.2– 15.4		23–66
Parallel current direct fired		6.1–16.4		65
Parallel current warm air	f	6.1–16.4		50
Countercurrent direct fired		6.1–16.4		60
Countercurrent warm air	f	6.1–16.4		45
Steam tube	h	6.1–16.4		85
Indirect fired	g	6.1–16.4		25
Tunnel				36–42
Pneumatic				
0.5 mm dia granules	o		6.2	26–63
1.0 mm			1.2	26–63
5 mm			0.25	26–63
Spray	m		0.1–3	21–50
Fluidized bed	n		50–160	20–55
Drum	l	1.4–5.1		36–73
Spiral agitated				
High moisture	i	1–3.1		36–63
Low moisture	i	0.1–0.5		36–63
Splash paddle	k		5.6	65–70
Scraped multitray	d	0.8–1.6		

[a]Efficiency is the ratio of the heat of evaporation to the heat input to the dryer. (Walas, 1988).

TABLE 9.3. Comparative Performances of Basic Dryer Types

	Basic Dryer Type					
	Tray	Conveyor	Rotary	Spray	Flash	Fluid Bed
Product	filter cake	clay	sand	TiO$_2$	spent grain	coal
Drying time (min)	1320	9.5	12	<1.0	<1.0	2.0
Inlet gas temperature (°F)	300	420	1650	490	1200	1000
Initial moisture (% dry basis)	233	25	6	100	150	16
Final moisture (% dry basis)	1	5.3	0.045	0	14	7.5
Product loading (lb dry/ft^2)	3.25	16.60	N.A.	N.A.	N.A.	21 in. deep
Gas velocity (ft/min)	500	295	700	50	2000	1000
Product dispersion in gas	slab	packed bed	gravity flow	spray	dispersed	fluid bed
Characteristic product shape	thin slab	extrusion	granules	spherical drops	grains	$\frac{1}{2}$-in. particles
Capacity [lb evap./(h)(dryer area)]	0.34	20.63	1.35[a]	0.27[a]	10[a]	285
Energy consumed (Btu/lb evap.)	3000	1700	2500	1300	1900	2000
Fan [hp/(lb evap./h)]	0.042	0.0049	0.0071	0.019	0.017	0.105

[a]lb evap./(h)(dryer, volume).
(Wentz and Thygeson, 1979: tray dryer from Perry, *Chemical Engineers' Handbook*, 4th ed., p. 20–7; conveyor and spray dryers from Proctor and Schwartz, Inc.; rotary, flash, and fluid bed dryers from Williams–Gardner, 1971, pp. 75, 149, 168, 193). (Walas, 1988).

in Figure 9.8(c). The heating medium may be steam, hot water, or hot oil. Moyers (2003) performed an interesting study for rating continuous tray and plate dryers for new services combining simulation and the specific drying rate equation comparing the Krauss Maffei plate dryer and the Wyssmont tray dryer.

Equipment developed essentially for movement of granular solids has been adapted to drying. Screw conveyors, for instance, have been used but are rarely competitive with belt conveyors, particularly for materials that tend to degrade when they are moved. From the point of view of drying, belt conveyors are of two types: with solid belts and air flow across the top of the bed, called convection drying, or with perforated belts and through circulation of the air. The screw conveyor of Figure 9.8(g) has indirect heating.

Solid belts are used for pastes and fine powders. Through circulation belts are applied to granules more than about 3 mm in narrowest dimension. When the feed is not in suitable granular form, it is converted in a preformer to a size range usually of 3–15 mm. Belts are made of chain mail mesh or metal with 2 mm perforations or slots of this width. Steam-heated air is the most common heat transfer medium; however, combustion gases may be used. A temperature limit of 620°F is recommended (*Perry's*, 1997, p.12.48) because of problems lubricating the conveyor, chain, and roller drives.

Several arrangements of belt dryers are shown in Figures 9.8(d)–(f). In the wet zone, air flow usually is upward, whereas in the drier and cooling zones it is downward in order to minimize dusting. The depth of material on the belt is 1–8 in. Superficial air

TABLE 9.4. Examples of Products Dried in Specific Kinds of Equipment

1. *Spray dryers*: rubber chemicals, sulfonates, inorganic phosphates, ceramics, kaolin, coffee, detergents, pharmaceuticals, pigments, inks, lignosulfonate wood waste, melamine and urea formaldehyde resins, polyvinyl chloride, microspheres, skim milk, eggs, starch, yeast, silica gel, urea, salts
2. *Drum dryers*: potatoes, cereals, buttermilk, skim milk, dextrins, yeasts, instant oat meal, polyacylamides, sodium benzoate, propionates, acetates, phosphates, chelates, aluminum oxide, *m*-disulfuric acid, barium sulfate, calcium acetate–arsenate-carbonate–hydrate-phosphate, caustic, ferrous sulfate, glue, lead arsenate, sodium benzene sulfonate, and sodium chloride
3. *Vacuum drum dryers*: syrups, malted milk, skim milk, coffee, malt extract, and glue
4. *Vacuum rotary dryers*: plastics, organic polymers, nylon chips, chemicals of all kinds, plastic fillers, plasticizers, organic thickeners, cellulose acetate, starch, and sulfur flakes
5. *Belt conveyor dryers*: yeast, charcoal briquettes, synthetic rubber, catalysts, soap, glue, silica gel, titanium dioxide, urea formaldehyde, clays, white lead, chrome yellow, and metallic stearates
6. *Pneumatic conveyor dryers*: yeast filter cake, starch, whey, sewage sludge, gypsum, fruit pulp, copper sulfate, clay, chrome green, synthetic casein, and potassium sulfate
7. *Rotary multitray dryer*: pulverized coal, pectin, penicillin, zinc sulfide, waste slude, pyrophoric zinc powder, zinc oxide pellets, calcium carbonate, boric acid, fragile cereal products, calcium chloride flakes, caffein, inorganic fluorides, crystals melting near 100°F, prilled pitch, electronic grade phosphors, and solvent-wet organic solids
8. *Fluidized bed dryer*: lactose base granules, pharmaceutical crystals, weed killer, coal, sand, limestone, iron ore, polyvinyl chloride, asphalt, clay granules, granular desiccant, abrasive grit, and salt
9. *Freeze dryers*: meat, seafood, vegetables, fruits, coffee, concentrated beverages, pharmaceuticals, veterinary medicines, and blood plasma
10. *Dielectric drying*: baked goods, breakfast cereals, furniture timber blanks, veneers, plyboard, plasterboard, water-based foam plastic slabs, and some textile products
11. *Infrared drying*: sheets of textiles, paper and films, surface finishes of paints and enamels, and surface drying of bulky nonporous articles.

Laboratory drying rate data of materials on trays are best obtained with constant air conditions. Along a belt conveyor or in a tray-truck tunnel, the moisture contents of air and stock change with position. Example 9.3 shows how constant condition drying tests can be adapted to belt conveyor operation. The effects of recycling moist air and of increasing the air velocity beyond that studied in the laboratory tests are studied in Example 9.4. Recycling does reduce drying time because of the increased air velocity, but it is not as effective in this regard as the same increase in the amount of fresh air. Recycling is practiced, however, to reduce heat consumption when the fresh air is cold and to minimize possible undesirable effects from over-rapid drying with low humidity air. Parallel current operation also avoids overrapid drying near the end. For parallel flow, the moisture balance of Example 9.4 becomes

$$H_g = \frac{97.4(R+1) + 1400(1.16 - W)}{7790(R+1)} \tag{9.16}$$

and would replace Eq. 1 in any computer program.

Figure 9.5. Residence time distribution in particle dryers. (a) Four types of dryers (*McCormick, 1979*). (b) Residence time distribution of air in a detergent spray tower; example shows that 27% (difference between the ordinates) has a residence time between 24 and 32 sec [*Place et al.*, Trans. Inst. Chem. Eng. **37,** *268* (*1959*)]. (c) Fluidized bed drying of two materials (*Vanacek et al.*, Fluidized Bed Drying, *1966*). (Walas, 1988).

velocities of 5 ft/sec usually are allowable. The multizone arrangement of Figure 9.8(f) takes advantage of the fact that the material becomes lighter and stronger and hence can be loaded more deeply as it dries. Each zone also can be controlled separately for air flow and temperature. The performance data of Table 9.9 cover a range of drying times from 11 to 200 min, and thermal efficiencies are about 50%.

TABLE 9.5. Specification Form for a Dryer[a]

1. Operation	mode	batch/continuous
	operating cycle	_____ h
2. Feed	(a) material to be dried	_____
	(b) feed rate	_____ kg/h
	(c) nature of feed	solution/slurry/sludge/granular/fibrous/sheet/bulky
	(d) physical properties of solids:	
	initial moisture content	_____ kg/kg
	hygroscopic-moisture content	_____ kg/kg
	heat capacity	_____ kJ/kg°C
	bulk density, wet	_____ kg/m³
	particle size	_____ mm
	(e) moisture to be removed:	
	chemical composition	_____
	boiling point at 1 bar	_____ °C
	heat of vaporization	_____ MJ/kg
	heat capacity	_____ kJ/kg°C
	(f) feed material is	scaling/corrosive/toxic/abrasive/explosive
	(g) source of feed	_____
3. Product	(a) final moisture content	_____ kg/kg
	(b) equilibrium-moisture content at 60% r.h.	_____ kg/kg
	(c) bulky density	_____ kg/m³
	(d) physical characteristics	granular/flaky/fibrous/powdery/sheet/bulky
4. Design restraints	(a) maximum temperature when wet	_____ °C
	when dry	_____ °C
	(b) manner of degradation	_____
	(c) material-handling problems,	
	when wet	_____
	when dry	_____
	(d) will flue-gases contaminate product?	_____
	(e) space limitations	_____
5. Utilities	(a) steam available at	_____ bar pressure (10^6 N/m²)
	maximum quantity	_____ kg/h
	costing	_____ $/kg
	(b) other fuel	_____
	at	_____ kg/h
	with heating value	_____ MJ/kg
	costing	_____ $/kg
	(c) electric power	_____ V
	frequency	_____ hz
	phases	_____
	costing	_____ $/kWh
6. Present method of drying		_____
7. Rate-of-drying data under constant external conditions:		
		____
		____
		____
or data from existing plant		
		____
		____
8. Recommended materials of construction		
	(a) parts in contact with wet material	_____
	(b) parts in contact with vapors	_____

[a]Questionnaires of several manufacturers are in Appendix C.

The kind of data desirable in the design of through-circulation drying are presented for a particular case by Nonhebel and Moss (1971, p. 147). They report on effects of extrusion diameters of the original paste, the bed depth, air linear velocity, and air inlet humidity, and apply these data to a design problem.

9.6. ROTARY CYLINDRICAL DRYERS

Rotating cylindrical dryers are suited for free-flowing granular materials that require drying times of the order of 1 hr or less. Materials that tend to agglomerate because of wetness may be preconditioned by mixing with recycled dry product.

Such equipment consists of a cylindrical shell into which the wet material is charged at one end and dry material leaves at the other end. Figure 9.9 shows some examples. Drying is accomplished by contact with hot gases in parallel or countercurrent flow or with heat transfer through heated tubes or double shells. Designs are available in which the tubes rotate with the shell or are fixed in space.

Diameters typically are 4–10 ft and lengths are 4–15 diameters. The product of rpm and diameter is typically between 25 and 35. Superficial gas velocities are 5–10 ft/sec; but lower values may be needed for fine products, and rates up to 35 ft/sec may be allowable for coarse materials. To promote longitudinal travel of the solid, the shell is mounted on a slope of 1 in 40 or 20.

Figure 9.6. Tray dryer arrangements, batch and continuous. Performance data are in Table 9.5. (a) Air flow across the surfaces of the trays. (b) Air circulation forced through the beds on the trays (*Proctor and Schwartz Inc.*). (c) Continuous drying of trays mounted on trucks that move through the tunnel; air flow may be in parallel or countercurrent (*P.W. Kilpatrick, E. Lowe, and W.B. Van Arsdel*, Advances in Food Research, *Academic, New York, 1955, Vol. VI, p. 342*). (Walas, 1988).

In a countercurrent dryer the exit temperature of the solid approaches that of the inlet gas. In a parallel current dryer, the exit gas is 10–20°C above that of the solid. For design purposes the temperature of the exit solid in parallel flow may be taken as 100°C.

Flights attached to the shell lift up the material and shower it as a curtain through which the gas flows. Cross sections of some dryers are shown in Figure 9.10. The shape of flights is a compromise

between effectiveness and ease of cleaning. The number is between 2 and 4 times the diameter of the shell in feet, and their depth is between $\frac{1}{12}$ and $\frac{1}{8}$ of the diameter. Holdup in the dryer depends on details of design and operation, but 7–8% is a usual figure. Cross-sectional holdup is larger at the wet end than at the dry end. An 85% free cross section commonly is adopted for design purposes; the rest is taken up by flights and settled and cascading solids.

Residence time depends on the nature of the material and mechanical features of the dryer. The performance data of Table 9.10 show a range of 7–90 min. A formula cited by Williams–Gardner (1971, p. 133) for the geometrical residence time θ, is

$$\theta = kL/nDS, \qquad (9.17)$$

where L is the length, D is the diameter, n is rpm, and S is the slope (in./ft). The coefficient k varies from 3 to 12 for various countercurrent single shell dryers. The formula may be of some value in predicting roughly the effects of changes in the quantities included in it.

The only safe way of designing a rotary dryer is based on pilot plant tests or by comparison with known performance of similar operations. Example 9.5 utilizes pilot plant data for upscaling a dryer. The design of Example 9.6 also is based on residence time and terminal conditions of solid and air established in a pilot plant.

When heating by direct contact with hot gases is not feasible because of contamination or excessive dusting, dryers with jacketed shells or other kinds of heat transfer surfaces are employed. Only enough air to entrain away the moisture is employed. The temperature of the solid approaches the boiling temperature of the water in the constant rate period. Figure 9.10 shows designs in which the heating tubes are fixed in space or are attached to the rotating shell. Table 9.10 gives some performance data.

Combined direct and indirect dryers pass the hot gases first through a jacket or tubes, and then wholly or in part through the open dryer. Efficiencies of such units are higher than of direct units, being in the range 60–80%. Table 9.10(d) shows performance data. Since the surfaces are hot, this equipment is not suitable for thermally sensitive materials and, of course, may generate dust if the gas rate through the open dryer is high.

In the Roto-Louvre design of Figure 9.10(b) the gas enters at the wall, flows first through the bed of particles and subsequently through the shower of particles. Performance data are in Tables 9.10(b) and (c).

A formula for the power required to rotate the shell is given by Wentz and Thygeson (1979):

$$P = 0.45W_t v_r + 0.12BDNf, \qquad (9.18)$$

where P is in watts, W_t is the weight (kg) of the rotating parts, v_r is the peripheral speed of the carrying rollers (m/sec), B is the holdup of solids (kg), D is diameter of the shell (m), N is rpm, and f is the number of flights along the periphery of the shell. Information about weights may be obtained from manufacturers catalogs or may be estimated by the usual methods for sizing vessels. Fan and driver horsepower are stated for the examples of Tables 9.10(a)–(c). The data of Table 9.10(a) are represented roughly by

$$P = 5 + 0.11DL, \qquad (9.19)$$

where P is in HP and the diameter D and length L are in feet.

9.7. DRUM DRYERS FOR SOLUTIONS AND SLURRIES

Solutions, slurries and pastes may be spread as thin films and dried on steam-heated rotating drums. Some of the usual arrangements

TABLE 9.6. Performance Data of Batch Tray and Tray–Truck Dryers

(a) Cross-Flow Operation

	Coated Tablets	PTFE	Aspirin Base Granules	Stearates	Chalk	Filter Cake	Filter Cake	Filter Cake
Capacity, wet charge (lb)	120	80	56	20,000	1800	3000	2800	4300
Number of trays	40	20	20	320	72	80	80	80
Tray area (ft^2)	140	70	70	4800	1130	280	280	280
Depth of loading (in.)	0.5	1.0	0.5	2.0	2.0	1.0	1.0	1.5
Initial moisture (% w/w basis)	25	25–30	15	71	46	70	70	80
Final moisture (% w/w basis)	nil	0.4	0.5	0.5	2.0	1.0	1.0	0.25
Maximum air temperature (°F)	113	284	122	200	180	300	200	200
Loading (lb/ft^2)	0.9	1.2	0.4	0.9	0.91	3.25	3.04	11.7
Drying time (hr)	12	5.5	14	24	4.5	22	45	12
Overall drying rate (lb/hr)	2.6	5.3	0.84	62.5	185	96.6	43.0	90
Evaporative rate (lb/hr/ft^2)	0.0186	0.05	0.008	0.013	0.327	0.341	0.184	0.317
Total installed HP	1	1	1	45	6	4	2	2

(Williams–Gardner, 1971, p. 75, Table 12: first three columns courtesy Calmic Engineering Co.; last five columns courtesy A.P.V.—Mitchell (Dryers) Ltd.) (Walas, 1988).

(b) Vacuum Dryers with Steam Heated Shelves

	Soluble Aspirin	Paint Pigment	Ferrous Glutinate	Ferrous Succinate	Lithium Hydroxide	Tungsten Alloy	Stabilized Diazamin
Capacity, wet product (lb/h)	44	30.5	41.6	52.5	36.8	12.8	4.6
Tray area (ft^2)	108	108	108	108	54	215	172
Depth of loading (in.)	1	2	0.5	1	1	0.5	0.75
Initial moisture (% w/w basis)	72.4	49.3	25	37.4	59	1.6	22.2
Final moisture (% w/w basis)	1.25	0.75	0.5	18.8	0.9	nil	0.5
Max temp (°F)	104	158	203	203	122	239	95
Loading [lb charge (wet) ft^2]	6.1	102	2.3	1.94	3.08	7.16	1.22
Drying time (hr)	15	36	6	4	4.5	12	48
Overall drying rate (lb moisture evaporated/ft^2/hr)	0.293	0.14	0.11	0.11	0.034	0.013	0.0058
Total installed HP	6	6	6	6	3	2	5
Vacuum (in. Hg)	29.5	28	27	27	27	29	22–23

(Williams–Gardner, 1971, p. 88, Table 15: courtesy Calmic Engineering Co.). (Walas, 1988).

(c) Vacuum Dryers with Steam-Heated Shelves

Material	Sulfur Black	Calcium Carbonate	Calcium Phosphate
Loading (kg dry material/m^2)	25	17	33
Steam pressure (kPa gauge)	410	410	205
Vacuum (mm Hg)	685–710	685–710	685–710
Initial moisture content (%, wet basis)	50	50.3	30.6
Final moisture content (%, wet basis)	1	1.15	4.3
Drying time (hr)	8	7	6
Evaporation rates (kg/sec m^2)	8.9×10^{-4}	7.9×10^{-4}	6.6×10^{-4}

(*Chemical Engineers' Handbook*, 1999, Table 12.13, p. 12.46).

(d) Through Circulation Dryers

Kind of Material	Granular Polymer	Vegetable	Vegetable Seeds
Capacity (kg product/hr)	122	42.5	27.7
Number of trays	16	24	24
Tray spacing (cm)	43	43	43
Tray size (cm)	91.4 × 104	91.4 × 104	85 × 98
Depth of loading (cm)	7.0	6	4
Physical form of product	crumbs	0.6-cm diced cubes	washed seeds
Initial moisture content (%, dry basis)	11.1	669.0	100.0
Final moisture content (%, dry basis)	0.1	5.0	9.9
Air temperature (°C)	88	77 dry-bulb	36
Air velocity, superficial (m/sec)	1.0	0.6–1.0	1.0
Tray loading (kg product/m^2)	16.1	5.2	6.7
Drying time (hr)	2.0	8.5	5.5
Overall drying rate (kg water evaporated/hr m^2)	0.89	11.86	1.14
Steam consumption (kg/kg water evaporated)	4.0	2.42	6.8
Installed power (kW)	7.5	19	19

(Proctor and Schwartz Co.). (Walas, 1988).

TABLE 9.6.—(continued**)**

(e) Tray and Tray–Truck Dryers

Material	Color	Chrome Yellow	Toluidine Red	Half-Finished Titone	Color
Type of dryer	2-truck	16-tray dryer	16-tray	3-truck	2-truck
Capacity (kg product/hr)	11.2	16.1	1.9	56.7	4.8
Number of trays	80	16	16	180	120
Tray spacing (cm)	10	10	10	7.5	9
Tray size (cm)	$60 \times 75 \times 4$	$65 \times 100 \times 2.2$	$65 \times 100 \times 2$	$60 \times 70 \times 3.8$	$60 \times 70 \times 2.5$
Depth of loading (cm)	2.5–5	3	3.5	3	
Initial moisture (%, bone-dry basis)	207	46	220	223	116
Final moisture (%, bone-dry basis)	4.5	0.25	0.1	25	0.5
Air temperature (°C)	85–74	100	50	95	99
Loading (kg product/m^2)	10.0	33.7	7.8	14.9	9.28
Drying time (hr)	33	21	41	20	96
Air velocity (m/sec)	1.0	2.3	2.3	3.0	2.5
Drying (kg water evaporated/hr m^2)	0.59	65	0.41	1.17	0.11
Steam consumption (kg/kg water evaporated)	2.5	3.0	—	2.75	
Total installed power (kW)	1.5	0.75	0.75	2.25	1.5

(Proctor and Schwartz Co.). (Walas, 1988).

TABLE 9.7. Performance of Agitated Batch Dryers (See Fig. 9.7)

(a) Double-Cone Tumbler

	Tungsten Carbide	Polyester Resin	Penicillin	Hydroquinone	Prussian Blue Pigment
Volatile ingredient	naphtha	water	acetone	water	water
Physical nature of charge	heavy slurry	pellets	powder	powder	filtercake
Dryer dia (ft)	2	2	2	2	2
Dryer capacity (ft^3)	2.5	2.5	2.5	2.5	2.5
Method of heating	hot water	steam	hot water	hot water	steam
Heating medium temperature (°F)	180	240	140	150	225
Vacuum (mm Hg abs)	40–84	12–18	40	50–100	40–110
Initial volatile content (% w/w basis)	18.0	0.34	27.9	5.0	83
Final volatile content (% w/w basis)	nil	0.01	nil	0.25	4.8
Weight of charge (lb)	640	130	55	61	142.5
Bulk density of charge (lb/ft^3)	256	51.5	21.5	26.5	58.5
Drying time (min)	155	215	90	50	480

(Courtesy Patterson Division, Banner Industries Inc.; Williams–Gardner, 1971). (Walas, 1988).

(b) Paddle, Ribbon, and Pan[a]

Material	Type of Dryer	Size of Dryer (mm) Length	Dia	Driving Motor (HP)	Wet Charge (kg)	Filling Ratio	Initial Moisture Content (%, Wet Basis)	Absolute Pressure in Dryer (mb)	Jacket Temp (°C)	Drying Time (hr)	Mean Overall Coeff. U_c (W/m °C)
Organic paste	HCRP	5500	1200		4000	0.36	30	200	80	15	35
Different fine	HCRP	3800	1350	15	2260	0.2	68	265	125	6	45
aromatic organic	HCRP	3800	1350	15	4660	0.4	75	265	125	8	60
compound crystals	HCRP	5500	1200		2100	0.2	6	200	125	4	25
Anthracene (water and pyridine)	HCRP	8900	1800	35	37000	0.72	76	665–1000	170	16	75
Dyestuff paste	HCSB	2750	1200	10	2000	0.3	70	265	105	14	30
Different organic	PVP		1800	15	1080	0.4	41	1000	125	32	35
paste	PVP		2450	25	800	0.4	35	665	125	$7\frac{1}{2}$	25
Different dyestuff	PVP		1800	15	1035	0.4	61	1000	125	11	135
pastes	PVP		2450	20–30	2400	0.7	64	470	125	12	115

[a] HCRP = paddle agitator; HCSP = ribbon agitator; PVP = pan with vertical paddles.
(Nonhebel and Moss, 1971). (Walas, 1988).

TABLE 9.7.—(continued)

(c) Pan Dryer

	Sodium Thiosulphate	Potassium Zeolite	Arsenic Pentoxide
Dryer diameter	6 ft 0 in.	2 ft 3 in.	8 ft 0 in.
Dryer depth	2 ft 0 in.	1 ft 0 in.	2 ft 0 in.
Capacity (lb product)	12 cwt	14 lb	$2\frac{1}{2}$ ton/day
Initial moisture (% w/w basis)	37	40	35
Final moisture (% w/w basis)	0	1	2–3
Method of heating	steam	steam	steam
Atmospheric (a) or vacuum (b)	(b) 26 Hg	(a) 60 lb/in.^{2}/gauge	(b)
Drying temperature: material (°F)			
Drying temperature: shelf (°F)		153 C	
Bulk density product (lb/ft^3)			
Drying time (hr/batch)	5	3	8
Material of construction	SS	MS	SS

[Courtesy A.P.V.—Mitchell (Dryers) Ltd., Williams–Gardner, 1971]. (Walas, 1988).

(a)

(b)

(c)
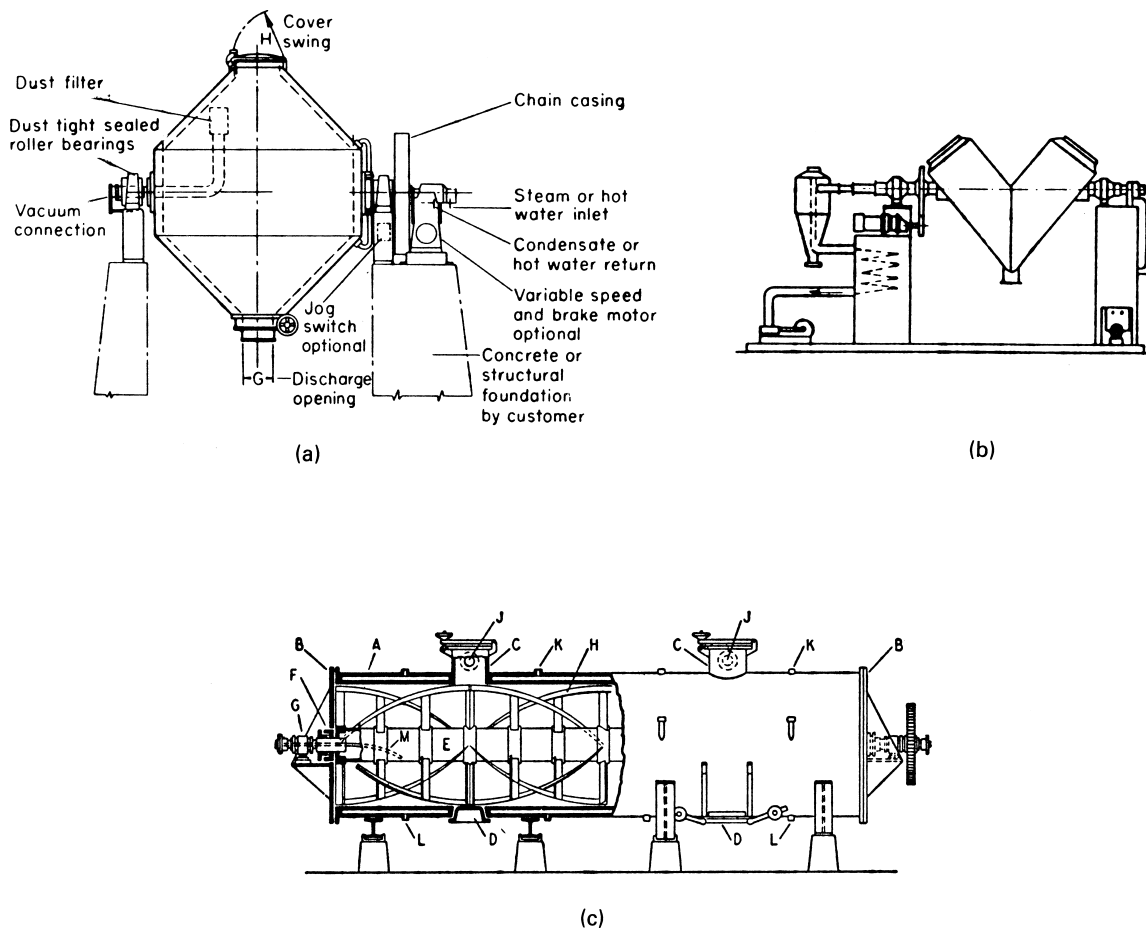
Figure 9.7. Tumbling and agitated heated dryers for atmospheric and vacuum batch operation. (a) Double cone tumbler; performance data in Table 9.7(a) (*Pennsalt Chem. Co.*). (b) V-shaped tumbler. (c) Ribbon agitated cylinder; performance data in Table 9.7(b). (*A*) jacketed shell; (*B*) heads; (*C*) charging connections; (*D*) discharge doors; (*E*) agitator shaft; (*F*) stuffing box; (*G*) shaft bearings; (*H*) agitator blades; (*J*) vapor outlets; (*K*) steam inlets; (*L*) condensate outlets; (*M*) discharge siphon for shaft condensate (*Buflovak Equip. Div., Blaw Knox Co.*) (d) Paddle agitated cylinder. Performance data in Table 9.7(b). (e) Horizontal pan with agitator blades. Data are Table 9.7(b) (Walas, 1988).

are shown on Figure 9.11. Twin drums commonly rotate in opposite directions inward to nip the feed, but when lumps are present that could damage the drums, rotations are in the same direction. Top feed with an axial travelling distributor is most common. Dip feed is shown in Figure 9.11(a) where an agitator also is provided to keep solids in suspension. When undesirable boiling of the slurry in the pan could occur, splash feed as in Figure 9.11(b) is employed. Example 9.7 describes some aspects of an industrial installation.

For mechanical reasons, drums larger than 5 ft diameter by 12 ft long are impractical. Performance data are found in Tables

(d)

(e)

Figure 9.7.—(*continued*)

(a)

(b)

(c)

1. Product

2. Heating or cooling medium

3. Housing

4. Conveying system
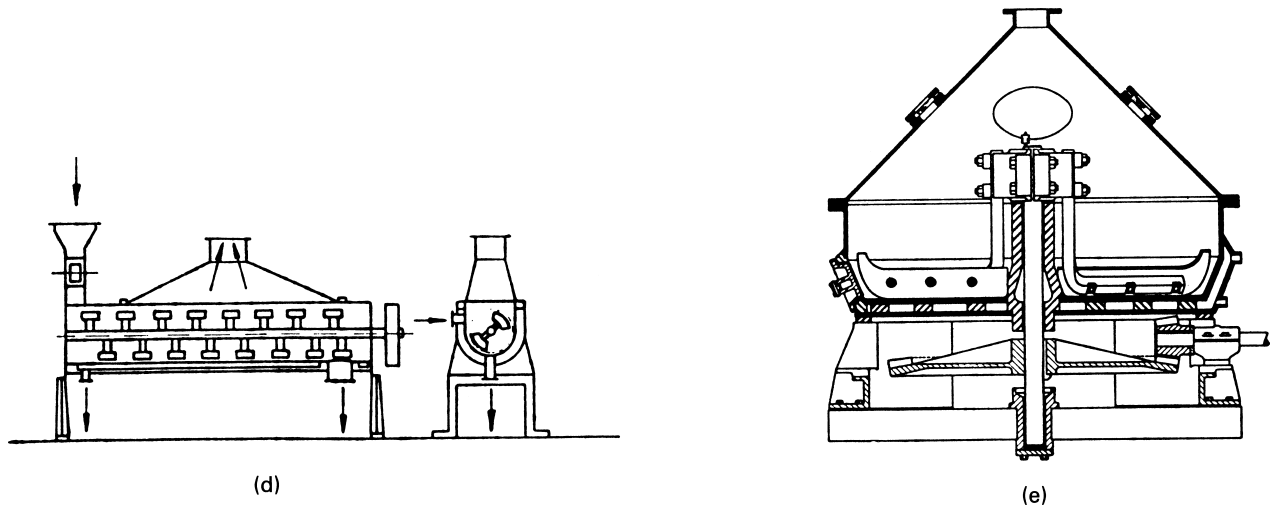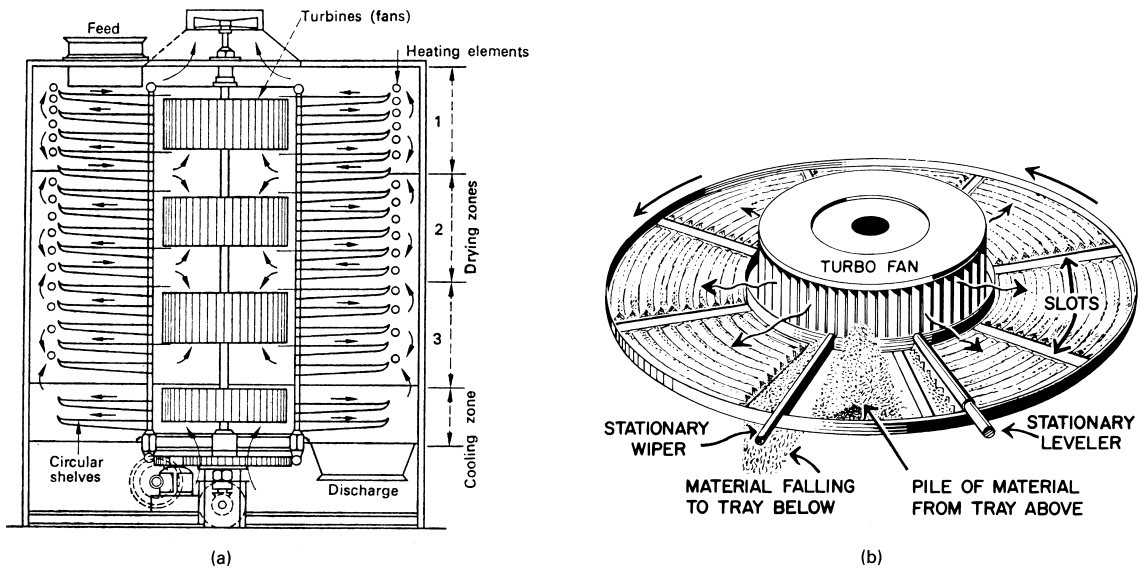
5. Plate

Figure 9.8. Rotary tray, through-circulation belt conveyor, and heated screw conveyor dryers. (a) Rotary tray dryer. (*Wyssmont Co.*). (b) Action of a rotating tray and wiper assembly. (*Wyssmont Co.*). (c) Krauss Maffei plate dryer. (d) A single conveyor belt with air upflow in wet zone and downflow in dry. (*Proctor and Schwartz Inc.*). (e) A two-stage straight-through belt conveyor dryer. (f) A three-belt conveyor dryer; as the material becomes dryer, the loading becomes deeper and the belt longer. (*Proctor and Schwartz Inc.*). (g) Screw conveyor dryer with heated hollow screw (*Bepex Corp.*). (Walas, 1988).

(d)

(e)

(f)

(g)
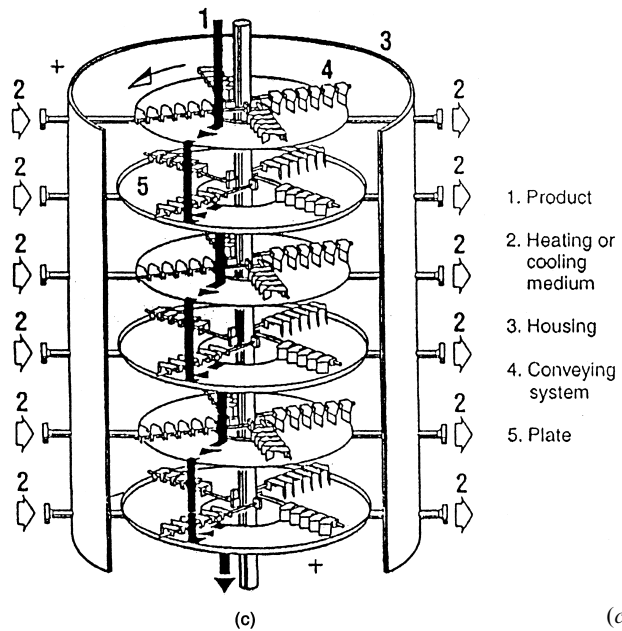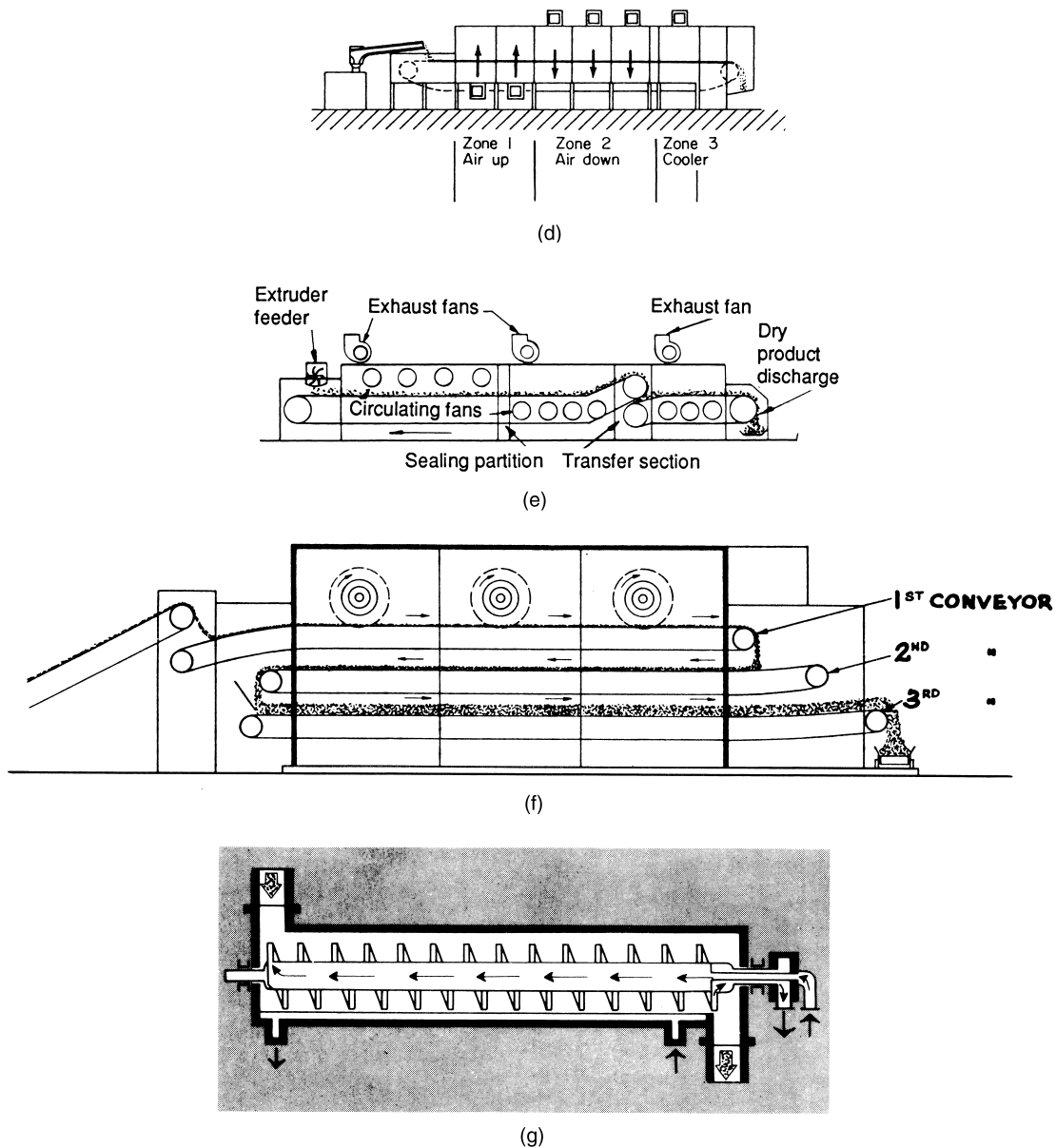
Figure 9.8.—(*continued*) Indirect-heated continuous plate dryer for atmospheric, gastight, or full-vacumm operation. (Courtesy of Krauss Maffei).

9.11 and 9.12. Pilot plant dryers may be 1 to 2 ft in diameter by 1 to 2 ft long.

The material comes off as flakes 1–3 mm or less thick. They are broken up to standard size of about $\frac{1}{4}$ in. square. That process makes fines that are recycled to the dryer feed. Drying times fall in the range of 3–12 sec. Many laboratory investigations have been made of drying rates and heat transfer coefficients, but it appears that the only satisfactory basis for sizing plant equipment is pilot plant data obtained with a drum of a foot or more in diameter. Usually plant performance is superior to that of pilot plant units because of steadier long time operation.

Rotation speeds of the examples in Table 9.12 show a range of 1–24 rpm. Thin liquids allow a high speed, thick pastes a low one. In Table 9.12(b) the evaporation rates group in the range 15–30 kg/ m² hr, but a few of the data are far out of this range. Efficiencies in

this type dryer is comparatively high, on the order of 1.3 lb steam/lb of water evaporated.

A safe estimate of power requirement for double drum dryers is approx 0.67 HP/(rpm)(100 sqft of surface). Maintenance can be as high as 10%/yr of the installed cost. Knives last from 1 to 6 months depending on abrasiveness of the slurry. Competitors for drum dryers are solid belt conveyors that can can handle greater thicknesses of pasty materials, and primarily spray dryers that have largely taken over the field.

9.8. PNEUMATIC CONVEYING DRYERS

Free-flowing powders and granules may be dried while being conveyed in a high velocity air stream. A pneumatic-conveyor dryer consists of a vertical or inclined drying leg, a fan to propel

TABLE 9.8. Performance of Rotary Tray and Pan Dryers

(a) Multitray Dryers at Atmospheric Pressure

	China Clay	Bread Crumbs	Cu–Ni Concentrate	Catalyst Pellets	Kaolin	Calcium Chloride	Urea	Vitamin Powder
Dryer height	—	—	—	23 ft	23 ft	47 ft	47 ft	12 ft
Dryer diameter	—	—	—	19 ft	19 ft	31 ft	15 ft	9 ft
Tray area (ft^2)	7000	2000 (drying) 1000 (cooling)	2900	—	—	—	—	—
Capacity (lb/product/hr)	31,000	1680	19,000	4200	10,000	24,000	5000	200
Initial moisture (% w/w basis)	30	36	22	45	35	25	20	20
Final moisture (% w/w basis)	10	5	5	18	5	1	0.2	5
Product temperature (°F)	160	100	200	—	—	—	—	—
Residence time (min)	40	40 (drying) 20 (cooling)	25	—	—	—	—	—
Evaporation rate (lb/ft^2/hr)	9.100	804	4060	2050	4600	11,000	100	37
Method of heating	external oil	steam	external oil	external gas	external oil	internal gas	external steam	external steam
Heat consumption (Btu/lb moisture evaporated)	1750	—	2200	1750	1850	1800	3500	2700
Installed HP	80	25	60	23	47	65	75	$2\frac{1}{2}$

(Williams–Gardner, 1971).
(First three columns courtesy Buell Ltd.; last five columns courtesy The Wyssmont Co., Inc.). (Walas, 1988).

(b) Multiple Vacuum Pan Dryer

	Sodium Hydrosulphite	Maneb	Melamine	Activated Carbon
Dryer diameter (pans) (m)	2	2	2	2
Number of pans	5	17	11	17
Area (approx)(m^2)	12.4	42.8	27.6	42.8
Dry product (lb/hr)	1100	660	1870	440
Initial moisture (% w/w)	4	23	11	62
Final moisture (% w/w)	0.1	0.5	0.03	3
Heating	hot water	steam 1.3 atm	steam 2.5 atm	steam 2.5 atm
Pan temperature (°C)	98	105	125	125
Evaporation rate (lb/ft^2/hr)	0.325	0.325	0.79	0.78
Drying time (min)	15	170	12	30

(Data of Krauss–Maffei-Imperial GmbH). (Walas, 1988).

TABLE 9.9. Performance of Through-Circulation Belt Conveyor Dryers [See Figures 9.8(c)–(e)]

(a) Data of A.P.V.—Mitchell (Dryers) Ltd.

	Fertilizers	Bentonite	Pigment	Nickel Hydroxide	Metallic Stearate
Effective dryer length	42 ft 6 in.	60 ft 0 in.	24 ft 0 in.	24 ft 0 in.	41 ft 3 in.
Effective band width	8 ft 6 in.	8 ft 6 in.	4 ft 0 in.	4 ft 0 in.	6 ft 0 in.
Capacity (lb product/hr)	2290	8512	100	125	125
Method of feeding / Feedstock preforming	oscillator	oscillator	extruder	extruder	extruder
Initial moisture (% w/w basis)	45.0	30	58.9	75	75
Final moisture (% w/w basis)	2.0	10.0	0.2	0.5	0.2
Drying time (min)	16	14	60	70	60
Drying rate (lb evaporated/ft^2/hr)	7.0	6.5	2.0	7.5	1.5
Air temperature range (°F)	—	—	—	—	—
Superficial air velocity (ft/min)	200	200	180	180	125
Heat consumption (Btu/lb evaporated)	—	—	—	—	—
Method of heating	direct oil	direct oil	steam	steam	steam
Fan installed HP	35	50	14	14	28

(Williams–Gardner, 1971; Walas, 1988).

TABLE 9.9.—(continued)

(b) Data of Krauss–Maffei–Imperial GmbH

	Aluminium Hydrate	Polyacrylic Nitrile	Sulfur	Calcium Carbonate	Titanium Dioxide
Effective dryer length	32 ft 9 in.	43 ft 0 in.	28 ft 0 in.	50 ft 0 in.	108 ft 0 in.
Effective band width	6 ft 6 in.	6 ft 6 in.	6 ft 6 in.	6 ft 3 in.	9 ft 6 in.
Capacity (lb product/hr)	615	2070	660	1800	6000
Method of feeding Feedstock preforming	grooved drum	extruder	extruder	extruder	extruder
Initial moisture (% w/w basis)	38.0	55.0	45.0	60.0	50.0
Final moisture (% w/w basis)	0.2	1.0	1.0	0.5	0.5
Drying time (min)	26	52	110	40	45
Drying rate (lb evaporated/hr/ft^2)	2.88	3.37	3.57	5.73	6.0
Air temperature range (°F)	233	186/130	194/230	320	314/392
Superficial air velocity (ft/min)	140	100/216	140	160	150
Heat consumption (lb steam/lb evaporated)	1.7–1.8	1.8–1.9	1.8–1.9	1.7–1.8	1.8–1.9
Method of heating	50 lb/in.^{2} steam	25 lb/in.^{2} steam	90 lb/in.^{2} steam	160 lb/in.^{2} steam	260 lb/in.^{2} steam
Fan installed hp (approx.)	25	65	20	35	80

(Williams–Gardner, 1971; Walas, 1988).

(c) Data of Proctor and Schwartz Inc.

Kind of Material	Inorganic Pigment	Cornstarch	Fiber Staple		Charcoal Briquettes	Gelatin	Inorganic Chemical
Capacity (kg dry product/hr)	712	4536	1724		5443	295	862
			Stage A	Stage B			
Approximate dryer area (m^2)	22.11	66.42	57.04	35.12	52.02	104.05	30.19
Depth of loading (cm)	3	4	—	—	16	5	4
Air temperature (°C)	120	115–140	130–100	100	135–120	32–52	121–82
Loading (kg product/m^2)	18.8	27.3	3.5	3.3	182.0	9.1	33
Type of conveyor (mm)	1.59 by 6.35 slots	1.19 by 4.76 slots	2.57-diameter holes, perforated plate		8.5 × 8.5 mesh screen	4.23 × 4.23 mesh screen	1.59 × 6.35 slot
Preforming method or feed	rolling extruder	filtered and scored	fiber feed		pressed	extrusion	rolling extruder
Type and size of preformed particle (mm)	6.35-diameter extrusions	scored filter cake	cut fiber		64 × 51 × 25	2-diameter extrusions	6.35-diameter extrusions
Initial moisture content (% bone-dry basis)	120	85.2	110		37.3	300	111.2
Final moisture content (% bone-dry basis)	0.5	13.6	9		5.3	11.1	1.0
Drying time (min)	35	24	11		105	192	70
Drying rate [kg water evaporated/(hr m^2)]	38.39	42.97	17.09		22.95	9.91	31.25
Air velocity (superficial)(m/sec)	1.27	1.12	0.66		1.12	1.27	1.27
Heat source per kg water evaporated [steam kg/kg gas (m^3/kg)]	gas 0.11	steam 2.0	steam 1.73		waste heat	steam 2.83	gas 0.13
Installed power (kW)	29.8	119.3	194.0		82.06	179.0	41.03

(*Perry's Chemical Engineers' Handbook,* 6th ed., McGraw-Hill, New York, 1984, Table 20-11, 20-28).

the gas, a suitable feeder for adding and dispersing particulate solids in the gas stream, a cyclone or other separation equipment, and an exhaust fan for the recovery of the final product. Figure 9.12 shows some of the many commercial equipment. Provision for recycling some of the product generally is included. Some of the materials being handled successfully in pneumatic dryers are listed in Table 9.4

Readily handled particles are in the size range 1–3 mm. When the moisture is mostly on the surface, particles up to 10 mm have been processed. Large particles are brought down to size in dispersion devices such as knife, hammer or roller mills.

Typical performance data are summarized in Table 9.13. In practice air velocities are 10–30 m/sec. The minimum upward velocity should be 2.5–3 m/sec greater than the free fall velocity of the largest particles. Particles in the range of 1–2 mm correspond to an air velocity of 25 m/sec. Since agglomerates may exist under drying conditions, the safest design is that based on pilot plant tests or prior experience.

Single pass residence times are 0.5–3 sec, but most commercial operations employ some recycling of the product so that average residence times are brought up to 60 sec. Recycling also serves to condition the feed if it is very wet. The spread of residence times in pneumatic dryers, as indicated by Figure 9.5(a), is broad, so feed that has a particularly wide size distribution may not dry uniformly. Recycling, however, assists uniformity, or several dryers in series or preclassification of particle sizes may be employed.

Since the contact time is short, heat-sensitive materials with good drying characteristics are particularly suited to this kind of dryer, but sticky materials obviously are not. Moreover, since attrition may be severe, fragile granules cannot be handled safely. Other kinds of dryers should be considered for materials that have substantial falling rate drying periods.

(a)

(b)

(c)
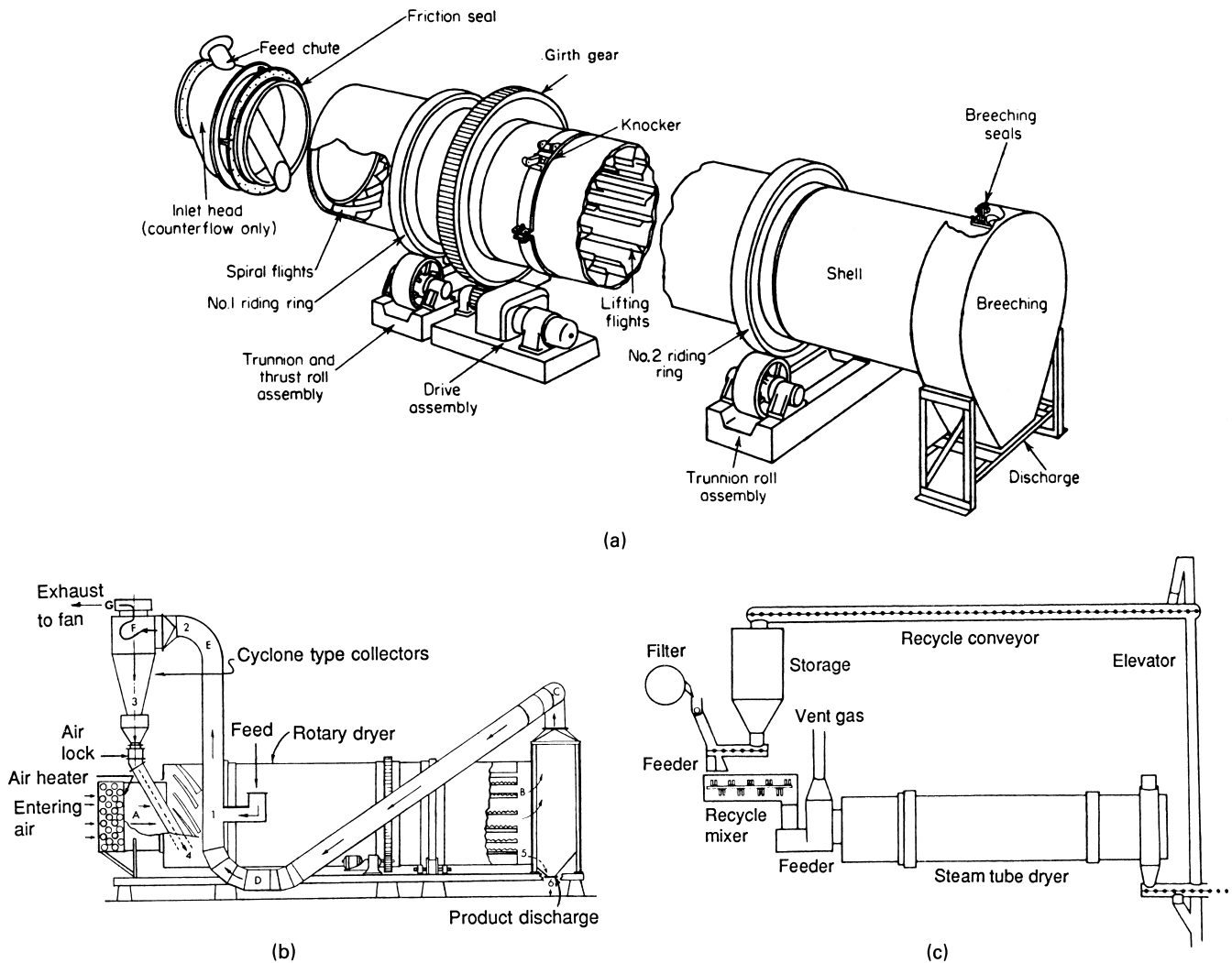
Figure 9.9. Rotary dryer assemblies. (a) Parts of the shell of a direct fired rotary dryer (*C.E. Raymond Bartlett Snow Co.*). (b) Assembly of a rotary dryer with pneumatic recycle of fines (*Standard Steel Corp.*). (c) Steam tube dryer with mechanical conveyor for partial recycle of product for conditioning of the feed. (Walas, 1988).

Pilot plant work is essential as a basis for full scale design. It may be directed to finding suitable velocities, temperatures and drying times, or it may employ more basic approaches. The data provided for Example 9.8, for instance, are of particle size distribution, partial pressure of water in the solution, and heat and mass transfer coefficients. These data are sufficient for the calculation of residence time when assumptions are made about terminal temperatures.

9.9. FLASH AND RING DRYERS

FLASH DRYERS

Flash dryers are the simplest gas suspension "pneumatic" dryers and require the least amount of space. The basic components of a flash dryer are an air heater with a gas duct, a vertical drying column (flash tube) with an expansion joint, a feed conveyor, a venturi feed section, a cyclone collector with a discharge valve, and a system fan (Papagiannes, 1992). A fan pushes air through a heater and into the bottom of the flash tube. The wet feed enters the tube

and is suspended in the air stream that carries the solid material to the collection equipment. Frequently, the flash tube has a venturi section so that the high gas velocity disperses the solid. Figure 9.12(a) is an example of a commercial unit and performance data are found in Table 9.13(a).

Various temperature-sensitive materials may be processed in this type dryer because of short material retention times and proper temperature control. Typical drying times are on the order of a few seconds. Flash dryers are most useful for moist, powdery, granular, and crystallized materials, including feeds that are wet and that are discharged from filtration equipment (Christiansen and Sardo, 2001). Because of the rapid drying process, they are often used to remove surface water, but they are not suitable for diffusion-controlled drying. Particle size of the product material is small, usually less than 500 microns, and the most suitable feed is that which can be fried, rather than a sticky material.

Flash dryers have several advantages over more complex gas-suspension dryers such as fluid-bed or rotary dryers. They are relatively simple and take up less space, as noted earlier, hence, they require a lower capital investment.
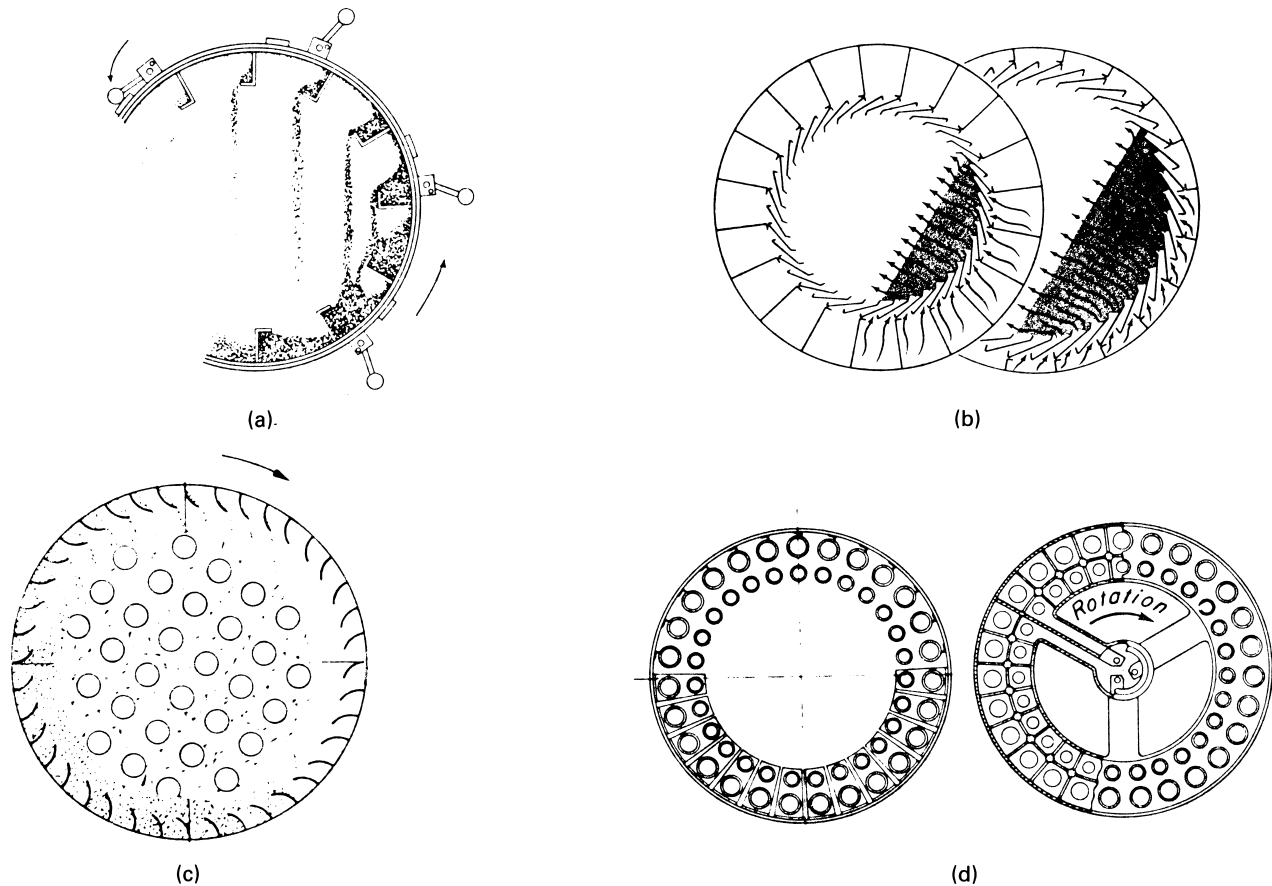
Figure 9.10. Cross sections of rotary dryers. (a) Action of the flights in cascading the drying material. The knockers are for dislodging material that tends to cling to the walls. (b) Cross section of chamber of rotolouvre dryer showing product depths and air flows at feed and discharge ends. The air enters at the wall and flows through the bed as well as through the cloud of showered particles (*Link-Belt Co*.). (c) Showering action in a dryer with fixed steam tubes and rotating shell. (d) Section and steam manifold at the end of a dryer in which the steam tubes rotate with the dryer. (Walas, 1988).

RING DRYERS

The ring dryer is a variation of the flash dryer design. The difference between the conventional flash dryer and the ring dryer is the integral centrifugal classifier (mill) in the latter unit. In a conventional flash dryer, the residence time is fixed. Because of the design features of the ring dryer, residence time is controlled by means of an adjustable internal mill that can simultaneously grind and dry the product to a specific size and moisture content. Fine particles that dry quickly leave without passing through the internal mill, whereas larger particles that are slower to dry have a greater residence time.

Figure 9.12(c) shows that material circulates through the ring-shaped path and the product is withdrawn through the cyclone and bag filter. Performance data for a typical ring dryer are found in Table 9.13(c).

9.10. FLUIDIZED BED DRYERS

Free-flowing granular materials that require relatively short drying times are particularly suited to fluidized bed drying. When longer drying times are necessary, multistaging, recirculation or batch operation of fluidized beds still may have advantages over other modes.

A fluidized bed is made up of a mass of particles buoyed up out of permanent contact with each other by a flowing fluid. Turbulent activity in such a bed promotes high rates of heat and mass transfer and uniformity of temperature and composition throughout. The basic system includes a solids feeding device, the fluidizing chamber with a perforated distributing plate for the gas, an overflow duct for removal of the dry product, a cyclone and other equipment for collecting fines, and a heater and blower for the gaseous drying medium.

Much ingenuity has been applied to the design of fluidized bed drying. Many different arrangements of equipment are illustrated and described in the comprehensive book of Kröll (1978) for instance. Figure 9.13(a) depicts the basic kind of unit and the other items are a few of the many variants. Tables 9.14 and 9.15 are selected performance data.

Fluid-bed dryers are useful for drying heat sensitive materials where exit temperatures should not exceed 200°F. Control of temperature in stable fluidization is easily maintained with essentially no hot spots in the bed.

Shallow beds are easier to maintain in stable fluidization and of course exert a smaller load on the air blower. Pressure drop in the air distributor is approximately 1 psi and that through the bed equals the weight of the bed per unit cross section. Some pressure drop data are shown in Table 9.14. The cross section is determined

EXAMPLE 9.5
Scale-Up of a Rotary Dryer

Tests on a laboratory unit come up with the stated conditions for drying a pelleted material at the rate of 1000 lb dry/hr:

Air
320 F
H = 0.013

160 F
H = 0.0428

W = 0.05 lb/lb
110 F

Stock
1000 lb/hr
W = 0.6 lb/lb
70 F
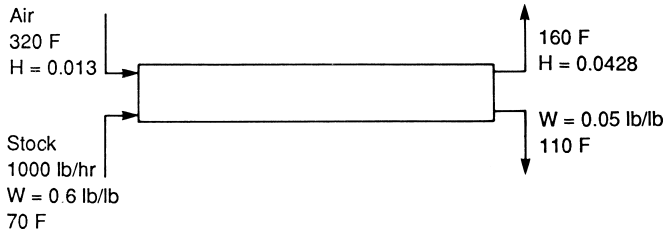
The residence time is 20 min. The speed is 3–4 rpm. On the average, 7.5% of the cross section is occupied by solid. Because of dusting problems, the linear velocity of the air is limited to 12 ft/sec. The diameter and length will be found. Since the inlet and outlet conditions are specified and the moisture transfer is known, the heat balance can be made. The heat capacity of the solid is 0.24:

$$\text{moisture evap} = 1000(0.6 - 0.05) = 550 \, \text{lb/hr}$$
$$\text{air rate} = 550/(0.0428 - 0.013) = 18,456 \, \text{lb/hr}$$

Off a psychrometric chart, the sp vol of the air is 15.9 cuft/(lb dry). The diameter is

$$D = \left(\frac{18,456(15.9)}{3600(12)(1 - 0.075)\pi/4}\right)^{1/2} = 3.06 \, \text{ft}, \quad \text{say} \ 3.0 \, \text{ft}.$$

The length is

$$L = \frac{30(20/60)}{0.075\pi D^2/4} = 18.9 \, \text{ft}.$$

EXAMPLE 9.6
Design Details of a Countercurrent Rotary Dryer

Pilot plants indicate that a residence time of 3 hr is needed to accomplish a drying with the conditions indicated on the sketch. For reasons of entrainment, the air rate is limited to 750 lbs dry/(hr)(sqft cross section). Properties of the solid are 50 lb/cuft and 0.22 Btu/(lb)(°F). Symbols on the sketch are A = dry air, S = dry solid, W = water:

136 F
A lb/hr

150 psig steam
290 F   60 F Air
H = 0.008

Stock
S = 1000
W = 334
60 F

S = 1000 lb/hr
W = 1 lb/hr
260 F
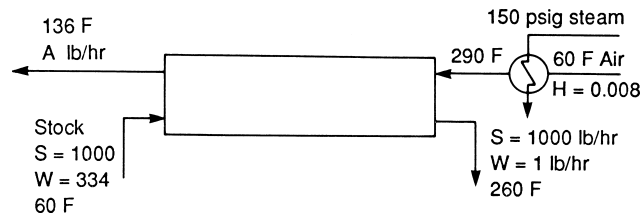
In terms of the dry air rate, A lb/hr, the average moist heat capacity is

$$C = 0.24 + 0.45[0.008 + \frac{1}{2}(333/A)] = 0.2436 + 74.93/A.$$

In the dryer, the enthalpy change of the moist air equals the sum of the enthalpy changes of the moisture and of the solid. Add 7% for heat losses. With steam table data,

$$(0.2436 + 74.93/A)A(290 - 136) = 1.07[333(1120.3) + 1(228)$$
$$+ 1000(0.22)(260 - 60) - 334(28)]$$
$$= 1.07(407,936) = 43,649],$$
$$\therefore A = 11,633 \, \text{lb/hr}.$$

The exit humidity is

$$H = 0.008 + 333/11,633 = 0.0366 \, \text{lb/lb},$$

which corresponds to an exit dewpoint of 96°F, an acceptable value.

With the allowable air rate of 750 lb/hr sqft, the diameter of the dryer is

$$D = \sqrt{11,633/750\pi/4} = 4.44 \, \text{ft}, \text{say} \ 4.5 \, \text{ft}.$$

Say the solid occupies 8% of the cross section. With a solids density of 50 lb/cuft, the dryer volume,

$$V = 3(1000/50)/0.08 = 750 \, \text{cuft},$$

and the length is

$$L = 750/(4.5)^2\pi/4 = 47.2 \, \text{ft}.$$

The standard number of flights is 2–4 times the diameter, or

$$\text{number} = (2 - 4)4.5 = 9 - 18, \text{ say} \ 12.$$

The product of rpm and diameter is 25–35

$$\therefore \text{rpm} = (25 - 35)/4.5 = 5.5 - 7.8, \text{ say} \ 6.7.$$

The steam heater duty is

$$Q_s = 11,633(0.2436)(290 - 60) = 651,733 \text{Btu/hr},$$
$$150 \, \text{psig steam},$$
$$\text{stm} = 651,733/857 = 760.5 \, \text{lb/hr}.$$

Evaporation efficiency is

$$\eta = 333/760.5 = 0.438 \, \text{lbwater/lb stm}.$$

The efficiency of the dryer itself is

$$\eta_d = 407,936/651,733 = 0.626 \, \text{Btu/Btu}.$$

TABLE 9.10. Performance Data of Rotary Dryers

(a) Direct Heated Dryers

	Sugar Beet Pulp[a]	Calcium Carbonate[a]	Blast Furnace Slag[a]	Lead Concentrate[b]	Sand[b]	Zinc Concentrate[b]	Ammonium Sulphate[c]	Fine Salt[c]	Crystals[d]	Chemicals[d]
Air flow	parallel	parallel	parallel	parallel	parallel	parallel	counter	counter	counter	indirect counter
Dryer length	9 ft 2 in.	6 ft 3 in.	7 ft 2 in.	4 ft 6 in.	4 ft 6 in.	7 ft 6 in.	9 ft 0 in.	5 ft 0 in.	10 ft 0 in.	4 ft 6 in.
Dryer length	46 ft 0 in.	34 ft 0 in.	40 ft 0 in.	35 ft 6 in.	32 ft 6 in.	60 ft 0 in.	40 ft 0 in.	40 ft 0 in.	60 ft 0 in.	27 ft 0 in.
Method of heating	oil	oil	oil	oil	gas	oil	gas	steam	steam	Louisville steam tube
Method of feed	screw	belt	belt	screw	chute	screw	conveyor	feeder	screw	screw
Initial moisture (% w/w)	82	13.5	33	14	5.65	18	2.5	5.0	7.0	1.5
Final moisture (% w/w)	10	0.5	nil	8	0.043	8	0.2	0.1	8.99	0.1
Evaporation (lb/hr)	34,000	6000	11,600	1393	701	8060	1120	400	1150	63
Capacity (lb evaporated/ft³ dryer volume)	11	6	7	2.5	1.35	2.3	0.5	0.52	0.245	—
Efficiency (Btu supplied/water evaporated)	1420	1940	1710	2100	2550	1850	1920	2100	1650	—
Inlet air temperature (°F)	1560	1560	1560	1300	1650	1500	400	280	302	—
Outlet air temperature (°F)	230	220	248	200	222	200	180	170	144	—
Residence time (av. min)	20	25	30	20	12	20	15	40	70	30/40
Fan HP	70	40	50	20	5	75	25	8	—	10
Motive HP	15	20	25	10	10	55	60	15	60	—
Fan capacity (std. air ft³/min)	45000	8500	18,000	2750	2100	12,000	18,500	6500	—	—

[a]Courtesy Buell Ltd.
[b]Courtesy Head Wrightson (Stockton) Ltd.
[c]Courtesy Edgar Allen Aerex Ltd.
[d]Courtesy Constantin Engineers Ltd.—Louisville Dryers; Williams–Gardner, 1971; Walas, 1988.

(b) Roto–Louvre Dryers

	Bone Meal	Sugar[a]	Sulfate of Ammonia[a]	Bread Crumbs	Bentonite
Dryer diameter	7 ft 6 in.	7 ft 6 in.	7 ft 6 in.	4 ft 6 in.	8 ft 10 in.
Dryer length	12 ft 0 in.	25 ft 0 in.	25 ft 0 in.	20 ft 0 in.	30 ft 0 in.
Initial moisture (% w/w basis)	17.0	1.5	1.0	37	45
Final moisture (% w/w basis)	7.0	0.03	0.2	2.5	11
Method of feed	screw	screw	chute	chute	chute
Evaporation rate (lb/hr)	1660	500	400	920	7100
Efficiency (Btu supplied/lb evaporation)	74.3	40	—	55	62.5
Method of heating	steam	steam	steam	gas	oil
Inlet air temperature (°F)	203	194	248	572	842
Outlet air temperature (°F)	122	104	149	158	176
Residence time, min	9.3	12.5	9.0	25.7	37.3
Fan HP (absorbed)	49.3	52.2	55	13.7	54.3
Motive HP (absorbed)	8	12.5	15	2.3	20.0
Fan capacity (ft³/min)					
Inlet	9560	18,000	16,000	5380	20,000
Outlet	14,000	22,300	21,000	5100	25,000

[a]Combined two-stage dryer-cooler.
(Courtesy Dunford and Elliott Process Engineering Ltd.; Williams–Gardner, 1971; Walas, 1988).

(c) Roto–Louvre Dryers

Material Dried	Ammonium Sulfate	Foundry Sand	Metallurgical Coke
Dryer diameter	2 ft 7 in.	6 ft 4 in.	10 ft 3 in.
Dryer length	10 ft	24 ft	30 ft
Moisture in feed (% wet basis)	2.0	6.0	18.0
Moisture in product (% wet basis)	0.1	0.5	0.5
Production rate (lb/hr)	2500	32,000	38,000
Evaporation rate (lb/hr)	50	2130	8110
Type of fuel	steam	gas	oil
Fuel consumption	255 lb/hr	4630 ft^3/hr	115 gal/hr
Calorific value of fuel	837 Btu/lb	1000 Btu/ft^3	150,000 Btu/gal
Efficiency (Btu supplied per lb evaporation)	4370	2170	2135
Total power required (HP)	4	41	78

(FMC Corp.; *Chemical Engineers' Handbook*, 1999, Table 12-25, p. 12–65).

(d) Indirect–Direct Double Shell Dryers

	Indirect–Direct Double Shell		
	Coal	Anhydrite	Coke
Dryer diameter	7 ft 6 in.	5 ft 10 in.	5 ft 10 in.
Dryer length	46 ft 0 in.	35 ft 0 in.	35 ft 0 in.
Initial moisture content (% w/w basis)	22	6.0	15
Final moisture (% w/w basis)	6	1.0	1.0
Evaporation rate (lb/hr)	5800	2300	1600
Evaporation—volume ratio (lb/ft^3/hr)	3.5	3.15	2.2
Heat source	coal	oil	oil
Efficiency (Btu supplied/lb water evaporated)	1250	1250	1340
Inlet air temperature (°F)	1200	1350	1350
Outlet air temperature (°F)	160	160	200

(Courtesy Edgar Allen Aerex Ltd.; Williams–Gardner, 1971; Walas, 1988).

(e) Steam Tube Dryers

	Class 1	Class 2	Class 3
Class of materials	high moisture organic, distillers' grains, brewers' grains, citrus pulp	pigment filter cakes, blanc fixe, barium carbonate, precipitated chalk	finely divided inorganic solids, water-ground mica, water-ground silica, flotation concentrates
Description of class	wet feed is granular and damp but not sticky or muddy and dries to granular meal	wet feed is pasty, muddy, or sloppy, product is mostly hard pellets	wet feed is crumbly and friable, product is powder with very few lumps
Normal moisture content of vet feed (% dry basis)	233	100	54
Normal moisture content of product (% dry basis)	11	0.15	0.5
Normal temperature of wet feed (K)	310–320	280–290	280–290
Normal temperature of product (K)	350–355	380–410	365–375
Evaporation per product (kg)	2	1	0.53
Heat load per lb product (kJ)	2250	1190	625
Steam pressure normally used (kPa gauge)	860	860	860
Heating surface required per kg product (m^2)	0.34	0.4	0.072
Steam consumption per kg product (kg)	3.33	1.72	0.85

(*Chemical Engineers' Handbook*, 1999, Table 12.23, p. 12.63).
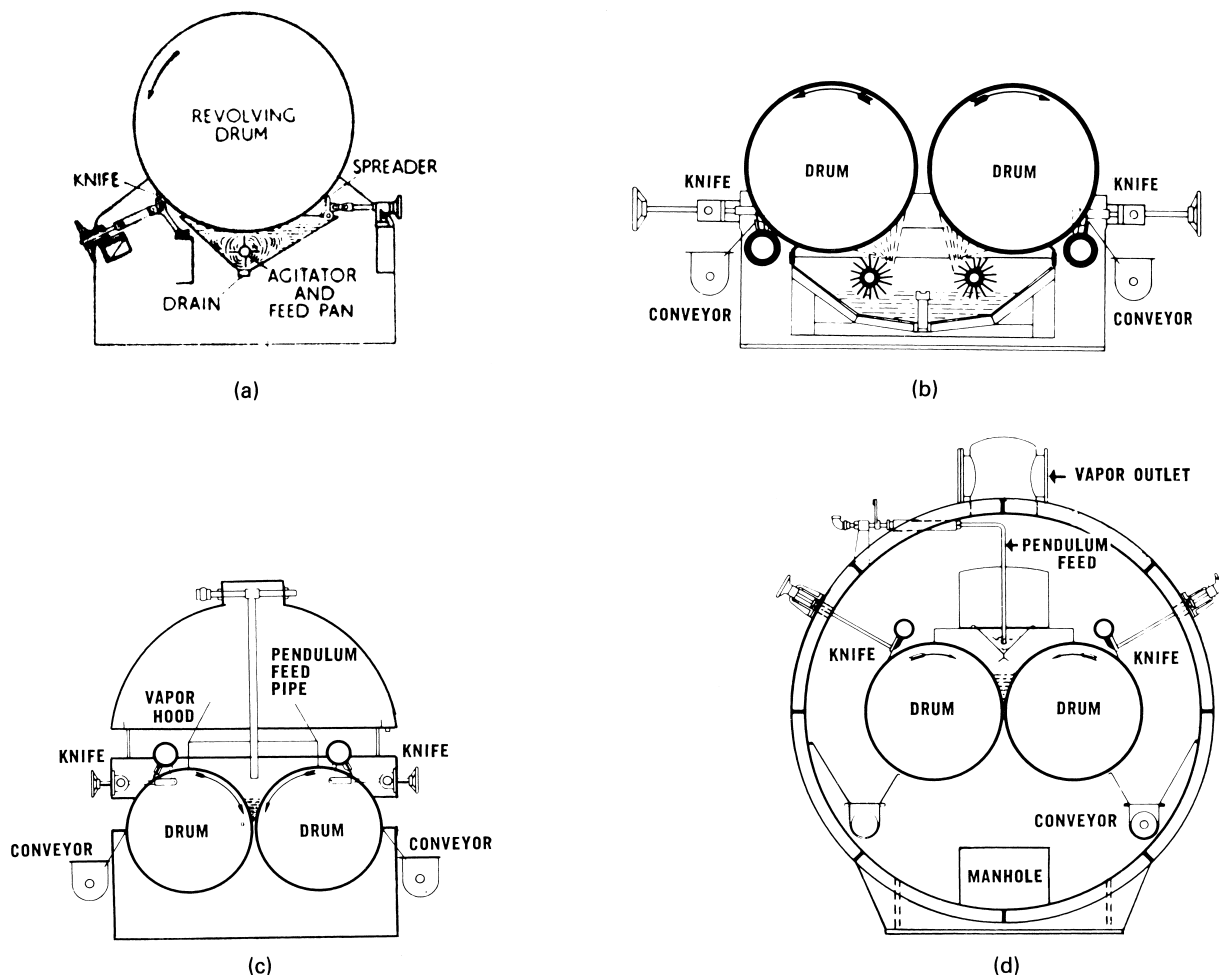
Figure 9.11. Drum dryers for solutions and thin slurries (*Buflovak Equip. Div., Blaw Knox Co.*). (a) Single drum dryer with dip feed and spreader. (b) Double drum dryer with splash feed. (c) Double drum dryer with top feed, vapor hood, knives and conveyor. (d) Double drum dryer with pendulum feed, enclosed for vacuum operation. (Walas, 1988).

by the gas velocity needed for fluidization as will be described. It is usual to allow 3–6 ft of clear height between the top of the bed and the air exhaust duct. Fines that are entrained are collected in a cyclone and blended with the main stream since they are very dry due to their small size. Normally entrainment is 5–10% but can be higher if the size distribution is very wide. It is not regarded as feasible to permit high entrainment and recycle back to the drying chamber, although this is common practice in the operation of catalytic cracking equipment.

Mixing in shallow beds is essentially complete; Figure 9.5(c) shows some test data in confirmation. The corresponding wide

distribution of residence times can result in nonuniform drying, an effect that is accentuated by the presence of a wide distribution of particle sizes. Multiple beds in series assure more nearly constant residence time for all particles and consequently more nearly uniform drying. The data of Table 9.14(b) are for multiple zone dryers. Figures 9.13(c) and (d) have additional zones for cooling the product before it leaves the equipment. Another way of assuring complete drying is a recirculation scheme like that of Figure 9.13(e). In batch operation the time can be made as long as necessary.

Stable fluidization requires a distribution of particle sizes, preferably in the range of a few hundred microns. Normally a size

EXAMPLE 9.7
Description of a Drum Drying System
A detergent drying plant handles 86,722 lb/day of a slurry containing 52% solids and makes 45,923 lb/day of product containing 2% water. The dryers are two sets of steam-heated double drums, each 3.5 ft dia by 10 ft, with a total surface of 440 sqft. Each drum is driven with a 10 HP motor with a variable speed transmission. Each

trolley top spreader has a 0.5 HP motor. Each side conveyor has a 1 HP motor and discharges to a common belt conveyor that in turn discharges to a bucket elevator that feeds a flaker where the product is reduced to flakes less than 0.25 in. square. Fines are removed in an air grader and recycled to the dryer feed tank.

TABLE 9.11. Performance Data of Drum Dryers

(a) Drum Dryers

	Yeast Cream	Stone Slop	Starch Solutions	Glaze	Zirconium Silicate	Brewers Yeast	Clay Slip
Feed solids (% by weight)	16	40	36	64	70	25	75
Product moisture (% w/w basis)	5.7	0.2	5	0.2	0.2	5	9
Capacity (lb prod./hr)	168	420	300–400	225	1120	146	4000
Dryer type (a) single, (b) twin, (c) double	(a)	(a)	(a)	(a)	(a)	(a)	(a)
Drum							
diameter	4 ft 0 in.	2 ft 6 in.	48 in.	18 in.	36 in.	28 in.	48 in.
length	10 ft 0 in.	5 ft 0 in.	120 in.	36 in.	72 in.	60 in.	120 in.
Type of feed method	top roller	dip	top roller	side	dip	center nip	side
Steam pressure (lb/in^2 gauge)	80	60	80	—	80	40	40
Atmospheric or vacuum	atmos.	atmos.	atmos.	atmos.	atmos.	atmos.	atmos.
Steam consumption (lb/lb evaporated)	—	—	1.3	1.3	—	—	1.35
Average effective area (%)	—	—	86	—	—	—	65
Evaporation/ft^2/hr	6.5	4	5	9	8.4	6	8.4

(Courtesy A.P.V. Mitchell Dryers, Ltd.; Williams–Gardner, 1971; (Walas, 1988).

(b) Drum Dryers in the Size Range 0.4 × 0.4–0.8 × 2.25 m[a]

Type of Dryer and Feed Size by Letter, A, B, or C	Drum Speed (rev/min)	Steam Press (bar, g)	Type of Material	Physical Form of Feed	Solids in Feed (%)	H$_2$O in Product (%)	Output of Dried Product (g/sec m^2)	Evaporation Rate of Water (g/sec m^2)
			inorganic salts					
Single (dip)	4.4	3.5[b]	alk. carbs	—	50	8–12	5.5	4.9
Single (splash)	1	3.0	Mg(OH)$_2$	thick slurry	35	0.5	1.9	1.5
Twin (splash) A	3	3.0	Fe(OH)$_3$	thin slurry	22	3.0	4.3	1.3
Double	3–8	5.0	Na Acetate	solution	20	0.4–10	2.0–7.0	8–24
Double and twin	7–9	2–3	Na$_2$SO$_4$	solution	24	0.15–5.5	4.7–6.1	11–12
Double and twin	5–9	4–6	Na$_2$HPO$_4$	solution	44	0.8–0.9	8.2–11.1	9–14
Twin (dip) A	5	5.5	organic salts	solution	27	2.8	1.9	5.2
Twin A	3	5.5	organic salts	solution	33	13.0	1.4	2.6
Twin B	2[c]	3.5	organic salts	solution	20	1.0	1.0	3.8
Twin C	5	5.5	organic salts	solution	39	0.4	3.9	6.1
Twin C	5$\frac{1}{2}$	5.5	organic salts	solution	42	1.0	2.1	4.6
Twin C	6	5.5	organic salts	solution	35	5.0	4.1	7.2
Twin (splash) A	3–5	5.0	organic salts	thin slurry	20	1.7–3.1	1.0–1.9	3.7–7.3
Double A	5$\frac{1}{2}$	6.0	organic salts	solution	11	—	1.1	9
Double B	6$\frac{1}{2}$	5–6	organic salts	solution	40	3	3.4	4.9
Twin (dip) A	5	5.5		thin slurry	30	1.2	2.4	5.5
Twin A	5	5.0	organic	viscous soln.	28	10.5	1.9	4.2
Double	2	3.0	compounds	viscous soln.	—	6.0	0.7	—
Double	4$\frac{1}{2}$	3.5		thin slurry	25	1.0	0.4–1.9	3.5–5.0
Twin (dip)	5	5.0	organic	(a) solution	25	0.5	0.3	0.8
Twin	10	5.5	compounds of	(b) thick slurry	30	2.5	2.0	4.6
Twin	10	5.5	low surface tension	(c) thick slurry	35	—	3.1	—
Double	11	5.5	similar letters	(b) thin paste	46	—	6.4	7.3
Double	12	5.5	for same	(c) thick paste	58	—	6.0	4.3
Double	11	5.5	compound	(a) solution	20	0.5	0.24	1.0

[a] Dryer dia and width (m): (A) 0.457 × 0.457; (B) 0.71 × 1.52; (C) 0.91 × 2.54.
[b] Plus external hot air flow.
[c] Stainless steel drum.
(Nonhebel and Moss, 1971; Walas, 1988).

of 4 mm or so is considered an upper limit, but the coal dryers of Tables 9.15(a) and (b) accommodate sizes up to 0.5 in. Large and uniformly sized particles, such as grains, are dried successfully in spouted beds [Fig. 9.13(f)]: Here a high velocity gas stream entrains the solid upward at the axis and releases it at the top for flow back through the annulus. Some operations do without the mechanical draft tube shown but employ a naturally formed central channel.

One way of drying solutions or pastes under fluidizing conditions is that of Figure 9.13(g). Here the fluidized mass is of auxiliary spheres, commonly of plastic such as polypropylene, into which the solution is sprayed. The feed material deposits uniformly on the spheres, dries there, and then is knocked off automatically as it leaves the drier and leaves the auxiliary spheres behind. When a mass of dry particles can be provided to start a fluidized bed drying process, solutions or pastes can be dried after deposition on the seed material as on the auxiliary spheres. Such a process is employed, for instance, for growing fertilizer granules of desired larger sizes, and has largely replaced rotary dryers for this purpose.

TABLE 9.12. Performance of Drum Dryers

(a) Single, Double drum and Vacuum Drums

Material	Method of Feed	Moisture Content, (% Wet Basis)		Steam Pressure, (lb/sq in.)	Drum Speed (rpm)	Feed Temp. (°F)	Capacity [lb product/ (hr)(sq ft)]	Vacuum (in. Hg)
		Feed	Product					
Double-drum dryer								
Sodium sulfonate	trough	53.6	6.4	63	$8\frac{1}{2}$	164	7.75	
Sodium sulfate	trough	76.0	0.06	56	7	150	3.08	
Sodium phosphate	trough	57.0	0.9	90	9	180	8.23	
Sodium acetate	trough	39.5	0.44	70	3	205	1.51	
Sodium acetate	trough	40.5	10.03	67	8	200	5.16	
Sodium acetate	trough	63.5	9.53	67	8	170	3.26	
Single-drum dryer								
Chromium sulfate	spray film	48.5	5.47	50	5	—	3.69	
Chromium sulfate	dip	48.0	8.06	50	4	—	1.30	
Chromium sulfate	pan	59.5	5.26	24	$2\frac{1}{2}$	158	1.53	
Chromium sulfate	splash	59.5	4.93	55	$1\frac{3}{4}$	150	2.31	
Chromium sulfate	splash	59.5	5.35	53	$4\frac{3}{4}$	154	3.76	
Chromium sulfate	dip	59.5	4.57	53	$5\frac{3}{4}$	153	3.36	
Vegetable glue	pan	60–70	10–12	20–30	6–7	—	1–1.6	
Calcium arsenate	slurry	75–77	0.5–1.0	45–50	3–4	—	2–3	
Calcium carbonate	slurry	70	0.5	45	2–3	—	1.5–3	
Twin-drum dryer								
Sodium sulfate	dip	76	0.85	55	7	110	3.54	
Sodium sulfate	top	69	0.14	60	$9\frac{1}{2}$	162	4.27	
Sodium sulfate	top	69	5.47	32	$9\frac{1}{2}$	116	3.56	
Sodium sulfate	splash	71	0.10	60	6	130	4.30	
Sodium sulfate	splash	71.5	0.17	60	12	140	5.35	
Sodium sulfate	splash	71.5	0.09	60	10	145	5.33	
Sodium phosphate	splash	52.5	0.59	58	$5\frac{1}{2}$	208	8.69	
Sodium phosphate	dip	55	0.77	60	$5\frac{1}{2}$	200	6.05	
Sodium sulfonate	top	53.5	8–10	63	$8\frac{1}{2}$	172	10.43	
Vacuum single-drum dryer								
Extract	pan	59	7.75	35	8	—	4.76	27.9
Extract	pan	59	2.76	35	6	—	1.92	27.9
Extract	pan	59	2.09	36	4	—	1.01	atmos.
Extract	pan	56.5	1.95	35	$7\frac{1}{2}$	—	3.19	22.7
Extract	pan	56.5	1.16	50	$2\frac{1}{2}$	—	0.75	atmos.
Skim milk	pan	65	2–3	10–12	4–5	—	2.5–3.2	
Malted milk	pan	60	2	30–35	4–5	—	2.6	
Coffee	pan	65	2–3	5–10	$11\frac{1}{2}$	—	1.6–2.1	
Malt extract	spray film	65	3–4	3–5	0.5–1.0	—	1.3–1.6	
Tanning extract	pan	50–55	8–10	30–35	8–10	—	5.3–6.4	
Vegetable glue	pan	60–70	10–12	15–30	5–7	—	2–4	

(*Perry's Chemical Engineers' Handbook*, 3rd ed. McGraw-Hill, New York, 1950).

A few performance data of batch fluid dryers are in Table 9.14(a). This process is faster and much less labor-intensive than tray drying and has largely replaced tray drying in the pharmaceutical industry which deals with small production rates. Drying rates of 2–10 lb/(hr)(cuft) are reported in this table, with drying times of a fraction of an hour to several hours. In the continuous operations of Table 9.15, the residence times are at most a few minutes.

Thermal efficiency of fluidized bed dryers is superior to that of many other types, generally less than twice the latent heat of the water evaporated being required as heat input. Power requirements are a major cost factor. The easily dried materials of Table 9.15(a) show evaporation rates of 58–103 lb/(hr)(HP installed) but the more difficult materials of Table 9.15(d) show only 5–18 lb/(hr) (HP installed). The relatively large power requirements of fluidized bed dryers are counterbalanced by their greater mechanical simplicity and lower floor space requirements.

Air rates in Table 9.15 range from 13 to 793 SCFM/sqft, which is hardly a guide to the selection of an air rate for a particular case. A gas velocity twice the minimum fluidization velocity may be taken as a safe prescription. None of the published correlations of minimum fluidizing velocity is of high accuracy. The equation of Leva (1959) appears to be as good as any of the later ones. It is

$$G_{mf} = 688D_p^{1.83}[\rho_g(\rho_s - \rho_g)]^{0.94}/\mu^{0.88}, \tag{9.20}$$

where G_{mf} is in lb/(hr)(sqft), ρ_g and ρ_s are densities of the gas and solid (lb/cuft), D_p is the particle diameter (in.), and μ is the gas viscosity (cP). In view of the wide scatter of the data on which this correlation is based, it appears advisable to find the fluidization velocity experimentally for the case in hand.

All aspects of fluidized bed drying must be established with pilot plant tests. The wide ranges of performance parameters in Tables 9.14 and 9.15 certainly emphasize this conclusion. A limited

TABLE 9.12.—(continued**)**

(b) Single and Double Drum with Various Feed Arrangements

Kind of Dryer, Kind of Stock	Moisture Content In (%)	Moisture Content Out (%)	Vapor Pressure Absolute (bar)	Rotation Speed (1/min)	Unit Product Capacity (kg/m² hr)	Drying Rate (kg/m² hr)
Single drum, dip feed						
Alkali carbonate	50	8 bis 12	3.5	4.4	20	17.8
Double drum, dip feed						
Organic salt solution	73	2.8	5.5	5	6.8	18.6
Organic compound, dilute slurry	70	1.2	5.5	5	8.6	19.6
Organic compound, solution	75	0.5	5.0	5	1.1	1.9
Single drum with spreading rolls						
Skim milk concentrate	50	4	3.8	24	15.8	14.2
Whey concentrate	45	4.3	5.0	16	10 bis 11.8	7.4 bis 8.8
Cuprous oxide	58	0.5	5.2	10	11.0	14.3
Single drum, splash feed						
Magnesium hydroxide, dense slurry	65	0.5	3.0	1	6.8	5.4
Double drum, splash feed						
Iron hydroxide, dilute slurry	78	3.0	3.0	3	15.4	4.7
Organic salt, dilute slurry	80	1.7 bis 3.1	5.0	3 bis 5	3.6 bis 6.8	13.3 bis 26.2
Sodium acetate	50	4.0	6.0	5	10.0	9.3
Sodium sulfate	70	2.3	7.8	5	18.0	40.4
Double drum, top feed						
Beer yeast	80	8.0	6.0	5	10.0	36.2
Skim milk, fresh	91.2	4.0	6.4	12	6.2	61.5
Organic salt solution	89	—	6.0	5.5	4	32.3
Organic salt solution	60	3	5 bis 6	6.5	12.2	17.7
Organic compound, dilute slurry	75	1	3.5	4.5	1.4 bis 6.8	12.6 bis 18
Double drum with spreading rolls						
Potato pulp	76.2	11.4	8	5	22.5	61.1

(Kröll, 1978, p. 348; Walas, 1988).

exploration of air rates and equipment size can be made on the basis of a drying rate equation and fluidization correlations from the literature. This is done in Example 9.9. A rough approximation of a drying rate equation can be based on through circulation drying of the granular material on a tray, with gas flow downward.

The vibrating conveyor dryer is a modification of the fluid bed dryer. The fluidization is maintained by a combination of pneumatic and mechanical forces. The heated gas enters beneath the conveying deck through ducts and passes up through a screen, perforations, or a slotted conveying deck. A combination pressure blower/exhaust fan system is employed to balance the pressure above the conveying deck and the atmosphere outside. The equipment provides economical heat transfer area, i.e., low capital cost as well as economical operating expenses. This dryer is suitable for free-flowing solids greater than 100 mesh having surface moisture only. The air velocities must be such as to fluidize the particles without creating excessive dust. Figure 9.13(h) is an example of a commercial unit.

TABLE 9.13. Performance Data of Pneumatic Conveying Dryers (Sketches in Fig. 9.12)

(a) Raymond Flash Dryer

	Fine Mineral	Spent Grain	Organic Chemical	Chicken Droppings	Fine Coal Filter Cake
Method of feed	pump	belt	screw	pump	screw
Material size, mesh	−100	—	−30	—	−30
Product rate (lb/hr)	27,000	9000	900	2300	2000
Initial moisture content (% w/w basis)	25	60	37	70	30
Final moisture content (% w/w basis)	nil	12	3	12	8.5
Air inlet temperature (°F)	1200	1200	450	1300	1200
Air outlet temperature (°F)	200/300	200/300	200/300	200/300	200/300
Method of heating	direct oil	direct oil	direct oil	direct oil	direct oil
Heat consumption (Btu/lb water evaporated)	1.6×10^3	1.9×10^3	3.1×10^3	1.9×10^3	1.4×10^3
Air recirculation	no	no	no	no	no
Material recirculation	yes	yes	no	yes	no
Material of construction	MS	MS/SS	MS	MS	MS
Fan capacity (std. ft³/min)	18,000	22,000	4300	8500	1500
Installed fan HP	110	180	30	50	10
Product exit temperature (°F)	200	—	200	—	135

(Courtesy International Combustion Products Ltd.; Williams–Gardner, 1971; Walas, 1988).

TABLE 9.13.—(continued**)**

(b) Buttner–Rosin Pneumatic Dryer

	Metallic Stearate	Starch	Adipic Acid	Fiber	Coal Filter Cake
Method of feed	sling	sling	screw	distributor	distributor
Material size	fine	fine	−30 mesh	−$\frac{1}{4}$ in.	−30 mesh
Product rate (lb/hr)	280	13,236	10,000	2610	67,200
Initial moisture (% w/w basis)	40	34	10	62.4	32
Final moisture (% w/w basis)	0.5	13	0.2	10	6
Air inlet temperature (°F)	284	302	320	752	1292
Air outlet temperature (°F)	130	122	149	230	212
Method of heating	steam	steam	steam	oil	PF
Heat consumption (Btu/lb/water evaporated)	2170	1825	2400	1720	1590
Air recirculation	no	no	no	no	yes
Material recirculation	yes	no	yes	yes	yes
Fan capacity (std. ft³/min)	1440	26,500	9500	12,500	27,000
Installed fan HP	15	220	65	60	250
Product exit temperature (°F)	104	95	120	140	158

(Courtesy Rosin Engineering Ltd.; Williams–Gardner, 1971; Walas, 1988).

(c) Pennsalt–Berks Ring Dryer

	Metal[a] Stearates	Spent[a] Grains	Sewage[b] Sludge	Starches	Polystyrene Beads
Method of Feed	belt feeder rotary valve	back mixer rotary valve	vibratory feeder rotary valve	cascading rotary valve screen	vibratory feeder rotary valve
Product rate (lb/hr)	240	1120	4300	5000	1000
Initial moisture (% w/w basis)	55	80	45	35	2.0
Final moisture (% w/w basis)	1	5	12	10	0.2
Air inlet temperature (°F)	250	500	600	300	175
Air outlet temperature (°F)	150	170	170	130	115
Method of heating	steam	gas	oil	steam	steam
Heat consumption (Btu/lb water evaporated)	2900	1800	1750	2000	5000
Air recirculation	no	no	no	no	no
Material recirculation	yes	yes	yes	no	no
Material of construction	SS	MSG	MS	MSG	SS
Fan capacity (std ft³/min)	3750	16,500	8250	15,000	900
Installed fan HP	20	75	60	60	7.5

[a] Ring dryer application.
(Courtesy Pennsalt Ltd.; Williams–Gardner, 1971; Walas, 1988).

(d) Various Pneumatic Dryers

Material	Location	Tube Dia (cm)	Tube Height (m)	Gas Rate (m³/hr) (NTP)	Gas Temp (°C) In	Gas Temp (°C) Out	Solid Rate (kg/hr)	Solid Temp (°C) In	Solid Temp (°C) Out	Moisture (%) In	Moisture (%) Out	Air/Solid Ratio (m³/hr) (NTP)	Air/Solid Ratio (kg/kg)	Water Evaporated (kg/hr)
Ammonium sulphate	Japan	18	1	1100	215	76	950	38.5	63	2.75	0.28	1.2	1.5	23.5
Sewage sludge filter cake	U.S.A.	—	—	1200	700	121	2270	15	71	80	10	5.3	7.2	1590
Coal 6 mm	U.S.A.	—	—	50,000	371	80	51,000	15	57	9	3	1.0	1.3	4350
Hexamethylene tetramine	Germany	30	38[a]	3600	93	50	2500	—	48	6–10	0.08–0.15	1.4	1.9	18.1

[a] 23 m vertical, 15 m horizontal.
(Nonhebel and Moss, 1971; Walas, 1988).
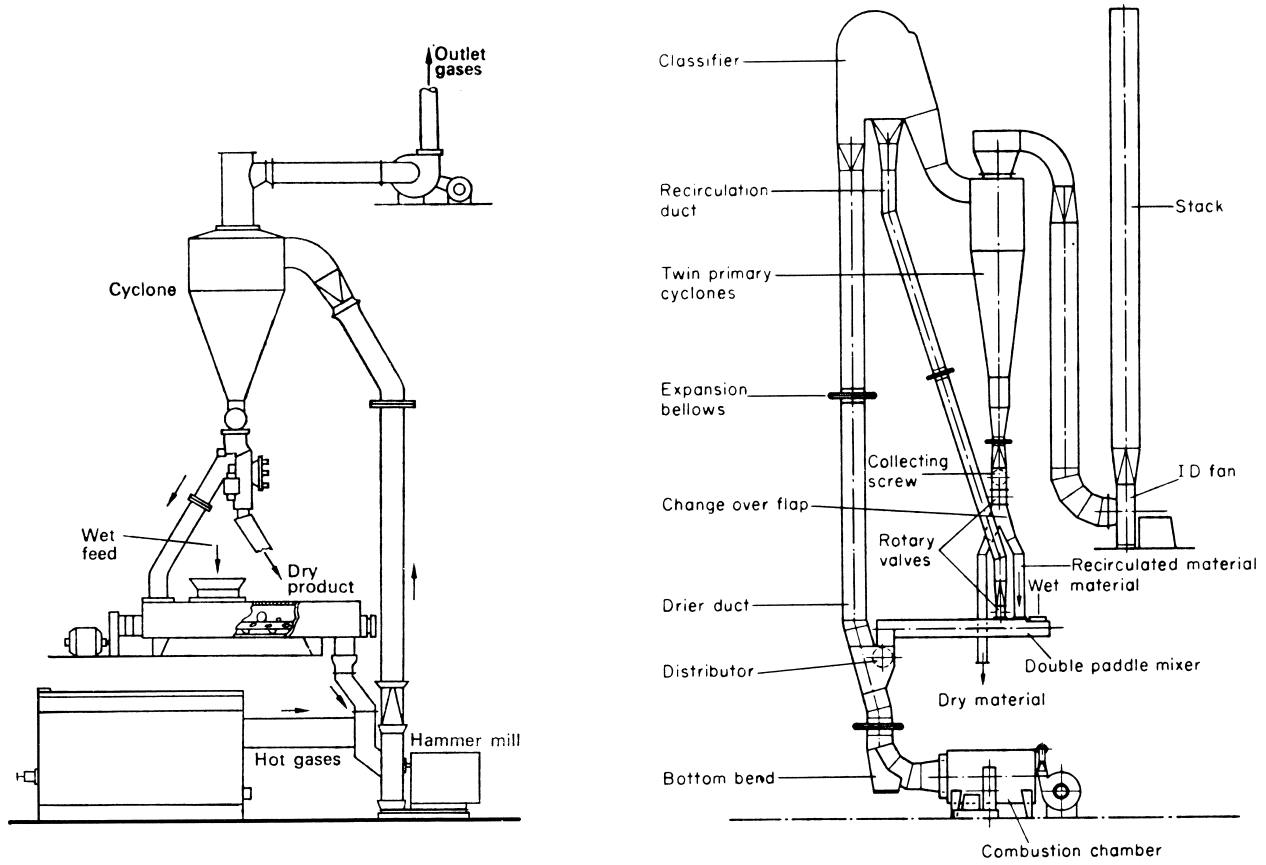
1. Fan
2. Ring duct
3. Manifold
4. Injector
5. Air outlet
6. Feeder
7. Filter
8. Heater
9. Cyclone
10. Disintegrator
11. Bag filter
12. Discharge

(a)

(b)
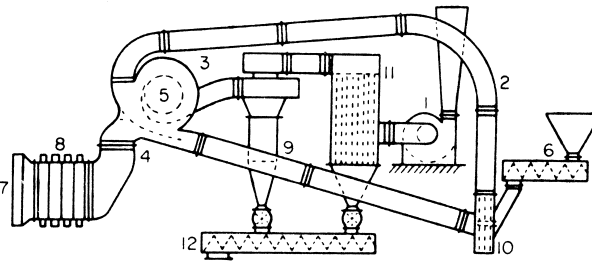
(c)
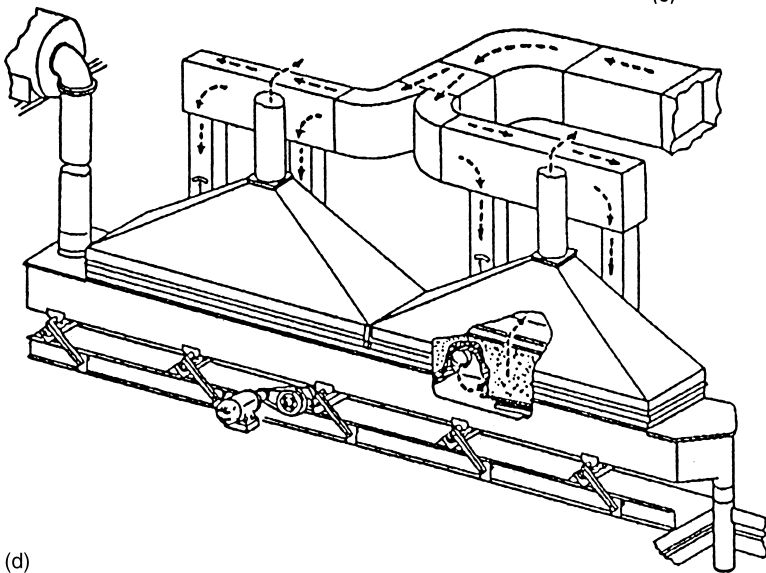
(d)

Figure 9.12. Examples of pneumatic conveying dryers; corresponding performance data are in Table 9.13. (a) Raymond flash dryer, with a hammer mill for disintegrating the feed and with partial recycle of product (*Raymond Division, Combustion Engineering*). (b) Buttner–Rosin pneumatic dryer with separate recycle and disintegration of large particles (*Rosin Engineering Ltd.*). (c) Berks ring dryer; the material circulates through the ring-shaped path, product is withdrawn through the cyclone and bag filter (*Pennsalt Chemical Co.*). (d) Vibrating conveyor dryer. (Courtesy of Carrier Vibrating Equipment, Inc.). (Walas, 1988).

EXAMPLE 9.8
Sizing a Pneumatic Conveying Dryer
A granular solid has a moisture content of 0.035 kg/kg dry material which is to be reduced to 0.001 kg/kg. The charge is at the rate of 9.72 kg/sec, is at 60°C and may not be heated above 90°C. Inlet air is at 450°C and has a moisture content of 0.013 kg/kg dry air. Specific gravity of the solid is 1.77 and its heat capacity is 0.39 cal/g °C. The settling velocity of the largest particle present, 2.5 mm dia, is 10 m/sec. Heat capacity of the air is taken as 0.25 cal/g °C and the latent heat at 60°C as 563 cal/g. Experimental data for this system are reported by Nonhebel and Moss (1971, pp. 240ff) and are represented by the expressions:
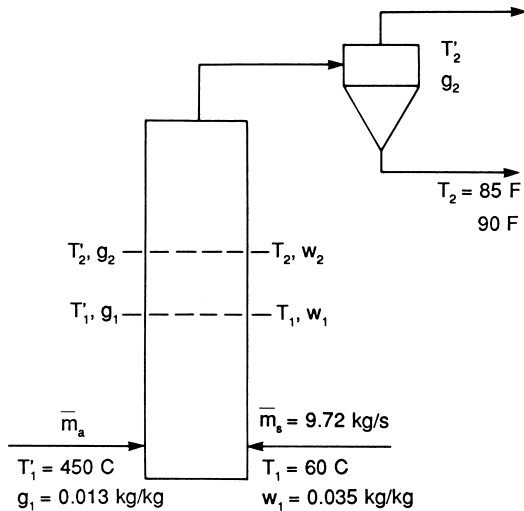
Heat transfer coefficient:

$ha = 0.47 \text{ cal}/(\text{kg solid})(°C)$.

Vapor pressure:

$P = \exp(13.7419 - 5237.0/T)$, atm, K.

Mass transfer coefficient:

$k_g a = \exp(-3.1811 - 1.7388 \ln w - 0.2553(\ln w)^2)$,

where w is the moisture content of the solid (kg/kg) in the units kg water/(kg solid)(atm)(sec).

In view of the strong dependence of the mass transfer coefficient on moisture content and the 35-fold range of that property, the required residence time and other conditions will be found by analyzing the performance over small decrements of the moisture content.

An air rate is selected on the assumption that the exit of the solid is at 85°C and that of the air is 120°C. These temperatures need not be realized exactly, as long as the moisture content of the exit air is below saturation and corresponds to a partial pressure less than the vapor pressure of the liquid on the solid. The amount of heat transferred equals the sum of the sensible heat of the wet solid and the latent heat of the lost moisture. The enthalpy balance is based on water evaporating at 60°C.

$\bar{m}_s[(0.39 + 0.001)(85 - 60) + (0.035 - 0.001)(85 - 60 + 563)]$
$= \bar{m}_a[(0.25 + 0.480(0.001))(450 - 120) + 0.48(0.034)(120 - 60)]$,

$\bar{m}_a = \dfrac{29.77\bar{m}_s}{83.64} = \dfrac{29.77(9.72)}{83.64} = \begin{cases} 3.46 \text{ kg/sec}, \\ 7.08 \text{ m}^3/\text{sec} \quad \text{at} 450° \text{ C}, \\ 3.85 \text{ m}^3/\text{sec} \quad \text{at} 120°\text{C}. \end{cases}$

At a tower diameter of 0.6 m,

$U = \dfrac{Q}{0.36\pi/4} = \begin{cases} 25.0 \text{ m/sec} \quad \text{at } 450°\text{C}, \\ 13.6 \, m/sec \quad at \, 120°C. \end{cases}$

These velocities are great enough to carry the largest particles with settling velocity of 10 m/sec.

Equations are developed over intervals in which $W_1 \rightarrow W_2$, $T_1 \rightarrow T_2$, and $T'_1 \rightarrow T'_2$.

The procedure outlined in steps through 5 is 8:

1. Start with known W_1, T_1, and T'_1.
2. Specify a moisture content W_2.
3. Assume a value T_2 of the solid temperature.
4. Calculate T'_2 from the heat balance.
5. Check the correctness of T_2 by noting if the times for heat and mass transfers in the interval are equal.

$\theta_h = \dfrac{Q}{ha(\Delta T)_{\text{lm}}} = \dfrac{Q}{0.47(\Delta T)_{\text{lm}}}$

$\theta_m = \dfrac{w_1 - w_2}{k_g a(\Delta P)_{\text{lm}}}$

Heat balance:

$\bar{m}_s[0.391(T_2 - T_1) + (W_1 - W_2)(T_2 - T_1 + 563)]$
$\quad = \bar{m}_a\{[0.25 + 0.48(0.001)](T'_1 - T'_2)$
$\quad\quad + 0.48(W_1 - W_2)(T'_2 - 60)\}$.

Substitute $\bar{m}_s / \bar{m}_a = 9.72/3.46 = 2.81$ and solve for T'_2.

$T'_2 = $
$\dfrac{\begin{array}{l} -0.25048 T'_1 + 28.8(W_1 - W_2) + 2.81 \\ \times[0.39(T_2 - T_1) + (W_1 - W_2)(T_2 - T_1 + 563)] \end{array}}{0.48(W_1 - W_2) - 0.25048}$. (1)

$g_1 = 0.013 + \dfrac{\bar{m}_s}{\bar{m}_a}(W_1 - 0.013) = 0.013 + 2.81(W_1 - 0.013)$. (2)

$P_1 = \dfrac{g_1}{18/29 + g_1} = \dfrac{g_1}{0.6207 + g_1}$ (partial pressure in air). (3)

$g_2 = 0.013 + 2.81(W_2 - 0.013)$. (4)

$P_2 = \dfrac{g_2}{0.6207 + g_2}$. (5)

$Pa_1 = \exp[13.7419 - 5237.9/(T_1 + 273.2)]$, vapor pressure. (6)

$Pa_2 = \exp[13.7419 - 5237.9/(T_2 + 273.2)]$. (7)

$(\Delta P)_{\text{lm}} = \dfrac{(Pa_1 - P_1) - (Pa_2 - P_2)}{\ln[(Pa_1 - P_1)/(Pa_2 - P_2)]}$. (8)

$(\Delta T)_{\text{lm}} = \dfrac{T'_1 - T_1 - (T'_2 - T_2)}{\ln[(T'_1 - T_1)/(T'_2 - T_2)]}$. (9)

$\Delta Q = 0.391(T_2 - T_1) + (W_1 - W_2)(T_2 - T_1 + 563)$,
per kg of solid. (10)

$\bar{W} = 0.5(W_1 + W_2)$. (11)

EXAMPLE 9.8—(*continued*)

$$k_g a = \exp[-3.1811 - 1.7388 \ln \bar{W} - 0.2553(\ln \bar{W})^2]. \quad (12)$$

$$\theta_h = \Delta Q/ha(\Delta T)_{lm} = \Delta Q/0.43(\Delta T)_{lm}, \text{ heating time.} \quad (13)$$

$$\theta_m = (W_1 - W_2)/k_g a(\Delta P)_{lm}, \text{ mass transfer time.} \quad (14)$$

$$Z = \theta_h - \theta_m \to 0 \text{ when the correct value of } T_2 \text{ has been selected.} \quad (15)$$

After the correct value of T_2 has been found for a particular interval, make $W_2 \to W_1$, $T_2 \to T_1$, and $T_2' \to T_1'$. Specify a decremented value of W_2, assume a value of T_2, and proceed. The solution is tabulated.

W	T	T1	θ(sec)
0.035	60	450	0
0.0325	73.04	378.2	0.0402
0.03	75.66	352.2	0.0581
0.025	77.41	315.3	0.0872
0.02	77.23	286.7	0.1133
0.015	76.28	261.3	0.1396
0.01	75.15	236.4	0.1687
0.005	74.67	208.4	0.2067
0.003	75.55	192.4	0.2317
0.001	79.00	165.0	0.2841

When going directly from 0.035 to 0.001,

$$T_2 = 80.28,$$
$$T_2' = 144.04,$$
$$\theta = 0.3279 \text{ sec.}$$

The calculation could be repeated with a smaller air rate in order to reduce its exit temperature to nearer 120°C, thus improving thermal efficiency.

In the vessel with diameter = 0.6 m, the air velocities are

$$u_a = \begin{cases} 25.0 \text{ m/sec at } 450° \text{ C inlet} \\ \underline{5.15 \text{ m/sec}} \quad \text{at } 165 °\text{C outlet} \end{cases}$$

20.1 m/sec average.

The vessel height that will provide the needed residence time is

$$H = \bar{u}_a\theta = 20.1(0.2841) = 5.70 \text{ m.}$$

Very fine particles with zero slip velocity will have the same holdup time as the air. The coarsest with settling velocity of 10 m/sec will have a net forward velocity of

$$\bar{u}_s = 20.1 - 10 = 10.1 \text{ m/sec,}$$

which corresponds to a holdup time of

$$\theta = 5.7/10.1 = 0.56 \text{ sec,}$$

which is desirable since they dry more slowly.

The procedure outlines in Steps 1 through 5 employing Eq. (1) through (15) will result in satisfactory fluid bed dryer design. The first step is to assume T_2 and then other quantities can be evaluated in order. A computer program using Fortran, MATHCAD, TK SOLVER, or other such programs may be used to solve this problem. Partial results for the first interval are:

$$W_1 = 0.035$$
$$W_2 = 0.0325$$
$$T_1 = 73.04$$
$$T_1' = 450$$
$$T_2 = 73.04$$
$$T_2' = 378.16969111$$

Time = 4.0228366079E-2

9.11. SPRAY DRYERS

Suitable feeds to a spray dryer are solutions or pumpable pastes and slurries. Such a material is atomized in a nozzle or spray wheel, contacted with heated air or flue gas and conveyed out of the equipment with a pneumatic or mechanical type of conveyor. Collection of fines with a cyclone separator or filter is a major aspect of spray dryer operation. Typical equipment arrangements and flow patterns are shown in Figure 9.14.

The action of a high speed spray wheel is represented by Figure 9.14(e); the throw is lateral so that a large diameter vessel is required with this form of atomization, as shown in Figure 9.14(a). The flow from nozzles is largely downward so that the dryer is slimmer and taller. Parallel flow of air and spray downward is the most common arrangement, but the right-hand figure of Figure 9.14(d) is in counterflow. Figure 9.14(c) has tangential input of cooling air. In some operations, the heated air is introduced tangentially; then the process is called mixed flow. Most of the entries in Table 9.16(a) are parallel flow; but the heavy duty detergent is in counterflow, and titanium dioxide is either parallel or mixed flow. Counterflow is thermally more efficient, results in less expansion of the product particles, but may be harmful to thermally sensitive products because they are exposed to high air temperatures as they leave the dryer. The flat bottomed dryer of Figure 9.14(c) contacts the exiting solids with cooling air and is thus adapted to thermally sensitive materials.

Two main characteristics of spray drying are the short drying time and the porosity and small, rounded particles of product.

Short drying time is a particular advantage with heat sensitive materials. Porosity and small size are desirable when the material subsequently is to be dissolved (as foods or detergents) or dispersed (as pigments, inks, etc.). Table 9.17 has some data on size distributions, bulk density, and power requirements of the several types of atomizers.

The mean residence time of the gas in a spray dryer is the ratio of vessel volume to the volumetric flow rate. These statements are made in the literature regarding residence times for spray drying:

Source	Time (sec)
Heat Exchanger Design Handbook (1983)	5–60
McCormick (1979)	20
Masters (1976)	20–40 (parallel flow)
Nonhebel and Moss (1971)	<60
Peck (1983)	5–30
Wentz and Thygeson (1979)	<60
Williams–Gardner (1971)	4–10 (<15 ft dia) / 10–20 (>15 ft dia)

Residence times of air and particles are far from uniform; Figure 9.5(a) and (b) is a sample of such data.

Because of slip and turbulence, the average residence times of particles are substantially greater than the mean time of the air, definitely so in the case of countercurrent or mixed flow. Surface moisture is removed rapidly, in less than 5 sec as a rule,

but falling rate drying takes much longer. Nevertheless, the usual drying operation is completed in 5–30 sec. The residence time distribution of particles is dependent on the mixing behavior and on the size distribution. The coarsest particles fall most rapidly and take longest for complete drying. If the material is heat-sensitive, very tall towers in parallel flow must be employed; otherwise, countercurrent or mixed flows with high air temperatures may suffice. In some cases it may be feasible to follow up incomplete spray drying with a pneumatic dryer.

Drying must be essentially completed in the straight sided zones of Figures 9.14(a) and (b). The conical section is for gathering and efficient discharge of the dried product. The lateral throw of spray wheels requires a vessel of large diameter to avoid accumulation of wet material on the walls; length to diameter ratios of 0.5–1.0 are used in such cases. The downward throw of nozzles permits small diameters but greater depths for a given residence time; *L/D* ratios of 4–5 or more are used.

ATOMIZATION

Proper atomization of feed is the key to successful spray drying. The three devices of commercial value are pressure nozzles, pneumatic nozzles, and rotating wheels of various designs. Usual pressures employed in nozzles range from 300 to 4000 psi, and orifice diameters are 0.012–0.15 in. An acceptably narrow range of droplet sizes can be made for a feed of particular physical properties by adjustment of pressure and diameter. Multiple nozzles are used for atomization in large diameter towers. Because of the expense of motive air or steam, pneumatic nozzles are used mostly in small installations such as pilot plants, but they are most suitable for dispersion of stringy materials such as polymers and fibers. The droplet size increases as the motive pressure is lessened, the range of 60–100 psi being usual. The action of a rotating wheel is indicated in Figure 9.14(e). Many different shapes of orifices and vanes are used for feeds of various viscosities, erosiveness, and clogging tendencies. Operating conditions are up to

(a)

(b)
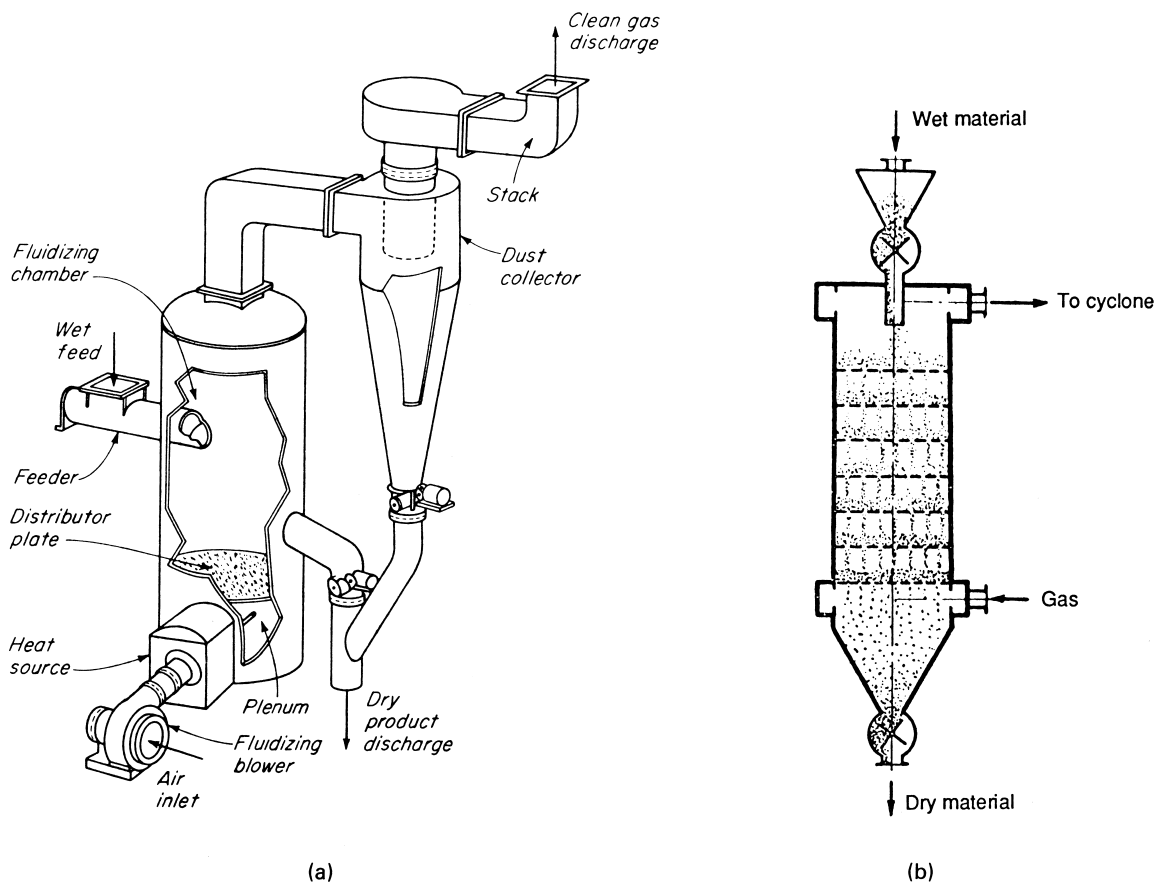
Figure 9.13. Fluidized bed dryers. (a) Basic equipment arrangement (McCabe, Smith and Harriott, Unit Operations in Chemical Engineering, 4th ed. *McGraw-Hill, New York*, 1985). (b) Multiple bed dryer with dualflow distributors; performance data are in Table 9.14(b) (*Romankov, in Davidson and Harrison*, Fluidisation, *Academic, New York, 1971*). (c) A two-bed dryer with the lower one used as cooler: (a, b, c) rotary valves; (d) drying bed; (e) cooling bed; (f, g) air distributors; (h, i) air blowers; (k) air filter; (l) air heater; (m) overflow pipe; (n) product collector (*Kroll, 1978*). (d) Horizontal multizone dryer: (a) feeder; (b) air distributor; (c) fluidized bed; (d) partitions; (e) dust guard; (f) solids exit; (g) drying zone; (h) cooling zone; (i, k) blowers; (l, m) air plenums; (n) air duct; (o) dust collector; (p) exhaust fan (*Kroll, 1978*). (e) Circulating fluidized bed used for removal of combined water from aluminum hydroxide: (a) feed; (b) fluidized bed; (c) solids exit; (d) fuel oil inlet; (e) primary air inlet; (f) secondary air inlet; (g) gas exit (*Kroll, 1978*). (f) Spouted bed with draft tube for drying coarse, uniform-sized granular materials such as grains [*Yang and Keairns*, AIChE Symp. Ser. **176**, *218* (*1978*), *Fig. 1*]. (g) Fluidized bed dryer for sludges and pastes. The fluidized solids are fine spheres of materials such as polypropylene. The wet material is sprayed in, deposits on the spheres and dries there. At the outlet the spheres strike a plate where the dried material is knocked off and leaves the dryer as flakes. The auxiliary spheres remain in the equipment: (a) feed; (b) distributor; (c) spheres loaded with wet material; (d) returning spheres; (e) striking plate; (f) hot air inlet; (g) air and solids exit (*Kroll, 1978*). (Walas, 1988).

(c)

(d)

(e)

(f)

(g)
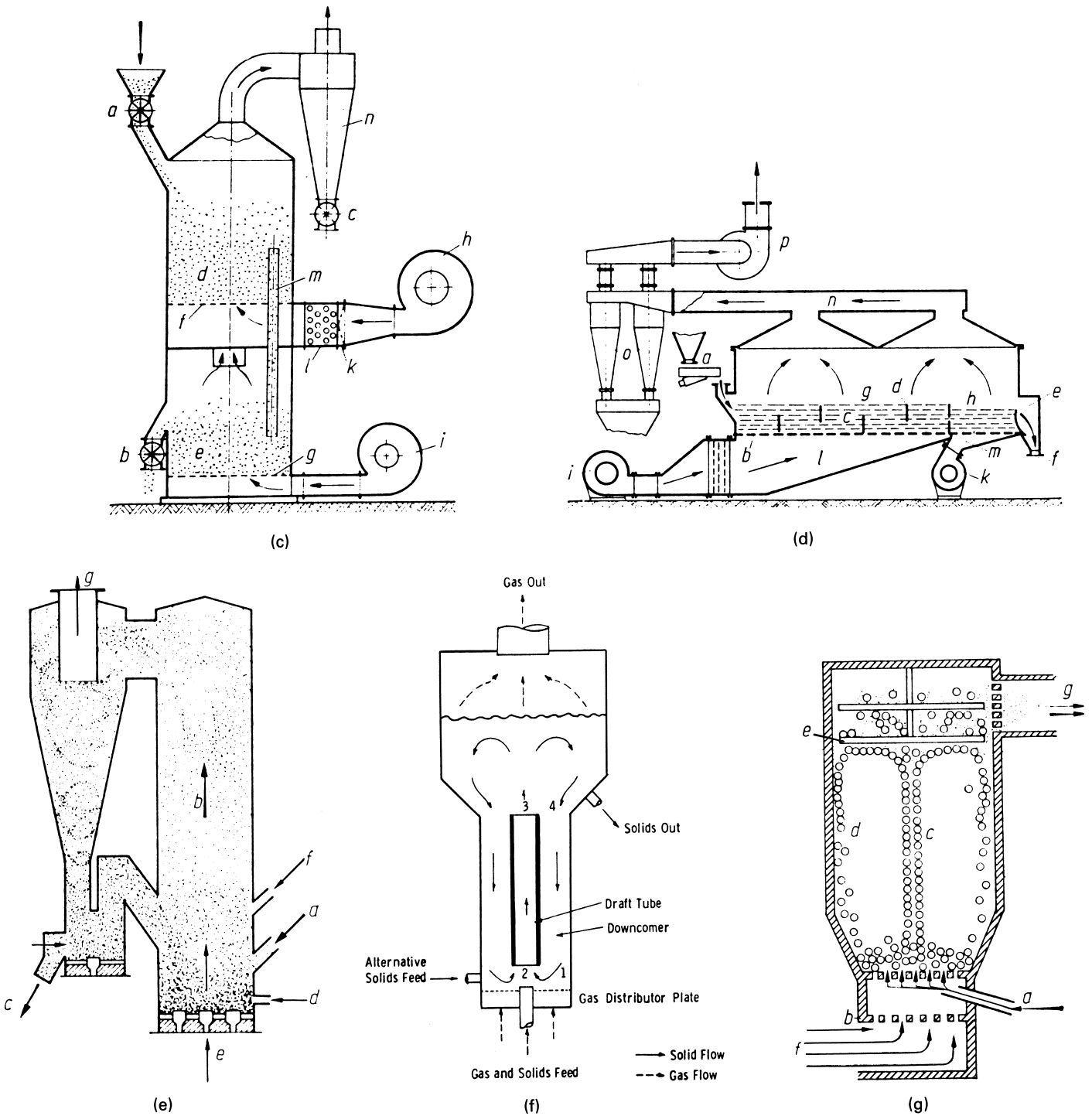
Figure 9.13.—(*continued*)

60,000 lb/hr per atomizer, speeds up to 20,000 rpm, and peripheral speeds of 250–600 ft/sec.

The main variables in the operation of atomizers are feed pressure, orifice diameter, flow rate and motive pressure for nozzles and geometry and rotation speed of wheels. Enough is known about these factors to enable prediction of size distribution and throw of droplets in specific equipment. Effects of some atomizer

characteristics and other operating variables on spray dryer performance are summarized in Table 9.18. A detailed survey of theory, design and performance of atomizers is made by Masters (1976), but the conclusion is that experience and pilot plant work still are essential guides to selection of atomizers. A clear choice between nozzles and spray wheels is rarely possible and may be arbitrary. Milk dryers in the United States, for example, are

TABLE 9.14. Performance Data of Fluidized Bed Dryers: Batch and Multistage Equipment

(a) Batch Dryers

	Ammonium Bromide	Lactose Base Granules	Pharmaceutical Crystals	Liver Residue	Weed Killer
Holding capacity (lb wet product)	100	104	160	280	250
Bulk density, dry (lb/ft^3)	75	30	20	30	35
Initial moisture (% w/w basis)	6	10	65	50	20–25
Final moisture (% w/w basis)	1	2	0.4	5.0	1.0
Final drying temperature (°F)	212	158	248	140	140
Drying time (min)	20	90	120	75	210
Fan capacity (ft^3/min at 11 in. w.g.)	750	1500	3000	4000	3000
Fan HP	5	10	20	25	20
Evaporation rate (lb H$_2$O/hr)	15	5.7	52	100	17

(Courtesy Calmic Engineering Co. Ltd.; Williams–Gardner, 1971; Walas, 1988).

(b) Multistage Dryers with Dual-flow Distributors [Equipment Sketch in Fig. 9.13(b)]

Function	Heater	Cooler	Drier	Cooler
Material	Wheat Grains	Wheat Grains	Slag	Quartz Sand
Particle size (diameter) (mm)	5 × 3	5 × 3	0.95	1.4
Material feed rate (metric tons/hr)	1.5	1.5	7.0	4.0
Column diameter (m)	0.90	0.83	1.60	1.70
Perforated trays (shelves):				
Hole diameter (mm)	20	20	20; 10	20
Proportion of active section	0.4	0.4	0.4; 0.4	0.4
Number of trays	10	6	1; 2	20
Distance between trays (mm)	20	20	25; 40	15
Total pressure drop on fluidized bed (kgf/m^2)	113	64	70[a]	40
Hydraulic resistance of material on one tray (kgf/m^2)	7.8	9.2	20; 10	1.8
Inlet gas temperature (°C)	265	38	300	20
Gas inlet velocity (m/sec)	8.02	3.22	4.60	0.74
Material inlet temperature (°C)	68	175	20	350
Material discharge temperature (°C)	175	54	170	22
Initial humidity (% on wet material)	25	—	8	—
Final humidity (% on wet material)	2.8	—	0.5	—
Blower conditions				
Pressure (kgf/m^2)	450	250	420	250
Throughput (m^3/min)	180	130	360	100
	(80°C)	(50°C)	(70°C)	(35°C)
Power consumption (HP)	50	20	75	7.5

[a]With grids and two distributor plates.
(Romankov, in Davidson and Harrison, *Fluidisation*, Academic, New York, 1971; Walas, 1988).

TABLE 9.15. Performance Data of Continuous Fluidized Bed Dryers

(a) Data of Fluosatatic Ltd.

	Coal	Sand	Silica Sand	Limestone	Iron Ore
Material size, mesh	$\frac{1}{2}$ – 0	−25−0	−18−0	$\frac{3}{16}$−0	−$\frac{3}{8}$−0
Method of feed	twin screw	bucket elev.	conv.	conv.	conv.
Product rate (lb product/hr)	448,000	22,400	112,000	67,000	896,000
Initial moisture (% w/w basis)	11	6	6	15	3
Final moisture (% w/w basis)	5.5	0.1	0.1	0.1	0.75
Residence time (min)	1	1.25	1.5	1.25	0.5
Dryer diameter (ft)	10	3.0	7.25	5.5	8.5
Fluid bed height (in.)	18	12	12	12	18
Air inlet temperature (°F)	1000	1200	1200	1200	1200
Air outlet temperature (°F)	170	212	212	212	212
Air quantity (ft^3/min std.)	40,000	2000	9000	13,000	45,000
Material exit temperature (°F)	140	220	220	220	220
Evaporation (lb/hr)	24,640	1430	6720	11,880	20,400
Method of heating	coal	gas	oil	oil	oil
Heat consumption (Btu/lb water evaporated)	1830	1620	1730	1220	2300
Fan installed HP	240	20	80	115	350

(Williams–Gardner, 1971; Walas, 1988).

TABLE 9.15.—(_continued_**)**

(b) Data of Head Wrightston Stockton Ltd.

	Coal	Silicious Grit	Glass Sand	Sand	Asphalt
Method of feed	screw feeder	chute	chute	chute	chute
Material size	$-\frac{1}{2}$ in.	$-\frac{1}{16}$ in.	−36 mesh	$-\frac{1}{16}$ in.	$-\frac{3}{16}$ in.
Product rate (lb product/hr)	190,000	17,920	15,680	33,600	22,400
Initial moisture (% w/w basis)	14	5	7	5	5
Final moisture (% w/w basis)	7	0	0	0	0.5
Residence time (min)	2	$1\frac{1}{2}$	3	3	10
Dryer diameter	7 ft 3 in.	3 ft 0 in.	4 ft 6 in.	6 ft 6 in.	8 ft 0 in.
Fluid bed height (in.)	21	12	12	12	24
Air inlet temperature (°F)	1000	1400	1400	1400	470
Air outlet temperature (°F)	135	230	230	230	220
Air quantity (ft³/min std)	20,000	2000	2000	3500	7000
Material exit temp (°F)	140	230	230	230	220
Evaporated rate (lb/hr)	11,200	896	1097	1680	1120
Method of heating	coke-oven gas	gas oil	town gas	gas oil	gas oil
Heat consumption (Btu/lb water evaporated)	2000	2250	2000	2200	1800
Fan installed HP	210	$32\frac{1}{2}$	18	30	90

(Williams–Gardner, 1971; Walas, 1988).

(c) Data of Pennsalt Ltd.

	Abrasive Grit	Clay Granules	Sand	Granular Desiccant	Household Salt
Product rate (lb/hr)	2200	1000	14,000	150	13,500
Initial moisture (% w/w basis)	9	22	6	25	4
Final moisture (% w/w basis)		3	dry	7	0.03
Air inlet temperature (°F)	580	160	325	300	390
Air outlet temperature (°F)	210	120	140	205	230
Method of heating	gas	steam	gas	gas	steam
Heat consumption (Btu/lb water evaporated)	2700	3800	2700	3600	5100
Bulk density (lb/ft³)	120	60	90	30	60
Average drying time (min)	2.5	30	3	24	4
Fan capacity (ft³/min std.)	2.5	1.35	1.05	0.84	1.05
Installed fan HP	10	45	25	5	50

(Williams–Gardner, 1971; Walas, 1988).

(d) Data of Rosin Engineering Ltd.

	Sodium Perborate	Weed Killer	PVC	Coal	Sand
Method of feed	screw	vibrator	screw	vibrator	vibrator
Material size	30–200 mesh	5–1 mm flake	60–120 mesh	3 mesh–zero	30–120 mesh
Product rate (lb product/hr)	11,400	5100	10,075	440,000	112,000
Initial moisture (% w/w basis)	3.5	14	2.0	8	8
Final moisture (% w/w basis)	0.0	0.2	0.2	1	0.2
Residence time (min)	1.5	11	30	0.3	0.45
Drier bed size (ft × ft)	22.5 × 5.5	18 × 4.5	23 × 6	16 × 6.6	12.5 × 3.2
Fluid bed height (in.)	4	3	18	5	6
Air inlet temperature (°F)	176	212	167	932	1202
Air outlet temperature (°F)	104	150	122	180	221
Air quantity (ft³/min std)	6600	14,200	5400	67,330	8000
Material exit temperature (°F)	104	205	122	180	212
Evaporation (lb/hr)	400	720	183	33,440	9750
Method of heating	steam	steam	steam	coke-oven gas	oil
Heat consumption (Btu/lb water evaporated)	2100	3060	4640	1970	2200
Fan installed HP	33	40	34	600	70

(Williams–Gardner, 1971; Walas, 1988).

EXAMPLE 9.9
Sizing a Fluidized Bed Dryer
A wet solid at 100°F contains $W = 0.3$ lb water/lb dry and is to be dried to $W = 0.01$. Its feed rate is 100 lb/hr dry. The air is at 350°F and has $H_{g0} = 0.015$ lb water/lb dry. The rate of drying is represented by the equation

$$-\frac{dW}{d\theta} = 60(H_s - H_g), \quad \text{(lb/lb)/min}.$$

The solid has a heat capacity 0.35 Btu/(lb)(°F), density 150 lb/cuft, and average particle size 0.2 μm (0.00787 in.). The air has a viscosity of 0.023 cP and a density of 0.048 lb/cuft. The fluidized bed may be taken as a uniform mixture. A suitable air rate and dimensions of the bed will be found:
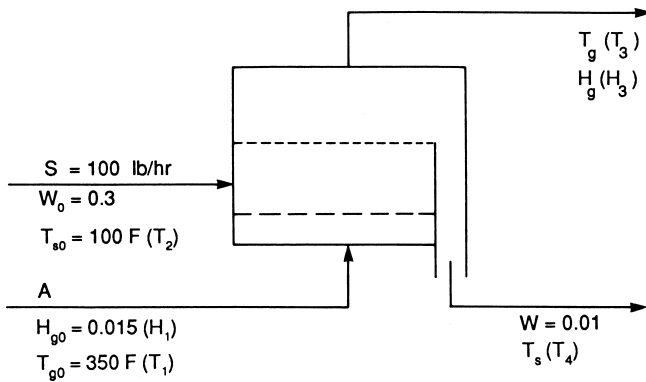
Symbols used in the computer program are in parentheses.
  Minimum fluidizing rate by Leva's Equation, Eq. 9–20

$$G_{mf} = \frac{688 D_p^{1.83}[0.048(150 - 0.048)]^{0.94}}{\mu^{0.88}}$$

$$= \frac{688(0.00787)^{1.83}[0.048(150 - 0.048)]^{0.94}}{(0.023)^{0.88}}$$

$$= 17.17 \text{ lb/(hr)(sqft)}.$$

Let $G_f = 2G_{mf} = 34.34$ lb/(hr)(sqft).

Expanded bed ratio

$$(L/L_0) = (G_f/G_{mf})^{0.22} = 2^{0.22} = 1.16.$$

Take voidage at minimum fluidization as

$$\varepsilon_{mf} = 0.40,$$
$$\therefore \varepsilon_f = 0.464.$$

Drying time:

$$\theta = \frac{W_o - W}{60(H_s - H_g)} = \frac{0.3 - 0.01}{60(H_s - H_g)}. \tag{1}$$

Since complete mixing is assumed, H_s and H_g are exit conditions of the fluidized bed.
  Humidity balance:

$$\dot{A}(H_g - H_{go}) = \dot{S}(W_0 - W),$$
$$H_g = 0.015 + 0.29\dot{S}/\dot{A}. \tag{2}$$

Average heat capacity:

$$C_g = \frac{1}{2}(C_{go} + C_g) = 0.24 + 0.45[(0.015 + H_g)/2]$$
$$= 0.2434 + 0.225 H_g. \tag{3}$$

Heat balance:

$$\dot{A}C_g(T_{go} - T_g) = \dot{S}[(C_s + W)(T_s - T_{s_0}) + \lambda(W_0 - W)],$$
$$(\dot{A}/\dot{S})C_g(350 - T_g) = 0.36(T_s - 100) + 900(0.29). \tag{4}$$

Adiabatic saturation line:

$$T_g - T_s = \frac{\lambda}{C_g}(H_s - H_g) = \frac{900}{C_g}(H_s - H_g). \tag{5}$$

Vapor pressure:

$$P_s = \exp[11.9176 - 7173.9/(T_s + 389.5)]. \tag{6}$$

Saturation humidity:

$$H_s = \frac{18}{29}\frac{P_s}{1 - P_s}. \tag{7}$$

Eliminate T_3 between Eqs. (4) and (5):

$$T_s = 350 - \frac{0.36(T_4 - 100) + 261}{RC_g}$$
$$= T_4 + \frac{900(H_4 - H_3)}{C_g}, \quad [T_3 \equiv T_g, \ T_4 \equiv T_s]. \tag{8}$$

Procedure: For a specified value of $R = \dot{A}/\dot{S}$, solve Eqs. (6), (7), and (8) simultaneously.

R	T_g	T_s	H_g	H_s	θ (min)
5	145.14	119.84	0.0730	0.0803	0.662
6	178.11	119.74	0.0633	0.0800	0.289
8	220.09	119.60	0.0513	0.0797	0.170
10	245.72	119.52	0.0440	0.0795	0.136
12	262.98	119.47	0.0392	0.0794	0.120

Take

$$R = 10 \text{ lb air/lb solid},$$
$$\dot{A} = 10(100) = 1000 \text{ lb/hr},$$
$$\theta = 0.136 \text{ min}.$$

Cross section:

$$\dot{A}/G_f = 1000/34.34 = 29.12 \text{ sqft}, \quad 6.09 \text{ ft dia}.$$

Avg density:

$$\frac{1}{2}(1/20.96 + 1/19.03) = 0.0501 \text{ lb/cuft}.$$

Linear velocity:

$$u = \frac{G_f}{\rho\varepsilon(60)} = \frac{34.34}{0.0501(0.464)(60)} = 24.62 \text{ fpm}.$$

Bed depth:

$$L = u\theta = 24.62(0.136) = 3.35 \text{ ft}.$$

Note: In a completely mixed fluidized bed, the drying time is determined by the final moisture contents of the air and solid.

When drying is entirely in the falling rate period with rate equation

$$-\frac{dW}{d\theta} = \frac{k(H_s - H_g)}{W_c} W, \quad W \leq W_c,$$

the drying time will be

$$\theta = \frac{W_c}{k(H_s - H_g)W}$$

where H_s, H_g, and W are final conditions. When the final W is small, 0.01 in the present numerical example, the single stage drying time will be prohibitive. In such cases, multistaging, batch drying, or some other kind of drying equipment must be resorted to.

Any appropriate computer program may be used to solve Eq. (1) through (8). For a specified value of R = A/S, Eq. (6), (7) and (8) may be solved simultaneously.

R	T_g	T_s	H_g	H_s	Time
5	145.1	119.84	.0730	.0803	.662
6	178.1	119.74	.0633	.0800	.289
8	220.1	119.61	.0513	.0797	.170
10	245.7	119.53	.0440	.0795	.136
12	263.0	119.47	.0392	.0794	.120
15	280.4	119.42	.0343	.0792	.108

equipped with nozzles, but those in Europe usually with spray wheels. Pneumatic nozzles may be favored for polymeric solutions, although data for PVC emulsions in Table 9.16(a) show that spray wheels and pressure nozzles also are used. Both pressure nozzles and spray wheels are shown to be in use for several of the applications of Table 9.16(a).

In a spray dryer, the feed material characteristics, in combination with the type of feed atomization, affect the surface characteristics, shape, density, and particle size of the product. Thin-shelled particles may shatter when they come in contact with high temperature drying gases or if the particles impact the walls and fittings in the ductwork. Of course, shattered particles are not usually a desired product (Papiagonnes, 1992).

Since atomization of the feed is a key characteristic of the process, under ideal conditions, spherical droplets will produce a product of spherical particles. This, then, is an advantage of the spray drying process. The feed usually has a high moisture content so that it can be pumped or atomized. Compared to other drying processes, the energy requirements of spray drying per unit mass of product are relatively high. For some applications, the product quality imparted by spray drying makes the high energy costs acceptable (Oakley, 1997).

APPLICATIONS

For direct drying of liquids, slurries, and pastes, drum dryers are the only competition for spray dryers, although fluidized bed dryers sometimes can be adapted to the purpose. Spray dryers are capable of large evaporation rates, 12,000–15,000 lb/hr or so, whereas a 300 sqft drum dryer for instance may have a capacity of only 3000 lb/hr. The spherelike sprayed particles often are preferable to drum dryer flakes. Dust control is intrinsic to spray dryer construction but will be an extra for drum dryers. The completely enclosed operation of spray dryers also is an advantage when toxic or noxious materials are handled.

THERMAL EFFICIENCY

Exit air usually is maintained far from saturated with moisture and at a high temperature in order to prevent recondensation of moisture in parallel current operation, with a consequent lowering of thermal efficiency. With steam heating of air the overall efficiency is about 40%. Direct fired dryers may have efficiencies of 80–85% with inlet temperatures of 500–550°C and outlet of 65–70°C. Steam consumption of spray dryers may be 1.2–1.8 lb steam/lb evaporated, but the small unit of Table 9.19(b) is naturally less efficient. A

10% heat loss through the walls of the dryer often is taken for design purposes. Pressure drop in a dryer is 15–50 in. of water, depending on duct sizes and the kind of separation equipment used.

DESIGN

The design of spray dryers is based on experience and pilot plant determinations of residence time, air conditions, and air flow rate. Example 9.10 utilizes such data for the sizing of a commercial scale spray dryer.

The smallest pilot unit supplied by Bowen Engineering has a diameter of 30 in. and straight side of 29 in., employs parallel flow, up to 25 ACFM, 150–1000°F, particle sizes 30–40 μm average, either pneumatic nozzle or spray wheel. The performance of this unit is given in Table 9.19. The magnitude of the ''product number'' is arrived at by pilot plant work and experience; it increases with increased difficulty of drying or thermal sensitivity or both. Although much useful information can be obtained on this small scale, Williams-Gardner (1971) states that data on at least a 7 ft dia dryer be obtained for final design of large capacity units.

9.12. COOLING TOWERS

Cooling water in process plants is most commonly and effectively obtained using a cooling tower. The principle of operation is the simultaneous transfer of mass and heat. Colburn (1939) introduced ''the idea of a unit of mass transfer which is a measure of the number of equilibrium changes to required to effect a given amount of diffusion.'' It is identical with the concept of a theoretical plate in distillation (Kern, 1950).

The cooling of the water occurs mostly by an exchange of the latent heat of vaporization of water and in part its sensible heat that raises both the dry-bulb and wet-bulb temperatures of the air. The heat that is transferred from the water to the air is then exhausted to the atmosphere.

The cooling tower has a packing or fill (see Figure 9.15) of wood or plastic material and is installed in such a manner that a drop of water does not fall the entire height of the tower but hits the fill. The splash that occurs forms a film and drops down to the next member of the fill. The stream of air flows across the water drops simultaneously cooling the water and humidifying the air. As the water flows down the tower, its temperature will drop below the dry-bulb temperature of the air entering the tower but it cannot go below the wet-bulb temperature although it approaches that temperature. The enthalpy difference between the film and the
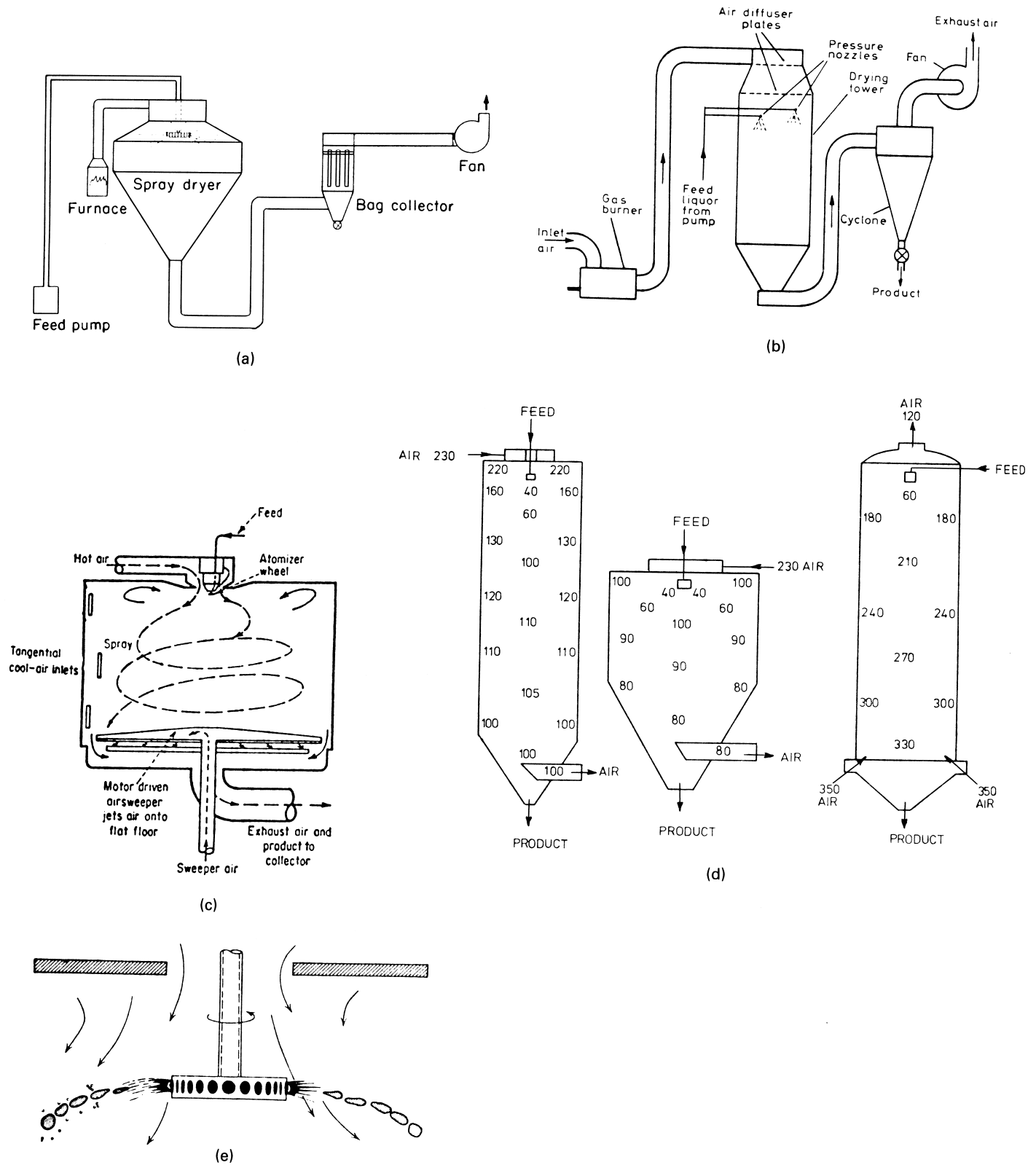
Figure 9.14. Spray dryer arrangements and behavior. (a) Spray dryer equipped with spray wheel; straight section $L/D = 0.5–1.0$ (*Proctor and Schwartz Inc.*). (b) Spray dryer equipped with spray nozzle; straight section $L/D = 4–5$ (*Nonhebel and Moss, 1971*). (c) Spray dryer for very heat sensitive products; flat bottom, side air ports and air sweeper to cool leaving particles. (d) Distribution of air temperatures in parallel and countercurrent flows (*Masters, 1976, p. 18, Fig. 1.5*). (e) Droplet-forming action of a spray wheel (*Stork–Bowen Engineering Co.*). (Walas, 1988).

TABLE 9.16. Performance Data of Spray Dryers

(a) Data of Kröll (1978)

Kind of Stock	Moisture Content		Spray Device	Flow Pattern	Air Temperature	
	In (%)	Out (%)			In (°C)	Out (°C)
Skim milk, d = 60 μm	48–55	4	wheel or nozzle	parallel	250	95–100
	50–60	4	170–200 bar	parallel	250	95–100
Whole milk	50–60	2.5	wheel or nozzle			
			100–140 bar	parallel	170–200	
Eggs, whole	74–76	2–4	wheel or nozzle	parallel	140–200	50–80
Eggs, yolks	50–55	2–4	wheel or nozzle	parallel	140–200	50–80
Eggs, whites	87–90	7–9	wheel or nozzle	parallel	140–200	50–80
Coffee, instant, 300 μm	75–85	3–3.5	nozzle	parallel	270	110
Tea, instant	60	2	nozzle, 27 bar	parallel	190–250	
Tomatoes	65–75	3–3.5	wheel	parallel	140–150	
Food yeast	76–78	8	wheel	parallel	300–350	100
Tannin	50–55	4	wheel	parallel	250	90
PVC emulsion, 90% > 80 μm < 60 μm	40–70	0.01–0.1	wheel or nozzle or pneumatic	parallel	165–300	
Melamine–urethane–formaldehyde resins	30–50	0	wheel 140–160 m/sec	parallel	200–275	65–75
Heavy duty detergents	35–50	8–13	nozzle, 30–60 bar	counter	350–400	90–110
Kaolin	35–40	1	wheel	parallel	600	120

(b) Performance of a Dryer 18 ft Dia by 18 ft High with a Spray Wheel and a Fan Capacity of 11,000 cfm at the Outlet[a]

Material	Air Temp (°F)		% Water in Feed	Evaporation Rate (lb/hr)
	In	Out		
Blood, animal	330	160	65	780
Yeast	440	140	86	1080
Zinc sulfate	620	230	55	1320
Lignin	400	195	63	910
Aluminum hydroxide	600	130	93	2560
Silica gel	600	170	95	2225
Magnesium carbonate	600	120	92	2400
Tanning extract	330	150	46	680
Coffee extract A	300	180	70	500
Coffee extract B	500	240	47	735
Magnesium chloride	810	305	53	1140 (to dihydrate)
Detergent A	450	250	50	660
Detergent B	460	240	63	820
Detergent C	450	250	40	340
Manganese sulfate	600	290	50	720
Aluminum sulfate	290	170	70	230
Urea resin A	500	180	60	505
Urea resin B	450	190	70	250
Sodium sulfide	440	150	50	270
Pigment	470	140	73	1750

[a]The fan on this dryer handles about 11,000 cuft/min at outlet conditions. The outlet-air temperature includes cold air in-leakage, and the true temperature drop caused by evaporation must therefore be estimated from a heat balance.

(Bowen Engineering Inc.; Walas, 1988).

surrounding air is the enthalpy driving force, Figure 9.16. The general equation representing this process is

$$dT/(h_s - h) = (K_G aV)/L = \text{NTU} \qquad (9.21)$$

where T_1 = entering warm water temperature
T_2 = leaving cool water temperature
dT = the water temperature difference

h_1 = enthalpy of the saturated air film at the bulk water temperature
h_2 = enthalpy of the air stream
K_G = mass transfer coefficient based on the gas phase
a = contact area
L = water rate
V = active cooling volume
NTU = number of transfer units

TABLE 9.17. Particle Diameters, Densities, and Energy Requirements

(a) Atomizer Performance

Type	Size Range (μm)	Power Input (kWh/1000 L)
Single fluid nozzle	8–800	0.3–0.5
Pneumatic nozzle	3–250	
Spray wheel	2–550	0.8–1.0
Rotating cup	25–950	

(b) Dry Product Size Range

Product	μm
Skim milk	20–250
Coffee	50–600
Eggs	5–500
Egg white	1–40
Color pigments	1–50
Detergents	20–2000
Ceramics	15–500

(c) Bulk Density of Sprayed Product as Affected by Air Inlet Temperature and Solids Content of Feed[a]
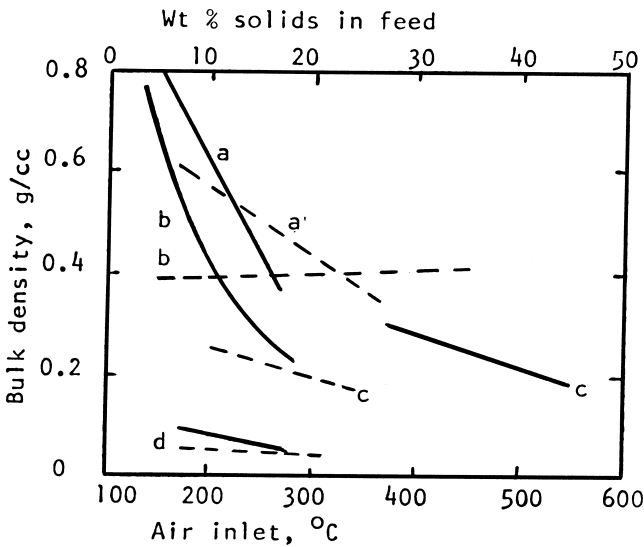
[a]The full lines are against temperature, the dashed ones against concentration: (a) sodium silicate; (b) coffee extract, 22%; (c) water dispersible dye, 19.5%; (d) gelatin.
[Data of Duffie and Marshall, *Chem. Eng. Prog.* **49,** 417 480 (1953)].

NTU is the number of transfer units or the tower characteristics based on the overall simultaneous heat and mass transfer, as defined by Eq. 9.21. For a more complete development of the NTU concept, see Chapter 13.

Figure 9.16, the enthalpy-temperature diagram, shows the relationship between the water and air as they exist in a counterflow cooling tower. The vertical difference at any given water temperature between the water operating line and the air operating line is the enthalpy driving force.
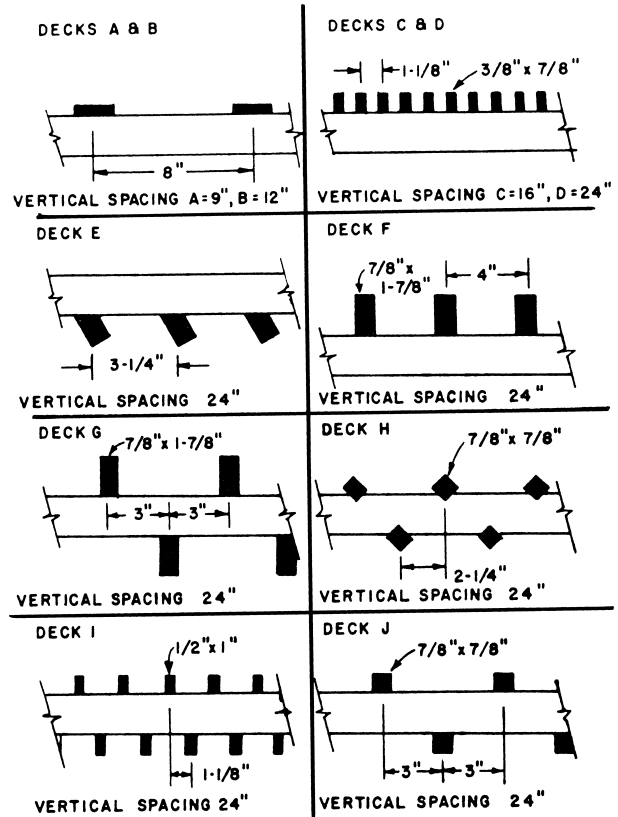
Factors in Eq. 9.38 for the Number of Decks

Deck Type	a	b
A	0.060	0.62
B	0.070	0.62
C	0.092	0.60
D	0.119	0.58
E	0.110	0.46
F	0.100	0.51
G	0.104	0.57
H	0.127	0.47
I	0.135	0.57
J	0.103	0.54

Figure 9.15. Kinds of fill made of redwood slats for cooling towers, and factors for determining the required number of decks with inlet water at 120°F. (*Cheremisinoff and Cheremisinoff, 1981*).

COOLING TOWER TERMINOLOGY

There are certain terms that are used with respect to cooling towers:

Dry-bulb temperature is the temperature indicated by a dry-bulb thermometer.
Wet-bulb temperature is the temperature to which air can be cooled adiabatically to saturation by the addition of water vapor.
Approach to the wet-bulb temperature is the temperature difference of the cold water leaving the tower and the wet-bulb temperature of the air.
Range is the number of degrees the water is cooled (i.e., the difference between the temperature of the hot and cold water).

TABLE 9.18. Effects of Variables on Operation of Spray Dryers

Variable Increased	Factors Increased	Factors Decreased
Chamber inlet temperature	*Feed rate* and thus: product rate, particle size (*b*), product moisture content, chamber wall build-up (*a*)	bulk density (*b*)
Chamber outlet temperature	product thermal degradation (*a*)	*feed rate* and thus: product rate particle size (*b*) product moisture content chamber wall build-up residence time
Gas volume rate	*feed rate* and thus: product rate, particle size (*b*), product moisture content, chamber wall build-up (*a*)	
Feed concentration Atomizer speed Atomizer disc diameter	product rate, bulk density (*b*), particle size (*b*)	
For stable lattices	bulk density	*particle size* and thus: product moisture content chamber wall build-up
For unstable lattices	coagulation (*a*) and thus: particle size, product moisture content, chamber wall build-up	
Atomizer vane depth	bulk density (*b*)	particle size (*b*) and thus: product moisture content, chamber wall build-up
Atomizer vane number Atomizer vane radial length		*For unstable lattices* particle size chamber wall build-up
Feed surface tension	bulk density (*b*)	particle size (*b*)
Chamber inlet gas humidity	product moisture content, chamber wall build-up (*a*)	

[a]This factor will only occur if a critical value of the variable is exceeded.
[b]Not for suspensions.
(Nonhebel and Moss, 1971; Walas, 1988).

Drift is the water that is lost from the tower as fine droplets entrained in the exhaust air. For mechanical draft towers, the value is less than 0.2% of the circulating water, but for natural draft towers the drift ranges between 0.3–1.0%.

Blowdown is the continuous or intermittent discharge of a certain amount of water from the tower to prevent the buildup of solids in the water due to evaporation. It is 2.5–3% of the water circulated to limit salt concentration.

Make-up water is the water to replace the circulating water that is lost by evaporation, drift, blowdown, or leakage. It is expressed as a percentage of the water circulated.

TABLE 9.19.—(*continued***)**

(b) Performance of the Pilot Unit as a Function of Product Number[a]

TABLE 9.19. Product Numbers and Performance of a 30 × 29 in. Pilot Plant Spray Dryer

(a) Product Numbers of Selected Materials

Material	Product number
1. COLOURS	
Reactive dyes	5–6
Pigments	5–11
Dispersed dyes	16–26
2. FOODSTUFFS	
Carbohydrates	14–20
Milk	17
Proteins	16–28
3. PHARMACEUTICALS	
Blood insoluble/soluble	11–22
Hydroxide gels	6–10
Riboflavin	15
Tannin	16–20
4. RESINS	
Acrylics	10–11
Formaldehyde resin	18–28
Polystyrene	12–15
5. CERAMICS	
Alumina	11–15
Ceramic colours	10

(Bowen Engineering Inc.).

[a]Example: For a material with product number = 10 and air inlet temperature of 500°F, the evaporation rate is 53 lb/hr, input Btu/lb evaporated = 1930, and the air outlet temperature is 180°F.
(Bowen Engineering).

EXAMPLE 9.10
Sizing a Spray Dryer on the Basis of Pilot Plant Data
Feed to a spray dryer contains 20% solids and is to be dried to 5% moisture at the rate of 500 lb/hr of product. Pilot plant data show that a residence time of 6 sec is needed with inlet air of 230°F, $H = 0.008$ lb/lb, and exit at 100°F. Ambient air is at 70°F and is heated with steam. Enthalpy loss to the surroundings is 10% of the heat load on the steam heater. The vessel is to have a 60° cone. Air rate and vessel dimensions will be found.

Enthalpy, humidity, and temperatures of the air are read off the psychrometric chart and recorded on the sketch.

Dry   475 pph
Water 1900 pph

70 F
H = 0.008
h = 28.0

230F
H = 0.008
h = 69.8
V = 17.6

$Q_{lost} = 0.1\,Q$

Air
100 F

Dry   475 pph
Water   23 pph
Total   500 pph
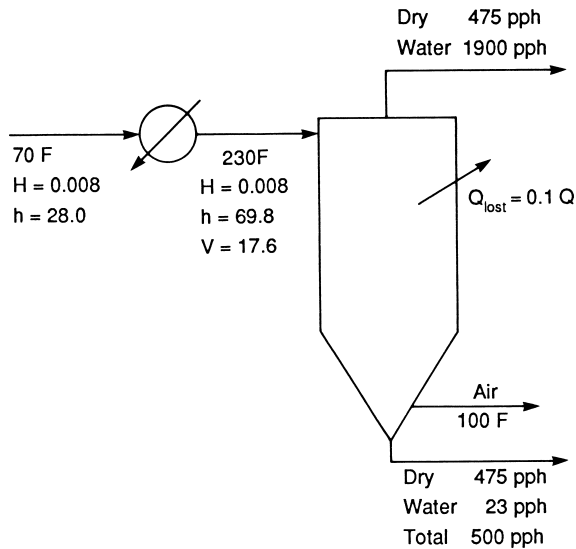
Enthalpy loss of air is

$$0.1(69.8 - 28.0) = 4.2\,\text{Btu/lb}.$$

Exit enthalpy of air is

$$h = 69.8 - 4.2 = 65.6.$$

At 100°F and this enthalpy, other properties are read off the psychrometric chart as

$$H = 0.0375\,\text{lb/lb},$$
$$V = 14.9\,\text{cuft/lb}.$$

Air rate is

$$A = \frac{1900 - 25}{0.0375 - 0.008} = 63,559\,\text{lb/hr}$$
$$\rightarrow \frac{63,559}{3600}\left(\frac{17.6 + 14.9}{2}\right) = 287\,\text{cfs}.$$

With a residence time of 6 sec, the dryer volume is

$$V_d = 287(6) = 1721.4\,\text{cuft}.$$

Make the straight side four times the diameter and the cone 60°:

$$1721.4 = 4D(\pi D^2/4) + \frac{0.866\pi D^3}{12} = 3.3683D^3,$$
$$\therefore D = 8.0\,\text{ft}.$$

Performance is the ability of a tower to cool water. It is expressed in terms of cooling a quantity of water from a specified hot water temperature to a specified water temperature that has a specific wet-bulb temperature.

TYPES OF COOLING TOWERS

The main types of cooling towers are represented in Figure 9.17. Their chief characteristics and pros and cons will be discussed.

Atmospheric spray tower is one in which the air movement depends on atmospheric conditions and the aspirating effect of spray nozzles, as in Figure 9.17(a). They are used for low-cooling loads and may not provide flexibility of operation or low-cooling water temperature. They are effective when the prevailing wind velocities are 5 miles/hr or more. Water drift losses are relatively large. These towers are of low capital investment and minimal operating expenses. The savings, because of the elimination of a tall chimney or fan power, are counterbalanced by their increased size because of low efficient cross flow and variation in wind velocities.

Chimney-assisted natural draft towers also do not have fans, as shown in Figure 9.17(b). Most have tall chimneys, a fill that occupies a small percentage of the tower and no fan. They depend on a stack or chimney to induce the airflow through the tower. The hyperboloidal shape has greater strength for a given wall thickness.

These towers are large, and the enlarged cross section at the top of the tower converts kinetic energy into pressure energy that assists in dispelling the humid air to the atmosphere. They are made of reinforced concrete.

Hyperbolic fan assisted towers may have as much as three times the capacity of the same sized natural draft towers in Figure 9.17(c). They provide greater control than the natural draft systems and may be turned on only at peak loads. A rule of thumb that Cheremisinoff and Cheremisinoff (1981) suggest for the relative sizing is that the fan assisted tower may be 2/3 the diameter and $\frac{1}{2}$ the height of the natural draft towers.

Counterflow-induced draft towers, Figure 9.17(d), are the most commonly used in the process industries. Mechanical draft towers are capable of greater control than natural draft and in some cases can cool water to below a 5°F approach. The flow of air is quite uniform at a high velocity and the discharge is positive so that there is a minimum of backflow of humid air into the tower. The elevated fan location creates some noise and structural problems. It has been reported that mechanical draft towers at low water rates (19,800 gpm) perform better than natural draft towers.

Crossflow-induced draft towers, Figure 9.17(e), offer less resistance to air flow and can operate at higher velocities, which means less power required than for countercurrent towers, but the shorter travel path makes them less efficient thermally. There is some saving in pumping costs because the tower is less high than other type towers and they are usually wider.
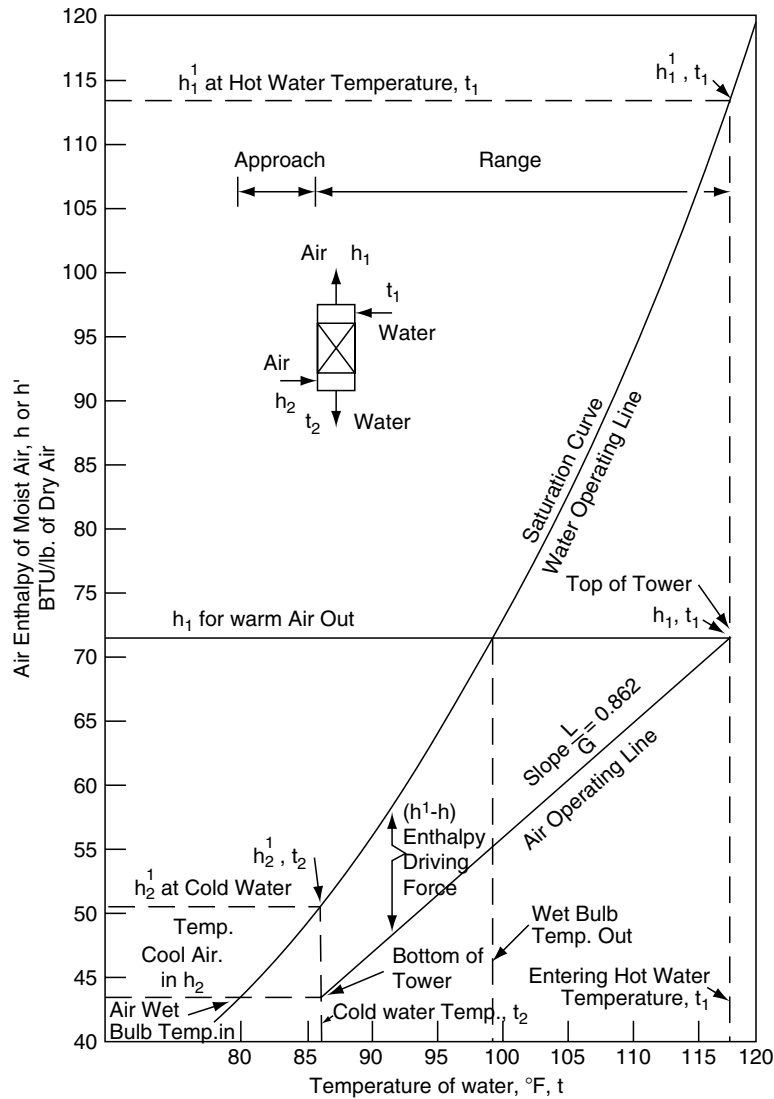
Figure 9.16. Driving force diagram for cooling tower.

Forced draft towers, Figure 9.17(f), locate the fan near ground level that requires simpler structural supports and perhaps lower noise level. A large space must be provided at the bottom for the air inlet. Because the air must make a 90° adjustment, the air distribution is poor. The humid air is discharged at a low velocity from the top of the tower and it tends to return to the tower, but the drift loss of water is less. The pressure drop on the discharge side of the fan that is less power demanding than that on the intake side of induced draft towers.

Wet-dry towers, Figure 9.17(g), employ heat transfer surface as well as direct contact between air and water. Air coolers are used widely for the removal of sensible heat from cooling water on a comparatively small scale when cooling tower capacity is limited. Since dry towers cost about twice as much as wet ones, combinations of wet and dry sometimes are applied, particularly when the water temperatures are high (near 160°F) so that the evaporation losses are prohibitive and the plumes are environmentally undesirable. The warm water flows first through tubes across which air is passed and then enters a conventional packed section where it is cooled further by direct contact with air. Separate dampers for air in the dry and wet sections can direct a greater load on the wet section in summer months.

SPECIFICATION AND MATERIALS OF CONSTRUCTION

The design of a cooling tower is best outsourced to the manufacturers/suppliers of that equipment with close cooperation between the process engineer and the supplier. A specification sheet, similar to Figure 9.18, is prepared by the process engineer for a given application.

Materials of construction for the cooling tower are often treated or untreated fir or redwood construction with the exception of the hyperbolic towers that are of reinforced concrete. Plastics and reinforced fiberglass have been used but there are temperature limitations on these materials.
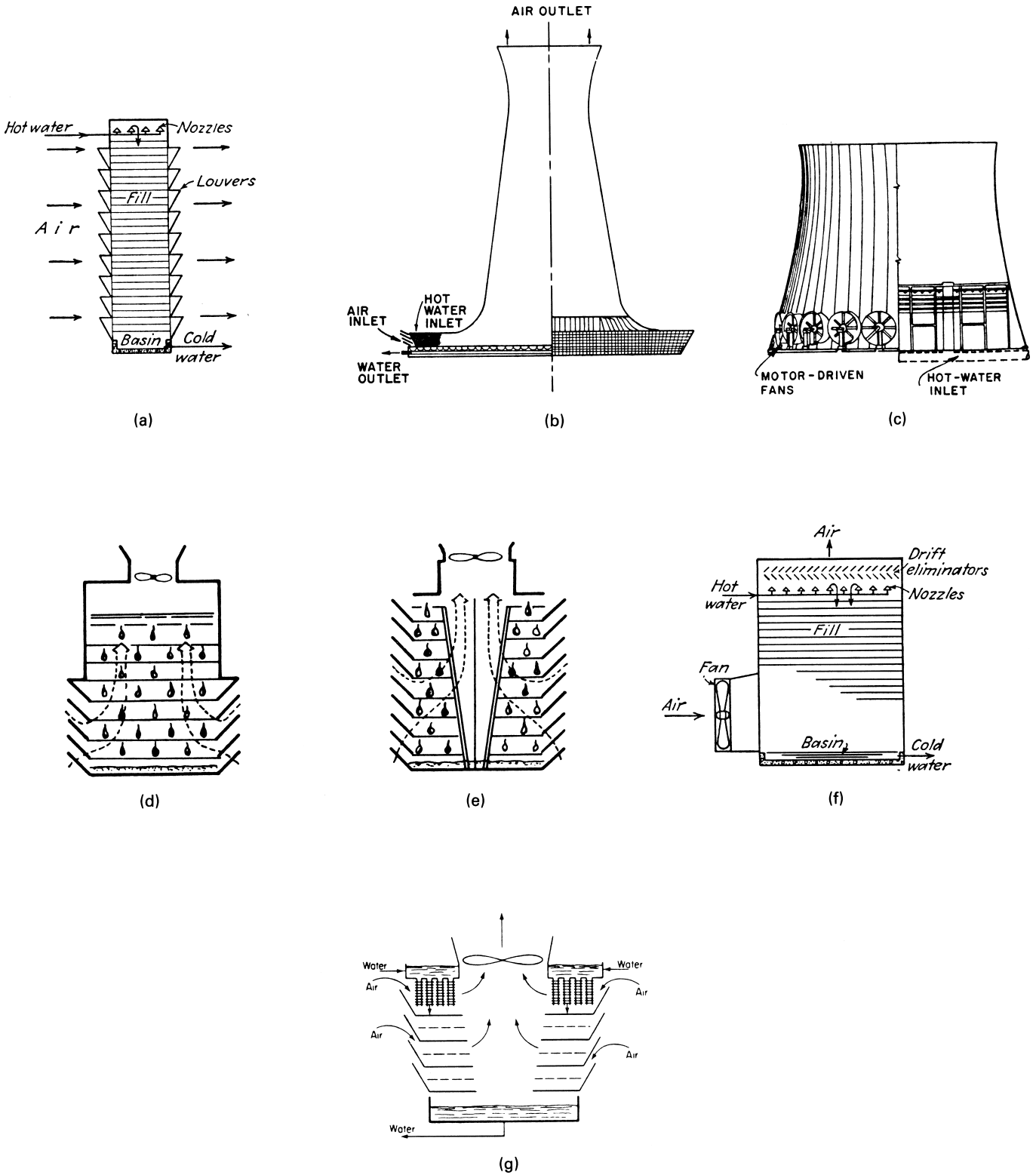
Figure 9.17. Main types of cooling towers. (a) Atmospheric, dependent on wind velocity. (b) Hyperbolic stack natural draft. (c) Hyperbolic assisted with forced draft fans. (d) Counterflow-induced draft. (e) Crossflow-induced draft. (f) Forced draft. (g) Induced draft with surface precooler for very hot water; also called wet/dry tower. [(*b*)–(*e*) *from Cheremisinoff and Cheremisinoff, 1981*); (Walas, 1988).

	SPEC. DWG. NO.
	A.
	Page of Pages
	Unit Price
	No. Units
	Item No.

Job No._____

_____

B/M No._____ **COOLING TOWER SPECIFICATIONS**

PERFORMANCE

Water Circulating Rese: _____ Spm. Temp. Fn: _____ °F Temp. Out: _____ °F
Cooling Duly _____Stu/Hrs Perform, Test Cose _____
*As Option of Owner _____

SELECTION

Manufacturer: _____ Models _____
Type: _____ No. of Calls: _____

DESIGN

Wet Bulb Temp: _____ *Fx Static Pumping Ht. _____ Ft. Elf. Cool. Vol. _____ Cu. Ft.
Fill Wetted Surf. _____ Sq.Fts. Total Wetted Surf. _____ Sq. Fts. EN. Splash Surf. _____ Cu. Ft.
No. of Fens Req'd. _____ Clm/Fen _____; SteNc Press _____ In. H2O;Normal BHP/Fen_____
Evaporation Less. Max, % _____ Saray Less. Max. % _____

MATERIALS OF CONSTRUCTION

Frame work _____ Casing _____ Fill _____
Fen Cylinder _____ Steirway _____
Salts Nutes, Mise, Hardware _____ Nails _____
Water Inlet Hdrs. _____ Mexxles _____ Basin _____
Fen Blade _____ Fen Hub _____ Fan Sheft. _____
Code for Lumber Grades _____ Code for Lumbar Strech Design _____
**Exceptions B1 and Lending, See Inquiry or P.O. _____

AUXILIARY EQUIPMENT

Fen	Manufacturer_____ Type _____
	Diameter _____ Fts. Speed _____ RPM: Tip Speed _____ Spm.
Geer	Manufacturer _____ Type _____ Size _____
	ReducNon Restle _____ Reted Cop. _____ BHP: Mechanical EN. _____%
Driver	Manufactuerer _____ Type _____ Speed _____ RPM
	Electric Power _____ BHP _____ Service Factor _____ Frame _____

REMARKS

By	Chk.d.	App.	Rev.	Rev.	Rev.
Date					

P.O.Tet _____

Figure 9.18. Cooling tower specifications form.

Figure 9.19. Typical cooling tower performance curves (*Cheremisinoff and Cheremisinoff, 1981*).

TESTING AND ACCEPTANCE

At the time of completion of an installation, the water and air conditions and the loads may not be exactly the same as those of the design specification. Acceptance tests performed then must be analyzed to determine if the performance is equivalent to that under the design specifications. Such tests usually are performed in accordance with recommendations of the Cooling Tower Institute.

The supplier generally provides a set of performance curves covering a modest range of variation from the design condition, of which Figure 9.19 is a sample. Some of the data commonly required with bids of cooling tower equipment are listed in Table 9.18. A 10-page example of a cooling tower requisition is found in Cheremisinoff and Cheremisinoff (1981).

REFERENCES

Drying

Chemical Engineering Buyers' Guide, Chemical Engineering, New York, 2003.
Chemical Engineers' Handbook, 7th ed., McGraw-Hill, New York, Table 12.2, p. 12.11; Table 12.13, p. 12.46, 1999.
O.B. Christiansen, and M.S. Sardo, Find the optimum flash dryer to remove surface moisture, *Chem. Eng. Prog.*, 54–58 (August 2001).
E.M. Cook, Process calculations for partial recycle dryers, *Chem. Eng.*, 82–89, (April 1996).
C.W. Hall, *Dictionary of Drying,* Dekker, New York, 1979.
R.B. Keey, *Drying Principles and Practice*, Pergamon, New York, 1972.
R.B. Keey, *Introduction to Industrial Drying Operations*, Pergamon, New York, 1978.
K. Kroll, *Trochner und Trochnungsverfahren*, Springer Verlag, Berlin, Germany, 1978.
M. Leva, *Fluidization*, McGraw-Hill, New York, 1959.
K. Masters, *Spray Drying,* George Godwin, London, England, 1976.
W.L. McCabe, J.C. Smith, and P. Harriott, *Unit Operations of Chemical Engineering*, 4th ed., McGraw-Hill, New York, 1985.
P.Y. McCormick, Drying in *Encyclopedia of Chemical Technology,* Wiley, New York, 1973, Vol. 8, pp. 75–113.

C.G. Moyers, Don't let dryer problems put you through the wringer, *Chem. Eng. Progr.*, 34–40 (December 1992).
C.G. Moyers, Evaluating dryers for new services, *Chem. Eng. Progr.*, 51–56 (December 2003).
A.S. Mujumdar, (Ed.), *Advances in Drying*, Hemisphere, New York, 1980–1984, 3 vols.
G. Nonhebel, and A.A.H. Moss, *Drying Solids in Chemical Industry,* Butterworths, London, England, 1971.
D.E. Oakley, Produce uniform particles in spray drying, *Chem. Eng. Progr.*, 48–54 (1997).
G.J. Papagiannes, Select the right dryer, *Chem. Eng. Progr.*, 20–27 (December 1992).
R.E. Peck, Drying solids, in *Encyclopedia of Chemical Processing and Design*, Dekker, New York, 1983, Vol. 17, pp. 1–29.
Perry's Chemical Engineers' Handbook, 7th ed., McGraw-Hill, New York, 1997.
E.U. Schlunder, Dryers, in *Heat Exchanger Design Handbook*, Hemisphere, New York, Sec. 3.13, 1983.
G.A. Schurr, Solids drying, in *Chemical Engineers' Handbook,* 6th ed., McGraw-Hill, New York, pp. 20.4–20.8, 1984.
S.M. Walas, *Chemical Process Equipment; Selection and Design,* Butterworth-Heinemann, Boston, 1988.
T.H. Wentz, and J.H. Thygeson, Drying of wet solids, in Schweitzer (Ed.), *Handbook of Separation Techniques for Chemical Engineers,* McGraw-Hill, New York, 1979.
L.A. Wenzel and R.R. White, *Ind. Eng. Chem.,* **43**, 1929 (1951).
A. Williams-Gardner, *Industrial Drying,* Leonard Hill, Glasgow, 1971.

Cooling Towers

Cooling Tower Fundamentals, The Marley Company, Kansas City, MO, 1967.
N.P. Cheremisinoff, and P.N. Cheremisinoff, *Cooling Towers: Selection, Design and Practice*, Ann Arbor Science, Ann Arbor, MI, 1981.
Cooling Tower Institute, *Performance Curves*, CTI, Spring, TX, 1967.
A.P. Colburn, *The Simplified Calculation of Diffusional Processes, General Considerations of Two Film Resistance*, Trans. A.I.Ch.E, **35**, 211 (1939).
A.S. Foust, et al., *Principles of Unit Operations*, Wiley, New York, 1980.
D.Q. Kern, *Process Heat Transfer*, McGraw-Hill, New York, 1950.
T.K. Sherwood, R.L. Pigford, and C.R.Wilke, *Mass Transfer*, McGraw-Hill, New York, 1975.
J.R. Singham, Cooling towers, in *Heat Exchanger Design Handbook*, Hemisphere, New York, Sec. 3.12, 1983.

10

MIXING AND AGITATION

*M*ixing—the movement of fluids and solids to enhance a process result—is accomplished by means of an agitation source. For example, the sun is the agitation source for mixing in the earth's atmosphere. Similarly, an air compressor and/or a mechanical mixer is the agitation source in any municipal wastewater treatment plant to enhance the process results of (1) solids suspension and (2) oxygen absorption from sparged or entrained air.

In its most general sense, the process of mixing is concerned with all combinations of phases, of which the most frequently occurring are

1. Gases with gases
2. Gases into liquids: gas dispersion
3. Gases with granular solids: fluidization, pneumatic conveying, drying
4. Liquids into gases: spraying and atomization
5. Liquids into liquids: dissolution, emulsification, dispersion
6. Liquids with granular solids: solids suspension, mass transfer, and dissolution
7. Pastes with each other and with solids
8. Solids with solids: mixing of powders

Interaction of three phases—gases, liquids, and solids—may also occur, as in the hydrogenation of a vegetable oil in the presence of a suspended solid nickel catalyst in a hydrogen-sparged, mechanically agitated reactor.

Three of the processes involving liquids—numbers 2, 5, and 6 in the preceding list—employ the same equipment; namely, tanks in which the liquid is circulated and subjected to a desired level of shear. Mixing involving liquids has been most extensively studied and is most important in practice; thus, fluid mixing will be given most coverage here. Many mixing process results can be designed a priori, by using the mixing literature without resorting to experimental studies. These include agitator power requirements, heat transfer, liquid-liquid blending, solids suspension, mass transfer to suspended particles, and many solid-solid applications. However, many other applications invariably involve experimental work followed by scale-up. These include liquid-liquid, gas-liquid, and fast competitive chemical reactions. Scale-up is addressed here, and, as we cover scaleup, the reader will discover that an understanding of mixing fundamentals is essential to the proper handling of scale-up.

This introduction would be incomplete without a short discussion of the place of this chapter in the toolbox of the practicing engineer. Today's engineer is faced with the daunting task of separating the truly practical and immediately useful design methods from the voluminous available literature. For example, the recent Handbook of Industrial Mixing (Paul et al., 2004) is comprised of 1,377 pages devoted only to the topic of Mixing and Agitation. Some of the coverage in that tome can be used with a minimum of effort; however, much of the coverage includes a literature survey with little emphasis on sifting the ''truly useful'' from the ''mundane and ordinary.'' It is our intent here to sift through the entire literature in the field of Mixing and Agitation and present only that material which is most useful to the busy practicing engineer and to present worked examples that apply the design methods.

In addition to the Handbook of Industrial Mixing there are at least 20 Mixing and Agitation books listed in the References. In today's electronic world there are also many web sites of equipment vendors that provide very valuable vendor design information. Among those sites are www.chemineer.com, www.clevelandmixer.com, www.lightnin-mixers.com, www.proquipinc.com, www.philadelphiamixers.com, and www.sulzerchemtech.com. All of these mentioned sites contain product information, but the Chemineer site (to a great extent) and the Lightnin site (to a lesser extent) contain useful design-oriented technical literature. The annual Chemical Engineering Buyer's Guide is a good source for vendor identificatrion.

10.1. A BASIC STIRRED TANK DESIGN

Figure 10.1 gives a ''typical'' geometry for an agitated vessel. "Typical" geometrical ratios are: D/T = 1/3; B/T = 1/12 (B/T = 1/10 in Europe); C/D = 1 and Z/T = 1. This so-called typical geometry is not economically optimal for all process results (e.g., optimal C/D for solids suspension is closer to C/D = 1/3 than to C/D = 1); as appropriate, the economical optimum geometry will be indicated later. Four "full" baffles are standard; they extend the full batch height, except baffles for dished bottoms, may terminate near the bottom head tangent line. Baffles are normally offset from the vessel wall about B/6. The typical batch is ''square''—that is, the batch height equals the vessel diameter (Z/T = 1). The vessel bottom and top heads can be either flat or dished. For axial flow impellers (discussed later) a draft tube, which is a centered cylinder with a diameter slightly larger than the impeller diameter and about two-thirds Z tall, is placed inside the vessel. Sterbacek and Tausk (1965, p. 283) illustrate about a dozen applications of draft tubes, and Oldshue (1983, pp. 469–492) devotes a chapter to their design.

OFF-CENTER ANGLED SHAFT ELIMINATES VORTEXING AND SWIRL

For axial flow impellers, the effect of full baffling can be achieved in an unbaffled vessel with an off-center and angled impeller shaft location. J. B. Fasano of Chemineer uses the following guideline: (1) vendors normally supply a $10°$ angled riser (2) at the vessel top, looking along the vessel centerline, move up (a) 0.19T and then (b) $0.17L_S$ to the right (3) position the agitator with the angled shaft pointing left. Vendors can help to provide optimum positioning.

An offset impeller location, illustrated in Figure 10.3(b) will not totally eliminate vortexing, but it will eliminate most swirl, give
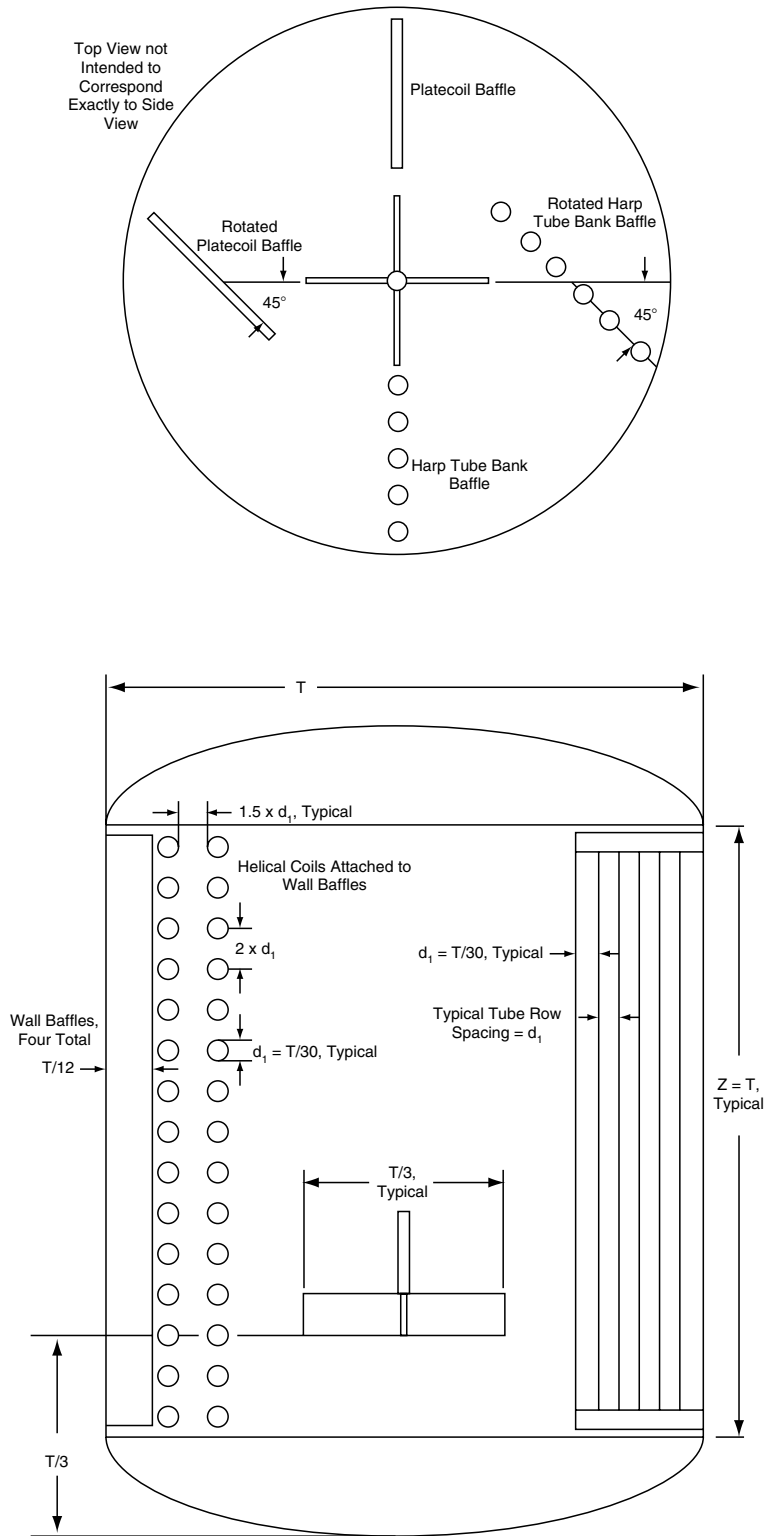
Figure 10.1. Agitated vessel standard geometry showing impeller, baffles, and heat transfer surfaces.

good top-to-bottom turnover, and keep the vortex from reaching the impeller.

INTERNAL HEAT TRANSFER SURFACES

Heat transfer surfaces—helical coils, harp coils, or platecoils—are often installed inside the vessel and jackets (both side wall and bottom head) so that the vessel wall and bottom head can be used as heat transfer surfaces. Figure 10.1 gives a suggested geometry for helical coils and harp coils.

IMPELLER SPEEDS

With 1750 rpm electric motors, standard impeller speeds (Paul et al., 2004, p. 352) are 4, 5, 6, 7.5, 9, 11, 13.5, 16.5, 20, 25, 30, 37, 45, 56, 68, 84, 100, 125, 155, 190, 230, 280, 350, and 1750. In addition, 1200 rpm electric motors are readily available.

IMPELLER TYPES

Twelve common impeller types are illustrated in Figure 10.2. Impellers (a) through (i) and (k) in Figure 10.2 are available worldwide. Impellers (j) (the Intermig) and (l) (the Coaxial [Paravisc Outside and Viscoprop inside]) are available only from Ekato. Key factors to aid in selection of the best impeller to enhance desired process result(s) are as follows:

(a) The three-bladed Marine Propeller (MP) was the first axial-flow impeller used in agitated vessels. It is often supplied with fixed and variable speed portable agitators up to 5 hp with impeller diameters (D) up to 6″. Above D = 6″, marine propellers are too heavy and too expensive to compete with hydrofoil impellers. They are usually applied at high speeds (up to 1750 rpm) in vessels up to 500 gal, with a viscosity limit of about 5000 cp. Lower N_{Re} limit: ~ 200.

(b) The impeller shown is the Chemineer HE-3 hydrofoil, high efficiency impeller, but all vendors have competitive impellers (e.g., Lightnin offers the A310 hydrofoil impeller). Hydrofoils are used extensively for high flow, low shear applications such as heat transfer, blending, and solids suspension at all speeds in all vessels. The economical optimum D/T ($0.4 > [D/T]_{optimum} > 0.6$) is greater for hydrofoils than for higher shear impellers. Lower N_{Re} limit: ~ 200.

(c) The 6-blade disk (the 6BD and, historically, the Rushton turbine) impeller is ancient; nevertheless, it still has no peer for some applications. It invests the highest proportion of its power as shear of all the turbine impellers, except those (e.g., the Cowles impeller) specifically designed to create stable emulsions. It is still the preferred impeller for gas-liquid dispersion for small vessels at low gas rates, it is still used extensively for liquid-liquid dispersions, and it is the only logical choice for use with fast competitive chemical reactions, as will be explained in a later section of this chapter. Lower N_{Re} limit: ~ 5.

(d) The 4-blade 45° pitched blade (4BP) impeller is the preferred choice where axial flow is desired and where there is a need for a proper balance between flow and shear. It is the preferred impeller for liquid-liquid dispersions and for gas dispersion from the vessel headspace (located about D/3 to D/2 below the free liquid surface), in conjunction with a lower 6BD or a concave blade disk inpeller. Lower N_{Re} limit: ~ 20.

(e) The 4-blade flat blade (4BF) impeller is universally used to provide agitation as a vessel is emptied. It is installed, normally fitted with stabilizers, as low in the vessel as is practical. An upper HE-3 or a 4BP is often installed at about $C/T = \frac{1}{2}$ to provide effective agitation at high batch levels. Lower N_{Re} limit: ~ 5

(f) The 6-blade disk-style concave blade impellers (CBI) [the Chemineer CD-6, which uses half pipes as blades, is shown] are used extensively and economically for gas dispersion in large vessels (in fermenters up to 100,000 gal) at high gas flow rates. The CBIs will handle up to 200% more gas without flooding than will the 6BD, and the gassed power draw at flooding drops only about 30%, whereas with a 6BD, the drop in power draw exceeds 50%.

(g) The sawtooth (or Cowles type) impeller is the ultimate at investing its power as shear rather than flow. It is used extensively for producing stable liquid-liquid (emulsions) and dense gas-liquid (foams) dispersions. It is often used in conjunction with a larger diameter axial-flow impeller higher on the shaft. Lower N_{Re} limit: ~ 10.

(h) The helical ribbon impeller and the Paravisc (l) are the impellers of choice when turbines and anchors cannot provide the necessary fluid movement to prevent stratification in the vessel. The turbine lower viscosity limit, for a Newtonian fluid, is determined primarily by the agitation Reynolds number ($Re = ND^2\rho/\mu$). For 6BD and 4BF turbines, Fasano et al., (1994, p. 111, Table 1) say $Re > 1$, and Hemrajani and Tatterson (in Paul (2004), 345) say $Re \sim 10$, although Novak and Rieger (1975, p. 68, Figure 5) indicate a 6BD is just as effective for blending as a helical ribbon above $Re \sim 1$. Using $Re = 5$ as the 6BD lower limit with T = 80″, D = 32″, N = 56 rpm, SG = 1, the upper viscosity limit for a 6BD is about $\mu = ND^2\rho/Re = (56/60)(0.0254 \times 32)^2(1, 000)/5 = 120\,Pa \cdot s = 120,000\,cp$. Thus, with this system, the helical ribbon is the impeller of choice for $\mu > \sim (100,000\,cP$. Lower N_{Re} limit: $= 0$.

(i) Anchor impellers are used for an intermediate range of $0.5 > Re > 10$ because they are much less expensive than helical ribbons and they sweep the entire vessel volume; whereas a turbine leaves stagnant areas near the vessel walls for $Re < 10$. Lower N_{Re} limit: ~ 2.

(j) The Ekato intermig impeller has reverse pitch on the inner and outer blades and they are almost always used with multiple impellers. They are used at high D/T and promote a more uniform axial flow pattern than other turbine impellers. They are advertised to be very effective for solids suspension, blending, and heat transfer in the "medium viscosity" range. Lower N_{Re} limit not given by Ekato (9), perhaps ~ 5.

(k) The hollow-shaft self-gassing impeller can, if properly designed, eliminate the need for a compressor by taking the headspace gas and pumping it through the hollow shaft and dispersing it into the batch as it leaves the hollow blades. As indicated in the Ekato Handbook, "Handbook of Mixing Technology" (2000, p. 164), the "self-gassing" hollow-shaft impeller is often used in hydrogenation vessels where the sparged hydrogen rate drops to very low levels near the end of batch hydrogenation reactions.

(l) According to Ekato (2000, p. 85), "The paravisc is particularly suitable for highly viscous and rheologically difficult media...." With products that are structurally viscous or have a pronounced flow limit or with suspensions having a low liquid content, the paravisc is used as the outer impeller of a coaxial agitator system." The Ekato viscoprop is a good choice for the counter-rotating inner impeller. There is not a lower N_{Re} limit. The coaxial, corotating agitator is an excellent choice for yield stress fluids and shear thinning fluids.

10.2. VESSEL FLOW PATTERNS

The illustrations in Figure 10.3 show flow patterns in agitated vessels. In unbaffled vessels with center mounting (Figure 10.3(a)) much swirl and vortexing is produced, resulting in poor

(a)

(b)

(c)

(d)

(e)

(f)

Double Ribbon

Bottam Scraper

(g)

(h)

(i)

(j)

(k)

(l)
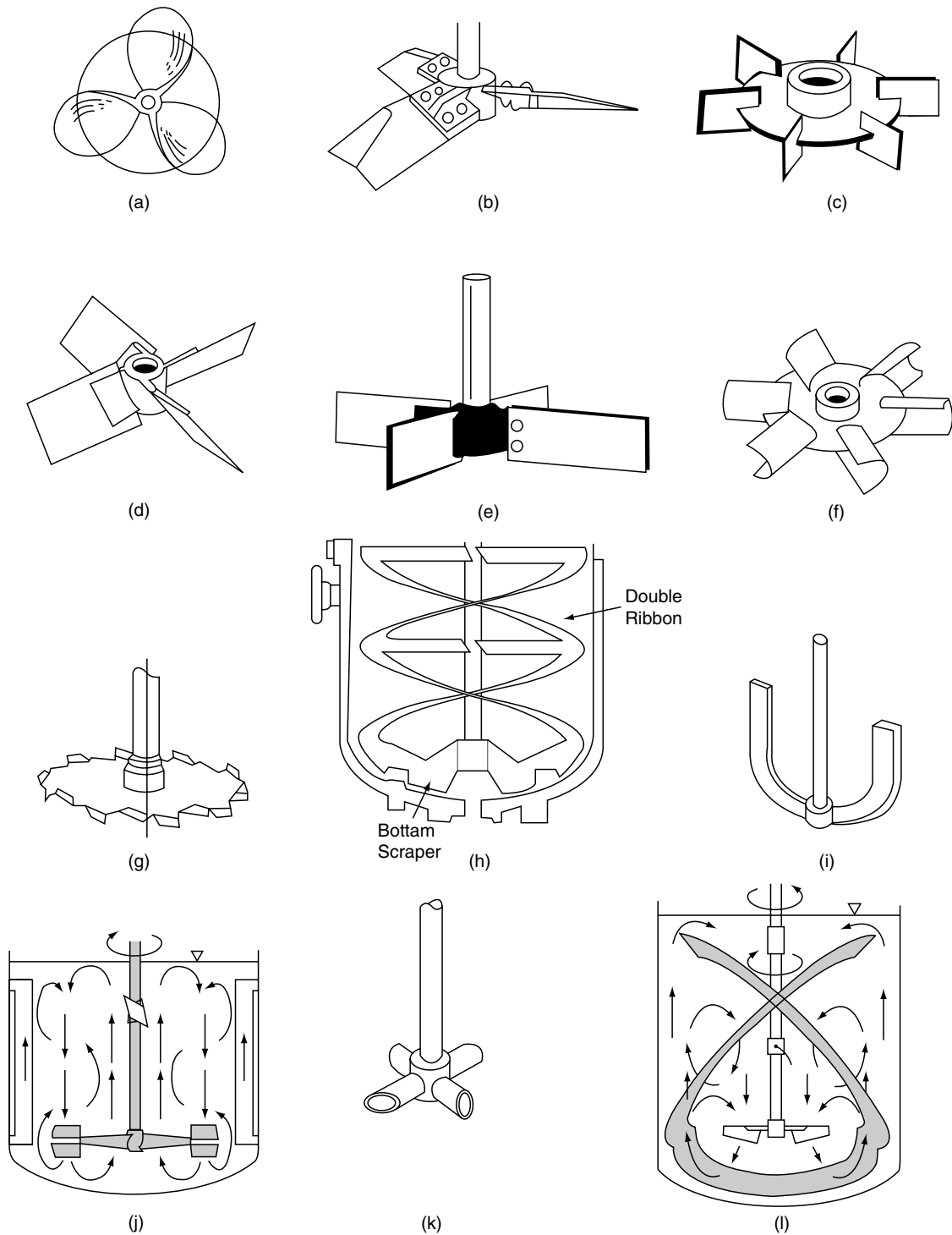
Figure 10.2. Representative impellers for fluid mixing in mechanically agitated vessels (descriptions are in the text).

top-to-bottom movement, reduced turbulence, and subsequent poor mixing. For these reasons, this system is never used in practice. Swirl and vortexing can be minimized by an offset location of the impeller (Figure 10.3(b)) or can be eliminated, to give the effect of full baffling, by an offset, angled positioning, as explained above. With full baffling, axial flow impellers give the full looping flow pattern, as illustrated in Figure 10.3(c), and with radial flow impellers the figure 8 flow pattern illustrated in Figure 10.3(d) is achieved. This flow pattern somewhat partitions the vessel into two zones, one above and another below the impeller. Mixing between zones is relatively rapid; however, for certain chemical reactions this zoning can be undesirable.
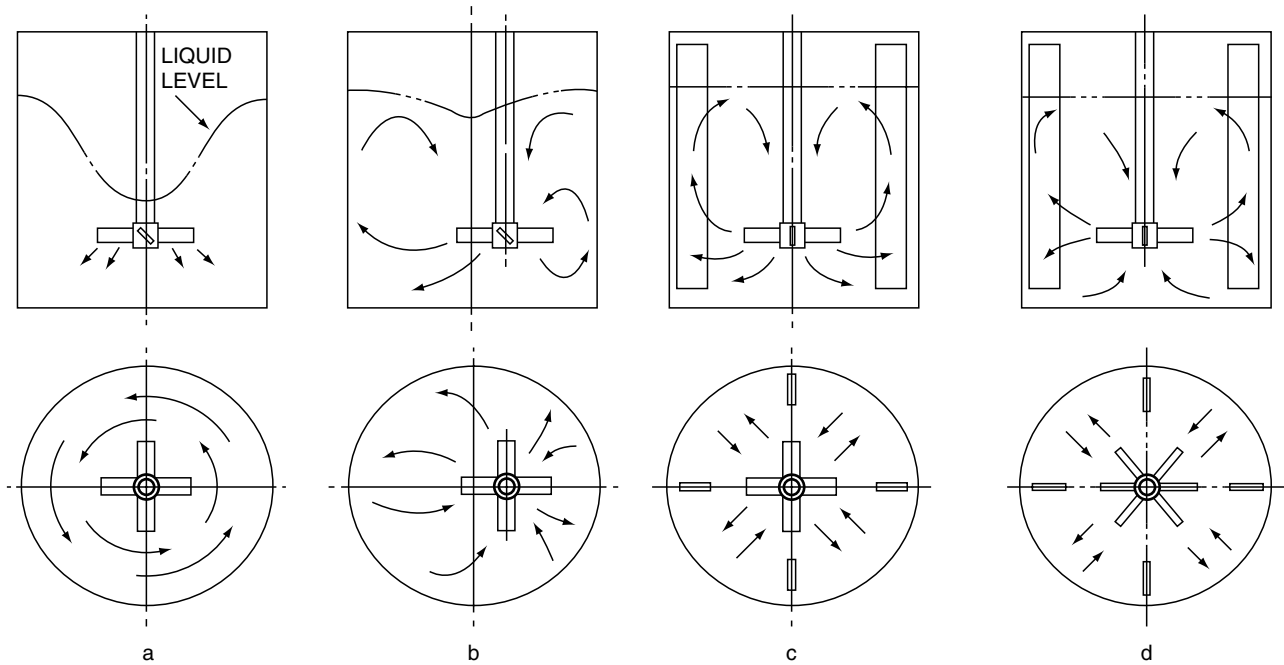
Figure 10.3. Agitator flow patterns. (a) Axial or radial impellers without baffles produce vortexes. (b) Offcenter location reduces the vortex. (c) Axial impeller with baffles. (d) Radial impeller with baffles.

10.3. AGITATOR POWER REQUIREMENTS

FOR A GIVEN SYSTEM GEOMETRY

For all impellers with Newtonian fluids, dimensional analysis indicates

$$N_P = f(N_{Re}, N_{Fr}, \text{Geometry}) \tag{10.1}$$

Thus, for geometrically similar systems

$$N_P = f(N_{Re}, N_{Fr}) \tag{10.2}$$

And, for geometrically similar fully baffled (or with anti-swirl impeller positioning)

$$N_P = f(N_{Re}) \tag{10.3}$$

Figure 10.4 presents the power correlations for the Chemineer Standard 4BP and HE-3 impellers as a function of D/T at a C/T of 1/3. Figure 10.5(a), (b), and (c) present power correlations for myriad impellers, with the figure title and figure caption explaining the details for each impeller. Figure 10.6 presents additional power correlations for six additional impellers in fully baffled vessels.

The application of the presented power correlations are illustrated in Examples 10.1 and 10.2.

EFFECT OF KEY GEOMETRICAL VARIABLE ON POWER DRAW

The effect of *impeller spacing* (S) is complex for S/D < 1, as indicated by Tatterson (1991, p. 39, Figure 2.6). However, S/D < 1 is not recommended in practice, and for S/D > 1, the power requirements of the individual impellers are additive to determine the total power requirement(s) of all impellers on a single shaft.

The effect of *off-bottom clearance* (C) is pronounced for all impellers, as indicated in Figure 10.7. For a 6BD (Rushton) impeller, the power draw (P) decreases as the impeller is moved closer to the vessel bottom from the typical impeller location of C/D = 1; for a 4BF turbine, P initially decreases as the impeller is moved down from C/D = 1, reaches a minimum at about C/D = 0.7 and then rises again as C/D drops below 0.7; and for a 4BP, the power draw continually increases as the impeller moves down from C/D = 1.

10.4. IMPELLER PUMPING

Agitation impellers act as caseless pumps. Measured pumping capacities for various impellers have been used to develop correlations of the flow number ($N_Q = Q/ND^3$), as a function of N_{Re} and system geometry. Figure 10.8 presents such a correlation for a 4BP and Figure 10.9 presents a pumping correlation for the HE-3.

Examples 10.3 and 10.4 determine the pumping capabilities of a 4BP and an HE-3.

10.5. TANK BLENDING

For $N_{Re} > \sim 200$ the high effeciency impellers (e.g., propeller, Chemineer HE-3, Lightnin A310, and others) are most economical. For $5 \sim< N_{Re} <\sim 200$, 4BF or 6BDs are most economical; however, once the flow regime becomes laminar, the Helical Ribbon or Paravisc are the preferred impellers. For competitive fast reactions, where rapid blending is extremely important, a six-blade disk impeller should be used so that the feed stream can be introduced at high velocity to the eye of the impeller. The disk forces the feed to immediately move outward along the disk and into the high shear zones around the impeller blade tips, where local blending is extremely rapid.

It is important to understand the experimental measurement of blend time. The early experimental work was done by using the
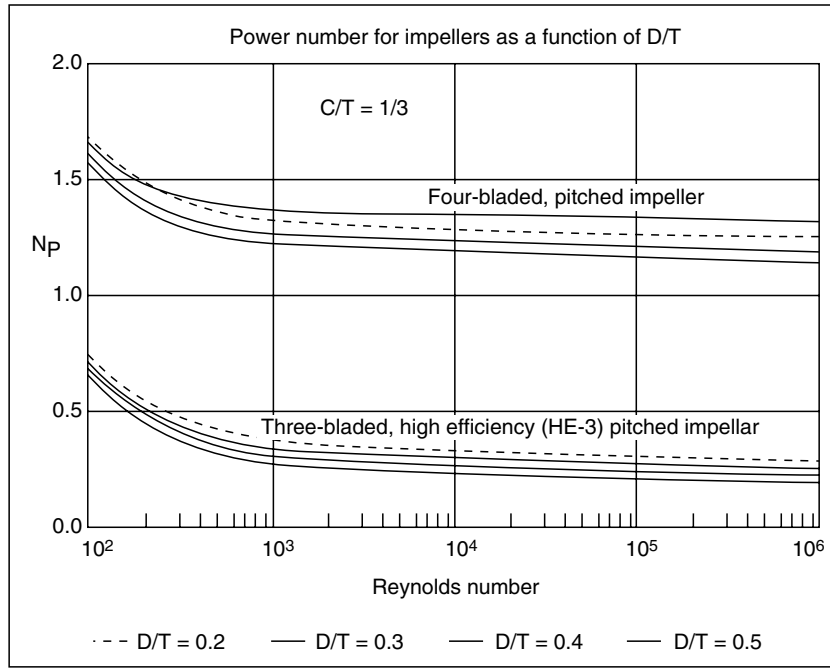
Figure 10.4. N_P vs. N_{Re} for 4BP and HE3 impellers as a function of (D/T) at (C/T) = 1/3. (D/T dependence: sequentially, from top curve going down to bottom curve: 4BP—0.5, 0.2, 0.3, 0.4; HE-3—0.2, 0.3, 0.4. 0.5) (*Chem. Eng.*, August 1984, p. 112).
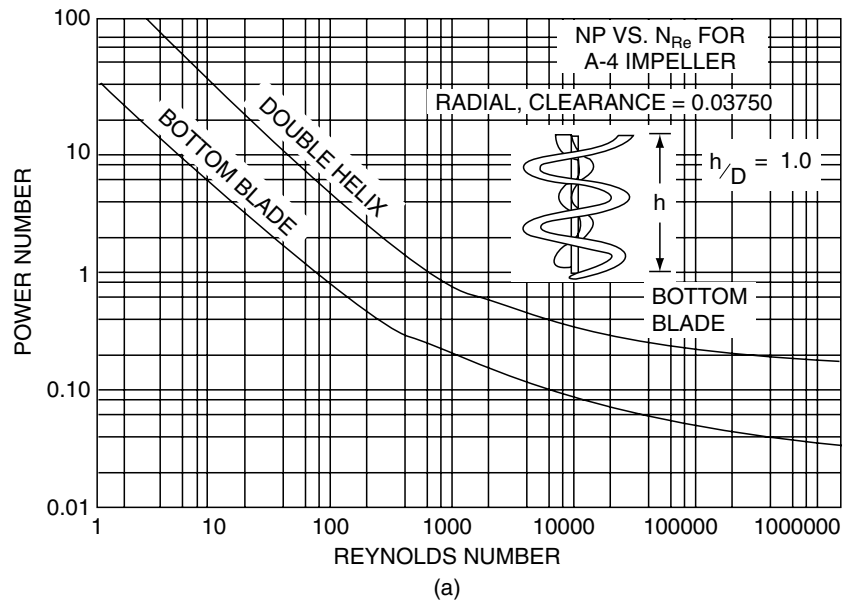
Figure 10.5. Power number, $N_P = Pg_c/N^3D^5\rho$, against Reynolds number, $N_{Re} = ND^2\rho/\mu$, for several kinds of impellers: (a) helical shape (*Oldshue, 1983*); (b) anchor shape (*Oldshue, 1983*); (c) several shapes: (1) propeller, pitch equalling diameter, without baffles; (2) propeller, $s = d$, four baffles; (3) propeller, $s = 2d$, without baffles; (4) propeller, $s = 2d$, four baffles; (5) turbine impeller, six straight blades, without baffles; (6) turbine impeller, six blades, four baffles; (7) turbine impeller, six curved blades, four baffles; (8) arrowhead turbine, four baffles; (9) turbine impeller, inclined curved blades, four baffles; (10) two-blade paddle, four baffles; (11) turbine impeller, six blades, four baffles; (12) turbine impeller with stator ring; (13) paddle without baffles (data of Miller and Mann); (14) paddle without baffles (data of White and Summerford). All baffles are of width 0.1D [*after Rushton, Costich, and Everett,* Chem. Eng. Prog. **46**(9), *467* (*1950*)].

human eye as a detector after injecting dye into the batch. Later work was done by injecting a tracer (e.g., KCl in an aqueous solution and detecting its local concentration by electrical conductivity) into a vessel and then measuring its concentration decay with time at an appropriate location in the vessel; this electronic method allows determination of blending uniformity with time.

The time required to achieve a certain degree of uniformity after a material is added to a tank is one of the most frequently

(b)

(c)
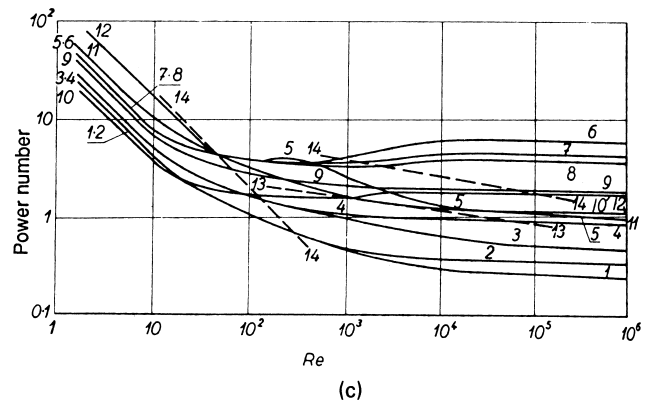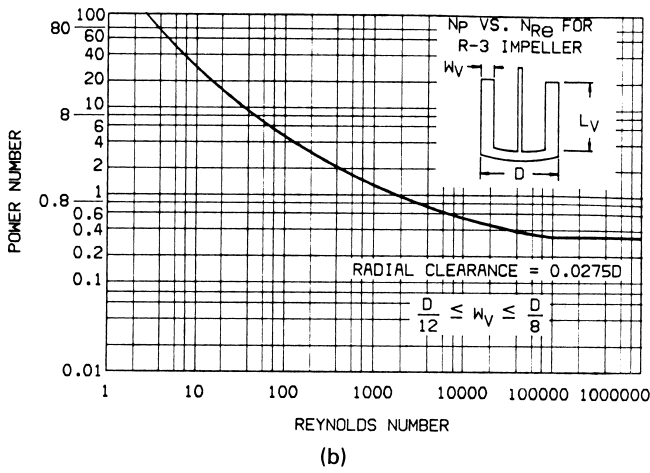
Figure 10.5.—(*continued*)
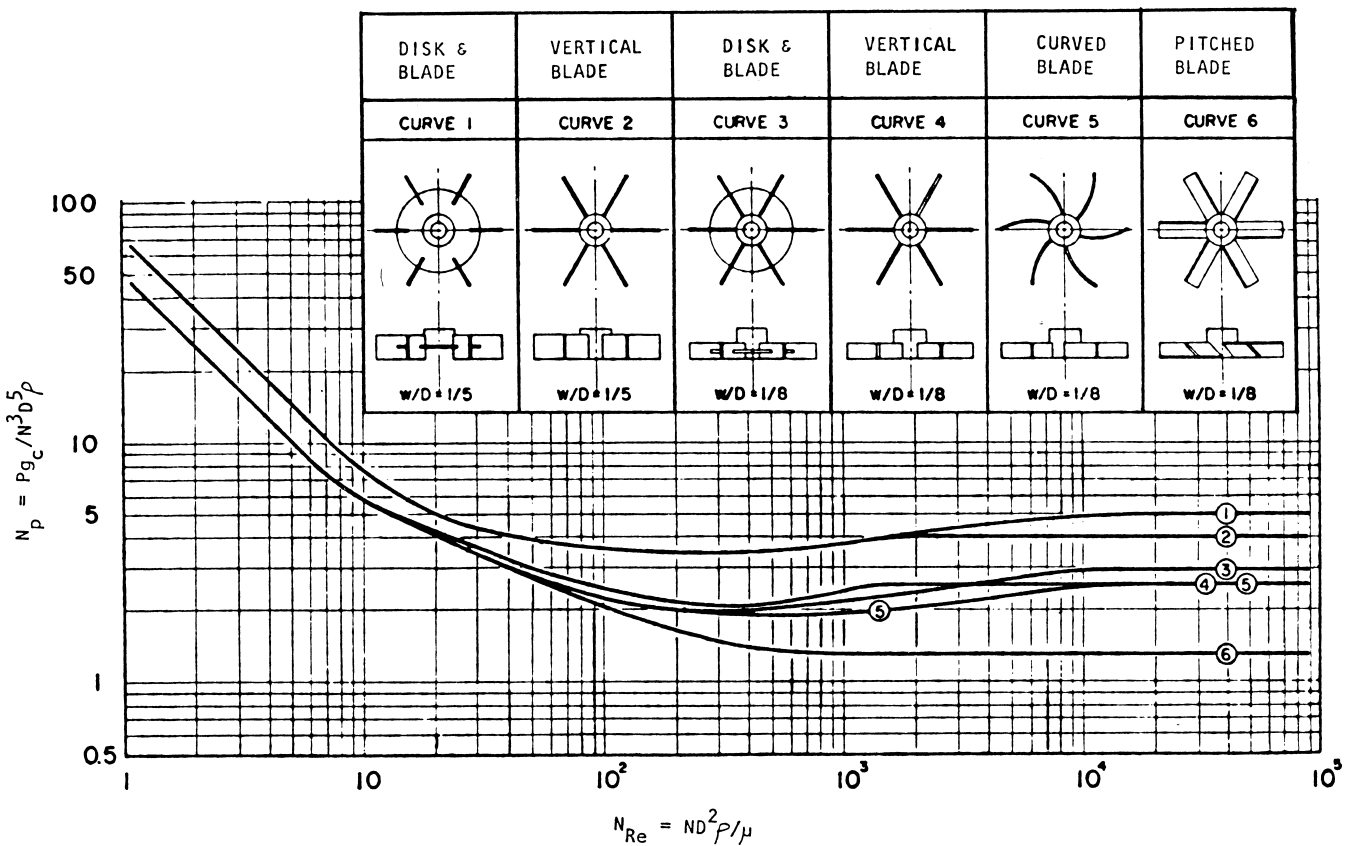
Figure 10.6. Power number against Reynolds number of some turbine impellers [*Bates, Fondy, and Corpstein*, Ind. Eng. Chem. Process. Des. Dev. **2**(4) *311 (1963)*].

specified process requirements. Fasano et al. (1994) explain the literature definition of mixing uniformity as

$$U = 1 - (\Delta C_{t,\max}/\Delta C_{t=0,\max}) \qquad (10.4)$$

Here, $\Delta C_{t,\max}$ is the peak deviation from the average tank concentration as C fluctuates and decays with time, i.e., $\Delta C_{t,\max} = (C_{t,\max} - C_\infty)$, where C_∞ is C at infinite time. Blending uniformity increases exponentially with time as follows:

$$U(t) = 1 - e^{-k_m t} \qquad (10.5)$$

where k_m is the mixing-rate constant. Equation 10.5 can be rearranged to yield an equation that relates the blend time (t) to U and agitation parameters as follows:

$$t_u = -\ln(1 - U)/k_m \qquad (10.6)$$

EXAMPLE 10.1
Impeller Power for a Specified Impeller at a Given Speed
A 32″ diameter 6BD impeller, located 32″ off the vessel bottom, is agitating water ($\mu = 1$ cP; $= 62.4\,\text{lb}_m/\text{ft}^3 = 1,000\,\text{kg/m}^3$) in an 80″ diameter vessel at 56 rpm. The batch height is 80″, giving a batch volume of 1,740 gal. The required power will be calculated.

$$N_{Re} = ND^2\rho/\mu = (56/60)(0.0254 \times 32)^2 1,000/(1/1,000)$$
$$= 616,000$$

From Figure 10.6, $N_P = 5$, thus

$$P = (N_P)\rho N^3 D^5 = (5)(1,000)(56/60)^3(.0254 \times 32)^5$$
$$= 1,442\,W = 1.93\,HP$$

This is a rather low specific power level of $1.93/1.74 = 1.11\,HP/1,000$ gal.

EXAMPLE 10.2
Impeller Power at High Viscosity
Let's take Example 10.1 and increase the viscosity to 123,000 cP, and recalculate P.

$$N_{Re} = 616,000(1/123,000) = 5$$

From Figure 10.6, $N_P = 16$, thus

$$P = 1.93(16/5) = 6.2\,HP$$

This is still a low power level of $6.2/1.74 = 3.55\,HP/1,000$ gal. With this agitator, a reasonable upper limit for agitator speed would be 100 rpm, for which the impeller power would be 22 HP with a specific power input of 13 HP/1,000 gal and $N_{Re} = 9$. This change would move up into the Reynolds number near the lower limit recommended by *Hemrajani and Tatterson* (in Paul (2004), 345). This example illustrates the great impact of fluid viscosity on (1) the power requirement of a 6BD and (2) the choice of an impeller style between a turbine and a helical ribbon impeller.

The dimensionless mixing-rate constant, k_m, in standard baffled tanks, is a function of impeller Reynolds number (N_{Re}) and geometry. For $N_{Re} > 10,000$, k_m is only a function of geometry, independent of N_{Re}. k_m is related to N, D, and T as follows (Fassano et al., 1994):

$$K_m = aN(D/T)_b(T/Z)^b \tag{10.7}$$

The correlation parameters a and b are given in Table 10.1. The a's and b's of Table 10.1 are for surface addition; however, blend times for similar fluids are relatively insensitive to addition location. Equation 10.7 is restricted to:

1. Newtonian fluids of nearly the same viscosity and density as the bulk fluid
2. Additions of 5%, or less, of the liquid volume of the vessel

3. Additions made to a vessel already undergoing agitation (blend times of stratified fluids can be considerably longer)

One can account for the increased blend time at a lower Reynolds number ($N_{Re} < 10,000$) and for the effects of fluids having different densities and viscosities using the following equation (Fasano et al., 1994):

$$T_u = t_{u,turb}f_{Re}f_\mu^* f_{\Delta\rho} \tag{10.8}$$

where $t_{U,turb}$ is determined from Eq. 10.6; the N_{Re} correction is given by Figure 10.10; the viscosity correction is given by Figure 10.11; and the density difference correction is given by Figure 10.12. Now let's do two examples (10.5 and 10.6) to calculate blend time.
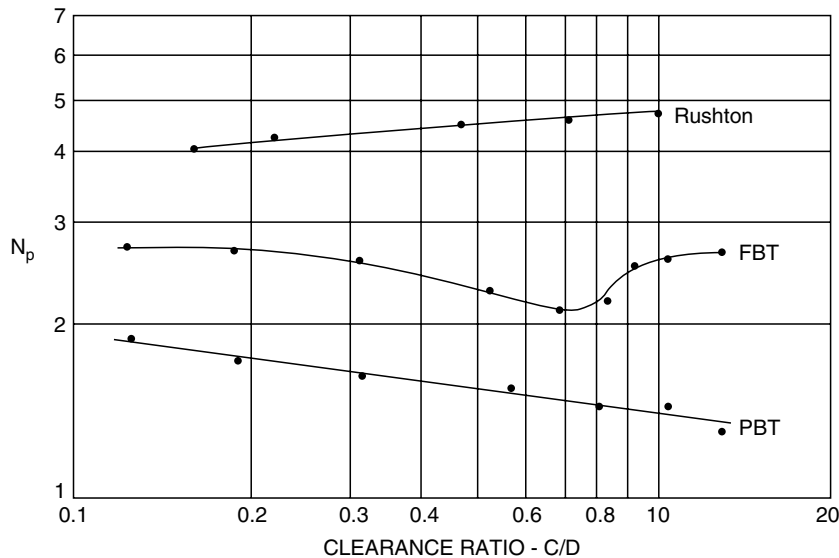
Figure 10.7. Effect of off-bottom clearance on N_P for turbines with full baffling (adapted from Bates, Fondy, and Corpstein, *I&EC Funds*, **2**, p. 310, 1963).
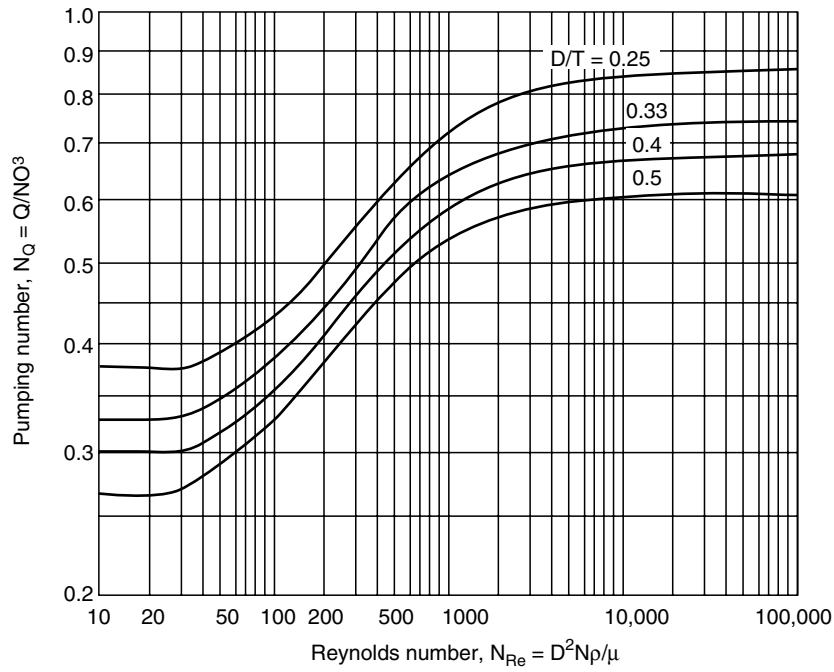
Figure 10.8. Flow number as a function of impeller Reynolds number for a pitched blade turbine with $N_P = 1.37$. D/T is the ratio of impeller and tank diameters. [*Dickey*, Chem. Eng., *102–110* (*26 April 1976*)].
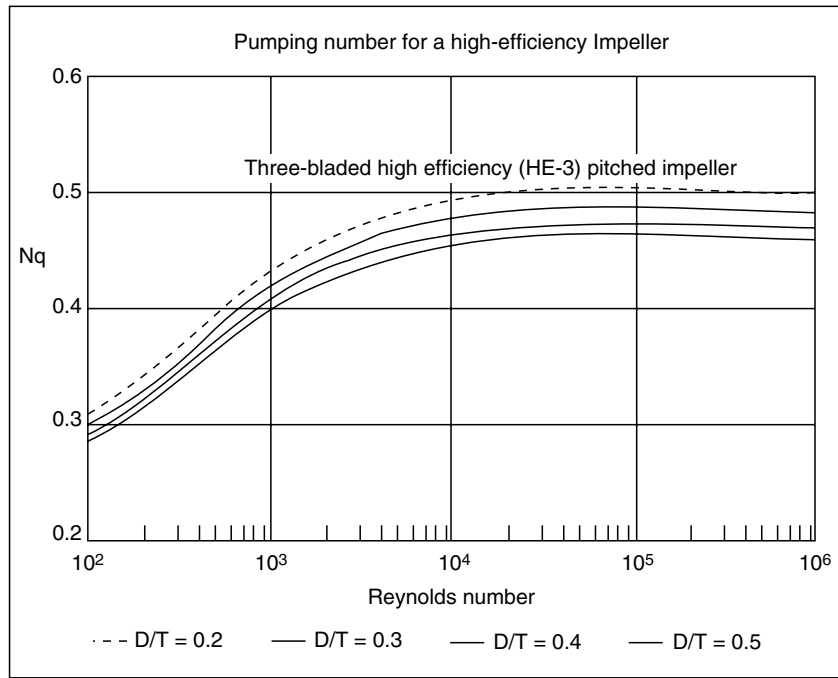
Figure 10.9. Flow number correlation for an HE-3 impeller [*Chem. Eng.*, p. 113 (August 1994)].

BLEND TIME FOR MULTIPLE IMPELLERS

An effective blending time constant ($k_{m,eff}$) can be estimated by the sum of the individual mixing-rate constants ($k_{m,i}$):

$$k_{m,eff} \approx \sum_{i=1}^{n} k_{m,i} \tag{10.9}$$

Each of the separate $k_{m,i}$ should be based on a particular impeller operating separately within the total volume.

EXAMPLE 10.3
Pumping Rate of a 4BP Impeller
Let's place a 32″ diameter 4BP impeller, operating at 125 rpm, in an 80″ diameter tank with C = 32″. We wish to determine the pumping rate with water in the vessel. We will first calculate P.

$$N_{Re} = ND^2\rho/\mu = (125/60)(0.0254 \times 32)^2 1,000/(1/1,000)$$
$$= 1,375,000$$

From Figure 10.4, $N_P = 1.2$, thus

$$P = (N_P)\rho N^3 D^5 = (1.2)(1,000)(125/60)^3(.0254 \times 32)^5$$
$$= 3,850\,W = 5.1\,HP(3HP/kGal)$$

From Figure 10.8, $N_Q = 0.68$, then

$$Q = (N_Q)ND^3 = 0.68(125/60)(0.0254 \times 32)^3 = 0.704\,m^3/s$$
$$= 24.9\,ft^3/s = 11,200\,gpm$$

TABLE 10.1. Mixing-Rate Constant (k_m) for Fully Turbulent Flow Regimes ($N_{Re} > 10,000$)

Mixing-Rate Constants		
Impeller style	**a**	**b**
Six-blade disc	1.06	2.17
Four-blade flat	1.01	2.30
Four-blade 45° pitched	0.0641	2.19
Three-blade high efficiency	0.272	1.67

EXAMPLE 10.4
Pumping Rate of an HE-3 Impeller
Let's check the pumping rate of an HE-3 impeller, for the application of Example 10.3, operating at the same HP and close to the same torque. To be entirely fair to the HE-3 impeller, we must make the comparison at constant HP and torque, because the operating cost of an agitator is directly related to HP and the first cost (the capital cost) is closely related to its torque, which primarily determines the gear reducer cost.
The torque requirement of the 4BP of Example 10.3 is

$$T = P/(2\pi N) = 3,850/(6.28 \times 125/60) = 294\,Nm$$

Let's try a 45″ diameter (D/T = 0.56) HE-3 operating at 125 rpm

$$N_{Re} = (1,375,000)(45/32) = 2,720,000$$

From Figure 10.4, $N_P = .21$, thus

$$P = (N_P)\rho N^3 D^5 = (0.21)(1,000)(125/60)^3(.0254 \times 45)^5$$
$$= 3,700\,W = 5\,HP$$

The torque requirement is $T = 3700/(6.28 \times 2.08) = 283$, which is close to T for the 4BP.
From Figure 10.9, $N_Q = 0.45$, then

$$Q = (N_Q)ND^3 = 0.45(125/60)(0.0254 \times 45)^3 = 1.4m^3/s$$
$$= 49.4\,ft^3/s = 22,200\,gpm$$

Thus, the high efficiency HE-3 impeller pumping capacity is twice that of the 4BP when compared at comparable torque and HP, which is a comparison at about the same overall cost.
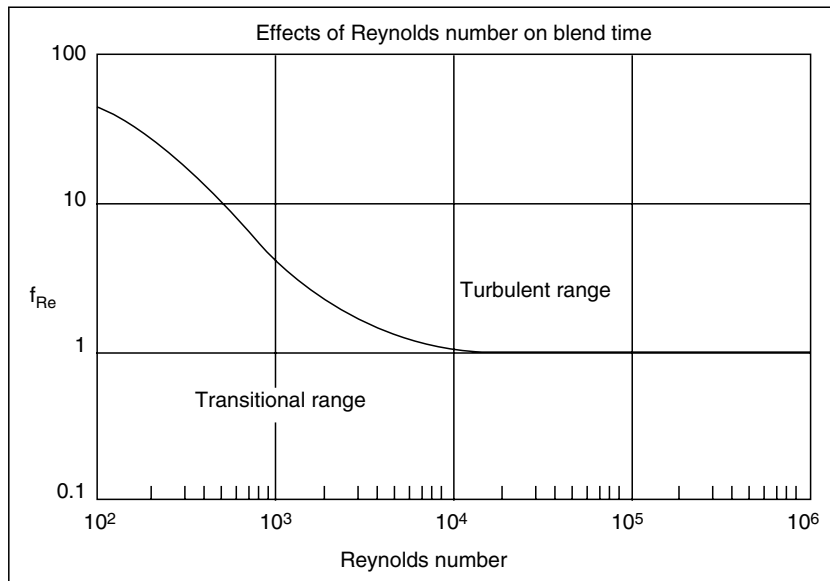
Figure 10.10. Effect of impeller Reynolds number on blend time for $N_{Re} < 10,000$.
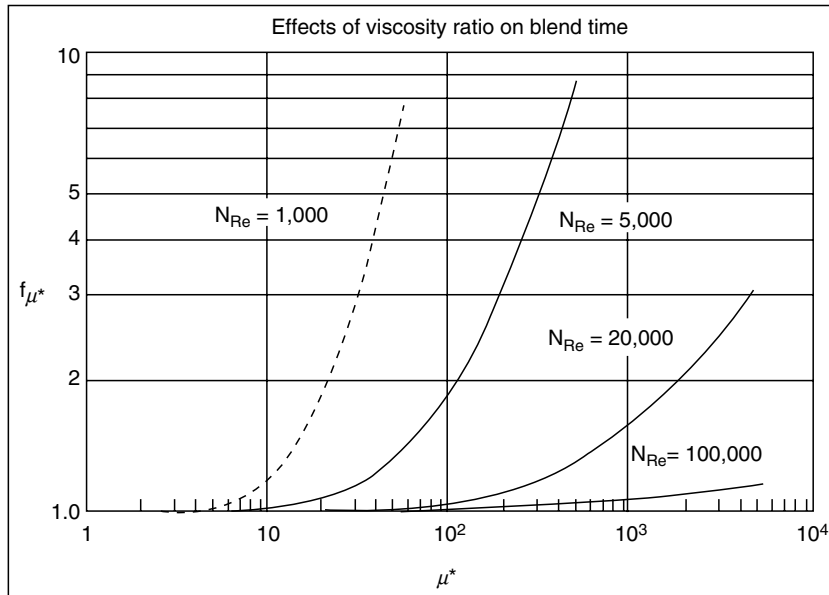
Figure 10.11. Effect of viscosity (μ^*) ratio on blend time.

10.6. HEAT TRANSFER

Guidance regarding the selection of an economical heat transfer system is

Type of Surface	+ wall → helical coils → harp coils → platecoils
Number of Coils, Plates, etc.	+ Helical coils: Use maximum of 2
	+ Up to 16 for harps and platecoils are effective
Position of Surface in Vessel	+ Helical coils inside and attached to baffles
	+ Harp coils and platecoils are baffles
Distance between Coil Banks	+ Minimum distance is twice the tube diameter
Spacing of Harps and Platecoils	+ Above ∼ 8, harps and platecoils are positioned at 45° to vessel diameter
Tube Spacing Harps and Helical Coils	+ Minimum spacing is one tube diameter
Reflux Cooling	+ Very economical when feasible
External Pumped-through Exchanger	+ Must be used when internal surface is too little or reflux cooling cannot be used
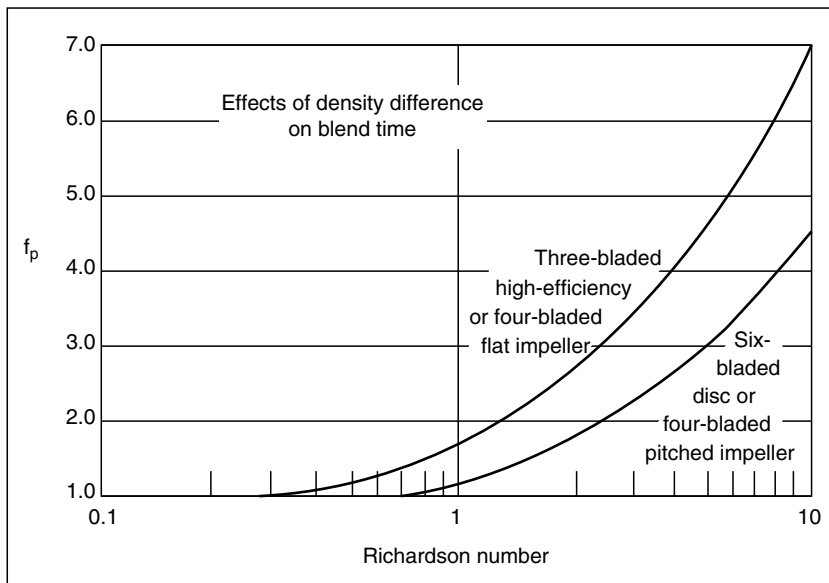
Figure 10.12. Effect of density difference on blend time.

EXAMPLE 10.5
Low Viscosity Blending with an HE-3 Impeller
Let's determine the blend time for the HE-3 impeller of Example 10.4 adding a few percent of a 10,000 cp additive. $D = 45''$; $T = 80''$; $D/T = 0.563$; $T/Z = 1$; $N = 125$ rpm $= 2.08$ rps; $\mu^* = 10,000$; SG additive $= 2$; $N_{Re} = 2,700,000$. Select a conservative uniformity of 99% (i.e., $U = 0.99$).

$$k_m = aN[D/T]^b[T/Z]^{0.5} = (0.272)2.08[0.563]^{1.67}[1]^{1/2} = 0.22$$

$$t_{U,turb} = -\ln(1 - U)/k_m = -\ln(1 - 0.99)/0.22 = 21 \text{ s}$$

Now apply the corrections for N_{Re}, μ^* and $\Delta\rho$. From Figure 10.10, $f_{Re} = 1$, and from Figure 10.11, $f_{\mu^*} = 1$. The Richardson number $(= \Delta\rho gZ/\rho N^2 D^2)$ is needed to determine f_ρ from Figure 10.12.

$$N_{Ri} = \Delta\rho gZ/\rho N^2 D^2 = (1,000)9.8(0.0254 \times 80)$$
$$/[1,000 \times 2.08^2 \times (0.0254 \times 45)^2] = 3.5$$

From Figure 10.12, $f_\rho = 3.7$, thus

$$t_U = t_{U,turb}f_{Re}f_\mu f_\rho = 21(1)(1)(3.7) = 78 \text{ s}$$

HEAT TRANSFER COEFFICIENTS

Most of the correlations were taken from Penney (1983) and from tables 5 and 6 in Fasano et al., (1994) for the HE-3 impeller and the bottom head. The correlation for heat transfer coefficients for helical ribbon impellers was taken from Ishibashi et al. (1979). The correlations given by Penney (1983) (p. 879) use the same sources.

Correlations for heat transfer coefficients are all of the form

$$N_{Nu} = K(N_{re}{}^a)(N_{pr}{}^b)(MuR^c)(G_{CORRECTION}) \tag{10.10}$$

The geometry correction ($G_{CORRECTION}$) takes account of the fact that any change in system geometry will affect the heat transfer correlation. This correction is handled algebraically by using what has been shown experimentally

$$G_{CORRECTION} = f(R_1{}^j, R_2{}^k, R_3{}^l, \ldots R_n{}^m) \tag{10.11}$$

Where the R's are geometrical dimensions ratios (e.g., d/T) ratioed to a standard experimental ratio (i.e., $[d/T]_{standard}$). Thus, for tube diameter (d), $R_d = [(d/T)/0.04]^{1/2}$.

The $[d/T]_{standard}$ was selected as 0.04 because most experimental data were taken with $d/T \sim 0.04$ (i.e., for $T = 50''$ in an experimental apparatus, $d \sim (0.04)(50) = 2''$) and, experimentally, $h \propto d^{1/2}$.

Individual heat transfer coefficient correlations are summarized in Table 10.2. Penney (1983) has given the recommended geometry for anchors and helical ribbons:

Geometric ratios	Anchor	Helical ribbon
P/D	∞	1/2
W/D	0.082	0.082
C/D	0.02	0.02
D/T	0.96	0.96

EXAMPLE 10.6
Medium/High Viscosity Blending with a 6BD Impeller
Let's go back to Example 10.2 and introduce a fed component with $SG = 1$ and $\mu = 120,000$ cp. Thus, this example will give us a good indication of what blending performance we can expect from a 6BD operating at $N_{Re} = 5$.

$$k_m = aN[D/T]^b[T/Z]^{0.5} = (1.06)0.93[0.4]^{2.17}[1]^{1/2} = 0.13$$

$$t_{U,turb} = -\ln(1 - U)/k_m = -\ln(1 - 0.99)/0.13 = 35 \text{ s}$$

Now apply the corrections for N_{Re}, μ^*, and $\Delta\rho$. From Figure 10.10, $f_{Re} \sim 1,000$ by extrapolation, $f_{\mu^*} = 1$; $N_{Ri} = 0$ & $f_\rho = 1$.

$$t_U = t_{U,turb}f_{Re}f_\mu f_\rho = 35(1,000)(1)(1) = 35,000 \text{ s} = 10 \text{ hours}$$

This is truly a long time and indicates that a 6BD will barely function at $N_{Re} = 5$. If the agitator speed is increased to 100 rpm and to $N_{Re} = 10$, then

$$t_U = 10(56/100)(600/1000) = 3.4 \text{ hours}$$

which is still a long time.

OVERALL HEAT TRANSFER COEFFICIENT (U)

The overall coefficient includes the following heat transfer resistances (1) process side film (2) process side fouling (3) wall resistances (4) utility side fouling, and (5) utility side film. The development of the relationship between U and these individual resistances is given in myriad heat transfer texts.

$$U = 1/[1/h + R_P + (\Delta X/k_m) + R_U + (1/h_U)]$$
$$\text{(for the jacket and bottom head)} \tag{10.12}$$

$$U = 1/[1/h_P + R_P + \{d_O/(2k)\}\ln(d_O/d_I)$$
$$+\{R_U + (1/h_U)\}\{d_O/d_I\}](\text{for a coil}) \tag{10.13}$$

HEAT-UP OR COOL-DOWN TIME

The transient heating or cooling time is calculated as follows (McCabe et al., 2001):

$$t = (Mc_p/UA)\ln[(T_U - T_I)/(T_U - T_F)] \tag{10.14}$$

Now let's do three heat transfer examples.

10.7. VORTEX DEPTH

The vortex depth predictive methods included here are for (1) unbaffled vessels and (2) a 4BP impeller with lower half baffles.

DRAWDOWN OF HEADSPACE GAS AND WETTING OF FLOATING SOLIDS USING PARTIAL BAFFLING

Partial baffling can be very effective to produce a votex, which can effectively drawdown gas from the headspace or rapidly move floating solids into the high shear zones surrounding the impeller blade tips. Figure 10.13 shows a 6BD operating in a vessel baffled with lower half baffles. A 6BD is effective in a partially baffled vessel, but the 4BP is a better choice. Figures 10.14(a) and (b) and 10.15 present correlations to predict the relative vortex, for a 4BP impeller, as a function of N_{Re}, N_{Fr}, D/T, and C/D. This data was

TABLE 10.2. Summary of Heat Transfer Coefficient Correlations for Agitated Vessels

IMP.	SURFACE	N_{Re} RANGE	K	a	b	c	GEOMETRY CORRECTION
RCI[+]	Wall & BH	> 100	0.54	2/3	1/3	0.14	
6BD	Wall	> 200	0.74	2/3	1/3	0.14	$(1/[Z/T])^{0.15}(L/L_S)^{0.2}$
6BD	BH	> 200	0.50	2/3	1/3	0.14	$(1/[Z/T])^{0.15}(L/L_S)^{0.2}$
6BD	Coil	> 200	0.03	2/3	1/3	0.14	$(1/[Z/T])^{0.15}(L/L_S)^{0.2}(1/[d/T])^{0.5}$
4BF	Wall	> 200	0.66	2/3	1/3	0.14	$(1/[Z/T])^{0.15}(L/L_S)^{0.2}$
4BF	BH	> 200	0.45	2/3	1/3	0.14	$(1/[Z/T])^{0.15}(L/L_S)^{0.2}$
4BF	Coil	> 200	0.027	2/3	1/3	0.14	$(1/[Z/T])^{0.15}(L/L_S)^{0.2}(1/[d/T])^{0.5}$
4BP	Wall	> 200	0.45	2/3	1/3	0.14	$(1/[Z/T])^{0.15}(L/L_S)^{0.2}$
4BP	BH	> 200	1.08	2/3	1/3	0.14	$(1/[Z/T])^{0.15}(L/L_S)^{0.2}$
4BP	Coil	> 200	0.023	2/3	1/3	0.14	$(1/[Z/T])^{0.15}(L/L_S)^{0.2}(1/[d/T])^{0.5}$
HE-3	Wall	> 200	0.31	2/3	1/3	0.14	$(1/[Z/T])^{0.15}(L/L_S)^{0.2}$
HE-3	BH	> 200	0.90	2/3	1/3	0.14	$(1/[Z/T])^{0.15}(L/L_S)^{0.2}(1/ZOT)$
HE-3	Coil	> 200	0.017	2/3	1/3	0.14	$(1/[Z/T])^{0.15}(L/L_S)^{0.2}(1/[d/T])^{0.5}$
M. PROP.	Wall	> 200	0.43	2/3	1/3	0.14	$(1/[Z/T])^{0.15}(L/L_S)^{0.2}$
M. PROP.	BH	> 200	0.90	2/3	1/3	0.14	$(1/[Z/T])^{0.15}(L/L_S)^{0.2}$
M. PROP.	Coil	> 200	0.016	2/3	1/3	0.14	$(1/[Z/T])^{0.15}(L/L_S)^{0.2}(1/[d/T])^{0.5}$
6BD	45° Harp Coils	> 100	0.021	0.67	0.4	0.27[*]	$(1/[Z/T])^{0.15}(L/L_S)^{0.2}([D/T]/[1/3])^{0.33}([d/T]/0/04)^{0.5}$
4BF	0° Harp Coils	> 100	0.06	0.65	0.3	0.4[*]	$(1/[Z/T])^{0.15}(L/L_S)^{0.2}([D/T]/[1/3])^{0.33}([d/T]/0/04)^{0.5}$
6BD	Plate Coils	> 100	0.031	0.66	0.33	0.5[*]	$(1/[Z/T])^{0.15}(L/L_S)^{0.2}$
Anchor	Wall	< 1	Not Recommended! Laminar Flow. No top-to-bottom turnover.				
''	''	> 12, < 100	0.69	1/2	1/3	0.14	
''	''	> 100	0.32	2/3	1/3	0.14	
Helical	Wall	< 13	0.94	1/3	1/3	0.14	*Note:* Double Helixp
Ribbon		>13, < 210	0.61	1/2	1/3	0.14	p/D = 1
		> 210	0.25	2/3	1/3	0.14	C/D = 0.02

Notes: + Pfaudler Retreat Curve Impeller.
[*]Petree and Small (*AIChE Symposium Series*, **74**, pp. 53–59, 1978) used the ratio of bulk to film viscosity. It is recommended that one use c = 0.14 and use the ratio of bulk to wall viscosity.

obtained by G. S. Spanel in laboratories at the University of Arkansas.

If possible, we prefer to approach the gas dispersion and solids wetting problem by doing experiments on a small scale and then scale up; such an experimental investigation of gas dispersion from a reactor headspace by using partial baffling is documented by Penney et al. (2000). Even with experimentation, a flexible baffling system must be designed. Sufficient flexibility can be achieved in metal vessels by (1) bolting in the baffles so that the degree of baffling can be varied by removing and reinstalling baffles and (2) *using a variable speed drive, which is a must.* It is not uncommon to use 100 HP variable speed drives in applications requiring gas headspace dispersion and/or drawdown of floating/lumping solids.

QUALITATIVE UNDERSTANDING OF VORTEX DEPTH

For any system the dimensionless vortex depth is a function of a Reynolds number (ratio of inertial to viscous forces) and the Froude number (ratio of inertial to gravity forces). Expressed mathematically,

$$X/D = f(N_{Re}, N_{Fr}, \text{Geometry}) \tag{10.15}$$

Figures 10.14(a) and (b) present this correlation for a 4BP impeller with the following range of geometry: Four lower baffles, $H_B/Z = 1/2$, $B/T = 1/12$; $D/T = 0.34 \& 0.53$; $C/D = 1/3, 1/2,$ and 1. These plots show how complex the relationship of Eq. 10.15 can be.

UNBAFFLED VESSELS

Unbaffled vessels are almost never used in practice because the swirling minimizes turbulence and inhibits top-to-bottom turnover,

resulting in very poor solids suspension and gas dispersion. It is, however, instructive to compare the vortex depth in partially baffled vessels with the vortex depth in unbaffled vessels (see Example 10.10). Rieger et al. (1979) have published vortex depth correlations for several impellers. Their correlations are given here:

For the high Galileo number range:

$$X/D = B_H(N_{Ga})^{0.069}(T/D)^{-0.38}(N_{Fr})^{1.14}(N_{Ga})^{0.008(T/D)^{0.008}} \tag{10.16}$$

For the low Galileo number range:

$$X/D = B_L(N_{Ga})^{0.33}(T/D)^{-1.18}(N_{Fr})^{3.38}(N_{Ga})^{-0.074(T/D)^{0.14}} \tag{10.17}$$

where the constants B_H and B_L are given in Table 10.3.

Anchor. The correlation for the anchor impeller is different and it is

$$X/D = 2.82(N_{Fr})^{1.07} \tag{10.18}$$

10.8. SOLID SUSPENSION

LEVEL OF SUSPENSION

For design purposes, three levels of solids suspension are defined:

1. On-bottom movement
2. Off-bottom suspension
3. Practical, uniform suspension

EXAMPLE 10.7
Overall Coefficient and Heat-Up Time for a Water Batch: Jacket

Let's use the HE-3 agitator of Example 10.4 and determine (1) the overall heat transfer coefficient (U) and (2) the batch heat-up time from 60 °F to 200°F. The vessel size is 1,740 gal (14,400 lb$_m$); the specific power input is 3HP/kGal; $N_{Re} = 2,720,000$; T = 80″; assume the wall is 1/4″ SS and the utility fluid is atmospheric steam at 212°F with a utility side coefficient of 1,000 Btu/hr ft^{2}F.

From Table 10.2: $N_{Nu} = K(N_{Re}^a)(N_{Pr}^b)(MuR^c)(G_{CORRECTION})$

$$N_{Nu} = 0.31 N_{Re}^{2/3} N_{Pr}^{1/3} MuR^{0.14}(1/[Z/T])^{0.15}(L/L_S)^{0.2}$$

$$N_{Nu} = 0.31(2.7E6)^{2/3}(5.9^{1/3})(1)^{0.14}(1/[1])^{0.15}(1)^{0.2} = 10,910$$

$$h_P = N_{Nu}(k)/T = 10,910(0.35)/(80/12) = 573 \, Btu/hr \, ft^2 F$$

$$U = 1/[1/h_P + R_P + (\Delta X/k_m) + R_U + (1/h_U)]$$
$$= 1/[1/572 + 0 + 0.0208/7.8 + 1/1,000]$$

$$U = 1/[0.0018 + 0.0027 + 0.001] = 1/0.0055$$
$$= 183; \%Rs: \, P\text{-}32\%, \, W\text{-}50\%, \, U\text{-}18\%$$

The time to heat from 60 to 200°F is given by Equation 10.14 with $A = \pi 6.67^2 = 140 \, ft^2$

$$t = (Mc_p/UA) \ln [(T_U\text{-}T_I)/(T_U\text{-}T_F)$$
$$= [(14,400)(1)$$
$$/(183)(140) \ln [(212\text{-}60)/(212\text{-}200)$$

$$t = 1.42 \, hr$$

On-bottom movement is not normally used for design purposes; off-bottom suspension—the most commonly used design criterion—was originally defined by Zwietering (1958) as the impeller speed (N_{js}), which suspends solids with no particles resting on the vessel bottom for > 1–2 s. *Uniform suspension* is defined as the highest practical level of solids uniformity. Practically speaking, 100% uniformity is not achievable because there is always a measurable layer of clear liquid at the very top of the batch.

On-bottom movement and uniform suspension have not been investigated as extensively as off-bottom suspension. Oldshue (1983) has recommended ratios of N_{js} and P_{js} for the three defined levels of suspension (see Table 10.4).

The relative *cloud height*, which is defined as the ratio of the level to which solids are suspended to the batch height

($R_{ch} = H_c/Z$), is addressed by Corpstein, Fasano and Myers (26, p. 141, Fig.5) and Bittrof and Kresta (25). Bitroff and Kresta have offered the following correlation for high efficiency (e.g., HE-3 and A310) impellers.

$$R_{ch} = (N/N_{js})[0.84 - 1.05(C/T) + 0.7(D/T)^2\{1 - (D/T)^2\}] \tag{10.19}$$

At $R_{ch} = 0.95$, D/T = 1/3 and C/T = $\frac{1}{4}$, which are reasonable for design, $N/N_{js} = 1.55$. This agrees well with the value obtained from Corpstein et al. (1994) of 1.45 and with the recommendation of Oldshue (1983), from Table 10.3, where $R_{ch} = 2.1/1.4 = 1.5$, provided *practical uniformity* is defined as a relative height (R_{ch}) of 0.95.

Zwietering's (1958) correlation, as modified by others, is recommended for prediction of N_{js} for off-bottom suspension. The dimensionless correlation is

$$N_{Re,js}^{0.1} N_{Fr,js}^{0.45}(d/D)^{0.2}B^{-0.13} = S[with N_{Re,js}$$
$$= NjsD^2\rho/\mu \& N_{Fr,js} = Njs^2D/g] \tag{10.20}$$

where

$$S = f(Geometry) = f(D/T, C/T, \, Head \, Style, \, etc.) \tag{10.21}$$

For ease of hand calculation, Zwietering wrote Eq. 10.20 in the following form:

$$S = N_{js}D^{0.85}/[\nu^{0.1}d_p^{0.2}(g\Delta\rho/\rho)^{0.45}B^{0.13}]$$
$$\rightarrow N_{JS} = S[\nu^{0.1}d_p^{0.2}(g\Delta\rho/\rho_1)^{0.45}B^{0.13}]/D^{0.85} \tag{10.22}$$

Particle diameter is included in the correlation as $(d_p/D)^{0.2}$. Chowdhury (1997; Penney et al., 1997) and others have found that N_{js} is virtually independent of (d_p/D) for $(d_p/D) > 0.01$. This is of no practical importance for large vessels where D could be 40″ and it would be unlikely to encounter particles larger than 0.4″ diameter; however, it could give underpowered agitators for scale-up from small vessels where the minimum D could be 2″ and the maximum d_p could be 0.2″, for a maximum $(d_p/D) = 0.1$, which is 10 times $(d_p/D) = 0.01$. Scale-up at equal P/V, which is typical for solids suspension, could give an N_{js} about $100/(10)^{0.2} = 60\%$ of the required N_{js}. Avoid this scale-up mistake by using accurate suspension correlations to determine N_{js} for plant vessels, when scaling-up from laboratory experiments where $(d_p/D) > 0.01$.

EXAMPLE 10.8
Overall Coefficient and Heat-Up Time for a Water Batch: Coil

Let's repeat Example 10.6 with a single helical coil of 3″ tubes, 1/4″ wall on 6″ centers with a coil diameter of 66″.

$$N_{Nu} = 0.017 N_{Re}^{2/3} N_{Pr}^{1/3} MuR^{0.14}(1/[Z/T])^{0.15}(L/L_S)^{0.2}$$

$$N_{Nu} = 10,910(0.017/0.31) = 600 [determined \, as \, (N_{Nu,Coil})$$
$$= (N_{Nu,Wall})(K_{Coil}/K_{wall})]$$

$$h_P = N_{Nu}(k)/T = 600(0.35)/(3/12) = 840 \, Btu/hr \, ft^2 \, F$$

$$U = 1/[1/h_P + R_P + d_O/\{2k_m\} \ln (d_O/d_{LM})$$
$$+ \{R_U + (1/h_U)\}\{d_O/d_I\}]$$

$$U = 1/[1/840 + 0 + (.25/\{2 \times 7.8\} \ln (3/2.5))$$
$$+ 0 + (1/1,000)(3/2.5)]$$

$$U = 1/[0.00121 + 0.00293 + 0.0012] = 1/0.00535 = 187$$

$$A = \pi(66/12)(80/6)[\pi(3/12)] = 181 \, ft^2$$

The coil outside heat transfer area is $(181/140 - 1)100 = 29\%$ greater than the jacket area.

$$t = (Mc_p/UA) \ln [(T_U - T_I)/(T_U - T_F)]$$
$$= [(14,400)(1)/(183)(140) \ln [(212\text{-}60)/(212\text{-}200)]$$

$$t = (1.42)(183/187)(140/181) = 1.07 \, hr.$$

<small>Example 10.9</small>
Helical Ribbon h and Heat-Up Time for a Viscous Batch: Wall
Let's work the design example by Bakker and Gates (1995, p. 31) for wall heat transfer. $T = 2.5\,m$, $Z = 2.5\,m$, $D/T = 0.95$; $D = 2.4\,m$; $\mu = 25\,Pa \cdot s$; $SG = 1.2$, $N = 16.4\,rpm$.

Let's assume the thermal properties of ethylene glycol: $k = 0.15\,Btu/hr\,ft\,F$, $C_P = 0.64\,Btu/lb_m\,F$. The ribbon is a single flight ($n_f = 1$) and the pitch is equal the impeller diameter ($P_t = D\,\&\,D/P_t = 1$).

$$N_{Re} = ND^2\rho/\mu = (16.4/60)(2.5)^2 1{,}200/25{,}000 = 76$$

Let also calculate the power requirement. Equation 24 in Bakker and Gates (1995) gives an equation for N_P as a function or N_{Re} and the system geometry.

$$N_P = (350/N_{Re})(D/P_t)^{1/2}(H/D)(\{W/D\}/0.1)$$
$$(\{D/24\}/(T\text{-}D))^{0.16}(n_f)^{1/2}$$
$$N_P = (350/76)(1)^{1/2}(1)(1)(\{2.4/24\}/\{2.5\text{-}2.4\})^{0.16}(1)^{1/2} = 4.61$$
$$P = (4.61)1{,}200(16.4/60)^3 2.4^5 = 9.16\,kW = 12.3\,HP$$

From Table 10.2 the correlation for the wall heat transfer coefficient is

$$N_{Nu} = 0.61(N_{Re})^{1/2}(N_{Pr})^{1/3}(\mu_B/\mu_W)^{0.14}$$

$$N_{Pr} = \mu_B C_P/k = [(25{,}000)(2.42)lb_m/hr\,ft](0.64\,Btu/lb_m F)$$
$$/(0.15\,Btu/hr\,ftF) = 2.58E5$$

$$N_{Nu} = hD/k = 0.61(76)^{1/2}(2.58E5)^{1/3}(\sim 1)^{0.14}$$
$$= (0.61)(8.72)(63.4) = 337$$

$$h = U = (337)(0.15\,Btu/hr\,ft\,F)/[(3.28)(2.5)ft]$$
$$= 6.2\,Btu/hr\,ftF$$

The time to heat from 60 to 200 F is given by Eq. 10.16 with $A = \pi 2.5^2 = 19.6\,m^2 = 211\,ft^2$. $M = (18)(1{,}200) = 21{,}600\,kg = 47{,}520 lb_m$

$$t = (MC_p/UA)\ln[(T_U - T_I)/(T_U - T_F)]$$
$$= [(47{,}520)(.64)/(6.2)(211\ rrb\ln[(212\text{-}60)/(212\text{-}200)]$$

$$t = 59\,hr$$

The heat transfer coefficients under laminar conditions are very low and heat-up times are so large as to be impractical. One would need to pump the batch contents through a well designed heat exchanger in a recycle loop to achieve reasonable heatup times.
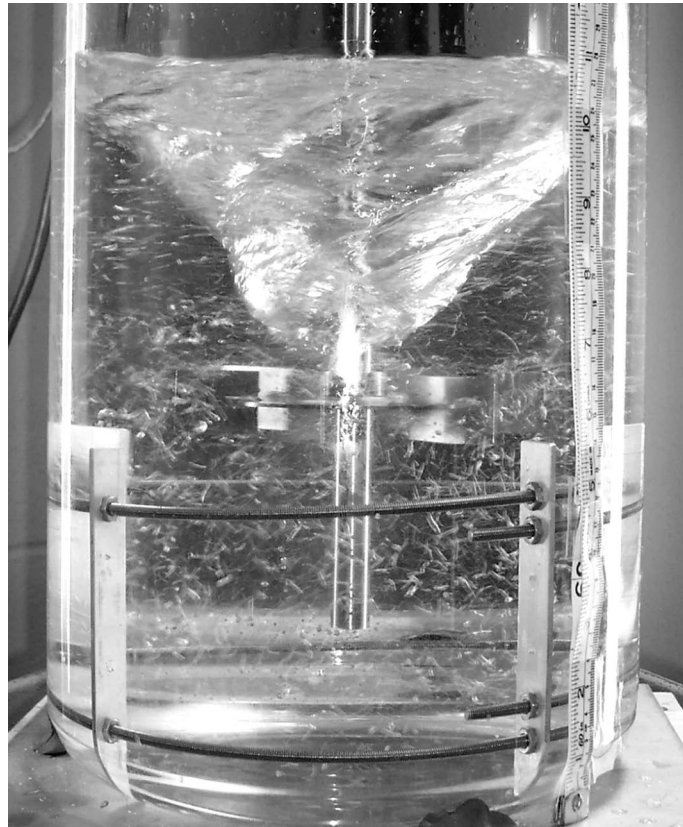
Figure 10.13. Vortex formation: 6BD in water at 262 rpm; 4 lower half baffles in 9.5″ vessel. (B/T = 1/12; Baffle Height = 4.75″, D/T = 0.526; C/T = 1; Z/T = 1; X/D = 0.7).
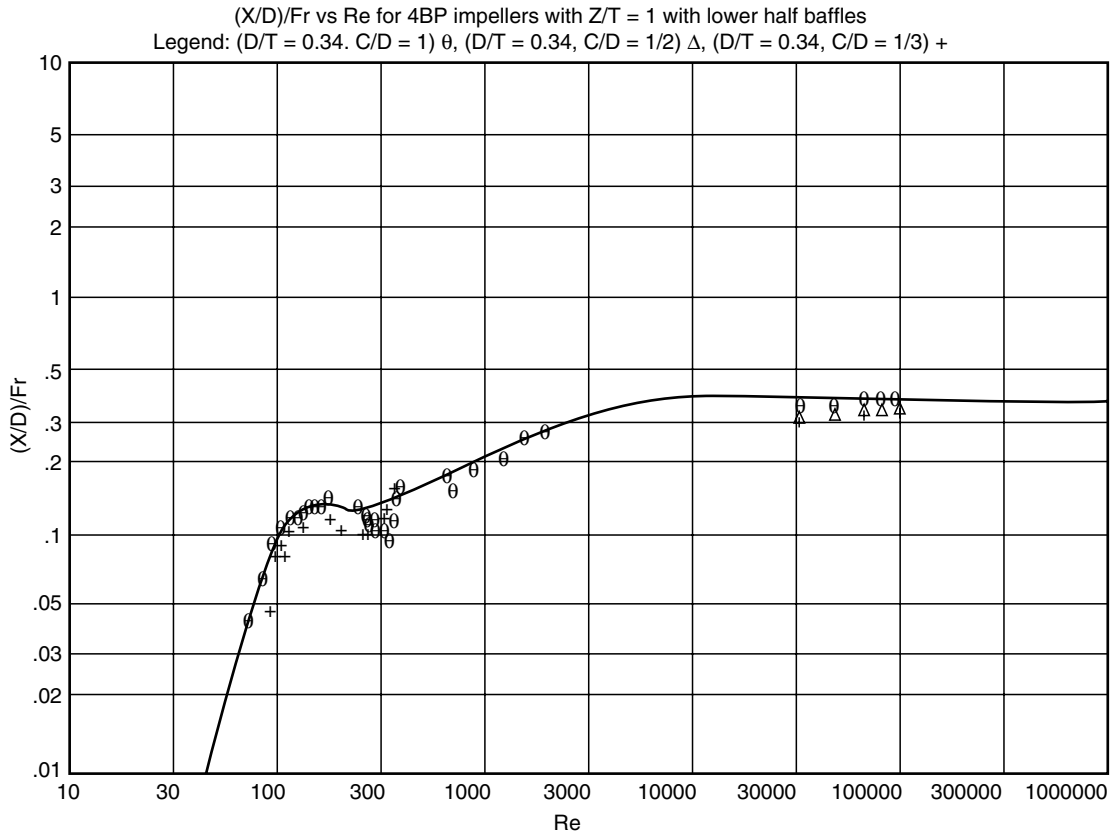
Figure 10.14(a). Correlation of relative vortex depth (X/D) for a 4BP impeller with lower half baffles. D/T = 0.34; C/D = 1/3, 1/2, 1 (by G. S. Spanel).
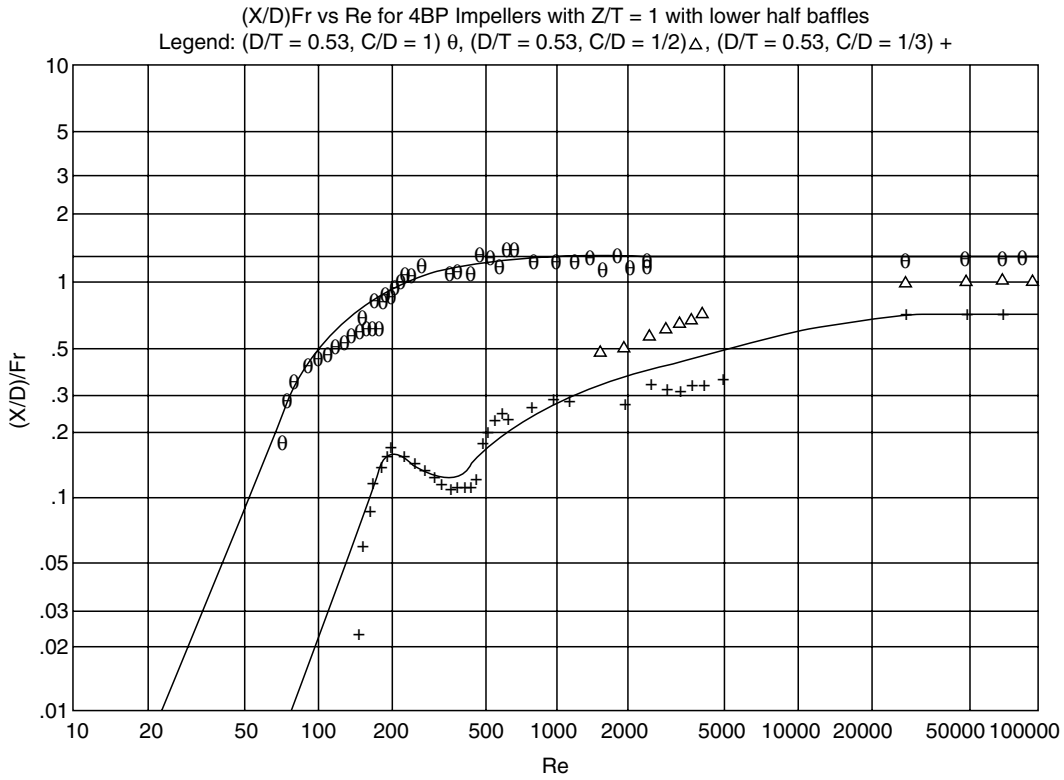
Figure 10.14(b). Correlation of relative vortex depth (X/D) for a 4BP impeller with lower half baffles. D/T = 0.53; C/D = 1/3, 1/2, 1 (by G. S. Spanel).

Effect of Solids Loading on Njs for Four Impellers
LEGEND: H - HE-3; P - 4BP; F - 4BF; D 6BD
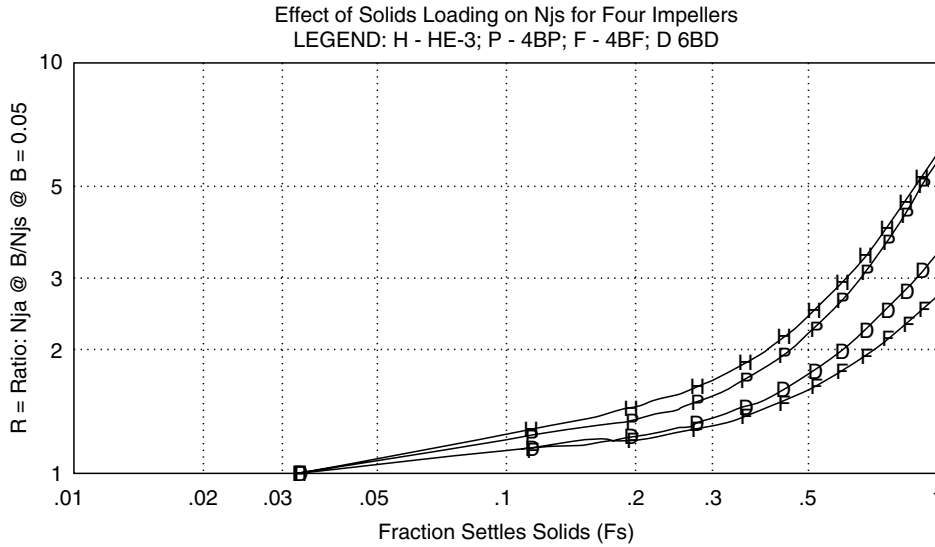
Figure 10.15. Solids loading effect on just suspended speed from Chowdhury (1997) and Penney et al. (1997).

The solids loading effect is accounted for by the term $B^{-0.13}$ in Eq. 10.24, where $B = 100(W_s/W_l)$. Inspection of Eq. 10.20 and 10.22 reveals that $N_{js} \rightarrow 0$ as $B \rightarrow 0$, which is not correct; thus, a lower limit must be placed on B. By experience, the lower limit of B for design purposes is 5; that is, $(W_S/W_L)100 = 5$. The weight fraction solids (X_s) for $B = 5$ is $X_s = B^*W_l/(W_s + W_l) = 5 \times 100/(5 + 100) = 0.0476$, and for a typical void fraction (ε) of 0.4 and a typical $\rho_s/\rho_l = 2.5$, the volume fraction solids at $B = 5$ is

$$X_s = (0.0476/\rho_s)/[0.0476/\rho_s + (1 - 0.0476)/\rho_l]$$
$$= 0.0476/[0.0476 + 0.9524(\rho_s/\rho_l) = 0.02.$$

Thus, the lower limit on B of 5 is a lower limit on X_s of about 0.02 or 2v% solids. (See Figure 10.15.)

Chowdhury (1997) determined that the best correlating parameter for solids loading is the fraction settled solids height (F_s), which is the settled solids height (H_s) ratioed to the batch height $(Z) = (H_s/Z)$. F_s is a logical correlating parameter as it has finite bounds: $0 < F_s > 1$. The Chowdhury/Penney/Fasano correction for solids loading can be used with the Zwietering method by

1. Computing $(N_{js})_Z$ by Eq. 10.22 at $B = 5$.
2. Applying the correction factor $R = N_{js}/(N_{js})_Z$ from Figure 10.15 to determine N_{js}. by the following procedure:

   (a) determine $X_v = (W_s/\rho_s)/(W_s/\rho_s + W_l/\rho_l)$ (10.23)
   (b) determine $F_s = V_s/(1-\varepsilon)/V = X_s(V)/(1-\varepsilon)/[(X_s(V)/(1-\varepsilon) + (1-X_s)V] = X_s/[X_s + (1-X_s)(1-\varepsilon)]$ (10.24)

EXAMPLE 10.10
Vortex Depth in an Unbaffled Vessel with a 4BF Impeller
Let's design a 4BP impeller operating in an 80″ diameter vessel with a batch depth of 80″ to give a vortex depth that just reaches the impeller with lower half baffles. Let's try a 40″ diameter 4BP impeller, 40″ off the vessel bottom, operating at 100 rpm.

$$N_{Fr} = N^2D/g = (155/60)^2(0.0254 \times 40)/9.8 = 0.7$$

$$N_{Re} = ND^2\rho/\mu = (100/60)(1.02)^2 1,000/0.001 = 1,700,000$$

From Figure 10.14(b), at $C/T = 1, (X/D)/N_{Fr} = 1.4$; thus

$$X/D = (1.4)(0.7) = 0.98; \text{ thus, } X = (X/D)0.98 = 40.$$

The vortex just touches the impeller. Let's check the power requirement.
From Figure 10.4, N_P 1.3, then $P = 1.3(1,000)(2.58)^3(1.02)^5 = 24,650W = 33$ HP
The impeller power requirement would decrease slightly, about 10 to 20%, because of the partial baffling; however, we would need to design for the fully-baffled condition.

This is a healthy power requirement of $33/(1,740/1000) = 19HP/1000$ gal. High power requirements are often required to achieve good headspace gas dispersion and to wet floating and lumping solids effectively. It would be worthwhile considering using narrower baffles, or perhaps two baffles, to increase the vortex depth while imparting sufficient power to disperse gas or solids.
Let's check the vortex depth in an unbaffled vessel operating at the same conditions.

$$N_{Ga} = N_{Re}^2/N_{Fr} = (1,700,000)^2/0.7 = 4.13 \times 10^{12}$$

From Eq. 10.18 and Table 10.3:

$$X/D = 1.13(4.17 \times 10^{12})^{0.069}(2)^{-0.38}$$
$$(0.7)^{1.14(4.17E12)^{\wedge} 0.008}$$
$$(2)^{\wedge 0.008} = 8.4; \text{ thus } X = 336''$$

This indicates the reduction in vortex depth achievable using a partially-baffled vessel.

TABLE 10.3. Values of Constants B_H and B_L in Equations 10.16 and 10.17.

Impeller	C/D	N_{Ga} Range	Equation	B_H or B_L
6BD	1	3E7 to 5E10	10.16	1.51
	1	2.6E5 to 3E7	10.17	0.055
	1/3	3E7 to 5E10	10.16	1.43
	1/3	3.4E5 to 3E7	10.17	0.046
6BF	1	8E46 to 1E10	10.16	1.52
	1	4E5 to 8E6	10.17	0.073
	1/3	8E6 to 1E10	10.16	1.57
	1/3	4.1E5 to 8E6	10.17	0.071
6BP	1	1E8 to 2E10	10.16	1.13
	1	5.6E5 to1E8	10.17	0.037
	1/3	1E8 to 2E10	10.16	1.04
	1/3	7.5E5 to1E8	10.17	0.029
3BP	1	1E8 to 1E10	10.16	0.84
	1	1.2E5 to1E8	10.17	0.019
	1/3	1E8 to 1E10	10.16	0.71
	1/3	1.2E5 to 1E8	10.17	0.013

TABLE 10.4. Process Ratios for Three Levels of Suspension at Various Settling Velocities

Degree of Suspension	Settling Velocity (ft/min)					
	0.1–6		4–8		16–60	
	$N_{R,js}$	$P_{R,js}$	$N_{R,js}$	$P_{R,js}$	$N_{R,js}$	$P_{R,js}$
On-Bottom Movement	1	1	1	1	1	1
Off-Bottom Susp.	1.3	2	1.4	3	1.7	5
Complete Uniformity	1.3	2	2.1	9	2.9	25

(c) determine $R = N_{js}/N_{js,\,B=5}$ from Figure 10.15, then compute $N_{js} = R(N_{js,B=5})$

The geometrical effects of (D/T) and (C/T) are accounted for as functionalities, which are applied to an S (i.e., S_{Std}) at a standard geometry (i.e., D/T = 1/3 and C/T = 1/4).

$$S = S_{Std}[f(C/T)f(D/T)] \qquad (10.25)$$

Table 10.5 presents S_{Std} for several impellers for the indicated standard geometry. Zwietering's original S values have been greatly modified and supplemented by later investigators (which includes all the references cited under the Solids Suspension heading under references, except the Zwietering citation). f(C/T) and f(D/T)] are

TABLE 10.5. S_{std} Values [*Note*: See Figures 10.16 and 10.17 for f(C/T) and f(D/T)]

IMPELLER	$(D/T)_{Std}$	$(C/T)_{Std}$	S_{Std} Bottom Style Flat	S_{Std} Bottom Style Dish
6BD	1/3	1/4	7	5.2
4BF	1/3	1/4	7.5	5.6
4BP	1/3	1/4	5	4.6
HE-3	1/3	1/4	9	8.2
MP	1/3	1/4	9	8.2
RCI	2/3	1/10	–	7
Anchor	0.96	0.02	7	7
H-Rib.	0.96	0.02	7	7

As an estimate, use the HE-3 correlation for **marine propellers**.

given in Figures 10.16 and 10.17. Now let's do a Solids Suspension example problem.

The style of vessel bottom affects N_{JS}, as indicated in Table 10.5. N_{js} is lower for dished-bottom vessels than for flat-bottom vessels. The reduction of N_{js} for a dished-bottom versus a flat-bottom is much more pronounced for radial-flow impellers (6BD and 4BF) axial flow impellers (4BP and HE-3).

10.9. SOLIDS DISSOLVING

The design method (developed by W. R. Penney at Monsanto in 1972 and presented at a St. Louis Local Section AIChE Meeting in 1973) assumes that dissolving occurs at a constant solute concentration. This assumption is realistic when

1. A relatively few particles are dissolving.
2. The size distribution includes a relatively small portion of large particles; thus, because the large particles dissolve more slowly than small particles (dissolving time varies about as the square of the particle diameter), the large particles will do most of their dissolving near the terminal concentration.
3. A conservative dissolving time, based on the terminal solute concentration, is adequate for design purposes.

Figure 10.18 is a qualitative description of a dissolving particle.

Let's develop the differential equation for dd_p/dt.

$$W = \text{Mass of Particle} = (\rho_S)(\pi d_p^3/6) \text{ thus} \qquad (10.26)$$

$$dW/dt = (dd_p/dt)(dW/dd_p) = (dd_p/dt)(3\rho_s \pi d^2/6)$$
$$= kA(\Delta C) = k\pi d_p^2 \Delta C$$

$$dd_p/dt = -2k\Delta C/\rho_s = -2k(C_s - C) \qquad (10.27)$$

To integrate d with t, we must relate the mass transfer coefficient (k) to the independent parameters of the system. Levins and Glastonbury (1972) have developed an accurate correlation to predict mass transfer coefficients for suspended particles in agitated vessels.

$$N_{Sh} = kd_p/\varsigma = 2 + 0.47(d_p^{4/3}\varepsilon^{1/3}/\nu)^{0.62}(D/T)^{0.17}(\nu/\varsigma)^{0.36} \qquad (10.28)$$

where ε is the rate of agitator energy input per unit mass of the batch

$$\varepsilon = N_P \rho_l N^3 D^5/(\rho_l V) \qquad (10.29)$$

By substituting k from Eq. 10.28 into Eq. 10.27, we obtain

$$dd_p/dt = -(2\Delta C/\rho_s)(\varsigma/d_p + 0.47(d_p^{4/3}\varepsilon^{1/3}/\nu)^{0.62} (D/T)^{0.17}(\nu/\varsigma)^{0.36} \qquad (10.30)$$

which can be made nondimensional as follows:

$$d(d_p/d_0)/d[(t\varsigma/d_0^2)(\Delta C/\rho_s) = 2[2/(d_p/d_0)$$
$$+0.47\{(d_p/d_0)^{4/3}d_0^{4/3}\varepsilon^{1/3}/\nu\}^{0.62}$$
$$\{1/(d_p/d_0)^{0.17}(D/T)^{0.17}(\nu/\varsigma)^{0.36}] \qquad (10.31)$$

Define

$$\chi = d_p/d_0; \quad Y = (\tau\varsigma/d_0^2)(\Delta C/\rho_S);$$
$$Z = (d_0^{4/3}\varepsilon^{1/3}/\nu)^{0.62}(D/T)^{0.17}(\nu/\varsigma)^{0.36} \qquad (10.32\text{--}10.34)$$

FIGURE 2. EFFECT OF C/T ON N$_{js}$ FOR FOUR IMPELLERS
PLOT OF f(C/T) VS C/T FOR 6BD (LINE); 4BF (-); (~); HE-3(+)
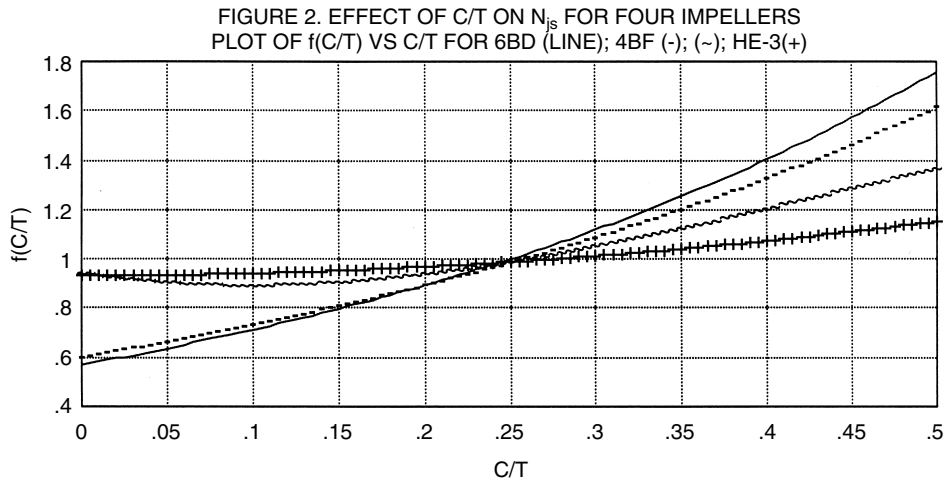
Figure 10.16. Effect of (C/T) on N$_{JS}$ [i.e., f(C/T)] for four impellers. [See Eq. 10.25 for definition of f(C/T)].

FIGURE 3. EFFECT OF D/T ON N$_{js}$ FOR FOUR IMPELLERS
PLOT OF f(D/T) VS D/T FOR 6BD (LINE); 4BF (-); 4BP (~); HE3 (+)
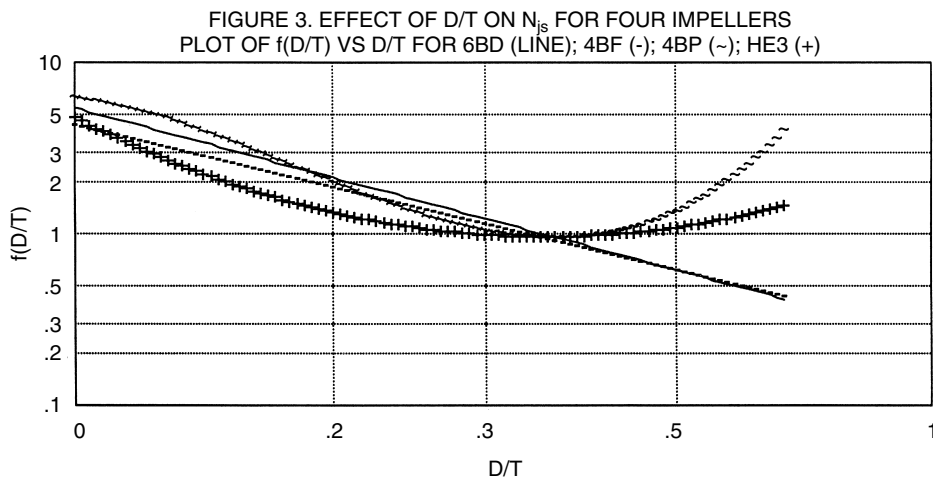
Figure 10.17. Effect of (D/T) on N$_{JS}$ [i.e., f(D/T)] for four impellers. [See Eq. 10.25 for definition of f(D/T)].

where the t in Y becomes the dissolving time ($= \tau$) in the definition of the dimensionless dissolving time (Y) when the particle dissolves (i.e., $d_p/d_0 = 0$). When Eq. 10.33, 10.34, and 10.35 are substituted into Eq. 10.31, the following dimensionless differential equation is obtained.

$$d\chi/dY = -(4/\chi + 0.94Z/\chi^{0.17} \qquad (10.35)$$

This expression was integrated numerically with an integration software package to determine the value of Y when χ became 0 (i.e., when $d/d_0 = 0$, when the particle is totally dissolved) for all values of Z. The relationship between Y and Z (when $\chi = 0$) determined from the integration is presented as Figure 10.19.

Here is the step-by-step procedure for using the design method:

1. Select C_b = *terminal concentration* after solids have dissolved.
2. Find the value of the *diffusivity* of the solute in the solvent and the *saturation concentration* of the solute in the solvent *from the literature*.

3. Design an agitator to give *off-bottom suspension* of the dissolving solids.
4. Calculate the impeller power per unit volume ($\varepsilon = P/\rho V$).
5. Calculate $Z[(d_0^{4/3}\varepsilon^{1/3}/v)^{0.62}(D/T)^{0.17}(v/\varsigma)^{0.36}]$.
6. Go to Figure 10.19 and determine the numerical value $Y[(\tau\varsigma/d_0^2)(\Delta C/\rho_S)]$.
7. From solute solubility data and saturated solution density data calculate the equilibrium concentration of solute (C^*).
8. Calculate the concentration driving force ($\Delta C = C^* - C_{b, \, final}$).
9. From Y, calculate the dissolving time as $[\tau = Yd_0^2\rho_S/(\varsigma\Delta C)]$. Let's now do a dissolving example problem.

10.10. GAS-LIQUID DISPERSIONS

Quantitative design methods will be presented only for the 6BD and the CD6 impellers because the literature is sparse for quantitative design methods for other impellers.

Impeller power requirements decrease as gas sparging increases. In (Bakker et al. (1994)), the ratio of gassed to ungassed power requirement is correlated in dimensionless form as

EXAMPLE 10.11
N_{js} and P_{js} for Suspension of AlCl$_3$ Crystals in Methylene Chloride
This is Example 10-2 the *Handbook of Industrial Mixing* (Paul et al., 2004). AlCl$_3$ crystals are suspended in methylene chloride. $\rho_s = 2440 \, kg/m^3 (SG_s = 2.44)$; $\rho_l = 1.326 \, kg/m^3$; $\mu = 1cP(0.001 \, Pa \cdot s)$; $d_p = 4\text{-}14$ mesh (5,000-1,000 μm, use the largest size $= 5,000 \, \mu$m); B $= 40$; $v = 0.001/1,326 = 7.541 \times 10^{-7} m^2/s$; 4BP impeller, T $= 85.5''$ (1.22 m); D $=$ T/3 $= 0.0724$ m; C/T $= 1/8$; $N_{js} = ?$ and $P_{js} = ?$. *The bottom head is DISHED*.

From Eq. 10.24, $N_{JS} = S[v^{0.1}d_p^{0.2}(g\Delta\rho/\rho_l)^{0.45}B^{0.13}]/D^{0.85}$
From Table 10.4, S_{Std} (at C/T $= 1/4$ and D/T $= 1/3$ and Dished Head) $= 4.6$
From Figure 10.16, f(C/T) $= 0.91$ and from Figure 10.17, f(D/T) $= 1$, thus

$$S = S_{Std}[f(C/T)f(D/T)] = 4.6(0.9)(1) = 4.14$$

$$N_{js} = 4.14(7.541 \times 10^{-7})^{0.1}[9.81(2.44-1.326)/1.326]^{0.45}$$
$$40^{0.13}(0.005)^{0.2}/(0.724^{0.85}) = 1.93 \, rps = 115.7 \, rpm$$

$$N_{Re} = ND^2\rho_l/\mu = 1.93(0.724)^2 1326/0.001$$
$$= 1,347,000; \text{thus, from Figure 10.6, } N_P = 1.2, \text{then}$$

$$P = (N_P)\rho_{slurry}N^3D^5 = (1.2)(1,326 \times 0.6 + 2440 \times 0.4)(1.93)^3$$
$$(.724)^5 = 2,275 \, W = 4 \, HP$$

For T $=$ Z $= 85.5'$ (2.17 m), V $= 2123$ gal; thus, the power input is relatively low at 1.89 HP/kGal.
Let's recalculate using the Chowdhury/Penney/Fasano correction for solids loading.

$$X_v = (W_s/\rho_s)/(W_s/\rho_s + W_l/\rho_l)$$
$$= (0.4/2.44)/(0.4/2.44 + 1/1.326) = 0.179$$

For these solids, let's assume $\varepsilon = 0.5$; thus,

$$F_s = X_s/[X_s + (1 - X_s)(1 - \varepsilon)]$$
$$= 0.179/[0.179 + (1-0.179)(1-0.5)] = 0.42$$

From Figure 10.15, R $= 1.8$. We need N_{js}, B $= 5 = 1.93(5/40)^{0.13}$
$= 1.473$ rps
Then $N_{js} = R(N_{js}, B = 5) = 1.8(1.473) = 2.65$ rps $= 159$ rpm

$$P = (N_P)\rho_{slurry}N^3D^5 = (1.2)(1,770)(2.65)^3(.724)^5$$
$$= 7,830 \, W = 10.5 \, HP(5 \, HP/kGal).$$

It appears that this solids loading of (X $= 40$, $X_v = 0.18$, and $F_s = 0.42$) justifies the use of the more tedious, but more accurate, Chowdhury/Penney/Fasano method for determining the effect of solids loading.

$$P_g = P_u[1 - (b - a\mu)N_{Fr}^d] \tanh(cN_A) \tag{10.36}$$

The correlational constants of Eq. 10.38 are given for 6BD and CD6 impellers in the following tabulation:

Impeller	a	b	c	d
6BD	0.72	0.72	24	0.25
CD-6	0.12	0.44	12	0.37

Ungassed power requirements were fully covered earlier. The turbulent regime power numbers for the 6BD and the CD-6 impeller are given in the following tabulation:

Impeller	Turbulent Regime Power Number
6BD	5.0
CD-6	3.2
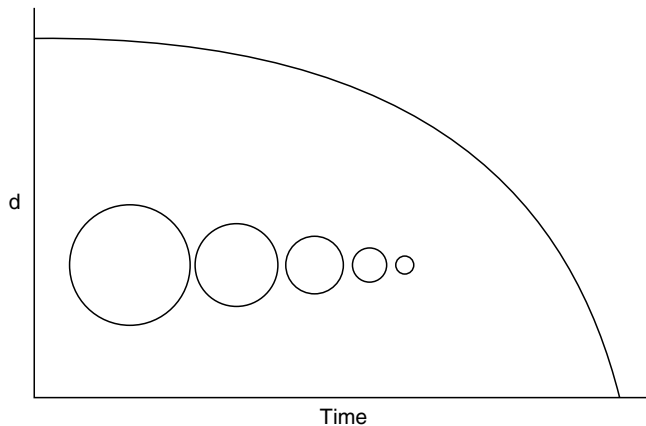
Figure 10.18. Variation of dissolving particle size with time.

High-efficiency impellers such as HE-3's and 4BP impeller are sometimes mounted above a 6BD or a CD-6. For these impellers, the effect of gassing on the power requirement is given in Bakker et al. (1994).

$$P_g = P_u[1 - (a + bN_{Fr})N_A^{(c+0.04N_{Fr})} \tag{10.37}$$

where $a = 5.3 \exp[-5.4(D/T)]$; $b = 0.47(D/T)^{1.3}$; $c = 0.64 - 1.1(D/T)$
The limits of applicability are: $0.4 < D/T < 0.65$; $0.05 < N_A < 0.35$; $0.5 < N_{Fr} < 2$
For the low range of aeration numbers (N_A), this correlation predicts ratios of P_g/P_u in the range of 0.3 to 0.68, which is lower than one normally expects. Thus, one is advised to use this correlation with a bit of caution. If the gassed power requirement seems somewhat low, a vendor should be consulted.
Impeller flooding is a phenomenon that limits the gas dispersion and mass transfer effectiveness of an impeller. Above the flood point (i.e., above the flooding gas sparging rate), gas effectively escapes the high shear zone around the impeller blade tips and is not dispersed effectively, and the mass transfer efficiency of the impeller decreases. In Bakker et al. (1994), a correlation is given for flooding of 6BD and the CD6 impellers.

$$N_{A,FL} = C_{FL}N_{Fr}(D/T)^{3.5} \tag{10.38}$$

The correlating constant, C_{FL}, is 30 for a 6BD and 70 for a CD-6; thus, the CD6 will effectively disperse $70/30 = 2.33$ times the gas flow that a 6BD will handle.
The volume fraction of gas within the batch (i.e., gas holdup) reduces the liquid volume thus, we must predict it for design purposes. Sensel et al. (1993) have developed a holdup correla-
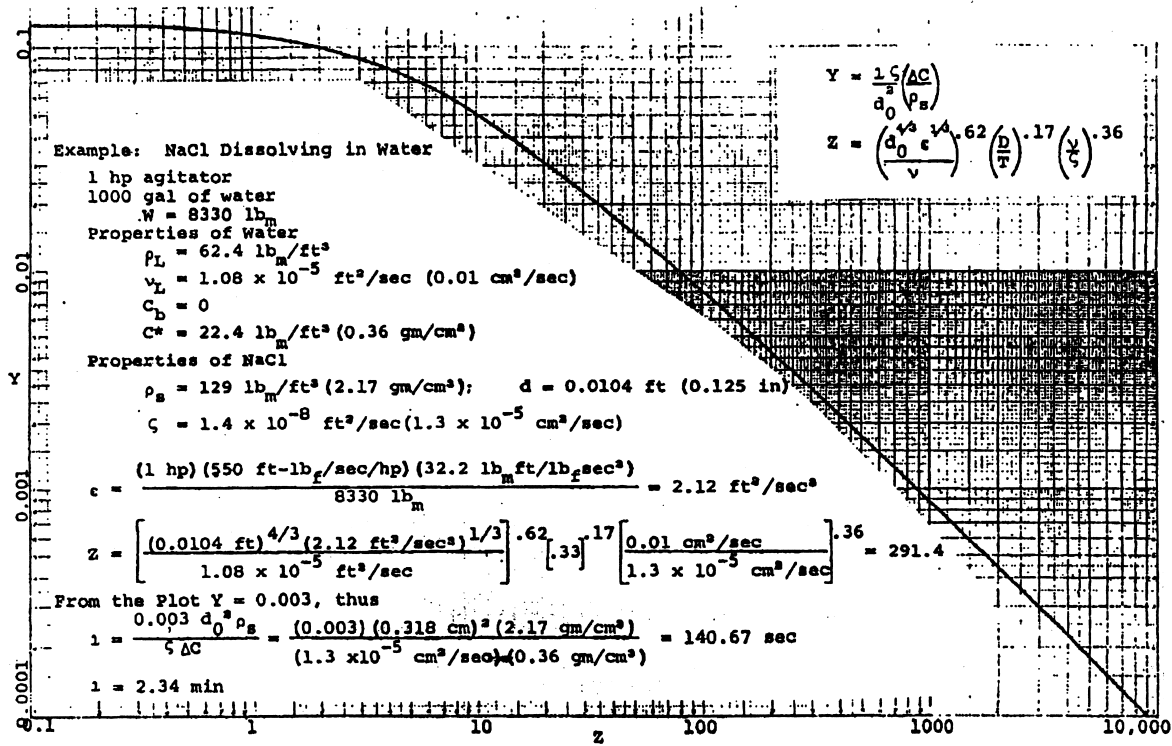
Figure 10.19. Penney dissolving plot—Particle dissolving time (τ) in agitated vessels.

tion, which was modified by Takriff (1996) to include the term $(D/T)^{2.5}$.

$$\alpha = 2.022(N_A N_{Fr})^{0.6}(D/T)^{2.5}$$

[From Takriff(1996), p.56, Equation 6.1-2]

(10.39)

Another gas holdup correlation is given by Bakker et al. (1994):

$$\alpha = 0.16(P_g/V_l)^{0.33}v_{sg}^{0.67}$$

(10.40)

where v_{sg} is the superficial gas velocity in the vessel

$$v_{sg} = Q_g/[(\pi/4)T^2]$$

(10.41)

Specifically, the holdup correlation above was developed from data with air-water systems agitated with a single impeller. However, the correlation will give reasonable results for other systems unless (1) coalescence inhibiting surfactants are present and (2) the viscosity exceeds several hundred centipoise. For higher viscosity liquids, vendors should be consulted.

EXAMPLE 10.12
Dissolving of NaCl in Water in an HE-3 Agitated Vessel
Let's illustrate the design procedure with a worked example for $1/8'$($d_{p,max} = 3{,}175\,\mu m$) sodium chloride solids dissolving in water in a 1,000 gal dished bottom vessel ($Z = T = 66.5''$) agitated with a $22''$ diameter HE-3 impeller operating at 218 rpm. The appropriate component properties are: $C_b = 0$; $C^* = 360\,kg/m^3(22.4\,lb_m/ft^3)$; $\nu = 1E\text{-}6\,m^2/s$ $(1.08E\text{-}5ft^2/s)$; $\rho_l = 1{,}000\,kg/m^3(62.4\,lb_m/ft^3)$; $\rho_s = 2{,}170\,kg/m^3(129\,lb_m/ft^3)$; $\varsigma = 1.3E\text{-}9\,m^2/s\,(1.4E\text{-}8ft^2/s)$. Let's select $C/T = 1/8$; thus, $C = 3''$.

$$N_{Re} = ND^2\rho_l/\mu = 3.6(0.56)^2 1{,}000/0.001 = 1{,}130{,}000$$

From Figure 10.4 $N_P = 0.25$

$$P = (N_P)\rho_{slurry}N^3D^5 = (0.3)(1{,}000)(3.6)^3(.56)^5$$
$$= 2{,}275\,W = 770\,W = 1\,HP\,(1\,HP/kGal)$$

Let's determine if this impeller will suspend the solids.
From Eq. 10.24, $N_{JS} = S[\nu^{0.1}d_p^{0.2}(g\Delta\rho/\rho_l)^{0.45}B^{0.13}]/D^{0.85}$

From Table 10.4, S_{Std} (at $C/T = 1/4$ & $D/T = 1/3$ & Dished Head) = 8.2.
From Figure 10.16, $f(C/T) = 0.99$ and from Figure 10.17, $f(D/T) = 1$, thus

$$S = S_{Std}[f(C/T)f(D/T)] = 8.2(0.96)(1) = 7.9$$

$$N_{js} = 7.9(1 \times 10^{-6})^{0.1}[9.81(2.17-1)/1]^{0.45}5^{0.13}(0.003175)^{0.2}$$
$$/(0.56^{0.85}) = 3.8\,rps = 228\,rpm$$

This impeller is adequate for solids suspension at about 220 rpm and 1 HP/kGal.

The step-by-step dissolving calculations are done on Figure 10.19 and the dissolving time is 141 s = 2.34 min. This can easily be verified experimentally. We routinely conduct a tabletop solids dissolving experiment in the AIChE Industrial Fluid Mixing Course using a $2''$ diameter 6BD in a $5''$ translucent vessel and, at the just suspended speed, the measured dissolving time for $1/8''$ rock salt varies from 2 to 3 minutes.

The *mass transfer rate* is given by

$$J = (k_L a)(C_l^* - C_l) = M/V \qquad (10.42)$$

where $k_L a$ is the *volumetric mass transfer coeffcient*.

C_l^* is the solute saturation concentration in equilibrium with the gas phase and C_l is the acutal bulk concentration of solute in the liquid phase. Thus, for absorption, where $C_l^* > C_l$, J is positive because the mass transfer is from the gas phase to the liquid phase; however, for stripping, where $C_l^* < C_l$, J is negative and the mass transfer is from the liquid to the gas phase. A correlation for $k_L a$ is given in Bakker et al. (1994).

$$k_L a = C_{kla}(P_g/V_l)^a v_{sg}{}^b \text{ For air-water:}$$
$$C_{kla} = 0.015 + -0.005; \text{ a } = 0.6: \text{ b } = 0.6 \qquad (10.43)$$

For systems other than air-water, testing is normally required. Now let's do two gas-liquid example problems. (Examples 10.13 and 10.14).

10.11. LIQUID-LIQUID (L-L) DISPERSIONS

Liquid-liquid dispersions are extremely difficult to understand and difficult to handle. Leng and Calabrese in Paul (2004) devote 114 pages to this topic and they do not even mention one of the most heavily researched topics—mass transfer in L-L systems. They do not mention mass transfer because one can do very little to predict it a priori; and, mass transfer, like most topics in the L-L area, must be approached experimentally followed by scale-up. The approach taken here can be summarized as:

1. Factors affecting equipment selection will be covered.
2. The fundamental phenomena will be explained in sufficient detail so the reader will understand scaleup considerations.
3. Scale-up procedures and techniques will be covered.

Proper impeller selection is a key to success in handling liquid-liquid systems. Of the impellers shown in Figure 10.3, the 6BD, 4BP, 4BF and Sawtooth (Cowles type) are all used to create liquid-liquid dispersions; however, only the Sawtooth and other high-speed, low-pumping designs are use to create stable liquid-liquid emulsions. Rotor-stator units (in-line versions are shown in Figure 10.20) are used to grind solids and create stable emulsion and pastes. The most widely used impeller for creating dispersions for mass transfer purposes is the 4BP impeller, which has a reasonable balance between the production of flow and shear, which balance is needed to effectively produce L-L dispersions. High efficiency impellers are not very suitable to create L-L dispersions because they are such efficient pumpers, with small shear zones near the blade tips; their shear zones occupy only a very small fraction of the vessel volume. The radial impellers (e.g., the 6BD and the 4BF) are used for liquid-liquid dispersions, but their creation of two zones in the vessel, one above and one below the impeller, can be detrimental to processes where the dispersed phase must be blended. However, the 4BF is almost always used for liquid-liquid dispersions if the impeller must be placed low in the vessel to provide agitation during pumpout; and, if used low in the vessel, radial impellers produce only one large circulation loop.

In glass-lined vessels, the 3 blade Pfaudler Retreat Curve Impeller (RCI) is often used for liquid-liquid dispersions; although the myriad of impeller styles currently available with glass

---

EXAMPLE 10.13
Case Study Problem Given by Bakker et al. (1994)
Problem: A recently built reactor, equipped with a flat-blade disc turbine, does not satisfy the process requirements. By examining the liquid surface, the operator suspects that the gas is rising straight through the impeller to the liquid surface. In other words, the impeller is flooded. The mass-transfer rate is usually lower when the impeller is flooded than when it is able to completely disperse the gas. Pertinent information about the reactor is:
T = 2 m; D = 0.8 m; N = 1.13 rps; Q_g = 0.12 m³/s; μ = 1 cP; ρ = 1,000 kg/m³; N_A = 0.21; N_{Fr} = 0.1.

Solution: One can calculate the aeration number ($N_{A,FL}$) at which the 6BD impeller is flooded. For the present example, $N_{A,FL} = 0.13$. The impeller operates at $N_A = 0.21$, which is significantly greater than the aeration number at which the flat-blade turbine is flooded. This confirms the suspicion of the operator that the impeller is flooded. Poor gas dispersion is most likely the cause of the unsatisfactory performance of the reactor.

To prevent the impeller from flooding, the gas flow rate can be decreased. However, this is undesirable because reduced gas flow rate leads to a lower mass-transfer rate. Therefore, it is decided to replace the flat-blade turbine with a concave-blade turbine that can handle larger gas flowrates. The gassed power draw of the flat-blade turbine is calculated to be 1,540 W.

At the given gassing rate, a 0.84-m-dia. concave-blade (CD6) turbine will draw the same power. Recalculating the aeration

number and the Froude number shows that this impeller is not flooded: $N_{Fr} = 0.12$; and N_A at 0.18 is less than $N_{A,FL}$ of 0.37. Thus, replacing the 0.80-m flat-blade turbine with a 0.84 m concave-blade turbine solves the flooding problems in the reactor.

Let's verify that Bakker et al. (1994) have done the calculations correctly.

$$N_A = Q/ND^3 = (0.12 \text{ m}^3/\text{s})/[(1.13 \text{ s}^{-1})\ 0.84^3] = 0.18 \text{ (O.K.)}$$
$$N_{Fr} = N^2D/g = (1.13 \text{ s}^{-1})^2 0.84 \text{ m}/9.8 \text{ m/s}^2$$
$$= 0.11(0.12 \sim 10\% \text{ high})$$

From a previous tabulation $N_P = 3.2$ for the CD6. The ungassed power draw is $P_U = 3.2(1000 \text{ kg/m}^3)(1.13 \text{ s}^{-1})^3(0.84, \text{ m})^5 = 1931$ kg m²/s³ = 1.93 kw.
The gassed power is calculated from Eq. 10.36.

$$P_G = 1.93\{1 - [0.44 - (0.12)(0.001)](0.11)^{0.37}\tanh[(12)(0.18)]$$
$$P_G = 1.93\{1 - (0.44)(0.442)(e^{2.16} - e^{-2.16})/(e^{2.16} + e^{-2.16})\}$$
$$= 1.93(0.8) = 1.54 \text{ kw}$$

Let's now compute the % of flood using Eq. 10.38.

$$N_{A,FL} = C_{FL}N_F(D/T)^{3.5} = (70)(0.11)(0.84/2)^{3.5}$$
$$= 0.37 \Rightarrow \% \text{ Flood} = 100(0.12/0.37) = 32\% \text{ of Flood}$$

EXAMPLE 10.14
Stripping of Oxygen from the Vessel of Example 10.13 with Nitrogen

The 2 m diameter vessel has a batch height (Z) of 2 m, giving a batch volume of 6.28 m^3. A water stream, which is saturated with oxygen in equilibrium with atmospheric air (i.e., saturation partial pressure = 0.22 atm), with a flow rate of 1.25 m^3/min, is being deoxygenated by stripping with pure nitrogen, which is entering the vessel, saturated with water vapor, at a rate of 0.12 m^3/s (7.2 m^3/min). Henry law constant for the oxygen in water is 4.01E4 atm/(mole fraction). The CD6 impeller operates as specified in Example 10.13. Determine the mole fraction of water in the exiting stream.

Mole fraction oxygen in entering water = 0.22 atm/[4.01 E4 atm/(mole fraction)] = 5.49E-6

Concentration of oxygen in the entering water $\sim=$ 5.49E-6 [(mol O_2)/(mol H_2O)]1000 kg/m^3/[18 kg/(mol H_2O)] = 0.0003 mol O_2/m^3

Molar flow rate O_2 entering with water = (0.0003 mol O_2/m^3) (1.25 m^3/min) = 0.00038 mol/min.

Molar flow rate of nitrogen = (7.2 m^3/min)(0.042 mol.m^3) = 0.3 molN_2/min.

If all of the O_2 were stripped into the N_2, then the O_2 partial pressure in the exiting gas stream would be 0.00038/ (0.00038 + 0.3) = 0.00127 atm; thus, initially, we can assume that the partial pressure in the exiting gas is 0, for practical purposes; then, from Eq. 10.43.

$$M = (k_La)(C^* - C_l)V = (k_La)(0 - C_l)V$$

[*Note*; *The transfer is from the liquid*.]

The mass transfer coefficient can be calculated from Eq. 10.42.

$$k_La = C_{kla}(Pg/V)^a(V_{sg})^b = 0.0I5(Pg/V)^{0.6}(v_{sg})^{0.6}$$

$$v_{sg} = (0.12\,m^3/s)/[(3.14/4)22\,m^2] = 0.038\,m/s$$

$$k_La = 0.015(1540/6.28)^{.6}(0.038)^{0.6} = (0.0\,15)(27.1)(0.14)$$
$$= 0.057\,s^{-1} = 3.41\,min^{-1}$$

$$M = (3.41\,min^{-1})(C_l,\,mol/m^3)(6.28\,m^3) = (21.4)C_l\,mol/min$$

The mass transfer rate can also be determined from a mass balance on the vessel:

$$M = O_{2,IN} - O_{2.OUT} = 0.0038 - 1.25C_l$$

We can now equate the two expressions for M:

$$21.4C_l = 0.0038 - 1.25C_l$$

$$C_l = 0.00038/(21.5 + 1.25) = 0.0000167\,mol/m^3$$

Fraction of O_2 Removed =

$$(0.0003\text{-}0.0000167)/0.0003 = 0.944$$

---

coatings (Paul et al., 2004, pp. 1030-1034) is decreasing the use of the PRC impeller. It is perhaps not as efficient as the 4BP; however, it performs very credibly in creating liquid-liquid dispersions because it has a large D/T and it is positioned near the vessel bottom.

The following considerations are most important in equipment selection, testing, and design and scale-up of L-L systems:

1. Which phase is dispersed?
2. What impeller speed is needed to suspend the dispersion?
3. Long time (equilibrium) drop size distribution.
4. Time variation of drop sizes as the equilibrium drop size is approached.
5. How do we scale-up to maintain *all the above from prototype to plant?*

Figure 10.20. Commercial in-line rotor stator mixers.

The question Which phase is dispersed? cannot be answered accurately without resorting to experiment. Experimental studies by Selker and Sleicher (1965) and Norato et al. (1998) indicate the complexity of the answer to this question. Selker and Sleicher have presented Figure 10.21, which shows that there is a very large *ambivalent region* where either phase can be the stable dispersed phase. (*In fact, in the laboratory it is not always readily apparent which phase is dispersed as one watches a break; however, invariably, the continuous phase remains hazy longer than the dispersed phase*.) Noratio et al. (1998) have shown that interfacial tension, phase viscosities, electrolytes, and so on, all affect the nature of the ambivalent region; thus, except at low volume fractions of either phase, experiments are needed to determine which phase is dispersed. There are techniques that can be used to enhance the dispersion of a particular phase: (1) the phase in which the impeller is initially located tends to be the continuous phase because the other phase is "dragged" into the impeller-located phase, (2) the phase that is fed to the vessel on a semi-batch basis tends to be the dispersed phase, and (3) the phase that is fed to a static mixer in a recycle loop tends to be the dispersed phase.

The two extremes of *coalescence (noncoalescing and coalescing)* greatly affect the nature of a dispersion. In the absence of coalescence (which can be inhibited and even stopped by the intentional of surfactants), droplet breakup and the approach to the equilibrium drop size distribution proceeds as follows:

1. The dispersed phase initially exists as large drops.
2. Drop breakup occurs as impeller pumping brings the drops through the high shear zones surrounding the impeller blade tips.
3. After sufficient cycles through the high shear zones, an equilibrium drop size is reached.
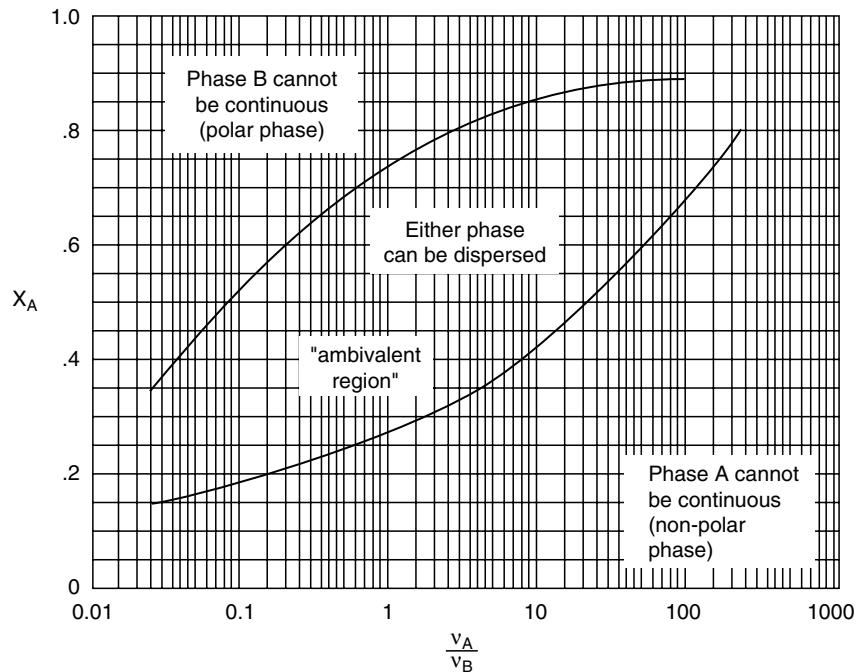
Figure 10.21. Chart for determining which phase is most likely to disperse for liquid-liquid dispersions in agitated vessels.

Fondy and Bates (1963) showed how noncoalescing systems were affected by agitation parameters. They found, for a given impeller style, that the equilibrium drop size was only a function of the impeller tip speed (Figure 10.22) and in Figure 10.23 they showed that a plot of drop size versus 1/t (t being agitation time), extrapolated to $t = \infty$ (i.e., $'t = \theta$) gave the equilibrium drop size. Their findings has a most important scale-up consequence: For *noncoalescing systems*, we can scale-up at equal impeller tip speed (i.e., ND = constant). However, beware! The approach to the equilibrium drop size depends on the blending in the vessel, which means that we must maintain equal blend time provided we want to create the dispersion just as fast in the plant and in the laboratory or pilot plant.

Unfortunately, the picture is much different for *coalescing* systems than for noncoalescing systems. For *coalescing systems*, drops break as they are pumped through the high shear zone surrounding the impeller blade tips; however, they coalesce and breakup, over and over again, in the hinterlands away from the impeller blade tips. So, if you were a drop within a vessel, what would your life be like? As you entered the vessel, if designed by a shrewd engineer, you would immediately enter the blade-tip high shear zone and you would be dispersed. As you left the high shear zone, you would immediately begin to bump into your siblings and coalesce into larger drops. You would spend a order-of-magnitude more time in the low shear zones of the vessel than in the impeller-tip zone because the impeller high shear zone is, at most, a few percent of the vessel volume. Your size in the low shear regions would be determined by a balance between coalescence rate and breakup rate. And the breakup rate in the low shear regions would be affected primarily by the average power dissipation in the vessel. On your first trip through the high shear zone you would still be rather fat; however, as you were pumped, time and again, through the high shear zone you would eventually reach your slim equilibrium size. You would find that the rate at which you moved through the high shear zone would be a strong function of the blending time of the vessel. Consequently,

if you dreamed of maintaining the same wonderful lifestyle in the plant as you enjoyed in the pilot plant, you would plead with your process design engineer to attempt the nearly impossible on scale-up and

1. Maintain tip speed constant. (You want the same exhilarating feeling at high shear in the plant as in the pilot plant!)
2. Maintain P/V constant. (You want the same sibling interaction [i.e., coalescence] and lazy breakup at low stress.)
3. Maintain blend time constant. (You can't wait to be exhilarated at high stress, time and time again as you pass through the high shear near the impeller tips.)

Chang (1990) has determined the distribution of drop sizes in an experimental vessel with time. A set of his data is presented in Figure 10.24. You will note that even though this is a laboratory vessel, the drop size is still changing after 3 hours. We need to predict the mean equilibrium (long time) drop size. For standard geometry Rushton turbines at D/T = 1/2, Calabrese et al. (1986) have published the following correlation:

$$d/D = [0.054(1 + 3\phi)N_{we}^{-3/5}] \, [1 + 4.42(1 - 2.5\phi) \\ N_{Vi}(d/D)^{1/3}]^{3/5} \qquad (10.44)$$

The dimensionless tank viscosity group ($N_{vi} = [\rho_c/\rho_d]^{1/2} \, \mu_d ND/\sigma$) accounts for the effects of density difference between the phases and for the dispersed phase viscosity.

Chang found that the ratio of drop size at a particular time to the equilibrium drop size was a function of the number of revolutions of the impeller. This finding indicates that *blend time is the proper scale-up criterion* to maintain constant temporal dependence of drop size.

Correlations for *just-suspended speed* have been developed by Nagata (1975), Skelland and Seksaria (1978), and van Heuven and Beek (1970).
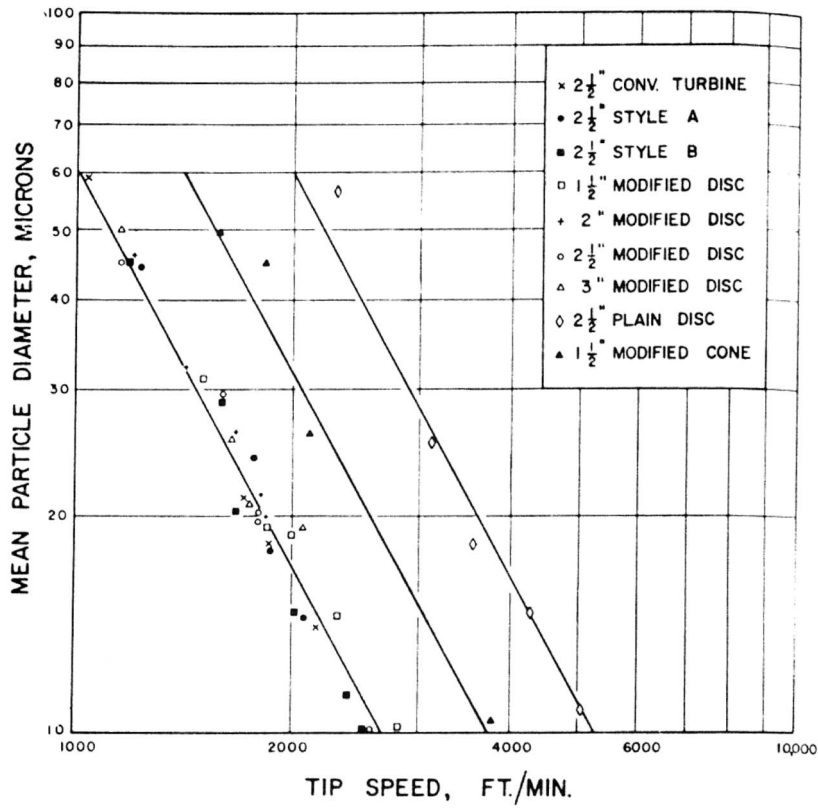
Figure 10.22. Mean particle diameter as a function of tip speed for various impellers (agitation time of 20 min). (From Fondy and Bates [1963]).
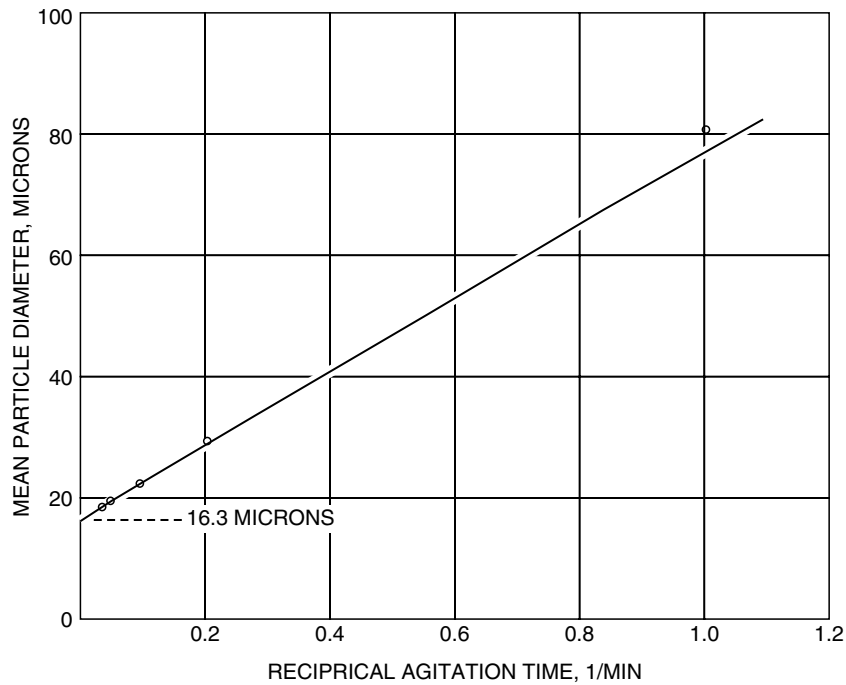
Figure 10.23. Particle diameter vs. reciprocal agitation time, 11/2 inch modified disk at 1850 rpm. (From Fondy and Bates [1963]).
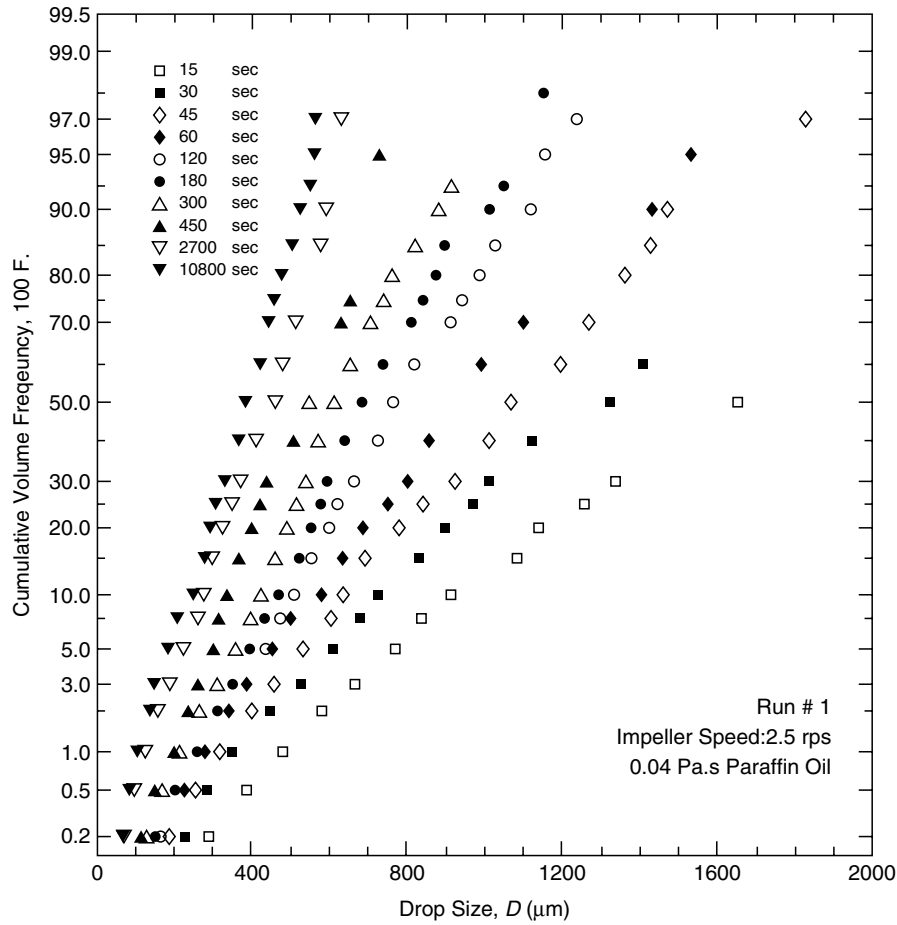
Figure 10.24. Effect of stirring time on drop size distribution. (From Chang [1990]).

The Nagata correlation is for a 4BF impeller with $D/T = 1/3$ & $C/D = 1/2$.

$$N_{js} = 610D^{-2/3}(\mu_c/\rho_c)^{1/9}[(\rho_c - \rho_d)/\rho_c]^{0.26} \quad (10.45)$$

The van Heuven and Beek correlation is for a 6BD with $D/T = 1/3$, $C/T = 1/3$.

$$N_{Fr} = N_{js}D/g = 36.1(N_{Re}N_{We})^{-0.2}(1 + 3.5\phi)^{2.34} \quad (10.46)$$

The Skelland and Seksaria correlation used five impellers and four impeller locations: midway in heavy phase (sets 1, 5, 9, 13), midway in the light phase (2, 6, 10, 14), at the interface (4,8,12,16), and two impellers each centered in each phase (3, 7, 11, 15).

$$(N_{js}D/g)^{1/2} = C_1(T/D)^{\alpha_1}(\mu_c/\mu_d)^{1/9}[(\rho_c - \rho_d)/\rho_c]^{0.25}N_{Go}^{-0.3} \quad (10.47)$$

The correlation parameters C_1 and α_1 are given in Table 10.6.

Experience has shown that these three correlations do not give agreement within a reasonable limit of +− 25%; thus, the recommended design procedure is to calculate N_{js} using all three methods and use for design either (1) the most conservative or (2) the value that is in agreement from at least two of the methods.

Another important consideration in designing an agitated system for creating an unstable dispersion is that the unstable dispersion must be broken to effect phase separation downstream of the agitated vessel. It is very important in scale-up to be cognizant of the fact that too much agitation (and too many surfactants) can be bad. Thus, one needs to scale-up with just right amount of agitation—not so little that the phases are not dispersed or the drops are too big but not so much that too small drops are created, which cause separation problems downstream.

Atemo-Obeng and Calabrese in Paul (2004) devote 26 pages to the coverage of *rotor-stator* devices. They have excellent coverage of available equipment and 1 page coverage of scale-up. Except for equipment selection and testing, scale-up is the real key in designing a rotor-stator unit because, as Myers, Reeder, Ryan, and Daly say ("Get a Fix on High Shear Mixing", *CEP*, pp. 33–42, November 1999) under the Heading "Need for Pilot-Scale Tests", "Virtually all high-shear mixing devices tend to be used in complex operations. . . . It is often difficult to quantify the level and duration of the shear needed to accomplish the production without damaging the final product. Therefore it is generally prudent to ensure a process result using laboratory or pilot-scale equipment." Bottomline: One must conduct experiments *and* scale-up. Atemo-Obeng and Calabrese in Paul (2004, p. 502) say about scale-up, "Vendors often design and scaleup rotor-stator mixers based on equal rotor tip speed, $V_{tip} = \pi ND$. . . . This criterion is equivalent to nominal shear rate in the rotor-stator gap (because) the gap width remains the same on scaleup." See rotor-stator scale-up Example 10.15.

TABLE 10.6. Correlation Constants for Equation 10.47.

	C_1	α_1	% av dev
Propeller			
1	15.3244	0.28272	11.24
Set 2	9.9687	0.55355	11.71
no. 3	15.3149	0.39329	12.28
—4	5.2413	0.92317	8.19
Pitched-blade turbine			
5	6.8231	1.05120	10.52
6	6.2040	0.81877	18.15
7	2.9873	1.59010	12.94
8	3.3545	0.87371	8.55
Flat-blade turbine			
9	3.1780	1.62474	6.49
10	*	*	*
11	3.9956	0.88099	11.00
12	*	*	*
Curved-blade turbine			
13	3.6108	1.46244	7.96
14	*	*	*
15	4.7152	0.80056	8.99
16	4.2933	0.54010	4.28
Overall	10.62		10.17

*Asterisks indicate there were insufficient data to correlate results. Sets 1, 5, 9, 13: impeller midway in denser phase, Z/4. Sets 2, 6, 10, 14: impeller midway in lighter phase, 3Z/4. Sets 3, 7, 11, 15: impeller at organic-water interface, Z/2. Sets 4, 8, 12, 16: two impellers, one midway in each phase, Z/4, 3Z/4. (Skelland and Seksaria, 1978).

Example 10.16 calculate N_{js}, which phase is dispersed and the equilibrium drop size for a liquid-liquid dispersion in an agitated vessel.'

10.12. PIPELINE MIXERS

The selection of the most economical static mixer depends primarily on the following parameters:

1. *The viscosities of the fluids*:
   a. The viscosity of the continuous phase determines the Reynolds number and the Reynolds number determines whether the flow is laminar or turbulent.
   b. For turbulent flow conditions ($N_{Re} > \sim 3000$) certain types of mixers [e.g., the Kenics HEV (Figure 10.25) and the Koch and SulzerChemtech SMV (Figure 10.27)] are cost effective. For laminar conditions ($N_{Re} < \sim 1000$), other types of mixers [e.g., the Kenics HEM (Figure 10.26)] and the Koch SMX (Figure 10.27) are cost effective.
2. *The viscosity ratio between the feeds to the mixer*: Widely varying viscosity ratios are much more difficult to blend than equal viscosities. The SMX mixer is the most effective mixer for widely varying viscosity ratios.
3. *The ratio of feed flow rates of the feed streams*: Widely varying feed ratios are much more difficult to blend than a feed ratio of unity.

EXAMPLE 10.15
Scale-Up of a Rotor-Stator Unit from 6″ Diameter to 18″ Diameter

Let's start with a 10 HP, 6″ nominal diameter by 1″ wide rotor, 1750 rpm test unit, like those shown in Figure 10.20, producing 5 gpm of product. The torque requirement of the test unit is $T = P/2\pi N = (5)550/(2\pi 29.2) = 15.5 \, ft \, lb_f$. What is the speed, torque, HP, and product capacity of an 18″ diameter by 3″ wide rotor plant unit?

The shear stress on the rotors will both be the same as they move at the same tip speeds; thus, he power requirement is expressed as

$$P = (Force)(Velocity) = \tau A(\pi DN)$$

However, the rotor shear stress (τ) remains constant from prototype to plant because the rotor tip speed and gap width remain constant, consequently

$$P_{plant}/P_{pilot \, plant} = (A_p)D_p N_p/[(A_{pp})D_{pp}N_{pp}$$
$$= (\pi D_p L_p)D_p N_p/[(\pi D_{pp}L_{pp})D_{pp}N_{pp}]$$

The rotor tip speed remains constant, thus $N_p = N_{pp}(D_{pp}/D_p)$ $= 1750(6/18) = 583 \, rpm$

$$P_{plant} = P_{pilot \, plant}(D_p/D_{pp})^2(L_p L_{pp})(N_p/N_{pp})$$
$$= 10(18/6)^2(3/1)(583/1750) = 90 \, HP$$

$$T_{plant} = P_{plant}/2\pi N_P = 45(550)/(2\pi 583/60) = 812 \, ft \, lb_f$$

$$T_{pilot \, plant} = (P_{pilot \, plant})/2\pi N_{PP} = 10(550)/(2\pi 1750/60)$$
$$= 30 \, ft \, lb_f$$

The throughput is proportional to the flow area through the rotors

$$GPM_p/GPM_{pp} = D_p L_p/(D_{pp}L_{pp}) \Rightarrow GPM_p$$
$$= (5)(18 \times 3)/(6 \times 1) = 20 \, gpm$$

EXAMPLE 10.16
Dispersed Phase? N_{js} and d_p for Acid/Benzene

Let's start with Example 7.1, page 300, in Nagata (1975). Benzene is nitrated with a mixed acit of SG = 1.55. As a reactor, a cylindrical mixing vessel, with T = Z = 80 cm is used and is agitated by a paddle (i.e., a 4BP impeller) D = T/3; L/D = 0.06; $\Phi = 90°$, $N_b = 4$, which is located at the middle height of the liquid. Calculate (1) the minimum agitator speed required to mix the liquid phases by an impeller located at the centerline of the vessel, (2) the maximum weight fraction of benzene for benzene to exist as the dispersed phase and (3) the equilibrium drop size for benzene. Assume the SG of benzene = 0.88 and the viscosity of the mixed acid is 30 cP. Let's assume the interfacial tension is 30 dyne/cm = 0.03 N/m.

From Eq. 10.47: $N_{js} = 610D^{-2/3}(\mu_c/\mu_d)^{1/9}[(\rho_c - \rho_d)/\rho_c]^{0.26}$

$$N_{js} = 750(0.8)^{(-2/3)}(0.03/1{,}550)^{(1/9)}[(1.55 - 0.88)/1.55]^{0.26}$$
$$= 210 \text{ rpm}$$

Let determine N_{js} from the Skelland and Seksaria (1978) correlation, Eq. 10.47:

$$(N_{js}D/g)^{1/2} = C_1(T/D)^{\alpha_1}(\mu_c/\mu_d)^{1/9}[(\rho_c - \rho_d)/\rho_c]^{0.25}N_{We}^{0.3}$$
$$(C_1 \text{ and } \alpha_1 \text{ from Table 10.6})$$

$$N_{Go} = \rho_c D^2 g/\sigma = 1{,}550(.8/3)^2 9.81/0.03 = 36{,}000$$

$$N_{js} = [9.81/(0.8/3)][3.35(3)^{0.87}(30/0.55)^{(1/9)}$$
$$\{(1.55 - 0.88)/1.55\}^{0.25}(36{,}000)^{-0.3}]^2 = 2.9 \text{ rps}$$

So the ratio of $N_{js,Nagata}/N_{js,Skelland} = 210/174 = 1.21$. This is about as good agreement as we can expect. Let's use the high value, 210 rpm, for subsequent calculations.

The acid is the continuous phase, now let's determine from Figure 10.21 how much of the benzene phase can be added before we enter the ambivalent region.

The viscosity ratio is: $\nu_A/\nu_B = (30/1550)/(0.6/600) = 20$. (A is the hydrocarbon phase.) From Figure 10.24, at the ambivalent region boundary, $X_A = 0.5$ to assure that "Phase A" (the benzene phase here) cannot be continuous (nonpolar phase).

$$X_A = W_A/\rho_A/(W_A/\rho_A + W_B/\rho_B)$$
$$= 1/(1 + [W_B/W_A][\rho_A/\rho_B]) = 0.5$$
$$W_B/W_A = (1/0.5 - 1)(600/1550) = 0.39$$

Thus, the highest tolerable weight fraction of benzene is $0.39/(1 + 0.39) = 0.28$.

Let's calculate the dispersed phase particle size from Eq. 10.44:

$$d/D = [0.054(1 + 3\phi)N_{we}^{-3/5}] [1 + 4.42(1 - 2.5\phi)N_{Vi}(d/D)^{1/3}]^{3/5}$$

$$N_{We} = \rho_c N^2 D^3/\sigma = 1{,}550(3.5)^2(.8/3)^3/0.03 = 12{,}000$$

$$N_{vi} = [\rho_c/\rho_d]^{1/2}\mu_d ND/\sigma = (1{,}550/600)^{1/2}0.0006^*$$
$$(3.5)(.8/3)/.03 = 0.03$$

Let's use a dispersed phase volume fraction of 0.2, which is the upper limit recommended by Calabrese et al. (1986) for Eq. 10.44. By inspection of equation 10.44, it appears that the term which includes N_{Vi} will be $\ll 1$; thus

$$d/D = [0.054(1 + 3 \times 0.2)(12{,}000)^{-3/5}] [1 + 0] = 0.00031$$

Let's check the full expression to determine if the viscosity term affects d:

$$d/D = [0.054(1 + 3 \times 0.2)(12{,}000)^{-3/5}]$$
$$[1 + 4.42(1 - 2.5 \times 0.2)0.03(0.00031)^{1/3}]^{3/5}$$

$$d/D = [0.054(1 + 3 \times 0.2)(12{,}000)^{-3/5}] [1 + 0.0045]^{3/5}$$
$$= 0.00031$$

$$d = (0.00031)0.267 = 0.000082$$

(The equilibrium Sauter mean drop size is 82 μm.)

---

4. *The size of the mixer*: Some mixers are difficult to manufacture in laboratory sizes down to 1/8″. This limitation precludes the use of most SMX mixers for D < 3/16″.

As explained well by Koch Engineering Company (1986), the most difficult blending applications are for conditions where flow ratios and viscosity ratio vary widely. Koch (p. 6 and Table 10.7, 1986) recommended relative mixer length required to blend miscible fluids in laminar conditions with widely varying feed and viscosity ratios. Note that the most difficult mixing task is blending a small stream of low viscosity fluid 1 into a large stream of viscous fluid 2 (e.g., $Q_1/Q_2 = Q/q = 0.001$ and $\mu_2/\mu_1 = 100{,}000$). For these extreme conditions, the required L/D for the SMX mixer is 20 diameters; whereas the required L/D for $Q_1/Q_2 = 1$ and $\mu_2/\mu_1 = 1{,}000$ is 11. Table 10.7 is recommended as a preliminary estimate for use in determining the effect of feed and viscosity ratios. Vendors must be contacted before the final decision is made regarding the handling widely varying feed and viscosity ratios. The *Chemical Engineering Buyer's Guide* is a good source for vendor identification.

DESIGN METHODS

We need to predict *pressure drop* and the *outlet coefficient of variation (COV_O)* to design a static mixer. Before addressing pressure drop, let's cover the definition of COV and relative coefficient of variation = COV_R = COV_{Outlet}/COV_{Inlet}. The coefficient of variation is a well-understood statistical concept; unfortunately, the use of this concept to quantify degree of mixing within a fluid, a fluid-solid, or a solid-solid system is not well understood. The best discussions of the use of this concept to quantify degree of mixing are given by Harnby et al. (1985) and Gray (1986), although Etchells and Myer in Paul (2004, Ch. 7) (19xx, Chapter 7) and Myers (1997) et al. (1997) explain the use of COV as a design tool. Let's take a simple example to illustrate COV. Assume student heights entering a classroom are distributed as follows: 58″, 60″, 62″, 64″, 66″, 68″, 70″, 72″, 74″, 76″, 78″. The mean height is 68″. The standard deviation of height is $[(10^2 + 8^2 + 6^2 + 4^2 + 2^2 + 0 + 2^2 + 4^2 + 6^2 + 8^2 + 10^2)/10]^{1/2} = [440/10]^{1/2} = 6.63″$. And, for this data set, $COV_I = \sigma/H_m = 6.63″/68″ = 0.098$. Now let's further assume that something happened in the classroom to stretch the small students and shrink the large students to give the following distribu-

TABLE 10.7. Koch Recommendations for the Effect of Viscosity Ratio ($\mu_2 : \mu_1$) and Flow Ratios (Q1:Q2) on Required Mixer Length

	L/D for $\sigma/\bar{x} = 0.05$	
$Q_1 : Q_2$	$\mu_2 : \mu_1 = 1000$	$\mu_2 : \mu_1 = 100000$
0.001	17	20
0.01	15	18
0.1	12	15
1	11	13
10	7	8
100	5	5
1000	5	5

Figure 10.25. The Kenics vortex tab mixer (HEV).

tion as they left the classroom: 63″, 64″, 65″, 66″, 67″, 68″, 69″, 70″, 71″, 72″, 73″. The mean height is still 68″, but $COV_O = [110/10]^{1/2}/68″ = 3.317″/68″ = 0.0488$. Thus, acting like a static mixer, the events in the classroom have given a relative $COV = COV_O/COV_I = COV_R = 0.49$.

We must now turn our attention to the calculation of the inlet COV. The most common condition of mixing at the inlet of a static mixer is two completely separated streams. COV_I for this condition is given by

$$COV_I = (Q/q)^{1/2} \quad (\text{where} Q/q = \text{volumetric flow ratio})$$

(10.48)

RELATIVE COEFFICIENT OF VARIATION FOR KENICS STATIC MIXERS

COV_R for the Kenics Helical Element Mixer (HEM) is presented in Figure 10.28 for low N_{Re}. COV_R for the HEV and the HEM are given in Figure 10.29 for high N_{Re}. Mathematical relationships for COV_R as a function of the Reynolds number and the number of tab rows ($N = N_{tr}$) for an HEV mixer and for number of elements ($N = N_e$) in an HEM mixer were provided by Julian Fasano of Chemineer.

$$COV_R = 10^{\wedge}(-0.0977*N) \quad N_{Re} < 100 \text{ HEM ONLY} \quad (10.49)$$

$$COV_R = 10^{\wedge}[(-0.27*N_{Re}^{\wedge}0.24)(0.0879*N + 0.763)]100 \atop < N_{Re} < 8,700$$

(10.50)

$$COV_R = 10^{\wedge}[(-1.65*N_{Re}^{\wedge}0.043)(0.0879*N + 0.763)]N_{Re} \atop > 8,700$$

(10.51)

COV_R is essentially the same for the Kenics HEM and HEV mixers when N_e in the HEM = N_{tr} in the HEV. Note, however, COV_R is not given for $N_{Re} < 1,000$ for the HEV because the HEV is an effective mixer only for fully turbulent conditions. Do not use the HEV for Reynolds numbers < 3,000 (Chemineer recommendation); however, Ethells and Meyer in Paul (2004, p. 432) say, "The Kenics HEV shows a weak Reynolds Number dependence, along with a length/number of element dependence. This vortex-generating mixer design is typically applied at a Reynolds Number above 10,000."

L/D = 1 for the standard HEV mixer; however, the L/D for the placing of the HEV into the piping system is nominally L/D = 4, because the HEV mixer produces vortexes, which provide mixing downstream of the mixer itself, and Kenics has specified that three pipe diameters of straight pipe must be attached to the exit of the mixer because the COV_R correlation they use is based on measurements made at an (X/D) of 3 downstream of the mixer exit proper.

A comparison of various static mixers for laminar applications is given in Figure 10.30 for an inlet $COV_I = 3$. This comparison is based on mixer L/D, which ignores the most important economic parameter: pressure drop. As an example of how misleading Figure 10.30 can be, $N_{Ne}N_{Re} = N_{\Delta P} = (\Delta PN_{\Delta P}/[\rho V^2\{L/D\}])[VD\rho/\mu] = 1,200$ for the Sulzer Chemtech Bulletin (p. 16) and, for the HEM, is only about 190. Thus, for the same L/D, mass flow, and ΔP, in laminar flow, $\Delta P \propto N_{\Delta P}/D^3$, the diameter of an SMX must be 1.84 times the diameter of an HEM to operate at the same pressure drop.
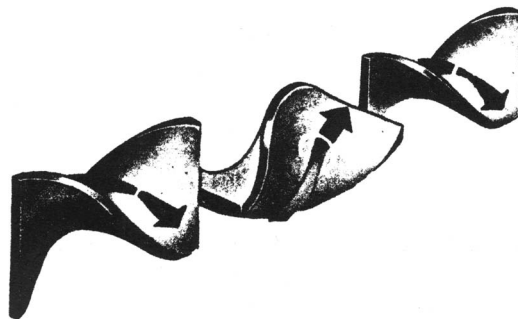
Figure 10.26. The Kenics helical element mixer (HEM).
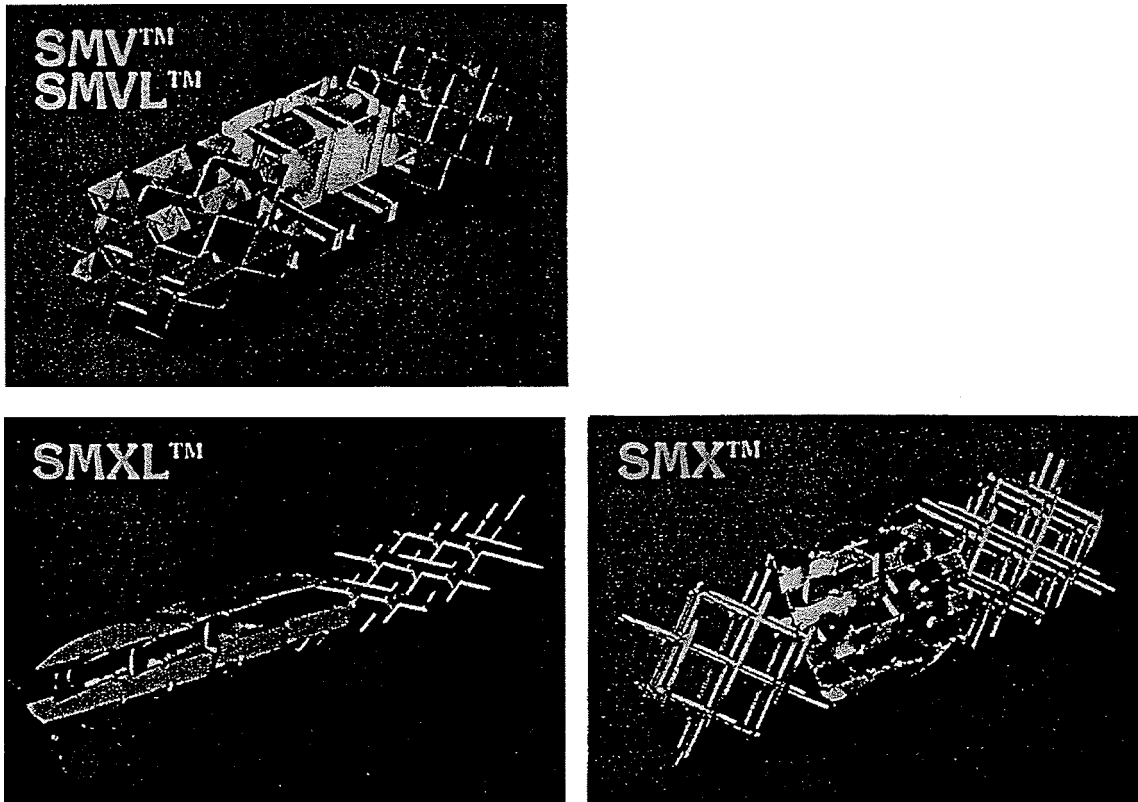
Figure 10.27. The Koch and Sulzer Chemtech SMV, SMX, and SMXL mixing elements.
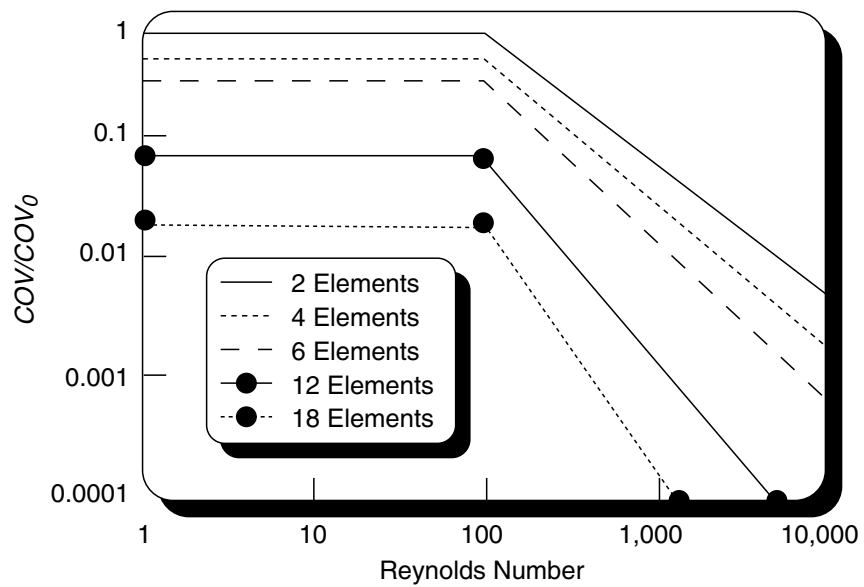
Figure 10.28. Relative coefficient of variation ($COV_R = COV_O/COV_I = COV/COV_0$) vs. Reynolds number ($N_{Re}$) and number of elements (N_e) for the Kenics HEM. (Myers et al. [1997]).

Mixing Performance of HEV's
At L/D = 3 Downstream
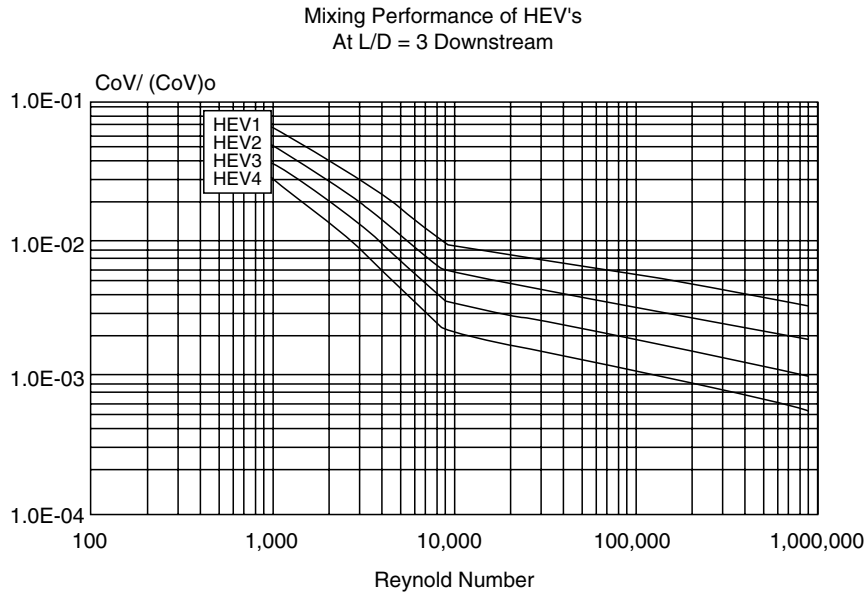
Figure 10.29. Relative coefficient of variation ($COV_R = COV_O/COV_I = COV/COV_0$) vs. Reynolds number ($N_{Re}$) and number of tab rows (N_{tr}) for the Kenics HEV and the number of elements (N_e) for the Kenics HEM. (Kenics Bulletin [1988]).

Detailed design methods for COV prediction is presented here for Kenics equipment because the design methods are readily available and space is limited in this text. Several other vendors supply equipment, which will perform all in-line blending tasks. Design information can be readily obtained by contacting individual vendors. However, it is advisable to have a workable design in hand before contacting vendors.

Most manufacturers of static mixers have published (either in sales literature or in the technical literature) design methods for *pressure drop*. The pressure drop design methods, from Myers et al. (1997) for the Kenics HEM and Kenics HEV mixers are presented. The Darcy friction factor for the standard HEV mixer, $N_{tr} = 2$, $L/D = 1$, (with $X/D = 3$ downstream pipe) is presented in Figure 10.31. The friction factor is not given below $N_{Re} = 1,000$ because the HEV mixer should not be used for $N_{Re} < 3,000$.

The friction factor is used in the Darcy-Weisbach equation for calculation of pressure drop for turbulent flow in an empty pipe. The mixer pressure drop is given by

$$\Delta P_{EP} = f(L/D)\rho V^2/(2g_C) \qquad (10.52)$$

The pressure drop for the Kenics HEM mixer (Myers et al., 1997) is correlated as a multiplication factor times the empty pipe pressure drop to obtain the pressure drop through the Kenics mixer as follows:

$$\Delta P_{MIXER} = K(\Delta P_{EP}) \qquad (10.53)$$

The pressure drop is a function of the number of elements (N_e), the Reynolds number (N_{Re}), the length to diameter ratio of each helical element (L_e/D), and the void fraction (VF) of the mixer. The void fraction must be considered because some HEM mixers, especially those made of plastic, have void fractions $\rightarrow$ 0.5. Figure 8 of Myers et al. (1997) gives K for the HEM as a function of Reynolds number for $L_e/D = 1$ and 1.5. Although the void fraction is not specified in Myers et al., the void fraction for most metal element HEM mixers above $1/4''$ diameter is about 0.9. The correlation for the effect of (L_e/D) and VF is

$$K = (K_{L_e/D=1, \ VF=0.9})(L_e/D)^{-m}(VF)^{-n} \qquad (10.54)$$

Figure 10.32 gives $K_{VF=0.9}$ as a function of (L_e/D) and N_{Re}. The effect of VF has not been published. The premise was made that ΔP is directly proportional to V in the laminar regime and V^2 in the turbulent regime. In the transition regime it was assumed that n varied linearly with $\ln(N_{Re})$. For use in Eq. 10.54, m and n are given in Figure 10.33. The validity of m and n have been determined experimentally by one set of experiments done by Taylor (1998) while doing a master's thesis using a $1/8''$ diameter mixer with ($L = /D = 0.83$) and VF = 0.678.

DROP SIZE FOR KENICS HEM MIXERS

The predictive method for drop size is given in the *Kenics Bulletin* (May 1988, p. 28, Fig. 5–1) and in Figure 10.34. The ratio of Sauter mean drop size to the mixer ID (d/D) is a function of the Weber Number ($V^2D\rho/\sigma$) and the ratio of dispersed phase to continuous phase viscosity (μ_d/μ_c). Now let's do two examples for static mixers.

10.13. COMPARTMENTED COLUMNS

This section provides the reader with the means to design a compartmented column to consider interstage backmixing. The predictive backmixing correlations are taken from Fasano et al. (1993), Lelli et al. (1972, 1976), Magelli et al. (1982), Takriff (1996), Takriff et al. (1996), Takriff et al. (1998), Takriff et al. (2000), and Takriff et al. (2000).

Figure 10.36 is a schematic of a vertical, multistage, mechanically agitated compartmented column (MSAC). The MSAC components are: (1) *Vessel*, (2) *Agitator Shaft*, (3) *Agitator Impellers*, (4) *Stage Dividers*, and (5) *Stage Divider Openings*. Mechanical design of MSACs is very important for successful application. For columns below about 3.3 meters (4 ft) diameter, the agitator, baffles, and stage dividers are often constructed as a single unit. This unit is installed in the vessel though a full body flange at the top of the vessel. To eliminate backmixing within the gap between
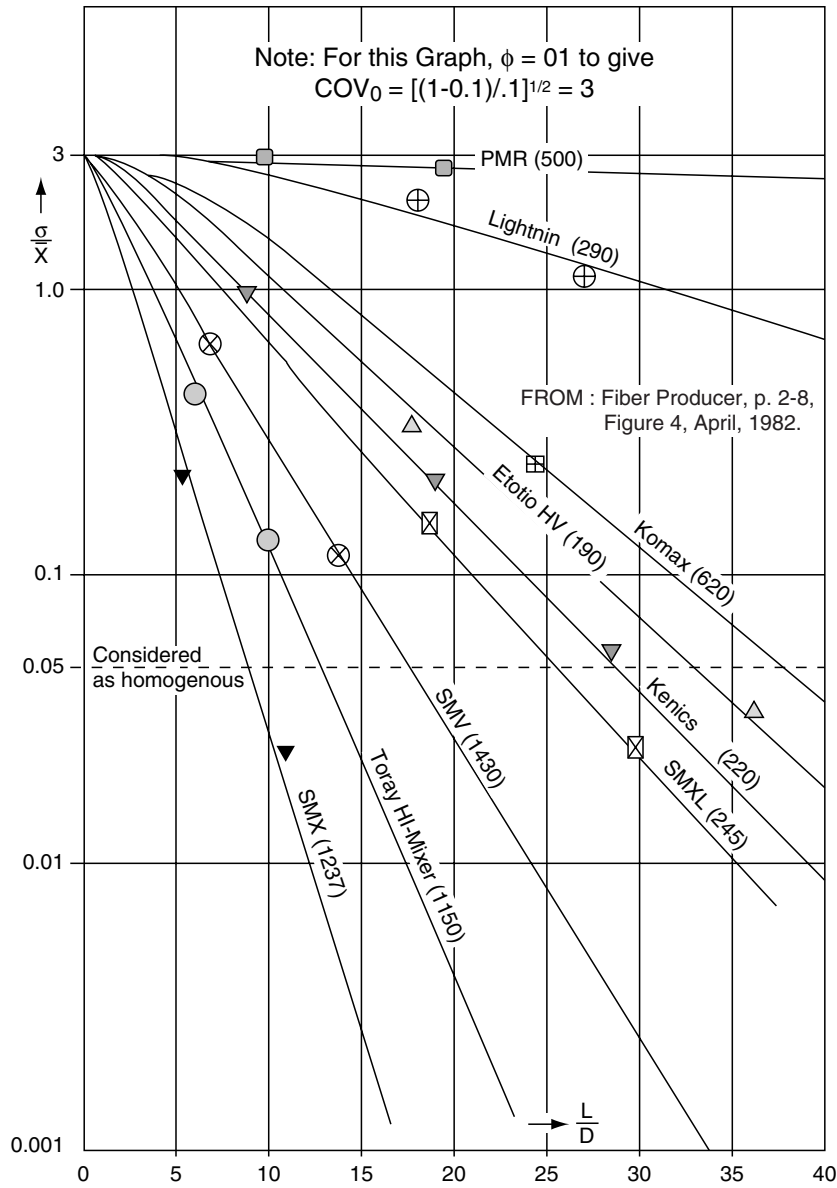
Figure 10.30. Comparison of the laminar regime blending performance of several pipeline static mixers as a function of mixer style and L/D of mixer. An inlet COV of 3 is assumed for the comparison basis. (Koch Engineering [1986]).
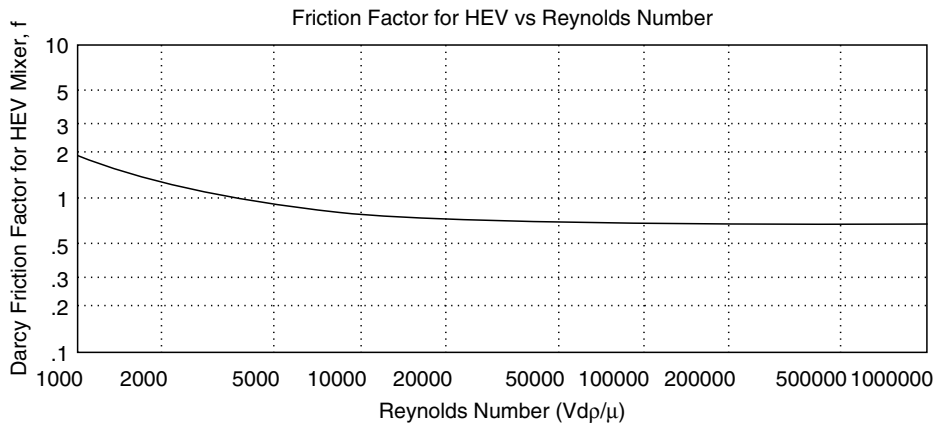
Figure 10.31. Darcy friction factor for the Kenics HEV mixer. (Myers et al. [1997, Fig. 9, p. 35])
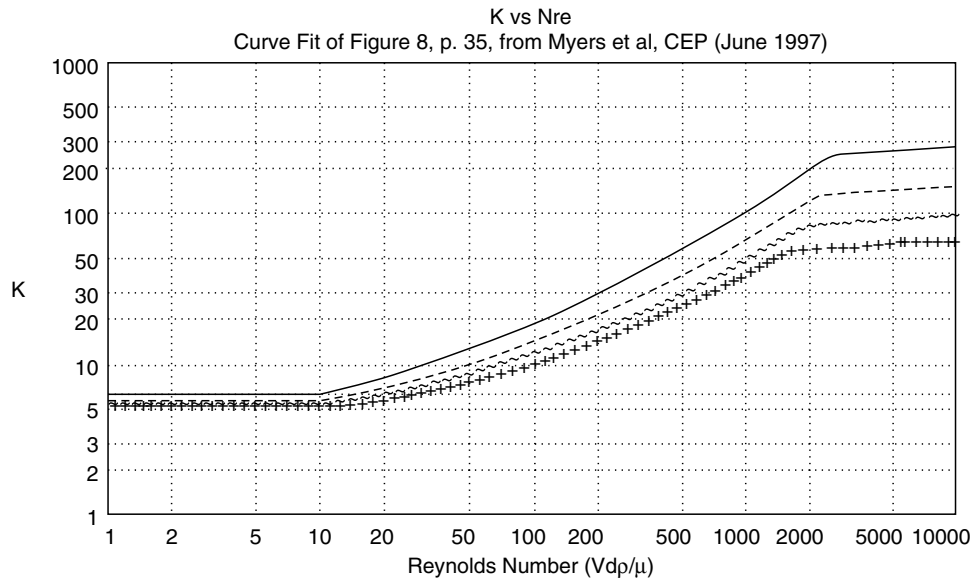
Figure 10.32. K vs Reynolds number and (L_e/D) for the Kenics HEM (from Myers et al. [1997, Fig. 8] with L_e/D for 0.5 and 0.75 added by WRP). *Legend*: (+L_e/D = 1.5), ($\sim$ L_e/D = 1), (−L_e/D = 0.75), (Line: L_e/D = 0.5).

the stage dividers and the vessel wall, a seal is normally provided between the stage divider and the vessel wall. This seal is normally constructed by attaching elastometric ring wipers to the stage dividers. Larger columns, of diameter exceeding 3.3 meters, are normally constructed like trayed distillation columns. The shaft and bottom shaft bearing are installed and then the stage dividers and impellers are individually installed, starting at the bottom stage. Alignment of the bottom bearing and the agitator shaft is one of the most important mechanical design considerations. Vendors must have demonstrated capability in the demanding manufacturing techniques for successful application.

For staged systems, backmixing is normally undesirable. The stage divider openings are the key to minimizing interstage backmixing. The openings must be sized properly and a draft tube, attached to the center opening, is often used. In efforts to minimize or eliminate interstage backmixing, we adjust the following two design parameters:

1. Stage divider opening in the absence of draft tubes
2. The diameter and length of draft tubes

We take full advantage of the following operational characteristics of MSACs:

1. In the absence of gas, with sufficient forward liquid flow, interstage backmixing is eliminated.
2. Counter to our normal intuitive sense, gas flow normally decreases interstage backmixing, and, in most cases, the reduction is dramatic.

By careful design of the MSAC we can normally eliminate, or certainly minimize, interstage backmixing by optimizing and/or taking advantage of the following:

1. Seal the opening between the stage divider and the vessel wall. *You must work with the vendor to accomplish this at reasonable cost.*
2. Use small stage divider openings in the absence of draft tubes. *Again, you must work with the vendor because dynamic movement of the shaft will limit the minimum size of the stage divider opening.*
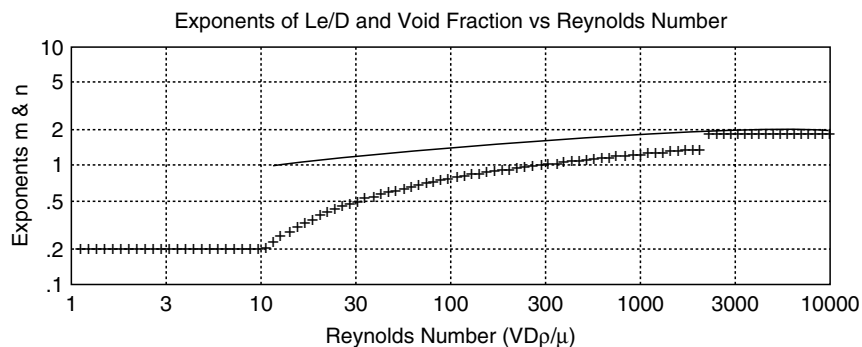
Figure 10.33. Exponents of (Le/D) and VF for HEM mixer in the relationship for ΔP. $\Delta P \propto (Le/D)^{-m}$ and $\Delta P \propto VF^{-n}$. LEGEND: + m, Line: n.

EXAMPLE 10.17
Blending of Ammonia and Air to Feed an Ammonia Burner
A pipeline mixer is being designed to blend ammonia (4000 SCFM) and air (20,000 SCFM) prior to entering an ammonia burner in a nitric acid plant. The mixer inlet pressure is 132.3 psig (i.e., 10 atm). The feed pipe (downstream of the mixer) entering the burner is 12″ diameter. The plant is being designed for an absolute minimum platinum loss. Average molecular weight = 24, gas density = 0.62 lb_m/ft^3, gas viscosity = 0.02 cp. Select a design value for the coefficient of variation of ammonia concentration entering the burner, and calculate the required length and pressure drop for a Kenics HEV Mixer.

Vendors normally select design COV = COV_O = 0.05. This is not adequate for this application; this author normally uses COV < 0.01 for design purposes.

$$V = 2400 \, cfm/[(\pi 1^2/4 \, ft^2)(60 \, s/min)] = 51 \, ft/s.$$

Try two rows of tabs (i.e., N_{tr} = 2), like the HEV shown in Figure 10.25. L/D = 1 for the mixer itself and X/D = 4 overall for the mixer plus tailpipe.

$$N_{Re} = VD\rho/\mu = (51)(1)(0.62)/[(2.42)(0.02)/3600] = 2.35 \times 10^6.$$

From Eq. 10.51 (and Fig. 10.29), $COV_R = COV_O/COV_I$ = 0.0013.

From Eq. 10.48, COV_I = [(1-4,000/24000)/(4000/24000)]$^{1/2}$ = 2.233

Then   COV = $COV_R(COV_I)$ = (0.00123)(2.233) = 0.0028, giving a uniformity of about 99.7 %, which is quite adequate, even for this demanding application.

With this low COV it may be possible to couple the HEV mixer directly to the reactor and not use 3 pipe diameters downstream of the mixer. To shorten the mixing system in this manner and maintain uniformity exceeding 99%, Kenics must guarantee the uniformity because the blending performance has only been published for L/D = 3 downstream of the mixer.

Using Eq. 10.52 and Figure 10.31, ΔP is calculated as follows:

$$\Delta P = 0.7(1/1)0.62(51)^2/[(2)(32.2)144] = 0.12 \, psi.$$

There is a voluminous literature regarding the use of mixing tees for pipeline mixing. Unfortunately, for this demanding application, an optimally designed mixing tee requires an L/D of about 100, as determined by Gray (1986, pp. 63–131, Chapter 13), who designed a pipeline mixer for about the same conditions as those used here. One hundred feet of feedpipe would normally be prohibitive for nitric acid plants.

EXAMPLE 10.18
Blending of Polyethylene Melt from an Extruder Using an HEM
The thermal homogenizer mixer for a polyethylene melt of 11,000 poise (i.e., 1,100,000 cp) is given as an example in the *Kinecs Bulletin* (1991). The 6 element (L_e/D = 1.5) HEM mixer is a 1.77″ ID.

The polyethylene mass flow rate is 150 lbm/hr and the melt density is 55 lb_m/ft^3; thus, the volumetric flow rate is (150 lb_m/hr)/(55 lb_m/ft^3) = 2.73 ft^3/hr. The experimental results for the inlet and outlet temperature profiles are given in Figure 10.35. Let's determine the blending performance of the mixer from correlations and then relate that to the experimental data.

$$N_{Re} = VD\rho/\mu = (2.73 \, ft^3/hr/0.0171 \, ft^2)(0.148 \, ft)(55 \, lb_m/ft^3)$$
$$/[(2.42)(1.1E6 \, lb_m/hr \, ft)] = (160 \, ft/hr)(0.148 \, ft)(55 \, lb_m/ft^3)$$
$$/(2.66E6 \, lb_m/hr\text{-}ft) = 0.0005$$

From Eq. 10.49, $COV_R = 10^{(-0.0977 \times 6)}$ = 0.26

We can also use the Koch chart on page II-D of these notes to estimate COV. The 6-element Kenics HEM, with an Element Length/Element Diameter = 1.5, will have an L/D of 9. From the figure on page II-D, the COV will be 0.9 for COV_{INLET} = 3; thus, $COV_R = COV/COV_0$ = 0.9/3 = 0.3.

Observe the experimental performance of the mixer from Figure 10.35. The experimental cross channel temperature profiles are given; however, to determine the COVs of the inlet and outlet stream we would also need the cross channel velocity profile. We would need the velocity profile because proper averaging must be done on a flowing enthalpy basis; that is, the averaging would have to be done as follows:

$$COV = [\{\Sigma[(\rho Cp V_i T_i)(r_i^2 - r_{i-1}^2)]^2\}/(N-1)]^{1/2}$$
$$/[R^2(\rho Cp V\{T\})_{AVG}}$$

Lacking the velocity profile we can only make a "ballpark" estimate of the COV_R of the mixer. We can use the approach in Paul (2004, p. 440) and use the maximum cross channel $\Delta Ts/T_{AVG}$ as a measure of the COV; thus, from Figure 10.35

$$COV_R = [382\text{-}379)/381]/[(402\text{-}362/381] = 0.15$$

This result compares favorably with the predicted COV_R = 0.26; and this result indicates that, for laminar conditions, one does not always need to design for very low COVs (e.g., 0.01) for the mixer to be quite effective. However, for most turbulent applications, it is prudent to use as a design basis COV =< 0.01.

The pressure drop can be calculated using Eq. 10.53 and Figure 10.32.

$$L = (1.77/12)(1.5)6 = 1.33 \, ft$$

From Figure 10.32, N_{Re} = 0.0005 and L_E/D = 1.5, K = 5.5. The flow is deeply laminar; thus, f = 64/N_{Re}; consequently,

$$\Delta P = 5.5 \times (64/[VD\rho/\mu])(L/D)(\rho V^2/2g_C)$$
$$\Delta P = 5.5 \times 32(L/D)V\mu/(Dg_c) = 5.5 \times 32 \times (6 \times 1.5)$$
$$\times (160/3,600 \, ft/s)(739 \, lb_m/ft\text{-}s)/[0.1475 \, ft(32.2 \, lb_m/lb_f \, ft/s^2)]$$
$$\Delta P = 10,960 \, lb_f/ft^2 = 76 \, psi.$$
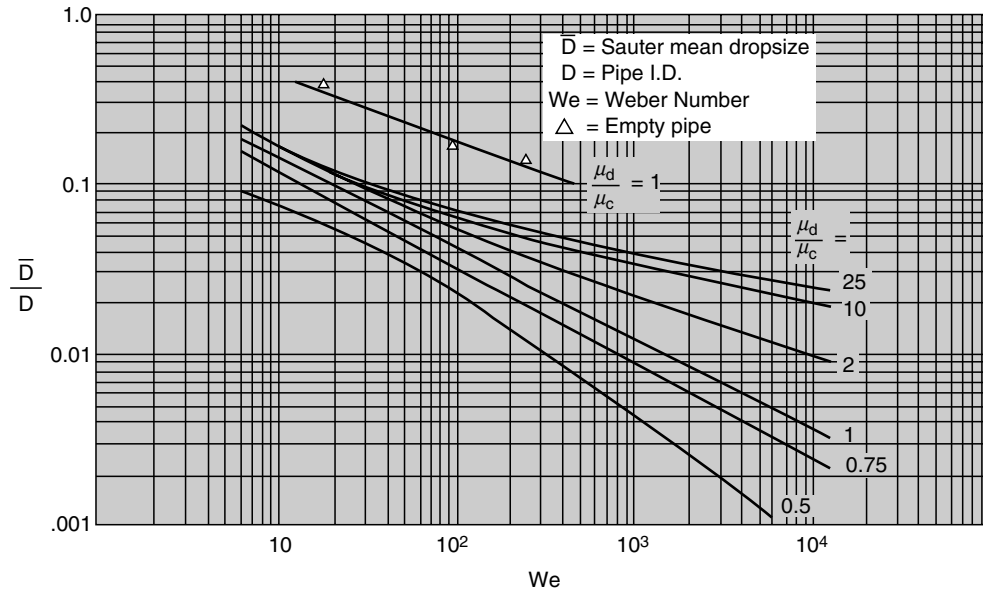
Figure 10.34. Dimensionless drop size correlation for a Kenics HEM pipeline mixer.
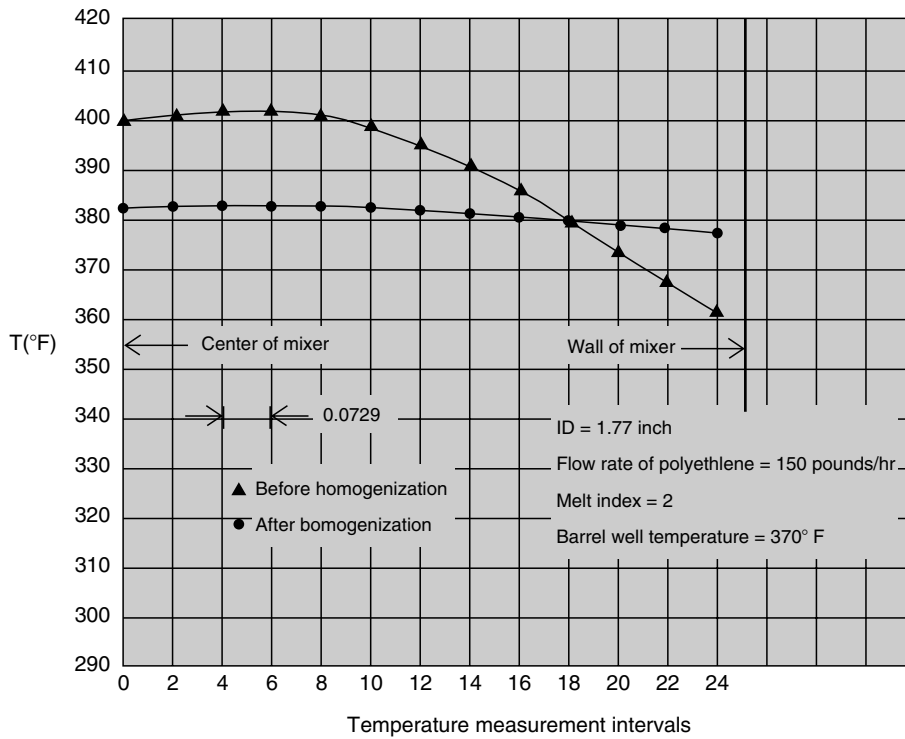
Figure 10.35. Temperature distributions before and after a 1.77 inch inside diameter six element Kenics HEM mixer performing thermal homogenization of polyethylene melt. The apparent viscosity of polyethylene used in the test was 11,000 poises. A homogeneous melt stream was obtained using a Kenics Mixer of six elements. It was found that thermal homogenization in the Kenics Mixer is independent of the initial radial temperature profiles and the size of the unit. A radial thermal gradient reduction from 100°F to less than 1°F was obtained in a PVC cast film production. In general, the unit delivers a polymer melt stream with less than a 3°F radial temperature gradient.

3. Use draft tubes.

4. Take advantage of the effect of forward flow through the stage divider opening to reduce backmixing and potentially eliminate it.

5. Take advantage of the fact that gas flow reduces backmixing.

The most common *stage divider openings* are (1) center opening and (2) center opening with draft tube. Less common openings are
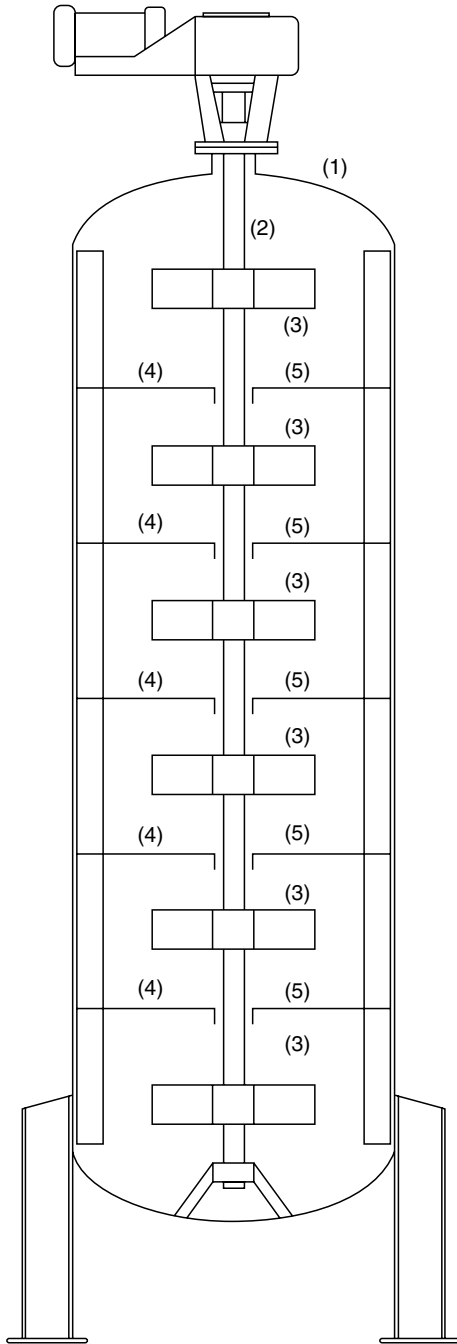
Figure 10.36. Compartmented, mechanically-agitated vertical column.

(1) ring opening between a disk attached to the shaft and an opening in the stage divider and (2) off-center holes. Without a wall-ring seal, the gap between the stage divider and the column wall is a stage divider opening.

All stage divider openings must be designed so that the column can be free draining. For this reason, draft tubes are often extended below the opening, or, if they extend above the stage divider, then small weep holes are drilled into the draft tube just above the stage divider. If a disk attached to the shaft is used to minimize back-

mixing (this feature is not recommended), then it is important that this disk be vertically aligned with the stage divider opening; otherwise, the vertical misalignment will increase backmixing (Xu, 1994).

The wall-ring opening is sometimes not sealed on smaller columns where additional backmixing can be tolerated. If the wall-ring opening is not sealed, then the thesis by Xu (1994) should be used to deternine the backmixing rate, because it is not included here.

DESIGN METHODS

In developing a predictive correlation for interstage backmixing, Xu (1994) first developed a backmixing correlation for zero forward flow. For a given interstage opening geometry, Xu determined that backmixing data were correlated in dimensionless form by the following relationship:

$$N_{b0} = f(N_{Re}) \tag{10.55}$$

For a *centered hole opening*, Figure 10.37 presents this correlation for (1) 6BD and (2) HE-3 impellers.

The effect of a *draft tube* on backmixing, for a center hole opening, is correlated in dimensionless form by

$$N_{b0}/N_{b0@L/Dh=0} = f(L/D_h) \tag{10.56}$$

where L is draft tube length and D_h is the hydraulic diameter of the stage divider opening.

Figure 10.38 presents the correlation for a 6BD and Figure 10.39 presents the correlation for an HE-3.

Forward liquid flow, in either direction through the stage divider opening, will act to decrease backmixing, and, at some finite rate of forward flow, the backmixing rate will reduce to zero. The effect of forward flow is correlated in dimensionless form by:

$$v_b/v_{b0} = f(v_f/v_{b0}) \tag{10.57}$$

where (v_b) is the backmixing velocity at any given forward flow velocity (v_f) through the stage divider opening. Figure 10.40 presents the correlation for the 6BD and the HE-3 impellers for a center hole, without a draft tube. Figure 10.41 presents the correlation for two different draft tube lengths. There is good agreement for all geometrical conditions for $v_b/v_{b0} < 0.5$, but there is not good agreement for lower backmixing ratios. Some of the data scatter is a result of inherent errors in backmixing rate measurements for very low backmixing rates. However, the economic penalty for a conservative design approach is not very great; therefore, for all designs using any draft tubes, the conservative curves of Figure 10.41 should be used.

The effect of *gas* has been considered by Takriff and various colleagues. With *countercurrent* flow of *liquid and gas* the column can flood. Flooding occurs at a constant liquid flow rate when the gas flow rate is increased to the point where all the liquid entering the top of the column cannot flow down the column counter to the upward flow of gas through the stage divider openings. The column is flooded when the excess liquid entering the column must flow out the top of the column with the gas.

Takriff and others have presented a dimensional corellation of $(U_{g,F})^{1/2}$ vs $(ND)(D/T)^{0.8}$ with v_f as a parameter, which allows prediction of the column flooding gas rate as a function of liquid flow and agitation parameters. Their correlation is presented here as Figure 10.42, where $U_{g,F}$ is the flooding velocity, m/s, and v_f is the forward liquid velocity, m/s, with both velocities based on the area of the stage divider opening.
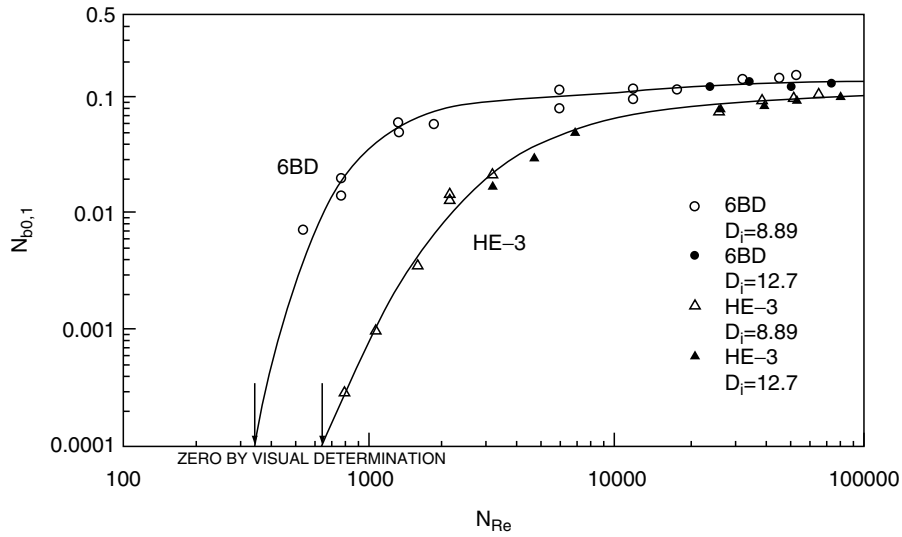
Figure 10.37. Backmixing correlation for center hole opening with zero forward flow.
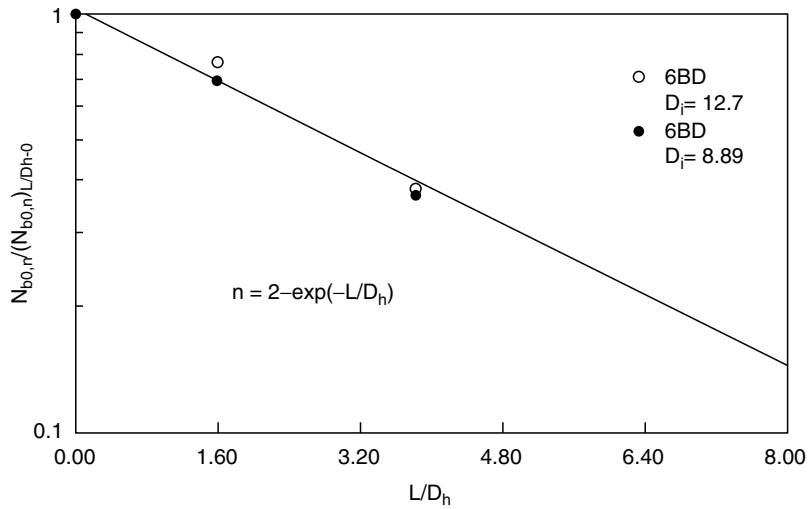
Figure 10.38. Effect of length to hydraulic diameter ratio on backmixing through a center draft tube with **6BD Impellers.**
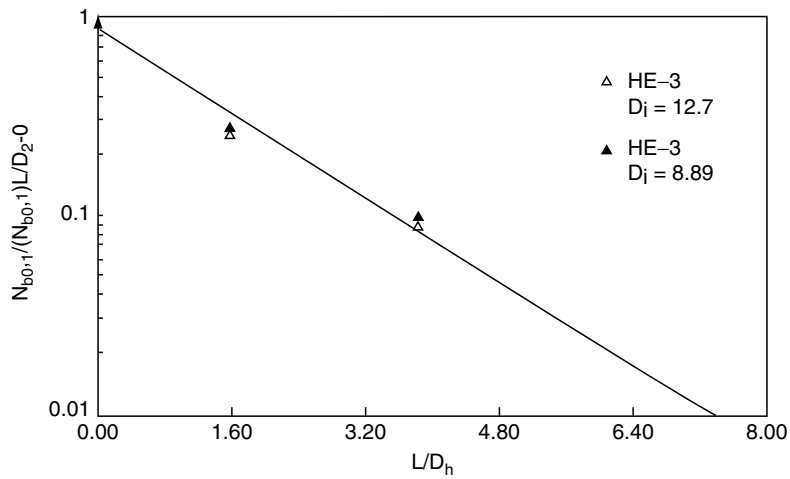
Figure 10.39. Effect of length to hydraulic diameter ratio on backmixing through a center draft tube with **HE-3 Impellers.**
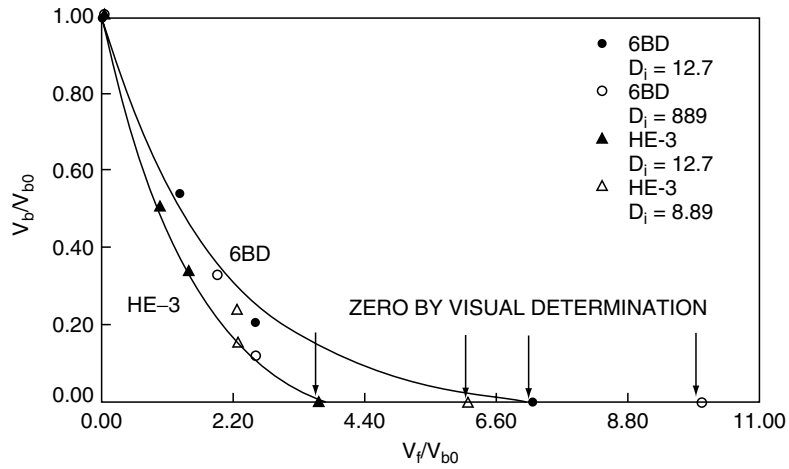
Figure 10.40. Correlation for the effect of forward flow on backmixing for center hole opening.
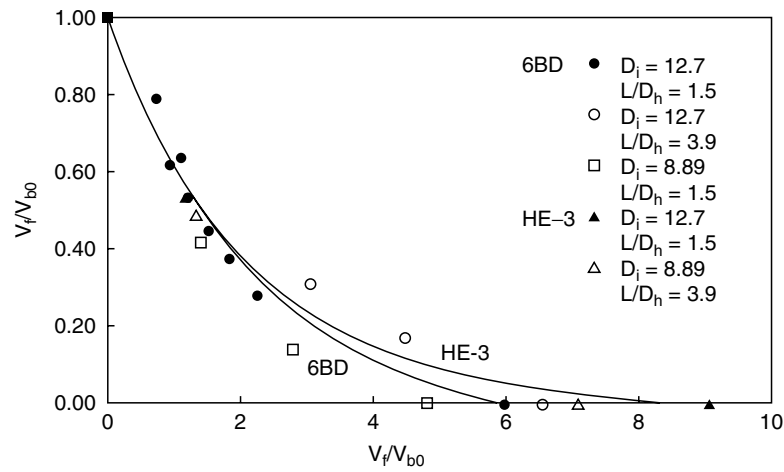
Figure 10.41. Effect of forward flow on backmixing for center draft tube
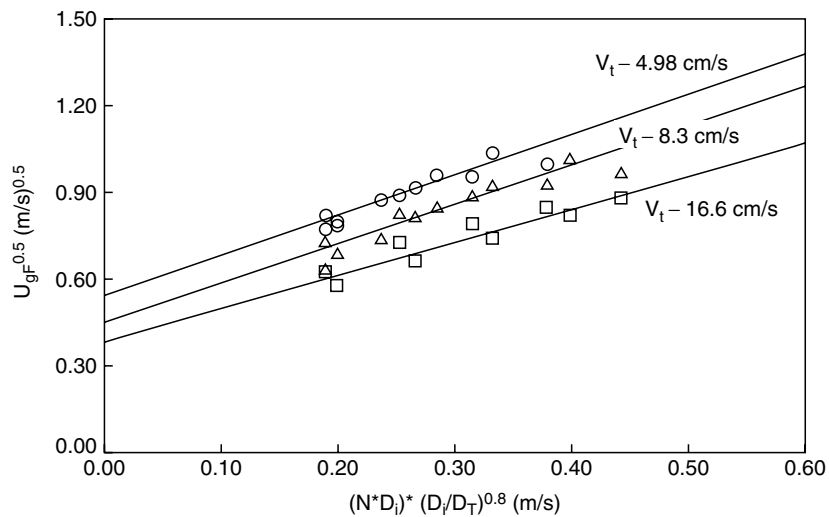
Figure 10.42. Impeller flooding correlation.

Takriff et al. have presented correlations for gas holdup in MSAC. Their correlation is presented in graphical form as Figure 10.43 and the equation of the graphical fit of the correlation is:

$$\alpha = H = 2.1(N_a N_{Fr})^{0.6}(D/T)^{2.5}$$

where N_a is the Aeration Number (Q_{gas}/ND^3) and N_{Fr} is the Froude number (ND_i^2/g).

For *cocurrent* gas-liquid flow, Takriff et al. have correlated the interstage backmixing using the following dimensional correlating method:

$$N_{bg} = f(U_{go}, v_f) \tag{10.58}$$

where

$$N_{bg} = 1/([ND_i](D_i/D_T)(D_T/Z)^{1/2}/v_{bg} + 5U_{go}/v_{bg}) \tag{10.59}$$

The backmixing correlation to account for the effect of gas flow for cocurrent flow of gas and liquid is presented as Figure 10.44.

For *contercurrent* gas-liquid flow, Takriff et al. developed the correlation of Figure 10.45. Now let's do an example problem for multistage column.

10.14. FAST COMPETITIVE/CONSECUTIVE (C/C) REACTIONS

Acid/base neutralization in the presence of organic substrates is the most commonly encountered example where poor mixing can promote undesired side reactions. The neutralization is the desired reaction; however, many organic species are very reactive under high concentrations of acid or base and under high feed concentration. Rapid mixing will promote the very fast neutralization reaction; slow mixing will allow organic species, in the presence of acids or bases, to react by substitution or decomposition, thereby producing side products. Fast C/C reaction systems are particularly prevalent in the pharmaceutical and specialty chemical industries; Paul (1990) has given several examples of fast C/C chemical reaction systems encountered in the pharmaceutical industry.

Fast C/C reactions are conducted in agitated vessels, agitated vessels with recycle loops, and continuous flow static mixers.

This section explains the strategies and procedures for handling fast competitive and/or consecutive (C/C) reactions in *agitated vessels* and *pipeline mixers*. This is a very important area of technology for the chemical process industries, and, in industrial practice, with few exceptions, it is almost *always approached as a scale-up problem* even though there is a very large body of literature related to predictive methods (Baldyga and Bourne, 1999; Knight, 1995). Unfortunately, the reaction kinetics is almost never known quantitatively; consequently, a fundamental approach is stymied. Determining the kinetics for fast reaction is a particularly daunting task, which few laboratories in the world are equipped to handle.

All previous experimental work for fast C/C reactions in *agitated vessels* has shown what one might suspect intuitively—*time scales in the prototype must be duplicated in the plant*. This leads to a conservative scale-up criterion of *constant blend time for agitated vessels and constant residence time for pipeline mixers* even though Patterson, Paul, Kresta and Ethells (in Pauls, (2004, p. 790) p. 790) say, "If experiments show a possibility of mixing reaction interactions and the rate of injection is important, consider multiple point injection. The feed time will have to be increased in large scale equipment." This author does not recommend multiple point injection, except to gain a small measure of conservatism. Increasing the feed time is expensive and not advised for certain reacting systems (e.g., the injection of strong caustic in an alkylpolyglyciside reactor over longer times leads to even more product degradation because the strong acid catalyst needs to be killed at an optimum time in the batch cycle).

By far *the best impeller choice is the 6BD* with the feed injected at rather high velocity into the eye of the impeller. The entering feed jet impinges against the disk of the impeller, which forces the feed to flow out along the disk and then immediately enter the high shear zone around the impeller blade tips. This mechanism of moving the feed immediately to the highest shear zone in the vessel—around the impeller blade tips—is ideal for promoting very rapid feed blending. Additionally, the high velocity feed jet and the impingement on the flat surface of the disk promotes rapid feed blending. With any other impeller and any other feed location, it is possible to miss the high shear zone with the feed with either too low or too high feed jet velocity.

The choice of the *optimum style of in-line mixer* is not nearly as certain as is the choice of the optimum style of agitator impeller. However, a firm recommendation can be made based on the experimental record and on judgment. There are several considerations that lead to the recommendation of the Kenics helical element mixer (HEM) as the most suitable mixer for handling fast consecutive reactions:
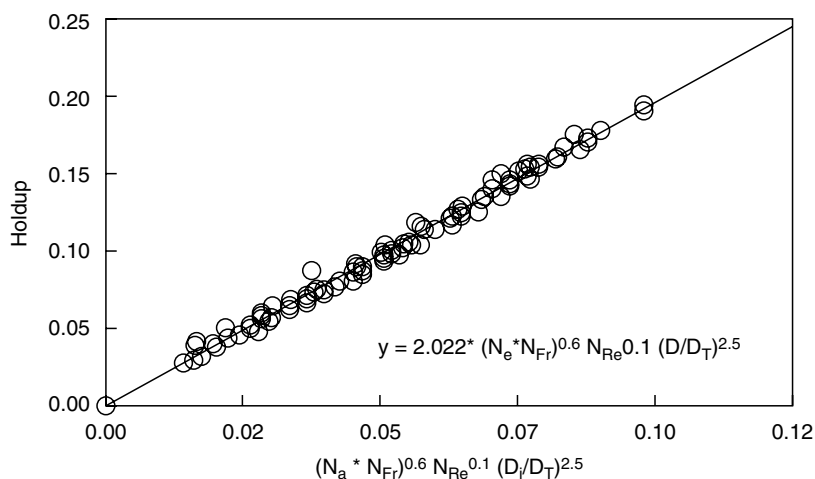
Figure 10.43. Gas Hold-up correlation
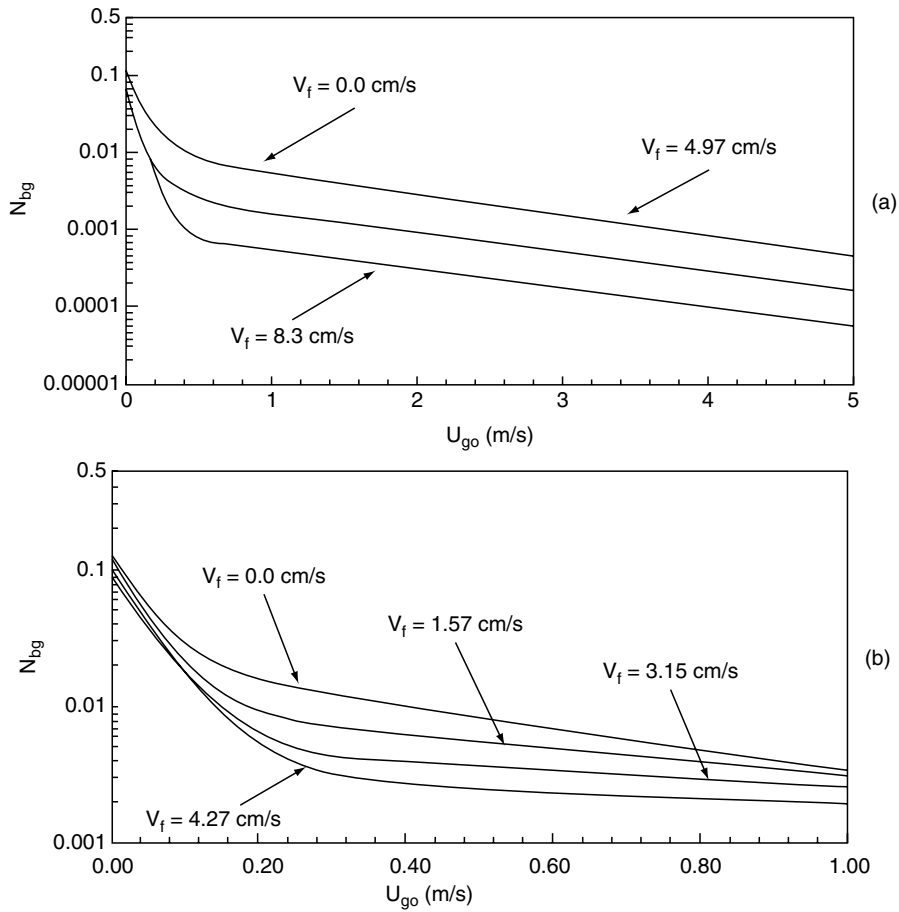
Figure 10.44. Design curve for the effect of gas flow on backmixing: (a) cocurrent flow; (b) countercurrent.
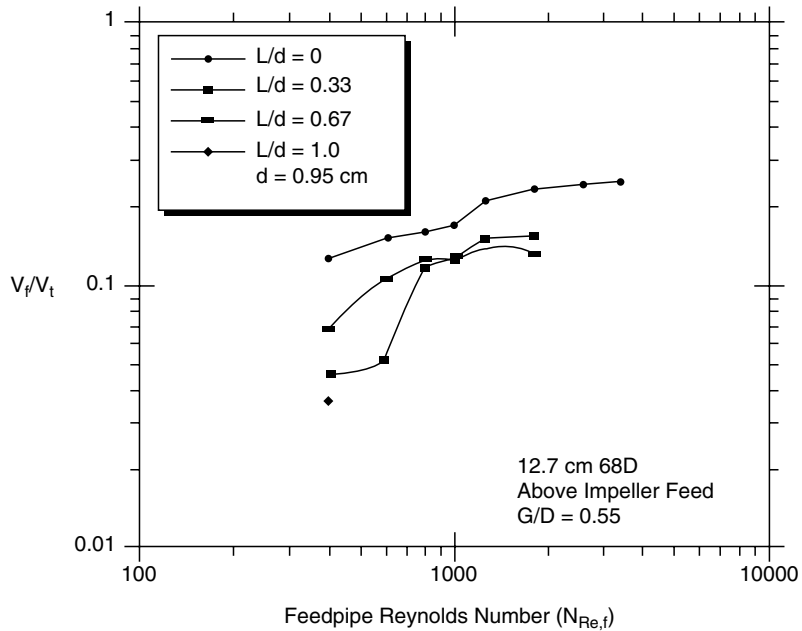
Figure 10.45. Ratio of Feedpipe Velocity to Impeller Tipspeed (v_f/v_t) vs. $N_{Re,f}$ for a 6BD impeller and above impeller feedpipe location Jo et al. (1994).

EXAMPLE 10.19
Staged Chemical Reactor
This example is a waste treatment application. It is the reaction of ethylchloroacetate with caustic

$$CH_2ClCOOC_2H_5(ECA) + NaOH \rightarrow C_2H_5OH$$
$$+ CH_2ClCOONa(NaA)$$
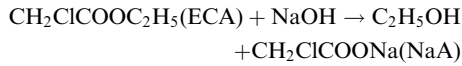
The second order reaction rate constant over the range of 275–299K is given in Baldyga and Bourne [1999, p. 654] as:

$$k = 2.5 \times 10^5 \exp(-3.891 \times 10^4/RT)\{m^3/(mols)\}$$

thus, at 25 C (298 K) the second order rate constant is

$$k_{298k} = 0.03\,m^3/(mols)$$

The premise of the practical problem is that a neutral aqueous stream is contaminated with ECA and the ECA must be neutralized with a stoichometric amount of caustic. ECA is an odorous compound at very low ambient concentrations. It would need to be completely neutralized before being sent to waste treatment. The reaction is to be done in a 15 stage MSAC; the quantitative details of the design are given here:

Input Variables

1. Number of stages = 15
2. Total mass flow to the reactor = 180,000 kg/hr (50 kg/s)
3. Total volumetric flow rate to the reactor = 0.05 m³/s
4. Concentrations of reactants in the feed: $C_{af} = C_{cf} = 70$ kg-mole/m³
5. Column inside diameter = T = 2 m
6. Stage height = 1 m
7. 6BD impeller; D = 2/3 m; impeller speed = 150 rpm
8. Diameter of stage divider opening = D_o = 1 m
9. Diameter of shaft = D_s = 0.15 m
10. Length of draft tube = 0
11. Volumetric flow rate of gas = Q_{gas} = 0

Output Parameters

1. Total agitator power = HP = 201
2. Total agitator per per unit reactor volume = HP/V = 16.2HP/1000 gal
3. Impeller tip speed = v_t = 5.23 m/s
4. Liquid velocity through stage divider opening = v_{fl} = 0.065 m/s
5. Backmixing velocity at zero forward flow = v_{b01} = 0.102 m/s
6. Backmixing velocity with forward flow = $vb0g$ = 0.074 m/s
7. Volumetric backmixing rate = Q_{b0g} = 0.057 m³/s
8. Ratio: Backmixing flow rate/Forward flow rate = R_b = 1.18
9. Total residence time of liquid in the reactor = τ = 942 min
10. {(1- Fractional Conversions) = X} of ECA & NaOH within column stages

Stage Number	$X = (1 - C_a$ or C_c/C_{af} or $C_{cf})$
1	0.08
2	0.0273
3	0.0134
4	0.0081
5	0.0055
6	0.004
7	0.0031
8	0.0025
9	0.0021
10	0.0017
11	0.0015
12	0.00133
13	0.00118
14	0.00108
15	0.00101

This design has a rather large stage divider opening. Let's see what we would need to do to reduce the backmixing to zero. From Figure 10.44, v_f/v_{b0} needs to exceed 7 to shut off backmixing. Thus, we need to increase the hole velocity by a factor of 7. $A_{flow} = \pi/4(1^2 - 0.15^2) = 0.767\,m^2$. Reduced A = 0.767/7 = 0.109 m². $D_o = [0.109 \times 4/\pi + 0.15^2]^{1/2} = 0.22$ m. This gives a clearance between the shaft and the divider opening of $(0.22 - 0.15)/2 = 0.033\,m = 1.3''$. This could be reasonable for this column.

Nomenclature *Only* for Staged Columns

D	Impeller diameter, m
D_h	Hydraulic diameter of stage divider opening $= (D_o/4)/(D_o + D_s)$
D_i	Impeller diameter on the figures in this chapter, m (*Note: This parameter is identified as D in the text material.*)
D_T	Column inside diameter on the figures in this chapter, m (*Note: This parameter is identified as T in the text material.*)
D_o	Diameter of the stage divider opening, m
D_s	Diameter of the agitator shaft, m
H	Gas stage holdup = (total volume – liquid volume)/total volume
L	Vertical length of draft tube, m
N	Impeller speed, m/s
Q_{gas}	Gas volumetric flow rate, m³/s
T	Column inside diameter, m
U_{go}	Superficial gas velocity through stage divider opening, m/s
U_{gF}	Flooding gas velocity through stage divider opening, m/s
v_b	Backmixing velocity through stage divider opening, m/s
v_{bg}	Gassed backmixing flow rate through stage divider opening, m/s
v_{b0}	Backmixing velocity at zero forward liquid through stage divider opening, m/s
v_f	Velocity of forward flow through stage divider opening, m/s
v_{go}	Superficial velocity of gas flow through stage divider opening, m/s
V_f	Forward velocity through the stage divider opening on the Figures, m/s (*Note: This parameter is identified as v_f in the text material.*
Z	Height of a compartment, m

Greek Characters

μ	Fluid viscosity, cp, mPs
ρ	Fluid density, kg/m³

Dimensionless Parameters

N_{b0}	Dimensionless backmixing parameter at $v_f = 0$ $\{v_{b0}/[ND(D/T)(T/Z)^{1/2}]\}$
N_{bg}	$1/([ND](D/T)(T/Z)^{1/2}/v_{bg} + 5v_{go}/v_{bg})$
$N_{b0@L/Dh=0}$	$= N_{b0}$ in the absence of a draft tube (i.e., at L = 0)
$U_{g,F}$	Flooding gas velocity through the stage divider opening, m/s
N_a	Aeration number (Q_{gas}/ND^3)
N_{Fr}	Froude number (Nd_i^2/g)
N_{Re}	Impeller Reynolds number ($ND^2\rho/\mu$)

1. The HEM can be purchased in sizes down to 1/8″. This is a great advantage for laboratory units.
2. The HEM will handle both laminar and turbulent flow regimes; the HEV will not. This is a very significant advantage when scaling-up from small diameter mixers in the laboratory (perhaps 1/8″) to large mixers in the plant. In the laboratory it may be that the flow regime is transition or laminar.
3. The geometry of the HEM is ideal for feeding the sidestreams so that initial feed mixing is rapid. The recommended feed point is midway along the third element. The feed is introduced in two locations on opposite sides of the mixer so that the feed enters normal (i.e., at right angles) to the midpoint of the third helical element. It is often introduced at high velocities, which causes the feed jet to penetrate halfway across the pipe and impinge against the helical tape. This impingement against the tape surface and subsequent flattening of the feed jet(s) provided rapid initial mixing, just like the flattening of the feed jet against the disk of a 6BD.

For *agitated vessels*, it is most important that the proper laboratory experimental program be implemented so that effective scale-up is accomplished. A more complete and comprehensive discussion (than the discussion presented here) of the proper laboratory experimental program is given by Penney and Fasano (1991). The key features of the recommended experimental program are:

1. *Select the proper size vessel and batch dimensions.*
   a. Penney and Fasano (1991) recommend a 4 liter (1 gallon) minimum size.
   b. Use a "square batch" (i.e., $T = Z = 6.77$ inch $= 17.2$ cm).
2. *Select the proper impeller, impeller position and ratio of impeller diameter to tank diameter ratio (D/T).*
   a. Use a 6BD placed $C/D = 1$, although C is of secondary importance.
   b. Use a relatively small ratio of impeller diameter to tank diameter (D/T) in the laboratory reactor to obtain a reasonable balance between blend time, impeller tip speed, and power input per unit volume. (For an in-depth discussion of these considerations, refer to the paper by Penney and Vo [1997].) Use $1/4 > D/T < 1/3$ in the laboratory unit and then perhaps increase D/T up to 1/2 in the plant reactor.
3. *Select the proper feedpipe position and feedpipe velocity.*
   a. The feedpipe should feed in a near vertical direction to the impeller eye (i.e., as near the center as reasonably possible and about $1/6 < G/D < 1/4$ above the impeller disk).
   b. The feedpipe velocity should be sufficiently great to prevent feedpipe backmixing (Jo et al., 1994; Jo, 1993). For a vertically oriented feedpipe feeding near the eye of a 6BD, feedpipe backmixing is prevented provided $v_f/v_t > 0.3$ (i.e., the feedpipe velocity exceeds 30% of the impeller tip speed).
4. *Conduct tests over a range of impeller speeds.*

Experiments must be conducted over a range of impeller speeds. It is important to operate at a speed sufficiently high so that the yield of the desired reaction(s) reaches an asymptotic high value or at least starts to level off at the highest speeds tested. For certain reactions this may not be possible because the rate of the slow reaction is so high that the yield of the desired reaction(s) continually improve as impeller speed is increased.

5. *Select the most economical scale-up speed.*

Chose an experimental impeller speed for scale-up purposes that gives a reasonable balance between:

a. High yield of the desired reaction(s) and
b. Economically reasonable agitator power requirements on the plant scale (*Note*: This is obviously an iterative process because one does not know anything about "economically reasonable power requirements for the plant agitator" until the plant agitator is sized the first time.)

The scale-up procedure for agitated vessels are straightforward:

1. Feed in the same location on both scales.
2. Maintain a high feedpipe velocity on both scales.
   a. It must be sufficiently high to prevent feedpipe backmixing.
3. Keep the time scales the same as you scale-up.
   a. Maintain the same feed time of the semi-batch feed.
   b. Maintain the same blend time of the agitator impeller.
4. Maintain reasonable geometrical similarity for the following parameters
   a. 6 BD impeller of standard dimensions.
   b. Impeller off-bottom clearance of $C/D = 1$.
   c. 4 longitudinal baffles, each 1/12 the tank diameter (i.e., $B/T = 1/12$).
   d. Feedpipe discharge to the eye of the impeller as close to the shaft and as close to the impeller disk as mechanically possible.
5. Normally break geometrical similarity with respect to impeller diameter.
   a. From $1/4 < D/T < 1/3$ in the prototype, use $1/3 < D/T < 1/2$ in the plant.

You will find other recommended procedures in the literature, some of which hint that one can scale-up at constant (P/V) rather than using constant t_b by

1. Increasing the number of feed points (i.e., increase the number of feedpipes)
2. Increasing the feed time of the semi-batch feed

This procedure is not conservative and its success has not been fully documented in the literature over a wide range of vessel sizes. It could be that this inexpensive alternate may be viable; however, an extensive experimental program is recommended before its implementation in scaling from a laboratory size vessel (perhaps 2 to 8 liters) to a reasonable plant size vessel (perhaps 2000 to 8000 liters). The scale-up procedures recommended here are those that have been shown to effect a successful scale-up for every case that has been technically documented. The procedure of scaling-up at constant blend time, constant feed time, with one feed point and a feedpipe velocity sufficiently high to prevent feedpipe backmixing, using a 6BD, is a procedure that will always produce equal yield results from laboratory to plan, which will maintain the desired yield of valuable products and, perhaps, prevent loss of job.

However, there are practical considerations other than scale-up that make these options highly viable. For example, if you are attempting to increase yields in a operating plant reactor, then adding additional feed points and/or increasing the feed time are logical changes that could improve yields. However, if this author were faced with scaling from a laboratory reactor, the multiple feed points and/or longer feed times would be tested in the laboratory and then scale-up would be accomplished using the same number of feed points and/or feed time in the plant reactor as those used in the laboratory reactor.

For a conservative *pipeline mixer scale-up*, use the following procedure:

1. Maintain equal time scales upon scale-up.

2. Use the same number of elements (9 is good) for the experimental and plant units.

3. Use two feed points, at the midpoint of the third element, at 90° to its surface.

4. Maintain geometrical similarity as much as reasonably possible. From practical procurement considerations, the smallest (about 1/8″ for the HEM), least expensive, and most readily available mixers have relatively shorter elements ($L_e/D < 1$) and lower void volumes (VF < 0.8); whereas plant-size units have relatively longer elements ($L_e/D \approx 1.5$) and larger void volume fractions (VF $\cong$ 0.9). Thus, if needed, scale-up may be accomplished by breaking geometrical similarity, but deviate only as needed.

5. Maintain equal residence time on scale-up (i.e., the volumetric flow rate divided by the mixer void volume remains constant on scale-up).

6. Increase the velocity of the entering wall jets by the ratio of linear dimension. (*Note*: This is of secondary importance; however, to maintain time scales the same, it needs to be done to the extent that it is technically feasible.)

It is not uncommon to scale-up from a 1/8 in. diameter unit in the laboratory to a unit exceeding 1 in. in diameter in the plant. The flow regime in the 1/8 unit may be in the transition regime or even in the laminar regime; whereas the flow regime in the plant unit may be fully turbulent. This scale-up, from the transition or laminar regime to the turbulent regime, is very likely conservative because the increasing turbulence in the plant mixer will promote better feed blending. The other alternative to scaling-up across flow regimes is to conduct experiments on the laboratory scale in a mixer of 3/16 in. or 1/4 in. (or larger where turbulent conditions can be reasonable obtained, and for which much more laboratory waste is generated). With the small 1/8 in. diameter mixers, one can increase the velocity to the extent that turbulent conditions are achieved; however, at such high velocities it may not be possible to scale-up to a large unit. For example, if 10 ft/sec velocity were required to achieve a Reynolds number of even 1000 in a 1/8 in. Kenics HEM unit with 9 elements (with a pitch/diameter ratio of 1), the length of this unit would be 1.125 in.; then the residence time would be 1.125/12/10 = 0.0094 sec. To obtain this residence time in a 1 in. diameter unit would require 10[1/(1/8)] = 80 ft/sec, which is unreasonable.

Therefore, one is often confronted with the real need to:

1. Use a small diameter mixer on the laboratory scale to minimize the production rate to minimize waste disposal and stay within the limits of typical laboratory feed tanks, feed pumps, and so on.

2. Scale-up across flow regime boundaries (i.e., scale-up from the transition or laminar regime in the laboratory to the turbulent regime in the plant).

The procedure outlined above is conservative because it is thought to be one that will always give equal or higher yield of the desired reaction(s) in the plant pipeline mixer reactors than in the laboratory pipeline mixer reactors.

There are other less stringent scale-up procedures mentioned in the literature (Baldyga and Bourne, 1999; Hearn, 1995); however, their validity have not been determined for practical applications in scaling from a typical laboratory size pipeline mixer reactor (perhaps 1/8 in. {0.3 cm} to 3/16 in. {0.5 cm}) to plant size reactors (perhaps 1/2 {1.25 cm} in. to 2 in. {5 cm}).

Let's now briefly look at one of the most important experimental fast competitive reactions. Let's select the Third Bourne Reaction (Bourne and Yu, 1994; Yu, 1993), which is the hydrolysis of ethylchloroacetate (ECA) reacting with NaOH in competition

with the parallel reaction of NaOH with HCl. The reactions, along with the first order reaction rate constants) are:

$$A + B \Rightarrow P_1 + P_2 \ [k = 1.3 \times 10^{11} \ \text{m}^3/\text{kg-mol s @ 25 C}]$$
(10.60)

$$A + C \Rightarrow Q_1 + Q_2 \ [k = 30.4 \ \text{m}^3/\text{kg-mol s @ 25 C}] \quad (10.61)$$
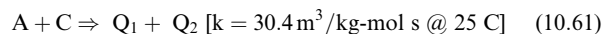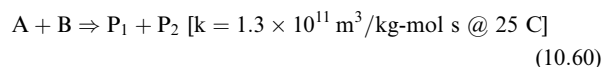
where:

A = sodium hydroxide (NaOH)
B = hydrochloric acid (HCl)
C = ethylchloroacetate ($CH_2ClCOOCH_2CH_3$ or ECA)
P_1 = sodium chloride (NaCl)
P_2 = water (H2O)
Q_1 = ethanol (EtOH)
Q_2 = sodium chloroacetate ($CH_2ClCOO^-Na^+$, i.e. NaECA)

With very rapid mixing, the yield of ethanol and NaCA are low; whereas with poor mixing, the yield of ethanol and NaCA are high. This reaction was used by Tipnis (1994; Tipnis et al., 1994) in an agitated vessel to determine how impeller speed, feedpipe location, and vessel size affected the yield of the instantaneous reaction (i.e., the neutralization of HCl with NaOH). The experiments were conducted by starting with equimolar amounts of HCl and ECA in a reaction vessel. To the vessel was added an NaOH solution on a semi-batch basis. The yield of the fast reaction was increased as impeller speed increased, as the feedpipe was moved toward the eye of the 6BD impeller, and as vessel size decreased. In fact, Tipnis's work was the definitive work to determine a scale-up procedure because he conducted experiments in 2, 20, 180, and 600 liter vessels. As will be discussed in the next section, Tipnis found that blend time was the proper scale-up criterion for the third Bourne reaction.

Knight (1995) and Colleagues (1995) used the third Bourne reaction to develop *scale-up methods for recycle loops on agitated vessels*. He added the NaOH solution at the entrance of a static mixer in a recycle loop on the agitated vessel. Knight showed that higher yields of the fast reaction (i.e., lower yields of the slower reaction which produces NaECA and ethanol) could be achieved by using the recycle loop as compared with the agitated vessel without any recycle loop.

DESIGN METHODS

Agitated Vessels. Figure 10.45 presents the correlation by Jo (1993) and Colleagues (1994) Penney and Fasano (60, 61) for determining the minimum feedpipe velocity needed to eliminate feedpipe backmixing for a feedpipe discharging vertically downward to the eye of a 6BD impeller positioned at $G/D = 0.55$ above the impeller disk. For conservative design, one uses the curve for zero backmixing into the feedpipe (i.e., the curve identified as L/d = 0). Note that for high feedpipe Reynolds numbers, the curve for L/d = 0 becomes asymptotic to $v_f/v_t = 0.3$. Thus, for plant vessels, with a 6BD with the feedpipe above the impeller, the feedpipe velocity must equal or exceed 30% of the impeller tipspeed. Note that for low feedpipe Reynolds numbers, in the laminar regime, the feedpipe velocity can be reduced to perhaps 15% of the impeller tip speed and still prevent feedpipe backmixing; however, even for laboratory vessels, where laminar conditions may occur in the feedpipe, it still makes sense to maintain the feedpipe velocity equal to or in excess of 30% of the impeller tipspeed.

Jo (1993) and Colleagues (1994) also presented correlations for a feedpipe in the radial position to a 6BD impeller and for radial and above positions for an HE-3 impeller.
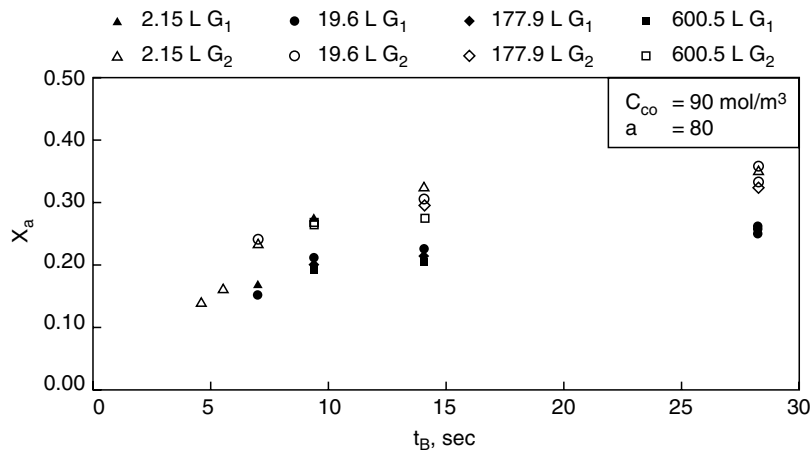
Figure 10.46. Yield data (X_Q = Fraction ECA converted to NaCA) for the 3rd Bourne Reaction as tested in 2, 20, 180 and 600 liter reactors correlated at X_Q vs blend time (6BD impeller used with feedpipe discharging downward to the eye of the impeller).

Scale-up to Maintain Equal Yields for Agitated Vessels. Tipnis (1994) and Colleagues (1994) have done the definitive work for scale-up of agitated vessels handling fast C/C reactions. They used the third Bourne reaction and determined that equal blend time correlated their yield results for vessel volumes of 2, 20, 180, and 600 liters. Figure 10.46 presents a portion of their results for an ECA feed concentration of 90 mol/m^3, a feed time of 15 min, a ratio of initial batch volume to fed volume (a) of 80 and two feedpipe discharge locations—one at G/D = 0.3 and another near the free surface at G/D = 1.34. Note that the yield data are very well correlated at equal blend times. Tipnis et al. (1994) also conducted experiments at other ECA feed concentrations and for other feed ratios and all the yield data were well correlated by equal blend time.

Scale-Up Agitated Vessels with Recycle Loops with Semi-Batch Feed to an In-Line Mixer in the Recycle Loop. Knight (1995) and Colleagues (1995) conducted a rather definitive study that determined the pertinent scale-up parameters for a static mixer in a recycle loop. They used a 20 liter semi-batch reactor agitated with

a 6BD. The third Bourne reaction was used and the caustic solution was fed into a Kenics helical element static mixer in a recycle loop. Mixer inside diameters of 3/16, 1/4, and 3/8 in. were tested. The pertinent scale-up parameters, in order of importance, were found to be:

1. Ratio of caustic feed molar rate to the recycle rate of HCl in the recycle loop.
2. Residence time in the mixer.
3. Feedpipe discharge velocity.

Figure 10.47 shows for the $\frac{1}{4}$ in. inside diameter mixer reactor the importance of the initial molar feed ratio. For relatively low initial molar feed ratios (below about 1.0) the recycle loop/static mixer system can actually give poorer performance than the agitated vessel without a recycle loop. The data indicate that this ratio should be kept above 3 to ensure that the recycle loop/static mixer system is used to fullest advantage. At recycle ratios of 2.4, the feedpipe velocity had a minor, although measurable, effect on the yield of the slowest reaction.
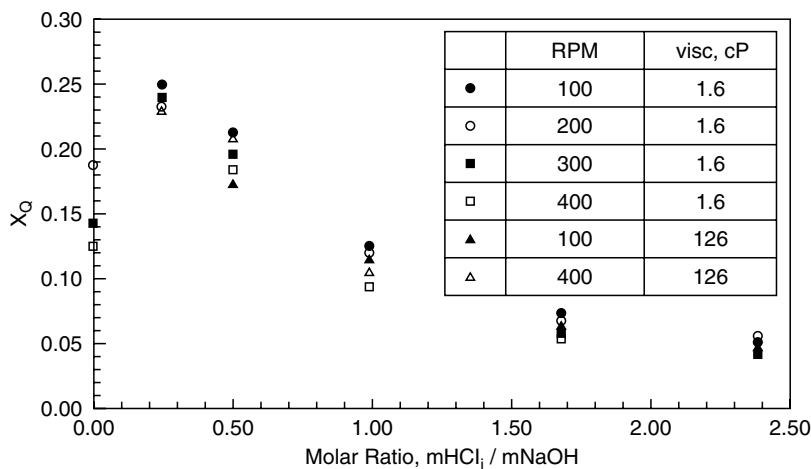
Figure 10.47. Yield data vs initial molar feed ratio for 3rd Bourne Reaction occurring in a 1/4 inch (0.64 cm) Kenics Helical Element Mixer used on a recycle loop on 20 liter semi-batch reactor agitated with a 6BD impeller.

The scale-up recommendations are as follows:

1. Use an initial recycle ratio (i.e., the ratio of the initial molar feed rate of the semi-batch chemical species [e.g., NaOH for the third Bourne Reaction] to the molar feed rate of the fastest reacting chemical species in the recycle loop [i.e., HCl for the third Bourne Reaction]) of at least 3:1.
2. Keep the residence time (= volumetric flow rate/void volume) in the static mixer constant.
3. Maintain a high feedpipe velocity both in the laboratory and plant reactors—perhaps 5–10 m/sec (1 to 30 ft/sec).
4. Scale-up at equal P/V in the agitated vessel and use a 6BD with feed to the impeller eye.

Pipeline Mixers used as Reactors for Fast C/C Reactions. Taylor (1996) and colleagues (1998) conducted a study to determine scale-up procedures for fast C/C reactions in pipeline mixers. They used the fourth Bourne reaction, which is the acid catalyzed hydrolysis of dimethoxypropane (DMP) to acetone and methanol. This is an extremely rapid reaction when catalyzed by HCl. The competitive reaction scheme, which is a unique one, is one in which NaOH reacts practically instantaneously with the HCl to remove the catalyst for the hydrolysis reaction. A water/ethanol solution of NaOH and DMP was fed as a main stream to a Kenics helical element mixer and an aqueous side stream containing slightly greater (abour 5% greater) than equimolar amount of NaOH was fed as the side stream. The product was analyzed by GC for methanol and acetone. For extremely rapid mixing, essentially no hydrolysis occurred; however, for slow mixing, essentially all the DMP is hydrolyzed because acidic conditions cause very rapid hydrolysis of the DMP.

Figure 10.48 presents data of yield (as a fraction of the DMP hydrolyzed) of the slow hydrolysis reaction versus residence time in the mixer. The correlation is not perfect; however, the results of this study indicate that, to be conservative, one must scale-up using equal residence time in static mixer.

The recommended procedure for doing a scale-up study and a scale-up are:

1. Use at least a 9 element Kenics helical element mixer (HEM).
2. Introduce the feed at two locations, 180 degrees apart around the mixer, at the midpoint of the third element. Position the third element in the tube so that the surface of the tape is normal to the radially entering feed ports.

3. Use a sideport velocity at least twice the mainstream velocity.
4. Conduct tests at several, perhaps 5, flow rates through the laboratory mixer.
5. Scale-up using one or more HEM mixers in parallel.
6. Select a flow rate for the laboratory mixer that gives acceptable yield.
7. Maintain equal residence time on scale-up.

Note: for equal residence time and geometrical similarity

$$t_{residence} = Q/V = Q/(\{VF\}\pi D^2 L/4) \propto Q/D^3$$

where VF is the void fraction, thus at constant residence time

$$D \propto Q^{1/3} \text{ i.e., } D_{plan}t;/D_{laboratory} = (Q_{plant}/Q_{laboratory})^{1/3}$$

8. As much as is feasible, maintain the same ratio of sideport to mainstream velocity on scale-up.

Let's now do examples for an agitated vessel and for a pipeline mixer.

10.15. SCALE-UP

This section covers the scale-up of agitated vessels. The quantitative scale-up relationships presented here are developed by starting with

1. The literature correlations for power requirements in both the laminar and turbulent flow regimes.
2. The literature correlations for various process results (e.g., heat transfer coefficients, blend time, solids suspension, and so on).

Start by using these correlations to develop algebraic relationships, for geometrically similar systems, between the impeller power per unit volume (P/V) required as a function of the vessel volume for various process results. The culmination of that analysis is presented as Figure 10.49, which presents $(P/V)_2/(P/V)_1$ versus V_2/V_1 for the various process results.

It is not always possible to maintain geometrical similarity while doing scale-up; heat transfer is an excellent example where it is often impossible to scale-up while maintaining geometrical similarity. Later is a discussion of key situations when geometrical similarity must be broken.
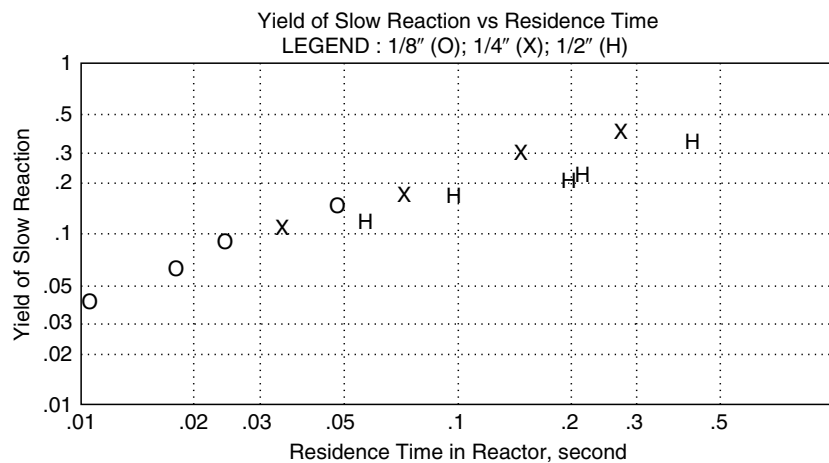
Figure 10.48. Yield of the Dimethoxypropane Hydrolysis Reaction vs Static Mixer Residence Time for three Kenics Helical Element Mixer of 1/8, 1/4 and 1/2 inch inside diameter.

EXAMPLE **10.20**
Semi-Batch Fast C/C Reaction in Agitated Reactor
Let's select laboratory run number 30 from Tipnis (1994) and colleagues (1994). The conditions are:

1. Third Bourne reaction; competitive reaction of NaOH with HCl and ECA.
2. Concentration of ECA in initial batch $= 90\,mol/m^3$.
3. ECA, HCL, and NaOH all stoichometrically equal at start of reaction.
4. Ratio of initial batch volume to semi-batch feed volume $= 80$.
5. Feed time of semi-batch feed $= 15$ minutes $= 900\,sec$.
6. The feedpipe discharges vertically downward very near the impeller shaft.
7. $G = 0.0173; G/D = 0.0173/0.0365 = 0.47$
8. $V = 2.15\,L$.
9. $T = Z = 0.1397\,m$.
10. $D = T/3 = 0.0365\,m$.
11. $C = Z/2 = 0.07\,m$.
12. Measured yield of NaCA (i.e., fraction ECA reacted with NaOH) $= 0.141$.

The plant reactor will be designed for the same yield of NaCA (i.e., $X_Q = 0.141$) from the slower reaction as obtained in the laboratory reactor. The plant reactor will be 2150 L (i.e., it will be 1000 times larger than the laboratory reactor). We don't need to maintain geometrical similarity in terms of D/T, so let's increase the D/T from 1/3 in the laboratory to 1/2 in the plant reactor. We know that we must maintain blend time the same in the plant reactor as in the laboratory reactor and we must design to eliminate backmixing into the plant feedpipe.

The details of the plant agitation system are given here:

1. $T = Z = 55''$
2. Standard 6BD impeller; $D/T = 1/2$, $D = 27.5''$
3. Blend time $= 4.71\,sec$ (*Note*: This variable was inputted on the Variable Sheet.)

4. $N = 249\,rpm$
5. $HP = 80; HP/V = 141\,HP/1000\,gal$ (*Note*: This is a very high power input.)

Note that HP/V in the laboratory reactor was only $2.5\,HP/1000\,gal$; whereas in the plant reactor it is $141\,HP/1000\,gal$. This scale-up is right on the verge of not being practical. For any larger plant reactor one would need to use a recycle loop with a static mixer to do a practical scale-up.

The feed pipe must now be designed. The impeller tip speed is $30\,ft/sec$; thus, the feedpipe velocity must be at least 30% of the impeller tip speed to avoid feedpipe backmixing. Thus, the feedpipe velocity must be $0.3 \times 30 = 9\,ft/sec = 2.74\,m/s$. The volume of semi-batch feed is $2150/80 = 27\,L$. This volume is fed over 15 minutes; thus, the feed rate of the semi-batch feed is:

$$Q_{feed} = 27/(15{}^*60) = 0.03\,L/s = 0.00003\,m^3/s$$

The feedpipe area is then determined

$$A_{feedpipe} = Q_{feed}/v_f = (0.00003\,m^3/s)/2.74\,m/s = 0.000011\,m^2$$

The feedpipe diameter is then determined

$$d = (4 \times 0.000011/\pi)^{1/2} = 0.00374\,m = 0.374\,cm = 0.15\,in$$

The feedpipe would be a pipe with a larger inside diameter than 0.15 in.; thus, it would normally be 1 to 2 in. inside diameter with a pipe cap on its discharge end. The pipe cap would have a 0.15 in. hole drilled in it. The discharge end of the feedpipe would be placed as close to the impeller shaft as possible (perhaps 2 in. away) and as close to the disk as possible. It should be feasible to place the end of the feedpipe about 3 in. above the disk for a $G/D = 3/27.5 = 0.11$.

It makes no sense to "beat around the bush" regarding the difficulty of scale-up. Often, scale-up is very difficult and expensive and in a few cases it is practically impossible. Listed here are the "easy" and "difficult" cases:

Easy Scale-Ups

1. Solids suspension
2. Gas-liquid mass transfer for sparged impellers
3. Equal bubble size in gas-liquid dispersions
4. Equal drop size in coalescing liquid-liquid dispersions
5. Equal drop size, without Time Restraints, for stable liquid-liquid dispersions
6. Equal heat transfer coefficients
7. Equal blend time in the laminar flow regime

Difficult Scale-Ups

1. Equal blend time in the turbulent flow regime
   a. This capability is needed to scale-up fast competitive reactions.
   b. This capability is needed to scale-up batch liquid-liquid dispersions and maintain the same drop size distribution with time as the batch progresses.
      (1) This is almost always pertinent for creating liquid-liquid dispersion in batch feed tanks.

   (2) This is always pertinent for fast competitive reactions in liquid-liquid systems.
2. Equal heat transfer capability per unit of batch volume
   a. This capability is normally needed for exothermic chemical reactions.
3. Equal mass transfer capability per unit of batch volume for gas dispersion from the vessel headspace.
4. Wetting of powders in a partially baffled vessel.

It is important that every process result, of any importance, be considered during scale-up. For example, one can easily ignore the importance of fast competitive reactions for neutralization reactions involving strong acids and bases with organic substrates because small laboratory reactors are so well agitated. It is not uncommon to have a blend time in the neighborhood of 2 to 3 sec in a 2 to 4 liter laboratory reactor, but is very expensive to achieve a blend time of 20 to 30 sec (an order of magnitude longer) in a 10,000 gallon reactor. Thus, one must be aware of all the potentially important process results for scaleup.

SCALE-UP ANALYSIS USING GEOMETRICAL SIMILARITY

Dependence of Agitator Power on Impeller Diameter (D) and Impeller Speed (N). As mentioned previously, scale-up is often accomplished by conducting laboratory experiments. These experi-

EXAMPLE **10.21**
Scale-up of a Static Mixer Reactor for the Fourth Bourne Reaction

This example uses Run 98 from Taylor's (1996) thesis as the laboratory experiment. The pertinent details of this run are given here:

1. Twelve element Kenics helical element mixer with an inside diameter of 1/8 in.
2. Feed of the HCl solution side feed through two ports, each 0.02 in. in diameter.
3. The feeds ports were 180 degrees apart; they fed to the center of the third element.
4. The third element surfaces, at its midpoint, were normal to the entering feed jets.
5. The mixer helical elements were of polypropylene construction; $L_e/D = 0.833$.
6. The void fraction of the mixer was 0.678.
7. For Run 98 the main stream (NaOH & DMP solution) flow rate was 3.47 gm/s.
8. For Run 98 the side stream(s) (HCl solution) total flow rate was 0.309 gm/s.
9. The viscosity of the 25% ethanol solution was 2.5 cp.
10. The specific gravity of the 25% ethanol solution was 0.968.
11. Fractional conversion of the hydrolysis reaction = 0.109.

The mixer velocity is 1.5 ft/s; the Reynolds number is 600; the calculated pressure drop is 3.1 psi; the residence time is 0.0437 sec; the turbulent energy dissipation rate is 1600 HP/1000 gal. The scale-up

results are are summarized next. Geometrical similarity was broken for scale-up. L_e/D was increased from 0.833 to 1.5 (an 80% increase) and the void fraction was increased from 0.678 to 0.9.

1. Scaleup ratio $= 8^3 = 512$.
2. Mixer diameter for geometrical similarity $= 1/8(512)^{1/3}$ $= 8/8 = 1\,in.$
3. Mixer diameter based on selected geometry $= 3/4\,in.$
   a. $L_e/D = 1.5$ (vs 0.833 for laboratory unit)
   b. Void fraction (VF) = 0.9 (vs. 0.678 for the laboratory unit)
4. Mixer overall length for 12 elements $= (3/4)(1.5)(12) = 13.5\,in.$
5. Residence time $= 0.0437\,sec$ (same as the laboratory mixer reactor).
6. Pressure drop $= 140\,psi$.
7. Velocity through mixer $= 21.2\,ft/s$.
8. Velocity of feed jets $= 68\,ft/s$.
9. Energy dissipation rate in mixer $= 72,000\,HP/1,000\,gal.$
10. Total mass flow rate through plant mixer $= 15,000\,lbm/hr$ ($\cong 120\,million\,lbm/year$).
11. The fractional conversion of the hydrolysis reaction will be the same as for the laboratory reactor (i.e., $X_Q = 0.109$).

The reader will note that this is about the limit of scale-up from a 1/8 in. mixer operating at a reasonable rate in the laboratory with water-like (in terms of physical properties) fluids. The velocities and pressure drops are getting high in the plant unit; higher velocities than those utilized here might cause erosion of the mixer elements.

ments are followed by scale-up based on previously determined (by experiment or by correlations) dependence of agitator speed on vessel and impeller diameter to obtain the various process results involved.

To develop algebraic scale-up equations, it is necessary to consider *geometrically similar systems*, (i.e., systems that are exactly the same except for scale). A cloned baby sheep is geometrically similar to its parent. We sometimes scale-up by breaking geometric similarity, but even then it is useful to use scale-up rules based on geometrical similarity to guide our efforts to break geometrical similarity.

Agitator Power Dependence on N and D. For the *fully turbulent* regime:

$$P \propto N^3 D^5 \tag{10.62}$$

Vessel volume (V) is related to impeller diameter (D), as given below for geometrically similar systems.

$$V \propto D^3 \tag{10.63}$$

then

$$P/V \propto N^3 D^2 \tag{10.64}$$

For the *fully laminar* regime:

$$P \propto N^2 D^3 \tag{10.65}$$

then

$$P/V \propto N^2 \tag{10.66}$$

Dependence of Process Result on Impeller Diameter (D) and Impeller Speed (N). For *geometrical similarity*, the Process Result desired can most often be expressed as a function of the impeller speed and the impeller diameter as:

$$R \propto N^c D^d \tag{10.67}$$

At constant process result (R) express the dependence of power per unit batch volume (P/V) on impeller diameter (D) and impeller speed (N).

Equations 10.62 and 10.65 can be expressed as follows:

$$P/V \propto N^a D^b \tag{10.68}$$

Rearranging Eq. 10.68

$$N \propto (P/V)^{1/a}/D^{(b/a)} \tag{10.69}$$

which is applicable for *geometrically similar* systems.

The substitution of Eq. 10.59 into Eq. 10.67 yields

$$R \propto (P/V)^{(c/a)}/D^{(b-ad/c)} \tag{10.70}$$

and by the use of Eq. 10.63, Eq. 10.70 can be modified to express R as a function of P/V and V:

$$R \propto (P/V)^{(c/a)}/V^{(b-ad/c)/3} \tag{10.71}$$

For a *constant process result* of **R**, Eq. 10.71 is an expression relating P/V and V, for *geometrically similar* systems. *For a constant process result upon scale-up* and by identifying one scale as

condition 1 and the other scale as condition 2, Eq. 10.71 becomes Eq. 10.72.

$$(P/V)_2/(P/V)_1 = (V_2/V_1)^{(b-ad/c)/3} \qquad (10.72)$$

This is the relationship that can be used to determine HP/V, and thus HP as scale-up is accomplished. For several Process Results, based on the most commonly accepted values of the exponents of N (i.e., c) and D (i.e., d) in Eq. 10.67 from the technical literature, in both laminar and turbulent regimes, the relationship between $(P/V)_2/(P/V)_1$ and (V_2/V_1) is graphed in Figure 10.49.

The following Process Results are easily maintained upon scale-up because equal (P/V) is a reasonable or conservative scaleup

criterion. Keep in mind that the scaleup methods presented here are all for *Geometrically Similar* systems:

EASY SCALEUP AT CONSTANT PROCESS RESULT

1. Blend Time, LAMINAR.
2. Heat Transfer Coefficient, TURBULENT
3. Solids Suspension, TURBULENT
4. Liquid Suspension, TURBULENT
5. Drop Size, TURBULENT
6. Volumetric Mass Transfer Coefficient, TURBULENT
7. Interstage Backmixing Velocity

Figure 1   P/V Scaleiup to Obtain Equal Physical or Process Result
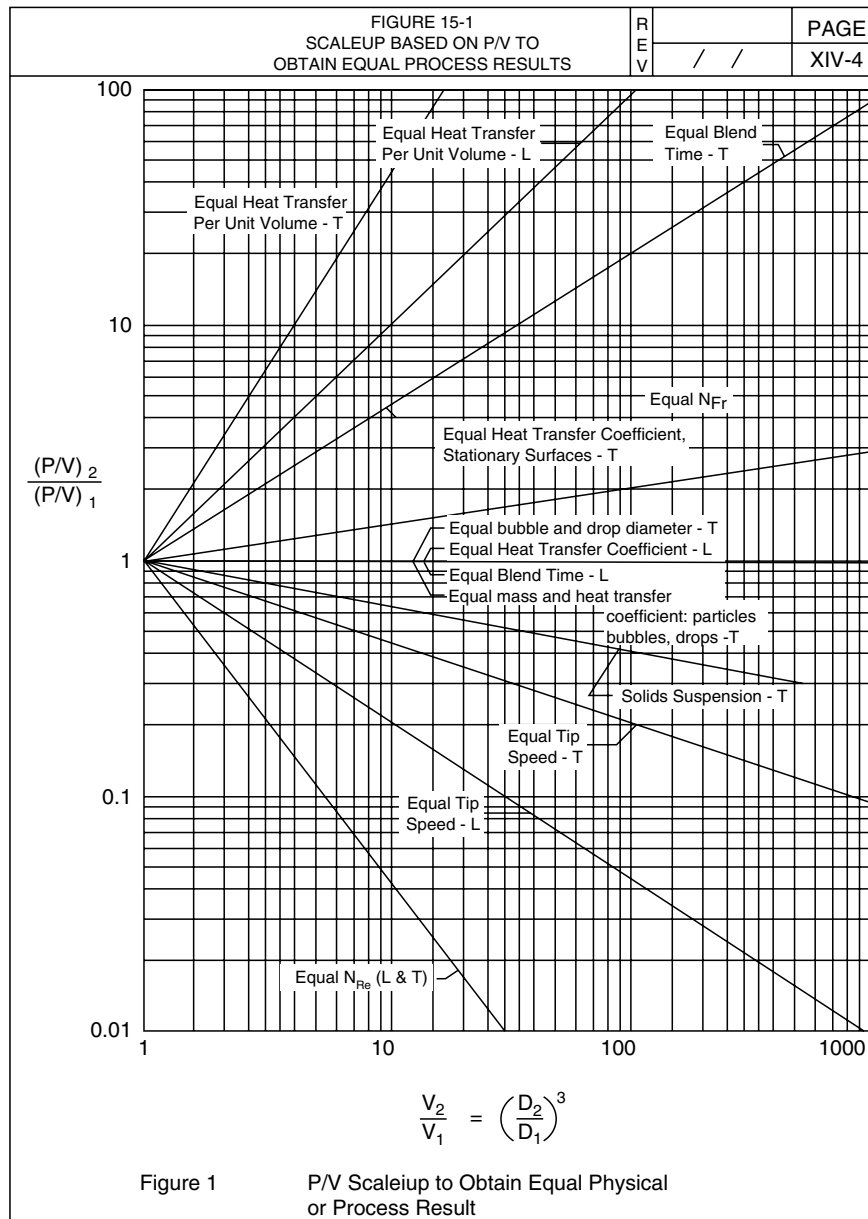
Figure 10.49. Penney Scaleup Chart for Various Process Results in Vessel Vessels.

DIFFICULT SCALEUPS AT CONSTANT PROCESS RESULT

1. Heat Transfer Coefficient, LAMINAR
2. Heat Removal per Volume, LAMINAR
3. Heat Removal per Volume, TURBULENT
4. Time to Achieve Drop Size, TURBULENT
5. Equal Blend Time, TURBULENT

Approaches to Handling Heat Transfer Scale-Up. One of the most difficult and the most frequently encountered scale-up problems for both LAMINAR and TURBULENT conditions is the maintaining of equal heat addition or removal capability upon scale-up. The following alternatives to increasing agitator power should be investigated in order to achieve equal heat removal capability upon scale-up:

1. Use internal pipes or coils. For laminar conditions, consider using a hollow agitator for additional heat transfer surface.
2. Use an external pumped-through heat exchanger.
3. Use small tubes in the plant unit (i.e., break geometrical similarity upon scale-up), and use a smaller ratio of tube diameter to impeller (or tank) diameter.
4. Use a refluxing component so that heat can be removed by evaporation and condensation of the solvent.

Recommendation for Handling Blending. To maintain equal bend time on scale-up is the most difficult scale-up of all. Fortunately, there are only a few process results: (1) handling fast competitive/consecutive reactions and (2) allowing time to achieve a drop size distribution, where equal blend time must be maintained.

Recommendations for Handling Blending Requirements for Fast Reactions. For handling fast reactions, if the power requirements are unreasonable to maintain equal blend time on scale-up, then one should consider two alternates: (1) inject the semi-batch feed into a recycle loop in the inlet of a static mixer and (2) do the reaction in-line while pumping out the vessel through an in-line mixer.

Recommendations to Handle Time to Approach Drop Size. Tests should be conducted at short cycle times (i.e., compared to those used in the plant) in the laboratory vessel. Dispersion times of 1 minute or less, on the low end, are reasonable for the laboratory vessel. But tests should be conducted over a range of dispersion times in order to determine how drop size (or drop size effects) change with dispersion time all the way up to the dispersion time required to achieve the long-term equilibrium drop size.

In the plant vessel the approach to the equilibrium drop size distribution will be longer than the time required in the laboratory. We do not yet know precisely how to scale-up to maintain the exact same temporal variation of drop size as vessel size changes all the way from the laboratory to the plant. The best we can do is to use blending time as a guide and scale-up with a reasonable degree of conservatism. Thus, the time required in the plant vessel should be determined based on scaling the laboratory results using equal blending uniformity in laboratory and plant. Consult the paper by Penney and Vo (1997) to get the details of a most difficult scale-up problem that handled a liquid-liquid chemical reaction in an agitated vessel.

NOMENCLATURE

(Note: The nomenclature for staged columns was given earlier in this chapter.)

A	Heat transfer area and surface area of particle and flow area, ft^2
B	Baffle width, ft
C	Impeller off-bottom clearance, ft
C_b	Concentration of dissolving component in bulk of the liquid, lb-mole/ft^3
C^*	Saturation concentration of dissolving component in solution (i.e., the concentration of dissolving component in the liquid at the particle surface, lb-mole/ft^3
COV	Coefficient of variation = standard deviation/mean
COV_I	Coefficient of variation at the inlet of a mixer
COV_O	Coefficient of variation at the outlet of a mixer
COV_R	Relative coefficient of variation across a mixer = COV_O/COV_I
Cp	Fluid specific heat, Btu/lb$_m$F
d	Pipe diameter of internal helical or harp coil and particle diameter, ft
d_0	Initial particle (when dissolving starts) diameter, ft
d_p	Mass mean particle diameter, ft
D	Impeller diameter, ft
f	Fanning friction factor, dimensionless
G	Distance between feedpipe end and impeller disk or impeller blade, ft
J	Volumetric flux of solute due to mass transfer, kg-mole/s-m^3
k	Fluid thermal conductivity (Btu/lb$_m$F) and particle mass transfer coefficient, ft/s
k_La	Volumetric mass transfer coefficient, 1/s
K	Ratio: pressure drop Kenics HEM/pressure drop empty pipe, same length
L	Height of the impeller blade parallel with the axis of rotation
L_e	Length of an individual element in a pipeline mixer, ft
L_S	Standard height of the impeller blade parallel to the axis of rotation (6BD: $L_S/D = 1/5$; 4BF: $L_S/D = 0.17$; 4*BP*: $L_S/D = 1/5$)
M	Mass of liquid in batch, lb$_m$
N	Impeller rotational speed, rpm or rps
N_B	Number of blades on an impeller
L_S	Shaft length from mounting flange to impeller, ft
N	Impeller rotational speed, rev./s
N_{js}	Just suspended speed for off-bottom suspension, rpm or rps
P	Impeller power requirement, ft lb$_f$/s or HP
P	Pitch of a propeller or a helical ribbon impeller (forward motion of the impeller in one rotation when moving in an internal screw thread)
P_g	Impeller gassed power requirement, HP
P_u	Impeller ungassed power requirement, HP
q	Volumetric flow rate of the minor stream, ft^3/s
Q	Volumetric flow rate of major stream, ft^3/s
S	Spacing between impellers on a shaft, ft
t	(1) Heating or cooling time from T_I to T_F and (2) time from start of dissolving, s
T	Vessel diameter, ft
T_F	The final temperature after cooling or heating of the batch is complete, F
T_I	The initial temperature of the batch before heating or cooling starts, F
T_U	The utility fluid temperature, F
U	Overall heat transfer coefficient, Btu/hr-ft^2-F
v_f	Feedpipe velocity, ft/s
v_{sg}	Superficial gas velocity = $Q_g/A_{V,CS}$
v_t	Inpeller tip speed = πDN, ft/s
V	Vessel volume, ft^3
VF	Void fraction in a pipeline mixer
W	Mass of a particle at time t, lb$_m$
W_l	Weight of liquid in a solid-liquid slurry, lb$_m$

W_s	Weight of solid in a solid-liquid slurry, lb_m
X	Vortex depth from static liquid level to the bottom of the vortex at the shaft, ft
Y	Dimensionless dissolving time $= (\tau\varsigma/d_0^2)(\Delta C/\rho_s)$
X_s	%: Solid weight in a slurry/Liquid weight in a slurry [= 100]
Z	(1) Batch height (ft) and (2) dissolving parameter $= (d_0^{4/3}\varepsilon^{1/3}/\nu)^{0.62}(D/T)^{0.17}(\nu/\varsigma)^{0.36}$

Greek Characters

α	Gas holdup
ΔC	Concentration driving force, $C^* - C_b$, lb-mole/ft^3
ε	(1)Void fraction and (2) impeller power input per unit of batch mass, ft-lb_f/s/lb_m
ς	Solute diffusivity, m^2/s
θ	Angle of impeller blade rotation axis (= 0 for flat blades and 45° for 4BP)
μ	Fluid viscosity, lb_m/hrft (subscripts: c—continuous, d—dispersed, l—liquid)
ν	Liquid kinematic viscosity, ft^2/s
ρ	Fluid density, lb_m/ft^3 (subscripts: c—continuous, d—dispersed, l—liquid, s—solid)
ρ_l	Liquid density, lb_m/ft^3
ρ_s	Solid density, lb_m/ft^3
σ	Interfacial tension, lb_f/ft (also standard deviation)
τ	Dissolving time (when d = 0), s
φ	Volume fraction dispersed phase

Dimensionless Number and Ratios

MuR	Viscosity ratio: bulk viscosity/wall viscosity $= (\mu_b/\mu_w)$
N_A	Aeration number, Q_g/ND^3
$N_{A,Flood}$	Aeration number at flooding, $Q_{g,Flood}/ND^3$
N_{Fr}	Impeller Froude number, N^2D/g
N_{Ga}	Galileo number, N_{Re}^2/N_{Fr}
N_{Go}	Goucher number, $\rho_c D^2 g/\sigma$ (Ratio: gravity to surface tension forces)
N_{Nu}	Nusselt number, hT/k or hd/k for vessel wall or internal pipe, respectively
N_{Pr}	Fluid Prandtl number, $\mu C_p/k$
N_Q	Aeration number, $Q/ND3$
N_P	Impeller power number, $P/\rho N^3 D^5$
N_{Re}	Impeller Reynolds number, $ND^2\rho/\mu$
N_{vi}	Viscosity group for liquid-liquid dispersions $[\rho_c/\rho_d]^{1/2}\mu_d ND/\sigma$
N_{We}	Weber number, $\rho_{cN^2D^3}/\sigma$
Y	$(\tau\varsigma/d_0^2)(\Delta C/\rho_s)$
Z	$(d_0^{4/3}\varepsilon^{1/3}/\nu)^{0.62}(D/T)^{0.17}(\nu/\varsigma)^{0.36}$
χ	d_p/d_0

REFERENCES

General

J. Baldyga and J. R. Bourne, *Turbulent Mixing and Chemical Reactions*, Wiley, New York, 1999.

R.S. Brodkey, *Turbulence in Mixing Operations*, Academic Press, New York, 1957.

Ekato (Company), *Handbook of Mixing Technology*, 2000.

N. Harnby, M.F. Edwards, and A.W. Nienow, *Mixing in the Process Industries*, Butterworths, London, 1985.

F.A. Holland and F.S. Chapman, *Liquid Mixing and Processing in Stirred Tanks*, Reinhold, New York, 1966.

R.J. McDonough, *Mixing in the Process Industries*, Van Nostrand Reinhold, New York, 1992.

S. Nagata, *Mixing—Principles and Applications*, Wiley, New York, 1975.

J.Y. Oldshue, *Fluid Mixing Technology*, McGraw-Hill, New York, 1983.

E.L. Paul, V.A. Atiemo-Obeng, and S.M. Kresta (Eds.), *Handbook of Industrial Mixing*, Wiley-Interscience, New York, 2004.

Z. Sterbacek, and P. Tausk, *Mixing in the Chemical Industry*, Pergamon, London, 1965.

G.B. Tatterson, *Fluid Mixing and Gas Dispersion in Agitated Vessels*, McGraw-Hill, New York, 1991.

G.B. Tatterson, *Scaleup and Design of Industrial Mixing Processes*, McGraw-Hill, New York, 1994.

V.W. Uhl, and J. B. Gray, (Eds.), *Mixing-Theory and Practice,* vols. I (1966), II (1967), III (1986) Academic Press, New York.

J.J. Ulbrecht and G.K. Patterson (Eds.), *Mixing of Liquids by Mechanical Agitation*, Gordon and Breach, New York, 1985.

M. Zlokarnik, *Section 25: "Stirring" in Ullmann's Encyclopedia of Industrial Chemistry*, Verlag Chemie, Weinheim, Germany, 1988.

Tank Blending

J.B. Fasano, A. Bakker, and W.R. Penney, "Advanced impeller—Geometry boosts liquid agitation," *Chem. Eng.*, 110–116 (August 1994).

V. Novak and F. Rieger, *The Chemical Engineering Journal*, No. 9, 63–70, (1975).

Heat Transfer

A. Bakker and L.E. Gates, "Properly choose agitators for viscous mixing," *CEP*, 25–34 (December 1995).

K. Ishibashi, A. Yamanaka, and N. Mitsuishi, "Heat transfer in agitated vessels with special types of impellers," *J. Chem. Eng. Japan*, **12**(3), 230–235 (1979).

W.L. McCabe, J. C. Smith, and P. Harriott, *Unit Operations of Chemical Engineering*, 6th ed., McGraw-Hill, New York, 2001.

W.R. Penney, Section 3.14 of *Heat Exchanger Design Handbook*, Hemisphere Publishing, 1983.

Vortex Depth

W.R. Penney, B.P. Deeth, M.F. Reeder, K.J. Myers, and J. B. Fasano, *Gas Dispersion from Vessel Headspace: Experimental Scale-Up Studies to Maintain Kla Constant,* written and presented at the Winter Annual AIChE Annual Meeting, Los Angeles, November 2000.

F. Rieger, P. Ditl, and V. Novak, "Vortex depth in mixed unbaffled vessels," *Chem. Eng. Sci.*, **34,** 397–401 (1979).

Solids Suspension

P.M. Armenante and E. Nagamine, *Solids Suspension in Agitated Vessels with Impellers Having Small Off-Bottom Clearances*, paper presented at the 1996 AIChE Annual Meeting, Chicago, 1996.

K.J. Bitterof and S.M. Kresta, "Prediction of cloud height for solids suspension in stirred tanks," *CHISA Proceedings*, Prague, August 2002.

N.H. Chowdhury, *Improved Predictive Methods for Solids Suspension in Agitated Vessels at High Solids Loadings*, PhD Dissertation, University of Arkansas, 1997.

R.R. Corpstein, J.B. Fasano, and K.J. Myers, "The high efficiency road to liquid-solid agitation," *Chem. Eng.*, 138–144 (October 1994).

K.J. Myers, R.R. Corpstein, A. Bakker, and J. S. Fasano, "Solids suspension agitator design with pitched blade and high efficiency impellers," *AIChE Symp. Series,* **90**(299), 186–190 (1994).

A.W. Nienow, "Suspension of solid paricles in turbine agitated baffled vessels," *CES*, **23,** 1453–1459 (1968).

W.R. Penney, N.H. Chowdhury, and J.B. Fasano, *Improved Predictive Methods for Solids Suspension in Agitated Vessels at High Solids Loading,* paper written and presented at the 1997 North American Mixing Conference at Williamsburg, VA, June 1997.

T.N. Zwietering, "Suspending of solid particles in liquid by agitators," *CES*, **8,** 244–253 (1958).

Solids Dissolving

D.M. Levins and J. Glastonbury, "Particle-liquid hydrodynamics and mass transfer in a stirred vessel," *Trans. Inst. Chem. Eng.*, **50,** 132–146 (1972).

Gas-Liquid Dispersions

A. Bakker, J. M. Smith, and K.J. Myers, "How to disperse gases in liquids," *Chem. Eng.* 98–104 (December 1994) and *Chemineer Bulletin* 5M-BK-4/97.

S.Y. Lee, and Y.P. Tsui, "Succeed at gas/liquid contacting," *Chem. Eng. Progress,* **95**(7) 23–49 (July 1999).

M.E. Sensel, K.J. Myers, and J. B. Fasano, "Gas dispersion at high aeration rates in low to moderately viscous systems," *AIChE Symposium Series*, No. 293, **89,** 76–84 (1993).

M.S. Takriff, *Column Flooding, Gas Holdup and Interstage Backmixing of an Aerated Multistage, Machanically Agitated, Compartmented Column*, PhD Dissertation, University of Arkansas, 1996.

Liquid-Liquid Dispersions

R.V. Calabrese, C.Y. Wang, and N.P. Bryner, "Drop breakup in turbulent stirred tank contactors," *AIChE J.*, **32**(4), 677–681 (April 1986).

K.C. Chang, *Analysis of Transient Drop Size Distributions in Dilute Agitated Liquid-Liquid Systems*, PhD Dissertation, University of Delaware, 1990.

P.L. Fondy and R.L. Bates, "Agitation of liquid systems requiring a high shear characteristic," *AIChE J.*, **9**(3) 338–342 (May 1963).

S. Nagata, *Mixing: Principles and Applications,* Wiley, New York, 1975, p. 299.

M.A. Norato, C. Tsouris, and L.I. Tavlarides, "Phase inversion studies in liquid-liquid dispersions," *Can. J. Chem. Eng.*, **76,** 486–494 (June 1998).

Selker A.H. and C.A. Sleicher, "Phase inversion in mixing of immisible liquids," *Can. J. Chem. Eng.*, 298–301 (December 1965).

A.H.P. Skelland and R. Seksaria, "Minimum impeller speeds for liquid-liquid dispersions in agitated vessels," *I&ECProcess Des. Dev.*, **17**(1) 56–61 (1978).

J.W. van Heuven, and W.J. Beek, *Ingenieur* (Utrecht), pp. 51–60, v. 82, n. 44, 1970; as reviewed by M. Zlokarnik in *Ullmann's Encyclopedia of Industrial Chemistry,* 5th ed., vol. B2, pp. 25–20.

Pipeline Mixers

J.B. Gray, in *Mixing: Theory and Practice*, vol. III, Academic Press, New York, 1986, Chapter 13, pp. 63–131.

Kenics Bulletin, "Kenics static mixers KETK series," May 1988.

Kenics Bulletin, "Kenics HEV mixer sets a new standard for turbulent mixing efficiency" from a paper by the same title presented at the 1991 NAMF Mixing Conference, Banff, Alberta, Canada.

K.J. Myers, A. Bakker and D. Ryan, "Avoid agitation by selecting static mixers," *CEP*, 28–38 (June 1997).

Koch Engineering Co., Bulletin KSM-6, "Static mixing technology," 1986.

Sulzer Chemtech Bulletin, "Mixing and reaction technology," identification number on back page: 23.27.06.40–I.99–50 US.

R.A. Taylor, *Scale-Up Methods for Fast Competitive Chemical Reactions in Pipeline Mixers*, MS Thesis, University of Arkansas, Fayetteville, 1998.

Staged Columns

J.B. Fasano, W.R. Penney, and B.C. Xu, *Design and Scaleup of Compartmented, Staged Process Equipment with Emphasis on Interstage Backmixing*, paper presented at 14th Bi-Annual Eng. Foundation Mixing Conf., Santa Barbara, CA, June 1993.

U. Lelli, F. Magelli, and C. Sama, "Backmixing in multistage mixer columns," *Chem. Eng. Sci.*, **27,** 1109–1116 (1972).

U. Lelli, F. Magelli, and C. Pasquali, "Multistage mixer columns—A contribution to fluid-dynamic studies," *Chem. Eng. Sci.*, **31,** 253–256 (1976).

F. Magelli, C. Pasquali, and U. Lelli, "Backmixing in multistage mixer columns—II," *Chem. Eng. Sci.*, **37,** 141–145 (1982).

M.S. Takriff, *Gas Holdup, Column Flooding and Interstage Backmixing of an Aerated Mechanically Agitated Compartmented Column*, PhD Thesis, University of Arkansas, 1996.

M.S. Takriff, W.R. Penney, and J.B. Fasano, Paper No. 107a, AIChE Annual Meeting, Chicago, November 1996.

M.S. Takriff, W.R. Penney, and J.B. Fasano, "Interstage backmixing of an aerated multistage, mechanically-agitated compartmented columns," *Can. J. Chem. Eng.*, **76,** 365–369 (June 1998).

M.S. Takriff, W.R. Penney, and J. B. Fasano, "Effect of inpeller diameter to vessel diameter ratio on gas holdup," *J. Kejuruteraan* (Malasia), n. 12, pp. 75–80, 2000.

M.S. Takriff, W.R. Penney, and J.B. Fasano, "The effects of design and operating parameters on the flooding of a gas-liquid mechanically-agitated, compartmented column," *J. Kejuruteraan* (Malasia), n. 12, pp. 99–104, 2000.

B.C. Xu, *Interstage Backmixing in Compartmented Agitated Columns*, PhD Thesis, University of Arkansas, 1994.

Fast Reactions

J. Baldyga, J.R. Bourne, and S.J. Hearn, "Interaction between chemical reactions and mixing on various scales," *Chem. Eng. Sci.*, **52**(4), 457–466 (1997).

J. Baldyga and J.R. Bourne, *Turbulent Mixing and Chemical Reactions*, Wiley, New York (1999).

J. Baldyga, J.R. Bourne, and S.J. Hearn, "Interaction between chemical reactions and mixing on various scales," *Chem. Eng. Sci.*, **52**(4) 457–466 (1997).

J. R. Bourne and S. Yu, "Investigation of micromixing in stirred tank reactors using parallel reactions," *Ind. Eng. Chem. Res.*, **33**(1) 41–55 (1994).

S. Hearn, *Turbulent Mixing Mechanisms in Motionless Mixers*, PhD Dissertation, University of Birmingham, Birmingham, England, UK, 1995.

M.C. Jo, *Experimental Determination of Conditions to Eliminate Feedpipe Backmixing*, MS Thesis, University of Arkansas, Fayetteville, 1993.

M.C. Jo, W.R. Penney, and J. B. Fasano, "Backmixing into reactor feed-pipes caused by turbulence in an agitated vessel," *AIChE Symposium Series*, **90**(299), pp. 41–49 (1994).

C.S. Knight, *Experimental Investigation of the Effects of a Recycle Loop/Static Mixer/Agitated Vessel System on Fast, Competitive-Parallel Reactions*, MS Thesis, University of Arkansas, 1995.

C.S. Knight, W.R. Penney, and J.B. Fasano, *Experimental Investigation of Effects of a Recycle Loop / Static Mixer / Agitated Vessel System on Fast Competitive-Parallel Reactions*, paper presented at Winter Annual AIChE Meeting, Miami Beach, 1995.

W.R. Penneyand and J.B. Fasano, "Cut reaction by-products by proper feed blending," *Chem. Eng. Prog.*, 46–52 (December 1991).

W.R. Penney and H.X. Vo, "Scale-up of liquid-liquid dispersions in agitated vessels to duplicate (1) time scales and (droplet size distribution)," Paper 150a, AIChE Annual Meeting, Los Angeles, 1997.

E. Paul, "Reaction systems for bulk pharmaceutical production," *Chemistry and Industry*, 320–325 (21 May 1990).

R.A. Taylor, *Scale-Up Methods for Fast Competitive Chemical Reactions in Pipeline Mixers*, MA Thesis, University of Arkansas, Fayetteville, 1996.

R.A. Taylor, W.R. Penney, and H.X. Vo, "Scale-up methods for fast competitive chemical reactions in pipeline mixers," paper number 188c, written and presented at the 1998 Annual AIChE Meeting at Miami Beach, 1998.

S.K. Tipnis, *Experimental Investigation of Scale-Up Procedures for Fast Chemical Reactions in Agitated Vessels*, MS Thesis, University of Arkansas, Fayetteville, 1994.

S.K. Tipnis, W.R. Penney, and J.B. Fasano, "An experimental investigation to determine a scale-up method for fast competitive parallel reactions in agitated agitated vessels," *AIChE Symp. Series 299*, **90,** 78–91 (1994).

B.M. Walker, *Einfluss der Temperatur-Segregation auf die Selektivitat raschablaufender Reaktionen*, PhD dissertation, Swiss Federal Institute of Technology, Zurich, Switzerland, 1996.

S. Yu, *Micromixing and Parallel Reactions*, PhD Dissertation, Swiss Federal Institute of Technology, Zurich, Switzerland, 1993.

Scale-up

W.R. Penney, ''Recent trends in mixing equipment,'' *Chem. Eng.*, 86–98 (March 22, 1971).

W.R. Penney and G.B. Tatterson, ''Scale-up relationships for mixing operations,'' *Food Technology*, 62–65 (February 1983).

G.B. Tatterson, ''Scale-up procedures and power consumption in agitated vessels,'' *Food Technology*, 65–70 (May 1981).

11

SOLID–LIQUID SEPARATION

S olid–liquid separation is concerned with mechanical processes for the separation of liquids and finely divided insoluble solids.

11.1. PROCESSES AND EQUIPMENT

Solid-liquid is not usually considered a "high-tech" operation. Much equipment for the separation of liquids and finely divided solids was invented independently in a number of industries and is of diverse character. These developments have occurred without benefit of any but the most general theoretical considerations. Even at present, the selection of equipment for specific solid–liquid separation applications is largely a process of scale-up based on direct experimentation with the process material.

The nature and sizing of equipment depends on the economic values and proportions of the phases as well as certain physical properties that influence relative movements of liquids and particles. Pressure often is the main operating variable so its effect on physical properties should be known. Table 11.1 is a broad classification of mechanical processes of solid–liquid separation. Clarification is the removal of small amounts of worthless solids from a valuable liquid. Filtration is applied to the recovery of valuable solids from slurries. Expression is the removal of relatively small contents of liquids from compressible sludges by mechanical means.

Whenever feasible, solids are settled out by gravity or with the aid of centrifugation. In dense media separation, like ore separations, an essentially homogeneous liquid phase is made by mixing in finely divided solids (less than 100 mesh) of high density; specific gravity of 2.5 can be attained with magnetite and 3.3 with ferrosilicon. Valuable ores and coal are floated away from gangue by such means. In flotation, surface active agents induce valuable solids to adhere to gas bubbles which are skimmed off. Magnetic separation

also is practiced when feasible. Thickeners are vessels that provide sufficient residence time for settling to take place. Classifiers incorporate a mild raking action to prevent the entrapment of fine particles by the coarser ones that are to be settled out. Classification also is accomplished in hydrocyclones with moderate centrifugal action.

Freely draining solids may be filtered by gravity with horizontal screens, but often filtration requires a substantial pressure difference across a filtering surface. An indication of the kind of equipment that may be suitable can be obtained by observations of sedimentation behavior or of rates of filtration in laboratory vacuum equipment. Figure 11.1 illustrates typical progress of sedimentation. Such tests are particularly used to evaluate possible flocculating processes or agents. Table 11.2 is a classification of equipment based on laboratory tests; test rates of cake formation range from several cm/sec to fractions of a cm/hr.

Figure 11.1. Sedimentation behavior of a slurry, showing loose and compacted zones (*Osborne, 1981*; Walas, 1988).

TABLE 11.1. Chief Mechanical Means of Solid–Liquid Separation

1. Settling
  a. by gravity
    i. in thickeners
    ii. in classifiers
  b. by centrifugal force
  c. by air flotation
  d. by dense media flotation
  e. by magnetic properties
2. Filtration
  a. on screens, by gravity
  b. on filters
    i.   by vacuum
    ii. by pressure
    iii. by centrifugation
3. Expression
  a. with batch presses
  b. with continuous presses
    i.   screw presses
    ii. rolls
    iii. discs

329

TABLE 11.2. Equipment Selection on the Basis of Rate of Cake Buildup

Process Type	Rate of Cake Buildup	Suitable Equipment
Rapid filtering	0.1–10 cm/sec	gravity pans; horizontal belt or top feed drum; continuous pusher type centrifuge
Medium filtering	0.1–10 cm/min	vacuum drum or disk or pan or belt; peeler type centrifuge
Slow filtering	0.1–10 cm/hr	pressure filters; disc and tubular centrifuges; sedimenting centrifuges
Clarification	negligible cake	cartridges; precoat drums; filter aid systems; sand deep bed filters

(Tiller and Crump, 1977; Flood, Parker, and Rennie, 1966; Walas, 1988).

Characteristics of the performance of the main types of commercial SLS equipment are summarized in Table 11.3. The completeness of the removal of liquid from the solid and of solid from the liquid may be important factors. In some kinds of equipment residual liquid can be removed by blowing air or other gas through the cake. When the liquid contains dissolved substances that are undesirable in the filter cake, the slurry may be followed by pure water to displace the residual filtrate. Qualitative cost comparisons also are shown in this table. Similar comparisons of filtering and sedimentation types of centrifuges are in Table 11.19.

Final selection of filtering equipment is inadvisable without some testing in the laboratory and pilot plant. A few details of such work are mentioned later in this chapter. Figure 11.2 is an outline of a procedure for the selection of filter types on the basis of appropriate test work. Vendors need a certain amount of information before they can specify and price equipment; typical inquiry forms are in Appendix C. Briefly, the desirable information is:

1. Flowsketch of the process of which the filtration is a part, with the expected qualities and quantities of the filtrate and cake.
2. Properties of the feed: amounts, size distribution, densities and chemical analyses.
3. Laboratory observations of sedimentation and leaf filtering rates.
4. Pretreatment options that may be used.
5. Washing and blowing requirements.
6. Materials of construction.

A major aspect of an SLS process may be conditioning of the slurry to improve its filterability. Table 11.4 summarizes common pretreatment techniques, and Table 11.5 lists a number of flocculants and their applications. Some discussion of pretreatment is in Section 11.4.

11.2. LIQUID-PARTICLE CHARACTERISTICS

As a first step, it is essential to know the characteristics of the particles as well as the liquids in a separation process. Most of these data are not found in handbooks or in the open literature. There is a need that the characteristics of both phases must be determined. What may be disturbing is that these properties might be time dependent, being affected by upstream conditions and the aging of the materials (Chow, 1997).

The size of the particle is the most important separation variable because it affects the particle filterability and its settling rate. The smaller the particles, the more difficult it is to separate from the liquid. So the first step is to determine the particle size. Some of the

equipment for particle measurement is a microscope, light-scattering size analyzers, and particle counters. The microscope permits a true image of the particles; it is inexpensive and easy to use. The other methods require a certain amount of experience or the results might be meaningless. Often, it is better to outsource particle size determination to a company that has performed these determinations.

Another important consideration is solids concentration, since this affects the type of separator to be used. In applications with low solids concentration (e.g., less than 50 ppm), sand filters or cartridge filters may be suitable. If the solids concentration is high, then cake filters are used. Electrical charges on particles affect the agglomeration of particles. Zeta potential measurements may be made but the results are unreliable and have not been used industrially.

The viscosity of the liquid phase is an important consideration. It is a known fact that the sedimentation velocity and the filtration rate vary inversely as the viscosity of the suspending liquid. Temperature, purity, and the amount of dissolved solids materially affect the viscosity value; therefore, it is essential that direct measurement of viscosity be made on the solid-liquid system.

Further, toxicity, volatility, and corrosiveness must be taken into account for environmental and safety reasons. Last, the particle shape and particle strength can be significant when considering the type of equipment to be specified.

11.3. THEORY OF FILTRATION

Filterability of slurries depends so markedly on small and unidentified differences in conditions of formation and aging that no correlations of this behavior have been made. In fact, the situation is so discouraging that some practitioners have dismissed existing filtration theory as virtually worthless for representing filtration behavior. Qualitatively, however, simple filtration theory is directionally valid for modest scale-up and may provide a structure on which more complete theory and data can be assembled in the future.

As filtration proceeds, a porous cake of solid particles is built up on a porous medium, usually a supported cloth. Because of the fineness of the pores the flow of liquid is laminar so it is represented by the equation

$$Q = \frac{dV}{dt} = \frac{A\Delta P}{\mu R}. \tag{11.1}$$

The resistance R is made up of those of the filter cloth R_f and that of the cake R_c which may be assumed proportional to the weight of the cake. Accordingly,

$$Q = \frac{dV}{dt} = \frac{A\Delta P}{\mu(R_f + R_c)} = \frac{A\Delta P}{\mu(R_f + \alpha cV/A)}, \tag{11.2}$$

α = specific resistance of the cake (m/kg),
c = wt of solids/volume of liquid (kg/m^3),
μ = viscosity (N sec/m^2)
P = pressure difference (N/m^2)
A = filtering surface (m^2)
V = volume of filtrate (m^3)
Q = rate of filtrate accumulation (m^3/sec).
t = time (sec)

R_f and α are constants of the equipment and slurry and must be evaluated from experimental data. The simplest data to analyze are those obtained from constant pressure or constant rate tests for which the equations will be developed. At constant pressure Eq. (11.2) is integrated as

$$\frac{A\Delta P}{\mu}t = R_f V + \frac{\alpha c}{2A}V^2 \tag{11.3}$$

TABLE 11.3. Comparative Performance of SLS Equipment[a]

	Product Parameters			Feed Conditions Favoring Use			Equipment Characteristics			Direct Costs		
	Solids in Liquid Product	Liquid in Solid Product	Wash[*] Possibilities	Solids Concentration	Solids Density	Particle Size	Power	Space	Holdup	Initial	Operating	Maintenance
Filtration												
Vacuum drum filter	F	G	E[d]	high to med.	—	medium	high	medium	medium	high	high	medium
Disc filters	F	G	P to F	medium	—	fine	high	medium	medium	med. to high	high	medium
Horizontal filter	F	G	G to E[d]	high to med.	—	coarse	high	medium	medium	medium	high	medium
Precoat filter	E	P[**]	P to F[**]	very low	—	slimy	high to med.	medium	medium	high	very high	medium
Leaf (Kelly) filter	G to E[d]	F	F to G	low	—	fine, slimy	med. to low	medium	medium	medium	very high	medium
Sedimentation												
Thickener	G to E	P	P	medium	dense	medium	low	very high	very high	med. to low	low	very low
Clarifier	G	P	very P	low	med. dense	fine	very low	very high	very high	med. to low	low	very low
Classifier	P	P	P to F	medium	dense	coarse	low	high	high	med. to low	low	low
Centrifugation												
Disc	F to G	P	P	low to med.	medium	fine	high	low	low	high	high	high
Solid bowl	P	F	P to F	med. to high	medium	med. to fine	high	low	low	med. to high	high	high
Basket	P to F	E	E[d]	med. to high	—	coarse	high	low	low	medium	high	high
Liquid cyclones												
Large	P	P to F	P	low to med.	high	medium	med. to low	low	low	very low	medium	high
Small multiple	P to F	P	very P	low	med. to high	fine	med. to low	low	low	low	medium	medium
Screens	P	P to F	P	med. to high	—	coarse to med.	low	very low	very low	very low	medium	med. to high
Ultrafiltration	E	P to F	P	low	—	very fine	med. to high	high	high	high	high	very high

[a] P = Poor. F = Fair. G = Good. E = Excellent. [*]Decantation wash always possible. [d]Displacement wash feasible. [**]Solids product contaminated by precoat material. (Purchas, 1981; Walas, 1988).

Laboratory routine	Final test work	Final sizing and process costing
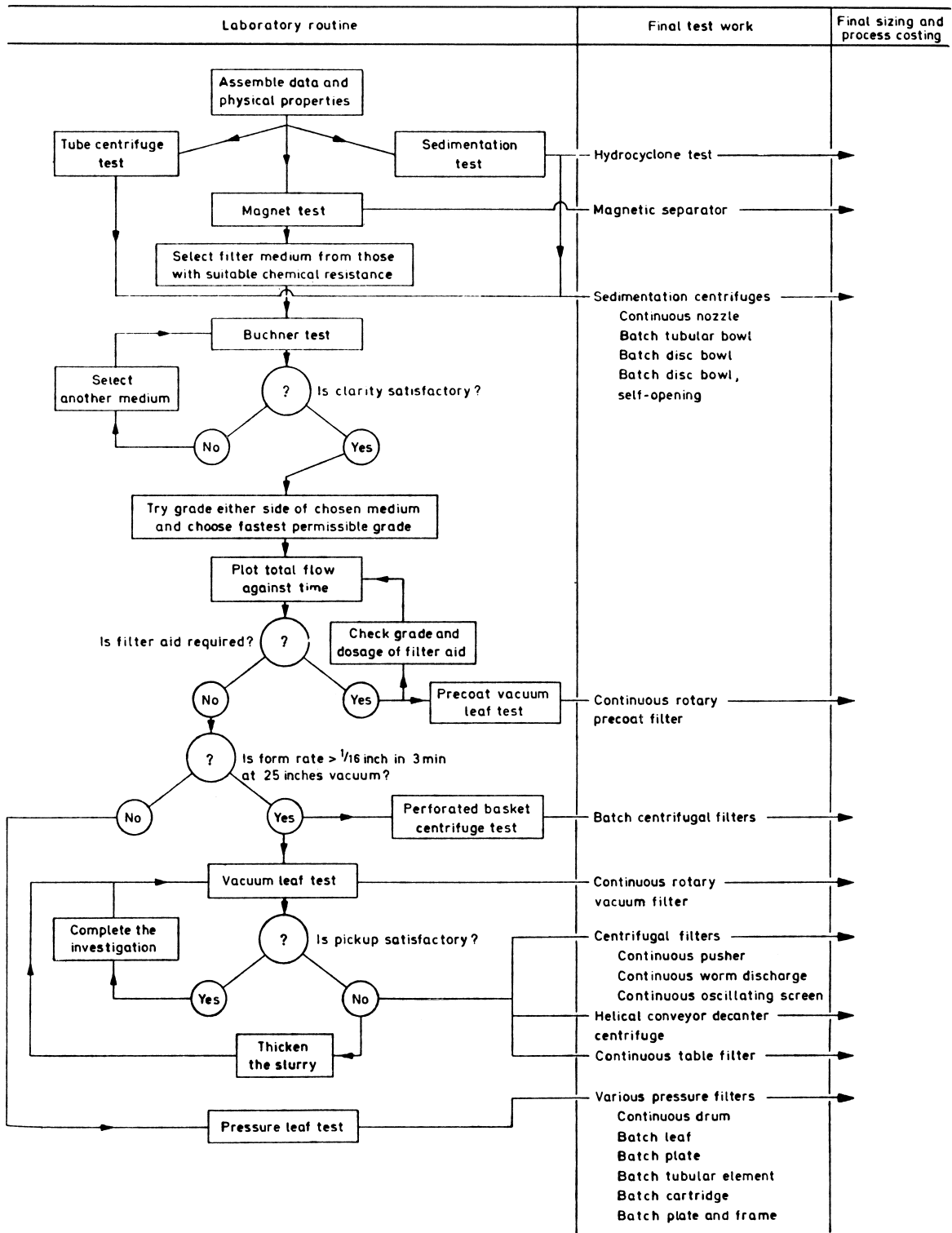
Figure 11.2. Experimental routine for aiding the selection of solid-liquid separation equipment. (*Davies, 1965; Walas, 1988*).

TABLE 11.4. Action and Effects of Slurry Pretreatments

Action On	Technique	Effects
1. Liquid	1. heating 2. dilution with solvent	reduction of viscosity, thereby speeding filtration and settling rates and reducing cake moisture content
	3. degassing and stripping	prevents gas bubbles forming within the medium or cake and impeding filtration
2. Solid particles	1. coagulation by chemical additives	destabilizes colloidal suspensions, allowing particles to agglomerate into microflocs
	2. flocculation by natural or forced convection	microflocs are brought into contact with each other to permit further agglomeration into large flocs
	3. aging	size of individual particles increases, e.g., by crystal growth
3. Concentration of solids	1. increase by appropriate first-stage device such as settling tank, cyclone flotation cell or filter/thickener	rate of filtration increased, especially if initial concentration <2%
	2. classify to eliminate fines, using sedimentation or cyclone	rate of filtration increased and cake moisture content reduced
	3. add filter aid (e.g., diatomite) or other solids to act as 'body aid'	rate of filtration increased by more porous cake and possibly by high total solid concentration
4. Solid/liquid interaction	1. heat treatment, e.g., Porteus process involving pressure cooking 2. freeze/thaw 3. ultrasonics 4. ionized radiation	physical methods which condition sludge and induce coagulation and/or flocculation
	5. addition of wetting agents	reduces the interfacial surface tension, improves the draining characteristics of the cake, and decreases the residual moisture content

(Purchas, 1981; Walas, 1988).

TABLE 11.5. Natures and Applications of Typical Flocculants

Trade Name	Composition	Type or Mechanism	Typical Application	Normal Range of pH Effectiveness	Normal Effective Concentration	Approx. Price per lb[a]	Manufacturer
Alum	$Al_2(SO_4)_3 \bullet XH_2O$	electrolytic and coagulation	water treatment	5–10	15 ppm	13¢	inorganic chemical manufacturers
Ferric sulfate	$Fe_3(SO_4)XH_2O$	electrolytic coagulation	water treatment and chemical processing	any	5–100 ppm	7–13¢	inorganic chemical manufacturers
Sodium CMC	sodium carboxy-methylcellulose	coagulation and bridging	mineral processing	3–9	0.03–0.5 lb/ton	$2.00	Hercules, DuPont, Dow
Separan	acrylamide polymer	bridging	chemical processing	2–10	0.2–10 ppm	$2.00	Dow
Fibrefloc	animal glue	electrolytic	waste treatment	1–9	5–30 ppm	18¢	Armour and Co.
Corn starch	corn starch	bridging	mineral processing	2–10	10 lb/ton	7¢	—
Polynox	polyethylene oxide	bridging	chemical processing	2–10	1–50 ppm	$2.75	Dow
Silica sol	activated silica sol	electrolytic coagulation	waste treatment	4–6	1–20 ppm	9¢ as sodium silicate	inorganic chemical manufacturers
Sodium aluminate	sodium aluminate	coagulation	water treatment	3–12	2–10 ppm	35¢	
Guar gum	guar gum	bridging	mineral processing	2–12	0.02–0.3 lb/ton	$1.10	General Mills
Sulfuric acid	H_2SO_4	electrolytic	waste treatment	1–5	highly variable	2.5–4¢	inorganic chemical manufacturers

[a] 2004 prices, for comparison only.
(Purchas, 1981; Walas, 1988).

and is recast into linear form as

$$\frac{t}{V/A} = \frac{\mu}{\Delta P} R_f + \frac{\mu \alpha c}{2 \Delta P} \frac{V}{A}. \tag{11.4}$$

The constants R_f and α are derivable from the intercept and slope of the plot of t/V against V. Example 11.1 does this. If the constant pressure period sets in when $t = t_0$ and $V = V_0$, Eq. (11.4) becomes

$$\frac{t - t_0}{V - V_0} = \frac{\mu}{A \Delta P} R_f + \frac{\mu \alpha c}{2 A^2 \Delta P} (V + V_0). \tag{11.5}$$

A plot of the left hand side against $V + V_0$ should be linear.

At constant rate of filtration, Eq. (11.2) can be written

$$Q = \frac{V}{t} = \frac{A \Delta P}{\mu (R_f + \alpha c V/A)} \tag{11.6}$$

and rearranged into the linear form

$$\frac{\Delta P}{Q} = \frac{\Delta P}{V/t} = \frac{\mu}{A} R_f + \frac{\mu \alpha c}{A^2} V. \tag{11.7}$$

The constants again are found from the intercept and slope of the linear plot of $\Delta P/Q$ against V.

After the constants have been determined, Eq. (11.7) can be employed to predict filtration performance under a variety of constant rate conditions. For instance, the slurry may be charged to a filter with a centrifugal pump with a known characteristic curve of output pressure against flow rate. Such curves often may be represented by parabolic relations, as in Example 11.2, where the data are fitted by an equation of the form

$$P = a - Q(b + cQ). \tag{11.8}$$

The time required for a specified amount of filtrate is found by integration of

$$t = \int_0^v dV/Q. \tag{11.9}$$

EXAMPLE 11.1
Constants of the Filtration Equation from Test Data
Filtration tests were performed on a $CaCO_3$ slurry with these properties:

$C = 135 \, \text{kg solid/m}^3 \, \text{liquid},$

$\mu = 0.001 \, \text{N sec/m}^2.$

The area of the filter leaf was $500 \, \text{cm}^2$. Data were taken of the volume of the filtrate (L) against time (sec) at pressures of 0.5 and 0.8 bar. The results will be analyzed for the filtration parameters:

(L)	V/A	0.5 bar		0.8 bar	
		t	t/(V/A)	t	t/(V/A)
0.5	0.01	6.8	680	4.8	480
1	0.02	19.0	950	12.6	630
1.5	0.03	36.4	1213	22.8	760
2	0.04	53.4	1335	35.6	890
2.5	0.05	76.0	1520	50.5	1010
3	0.06	102.0	1700	69.0	1150
3.5	0.07	131.2	1874	88.2	1260
4	0.08	163.0	2038	112.0	1400
4.5	0.09			—	—
5	0.10			165.0	1650

The units of V/A are m^3/m^2. Equation (11.2) is

$$\frac{d(V/A)}{dt} = \frac{\Delta P}{\mu (R_f + \alpha C V/A)},$$

whose integral may be written

$$\frac{R_f}{\Delta P/\mu} + \frac{\alpha C}{2(\Delta P/\mu)} \frac{V}{A} = \frac{t}{V/A}.$$

Intercepts and slopes are read off the linear plots. At 0.5 bar,

$$\Delta P/\mu = 0.5(10^5)/0.001 = 0.5(10^8),$$

$$R_f = 600 \Delta P/\mu = 3.0(10^{10}) \, \text{m}^{-1},$$

$$\alpha = [18,000(2)/C] \Delta P/\mu = 36,000(0.5)(10^8)/135$$
$$= 1.333(10^{10}) \quad \text{m/kg}.$$

At 0.8 bar,

$$\Delta P/\mu = 0.8(10^8),$$

$$R_f = 375(0.8)(10^8) = 3(10^{10}) \quad \text{m}^{-1},$$

$$\alpha = 12,750(2)(0.8)(10^8)/135 = 1.511(10^{10}) \quad \text{m/kg}.$$

Fit the data with Almy–Lewis equation, Eq. (11.24),

$$\alpha = kp^n,$$

$$n = \frac{\ln(\alpha_1/\alpha_2)}{\ln(P_1/P_2)} = \frac{\ln(1.511/1.333)}{\ln(0.8/0.5)} = 0.2664,$$

$$k = 1.511(10^{10})/0.8^{0.2664} = 1.604(10^{10}),$$

$$\therefore \alpha = 1.604(10^{10})P^{0.2664}, \, \text{m/kg}, \, P \, \text{in bar}.$$
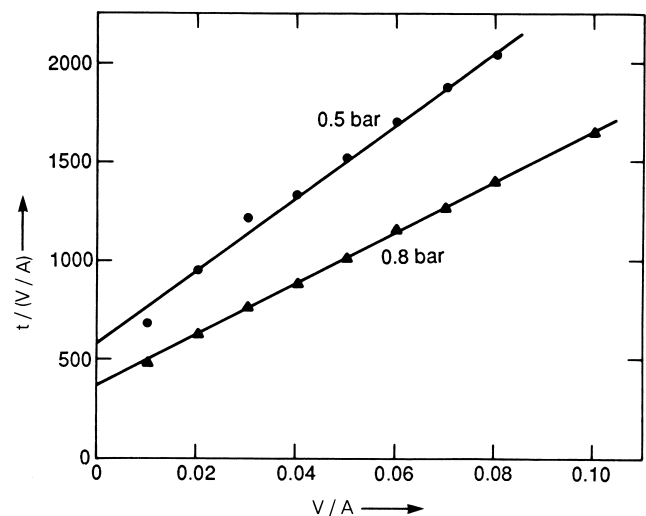
Basic filtration Eq. (11.2) is solved for the amount of filtrate,

$$V = \frac{A}{\mu c \alpha}\left(\frac{A\Delta P}{Q} - \mu R_f\right). \tag{11.10}$$

Equations (11.8) and (11.10) are solved simultaneously for ΔP and Q at specified values of V and the results tabulated as follows:

V	ΔP	Q	1/Q	t
0	—	—	—	0
—	—	—	—	—
V_{final}	—	—	—	t_{final}

Integration is accomplished numerically with the Simpson or trapezoidal rules. This method is applied in Example 11.2.

When the filtrate contains dissolved substances that should not remain in the filter cake, the occluded filtrate is blown out; then the cake is washed by pumping water through it. Theoretically, an amount of wash equal to the volume of the pores should be sufficient, even without blowing with air. In practice, however, only 30–85% of the retained filtrate has been found removed by one-displacement wash. Figure 11.3(b) is the result of one such test. A detailed review of the washing problem has been made by Wakeman (1981, pp. 408–451).

The equations of this section are applied in Example 11.3 to the sizing of a continuous rotary vacuum filter that employs a washing operation.

COMPRESSIBLE CAKES

Resistivity of filter cakes depends on the conditions of formation of which the pressure is the major one that has been investigated at length. The background of this topic is discussed in Section 11.4,

but here the pressure dependence will be incorporated in the filtration equations. Either of two forms of pressure usually is taken,

$$\alpha = \alpha_0 P^n \tag{11.11}$$

or

$$\alpha = \alpha_0(1 + kP)^n. \tag{11.12}$$

The first of these does not extrapolate properly to resistivity at low pressures, but often it is as adequate as the more complex one over practical ranges of pressure.

Since the drag pressure acting on the particles of the cake varies from zero at the face to the full hydraulic pressure at the filter cloth, the resistivity as a function of pressure likewise varies along the cake. A mean value is defined by

$$\frac{1}{\bar{\alpha}} \simeq \left(\frac{1}{\alpha}\right)_{mean} = \frac{1}{\Delta P_c}\int_0^{\Delta P_c}\frac{dP}{\alpha} \simeq \frac{1}{\Delta P}\int_0^{\Delta P}\frac{dP}{\alpha}, \tag{11.13}$$

where ΔP_c is the pressure drop through the cake alone. In view of the roughness of the usual correlations, it is adequate to use the overall pressure drop as the upper limit instead of the drop through the cake alone.

With Eq. (11.12) the mean value becomes

$$\bar{\alpha} = \frac{\alpha_0 k(1-n)\Delta P}{(1+k\Delta P)^{1-n} - 1}. \tag{11.14}$$

The constants α_0, k, and n are determined most simply in compression-permeability cells as explained in Section 11.5, but those found from filtration data may be more appropriate because the mode of

---

EXAMPLE 11.2
Filtration Process with a Centrifugal Charge Pump
A filter press with a surface of $50\,m^2$ handles a slurry with these properties:

$$\mu = 0.001\,\text{N sec/m}^2,$$
$$C = 10\,\text{kg/m}^3,$$
$$\alpha = 1.1(10^{11})\text{m/kg},$$
$$R_f = 6.5(10^{10})\text{m}^{-1}.$$

The feed pump is a centrifugal with a characteristic curve represented by the equation

$$\Delta P = 2 - Q(0.00163Q - 0.02889),\ \text{bar} \tag{1}$$

with Q in $\frac{m^3}{hr}$. Find (a) the time required to obtain $50\,m^3$ of filtrate; (b) the volume, flow rate, and pressure profiles. Equation (11.2) of the text solved for V becomes

$$V = \frac{A}{\alpha\mu C}\left(\frac{A\Delta P}{Q} - \mu R_f\right) = \frac{50}{1.1(10^9)}\left[\frac{50(10^5)\Delta P}{Q/3600} - 6.5(10^7)\right]$$
$$= 818.1\left(\frac{\Delta P}{Q} - 0.0036\right). \tag{2}$$

Equations (1) and (2) are solved simultaneously to obtain the tabulated data. The time is found by integration with the trapezoidal rule:

$$t = \int_0^{50}\frac{dV}{Q}$$

V	ΔP	Q	t (hr)
0	0.1576	43.64	0
10	0.6208	39.27	0.24
20	0.9896	35.29	0.51
30	1.2771	31.71	0.81
40	1.4975	28.53	1.14
50	1.6648	25.72	1.51
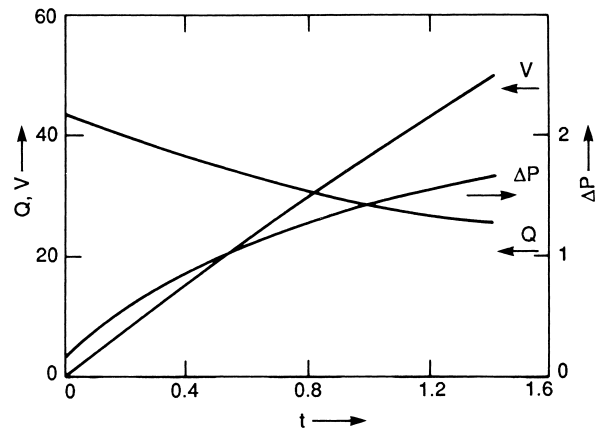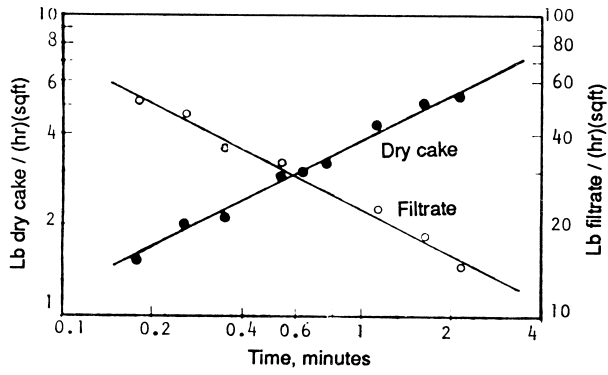
(a)
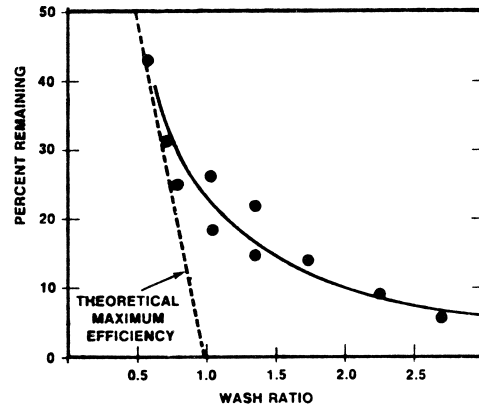
(b)
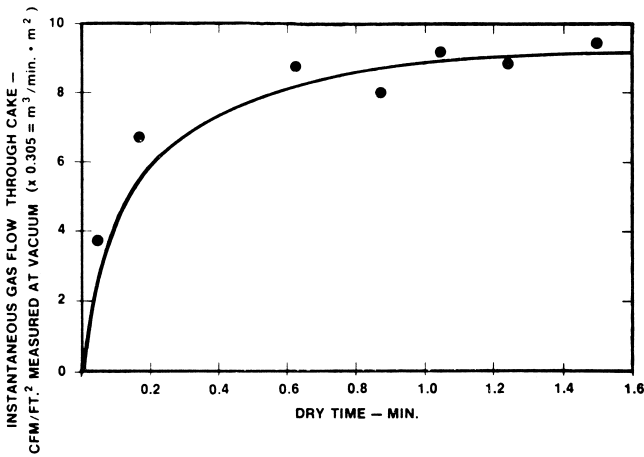
(c)
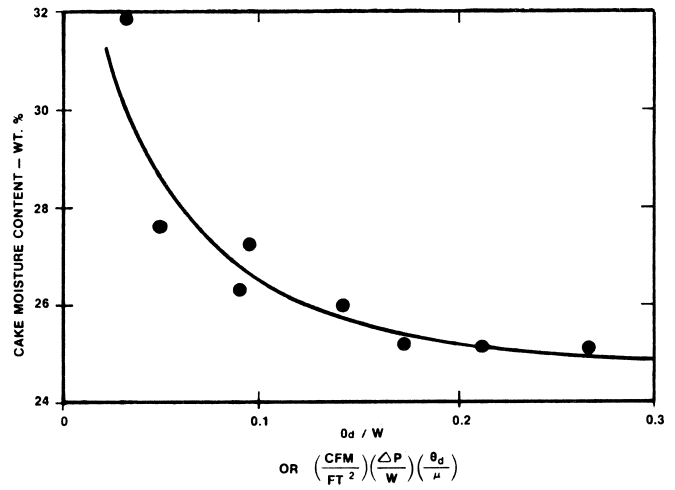
(d)

Figure 11.3. Laboratory test data with a vacuum leaf filter. (a) Rates of formation of dry cake and filtrate. (b) Washing efficiency. (c) Air flow rate vs. drying time. (d) Correlation of moisture content with the air rate, pressure difference ΔP, cake amount W lb/sqft, drying tin θ_d min and viscosity of liquid. (*Dahlstrom and Silverblatt, 1977*; Walas, 1988).

EXAMPLE 11.3
Rotary Vacuum Filter Operation
A TiO$_2$ slurry has the properties

$c = 200\,$kg solid/m^2 liquid,

$\rho_s = 4270\,$kg/m^3,

$\mu = 0.001/3600\,$N hr/m^2,

$\alpha = 1.6(E12)$m/kg (item 4 of Fig.11.2),

$\varepsilon = 0.6$.

Cloth resistance is $R_f = 1(E10)$m^{-1}. Normal peripheral speed is about 1 m/min. Filtering surface is 1/3 of the drum surface and washing surface is 1/6 of the drum surface. The amount of wash equals the pore space of the cake. The cake thickness is to be limited to 1 cm. At suitable operating pressures, find the drum speed in rph and the drum diameter:

$$\text{cake thickness} = 0.01\,\text{m} = \frac{c}{\rho_s(1-\varepsilon)}\frac{V_f}{A}$$
$$= \frac{200}{4270(0.4)}\frac{V_f}{A},$$

$$\frac{V_f}{A} = \frac{0.01(4270)(0.4)}{200} = 0.0854\,\text{m}^3/\text{m}^2,$$

wash liquid = pore volume
$$= 0.01(0.6) = 0.006\,\text{m}^3.$$

With the pressure difference in bar,

$$\frac{d(V/A)}{dt} = \frac{10^5\Delta P_b}{(0.001/3600)[10^{10} + 160(10^{10})V/A]}$$
$$= \frac{36\Delta P_b}{1 + 160V/A}.$$

EXAMPLE 11.3—(*continued***)**

The integral at constant pressure is

$$80(V_f/A)^2 + V_f/A = 36\Delta P_b t_f. \tag{3}$$

With $V_f/A = 0.0854$,

$$\Delta P_b t_f = 0.01858,$$

$$t_f = 0.01858/\Delta P_b = 1/3\dot{n}_f \tag{4}$$

$$\dot{n}_f = 17.94\Delta P_b, \tag{5}$$

where $\dot{n}_f$ is the rph speed needed to make the 1 cm thick cake. From Eq. (2) the washing rate is

$$r_w = \frac{36\Delta P_b}{1 + 160(0.0854)} = 2.455\Delta P_b. \tag{6}$$

Washing time:

$$t_w = \frac{0.006}{2.455\Delta P_b} = \frac{0.00244}{\Delta P_b} \geq \frac{1}{\dot{n}_w}, \tag{7}$$

$$\dot{n}_w \leq 68.3\Delta P_b \tag{8}$$

Comparing (5) and (8), it appears that an rph to meet the filtering requirements is $68.3/17.94 = 3.8$ times that for washing and is the controlling speed.

With a peripheral speed of 60 m/hr

$$60 = \pi Dn,$$
$$D = 60/\pi n = 19.1/\dot{n}. \tag{9}$$

The parameters at several pressures are

ΔP_b(bar)	0.2	0.4	0.6	0.8
$\dot{n}$(rph)	3.59	7.18	10.76	14.35
D(m)	5.3	2.66	1.78	1.33

If the peripheral speed were made 1.22 m/min, a drum 1.0 m dia would meet the requirements with $\Delta P = 0.8$ bar. Another controllable feature is the extent of immersion which can be made greater or less than 1/3. Sketches of a rotary vacuum filter are in Figure 11.12.

---

formation of a cake also affects its resistivity. Equations (11.14) and (11.2) together become

$$\frac{d(V/A)}{dt} = \frac{\Delta P}{\mu}\left[R_f + \frac{\alpha_0 ck(1-n)\Delta P}{(1+k\Delta P)^{n-1} - 1}\frac{V}{A}\right]^{-1}, \tag{11.15}$$

which integrates at constant pressure into

$$\frac{2t}{V/A} = \frac{2\mu}{\Delta P}R_f + \frac{\alpha_0 ck\mu(1-n)}{(1+k\Delta P)^{1-n} - 1}(V/A) \tag{11.16}$$

The four unknown parameters are α_0, k, n, and R_f. The left-hand side should vary linearly with V/A. Data obtained with at least three different pressures are needed for evaluation of the parameters, but the solution is not direct because the first three parameters are involved nonlinearly in the coefficient of V/A. The analysis of constant rate data likewise is not simple.

The mean resistivity at a particular pressure difference can be evaluated from a constant pressure run. From three such runs—ΔP_1, ΔP_2, and ΔP_3—three values of the mean resistivity—$\bar{\alpha}_1$, $\bar{\alpha}_2$, and $\bar{\alpha}_3$—can be determined with Eq. (11.2) and used to find the three constants of the expression for an overall mean value,

$$\bar{\alpha} = \alpha_0(1 + k\Delta P)^n, \tag{11.17}$$

which is not the same as Eq. (11.12) but often is as satisfactory a representation of resistivity under practical filtration conditions. Substituting Eq. (11.17) into Eq. (11.2), the result is

$$\frac{d(V/A)}{dt} = \frac{\Delta P}{\mu[R_f + \alpha_0 c(1 + k\Delta P)^n(V/A)]}. \tag{11.18}$$

Integration at constant pressure gives the result

$$\frac{\alpha_0 c\mu(1 + k\Delta P)^n}{2\Delta P}\frac{V}{A} + \mu R_f/\Delta P = \frac{t}{V/A}. \tag{11.19}$$

Eq. (11.19) could be written in terms of $\bar{\alpha}$ from Eq. (11.17) and would then have the same form as Eq. (11.2), but with only R_f as a

parameter to be found from a single run at constant pressure. In Example 11.1, the mean resistivity is found from the simpler equation

$$\bar{\alpha} = \alpha_0(\Delta P)^n. \tag{11.20}$$

Analysis of the filtration of a compressible material is treated in Example 11.4.

11.4. RESISTANCE TO FILTRATION

The filtration equation

$$\frac{Q}{A} = \frac{\Delta P}{\mu(R_f + \alpha c V/A)} \tag{11.2}$$

considers the overall resistance to flow of filtrate to be made up of contributions from the filter medium R_f, and from the cake with specific resistance α.

FILTER MEDIUM

In practice, a measured R_f includes the effects of all factors that are independent of the amount of the cake; in a plate-and-frame press, for instance, piping and entrance and exit losses will be included, although most of the resistance usually is due to the medium itself. Aging and the resulting increase in resistance is a recognized behavior, particularly of media made of fibers. Particles are gradually occluded in the media so thoroughly that periodic cleaning cannot restore the original condition. The media must be replaced. The degree of penetration of the medium depends on the porosity, the pore sizes, particles sizes, and velocity. Normally R_f is found to depend on the operating pressure; like the plots of Example 11.1, the two intercepts may correspond to different values of R_f at the two pressures.

Data for some filter media are shown in Table 11.6. Although these porosities and permeabilities are of unused materials, the relative values may be useful for comparing behaviors under

EXAMPLE 11.4
Filtration and Washing of a Compressible Material
A kaolin slurry has the properties

$$c = 200 \text{kg solid/m}^3 \text{ filtrate},$$

$$\mu = 0.001 \text{ N sec/m}^2, 2.78(E-7)\text{N hr/m}^2,$$

$$\rho_s = 200 \text{ kg/m}^3,$$

$$\alpha = 87(E10)(1 + P/3.45)^{0.7}\text{m/kg with} P \text{ in bar},$$

$$\varepsilon = 1 - 0.460(1 + P/3.45)^{0.12}.$$

The equations for α and ε are taken from Table 11.8.

Filtration will proceed at a constant rate for 15 min, the pressure will rise to 8 bar and filtration will continue at this pressure until the end of the operation. Filter cloth resistance is $R_f = 1(10^{10})\text{m}^{-1}$. The down time per batch is 1 hr.

a. Find the maximum daily production of filtrate.
b. The filtrate will be blown and then washed with a volume of water equal to the pore space of the cake. Find the maximum daily production of filtrate under these conditions.

Part (a)
Basis 1 m^2 of filtering surface. At $P = 8(10^5)$Pa

$$\alpha = 87(10^{10})(1 + 8/3.45)^{0.7} = 2.015(10^{12}) \text{ m/kg},$$

$$\varepsilon = 1 - 0.46(1 + 8/3.45)^{0.12} = 0.47,$$

$$\mu c\alpha = (0.001/3600)(200)(2.015)(10^{12}) = 1.12(10^8) \text{ N hr/m}^4.$$

The filtration equation (11.2) is

$$\frac{dV}{dt} = \frac{A\Delta P}{\mu(R_f + \alpha CV/A)} = \frac{\Delta P}{(0.001/3600)[10^{10} + 2.015(10^{12})(200)V]}$$

$$= \frac{\Delta P}{2780 + 1.12(10^8)V}.$$

The rate when $t = 0.25h$ and $\Delta P = 8(10^5)$ Pa,

$$Q = \frac{8(10^5)}{2780 + 1.12(10^8)Qt} = \frac{8(10^5)}{2780 + 0.28(10^8)Q}$$

$$= 0.1691 \text{ m}^3/\text{m}^2\text{hr}.$$

The amount of filtrate at this time is

$$V_0 = Qt = 0.1691(0.25) = 0.0423 \text{ m}^3.$$

The integral of the rate equation at constant P is

$$V_o \int_{\frac{dV}{dt}}^{V_f} 2780(V_f - 0.0423) + 0.56(10^8)(V_f^2 - (0.00423)^2]$$

$$= 8(10^5)(t_f - 0.25).$$

Filtering period is

$$t_f = 0.25 + 0.0035(V_f - 0.0423) + 70.0(V_f^2 - 0.0018).$$

Daily production rate,

$$R_d = \text{(no of batches/day)(filtrate/batch)}$$

$$= \frac{24V_f}{t_d + t_f} = \frac{24V_f}{1 + t_f}, \text{m}^3/(\text{m}^2)(\text{day})$$

$$= \frac{24V_f}{1.25 + 0.0035(V_f - 0.0423) + 70(V_f^2 - 0.0018)}.$$

The tabulation shows that R_d is a max when $V_f = 0.127$.

V_f	t_f	R_d
0.12		1.3507
0.126		1.3526
0.127	1.2533	1.3527 (max)
0.128		1.3526
0.129		1.3525
0.130		1.3522

Part (b)
Amount of wash liquid $= \dfrac{cV_f\varepsilon}{\rho_s(1-\varepsilon)} = \dfrac{200(0.47)V_f}{2500(0.53)} = 0.0709V_f,$

wash rate = filtering rate at the conclusion of the filtration

$$= \frac{\Delta p}{\mu(R_f + \alpha cV_f)} = \frac{8(10^5)}{2780 + 1.12(10^8)V_f}, \text{ m}^3/\text{hr},$$

$$t_w = \text{wash time} = \frac{0.709V_f[2780 + 1.12(10^8)V_f]}{8(10^5)}$$

$$= V_f(0.000246 + 9.926V_f),$$

$$R_d = \frac{24V_f}{1 + t_f + t_w}$$

$$= \frac{24V_f}{[1 + 0.0035(V - 0.0423) + 7010(V_f^2 - 0.0018)}$$

$$+ V_f(0.000246 + 9.926V_f)].$$

The optimum operation is found by trial:

$$V_f = 0.105, (\text{m}^3)$$
$$t_f = 1.0805, (\text{hr}) \text{ filtration time}$$
$$t_w = 0.1095, (\text{hr}) \text{ wash time}$$
$$R_d = 1.1507(\text{ max }), \text{ daily production rate, (m}^3/\text{day})$$

---

filtration conditions. Permeability K_p normally is the property reported rather than the resistivity that has been discussed here. It is defined by the equation

$$Q/A = K_p\Delta P/\mu L, \tag{11.21}$$

where L is the thickness. The relation to the resistivity is

$$R_f = L/K_p. \tag{11.22}$$

Thus the filtration resistivity of the medium includes its thickness. Typical measured values of R_f are of the order of 10^{10}m^{-1}; for comparison, the fine filter sheet of Table 11.6, assuming it to be 1 mm thick, has $L/K_p = 0.001/0.15(10^{-12}) = 0.7(10^{10})\text{m}^{-1}$.

CAKE RESISTIVITY

A fundamental relation for the flow resistance of a bed of particles is due to Kozeny (1927):

TABLE 11.6. Porosities and Permeabilities of Some Filter Media

Porosity (%)

Wedge wire screen	5–10
Perforated sheet	20
Wire mesh:	
Twill weave	15–25
Square	30–35
Porous plastics, metals, ceramics	30–50
Crude kieselguhr	50–60
Porous ceramic, special	70
Membranes, plastic foam	80
Asbestos/cellulose sheets	80
Refined filter aids (diatomaceous earth expanded perlite)	80–90
Paper	60–95
Scott plastic foam	97

Permeability, $10^{12}K_p(m^2)$ (compare Eq. (11.22))

Filter aids	
Fine	0.05–0.5
Medium	1–2
Coarse	4–5
Cellulose fibre pulp	1.86
Cellulose fibre + 5% asbestos	0.34
Filter sheets	
Polishing	0.017
Fine	0.15
Clarifying	1.13
Sintered metal	
3 μm pore size	0.20
8 μm pore size	1.0
28 μm pore size	7.5
75 μm pore size	70

(Purchas, 1981; Walas, 1988).

$$\alpha = Ks_0^2(1-\varepsilon)/\varepsilon^3,$$

$K =$ approximately 5 at low porosities,

$s_0 =$ specific surface of the particles, $\qquad$ (11.23)

$\rho_s =$ density of the particles,

$\varepsilon =$ porosity, volume voids/volume of cake.

Because the structure of a cake is highly dependent on operating conditions and its history, the Kozeny equation is only of qualitative value to filtration theory by giving directional effects.

At increasing pressures, the particles or aggregates may be distorted and brought closer together. The rate of flow also may affect the structure of a cake: at low rates a loose structure is formed, at higher ones fine particles are dragged into the previously formed bed. The drag pressure at a point in a cake is the difference between the pressure at the filter medium and the pressure loss due to friction up to that point. As the drag pressure at a distance from the filter cloth increases, even at constant filtering pressure, the porosity and resistance adjust themselves continuously. Figure 11.4(a) shows such effects of slurry concentration and filtering rates on the parameters of the correlating equation, the Almy–Lewis equation:

$$\alpha = \alpha_0(\Delta P)^n. \qquad (11.24)$$

The measurements were obtained with a small filter press. Clearly, the resistivity measured at a particular rate is hardly applicable to predicting performance at another rate or at constant pressure.

COMPRESSIBILITY–PERMEABILITY (CP) CELL MEASUREMENTS

The probable success of correlation of cake resistivity in terms of all the factors that have been mentioned has not been great enough to have induced any serious attempts of this nature, but the effect of pressure has been explored. Although the α's can be deduced from filtration experiments, as done in Example 11.1, a simpler method is to measure them in a CP cell as described briefly later in this chapter. Equation (11.24) for the effect of pressure was proposed by Almy and Lewis (1912). For the materials of Figure 11.4(b), for instance, it seems to be applicable over at least moderate stretches of pressure. Incidentally, these resistances are not represented well by the Kozeny porosity function $(1 - \varepsilon)/\varepsilon^3$; for substance 6, the ratio of resistivities at 100 and 1 psia is 22 and the ratio of the porosity functions is 2.6. The data of Table 11.7 also show a substantial effect of pressure on resistivity.

Since the drag pressure varies along the cake as a result of friction, porosity and resistivity also will vary with position. Figure 11.5(b) shows such data at three different overall pressures. The axial profile of the normalized pressure, P_{local}/P_{face}, appears to be a unique function of fractional distance along the cake, independent of the filtering pressure. The resistivity will vary along the cake just as the porosity does. As the cake builds up, moreover, the drag pressure, porosity, and resistivity at a particular distance from the filter medium also will vary. Consequently, since the resistivity does not necessarily change linearly with position, any mean value also is likely to vary as the cake builds up. Thus, in the filtration equation even a mean value of α has to be expressed as a function of P and V. The proper mathematical representation of a filtration process is by means of an integro-differential equation with a moving boundary (the face of the cake). Such an analysis was made by Wakeman (1978) and a similar one by Tiller, Crump, and Ville (1979). At present, unfortunately, such a mathematical approach to filtration problems is more of academic than practical value. One of the factors that is not taken into account is the effect of flow rate on the formation and stability of loose cake structures; such behavior normally is not reproducible.

ANOTHER FORM OF PRESSURE DEPENDENCE

Equation (11.24) cannot be entirely valid because it predicts zero resistivity at zero pressure, whereas cakes do have structures and significant resistivities even at minimal operating pressures. Modified Eq. (11.12) is extrapolatable, and is rewritten here as

$$\alpha = \alpha_0(1 + kP)^n \qquad (11.25)$$

with a similar one for porosity

$$\varepsilon = 1 - (1 - \varepsilon_0)(1 + kP)^n. \qquad (11.26)$$

Some data fitted to these equations by Tiller et al. (1979) are in Table 11.8; here the constant k is the same for both α and ε, although this is not necessarily generally the case. Unfortunately, these data show that the parameters are not independent of the pressure range. Apparently the correlation problem has not been solved. Perhaps it can be concluded that insofar as the existing filtration theory is applicable to real filtering behavior, the approximation of Almy and Lewis may be adequate over the moderate ranges or pressures that are used commonly, somewhere between 0.5 and 5 atm.
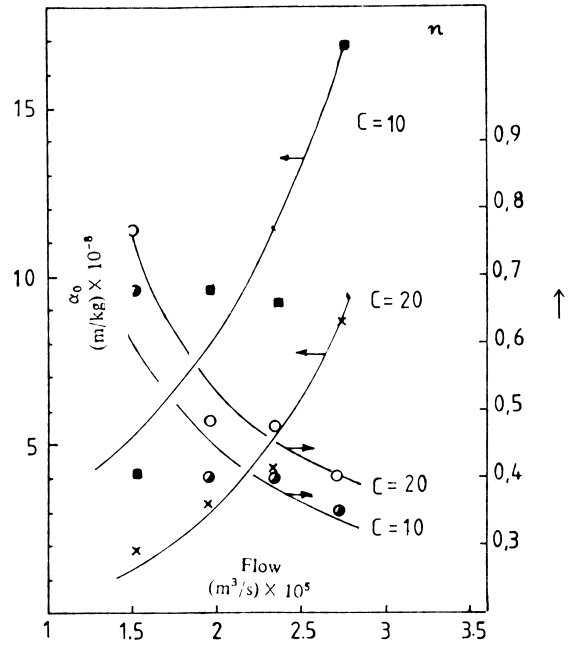
(a)
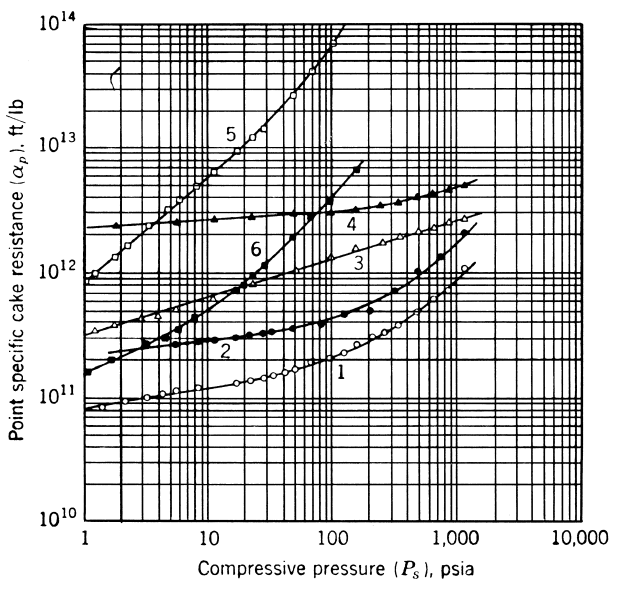
1—Superlite CaCO₃ (flocculated), pH = 9.8
2—Superlite CaCO₃, pH = 10.3
3—R-110 grade TiO₂ (flocculated), pH = 7.8
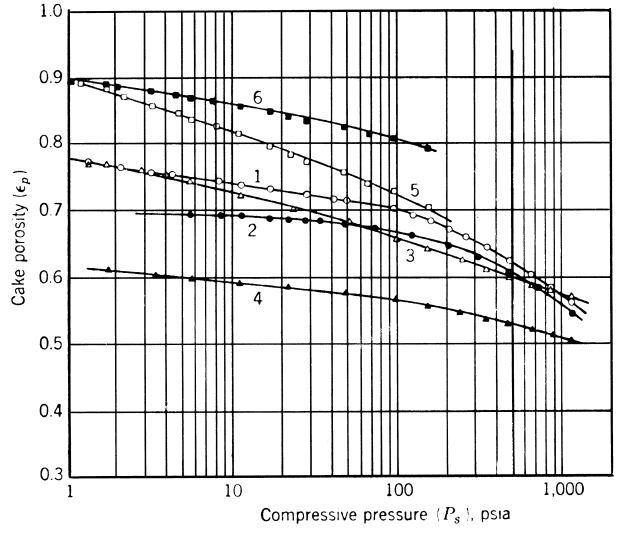
4—R-110 grade TiO₂, pH = 3.5
5—Zns, Type B, pH = 9.1
6—ZnS, Type A, pH = 9.1

(b)

(c)

Figure 11.4. Data of compressibilities and porosities of filter cakes. (a) Parameters of the correlation $\alpha = \alpha_0(\Delta P)^n$ for resistivity of $CaSiO_3$ filter cakes at two rates and two concentrations. (*Rushton and Katsoulas, 1984*). (b) Resistivity as a function of pressure measured in a compressibility-permeability (CP) cell. (Grace, 1953). (c) Porosity as a function of pressure for the same six materials. (Grace, 1953; Walas 1988).

TABLE 11.7. Specific Resistances of Some Filter Cakes

Material	Filtration Pressure psi	Resistance SI Units, m/kg
High grade kieselguhr	—	1.64×10^9
Ordinary kieselguhr	25	1.15×10^{11}
	100	1.31×10^{11}
Carboraffin charcoal	1.4	3.14×10^{10}
	10	5.84×10^{10}
Calcium carbonate	25	2.21×10^{11}
(precipitated)	100	2.68×10^{11}
Ferric oxide (pigment)	25	8.04×10^{11}
	100	14.12×10^{11}
Mica clay	25	4.81×10^{11}
	100	8.63×10^{11}
Colloidal clay	25	5.10×10^{12}
	100	6.47×10^{12}
Magnesium hydroxide	25	3.24×10^{12}
(gelatinous)	100	6.97×10^{12}
Aluminium hydroxide	25	2.16×10^{13}
(gelatinous)	100	4.02×10^{13}
Ferric hydroxide	25	1.47×10^{13}
(gelatinous)	100	4.51×10^{13}
Thixotropic mud	80	6.77×10^{14}
Theoretical figures for rigid spheres:		
$d = 10\,\mu m$	—	6.37×10^9
$d = 1\,\mu m$	—	6.37×10^{11}
$d = 0.1\,\mu m$	—	6.37×10^{13}

(Carman, 1938; Walas 1988).

PRETREATMENT OF SLURRIES

Since the sizes of particles and agglomerates of the slurry are a main determinant of a rate of filtration, any methods of influencing these sizes are of great practical value. For example, Figures 11.4(b) and 11.4(c) show $CaCO_3$ and TiO_2 each to be precipitated at two different values of pH with resultant great differences in resistivity and porosity. At 10 psia, for instance, the resistivities of the two $CaCO_3$'s are in the ratio of 5, with corresponding differences in rate of filtration. Pretreatment of a slurry to enhance coagulation and particle growth is an important aspect of filter process design. Another method of long standing for improving filtration behavior is the formation of an open cake structure by addition of relatively large and rigid particles of a filter aid. The common methods of pretreatment are listed in Table 11.4, and some chemical flocculants that are of practical value are described in Table 11.5. These effects cannot be predicted safely and must be measured.

11.5. THICKENING AND CLARIFYING

When dilute slurries are encountered on a large scale, it is more economical to concentrate them before filtering. This is accomplished by sedimentation or thickening in tanks for an appropriate period. Typical designs of thickeners are sketched in Figure 11.6. The slurry is introduced at the top center, clear liquid overflows the top edge, whereas the solids settle out and are worked gradually towards the center with slowly rotating rakes towards the discharge port at the bottom center. The concentrated slurry then is suitable

(a)

(b)
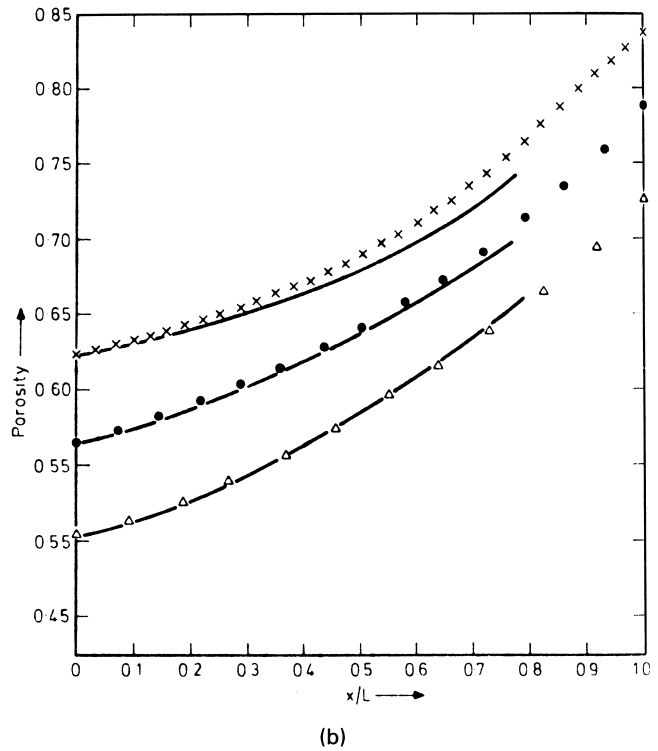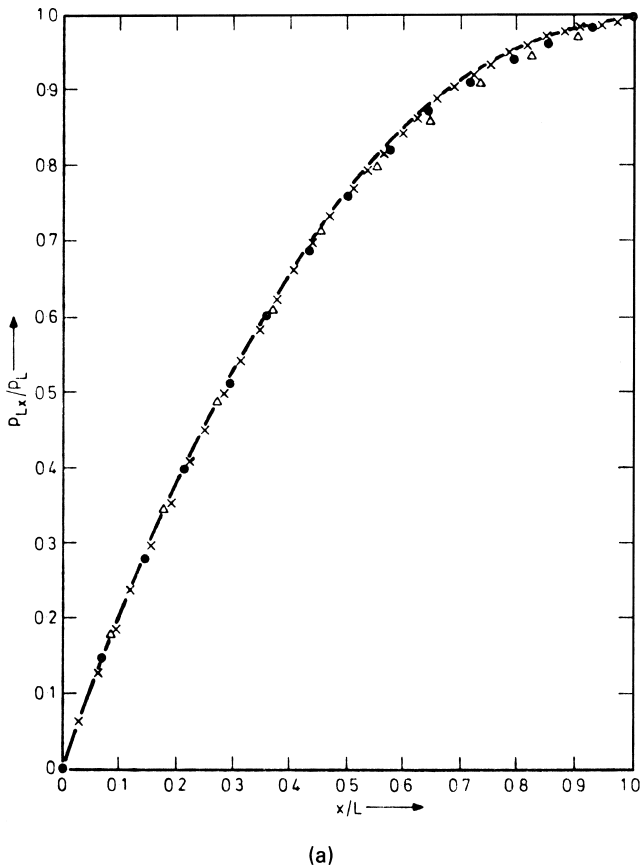
Figure 11.5. Axial distribution of pressure and porosity of an ignition-plug clay measured in a CP cell. (a) Normalized pressure distribution a function of normalized distance [(----) experimental filtration data; theoretical curves: $(\times)\ \Delta P = 98\,\text{kNm}^{-2}$; $(\bullet)\ \Delta P = 294\,\text{kNm}^{-2}$; $(\triangle)P = 883\,\text{kNm}^{-2}$]. (b) Porosity distributions at three pressures. The curves are by Wakeman (1978). (Walas, 1988).

TABLE 11.8. Parameters of Equations for Resistivity α and Porosity ϵ of Some Filter Cakes

$$\alpha = \alpha_0 \left(1 + \frac{p_s}{p_a}\right)^n$$

$$(1 - \varepsilon) = (1 - \varepsilon_0)\left(1 + \frac{p_s}{p_a}\right)^{\beta*}$$

Material	Pressure range, kPa	p_a, kPa	α_0, m kg^{-1} × 10^{-10}	n	$(1-\varepsilon_0)$	β^*
CaCO$_3$ (ref. 7)	3–480	1	11	0.15	0.209	0.06
CaCO$_3$ (ref. 8)	7–550	7	5.1	0.2	0.225	0.06
	550–7000	790	8.1	0.9	0.263	0.22
Darco-B (ref. 8)	7–275	1.7	1.1	0.4	0.129	0.08
	275–7000	520	4.7	1.8	0.180	0.18
Kaolin-Al$_2$SO$_4$ (ref. 8)	7–415	7	43	0.3	0.417	0.04
	415–7000	345	87	0.7	0.460	0.12
Solka-Floc (ref. 8)	7–275	2.75	0.00058	1.0	0.132	0.16
	275–7000	260	0.13	2.0	0.237	0.26
Talc-C (ref. 8)	7–1400	5.5	4.7	0.55	0.155	0.16
	1400–7000	1400	35	1.8	0.339	0.25
TiO$_2$ (ref. 8)	7–7000	7	18	0.35	0.214	0.1
Tungsten (ref. 8)	7–480	7	0.39	0.15	0.182	0.05
	480–7000	520	0.38	0.9	0.207	0.22
Hong Kong	1–15	1	42	0.35	0.275	0.09
pink kaolin (ref. 9)	15–1000	12	70	0.55	0.335	0.1
Gairome clay (ref. 10)	4–1000	3.4	370	0.55	0.309	0.09

(Tiller et al, 1979; Walas, 1988).

for filtration or other further processing. Clarifiers are similar devices, primarily for recovering clear liquids from dilute suspensions. Some characteristics of sedimentation equipment are given in Table 11.3 and typical applications are listed in Tables 11.9. Sedimentation rates often are assisted by addition of flocculating agents, some of which are listed in Table 11.5. Specifically, pilot plant testing is advisable when

1. The expecting filtering area is expected to be substantial, measured in tens of m^2.
2. Cake washing is critical.
3. Cake drying is critical.
4. Cake removal may be a problem.
5. Precoating may be needed.

11.6. LABORATORY TESTING AND SCALE-UP

Laboratory filtration investigations are of three main kinds:

1. observation of sedimentation rates;
2. with small vacuum or pressure leaf filters;
3. with pilot plant equipment of the types expected to be suitable for the plant.

Sedimentation tests are of value particularly for rapid evaluation of the effects of aging, flocculants, vibration, and any other variables that conceivably could affect a rate of filtration. The results may suggest what kinds of equipment to exclude from further consideration and what kind is likely to be worth investigating. For instance, if sedimentation is very rapid, vertical leaves are excluded, and top feed drums or horizontal belts are indicated; or it may be indicated that the slurry should be preconcentrated in a thickener before going to filtration. If the settling is very slow, the use of filter aids may be required, etc. Figure 11.1 illustrates typical sedimentation behavior. Figure 11.2 summarizes an experimental routine.

Vacuum and pressure laboratory filtration assemblies are shown in Figure 11.7. Mild agitation with air sometimes may be preferable to the mechanical stirrer shown, but it is important that any agglomerates of particles be kept merely in suspension and not broken up. The test record sheet of Figure 11.8 shows the kind of data that normally are of interest. Besides measurements of filtrate and cake amounts as functions of time and pressure, it is desirable to test washing rates and efficiencies and rates of moisture removal with air blowing. Typical data of these kinds are shown in Figure 11.3. Detailed laboratory procedures are explained by Bosley (1977) and Dahlstrom and Silverblatt (1977). Test and scale-up procedures for all kinds of SLS equipment are treated in the book edited by Purchas (1977).

Before any SLS equipment of substantial size is finally selected, it is essential to use the results of pilot plant tests for guidance. Although many vendors are in a position to do such work, pilot equipment should be used at the plant site where the slurry is made. Because slurries often are unstable, tests on shipments of slurry to the vendors pilot plant may give misleading results. It may be possible to condition a test slurry to have a maximum possible resistivity, but a plant design based on such data will have an unknown safety factor and may prove uneconomical.

COMPRESSION–PERMEABILITY CELL

Such equipment consists of a hollow cylinder fitted with a permeable bottom and a permeable piston under controlled pressure. Slurry is charged to the CP cell, cake is formed with gentle suction, and the piston is lowered to the cake level. The rate of flow of filtrate at low head through the compressed cake is measured at a series of pressures on the piston. From the results the resistivity of the cake becomes known as a function of pressure. The data of Figures 11.4(b) and (c) were obtained this way; those of Figure 11.4(a) by filtration tests.
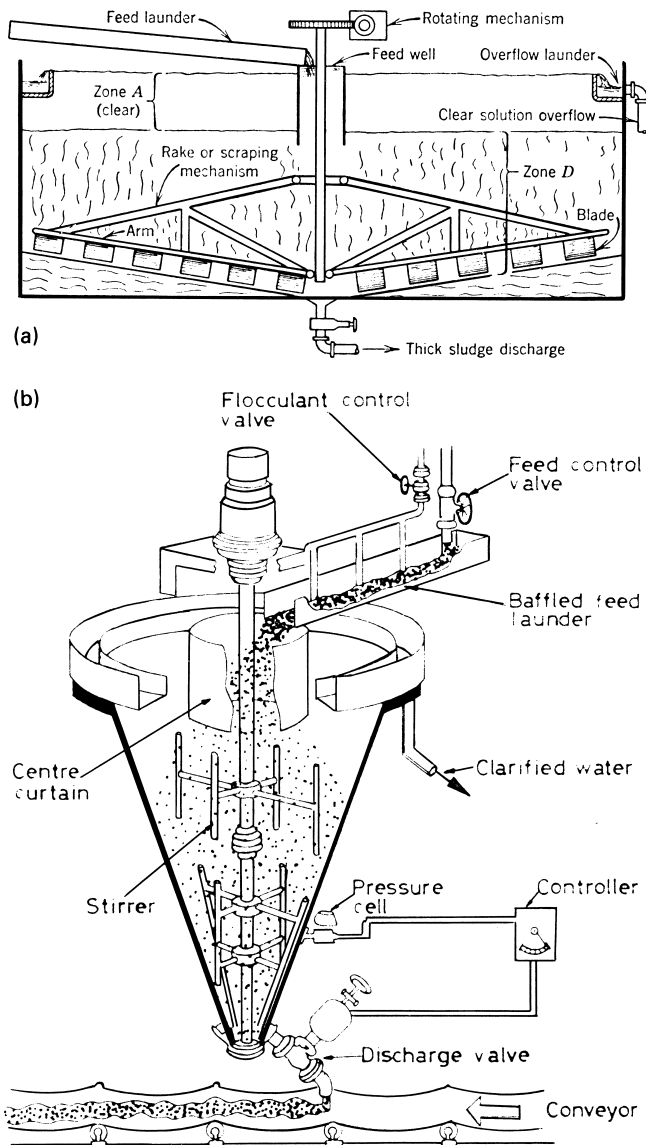
Figure 11.6. Thickeners for preconcentration of feed to filters or for disposal of solid wastes [see also the rake classifier of Fig. 12.2(e)]. (a) A thickener for concentrating slurries on a large scale. The rakes rotate slowly and move settled solids towards the discharge port at the center. Performance data are in Table 11.11. (*Brown, 1950*). (b) Deep cone thickener developed for the National Coal Board (UK). In a unit about 10 ft dia the impellers rotate at about 2 rpm and a flow rate of 70 m³/sec with a solids content of 6 wt %, concentrates to 25–35 wt %. (*Svarousky, 1981*; Walas, 1988).

There is much evidence, however, that the resistivity behavior of a cake under filtration conditions may be different from that measured in a CP cell. The literature is reviewed by Wakeman (1978). CP cell data are easily obtained and may be of value in a qualitative sense as an indication of the sensitivity of resistivity to pressure, but apparently are not of acceptable engineering accuracy for the design of filtration equipment. The deduction of resistivities from filtration tests is illustrated in Example 11.1.

THE STANDARD CAKE FORMATION TIME CONCEPT (SCFT)

No serious attempt has yet been made to standardize filtration tests and to categorize filtration behavior in generally accepted terms. A possibly useful measure of filterability, however, has been proposed by Purchas (1977; 1981). The time in minutes required to form a cake 1 cm thick when the cell is operated with a differential of 500 Torr (0.67 bar) is called the Standard Cake Formation Time (SCFT), t_F. The pressure of 500 Torr is selected because it is obtained easily with common laboratory equipment. The procedure suggested is to make a series of tests at several cake thicknesses and to obtain the SCFT by interpolation, rather than to interrupt a single test to make observations of cake thickness. A direct relation exists, of course, between the SCFT and resistivity α; some examples are

Material	α (m/kg)	SCFT t_F (min)
Filter aid	1.64(E9)	0.26
CaCO$_3$	2.21(E11)	34.6
Colloidal clay	5.10(E12)	798

Full scale filtration equipment requirements can be estimated quickly in terms of t_F. For instance, when the resistance of the filter medium is neglected, the constant pressure Eq. (11.3) may be written as

$$\Delta Pt = \frac{\alpha c}{2}\left(\frac{V}{A}\right)^2 = \frac{\alpha c}{2}\left[\frac{(1-\varepsilon)L}{c}\right]^2, \tag{11.27}$$

where L is the thickness of the cake in meters. Upon rationing in the SCFT data for 0.01 m,

$$\frac{\Delta Pt}{0.67 t_F} = (100L)^2, \tag{11.28}$$

with ΔP in bar. From this relation the filtering time, t, minutes, can be found at a specified pressure and cake thickness and when t_F is known.

SCALE-UP

Sizing of full-scale equipment on the basis of small-scale tests requires a consideration of possible ranges of at least the following variables:

1. filterability as measured by cake and medium resistivity;
2. feed rate and concentration;
3. operating conditions, particularly pressure and high initial rates;
4. behavior of the filter cloth with time.

Safety factors for scale up from laboratory leaf tests are difficult to generalize. On the basis of pilot plant work, adjustments of 11–21% are made to plate-and-frame filter areas or rates, and 14–20% to continuous rotary filters.

The performance of solid–liquid separation equipment is difficult to predict by the engineer without some specific experience in this area. Unfortunately, it must be again recommended that the advice of experienced vendors should be sought, as well as that expert consultants.

11.7. ILLUSTRATIONS OF EQUIPMENT

Equipment for solid–liquid separation is available commercially from many sources. The names and addresses of suppliers in the United States and abroad are listed by Purchas (1981).

TABLE 11.9. Performances of Sedimentation Equipment

(a) Thickeners[a]

	% solids		Unit area, sq. ft./ton day
	Feed	Underflow	
Alumina, Bayer process:			
Red-mud primary settlers	3–4	10–25	20–30
Red-mud washers	6–8	15–20	10–15
Red-mud final thickener	6–8	20–35	10–15
Trihydrate seed thickener	2–8	30–50	12–30
Cement, West process	16–20	60–70	15–25
Cement kiln dust	9–10	45–55	3–18
Coral	12–18	45–55	15–25
Cyanide slimes	16–33	40–55	5–13
Lime mud:			
Acetylene generator	12–15	30–40	15–33
Lime-soda process	9–11	35–45	15–25
Paper industry	8–10	32–45	14–18
Magnesium hydroxide from brine	8–10	25–50	60–100
Metallurgical (flotation or gravity concentration):			
Copper concentrates	14–50	40–75	2–20
Copper tailings	10–30	45–65	4–10
Lead concentrates	20–25	60–80	7–18
Zinc concentrates	10–20	50–60	3–7
Nickel:			
Leached residue	20	60	8
Sulfide concentrate	3–5	65	25
Potash slimes	1–5	6–25	40–12
Uranium:			
Acid leached ore	10–30	25–65	2–10
Alkaline leached ore	20	60	10
Uranium precipitate	1–2	10–25	50–12

(b) Clarifiers

Application	Overflow rate, gal./min., sq. ft.	Detention tin hr.
Primary sewage treatment (settleable-solids removal)	0.4	2
Secondary sewage treatment (final clarifiers—activated sludge and trickling filters)	0.55–0.7	1.5–2
Water clarification (following 30-min. flocculation)	0.4–0.55	3
Lime and lime-soda softening (high rate—upflow units)	1.5	2
Industrial wastes	Must be tested for each application	

[a] See also Table 14.7.
(*Perry,* 1963) (Walas, 1988)

Classifications of vendors with respect to the kind of equipment are given in *Chemical Engineering Buyers' Guide* (2004).

The variety of solid–liquid separation equipment is so great that only a brief selection can be presented here. The most extensive modern picture gallery is in the book of Purchas 1981. The older encyclopedia of Kieser (Spamer-Springer, Berlin, 1937, Vol. 2) has 250 illustrations in 130 pages of descriptions; the pictures do not appear to have aged particularly. Illustrations in manufacturers catalogs are definitive and often reveal the functioning as well as aspect of the equipment. The selected figures of this chapter are primarily line drawings that best reveal the functioning modes of the equipment.

(a)

(b)
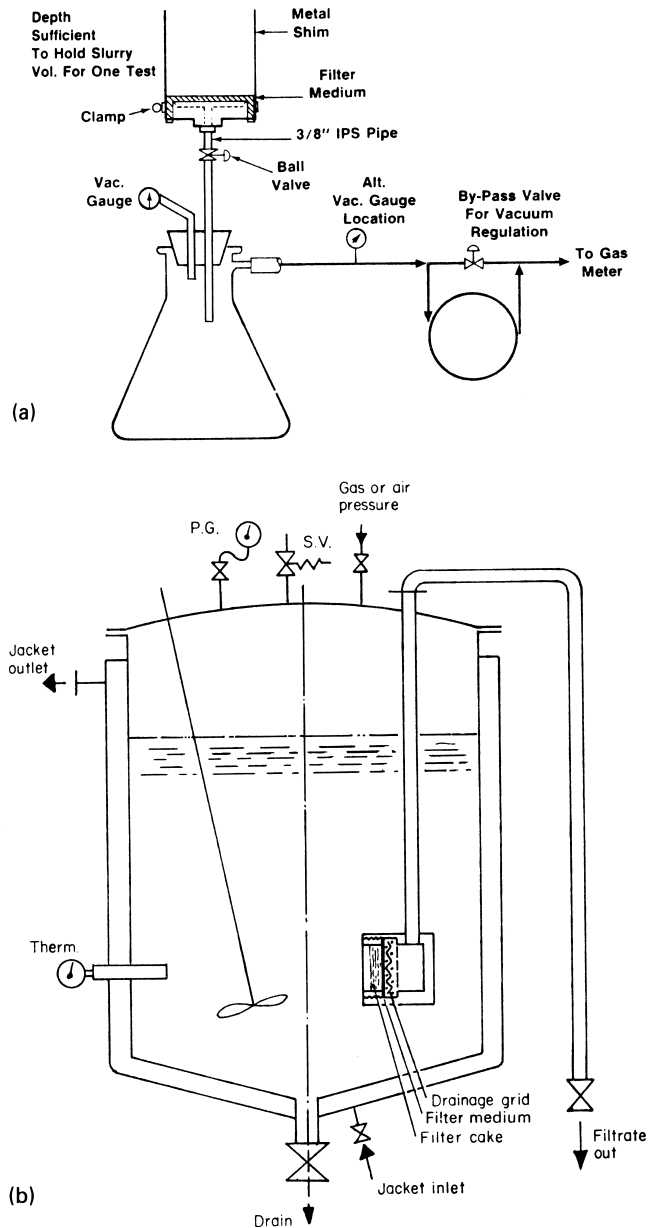
Figure 11.7. Two types of laboratory filter arrangements. (a) Vacuum test filter arrangement; standard sizes are 0.1, 0.05, or 0.025 sqft. (*Dahlstrom and Silverblatt, 1977*). (b) Laboratory pressure filter with a vertical filtering surface and a mechanical agitator; mild air agitation may be preferred. (*Bosley, 1977*; Walas, 1988).

Figure 11.9 shows two models of sand filters whose purpose is to remove small contents of solids from large quantities of liquids. City water plants often use large-scale sand filters for this application. The solids deposit both on the surface of the bed and throughout the bed. They are removed intermittently by shutting off the main flow and backwashing with liquid. The concentrated sludge then must be disposed of in accordance with environmental regulations. Beds of charcoal are employed similarly for clarification of some organic liquids; they combine adsorption and mechanical separation.

Clarification of a large variety of liquids is accomplished with cartridge filters which come in a large variety of designs. Usually

FILTRATION LEAF TEST DATA SHEET — VACUUM AND PRESSURE

Company _____ Mat'l as Received: Date _____ Test No. _____
Address _____ Solids: _____ % Date Tested _____
_____ Analysis _____ By _____
_____ Liquid: _____ % Location _____
Filter Type _____ Leaf Size _____ Ft.² Analysis _____
Used Shim: No _____ Yes _____ Precoat Forming Liquid _____ Temp. _____ °F/°C

Run No.	Filter Media and/or Precoat Type	Feed Temp., °F/°C	% Solids in Feed		Vacuum - in. Hg. Pressure - PSI.				TIME MIN.				Air Flow		Filtrate			Wash				Cake Weights			
			As Prepared	Back Calculated	Form	Wash	Dry	After Cake Cracks	Form	Dewater	Wash	Dry	To Crack or Gas Breakthrough After Form Wash	(1) Temp., °F °C	ML.	Clarity	Precoat Penetration	ML.	Temp., °F/°C	Cake/Precoat Thickness, In.	Dia. of Shaved Area, in.	Tare GMS.	Wet & Tare GMS.	Dry & Tare GMS.	Dish No.

CAKE DISCHARGE		REAGENT TREATMENT	
RUNS	COMMENT	RUNS	COMMENT

REMARKS: (1) Record Basis of Observation in Space Provided.

Figure 11.8. A filtration leaf test data sheet. (*Dahlstrom and Silverblatt, 1977*; Walas, 1988).

(a)   (b)

Figure 11.9. Deep bed sand filters for removal of small contents of solids from large quantities of liquids. Accumulations from the top and within the bed are removed by intermittent backwashing. Charcoal may be used instead of sand for clarifying organic liquids. (a) Gravity operation. (b) Pressure operation. (Walas, 1988).

the cartridges are small, but liquid rates in excess of 5000 gpm have been designed for. The filtering surface may be a fine metal screen or an assembly of closely spaced disks whose edge face functions as the filtering surface, or woven or matted fibers. The operation is intermittent, with either flushing back of the accumulated solids or replacement of the filtering elements in the body of the cartridge, or in some instances the solids are scraped off the filtering surface with a built-in mechanism and then flushed out in concentrated form. The variety of cartridge filters are described in detail in books by Warring (1981), Purchas (1981), and Cheremisinoff and Azbel (1983). Table 11.10 is a selected list of some of their applications and the minimum sizes of particles that are removed.

Figure 11.6 is of two types of sedimentation equipment, and Figure 12.2(e) of another. They are used for clarifying a valuable liquid or for preparing a concentrated slurry for subsequent filtration. They depend on gravitational sedimentation. Removal is assisted by rake action, or by the conical sides of the vessel of Figure 11.6(b).

Figure 11.10 is of the main kinds of filters that can be operated at superatmospheric pressures which may be necessary with otherwise slow filtering slurries. Commercial sizes are listed in Table 11.11. They all operate on intermittent cycles of cake formation, washing, dewatering with air blowing and cake removal. The plate-and-frame design of Figure 11.10(a) is the most widely recognized type. In it, cake removal is effected after separating the plates. The horizontal plate design of Figure 11.10(b) is popular in smaller sizes under, 2 ft dia or so; the plates are lifted out of the casing for cake removal. The other units all have fixed spacings between the leaves. From them the cakes may be blown back with air or flushed back or scraped off manually. The Vallez unit of Figure 11.10(f) ordinarily does not require the case to be opened for cleaning.

Figure 11.11 is of continuous horizontal filtering equipment that operate primarily with vacuum, although they could be housed in pressure-tight casings for operation at superatmospheric pressure or with volatile liquids. Both the belt and the rotary units are well suited to rapidly settling and free draining slurries. In comparison with rotary drum vacuum filters, the horizontal equipment of Figure 11.11(c) has the merit of more readily accessible piping, a real advantage from a servicing point of view.

Figure 11.12 represents the main kinds of rotary drum filters. Commercial sizes are listed in Table 11.14. The flowsketch of Figure 11.12(a) identifies the main auxiliaries required for this kind of filtration process. Feed to the drum may be dip-type as in Figure 11.12(b), but top feed designs also are widely used. The unit with internal filtering surface of Figure 11.12(c) is suited particularly to rapidly settling solids and has been adapted to pressure operation.

Cake removal usually is with a scraper into a screw or belt conveyor, but Figure 11.12(d) depicts the use of a drum with a filtering belt that is subject to a continual cleaning process. Some filters have a multi parallel string discharge assembly whose path follows that of the belt shown.

The double drum filter of Figure 11.12(e) has obvious merit particularly when top feeding is desirable but it is only infrequently used nowadays. Disk filters of the type of Figure 11.12(f) are the most widely used rotary type when washing of the cake is not necessary.

Figure 11.13 is of a variety of devices that utilize centrifugal force to aid in the separation of solid and liquid mixtures. Figure 11.13(a) performs cake removal at reduced rotating speed, whereas the design of Figure 11.13(d) accomplishes this operation without slowing down. The clarifying centrifuge of Figure 11.13(e) is employed for small contents of solids and is cleaned after shutdown. The units of Figures 11.13(b) and (c) operate continuously,

TABLE 11.10. Application of Cartridge Filters in Industry and Typical Particle Size Ranges Removed

Industry and Liquid	Typical Filtration Range
Chemical Industry	
Alum	60 mesh–60 μm
Brine	100–400 mesh
Ethyl Alcohol	5–10 μm
Ferric Chloride	30–250 mesh
Herbicides/Pesticides	100–700 mesh
Hydrochloric Acid	100 mesh to 5–10 μm
Mineral Oil	400 mesh
Nitric Acid	40 mesh to 5–10 μm
Phosphoric Acid	100 mesh to 5–10 μm
Sodium Hydroxide	1–3 to 5–10 μm
Sodium Hypochlorite	1–3 to 5–10 μm
Sodium Sulfate	5–10 μm
Sulfuric Acid	250 mesh to 1–3 μm
Synthetic Oils	25–30 μm
Petroleum Industry	
Atmospheric Reduced Crude	25–75 μm
Completion Fluids	200 mesh to 1–3 μm
DEA	250 mesh to 5–10 μm
Deasphalted Oil	200 mesh
Decant Oil	60 mesh
Diesel Fuel	100 mesh
Gas Oil	25–75 μm
Gasoline	1–3 μm
Hydrocarbon Wax	25–30 μm
Isobutane	250 mesh
MEA	200 mesh to 5–10 μm
Naphtha	25–30 μm
Produced Water for Injection	1–3 to 15–20 μm
Residual Oil	25–50 μm
Seawater	5–10 μm
Steam Injection	5–10 μm
Vacuum Gas Oil	25–75 μm
All Industries	
Adhesives	30–150 mesh
Boiler Feed Water	5–10 μm
Caustic Soda	250 mesh
Chiller Water	200 mesh
City Water	500 mesh to 1–3 μm
Clay Slip (ceramic and china)	20–700 mesh
Coal-Based Synfuel	60 mesh
Condensate	200 mesh to 5–10 μm
Coolant Water	500 mesh
Cooling Tower Water	150–250 mesh
Deionized Water	100–250 mesh
Ethylene Glycol	100 mesh to 1–3 μm
Floor Polish	250 mesh
Glycerine	5–10 μm
Inks	40–150 mesh
Liquid Detergent	40 mesh
Machine Oil	150 mesh
Pelletizer Water	250 mesh
Phenolic Resin Binder	60 mesh
Photographic Chemicals	25–30 μm
Pump Seal Water	200 mesh to 5–10 μm
Quench Water	250 mesh
Resins	30–150 mesh
Scrubber Water	40–100 mesh
Wax	20–200 mesh
Wellwater	60 mesh to 1–3 μm

(Courtesy of Ronningen Petter Corp., Portage, MI; Cheremisinoff and Azbel, 1983; Walas, 1988).

(a)

(b)

(c)

(d)
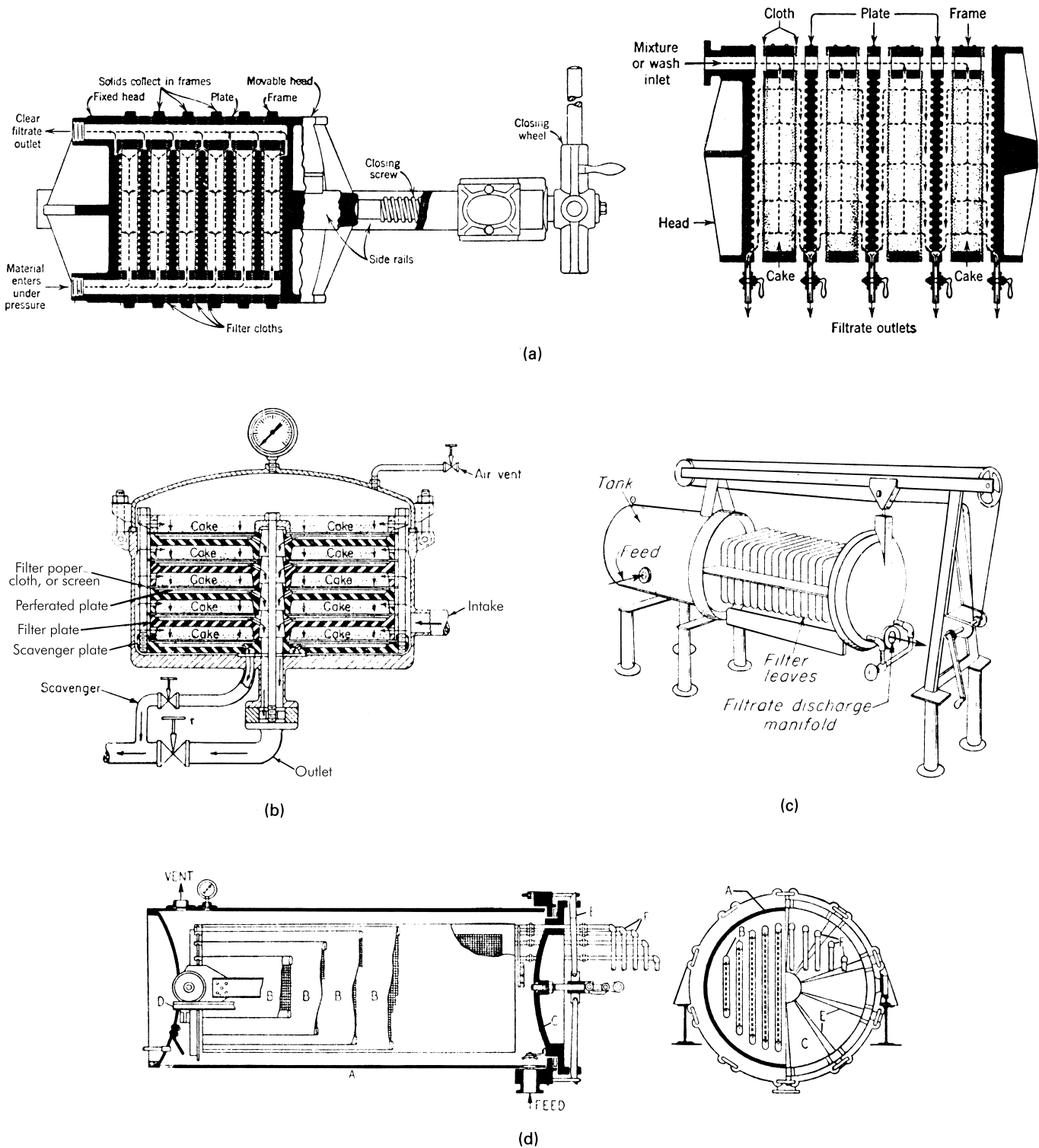
Figure 11.10. Pressure filters for primarily discontinuous operation. (a) Classic plate-and-frame filter press and details; the plates are separated for manual removal of the cake. (*T. Shriver Co.*). (b) Horizontal plate filter; for cleaning, the head is removed and the plates are lifted out of the vessel. (*Sparkler Mfg. Co.*). (c) Pressure leaf filter; the leaf assembly is removed from the shell and the cake is scraped off without separating the leaves (*Ametek Inc.*). (d) The Kelly filter has longitudinal leaves mounted on a carriage; for cleaning, the assembly is slid out of the shell. (*Oliver United Filters*). (e) The Sweetland filter has circular leaves and a split casing; the lower half of the casing is dropped to allow access for removal of the cake. (*Oliver United Filters*). (f) The Vallez filter has circular leaves rotating at about 1 rpm to promote cake uniformity when the solids have a wide size range; removal of blown-back or washed back cake is accomplished with a built-in screw conveyor without requiring the shell to be opened. (*Goslin–Birmingham Co.*). (g) Cartridge filter (Walas, 1988).
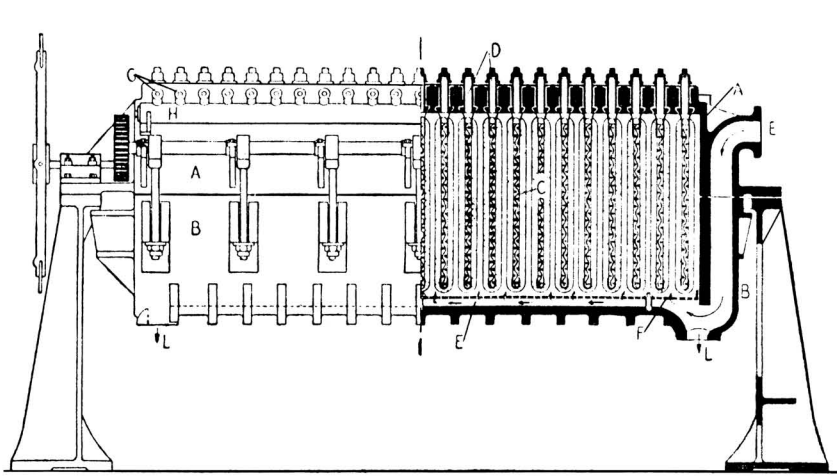
(e)
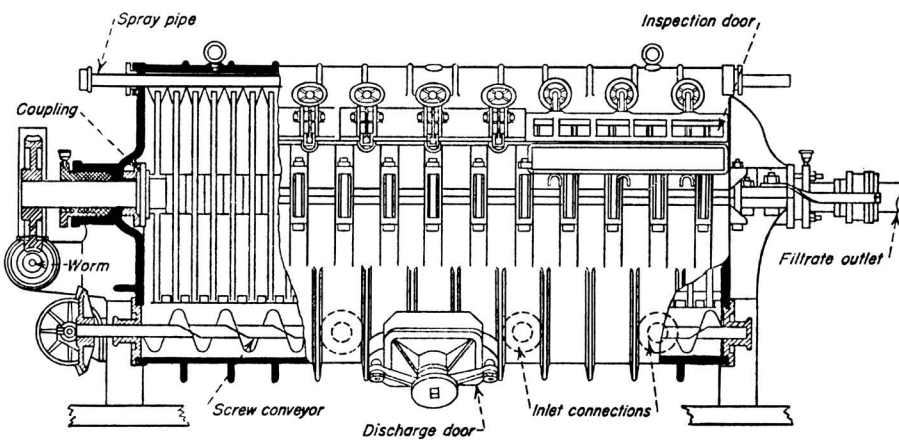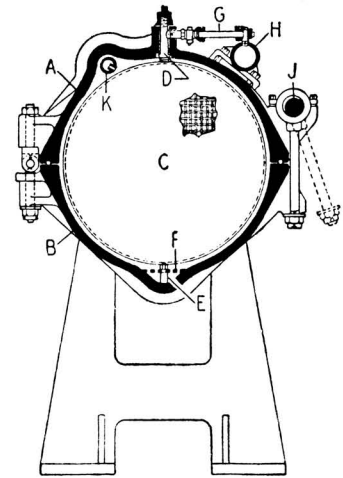
(f)

(g) Courtesy of Cuno, Inc.

Figure 11.10. —(*continued*)
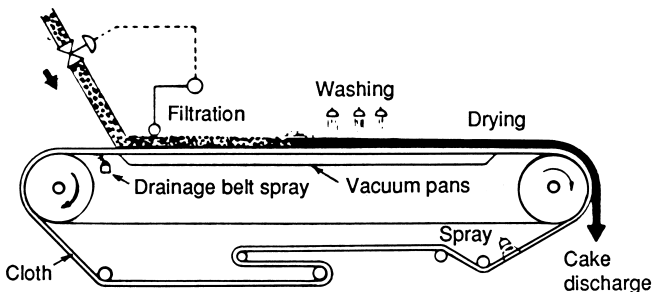
(a)
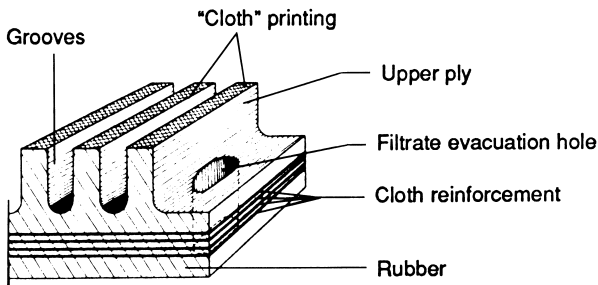
(b)
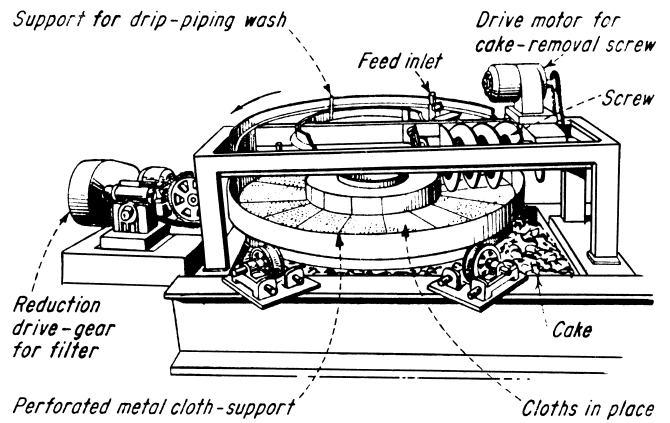
(c)

Figure 11.11. Continuous horizontal vacuum filters especially suited to free settling and draining solids. (a) Principle of the conveyor belt filter; units may operate up to 0.5 m/sec with a cycle time up to 10 min and produce cake thicknesses up to 15 cm. (b) Showing the construction of a grooved rubber belt support for the filter cloth of the belt filter. (*Purchas, 1981*). (c) Rotating horizontal vacuum filter; the unit has readily accessible piping and is amenable to thorough washing of free draining solids (*Dorr–Oliver Inc.*; Walas, 1988).

TABLE 11.11. Sizes of Commercial Discontinuous Pressure Filters

(a) Approximate Area and Cake Capacity for Various Sizes of Plate and Frame Filters

Size of filter plate (mm)	Effective Filtration area per Chamber (m^2)		Cake-Holding Capacity per Chamber per 25 mm of Chamber Thickness *l*	
	Cast Iron	Wood	Cast Iron	Wood
250	0.096	0.054	1.2	0.6
360	0.2	0.123	2.5	1.43
470	0.35	0.21	4.4	2.5
630	0.66	0.45	8.3	5.4
800	1.1	0.765	13.7	9.3
1000	1.74	1.2	21.62	14.6
1200	2.5	1.76	31.4	21.36
1450	3.7	2.46	46.24	30.2

(b) Sizes of Kelly Filters (in.)

	30 × 49	40 × 108	48 × 120	60 × 108
Number of frames	6	8	10	12
Spacing between frames (in.)	4	4	4	4
Filter area (sqft)	50	250	450	650

(c) Standard Sweetland Filter

No.	ID[b] (in.)	Length of Shell (in.)	No. Leaves 2 in. Space	No. Leaves 4 in. Space	Filter Area 2 in. Spacing (sqft)	Filter Area 4 in. Spacing (sqft)	Total Weight[c] of Filter (lbs)
1	10	$20\frac{1}{2}$	9	5	8	$4\frac{1}{2}$	550
2	16	$36\frac{1}{2}$	18	9	46	23	2150
5	25	61	30	15	185	92	7300
7	25	82	41	20	252	123	9350
10	31	109	54	27	523	262	16500
12	37	145	72	36	1004	502	29600

(d) Vallez Filter (Largest Size Only, 20 ft Long, 7 ft high, 7 ft wide)[d]

Spacing of Leaves (in.)	No. of Leaves	O.D. of Leaf (in.)	Filter Area (sqft)	Cake Capacity (cuft)
3	52	52	1232	65
4	39	52	924	72
5	31	52	734	79
6	23	52	646	92

(e) Characteristics of Typical Vertical-Tank Pressure Leaf Filters[e]

Tank Diam (in.)	Filter Area (sqft)	No. of Leaves	Leaf Spacing (in.)	Max. Cake Capacity (cuft)	Tank Volume (gal)	Approx. Overall Height (ft)	Approx. Shipping Weight (lb)
18	19	5	3	1.8	38	5.5	625
18	24	5	3	2.3	45	6.0	650
18	27	7	2	1.7	38	5.5	650
18	35	7	2	2.2	45	6.0	675
30	80	9	3	7.2	128	6.5	1125
30	95	9	3	8.7	132	7.0	1200
30	110	12	2	6.6	128	6.5	1180
30	125	12	2	8.0	132	7.0	1275
48	320	16	3	30.0	435	8.8	2900
48	370	16	3	35.0	500	9.3	3050
48	440	21	2	28.0	435	8.8	3125
48	510	21	2	32.0	500	9.3	3325

[a] F. H. Schule, Ltd.
[b] Diameter of leaf 1 in. less.
[c] Filled with water.
[d] There are smaller sizes with leaves the outside diameters of which are $44\frac{1}{2}$, 36, 30, and 22 in.; for the 30 in. leaves, four lengths of shell are available.
[e] T. Shriver & Co., Inc.

Hydrocyclones generate their own, mild centrifugal forces. Since the acceleration drops off rapidly with diameter, hydrocyclones are made only a few inches in diameter. For large capacities, many units are used in parallel. The flow pattern is shown schematically in Figure 11.13(f). The shapes suited to different applications are indicated in Figure 11.13(g). In Fig. 11.13(h), the centrifugal action in a hydrocyclone is assisted by a high speed impeller. This assistance, for example, allows handing of 6% paper pulp slurries in comparison with only 1% in unassisted units. Hydrocyclones are perhaps used much more widely for separation than for slurries.

There are certain parameters that influence the ability of a hydroclone to perform a separation. These are particle size, particle shape, solids loading, inlet velocity, the split desired between underflow (solids discharge) and overflow (liquid discharge), density of solids and liquid, as well as liquid viscosity. Day (1973) published a performance plot incorporating particle size, viscosity of the fluid phase, specific gravity differences between liquid and solid, and feed conditions. It is suggested that this plot be used only as a preliminary guide and that final sizing of a hydroclone be determined by tests on the proposed slurry and consultation with an equipment vendor (Jacobs and Penney, 1987). Salcudean et al. (2003) suggested that modeling and simulation of hydroclone behavior can significantly reduce design and operation uncertainties.

11.8. APPLICATIONS AND PERFORMANCE OF EQUIPMENT

Data of commercially available sizes of filtration equipment, typical applications, and specific performances are available only to a limited extent in the general literature, but more complete in manufacturers' literature. Representative data are collected in this section and summarized in tabular form. One of the reasons why more performance data have not been published is the difficulty of describing each system concisely in adequate detail. Nevertheless, the limited listings here should afford some perspective of the nature and magnitude of some actual and possibly potential applications.

the former with discharge of cake by a continuous helical screw, the latter by a reciprocating pusher mechanism that operates at 30–70 strokes/min and is thus substantially continuous.

Table 11.13 is a list of typical applications of industrial filters and Table 11.15 contains performance data for horizontal belt filters.

Hydroclones were introduced in 1891 to remove sand from water. They function like a gas-solid cyclone, have no moving parts, and rely on centrifugal force for separation, clarification, and dewatering processes. Hydroclones find use in concentrating slurries, in classifying solids in liquid suspensions, and in washing solids. They may be used alone or in conjunction with clarifiers, thickeners, or filters (Besendorfer, 1996).

(a)

(b)

(c)

Figure 11.12. Continuous rotary drum filters. (a) Flowsketch of continuous vacuum filtration with a rotary drum filter. The solids are taken away with a screw or belt conveyor. (*McCabe and Smith, 1956*). (b) Cross section of a dip-type rotary drum filter showing the sequence of cake formation, washing, dewatering and cake removal; units also are made with top feed. (*Oliver United Filters*). (c) Cross section of a rotary drum filter with internal filtering surface, suited particularly to free settling slurries. (*Oliver United Filters*). (d) Rotary filter with a filtering belt that is discharged and cleaned away from the drum; in the similarly functioning string discharge filters, the filtering cloth remains on the drum but the string assembly follows the path shown here for the belt. (e) Double drum filter, particularly suited to rapidly settling slurries, and may be adapted to cake washing which is not shown in this unit. (*System Gerlach, Nordhausen, E. Germany*). (f) Vacuum disk filter, the main kind in use when cake washing is not required. (*Dorr–Oliver Inc.*; Walas, 1988).
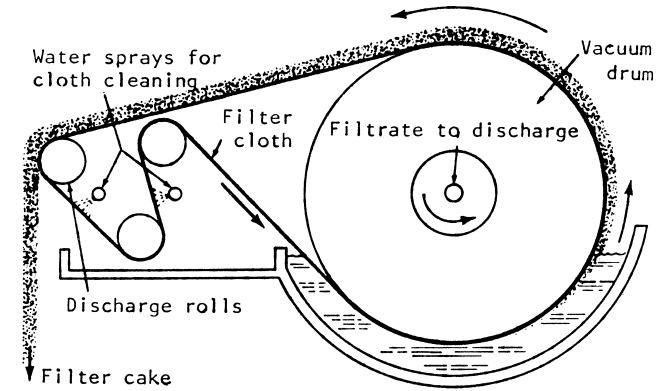
(d)
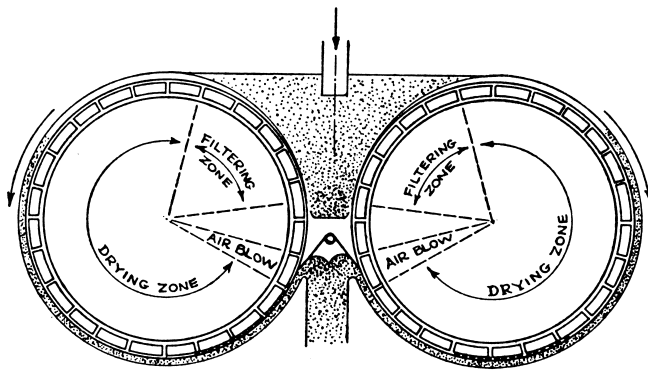
(e)
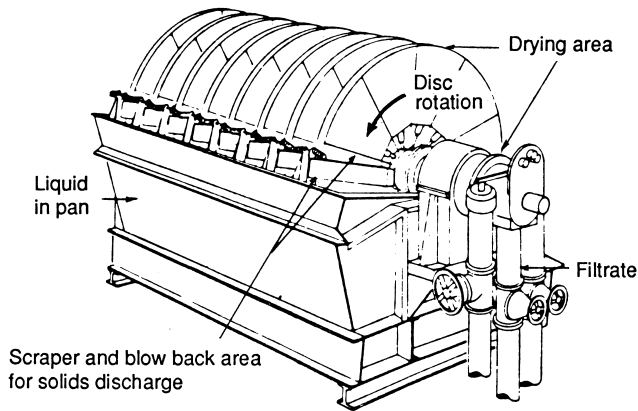
(f)

Figure 11.12. —(*continued*)

TABLE 11.12. Sizes of Commercial Continuous Vacuum Filters

(a) Horizontal Belt Filters[a]

Series	Ft² Range	No. Vac. Pans
2600	10–45	1
4600	45–200	1
6900	150–700	1
9600	130–500	2
13,600	600–1200	2

(Eimco).

(b) Rotary Drum, Disk, and Horizontal Filters

Rotary Drum Component Filters[b]

Filter Surface Area (sqft)

Drum[c] Diam (ft)	Length (ft)										
	4	6	8	10	12	14	16	18	20	22	24
6	76	113	151	189	226						
8			200	250	300	350	400				
10				310	372	434	496	558	620		
12					456	532	608	684	760	836	912

Disk Component Filters[d]

Disk diam (ft)[e]	6	7	8	9	10	11
Number of disks						
Min.	2	3	4	5	6	7
Max.	8	9	10	11	12	13
Filtering area per disk (sqft)	47	67	90	117	147	180

Horizontal Filters

Dia (ft)[f]	6	8	10	13	15	16	17	18	19	20	22	24
Area (sqft)												
Nom	28	50	78	133	177	201	227	254	283	314	380	452
Eff	25	45	65	120	165	191	217	244	273	304	372	444

[a]Filtrate 10–1600 lb/(hr) (sqft).
[b]Adaptable to knife, wire, string, belt, or roll discharge.
[c]All-plastic construction filters also available in 3 and 4 ft drum dia, providing filter areas of 9 to 100 sqft.
[d]All disks are composed of 10 sectors. Disk spacing is 16 in.
[e]The American filter, a similar disk filter, also available in 4 ft diameter, with 20 sqft disk.
[f]Also available in 3, 4, and 11.5 ft diameter.
(Dorr–Oliver Inc.; Walas, 1988).
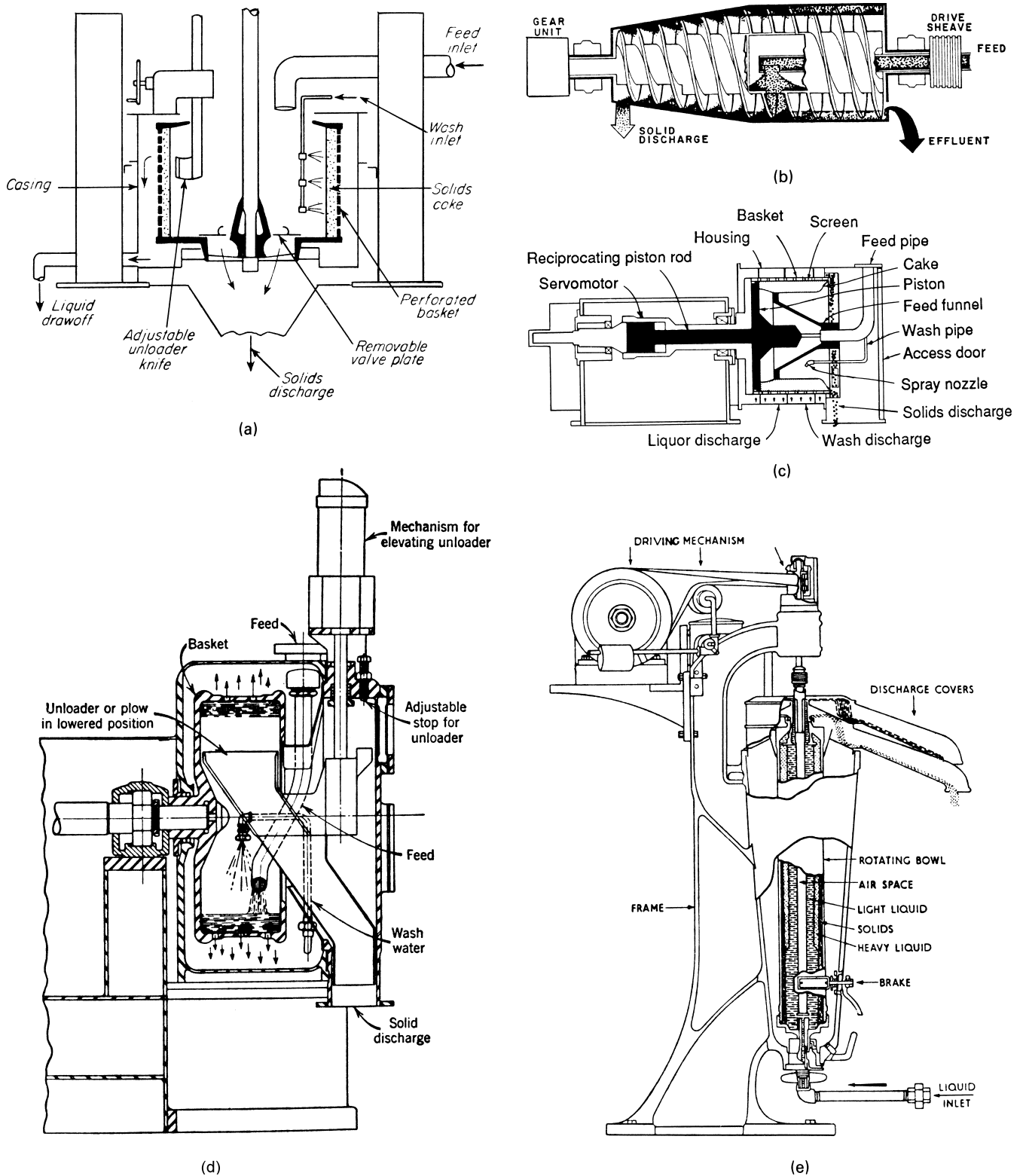
Figure 11.13. Filtering centrifuges. (a) Top suspended batch centrifugal filter; the cake is scraped off the screen intermittently at lower rotation speeds of 50 rpm or so, cake thicknesses of 2–6 in., cycle time per load 2–3 min. (*McCabe and Smith, 1956*). (b) A solid bowl centrifugal filter with continuous helical screw discharge of the cake (*Bird Machine Co.*). (c) Pusher type of centrifuge in which the cake is discharged with a reciprocating pusher mechanism that operates while the machine is at full speed. (*Baker–Perkins Co.*). (d) Horizontal centrifugal with automatic controls for shutting off the feed, washing the cake and scraping it off, all without slowing down the rotation. (*Baker–Perkin Co.*). (e) Supercentrifuge for removing small contents of solids from liquids; dimensions 3–6 in. by 5 ft, speed 1000 rps, acceleration 50,000 g, 50–500 gal/hr, cleaned after shutdown. (f) Pattern of flow in a hydrocyclone. (g) The shape of hydrocyclone adapted to the kind of service. (h) Centrifugal action of a cyclone assisted by a high space speed impeller. (*Voight Gmbh*). (Walas, 1988).
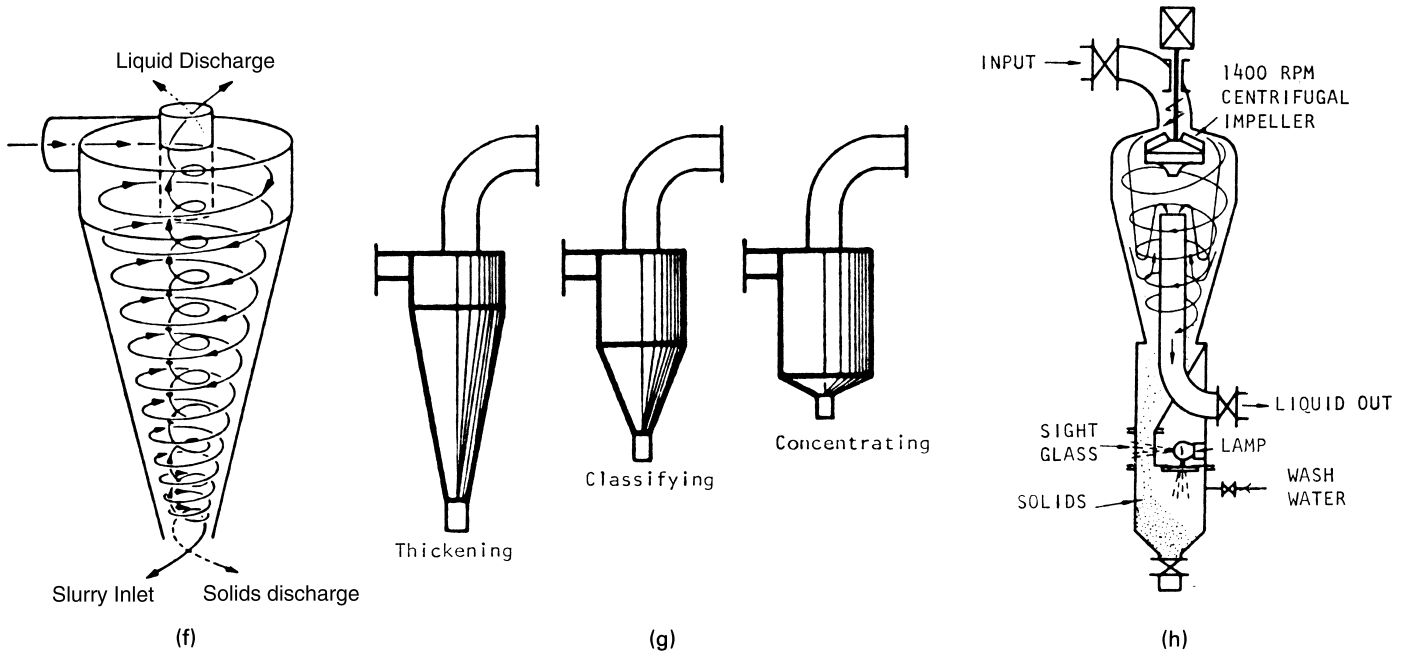
Figure 11.13.—(*continued*)

TABLE 11.13. Typical Applications of Industrial Filters

Material	Characteristics	Filtrate Rate kg/(m²)(hr)	Equipment Type[a]					Vacuum (Torr)	Pressure (atm)
			A	B	C	D	E		
Flotation concentrates	minerals, <0.3 m	300–1000	—	—	×	—	×	450–600	—
Sedimentation concentrates	> 0.3 mm	6000–42,000	—	—	×	—	×	50–150	—
Crystals and granules	0.05–0.3 mm	600–2000	—	—	×	—	×	100–300	—
Beverages, juices	worthless solids, use filter aids	150–5000	×	×	—	—	—	—	2.5–3.5
Pigments	smeary, sticky, 0.06 mm	120–300	—	—	×	×	—	500–680	—
		batch mode	×	×	—	—	—		2.5–4
Limestone, oxide minerals	fine, high density	200–1000	—	—	×	—	—	450–600	—
		batch mode	×	×	—	×	—	—	2.5–4
Cane sugar mud	fibrous, viscous		×	×	×	—	—	—	—
Mineral oils	high viscosity, 1–20% bleaching clays	100–1000	—	×	—	—	—	—	4
Liquid fuels	low viscosity, bleaching clays	800–2500	—	×	—	—	—	—	<4
Varnishes, lacquers	cloudy, viscous, solid adsorbents	15–18	×	—	—	—	—	—	1
Fats, oils, waxes	worthless solids, 50–70°C	500–800	×	×	—	—	—	—	—
Sewage sludge	colloidal, slimy	15–150	—	—	×	—	—	550–600	—
Pulp and paper	fibrous, free filtering	150–500	—	—	×	—	—	150–500	—
Cement	fine limestone, shale, clay, etc	300–1000	—	—	×	—	—	450–630	—

[a]Equipment type: (A) filter press; (B) leaf pressure filters, such as Kelly, Sweetland, etc.; (C) continuous vacuum filter; (D) batch rotary filter; (E) continuous rotary filter. (Walas, 1988).

TABLE 11.14. Design and Operating Factors for Continuous Vacuum Filters

(a) Typical Factors for Cycle Design

Filter type	Submergence[a]		Total under[b] Active Vac or Pressure	Max[c] for Washing	% of Cycle Max for[d] Dewatering Only	Required for Cake Discharge
	Apparent	Effective Maximum				
Drum						
Standard scraper	35	30	80	29	50–60	20
Roll discharge	35	30	80	29	50–60	20
Belt	35	30	75	29	45–50	25
Coil or string	35	30	75	29	45–50	25
Precoat	35, 55, 85	35, 55, 85	93	30	10	5
Horizontal belt	as req'd	as req'd	lengthen as req'd	as req'd	as req'd	0
Horizontal table	as req'd	as req'd	80	as req'd	as req'd	20
Tilting pan	as req'd	as req'd	75	as req'd	as req'd	25
Disc	35	28	75	none	45–50	25

[a]Total available for effective subm., cake washing, drying, etc. (Purchas, 1981).
[b]Value for bottom feed filters assume no trunnion stuffing boxes, except for precoat. Consult manufacturers for availability of higher submergences. (Purchas, 1981).
[c]Maximum washing on a drum filter starts at horizontal centerline on rising side and extends to 15 past top dead center. (Purchas, 1977).
[d]Dewatering means drainage of liquor from cake formed during submergence. (Walas, 1988).

(b) Typical Air Flow Rates

Type of Filter	Air Flow at 500 Torr Vacuum [m^3/(h)(m^2)]
Rotary drum	50–80
Precoat drum	100–150
Nutsche	30–60
Horizontal belt or pan	100–150

(c) Minimum Cake Thickness for Effective Discharge

Filter Type	Minimum Design Thickness	
	(in.)	(mm)
Drum		
Belt	1/8–3/16	3–5
Roll discharge	1/32	1
Std scrapter	1/4	6
Coil	1/8–3/16	3–5
String discharge	1/4	6
Precoat	0–1/8 max	0–3 max
Horizontal belt	1/8–3/16	3–5
Horizontal table	3/4	20
Tilting pan	3/4–1	20–25
Disc	3/8–1/2	10–13

[(a, b) Purchas, 1981; (c) Purchas, 1997] (Walas, 1988)

TABLE 11.15. Typical Performance Data for Horizontal Belt Filters

Application	Filter area, m^2	Slurry feed characteristics			Wash ratio (wt/wt based on dry solids)	Solubles recovery %	Final cake moisture %
		% solids	pH	t/hr			
Dewatering metallic concentrates	8	40	—	20	—	—	7
Brine precipitate sludge	25	12	—	1	8	90	50
Calcine leach	60	45	10	78	1	99.7	14
Uranium leach pulp	120	50	1–2	300	0.4	99.3	18
Cyanide leach gold pulp	120	50	10–11	80	0.6	99.6	20

(Purchas, 1981; Walas, 1988).

TABLE 11.16. Examples of Filter Press Performance for Dewatering of Wastes in Municipal, Potable Water and Industrial Effluents

Type of Material	Nature and level of conditioning	Filtration cycle time (Hr)	Solids feed Wt/Wt (%)	Cake Wt/Wt (%)	Cake thickness (mm)	Remarks
Fine waste slurry	Polyelectrolytes 0.05–0.3 lb/ton	0.5–2	15–35	75–82	25–40	More than 80% below
Frothed tailings	Polyelectrolytes 0.05–0.3 lb/ton	1–2.5	15–35	73–80	25–40	240BS mesh
Primary sewage sludge	5–25% lime with 5–15% copperas, 5–25%	3–7	4–7	40–55	25–32	
	lime and 3–6% ferric chloride	1.5–2	3–6	35–50	25–32	
Digested sewage sludge	or 1.2% ACH(Al$_2$O$_3$)	2–3				
Heat treated sludge		1–2	12–15	50–70	32	
Mixed sewage sludge including surplus activated	Up to 3% aluminium chlorohydrate (Al$_2$O$_3$ basic)	3–6	up to 4	30–45	32	Proportion of surplus activ. sludge is 40% by weight
	or 30% lime with 30% copperas or 3–8% FECl$_3$	2–4	up to 4	30–40	25	
Paper Mill Humus sludge	1% ACH	8	0.5–1.5	30–45	25	
Paper Mill pool effluent sludge	10% lime, 10% copperas of 1% FECl$_3$	1–3	1–1.5	40–55	25	
Pickling and plating sludge	Up to 10% lime if required	1.5–3	2–3	30–45	25–32	
Potable water treatment sludge	In some instances no conditioning is required 0.2–1.5% polyelectrolyte (Frequently it is possible to decant large quantities of clarified water after conditioning and before filtration).	3–8	0.5–3	25–35	19–25	
Brine sludge		1.5–3	10–25	60–70	20–25	
Hydroxide sludge	1 mg/l polyelectrolyte or 10% lime	1.5–3	0.5–1.5	35–45	25–32	
Lead hydroxide sludge		0.5	45	80	32	

(Edwards and Jones Ltd.; Walas, 1988).

TABLE 11.17. Operating Data of Some Vacuum Filter Applications

Application	Type of vacuum filter frequency used[b]	Solids content of feed, wt/wt	Solids handling rate, kg dry solids h^{-1}m^{-2} filter surface[c]	Moisure content of cake, wt/wt	Air flow m^{3}h^{-1}m^{-2} filter surface[d]	Vacuum, mmHg
Chemicals						
Alumina hydrate	Top feed drum	40	450–750	15	90	125
Barium nitrate	Top feed drum	80	1250	5	450	250
Barium sulphate	Drum	40	50	30	18	500
Bicarbonate of soda	Drum	50	1750	12	540	300
Calcium carbonate	Drum	50	125	22	36	500
Calcium carbonate (precipitated)	Drum	30	150	40	36	550
Calcium sulphate	Tipping pan	35	600	30	90	450
Caustic lime mud	Drum	30	750	50	108	375
Sodium hypochlorite	Belt discharge drum	12	150	30	54	500
Titanium dioxide	Drum	30	125	40	36	500
Zinc stearate	Drum	5	25	65	54	500
Minerals						
Frothed coal (coarse)	Top feed drum	30	750	18	72	300
Frothed coal (fine)	Drum or disc	35	400	22	54	375
Frothed coal tailings	Drum	40	200	30	36	550
Copper concentrates	Drum	50	300	10	36	525
Lead concentrates	Drum	70	1000	12	54	550
Zinc concentrates	Drum	70	750	10	36	500
Flue dust (blast furnace)	Drum	40	150	20	54	500
Fluorspar	Drum	50	1000	12	90	375

Notes:
[a] The information given should only be used as a general guide, for slight differences in the nature, size range and concentration of solids, and in the nature and temperature of liquor in which they are suspended, can significantly affect the performance of any filter.

[b] It should not be assumed that the type of filter stated is the only suitable unit for each application. Other types may be suitable, and the ultimate selection will normally be a compromise based on consideration of many factors regarding the process and the design features of the filter.

[c] The handling rate (in kg h^{-1}m^{-2}) generally refers to dry solids except where specifically referred to as filtrate.

[d] The air volumes stated are measured at the operating vacuum (i.e. they refer to attenuated air).

(Osborne, 1981; Walas, 1988).

TABLE 11.18. Typical Performance Data of Rotary Vacuum Filters

Material	Approximate particle size	Feed solids conc. wt %	Filtration rate (9) kg/(m²)(hr)	Vacuum Pump (9)	
				m³/(m²)(min)	mm Hg
Disc filter					
Flotation coal	33–43%–200 mesh	22–26	300–600	1.5	500
Copper concentrates	90%–200 mesh	60–70	250–450	0.5	500
Magnetic concentrates	80–95%–325 mesh	55–65	1000–2000	2.5–3.0	600–650
Coal refuse	35–50%–250 mesh	35–40	100–125	0.6	500
Magnesium hydroxide	15 microns av. size	10–15	40–60	0.6	500
Drum filter					
(1) Sugar cane mud	Limed for flocculation	7–18 by vol.	25–75	0.2	500
CaCO₃ mud recausticising	—	35–40	500–600	1.8–2	250–380
(2) Corn starch	15–18 microns, av. size	32–42	110–150	0.9–1	560
Sewage sludge					
Primary	Flocculated	5–8	15–30	0.5	500
Primary digested	Flocculated	4–7	10–20	0.5	509
(3) Leached uranium ore	50–60%–200 mesh Flocculated	50–60	150–220	0.5–	500
Kraft pulp	Long fibre	1–11	220–300	Barometric leg	
(4) Kaolin clay	98–75%–2 micron	25–35	30–75	0.5	600
Belt drum filter					
(5) Sugar cane mud	Seperan flocculated	7–18 by vol.	90–250	0.2	500
Sewage sludge					
Primary	Flocculated	5–8	30–50	0.5	500
Primary digested	Flocculated	4–7	15–35	0.5	500
Corn gluten	Self flocculating	16–20 oz/U.S. gal	15–30	0.6	500
Corn starch	15–18 microns, av. size	32–42	180–250	0.9–1	500
(3) Gold cyanide leached off	65%–200 mesh	50–60	300–600	0.5	500
(3) Spent vegetable carbon	98%–325 mesh	100–130 gm/litres	30–50	1.5	500
Dextrose processing					
Steel mill dust	20–40%–2 microns	40–50	170–300	0.6–1.2	500
(3) Sodium hypochlorite	Fine	12	150	0.9	500
Top feed drum					
Iron ore concentrates	2–4%–200 mesh 8 mesh top size	35	6300–7300	15	150
(6) Sodium Chloride	5–10%–100 mesh	25–35	1000–1500	30	150
Bone char	1%–70 mesh	8–20	1200–1700	40	90
(6) Ammonium sulphate	5–15%–35 mesh	35–40% by vol.	1000–1700	45–60	75
Tilting pan filter					
(7) Gypsum from digested phosphate rock	40–50 micron av.	35–40	600–900	1.2–1.5	500
(8) Leached cobalt residue	—200 mesh	45–50	250	3	380
(8) Alumina-silica gel catalyst	—	12	270	0.9	500
(7) Pentaerythritol	—	30–40	75–100	3.6	500

Notes: (1) Filtrate very dirty—must be recirculated back to clarifier—cake washed.
      (2) String discharge filter.
      (3) Cake washed.
      (4) Roller discharge drum filter.
      (5) Filtrate very clean—goes directly to evaporation—cake washed.
      (6) top feed filter drier.
      (7) Two or three stages of counter-current washing.
      (8) Three stages of counter-current washing.
      (9) Based on total filter area.
        (Data of Envirotech Corp.). (Walas, 1988).

TABLE 11.19. Data of Centrifugal Filters and Sedimentation Centrifuges (*Purchas, 1977*)

(a) Operating Ranges of Main Types of Centrifugal Filters

Type of Centrifuge	Continuous	Automatically Discharged at Full Speed	Automatically Discharged at Reduced Speed	g-Factor Range (F_c)	Minimum Solid Concentration in Feed [% by Volume (C_v)	Possibility of Washing	Minimum Particle Size, mm	Minimum Filtrability Coefficient (k) (m/sec)	Maximum Retention Time (Sec)
Oscillating	x			30–120	40	no	0.3	5×10^{-4}	6
Tumbler	x			50–300	40	no	0.2	2×10^{-4}	6
Worm Screen	x			500–3000	20	poor	0.06	1×10^{-5}	15
Pusher	x			300–2000	30	good	0.08	5×10^{-5}	60
Peeler		x	x	300–1600	5	very good	0.01	2×10^{-7}	as wanted
Pendulum			x	200–1200	5	very good	0.005	1×10^{-7}	as wanted

(Hultsch and Wilkesmann; Purchas, 1977; Walas, 1988). (*continued*)

TABLE 11.19.—(*continued*)

(b) Criteria for Selection of Sedimentation Centrifuges

Parameter	Tubular Bowl	Skimmer Pipe	Disc	Scroll
Solids concentration. vol./vol.	<1%	up to about 40%	up to about 20%	any as long as it remains pumpable
Particle size range processable for density difference under 1 g/cc and liquor viscosity 1 cP	$\frac{1}{2}$-50 μm	10 μm–6 mm	1–400 μm	5 μm–6 mm
Settling time of 1 litre under 1 g	Few hours to infinity	$\frac{1}{2}$ hr to days	several hours	$\frac{1}{2}$–1 hr
Settling time of 50 cc at 2000 g	5–15 min	1–5 min	5–10 min	1–5 min
Approximation maximum throughput for largest machine	5000 litre/hr	15,000 litre/hr	100,000 litre/hr	70,000 litre/hr
Approximation nominal throughput for largest machine	1250 litre/hr	12,000 litre/hr	40,000 litre/hr	30,000 litre/hr
Nature of bottle spun solids	Can be any consistency	Must be fluid to pasty	Must not be too cohesive	Preferably compact and cohesive
Batch or continuous	Batch	Semi	Semi or continuous	Continuous
Floc applicable	Possibly but not usual	Yes	No	Yes
g levels used	Up to 18,000. 60,000 Laboratory model	Up to 1600	4500–12,000	500–4000
Maximum sigma value $\times 10^7$ cm^2	5	4	10	14

(F. A. Records; Walas, 1988).

Performance often is improved by appropriate pretreatment of the slurry with flocculants or other means. An operating practice that is receiving increased acceptance is the delaying of cake deposition by some mechanical means such as scraping, brushing, severe agitation, or vibration. In these ways most of the filtrate is expelled before the bulk of the cake is deposited. Moreover, when the cake is finally deposited from a thickened slurry, it does so with an open structure that allows rapid filtration. A similar factor is operative in belt or top feed drum filters in which the coarse particles drop out first and thus form the desirable open structure. A review of such methods of enhancement of filtration rates is by Svarovsky (1981).

The relative suitability of the common kinds of solid–liquid separation applications is summarized in Table 11.3. Filtration is the most frequently used operation, but sedimentation as a method of pretreatment and centrifugation for difficulty filterable materials has many applications. Table 11.14 gives more detail about the kinds of filters appropriate to particular services.

Representative commercial sizes of some types of pressure filters for operation in batch modes are reported in Table 11.11. Some of these data are quite old, and not all of the equipment is currently popular; thus manufacturers should be consulted for the latest information. Commercially available size ranges of continuous belt, rotary drum, rotary disk, and horizontal rotary filters are listed in Table 11.12. For the most part these devices operate with vacua of 500 Torr or less.

Cycle times, air rates, and minimum cake thicknesses in operation of rotary drum filters are stated in Table 11.14. A few special applications of horizontal belt filters are given in Table 11.15, but in recent times this kind of equipment has taken over many of the traditional functions of rotary drum filters. Belt filters are favored particularly for freely filtering slurries with wide range of particle sizes.

The applications listed in Table 11.17 and 11.18 are a few of those of rotary drum, rotary disk, and tipping or tilting pan filters. The last type employs a number of vacuum pans on a rotating circular track; after the cake is formed, the pans are blown back with air and then tipped to discharge the cake. The data of these tables include particle size range, moisture content of the cake, filtering rate, solids handling rate, vacuum pump load and degree of vacuum. Clearly a wide range of some of these variables occurs in practice.

SEDIMENTATION AND CLASSIFICATION EQUIPMENT

Sedimentation equipment is employed on a large scale for mineral and ore processing. These and other applications are listed in Table 11.9(a). The clarification operations of Table 11.9(b) are of water cleaning and sewage treatment. The sludges that are formed often are concentrated further by filtration. Such applications are listed in Table 11.16 along with other common applications of plate-and-frame filter presses. Sludge filter cakes are compressible and have high resistivity so that the elevated pressures at which presses can be operated are necessary for them. Among the kinds of data given here are modes of conditioning the slurries, slurry concentrations, cake characteristics, and cycle times.

Clarification of a great variety of industrial liquids is accomplished on smaller scales than in tank clarifiers by application of cartridge filters; some of these applications are listed in Table 11.10. Cartridge filters are available in a wide variety of designs—vertical and horizontal as well as single and multiple cartridge models. They are the most common filters for clarification purposes. Further, the cartridge element may be made of ceramic, porous metal, resin-treated paper, thermally bonded polypropylene, and wound fibers. Cartridge filters are operated until the pressure drop across the element becomes undesirable at which time the paper and fiber elements are discarded and the metal and ceramic elements are cleaned for reuse. There are certain models on the market using ceramic or metallic elements that may be back flushed to clean these elements without opening the filter. Some metallic and ceramic filter elements have been designed to operate at temperatures in excess of 250°C. See Figure 11.10(g).

CENTRIFUGAL FILTERS AND CENTRIFUGES

Characteristics of centrifugal filters and sedimentation centrifuges are in Table 11.19. The filtering types are made to handle from less than 5 tons/hr to more than 100 tons/hr of solids, with *g*-levels ranging from 30 to 3000. For sedimentation types, the *g*-levels listed

range up to 18,000, but high values can be used only with small diameter equipment because of metal strength limitations. Capacity of sedimentation types is measured in terms of liquid rates, the maximum listed here being 100,000 L/hr. An outstanding feature of centrifugal separators is the small sizes of particles that can be handled satisfactorily; the values in the table cover the range 1–400 μm. Short retention time is a feature of centrifuge operation that may be of interest when unstable materials need to be processed.

Figure 11.13 shows schematic diagrams of various types of filtering centrifuges. In Figure 11.13(a) a top suspended batch centrifuge is shown but there are also models that are not suspended but have the drive mechanism beneath the centrifuge.

REFERENCES

C. Almy, and W.K. Lewis, Factors determining the capacity of a filter press, *Ind. Eng. Chem.,* **4**, 528 (1912).

C. Besendorfer, Exert the force of hydroclones, *Chem. Eng*., 108–114 (September 1996).

R. Bosley, Pressure vessel filters, in Purchas, 1977, pp. 367–401.

G.G. Brown, *Unit Operations*, Wiley, New York, 1950.

P. C. Carman, *Trans. Inst. Chem. Eng*, London, 15, 150 (1937).

Chemical Engineering Buyers' Guide, Chemical Week, New York, 2004.

Chemical Engineers' Handbook, 4th ed., McGraw-Hill, New York, 1963, pp. 19.40, 19.52.

W. Chow, *Chem. Eng*., 66–72, February 1997.

N. P. Cheremisinoff, and D. Abel, *Liquid Filtration,* Ann Arbor Science, Ann Arbor MI, 1981.

D. A. Dahlstrom, and C.E. Silverblatt, Continuous filters, in Purchas, 1977, pp. 445–492.

E. Davies, Filtration equipment for solid-liquid separation, *Trans. Inst. Chem. Eng,* **43**(8) (1965).

R. W. Day, *Chem. Eng. Prog.,* **69**(9) (1973).

J. E. Flood, H.E. Parker, and F.W. Rennie, Solid-liquid separation, *Chem. Eng*., 63–181 (June 30, 1966).

M. P. Freeman, and J.A. Fitzpatrick (Eds.), *Theory, practice and principles for physical separations*, Proceedings of the Engineering Foundation Conference, Pacific Grove CA, October–November 1977.

C. Gelman, H. Green, and T.H. Meltzer, Microporous membrane filtration, in Cheremisnoff and Azbel, 1981, pp. 343–376.

C. Gelman, and R.E.Williams, Ultrafiltration, in Cheremisnoff and Azbel, 1981, pp. 323–342.

H. P. Grace, *Chem. Eng. Prog.,* **49**, 303, 367, 427 (1953).

J. Gregory, (Ed.), *Solid-Liquid Separation*, Ellis Horwood, Chichester, England, 1984.

K. J. Ives, Deep bed filtration, in Svarovsky, 1981, pp. 284–301.

L. J. Jacobs, and W. R. Penney, in R.W. Rosseau, *Handbook of Separation Processes,* Wiley, New York, 1987, Chapter 3.

J. Kozeny, *Ber. Wien. Akad*., **135a**, pp. 271–278 (1927).

W. L. McCabe, and J.C. Smith, *Unit Operations of Chemical Engineering*, 1st ed., McGraw-Hill, New York, 1956.

D. G. Osborne, Gravity thickening, in Svarovsky, 1981, pp. 120–161.

D. G. Osborne, Vacuum filtration, in Svarovsky, 1981, pp. 321–357.

D. B. Purchas, (Ed.), *Solid-Liquid Separation Equipment Scale-up,* Uplands Press, London, 1977.

D. B. Purchas, *Solid-Liquid Separation Technology*, Uplands Press, London, 1981.

A. Rushton, and C. Katsoulas, Practical and theoretical aspects of constant pressure and constant rate filtration, in Gregory, 1984, pp. 261–272.

M. Salcudean, I. Gartshore, and E.C. Statie, Test hydroclones before they are built, *Chem. Eng*., 66–72 (April 2003).

L. Svarovsky, (Ed.), *Solid-Liquid Separation*, Butterworths, London, 1981.

F. M. Tiller, (Ed.), *Theory and Practice of Solid-Liquid Separation,* University of Houston, 1978.

F. M. Tiller, and J.R. Crump, Solid-liquid separation: An overview, *Chem. Eng. Prog.*, **73**(10), 65–75 (1977).

F. M. Tiller, J.R. Crump, and C. Ville, Filtration theory in its historical perspective: A revised approach with surprises, Second World Filtration Congress, The Filtration Society, London, 1979.

R.J. Wakeman, A numerical integration of the differential equations describing the formation of and flow in compressible filter cakes, *Trans. Inst. Chem. Eng.*, **56**, 258–265 (1978).

R.J. Wakeman, Filter cake washing, in Svarovsky, 1981, pp. 408–451.

R.H. Warring, *Filters and Filtration Handbook*, Gulf, Houston, 1981.

Wu Chen, Solid-liquid seperation via filtration, Chem. Eng., 66–72 (February 1997).

Solids Separation Process, International Symposium, Dublin, April 1980, EFCE Publication Series No. 9. Institute of Chemical Engineers, Symposium Series., No., Rugby, England, 1980.

12

DISINTEGRATION, AGGLOMERATION, AND SIZE SEPARATION OF PARTICULATE SOLIDS

*F*rom the standpoint of chemical processing, size reduction of solids is most often performed to make them more reactive chemically or to permit recovery of valuable constituents. Common examples of comminution are of ores for separation of valuable minerals from gangue, of limestone and shale for the manufacture of cement, of coal for combustion and hydrogenation to liquid fuels, of cane and beets for recovery of sugar, of grains for recovery of oils and flour, of wood for the manufacture of paper, of some flora for recovery of natural drugs, and so on.

Since the process of disintegration ordinarily is not highly selective with respect to size, the product usually requires separation into size ranges that are most suitable to their subsequent processing. Very small sizes are necessary for some applications, but in other cases intermediate sizes are preferred. By-product fines are frequently briquetted

with a binder for ease of handling. Agglomeration in general is practiced when larger sizes are required for ease of handling, or to reduce dust nuisances, or to densify the product for convenient storage or shipping, or to prepare products in final form as tablets, granules, or prills.

Comminution and size separation are characterized by the variety of equipment devised for them. Examples of the main types are described in this chapter with a few case studies. For equipment, it is essential to consult manufacturers' catalogs for details of construction, sizes, capacities, space, and power requirements. Textbooks give general information for these operations but there are few generalizations for the prediction of equipment characteristics. A list of manufacturers of this equipment may be found in the Chemical Engineering Equipment Buyers' Guide 2004 (2003) as well as on the Internet.

12.1. SCREENING

Separation of mixtures of particulate solids according to size may be accomplished by a series of screens with openings of standard sizes. Table 12.1 compares several such standards. The U.S. Standard sieves correspond to those recommended by the International Standards Organization (ISO) as an International Standard. The distribution of sizes of a given mixture often is important.

In sieve analysis, standard screens with precise screen openings are arranged in a stack from the coarsest to the finest with a pan below the bottom sieve to collect the fines. The material is introduced on the top screen and the stack of sieves is vibrated such that the material will stratify by particle size through the sieves.

After a given time period, the stack is disassembled, and the weight of the material retained on each screen is measured and expressed as a percentage of the total. A typical sieve analysis is found in Table 12.2.

Although sieving is probably the most frequently used method of particle-sized analysis, it has some major disadvantages:

- In weaving the wire, there are wide tolerances, especially for the fine mesh.
- The mesh is often damaged in use, as they are fragile.
- The particles must be uniformly distributed on the sieve (Snow et al., 1999).

Other new measurement techniques, such as laser-diffraction, light-diffraction, photon spectroscopic, video-imaging, and various scanning methods are available and give more reliable results.

The distribution of sizes of a product varies with the kind of disintegration equipment. Typical distribution curves in normalized form are presented in Figure 12.1, where the size is given as a percentage of the maximum size normally made in that equipment. The more concave the curves, the greater the proportion of fine material. According to these correlations, for example, the percentages of material greater than 50% of the maximum size are 50% from rolls, 15% from tumbling mills, and only 5% from closed

circuit conical ball mills. There are several ways of recording particle size distribution. The data in Figure 12.2(a) is plotted as cumulative weight percent retained on or passed through a screen against sieve aperture. See Figure 12.2(b).

Cumulative data are often represented closely by the Rosin-Remmler-Sperling (RRS) equation:

$$y = 100 \exp\left[-(d/d_m)^n\right] \tag{12.1}$$

where d = diameter
d_m = mean diameter corresponding to $y = 100/e = 36.8\%$
n = uniformity factor
the greater the value of n, the more nearly uniform the distribution.

The log-log plot of this equation should be linear, Figure 12.2(b). In Chapter 16, plots of commercial crystallization data deviate somewhat from linearity at the large particle diameters.

Two other single numbers are used to characterize size distributions. They are:

1. Median aperture, MA, or d_{50}, is the screen opening through which 50% of the material passes, or
2. Coefficient of variation defined by the following equation:

$$CV = [(100)(d_{16} - d_{84})]/(2d_{50}) \tag{12.2}$$

The origin of this concept is that the fraction of the total area under a normal distribution curve between 16 and 84% points is twice the standard deviation. The smaller the CV, the more uniform the particle sizes. This information is also used in describing particle sizes in crystallization processes.

The screening capacity of a system is always specified in terms of feed rate to the screen rather than product rate of the machine. The capacity is reported in lb/hrft^2 of the screen area. Loadings will vary considerably depending on the application. Commercial

TABLE 12.1. Comparison Table of United States, Tyler, Canadian, British, French, and German Standard Sieve Series

U.S.A. (1)		TYLER (2)	CANADIAN (3)		BRITISH (4)		FRENCH (5)		GERMAN (6)
*Standard	Alternate	Mesh Designation	Standard	Alternate	Nominal Aperture	Nominal Mesh No.	Opg. M.M.	No.	Opg.
125 mm	5″		125 mm	5″					
106 mm	4.24″		106 mm	4.24″					
100 mm	4″		100 mm	4″					
90 mm	3 1/2″		90 mm	3 1/2″					
75 mm	3″		75 mm	3″					
63 mm	2 1/2″		63 mm	2 1/2″					
53 mm	2.12″		53 mm	2.12″					
50 mm	2″		50 mm	2″					
45 mm	1 2/4″		45 mm	1 2/4″					
37.5 mm	1 1/2″		37.5 mm	1 1/2″					
31.5 mm	1 1/4″		31.5 mm	1 1/4″					
26.5 mm	1.06″	1.05″	26.5 mm	1.06″					
25.0 mm	1″		25.0 mm	1″					25.0 mm
22.4 mm	7/8″	.883″	22.4 mm	7/8″					
19.0 mm	2/4″	.742″	19.0 mm	2/4″					20.0 mm
									18.0 mm
16.0 mm	5/8″	.624″	16.0 mm	5/8″					16.0 mm
13.2 mm	.530″	.525″	13.2 mm	.530″					
12.5 mm	1/2″		12.5 mm	1/2″					12.5 mm
11.2 mm	7/16″	.441″	11.2 mm	7/14″					
									10.0 mm
9.5 mm	2/8″	.371″	9.5 mm	2/8″					
8.0 mm	3/16″	2 1/2	8.0 mm	3/14″					8.0 mm
6.7 mm	.265″	3	6.7 mm	.265″					
6.3 mm	1/4″		6.3 mm	1/4″					6.3 mm
5.6 mm	No. 3 1/2	3 1/2	5.6 mm	No. 3 1/2			5.000	38	5.0 mm
4.75 mm	4	4	4.75 mm	4					
4.00 mm	5	5	4.00 mm	5			4.000	37	4.0 mm
3.35 mm	6	6	3.35 mm	6	3.35 mm	5			
2.80 mm	7	7	2.80 mm	7	2.80 mm	6	3.150	36	3.15 mm
2.36 mm	8	8	2.36 mm	8	2.40 mm	7	2.500	35	2.5 mm
2.00 mm	10	9	2.00 mm	10	2.00 mm	8	2.000	34	2.0 mm
1.70 mm	12	10	1.70 mm	12	1.68 mm	10	1.600	33	1.6 mm
1.40 mm	14	12	1.40 mm	14	1.40 mm	12			
							1.250	32	1.25 mm
1.18 mm	16	14	1.18 mm	16	1.20 mm	14			
1.00 mm	18	16	1.00 mm	18	1.00 mm	16	1.000	31	1.0 mm
850 μm	20	20	850 μm	20	850 μm	18			
710 μm	25	24	710 μm	25	710 μm	22	.800	30	800 μm
							.630	29	630 μm
600 μm	30	28	600 μm	30	600 μm	25			
500 μm	35	32	500 μm	35	500 μm	30	.500	28	500 μm
425 μm	40	35	425 μm	40	420 μm	36			
							.400	27	400 μm
355 μm	45	42	355 μm	45	355 μm	44			
							.315	26	315 μm
300 μm	50	48	300 μm	50	300 μm	52			
250 μm	60	60	250 μm	60	250 μm	60	.250	25	250 μm
212 μm	70	65	212 μm	70	210 μm	72			
							.200	24	200 μm
180 μm	80	80	180 μm	80	180 μm	85			
							.160	23	160 μm
150 μm	100	100	150 μm	100	150 μm	100	.125	22	125 μm
125 μm	120	115	125 μm	120	125 μm	120			
106 μm	140	150	106 μm	140	105 μm	150	.100	21	100 μm
90 μm	170	170	90 μm	170	90 μm	170			90 μm
75 μm	200	200	75 μm	200	75 μm	200	.080	20	80 μm
									71 μm
63 μm	230	250	63 μm	230	63 μm	240	.063	19	63 μm
									56 μm
53 μm	270	270	53 μm	270	53 μm	300			
							.050	18	50 μm
45 μm	325	325	45 μm	325	45 μm	350			45 μm
							.040	17	40 μm
38 μm	400	400	38 μm	400					

(1) U.S.A. Sieve Series—ASTM Specification E-11-70
(2) Tyler Standard Screen Scale Sieve Series.
(3) Canadian Standard Sieve Series 8-GP-1d.
(4) British Standards Institution, London BS-410-62.
(5) French Standard Specifications, AFNOR X-11-501.
(6) German Standard Specification D1N 4188.
*These sieves correspond to those recommended by ISO (International Standards Organization) as an International Standard and this designation should be used when reporting sieve analysis intended for international publication.

TABLE 12.2. A Typical Sieve Analysis

B.S. Mesh Number	Sieve Aperture μm	Fractional Weight Percent Retained	Cumulative Weight Percent Oversize	Cumulative Weight Percent Undersize
7	2360	1·2	1·2	98·8
10	1700	2·9	4·1	95·9
14	1180	18·8	22·9	77·1
18	850	28·8	51·7	48·3
25	600	22·0	73·7	26·3
36	425	11·1	84·8	15·2
52	300	6·0	90·8	9·2
72	212	3·9	94·7	5·3
100	150	1·8	96·5	3·5
150	106	1·3	97·8	2·2
>150	—	2·2	—	—

screens of different manufacturers can have very different loading capacities, even in the same application.

In order to handle large lumps, separators are made of sturdy parallel bars called grizzlies. Punched plates are used for intermediate sizes and woven screens for the smallest. Screening is best performed dry, unless the feed is the product of wet grinding or is overly dusty and an equipment cover is not feasible. Wetting sometimes is used to prevent particles from sticking together. Types of screens and other classifiers to cover a range of sizes are shown in Figure 12.3. Usually some kind of movement of the stock or equipment is employed to facilitate the separations.

REVOLVING SCREENS OR TROMMELS

One type is shown in Figure 12.3(a). They are perforated cylinders rotating at 15–20 rpm, below the critical velocity. The different-sized perforations may be in series as shown or they may be on
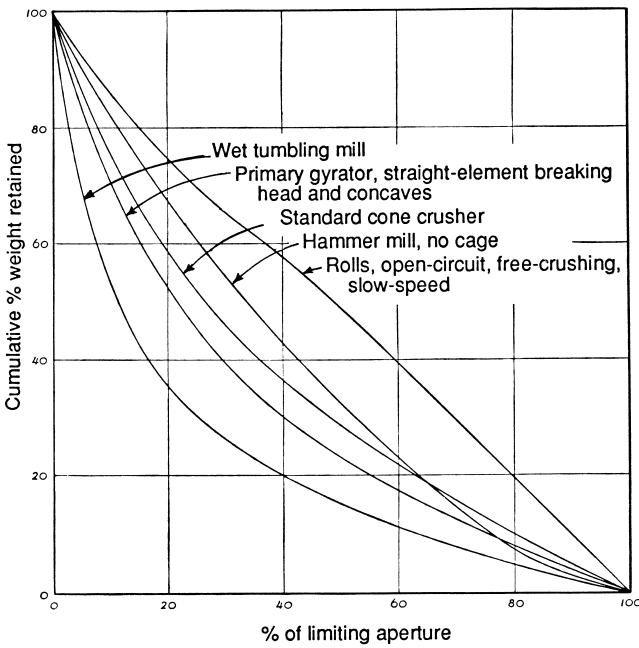
(a)
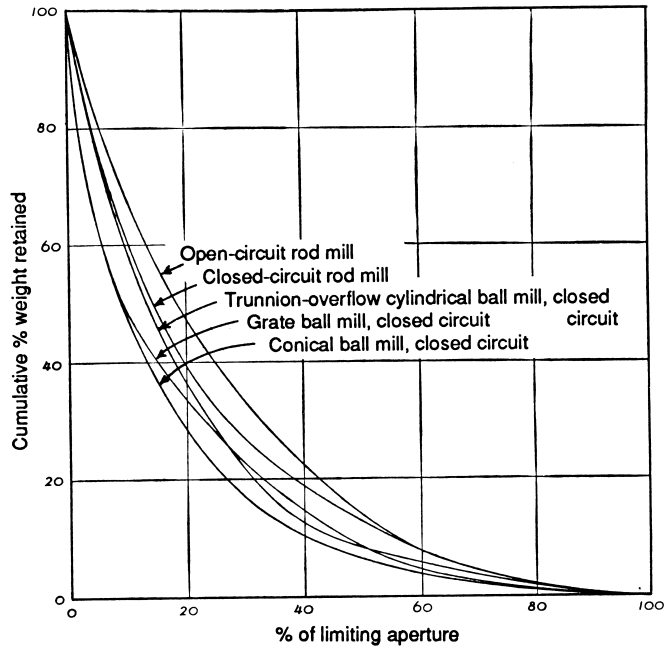
(b)
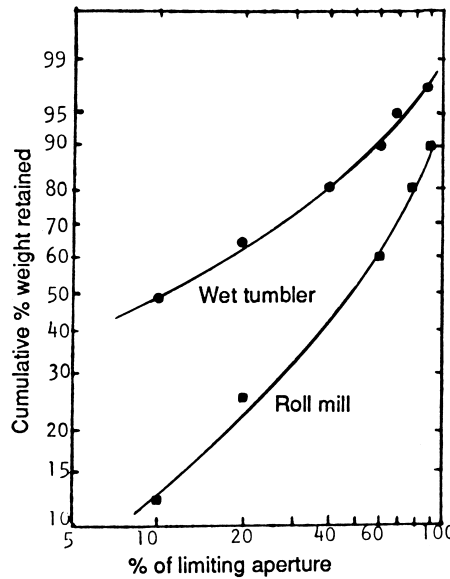
(c)

Figure 12.1. Normalized cumulative size distribution curves of comminuted products. (a) From various kinds of crushing equipment. (b) From rod and ball mills. (c) RRS plots of two curves. (*Taggart, 1951*) (Walas, 1988)

(a) Cumulative wt. % retained or passed
against sieve aperture

(b) Log-log plot according to
the RRS Equation

(c) Differential Polygon
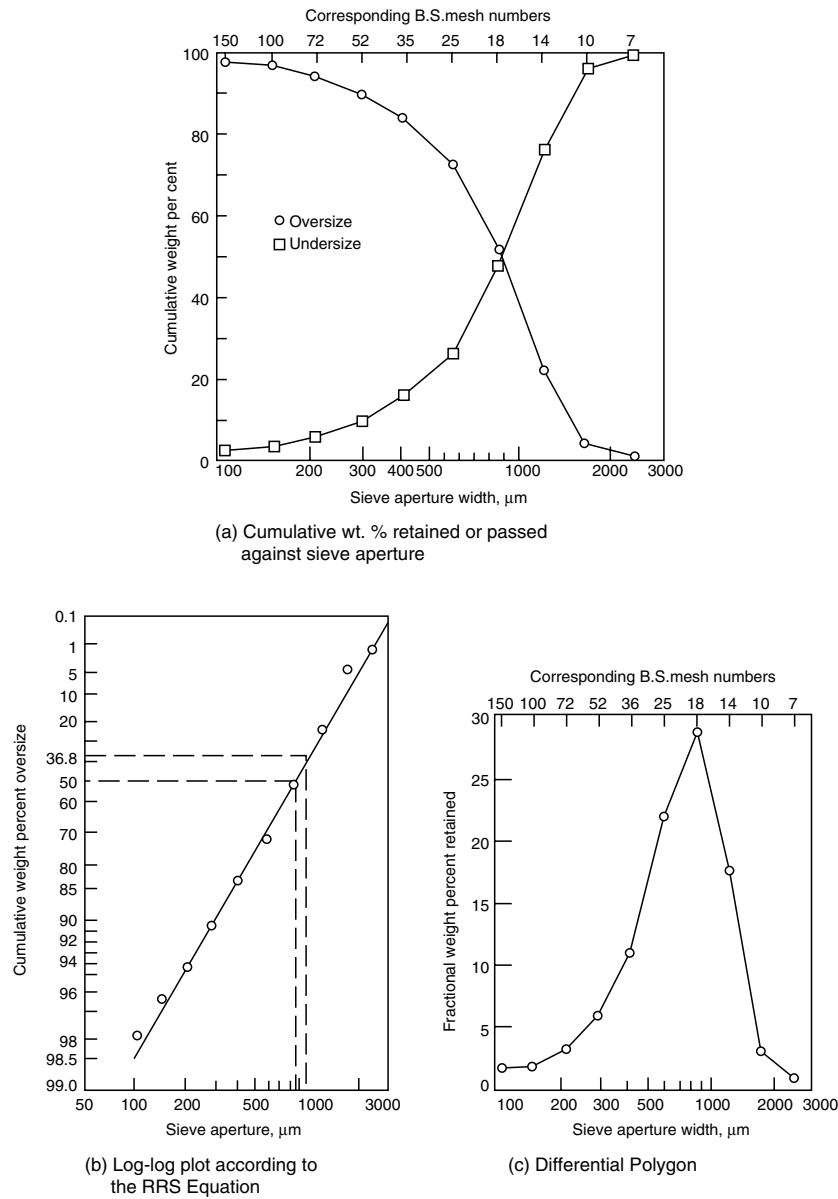
Figure 12.2. Several ways of recording sieve analysis data

concentric surfaces. They are suitable for wet or dry separation in the range of 60–10 mm. Vertically mounted centrifugal screens run at 60–80 rpm and are suitable for the range of 12–0.4 mm.

Examples of performance are: (1) a screen 3 ft dia by 8 ft long with 5-mesh screen at 2 rpm and an inclination of 2° has a capacity of 600 cuft/hr of sand; (2) a screen 9 ft dia by 8 ft long at 10 rpm and an inclination of 7° can handle 4000 cuft/hr of coke.

Flat screens are vibrated or shaken to force circulation of the bed of particles and to prevent binding of the openings by oversize particles. Usually several sizes are arranged vertically as in Figures 12.3(b) and (c), but sometimes they are placed in line as in the cylindrical screen of Figure 12.3(a). Inclined screens vibrate at 600–7000 strokes/min. They are applicable down to 38 μm or so, but even down to 200 mesh at greatly reduced capacity. Horizontal screens have a vibration component in the horizontal direction to convey the material along; they operate in the range of 300–3000 strokes/min.

Shaking or reciprocating screens are inclined slightly. Speeds are in the range of 30–1000 strokes/min; the lower speeds are used for coal and nonmetallic minerals down to 12 mm, and higher speeds may size down to 0.25 mm. The bouncing rubber balls of Figure 12.3(c) prevent permanent blinding of the perforations.

Rotary sifters are of either gyratory or reciprocating types. They operate at 500–600 rpm and are used for sizes of 12 mm– 50 μm, but have low capacity for fine sizes.

CAPACITY OF SCREENS

For coarse screening, the required area per unit of hourly rate may be taken off Figure 12.4. More elaborate calculation procedures that take into account smaller sizes and design features of the equipment appear in the following references:
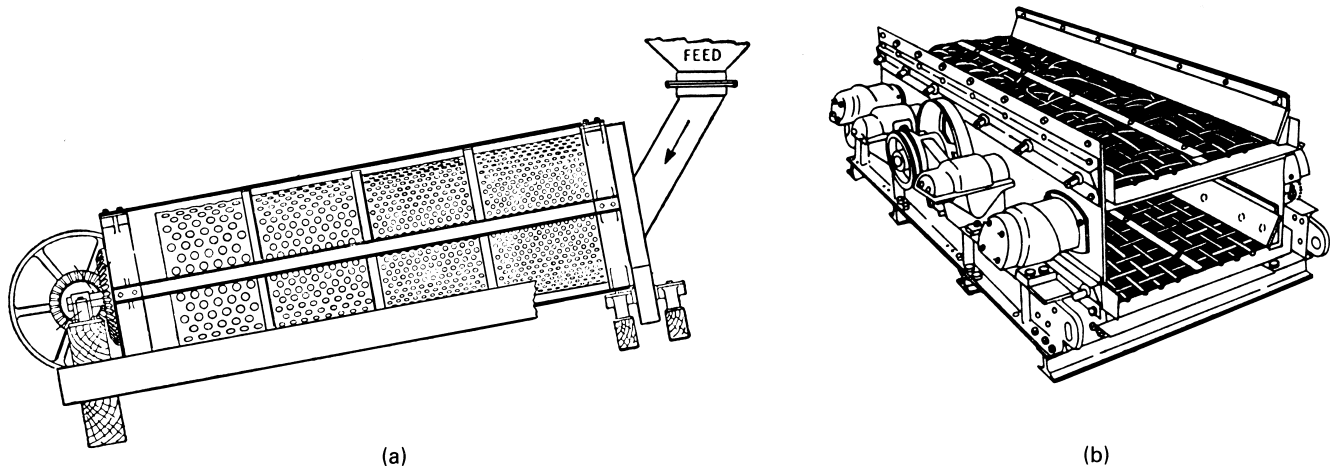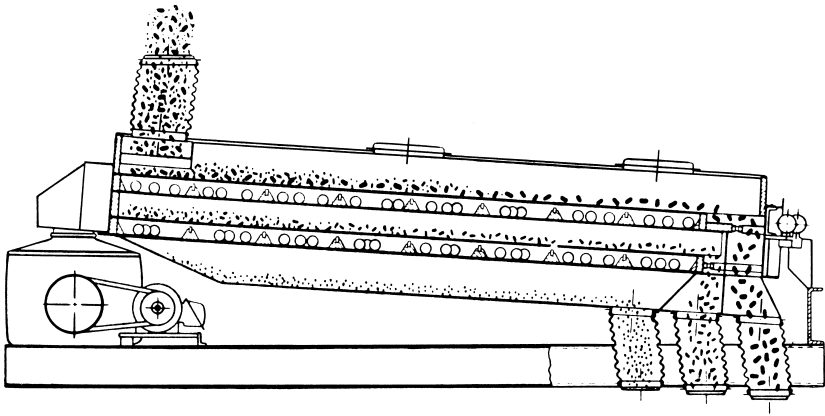
Model Number	Screen Size per Surface	Capacity in Tons per Hour		Motor	
		Pellets	Crumbles	HP	RPM
203	30" x 60"	13	8	2	1800
43*	40" x 84"	25	15	2	1800
83*	40" x 120"	35	23	3	1800
523	60" x 120"	50	34	7.5	1200
73	80" x 144"	85	55	10	1200
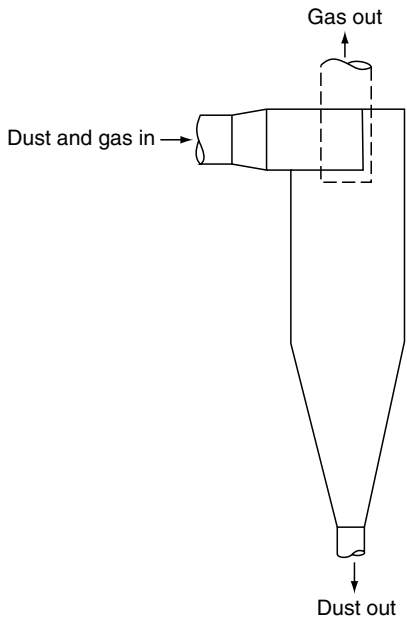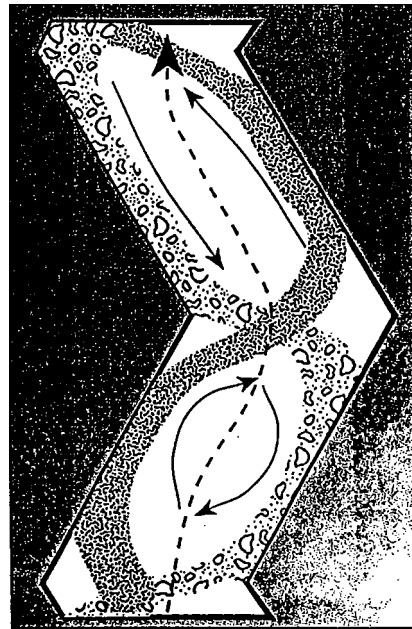
Figure 12.3. Equipment for classifying particulate solids by size from more than 0.5 in to less than 150 mesh. (a) Rotating cylinder (trammel) for sizing particles greater than 0.5 in., 2–10 rpm, 10–20° inclination. (b) Heavy duty vibrating screen, 1200–1800 vib/min (*Tyler-Niagara, Combustion Engineering, Inc.*). (c) Three-product reciprocating flat screen, 500–600 rpm, with bouncing rubber balls to unbind the openings, dry products to 100 mesh (*Rotex Inc.* (d) Cyclone separator. (e) Gravity air classifier, (f) Air classifier for products less than 150 mesh. Feed enters at A, falls on rotating plate B, fines are picked up by air suction fans C, transferred to zone D where they separate out and fall to the discharge, and air recirculates back to the fans *C (Sturtevant Mill Co.*). (g) Dorr drag rake wet classifer. (h) Hydroclone (Walas, 1988). (i) Turbine wheel classifer (Crawley et al., 2002). (j) Laser diffraction classifier (Crawley et al., 2002).

(f)

(g)

(i)

(h)

1. Photodiode
2. X-Y alignment stage
3. Lens
4. Window (receiver)
5. Window purge air
6. Automatic valve (outlet)
7. Laser diode
8. Sample return
9. Window (transmitter)
10. Instrument support bracket
11. Process flow
12. Sample probe
13. Triclamp
14. Automatic valve (inlet)
15. Motive air
16. Venturi

(j)

Figure 12.3.—(*continued*)

(a)

Cyclone capacity - US GPM,   (I US GPM = 227.1 $m^3 h^{-1}$)
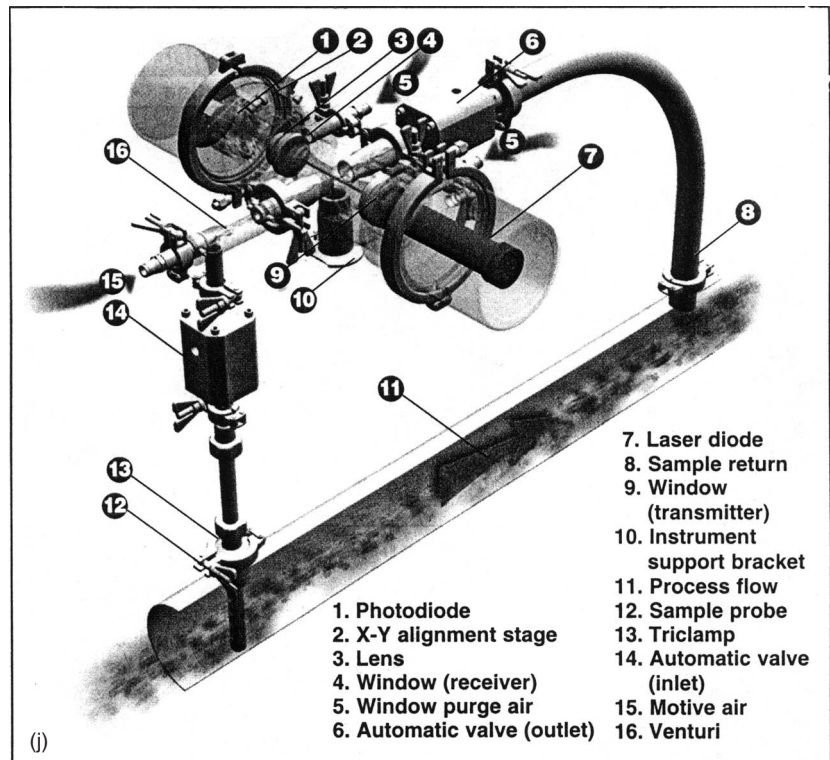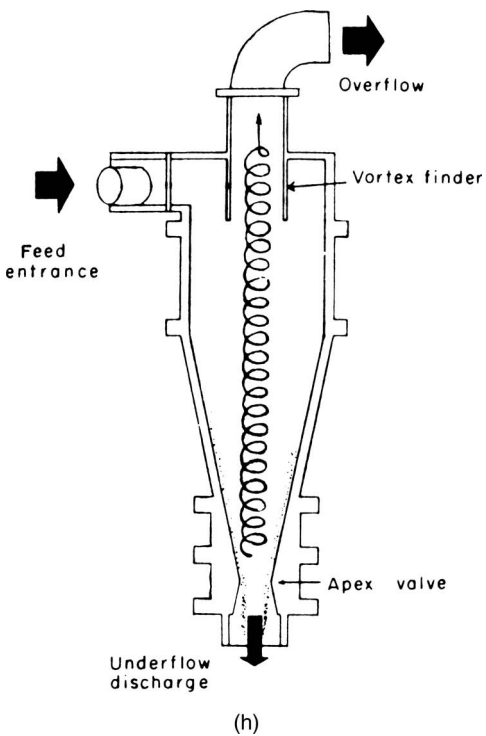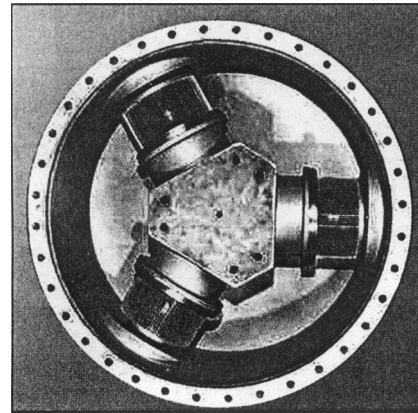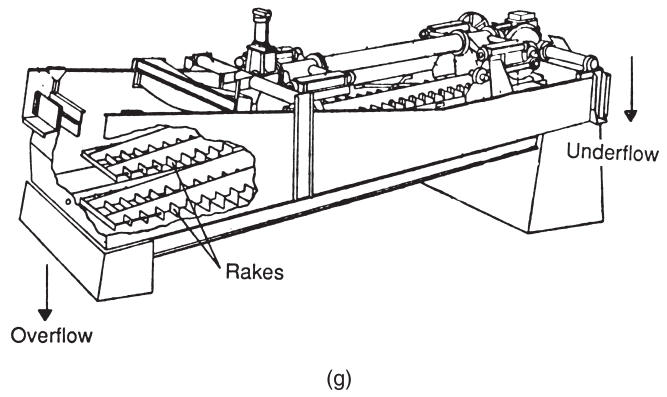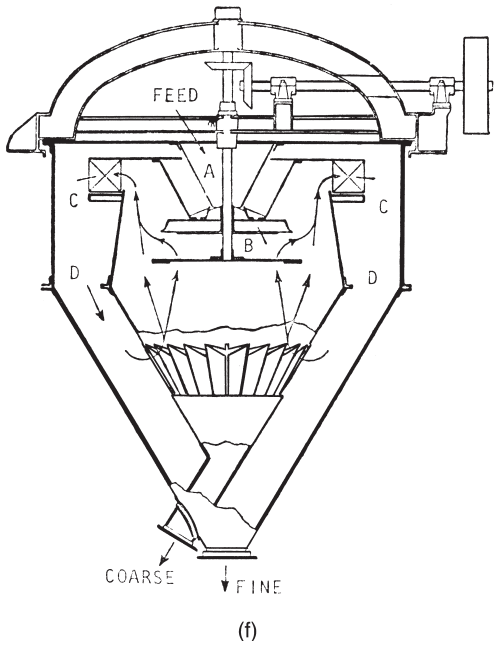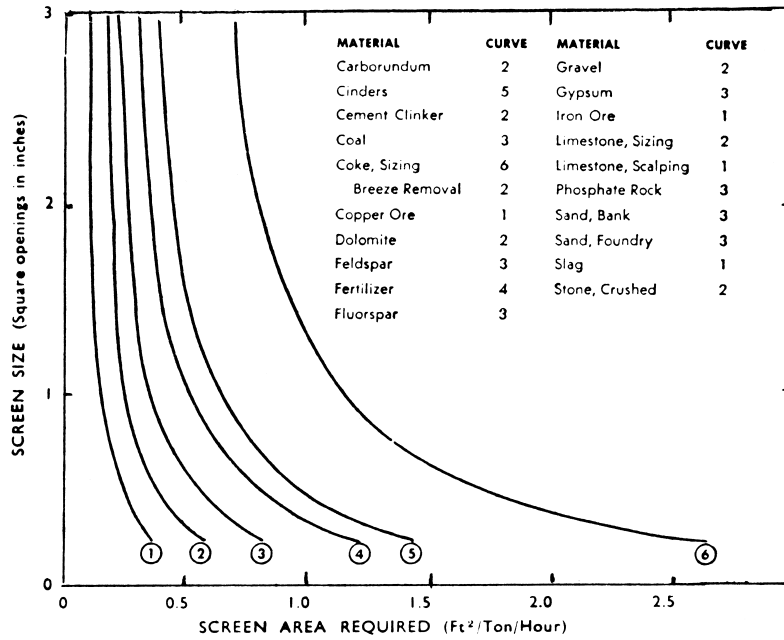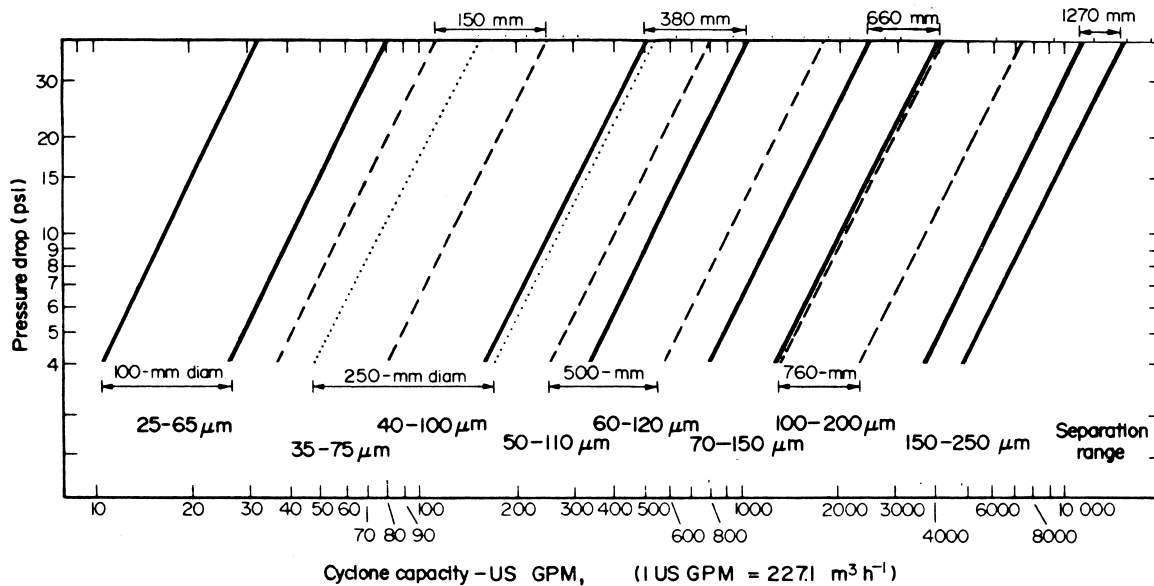
(b)

Figure 12.4. Performances of screens and hydrocyclones. (a) Capacities of screens for various products. (b) Capacity, separation range and pressure drop of hydrocyclones. Example: A 380 mm dia vessel has a separation range of 50–110 μm, and can handle between 200 and 450 gpm at a pressure drop of 7.5 psi. (Walas, 1988).

Mathews, *Chem. Eng.* 76 (10 July 1972) and presented in *Chemical Engineers' Handbook*, McGraw-Hill, New York, 1984, p. 21.17.

Kelly and Spottiswood, *Introduction to Mineral Processing*, 1982, p. 193.

V.K. Karra, Development of a model for predicting the screening performance of a vibrating screen, *CIM Bull.* **72**, 167–171 (Apr. 1979).

Karra (1979) has developed equations that are suitable for use on a computer.

OTHER METHODS FOR SIZE SEPARATION

In *sedimentation* methods, dependent on gravity, particle size is determined from settling velocity and under size fraction is determined by changes in concentration in a settling suspension (Snow et al., 1999). Stokes Law relates particle size to settling velocity:

$$d_s = \{(18\eta\mu)/[(\rho_s - \rho_f)g]\}^{0.5} \tag{12.3}$$

where η = viscosity

$\quad\mu$ = particle settling velocity

$\quad\rho_s$ = particle density

$\quad\rho_f$ = fluid density

$\quad g$ = acceleration of gravity

There are several *scanning* methods that measure particles individually in a fluid stream. These methods include field scanning, light diffraction, and photon spectroscopy methods. They are described briefly in *Perry's Handbook* (Snow et al., 1999).

In *elutriation* methods, particles are classified in a column by a rising fluid stream. A series of cyclones are used to separate particles into different size ranges. Gas adsorption of a gas on a powder is another method for determining surface area. Measurements are usually interpreted by using the Braunauer, Emmett, and Teller (BET) theory.

12.2. COMMERCIAL CLASSIFICATION WITH STREAMS OF AIR OR WATER

Air classifiers can handle a variety of fine as well as coarse powders like cement, alumina, inorganic chemicals, limestone, plastic particles, fine chemicals, and pharmaceuticals. The equipment in Figures 12.3(d) and 12.3(e) employ devices that throw particles into an air space from which the finer particles are removed and subsequently recovered.

Hickson (1992) defined *classification* as a means for "sorting out of particles to achieve a desired degree of uniformity." The term *separation* usually refers to dissimilar materials, whereas *classification* applies to different "grades" or sizes of the same material. These definitions will apply in this section.

Particle characteristics affect classification. The particles should be

uniform and homogeneous

spherical and smooth

dry and easily dispersible

As the name implies, air classifiers operate on the basis of air flow. It is an elutriation process in which the separation occurs using air. Fine particles rise in the air stream and the coarse particles that are too heavy to be carried upward fall under the influence of gravity. The cut point in a classification system can be adjusted by the air velocity within the unit.

The equipment to perform air classification is a combination of a mill with the grinding and air classification system integrated into a single unit. In general, fine material is continuously discharged when it reaches the desired product fineness and the coarse material continues to be ground. There are many types of air classifiers on the market today. They can be broadly classified into static units that have no moving parts and dynamic units using a variety of devices to create a vortex. Static units include cyclone separators and gravity air separators, as shown in Figure 12.3(d) and 12.3(e). A gravity air classifier is a static device; that is, it has no moving parts. It is usually a single zig-zag classifying channel like Figure 12.3(e), and it is used for crude separations that let the classifier separate materials that cannot be sieved effectively (Hixon, 1992). Dynamic devices are spiral separators, single- or multiturbine wheel classifiers (see Figure 12.3(i)), high-energy dispersion, and laser classifiers. The newest classification equipment is an on-line laser, Figure 12.3(j), which is often combined with a mill, static cyclone, and turbine classifier to control particle size. Table 12.3 shows the ranges of operation of classifiers.

Improved designs enhance the economics of a process to produce finer, better quality products with

- sharp particle size distribution from the grinding operation
- better efficiency
- reduction of the load on the grinding mill
- production of many grades from the same feedstock
- ability to produce new products with a higher value added

Chemical Engineering Buyers' Guide 2004 (2003) lists more than 30 manufacturers of such equipment.

WET CLASSIFIERS

There are used to make two product size ranges, oversize and undersize, with some overlap. The break commonly is between 28 and 200 mesh. A considerable variety of equipment of this nature is available, and some 15 kinds are described by Kelly and Spottiswood (1982, pp. 200–201). Two of the most important kinds, the drag rake classifier and the hydrocyclone, will be described here.

The classifier of Figure 12.3(g) employs two set of rakes that alternately raise, lower, and move the settled solids up the incline to the discharge. Movement of the rakes is sufficient to keep the finer particles in suspension and discharge them at the lower end. More construction detail of the Dorr classifier may be found in older books, for example, the Third edition of the *Chemical Engineers' Handbook*. The stroke rate may be 9/min when making separation at 200 mesh and up to 32/min for 28 mesh rapid settling sands. Widths range from 1 to 20 ft, lengths to 40 ft, capacity of 5–850 tons slurry/hr, loads from 0.5 to 150 HP. The solids content of the feed is not critical, and that of the overflow may be 2–20% or more.

Hydrocyclones, also called hydroclones, employ self-generated mild centrifugal forces to separate the particles into groups of predominantly small and predominantly large ones. Because of bypassing, the split of sizes is not sharp. The characteristic diameter of the product is taken as d_{50}, the diameter than which 50 wt % of the material is greater or less. The key elements of a hydrocyclone are identified on Figure 12.3(h). A typical commercial unit has an inlet area about 7% of the cross-sectional area between the vessel wall and the vortex finder, a vortex finder with diameter 35–40% that of the vessel, and an apex diameter not less than 25% that of the vortex finder. For such a unit, the equation for the cut point is

$$d_{50} = \frac{13.2D^{0.675}\exp(-0.301 + 0.0945V - 0.00356V^2 + 0.0000684V^3)}{(\Delta P)^{0.3}(S-1)^{0.5}}$$

$$(12.4)$$

and the slurry flow rate is

$$Q = 0.7(\Delta P)^{0.5}D^2 \tag{12.5}$$

in the units d_{50} μm, vessel diameter D in inches, V = vol % of solids in the feed, ΔP is the pressure drop in psi, S = specific gravity, and Q is the flow rate in gpm (Mular and Jull, in Mular and Bhappu 1978, p. 397). Performance characteristics of one line of commercial hydrocyclones are shown in Figure 12.4(b). Comparison of the chart and equations is made in Example 12.1.

Hydrocyclones are small and inexpensive separators for handling feeds up to about 600 cuft/min and removing particles in the range of 300–5 μm from dilute suspensions. Large diameters (up to about 24 in.) have greater volumetric capacity but also a greater cutpoint on particle diameter. Series and parallel arrangements may be made for any desired compromise between these quantities. In comparison with drag rake classifiers, hydroclones are smaller, cost about the same to operate but have lower costs

TABLE 12.3. Range of classifier operation

Type	Size Range
Static gravity units	> 1,000 microns
Cyclone separator	20–300 microns
Spiral separator	3–80 microns
Turbine classifiers (single and multiple wheel units)	5–150 microns
High energy dispersion	<5 microns
Laser classifiers	<5 microns

(*Chemical Engineering*, pp. 54–60, April 2002).

for capital and installation. They are preferred in closed circuit grinding.

12.3. SIZE REDUCTION

The term *crushing* is commonly thought of as the size reduction of large lumps of a feed stock, and *grinding* is regarded as the reduction of larger particles to smaller ones, although the distinction is not sharp. The process of size reduction results in a range of product sizes whose description is often reported as a cumulative size distribution. Frequently, the product is reported as a given percentage passing a certain screen size. Another term associated with crushing and grinding is *grindability*. It is defined as the amount of product from a particular mill meeting a particular specification in a unit of grinding time, such as tons per hour passing a 200 mesh screen (*Chemical Engineers' Handbook*, 1999). Grindability is used to evaluate the size and type of mill needed to produce a product of a given size. It can only be used for rough sizing of a mill. Important factors that affect grindability are hardness, elasticity, toughness, and cleavage. The "hardness" of a material is measured by the Moh scale and is a fairly good indication of the abrasiveness of a material. Materials may range from soft, like talc and gypsum, to hard materials, like quartz and granite.

Some equipment employs impact, as in hammer mills and others employ "nipping" (i.e., the crushing of a feed between rolls or jaws). Within limits, kinetic energy as well as the dimensions and design of the crushing elements can be selected to obtain the desired particle reduction ratio. Because of the deformability of solid

materials, there is a theoretical limit to the size that particles can be crushed. Walas (1988) mentions the limits as 1 μm for quartz and 3–5 μm for limestone. There is, however, no practical lower limit, since these products can be much smaller.

In practical operations, about 1% of the input energy to the mill results as new surface energy of the product. Empirical relations for power consumption based on the extent of the size reduction have been developed for such a relationship is

$$W = 10W_i(1/d^{0.5} - 1/d_i^{0.5})\text{KWH/ton} \tag{12.6}$$

where d and d_i are final and initial diameters (μm) corresponding to 80% cumulative passing a given screen size.

Bond (1952) postulated that the work required to reduce large feed particles, d_i, to particles of diameter, d, is given by Equation 12.6. He also proposed a work index, W_i, which is defined as the gross energy requirement in KWH/ton of feed needed to reduce the feed, d_i, to a size that 80% of the material passes a 100 μm screen. Table 12.4 is a list of typical work index values. Example 12.2 compares a result from this equation with direct data from a manufacturer's catalog.

Characteristics of the main types of size reduction equipment are listed in Table 12.5, including sizes of feed and product, capacity, power consumption, and average reduction ratio. Coarse size reduction equipment operates with reduction ratios less than 10, fine ones with ratios of 100 or more. Sometimes several operations in series are necessary to reduce very large material to small particles, as shown in closed-circuit grinding in Figure 12.5(b) that has three stages of crushing and two stages of classification.

Toughness, hardness, and temperature sensitivity are some of the properties that influence choice of equipment and operating conditions. Fibrous materials require cutting rather than crushing action. Temperature-sensitive materials such as plastics and rubber need to be cooled with ambient or refrigerated air. Cryogenic processing that involves immersion of the material in liquid nitrogen is employed even for such prosaic materials as scrap automobiles and rubber tires; the low temperatures enhance brittleness and result in lowered power consumptions.

The kinds of equipment used for certain materials are identified in Table 12.6. Usually several kinds are more or less equally suited. Then the choice may be arbitrary and based on experience or on marginal considerations. Table 12.7 presents a broader range of materials that are being ground in four of the principal kinds of

---

EXAMPLE 12.1
Sizing a Hydrocyclone

A hydrocyclone assembly is required to handle 10,000 gpm of slurries of a solid with specific gravity 2.9 with a cutoff point of $d_{50} = 100$ μm. The allowable pressure is $\Delta P = 5$ psi. Several slurry concentrations V will be examined. Substituting into Eq. 12.4 with z the function of V in parentheses,

$$100 = \frac{13.2D^{0.675}e^z}{5^{0.3}1.9^{0.5}},$$

whence

$$D = (16.92/e^z)^{1.4815}.$$

The corresponding capacity Eq. (12.5) of one hydrocyclone is

$$Q = 0.7(5)^{0.5}D^2.$$

The results are tabulated following at several values of V:

		D			
V	e^z	in.	mm	Q	No. Units in Parallel
5	1.0953	57.7	1466	5214	2
10	1.4282	39.0	989	2375	4
20	2.0385	23.0	584	828	12
30	3.2440	11.6	293	209	48

From Figure 12.4(b), with 5 psi a 660 mm unit will handle 1000 gpm and have a cutoff between 50 and 150 μm. This corresponds to the calculated data with V about 19 vol %. For a more detailed study of hydrocyclone sizing, Mular and Bhappu (1980, pp. 376–403) may be consulted. The pressure drop can be adjusted to compensate for changes in slurry concentration.

TABLE 12.4 Typical Values of the Work Index W_i kWh/ton, of Eq. (12.3)

Material	Work Index W_i	Material	Work Index W_i
All materials tested	13.81	Kyanite	18.87
Andesite	22.13	Lead ore	11.40
Barite	6.24	Lead-zinc ore	11.35
Basalt	20.41	Limestone	11.61
Bauxite	9.45	Limestone for cement	10.18
Cement clinker	13.49	Manganese ore	12.46
Cement raw material	10.57	Magnesite, dead burned	16.80
Chrome ore	9.60	Mica	134.50
Clay	7.10	Molybdenum	12.97
Clay, calcined	1.43	Nickel ore	11.88
Coal	11.37	Oil shale	18.10
Coke	20.70	Phosphate fertilizer	13.03
Coke, fluid petroleum	38.60	Phosphate rock	10.13
Coke, petroleum	73.80	Potash ore	8.88
Copper ore	13.13	Potash salt	8.23
Coral	10.16	Pumice	11.93
Diorite	19.40	Pyrite ore	8.90
Dolomite	11.31	Pyrrhotite ore	9.57
Emery	58.18	Quartzite	12.18
Feldspar	11.67	Quartz	12.77
Ferro-chrome	8.87	Rutile ore	12.12
Ferro-manganese	7.77	Sandstone	11.53
Ferro-silicon	12.83	Shale	16.40
Flint	26.16	Silica	13.53
Fluorspar	9.76	Silica sand	16.46
Gabbro	18.45	Silicon carbide	26.17
Galena	10.19	Silver ore	17.30
Garnet	12.37	Sinter	8.77
Glass	3.08	Slag	15.76
Gneiss	20.13	Slag, iron blast furnace	12.16
Gold ore	14.83	Slate	13.83
Granite	14.39	Sodium silicate	13.00
Graphite	45.03	Spodumene ore	13.70
Gravel	25.17	Syenite	14.90
Gypsum rock	8.16	Tile	15.53
Ilmenite	13.11	Tin ore	10.81
Iron ore	15.44	Titanium ore	11.88
Hematite	12.68	Trap rock	21.10
Hematite—Specular	15.40	Uranium ore	17.93
Oolitic	11.33	Zinc ore	12.42
Limanite	8.45		
Magnetite	10.21		
Taconite	14.87		

[F.C. Bond, Bri. Chem. Eng. **6**, 378–385, 543–548 (1961)].

Power Requirement for Grinding

Cement clinker is to be reduced from an initial $d_{80} = 1500\,\mu\text{m}$ to a final d_{80} of $75\,\mu\text{m}$. From Table 12.4 the work index is $W_i = 13.49$. Substituting into Eq. (12.6),

$$W = 10(13.49)(1/\sqrt{75} - 1/\sqrt{1500}) = 12.1\,\text{kW/(ton/hr)}.$$

According to Table 12.8(b), a 3 ft × 24 in. ball mill requires 10 HP for a rate of 0.5 tons/hr, or 14.9 kW/(ton/hr), a rough check of the result from the equation.

fine grinders. Performances of ring roller, attrition, and cutter mills with some materials are given with Table 12.9. Additional operating data arranged by material are referred to in Table 12.12.

Open-circuit grinding occurs when no attempt is made to return the oversize material to the mill for further size reduction. *Closed-circuit* grinding employs a means whereby only material smaller than a specified size appears in the product. A less precise mode of operation employs an air stream through the equipment at such a rate that only the appropriately fine material is withdrawn and the rest remains until it is crushed to size. Ball mills sometimes are operated in this fashion, and also the ring-roller mill of Figure 12.5(a). For closer size control, all of the crushed material is withdrawn as it is formed and classified externally into product and recycle. The other examples of Figure 12.5 illustrate several such schemes.

Wet grinding with water is practiced when dusting is a problem, or when subsequent processing is to be done wet, as of ores that are later subjected to separation by flotation or sink-float processes. Removal of a slurry from a ball mill is easier than of dry material; there are cases where this advantage is controlling. Because of the lubricating effect of the water, power consumption of wet milling is less per ton, but this advantage may be outweighed by corrosion of the equipment.

12.4. EQUIPMENT FOR SIZE REDUCTION

Some of the many kinds of size reduction equipment are described in this section. The best source for complete equipment descriptions is manufacturers' catalogs. They often provide technical or expected performance data. Compilations of typical performance information may also be found in the *Chemical Engineers' Handbook*, especially the earlier editions. *Chemical Engineers' Buyers' Guide* 2004 (2003) is a source of the companies that manufacture size reduction equipment.

TABLE 12.5. Operating Ranges for Commonly Used Size Reduction Equipment

Equipment	Size of Feed (mm)	Size of Product (mm)	Reduction Ratio	Capacity (tons/hr)	Power Consumption (kW)
Gyratory crushers	200–2000	25–250	8	100–500	100–700
Jaw crushers	100–1000	25–100	8	10–1000	5–200
Cone crushers	50–300	5–50	8	10–1000	20–250
Impact breakers	50–300	1–10	40	10–1000	100–2000
Rod mills	5–20	0.5–2	10	20–500	100–4000
Ball mills	1–10	0.01–0.1	100	10–300	50–5000
Hammer mills	5–30	0.01–0.1	400	0.1–5	1–100
Jet mills	1–10	0.003–0.05	300	0.1–2	2–100
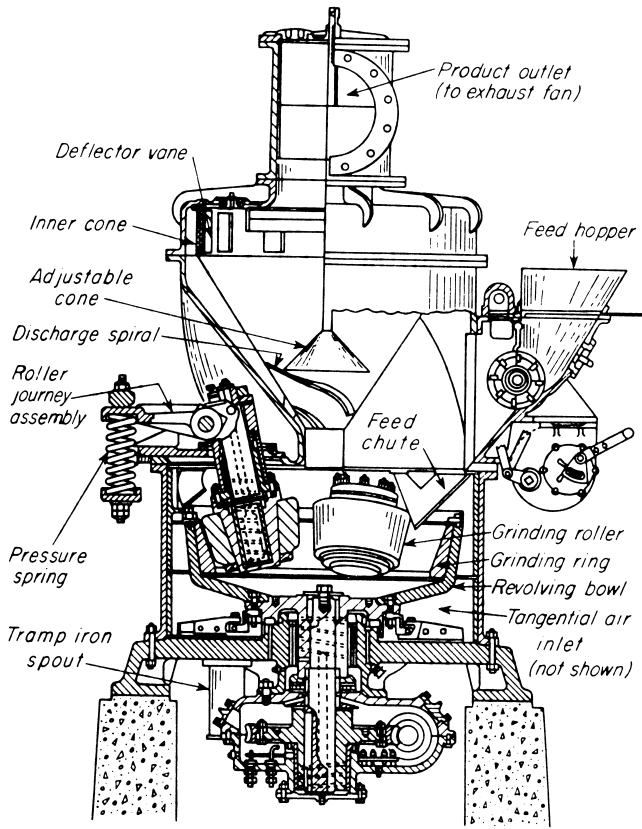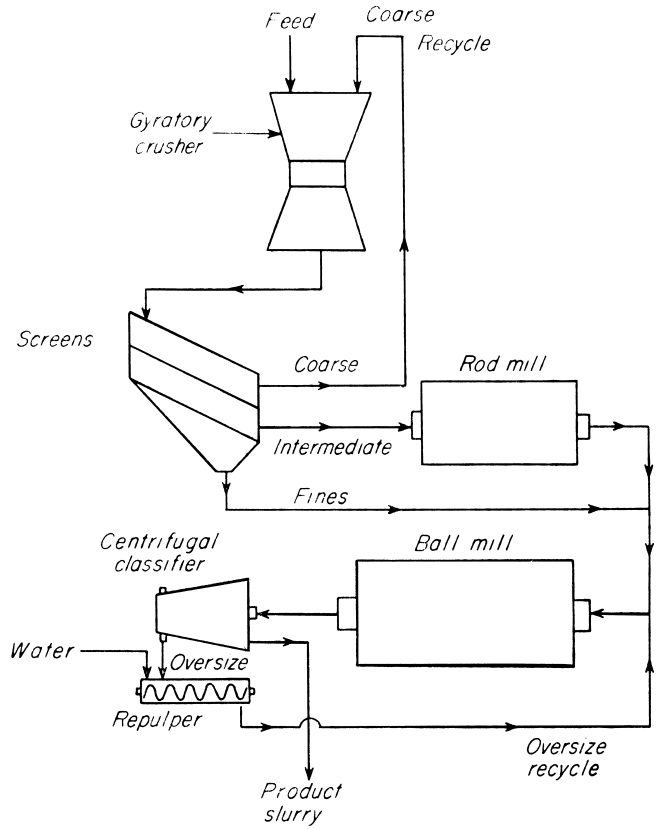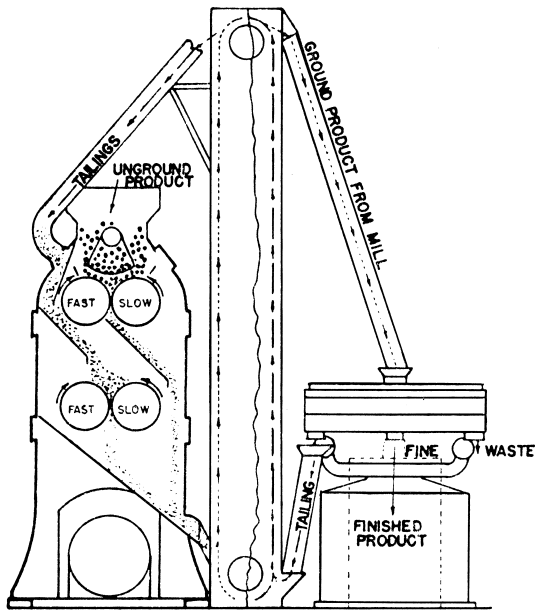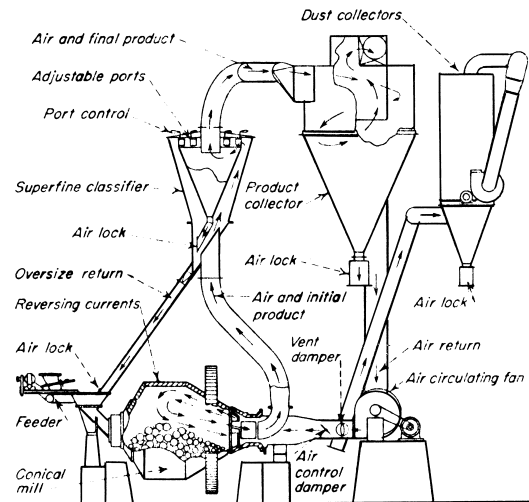
Figure 12.5. Closed-circuit grinding processes, in which coarse products are captured and recirculated until they are brought down to size. (a) Ring-roller mill (Raymond) with built-in air classification; crushing action is by rotating vertical rolls acting on a revolving bowl ring. (b) Flowsketch of closed-circuit grinding with three stages of grinding and two of classifying. (*McCabe and Smith*, Unit Operations, *McGraw-Hill, New York, 1976*). (c) A two-pair high roller mill; recycle is reground in the lower rolls; Table 12.7(c) lists materials ground by this equipment. (d) A Hardinge conical ball mill in a closed circuit with an air classifier and dust collectors (Walas, 1988).

A key consideration in the selection of size reduction equipment is the trade-off between the capital cost of the equipment and the operating expenses. This equipment is large, hence a high capital investment, and large quantities of utilities are required, resulting in high operating expenses.

JAW CRUSHERS

Crushers are slow-speed machines for the coarse reduction of large quantities of solids. Large lumps of solids up to several feet in diameter are crushed in jaw or gyratory crushers. Figure 12.6(a) is an example of one type of jaw crusher, the Blake crusher, and is suitable for hard, abrasive, and sticky feeds. In this type of unit, the movable jaw is pivoted at the top and an eccentric drives the machine. Through repeated movement, material is ground and falls out the bottom of the unit, producing a minimum of fines. If the feed has a large amount of cohesive material, like clays, the crusher may have a tendency to pack the fines in the outlet of the crusher. Operating and capacity data for Blake crushers are found in Table 12.10(a).

Jaw crushers are used as primary crushers and are often followed by other types of crushers. Blake crushers come in various sizes from about 10 to 400 HP. Smaller jaw crushers are manufactured with capacities of 1 to 10 HP.

GYRATORY CRUSHERS

The principle of operation is similar to that of a mortar and pestle used in chemistry laboratories. A cone-shaped part (the pestle) rotates within a tapered bowl (the mortar). The motion of the cone-shaped part against the tapered part causes attrition, since the space between the two parts varies, thereby causing material to be trapped between the two parts. Figure 12.7(a) is an example of a gyratory crusher. They are used on large hard-core and mineral crushing operations and are available in sizes up to 1000 HP. Very large lumps are often pre-crushed before being fed to a gyratory crusher. Gyratory crushers are more suited to clabby feeds and make a rounded product

ROLL CRUSHERS

Roll crushers are available as smooth or toothed rolls. Figure 12.6(b) is an example of a smooth-roll crusher and Table 12.10(b) presents data for a double tooth-roll crusher for coal. For smooth rolls, the feed size is limited by the angle of nip, which depends on surface conditions but it is approximately 16 degrees. Table 12.10(c) contains additional operating data for roll crushers. The relation between the diameters of the roll d_r and feed d_f and the gap d_0 between the rolls is given by

$$d_r = (0.961d_f - d_0)/0.039. \qquad (12.7)$$

For example, with $d_f = 1$ in. and $d_0 = 0.25$ in., the roll diameter is figured as 18 in. Table 12.10(b) lists 16 in. as the smallest size suitable for this service, which appears to be somewhat marginal in comparison with the calculated result. According to the equation, 1 in. lumps could be nipped by 16 in. rolls with a spacing of 0.34 in. It is not possible to state who is correct, the formula or the manufacturer.

Figure 12.6(b) shows a smooth roll assembly. Usually only one of the rolls is driven and one is spring mounted to prevent damage by uncrushable material in the feed. Reduction ratios shown in Table 12.10(c) range only between 2:1 and 4:1. The proportion of fines is comparatively small. Sets of rolls in series with decreasing settings are used to achieve overall high reduction ratios. The rolls of a pair can be driven at the same or different speeds, within a range of 50–200 rpm. The capacity generally is about 25% of the maximum corresponding to a continuous ribbon of material passing between the rolls. A sample listing of materials that are ground in roll mills is in Table 12.7(a). In the arrangement of Figure 12.5(c) the upper pair of rolls is the primary crusher whereas the lower pair works on recycle of the oversize.

TUMBLING MILLS

These mills consist of vessels rotating on a horizontal axis and are charged with a mass of relatively small elements that tumble and crush the process material as the element falls. Their function is to mix as well as grind. Figure 12.5(b) shows a closed-circuit arrangement with a ball mill. The crushing elements most commonly used are balls of several sizes, ceramic pebbles, rods the length of the shell, or a range of process material (made to grind itself). Ball, pebble, rod, and tube mills are in this category and will be discussed in the following sections.

The mode in which the material grinds itself is called *autogeneous grinding*. Such operation can achieve size reduction from 25 cm to 0.1 mm in one step. Autogeneous mills operate at 80 to 85% of the critical speed, which is the speed at which the grinding media are thrown to the wall and cling to it. They are desirable for mineral treatment because they release the mineral content without overgrinding, which could complicate a subsequent flotation process, for instance. Materials for which the process is used are friable and grainy, such as silica rock, bauxite, cement clinker, limestone, hematite, and others. In comparison with ball milling, steel consumption is largely eliminated but energy costs are greater by 25 and 100% because of lower impact forces with low density materials.

TABLE 12.6. Size Reduction Equipment Commonly Used in the Chemical Process Industries

Material	Equipment
Asbestos and mica	roll crushers, hammer, and jet mills
Cement	gyratory, jaw and roll crushers, roller, and ball mills
Clays	pan crushers, ring-rollers, and bead mills
Coal	roll crushers, pulverizers, ball, ring-roller, and bowl mills
Coke	rod, ball, and ring-roller mills
Colors and pigments	hammer, jet, and ring-roller mills
Cosmetics and pharmaceuticals	dispersion and colloid mills
Cotton and leather	rotary cutters
Flour and feed meal	roller, attrition, hammer, and pin mills
Graphite	ball, tub, ring-roller, and jet mills
Hard rubber	roller mills
Lime and Shells	hammer and ring-roller mills
Metallic minerals	gyratory and jaw crushers, tumbling mills
Paper and plastics	cutters and slitters
Phosphates	ball and ring-roller mills
Polymers	pulverizers, attrition mills
Pressed cakes	hammer and attrition mills
Refractories	gyratory and jaw crushers, pan and ball mills
Salts	cage and hammer mills
Soaps	hammer, multicage, and screen mills
Starch	hammer and pin mills
Stone and aggregate	gyratory, jaw, and roll crushers
Sulfur	ring-roller mills
Talc and soapstones	roll crushers, ring-roller, pebble, and jet mills

TABLE 12.7. Materials that Have Been Ground in Particular Kinds of Mills

(a) Crusher Rolls

ammonium nitrate	feedstuffs
asbestos	flaxseed
barley malt	floor tile
bauxite	flour
beet pulp	fuller's earth
bone	glue
casein	grains
catalyst beads	gun powder
cereals	insulating materials
charcoal	iron oxide
cheese	lumpy chemicals and flour
chemicals	magnesium oxide
coal	malt
cocoa cakes	malted milk
coconut shells	meat scraps
coffee	mustard seed
cork	oil bearing seeds
corn	pelletized feeds
corn cobs	pepper
corn meal	pharamaceuticals
cottonseed	plastics
cracker meal	reclaim rubber
crackings	resin
crimping grains	salt
dog food cakes	soy beans
DDT	spices
dolomite lime	sponge iron
dried biscuits	starch
dried apple pulp	uranium concentrates

(b) Disc Attrition Mills

alloy powders	gum arabic
alum	hops
aluminum chips	leather
apples, dried	metal powder
asbestos	mica
bark	nuts and shells
borax	oil cake
brake lining scrap	paris green
brass chips	peanuts and hulls
caustic soda	pepper
cereals	phosphates
chalk	plaster
charcoal	potash
chemical salts	potatoes
chips	pumice
cloves	rice and hulls
cocoa	roots
coconut shells	rosin
copper powders	rubber
copra	sawdust
cork	salt
corn	suds
cottonseed and hulls	soy beans
drugs	spices
dye stuffs	starch
egg shells	shavings
feathers	tankage
fertilizers	tobacco stems
fish meal	wood pulp
glue	

(c) Roller Mills

alum	hematite
barytes	insecticide roots
bentonite	kaolin
clay	lime
cement clinker	limestone
chalk	mica
cocoa	phosphate rock
DDT	resins
dolomite	soy bean cake
feldspar	sulfur
graphite	talc
gypsum	titanium dioxide

(d) Hammer Mills

aluminum tristearate	graphite
animal glue	guar gum
antioxidants	gum acacia
asbestos	gypsum
asphalt	irish moss
aspirin	lactose
bagasse	lead, red
barley	licorice root
bentonite, dried	lime, hydrated
bone char	mica
brewer's yeast	milo grain
calcium carbonate	oats, rolled
calcium phosphate	oyster shells
carbon black	pentaerythritol
cellulose acetate	perlite
cinnamon	pigments
clay	plastic molding compounds
coal	potato flour
cocoa cake	pyrethrum
cocoa-sugar mixtures	saccharin
coconut shells	sage
corn meal	soya flour
cottonseed cake	sugar
diatomaceous earth	talc
dyestuffs	tobacco stems
etching powder	vermiculite
ginger	

(e) Fluid Jet Mills

aluminum	molybdenum disulfide
aluminum oxide	nephelene syenite
antibiotics	phenolics
asbestos	PVC
barytes	pyrethrum
benzene hexachloride	resins
carbon	rotenone
carborundum	salts
coal	shellacs
cocoa	silica gel
cryolite	silicon
DDT	silicon carbide
dieldrin	sugar
fatty acids	sulfa drugs
feldspar	sulfur
ferrochrome	talc
frits	titanium dioxide
fuller's earth	toluidine red
graphite	vanilla beans
iron oxide	vitamins
lead oxide	waxes
mica	yeast

(After Mead, ''Encyclopedia of Chemical Process Equipment,'' Reinhold, NY, 1964).

TABLE 12.8. Performance of Ball, Pebble, and Rod Mills in Continuous and Batch Modes

(a) Capacities of Some Straight-Sided Ball Mills on Quartz to Various Meshes

Denver Ball Mill Size Dia. × Lgt. (ft)	Capacity (tons per 24 hrs) Medium-hard Quarts					Rpm Mill	Horsepower	
	2-in to 35 mesh	1-in to 48 mesh	1/2-in to 65 mesh	1/2-in to 100 mesh	1/4-in to 200 mesh		To Run	Of Motor
3 × 2	15	11	9	6		33	7 1/2	10
3 × 3	20	16	14	9		33	10	15
3 × 4	25	21	19	12	7	33	12	15
3 × 6	35	31	29	18	9	33	17 1/2	20
3 × 9	50	46	44	27	13	33	24	25
4 × 3	42	34	30	22	12	28	17	20
4 × 5	63	55	50	31	16	28	28	30
4 × 10	116	108	103	62	26	28	49	50
5 × 3	77	63	55	40	22	26	34	40
5 × 6	130	116	110	67	33	26	57	60
5 × 12	250	236	224	136	54	26	103	125

(Denver Equipment Co.).

(b) Hardinge Conical Ball Mills in Continuous Wet Grinding; Dry Grinding Rates Are 10–20% Less

Size	Weight of		Weight of Balls Maximum (lbs)	Rpm*	Motor (max. hp)	Capacity (tons per 24 hrs)		
	Mill	Lining				1 1/2-in to 10 mesh	1/2-in to 100 mesh	1/4-in to 98% −325 mesh
3′ × 24″	3,050	2,400	2,400	39.8	10	32	12	4
5′ × 22″	10,200	8,000	8,300	30.4	40	140	49	19
6′ × 36″	17,100	11,700	17,500	27.7	75	282	97	38
8′ × 48″	29,000	23,000	43,500	23.8	200	820	274	108
10′ × 66″	50,600	35,000	83,500	21.2	450	1,900	632	249

(Hardinge Co.).

(c) Hardinge Conical Pebble Mills in Continuous Wet Grinding; Dry Grinding Rates Are 10–20% Less

Size	Weight of		Weight of Balls Maximum (lbs)	Rpm*	Motor (max. hp)	Capacity (tons per 24 hrs)		
	Mill	Lining				1 1/2-in to 10 mesh	1/2-in to 100 mesh	1/4-in to 98% −325 mesh
3′ × 24″	3,000	1,300	700	40.4	5	15	5.5	2.1
5′ × 22″	9,600	4,000	2,300	31.2	15	54	19	7.5
6′ × 36″	16,500	6,500	4,800	28.2	30	117	42	17
8′ × 48″	19,400	12,300	12,700	24.1	75	326	117	45
10′ × 66″	35,900	16,800	25,500	21.4	150	675	242	95

(Hardinge Co.).

(d) Pebble and Balls Mills for Batch Grinding of Sand of 100 lb/cuft; Pebble Charge 50 vol %, Steel Ball Charge 33 vol %

Mill No.	I.D. of Steel Cylinder	Pebble Mills			Ball Mills— Capacity.	
		Capacity, Grinding Porcelain	Dry (lbs) Buhrstone	Approx. rpm	Dry Grinding (lbs)	Rpm
8 1/2A	24 × 24″	104	9C	40	188	36
8 1/2 C	24 × 36″	164	145	40	280	36
6 A	30 × 36″	273	245	36	140	32
5	36 × 42″	440	440	32	740	29
4 1/2	42 × 48″	720	720	29	1152	27
2 A	60 × 60″	1916	1890	19	2936	17
1 A	72 × 72″	3456	3410	16	5076	14
1 C	72 × 120″	5900	5850	16	8460	14

(Paul Abbe Co.).
Data in TABLE 12.8 from Walas (1988).

(e) Performance of Marcy Rod Mills

Size, ft.	Rod charge, tons	Hp. to run	Mill speed, r.p.m.	Capacity, tons/24 hr.				
				No. 8 sieve	No. 20 sieve	No. 35 sieve	No. 48 sieve	No. 65 sieve
2 × 4	0.9	4– 6	38	28	15	12	10	7
3 × 6	3.6	18– 22	30	105	80	65	50	40
4 × 8	7.6	44– 48	25	240	180	145	120	90
5 × 10	14.5	85– 95	21	525	390	315	260	195
6 × 12	24.1	135–150	17¼	855	640	510	425	320
7 × 15	42.1	225–250	15	1600	1200	965	800	600
8 × 12	43.4	230–250	13.2	1675	1250	1000	830	625
9 × 12	54.7	310–340	12.5	2240	1680	1350	1115	835

(Mine and Smelter Division, Kennedy Van Saun Co).
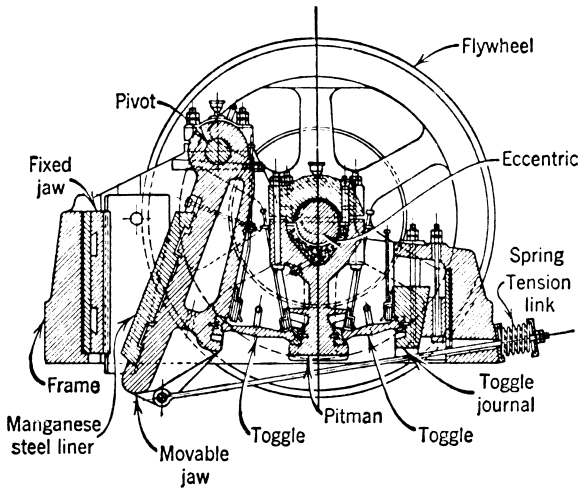
(a)
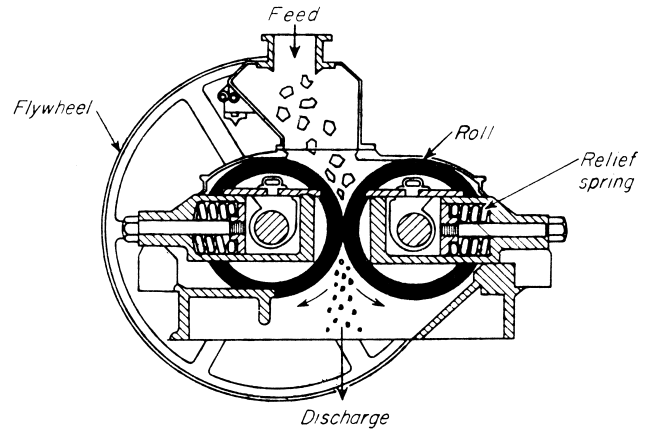
(b)
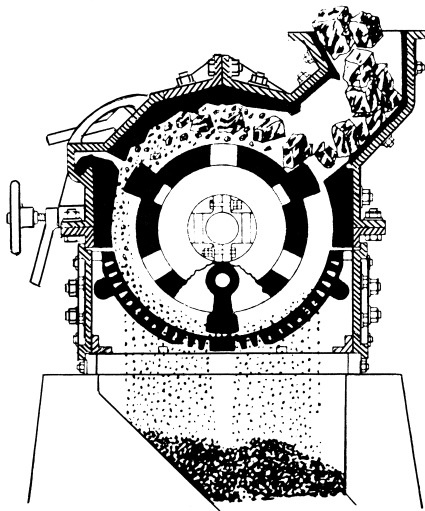
(c)
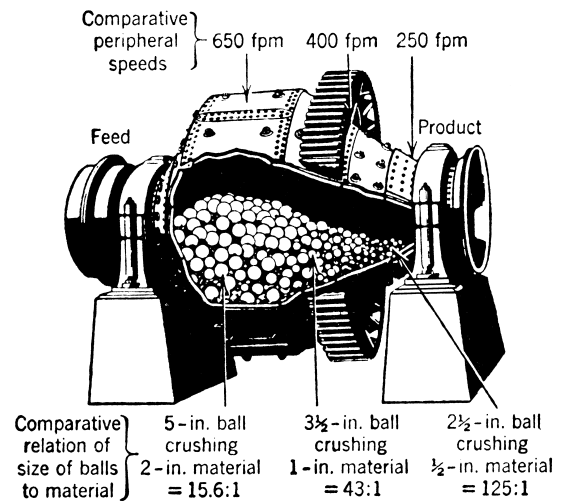
(d)
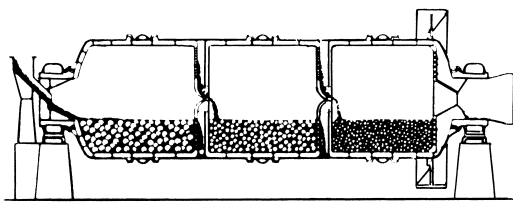
(e)
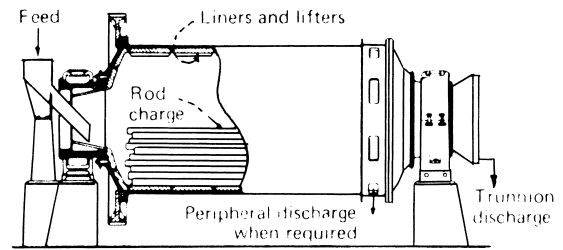
(f)

Figure 12.6. Jaw, roll, impact, and tumbling equipment for size reduction. (a) Blake-type jaw crusher operates at 200–300 strokes/min (*Allis–Chalmers Co.*). (b) Smooth roll crusher, for which operating data are in Table 12.16(b)(c). (c) Swing hammer mill; operating data in Table 12.11(a). (d) View of a conical ball mill, showing distributions of balls and material and crushing ranges; data in Table 12.8(b). (e) Tube mill with three compartments, length to diameter ratio 3–5. (f) Rod mill in a cylindrical tumbler, $L/D = 1.2$–1.6; data in Table 12.8(e). (Walas, 1988).

TABLE 12.9. Some Other Kinds of Disintegrators

(a) Ring Roller Mills to Make Down to 100 Mesh

Barytes, 8 to 10 tons/hr to 40 mesh
Coal, 5 to 6 tons/hr to 40 mesh
Coke (96 hour) $3\frac{1}{2}$ to 4 tons/hr to 20 mesh
Fire clay, 8 to 11 tons/hr
Florida pebble, 7 t. to 85%–60 mesh
Florida pebble, 3 t. to 95%–100 mesh

Gannister, 10 to 12 tons/hr to 14 mesh
Iron borings, 8 to 10 tons/hr to 20 mesh
Limestone, 8 to 12 tons/hr to 20 mesh
Limestone, 3 to 4 tons/hr to 85%–200 mesh
Manganese, 2 to 4 tons/hr to 80 mesh
Marble, 3 to 4 tons/hr to 95%–100 mesh
Oyster shells, 4 to 5 tons/hr to 60 mesh

    The No. 2 mill has 50 per cent larger capacities
    The No. 0 capacity is approximately 35 per cent of the figures for No. $1\frac{1}{2}$ in this table.
    Size of feed: 1″ to $1\frac{1}{2}″$.

DIMENSIONS AND SPEEDS FOR STURTEVANT RING ROLL MILLS

Size	Ring Diam. × Face	Rolls Diam. × Face	Ring Speed (rpm)	Horsepower
No. 0	24″ × 7″	14″ × 7″	125	8 to 15
No. $1\frac{1}{2}$	45″ × 8″	16″ × $10\frac{1}{2}$	64	45 to 50
No. 2	44″ × 14″	18″ × 14″	70	75

    (Sturtevant Mill Co.).

(b) Attrition Mills for Tough Organic Materials

Material	Size-reduction details	Unit[*]	Capacity lb./hr.	Hp.
Alkali cellulose	Shredding for xanthation	B	4,860	5
Asbestos	Fluffing and shredding	C	1,500	50
Bagasse	Shredding	B	1,826	5
Bronze chips	$\frac{1}{8}$ in. to No. 100 sieve size	A	50	10
Carnauba wax	No. 4 sieve to 65% < No. 60 sieve	D	1,800	20
Cast-iron borings	$\frac{1}{4}$ in. to No. 100 sieve	A	100	10
Cast-iron turnings	$\frac{1}{4}$ in. to No. 100 sieve	E	500	50
Cocoanut shells	$2 \times 2 \times \frac{1}{4}$ in. to 5/100 sieve	B	1,560	17
	5/100 sieve to 43% < No. 200 sieve	D	337	20
Cork	2/20† sieve to 20/120 < No. 200 sieve	D	145	15
Corn cobs	1 in. to No. 10 sieve	F	1,500	150
Cotton seed oil and solvent	Oil release from 10/200 sieve product	B	2,400	30
Mica	$4 \times 4 \times \frac{1}{4}$ in. to 3/60 sieve	B	2,800	6
	8/60 to 75% < 60/200 sieve	D	510	7.5
Oil-seed cakes (hydraulic)	$1\text{-}\frac{1}{2}$ in. to No. 16 sieve	F	15,000	100
Oil-seed residue (screw press)	1 in. to No. 16 sieve size	F	25,000	100
Oil-seed residue (solvent)	$\frac{1}{4}$ in. to No. 16 sieve	F	35,000	100
Rags	Shredding for paper stock	B	1,440	11
Ramie	Shredding	B	820	10
Sodium sulfate	35/200 sieve to 80/325 sieve	B	11,880	10
Sulfite pulp sheet	Fluffing for acetylation, etc.	C	1,500	50
Wood flour	10/50 sieve to 35% < 100 sieve	D	130	15
Wood rosin	4 in. max. to 45% < 100 sieve	B	7,200	15

    [*]A—8 in. single-runner mill
     B—24 in. single-runner mill
     C—36 in. single-runner mill
     D—20 in. double-runner mill
     E—24 in. double-runner mill
     F—36 in. double-runner mill
    [†]2/20, or smaller than No. 2 and larger than No. 20 sieve size.
    (Sprout-Waldron Co.).

TABLE 12.9.—(*continued*)

(c) Rotary Cutters for Fibrous Materials

Material	Screen Opening	Feed Rate, lb./hr.	Hp.	Air	Remarks on Product
Amosite asbestos pencils	$1\frac{1}{2}''$	1000	11	Yes	Finer fiber bundles average length 2″
Cellophane bags	$\frac{11}{32}''$	200	10	Yes	Finer than $\frac{5}{16}''$
Cork	$\frac{3}{16}''$	525	16	Yes	90% 4/24″ sieve
Chemical cotton	60 mesh	120	15	Yes	Flock; 35% under No. 100 sieve
Leather scrap	$\frac{3}{4}''$	600	20	Yes	Precutting before shredding
Fiberglass	$\frac{3}{16}''$	300	18	Yes	1″ (approx.) lengths
Waste paper	$\frac{5}{16}''$	338	13	Yes	Through No. 4 sieve and finer
Sheet pulp	40 mesh	150	15	Yes	Flock; 85%, 40/100 sieve
Tenite scrap	$\frac{5}{16}''$	340	12	No	Granulated for reuse
Vinylite scrap	$\frac{7}{32}''$	300	15	Yes	35%, 6/10 sieve; granular
$\frac{1}{3}''$ Geon sheet	$\frac{5}{16}''$	540	11	No	99%, 4/20 sieve; for molding granules
Cotton rags	$\frac{3}{4}''$	500	11	Yes	No linting
Buna scrap	10 mesh	264	12	Yes	Granular
Neoprene scrap	30 mesh	90	14	Yes	20°F, temperature rise
Soft-wood chips	$\frac{1}{8}''$	960	12	Yes	90%, 10/50 sieve
Hard-wood chips	$\frac{1}{16}''$	290	11	Yes	83%, 20/100 sieve

[*]90 per cent 4/24 sieve, *i.e.*, 90 per cent is through No. 4 and on No. 24 sieve.
(Sprout-Waldron Co.). Data in TABLE 12.9 from Walas (1988).

TABLE 12.10. Performance of Jaw and Roll Crushers

(a) Capacities and Data on Blake Type Jaw Crushers (Selected Items)[a]

Size of Jaw Opening (in.)	Capacity (tons/hr) (1 ton to 20 cuft Capacity) Open Side Setting (in.)						Jaw Motion (in.)	Horse Power Req.	rpm
	1	1½	2	2½	3	4			
10 × 7	7	9	12				A } $\frac{5}{8}$	$7\frac{1}{2}$	300
	8	12	16				B }		
20 × 10	15	20	24	31			A } $\frac{5}{8}$	15	275
	24	32	40	49			B }		
30 × 18			38	45	61		A } $\frac{11}{16}$	40	250
			48	60	74	102	B }		

[a]A-straight jaw plates; B-nonchoking jaw plates.
[*](Data supplied by Allis–Chalmers Mfg. Co., Milwaukee, WI).

(b) Double Toothed-Roll Crushers on Coal

Roll Size (in.)		Maximum Size Lump (in.)	Roll (rpm)	Capacity (TPH) Reducing to $1\frac{1}{4}$ to 2	Minimum Motor (HP)
Dia	Face				
18	18	4	150	39–67	8
18	20	4	150	46–75	8–10
18	24	4	150	52–88	10–12
24	18	14	125	46–74	12–18
24	20	14	125	54–82	15–20
24	24	14	125	62–98	15–20

(Stephens–Adamson Co.) Data in TABLE 12.10 from Walas (1988).

HAMMER MILLS

Hammer mills employ rotating elements that beat the material until it is small enough to pass through a screen located at the bottom of the mill casing as shown in Fig. 12.6(c). The length-to-diameter ratio of these mills is about 1 to 1. A rotating shaft is horizontally oriented and the shaft is outfitted with sets of swing hammers. The grinding action results from impact and attrition between the lumps of material being ground, the housing, and the hammers. The product size is determined by the speed of the hammers and the size of the screen openings. Table 12.11(a) shows the former effect. The units in this table operate at speeds up to 900 rpm and make size reductions of 40 to 1. Smaller units in Table 12.11(b) operate at

(c) Relation of Capacity, Size of Feed, Roll Setting, and Speed of Rolls for Sturtevant Balanced Crushing Rolls; Screening in Closed Circuit (Average Rock, Which Can Be Nipped at Speeds Named)

Size of Roll Dia × Face (in.)	Feed Cubes (in.)	Roll Setting (in.)	Speed (rpm)	Capacity (tons/hr)
16 × 10	1.25	0.61	200	26.6
	1	0.25	212	11.6
	0.75	0.2	225	9.8
	0.50	0.125	245	6.67
	0.25	0.065	272	3.86
24 × 15	2	1	115	56.4
	1.5	0.54	130	34.4
	1	0.25	140	17.15
	0.75	0.2	150	14.7
	0.5	0.125	163	10
36 × 20	3	1.5	59	87
	2.5	1	62	61
	2	0.5	70	34.2
	1.5	0.37	78	29.2
	1	0.25	85	20.9

(Sturtevant Mill Co.).

(a)

(b)

(c)

(d)

(e)

(f)

(g)
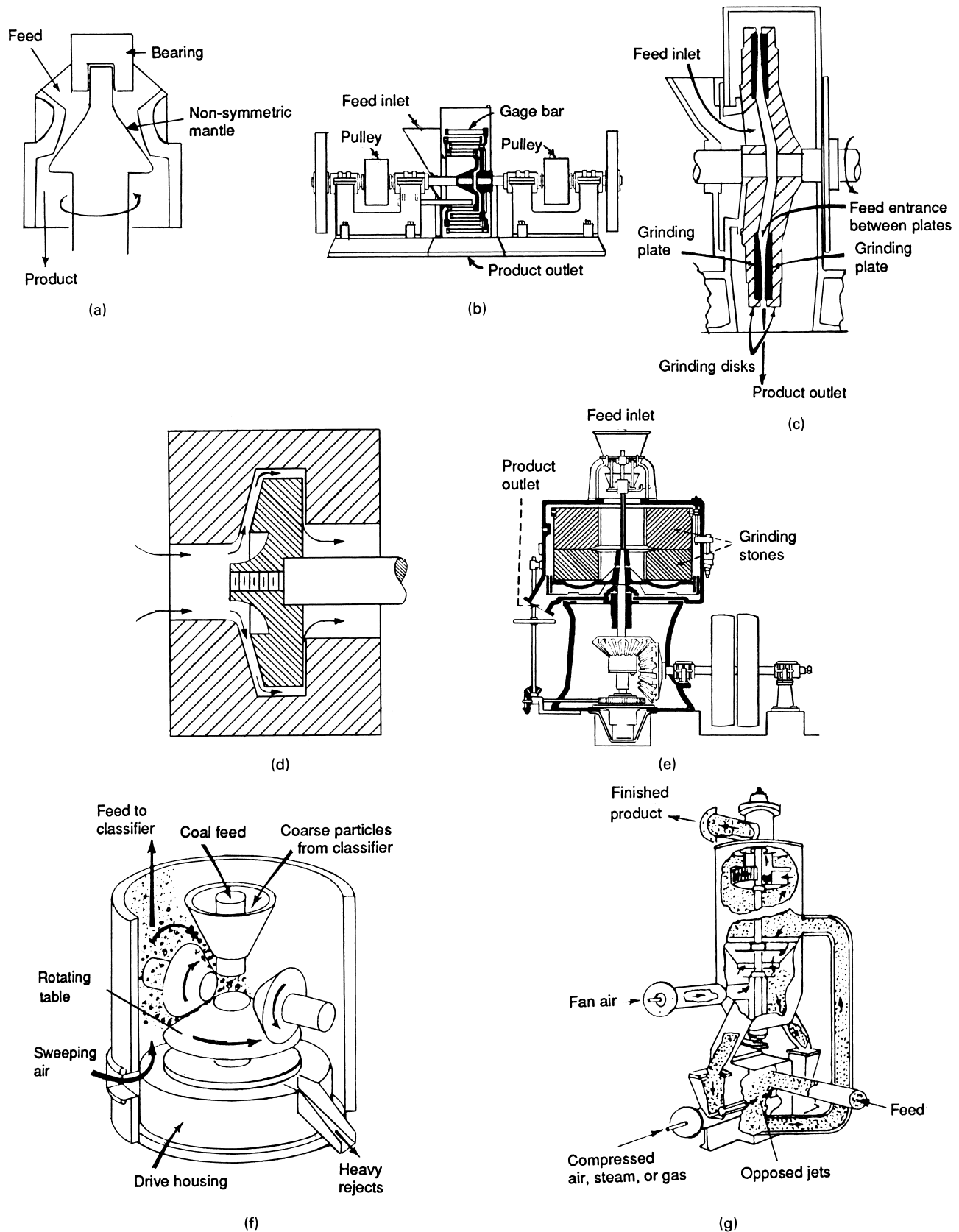
Figure 12.7. Examples of mostly less common devices for size reduction. (a) Schematic of a gyratory crusher for very large lumps. (b) Squirrel-cage disintegrator with four cages. (c) Disc-type attrition mill, rotating at 1200–7000 rpm, clearances adjustable by increments of 0.001 in. (d) Schematic of colloid mill, clearance adjustable between 0.001 and 0.050 in., peripheral speeds to 10,000 ft/min. (e) Buhrstone attrition mill, used for making flour and grinding paints, printers inks and pharmaceuticals. (f) Roller or spindle mill; the crushed material is thrown outwards and removed with an air stream. (g) Majac fluid energy mill making a −200 mesh product; opposed air jets cause high speed collisions and disintegration of the material. (Walas, 1988).

TABLE 12.11. Performance of Impact Disintegrators

(a) Hammer Mills

	tons/hr		
	Limestone, $\frac{1}{8}$ in. Slots	Limestone, $\frac{1}{4}$ in. Slots	Burnt lime, $\frac{1}{4}$ in. Slots
0 Swing-sledge	2–4	4–7	7–9
1 Swing-sledge	6–10	12–15	18–20
2 Swing-sledge	12–15	20–30	60–70
00 Hinged-hammer pulverizer	1–2	2–4	4–6

Approximate Screen Analysis of Product, Reducing 3 in. Limestone

	Passing through Mesh Stated			
Grate Spacing (in.)	$\frac{1}{4}$ in.	10 mesh	50 mesh	100 mesh
$\frac{1}{4}$ $\frac{1}{8}$	99.8%	85% 99	50% 70	40% 60

$\frac{1}{8}$ in. slots means that the grating space was $\frac{1}{8}$ in.

Dimensions and Speeds

	Length	Width	Inside Diameter	Inside Width	Feed Opening	Pulley Speed (rpm)	Approx. HP
0 Swing-sledge	4ft 3 in.	4ft 1in.	24 in.	10 in.	13 × 11 in.	1200–1500	12
1 Swing-sledge	5ft 1 in.	5ft 8 in.	30 in.	20 in.	17 × 20 in.	1000–1300	40
2 Swing-sledge	6 ft	7 ft	36 in.	30 in.	20 × 30 in.	1000–1200	75
00 Hinged-hammer pulverizer	2 ft 5 in.	3 ft	16 in.	11 in.	12 × 12 in.	1200–3600	5–20
0–24 in. Hinged hammer pulverizer	3 ft 7 in.	5 ft 8 in.	24 in.	24 in.	$12\frac{1}{2}$ × 24 in.	1000–1200	15–20

(Data supplied by Sturtevant Mill Co., Boston, MA).

(b) High Speed "Mikro-Pulverizer"

Material	Mesh Fineness	No. 1 (5 HP)	No. 2 (15 HP)	No. 3 (40 HP)	No. 4 (75 HP)
Aluminum Hydrate	99.8% through 200	600	1,800	4,800	9,000
Ball Clay	98% through 325	600	1,800	4,800	9,000
Calcium Arsenate	99% through 300	1,250	3,750	10,000	18,750
Bituminous Coal	70% through 200	500	1,500	4,000	7,500
Carbon Black	99.99% through 325	450	1,350	3,600	6,750
Cellulose Acetate (Pulp)	94% through 40	200	600	1,600	3,000
Chrome Yellow	99.9% through 200	1,250	3,750	10,000	18,750
Dry Color Slurry	Smooth Slurry	800	2,400	6,400	12,000
Face Powder Mixture	Good Blend	600	1,800	4,800	9,000
Gypsum, Raw	88% through 100	1,650	5,000	13,200	24,750
Iron Blue	95% through 325	750	2,250	6,000	11,250
Kaolin	99.9% through 325	750	2,250	6,000	11,250
Malted Milk	99% through 20	625	1,875	5,000	9,400
Molding Compound	90% through 16	750	2,250	6,000	11,250
Soap Powder	96% through 20	1,500	4,500	12,000	22,500
Soybean Flake	94% through 100	300	900	2,400	4,500
Sugar	99% through 100	600	1,800	4,800	9,000
Tile Clay Body	100% through 16	1,650	5,000	13,200	24,750
Titanium Dioxide	99.8% through 325	600	1,800	4,800	9,000
White Lead	99.99% through 325	1,000	3,000	8,000	15,000
Zinc Oxide	99.9% through 325	600	1,800	4,800	9,000

Top Rotor Speeds— Approximate Idle Loads		
Unit	Speed	HP
No. 1	9,600 RPM	11/2
No. 2	6,900 RPM	4
No. 3	4,600 RPM	12
No. 4	3,450 RPM	18

(Pulverizing Machinery Co.).

(c) Steam- or Air-Operated Jet Mills

Material	Mill Diameter	Grinding Type	Medium Flow	Solid Feed Rate	Approx. Avg. Particle Size (μ)
Titanium Dioxide	30″	steam	4000 lbs/hr	2250 lbs/hr	less than 1
Sulfur	24″	air	1000 cfm	1300 lbs/hr	3–4
Talc (varies)	30″	steam	4000 lbs/hr	2000 lbs/hr	2
Iron Oxide Pigment	30″	steam	4000 lbs/hr	1000 lbs/hr	2–3
Cryotite	30″	steam	4000 lbs/hr	1000 lbs/hr	3
Barytes	30″	steam	4000 lbs/hr	1800 lbs/hr	3–4
Fuller's Earth	20″	steam	1200 lbs/hr	600 lbs/hr	3–4, 5 top
Anthracite Coal	20″	air	1000 cfm	1000 lbs/hr	5–6
DDT (50%)	24″	air	1000 cfm	1400 lbs/hr	3–4
Procaine-Peniciltin	8″	air	100 cfm	25 lbs/hr	5.20 top

(Sturtevant Mill Co.). (Data in TABLE 12.11 from Walas (1988).

faster speeds and make very fine powders. Streams of ambient or refrigerated air may be used to reduce the heating effect. Even under these conditions softening materials like natural resins can be ground satisfactorily.

Hammer mills are the principal equipment in cryogenic processing when products of 50–100 mesh are adequate. Scrap automobiles and rubber tires are chilled with liquid nitrogen to be made brittle to facilitate grinding (Walas, 1988).

This equipment is particularly suited for crushing soft, friable materials to cube-shaped products with small proportions of fines. For fibrous materials, the screen is provided with cutting edges. Some data are in Table 12.9(c). A list of materials that are handled in hammer mills is found in Table 12.6(a), and other products are referred to in Table 12.11.

TUBE MILLS

Tube mills are of uniform diameter with a ratio of length to diameter about 3 to 5. Because of the greater length and a corresponding greater residence time, a finer product is obtained. Tube mills often have several compartments separated by perforated partitions. As the material passes through the mill, the size is reduced, starting with preliminary grinding, and the finished product is obtained at the discharge end of the mill. Figure 12.6(e) is an example of a tube mill.

Ball mills serve as a final stage of comminution. Balls have a greater ratio of surface area to weight than rods so they are better suited to fine grinding. The length to diameter ratio ranges from less than 1 to about 1.5. Rotation speed is greater than that of rod mills, being 70–80% of critical. Mills that are subjected to vibration can operate above the critical speed. The bulk volume of balls is about 50% of the mill volume.

The Denver ball mills for which operating data are shown in Table 12.8(a) normally are charged with equal weights of 2-, 3-, and

TABLE 12.12. Mill Performance Data for Grinding of Specific Products

Material	Equipment	Handbook Table No.
Anthracite	ball mill CC	46
Barite	wet Hardinge ball mill	35
Cement clinker	three-compartment wet tube mill	42
Fertilizers	hammer mill	41
Fuller's earth	roller	48
Grain	attrition	32
Gypsum rock	ring-roller	45
Iron oxide	ring-roller	47
Limestone	ring-roller	34
Limestone	wet Hardinge ball mill	35
Metal stearates	hammer mill	50
Oyster shells	hammer mill	38
Phosphates	ball mill	39–40
Quicklime	ball mill CC	44
Rubber	roller mill	51
Seed cake	hammer mill	33
Siliceous refractories	pebble mill	36
Slate	three-compartment wet tube mill	43
Sodium carbonate	roller	48
Sulfur	ring-roller	49

Note: CC is closed circuit grinding; the ring-roller mill has built-in air classification.

(From *Chemical Engineers' Handbook*, 6th ed., McGraw-Hill, New York, 1984, pp. 8.48–8.60; Walas, 1988).

4-in. balls; or for finer grinding, with equal weights of 1.5-, 2-, and 3-in. balls. Figure 12.6(d) is of the widely used conical shape of mill in which a range of sizes of balls group themselves axially during operation. The balls range from 5 in. down, the large ones for crushing the large lumps and the small ones acting on the small lumps. The performance data of Table 12.8(b) are for wet grinding; dry grinding capacities are 10–20% less. Segregation of balls by size also is achieved in cylindrical shapes with spiral twists in the liner profile.

ROD MILLS

Rod mills are single-compartment mills partially filled with rods rotating horizontally. They are capable of taking relatively large material, 50 mm, and reducing it to 300 mesh, minimizing the amount of fine material. They can produce a product of relatively narrow size range. The ratio of rod length to vessel diameter is 1.4 to 1.6. Ratios below 1.25 often result in tangling of the rods. Rods in use range from 25 to 150 mm diameter; smaller ones tend to bend and break. The maximum rod length is about 6 m; above this, they tend to bend. About 45% of the bulk volume of the mill is occupied by rods. Figure 12.6(f) is a typical rod mill, and typical operating data are found in Table 12.8(e). Because the coarse feed tends to spread the rods at the feed end, grinding takes place preferentially on the large particles and results in a product of relatively narrow size range. Rod mills are nearly always run in open circuit grinding.

PEBBLE MILLS

Pebble mills are single-compartment tube mills with ceramic balls as the grinding medium. They are used in applications for grinding and mixing of light-colored pigments, food products, and pharmaceuticals where iron contamination must be avoided. The grinding rate is approximately proportional to the weight of the balls. In comparison to steel ball mills, the grinding rate with ceramic balls is only about 1/3 to 1/2 that with steel balls. Data in Tables 12.8(c) and 12.8(d) confirm this statement. Any degree of fineness can be obtained using batch grinding along with sufficient time. Since the grinding rate is roughly proportional to the weight of the balls, the grinding rate with pebbles is only about 1/3 that with steel balls of the same volume. This is clear from data in Table 12.8(b).

ROLLER MILLS

Roller mills, Figures 12.5(a) and 12.7(f), employ cylindrical or tapered surfaces that roll against flatter surfaces, crushing nipped particles. In Figure 12.5(a), spring-loaded rolls are forced against a revolving bowl ring and crush the material that is thrown between them with a plow-like device. In an alternative design, the ring is stationary and a roll assembly is rotated and is maintained in contact with the ring by centrifugal force. Some ring-roller mills are equipped with built-in classification systems, such as that shown in Figure 12.5(d). The performance data of Table 12.9(a) are for products ranging from 14 to 200 mesh, with appropriate control of air rates. Ring roller mills are used for grinding materials from coal to hard rock. Some applications are cited in Tables 12.7(c), 12.9(a), and 12.12.

DISC-TYPE ATTRITION MILLS

Disc-type attrition mills have surfaces that rotate past each other at high speeds with close tolerances. One or both discs may be rotated usually in opposite directions but also may rotate in the same direction. These mills are the modern version of the early Buhrstone mills. Clearances between the discs may be adjusted with springs. The grinding plates may be an abrasive or steel. Feed material

enters a chute near the axis, passes between the grinding plates, and is discharged at the periphery of the plates. These mills are used on a wide range of materials found in Table 12.7(b) and Table 12.9(b).

Disc-type attrition mills are employed in the food industry for grinding cereals and grains as well as in the pharmaceutical industry. Other applications include the grinding of paint pigments and inks. Buhrstone mills are an ancient example of a disc attrition mill.

COLLOID MILLS

Colloid mills are used to grind and disperse solids in liquids and to prepare emulsions. They operate on the principle of high-speed fluid shear to grind the feed material. Another application is in the manufacture of lubricating greases by dispersion of calcium stearate in hydrocarbon oils. In the paint industry, colloid mills are used to incorporate pigments in liquid vehicles. In the food industry, the mills are used to make purees, sauces, ointments, creams, lotions, and other products.

FLUID JET PULVERIZERS

In general, this class of mills uses high-speed gas jets to cause the collision and disintegration of particles. One class admits the high-velocity around the periphery of the grinding and classification chambers. Another type has opposed jets and a classifier. The fineness of the product depends on the classifier speed and the amount of fan air delivered to the classifier. Other variables include the nozzle pressure and the position of the jets. Each fluid jet pulverizer has a classifier and a fan to return large particles to the jet stream. These mills are used primarily for specialty grinding of high-value materials.

Two mills in this category are the Majac mill manufactured by Hosokawa, seen in Figure 12.7(g), and the Micronizer manufactured by Sturtevant. Performance data for Micronizer are found in Table 12.11(b), but both mills are expected to achieve similar results.

12.5. PARTICLE SIZE ENLARGEMENT

Size enlargement is generally considered to be a process in which small particles are combined into larger masses but the individual particles can still be distinguished. *Agglomeration* is the formation of aggregates of material due to the fact that particles tend to stick together.

For many purposes, materials of intermediate sizes are the most desirable forms, neither too small nor too large. Examples are catalyst beds of very small granules that exhibit too great resistance to the flow of reacting fluids or too small particles in suspensions that settle out or filter too slowly. The benefits of size enlargement and examples are presented in Table 12.13.

Binders are frequently used to assist in the agglomeration process. They make a difference in the performance of the end product. Gantner (2003) pointed out that there are six types of binding mechanisms:

1. Sinter bridges
2. Chemical reaction
3. Liquid bridges
4. Molecular forces
5. Interlocking
6. Matrix binders

Sinter bridges are formed when particles are partially melted, due to heat, and then resolidify as agglomerates. A second method is by chemical reaction or by the use of a viscous or hardening binder.

TABLE 12.13. Benefits of Size Enlargement and Examples of Such Applications

Benefit	Examples of Application
1. Production of useful structural forms and shapes	pressing of intricate shapes in powder metallurgy; manufacture of spheres by planetary rolling
2. Preparation of definite quantity units	metering, dispensing, and administering of drugs in pharmaceutical tablets
3. Reduced dusting losses	briquetting of waste fines
4. Creation of uniform, non-segregating blends of fine materials	sintering of fines in the steel industry
5. Better product appearance	manufacture of fuel briquets
6. Prevention of caking and lump formation	granulation of fertilizers
7. Improvement of flow properties	granulation of ceramic clay for pressing operations
8. Greater bulk density to improve storage and shipping of particulates	pelleting of carbon black
9. Reduction of handling hazards with irritating and obnoxious materials	flaking of caustic
10. Control of solubility	production of instant food products
11. Control of porosity and surface-to-volume ratio	pelleting of catalyst supports
12. Increased heat transfer rates	agglomeration of ores and glass batch for furnace feed
13. Removal of particles from liquids	pellet flocculation of clays in water using polymeric bridging agents
14. Fractionation of particle mixtures in liquids	selective oil agglomeration of coal particles from dirt in water
15. Lower pressure drop in packed beds	reactors with granular catalysts

Liquid bridges occur when a liquid is sprayed to wet the surface of the particles, then they collide with other particles and the liquid connects the particles. Molecular, electrical, or magnetic forces between particles is another binding mechanism. Interlocking occurs when irregular-shaped particles collide and lock together. A matrix binder has particles that are imbedded in a continuous matrix of the binder.

Binders must be thoroughly mixed with the material to be effective, through perhaps premixing before agglomeration, but this depends on the type of agglomeration process. Holley (1981) wrote a classic article on binders and binding systems.

A number of processes are used industrially for particle size enlargement and are defined as follows:

1. *Compaction* is achieved either by compression or extrusion. *Compression* is either done in a mold to give the final desired shape or done in a sheet or block that may be later broken into proper sizes. *Extrudates* are formed under pressure in dies of various cross sections; as they leave the die, they are broken or cut to size.

2. *Agglomeration* is accomplished by tumbling or other agitated conditions, with or without the use of binders. Size is controlled either by adjusting the residence time or by the gradual feed and binder, slurry, or solution.
3. *Globulation* is the formation of droplets of solution, slurry, or melt followed by solidification by prilling, spray drying, or fluid bed techniques. Control of particle size is best achieved in fluidized beds.
4. *Heat bonding* is of two types: In *nodulization*, the material is tumbled while being heated to give hard, rounded granules. *Sintering* forms a product as an integrated mass that is subsequently broken to size.
5. *Flocculation* occurs in the coagulation and growth of particles in dilute slurries to assist in subsequent sedimentation and filtration.

These processes may be carried out batchwise or continuously. In batch processing, there are some advantages—namely, that any contamination can be easily traced and identified but the production rate is slow. Continuous processing has obvious economic advantages when the production rate is large and product specifications are relatively constant (Gantner, 2003). In continuous processing, the product tends to be uniform and the labor is less than in batch processing.

In any particular industry, more than one of the above processes may be used. For example, in the manufacture of specialty solid catalysts, rotating pan granulators may be employed (Figure 12.8). Perhaps, if the rheological properties are favorable, the material could be extruded (Figure 12.11[e]), cut into short cylinders, and subsequently tumbled into rounded shapes (Figure 12.10). Small spherical beads of catalysts are made in a moving-bed process by precipitation or coagulation in an immiscible fluid. Pellets or rings are made on tabletting machines (Figure 12.9). This process is more expensive than extrusion but the product is more uniform. Ammonia synthesis catalysts are made by sintering (Figure 12.12) or fusion of several ingredients, then crushed and used as irregular lumps of size ranges, such as 1.5–3, 6–10, and 12–21 mm.

In the following sections, the main type of equipment for particle size enlargement will be discussed and illustrated.

TUMBLERS

Particles may be agglomerated by spraying lightly with a liquid binder that may be water or a concentrated solution of the material. The liquid is sprayed at certain points in a rotating disk or drum where smaller particles congregate, and as the material agglomerates and the particles become larger they roll out of the machine. The growth may be due to agglomeration of small particles or to layering of material evaporated from the sprayed solution. The drum or disc equipment usually produces a rounded product due to the rolling action. The product density and the dissolution rate are dependent on the type of binder used. Usually the tumbling action is less intensive and only enough to expose the material to the sprays. The sprays are fine and are applied to the surface of the bed of particles. The tumbling action distributes the liquid uniformly through the mass.

A disk-type granulator (Figure 12.8) is a shallow pan, inclined at an angle, that rotates at slow speeds, 10–30 rpm. Pans are made with a ratio of pan diameter to collar height of 3 to 5. As the rotation proceeds, fresh solids and spray are injected continuously where the finer particles tend to settle to the bottom of the unit and larger agglomerated particles roll out of the equipment as they become larger. Because of the size stratification, the product from this equipment is more uniform than that made in a rotating drum granulator (Walas, 1988). Some performance data in addition to that found in Figure 12.8 are:

Material	Diameter (mm)	kg/(min)(m^2)
Iron ore	10–25	11.4
Cement flour		18.0
Fertilizer	1.6–3.3	14.3

Rolling drum granulators, Figure 12.10, are largely free of internals but provide sufficient turnover to effect good distribution of the spray throughout the mass. If heavy sprays and little tumbling action are used, the product will be non-uniform. Fertilizer granules have been made this way resulting in larger, more dense and harder product than those made by prilling. In this industry, the trend has been to replace drum granulators with prilling towers and those in turn with fluid-bed granulators.

BRIQUETTING AND ROLL COMPACTORS

Briquetting is used to achieve a product of uniform shape and density. This process takes place on a two-roll compactor in which feed enters at the top of the unit. Finely divided material is agglomerated at high rates and at low costs by roll compression. High pressure is applied in the region between the rolls and the feed. The rolls have individual cavities or pockets to form the desired briquette shape. The product formed is low cost, rough in shape, and not of highly uniform weight. If a smooth appearance and weight uniformity are required, then tabletting is the process to be used. Table 12.17 and Table 12.18 list the wide variety of materials that have been compacted by rolls. Equipment for compacting, briquetting, and pelletizing is shown in Figure 12.11.

The production of briquettes may require little or no binders but when they are used, strength is conferred to the agglomerates and the addition of lubricants may reduce friction during the operation. Table 12.14 is a list of some binders that have been used. The lubricants may be liquids such as water, glycerine, lubricating oils and solid waxes, metallic stearates, starch, and talc.

TABLETTING

Rotary compression equipment, Figure 12.9(a), converts powders and granules into hard tablets of quite uniform weight, most notably pharmaceuticals, but also some solid catalyst formulations. A powder is loaded into a die where it is retained by a lower punch; then it is compressed by the upper punch and ultimately ejected by raising both punches.

Most tablets formed are small; the largest (shown in Figure 12.15) is 1-3/16 in. in diameter and the greatest depth is 1-3/8 in. There are some machines that make large tablets, say 4 in. in diameter and exert a force of 100 tons. The U.S. Pharmacopeia specifies the degree of weight uniformity. For example, in a sample of 20 tablets, only two may differ from the mean percentage stated below and only one may deviate by twice the percentage stated.

Weight of tablet (mg)	% Deviation
Equal to or less than 13	15.0
13–130	10.0
130–324	7.5
More than 324	5.0

Coarse powders and granules fed to tabletting machines produce greater weight uniformity. Too many fines will cause the tablets to disintegrate upon ejection. For pharmaceuticals, a limited amount of additives are allowed to facilitate tabletting. Examples are magnesium stearate as a lubricant (up to 2%) and corn starch (up to 5%) as a binder. Preparation of additive mixes are best made in powder blenders and fixed by granulation.

(a)

(b)
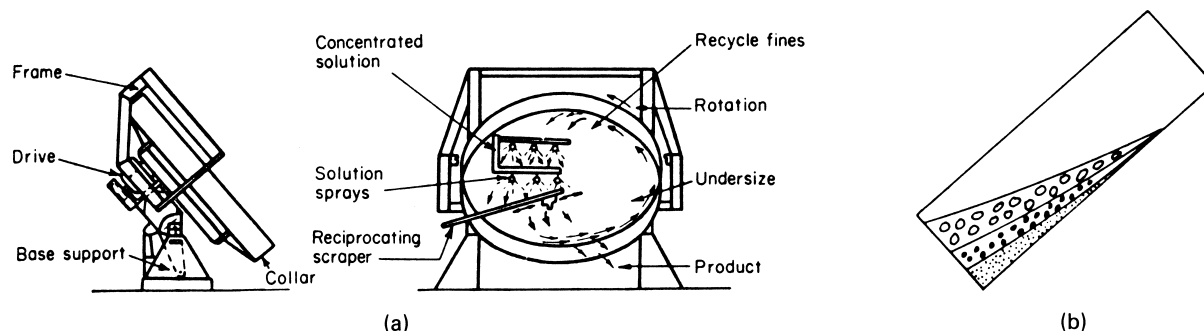
Dish size (m)	Motor (kW)	Capacity (kg s⁻¹)	Material	Remarks
0·36	0·18	0·013	Tungsten carbide	16 × 60 mesh micropellets
0·36	0·18	0·0044	Alumina	
0·99	0·55	0·13	Phosphate rock	85% 4 × 30 mesh product
0·99	0·55	0·076	Bituminous coal filter cake	Feed to pan dryer
0·99	0·55	0·076	Beryl ore mix	Feed to sinter belt
0·99	0·55	0·15	Copper precipitate	
1·37	2·2	0·28	Frit enamel mix	Feed to furnace
2·59	11	8·5	Zinc concentrate sinter mix	Micropelletized sinter machine feed
2·59	11	0·85	Chromate	For electric ore furnace
2·59	7·3	0·93	Bituminous coal fines	For coking furnace
3·05	15	1·7–2·3	Raw shale fines	For expanding in rotary kiln
3·05	18	2·8	Bituminous coal filter cake	
3·66	22	3·4	Zinc sulphide ore	For fluid bed roasting of 4 × 30 mesh pellets
4·27	37	11	Nitrogen fertilizer material	Feed: hot melt and recycle
5·49	44	11	Magnetite ore	Feed to travelling grate — indurating section

(c)

Disk size, ft.	70 lb./cu. ft. material Pelletizing Approx. capacity, tons/hr.	70 lb./cu. ft. material Pelletizing Horse-power	125 lb./cu. ft. Pelletizing Approx. capacity, tons/hr.	125 lb./cu. ft. Pelletizing Horse-power
18	30	40	40	50
15	18	25	25	30
12	10	12	15	16
9	5	6	10	7½
6	3	3	5	5
3¼	½	1	1	1

Diameter (m)	3·6	4
Depth (cm)	91	91
Speed (rpm)	17·5	14·0
Drive (kW)		
Installed	30	37
Used	26	25–30
Feed rate (kg s⁻¹)	7·1	8·5–10·1
Moisture (%)	12·5–13·5	12·5–13·5
Granule porosity (%)	26	26
Granule compressive strength (kg)	2·7–6·7	2·7–6·7
Powder feed position	Bottom centre	
Water feed positions		
Main	Jets above powder feed	
Secondary	Fine sprays in top section of pan	

(d)

(e)

Figure 12.8. Rotating disk granulator applications and performance. (*Sherrington and Oliver, 1981*). (a) Edge and face view of a disk granulator, diameters to 25 ft, Froude no. $n^2 D/g_c = 0.5$–0.8. (b) Stratification of particle sizes during rotation. (c) Typical applications of disk granulation. (*Dravo Corp.*). (d) Capacity and power. (*Dravo Corp.*). (e) Performance on cement kiln feed. (Walas, 1988).

Machines commonly used are found in Figure 12.9. Maximum forces for small tablets are 10 tons but up to 100 tons may be required for tablets 2-1/2 to 4 in. in diameter.

EXTRUSION PROCESSES

Powders, pastes, and melts are pelletized by extrusion through a die followed by cutting. Binders and lubricants may be incorporated in the feed but the process is not feasible for abrasive materials.

Economically feasible power requirements correspond to the range of 100–200 lb/HPhr. The main types of these machines are found in Figures 12.11 (d&e) and 12.16.

The product formed in an extrusion process are cylindrical-shaped pellets. Very few fines result, because the dies forming the pellets are at the exit of the extruder. Equipment is also available, called a spheronizer, that can produce spherical products.

A wide variety of extruders are available on the market, including basket extruders, screw extruders, gear pelletizers, and

(a)
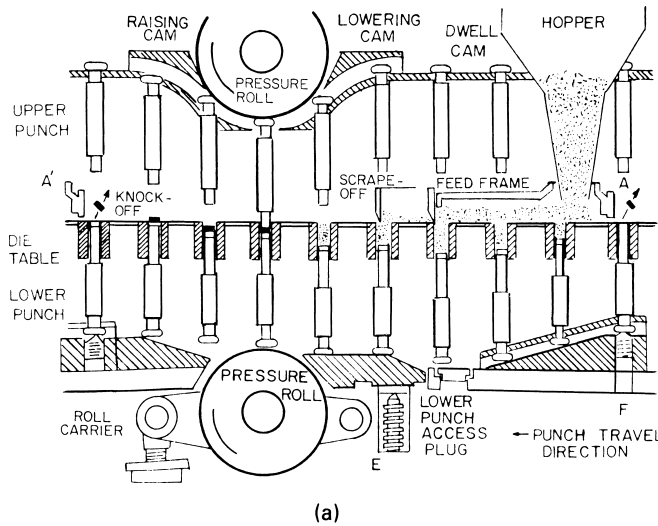
Number of tooling stations	27	33	45
Output (tablets/min)	1,000–2,700	1,200–3,300	1,600–4,500
Max. tablet diameter (in.)	$1\frac{3}{16}$	$1\frac{1}{16}$	$\frac{3}{4}$
Fill depth (in.):			
Standard	$0-\frac{11}{16}$	$0-\frac{11}{16}$	$0-\frac{11}{16}$
Optional	$\frac{11}{16}-1\frac{3}{8}$	$\frac{11}{16}-1\frac{3}{8}$	$\frac{11}{16}-1\frac{3}{8}$
Max. operating pressure (tons)	10	10	10
Pressure release adjustment (tons)	0–10	0–10	0–10
Upper punch entrance (in.)	$\frac{3}{16}-\frac{7}{16}$	$\frac{3}{16}-\frac{7}{16}$	$\frac{3}{16}-\frac{7}{16}$

(b)

Series	37	45	55	61
Number of stations	37	45	55	61
Max. operating pressure (tons)	10	6.5	6.5	6.5
Max. depth of fill (in.)	$\frac{13}{16}$	$\frac{11}{16}$	$\frac{11}{16}$	$\frac{11}{16}$
Max. tablet diameter (in.)	1	$\frac{5}{8}$	$\frac{7}{16}$	$\frac{7}{16}$
Output (tablets/min)	888–3,552	2,050–8,200	2,500–10,000	2,775–11,100

(c)

Figure 12.9. Operation and specifications of rotary tabletting machines. (a) Action of the punches of a rotary tabletting machine. (b) Specifications of a Sharples Model 328. (c) Specifications of a Manesty Rotapress Mk 11. (Walas, 1988).

pellet mills. Frequently, extruders will have internal devices to aid in the mixing and will have die plates at the discharge end of the extruder. In general, extruders can be divided into low-pressure and high-pressure units. In the former group are basket extruders, Figure 12.16(c), that produce a product of medium hardness and low to medium dispersion and dissolution rates. Particles from a high-pressure extruder display limited solubility and have a high degree of hardness. Figure 12.11(d) is an example of a gear-type pelletizer in which material is fed at the top and pushed through the gap by the opposing tooth.

Screw extruders are built with a single screw, as shown in Figures 12.11(e) and 12.16. The die at the extruder exit may have multiple holes. To make pellets, the extrudate goes to cutting machines. The extrusion of plastics is described by Schwartz and Goodman (1982).

Ring mills consist of a power-driven rotating ring with radial holes, friction rolls to force the material holes and knives to cut the extrudate to the desired lengths. See Figure 12.16(a). The feed is charged with screw feeders into spaces between the rolls and feed distributor flights. The force of compaction is due to flow friction through the die. Different flow and compression characteristics are possible by varying the thickness of the ring. The life of the dies in a ring mill is measured in hours. An example of large-scale production is the preparation of animal feeds, but small-scale applications are also possible. Some applications are cited in Table 12.19. A survey of this literature is made by Sherrington and Oliver (1981).

PIN-PADDLE MIXERS (MIXING AGGLOMERATION)

Pin or paddle mixers provide instant mixing agglomeration and produce a product that has excellent flow properties and of sizes up to 6 mesh (Gantner, 2003). Paddle mixing equipment, Figure 12.13, has been used in the manufacture of fertilizers, chemicals, detergents, and some food products, and the products formed are less porous, more granular, and have a lower dispersability. Fertilizers can then be compacted, if desirable, for a slower dissolving product.

Sticky, very fine, and highly aerated materials can be granulated in drums with pins and pegs instead of paddles. In Figure
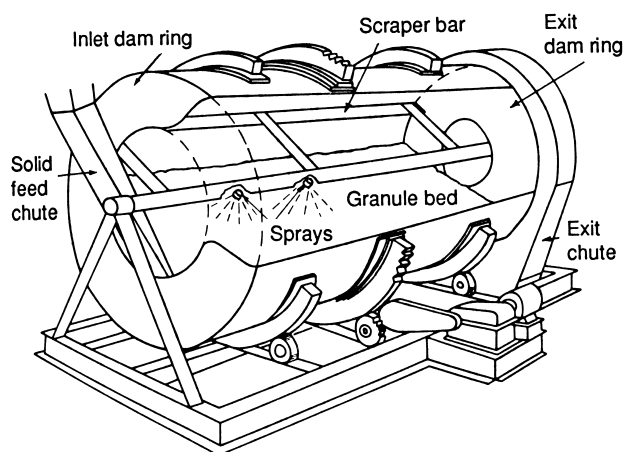
(a)
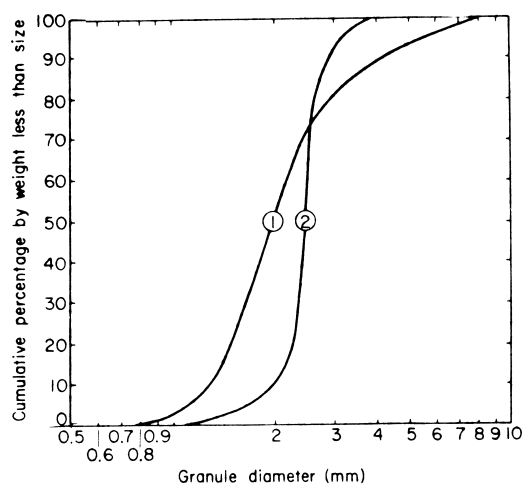
(b)

Application	Diameter (ft)	Length (ft)	Installed Power (HP)	rpm	Approximate[a] Capacity (tons/hr)
Fertilizer granulation	5	10	15	10–17	7.5
	8[b]	16	75	8–14	40
Iron ore balling	9	31	60	12–14	54
	12	33	75	10	98

[a] Capacity excludes recycle; actual drum throughput may be much higher.
[b] Inclination 2°.

(c)

Figure 12.10. Rolling drum granulator sketch and performance. (a) Sketch of a rolling drum granulator. (*Sherrington and Oliver, 1981*). (b) Effect of rotational speed on size distribution: (1) at 20% of critical speed; (2) at 50%. (c) Performance data on commercial units. (*Capes and Fouda, 1984*; Walas, 1988).

TABLE 12.14. List of Agglomerated Products and Their Binders

Material	Binder	Agglomeration Equipment
Activated Charcoal	Lignosulfonate	Turbulator[*]
Alumina	Water	Turbulator[*]/Disc
Animal Feed	Molasses	Ring Extruder
Boric Acid	Water	Disc Pelletizer
Carbon Black & Iron Powder	Alcohol-Carbowax	Turbulator[*]
Carbon, Synthetic Graphite	Sodium Silicate	Turbulator[*]/Disc
Cement, Raw Mix	Water	Disc Pelletizer
Cement Kiln Dust	Water	Turbulator[*]/Disc
Charcoal	Starch Gel	Briquetter
Chrome Carbide	Alcohol	Disc Pelletizer
Clay, Attapulgite	Water	Turbulator[*]/Disc
Clay, Bentonite	Water	Turbulator[*]
Coal, Anthracite	Pitch	Briquetter
Coal, Bituminous	Lignosulfonate	Disc Pelletizer
Coal Dust	Water	Turbulator[*]
Coke, Petroleum	Pitch	Briquetter
Continuous Casting Flux	Water	Turbulator[*]/Disc
Copper Smelter Dust	Sodium Silicate	Turbulator[c]
Copper Sulphite Concentrate	Sodium Silicate	Disc Pelletizer
Detergent Dust	Water	Disc Pelletizer
Dolomite Kiln Dust	Water	Turbulator[*]/Disc
Dye Pigment	Lignosulfonate	Turbulator[*]/Disc
Electric Furnace Dust	Water	Turbulator[*]/Disc
Fertilizer	Ammonia	Drum
Flourspar	Sodium Silicate	Disc Pelletizer

(*continued*)

TABLE 12.14.—(continued**)**

Material	Binder	Agglomeration Equipment
Flourspar	Lime-Molasses	Briquetter
Flyash (boiler)	Water	Turbulator*/Disc
Flyash (high carbon)	Lignosulfonate	Briquetter
Glass Batch	Caustic Soda	Disc Pelletizer
Glass Batch	Water	Briquetter
Herbicide	Lignosulfonate-Water	Turbulator*/Disc
Herbicide	Clay-Carbowax	Briquetter
Iron Ore	Bentonite-water	Drum
Lignite	Gilsonite-Water	Turbulator*/Disc
Limestone	Clay-Water	Turbulator*
Manganese Ore	Lime-Molasses	Briquetter
Manganese Oxide	Sulfuric Acid	Turbulator*/Disc
Phosphate Rock	Phosphoric Acid	Turbulator*/Disc
Plastic Powder	Alcohol	Disc Pelletizer
Potash Fines	Water	Disc Pelletizer
Sodium Borate	Sulfuric Acid	Turbulator*/Disc
Sulfur Powder	Clay	Compactor
Tungsten Carbide	Alcohol	Disc Pelletizer
Zeolite	Clay-Water	Turbulator*/Disc

(Walas, 1988).

TABLE 12.15. Moisture Requirements for Successful Granulation in Tumbling Machines

Raw Material	Approximate Size Analyses of Raw Material, less than Indicated Mesh	Moisture Content of Balled Product (% H_2O)
Precipitated calcium carbonate	200	29.5–32.1
Hydrated lime	325	25.7–26.6
Pulverized coal	48	20.8–22.1
Calcined ammonium metavananaite	200	20.9–21.8
Lead–zinc concentrate	20	6.9–7.2
Iron pyrite calcine	100	12.2–12.8
Specular hematite concentrate	150	9.4–9.9
Taconite concentrate	150	9.2–10.1
Magnetic concentrate	325	9.8–10.2
Direct shipping open pit ores	10	10.3–10.9
Underground iron ore	0.25 in.	10.4–10.7
Basic oxygen converter fume	1 μm	9.2–9.6
Row cement meal	150	13.0–13.9
Utilities–fly ash	150	24.9–25.8
Fly ash–sewage sludge composite	150	25.7–27.1
Fly ash–clay slurry composite	150	22.4–24.9
Coal–limestone composite	100	21.3–22.8
Coal–iron ore composite	48	12.8–13.9
Iron ore–limestone composite	100	9.7–10.9
Coal–iron ore–limestone composite	14	13.3–14.8

(Walas, 1988).

12.14, the material enters at one end, is immediately wetted, and emerges as pellets at the other end. Residence times are under one minute. The data with this figure show that the bulk density of carbon black, for example, is increased by a factor of 11 with about 50% binder in the product.

The process often involves the use of liquid sprays and the particles produced may be of irregular shape, but the resulting product has a medium to high dissolution rate because of increased porosity and lower density.

PRILLING

In this process, a molten material is disintegrated into droplets that are allowed to fall and solidify in contact with an air stream. The process mechanism is simpler in that no evaporation occurs and the resulting product is less porous and stronger. A sketch of a prilling process is in Figure 12.17. A partial list of prillable materials is found in Table 12.20.

Materials suitable for prilling are those that melt without decomposition, have a low heat of solidification, and have a high enough melting point to permit the use of ambient conditions for cooling. Many of the materials have a high viscosity, so spray wheels are preferred to spray nozzles. The tower cross section may be rectangular to accommodate several spray wheels for large production capacity. To prevent clogging, the spray wheels are equipped with scrapers. An alternate method for obtaining prills is to force the liquid melt through holes in a pipe. The product formed is rounded, individual particles due to high surface tension.

Prilled granules are usually less dense than those made in drum or fluidized bed granulators. The latter processes can make large prills economically. Very tall towers are needed to ensure solidification before the prills reach the bottom. Size distribution depends on the character of the atomization but can be moderately uniform. Some commercial data of cumulative percent less than size are:

% less than size	0	5	50	95	100
Die (mm)	1.2	1.6	2.4	3.5	4.8

Cooling of the prills can be accomplished more economically in either drums or fluidized beds than in providing additional prill tower height. Fluid-bed coolers are cheaper and preferred because dusting problems are more easily controlled. After cooling, the product is screened and the fines may be recycled to the melter.

Dimensional and some operating data for prilling urea and ammonium nitrate are found in Table 12.20(b). Because of the size and expense of the towers, prilling is not a competitive process
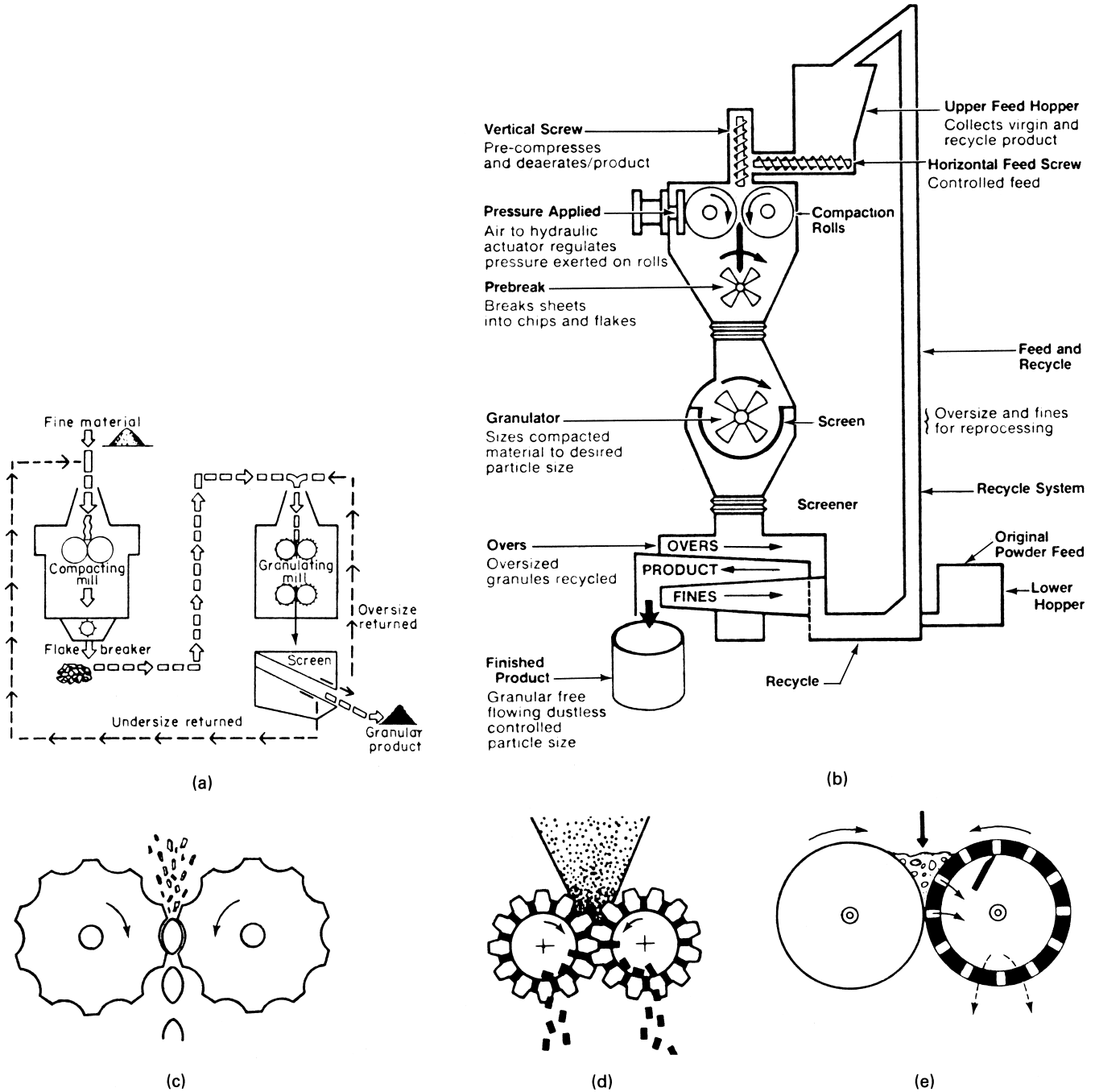
Figure 12.11. Equipment for compacting, briquetting, and pelleting. (a) Flowsketch of a process for compacting fine powders, then granulating the mass. (b) Integrated equipment for roll compacting and granulating. (c) A type of briquetting rolls. (d) A gear pelleter. (e) A double roll extruder. (Walas, 1988).
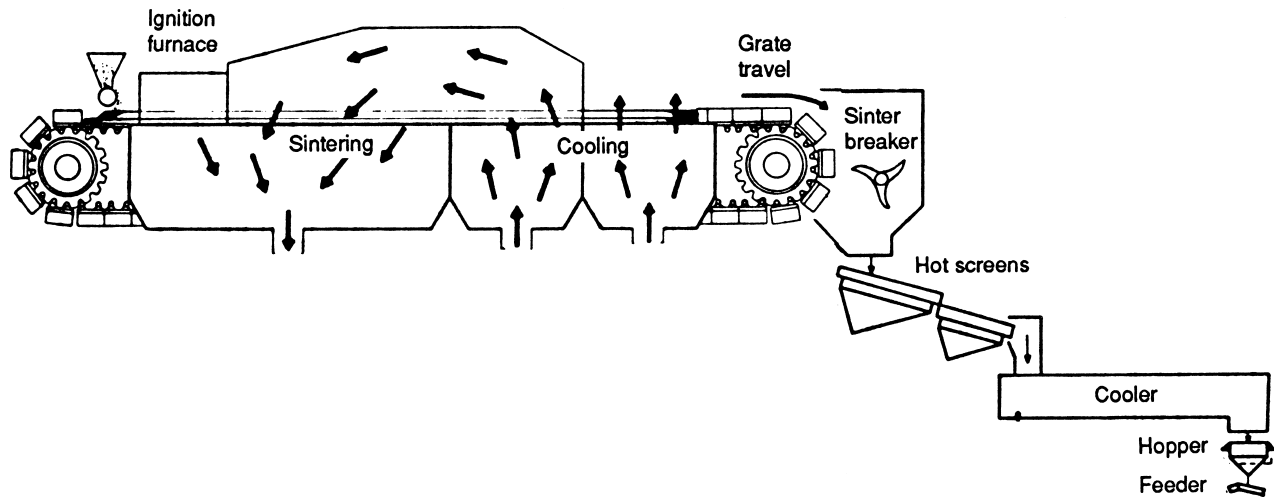
Figure 12.12. Flowsketch and operation of a sintering process.

TABLE 12.16. Industries that Employ Disk Granulators and Some of the Products They Process

Industry	Typical Application
Steel	Electric Furnace Baghouse Dust, BOF Dust, OH Dust, Coke Fines, Raw Materials, Iron Ore Pelletizing
Foundry	Baghouse Dust, Mold Sand Fines
Ferroalloy	Silicon, Ferrosilicon, Ferromanganese, Ferrochrome
Copper	Concentrates, Smelter Dust, Precipitates
Lead/Zinc	Concentrates, Sinter Mix, Flue Dust, Drosses
Other Metals	Tungsten, Molybdenum, Antimony, Brass, Tin, Berrylium, Precious Metals, Aluminum, Silicon, Nickel
Glass	Glass Rawmix, Furnace Dust, Glass Powder
Ceramics	Alumina, Catalyst, Molecular Sieves, Substrates, Insulator Body, Tilemix, Press Feed, Proppants, Frits, Colors
Refractories	Bauxite, Alumina, Kiln Dust, Blends
Cement/Lime	Raw Meal, Kiln Dust
Chemicals	Soda Ash, Sodium Sulfate, Detergents, Cleaners, Zinc Oxide, Pigments, Dyes, Pharmaceutical Compounds, Industrial Carbons, Carbon Black
Ag-Chemicals	Fertilizers, Pesticides, Herbicides, Insecticides, Soil Conditioners, Aglime, Dolomite, Trace Minerals, N-P-K raw Materials
Foods	Instant Drink Mix, Powdered Process Foods, Sugar, Sweetners, Confectionary Mix
Coal	Coal Fines
Power	Coal Fines, Fly Ash, FGD Sludge, Boiler Ash, Wood Ash
Nonmetallic Minerals	Clay, Talc, Kaolin, Fluorspar, Feldspar, Diatomaceous Earth, Fullers Earth, Perlite
Pulp, Paper, Wood	Paper Dust, Wood Fines, Sander Dust, Boiler Ash
Solid Waste	Incinerator Ash, Refuse Fines, Mixed Refuse, Dried Sludge

(Koerner and MacDougal, 1983; Walas, 1988).

when compared to other granulation processes, until the production rate exceeds 200 tons/day.

FLUIDIZED AND SPOUTED BEDS

Agglomeration can be performed in a standard fluidized bed such as seen in Figure 12.18. Some fluid-bed units are designed to take the product from a solution to product from a solution to an agglomerate in one step. "If the feed is a slurry, it can be sprayed into the middle of a cylindrical agglomerator and the product dries as it falls. Air may be blown up from the bottom of the vessel, fluidizing the newly formed granules. As the granule falls, more liquid deposits on the solid forming layers similar to the skin of onions" (Gantner, 2003). Granules formed by layering are smoother and harder. Large agglomerates are obtained when the ratio of droplet/granule diameters decreases. Increase in the rate of the fluidizing gas and in the temperature of the bed decreases penetration and wetting of the bed, and hence leads to smaller granule sizes. A narrower and more concentrated spray wets a smaller proportion of the particles, thus leading to a larger size product. The bed is often cylindrical with a conical bottom so that larger particles are lifted off the bottom and recirculated more thoroughly.
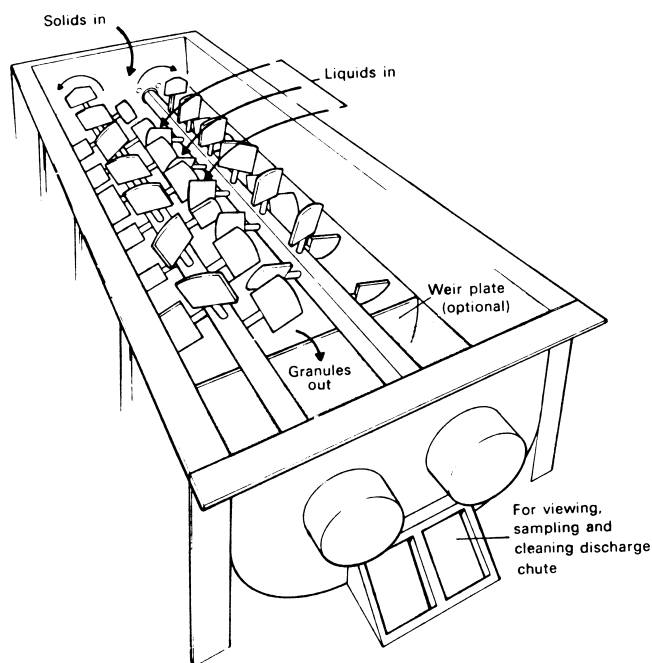
Blunger dimensions

Length (m)	4·5
Width (m)	1·4
Height (m)	1·07
Screw diameter (m)	0·8
Pitch (m)	1·7
Shaft speed (rpm)	55
Capacity (kg s^{-1})	23–25
Installed power (kW)	104

(a)

MODEL	MATERIAL BULK DENSITY LB/FT^3	APPROXIMATE CAPACITY (TONS/HR)	SIZE (WIDTH × LENGTH) (FT)	SPEED (RPM)	DRIVE (HP)
A	25	8	2 × 8	56	15
	50	15	2 × 8	56	20
	75	22	2 × 8	56	25
	100	30	2 × 8	56	30
B	25	30	4 × 8	56	30
	50	60	4 × 8	56	50
	75	90	4 × 8	56	75
	100	120	4 × 8	56	100
C	25	30	4 × 12	56	50
	50	60	4 × 12	56	100
	75	90	4 × 12	56	150
	100	120	4 × 12	56	200
	125	180	4 × 12	56	300

(b)

Figure 12.13. Paddle blending granulator and typical performance. (a) Sketch of a double paddle trough granulator (*Sherrington and Oliver, 1984*). (b) Performance in granulation of fertilizers. (Walas, 1988).

A wide range of operating conditions used commercially as well as performance data are found in Table 12.21. Batch fluidization is used for smaller or intermittent production rates, when residence times must be long or when there is frequent changeover, as in a multipurpose production facility. Further, in batch processing, it is easier to trace any contamination or off-specification products. A batchwise arrangement to make granules for feed to pharmaceutical tabletting equipment is found in Figure 12.18(a) and in Table 12.21(a). This equipment has an elaborate filter system to prevent the escape of fine particles, thereby assuring their eventual growth. Continuous operation is useful when the production rate is large and the product specifications are uniform. Labor expenses are lower and the end product tends to be more uniform in continuous operations. A continuous process for the recovery of sodium sulfate pellets from the incineration of paper mill wastes is shown in Figure 12.18(b) and operating data are in Table 12.21(b). Multicomponent equipment in Figure 12.18(c) permits improved control of process conditions and may assure a narrower size distribution because of the approach to plug flow. Some fluid-bed dryers (Figure 9.13) can be equipped with sprays and adapted for granulation.
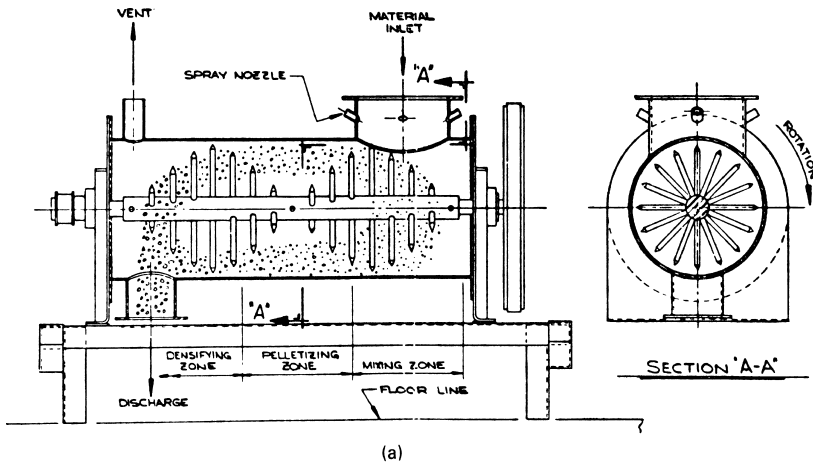
Carbon black feed	
Rate, Mg/day	26.3[a]
Bulk density, kg/m^3	51.3
Pellets produced	
Wet basis	
Production rate, kg/h	2108.3
Bulk density, kg/m^3	562.3
Densification ratio	11.0
Dry basis	
Production rate, kg/h	1096.3
Bulk density, kg/m^3	394.1
Binder	
Specific gravity	1.05
Injection rate, kg/h	1011.5
Use ratio, weight of binder to	
weight of wet pellets	0.92
Power Consumption[b]	
Rate, kW	18.5
Per Mg of wet pellets, kWh	15.0[c]
Production quality	
Rotap test (5 min), %	1.4 (avg. of 45 samples)
Crushing strength, g	25 (avg. of 73 samples)

[a]Average from 5-day test, plus subsequent production.
[b]Ammeter readings.
[c]Cold shell.

(b)

Figure 12.14. Pin mixers which operate at high speed for granulation of fine and aerated powders. (a) Pinmixer for the granulation of wetted fine powders. (b) Performance of a pinmixer, dimensions 0.67 m dia by 2.54 m, for pelleting a furnace oil carbon black. (Walas, 1988).
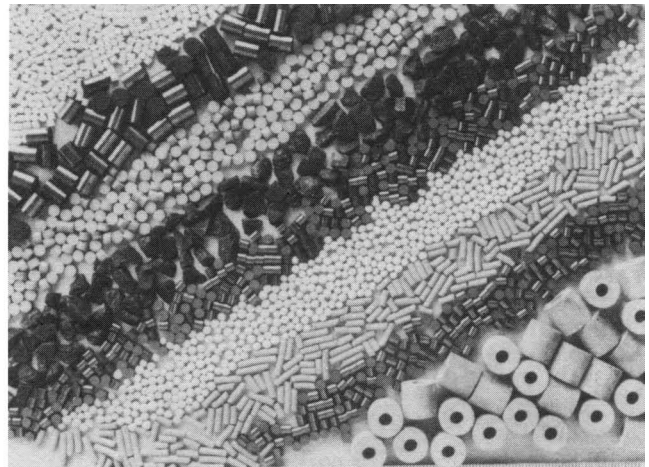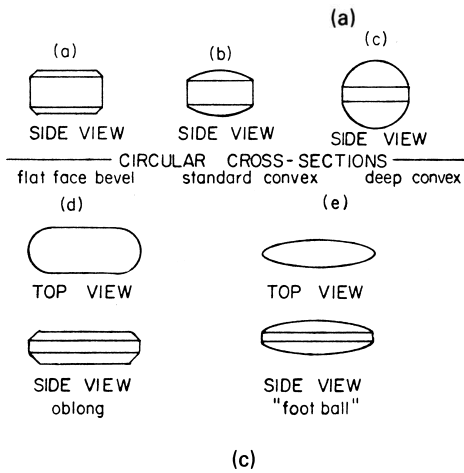
Figure 12.15. Common shapes and sizes of pellets made by some agglomeration techniques. (a) Sizes and shapes of briquets made on roll-type machines. (b) Catalyst pellets made primarily by extrusion and cutting. (c) Some of the shapes made with tabletting machines. (Walas, 1988).

TABLE 12.17. Alphabetical List of Some of the Materials that Have Been Successfully Compacted by Roll Presses

Acrylic resins, activated carbon, adipic acid, alfalfa, alga powder, alumina, aluminium, ammonium chloride, animal feed, anthracite, asbestos
Barium chloride, barium sulfate, battery masses, bauxite, bentonite, bitumen, bone meal, borax, brass turnings
Cadmium oxide, calcined dolomite, calcium chloride, calcium oxide, carbomethylcellulose (CMC), carbonates, catalysts, cellulose acetate, ceramics, charcoal, clay, coal, cocoa powder, coffee powder, coke, copper, corn starch
Detergents, dextrine, dimethylterephthalate (DMT), dolomite, ductile metals, dusts, dyes
Earthy ores, eggshells, elastomers, emulsifiers, epoxy resins
Feldspar, ferroalloys, ferrosilicium, fertilizers, flue dusts, fluorspar, fly ash, foodstuffs, fruit powders, fruit wastes, fungicides
Gipsum, glass making mixtures, glass powder, grain waste, graphite, gray iron chips and turnings
Herb teas, herbicides, hops, hydrated lime
Ice, inorganic salts, iron oxide, iron powder, insecticides
Kaolin, kieselgur, kieserite
Lead, lead oxide, leather wastes, LD-dust, lignite, lime, limestone, lithium carbonate, lithium fluoride, lithium hydroxide
Magnesia, magnesium carbonates, magnetite, maleic anhydrate, manganese dioxide, metal powders, molding compounds, molybdenum, monocalciumphosphate (MCP)
Naphthalene, nickel powders, nickel ores, niobium oxide
Ores, organic chlorides, organic silicates, oil shale, oyster shells
Pancreas powder, penicillin, pharmaceuticals, phosphate ores, plastics, polyvinylchloride (PVC), potash, potassium compounds, protein pigments, pyrites, pyrocatechol
Raisin seeds, reduced ores, refractory materials, rice starch, rock salt
Salts, sawdust, scrap metals, shales, silicates, soda ash, sodium chloride, sodium compounds, sodium cyanide, sponge iron, steel turnings, stone wool, sugar, sulfur
Teas, tin, titanium sponge, turnings
Urea, urea formaldehyde
Vanadium, vermiculite, vitamins
Waxes, welding powder, wood dust, wood shavings
Yeast (dry)
Zinc oxide, zirconium sand

(Walas, 1988).

TABLE 12.18. Roll Pressing Equipment Offered by Two Manufacturers

(a)

Model	Roll dia./mm	Max. roll width/mm	Position of rolls/feeder	Max. force/ metric tons	Overload system	Approx. capacity/ kg^{-1}	Feeder type	Press drive/ kW	Feeder drive/ kW	Roll shapes	Max. feed temp. /°C
L 200/50	200	50	horiz./vert. or vert./horiz.	~10	None	10–100	screw	3/4	0·5	smooth/corrugated/ pocketed	80
K 26/100	200	100	horizontal/vertical	~20	''	100–200	''	11	3	''	80
K 27/200	300	200	''	~40	''	200–500	''	22	7·5	''	80
K 27/300	300	300	''	~80	hydraulic	500–1 000	''	30	7·5	''	80
CS 25	230	65	''	25	''	100–300	''	7	3	''	120
CS 50	406	119	''	50	''	300–1 000	''	15	5	''	150
MS 75	500	230	''	75	''	1 000–10 000	''	22	7·5	''	120
MS 150	500	280	''	150	''	3 000–15 000	''	75	11	''	1 000
MS 200	710	460	''	200	''	up to 50 000	''	300	15	''	1 000
MS 300	710	550	''	300	''	up to 60 000	screw(s)	400	15	''	1 000
MS 350	910	250	''	350		up to 40 000	screw	250	15	''	1 000

(b)

B 100	130	50	vertical/horizontal	10	hydraulic	20	screw			smooth/corrugated/pocketed	ambient
B 150	200	75	''	20	''	200	''			''	''
B 220	300	75	''	30	''	1 500	''			''	''
B 300	380	100	''	60	''	3 000	''	as required		''	''
B 400	460	150	''	125	''	5 000	''			''	''
B 500	610	200	''	250	''	15 000	''			''	''
D 100	130		''	20	''	50	''			''	''
D 150	200		''	40	''	200	''			''	''
D 300	330		''	70	''	3 000	''			''	''
DH 400	520		horizontal/vertical	140	''	6 000	''			''	800
DH 500	710		''	270	''	20 000	''			''	800
DH 600	920		''	500	''	50 000	''			''	800

(Walas, 1988).

TABLE 12.19. Some Applications of Rotating Ring Pelletizers (see Figure 12.15(b))

Material	Reason To Pellet	LB/HP/HR (KG/KW/HR)	Pellet Size (Inches Diameter) (Millimeter Dia.)
Asbestos Shorts	Density, Reduce Dust In at 20 lb/ft3 (320 kg/m3) Out at 65 lb/ft3 (1041 kg/m3)	45 (27)	3/8″ (9.5 mm)
Acrylamide-Dry Wet	Handling	80 (49) 170 (103)	1/4″ (6.4 mm)
Bagasse	Densify, Reduce Dust In at 5 lb/ft3 (80 kg/m3) Out at 30 lb/ft3 (480 kg/m3)	80 (49)	3/8″ (9.5 mm)
Bauxite	Handling	300 (182)	1/2″ (12.8 mm)
Brewers Grain (Spent)	Densify, Handling In at 13 lb/ft3 (208 kg/m3) Out at 36 lb/ft3 (577 kg/m3)	150 (91)	1/4″ (6.4 mm)
Clay Base Material	Handling, Densify, Calcine	100–300 (81–182)	1/8″ to 3/4″ (3.2 mm to 19 mm)
Cryolite Filter Cake	Handling	100 (61)	3/8″ (9.5 mm)
Domolite	Handling	200 (122)	1/4″ to 3/16″ (6.4 mm to 4.8 mm)
Herbicide	Handling, Control, Solubility	150 (91)	12/64″ (4.8 mm)
Insecticide	Defined Form, Reduce Dust	120 (73)	1/8″ (3.2 mm)
Iron Oxide	Calcining, Reduce Dust	50–100 (30–61)	1/8″ to 1/4″ (3.2 mm to 6.4 mm)
Lignite	Eliminate Fines	100 (61)	1/8″ to 1/4″ (3.2 mm to 6.4 mm)
Nylon Film Scrap	Densify	60 (36)	1/8″ (3.2 mm)
Paper Scrap	Densify	83 (50)	1/2″ (12.7 mm)
Phenolic Molding Compound	Reduce Dust, Handling	60 (36)	1/8″ (3.2 mm)
Polyethelyene Film	Densify from 5 lb/ft3 (80 kg/m3) to 20 lb/ft3 (320 kg/m3)	30 (18)	1/8″ to 3/16″ (3.2 mm to 4.8 mm)
Polystyrene Foam	Densify from 4 lb/ft3 (64 kg/m3) to 24 lb/ft3 (384 kg/m3)	164 (100)	1/8″ (3.2 mm)
Polypropylene Film	Densify	40 (24)	1/8″ (3.2 mm)
Rubber Accelerator	Reduce Dust, Handling	192 (117)	12/64″ (4.8 mm)
Starch	Handling	75 (46)	12/64″ (4.8 mm)
Sawdust	Burn	60 (36)	1/4″ (6.4 mm)
Salt	Handling, Reduce Dust	70 (43)	1/8″ (3.2 mm)

(Walas, 1988).

(a)
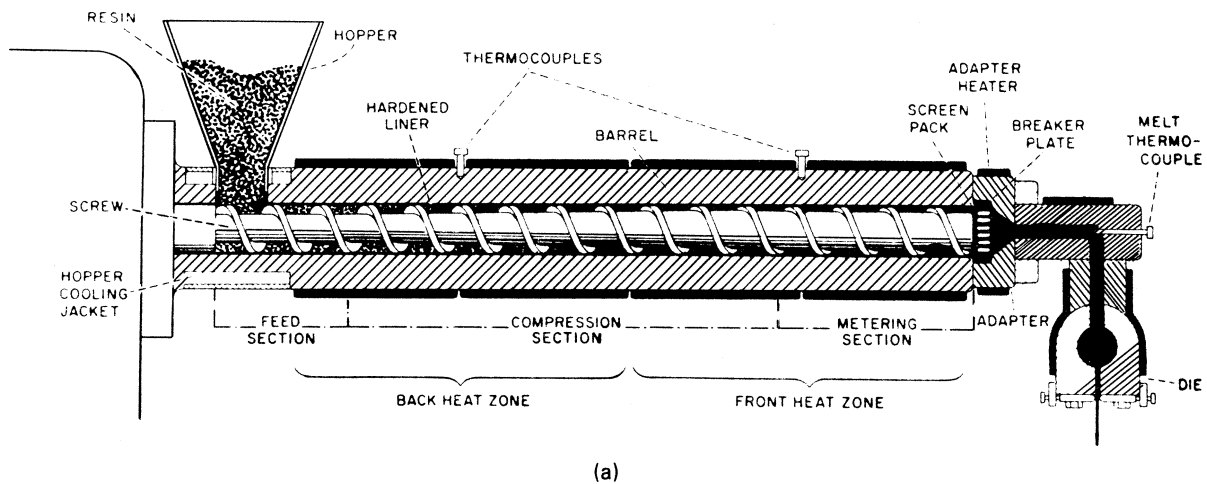
Figure 12.16. Two types of extrusion pelleting equipment. (a) Screw-type extruder for molten plastics: The die is turned 90° in the illustration from its normal position for viewing purposes. The extruded material is cooled and chopped subsequently as needed. (b) Ring extruders: material is charged with screw conveyors to the spaces between the inner rolls and the outer perforated ring, the ring rotates, material is forced through the dies and cut off with knives. (Walas, 1988). (c) BEPEX basket extruder (Courtesy of Hoso Kawa. BEPEX Gmblh).

(b)
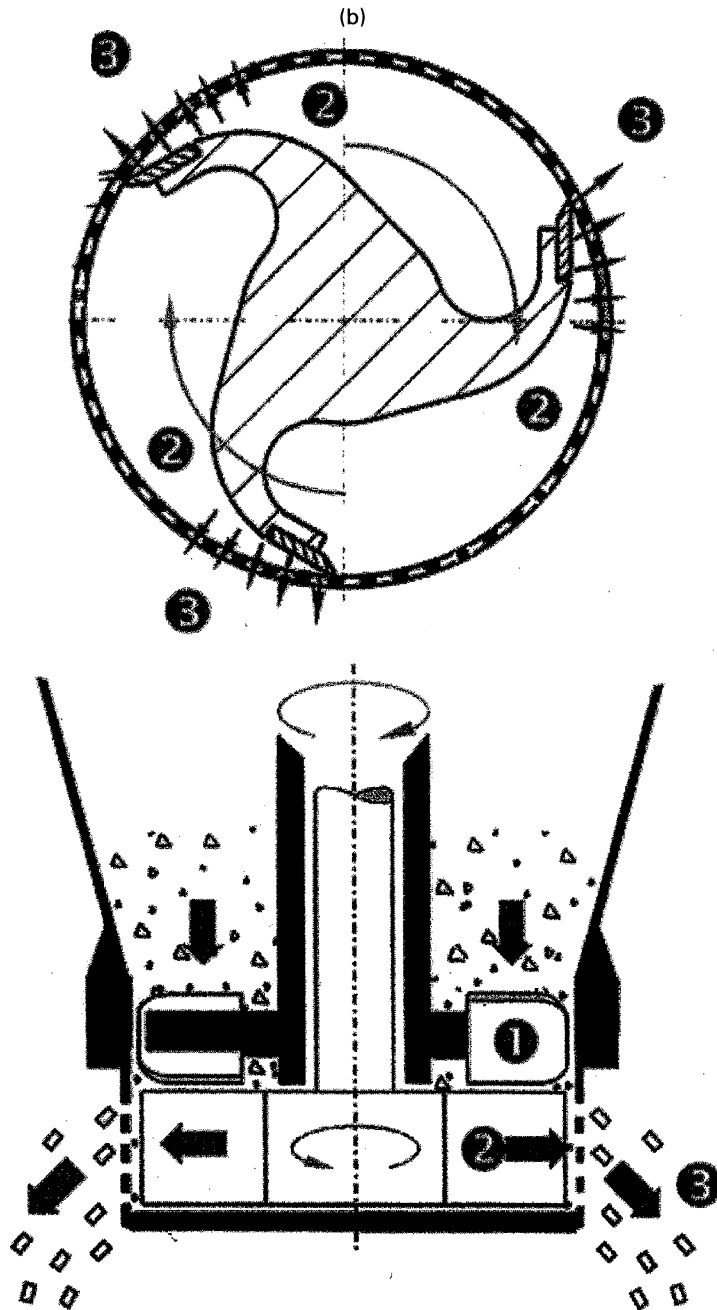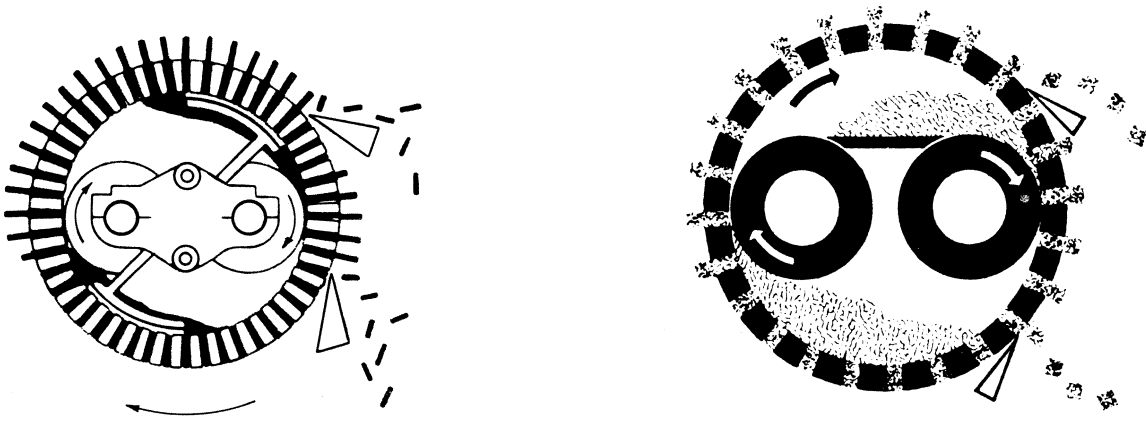
Figure 12.16.—(*continued*)

TABLE 12.20. List of Typical Prillable Materials and Performances of Some Prilling Operations

(a) List of Typical Prillable Materials

Adhesives	Pentachlorophenol
Adipic Acid	Petroleum wax
Alpha naphthol	Phenolic resins–Novalak resin
Ammonium nitrate and additives	Pine rosin
Asphalt	Polyethylene resins
Bisphenol-A	Polystyrene resins
Bitumen	Polypropylene–maleic anhydride
Carbon pitch	Potassium nitrate
Caustic soda	Resins
Cetyl alcohol	Sodium glycols
Coal-derived waxes	Sodium nitrate
Coal tar pitch	Sodium nitrite
Dichloro-benzidine	Sodium sulphate
Fatty acids	Stearic acid
Fatty alcohols	Stearyl alcohol
Epoxy resins	Substituted aliphatics
Hydrocarbon resins	Substituted amides
High-melting inorganic salts	Sulphur
Ink formulations	Urea and additives
Lauric acid	Urea–sulphur mix
Myristic acid	Wax–resin blends
Myristyl alcohol	
Paraffins	

(b) Data for the Prilling of Urea and Ammonium Nitrate

Tower size		
Prill tube height, ft	130	
Rectangular cross section, ft	11 by 21.4	
Cooling air		
rate, lb/h	360,000	
inlet temperature	ambient	
temperature rise, °F	15	
Melt		
Type	Urea	Ammonium Nitrate
rate, lb/h	35,200 (190 lb H_2O)	43,720 (90 lb H_2O)
inlet temperature, °F	275	365
Prills		
outlet temperature, °F	120	225
size, mm	approximately 1 to 3	

(Walas, 1988).

TABLE 12.21. Performance of Fluidized Bed and Spouted Bed Granulators

(a) Batch Fluidized Bed Granulator to Make Feed to Pharmaceutical Tablets; the Sketch Is in Figure 12.17(a)

	Approximate Range
Batch load, dry basis, lb	20 to 400[a]
Volume of container for static bed, ft^3	2 to 15
Fluidizing air fan, hp	5 to 25
Air (Steam) heating capacity, Btu/h	70,000 to 600,000
Drying air temperature, °C	40 to 80
Granulating liquid spray[b]	Two fluid nozzle
Air volume	$\frac{1}{2}$ to 2 SCFM
Liquid volume	500 to 1500 cm^3/min
Batch processing time, min	30 to 50
Average granule size	24 to 8 mesh

[a]Batch capacity exceeds 1500 lb in the largest modern units.
[b]Typical granulating liquids are gelatin or sodium carboxymethyl cellulose solutions.
(Walas, 1988).

TABLE 12.21.—(*continued*)

(b) Performance of Fluidized Bed Granulation of Two Waste Products; Sketch Is in Figure 12.17(b) for Paper Mill Waste

Type of Sludge	Incinerator Size	Bed Temperature	Capacity	Granular Product Composition
Oil refinery waste sludge (85–95% water)	40 ft high; 20 ft ID at base increasing to 28 ft at top	1330°F	31 × 10³ lb/hr of sludge	Start-up material was silica sand; replaced by nodules of various ash components such as CaSO₄, Na, Ca, Mg silicates, Al₂O₃ after operation of incinerator.
Paper mill waste liquor[a] (40% solids)	20 ft ID at top	1350°F	31 × 10³ lb/hr	Sulfur added to produce 90–95% Na₂SO₄ and some Na₂CO₃

(Walas, 1988).

(c) Applications of Spouted Bed Granulations

Material	Feed solution Moisture content (%)	Feed solution Temperature (°C)	Product Size (mm)	Product Moisture (%)	Gas temperature Inlet (°C)	Gas temperature Outlet (°C)	Gas flow rate (m³s⁻¹)	Capacity (kgh⁻¹)
Complex fertilizer	27	15	3–3·5	2·4	170	70	13·9	4000
Potassium chloride	68	15	4–5	–	200	60	13·9	1000
Ammonium nitrate	4	175	2·5–4	0·2	15	55	13·9	9500
Sulphur	–	135	2–5	–	15	–	1·1 × 10⁻²	40
Inorganic pigments, e.g. natural sienna	45	–	3–5	–	280	100		
Organic dyes, e.g. acid blue black	63	–	1–3	6·5	226	154		
Ammonium sulphate	60	70	∼2	–	190	83	∼1·3 × 10⁻²	∼2·7
Sodium chloride	77	–	∼4·5	–	120	70	∼1·8 × 10⁻²	∼1·2

(Walas, 1988).
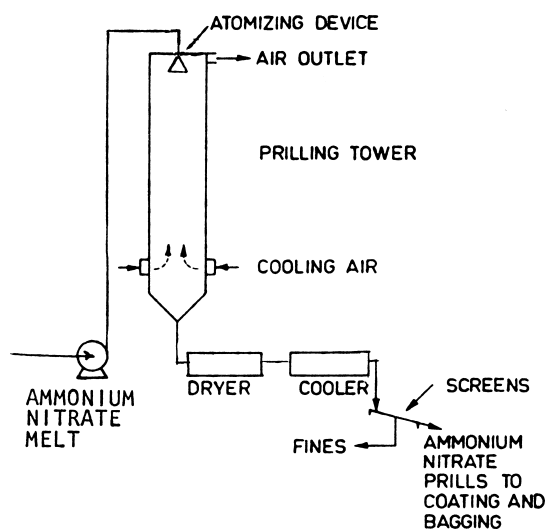
Figure 12.17. A prilling tower for ammonium nitrate, product size range 0.4–2.0 mm. The dryer is not needed if the moisture content of the melt is less than about 0.5%. (Walas, 1988).
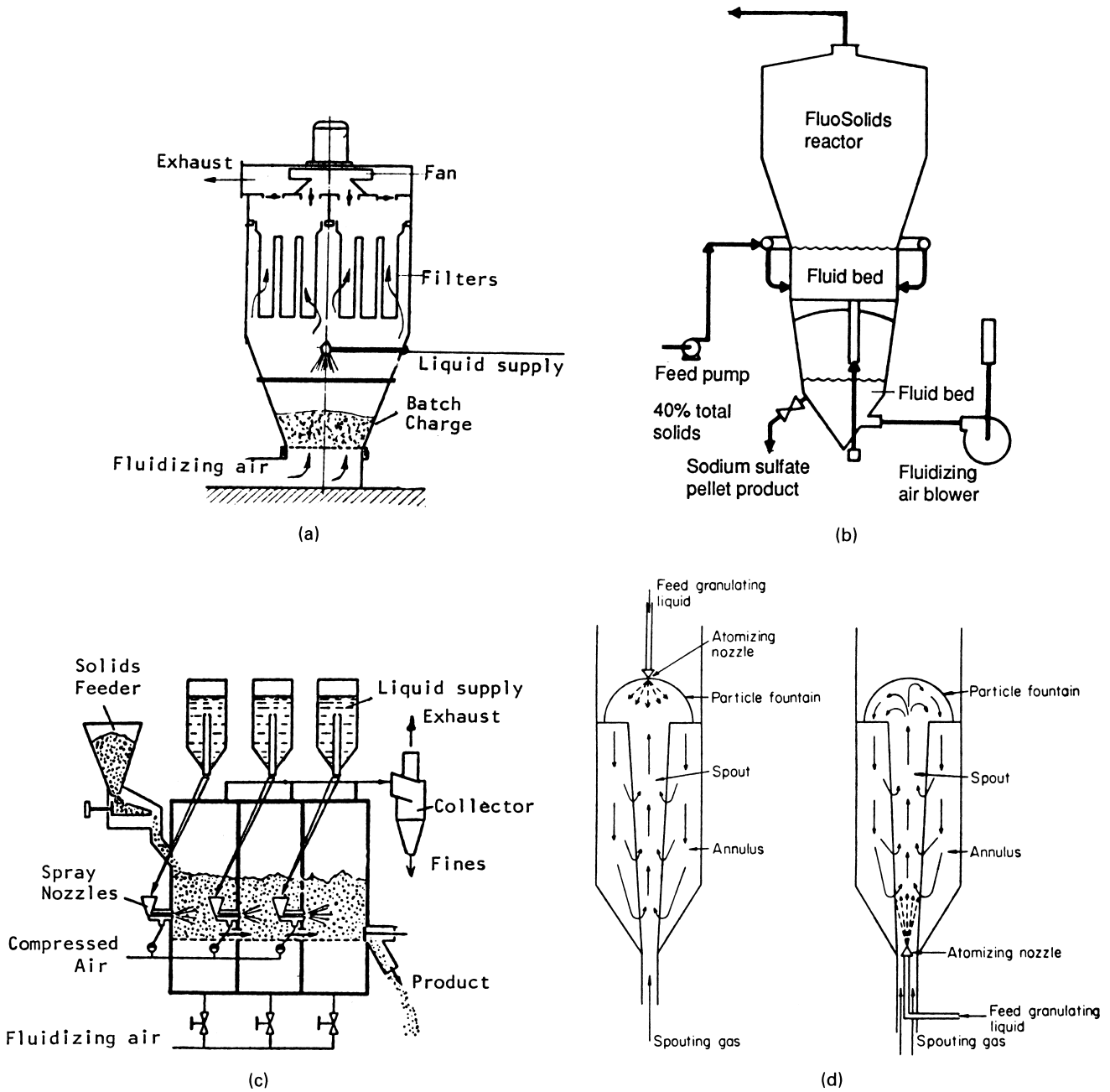
Figure 12.18. Fluidized bed and spouted bed granulators. (a) A batch fluidized bed granulator used in the pharmaceutical industry; performance data in Table 12.21(a). (b) Part of a fluidized bed incineration process for paper mill waste recovering sodium sulfate pellets; performance data in Table 12.21(b). (c) A three-stage fluidized bed granulator for more complete control of process conditions and more nearly uniform size distribution. (d) Two modes of injection of spray to spouted beds, into the body on the left and at the top on the right; performance data in Table 12.21(c). (Walas, 1988).

Spouted beds are applicable when granule size is larger than those that can be fluidized smoothly. Two arrangements are shown in Figure 12.18(d). Particles grow primarily by deposition from evaporated liquid that wets them as they flow up the spout and down the annulus. Performance data are given in Table 12.21(c). The diameter of the spout can be deduced from given gas rates and the entraining velocities of the particles being made. Figure 9.13(f) is a sketch of a spouted bed arrangement. Example 9.9 is devoted to sizing a fluidized bed dryer but many aspects of that design are applicable to a granulation process.

SINTERING AND THERMAL PROCESSES

The sintering process was originally developed to salvage iron ore fines that could not be charged to a blast furnace. The fines are mixed with a flux, such as 14–25% calcite or dolomite and 2.5–5% solid fuel, and conveyed to an ignition furnace, burned and fused together, cooled, and crushed to appropriate size. Very large equipment was required because of the large number of fines. Figure 12.12 is a sketch of this process.

Nodulizing is another process of size enlargement by fusion. A rotary kiln like those used in the cement industry is employed. The product formed is uniform with a hard surface and is more dense than the sintering process. Agglomeration by partial melting requires a feed in powder form.

Sintering of powdered metals such as aluminum, beryllium, tungsten, and zinc, as well as ceramics, under pressure is widely practiced as a shaping process, but that is different from the sintering process described here.

REFERENCES

Size Reduction and Classification

C. F. Bond, *Brit. Chem. Eng.*, **6**, 378–385, 543–548 (1961).

F. C. Bond, *Trans. Am. Inst. Mining and Metallurgical, Pet, Eng.*, 193, 484 (1952).

Chemical Engineering Buyers' Guide 2004, Chemical Engineering, New York, 2003.

G. A. Crawley, A. Malcolmson, I. Crosley, and A. McLeish, *Chemical Engineering*, pp. 54–60, April 2002.

L. Hixon, Sizing up air classifiers, *Chem. Eng. Progr.*, 59–62 (1992).

V. K. Karra, Development of a model for predicting the screening performance of a vibrating screen, *CIM Bull.*, **72,** 167–171 (April 1979).

E. G. Kelley, and D.J. Spottswood, *Introduction to Mineral Processing,* Wiley, New York, 1982, p. 193.

C. W. Mathews, *Chem. Eng.*, 76, July 10, 1972, and in *Chemical Engineers' Handbook*, 6th ed., McGraw-Hill, New York, 1984, p. 21.17.

W. L. McCabe, J.C. Smith, and P. Harriott, *Unit Operations of Chemical Engineering,* 4th ed., McGraw-Hill, New York, 1985.

A. L. Mular, and R.B. Bhappu (Eds.), *Mineral Processing Plant Design*, AIMME, New York, 1980.

R. H. Snow, et al., Size reduction and size enlargement, *Chemical Engineers' Handbook*, 7th ed., McGraw-Hill, New York, 1999.

G. C. Sresty, Crushing and grinding equipment, *Chemical Engineers' Handbook,* 6th ed., McGraw-Hill, New York, 1984, pp. 8.9–8.59.

S. M. Walas, *Chemical Process Equipment: Selection and Design*, Butterworth, Woburn, MA, 1988.

Agglomeration and Size Enlargement

C. E. Capes, *Particle Size Enlargement*, Elsevier, New York, 1980.

C. E. Capes, Size enlargement, in *Chemical Engineers' Handbook,* 6th ed., McGraw-Hill, New York, 1984, pp. 8.60–8.72.

C. E. Capes, and A.E. Fouda, Prilling and other spray methods, in Fayed and Otten, 1984, pp. 294–307.

J. T. Cartensen, Tabletting and pellitization in the pharmaceutical industry, in Fayed and Otten, 1984, pp. 252–268.

M. E. Fayed, and L. Otten (Eds.), *Handbook of Powder Science and Technology*, Van Nostrand Reinhold, New York, 1984.

S. Gantner, *Chemical Engineering*, pp. 36–39 (May 2003).

C. A. Holley, Binders and binding systems for agglomeration, *IBA Proceedings*, 17th Brenn Conference, August 1981.

Hosokawa BEPEX GmbH, *Bextruder Catalog*, Leingarten, Germany, 2003.

R. M. Koerner, and J.A. MacDougal (Eds.), *Briquetting and Agglomeration,* Institute for Briquetting and Agglomeration, Erie, PA, 1983.

R. A. Limons, Sintering iron ore, in Fayed and Otten, 1984, pp. 307–331.

S. Schwartz and S. Goodman, *Plastics Materials and Processes,* Van Nostrand Reinhold, New York, 1982.

P. A. Sherrington, and R. Oliver, *Granulation*, Heyden, London, 1981.

N. E. Stanley-Wood, (Ed.), *Enlargement and Compaction of Particulate Solids*, Butterworths, London, 1983.

13

DISTILLATION AND GAS ABSORPTION

*T*he feasibility of separation of mixtures by distillation, absorption, or stripping depends on the fact that the compositions of vapor and liquid phases are different from each other at equilibrium. The vapor or gas phase is said to be richer in the more volatile or lighter or less soluble components of the mixture. Distillation employs heat to generate vapors and cooling to effect partial or total condensation as needed. Gas absorption employs a liquid of which the major components are essentially nonvolatile and which exerts a differential solvent effect on the components of the gas. In a complete plant, gas absorption is followed by a stripping operation for regeneration and recycle of the absorbent and for recovering the preferentially absorbed substances. In reboiled absorbers, partial stripping of the lighter components is performed in the lower part of the equipment. In distillation, absorption, or rectification and stripping are performed in the same equipment. Figures 13.1 and 13.2 show the basic types of equipment.

These distinctions between the two operations are partly traditional. The equipment is similar, and the mathematical treatment, which consists of material and energy balances and phase equilibrium relations, also is the same for both. The fact, however, that the bulk of the liquid phase in absorption-stripping plants is nonvolatile permits some simplifications in design and operation.

Equipment types are of two kinds, tray-type or packed, stagewise or continuous. The trays function as individual stages and produce stepwise changes in concentration. In packed towers concentration changes occur gradually. Until recently packed towers were used only in small equipment and where their construction was an advantage under corrosive conditions or when low pressure drop was mandatory. The picture now has changed and both types often are competitive over a wide range of sizes.

13.1. VAPOR-LIQUID EQUILIBRIA

This topic is concerned with the relations between vapor and liquid compositions over a range of temperature and pressure. Functionally, the dependence of the mol fraction y_i of component i in the vapor phase depends on other variables as

$$y_i = f(T, P, x_1, x_2, \ldots, x_n). \tag{13.1}$$

The dependence on composition alone often is approximated by

$$y_i = K_i x_i, \tag{13.2}$$

where K_i, the vaporization equilibrium ratio (VER), is a function of temperature, pressure, and composition. Equation (13.2) can be viewed, as suggested by Raoult's law,

$$y_i = (P_i^{\text{sat}}/P)x_i \tag{13.3}$$

with

$$(K_i)_{\text{ideal}} = P_i^{\text{sat}}/P, \tag{13.4}$$
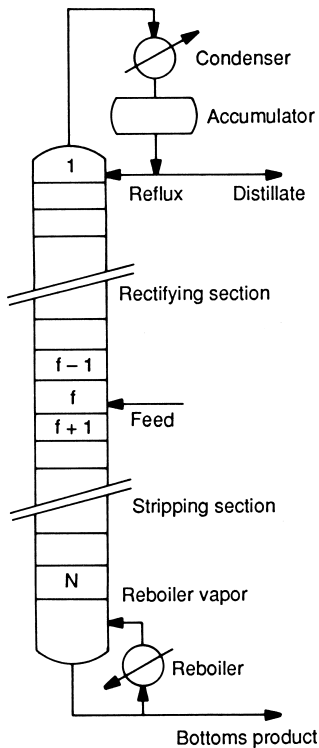
Figure 13.1. Distillation column assembly.
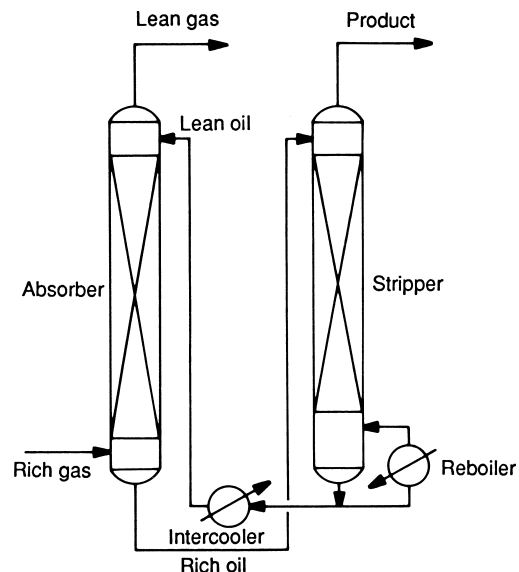
Figure 13.2. Absorber-stripper assembly.

397

where P_i^{sat} is the vapor pressure of component I, and P is the system total pressure. A number of correlations for VER have been developed for hydrocarbon systems that form relatively ideal solutions, but for most chemical systems, Eq. (13.4) must be corrected. At lower pressures (below about 5 atm), the correction factor is a liquid phase activity coefficient γ_i^L (sometimes called a "Raoult's law correction factor").

A more rigorous expression is derived by noting that at equilibrium, partial fugacities of each component are the same in each phase, that is

$$f_i^v = f_i^L \tag{13.5}$$

or, in terms of fugacity and activity coefficients,

$$y_i \phi_i^v P = \gamma_i^L x_i \phi_i^L P_i^{sat} \tag{13.6}$$

and the VER becomes

$$K_i = \frac{y_i}{x_i} = \frac{\gamma_i^L \phi_i^{sat} P_i^{sat}}{\phi_i^v P} \tag{13.7}$$

Additionally, small corrections for pressure, called Poynting factors, belong in Eq. (13.6) but are omitted here. The new terms are:

ϕ_i^{sat} = fugacity coefficient of the pure component at its vapor pressure,

ϕ_i^v = partial fugacity coefficient in the vapor phase.

Equations for fugacity coefficients are derived from equations of state or are approximated from activity coefficient charts as functions of reduced temperature and pressure. Table 13.1 includes them for the popular Soave equation of state. At pressures below 5–6 atm, the ratio of activity coefficients in Eq. (13.7) often is near unity. Then the VER becomes

$$K_i = \gamma_i^L P_i^{sat} / P \tag{13.8}$$

which is independent of the nature of the vapor phase.

Values of the activity coefficients are deduced from experimental data of vapor-liquid equilibria and correlated or extended by any one of several available equations. Values also be calculated approximately from structural group contributions by methods called UNIFAC and ASOG. For more than two components, the correlating equations favored nowadays are the Wilson, the NRTL, and UNIQUAC, and for some applications a solubility parameter method. The first and last of these are given in Table 13.2. Calculations from measured equilibrium compositions are made with the rearranged equation

$$\gamma_i = \frac{\phi_i^v P}{\phi_i^{sat} P_i^{sat}} \frac{y_i}{x_i} \tag{13.9}$$

$$\simeq \frac{P}{P_i^{sat}} \frac{y_i}{x_i}. \tag{13.10}$$

The last approximation usually may be made at pressures below 5–6 atm. Then the activity coefficient is determined by the vapor pressure, the system pressure, and the measured equilibrium compositions.

Since the fugacity and activity coefficients are mathematically complex functions of the compositions, finding corresponding compositions of the two phases at equilibrium when the equations are known requires solutions by trial. Suitable procedures for making flash calculations are presented in the next section, and in

TABLE 13.1. The Soave Equation of State and Fugacity Coefficients

Equation of State

$$P = \frac{RT}{V - b} - \frac{a\alpha}{V(V + b)}$$

$$z^3 - z^2 + (A - B - B^2)z - AB = 0$$

Parameters

$a = 0.42747 R^2 T_c^2 / P_{c'}$
$b = 0.08664 R T_c / P_c$
$\alpha = [1 + (0.48508 + 1.55171\omega - 0.15613\omega^2)(1 - T_r^{0.5})]^2$
$\alpha = 1.202 \exp(-0.30288 T_r)$ and for hydrogen
    (Graboski and Daubert, 1979)
$A = a\alpha P / R^2 T^2 = 0.42747 \alpha P_r / T_r^2$
$B = bP / RT = 0.08664 P_r / T_r$

Mixtures

$a\alpha = \Sigma\Sigma y_i y_j (a\alpha)_{ij}$
$b = \Sigma y_i b_i$
$A = \Sigma\Sigma y_i y_j A_{ij}$
$B = \Sigma y_i B_i$

Cross parameters

$(a\alpha)_{ij} = (1 - k_{ij})\sqrt{(a\alpha)_i (a\alpha)_j}$

k_{ij} in table
$k_{ij} = 0$ for hydrocarbon pairs and hydrogen

Correlations in Terms of Absolute Differences between Solubility Parameters of the Hydrocarbon, δ_{HC} and of the Inorganic Gas

Gas	k_{ij}
H_2S	$0.0178 + 0.0244\|\delta_{HC} - 8.80\|$
CO_2	$0.1294 - 0.0292\|\delta_{HC} - 7.12\|^2 - 0.0222\|\delta_{HC} - 7.12\|^2$
N_2	$-0.0836 + 0.1055\|\delta_{HC} - 4.44\| - 0.0100\|\delta_{HC} - 4.44\|^2$

Fugacity Coefficient of a Pure Substance

$$\ln\phi = z - 1 - \ln\left[z\left(1 - \frac{b}{V}\right)\right] - \frac{a\alpha}{bRT} \ln\left(1 + \frac{b}{V}\right)$$

$$= z - 1 - \ln(z - B) - \frac{A}{B} \ln\left(1 + \frac{B}{z}\right)$$

Fugacity Coefficients in Mixtures

$$\ln\phi_i = \frac{b_i}{b}(z - 1) - \ln\left[z\left(1 - \frac{b}{V}\right)\right]$$
$$+ \frac{a\alpha}{bRT}\left[\frac{b_i}{b} - \frac{2}{a\alpha}\sum_j y_j (a\alpha)_{ij}\right] \ln\left(1 + \frac{b}{V}\right)$$
$$= \frac{B_i}{B}(z - 1) = \ln(z - B) + \frac{A}{B}\left[\frac{B_i}{B} - \frac{2}{a\alpha}\sum_j y_j (a\alpha)_{ij}\right] \ln\left(1 + \frac{B}{2}\right)$$

(Walas, 1985).

greater detail in some books on thermodynamics, for instance, the one by Walas (1985). In making such calculations, it is usual to start by assuming ideal behavior, that is,

$$\hat{\phi}_i^v / \phi_i^{\text{sat}} = \gamma_i = 1. \tag{13.11}$$

After the ideal equilibrium compositions have been found, they are used to find improved values of the fugacity and activity coefficients. The process is continued to convergence.

RELATIVE VOLATILITY

The compositions of vapor and liquid phases of a binary system at equilibrium sometimes can be related by a constant relative volatility which is defined as

$$\alpha_{12} = \frac{y_1}{x_1} \Big/ \frac{y_2}{x_2} = \left(\frac{y_1}{1 - y_1}\right) \Big/ \left(\frac{x_1}{1 - x_1}\right). \tag{13.12}$$

Then

$$\frac{y_1}{1 - y_1} = \alpha_{12} \frac{x_1}{1 - x_1}. \tag{13.13}$$

In terms of vaporization equilibrium ratios,

$$\alpha_{12} = K_1 / K_2 = \gamma_1^L P_1^{\text{sat}} / \gamma_2 P_2^{\text{sat}}, \tag{13.14}$$

and when Raoult's law applies ($\gamma^L = 1.0$) the relative volatility is the ideal value,

$$\alpha_{\text{ideal}} = P_1^{\text{sat}} / P_2^{\text{sat}}. \tag{13.15}$$

Usually the relative volatility is not truly constant but is found to depend on the composition, for example,

$$\alpha_{12} = k_1 + k_2 x_1. \tag{13.16}$$

Other relations that have been proposed are

$$\frac{y_1}{1 - y_1} = k_1 + k_2 \left(\frac{x_1}{1 - x_1}\right) \tag{13.17}$$

and

$$\frac{y_1}{1 - y_1} = k_1 \left(\frac{x_1}{1 - x_1}\right)^{k_2}. \tag{13.18}$$

A variety of such relations is discussed by Hala (*Vapor–Liquid Equilibria*, Pergamon London, 1967). Other expressions can be deduced from Eq. (13.14) and some of the equations for activity coefficients, for instance, the Scatchard-Hildebrand of Table 13.2.
Then

$$\alpha_{12} = \frac{y_1}{x_1} \Big/ \frac{y_2}{x_2} = \frac{P_1^{\text{sat}}}{P_2^{\text{sat}}} \exp\left\{\frac{(\delta_1 - \delta_2)^2}{RT}[V_1(1 - \phi_1)^2 - V_2\phi_1^2]\right\}, \tag{13.19}$$

where

$$\phi_1 = \frac{V_1 x_1}{V_1 x_1 + V_2 x_2} \tag{13.20}$$

is the volume fraction of component 1 in the mixture.

Beyond a certain complexity these analytical relations between vapor and liquid compositions lose their utility. The simplest one, Eq. (13.13), is of value in the analysis of multistage separating equipment. When the relative volatility varies modestly from stage to stage, a geometric mean often is an adequate value to use. Applications are made later. Example 13.1 examines two ways of interpreting dependence of relative volatility on composition.

BINARY $x - y$ DIAGRAMS

Equilibria between the components of a binary mixture are expressed as a functional relation between the mol fractions of the usually more volatile component in the vapor and liquid phases,

$$y = f(x). \tag{13.21}$$

The definition of relative volatility, Eq (13.13) is rearranged into this form:

$$y = \frac{\alpha x}{1 + (\alpha - 1)x} \tag{13.22}$$

Representative $x - y$ diagrams appear in Figure 13.3; one should note that the y and x scales are in weight percent, not the usual mole percent. Generally they are plots of direct experimental data, but they can be calculated from fundamental data of vapor pressure and activity coefficients. The basis is the bubblepoint condition:

$$y_1 + y_2 = \frac{\gamma_1 P_1^{\text{sat}}}{P} x_1 + \frac{\gamma_2 P_2^{\text{sat}}}{P}(1 - x_1) = 1. \tag{13.23}$$

In order to relate y_1 and x_1, the bubblepoint temperatures are found over a series of values of x_1. Since the activity coefficients depend on the composition of the liquid and both activity coefficients and vapor pressures depend on the temperature, the calculation requires a respectable effort. Moreover, some vapor-liquid measurements must have been made for evaluation of a correlation of activity coefficients. The method does permit calculation of equilibria at several pressures since activity coefficients are substantially independent of pressure. A useful application is to determine the effect of pressure on azeotropic composition (Walas, 1985, p. 227).

13.2. SINGLE-STAGE FLASH CALCULATIONS

The problems of interest are finding the conditions for onset of vaporization, the bubble-point; for the onset of condensation, the dewpoint; and the compositions and the relative amounts of vapor and liquid phases at equilibrium under specified conditions of temperature and pressure or enthalpy and pressure. The first cases examined will take the K_i to be independent of composition. These problems usually must be solved by iteration, for which the Newton–Raphson method is suitable. The dependence of K on temperature may be represented adequately by

$$K_i = \exp[A_i - B_i/(T + C_i)]. \tag{13.24}$$

An approximate relation for the third constant is

$$C_i = 18 - 0.19T_{bi}, \tag{13.25}$$

where T_{bi} is the normal boiling point in $^\circ$K. The dependence of K on pressure may be written simply as

$$K_i = a_i P^{bi}. \tag{13.26}$$

TABLE 13.2. Activity Coefficients from Solubility Parameters and from the Wilson Equation

Binary Mixtures		
Name	**Parameters**	**$\ln \gamma_1$ and $\ln \gamma_2$**
Scatchard–Hildebrand	δ_1, δ_2	$\dfrac{V_1}{RT}(1 - \phi_1)^2(\delta_1 - \delta_2)^2$
		$\dfrac{V_2}{RT}\phi_1^2(\delta_1 - \delta_2)^2$
Wilson	$\phi_1 = V_1 x_1/(V_1 x_1 + V_2 x_2)$ $\lambda_{12}, \lambda_{21}$	$-\ln(x_1 + \Lambda_{12}x_2) + x_2\left(\dfrac{\Lambda_{12}}{x_1 + \Lambda_{12}x_2} - \dfrac{\Lambda_{21}}{\Lambda_{21}x_1 + x_2}\right)$
		$-\ln(x_2 + \Lambda_{21}x_1) - x_1\left(\dfrac{\Lambda_{12}}{x_1 + \Lambda_{12}x_2} - \dfrac{\Lambda_{21}}{\Lambda_{21}x_1 + x_2}\right)$
	$\Lambda_{12} = \dfrac{V_2^L}{V_1^L}\exp\left(-\dfrac{\lambda_{12}}{RT}\right)$	$\Lambda_{21} = \dfrac{V_1^L}{V_2^L}\exp\left(-\dfrac{\lambda_{21}}{RT}\right)$

V_i^L molar volume of pure liquid component i.

Ternary Mixtures

$$\ln \gamma_1 = 1 - \ln(x_1\Lambda_{i1} + x_2\Lambda_{i2} + x_3\Lambda_{i3}) - \frac{x_1\Lambda_{1i}}{x_1 + x_2\Lambda_{12} + x_3\Lambda_{13}}$$

$$-\frac{x_2\Lambda_{2i}}{x_1\Lambda_{21} + x_2 + x_3\Lambda_{23}} - \frac{x_3\Lambda_{3i}}{x_1\Lambda_{31} + x_2\Lambda_{32} + x_3}$$

$$\Lambda_{ii} = 1$$

Multicomponent Mixtures		
Equation	**Parameters**	**$\ln \gamma_i$**
Scatchard–Hildebrand	δ_i	$\dfrac{V_i}{RT}\left[\delta_i - \sum_j \dfrac{x_j V_j \delta_j}{\sum_k x_k V_k}\right]^2$
Wilson	$\Lambda_{ij} = \dfrac{V_j^L}{V_i^L}\exp\left(-\dfrac{\lambda_{ij}}{RT}\right)$ $\Lambda_{ij} = \Lambda_{jj} = 1$	$-\ln\left(\sum_{j=1}^{m} x_j\Lambda_{ij}\right) + 1 - \sum_{k=1}^{m}\dfrac{x_k\Lambda_{ki}}{\sum_{j=1}^{m} x_j\Lambda_{kj}}$

Linear expressions for the enthalpies of the two phases are

$$h_i = a_i + b_i T, \tag{13.27}$$

$$H_i = c_i + d_i T, \tag{13.28}$$

assuming negligible heats of mixing. The coefficients are evaluated from tabulations of pure component enthalpies. First derivatives are needed for application of the Newton-Raphson method:

$$\partial K_i/\partial T = B_i K_i/(T + C_i)^2, \tag{13.29}$$

$$\partial K_i/\partial P = b_i K_i/P. \tag{13.30}$$

BUBBLE-POINT TEMPERATURE AND PRESSURE

The temperature at which a liquid of known composition first begins to boil is found from the equation

$$f(T) = \sum K_i x_i - 1 = 0, \tag{13.31}$$

where the K_i are known functions of the temperature. In terms of Eq. (13.24) the Newton–Raphson algorithm is

$$T = T - \frac{-1 + \sum K_i x_i}{\sum [B_i K_i x_i/(T + C_i)^2]}. \tag{13.32}$$

Similarly, when Eq. (13.26) represents the effect of pressure, the bubble-point pressure is found with the N-R algorithm:

$$f(P) = \sum K_i x_i - 1 = 0, \tag{13.33}$$

$$P = P - \frac{-1 + \sum a_i P^{b_i} x_i}{\sum a_i b_i P_i^{b_i-1} x_i}. \tag{13.34}$$

DEWPOINT TEMPERATURE AND PRESSURE

The temperature or pressure at which a vapor of known composition first begins to condense is given by solution of the appropriate equation,

$$f(T) = \sum y_i/K_i - 1 = 0, \tag{13.35}$$

EXAMPLE 13.1
Correlation of Relative Volatility
Data for the system ethanol + butanol at 1 atm are taken from the collection of Kogan (1966, #1038). The values of $x/(100 - x)$, $y/(100 - y)$, and α are calculated and plotted. The plot on linear coordinates shows that relative volatility does not plot linearly with x, but from the linear log–log plot it appears that

$$\frac{y}{100 - y} = 4.364\left(\frac{x}{100 - x}\right)^{1.045} \text{ or } \alpha = 4.364\left(\frac{x}{100 - x}\right)^{0.045}.$$

x	y	x	y
0	0	39.9	74.95
3.45	12.5	53.65	84.3
6.85	22.85	61.6	88.3
10.55	32.7	70.3	91.69
14.5	41.6	79.95	95.08
18.3	49.6	90.8	97.98
28.4	63.45	100.0	100.0

x	α	$x/100 - x$	$y/100 - y$
3.5	4.00	0.04	0.14
6.9	4.03	0.07	0.30
10.6	4.12	0.12	0.49
14.5	4.20	0.17	0.71
18.8	4.25	0.23	0.98
26.4	4.38	0.40	1.74
39.9	4.51	0.66	2.99
53.7	4.64	1.16	5.37
61.6	4.70	1.60	7.55
70.3	4.66	2.37	11.03
80.0	4.85	3.99	19.33
90.8	4.91	9.87	48.50
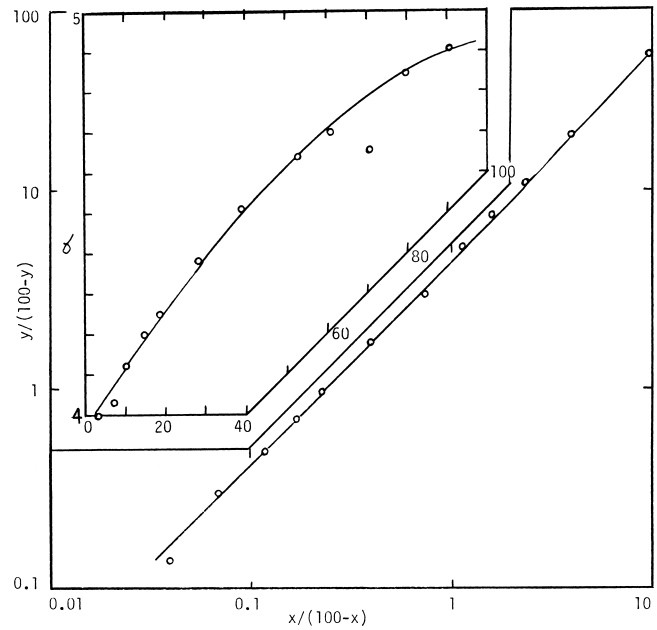
$$f(P) = \sum y_i/K_i - 1 = 0. \tag{13.36}$$

In terms of Eqs. (13.24) and (13.26) the N–R algorithms are

$$T = T + \frac{-1 + \sum y_i/K_i}{\sum [(y_i/K_i^2)\partial K_i/\partial T]} = T + \frac{-1 + \sum y_i/K_i}{\sum [B_i y_i/K_i(T + C_i)^2]}, \tag{13.37}$$

$$P = P + \frac{-1 + \sum y_i/K_i}{\sum [(y_i/K_i^2)\partial K_i/\partial P]} = P + \frac{(-1 + \sum y_i/K_i)P}{\sum (b_i y_i/K_i)}. \tag{13.38}$$

FLASH AT FIXED TEMPERATURE AND PRESSURE

At temperatures and pressures between those of the bubblepoint and dewpoint, a mixture of two phases exists whose amounts and compositions depend on the conditions that are imposed on the system. The most common sets of such conditions are fixed T and P, or fixed H and P, or fixed S and P. Fixed T and P will be considered first.

For each component the material balances and equilibria are:

$$Fz_i = Lx_i + Vy_i, \tag{13.39}$$

$$y_i = K_i x_i. \tag{13.40}$$

On combining these equations and introducing $\beta = V/F$, the fraction vaporized, the flash condition becomes

$$f(\beta) = -1 + \sum x_i = -1 + \sum \frac{z_i}{1 + \beta(K_i - 1)} = 0, \tag{13.41}$$

and the corresponding N–R algorithm is

$$\beta = \beta + \frac{-1 + \sum [z_i/(1 + \beta(K_i - 1))]}{\sum \{(K_i - 1)z_i/[1 + \beta(K_i - 1)]^2\}}. \tag{13.42}$$

After β has been found by successive approximation, the phase compositions are obtained with

$$x_i = \frac{z_i}{1 + \beta(K_i - 1)}, \tag{13.43}$$

$$y_i = K_i x_i. \tag{13.44}$$

A starting value of $\beta = 1$ always leads to a converged solution by this method.

FLASH AT FIXED ENTHALPY AND PRESSURE

The problem will be formulated for a specified final pressure and enthalpy, and under the assumption that the enthalpies are additive (that is, with zero enthalpy of mixing) and are known functions of temperature at the given pressure. The enthalpy balance is

$$H_F = (1 - \beta)\sum x_i H_{iL} + \beta \sum y_i H_{iV} \tag{13.45}$$
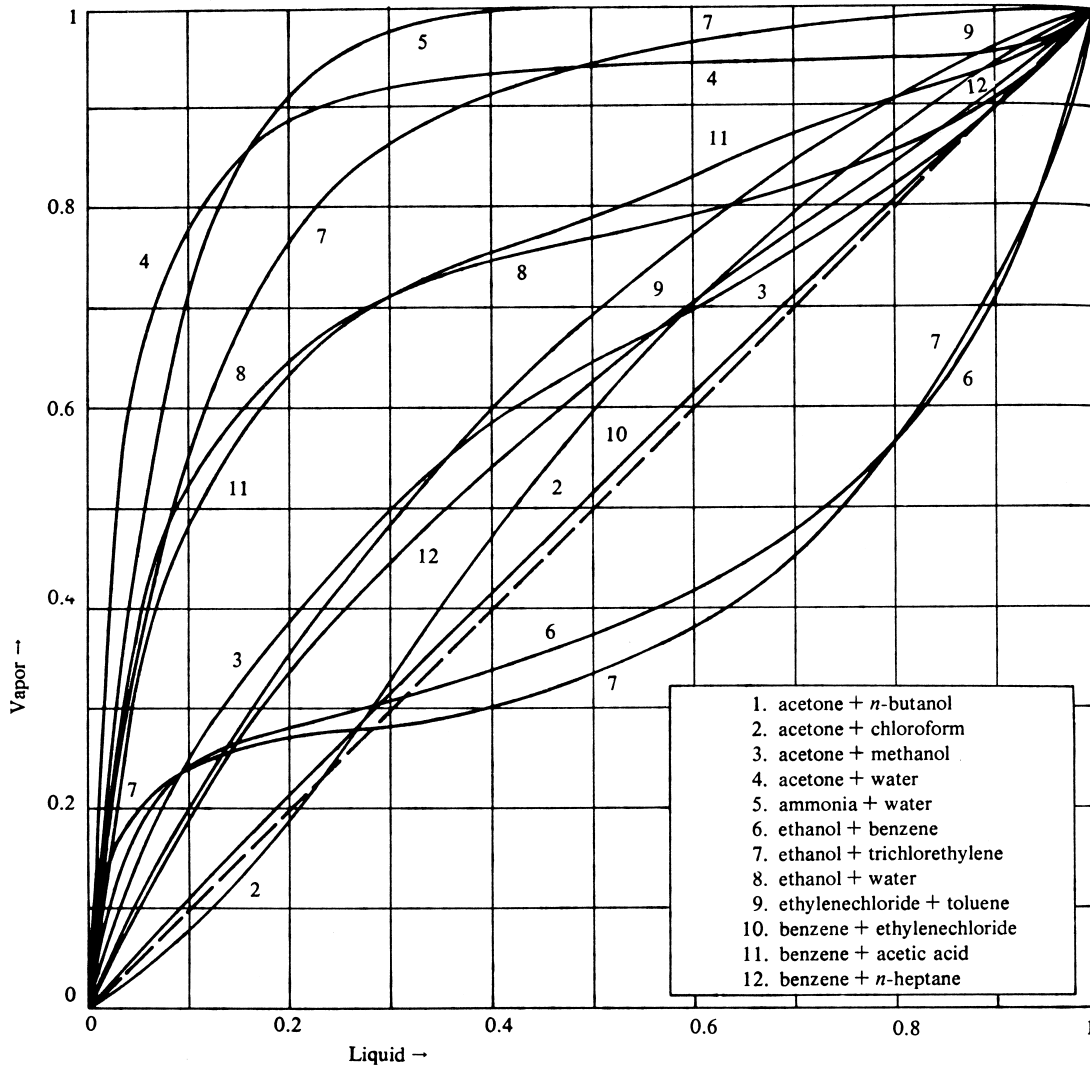
Figure 13.3. Some vapor-liquid composition diagrams at essentially atmospheric pressure. This is one of four such diagrams in the original reference (*Kirschbaum, 1969*). Compositions are in weight fractions of the first-named.

$$= (1 - \beta) \sum \frac{z_i H_{iL}}{1 + \beta(K_i - 1)} + \beta \sum \frac{K_i z_i H_{iV}}{1 + \beta(K_i - 1)}. \qquad (13.46)$$

This equation and the flash Eq. (13.41) constitute a set:

$$f(\beta, T) = -1 + \sum \frac{z_i}{1 + \beta(K_i - 1)} = 0, \qquad (13.47)$$

$$g(\beta, T) = H_F - (1 - \beta) \sum \frac{z_i H_{iL}}{1 + \beta(K_i - 1)} - \beta \sum \frac{K_i z_i H_{iV}}{1 + \beta(K_i - 1)} = 0, \qquad (13.48)$$

from which the phase split β and temperature can be found when the enthalpies and the vaporization equilibrium ratios are known functions of temperature. The N–R method applied to Eqs. (13.47 and 13.48) finds corrections to initial estimates of β and T by solving the linear equations

$$h \frac{\partial f}{\partial \beta} + k \frac{\partial f}{\partial T} + f = 0, \qquad (13.49)$$

$$h \frac{\partial g}{\partial \beta} + k \frac{\partial g}{\partial T} + g = 0, \qquad (13.50)$$

where all terms are evaluated at the assumed values (β_0, T_0) of the two unknows. The corrected values, suitable for the next trial if that is necessary, are

$$\beta = \beta_0 + h, \qquad (13.51)$$

$$T = T_0 + K. \qquad (13.52)$$

Example 13.2 applies these equations for dewpoint, bubblepoint, and flashes.

EQUILIBRIA WITH Ks DEPENDENT ON COMPOSITION

The procedure will be described only for the case of bubblepoint temperature for which the calculation sequence is represented on Figure 13.4. Equations 13.7 and 13.31 are combined as

$$f(T) = \sum \frac{\gamma_i \phi_i^{\mathrm{sat}} P_i^{\mathrm{sat}}}{\hat{\phi}_i P} x_i - 1 = 0. \qquad (13.53)$$

EXAMPLE 13.2
Vaporization and Condensation of a Ternary Mixture
For a mixture of ethane, n-butane, and n-pentane, the bubblepoint and dewpoint temperatures at 100 psia, a flash at 100°F and 100 psia, and an adiabatic flash at 100 psia of a mixture initially liquid at 100°F will be determined. The overall composition z_i, the coefficients A, B, and C of Eq. (13.21) and the coefficients a, b, c, and d of Eqs. (13.27) and (13.28) are tabulated:

Coefficients

	z	A	B	C	a	b	c	d
C_2	0.3	5.7799	2167.12	−30.6	122	0.73	290	0.45
nC_4	0.3	6.1418	3382.90	−60.8	96	0.56	267	0.34
nC_5	0.4	6.4610	3978.36	−73.4	90	0.55	260	0.40

The bubble-point temperature algorithm is

$$T = T - \frac{-1 + \Sigma K_i x_i}{\Sigma [B_i K_i x_i / (T + C_i)^2]}, \tag{13.32}$$

and the dewpoint temperature algorithm is

$$T = T + \frac{-1 + \sum y_i / K_i}{\sum [B_i y_i / K_i (T + C_i)^2]}. \tag{13.33}$$

Results of successive iterations are

Bubble-point	Dewpoint
1000.0000	700.0000
695.1614	597.8363
560.1387	625.9790
506.5023	635.3072
496.1742	636.0697
495.7968	636.0743
495.7963	636.0743

The algorithm for the fraction vapor at specified T and P is

$$\beta = \frac{V}{F} = \beta + \frac{-1 + \Sigma z_i / (1 + \beta(K_i - 1))}{\Sigma (K_i - 1) z_i / (1 + \beta(K_i - 1))^2}, \tag{13.42}$$

and the equations for the vapor and liquid compositions are

$$x_i = z_i / (1 + \beta(K_i - 1)), \tag{13.43}$$

$$y_i = K_i x_i. \tag{13.44}$$

Results for successive iterations for β and the final phase compositions are

β		z_i	x_i	y_i
1.0000	C_2	0.3	0.1339	0.7231
0.8257	nC_4	0.3	0.3458	0.1833
0.5964	nC_5	0.4	0.5203	0.0936
0.3986				
0.3038				
0.2830				
0.2819				

Adiabatic flash calculation: Liquid and vapor enthalpies off charts in the API data book are fitted with linear equations

$$h = a + bT(°F), \tag{13.27}$$

$$H = c + dT(°F). \tag{13.28}$$

The inlet material to the flash drum is liquid at 100°F, with $H_0 = 8,575.8$ Btu/lb mol. The flash Eq. (13.42) applies to this part of the example. The enthalpy balance is

$$\begin{aligned} H_0 &= 8575.8 \\ &= (1 - \beta)\Sigma M_i x_i h_i + \beta\Sigma M_i y_i H_i \end{aligned} \tag{13.45}$$

$$= (1 - \beta)\Sigma \frac{M_i z_i h_i}{1 + \beta(K_i - 1)} + \beta\Sigma \frac{K_i M_i z_i H_i}{1 + \beta(K_i - 1)}. \tag{13.46}$$

The procedure consists of the steps.

1. Assume T.
2. Find the K_i, h_i, and H_i.
3. Find β from the flash equation (13.42).
4. Evaluate the enthalpy of the mixture and compare with H_0, Eq. (13.46).

The results of several trials are shown:

T (°R)	β	H
530.00	0.1601	8475.70
532.00	0.1681	8585.46
531.82	0.1674	8575.58 ∼ 8575.8, check.

The final VERs and the liquid and vapor compositions are:

	K	x	y
C_2	4.2897	0.1935	0.8299
nC_4	0.3534	0.3364	0.1189
nC_5	0.1089	0.4701	0.0512

The numerical results were obtained with short computer programs which are given in Walas (1985, p. 317).

The liquid composition is known for a bubble-point determination, but the temperature is not at the start, so that starting estimates must be made for both activity and fugacity coefficients. In the flow diagram, the starting values are proposed to be unity for all the variables. After a trial value of the temperature is chosen, subsequent calculations on the diagram can be made directly. The correct value of T has been chosen when $\sum y_i = 1$.

Since the equations for fugacity and activity coefficients are complex, solution of this kind of problem is feasible only by computer. Reference is made in Example 13.3 to such programs. There also are given the results of such a calculation which reveals the magnitude of deviations from ideality of a common organic system at moderate pressure.

13.3. EVAPORATION OR SIMPLE DISTILLATION

As a mixture of substances is evaporated, the residue becomes relatively depleted in the more volatile constituents. A relation for

1. Read P, x_i

2. $\hat{\phi}_i = \gamma_i = 1$

3. Assume T

4. ϕ_i^s, P_i^s, $(PF)_i$

5. K_i

12. $\hat{\phi}_i$, γ_i

6. $\Sigma\, y_i$

11. Normalize y_i

7. First trial? —— YES

8. $\Sigma\, y_i = $ constant? —— NO

NO

9. $\Sigma\, y_i = 1$?

YES

10. E N D
Print T, y_i
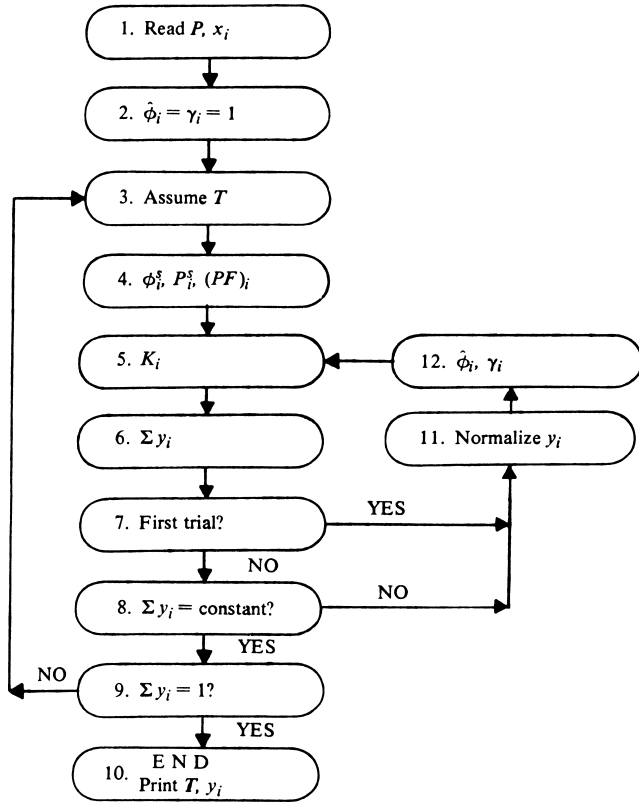
Figure 13.4. Calculation diagram for bubblepoint temperature. (*Walas, 1985*).

binary mixtures due to Rayleigh is developed as follows: The differential material balance for a change dL in the amount of liquid remaining is

$$-y\, dL = d(LX) = L\, dx + X\, dL. \qquad (13.54)$$

Upon rearrangement and integration, the result is

$$\ln\left(\frac{L}{L_0}\right) = \int_{x_0}^{x} \frac{dx}{x - y}. \qquad (13.55)$$

In terms of a constant relative volatility

$$y = \frac{\alpha x}{1 + (\alpha - 1)x'} \qquad (13.56)$$

the integral becomes

$$\ln\frac{L}{L_0} = \frac{1}{x - 1}\ln\frac{x(1 - x_0)}{x_0(1 - x)} + \ln\frac{1 - x_0}{1 - x}. \qquad (13.57)$$

MULTICOMPONENT MIXTURES

Simple distillation is not the same as flashing because the vapor is removed out of contact with the liquid as soon as it forms, but the process can be simulated by a succession of small flashes of residual liquid, say 1% of the original amount each time. After n intervals, the amount of residual liquid F is

$$F = L_0(1 - 0.01n) \qquad (13.58)$$

and

$$\beta = \frac{V}{F} = \frac{0.01 L_0}{(1 - 0.01n)L_0} = \frac{0.01}{1 - 0.01n}. \qquad (13.59)$$

Then the flash equation (13.41) becomes a function of temperature,

$$f(T_n) = -1 + \sum \frac{z_i}{1 + 0.01(K_i - 1)/(1 - 0.01n)} = 0. \qquad (13.60)$$

Here z_i is the composition at the end of interval n and K_i also may be taken at the temperature after interval n. The composition is found by material balance as

$$Lz_i = L_0(1 - 0.01n)z_i = L_0\left[z_{i0} - 0.01\sum_{k=1}^{n} y_{ik}\right], \qquad (13.61)$$

where each composition y_{ik} of the flashed vapor is found from Eqs. (13.43) and (13.44)

$$y_i = K_i x_i = \frac{K_i z_i}{1 + 0.01(K_i - 1)/(1 - 0.01n)} \qquad (13.62)$$

and is obtained during the process of evaluating the temperature with Eq. (13.60). The VERs must be known as functions of temperature, say with Eq. (13.24).

13.4. BINARY DISTILLATION

Key concepts of the calculation of distillation are well illustrated by analysis of the distillation of binary mixtures. Moreover, many real systems are essentially binary or can be treated as binaries made up of two pseudo components, for which it is possible to calculate upper and lower limits to the equipment size for a desired separation.

EXAMPLE 13.3
Bubble-Point Temperature with the Virial and Wilson Equations
A mixture of acetone (1) + butanone (2) + ethylacetate (3) with the composition $x_1 = x_2 = 0.3$ and $x_3 = 0.4$ is at 20 atm. Data for the system such as vapor pressures, critical properties, and Wilson coefficients are given with a computer program in Walas (1985, p. 325). The bubblepoint temperature was found to be 468.7 K. Here only the properties at this temperature will be quoted to show deviations from ideality of a common system. The ideal and real K_i differ substantially.

Component	ϕ^{sat}	$\hat{\phi}^{\mathrm{v}}$	$\phi^{\mathrm{sat}}/\hat{\phi}^{\mathrm{v}}$	γ
1	0.84363	0.84353	1.00111	1.00320
2	0.79219	0.79071	1.00186	1.35567
3	0.79152	0.78356	1.00785	1.04995

Component	K_{ideal}	K_{real}	y
1	1.25576	1.25591	0.3779
2	0.72452	0.98405	0.2951
3	0.77266	0.81762	0.3270

The calculational base consists of equilibrium relations and material and energy balances. Equilibrium data for many binary systems are available as tabulations of x vs. y at constant temperature or pressure or in graphical form as on Figure 13.3. Often they can be extended to other pressures or temperatures or expressed in mathematical form as explained in Section 13.1. Sources of equilibrium data are listed in the references. Graphical calculation of distillation problems often is the most convenient method, but numerical procedures may be needed for highest accuracy.

MATERIAL AND ENERGY BALANCES

In terms of the nomenclature of Figure 13.5, the balances between stage n and the top of the column are

$$V_{n+1}y_{n+1} = L_nx_n + Dx_D, \tag{13.63}$$

$$V_{n+1}H_{n+1} = L_nh_n + Dh_D + Q_c \tag{13.64}$$

$$= L_nh_n + DQ', \tag{13.65}$$

where

$$Q' = h_D + Q_c/D \tag{13.66}$$
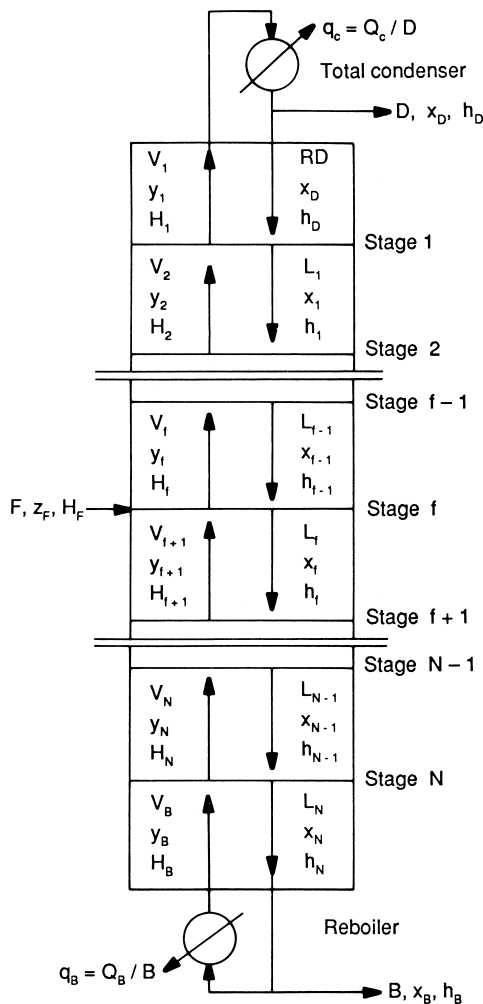
Figure 13.5. Model of a fractionating tower.

is the enthalpy removed at the top of the column per unit of overhead product. These balances may be solved for the liquid/vapor ratio as

$$\frac{L_n}{V_{n+1}} = \frac{y_{n+1} - x_D}{x_n - x_D} = \frac{Q' - H_{n+1}}{Q' - h_n} \tag{13.67}$$

and rearranged as a combined material and energy balance as

$$\frac{L_n}{V_{n+1}} = \frac{y_{n+1} - x_D}{x_n - x_D}x_n + \frac{H_{n+1} - h_n}{Q' - h_n}x_D. \tag{13.68}$$

Similarly the balance between plate m below the feed and the bottom of the column can be put in the form

$$y_m = \frac{Q'' - H_m}{Q'' - h_{m+1}}x_{m+1} + \frac{h_{m+1} - H_m}{h_{m+1} - Q''}x_B, \tag{13.69}$$

where

$$Q'' = h_B - Q_b/B \tag{13.70}$$

is the enthalpy removed at the bottom of the column per unit of bottoms product.

For the problem to be tractable, the enthalpies of the two phases must be known as functions of the respective phase compositions. When heats of mixing and heat capacity effects are small, the enthalpies of mixtures may be compounded of those of the pure components; thus

$$H = yH_a + (1 - y)H_b, \tag{13.71}$$

$$h = xh_a + (1 - x)h_b, \tag{13.72}$$

where H_a and H_b are vapor enthalpies of the pure components at their dewpoints and h_a and h_b are corresponding liquid enthalpies at their bubblepoints.

Overall balances are

$$F = D + B, \tag{13.73}$$

$$Fz_F = Dx_D + Bx_B, \tag{13.74}$$

$$FH_F = Dh_D + Bh_B. \tag{13.75}$$

In the usual distillation problem, the operating pressure, the feed composition and thermal condition, and the desired product compositions are specified. Then the relations between the reflux rates and the number of trays above and below the feed can be found by solution of the material and energy balance equations together with a vapor–liquid equilibrium relation, which may be written in the general form

$$f(x_n, y_n) = 0. \tag{13.76}$$

The procedure starts with the specified terminal compositions and applies the material and energy balances such as Eqs. (13.63) and (13.64) and equilibrium relations alternately stage by stage. When the compositions from the top and from the bottom agree closely, the correct numbers of stages have been found. Such procedures will be illustrated first with a graphical method based on constant molal overflow.

CONSTANT MOLAL OVERFLOW

When the molal heats of vaporization of the two components are equal and the tower is essentially isothermal throughout, the molal

flow rates L_n and V_n remain constant above the feed tray, and L_m and V_m likewise below the feed. The material balances in the two sections are

$$y_{n+1} = \frac{L_n}{V_{n+1}} x_n + \frac{D}{V_{n+1}} x_D, \tag{13.63}$$

$$y_m = \frac{L_{m+1}}{V_m} x_{m+1} - \frac{B}{V_m} x_B. \tag{13.77}$$

The flow rates above and below the feed stage are related by the liquid–vapor proportions of the feed stream, or more generally by the thermal condition of the feed, q, which is the ratio of the heat required to convert the feed to saturated vapor and the heat of vaporization, that is,

$$q = (H_F^{\text{sat}} - H_F)/(\Delta H)_{\text{vap}}. \tag{13.78}$$

For instance, for subcooled feed $q > 1$, for saturated liquid $q = 1$, and for saturated vapor $q = 0$. Upon introducing also the reflux ratio

$$R = L_n/D, \tag{13.79}$$

the relations between the flow rates become

$$L_m = L_n + qF = RD + qF, \tag{13.80}$$

$$V_m = L_m - B = RD + qF - B. \tag{13.81}$$

Accordingly, the material balances may be written

$$y = \frac{R}{R+1} x_n + \frac{1}{R+1} x_D, \tag{13.82}$$

$$y_m = \frac{RD + qF}{RD + qF - B} x_{m+1} - \frac{B}{RD + qF - B} x_B. \tag{13.83}$$

The coordinates of the point of intersection of the material balance lines, Eqs. (13.82) and (13.83), are located on a "q-line" whose equation is

$$y = \frac{q}{q-1} x + \frac{1}{q-1} x_F. \tag{13.84}$$

Figure 13.6 (b) shows these relations.

BASIC DISTILLATION PROBLEM

The basic problem of separation by distillation is to find the numbers of stages below and above the feed stage when the quantities x_F, x_D, x_B, F, D, B, and R are known together with the phase equilibrium relations. This means that all the terms in Eqs. 13.82 and 13.85 are to be known except the running x's and y's. The problem is solved by starting with the known compositions, x_D and x_B, at each end and working one stage at a time towards the feed stage until close agreement is reached between the pairs (x_n, y_n) and (x_m, y_m). The procedure is readily implemented on a programmable calculator; a suitable program for the enriching section is included in the solution of Example 13.4. A graphical solution is convenient and rapid when the number of stages is not excessive, which depends on the scale of the graph attempted.

Figure 13.6 illustrates various aspects of the graphical method. A minimum number of trays is needed at total reflux, that is, with no product takeoff. Minimum reflux corresponds to a separation requiring an infinite number of stages, which is the case when the

equilibrium curve and the operating lines touch somewhere. Often this can occur on the q-line, but another possibility is shown on Figure 13.6(e). The upper operating line passes through point (x_D, x_D) and $x_D/(R + 1)$ on the left ordinate. The lower operating line passes through the intersection of the upper with the q-line and point (x_B, x_B). The feed tray is the one that crosses the intersection of the operating lines on the q-line. The construction is shown with Example 13.5. Constructions for cases with two feeds and with two products above the feed plate are shown in Figure 13.7.

Optimum Reflux Ratio. The reflux ratio affects the cost of the tower, both in the number of trays and the diameter, as well as the cost of operation which consists of costs of heat and cooling supply and power for the reflux pump. Accordingly, the proper basis for choice of an optimum reflux ratio is an economic balance. The sizing and economic factors are considered in a later section, but reference may be made now to the results of such balances summarized in Table 13.3. The general conclusion may be drawn that the optimum reflux ratio is about 1.2 times the minimum, and also that the number of trays is about 2.0 times the minimum. Although these conclusions are based on studies of systems with nearly ideal vapor-liquid equilibria near atmospheric pressure, they often are applied more generally, sometimes as a starting basis for more detailed analysis of reflux and tray requirements.

Azeotropic and Partially Miscible Systems. Azeotropic mixtures are those whose vapor and liquid equilibrium compositions are identical. Their x–y lines cross or touch the diagonal. Partially miscible substances form a vapor phase of constant composition over the entire range of two-phase liquid compositions; usually the horizontal portion of the x–y plot intersects the diagonal, but those of a few mixtures do not, notably those of mixtures of methylethylketone and phenol with water. Separation of azeotropic mixtures sometimes can be effected in several towers at different pressures, as illustrated by Example 13.6 for ethanol-water mixtures. Partially miscible constant boiling mixtures usually can be separated with two towers and a condensate phase separator, as done in Example 13.7 for n-butanol and water.

UNEQUAL MOLAL HEATS OF VAPORIZATION

Molal heats of vaporization often differ substantially, as the few data of Table 13.4 suggest. When sensible heat effects are small, however, the condition of constant molal overflow still can be preserved by adjusting the molecular weight of one of the components, thus making it a pseudocomponent with the same molal heat of vaporization as the other substance. The x–y diagram and all of the compositions also must be converted to the adjusted molecular weight. Example 13.5 compares tray requirements on the basis of true and adjusted molecular weights for the separation of ethanol and acetic acid whose molal heats of vaporization are in the ratio 1.63. In this case, the assumption of constant molal overflow with the true molecular weight overestimates the tray requirements. A more satisfactory, but also more laborious, solution of the problem takes the enthalpy balance into account, as in the next section.

MATERIAL AND ENERGY BALANCE BASIS

The enthalpies of mixtures depend on their compositions as well as the temperature. Enthalpy–concentration diagrams of binary mixtures, have been prepared in general form for a few important systems. The most comprehensive collection is in Landolt-Börnstein [**IV4b**, 188, (1972)] and a few diagrams are in *Perry's Chemical Engineers' Handbook*, for instance, of ammonia and water, of ethanol and water, of oxygen and nitrogen, and some others. Such diagrams are named after Merkel.
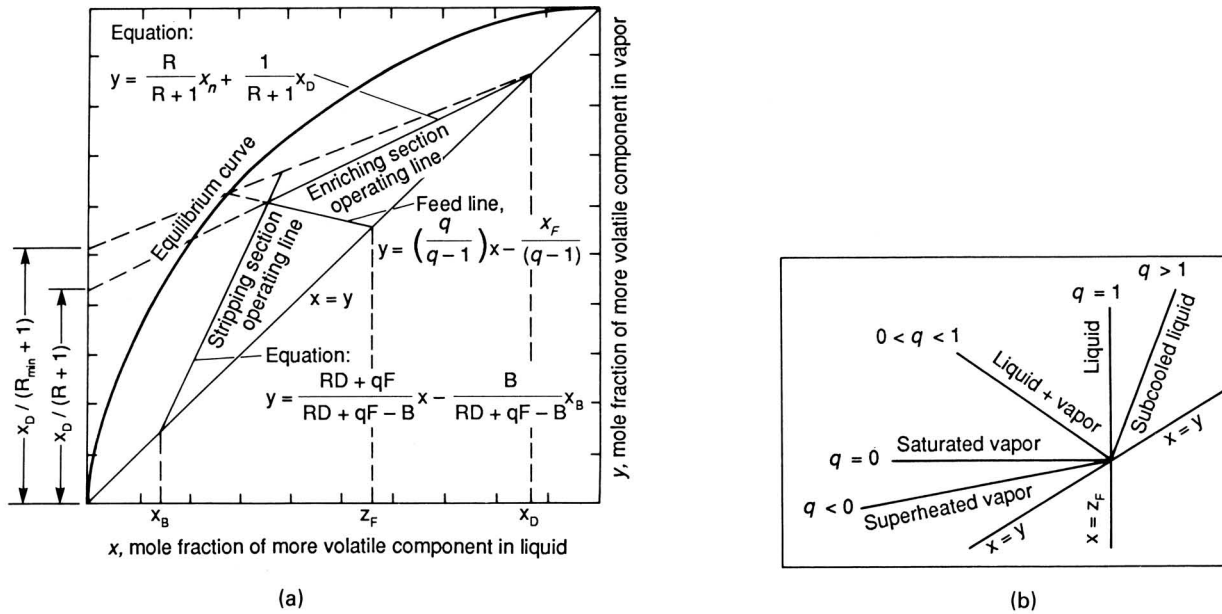
Figure 13.6. Features of McCabe–Thiele diagrams for constant modal overflow. (a) Operating line equations and construction and minimum reflux construction. (b) Orientations of q-lines, with slope $= q/(q-1)$, for various thermal conditions of the feed. (c) Minimum trays, total reflux (d) Operating trays and reflux. (e) Minimum reflux determined by point of contact nearest x_D.

For purposes of distillation calculations, a rough diagram of saturated vapor and liquid enthalpy concentration lines can be drawn on the basis of pure component enthalpies. Even with such a rough diagram, the accuracy of distillation calculation can be much superior to those neglecting enthalpy balances entirely. Example 13.8 deals with preparing such a Merkel diagram.

A schematic Merkel diagram and its application to distillation calculations is shown in Figure 13.8. Equilibrium compositions of vapor and liquid can be indicated on these diagrams by tielines, but are more conveniently used with associated x–y diagrams as shown with this figure. Lines passing through point P with coordinates (x_D, Q) are represented by Eq. (13.68) and those through point Q with coordinates (x_B, Q'') by Eq. (13.69). Accordingly, any line through P to the right of PQ intersects the vapor and liquid enthalpy lines in corresponding (x_n, y_{n+1}) and similarly the intersections of random lines through Q determine corresponding

(x_{m+1}, y_m). When these coordinates are transferred to the x–y diagram, they determine usually curved operating lines. Figure 13.8 (b) illustrates the stepping off process for finding the number of stages. Points P, F, and Q are collinear.

The construction for the minimum number of trays is independent of the heat balance. The minimum reflux corresponds to a minimum condenser load Q and hence to a minimum value of $Q' = h_D + Q_c/D$. It can be found by trial location of point P until an operating curve is found that touches the equilibrium curve.

ALGEBRAIC METHOD

Binary systems of course can be handled by the computer programs devised for multicomponent mixtures that are mentioned later. Constant molal overflow cases are handled by binary computer programs such as the one used in Example 13.4 for the enriching section which employ repeated alternate application of material

EXAMPLE 13.4
Batch Distillation of Chlorinated Phenols
A mixture of chlorinated phenols can be represented as an equivalent binary with 90% 2,4-dichlorphenol (DCP) and the balance 2,4,6-trichlorphenol with a relative volatility of 3.268. Product purity is required to be 97.5% of the lighter material, and the residue must be below 20% of 2,4-DCP. It is proposed to use a batch distillation with 10 theoretical stages. Vaporization rate will be maintained constant.

a. For operation at constant overhead composition, the variations of reflux ratio and distillate yield with time will be found.
b. The constant reflux ratio will be found to meet the overhead and bottoms specifications.

a. At constant overhead composition, $y_D = 0.975$: The composition of the residue, x_{10}, is found at a series of reflux ratios between the minimum and the value that gives a residue composition of 0.2.

```
10    ! Example 13.4. Distillation at constant Yd
20    A = 3.268
30    OPTION BASE 1
40    DIM X(10), Y(12)
50    Y(1) = .975
60    INPUT R
70    FOR N=1 TO 10
80    X(N)=1 / (A/Y(N)−A+1)
90    Y(N + 1) = 1/(R + 1) ∗ (R ∗ X(N) + Y(1))
100   NEXT N
110   Z = (Y(1) −.9)/(Y(1)−X(10) )! = L/Lo
120   I = (R + 1)/(Y(1) − X(10))² ! Int egrand of Eq 4
130   PRINT USING 140; R, X (10), Z, I
140   IMAGE D.DDDD, 2X, .DDDD, 2X, D.D DDD, 2X, DDD.DDDDD
150   GOTO 60
160   END
```

With $q = 1$ and $x_n = 0.9$,

$$y_n = \frac{\alpha x_n}{1 + (\alpha - 1)x_n} = \frac{3.268(0.9)}{1 + 2.268(0.9)} = 0.9671,$$

$$R_m/(R_m + 1) = \frac{0.975 - 0.9671}{0.975 - 0.9} = 0.1051,$$

$$\therefore R_m = 0.1174.$$

The btms compositions at a particular value of R are found by successive applications of the equations

$$x_n = \frac{y_n}{\alpha - (\alpha - 1)y_n}, \tag{1}$$

$$y_{n+1} = \frac{R}{R + 1}x_n + \frac{1}{R + 1}y_D. \tag{2}$$

Start with $y_1 = y_D = 0.975$. The calculations are performed with the given computer program and the results are tabulated. The values of L/L_0 are found by material balance:

$$L/L_0 = (0.975 - 0.900)/(0.975 - x_L) \tag{3}$$

The values of V/L_0 are found with Eq. 13.110

$$\begin{aligned} \frac{V}{L_0} &= (y_D - x_{L_0}) \int_{x_{L_0}}^{x_L} \frac{R + 1}{(y_D - x_L)^2} dx_L \\ &= (0.975 - 0.900) \int_{0.9}^{x_L} \frac{R + 1}{(0.975 - x_L)^2} dx_L. \end{aligned} \tag{4}$$

From the tabulation, the cumulative vaporization is

$$V/L_0 = 1.2566.$$

The average reflux ratio is

$$\overline{R} = \frac{V - D}{D} = \frac{V}{D} - 1 = \frac{V}{L_0 - L} - 1 = \frac{V/L_0}{1 - L/L_0} - 1$$

$$= \frac{1.2566}{1 - 0.0968} - 1 = 0.3913.$$

R	X_L	L/L_o	Integrand	V/L_o	$t/\bar{t}$
.1174	.9000	1.0001	198.69073	0.0000	0.000
.1500	.8916	.8989	165.17980	.1146	.091
.2000	.8761	.7585	122.74013	.2820	.224
.2500	.8571	.6362	89.94213	.4335	.345
.3000	.8341	.5321	65.43739	.5675	.452
.3500	.8069	.4461	47.75229	.6830	.544
.4000	.7760	.3768	35.33950	.7793	.620
.4500	.7422	.3222	26.76596	.8580	.683
.5000	.7069	.2797	20.86428	.9210	.733
.6000	.6357	.2210	13.89632	1.0138	.807
.7000	.5694	.1849	10.33322	1.0741	.855
.8000	.5111	.1617	8.36592	1.1150	.887
.9000	.4613	.1460	7.20138	1.1440	.910
1.0000	.4191	.1349	6.47313	1.1657	.928
1.2000	.3529	.1206	5.68386	1.1959	.952
1.4000	.3040	.1118	5.32979	1.2160	.968
1.6000	.2667	.1059	5.18287	1.2308	.979
1.8000	.2375	.1017	5.14847	1.2421	.988
2.0000	.2141	.0986	5.18132	1.2511	.996
2.1400	.2002	.0968	5.23097	1.2566	1.000

EXAMPLE 13.4—(*continued*)

This is less than the constant reflux, $R = 0.647$, to be found in part b.

At constant vaporization rate, the time is proportional to the cumulative vapor amount:

$$\frac{t}{\bar{t}} = \frac{V}{V_{\text{final}}} = \frac{V/L_0}{1.2566}. \tag{5}$$

Also

$$D/L_0 = 1 - L/L_0. \tag{6}$$

From these relations and the tabulated data, D/L_0 and R are plotted against reduced time $t/\bar{t}$.

b. At constant reflux: A reflux ratio is found by trial to give an average overhead composition $\bar{y}_D = 0.975$ and a residue composition $x_L = 0.2$. The average overhead composition is found with material balance

$$\bar{y}_D = [x_{L_0} - (L/L_0)x_L]/(1 - L/L_0). \tag{7}$$

The value of L/L_0 is calculated as a function of y_D from

$$\ln\frac{L}{L_0} = \int_{0.9}^{x_L} \frac{1}{y_D - x_L} dx_L. \tag{8}$$
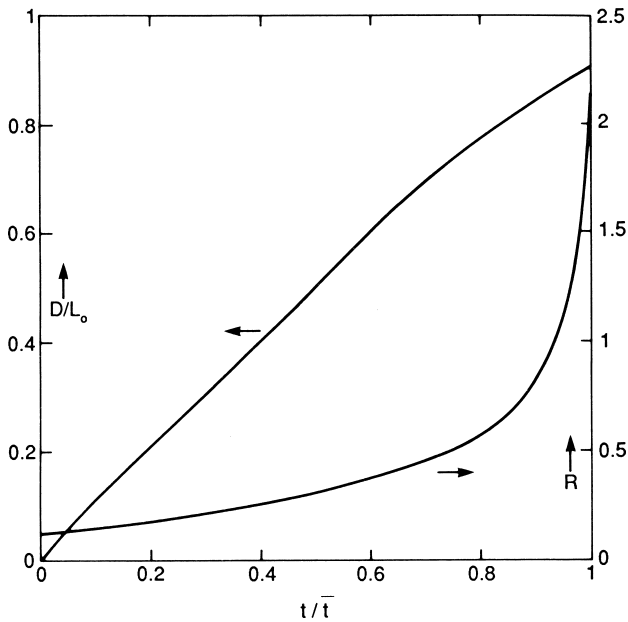

```
 10    ! Example 13.4. Distillation at constant reflux
 20    A = 3.268
 30    OPTION BASE 1
 40    DIM X(10), Y(11)
 50    INPUT R ! reflux ratio
 60    INPUT Y(1)
 70    FOR N = 1 TO 10
 80    X(N) = 1/(A/Y(N) − A + 1)
 90    Y(N + 1) = 1/(R + 1)*(R*X(N) + Y(1))
100    NEXT N
110    I = 1/(Y(1) − X(10))
120    DISP USING 130 ; Y(1), X(10), I
130    IMAGE .DDDDD,2X, .DDDD, 2X, DD. DDDD
140    GOTO 60
150    END
```

At a trial value of R, values of x_{10} are found for a series of assumed y_D's until x_{10} equals or is less than 0.20. The given computer program is based on Eqs. (1) and (2). The results of two trials and interpolation to the desired bottoms composition, $x_L = 0.200$, are

R	0.6	0.7	0.647
x_L	0.2305	0.1662	0.200

y_D	x_L	$1/(y_D - x_L)$	L/L_0	$\bar{y}_D$
		Reflux ratio $R = 0.6$		
0.99805	0.9000	10.2035		
0.99800	0.8981	10.0150	0.9810	
0.99750	0.8800	8.5127	0.8295	
0.99700	0.8638	7.5096	0.7286	
0.99650	0.8493	6.7917	0.6568	
0.99600	0.8361	6.2521	0.6026	
0.99550	0.8240	5.8314	0.5602	
0.99500	0.8130	5.4939	0.5263	
0.99400	0.7934	4.9855	0.4750	
0.99300	0.7765	4.6199	0.4379	
0.99200	0.7618	4.3436	0.4100	
0.99100	0.7487	4.1270	0.3879	
0.99000	0.7370	3.9522	0.3700	
0.98500	0.6920	3.4135	0.3135	
0.98000	0.6604	3.1285	0.2827	
0.97500	0.6357	2.9471	0.2623	
0.97000	0.6152	2.8187	0.2472	
0.96500	0.5976	2.7217	0.2354	
0.96000	0.5819	2.6450	0.2257	
0.95500	0.5678	2.5824	0.2176	
0.95000	0.5548	2.5301	0.2104	
0.90000	0.4587	2.2662	0.1671	
0.85000	0.3923	2.1848	0.1441	
0.80000	0.3402	2.1751	0.1286	
0.75000	0.2972	2.2086	0.1171	
0.70000	0.2606	2.2756	0.1079	0.9773
0.65000	0.2286	2.3730	0.1001	0.9746
0.60000	0.2003	2.5019	0.0933	0.9720
		Reflux ratio $R = 0.7$		
0.99895	0.9000	10.1061		
0.99890	0.8963	9.7466	0.9639	
0.99885	0.8927	9.4206	0.9312	
0.99880	0.8892	9.1241	0.9015	
0.99870	0.8824	8.5985	0.8488	
0.99860	0.8758	8.1433	0.8032	
0.99840	0.8633	7.4019	0.7288	
0.99820	0.8518	6.8306	0.6716	
0.99800	0.8410	6.3694	0.6254	
0.99700	0.7965	4.9875	0.4857	
0.99600	0.7631	4.2937	0.4160	
0.99500	0.7370	3.8760	0.3739	
0.99400	0.7159	3.5958	0.3456	
0.99300	0.6983	3.3933	0.3249	
0.99200	0.6835	3.2415	0.3094	
0.99100	0.6076	2.6082	0.2969	
0.99000	0.6594	3.0248	0.2869	
0.98000	0.5905	2.5674	0.2366	
0.97000	0.5521	2.3929	0.2151	
0.96000	0.5242	2.2946	0.2015	
0.95000	0.5013	2.2287	0.1913	
0.94000	0.4816	2.1815	0.1832	
0.93000	0.4639	2.1455	0.1763	
0.92000	0.4479	2.1182	0.1704	
0.91000	0.4334	2.0982	0.1652	
0.90000	0.4193	2.0803	0.1605	
0.85000	0.3611	2.0454	0.1423	
0.80000	0.3148	2.0610	0.1294	
0.75000	0.2761	2.1101	0.1194	
0.70000	0.2429	2.1877	0.1112	
0.65000	0.2137	2.2920	0.1041	
0.60000	0.1877	2.4254	0.0979	0.9773
0.55000	0.1643	2.5927	0.0923	0.9748
0.50000	0.1431	2.8019	0.0872	0.9723

EXAMPLE **13.5**
Distillation of Substances with Widely Different Molal Heats of Vaporization

The modal heats of vaporization of ethanol and acetic acid are 9225 and 5663 cal/g mol. A mixture with ethanol content of $x_F = 0.50$ is to be separated into products with $x_B = 0.05$ and $x_D = 0.95$. Pressure is 1 atm, feed is liquid at the boiling point, and the reflux ratio is to be 1.3 times the minimum. The calculation of tray requirements is to be made with the true molecular weight, 60.05, of acetic acid and with adjustment to make the apparent molal heat of vaporization the same as that of ethanol, which becomes

$$60.05(9225/5663) = 98.14.$$

The adjusted mol fractions, x' and y', are related to the true ones by

$$x' = \frac{x}{x + 0.6119(1 - x)}, \quad y' = \frac{y}{y + 0.6119(1 - y)}.$$

The experimental and converted data are tabulated following and plotted on McCabe–Thiele diagrams. The corresponding compositions involved in this distillation are:

$$x_B = 0.05, \ x'_B = 0.0792$$

$$x_F = 0.50, \ x'_F = 0.6204$$

$$x_D = 0.95, \ x'_D = 0.9688$$

x	y	x'	y'
0.0550	0.1070	0.0869	0.1638
0.0730	0.1440	0.1140	0.2156
0.1030	0.1970	0.1580	0.2862
0.1330	0.2740	0.2004	0.3815
0.1660	0.3120	0.2454	0.4257
0.2070	0.3930	0.2990	0.5141
0.2330	0.4370	0.3318	0.5592
0.2820	0.5260	0.3909	0.6446
0.3470	0.5970	0.4648	0.7077
0.4600	0.7500	0.5820	0.8306
0.5160	0.7930	0.6353	0.8623
0.5870	0.8540	0.6990	0.9053
0.6590	0.9000	0.7595	0.9363
0.7280	0.9340	0.8139	0.9586
0.6160	0.9660	0.8788	0.9789
0.9240	0.9900	0.9521	0.9939

In terms of the true molecular weight, minimum reflux is given by

$$x_D/(R_{min} + 1) = 0.58,$$

whence

$$R_m = 0.6379,$$

$$R = 1.3(0.6379) = 0.8293,$$

$$x_D/(R + 1) = 0.5193,$$

$$x'_D/(R + 1) = 0.5296.$$

Taking straight operating lines in each case, the numbers of trays are

$N = 11.0$ with true molecular weight of acetic acid,
$N' = 9.8$ with adjusted molecular weight.

In this case it appears that assuming straight operating lines, even though the molal heats of vaporization are markedly different, results in overestimation of the number of trays needed for the separation.
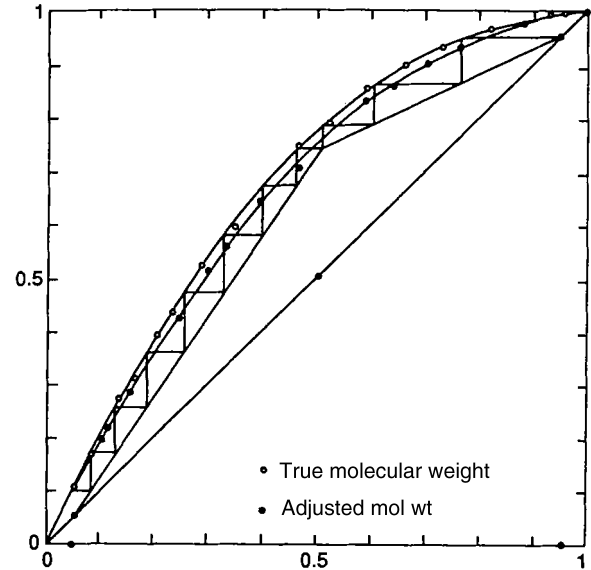
a. Construction with true molecular weight, $N = 11$.
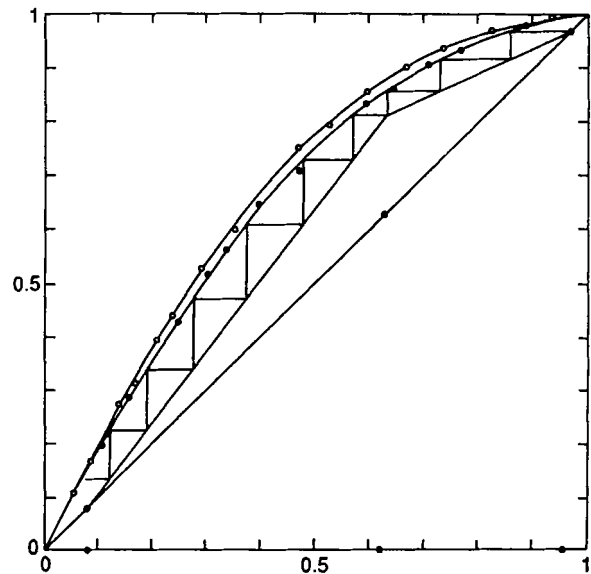
b. Construction with adjusted molecular weight, $N = 9.8$.
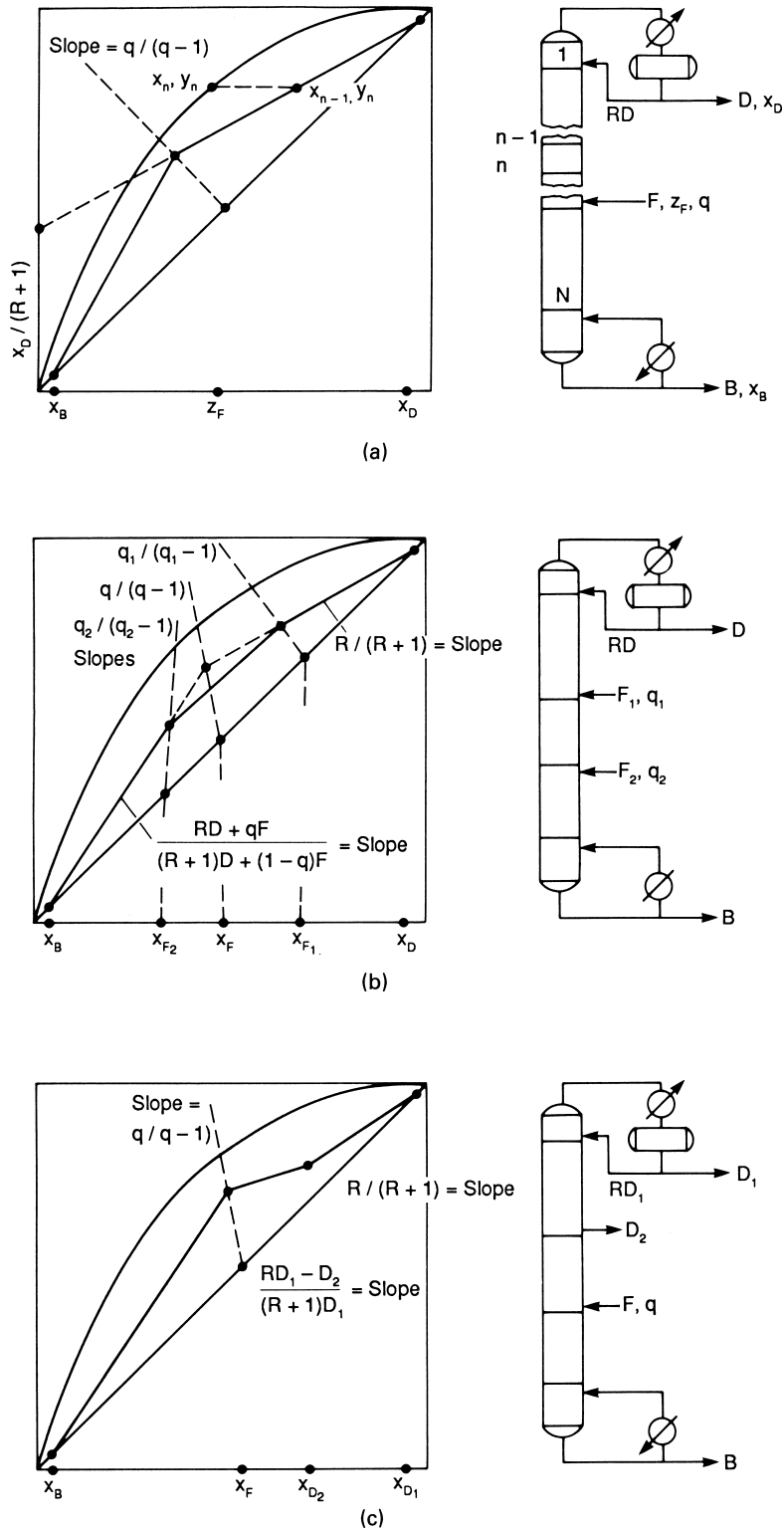
Figure 13.7. Operating and q-line construction with several feeds and top products. (a) One feed and one overhead product. (b) Two feeds and one overhead product. (c) One feed and two products from above the feed point.

TABLE 13.3. Economic Optimum Reflux Ratio for Typical Petroleum Fraction Distillation Near 1 atm[a]

	Factor for Optimum Reflux $f = (R_{opt}/R_m)-1$ $R_{opt} = (1+f)R_m$								Factor for Optimum Trays N_{opt}/N_m		
	$N_m = 10$ R_m			$N_m = 20$ R_m			$N_m = 50$ R_m		$N_m = 10$ R_m	$N_m = 20$ R_m	$N_m = 50$ R_m
	1	3	10	1	3	10	1	10	1 to 10	1 to 10	1 to 10
Base case	0.20	0.12	0.10	0.24	0.17	0.16	0.31	0.21	2.4	2.3	2.1
Payout time 1 yr	0.24	0.14	0.12	0.28	0.20	0.17	0.37	0.24	2.2	2.1	2.0
Payout time 5 yr	0.13	0.09	0.07	0.17	0.13	0.10	0.22	0.15	2.7	2.5	2.2
Steam cost $0.30/M lb	0.22	0.13	0.11	0.27	0.16	0.14	0.35	0.22	2.3	2.1	2.0
Steam cost $0.75/M lb	0.18	0.11	0.09	0.21	0.13	0.11	0.29	0.19	2.5	2.3	2.1
$G_a = 50$ lb mole/(hr)(sqft)	0.06	0.04	0.03	0.08	0.06	0.05	0.13	0.08	3.1	2.8	2.4

[a] The ''base case'' is for payout time of 2 yr, steam cost of $0.50/1000 lb, vapor flow rate $G_a = 15$ lb mol/(hr)(sqft). Although the capital and utility costs are prior to 1975 and are individually far out of date, the relative costs are roughly the same so the conclusions of this analysis are not far out of line. Conclusion: For systems with nearly ideal VLE, R is approx. $1.2R_{min}$ and N is approx. $2.0N_{min}$.
(Happel and Jordan, *Chemical Process Economics*, Dekker, New York, 1975).

balance and equilibrium stage-by-stage. Methods also are available that employ closed form equations that can give desired results quickly for the special case of constant or suitable average relative volatility.

Minimum Trays. For a binary system, this is found with the Fenske–Underwood equation,

$$N_{min} = \frac{\ln[x_D(1-x_B)/x_B(1-x_D)]}{\ln \alpha} \quad (13.85)$$

Minimum Reflux. Underwood's method employs two relations. First an auxiliary parameter θ is found in the range $1 < \theta < \alpha$ by solving

$$\frac{\alpha x_F}{\alpha - \theta} + \frac{1 - x_F}{1 - \theta} = 1 - q \quad (13.86)$$

$$(1-q)\theta^2 + [(\alpha-1)x_F + q(\alpha+1) - \alpha]\theta - \alpha q = 0, \quad (13.87)$$

or in two important special cases:

when $q = 0$, $\theta = \alpha - (\alpha-1)x_F$, $\quad (13.88)$

when $q = 1$, $\theta = \dfrac{\alpha}{(\alpha-1)x_F + 1}$. $\quad (13.89)$

Then R_m is found by substitution into

$$R_m = -1 + \frac{\alpha x_D}{\alpha - \theta} + \frac{1 - x_D}{1 - \theta}. \quad (13.90)$$

Formulas for the numbers of trays in the enriching and stripping sections at operating reflux also are due to Underwood (*Trans. Inst. Chem. Eng.* **10**, 112–152, 1932). For above the feed, these groups of terms are defined:

$$K_1 = L_n/V_n = R/(R+1), \quad (13.91)$$

$$\phi_1 = K_1(\alpha-1)/(K_1\alpha - 1). \quad (13.92)$$

Then the relation between the compositions of the liquid on tray 1 and that on tray n is

$$(K_1\alpha)^{n-1} = \frac{1/(1-x_1) - \phi_1}{1/(1-x_n) - \phi_1}. \quad (13.93)$$

EXAMPLE 13.6
Separation of an Azeotropic Mixture by Operation at Two Pressure Levels
At atmospheric pressure, ethanol and water form an azeotrope with composition $x = 0.846$, whereas at 95 Torr the composition is about $x = 0.94$. As the diagram shows, even at the lower pressure the equilibrium curve hugs the $x = y$ line. Accordingly, a possibly feasible separation scheme may require three columns, two operating at 760 Torr and the middle one at 95 Torr, as shown on the sketch. The basis for the material balance used is that 99% of the ethanol fed to any column is recovered, and that the ethanol-rich products from the columns have $x = 0.8$, 0.9, and 0.995, resp.

Although these specifications lead to only moderate tray and reflux requirements, in practice distillation with only two towers and the assistance of an azeotropic separating agent such as benzene is found more economical. Calculation of such a process is made by Robinson and Gilliland (1950, p. 313).
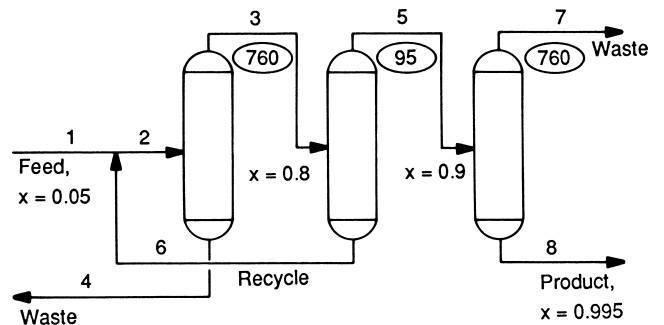
	1	2	3	4	5	6	7	8
Ethanol	5	5.05000	4.9995	0.05050	4.949500	0.049995	0.04950	4.90000
Water	95	95.69992	1.24987	94.45005	0.54994	0.69993	0.52532	0.02462

EXAMPLE **13.6**—(*continued*)
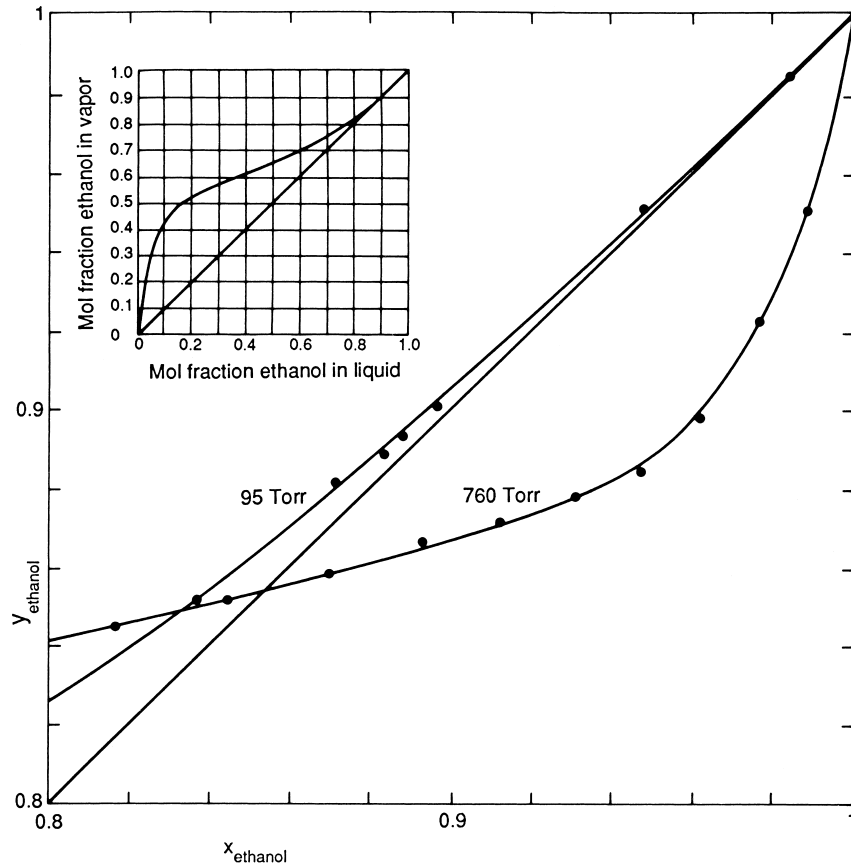
Ethanol-water vapor-liquid equilibria at 95 and 760 Torr.

EXAMPLE **13.7**
Separation of a Partially Miscible Mixture
Water and *n*-butanol in the concentration range of about 50–98.1 mol % water form two liquid phases that boil at 92.7°C at one atm. On cooling to 40°C, the hetero-azeotrope separates into phases containing 53 and 98 mol % water.

A mixture containing 12 mol % water is to be separated by distillation into products with 99.5 and 0.5 mol % butanol. The accompanying flowsketch of a suitable process utilizes two columns with condensing-subcooling to 40°C. The 53% saturated solution is refluxed to the first column, and the 98% is fed to the second column. The overhead of the second column contains a small amount of butanol that is recycled to the condenser for recovery. The recycle material balance is shown with the sketch.

The three sets of vapor–liquid equilibrium data appearing on the $x - y$ diagram show some disagreement, so that great accuracy cannot be expected from determination of tray requirements, particularly at the low water concentrations. The upper operating line in the first column is determined by the overall material balance so it passes through point (0.995, 0.995), but the initial point on the operating line is at $x = 0.53$, which is the composition of the reflux. The construction is shown for 50% vaporized feed. That result and those for other feed conditions are summarized:

q	R_m	$R_m = 1.3R_m$	N
1	2.02	2.62	12
0.5	5.72	7.44	8
0	9.70	12.61	6
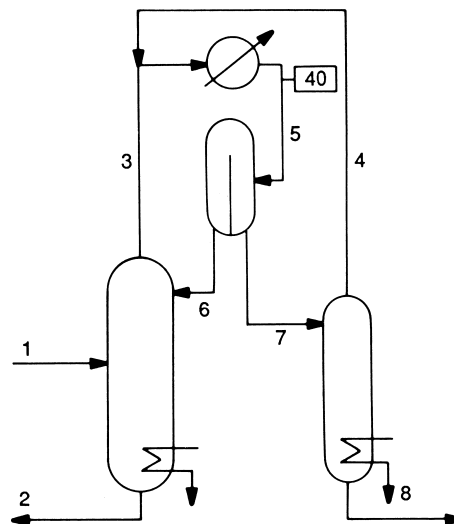
	1	2	3	4	5	6	7	8
Water	12	0.44	18.4139	0.7662	19.1801	6.8539	12.3262	11.56
Butanol	88	87.94	6.1379	0.1916	6.3295	6.0779	0.2516	0.06
	100	88.38	24.5518	0.9578	25.5096	12.9318	12.5778	11.62
% Water	12	0.5	75	80	75.19	53	98	99.5

EXAMPLE 13.7—(*continued*)
In the second column, two theoretical trays are provided and are able to make a 99.6 mol % water waste, slightly better than the 99.5 specified. The required L/V is calculated from compositions read off the diagram:

$$L/V = (0.966 - 0.790)/(0.996 - 0.981) = 13.67.$$

If live steam were used instead of indirect heat, the bottoms concentration would be higher in water. This distillation is studied by Billet (1979, p. 216). Stream compositions are given below the flowsketch.
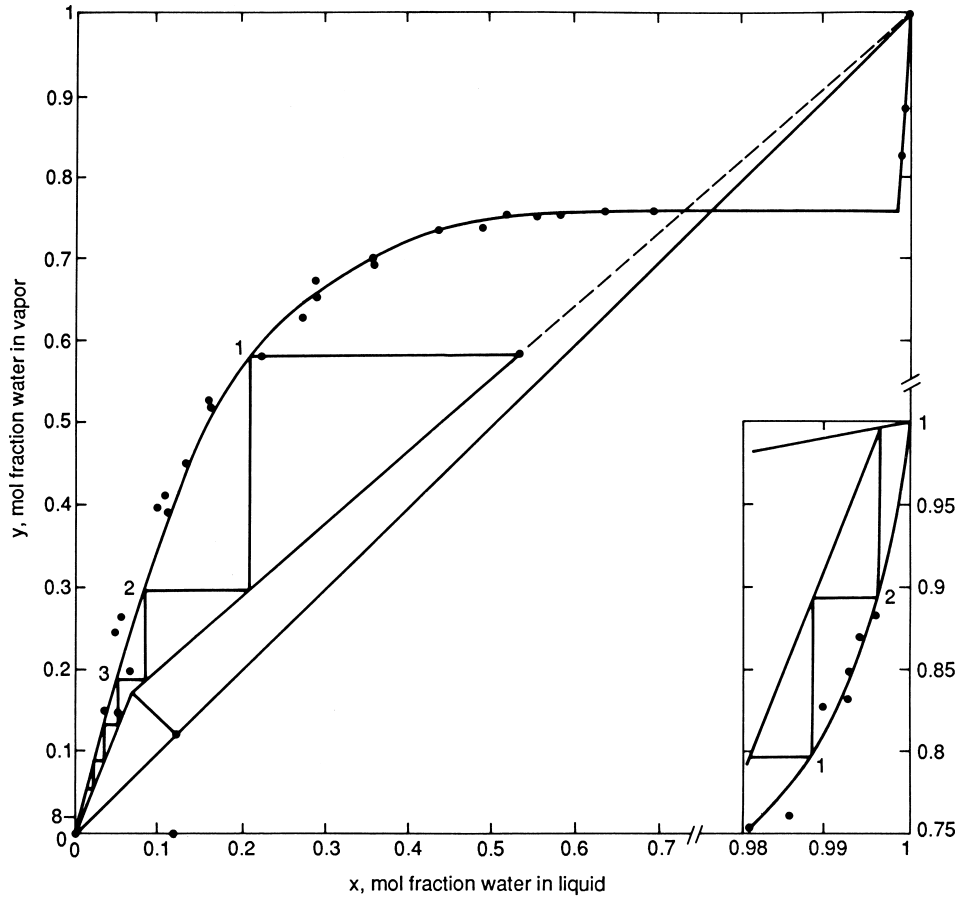
Equilibrium stage requirements for the separation of water and n-butanol.

Since the overhead composition x_D is the one that is specified rather than that of the liquid on the top tray, x_1, the latter is eliminated from Eq. (13.93). The relative volatility definition is applied

$$\frac{\alpha x_1}{1 - x_1} = \frac{x_D}{1 - x_D}, \tag{13.94}$$

from which

$$\frac{1}{1 - x_1} = \frac{x_D + \alpha(1 - x_D)}{\alpha(1 - x_D)}. \tag{13.95}$$

With this substitution, Eq. (13.93) becomes

$$(K_1\alpha)^{n-1} = \frac{[x_D + \alpha(1 - x_D)]/\alpha(1 - x_D) - \phi_1}{1/(1 - x_n) - \phi_1}. \tag{13.96}$$

The number of trays above the feed plus the feed tray is obtained after substituting the feed composition x_F for x_n.
    Below the feed,

$$K_2 = V_m/L_m = (RD + qF - B)/(RD + qF), \tag{13.97}$$

$$\phi_2 = (\alpha - 1)/(K_2\alpha - 1). \tag{13.98}$$

The relation between the compositions at the bottom and at tray m is

$$(K_2\alpha)^m = \frac{1/x_B - \phi_2}{1/x_m - \phi_2}. \tag{13.99}$$

The number of trays below the feed plus the feed tray is found after replacing x_m by x_F. The number of trays in the whole column then is

TABLE 13.4. Molal Heats of Vaporization at Their Normal Boiling Points of Some Organic Compounds That May Need To Be Separated from Water

| Compound | NBP (°C) | cal/g mol | Molecular Weight | |
			True	Adjusted[a]
Water	100	9717	18.02	18.02
Acetic acid	118.3	5663	60.05	103.04
Acetone	56.5	6952	58.08	81.18
Ethylene glycol	197	11860	62.07	50.85
Phenol	181.4	9730	94.11	94.0
n-Propanol	97.8	9982	60.09	58.49
Ethanol	78.4	9255	46.07	48.37

[a]The adjustment of molecular weight is to make the molal heat of vaporization the same as that of water.

$$N = m + n - 1. \tag{13.100}$$

Example 13.9 applies these formulas.

13.5. BATCH DISTILLATION

A batch distillation plant consists of a still or reboiler, a column with several trays, and provisions for reflux and for product collection. Figure 13.9 (c) is a typical equipment arrangement with con-trols. The process is applied most often to the separation of mixtures of several components at production rates that are too small for a continuous plant of several columns equipped with individual reboilers, condensers, pumps, and control equipment. The number of continuous columns required is one less than the number of components or fractions to be separated. Operating conditions of a typical batch distillation making five cuts on an 8-hr cycle are in Figure 13.10.

Operation of a batch distillation is an unsteady state process whose mathematical formulation is in terms of differential equations since the compositions in the still and of the holdups on individual trays change with time. This problem and methods of solution are treated at length in the literature, for instance, by Holland and Liapis (*Computer Methods for Solving Dynamic Separation Problems*, 1983, pp. 177–213). In the present section, a simplified analysis will be made of batch distillation of binary mixtures in columns with negligible holdup on the trays. Two principal modes of operating batch distillation columns may be employed:

1. With constant overhead composition. The reflux ratio is adjusted continuously and the process is discontinued when the concentration in the still falls to a desired value.
2. With constant reflux. A reflux ratio is chosen that will eventually produce an overhead of desired average composition and a still residue also of desired composition.

EXAMPLE 13.8
Enthalpy–Concentration Lines of Saturated Vapor and Liquid of Mixtures of Methanol and Water at a Pressure of 2 atm
A basis of 0°C is taken. Enthalpy data for methanol are in *Chemical Engineers' Handbook* (McGraw-Hill, New York, 1984, p. 3.204) and for water in Keenan et al. (*Steam Tables: SI Units*, Wiley, New York, 1978).

Methanol: $T = 82.8°C$
$H_v = 10{,}010 \,\text{cal/g mol}$,
$h_L = 1882 \,\text{cal/g mol}$,
$\Delta H_v = 8128 \,\text{cal/g mol}$,
$C_p = 22.7 \,\text{cal/g mol°C}$.
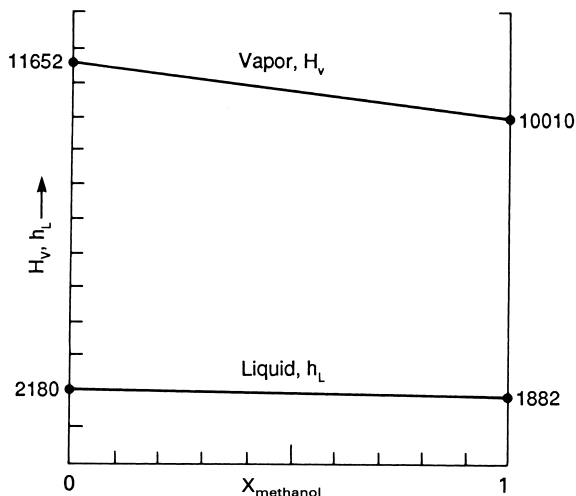
Water: $T = 120.6°C$
$H_v = 11{,}652 \,\text{cal/g mol}$,
$h_L = 2180 \,\text{cal/g mol}$,
$\Delta H_v = 9472 \,\text{cal/g mol}$,

Experimental $x - y$ data are available at 1 and 3 atm (Hirata et al., 1976, #517, #519). Values at 2 atm can be interpolated by eye. The lines show some overlap. Straight lines are drawn connecting enthalpies of pure vapors and enthalpies of pure liquids. Shown is the tie line for $x = 0.5, y = 0.77$.
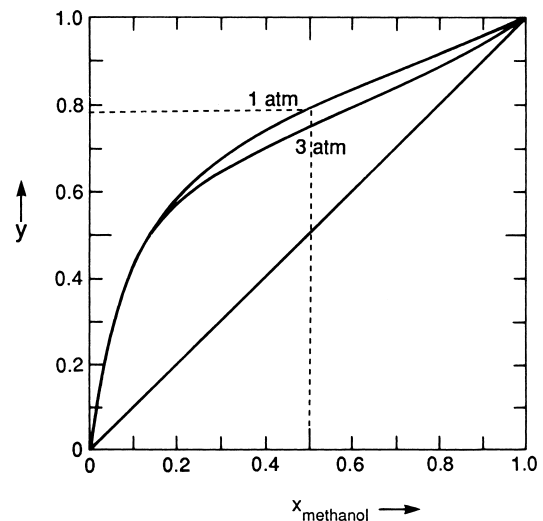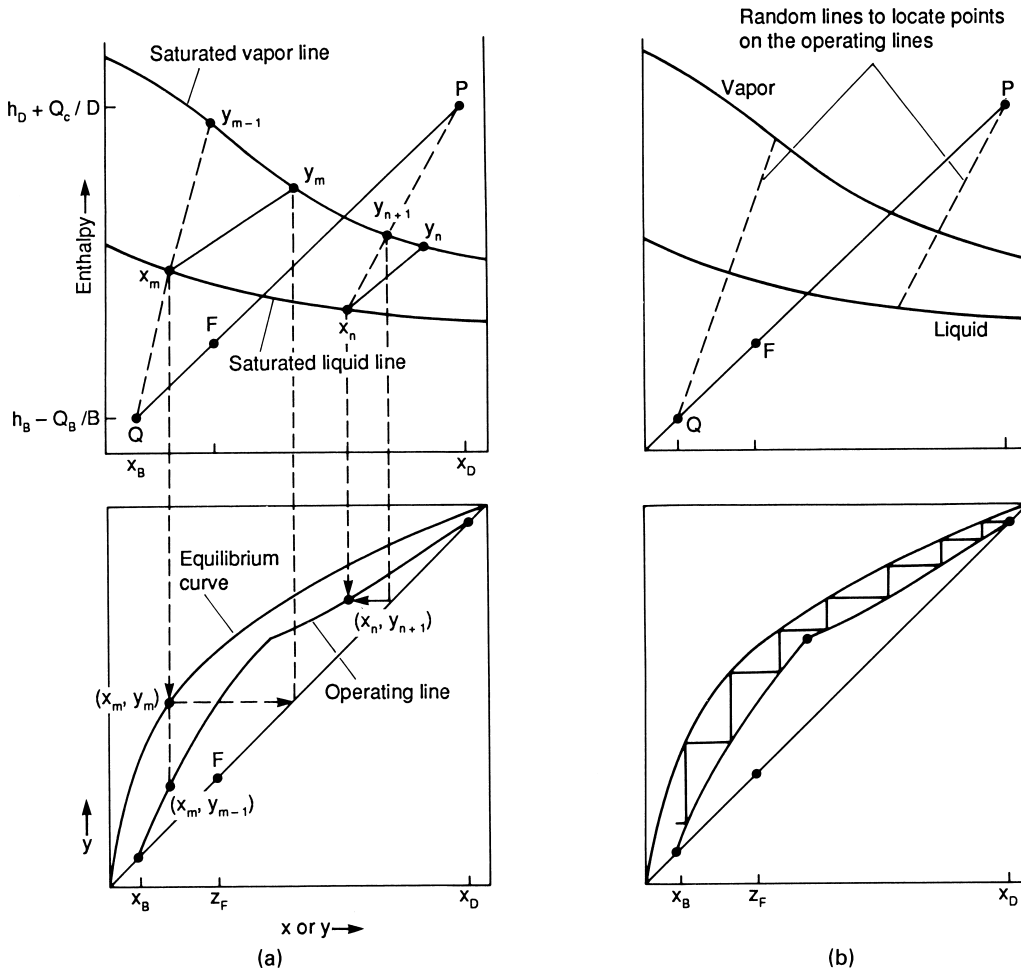
Figure 13.8. Combined McCabe–Thiele and Merkel enthalpy–concentration diagrams for binary distillation with heat balances. (a) Showing key lines and location of representative points on the operating lines. (b) Completed construction showing determination of the number of trays by stepping off between the equilibrium and operating lines.

Both modes usually are conducted with constant vaporization rate at an optimum value for the particular type of column construction. Figure 13.9 represents these modes on McCabe–Thiele diagrams. Small scale distillations often are controlled manually, but an automatic control scheme is shown in Figure 13.9(c). Constant overhead composition can be assured by control of temperature or directly of composition at the top of the column. Constant reflux is assured by flow control on that stream. Sometimes there is an advantage in operating at several different reflux rates at different times during the process, particularly with multicomponent mixtures as on Figure 13.10.

MATERIAL BALANCES

Assuming negligible holdup on the trays, the differential balance between the amount of overhead, dD, and the amount L remaining in the still is

$$y_D \, dD = -y_D \, dL = -d(Lx_L) = -L \, dx_L - x_L \, dL, \qquad (13.101)$$

which is integrated as

$$\ln(L/L_0) = \int_{x_{L_0}}^{x_L} \frac{1}{y_D - x_L} \, dx_L. \qquad (13.102)$$

The differences $y_D - x_L$ depend on the number of trays in the column, the reflux ratio, and the vapor–liquid equilibrium relationship. For constant molal overflow these relations may be taken as

$$y_{n+1} = \frac{R}{R+1} x_n + \frac{1}{R+1} y_D, \qquad (13.103)$$

$$y_n = f(x_n). \qquad (13.104)$$

When the overhead composition is constant, Eq. 13.102 is integrable directly, but the same result is obtained by material balance,

$$\frac{L}{L_0} = \frac{y_D - x_{L_0}}{y_D - x_L}. \qquad (13.105)$$

With variable overhead composition, the average value is represented by the same overall balance,

$$\bar{y}_D = \frac{x_{L_0} - (L/L_0)x_L}{1 - (L/L_0)}, \qquad (13.106)$$

but it is also necessary to know what reflux will result in the desired overhead and residue compositions.

EXAMPLE **13.9**
Algebraic Method for Binary Distillation Calculation
An equimolal binary mixture which is half vaporized is to be separated with an overhead product of 99% purity and 95% recovery. The relative volatility is 1.3. The reflux is to be selected and the number of trays above and below the feed are to be found with the equations of Section 13.4.6.
The material balance is

Component	F	D	x_D	B	X_B
1	50	49.50	0.99	0.50	0.0100
2	50	0.48	0.01	49.52	0.9900
Total	100	49.98		50.02	

Minimum no. of trays,

$$N_m = \frac{\ln(0.99/0.01)(0.99/0.01)}{\ln 1.3} = 35.03.$$

For minimum reflux, by Eqs. (13.87) and (13.90),

$$0.5\theta^2 + [0.3(0.5) + 0.5(2.3) - 1.3]\theta - 1.3(0.5) = 0,$$

$$\theta^2 = 1.3,$$

$$\theta = 1.1402,$$

$$R_m = -1 + \frac{1.3(0.99)}{1.3 - 1.1402} + \frac{0.01}{1 - 0.1402} = 6.9813,$$

$$R = 1.2R_m = 8.3775,$$

$$K_1 = \frac{R}{R+1} = 0.8934,$$

$$\phi_1 = \frac{0.8934(1.3 - 1)}{0.8934(1.3) - 1} = 1.6608,$$

$$\frac{1}{1 - x_1} = \frac{0.99 + 1.3(0.01)}{1.3(0.01)} = 77.1538,$$

$$(K_1\alpha)^{n-1} = (1.1614)^{n-1} = \frac{77.1538 - 1.6608}{1/(1 - 0.5) - 1.6608} = 222.56,$$

$$\therefore n = 37.12,$$

$$K_2 = \frac{8.3775(49.98) + 0.5(100) - 50.02}{468.708} = 0.8933,$$

$$\phi_2 = \frac{1.3 - 1}{0.8933(1.3) - 1} = 1.8600,$$

$$[0.8933(1.3)]^m = \frac{1/0.01 - 1.8600}{1/0.5 - 1.8600} = 701.00,$$

$$\therefore m = 43.82,$$

$$\therefore N = m + n - 1 = 37.12 + 43.82 - 1 = 79.94 \text{ trays.}$$

For constant overhead composition at continuously varied reflux ratios, the total vaporization is found as follows. The differential balance is

$$dD = dV - dL = (1 - dL/dV)dV \tag{13.107}$$

The derivative dL/dV is the slope of the operating line so that

$$1 - \frac{dL}{dV} = 1 - \frac{R}{R+1} = \frac{1}{R+1}. \tag{13.108}$$

Substitution from Eqs. (13.102), (13.105), and (13.108) into Eq. (13.107) converts this into

$$dV = L_0(x_{L_0} - \bar{y}_D)\frac{R+1}{(x_L - \bar{y}_D)^2}dx_L, \tag{13.109}$$

from which the total amount of vapor generated up to the time the residue composition becomes x_L is

$$V = L_0(x_{L_0} - \bar{y}_D)\int_{x_{L_0}}^{x_L}\frac{R+1}{(x_L - \bar{y}_D)^2}dx_L. \tag{13.110}$$

(a)

(b)
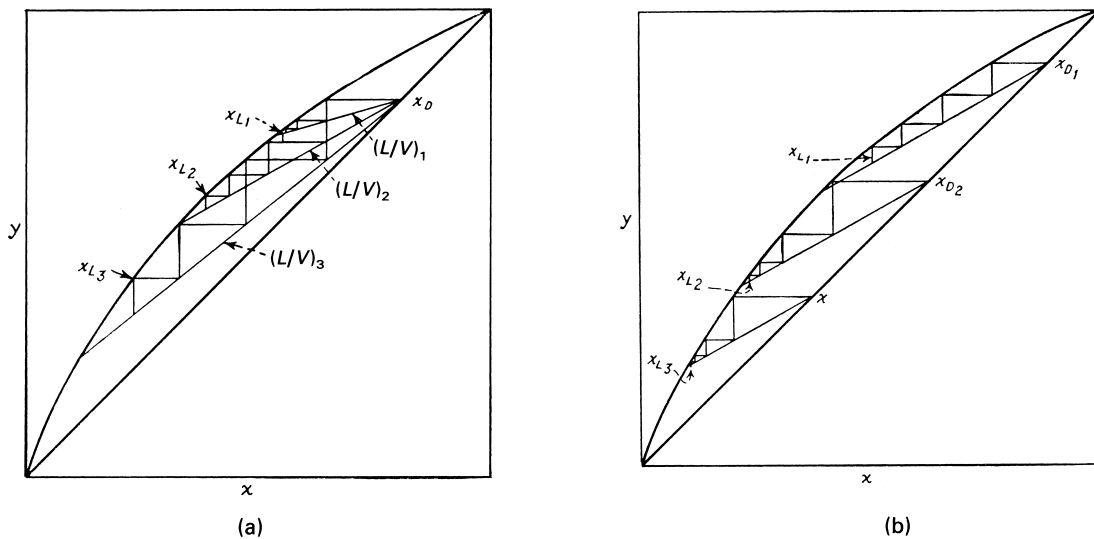
Figure 13.9. Batch distillation: McCabe–Thiele constructions and control modes. (a) Construction for constant overhead composition with continuously adjusted reflux rate. (b) Construction at constant reflux at a series of overhead compositions with an objective of specified average overhead composition. (c) Instrumentation for constant vaporization rate and constant overhead composition. For constant reflux rate, the temperature or composition controller is replaced by a flow controller.

(c)
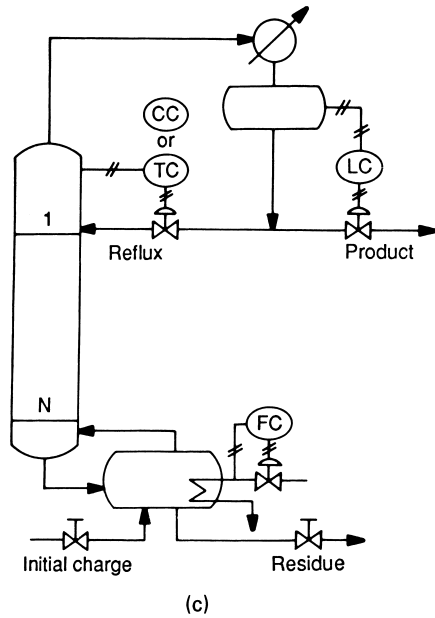
Figure 13.9.—(*continued*)
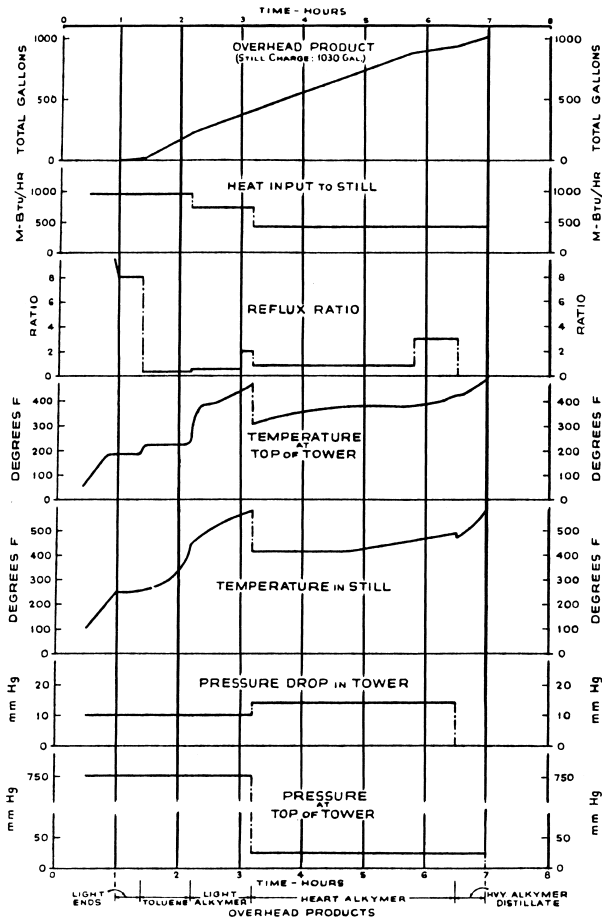
Figure 13.10. Operation of a batch distillation with five cuts.

At constant vaporization rate the time is proportional to the amount of vapor generated, or

$$t/\bar{t} = V/V_{\text{total}}. \tag{13.111}$$

Hence the reflux ratio, the amount of distillate, and the bottoms composition can be related to the fractional distillation time. This is done in Example 13.4, which studies batch distillations at constant overhead composition and also finds the suitable constant reflux ratio that enables meeting required overhead and residue specifications. Although the variable reflux operation is slightly more difficult to control, this example shows that it is substantially more efficient thermally—the average reflux ratio is much lower—than the other type of operation.

Equation (13.96) can be used to find the still composition—x_n in that equation—at a particular reflux ratio in a column-reboiler combination with n stages. Example 13.4 employs instead a computer program with Equations (13.103) and (13.104). That procedure is more general in that a constant relative volatility need not be assumed, although that is done in this particular example.

13.6. MULTICOMPONENT SEPARATION: GENERAL CONSIDERATIONS

A tower comprised of rectifying (above the feed) and stripping (below the feed) sections is capable of making a more or less sharp separation between two products or pure components of the mixture, that is, between the light and heavy key components. The *light key* is the most volatile component whose concentration is to be controlled in the bottom product and the *heavy key* is the least volatile component whose concentration is to be controlled in the overhead product. Components of intermediate volatilities whose distribution between top and bottom products is not critical are called *distributed keys*. When more than two sharply separated products are needed, say n top and bottom products, the number of columns required will be $n - 1$.

In some cases it is desirable to withdraw sidestreams of intermediate compositions from a particular column. For instance, in petroleum fractionation, such streams may be mixtures of suitable boiling ranges or which can be made of suitable boiling range by stripping in small auxiliary columns. Other cases where intermediate streams may be withdrawn are those with minor but critical impurities that develop peak concentrations at these locations in the column because of inversion of volatility as a result of concentration gradient. Thus, pentyne-1 in the presence of n-pentane in an isoprene-rich C_5 cracked mixture exhibits this kind of behavior and can be drawn off as a relative concentrate at an intermediate point. In the rectification of fermentation alcohol, whose column profile is shown in Figure 13.11(a), undesirable esters and higher alcohols concentrate at certain positions because their solubilities are markedly different in high and low concentrations of ethanol in water, and are consequently withdrawn at these points.

Most distillations, however, do not develop substantial concentration peaks at intermediate positions. Figure 13.11(b) is of normal behavior.

SEQUENCING OF COLUMNS

The number n of top and bottom products from a battery of $n - 1$ columns can be made in several different ways. In a direct method, the most volatile components are removed one-by-one as overheads in successive columns with the heaviest product as the bottoms of the last column. The number of possible ways of separating components goes up sharply with the number of products, from two arrangements with three products to more than 100 with
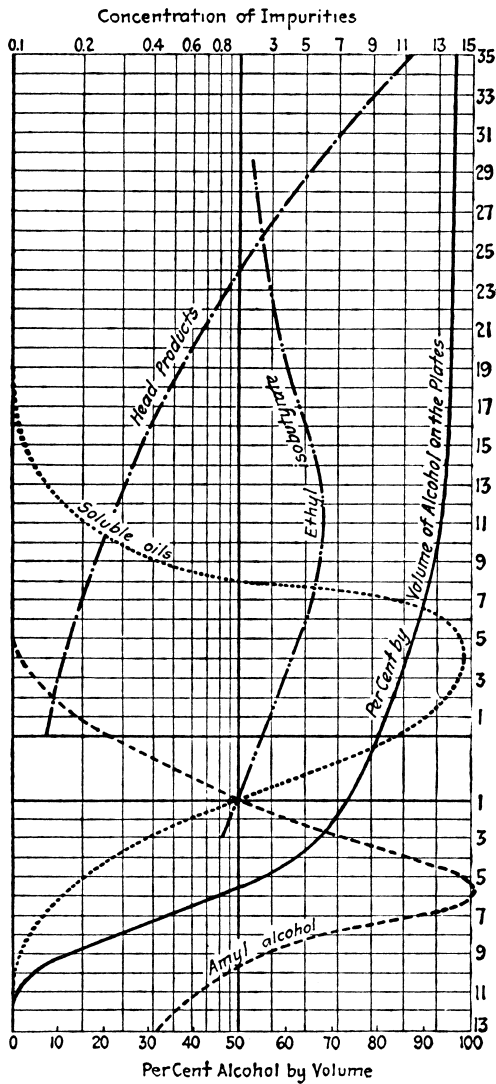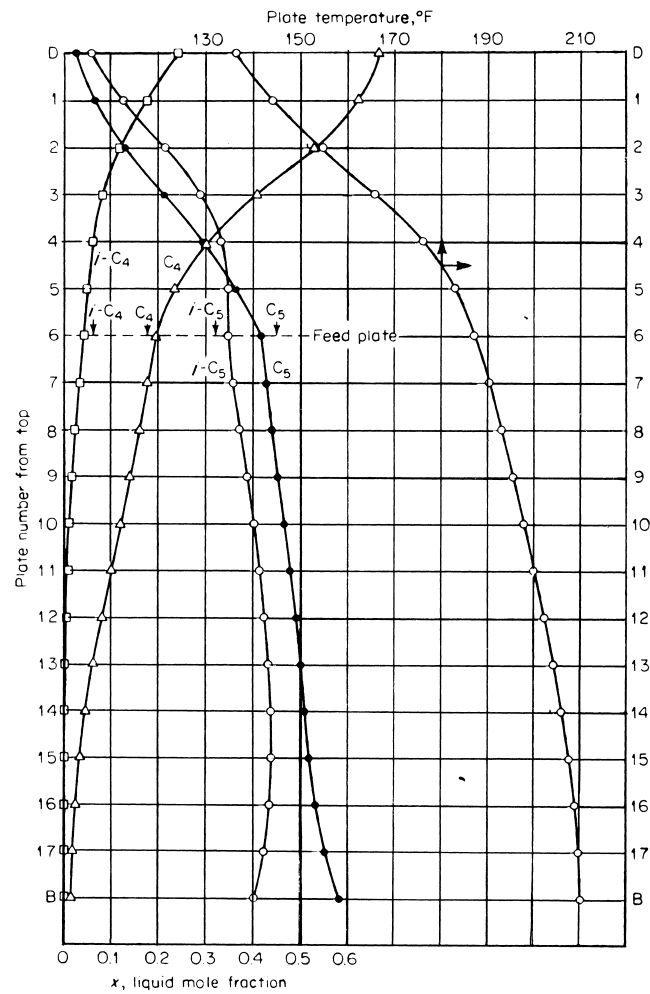
Figure 13.11. Concentration profiles in two kinds of distillations. (a) Purifying column for fermentation alcohol; small streams with high concentrations of impurities are withdrawn as sidestreams (*Robinson and Gilliland, 1939*). (b) Typical concentration profiles in separation of light hydrocarbon mixtures when no substantial inversions of relative volatilities occur (*Van Winkle*, Distillation, *McGraw-Hill, New York, 1967*).

seven products. Table 13.5 identifies the five possible arrangements for separating four components with three columns. Such arrangements may differ markedly in their overall thermal and capital cost demands, so in large installations particularly a careful economic balance may be needed to find the best system.

TABLE 13.5. The Five Possible Sequences for the Separation of Four Components ABCD by Three Columns

Column 1		Column 2		Column 3	
Ovhd	Btms	Ovhd	Btms	Ovhd	Btms
A	BCD	B	CD	C	D
A	BCD	BC	D	B	C
AB	CD	A	B	C	D
ABC	D	A	BC	B	C
ABC	D	AB	C	A	B

The literature of optimum sequencing of columns is referenced by King (1980, pp. 711–720) and Henley and Seader (1981, pp. 527–555). For preliminary selection of near optimal sequences, several rules can be stated as guides, although some conflicts may arise between recommendations based on the individual rules. Any recommended cases then may need economic evaluations.

1. Perform the easiest separation first, that is, the one least demanding of trays and reflux, and leave the most difficult to the last.
2. When neither relative volatility nor concentration in the feed varies widely, remove the components one-by-one as overhead products.
3. When the adjacent ordered components in the process feed vary widely in relative volatility, sequence the splits in the order of decreasing relative volatility.

4. When the concentrations in the feed vary widely but the relative volatilities do not, sequence the splits to remove components in the order of decreasing concentration in the feed.

NUMBER OF FREE VARIABLES

The performance of a given column or the equipment requirements for a given separation are established by solution of certain mathematical relations. These relations comprise, at every tray, heat and material balances, vapor–liquid equilibrium relations, and mol fraction constraints. In a later section, these equations will be stated in detail. For now, it can be said that for a separation of C components in a column of n trays, there still remain a number, $C + 6$, of variables besides those involved in the cited equations. These must be fixed in order to define the separation problem completely. Several different combinations of these $C + 6$ variables may be feasible, but the ones commonly fixed in column operation are the following:

Item	Name	Number of Variables
1	feed rate	1
2	feed composition	$C - 1$
3	feed enthalpy	1
4	ratio of overhead and feed rates	1
5	reflux enthalpy	1
6	reflux ratio, L/D or L/V	1
7	number of trays	1
8	column pressure	1
		$C + 6$

A common alternate specification is of the overhead and bottoms compositions expressed through distribution of the keys (two variables) as a replacement of items 4 and 7.

13.7. ESTIMATION OF REFLUX AND NUMBER OF TRAYS (FENSKE–UNDERWOOD–GILLILAND METHOD)

The first step in the design of distillation equipment is specification of the required distribution of light and heavy key components. Then the specific operating conditions and equipment size are established, ultimately on the basis of an economic balance or simply by exercise of judgment derived from experience. The design parameters that need to be determined include intermediate ones such as limiting reflux and trays that are needed for establishing a working design. These design parameters are the following:

1. Minimum number of theoretical trays,
2. Distribution of nonkeys between the overhead and bottoms products,
3. Minimum reflux,
4. Operating reflux,
5. Number of theoretical trays,
6. Location of the feed tray,
7. Tray efficiencies.

In packed towers, the variation of conditions from top to bottom is continuous and not interrupted as at trays. Nevertheless, it is convenient to speak of packing heights equivalent to a theoretical tray (HETP), so that tray tower theory can be applied to the design of packed towers.

All of the values of this list can be established at least approximately by rapid shortcut methods. In some instances such values may be useful as final ones, but ordinarily they are for exploratory purposes or as a starting basis for a computer design. Computer design of fractionation is an iterative process which depends for rapid convergence on good starting estimates of the principal quantities.

The background of shortcut methods is well treated in the books of King (1980) and Seader and Henley (1998). Here attention will be directed to application of the techniques. These shortcut methods assume constant molal overflow in the rectifying and stripping zones and constant relative volatilities, which may be taken at the conditions of the feed tray or as a geometric mean of the values at the top and bottom of the column. Since the top conditions are not known completely in advance, evaluation of a mean relative volatility is an iterative process that can be started with the value at the feed tray or at the feed condition. Particular modes of variation of α sometimes are assumed. The method of Winn assumes that the vaporization equilibrium ratios vary as

$$K_{1k} = \beta K_{hk}^{\delta} \tag{13.112}$$

or

$$\alpha = K_{1k}/K_{hk} = \beta K_{hk}^{\delta-1} \tag{13.113}$$

The constants β and δ for the conditions of the tower are deduced from log–log plots of K's, which usually are available for hydrocarbons and natural gas constituents but can be evaluated from

$$K = \gamma P^{\text{sat}}/P, \tag{13.114}$$

with activity coefficient γ of unity if no better information is known.

MINIMUM TRAYS

This is found from the relative volatility and the distribution of the keys between the overhead and bottoms by the Underwood–Fenske equation

$$N_m = \frac{\ln\left[(x_D/x_B)_{1k}/(x_D/x_B)_{hk}\right]}{\ln(\alpha_{1k}/\alpha_{hk})} = \frac{\ln\left[(d/b)_{1k}/(d/b)_{hk}\right]}{\ln(\alpha_{1k}/\alpha_{hk})}. \tag{13.115}$$

In terms of the variation of VERs according to Eq. (13.112),

$$N_m = \frac{\ln\left[(d/b)_{1k}/(d/b)_{hk}^{\delta}\right]}{\ln\beta} \tag{13.116}$$

DISTRIBUTION OF NONKEYS

A convenient approximation is that the distributions of nonkeys require the minimum number of trays as given by Eq. (13.115). Designating the nonkey by subscript nk, that equation becomes

$$\ln(d/b)_{nk} = \ln(d/b)_{1k} + N_m \ln(\alpha_{nk}/\alpha_{1k}) \tag{13.117}$$

or

$$(d/b)_{nk} = (d/b)_{1k}(\alpha_{nk}/\alpha_{1k})^{N_m}. \tag{13.118}$$

The distribution of nonkeys actually depends somewhat on the reflux ratio. For instance, in the case of Example 13.10, the distributions at minimum trays (total reflux) and minimum reflux are substantially different. Often it turns out, however, that the distributions predicted by Eq. (13.118) are close to those at finite reflux whenever R is near $1.2R_m$, which is often near the economic value for the reflux ratio. Further discussion of this topic is by Hengstebeck (1961) and Stupin and Lockhart (1982) whose work is summarized by King (1980, p. 434). Knowledge of the complete distribution is needed for estimation of top and bottom temperatures and for determination of the minimum reflux by the method to be cited.

EXAMPLE 13.10
Shortcut Design of Multicomponent Fractionation

A mixture of the given composition and relative volatilities has a thermal condition $q = 0.8$ and a pressure of 10 atm. It is to be fractionated so that 98% of component C and 1% of component E will appear in the overhead. The tray and reflux requirements are to be found. In the following table, the quantities in brackets are calculated in the course of the solution. f_i, d_i, and b_i are the mols of component i per mol of total feed.

	α	f	d	b
A	3.1	0.03	[0.0300]	[1.5($E-5$)]
B	2.6	0.07	[0.0698]	[0.0002]
C lk	2.2	0.15	0.147	0.0030
D	1.3	0.33	[0.0481]^a	[0.2819]^a
D hk	1.0	0.30	0.003	0.297
F	0.8	0.12	[0.0000]	[0.1200]

^{a}The corrected distribution of component D will be found along with the minimum reflux.

The minimum number of trays is

$$N_m = \frac{\ln\left[\dfrac{0.147}{0.003}\Big/\dfrac{0.003}{0.297}\right]}{\ln 2.2} = 10.76$$

The distribution of component A is found as

$$\left(\frac{d}{b}\right)_i = \left(\frac{f-b}{b}\right)_i = \left(\frac{d}{b}\right)_{lk}\left(\frac{\alpha_i}{\alpha_{lk}}\right)^{N_m}$$

$$= \frac{0.147}{0.003}\left(\frac{3.1}{2.2}\right)^{10.76} = 1962,$$

$$b_i = \frac{f_i}{1+(d/b)_i} = \frac{0.03}{1+1962} = 1.5(E-5),$$

$$d_i = f_2 - b_i = 0.03 - 1.5(E-5) = 0.300.$$

Distributions of the other components are found in the same way.

Since component D is distributed, two values of θ are found from Eq. (13.119).

$$\frac{3.1(0.03)}{3.1-\theta} + \frac{2.6(0.7)}{2.6-\theta} + \frac{2.2(0.15)}{2.2-\theta} + \frac{1.3(0.33)}{1.3-\theta}$$

$$+ \frac{1(0.3)}{1-\theta} + \frac{0.8(0.12)}{0.8-\theta} = 1 - 0.8,$$

$$\therefore \theta_1 = 1.8817,\ \theta_2 = 1.12403.$$

The overhead content d_D of component D and the minimum reflux are found from the two equations

$$(R_m + 1)D = (R_m + 1)(0.2498 + d_D)$$

$$= \frac{3.1(0.03)}{3.1-\theta_1} + \frac{2.6(0.07)}{2.6-\theta_1} + \frac{2.2(0.147)}{2.2-\theta_1}$$

$$+ \frac{1.3d_D}{1.3-\theta_1} + \frac{0.003}{1-\theta_1}$$

$$= \frac{3.1(0.03)}{3.1-\theta_2} + \frac{2.6(0.007)}{2.6-\theta_2} + \frac{2.2(0.147)}{2.2-\theta_2}$$

$$+ \frac{1.3d_D}{1.3-\theta_2} + \frac{0.003}{1-\theta_2}.$$

Upon substituting $\theta_1 = 1.8817$, $\theta_2 = 1.12403$,

$$d_D = 0.09311,$$
$$D = 0.2498 + 0.09311 = 0.3429,$$
$$(R_m + 1)D = 1.1342,$$
$$R_m = 2.3077.$$

Let $R = 1.2\ R_m = 1.2(2.3077) = 2.7692$. Apply Eq. (13.123):

$$X = \frac{R - R_m}{R + 1} = \frac{0.2(2.3077)}{3.7692} = 0.1225,$$

$$Y = 0.5313$$

$$N = \frac{N_m + Y}{1 - Y} = \frac{10.76 + 0.5313}{1 - 0.5313} = 24.1.$$

Feed plate location:

$$\frac{N_{above}}{N_{below}} = \frac{\ln\left(\dfrac{0.147}{0.15}\Big/\dfrac{0.003}{0.300}\right)}{\ln\left(\dfrac{0.15}{0.003}\Big/\dfrac{0.3}{0.297}\right)} = 1.175.$$

Since $N_{above} + N_{below} = 24.1$,

$$\text{feed tray} = \frac{24.1}{1 + 1/1.175} = 13 \text{ from the top.}$$

For comparison, apply Eqs. (13.129) and (13.130):

$$\frac{N_r^*}{24 - N_r^*} = \left[\frac{0.6572}{0.3428}\left(\frac{0.30}{0.15}\right)\left(\frac{0.003/0.6572}{0.003/0.3428}\right)^2\right]^{0.206}$$

$$= 1.0088,$$

$$N_r^* = 12.05,$$

$$N_r = 12.05 - 0.5\log 24 = 10.46 \text{ from the top.}$$

Presumably 10.46 from the top is more accurate than 13.0, but it also may be in error because of the approximate fashion in which the distributions of nonkeys were found.

Note that the predicted distributions of component D do not agree closely.

	d	b
From minimum trays	0.0481	0.2819
From minimum reflux	0.09303	0.2370

MINIMUM REFLUX

The method of Underwood employs auxiliary parameters θ derived from the equation

$$\sum_{i=1}^{C} \frac{\alpha_i x_{Fi}}{\alpha_i - \theta} = 1 - q, \qquad (13.119)$$

where q is the thermal condition of the feed and the summation extends over all the components in the feed. The only roots required are those in numerical value between the relative volatilities of the light and heavy keys. For instance, if there is one distributed component, subscript $_{dk}$, the required roots θ_1 and θ_2 are in the ranges

$$\alpha_{1k} > \theta_1 > \alpha_{dk},$$
$$\alpha_{dk} > \theta_2 > \alpha_{hk}.$$

Then the minimum reflux and the distribution of the intermediate component are found from the two equations that result from substitution of the two values of θ into Underwood's second equation

$$R_m + 1 = \frac{1}{D} \sum \frac{\alpha_i d_i}{\alpha_i - \theta}. \qquad (13.120)$$

The number of values of θ and the number of Eqs. (13.120) is equal to 1 plus the number of components with relative volatilities between those of the light and heavy keys. When there is no distributed component, Eq. (13.120) may be used in terms of mol fractions and only a single form is needed for finding the minimum reflux,

$$R_m + 1 = \sum \frac{\alpha_i x_{iD}}{\alpha_i - \theta}. \qquad (13.121)$$

Occasionally the minimum reflux calculated by this method comes out a negative number. That, of course, is a signal that some other method should be tried, or it may mean that the separation between feed and overhead can be accomplished in less than one equilibrium stage.

OPERATING REFLUX

As discussed briefly in Section 13.4, the operating reflux is an amount in excess of the minimum that ultimately should be established by an economic balance between operating and capital costs for the operation. In many cases, however, as stated there the assumptions $R = 1.2R_m$ often is close to the optimum and is used without further study unless the installation is quite a large one.

ACTUAL NUMBER OF THEORETICAL TRAYS

An early observation by Underwood (*Trans. Inst. Chem. Eng.* **10,** pp. 112–152, 1932) of the plate–reflux relation was

$$(R - R_m)(N - N_m) = \text{const}, \qquad (13.122)$$

but no general value for the constant was possible. Several correlations of calculated data between these same variables have since been made. A graphical correlation made by Gilliland (*Ind. Eng. Chem.* **32,** 1101, 1940) has found wide acceptance because of its fair accuracy and simplicity of use (Fig. 13.12). Of the several representations of the plot by equations, that of Molokanov et al. [*Int. Chem. Eng.* **12,** 209–212 (1972)] is accurate:

$$Y = \frac{N - N_{\min}}{N + 1} = 1 - \exp\left[\left(\frac{1 + 54.4X}{11 + 117.2X}\right)\left(\frac{X - 1}{X^{0.5}}\right)\right], \qquad (13.123)$$

An alternate relationship due to Rusche (1999) is easier to use:

$$Y = 1.0 - 0.1256X - 0.8744X^{0.291} \qquad (13.124)$$

where

$$X = \frac{R - R_{\min}}{R + 1}, \qquad (13.125)$$

from which the number of theoretical trays is

$$N = \frac{N_m + Y}{1 - Y}. \qquad (13.126)$$

The Gilliland correlation appears to be conservative for feeds with low values of q (the thermal condition of the feed), and can be in error when there is a large difference in tray requirements above and below the feed. The principal value of the correlation is for preliminary exploration of design variables which can be refined by computer calculations. Although it is often used for final design, that should be done with caution.

FEED TRAY LOCATION

Particularly when the number of trays is small, the location of the feed tray has a marked effect on the separation in the column. An estimate of the optimum location can be made with the Underwood-Fenske equation (13.115), by applying it twice, between the overhead and the feed and between the feed and the bottoms. The ratio of the numbers of rectifying N_r and stripping N_s trays is

$$\frac{N_r}{N_s} = \frac{\ln[(d/f)_{1k}/(d/f)_{hk}]}{\ln[(f/b)_{1k}/(f/b)_{hk}]} \qquad (13.127)$$

$$= \frac{\ln[(x_d/x_f)_{1k}/(x_d/x_f)_{hk}]}{\ln[(x_f/x_b)_{1k}/(x_f/x_b)_{hk}]}. \qquad (13.128)$$

An improved relation that, however, requires more information is due to Akashah, Erbar, and Maddox [*Chem. Eng. Commun.* **3,** 461 (1979)]:

$$N_r = N_r^* - 0.5\log(N_t), \qquad (13.129)$$

where N_t is the total number of trays in the column and N_r^* is given by the empirical Kirkbride (*Petrol. Refiner* **23** (9), 321, 1944) equation,

$$\frac{N_r^*}{N_t - N_r^*} = \left[\frac{B}{D}\left(\frac{x_{1k}}{x_{hk}}\right)_f \left(\frac{x_{B1k}}{x_{Dhk}}\right)^2\right]^{0.206}. \qquad (13.130)$$

Example 13.10 shows how theoretical stages and feed tray location are determined by the foregoing method.

TRAY EFFICIENCIES

The calculations made thus far are of theoretical trays, that is, trays on which vapor-liquid equilibrium is attained for all components. Actual tray efficiencies vary widely with the kind of system, the flow rates, and the tray construction. The range can be from less than 10% to more than 100% and constitutes perhaps the greatest

uncertainty in the design of distillation equipment. For hydrocarbon fractionation a commonly used efficiency is about 60%. Section 13.14 discusses this topic more fully.

13.8. ABSORPTION FACTOR SHORTCUT METHOD OF EDMISTER

This method finds the product distribution ratio b/d for each component in a column with known numbers of trays above and below the feed and with a known reflux ratio. The flowsketch and nomenclature appear on Figure 13.13.

An absorption factor for each component i on each tray j is defined as

$$A_{ij} = L_j/V_j K_{ij}, \tag{13.131}$$

but usually it is understood to apply to a specific component so the subscript i is dropped and the absorption factors on tray j become

$$A_j = L_j/V_j K_j. \tag{13.132}$$

Similarly a stripping factor for each component is defined as

$$S_j = K_j V_j/L_j. \tag{13.133}$$

The ratio of bottom and overhead flow rates for each component is

$$\frac{b}{d} = \frac{\phi_1 + (L_d/DK_d)\phi_2 - (1-q)F}{\psi_1 + (V_b/B)\psi_2 - 1}, \tag{13.134}$$

with which the individual flow rates of each component are found

$$b_i = \frac{f_i}{1 + (b/d)_i}, \tag{13.135}$$

$$d_i = f_i - b_i. \tag{13.136}$$

The function ϕ and ψ are defined as

$$\phi_1 = \frac{A_e^{n+1} - 1}{A_e - 1}, \tag{13.137}$$

$$\phi_2 = (A_1 A_n)^{n/2}, \tag{13.138}$$

$$\psi_1 = \frac{S_e^{m+1} - 1}{S_e - 1}, \tag{13.139}$$

$$\psi_2 = (S_1 S_m)^{m/2}. \tag{13.140}$$

The effective absorption and stripping factors in each zone are approximately

$$A_e = -0.5 + \sqrt{A_n(A_1 + 1) + 0.25}, \tag{13.141}$$

$$S_e = -0.5 + \sqrt{S_m(S_1 + 1) + 0.25}. \tag{13.142}$$

A certain number of initial estimates must be made when applying Edmister's method which are improved by iteration.

1. Initial estimates must be made of the top and bottom temperatures so that the A_1 and S_1 can be estimated. These estimates will be adjusted by bubblepoint calculations after b and d have been found by the first iteration.
2. The temperature at the feed zone may be found by taking a linear temperature gradient.

3. Estimates must be made of V/L at the top and bottom and the feed zone. In distillation problems, assumption of constant molal overflow in each zone probably is within the accuracy of the method. In stripping or absorption columns, first iteration evaluations of the amounts of stripping or absorption will provide improved estimates of V/L at the key points in the columns.

A distillation problem is worked out by this method by Edmister [*Pet. Eng.*, 128–142 (Sept. 1948)]. The method is developed there.

For independent absorbers and strippers, the Kremser-Brown formulas apply. The fraction absorbed is

$$\phi_a = \frac{A_e^{n+1} - A_e}{A_e^{n+1} - 1}, \tag{13.143}$$

and the fraction stripped is

$$\phi_s = \frac{S_e^{m+1} - S_e}{S_e^{m+1} - 1}. \tag{13.144}$$

An absorber is calculated by this method in Example 13.11.

13.9. SEPARATIONS IN PACKED TOWERS

Continuous changes in compositions of phases flowing in contact with each other are characteristic of packed towers, spray or wetted wall columns. The theory of mass transfer between phases and separation of mixtures under such conditions is based on a two-film theory. The concept is illustrated in Figure 13.14(a).

In its simplest form, the rate of mass transfer per unit area across these films is

$$N/A = k_G(y - y^*) = k_L(x^* - x). \tag{13.145}$$

Two special cases are commonly recognized.

1. Equimolar counterdiffusion between the phases, as in distillation with McCabe-Thiele approximations.
2. Unidirectional diffusion through a stagnant film or boundary layer, as in absorption or stripping processes involving transfer of a single component between liquid and vapor phases. Since there is a concentration gradient of the diffusing substance in the film or boundary layer, a correction is applied to the mass transfer coefficient. It is shown in texts on mass transfer (e.g., Hines and Maddox, 1985) that the effective coefficient for the film is

$$(k_G)_{\text{effective}} = k_G/(y - y^*)_{\text{log mean}}, \tag{13.146}$$

where

$$(y - y^*)_{\text{log mean}} = \frac{(1-y) - (1-y^*)}{\ln[(1-y)/(1-y^*)]} = \frac{(y^* - y)}{\ln[(1-y)/(1-y^*)]}. \tag{13.147}$$

MASS TRANSFER COEFFICIENTS

Numerous investigations have been conducted of mass transfer coefficients in vessels with a variety of kinds of packings. Many of the more acceptable results are cited in books on mass transfer, for instance, those of Sherwood et al. (1975), Cussler (*Diffusion*, Cambridge, 1984), and Hines and Maddox (1985). A convenient correlation of mass transfer coefficients in granular beds covering both liquid and vapor films is that of Dwivedi and

EXAMPLE 13.11
Calculation of an Absorber by the Absorption Factor Method

A mixture of a given composition is to have 60% of its n-butane removed by scrubbing with an oil in a 4-tray tower operating essentially isothermally at a pressure of 4 atm. The oil feed rate per 100 mol of feed gas will be found. The data are

	z_f	K	ϕ
C_1	0.253	54	
C_2	0.179	14	
C_3	0.222	3.5	
nC_4	0.240	0.5	0.600
nC_5	0.105	0.2	
	1.000		

The Kremser–Brown formula (Eq.(13.143)) for the fraction absorbed is applied to nC_4:

$$\phi = (A_e^5 - A_e)/(A_e^5 - 1) = 0.6,$$

$$\therefore A_e = 0.644, \text{ by trial.}$$

Estimate that 27 mol of gas is absorbed. Let L_d represent the lean oil rate: For nC_4

$$A_1 = \frac{L_d}{KV_1} = \frac{L_d}{0.5(73)}, \quad A_n = \frac{L_d + 27}{0.5(100)}.$$

Substitute into Eq. (13.141),

$$A_e = -0.5 + \left[\frac{(L_d + 27)}{50}\left(\frac{L_d}{36.5} + 1\right) + 0.25\right]^{1/2} = 0.644,$$

$$\therefore L_d = 12.46, \text{ by trial.}$$

For the other components,

$$A_e = -0.5 + \left[\frac{12.46 + 27}{100K}\left(\frac{12.46}{73K} + 1\right) + 0.25\right]^{1/2},$$

$$\phi = \frac{A_e^5 - A_e}{A_e^5 - 1},$$

$$b = 100 z_f \phi.$$

The results are tabulated and show that the calculated value, 27.12, is close to the assumed, 27.00.

	z_f	K	A_e	ϕ	b
C_1	0.253	54	0.00728	0.00728	0.18
C_2	0.179	14	0.02776	0.02776	0.50
C_3	0.222	3.5	0.1068	0.1068	2.37
nC_4	0.240	0.5	0.644	0.600	14.40
nC_5	0.105	0.2	1.4766	0.9208	9.67
	1.000				27.12

Upadhyay [*Ind. Eng. Chem. Process Des. Dev.* **16,** 157 (1977)], namely,

$$\varepsilon j_d = \frac{0.765}{\text{Re}^{0.82}} + \frac{0.365}{\text{Re}^{0.386}} \tag{13.148}$$

$$j_d = (\text{Sh})/(\text{Re})(\text{Sc})^{2/3} \quad \text{(Chilton–Colburn factor)}, \tag{13.149}$$

$$\text{Sh} = kd/\mathcal{D} \quad \text{(Sherwood number)}, \tag{13.150}$$

$$\text{Sc} = \mu/\rho\mathcal{D} \quad \text{(Schmidt number)}, \tag{13.151}$$

$$\text{Re} = du\rho/\mu = 4w/\pi d^2\mu \quad \text{(Reynolds number)}, \tag{13.152}$$

where

d = particle diameter,
$\mathcal{D}$ = diffusivity of the substance being transferred,
k = mass transfer coefficient,

Figure 13.12. Gilliland relationship between actual reflux ratio R, minimum reflux ratio R_m, theoretical stages N and minimum theoretical stages N_m.

$$-dN = d(Gy) = Gdy = k_G a(y - y^*)dz \tag{13.155}$$

$$= d(Lx) = Ldx = k_L a(x^* - x)dz, \tag{13.156}$$

where a is the interfacial surface per unit volume of the packed bed.

These equations relate the interfacial concentrations (x^*, y^*) to those in the bulks of the liquid and gas phases (x, y); thus

$$\frac{y^* - y}{x^* - x} = -\frac{k_L}{k_G}. \tag{13.157}$$

The bulk concentrations (x, y) are related by the material balance Eq. (13.144), and the equilibrium concentrations (x^*, y^*) from experimental data in graphical, tabular, or equation form,

$$y^* = f(x^*) \tag{13.158}$$

for instance, at constant relative volatility,

$$y^* = \frac{\alpha x^*}{1 + (\alpha - 1)x^*}. \tag{13.159}$$

Corresponding points (y, y^*) in a column where the ratio k_L/k_G is k are found as follows: At a particular composition x, the value of y is known from Eq. (13.154). Then corresponding values (x^*, y^*) are related linearly by Eq. (13.157). Substitution into Eq. (13.158) then will establish the value of y^* corresponding to the selected y. The terms HTU_{OG} and HETP are sometimes used interchangeably, but they are nearly the same only when the ratio $K_L K_G$ is a large number, i.e., gas side resistance dominates. Example 13.12 studies this difference.

By rearrangements of Eqs. (13.155) and (13.156) the height of the column is given by

$$Z = \frac{G}{k_G a} \int_{y_1}^{y_2} \frac{dy}{y^* - y} \tag{13.160}$$

$$= \frac{L}{k_L a} \int_{x_1}^{x_2} \frac{dx}{x - x^*}. \tag{13.161}$$

The integrals in these equations are measures of the difficulty of the separation. Under some conditions they are roughly equal to the number of theoretical trays for the same change in concentration (y_1, y_2) or (x_1, x_2). Accordingly, they are called numbers of transfer units.

$$NTU_G = \int_{y_1}^{y_2} \frac{dy}{y^* - y'}, \tag{13.162}$$

$$NTU_L = \int_{x_1}^{x_2} \frac{dx}{x - x^*}. \tag{13.163}$$

Consequently, it is natural to call the coefficients of the integrals the height of a transfer unit. For distillation,

$$HTU_G = G/k_G a \tag{13.164}$$

$$HTU_L = L/k_L a \tag{13.165}$$

Thus, the required height of the packed section is, from Eqs. (13.162–13.165),

$$Z = (NTU_G)(HTU_G) = (NTU_L)(HTU_L) \tag{13.166}$$

However, Eq. (13.166) can be used only when there is no resistance to mass transfer in one of the phases. For resistance in both phases, the individual HTU values can be combined:

$$HTU_{OG} = HTU_G + \lambda(HTU_L) \tag{13.167}$$

Figure 13.13. Sketch and nomenclature for the absorption factor method.

u = linear velocity of the fluid,
w = mass rate of flow of the fluid,
ε = fractional voidage between particles,
ρ = density of the fluid,
μ = viscosity of the fluid.   (13.152)

Most of the properties change somewhat from one end to the other of industrial columns for effecting separations, so that the mass transfer coefficients likewise vary. Perhaps the property that has the most effect is the mass rate of flow which appears in the Reynolds number. Certainly it changes when there is a substantial transfer of material between the two phases in absorption or stripping; and even under conditions of constant molal overflow in distillation processes, the mass rate of flow changes because of differences of the molecular weights of the substances being separated. As a practical expedient, however, mass transfer coefficients are evaluated at mean conditions in a column.

DISTILLATION

Only the important case of constant molal overflow will be considered. the material balance around the lower end of the column of Figure 13.14 (b) is

$$Gy + L_1 x_1 = G_1 y_1 + Lx, \tag{13.153}$$

which becomes at constant molal overflow

$$y = \frac{L}{G}x + \left(y_1 - \frac{L}{G}x_1\right). \tag{13.154}$$

The rate balance on an element of height dz of a column of unit cross section is

Figure 13.14. Mechanism, nomenclature, and constructions for absorption, stripping and distillation in packed towers. (a) Two-film mechanism with equilibrium at the interface. (b) Sketch and nomenclature for countercurrent absorption or stripping in a packed tower. (c) Equilibrium and material balance lines in absorption, showing how interfacial concentrations are found. (d) Equilibrium and material balance lines in stripping, showing how interfacial concentrations are found. (e) Equilibrium and material balance lines in distillation, showing how interfacial concentrations are found.

where HTU_{OG} is an overall coefficient representing the resistance to mass transfer in both phases, and based on gas phase concentrations, and λ is the stripping factor, $\left(\frac{K_i V}{L}\right)$

The coefficients may be related as follows:

$$\frac{1}{K_{OG}} = \frac{1}{k_G} + \frac{H_i}{k_L} \qquad (13.168)$$

where H_i is a Henry's law constant, related to the VER: $H_i = K_i P$, with units consistent with the mass transfer expressions. The value of NTU_{OG} is based on the total driving force:

$$NTU_{OG} = \int_{y_1}^{y_2} \frac{dy}{y^* - y} \tag{13.169}$$

where $-(y^* - y)$ is the total gas concentration difference, bulk gas concentration to an equilibrium value based on bulk liquid concentration.

The required height of a separation in which both phases play a role, follows Eq. (13.166):

$$Z = (HTU_{OG})(NTU_{OG}) \tag{13.170}$$

EXAMPLE 13.12
Numbers of Theoretical Trays and of Transfer Units with Two Values of k_L/k_G for a Distillation Process
An equimolal mixture at its boiling point is to be separated into 95 and 5% contents of the lighter component in the top and bottoms products. The relative volatility is $\alpha = 2$, the minimum reflux is 1.714, and the operating reflux is 50% greater. The two values of k_L/k_G to be examined are -1 and ∞.

The relation between interfacial and bulk concentrations is that of Eq. (13.157), $(y^* - y)/(x^* - x) = -k_L/k_G$. At a series of values of x, corresponding values of y^* and y may be read off with the graphical constructions shown on Figures (b) and (c) of this example. The values for slope $= -1$ are tabulated, but those for slope $= \infty$ are calculated from the equations of the equilibrium and operating lines and are not recorded. The integrands of Eq. (13.160) also are tabulated for both cases, and the numbers of transfer units are obtained by integration with the trapezoidal rule:

$$NTU_{OG} = \int_{y_1}^{y_2} \frac{dy}{y^* - y}$$

a. The number of theoretical trays stepped off on the McCabe-Thiele diagram is 16.2.
b. With $k_L/k_G = 1$, the number of transfer units is 30.7.
c. With $k_L/k_G = \infty$, the number of transfer units is 15.4.

(b) Construction with $k_L/k_G = 1$, showing takeoff of vapor concentrations in the bulk, y, and at the interface, y^*. Number of transfer found by integration = 15.4.
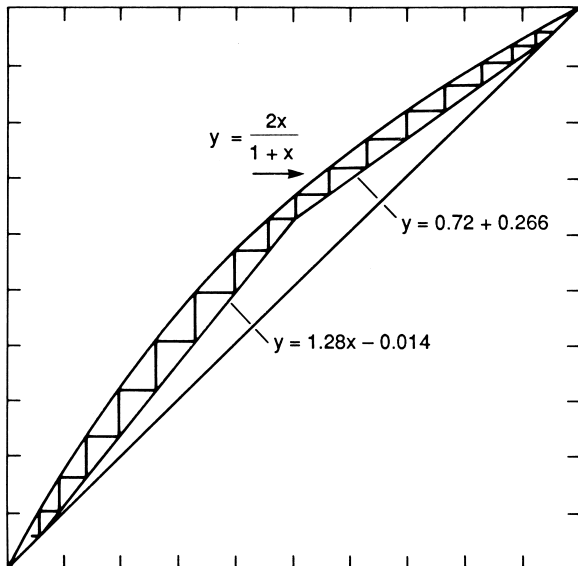
(a) McCabe-Thiele construction showing that 16.2 trays are needed to contain 95 and 5% of the lighter substance in the products from a 50% boiling liquid feed.
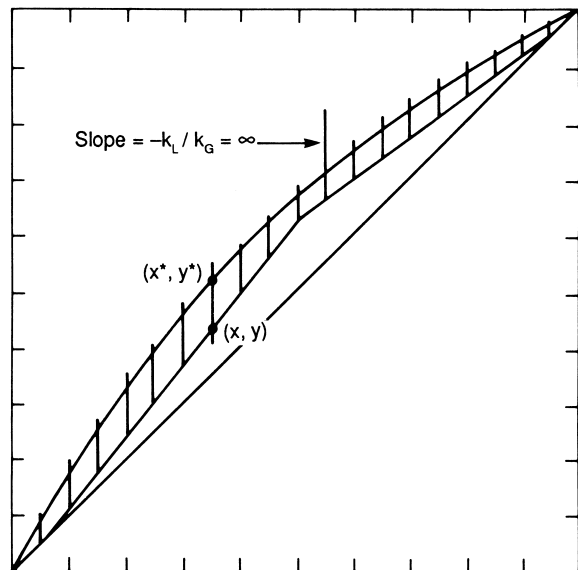
(c) Construction with $k_L/k_G = \infty$. Number of transfer units found by integration = 30.6.

(continued)

EXAMPLE 13.12—(*continued*)

Within the accuracy of the trapezoidal rule integration and of the graphical determination of the number of trays, the numbers 16.2 and 15.4 are substantially the same. The infinite value of the ratio of mass transfer coefficients k_L/k_G means that all of the resistance to mass transfer is in the gas film:

x	y	y_1^*	$1/(y_\infty^* - y)$	$1/(y_1^* - y)$
0.05	0.05	0.068	22.105	55.56
0.10	0.114	0.149	14.745	28.57
0.15	0.178	0.209	12.067	32.26
0.2	0.242	0.279	10.949	27.03
0.25	0.306	0.345	10.638	25.64
0.3	0.370	0.411	10.924	24.39
0.35	0.434	0.474	11.832	25.00

x	y	y_1^*	$1/(y_\infty^* - y)$	$1/(y_1^* - y)$
0.4	0.498	0.536	13.619	26.31
0.45	0.526	0.593	17.039	32.26
0.5	0.626	0.648	24.590	45.45
0.55	0.662	0.687	20.974	40.00
0.6	0.698	0.728	19.231	33.33
0.65	0.734	0.763	18.560	34.48
0.7	0.770	0.798	18.681	35.71
0.75	0.806	0.832	19.533	38.46
0.8	0.842	0.870	21.327	35.71
0.85	0.878	0.902	24.439	41.67
0.9	0.914	0.933	29.969	52.63
0.95	0.950	0.965	41.053	66.67

The concepts of NTU and HTU are defined only for binary distillations and transfer of a single component in absorption and stripping. For multicomponent mixture separations, the term *height equivalent to a theoretical plate (HETP)* is often used:

$$Z = (HETP)(N_t) \tag{13.171}$$

Thus, for multicomponent mixtures, the required number of theoretical stages N_t is calculated, and the *HETP* for the key components is estimated from the approximate relationship,

$$HETP = \left(\frac{\ln \lambda}{\lambda - 1}\right) HTU_{OG} \tag{13.172}$$

Packings for columns are available in a variety of shapes and sizes. Modern models for predicting their efficiency utilize the transfer unit concept. For the multicomponent case, NTU values are found from theoretical stages:

$$NTU_{OG} = \left(\frac{\ln \lambda}{\lambda - 1}\right) N_t \tag{13.173}$$

The terms HTU_{OG} and HETP are sometimes used interchangeably, but they are nearly the same only when the ratio k_L/k_G is a large number, *i.e.*, gas side resistance dominates. Example 13.12 studies this difference.

ABSORPTION OR STRIPPING

Neither mass nor molal flow rates are constant in these operations. In cases where essentially only one component is being transferred between phases, it is sometimes convenient to recognize the flow rates G' and L' of solute-free phases. They are related to the total flow rates by

$$G' = G(1 - y) = G_1(1 - y_1), \tag{13.174}$$
$$L' = L(1 - x) = L_1(1 - x_1). \tag{13.175}$$

The material balance around the lower end of the column of Figure 13.14 (b),

$$Gy + L_1 x_1 = G_1 y_1 + Lx \tag{13.176}$$

can be written

$$\frac{y}{1-y} = \frac{L'}{G'}\left(\frac{x}{1-x}\right) + \left(\frac{y_1}{1-y_1} - \frac{L'}{G'}\frac{x_1}{1-x_1}\right) \tag{13.177}$$

or in the linear form

$$Y = \frac{L'}{G'}X + \left(Y_1 - \frac{L'}{G'}X_1\right) \tag{13.178}$$

with the substitutions

$$X = \frac{x}{1 - x'} \tag{13.179}$$

$$Y = \frac{y}{1 - y}. \tag{13.180}$$

The equilibrium curve also can be transformed into these coordinates. These transformations are useful for graphical determinations of numbers of theoretical trays rather than for determination of numbers of transfer units. Example 13.13 employs both sets of units.

The rate balance on an element of height dz of a column of unit cross section, as in Figure 13.14(b), is

$$-dN = d(Gy) = (k_G)_{eff}a(y - y^*)dz \tag{13.181}$$

$$= d(Lx) = (k_L)_{eff}a(x^* - x)dz. \tag{13.182}$$

Expanding the differential of Eq. (13.163),

$$d(Gy) = d\left(\frac{G'}{1-y}\right) = \frac{G'}{(1-y)^2}dy = \frac{G}{1-y}dy. \tag{13.183}$$

Introducing Eqs. (13.146) and (13.183) into Eq. (13.181) and integrating, the height becomes

$$Z = \left(\frac{G}{k_G a}\right)_{mean}\int_{y_1}^{y_2} \frac{(y - y^*)_{1m}}{(1-y)(y-y^*)}dy. \tag{13.184}$$

On replacing the log mean term by Eq. (13.147), the result becomes

$$Z = \left(\frac{G}{k_g a}\right)_m \int_{y_1}^{y_2} \frac{1}{(1-y)\ln[(1-y)/(1-y^*)]}dy. \tag{13.185}$$

The variable flow rate G is used here instead of the constant G' because the mass transfer coefficient k_G depends more directly on G. As used in Eqs. (13.184) and (13.185), a mean value of the

coefficient is preferred in practice in preference to accounting for its variation within the integral.

The integrals are defined as numbers of transfer units for absorption or stripping,

$$\text{NTU}_G = \int_{y1}^{y2} \frac{1}{(1-y)\ln[(1-y)/(1-y^*)]} dy, \qquad (13.186)$$

$$\text{NTU}_L = \int_{x1}^{x2} \frac{1}{(1-x)\ln[(1-x)/(1-x^*)]} dx, \qquad (13.187)$$

and the heights of transfer units are

$$\text{HTU}_G = (G/k_G a)_{\text{mean}}, \qquad (13.188)$$

$$\text{HTU}_L = (L/k_L a)_{\text{mean}}. \qquad (13.189)$$

and the overall values may be obtained from Eq. (13.167) and from

$$1/NTU_{OG} = 1/NTU_G + \lambda(1/NTU_L) \qquad (13.190)$$

HTUs vary with the type and size of packing, the flow rates, the distribution of flow across the cross section, and sometimes with the packing height and column diameter. They are necessarily experimental data. Some of these data are discussed at the end of this chapter.

The way in which interfacial concentrations y^* are related to the bulk concentrations y required for evaluation of the integrand of Eq. (13.184) is explained in Example 13.13, which finds trays and transfer units for an absorption problem.

13.10. BASIS FOR COMPUTER EVALUATION OF MULTICOMPONENT SEPARATIONS

Until the advent of computers, multicomponent distillation problems were solved manually by making tray-by-tray calculations of heat and material balances and vapor–liquid equilibria. Even a partially complete solution of such a problem required a week or more of steady work with a mechanical desk calculator. The alternatives were approximate methods such as those mentioned in Sections 13.7 and 13.8 and pseudobinary analysis. Approximate methods still are used to provide feed data to iterative computer procedures or to provide results for exploratory studies.

The two principal tray-by-tray procedures that were performed manually are the Lewis and Matheson and Thiele and Geddes. The former started with estimates of the terminal compositions and worked plate-by-plate towards the feed tray until a match in compositions was obtained. Invariably adjustments of the amounts of the components that appeared in trace or small amounts in the end compositions had to be made until they appeared in the significant amounts of the feed zone. The method of Thiele and Geddes fixed the number of trays above and below the feed, the reflux ratio, and temperature and liquid flow rates at each tray. If the calculated terminal compositions are not satisfactory, further trials with revised conditions are performed. The twisting of temperature and flow profiles is the feature that requires most judgement. The Thiele–Geddes method in some modification or other is the basis of most current computer methods. These two forerunners of current methods of calculating multicomponent phase separations are discussed briefly with calculation flowsketches by Hines and Maddox (1985).

Computer programs for multistage operations embodying heat and material balances and sophisticated phase equilibrium relations are best left to professionals. Most such work is done by service organizations that specialize in chemical engineering process calculations or by specialists in engineering organizations. A few valuable programs appear in the open literature:

1. A Wang–Henke program appears in J. Christensen (Ed.) (*Stagewise Computations—Computer Programs for Chemical Engineering Education*, Sterling Swift Publishing, Manchaia, TX, 1972).
2. A Naphthali–Sandholm program appears in Fredenslund, Gmehling, and Rasmussen (*Vapor–Liquid Equilibria Using UNIFAC*, Elsevier, New York, 1977).
3. A Newton–Raphson SC (simultaneous correction) program of Newman is reproduced by King (*Separation Processes*, McGraw-Hill, New York, Appendix E).

Abundant descriptions of the theoretical basis and procedures for computer methods appear in recent literature and are summarized in books by King (1980, Chapter 10), Seader and Henley (1998, Chapter 15), and Kister (1992, Chapter 4). The present chapter will be devoted to the basic equations, the kinds of process specifications that can be made and met, and convergence criteria applicable to iterative calculations of problems of distillation, absorption, and stripping. To a certain extent, the same methods are applicable to liquid–liquid extraction and other phase separation processes.

SPECIFICATIONS

The variables most commonly fixed in operations of distillation columns are listed in Section 13.6. Detailed calculation processes of column performance may require other intermediate or tentative specifications whose nature depends on the particular computer algorithm used. These specifications are identified with the descriptions of the three chief methods of this section.

THE MESH EQUATIONS

The letters of this acronym refer to *M*aterial balances, *E*quilibria between vapor and liquid, *S*ummations of mol fractions to unity, and *H*eat or enthalpy balances. The quantities and notation pertaining to a single equilibrium stage and to an assembly of them are represented on Figure 13.15. In the simplest case a distillation stage exchanges two inlet and two outlet streams with adjacent stages. In addition, some stages will have in or out material or heat flows. Computer programs can be written in general form to include these factors on each stage to accommodate multiple feeds, side streams, and intermediate condensing or boiling. Enthalpy transfers sometimes are effected with hollow trays through which a heat transfer medium is circulated, or commonly by pumping a sidestream through an external heat exchanger and returning it to the column. The latter practice is particularly common for petroleum fractionation as an aid in controlling the wide range of vapor rates that accompany the difference of 500–600°F between top and bottom of a crude oil fractionator. Side reflux of this kind requires more trays than all top reflux, but an overall benefit in equipment cost results because of diameter reduction.

For every component, C in number, on every stage, N in number, there are material, equilibrium, and energy balances, and the requirement that the mol fractions of liquid and vapor phases on each tray sum to unity. The four sets of these equations are:

1. *M* equations—*M*aterial balance for each component (C equations for each stage):

$$\begin{aligned} M_{ij} = L_{j-1}x_{i,j-1} &+ V_{j+1}y_{i,j+1} + F_j z_{ij} \\ &- (L_j + U_j)x_{ij} - (V_j + W_i)y_{ij} = 0. \end{aligned} \qquad (13.191)$$

EXAMPLE 13.13
Trays and Transfer Units for an Absorption Process
The solute content of a gas with $y_1 = 0.40$ is to be reduced to $y_2 = 0.05$. The entering solvent is solute-free, $x_1 = 0$, and is to leave with $x_2 = 0.19$. The equilibrium relationship is represented by the equation

$$y^* = x^*(1 + 5x^*),$$

and the ratio of mass transfer coefficients is $k_L/k_G = 1$.
In terms of solute-free coordinates, the equation of the material balance line is

$$Y = 2.6176X + 0.0526,$$

calculated with the given terminal concentrations. In terms of mol fractions the material balance line is curved, with equation

$$y = \frac{2.6176x/(1-x) + 0.0526}{2.6176x/(1-x) + 1.0526}.$$

The equation of the equilibrium curve in solute-free coordinates is

$$\frac{Y}{1+Y} = \frac{X}{1+X}\left(1 + \frac{5X}{1+X}\right).$$

Constructions for the numbers of trays in both sets of coordinates are made. They agree within the accuracy of graphical constructions on this scale, $N = 4.7$ with (x, y) and $N = 4.5$ with (X, Y).

For the transfer unit determination with the given ratio of mass transfer coefficients, corresponding values of $(y, y*)$ are found by intersections of the material balance and equilibrium lines with lines whose slopes are $-k_L/k_G = -1$ as indicated on Figure (a) and in detail with Example 13.12. These values are tabulated together with the corresponding integrands. The number of transfer units is found by trapezoidal rule integration of

$$(NTU)_G = \int_{0.05}^{0.40} \frac{dy}{(1-y)\ln[(1-y^*)/(1-y)]}.$$
$$= 6.52$$

(a)

(b)
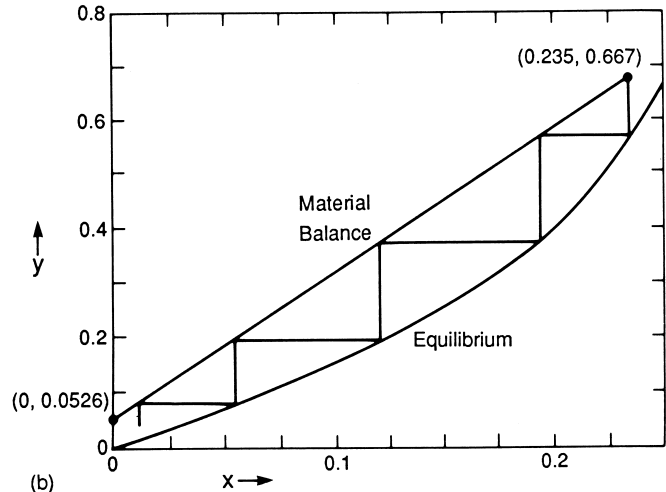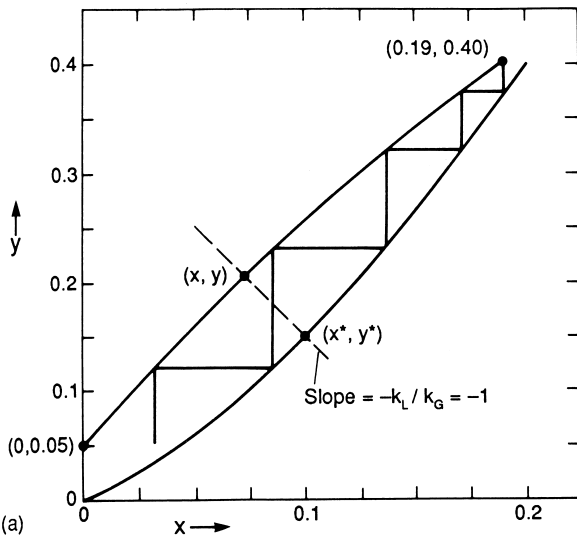
The two values of N should be the same, but there is a small disagreement because of construction inaccuracies on this scale: (a) construction with mol fraction coordinates, $N = 4.7$; (b) construction with solute-free coordinates, $N = 4.5$.

Within the accuracy of the trapezoidal rule integration and of the graphical determination of the number of trays, the numbers 16.2 and 15.4 are substantially the same. The infinite value of the ratio of mass transfer coefficients k_L/k_G means that all of the resistance to mass transfer is in the gas film:

x	y	y*	Integrand
0	0.05	0.009	24.913
0.01	0.0733	0.020	19.296
0.02	0.0959	0.036	17.242
0.03	0.1178	0.052	15.757
0.04	0.1392	0.069	14.818
0.05	0.1599	0.086	14.119
0.06	0.1801	0.102	13.405
0.07	0.1998	0.122	13.469
0.08	0.2189	0.141	13.467
0.09	0.2375	0.160	13.548

x	y	y*	Integrand
0.10	0.2556	0.180	13.888
0.11	0.2733	0.202	14.703
0.12	0.2906	0.224	15.709
0.13	0.3074	0.246	16.998
0.14	0.3237	0.268	18.683
0.15	0.3397	0.290	20.869
0.16	0.3553	0.312	23.862
0.17	0.3706	0.335	28.877
0.18	0.3854	0.358	37.304
0.19	0.4000	0.381	53.462
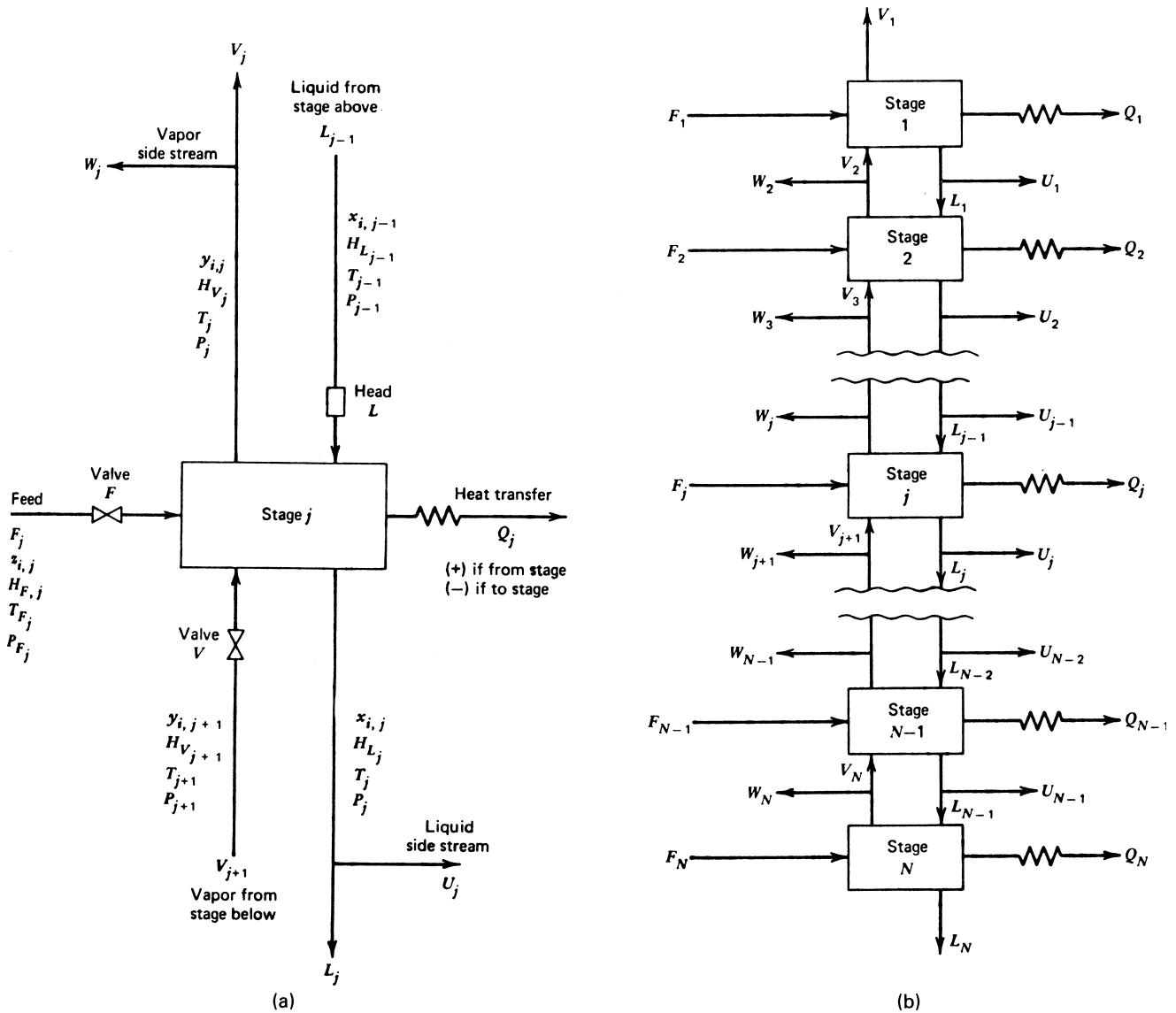
Figure 13.15. Flow patterns and nomenclature of a single equilibrium stage and a cascade of them (*after Henley and Seader, 1981*). (a) A single equilibrium stage. (b) An assembly of N stages.

2. *E* equations—phase *E*quilibrium relation for each component (*C* equations for each stage):

$$E_{i,j} = y_{ij} - K_{ij}x_{ij} = 0, \qquad (13.192)$$

where K_{ij} is the phase equilibrium ratio.

3. *S* equations—mole fraction *S*ummations (one for each stage):

$$(S_y)_j = \sum_{i=1}^{C} y_{ij} - 1.0 = 0, \qquad (13.193)$$

$$(S_x)_j = \sum_{i=1}^{C} x_{ij} - 1.0 = 0. \qquad (13.194)$$

4. *H* equation—energy balance (one for each stage):

$$H_j = L_{j-1}H_{Lj-1} + V_{j+1}Hv_{j+1} + F_jH_{Fj} - (L_j + U_j)H_{Lj}$$
$$-(V_j + W_j)H_{vj} - Q_j = 0 \qquad (13.195)$$

where kinetic and potential energy changes are ignored.

In order to simplify these equations, the liquid rate at each stage is eliminated with the substitutions

$$L_j = V_{j+1} + \sum_{m=1}^{j}(F_m - U_m - W_m) - V_1, \qquad (13.196)$$

and the vapor compositions by the equilibrium relations

$$y_{ij} = K_{ij}x_{ij}. \qquad (13.197)$$

Three other variables occurring in the MESH equations are functions of more fundamental variables, namely,

$$K_{ij} = K(T_j, P_j, x_{ij}, y_{ij}), \qquad (13.198)$$

$$H_{LJ} = H_L(T_j, P_j, x_j), \qquad (13.199)$$

$$H_{vj} = H_v(T_j, P_j, y_j). \qquad (13.200)$$

The reboiler load is determined by the overall energy balance,

$$Q_N = \sum_{j=1}^{N} (F_j H_{F_j} - U_j H_{L_j} - W_j H_{v_j})$$
$$- \sum_{j=1}^{N-1} Q_j - V_1 H_{v_1} - L_N H_{L_N}. \qquad (13.201)$$

When all of the following variables are specified,

N, F_j, z_{ij}, T_j, P_j, U_j, W_j, and Q_j (except Q_1 and Q_N),
  for $i = 1$ to C and $j = 1$ to N,

the MESH equations reduce in number to $N(2C + 3)$ in the same number of variables, and are hence in principle solvable. The equations are nonlinear, however, and require solution by some iterative technique, invariably involving linearization at some stage in the calculation process.

Almost all computer programs employed currently adopt the Thiele–Geddes basis; that is, they evaluate the performance of a column with a specified feed, bottoms/overhead ratio, reflux ratio, and numbers of trays above and below the feed. Specific desired product distributions must be found by interpolation between an appropriate range of exploratory runs. The speed and even the possibility of convergence of an iterative process depends on the values of starting estimates of the variables to be established eventually. Accordingly, the best possible starting estimates should be made by methods such as those of Sections 13.7 and 13.8, or on the basis of experience.

After values of the variables T_j and V_j, called tear variables, are specified, Eqs. (191)ff become a linear set in the x_{ij} variables. Initial estimates of the vapor flows are made by assuming constant molal overflow modified by taking account of external inputs and outputs, and those of the temperatures by assuming a linear gradient between estimated top and bottom temperatures. Initially, also, the K_{ij} are taken as ideal values, independent of composition, and for later iterations the compositions derived from the preceding one may be used to evaluate corrected values of K_{ij}. With appropriate substitutions,

$$A_j x_{i,j-1} + B_j x_{ij} + C_j x_{i,j+1} = D_j, \qquad (13.202)$$

where

$$A_j = V_j + \sum_{m=1}^{j-1} (F_m - W_m - U_m) - V_1, \; 2 \le j \le N, \qquad (13.203)$$

$$B_j = - \left[V_{j+1} + \sum_{m=1}^{j} (F_m - W_m - U_m) - V_1 + U_j + (V_j + W_j) K_{i,j} \right],$$
$$1 \le j \le N \qquad (13.204)$$

$$C_j = V_{j+1} K_{i,j+1}, \; 1 \le j \le N - 1, \qquad (13.205)$$

$$D_j = -F_j z_{ij}, \; 1 \le j \le N, \qquad (13.206)$$

the modified MESH equations can be written as a tridiagonal matrix, thus

The tridiagonal matrix is readily solved by computer by a method due to Thomas which is explained by Wang and Henke [*Hydrocarbon Proc.* **45**(8), 155–163 (1966)] and by Henley and Seader (1981). A FORTRAN program is given by Gerald and Wheatley [*Appl. Numer. Anal.*, 146, (1984)] and King (1980, Appendix E). A program in BASIC language is by Pachner (*Handbook of Numerical Analysis Applications*, McGraw-Hill, New York, 1984, Program P103).

After solution of the matrix for the liquid phase mol fractions x_{ij}, the next step is to make improved estimates of T_j and V_j for the next iteration. Three different procedures have been commonly employed for proceeding to succeeding trials, differing in simplicity or particular merit for certain kinds of problems.

1. BP (bubble-point) methods. Temperatures are corrected iteratively by determinations of bubblepoints. The method is satisfactory for mixtures with relatively narrow ranges of volatilities. The parent program of this type is that of Wang and Henke (1966) which is flowsketched on Figure 13.16 and described in the next section. The availability of a FORTRAN program was cited earlier in this section.
2. SR (sum-rates) method. The new liquid flow rates are taken proportional to the nonnormalized sums of mol fractions, the vapor rates by subsequent material balances, and the new temperatures by enthalpy balances. A flowsketch of the calculation process is in Figure 13.17, and a brief description also is given subsequently. This method is particularly suited to separations involving substances with widely differing volatilities, as in absorbers and strippers, where the bubblepoint method breaks down.
3. SC (simultaneous correction) method. The MESH equations are reduced to a set of $N(2C + 1)$ nonlinear equations in the mass flow rates of liquid components l_{ij} and vapor components v_{ij} and the temperatures T_j. The enthalpies and equilibrium constants K_{ij} are determined by the primary variables l_{ij}, v_{ij}, and T_j. The nonlinear equations are solved by the

<u>Start</u>

Specify: all F_j, $z_{i,j}$, feed conditions (T_{F_j}, P_{F_j}, or H_{F_j}),

P_j, U_j, W_j; all Q_j except Q_1 and Q_N;

N; L, (reflux rate), V_1 (vapor distillate rate)

Set k = 1 (to begin first iteration)

1 | Initialize tear variables T_j, V_j

2 | Compute x from 13.198 by Thomas method

Set k = k + 1 (to begin next iteration)

Tridiagonal matrix equation evaluations (one component at a time)

3 | Normalize $x_{i',j}$ for each stage

$$x_{i,j} = x_{i,j} \bigg/ \sum_{i=1}^{C} x_{i,j}$$

4 | Compute new T_j from bubble-point, then $y_{i,j} = K_{i,j} x_{i,j}$

$$\sum_{i=1}^{C} K_{i,j} x_{i,j} - 1.0 = 0$$

8 | Adjust tear variables

5 | Compute Q_1, from 13.186 and Q_N from 13.201

Sequential evaluations (one equation at a time)

6 | Compute new V_j from 13.214 L_j from 13.196

7 | No — Not converged

$$\mathcal{T} = \sum_{j=1}^{N} [T_j^{(k)} - T_j^{(k-1)}]^2 \leq 0.01\ N\ ?$$

Yes — Converged → <u>Exit</u>

Figure 13.16. Algorithm of the BP (bubble-point) method for distillation separations [*Wang and Henke*, Hydrocarbon Processing **45**(*8, 155–166 (1963)*)); Seader and Henley, 1998].

Newton–Raphson method. A convergence criterion is made up of deviations from material, equilibrium, and enthalpy balances simultaneously, and corrections for the next iterations are made automatically. The method is applicable to distillation, absorption and stripping in single and multiple columns. The calculation flowsketch is in Figure (13.17). A brief description of the method also will be given. The availability of computer programs in the open literature was cited earlier in this section.

THE WANG–HENKE BUBBLE-POINT METHOD

The procedure is outlined in Figure 13.16. The input data are listed above Box 1 and include all external material and enthalpy flows except condenser and reboiler loads, the number of trays, the reflux rate, and the reboiler load. The process is iterative, starting with estimates of temperature and vapor flow rates on each tray and making successive improvements in these values until a convergence criterion on temperatures is satisfied.

Box 1. Initial estimates of the temperature are made by taking linear variation between estimated overhead dewpoint and bottoms bubblepoint. The vapor rates are estimated on the basis of constant molal overflow with due regard to input or output sidestreams.

Box 2. The system represented by the matrix Eq. (13.207) consists of linear equations that are solved for the liquid mol fractions x_{ij}.

Box 3. In general the mol fractions will not sum to unity, so that they are normalized as

$$(x_{ij})_{\text{normalized}} = x_{ij} \bigg/ \sum_{i=1}^{C} x_{ij}. \tag{13.208}$$
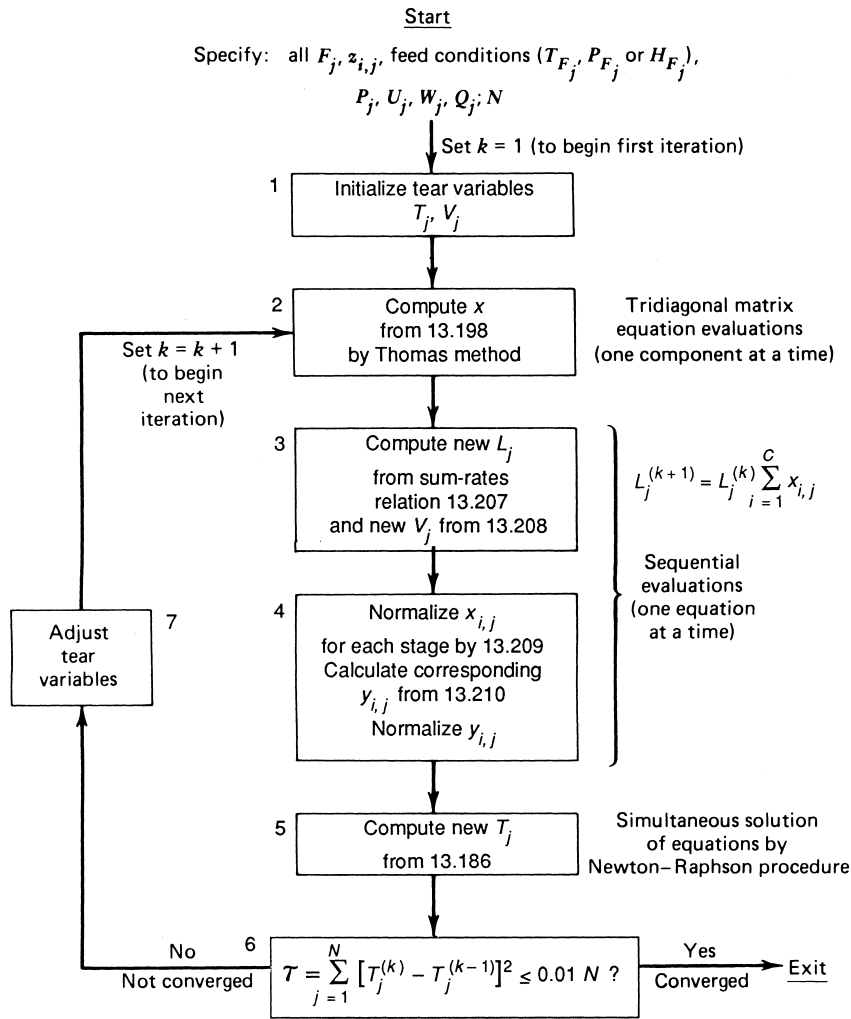
Figure 13.17. Algorithm for the SR (sum rates) method for absorbers and strippers [*Birnigham and Otto*, Hydrocarbon Processing **46**(*10*), *163–170* (*1967*); Seader and Healey, 1998].

Box 4. New values of the stage temperatures T_j are calculated as bubblepoints with the normalized x_{ij}. Initially the effect of vapor compositions y_{ij} on K_{ij} is ignored and the vapor compositions are found with

$$y_{ij} = K_{ij}x_{ij}. \tag{13.209}$$

Subsequently, the values of y_{ij} from the previous iteration can be used in the evaluation of K_{ij}.

Box 5. The enthalpies H_{vj} and H_{Lj} can be evaluated with Eqs. (13.199) and (13.200) since T_j, P_j, x_{ij}, and y_{ij} have been estimated. The condenser load Q_1 is figured with Eq. (13.195) and the reboiler load Q_N with Eq. (13.201).

Box 6. The new vapor rates V_j are found with the heat balances, Eqs. (13.210)–(13.214), and the new liquid rates with Eq. (13.196):

$$\alpha_j V_j + \beta_j V_{j+1} = \gamma_j, \tag{13.210}$$

where

$$\alpha_j = H_{L_{j-1}} - H_{V_j}, \tag{13.211}$$

$$\beta_j = H_{V_{j+1}} - H_{L_j}, \tag{13.212}$$

$$\gamma_j = \left[\sum_{m=1}^{j-1}(F_m - W_m - U_m) - V_1\right](H_{L_j} - H_{L_{j-1}}) \\ + F_j(H_{L_j} - H_{F_j}) + W_j(H_{V_j} - H_{L_j}) + Q_j, \tag{13.213}$$

$$V_j = \frac{\gamma_{j-1} - \alpha_{j-1}V_{j-1}}{\beta_{j-1}}. \tag{13.214}$$

Box 7. The convergence criterion imposes a tolerance on the differences between successive iterations of the temperatures

$$\tau = \sum_{1}^{N}(T_j^{(k)} - T_j^{(k-1)})^2 \leq 0.01N. \tag{13.215}$$

Box 8. If the criterion is not satisfied, the values of T_j found in Box 4 and the vapor rates V_j of Box 6 are the new starting values to be input to Box 2.

THE SR (SUM-RATES) METHOD

In this method, temperatures for succeeding iterations are found by enthalpy balances rather than by bubblepoint determinations, after new values of the liquid and vapor flow rates have been estimated from solution of the equations for the liquid mol fractions. This procedure is suited to absorption and stripping problems for which the BP method breaks down because of the wide range of relative volatilities involved. The algorithm appears in Figure 13.17. Input data are the same as for the BP method.

Box 1. Initial temperatures and vapor flow rates are estimated in the same way as in the BP method.

Box 2. The mol fractions are found by solution of the tridiagonal matrix as in the BP method.

Box 3. At this point the x_{ij} are not normalized but their sum is applied to estimate new liquid flow rates from the relation

$$L_j^{(k+1)} = L_j^{(k)} \sum_{i=1}^{C} x_{ij}. \tag{13.216}$$

The corresponding vapor rates are obtained by the material balance, which is a rearrangement of Eq. (13.196),

$$V_j = L_{j-1} - L_N + \sum_{m=j}^{N} (F_m - W_m - U_m). \tag{13.217}$$

Box 4. Then the x_{ij} are normalized by

$$(x_{ij})_{\text{normalized}} = x_{ij} / \sum_{i=1}^{C} x_{ij}; \tag{13.218}$$
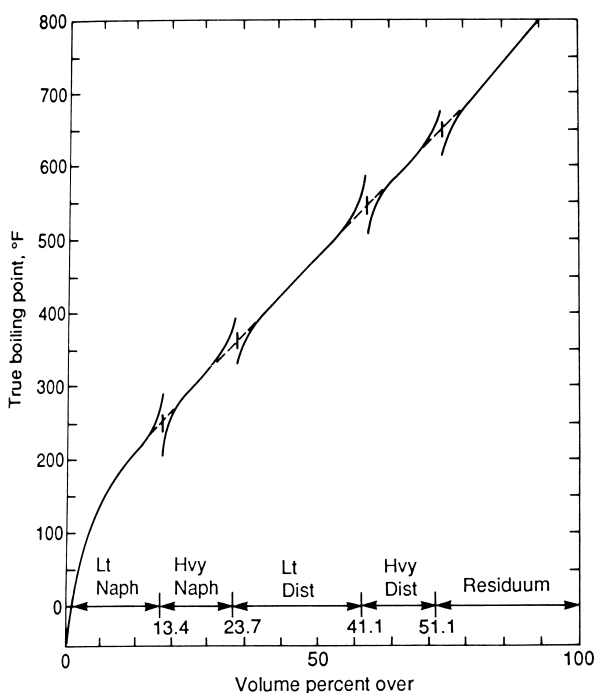
Figure 13.18. True boiling point (TBP) curve of a crude oil, with superimposed TBP curves of five fractions into which it is separated by a typical fractionating system like that of Figure 13.20. The separations are not sharp, with as much as 50°F difference between the end point of a light product and the initial of the next heavier one. It is common to speak of the gap between the 95 and 5% points rather than the end points.

the values of y_{ij} are obtained by

$$y_{ij} = K_{ij} x_{ij} \tag{13.219}$$

and also normalized,

$$y_{ij} = y_{ij} / \sum_{i=1}^{C} y_{ij}. \tag{13.220}$$

When the K_{ij} depend on the vapor phase compositions, values of y_{ij} from the previous iteration are used.

Box 5. New temperatures are calculated from the enthalpy balances Eq. (13.195). The temperature is implicit in these equations because of its involvement in the enthalpies and the K_{ij}. Accordingly, the temperature must be found by the Newton–Raphson method for simultaneous nonlinear equations.

Box 6. The convergence criterion is

$$\tau = \sum (T_j^{(k)} - T_j^{(k-1)})^2 \leq 0.01N? \tag{13.221}$$

Box 7. If the convergence criterion is not satisfied, the values of V_j from Box 3 and the temperatures from Box 5 are input to Box 2.

SC (SIMULTANEOUS CORRECTION) METHOD

A brief description of this procedure is abstracted from the fuller treatment of Seader and Henley (1998). The MESH equations 13.191–13.195 in terms of mol fractions are transformed into equations with molal flow rates of individual components in the liquid phase l_{ij} and vapor phase v_{ij} as the primary variables. The relations between the transformed variables are in this list:

$$L_j = \sum_{i=1}^{C} l_{ij}, \quad V_j = \sum_{i=1}^{C} v_{ij}, \quad x_{i,j} = \frac{l_{i,j}}{L_i}, \quad y_{ij} = \frac{v_{ij}}{V_i},$$

$$f_{ij} = F_j z_{ij}, \quad s_j = U_j / L_j, \quad S_j = W_j / V_j. \tag{13.222}$$

The balance equations become three groups totalling $N(2C + 1)$ in number:

Material balance:

$$M_{i,j} = l_{i,j}(1 + s_j) + v_{ij}(1 + S_j) - l_{ij-1} - v_{ij+1} - f_{ij} = 0. \tag{13.223}$$

Phase equilibria:

$$E_{i,j} = K_{ij} l_{ij} \frac{\sum_{\kappa=1}^{C} v_{\kappa j}}{\sum_{\kappa=1}^{C} l_{\kappa j}} - v_{ij} = 0. \tag{13.224}$$

Energy balance:

$$H_j = H_{L_j}(1 + s_j) \sum_{i=1}^{C} l_{ij} + H_{V_j}(1 + S_j) \sum_{i=1}^{C} v_{ij} - H_{L_{j-1}} \sum_{i=1}^{C} l_{ij-1}$$

$$- H_{V_{j+1}} \sum_{i=1}^{C} v_{ij+1} - H_{F_j} \sum_{i=1}^{C} f_{ij} - Q_j = 0. \tag{13.225}$$

When N and all f_{ij}, P_F, P_j, s_j, S_j, and Q_i are specified, there remain $N(2C + 1)$ unknowns, the same as the number of MESH equations (13.223–13.225). They are nonlinear equations in the primary variables l_{ij}, v_{ij}, and T_j for $i = 1$ to C and $j = 1$ to N. The T_j are involved implicitly in equations for the enthalpies and equilibrium constants.

The convergence criterion adopted is

$$\tau_3 = \sum_{j=1}^{N} \left\{ (H_j)^2 + \sum_{i=1}^{C} [(M_{ij})^2 + (E_{ij})^2] \right\} \leq \varepsilon_3$$

$$= N(2C+1) \left(\sum_{j=1}^{N} F_j^2 \right) 10^{-10}. \qquad (13.226)$$

It will ensure that the converged variables will be accurate to generally at least four significant figures.

The algorithm of the procedure is in Figure 13.19.

Box 1. Initial estimates of the stage temperatures are taken from linear variations between estimated overhead dewpoint and bottoms bubblepoint temperatures. Those of the vapor rates are based on the assumption of constant molal overflow with due regard to sidestreams, and those of the liquid rates are made consistent with the material flow balances.

Box 2. With the initializations of Box 1, the matrix of the MESH equations is tridiagonal like Eq. (13.207) and may be solved for the l_{ij} and v_{ij} by the Thomas algorithm.

Box 3. Evaluate the discrepancy function made up of deviations from zero of the mass M, equilibrium E, and enthalpy H functions of Eqs. (13.223)–(13.225):

$$\tau_3 = \sum_{j=1}^{N} \left\{ (H_j)^2 + \sum_{i=1}^{C} [(M_{ij})^2 + (E_{ij})^2] \right\}. \qquad (13.227)$$

Box 4. The discrepancy function τ_3 is compared with the tolerance ε_3

$$\varepsilon_3 = N(2C+1) \left(\sum_{j=1}^{N} F_j^2 \right) 10^{-10}. \qquad (13.228)$$

If $\tau_3 \leq \varepsilon_3$, the process has converged and final data are evaluated in Boxes 5 and 6. If $\tau_3 > \varepsilon_3$, proceed to the next iteration by way of Box 7.

Box 5. The total flow rates are found by summing up the component flow rates

$$L_j = \sum_{i=1}^{C} l_{ij} \qquad (13.229)$$
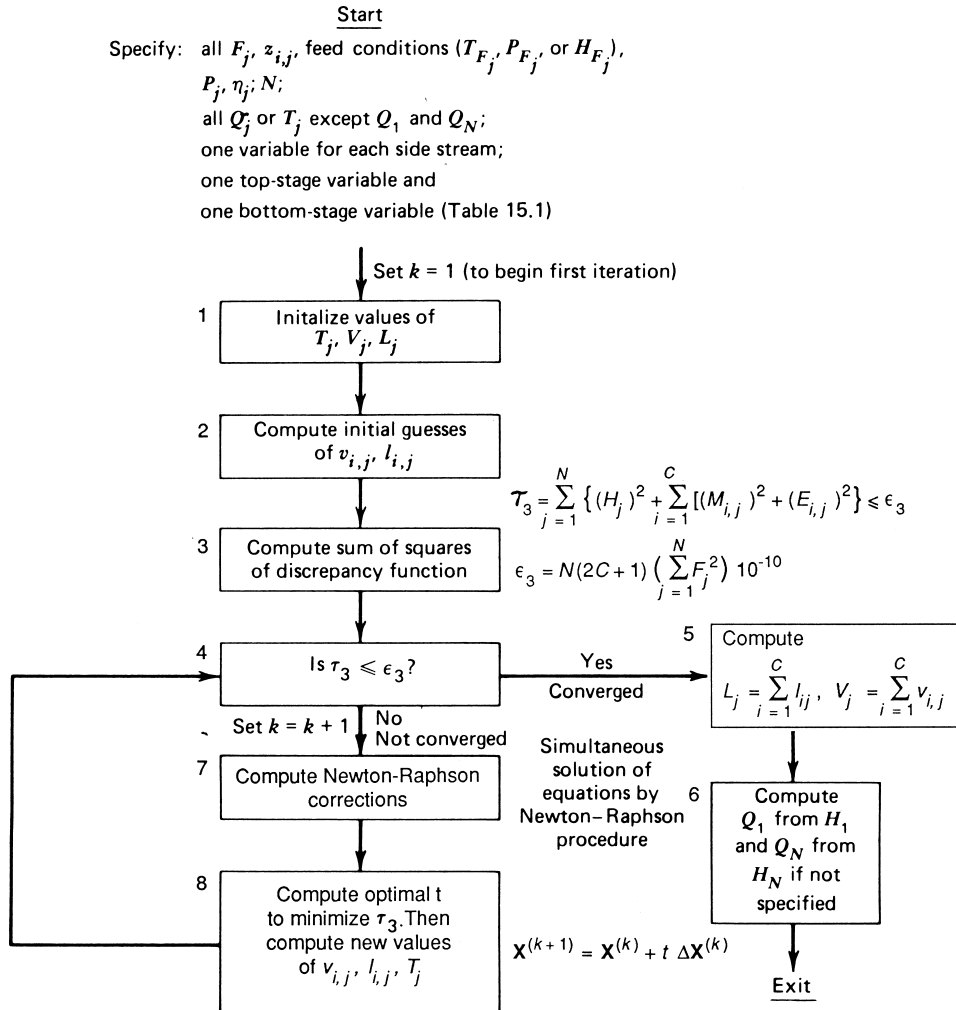
Figure 13.19. Algorithm of the SC (simultaneous correction) method for all multistage separations of fluid mixtures [*Naphthali and Sandholm*, AIChE J. **17**, *148* (*1971*); Seader and Henley, 1998].
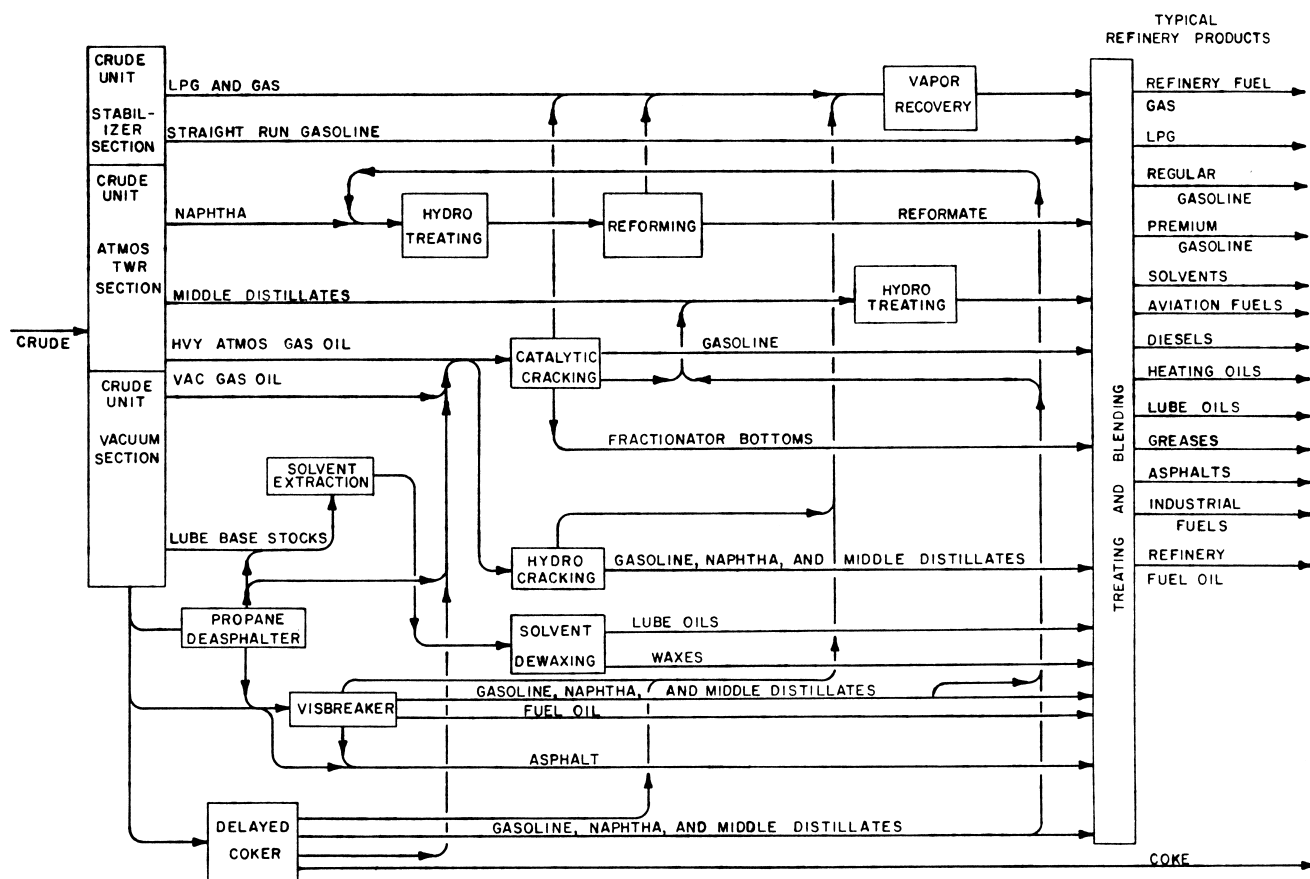
Figure 13.20. Petroleum refinery block diagram. Several of the processes identified by blocks include distillation or are followed by distillation (*Gary and Handwerk*, Petroleum Refining, *Dekker, New York, 1975*).

and

$$V_j = \sum_{i=1}^{C} v_{ij}. \tag{13.230}$$

Box 6. Evaluate condenser and reboiler loads by heat balances if they have not been specified.

Box 7. When $\tau_3 > \varepsilon_3$, corrections to the l_{ij}, v_{ij}, and T_j are calculated from the nonlinear MESH equations by the Newton–Raphson method. In these equations the enthalpies and equilibrium constants usually are nonlinear functions of the temperatures.

Box 8. Employ a process for evaluating the optimum fraction of a calculated correction of each variable to be applied to the next trial. That is,

$$(\Delta a)_{\text{optimum}} = t(\Delta a)_{\text{calculated}}, \quad 0 < t \leq 1. \tag{13.231}$$

The selection process is described by Henley and Seader. The optimally corrected values of l_{ij}, v_{ij}, and T_j are input to Box 4 for the next iteration.

13.11. SPECIAL KINDS OF DISTILLATION PROCESSES

Conditions sometimes exist that may make separations by distillation difficult or impractical or may require special techniques. Natural products such as petroleum or products derived from vegetable or animal matter are mixtures of very many chemically unidentified substances. Thermal instability sometimes is a problem. In other cases, vapor–liquid phase equilibria are unfavorable. It is true that distillations have been practiced successfully in some natural product industries, notably petroleum, long before a scientific basis was established, but the designs based on empirical rules are being improved by modern calculation techniques. Even unfavorable vapor–liquid equilibria sometimes can be ameliorated by changes of operating conditions or by chemical additives. Still, it must be recognized that there may be superior separation techniques in some cases, for instance, crystallization, liquid–liquid extraction, supercritical extraction, foam fractionation, dialysis, reverse osmosis, membrane separation, and others. The special distillations exemplified in this section are petroleum, azeotropic, extractive, and molecular distillations.

PETROLEUM FRACTIONATION

Crude oils are mixtures of many substances, mostly unidentified chemically, that cover a boiling range of less than 0°F to more than 1000°F. Lower molecular weight substances are identifiable and may be recovered as pure substances, but the usual products of petroleum fractionation are mixtures with relatively narrow boiling ranges that have found consumer acceptance as final products or are suitable for further processing in the plant. On the typical refinery flow diagram of Figure 13.20, several of the processes represented as blocks either involve or are followed by distillation.

Important properties of petroleum and its fractions are measured by standardized procedures according to the API or ASTM.

A particularly distinctive property is the true boiling point (TBP) curve as a function of the volume percent distilled under standardized conditions. Figure 13.18 is the TBP curve of a whole crude on which are superimposed curves of products that can be taken off sidestreams from a main distillation column, as in Figure 13.20. As samples of the distillate are collected, their densities and other properties of interest also are measured. The figure with Example 13.14 is of such measurements.

A representative petroleum fractionation process is summarized on Figure 13.20. Steam stripping of the sidestreams removes light ends and narrows the 95–5% temperature gap discussed in Example 13.14. The only source of heat supply to the column is at the feed point. A sufficient portion of the feed must be vaporized to be equivalent to the sum of all the products removed from the column above the feed point. Usually an additional amount of 2–5%, called overflash, may be needed to cover heat losses and reflux requirements. Because of the large temperature gradient and the high temperatures, the vapor volumes are large and also change greatly as the temperature falls along the column and sidestreams are withdrawn. Optimization of the size and cost of the fractionator usually requires removal of heat and provision of reflux at intermediate points rather than exclusively at the top as in most distillations, despite the need for additional trays to maintain efficient fractionation. The vapor rates at sidestream drawoffs usually are critical ones so they are checked by heat balances. Empirical rules have been developed for reflux ratios at drawoffs that ensure quality of these products.

The older, empirical practices for the design and operation of petroleum fractionators are stated in books such as that of Nelson (*Petroleum Refinery Engineering*, McGraw-Hill, New York, 1958). Some such rules are collected in Table 13.6. A coverage of this subject is by Watkins (*Petroleum Refinery Distillation*, 1979), and an estimation procedure for distillations of naphthas without sidestreams is described by Broughton and Uitti [*Encycl. Chem. Process. Des*. **16,** 186–198 (1982)]. An engineer versed in these techniques can prepare a near optimum design in a few days. For the most part, nowadays, only rough estimates of tray numbers and heat balances need be made as starting estimates for eventual computer design of the process.

The basis of the fractionation design is the true boiling point curve. This is replaced by a stepped curve made up of fractions boiling over ranges of 10–25°F. The lighter components up to pentanes or hexanes are treated as such, but the other components are pseudocomponents characterized by their average boiling points, specific gravities, molecular weights, and other properties necessary to calculation of the distillation behavior. For full range crude oil fractionation, as many as 50 pseudocomponents may be required to represent the real TBP curve. In the case of naphtha fractionators without sidestreams, 20 pseudocomponents may be sufficient. Calculated compositions of products in terms of pseudocomponents can be reconstituted into smooth TBP curves to ensure that conventional specifications such as initial and final boiling points are met. The operation of converting a mixture characterized by TBP and specific gravity curves into a mixture of a discrete number of components with compositions expressed in mol fractions is performed in Example 13.14.

EXTRACTIVE DISTILLATION

In such a process an additive or solvent of low volatility is introduced in the separation of mixtures of low relative volatilities or for concentrating a mixture beyond the azeotropic point. From an extractive distillation tower, the overhead is a finished product and the bottoms is an extract which is separated down the line into a product and the additive for recycle. The key property of the additive is that it enhances the relative volatilities of the substances to be separated. From a practical point of view, the additive should be stable, of low cost, require moderate reboiler temperatures particularly for mixtures subject to polymerization or thermal degradation, effective in low to moderate concentrations, and easily recoverable from the extract. Some common additives have boiling points 50–100°C higher than those of the products.

Selection of an Additive. Ultimately the choice of an extractive distillation solvent will require a certain amount of experimental work, but some screening process should be employed to limit its scope. Examination of solvents that are being used or have been studied for successful commercial operations is a starting point. Some rules involving similarities or differences in polarities or hydrogen bonding have been proposed. The less soluble of a pair of substances usually will have the enhanced volatility. Accordingly, a comparison of solubility parameters may be a guide: A good additive should have a solubility parameter appreciably different from one of the components and closer to that of the other. Such an explanation may be correct for the enhancement of the volatility of isooctane (7.55) relative to that of toluene (8.91) in the presence of phenol (12.1) or aniline (11.5), both of which are commercially feasible additives. The data of Figure 13.22(a) do show that the volatility of isooctane is enhanced by the presence of phenol. The numbers in parentheses are the solubility parameters. In the case of acetone (9.8), chloroform (9.3), and methyl-isobutylketone (8.3), the data of Figure 13.22(b) show that chloroform has the enhanced volatility, although its solubility parameter is closer to that of the solvent. A possible interpretation of the data is that association of the ketones as a consequence of their hydrogen bonding capabilities reduces the volatility of the acetone. Explanations of the effects of dissolved solids, as in Figures 13.22(c) and (d), are more obscure, although a substantial number of other cases also is known.

Measurements of binary vapor-liquid equilibria can be expressed in terms of activity coefficients, and then correlated by the Wilson or other suitable equation. Data on all possible pairs of components can be combined to represent the vapor–liquid behavior of the complete mixture. For exploratory purposes, several rapid experimental techniques are applicable. For example, differential ebulliometry can obtain data for several systems in one laboratory day, from which infinite dilution activity coefficients can be calculated and then used to evaluate the parameters of correlating equations. Chromatography also is a well-developed rapid technique for vapor–liquid equilibrium measurement of extractive distillation systems. The low-boiling solvent is deposited on an inert carrier to serve as the adsorbent. The mathematics is known from which the relative volatility of a pair of substances can be calculated from the effluent trace of the elutriated stream. Some of the literature of these two techniques is cited by Walas (1985, pp. 216–217).

Some Available Data. A brief list of extractive distillation processes of actual or potential commerical value is in Table 13.7; the column of remarks explains why this mode of separation is adopted. The leading applications are to the separation of close-boiling aromatic, naphthenic, and aliphatic hydrocarbons and of olefins from diolefins such as butadiene and isoprene. Miscellaneous separations include propane from propylene with acrylonitrile as solvent (DuPont, U.S. Pat. 2,980,727) and ethanol from isopropanol with water as solvent [Figure 13.23 (b)].

Earlier explorations for appropriate solvents may have been conducted by the Edisonian technique of trying whatever was on the laboratory shelves. An extensive list of mixtures and the extractive distillation solvents that have been studied is in the book of

EXAMPLE 13.14
Representation of a Petroleum Fraction by an Equivalent Number of Discrete Components

The true boiling point and specific gravity variation with the volume percent distilled are found by standard ASTM procedures. In the present case, the smooth TBP curve is replaced by a stepped curve of eleven pseudo components characterized by their 50% boiling points and specific gravities. Their molecular weights are

obtained with the general correlation of Figure (c); then the mol fractions are calculated. Vaporization equilibrium ratios and relative volatilities can be read off equilibrium value charts, which are available for higher boiling ranges than this one. Then any required distillation can be calculated by any suitable standard method.
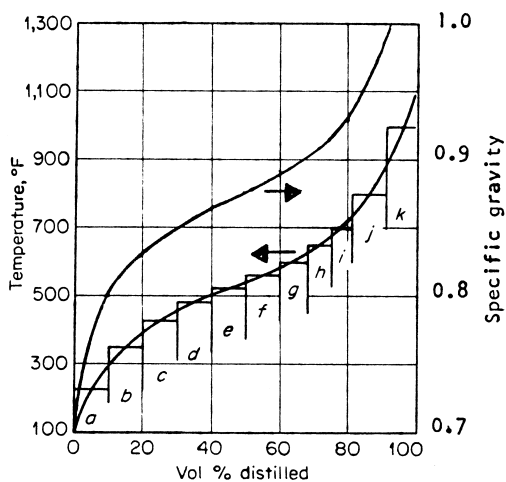
(a)

Component	Vol %	TBP 50% t, F	ρ, g/cu cm	Mol. weight	Mol. frac.
a	10	225	0.745	102	0.1730
b	10	350	0.815	141	0.1370
c	10	430	0.842	165	0.1215
d	10	485	0.860	192	0.0990
e	10	528	0.870	210	0.0987
f	10	565	0.880	227	0.0920
g	8	600	0.896	242	0.0705
h	7	650	0.913	270	0.0562
i	6	700	0.930	300	0.0434
j	10	800	0.955	353	0.0641
k	9	1000	1.030	485	0.0450
					1.0000

(b)
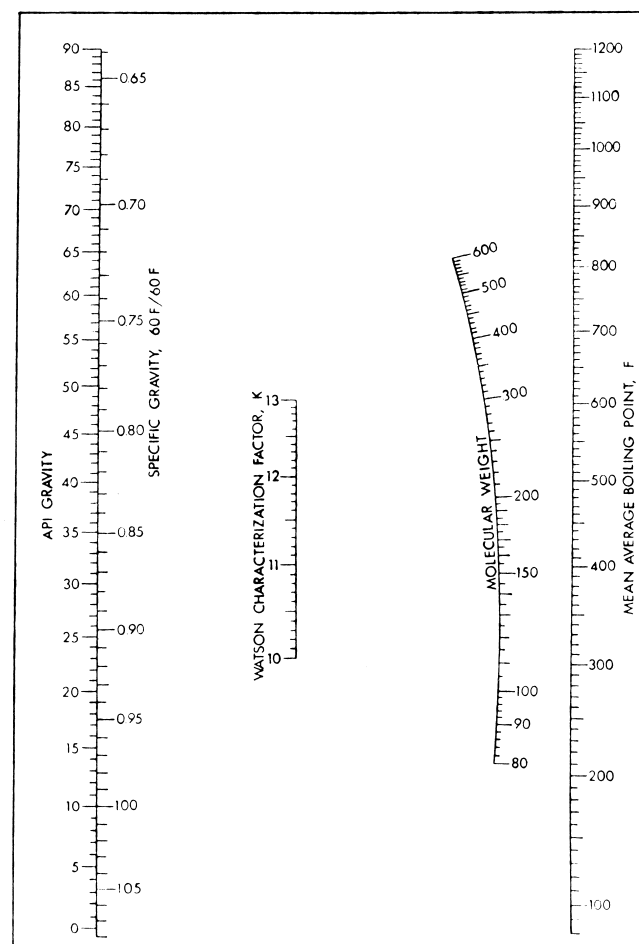
(c)

(a) Experimental true boiling point and specific gravity curves, and the equivalent stepped curve. (b) Mol fraction composition of the 11 pseudo components with equivalent vaporization behavior. (c) Standard correlations of properties of petroleum fractions.

Kogan (*Azeotropic and Extractive Distillation*, Leningrad, 1971, pp. 340–430, in Russian).

Some of the many solvents that have been examined for certain hydrocarbon separations are listed in Table 13.8; part (c) for *n*-butane and butene-2 separations includes data showing that

addition of some water to the solvent enhances the selectivity. The diolefins butadiene and isoprene are available commercially as byproducts of cracking operations and are mixed with other close-boiling saturated, olefinic and acetylenic hydrocarbons, often as many as 10–20 different ones. The most widely used
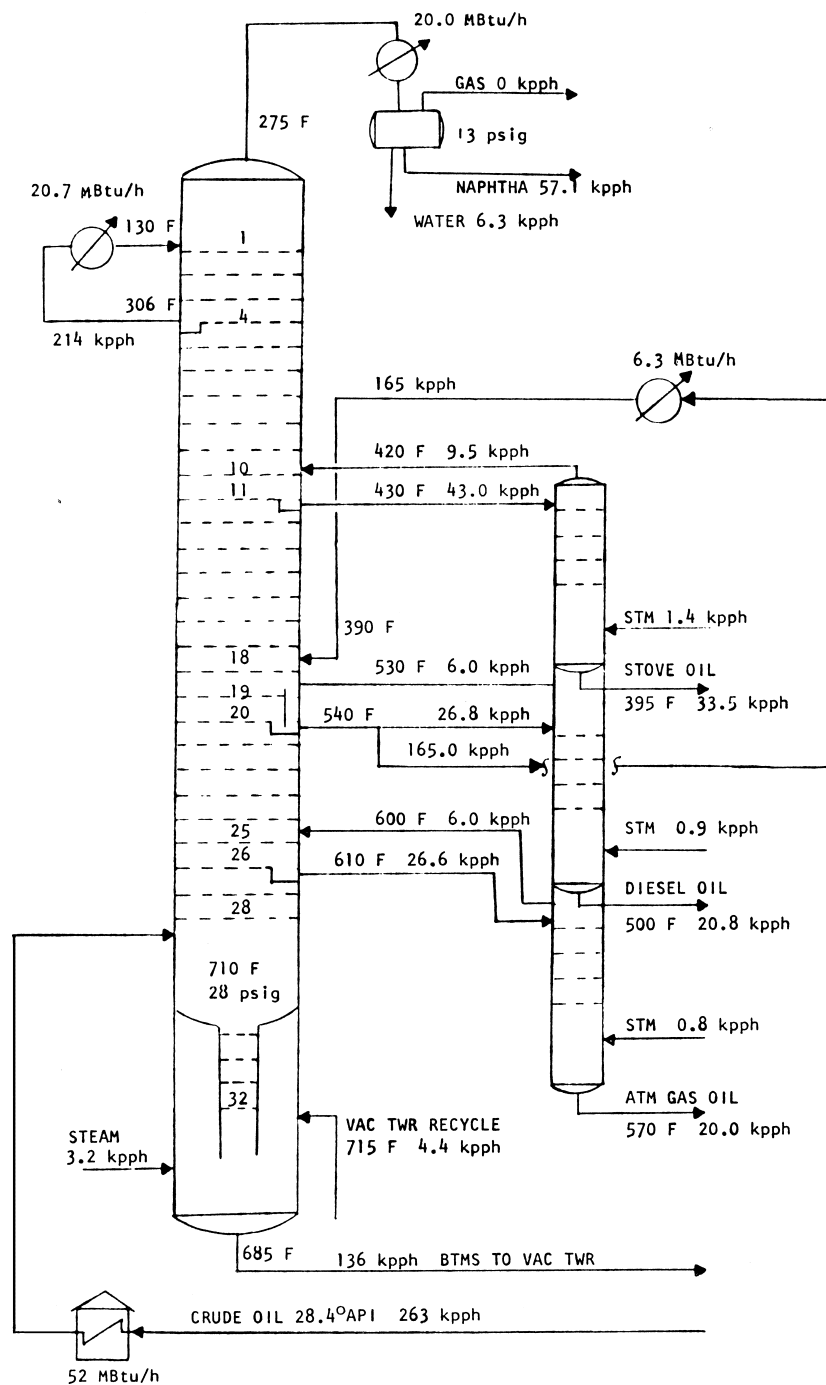
Figure 13.21. Material and energy flows in distillation of 20,000 BPSD (263,000 lb/hr) of 28.4° API crude oil into five products. The main tower is 11 ft dia by 94 ft TT, and the stripper is 3 ft dia by 54 ft TT.

extractive solvents are *n*-methylpyrrolidone (NMP), dimethylformamide (DMF), furfural and acetonitrile (ACN), usually with 10–20% water to improve selectivity, although at the expense of reduced solvent power and the consequent need for a greater proportion of solvent. A few of the many available data for these important separations appear in Figure 13.22 (f) and Table 13.9. They show the effects of hydrocarbon proportions, the content of solvent, and the concentration of water in the solvent. Sufficient

data are available for the major pairs of commercial mixtures to permit evaluation of parameters of the Wilson or other equations for activity coefficients in multicomponent mixtures, and thus to place the design of the equipment on a rational basis. Another distinction between possible additives is their solvent power. Table 13.10, for example, shows that diolefins are much more soluble in DMF than in ACN, and thus DMF circulation need be less.

TABLE 13.6. Some Rules for Design and Operation of Petroleum Fractionators

(a) Draw Tray Temperature T_{dt} as a Function of the Bubblepoint T_{bp} of the Stream:

$$T_{dt} = \begin{cases} \exp\,(0.0040\,T_{bp} + 4.404), & 200 \leq Tbp \leq 325\ °F \\ \exp\,(0.002952\,T_{bp} + 4.744), & 325 \leq Tbp \leq 600\ °F \end{cases}$$

(b) Gap and Overlap of Top and Sidestream Products in Terms of Reflux and Plates
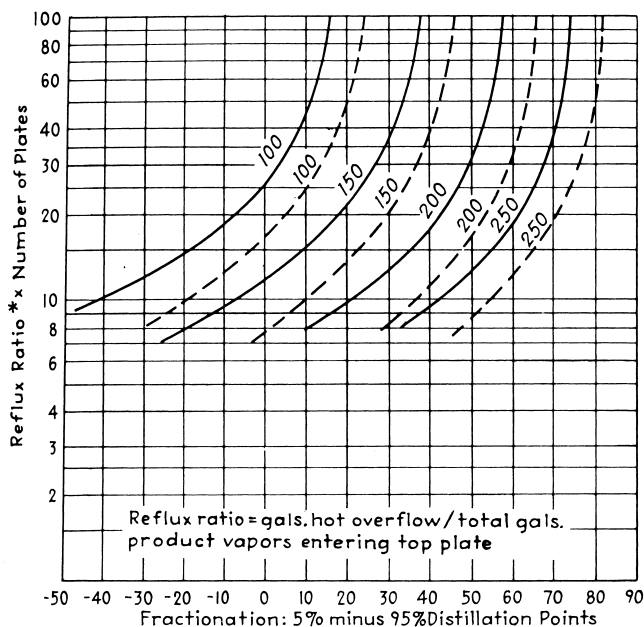
(c) Gap and Overlap between Sidestream Products in Terms of Reflux and Plates
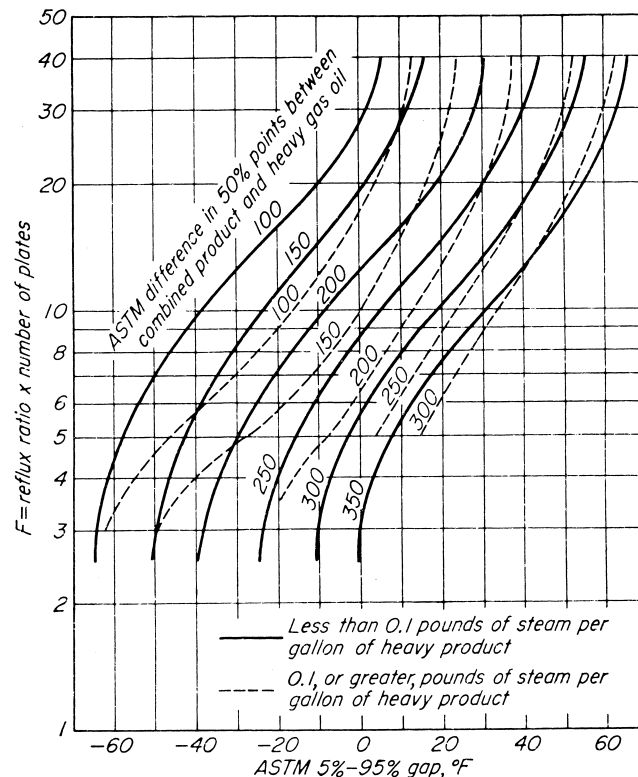
Numbers on the streams are °F differences between the 50% points of the streams. Dashed lines are with stripping steam, full ones without [Packie, *Trans. AIChE* **37**, 51 (1941)].

(d) Number of Trays between Drawoffs

Separation	Number of Trays
Light naphtha to heavy naphtha	6 to 8
Heavy naphtha to light distillate	6 to 8
Light distillate to heavy distillate	4 to 6
Heavy distillate to atmospheric gas oil	4 to 6
Flash zone to first draw tray	3 to 4
Steam and reboiled stripping sections	4

(e) Normal Stripping Steam Usage

Product	lb Steam/gal
Naphtha	0.2–0.5
Kerosene or diesel fuel	0.2–0.6
Gas oil	0.1–0.5
Neutral oils	0.4–0.9
Topped crude oil	0.4–1.2
Residual cylinder stock	1.0 up

(f) Superficial Linear Velocities in Towers

Operation	Pressure (psia or mm)	Tray Spacing (in.)	Superficial Tower Velocity (ft/sec)
Topping	17 lb	22	2.6–3.3
Cracking	40 lb	22	1.5–2.2
Pressure dist. rerun	20 lb	22	2.8–3.7[a]
Solution rerun	25 lb	22	2.8–3.5
Pressed dist. rerun	25 lb	22	2.8–3.9[a]
Pressed dist. rerun	60 mm	24	6.0–9.0
Vacuum	30 mm	30	9.0–12.0
Vacuum	90 mm	24	5.0–8.0
Stabilizer	160 lb	18	2.2–2.8
Nat. gaso. absorber	50 lb	14	1.0–1.3
Nat. gaso. absorber	400 lb	18	0.5–0.8

[a] Greatly dependent on quantity of steam.

(g) Pressure Drop 0.1–0.2 psi/tray

(h) Overflash into Tower Feed Zone is 2–5%

(a)

(b)

(c)

(d)

(e)

(f)
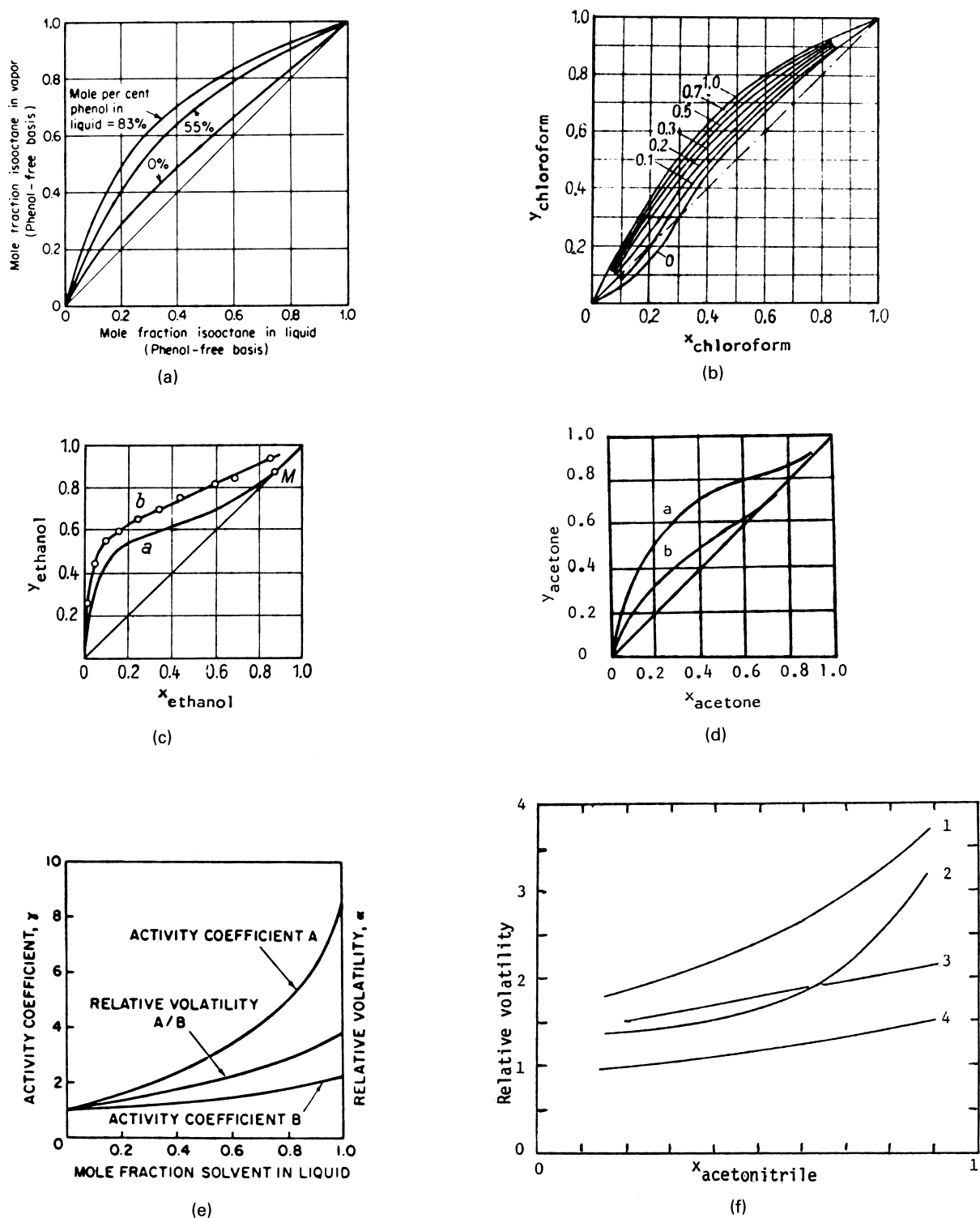
Figure 13.22. Examples of vapor–liquid equilibria in presence of solvents. (a) Mixture of i-octane and toluene in the presence of phenol. (b) Mixtures of chloroform and acetone in the presence of methylisobutylketone. The mole fraction of solvent is indicated. (c) Mixture of ethanol and water: (a) without additive; (b) with $10\,\mathrm{gCaCl_2}$ in $100\,\mathrm{mL}$ of mix. (d) Mixture of acetone and methanol: (a) in $2.3M$ $CaCl_2$; (b) salt-free. (e) Effect of solvent concentration on the activity coefficients and relative volatility of an equimolal mixture of acetone and water (*Carlson and Stewart, in Weissbergers Technique of Organic Chemistry IV, Distillation, 1965*). (f) Relative volatilities in the presence of acetonitrile. Compositions of hydrocarbons in liquid phase on solvent-free basis: (1) 0.76 isopentane + 0.24 isoprene; (2) $0.24iC_5 + 0.76\,\mathrm{IP}$; (3) $0.5iC_5 + 0.5$ 2-methylbutene-2; (4) 0.25–0.76 2MB2 + 0.75–$0.24\,\mathrm{IP}$ [*Ogorodnikov et al., Zh. Prikl. Kh.* **34**, *1096–1102 (1961)*].

TABLE 13.7. Examples of Extractive Distillation Processes for the Separation of Ideal, Nonideal, and Azeotropic Systems

Additive	Mixture To Be Separated	ΔT (°C)[a]	Remarks
Aniline	n-heptane–methylcyclohexane	2.7	ideal mixture ($\alpha = 1.07$)
	benzene–cyclohexane	0.7	azeotrope
	n-heptane–toluene	12.8 ⎫	
			non-ideal mixtures;
Phenol	n-heptane–toluene	12.8 ⎬	asymptotic approach of
	iso-octane–toluene	11.4	equilibrium curve to
	methylcyclohexane–toluene	9.5 ⎭	diagonal
Ethyleneglycol monobutylether	methylethylketone–water	20.4	azetrope
Diethylether	ethanol–water	21.6	azeotrope
Higher ketones and alcohols	acetone–methanol	8.5	azeotrope
Higher esters and alcohols	ethylacetate–ethanol	1.3	azeotrope
Higher ketones and chloro compounds	acetone–chloroform	5.0	azetrope

[a] ΔT is the difference in atmospheric boiling points, °C.
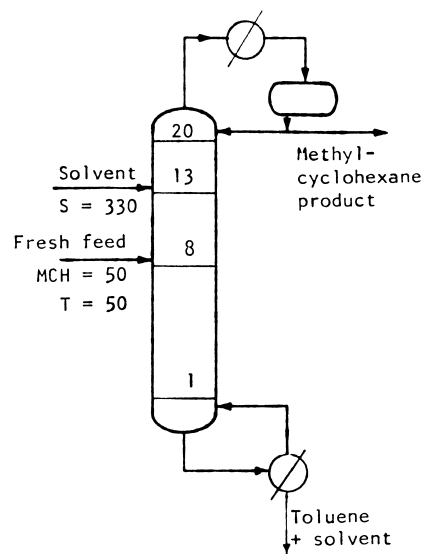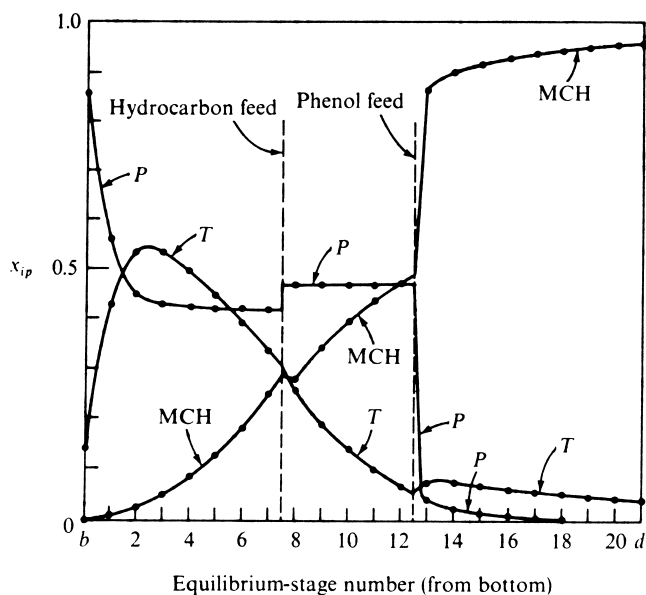
(a)
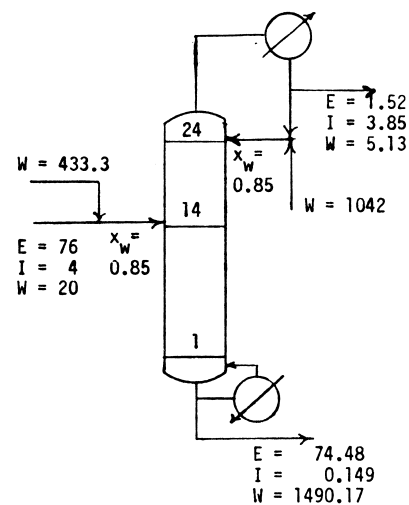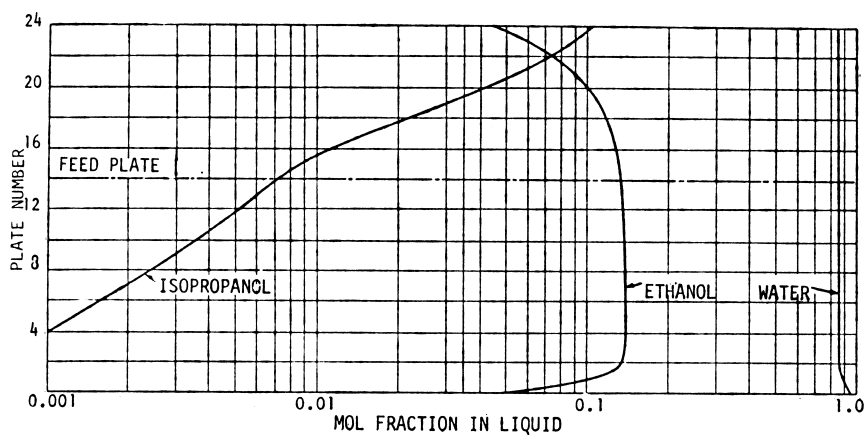
(b)

Figure 13.23. Composition profiles and flowsketches of two extractive distillation processes. (a) Separation of methylcyclohexane and toluene with phenol as solvent (*data calculated by Smith, 1963*). (b) Separation of aqueous ethanol and isopropanol, recovering 98% of the ethanol containing 0.2 mol% isopropanol, employing water as the solvent. Flow rates are in mols/hr (*data calculated by Robinson and Gilliland, 1950*).

Calculation Methods. An often satisfactory approximation is to take the mixture in the presence of the solvent to be a pseudo-binary of the keys on a solvent-free basis, and to employ the McCabe–Thiele or other binary distillation method to find tray and reflux demands. Since the relative volatility varies with concentration of the solvent, different equilibrium curves are used for above and below the feed based on average loads in those zones. Figure 13.24 is of such a construction.

When data of activity coefficients of all pairs of components are known, including those with the solvent, any of the standard calculation procedures for multicomponent distillation, which include ternaries, may be used. Composition profiles found by tray-by-tray calculations in two cases appear in Figure 13.24.

To the number of trays found by approximate methods, a few trays are added above the solvent feed point in order to wash back any volatilized solvent. Nonvolatility is a desirable property, but most otherwise suitable solvents do have appreciable volatilities.

Extractive Distillation Recovery of Isoprene. A typical flow-sketch and material balance of distillation and solvent recovery towers for extracting isoprene from a mixture of cracked products with aqueous acetonitrile appears in Figure 13.25. A description of the flowsheet of a complete plant is given in Example 2.9. In spite of the fact that several trays for washing by reflux are provided, some volatilization of solvent still occurs so that the complete plant also has water wash columns on both hydrocarbon product streams. A further complication is that acetonitrile and water form an azeotrope containing about 69 mol % solvent. Excess water enters the process in the form of a solution to control poly-

TABLE 13.8 Relative Volatilities of Three Binary Systems and Their Enhancement in the Presence of Several Solvents

(a) *n*-Heptane/Methylcyclohexane with Relative Volatility of 1.07

Solvent	Mole per cent in liquid phase	T, °C. (av.)	Av. rel. volatility, α_S	Improvement factor, α_S/α	Ref. No.
Aniline	92	139	1.52	1.42	1
	78	121	1.40	1.31	1
	70	110	1.27	1.19	2
	58	113	1.26	1.18	1
Furfural	79	—	1.35	1.26	1
Phenol.	81	—	1.31	1.24	1
Nitrobenzene	82	—	1.31	1.24	1
Dichlorodiethyl ether . . .	81	—	1.28	1.20	1
Aminocyclohexane	76	—	1.16	1.08	1
Pyridine	70	—	1.4	1.31	2
Ethanol	70	—	1.3	1.21	2
n-Butanol	70	—	1.3	1.21	2
tert-Butanol	70	—	1.25	1.17	2
Acetic acid	70	—	1.27	1.19	2
None	—	—	1.07	1.00	2

[1] Griswold, Andres, Van Berg, and Kasch, *Ind. Eng. Chem.*, 38, 66 (1946).
[2] Fenske, Carlson, and Quiggle, *Ind. Eng. Chem.*, 39, 1322 (1947).

(b) Cyclohexane/Benzene with Relative Volatility of 1.02

Solvent	Mole per cent in charge	T, °C.	Relative volatility, α_S	Improvement factor, α_S/α
Acetic acid	69.0	84	1.75	1.78
Methanol	67.3	53	1.58	1.61
Ethanol	67.3	65	1.36	1.38
n-Propanol	70.5	79	1.26	1.28
Isopropanol	67.9	70	1.22	1.24
Dioxane	67.4	86	1.75	1.78
Chlorex (dichlorodiethyl ether) . . .	67.5	105	2.31	2.36
Methyl Cellosolve	66.7	85	1.84	1.88
Cellosolve.	67.5	95	1.58	1.61
Carbitol.	66.8	87	1.99	2.03
Acetone	66.3	55	2.03	2.07
Methyl ethyl ketone.	65.1	72	1.78	1.81
Diacetone	67.3	89	1.82	1.85
Pyridine	66.9	93	1.83	1.86
Aniline	66.8	93	2.11	2.16
Nitromethane.	67.8	74	3.00	3.06
Nitrobenzene	68.2	102	2.25	2.30
Acetonitrile.	67.3	65	2.85	2.92
Furfural.	67.1	79	3.10	3.16
Phenol.	66.8	92	2.01	2.05

Updike, Langdon, and Keyes, *Trans. Am. Inst. Chem. Engrs.*, 41, 717 (1945).

(c) Butane/2-Butene with Relative Volatility of about 1.08.[a] The asterisks denote that data are included for both dry and wet solvents

Solvent	Vol/vol HC	Temperature, °F	$\alpha = \gamma c_4 / \gamma c_{4-}$
Hydroxyethylacetate	4	133	1.54
Methylsalicylate	2	156	1.46
Dimethylphthalate	2	142	1.41
Ethyl oxalate	2	154	1.38
Carbitolacetate	2	160	1.35
Diethyl carbonate	2	172	1.28
Amylacetate	2	180	1.21
* Acetonitrile	2	137	1.49
Butyronitrile	2	161	1.42
Acrylonitrile	2	156	1.23
Acetonyl acetone	2	141	1.43
Cyclohexanone	2	171	1.32
Acetophorone	2	145	1.31
Methylhexyl ketone	2	166	1.27
Methylamyl ketone	2	173	1.23
Methylisobutyl ketone	2	171	1.23
Methyldiisobutyl ketone	2	177	1.18
Nitromethane	1.8	134	1.60
Nitroethane	2	146	1.46
1-Chloro-1-nitropropane	2	155	1.46
Nitrobenzene	2	150	1.41
o-Nitrotoluene	2	155	1.38
o-Nitroanisole	2	130	1.30
n-Formylmorpholine	4.6	133	1.60
Morpholine	2	160	1.41
Pyridine	2	176	1.35
Quinoline	2	148	1.33
Picoline	2	188	1.29
Benzyl alcohol	3	144	1.48
* Phenol	2	138	1.47
Diacetone alcohol	2	146	1.32
Butyl alcohol	2	152	1.21
2-Ethyl butyl alcohol	2	161	1.20
o-Hexanol	2	159	1.18
tert-Butyl alcohol	2	154	1.16
Benzaldehyde	2	145	1.42
* Furfural	3	158	1.40
3,4-Diethoxybenzaldehyde	2	125	1.11
Butyraldehyde	2	165	1.09
* Aniline	3	130	1.65
o-Chloroaniline	2	152	1.44
Methylaniline	2	146	1.42
o-Toluidine	2	148	1.38
Dimethyl aniline	2	169	1.37
n-Tributyl amine	2	176	1.09
Cellosolve	2	152	1.40
Dichloroethylether	2	152	1.39
Anisole	2	175	1.28
Butyl Cellosolve	2	163	1.24
Diethyl Cellosolve	2	179	1.23
Diethyl carbitol	2	173	1.23
n-Butylether	2	197	1.10
Solvents with water			
* Furfural, 96 wt %	3.7	128	1.78
* Aniline, 96.5 wt %	4.4	132	1.77
Methylacetoacetate (90 vol %)	3.6	134	1.67
* Phenol (90 vol %)	2.5	133	1.66
Acetonylacetone (95 vol %)	3	128	1.58
* Acetonitrile (90 vol %)	4	133	1.58
Benzyl alcohol (95 vol %)	2.5	133	1.51
o-Chlorophenol (90 vol %)	5.0	180	1.50

[Data from Hess, Narragon, and Coghlin, *Chem. Eng. Prog. Symp. Ser.* **2**, 72–96 (1952)].

TABLE 13.9. Relative Volatilities of C$_4$ and C$_5$ Hydrocarbons in Various Solvents

(a) Volatilities of Butenes Relative to Butadiene at 40°C

Mole Fraction Hydro-carbons in Solution	DMF with 12% H$_2$O			Acetonitrile					
				Dry			13% H$_2$O		
	1-Butene	*trans*-2-Butene	*cis*-2-Butene	1-Butene	*trans*-2-Butene	*cis*-2-Butene	1-Butene	*trans*-2-Butene	*cis*-2-Butene
0.05	2.10	1.66	1.6	—	—	—	1.86	1.47	1.41
0.10	1.90	1.62	1.43	1.81	1.44	1.37	1.73	1.38	1.31
0.15	2.15	1.65	1.40	1.83	1.50	1.35	1.73	1.43	1.20

[Galata, Kofman, and Matveeva, *Chem. Chem. Tech.* (in Russian) **2,** 242–255 (1962)].

(b) Volatilities at Infinite Dilution and 20°C Relative to Butadiene

Compound	Solvent				
	None	Furfural	DMF	NMP	ACN
n-Butane	0.88	3.0	3.04	3.84	3.41
Isobutylene	1.03	2.03	2.00	2.45	2.20
Butene-1	1.01	1.97	1.95	2.44	2.16
t-Butene-2	0.86	1.42	1.54	2.02	1.70
c-Butene-2	—	1.29	1.40	1.76	1.56

(Evans and Sarno, Shell Development Co.).

(c) Enhancement of Relative Volatilities of C$_4$ and C$_5$ Hydrocarbons

Class and Name of Hydrocarbons	No. Solvent α_o	α/α_0 in Presence of Solvent		
		Furfural	DMF	ACN
Alkanes/alkenes				
n-Butane/1-butene	0.83	1.53	1.83	1.70
i-Butene/1-butene	1.14	1.52	1.83	1.70
i-Pentane/2-methyl-1-butene	1.08	1.66	1.85	—
n-Pentane/2-methyl-1-butene	0.84	1.61	1.80	—
Alkanes/dienes				
1-Butene/butadiene	1.04	1.57	1.91	1.69
Trans-2-butene/butadiene	0.83	1.44	1.85	1.71
cis-2-butene/butadiene	0.76	1.41	1.84	1.71
2-Methyl-2-butene/isoprene	0.87	1.45	1.84	—
Isoprene/3-methyl-1-butene	0.88	—	1.37	—

(Galata et al., loc cit.)

TABLE 13.10. Solubilities (wt %) of Classes of C$_4$ and C$_5$ Hydrocarbons in Various Solvents

Compounds	DMF with		ACN with		Furfural with
	8% Water	12% Water	8% Water	12% Water	4% Water
Saturated	7	5	14	9	7
Olefins	18	13	32	22	18
Diolefins	58	41	32	22	24
Acetylenes	69	50	—	—	—

[Galata, Kofman, and Matveeva, *Chem. Chem. Tech.* (in Russian) **2,** 242–255 (1962)].

merization of the unsaturates in the hotter parts of the towers and reboilers.

Two feasible methods for removal of as much water as desired from the azeotrope are depicted on Figure 13.26. The dual pressure process takes advantage of the fact that the azeotropic composition is shifted by change of pressure; operations at 100 and 760 Torr result in the desired concentration of the mixture. In the other method, trichlorethylene serves as an entrainer for the water. A ternary azeotrope is formed that separates into two phases upon condensation. The aqueous layer is rejected, and the solvent layer is recycled to the tower. For economic reasons, some processing beyond that shown will be necessary since the aqueous layer contains some acetonitrile that is worth recovering or may be regarded as a pollutant.

AZEOTROPIC DISTILLATION

The objective of azeotropic distillation is the separation or concentration beyond the azeotropic point of mixtures with the aid of an entrainer to carry some of the components overhead in a column. An azeotrope is a constant boiling mixture with vapor and liquid phases of the same composition. A related class of systems is that of partially miscible liquids that also boil at constant temperature. The two phases exert their individual vapor pressures so that the boiling temperature and vapor composition remain constant over the full range of immiscibility, but the compositions of vapor and overall liquid phases are only accidentally the same. In most cases of immiscible liquids, the horizontal portion of an $x - y$ diagram crosses the $x = y$ line, for instance, the system of *n*-butanol and water of Example 13.5. The system of methylethylketone and water is one of the few known exceptions for which the immiscible boiling range does not cross the $x = y$ line of Figure 13.28(b). Artificial systems can be constructed with this behavior. Thus Figures 13.28(c) and (d) are of diagrams synthesized with two different sets of parameters of the Margules equation for the activity coefficients; one of the $x - y$ lines crosses the diagonal and the other does not. Figure 13.28(a) for acetone and water is representative of the most common kind of homogeneous azeotropic behavior.

The overhead stream of the distillation column may be a low-boiling binary azeotrope of one of the keys with the entrainer or more often a ternary azeotrope containing both keys. The latter kind of operation is feasible only if condensation results in two liquid phases, one of which contains the bulk of one of the key components and the other contains virtually all of the entrainer which can be returned to the column. Figure 13.29(a) is of such a flow scheme. When the separation resulting from the phase split is not complete, some further processing may make the operation technically as well as economically feasible.
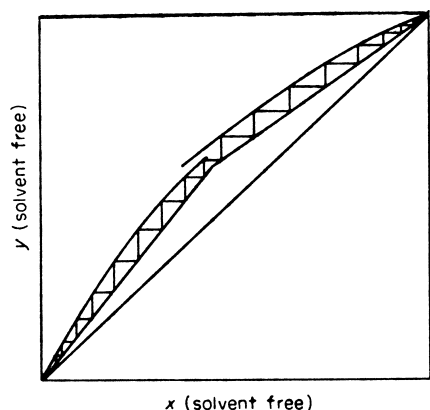
Figure 13.24. Illustrating McCabe–Thiele construction of pseudo-binary extractive distillation with smaller relative volatility below the feed plate.

Data of Azeotropes. The choice of an azeotropic entrainer for a desired separation is much more restricted than that of solvents for extractive distillation, although many azeotropic data are known. The most modern and extensive compilation is that of Gmehling et al. (1994), a two-volume set that includes many ternary and some quaternary azeotropes. Probably the most available

compilation, though less extensive, is by Horsley (1973). A large listing has been compiled by Ogorodnikov et al. (1971) and is in Russian. Shorter lists of azeotropes are given in all editions of *Perry's Handbook, Lange's Handbook of Chemistry*, and *Handbook of Chemistry and Physics*. Data for some ternary systems are in Table 13.11.

Commercial Examples. The small but often undesirable contents of water dissolved in hydrocarbons may be removed by distillation. In drying benzene, for instance, the water is removed

(a)

Fractionator
10.5' dia. x 173' TT
24" tray spacing

Stripper
10.5' dia. x 145' TT
24" tray spacing

Component	1	2	3	4	5
Pentanes & Olefins	13,600	13,430	170	170	0
Isoprene	17,435	488	17,112	16,947	165
Pentadienes +	15,090	160	66,363	14,930	51,433
ACN	0	2200	275,228	900	277,428
Water	0	0	41,350	0	41,350
	46,125	16,278	400,223	32,947	370,376

Figure 13.25. Flowsketch for the recovery of isoprene from a mixture of C₅s with aqueous acetonitrile. Flow quantities in lb/hr, pressures in psia, and temperatures in °F. Conditions are approximate. (Data of The C. W. Nofsinger Co.)

(b)

Figure 13.26. Separation of the azeotropic mixture of acetonitrile and water which contains approximately 69 mol% or 79.3 wt% of acetonitrile. (*Pratt*, Countercurrent Separation Processes, *Elsevier, New York, 1967, pp. 194, 497*). (a) A dual pressure process with the first column at 100 Torr and the second at 760 Torr. (b) Process employing trichlorethylene as entrainer that in turn separates into two phases upon condensation.
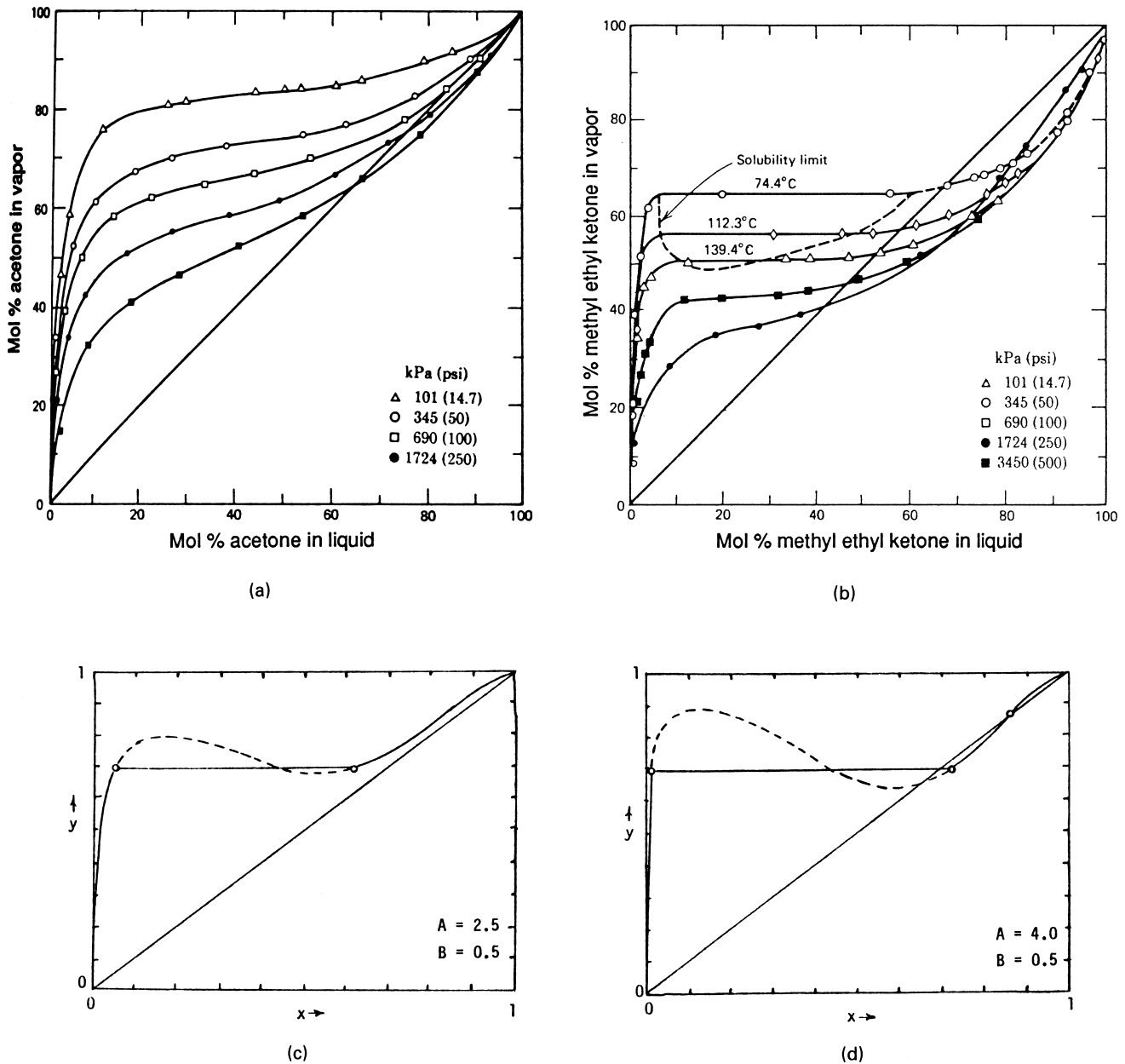
Figure 13.27. Vapor–liquid equilibria of some azeotropic and partially miscible liquids. (a) Effect of pressure on vapor–liquid equilibria of a typical homogeneous azeotropic mixture, acetone and water. (b) Uncommon behavior of the partially miscible system of methylethylketone and water whose two-phase boundary does not extend byond the $y = x$ line. (c) $x - y$ diagram of a partially miscible system represented by the Margules equation with the given parameters and vapor pressures $P_1^0 = 3$, $P_2^0 = 1$ atm; the broken line is not physically significant but is represented by the equation. (d) The same as (c) but with different values of the parameters; here the two-phase boundary extends beyond the $y = x$ line.

overhead in the azeotrope, and the residual benzene becomes dry enough for processing such as chlorination for which the presence of water is harmful. The benzene phase from the condenser is refluxed to the tower. Water can be removed from heavy liquids by addition of some light hydrocarbon which then is cooked out of the liquid as an azeotrope containing the water content of the original heavy liquid. Such a scheme also is applicable to the breaking of aqueous emulsions in crude oils from tar sands. After the water is removed azeotropically, solids originally dissolved or entrained in the aqueous phase settle out readily from the dry hydrocarbon phase. Even in the evaporation of water from caustic,

the addition of kerosene facilitates the removal of water by reducing the temperature to which the pot must be heated.

The separation of the azeotrope acetonitrile/water can be accomplished without an entrainer as shown in Figure 13.26(a). Two columns are required, operating at two different pressures. A single column suffices if trichloroethylene is added as an entrainer, shown in Figure 13.26(b).

Ordinary rectification for the dehydration of acetic acid requires many trays if the losses of acid overhead are to be restricted, so that azeotropic processes are used exclusively. Among the entrainers that have been found effective are ethylene dichloride,
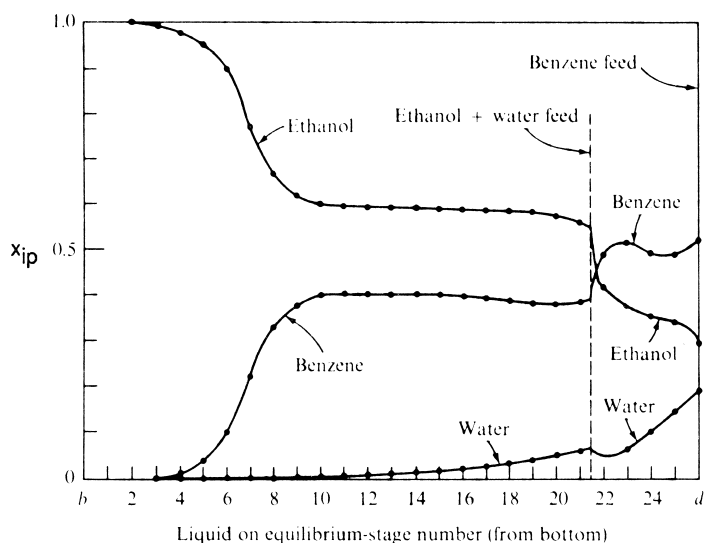
(a)
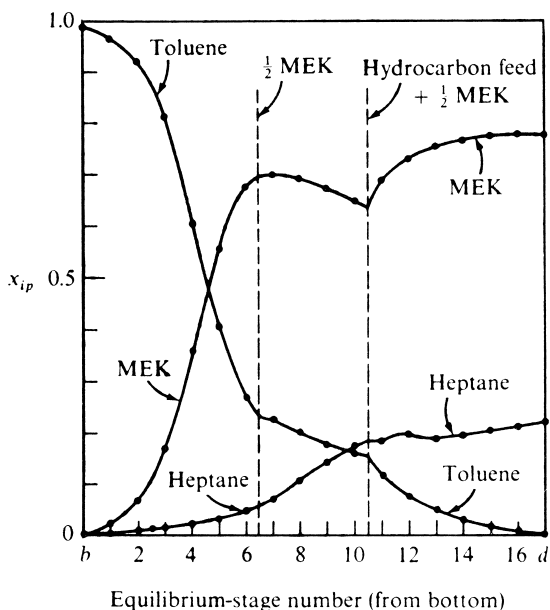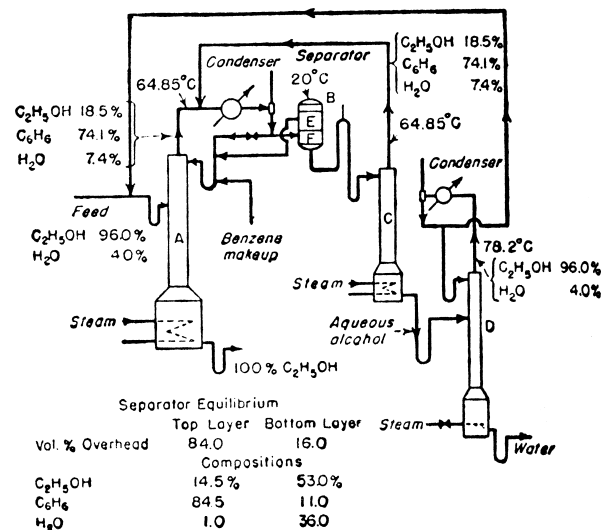
(b)
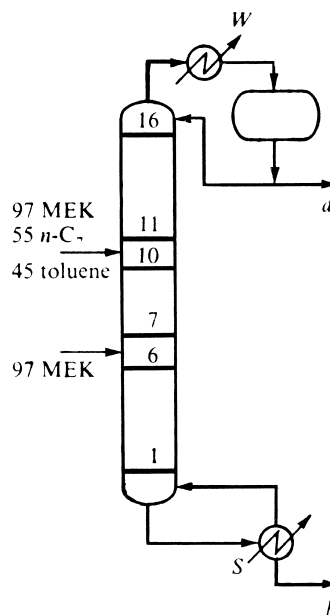
Figure 13.28. Composition profiles and flowsketches of two azeotropic distillation processes (*adapted by King, 1980*). (a) Separation of ethanol and water with benzene as entrainer. Data of the composition profiles in the first column were calculated by Robinson and Gilliland, (1950); the flowsketch is after Zdonik and Woodfield (*in* Chemical Engineers' Handbook, *McGraw-Hill, New York, 1950, p. 652*). (b) Separation of *n*-heptane and toluene with methylethylketone entrainer which is introduced in this case at two points in the column (*data calculated by Smith, 1963*).

n-propyl acetate, and *n*-butyl acetate. Water contents of these azeotropes are 8, 14, and 28.7 wt %, respectively. Accordingly, the *n*-butyl acetate is the most thermally efficient of these agents. The *n*-propyl acetate has been used in large installations, in the first stage as solvent for extraction of acetic acid and then as azeotropic entrainer to remove the accompanying water. Extractive distillation with a high boiling solvent that is immiscible with water upon condensation is technically feasible for acetic acid drying but is a more expensive process.

Ethanol forms an azeotrope containing 5 wt% water. In older installations, dissolved salts were employed to break the azeotrope. Typical data are in Figure 13.27 (c). Several substances form ternary azeotropes with ethanol and water, including benzene, gasoline, trichlorethylene. The first is not satisfactory because of slight decomposition under distillation conditions. A flowsketch of a process employing benzene is in Figure 13.28(a). In a modernization of the benzene process (Raphael Katzen Associates, Cincinnati, OH), a high purity ethanol is made by controlling the distillation so that

TABLE 13.11. Selected Ternary Aezotropic Systems at Atmospheric Pressure

(a) Systems with Water and Alcohols

	B.P. 760 mm.		% By weight		
	Other component	Azeotrope	Water	Alcohol	Other component
A—Ethyl Alcohol (B.P. 78.3°)					
Ethyl acetate (6)	77.1	70.3	7.8	9.0	83.2
Diethyl formal (7)	87.5	73.2	12.1	18.4	69.5
Diethyl acetal (8)	103.6	77.8	11.4	27.6	61.0
Cyclohexane	80.8	62.1	7	17	76
Benzene (4)	80.2	64.9	7.4	18.5	74.1
Chloroform	61.2	55.5	3.5	4.0	92.5
Carbon tetrachloride	76.8	61.8	4.3	9.7	86.0
Ethyl iodide	72.3	61	5	9	86
Ethylene chloride	83.7	66.7	5	17	78
B—n-Propyl Alcohol (B.P. 97.2°)					
n-Propyl formate (6)	80.9	70.8	13	5	82
n-Propyl acetate (6)	101.6	82.2	21.0	19.5	59.5
Di-*n*-propyl formal (7)	137.4	86.4	8.0	44.8	47.2
Di-*n*-propyl acetal (8)	147.7	87.6	27.4	51.6	21.0
Di-*n*-propyl ether (7)	91.0	74.8	11.7	20.2	68.1
Cyclohexane	80.8	66.6	8.5	10.0	81.5
Benzene (4)	80.2	68.5	8.6	9.0	82.4
Carbon tetrachloride	76.8	65.4	5	11	84
Diethyl ketone	102.2	81.2	20	20	60
C—Isopropyl Alcohol (B.P. 82.5°)					
Cyclohexane	80.8	64.3	7.5	18.5	74.0
Benzene (4)	80.2	66.5	7.5	18.7	73.8
D—n-Butyl Alcohol (B.P. 117.8°)					
n-Butyl formate (6)	106.6	83.6	21.3	10.0	68.7
n-Butyl acetate (6)	126.2	89.4	37.3	27.4	35.3
Di-*n*-butyl ether (7)	141.9	91	29.3	42.9	27.7
E—Isobutyl Alcohol (B.P. 108.0°)					
Isobutyl formate (6)	94.4	80.2	17.3	6.7	76.0
Isobutyl acetate	117.2	86.8	30.4	23.1	46.5
F—tert-Butyl Alcohol (B.P. 82.6°)					
Benzene (4)	80.2	67.3	8.1	21.4	70.5
Carbon tetrachloride (9)	76.8	64.7	3.1	11.9	85.0
G—n-Amyl Alcohol (B.P. 137.8°)					
n-Amyl formate (6)	131.0	91.4	37.6	21.2	41.2
n-Amyl acetate (6)	148.8	94.8	56.2	33.3	10.5
H—Isoamyl Alcohol (B.P. 131.4°)					
Isoamyl formate (6)	124.2	89.8	32.4	19.6	48.0
Isoamyl acetate (6)	142.0	93.6	44.8	31.2	24.0
I—Allyl Alcohol (B.P. 97.0°)					
n-Hexane	69.0	59.7	5	5	90
Cyclohexane	80.8	66.2	8	11	81
Benzene	80.2	68.2	8.6	9.2	82.2
Carbon tetrachloride	76.8	65.2	5	11	84

(Lange, *Handbook of Chemistry*, McGraw-Hill, New York, 1979).

the lower 10 trays or so are free of benzene. Another entrainer, diethyl ether, has the desirable property of forming an azeotrope with water but not with ethanol. The water content of the azeotrope is small so that the operation is conducted at 8 atm to shift the composition to a higher value of 3% water. In small installations, drying with molecular sieves is a competitive process. Separations with membranes of both vapor and liquid phases, supercritical extraction with carbon dioxide and many other techniques have been proposed for removal of water from ethanol.

Formic acid can be dehydrated with propyl formate as entrainer. Small contents of formic acid and water in acetic acid can be entrained away with chloroform which forms binary azeotropes with water and formic acid but no other azeotropes in this system.

Some hydrocarbon separations can be effected azeotropically. Figure 13.28(b) shows an operation with methylethylketone which entrains *n*-heptane away from toluene. Hexane in turn is an effective entrainer for the purification of methylethylketone by distilling the latter away from certain oxide impurities that arise during the synthesis process.

Design. When the vapor–liquid equilibria are known, in the form of UNIQUAC parameters for instance, the calculation of azeotropic distillation may be accomplished with any of the standard multicomponent distillation procedures. The Naphthali–Sandholm algorithm (Fig. 13.19) and the θ-method of Holland (1981) are satisfactory. Another tray-by-tray algorithm is illustrated for azeotropic distillation by Black, Golding, and Ditsler [*Adv. Chem. Ser.*

Table 13.11.—(continued**)**

(b) Other Systems

Component A Mole % A = 100 − (B + C)	Components B and C	Mole % B and C	Temp., °C.
Water	Carbon tetrachloride	57.6	61.8
	Ethanol	23.0	2 phase
	Trichloroethylene	38.4	67.25
	Ethanol	41.2	2 phase
	Trichloroethylene	49.2	71.4
	Allyl alcohol	17.3	2 phase
	Trichloroethylene	51.1	71.55
	Propyl alcohol (n)	16.6	2 phase
	Ethanol	12.4	70.3
	Ethyl acetate	60.1	
	Ethanol	22.8	64.86
	Bensene	53.9	
	Allyl alcohol	9.5	68.3
	Benzene	62.2	
	Propyl alcohol (n)	8.9	68.48
	Benzene	62.8	
Carbon disulfide	Methanol	24.1	33.92
	Ethyl bromide	35.4	
Methyl formate	Ethyl bromide	23.8	16.95
	Isopentane	31.0	
	Ethyl ether	7.2	20.4
	Pentane (n)	48.2	
Propyl lactate (n)	Phenetol	35.2	163.0
	Menthene	34.1	

115, 64 (1972)]. A procedure coupling the tower, decanter, and stripper of Figure 13.28(a) is due to Prokopakis and Seider [*AIChE J*. **29,** 49 (1983)]. Two sets of composition profiles obtained by tray-by-tray calculations appear in Figures 13.28 (a) and (b).

MOLECULAR DISTILLATION

This process is an evaporation that is conducted at such low pressures that the distance between the hot and condensing surfaces is less than the mean free path of the molecules. Each unit is a single stage, but several units in series are commonly employed. Molecular distillation is applied to thermally sensitive high molecular weight materials in the range of 250–1200 molecular weights, such as oils, fats, waxes, essential oils and scents, vitamins and hormone concentrates, and to the deodorization of high molecular weight materials.

Operating pressures are in the range of 1 m Torr. For example, the mean free paths of normal triglycerides of 800 molecular weight are

P(m Torr)	Path (mm)
8	7
3	25
1	50

The theoretical Langmuir equation for the rate of evaporation is

$$w' = 2100P^0\sqrt{M/T} \text{ kg/m}^2\text{hr} \tag{13.232}$$

with the vapor pressure P^0 in Torr, the temperature in K, and with M as the molecular weight. Industrial apparatus may have 80–90% of these rates because of inefficiencies. Some numerical values at 120°C are:

Compound	M	P^0 (Torr)	w' (kg/m²hr)
Stearic acid	284	35.0	1.87
Cholesterin	387	0.5	2.02
Tristearin	891	0.0001	2.74

From Langmuir's equation it is clear that it is possible to separate substances of the same vapor pressure but different molecular weights by molecular distillation.

Apparatus and Operating Conditions. The main kinds of commercial units are illustrated in Figure 13.29. In the falling film type, the material flows by gravity as a thin film on a vertical heated cylinder, evaporates there, and is condensed on a concentric cooled surface. Diameters range from 2 to 50 cm, heights 2 to 10 m, and feed rates from 1 to 60 L/hr. In order to prevent channelling, the surface of the evaporator is made rough or other means are employed. The cross section of a wiped film commercial still is shown in Figure 13.29(b). Contact times in commercial apparatus may be as low as 0.001 sec.

In the centrifugal still, the material that is charged to the bottom creeps up the heated, rotating conical surface as a thin film, is evaporated, and then condensed and discharged (Figure 13.29(d)). The film thickness is 0.05–0.1 mm. Rotors are up to about 1.5 m dia and turn at 400–500 rpm. Evaporating areas are up to 4.5 m² per unit, feed rates range from 200 to 700 L/hr, and distillates range from 2 to 400 L/hr, depending on the service. From three to seven stills in series are used for multiple redistillation of some products. Two stills 1.5 m dia can process a tank car of oil in 24 hr. A typical pumping train for a large still may comprise a three-stage steam ejector, two oil boosters and a diffusion pump, of capacity 1000–5000L/sec, next to the still. Equivalent mechanical pumps may be employed instead of the ejectors, depending on the economic requirements.

The evaporator of Figure 13.29(c) is for service intermediate between those of ordinary film evaporators and molecular stills, with greater clearances and higher operating pressures than in the latter equipment. The rotating action permits handling much more viscous materials than possible in film evaporators.

13.12. TRAY TOWERS

Contacting of vapor and liquid phases on trays is either in countercurrent flow or with cross flow of liquid against vapor flow upward. The spacing of trays is determined partly by the necessity of limiting carryover of entrainment from one tray to another, and is thus related to the vapor velocity and the diameter of the vessel. For reasons of accessibility of trays to periodic servicing, however, their spacing commonly is 20–24 in. Then workmen can go up or down the tower through removable sections of the trays and have enough room to work in. For the same reason, tray diameters are restricted to a minimum of 30 in. When a smaller size is adequate, cartridge trays that can be lifted out of the vessel as a group, as in Figure 13.30(b), or packed towers are adopted. A data sheet for recording key data of a tray tower is in Table 13.12. The tedious calculations of many mechanical details of tray construction usually are relegated to computers.

COUNTERCURRENT TRAYS

The three main kinds of trays with countercurrent flow of liquid and gas are:

Dualflow, with round holes in the 1/8–1/2 in. range, extensively tested by Fractionation Research Inc. (FRI).

Turbogrid, with slots 1/4–1/2 in. wide, developed by Shell Development Co.

Ripple trays, made of perforated corrugated sheets, with vapor flow predominantly through the peaks and liquid through the valleys, developed by Stone and Webster.

(a)

(b)

(c)

(d)
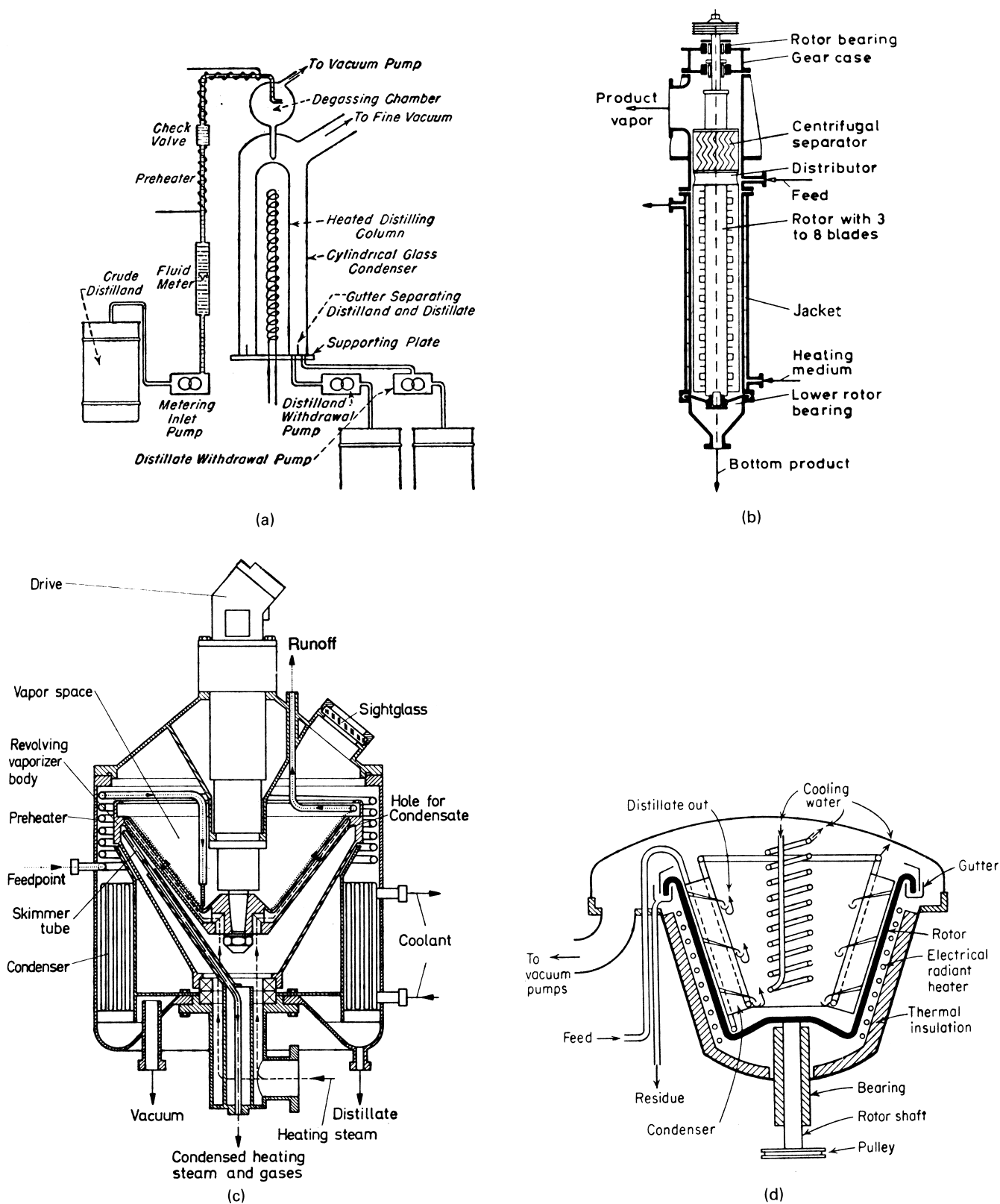
Figure 13.29. Molecular distillation and related kinds of equipment. (a) Principle of the operation of the falling film still (Chemical Engineers Handbook, *McGraw-Hill, New York, 1973*). (b) Thin-layer evaporator with rigid wiper blades (*Luwa Co., Switzerland*). (c) The Liprotherm rotating thin film evaporator, for performance intermediate to those of film evaporators and molecular stills (*Sibtec Co., Stockholm*). (d) Centrifugal molecular still [*Hickman*, Ind. Eng. Chem. **39**, *686* (*1947*)].
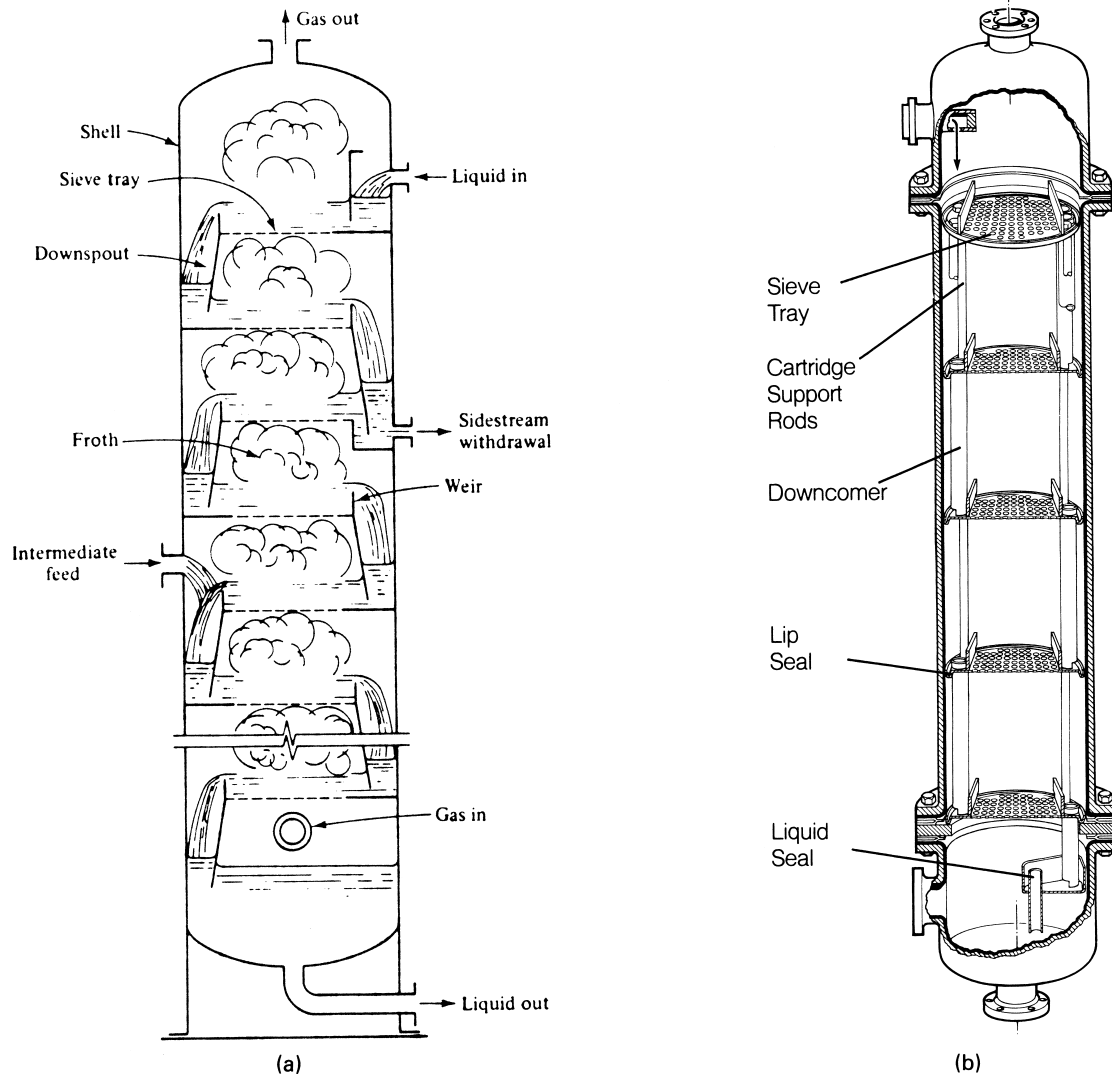
Figure 13.30. Assembled sieve tray towers. (a) Flowsketch of a sieve tray tower (*Treybal, 1980*). (b) Cartridge type sieve tray tower in small diameters (*Pfaudler Co.*).

Although some of the vapor and liquid flows through the openings are continuous, the bulk of the flows pass alternately with a surging action. The absence of downcomers means a greater bubbling area and consequently a greater vapor handling capacity, and also allows a close spacing to be used, as little as 9 in. in some applications. The action in such cases approaches those of towers filled with structured packings. Their turndown ratio is low, that is, the liquid drains completely off the tray at lowered vapor rates. Consequently, countercurrent trays have never found widespread use.

The FRI data for dualflow trays have been used to form a tentative design method (Garcia and Fair, 2002). Data for Turbogrid trays have been included in the model. A generalized chart for predicting allowable vapor velocity, similar to that for cross flow trays given in Fig. 13.32(b), is included.

On crossflow trays, the path of liquid is horizontal from downcomer to weir and in contact with vapor dispersed through openings in the tray floor. Such flows are illustrated in Figures 13.30 and 13.31. Depending on the rate and on the diameter, the liquid flow

may be single, double, or four-pass. A common rule for dividing up the flow path is a restriction of the liquid rate to a maximum of about 8 gpm/in. of weir length. Usually towers 5 ft dia and less are made single pass. Since efficiency falls off as the flow path is shortened, a maximum of two passes sometimes is specified, in which case flow rates may approach 20 gpm/in. of weir.

The main kinds of cross flow trays with downcomers in use are sieve, valve, and bubblecap.

SIEVE TRAYS

A liquid level is maintained with an overflow weir while the vapor comes up through the perforated floor at sufficient velocity to keep most of the liquid from weeping through. Hole sizes may range from 1/8 to 1 in., but are mostly 1/4–1/2 in. Hole area as a percentage of the active cross section is 5–15%, commonly 10%. The precise choice of these measurements is based on considerations of pressure drop, entrainment, weeping, and mass transfer efficiency. The range of conditions over which tray operation is

TABLE 13.12. Tray Design Data Sheet

Item No. or Service				
Tower diameter, I.D.				
Tray spacing, inches				
Total trays in section.				
Max. Δ P, mm Hg.				
Conditions at Tray No				
Vapor to tray, °F.				
Pressure, ...				
Compressibility				
°Density, lb./cu. ft.				
°Rate, lb./hr.				
cu.ft./sec. (cfs)				
cfs $\sqrt{D_v/(D_L - D_V)}$				
Liquid from tray, °F				
Surface tension				
Viscosity, cp				
°Density, lb./cu. ft.				
°Rate, lb./hr.				
GPM hot liquid				

Foaming tendency. . . . . None_____Moderate_____High_____Severe_____

  °These values are required in this form for direct computer input.

Notes
1. Tray numbering: top to bottom_____; bottom to top_____.
2. Number of flow paths or passes_____.
3. Minimum rate as a % of design rate_____.
4. Allowable downcomer velocity_____ft/sec.
5. Bottom tray downcomer: total drawoff_____other_____.
6. Adjustable weir required: yes_____; no_____.
7. Tray material and thickness_____.
8. Valve or cap material_____.

satisfactory and the kinds of malfunctions that can occur are indicated roughly in Figure 13.32(a) and the behavior is shown schematically on Figure 13.31(c).

The required tower diameter depends primarily on the vapor rate and density and the tray spacing, with a possibly overriding restriction of accommodating sufficient weir length to keep the gpm/in. of weir below about 8. Figure 13.32(b) is a correlation for the flooding velocity. Allowable velocity usually is taken as 80% of the flooding value. Corrections are indicated with the figure for the fractional hole area other than 10% and for surface tension other than 20 dyn/cm. Moreover, the correction for the kind of operation given with Figure 13.33 for valve trays is applicable to sieve trays.

Weir heights of 2 in. are fairly standard and weir lengths about 75% of the tray diameter. For normal conditions downcomers are sized so that the depth of liquid in them is less than 50% and the residence time more than 3 sec. For foaming and foam-stable systems, the residence time may be two to three times this value. The topic of tray efficiency is covered in detail in Section 13.6, but here it can be stated that they are 80–90% in the vicinity of $F = u_v\sqrt{\rho_v} = 1.0(\text{ft/sec})(\text{lb/cuft})^{1/2}$ for mixtures similar to water with alcohols and to $C_6 - C_7$ hydrocarbons.

A detailed design of a tray includes specification of these items:

1. Hole dia, area, pitch and pattern.
2. Blanking of holes for less than eventual load.
3. Downcomer type, size, clearance, and weir height.
4. Tray thickness and material.
5. Pressure drop.
6. Turndown ratio before weeping begins.
7. Liquid gradient.

Correlations for checking all of these specifications are known. An example is worked out by Fair (in Smith, 1963, Chap. 15). The basis is holes 3/16 in. dia, fractional open area of 0.10, weir height of 2 in. and tray spacing 24 in.

The correlation of Figure 13.32 has no provision for multipass liquid flow. Corrections could be made by analogy with the valve tray correlation, as suggested at the close of Example 13.15.

VALVE TRAYS

The openings in valve trays are covered with liftable caps that adjust themselves to vapor flow. Illustrations of two kinds of valves are in Figure 13.31(b). The caps rest about 0.1 in. above the floor and rise to a maximum clearance of 0.32 in. The commonest hole diameter is 1.5 in. but sizes to 6 in. are available. Spacing of the standard diameter is 3–6 in. With 3 in. spacing, the number of valves is 12–14/sqft of free area. Some of the tray cross section is taken up by the downcomer, by supports, and by some of the central manway structure.

In spite of their apparent complexity of construction in comparison with sieve trays, they usually are less expensive than sieve trays because of their larger holes and thicker plates which need less support. They are more subject to fouling and defer to sieves for such services.

Tray diameters may be approximated with Figure 13.32(b)

Factors for correcting the allowable volumetric rate for various degrees of foaming are given with the figure.

Formulas and procedures for calculation of detailed tray specifications may be obtained from the manufacturers of valve trays.
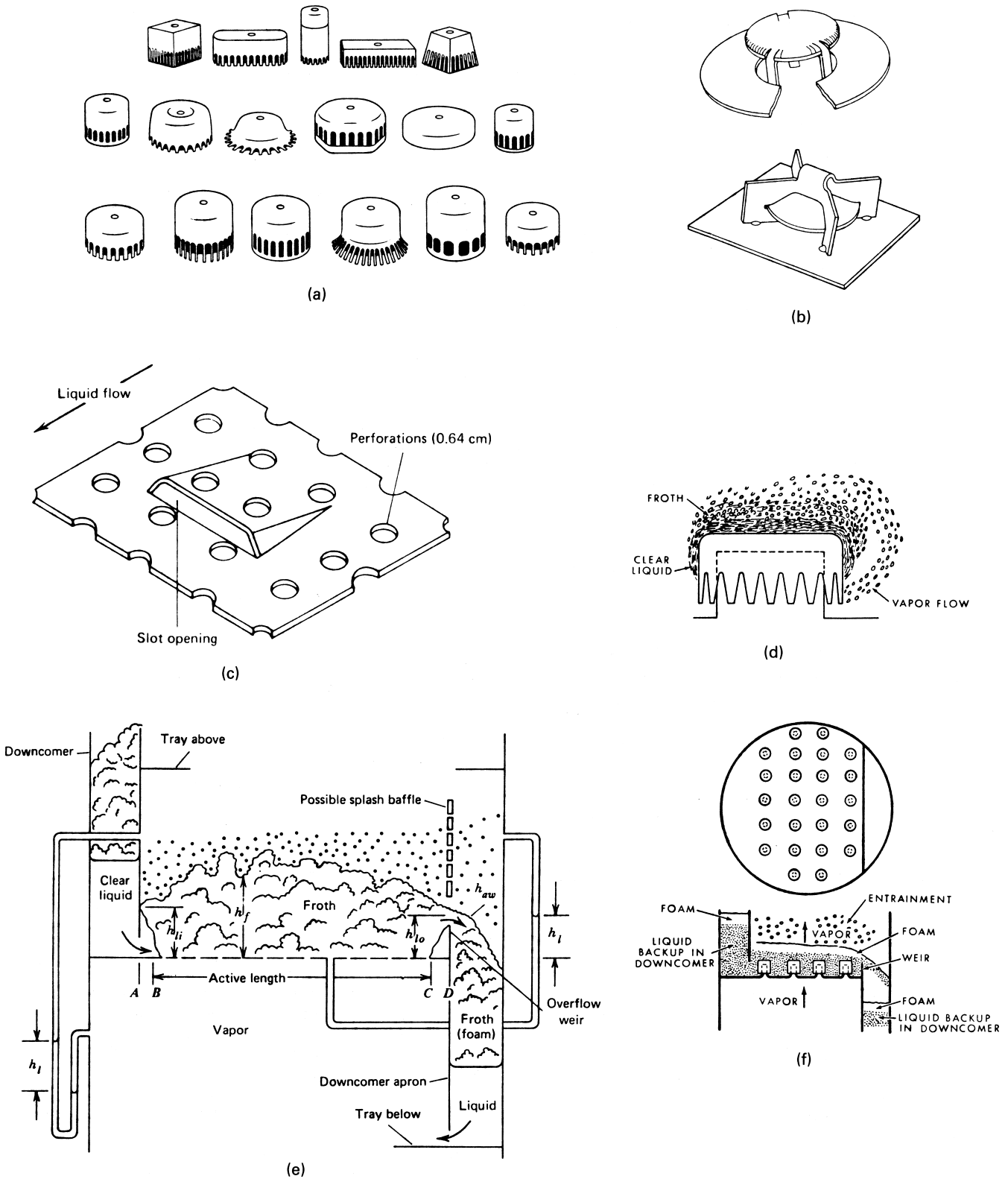
Figure 13.31. Internals and mode of action of trays in tray towers. (a) Some kinds of bubblecaps (*Glitsch*). (b) Two kinds of valves for trays. (c) Vapor directing slot on a Linde sieve tray [*Jones and Pyle* Chem. Eng. Prog. **71**, *66* (*1975*)]. (d) Vapor flow through a bubblecap. (e) Sieve tray phenomena and pressure relations; h_h is the head in the downcomer, h_l is the equivalent head of clear liquid on the tray, h_f is the visible height of froth on the tray, and h_t is the pressure drop across the tray (*Bolles, in Smith, 1963*). (f) Assembly of and action of vapor and liquid on a bubblecap tray.
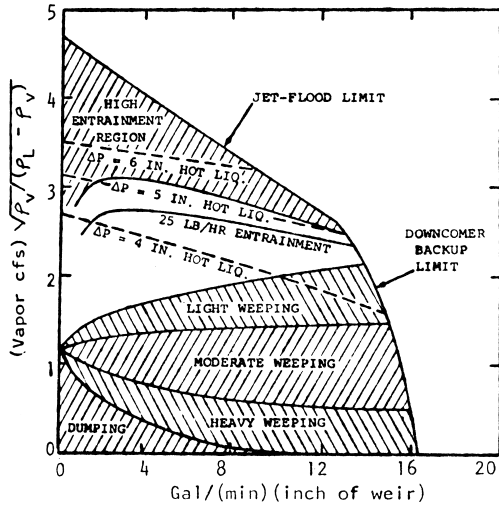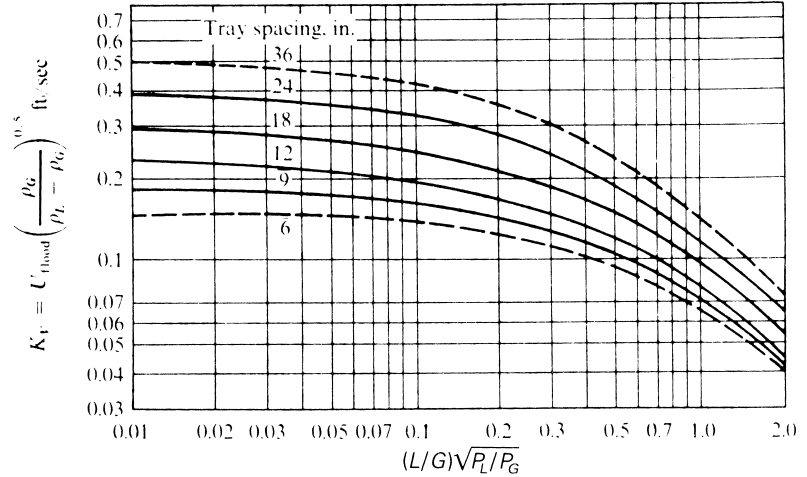
Figure 13.32. Operating ranges of malfunctions and flooding velocity correlation of sieve trays. (a) Performance of a typical sieve tray, showing ranges of weeping, dumping, entrainment, and flooding. (b) Correlation of flooding at various tray spacings. For normal operation, take 80% of the flooding rate as a design condition. To correct for surface tension (dyn/cm), multiply the ordinate by $(\sigma/20)^{0.2}$. To correct for other than 10% hole area, multiply the ordinate by 0.9 for 8% and by 0.8 for 6% [*after Fair*, Sect. 14 in *Perry's Handbook*, 1997].

For example, Koch-Glitsch Co. makes available a tray design manual that includes a completely solved example problem.

BUBBLECAP TRAYS

Bubblecap assemblies serve to disperse the vapor on the tray and to maintain a minimum level of liquid on the tray. A few of the many kinds that have been used are shown in Fig. 13.31, together with their mode of action on a tray. The most used sizes are 4 or 6 in. diameter round caps, although for special services (such as cryogenic distillation) smaller sizes (down to 1 in.) have been used. Because of their greater cost, weight, higher pressure drop, and creation of a hydraulic gradient across the tray, bubblecaps are rarely used these days. Since they maintain a positive seal on the tray, they are sometimes used for low liquid flow situations and for reactive distillations involving reactions in the liquid phase.

The allowable vapor velocity for bubblecap trays is about the same as for sieve trays, and Figure 13.32(b) may be used. The most complete published source of design and performance prediction of these trays is given by W. L. Bolles (in Smith, 1963).

Example 13.15 shows the calculation of tray diameter.

A factor that is of concern with bubblecap trays is the development of a liquid gradient from inlet to outlet which results in corresponding variation in vapor flow across the cross section and usually to degradation of the efficiency. With other kinds of trays this effect rarely is serious. Data and procedures for analysis of this behavior are summarized by Bolles (in Smith, 1963, Chap. 14). There also are formulas and a numerical example of the design of all features of bubblecap trays. Although, as mentioned, new installations of such trays are infrequent, many older ones still are in operation and may need to be studied for changed conditions.

EXAMPLE 13.15
Diameter of a Sieve Tray Column

A C_3 splitter has 24 in. tray spacing and will operate at 80% of flooding. These data are applicable:

$W_v = 271,500\,\text{lb/hr of vapor,}$

$Q_v = 27.52\,\text{cfs of vapor,}$

$W_L = 259,100\,\text{lb/hr of liquid,}$

$Q_L = 1100\,\text{gpm,}$

$\rho_V = 2.75\,\text{lb/cuft,}$

$\rho_L = 29.3\,\text{lb/cuft.}$

Use Figure 13.32 (b):

abscissa $= (259,100/271,500)\sqrt{2.75/29.3} = 0.2924,$
ordinate, $C = 0.24,$

$$u_G = C\sqrt{(\rho_L - \rho_V)/\rho_V} = 0.24\sqrt{29.3/2.75 - 1} = 0.746\,\text{fps.}$$

Allowable velocity at 80% of flooding,

$$u_G = 0.8(0.746) = 0.597\,\text{fps,}$$

$$\therefore D = \sqrt{Q_v/(\pi/4)u_G} = \sqrt{27.52/(\pi/4)(0.597)} = 7.67\,\text{ft.}$$

The correlations for sieve (and bubblecap) trays have no provision for multipass flow of liquid. Their basic data may have been obtained on smaller towers with liquid flow equivalent to two-pass arrangement in towers 8 ft dia. The sieve tray correlation velocity should take into account the loss of vapor flow area due to downcomers.

13.13. PACKED TOWERS

In comparison with tray towers, packed towers are used whenever low pressure drop is desirable, whenever low holdup is necessary, and whenever plastic or ceramic construction is required. In addition, some of the newer structured (ordered) packings can provide more theoretical stages per unit of tower height than can trays. Especially in large diameter towers, liquid and vapor distribution are important considerations that are lacking for tray towers. In large towers, the cost of packing and other required internals, such as liquid distributors and redistributors, can be much greater than the cost of crossflow trays.

Depth of plastic random packings may be limited by the deformability of the packing elements to 10–15 ft. For metal random packings, this height can be 20–25 ft. For both random and structured packings, the height between redistributors is limited to 20–25 ft. because of the tendency of the phases to maldistribute.

The various kinds of internals of packed towers are represented in Figure 13.33, the individual parts of which may be described one-by-one:

(a) is an example of a column showing the inlet and outlet connections and a variety of possible packings. Note that both random and dumped packings are present as well as structured (ordered) packings.

(b) is a combination packing support and vapor distributor used for beds of random packings. The serrated shape is used to increase the area for vapor flow.

(c) is a trough-type distributor that is suitable for liquid rates in excess of 2 gpm/sqft in towers 1 ft in diameter and larger. In specialized forms, this type of distributor can be used in very large towers where caution must be taken to ensure levelness of the device. Also, care must be taken not to starve the far notches from their equal share of liquid flow. Trough distributors can be fabricated form ceramic, plastic, or metal materials.

(d) is an example of a perforated pipe distributor, which is available in a variety of shapes. It is a very efficient type over a wide range of liquid rates but suffers from its likelihood of plugging from even minute-size solids in the liquid feed. In some large towers, spray nozzles may replace the perforations.

(e) is a device to redistribute liquid, which has a tendency to flow toward the wall. It is sometimes called a wall wiper, and for structured packing elements, it is an integral part of the element.

(f) is a holddown grid to keep low density packings in place and to prevent fragile random packings, such as those made of carbon, for instance, from disintegrating because of mechanical disturbances at the top of the bed.

KINDS OF PACKINGS

The broad classes of packings for vapor-liquid contacting are either random or structured. The former are small, hollow structures with large surface per unit volumes that are usually randomly dumped into the tower. Structured packings are normally layers of elements fabricated form expanded metal, woven wire screen, or sheet metal, and are stacked into the tower very carefully.

The first of the widely used random packings were Raschig rings which are hollow cylinders of ceramics, plastics, or metal. They were an economical replacement for the crushed rock often used then. Because of their simplicity and their early introduction, Raschig rings have been investigated thoroughly and many data of their performance have been obtained which are still useful, for

example, in defining the lower limits of mass transfer efficiency that can be realized with improved packings.

Several kinds of rings are shown in Figure 13.34. They are being made in a variety of internal structure and surface modifications. Pall rings in metal and plastics are perhaps the most widely used packings. One brand, ''Hy-Pak,'' has corrugated walls and more intrusions than the standard designs shown in the figure. Cascade minirings, with height less than the diameter, appear to have improved efficiency in comparison with some other pall rings. Saddles are more efficient because of greater surface and improved hydrodynamics. In plastic construction, Figure 13.34(h), they are made with a variety of holes and protrusions to enlarge the specific surface. When ceramic construction is necessary, saddles are the preferred packings.

Table 13.13 shows dimensional characteristics of some important random packings. A survey of efficiencies of random-packed beds is in Table 13.14. Whenever possible, the ratio of tower and random packing diameters should be at least 10. As a rough guide, 1 in. packing is used for gas rates of about 500 cfm and 2 in. for gas rates of 2000 cfm or more.

Structured packings have replaced trays and random packings as their cost has decreased and more is known of their performance behavior. Initially thought to be appropriate only for high vacuum distillations, they are now used for absorbers, strippers, and pressure distillations. Because of their open structure (over 90% voids) and large specific surface areas, their mass transfer efficiency is high when proper distribution of liquid and gas over the cross section can be maintained. Table 13.15 shows a comparison of features of several commercial makes of structured packings.

Ultimately, the choice of packing is based on pressure drop, mass transfer efficiency, and cost. Structured packings made from sheet metal now cost less than \$100 per cubic foot. The hydraulics of packed beds will be discussed later in this section.

Ultimately, the choice of packing is based on pressure drop and mass transfer efficiency. Since packings of individual manufacturers differ in detail, the manufacturers pressure drop data should be used. A few such data are in Figure 13.36. Mass transfer efficiency is discussed in the next section.

The main operating limitation of a packed column is the onset of flooding. Then the interstices tend to fill with liquid, the gas flow becomes unstable, and the pressure drop rises sharply. Correlations for predicting flooding are combined with pressure drop observations to produce the general model shown in Fig. 13.36, taken from R. F. Strigle (*Packed Tower Design and Applications*, 1994). More detailed and mechanistic methods for predicting pressure drop are given by Stichlmair et al. (1989) for random packings and are summarized by Fair et al. (2000) for structured packings.

The use of Fig. 13.36 requires a value of the packing factor F_p, which may be taken from Table 13.13 or 13.15. The abscissa term is the same as that for tray columns. It is sensible to use a value of about 80% of the maximum curve (equivalent to 1.5 in. H_2O/ft, or 125 mm H_2O/m) for design purposes. The corresponding ordinate term then allows deduction of the value of C_s, defined as $C_s = U_s[\rho_g/(\rho_L - \rho_g)]^{0.5}$, where U_s is the allowable superficial velocity of vapor or gas through the column. Also, ν = liquid kinematic viscosity = centistokes (centipoises/density, gm/ml). Example 13.16 shows how Fig. 13.36 is used.

LIQUID DISTRIBUTION

Liquid introduced at a single point at the top of a packed bed migrates towards the walls. Relatively high liquid rates, as in distillation operations where the molal flow rates of both phases are roughly comparable, tend to retard this migration. When liquid
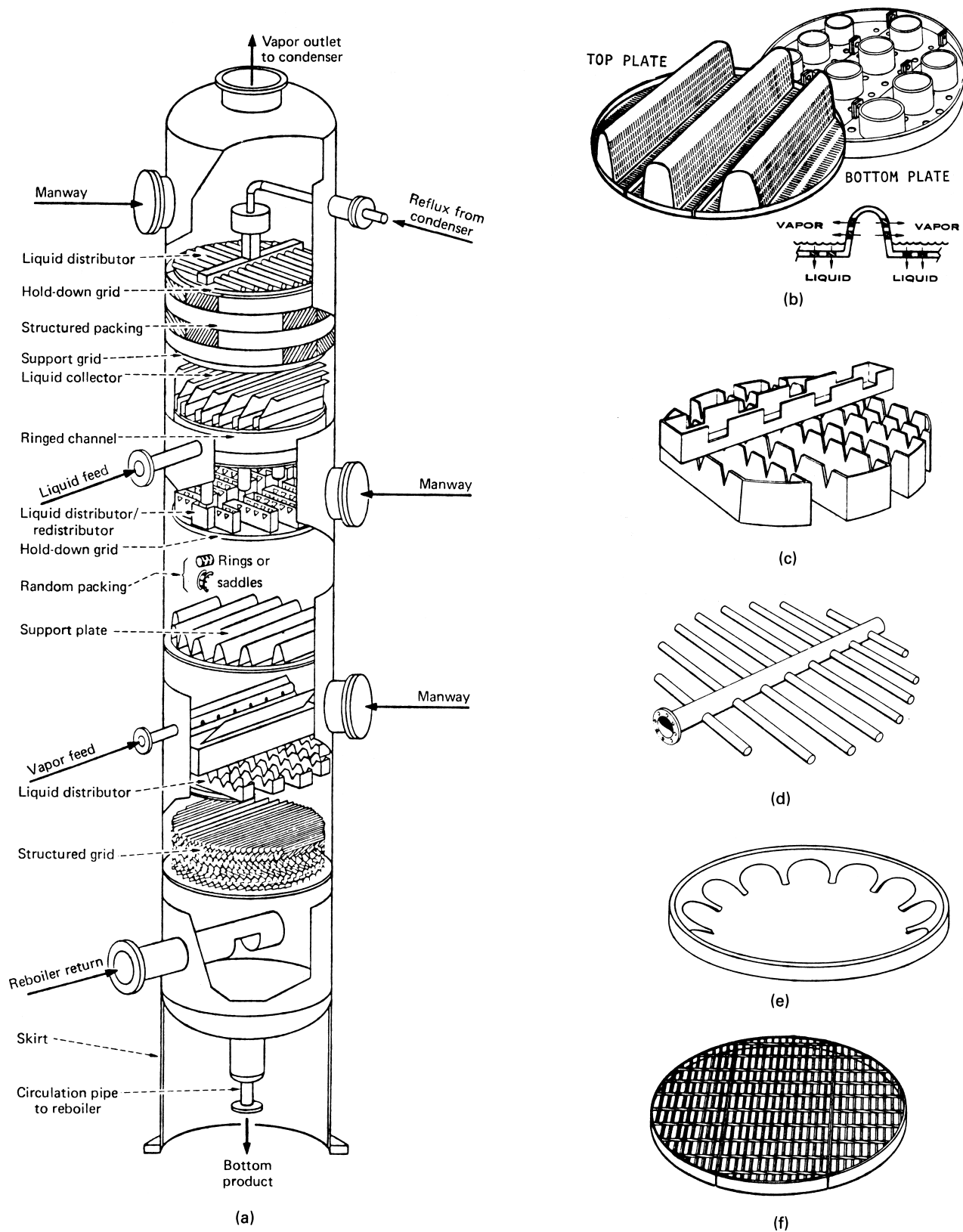
Figure 13.33. Packed column and internals. (a) Example packed column with a variety of internals [*Chen,* Chem. Eng. **40,** (*5 Mar. 199* (b) Packing support and redistributor assembly. (c) Trough-type liquid distributor. (d) Perforated pipe distributor. (e) Rosette distributor for small towers. (f) Hold-down plate, particularly for low density packing.
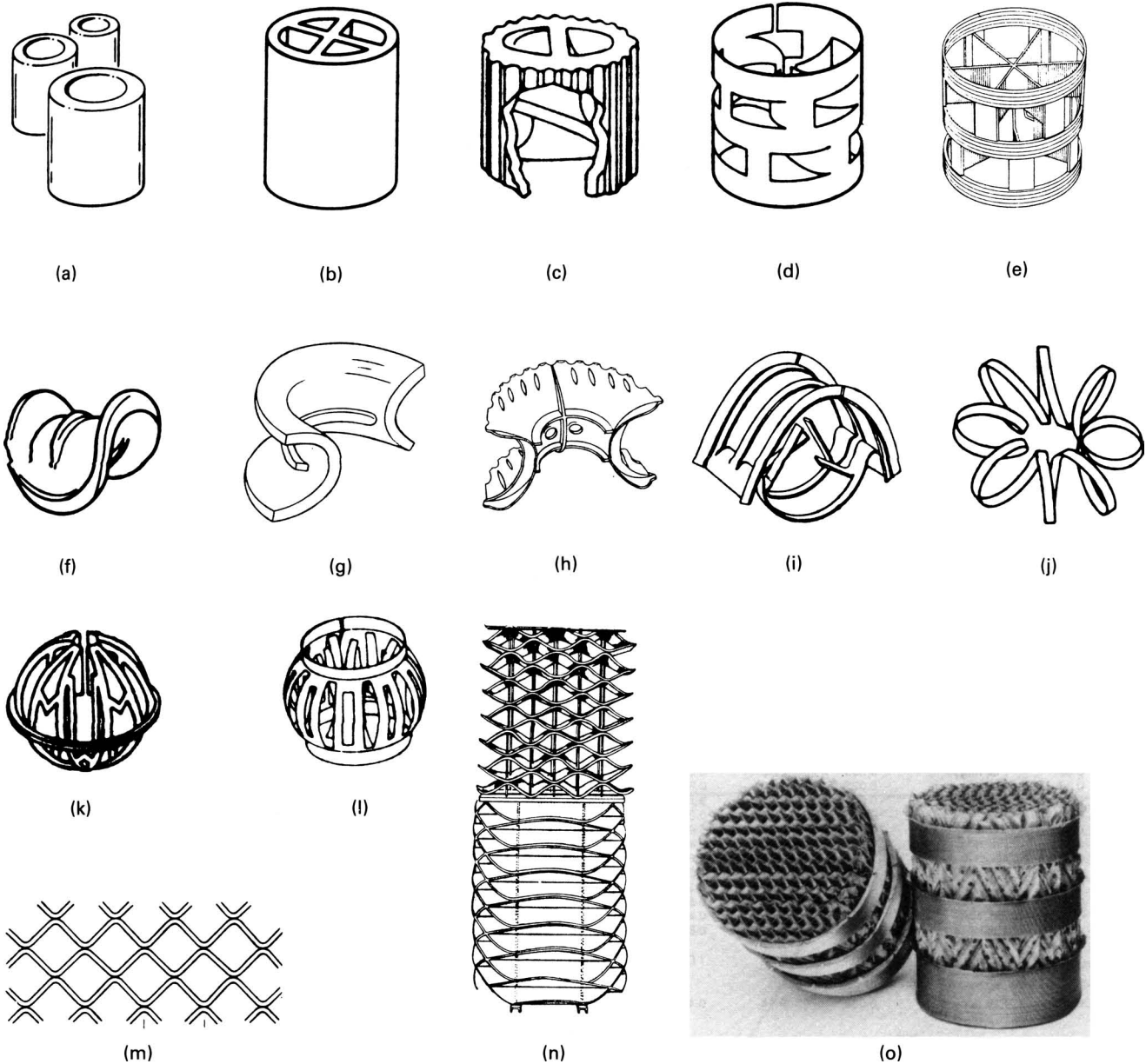
Figure 13.34. Some kinds of tower packings: (a) Raschig ring; (b) partition or Lessing ring; (c) double spiral ring; (d) metal pall ring; (e) plastic pall ring; (f) ceramic Berl saddle; (g) ceramic intalox saddle (*Koch-Glitsch Co.*); (h) plastic intalox saddle (*Koch-Glitsch Co.*); (i) metal intalox saddle (*Koch-Glitsch Co.*); (j) *Tellerette (Chem-Pro Co.*); (k) plastic tripak (*Jaeger Products Co.*); (l) metal tripak (*Jaeger Products Co.*); (m) section through expanded metal packing; (n) sections of expanded metal packings placed alternately at right angles (*Denholme Co.*); (o) structured packing elements for small columns, with wall wipers at the periphery.

rates are low, the maldistribution is more serious. In any event good distribution must be provided initially. A common rule is that the number of liquid streams should be 3–5/sqft in towers larger than 3 ft dia, and several times this number in smaller towers. Some statements about redistribution are made at the beginning of this section.

LIQUID HOLDUP

The amount of liquid holdup in the packing is of interest when the liquid is unstable or when a desirable reaction is to be carried out in the vessel. A correlation for Raschig rings, Berl saddles, and intalox

saddles is due to Leva (*Tower Packings and Packed Tower Design,* U.S. Stoneware Co., Akron, OH, (1953):

$$L_w = 0.004(L/D_p)^{0.6}, \text{ cuft liquid/cuft bed} \tag{13.232a}$$

with L in lb liquid/(hr)(sqft) and D_p is packing size (in.). For instance, when $L = 10,000$ and $D_p = 2$, then $L_w = 0.066$ cuft/cuft.

PRESSURE DROP

An approximate method for determining pressure drop in beds of random or structured packings has been given (Figure 13.35). All

Table 13.13. Characteristics of Random Packings

Name	Material	Nominal Size, mm	Surface area m^2/m^3	% Voids	Packing factor, m^{-1}	Vendor
*Intalox saddles	M	(No. 25)		97	135	Koch-Glitsch, Inc.
''IMTP''		(No. 40)		97	24	Wichita, Kansas USA
		(No. 50)		98	59	
*Pall rings	M	16	—	92	266	(Generic)
		25	205	94	184	
		38	130	95	131	
		50	115	96	88	
		90	92	97	59	
*Pall rings	P	16	340	87	310	(Generic)
		25	205	90	180	
		50	130	91	131	
		90	100	92	85	
Berl saddles	C	13	465	62	790	(Generic)
		25	250	68	360	
		38	150	71	215	
Intalox saddles	C	13	625	78	660	Koch-Glitsch, Inc.
		25	255	77	197	Wichita, Kansas USA
		50	118	79	98	
		75	92	80	70	
Intalox saddles	P	25	206	91	131	Koch-Glitsch, Inc.
		50	108	93	92	Wichita, Kansas USA
		75	88	94	59	
Raschig rings	C	13	370	64	1900	(Generic)
		25	190	74	587	
		38	120	68	305	
		50	92	74	213	
		75	62	75	121	
Raschig rings	M	19	245	80	730	(Generic)
		25	185	86	470	
		38	130	90	270	
		50	95	92	187	
		75	66	95	105	

*Through-flow packing
Materials of construction: C = ceramic; M = metal; P = plastic (usually polypropylene)

TABLE 13.14. Survey of Efficiencies of Random Packed Beds

System	Dia. m	Packing Type	Size, m	Bed Depth m	HETP, m	HTU, m	System press., kPa
Hydrocarbons							
Absorber	0.91	Pall rings	0.05	7.0	0.85	—	5.964
L. O. top fractionator	0.91	Pall rings	0.05	5.2	0.76	—	1.083
L. O. bottom fractionator	1.22	Pall rings	0.05	5.2	0.85	—	1.083
Deethanizer top	0.46	Pall rings	0.038	6.1	0.88	—	2.069
Deethanizer bottom	0.76	Pall rings	0.05	5.5	1.01	—	2,069
Depropanizer top	0.59	Pall rings	0.038	4.88	0.98	—	1,862
Depropanizer bottom	0.59	Pall rings	0.038	7.32	0.73	—	1,862
Debutanizer top	0.50	Pall rings	0.038	3.66	0.73	—	621
Debutanizer bottom	0.50	Pall rings	0.038	5.49	0.61	—	621
Pentane-isopentane	0.46	Pall rings	0.025	2.74	0.46	—	101
Light/heavy naphtha	0.38	Pall rings	0.025	3.05	0.62	0.54	13
	0.38	Intalox	0.025	3.05	0.76	0.61	13
	0.38	Raschig rings	0.025	3.05	0.71	0.52	13
Iso-octane/toluene	0.38	Pall rings	0.025	3.05	0.43	0.45	13
	0.38	Pall rings	0.025	3.05	0.53	0.51	13
Gas plant absorber	1.22	Pall rings	0.025	7.0	0.88	—	6,206

manufacturers make available pressure drop data for their packings, usually only for the air-water system. Samples of such data are given in Figures 13.36 and 13.37.

13.14. EFFICIENCES OF TRAYS AND PACKINGS

The numbers of theoretical or equilibrium stages needed for a given vapor-liquid separation process can be evaluated quite pre-

TABLE 13.14.—(*continued***)**

System	Dia. m	Packing Type	Size, m	Bed Depth m	HETP, m	HTU, m	System press., kPa
Hydrocarbons/water							
Acetone	0.36	Intalox	0.025	3.96	0.46	—	101
	0.46	Pall rings	0.025	8.38	0.37	—	101
Methanol (batch)	0.61	Intalox	0.038	4.27	—	0.76	101
Methanol	0.41	Pall rings	0.025	4.27	—	0.52	101
	0.30	Intalox	0.025	8.23	0.46	—	101
Isopropanol	0.53	Plastic pall	0.038	4.88	—	0.84	101
	0.33	Intalox	0.025	6.40	—	0.76	101
	0.46	Intalox	0.025	3.35	0.48	—	101
Ethylene glycol	1.07	Pall rings	0.038	4.88	0.91	—	31
Propylene glycol	0.25	Intalox	0.013	1.83	—	0.86	101
Furfural	0.51	Intalox	0.038	5.49	0.61	—	101
Formic acid	0.91	Pall rings	0.05	10.67	0.76	—	101
Acetone (absorption)	0.61	Intalox	0.038	5.49	—	0.46	101
Benzolchloride/benzene/steam	0.61	Pall rings	0.025	5.18	—	1.07	101
Tall oil/steam	3.66	Intalox	0.05	10.46	0.76	—	101
Methylisobutyl ketone/steam	1.07	Intalox	0.038	8.53	1.22	—	101
Acetone	0.38	Intalox	0.05	2.90	0.53	0.47	101
	0.38	Pall rings	0.038	2.90	0.46	0.55	101
	0.38	Pall rings	0.025	2.90	0.44	0.34	101
	0.38	Intalox	0.025	2.90	0.52	0.32	101
	0.38	Berl	0.025	2.90	0.52	0.34	101
	0.38	Cer. Raschig	0.025	2.90	1.05	0.36	101
	0.38	Raschig rings	0.025	2.90	0.52	0.36	101
	0.38	Pall rings	0.016	2.90	0.40	0.32	101
Methanol	0.38	Pall rings	0.025	2.90	0.66	0.67	101
Polar hydrocarbons							
Methyl furan/methyl tetra-hydrofuran	0.61	Intalox	0.038	14.63	0.53	—	101
Benzoic acid/toluene	0.61	Intalox	0.038	6.40	0.46	—	101
Methone (5, 5 dimethyl 1, 3 cyclohexanedione), batch	0.56	Pall rings	0.038	9.75	0.49	—	101
Monochloro acetic acid/acetic anhydride	0.25	Intalox	0.025	2.74	—	0.86	8.0
Tar acid distillation (batch)	0.46	Pall rings	0.038	9.14	0.49	—	13
Cresols (batch)	0.46	Pall rings	0.038	9.14	0.85	—	13
Benzene/monochloro-benzene	0.38	Intalox	0.038	2.90	1.80	0.52	101
	0.38	Intalox	0.025	2.90	1.13	0.76	101
Methylethylketone/toluene	0.38	Pall rings	0.025	2.90	0.35	0.29	101
	0.38	Raschig rings	0.025	2.90	0.30	0.31	101
	0.38	Intalox	0.025	2.90	0.23	0.27	101
	0.38	Berl	0.025	2.90	0.31	0.31	101
	0.38	Cer. Raschig	0.025	2.90	0.46	0.30	101
	0.38	Pall rings	0.025	2.90	0.40	0.28	101
	0.38	Raschig rings	0.025	2.90	0.35	0.30	101
	0.38	Intalox	0.025	2.90	0.29	0.26	101
	0.38	Berl	0.025	2.90	0.34	0.29	101
	0.38	Cer. Raschig	0.025	2.90	0.31	0.27	101
Phenol/ortho-creosol	0.46	Pall rings	0.038	9.14	0.49	—	13
Fatty acid	0.76	Pall rings	0.038	12.19	0.85	—	4.94
Benzene/monochloro-benzene	1.83	Intalox	0.038	9.75	1.07	—	13
DMPC/DMPC cresols/DBOC batch	0.46	Pall rings	0.038	9.14	0.49	—	2.67
$CH_3Cl/CH_3Cl_2/CHCl_3/CCl_4$	0.48	Intalox	0.025	20.73	0.46	—	101
Methylene/light ends	0.46	Intalox	0.025	13.41	0.46	—	101
Methylene/product	0.64	Intalox	0.038	13.72	0.46	—	101
Chloroform/product	0.56	Intalox	0.038	27.43	0.46	—	101

[Eckert, *Chem. Eng. Prog.* **59**(5) 76 (1963)].

cisely when the equilibrium data are known, but in practice, equilibrium is not attained completely on trays, and the height of packing equivalent to a theoretical stage is a highly variable quantity. In a few instances, such as in large diameter towers (10 ft or so), a significant concentration gradient exists along the path of the liquid flow, so that the amount of mass transfer may correspond to more than that calculated from the average terminal compositions.

For trays, it is convenient to express efficiency on an overall basis:

$$E_{oc} = N_t/N_{act} \qquad (13.233)$$

Where E_{oc} is the overall column efficiency. For packed columns, a related term is used:

Table 13.15. Characteristics of Structured Packings

Name	Material	Nominal Size	Surface area m^2/m^3	% Voids	Packing factor, m^{-1}	Vendor
Flexipac	S	1	558	91	108	Koch-Glitsch
		2	223	93	72	Wichita, Kansas USA
		3	134	96	52	
Intalox	S	1T	315	95	66	Koch-Glitsch
		2T	213	97	56	Wichita, Kansas USA
Max-Pak	S		229	95	39	Jaeger Products Houston, Texas USA
Mellapak	S	125Y	125	97	33	Sulzer Chemtech Tulsa, Oklahoma USA;
		125X*	125	97		Winterthur, Switzlerland
		250Y	250	95	66	
		250X*	250	95		
		350Y	350	93	75	
		500X*	500	91	25	
Sulzer	G	AX*	250	95		Sulzer Chemtech
		BX*	492	90	69	
		CY	700	85		
Montz-Pak	S	B1-125	125	97		Julius Montz
		B1-125.6*	125	97	72	Hilden, Germany
		B1-250	250	95		
		B1-250.6*	250	95		
		B1-350	350	93		
	G	A3-500	500	91		
	E	BSH-250	250	95		
		BSH-500	500	91		
Ralupak	S	250YC*250		95		Raschig AG Ludwigshafen, Germany

NOTES: Asterisk denotes 60=degree corrugation angle (with the horizontal); all others 45 degrees. Packing factors from Kister & Gill (*Chem. Eng. Prog.* **87** (2) 32 (1991), and Houston AIChE Meeting, March 19–23, 1995.
Material of construction: C = ceramic; E = expanded metal; G = metal gauze; S = sheet metal

$$HETP = Z/N_t \qquad (13.234)$$

where $HETP$ = height equivalent to a theoretical plate (stage) and Z is the packed height. If the transfer unit approach is being used, N_t and NTU_{og} are related by Eq. (13.173). The main factors affecting E_{oc} and $HETP$ are geometrical configuration of the tray or packing, flow rates, vapor-liquid equilibrium ratio, and physical properties of the vapor and liquid.

TRAYS

In spite of all the effort that has been expended on this topic, the prediction of mass transfer efficiency on crossflow trays is still not on a satisfactory basis for rigorous design. However, if only an approximate value of efficiency is needed, as in conceptual design, the O'Connell (1946) method is satisfactory. As shown in Figure 13.38(a), a number of overall efficiency values have been correlated

EXAMPLE 13.16
Hydraulic Performance of a Packed Column
For the system of Example 13.15, a packed column will be analyzed for (a) 2-in. metal pall rings and (b) Mellapak 250Y structured packing. From Table 13.13, F_p for pallrings = 131 m^{-1} or 40 ft^{-1}. From Table 13.15, F_p for Mellapak 250Y = 66 m^{-1} or 20.1 ft^{-1}. The liquid viscosity is 0.20 centipoises = 0.43 centistokes.

(a) *Pall rings.* Use the correlation of Figure 13.36:

$abscissa = L/G[\rho_v/(\rho_L - \rho_v)]^{0.5}$

= 0.307 (as in previous example)

for 80% flood, $\Delta P = 0.8(1.5) = 1.2$ inH_2O/ft.

$ordinate = 1.15 ft^{0.5}/s = C_s F_p^{0.5} v^{0.05}$

$\therefore C_s = 1.15/(40^{0.5} \times 0.43^{0.05}) = 0.189 = U_s[(26.55 - 2.75)/2.75]$

$U_s = 0.589$ ft/s

volumetric flow = $Q_v = 271,500/[(3600)(2.75)] = 27.42$ cfs

cross section of column = 46.56 ft2

$\therefore$ column diameter = 7.70 ft

(b) *Mellapak 250 Y*
For same abscissa and ordinate,

$C_s = 1.15/[(20.1^{0.5} \times 0.43^{0.05}) = 0.267$

$U_s = 0.833$ ft/s

Cross section of column = 32.93 ft^2

$\therefore$ column diameter = 6.48 ft

Recapitulation: For this problem, column diameters are:

Sieve tray	7.67 ft
Pall rings	7.70 ft
Mellapak 250Y	6.48 ft
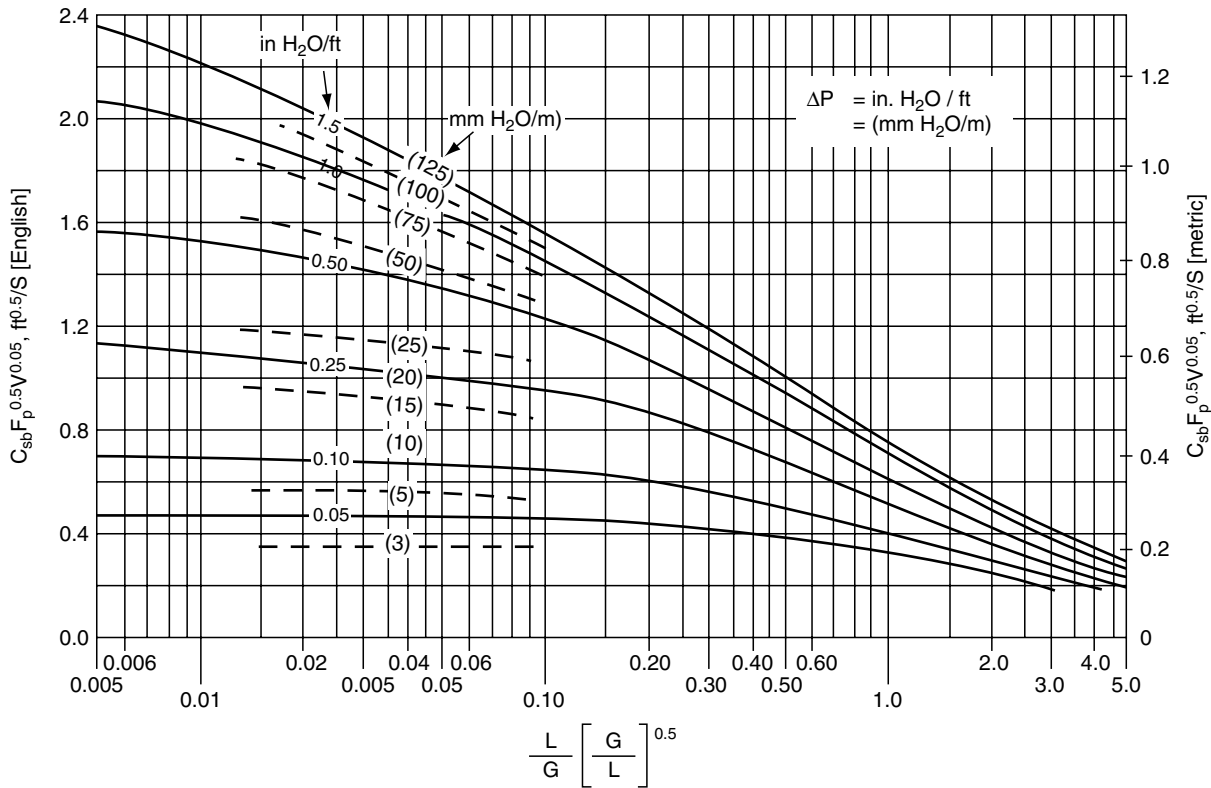
Figure 13.35. Generalized chart for estimating pressure drop and maximum capacity of packings (Strigle, 1994)

against the product $\mu_L \alpha$, where μ_L is the liquid viscosity on the tray (in centipoises) and α is the relative volatility. In Figure 13.38(b), efficiency values for absorber-strippers are shown, with the correlating parameter related to that in the upper figure. Fitting equations for the curves are given on the charts. For the curve in 13.38(a), Doherty and Malone (2001) have given an approximate equation:
where μ_{Lo} is taken as 1.0 centipoise.

$$\frac{E_{oc} - 0.24}{0.76} = \exp\left(-\sqrt{\alpha \frac{\mu_L}{\mu_{L0}}}\right) \tag{13.235}$$

For more rigorous prediction of tray efficiency, the first effort was made by the AIChE Research Committee resulting in a semi-empirical method for bubblecap trays (*AIChE Bubble-Tray Manual*, 1958), based on the two-film model and small air-water simulation studies. The product of the method is the so-called point efficiency E_{og} that applies to a point on the tray and is related through corrections to the overall efficiency E_{oc}, as shown in Figure 13.39. The reference gives methods for converting point efficiency top overall tray efficiency E_{mv} (Murphree efficiency) and on to overall column efficiency E_{oc}, accounting for the amount of liquid entrainment (if any) from tray to tray. Chan and Fair (1984a) used a large database of large column efficiencies to extend the AIChE approach to sieve trays.

Recent efforts have attempted to address quantitatively the complex fluid mechanics on trays, although the effects of geometry, flow rates, and physical properties on interfacial area and transfer rate are not completely understood. Prado and Fair (1990) made the first attempt, using such variables as bubble size distribution, residence times, and vapor/liquid diffusional phenomena. Garcia

and Fair (2000) extended this work to a large database of commercial efficiencies. The latter two methods require a special computer program for calculating efficiencies. The Chan/Fair model is commonly used for final design, if the systems involved are fairly simple and straightforward. For situations involving highly nonideal or complex mixtures (e.g., in azeotropic distillations), another method is being used: scaleup from laboratory distillation data using the design mixture. This method involves setting up a laboratory Oldershaw column, which contains small sieve trays (typically 1 or 2 in. in diameter), and running the column under proposed design conditions. For atmospheric pressure and below, glass equipment is used; for higher pressures, metal columns with the same dimensions are used. Oldershaw equipment is off-the-shelf from a number of laboratory supply houses. The approach is discussed by Fair et al. (1983). and Fair et al. (2002) have provided an update with new data. As in the case of the computational methods, values of the point efficiency are provided from Oldershaw experiments.

Pressure Drop. Since efficiency depends on hydraulic factors, a method will first be given for estimating pressure drop across a sieve tray. The total drop across the tray is taken as the sum of the drop through the holes plus the drop through the aerated mixture:

$$h_t = h_d + h_L \tag{13.236}$$

where h is the hydraulic head of liquid. The drop through the holes ("dry drop") is obtained from the orifice equation:

$$h_d = 92.8(\rho_G/\rho_L)U_h^2 \tag{13.237}$$
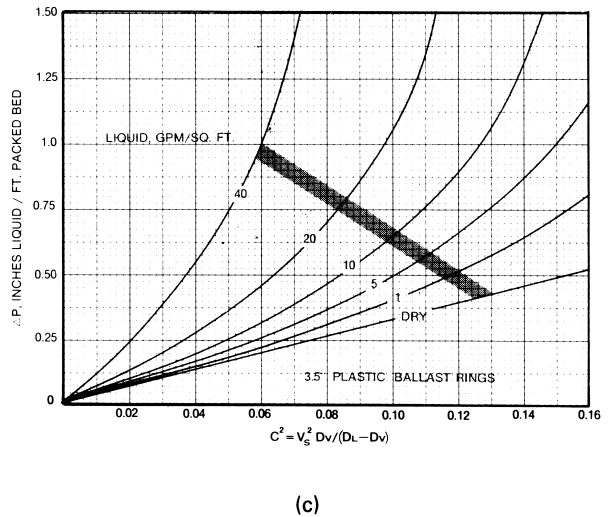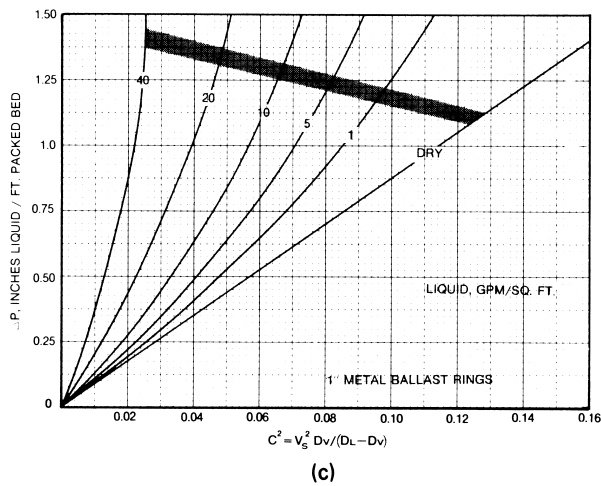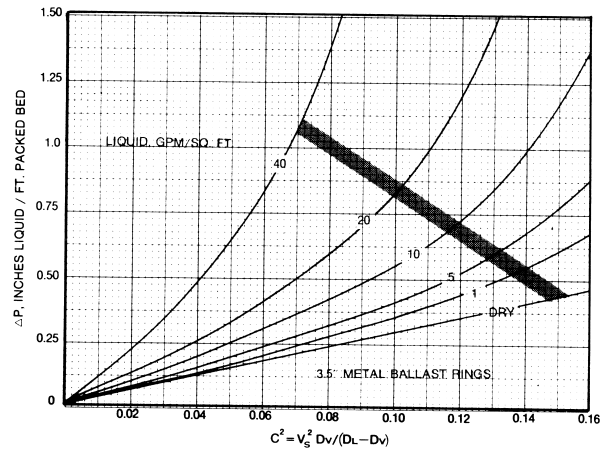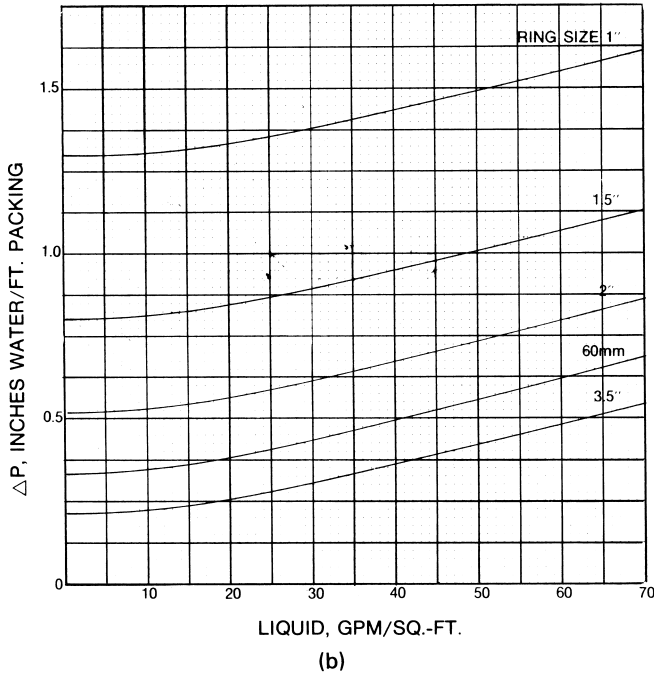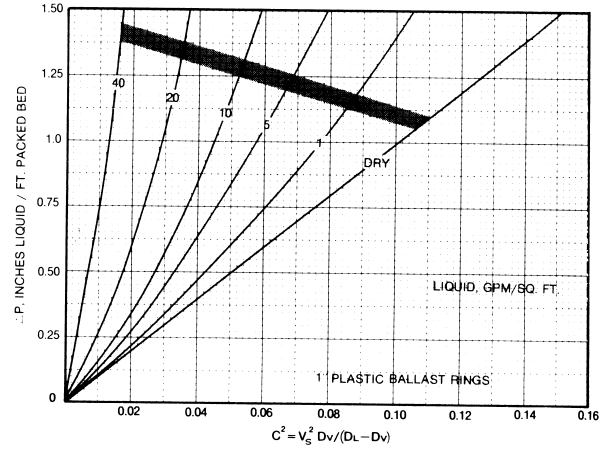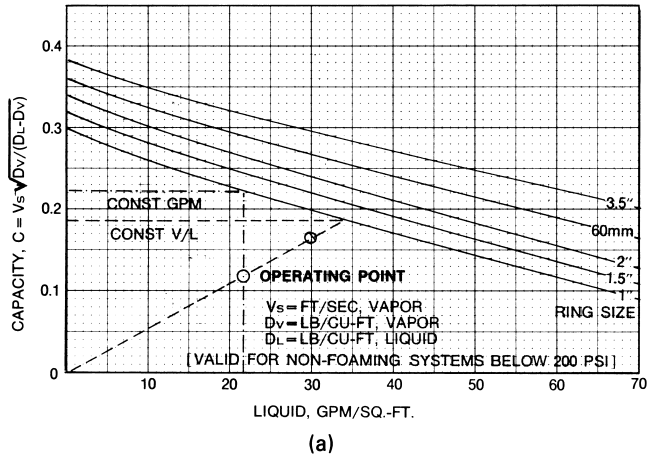
Figure 13.36. Capacity and pressure drop in beds of pall rings Koch-Glitsch, Inc. (a) Capacity chart for pall rings. V_s = vapor velocity (ft/sec). Example with 1 in. rings,

$$\text{fractional loading} = C/C_F$$

$$= \begin{cases} 10.161/0.188 = & 0.856 \text{ at constant } V/L \\ 0.161/0.200 = & 0.805 \text{ at constant gpm.} \end{cases}$$

(b) Pressure drop at 85% of flooding. (c) Pressure drops with 1 and 3.5 in. metal and plastic rings at a range of flow rates.
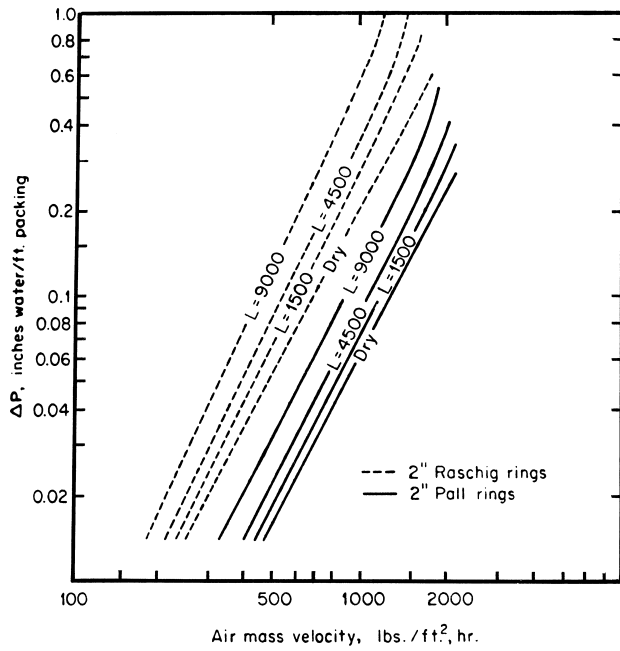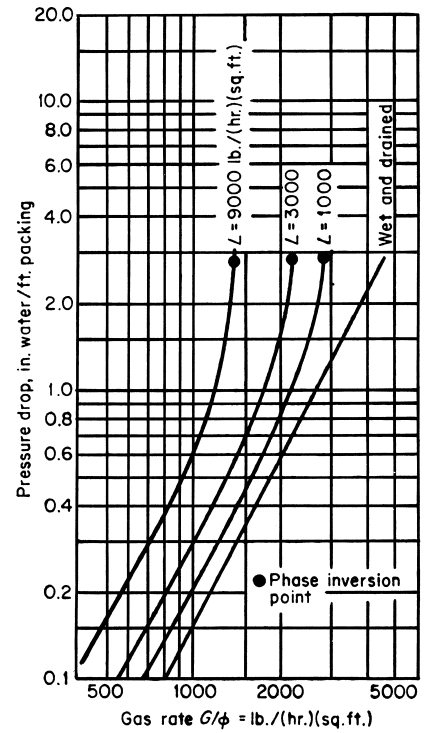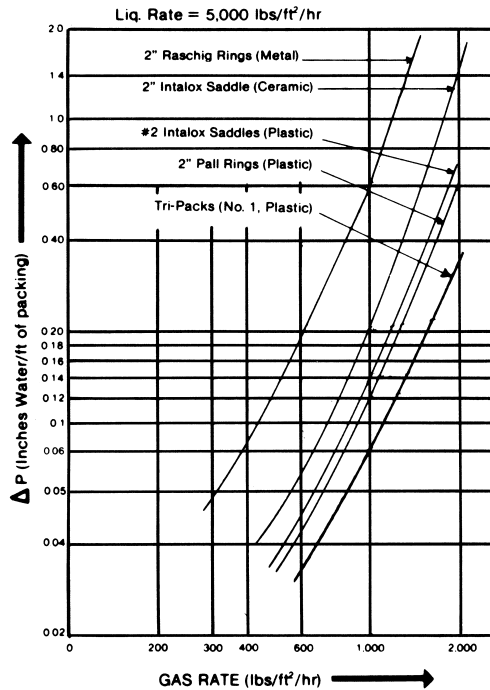
Figure 13.37. Comparison of pressure drops through several kinds of packed beds. (a) 2 in. Raschig and pall rings [*Eckert et al.*, Chem. Eng. Prog. **54**(*1*), *70* (*1958*)]. (b) 1 in. Tellerettes [*Teller and Ford*, Ind. Eng. Chem. **50**, *1201* (*1958*)]. (c) 2 in. plastic Tripack and other 2 in. packings (*Polymer Piping and Metals Co.*).
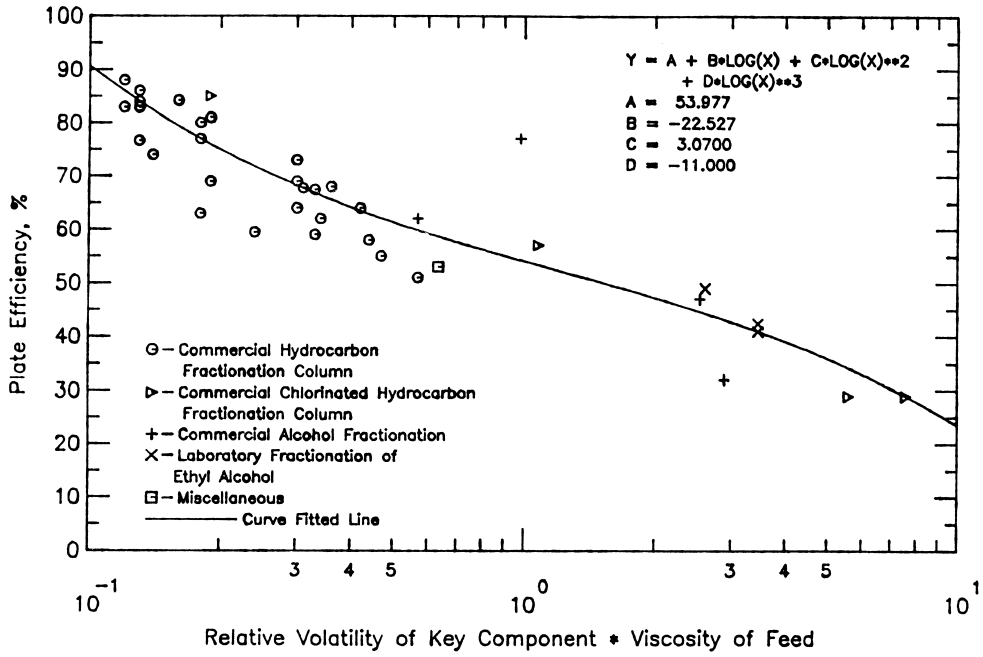
(a)
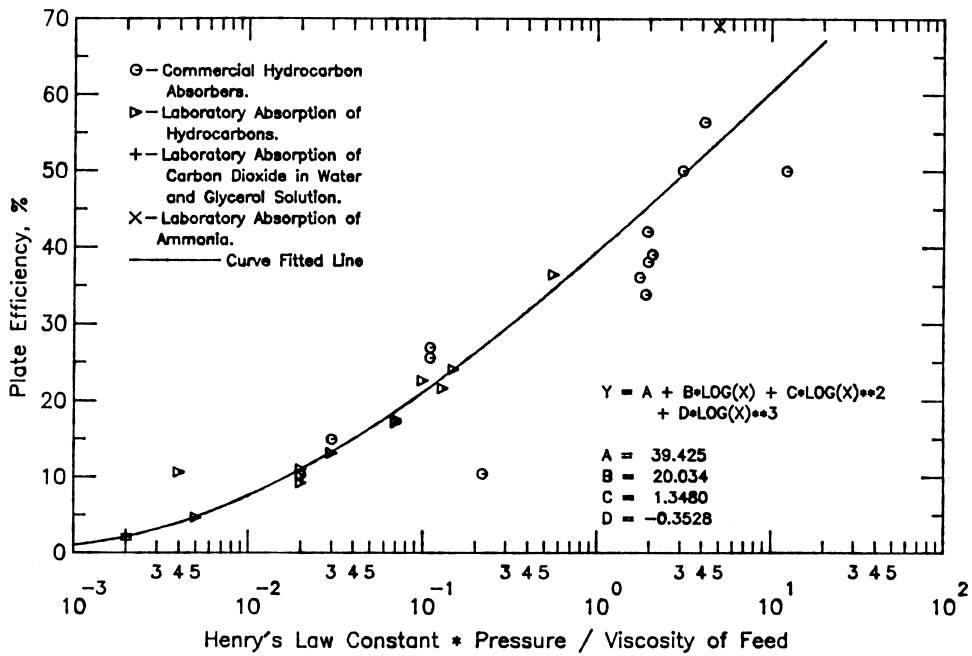
(b)

Figure 13.38. Efficiencies of fractionators and absorber-strippers. The original curves of O'Connell [Trans. AIChE **42**, *741 1946*)] have been replotted and fitted with equations, as shown on the figures, by S. Negahban (*University of Kansas, 1985*). (a) Fractionators (the viscosity μ is in cP). (b) Absorbers and strippers; H = Henry's law constant in lb mol/(cuft)(atm), P is in atm, and μ is in cP.

where h is in mm liquid and U_h, the hole velocity, is in m/s. Eq. (13.237) utilizes an orifice coefficient of 0.75; for other values and more details on the methodology, see Fair, 1997.

The liquid holdup term h_L is obtained from

$$h_L = \beta(h_w + h_{ow}) \tag{13.238}$$

where β is an aeration factor, h_w is the weir height, and h_{ow} is the crest over the outlet weir. An average value of β may be taken as 0.5. The crest is obtained from the weir equation:

$$h_{ow} = 664(q/L_w)^{2/3} \tag{13.239}$$
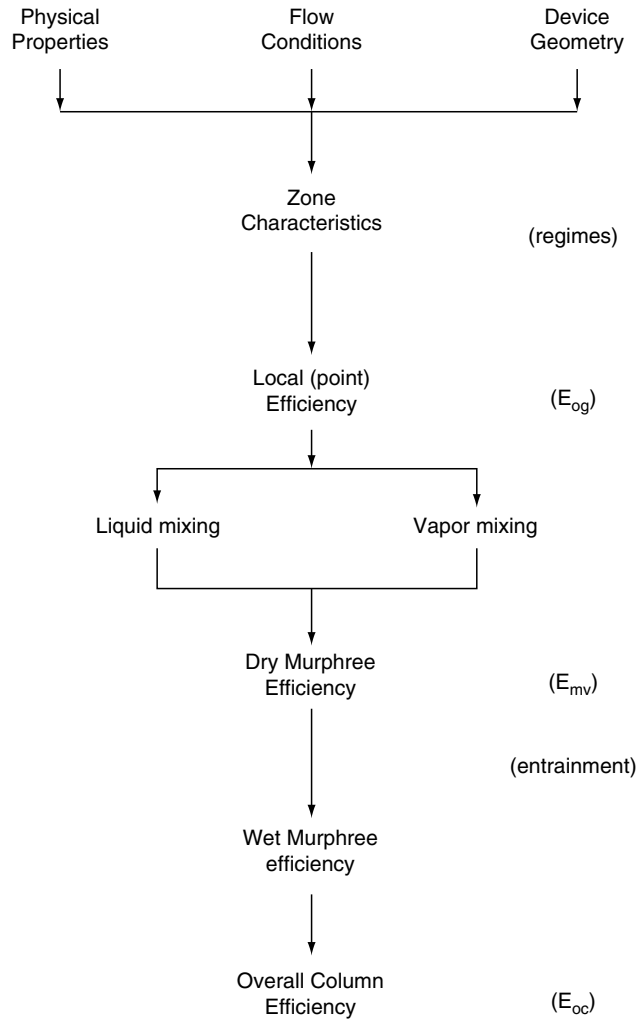
Figure 13.39. Relationships between the different efficiencies.

where q = liquid flow rate, m^3/s and L_w = weir length, m.

One should note the above reference for more detailed hydraulic calculation methodology.

Efficiency Calculation. The Chan/Fair approach will be described here. First, the vapor phase volumetric mass transfer coefficient is calculated:

$$k_g a = \frac{316 D_g^{0.5}(1030f - 867f^2)}{(h_L)^{0.5}} s^{-1} \tag{13.240}$$

Next, the liquid phase volumetric coefficient is calculated:

$$k_L a = (0.40 F_{va} + 0.17)[3.875(10^8)D_L]^{0.5} s^{-1} \tag{13.241}$$

where

D_g, D_L = vapor and liquid phase diffusion coefficients, m^2/s
h_L = liquid holdup, mm
f = fractional approach to flood
F_{va} = active area F-factor, $U_a \rho_g^{0.5}$ (active area = bubbling area of tray)

Residence times for liquid and vapor in the two-phase mixture on the tray (called froth) are determined from

$$t_g = \frac{\text{volume of vapor space within the froth}}{\text{volumetric flow rate of vapor}} = \frac{A_a \varepsilon Z_f}{Q_v} \tag{13.242}$$

$$t_L = \frac{\text{volume of liquid space within the froth}}{\text{volumetric flow rate of liquid}} = \frac{A_a(1 - \varepsilon)Z_f}{q_L} \tag{13.243}$$

where

Z_f = height of froth (from Figure 13.40)
A_a = active area of tray
ε = void fraction of froth = $1 - h_L/Z_f$

Gas and liquid phase transfer units are next calculated:

$$(NTU)_g = (k_g a)(t_g) \tag{13.244}$$

$$(NTU)_L = (k_L a)(t_L) \tag{13.245}$$

which leads to a value of the point efficiency:

$$1/(NTU)_{og} = 1/(NTU)_g + \lambda/(NTU)_L \tag{13.246}$$

$$E_{og} = 1 - \exp\lfloor -(NTU)_{og}\rfloor \tag{13.247}$$
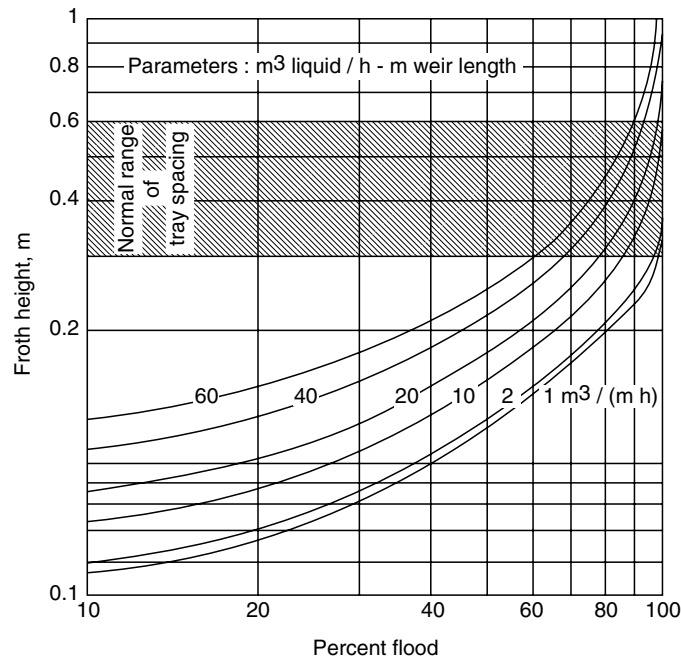
Figure 13.40. Chart for estimating the height of froth on a sieve tray. (Stichlmair and Fair, 1998).

where
λ = stripping factor (see Eq. 13.167)
E_{og} = point efficiency, fractional

Conversion to Murphree Tray Efficiency. For complete liquid mixing on the tray, as found in small columns (e.g., Oldershaws) and in some vacuum columns where the volumetric flow of vapor is much higher than that of the liquid, $E_{og} = E_{mv}$. For the opposite case of plug flow of liquid across the tray,

$$E_{mv} = 1/\lambda\left(\exp\left[\lambda E_{og} - 1\right]\right) \tag{13.248}$$

For a condition between complete mixing and plug flow, diffusional models such as that of Bennett and Grimm (1991) are used. For conservative work, the complete mixing model is appropriate.

Conversion to Overall Column Efficiency. The value of E_{oc} is most used and understood (see Eq. 13.233). At total reflux, E_{oc} and E_{mv} are about equal. Otherwise,

$$E_{oc} = \frac{\ln\left[1 + E_{mv}(\lambda - 1)\right]}{\ln \lambda} \tag{13.249}$$

where λ is the stripping factor, for distillation taken as m (V/L), with m being the slope of the equilibrium curve. When the relative volatility is high, this slope varies greatly between the top and bottom of the column.

Entrainment Corrections. Above about 80% of flood, the recirculation of liquid as entrainment between trays undermines the countercurrent action of the tray column, and efficiency therefore suffers. This is a particular problem in vacuum distillation where it may be optimum to allow a certain amount of liquid entrainment in initial design. Figure 13.41 shows an approximate method for entrainment correction to column efficiency or Murphree efficiency. The abscissa scale is the same parameter used for flooding prediction (Figure 13.32(b)). The ordinate value is used to correct from a "dry" to a "wet" efficiency (with entrainment):

$$E_{wet} = \frac{E_{dry}}{1 + E_{dry}\psi/(1 - \psi)} \tag{13.250}$$

Representative Efficiencies of Larger Columns. Table 13.16 and Figure 13.42 show efficiencies for several different tray types and systems being separated. It is clear that vapor velocity has an effect on efficiency, especially at high loadings when entrainment occurs. At low velocities, sieve and valve trays tend to weep liquid through the perforations, and this recycle of liquid affects efficiency. For bubblecap trays, with their built-in liquid seal, the loss of efficiency at low loading results from poor dispersion. It may be noted that most of the test data are based on total reflux operation, and thus at low vapor loadings, liquid loadings are low also.

Multicomponent Systems. Most efficiency models and test data are based on binary systems. For multicomponent systems it is often possible to use the key components as a pseudobinary system. Chan and Fair (1984b) found that selection of the two components should be based on the dominant pair (if not the key components). Rigorous treatments of multicomponent separations are given by Taylor and Krishna (1993).

Example 13.17 shows a comparison between efficiencies calculated by the O'Connell and Chan/Fair methods.

PACKED TOWERS

As discussed earlier, Eqs. 13.164–13.173 form the basis for prediction or evaluation of packed column mass transfer efficiency. The simplest, and often most useful, criterion for packed bed efficiency is the HETP (height equivalent to a theoretical plate). It is the bed height in which one theoretical stage may be accomplished. However, it is an empirical term and can relate only to mass transfer rate after being converted to the HTU (height of a transfer unit) value. Still, many designers prefer to couple an HETP value with the required number of stages to obtain the needed bed height. Many vendors of packings can supply approximate values of HETP, taken from experience. Fortunately, the more fundamental HTU
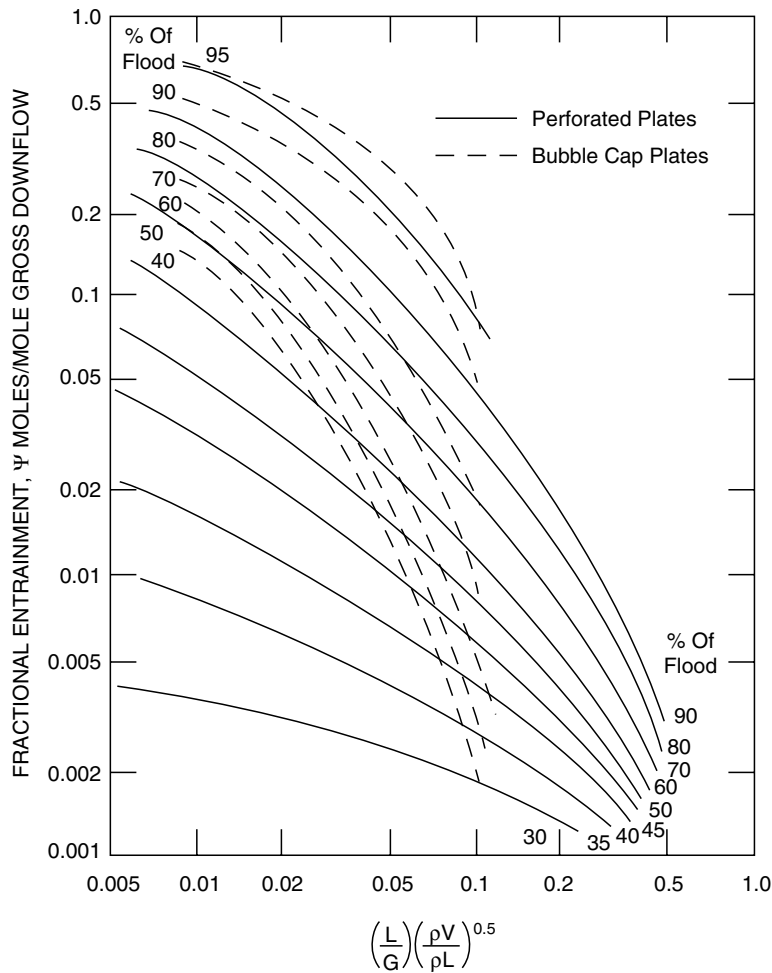
Figure 13.41. Chart for estimating entrainment parameter as a function of flow parameter and approach to entrainment flood.

approach, used in all modern mass transfer models, allow conversion to HETP values (Eqs. 13.172 and 13.173). In the sections to follow, predictive models for transfer efficiency will be limited to the transfer unit approach.

Random Packings. In a 1960 paper, Cornell et al. correlated available packed column efficiencies using a two-film concept and a rather limited database, especially for larger columns. Their correlation was updated by Bolles and Fair (1982), who used a much larger database and column diameters up to 4 ft (1.2 m). Several sizes of ceramic Raschig rings, metal Raschig rings, metal pall rings, and ceramic Berl saddles were included in the database. For the liquid phase,

$$(HTU)_L = \phi (Sc_L)^{0.5}(C)(Z/10)^{0.15} \tag{13.251}$$

For the gas or vapor phase,

$$(HTU)_G = \frac{\psi (Sc_G)^{0.5} \left(\frac{d_c}{12}\right)^m \left(\frac{Z}{10}\right)^{1/3}}{[L_m f_1 f_2 f_3]^{0.6}} \tag{13.252}$$

where

HTU_L, HTU_G = heights of transfer units, ft.
ϕ and ψ = parameters in Figures 13.43 and 13.44

Sc_L and Sc_G = dimensionless Schmidt numbers ($= \mu/(\rho D)$ for each phase
C = flooding correction factor from Figure 13.45
Z = height of packed section (between distributors), ft
d_c = column diameter, in.
L_m = liquid flow mass velocity, lb/(hr-ft^2)
f_1 = liquid viscosity correction = $(\mu_1/1.005)^{0.16}$, μ_L in cP
f_2 = liquid density correction = $(1.00/\rho_L)^{1.25}$, ρ_L in g/cm^3
f_3 = surface tension correction = $(72.8/\sigma)^{0.8}$, σ in dyn/cm
m = exponent = 1.24 for rings and 1.11 for saddles

The Bolles/Fair correlation does not include some of the newer, "through-flow" random packings, such as intalox metal tower packing (IMTP), Nutter rings, cascade mini-rings, and Fleximax rings. A model by Wagner et al. (1997) covers these packings as well as pall rings and metal Raschig rings. This model is difficult to use without access to the computer program, and reasonable results can be obtained from the Bolles/Fair model if the approach to flood is adjusted for the higher capacities of the "through-flow" elements.

Figures 13.46 and 13.47 show representative efficiency and pressure drop data for different random packings.

Structured Packings. A number of models for predicting mass transfer efficiency of a given structured packing have been

TABLE 13.16. Efficiency Data of Some Operations with Bubblecap, Ripple, and Turbogrid Trays

Disperser	System	Column diameter, ft	Tray spacing, in	Pressure, psia	Static submergence, in	Efficiency, % E_{mo}^*	Efficiency, % $E_{oc}^\dagger$	Remarks	Ref.
Bubble cap	Ethanol-water	1.31	10.6	14.7	1.18	83–87	......	......	1
		1.31	16.3	14.7	1.18	84–97	......	......	
		2.5	14	14.7	1.2	80–85	......	......	2
	Methanol-water	3.2	15.7	14.7	1.0	90–95	......	......	3
	Ethyl benzene-styrene	2.6	19.7	1.9	0.2	55–68	......	......	4
	Cyclohexane–n-heptane	4.0	24	14.7	0.25	65–90	......	......	5
				24	4.25	65–90	......		
				50		65–90			
	Cyclohexane–n-heptane	4.0	24	5	0.6	65–85	......	Tunnel caps	6
				24		75–100	......		
	Benzene-toluene	1.5	15.7	14.7	1.5	70–80	......	......	7
	Toluene-isooctane	5.0	24	14.7	0.4	......	60–80	......	8
Ripple sieve	Methanol-water	3.2	15.7	14.7	......	70–90	......	10.8% open	3
	Ethanol-water	2.5	14	14.7	1.0	75–85		10.4%	2
	Methanol-water	3.2	15.7	14.7	1.57	90–100		4.8% open	3
	Ethyl benzene–styrene	2.6	19.7	1.9	0.75	70		12.3% open	9
	Benzene-toluene	1.5	15.7	14.7	3.0	60–80		18% open	7
	Methyl alcohol–n-propyl alcohol– sec-butyl alcohol	6.0	18	18	1.38	......	64	......	10
	Mixed xylenes +C$_8$-C$_{10}$ paraffins and naphthenes	13.0	21	25	1.25	......	86	......	5
	Cyclohexane–n-heptane	4.0	24	5	2.0	60–70	......	14% open	13
				24		80	......	14% open	13
		4.0	24	5	2.0	70–80	......	8% open	12
	Isobutane-n-butane	4.0	24	165	2.0	110	......	14% open	13
		4.0	24	165	2.0	120	......	8% open	12
		4.0	24	300	2.0	110	......	8% open	12
		4.0	24	400	2.0	100	......	8% open	12
Turbogrid valve	Methanol-water	3.2	15.7	14.7	......	70–80	......	14.7% open	3
	Ethanol-water	2.5	14	14.7	1.0	75–85	......	......	2
	Ethyl benzene–styrene	2.6	19.7	1.9	0.75	75–85	......	......	4
	Cyclohexane–n-heptane	4.0	24	20	3.0	......	50–96	Rect. valves	11
	n-Butane-isobutene	4.0	24	165	3.0	......	104–121	Rect. valves	11
	Benzene-toluene	1.5	15.7	14.7	3.0	75–80	......	......	7

References
1. Kirschbaum, *Z. Ver. Dtsch. Ing. Beth. Verfahrenstech.*, (5), 131 (1938); (3), 69 (1940).
2. Kirschbaum, *Distillier-Rektifiziertechnik*, 4th ed., Springer-Verlag. Berlin and Heidelberg, 1969.
3. Kastanek and Standart, *Sep. Sci*, 2, 439 (1967).
4. Billet and Raichle, *Chem. Ing. Tech.*, 38, 825 (1966); 40, 377 (1968).
5. AIChE Research Committee, *Tray Efficiency in Distillation Columns*, final report, University of Delaware, Newark, 1958.
6. Raichle and Billet, *Chem. Ing. Tech.*, 35, 831 (1963).
7. Zuiderweg, Verburg, and Gilissen, *Proc. Intn. Symp.*, Brighton, England, 1960.
8. Manning, Marple, and Hinds, *Ind. Eng. Chem.*, 49, 2051 (1957).
9. Billet, *Proc. Intn. Symp.*, Brighton, England, 1970.
10. Mayfield, Church, Green, Lee, and Rasmussen, *Ind. Eng. Chem.*, 44, 2238 (1952).
11. Fractionation Research, Inc., ''Report of Tests of Nutter Type B Float Valve Tray,'' July 2, 1964, from Nutter Engineering Co., Tulsa.
12. Sakata and Yanagi, *Inst. Chem. Eng. Symp. Ser.*, no. 56, 3.2/21 (1979).
13. Yanagi and Sakata, *Ind. Eng. Chem. Process Des. Dev.* 21, 712 (1982).
*See Eq. (18–32).
†See Eq. (18–28).
NOTE: To convert feet to meters, multiply by 0.3048; to convert inches to centimeters, multiply by 2.54; and to convert pounds-force per square inch to kilopascals, multiply by 6.895.
(*Chemical Engineers' Handbook*, McGraw-Hill, New York, 1984).

published since 1985. Because of the ordered geometry of the bed, the models are mechanistic and semi-theoretical. The first, by Bravo et al (1985) dealt only with Sulzer BX packing (see Table 13.15) which is a high-efficiency material made from wire gauze. The second, by Rocha et al. (1996) was an extension of the Bravo model, and covered a number of structured packing types, including those fabricated from sheet metal (e.g., Flexipac, Mellapak, and Montz-Pak). Concurrently, a somewhat different model was de-

veloped by Olujic at Delft University (1997). Fair et al. (2000) compared the Rocha and Olujic models against an extensive set of experimental data. The two models gave equal fits to the data. Since the Rocha model is somewhat easier to use, it will be described here.

Shortcut method. For orientation and conceptual design, a shortcut method for structured packing efficiency should be con-
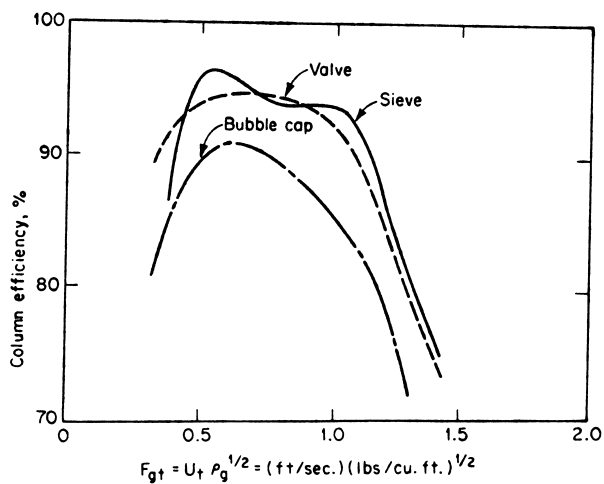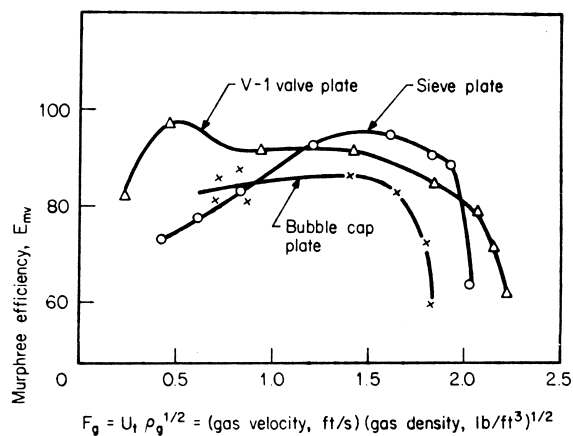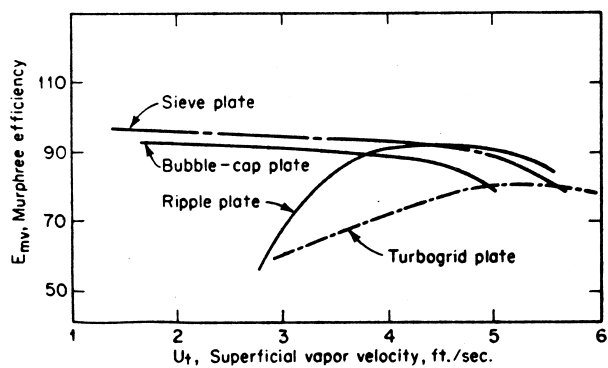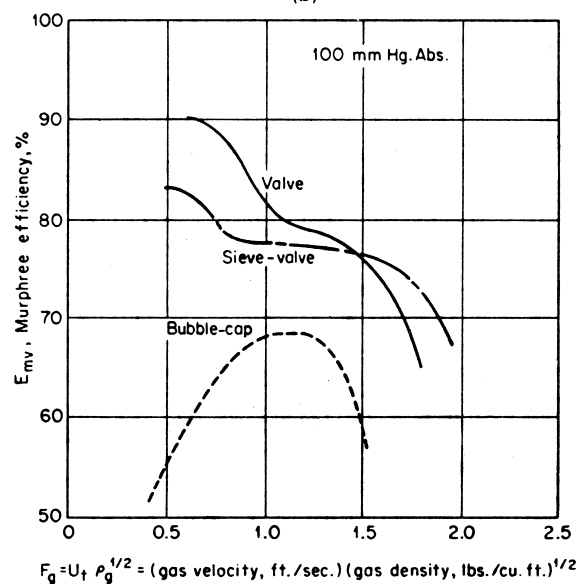
Figure 13.42. Efficiencies of some fractionations with several types of trays as a function of vapor factor $F = u\sqrt{\rho}$ or linear velocity. (a) Data of methanol/water in a column 3.2 ft dia [*data of Kastanek, Huml, and Braun*, Inst. Chem. Eng. Symp. Ser. **32**(*5*), *100 (1969)*]. (b) System cyclohexane/*n*-heptane in a 4 ft dia sieve column [*Sakata and Yanagi*, Inst. Chem. Eng. Symp. Ser. **56**, *3.2/21 (1979)*]; valve tray data (*Bulletin 160, Glitsch Inc., 1967*). (c) Methanol/water [*Standart et al.*, Br. Chem. Eng. **11**, *1370 (1966)*; Sep. Sci. **2**, *439 (1967)*]. (d) Styrene/ethylbenzene at 100 Torr [*Billet and Raichle*, Chem. Ing. Tech. **38**, *825 (1966)*; **40**, *377 (1968)*]. (e) Ethanol/water (*Kirschbaum*, Destillier und Rektifiziertechnik, *Springer, Berlin, 1969*). (f) Methanol/water [*Kastanek, Huml, and Braun*, Inst. Chem. Eng. Symp. Ser. **32**, *5.100, (1969)*].

sidered. Lockett (1998) generated the source data from the Rocha et al. model, described below, and expressed the result in terms of the *HETP*. At total reflux and $\lambda = m/(L/V) = 1.0$,

$$HETP = A_1 + B_1(F_{s,80}) \tag{13.253}$$

where $F_{s,80} = U_s\rho_g$ = superficial F-factor at 80% of flood.
The constants for Eq. (13.253) are:

	A_1	B_1	$a_p, m^2/m^3$
Flexipac 1	0.018	0.106	443
Flexipac 2	0.023	0.156	223
Flexipac 3	0.061	0.235	111

and *HETP* is in meters. The basis of $\lambda = 1.0$ is not overly restrictive, since many distillation columns have an average λ close to unity. Packings other than those listed may be used on an equivalent surface basis (see Table 13.15). Lockett suggests another useful approximation,

$$HETP = \frac{2450 F_{s,80}}{a_p^{0.5}} \tag{13.254}$$

Mechanistic model. The mechanistic model begins with the work of Bravo et al. (1985). They found that earlier data from wetted-wall columns for countercurrent flow in vertical, round

(e)

1: Uniflux plate, $F_c = 0.1455$, $h_w = 70$ mm
2: Kittel plate, $F_c = 0.213$, elliptic slot 14.5×8 mm
3: Ripple plate, $F_c = 0.1082$, $d = 3.0$ mm
4: Bubble-cap plate, $F_c = 0.099$, $h_w = 60$ mm
5: Sieve plate, $F_c = 0.042$, $h_w = 40$ mm, $d = 4.0$ mm
6: APV–West plate, $F_c = 0.1072$, $h_w = 45$ mm
7: Glitsch valve plate, A1, $F_c = 0.14$, $h_w = 50$ mm
8: Turbogrid, set IV, $F_c = 0.147$, $d = 4.5$ mm

(f)
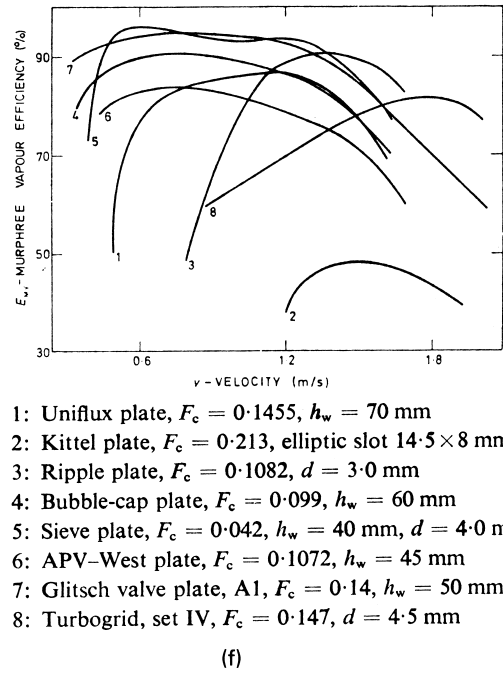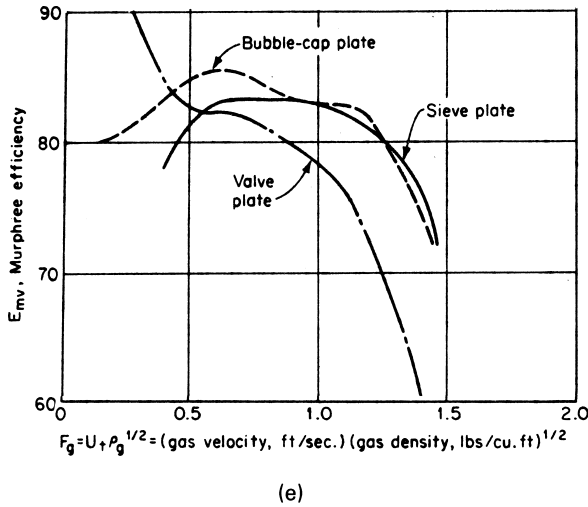
Figure 13.42.—(*continued*)

columns agreed well with the results from structured packing experiments. The agreement confirmed that the gauze surface is essentially completely wetted, enabling the interfacial area to be equated to the specific surface area of the packing. The final model for the gas phase mass transfer coefficient was obtained from dimensionless groups:

$$Sh_g = 0.0338(Re_g)^{0.8}(Sc_g)^{0.333} \tag{13.255}$$

where

$$Sh_g = \text{Sherwood number} = (k_g d_{eq}/D_g) \tag{13.256}$$

$$Re_g = \text{Reynolds number} = (d_{eq}\rho_g/\mu_g)(U_{g,eff} + U_{L,eff}) \tag{13.257}$$

$$Sc_g = \text{Schmidt number} = (\mu_g/\rho_g D_g) \tag{13.258}$$

The effective gas and liquid rates, $U_{g,eff}$ and $U_{L,eff}$, take into account the flow angles, void fractions, and film thicknesses that derive from gross flow rates and packing geometry. The equivalent diameter is taken as the width of a corrugation.

For the liquid phase, a penetration model is used, with the exposure time based on flow across the corrugation side of the packing. Thus,

$$k_L = 2\sqrt{\frac{D_L U_{L,eff}}{\pi S}} \, \text{m/s} \tag{13.259}$$

where S is the width of the side of a corrugation.

Heights of transfer units for the individual phases were obtained from Eq. 13.164 and 13.165, and Eq. 13.167 provides the height of an overall transfer unit. For the gauze packings, with spreading aided by capillary action, interfacial area $a = a_p$ (specific surface area from Table 13.15). For sheet metal packings, which do not promote as much liquid spreading, empirical correction factors were proposed by Fair and Bravo (1990):

$$a/a_p = 0.50 + 0.0058(\% \, flood) \tag{13.260}$$

The Rocha model follows the Bravo model, but is more complicated and usually requires a computer program for effective use. Only a brief summary of it follows. The gas phase mass transfer coefficient is obtained through the Sherwood number, as in Eq. (13.255):

$$Sh_g = \frac{k_g S}{D_g} = 0.54\left[\frac{(U_{g,eff} + U_{L,eff})}{\mu_g}\right]^{0.8} Sc_g^{1/3} \tag{13.261}$$

The liquid phase mass transfer coefficient k_L is obtained from Eq. 13.253. The effective interfacial area a is obtained from the rather complex relationship

$$\frac{a_i}{a_p} = F_{SE}\frac{29.12(We_L Fr_L)^{0.15}S^{0.359}}{Re_L^{0.2}\varepsilon^{0.6}(1 - 0.93\cos\gamma)(\sin\theta)^{0.3}} \tag{13.262}$$

where

S = length of side of corrugation = equivalent diameter, m
F_{SE} = factor to account for surface texturing
θ = corrugation angle, measured from the horizontal, deg
γ = contact angle, liquid/surface, deg, estimated from $\cos\gamma = 5.211 \cdot 10^{-16.835\sigma}$
σ = surface tension, mN/m

In many cases, the simpler Eq. (13.260) is sufficient.

The effective velocities of the phases are computed from

$$U_{g,eff} = \frac{U_{gs}}{\varepsilon(1 - h_t)\sin\theta} \tag{13.263}$$

$$U_{L,eff} = \frac{U_{Ls}}{\varepsilon h_t \sin\theta} \tag{13.264}$$

where h_t is total liquid holdup, vol. liquid per vol. packed bed. Values of h_t are obtained from complex relationships, but

EXAMPLE 13.17
Tray Efficiency for the Separation of Acetone and Benzene, by (a) O'Connell Method (b) Chan/Fair Method.

Operating data:

Acetone mole fraction, $x_1 = 0.637$
Benzene mole fraction, $x_2 = 0.363$
Temperature $= 166°F$
Superficial vapor mass velocity G (lb/hr-sqft) $= 2920$
Superficial vapor velocity $U_v = 18,433\,\text{ft/hr} = 5.12\,\text{ft/s} = 1.56\,m/s$
Volumetric flow of vapor $= Q_v = (1.56)(1.149) = 1.79\,\text{m}^3/\text{s}$
Liquid/vapor molar ratio $= 0.80$ (above the feed)
Volumetric flow of liquid $= q_L = 0.80(0.159/47.73)(1.79) = 0.00477\,m^3/s$

Geometry:

Weir height $h_w = 2.0\,\text{in.} = 51\,\text{mm}$
Weir length $= L_w = 2.88\,\text{ft} = 0.871\,\text{m}$
Fraction hole area, based on total cross section, FA $= 0.063$
Downcomer area $= 10\%$; active area $= 80\%$ (of total tower cross section)
Active area $= 0.80(12.56) = 10.05\,\text{sqft} = 0.919\,\text{m}^2$
Fraction hole area based on active area $= 0.079$
Tray spacing $= 24\,\text{in.} = 0.61\,\text{m}$
Column diameter $= 4.0\,\text{ft} = 1.21\,\text{m}$

Physical properties:

$\rho_G = 0.159\,lb/cuft = 2.55\,kg/m^3$
$\rho_L = 47.73\,lb/cuft = 765\,kg/m^3$
$\mu_L = 0.609\,lb/ft/hr = 0.252\,cP$
$\sigma = 18.96\,\text{dyn/cm} = 5.417(105)\text{lb/sqft/hr}$
Liquid diffusivity $= 2.32(10\text{-}4)\text{sqft/hr} = 5.99(10^{-9})\text{m}^2/\text{s}$
Vapor diffusivity $= 0.247\text{sqft/hr} = 6.38(10^{-6})\text{m}^2/\text{s}$
Slope of equilibrium curve $= 1.10$; $\lambda = 1.10/0.8 = 1.38$
Average relative volatility for column $= 2.30$

Efficiency calculations:

(a) Method of O'Connell: $\mu_L \alpha = 0.252(2.30) = 0.58$.
From Fig. (13.39), $E_{oc} = 0.56$ or 56%
(b) Method of Chan and Fair:
Abscissa for flood chart (Fig. 13.32 (b)) $= 0.37\,\text{ft/s}$
From which, U_s, *flood* $= 6.40\,\text{ft/s}$
Percent flood $= 5.12/6.40 \times 100 = 80\%$

Liquid flow $= 0.00483\,\text{m}^3/\text{s} = 17.4\,\text{m}^3/\text{hr}$
Weir crest (Eq. 13.239) $= h_{ow} = 664(q/L_w)^{2/3} = 664(0.00483/0.871)^{2/3} = 21\,\text{mm}$
Liquid holdup (Eq. 13.238) $= h_L = \beta(h_w + h_{ow}) = 0.5(51 + 21) = 36\,\text{mm} = 0.036\,\text{m}$
Froth height (Fig. 13.41) $= Z_f = 0.30\,\text{m} = 11.8\,\text{in.}$
Void fraction, vapor in froth (Eq. 13.242) $= \varepsilon = 1 - h_L/Z_f = 1 - 0.042/0.3 = 0.89$
Void fraction, liquid in froth $= 1 - 0.89 = 0.11$
Vapor residence time in froth (Eq. 13.242) $= t_g = (A_a\varepsilon Z_f)/Q_g = [(0.919)(0.89)(0.30)/(1.79) = 0.137\,\text{s}$
Liquid residence time in froth (Eq. 13.243) $= t_L = 0.919)(0.11)(0.30)/(0.00477) = 6.36\,\text{s}$
Vapor phase coefficient (Eq. 13.240)

$$k_g a = \frac{316(6.38 \times 10^{-6})^{0.5}(1030 \times 0.80 - 867 \times 0.64)}{(36)^{0.5}} = 35.8\,s^{-1}$$

Liquid phase coefficient (Eq. 13.241):

$$F_{va} = U_a \rho_g^{0.5} = (Q_g/A_a)(\rho_g^{0.5}) = 3.11\,\text{m/s}(\text{kg/m}^3)^{0.5}$$

$$k_L a = (0.40 F_{va} + 0.17)(3.875 \times 10^8 D_L)^{0.5}$$
$$= (0.40 \times 3.11 + 0.17)\{0.387 \times 5.99\}^{0.5} = 2.15\,s^{-1}$$

Transfer units: Eqs. (13.244–13.246):
$NTU_g = 35.8(0.137) = 4.90$;
$NTU_L = 2.15(6.36) = 13.67$
$NTU_{og} = 3.61$
Point efficiency (Eq. 13.248) $= E_{og} = 1 - \exp[-3.61] = 1 - 0.027 = 0.973(97.3\%)$

Comment:

The calculated point efficiency must be converted to overall column efficiency, which will lower its value and make it closer to the O'Connell prediction. The calculated value of E_{og} is slightly higher than obtained experimentally ($E_{og} = 0.83$–0.92) at the University of Delaware for bubblecap trays (Annual Progress Report of Research Committee, *Tray Efficiencies in Distillation Columns*, AIChE, New York, 1955).

Table 13.17 lists typical values. Values of a_p, F_{SE}, ε, S, and θ for representative structured packings are given in Table 13.18.

Scale-up of structured packing efficiency. As noted earlier, tests in an Oldershaw column as small as 25 mm diameter can often be converted to commercial scale designs. For random packings, a minimum test column diameter of 100 mm is recommended. For structured packings it appears possible to go as small as 25 mm for scale-up studies. This is because scaled-down versions of some of the packings are available in sizes of 25 and 50 mm diameter. Hufton et al. (1988) used a 23-mm diameter Sulzer BX laboratory packing and found that the original Bravo model (Eq. 13.255) worked well, so long as the actual geometric dimensions of the laboratory packing were used. Thus, one might run the system at hand in, say, a 26-mm column, using small structured packing, and scale up to the large size using the efficiency model for the packing.

Structured packing performance. The most common type of structured packing has a specific surface area in the range of 225–250 m^2/m^3, a corrugation angle of 45 degrees and is fabricated from thin-gauge sheet metal; this is often called a "No. 2 packing." The metal may have a textured surface to promote liquid spreading, and may have perforations to equalize pressure (as well as promote spreading). Alternate materials to sheet metal are expanded metal and wire gauze.

Performance tests are usually run at total reflux with several standard test mixtures. The following four figures portray total reflux data taken at the Separations Research Program at the University of Texas at Austin. The test mixture is cyclohexane/n-heptane. Figures 13.48 and 13.49 are taken from Olujic et al. (2003) and Figures 13.50 and 13.51 are from Olujic et al. (2000).

Figure 13.48 shows the effect of operating pressure on the efficiency and pressure drop of a No. 2 packing (Montz-Pak B1-250M). The highest efficiency (lowest HETP) occurs at the highest pressure tested. Figure 13.49 shows a comparison between packings with surface areas of 250 and 350 m^2/m^3 at atmospheric pressure. The higher surface area provides higher efficiency but also higher pressure drop and lower capacity. Figure 13.50 shows the effect
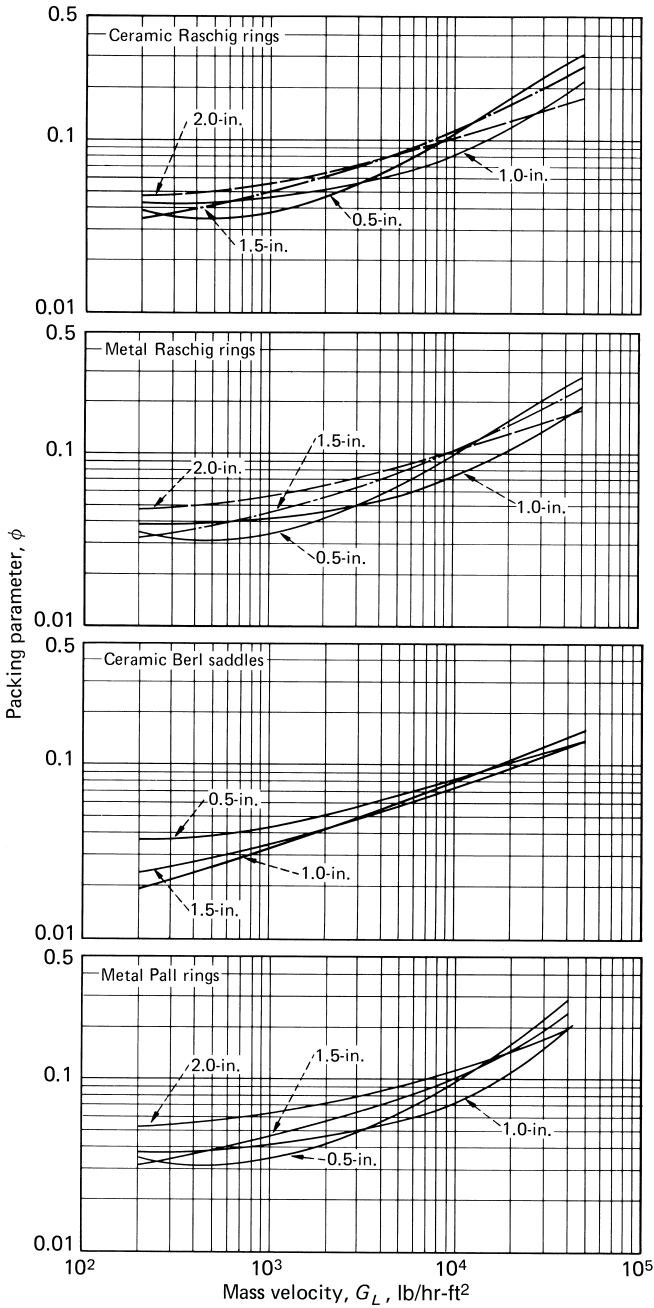
Figure 13.43. Liquid phase parameters for the Bolles/Fair correlation for random packing efficiency.

Figure 13.44. Vapor or gas phase parameters for the Bolles/Fair correlation for random packing efficiency.

of surface treatment for high surface area packing. BSH-400 is fabricated from expanded metal, and B1-400 from sheet metal. It is apparent that the expanded metal surface creates a slightly greater surface wettability. Finally, Figure 13.51 shows the effect of corrugation angle for a 400-m^2/m^3 packing fabricated from sheet metal. The 60-degree packing provides lower efficiency but also (not shown) lower pressure drop.

These figures are included to show that the variables of surface area, surface material, corrugation inclination, and operating pressure influence the efficiency, pressure drop, and capacity of structured packings. The packings shown in the figures are from one manufacturer, and differences between manufacturers can exist depending on the geometry and method of fabrication. Thus, the serious designer should obtain performance information (including design computer programs) as well as cost information from the manufacturer or vendor before going to final design.
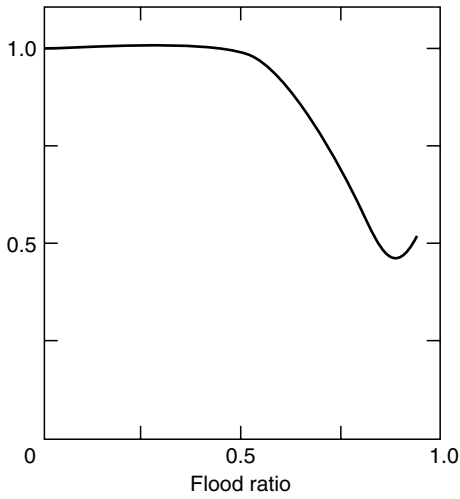
Figure 13.45. Flooding correction factor for liquid phase mass transfer Bolles/Fair correlation for random packing efficiency.

Example 13.18 is included to show the predicted mass transfer efficiency of an acetone-water column in which structured packing is used. Of particular interest are the results from Eqs. 13.255, 13.259, 13.261 and 13.262 are used to determine transfer units. The value of HETP is calculated using Eq. 13.172. Plug flow of the phases is usually assumed, although extreme ratios of the flowing phases can cause some back mixing.

(a) Lockett shortcut method (Eq (13.253):

for $F_{gs} = 2.49 \text{ m/s(kg/m}^3)^{0.5}$, and Flexipac 2,

$$HETP = A_1 + B_1(F_{gs}) = 0.023 + 0.156(2.49) = \underline{0.41 \text{ m}}$$
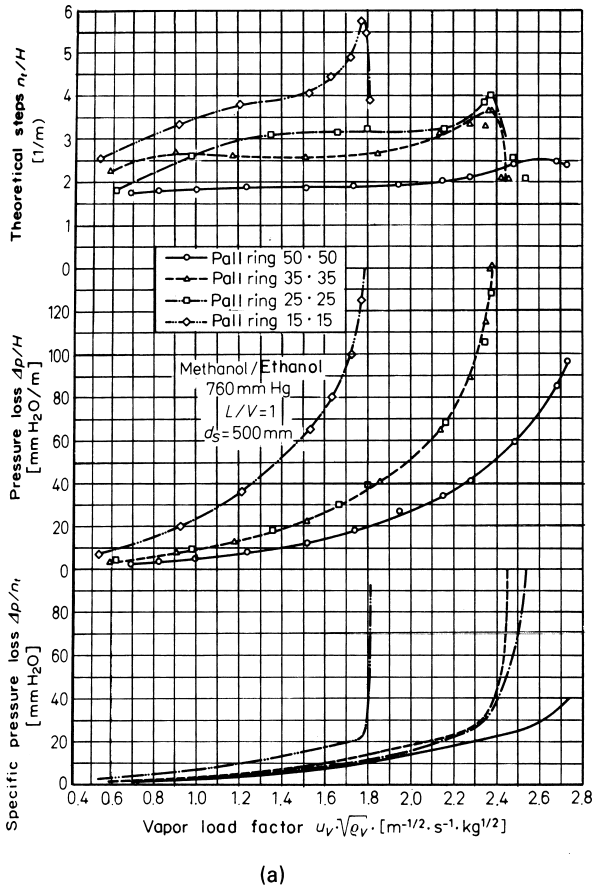
(a)
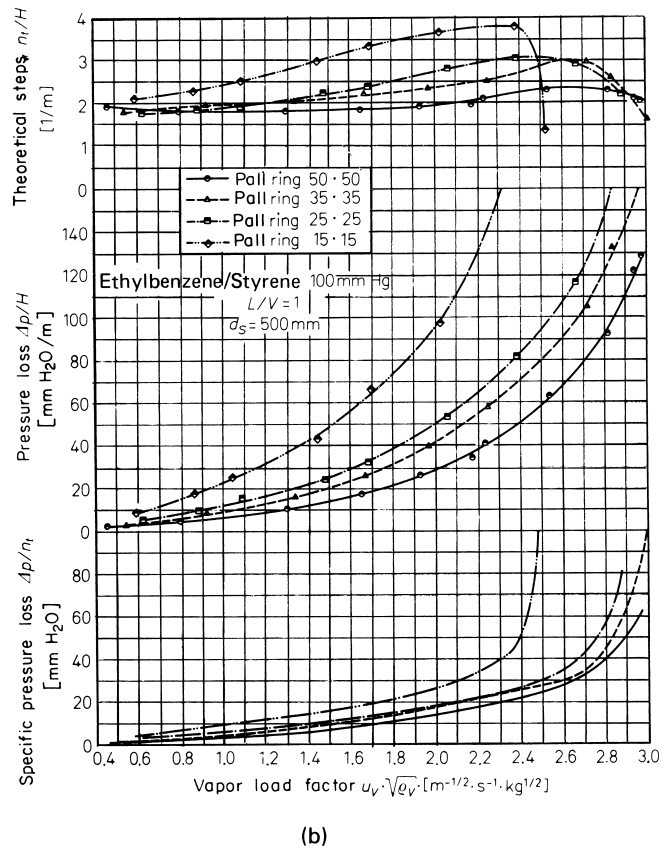
(b)

Figure 13.46. Number of stages per meter (reciprocal of HETP), pressure loss per meter and pressure loss per theoretical stage in a 500 mm dia column filled with metal pall rings. Other charts in the original show the effects of packing height and column diameter, as well as similar data for Raschig rings (*Billet, 1979*). (a) Methanol/ethanol at 760 Torr and total reflux in a column 500 mm dia. (b) Ethylbenzene/styrene at 100 Torr and total reflux in a column 500 mm dia.

(a)

(b)

Figure 13.47. Data of HETP, HTU, and $K_g a$ for several systems and kinds of tower random packings. (a) $K_g a$ for absorption of ammonia in NaOH with various packings (*Polymer Piping and Materials Co.*). (b) HETP of several packings as functions of the gas rate (*I. Eastham, cited by Coulson and Richardson, 1978*, Vol. *2*, p. *515*). (c) HETP for ethylbenzene/styrene at 100 Torr; curve 1 for 2 in. metal pall rings [*Billet, Chem. Eng. Prog.* **63**(*9*), *55* (*1967*)]; curve 2 for 1 in. metal pall rings (*Billet*, loc. cit.); curve 3 for Sulzer packing (*Koch Engineering Co.*). (d) $K_g a$ for absorption of CO_2 in NaOH with various packings; CMR are cascade mini rings which are pall rings with heights about one-half the diameters (*Mass Transfer International*). (e) HTU for absorption of ammonia from air with water [*Teller, Chem. Eng. Prog.* **50**, *70*, (*1954*). (f) HTU for absorption of ammonia from air with water (*Wen, S. M. Thesis, University of West Virginia, 1953*). (g) Typical HETP for distillation with 2 in. metal pall ("ballast") rings (*redrawn from Bulletin 217, Glitsch Inc.*).

$$F_s = V_s \sqrt{\rho_v} \text{ (LB }^{1/2}\text{/SEC-FT }^{1/2}\text{)}$$

(c)

NB
The differential performance between No3 Metal CMR and the other rings in this test is increased by a further 10/15% in K_2CO_3 systems. This is confirmed by extensive feed-back data from operating plants up to 13 ft (4 m) diameter.

—··—— No 3 METAL CMR
------ No 2 Hy-Pak®
———— 2 in METAL PALL RING

COLUMN DIA	= 30 ins
PACKED HEIGHT	= 10 ft
GAS RATE	= 900 lbs/ft² hr
GAS CONC	= 1% CO_2
LIQUID CONC	= 4% NaOH
LIQUID TEMP	= 75°F
CARBONATE CONC	= 25%

(d)

Figure 13.47.—(*continued*)
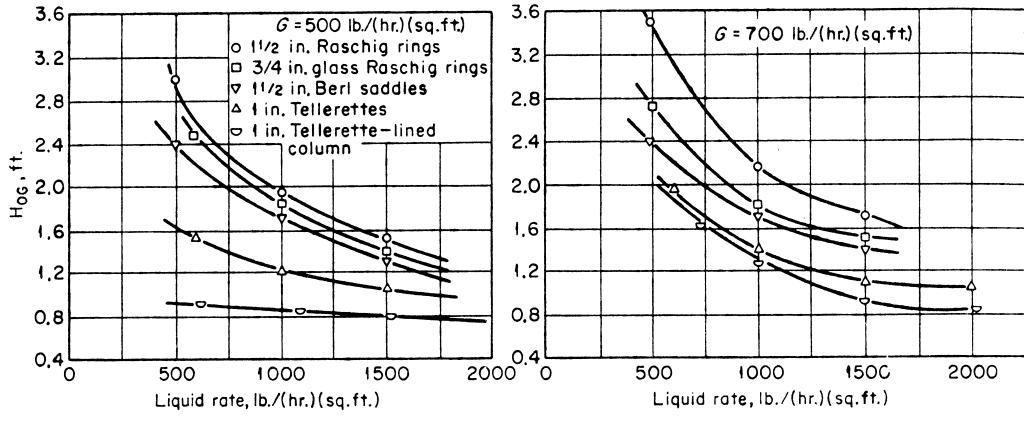
(e)
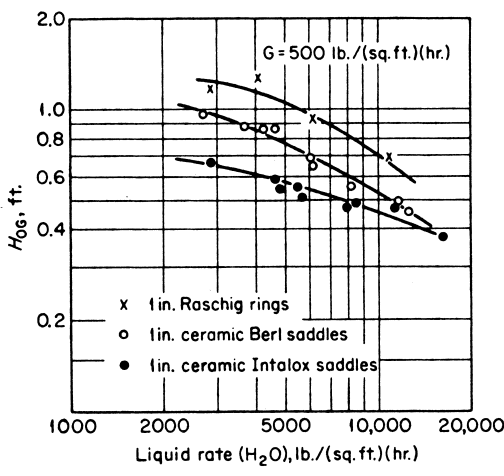
(f)
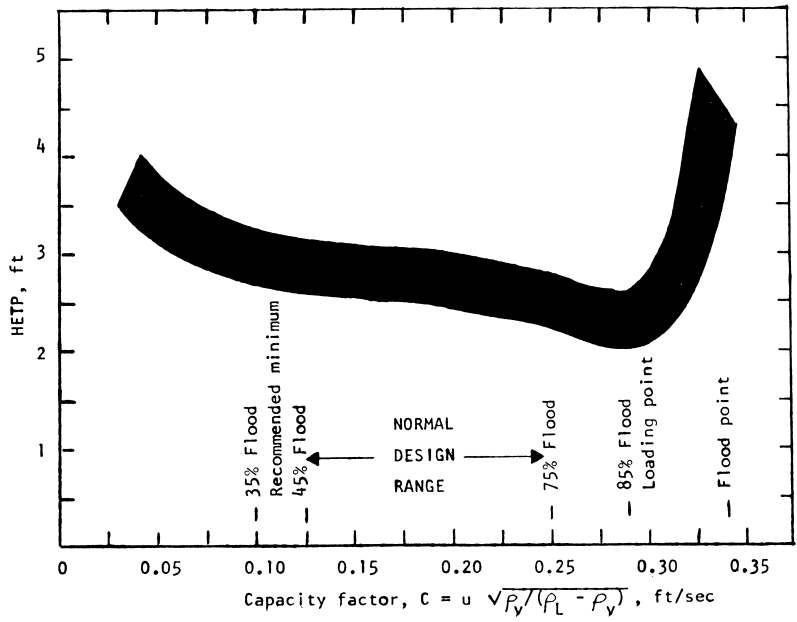
(g)

Figure 13.47.—(*continued*)

TABLE 13.17. Values of Liquid Holdup for Three Sizes of Structured Packings

Type	Area, m^2/m^3	U_{Ls} m/s	Total Holdup	Max. Gas F-factor $m/s(kg/m^3)^{0.5}$
1	500–560	0.007	0.07	1.5
		0.021	0.11	1.0
		0.035	0.15	0.9
2	225–250	0.007	0.04	3.0
		0.021	0.07	2.5
		0.035	0.10	2.0
3	135–150	0.007	0.07	4.0
		0.021	0.11	3.0
		0.035	0.15	2.0

Note: h_t = total holdup, vols. liquid/vol. of bed.

TABLE 13.18. Values of Parameters for Equations 13.259–13.261

	$a_p(m^2/m^3)$	$F_{SE}(-)$	$\varepsilon(-)$	$S(m)$	θ (deg)
Flexipac 2	223	0.350	0.91	0.018	45
Gempak 2A	223	0.344	0.95	(0.018)	45
Intalox 1T	315	0.415	0.95	0.0152	45
Intalox 2T	213	0.415	0.97	0.0221	45
Jaeger Maxpak	229	0.364	0.95	0.0175	45
Mellapak 250Y	250	0.350	0.95	(0.018)	45
Mellapak 500Y	500	0.350	0.91	(0.009)	45
Sulzer BX	492	(0.350)	0.90	0.0090	60

Note: Numbers in parentheses are estimated.
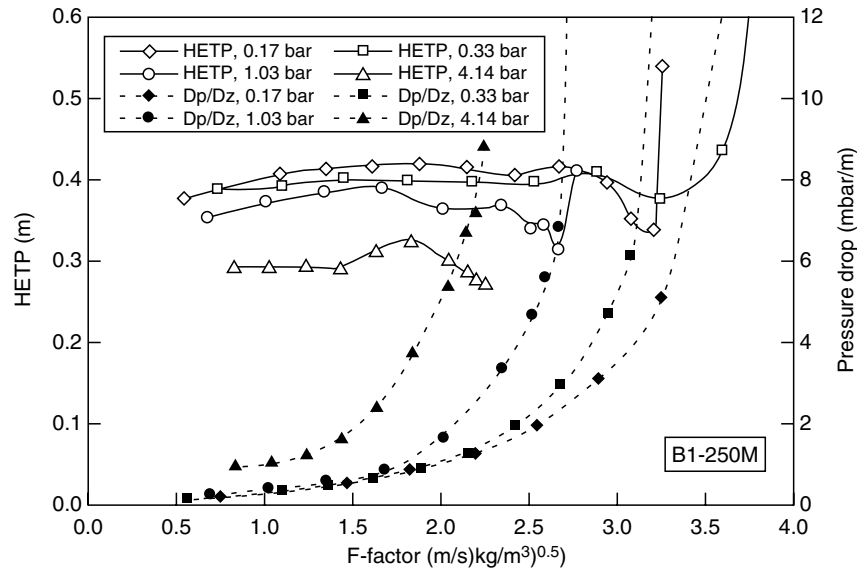
Figure 13.48. Effect of operating pressure on the hydraulic and mass transfer performance of Montz-Pak B1-250M. Total reflux, cyclohexane/n-heptane, column diameter = 0.43 m, bed height = 3.3 m. (Olujic et al., 2003).
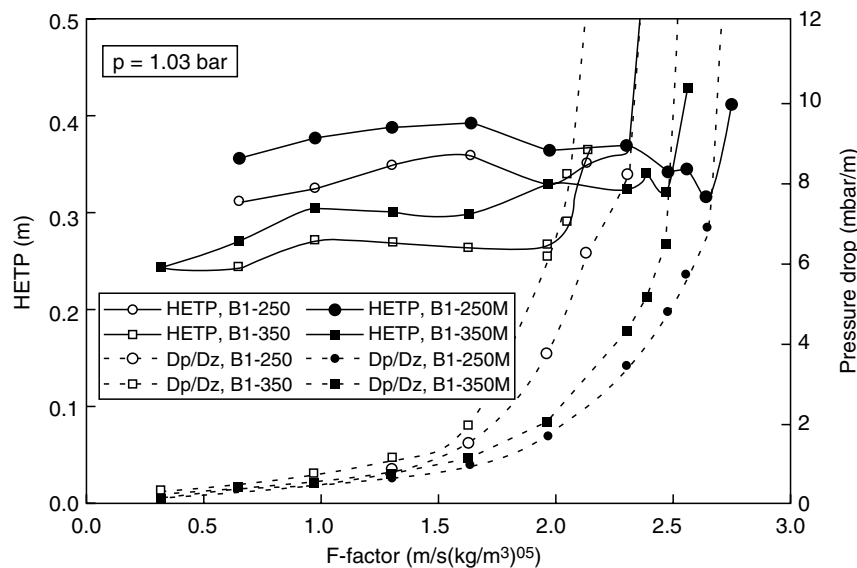
Figure 13.49. Comparison of total reflux distillation performance of high-performance packings of $250\,m^2/m^3$ and $350\,m^2/m^3$ surface areas, at 1.03 bar pressure. Cyclohexane/n-heptane, column diameter = 0.43 m, bed height = 3.3 m. (Olujic et al., 2003).

EXAMPLE 13.18
Mass Transfer Efficiency for the Separation of Acetone and Benzene, Using a Type 2 Structured Packing. Use same condition as for Example 13.17, including column diameter = 4.0 ft = 1.21 m. Use the mechanistic model of Rocha et al. and compare the result with the shortcut method of Lockett.

Operating data:
Acetone mole fraction, $x_1 = 0.637$
Benzene mole fraction, $x_2 = 0.363$
Temperature = $166°F = 74.4°C$
Superficial vapor mass velocity G (lb/hr-sqft) = 2920
Superficial vapor velocity $U_v = 18,433$ ft/hr = 5.12 ft/s = 1.56 m/s
Volumetric flow of vapor = $Q_v = (1.56)(1.149) = 1.79$ m³/s
Liquid/vapor molar ratio = 0.80 (above the feed)
Volumetric flow of liquid = $q_L = 0.80(0.159/47.73)(1.79)$ = 0.00477 m³/s

Geometry:
Column diameter = 4.0 ft = 1.21 m (compare with 3.5 ft = 1.07 m)
Packing properties (Table 13.18, Flexipac 2):

Surface area = $a_p = 233$ m²/m³
Percent voids = 95
$F_{SE} = 0.350$
S = 0.018 m
Packing factor = 72 m⁻¹ (Table 13.15)

Physical properties:
$\rho_G = 0.159$ lb/cuft = 2.55 kg/m³
$\rho_L = 47.73$ lb/cuft = 765 kg/m³
$\mu_L = 0.609$ lb/ft/hr = 0.252 cP
$\mu_g = 0.01452$ lb/ft/hr = 0.0060 cP
$\sigma = 18.96$ dyn/cm = 5.417(105) lb/sqft/hr
Liquid diffusivity = 2.32(10-4) sqft/hr = 5.99(10⁻⁹) m²/s
Vapor diffusivity = 0.247 sqft/hr = 6.38(10⁻⁶) m²/s
Slope of equilibrium curve = 1.10; $\lambda = 1.10/0.8 = 1.38$

	Column diameter	
Flooding Calculations	**1.21 m (4.0 ft)**	**1.067 m (3.5 ft)**
Superficial Vapor Velocities		
At the Flood Point	2.6393 m/s	2.4436 m/s
At Design Conditions	1.5566 m/s	2.0018 m/s
Column Diameter	1.2100 m	1.0670 m
Flooding Factor (%)	58.98	81.92
Pressure Drop Calculations		
Friction Factor	0.1534	0.1520
Fractional Liquid Holdup	0.0556	0.0705
Dry Pressure Drop	0.0012 bar/m	0.0019 bar/m
Wet Pressure Drop	0.0023 bar/m	0.0042 bar/m
Flood Pressure Drop	0.0103 bar/m	0.0103 bar/m
Mass Transfer Calculations		
Stripping Factor	1.3759	1.3759
Effective Interfacial Area	164.5441 1/m	181.9614 1/m
Ae/Ap	0.7379	0.8160
Mass Transfer Coefficient-Liquid	2.1718E-04 m/s	2.1866E-04 m/s
Mass Transfer Coefficient-Vapor	3.7442E-02 m/s	4.6015E-02 m/s
Height of a Transfer Unit -Liquid	0.1161 m	0.1341 m
Height of a Transfer Unit -Vapor	0.2527 m	0.2391 m
Overall Height of a Vapor Transfer Unit	0.4124 m	0.4236 m
Number of Transfer Units	9.6996	9.4436
HETP—Plug Flow	0.3501 m	0.3596 m

(b) Mechanistic model of Rocha et al. (1996):

The output of a computer program (DISTIL 2.0) is shown in the chart within this example. Two column sizes have been used, in order to bracket the 80% flood case. The results are summarized as:

Column diameter, ft	4.0	3.5
Column diameter, m	1.21	1.07
Percent flood	59.0	81.9
Effective area, m⁻¹	165	182
$(HTU)_{og}$,m	0.41	0.42
HETP, m	0.35	0.36

(c) Comments:

As expected, the Type 2 packing has a higher capacity than the sieve tray with 24-inch spacing (Example 13.17). The sieve tray has an expected overall efficiency in the range of 80–90%, or an equivalent HETP of 24/0.9 = 26.7 in. to 24/0.8 = 30 in. This range of HETP = 0.68–0.76 m does not approach the efficiency of structured packing.
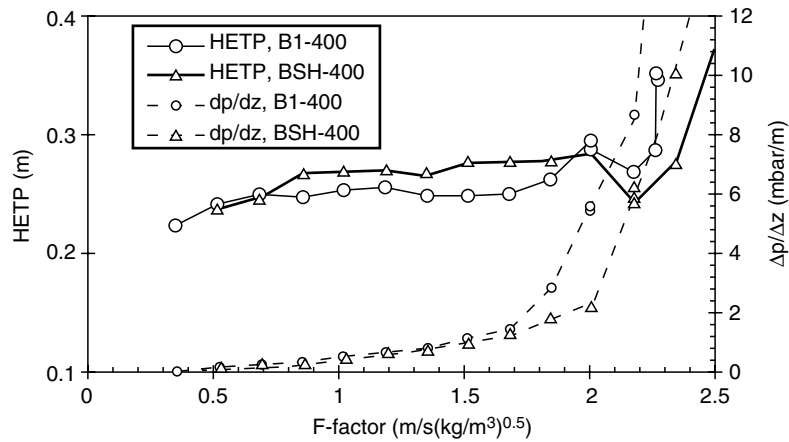
Figure 13.50. Effect of surface design on the total reflux performance of a 400 m^2/m^3 packing. B1-400 is made from sheet metal; BSH-400 is made from expanded metal. Pressure = 1.03 bar, column diameter = 0.43 m. (Olujic et al., 2000).
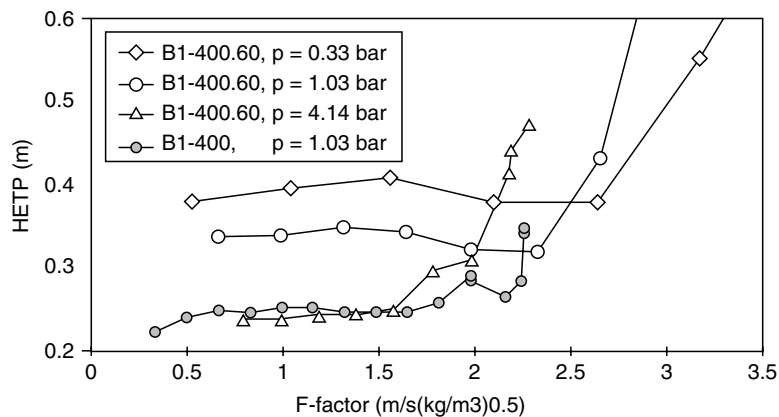
Figure 13.51. Effect of corrugation angle on the mass transfer performance of a high-area structured packing, operated at total reflux. B1-400 has the standard 45-degree angle, whereas 400.60 has a 60-degree angle (with the horizontal). Cyclohexane/n-heptane, column diameter = 0.43 m, bed height = 3.3 m. (Olujic et al., 2000).

REFERENCES

General

American Institute of Chemical Engineers, *Bubble-Tray Design Manual*, AIChE, New York, 1958.

R. Billet, *Distillation Engineering*, Chemical Publishing, New York, 1979.

M.F. Doherty and M.F. Malone, *Conceptual Design of Distillation Systems*, McGraw-Hill, New York, 2001.

J.R. Fair, Liquid-gas systems, in *Perry's Chemical Engineers' Handbook*, 5th ed., McGraw-Hill, New York, 1984, Section 18.

J.R. Fair, Gas absorption and gas-liquid system design, in *Perry's Chemical Engineers' Handbook*, 7th ed., McGraw-Hill, New York, 1997, Section 14.

J. Gmehling, J. Menke, J. Krafczyk, and K. Fischer, *Azeotropic Data*, VCH, Weinheim, New York, 1994.

J. Gmehling, U. Onken, et al., *Vapor-Liquid Equilibrium Data Collection*, DECHEMA, Frankfurt/Main, Germany, 1979–date (continuing series).

R.J. Hengstebeck, *Distillation*, Reinhold, New York, 1961.

E.J. Henley and J.D. Seader, *Equilibrium Stage Processes in Chemical Engineering*, Wiley, New York, 1981.

A.L. Hines and R.N. Maddox, *Mass Transfer Fundamentals and Applications*, Prentice-Hall, Englewood Cliffs, NJ, 1985.

M. Hirata, S. Ohe, and E. Hala, *Computer-Aided Data Book of Vapor-Liquid Equilibria*, Elsevier, Amsterdam, 1975.

C.D. Holland, *Fundamentals of Multicomponent Distillation*, McGraw-Hill, New York, 1981.

L.H. Horsley, *Azeotropic Data—III*, American Chemical Society, Washington, 1973.

C.J. King, *Separation Processes*, 2nd ed., McGraw-Hill, New York, 1980.

E. Kirschbaum, *Destillier und Rektifiziertechnik*, Springer, Berlin, 1969.

H.Z. Kister, *Distillation—Design*, McGraw-Hill, New York, 1992.

V.B. Kogan, et al., *Equilibria between Vapor and Liquid (in Russian)*, Izdatelstvo Nauka, Moscow, 1966.

L. Ogorodnikov, and V.B. Kogan, *Handbook of Azeotropic Mixtures* (in Russian), 1971.

R.H. Perry and D. Green (Eds.), *Perry's Chemical Engineers' Handbook*, 7th ed., McGraw-Hill, New York, 1997.

B. Poling, J. Prausnitz, and J. O'Connell, *The Properties of Gases and Liquids*, 5th ed., McGraw-Hill, New York, 2000.

C.S. Robinson, *Elements of Fractional Distillation*, McGraw-Hill, New York, 1939.

C.S. Robinson and E.R. Gilliland, *Elements of Fractional Distillation*, 2nd ed., McGraw-Hill, New York, 1950.

J.D. Seader, Distillation, in *Chemical Engineers' Handbook*, McGraw-Hill, New York, 1984, Section 13.

J.D. Seader and E.J. Henley, *Separation Process Principles*, Wiley, New York, 1998.

T.K. Sherwood, R.L. Pigford and C.R. Wilke, *Mass Transfer*, McGraw-Hill, New York, 1975.

B.D. Smith, *Design of Equilibrium Stage Processes*, McGraw-Hill, New York, 1963.

J. Stichlmair and J.R. Fair, *Distillation—Principles and Practice*, Wiley-VCH, New York, 1998.

R.F. Strigle, Jr., *Packed Tower Design and Applications—Random and Structured Packings*, 2nd ed., Gulf, Houston, 1994.

R. Taylor and R. Krishna, *Multicomponent Mass Transfer*, Wiley, New York, 1993.

R.E. Treybal, *Mass Transfer Operations*, McGraw-Hill, New York, 1980.

S.M. Walas, *Phase Equilibria in Chemical Engineering*, Butterworths, Reading, MA, 1985.

Cited References

D.L. Bennett and H.J. Grimm, *AIChE J.*, **37**, 589 (1991).

W.L. Bolles, in B.D. Smith, *Design of Equilibrium Stage Processes*, New York, McGraw-Hill, 1963, Chapter 15.

W.L. Bolles and J.R. Fair, *Chem. Eng.* **89**(14), 109 (1982).

J.L. Bravo, J.A. Rocha and J.R. Fair, *Petroleum Proc.* **64**(1) 91 (1985).

H. Chan and J.R. Fair, *Ind. Eng. Chem., Proc. Des. Devel.*, **23**(4) 814 (1984a).

H. Chan and J.R. Fair, *Ind. Eng. Chem., Proc. Des. Devel.*, **23**(4) 820 (1984b).

D. Cornell, W.G. Knapp, and J.R. Fair, *Chem. Eng. Prog.*, **56**(7) 68 (1960).

J.R. Fair and J.L. Bravo, *Chem. Eng. Prog.*, **86**(1) 19 (1990).

J.R. Fair, H.R. Null and W.L. Bolles, *Ind. Eng. Chem., Proc. Des. Devel.*, **22**, 53 (1983).

J.R. Fair, B.E. Reeves and A.F. Seibert, The Oldershaw column: Useful for solving distillation problems, *Proc. AIChE Meeting*, New Orleans, March 2002.

J.R. Fair, A.F. Seibert, M. Behrens, P.P. Saraber, and Z. Olujic, *Ind. Eng. Chem. Res.*, **39**, 1788 (2000).

J.A. Garcia and J.R. Fair, *Ind. Eng. Chem. Res.*, **39**, 1809, 1818 (2000).

J.A. Garcia and J.R. Fair, *Ind. Eng. Chem. Res.*, **41**, 1632 (2002).

J.R. Hufton, J.L. Bravo and J.R. Fair, *Ind. Eng. Chem. Res.*, **27**, 2096 (1988).

M.J. Lockett, *Chem. Eng. Prog.*, **94**(1) 60 (1998).

H.E. O'Connell, *Trans. AIChE*, **42**, 741 (1946).

Z. Olujic, *Chem. Biochem. Eng. Q.*, **11**, 31 (1997).

Z. Olujic, A.F. Seibert and J.R. Fair, *Chem. Eng. Proc.*, **39**, 335 (2000).

Z. Olujic, A.F. Seibert, B. Kaibel, H. Jansen, T. Rietfort and E. Zich, *Chem. Proc. Eng.*, **42**, 55 (2003).

M. Prado and J.R. Fair, *Ind. Eng. Chem. Res.*, **29**, 1031 (1990).

J.A. Rocha, J.L. Bravo and J.R. Fair, *Ind. Eng. Chem. Res.*, **35**, 1660 (1996).

F.A. Rusche, *Hydrocarbon Proc.*, **78**(12), 41 (1999).

W.J. Stupin and F.J. Lockhart, Distillation, Thermally Coupled, *Encyclopedia of Chemical Processing and Design*, Dekker, New York, 1982, Vol. 16, 279–299.

I. Wagner, J. Stichlmair, and J. R. Fair, *Ind. Eng. Chem. Res.* **36**, 227 (1997).

14

EXTRACTION AND LEACHING

*E*xtraction is a process for the separation of one or more components through intimate contact with a second immiscible liquid called a solvent. If the components in the original solution distribute themselves differently between the two phases, separation will occur. Separation by extraction is based on this principle. When some of the original substances are solids, the process is called leaching. In a sense, the role of solvent in extraction is analogous to the role of enthalpy in distillation. The solvent-rich phase is called the extract, and the carrier-rich phase is called the raffinate. A high degree of separation may be achieved with several extraction stages in series, particularly in countercurrent flow.

Processes of separation by extraction, distillation, crystallization, or adsorption sometimes are equally possible. Differences in solubility, and hence of separability by extraction, are associated with differences in chemical structure, whereas differences in vapor pressure are the basis of separation by distillation. Extraction often is effective at near-ambient temperatures, a valuable feature in the separation of thermally unstable natural mixtures or pharmaceutical substances such as penicillin.

The simplest separation by extraction involves two immiscible liquids. One liquid is composed of the carrier and solute to be extracted. The second liquid is solvent. Equilibria in such cases are represented conveniently on triangular diagrams, either equilateral or right-angled, as for example on Figures 14.2 and 14.3. Equivalent representations on rectangular coordinates also are shown. Equilibria between any number of substances are representable in terms of activity coefficient correlations such as the UNIQUAC or NRTL. In theory, these correlations involve only parameters that are derivable from measurements on binary mixtures, but in practice the resulting accuracy may be poor and some multicomponent equilibrium measurements also should be used to find the parameters. Finding the parameters of these equations is a complex enough operation to require the use of a computer. An extensive compilation of equilibrium diagrams and UNIQUAC and NRTL parameters is that of Sorensen and Arlt (1979–1980). Extensive bibliographies have been compiled by Wisniak and Tamir (1980–1981).

The highest degree of separation with a minimum of solvent is attained with a series of countercurrent stages.

Such an assembly of mixing and separating equipment is represented in Figure 14.4(a), and more schematically in Figure 14.4(b). In the laboratory, the performance of a continuous countercurrent extractor can be simulated with a series of batch operations in separatory funnels, as in Figure 14.4(c). As the number of operations increases horizontally, the terminal concentrations E_1 and R_3 approach asymptotically those obtained in continuous equipment. Various kinds of more sophisticated continuous equipment also are widely used in laboratories; some are described by Lo et al. (1983, pp. 497–506). Laboratory work is of particular importance for complex mixtures whose equilibrium relations are not known and for which stage requirements cannot be calculated.

In mixer-separators the contact times can be made long enough for any desired approach to equilibrium, but 80–90% efficiencies are economically justifiable. If five stages are required to duplicate the performance of four equilibrium stages, the stage efficiency is 80%. Since mixer-separator assemblies take much floor space, they usually are employed in batteries of at most four or five units. A large variety of more compact equipment is being used. The simplest in concept are various kinds of tower arrangements. The relations between their dimensions, the operating conditions, and the equivalent number of stages are the key information.

Calculations of the relations between the input and output amounts and compositions and the number of extraction stages are based on material balances and equilibrium relations. Knowledge of efficiencies and capacities of the equipment then is applied to find its actual size and configuration. Since extraction processes usually are performed under adiabatic and isothermal conditions, in this respect the design problem is simpler than for thermal separations where enthalpy balances also are involved. On the other hand, the design is complicated by the fact that extraction is feasible only of nonideal liquid mixtures. Consequently, the activity coefficient behaviors of two liquid phases must be taken into account or direct equilibrium data must be available. In countercurrent extraction, critical physical properties such as interfacial tension and viscosities can change dramatically through the extraction system. The variation in physical properties must be evaluated carefully.

14.1. INTRODUCTION

The simplest extraction system is made up of three components: the *solute* (material to be extracted); the *carrier*, or nonsolute portion of the feed; and the *solvent*, which should have a low solubility in the carrier. Figure 14.1 illustrates a countercurrent extraction with a light-phase solvent. The diagram can be inverted for a heavy-phase solvent.

The carrier-rich liquid leaving the extractor is referred to as the *raffinate* phase and the solvent-rich liquid leaving the extractor is the *extract* phase. The solvent may be the *dispersed* phase or it may be the *continuous* phase; the type of equipment used may determine which phase is to be dispersed in the other phase.

In general, distillation is used to purify liquid mixtures. However, liquid extraction should be considered when the mixture involves a:

- Low relative volatility (< 1.3)
- Removal of a nonvolatile component
- High heat of vaporization
- Thermally-sensitive components
- Dilute concentrations
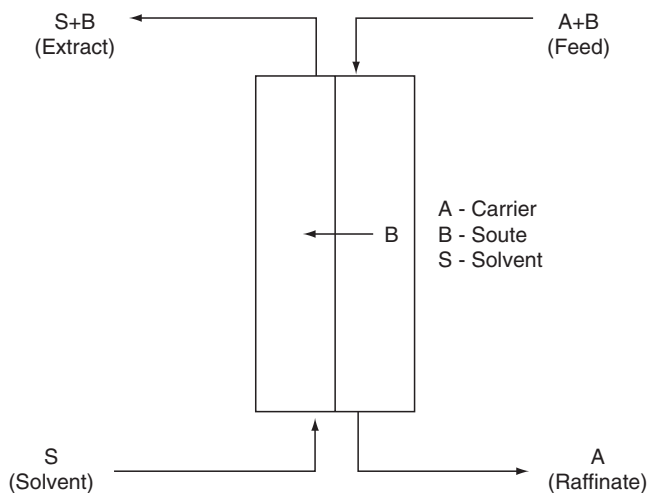
Figure 14.1. Solvent extraction process

Liquid extraction is utilized by a wide variety of industries. Applications include the recovery of aromatics, decaffeination of coffee, recovery of homogeneous catalysts, manufacture of penicillin, recovery of uranium and plutonium, lubricating oil extraction, phenol removal from aqueous wastewater, and extraction of acids from aqueous streams. New applications or refinements of solvent extraction processes continue to be developed.

Extraction is treated as an equilibrium-stage process. Ideally, the development of a new extraction process includes the following steps:

- Select solvent.
- Obtain physical properties, including phase equilibria.
- Obtain material balance.
- Obtain required equilibrium stages.
- Develop preliminary design of contactor.
- Obtain pilot data and stage efficiency.
- Compare pilot data with preliminary design.
- Determine effects of scale-up and recycle.
- Obtain final design of system, including the contactor.

The ideal solvent would be easily recovered from the extract. For example, if distillation is the method of recovery, the solvent-solute mixture should have a high relative volatility, low heat of vaporization of the solute, and a high equilibrium distribution coefficient. A high distribution coefficient will translate to a low solvent requirement and a low extract rate fed to the solvent recovery column. These factors will minimize the capital and operating costs associated with the distillation system. In addition to the recovery aspects, the solvent should have a high selectivity (ratio of distribution coefficients), be immiscible with the carrier, have a low viscosity, and have a high density difference (compared to the carrier) and a moderately low interfacial tension.

The critical physical properties that affect extractor performance include phase equilibria, interfacial tension, viscosities, densities, and diffusion coefficients. In many extraction applications, these properties may change significantly with changes in chemical concentration. It is important that the effect of chemical concentration on these physical properties be understood.

The required equilibrium stages and solvent-to-feed ratio is determined by the phase equilibria, as discussed in Section 14.2. The interfacial tension will affect the ease in creating drop size and interfacial area for mass transfer. Jufu et al. (1986) provide a

reliable method for predicting the interfacial tension. It should be noted that impurities and minor components can change the interfacial tension significantly.

A high density difference promotes phase settling and potentially higher throughputs. High viscosities restrict throughput if the viscous phase is continuous, and result in poor diffusion and low mass transfer coefficients. The liquid molecular diffusion coefficient has a strong dependence on viscosity. In some applications, increasing the operating temperature may enhance the extractor performance.

14.2. EQUILIBRIUM RELATIONS

On a ternary equilibrium diagram like that of Figure 14.2, the limits of mutual solubilities are marked by the binodal curve and the compositions of phases in equilibrium by tielines. The region within the dome is two-phase and that outside is one-phase. The most common systems are those with one pair (Type I, Figure 14.2) and two pairs (Type II, Figure 14.5) of partially miscible substances. For instance, of the approximately 800 sets of data collected and analyzed by Sorensen and Arlt (1979) and Arlt et al. (1987), 75% are Type I and 20% are Type II. The remaining small percentage of systems exhibit a considerable variety of behaviors, a few of which appear in Figure 14.5. As some of these examples show, the effect of temperature on phase behavior of liquids often is very pronounced.

Both equilateral and right triangular diagrams have the property that the compositions of mixtures of all proportions of two mixtures appear on the straight line connecting the original mixtures. Moreover, the relative amounts of the original mixtures corresponding to an overall composition may be found from ratios of line segments. Thus, on the figure of Example 14.2, the amounts of extract and raffinate corresponding to an overall composition M are in the ratio $E_1/R_N = MR_N/E_1M$.

Experimental data on only 28 quaternary systems were found by Sorensen and Arlt (1979) and Arlt et al. (1987), and none of more complex systems, although a few scattered measurements do appear in the literature. Graphical representation of quaternary systems is possible but awkward, so that their behavior usually is analyzed with equations. To a limited degree of accuracy, the phase behavior of complex mixtures can be predicted from measurements on binary mixtures, and considerably better when some ternary measurements also are available. The data are correlated as activity coefficients by means of the UNIQUAC or NRTL equations. The basic principle of application is that at equilibrium the activity of each component is the same in both phases. In terms of activity coefficients this condition is for component i,

$$\gamma_i x_i = \gamma_i^* x_i^*, \tag{14.1}$$

where* designates the second phase. This may be rearranged into a relation of distributions of compositions between the phases,

$$x_i^* = (\gamma_i/\gamma_i^*)x_i = K_i x_i, \tag{14.2}$$

where K_i is the distribution coefficient. The activity coefficients are functions of the composition of the mixture and the temperature. Applications to the calculation of stage requirements for extraction are described later.

The distribution coefficient K_i is the ratio of activity coefficients and may be estimated from binary infinite dilution coefficient data.

$$K_i = \frac{\gamma_i^\infty}{\gamma_i^{*,\infty}} \tag{14.3}$$
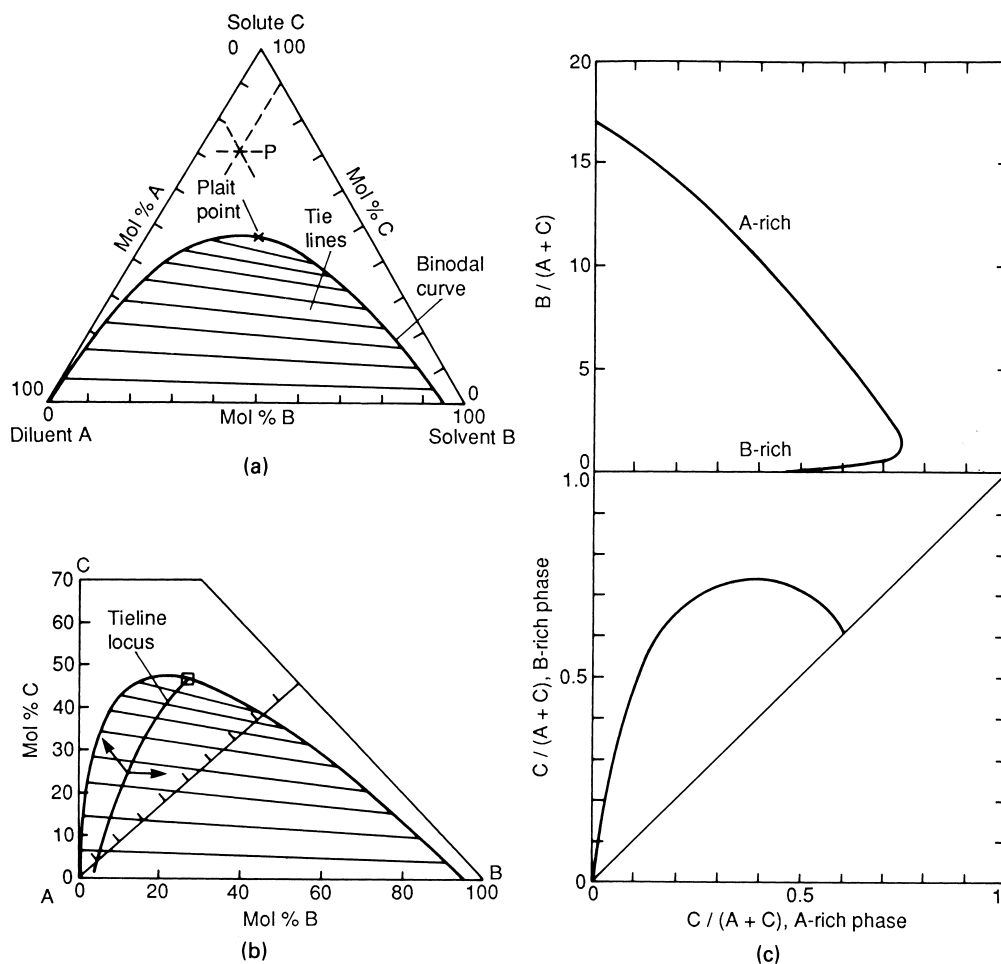
Figure 14.2. Equilibria in a ternary system, type 1, with one pair of partially miscible liquids; A = 1-hexene, B = tetramethylene sulfone, C = benzene, at 50°C (*R.M. De Fre, thesis, Gent, 1976*). (a) Equilateral triangular plot; point *P* is at 20% A, 10% B, and 70% C. (b) Right triangular plot with tielines and tieline locus, the amount of A can be read off along the perpendicular to the hypotenuse or by difference. (c) Rectangular coordinate plot with tieline correlation below, also called Janecke and solvent-free coordinates.

Binary interaction parameters (A$_{ij}$) and infinite dilution activity coefficients are available for a wide variety of binary pairs. Therefore the ratio of the solute infinite dilution coefficient in solvent-rich phase to that of the second phase (*) will provide an estimate of the equilibrium distribution coefficient. The method can provide a reasonable estimate of the distribution coefficient for dilute cases.

$$\mathrm{RT}\ln\left\{\gamma_{i,j}^{\infty}\right\} = A_{i,j} \qquad (14.4)$$

$$K_i = \frac{\gamma_i^{\infty}}{\gamma_i^{*,\infty}} = \frac{e^{A_{ij}/RT}}{e^{A_{ij}^{*}/RT}} \qquad (14.5)$$

See Example 14.1

Extraction behavior of highly complex mixtures usually can be known only from experiment. The simplest equipment for that purpose is the separatory funnel, but complex operations can be simulated with proper procedures, for instance, as in Figure 14.4(c). Elaborate automatic laboratory equipment is in use. One of them employs a 10,000–25,000 rpm mixer with a residence time of 0.3–5.0 sec, followed by a highly efficient centrifuge and two

chromatographs for analysis of the two phases (Lo et al., 1983, pp. 507).

Compositions of petroleum mixtures sometimes are represented adequately in terms of some physical property. Three examples appear in Figure 14.6. Straight line combining of mixtures still is valid on such diagrams.

Basically, compositions of phases in equilibrium are indicated with tielines. For convenience of interpolation and to reduce the clutter, however, various kinds of tieline loci may be constructed, usually as loci of intersections of projections from the two ends of the tielines. In Figure 14.2 the projections are parallel to the base and to the hypotenuse, whereas in Figures 14.3 and 14.7 they are horizontal and vertical.

Several tieline correlations in equation form have been proposed, of which three may be presented. They are expressed in weight fractions identified with these subscripts:

CA solute C in diluent phase A
CS solute C in solvent phase S
SS solvent S in solvent phase S
AA diluent A in diluent phase A
AS diluent A in solvent phase S
SA solvent S in diluent phase A.

EXAMPLE 14.1
Estimate the distribution coefficient for transferring acetone from water into benzene at 25°C. The concentration of acetone in benzene is assumed to be dilute.

For acetone/benzene, $A_{i,II}/RT = 0.47$

For acetone/water, $A_{i,II}/RT = 2.27$

$$K_i = \frac{e^{2.27}}{e^{0.47}} = \frac{9.68}{1.6} = 6.05(mol/mol) = 1.39(wt/wt)$$

Experimental values range 1.06–1.39. Distribution coefficient data for dilute solute concentrations have been compiled by Treybal in *Perry's Handbook*. A sampling of the data presented by Treybal and additional distribution coefficient data are given in Table 14.1.

TABLE 14.1. Distribution Coefficients of Dilute Solute Systems.

Component A = Carrier, component B = solute, and component S = extraction solvent. K₁ is the distribution coefficient (wt/wt)

Component B	Component S	Temp., °C.	K_1	Ref.
A = ethylene glycol				
Acetone	Amyl acetate	31	1.838	38
Acetone	n-Butyl acetate	31	1.940	38
Acetone	Ethyl acetate	31	1.850	38
A = furfural				
Trilinolein	n-Heptane	30	47.5	5
Triolein	n-Heptane	30	95	5
A = n-hexane				
Toluene	Sulfolane	25	0.336	4
Xylene	Sulfolane	25	0.302	4
A = n-octane				
Toluene	Sulfolane	25	0.345	4
Xylene	Sulfolane	25	0.245	4
A = water				
Acetaldehyde	n-Amyl alcohol	18	1.43	31
Acetaldehyde	Furfural	16	0.967	31
Acetic acid	1-Butanol	26.7	1.613	41
Acetic acid	Cyclohexanol	26.7	1.325	41
Acetic acid	Di-n-butyl ketone	25–26	0.379	32
Acetic acid	Diisopropyl carbinol	25–26	0.800	32
Acetic acid	Ethyl acetate	30	0.907	11
Acetic acid	Isopropyl ether	20	0.248	12
Acetic acid	Methyl acetate		1.273	29
Acetic acid	Methyl cyclohexanone	25–26	0.930	32
Acetic acid	Methylisobutyl ketone	25	0.657	40
		25–26	0.755	32
Acetic acid	Toluene	25	0.0644	49
Acetone	n-Butyl acetate		1.127	29
Acetone	Chloroform	25	1.830	15
		25	1.720	2
Acetone	Dibutyl ether	25–26	1.941	32
Acetone	Diethyl ether	30	1.00	19
Acetone	Ethyl acetate	30	1.500	46
Acetone	Ethyl butyrate	30	1.278	46
Acetone	n-Hexane	25	0.343	45
Acetone	Methyl acetate	30	1.153	46
Acetone	Methylisobutyl ketone	25–26	1.910	32
Acetone	Toluene	25–26	0.835	32
Aniline	n-Heptane	25	1.425	14
		50	2.20	14
Aniline	Methylcyclohexane	25	2.05	14
		50	3.41	14
Aniline	Toluene	25	12.91	43
tert-Butanol	Ethyl acetate	20	1.74	3
Butyric acid	Methyl butyrate	30	6.75	28
Citric acid	25% Triisooctylamine/Chloroform	25	14.1	24
Citric acid	25% Triisooctylamine/1-Octanol	25	41.5	24
p-Cresol	Methylnaphthalene	35	9.89	35
Ethanol	n-Butanol	20	3.00	10

TABLE 14.1.—(continued**)**

Component B	Component S	Temp., °C.	K_1	Ref.
Ethanol	Di-n-propyl ketone	25–26	0.592	32
Ethanol	3-Heptanol	25	0.783	33
Ethanol	n-Hexanol	28	1.00	22
Ethanol	sec-Octanol	28	0.825	22
Ethylene glycol	Furfural	25	0.315	6
Formic acid	Methylisobutyl carbinol	30	1.218	36
Furfural	Toluene	25	5.64	18
Lactic acid	iso-Amyl alcohol	25	0.352	48
Lactic acid	25% Triisooctylamine/Chloroform	25	19.2	24
Lactic acid	25% Triisooctylamine/1-Octanol	25	25.9	24
Malic acid	25% Triisooctylamine/Chloroform	25	30.7	24
Malic acid	25% Triisooctylamine/1-Octanol	25	59.0	24
Methanol	n-Butanol	0	0.600	27
Methanol	p-Cresol	35	0.313	35
Methanol	Ethyl acetate	0	0.0589	3
		20	0.238	3
Methanol	n-Hexanol	28	0.565	20
Methanol	Phenol	25	1.333	35
Methyl-n-butyl ketone	n-Butanol	37.8	53.4	17
Methylethyl ketone	Cyclohexane	25	1.775	16
Methylethyl ketone	n-Heptane	25	1.548	44
Methylethyl ketone	n-Hexane	25	1.775	44
		37.8	2.22	17
Methylethyl ketone	1,1,2-Trichloroethane	25	3.44	30
Methylethyl ketone	Trichloroethylene	25	3.27	30
Methylethyl ketone	2,2,4-Trimethylpentane	25	1.572	26
Oxalic acid	25% Triisooctylamine/Chloroform	25	25.5	24
Oxalic acid	25% Triisooctylamine/1-Octanol	25	46.0	24
Phenol	Ethyl acetate	25	0.048	1
Phenol	Isoamyl acetate	25	0.046	1
Phenol	Isopropyl acetate	25	0.040	1
iso-Propanol	Carbon tetrachloride	20	1.405	9
iso-Propanol	Diisopropyl ether	25	0.406	13
n-Propanol	iso-Amyl alcohol	25	3.34	7
n-Propanol	n-Butanol	37.8	3.61	25
n-Propanol	Ethyl acetate	0	1.419	3
		20	1.542	3
n-Propanol	n-Heptane	37.8	0.540	25
n-Propanol	n-Propyl acetate	20	1.55	42
Propionic acid	Ethyl acetate	30	2.77	39
Propionic acid	Ethyl butyrate	26	1.470	39
Propionic acid	Ethyl propionate	28	0.510	39
Propionic acid	Methyl butyrate	30	2.15	28
Propionic acid	Methylisobutyl carbinol	30	3.52	36
Propionic acid	Monochlorobenzene	30	0.513	23
Propionic acid	Toluene	31	0.515	37
Propionic acid	Trichloroethylene	30	0.496	23
Pyridine	Monochlorobenzene	25	2.10	34
Pyridine	Toluene	25	1.900	47
Pyridine	Xylene	25	1.260	47
Sodium chloride	1-Methyldodecyl amine	30	0.693	8
Sodium chloride	1-Methyloctyl amine	30	0.589	8
A = Salt water				
Citric acid	2-Butanol	25	0.534	21

*Concentrations in lb.-moles./cu. ft.
†Concentrations in volume fraction.

References for Table 14.1:
1. Alberty and Washburn, *J. Phys. Chem.*, 49, 4 (1945).
2. Baker, *J. Phys. Chem.*, 59, 1182(1955)
3. Bancroft and Hubard, *J. Am. Chem. Soc.,* 64, 347 (1942).
4. Barbaudy, *Compt. rend.,* 182, 1279 (1926).
5. Beech and Glasstone, *J. Chem. Soc.,* 1938, 67.
6. Berg, Manders, and Switzer, *Chem. Eng. Progr.,* 47, 11 (1951).
7. Bergelin, Lockhart, and Brown, *Trans. Am. Inst. Chem. Engrs.,* 39, 173 (1943).
8. Berndt and Lynch, *J. Am. Chem. Soc.,* 66, 282 (1944).
9. Blumberg, Cejtlin, and Fuchs, *J. Appl. Chem.,* 10, 407 (1960).
10. Boobar et al., *Ind. Eng. Chem.,* 43, 2922 (1951).
11. Briggs and Comings, *Ind. Eng. Chem.,* 35, 411 (1943).
12. Buchanan, *Ind. Eng. Chem.,* 44, 2449 (1952).
13. Chang and Moulton, *Ind. Eng. Chem.,* 45, 2350 (1953).
14. Charles and Morton. *J. Appl. Chem.,* 7, 39 (1957).
15. Church and Briggs, *J. Chem. Eng. Data,* 9, 207 (1964).
16. Colbum and Phillips, *Trans. Am. Inst. Chem. Engrs.,* 40, 333 (1944).
17. Conti, Othmer, and Gilmont, *J. Chem. Eng. Data,* 5, 301 (1960).
18. Conway and Norton, *Ind. Eng. Chem.,* 43, 1433 (1951).
19. Conway and Phillips, *Ind. Eng. Chem.,* 46, 1474 (1954).
20. Coull and Hope, *J. Phys. Chem.,* 39, 967 (1935).

21. Crittenden and Hixson, *Ind. Eng. Chem.,* **46,** 265 (1954).
22. Crook and Van Winkle, *Ind. Eng. Chem.,* **46,** 1474 (1954).
23. Cumming and Morton, *J. Appl. Chem.,* **3,** 358 (1953).
24. Davison, Smith, and Hood, *J. Chem. Eng. Data,* **11,** 304 (1966).
25. Denzler, *J. Phys. Chem.,* **49,** 358 (1945).
26. Drouillon, *J. chim. phys.,* **22,** 149 (1925).
27. Durandet and Gladel, *Rev. Inst. Franc. Pétrole,* **9,** 296 (1954).
28. Durandet and Gladel, *Rev. Inst. Franc. Pétrole,* **11,** 811 (1956).
29. Durandet, Gladel, and Graziani, *Rev. Inst. Franc. Pétrole,* **10,** 585 (1955).
30. Eaglesfield, Kelly, and Short, *Ind. Chemist,* **29,** 147, 243 (1953).
31. Elgin and Browning, *Trans. Am. Inst. Chem. Engrs.,* **31,** 639 (1935).
32. Fairburn, Cheney, and Chernovsky, *Chem. Eng. Progr.,* **43,** 280 (1947).
33. Forbes and Coolidge, *J. Am. Chem. Soc.,* **41,** 150 (1919).
34. Fowler and Noble, *J. Appl. Chem.,* **4,** 546 (1954).
35. Frere, *Ind. Eng. Chem.,* **41,** 2365 (1949).
36. Fritzsche and Stockton, *Ind. Eng. Chem.,* **38,** 737 (1946).
37. Fuoss, *J. Am. Chem. Soc.,* **62,** 3183 (1940).
38. Garner, Ellis, and Roy, *Chem. Eng. Sci.,* **2,** 14 (1953).
39. Gladel and Lablaude, *Rev. Inst. Franc. Pétrole,* **12,** 1236 (1957).
40. Griswold, Chew, and Klecka, *Ind. Eng. Chem.,* **42,** 1246 (1950).
41. Griswold, Chu, and Winsauer, *Ind. Eng. Chem.,* **41,** 2352 (1949).
42. Griswold, Klecka, and West, *Chem. Eng. Progr.,* **44,** 839 (1948).
43. Hand, *J. Phys. Chem.,* **34,** 1961 (1930).
44. Henty, McManamey, and Price, *J. Appl. Chem.,* **14,** 148 (1964).
45. Hirata and Hirose, *Kagalau Kogaku,* **27,** 407 (1963).
46. Hixon and Bockelmann, *Trans. Am. Inst. Chem. Engrs.,* **38,** 891 (1942).
47. Hunter and Brown, *Ind. Eng. Chem.,* **39,** 1343 (1947).
48. Jeffreys, *J. Chem. Eng. Data,* **8,** 320 (1963).
49. Johnson and Bliss, *Trans. Am. Inst. Chem. Engrs.,* **42,** 331 (1946).
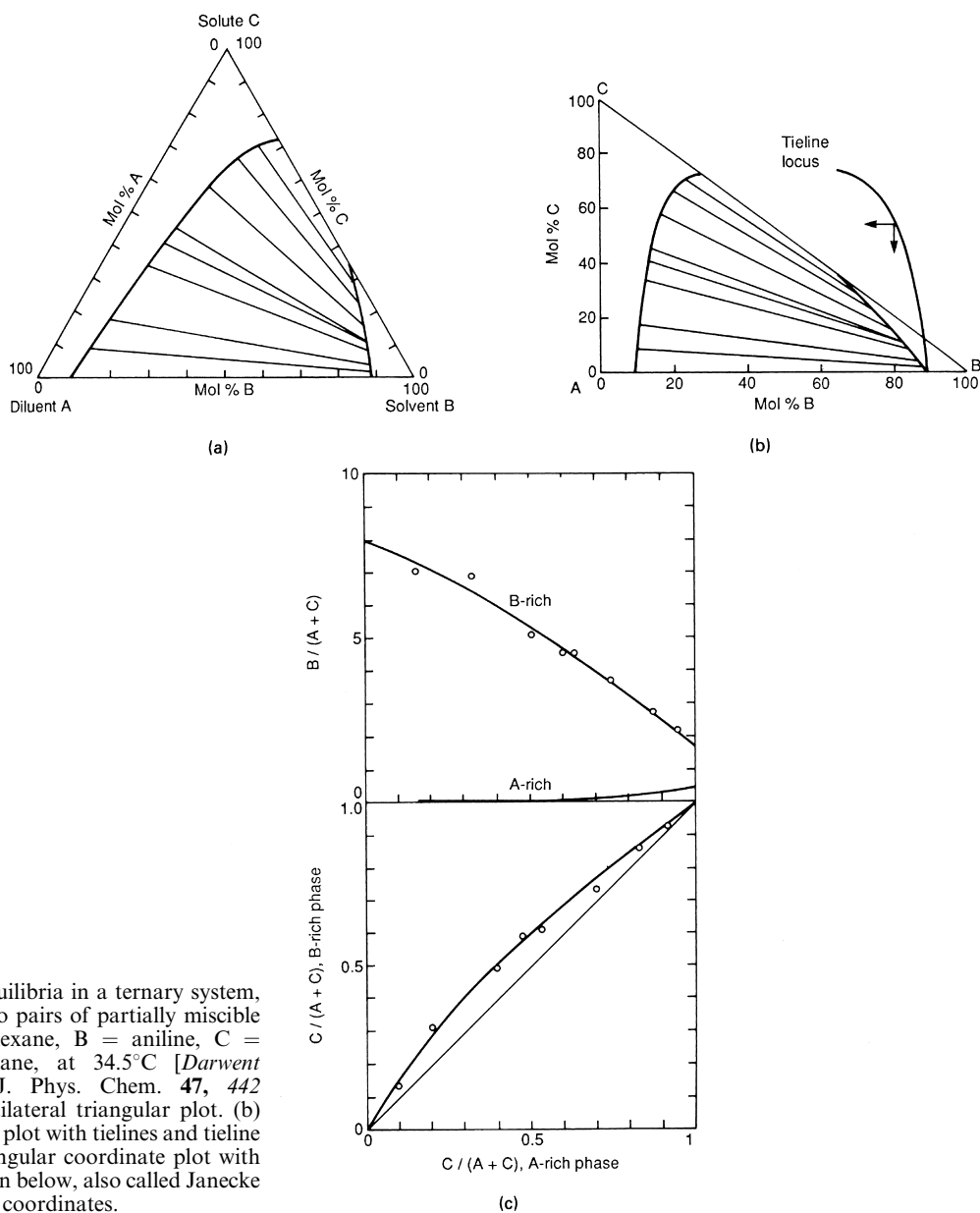
Figure 14.3. Equilibria in a ternary system, type II, with two pairs of partially miscible liquids; A = hexane, B = aniline, C = methylcyclopentane, at 34.5°C [*Darwent and Winkler*, J. Phys. Chem. **47,** *442* (*1943*)]. (a) Equilateral triangular plot. (b) Right triangular plot with tielines and tieline locus. (c) Rectangular coordinate plot with tieline correlation below, also called Janecke and solvent-free coordinates.

(a)

(b)

S = Fresh solvent R = Raffinate
F = Feed to be extracted E = Extract

(c)
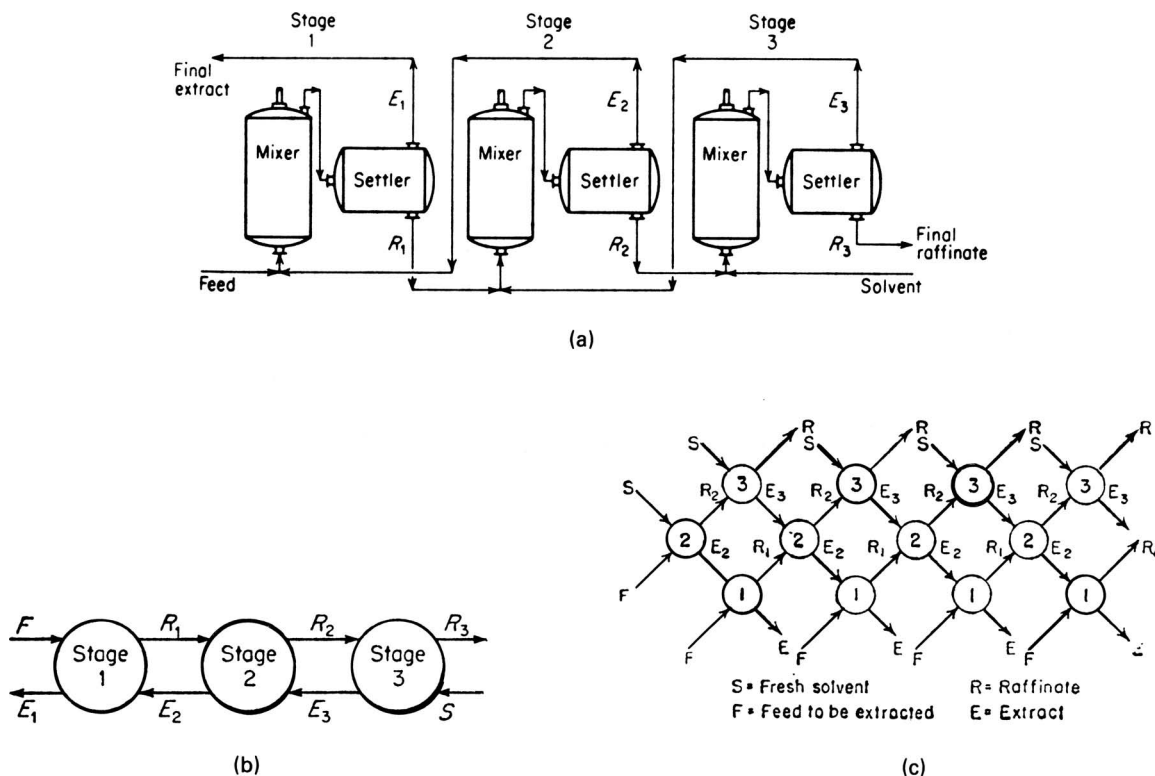
Figure 14.4. Representation of countercurrent extraction batteries. (a) A battery of mixers and settlers (or separators). (b) Schematic of a three-stage countercurrent battery. (c) Simulation of the performance of a three-stage continuous countercurrent extraction battery with a series of batch extractions in separatory funnels which are designated by circles on the sketch. The numbers in the circles are those of the stages. Constant amounts of feed F and solvent S are mixed at the indicated points. As the number of operations is increased horizontally, the terminal compositions E_1 and R_3 approach asymptotically the values obtained in continuous countercurrent extraction (*Treybal, 1963, p. 360*).

(a)

(b)
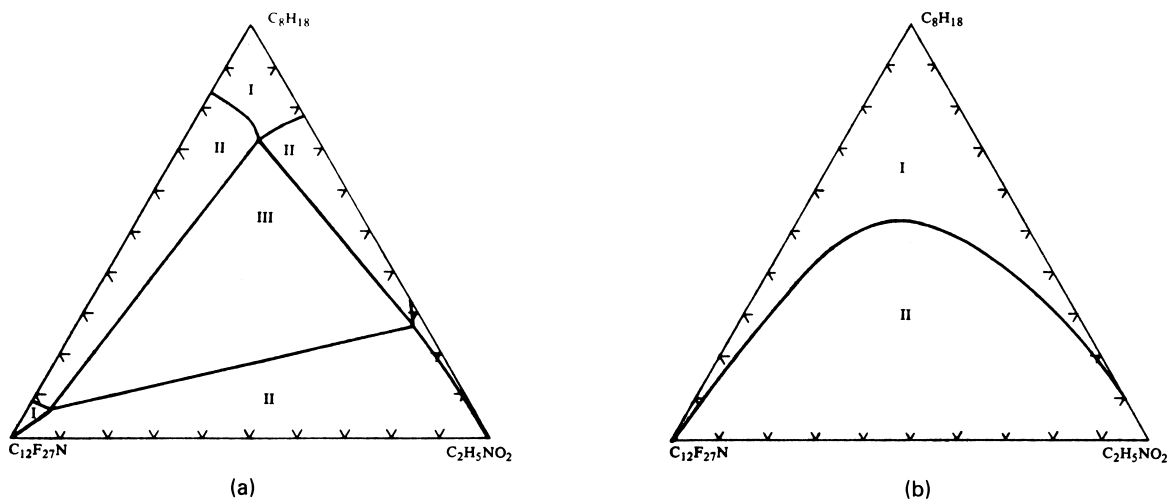
Figure 14.5. Less common examples of ternary equilibria and some temperature effects. (a) The system 2,2,4-trimethylpentane + nitroethane + perfluorobutylamine at 25°C; the Roman numerals designate the number of phases in that region [*Vreeland and Dunlap*, J. Phys. Chem. **61**, *329 (1957)*]. (b) Same as (a) but at 51.3°C. (c) Glycol + dodecanol + nitroethane at 24°C; 12 different regions exist at 14°C [*Francis*, J. Phys. Chem. **60**, *20 (1956)*]. (d) Docosane + furfural + diphenylhexane at several temperatures [*Varteressian and Fenske*, Ind. Eng. Chem. **29**, *270 (1937)*]. (e) Formic acid + benzene + tribromomethane at 70°C; the pair formic acid/benzene is partially miscible with 15 and 90% of the former at equilibrium at 25°C, 43 and 80% at 70°C, but completely miscible at some higher temperature. (f) Methylcyclohexane + water + -picoline at 20°C, exhibiting positive and negative tieline slopes; the horizontal tieline is called solutropic (*Landolt-Börnstein II2b*).

(c)

(d)

(e)

(f)
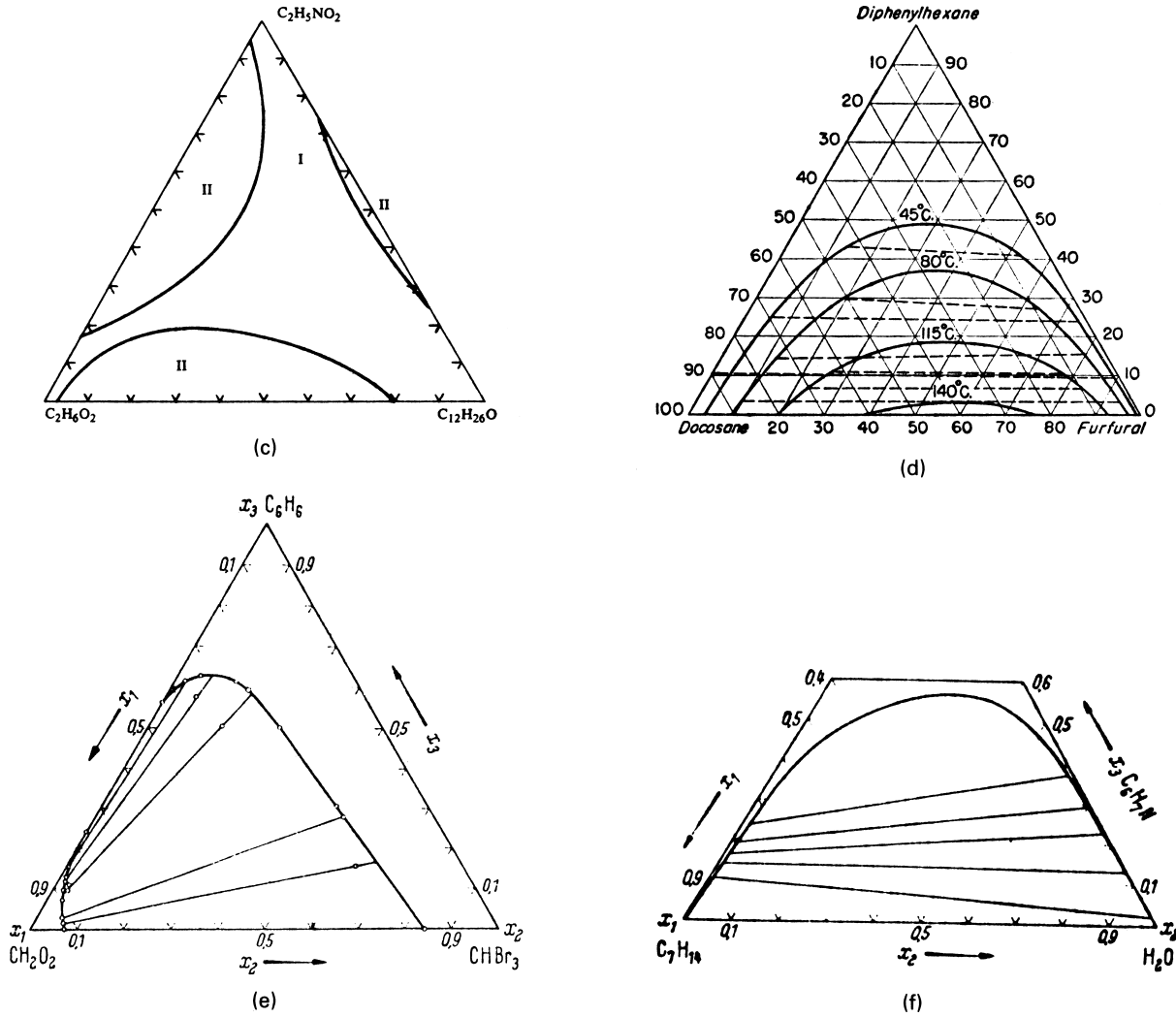
Figure 14.5.—(*continued*)

Ishida, *Bull. Chem. Soc. Jpn.* **33,** 693 (1960):

$$X_{CS}X_{SA}/X_{CA}X_{SS} = K(X_{AS}X_{SA}/X_{AA}X_{SS})^n. \tag{14.6}$$

Othmer and Tobias, *Ind. Eng. Chem.* **34,** 693 (1942):

$$(1 - X_{SS})/X_{SS} = K[(1 - X_{AA})/X_{AA}]^n. \tag{14.7}$$

Hand, *J. Phys. Chem.* **34,** 1961 (1930):

$$X_{CS}/X_{SS} = K(X_{CA}/X_{AA})^n. \tag{14.8}$$

These equations should plot linearly on log–log coordinates; they are tested in Example 14.2.

A system of plotting both binodal and tieline data in terms of certain ratios of concentrations was devised by Janecke and is illustrated in Figure 14.2(c). It is analogous to the enthalpy–concentration or Merkel diagram that is useful in solving distillation problems. Straight line combining of mixture compositions is valid in this mode. Calculations for the transformation of data are made most conveniently from tabulated tieline data. Those for Figure 14.2 are made in Example 14.3. The *x–y* construction shown in Figure 14.3 is the basis for a McCabe–Thiele construction

for finding the number of extraction stages, as applied in Figure 14.8.

14.3. CALCULATION OF STAGE REQUIREMENTS

Although the most useful extraction process is with countercurrent flow in a multistage battery, other modes have some application. Calculations may be performed analytically or graphically. On flowsketches for Example 14.2 and elsewhere, a single box represents an extraction stage that may be made up of an individual mixer and separator. The performance of differential contactors such as packed or spray towers is commonly described as the height equivalent to a theoretical stage (HETS) in ft or m.

SINGLE STAGE EXTRACTION

The material balance is

$$\text{feed} + \text{solvent} = \text{extract} + \text{raffinate}, \quad F + S = E + R. \tag{14.9}$$

This nomenclature is shown with Example 14.4. On the triangular diagram, the proportions of feed and solvent locate the mix point *M*. The extract *E* and raffinate *R* are located on opposite ends of the tieline that goes through *M*.
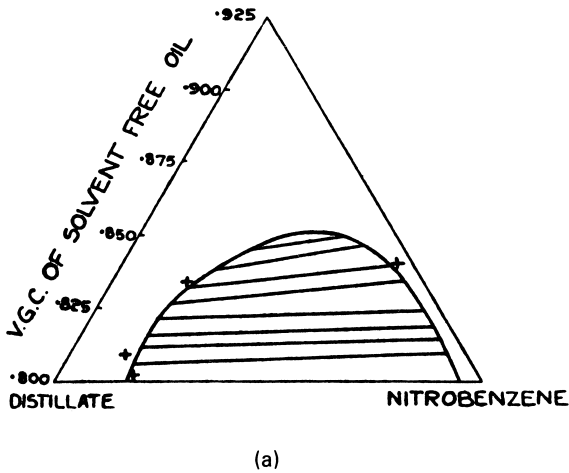
(a)
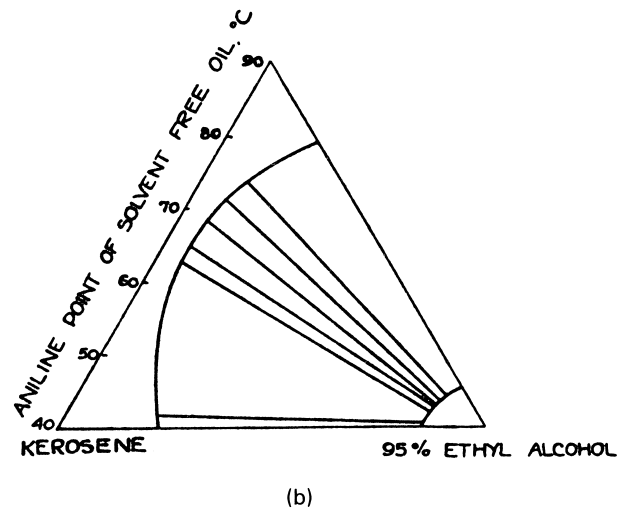
(b)
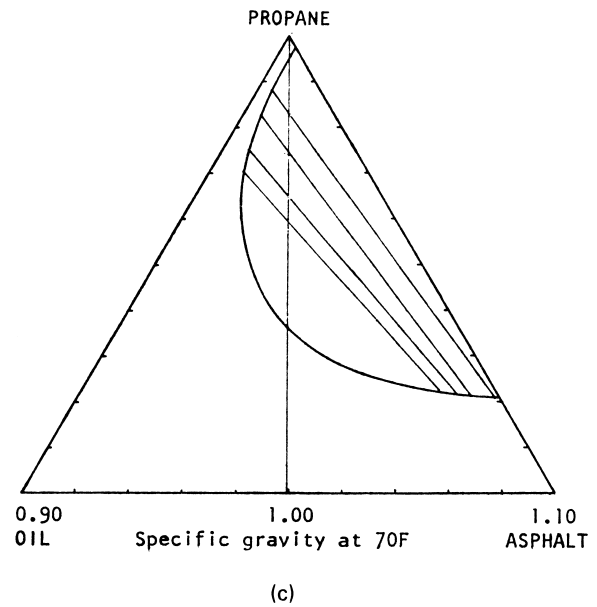
(c)

Figure 14.6. Representation of solvent extraction behavior in terms of certain properties rather than direct compositions [*Dunstan et al.*, Sci. Pet., *1825–1855 (1938)*]. (a) Behavior of a naphthenic distillate of VGC = 0.874 with nitrobenzene at 10°C. The viscosity-gravity constant is low for paraffins and high for naphthenes. (b) Behavior of a kerosene with 95% ethanol at 17°C. The aniline point is low for aromatics and naphthenes and high for paraffins. (c) Behavior of a dewaxed crude oil with liquid propane at 70°F, with composition expressed in terms of specific gravity.

CROSSCURRENT EXTRACTION

In this process the feed and subsequently the raffinate are treated in successive stages with fresh solvent. The sketch is with Example 14.4. With a fixed overall amount of solvent the most efficient process is with equal solvent flow to each stage. The solution of Example 14.4 shows that crosscurrent two stage operation is superior to one stage with the same total amount of solvent.

IMMISCIBLE SOLVENTS

The distribution of a solute between two mutually immiscible solvents can be represented by the simple equation,

$$Y = K'X, \qquad (14.10)$$

where

X = mass of solute/mass of diluent,
Y = mass of solute/mass of solvent.

When K' is not truly constant, some kind of mean value may be applicable, for instance, a geometric mean, or the performance of the extraction battery may be calculated stage by stage with a different value of K' for each. The material balance around the first stage where the raffinate leaves and the feed enters and an intermediate stage k (as in Figure 14.9, for instance) is

$$EY_F + RX_{k-1} = EY_k + RX_n. \qquad (14.11)$$

In terms of the extraction ratio,

$$A = K(E/R), \qquad (14.12)$$

the material balance becomes

$$(A/K)Y_F + X_{k-1} = AX_k + X_n. \qquad (14.13)$$

When these balances are made stage-by-stage and intermediate compositions are eliminated, assuming constant A throughout,

Figure 14.7. Construction of points on the distribution and operating curves: Line *ab* is a tieline. The dashed line is the tieline locus. Point *e* is on the equilibrium distribution curve, obtained as the intersection of paths *be* and *ade*. Line *Pfg* is a random line from the difference point *P* and intersecting the binodal curve in *f* and *g*. Point *j* is on the operating curve, obtained as the intersection of paths *gj* and *fhj*.

the result relates the terminal compositions and the number of stages. The expression for the fraction extracted is

$$\phi = \frac{X_F - X_n}{X_F - Y_S/K} = \frac{A^{n+1} - A}{A^{n+1} - 1}. \tag{14.14}$$

This is of the same form as the Kremser-Brown equation for gas absorption and stripping and the Turner equation for leaching. The solution for the number of stages is

$$n = -1 + \frac{\ln\left[(A - \phi)/(1 - \phi)\right]}{\ln A}. \tag{14.15}$$

When A is the only unknown, it may be found by trial solution of these equations, or the Kremser-Brown stripping chart may be used. Example 14.5 applies these results.

EXAMPLE 14.2
The Equations for Tieline Data
The tieline data of the system of Example 14.2 are plotted according to the groups of variables in the equations of Ishida, Hand, and Othmer and Tobias with these results:

Ishida: $y = 1.00x^{0.67}$ [Eq.(14.3)],

Hand: $y = 0.078x^{1.11}$ [Eq.(14.5)],

Othmer and Tobias: $y = 0.88x^{0.90}$ [Eq.(14.4)].

The last correlation is inferior for this particular example as the plots show.

x_{AA}	x_{CA}	x_{SA}	x_{AS}	x_{CS}	x_{SS}
98.945	0.0	1.055	5.615	0.0	94.385
92.197	6.471	1.332	5.811	3.875	90.313
83.572	14.612	1.816	6.354	9.758	83.889
75.356	22.277	2.367	7.131	15.365	77.504
68.283	28.376	3.341	8.376	20.686	70.939
60.771	34.345	4.884	9.545	26.248	64.207
54.034	39.239	6.727	11.375	31.230	57.394
47.748	42.849	9.403	13.505	35.020	51.475
39.225	45.594	15.181	18.134	39.073	42.793

$\dfrac{10^4 x_{AS} x_{SA}}{x_{AA} x_{SS}}$	$\dfrac{x_{CS} x_{SA}}{x_{CA} x_{SS}}$	$\dfrac{1}{x_{AA}} - 1$	$\dfrac{1}{x_{SS}} - 1$	x_{CA}/X_{AA}	x_{CS}/x_{SS}
6.34	0	0.0107	0.0595	0	0
9.30	0.0088	0.0846	0.1073	0.070	0.043
16.46	0.0129	0.1966	0.1928	0.178	0.116
28.90	0.0211	0.3270	0.2903	0.296	0.198
58.22	0.0343	0.4645	0.4097	0.416	0.292
119.47	0.0581	0.6455	0.5575	0.565	0.409
339.77	0.0933	0.8507	0.7423	0.726	0.544
516.67	0.1493	1.0943	0.9427	0.897	0.680
1640	0.3040	1.5494	1.3368	1.162	0.913

EXAMPLE 14.3
Tabulated Tieline and Distribution Data for the System A = 1-Hexene, B = Tetramethylene Sulfone, C = Benzene, Represented in Figure 14.1
Experimental tieline data in mol %:

	Left Phase			Right Phase	
A	**C**	**B**	**A**	**C**	**B**
98.945	0.0	1.055	5.615	0.0	94.385
92.197	6.471	1.332	5.811	3.875	90.313
83.572	14.612	1.816	6.354	9.758	83.888
75.356	22.277	2.367	7.131	15.365	77.504
68.283	28.376	3.341	8.376	20.686	70.938
60.771	34.345	4.884	9.545	26.248	64.207
54.034	39.239	6.727	11.375	31.230	57.394
47.748	42.849	9.403	13.505	35.020	51.475
39.225	45.594	15.181	18.134	39.073	42.793

Calculated ratios for the Jänecke coordinate plot of Figure 14.1:

Left Phase		Right Phase	
B	**C**	**B**	**C**
$\overline{A+C}$	$\overline{A+C}$	$\overline{A+C}$	$\overline{A+C}$
0.0108	0	16.809	0
0.0135	0.0656	9.932	0.4000
0.0185	0.1488	5.190	0.6041
0.0248	0.2329	3.445	0.6830
0.0346	0.2936	2.441	0.7118
0.0513	0.3625	1.794	0.7333
0.0721	0.4207	1.347	0.7330
0.1038	0.4730	1.061	0.7217
0.1790	0.5375	0.748	0.6830

The $x - y$ plot like that of Figure 14.7 may be made with the tieline data of columns 5 and 2 expressed as fractions or by projection from the triangular diagram as shown.

Equation 14.15 may be rewritten:

$$N_s = \frac{\ln\left\{\frac{(X_f - Y_s/K')}{(X_r - Y_s/K')}\left(1 - \frac{1}{A}\right) + \frac{1}{A}\right\}}{\ln\{A\}} \qquad (14.16)$$

where:

X_f = mass (or moles) of solute in feed/mass (or moles) of diluent

X_r = mass (or moles) of solute in raffinate/mass (or moles) of diluent

Y_s = mass (or moles) of solute in entering solvent/mass (or moles) of solvent

K' = distribution coefficient, $Y = K'X$ wt/wt (or mol/mol)

E/R = mass (or mole) ratio of extract to raffinate on a solute free basis

$A = EK'/R$

14.4. COUNTERCURRENT OPERATION

In countercurrent operation of several stages in series, feed enters the first stage and final extract leaves it, and fresh solvent enters the last stage and final raffinate leaves it. Several representations of such processes are in Figure 14.4. A flowsketch of the process together with nomenclature is shown with Example 14.6. The overall material balance is

$$F + S = E_1 + R_N = M \qquad (14.16)$$

or

$$F - E_1 = R_N - S = P. \qquad (14.17)$$

(a)
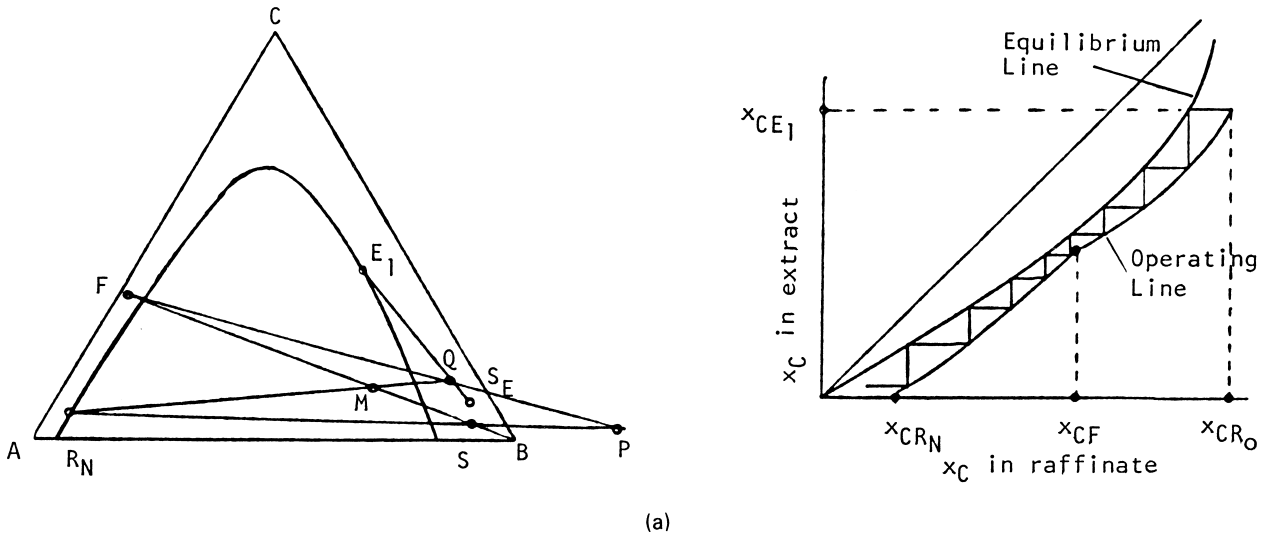
Figure 14.8. Locations of operating points P and Q for feasible, total, and minimum extract reflux on triangular diagrams, and stage requirements determined on rectangular distribution diagrams. (a) Stages required with feasible extract reflux. (b) Operation at total reflux and minimum number of stages. (c) Operation at minimum reflux and infinite stages.
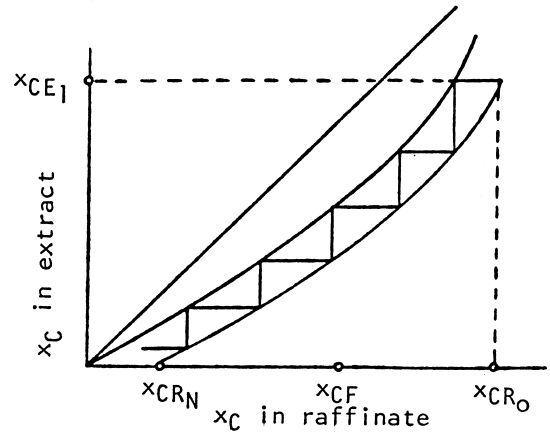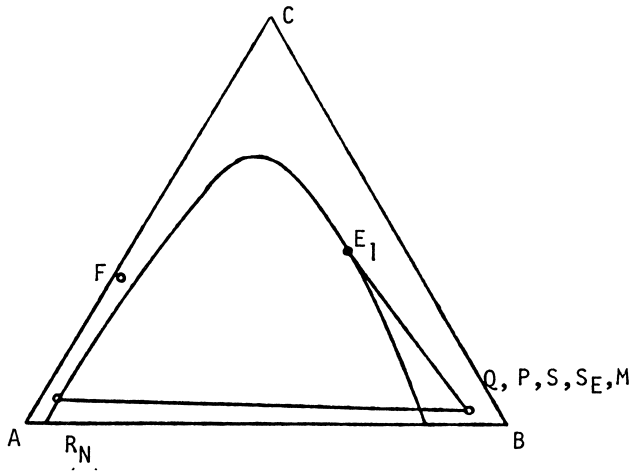
(b)
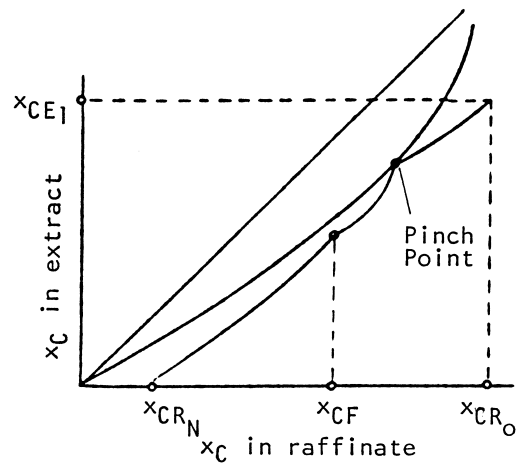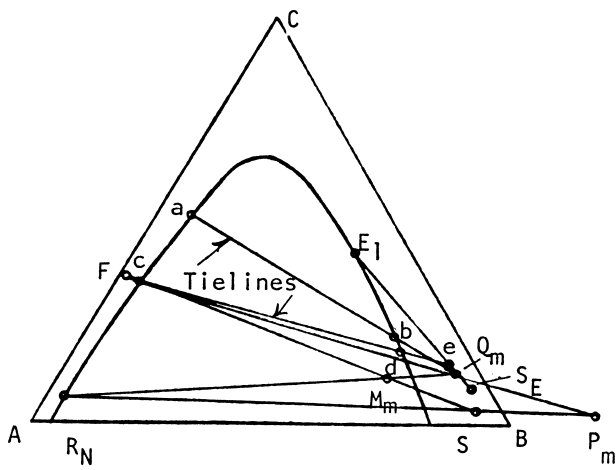
(c)

Figure 14.8.—(*continued*)

The intersection of extended lines FE_1 and $R_N S$ locates the operating point P. The material balance from stage 1 through k is

$$F + E_{k+1} = E_1 + R_k \qquad (14.18)$$

or

$$F - E_1 = R_k - E_{k+1} = P. \qquad (14.19)$$

Accordingly, the raffinate from a particular stage and the extract from a succeeding one are on a line through the operating point P. Raffinate R_k and extract E_k streams from the same stage are located at opposite ends of the same tieline.

The operation of finding the number of stages consists of a number of steps:

1. Either the solvent feed ratio or the compositions E_1 and R_N serve to locate the mix point M.
2. The operating point P is located as the intersection of lines FE_1 and $R_N S$.
3. When starting with E_1, the raffinate R_1 is located at the other end of the tieline.
4. The line PR_1 is drawn to intersect the binodal curve in E_2.

The process is continued with the succeeding values R_2, E_3, R_3, E_4, . . . until the final raffinate composition is reached.

When number of stages and only one of the terminal compositions are fixed, the other terminal composition is selected by trial until the stepwise calculation finds the prescribed number of stages. Example 14.7 applies this kind of calculation to find the stage requirements for systems with Types I and II equilibria.

Evaluation of the numbers of stages also can be made on rectangular distribution diagrams, with a McCabe–Thiele kind of construction. Example 14.6 does this. The Janecke coordinate plots like those of Figures 14.2 and 14.3 also are convenient when many stages are needed, since then the triangular construction may become crowded and difficult to execute accurately unless a very large scale is adopted. The Janecke method was developed by Maloney and Schubert [*Trans. AIChE* **36,** 741 (1940)]. Several detailed examples of this kind of calculation are worked by Treybal (1963), Oliver (*Diffusional Separation Processes*, Wiley, New York, 1966), and Laddha and Degaleesan (1978).

MINIMUM SOLVENT/FEED RATIO

Both maximum and minimum limits exist of the solvent/feed ratio. The maximum is the value that locates the mix point M on the

EXAMPLE 14.4
Single Stage and Cross Current Extraction of Acetic Acid from Methylisobutyl Ketone with Water

The original mixture contains 35% acetic acid and 65% MIBK. It is charged at 100 kg/hr and extracted with water.

a. In a single stage extractor water is mixed in at 100 kg/hr. On the triangular diagram, mix point M is midway between F and S. Extract and raffinate compositions are on the tieline through M. Results read off the diagram and calculated with material balance are

b. The flowsketch of the crosscurrent process is shown. Feed to the first stage and water to both stages are at 100 kg/hr. The extract and raffinate compositions are on the tielines passing through mix points M_1 and M_2. Point M is for one stage with the same total amount of solvent. Two stage results are:
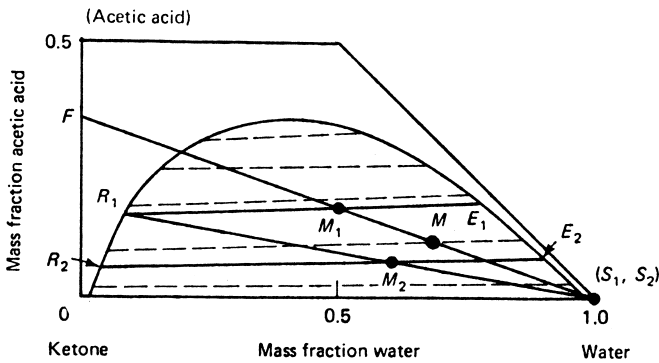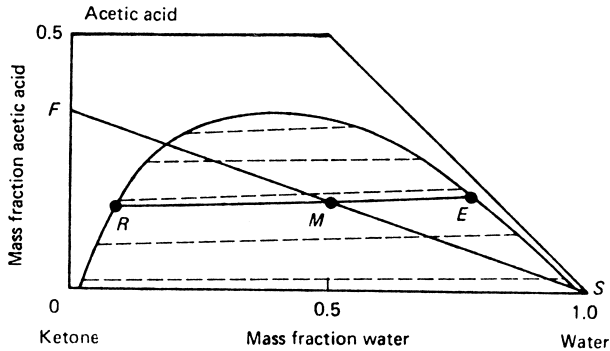
	E	R
Acetic acid	0.185	0.16
MIBK	0.035	0.751
Water	0.78	0.089
kg/hr	120	80

	E_1	R_1	E_2	R_2
Acetic acid	0.185	0.160	0.077	0.058
MIBK	0.035	0.751	0.018	0.902
Water	0.780	0.089	0.905	0.040
kg/hr	120	80	113.4	66.6
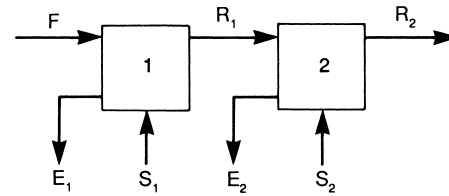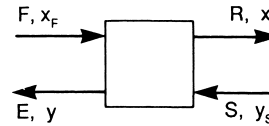
binodal curve near the solvent vertex, such as point M_{max} on Figure 14.8(b). When an operating line coincides with a tieline, the number of stages will be infinite and will correspond to the minimum solvent/feed ratio. The pinch point is determined by the intersection of some tieline with line $R_N S$. Depending on whether the slopes of the tielines are negative or positive, the intersection that is closest or farthest from the solvent vertex locates the operating point for minimum solvent. Figure 14.10 shows the two cases. Frequently, the tieline through the feed point determines the minimum solvent quantity, but not for the two cases shown.

For dilute solutions and a high degree of solute removal, the minimum solvent to feed ratio (S_{min}/F) may be estimated from the inverse of the distribution coefficient.

$$\frac{S_{min}}{F} \approx \frac{1}{K}$$

EXTRACT REFLUX

Normally, the concentration of solute in the final extract is limited to the value in equilibrium with the feed, but a countercurrent stream that is richer than the feed is available for enrichment of the extract. This is essentially solvent-free extract as reflux. A flowsketch and nomenclature of such a process are given with Example 14.8. Now there are two operating points, one for above the feed and one for below. These points are located by the following procedure:

1. The mix point is located by establishing the solvent/feed ratio.
2. Point Q is at the intersection of lines $R_N M$ and $E_1 S_E$, where S_E refers to the solvent that is removed from the final extract, and may or may not be of the same composition as the fresh solvent S. Depending on the shape of the curve, point Q may be inside the binodal curve as in Example 14.8, or outside as in Figure 14.8.
3. Point P is at the intersection of lines $R_N M$ and $E_1 S_E$, where S_E refers to the solvent removed from the extract and may or may not be the same composition as the fresh solvent S.

Determination of the stages uses Q as the operating point until the raffinate composition R_k falls below line FQ. Then the operation is continued with operating point P until R_N is reached.

EXTRACT

E_1, y_{i1}

F_1, z_{i1} → 1

R_1, x_{i1}

E_2, y_{i2}

$R_{k-1}, x_{i,k-1}$

E_k, y_{ik}

F_k, z_{ik} → k ---→ U_k, w_{ik}

R_k, x_{ik}

$E_{k+1}, y_{i,k+1}$

$R_{N-1}, x_{i,N-1}$

E_N, y_{iN}

F_N, z_{iN} → N

R_N, x_{iN}

RAFFINATE
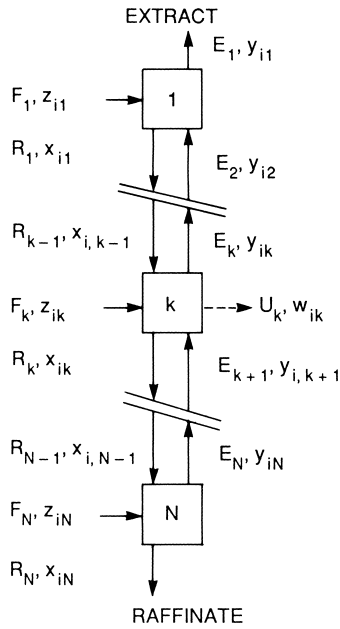
Figure 14.9. Model for liquid–liquid extraction. Subscript i refers to a component: $i = 1, 2, \ldots, c$. In the commonest case, F_1 is the only feed stream and F_N is the solvent, or F_k may be a reflux stream. Withdrawal streams U_k can be provided at any stage; they are not incorporated in the material balances written here.

MINIMUM REFLUX

For a given extract composition E_1, a pinch point develops when an operating line through either P or Q coincides with a tieline. Frequently, the tieline that passes through the feed point F determines the reflux ratio, but not on Figure 14.8(c). The tieline that intersects line FS_E nearest point S_e locates the operating point Q_m for minimum reflux. In Figure 14.8(c), intersection with tieline $Fcde$ is further away from point S_E than that with tieline abQ_m, which is the one that locates the operating point for minimum reflux in this case.

MINIMUM STAGES

As the solvent/feed ratio is increased, the mix point M approaches the solvent point S, and poles P and Q likewise do so. At total reflux all of the points P, Q, S, S_E, and M coincide; this is shown in Figure 14.8(b).

Examples of triangular and McCabe-Thiele constructions for feasible, total, and minimum reflux are shown in Figure 14.8.

Naturally, the latter constructions are analogous to those for distillation since their forms of equilibrium and material balances are the same. References to the literature where similar calculations are performed with Janecke coordinates were given earlier in this section.

Use of reflux is most effective with Type II systems since then essentially pure products on a solvent-free basis can be made. In contrast to distillation, however, extraction with reflux rarely is beneficial, and few if any practical examples are known. A related kind of process employs a second solvent to wash the extract countercurrently. The requirements for this solvent are that it be

---

EXAMPLE 14.5
Extraction with an Immiscible Solvent

A feed containing 5% of propionic acid and 95% trichlorethylene is to be extracted with water. Equilibrium distribution of the acid between water (Y) and TCE (X) is represented by $Y = K'X$, $K' = 0.38$. Section 14.4 is used.

a. The ratio of E/R of water to TCE needed to recover 95% of the acid in four countercurrent stages will be found:

$$X_f = 0.05/0.95 = 0.0526$$

$$X_r = 0.0025/0.95 = 0.00263$$

$$Y_s = 0$$

$$N_s = \frac{\ln\left\{\left(\frac{0.0526 - 0/0.38}{0.00263 - 0/0.38}\right)\left(1 - \frac{1}{A}\right) + \frac{1}{A}\right\}}{\ln\{A\}} = 4.0$$

by trial and error, $A = 1.734$

Therefore $E/R = 1.734/0.38 = 4.56$

b. Determine the number of stages needed to recover 95% of the acid with a $E/R = 3.5$.

$$A = (3.5)(0.38) = 1.33$$

$$N_s = \frac{\ln\left\{\left(\frac{0.0526 - 0/0.38}{0.00263 - 0/0.38}\right)\left(1 - \frac{1}{1.33}\right) + \frac{1}{1.33}\right\}}{\ln\{1.33\}} = 6.11 \text{ stages}$$

F, x_F → 1 → E_1, Y_1

R_1, x_1

E_2, Y_2

R_{m-1}, X_{m-1}

E_m, Y_m

m

R_m, x_m

E_{m+1}, Y_{m+2}

m + 1

R_{m+1}, x_{m+1}

E_{m+2}, Y_{m+2}

R_{n-1}, x_{n-1}

E_n, Y_n

n

R_n, x_n ← S, y_s
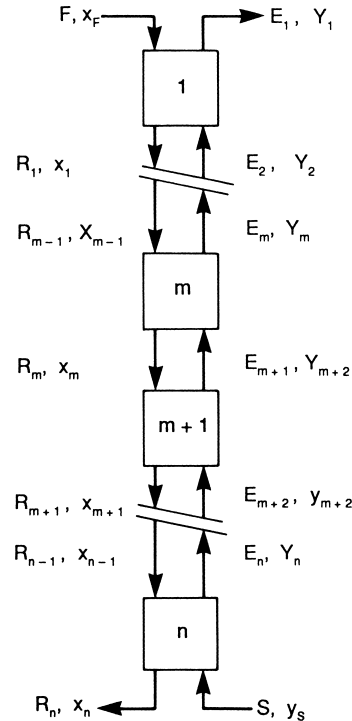
EXAMPLE **14.6**
Countercurrent Extraction Represented on Triangular and Rectangular Distribution Diagrams

The specified feed F and the desired extract E_1 and raffinate R_N compositions are shown. The solvent/feed ratio is in the ratio of the line segments MS/MF, where the location of point M is shown as the intersection of lines $E_1 R_N$ and FS.

Phase equilibrium is represented by the tieline locus. The equilibrium distribution curve is constructed as the locus of intersections of horizontal lines drawn from the right-hand end of a tieline with horizontals from the left-hand end of the tielines and reflected from the 45° line.

The operating curve is drawn similarly with horizontal projections from pairs of random points of intersection of the binodal curve by lines drawn through the difference point P. Construction of these curves also is explained with Figure 14.7.

The rectangular construction shows that slightly less than eight stages are needed and the triangular that slightly more than eight are needed. A larger scale and greater care in construction could bring these results closer together.
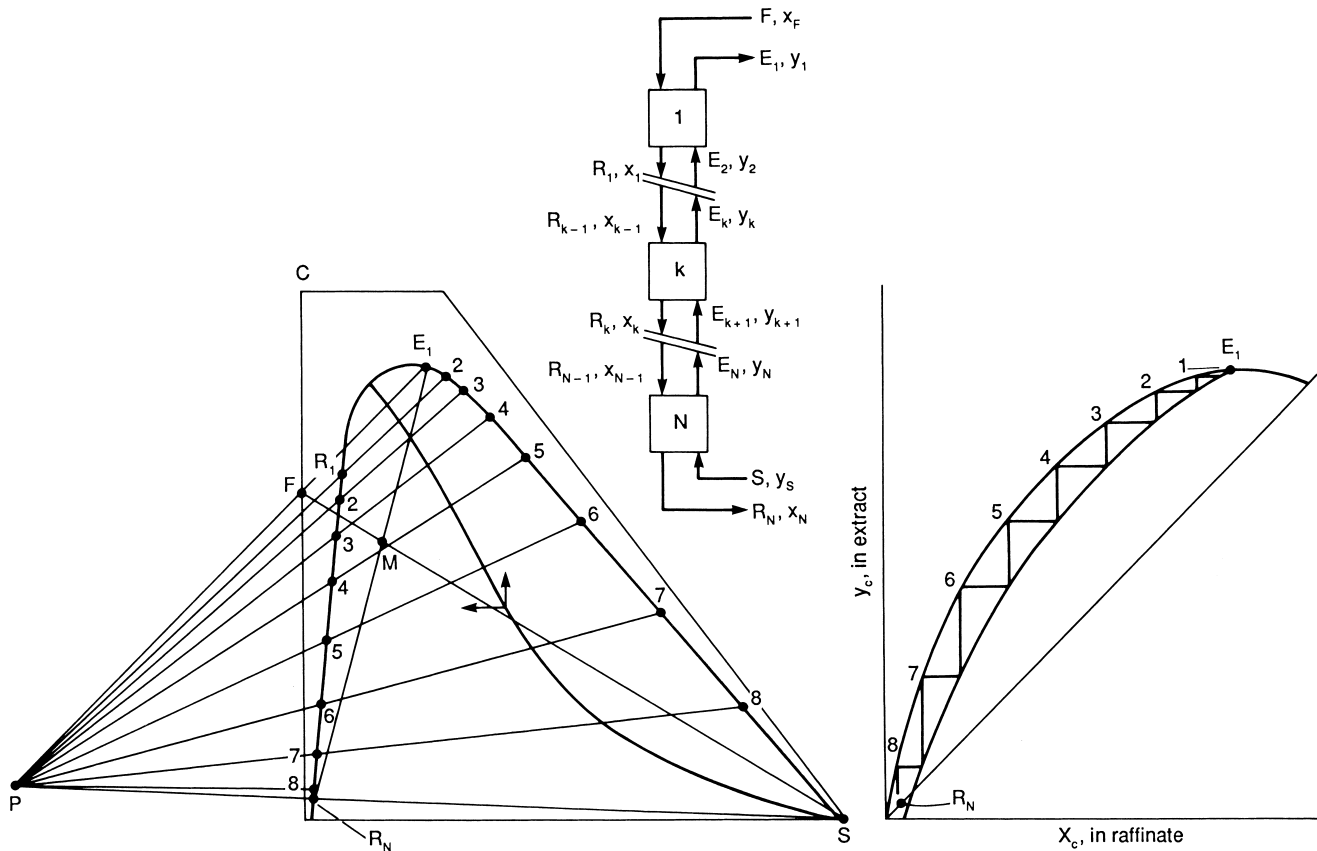
only slighly soluble in the extract and easily removable from the extract and raffinate. The sulfolane process is of this type; it is described, for example, by Treybal (1980) and in more detail by Lo et al. (1983, pp. 541–545).

Fractional extraction involves the use of two solvents and represents the most powerful separation means in extraction (Treybal, 1963). As shown in Figure 14.11, the feed is introduced near the middle of the countercurrent cascade consisting of $n + n'$ stages. Solvent 1 is fed to the top of the cascade, while solvent 2 is fed to the bottom of the cascade. Reflux at either or both ends of the cascade may or may not be used. In general, one solvent is aqueous or polar and the second solvent is a nonpolar hydrocarbon. A batch method of simulating a continuous countercurrent six-stage fractional extraction process is shown in Figure 14.11 (Treybal, 1963). Applications are shown in Table 14.2. Stage calculation methods and additional information on fractional extraction may be found in Treybal (1963).

14.5. LEACHING OF SOLIDS

Leaching is the removal of solutes from admixture with a solid by contracting it with a solvent. The solution phase sometimes is called the overflow, but here it will be called extract. The term underflow or raffinate is applied to the solid phase plus its entrained or occluded solution.

Equilibrium relations in leaching usually are simpler than in liquid–liquid equilibria, or perhaps only appear so because few measurements have been published. The solution phase normally contains no entrained solids so its composition appears on the hypotenuse of a triangular diagram like that of Example 14.9. Data for the raffinate phase may be measured as the holdup of solution by the solid, K lb solution/lb dry (oil-free) solid, as a function of the concentration of the solution, y lb oil/lb solution. The corresponding weight fraction of oil in the raffinate or underflow is

EXAMPLE 14.7
Stage Requirements for the Separation of a Type I and a Type II System

a. The system with A = heptane, B = tetramethylene sulfone, and C = toluene at 50°C [Triparthi, Ram, and Bhimeshwara, *J. Chem. Eng. Data* **20,** 261 (1975)]: The feed contains 40% C, the extract 70% C on a TMS-free basis or 60% overall, and raffinate 5% C. The construction shows that slightly more than two equilibrium stages are needed for this separation. The compositions of the streams are read off the diagram:

	Feed	**Extract**	**Raffinate**
Heptane	60	27	2
TMS	0	13	93
Toluene	40	60	5
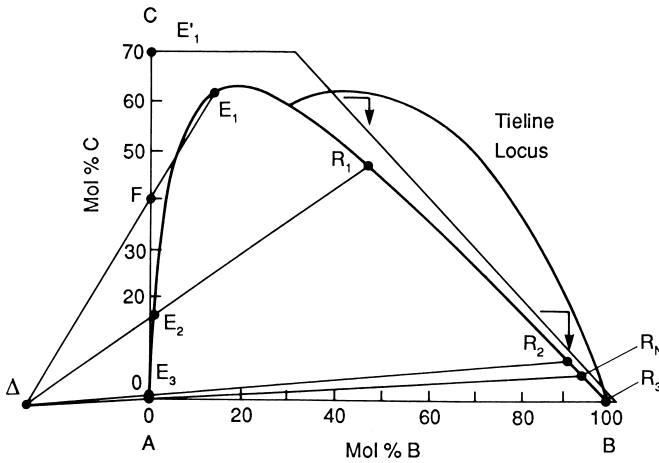
The material balance on heptane is

$$40 = 0.6E + 0.05(100 - E),$$

whence $E = 63.6\,\text{lb}/100\,\text{lb feed}$, and the TMS/feed ratio is

$$0.13(63.6) + 0.93(36.4) = 42\,\text{lb}/100\,\text{lb feed}.$$

b. The type II system with A = octane, B = nitroethane, and C = 2,2,4-trimethylpentane at 25°C [Hwa, Techo, and Ziegler, *J. Chem. Eng. Data* **8,** 409 (1963)]: The feed contains 40% TMP, the extract 60% TMP, and the raffinate 5% TMP. Again, slightly more than two stages are adequate.
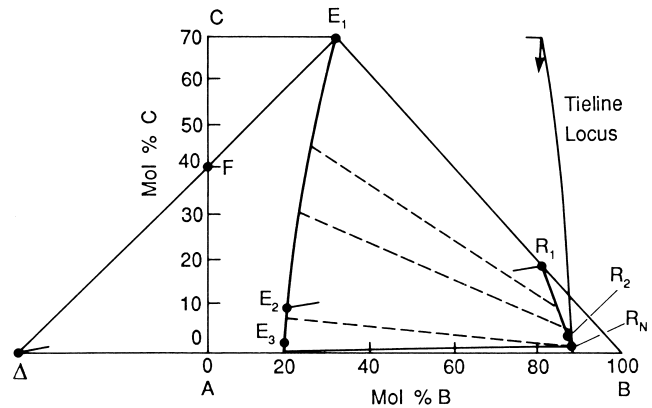
$$x = Ky/(K + 1). \tag{14.20}$$

Since the raffinate is a mixture of the solution and dry solid, the equilibrium value in the raffinate is on the line connecting the origin with the corresponding solution composition y, at the value of x given by Eq. (14.20). Such a raffinate line is constructed in Example 14.9.

Material balance in countercurrent leaching still is represented by Eqs. (14.17) and (14.19). Compositions R_k and E_{k+1} are on a line through the operating point P, which is at the intersection of lines FE_1 and SR_N. Similarly, equilibrium compositions R_k and E_k are on a line through the origin. Example 14.9 evaluates stage requirements with both triangular diagram and McCabe–Thiele

(a)

(b)
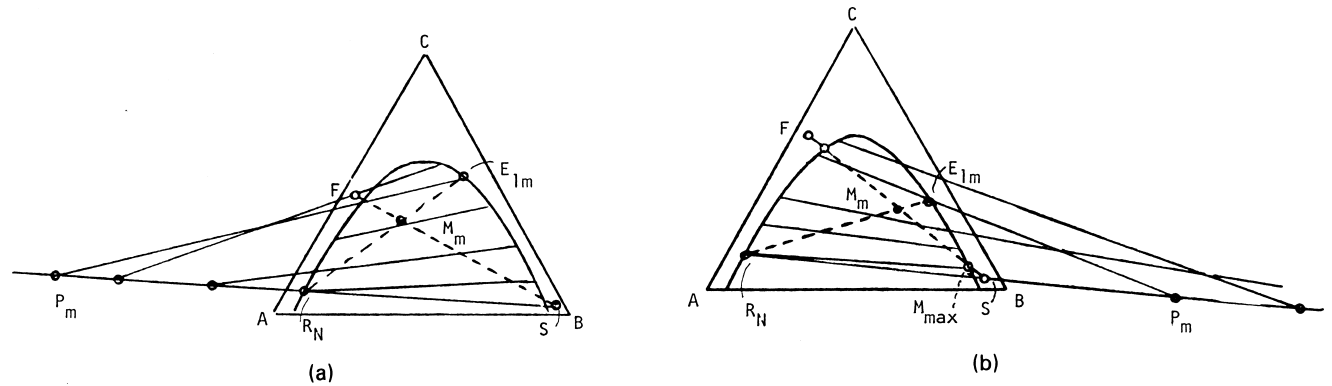
Figure 14.10. Minimum solvent amount and maximum extract concentration. Determined by location of the intersection of extended tielines with extended line $R_N S$. (a) When the tielines slope down to the left, the furthest intersection is the correct one. (b) When the tielines slope down to the right, the nearest intersection is the correct one. At *maximum* solvent amount, the mix point M_m is on the binodal curve.

<small>Example **14.8**</small>
Countercurrent Extraction Employing Extract Reflux

The feed F, extract E_1, and raffinate R_N are located on the triangular diagram. The ratio of solvent/feed is specified by the location of the point M on line SF.

Other nomenclature is identified on the flowsketch. The solvent-free reflux point R_0 is located on the extension of line SE_1. Operating point Q is located at the intersection of lines SR_0 and $R_N M$. Lines through Q intersect the binodal curve in compositions of raffinate and reflux related by material balance: for instance, R_n and E_{n+1}. When the line QF is crossed, further constructions are

made with operating point P, which is the intersection of lines FQ and SR_N.

In this example, only one stage is needed above the feed F and five to six stages below the feed. The ratio of solvent to feed is

$$S/F = FM/MS = 0.196,$$

and the external reflux ratio is

$$r = E_{1R}/E_{1P} = (R_0 S/R_0 E_1)(QE_1/SQ) = 1.32.$$
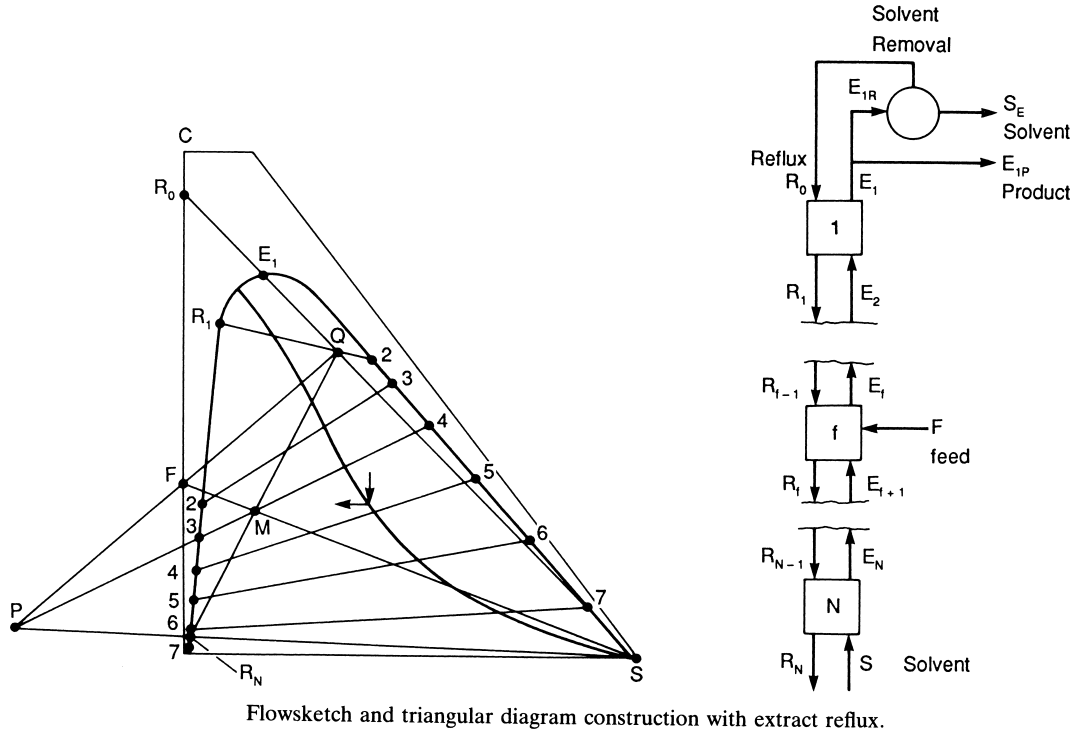
Flowsketch and triangular diagram construction with extract reflux.

constructions. The mode of construction of the McCabe–Thiele diagram is described there.

These calculations are of equilibrium stages. The assumption is made that the oil retained by the solids appears only as entrained solution of the same composition as the bulk of the liquid phase. In some cases the solute may be adsorbed or retained within the interstices of the solid as solution of different concentrations. Such deviations from the kind of equilibrium assumed will result in stage efficiencies less than 100% and must be found experimentally.

14.6. NUMERICAL CALCULATION OF MULTICOMPONENT EXTRACTION

Extraction calculations involving more than three components cannot be done graphically but must be done by numerical solution of equations representing the phase equilibria and material balances over all the stages. Since extraction processes usually are adiabatic and nearly isothermal, enthalpy balances need not be made. The solution of the resulting set of equations and of the prior determination of the parameters of activity coefficient correlations requires computer implementation. Once such pro-

grams have been developed, they also may be advantageous for ternary extractions, particularly when the number of stages is large or several cases must be worked out. Ternary graphical calculations also could be done on a computer screen with a little effort and some available software.

The notation to be used in making material balances is shown on Figure 14.9. For generality, a feed stream F_k is shown at every stage, and a withdrawal stream U_k also could be shown but is not incorporated in the balances written here. The first of the double subscripts identifies the component i and the second the stage number k; a single subscript refers to a stage.

For each component, the condition of equilibrium is that its activity is the same in every phase in contact. In terms of activity coefficients and concentrations, this condition on stage k is written:

$$\gamma_{ik}^E y_{ik} = \gamma_{ik}^R x_{ik} \qquad (14.21)$$

or

$$y_{ik} = K_{ik} x_{ik}, \qquad (14.22)$$
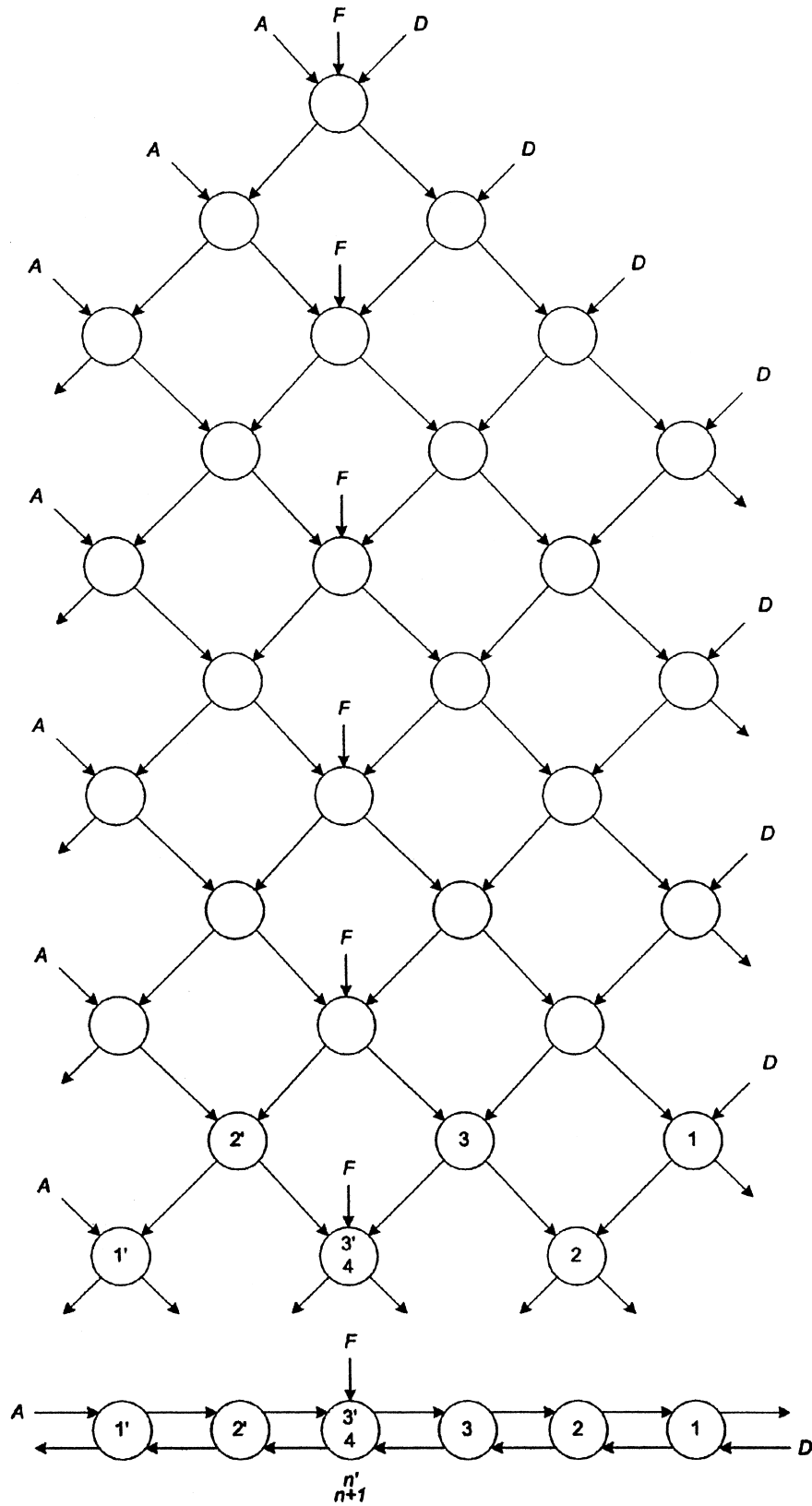
Figure 14.11. Rocha et al. (1986) provide additional descriptions of equipment options and relative costs.

TABLE 14.2. Applications of Fractional Extraction (Treybal 1963)

Application	Solvent 1	Solvent 2
Separation of p- and o- chloronitrobenzene	heptane	86.7% aqueous methanol
Separation of p- and o-methoxyphenol	50%gasoline, 50% benzene	60% aqueous ethanol
Separation of o-, m- and p-nitroaniline	benzene	water
Separation of weak acids or bases	Organic solvent	water

EXAMPLE 14.9
Leaching of an Oil-Bearing Solid in a Countercurrent Battery
Oil is to be leached from granulated halibut livers with pure ether as solvent. Content of oil in the feed is 0.32 lb/lb dry (oil-free) solids and 95% is to be recovered. The economic upper limit to extract concentration is 70% oil. Ravenscroft [*Ind. Eng. Chem.* **28,** (1934)] measured the relation between the concentration of oil in the solution, y, and the entrainment or occlusion of solution by the solid phase, K lb solution/lb dry solid, which is represented by the equation

$$K = 0.19 + 0.126y + 0.810y^2.$$

The oil content in the entrained solution then is given by

$$x = K/(K + 1)y, \text{ wt fraction,}$$

and some calculated values are

y	0	0.1	0.2	0.3	0.4	0.5	0.6	0.7	0.8
x	0	0.0174	0.0397	0.0694	0.1080	0.1565	0.2147	0.2821	0.3578

Points on the raffinate line of the triangular diagram are located on lines connecting values of y on the hypotenuse (solids-free) with the origin, at the values of x and corresponding y from the preceding tabulation.

Feed composition is $x_F = 0.32/1.32 = 0.2424$.
Oil content of extract is $y_1 = 0.7$.
Oil content of solvent is $y_s = 0$.
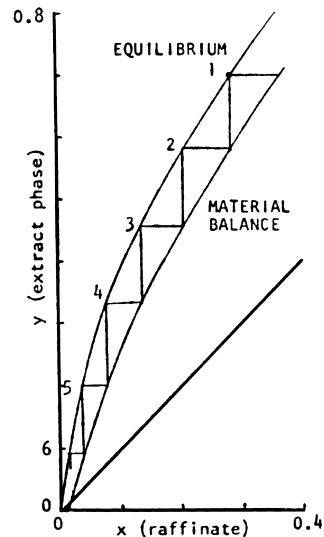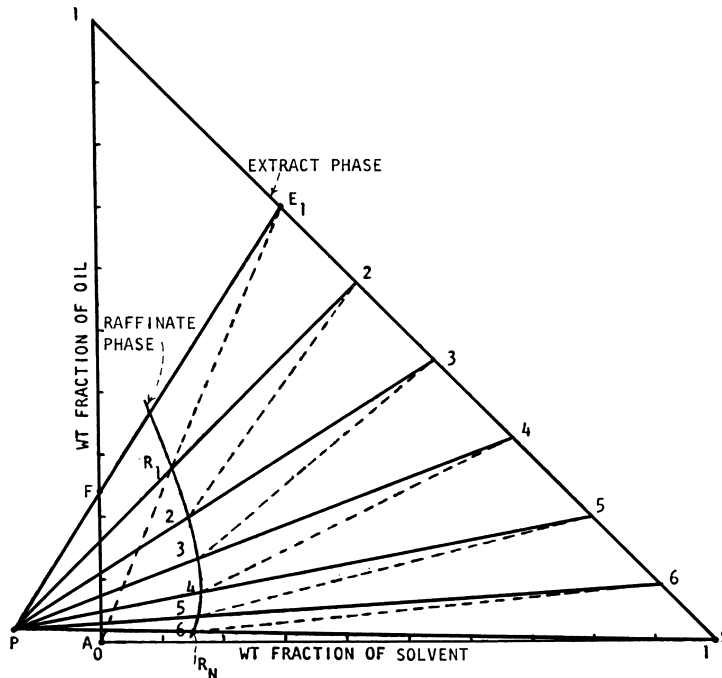
Amount of oil in the raffinate is $0.32(0.05) = 0.016$ lb/lb dry, and the corresponding entrainment ratio is

$$K_N = 0.016/y_N = 0.19 + 0.126y_N + 0.81y_N^2.$$

Solving by trial,

$$y_N = 0.0781,$$
$$K_N = 0.2049,$$
$$x_N = 0.0133 \text{ (final raffinate composition).}$$

The operating point P is at the intersection of lines FE_1 and SR_N. The triangular diagram construction shows that six stages are needed.

The equilibrium line of the rectangular diagram is constructed with the preceding tabulation. Points on the material balance line are located as intersections of random lines through P with these results:

y	0	0.1	0.2	0.3	0.4	0.5	0.6	0.7
x	0.013	0.043	0.079	0.120	0.171	0.229	0.295	0.368

The McCabe–Thiele construction also shows that six stages are needed.

Point P is at the intersection of lines E_1F and SR_N. Equilibrium compositions are related on lines through the origin, point A. Material balance compositions are related on lines through the operating point P.

where

$$K_{ik} = \gamma_{ik}^R / \gamma_{ik}^E \tag{14.23}$$

is the distribution ratio. The activity coefficients are functions of the temperature and the composition of their respective phases:

$$\gamma_{ik}^E = f(T_k, y_{1k}, y_{2k}, \ldots, y_{ck}), \tag{14.24}$$

$$\gamma_{ik}^R = f(T_k, x_{1k}, x_{2k}, \ldots, x_{ck}). \tag{14.25}$$

The most useful relations of this type are the NRTL and UNIQUAC which are shown in Table 14.3.

Around the kth stage, the material balance is

$$R_{k-1}x_{i,k-1} + E_{k+1}y_{i,k+1} + F_k z_{ik} - R_k x_{ik} - E_k y_{ik} = 0. \tag{14.26}$$

When combined with Eq. (14.19), the material balance becomes

$$R_{k-1}x_{i,k-1} - (R_k + E_k K_{ik})x_{ik} + E_{k+1}K_{i,k+1}x_{i,k+1} = -F_k z_{ik}. \tag{14.27}$$

In the top stage, $k = 1$ and $R_0 = 0$ so that

$$-(R_1 + V_1 K_{i1})x_{i1} + E_2 K_{i2}x_{i2} = -F_1 z_{i1}. \tag{14.28}$$

In the bottom stage, $k = N$ and $E_{N+1} = 0$ so that

$$R_{N-1}x_{i,N-1} - (R_N + E_N K_{iN})x_{iN} = -F_N z_{iN}. \tag{14.29}$$

The overall balance from stage 1 through stage k is

$$R_k = E_{k+1} - E_1 + \sum_{1}^{k} F_k, \tag{14.30}$$

which is used to find raffinate flows when values of the extract flows have been estimated.

TABLE 14.3. NRTL and UNIQUAC Correlations for Activity Coefficients of Three-Component Mixtures[a]

NRTL

$$\ln \gamma_i = \frac{\tau_{1i}G_{1i}x_1 + \tau_{2i}G_{2i}x_2 + \tau_{3i}G_{3i}x_3}{G_{1i}x_1 + G_{2i}x_2 + G_{3i}x_3}$$
$$+ \frac{x_1 G_{i1}}{x_1 + G_{12}x_2 + G_{13}x_3} \left[\tau_{i1} - \frac{x_2 \tau_{21} G_{21} + x_3 \tau_{31} G_{31}}{x_1 + x_2 G_{21} + x_3 G_{31}} \right]$$
$$+ \frac{x_2 G_{i2}}{G_{12}x_1 + x_2 + G_{32}x_3} \left[\tau_{i2} - \frac{x_1 \tau_{12} G_{12} + x_3 \tau_{32} G_{32}}{x_1 G_{12} + x_2 + x_3 G_{32}} \right]$$
$$+ \frac{x_3 G_{i3}}{G_{13}x_1 + G_{23}x_2 + x_3} \left[\tau_{i3} - \frac{x_1 \tau_{13} G_{13} + x_2 \tau_{23} G_{23}}{G_{13}x_1 + G_{23}x_2 + x_3} \right]$$

$\tau_{ii} = 0$

$G_{ii} = 1$

UNIQUAC

$$\ln \gamma_i = \ln \frac{\phi_i}{x_i} + 5q_i \ln \frac{\theta_i}{\phi_i} + I_i - \frac{\phi_i}{x_i}(x_1 I_1 + x_2 I_2 + x_3 I_3) + q_i[1 - \ln(\theta_1 \tau_{1i} + \theta_2 \tau_{2i} + \theta_3 \tau_{3i})]$$
$$- \frac{\theta_1 \tau_{i1}}{\theta_1 + \theta_2 \tau_{21} + \theta_3 \tau_{31}} - \frac{\theta_2 \tau_{i2}}{\theta_1 \tau_{12} + \theta_2 + \theta_3 \tau_{32}} - \frac{\theta_3 \tau_{i3}}{\theta_1 \tau_{13} + \theta_2 \tau_{23} + \theta_3}$$

$\tau_{ii} = 1$

$$\phi_i = \frac{r_i x_i}{r_1 x_1 + r_2 x_2 + r_3 x_3}$$

$$\theta_i = \frac{q_i x_i}{q_1 x_1 + q_2 x_2 + q_3 x_3}$$

$I_i = 5(r_i - q_i) - r_i + 1$

---

[a]NRTL equation: There is a pair of parameters g_{jk} and g_{kj} for each pair of substances in the mixture; for three substances, there are three pairs. The other terms of the equations are related to the basic ones by

$\tau_{jk} = g_{jk}/RT$,
$G_{jk} = \exp(-\alpha_{jk}\tau_{jk})$.

For liquid–liquid systems usually, $\alpha_{jk} = 0.4$.
UNIQUAC equation: There is a pair of parameters u_{jk} and u_{kj} for each pair of substances in the mixture:
$\tau_{jk} = \exp(-u_{jk}/RT)$.

The terms with single subscripts are properties of the pure materials which are usually known or can be estimated.
The equations are extended readily to more components.
(See, for example, Walas, 1985).

For all stages for a component i, Eqs. (14.27)–(14.29) constitute a tridiagonal matrix which is written

$$
\begin{bmatrix}
B_1 & C_1 & & & & \\
A_2 & B_2 & C_2 & & & \\
& A_j & B_j & C_j & & \\
& & A_{N-1} & B_{N-1} & C_{N-1} & \\
& & & & A_N & B_N
\end{bmatrix}
\begin{bmatrix}
x_{i1} \\
x_{i2} \\
x_{ij} \\
x_{iN-1} \\
x_{iN}
\end{bmatrix}
=
\begin{bmatrix}
D_1 \\
D_2 \\
D_j \\
D_{N-1} \\
D_N
\end{bmatrix}
$$
(14.31)

When all of the coefficients are known, this can be solved for the concentrations of component i in every stage. A straightforward method for solving a tridiagonal matrix is known as the Thomas algorithm to which references are made in Sec. 13.10. "Basis for Computer Evaluation of Multicomponent Separations: Specifications."

INITIAL ESTIMATES

Solution of the equations is a process in which the coefficients of Eq. (14.31) are iteratively improved. To start, estimates must be made of the flow rates of all components in every stage. One procedure is to assume complete removal of a "light" key into the extract and of the "heavy" key into the raffinate, and to keep the solvent in the extract phase throughout the system. The distribution of the keys in the intermediate stages is assumed to vary linearly, and they must be made consistent with the overall balance, Eq. (14.30), for each component. With these estimated flowrates, the values of x_{ik} and y_{ik} are evaluated and may be used to find the activity coefficients and distribution ratios, K_{ik}. This procedure is used in Example 14.10.

PROCEDURE

The iterative calculation procedure is outlined in Figure 14.12. The method is an adaptation to extraction by Tsuboka and Katayama (1976) of the distillation calculation procedure of Wang and Henke [*Hydrocarb. Proc.* **45**(8), 155–163 (1967)]. It is also presented by Henley and Seader (1981, pp. 586–594).

1. The initial values of the flowrates and compositions x_{ik} and y_{ik} are estimated as explained earlier.
2. The values of activity coefficients and distribution ratios are evaluated.
3. The coefficients in the tridiagonal matrix are evaluated from Eqs. (14.27)–(14.29). The matrix is solved once for each component.
4. The computed values of iteration $(r+1)$ are compared with those of the preceding iteration as

$$
\tau_1 = \sum_{i=1}^{C} \sum_{k=1}^{N} |x_{ik}^{(r+1)} - x_{ik}^{(r)}| \leq \varepsilon_1 = 0.01NC.
$$
(14.32)

The magnitude, $0.01NC$, of the convergence criterion is arbitrary.

5. For succeeding evaluations of activity coefficients, the values of the mol fractions are normalized as

$$
(x_{ik})_{\text{normalized}} = x_{ik} \Big/ \sum_{i=1}^{C} x_{ik},
$$

$$
(y_{ik})_{\text{normalized}} = y_{ik} \Big/ \sum_{i=1}^{C} y_{ik}.
$$
(14.33)

6. When the values of x_{ik} have converged, a new set of y_{ik} is calculated with

$$
y_{ik} = K_{ik} x_{ik}.
$$
(14.34)

7. A new set of extract flow rates is calculated from

$$
E_k^{(s+1)} = E_k^{(s)} \sum_{i=1}^{C} y_{ik},
$$
(14.35)

where s is the outer loop index number.

8. The criterion for convergence is

$$
\tau_2 = \sum_{k=1}^{N} (1 - E_k^{(s)}/E_k^{(s+1)})^2 \leq \varepsilon_2 = 0.01N.
$$
(14.36)

The magnitude, $0.01N$, of the convergence criterion is arbitrary.

9. If convergence has not been attained, new values of R_k are calculated from Eq. (14.30).
10. Distribution ratios K_{ik} are based on normalized values of x_{ik} and y_{ik}.
11. The iteration process continues through the inner and outer loops.

Solutions of four cases of three- and four-component systems are presented by Tsuboka and Katayama (1976); the number of outer loop iterations ranged from 7 to 41. The four component case worked out by Henley and Seader (1981) is summarized in Example 14.10; they solved two cases with different water contents of the solvent, dimethylformamide.

14.7. EQUIPMENT FOR EXTRACTION

Equipment for extraction and leaching must be capable of providing intimate contact between two phases so as to effect transfer of solute between them and also of ultimately effecting a complete separation of the phases. For so general an operation, naturally a substantial variety of equipment has been devised. A very general classification of equipment, their main characteristics and industrial applications is in Table 14.4. A detailed table of comparisons and ratings of 20 kinds of equipment on 14 characteristics has been prepared by Pratt and Hanson (in Lo et al., 1983, p. 476). Some comparisons of required sizes and costs are in Table 14.5. Rocha et al. (1986) provide additional descriptions of equipment options and relative costs.

Selected examples of the main categories of extractors are represented in Figures 14.13 through 14.17. Their capacities and performance will be described in general terms insofar as possible, but sizing of liquid–liquid extraction equipment always requires some pilot plant data or acquaintance with analogous cases. Little detailed information about such analogous situations appears in the open literature. Engineers familiar with particular kinds of equipment, such as their manufacturers, usually can predict performance with a minimum amount of pilot plant data.

In general, performance data published in the literature are usually obtained from small laboratory equipment. As a result, efficiency and flooding correlations should be used with caution. The limits of models should be checked. For example, since most published packed extractor data are based on small diameter columns, the packings studied are usually small with a high specific surface area. The extrapolation of models primarily based on such high specific surface areas to larger packings with much lower areas

Trial Estimates and Converged Flow Rates and Compositions in All Stages of an Extraction Battery for a Four-Component Mixture

Benzene is to be recovered from a mixture with hexane using aqueous dimethylformamide as solvent in a five-stage extraction battery. Trial estimates of flow rates for starting a numerical solution are made by first assuming that all of the benzene and all of the solvent ultimately appear in the extract and all of the hexane appears in the raffinate. Then flow rates throughout the battery are assumed to vary linearly with stage number. Table 1 shows these estimated flowrates and Table 2 shows the corresponding mol fractions. Tables 3 and 4 shows the converged solution made by Henley and Seader (1981, p. 592); they do not give any details of the solution but the algorithm of Figure 14.12 was followed.

TABLE 1. Estimated mol/hr

Stage	Extract Total	H	B	D	W	Raffinate Total	H	B	D	W
0	—									
1	1100	0	100	750	250	400	300	100	0	0
2	1080	0	80	750	250	380	300	80	0	0
3	1060	0	60	750	250	360	300	60	0	0
4	1040	0	40	750	250	340	300	40	0	0
5	1020	0	20	750	250	320	300	20	0	0
N + 1	1000	0	0	750	250	300	300	0	0	0

TABLE 2. Estimated Mol Fractions

Stage j	y_{ij} H	B	D	W	x_{ij} H	B	D	W
1	0.0	0.0909	0.6818	0.2273	0.7895	0.2105	0.0	0.0
2	0.0	0.0741	0.6944	0.2315	0.8333	0.1667	0.0	0.0
3	0.0	0.0566	0.7076	0.2359	0.8824	0.1176	0.0	0.0
4	0.0	0.0385	0.7211	0.2404	0.9375	0.0625	0.0	0.0
5	0.0	0.0196	0.7353	0.2451	1.0000	0.0	0.0	0.0

TABLE 3. Converged Mol Fractions

Stage j	y_{ij} H	B	D	W	x_{ij} H	B	D	W
1	0.0263	0.0866	0.6626	0.2245	0.7586	0.1628	0.0777	0.0009
2	0.0238	0.0545	0.6952	0.2265	0.8326	0.1035	0.0633	0.0006
3	0.0213	0.0309	0.7131	0.2347	0.8858	0.0606	0.0532	0.0004
4	0.0198	0.0157	0.7246	0.2399	0.9211	0.0315	0.0471	0.0003
5	0.0190	0.0062	0.7316	0.2432	0.9438	0.0125	0.0434	0.0003

TABLE 4. Converged mol/hr

	Extract	Raffinate
Hexane	29.3	270.7
Benzene	96.4	3.6
DMF	737.5	12.5
Water	249.0	0.1
Total	1113.1	286.9

can yield poor results. Such models can be checked by looking at limits where the specific surface approaches zero.

Most laboratory extraction columns operate close to true countercurrent flow. However, large diameter columns promote significant axial mixing, which reduces the overall concentration driving force and the apparent performance. Mixing studies at the University of Texas at Austin confirmed that significant continuous phase axial mixing occurred in a 42.8 cm diameter packed column, while little axial mixing was present in 10.2 cm diameter column with the same system and packing (Becker, 2003).

In addition, most published laboratory data are obtained using very pure chemicals. Unfortunately, most industrial extraction systems contain impurities that are often surface active. These impurities can greatly reduce the rate of mass transfer and can also inhibit coalescence and settling.

With regard to equipment design, it is critically important to work closely with equipment vendors or others experienced in scale-up. Published models should be considered as tools for an initial engineering design only, and a not as a replacement for pilot testing and consulting with those experienced in extractor design.

CHOICE OF DISPERSE PHASE

Customarily the phase with the highest volumetric rate is dispersed since a larger interfacial area results in this way with a given droplet size. In equipment that is subject to backmixing, such as spray and packed towers but not sieve tray towers, the disperse phase is made the one with the smaller volumetric rate. When a substantial

difference in resistances of extract and raffinate films to mass transfer exists, the high phase resistance should be compensated for with increased surface by dispersion. From this point of view, Laddha and Degaleesan (1978, pp. 194) point out that water should be the dispersed phase in the system water + diethylamine + toluene. The dispersed phase should be the one that wets the material of construction less well. Since the holdup of continuous phase usually is greater, the phase that is less hazardous or less expensive should be continuous. It is best usually to disperse a highly viscous phase.

MIXER-SETTLERS

The original and in concept the simplest way of accomplishing extractions is to mix the two phases thoroughly in one vessel and then to allow the phases to separate in another vessel. A series of such operations performed with series of countercurrent flows of the phases can accomplish any desired degree of separation. Mixer-settlers have several advantages and disadvantages, for instance:

Pros. The stages are independent, can be added to or removed as needed, are easy to start up and shut down, are not bothered by suspended solids, and can be sized for high (normally 80%) efficiencies.

Cons. Emulsions can be formed by severe mixing which are hard to break up, pumping of one or both phases between tanks may be required, independent agitation equipment and large floor space needs are expensive, and high holdup
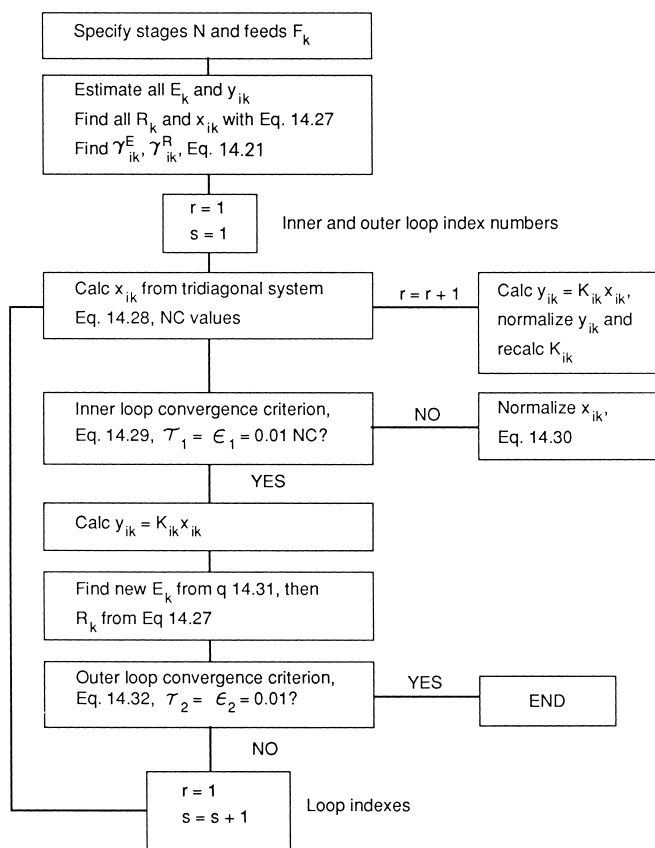
Figure 14.12. Algorithm for computing flows and compositions in an extraction battery of a specified number of stages (*after Henley and Seader, 1981*).

TABLE 14.4. Features and Industrial Applications of Liquid–Liquid Extractors

Types of Extractor	General Features	Fields of Industrial Application
Unagitated columns	Low capital cost	Petrochemical
	Low operating and maintenance cost	Chemical
	Simplicity in construction	
	Handles corrosive material	
Mixer-settlers	High-stage efficiency	Petrochemical
	Handles wide solvent ratios	Nuclear
	High capacity	Fertilizer
	Good flexibility	Metallurgical
	Reliable scale-up	
	Handles liquids with high viscosity	
Pulsed columns	Low HETS	Nuclear
	No internal moving parts	Petrochemical
	Many stages possible	Metallurgical
Rotary-agitation columns	Reasonable capacity	Petrochemical
	Reasonable HETS	Metallurgical
	Many stages possible	Pharmaceutical
	Reasonable construction cost	Fertilizer
	Low operating and maintenance cost	
Reciprocating-plate columns	High throughput	Pharmaceutical
	Low HETS	Petrochemical
	Great versatility and flexibility	Metallurgical
	Simplicity in construction	Chemical
	Handles liquids containing suspended solids	
	Handles mixtures with emulsifying tendencies	
Centrifugal extractors	Short contacting time for unstable material	Pharmaceutical
	Limited space required	Nuclear
	Handles easily emulsified material	Petrochemical
	Handles systems with little liquid density difference	

(Reprinted by permission from T. C. Lo, Recent Developments in Commercial Extractors, Engineering Foundation Conference on Mixing Research, Rindge, N.H., 1975).

of valuable or hazardous solvents exists particularly in the settlers.

Some examples of more or less compact arrangements of mixers and settlers are in Figures 14.13 and 14.16(c). Mixing equipment is described in Chapter 10 where rules for sizing, blending, mixing intensity, and power requirements are covered, for instance Figure 10.3 for blend times in stirred tanks. Mixing with impellers in tanks is most common, but also is accomplished with pumps, jet mixers [Fig. 14.13(b)], line mixers and static mixers. Capacities of line mixers are fond in Section 10.12, Pipeline Mixers, and of static mixers are stated in manufacturers catalogs. A procedure for estimating mixing efficiencies from basic correlations is illustrated by Laddha and Degaleesan (1978, p. 424).

Separation of the mixed phases is accomplished by gravity settling or less commonly by centrifugation. It can be enhanced by inducing coalescence with packing or electrically, or by shortening the distance of fall to a coalesced phase. Figures 14.13(d), 18.2, and 18.3 are some examples. Chapter 18 deals with some aspects of the separation of liquid phases.

A common basis for the design of settlers is an assumed droplet size of 150 μm, which is the basis of the standard API design method for oil–water separators. Stokes law is applied to find the settling time. In open vessels, residence times of 30–60 min or superficial velocities of 0.5–1.5 ft/min commonly are provided. Longitudinal baffles can cut the residence time to 5–10 min. Coalescence with packing or wire mesh or electrically cut these times substantially. A chart for determining separation of droplets of water with a plate pack of 3/4 in. spacing is reproduced by

Hooper and Jacobs (in Schweitzer, 1979, 1.343–1.358). Numerical examples of settler design also are given in that work. For especially difficult separations or for space saving, centrifuges are applied. Liquid hydrocyclones individually have low efficiencies, but a number in series can attain 80–85% efficiency overall. Electrical coalescence is used commonly for separation of brine from crude oil; the subject is treated by Waterman (*Chem. Eng. Prog.* **61**(10), 51 1965).

A control system for a mixer-settler is represented by Figure 3.19.

SPRAY TOWERS

These are empty vessels with provisions for introducing the liquids as dispersed or continuous phases and for removing them. Figure 14.14(a) shows both phases dispersed, which may be demanded when substantial changes in volumetric or physical properties result from solute transfer. Capacities of spray towers are high because of their openness, and they are not bothered by suspended solids. Backmixing is severe in towers of more than a few inches in diameter. Without operating experience to the contrary, even

TABLE 14.5. Comparisons of Performance and Costs of Extraction Equipment

(a) Some Comparisons and Other Performance Data

System	Equipment	Total Flow Capacity (Imp. gal/hrft²)	
		Pilot Plant	Plant
Co–Ni–D2EHPA H₂SO₄	Mixco agitated	(4 in.) 300	(60 in.) 170
	Karr reciprocating sieve plate pulse	(3 in.) 900	
		(2 in.) 900	
Zr–Hf–TBP HNO₃	Mixco agitated		(30 in.) 184
	sieve plate pulse (steel)	(2 in.) 500	
	sieve plate pulse (Teflon)	(2 in.) 1345	(10 in.) 1345
	RDC		(30 in.) 135
Hf–Zr–MIBK SCN⁻	spray column		(4 in.) 2450
Rare earths– D2EHPA H₂SO₄	Podbielniak centrifuge		(4 feed dia) 30,000 gal/hr
U–amine–solvent-in-pulp H₂SO₄	sieve plate pulse	(2 in.) 600	(10 in.) 900
Cu–Lix 64N H₂SO₄	mixer settlers		60–120
Cu–Ni–amine HCl	mixer settlers		60–120

(b) Cost Comparison, 1970 Prices, for Extraction of 150 gpm of Aqueous Feed Containing 5 g/L of Cu with 100 gpm Solvent, Recovering 99% of the Copper

Contactor	Equipment Required				
	No.	Dia. (ft)	Length (ft)	Equip. Cost $ × 1000	Total cost $ × 1000
Mixer settler	2	—	—	60	151.2
Mixco	3	5	16	100	246.7
Pulse	1	5	60	160	261.5
Kenics	3	2	28	230	336.1
Podbielniak		3–D36	—	300	378.0
Graesser	15	5	3.0	88	308.0

[a] Mixers have 150 gal capacity, settlers are 150 sqft by 4 ft deep with 9 in. solvent layer.
(Ritcey and Ashbrook, 1979, Vol. II).

towers 20–40 ft high cannot be depended upon to function as more than single stages.

Commercially, spray towers are suitable for liquid-liquid processes in which rapid, irreversible chemical reactions occur, as in neutralization of waste acids. The substantial literature of flooding, holdup, mass transfer and axial mixing in small spray towers is reviewed by Laddha and Degaleesan (1978, pp. 221–255) and more briefly by Cavers (in Lo et al., 1983, pp. 320–328).

PACKED TOWERS

Since mass transfer in packed or spray towers occurs differentially rather than stagewise, their performance should be expressed in terms of the number of transfer units (NTU) rather than the number of theoretical stages (NTS). For dilute systems, the number of transfer units is given in terms of the terminal concentrations and the equilibrium relation by

$$\text{NTU} = \int_{x_1}^{x_2} \frac{dx}{x - x_{\text{equilib}}}. \tag{14.37}$$

In order to permit sizing a tower, data must be available of the height of a transfer unit (HTU). This term often is used interchangeably with the height equivalent to a theoretical stage (HETS), but strictly they are equal only for dilute solutions when the ratio of the extract and raffinate flow rates, E/R, equals the distribution coefficient, $K = x_E/x_R$ (Treybal, 1963, p. 350). Extractor performance also is expressible in terms of mass transfer coefficients, for instance, $K_E a$, which is related to the number and height of transfer units by

$$\frac{K_E a \Delta C}{E/S} = \frac{\text{NTU}}{Z} = \frac{1}{\text{HTU}}, \tag{14.38}$$

where E/S is the extract flow rate per unit cross section and ΔC is mean concentration difference of the solute. Correlations of this quantity based on data from towers of 1–2 in. dia have been made, for example, by Laddha and Degaleesan (1978). They may be of qualitative value in predicting performance of commercial equipment when combined with some direct pilot plant information. In commercial packed towers, an HETS of 3–5 ft is possible. However, large-scale packed columns are susceptible to axial mixing. As a result, bed heights should be limited to 5–10 ft and frequent redistribution is recommended. The redistributor allows re-formation of drops and limits axial mixing.

The University of Texas at Austin has performed extensive testing of commercial scale packing using a 42.8-cm diameter column (Seibert et al., 1990; Becker, 2003). Rigorous mechanistic models have been developed that compare well with larger-scale data. An approximation of the rigorous design method is given here. The approximation is based on extraction factors near unity.

$$\text{HETP} = f_1 + f_2 \tag{14.39}$$

$$f_1 = A \bullet B \left[\frac{U_c}{U_d}\right]^{0.8} \left[\frac{\sigma^2}{e^{\sqrt{a_p}} \Delta \rho}\right]^{0.25} \left[\mu_d^{0.5} \; \mu_c^{0.35}\right] \tag{14.40}$$

$$f_2 = Z_p \left[1 - \exp\left\{-C\left(\frac{D}{42}\right)^{0.3} \left(\frac{\mu_c^{0.5}}{a_p}\right)\left(\frac{U_d}{U_c}\right)\right\}\right] \tag{14.41}$$

Where

A = 60 for mass transfer c → d
 = 85 for mass transfer d → c
a_p = specific surface of the packing, cm²/cm³
B = 1 for clean chemical system, no surface active impurities
 = 1.5 for chemical system with surface active impurities
C = 0.1 for structured packing with intermediate dualflow trays
 = 0.2 for structured packing with no plate
 = 0.3 for random packing
D = column diameter, cm
U_c = superficial velocity of the continuous phase, cm/s
U_d = superficial velocity of the dispersed phase, cm/s
Z_p = packed height between distributors
σ = interfacial tension, dynes/cm
$\Delta \rho$ = density difference, g/cm³
ρ_c = density of the continuous phase, g/cm³
μ_d = viscosity of the dispersed phase, cP
μ_c = viscosity of the continuous phase, cP
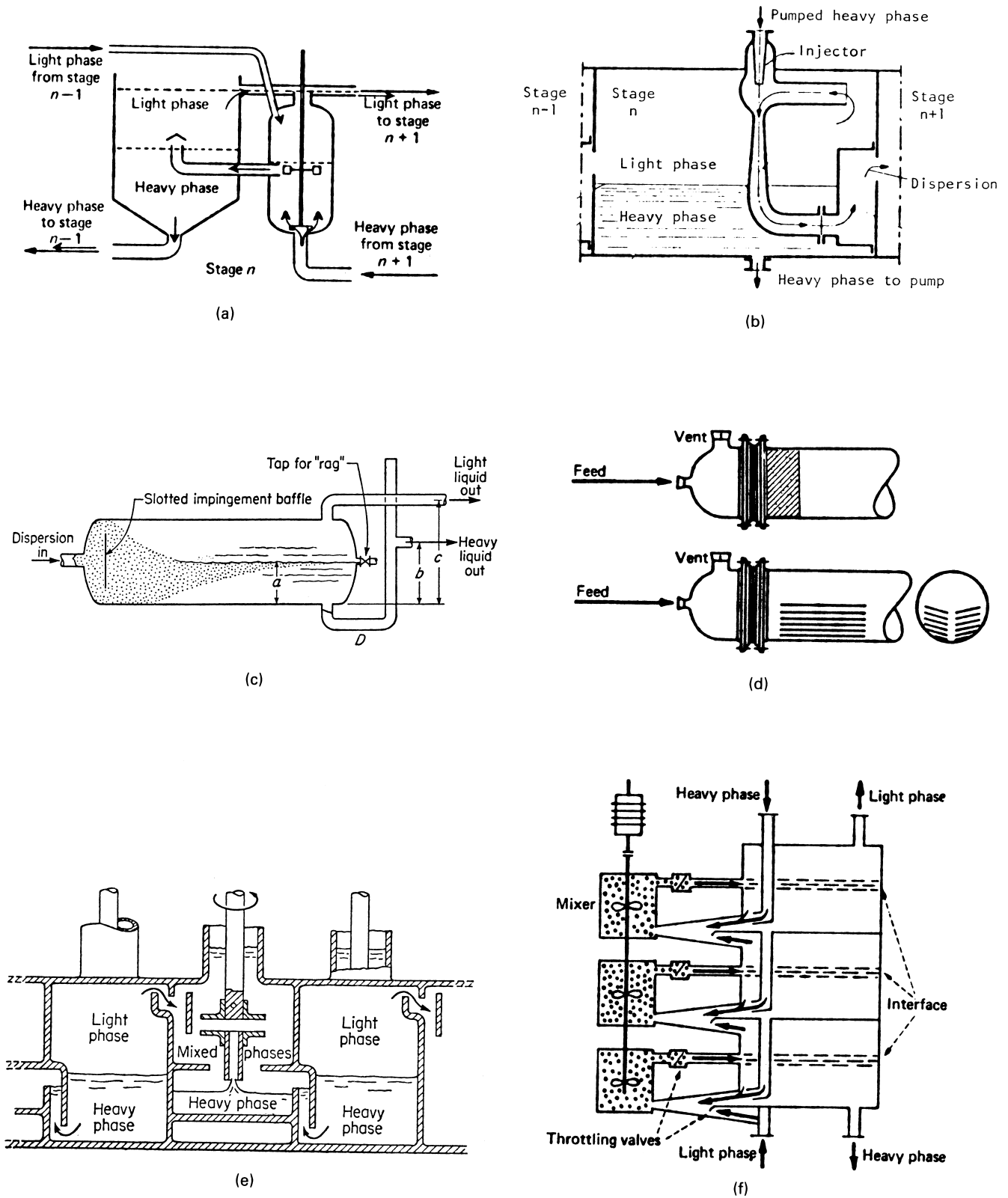
Figure 14.13. Some types and arrangements of mixers and settlers. (a) Kemira mixer-settler (*Mattila*, Proc. Solvent Extraction Conference, *ISEC 74, Inst. Chem. Eng., London, 1974*); (b) Injection mixer and settler (*Ziolkowski, 1961*). (c) Gravity settler; "rag" is foreign material that collects at the interface. (d) Provisions for improving rate of settling: (top) with packing or wire mesh; (bottom) with a nest of plates. (e) Compact arrangement of pump mixers and settlers [*Coplan et al.*, Chem. Eng. Prog. **50**, *403* (*1954*)]. (f) Vertical arrangement of a battery of settlers and external mixers (*Lurgi Gesellschaften*).
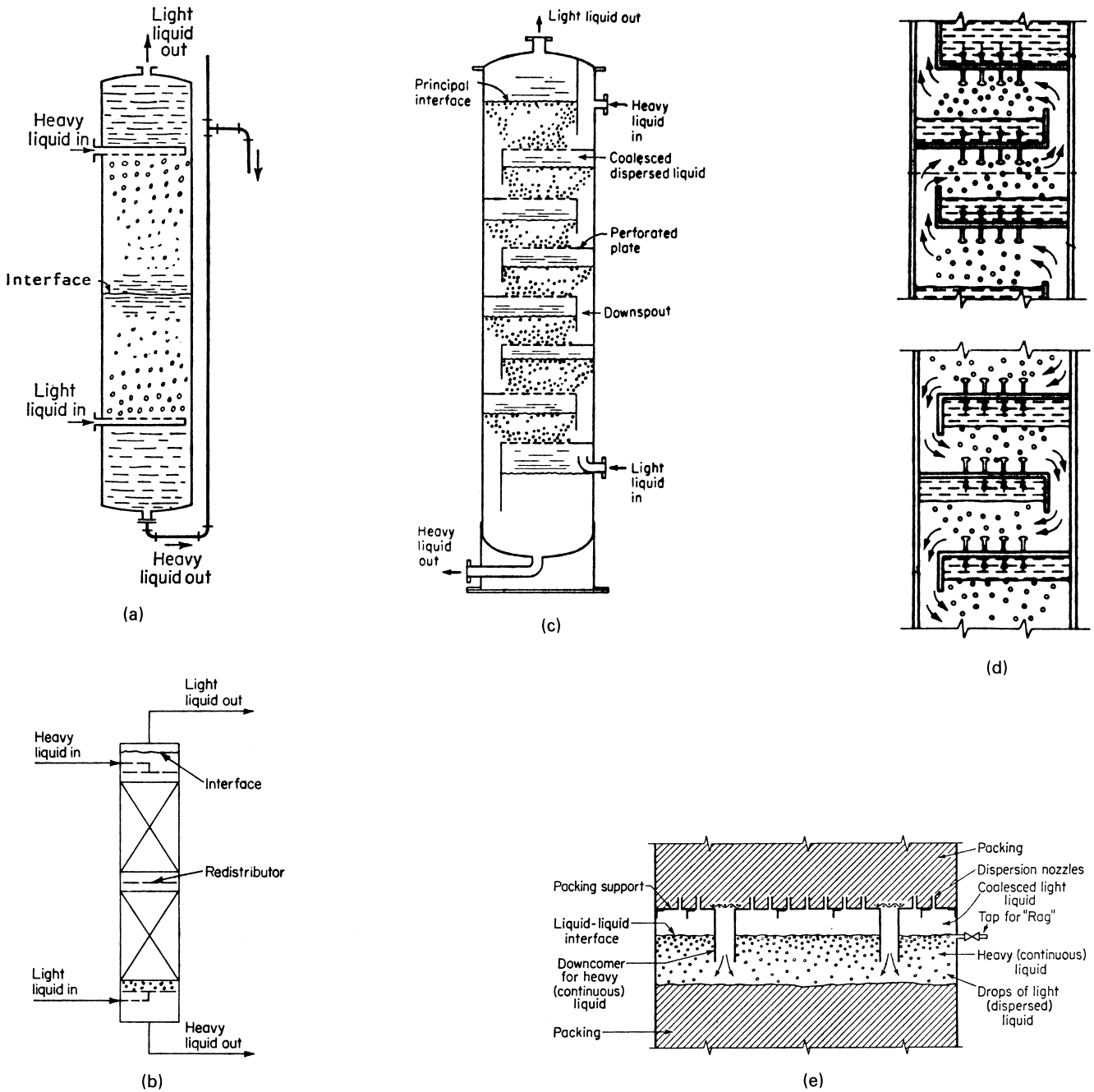
Figure 14.14. Tower extractors without agitation. (a) Spray tower with both phases dispersed. (b) Two-section packed tower with light phase dispersed. (c) Sieve tray tower with light phase dispersed. (d) Sieve tray construction for light phase dispersed (left) and heavy phase dispersed (right). (e) Redistributor for packed tower with light phase dispersed (*Treybal, 1963*).

Packed towers are best employed when 3–6 equilibrium stages suffice, there is an interfacial tension of 15 dynes/cm or less, and the desired dispersed-to-continuous phase ratio is between 0.3 and 3. Packed columns provide the advantages of excellent interface control, low dispersed phase hold-up, and potentially high capacity.

Published data indicate that it is best that the continuous phase preferentially wets the packing surface, which allows the dispersed phase to travel through the column as drops. In general, a metal or ceramic packing material should be used with a continuous aque-

ous phase, whereas a thermoplastic material should be used with an organic continuous phase.

In recent years, high performance random packings and structured packings have been utilized in extraction. These packings are similar to those used in distillation service, such as Pall rings and IMTP. Structured packings are also popular. In some cases, dual-flow plates are placed between elements of structured packings for the purpose of enhancing flow distribution and reducing axial mixing.
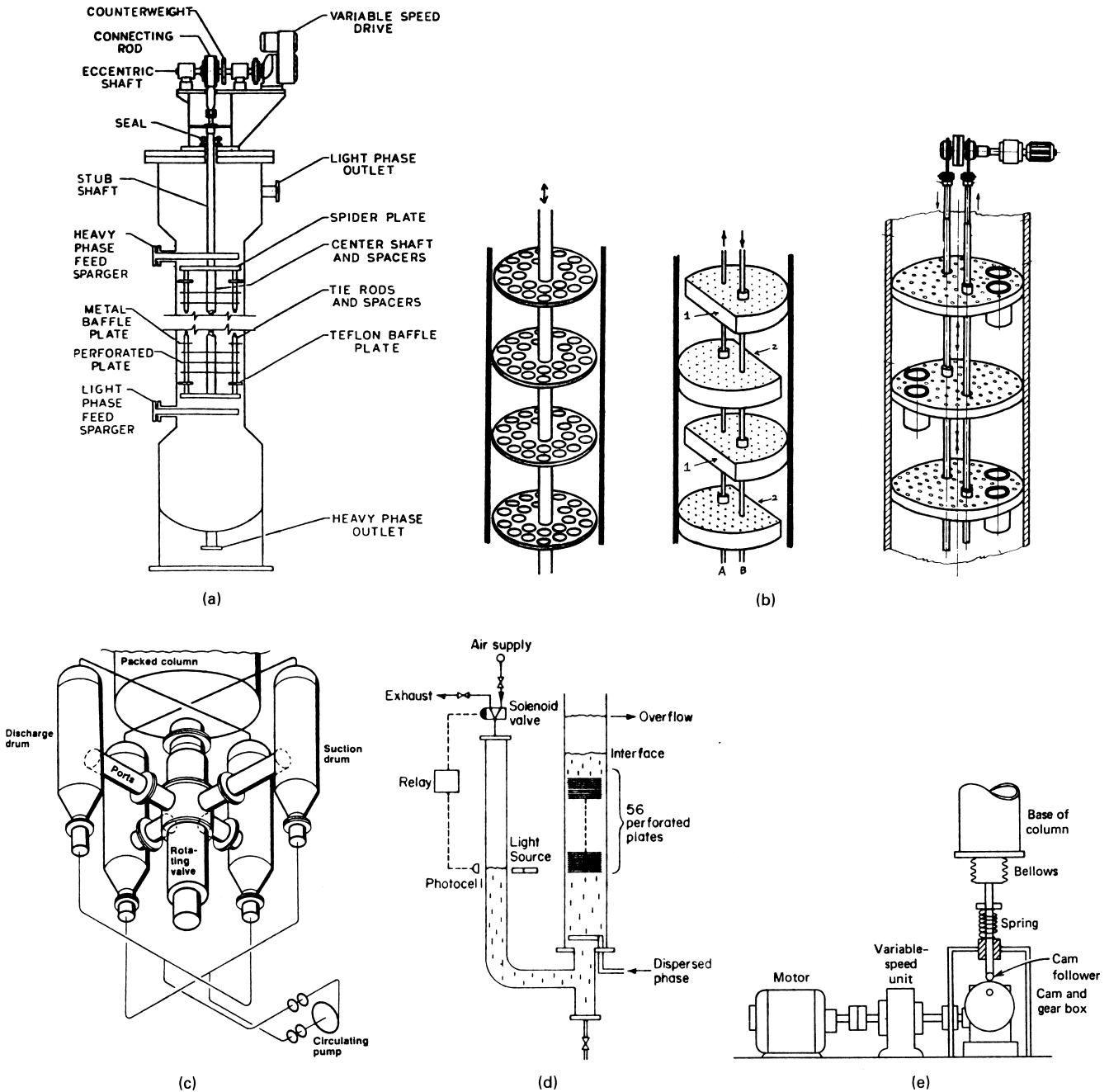
Figure 14.15. Towers with reciprocating trays or with pulsing action. (a) Assembly of a 36 in. Karr reciprocating tray column (*Chem. Pro. Co.*). (b) Sieve trays used in reciprocating trays columns; (left) large opening trays for the Karr column; (middle) countermotion trays with cutouts; (right) countermotion trays with downpipes for heavy phase. (c) Rotary valve pulsator, consisting of a variable speed pump and a rotary valve that alternately links the column with pairs of suction and discharge vessels. (d) Sieve tray tower with a pneumatic pulser [Proc. Int. Solv. Extr. Conf. **2**, *1571 (1974)*]. (e) A pulser with a cam-operated bellows.

$$\frac{1}{U_{cf}} = \frac{5.63}{\varepsilon U_{so}} + \frac{5.21\left(U_{df}\,U_{cf}\right)}{\varepsilon U_{so}\cos^2\left(\frac{\pi\zeta}{4}\right)} \qquad (14.42)$$

$$d_{vs} = 1.15\eta\sqrt{\frac{\sigma}{\Delta\rho g}} \qquad (14.44)$$

Where:

n = 1.0 for mass transfer c → d or no mass transfer
= 1.4 for mass transfer d → c
σ = interfacial tension, dynes/cm
$\Delta\rho$ = density difference, g/cm^3
g = 980 cm/s^2

$$\zeta = \frac{a_p \cdot d_{vs}}{2} \qquad (14.43)$$

The equilibrium Sauter mean drop diameter (d_{vs}) is estimated:
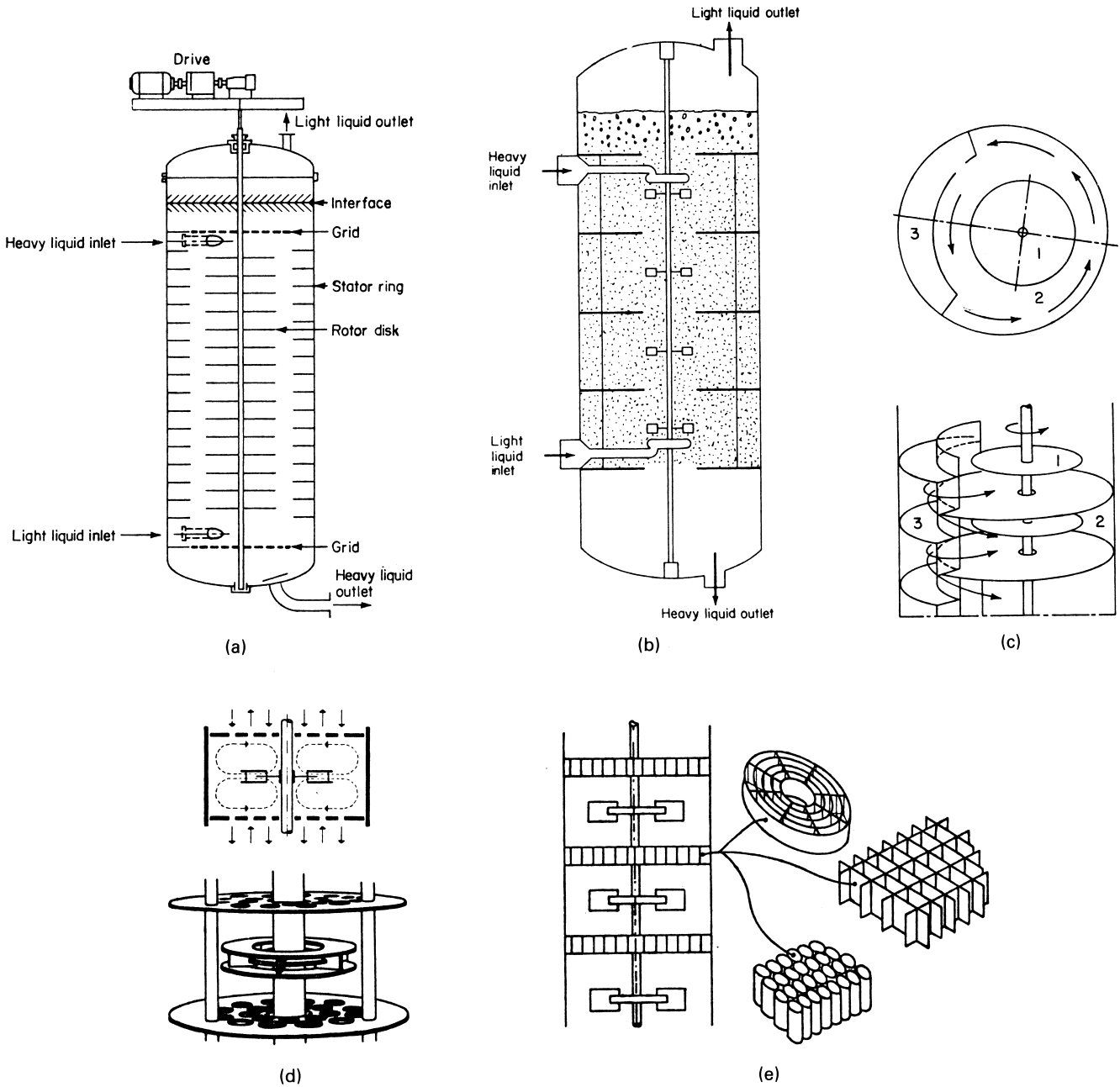
Figure 14.16. Tower extractors with rotary agitators. (a) RDC (rotating disk contactor) extraction tower (*Escher B.V., Holland*). (b) Oldshue–Rushton extractor with turbine impellers and stator rings (*Mixing Equip. Co.*). (c) ARD (asymmetric rotating disk) extractor: (1) rotating disk rotor; (2) mixing zone; (3) settling zone (*Luwa A.G.*). (d) Kuhni extractor, employing turbine impellers and perforated partitions (*Kühni Ltd.*). (e) EC (enhanced coalescing) extractor [*Fischer et al.*, Chem. Ing. Tech., *228* (*Mar. 1983*)]. (f) Model of Scheibel extractor employing baffled mixing stages and wire mesh separating zones (*E.G. Scheibel Inc.*). (g) Model of Scheibel extractor employing shrouded turbine impellers and flat stators, suited for larger diameter columns (*E.G. Scheibel Inc.*).

The empirical model of Grace et al. (1976) is recommended for estimating the characteristic drop velocity (U_{so}).

$$\frac{N_{Re}}{P^{0.149}} = 0.94H^{0.757} - 0.857 \quad H \leq 59.3 \tag{14.45}$$

$$\frac{N_{Re}}{P^{0.149}} = 3.42H^{0.441} - 0.857 \quad H > 59.3 \tag{14.46}$$

where the dimensionless groups are defined as:

$$P = \frac{\rho_c^2 \sigma^3}{\mu_c^4 g \Delta \rho} \tag{14.47}$$

$$H = \left[\frac{4d_{vs}^2 g \Delta \rho}{3\sigma}\right] \left[\frac{\mu_w}{\mu_c}\right]^{0.14} P^{0.149} \tag{14.48}$$

(f)

(g)
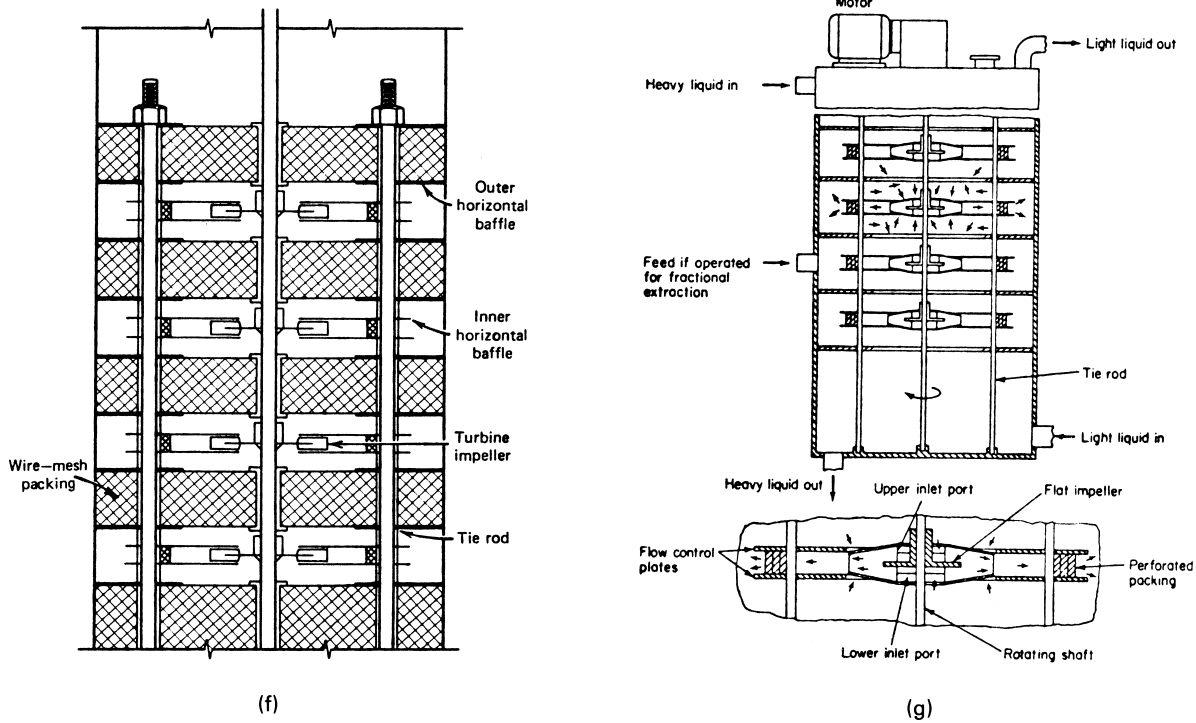
Figure 14.16.—(*continued*)

$$N_{Re} = \frac{d_{vs}\rho_c U_{so}}{\mu_c} \tag{14.49}$$

and

μ_c = viscosity of the continuous phase, g/cm-s(= cP/100)
μ_w = reference viscosity = 0.009, g/cm-s

In the absence of packing, equation 14.42 can be rewritten to predict flooding in a spray column:

$$\frac{1}{U_{cf}} = \frac{5.63}{U_{so}} + \frac{5.21(U_{df}/U_{cf})}{U_{so}} \tag{14.50}$$

$$U_{cf} = \frac{0.178U_{so}}{1 + 0.925(U_{df}/U_{cf})} \tag{14.51}$$

where U_{cf} and U_{df} are the superficial velocities for the continuous and dispersed phases at the flooding point.

Dispersed phase loadings should not exceed 25 gal/min-ft^2 For most packed column applications, the maximum dispersed phase loadings will range 10 to 20 gal/min-ft^2. Dispersion is best accomplished with perforated plates with a hole size range of 3/16 to 1/4 in. Velocities though the holes should not exceed 0.8 ft/s, but if short riser tubes are employed, the velocities can be as high as 1.5 ft/s.

SIEVE TRAY TOWERS

Sieve tray extractors are popular in the chemical and petrochemical industries. The trays minimize axial mixing, which results in good scale-up from laboratory data. The dispersed phase drops re-form at the each perforation, rise (or fall) near their terminal velocity, and then coalesce underneath (or above) the tray, as shown in Figure 14.14(d). The coalesced layer is important to prevent axial mixing of the continuous phase and to allow re-formation of the drops, which enhances mass transfer. The continuous phase passes through the downcomer (or upcomer) and across the sieve tray. The height of the coalesced layer depends on the combined pressure drop of the dispersed phase through the perforations and the continuous phase through the downcomer (or upcomer). In commercial sieve tray extractors, the height of the coalesced layer should be designed for 1 to 2 inches. In general, the pressure drop should be balanced between the downcomer and orifice. In some cases, the inlet area of the downcomer is larger than the outlet to minimize entrainment of dispersed phase into the downcomer.

$$h = \frac{\Delta P_o + \Delta P_{dow}}{g\Delta\rho} \tag{14.52}$$

The orifice pressure drop may be calculated using the predicted model of Pilhofer and Goedl (1977).

$$\Delta P_o = \frac{1}{2}\left(1 - \frac{0.71}{\log Re}\right)^{-2}\rho_d U_o^2 + 3.2\left(\frac{d_o^2 g\Delta\rho}{\sigma}\right)^{0.2}\frac{\sigma}{d_o} \tag{14.53}$$

The downcomer pressure drop may be estimated:
where:

$$\Delta P_{dow} = \frac{4.5\rho_c U_{dow}^2}{2} \tag{14.54}$$

d_o = hole diameter, cm
g = acceleration due to gravity, cm/s^2
U_o = average hole velocity, cm/s
U_{dow} = average velocity in downcomer, cm/s
Re = orifice Reynolds number, (= $d_o U_o \rho_d/\mu_d$)
ΔP_o = orifice pressure drop, g/cm-s^2
ΔP_{dow} = downcomer pressure drop, g/cm-s^2
$\Delta\rho$ = density difference, g/cm^3

(a)

(b)

(c)
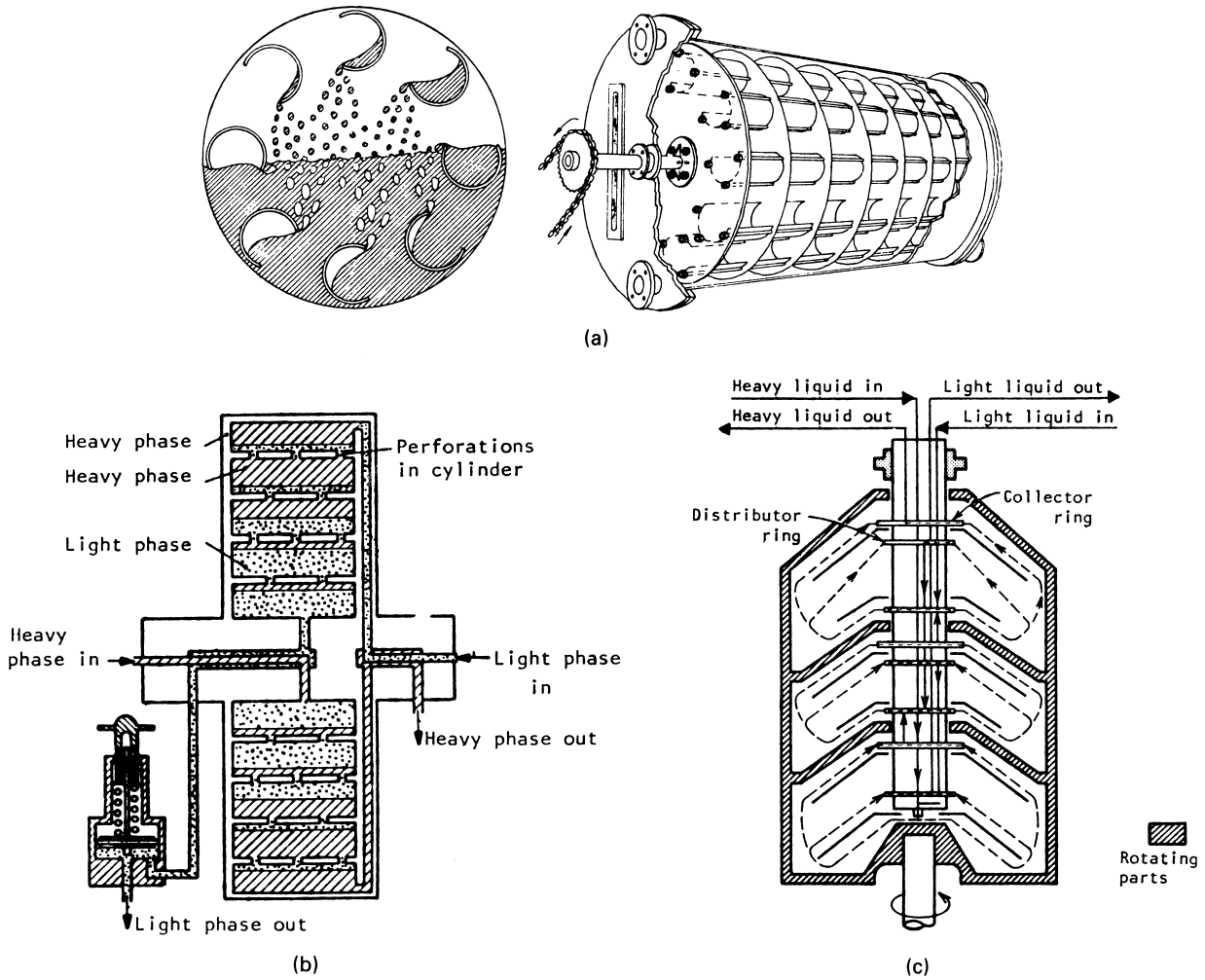
Figure 14.17. A horizontal rotating extractor and two kinds of centrifugal extractors. (a) The RTL (formerly Graesser raining bucket) horizontal rotating extractor; both phases are dispersed at some portion of the rotation (*RTL S. A., London*). (b) Operating principle of the Podbielniak centrifugal extractor; it is made up of several concentric perforated cylinders (*Baker–Perkins Co.*). (c) The Luwesta centrifugal extractor (schematic diagram) (*Luwa Corp.*).

ρ_d = density of the dispersed phase, g/cm^3
σ = interfacial tension, dynes/cm
μ_d = viscosity of the dispersed phase, g/cm-s (= cP/100)

Hole diameters are generally smaller than for vapor-liquid contacting, being 3–8 mm, usually on a triangular pitch of 2–3 hole diameters, and occupy 4–15% of the available tray area. The area at a downcomer or riser is not perforated, nor is the area at the support ring, which may be 1 to 2 inches wide. Velocities through the holes are kept below 25 cm/s to minimize formation of small drops. Likewise, the average drop velocity should be sufficient to ensure complete operation of holes. Eldridge (1986) confirmed the Weber number (We) of at least 2 is required to have complete hole operation.

$$We = \frac{p_d U_o^2 d_o}{\sigma} > 2 \qquad (14.55)$$

Diameter of the Tower. The cross section of the tower must be large enough to accommodate the downcomer and the perforated

zone. The ultimate capacity of a sieve tray tower should approach that of a spray column. The capacity of an existing tower can also be limited by the total pressure drop through the perforated zone and downcomer. In addition, for applications of high dispersed-to-continuous phase flow ratios, the maximum capacity may be limited by inadequate drop coalescence at the main operating interface. In such cases, a structured packing that is preferentially wetted by the dispersed phase may be added to the region of the main operating interface. In large diameter sieve tray extractors, the crossflow velocity may be large enough to slow the vertical rise (or fall) of the drops. In this case, multiple downcomer (or upcomer) trays may be used to reduce the radial velocity of the continuous phase and increase the column capacity by 10 to 15% (Seibert et al., 2002).

Tray Efficiency. A rough correlation for tray efficiency is due to Treybal (1963); as modified by Krishnamurty and Rao [*Ind. Eng. Chem. Process. Des. Dev.* **7**, 166 (1968)] it has the form

$$E = (0.35 Z_T^{0.5}/\sigma d_0^{0.35})(V_D/V_C)^{0.42}, \qquad (14.56)$$

where the interfacial tension σ is in dyn/cm and the tray spacing Z_T and hole diameter d_0 are in ft. Efficiencies and capacities of several kinds of extractors are summarized in Figure 14.18.

Application of the rules given here for sizing extraction towers without mechanical agitation is made in Example 14.11. The results probably are valid within only about 25%. The need for some pilot plant information of the particular system is essential.

The sieve tray extractor is amenable to mechanistic modeling. Seibert and Fair (1993) provide a rigorous model for the prediction of efficiency.

Other Static Extractors. Baffle trays are also utilized in extraction for the processing when significant solids are present. In general, short tray spacings are used (4–6 inches). The baffles are generally segmental with a side-to-side arrangement. The capacity and efficiency are dependent on the available open area. In general, the dispersed phase flows as a stream across the tray. In some cases, drops are also present. These trays are best suited for processing slurries and with systems that have a low interfacial tension.

The application of hollow fiber extractor technology to extraction is relatively new. These contactors resemble a shell- and-tube heat exchanger and are comprised of bundles of microporous hollow fibers, usually made of polyethylene or polypropylene. Since a liquid-liquid interface can be immobilized within the large pores of the fiber walls, a very large area for mass transfer is available. These devices are best suited for very high distribution coefficient systems where solute transfer is into the organic phase. The organic solvent should be chemically compatible with the device, feed should not contain solids, and only a few equilibrium stages of separation are required.

PULSED PACKED AND SIEVE TRAY TOWERS

A rapid reciprocating motion imparted to the liquid in a tower results in improved mass transfer. This action can be accomplished without parts and bearings in contact with the process liquids and consequently has found favor for handling hazardous and corrosive liquids as in nuclear energy applications. Most of the applications still are in that industry, but several other installations are listed by Lo et al. (1983, pp. 345, 366). Packed columns up to 3 m dia and 10 m high with throughputs in excess of 200 m^3/hr are in use.

Both packed and perforated plate towers are in use. The most commonly used packing is 1 in. Raschig rings. A "standard" geometry for the plates is 3 mm dia holes on triangular spacing to give 23% open area, plate thickness of 2 mm, and plate spacing of 50 mm. Reissinger and Schröter (1978) favor 2 mm holes and 100 mm plate spacing. The action of the plates is to disperse the heavy phase on the upstroke and the light phase on the down stroke.

Pulsing is uniform across the cross section, and accordingly the height needed to achieve a required extraction is substantially independent of the diameter as long as hydrodynamic similarity is preserved. Although correlations for flooding, holdup, and HTU are not well generalized, a major correlating factor is the product of frequency f and amplitude A_p; in practical applications fA_p is in the range of 20–60 mm/sec.

One large user has standardized on a frequency of 90 cycles/min and amplitudes of vibration of 6–25 mm. Three kinds of pulsing modes are shown in Figures 14.15(c)–(e). The rotary valve pulsator consists of two reservoirs each on the suction and discharge of a variable speed centifugal pump and hooked to a rotating valve. Pneumatic and reciprocating pump pulsers also are popular.

Extraction efficiency can be preserved over a wide range of throughputs by adjusting the product fA_p. A comparison of several

correlations of HTU made by Logsdail and Slater (in Lo et al., 1983, pp. 364) shows a four- to five-fold range, but a rough conservative rule can be deduced from these data, namely

$$\text{HTU} = 3.7/(fA_p)^{1/3}, \ 20 \leq fA_0 \leq 60 \ \text{mm/sec}, \tag{14.57}$$

which gives an HTU of 1 m at $fP_p = 50$ mm/sec. In small diameter extractors, data for HETS of 0.2–0.5 m or less have been found, as appear in Figure 14.18.

Flooding, holdup, and mass transfer rates are highly interdependent and are not simply related. Reissinger and Schröter (1978) state that tray towers in comparison with other types have good efficiencies at 60 m^3/m^2 hr at frequencies of 60–90/min and amplitudes of 10 mm. Packed towers have about 2/3 the capacities of tray towers. Also in comparison with unagitated towers, which are limited to interfacial tensions below 10 dyn/cm, pulsed towers are not limited by interfacial tension up to 30–40 dyn/cm. Some further comparisons are made in Tables 14.5 and 14.6 and Figure 14.18.

RECIPROCATING TRAY TOWERS

Desirable motion can be imparted to the liquids by reciprocating motion of the plates rather than by pulsing the entire liquid mass. This mode employs much less power and provides equally good extraction efficiency. A 30 in. dia tower 20 ft high is sufficiently agitated with a 1.5 HP motor. Some arrangements of such extractors are shown in Figure 14.15.

The holes of reciprocating plates are much larger than those of pulsed ones. Typical specifications of such extractors are: Holes are 9/16 in. dia, open area is 50–60%, stroke length 0.5–1.0 in., 100–150 strokes/min at 0.75 in. stroke length, plate spacing normally 2 in. but may vary from 1–6 in. when the physical properties vary significantly in different parts of the tower. In towers about 30 in. dia, HETS is 20–25 in. and throughputs are up to 40 m^3/m^2 hr (2000 gal/hr sqft). Scaleup formulas for HETS and reciprocating speed, fA_p, are stated by the manufacturer, Chem Pro Corp.:
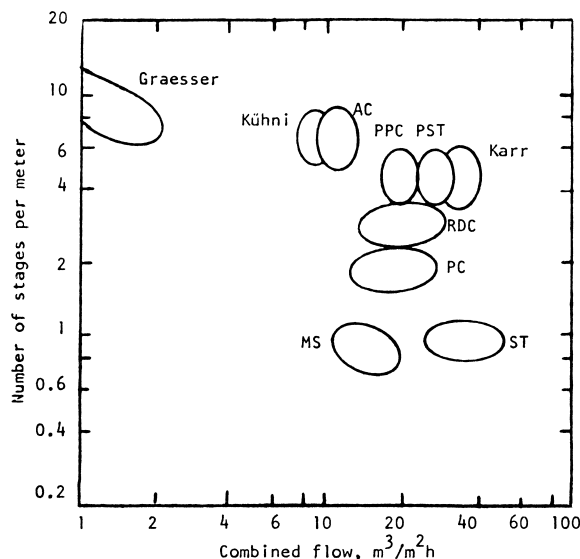
Figure 14.18. Efficiency and capacity range of small diameter extractors, 50–150 mm dia. Acetone extracted from water with toluene as the disperse phase, $V_d/V_c = 1.5$. Code: AC = agitated cell; PPC = pulsed packed column; PST = pulsed sieve tray; RDC = rotating disk contactor; PC = packed column; MS = mixersettler; ST = sieve tray [*Stichlmair*, Chem. Ing. Tech. **52**(*3*), 253–255 (*1980*)].

EXAMPLE 14.11
Sizing of Spray, Packed, or Sieve Tray Towers
Determine the capacity and efficiency of the tower, given the following:

$Q_d = 600\,\text{ft}^3/\text{hr} = 4{,}719\,\text{cm}^3/\text{s}$
$Q_c = 500\,\text{ft}^3/\text{hr} = 3{,}933\,\text{cm}^3/\text{s}$
$\rho_d = 50\,\text{lb}/\text{ft}^3 = 0.80\,\text{g}/\text{cm}^3$
$\rho_c = 60\,\text{lb}/\text{ft}^3 = 0.96\,\text{g}/\text{cm}^3$
$\mu_d = 0.5\,\text{cP}$
$\mu_c = 1.0\,\text{cP}$
$\sigma = 10\,\text{dyne}/\text{cm}$
$d_o = 0.25\,\text{in} = 0.635\,\text{cm}$ (hole diameter for sieve tray case)
$d_{vs} = 0.41\,\text{cm}$ (Sauter mean drop diameter)

Characteristic drop velocity: Use method of Grace et al. (Eqs 14.45–14.49)

$$P = \left[\frac{\rho_c^2 \sigma^3}{\mu_c^4 g \Delta\rho}\right] = \frac{(0.96)^2 (10)^3}{(0.01)^4 (981)(0.16)} = 5.87 \bullet 10^8$$

$$H = \left[\frac{4(0.41)^2 (981)(0.16)}{3(10)}\right]\left[\frac{0.009}{0.01}\right]^{0.14} (5.87 \bullet 10^8)^{0.149} = 70.2$$

$$H = 70.2 > 59.3$$

$$\frac{N_{Re}}{P^{0.149}} = 3.42 H^{0.441} - 0.857\ H > 59.3$$

$$N_{RE} = \left[3.42\,(70.2)^{0.441} - 0.857\right]\left[5.87 \bullet 10^8\right]^{0.149}$$

$$N_{RE} = 434$$

$$U_{so} = \frac{434\,\mu_c}{d_{vs}\rho_c}$$

$$U_{so} = \frac{434(0.01)}{(0.41)(0.96)}$$

$$U_{so} = 11.0\,\text{cm/s} \qquad \text{(Characteristic Drop Velocity)}$$

Spray tower: The flooding velocity is found from Equation 14.51.

$$U_{cf} = \frac{0.178(11.0)}{1 + 0.925(4719/3933)} = 0.928\,\text{cm/s}$$

Designing for 60% of flood, $U_c = (0.6)(0.928) = 0.56\,\text{cm/s}$
Required Area $= 3933/0.56 = 7023\,\text{cm}^2$

Required Diameter $= \sqrt{\frac{4(7023)}{\pi}} = 94.6\,\text{cm}(3.1\,\text{ft})$

To accommodate four stages, a total height of 100 ft. or so would be needed. Two towers each 3.1 ft dia by 50 ft high may be suitable.
Packed Tower: Flooding velocity is obtained using Equations 14.42–14.43. For one inch metal Pall rings,

$$a_p = 2.07\,\text{cm}^2/\text{cm}^3, \varepsilon = 0.94$$

$$\zeta = \frac{2.07 \cdot 0.41}{2} = 0.42$$

$$\frac{1}{U_{cf}} = \frac{5.63}{(0.94)(11.0)} + \frac{5.21(4719/3933)}{(0.94)(11.0)\cos^2\left(\frac{\pi(0.42)}{4} \bullet \frac{180}{\pi}\right)} = 1.21$$

$$U_{cf} = 0.82\,\text{cm/s}$$

Designing for 60% of flood, $U_c = (0.6)(0.82) = 0.49\,\text{cm/s}$
Required Area $= 3933/0.49 = 8027\,\text{cm}^2$

Required Diameter $= \sqrt{\frac{4(8027)}{\pi}} = 101\,\text{cm}(3.3\,\text{ft})$

The HETS is calculated from Equations 14.39–14.41. A bed height of 10 ft (between redistributors) is used.

$$\text{HETP} = f_1 + f_2$$

$$f_1 = 60 \bullet 1.5 \left[\frac{0.49}{0.59}\right]^{0.8} \left[\frac{10^2}{(e^{2.07})(0.16)}\right]^{0.25} \left[(0.5^{0.5})(1.0)^{0.35}\right] = 163\,\text{cm}$$

$$f_2 = 305\left[1 - \exp\left\{-0.3\left(\frac{101}{42}\right)^{0.3}\left(\frac{(1.0)^{0.5}}{2.07}\right)\left(\frac{0.59}{0.49}\right)\right\}\right] = 62\,\text{cm}$$

$$\text{HETP} = 163 + 62 = 225\,\text{cm}(7.4\,\text{ft})$$

Therefore three beds will provide approximately 4 stages. The tower will be 3.4 ft in diameter with three beds (total of 30 ft of packing), two redistributors (6 ft), and two settling zones on ends of column (8 ft each); height will be 52 ft.
Sieve tray tower: Design is based on a coalesced layer of 1 inch ($h = 2.54\,cm$) with 50% of pressure drop through perforations and 50% through downcomer. An 18-inch tray spacing is used.
Therefore, the orifice pressure drop is calculated using equation 14.53.

$$\Delta Po = (0.5)(2.54)(981)(0.16) = 199\,\text{g/cm-s}^2$$

$$199 = \frac{1}{2}\left(1 - \frac{0.71}{\log\left(\frac{(0.8)(0.635)(U_o)}{0.005}\right)}\right)^{-2}(0.8)U_o^2$$
$$+ 3.2\left(\frac{(0.635)^2(981)(0.16)}{10}\right)^{0.2}\frac{10}{0.635}$$

by trial and error, $U_o = 13.8\,\text{cm/s}$
Area required for perforations $= 4719/13.8 = 342\,\text{cm}^2$
Number of perforations $= \frac{342}{\frac{\pi}{4}(0.635)^2} = 1080$

$$\text{Weber Number} = \frac{(0.635)(13.8^2)(0.8)}{10} = 9.7 > 2$$

(Therefore all perforations will be active.)
The downcomer pressure drop is calculated using equation 14.55.

$$199 = 4.5(0.96)\frac{U_{dow}^2}{2}$$
$$U_{dow} = 9.5\,\text{cm/s}$$

Therefore the downcomer area $= 3933/9.5 = 414\,cm^2$.
The tray will be designed so that the flooding velocity within the active area approaches the ultimate capacity (spray column). The total active area required for 60% of flood $= 7023\,\text{cm}^2$.
The total area occupied by the downcomer region $= 2(414) = 828\,\text{cm}^2$.
Therefore the total column area $= 7023 + 828 = 7851\,\text{cm}^2$.

$$\text{Required Column Diameter} = \sqrt{\frac{4(7851)}{\pi}} = 100\,\text{cm}(3.3\,\text{ft}).$$

The tray efficiency is calculated from Equation (14.57):

$$E = \frac{0.35(1.5)^{0.5}}{10(0.0208)^{0.35}}(4719/3933)^{0.42} = 0.18 = 18\%$$

Number of trays $= 4/0.18 = 22$ trays
The tower will be 3.3 ft in diameter with 22 sieve trays, contacting height of 33 ft and two settling zones on ends of column (8 ft each), yielding a total height of 49 ft.
Summary:

	Height, ft	Diameter, ft
Spray*	100	3.1
Packed	52	3.3
Sieve Tray	49	3.3

*Two towers in series may be

$$(HETS)_2/(HETS)_1 = (D_2/D_1)^{0.36}, \qquad (14.58)$$

$$(fA_p)_2/(fA_p)_1 = (D_1/D_2)^{0.14}. \qquad (14.59)$$

The performance of a reciprocating tower is compared with several other small extractors in Figure 14.18.

An extractor with countermotion of alternate plates is known as the VPE (vibrating plate extractor). Figure 14.15(c) shows the arrangement. This model also is constructed with segmented plates or with downcomers for passage of the continuous phase. At least during some portion of the cycle, the light phase coalesces and is trapped below the tray, just as in static tray extractors. The capacity of these units is greater than of those with full trays and the efficiency remains high. Some data (Lo et al., 1984, p. 386) indicate that some commercial extractions are completed satisfactorily in towers 4–8 m high at rates of 35–100 m^3/m^2 hr.

ROTATING DISK CONTACTOR (RDC)

The concept of arranging a battery of mixer-settlers in a vertical line in a single shell has been implemented in a variety of ways. In the RDC (Rotary Disk Contactor) extractor, the impellers are flat disks, the mixing zones are separated by partial diametral baffles called stators, but distinct settling zones are not provided. Figure 14.16(a) is a sketch. Because of its geometrical simplicity and its effectiveness, the RDC is one of the most widely employed of agitated extractors. The situations in which it may not be suitable are when only a few stages are needed, in which case mixer-settlers will be satisfactory and cheaper; or when their large holdup and long residence times may be harmful to unstable substances; or for systems with low interfacial tensions and low density differences because then stable emulsions may be formed by the intense agitation.

According to the comparisons of small units in Figure 14.18, the RDC is intermediate in stage efficiency and throughput. The value of HETS = 0.3 m from this figure compares roughly with the HTU = 0.4 or 0.75, depending on which phase is dispersed, of the pilot plant data of Example 14.12.

The design procedure used by Kosters, of Shell Oil Co., who developed this equipment, requires pilot plant measurements on the particular system of HTU and slip velocity as functions of power input. The procedure for scaleup is summarized in Table 14.5, and results of a typical design worked out by Kosters (in Lo et al., 1983, pp. 391–405) are summarized in Example 14.12. Scale-up by this method is said to be reliable in going from 64 mm dia to 4–4.5 m dia. The data of Figure 14.19 are used in this study.

OTHER ROTARY AGITATED TOWERS

One of the first agitated tower extractors was developed by Scheibel (*AIChE. J.* **44**, 681, 1948). The original design, like Figure 14.16(f), employed settling zones packed with wire mesh, but these were found unnecessary in most cases and now flat partitions between mixing zones are used. The Mixco [Figure 14.16(b)] and Scheibel–York [Figure 14.14(g)] units differ primarily in the turbine impellers, the Mixco being open and the other shrouded. In spite of the similarity of their equipment, the manufacturers have possibly different ranges of experience. Since extractor selection is not on an entirely rational basis, a particular body of experience may be critical for fine tuning.

Enhanced coalescing between stages is provided in the designs of Figure 14.16(e). The Kühni extractor of Figure 14.16(d) employs shrouded turbine impellers and perforated plate partitions between compartments and extending over the entire cross section. The ARD (asymmetric rotating disk) extractor has lateral spaces for settling between agitation zones.

Some performance data are cited for the Kühni by Ritcey and Ashbrook (1979, p. 102):

% Free Cross Section	m^3/m^2hr	HETS (m)
10	10	0.08
40	50	0.20

Although not all equipment is compared, Figure 14.18 shows the Kühni to have a high efficiency but somewhat lower capacity than the RDC and other units.

Most of these types of equipment have at least several hundred installations. The sizing of full scale equipment still requires pilot planting of particular systems. The scaleup procedures require geometrical and hydrodynamic similarities between the pilot and full scale plants. Hydrodynamic similarity implies equalities of droplet diameters, fractional holdups, and linear superficial velocities. Also preserved are the specific radial discharge rates, defined by Q/DH = (volumetric flow rate)/(vessel dia) (compartment height).

A detailed design of an ARD extractor based on pilot plant work is presented by Misek and Marek (in Lo et al., 1983, pp. 407–417). The design and operating parameters of the ARD extractor are related to the vessel diameter D (mm); thus:

Free cross section = 25%
Disk diameter = 0.49D.
Chamber height = 1.3 $D^{0.67}$.
Agitator rpm = $15,000/D^{0.78}$.

A manufacturer's bulletin on a 150 mm dia ARD extractor gives HETS = 0.4 m and capacity 15 m^3/m^2 hr.

Less specific information about the other kinds of extractors mentioned here is presented by Lo et al. (1983, pp. 419–448) but no integrated examples. The information perhaps could be run down in the abundant literature cited there, or best from the manufacturers.

OTHER KINDS OF EXTRACTORS

Some novel types and variations of basic types of extractors have been developed, most of which have not found wide acceptance, for instance pulsed rotary towers. The literature of a few of them is listed by Baird (in Lo et al., 1983, pp. 453–457). Here the extractors illustrated in Figure 14.17 will be described.

Graesser Raining Bucket Contactor. The Graesser "raining bucket" contactor consists of a horizontal rotating shell with a shaft that carries a number of diametral partitions extending to the wall. Between the partitions are buckets that carry the liquid and cascade it through each phase. No attempt is made to effect dispersion beyond simply emptying the buckets. The light and heavy phases are alternately both dispersed. They are introduced and withdrawn at opposite ends. The speed of rotation can vary between 0.25–40 rpm depending on the Graesser diameter and viscosities of the phases. The performance will vary depending on the physical properties of the extraction system.

A commercial unit 5 ft dia by 18 ft long has 26 × 7-in. wide compartments each with 16 × 8-in. buckets and provides six theoretical stages. A unit 12 in. dia by 3 ft long has a capacity of 30 gal/hr at 8 rpm. A unit 6 ft dia has a capacity of 6000 gal/hr at 1.4 rpm.

Centrifugal Contactors. These devices have large capacities per unit, short residence times, and small holdup. They can handle systems that emulsify easily or have small density differences or large interfacial tensions or need large ratios of solvent to feed. Some types are employed as separators of mixtures made in other

TABLE 14.6. Maximum Loads and Diameters of Extractors

Column Type	Maximum Load $(m^3/(m^2)\ (h))$	Maximum Column Diameter (m)	Maximum Throughput (m^3/h)
Graesser contactor	<10	7.0	380
Scheibel	<20	1.0	16
Asymmetric rotating-disk	≈25	3.2–5.0	200
Lurgi tower	≈30	8.0	1500
Pulsed packed	≈40	2.8	250
Rotating-disk contactor	≈40	4.0	500
Kühni	≈50	3.0	350
Pulsed sieve-tray extractor	≈60	3.0	420
Karr	80–100	1.0	<80

These data apply at a high interfacial tension (30–40 dyn/cm), a viscosity similar to water, an inlet ratio of the phases of 1:1 parts by volume, and a density difference of approximately $0.6\,g/cm^3$.
(Reissinger and Schröter, 1978).

equipment, others as both mixers and settlers, and some as differential contactors.

The Podbielniak contactor is a differential type. It is constructed of several perforated concentric cylinders and is shown schematically in Figure 14.17(b). Input and removal of the phases at each section are accomplished through radial tubes. The flow is countercurrent with alternate mixing and separating occurring respectively at the perforations and between the bands. The position of the interface is controlled by the back pressure applied on the light phase outlet.

EXAMPLE 14.12
Design of a Rotating Disk Contactor

A hydrocarbon mixture containing 10% aromatics and at the rate of $55.5\,m^3/hr$ is to be treated with a solvent at the rate of $173.6\,m^3/hr$. Ten stages are needed for the extraction. Pilot plant data are available for the HTU and the slip velocity; they are shown on the graphs for solvent either continuous or dispersed. The procedure of Table 14.7 was applied by Kosters (in Lo et al., 1983, pp. 391–405) with the following results:

	Solvent Continuous	Solvent Dispersed
Vessel dia (m)	2.1	1.7
Stator dia (m)	1.47	1.19
Rotor dia (m)	1.26	1.02
HTU (m)	0.41	0.75
$(HTU)_{off}$ (m)	0.663	1.107
Number of compartments	40	81
Compartment height (m)	0.20	0.17
Total height (m)	10.4	15.7
Rotor speed (rpm)	15–60	15–70
Power (theoretical kW)	4.6	2.8
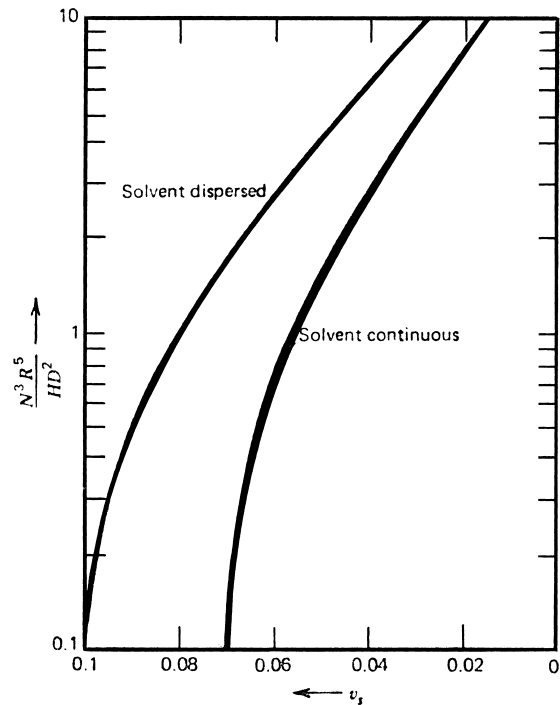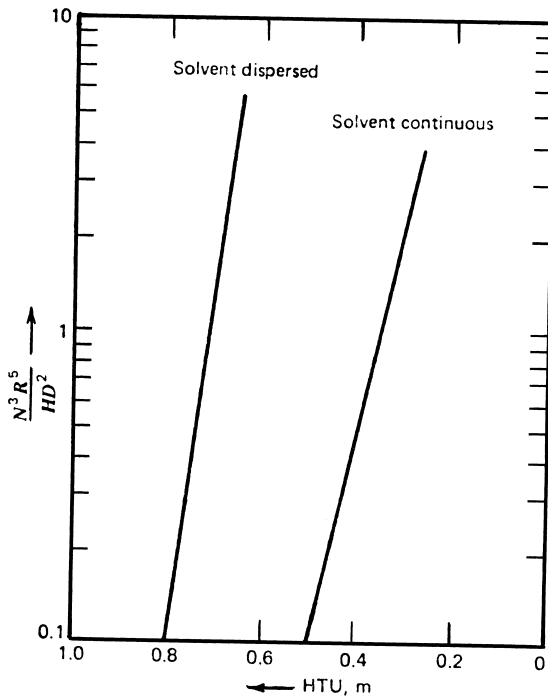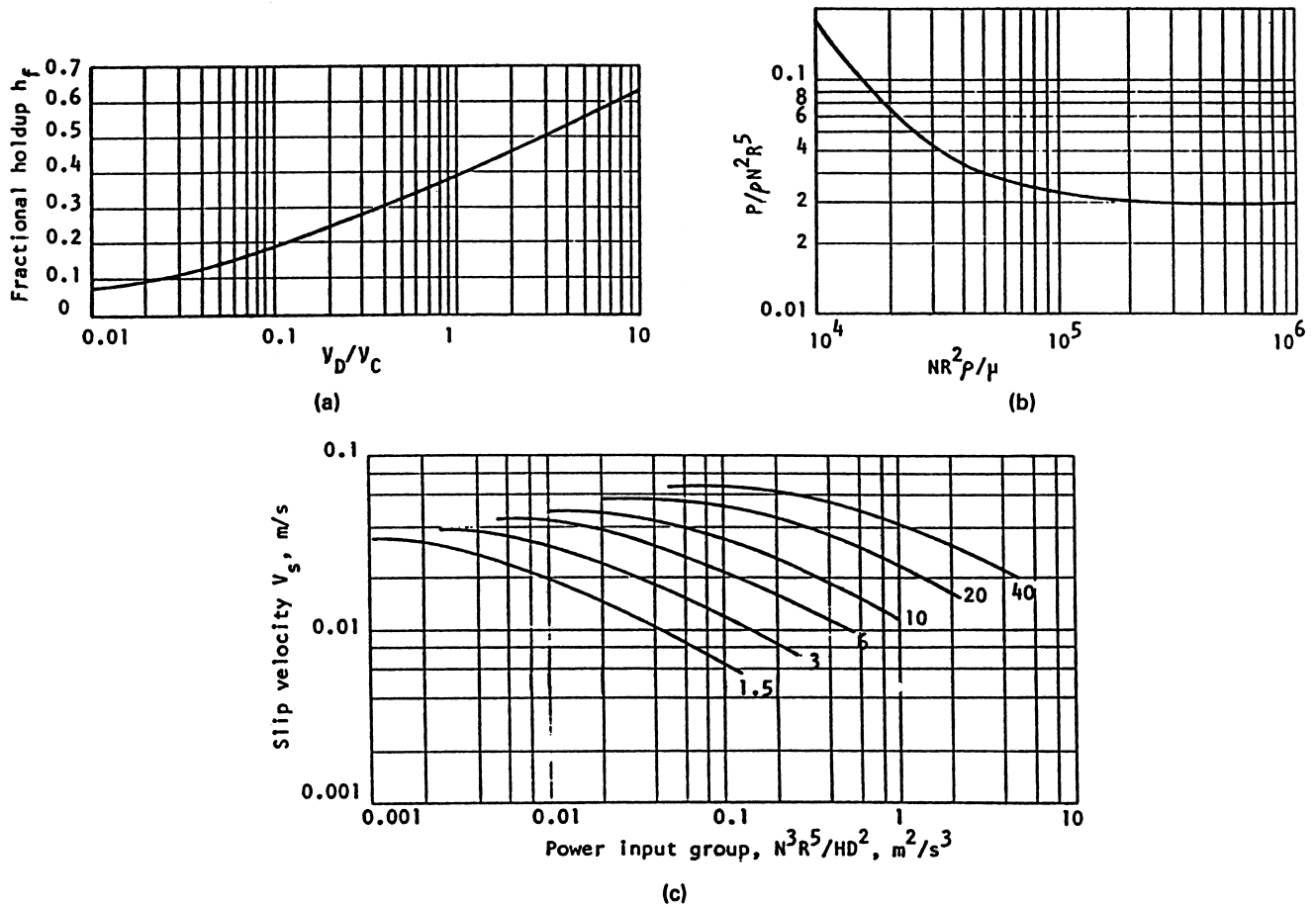
Figure 14.19. Holdup at flooding, power input, and slip velocity in an RDC (*Kosters, in Lo, Baird, and Hanson, 1983*). (a) Fractional holdup at flooding, h_f, as a function of flow ratio of the phases. (b) Power input to one rotor as a function of rotation speed N and radius R. (c) Slip velocity versus power input group for density difference of 0.15 g/mL, at the indicated surface tensions (dyn/cm).

TABLE 14.7. Formulas for Sizing and RDC

1. Stator opening diameter, $S = 0.7D$, where D is vessel diameter
2. Rotor diameter, $R = 0.6D$
3. Height to diameter ratio of a compartment:

D (m)	0.5–1.0	1.0–1.5	1.5–2.5	2.5
H/D	0.15	0.12	0.1	0.08–0.1

4. Power input, Figure 14.20(a)
5. Fractional holdup at flooding, h_f, from Figure 14.20(b)
6. Slip velocity V_s preferably is obtained experimentally, but is given approximately by Figure 14.20(c)
7. Superficial velocity of the continuous phase at flooding,

$$V_{Cf} = \frac{V_s \exp(-h_f)}{V_D/V_C h_f + 1/(1-h_f)},$$

where V_C and V_D are the superficial velocities of the continuous and dispersed phases
8. Holdup h at an operating velocity $V_{C'}$ say 70–80% of flooding,

$$V_C = \frac{V_s \exp(-h)}{V_D/V_C h + 1/(1-h)};$$

solve by trial for h when other quantities are specified

9. Effective height of a transfer unit,

$$(\text{HTU})_{\text{off}} = (\text{HTU})_{\text{pilot plant}} + \text{HDU}$$

in terms of a value obtained in a pilot plant and a calculated height of a diffusion unit (HDU)
10. Height of a diffusion unit, $\text{HDU} = H(1/\text{Pe}_C + 1/\text{Pe}_D)$
11. Factors E_C and E_D for evaluating the Peclet numbers,

$$E_C = 0.5V_C H + 0.012RNH(S/D)^2$$
$$E_D = E_C[4.2(10^5)(V_D/h)^{3.3}/D^2];$$

when the correction in brackets is less than unity, make $E_{D_E} = E_C$
12. The Peclet numbers are

$$1/\text{Pe}_C = E_C(1-h)/HV_C,$$
$$1/\text{Pe}_D = E_D h/HV_D$$

13. Final expression for height of a diffusion unit is
$$\text{HDU} = E_c(1-h)/V_C + E_d h/V_D$$

(W.C.G. Kosters, Shell Oil Co.).

Residence time can be as short as 10 sec. One 750 gpm unit is said to have a total liquid holdup of 200 gal. From 3–10 stages per unit have been reported, although Table 14.8 shows a range of 1.8–7.7. A 65 in. dia casing can accommodate throughputs up to 25,000 gal/hr. An economic comparison of a Podbielniak with other extractors is made in Table 14.5(b). Although its basic cost is high, it requires few auxiliaries so that the overall cost of an extraction plant is not drastically out of line in every instance. Nevertheless, this equipment is used primarily when short residence time and other characteristic features are indispensable.

Other kinds of centrifugals also are used widely. Some are described by Hafez (in Lo et al., 1983, pp. 459–474) and performance data are presented in Table 14.8. Characteristics of centrifu-

gals that are used primarily for removal of solids from slurries are summarized in Table 11.18.

LEACHING EQUIPMENT

In leaching processes, finely divided solids are contacted with solvents to remove soluble constituents. Usually some kind of multistage and countercurrent operation is desirable. The most bothersome aspect is handling of the wet solids.

In the leaching battery of Figure 14.20(a), the solids are transported between vessels with slurry pumps and are mixed in line with countercurrent solution from the next stage. For the process to be effective, the solids must settle freely. The tanks have sloped

TABLE 14.8. Performance of Centrifugal Extractors

SPECIFICATIONS[a]

Extractor	Model	Volume, m^3	Capacity, m^3/hr	rpm	Motor Mounting	Motor Power, kW	Diameter, m
Podbielniak	E 48	0.925	113.5	1,600	Side	24	1.2
Quadronic	Hiatchi 4848	0.9	72	1,500	Side	55	1.2
α-Laval	ABE 216	0.07	21	6,000	Top	30	
UPV			6	1,400	Bottom	14	
Luwesta	EG 10006		5	4,500	Bottom		
Robatel SGN	LX6 70NL	0.072	3.5	1,600	Top, side		1.3
Robatel BXP	BXP 800	0.220	50	1,000	Top	15	0.8
Westfalia	TA 15007	0.028	30	3,500	Top	63	0.7
SRL/ANL		0.003	0.05	3,500	Top		0.1
MEAB	SMCS-10	0.00012	0.3	22,000	Bottom		

[a] Operating pressures are in the range 300–1750 kPa; operating temperatures cover a very wide range; operating flow ratios cover the range $\frac{10}{1} - \frac{1}{10}$ easily.

PERFORMANCE

Extractor	System	rpm	$R = Q_h/Q_l$	Q_t, m^3/hr	Flooding, %	Number of Theoretical Stages
Podbielniak						
B-10	Kerosene-NBA[a]-water	3000	0.5	5.1	73	6–6.5
D-18	Kerosene-NBA-water	2000	0.5	11.1	58	5–5.5
A-1	Oil-aromatics-phenol[b]	5000	3.5	0.01–0.02	33–66	5–7.7
9000	Broth-penicillin B-pentacetate	2900	4.4	7.5		1.8
		2900	3.4	7.5	2.04	
		2900	2.4	7.5	2.21	
9500	Some system	2900	3.5	7.5	2.04	
		2700	3.5	7.5	2.19	
		2500	3.5	7.5		2.30
		2300	3.5	7.5		2.36
	Oil-aromatics-furfural	2000	4.0	12.0	90	3–6
A-1	IAA[c]-boric acid-water	5000	1–0.3	0.01–0.03	44–95	3.5–7.7
		3000	1.0	0.01	44	2.3
		4075	1.0	0.01	44	2.8
		4600	1.0	0.01	44	2.96
UPV	Oil-aromatics-phenol[b]	1400	0.8–1.2	6	75	2–5.8
Robatel SGN						
LX-168N	Uranyl nitrate-30% TBP	1500	1–0.2	2.1–4.5		7
LX-324	Some system	3100	1.6	24–63		3.4–3.9
SRL single stage	Uranyl nitrate-Ultrasene	1790	0.5–1.5	6.4–12	33–96	0.92–0.99
ANL single stage	Uranyl nitrate-TBP/dodacane	3500	0.3–4	0.8–1.6	50	0.97–1

[a] Normal butyl amine.
[b] Containing 1.7–5% water.
[c] Isoamyl alcohol.
[d] Number of theoretical and actual stages.
(M. Hafez, in Lo et al., 1983, pp. 459–474).

(a)

(b)

(c)
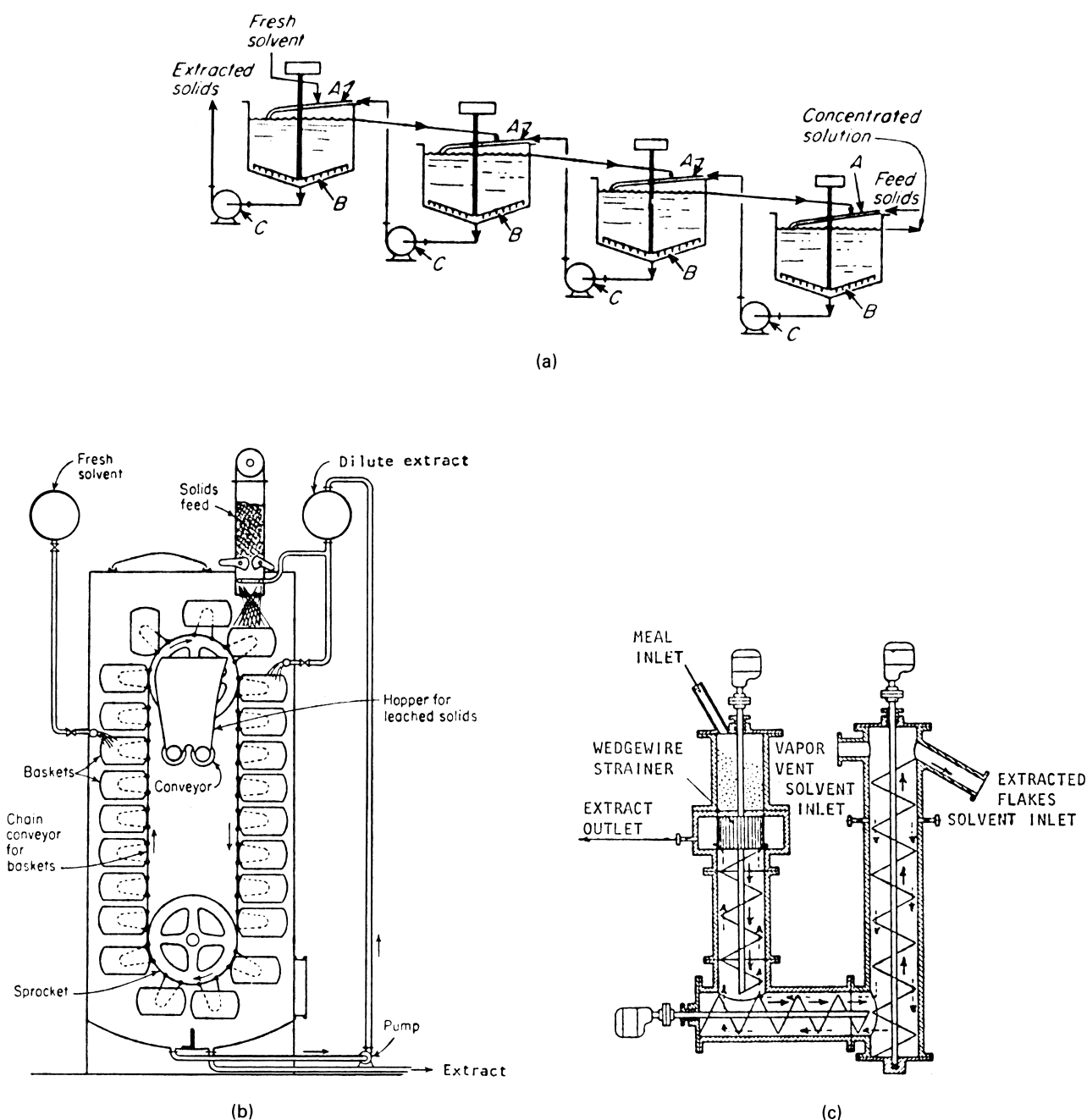
Figure 14.20. Continuous leaching equipment. (a) A battery of thickeners of the type shown, for example, in Figure 13.9(a), used in countercurrent leaching. The slurry is pumped between stages counter to the liquid flow: (*A*) mixing line for slurry and solution; (*B*) scraper arms; (C) = slurry pumps. (b) A bucket elevator with perforated buckets used for continuous extraction, named the Bollmann or Hansa–Muehle system [*Goss*, J. Am. Oil Chem. Soc. **23**, *348 (1946)*]. (c) A countercurrent leaching system in which the solid transport is with screw conveyors; a similar system is named Hildebrandt. (d) The Bonotto multi-tray tower extractor. The trays rotate while the solid is scraped and discharged from tray to tray. The solid transport action is similar to that of the rotary tray dryer of Figure 9.8(a) [*Goss*, J. Am. Oil Chem. Soc. **23**, *348 (1946)*]. (e) Rotocel extractor, which consists of about 18 wedge-shaped cells in a rotating shell. Fresh solvent is charged to the last cell and the drained solutions are pumped countercurrently to each cell in series (*Blaw-Knox Co.*).

bottoms and slowly moving rakes that scrape the solids towards the center discharge. Units employed for treating ores, for example, are very large, 100–200 ft dia. A few performance data of settlers are in Table 14.9.

Solids being extracted remain fixed in the cells of the battery of Figure 14.21(b). Fresh solvent is charged to the cell that is most

nearly exhausted and next to be taken off stream, then solution proceeds through the other cells in series and leaves as finished extract from the cell that has been charged most recently. For sugar beet extraction a battery normally consists of 10–14 cells. Cells have volumes ranging from 4–12 m^3 and height to diameter ratios as high as 1.5. Since leaching is faster at elevated temperatures, the

(d)

(e)
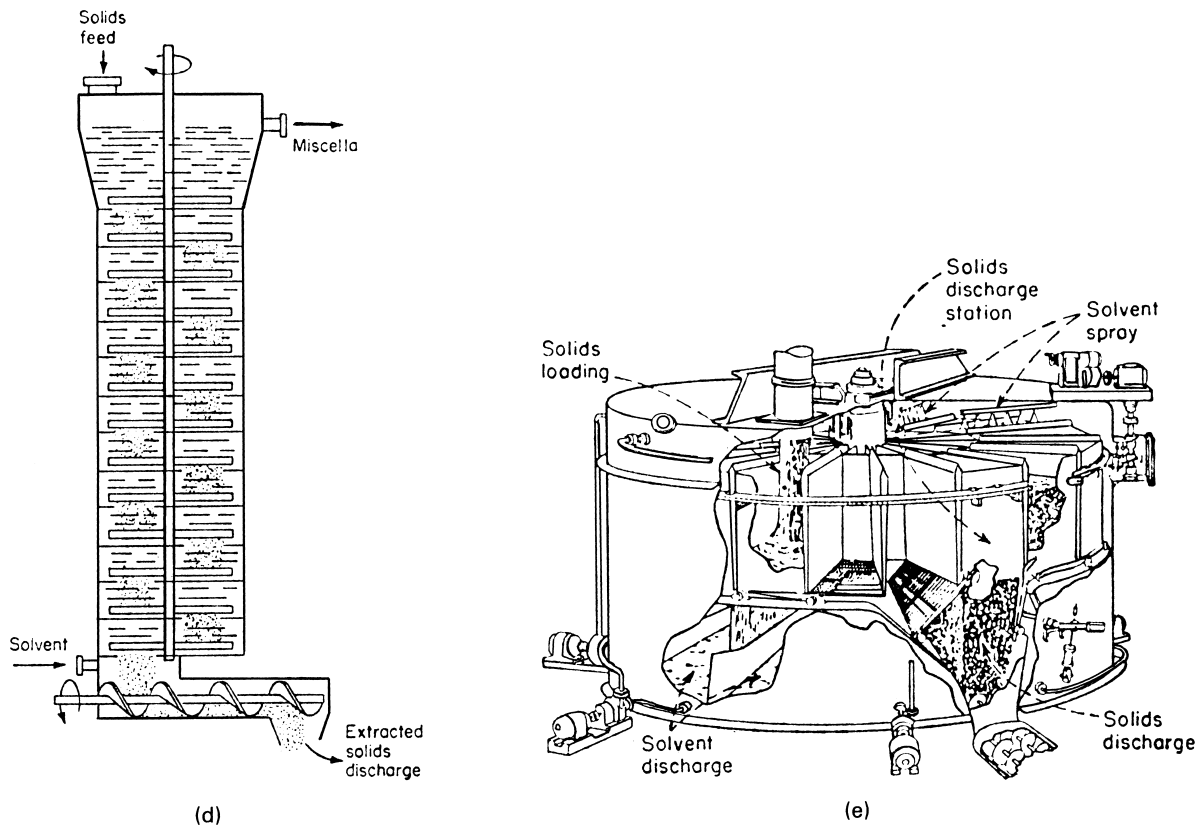
Figure 14.20.—(*continued***)**

solutions are heated between cells. Leaching time is 60–100 min. The amount of solution made is 110 kg/100 kg beets and contains 13–16% sugar. Various kinds of barks and seeds also are extracted in this kind of equipment. Further details of the equipment arrangement are given by Badger and McCabe (*Elements of Chemical Engineering*, McGraw-Hill, New York, 1936).

Continuous transport of the solids against the solution is employed in several kinds of equipment, including screw, perforated belt, and bucket conveyors. One operation carries a bed of seeds 3–4 ft thick on a perforated belt that moves only a few feet per minute. Fresh solvent is applied 1/5 to 1/3 of the distance from the discharge, percolates downward, is collected in pans, and is redistributed by pumps countercurrently to the travel of the material.

The vertical bucket elevator extractor of Figure 14.20(b) stands 40–60 ft high and can handle as much as 50 tons/hr with

1–2 HP. The buckets have perforated bottoms. As they start to descend, they are filled with fresh flaked material and sprayed with dilute intermediate extract. The solution percolates downward from bucket to bucket. As the travel turns upward, the buckets are subjected to countercurrent extraction with solution from fresh solvent that is charged about 1/3 the distance from the top. There is sufficient travel time for drainage before discharge of the spent flakes.

Countercurrent action is obtained in the Bonotto extractor of Figure 14.20(d). It has a number of trays arranged in vertical line and provided with scrapers to discharge solids through staggered openings in the trays. The principle of this mode of solid transport is similar to that of Figure 9.8(b). Solvent is charged at the bottom of the tower and leaves at the top, and the spent solid is removed with a screw conveyor.

TABLE 14.9. Performance of Settling Tanks

No.	Size (ft)	Slurry	Mesh	Rate of Feed (tons/day)	Solids in Feed	Solids in Under-flow (%)	Remarks
4	6 × 5	Paint pigment	300	39	5.7%	33	Solubles washed out
3	16 × 8	Iron oxide	300	162	10	33	C.C.D. washing
1	20 × 8	Zinc, copper, lead ore	99.5% −200	400	20	40	
2	25 × 10	Calcium carbonate	200	450 each	10	38	Feed is 14°Bé caustic liquor
1	40 × 10	Flotation tailings	65% −200	800	20	55	To recover the water
1	40 × 12	Flotation mill concentrates		1050	25	56	

(Hardinge Co.).
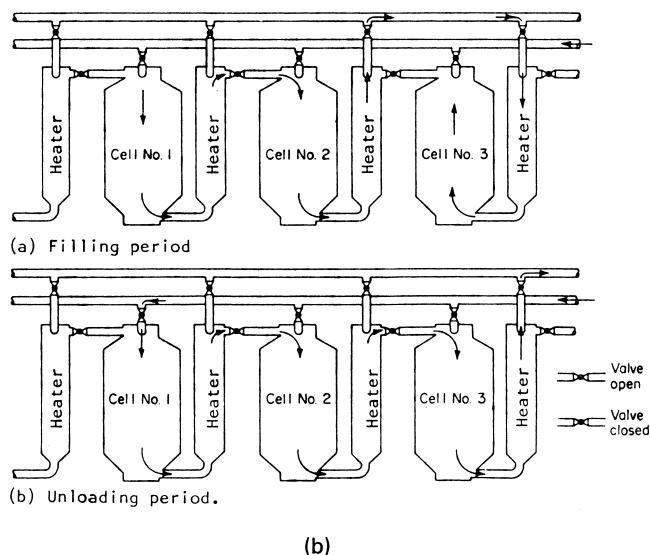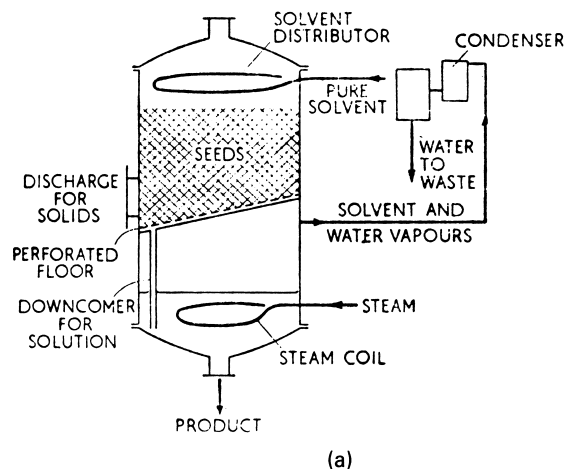
Figure 14.21. Single tank and battery of tanks as equipment for batch leaching. (a) A single tank extractor of the type used for recovering the oil from seeds. (b) Principle of the leaching battery. Cells are charged with solid and solvent is pumped through heaters and cells in series. In the figure, cell 1 has been exhausted and is being taken off stream and cell 3 has just been charged. (*Badger and McCabe*, Elements of Chemical Engineering, *McGraw-Hill, New York, 1936*.)

Few performance data of leaching equipment have found their way into the open literature, but since these processes have long been exploited, a large body of information must be in the files of manufacturers and users of such equipment.

14.8. PILOT-TESTING

It is highly recommend that all new extraction processes be pilot-tested before commercialization. Design models are especially useful when coupled with experimental verification. Use pilot tests to address four critical issues:

1. Demonstrate the full separation process.
2. Detect the effects of impurity buildup in the extraction loop.
3. Carefully analyze pilot data and evaluate scale-up of the contacting device (e.g., the packing material).
4. Evaluate solvent recovery.

In general, an extraction process involves an extractor and a solvent-recovery operation. The recovered solvent is recycled back to the extractor, making an extraction loop necessary. The feasibility of the loop must be demonstrated. This is especially important for chemical systems with complex and poorly understood phase equilibria. For example, a systems where the slope of the equilibrium line changes significantly with solute concentration may be prone to pinching.

If the solvent is nonvolatile, it can cause accumulation of heavy impurities in an extraction loop that are surface-active. Even in trace concentrations, these culprits can have a devastating effect on extractor performance. They can reduce the coalescing rates of drops—and thus reduce column capacity. Since most flooding models are based on pure-component tests, these models tend to be overly optimistic. Relative to a clean system, the presence of impurities can lower column capacity by 20% or more and efficiency by as much as 60%.

Pilot-testing of the extractor is useful for detecting other unforeseen problems. One should create an experimental design using available mass-transfer and hydraulic models, and then use an experimental vessel that permits viewing, if at all possible. Tests should vary the design solvent-to-feed ratio at a variety of loadings. In particular, the mechanisms and location of the flooding condition should be noted.

After successful completion of the pilot tests, the data should be analyzed carefully and compared against those predicted by the models. All deviations should be address carefully and then resolved before the commercial system is designed. For column-type extractors, the designer should not fail to allow for axial mixing effects. Axial mixing will reduce the concentration difference between the phases, and as a result, reduce the apparent efficiency of the contacting device. Axial mixing can be especially critical in the design of commercial-scale columns. Vendors of extraction equipment can be especially helpful regarding scale-up of their devices.

REFERENCES

W. Arlt, M. Macedo, P. Rasmussen, and J.M. Sorensen, *Liquid-Liquid Equilibrium Data Collection*, vol. V, Parts 1–4, DECHEMA Chemistry Data Series, Frankfurt, 1987.

P.J. Bailes, C. Hanson, M.A. Hughes, and M.W.T. Pratt, Extraction, liquid–liquid, *Encycl. Chem. Process. Des.* **21**, 19–125 (1984).

O. Becker, *Chemical Engineering and Technology*, **26**(1), 3 (2003).

S.W. Briggs and E.W. Comings, Ind. Chem., **35**(4), 1943.

A.E. Dunstan et al. (Eds.), in *Science of Petroleum*, Solvent extraction methods of refining, 1817–1929, Oxford University Press, Oxford, 1938, Section 28.

R.B. Eldridge, Ph.D. Dissertation, The University of Texas at Austin, 1986.

J.R. Grace, T. Wairegi, and T.H. Nguyen, *Trans. Instn. Chem. Engrs.* **54**, 167 (1976).

C. Hanson (Ed.), *Recent Advances in Liquid–Liquid Extraction*, Pergamon, New York, 1971.

E.J. Henley and J.D. Seader, *Equilibrium-Stage Separation Operations in Chemical Engineering*, Wiley, New York, 1981.

F. Jufu, L. Buqiang, and W. Zihao, *Chemical Engineering Science*, **41**(10), 2673 (1986).

A.E. Karr, Design scale up and application of the reciprocating plate extraction column, *Sep. Sci. Technol.* **15**, 877–905 (1980).

G.S. Laddha and T.E. Degaleesan, *Transport Phenomena in Liquid Extraction*, Tata McGraw-Hill, New York, 1978.

T.C. Lo, M.H.I. Baird, and C. Hanson, Eds., *Handbook of Solvent Extraction*, Wiley, New York, 1983.

T. Pilhofer, and R. Goedl, *Chem. Eng. Tech*. **49**, 431 (1977).

K.H. Reissinger and J. Schröter, Selection criteria for liquid–liquid extractors, *Chem. Eng*., 109–118 (6 Nov. 1978); also *Encycl. Chem. Process. Des*. **21**, 125–149 (1984).

G.M. Ritcey and A.W. Ashbrook, *Solvent Extraction with Applications to Process Metallurgy*, Elsevier, New York, 1979, Parts I, II.

L.A. Robbins, Liquid–liquid extraction, in Ref. 13, pp. 1.256–1.282; in *Chemical Engineers' Handbook*, McGraw-Hill, New York, 1984, pp. 15.1–15.20, 21.56–21.83.

J.A. Rocha, J.R. Fair, and J.L. Humphrey, *Ind. Eng. Chem. Proc. Des. Dev*. **25**, 862 (1986).

H. Sawistowski and W. Smith, *Mass Transfer Process Calculations*, Wiley, New York, 1963.

P.A. Schweitzer, Ed., *Handbook of Separation Techniques for Chemical Engineers*, McGraw-Hill, New York, 1979.

A.F. Seibert, and J.R. Fair, *Ind. Eng. Chem. Res*., **32**, 2213 (1993).

A.F. Seibert, J.R. Fair, and J.L. Bravo, *ISEC2002 Proceedings*, Vol. **2**, 1328 (2002).

A.F. Seibert, B.E. Reeves, and J.R. Fair, *Ind. Eng. Chem. Res*., **29**(9), 1901 (1990).

J.M. Sorensen and W. Arlt, *Liquid–Liquid Equilibrium Data Collection*, DECHEMA, Frankfurt/Main, Germany, 1979–1980.

R.E. Treybal, *Liquid Extraction*, McGraw-Hill, New York, 1951, 1963.

R.E. Treybal, *Mass Transfer Operations*, McGraw-Hill, New York, 1980.

T. Tsuboka and T. Katayama, Design algorithm for liquid-liquid separation processes, *J. Chem. Eng. Jpn*. **9**, 40–45 (1976).

S.M. Walas, *Phase Equilibria in Chemical Engineering*, Butterworths, Stoneham, MA, 1985.

J. Wisniak and A. Tamir, *Liquid–Liquid Equilibrium and Extraction Bibliography*, Elsevier, New York, 1980.

J. Wisniak and A. Tamir, *Phase Diagrams: A Literature Source Book*, Elsevier, New York, 1981.

Z. Ziolkowski, *Liquid Extraction in the Chemical Industry* (in Polish), PWT, Warsaw, 1961.

15

ADSORPTION AND ION EXCHANGE

Separation of the components of a fluid can be effected by contacting them with a solid that has a preferential attraction for some of them. Such processes are quantitatively significant when the specific surfaces of the solids are measured in hundreds of m²/g. Suitable materials are masses of numerous fine pores that were generated by expulsion of volatile substances. The most important adsorbents are activated carbon, prepared by partial volatilization or combustion of a carbonaceous body, and activated alumina, silica gel, and molecular sieves which are all formed by expulsion of water vapor from a solid. The starting material for silica gel is a coagulated silicic acid and that for molecular sieves is hydrated aluminum silicate crystals that end up as porous crystal structures. Porous glasses made by leaching with alkai have some application in chromatography. Physical properties of common adsorbents are listed in Tables 15.1 and 15.2. Representative manufacturing processes are represented on Figure 15.1.

The amount of adsorption is limited by the available surface and pore volume, and depends also on the chemical natures of the fluid and solid. The rate of adsorption also depends on the amount of exposed surface but, in addition, on the rate of diffusion to the external surface and through the pores of the solid for accessing the internal surface which comprises the bulk of the surface. Diffusion rates depend on temperature and differences in concentration or partial pressures. The smaller the particle size, the greater is the utilization of the internal surface, but also the greater the pressure drop for flow of bulk fluid through a mass of the particles.

Adsorption and ion exchange are considered together because they share many common features, including design concepts and, in some cases, operating cycles, although ion exchange operating cycles are somewhat more complex.

In ion exchange equipment, cations or anions from the fluid deposit in the solid and displace equivalent amounts of other ions from the solid. Suitable solids are not necessarily porous; the ions are able to diffuse through the solid material. A typical exchange is that of H^+ or OH^- ions from the solid for some undesirable ions in the solution, such as Ca^{++} or SO_4^{--}. Eventually all of the ions in the solid are replaced, but the activity is restored by contacting the exhausted solid with a high concentration of the desired ion, for example, a strong acid to replace lost hydrogen ions.

For economic reasons, saturated adsorbents and exhausted ion exchangers must be regenerated. Most commonly, saturation and regeneration are performed alternately and intermittently, but equipment can be devised in which these processes are accomplished continuously by countercurrent movement of the solid and fluid streams. Only a few such operations have proved economically feasible. The UOP and Toray processes for liquid adsorption are not true continuous processes but are effectively such.

Desorption is accomplished by elevating the temperature, or reducing the pressure, or by washing with a suitable reagent. The desorbed material may be recovered as valuable product in concentrated form or as a waste in easily disposable form. Adsorbent carbons used for water treating often must be regenerated by ignition in a furnace. Relatively small amounts of adsorbents that are difficult to regenerate are simply discarded.

15.1. ADSORPTION EQUILIBRIA

The amount of adsorbate that can be held depends on the concentration or partial pressure and temperature, on the chemical nature of the fluid, and on the nature, specific surface, method of preparation, and regeneration history of the solid. For single adsorbable components of gases, the relations between amount adsorbed and the partial pressure have been classified into the six types shown in Figure 15.2. Many common systems conform to Type I, for example, some of the curves of Figure 15.3. Adsorption data are not highly reproducible because small contents of impurities and the history of the adsorbent have strong influences on their behavior.

One of the simplest equations relating amount of adsorption and pressure with some range of applicability is that of Freundlich,

$$w = aP^n \tag{15.1}$$

and its generalization for the effect of temperature

$$\omega = aP^n \exp(-b/T). \tag{15.2}$$

The exponent n usually is less than unity. Both gas and liquid adsorption data are fitted by the Freundlich isotherm. Many liquid data are fitted thus in a compilation of Landolt-Börnstein, (1956) but their gas data are presented in graphical form only (LB IV 4/b, 1972, pp. 121–187). The effect of temperature also is correlated by a theory of Polanyi, whereby all data of a particular system fall on the same curve; Figure 15.4 is an example. For isothermal data, a combination of the Freundlich and Langmuir equations was developed by Yon and Turnock (1971).

$$w = kP^n/(1 + kP^n). \tag{15.3}$$

Individual components of multicomponent mixtures compete for the limited space on the adsorbent. Equilibrium curves of binary mixtures, when plotted as x vs. y diagrams, resemble those of vapor–liquid mixtures, either for gases (Fig. 15.5) or liquids (Fig. 15.6). The shapes of adsorption curves of binary mixtures, Figure 15.7, are varied; the total adsorptions of the components of the pairs of Figure 15.7 would be more nearly constant over the whole range of compositions in terms of liquid volume fractions rather than the mol fractions shown. Fig 15.8 shows the variation of isosteric parts of adsorption between polar and nonpolar adsorbates.

Higher molecular weight members of homologous series adsorb preferentially on some adsorbents. The desorption data of

TABLE 15.1. Physical Properties of Adsorbents

	Particle Form[*]	Mesh Size	Effective Diameter D_p, ft.	Bulk Density P_b, Lb/cu.ft.	External Void Fraction F_a	External Surface a_v, sq.ft.	Specific Heat C_x, Btu/lb °F	Reactivation Temperature °F	Examples
Activated Carbon . . .	P	4 × 6	0.0128	30	0.34	310	0.25	200–1000	Columbia L
	P	6 × 8	0.0092	30	0.34	446	''	'' ''	'' ''
	P	8 × 10	0.0064	30	0.34	645	''	'' ''	'' ''
	G	4 × 10	0.0110	30	0.40	460	0.25	'' ''	Pittsburgh BPL
	G	6 × 16	0.0062	30	0.40	720	''	'' ''	''
	G	4 × 10	0.0105	28	0.44	450	''	'' ''	Witco 256
Silica Gel	G	3 × 8	0.0127	45	0.35	230	0.22	250–450	Davison 03
	G	6 × 16	0.0062	45	0.35	720	''	'' ''	'' ''
	S	4 × 8	0.0130	50	0.36	300	0.25	300–450	Mobil Sorbead R
Activated Alumina . .	G	4 × 8	0.0130	52	0.25	380	0.22	350–600	Alcoa Type F
	G	8 × 14	0.0058	52	0.25	480	''	'' ''	'' '' ''
	G	14 × 28	0.0027	54	0.25	970	''	'' ''	'' '' ''
	S	(1/4″)	0.0208	52	0.30	200	0.22	350–1000	Alcoa Type H
	S	(1/8″)	0.0104	54	0.30	400	''	'' ''	'' '' ''
Molecular Sieves . . .	G	14 × 28	0.0027	30	0.25	970	0.23	300–600	Davison, Linde
	P	(1/16″)	0.0060	45	0.34	650	''	'' ''	''
	P	(1/8″)	0.0104	45	0.34	400	''	'' ''	''
	S	4 × 8	0.0109	45	0.37	347	''	'' ''	''
	S	8 × 12	0.0067	45	0.37	565	''	'' ''	''

[*]P = pellets; G = granules; S = spheroids
(Fair, 1969; Walas, 1988).

TABLE 15.2. Data of Molecular Sieves

(a) Structures and Applications

Framework	Cationic Form	Formula of Typical Unit Cell	Window	Effective Channel Diameter (Å)	Application
A	Na	$Na_{12}[(AlO_2)_{12}(SiO_2)_{12}]$	8-ring (obstructed)	3.8	Desiccant. CO_2 removal from natural gas
	Ca	$Ca_5Na_2[(AlO_2)_{12}(SiO_2)_{12}]$	8-ring (free)	4.4	Linear paraffin separation. Air separation
	K	$K_{12}[(AlO_2)_{12}(SiO_2)_{12}]$	8-ring (obstructed)	2.9	Drying of cracked gas containing C_2H_4, etc.
X	Na	$Na_{86}[(AlO_2)_{86}(SiO_2)_{106}]$	12-ring	8.4	Pressure swing H_2 purification
	Ca	$Ca_{40}Na_6[(AlO_2)_{86}(SiO_2)_{106}]$	12-ring	8.0	Removal of mercaptans from natural gas
	Sr, Ba[a]	$Sr_{21}Ba_{22}[(AlO_2)_{86}(SiO_2)_{106}]$	12-ring	8.0	Xylene separation
Y	Na	$Na_{56}[(AlO_2)_{56}(SiO_2)_{136}]$	12-ring	8.0	Xylene separation
	K	$K_{56}[(AlO_2)_{56}(SiO_2)_{136}]$	12-ring	8.0	Xylene separation
Mordenite	Ag	$Ag_8[(AlO_2)_8(SiO_2)_{40}]$	12-ring	7.0	I and Kr removal from nuclear off-gases[32–34]
	H	$H_8[(AlO_2)_8(SiO_2)_{40}]$			
Silicalite	—	$(SiO_2)_{96}$	10-ring	6.0	Removal of organics from water
ZSM-5	Na	$Na_3[(AlO_2)_3(SiO_2)_{93}]$	10-ring	6.0	Xylene separation[31]

[a]Also K-BaX.
(Ruthven, 1984; Walas, 1988).

Figure 15.12b attest to this, the hydrogen coming off first and the pentane last. In practical cases it is not always feasible to allow sufficient time for complete removal of heavy constituents so that the capacity of regenerated adsorbent becomes less than that of fresh, as Figure 15.9 indicates. Repeated regeneration causes gradual deterioration of adsorbent; Figure 15.10 reports this for a molecular sieve operation.

Representation and generalization of adsorption equilibria of binary and higher mixtures by an equation is desirable, but less progress has been made for such systems than for vapor–liquid or liquid–liquid equilibria. The Yon and Turnock equations (1971) applied to components 1 and 2 of binary mixtures are

$$w_1/w_{1,\text{sat}} = k_1 P_1^{n_1} \theta, \tag{15.4}$$

$$w_2/w_{2,\text{sat}} = k_2 P_2^{n_2} \theta, \tag{15.5}$$

$$\theta = 1/(1 + k_1 P_1^{n_1} + k_2 P_2^{n_2}). \tag{15.6}$$

TABLE 15.2.—(continued**)**

(b) Typical Properties of Union Carbide Type X Molecular Sieves

Basic Type	Nominal pore Diameter, Angstroms	Available Form	Bulk Density, lb/ft³	Heat of Adsorption (max), Btu/lb H₂O	Equilibrium H₂O capacity, % wt	Molecules Adsorbed	Molecules Excluded	Applications
3A	3	Powder	30	1800	23	Molecules with an effective diameter < 3 Å, including H_2O and NH_3	Molecules with an effective diameter > 3 Å, e.g., ethane	The preferred molecular sieve adsorbent for the commercial dehydration of unsaturated hydrocarbon streams such as cracked gas, propylene, butadiene, and acetylene. It is also used for drying polar liquids such as methanol and ethanol.
		1/16-in pellets	44		20			
		1/8-in pellets	44		20			
4A	4	Powder	30	1800	28.5	Molecules with an effective diameter < 4 Å, including ethanol, H_2S, CO_2, SO_2, C_2H_4, C_2H_6, and C_3H_6	Molecules with an effective diameter > 4 Å, e.g., propane	The preferred molecular sieve adsorbent for static dehydration in a closed gas or liquid system. It is used as a static desiccant in household refrigeration systems; in packaging of drugs, electronic components and perishable chemicals; and as a water scavenger in paint and plastic systems. Also used commercially in drying saturated hydrocarbon streams.
		1/16-in pellets	45		22			
		1/8-in pellets	45		22			
		8 × 12 beads	45		22			
		4 × 8 beads	45		22			
		14 × 30 mesh	44		22			
5A	5	Powder	30	1800	28	Molecules with an effective diameter < 5 Å, including n-C_4H_9OH, † n-C_4H_{10}, † C_3H_5 to $C_{22}H_{46}$, R-12	Molecules with an effective diameter > 5 Å, e.g., iso compounds and all 4-carbon rings	Separates normal paraffins from branched-chain and cyclic hydrocarbons through a selective adsorption process.
		1/16-in pellets	43		21.5			
		1/8-in pellets	43		21.5			
10X	8	Powder	30	1800	36	Iso paraffins and olefins, C_6H_6, molecules with an effective diameter < 8 Å	Di-n-butylamine and larger	Aromatic hydrocarbon separation.
		1/16-in pellets	36		28			
		1/6-in pellets	36		28			
13X	10	Powder	30	1800	36	Molecules with an effective diameter < 10 Å	Molecules with an effective diameter > 10 Å, e.g., $(C_4F_9)_3N$	Used commercially for general gas drying, air plant feed purification (simultaneous removal of H_2O and CO_2), and liquid hydrocarbon and natural gas sweetening (H_2S and mercaptan removal).
		1/16-in pellets	38		28.5			
		1/8-in pellets	38		28.5			
		8 × 12 beads	42		28.5			
		4 × 8 beads	42		28.5			
		14 × 30 mesh	38		28.5			

(Kovach, 1978; Walas, 1988).

They have been found useful as an empirical correlation method for adsorption on molecular sieves (Maurer, 1980). Other attempts at prediction or correlation of multicomponent adsorption data are reviewed by Ruthven (1984). In general, however, multicomponent equilibria are not well correlatable in general form so that design of equipment is best based on direct laboratory data with the exact mixture and the exact adsorbent at anticipated pressure and temperature.

Adsorption processes are sensitive to temperature, as the data of Figures 15.3, 15.5, and 15.11 show. Thus practical adsorption process are complicated by the substantial heats of adsorption that necessarily develop. These are of the same order of magnitude as heats of condensation. Some data are in Figure 15.8.

15.2. ION EXCHANGE EQUILIBRIA

Ion exchange is a chemical process that can be represented by a stoichiometric equation, for example, when ion A in solution replaces ion B in the solid phase,

$$A(solution) + B(solid) \rightleftharpoons A(solid) + B(solution) \qquad (15.7)$$

or

$$A + \bar{B}/\bar{A} + B, \qquad (15.8)$$
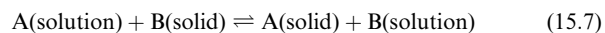
where the overstrike designates a component in the solid phase. The equilibrium constant is called the selectivity, designated by K_{AB},

(a)

(b)

(c)
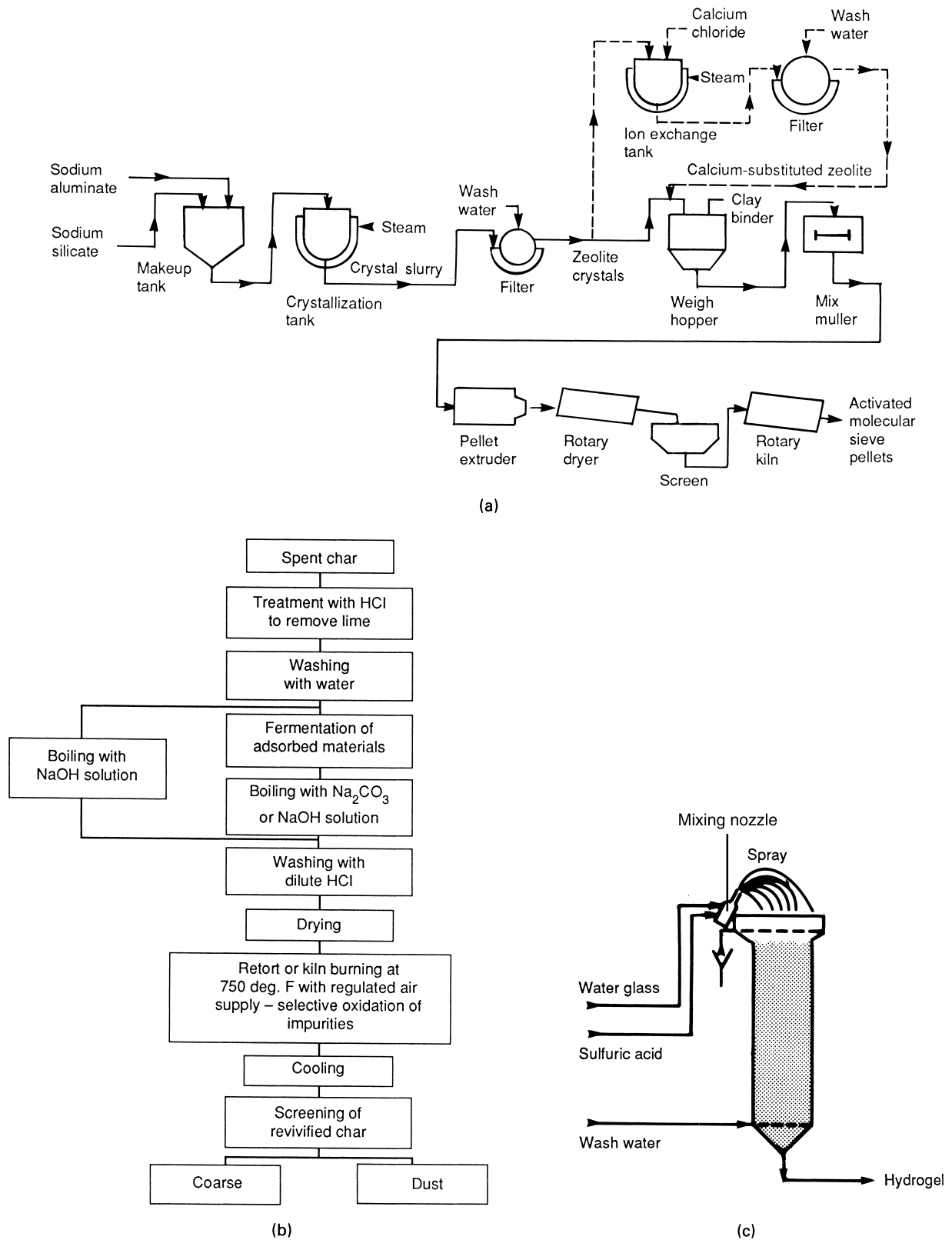
Figure 15.1. Processes for making adsorbents. (a) Flowsketch of a process for making molecular sieve adsorbents. (b) Process for reactivation of bone char. (c) Silica gel by the BASF process. The gel is formed and solidifies in air from sodium silicate and sulfuric acid, then is washed free of sodium sulfate with water (*Ullmann, Encyclopedia of Chemical Technology, Verlag Chemie, Weinheim, Germany*).
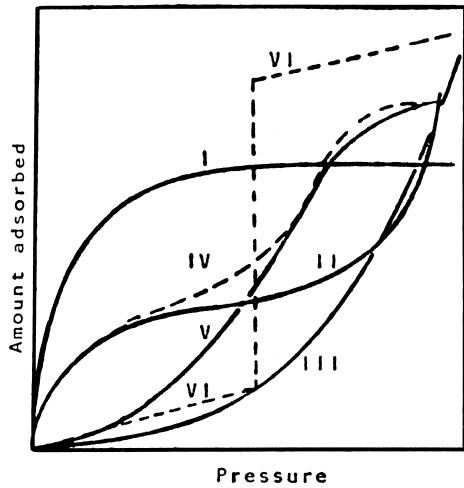
Figure 15.2. Types of adsorption isotherms: (I) monomolecular layer; (II and III) multimolecular layers; (IV and V) multimolecular layers and condensation in pores; (VI) phase transition of a monomolecular layer on the surface (*after Brunauer 1945*). (Walas, 1988).

Figure 15.4. Polanyi characteristic curve for effect of temperature on adsorption of *n*-butane on silica gel [*Al-Sahhat* (*1981*)]. (Walas, 1988).

$$K_{AB} = C_{\bar{A}} C_B / C_A C_{\bar{B}} \tag{15.9}$$

$$= x_{\bar{A}} x_B / x_A x_{\bar{B}} \tag{15.10}$$

$$= \left[\frac{x_{\bar{A}}}{1 - x_{\bar{A}}} \right] / \left[\frac{x_A}{1 - x_A} \right]. \tag{15.11}$$

The last equation relates the mol fractions of the ion originally in the solution at equilibrium in the liquid (x_A) and solid ($x_{\bar{A}}$) phases.

The residual mol fraction in the liquid phase corresponding to a given mol fraction or degree of saturation in the solid phase is

$$x_A = \frac{1}{1 + K_{AB}(1 - x_{\bar{A}})/x_{\bar{A}}}. \tag{15.12}$$

Approximate values of the selectivity of various ions are shown in Table 15.4 (b)(c) for a particular pair, K_{AB} is the ratio of tabulated values for each.

When the exchanged ion D is divalent, the reaction is

$$D + 2\bar{B} \rightleftharpoons \bar{D} + 2B, \tag{15.13}$$

Figure 15.3. Effects of temperature, pressure, and kind of adsorbent on the amount of ethane adsorbed: (1) activated carbon at 25°C; (2) type 4A molecular sieve (MS) at 0°C; (3) type 5A MS at 25°C; (4) type 4A MS at 25°C; (5) type 4A MS at 75°C; (6) silica gel at 25°C; (7) type 4A MS at 150°C. (*Data from Union Carbide Corp.*) (Walas, 1988).
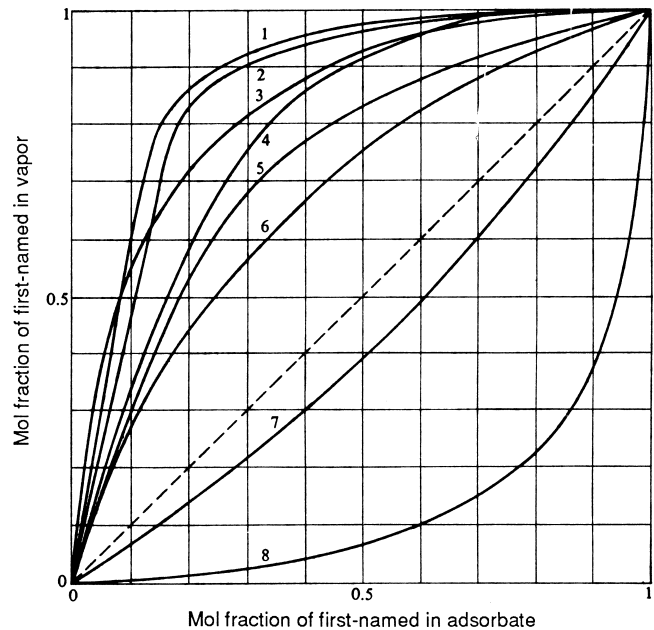
Figure 15.5. Adsorption of binary mixtures: (1) ethane + ethylene. Type 4A MS 25°C, 250 Torr; (2) ethane + ethylene. Type 4A MS, 25°C, 730 Torr; (3) ethane + ethylene. Type 4A MS, 75°C, 730 Torr; (4) carbon dioxide + hydrogen sulfide. Type 5A MS, 27°C, 760 Torr; (5) *n*-pentane + *n*-hexane, type 5A MS, 100°C, 760 Torr; (6) ethane + ethylene, silica gel, 25°C, 760 Torr; (7) ethane + ethylene, Columbia G carbon, 25°C, 760 Torr; (8) acetylene + ethylene. Type 4A MS, 31°C, 740 Torr. (*Data from Union Carbide Corp.*) (Walas, 1988).
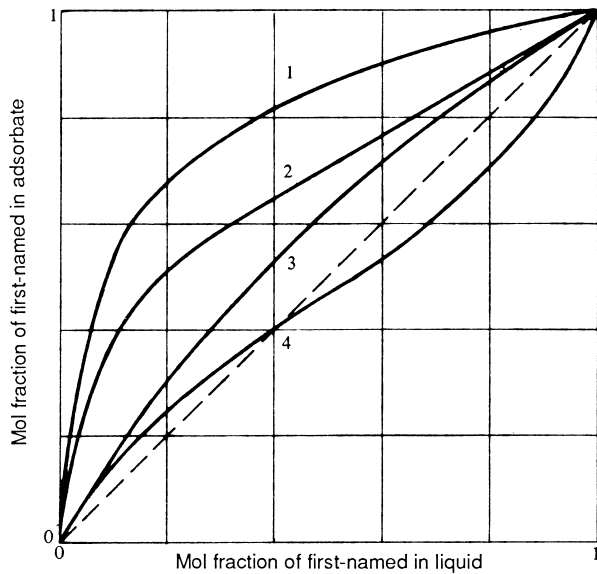
Figure 15.6. Binary liquid adsorption equilibria on $X - Y$ diagrams: (1) toluene + iso-octane on silica gel (Eagle and Scott, 1950); (2) toluene + iso-octane on charcoal (Eagle and Scott, 1950); (3) ethylene dichloride + benzene on boehmite (Kipling); (4) ethylene dichloride + benzene on charcoal (Kipling). (*Kipling, 1957*), (Walas, 1988).

and the equilibrium constant or selectivity is given by

$$(\bar{C}/C)K_{DB} = x_B^2 x_{\bar{D}} / x_B^2 x_D \tag{15.14}$$

$$= (x_{\bar{D}}/x_D)[(1 - x_D)/(1 - x_{\bar{D}})]^2, \tag{15.15}$$
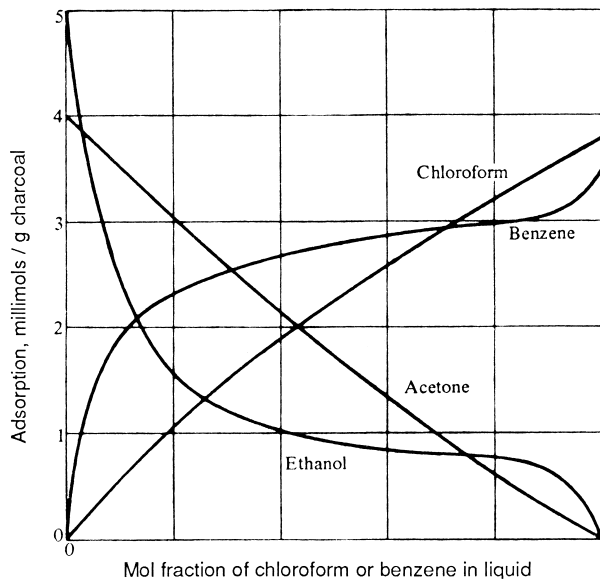
Figure 15.7. Adsorption of liquid mixtures on charcoal. Chloroform + acetone and benzene + ethanol. The ordinate gives the amount of each individual substance that is adsorbed, the abscissa the mol fraction of chloroform (mixed with acetone) or the mol fraction of benzene (mixed with ethanol). (*Data gathered by Kipling, 1965*). (Walas, 1988).
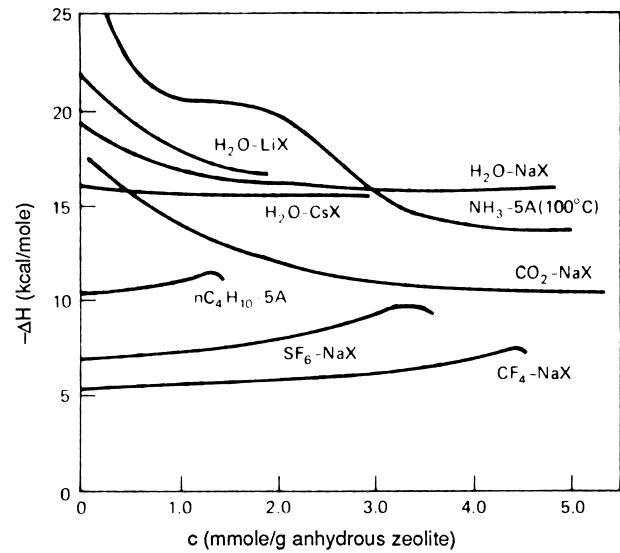
Figure 15.8. Variation of isosteric heat of adsorption with coverage showing the difference in trends between polar and nonpolar sorbates. $nC_4H_{10} - 5A$ (data of Schirmer et al.); $CF_4 - NaX$, $SF_6 - NaX$ (data of Barrer and Reucroft); $CO_2 - NaX$, (data of Huang and Zwiebel), $NH_3 - 5A$ (data of Schirmer et al.); $H_2O - LiX$, NaX, and CsX, (data of Avgul et al.). (*Ruthuen, 1976*). (Walas, 1988).

where C and $\bar{C}$ are the total concentrations of the two kinds of ions in the solution and in the solid, respectively.

Example 15.1 is concerned with such an exchange and regeneration process.

15.3. ADSORPTION BEHAVIOR IN PACKED BEDS

Adsorption is performed most commonly in fixed vertical beds of porous granular adsorbents. Flow of adsorbing fluid usually is down through the bed, that of regenerant usually is upward. Moving and fluidized beds have only a limited application in the field.

If the time is sufficient, the adsorbent nearer the inlet of the fluid becomes saturated at the prevailing inlet fluid concentration but a concentration gradient develops beyond the saturation zone. Figure 15.9 depicts this behavior. The region of falling concentration is called the mass transfer zone (MTZ). The gradient is called the adsorption wave front and is usually S-shaped. When its leading edge reaches the exit, breakthrough is said to have been attained. Practically, the breakthrough is not regarded as necessarily at zero concentration but at some low value such as 1% or 5% of the inlet concentration that is acceptable in the effluent. A hypothetical position, to the left of which in Figure 15.9(b) the average adsorbate content equals the saturation value, is called the stoichiometric front. The distance between this position and the exit of the bed is called the length of unused bed (LUB). The exhaustion time is attained when the effluent concentration becomes the same as that of the inlet, or some practical high percentage of it, such as 95 or 99%.

The shape of the adsorption front, the width of the MTZ, and the profile of the effluent concentration depend on the nature of the adsorption isotherm and the rate of mass transfer. Practical bed depths may be expressed as multiples of MTZ, values of 5–10 multiples being economically feasible. Systems that have linear adsorption isotherms develop constant MTZs whereas MTZs of convex ones (such as Type I of Figure 15.2 become narrower, and those of concave systems become wider as they progress through
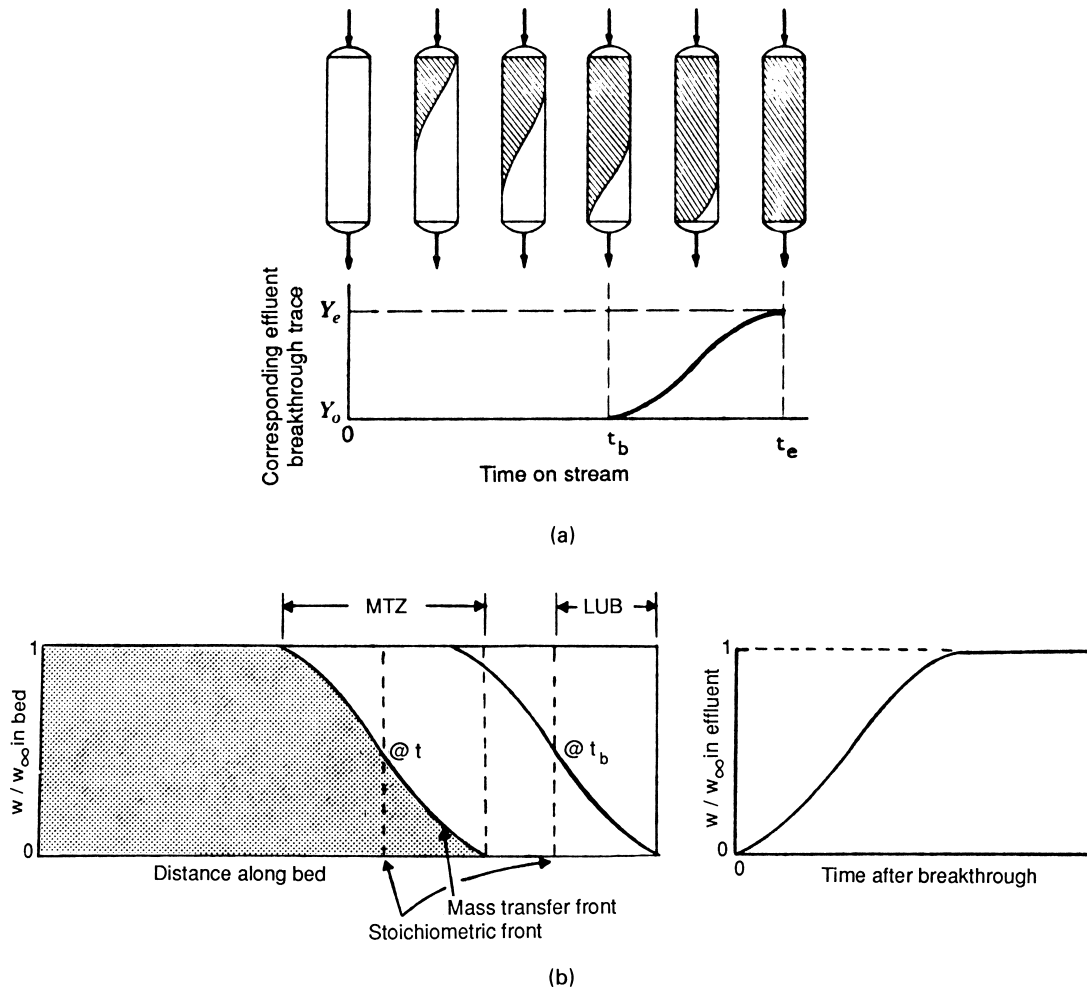
Figure 15.9. Concentrations in adsorption beds as a function of position and of effluent as a function of time. (a) Progress of a stable mass transfer front through an adsorption bed and of the effluent concentration (*Lukchis, 1973*). (b) The mass transfer zone (MTZ), the length of unused bed (LUB), stoichiometric front, and profile of effluent concentration after breakthrough.

the bed. The last types are called unfavorable isotherms; separations in such cases usually are accomplished more economically by some other kind of process. The narrower the MTZ, the greater the degree of utilization of the bed.

The rate of mass transfer from fluid to solid in a bed of porous granular adsorbent is made up of several factors in series:

1. Diffusion to the external surface.
2. Deposition on the surface.
3. Diffusion in the pores.
4. Diffusion along the surface.

Various combination of shapes of isotherms and mass transfer factors have been taken into account by solutions of the problem in the literature. One of the simpler cases was adopted by Hougen and Marshall (1947, see Figure 15.13), who took a linear isotherm and diffusion to the external surface as controlling the rate. They developed the solution in analytical form, of which several approximations that are easier to use are mentioned for instance by Vermeulen et al. (1984, p. 16.28). A graphical form of the solution appears in Figure 15.13. This shows the effluent concentration

ratio, C/C_0, in terms of a time parameter τ, at a number of values of a parameter Z', which involves the bed length Z. In Example 15.2, this chart is used to find the concentration profile of the effluent, the break and exhaustion times, and the % utilization of the adsorbent bed. In this case, the model affords a fair comparison with experimental data.

Many investigations have been conducted of the mass transfer coefficient at the external surfaces of particles and of other diffusional mechanisms. Some of the correlations are discussed in Chapters 13 and 17. A model developed by Rosen (1954) takes into account both external film and pore diffusional resistance to mass transfer together with a linear isotherm. A numerical example is worked out by Hines and Maddox (1985, p. 485).

In the model developed by Thomas (1944), the controlling mechanism is the surface kinetics represented by the Langmuir isotherm. Extensions of this work by Vermeulen et al. (1984) incorporate external surface and pore diffusional resistances.

No comprehensive comparisons of the several models with each other and with experimental data appear to have been published.

(1) At end of adsorption.

(2) At end of regeneration.

(3) Useful capacity of cycle.
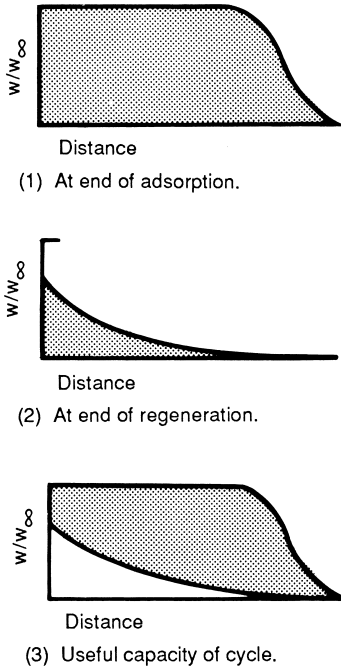
Figure 15.10. Incomplete regeneration of adsorbent bed by a thermal-swing cycle.
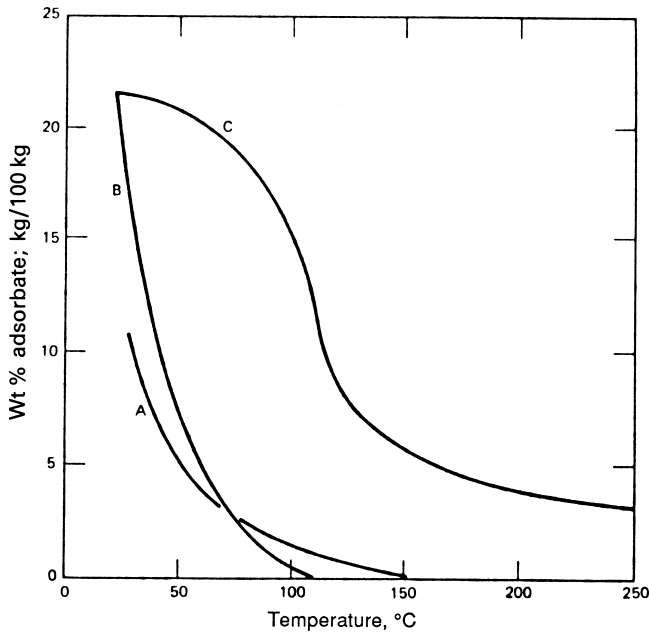
Figure 15.11. Effect of temperature on molecular sieve type 5A, silica gel and activated alumina at water vapor pressure, 13.3 kPa (100 mm Hg). A, molecular sieve type 5A; B, silica-type adsorbent; C, alumina-type adsorbent. (*Chi and Cummings, 1978*; Walas, 1988).

TABLE 15.3. Gas Phase Adsorption Cycles, Steam Requirements, and Operation

(a) Typical Cycle Times for Adsorber Operation

	High Pressure Gas Dryer		Organic Solvent Recovery Unit	
	A	B	A	B
Onstream	24	24	2.00	1.00
Depressure/purge	2	1	.....	.....
Hot gas	10	13	.....	.....
Steam	...	...	0.75	0.67
Hot gas	...	...	0.33	.....
Cold gas	5	8	0.42	0.33
Pressure/standby	7	2	0.50	.....
	24	24	2.00	1.00

(Fair, 1969; Walas, 1988).

(b) Steam/Solvent Ratios and Amount of Adsorbate for a Coconut-Shell Carbon 6–12 Mesh, 1200 m^2/g
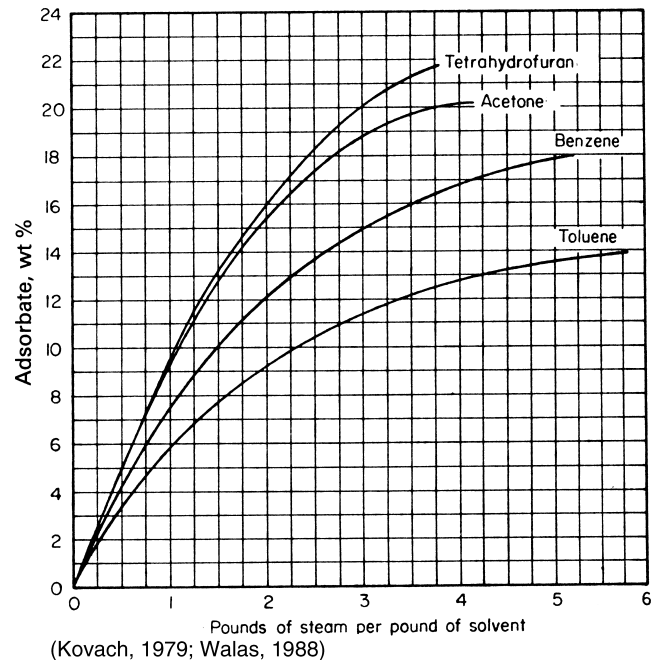
(Kovach, 1979; Walas, 1988)

(c) Typical Operating Parameters for Gas Phase Adsorption

	Range	Design
Superficial gas velocity	20 to 50 cm/s (40 to 100 ft/min)	40 cm/s (80 ft/min)
Adsorbent bed depth	3 to 10 MTZ	5 MTZ
Adsorption time	0.5 to 8 h	4 h
Temperature	−200 to 50°C	
Inlet concentration		
Adsorption base	100 to 5000 vppm	
LEL base	40%	
Adsorbent particle size	0.5 to 10 mm	4 to 8 mm
Working charge	5 to 20% wt	10%
Steam solvent ratio	2:1 to 8:1	4:1
Adsorbent void volume	38 to 50%	45%
Steam regeneration temperature	105 to 110°C	
Inert gas regenerant temperature	100 to 300°C	
Regeneration time	1/2 adsorption time	
Number of adsorbers	1 to 6	2 to 3

(Kovach, 1979; Walas, 1988).

TABLE 15.4. Properties of Ion-Exchange Materials

(a) Physical Properties

Material	Shape* of particles	Bulk wet density (drained). kg/L	Moisture content (drained). % by weight	Swelling due to exchange. %	Maximum operating temperature. [†] °C	Operating pH range	Exchange capacity Dry, equvialent/kg	Exchange capacity Wet, equivalent/L
Cation exchangers: strongly acidic								
Polystyrene sulfonate								
Homogeneous (gel) resin	S				120–150	0–14		
4% cross-linked		0.75–0.85	64–70	10–12			5.0–5.5	1.2–1.6
6% cross-linked		0.76–0.86	58–65	8–10			4.8–5.4	1.3–1.8
8–10% cross-linked		0.77–0.87	48–60	6–8			4.6–5.2	1.4–1.9
12% cross-linked		0.78–0.88	44–48	5			4.4–4.9	1.5–2.0
16% cross-linked		0.79–0.89	42–46	4			4.2–4.6	1.7–2.1
20% cross-linked		0.80–0.90	40–45	3			3.9–4.2	1.8–2.0
Macroporous structure 10–12% cross-linked	S	0.81	50–55	4–6	120–150	0–14	4.5–5.0	1.5–1.9
Sulfonated phenolic resin	G	0.74–0.85	50–60	7	50–90	0–14	2.0–2.5	0.7–0.9
Sulfonated coal	G							
Cation exchangers: weakly acidic								
Acrylic (pK 5) or methacrylic (pK 6)								
Homogeneous (gel) resin	S	0.70–0.75	45–50	20–80	120	4–14	8.3–10	3.3–4.0
Macroporous	S	0.67–0.74	50–55	10–100	120		∼8.0	2.5–3.5
Phenolic resin	G	0.70–0.80	∼50	10–25	45–65	0–14	2.5	1.0–1.4
Polystyrene phosphonate	G, S	0.74	50–70	< 40	120	3–14	6.6	3.0
Polystyrene aminodiacetate	S	0.75	68–75	< 100	75	3–14	2.9	0.7
Polystyrene amidoxime	S	∼0.75	58	10	50	1–11	2.8	0.8–0.9
Polystyrene thiol	S	∼0.75	45–50		60	1–13	∼5	2.0
Cellulose								
Phosphonate	F						∼7.0	
Methylene carboxylate	F, P, G						∼0.7	
Greensand (Fe silicate)	G	1.3	1–5	0	60	6–8	0.14	0.18
Zeolite (Al silicate)	G	0.85–0.95	40–45	0	60	6–8	1.4	0.75
Zirconium tungstate	G	1.15–1.25	∼5	0	> 150	2–10	1.2	1.0
Anion exchangers: strongly basic								
Polystyrene-based								
Trimethyl benzyl ammonium (type I)								
Homogeneous, 8% CL	S	0.70	46–50	∼20	60–80	0–14	3.4–3.8	1.3–1.5
Macroporous, 11% CL	S	0.67	57–60	15–20	60–80	0–14	3.4	1.0
Dimethyl hydroxyethyl ammonium (type II)								
Homogeneous, 8% CL	S	0.71	∼42	15–20	40–80	0–14	3.8–4.0	1.2
Macroporous, 10% CL	S	0.67	∼55	12–15	40–80	0–14	3.8	1.1
Acrylic-based								
Homogeneous (gel)	S	0.72	∼70	∼15	40–80	0–14	∼5.0	1.0–1.2
Macroporous	S	0.67	∼60	∼12	40–80	0–14	3.0–3.3	0.8–0.9
Cellulose-based								
Ethyl trimethyl ammonium	F				100	4–10	0.62	
Triethyl hydroxypropyl ammonium					100	4–10	0.57	
Anion exchangers: intermediately basic (pK 11)								
Polystyrene-based	S	0.75	∼50	15–25	65	0–10	4.8	1.8
Epoxy-polyamine	S	0.72	∼64	8–10	75	0–7	6.5	1.7
Anion exchangers: weakly basic (pK 9)								
Aminopolystyrene								
Homogeneous (gel)	S	0.67	∼45	8–12	100	0–7	5.5	1.8
Macroporous	S	0.61	55–60	∼25	100	0–9	4.9	1.2
Acrylic-based amine								
Homogeneous (gel)	S	0.72	∼63	8–10	80	0–7	6.5	1.7
Macroporous	S	0.72	∼68	12–15	60	0–9	5.0	1.1
Cellulose-based								
Aminoethyl	P						1.0	
Diethyl aminoethyl	P						∼0.9	

* Shapes: C, cylindrical pellets; G, granules; P, powder; S, spheres.

† When two temperatures are shown, the first applies to H form for cation, or OH form for anion, exchanger; the second, to salt ion.

NOTE: To convert kilograms per liter to pounds per cubic foot, multiply by 6.238×10^1; °F = % °C + 32.

(*Chemical Engineers' Handbook*, McGraw-Hill, 6th ed. New York, 1984; a larger table complete with trade names is in the 5th edition, 1973). (Walas, 1988)

TABLE 15.4.—(continued)

(b) Selectivity Scale for Cations on 8% Crosslinked Resin

Li^+	1.0	Zn^{2+}	3.5
H^+	1.3	Co^{2+}	3.7
Na^+	2.0	Cu^{2+}	3.8
NH_4^+	2.6	Cd^{2+}	3.9
K^+	2.9	Be^{2+}	4.0
Rb^+	3.2	Mn^{2+}	4.1
Cs^+	3.3	Ni^{2+}	3.9
Ag^+	8.5	Ca^{2+}	5.2
UO_2^{2+}	2.5	Sr^{2+}	6.5
Mg^{2+}	3.3	Pb^{2+}	9.9
		Ba^{2+}	11.5

(Bonner and Smith, 1957). (Walas, 1988)

(c) Approximate Selectivity Scale for Anions on Strong-Base Resins

I^-	8	HCO_3^-	0.4
NO_3^-	4	CH_3COO^-	0.2
Br^-	3	F^-	0.1
HSO_4^-	1.6	OH^- (Type I)	0.05–0.07
NO_2^-	1.3	SO_4^{2-}	0.15
CN^-	1.3	CO_3^{2-}	0.03
Cl^-	1.0	HPO_4^{2-}	0.01
BrO_3^-	1.0		
OH^- (Type III)	0.65		

(Bonner and Smith, J. 1957). (Walas, 1988).

EXAMPLE 15.1
Application of Ion Exchange Selectivity Data

The $SO_4^=$ ion of an aqueous solution containing $C = 0.018$ eq/L is to be replaced with Cl^- ion from a resin with $\bar{C} = 1.2$ eq/L. The reaction is

$$SO_4^=(\text{solution}) + 2Cl^-(\text{resin}) \rightleftharpoons SO_4^=(\text{resin}) + 2Cl^-(\text{solution}),$$

$$D + 2\bar{B} \rightleftharpoons \bar{D} + 2B.$$
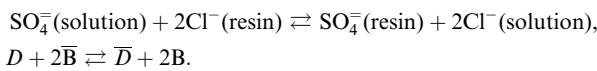
From Table 15.4(c) the selectivity ratio $K_{DB} = 0.15/1.0 = 0.15$, and

$$K_{DB}\bar{C}/C = 0.15(1.2)/0.018 = 10.$$

Then Eq. (15.15) becomes

$$x_{\bar{D}}^-/(1 - x_{\bar{D}})^2 = 10x_D/(1 - x_D)^2.$$

For several values of mol fraction x_D of $SO_4^=$ in solution, the corresponding mol fractions $x_{\bar{D}}$ in the resin are calculated and tabulated:

$x_{SO_4^-}$	
In Solution	**In Resin**
1	1
0.1	0.418
0.05	0.284
0.01	0.0853

Moreover, they are all based on isothermal behavior and approximations of adsorption isotherms and have not been applied to multicomponent mixtures. The greatest value of these calculation methods may lie in the prediction of effects of changes in basic data such as flow rates and slopes of adsorption isotherms after experimental data have been measured of breakthroughs and effluent concentration profiles. In a multicomponent system, each substance has a different breakthrough which is affected by the presence of the other substances. Experimental curves such as those of Figure 15.14 must be the basis for sizing an adsorber.

Since taking samples of adsorbent from various positions in the bed for analysis is difficult, it is usual to deduce the shape of the adsorption front and the width of the MTZ from the effluent concentration profile which may be monitored with a continuous analyzer-recorder or by sampling. The overall width of the MTZ, for instance, is given in terms of the exhaustion and breakthrough times and the superficial velocity, u_s, as

$$\text{width} = u_s(t_e - t_b)/\varepsilon,$$

where ε = bed voidage
   u_s = superficial velocity
   t_b = time to breakthrough

REGENERATION

Adsorbents are restored to essentially their original condition for reuse by desorption. Many hundreds of cycles usually are feasible, but eventually some degradation occurs, as in Figure 15.15 for instance, and the adsorbent must be discarded.

The most common method of regeneration is by purging the bed with a hot gas. Operating temperatures are characteristic of the adsorbent; suitable values at atmospheric pressure are shown in Table 15.1. The exit temperature of the gas usually is about 50°F

For regeneration of the resin, a 12% solution of NaCl will be used; its ion concentration is 2.23 eq/L. Other values for the system remain at $\bar{C} = 1.2$ eq/L and $K_{DB} = 0.15$. Accordingly,

$$K_{DB}\bar{C}/C = 0.15(1.2)/2.23 = 0.0807$$

and Eq. (15.15) becomes

$$x_{\bar{D}}/(1 - x_{\bar{D}})^2 = 0.0807x_D/(1 - x_D)^2.$$

The values of $x_{SO_4^-}$ in the liquid phase will be calculated for several values in the resin. Those results will be used to find the minimum amount of regenerant solution needed for each degree of regeneration

$x_{SO_4^-}$		
In Resin	**In Solution**	**L regenerant/L resin**
0.1	0.455	1.06
0.05	0.319	1.60
0.01	0.102	5.22

Sample calculation for the last entry of the table: The equivalents of SO_4^- transferred from the resin to the solution are

$$0.99(1.2) = 1.188 \text{eq/L}.$$

The minimum amount of solution needed for this regeneration is

$$\frac{1.188}{0.102(2.23)} = 5.22\text{L solution/Liter}.$$
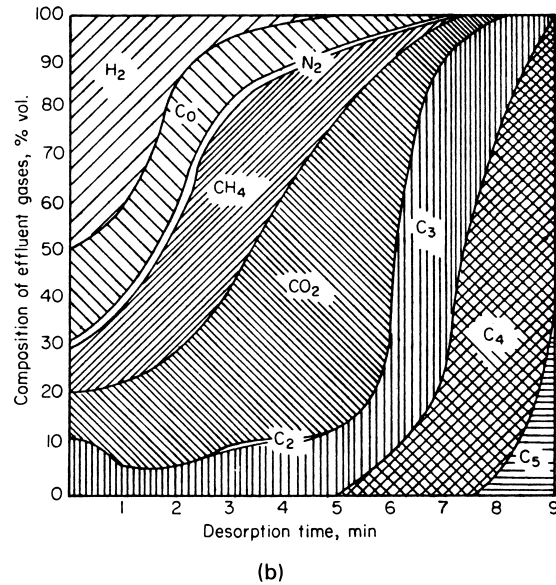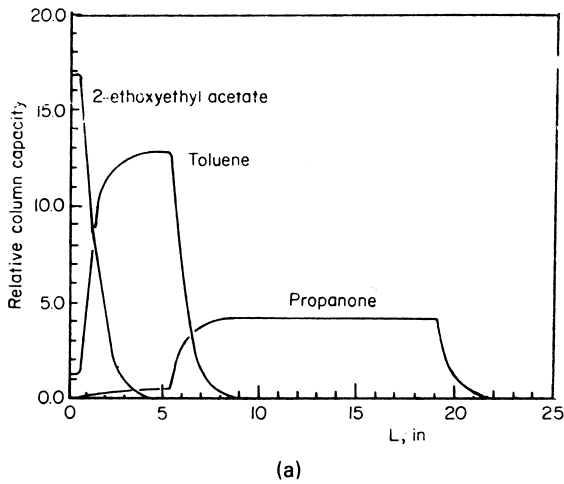
Figure 15.12. Multicomponent mixtures, adsorption, and desorption. (a) Concentrations of the components of a ternary mixture in continuous adsorption, as in a moving bed unit (*Kouach, 1979*). (b) Composition of a desorbed stream consisting of several components as a function of time. (Walas, 1988).
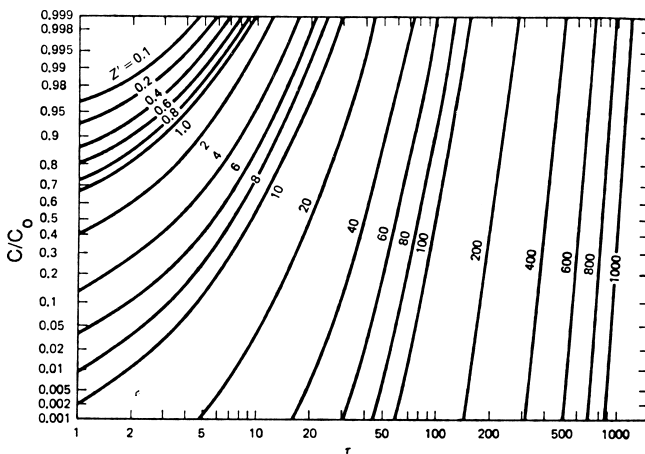
Figure 15.13. Dependence of the concentration ratio, C/C_0 of the effluent from an adsorber on parameters of bed length and time; for the case of a linear isotherm, zero initial adsorbate content and constant inlet composition C_0.

$Z' = (K_f a/\varepsilon u_i)Z$, bed length parameter,

$\tau = (K_f a/K_D \rho_b)(t - Z/u_i)$, time parameter,

$K_D = q/C$, coefficient of linear adsorption isotherm,

u_i = interstitial velocity in the bed,

ε = voidage of the bed,

Z = length of the bed,

$K_f a$ = mass transfer coefficient, $(L^3 \text{ fluid})/(L^3 \text{ bed})(\text{time})$.

(Hougen and Watson, 1947; Hougen and Marshall, 1947; Vermeulen et al., 1984, p. 16.29; Walas, 1988).

higher than that of the end of the bed. Typical cycle times for adsorption and regeneration and steam/adsorbent ratios are given in Table 15.3. Effluent composition traces of a multicomponent system are in Figure 15.12. Complete removal of adsorbate is not

always economically feasible, as suggested by Table 15.3(b). The effect of incomplete removal on capacity is shown schematically by Figure 15.10. Sufficient heat must be supplied to warm up the adsorbent and the vessel, to provide heat of desorption and enthalpy absorption of the adsorbate, and to provide for heat losses to the surroundings. Table 15.3(c) suggests that regeneration times be about one-half the adsorption times. For large vessels, it may be worthwhile to make the unsteady heating calculation by the general methods applicable to regenerators, as presented, for instance, by Hausen (1983).

Purging of the adsorbate with an inert gas at much reduced pressure is feasible in high pressure adsorption plants. The adsorption of Example 15.2, for instance, is conducted at 55 atm, so that regeneration could be accomplished at a pressure of only a few atmospheres without heating. If the adsorbate is valuable, some provision must be made for recovering it from the desorbing gas.

Ignition of adsorbents in external furnaces is practiced to remove some high molecular weight materials that are difficult to volatilize. This is done, for example, for reactivation of carbon from water treating for trace removal of impurities such as phenol. Caustic solution can convert the phenol into soluble sodium phenate in readily disposable concentrated form as an alternate process for regeneration.

Displacement of the adsorbate with another substance that is in turn displaced in process is practiced, for instance, in liquid phase recovery of paraxylene from other C_8 aromatics. In the Sorbex process, suitable desorbents are toluene and paradiethylbenzene. This process is described later.

15.4. GAS ADSORPTION CYCLES

Commercial processes have been arbitrarily divided into two groups: purifications and bulk separations. In purification processes, relatively dilute streams of adsorbate (e.g., 10 weight percent or less) are absorbed, whereas in bulk separations, 10 weight percent or more is adsorbed. Different adsorption cycles are used for each group.

EXAMPLE 15.2
Adsorption of *n*-Hexane from a Natural Gas with Silica Gel
Hexane is to be recovered from a natural gas with silica gel. Molecular weight of the gas is 17.85, the pressure is 55.4 atm, temperature is 94°F, and the content of *n*-hexane is 0.853 mol % or 0.0982 lb/cuft. The bed is 43 in. deep and the superficial velocity is 11.4 ft/min. Other data are shown with the sketch:

0.0982 lb/cuft
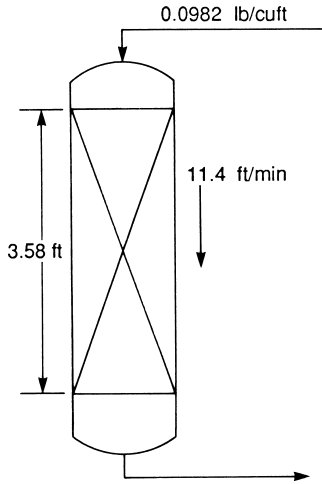
11.4 ft/min

3.58 ft

$Z = 3.58$ ft, bed depth,
$u_s = 11.4$ ft/min, superficial velocity,
$D_p = 0.01$ ft, particle diameter,
$a = 284$ sqft/cuft, packing external surface,
$\rho_b = 52$ lb/cuft, bed density,
$\varepsilon = 0.35$ bed voidage.

From these and physical property data, the Schmidt and Reynolds numbers are calculated as

Sc = 1.87, Re = 644.

The equation of Dwivedi and Upadhyay, Eq. (13.148), is applicable:

$$J_d = \frac{k_g}{u_s} Sc^{2/3} = \frac{1}{\varepsilon} \left(\frac{0.765}{Re^{0.82}} + \frac{0.365}{Re^{0.386}} \right),$$

$$\therefore k_g = \frac{11.4}{0.35(1.87)^{2/3}}(0.0038 + 0.0301) = 0.7268 \text{ ft/min},$$

$$k_g a = 0.7268(284) = 206.4 \text{cuft gas/solid)(min)}.$$

Saturation content of adsorbate is 0.17 lb/lb solid. Accordingly, the coefficient of the linear adsorption isotherm is

$$k_d = \frac{0.17}{0.0982} = 1.731 \frac{\text{lb hexane/lb solid}}{\text{lb hexane/cuft gas}}.$$

Use the Hougen–Marshall chart (Fig. 15.13):

$$Z' = \frac{k_g a Z}{u_s} = \frac{206.4(3.58)}{11.4} = 64.82,$$

$$t = \frac{k_d \rho_b}{k_g a}\tau + \frac{z}{u_s/\varepsilon} = \frac{1.731(52)}{206.4}\tau + \frac{3.58}{11.4/0.35}.$$
$$= 0.436\tau + 0.11 \text{ min}$$

Values of τ are read off Figure 15.13 and converted into values of t:

C/C_0	τ	t (min)
0.01	40	17.56
0.05	45	19.74
0.1	50	21.92
0.2	53	23.23
0.4	60	26.28
0.6	65	28.46
0.8	73	31.95
0.9	79	34.57
0.95	82	35.87
0.99	92	40.24

The total amount adsorbed to the breakpoint, at $C/C_0 = 0.01$, per sqft of bed cross section is

0.0982(11.4)(17.56) = 19.66 lb/sqft cross section.

The saturation amount for the whole bed is

3.58(0.17)(52) = 31.65 lb/sqft cross section.

Accordingly,

utilization of bed = (19.66/31.65)(100%) = 62.1%.

The calculated concentration profile is compared in the figure with experimental data, Run 117, of McLeod and Campbell, *Soc. Pet. Eng. J.*, 166 (June 1966):
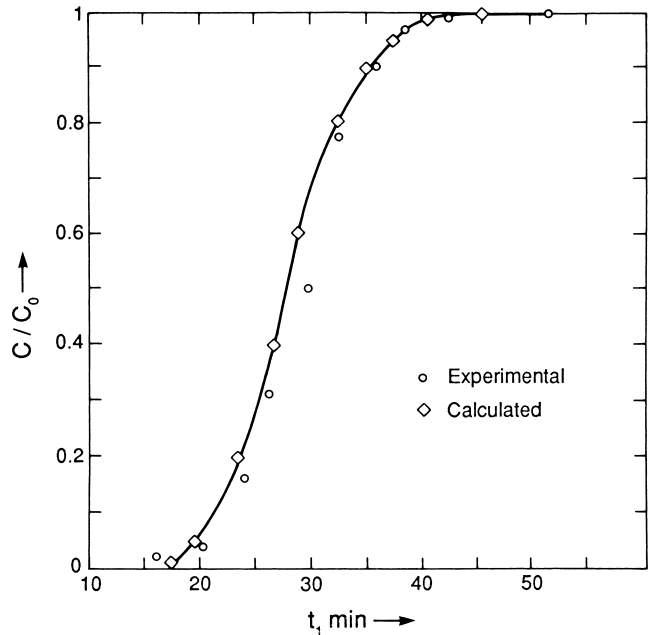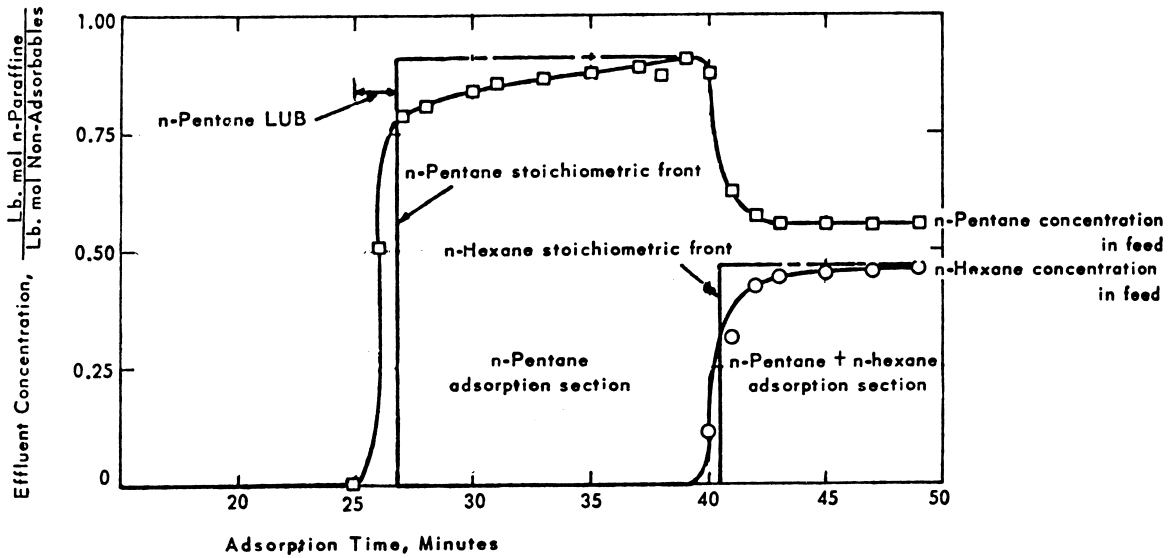
Figure 15.14. Breakthrough curves in the adsorption of a mixture of hydrocarbons with composition *n*-butane 0.4 mol %, *n*-pentane 25.9, *n*-hexane 23.9 iso and cyclic hydrocarbons 49.8 mol % (*Lee, 1972*; Walas, 1988).

TEMPERATURE-SWING CYCLE (TSA)

Temperature-swing adsorption processes have to identical, parallel adsorption beds. One of the beds is in the adsorption cycle while the other bed is being regenerated by heating with a regenerating gas. The two beds generally operate 180 degrees out of phase (Knaebel, 1999).

A stream with a small amount of adsorbate having a partial pressure, P_1, is passed through the adsorbent bed at an initial temperature, T_1 (see Figure 15.16). As time passes, equilibrium is established and is represented by adsorbate loading, X_1. It is usually expressed as mass or moles of adsorbate per unit mass of adsorbent. When the adsorbate is loaded, the temperature of the

bed is increased to T_2, and more feed is introduced to the bed. Desorption begins and a new equilibrium, X_2, is established. The net bed removal is $X_1 - X_2$. This description thus far of the TSA cycle is idealized because equilibrium loadings are not attained in
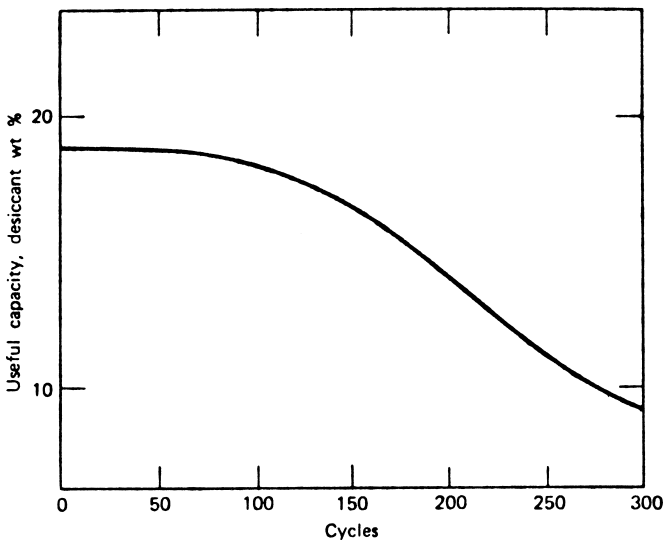
Figure 15.15. Capacity decline with service of a molecular sieve (*plant data, Davison Sieve 562*). Flow, 8150 kg mol; pressure, 3600 kPa (36 atm); temperature, 15°C; water content, 96 kg/hr; minimum cycle time, 24 hr. (*Chi and Cummings, 1978*). (Walas, 1988).
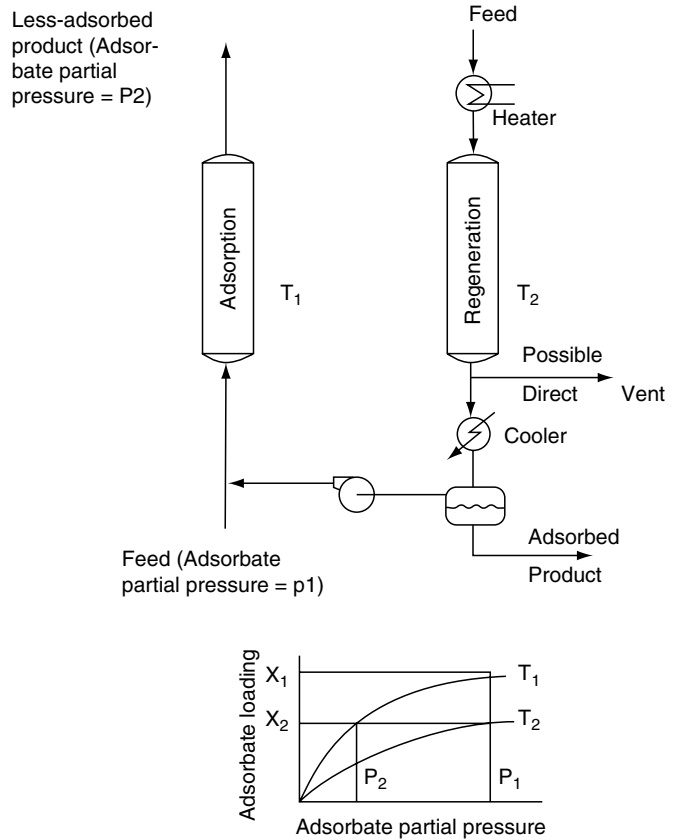
Figure 15.16. Temperature-swing cycle. (Keller et al., 1987).

practice. When the bed is cooled to T_1, a new equilibrium is established and feed is again introduced to the bed and purification will occur down to P_2 (Keller et al., 1987).

The process to heat, desorb and cool an adsorption bed is time consuming since it may take from a few hours to as much as a day to complete the cycle. The TSA cycle also requires a large amount of energy per unit of adsorbate. In general, the smaller the amount of adsorbate in the feed, the higher the energy cost per unit mass of feed (Knaebel, 1999).

PRESSURE-SWING CYCLE (PSA)

In the PSA cycle, the regeneration step takes place by lowering the pressure on the bed and purging the adsorbent. The lower pressure shifts the adsorption equilibrium and affects the regeneration of the adsorbent. In the PSA cycles, the time required to depressure, regenerate, and increase the pressure on the bed is of the order of minutes. Because of the short time cycle, the PSA process is attractive for bulk separations (see Figure 15.17).

The PSA process, like the TSA process, requires two (or more) beds operating out of phase so that feed can be admitted to one of the beds continuously. Pressure equalization, followed by blow-down of the impure gas from one of the adsorbers whose pressure is less, leads to energy efficiency (Knaebel, 1999).

INERT-PURGE CYCLE

Inert gas may be introduced to the adsorber be to remove adsorbate instead of increasing the temperature as in the TSA cycle. The use of an inert lowers the partial pressure of the adsorbate and therefore the concentration of the adsorbate is lowered. It has been demonstrated that if enough inert gas is used, it is possible to remove essentially all the adsorbate. Instead of an inert gas, the purge may be a slip stream of some of the less adsorbed product (see Figure 15.18).

During the adsorption step, the temperature of the bed increases due to the heat of adsorption and then the bed is cooled during regeneration. As the bed temperature increases, the bed capacity is reduced.

In comparing this process cycle with the TSA cycle, the cycle time is materially reduced.

COMBINED CYCLES

As has been discussed in the foregoing sections, it is possible to combine cycles to take advantage of certain efficiencies. For example, in the TSA cycle, combining it with an inert gas purge, the time cycle is reduced. In the PSA cycle, it is possible to use a part of the adsorbed product as a low pressure purge to reduce energy requirements.

15.5. ADSORPTION DESIGN AND OPERATING PRACTICES

When continuous operation is necessary, at least two adsorbers are employed, one on adsorption and the other alternately on regeneration and cooling. In cases where breakthrough is especially harmful, three vessels are used, one being regenerated, the other two onstream with the more recently regenerated vessel downstream, as in Figure 15.19.

Figure 15.17. Pressure-swing cycle. (Keller et al., 1987).
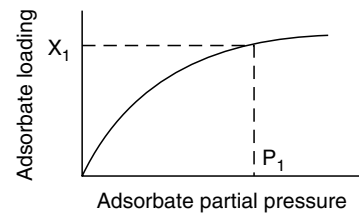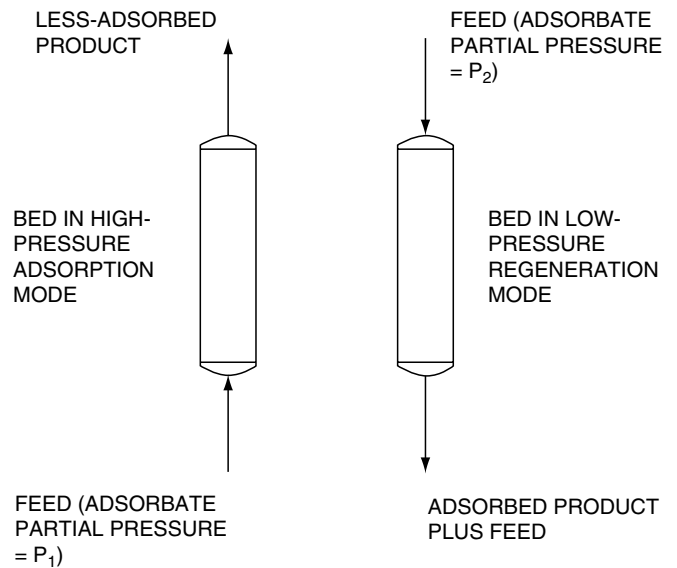
Figure 15.18. Inert-purge cycle. (Keller et al., 1987).
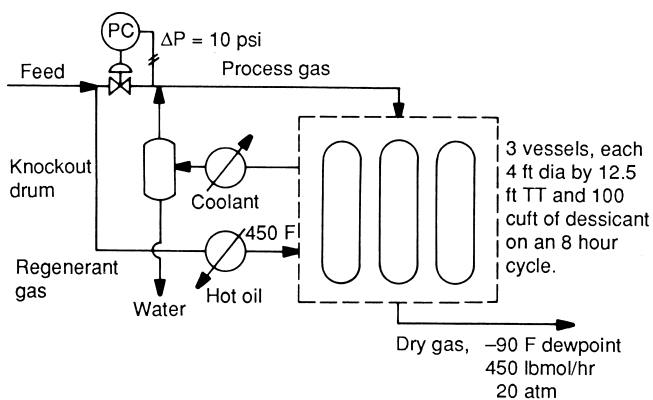
Figure 15.19. A three-vessel drying system for a cracked light hydrocarbon stream. Valve operation usually is on automatic timer control. Recycled process gas serves as regenerant.

Beds usually are vertical; adsorbers 45 ft high and 8–10 ft dia are in use. When pressure drop must be minimized, as in the recovery of solvents from atmospheric air, horizontal vessels with shallow beds are in common use. Process gas flow most often is downward and regenerant gas flow is upward to take advantage of counterflow effects. Upflow rates are at most about one-half the fluidizing velocity of the particles. Vertical and horizontal types are represented on Figure 15.20.

A major feature of adsorber design is the support for the granular adsorbent, preferably one with a low pressure drop. The combination of Figure 15.21(a) of grid, screens, and support beams is inexpensive to fabricate and maintain, has a low heat capacity and a low pressure drop. The construction of Figure 15.21(b) is suited to adsorbers that must be dumped frequently. Supports of layers of ceramic balls or gravel or anthracite, resting on the bottom of the vessel, are suited to large vessels and when corrosion-resistant construction is required. Typical arrangements are shown in Figures 17.26 and 17.27. The successive layers increase in diameter by factors of 2–4 up to 1 in. or so. Holddown balls also may be provided at the top to prevent disturbance of the top layer of adsorbent by incoming high velocity gas or entrainment by upflowing gases. When regeneration is by heating, a drawback of the ball support arrangement is their substantial heat capacity, which slows up the heating rate and subsequent cooling to process temperature.

Representative values and ranges of operating parameters are summarized in Table 15.3. Cycle times for some adsorptions are adjusted to work shift length, usually multiples of 8 hr. When cycle times are short, as for solvent recovery, automatic opening and closing of valves is necessary.

Steam rates for regeneration of a particular adsorbent carbon are shown in Table 15.3(b). Steam/solvent ratios as high as 8 sometimes are necessary.

Data for liquid phase adsorption are typified by water treating for removal of small but harmful amounts of impurities. Some conditions are stated by Bernardin [*Chem. Eng.*, (18 Oct. 1976)]. Water flow rates are 5–10 gpm/sqft. When suspended solids are present, the accumulation on the top of the bed is backwashed at 15–20 gpm/sqft for 10–20 min/day. The adsorbent usually is not regenerated in place but is removed and treated in a furnace. Accordingly, a continuous operation is desirable, and one is simulated by periodic removal of spent adsorbent from the bottom of the vessel with a design like that of Figure 15.21(b) and replenishing of fresh adsorbent at the top. The pulses of spent and fresh carbon

are 2–10% of the total bed. Height to diameter ratio in such units is about 3.

A carbon adsorber for handling 100,000 gal/day of water consists of two vessels in series, each 10 ft dia by 11 ft sidewall and containing 20,000 lb of activated carbon. Total organic carbon is reduced from 650 mg/L to 25 mg/L, and phenol from 130 mg/L to less than 0.1 mg/L.

The capacity of regeneration furnaces is selected so that they operate 80–90% of the time. In multiple-hearth furnaces the loading is 70–80 lb/(sqft)(day). In countercurrent direct fired rotary kilns, a 6% volumetric loading is used with 45 min at activation temperature.

Details of the design and performance of other commercial liquid phase adsorptions are proprietary.

15.6. PARAMETRIC PUMPING

In liquid-phase adsorption, an approach to bulk-liquid separations is a technique known as *parametric pumping*. The process fluid is pumped through a particular kind of packed bed in one direction for a while, then in the reverse direction. Each flow direction is at a different level of an operating parameter, such as temperature, pressure, or pH, to which the transfer process is sensitive. Such a periodic and synchronized variation of the flow direction and some operating parameter was given the name of *parametric pumping* by Wilhelm (1968). A difference in concentrations of an adsorbable-desorbable component, for instance, may develop at the two ends of the equipment as the number of cycles progresses. The result is that the more strongly adsorbed components concentrate at the end of the bed toward where the adsorptivity is low, and the less strongly adsorbed components concentrate at the opposite end. High degrees of separation have been demonstrated in some cases. One advantage is that in thermally driven processes, where the temperature is high, no displacement liquid is needed; therefore, no downstream distillation recovery is required.

A schematic of a batch parametric pumped adsorption process is sketched in Figure 15.22(a), and Figure 15.22(b) shows the synchronized temperature levels and flow directions. At the start, the interstices of the bed and the lower reservoir are filled with liquid of the initial composition and with the same amount in both. The upper reservoir is empty. The bed is kept cold while the liquid is displaced from the interstices into the upper reservoir by liquid pumped from the lower reservoir. Then the temperature of the bed is raised and liquid is pumped down through the bed. Adsorption occurs from the cold liquid and desorption from the hot liquid. For the system of Figure 15.22(c), the separation factor is defined as the ratio of concentrations of the aromatic component in the upper and lower reservoirs; very substantial values were obtained in this case. Data of partial desalination of a solution with an ion exchange resin are in Figure 15.22(d), but here the maximum separation ratio is only about 10.

An intermittent—simulated continuous—operation is described in Figure 15.23. Feed input and product withdrawals are accomplished with periodic openings and closings of valves without shutting down the equipment at any time. Other modes of operation can be devised.

Theoretical studies also have applied this cycling principle to liquid-liquid extraction processes with immobilized solvents, and to reversible chemical reactions. Comprehensive reviews of the literature of cycling zone separations have been made by Sweed (1972), Wankat (1974), and Wankat et al. (1976).

Although parametric pumping appeared on the academic scene in 1966, no commercial installations have been made, at least no widely publicized ones.
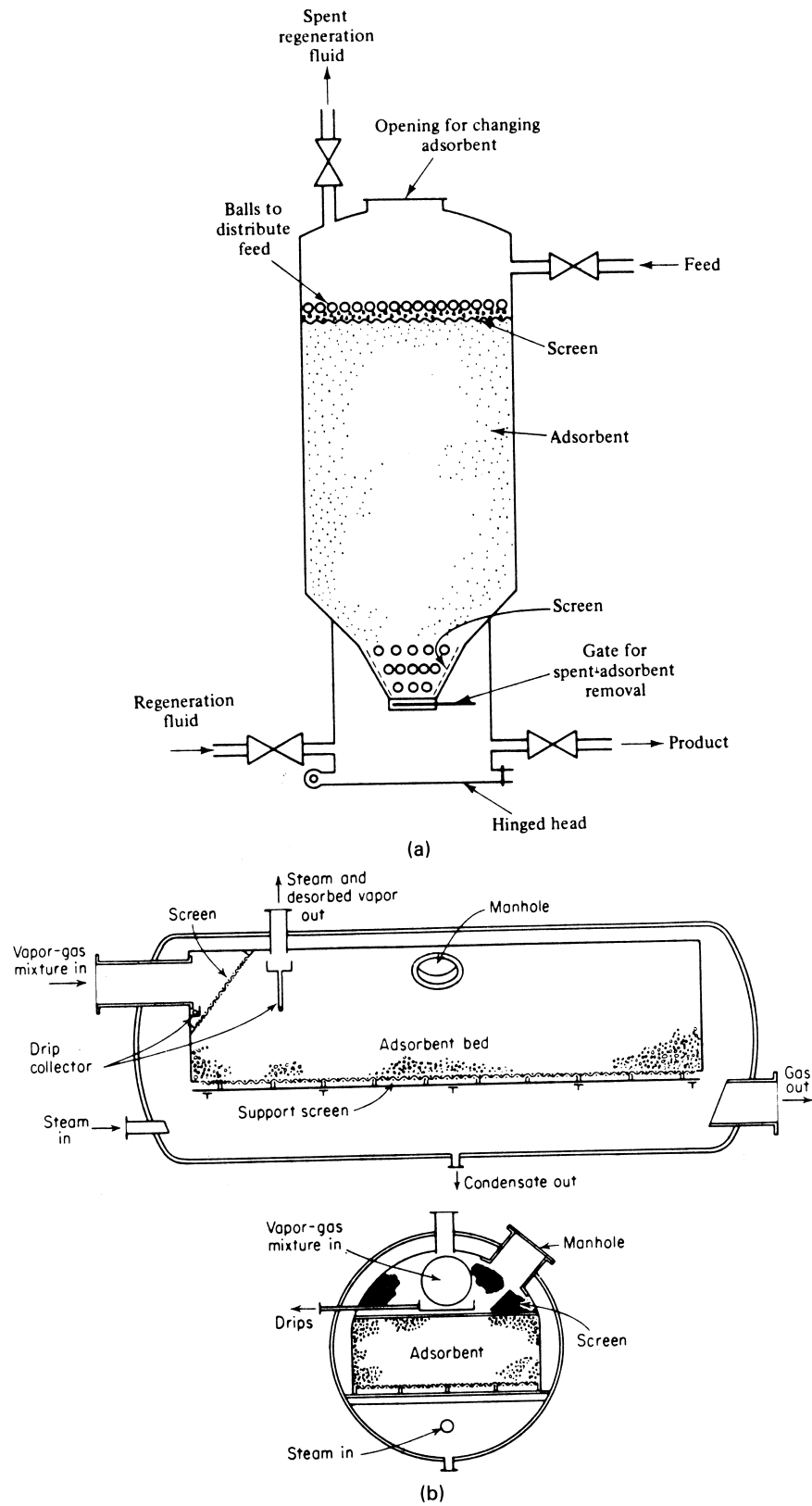
Figure 15.20. Two designs of fixed bed gas adsorbers. (a) Vertical bed with balls on top for hold-down and distribution of feed (*Johnston* (*27 Nov. 1972*). (b) Horizontal fixed bed for low pressure drop operation [*Treybal, 1980*; *Logan, U.S. Pat. 2,180,712* (1939; Walas, 1988)].
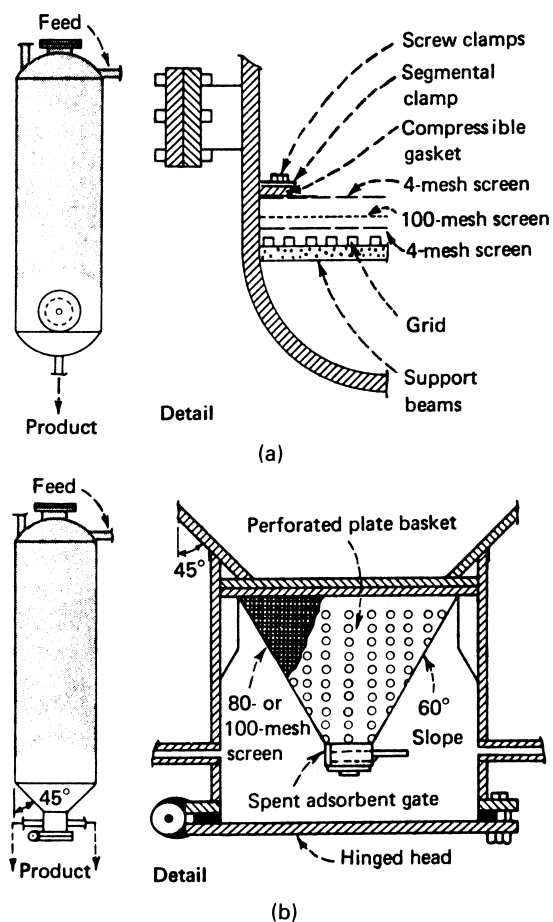
Figure 15.21. Two types of supports for adsorbent beds [*Johnston, (27 Nov. 1972)*]. See also Figures 17.23 and 17.24. (a) Common type of flat screen support. (b) Conical-type of support suited to frequent removal of adsorbent. (Walas, 1988).

15.7. ION EXCHANGE DESIGN AND OPERATING PRACTICES

Ion exchange processes function by replacing undesirable ions of a liquid with ions such as H^+ or OH^- from a solid material in which the ions are sufficiently mobile, usually some synthetic resin. Eventually the resin becomes exhausted and may be regenerated by contact with a small amount of solution with a high content of the desired ion. Resins can be tailored to have selective affinities for particular kinds of ions, for instance, mercury, boron, ferrous iron, or copper in the presence of iron. Physical properties of some commercial ion exchange resins are listed in Table 15.4 together with their ion exchange capacities. The most commonly used sizes are $-20 + 50$ mesh (0.8–0.3 mm) and $-40 + 80$ mesh (0.4–0.18 mm).

Rates of ion exchange processes are affected by diffusional resistances of ions into and out of the solid particles as well as resistance to external surface diffusion. The particles are not really solid since their volume expands by 50% or more. For monovalent exchanges in strongly ionized resins, half times with intraparticle diffusion controlling are measured in seconds or minutes. For film diffusion, half times range from a few minutes with $0.1N$ solutions up to several hours with $0.001N$ solutions. Film diffusion rates also vary inversely with particle diameter. A rough rule is that film diffusion is the controlling mechanism when concentrations are below 0.1–$1.0N$, which is the situation in many commercial instances. Then the design methods can be same as for conventional adsorbers.

Ion exchange materials have equilibrium exchange capacities of about 5 meq/g or 2.27 g eq/lb. The percentage of equilibrium exchange that can be achieved practically depends on contact time, the concentration of the solution, and the selectivity or equilibrium constant of the particular system. The latter factor is discussed in Section 15.2 with a numerical example.

Commercial columns range up to 6 m dia and bed heights from 1 to 6 m, most commonly 1–3 m. Freeboard of 50–100% is provided to accommodate bed expansion when regenerant flow is upward. The liquid must be distributed and withdrawn uniformly over the cross section. Perforated spiders like those of Figure 15.25 are suitable. The usual support for the bed of resin is a bed of gravel or layers of ceramic balls of graded sizes as in Figure 17.27. Balls sometimes are placed on top of the bed to aid in distribution or to prevent disturbance of the top level. Since the specific volume of the material can change 50% or more as a result of water absorption and ion–ion exchange, the distributor must be located well above the initial charge level of fresh resin.

Liquid flow rates may range from 1 to 12 gpm/sqft, commonly 6–8 gpm/sqft. When the concentration of the exchange ion is less than 50 meq/L, flow rates are in the range of 15–80 bed volumes (BV)/hr. For demineralizing water with low mineral content, rates as high as 400 BV/hr are used. Regenerant flow rates are kept low, in the range of 0.5–5.0 BV/hr, in order to allow attainment of equilibrium with minimum amounts of solution.

The ranges of possible operating conditions that have been stated are very broad, and averages cannot be depended upon. If the proposed process is similar to known commercial technology, a new design can be made with confidence. Otherwise laboratory work must be performed. Experts claim that tests on columns 2.5 cm dia and 1 m bed depth can be scaled up safely to commercial diameters. The laboratory work preferably is done with the same bed depth as in the commercial unit, but since the active exchange zone occupies only a small part of a normal column height, the exchange capacity will be roughly proportional to the bed height, and tests with columns 1 m high can be dependably scaled up. The laboratory work will establish process flow rates, regenerant quantities and flow rates, rinsing operations, and even deterioration of performance with repeated cycles.

Operating cycles for liquid contacting processes such as ion exchange are somewhat more complex than those for gas adsorption. They consist of these steps:

1. Process stream flow for a proper period.
2. A rinse for recovering possibly valuable occluded process solution.
3. A backwash to remove accumulated foreign solids from the top of the bed and possibly to reclassify the particle size distribution.
4. The flow of regenerant for a proper period.
5. Rinse to remove occluded regenerant.

As complex a cyclic process as this may demand cycle times of more than a few hours. Very high ion concentrations or high volumetric rates may require batteries of vessels and automatic switching of the several streams, or continuously operating equipment. Several continuous ion exchange plants are being operated successfully. The equipment of Figure 15.25 employs pulsed transfer of solid between exchange and regenerant zones as often as every 4 min to every 20 or 30 min. Attrition of the resin may require replacement of as much as 30% of the resin each year in water conditioning applications.

(a)

(b)

(c)

(d)
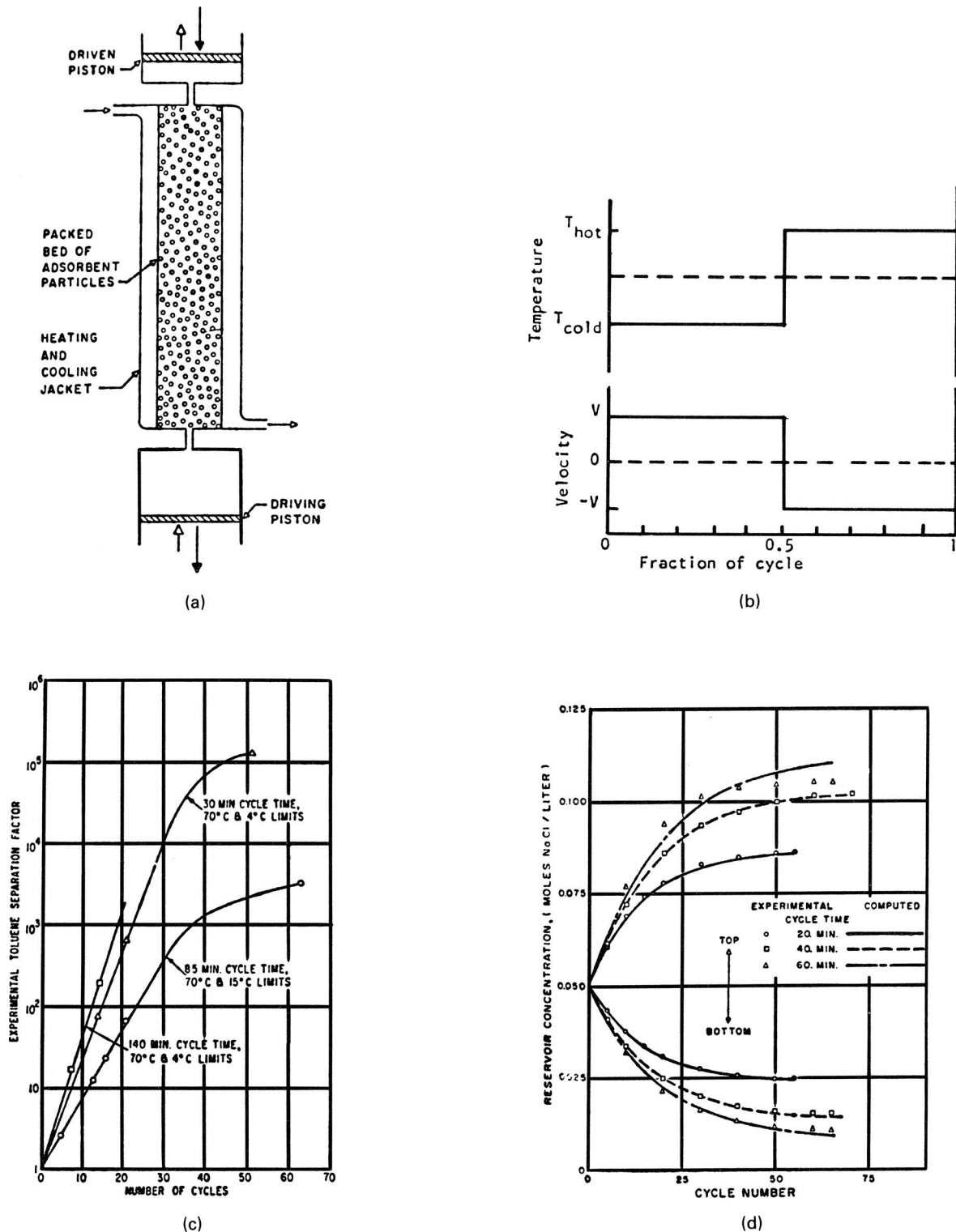
Figure 15.22. Batch parametric processing of solid–liquid interactions such as adsorption or ion exchange. The bottom reservoir and the bed interstices are filled with the initial concentration before pumping is started. (a) Arrangement of adsorbent bed and upper and lower reservoirs for batch separation. (b) Synchronization of temperature levels and directions of flow (positive upward). (c) Experimental separation of a toluene and n-heptane liquid mixture with silica gel adsorbent using a batch parametric pump. (*Reprinted from Wilhelm, 1968, with permission of the American Chemical Society*). (d) Effect of cycle time τ on reservoir concentrations of a closed system for an NaCl-H$_2$O solution with an ion retardation resin adsorbent. The column is initially at equilibrium with 0.05M NaCl at 25°C and $\alpha = 0.8$. The system operates at 5° and 55°C. (*Sweed and Gregory, 1971*).
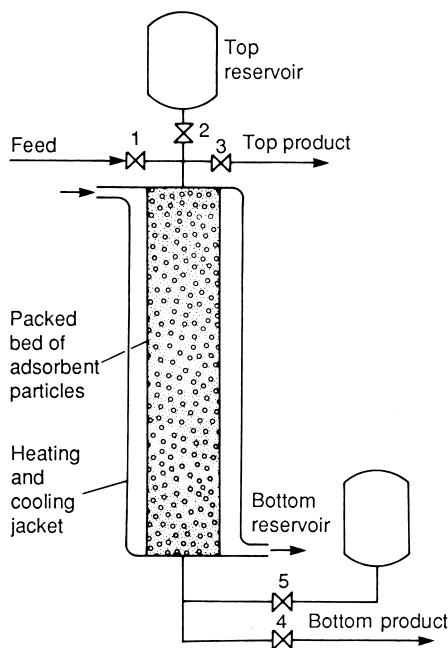
Valve							
1	**2**	**3**	**4**	**5**	T_h	T_c	**Process**
V_1	—	—	V_1	—		*	feed supplied, btm product removed cold
V_2	—	—	—	V_2		*	feed supplied, btm reservoir chgd. cold
—	V_3	—	—	V_3		*	top reservoir dschgd., btm reservoir chgd. cold
—	—	V_4	—	V_4	*		top product dschgd. hot, btm reservoir dschgd. hot
—	V_5	—	—	V_5	*		top reservoir chgd., btm reservoir dschgd. hot

Figure 15.23. Parametric cycle operating intermittently in five periods; valves that are open each time are identified with their flow rates V_{i}, and the low and high temperature levels are identified with an asterisk in the proper column.

Fluidized bed units such as the multistage unit of Figure 15.25 suffer from some loss of efficiency because the intense mixing eliminates axial concentration gradients. They do have the merit, however, of not being bothered by the presence of foreign solid particles.

The economic break between fixed bed and continuous operation has been estimated as ion concentrations of $0.5N$, or flow rates above 300 gpm, or when three or more parallel beds are required to maintain continuous operation. The original application of continuous ion exchange was to treatment of radioactive wastes, but some installations of ordinary water treating have been made.

Resin requirements for two extremes of ion concentration are analyzed in Example 15.3. The high concentration stream clearly is a candidate for continuous ion exchange. Manufacturers and distributors of ion exchange resins are Dow, Rohm and Haas, Bayer, Kasai, Sybron Chemical and Purolite.

ELECTRODIALYSIS

In this process, dissolved electrolytes are removed by application of electromotive force across a battery of semipermeable membranes constructed from cation and anion exchange resins. The cation membrane passes only cations and the anion membrane only anions. The two kinds of membranes are stacked alternately and

separated about 1 mm by sheets of plastic mesh that are still provided with flow passages. When the membranes and spacers are compressed together, holes in the corners form appropriate conduits for inflow and outflow. Membranes are 0.15–0.6 mm thick. A commercial stack may contain several hundred compartments or pairs of membranes in parallel. A schematic of a stack assembly is in Figure 15.26. Properties of commercially produced membranes are in Table 15.5 and performance data are in Table 15.6.

Membranes may be manufactured by mixing powdered ion exchange resin with a solution of binder polymer and pouring the heated mixture under pressure onto a plastic mesh or cloth. The concentration of the ion exchanger is normally 50–70%. They are chiefly copolymers of styrene and divinylbenzene, sulfonated with sulfuric acid for introduction of the cation exchange group.

Standard cell sizes are up to 30 by 45 in. In an individual stack the compartments are in parallel, but several stacks in series are employed to achieve a high degree of ion exchange. The ion exchange membrane is not depleted and does not need regeneration. The mechanism is that an entering cation under the influence of an emf replaces an H^+ ion from the resin and H^+ from solution on the opposite face of membrane replaces the migrating cation.

Table 15.6 shows that pressures drops may be as high as 900 psi. Flow rates in a single stage are about 1 gal/(hr)(sqft of available membrane surface). The process is distinguished by very low power requirements: the desalination of sea water, for instance, consumes 11–12 kWh/1000 gal. One stage effects a reduction of about 50% in salt content, so several stages in series are used for high performance. A flow sketch of a three-stage electrodialysis plant is in Figure 15.26(c).

Like many other specialities, electrodialysis plants are purchased as complete packages from a few available suppliers. Membrane replacement is about 10% per year. Even with prefiltering the feed, cleaning of membranes may be required at intervals of a few months. The comparative economics of electrodialysis for desalting brackish waters is discussed by Belfort (1984): for lower salinities, electrodialysis and reverse osmosis are competitive, but for higher ones electrodialysis is inferior. Electrodialysis has a number of important unique applications, for removal of high contents of minerals from foods and pharmaceuticals, for recovery of radioactive and other substances from dilute solutions, in electro-oxidation reduction processes and others.

15.8. PRODUCTION SCALE CHROMATOGRAPHY

When a mixture of two substances is charged to a chromatographic column, one of them may be held more strongly than the other. Elution with an inert fluid will remove the more lightly held substance first, then the other. Separations even between very similar substances can be very sharp. Figure 15.33(a) is an example of a chromatogram. Only fluid–solid chromatography is an adsorptive process, but gas–liquid and liquid–liquid are used more frequently since liquids with suitable absorption properties are easier to find than solid adsorbents. The active sorbent is a high-boiling solvent deposited on a finely divided inert solid carrier. The process is one of absorption, but the behavior is much like that of adsorption. The principal application is to chemical analysis. Relative retention times on various sorbents are key data which are extensively tabulated, for instance in Meites (1963).

Chromatographic separations are necessarily intermittent with alternate injections and elutions, although a measure of continuity can be achieved with an assembly of several units, or with suitably sized surge tanks. A process flowsketch appears in Figure 15.33(b). Information on production scale chromatography is provided by Conder (1973). Only separations difficult to achieve by other means are economical with chromatography.

(a)

(b)
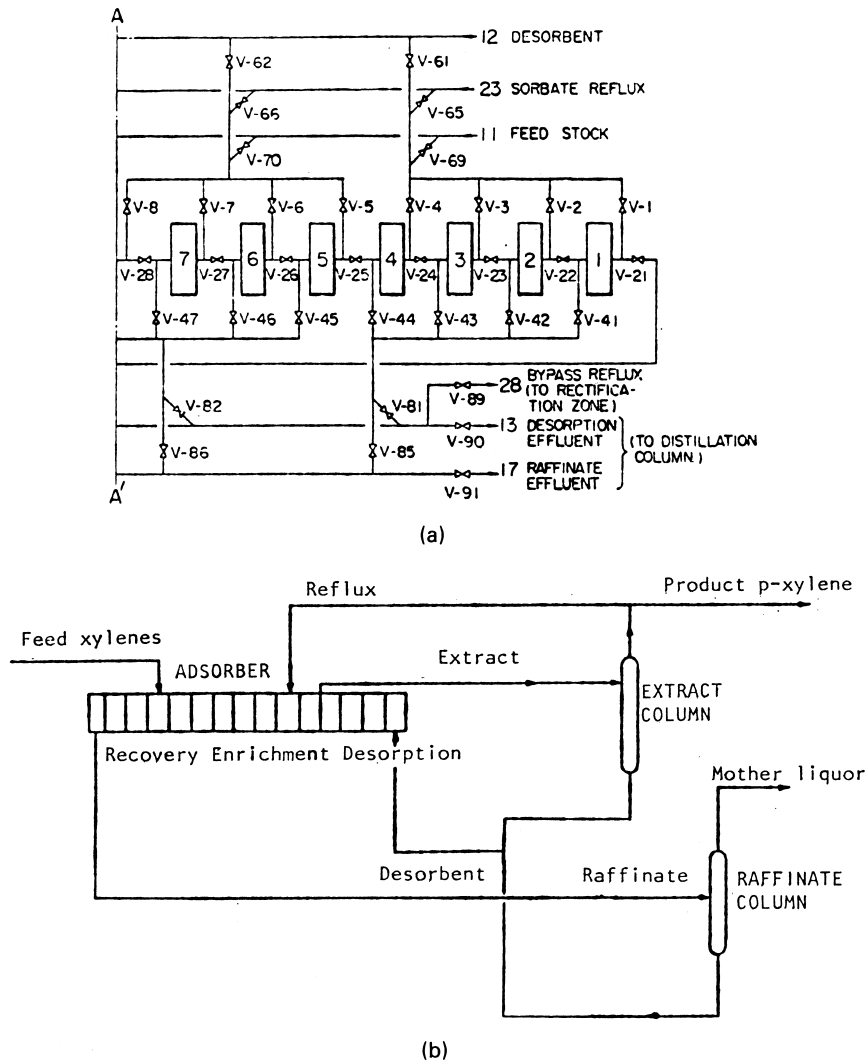
Figure 15.24. The Toray simulated continuous adsorption process. (**a**) Showing the main valving for a seven-chamber adsorption system (*Otani et al., U.S. Pat. 3,761,533, 25 Sep. 1973*). (**b**) Flowsketch for recovery of paraxylene by continuous adsorption (*Otani et al.*, 1971). (Walas, 1988).

Individual drums are provided for each product fraction. A detector monitors the separation and provides signals for controlling the injection and collection sequence. The operation of partial condensers for the dilute eluted streams presents challenges because of aerosol formations. When a valuable carrier such as nitrogen is used, it must be cleaned up and recycled.

A 1968 estimate of the cost breakdown for a plant with a column 4 ft dia by 15 ft high and a throughput of 200–920 tons/yr has been converted to a percentage basis in Table 15.7 because of its age. The costs are said to not vary greatly with throughput or the nature of the separation, although this analysis has been made specifically for the separation of α- and β-pinenes. The temperature was 165°C and the solvent was Carbowax 20M. The design was based on data in a 4 in. dia column which had a capacity of 200–1500 mL/hr.

Some of the materials for which chromatographic separation should be considered are essential oils, terpenoids, steroids, alkaloids, pharmaceuticals, metal chelates, isotopes, and close-boiling isomers. For easy separations, vacuum distillation, liquid–liquid

extraction, and fractional crystallization are less expensive. Operating data are proprietary and difficult to obtain.

15.9. EQUIPMENT AND PROCESSES

Adsorbents are made in pellet form by extrusion or pressing or in granular form by crushing and classification of larger masses or in spherical or globular form by precipitation in an inert gaseous or liquid medium. Typical processes for some adsorbent preparations are represented in Figure 15.1. The BASF process of Figure 15.1(c) for silica gel employs a special mixing nozzle in which water glass is mixed intermittently with a stream of sulfuric acid to form an unstable sol that is sprayed directly into air where the globules solidify immediately. Mixing time in the nozzle is 0.1–1.0 sec. The sodium sulfate is washed out in a tower to which the particles fall. The process of initial activation or reactivation is shown in Figure 15.1(b) for bone char. In general a heating process, sometimes combined with oxidation, is required to drive gases out of the solid mass and thus to make it porous.
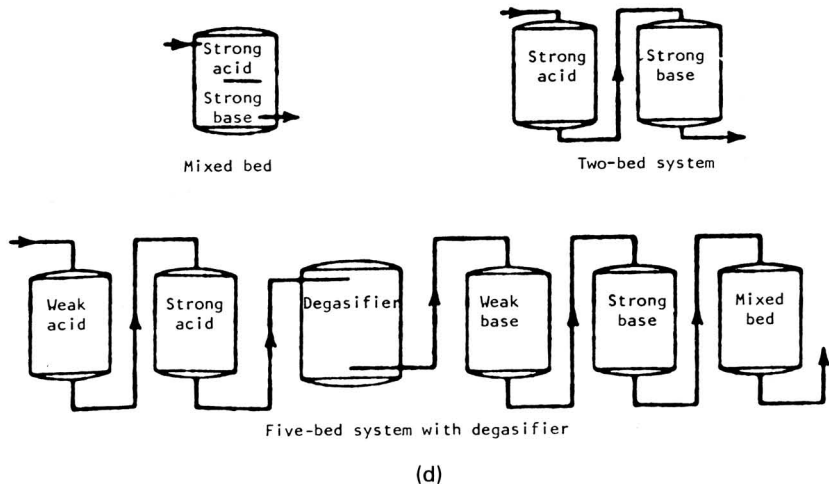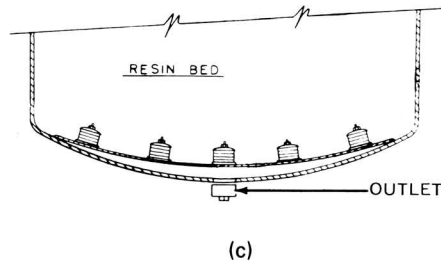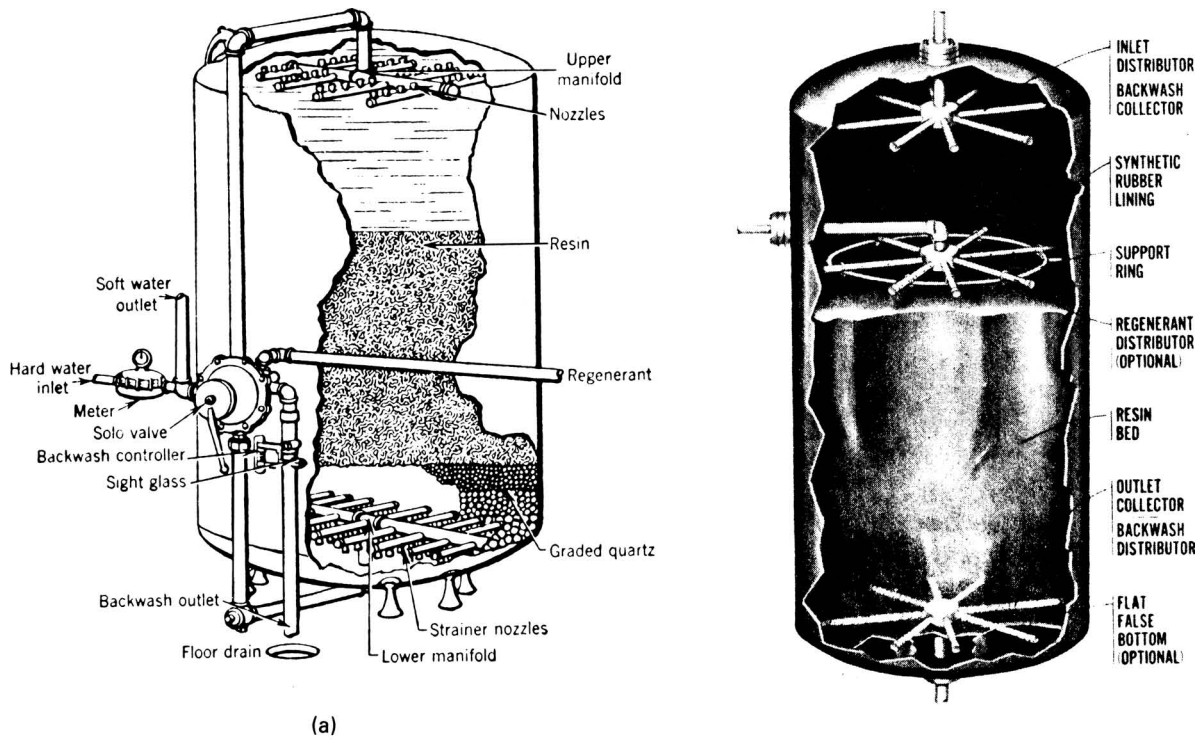
Figure 15.25. Fixed bed ion exchange vessels and arrangements. (a) Typical design of a water softener, showing bed support, distributor, and effluent collector. (b) Vessel with radial-type distributors and collectors (*Illinois Water Treatment Co.*). (c) A double-dish underdrain system (*Permutit Co.*). (d) Some arrangements of vessels for cation and anion exchange. (Walas, 1988).

EXAMPLE 15.3
Size of an Ion Exchanger for Hard Water
A hard water contains 120 ppm of $CaCO_3$, 90% of which is to be removed with a hydrogen exchange resin of capacity 5 meq/g. By the method of Example 15.1 it is ascertained that under these conditions 98% of H^+ ion of the resin will be replaced by the Ca^{++} at equilibrium. The minimum amount of resin will correspond to the equilibrium value. That amount will be calculated for treating 100 gpm of water on a 24 hr cycle. The mol wt of $CaCO_3 = 100.06$.

$$\text{resin capacity} = 0.98(0.005)(100.06)$$
$$= 0.490 \text{ lb } CaCO_3/\text{lb resin,}$$

$$CaCO_3 \text{ removed} = 0.9(8.34)(100)(1440)(120)(10^{-6})$$
$$= 129.7 \text{ lb}/24 \text{ hr,}$$

$$\text{resin needed} = 129.7/0.49$$
$$= 264.7 \text{ lb, or } 4.71 \text{ cuft of resin with sp gr} = 0.9.$$

For comparison, the amount of resin needed to remove the Na^+ from a 3.5% solution of NaCl at the rate of 100 gpm in 24 hr will be found:

$$\text{resin capacity} = 5 \text{ meq/g} = 0.005 \text{ lb mol/lb,}$$
$$Na^+ \text{removed} = 0.035(8.34)(100)(1440)/58.5$$
$$= 718.5 \text{ lb mol/day.}$$

Accordingly,

$$\text{resin} = 718.5/0.005 = 142,700 \text{ lb,}$$

pointing out that a fixed bed unit on such a long cycle may not be practical for such a high concentration of ion to be exchanged.

GAS ADSORPTION

The usual equipment for gas adsorption is a number of vessels containing fixed beds of the adsorbent, at least two vessels for achieving overall continuous operation. Figure 15.20 shows suitable vertical and horizontal vessels. The vertical ones are less likely to form channels and usually are favored. Bed depths as high as 45 ft are in use. Horizontal vessels are preferred when pressure drops must be kept low, as in recovery of solvents from air in printing or paint establishments. Modes of support of granular beds are shown in Figures 15.21, and 17.27.

A three-bed adsorption unit is illustrated in Figure 15.19. It is used to dry the feed to a distillation column with a top temperature of $-70°F$; thus a water dewpoint of $-90°F$ is required. One of the vessels always is on regeneration and cooling down, and the other two in series on adsorption, with the more recently reactivated one

downstream. A bleed off the process stream is diverted to use as regenerant. After the gas leaves the vessel being regenerated, the water is condensed out by cooling and the gas returns to the process downstream of a control valve that maintains a 10 psi differential.

Normally adsorption is conducted at or as near ambient temperature as possible and regeneration is at 350–500°F. A process developed by Union Carbide Corp, the AHR process (adsorption heat recovery), allows the temperature to rise to 200–400°F as a result of the heat of adsorption and effects the desorption at comparable temperatures with a stream of inert gas such as nitrogen or carbon dioxide which is recycled after the water is condensed out. The process is applied to removal of as much as 20% of water from ethanol with cycle times of the order of 1 hr, instead of the common 24 hr, even for much smaller contents of water (Anon, April 15, 1985).
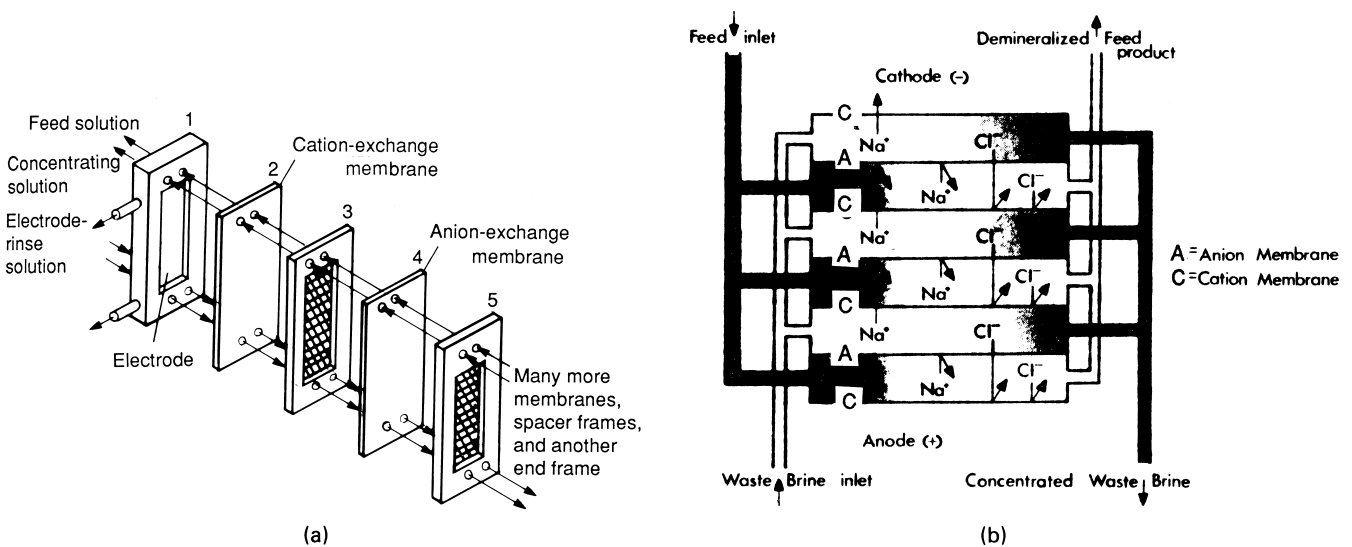
Figure 15.26. Electrodialysis equipment and processes. (a) View of the components of an electrodialysis stack (*Lacey, 1978*). (b) Flow pattern through an electrodialyzer for removal of NaCl from water (*Ionics Inc.*). (c) Electroreduction with the use of an ion exchange diaphragm. (d) Flowsketch of a three-stage electrodialysis for treatment of brackish water (*Rogers, in Belfort, 1984*). (Walas, 1988).

(c)

(d)
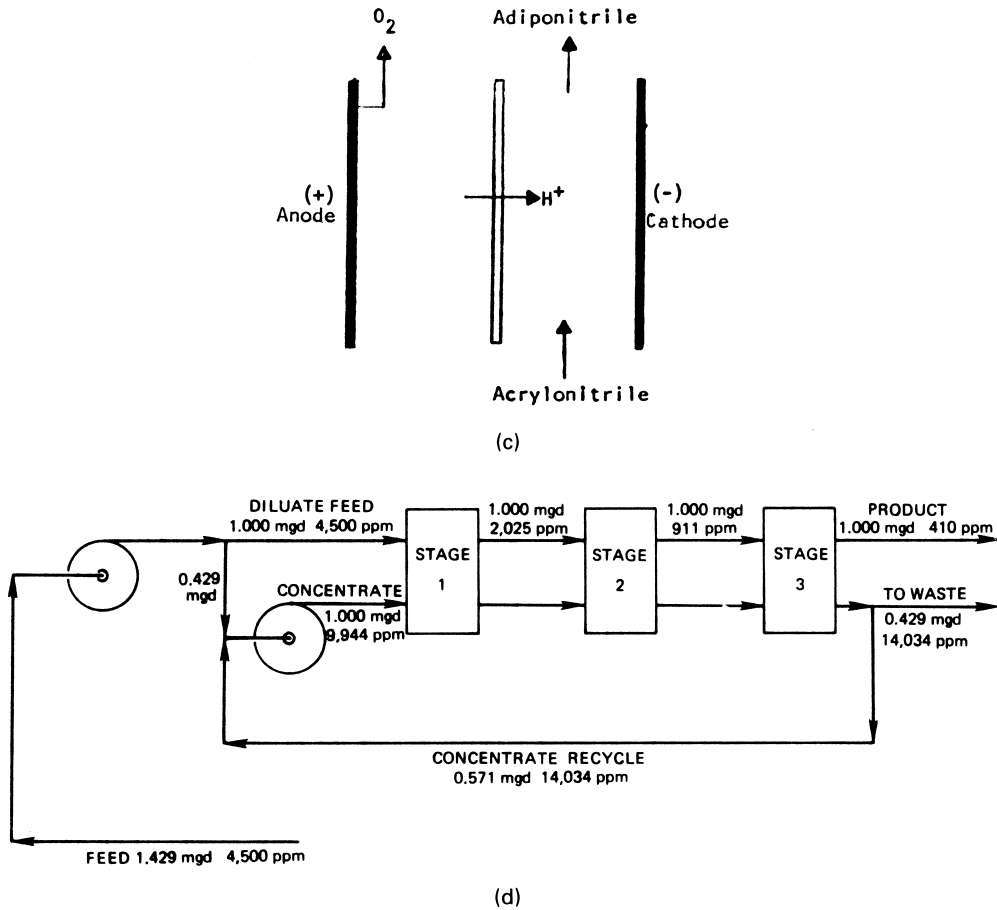
Figure 15.26.—(*continued*)

TABLE 15.5. Properties of Membranes for Electrodialysis

Manufacturer	Name of membranes	Membrane	Thickness (mm)	Capacity (meq/gm)	Electrical resistance (Ωcm^2 in 0.1 N NaCl)	Reinforcement
Ionac Chemical Co. New Jersey	Ionac	MC-3142	0.15	1.06	9.1	Yes
		MC-3470	0.35	1.05	10.5	Yes
		MA-3148	0.17	0.93	10.1	Yes
		MA-3475	0.40	1.13	23	Yes
		IM-12	0.13	—	4	Yes
American Machine and Foundry Connecticut	A.M.F.	C-60	0.30	1.5	6	No
		A-60	0.30	1.6	5	No
Ionics Inc. Massachusetts	Nepton	CR61 AZL 183	0.60	2.7	9	Yes
		AR 111 BZL 183	0.60	1.8	14	Yes
Asahi Glass Co. Ltd. Tokyo, Japan	Selemion	CMV	0.15	1.4	6.1	Yes
		AMV	0.14		4.0	Yes
Tokuyama Soda Ltd. Tokyo, Japan	Neosepta	CL 25 T	0.16	1.8–2.0	3.5	Yes
		AV 4 T	0.15	1.5–2.0	4.0	Yes
Asahi Chemical Industry Co. Ltd. Tokyo, Japan	A.C.I. or Acipex	DK 1	0.23	2.6	6.5	Yes
		DA 1	0.21	1.5	4.5	Yes
Ben-Gurion University of the Negev, Research & Development Authority Beersheva, Israel	Neginst	NEGINST-HD	0.35	0.8	12	Yes
		NEGINST-HD	0.35	0.8	10	No
		NEGINST-HC	0.2	1.6	6	No
		NEGINST-HC	0.2	1.7		

(Belfort, 1984; Walas, 1988).

TABLE 15.6. Performance of Electrodialysis Equipment on Treatment of 3000 ppm Brackish Water

	Single stack, MK II, four stages	Single stack, MK III, three stages	Single stack, MK III, one stage	Three stacks in series, MK III
Typical hydraulic flow rate				
U.S. gal/24-h day	16,700	55,600	166,700	166,700
U.S. gal/min	11.6	38.6	116	116
Pressure drop at typical flow, lb/in^2	47	44	14	42
Number of membranes	540	900	900	2,700
Size of membranes, in × in	18 × 20	18 × 40	18 × 40	18 × 40
Total area of membranes, ft^2	1,350	4,500	4,500	13,500
% total area available for transfer	62	64	64	64
Approximate weight, lb	1,300	2,800	2,800	8,400
Approximate overall height, including legs	4'6″	6'10″	6'8″	6'8″
Demineralization per pass (25°C, high-Cl water, typical flow), %	88.5	88.3	52	90.0
Current required for 3000-ppm feed, A	Stages 1 and 2: 19 Stages 3 and 4: 8	Stages 1 and 2: 36 Stage 3: 12	46	Stage 1: 46 Stage 2: 24 Stage 3: 12
Voltage required for 3000-ppm feed†	Stages 1 and 2: 180 Stages 3 and 4: 150	Stages 1 and 2: 350 Stage 3: 150	640	Stage 1: 640 Stage 2: 500 Stage 3: 420
Direct-current kW/stack for 3000-ppm feed†	4.6	14.1	29	Stage 1: 29 Stage 2: 12 Stage 3: 5
Direct-current kWh/1000 gal product ‡ for 3000-ppm feed†	7.4	6.8	4.7	7.4

*Ionics, Incorporated, Watertown, Mass, 1979. These units use the EDR process, in which polarity and fluid flow are periodically reversed. In general, addition of acid and antiprecipitant to the feed is not necessary in this process.
†For typical brackish water containing a high proportion of sodium chloride.
‡Approximately 10% of flow wasted during reversal.
(Spiegler, 1984; Walas, 1988).

Continuous fluidized bed equipment has been utilized for gas adsorption, but usually attrition losses of comparatively expensive adsorbents have been prohibitive and the loss of efficiency because of axial mixing has been a serious handicap. Drying equipment such as those of Figure 9.13 presumably can be operated in reverse to recover valuable substances from a vapor phase, and the forward mode applied for regeneration in associated equipment. Other possibly suitable fluidized bed configurations are those of the reactors of Figures 17.32(a), (c), and (d).

Moving bed gas adsorbers also have been proposed and used, patterned after moving bed gas oil crackers. In the Hypersorber of Figure 15.28, flows of gas and solids are countercurrent in a single vessel. After saturation, the solid is stripped with steam and removed at the bottom of the tower, and gas is lifted to cooling and adsorption zones. The control mechanism for solids flow and typical performance for ethylene recovery from cracked gases also are shown with the figure. Partly because of attrition losses and the advent of competitive processes for ethylene recovery, the Hyper-
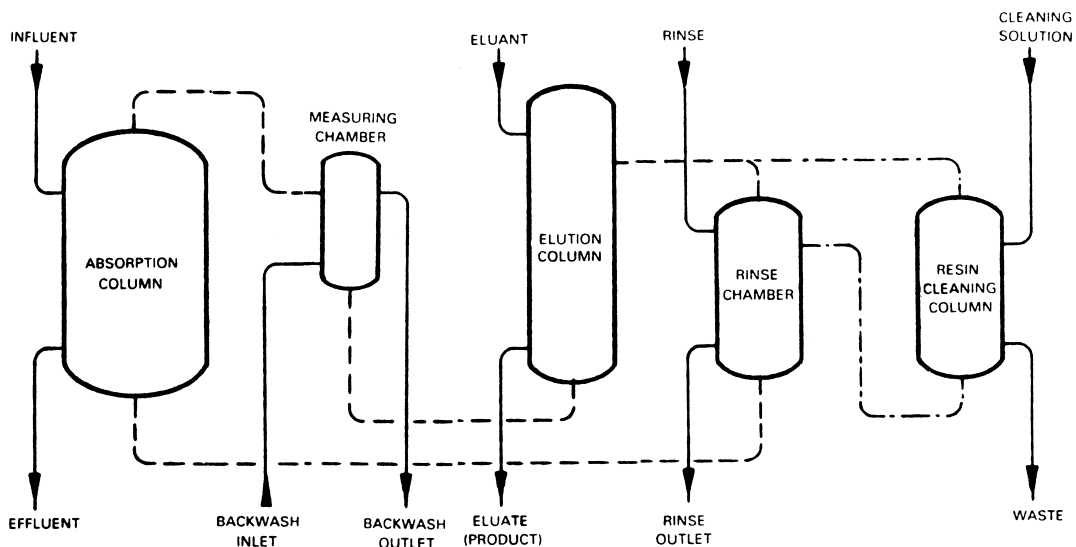
Figure 15.27. A process for recovering uranium from mine waters. The absorption column is 2.16 m dia, water flow rate is 28.5 m/hr, resin transfer off the top of the absorption column is 87 L every 3 hr, inlet concentration 3–6 mg U/L, outlet 0.002–0.009 mg U/L (*Himsley and Bennett, in Naden and Streat, 1984; U.S. Pat. 4,018,677*; Walas, 1988).

TABLE 15.7. Economic Data for a Chromatographic Process with Throughput of 400–920 tons/yr, with Column 4 ft dia by 15 ft high[a]

Equipment Cost	Percent	Annual Operating Cost	Percent
Feed preparation and injection	9.4	Maintenance and taxes	19.9
Column	13.1	Operating labor	13.7
Detection and control	2.6	Utilities and supplies	5.7
Fraction collection and heat exchange	18.7	Packing replacement	40.8
Carrier recycle	11.2	Depreciation (10 year)	19.9
			100
Process piping and building	16.5		
Engineering and construction	28.5		
	100		

[a]Data are given only on percentage bases because of their age. (Abcor Inc., 1968).

(a)

(b)
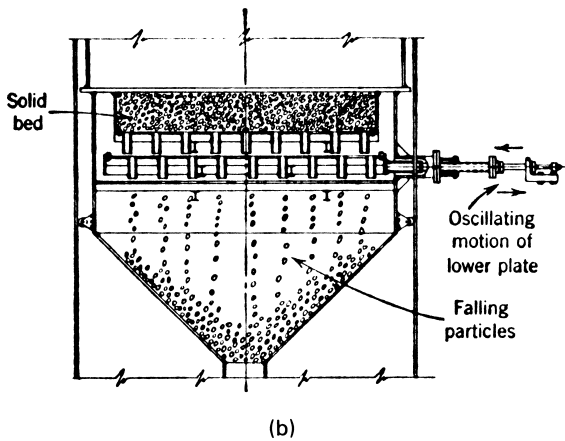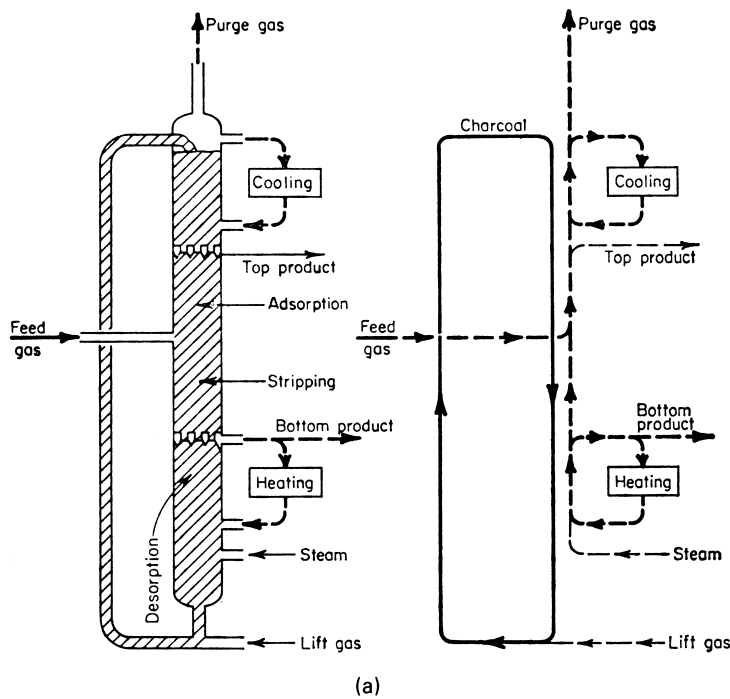
Component	Compositions, vol %			
	Feed gas	Bottoms	Overhead	Purge gas
Hydrogen	39.8	.....	31.6	61.8
Nitrogen	1.7	.....	1.4	2.5
Carbon monoxide	0.9	.....	0.8	1.3
Oxygen	0.1	0.1	0.1	0.2
Methane	51.3	.....	66.1	33.7
Carbon dioxide	0.2	2.9	.....	0.1
Acetylene	0.2	3.6		
Ethylene	5.8	92.7	.....	0.4
Ethane	Tr.	0.7		
Total	100.0	100.0	100.0	100.0

(c)

Figure 15.28. Hypersorber continuous moving bed gas phase adsorption system (*See Mantell, 1951*) (a) Schematic pattern of flows of gas and solid adsorbent (*Hengstebeck, 1959*). (b) Solid flow rate control mechanism. (c) Typical separation performance. (Walas, 1988).

sorber was abandoned after a few years. The simpler Nofsinger moving bed adsorber of Figure 15.29 also has not proved commercially attractive.

LIQUID PHASE ADSORPTION

A major application of liquid phase adsorption is to the removal of relatively small amounts of impurities or color bodies in water treating, sugar refining, and other processes. Both batch and continuous equipment are illustrated in Figure 15.30. The batch process consists of slurrying the liquid with powdered adsorbent and then separating the two phases by filtration. The saturated adsorbent—carbon from water treating or fullers earth from oil treating—is regenerated by ignition as in the flow diagram of Figure 15.30(a), or sometimes by treatment with suitable reactive solvents such as sodium hydroxide for adsorbed phenol from water. In the semicontinuous process of Figure 15.30(b), pulses of adsorbent are withdrawn periodically from the bottom and fresh material is charged in at the top. The pulses are 2–10% of the volume of the bed. Some data of adsorbent treating of water were given in Section
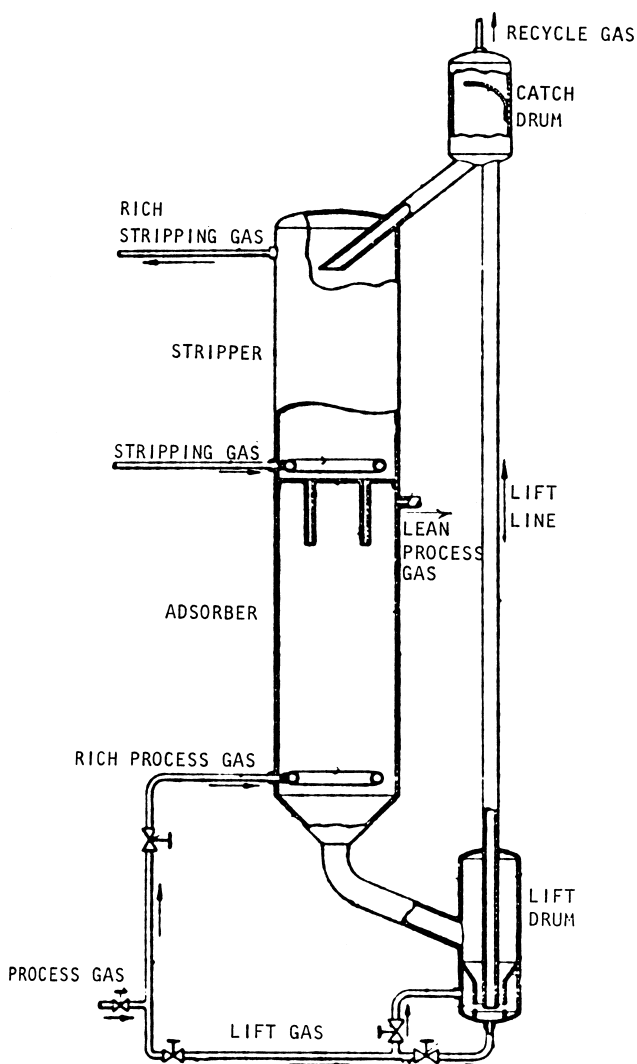
Figure 15.29. Nofsinger continuous moving bed adsorber (*Spangler and Price, U.S. Pat. 3,442,066, 6 May 1969*).

15.5. Attrition losses in moving beds for liquid treating are less than for gas treating. In the similar process of ion exchange of Figure 15.30(a)(b), ion exchange losses of 30% per year are mentioned.

The successful simulation of continuous moving bed adsorption process developed by UOP (Universal Oil Products) is illustrated in Figure 15.31. For the process being simulated, part (a) of the figure shows flows of adsorbent and fluids and the composition profiles along the tower. The simulated process employs 12 fixed beds in a single vessel, in which input and output streams are individually controlled. The points of entry and withdrawal of the four external streams—feed, extract, raffinate, adsorbent—are controlled with a single special rotary valve. Periodically each stream is switched to the adjacent bed so that the four liquid access positions are always maintained the same distance apart. Satisfactory operation is assured by uniform feeds and withdrawals and flushing of lines between their uses for regeneration and other purposes. The internal constructions of the tower, such as the mechanism of feed and withdrawal at individual beds, are not revealed in the literature. As of 1984, some 60 large capacity installations for various hydrocarbon isomer separations with molecular sieves have been made. The largest column mentioned is 22 ft dia. The distribution across the cross section has been worked out so that scale-up from 3 in. to commercial size is reliable. The process is described briefly in articles by Broughton (1978; 1984) and in several patents listed in the first of these articles.

A variant of this process developed by Toray industries is illustrated in Figure 15.24. The beds are individual rather than in a single shell and utilize individual on-off valves. One application, to the separation of aromatics, is mentioned in the literature [Otani, (17 Sept. 1973)].

ION EXCHANGE

Because of the large volumes of dilute electrolytes that sometimes need to be treated, continuous processing with ion exchange materials is more common than liquid phase adsorption, although fixed bed processes still are predominant. Typical arrangements of fixed beds appear in Figure 15.25. Any particular ion exchange resin is capable of exchanging only cations or anions. The two kinds of resins may be mixed and incorporated in the same vessel or they may be used separately in their own vessels. Cation exchange resins may be strongly or weakly acid, and anion exchange resins, strongly or weakly basic. The choice of an ion exchange system depends on the composition of the feed, the product quality required, the scale of the operation, and the economics of the process. Three of the many possible arrangements of vessels are sketched in Figure 15.25(d). Series combinations of vessels are employed when leakage is highly undesirable. The inlet to the last stage is monitored and the information is taken as a guide to transfer of the first vessel in line to regeneration.

All of the continuous processes of Figures 15.32 and 15.27 employ intermittent transfer of spent resin out of the primary vessel to regeneration facilities. Although all of the operations of exchange, rinsing, and regeneration can be performed in elegantly designed equipment such as Figure 15.32(a), greater flexibility is inherent in a multivessel plant such as Figure 15.27. This is of an operating plant for which some size and operating data are given here, and more appear in the reference article.

Performances of four fluidized bed ion exchange plants are described by Cloete (in Naden and Streat, 1984, pp. 661–667). One of the exchange columns is 4.85 m dia, has 12 stages each 1 m high, with perforated trays having holes 12 mm dia with a capacity of 640 m³/hr of uranium mine waters.

(a)

(b)
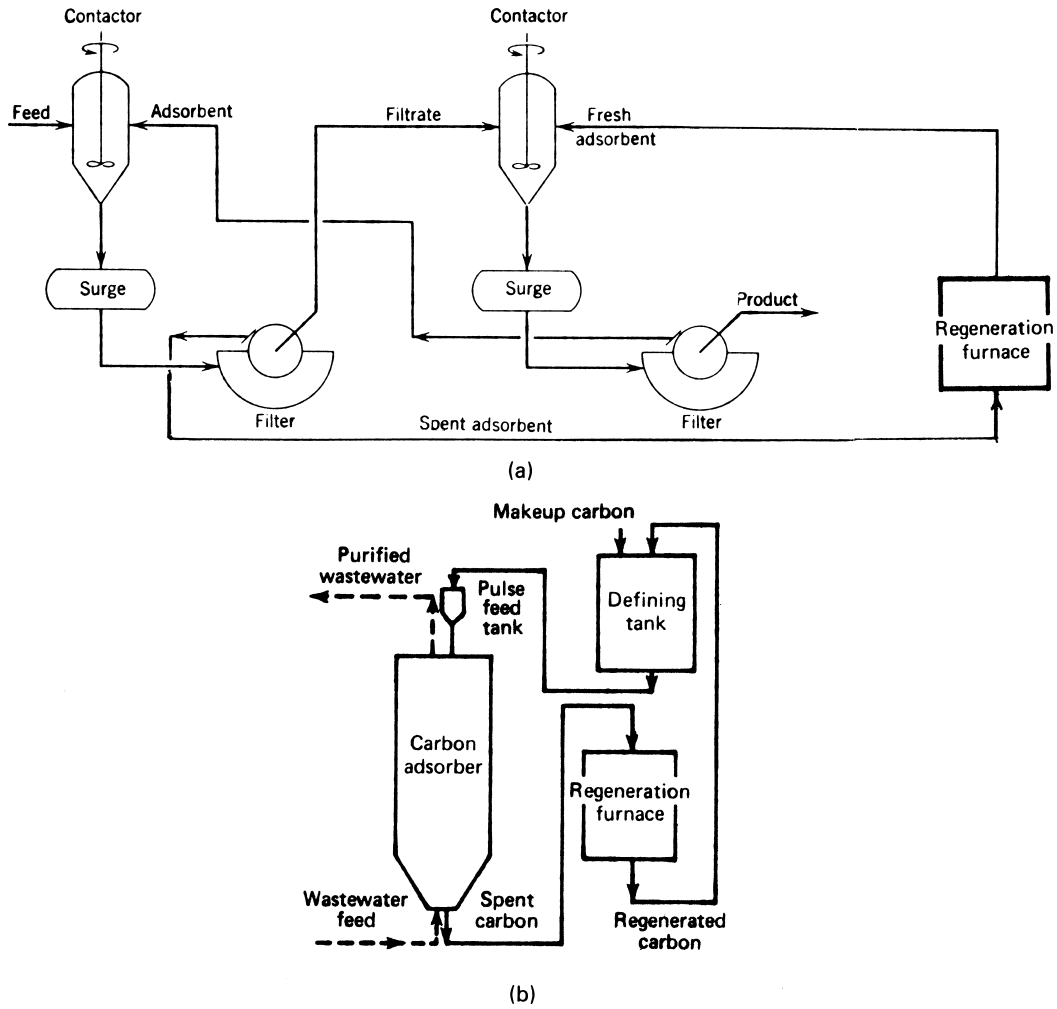
Figure 15.30. Liquid phase adsorption processes for water treated with activated carbon and petroleum treated with clay adsorbents. (a) A two-stage slurry tank and filter process. (b) Continuous pulsed bed operation, individual pulses 2–10% of bed volume as needed. (Walas, 1988).

(a)
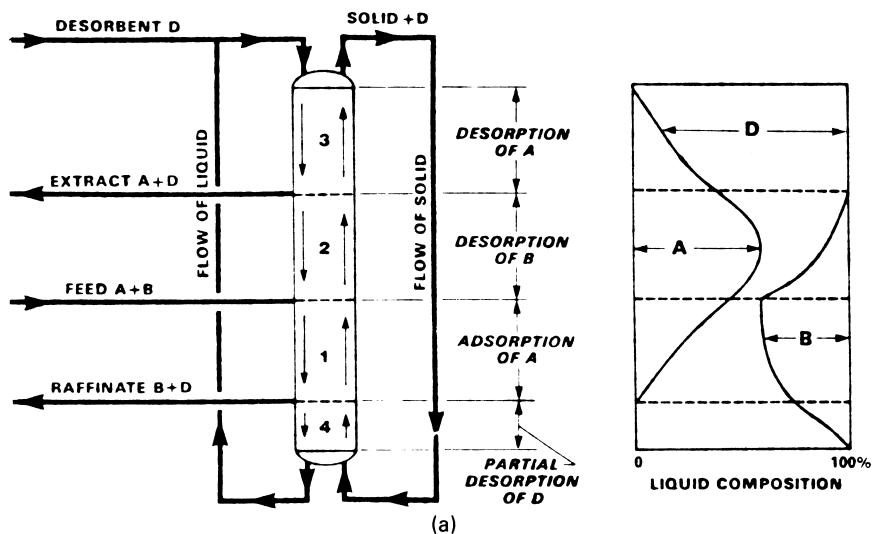
Figure 15.31. Continuous and UOP simulated continuous moving bed liquid adsorption processes (*Broughton, 1984–1985*). (a) Continuous moving bed liquid adsorption process flows and composition profiles. (b) UOP Sorbex simulated moving bed adsorption process. (Walas, 1988).

(b)

Figure 15.31.—(*continued*)

Figure 15.32. Continuous ion exchange equipment. (a) The Higgins moving bed unit; the consolidated resin bed is recirculated upwards with a hydraulic pulse. [*U.S. Pat. 3,580,842, (25 May 1942)*]. (b) Operating sequence in the Higgins contactor. The double-acting piston simultaneously sucks liquid from the top of the column and delivers it to the bottom: (a) solution pumping for several minutes; (b) resin movement for 3–5 sec; (c) solution pumping for several minutes (*Coulson and Richardson, 1979*). (c) In the Asahi system, resin is transferred between the adsorber and the regenerator at 10–60 min intervals (*Asahi., U.S. Pat. 3,152,072*). (d) The Himsley multistage slurry adsorber; the resin is pumped as a slurry, one stage at a time into and from the regenerator [*Himsley, Can. Pat. 980,467, (23 Dec. 1975)*]. (Walas, 1988).

Figure 15.32.—(*continued*)

Ion exchange resins are used widely as heterogeneous catalysts of processes that require acid or base catalysis, for example, hydration of propylene to isopropanol, reaction of isobutylene with acetonitrile, and many others. The same kind of equipment is suitable as for ion exchange, but usually regeneration is not necessary, although some degradation of the resin naturally occurs over a period of time.

ION EXCHANGE MEMBRANES AND ELECTRODIALYSIS

There is one basic design of electrodialysis equipment for demineralization appears to be in use. This is an assembly of alternate cation and anion ion exchange sheets separated by spacers in groups of several hundred clamped together between electrodes. The assembly physically resembles a plate-and-frame filter press.
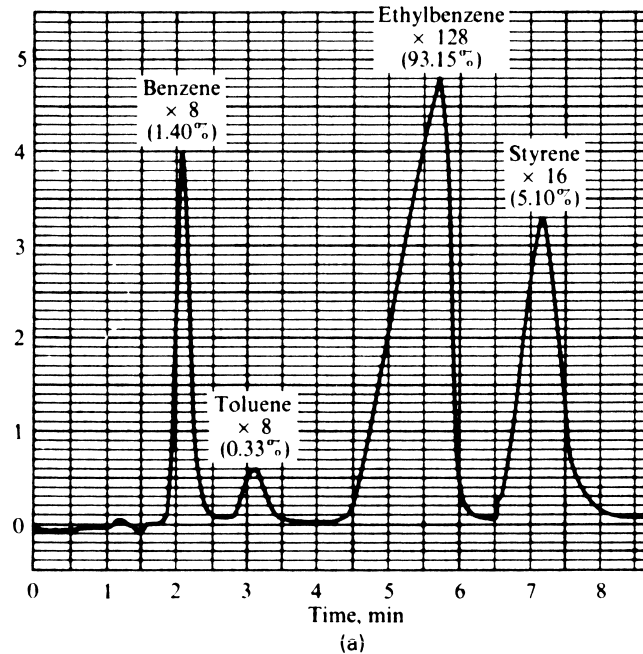
Figure 15.33. Chromatographic separations. (a) Typical chromatogram produced by gas–liquid chromatography. (b) Flowsketch of a production scale chromatographic unit (*Ryan, Timmins, and O'Donnell, Aug. 1968*). (Walas, 1988).

(b)
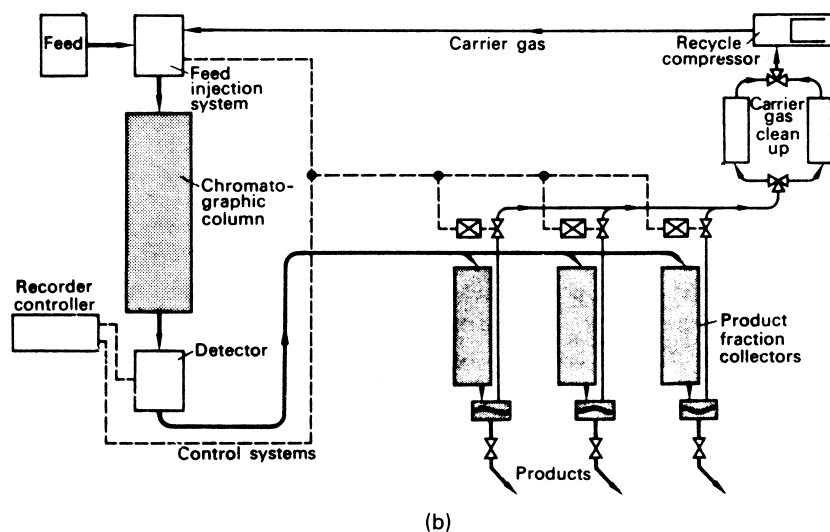
Figure 15.33.—(*continued*)

TABLE 15.8. Examples of Chromatographic Separations in a Column 125 mm dia

(a) Five Separations

Case	Mixture	Charge (mol %)	Product (mol %)	Temperature (°C)/ Pressure (Torr)	Remarks
1	Pentane	99.3	99.995	225/760	extreme purification
	Isopentane	0.7	50 ppm		
2	Benzyl alcohol	99.5	99.6	150/50	selective removal of small impurities
	Benzyl aldehyde	0.1			
	Others	0.4			
3	α-Pinene	70.0	99/2	160/760	simultaneous purification of two materials
	β-Pinene	30.0	1/98		
4	Essence of cloves			220/760	recovery of a thermally sensitive natural product
	Eugenol	75	99.8		
5	Bromo-3-thiophene	91.6	99.0	150/760	a difficult separation of position isomers
	Bromo-2-thiophene	4.6	1.0		
	Others	3.8			

(Bonmati and Guiochon, Sept/Oct 1976; Walas, 1988).

(b) Details of the Separation of α-Pinene and β-Pinene

Operating Conditions	Other Data			ELF–SRTI Process	
Column					
diameter (mm)	100		305	125	400
Length (m)	2.7		unknown	1.5	1.5
Baffles	yes		yes	no	no
Programmer		peak deflection		time-based	
Carrier gas	He		He	He	H_2
Velocity (cm/sec)	9.2		—	9.5	9
Temperature (°C)	160		160	160	160
Cycle (sec)	80		—	80	65
Purity		98.5–98.6		99.1–97.8	
Productivity (kg/day)	19		160	40	540

(Walas, 1988).

Figures 15.26(a) and (b) show such assemblies, and some dimensional data were stated in Section 15.7, Electrodialysis.

The concentrates of salt solutions made by electrodialysis of seawater are suited as feed to the evaporators of salt manufacturing plants with considerable savings in overall energy requirements. Other applications also are based on the concentrating effects of electrodialysis, for instance, tenfold increases of concentrations of depleted streams from nickel and copper plating plants are made routinely.

In applications such as the electroreduction of Figure 15.26(c) and electrolysis of brine to caustic and chlorine, single membranes serve as diaphragms between electrodes, permitting passage of ions but retarding diffusion and mixing of feed and product solutions.

CHROMATOGRAPHIC EQUIPMENT

The components of a commercial process employing chromatographic separation are represented on the flowsketch of Figure 15.33(b). The process is intermittent with very short cycles. The cost breakdown of a plant for the separation of α- and β-pinenes is given in Table 15.7. Other data for the same separation, however, are presented in Table 15.8. The largest column considered there, 0.4 m dia, has a production rate of 4300 kg/(m^2)(day), with cycle times of about 1 min. Valentin (1981) refers to literature where columns of 1 and 2 m dia are described and mentions that diameters up to 5 m are feasible and may have throughputs of 10,000 metric tons/yr.

REFERENCES

Adsorption

Al-Sahat et al., *Ind. Eng. Chem. Des. Dev.*, **20**, 658 (1981).

R.A. Anderson, Adsorption (general), *Encycl. Chem. Process Des.*, **2**, 174–213 (1977).

Anon., *Chem. Eng.*, **17**, April 15, 1985.

F.E. Bernardin, *Chem. Eng.*, October 18, 1976, 77–82.

Bonner and Smith, *J. Phys. Chem.*, **61**, p. 336 (1957).

G.B. Broughton, Adsorption separation (liquids), *Encyc. Chem. Technol.* **1**, 563–581 (1978).

G.B. Broughton, Production scale adsorption of liquid mixtures by simulated moving bed technology, *Sep. Sci. Technol.*, **19**, 723–736 (1984–1985).

S. Brunauer, *Physical Adsorption*, Princeton University Press, Princeton, NJ, 1945.

C.H. Chi, and W.P. Cummings, Adsorptive separation (gases), *Encycl. Chem. Technol.*, **1**, 544–563 (1978).

J.M. Coulson and J.F. Richardson, *Chemical Engineering*, Vol. 3, 520 (1979).

J.R. Fair, Sorption processes, *Chem. Eng.*, 90–110 (14 July 1969).

Hansen, *Heat Transfer in Counterflow, Parallelflow and Crossflow*, McGraw-Hill, New York, 1983.

R.J. Hengstebeck, *Petroleum Processing*, McGraw-Hill, New York, 1959.

A.L. Hines, and R.N. Maddox, *Mass Transfer Fundamentals and Applications*, Prentice-Hall, Englewood Cliffs, NJ, 1985.

O.A. Hougen and K.M. Watson, *Chemical Process Principles*, Vol. 3, Wiley, New York, 1947, p. 1056.

O.A. Hougen and Marshall, *Chem. Eng. Prog.*, **43**, 197 (1947).

W.A. Johnston, *Chem. Eng.*, **79**, 87–92, (27 November 1972).

G.E. Keller, R.A. Anderson, and C.M. Yon, in Rousseau (Ed.), *Handbook of Separation Process Technology*, Wiley, New York, 1987.

Kipling, *Proceedings of the Second International Congress on Surface Activity*, Vol. III, 1959, p. 462.

K.S. Knaebel, The basics of adsorber design, *Chem. Eng.*, 92–103 (April 1999).

Kovach, Gas adsorption, in Schweitzer (Ed.), *Handbook of Separation Processes for Chemical Engineers*, McGraw-Hill, New York, 1979, pp. 3.3–3.47.

L.M. Landholt-Bornstein, *Numerical Data and Functional Relationships in Science and Technology*, **II**/3, Springer, New York, 1956, pp. 525–528.

M.N.Y. Lee, Novel separations with molecular sieve adsorption, in *Recent Developments in Separation Science*, **II**, CRC Press, Boca Raton, FL, 1972, pp. 75–110.

C.M. Lukchis, Adsorption systems, *Chem. Eng.*, (11 June 1973); (9 July 1973); 6 August 1973).

C.L. Mantel, *Adsorption*, McGraw-Hill, New York, 1951.

J.J. Maurer, *Am. Chem. Soc. Symp. Ser.*, **135**, 73 (1980).

S. Otani et al., *Chem. Economy Eng. Rev.*, **3**(6), 56–59 (1970).

S. Otani et al., *Chem. Eng.*, **80**(9), 106 (17 September 1973).

J.B. Rosen, *Ind. Eng. Chem.*, **46**, 1590 (1954).

R.W. Rousseau (Ed.), *Handbook of Separation Process Technology*, Wiley, New York, 1987.

D.M. Ruthven, *Separation Purification Methods*, **5**(2), 189 (1976).

D.M. Ruthven, *Principles of Adsorption and Adsorption Processes*, Wiley, New York, 1984.

J.M. Ryan, R.S. Timmins and J.F. O'Donnell, *Chem. Eng. Prog.*, **64**, 53 (August 1968).

J.J. Thomas, *J. Am. Chem. Soc.*, **66**, 1664 (1944).

R. Treybal, *Mass Transfer Operations*, McGraw-Hill, New York, 1980.

D.G. Vilman, *Encyclopedia of Chemical Technology*, Verlag Chemic, Weinheim, Germany, 1994.

T. Vermeulen, et al., Adsorption design, *Encycl. Chem. Process Des*, **2**, 162–174 (1984). Adsorption separation, *Encycl. Chem. Technol.* **1**, 531–544 (1978); Adsorption and ion exchange, in *Chemical Engineer's Handbook,* 6th ed., McGraw-Hill, New York, 1984, Sec 16.

C.M. Yon and L. Turnock, *Chem. Eng. Prog. Symposium Series,* **117**, 67 (1971).

Parametric Pumping

G.E. Keller et al., in *Handbook of Separation Process Technology,* Wiley, New York, 1987, p. 667.

N.H. Sweed, N. Li (Ed.), in *Recent Developments in Separation Science* Am. Chem. Soc., Symposium Series, No. 141, 1973.

N.H. Sweed, and Gregory, *A.I.Ch.E.J.* **17**, 171 (1971).

P.C. Wankat, Cyclic separation processes, *Sep. Sci.*, **9**(2), 85–116 (1974).

P.C. Wankat, J.C.D. Ore, and W.C. Nelson, Cyclic zone separations, in *Separation and Purification Methods,* Vol. 4, pp. 215–266, CRC Press, Boca Raton, FL., 1976.

R.H. Wilhelm et al., *Ind. Eng. Chem. Fundam.*, **5**, 141–144 (1966); **7**, 337–349 (1968).

Ion Exchange

R.E. Anderson, Ion exchange separation, in Schweitzer, (Ed.), *Handbook of Separation Techniques for Chemical Engineers,* McGraw-Hill, New York, 1979, pp. 1.359–1.414.

Himsley and Bennett, in Naden and Streat (Eds.), 1984, pp. 144–168.

D. Naden and M. Streat (Eds.), *Ion Echange Technology*, Horwood, Chichester, England, 1984.

T. Vermeulen, Adsorption and ion exchange, in *Chemical Engineer's Handbook,* McGraw-Hill, New York, 1984, Sec. 16.

R.M. Wheaton and E.J. Le Fevre, Ion exchange, *Encycl. Chem. Technol.*, **13**, 678–705 (1981).

Electrodialysis and Ion Exchange Membranes

Anon., *Chem. Eng.* April 15, 1985, 17

G. Belfort, (Ed.), *Synthetic Membrane Processes,* Academic, New York, 1984.

D.S. Flett (Ed.), *Ion Exchange Membranes*, Horwood, Chichester, England, 1983.

R.E. Lacey, Ion exchange separations, in Schweitzer (Ed.), *Handbook of Separation Techniques for Chemical Engineers,* McGraw-Hill, New York, 1979, pp. 1.449–1.465.

K.S. Spiegler, Electrodialysis, in *Chemical Engineers' Handbook,* McGraw-Hill, New York, 1984, pp. 17.37–17.45.

H. Strathmann, Electrodialysis and its application in the chemical process industry, *Sep. Purification Methods,* **14**(1), 41–66 (1985).

Chromatography

R. Bonmati and G. Guiochon, *Pqrfums Cosmetiques Aromes,* 37–59 (September/October 1976).

J.R. Conder, Production scale gas chromatography, in H. Purcell (Ed.), *New Developments in Gas Chromatography*, Wiley, New York, 1973.

L. Meites, (Ed.) *Handbook of Analytical Chemistry*, McGraw-Hill, New York, 1963.

A.E. Rodriques and D. Tondeur (Eds.), *Percolation Processes: Theory and Applications*, Sijthoff and Noordhoff, Alphen aan den Rijn, Netherlands, 1981.

Valebntin, in Rodriques and Tondeur (Eds.), *Percolation Processes: Theory and Applications,* Sijthoff and Noorhoff, Alphen aan den Rijn, Netherlands, 1981.

16

CRYSTALLIZATION FROM SOLUTIONS AND MELTS

rystals are solids composed of atoms arranged in an orderly repetitive array. Thus, the interatomic distances in a crystal of any definite compound are constant and are characteristic of that material. Crystallization is an important unit operation because the process of crystallization is capable of producing very high purity products from solutions containing significant amounts of impurities with very low energy input compared to other unit operations such as distillation. The crystals produced have a good appearance with high bulk density and good handling characteristics, so drying requirements are minimized due to the low moisture content of the cake off of a centrifuge or filter.

Crystals can be stored for long periods of time compared to agglomeration or compaction, which have much shorter storage lives before breaking down.

Dissolved or molten substances are recoverable in solid form by precipitation upon cooling or upon removal of the solvent or by addition of precipitating agents or by reaction between solutions or a solution and a gas. For convenience a distinction is made between two kinds of processes:

1. In solution crystallization, the crystals are separated away from a solvent, often water. In the case of inorganic solids particularly, the operating temperature is far below their melting points.
2. In melt crystallization, two or more substances of comparable melting points are separated by some degree of cooling. The degree of completeness of such separations depends on the phase equilibrium relations. When the crystals must be refined to remove occluded substances, the recovered material may leave the process in molten form. Subsequently, it may be solidified as flakes or sprayed granules.

The design of crystallizers is based on knowledge of phase equilibria, solubilities, rates and amounts of nuclei generation, and rates of crystal growth. Each system is unique in most of these respects and not often predictable. The kind of information needed for design of a continuous crystallizer is indicated by the data supplied for Example 16.1 and as listed in greater detail below.

Significant advances in the theory of crystallization have occurred. Due to the complex nature of crystallization, the theory of crystallization can best be used to troubleshoot and improve the operation of an existing crystallizer. Attempts to design a new crystallizer from the theory alone will not lead to the best commercial design. It is necessary to have experienced crystallizer designers incorporate their knowledge about their equipment and their experience with scaling up to achieve the commercial crystallizer design that will best meet the requirements. Testwork is required to make the required guarantees. Depending on the experience with the product being produced from the process, this testwork may involve pilot plant, bench scale, and or a demonstration plant. The information required for the proper design of the crystallizer is either developed by the designer based on the testwork or the designer's prior knowledge and input from the process supplier as follows:

1. Solubility data for the product in the particular solvent at the level of impurities that will be present in the purge as a function of possible operating temperatures.
2. Physical property data for the product and solutions, including the heat of crystallization, specific heats, specific gravities, viscosities, vapor pressures over the solution at the operating temperatures, and thermal conductivities.
3. The effect of residence time on the decomposition of the product in the case of organic products.
4. The composition of the feed solutions and/or gases along with their temperatures.
5. The required instantaneous production rate.
6. The crystal size distribution, crystal habit (shape or morphology), and bulk density.
7. Crystal retention time.
8. The utilities available to operate the crystallizer, such as steam pressure and temperature, condensing water, or brine temperature (if brine its physical properties), electricity, and so on, and the cost of these utilities.
9. Level of allowable supersaturation. (Organics such as dextrose, citric acid, lactose, fructose, etc., exhibit high levels of supersaturation in the presence of significant amounts of product crystals, which affects their yields from the feed solution. In the case of lactose, the yield can be significantly increased by holding the slurry after the crystallizer for 24 hours before separating the crystals from the solution.)
10. Effects of additives, impurities, and pH on the crystal habit, crystal size distribution, crystal purity, and crystal hardness.
11. Materials of construction.
12. Factors to use in evaluating the design, such as the number of effects or stages, payout period, etc.
13. If the vapor generated in the crystallizer is not water, its enthalpy, specific volume, and viscosity are required as a function of the operating temperature and pressure.
14. Heat transfer characteristics.
15. Factors based on the designer's experience for selecting the allowable vapor velocity, circulation rate, operating slurry density, mixing parameters, circulating device characteristics, geometry, temperature rise or drop, feed locations, product withdrawal location, required instrumentation for controlling the crystallizer, operating cycle, etc.
16. Some products, such as boric acid, sublime. If this is the case, it is therefore necessary to know the amount of product in the overhead vapor as a function of the solution temperature, pressure over the solution, and solution composition.
17. Details about products that can crystallize in alpha or beta forms, such as the effect of time and temperature.

18. *Other factors that can influence the design, such as space limitations, tendency for the solution to foam, and so on. In this chapter will discuss the main concepts associated with crystallization practice, and will describe* the main types of equipment used nowadays, together with some indications of their performance and applicability.

16.1. SOME GENERAL CRYSTALLIZATION CONCEPTS

The following concepts should be kept in mind when evaluating crystallizer performance:

1. Crystal growth rates are higher at higher temperatures.
2. Additives or the level of impurities are only effective within a narrow range. Crystal habit can be poorer at too high a level of impurities and the habit may not be affected at all at too low a level of impurities.
3. The incorrect amount or type of impurities can cause cycling of the crystal size.
4. Seeding a crystallizer with fines will lower the crystal size. Therefore, the feed to the crystallizer should be free of fines to grow larger crystals. When the design uses a number of stages of crystallizers in series, the crystal size will be smaller in every stage after the first stage due to the fines in the feed and the lower growth rate at lower temperatures.
5. Crystals grown contain occlusions. These occlusions can result in a lower product purity and crystals that can be more easily broken. Crystals grown with the right level of impurities present in solution can be less prone to breakage and can be purer.
6. Longer crystal retention times can result in less liquor occlusions in the crystals.
7. It is important to operate the crystallizer at low levels of supersaturation. Supersaturation can be lowered by operating at higher slurry densities, longer crystal retention times, higher crystallizer circulation rates, and good mixing of the feed solution (multiple feed injection points or other feed dispersion devices may be desirable). The type and level of impurities can also affect the level of supersaturation.
8. Cycling of the crystal size in a crystallizer can be reduced by periodically or continuously injecting a slurry of crystals equivalent to 5 to 40% of the production rate in the crystallizer and having a crystal size distribution at least equivalent to the average crystal size produced in the crystallizer.
9. Some product crystals are more prone to mechanical attrition by the circulating device and/or transfer pumps or a centrifuge. Larger crystals in these cases can be obtained by operating at shorter retention times, lower slurry densities, or careful selection of the circulating device, centrifuge, or transfer pumps. Sodium sulfate, citric acid, and sodium carbonate monohydrate are examples of products that fall into this category. Four-bladed axial flow pumps result in higher crystal breakage than three-bladed axial flow pumps.
10. Crystal size is determined by screening the dried product crystals. Products that exhibit a tendency to stick to vibratory screeners must either be screened for a minimum of 20 minutes on a vibratory screener or screened using an air sifter. Fructose and dextrose exhibit this tendency.
11. Crystal samples out of a crystallizer must be separated from the solution and dried. The separation from the solution typically is done on a laboratory centrifuge or on a Buchner Funnel. The separated crystals are typically washed with alcohol on the separation device and air dried before screening. Some products require special separation techniques to avoid fines precipitation or agglomeration during separation of the crystals from the slurry. Glaubers salt, for instance, can be properly separated by first washing the solution off of the crystals with car brake fluid and then alcohol washing the crystals. Solutions such as dextrose highly supersaturate. This supersaturation must be removed before crystal separation can be properly effected. This can be done by mixing a saturated solution of dextrose with the slurry in equal proportions before separating the crystals from the solution. This is followed by alcohol washing. Normally, ethanol or methanol alcohols are used. In some cases, acetone is used instead of alcohol.
12. Continuous crystallizers must operate steadily at equilibrium to achieve the design requirements. This means the feed rate, production rate, slurry density, operating temperature, liquid level, and so on, should held constant as a function of time. To accomplish this result requires the crystallizer to be isolated from upstream or downstream variations and the instruments need to be continuously calibrated. To help accomplish this objective, a 12- to 24-hour agitated feed tank needs to be installed before the crystallizer.
13. The feed to the crystallizer should be slightly unsaturated.
14. The feed to the crystallizer and any heat exchanger on the crystallizer need to be submerged from flashing to prevent salting and fines formation.
15. The steam to the heat exchanger should be desuperheated.
16. Batch crystallizers are self-cleaning due to injection of new unsaturated feed solution at the start of every batch, which, with agitation, dissolves any buildup.
17. Batch crystallizers tend to have a broader crystal size distribution than continuous crystallizers. To help narrow the crystal size distribution you must either cool slowly through the initial crystallization temperature or seed at the initial crystallization temperature.
18. If the solubility of the product in the solvent increases with temperature (normal solubility), heating the solution containing fines or the slurry will dissolve crystals. When heating, the supersaturation is relieved first, followed by dissolving the finer crystals. Fines destruction can also be accomplished by adding a solvent or unsaturated solution or steam. The temperature of the slurry must not be allowed to drop in these cases.
19. Any heat exchangers on the crystallizer should use a minimum of 1.25 inch diameter tubes and a minimum of 5 ft/sec tube velocities. Larger diameter tubes can result in longer operating cycles. Properly designed plate heat exchangers can be used in place of shell and tube heat exchangers. When handling crystals, the gap between plates is very important to prevent plugging.
20. Crystallizers should operate with a minimum of 10% by weight crystals in suspension (slurry density).
21. Surface-cooled heat exchangers must be designed using large diameter tubes, low temperature drops, and low ΔTs between the cooling media and the slurry to obtain reasonable operating cycles. The steepness of the solubility curve determines these parameters.
22. Mixed suspension, mixed product removal crystallizers (MSMPR) normally have much longer operating cycles than

OSLO crystallizers because MSMPR crystallizers operate with much higher slurry densities and lower levels of supersaturation. Forced circulation and DTB crystallizers are examples of MSMPR crystallizers. An OSLO crystallizer operating at high slurry densities with the slurry circulated to the vaporizer will perform like an MSMPR crystallizer.

23. Crystal agglomeration (crystals sticking together) normally occurs in the crystal separator and/or dryer. Ammonium chloride and borax can form agglomerates in the crystallizer depending on the type and amount of impurities present as well as the level of supersaturation.

16.2. IMPORTANCE OF THE SOLUBILITY CURVE IN CRYSTALLIZER DESIGN

Figure 16.1 shows four different solubility curves. It is important for the crystallizer designer to know the shape of the solubility curve to properly design the crystallizer.

CURVE 1

Solubility Curve 1 exhibits normal solubility. Yield can be obtained by cooling a saturated solution, evaporating the solvent, or salting out (adding a compound that goes into the solution while the product comes out of solution). Heat exchangers on the crystallizer can be designed using higher temperature increases and ΔTs between the heating media and the slurry. Ammonium sulfate and potassium chloride exhibit this type of solubility.

CURVE 2

Curve 2 shows that the solubility of the solute in the solvent does not change with temperature. Yield can be obtained by evaporating the solvent or salting out. Heat exchangers on the crystallizer can be designed using higher temperature increases and ΔTs between the heating media and the slurry. Sodium chloride exhibits this type of solubility.

CURVE 3

Curve 3 shows that as the temperature increases, the solubility decreases. This is inverse solubility. Yield is obtained by evaporating the solvent or salting out. Heat exchangers must be designed using lower temperature increases and lower ΔTs between the heating media and the slurry. Sodium sulfate and sodium carbonate monohydrate exhibit this type of solubility.

CURVE 4

Curve 4 exhibits very steep solubility. Yield is obtained by cooling the feed solution. To prevent fines formation, the cooling must exactly follow the solubility curve. This is done automatically in batch crystallizers. Continuous crystallizers in series must have the crystallizer stage temperatures selected so as not to cross the solubility curve. Benzoic acid and DMT exhibit this type of solubility.

16.3. SOLUBILITIES AND EQUILIBRIA

The variation of the solubilities of most substances with temperature is fairly regular, and usually increases with temperature. When water is the solvent, breaks may occur in solubility curves because of the formation of hydrates. Figure 16.2(a) shows such breaks, and they can be also discerned in Figures 16.2(b) and (c). Unbroken lines usually are well enough represented by second degree polyno-

mials in temperature, but the Clapeyron-type equation with only two constants, $\ln x = A + B/T$, is of good accuracy, as appears for some cases on Figure 16.2(b).

A convenient unit of solubility is the mass of solute per unit mass of solvent, or commonly g solute/100 g solvent. Interconversions with molal units and mol fractions are made readily when densities of the solutions are known.

Under quiescent conditions a concentration substantial in excess of normal solubility or a temperature lower than the normal saturation temperature can be maintained. The maximum supersaturation appears to be a fairly reproducible quantity, but is reduced or even eliminated by stirring or by the introduction of dust or seed crystals. Some data are shown in Figure 16.2(c) and in Table 16.1. They are expressed as $\Delta C = C - C_{\text{sat}}$ or as $\Delta C / C_{\text{sat}}$ or as $\Delta T = T - T_{\text{sat}}$. According to the data of Table 16.1(d), subcooling correlates roughly with the heat of solution. The increments ΔC and ΔT can be quite substantial quantities.

The several regions of varying stability are represented by Figure 16.2(d). At concentrations above or temperatures below those represented by the supersaturation line, nuclei form and crystals grow spontaneously, although the rates of these processes do depend on the depth of penetration of the unstable region. Little control can be exercised on behavior in this region. In the metastable region, growth of crystals will occur even under quiescent conditions when dust or seeds are introduced and nuclei can be generated by agitation. Behavior in the metastable region is largely controllable so that it is the practical operating region for production of crystals of significant sizes.

Practically feasible extents of supersaturation or subcooling are fairly small and depend on the substance and the temperature. Some data appear in Table 16.2. Since the recommended values are one-half the maxima listed, they rarely are more than 2°C or so. This means that very high circulation rates through heat exchangers are needed. Thus, in the urea process of Example 16.1, the temperature rise is 2°F, and the volumetric circulation rate is about 150 times the fresh feed rate.

PHASE DIAGRAMS

Equilibria between liquid and solid phases over wide ranges of temperature are represented compactly on phase diagrams. The effect of moderate pressure on condensed phases is negligible. Aqueous systems often are complicated by the formation of hydrates, and other substances also may form intermolecular compounds. Of the substances of Figure 16.3, KCl does not form a hydrate, but NaCl and $MgSO_4$ do. Mixtures always have lower melting points than those of the pure components. The lowest temperature and the corresponding composition at which a liquid phase can be present identify the eutectic ("easy melting"), for example, point C on Figure 16.3(a) and point B on Figure 16.3(b). Binary and ternary eutectics also are identified on the ternary diagram [Figure 16.3(f)].

The effects of evaporation or chilling on the amounts and compositions of the liquid and solid phases can be followed on the diagrams. Example 16.2 does this. Mixtures that form eutectics cannot be separated completely by chilling. The amount and nature of a separated solid phase depends on the temperature and the overall composition. Examples 16.2(c) and (d) make such calculations. Mixtures that are completely miscible in both liquid and solid phases, such as Figure 16.3(d), can be separated essentially completely in multistage equipment, although such processes are not often feasible. The possible extent of separation of multicomponent mixtures can be interpreted with a phase diagram like those of Figure 16.3(f) and Example 16.3. Phase diagrams are
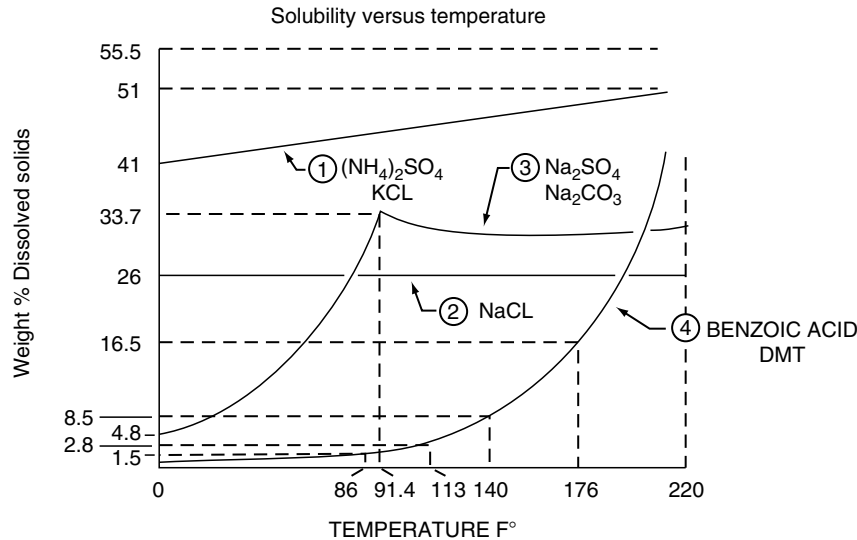
Figure 16.1. Solubility versus temperature.

EXAMPLE 16.1
Design of a Crystallizing Plant

A plant is to make 10,000 lb/hr of urea crystals from a solution that contains 75% dissolved salt. The material balance and operating conditions are shown on the sketch. Key crystallization data are given by Bennett (1981, p. 452) as

1. The residence time is 3.4 hr.
2. The temperature rise across the heater is 2°F.
   Other information deduced from pilot plant work is:
3. The feed contains 75% solids, but 1200 lb/hr of wash water from the centrifuge also is returned to the crystallizer.
4. The liquor contains 66.8% dissolved urea and has a specific gravity of 1.17 at the operating temperature of 130°F.
5. The slurry contains 28 lb crystals/cuft and has a specific gravity of 1.354.
6. A purge stream amounting to 7% of the feed liquor is withdrawn as shown on the sketch.
7. The pressure is 60 Torr, at which the saturation temperature of steam is 106°F. The superheat of 24°F is neglected in figuring the vapor density and velocity.
8. Depth of liquid in the vessel should not exceed 10 ft and the vapor velocity should not exceed that given by the equation, $u = 0.06\sqrt{\rho_L/\rho_g - 1}$. A wire mesh deentrainer is not feasible because of encrustation.
9. Heat capacity of the solid is 0.62 Btu/(lb)(°F) and the heat of crystallization is 104 Btu/lb.
10. For sizing the vacuum ejector, air leakage is estimated at 25 lb/hr and carbon dioxide is 34 lb/hr.
11. The coefficient of heat transfer in the exchanger is 200 Btu/(hr)(sqft)(°F).

Calculations:

vapor rate = 4471(296)/3600 = 367.6 cfs,
slurry holdup = 10,000(3.4)/28 = 1214.3 cuft,
$u_{max} = 0.06\sqrt{84.5/0.0034 - 1} = 9.46$fps,
$D_{min} = \sqrt{367.6/9.46(\pi/4)} = 7.03$ft.

The corresponding liquid depth is

$$h = 1214.3/(\pi/4)D^2 = 31.0\text{ft},$$

which is too great a value.

Try $D = 12.5$ ft:
dished head capacity = 152 cuft (Figure 18.5),

straight side = $(1214.3 - 152)/(12.5)^2(\pi/4) = 8.66$ ft, say 9.0 ft.

Together with the depth of liquid in the dished head, the total depth will be close to the 10 ft specified as the maximum. From Figure 18.5, a free board of 5.5 ft is adequate in the absence of a deentraining pad. Accordingly, the vessel will have a diameter of 12.5 ft, a straight side of 14.5 ft, and dished heads designed for full vacuum. The sketch is to scale.

Sufficient data are given for finding the heat balance and the liquor circulation rate, and for sizing the auxiliaries such as lines, pump, heat exchanger and vacuum system, but those calculations will not be made.

Code: W = water, U = urea.
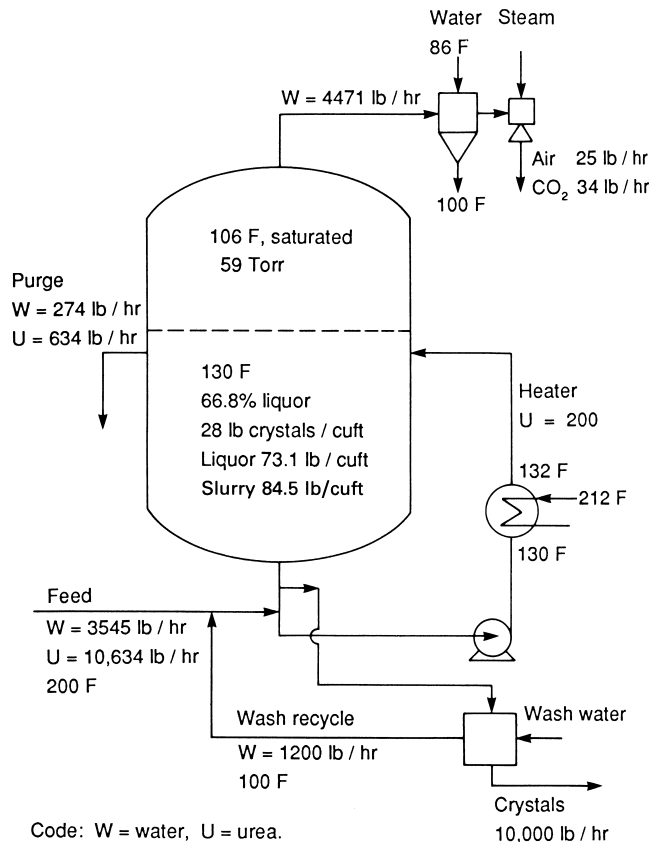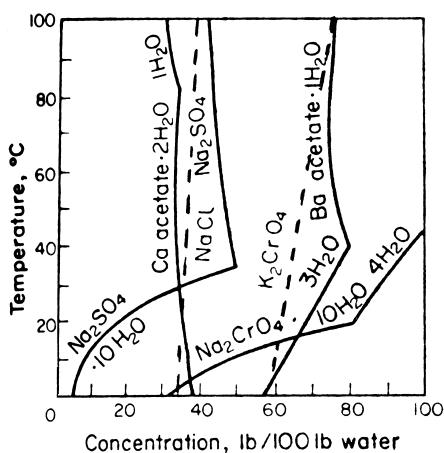
(a)
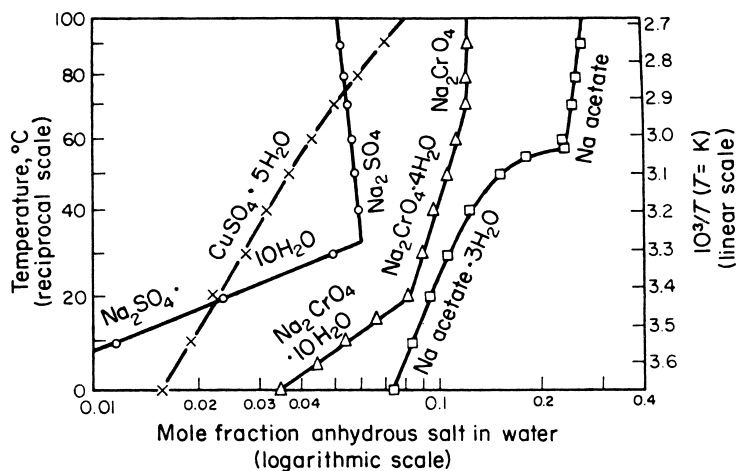
(b)
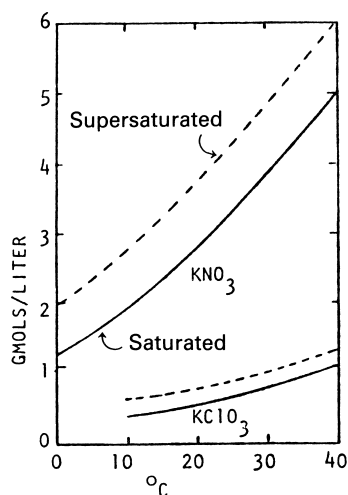
(c)
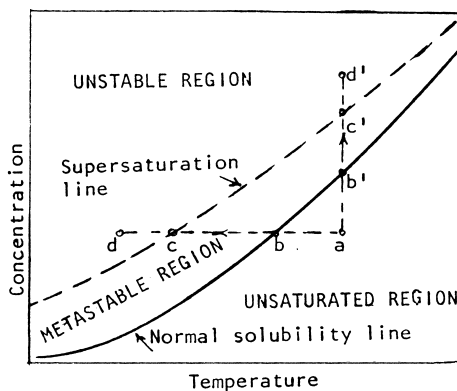
(d)

Figure 16.2. Solubility relations. (a) Linear plot of solubilities against temperature (*Mullin, 1972*). (b) Solubility against temperature plotted according to the equation $z = \exp(A + B/T)$ (*Mullin, 1972*). (c) Normal and supersolubilities of two salts (*data collected by Khamskii, 1969*). (d) Identification of regions on solubility plots. In the unstable region, nucleation and growth are spontaneous. In the metastable region growth can occur on externally introduced particles. Along $a - d$ to the left or along $a - d'$ upwards, nucleation and growth can start at c or c', but a substantial nuclei growth rate will not be achieved until d or d' are reached.

fairly plentiful, but published ones usually seem to be of the system they were interested in and not of the one you are interested in. Fortunately, nowadays phase diagrams can be developed at moderate cost and expenditure of time with differential scanning calorimeters.

Estimates of phase diagrams can be made on the assumption of ideal behavior or with activity coefficient data based on binary measurements that are more easily obtained. In such cases, clearly, it should be known that intermolecular compounds do not form. The freezing behaviors of ideal mixtures over the entire range of temperatures can be calculated readily. The method is explained for example by Walas (1985, Example 8.9).

In handling many crystallization problems, such as the concentration and crystallization of waste solutions, many ions can be present. Software is available, such as that distributed by OLI Systems, Inc., which can predict which compounds will form and crystallize as the solution is concentrated at a given temperature.

ENTHALPY BALANCES

Although the thermal demands of crystallization processes are small compared with those of possibly competitive separation processes such as distillation or adsorption; nevertheless, they must be known. For some important systems, enthalpy–composition diagrams have been prepared, like those of Figure 16.4, for instance. Calculations also may be performed with the more widely available data of heat capacities and heats of solution. The latter are most often recorded for infinite dilution, so that their utilization will result in a conservative heat balance. For the case of Example 16.3, calculations with the enthalpy–concentration diagram and with heat of solution and heat capacity data are not far apart.

16.4. CRYSTAL SIZE DISTRIBUTION

Crystal size distribution (CSD) is measured with a series of standard screens. The openings of the various mesh sizes according to the

TABLE 16.1. Data of Supersaturation and Subcooling of Solutions

(a) Maximum Supersaturation of Solutions at 20°C, $\beta = \Delta C/C_0$

Solute	Tovbin and Krasnova's data [144]	Gorbachev and Shlykov's data [34]	Fisher's data [152]*
KCl.	0.095	0.39	—
K Br	0.056	0.102	—
KI.	0.029	—	—
KClO$_3$	0.41	—	—
KNO$_3$.	0.36	1.08	—
NH$_4$NO$_3$	0.10	—	—
NaNO$_3$	0.064	—	—
Mg(NO$_3$)$_2$	0.93	—	—
K$_2$SO$_4$	0.37	—	0.34
K$_2$C$_2$O$_4$	0.41	—	—
K$_2$CrO$_4$	0.093	—	—
K$_2$Cr$_2$O$_7$	0.62	—	0.32
Ba(NO$_3$)$_2$.	0.40	—	—
CuSO$_4$.	1.50	—	—
HgCl$_2$.	0.43	—	—
K$_3$Fe(CN)$_6$	0.13	—	—
K$_4$Fe(CN)$_6$	0.54	—	—
KBrO$_3$	—	2.71	—
KIO$_3$.	—	1.60	—
Na$_2$C$_2$O$_4$	—	—	0.86
(NH$_4$)$_2$C$_2$O$_4$ · H$_2$O	—	—	0.36

*Fisher's results were obtained at 25°C.

(b) Temperature Dependence of the Maximum Supersaturation of Salt Solutions

Solute	t_1°C	C_0, moles/liter	C, moles/liter	$a = C - C_0$	β
KNO$_3$	0	1.25	2.03	0.78	0.62
	10	1.96	2.78	0.81	0.41
	20	2.76	3.75	0.99	0.36
	30	3.83	4.84	1.01	0.26
	40	4.97	6.00	1.03	0.20
KCl	0	3.33	3.88	0.55	0.16
	10	3.72	4.12	0.40	0.11
	20	4.03	4.42	0.39	0.095
	30	4.29	4.45	0.16	0.037
	40	4.45	4.58	0.13	0.029
KClO$_3$	10	0.40	0.65	0.25	0.62
	20	0.58	0.82	0.24	0.41
	30	0.80	1.05	0.25	0.32
	40	1.11	1.32	0.21	0.19
K$_2$CrO$_4$	10	2.68	2.96	0.28	0.11
	20	2.74	3.00	0.26	0.093
	30	2.82	3.03	0.21	0.073
	40	2.98	3.07	0.19	0.065

(c) Maximum Supercooling of Salt Solutions at Various Temperatures

Solute	Heat of solution λ, cal/mole	$t_0 - t$, °C	$\lambda(t_0 - t)$, $cal \cdot mole^{-1}$, $°^{-1}$
KCl.	4046	19.6	78897
KBr	5080	16.3	80804
KI.	5110	15.5	79205
KBrO$_3$	9760	8.8	84788
KIO$_6$.	6780	13.5	91490
KClO$_3$ . . .	9950	6.6	65670
KNO$_3$. . . .	8800	13.0	114400
KClO$_4$ . . .	12100	6.3	76230
KCNS . . .	6100	13.0	79300
NaNO$_3$ . .	5030	13.0	65399
NaClO$_3$ . .	5600	12.0	67200
NaCl	12200	51.0	62220
NH$_4$Cl . . .	3880	20.0	77600
(NH$_4$)$_2$SO$_4$	2370	24.0	56880
NH$_4$NO$_3$.	6320	10.3	65016
HgCl$_2$. . . .	3300	25.0	82500
CuSO$_4$. . .	2750	36.7	80925
NaClO$_4$ . .	3600	20.0	72000
NH$_4$ClO$_4$.	6360	12.0	76320
Ba(ClO$_4$)$_2$	9400	9.0	84600

(d) Dependence of the Maximum Supercooling of Solutions on Heat of Solution

Solute	t_0, °C	t_1°C	$0 = t_0 - t$, °C	Solute	t_0, °C	t_1°C	$0 = t_0 - t$, °C
KNO$_3$	20	−1.0	21.0	KBr	10.5	−1.8	12.3
	30	8.9	21.1		20	8.0	12.0
	40	18.9	21.1		30	17.8	12.2
	50	28.8	21.2		40	28.0	12.0
	60	38.8	21.2		50	37.9	12.1
	70	48.9	21.1		60	47.7	12.3
					80	67.7	12.3
KCl	50	6.7	43.3	K$_2$SO$_4$	90	3.0	87.0
	60	16.6	43.4		100	13.0	87.0
	70	26.7	43.3				
	80	36.7	43.3				
	90	46.6	43.4				

(Khamskii, 1969).

way. Some theoretical cumulative and differential distribution curves of similar nature are shown in Figure 16.7; the abscissas are proportional to the crystal length.

Cumulative data often are represented closely by the Rosin–Rammler–Sperling (RRS) equation

$$y = 100 \exp[-(d/d_m)^n], \qquad (16.1)$$

where d is the diameter, d_m is a mean diameter corresponding to $y = 100/e = 36.8\%$ and n is called the uniformity factor. The greater n, the more nearly uniform the distribution. The log–log plot of this equation should be linear. On Figure 16.5 (c) the scatter about the straight line is small, but several of the plots of commercial data of Figure 16.7 deviate somewhat from linearity at the larger diameters.

Two other single numbers are used to characterize size distributions. The median aperture, MA or d_{50}, is the screen opening through which 50% of the material passes. The coefficient of variation is defined by the equation

Tyler Standard are listed in Example 6.7 and according to the British Standard in Figure 16.5. Table 12.1 is a complete listing. The size of a crystal is taken to be the average of the screen openings of successive sizes that just pass and just retain the crystal.

The cumulative wt % either greater or less than a specified screen opening is recorded. The amount of a size less than a particular screen opening and greater than the next smaller size is called the differential amount. Typical size distribution data on Figure 16.5 are plotted in two cumulative modes, greater than or less than, and as differential polygons or histograms. For some purposes the polygon may be smoothed and often is shown that

TABLE 16.2. Maximum Allowable Supercooling ΔT (°C) and Corresponding Supersaturation ΔC (g/100 g water) at 25°C[a]

Substance	ΔT	ΔC
NH_4 alum	3.0	1.0
NH_4Cl	0.7	0.3
NH_4NO_3	0.6	3.0
$(NH_4)_2SO_4$	1.8	0.5
$NH_4H_2PO_4$	2.5	2.3
$CuSO_45H_2O$	1.4	1.0
$FeSO_47H_2O$	0.5	0.6
Kalum	4.0	1.0
KBr	1.1	0.6
KCl	1.1	0.3
KI	0.6	0.4
KH_2PO_4	9.0	4.6
KNO_3	0.4	0.6
KNO_2	0.8	0.8
K_2SO_4	6.0	1.3
$MgSO_47H_2O$	1.0	1.3
$NiSO_47H_2O$	4.0	4.4
$NaBr2H_2O$	0.9	0.9
$Na_2CO_310H_2O$	0.6	2.8
$Na_2CrO_410H_2O$	1.6	0
NaCl	4.0	0.2
$Na_2B_4O_710H_2O$	4.0	0.9
NaI	1.0	1.7
$NaHPO_412H_2O$	0.4	1.5
$NaNO_3$	0.9	0.7
$NaNO_2$	0.9	0.6
$Na_2SO_410H_2O$	0.3	0.7
$Na_2S_2O_35H_2O$	1.0	2.2
Urea	2.0	

[a] Working values usually are not more than one-half the maxima. (After Mullin, 1972).

$$CV = 100(d_{16} - d_{84})/2d_{50}. \tag{16.2}$$

The origin of this concept is that the fraction of the total area under a normal distribution curve between the 16 and 84% points is twice the standard deviation. The smaller CV, the more nearly uniform the crystal sizes. Products of DTB crystallizers, for instance, often have CVs of 30–50%. The number is useful as a measure of consistency of operation of a crystallizer. Some details are given by Mullin (1972, pp. 349, 389).

16.5. THE PROCESS OF CRYSTALLIZATION

The questions of interest are how to precipitate the crystals and how to make them grow to suitable sizes and size distributions. Required sizes and size distributions are established by the need for subsequent recovery in pure form and ease of handling, and by traditional commercial practices or consumer preferences.

CONDITIONS OF PRECIPITATION

The most common methods of precipitating a solid from a solution are by evaporation of the solvent or by changing to a temperature at which the solubility is lower. Usually solubility is decreased by lowering the temperature. Some examples are in Figure 16.2. The limit of removal is determined by the eutectic composition. According to the data of Figure 16.3, for instance, a 24.6% solution of KCl will solidify completely at −11°C and a 3.5% solution of $MgSO_4$ will do so at 4°C; these values represent the limits to which salt is recoverable by chilling. Complete recovery, however, is accomplished by evaporation.

A precipitate may be formed as a result of chemical reaction between separately soluble gases or liquids. Commercial examples are productions of sodium sulfate, ammonium sulfate, and ammonium phosphate.

Precipitation also can be induced by additives, a process generally called salting out because salts with ions common to those whose precipitation is desired are often used for this purpose. For instance, ammonium chloride is recovered from spent Solvay liquors by addition of sodium chloride and the solubility of $BaCl_2$ can be reduced from 32% to 0.1% by addition of 32% of $CaCl_2$. Other kinds of precipitants also are used, for instance, alcohol to precipitate aluminum sulfate from aqueous solutions.

Foreign substances even in minute amounts may have other kinds of effects on crystallization: They may inhibit or accelerate growth rate or change the shape of crystals, say from rounded to needlelike, or otherwise. One of the problems sometimes encountered with translating laboratory experience to full scale operation is that the synthetic liquors used in the laboratory may not contain the actually occurring impurities, and thus give quite different performance. Substances that modify crystal formation are very

EXAMPLE 16.2
Using the Phase Diagrams of Figure 16.3
a. Evaporation of a solution of $MgSO_4$ at 30°C: As water is removed, the composition moves along the horizontal. When the salt concentration reaches about 6%, precipitation of heptahydrate begins and is completed at about 13%. Between 13 and 14% salt, the precipitate is a mixture of solid hepta and solid hexa hydrates. Beyond 14%, the mixture consists of mixtures of solid hepta and mono hydrates in proportions determined by the amount of water present overall.
b. Chilling of a 6% solution of $MgSO_4$: precipitation of heptahydrate begins at about 35°C. At about 2°C, the mixture consists of solid dodecahydrate and unsaturated solution. Below −4°C complete solidification exists; the product is a mixture of pure dodecahydrate and an intimate eutectic mixture of ice and dodeca crystals.

c. Recovery of pyridine: As appears on the diagram of Figure 16.3(e), the eutectic contains 33% formamide and 67% pyridine. When the mixture contains 80% pyridine, the maximum possible recovery of pure pyridine is

$$P = (0.8 - 0.67)/(1 - 0.67) = 0.39, \text{ or } 39\%.$$

d. Recovery of formamide: When the mixture of Figure 16.3(e) contains 80% formamide, the maximum recovery of the pure material is

$$F = (0.8 - 0.33)/(1 - 0.33) = 0.70, \text{ or } 70\%.$$

e. At 50°C, the liquid phase of Figure 16.2(d) contains 35% and the solid phase 74% of β-chloronaphthalene.
f. The progress of crystallization of a ternary mixture such as that of Figure 16.3(f) is described in Example 16.8.

(a)

(b)

(c)

(d)

(e)

(e)

(f)
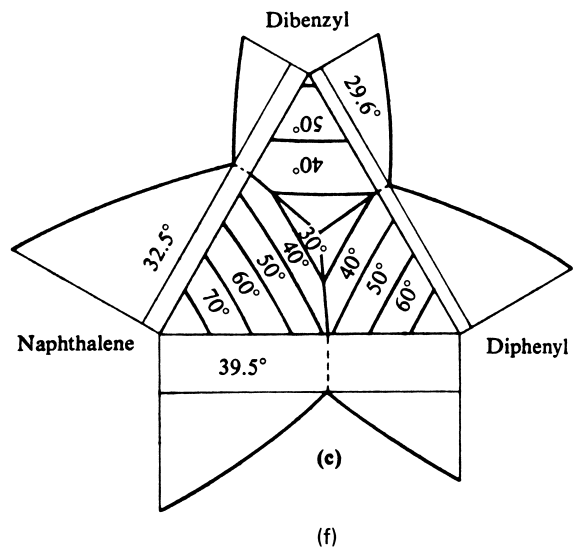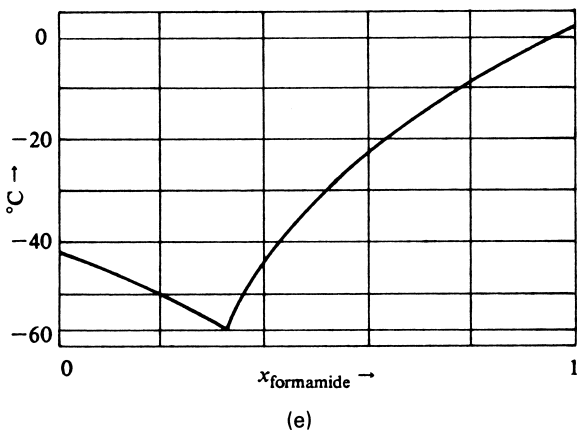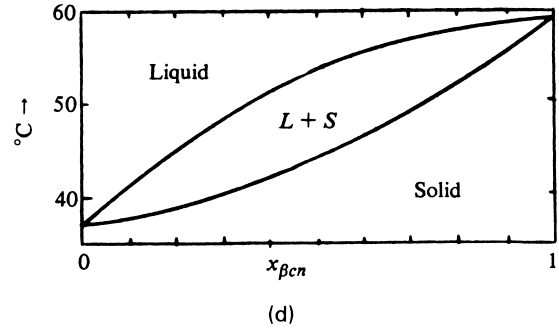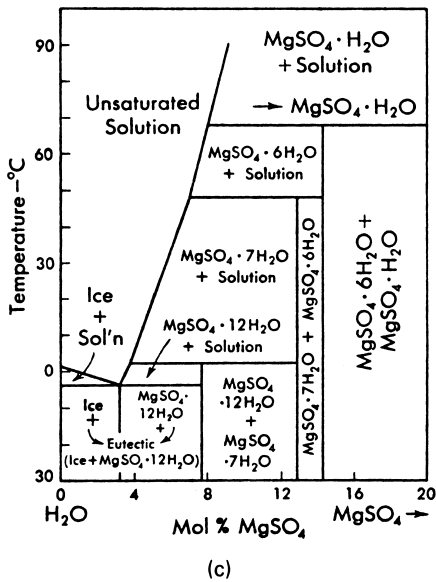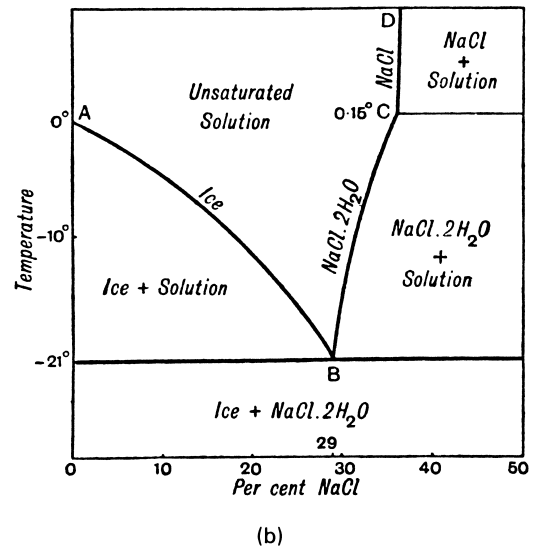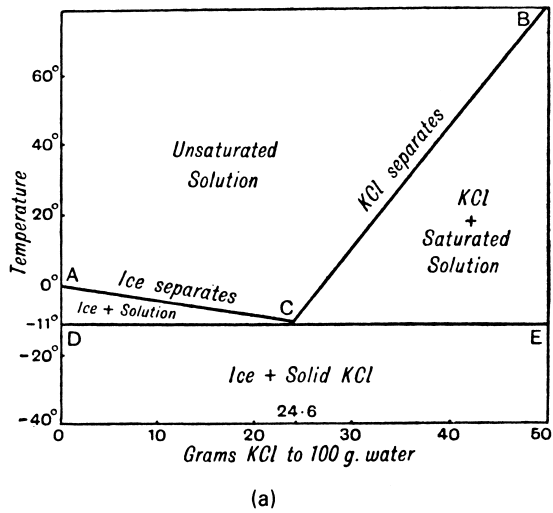
Figure 16.3. Some phase diagrams. (a) The water end of the system potassium chloride and water. (b) The water end of the system sodium chloride and water. (c) The water end of the system magnesium sulfate and water; the heptahydrate goes to the mono at 150°C, and to anhydrous at 200°C. (d) β-methylnaphthalene and β-chloronaphthalene form solid solutions. (e) Mixtures of formamide and pyridine form a simple eutectic. (f) These mixtures form binary eutectics at the indicated temperatures and a ternary eutectic at mol fractions 0.392 dibenzyl, 0.338 diphenyl, and 0.27 naphthalene.

EXAMPLE 16.3
Heat Effect Accompanying the Cooling of a Solution of MgSO₄
A 30% solution of MgSO₄ is cooled from 150F to 50F. Data of the
initial and final conditions are taken off the equilibrium diagram,
Figure 16.4(b). At the lower temperature, 27% of the mixture
crystallizes out as the heptahydrate.

		Final (at 50°F)		
	Original at 150°F	Total	Liquid	Solid
Water (lb)	38.6	38.6	38.6	—
MgSO₄.7H₂O (lb)	61.4	61.4	34.4	27.0
Total (lb)	100	100	73.0	27.0
H (Btu/lb)	−3	−82	−53	−161

Accordingly the change in enthalpy is

$$\Delta H = -82 - (-3) = -79 \text{ Btu/lb}.$$

This value will be compared with a calculation using data of
heat capacities and heat of solution. From *Perry's Chemical
Engineers' Handbook* (1997), the heat solution of the heptahyd-
rate is −39.2 Btu/lb and its heat capacity is 0.36 Btu/(lb)
(°F). The enthalpy change of the cooling and crystallization
process is

$$\Delta H = [0.386 + 0.614(0.36)](50 - 150) + 0.27(-39.2)$$
$$= -71.3 \text{ Btu/lb},$$

which is a poor check of the value found with the aid of the
equilibrium diagram. Possible sources of error of the second
method include the use of heat of solution at infinite dilution
instead of the prevailing concentration and the assumption that
the heat capacities are additive.
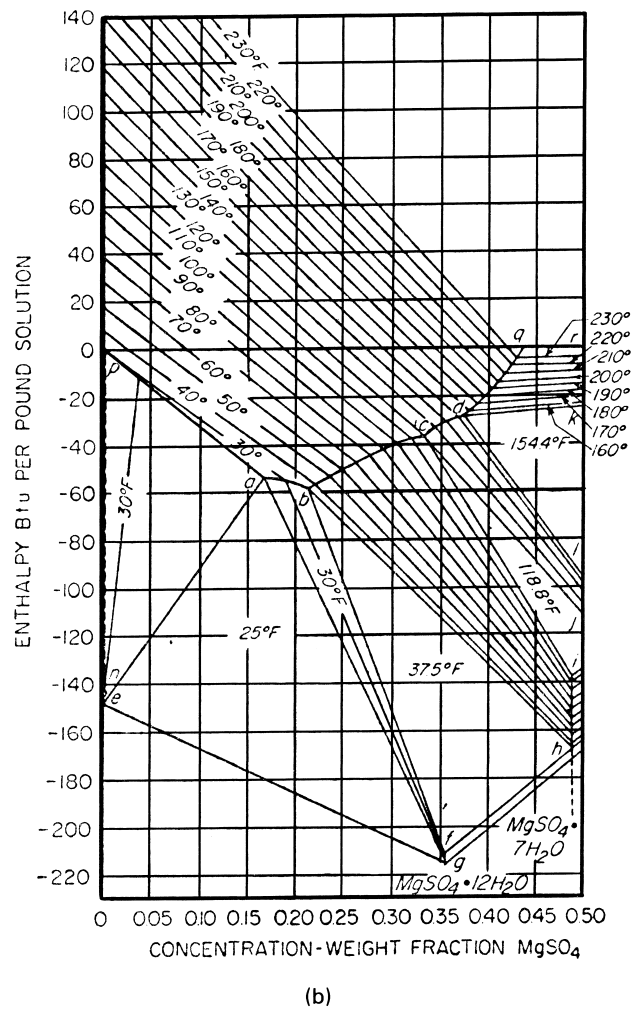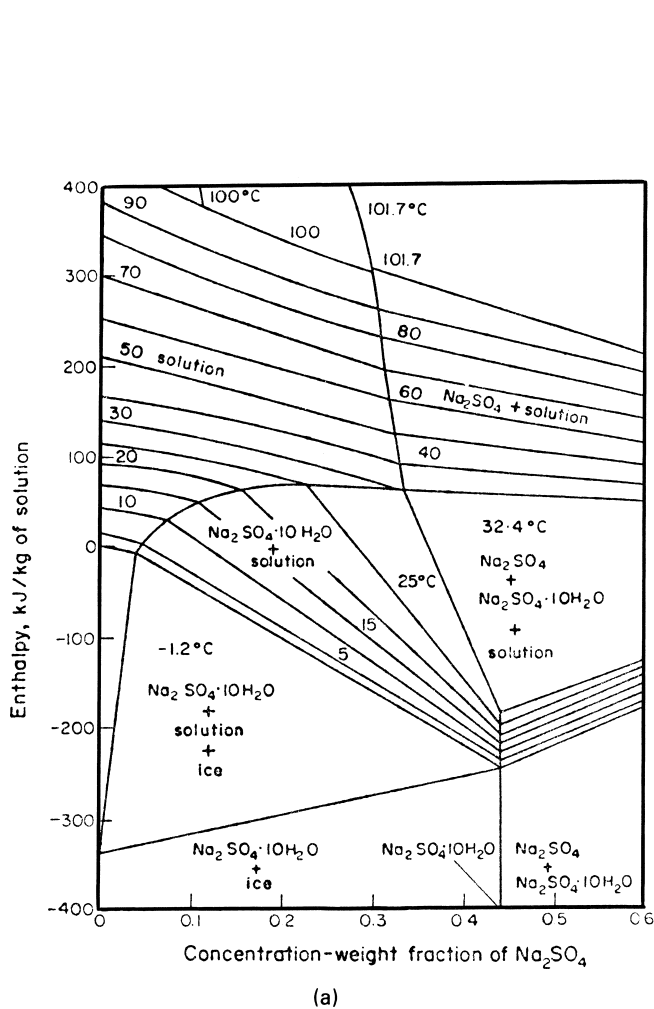
Figure 16.4. Enthalpy–composition diagrams of some salt solutions. Several other diagrams are in the compilation of Landolt-Börnstein,
IV 4b, 1972, pp. 188–224. (a) sodium sulfate/water; (b) magnesium sulfate/water (*after* Chemical Engineers' Handbook, *1963 edition,*
McGraw-Hill, New York); (c) sodium carbonate/water.
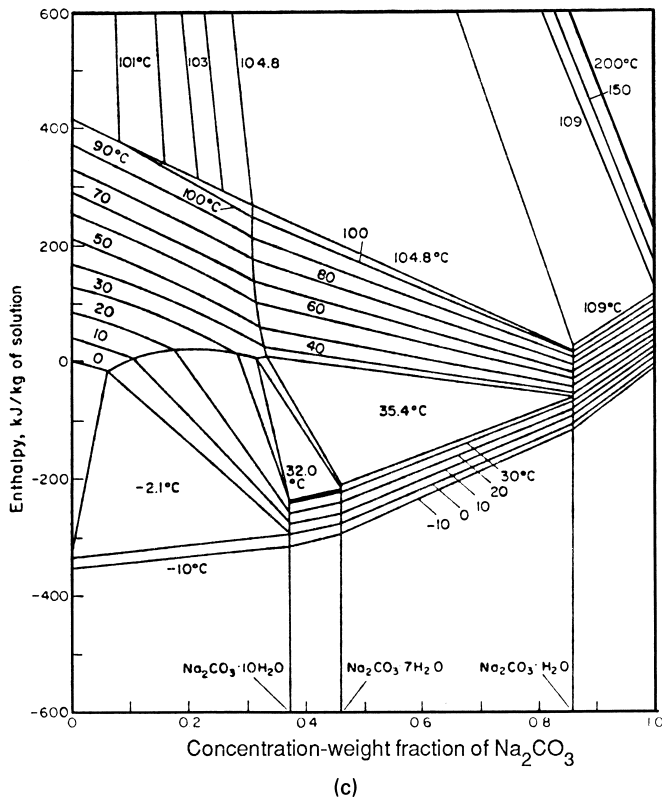
Figure 16.4.—(*continued*)

important industrially and many such materials have been the subject of patents.

SUPERSATURATION

A saturated solution is one that is in equilibrium with the solid phase and will remain unchanged indefinitely at a particular tem-

perature and composition of other constituents. Greater than normal concentrations also can be maintained in what is called a supersaturated condition which is metastable. Metastability is sensitive to mechanical disturbances such as agitation, ultrasonics, and friction and the introduction of solid particles. Under those conditions, solids will separate out until a lower level of supersaturation is achieved. Supersaturation cannot be completely eliminated, although in some cases the saturation curve can be closely approached. When great care is taken, the metastable state is reproducible. A thermodynamic interpretation of metastability can be made in terms of the Gibbs energy of mixtures. In Figure 16.6(a), the solid line $a - b$ is of unsaturated solution and the straight line $b - e$ is of mixtures of all proportions of pure solid and saturated solution represented by point b. Points c and d are at the points of inflection of the plot and represent the limits of metastability. Thus line $b - c$ represents the range of concentrations between the saturated and supersaturated values.

Several measures of supersaturation are being used in terms of the saturation concentration C_0; thus

$$\alpha = \Delta C_s = C - C_0, \text{ the difference in concentrations,}$$

$$\beta = \Delta C_s / C, \qquad \text{the relative difference}$$

$$\gamma = C / C_0 = \beta + 1, \text{ the concentration ratio,}$$

with similar definitions for subcooling or superheating. The data of Figure 16.2(c) and Table 16.2 show that excess concentration and metastable cooling can be quite substantial amounts.

GROWTH RATES

Crystallization can occur only from supersaturated solutions. Growth occurs first by formation of nuclei and then by their gradual growth. At concentrations above supersaturation, as at point d' on Figure 16.2(d), nucleation is conceived to be spontaneous and rapid. In the metastable region, nucleation is caused by

B.S. mesh number	Sieve aperture, μm	Fractional weight per cent retained	Cumulative weight per cent oversize	Cumulative weight per cent undersize
7	2360	1·2	1·2	98·8
10	1700	2·9	4·1	95·9
14	1180	18·8	22·9	77·1
18	850	28·8	51·7	48·3
25	600	22·0	73·7	26·3
36	425	11·1	84·8	15·2
52	300	6·0	90·8	9·2
72	212	3·9	94·7	5·3
100	150	1·8	96·5	3·5
150	106	1·3	97·8	2·2
>150	—	2·2	—	—

(a)

(b)

Figure 16.5. Several ways of recording the same data of crystal size distribution (CSD) (*Mullin, 1972*). (a) The data. (b) Cumulative wt % retained or passed, against sieve aperture. (c) Log–log plot according to the RRS equation $P = \exp[(-d/d_m)^n]$; off this plot, $d_{50\%} = 850, d_m = 1000, n = 1.8$. (d) Differential polygon. (e) Differential histogram.
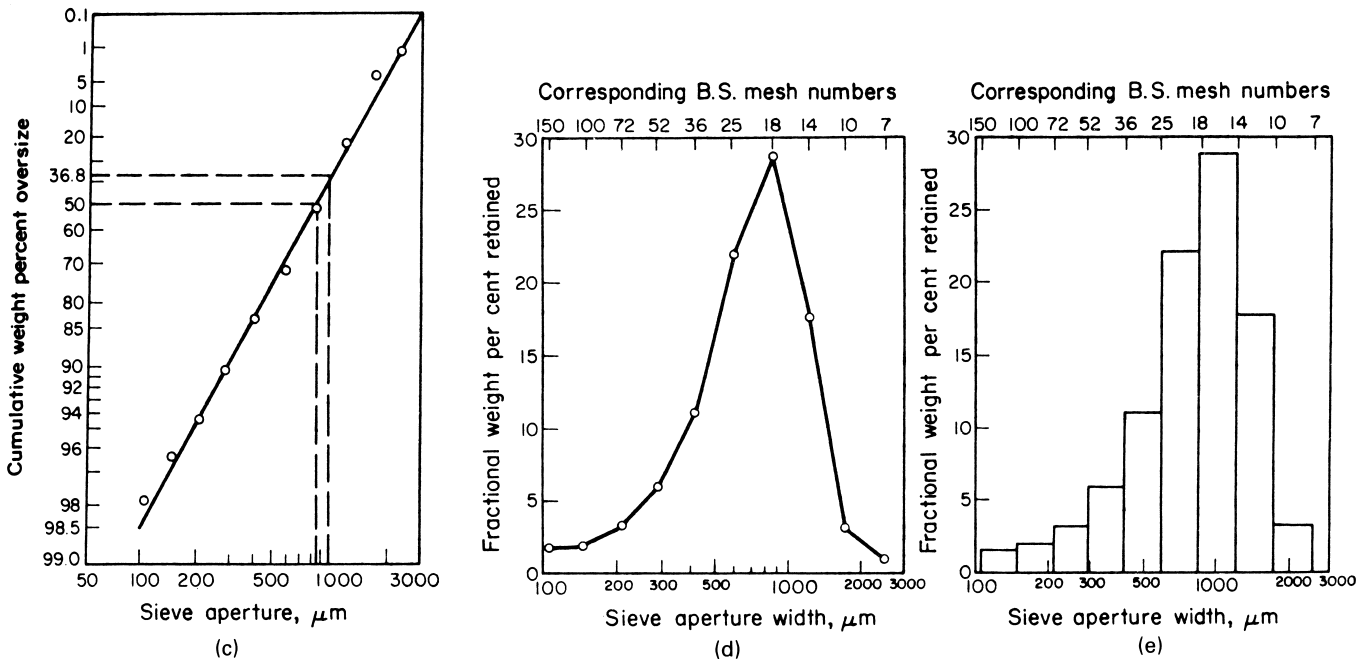
Figure 16.5.—(*continued*)
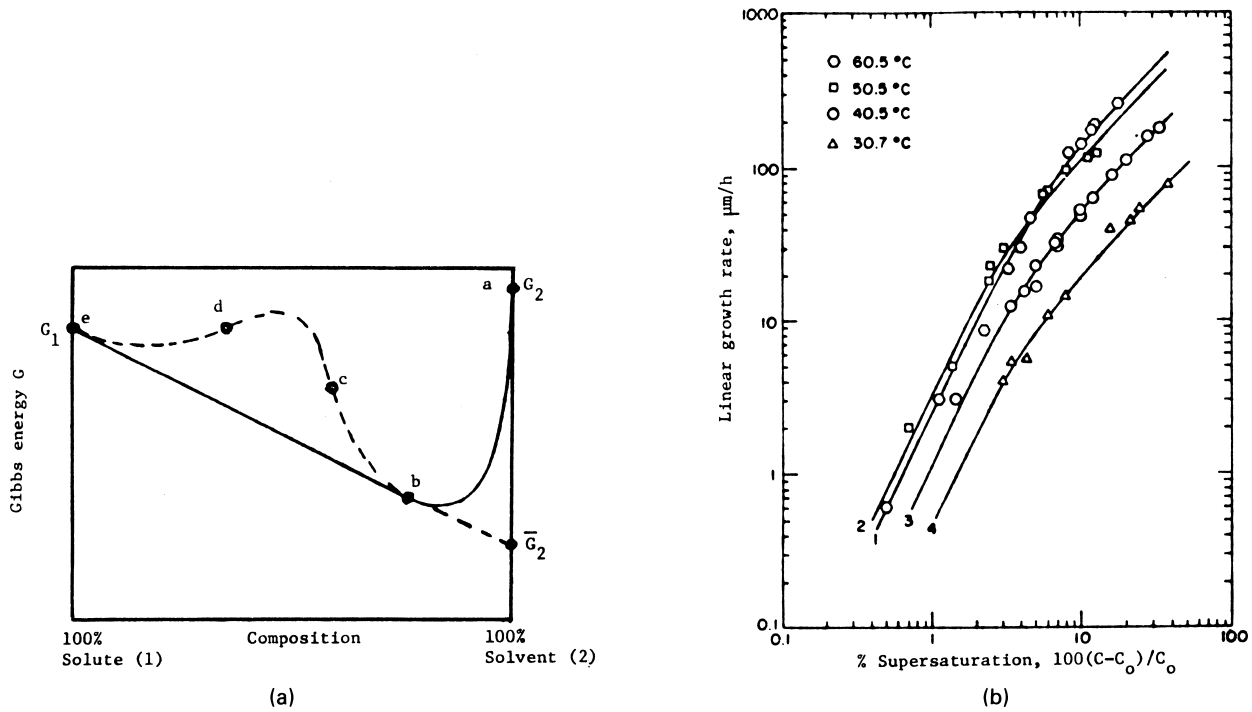
Figure 16.6. Supersaturation behavior. (a) Schematic plot of the Gibbs energy of a solid solute and solvent mixture at a fixed temperature. The true equilibrium compositions are given by points *b* and *e*, the limits of metastability by the inflection points *c* and *d*. For a salt–water system, point *d* virtually coincides with the 100% salt point *e*, with water contents of the order of 10^{-6} mol fraction with common salts. (b) Effects of supersaturation and temperature on the linear growth rate of sucrose crystals [*data of Smythe (1967) analyzed by Ohara and Reid, 1973*].
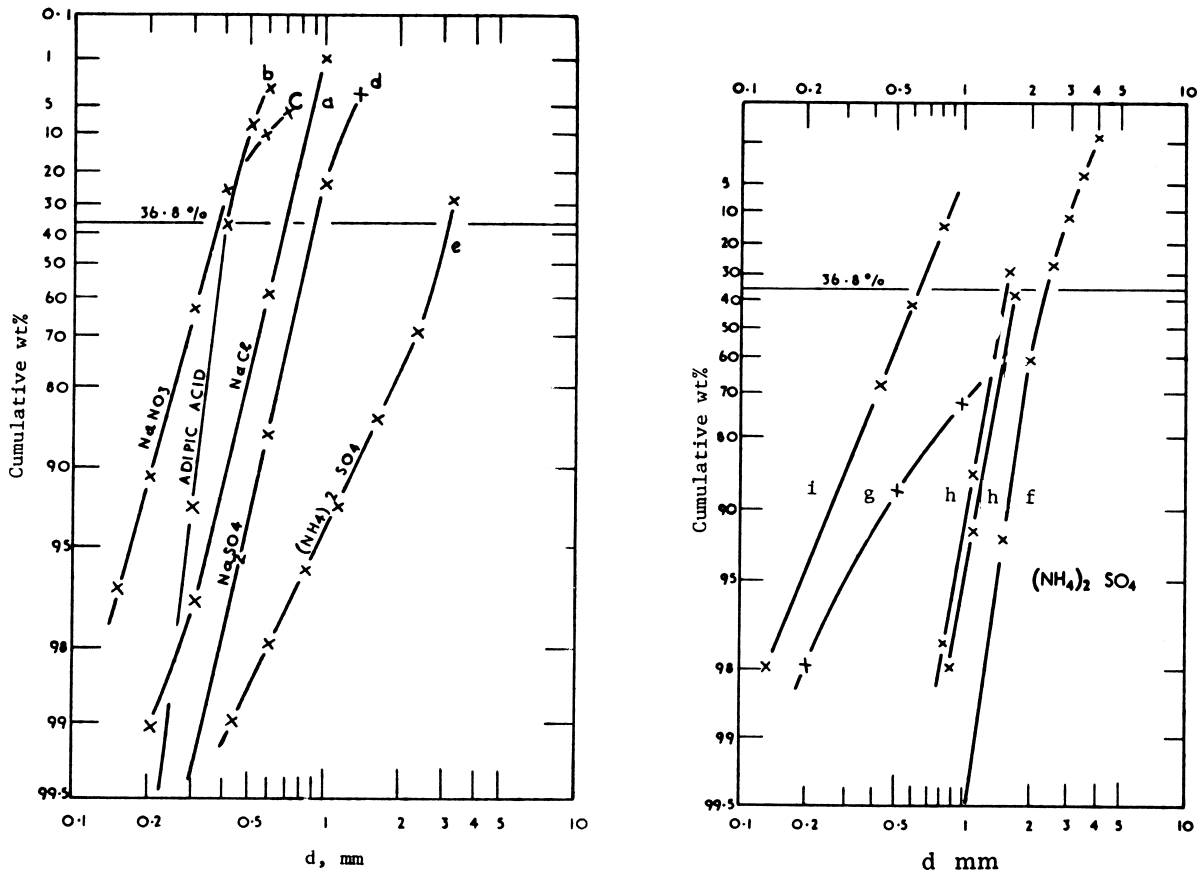
Figure 16.7. Crystal size distributions of several materials in several kinds of crystallizers (*Bamforth, 1965*).

Code	Crystallizer	Substance	d_m	n
a	Escher-Wyss	NaCl	0.7	4.7
b	Giavanola	adipic acid	0.4	8.1
c	Matusevich	NaNO$_3$	0.37	4.0
d	Kestner	Na$_2$SO$_4$	0.92	4.7
e	Oslo-Krystal	(NH$_4$)$_2$SO$_4$	3.2	2.1
f	Oslo-Krystal	(NH$_4$)$_2$SO$_4$	2.35	6.0
g	Sergeev	(NH$_4$)$_2$SO$_4$	—	1.5(?)
h	DTB	(NH$_4$)$_2$SO$_4$	1.6	5.7
i	Standard saturator	(NH$_4$)$_2$SO$_4$	0.62	2.6

The parameters are those of the RRS equation, Eq. 16.1.

mechanical shock or friction and secondary nucleation can result from the breakup of already formed crystals. It has been observed that the rate depends on the extent of supersaturation; thus

$$\frac{dC_N}{d\theta} = k(C - C_0)^m. \tag{16.3}$$

Values of the exponent m have been found to range from 2 to 9, but have not been correlated to be of quantitative value for prediction.

Nucleation rates are measured by counting the numbers of crystals formed over periods of time.

The growth rates of crystals depend on their instantaneous surface and the linear velocity of solution past the surface as well as the extent of supersaturation, and are thus represented by the equation

$$\frac{dW_c}{d\theta} = kuA(C - C_0)^n. \tag{16.3'}$$

Values of the exponent have been found of the order of 1.5, but again no correlation of direct use to the design of crystallizers has been achieved. The sucrose growth data of Figure 16.6(b) are not quite log–log linear as predicted by this equation.

In laboratory and commercial crystallizations, wide size distributions usually are the rule, because nuclei continue to form throughout the process, either spontaneously or by breakage of already formed crystals. Large crystals of more or less uniform size are desirable. This condition is favored by operating at relatively low extents of supersaturation at which the nucleation rate is low but the crystals already started can continue to grow. The optimum extent of supersaturation is strictly a matter for direct experimentation in each case. As a rough guide, the data for allowable subcooling and corresponding supersaturation of Table 16.2 may serve. Since the recommended values are one-half the maxima shown, it appears that most crystallizations under commercial conditions should operate with less than about 2°C

<small>EXAMPLE 16.4</small>
Deductions from a Differential Distribution Obtained at a Known Residence Time

The peak of the differential distribution obtained with a residence time of $\bar{t} = 2$hr corresponds to $L_{pr} = 1.2$ mm. Assuming ideal mixing, $L_{pr}/G\bar{t} = 1.2/2G = 3$, and $G = 0.2$ mm/h. With this knowledge of G, crystal size distributions could be found at other residence times.

---

subcooling or the corresponding supersaturation. The urea crystallizer design of Example 16.1 is based on 2°F heating.

Growth rates of crystals also must be measured in the laboratory or pilot plant, although the suitable condition may be expressed simply as a residence time. Table 16.3 gives some growth rate data at several temperatures and several extents of supersaturation for each substance. In most instances the recommended supersaturation measured as the ratio of operating to saturation concentrations is less than 1.1. It may be noted that at a typical rate of increase of diameter of 10^{-7} m/sec, the units used in this table, the time required for an increase of 1 mm is 2.8 hr.

Batch crystallizers often are seeded with small crystals of a known range of sizes. The resulting crystal size distribution for a given overall weight gain can be estimated by an approximate relation known as the McCabe Delta-L Law, which states that each original crystal grows by the same amount ΔL. The relation between the relative masses of the original and final size distributions is given in terms of the incremental ΔL by

$$R = \frac{\sum w_i (L_{0i} + \Delta L)^3}{\sum w_i L_{0i}^3}. \tag{16.4}$$

When R is specified, ΔL is found by trial, and then the size distribution is evaluated. Example 16.5 does this.

Some common substances for which crystallization data are reported in the literature and in patents are listed in Table 16.4.

16.6. THE IDEAL STIRRED TANK

All continuous crystallizers are operated with some degree of mixing, supplied by internal agitators or by pumparound. The important limiting case is that of ideal mixing in which conditions are uniform throughout the vessel and the composition of the effluent is the same as that of the vessel content. In crystallization literature, this model carries the awkward name MSMPR (mixed suspension mixed product removal). By analogy with the terminology of chemical reactors it could be called CSTC (continuous stirred tank crystallizer). Several such tanks in series would be called a CSTC battery. A large number of tanks in series would approach plug flow, but the crystal size distribution still would not be uniform if nucleation continued along the length of the crystallizer.

The process to be analyzed is represented by Figure 16.8. What will be found are equations for the cumulative and differential size distributions in terms of residence time and growth rate. The principal notation is summarized here.

Q = volumetric feed rate,
V_c = volume of holdup in the tank
n = number of crystals per unit volume

TABLE 16.3. Mean Overall Growth Rates of Crystals (m/sec) at Each Face[a]

Crystallising substance	°C	S	$\bar{v}$(m/s)
$(NH_4)_2SO_4 \cdot Al_2(SO_4)_3 \cdot 24H_2O$	15	1·03	$1 \cdot 1 \times 10^{-8*}$
	30	1·03	$1 \cdot 3 \times 10^{-8*}$
	30	1·09	$1 \cdot 0 \times 10^{-7*}$
	40	1·08	$1 \cdot 2 \times 10^{-7*}$
NH_4NO_3	40	1·05	$8 \cdot 5 \times 10^{-7}$
$(NH_4)_2SO_4$	30	1·05	$2 \cdot 5 \times 10^{-7*}$
	60	1·05	$4 \cdot 0 \times 10^{-7}$
	90	1·01	$3 \cdot 0 \times 10^{-8}$
$NH_4H_2PO_4$	20	1·06	$6 \cdot 5 \times 10^{-8}$
	30	1·02	$3 \cdot 0 \times 10^{-8}$
	30	1·05	$1 \cdot 1 \times 10^{-7}$
	40	1·02	$7 \cdot 0 \times 10^{-8}$
$MgSO_4 \cdot 7H_2O$	20	1·02	$4 \cdot 5 \times 10^{-8*}$
	30	1·01	$8 \cdot 0 \times 10^{-8*}$
	30	1·02	$1 \cdot 5 \times 10^{-7*}$
$NiSO_4 \cdot (NH_4)_2SO_4 \cdot 6H_2O$	25	1·03	$5 \cdot 2 \times 10^{-9}$
	25	1·09	$2 \cdot 6 \times 10^{-8}$
	25	1·20	$4 \cdot 0 \times 10^{-8}$
$K_2SO_4 \cdot Al_2(SO_4)_3 \cdot 24H_2O$	15	1·04	$1 \cdot 4 \times 10^{-8*}$
	30	1·04	$2 \cdot 8 \times 10^{-8*}$
	30	1·09	$1 \cdot 4 \times 10^{-7*}$
	40	1·03	$5 \cdot 6 \times 10^{-8*}$
KCl	20	1·02	$2 \cdot 0 \times 10^{-7}$
	40	1·01	$6 \cdot 0 \times 10^{-7}$
KNO_3	20	1·05	$4 \cdot 5 \times 10^{-8}$
	40	1·05	$1 \cdot 5 \times 10^{-7}$
K_2SO_4	20	1·09	$2 \cdot 8 \times 10^{-8*}$
	20	1·18	$1 \cdot 4 \times 10^{-7*}$
	30	1·07	$4 \cdot 2 \times 10^{-8*}$
	50	1·06	$7 \cdot 0 \times 10^{-8*}$
	50	1·12	$3 \cdot 2 \times 10^{-7*}$
KH_2PO_4	30	1·07	$3 \cdot 0 \times 10^{-8}$
	30	1·21	$2 \cdot 9 \times 10^{-7}$
	40	1·06	$5 \cdot 0 \times 10^{-8}$
	40	1·18	$4 \cdot 8 \times 10^{-7}$
NaCl	50	1·002	$2 \cdot 5 \times 10^{-8}$
	50	1·003	$6 \cdot 5 \times 10^{-8}$
	70	1·002	$9 \cdot 0 \times 10^{-8}$
	70	1·003	$1 \cdot 5 \times 10^{-7}$
$Na_2S_2O_3 \cdot 5H_2O$	30	1·02	$1 \cdot 1 \times 10^{-7}$
	30	1·08	$5 \cdot 0 \times 10^{-7}$
Citric acid monohydrate	25	1·05	$3 \cdot 0 \times 10^{-8}$
	30	1·01	$1 \cdot 0 \times 10^{-8}$
	30	1·05	$4 \cdot 0 \times 10^{-8}$
Sucrose	30	1·13	$1 \cdot 1 \times 10^{-8*}$
	30	1·27	$2 \cdot 1 \times 10^{-8*}$
	70	1·09	$9 \cdot 5 \times 10^{-8}$
	70	1·15	$1 \cdot 5 \times 10^{-7}$

[a] The supersaturation is expressed by $S = C/C_0$, with C the amount dissolved and C_0 the normal solubility (kg crystals/kg water). The mean growth velocity is that at one face of the crystal; the length increase is $G = 2\bar{v}$ (m/sec). Data are for crystals in the size range 0.5–1.0 mm in the presence of other crystals. The asterisk denotes that the growth rate probably is size-dependent.
(Mullin, 1972).

L = length of the crystal
G = linear growth rate of the crystal
t = time
$\bar{t} = V_c/Q$, mean residence time
$x = L/G\bar{t}$, reduced time
ϕ_m = cumulative mass distribution
n^0 = zero side nuclei concentration, also called zero size population density

EXAMPLE 16.5
Batch Crystallization with Seeded Liquor

Seed crystals with this size distribution are charged to a batch crystallizer:

L_0, length (mm)	0.251	0.178	0.127	0.089	0.064
w (wt fraction)	0.09	0.26	0.45	0.16	0.04

On the basis of the McCabe ΔL law, these results will be found:

a. The length increment that will result in a 20-fold increase in mass of the crystals.
b. The mass growth corresponding to the maximum crystal length of 1.0 mm.

When L is the increment in crystal length, the mass ratio is

$$R = \frac{\sum w_i(L_{0i} + L)^3}{\sum w_i L_{0i}^3} = \frac{\sum w_i(L_{0i} + L)^3}{0.09346} = 20$$

a. By trial, the value of $L = 0.2804$ mm.
b. When $L = 1 - 0.251 = 0.749$, $R = 181.79$.
A computer program may be written to solve this equation.
The size distributions are tabulated.

W	L₀	L₀ + L
.090	.251	.2510
.260	.178	.1780
.450	.127	.1270
160	.089	.0890
.040	.064	.0640

INCREMENT L = 0
SUMMATION = .00393458126
WEIGHT RATIO = 1.00000032024

.090	.251	.5314
.260	.178	4584
.450	.127	4074
.160	.089	3694
.040	.064	3444

INCREMENT L = .2804
SUMMATION = 7.86768511336E–2
WEIGHT RATIO = 19.9962514763

.090	.251	1.0000
.260	.178	.9270
.450	.127	.8760
.160	.089	.8380
.040	.064	.8130

INCREMENT L = .749
SUMMATION = .71526668218
WEIGHT RATIO = 181.789843434

B^0 = nucleation rate
a_v = volume shape factor = volume of crystal/(length)^3

Randolph measured 0.70 for cubes and 0.60 for Borax tabloids. The measurement is made by screening and then weighing the mass of crystals on each screen and then counting the number of crystals corresponding to the retained mass on the screen.

The case being considered is that in which the feed contains no nuclei but they are generated in the tank. The balance on the number of crystals is
     rate of generation = rate of efflux
or

$$V_c\frac{dn}{dt} = Qn \tag{16.5}$$

Upon substituting for the linear growth rate

$$G = dL/dt \tag{16.6}$$

and rearranging,

$$\frac{dn}{n} = \frac{Q}{V_c}dt = \frac{Q}{V_c G}dL = \frac{dL}{\bar{t}G} = dx \tag{16.7}$$

where

$$\bar{t} = V_c/Q \tag{16.8}$$

is the mean residence time and

$$x = L/G\bar{t} = t/\bar{t} \tag{16.9}$$

is the dimensionless time. Integration of the equation

$$\int_0^n \frac{dn}{n} = \frac{1}{G\bar{t}}\int_0^L dL \tag{16.10}$$

is

$$n = n^0 \exp(-L/G\bar{t}) = n^0\exp(-x), \tag{16.11}$$

where

$$n^0 = \lim_{L \to 0}\frac{dn}{dL} \tag{16.12}$$

is the concentration of crystals of zero length which are the nuclei; it also is called the zero size population density.

TABLE 16.4. Some Common Substances for which Crystallization Data Are Reported in the Literature and in Patents[a]

Compound	Remark or aspect referred to
Ag–halides	
Ag_2CrO_4	growth kinetics
AlF_3	
Al_2O_3–corundum	
$Al\,NH_4(SO_4)_2$	
$AlK(SO_4)_2$	influence of supersaturation
$Al(OH)_3$	
H_3BO_3	
$Na_2B_4O_7$	oleic acid conducive
$BaSO_4$	nucleation
	growth
	habit
$BaCO_3$	
$BaTiO_4$	
$CaSO_4$	citrates, SO_4', elevated temp.
$CaCO_3$	metaphosphate conducive
$CaCl_2$	
$Ca(NO_3)_2$	
$K_2Cr_2O_7$	rhythmic crystallisation
$CuSO_4$	excess H_2SO_4 detrimental
$CuCl_2$	
$FeSO_4$	
H_2O	nucleation
	growth
NH_4J	nucleation
K-halides	Pb^{2+}, Zn^{2+} conducive
KH_2PO_4	
KNO_3	
K_2SO_4	
K_2CrO_4	
$MgSO_4$	$t = 45°C$, borax conducive
$MgCl_2$	
$MnCl_2$	
LiF	
LiCl	
Li_2SO_4	
NaCl	Pb, Fe, Al, Zn conducive; caking inhibited by ferrocyanides; urea leads to octahedral prisms
Na_2CO_3	Na_2SO_4 conducive
$NaHCO_3$	
Na_2SO_4	wetting agents conducive
$Na_2S_2O_3$	
$NaClO_3$	
NaCN	
NH_4NO_3	paraffin, urea, dyes methods of crystallising effect of additives: conducive
$(NH_4)_2SO_4$	urea, Fe^{2+}, Mg^{2+}, tannin, pH5; Al^{3+} and Fe^{3+} lead to needle formation removal of admixtures crystal growth methods of crystallising
$(NH_4)_2S_2O_5$	
NH_4HCO_3	coarse grained, stabilisation
NH_4Cl	Zn^{++}, Pb^{++}, NH_4^+, wood extract
H_3PO_4	
$NH_4H_2PO_4$	Fe^{3+} and NH_4^+ conducive
$(NH_4)_2HPO_4$	
$NiSO_4$	
$Pb(NO_3)_2$	
$PbCO_3$	
$SrSO_4$	
$ZnSO_4$	
anthracene	
adipic acid	
sugars	

Compound	Remark or aspect referred to
citric acid	
phenols	
xylenes	
naphthalene	
paraffin	
urea	methods and parameters of crystallisation NH_4Cl, $MgCO_3$ glyoxal, cyanuric acid surface-active agents
Na-acetate	
NaK-tartarate	
pentaerythrite	
pepsine	
terephthalic acid	

[a](The references, some 400 in number, are given by Nyvlt, 1971, Appendix A).

The nucleation rate is

$$B^0 = \lim_{L \to 0} \frac{dn}{dt} = \lim_{L \to 0}\left(\frac{dL}{dt}\frac{dn}{dL}\right) \tag{16.13}$$

$$= Gn^0. \tag{16.14}$$

The number of crystals per unit volume is

$$n_c = \int_0^\infty n\,dL = \int_0^\infty n^0 \exp(-L/G\bar{t})dL = n^0 G\bar{t}. \tag{16.15}$$

The total mass of crystals per unit volume is

$$m_c = \int_0^\infty mn\,dL = \int_0^\infty a_v\rho_c L^3 n^0 \exp(-L/G\bar{t})dL$$
$$= 6a_v\rho_c n^0(G\bar{t})^4, \tag{16.16}$$
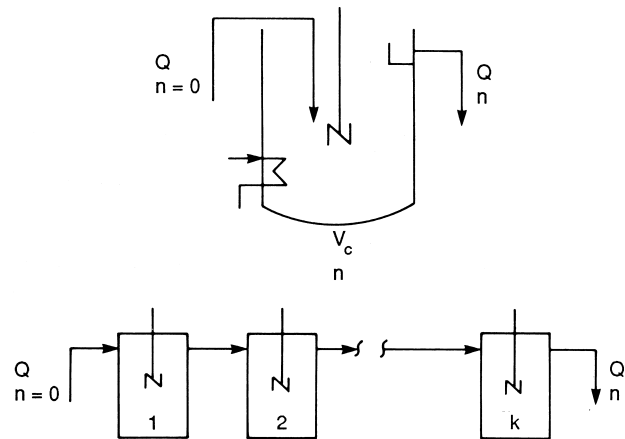
Figure 16.8. Material balancing of continuous stirred tank crystallizers (CSTC). (a) The single stage CSTC. (b) Multistage battery with overall residence time $t = (1/Q)\sum_1^k V_{ci}$.

where a_v is the volumetric shape factor and ρ_c the crystal density. Accordingly, the number of crystals per unit mass is

$$n_c/m_c = 1/6 a_v \rho_c (G\bar{t})^3. \tag{16.17}$$

The mass of crystals per unit volume with length less than L or with dimensionless residence time less than x is

$$m_L = \int_0^L mn \, dL = a_v \rho_c (G\bar{t})^4 n^0 \int_0^x x^3 e^{-x} \, dx. \tag{16.18}$$

The value of the integral is

$$\int_0^x x^3 e^{-x} \, dx = 6[1 - e^{-x}(1 + x + x^2/2 + x^3/6)]. \tag{16.19}$$

This expression has a maximum value at $x = 3$ and the corresponding length L_{pr} is called the predominant length

$$L_{pr} = 3G\bar{t}. \tag{16.20}$$

The cumulative mass distribution is

$$\phi_m = m_L/m_c = 1 - e^{-x}(1 + x + x^2/2 + x^3/6), \tag{16.21}$$

and the differential mass distribution is

$$d\phi_m/dx = x^3 e^{-x}/6, \tag{16.22}$$

which has a maximum value of 0.224 at $x = 3$.

The nucleation rate must generate one nucleus for every crystal present in the product. In terms of M', the total mass rate of production of crystals,

$$B^0 = \frac{M'}{n_c/m_c} = \frac{M'}{6 a_v \rho_c (G\bar{t})^3} = \frac{1.5 M'}{a_v \rho_c L_{pr}^3}. \tag{16.23}$$

The principal quantities related by these equations are ϕ_m, $d\phi_m/dx$, L, L_{pr}, $\bar{t}$, n^0, and B^0. Fixing a certain number of these will fix the remaining one. Size distribution data from a CSTC are analyzed in Example 16.6. In Example 16.7, the values of the predominant length L_{pr} and the linear growth rate G are fixed. From these values, the residence time and the cumulative and differential mass distributions are found. The effect of some variation in residence time also is found. The values of n^0 and B^0 were found, but they are ends in themselves. Another kind of condition is analyzed in Example 16.4.

MULTIPLE STIRRED TANKS IN SERIES

Operation in several tanks in series will provide narrower size distributions. Equations were developed by Nyvlt (1971) for two main cases. With generation of nuclei in the first stage only, the cumulative and differential distributions for k stages are

$$\phi_m = 1 - e^{-kx} \sum_{j=0}^{k+2} \frac{n^j x^j}{j!}, \tag{16.24}$$

$$\frac{d\phi_m}{dx} = \frac{k(kx)^{k+2}}{(k+2)!} e^{-kx}. \tag{16.25}$$

The multistage distributions are plotted in Figure 16.9 for several values of the number of stages. Maxima of the differential distributions occur at

$$x_{max} = 1 + 2/k, \tag{16.26}$$

and the values of those maxima are represented by

$$\left(\frac{d\phi_m}{dx}\right)_{max} = \frac{k^{k+3}(1 + 2/k)^{k+2}}{(k+2)!} \exp[-(k+2)]. \tag{16.27}$$

Some numerical values are:

k	1	2	3	4	5	10
x_{max}	3	2	1.67	1.5	1.4	1.2
$(d\phi_m/dx)_{max}$	0.224	0.391	0.526	0.643	0.745	1.144

Nyvlt (1971) also develops equations for multistage crystallizers in which nuclei form at the same rate in all stages. For two such stages, the cumulative distribution is represented by

$$\begin{aligned} \phi_m =\, &1 - 0.5 e^{-x}[1 + x + x^2/2 + x^3/6] \\ &- 0.5 e^{-2x}[1 + 2x + 2x^2 + (4/3)x^3 + (2/3)x^4]. \end{aligned} \tag{16.28}$$

A comparison of two-stage crystallizers with nucleation in the first stage only and with nucleation in both stages appears in Figure 16.10. The uniformity of crystal size is not as good with nucleation proceeding in every stage; the difference is especially pronounced at larger numbers of stages, which are not shown here but are by Nyvlt (1971).

As in the operation of chemical reactors, multistaging requires shorter residence time for the same performance. For the same L/G ratio, the relative crystallization times of k stages and one stage to reach the peaks are given by Eq. (16.26) as

$$\bar{t}_k/\bar{t}_1 = (1 + k/2)/3, \tag{16.29}$$

which is numerically 0.4 for five stages. Not only is the time shortened, but the size distribution is narrowed. What remains is how to maintain substantial nucleation in only the first stage. This could be done by seeding the first stage and then operating at such low supersaturation that spontaneous nucleation is effectively retarded throughout the battery. Temperature control also may be feasible.

APPLICABILITY OF THE CSTC MODEL

Complete mixing, of course, is not practically realizable and in any event may have a drawback in that intense agitation will cause much secondary nucleation. Some rules for design of agitation of solid suspensions are discussed in Chapter 10.

Equations can be formulated for many complex patterns, combinations of mixed and plug flow, with decanting of supernatant liquor that contains the smaller crystals and so on. A modification to the CSTC model by Jancic and Garside (1976) recognizes that linear crystal growth rate may be size-dependent; in one instance they find that

$$G = G^0 (1 + L/G^0 \bar{t})^{0.65}. $$

Other studies have tried to relate sizes of draft tubes, locations and sizes of baffles, circulation rate, and so on to crystallization

EXAMPLE 16.6
Analysis of Size Distribution Data Obtained in a CSTC
Differential distribution data obtained from a continuous stirred tank crystallizer are tabulated.

W	L	$\sum w/L^3$
0.02	0.340	0.5089
0.05	0.430	1.1377
0.06	0.490	1.6477
0.08	0.580	2.0577
0.10	0.700	2.3493
0.13	0.820	2.5851
0.13	1.010	2.7112
0.13	1.160	2.7945
0.10	1.400	2.8310
0.09	1.650	2.8510
0.04	1.980	2.8562
0.03	2.370	2.8584

The last column is of the summation $\sum_0^L w_i/L_i^3$ at corresponding values of crystal length L. The volumetric shape factor is $a_v = 0.866$, the density is 1.5 g/mL, and the mean residence time was 2.0 hr. The linear growth rate G and the nucleation rate B^0 will be found.

The number of crystals per unit mass smaller than size L is

$$N = \frac{1}{a_v \rho} \sum_0^L \frac{w_i}{L_i^3}. \tag{1}$$

It is also related to the CSTC material balance by

$$dN/dL = n = n^0 \exp(-L/G\bar{t}). \tag{2}$$

Integration of Eq. (2) is

$$N = \int_0^L n^0 \exp(-L/G\bar{t})dL = G\bar{t}n^0[1 - \exp(-L/G\bar{t})]. \tag{3}$$

Combining Eqs. (1) and (3),

$$\sum w_i/L_i^3 = a_v \rho G\bar{t}n^0[1 - \exp(-L/G\bar{t})]. \tag{4}$$

The two unknowns G and n^0 may be found by nonlinear regression with the 12 available data for L_i. However, two representative values of L_i are taken here, and the unknowns are solved for simultaneous solution of two equations. When

$$L = 0.58, \sum = 2.0577,$$
$$L = 1.40, \sum = 2.8310.$$

Substituting into Eq. (4) and rationing,

$$\frac{2.8310}{2.0577} = \frac{1 - \exp(-1.4/G\bar{t})}{1 - \exp(-0.58/G\bar{t})};$$

by trial,

$$G\bar{t} = 0.5082$$
$$G = 0.5082/2 = 0.2541.$$

With $L = 1.4$ in Eq. (4),

$$2.8310 = 0.866(1.5)(0.5082)n^0[1 - \exp(-1.4/0.5082)],$$

from which

$$n^0 = 4.58 \text{ nuclei/mm}^4$$
$$= 4.58(10)^{12} \text{nuclei/m}^4.$$

Accordingly,

$$B^0 = Gn^0 = 0.2541(10)^{-3}(4.58)(10)^{12} = 1.16(10)^9 \text{nuclei/m}^3 \, hr.$$

The cumulative mass size distribution is represented by

$$\phi_m = 1 - e^{-x}(1 + x + x^2/2 + x^3/6)$$

with

$$x = L/G\bar{t} = L/0.5082.$$

This distribution should be equivalent to the original one, but may not check closely because the two points selected may not have been entirely representative. Moreover, although the data were purportedly obtained in a CSTC, the mixing may not have been close to ideal.

---

behavior. So far the conclusions are not general enough to do a designer much good. A possibly useful concept, the separation index (SI), is mentioned by Mullin (1976, p. 293):

SI = (kg of 1 mm equivalent crystals)/m³ hr.

For inorganic salts in water at near ambient temperature, a value of SI in the range of 100–150 kg/m³/hr may be expected. An illustration of the utilization of pilot plant data and plant experience in the design of a urea crystallizer is in Example 16.1.

In general, the design policy to be followed is to utilize as much laboratory and pilot plant information as possible, to work it into whatever theoretical pattern is applicable, and to finish off with a comfortable safety factor. There may be people who know how they should be consulted.

16.7. KINDS OF CRYSTALLIZERS

The main kinds of crystallizers are represented in Figures 16.11 and 16.12. They will be commented on in order. Purification of products of melt crystallization is treated separately.

Batch crystallizers are used primarily for production of fine chemicals and pharmaceuticals at the rate of 1–100 tons/week. The one exception is the sugar industry that still employs batch vacuum crystallization on a very large scale. In that industry, the syrup is concentrated in triple- or quadruple-effect evaporators, and crystallization is completed in batch vacuum pans that may or may not be equipped with stirrers [Figure 16.12(g)].

Natural circulation evaporators like those shown on Figure 8.16 may be equipped for continuous salt removal and thus adapted to crystallization service. For large production rates, however, forced circulation types such as the crystallizer of Figure 16.11(d), with some control of crystal size, are the most often used. The lower limit for economic continuous operation is 1–4 tons/day of crystals, and the upper limit in a single vessel is 100–300 tons/day, but units in parallel can be used for unlimited capacity.

Many special types of equipment have been developed for particular industries, possibly extreme examples being the simple open ponds for solar evaporation of brines and recovery of salt, and the specialized vacuum pans of the sugar industry that operate with syrup on the tubeside of calandrias and elaborate internals to eliminate entrainment. Some modifications of basic types of

EXAMPLE 16.7
Crystallization in a Continuous Stirred Tank with Specified Predominant Crystal Size

Crystals of citric acid monohydrate are to made in a CSTC at 30°C with predominant size $L_{pr} = 0.833$ mm (20 mesh). The density is 1.54 g/mL, the shape factor $a_v = 1$ and the solubility is 39.0 wt %. A supersaturation ratio $C/C_0 = 1.05$ is to be used.

Take the growth rate, $G = 2\bar{v}$, to be one-half of the value given in Table 16.3:

$$G = dL/d\theta = 4(10^{-8})\,\text{m/sec}, \; 0.144\,\text{mm/hr}.$$

The predominant size is related to other quantities by

$$L_{pr} = 0.833 = 3G\bar{t},$$

from which

$$\bar{t} = 0.833/(3)(0.144) = 1.93\text{hr}.$$

For a mass production rate of 15 kg/hr of crystals, $C = 15$, the nucleation rate is

$$B^0 = \frac{1.5C}{a_v \rho_c L_{pr}^3} = \frac{1.5(15)}{1(1.5)[0.833(E-3)]^3}$$
$$= 2.595(10)^{10}\,\text{nuclei/m}^3\text{hr}.$$

The zero size concentration of nuclei is

$$n^0 = B^0/G = 2.595(10)^{10}/(4)(10^{-8}) = 6.49(10)^{17}\; \text{nuclei/m}^4.$$

Accordingly, the equation of the population density is

$$n = n^0 \exp(-L/G\bar{t}) = \exp(41.01 - 360L).$$

The cumulative mass distribution is

$$\phi_m = 1 - e^{-x}(1 + x + x^2/2 + x^3/6),$$

where

$$x = L/G\bar{t} = 3.60L, \qquad \text{with } L \text{ in mm.}$$

The differential distributions are differences between values of ϕ_m at successive values of crystal length L. The tabulation shows cumulative and differential distributions at the key $\bar{t} = 1.93$ hr, and also at 1.5 and 3.0 hr. The differential distributions are plotted and show the shift to larger sizes as residence time is increased, but the heights of the peaks are little affected.

Mesh	mm	$\bar{t} = 1.5$ h Cum	Diff	$\bar{t} = 1.93$ h Cum	Diff	$\bar{t} = 3.0$ h Cum	Diff
0	0	1.0000	.0002	1.0000	.0020	1.0000	.0517
6	3.327	.9998	.0010	.9980	.0068	.9483	.0623
7	2.794	.9989	.0041	.9912	.0185	.8859	.0913
8	2.362	.9948	.0136	.9728	.0424	.7947	.1226
9	1.981	.9812	.0350	.9304	.0778	.6720	.1410
10	1.651	.9462	.0603	.8526	.1021	.5310	.1260
12	1.397	.8859	.0983	.7505	.1322	.4051	.1183
14	1.168	.7876	.1152	.6183	.1278	.2868	.0873
16	.991	.6724	.1343	.4905	.1268	.1995	.0693
20	.833	.5381	.1304	.3637	.1071	.1302	.0482
24	.701	.4076	.1157	.2565	.0845	.0820	.0323
28	.589	.2919	.0929	.1720	.0614	.0497	.0204
32	.495	.1990	.0684	.1106	.0416	.0293	.0123
35	.417	.1306	.0483	.0690	.0274	.0169	.0074
42	.351	.0823	.0324	.0416	.0173	.0096	.0043
48	.295	.0499	.0312	.0243	.0108	.0053	.0025
60	.246	.0287	.0119	.0135	.0058	.0028	.0013
65	.208	.0168	.0073	.0077	.0034	.0015	.0007
80	.175	.0095	.0043	.0042	.0019	.0008	.0004
100	.147	.0052	.0037	.0023	.0016	.0004	.0003
150	.104	.0015	.0011	.0006	.0005	.0001	.0001
200	.074	.0004	.0004	.0002	.0002	.0000	.0000
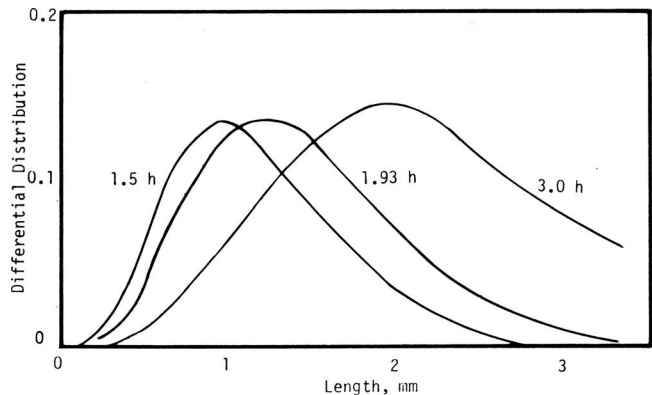
crystallizers often carry the inventor's or manufacturer's name. For their identification, the book of Bamforth (1965) may be consulted.

The basic equipment descriptions following carry the letter designations of Figure 16.11.

(a) Jacketed pipe scraped crystallizers. These are made with inner pipe 6–12 in. dia and 20–40 ft long, often arranged in tiers of three or more connected in series. Scraper blades rotate at 15–30 rpm. Temperatures of −75 to +100°F have been used and viscosities in excess of 10,000 cP present no problems. Although the action is plug flow with tendency to uniform crystal size, the larger particles settle to the bottom and grow at the expense of the smaller ones that remain suspended, with the result that a wide range of sizes is made. Capacity is limited by rates of heat transfer; coefficients of 10–25 Btu/(hr)(sqft)(°F) usually are attainable. Higher coefficients are obtainable in Votators (Cherry Burrell Co.) that have more intense scraping action. Pilot units of 4 in. by 4 ft and larger are made.

(b) Swenson–Walker type. In comparison with jacketed pipes, they have the advantage of being more accessible for cleaning. The standard unit is 24 in. wide, 26 in. high, and 10 ft long. Four units in line may be driven off one shaft. Capacity is limited by heat transfer rates which may be in the range of 10–25 Btu/(hr)(sqft)(°F), with an effective area of 3 sqft/ft of length. According to data in *Chemical Engineers' Handbook* (3rd ed., McGraw-Hill, New York, 1950, p. 1071), a 40 ft unit is able to produce 15 tons/day of trisodium phosphate, and a 50 ft unit can make 8 tons/day of Glaubers salt. The remarks about crystal size distribution made under item (a) apply here also.

(c) Batch stirred and cooled types. Without agitation, crystallization time can be 2–4 days; an example is given in *Chemical*

(a)

(b)
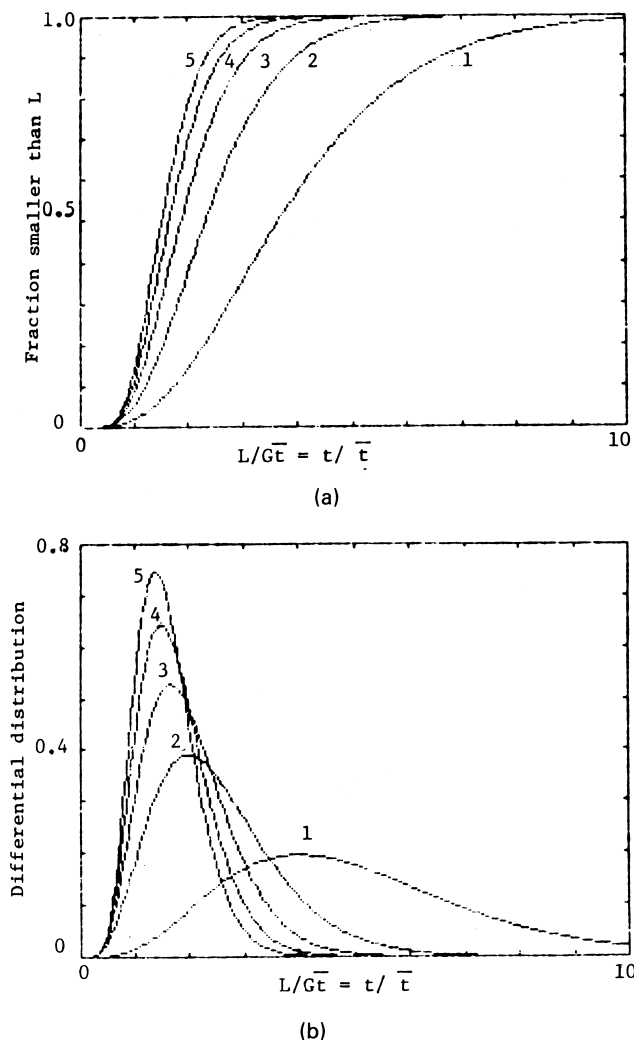
Figure 16.9. Theoretical crystal size distributions from an ideal stirred tank and from a series of tanks with generation of nuclei only in the first tank. Equations of the curves and for the peak values are in the text. (a) Cumulative distributions. (b) Differential distributions.

Figure 16.10. Cumulative size distribution in continuous stirred tanks. (a) one tank; (b) two tanks in series, nucleation in both; (c) two tanks in series, nucleation in only the first.

Engineer's Handbook (1950, p. 1062). With agitation, times of 2–8 hr are sometimes cited. The limitation is due to attainable rates of heat transfer. Without encrustation of surfaces by crystals, coefficients of 50–200 Btu/(hr)(sqft)(°F) are realizable, but temperature differences are maintained as low as 5–10°F in order to keep supersaturation at a level that prevents overnucleation. Stirring breaks corners off crystals and results in secondary nucleation so that crystal size is smaller than in unagitated tanks. Larger crystal sizes are obtained by the standard practice of seeding with an appropriate range of fine crystals. Calculation of the performance of such an operation is made in Example 16.5. Teflon heat transfer tubes that are thin enough to flex under the influence of circulating liquid cause a continual descaling that maintains good heat transfer consistently, 20–65 Btu/(hr)(sqft)(°F). Circulating types such as Figure 16.11(d) and (e) often are operated in batch mode, the former under vacuum if needed. High labor costs keep application of batch crystallizers to small or specialty production.

(d) Circulating evaporators. Some units are built with internal coils or calandrias and are simply conventional evaporators with provisions for continual removal of crystals. Forced circulation and external heat exchangers provide better temperature control. High velocities in the tubes keep the surfaces scoured. Temperature rise is limited to 3–10°F per pass in order to control supersaturation and nucleation. Operation under vacuum often is practiced. When the boiling point elevation is not excessive, the off vapors may be recompressed and used again for heating purposes. Multiple effect units in series for thermal economy may be used for crystallizing evaporators as they are for conventional evaporation. Pilot units of 2 ft dia are made, and commercial units up to 40 ft dia or so.

(e) Circulating cooling crystallizers. Such operations are feasible when the solubility falls sharply with decreasing temperature. Coolers usually are applied to smaller production rates than the evaporative types. Cooling is 1–2°F per pass and temperature differences across the tubes are 5–15°F.

(f) Swenson Fluid Bed crystallizer. This crystallizer is an improved circulating cooling crystallizer. An inert gas stream like air is recirculated by means of a blower. The gas stream suspends the product crystals and flows around tubes in the product slurry. A cooling media is pumped through the inside of the tubes. The feed solution enters near the liquid level and is cooled to the end temperature. The product crystal slurry is removed continuously via downpipes through the bottom of the crystallizer. The heat transfer coefficient in this crystallizer is two to three times as high as in the circulating cooling crystallizer. Higher ΔTs can be utilized while still achieving a reasonable operating cycle. Larger crystals are produced than in the conventional circulating cooling crystallizer since there is less mechanical attrition of the crystals.

The special designs of Figure 16.12 mostly feature some control of crystal size. They are discussed in order.

(a) Draft tube baffle (DTB) crystallizer. The growing crystals are circulated from the bottom to the boiling surface with a slow moving propeller. Fine crystals are withdrawn from an annular space, redissolved by heating to destroy unwanted nuclei and returned with the feed liquor. The temperature rise caused by mixing of heated feed and circulating slurry is 1–2°F. The fluidized bed of large crystals occupies 25–50% of the vessel active volume. Holdup time is kept sufficient for crystal growth to the desired size. Products such as KCl, $(NH_4)_2SO_4$, and $(NH_4)H_2PO_4$ can be made in this equipment in the range of 6–20 mesh. Reaction and crystallization can be accomplished simultaneously in DTB units. The reactants can be charged into the recirculation line or into the draft tube. Examples are the production of ammonium sulfate from ammonia and sulfuric acid and the neutralization of waste
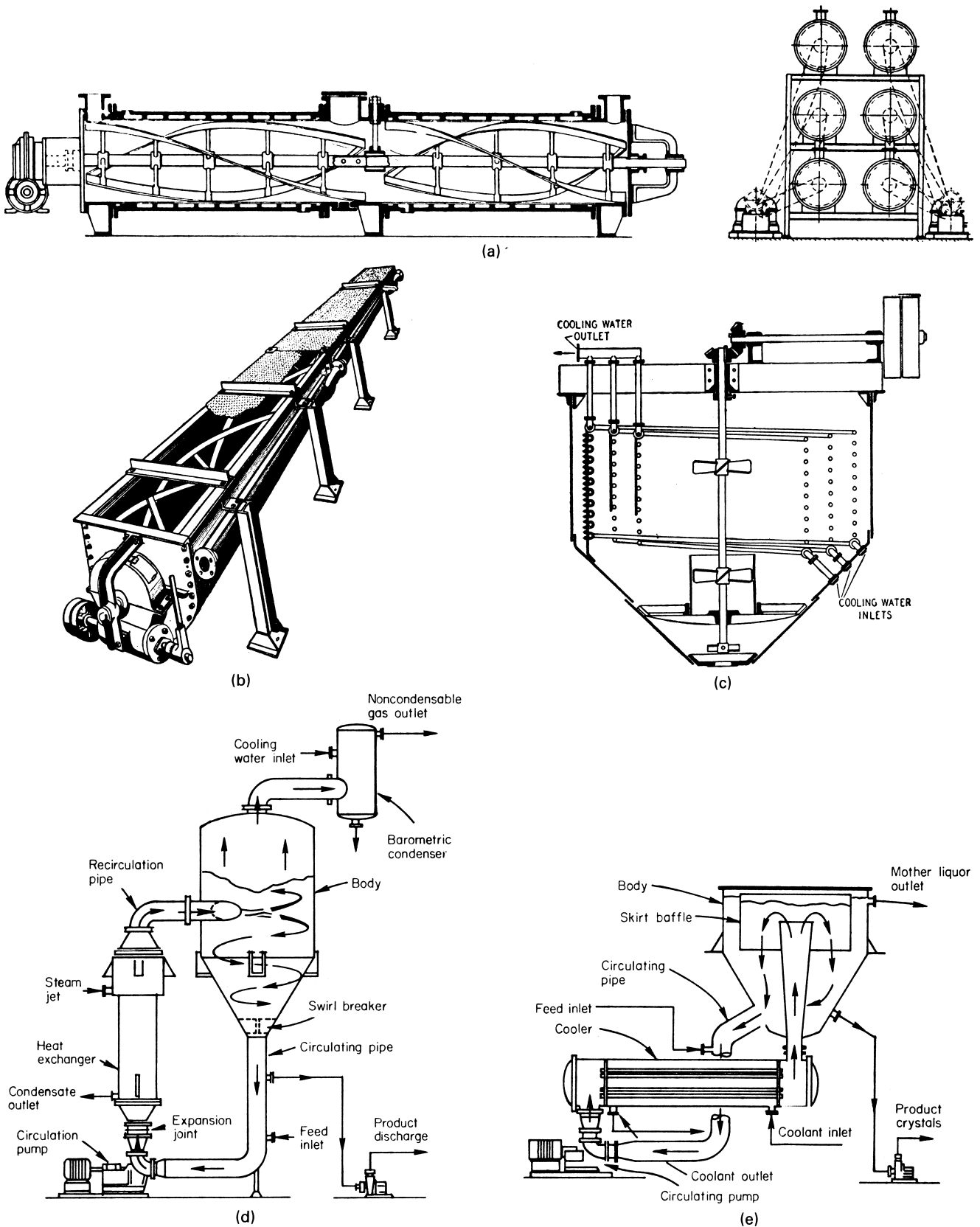
Figure 16.11. Basic types of batch and continuous crystallizers. (a) Jacketed scraped pipe and assembly of six units (*Riegel, 1953*). (b) Swenson–Walker jacketed scraped through (*Swenson Evaporator Co., Riegel, 1953*). (c) Batch stirred tank with internal cooling coil (*Badger and McCabe*, Elements of Chemical Engineering, *McGraw-Hill, New York, 1936*). (d) Crystallization by evaporation, with circulation through an external heater (Swenson Technology Inc.). (e) Crystallization by chilling, with circulation through an external cooler. (Swenson Technology Inc.). (f) Fluid bed crystallizer, crystallization by chilling with an inert gas suspending the product crystals (Swenson Technology Inc.).

(f)
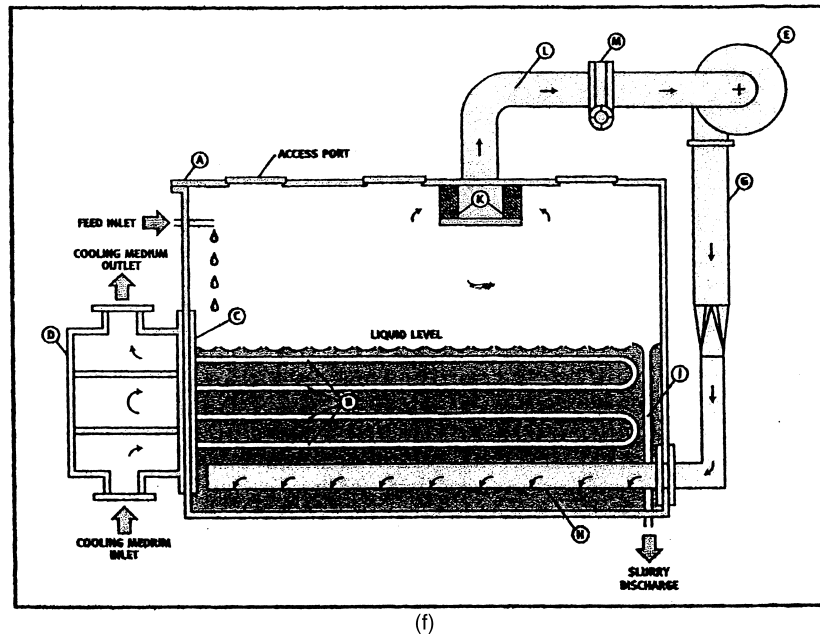
Figure 16.11.—(*continued*)

(a)

(b)
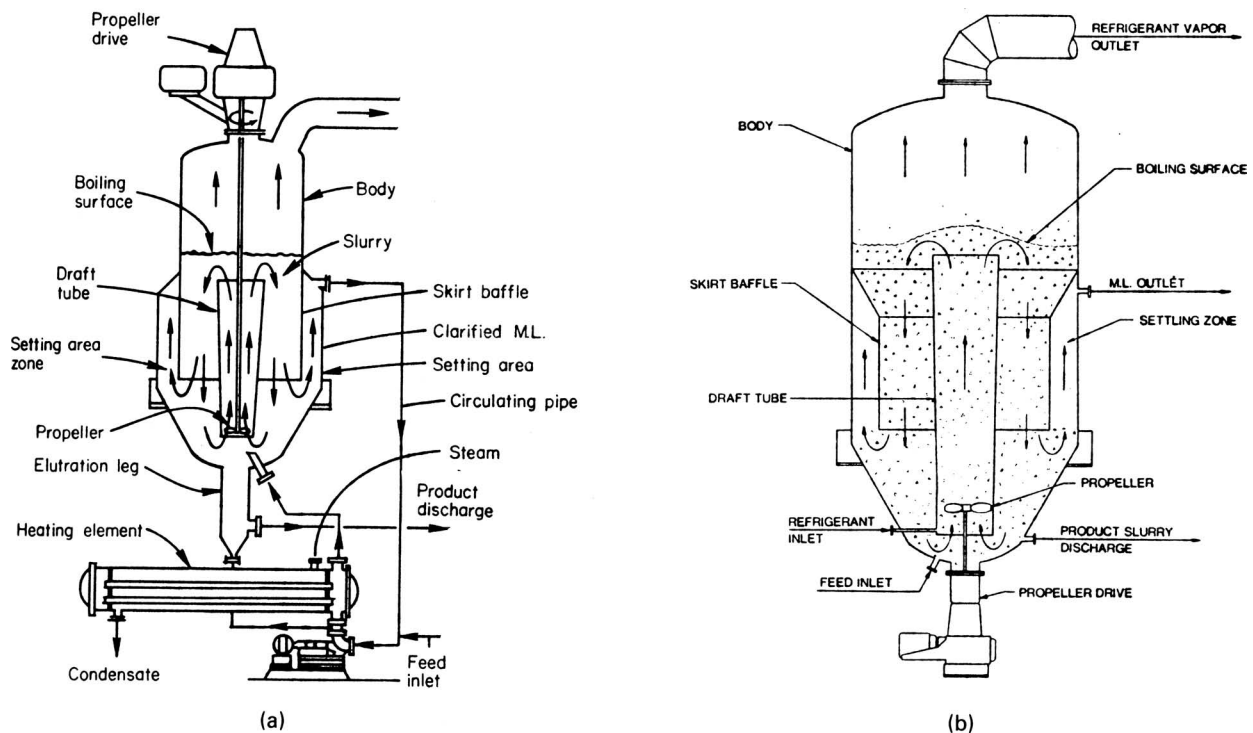
Figure 16.12. Examples of special kinds of crystallizers. (a) Swenson draft tube baffle (DTB) crystallizer; crystals are brought to the surface where growth is most rapid, the baffle permits separation of unwanted fine crystals, resulting in control of size. (b) Swenson direct chilling by contact with immiscible refrigerant, attains very low temperatures and avoids encrustation of heat transfer surfaces. Freons and propane are in common use. (c) Oslo "Krystal" evaporative classifying crystallizer. Circulation is off the top, the fine crystals are destroyed by heating, large crystals grow in the body of the vessel. (d) Twinned crystallizer. When one chamber is maintained slightly supersaturated and the other slightly subsaturated, coarse crystals can be made. (*Nyvlt, 1971*). (e) APV–Kestner long tube salting evaporator; large crystals (0.5 mm or so) settle out. (f) Escher-Wyss or Tsukushima DP (double propeller) crystallizer. The double propeller maintains upward flow in the draft tube and downward flow in the annulus, resulting in highly stable suspensions. (g) A vacuum pan for crystallization of sugar (*Honolulu Iron Works*).

(c)

(d)

(e)

(f)

1 Thickening zone	10 Heater or cooler
2 Draft tube	11 Solution return
3 Evaporation chamber	12 Elutriation liquid feed
4 Double-acting circulation propeller	13 Slurry discharge pump
5 Crystal growth zone	14 Elutriation zone
6 Grading zone	15 Vapour outlet
7 Settling zone	16 Overflow
8 Circulation pipe	17 Variable-speed drive
9 Circulation pump	

(g)
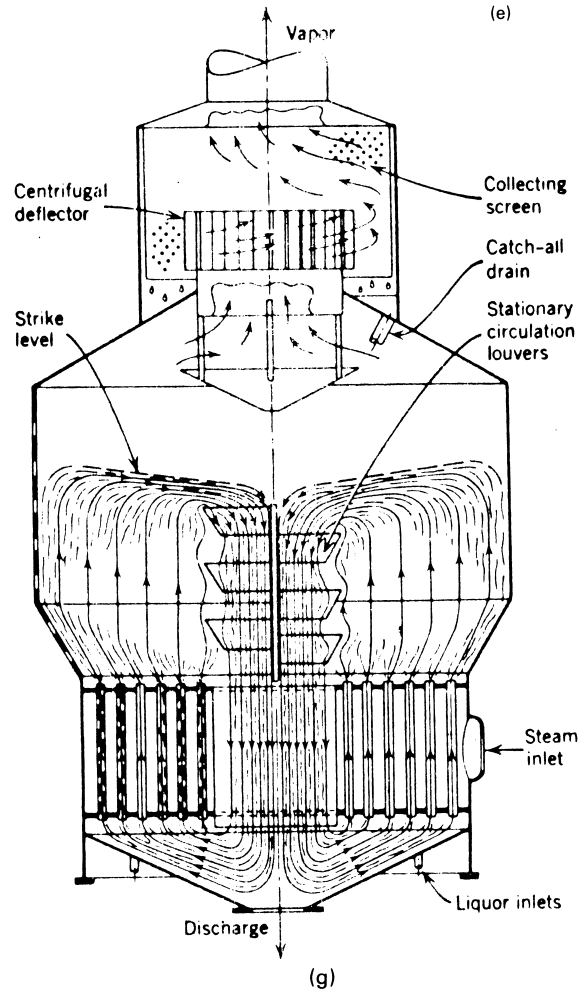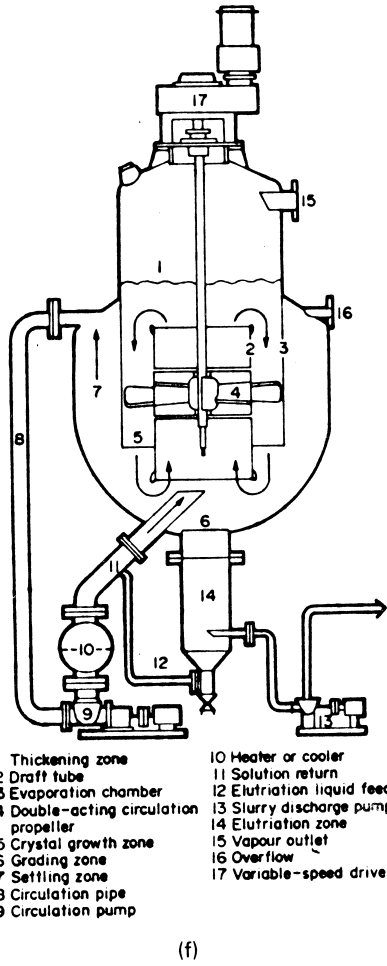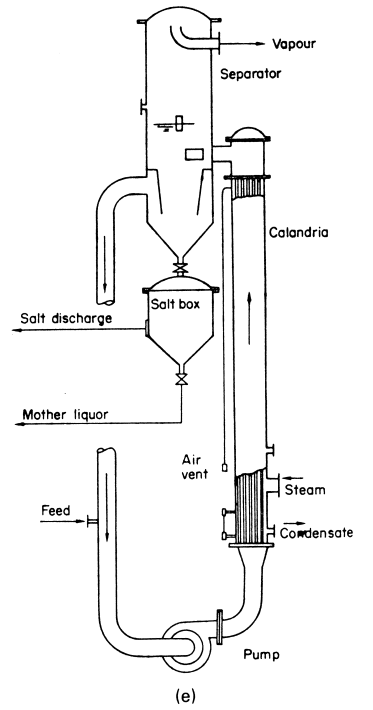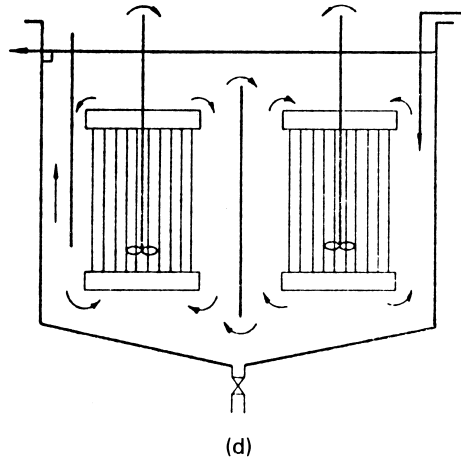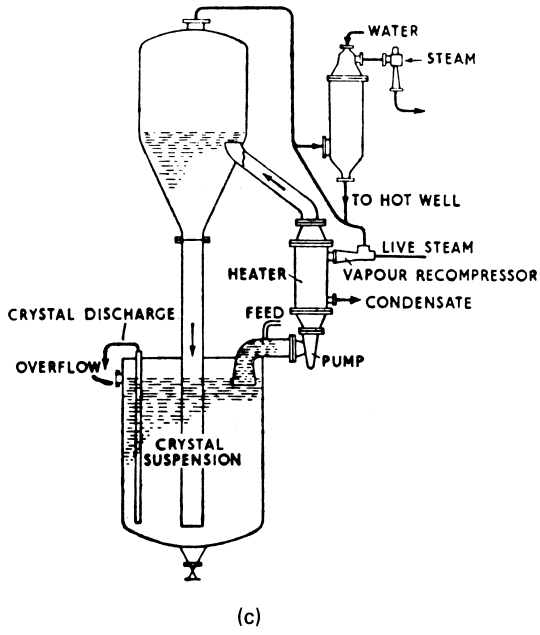
Figure 16.12.—(*continued*)

acids with lime. The heat of reaction is removed by evaporation of water.

(b) Direct contact refrigeration. Such equipment is operated as low as −75°F. Essentially immiscible refrigerant is mixed with the liquor and cools it by evaporation. The effluent refrigerant is recovered, recompressed, and recycled. Direct contacting eliminates the need for temperature difference across a heat transfer tube which can be economically more than 5–15°F, and also avoids scaling problems since the liquor must be on the outside of the tubes when refrigerant is used. Examples are crystallization of caustic with freon or propane and of p-xylene with propane refrigerant.

(c) Oslo "Krystal" evaporative classifying crystallizer. The supernatant liquid containing the fines is circulated through the external heater where some of the fines are redissolved because of the temperature rise. The settled large crystals are withdrawn at the bottom. The recirculation rate is much greater than the fresh feed rate. In one operation of $MgSO_4.7H_2O$ crystallization, fresh feed saturated at 120°C is charged at 2000 kg/hr to the vessel maintained at 40°C and is mixed with a recirculated rate of 50,000 kg/hr to produce a mixture that is temporarily at 43°C, which then evaporates and cools. Vessel sizes as large as 15 ft dia and 20 ft high are mentioned in the literature. The same principle is employed with cooling type crystallization operations.

(d) Twinned crystallizer. Feed is to the right chamber. The rates of recirculation and forward feed are regulated by the position of the center baffle. Improved degree of uniformity of crystal size is achieved by operating one zone above saturation temperature and the other below. Fine particles are dissolved and the larger ones grow at their expense. Even with both zones at the same temperature, the series operation of two units in series gives more nearly uniform crystal size distribution than can be made in a single stirred tank. It is not stated if any such crystallizers are operated outside Nyvlt's native land, Czechoslovakia, that also produces very fine tennis players (Lendl, Mandlikova, Navratilova, Smid, and Sukova).

(e) APV-Kestner long tube vertical evaporative crystallizers are used to make small crystals, generally less than 0.5 mm, of a variety of substances such as NaCl, Na_2SO_4, citric acid, and others; fine crystals recirculate through the pump and heater.

(f) Escher-Wyss (Tsukushima) double propeller maintains flow through the draft tube and then annulua and maintains highly stable suspension characteristics.

(g) Sugar vacuum pan. This is an example of the highly specialized designs developed in some long-established industries. Preconcentration is effected in multiple effect evaporators; then crystallization is accomplished in the pans.

16.8. MELT CRYSTALLIZATION AND PURIFICATION

Some mixtures of organic substances may be separated advantageously by cooling and partial crystallization. The extent of such recovery is limited by the occurrence of eutectic behavior. Examples 16.2 and 16.8 consider such limitations. Sometimes these limitations can be circumvented by additions of other substances that change the phase equilibria or may form easily separated compounds with one of the constituents that are subsequently decomposed for recovery of its constituents.

Thus the addition of n-pentane to mixtures of p-xylene and m-xylene permits complete separation of the xylenes which form a binary eutectic with 11.8% para. Without the n-pentane, much para is lost in the eutectic, and none of the meta is recoverable in pure form. A detailed description of this process is given by Dale (1981), who calls it extractive crystallization. Other separation processes depend on the formation of high melting molecular compounds or clathrates with one of the constituents of the mixture. One example is carbon tetrachloride that forms a compound with p-xylene and alters the equilibrium so that its separation from m-xylene is facilitated. Hydrocarbons form high-melting hydrates with water; application of propane hydrate formation for the desalination of water has been considered. Urea forms crystalline complexes with straight chain paraffins such as the waxy ingredients of lubricating oils. After separation, the complex may be decomposed at 75–80°C for recovery of its constituents. This process also is described by Dale (1981). Similarly thiourea forms crystalline complexes with isoparaffins and some cyclic compounds.

Production rates of melt crystallization of organic materials usually are low enough to warrant the use of scraped surface crystallizers like that of Figure 16.11(a). A major difficulty in the production of crystals is the occlusion of residual liquor on them which cuts the overall purity of the product, especially so because of low temperatures near the eutectic and the consequent high viscosities. Completeness of removal of occluded liquor by centrifugation or filtration often is limited because of the fragility and fineness of the organic crystals.

MULTISTAGE PROCESSING

In order to obtain higher purity, the first product can be remelted and recrystallized, usually at much higher temperatures than the eutectic so that occlusion will be less, and of course at higher concentration. In the plant of Figure 16.13, for instance, occlusion from the first stage is 22% with a content of 8% p-xylene and an overall purity of 80%; from the second stage, occlusion is 9% with a PX content of 42% but the overall purity is 95% PX; one more crystallization could bring the overall purity above 98% or so.

Because the handling of solids is difficult, particularly that of soft organic crystals, several crystallization processes have been developed in which solids do not appear outside the crystallizing equipment, and the product leaves the equipment in molten form. For organic substances, crystalline form and size usually are not of great importance as for products of crystallization from aqueous solutions. If needed, the molten products can be converted into flakes or sprayed powder, or in extreme cases they can be recrystallized out of a solvent.

THE METALLWERK BUCHS PROCESS

The Metallwerk Buchs (MWB) process is an example of a batch crystallization that makes a molten product and can be adapted to multistaging when high purities are needed. Only liquids are transferred between stages; no filters or centrifuges are needed. As appears on Figure 16.14, the basic equipment is a vertical thin film shell-and-tube heat exchanger. In the first phase, liquor is recirculated through the tubes as a film and crystals gradually freeze out on the cooled surface. After an appropriate thickness of solid has accumulated, the recirculation is stopped. Then the solid is melted and taken off as product or transferred to a second stage for recrystallization to higher purity.

PURIFICATION PROCESSES

As an alternative to multistage batch crystallization processes with their attendant problems of material handling and losses, several types of continuous column crystallizers have been developed, in which the product crystals are washed with their own melts in countercurrent flow. Those illustrated in Figures 16.15–16.18 will be described. Capacities of column purifiers as high as 500 gal/(hr) (sqft) have been reported but they can be less than one-tenth as much. Lengths of laboratory size purifiers usually are less than three feet.

Crystallization from a Ternary Mixture
The case is that of mixtures of the three isomeric nitrotoluenes for which the equilibrium diagram is shown. Point *P* on the diagram has the composition 0.885 para, 0.085 meta, and 0.030 ortho. The temperature at which crystals begin to form must be found experimentally or it may be calculated quite closely from the heats and temperatures of fusion by a method described for instance by Walas (Example 8.9, 1985). It cannot be found with the data shown on the diagram. In the present case, incipient freezing is at 46°C, with para coming out at point *P* on the diagram. As cooling continues, more and more pure para crystals form. The path is along straight line *PS* which corresponds to constant proportions of the other two isomers since they remain in the liquid phase. At point *S*, −13°C, which is on the eutectic trough of meta and ortho, the meta also begins to precipitate. Para and meta continue to precipitate along the trough until the ternary eutectic *E* is reached at −40°C when complete solidification occurs. The cooling path is shown on the phase diagram. The recovery of pure para at equilibrium at various temperatures and the composition of the liquid phase are tabulated. (Coulson and Warner, 1949).
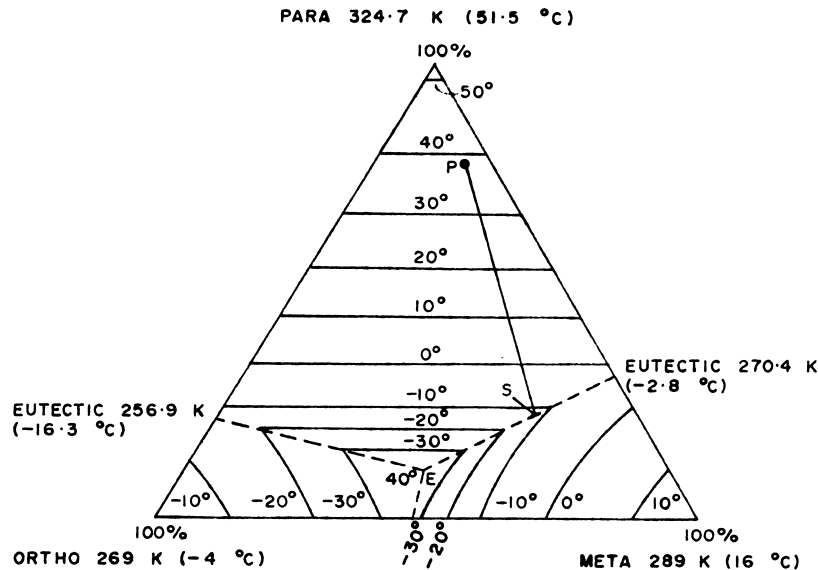
Temperature, °C	Para-deposited, kg	Mother liquor, kg	Composition of mother liquor (per cent by weight)		
			O	*M*	*P*
46	0	100	3·0	8·5	88·5
40	39·6	60·4	5·0	14·0	81·0
30	66·7	33·3	8·7	24·8	66·5
20	75·0	25·0	12·0	34·0	54·0
10	79·6	20·4	14·7	41·6	43·7
0	82·3	17·7	16·7	48·0	35·3
−10	84·8	15·2	17·0	53·9	27·1

Schildknecht Column [Fig. 16.15(a)]. This employs a rotating spiral or screw to move the solids in the direction against the flow of the fluid. The conveyor is of open construction so that the liquid can flow through it but the openings are small enough to carry the solids. Throughputs of 50 L/hr have been obtained in a 50 mm dia column. Because of the close dimensional tolerances that are needed, however, columns larger than 200 mm dia have not been successful. Figure 16.15(a) shows a section for the formation of the crystals, but columns often are used only as purifiers with feed of crystals from some external source.

Philips Crystallization Process [Fig. 16.15(b)]. The purifying equipment consists of a vessel with a wall filter and a heater at the bottom. Crystals are charged from an external crystallizer and forced downwards with a reciprocating piston or with pulses from a pump. The washing liquid reflux flows from the melting zone where it is formed upward through the crystal bed and out through the wall filter. Pulse displacement is 0.3–0.6 cm/sq cm of column cross section, with a frequency of 200–250/min. For many applications reflux ratios of 0.05–0.60 are suitable. Evaluation of the proper combination of reflux and length of purifier must be made empirically.

From a feed containing 65% *p*-xylene, a column 1000 sqcm in cross section can make 99% PX at the rate of 550 kg/hr, and 99.8% PX at 100 kg/hr; this process has been made obsolete, however, by continuous adsorption with molecular sieves. Similarly, a feed of
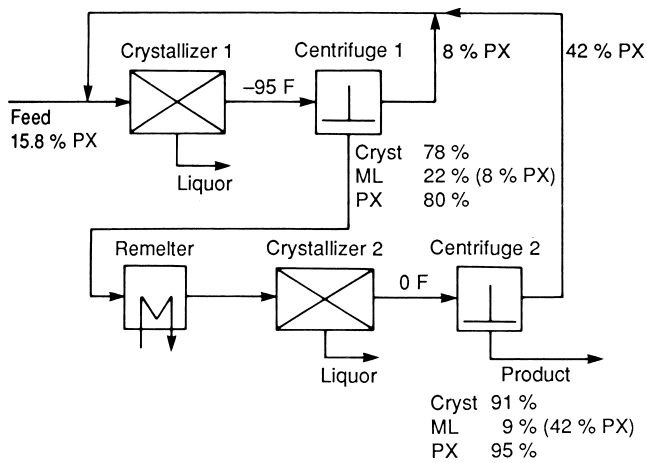
Figure 16.13. Humble two-stage process for recovery of *p*-xylene by crystallization. Yield is 82.5% of theoretical. ML = mother liquor, PX = *p*-xylene (*Haines, Powers and Bennett, 1955*).
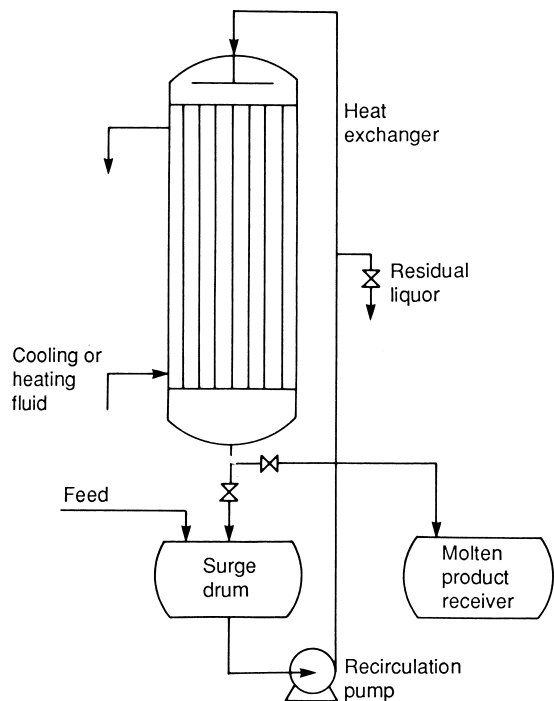
Figure 16.14. MWB (Metallwerk Buchs) batch recirculating crystallizer, with freezing on and melting off insides of thin film heat exchanger tubes; adaptable to multistage processing without external solids handling (*Mützenberg and Saxer, 1971*).

83 mol % of 2- methyl- 5- vinyl pyridine has been purified to 95% at the rate of 550 g/hrcm^2 and 99.7% at 155 g/hrcm^2. At one time, columns of more than 60 cm dia were in operation.

Brodie Crystallizer-Purifier [Fig. 16.15(c)]. This equipment combines a horizontal scraped surface crystallizer with a vertical purifying section. The capacity and performance of the purifier depends strongly on the sizes of the crystals that enter that zone. In order to ensure adequate crystal size, residence times in the crystallizing zone as long as 24 hr may be needed. No data of

residence times are stated in the original article. Some operating data on the recovery of para- dichlorbenzene from a mixture containing 75% of this material are reported for a purifier that is 1.14 sqft cross section as follows, as well as data for some other materials.

Reflux ratio	2	0.5	0.25
Feed rate (gal/hr)	29	60	90
Residue rate (gal/hr)		20	30
Product rate (gal/hr)	20	40	60
PDCB in residue (%)		25	25
Product purity (%)	99.997	99.99	99.5

TNO Bouncing Ball Purifier (Fig. 16.16). The basis for this design is the observation that small crystals melt more readily and have a greater solubility than large ones. The purifier is a column with a number of sieve trays attached to a central shaft that oscillates up and down. As the slurry flows through the tower, bouncing balls on each tray impact the crystals and break up some of them. The resulting small crystals melt and enrich the liquid phase, thus providing an upward refluxing action on the large crystals that continue downward to the melting zone at the bottom. Reflux is returned from the melting zone and product is taken off.

Specifications of a pilot plant column are:

diameter, 80 mm,
hole size, 0.6 × 0.6 mm,
number of balls/tray, 30,
diameter of balls, 12 mm,
amplitude of vibration, 0.3 mm,
frequency, 50/sec,
number of trays, 13,
tray spacing, 100 mm.

For the separation of benzene and thiophene that form a solid solution, a tray efficiency of more than 40% could be realized. Flow rates of 100–1000 kg/m^2 hr have been tested. The residence time of crystals was about 30 min per stage. Eutectic systems also have been handled satisfactorily. A column 500 mm dia and 3 m long with 19 trays has been built; it is expected to have a capacity of 300 tons/yr.

Kureha Double-Screw Purifier (Fig. 16.17). This unit employs a double screw with intermeshing blades that express the liquid from the crystal mass as it is conveyed upward. The melt is formed at the top, washes the rising crystals countercurrently, and leaves as residue at the bottom. A commercial unit has an effective height of 2.6 m and a cross section of 0.31 m^2. When recovering 99.97% p-dichlorbenzene from an 87% feed, the capacity is 7000 metric tons/yr. The feed stock comes from a tank crystallizer and filter. Data on other eutectic systems are shown, and also on separation of naphthalene and thiophene that form a solid solution; a purity of 99.87% naphthalene is obtained in this equipment.

Brennan–Koppers Purifier (Fig. 16.18). This equipment employs top melting like the Kureha and wall filters like the Philips. Upward movement of the crystals is caused by drag of the flowing fluid. The crystal bed is held compact with a rotating top plate or piston that is called a harvester. It has a corrugated surface that scrapes off the top of the top of the bed and openings that permit the crystals to enter the melting zone at any desired rate. The melt flows downward through the openings in the harvester, washes the upwardly moving crystals, and leaves through the sidewall filter as residue. The movement of crystals is quite positive and not as

(a)

(b)

(c)
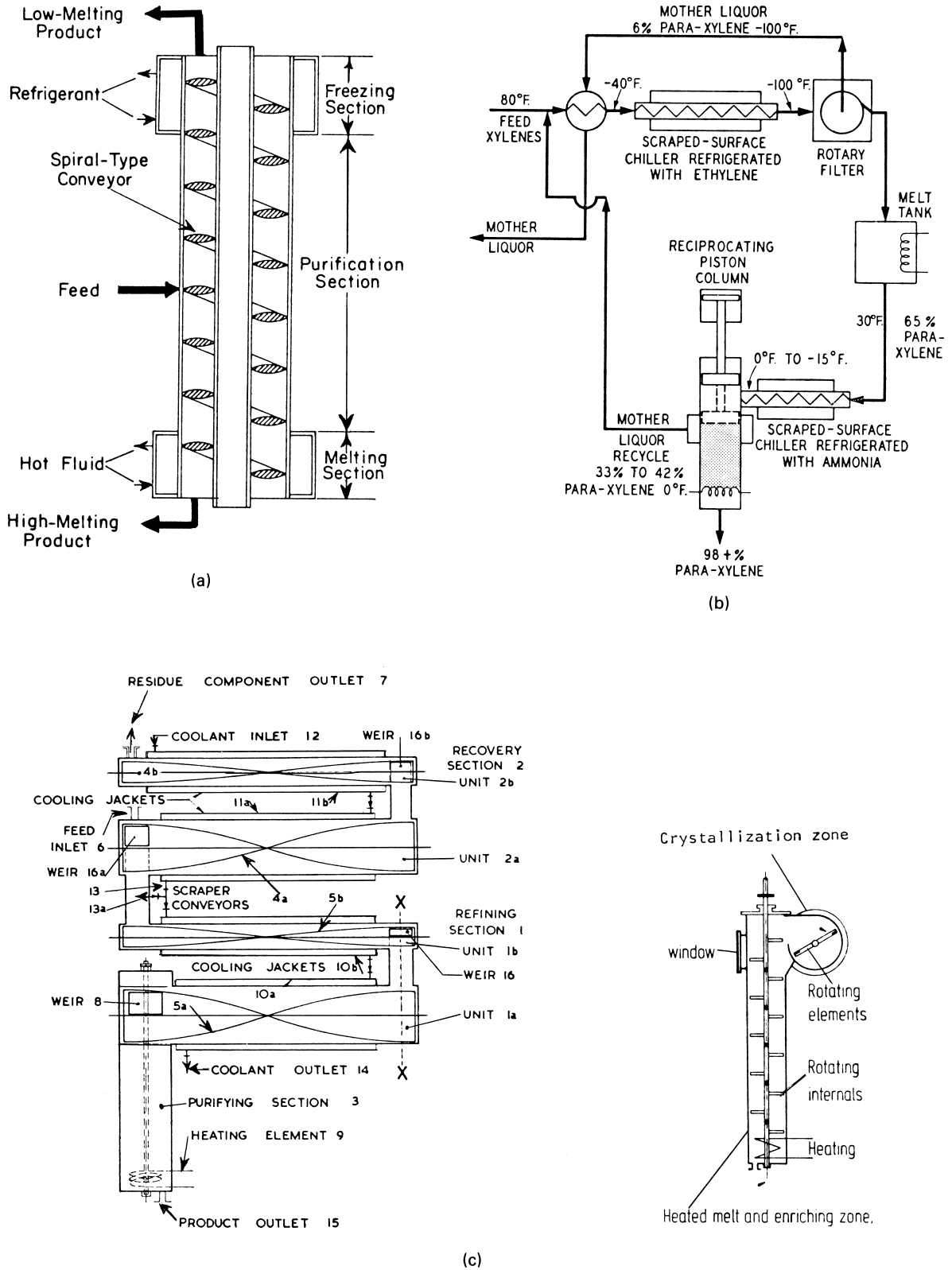
Figure 16.15. Three types of crystal purifiers with different ways of transporting the crystals. (a) Spiral or screw conveyor type, laboratory scale, but successful up to 200 mm dia [*Schildknecht, (1961)*]. (b) Philips purifier with reciprocating piston or pulse pump drive [*McKay, Dale, and Weedman, (1960)*]. (c) Combined crystallizer and purifier, gravity flow of the crystals; purifier details on the right (*Brodie, 1971*).
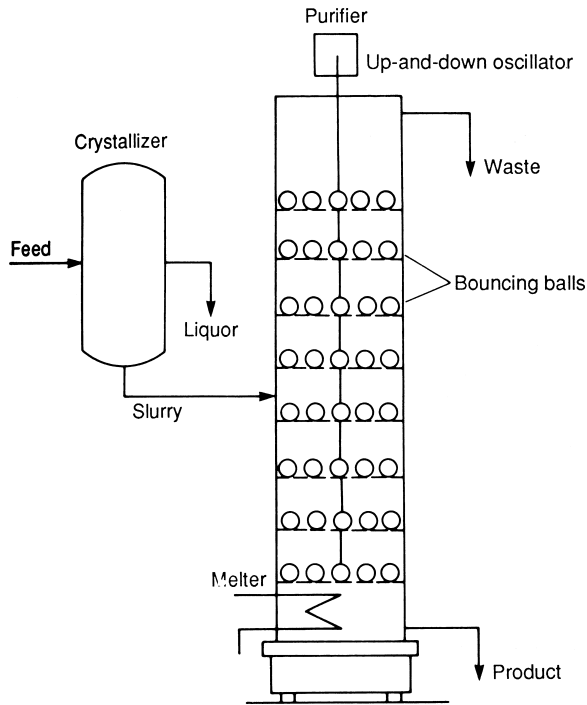
Figure 16.16. TNO Crystal Purifier (*Arkenbout et al., 1976, 1978*).

dependent on particle size as in some other kinds of purifiers. Data are given in the patent (U.S. Pat. 4,309,878) about purification of 2,6- ditertiary butyl para cresol; the harvester was operated 40–60 rpm and filtration rates of 100 lb/(hr)(sqft) were obtained. Other information supplied directly by E.D. Brennan are that a 24 in. dia unit stands 9 ft high without the mixer and that the following performances have been achieved:

	Diameter (in.)	Purity (wt %)		Prod. Rate (lb/hr/ft²)
		Feed	Product	
A. Pilot plant tests				
Acetic acid	3	83	99.85	100
p- Dichlorbenzene	6	70	99.6	380
Naphthalene (high sulfur)	6	68	98	220
Di- t- butyl- p- cresol	3	85	99.1	210
	6	85	99.1	230
B. Commercial operation				
Di- t- butyl- p- cresol	24	90	99.5	340

All feeds were prepared in Armstrong scraped surface crystallizers

1. KCP Column
2. Screw Conveyer
3. Melter
4. Bottom Filter Plate
5. Feed Charger
6. Output of Product
7. Outlet of Bottom Liquid
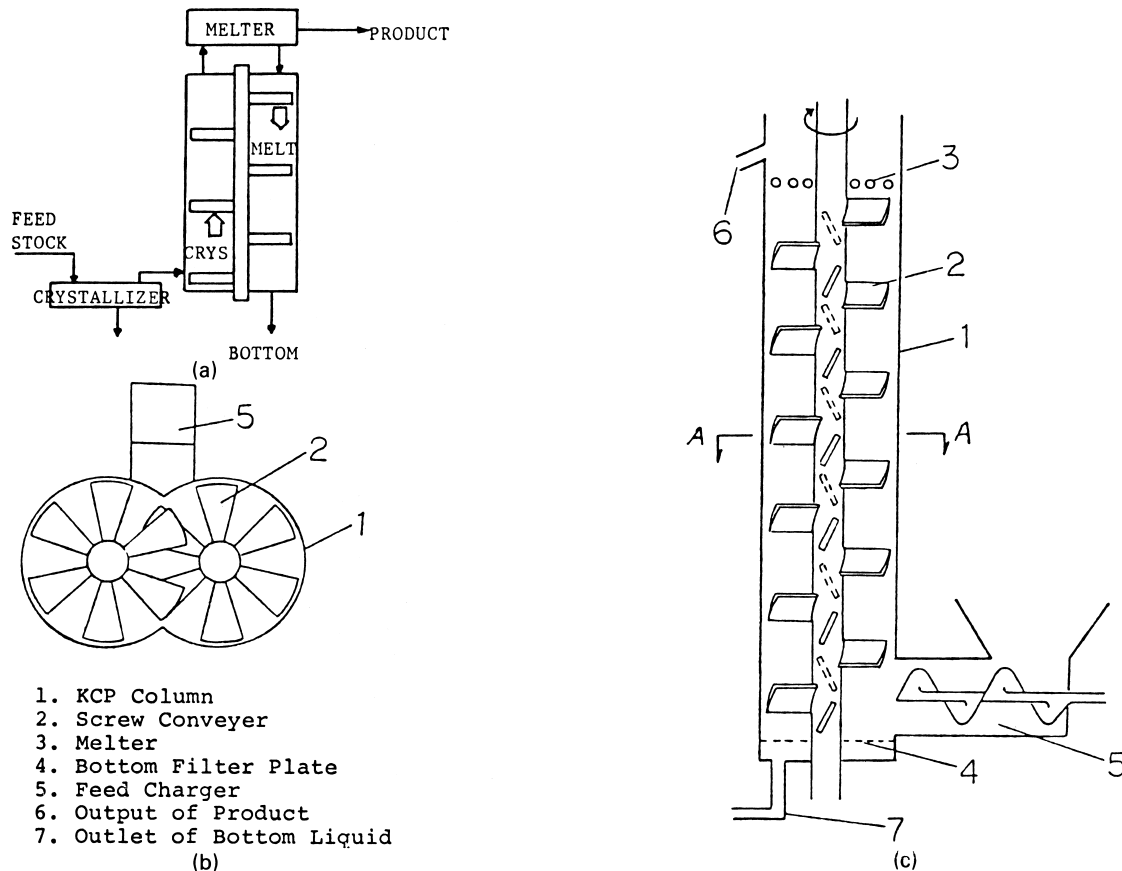
Figure 16.17. Kureha continuous crystal purifier (KCP column) (*Yamada, Shimizu, and Saitoh, in Jancic and DeJong, 1982, pp. 265–270*). (a) Flowsketch. (b) Dumbbell-shaped cross section at AA. (c) Details of column and screw conveyor.
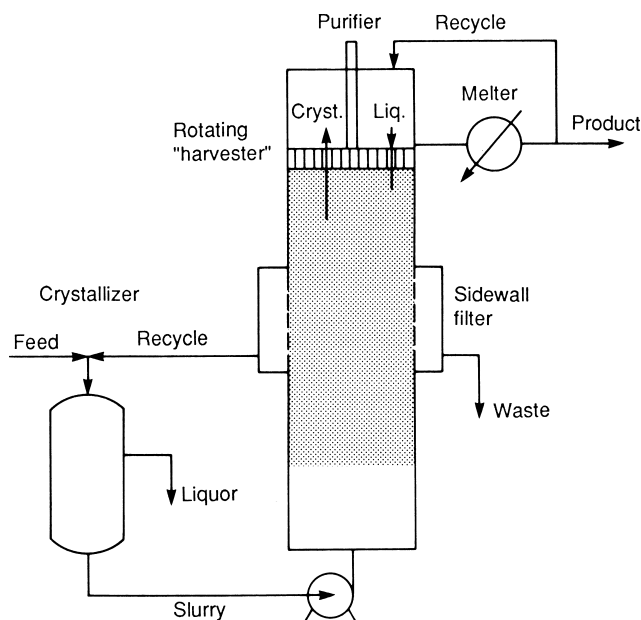
Figure 16.18. Brennan–Koppers crystal purifier (*Brennan, 1982*).

REFERENCES

Crystallization from Solutions

W.L. Badger and W.L. McCable, *Elements of Chemical Engineering*, McGraw-Hill, New York, 1936.

A.W. Bamforth, *Industrial Crystallization*, Leonard Hill, London, 1965.

R.C. Bennett, Crystallization design, *Encycl. Chem. Process. Des.* **13**, 421–455 (1981).

R.C. Bennett, Crystallization from solution, in *Chemical Engineers' Handbook*, McGraw-Hill, New York, 1984, pp. 19.24–19.40.

G.D. Botsaris and K. Toyokura, *Separation and Purification by Crystallization*, American Chemical Society, 1997.

E.D. DeJong and S.I. Jancic, *Industrial Crystallization 1978*, North-Holland, Amsterdam, 1979.

J. Garside and R.J. Davey, *From Molecules to Crystallizers*, Oxford University Press, Oxford, England, 2001.

Industrial Crystallization, Symposium of Inst. Chem. Eng., Inst. Chem. Eng, London, 1969.

S.I. Jancic and E.J. DeJong (Eds.), *Industrial Crystallization 1981*, North-Holland, Amsterdam, 1982.

S.I. Jancic and J. Garside, in Mullin (Ed.), 1976, p. 363.

A.G. Jones, *Crystallization Process Systems*, Butterworth-Heinemann, 2002.

D. Kashchiev, *Nucleation*, Elsevier Science & Technology Books, 2000.

E.V. Khamskii, *Crystallization from Solution*, Consultants Bureau, New York, 1969.

A. Mersmann and A. Mersmann, *Crystallization Technology Handbook*, Marcel Dekker, New York, 2001.

J.W. Mullin, *Crystallization*, Butterworths, London, 1972.

J.W. Mullin, *Crystallization*, Elsevier Science & Technology Books, 2001.

J.W. Mullin, Ed., *Symposium on Industrial Crystallization*, Plenum, New York, 1976.

J.W. Mullin, Crystallization, *Encycl. Chem. Technol.* **7** (1978, pp. 243–285).

J.W. Mullin, Bulk crystallization, in Pamplin (Ed.), *Crystal Growth* Pergamon, New York, 1980, pp. 521–565.

A. Myerson, J. Joseph, V.J. Jacovs, and A.S. Myerson, *Handbook of Industrial Crystallization*, Butterworth-Heinemann, 2001.

J. Nyvlt, Crystallization as a unit operation in chemical engineering, in Industrial Crystallization, 1969, pp. 1–23.

J. Nyvlt, *Industrial Crystallization from Solutions*, Butterworths, London, 1971.

J. Nyvlt, *Industrial Crystallization: The Present State of the Art*, Verlag Chemie, Weinheim, 1978.

M. Ohara and R. C. Reid, *Modelling Crystal Growth Rates from Solution*, Prentice-Hall, Englewood Cliffs, NJ, 1973.

A.D. Randolph and M.A. Larson, *Theory of Particulate Processes*, Academic, New York, 1971.

E.R. Riegel, *Chemical Process Machinery*, Reinhold, New York, 1953.

G. Singh, Crystallization from Solution, in Schweitzer (Ed.), *Handbook of Separation Techniques for Chemical Engineers*, McGraw-Hill, New York, 1979, pp. 2.151–2.182.

S.M. Walas, *Phase Equilibria in Chemical Engineering*, Butterworth, Stoneham, MA, 1985.

Melt Crystallization

R. Albertins, W.C. Gates, and J.E. Powers, Column crystallization, in Zief and Wilcox, *Fractional Solidification*, 1967, pp. 343–367.

G.J. Arkenbout, *Melt Crystallization Technology*, CRC Press. 1995.

G.J. Arkenbout, Progress in continuous fractional crystallization, *Sep. Purification Methods* 7(1), 99–134 (1978).

G.J. Arkenbout, A. vanKujik, and W.M. Smit, Progress in continuous fractional crystallization, in J.W. Mullin (Ed. 1976, pp. 431–435.

E.D. Brennan (Koppers Co.), Process and Apparatus for Separating and Purifying a Crystalline Material, U.S. Pat. 4, 309,878 (12 Jan. 1982).

J.A. Brodie, A continuous multistage melt purification process, *Mech. Chem. Eng. Trans., Inst. Eng. Australia*, 37–44 (May 1971).

Coulson and Warner, *A Problem in Chemical Engineering Design*, Inst. of Chem. Eng. Rugby, England (1949).

G.H. Dale, Crystallization: extractive and adductive, *Encycl. Chem. Process. Des.* **13**, 456–506 (1981).

R.A. Findlay, Adductive crystallization, in Schoen (Ed.), *New Chemical Engineering Separation Techniques*, Wiley-Interscience, New York, 1958.

R.A. Findlay and J.A. Weedman, Separation and purification by crystallization, in *Advances in Petroleum Chemistry and Refining*, Wiley-Interscience, New York, 1958, Vol. 1, pp. 118–209.

H.W. Haines, J.M. Powers, and R.B. Bennett, Separation of xylenes, *Ind. Eng. Chem.* **47**, 1096 (1955).

J.D. Henry and C.C. Moyers, Crystallization from the melt, in *Chemical Engineers' Handbook*, McGraw-Hill, New York, 1984, pp. 17.2–17.12.

D.L. McKay, Phillips fractional solidification process, in Zief and Wilcox 1967, pp. 427–439.

McKay, Dale, and Weedman, *Ind. Eng. Chem.*, **52**, 197 (1960).

A.B. Mützenberg and K. Saxer, The MWB crystallizer, *Dechema Monographien* **66**, 313–320 (1971).

Schildknecht, *Z. Anal. Chem.*, **181**, 254 (1961).

J. Yamada, C. Shimizu, and S. Saitoh, Purification of organic chemicals by the Kureha Continuous Crystal Purifier, in Jancic and DeJong, 1982, pp. 265–270.

M. Zief and W.R. Wilcox, *Fractional Soldification*, Dekker, New York, 1967, Vol. 1.

17

CHEMICAL REACTORS

*I*n this chapter, the principles of chemical kinetics and catalysis are discussed. The basic rate equations are presented along with descriptions of operating modes and the wide variety of equipment that is suitable as chemical reactors. Few rules are generally applicable to the design of equipment for chemical reactions. The broad classes of reactors include stirred tanks, empty or packed beds in tubes, vessels and shell-and-tube devices, and highly specialized configurations in which heat transfer may be provided. Many design factors in individual cases are balanced to achieve economic optima. The general rules of other chapters for design of pressure vessels, heat

exchangers, agitators, and so on, apply to chemical reactors.

The literature in this field is so abundant that only the most significant research that has resulted in commercialization is presented. The material reported is satisfactory for design purposes, although newer techniques are reported in the literature but may not be better than what is presented in this chapter.

Examples of commercial reactors successfully employed in industry are presented but by no means is this to be construed to be a comprehensive treatment. Due to space constraints, the editors had to make decisions concerning what was to be included in the chapter.

17.1. DESIGN BASIS AND SPACE VELOCITY

DESIGN BASIS

Although the intent of this chapter is not detailed design, it is in order to state what is included in a proper design basis, for example at least these items:

1. Stoichiometry of the participating reactions.
2. Thermal and other physical properties.
3. Heats of reaction and equilibrium data.
4. Rate of reaction, preferably in equation form, relating it to composition, temperature, pressure, impurities, catalysts and so on. Alternately tabular or graphical data relating compositions to time and the other variables listed.
5. Activity of the catalyst as a function of onstream time.
6. Mode of catalyst reactivation or replacement.
7. Stability and controllability of the process.
8. Special considerations of heat and mass transfer.
9. Corrosion and safety hazards.

REACTION TIMES

In practical cases reaction times vary from fractions of a second to many hours. The compilation of Table 17.1 of some commercial practices may be a basis for choosing by analogy an order of magnitude of reactor sizes for other processes.

For ease of evaluation and comparison, an apparent residence time often is used instead of the true one; it is defined as the ratio of the reactor volume to the inlet volumetric flow rate,

$$\bar{t}_{\mathrm{app}} = V_r/V_o'$$

On the other hand, the true residence time must be found by integration,

$$\bar{t} = \int dV_r/V' = \int dn'/rV'.$$

Since the rate of reaction r and the volumetric flow rate V' at each position depend on T, P, and local molal flow rate n' of the key component of the reacting mixture, finding the true residence time is an involved process requiring many data. The easily evaluated apparent residence time usually is taken as adequate for rating sizes of reactors and for making comparisons.

A related concept is that of space velocity which is the ratio of a flow rate at STP ($60°F$, 1 atm usually) to the size of the reactor. The most common versions of space velocities in typical units are:

GHSV (gas hourly space velocity) = (volumes of feed as gas at STP/hr)/(volume of the reactor or its content of catalyst) = (SCFH gas feed)/cuft.

LHSV (liquid hourly space velocity) = (Volume of liquid feed at $60°F$/hr)/volume of reactor or catalyst) = (SCFH liquid feed)/cuft.

WHSV (weight hourly space velocity) = (lb of feed/hr)/(lb of catalyst). Other combinations of units of the flow rate and reactor size often are used in practice, for instance.

BPSD/lb = (barrels of liquid feed at $60°F$ per stream day)/(lb catalyst), but it is advisable to write out such units in each case to avoid confusion with the standard meanings of the given acronyms. Since the apparent residence time is defined in terms of the actual inlet conditions rather than at standard T and P, it is not the reciprocal of GHSV or LHSV, although the units are the same.

17.2. RATE EQUATIONS AND OPERATING MODES

The equations of this section are summarized and extended in Table 17.2. The term ''rate of reaction'' used here is the rate of decomposition per unit volume,

$$r_a = -\frac{1}{V}\frac{dn_a}{dt}, \text{ mol/(unit time)(unit volume).} \quad (17.1)$$

A rate of formation will have the opposite sign. When the volume is constant, the rate is the derivative of the concentration

$$r_a = -\frac{dC_a}{dt}, \text{ at constant volume.} \quad (17.2)$$

In homogeneous environments the rate is expressed by the law of mass action in terms of powers of the concentrations of the reacting substances

$$r_a = -\frac{1}{V}\frac{dn_a}{dt} = kC_a^\alpha C_b^\beta \cdots. \quad (17.3)$$

When the reaction mechanism truly follows the stoichiometric equation

TABLE 17.1. Residence Times and/or Space Velocities in Industrial Chemical Reactors

Product (raw materials)	Type	Reactor phase	Catalyst	Conditions T,°C	P, atm	Residence time or space velocity	Source and page
1. Acetaldehyde (ethylene, air)	FB	L	Cu and Pd chlorides	50–100	8	6–40 min	[2] 1, [7] 3
2. Acetic anhydride (acetic acid)	TO	L	Triethyl phosphate	700–800	0.3	0.25–5 s	[2]
3. Acetone (i-propanol)	MT	LG	Ni	300	1	2.5 h	[1] 1 314
4. Acrolein (formaldehyde, acetaldehyde)	FL	G	MnO, silica gel	280–320	1	0.6 s	[1] 1 384, [7] 33
5. Acrylonitrile (air, propylene, ammonia)	FL	G	Bi phosphomolybdate	400	1	4.3 s	[3] 684, [2] 47
6. Adipic acid (nitration of cyclohexanol)	TO	L	Co naphthenate	125–160	4–20	2 h	[2] 51, [7] 49
7. Adiponitrile (adipic acid)	FB	G	H_3BO_3 H_3PO_4	370–410	1	3.5–5 s 350–500 GHSV	[1] 2 152 [7] 52
8. Alkylate (i-C_4, butenes)	CST	L	H_2SO_4	5–10	2–3	5–40 min	[4] 223
9. Alkylate (i-C_4, butenes)	CST	L	HF	25–38	8–11	5–25 min	[4] 223
10. Allyl chloride (propylene, Cl_2)	TO	G	N.A.	500	3	0.3–1.5 s	[1] 2 416, [7] 67
11. Ammonia (H_2, N_2)	FB	G	Fe	450	150	28 s 7,800 GHSV	[6] 61
12. Ammonia (H_2, N_2)	FB	G	Fe	450	225	33 s 10,000 GHSV	[6] 61
13. Ammonia oxidation	Flame	G	Pt gauze	900	8	0.0026 s	[6] 115
14. Aniline (nitrobenzene, H_2)	B	L	$FeCl_2$ in H_2O	95–100	1	8 h	[1] 3 289
15. Aniline (nitrobenzene, H_2)	FB	G	Cu on silica	250–300	1	0.5–100 s	[7] 82
16. Aspirin (salicylic acid, acetic anhydride)	B	L	None	90	1	>1 h	[7] 89
17. Benzene (toluene)	TU	G	None	740	38	48 s 815 GHSV	[6] 36, [9] 109
18. Benzene (toluene)	TU	G	None	650	35	128 s	[1] 4 183, [7] 98
19. Benzoic acid (toluene, air)	SCST	LG	None	125–175	9–13	0.2–2 h	[7] 101
20. Butadiene (butane)	FB	G	Cr_2O_3, Al_2O_3	750	1	0.1–1 s	[7] 118
21. Butadiene (1-butene)	FB	G	None	600	0.25	0.001 s 34,000 GHSV	[3] 572
22. Butadiene sulfone (butadiene, SO_2)	CST	L	t-butyl catechol	34	12	0.2 LHSV	[1] 5 192
23. i-Butane (n-butane)	FB	L	$AlCl_3$ on bauxite	40–120	18–36	0.5–1 LHSV	[4] 239, [7] 683
24. i-Butane (n-butane)	FB	L	Ni	370–500	20–50	1–6 WHSV	[4] 239
25. Butanols (propylene hydroformylation)	FB	L	PH_3-modified Co carbonyls	150–200	1,000	100 g/L-h	[1] 5 373
26. Butanols (propylene hydroformylation)	FB	L	Fe pentacarbonyl	110	10	1 h	[7] 125
27. Calcium stearate	B	L	None	180	5	1–2 h	[7] 135
28. Caprolactam (cyclohexane oxime)	CST	L	Polyphosphoric acid	80–110	1	0.25–2 h	[1] 6 73, [7] 139
29. Carbon disulfide (methane, sulfur)	Furn.	G	None	500–700	1	1.0 s	[1] 6 322, [7] 144
30. Carbon monoxide oxidation (shift)	TU	G	Cu-Zn or Fe_2O_3	390–220	26	4.5 s 7,000 GHSV	[6] 44
30′. Port. cement	Kiln	S		1400–1700	1	10 h	[11]
31. Chloral (Cl_2, acetaldehyde)	CST	LG	None	20–90	1	140 h	[7] 158
32. Chlorobenzenes (benzene, Cl_2)	SCST	LG	Fe	40	1	24 h	[1] 8 122
33. Coking, delayed (heater)	TU	LG	None	490–500	15–4	250 s	[1] 10 8
34. Coking, delayed (drum, 100 ft max.)	B	LG	None	500–440	4	0.3–0.5 ft/s vapor	[1] 10 8
35. Cracking, fluid-catalytic	FL	G	SiO_2, Al_2O_3	470–540	2–3	0.5–3 WHSV	[4] 162
36. Cracking, hydro-(gas oils)	FB	LG	Ni, SiO_2, Al_2O_3	350–420	100–150	1–2 LHSV	[11]
37. Cracking (visbreaking residual oils)	TU	LG	None	470–495	10–30	450 s 8 LHSV	[11]
38. Cumene (benzene, propylene)	FB	G	H_3PO_4	260	35	23 LHSV	[11]

TABLE 17.1.—(*continued***)**

Product (raw materials)	Type	Reactor phase	Catalyst	Conditions T,°C	P, atm	Residence time or space velocity	Source and page
39. Cumene hydroperoxide (cumene, air)	CST	L	Metal porphyrins	95–120	2–15	1–3 h	[7] 191
40. Cyclohexane (benzene, H_2)	FB	G	Ni on Al_2O_3	150–250	25–55	0.75–2 LHSV	[7] 201
41. Cyclohexanol (cyclohexane, air)	SCST	LG	None	185–200	48	2–10 min	[7] 203
42. Cyclohexanone (cyclohexanol)	CST	L	N.A.	107	1	0.75 h	[8] (1963)
43. Cyclohexanone (cyclohexanol)	MT	G	Cu on pumice	250–350	1	4–12 s	[8] (1963)
44. Cyclopentadiene (dicyclopentadiene)	TU	G	None	220–300	1–2	0.1–0.5 LHSV	[7] 212
45. DDT (chloral, chlorobenzene)	B	L	Oleum	0–15	1	8 h	[7] 233
46. Dextrose (starch)	CST	L	H_2SO_4	165	1	20 min	[8] (1951)
47. Dextrose (starch)	CST	L	Enzyme	60	1	100 min	[7] 217
48. Dibutylphthalate (phthalic anhydride, butanol)	B	L	H_2SO_4	150–200	1	1–3 h	[7] 227
49. Diethylketone (ethylene, CO)	TO	L	Co oleate	150–300	200–500	0.1–10 h	[7] 243
50. Dimethylsulfide (methanol, CS_2)	FB	G	Al_2O_3	375–535	5	150 GHSV	[7] 266
51. Diphenyl (benzene)	MT	G	None	730	2	0.6 s 3.3 LHSV	[7] 275, [8] (1938)
52. Dodecylbenzene (benzene, propylene tetramer)	CST	L	$AlCl_3$	15–20	1	1–30 min	[7] 283
53. Ethanol (ethylene, H_2O)	FB	G	H_3PO_4	300	82	1,800 GHSV	[2] 356, [7] 297
54. Ethyl acetate (ethanol, acetic acid)	TU, CST	L	H_2SO_4	100	1	0.5–0.8 LHSV	[10] 45, 52, 58
55. Ethyl chloride (ethylene, HCl)	TO	G	$ZnCl_2$	150–250	6–20	2 s	[7] 305
56. Ethylene (ethane)	TU	G	None	860	2	1.03 s 1,880 GHSV	[3] 411, [6] 13
57. Ethylene (naphtha)	TU	G	None	550–750	2–7	0.5–3 s	[7] 254
58. Ethylene, propylene chlorohydrins (Cl_2, H_2O)	CST	LG	None	30–40	3–10	0.5–5 min	[7] 310, 580
59. Ethylene glycol (ethylene oxide, H_2O)	TO	LG	1% H_2SO_4	50–70	1	30 min	[2] 398
60. Ethylene glycol (ethylene oxide, H_2O)	TO	LG	None	195	13	1 h	[2] 398
61. Ethylene oxide (ethylene, air)	FL	G	Ag	270–290	1	1 s	[2] 409, [7] 322
62. Ethyl ether (ethanol)	FB	G	WO_3	120–375	2–100	30 min	[7] 326
63. Fatty alcohols (coconut oil)	B	L	Na, solvent	142	1	2 h	[8] (1953)
64. Formaldehyde (methanol, air)	FB	G	Ag gauze	450–600	1	0.01 s	[2] 423
65. Glycerol (allyl alcohol, H_2O_2)	CST	L	H_2WO_4	40–60	1	3 h	[7] 347
66. Hydrogen (methane, steam)	MT	G	Ni	790	13	5.4 s 3,000 GHSV	[6] 133
67. Hydrodesulfurization of naphtha	TO	LG	Co-Mo	315–500	20–70	1.5–8 LHSV 125 WHSV	[4] 285, [6] 179, [9] 201
68. Hydrogenation of cottonseed oil	SCST	LG	Ni	130	5	6 h	[6] 161
69. Isoprene (i-butene, formaldehyde)	FB	G	HCl, silica gel	250–350	1	1 h	[7] 389
70. Maleic anhydride (butenes, air)	FL	G	V_2O_5	300–450	2–10	0.1–5 s	[7] 406
71. Melamine (urea)	B	L	None	340–400	40–150	5–60 min	[7] 410
72. Methanol (CO, H_2)	FB	G	ZnO, Cr_2O_3	350–400	340	5,000 GHSV	[7] 421
73. Methanol (CO, H_2)	FB	G	ZnO, Cr_2O_3	350–400	254	28,000 GHSV	[3] 562
74. o-Methyl benzoic acid (xylene, air)	CST	L	None	160	14	0.32 h 3.1 LHSV	[3] 732
75. Methyl chloride (methanol, Cl_2)	FB	G	Al_2O_3 gel	340–350	1	275 GHSV	[2] 533
76. Methyl ethyl ketone (2-butanol)	FB	G	ZnO	425–475	2–4	0.5–10 min	[7] 437
77. Methyl ethyl ketone (2-butanol)	FB	G	Brass sphereś	450	5	2.1 s 13 LHSV	[10] 284
78. Nitrobenzene (benzene, HNO_3)	CST	L	H_2SO_4	45–95	1	3–40 min	[7] 468
79. Nitromethane (methane, HNO_3)	TO	G	None	450–700	5–40	0.07–0.35 s	[7] 474
80. Nylon-6 (caprolactam)	TU	L	Na	260	1	12 h	[7] 480
81. Phenol (cumene hydroperoxide)	CST	L	SO_2	45–65	2–3	15 min	[7] 520
82. Phenol (chlorobenzene, steam)	FB	G	Cu, Ca phosphate	430–450	1–2	2 WHSV	[7] 522
83. Phosgene (CO, Cl_2)	MT	G	Activated carbon	50	5–10	16 s 900 GHSV	[11]
84. Phthalic anhydride (o-xylene, air)	MT	G	V_2O_5	350	1	1.5 s	[3] 482, 539, [7] 529
85. Phthalic anhydride (naphthalene, air)	FL	G	V_2O_5	350	1	5 s	[9] 136, [10] 335

(continued)

TABLE 17.1.—(continued**)**

Product (raw materials)	Type	Reactor phase	Catalyst	T,°C	P, atm	Residence time or space velocity	Source and page
86. Polycarbonate resin (bisphenol-A, phosgene)	B	L	Benzyltri-ethylammonium chloride	30–40	1	0.25–4 h	[7] 452
87. Polyethylene	TU	L	Organic peroxides	180–200	1,000–1,700	0.5–50 min	[7] 547
88. Polyethylene	TU	L	Cr_2O_3, Al_2O_3, SiO_2	70–200	20–50	0.1–1,000 s	[7] 549
89. Polypropylene	TO	L	R_2AlCl, $TiCl_4$	15–65	10–20	15–100 min	[7] 559
90. Polyvinyl chloride	B	L	Organic peroxides	60	10	5.3–10 h	[6] 139
91. i-Propanol (propylene, H_2O)	TO	L	H_2SO_4	70–110	2–14	0.5–4 h	[7] 393
92. Propionitrile (propylene, NH_3)	TU	G	CoO	350–425	70–200	0.3–2 LHSV	[7] 578
93. Reforming of naphtha (H_2/hydrocarbon = 6)	FB	G	Pt	490	30–35	3 LHSV 8,000 GHSV	[6] 99
94. Starch (corn, H_2O)	B	L	SO_2	25–60	1	18–72 h	[7] 607
95. Styrene (ethylbenzene)	MT	G	Metal oxides	600–650	1	0.2 s 7,500 GHSV	[5] 424
96. Sulfur dioxide oxidation	FB	G	V_2O_5	475	1	2.4 s 700 GHSV	[6] 86
97. t-Butyl methacrylate (methacrylic acid, i-butane)	CST	L	H_2SO_4	25	3	0.3 LHSV	[1] 5 328
98. Thiophene (butane, S)	TU	G	None	600–700	1	0.01–1 s	[7] 652
99. Toluene diisocyanate (toluene diamine, phosgene)	B	LG	None	200–210	1	7 h	[7] 657
100. Toluene diamine (dinitrotoluene, H_2)	B	LG	Pd	80	6	10 h	[7] 656
101. Tricresyl phosphate (cresyl, $POCl_3$)	TO	L	$MgCl_2$	150–300	1	0.5–2.5 h	[2] 850, [7] 673
102. Vinyl chloride (ethylene, Cl_2)	FL	G	None	450–550	2–10	0.5–5 s	[7] 699

Abbreviations

Reactors: batch (B), continuous stirred tank (CST), fixed bed of catalyst (FB), fluidized bed of catalyst (FL), furnace (Furn.), multitubular (MT), semicontinuous stirred tank (SCST), tower (TO), tubular (TU).

Phases: liquid (L), gas (G), both (LG).

Space velocities (hourly): gas (GHSV), liquid (LHSV), weight (WHSV).

Not available (N.A.)

REFERENCES

1. J.J. McKetta (Ed.), *Encyclopedia of Chemical Processing and Design*, Marcel Dekker, New York, 1976 to date (referenced by volume).
2. W.L. Faith, D.B. Keyes, and R.L. Clark, *Industrial Chemicals*, revised by F.A. Lowenstein and M.K. Moran, Wiley, New York, 1975.
3. G.F. Froment and K.B. Bischoff, *Chemical Reactor Analysis and Design*, Wiley, New York, 1979.
4. R.J. Hengstebeck, *Petroleum Processing*, McGraw-Hill, New York, 1959.
5. V.G. Jenson and G.V. Jeffreys, *Mathematical Methods in Chemical Engineering*, 2nd ed., Academic Press, New York, 1977.
6. H.F. Rase, *Chemical Reactor Design for Process Plants: Vol. 2, Case Studies*, Wiley, New York, 1977.
7. M. Sittig, *Organic Chemical Process Encyclopedia*, Noyes, Park Ridge, N.J., 1969 (patent literature exclusively).
8. Student Contest Problems, published annually by AIChE, New York (referenced by year).
9. M.O. Tarhan, *Catalytic Reactor Design*, McGraw-Hill, New York, 1983.
10. K.R. Westerterp, W.P.M. van Swaaij, and A.A.C.M. Beenackers, *Chemical Reactor Design and Operation*, Wiley, New York, 1984.
11. Personal communication (Walas, 1985).

$$v_a A + v_b B + \cdots \rightarrow \text{products},\qquad(17.4)$$

the exponents are the stoichiometric coefficients; thus,

$$r_a = k(C_a)v_a(C_b)v_b \cdots,\qquad(17.5)$$

but α, β, ... often are purely empirical values—integral or noninte-gral, sometimes even negative.

The coefficient k is called the specific rate coefficient. It is taken to be independent of the concentrations of the reactants but does depend primarily on temperature and the nature and concen-tration of catalysts. Temperature dependence usually is represented by

$$k = k_\infty \exp(-E/RT) = \exp(a' - b'/T),\qquad(17.6)$$

where E is the energy of activation.

Specific rates of reactions of practical interest cannot be found by theoretical methods of calculation nor from correlations in terms of the properties of the reactants. They must be found empirically in every case together with the complete dependence of the rate of reaction on concentrations, temperature, and other pertinent factors. The analysis of experimental data will be ignored here since the emphasis is placed on the use of known rate equa-tions.

Integration of the rate equation is performed to relate the composition to the reaction time and the size of the equipment. From a rate equation such as

$$-\frac{dC_a}{dt} = kC_a^\alpha C_b^\beta C_c^\gamma,\qquad(17.7)$$

TABLE 17.2. Basic Rate Equations

1. The reference reaction is

$$v_a A + v_b B + \cdots \rightarrow v_r R + v_s S + \cdots$$

$$\Delta v = v_r + v_s + \cdots - (v_a + v_b + \cdots)$$
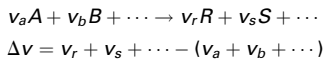
2. Stoichiometric balance for any component i,

$$n_i = n_{i0} \pm (v_i/v_a)(n_{a0} - n_a)$$

$$\begin{cases} + & \text{for product (right-hand side, RHS)} \\ - & \text{for reactant (left-hand side, LHS)} \end{cases}$$

$$C_i = C_{i0} \pm (v_i/v_a)(C_{a0} - C_a), \text{ at constant } T \text{ and } V \text{ only}$$

$$n_t = n_{t0} + (\Delta v/v_a)(n_{a0} - n_a)$$

3. Law of mass action

$$r_a = -\frac{1}{V_r}\frac{dn_a}{dt} = kC_a^{v_a}C_b^{v_b}\cdots$$

$$= kC_a^{v_a}[C_{b0} - (v_b/v_a)(C_{a0} - C_a)]^{v_b}\cdots$$

$$r_a = kC_a^{\alpha}[C_{b0} - (v_b/v_a)(C_{a0} - C_a)]^{\beta}\cdots$$

where it is not necessarily true that $\alpha = v_{a'}$ $\beta = v_{b'}\cdots$

4. At constant volume, $C_a = n_a/V_r$

$$kt = \int_{C_a}^{C_{a0}} \frac{1}{C_a^{\alpha}[C_{b0} - (v_b/v_a)(C_{a0} - C_a)]^{\beta}\cdots} dC_a$$

$$kt = \int_{n_a}^{n_{a0}} \frac{V_{\cdots}^{-1+\alpha+\beta}}{n_a^{\alpha}[n_{b0} + (v_b/v_a)(n_{a0} - n_a)]^{\beta}\cdots} dn_a$$

Completed integrals for some values of α and β are in Table 17.3

5. Ideal gases at constant pressure:

$$V_r = \frac{n_t RT}{P} = \frac{RT}{P}\left[n_{t0} + \frac{\Delta v}{v_a}(n_{a0} - n_a)\right]$$

$$r_a = kC_a^{\alpha}$$

$$kt = \left(\frac{RT}{P}\right)^{\alpha-1}\int_{n_a}^{n_{a0}} \frac{[n_{t0} + (\Delta v/v_a)(n_{a0} - n_a)]^{\alpha-1}}{n_a^{\alpha}} dn_a$$

6. Temperature effect on the specific rate:

$$k = k_{\infty}\exp(-E/RT) = \exp(a' - b'/T)$$

$$E = \text{energy of activation}$$

7. Simultaneous reactions: The overall rate is the algebraic sum of the rates of the individual reactions. For example, take the three reactions:

1. $A + B \overset{k_1}{=} C + D.$
2. $C + D \overset{k_2}{=} A + B.$
3. $A + C \overset{k_3}{=} E.$

The rates are related by:

$$r_a = r_{a1} + r_{a2} + r_{a3} = k_1 C_a C_b - k_2 C_c C_d + k_3 C_a C_c$$

$$r_b = -r_d = k_1 C_a C_b - k_2 C_c C_d$$

$$r_c = -k_1 C_a C_b + k_2 C_c C_d + k_3 C_a C_c$$

$$r_e = -k_3 C_a C_c$$

The number of independent rate equations is the same as the number of independent stoichiometric relations. In the present example, reactions 1 and 2 are a reversible reaction and are not independent. Accordingly, C_c and C_d, for example, can be eliminated from the equations for r_a and r_b which then become an

integrable system. Usually only systems of linear differential equations with constant coefficients are solvable analytically. Many such cases are treated by Rodiguin and Rodiguina, 1964.

8. Mass transfer resistance:

$$C_{ai} = \text{interfacial concentration of reactant A}$$

$$r_a = -\frac{dC_a}{dt} = k_d(C_a - C_{ai}) = kC_{ai}^{\alpha} = k\left(C_a - \frac{r_a}{k_d}\right)^{\alpha}$$

$$kt = \int_{C_a}^{C_{a0}} \frac{1}{(C_a - r_a/k_d)^{\alpha}} dC_a$$

The relation between r_a and C_a must be established (numerically if need be) from the second line before the integration can be completed

9. Solid-catalyzed reactions, some Langmuir-Hinshelwood mechanisms for the reference reaction $A + B \rightarrow R + S$.

1. Adsorption rate of A controlling

$$r_a = -\frac{1}{V}\frac{dn_a}{dt} = kP_a\theta_v$$

$$\theta_v = 1/\left[1 + \frac{K_a}{K_e}\frac{P_r P_s}{P_b} + K_b P_b + K_r P_r + K_s P_s + K_I P_I\right]$$

$$K_e = P_r P_s/P_a P_b \text{ (equilibrium constant)}$$

/ is an adsorbed substance that is chemically inert

2. Surface reaction rate controlling:

$$r = kP_a P_b\theta_v^2$$

$$\theta_v = 1/\left(1 + \sum K_j P_j\right),$$

summation over all substances absorbed

3. Reaction $A_2 + B \rightarrow R + S$, with A_2 dissociated upon adsorption and with surface reaction rate controlling:

$$r_a = kP_a P_b\theta_v^3$$

$$\theta_v = 1/(1 + \sqrt{K_a P_a} + K_b P_b + \cdots)$$

4. At constant P and T the P_i are eliminated in favor of n_i and the total pressure by

$$P_a = \frac{n_a}{n_t}P$$

$$P_i = \frac{n_i}{n_t}P = \frac{n_{i0} \pm (v_i/v_a)(n_{a0} - n_a)}{n_{t0} + (\Delta v/v_a)(n_{a0} - n_a)}P$$

$$\begin{cases} + & \text{for products, RHS} \\ - & \text{for reactants, LHS} \end{cases}$$

$$V = \frac{n_t RT}{P}$$

$$kt = \int_{n_a}^{n_{a0}} \frac{1}{VP_a P_b\theta_v^2}, \text{ for a case (2) batch reaction}$$
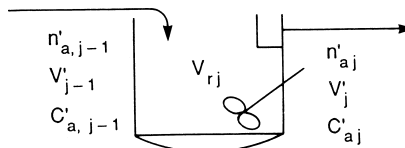
TABLE 17.2.—(*continued*)

10. A continuous stirred tank reactor battery (CSTR)
Material balances:

$$n'_{a0} = n'_a + r_{a1} V_{r1}$$

$$\vdots$$

$$n'_{a,j-1} = n'_{aj} + r_{aj} V_{rj}, \text{ for the } j\text{th stage}$$

For a first order reaction, with $r_a = kC_{a'}$

$$\frac{C_{aj}}{C_{a0}} = \frac{1}{(1 + k_1 \bar{t}_1)(1 + k_2 \bar{t}_2) \cdots (1 + k_j \bar{t}_j)} = \frac{1}{(1 + k\bar{t}_i)^j},$$

for *j* tanks in series with the same temperatures and residence times $\bar{t}_i = V_{ri}/V'_i$, where V' is the volumetric flow rate

11. Plug flow reactor (PFR):

$$r_a = -\frac{dn'_a}{dV_r} = kC_a^\alpha C_b^\beta \cdots$$
$$= k(n'_a/V')^\alpha (n'_b/V')^\beta \cdots$$
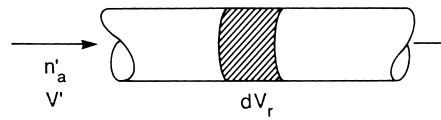
12. Material and energy balances for batch, CSTR and PFR are in Tables 17.4, 17.5, and 17.6
13. Notation

A, B, R, S are participants in the reaction; the letters also are used to represent concentrations

$C_i = n_i/V_r$ or n'_i/V', concentration
n_i = mols of component *i* in the reactor
n'_i = molal flow rate of component *i*
V_r = volume of reactor
V' = volumetric flow rate
ν_i = stoichiometric coefficient
r_i = rate of reaction of substance *i* [mol/(unit time)(unit volume)]
α, β = empirical exponents in a rate equation

the concentrations C_b and C_c first must be eliminated with the aid of the stoichiometric equation of the process. Item 4 of Table 17.2 is an example. When several reactions occur simultaneously, the overall rate of a particular participant is the algebraic sum of its rates in individual reactions. Item 7 of Table 17.2 is an example. The number of differential equations representing the reacting system is the same as the number of independent stoichiometric equations; appropriate concentrations are eliminated with stoichiometry to develop an integrable set of equations. Integrals of common isothermal, constant volume rate equations are summarized in Table 17.3, and a simple case of a process at constant pressure is item 5 of Table 17.3.

An overall conversion rate may depend on rates of mass transfer between phases as well as chemical rates. In the simplest case, mass transfer and chemical transformation occur in series; advantage is taken of the equality of these two rates at steady state conditions to eliminate interfacial concentrations from the rate equations and thus to permit integration. Item 8 of Table 17.2 is an example.

Rates of fluid phase reactions catalyzed by solids also can be represented at least approximately by powers of the concentrations. A more fundamental approach, however, takes into account mechanisms of adsorption and of reaction on the catalyst surface. A few examples of resulting equations are in item 9 of Table 17.2.

Practical solid-catalyzed rate processes also may be influenced by rates of diffusion to the external and internal surfaces. In the latter case the rate equation is modified by inclusion of a catalyst effectiveness to become

$$r_a = k\eta f(C_a). \tag{17.8}$$

The effectiveness, η, is a measure of the utilization of the internal surface of the catalyst and C_a is the concentration of the reactant, *a*, at the external catalyst surface. It depends on the dimensions of the catalyst particle and its pores, on the diffusivity, specific rate, and heat of reaction. With a given kind of catalyst, the only control is particle size to which the effectiveness is proportional; a compromise must be made between effectiveness and pressure drop. In simple cases η can be related mathematically to its parameters, but in such important practical cases as ammonia synthesis its dependence on parameters is complex and strictly empirical. Section 17.5 deals with this topic.

Reaction processes may be conducted under nonflow or steady flow conditions. One mode of the latter is tubular flow or, in the limiting case, plug flow, in which all molecules have substantially the same residence time. The rate equation for a plug flow reactor (PFR) is

$$r_a = -\frac{dn'_a}{dV_r} = kC_a^\alpha C_b^\beta \cdots = k\left(\frac{n'_a}{V'}\right)^\alpha \left(\frac{n'_b}{V'}\right)^\beta \cdots, \tag{17.9}$$

where V_r is the reactor volume and the primes (′) designate flow rates. Flow reactions of gases take place at substantially constant pressure so that V' will depend on the extent of conversion if there is a change in the number of mols. Item 11 of Table 17.2 is an example of the rate equation for such conditions.

The other mode of flow reaction employs one or more stirred tanks in series, which is called a continuous stirred tank (CSTR) battery. The rate of reaction in a single tank is

$$r_a = \frac{n'_{a0} - n'_a}{V_r} \simeq \frac{C_{a0} - C_a}{V_r/V'} = \frac{C_{a0} - C_a}{\bar{t}} = kC_a^\alpha C_b^\beta \cdots. \tag{17.10}$$

The relation in terms of concentrations is valid if the volumetric rates into and out of the tank are substantially the same. Stirring is assumed sufficient to maintain uniform composition and temperature in the tank; then the effluent conditions are the same as those of the tank. Relations for several tanks in series are in item 10 of Table 17.2.

17.3. MATERIAL AND ENERGY BALANCES OF REACTIONS

All chemical reactions are accompanied by some heat effects so that the temperature will tend to change, a serious result in view of the sensitivity of most reaction rates to temperature. Factors of equipment size, controllability, and possibly unfavorable product distribution of complex reactions often necessitate provision of means of heat transfer to keep the temperature within bounds. In practical operation of nonflow or tubular flow reactors, truly isothermal conditions are not feasible even if they were desirable. Individual continuous stirred tanks, however, do maintain substantially

TABLE 17.3. Some Isothermal Rate Equations and Their Integrals

1. $A \rightarrow$ products:

$$-\frac{dA}{dt} = kA$$

$$\frac{A}{A_0} = \begin{cases} \exp[-k(t-t_0)], & \alpha = 1 \\ \left[\frac{1}{1+kA_0^{\alpha-1}(t-t_0)}\right]^{1/(\alpha-1)}, & \alpha \neq 1 \end{cases}$$

2. $A + B \rightarrow$ products:

$$-\frac{dA}{dt} = kAB = kA(A + B_0 - A_0)$$

$$k(t-t_0) = \frac{1}{B_0 - A_0} \ln \frac{A_0(A + B_0 - A_0)}{AB_0}$$

3. Reversible reaction $A \underset{k_3}{\overset{k_1}{\rightleftharpoons}} B$:

$$-\frac{dA}{dt} = k_1 A - k_2(A_0 + B_0 - A) = (k_1 + k_2)A - k_2(A_0 + B_0)$$

$$(k_1 + k_2)(t - t_0) = \ln \frac{k_1 A_0 - k_2 B_0}{(k_1 + k_2)A - k_2(A_0 + B_0)}$$

4. Reversible reaction, second order, $A + B \underset{k_3}{\overset{k_1}{\rightleftharpoons}} R + S$

$$-\frac{dA}{dt} = k_1 AB - k_2 RS = k_1 A(A + B_0 - A_0)$$

$$- k_2(A_0 + R_0 - A)(A_0 + S_0 - A)$$

$$= \alpha A^2 + \beta A - \gamma$$

$$\alpha = k_1 - k_2$$

$$\beta = k_1(B_0 - A_0) + k_2(2A_0 + R_0 + S_0)$$

$$\gamma = k_2(A_0 + R_0)(A_0 + S_0)$$

$$q = \sqrt{\beta^2 + 4\alpha\gamma}$$

$$k(t - t_0) = \begin{cases} \frac{2\alpha A_0 + \beta}{2\alpha A + \beta}, & q = 0 \\ \frac{1}{q} \ln\left[\left(\frac{2\alpha A_0 + \beta - q}{2\alpha A_0 + \beta + q}\right)\left(\frac{2\alpha A + \beta + q}{2\alpha A + \beta - q}\right)\right], & q \neq 0 \end{cases}$$

5. The reaction $v_a A + v_b B \rightarrow v_r R + v_s S$ between ideal gases at constant T and P

$$-\frac{dn_a}{dt} = \frac{kn_a^\alpha}{V^{\alpha-1}}$$

$$V = n_t \frac{RT}{P} = \left[n_{t0} + \frac{\Delta v}{v_a}(n_{a0} - n_a)\right] \frac{RT}{P}$$

$$k(t - t_0) = \begin{cases} \int_{n_a}^{n_{a0}} \frac{V^{\alpha-1}}{n_a^\alpha} dn_a, & \text{in general} \\ \frac{RT}{P}\left[n_{b0} + \frac{\Delta v}{v_a}\left(\frac{1}{n_a} - \frac{1}{n_{a0}}\right) - \frac{\Delta v}{v_a} \ln\left(\frac{n_{a0}}{n_a}\right)\right], & \text{when } \alpha = 2 \end{cases}$$

6. Equations readily solvable by Laplace transforms. For example:

$$A \underset{k_3}{\overset{k_1}{\rightleftharpoons}} B \overset{k_2}{\rightarrow} C$$
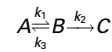
Rate equations are

$$-\frac{dA}{dt} = k_1 A - k_2 B$$

$$-\frac{dB}{dt} = -k_1 A + (k_2 + k_3)B$$

$$-\frac{dC}{dt} = -k_2 B$$

Laplace transformations are made and rearranged to

$$(s + k_1)\bar{A} + k_3\bar{B} = A_0$$

$$- k_1\bar{A} + (s + k_2 + k_3)\bar{B} = B_0$$

$$- k_2\bar{B} + s\bar{C} = C_0$$

These linear equations are solved for the transforms as

$$D = s^2 + (k_1 + k_2 + k_3)s + k_1 k_2$$

$$\bar{A} = [A_0 s + (k_2 + k_3)A_0 + k_3 B_0]/D$$

$$\bar{B} = [B_0 s + k_1(A_0 + B_0)]/D$$

$$\bar{C} = (k_2\bar{B} + C_0)/s$$

Inversion of the transforms can be made to find the concentrations A, B, and C as functions of the time t. Many such examples are solved by Rodiguin and Rodiguina, 1964).

---

uniform temperatures at steady state when the mixing is intense enough; the level is determined by the heat of reaction as well as the rate of heat transfer provided.

In many instances the heat transfer aspect of a reactor is paramount. Many different modes have been and are being employed, a few of which are illustrated in Section 17.6. The design of such equipment is based on material and energy balances that incorporate rates and heats of reaction together with heat transfer coefficients. Solution of these balances relates the time, composition, temperature, and rate of heat transfer. Such balances are presented in Tables 17.4–17.7 for four processes:

1. Nonflow reactors.
2. Continuous stirred tanks.
3. Plug flow reactors.
4. Flow reactor packed with solid catalyst.

The data needed are the rate equation, energy of activation, heat of reaction, densities, heat capacities, thermal conductivity, diffusivity, heat transfer coefficients, and usually the stoichiometry of the process. Simplified numerical examples are given for some of these cases. Item 4 requires the solution of a system of partial differential equations that cannot be made understandable in concise form, but some suggestions as to the procedure are made.

17.4. NONIDEAL FLOW PATTERNS

The CSTR with complete mixing and the PFR with no axial mixing are limiting behaviors that can be only approached in practice. Residence time distributions in real reactors can be found with tracer tests.

RESIDENCE TIME DISTRIBUTION

In the most useful form the test consists of a momentary injection of a known amount of inert tracer at the inlet of the operating vessel and monitoring of its concentration at the outlet. The data are used most conveniently in reduced form, as $E = C/\bar{C}_0$ in terms of $t_r = t/\bar{t}$, where

C = concentration of tracer at the outlet,
$\bar{C}_0$ = initial average concentration of tracer in the vessel,
$\bar{t} = V_r/V'$ = average residence time.

The plotted data usually are somewhat skewed bell-shapes. Some actual data are shown in Figure 17.1 together with lines for ideal CSTR and PFR. Such shapes often are represented

TABLE 17.4. Material and Energy Balances of a Nonflow Reaction

Rate equations:

$$r_a = -\frac{1}{V_r}\frac{dn_a}{d\theta} = kC_a^\alpha = k\left(\frac{n_a}{V_r}\right)^\alpha \tag{1}$$

$$k = \exp\left(a' - b'/T\right) \tag{2}$$

Heat of reaction:

$$\Delta H_r = \Delta H_{r298} + \int_{298}^{T}\Delta C_p\,dT \tag{3}$$

Rate of heat transfer:

$$Q' = UA(T_s - T) \tag{4}$$

(the simplest case is when UA and T_s are constant)
Enthalpy balance:

$$\frac{dT}{dn_a} = \frac{1}{\rho V_r \bar{C}_p}\left[\Delta H_r + \frac{UA(T_s - T)}{V_r k(n_a/V_r)}\right] \tag{5}$$

$$\frac{dT}{dC_a} = \frac{1}{\rho \bar{C}_p}\left[\Delta H_r + \frac{UA(T_s - T)}{V_r k C_a}\right] \tag{6}$$

$$T = T_0 \text{ when } C_a = C_{a0} \tag{7}$$

$$\bar{C}_p = \frac{1}{\rho V_r}\sum n_i C_{pi} \tag{8}$$

Solve Eq. (6) to find $T = f(C_a)$; combine Eqs. (1) and (2) and integrate as

$$\theta = \int_{C_a}^{C_{a0}} \frac{1}{C_a^\alpha \exp\left[a' - b'/f(C_a)\right]}\,dC_a \tag{9}$$

Temperature and time as a function of composition are shown for two values of UA/V_r for a particular case represented by

$$\frac{dT}{dC_a} = \frac{1}{50}\left[5000 + 5T + \frac{UA(300 - T)}{V_r k C_a^2}\right]$$

$$k = \exp\left(16 - 5000/T\right)$$

$$T_0 = 350$$

$$C_{a0} = 1$$
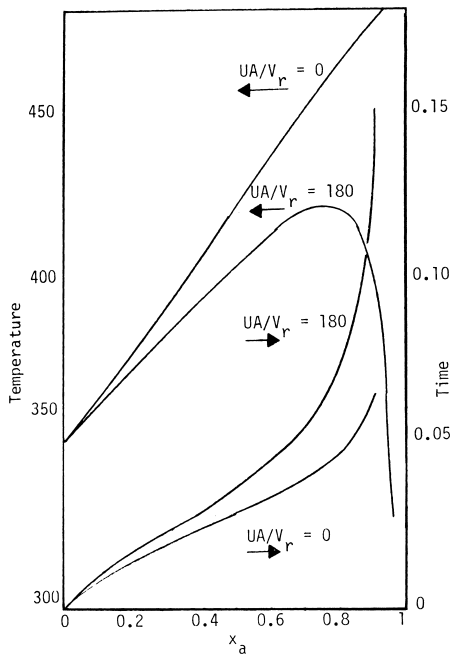
TABLE 17.5. Material and Energy Balance of a CSTR

The sketch identifies the nomenclature
Mean residence time:

$$\bar{t} = V_r/V' \tag{1}$$

Temperature dependence:

$$k = \exp\left(a' - b'/T\right) \tag{2}$$

Rate equation:

$$r_a = kC_a^\alpha = kC_{a0}^\alpha(1 - x)^\alpha, \quad x = (C_{a0} - C_a)/C_{a0} \tag{3}$$

Material balance:

$$C_{a0} = C_a + k\bar{t}C_a \tag{4}$$

$$x = k\bar{t}C_{a0}^{\alpha-1}(1 - x)^\alpha \tag{5}$$
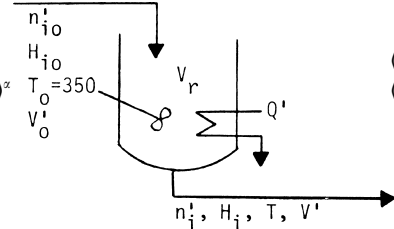
Enthalpy balance:

$$\sum n_i' H_i - \sum n_{i0}' H_{i0} = Q' - \Delta H_r(n_{a0}' - n_a') \tag{6}$$

$$H_i = \int_{298}^{T} C_{pi}\,dT \tag{7}$$

$$\Delta H_r = \Delta H_{r298} + \int_{298}^{T}\Delta C_p\,dT \tag{8}$$

For the reaction $aA + bB \rightarrow rR + sS$,

$$\Delta C_p = rC_{pr} + sC_{ps} - aC_{pa} - bC_{pb} \tag{9}$$

When the heat capacities are equal and constant, the heat balance is

$$\bar{C}_p \rho V'(T - T_0) = Q' - \Delta H_{r298}V'(C_{a0} - C_a) \tag{10}$$

Example:

$$k = \exp\left(16 - 5500/T\right)$$
$$C_{a0} = 5\,\text{g mol/L}$$
$$V' = 2000\,\text{L/hr}$$
$$\Delta H_r = -5\,\text{kcal/g mol}$$
$$\rho C_p = 0.9\,\text{kcal/(L)(K)}$$
$$\alpha = 2$$
$$T_0 = 350$$

$\bar{t}$	x = 0.90		x = 0.95	
	T	Q'	T	Q'
1	419.5	80	471.3	171
2	398.5	42	444.9	123
3	387.1	22	430.8	98
4	379.4	8	421.3	81
5	373.7	−2	414.2	68
6	369.1	−11	408.6	58
7	365.3	−17	404.0	50
8	362.1	−23	400.0	43
9	359.3	−28	396.6	36
10	356.9	−33	393.6	31

Eqs. (2) and (5) combine to

$$T = \frac{5500}{16 - \ln\left[x/5\bar{t}(1 - x)^2\right]}$$

and Eq. (10) becomes

$$Q' = 2[0.9(T - 350) - 25x], \text{ Mcal/hr}$$

The temperature and the rate of heat input Q' are tabulated as functions of the residence time for conversions of 90 and 95%

TABLE 17.6. Material and Energy Balances of a Plug Flow Reactor (PFR)

The balances are made over a differential volume dV_r of the reactor
Rate equation:

$$dV_r = \frac{-dn'_a}{r_a} \tag{1}$$

$$= -\frac{1}{k}\left(\frac{V'}{n'_a}\right)^{\alpha} dn'_a \tag{2}$$

$$= -\exp\left(\frac{-a'+b'}{T}\right)\left(\frac{n'_t RT}{Pn'_a}\right)^{\alpha} dn'_a \tag{3}$$

Enthalpy balance:

$$\Delta H_r = \Delta H_{r298} + \int_{298}^{T} \Delta C_p \, dT \tag{4}$$

$$dQ = U(T_s - T)\, dA_p = \frac{4U}{D}(T_s - T)\, dV_r$$
$$= -\frac{4U(T_s - T)}{Dr_a}\, dn'_a \tag{5}$$

$$dQ + \Delta H_r dn'_a = \sum n_i dH_i = \sum n_i C_{pi} dT \tag{6}$$

$$\frac{dT}{dn'_a} = \frac{\Delta H_r - 4U(T_s - T)/Dr_a}{\sum n_i c_{pi}} = f(T, T_s, n'_a) \tag{7}$$
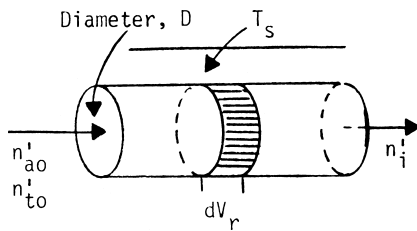
At constant T_s, Eq. (7) may be integrated numerically to yield the temperature as a function of the number of mols

$$T = \phi(n'_a) \tag{8}$$

Then the reactor volume is found by integration

$$V_r = \int_{n'_a}^{n'_{a0}} \frac{1}{\exp\left[a' - b'/\phi(n'_a)\right][Pn'_a/n'_t R\phi(n'_a)]^{\alpha}} \, dn'_a \tag{9}$$

Adiabatic process:

$$dQ = 0 \tag{10}$$
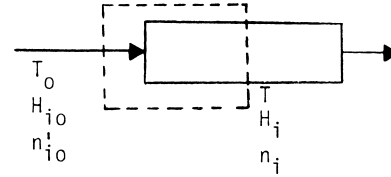
The balance around one end of the reactor is

$$\sum n_{i0} H_{i0} - \sum H_{r0}(n'_{a0} - n'_a) = \sum n_i H_i = \sum n_i \int C_{pi} dT \tag{11}$$

With reference temperature at T_0, enthalpies $H_{i0} = 0$

$$\Delta H_{r0} = \Delta H_{r298} + \int_{298}^{T_0} \Delta C_p dT \tag{12}$$

Substituting Eq. (12) into Eq. (10)

$$\left[-\Delta H_{r298} + \int_{298}^{T_0} \Delta C_p dT\right](n'_{a0} - n'_a) = \sum n_i \int_{T_0}^{T} C_{pi} dT \tag{13}$$

Adiabatic process with $\Delta C_p = 0$ and with constant heat capacities

$$T = T_0 - \frac{\Delta H_{r298}(n'_{a0} - n'_a)}{\sum n_i C_{pi}} \tag{14}$$

This expression is substituted instead of Eq. (8) to find the volume with Eq. (9)

---

approximately by the Erlang statistical distribution which also is the result for an n-stage stirred tank battery,

$$E(t_r) = \frac{C}{C_0} = \frac{n^n t_r^{n-1}}{(n-1)!} \exp(-nt_r), \tag{17.11}$$

where n is the characterizing parameter; when n is not integral, $(n-1)!$ is replaced by the gamma function $\Gamma(n)$. C_0 is the initial average concentration. The variance,

$$\sigma^2 = \int_0^{\infty} E(t_r - 1)^2 \, dt_r = 1/n \tag{17.12}$$

of this distribution is a convenient single parameter characterization of the spread of residence times. This quantity also is related to the Peclet number, $\text{Pe} = uL/D_e$, by

$$\sigma^2 = 2/\text{Pe} - [1 - \exp(-\text{Pe})]/\text{Pe}^2, \tag{17.13}$$

where
u = linear velocity in the axial direction,
L = distance in the axial direction,

D_e = axial eddy diffusivity or dispersion coefficient.

At large values of Pe, the ratio Pe/n approaches 2.
The superficial Peclet number in packed beds,

$$\text{Pe} = u_0 d_p / D_e$$

is very roughly correlated (Wen and Fan, 1975) in terms of the dimensionless groups $\text{Re} = u_0 d_p \rho / \mu$ and $\text{Sc} = \mu/\rho D_m$, where

d_p = particle diameter,

D_m = molecular diffusivity,

ε = fraction voids in the bed.

The correlations are

$$\varepsilon \text{Pe} = 0.20 + 0.011 \text{Re}^{0.48}, \text{ for liquids, standard deviation 46\%,} \tag{17.14}$$

$$\frac{1}{\text{Pe}} = \frac{0.3}{\text{Re Sc}} + \frac{0.5}{1 + 3.8/\text{Re Sc}}, \text{ for gases.} \tag{17.15}$$

TABLE 17.7. Material and Energy Balances of a Packed Bed Reactor

Diffusivity and thermal conductivity are taken appreciable only in the radial direction

Material balance equation:

$$\frac{\partial x}{\partial z} - \frac{D}{u}\left(\frac{\partial^2 x}{\partial r^2} + \frac{1}{r}\frac{\partial x}{\partial r}\right) - \frac{\rho}{u_0 C_0} r_c = 0 \tag{1}$$

Energy balance equation:

$$\frac{\partial T}{\partial z} - \frac{k}{GC_p}\left(\frac{\partial^2 T}{\partial r^2} + \frac{1}{r}\frac{\partial T}{\partial r}\right) + \frac{\Delta H_r \rho}{GC_p} r_c = 0 \tag{2}$$

At the inlet:

$$x(0,r) = x_0 \tag{3}$$
$$T(0,r) = T_0 \tag{4}$$

At the center:

$$r = 0, \frac{\partial x}{\partial r} = \frac{\partial T}{\partial r} = 0 \tag{5}$$

At the wall:

$$r = R, \frac{\partial x}{\partial r} = 0 \tag{6}$$

$$\frac{\partial T}{\partial r} = \frac{U}{k}(T' - T) \tag{7}$$

When the temperature T' of the heat transfer medium is not constant, another enthalpy balance must be formulated to relate T' with the process temperature T.

A numerical solution of these equations may be obtained in terms of finite difference equivalents, taking m radial increments and n axial ones. With the following equivalents for the derivatives, the solution may be carried out by direct iteration:

$$r = m(\Delta r)$$
$$z = n(\Delta z) \tag{8}$$
$$\frac{\partial T}{\partial z} = \frac{T_{m,n+1} - T_{m,n}}{\Delta z} \tag{9}$$
$$\frac{\partial T}{\partial r} = \frac{T_{m+1,n} - T_{m,n}}{\Delta r} \tag{10}$$
$$\frac{\partial^2 T}{\partial r^2} = \frac{T_{m+1,n} - 2T_{m,n} + T_{m-1,n}}{(\Delta r)^2} \tag{11}$$

Expressions for the x-derivatives are of the same form:
r_c = rate of reaction, a function of s and T
G = mass flow rate, mass/(time)(superficial cross section)
u = linear velocity
D = diffusivity
k = thermal conductivity

There are no direct correlations of the variance (or the corresponding parameter n) in terms of the geometry and operating conditions of a vessel. For this reason the RTD is not yet a design tool, but it does have value as a diagnostic tool for the performance of existing equipment on which tracer tests can be made. RTDs obtained from tracer tests or perhaps estimated from dispersion coefficient data or correlations sometimes are applicable to the
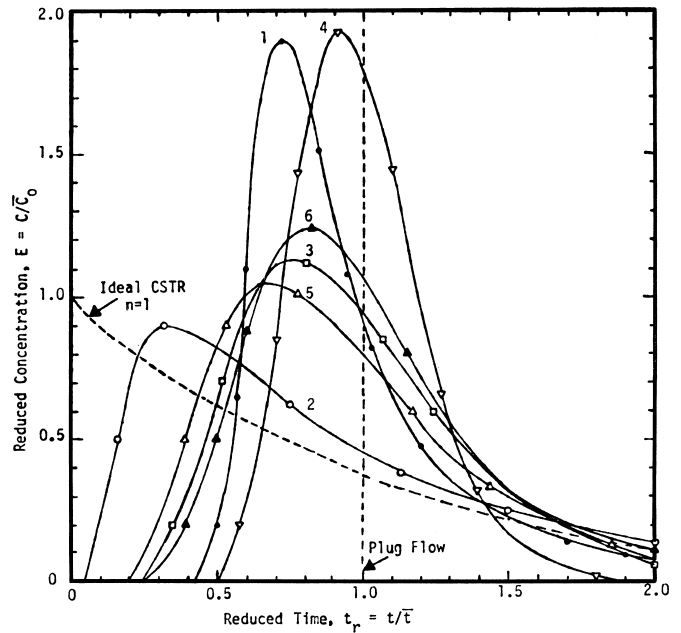
No.	Code	Process	σ^2	n	Pe
1	○	aldolization of butyraldehyde	0.050	20.0	39.0
2	●	olefin oxonation pilot plant	0.663	1.5	1.4
3	□	hydrodesulfurization pilot plant	0.181	5.5	9.9
4	▽	low temp hydroisomerization pilot	0.046	21.6	42.2
5	△	commercial hydrofiner	0.251	4.0	6.8
6	▲	pilot plant hydrofiner	0.140	7.2	13.2

Figure 17.1. Residence time distributions of some commercial and pilot fixed bed reactors. The variance, the equivalent number of CSTR stages, and the Peclet number are given for each.

prediction of the limits between which a chemical conversion can take place in the vessel.

CONVERSION IN SEGREGATED AND MAXIMUM MIXED FLOWS

In some important cases, limiting models for chemical conversion are the segregated flow model represented by the equation

$$\bar{C}/C_0 = 1 - x = \int_0^\infty (C/C_0)_{\text{batch}} E(t_r)\, dt_r$$
$$= \int_0^\infty (C/C_0)_{\text{batch}} E(t)\, dt \tag{17.16}$$

and the maximum-mixedness model represented by Zwietering's equation. For a rate equation $r_c = kC^\alpha$ this equation is

$$\frac{dx}{dt_r} - kC_0^{\alpha-1}x^\alpha + \frac{E(t_r)}{1 - \int_0^{t_r} E(t_r)\, dt_r}x = 0, \tag{17.17}$$

with the boundary condition

$$dx/dt_r = 0 \text{ when } t_r \to \infty, \tag{17.18}$$

which is used to find the starting value x_∞ from

$$kC_0^{\alpha-1}x_\infty - \frac{E(t_r)}{1 - \int_0^\infty E(t_r)\, dt_r}x_\infty = 0. \tag{17.19}$$

Numerical integration of the equation is sufficiently accurate by starting at $(x_\infty, t_r \simeq 4)$ and proceeding to $t_r = 0$ at which time the value of x is the conversion in the reactor with residence time distribution $E(t_r)$.

With a given RTD the two models may correspond to upper and lower limits of conversion or reactor sizes for simple rate equations; thus

	Conversion Limit	
Reaction Order	Segregated	Max–Mix
More than 1	upper	lower
Less than 1	lower	upper
Complex	?	?

Relative sizes of reactors based on the two models are given in Figure 17.2 for second- and half-order reactions at several conversions. For first order reactions the ratio is unity. At small values of the parameter n and high conversions, the spread in reactor sizes is very large. In many packed bed operations, however, with proper initial distribution and redistribution the value of the parameter n is of the order of 20 or so, and the corresponding spread in reactor sizes is modest near conversions of about 90%. In such cases the larger predicted vessel size can be selected without undue economic hardship.

The data also can be rearranged to show the conversion limits for a reactor of a given size.

When the rate equation is complex, the values predicted by the two models are not necessarily limiting. Complexities can arise from multiple reactions, variation of density or pressure or temperature, incomplete mixing of feed streams, minimax rate behavior as in autocatalytic processes, and possibly other behaviors. Sensitivity of the reaction to the mixing pattern can be established in such cases, but the nature of the conversion limits will not be ascertained. Some other, possibly more realistic models will have to be devised to represent the reaction behavior. The literature has many examples of models but not really any correlations (Naumann and Buffham, 1983; Wen and Fan, 1975; Westerterp et al., 1984).

CONVERSION IN SEGREGATED FLOW AND CSTR BATTERIES

The mixing pattern in an n-stage CSTR battery is intermediate between segregated and maximum mixed flow and is characterized by residence time distribution with variance $\sigma^2 = 1/n$. Conversion in the CSTR battery is found by solving n successive equations

$$\frac{C_{j-1}}{C_0} = \frac{C_j}{C_0} + \frac{k\bar{t}}{n} C_0^{\alpha-1}\left(\frac{C_j}{C_0}\right)^\alpha \text{ for } j = 1 - n \tag{17.20}$$

for $C_n/C_0 = 1 - x$. The ratio of required volumes of CSTR batteries and segregated flow reactors is represented by Figure 17.3 for several values of n over a range of conversions for a second order reaction. Comparison with the maximum mixed/segregated flow relation of Figure 17.2 shows a distinct difference between the two sets of ratios.

DISPERSION MODEL

Although it also is subject to the limitations of a single characterizing parameter which is not well correlated, the Peclet number, the dispersion model predicts conversions or residence times unambiguously. For a reaction with rate equation $r_c = kC^\alpha$, this model is represented by the differential equation

$$\frac{1}{\text{Pe}}\frac{d^2x}{dz^2} - \frac{dx}{dz} + k\bar{t}C_0^{\alpha-1}(1-x)^\alpha = 0 \tag{17.21}$$

with the boundary conditions

$$\text{at } z = 0, \left(1 - x + \frac{1}{\text{Pe}}\frac{dx}{dz}\right)_0 = 1, \tag{17.22}$$

$$\text{at } z = 1, \frac{dx}{dz} = 0, \tag{17.23}$$

where

$x = 1 - C/C_0$, fractional conversion,

$z = $ axial distance/length of reactor.

An analytical solution can be found only for a first-order reaction. The two-point boundary condition requires a special numerical procedure. Plots of solutions for first and second order reactions are shown in Figures 17.4 and 17.5.

LAMINAR AND RELATED FLOW PATTERNS

A tubular reactor model that may apply to viscous fluids such as polymers has a radial distribution of linear velocities represented by

$$u = (1 + 2/m)\bar{u}(1 - \beta^m), \tag{17.24}$$
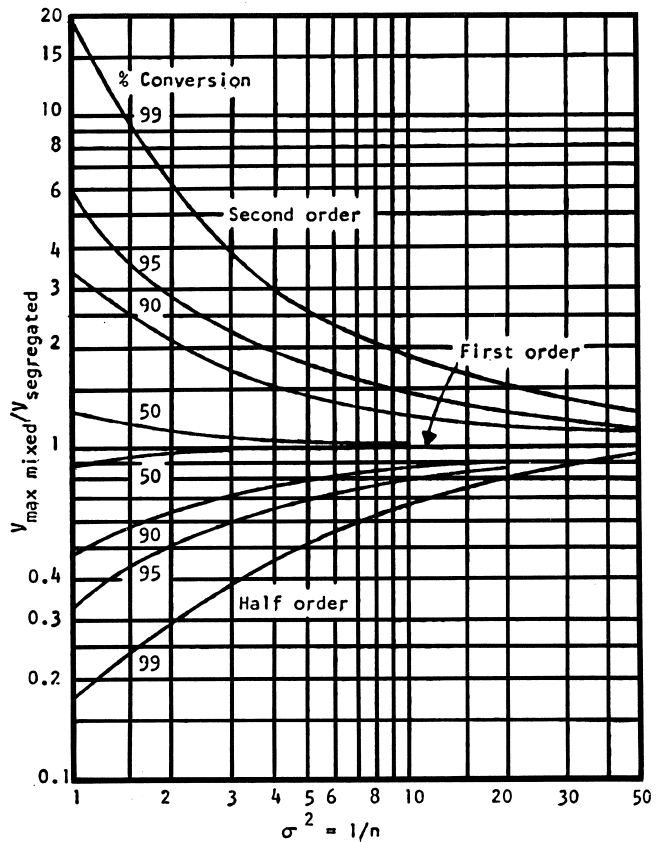
Figure 17.2. Relative volumes of maximum-mixed and segregated flow reactors with the same RTDs identified by $n = 1/\sigma^2$, as a function of conversion for second- and half-order reactions. For first-order reactions the ratio is unity throughout.
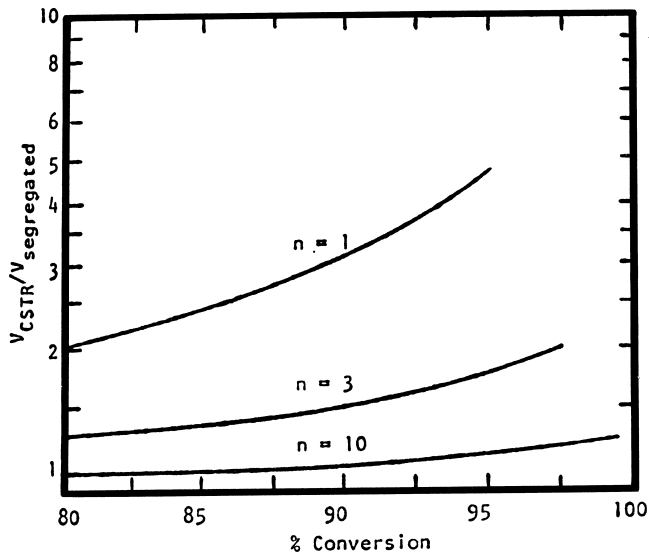
Figure 17.3. Ratio of volumes of an *n*-stage CSTR battery and a segregated flow reactor characterized by a residence time distribution with variance $\sigma^2 = 1/n$. Second-order reaction.

where $\beta = r/R$. When $m = 2$, the pattern is Poiseuille or laminar flow, and, when m is infinite, it is plug flow. The residence time along a streamline is

$$t = \bar{t}/(1 + 2/m)(1 - \beta^m). \tag{17.25}$$

The average conversion over all the stream lines is

$$\frac{\bar{C}}{C_0} = \frac{1}{\pi R^2} \int \left(\frac{C}{C_0}\right)_{\text{streamline}} d(\pi r^2) = 2 \int_0^1 \left(\frac{C}{C_0}\right)_{\text{streamline}} \beta \, d\beta. \tag{17.26}$$

For first-order reaction, for example

$$\frac{\bar{C}}{C_0} = 2 \int_0^1 \exp\left[\frac{-k\bar{t}}{(1 + 2/m)(1 - \beta^m)}\right] \beta \, d\beta \tag{17.27}$$

and for second-order

$$\frac{\bar{C}}{C_0} = 2 \int_0^1 \frac{1}{1 + kC_0\bar{t}/(1 + 2/m)(1 - \beta^m)} \beta \, d\beta. \tag{17.28}$$

These integrals must be evaluated numerically. Variation in residence time will contribute, for example, to the spread in molecular weight distribution of polymerizations.

17.5. SELECTION OF CATALYSTS

A catalyst is a substance that increases a rate of reaction by participating chemically in intermediate stages of reaction and is liberated near the end in a chemically unchanged form. Over a period of time, however, permanent changes in the catalyst—deactivation—may occur. Inhibitors are substances that retard rates of reaction. Many catalysts have specific actions in that they influence only one reaction or group of definite reactions. An outstanding example is the living cell in which there are several hundred different catalysts, called enzymes, each one favoring a specific chemical process.

The mechanism of a catalyzed reaction—the sequence of reactions leading from the initial reactants to the final products—is changed from that of the uncatalyzed process and results in a lower overall energy of activation, thus permitting a reduction in the temperature at which the process can proceed favorably. The equilibrium condition is not changed since both forward and reverse rates are accelerated equally. For example, a good hydrogenation catalyst also is a suitable dehydrogenation accelerator; the most favorable temperature will be different for each process, of course.

A convenient classification is into homogeneous and heterogeneous catalysts. The former types often are metal complexes that are soluble in the reaction medium, but acids and bases likewise have a long known history of catalytic action. The specific action of
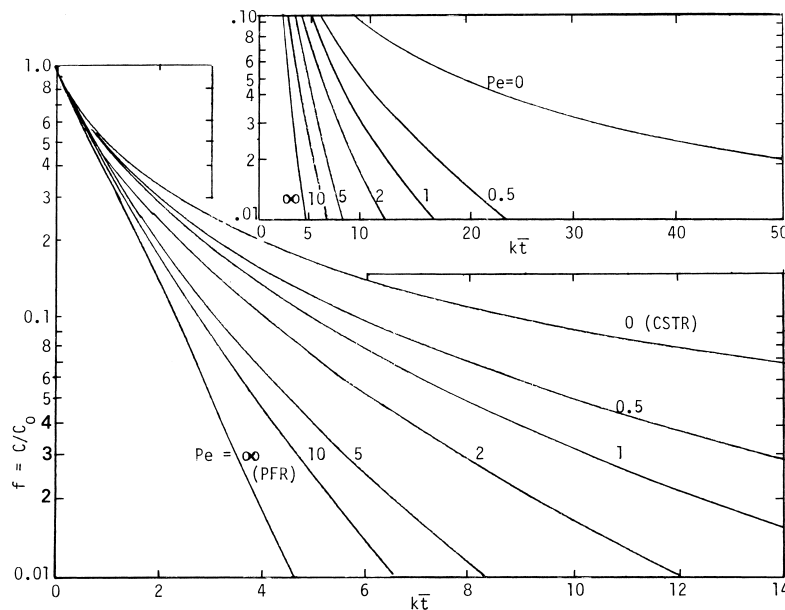
Figure 17.4. Dispersion model. Conversion of first-order reaction as function of the Peclet number.
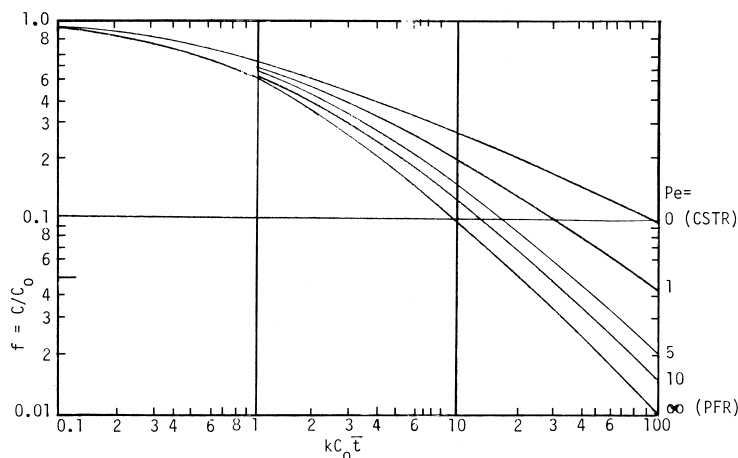
Figure 17.5. Second-order reaction with dispersion identified by the Peclet number, Pe = uL/D_L.

a particular metal complex can be altered by varying the ligands or coordination number of the complex or the oxidation state of the central metal atom. Advantages of homogeneous catalysts are their specificity and low temperature and pressure requirements. Their main drawbacks are difficulty of recovery from the process fluid, often rapid degradation, and relatively high cost. Classic examples of homogeneous catalysis are the inversion of sugar with mineral acids, olefin alkylation with hydrofluoric acid, and the use of ammonia in the Solvay process and of nitrogen oxides in the Chamber process. A modern development is the synthesis of acetic acid from methanol and CO in the presence of homogeneous rhodium complexes.

The problem of separating the catalyst at the end of the operation can be eased in some cases by attaching the catalyst to a solid support, for instance, liquid phosphoric acid in the pores of a solid carrier for the vapor phase synthesis of cumene and the fairly wide application of enzymes that are attached (immobilized) by various means to solid polymers. Some metal ligands also are being combined with solid polymers.

HETEROGENEOUS CATALYSTS

By far the greatest tonnages of synthetic chemicals are manufactured in fluid phases with solid catalysts. Such materials are cheap, are easily separated from the reaction medium, and are adaptable to either flow or nonflow reactors. Their drawbacks are a lack of specificity and often high temperature and pressure requirements. The principal components of most heterogeneous catalysts are three in number:

1. A catalytically active substance or mixture.
2. A carrier of more or less large specific surface on which the catalyst proper is deposited as a thin film, either for economy when the catalyst is expensive or when the catalyst itself cannot be prepared with a suitable specific surface.
3. Promoters, usually present in relatively small amount, which enhance the activity or retard degradation.

Some composite catalysts are designed to promote several reactions of a sequence leading to the final products. A basic catalyst often can be selected with general principles, but subsequent fine tuning of a commercially attractive design must be done in a pilot plant or sometimes on a plant scale.

Analogy to what is known to be effective in chemically similar problems usually provides a start for catalyst design, although a

scientific basis for selection is being developed. This involves a study in detail of the main possible intermediate reactions that could occur and of the proton and electron receptivity of the catalyst and possible promoters, as well as reactant bond lengths and crystals lattice dimensions. Several designs are made from this fundamental point of view in the book of Trimm (1980). A thorough coverage of catalytic reactions and catalysts arranged according to the periodic table is underway in a series edited by Roiter (1968–date). Industrial catalyst practice is summarized by Thomas (1970) who names manufacturers of specific catalysts. Specific processes and general aspects of catalysis are covered in three books edited by Leach (1983–1985): In a chapter by Wagner, there are lists of 40 catalysts with the kinds of processes for which they are effective and of 49 catalytic processes with the homogeneous or heterogeneous catalysts that have been used with them. Many industrial processes are described by Satterfield (1980). Cracking, reforming, partial oxidation, hydrodesulfurization, and catalysis by transition-metal complexes are treated in detail by Gates et al. (1979) and the catalytic conversion of hydrocarbons by Pines (1981). The mechanisms and other aspects of organic catalysis are described in one of the volumes of the series edited by Bamford and Tipper (1978). A vast literature exists for enzyme processes; that technology is well reviewed in two articles in *Ullmann's Encyclopedia* (Biotechnologie, Enzyme) as well as by Bailey and Ollis (1986). In the present text, Table 17.1 identifies the catalyst used in most of the 100 processes listed.

Intermediate processes of catalyzed organic reactions may involve neutral free radicals R·, positive ions R^+, or negative ions R^- as short-lived reactants. A classification of catalysts and processes from the point of view of elementary reactions between reagents and catalysts is logically desirable but has not yet been worked out. However, there is a wealth of practice more or less completely documented, some proprietary but available at a price. The ensuing discussions are classified into kinds of catalysts and into kinds of processes.

KINDS OF CATALYSTS

To a certain extent, it is known what kinds of reactions are speeded up by certain classes of catalysts, but individual members of the same class may differ greatly in activity, selectivity, resistance to degradation, and cost. Even small differences in these properties can mean large sums of money on the commercial scale. Solid catalysts, the most usual kind, are not particularly specific or selective, so that there is a considerable crossing of lines in

classifications between kinds of catalysts and kinds of reactions they favor. Nevertheless, leading relations can be brought out.

Strong acids are able to donate protons to a reactant and to take them back. Into this class fall the common acids, aluminum halides, and boron trifluoride. Also acid in nature are silica, alumina, aluminosilicates, metal sulfates and phosphates, and sulfonated ion exchange resins. The nature of the active sites on these kinds of solids still is not completely understood. The majority of reactions listed subsequently are catalytically influenced to some extent by acidic substances. Zeolites are dehydrated aluminosilicates with small pores of narrow size distribution, to which is due their highly selective catalytic action since only molecules small enough to enter the pores can react. In cracking operations they are diluted to 10–15% in silica–alumina to restrain their great activity; the composite catalyst still is very active but makes less carbon, makes lower amounts of C_3–C_4 products, and has a longer life. Their greater activity has led to the supplanting of fluidized bed crackers by riser-tube reactors. When zeolites are incorporated in reforming catalysts, they crack isoparaffins into straight chains that enter the pores and convert into higher octane substances.

Base catalysis is most effective with alkali metals dispersed on solid supports or in the homogeneous form as aldoxides, amides, and so on. Small amounts of promoters may be added to form organoalkali compounds that really have the catalytic power. Basic ion exchange resins also are useful. Some base-catalyzed processes are isomerization and oligomerization of olefins, reaction of olefins with aromatics, and hydrogenation of polynuclear aromatics.

Metal oxides, sulfides, and hydrides form a transition between acid–base and metal catalysts. They catalyze hydrogenation–dehydrogenation as well as many of the reactions catalyzed by acids such as cracking and isomerization. Their oxidation activity is related to the possibility of two valence states which allow oxygen to be released and reabsorbed alternately. Common examples are oxides of cobalt, iron, zinc, and chromium; and hydrides of precious metals which can release hydrogen readily. Sulfide catalysts are more resistant than metallic catalysts to formation of coke deposits and to poisoning by sulfur compounds; their main application is to hydrodesulfurization.

Metals and alloys. The principal industrial metallic catalysts are found in periodic group VIII which are transition elements with almost completed 3d, 4d, and 5d electron orbits. According to one theory, electrons from adsorbed molecules can fill the vacancies in the incomplete shells and thus make a chemical bond. What happens subsequently will depend on the operating conditions. Platinum, palladium, and nickel, for example, form both hydrides and oxides; they are effective in hydrogenation (vegetable oils, for instance) and oxidation (ammonia or sulfur dioxide, for instance). Alloys do not always have catalytic properties intermediate between those of the pure metals since the surface condition may be different from the bulk and the activity is a property of the surface. Addition of small amounts of rhenium to Pt/Al_2O_3 results in a smaller decline of activity with higher temperature and slower deactivation rate. The mechanism of catalysis by alloys is in many instances still controversial.

Transition-metal organometallic catalysts in solution are effective for hydrogenation at much lower temperatures than metals such as platinum. They are used for the reactions of carbon monoxide with olefins (hydroformylation) and for some oligomerizations. The problem of separating the catalyst from solution sometimes is avoided by anchoring or immobilizing the catalyst on a polymer support containing pendant phosphine groups and in other ways.

KINDS OF CATALYZED ORGANIC REACTIONS

A fundamental classification of organic reactions is possible on the basis of the kinds of bonds that are formed and destroyed and the natures of eliminations, substitutions, and additions of groups. Here a more pragmatic list of 20 commercially important individual kinds or classes of reactions will be discussed.

1. Alkylations, for example, of olefins with aromatics or isoparaffins, are catalyzed by sulfuric acid, hydrofluoric acid, BF_3, and $AlCl_3$.
2. Condensations of aldehydes and ketones are catalyzed homogeneously by acids and bases, but solid bases are preferred, such as anion exchange resins and alkali or alkaline earth hydroxides or phosphates.
3. Cracking, a rupturing of carbon—carbon bonds, for example, of gas oils to gasoline, is favored by silica–alumina, zeolites, and acid types generally.
4. Dehydration and dehydrogenation combined utilizes dehydration agents combined with mild dehydrogenation agents. Included in this class of catalysts are phosphoric acid, silica–magnesia, silica–alumina, alumina derived from aluminum chloride, and various metal oxides.
5. Esterification and etherification may be accomplished by catalysis with mineral acids of BF_3; the reaction of isobutylene with methanol to make MTBE is catalyzed by a sulfonated ion exchange resin.
6. Fischer–Tropsch oligomerization of CO + hydrogen to make hydrocarbons and oxygenated compounds. Iron promoted by potassium is favored, but the original catalyst was cobalt which formed a carbonyl in process.
7. Halogenation and dehalogenation are catalyzed by substances that exist in more than one valence state and are able to accept and donate halogens freely. Silver and copper halides are used for gas-phase reactions, and ferric chloride commonly for liquid phase. Hydrochlorination (the absorption of HCl) is promoted by $BiCl_3$ or $SbCl_3$ and hydrofluorination by sodium fluoride or chromia catalysts that fluoride under reaction conditions. Mercuric chloride promotes addition of HCl to acetylene to make vinyl chloride.
8. Hydration and dehydration employ catalysts that have a strong affinity for water. Alumina is the principal catalyst, but also used are aluminosilicates, metal salts, and phosphoric acid or its metal salts on carriers and cation exchange resins.
9. Hydrocracking is catalyzed by substances that promote cracking and hydrogenation together. Nickel and tungsten sulfides on acid supports and zeolites loaded with palladium are used commercially.
10. Hydrodealkylation, for example, of toluene to benzene, is promoted by chromia–alumina with a low sodium content.
11. Hydrodesulfurization uses sulfided cobalt/molybdena/alumina, or alternately with nickel and tungsten substituted for Co and Mo.
12. Hydroformylation, or the oxo process, is the reaction of olefins with CO and hydrogen to make aldehydes. The catalyst base is cobalt naphthenate which transforms to cobalt hydrocarbonyl in place. A rhodium complex that is more stable and functions at a lower temperature also is used.
13. Hydrogenation and dehydrogenation employ catalysts that form unstable surface hydrides. Transition-group and bordering metals such as Ni, Fe, Co, and Pt are suitable, as well as transition group oxides or sulfides. This class of reactions includes the important examples of ammonia and methanol syntheses, the Fischer–Tropsch and oxo and synthol

processes and the production of alcohols, aldehydes, ketones, amines, and edible oils.

14. Hydrolysis of esters is accelerated by both acids and bases. Soluble alkylaryl sulfonic acids or sulfonated ion exchange resins are satisfactory.

15. Isomerization is promoted by either acids or bases. Higher alkylbenzenes are isomerized in the presence of $AlCl_3/HCl$ or BF_3/HF; olefins with most mineral acids, acid salts, and silica alumina; saturated hydrocarbons with $AlCl_3$ or $AlBr_3$ promoted by 0.1% of olefins.

16. Metathesis is the rupture and reformation of carbon—carbon bonds, for example of propylene into ethylene plus butene. Catalysts are oxides, carbonyls or sulfides of Mo, W, or rhenium.

17. Oxidation catalysts are either metals that chemisorb oxygen readily such as platinum or silver, or transition metal oxides that are able to give and take oxygen by reason of their having several possible oxidation states. Ethylene oxide is formed with silver, ammonia is oxidized with platinum, and silver or copper in the form of metal screens catalyze the oxidation of methanol to formaldehyde.

18. Polymerization of olefins such as styrene is promoted by acid or base catalysts or sodium; polyethylene is made with homogeneous peroxides.

19. Reforming is the conversion primarily of naphthenes and alkanes to aromatics, but other chemical reactions also occur under commercial conditions. Platinum or platinum/rhenium are the hydrogenation–dehydrogenation component of the catalyst and alumina is the acid component responsible for skeletal rearrangements.

20. Steam reforming is the reaction of steam with hydrocarbons to make a manufactured gas containing mostly methane with trace amounts of ethylene, ethane, and hydrogen. For the manufacture of this gas, a representative catalyst composition contains 13 wt % Ni, 12.1 wt % U, and 0.3 wt % K; it is particularly resistant to poisoning by sulfur. To make hydrogen, the catalyst contains oxides of Ni, Ca, Si, Al, Mg, and K. Specific formulations are given by Satterfield (1980).

PHYSICAL CHARACTERISTICS OF SOLID CATALYSTS

Although a few very active solid catalysts are used as fine wire mesh or other finely divided form, catalysts are mostly porous bodies whose total surface is measured in m^2/g. These and other data of some commercial catalysts are shown in Table 17.8. The physical characteristics of major importance are as follows.

1. *Particle size*. In gas fluidized beds the particle diameters average less than 0.1 mm; smaller sizes impose too severe loading on entrainment recovery equipment. In slurry beds the particles can be about 1 mm dia. In fixed beds the range is 2–5 mm dia. The competing factors are that the pressure drop increases with diminishing diameter and the accessibility of the internal surface decreases with increasing diameter. With poorly thermally conducting materials, severe temperature gradients or peaks arise with large particles that may lead to poor control of the reaction and the development of undesirable side reactions like carbonization.

2. *Specific surface*. Solid spheres of 0.1 mm dia have a specific surface of 0.06 m^2/mL and an activated alumina one of about 600 m^2/mL. Other considerations aside, a large surface is desirable because the rate of reaction is proportional to the amount of accessible surface. Large specific surfaces are associated with pores of small diameters and are substantially all internal surface.

3. *Pore diameters and their distribution*. Small pores limit accessibility of internal surface because of increased resistance to diffusion of reactants into the pores. Diffusion of products outward also is slowed down and may result in degradation of those products. When the catalyst is expensive, the inaccessible internal surface is a liability. A more or less uniform pore diameter is desirable, but the distribution usually is statistical and only molecular sieves have nearly uniform pores. Those catalyst granules that are extrudates of compacted masses of smaller particles have bimodal pore size distribution, between the particles and within them. Clearly a compromise between large specific surface and its accessibility as measured by pore diameter is required in some situations.

4. *Effective diffusivity*. Resistance to diffusion in a catalyst pore is due to collisions with other molecules and with the walls of the pore. The corresponding diffusivities are called bulk diffusivity and Knudsen diffusivity D_K. Many data and correlations of the former type exist; the latter is calculable from the following formula (Satterfield, 1970, p. 42):

$$D_K = \frac{19,400\theta^2}{S_g \rho_p} \left(\frac{T}{M}\right)^{1/2},$$

where

θ = fraction porosity,
S_g = specific surface per unit mass,
ρ_p = density,
T = temperature (K),
M = molecular weight.

This equation applies to uniform cylindrical pores whose length equals the thickness of the catalyst through which the diffusion takes place. The actual diffusivity in common porous catalysts usually is intermediate between bulk and Knudsen. Moreover, it depends on the pore size distribution and on the true length of path. Two tortuosity factors are defined:

τ_p = ratio of measured diffusivity to that calculated with the known pore size distribution and bulk diffusivity and the thickness of the catalyst mass.

τ_m = ratio of measured diffusivity to that calculated from the Knudsen formula with a mean pore diameter.

The data of Table 17.8 exhibit a fairly narrow range of τ_p, an average of about 4, but there seems to be no pattern to τ_m, which is not surprising since the diffusions actually are intermediate between bulk and Knudsen in these cases. In order to be able to calculate the effective diffusivity, it is necessary to know the pore size distribution, the specific surface, the porosity, and bulk diffusivity in the reaction mixture under reaction conditions. Such a calculation is primarily of theoretical interest. Practically it is more useful to simply measure the diffusivity directly, or even better to measure the really pertinent property of catalyst effectiveness as defined next.

CATALYST EFFECTIVENESS

Catalyst effectiveness is a measure of the extent of utilization of internal surface; it is the ratio of a rate of reaction actually achieved with the catalyst particle to the rate that would prevail if all of the internal surface were exposed to the reactant concentration at the external surface of the particle. The rate equation accordingly is modified to

TABLE 17.8. Physical Properties of Some Commercial Catalysts and Carriers[a]

Designation	Nominal Size	Surface Area (m^2/g)	Total Void Fraction	$D_{eff}^b \times 10^3$ (cm^2/sec}	Average Tortuosity Factor τ_p Parallel-Path Pore Model	$r_e = 2V_e/S_e$(Å)	τ_m Based on Average Pore Radius
T-126	$3/16 \times 1/8$ in.	197	0.384	29.3	3.7 ± 0.2	29	0.45
T-1258		302	0.478	33.1	3.8 ± 0.2	23.6	0.41
T-826		232	0.389	37.7	3.9 ± 0.1	21.4	0.26
T-314		142	0.488	20.0	7.1 ± 0.9	41.5	1.2
T-310		154	0.410	16.6	$3.8 + 0.1$	34.3	0.67
G-39	$3/16 \times 3/16$ in.	190	0.354	17.5	4.8 ± 0.3	22.4	0.53
G-35		—	0.354	18.2	4.9 ± 0.1		—
T-606		—	0.115	27.7	2.9 ± 0.2		—
G-58		6.4	0.389	87.0	2.8 ± 0.3	543.	2.87
T-126	$1/4 \times 1/4$ in.	165	0.527	38.8	3.6 ± 0.3	49.0	0.79
T-606		—	0.092	0.71	79 ± 28		—
G-41		—	0.447	21.9	4.4 ± 0.1		—
G-52		—	0.436	27.4	$3.9 + 0.2$		—
G-56	$1/2 \times 1/2$ in.	42	0.304	8.1	11.1 ± 1.1	84.	3.74
BASF	5×5 mm	87.3	0.500	11.8	$7.3 + 0.7$	41.	2.05
Harshaw	$1/4 \times 1/4$ in.	44	0.489	13.3	7.2 ± 0.1	91.	3.95
Haldor Topsøe	$1/4 \times 1/4$ in.	143	0.433	15.8[e]	2.8	25.8	0.83

Catalyst	Description
T-126	Activated γ-alumina
T-1258	Activated γ-alumina
T-826	3% CoO, 10% MoO$_3$, and 3% NiO on alumina
T-314	About 8–10% Ni and Cr in the form of oxides on an activated alumina
T-310	About 10–12% nickel as the oxide on an activated alumina
T-606	Specially compounded refractory oxide support
G-39	A cobalt-molybdenum catalyst, used for simultaneous hydrodesulfurization of sulfur compounds and hydrogenation of olefins
G-35	A cobalt-molybdenum catalyst supported on high-purity alumina, used for hydrodesulfurization of organic sulfur compounds
G-41	A chromia-alumina catalyst, used for hydrodealkylation and dehydrogenation reactions
G-58	Palladium-on-alumina catalyst, for selective hydrogenation of acetylene in ethylene
G-52	Approximately 33 wt % nickel on a refractory oxide support, prereduced. Used for oxygen removal from hydrogen and inert gas streams
G-56	A nickel-base catalyst used for steam reforming of hydrocarbons
BASF	A methanol synthesis catalyst, prereduced
Harshaw	A methanol synthesis catalyst, prereduced
Haldor Topsøe	A methanol synthesis catalyst, prereduced

[a] The measured effective diffusivities are those of hydrogen in nitrogen at room temperature and pressure except that of Haldor Topsoe which is of helium in nitrogen.
[Satterfield and Cadle, 1968].

$$r = knf(C_s), \tag{17.30}$$

where η is the catalyst effectiveness and C_s is the concentration of the reactant at the external surface. For isothermal reactions, η

always is less than unity, but very large values can develop for exothermic reactions in poorly conducting catalysts.

A great deal of attention has been devoted to this topic because of the interesting and often solvable mathematical problems that it presents. Results of such calculations for isothermal zero-, first-, and second-order reactions in uniform cylindrical pores are summarized in Figure 17.6. The abscissa is a modified Thiele modulus whose basic definition is

$$\phi = R/k_v C_s^{n-1}/D_{eff}, \tag{17.31}$$

where R is a linear dimension (the radius of a sphere, for example), k_v the specific rate on a volumetric basis, C_s the surface concentration, n the order of the reaction, and D_{eff} the effective diffusivity. For nonisothermal reactions, those with variable volume and with rate equations of the Langmuir–Hinshelwood or other complex types, additional parameters are involved. Although such calculations can be made, they still require measurements of effective diffusivity as well as a number of unverifiable assumptions. Accordingly in practical cases it is preferable to make direct measurements of catalyst effectiveness and to correlate them with operating parameters. The effectiveness is deduced by comparing conversion with the reference particle size with those with successively small particle sizes until the effect disappears. Two examples are presented to illustrate the variables that are taken into account and the magnitudes of the effects.

For synthesis of ammonia the effectiveness has been measured by Dyson and Simon (1968) and correlated by the equation

$$\eta = b_0 + b_1 T + b_2 x + b_3 T^2 + b_4 x^2 + b_5 T^3 + b_6 x^3, \tag{17.32}$$

where T is in K, x is fractional conversion of nitrogen, and the b_i depend on pressure as given in this table:

Pressure (atm)	b_0	b_1	b_2	b_3	b_4	b_5	b_6
150	−17.539096	0.07697849	6.900548	-1.082790×10^{-4}	−26.42469	4.927648×10^{-3}	38.93727
225	−8.2125534	0.03774149	6.190112	-5.354571×10^{-5}	−20.86963	2.379142×10^{-3}	27.88403
300	−4.6757259	0.02354872	4.687353	-3.463308×10^{-5}	−11.28031	1.540881×10^{-3}	10.46627
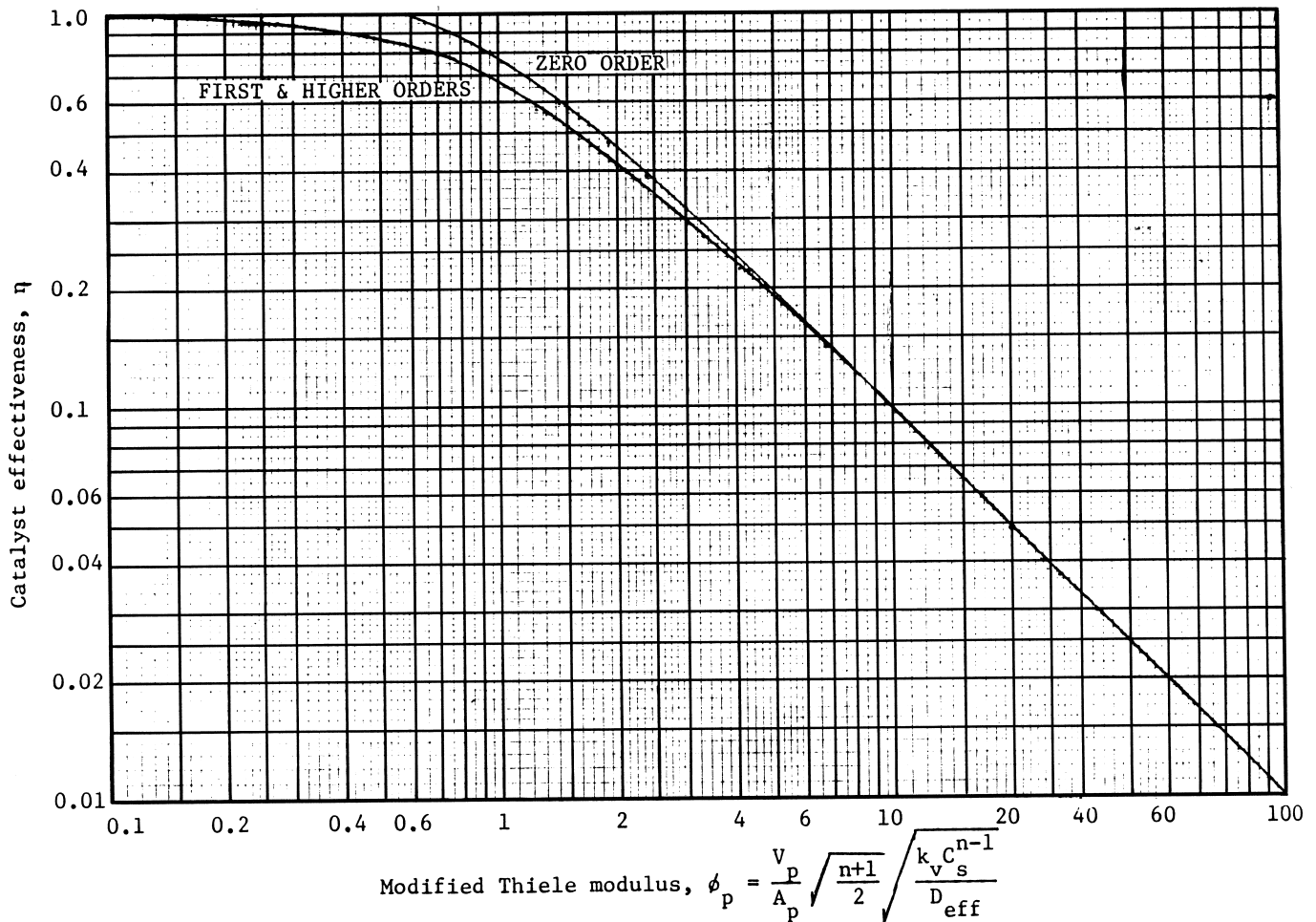
Figure 17.6. Generalized chart of catalyst effectiveness for reactions of order n in particles with external surface A_p and volume V_p. The upper curve applies exactly to zero-order reaction in spheres, and the lower one closely for first- and second-order reactions in spheres.

The reference mixture has $H_2/N_2 = 3$ and contains 12.7% inert; other ratios had slightly different effectiveness. The particle diameters are 6–10 mm. Some calculations from this equation at 225 atm are:

T	x	η
700	0.25	0.81
700	0.10	0.57
650	0.25	0.91

For oxidation of sulfur dioxide, measurements of effectiveness were made by Kadlec, Pour, and Regner (1968) whose data are shown following. They are at atmospheric pressure. The initial content of SO_2 and the conversion have little effect on the result. Both increase in size of granule and temperature lower the effectiveness, although the effect of temperature is somewhat erratic.

The rate equations of both these processes are quite complex, and there is little likelihood that the effectiveness could be deduced mathematically from fundamental data as functions of temperature, pressure, conversion, and composition, which is the kind of information needed for practical purposes. Perhaps the only estimate that can be made safely is that, in the particle size range below 1 mm or so, the effectiveness probably is unity. The penetration of small pores by liquids is slight so that the catalysts used in

liquid slurry systems are of the low specific surface type or even nonporous.

Experimentally Determined Effectiveness Factors

°C	% SO$_2$	0.4	0.5	0.6	0.7	0.8	0.9
				Conversion			

Irregular grain shape, fraction 5–6 mm

460	7	0.84	0.84	0.82	0.83	0.82	0.81
480	7	0.60	0.62	0.62	0.62	0.60	0.60
500	7	—	0.54	0.51	0.50	0.50	0.52
520	7	—	0.35	0.35	0.35	0.38	0.38

Cylindrical granules of 6 mm diameter and 12 mm length

460	7	0.57	0.57	0.59	0.60	0.60	0.60
	10	0.58	0.62	0.63	0.63	0.62	0.62
480	7	0.53	0.54	0.56	0.57	0.56	0.57
	10	0.44	0.45	0.45	0.46	0.45	0.47
500	7	0.25	0.25	0.27	0.28	0.27	0.31
	10	0.26	0.27	0.30	0.30	0.31	0.30
520	7	—	0.21	0.21	0.22	0.22	0.23
	10	—	0.20	0.21	0.21	0.22	0.24

17.6. TYPES AND EXAMPLES OF REACTORS

Almost every kind of holding or contacting equipment has been used as a chemical reactor at some time, from mixing nozzles and centrifugal pumps to the most elaborate towers and tube assemblies. This section is devoted to the general characteristics of the main kinds of reactors, and also provides a gallery of selected examples of working reactors.

The most obvious distinctions are between nonflow (batch) and continuous operating modes and between the kinds of phases that are being contacted. A classification of appropriate kinds of reactors on the basis of these two sets of distinctions is in Figure 17.7.

When heterogeneous mixtures are involved, the conversion rate often is limited by the rate of interphase mass transfer, so that a large interfacial surface is desirable. Thus, solid reactants or catalysts are finely divided, and fluid contacting is forced with mechanical agitation or in packed or tray towers or in centrifugal pumps. The rapid transfer of reactants past heat transfer surfaces by agitation or pumping enhances also heat transfer and reduces harmful temperature gradients.

Batch processing is used primarily when the reaction time is long or the required daily production is small. The same batch equipment often is used to make a variety of products at different times. Otherwise, it is not possible to generalize as to the economical transition point from batch to continuous operation. One or more batch reactors together with appropriate surge tanks may be used to simulate continuous operation on a daily or longer basis.

STIRRED TANKS

Stirred tanks are the most common type of batch reactor. Typical proportions are shown on Figures 17.8 and 10.1, and modes of level control on Figure 3.6. Stirring is used to mix the ingredients initially, to maintain homogeneity during reaction, and to enhance heat transfer at a jacket wall or internal surfaces. The reactor of Figure 17.9(b) employs a pumparound for mixing of the tank contents and for heat transfer in an external exchanger. Pumparound or recycle in general may be used to adapt other kinds of vessels to service as batch mode reactors; for example, any of the packed vessels of Figure 17.13(a)–(e). A pumparound tubular flow reactor is employed for the polymerization of ethylene. As the polymer is formed, it is bled off at a much lower rate than that of the recirculation, so that in a sense the action of this equipment approaches batch operation.

Some special industrial stirred reactors are illustrated in Figure 17.10: (b) is suitable for pasty materials, (c) for viscous materials, and the high recirculation rate of (d) is suited to intimate contacting of immiscible liquids such as hydrocarbons with aqueous solutions.

Many applications of stirred tank reactors are to continuous processing, either with single tanks or multiple arrangements as in Figures 17.9(c)–(d). Knowledge of the extent to which a stirred tank does approach complete mixing is essential to being able to predict its performance as a reactor. The other limiting case is that of plug flow, in which all nonreacting molecules have the same residence time. Deviations from the limiting cases of complete mixing (in a CISTR) and no axial mixing (in a PFR) are evaluated with residence time distributions (RTDs) based on analyses of tracer tests.

CODE: ☐ Commonly used ▨ Rarely used ⊠ Not feasible
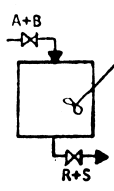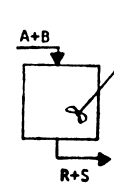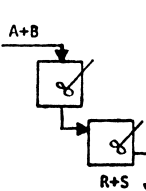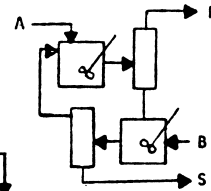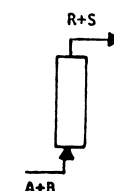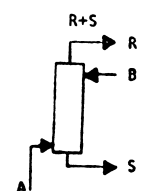
MODE	BATCH	CONTINUOUS				
REACTOR TYPE	Tank	Tank	Tank battery		Tubular	
Phase \ Flow type	Agitated	Agitated	Parallel	Counter	Parallel	Counter
Gaseous				⊠		⊠
Liquid				⊠		⊠
Gas-liquid	Gas continuous					
Liquid-liquid						
Gas-solid						
Liquid-solid						
Gas-liquid-solid						

Figure 17.7. Classification of reactors according to the mode of operation and the kinds of phases involved.
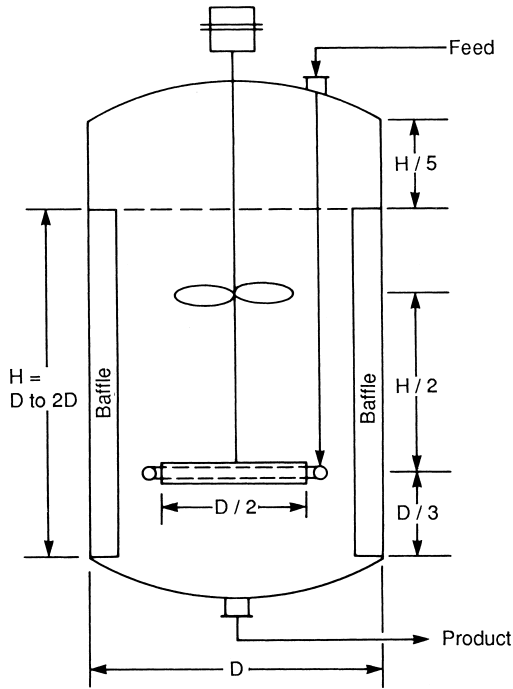
Figure 17.8. Typical proportions of a stirred tank reactor with radial and axial impellers, four baffles, and a sparger feed inlet.

At present, RTD behavior has not been well correlated with operating or design factors, but the technique is of diagnostic value with existing equipment. CISTR (continuous ideal stirred tank reactor) behavior is approached when the mean residence time is 5–10 times the mixing time, which is in turn the length of time needed to achieve homogeneity of a mixture of several inputs. Often this is achieved by 50–200 revolutions of a properly designed stirrer. Although mixing times have been the subject of many studies in the literature (Westerterp et al., 1984, p. 254) (see Table 17.1), no useful generalizations have been deduced. The mixing time depends on the geometry and the speed and power of the agitator. A propeller above and a turbine below on the same shaft, baffles attached to the wall of the tank, and possibly a draft tube around the shaft for effective recirculation of the contents constitute a basic design. However, rational design of mixing equipment is possible but in critical cases experts should be consulted. Chapter 10 also deals with this topic.

Power input per unit volume and impeller tip speeds are often used measures of the intensity of stirring, assuming correct proportions of the vessel and proper baffling. Appropriate ranges for some reaction conditions are as tabulated:

Operation	kW/m^{3a}	Tip speed (m/sec)
Blending	0.05–0.1	
Homogeneous reaction	0.1–0.3	2.5–3.3
Reaction with heat transfer	0.3–1.0	3.5–5.0
Gas–liquid, liquid–liquid	1–2	5–6
Slurries	2–5	

^{a}1 kW/m^3 = 5.08 HP/1000 gal

(a)

(b)

(c)

(d)
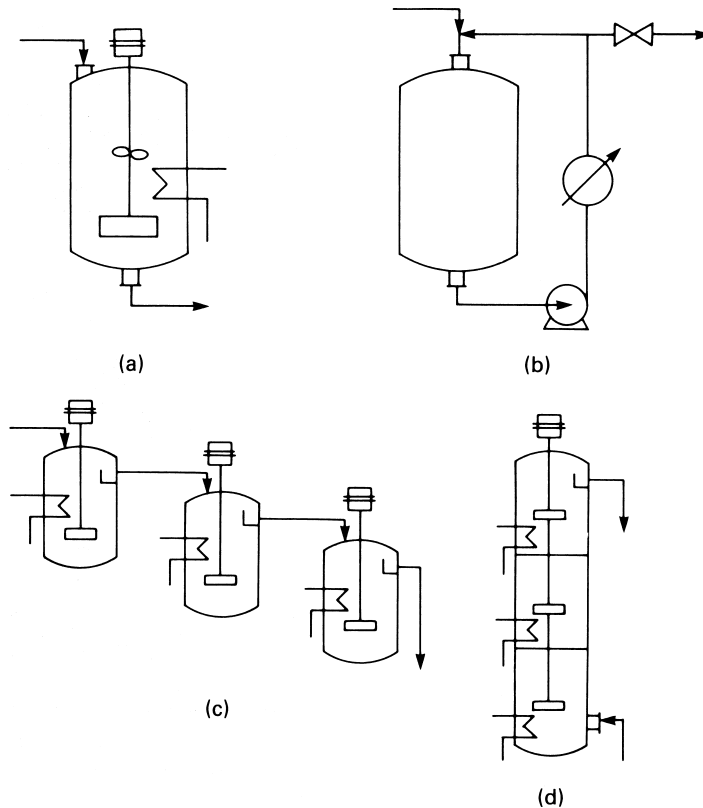
Figure 17.9. Stirred tank reactors, batch and continuous. (a) With agitator and internal heat transfer surface, batch or continuous. (b) With pumparound mixing and external heat transfer surface, batch or continuous. (c) Three-stage continuous stirred tank reactor battery. (d) Three-stage continuous stirred tank battery in a single shell.

Heat transfer coefficients in stirred tank operations are discussed in Section 17.7.

For a given load and conversion, the total volume of a CSTR (continuous stirred tank reactor) battery decreases with the number of stages, sharply at first and then more slowly. When the reaction is first order, for example, $r = kC$, the ratio of total reactor volume V_r of n stages to the volumetric feed rate V'_0 is represented by

$$kV_r/V'_0 = n[(C_0/C)^{1/n} - 1]. \qquad (17.33)$$

At conversions of 95 and 99%, some values from this equation are

n	1	2	3	4	5	10
kV_r/V'_0 at 95%	19	6.9	5.1	4.5	5.1	3.5
kV_r/V'_0 at 99%	99	18.0	10.9	9.7	7.6	5.9

Since the cost of additional controls, agitators, and pumps can counterbalance the savings in volume, four or five tanks in a battery normally prove to be an optimum number, but a larger number of stages may be economical with a single shell design like Figure 17.9(d), particularly when the stages are much less efficient than ideal ones.

For some purposes it is adequate to assume that a battery of five or so CSTRs is a close enough approximation to a plug flow reactor. The tubular flow reactor is smaller and cheaper than any comparable tank battery, even a single shell arrangement. For a first order reaction the ratio of volumes of an n-stage CSTR and a PFR is represented by

$$(V_r)_{\mathrm{CSTR}}/(V_r)_{\mathrm{PFR}} = n[(C_0/C)^{1/n} - 1]/\ln(C_0/C). \qquad (17.34)$$

For example, when $n = 5$ and conversion is 99%, the ratio is 1.64. For second-order and other-order reactions a numerical solution for the ratio is needed, one of which is represented by Figure 17.12. For a second order reaction the ratio is 1.51 at 99% conversion with five stages.

A further difference between CSTR batteries and PFRs is that of product distributions with complex reactions. In the simple case, $A \to B \to C$ for example, a higher yield of intermediate product B is obtained in a PFR than in a single CSTR. It is not possible to generalize the results completely, so that the algebra of each individual reacting system must be solved to find the best mode.

TUBULAR FLOW REACTORS

The ideal behavior of tubular flow reactors (TFR) is plug flow, in which all nonreacting molecules have equal residence times. Any backmixing that occurs is incidental, the result of natural turbulence or that induced by obstructions to flow by catalyst granules or tower packing or necessary internals of the vessels. The action of such obstructions can be two-edged, however, in that some local backmixing may occur, but on the whole a good approach to plug flow is developed because large scale turbulence is inhibited. Any
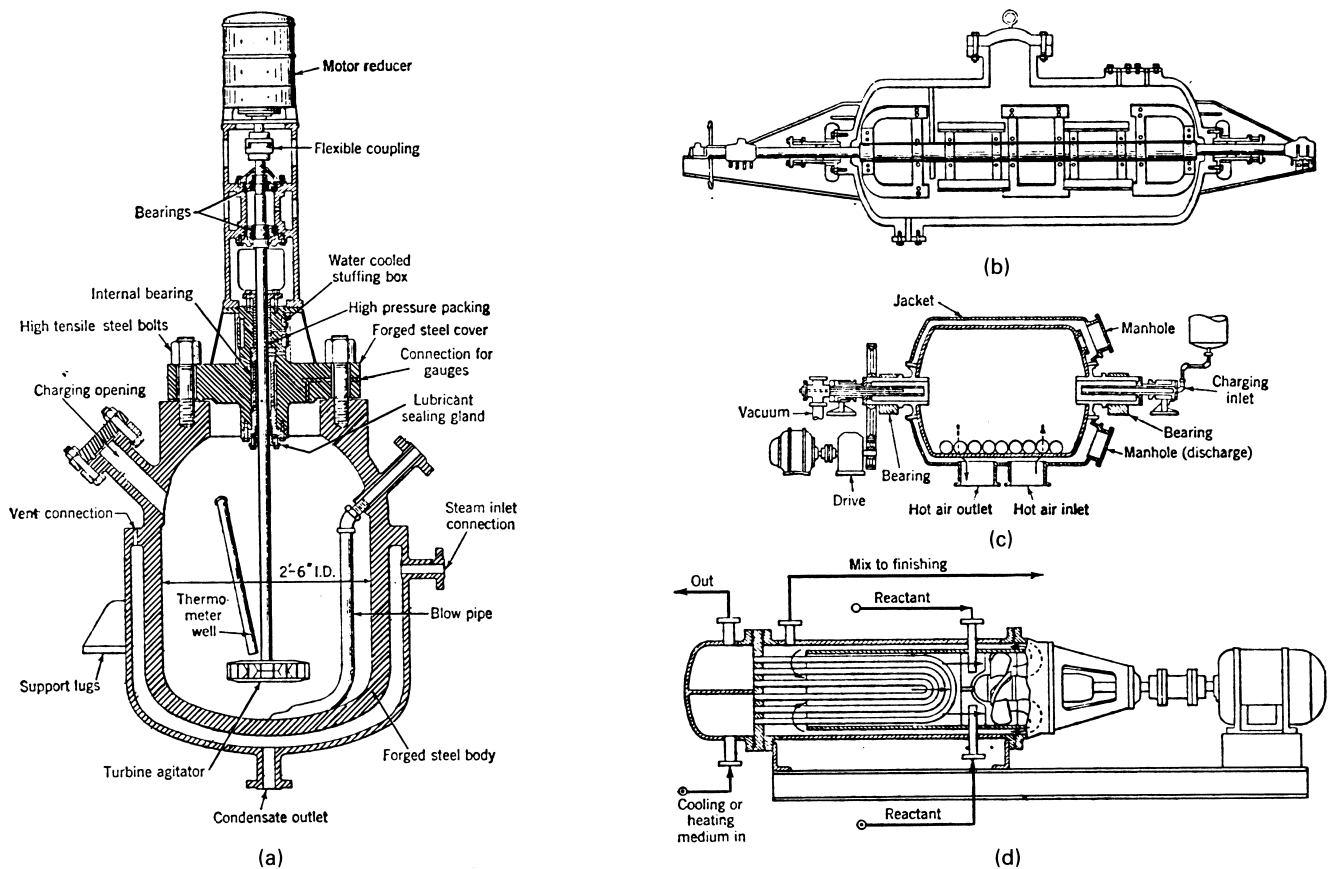
Figure 17.10. Several modes of mixing in commercial tank reactors. (a) Steam-jacketed autoclave, 120 gal, 200 psig, 300°F (*courtesy Blaw-Knox Co.*). (b) Horizontal autoclave, 650 gal, 100 psig (*courtesy Blaw-Knox Co.*). (c) Ball-mill sulfonator [*Groggins. Courtesy McGraw-Hill, New York*]. (d) Horizontal heat-exchange reactor (*courtesy Stratford Engineering Corp. patents issued*).
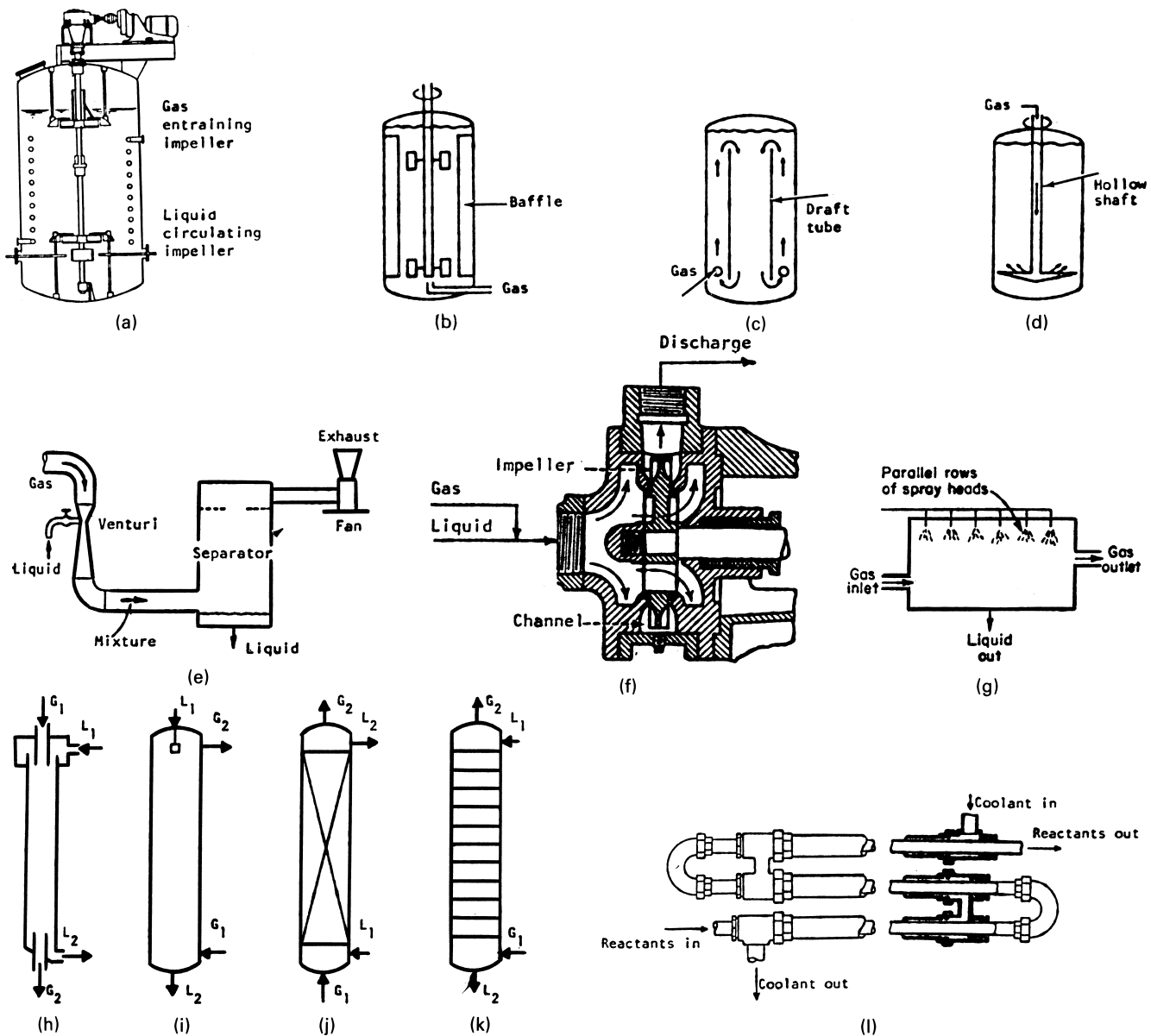
Figure 17.11. Types of contactors for reacting gases with liquids; many of these also are suitable for reacting immiscible liquids. Tanks: (a) with a gas entraining impeller; (b) with baffled impellers; (c) with a draft tube; (d) with gas input through a rotating hollow shaft. (e) Venturi mixer for rapid reactions. (f) Self-priming turbine pump as a mixer-reactor. (g) Multispray chamber. Towers: (h) parallel flow falling film; (i) spray tower with gas as continuous phase; (j) parallel flow packed tower; (k) counter flow tray tower. (l) A doublepipe heat exchanger used as a tubular reactor.

required initial blending of reactants is accomplished in mixing nozzles or by in-line mixers such as those of Figures 10.20. As a result of chemical reaction, gradients of concentration and temperature are developed in the axial direction of TFRs.

TFRs may be of pipe diameters ranging from 1 to 15 cm or so, or they may be vessels of diameters measured in meters. Figure 17.13 is of a variety of vessel configurations. Single tube reactors more than 1000 m long are used, in which case they are trombone-shaped as on Figures 17.14(f) and 17.15(c). The selection of diameter is a result of compromise between construction cost, pumping cost, and required heat transfer. In some cases it may be necessary to avoid the laminar flow region, which is below Reynolds numbers of 2300–4000 or so, if the reaction is complex and a spread of residence times is harmful.

When many tubes in parallel are needed, a shell-and-tube construction like that of heat exchangers is employed; the vessel then may be regarded as a heat exchanger in which a reaction occurs incidentally. Heat transfer to single tubes is accomplished with jackets in Figure 17.14(f) and in a fired heater in Figure 17.15(c). Some of the many designs of fired heaters that are suitable for pyrolysis and other high temperature reactions are illustrated on Figure 17.16. In the process for making phenol, monochlorbenzene, and aqueous caustic are reacted at 320°C and 200 atm in multipass tubes of 10 cm dia or so in a fired heater.

In general, the construction of TFRs is dictated by the need for accommodation of granular catalysts as well as for heat transfer. Some of the many possible arrangements are illustrated on Figure 17.13 and elsewhere in this section.
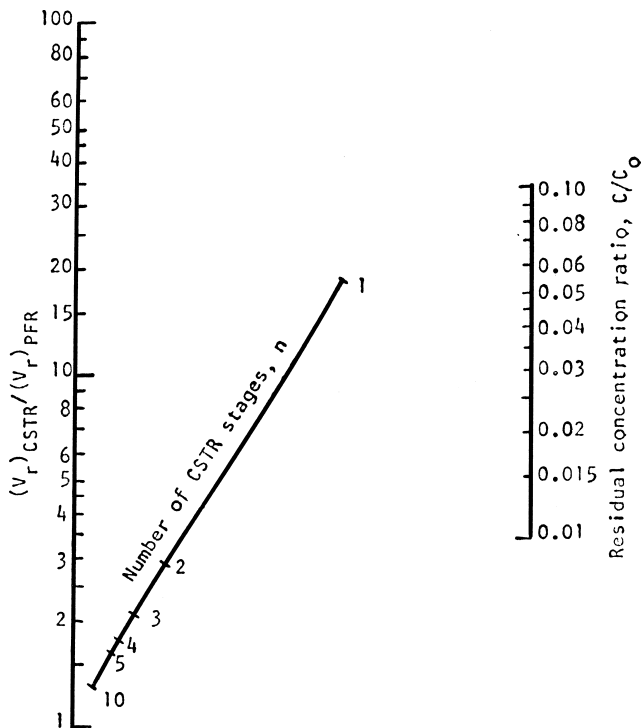
Figure 17.12. Ratio of volumes of an n-stage CSTR battery and a plug flow reactor as a function of residual concentration ratio C/C_0 with a rate equation $r = kC^2$.

Some unusual flow reactors are shown in Figure 17.14. The residence times in the units for high temperature pyrolysis to make acetylene and ethylene and for the oxidation of ammonia are measured in fractions of a second; acetic anhydride is made by mixing reactants quickly in a centrifugal pump; NO is formed at very high temperature in an electric furnace; and ethylene is polymerized at high or low pressures in the two units shown.

GAS–LIQUID REACTIONS

Except with highly volatile liquids, reactions between gases and liquids occur in the liquid phase, following a transfer of gaseous participants through gas and liquid films. The rate of mass transfer always is a major or limiting factor in the overall transformation process. Naturally the equipment for such reactions is similar to that for the absorption of chemically inert gases, namely towers and stirred tanks. Figure 17.11 illustrates schematically types of gas–liquid reactors. Figure 17.17 shows specific examples of such reactors: In the synthesis of butynediol, acetylene at high pressure is bubbled into aqueous formaldehyde at several positions along a tower in (a). The heat of absorption of nitrogen oxides in water to make nitric acid is removed in two ways in the equipment of (b) and (e). Fats are hydrogenated in a continuous multistage stirred reactor in (c) and under batch conditions in a coil-cooled stirred tank in (d). A thin film reactor is used for the sulfonation of dodecylbenzene with SO_3 in (f). Hydrogen is recirculated with a hollow-shaft agitator to convert nitrocaprolactam in (g). A shell-and-tube design is used for the reaction of ammonia and adipic acid in (h).

Reactions between gases and liquids may involve solids also, either as reactants or as catalysts. Table 17.9 lists a number of examples. The lime/limestone slurry process is the predominant one for removal of SO_2 from power plant flue gases. In this case

it is known that the rate of the reaction is controlled by the rate of mass transfer through the gas film.

Some gases present in waste gases are recovered by scrubbing with absorbent chemicals that form loose compounds; the absorbent then may be recovered for reuse by elevating the temperature or lowering the pressure in a regenerator. Such loose compounds may exert appreciable back pressure in the absorber, which must be taken into account when that equipment is to be sized.

In all cases, a limiting reactor size may be found on the basis of mass transfer coefficients and zero back pressure, but a size determined this way may be too large in some cases to be economically acceptable. Design procedures for mass transfer equipment are in other chapters of this book. Data for the design of gas–liquid reactors or chemical absorbers may be found in books such as those by Astarita, Savage, and Bisio (1983) and Kohl and Nielsonfeld (1979).

FIXED BED REACTORS

The fixed beds of concern here are made up of catalyst particles in the range of 2–5 mm dia. Vessels that contain inert solids with the sole purpose of improving mass transfer between phases and developing plug flow behavior are not in this category. Other uses of inert packings are for purposes of heat transfer, as in pebble heaters and induction heated granular beds—these also are covered elsewhere.

The catalyst in a reactor may be loaded in several ways, as:

1. a single large bed,
2. several horizontal beds,
3. several packed tubes in a single shell,
4. a single bed with imbedded tubes,
5. beds in separate shells.

Some of the possibilities are illustrated in Figures 17.13 and 17.18. Variations from a single large bed are primarily because of a need for control of temperature by appropriate heat transfer, but also for redistribution of the flow or for control of pressure drop. There are few fixed bed units that do not have some provision for heat transfer. Only when the heat of reaction is small is it possible to regulate the inlet temperature so as to make adiabatic operation feasible; butane dehydrogenation, for example, is done this way.

Because of their long industrial histories and worldwide practice, the sulfuric acid and ammonia industries have been particularly inventive with regard to reactors. A few designs for SO_2 oxidation are illustrated in Figure 17.19. Their dominant differences are in modes of temperature control to take advantage of high rates of reaction at high temperature and favorable equilibrium conversion at lower temperatures. Figure 17.19(g) shows the temperature profile achieved in that equipment, and Figure 17.20 presents patterns of temperature control in the production of SO_3, ammonia, and methanol.

A selection of ammonia reactors is illustrated in Figures 17.21 and 17.22. These vessels incorporate particularly elaborate means for temperature regulation. The basic flow pattern is indicated in Figure 17.21(a), and some temperature profiles in Figures 17.21(d) and 17.22 (d) and 17.23 (c) and (d). For modern high capacity performance in single units, reactors with short travel paths through the catalyst and pressures below 200 atm are favored. Comparative performance data over a range of conditions appear in Figure 17.22.

Thermal effects also are major factors in the design of reactors for making synthetic fuels. The units of Figure 17.24 for synthesis of methanol and gasoline are typical fixed bed types.
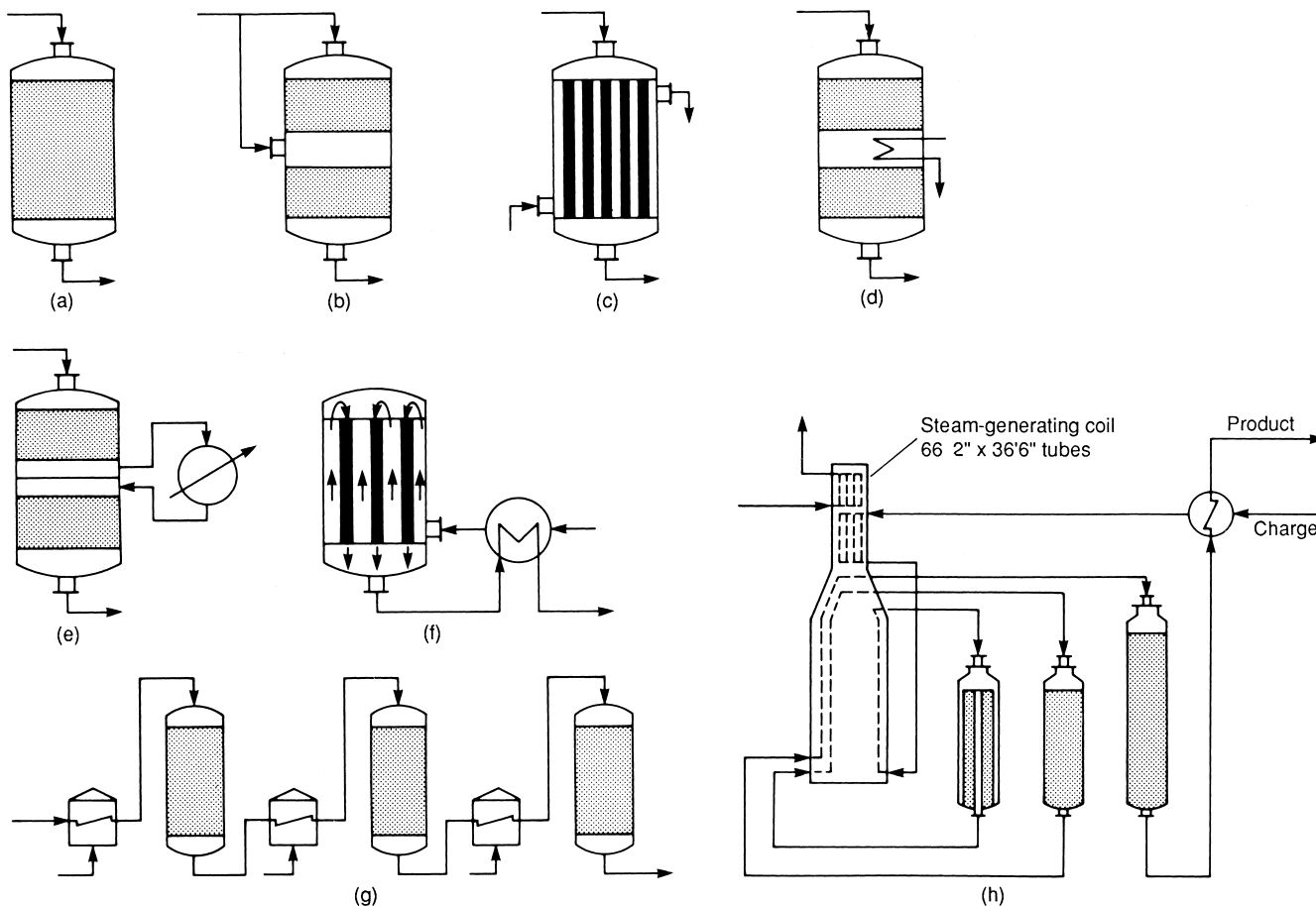
Figure 17.13. Multibed catalytic reactors: (a) adiabatic; (b) interbed coldshot injection; (c) shell and tube; (d) built-in interbed heat exchanger; (e) external interbed exchanger; (f) autothermal shell, outside influent-effluent heat exchanger; (g) multishell adiabatic reactor with interstage fired heaters; (h) platinum-catalyst, fixed bed reformer for 5000 bpsd charge rate; reactors 1 and 2 are 5.5 ft dia by 9.5 ft high and reactor 3 is 6.5 × 12.0 ft.

Catalytic reformers upgrade low octane naphthas into gasoline in the presence of hydrogen to retard deposition of carbon on the catalyst. Temperatures to 500°C and pressures to 35 atm are necessary. Representative reactors are shown in Figure 17.25. Feedstocks to such units usually must be desulfurized; a reactor like that of Figure 17.26 hydrogenates sulfur compounds to hydrogen sulfide, which is readily removed.

Fluid flow through fixed bed reactors usually is downward. Instead of screens for supporting catalyst in the vessel, a support of graduated sizes of inert material is used, as illustrated in Figure 17.27. Screens become blinded by the small particles of catalyst. A similar arrangement is used at the top to prevent disturbance of the catalyst level by the high velocity fluids.

MOVING BEDS

In such vessels granular or lumpy material moves vertically downward as a mass. The solid may be a reactant or a catalyst or a heat carrier. The reactor of Figure 17.28(a) was used for the fixation of nitrogen in air at about 4000°F. The heat-carrying pebbles are heated by direct contact with combustion gases, dropped into a reaction zone supplied with reacting air, and then recycled with elevators to the reheating zone. The treated air must be quenched at the rate of about 25,000°F/sec to retain a concentration of about 1% nitrogen oxides. In another such operation, two units are used in parallel, one being heated while the other is reacting.

The pebble heater, Figure 17.28(b), is used in the same manner; its application to the pyrolysis of oils to make ethylene also did not prove competitive and has been abandoned.

Units like that of Figure 17.28(c) were employed at one time in the catalytic cracking of gas oils. The catalyst is transferred between regenerating and reacting zones with bucket elevators or air lifts. Some data for this equipment are given with the figure.

Two examples in which the solid itself is reactive are the shale oil retorts of Figure 17.29. Crushed oil shale is charged at the top, air and gaseous fuel at the bottom. When the shale moving downward reaches a temperature of 900°F, the kerogen decomposes into oil vapor, gas, and carbonaceous residue. There are many designs of pilot plant retorts, but the only commercial units at present are in the USSR and China.

KILNS AND HEARTH FURNACES

These units are primarily for high temperature services, the kilns up to 2500°F and the furnaces up to 4000°F. Usual construction is steel-lined with ceramics, sometimes up to several feet in thickness.

Vertical kilns are used for materials that do not fuse or soften, as for the burning of limestone or dolomite. Many such operations are batch: the fresh solid is loaded into the kiln, heated with

combustion products until reaction is complete, and then dumped. The lime kiln of Figure 17.30(c), however, operates continuously as a moving bed reactor. These vessels range in size from 8 to 15 ft dia and are 50–80 ft high. For calcination of lime the peak temperatures are about 2200°F, although decomposition proceeds freely at 1850°F. Fuel supply may be coke mixed with the limestone if the finished lime can tolerate the additional ash, or gaseous or liquid

fuels. Space velocity is 0.8–1.5 lb CaO/(hr)(cuft of kiln), or 45–100 lb CaO/(hr)(sqft of kiln cross section), depending on the size and modernity of the kiln, the method of firing, and the lump size which is in the range of 4–10 in.

Rotary kilns have many applications as reactors: between finely divided solids (cement), between liquids and solids (salt cake from salt and sulfuric acid), between gases and solids, and
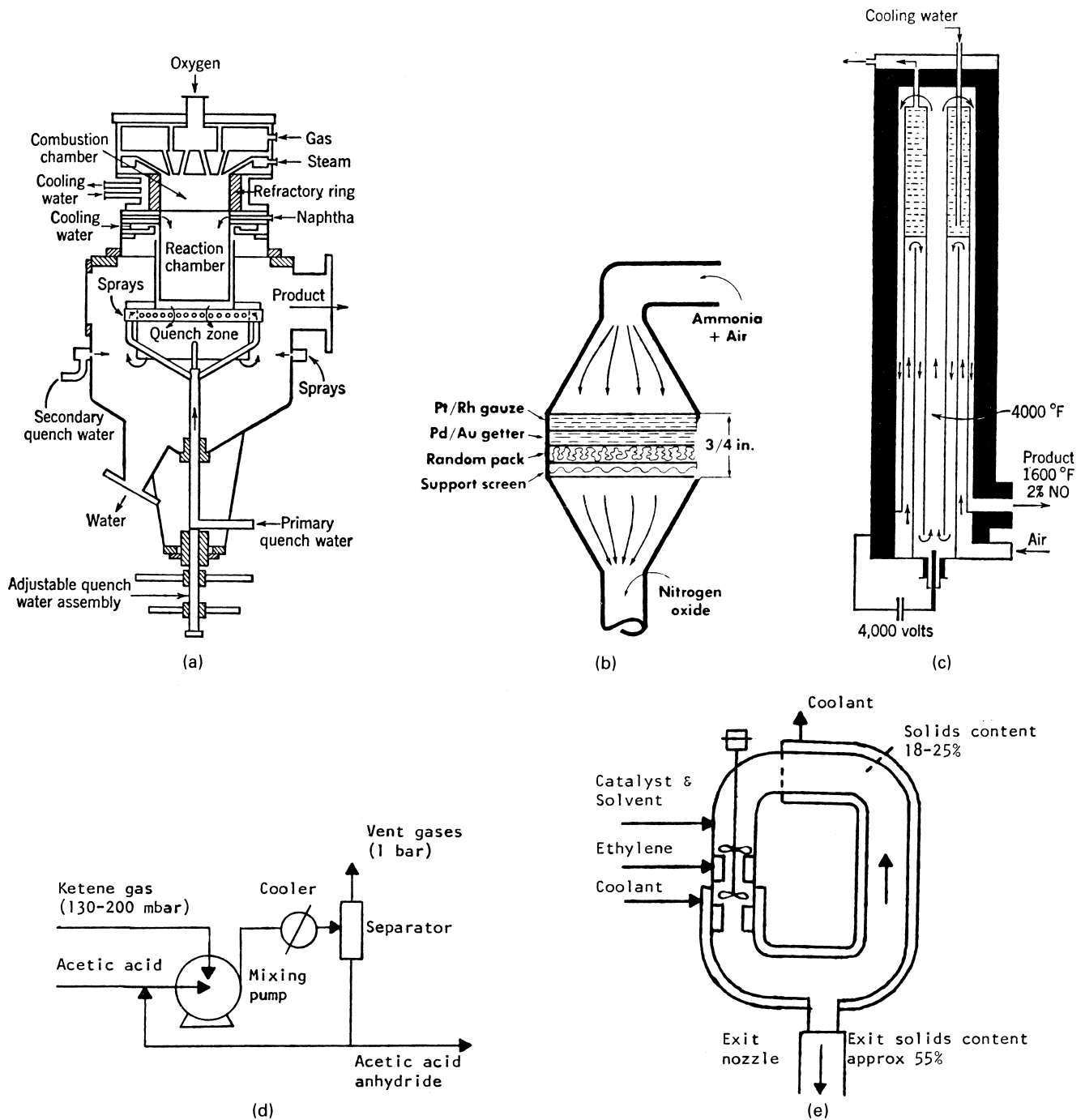
Figure 17.14. Some unusual reactor configurations. (a) Flame reactor for making ethylene and acetylene from liquid hydrocarbons [*Patton et al, (1958)*]. (b) Shallow bed reactor for oxidation of ammonia, using Pt-Rh gauze [*Gillespie and Kenson, (Oct. 1971)*]. (c) Schoenherr furnace for fixation of atmospheric nitrogen. (d) Production of acetic acid anhydride from acetic acid and gaseous ketene in a mixing pump. (e) Phillips reactor for low pressure polymerization of ethylene (closed loop tubular reactor). (f) Polymerization of ethylene at high pressure.

(f)
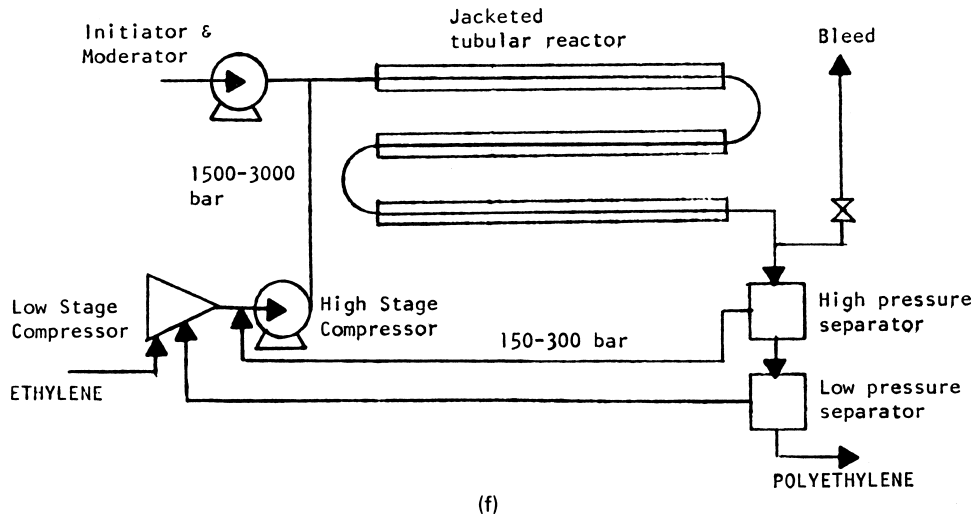
Figures 17.14.—(*continued*)

(a)   **(b)**   **(c)**
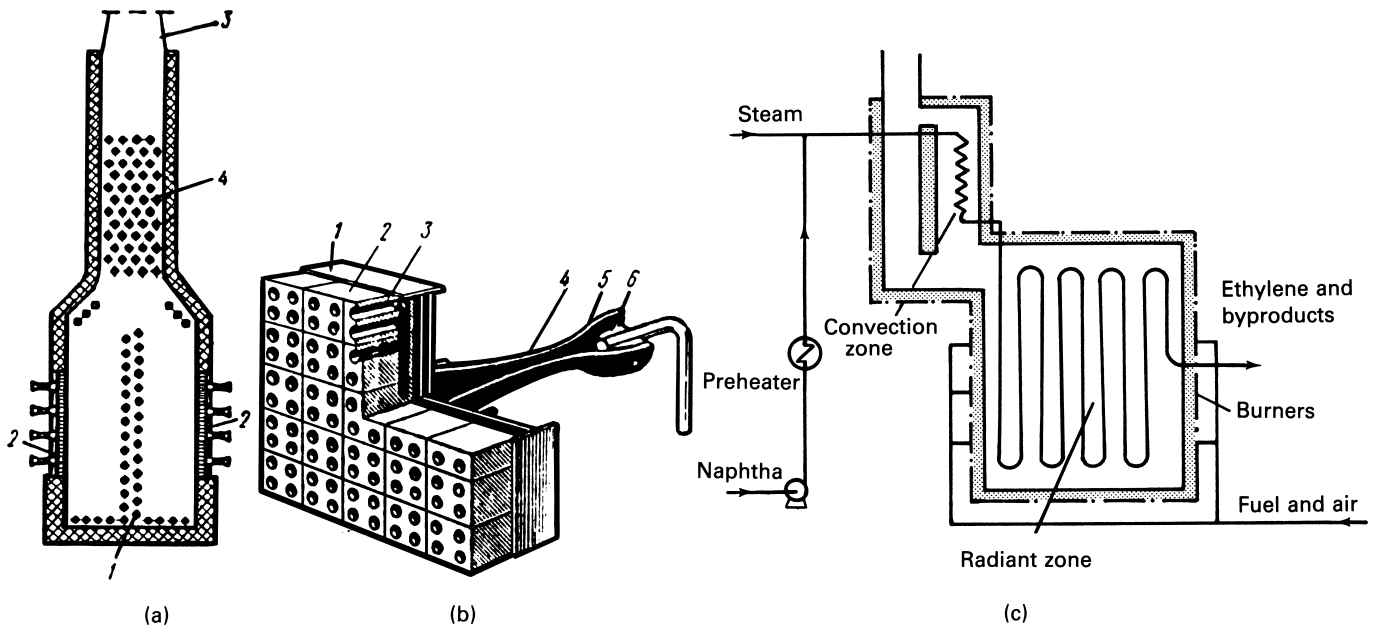
Figure 17.15. A fired heater as a high temperature reactor. (a) Arrangement of tubes and burners: (1) radiant tubes; (2) radiant panel burners; (3) stack; (4) convection chamber tubes (*Sukhanov, 1982*). (b) Radiant (surface-combustion) panel burner: (1) housing; (2) ceramic perforated prism; (3) tube; (4) injector; (5) fuel gas nozzle; (6) air throttle (*Sukhanov, 1982*). (c) Fired tubular cracking furnace for the preparation of ethylene from naphtha.

for the decomposition of solids (SO_3 and lime from $CaSO_4$). The kiln is a long narrow cylinder with a length-to-diameter ratio of 10–20. General purpose kilns are 100–125 ft long, but cement kilns as large as 12 ft dia by 425 ft long are operated. An inclination to the horizontal of 2–5 deg is sufficient to move the solid along. Speed of rotation is 0.25–2 rpm. Lumps up to 1 in. dia or fine powders are usual. Heating mostly is with combustion gases, but some low temperature heating may be accomplished through heated jackets. Figures 17.30(a) and (c) show the temperature profiles of gas and stock in a cement kiln and space velocities of a number of kiln processes.

Multiple-hearth furnaces are suited to continuous handling of solids that exhibit a limited amount of fusion or sintering. In the kind shown on Figure 17.30(e), the scrapers rotate, in other kinds

the plates rotate, and in still others the scrapers oscillate and discharge the plates at each stroke. Material is charged at the top, moves along as rotation proceeds, and drops onto successively lower plates while combustion gases or gaseous reactants flow upward. This equipment is used to roast ores, burn calcium sulfate or bauxite, and reactivate the absorbent clays of the petroleum industry. A reactor with nine trays, 16 ft dia and 35 ft high can roast about 1,250 lb/hr of iron pyrite, at a residence time of about 4–5 hr.

Hearth furnaces consist of one or more flat or concave pans, either moving or stationary, usually equipped with scraper-stirrers. Although such equipment is used mostly for ore treating and metallurgical purposes, a few inorganic chemical processes utilize them, for example, Leblanc soda ash, sodium sulfide from salt cake
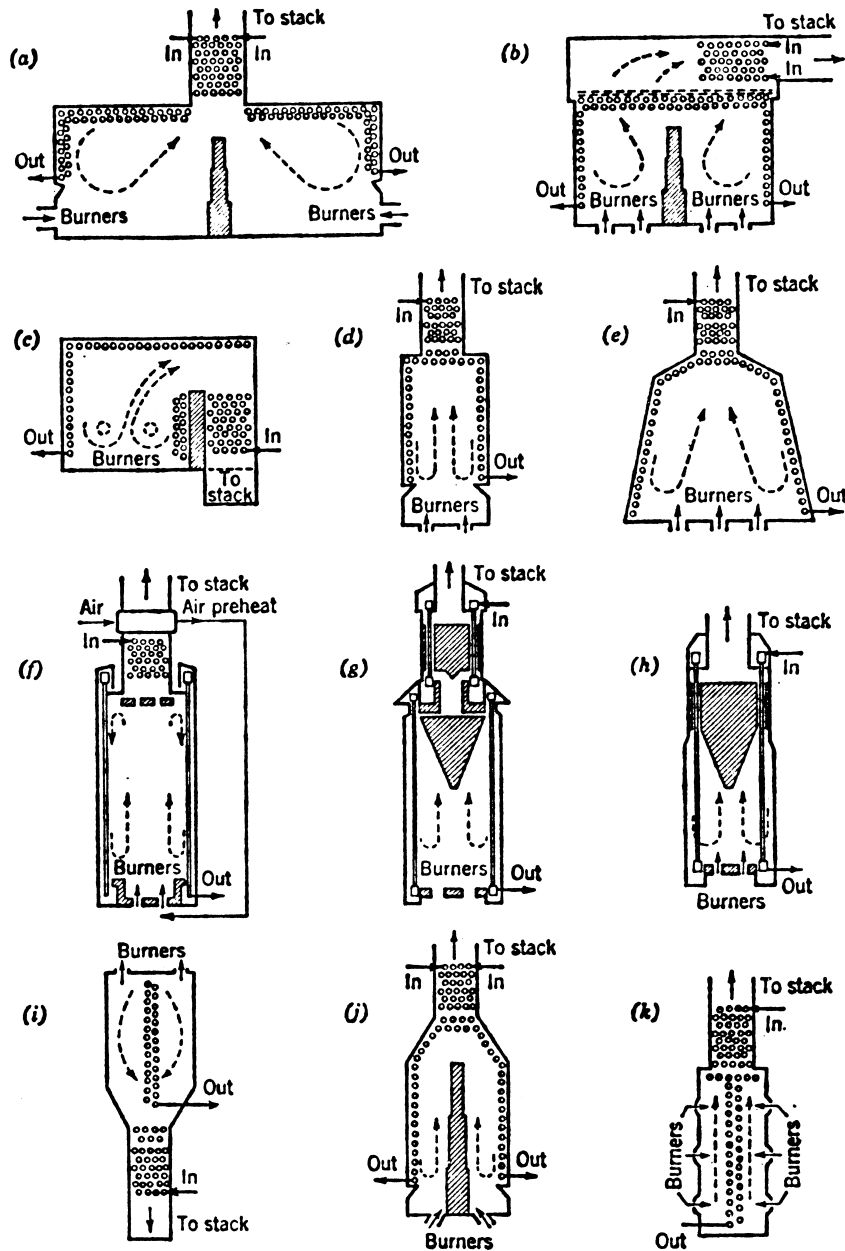
Figure 17.16. Basic types of tubular furnaces [*Nelson, 1958. Courtesy McGraw-Hill, New York*].

and coal, sodium sulfate and hydrogen chloride from salt and sulfuric acid, and sodium silicate from sand and soda ash. A kind of salt-cake furnace is shown in Figure 17.30(d). Salt and sulfuric acid are charged continuously to the center of the pan, and the rotating scrapers gradually work the reacting mass towards the periphery where the sodium sulfate is discharged over the edge. The products leave at about 1000°F. Pans of 11–18 ft dia can handle 6–10 tons/24 hr of salt. For comparison, a Laury horizontal rotating cylindrical kiln, 5 × 22 ft, has a capacity of 1 ton/hr of salt cake.

Very high temperature operations such as those of production of glass or metals utilize single-hearth furnaces, often with heat regenerators for fuel economy. The Siemens-Martin furnace of Figure 17.30 (f) with a hearth 13 ft wide and 40 ft long has a production rate of 10 tons/hr of steel with a residence time of

10 hr. The hearth volume is about 5000 cuft and the total regenerator volume is about 25,000 cuft.

FLUIDIZED BED REACTORS

This term is restricted here to equipment in which finely divided solids in suspension interact with gases. Solids fluidized by liquids are called slurries. Three phase fluidized mixtures occur in some coal liquefaction and petroleum treating processes. In dense phase gas–solid fluidization, a fairly definite bed level is maintained; in dilute phase systems the solid is entrained continuously through the reaction zone and is separated out in a subsequent zone.

The most extensive application of fluidization has been to catalytic cracking of petroleum fractions. Because the catalyst
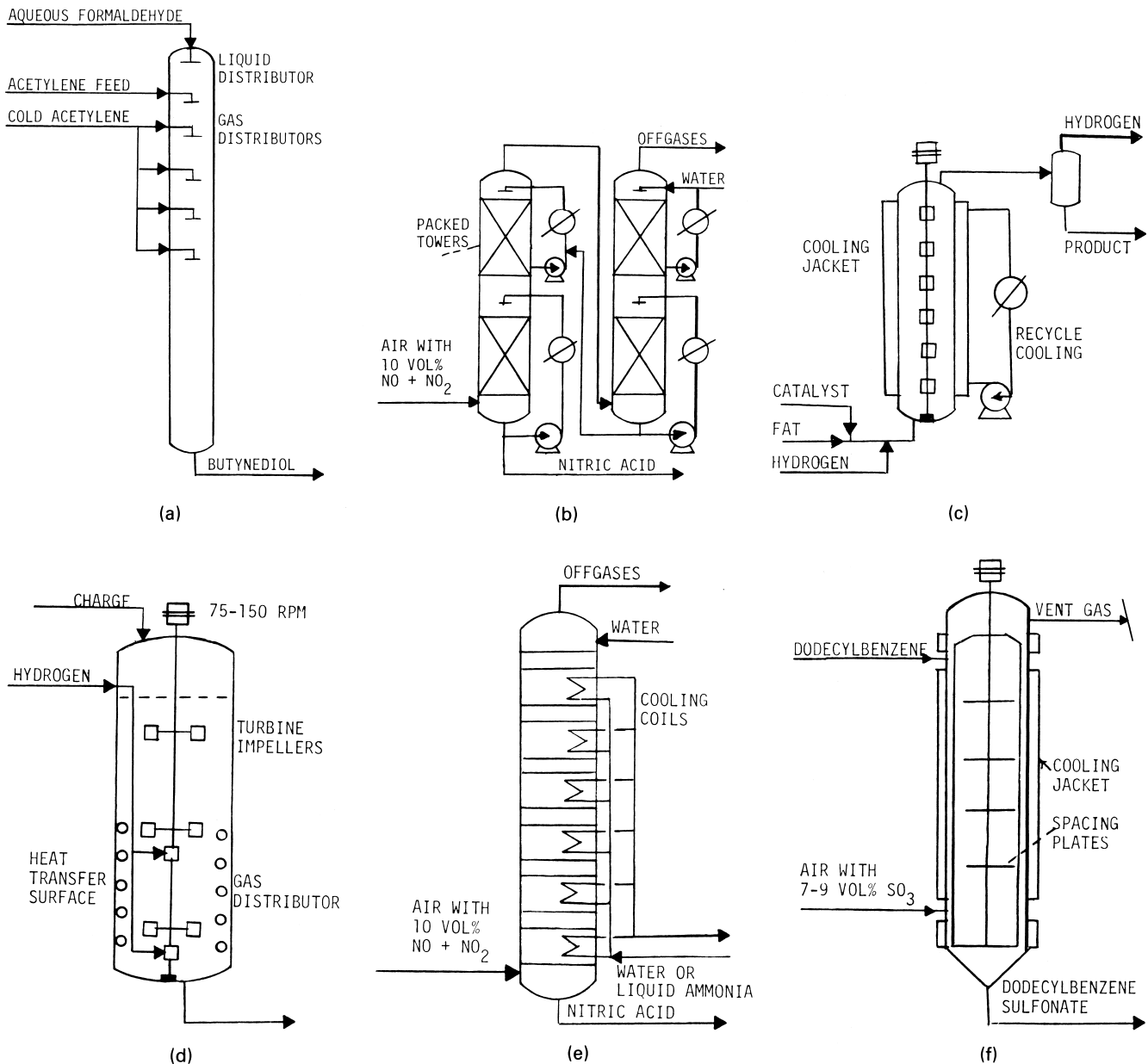
Figure 17.17. Examples of reactors for specific liquid–gas processes. (a) Trickle reactor for synthesis of butinediol 1.5 m dia by 18 m high. (b) Nitrogen oxide absorption in packed columns. (c) Continuous hydrogenation of fats. (d) Stirred tank reactor for batch hydrogenation of fats. (e) Nitrogen oxide absorption in a plate column. (f) A thin film reactor for making dodecylbenzene sulfonate with SO_3. (g) Stirred tank reactor for the hydrogenation of caprolactam. (h) Tubular reactor for making adiponitrile from adipic acid in the presence of phosphoric acid.

degrades in a few minutes, it is circulated continuously between reaction and regeneration zones. Figure 17.31(a) is a version of such equipment. The steam stripper is for the removal of occluded oil before the catalyst is to be burned. The main control instrumentation of a side-by-side system is shown in Figure 3.19 h (Walas 1988).

Fluid catalytic vessels are very large. Dimensions and performance of a medium capacity unit (about 50,000 BPSD, 60 kg/sec) are shown with the figure. Other data for a reactor to handle 15,000 BPSD are a diameter of 25 ft and a height of 50 ft. Catalyst holdup and other data of such a reactor are given by Kraft, Ulrich, and O'Connor (in Othmer, 1956) as follows:

Item	Quantity
Unit charge, nominal	15,000 BPSD
Catalyst inventory, total	250 tons
Catalyst inventory, regenerator bed	100 tons
Superficial velocity, regenerator	2.5 fps
Bed density, regenerator	28.0 lb/cuft
Flue gas plus solids density, cyclone inlet	0.5 lb/cuft
Catalyst circulation rate, unit	24.0 tons/min
Catalyst circulation rate, to cyclones	7.0 tons/min
Catalyst loss rate, design expectation	2.0 tons/day

Figure 17.31(b) is of a unit in which most of the cracking occurs in a transfer line, an operation that became feasible with the

(g)

(h)
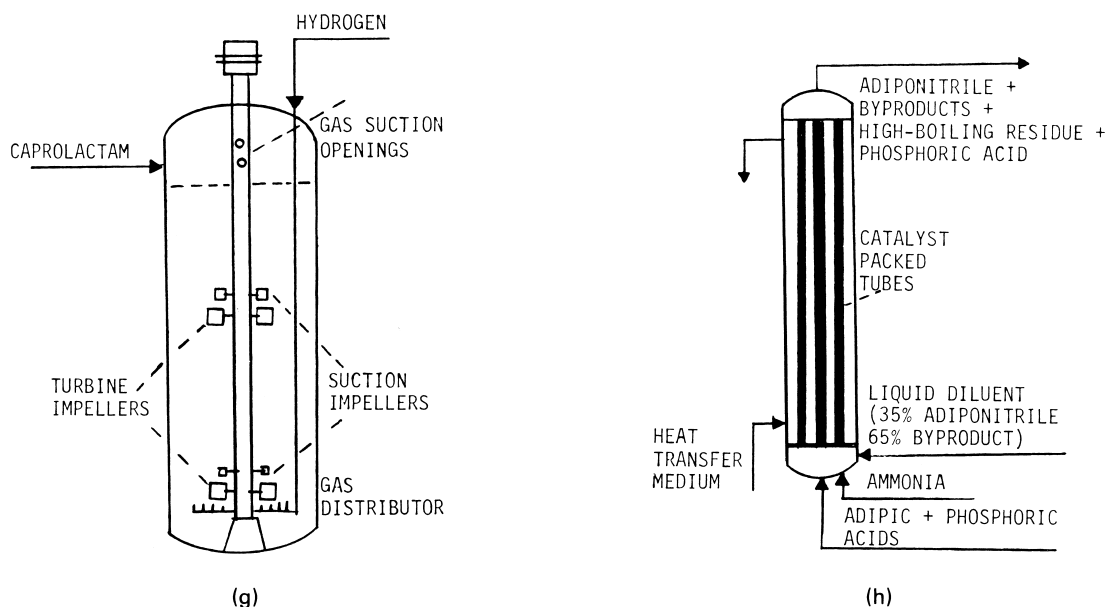
Figure 17.17.—(*continued*)

TABLE 17.9. Examples of Fluidized Bed Processes

A. Catalytic Processes

1. Oil cracking and reforming
2. Recovery of high concentrations of benzene from gas oils
3. Olefin production from crude oil
4. Chlorine by oxidation of HCl
5. Acetylene from methane
6. Preparation of unsaturated aldehydes
7. Reduction of nitro compounds to amines
8. Oxidation of SO_2 to SO_3
9. Phthalic anhydride from naphthalene or *o*-xylene
10. Maleic acid anhydride from benzene
11. Formaldehyde from methanol
12. Chlorination of methane and ethylene
13. Fischer–Tropsch synthesis of gasoline
14. Hydrogenation of ethylene
15. Oxidation of ammonia
16. Ethylene oxide from ethylene
17. Butadiene from ethanol
18. Dehydrogenation of isopropanol
19. Isomerization of *n*-butane
20. Post-chlorination of PVC
21. Decomposition of ozone
22. Preparation of chlorinated hydrocarbons
23. Preparation of melamine resins
24. Isoprene synthesis
25. Reduction of vinyl acetate
26. Preparation of acrylonitrile

B. Noncatalytic Processes

1. Gasification of coal
2. Fluid bed coking
3. Pyrolytic cracking of methane
4. Preparation of activated carbon
5. Ethylene by cracking of petroleum fractions
6. Combustion of coal
7. Burning of oil shale

8. Combustion of municipal and industrial wastes
9. Burning of black liquor (paper industry)
10. Roasting of sulfides of iron, copper, and zinc
11. Combustion of sulfur in a sand bed
12. Decomposition of waste sulfuric acid and sulfates
13. Cracking of chlorides such as $FeCl_2$, $NiCl_3$, and $AlCl_3$
14. Volatilization of rhenium
15. Burning of limestone and dolomite
16. Cement burning
17. Reduction of iron ores and metallic oxides
18. Chlorination of ores of aluminum, titanium, nickel, cobalt, and tin
19. Chlorination of roasted pyrites and iron ores
20. Chlorination of lime
21. Calcination of aluminum hydroxide to alumina
22. Preparation of aluminum sulfate from bauxite
23. Preparation of fluorides aluminum trifluoride, uranium tetra- and hexafluorides
24. Preparation of pure tungsten from the fluoride
25. Calcination of phosphates
26. Preparation of phosphorus oxychloride
27. Preparation of carbon disulfide
28. Preparation of hydrazine
29. Preparation of nitric acid
30. Preparation of nitrates of ammonia and sodium
31. Preparation of sodium carbonate
32. Preparation of hydrogen cyanide
33. Hydrochlorination of uranium fuel elements
34. Preparation of uranium trioxide from the nitrate
35. Recovery of uranium from nuclear fuels
36. Removal of fluorine from offgases of aluminum electrolysis
37. Heating of heat transfer media such as sand
38. Cooling of granular masses such as fertilizers
39. Drying of finely divided materials such as flotation ores and raw phosphates
40. Coating of fuel elements by pyrolytic cracking of chlormethylsilanes
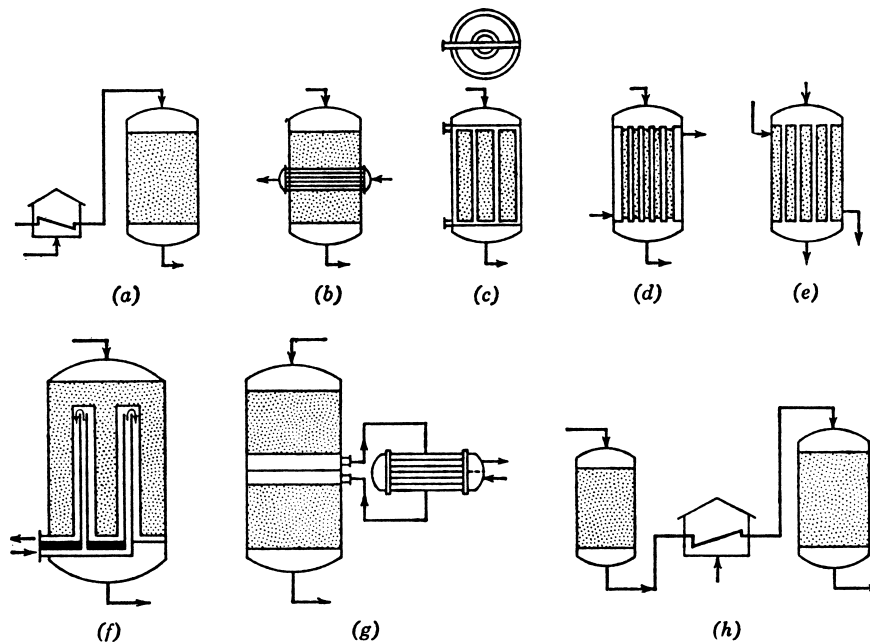
Figure 17.18. Heat transfer in fixed-bed reactors: (a) adequate preheat; (b) internal heat exchanger; (c) annular cooling spaces; (d) packed tubes; (e) packed shell; (f) tube and thimble; (g) external heat exchanger; (h) multiple shell, with external heat transfer (*Walas, 1959*).

development of highly active zeolite catalysts. The reaction is completed in the upper zone, but the main function of that zone is to separate product and spent catalyst. In contrast to the dense-phase bed of a large reactor, in which mixing can approach ideality, the dilute phase transfer line is more nearly in plug flow. Accordingly, a much smaller reaction zone suffices; moreover, superior product distribution and greater gasoline yield result. Similar reactor configurations are shown in Figures 17.31(c) and (d) of other petroleum processes.

The mechanism of interaction between catalyst and gas in a large fluidized bed is complex and is not well correlated with design factors. In the bed itself, large bubbles of a foot or more in diameter form and are irrigated with a rain of catalyst particles. This process occurs in parallel with a well-mixed fluidized bed. Above the bed level and before the entrained catalyst is recovered in cyclones, the reaction continues in dilute phase plug flow. Since even the physical behavior of fluidized beds is not well understood, the design of such

reactors is done largely on the basis of fairly large pilot plants and by analogy with earlier experience in this area.

The earliest fluidized process was the noncatalytic Winkler process for gasification of coal in 1921. Other noncatalytic processes, and some catalytic ones, are listed in Table 17.9. A few noncatalytic reactors are shown in Figure 17.32. Cracking of naphthas to ethylene with circulating hot sand as the heat carrier is shown in part (a); at the operating temperature of 720–850°C, much carbon deposits on the sand but is not at all harmful as it would be on the surfaces of tubular cracking units. In the dilute phase process of calcination of alumina, part (b), the circulating solid is the product itself; combustion products from sprays of oil and auxiliary air furnish the motive power. The calcining unit for lime of part (c) is an example of a successful multistage reactor; residence time in the calcining zone is 2 hr, in the cooling zone 0.5 hr, and in each of the preheating zones 1 hr. Multibed units for petroleum operations have not been feasible, but some units have
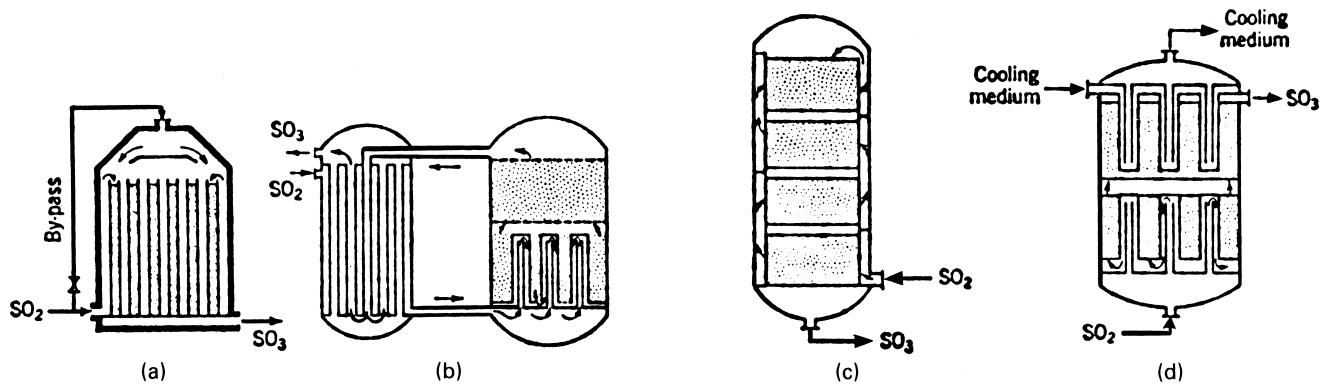
Figure 17.19. Reactors for the oxidation of sulfur dioxide: (a) Feed–product heat exchange. (b) External heat exchanger and internal tube and thimble. (c) Multibed reactor, cooling with charge gas in a spiral jacket. (d) Tube and thimble for feed against product and for heat transfer medium. (e) BASF-Knietsch, with autothermal packed tubes and external exchanger. (f) Sper reactor with internal heat transfer surface. (g) Zieren-Chemiebau reactor assembly and the temperature profile (*Winnacker-Weingartner, 1950–1954*).

(e)

(f)

(g)
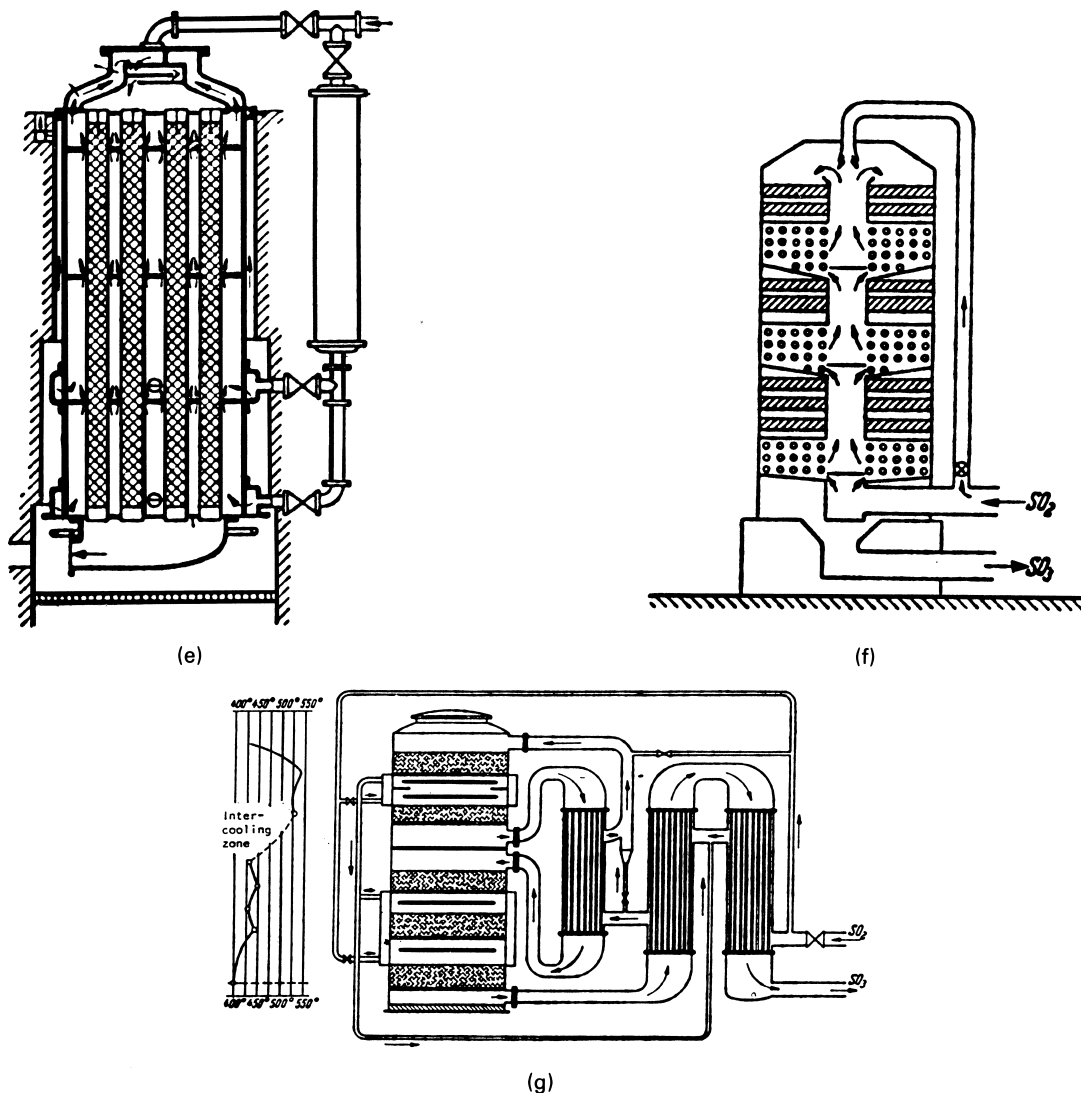
Figure 17.19.—(*continued*)

been built with a degree of baffling that simulates staging in a rough fashion. The catalyst of the phthalic anhydride reactor of part (d) does not need to be regenerated so the fluidized bed remains in place; since the reaction is highly sensitive to temperature, the oxidation is kept under control with much imbedded heat transfer surface and by cold injections. A typical coal gasifier appears in part (e); a thirtyfold circulation of spent char is employed along with the fresh feed to counteract the agglomeration tendency of many coals. The H-Coal reactor of part (f) operates with a three-phase mixture. The catalyst does not circulate but bubbles in place. Activity is maintained by bleeding off and replenishing 1–2% of the catalyst holdup per day. Operating conditions are 450°C and 3000 psig. Both coal and heavy petroleum residua are handled successfully. The unit is known as an "ebullating bed."

The literature of fluidization phenomena and technology is extensive. A good although dated bibliography is in *Ullmann's Encyclopedia* (1973, Vol. 3, pp. 458–460). The book by Cheremisinoff and Cheremisinoff (1984) has more than 500 abstracts of articles on fluidization hydrodynamics, mixing and heat transfer, but

little on reactor technology. Other literature on fluidization is cited in the References of Chapter 6.

17.7. HEAT TRANSFER IN REACTORS

Maintenance of proper temperature is a major aspect of reactor operation. The illustrations of several reactors in this chapter depict a number of provisions for heat transfer. The magnitude of required heat transfer is determined by heat and material balances as described in Section 17.3. The data needed are thermal conductivities and coefficients of heat transfer. Some of the factors influencing these quantities are associated in the usual groups for heat transfer; namely, the Nusselt, Stanton, Prandtl, and Reynolds dimensionless groups. Other characteristics of particular kinds of reactors also are brought into correlations. A selection of practical results from the abundant literature will be assembled here. Some modes of heat transfer to stirred and fixed bed reactors are represented in Figures 17.33 and 17.18, and temperature profiles in several industrial reactors appear in Figures 17.21, 17.23, 17.30, 17.34, and 17.35.

(a)

(b)

(c)
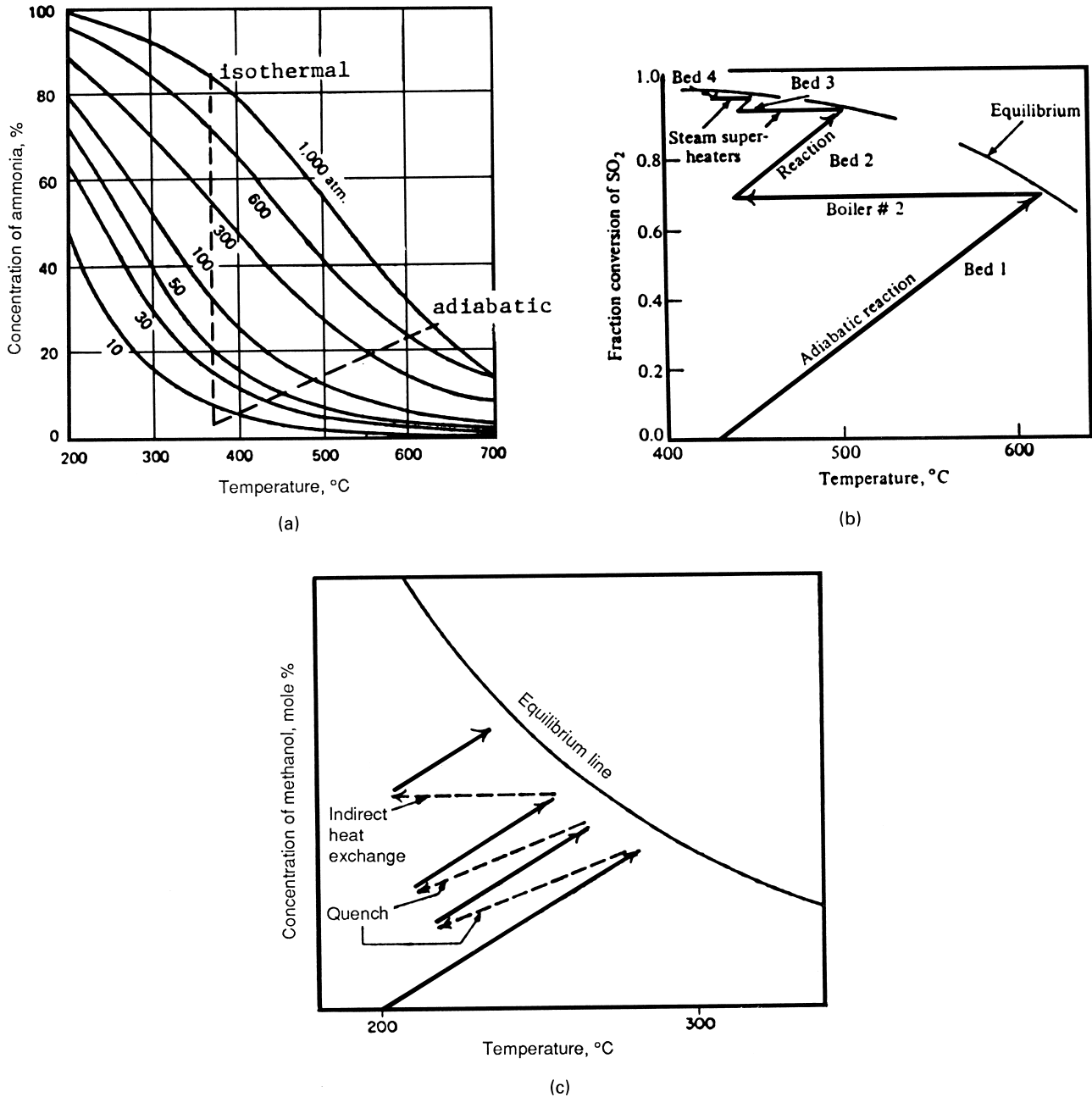
Figure 17.20. Control of temperature in multibed reactors so as to utilize the high rates of reaction at high temperatures and the more favorable equilibrium conversion at lower temperatures. (a) Adiabatic and isothermal reaction lines on the equilibrium diagram for ammonia synthesis. (b) Oxidation of SO_2 in a four-bed reactor at essentially atmospheric pressure. (c) Methanol synthesis in a four bed reactor by the ICI process at 50 atm; not to scale; 35% methanol at 250°C, 8.2% at 300°C, equilibrium concentrations.

STIRRED TANKS

Values of overall coefficients of heat transfer are collected in Tables 17.10–17.12. Two sets of formulas for tank-side film coefficients are in Tables 17.13 and 17.14. They relate the Nusselt number to the Reynolds and Prandtl numbers and several other factors. In the equation for jacketed tanks, for example,

$$h_0(\text{jacket})\frac{T}{k} = 0.85\left(\frac{D^2 N\rho}{\mu}\right)^{0.66}\left(\frac{C_p\mu}{k}\right)^{0.33}\left(\frac{\mu}{\mu_s}\right)^{0.14}$$
$$\times \left(\frac{Z}{T}\right)^{-0.56}\left(\frac{D}{T}\right)^{0.13}$$

$$(17.35)$$
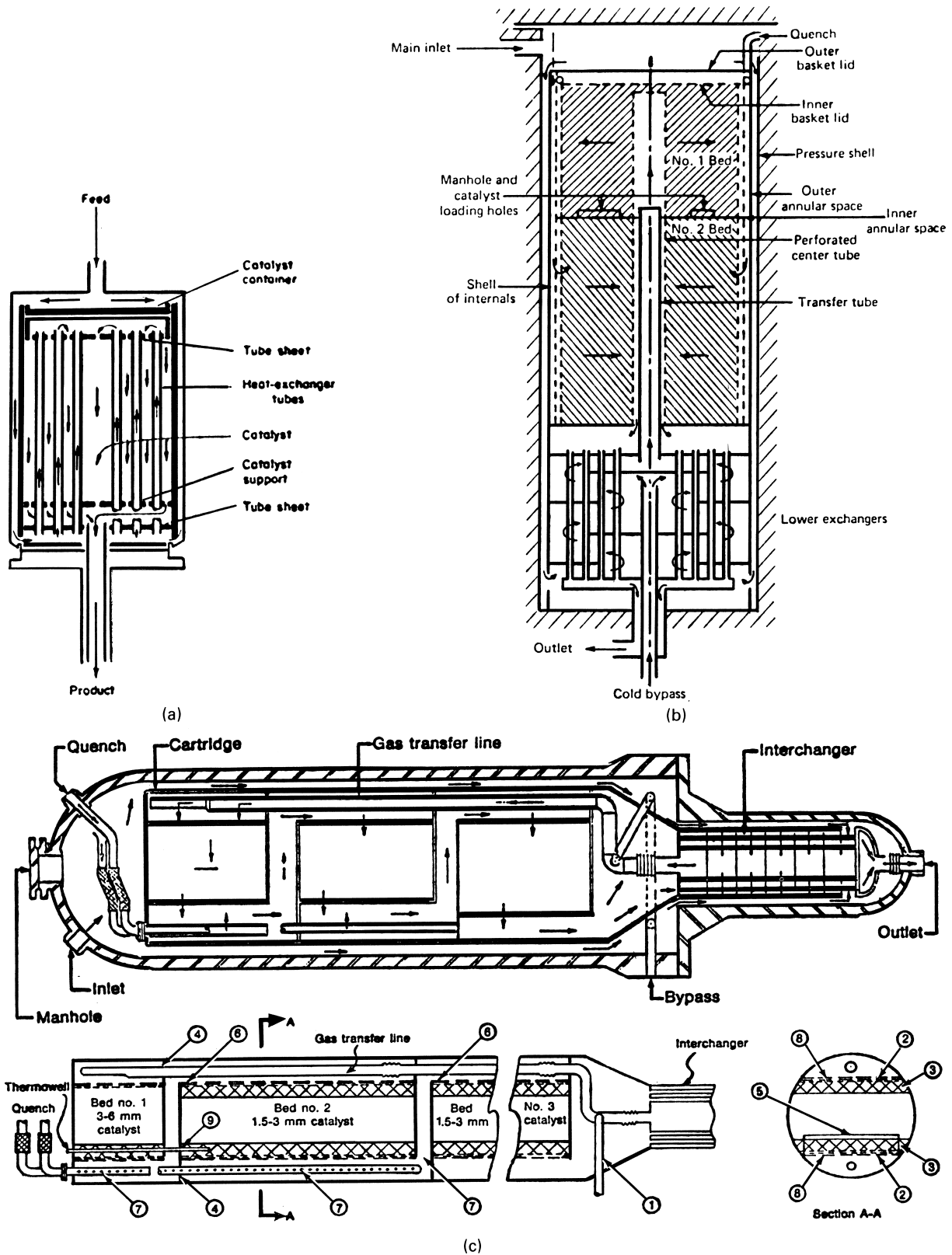
Figure 17.21. Some designs of ammonia synthesis converters. (a) Principle of the autothermal ammonia synthesis reactor. Flow is downwards along the wall to keep it cool, up through tubes imbedded in the catalyst, down through the catalyst, through the effluent-influent exchanger and out. (b) Radial flow converter with capacities to 1800 tons/day (*Haldor Topsoe Co., Hellerup, Denmark*). (c) Horizontal three-bed converter and detail of the catalyst cartridge. Without the exchanger the dimensions are 8 × 85 ft, pressure 170 atm, capacity to 2000 tons/day (*Pullman Kellogg*). (d) Vessel sketch, typical temperature profile and typical data of the ICI quench-type converter. The process gas follows a path like that of part (a) of this figure. Quench is supplied at two points (*Imperial Chemical Industries*).

Figure 17.21.—(*continued*)

Typical Data for ICI Quench Converters of Various Sizes

Capacity (short tpd)	660	990	1100	1650
Pressure (psig)	4700	3200	4250	3220
Inlet gas composition (%)				
Ammonia	4.0	3.0	3.2	1.4
Inerts	15.0	12.0	15.0	12.0
Inlet gas flow (MM scfh)	10.6	18.0	18.5	24.5
Catalyst volume (ft^3)	740	1170	1100	2400
Pressure vessel				
Internal diameter (in.)	80	96	95	109
Length (in.)	437	493	472	700
Weight (short ton)				
Cartridge shell	14.2	34.2	22.8	56.4
Heat exchanger	15.5	30.0	25.4	23.8
Pressure vessel (less cover)	130	128	182	240

Typical Data for an ICI Quench Converter of 1300 Short Tons/Day Capacity

Pressure (psig)	2200	3200	4000	4700
Inlet gas flow (MM scfh)[a]	25.8	21.2	19.8	19.0
Catalyst volume (ft^3)	2600	1730	1320	1030
Pressure vessel				
Internal diameter (in.)	120	102	96	89
Length (in.)	663	606	528	488
Weight (short ton)				
Cartridge shell	68.5	40.8	29.2	23.6
Heat exchanger	37.1	25.4	20.7	17.9
Pressure vessel (less cover)	186	184	187	189
Converter pressure drop (psi)	140	104	87	91

[a] Composition: 2% NH$_3$, 12% inerts (CH$_4$ + A), 21.5% N$_2$, 64.5% H$_2$ by vol.

(d)

the rpm, the tank and impeller diameters, and the liquid depth as well as a viscosity ratio are involved. Table 17.14 identifies the kind of impeller that was used in the investigation, but in general test results have shown that approximately the same heat transfer coefficient is obtained with flat-blade turbines, pitched-blade turbines, or propellers. Axial flow turbines produce the most circulation for a given power input and heat transfer is related directly to the flow, so that this kind of impeller usually is favored. From Eq. (17.35), the coefficient is proportional to the 0.66 power of the rpm, $N^{0.66}$, and from Chapter 10, the power input at high Reynolds numbers varies as the cube root of N. Accordingly it appears that the coefficient is proportional to the 0.22 exponent of the power input to the stirred tank,

$$h \propto P^{0.22}$$

and consequently that the coefficient of heat transfer is little affected by large increases of power input.

Since most of the literature in this area is relatively old, practitioners apparently believe that what has been found out is adequate or is kept confidential. Table 17.14 has the recommended formulas.

PACKED BED THERMAL CONDUCTIVITY

The presence of particles makes the effective conductivity of a gas greater than the molecular conductivity by a factor of 10 or more. The nature of the solid has little effect at Reynolds numbers above 100 or so; although the effect is noticeable at the lower values of Re, it has not been completely studied. Besides the Reynolds, Prandtl,

and Peclet numbers, the effective diffusivity depends on the molecular conductivity, porosity, particle size, and flow conditions. Plots in terms of Re, Pr, and Pe (without showing actual data points) are made by Beek (1962, Fig. 3), but the simpler plots obtained by a number of investigators in terms of the Reynolds number alone appear on Figure 17.36(a). As Table 17.15 shows, most of the data were obtained with air whose Pr = 0.72 and k_f = 0.026 kcal/(m)(hr)(°C) at about 100°C. Accordingly, the data could be generalized to present the ratio of effective and molecular conductivities as

$$k_e/k_f = 38.5 k_e. \tag{17.36}$$

Equations of the highest and lowest lines on this figure then may be written

$$k_e/k_f = 8.08 + 0.1027 \text{Re} \quad \text{(Kwong and Smith),} \tag{17.37}$$

$$k_e/k_f = 13.85 + 0.0623 \text{Re} \quad \text{(Quinton and Storrow).} \tag{17.38}$$

At higher temperatures, above 300°C or so, radiation must contribute to the effective conductivity, but there are so many other uncertainties that the radiation effect has not been studied at length.

HEAT TRANSFER AT WALLS, TO PARTICLES, AND OVERALL

The correlations cited in Tables 17.16 and 17.18 are of the Nusselt number in terms of the Reynolds and Prandtl numbers, or of the Reynolds alone. They are applicable only above specified Reynolds
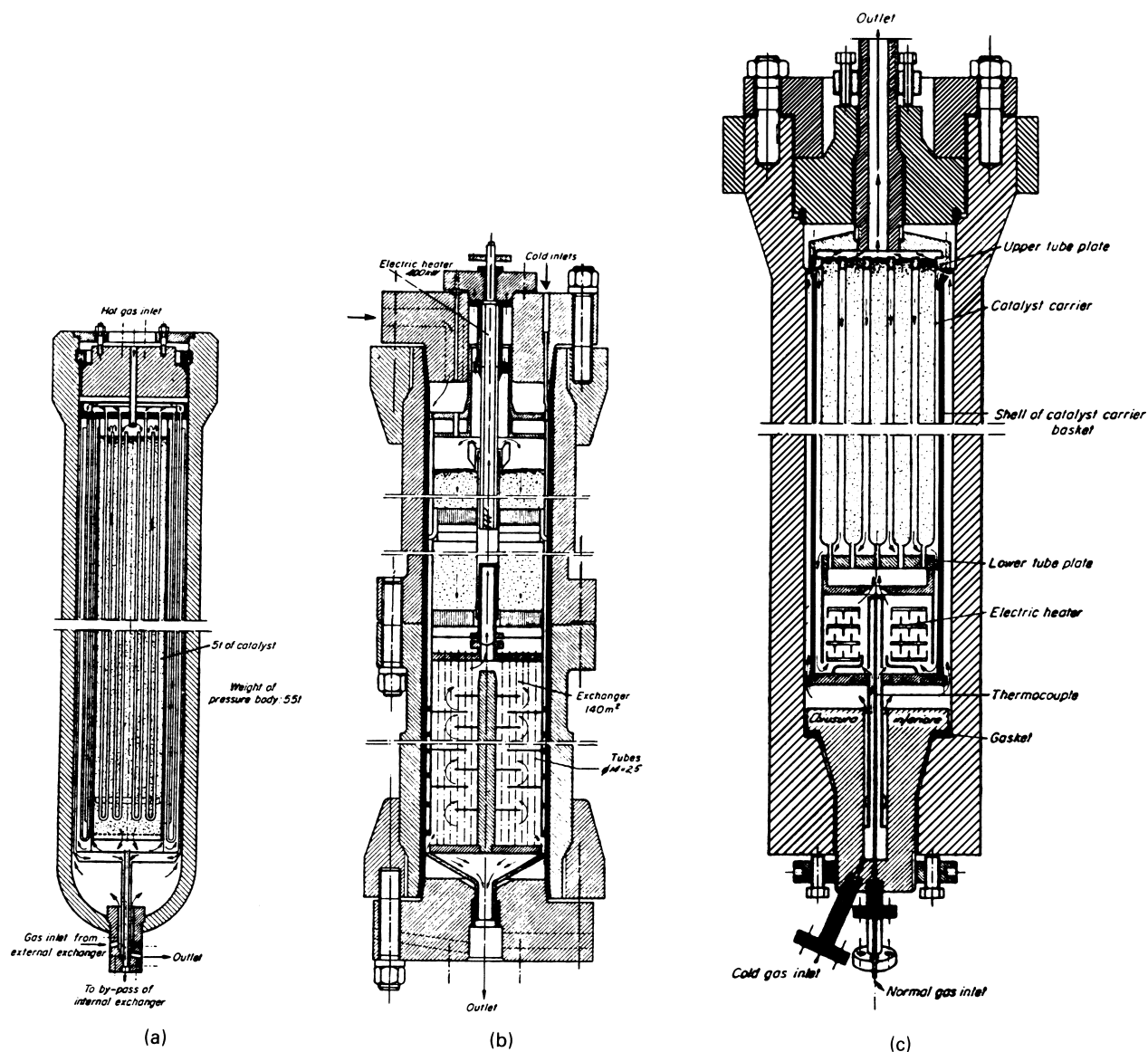
Figure 17.22. Representative ammonia converters operating at various pressures and effluent concentrations (*Vancini, 1971*). (a) Original Uhde design operating at 125 atm; typical dimensions, 1.4 × 7 m. (b) Haber–Bosch–Mittasch converter operating at 300 atm; typical dimensions, 1.1 × 12.8 m. (c) Claude converter operating at 1000 atm; typical dimensions 1.2 × 7 m. (d) Fauser–Montecatini (old style) converter operating at 300 atm with external heat exchange, showing axial profiles of temperature and ammonia concentration.

Comparison of Performance

Process	Pressure (bar)	Effluent ammonia (%)	TPD/m^3	Catalyst life (yr)
Uhde	125	7–8	10	> 2
Haber-Bosch	300	13–15	25	2
Claude	1000	22–24	120	0.25
Fauser	300	12–17	25	2
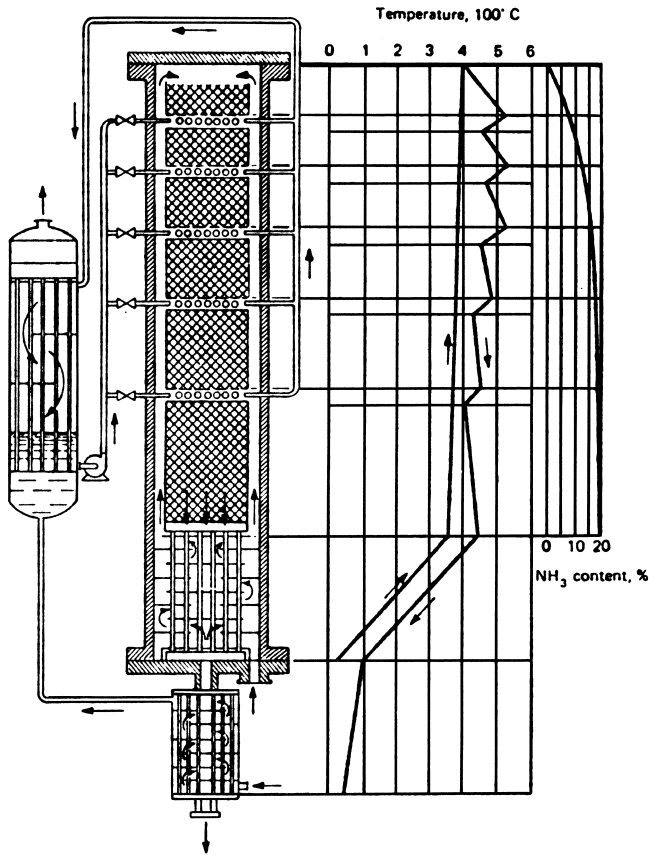
(d)

Figure 17.22.—(*continued*)

(b)

(a)
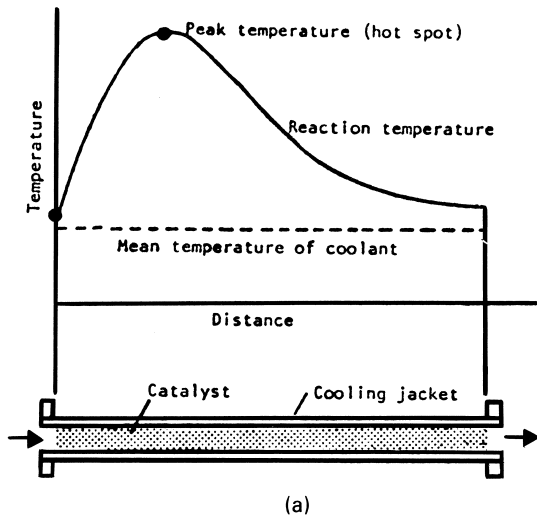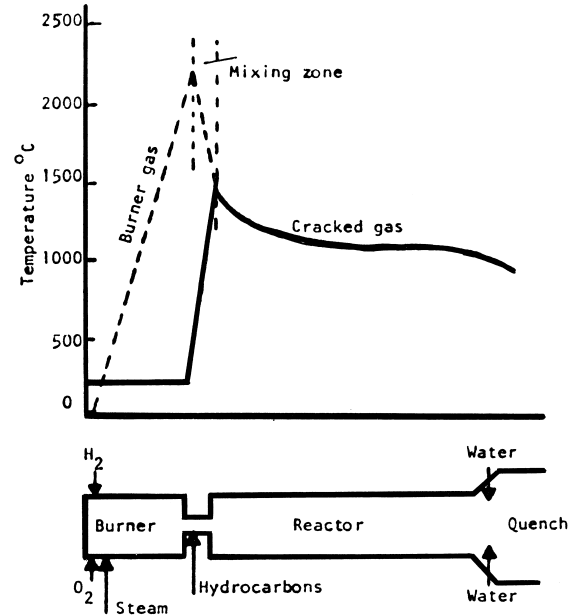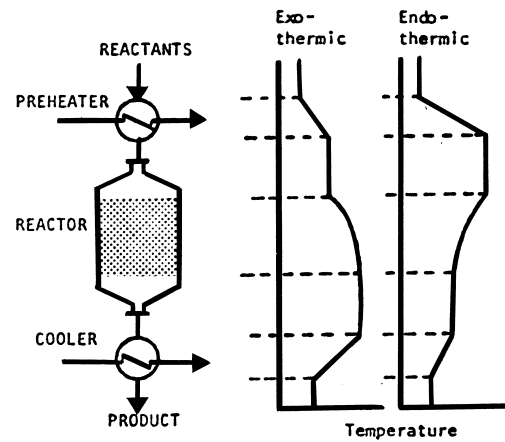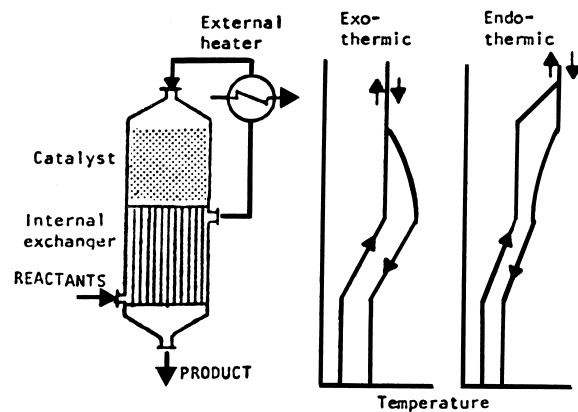
Figure 17.23. Representative temperature profiles in reaction systems (see also Figs. 17.20, 17.21(d), 17.22(d), 17.30(c), 17.34, and 17.35). (a) A jacketed tubular reactor. (b) Burner and reactor for high temperature pyrolysis of hydrocarbons (*Ullmann, 1973, Vol. 3, p. 355*); (c) A catalytic reactor system in which the feed is preheated to starting temperature and product is properly adjusted; exo- and endothermic profiles. (d) Reactor with built-in heat exchange between feed and product and with external temperature adjustment; exo- and endothermic profiles.

(c)

(d)

(a)

(b)

(c)

(d)
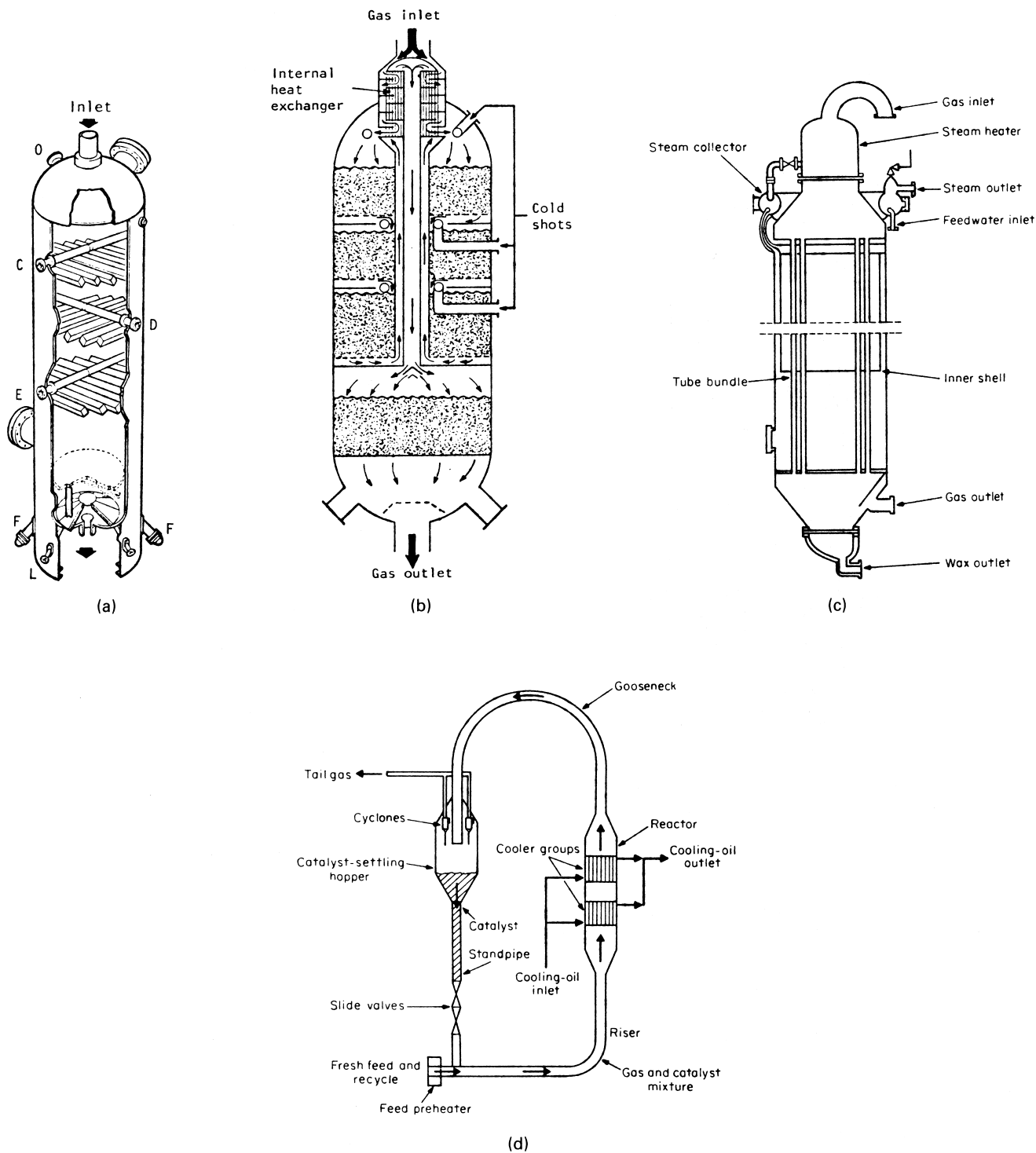
Figure 17.24. Types of reactors for synthetic fuels (*Meyers, 1984*). (a) ICI methanol reactor, showing internal distributors. C, D and E are cold shot nozzles, F = catalyst dropout, L = thermocouple, and O = catalyst input. (b) ICI methanol reactor with internal heat exchange and cold shots. (c) Fixed bed reactor for gasoline from coal synthesis gas; dimensions 10×42 ft, 2000 2-in. dia tubes packed with promoted iron catalyst, production rate 5 tons/day per reactor. (d) Synthol fluidized bed continuous reactor system for gasoline from coal synthesis gas.
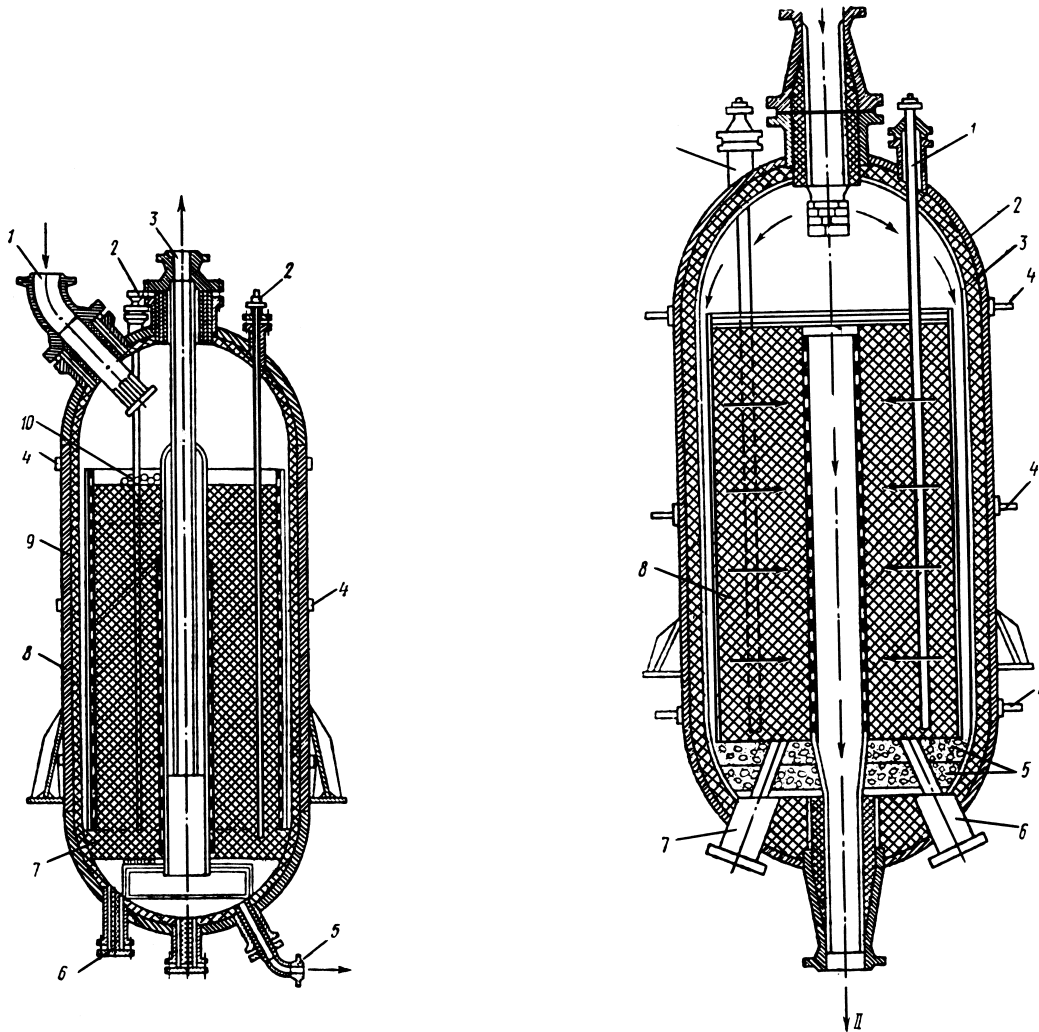
Figure 17.25. Catalytic reforming reactors of axial and radial flow types. The latter is favored because of lower pressure drop (*Sukhanov, 1982*). (a) Axial flow pattern. (b) Radial flow pattern.

numbers, about 40 in most cases; clearly they do not predict correctly the coefficient of natural convection, at Re = 0.

Wall coefficients are obtainable from particle–fluid data by a rule of Beek (1962),

$$h_w = 0.8h_p. \tag{17.39}$$

This is how Eq. (8) of Table 17.18 is deduced; Eq. (9) represents the same data but is simply a curve fit of Figure 17.36(c) at an average value Pr = 0.65.

Data of heat transfer between particle and fluid usually are not measured directly because of the experimental difficulties, but are deduced from measurements of mass transfer coefficients assuming the Colburn analogy to apply,

$$(\text{Sherwood})(\text{Schmidt})^{2/3} = (\text{Nusselt})(\text{Prandtl})^{2/3}$$
$$= \text{function of Reynolds.} \tag{17.40}$$

Thus, in Figure 17.36(c), if the Nusselt number is replaced by the Sherwood and the Prandtl by the Schmidt, the relation will be equally valid for mass transfer.

The ratio, L/D, of length to diameter of a packed tube or vessel has been found to affect the coefficient of heat transfer. This is a dispersion phenomenon in which the Peclet number, uL/D_{disp}, is involved, where D_{disp} is the dispersion coefficient. Some 5000 data points were examined by Schlünder (1978) from this point of view; although the effect of L/D is quite pronounced, no clear pattern was deduced. Industrial reactors have L/D above 50 or so; Eqs. (6) and (7) of Table 17.18 are asymptotic values of the heat transfer coefficient for such situations. They are plotted in Figure 17.36(b).

Most investigators have been content with correlations of the Nusselt with the Reynolds and Prandtl numbers, or with the Reynolds number alone. The range of numerical values of the Prandtl number of gases is small, and most of the investigations have been conducted with air whose Pr = 0.72 at 100°C. The effect of Pr is
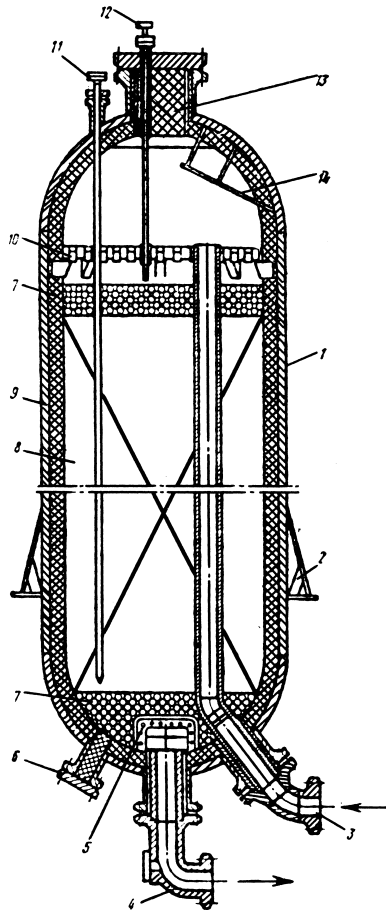
Figure 17.26. Reactor for hydrofining diesel oils, with ceramic lining (*Sukhanov, 1982*).

Figure 17.27. Catalyst packed adiabatic reactor, showing application of ceramic balls of graduated sizes for support at the bottom and hold-down at the top (*Rase, 1977*).

small on Figure 17.36(c), and is ignored on Figure 17.36(b) and in some of the equations of Tables 17.17 and 17.18.

The equations of Table 17.18 are the ones recommended for coefficients of heat transfer between wall and fluid in packed vessels.

For design of equipment like those of Figure 17.28, coefficients of heat transfer between particle and fluid should be known. Direct measurements with this objective have been made with metallic packings heated by electrical induction or current. Some correlations are given in Table 17.17. Glaser and Thodos (1958) correlated such data with the equation

$$(h_p/C_p G)(C_p \mu/k)^{2/3} = \frac{0.535}{(\mathrm{Re}')^{0.3} - 1.6}, \ 100 < \mathrm{Re}' < 9200,$$

$$(17.41)$$

where

$$\mathrm{Re}' = \phi \sqrt{a_p} G/\mu(1 - \varepsilon),$$

a_p = surface of a single particle,

ϕ = sphericity of the particle.

The equations of Table 17.18 also could be used by taking $h_p = 1.25 h_w$. In moving bed catalyst regenerators, heat fluxes of

the order of 25,000 Btu/(hr)(cuft) have been estimated to occur between fluid and particle. Fluid and particle temperatures consequently differ very little.

FLUIDIZED BEDS

A distinctive feature of fluidized beds is a high rate of heat transfer between the fluid and immersed surfaces. Some numerical values are shown on Figure 17.37. For comparison, air in turbulent flow in pipelines has a coefficient of about 25 Btu/(hr)(sqft)(°F). (a) is of calculations from several correlations of data for the conditions identified in Table 17.19; (b) shows the effect of diameters of quartz particles; and (c) pertains to 0.38 mm particles of several substances.

Temperature in a fluidized bed is uniform unless particle circulation is impeded. Gas to particle heat flow is so rapid that it is a minor consideration. Heat transfer at points of contact of particles is negligible and radiative transfer also is small below 600°C. The mechanisms of heat transfer and thermal conductivity have been widely studied; the results and literature are reviewed, for example, by Zabrodsky (1966) and by Grace (1982, pp. 8.65–8.83).

Heat transfer behavior is of importance at the walls of the vessel where it determines magnitudes of heat losses to the surroundings and at internal surfaces used for regulation of the operating temperature. The old correlations for heat transfer coefficients of Wender and Cooper (1958) (shown on Fig. 17.38) and those of Vreedenburg (1960) still are regarded as perhaps the best. (See Table 17.20.) A fair amount of scatter of the data obtained by various investigators is evident in Figure 17.38. Vreedenburg utilized additional data in his correlating, and, consequently, his figures show even more scatter. On Figure 17.37(a)
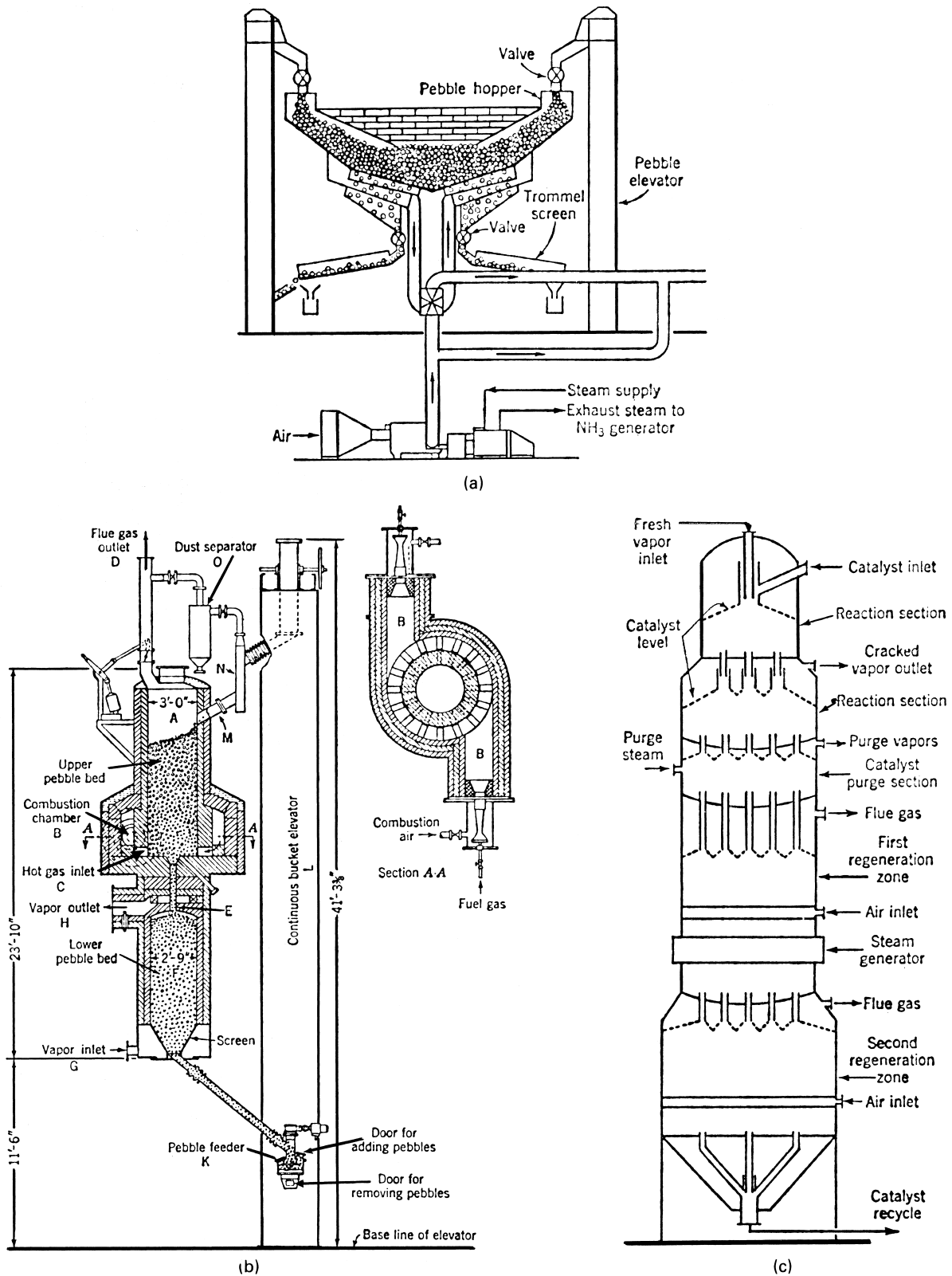
Figure 17.28. Reactors with moving beds of catalyst or solids for heat supply. (a) Pebble reactor for direct oxidation of atmospheric nitrogen; two units in parallel, one being heated with combustion gases and the other used as the reactor (*Ermenc,* (*1956*). (b) Pebble heater which has been used for making ethylene from heavier hydrocarbons (*Batchelder and Ingols, 1951*). (c) Moving bed catalytic cracker and regenerator; for 20,000 bpsd the reactor is 16 ft dia, catalyst circulation rate 2–7 lbs/lb oil, attrition rate of catalyst 0.1–0.5 lb/ton circulated, pressure drop across air lift line is about 2 psi (*L. Berg, in Othmer, 1956*).

(a)

(b)
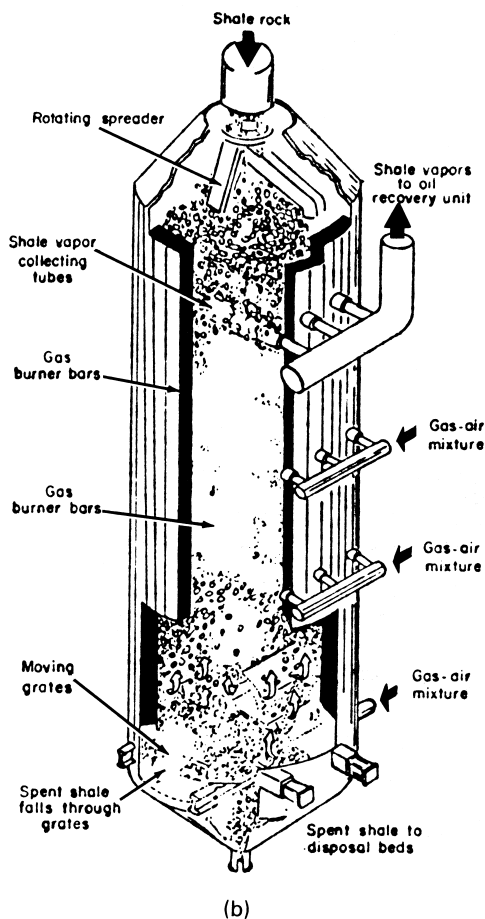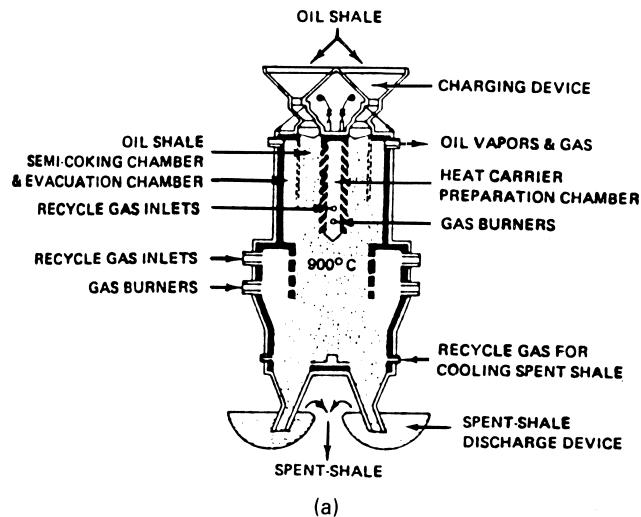
Figure 17.29. Moving bed reactors for cracking and recovery of shale oil. (a) Kiviter retort, USSR 200–300 tons/day (*J.W. Smith, in Meyers, 1984*). (b) Paraho retort for shale oil recovery (*Paraho Oil Shale Demonstration, Grand Junction, CO*).

also there is much disagreement; but if lines 8 and 9 by the same investigators and part of line 3 are ignored, the agreement becomes fair.

Some opinion is that the correlations for vertical tubes should be taken as standard. Coefficients at the wall appear to be about 10% less than at vertical tubes on the axis of the vessel and those for horizontal tubes perhaps 5–6% less (Korotjanskaja et al., 1984, p. 315).

As appears on Figure 17.37(c), a peak rate of heat transfer is attained. It has been correlated by Zabrodsky et al. (1976) for particles smaller than 1 mm by the equation

$$h_{max}d_s/k_g = 0.88 Ar^{0.213}, \quad 100 < Ar < 1.4 \times 10^5, \qquad (17.42)$$

$$Ar = g\rho_g(\rho_s - \rho_g)d_s^3/\mu_g^2. \qquad (17.43)$$

17.8. CLASSES OF REACTION PROCESSES AND THEIR EQUIPMENT

In this section, industrial reaction processes are classified primarily with respect to the kinds of phases participating, and instances are given of the kind of equipment that has been found suitable. As always, there is much variation in practice because of local or historical or personal circumstances which suggests that a certain latitude in new plant design is possible.

HOMOGENEOUS GAS REACTIONS

Ethylene is made by pyrolysis of hydrocarbon vapors in tubes of 50–100 mm dia and several hundred meters long with a reaction time of several seconds; heat is supplied by mixing with superheated steam and by direct contact of the tube with combustion gases.

Reactors to make polyethylene are 34–50 mm dia with 10–20 m long turns totalling 400–900 m in length. The tube is jacketed and heated or cooled at different positions with pressurized water.

A flow reactor is used for the production of synthesis gas, $CO + H_2$, by direct oxidation of methane and other hydrocarbons in the presence of steam. Preheated streams are mixed and react in a flow nozzle. Burning and quenching are performed in different zones of a ceramic-lined tower.

HOMOGENEOUS LIQUID REACTIONS

Almost innumerable instances of such reactions are practiced. Single-batch stirred tanks, CSTR batteries, and tubular flow reactors are all used. Many examples are given in Table 17.1. As already pointed out, the size of equipment for a given purpose depends on its type. A comparison has been made of the production of ethyl acetate from a mixture initially with 23% acid and 46% ethanol; these sizes were found for 35% conversion of the acid (Westerterp, 1984, pp. 41–58):

Reactor	$V_r/V_o'[m^3/(kg/day)]$
Batch (1/3 downtime)	1.04
PFR	0.70
CSTR	1.22
3-stage CSTR	0.85

Some of the homogeneous liquid systems of Table 17.1 are numbers 2, 16, 22, 28, 42, 53, 54, and 96, some in batch, mostly continuous.

(a)

Process	Lb/(hr)(cuft of kiln)
Cement, dry process	1.1–2.6
Cement, wet process, 44% water	0.7–1.7
Limestone calcination	1.1–2.1
Dolomite calcination	1.0–1.4
Alumina preparation	1.2–1.7
Barium sulfide preparation	0.9–2.0
Ignition of inorganic pigments	0.4–4.6
Iron pyrite roasting	0.7–0.9

(b)

(c)

(d)

(e)

(f)
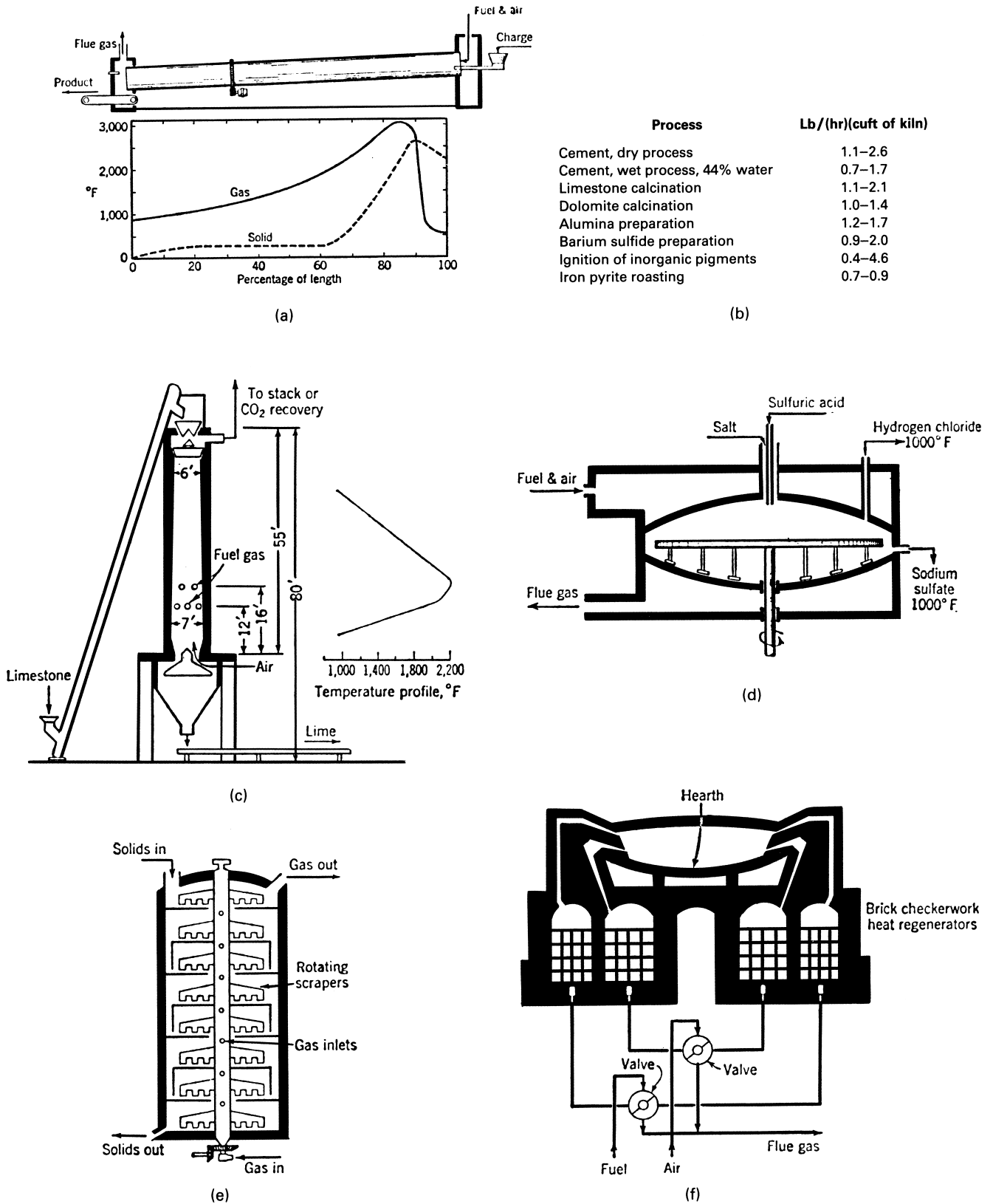
Figure 17.30. Kilns and hearth furnaces (*Walas, 1959*). (a) Temperature profiles in a rotary cement kiln. (b) Space velocities in rotary kilns. (c) Continuous lime kiln for production of approximately 55 tons/24 hr. (d) Stirred salt cake furnace operating at 1000°F, 11–18 ft dia, 6–10 tons salt/24 hr. (e) Multiple-hearth reactor; one with 9 trays, 16 ft dia and 35 ft high roasts 1250 lb/hr iron pyrite. (f) Siements–Martin furnace and heat regenerators; a hearth 13 ft wide and 40 ft long makes 10 tons/hr of steel with a residence time of 10 hr.

Typical FCC Operating Parameters

Parameter	Value
Feed capacity, kg/s	60 fresh; 95 total
Reactor diameter, m	6.7
Bed depth of reactor, m	Variable 0–1.6
Reactor dilute-phase velocity, m/s	0.75
Reactor temperature, °C	520
Stripper diameter, m	3.3
Stripper height, m	11
U-bend diameter, m	0.86
Catalyst circulation rate, kg/s	450
Regenerator diameter, m	10.7
Regenerator bed depth, m	6.64
Regenerator gas velocity, m/s	0.64
Height of regenerator cyclones inlet above bed, m	10.3
Regenerator temperature, °C	670
Regenerator pressure, kN/m^3 gauge	170
Catalyst inventory in regenerator, Mg	190
Entrainment to regenerator cyclones (estimated), kg/s	260
Catalyst losses in regenerator flue gas, g/s	15

(a)

(b)

Figure 17.31. Fluidized bed reactor processes for the conversion of petroleum fractions. (a) Exxon Model IV fluid catalytic cracking (FCC) unit sketch and operating parameters. (*Hetsroni, 1982*). (b) A modern FCC unit utilizing active zeolite catalysts; the reaction occurs primarily in the riser which can be as high as 45 m. (c) Fluidized bed hydroformer in which straight chain molecules are converted into branched ones in the presence of hydrogen at a pressure of 1500 atm. The process has been largely superseded by fixed bed units employing precious metal catalysts (*Hetsroni, 1982*). (d) A fluidized bed coking process; units have been built with capacities of 400–12,000 tons/day.
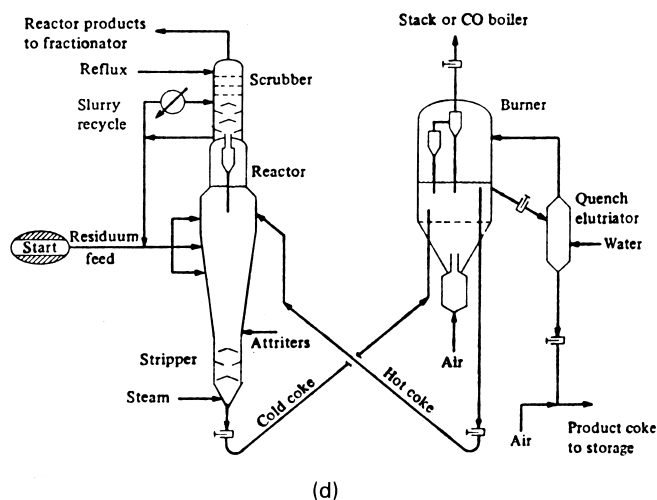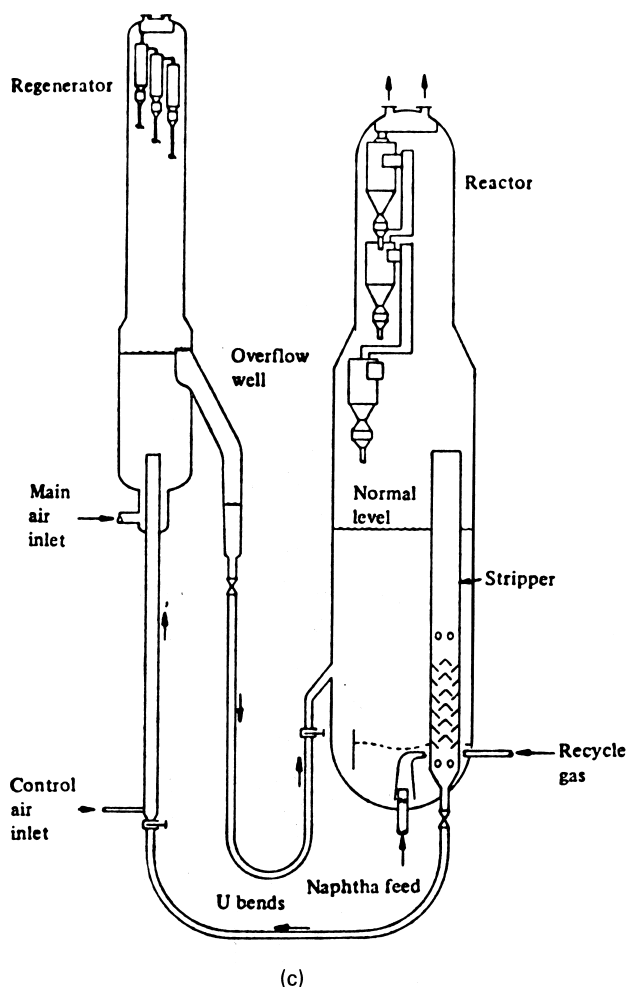
Figure 17.31.—(*continued*)

LIQUID-LIQUID REACTIONS

Such reactions can take place predominantly in either the continuous or disperse phase or in both phases or mainly at the interface. Mutual solubilities, distribution coefficients, and the amount of interfacial surface are factors that determine the overall rate of conversion. Stirred tanks with power inputs of 5–10 HP/1000 gal or extraction-type equipment of various kinds are used to enhance mass transfer. Horizontal TFRs usually are impractical unless sufficiently stable emulsions can be formed, but mixing baffles at intervals are helpful if there are strong reasons for using such equipment. Multistage stirred chambers in a single shell are used for example in butene–isobutane alkylation with sulfuric acid catalyst. Other liquid–liquid processes listed in Table 17.1 are numbers 8, 27, 45, 78, and 90.

GAS-LIQUID REACTIONS

Intimate contacting between chemically reacting gas and liquid phases is achieved in a variety of equipment, some examples of which follow

a. Tanks equipped with turbine agitators with or without internal gas recirculation. An example is air oxidation of cyclohexane to cyclohexanol and cyclohexanone.

b. Bubble towers with parallel flow of the phases, gas dispersed, with or without trays or packing. In such equipment isobutene from a mixture of C_4 hydrocarbons forms tertiary butanol in contact with aqueous sulfuric acid.

c. Countercurrent flow of the two phases in tray or packed towers, as in ordinary absorption processes. Absorption of nitrogen oxides in water to make nitric acid is a prime example.

d. Tubular or multitubular reactors are usable when the volumetric rate of the gas is so much greater than that of the liquid that substantial mixing of phases exists. Adipic acid nitrile is made from gaseous ammonia and liquid adipic acid with a volumetric ratio of 1500; the residence time of the gas phase is about 1 sec, and that of the liquid 180–300 sec.

e. Liquid ejector for entraining the gas. This is used to remove dilute acid or other impurities from waste air by scrubbing with aqueous solutions; the liquid is recirculated so that a gas/liquid volumetric ratio of 100–200 is maintained.

f. Pumps of centrifugal or turbine types are effective mixing devices and can constitute a reactor when the needed residence time is short. Such a device is used, for instance, to make acetic anhydride from acetic acid and ketene (Spes, 1966).

g. Thin film reactors are desirable when the liquid viscosity is high, the reaction is highly exothermic and short reaction times are adequate. Such a process is the sulfonation of dodecylbenzene with dilute SO_3 (Ujhidy et al., 1966).

(a)

(b)

(c)

(d)
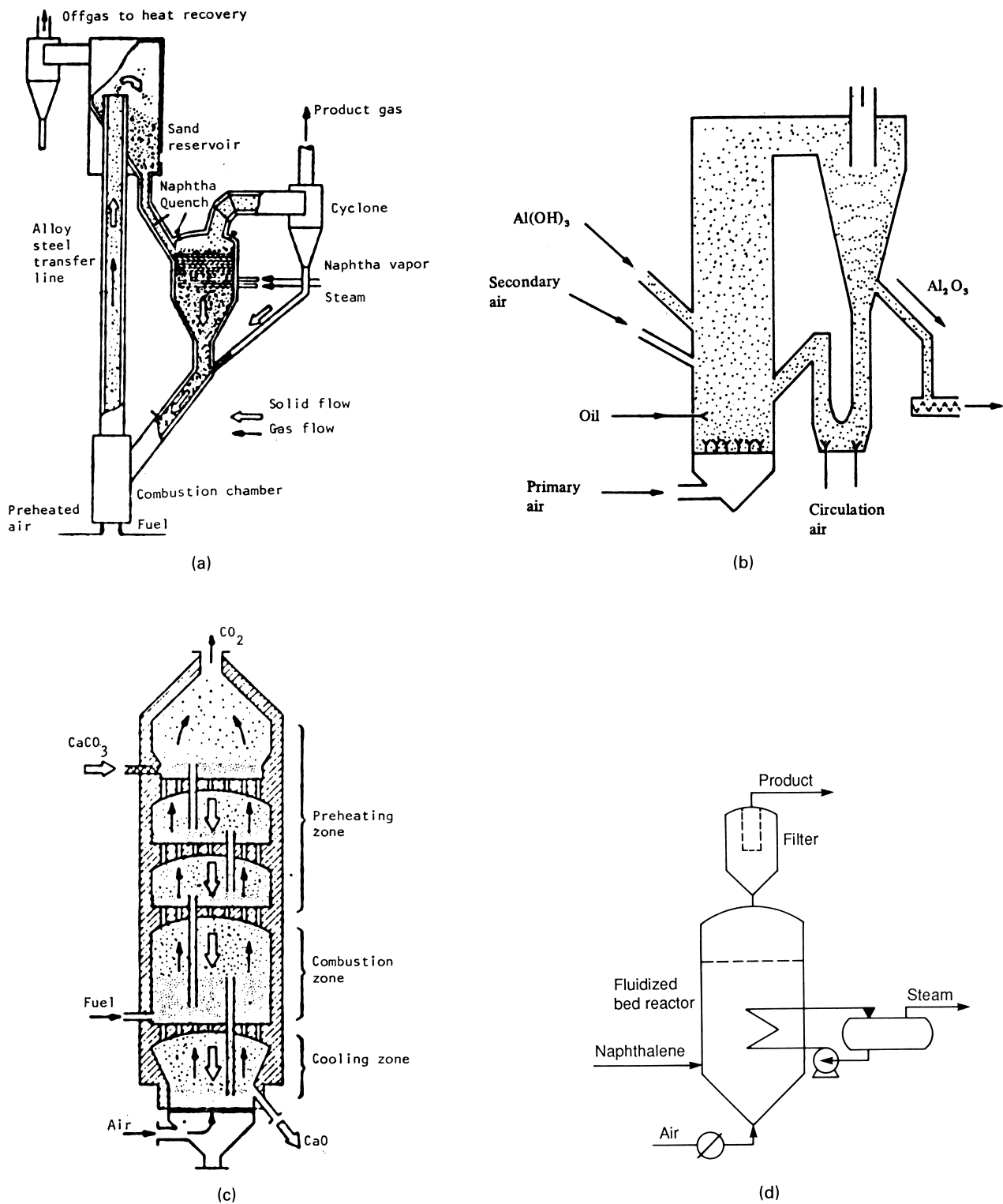
Figure 17.32. Other fluidized bed reaction systems. (a) Cracking of naphtha to ethylene with circulating hot sand at 720–850°C (*Lurgi*). (b) Circulating fluidized bed process for production of alumina by calcination (*Lurgi*). (c) Multibed reactor for calcination of limestone (*Dorr-Oliver*). (d) Synthesis of phthalic anhydride; cooling surface is in the bed (*Badger-Sherwin-Williams*). (e) Coal gasifier with two beds to counteract agglomeration, with spent char recirculating at 20–30 times the fresh feed rate (*Westinghouse*). (f) Ebbulating bed reactor of the H-Coal and H-Oil process for converting these materials at high temperature and pressure into gas and lighter oils (*Meyer, 1984*).

(e)

(f)
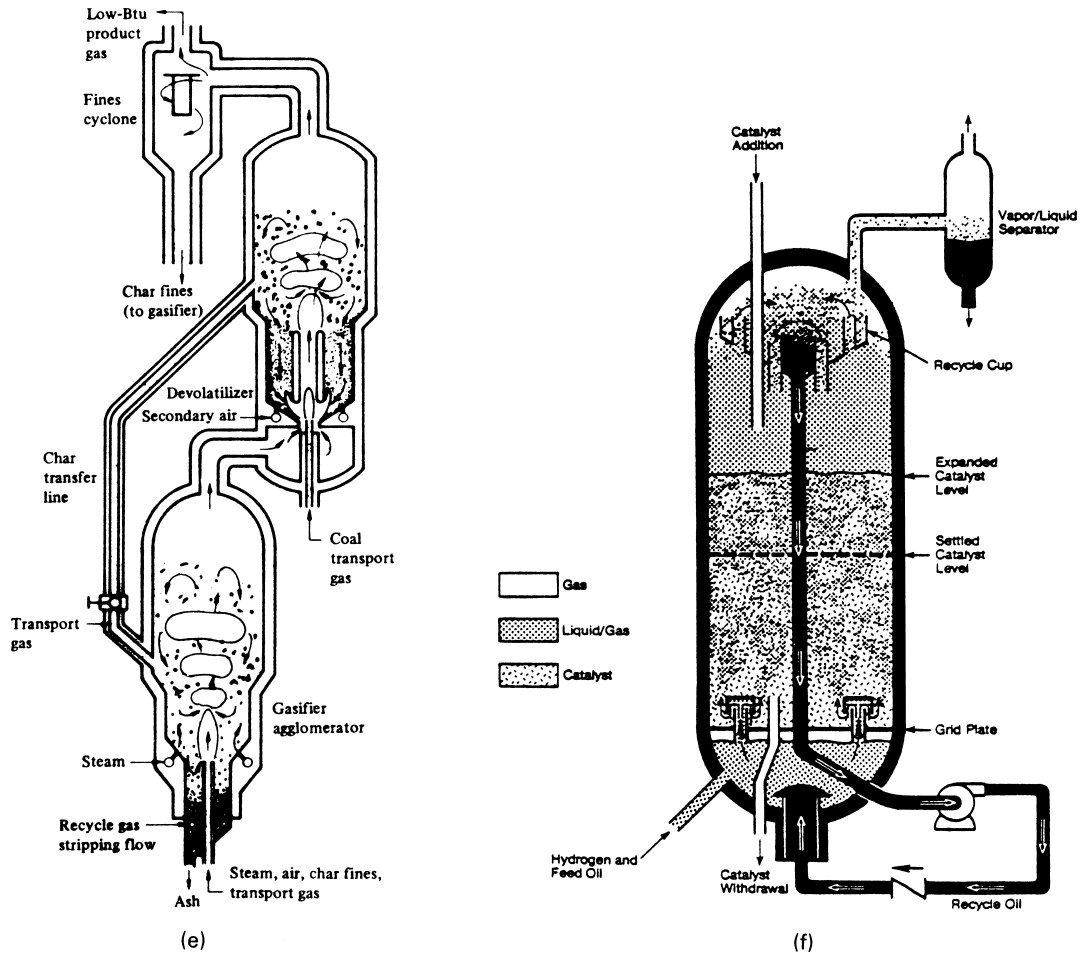
Figure 17.32.—(*continued*)

(a)   *(b)*   *(c)*

(d)   *(e)*   *(f)*
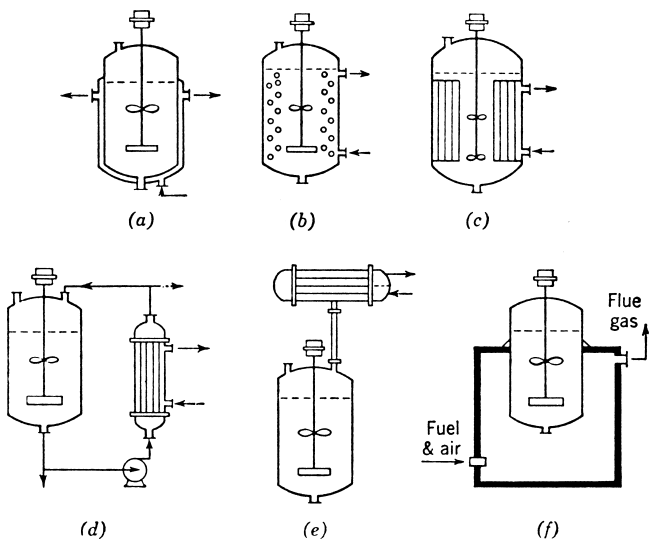
Figure 17.33. Heat transfer to stirred-tank reactors: (a) jacket; (b) internal coils; (c) internal tubes; (d) external heat exchanger; (e) external reflux condenser; (f) fired heater (*Walas, 1959*).
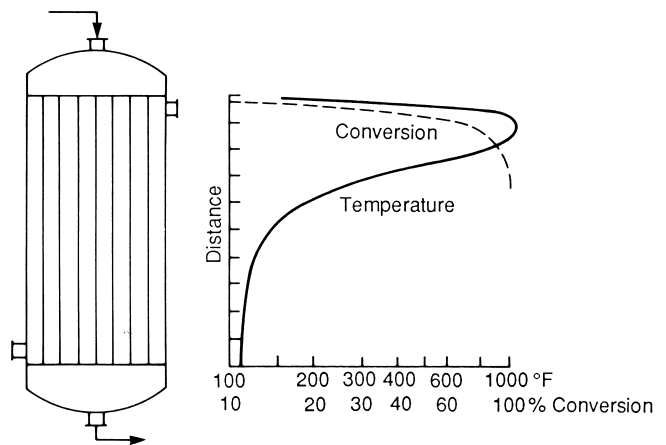
Figure 17.34. Temperature and conversion profiles in a water-cooled shell-and-tube phosgene reactor, 2-in. tubes loaded with carbon catalyst, equimolal CO and Cl_2.
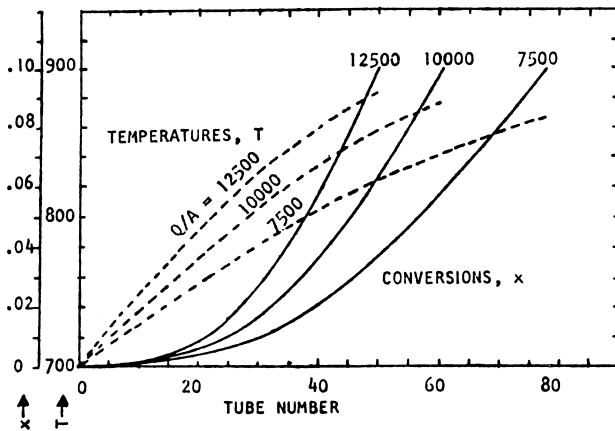
Figure 17.35. Temperature and conversion profiles of mild thermal cracking of a heavy oil in a tubular furnace with a back pressure of 250 psig and at several heat fluxes [Btu/hr(sqft)].

h. Packed tower reactors in parallel flow are operated either top-to-bottom or bottom-to-top. Distribution, holdup, and pressure drop behavior can be predicted from mass transfer correlations. Downflow towers have lower pressure drop, but upflow of liquid assures greater liquid holdup and longer contact time which often are advantages.

NONCATALYTIC REACTIONS WITH SOLIDS

The chief examples are smelting for the recovery of metals from ores, cement manufacture, and lime burning. The converters, roasters, and kilns for these purposes are huge special devices, not usually adaptable to other chemical applications. Shale oil is recovered from crushed rock in a vertical kiln on a batch or continuous basis—moving bed in the latter case—sometimes in a hydrogen-rich atmosphere for simultaneous denitrification and desulfurization. The capacity of ore roasters is of the order of 300–700 tons/(day)(m^3 of reactor volume). Rotary kilns for cement have capacities of 0.4–1.1 tons/(day)(m^3); for other purposes the range is 0.1–2.

FLUIDIZED BEDS OF NONCATALYTIC SOLIDS

Fluidized bed operations sometimes are alternates to those with fixed beds. Some of the successful processes are fluid bed combustion of coal, cracking of petroleum oils, ethylene production from gas oils in the presence of fluidized sand as a heat carrier, fluidized bed coking, water–gas production from coal (the original fluidized bed operation), recovery of shale oil from rock, reduction of iron ore with hydrogen at 30 atm pressure, lime burning, HCN from coke + ammonia + propane in a fluidized electric furnace, and many others. Many of these processes have distinct equipment configurations and space velocities that cannot be generalized, except insofar as general relations apply to fluidized bed stability, particle size distribution, heat transfer, multistaging, and possibly other factors.

CIRCULATING GAS OR SOLIDS

High temperatures are generated by direct or indirect contact with combustion gases. A circulating bed of granular solids heated in this way has been used for the fixation of nitrogen from air in the range of 2300°C. Pebble heaters originally were developed as pyrolysis reactors to make ethylene, but are no longer used for this purpose. Pebbles are 5–10 mm dia, temperatures of 1700°C are readily attained, heat fluxes are in the vicinity of 15,000 Btu/(hr)(°F)(cuft of pebbles) and contact times are fractions of a second. These characteristics should be borne in mind for new processes, although there are no current examples. Induction heating of fluidized particles has been used to transfer heat to a reacting fluid; in this process the solid remains in the reactor and need not circulate through a heating zone.

FIXED BED SOLID CATALYSIS

This kind of process is used when the catalyst maintains its activity sufficiently long, for several months or a year or two as in the cases of some catalytic reforming or ammonia synthesis processes. A few processes have operated on cycles of reaction and regeneration of less than an hour or a few hours. Cycle timers on automatic valves make such operations completely automatic. A minimum of three vessels usually is needed: One on-stream, one being regenerated, and the last being purged and prepared for the next cycle. Adsorption processes are conducted this way. The original Houdry cracking process employed 10 min on-stream. One catalytic reforming process employs seven or so reactors with one of them down every week. Regeneration usually is done in place, but eventually the catalyst must be removed and replaced. Platinum and other precious metals are recovered from the catalyst carriers in the factory.

A granular catalyst sometimes serves simultaneously as tower packing for reaction and separation of the participants by distillation, particularly when the process is reversible and removal of the product is necessary for complete conversion to take place. This is the case of the reaction of methanol and isobutene to make methyl tertiary-butyl ether (MTBE) in the presence of granular acid ion exchange resin catalyst. MTBE is drawn off the bottom of the tower and excess methanol off the top. Such a process is applicable when the reaction can be conducted satisfactorily at boiling temperatures; these can be adjusted by pressure.

A variety of provisions for temperature control of fixed beds is described in Section 17.6 and following.

a. Single beds are used when the thermal effects are small. Jacketed walls usually are inadequate for heat transfer to beds, but embedded heat transfer tubes sometimes are used.
b. Multitubular units with catalyst in tubes and heat transfer medium on the shell side are popular. A reactor for making phosgene from carbon monoxide and chloride has 2-in. dia tubes 8 ft long filled with activated carbon catalyst and cooling water on the shell side.
c. Multibed units with built-in interstage heat transfer surface. Economical when the amount of surface is not large. In comparison with type (d) of Figure 17.13, this design may have more difficult maintenance, less flexibility and higher cost because of the shortness of the tubes that may have to be used. The Sper-Rashka converter for SO$_2$ oxidation has three beds and three large internal exchangers in a single shell (Ullmann, 3rd ed., 1964, Vol. 15, p. 456).
d. Multibed units with external heat exchangers. Several variations of this design with steam generation or feed gas as means of cooling are used for the catalytic oxidation of SO$_2$.
e. Multibed unit with interstage injection of temperature controlled process fluid or inert fluid for temperature control of the process. In the synthesis of cumene from propylene and benzene in the presence of supported phosphoric acid catalyst, interstage injection of cold process gas and water is used for temperature control and maintenance of catalyst activity (Figure 17.18(g)).

TABLE 17.10. Overall Heat Transfer Coefficients in Agitated Tanks [U Btu/(hr)(sqft)(°F)]

Fluid Inside Jacket	Fluid In Vessel	Wall Material	Agitation	U
Steam	water	enameled cast iron	0–400 rpm	96–120
Steam	milk	enameled C.I.	none	200
Steam	milk	enameled C.I.	stirring	300
Steam	milk boiling	enameled C.I.	none	500
Steam	milk	enameled C.I.	200 rpm	86
Steam	fruit slurry	enameled C.I.	none	33–90
Steam	fruit slurry	enameled C.I.	stirring	154
Steam	water	C.I. and loose lead lining	agitated	4–9
Steam	water	C.I. and loose lead lining	none	3
Steam	boiling SO$_2$	steel	none	60
Steam	boiling water	steel	none	187
Hot water	warm water	enameled C.I.	none	70
Cold water	cold water	enameled C.I.	none	43
Ice water	cold water	stoneware	agitated	7
Ice water	cold water	stoneware	none	5
Brine, low velocity	nitration slurry	—	35–58 rpm	32–60
Water	sodium alcoholate solution	''Frederking'' (cast-incoil)	agitated, baffled	80
Steam	evaporating water	copper	—	381
Steam	evaporating water	enamelware	—	36.7
Steam	water	copper	none	148
Steam	water	copper	simple stirring	244
Steam	boiling water	copper	none	250
Steam	paraffin wax	copper	none	27.4
Steam	paraffin wax	cast iron	scraper	107
Water	paraffin wax	copper	none	24.4
Water	paraffin wax	cast iron	scraper	72.3
Steam	solution	cast iron	double scrapers	175–210
Steam	slurry	cast iron	double scrapers	160–175
Steam	paste	cast iron	double scrapers	125–150
Steam	lumpy mass	cast iron	double scrapers	75–96
Steam	powder (5% moisture)	cast iron	double scrapers	41–51

(LIGHTNIN Technology Seminar, Mixing Equipment Co., 1982).

TABLE 17.11. Jacketed Vessels Overall Heat Transfer Coefficients

Jacket Fluid	Fluid in Vessel	Wall Material	Overall U[*]	
			Btu/(h · ft^2 · °F)	J/(m^2 · s · K)
Steam	Water	Stainless steel	150–300	850–1700
Steam	Aqueous solution	Stainless steel	80–200	450–1140
Steam	Organics	Stainless steel	50–150	285–850
Steam	Light oil	Stainless steel	60–160	340–910
Steam	Heavy oil	Stainless steel	10–50	57–285
Brine	Water	Stainless steel	40–180	230–1625
Brine	Aqueous solution	Stainless steel	35–150	200–850
Brine	Organics	Stainless steel	30–120	170–680
Brine	Light oil	Stainless steel	35–130	200–740
Brine	Heavy oil	Stainless steel	10–30	57–170
Heat-transfer oil	Water	Stainless steel	50–200	285–1140
Heat-transfer oil	Aqueous solution	Stainless steel	40–170	230–965
Heat-transfer oil	Organics	Stainless steel	30–120	170–680
Heat-transfer oil	Light oil	Stainless steel	35–130	200–740
Heat-transfer oil	Heavy oil	Stainless steel	10–40	57–230
Steam	Water	Glass-lined CS	70–100	400–570
Steam	Aqueous solution	Glass-lined CS	50–85	285–480
Steam	Organics	Glass-lined CS	30–70	170–400
Steam	Light oil	Glass-lined CS	40–75	230–425
Steam	Heavy oil	Glass-lined CS	10–40	57–230
Brine	Water	Glass-lined CS	30–80	170–450
Brine	Aqueous solution	Glass-lined CS	25–70	140–400
Brine	Organics	Glass-lined CS	20–60	115–340
Brine	Light oil	Glass-lined CS	25–65	140–370
Brine	Heavy oil	Glass-lined CS	10–30	57–170
Heat-transfer oil	Water	Glass-lined CS	30–80	170–450
Heat-transfer oil	Aqueous solution	Glass-lined CS	25–70	140–400
Heat-transfer oil	Organics	Glass-lined CS	25–65	140–370
Heat-transfer oil	Light oil	Glass-lined CS	20–70	115–400
Heat-transfer oil	Heavy oil	Glass-lined CS	10–35	57–200

[*]Values listed are for moderate nonproximity agitation. CS = carbon steel.
(*Perry's Chemical Engineers' Handbook*, 6th ed., McGraw-Hill, New York, 1984, Table 10-14, p. 10–46).

TABLE 17.12. Overall Heat Transfer Coefficients with Immersed Coils [U expressed in Btu/(h · ft^2 · °F)]

Type of coil	Coil spacing, in. †	Fluid in coil	Fluid in vessel	Temp. range, °F.	U‡ without cement	U with heat-transfer cement
3/8 in. o.d. copper tubing attached with bands at 24-in. spacing	2	5 to 50 lb./sq. in gage steam	Water under light agitation	158–210	1–5	42–46
	3 1/8			158–210	1–5	50–53
	6 1/4			158–210	1–5	60–64
	12 1/2 or greater			158–210	1–5	69–72
3/8 in. o.d. copper tubing attached with bands at 24-in. spacing	2	50 lb./sq. in. gage steam	No. 6 fuel oil under light agitation	158–258	1–5	20–30
	3 1/8			158–258	1–5	25–38
	6 1/4			158–240	1–5	30–40
	12 1/2 or greater			158–238	1–5	35–46
Panel coils		50 lb./sq. in. gage steam	Boiling water	212	29	48–54
		Water	Water	158–212	8–30	19–48
		Water	No. 6 fuel oil	228–278	6–15	24–56
		Water	Water	130–150	7	15
			No. 6 fuel oil	130–150	4	9–19

Data courtesy of Thermon Manufacturing Co.
†External surface of tubing or side of panel coil facing tank.

TABLE 17.13. Summary of Heat-Transfer Coefficients on the Agitated Side

General Equation: $\frac{h(L)}{\lambda_f} = \alpha \left(\frac{\rho N D_l^2}{\mu}\right)^m \left(\frac{c_p \mu}{\lambda_f}\right)^b \left(\frac{\mu_b}{\mu_w}\right)^c$ (other terms)

Agitator Type	Transfer Surface	Approx. Reynolds Number Range	L	α	m	b	c	Other Terms	Additional Comments	Ref.
Turbine 6-blade, flat (baffled)	jacket	$10–10^5$	D	0.73	0.65	0.33	0.24	—	Use for standard configuration. See p. 357 for details	1,25
	coil	$400 - 1.5 \times 10^6$	d_{ct}	0.17	0.67	0.37	See Note 1	$\left(\frac{D_1}{D}\right)^{0.1}\left(\frac{d_{et}}{D}\right)^{0.5}$	See Note 2. Applies for standard configuration with $D_c/D = 0.7$ and	29
	vertical baffle-type	$10^3 - 2 \times 10^6$	d_{ct}	0.09	0.65	0.33	0.4	$\left(\frac{D_1}{D}\right)^{0.33}\left(\frac{2}{n_{bv}}\right)^{0.2}$	$S_c/d_{ct} = 2 - 4; Z_c/D = 0.15$	32
6-blade, retreating blade (curved blade)	jacket	$10^3 - 10^6$	D	0.68	0.67	0.33	0.14		Revised. See Note 3	27,30
no baffles	coil	$10^3 - 10^6$	d_{ct}	1.40	0.62	0.33	0.14	—	Revised	27,30
6-blade, 45° pitched	jacket	20–200	D	0.44^a	0.67	0.33	0.24	—	Baffles have no effect in Reynolds number range studied in 12-in diameter vessel	33
3-blade retreating	jacket	$2 \times 10^4 - 2 \times 10^6$	D	0.37^b	0.67	0.33	0.14	—	For glass-lined vessels with finger-type baffle	27
Propeller	jacket	2×10^3	D	0.54	0.67	0.25	0.14	—	Limited data, but a large 5 ft diameter tank used, marine-type impeller used at 45° pitch and located at the midpoint of tank. No baffles used	34
Paddle	jacket	$600 - 5 \times 10^5$	D	0.112	0.75	0.44	0.25	$\left(\frac{D}{D_l}\right)^{0.40}\left(\frac{w_l}{D_l}\right)^{0.13}$		26,35
	coil	$3 \times 10^2 - 2.6 \times 10^5$	d_{ct}	0.87	0.62	0.33	0.14			37
Anchor	jacket	10–300	D	1.0	0.5	0.33	0.18	—		34,36
		300–40,000	D	0.36	0.67	0.33	0.18	—		34,36

Notes.
1. $\ln c = -0.202 \ln \mu - 0.357$, with μ in cp.
2. For unbaffled case with coils use 0.65 of h calculated for baffled case (29).
3. With baffles and $N_{Re} < 400$ use value calculated. In fully developed turbulent region baffles increase calculated h by approximately 37% (1)

New nomenclature: d_{ct} is outside tube diameter of coil, D_c is coil diameter, n_{bv} is number of vertical baffle-type coils, S_c is coil spacing, w_1 is impeller blade width, and Z_c is height of coil from tank bottom.
^{a}For impeller 4 $\frac{1}{2}$ -in. from bottom, 0.535 for impeller 11-in from bottom
^{b}For steel impeller, 0.33 for glassed-steel impeller
(Rase, 1977, Vol. 1).

TABLE 17.14. Equations for Heat Transfer Coefficients inside Stirred Tanks[a]

1. To jackets, with paddles, axial flow, and flat blade turbines[1,6,7]

$$h_0(\text{jacket})\frac{T}{k} = 0.85\left(\frac{D^2 N\rho}{\mu}\right)^{0.66}\left(\frac{C_p\mu}{k}\right)^{0.33}$$
$$\times\left(\frac{\mu}{\mu_s}\right)^{0.14}\left(\frac{Z}{T}\right)^{-0.56}\left(\frac{D}{T}\right)^{0.13}$$

2. To helical coils[3,5]

$$h_0(\text{coil})\frac{D}{k} = 0.17\left(\frac{D^2 N\rho}{\mu}\right)^{0.67}\left(\frac{C_p\mu}{k}\right)^{0.37}$$
$$\times\left(\frac{D}{T}\right)^{0.1}\left(\frac{d}{T}\right)^{0.5}\left(\frac{\mu}{\mu_s}\right)^{m}$$
$$m = 0.714/\mu^{0.21},\ \mu\ \text{in}\ cP$$

3. To vertical tubes[2]

$$h_0(\text{tubes})\frac{D}{K} = 0.09\left(\frac{D^2 N\rho}{\mu}\right)^{0.65}\left(\frac{C_p\mu}{k}\right)^{0.3}$$
$$\times\left(\frac{D}{T}\right)^{0.33}\left(\frac{2}{n_b}\right)^{0.2}\left(\frac{\mu}{\mu_s}\right)^{0.14}$$

4. To plate coils[4]

$$h_0(\text{plate coil})\frac{L}{K} = 0.1788\left(\frac{ND^2\rho}{\mu}\right)^{0.448}\left(\frac{C_p\mu}{k}\right)^{0.33}\left(\frac{\mu}{\mu_f}\right)^{0.50}$$
$$\text{for}\ N_{Re} < 1.4\times 10^3$$

$$h_0(\text{plate coil})\frac{L}{K} = 0.0317\left(\frac{ND^2\rho}{\mu}\right)^{0.658}\left(\frac{C_p\mu}{k}\right)^{0.33}\left(\frac{\mu}{\mu_f}\right)^{0.50}$$
$$\text{for}\ N_{Re} > 4\times 10^3$$

[a] Nomenclature: d = tube diameter, D = impeller diameter, L = plate coil height, N = impeller rotational speed, n_b = number of baffles or of vertical tubes acting as baffles, T = tank diameter, Z = liquid height.

REFERENCES FOR TABLE 17.14

G. Brooks and G.-J. Su, *Chem. Eng. Prog.* **54** (October 1959).
I.R. Dunlap and J.H. Rushton, *Chem. Eng. Prog. Symp. Ser.* **49**(5), 137 (1953).
J.Y. Oldshue and A.T. Gretton, *Chem. Eng Prog.* **50**(12), 615 (1954).
D.K. Petree and W.M. Small, *AIChE Symp. Series.* **74**(174) (1978).
A.H.P. Skelland, W.K. Blake, J.W. Dabrowski, J.A. Ulrich, and T.F. Mach, *AIChE. J.* **11**(9) (1965).
F. Strek, *Int. Chem. Eng.* **5**, 533 (1963).
V.W. Uhl and J.B. Gray, *Mixing Theory and Practice*, Academic, New York, 1966, Vol. 1.
(Recommended by Oldshue, 1983).

(a)

(b)

(c)

Figure 17.36. Effective thermal conductivity and wall heat transfer coefficient of packed beds. $Re' = d_p G/\mu$, $d_p = 6V_p/A_p$, ε = porosity. (a) Effective thermal conductivity in terms of particle Reynolds number. Most of the investigations were with air of approx. $k'_f = 0.026$, so that in general $k'_e/k'_f = 38.5k'_e$ (*Froment*, 1970). (b) Heat transfer coefficient at the wall. Recommendations for L/d_p above 50 by Doraiswamy and Sharma are line H for cylinders, line J for spheres. (c) Correlation of Gnielinski (*cited by Schlünder, 1978*) of coefficient of heat transfer between particle and fluid. The wall coefficient may be taken as $h_w = 0.8h_p$.
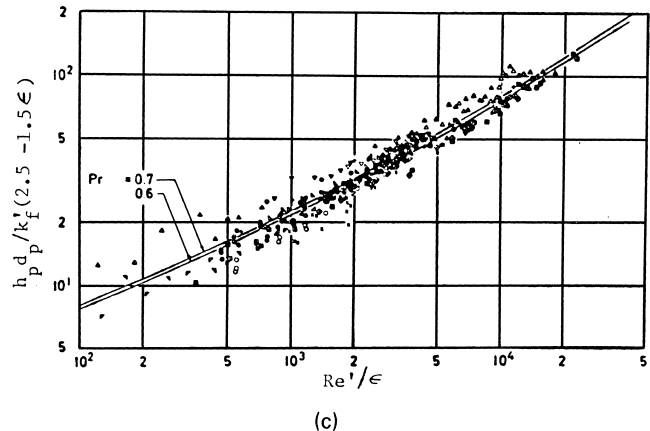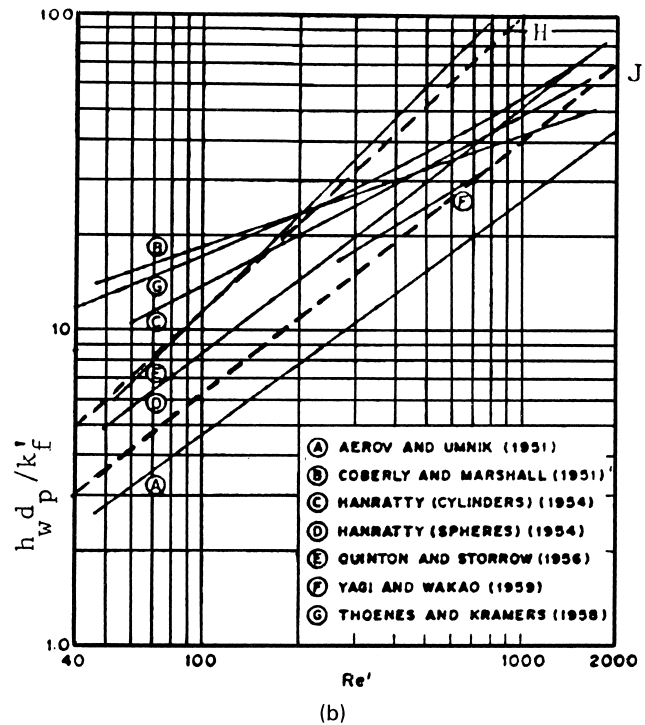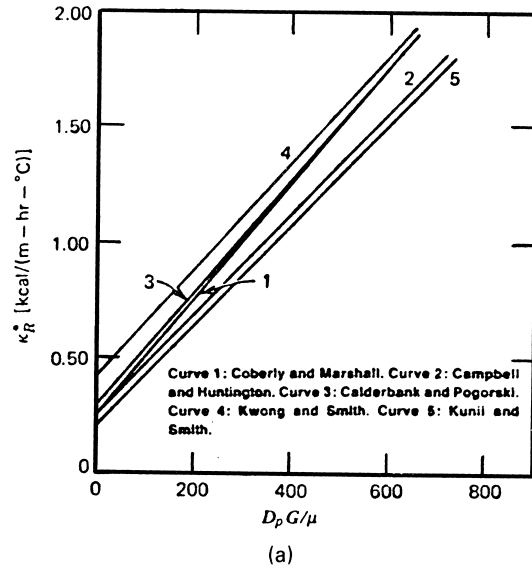
TABLE 17.15. Data for the Effective Thermal Conductivity, K_r (kcal/mh°C), and the Tube Wall Film Coefficient, h_w (kcal/m²h°C), in Packed Beds[a]

Authors	Method of Measurement	Heating or Cooling of Gas	Gas	Particles		
				Material	Shape	Diameter D_p, mm
Bakhurov and Boreskov (1947)	Radial temperature and concentration profiles	C	Air	Glass, porcelain, metals, etc.	Spheres, rings, cylinders, granules	3–19
Brötz (1951)	ʺ	H	N_2, CO_2, H_2	Glass, catalyst	Spheres, granules	2–10
Bunnell, Irvin, Olson, and Smith (1949)	Radial temperature profiles	C	Air	Alumina	Cylinders	3
Campbell and Huntington (1952)	ʺ	H, C	Air, natural gas (82% CH_4)	Glass, alumina, aluminum	Spheres, cylinders	5–25
Coberly and Marshall (1951)	ʺ	H	Air	Celite	Cylinders	3–12
Maeda (1952)	ʺ	C	Air	Catalyst	Cylinders	3–10
Quinton and Storrow (1956)	ʺ	H	Air	Glass	Spheres	4.4
Aerov and Umnik (1951b, c)	Packed bed heat exchanger. Single radial temperature	C	Air, CO_2, H_2	Glass, catalyst, porcelain, sand	Spheres, tablets, rings	0.4–10
Hougen and Piret (1951) Molino and Hougen (1952)	Packed bed heat exchanger	C H	Air	Celite	Spheres, cylinders	2–12
Kling (1938b)	ʺ	H	Air	Steel, glass	Spheres	3–4
Verschoor and Schuit (1950)	ʺ	H	Air, H_2	Lead, glass, etc.	Spheres, cylinders, granules	3–10
Bernard and Wilhelm (1950)	Mass diffusion		(Water)	Glass, lead, alumina, etc.	Spheres, cylinders, granules	1–8

f. Autothermal multitubular unit with heat interchange between feed on the shell side and reacting gas in the packed tubes and between feed and reacted gas in an external or built-in exchanger. Many complex variations of this design have been or are being used for ammonia synthesis.

g. Multibed units in individual shells with interstage heat transfer. From three to seven stages are adopted by different processes for the catalytic reforming of naphthas to gasoline.

FLUIDIZED BED CATALYSIS

Such processes may be conducted to take advantage of the substantial degree of uniformity of temperature and composition and high rates of heat transfer to embedded surfaces. Orthophthalic anhydride is made by oxidation of naphthalene in a fluidized bed of V_2O_5 deposited on silica gel with a size range of 0.1–0.3 mm with a contact time of 10–20 sec at 350–380°C. Heat of reaction is removed by generation of steam in embedded coils. No continuous regeneration of catalyst is needed. Acrylonitrile and ethylene dichloride also are made under conditions without the need for catalyst regeneration.

From the standpoint of daily capacity, the greatest application of fluidized bed catalysis is to the cracking of petroleum fractions into the gasoline range. In this process the catalyst deactivates in a few minutes, so that advantage is taken of the mobility of fluidized catalyst to transport it continuously between reaction and regeneration zones in order to maintain its activity; some catalyst also must be bled off continuously to maintain permanent poisons such as heavy metal deposits at an acceptable level.

Several configurations of reactor and regenerator have been in use, two of which are illustrated in Figures 17.31(a) and (b). Part (a) shows the original arrangement with separate vessels side by side for the two operations. The steam stripper is for removal of occluded oil from the catalyst before it is burned. In other designs the two vessels are in vertical line, often in a single shell with a partition. Part (b) is the design of transfer line cracking which employs highly active zeolite catalysts that are effective at short contact times. The upper vessel is primarily a catalyst disengaging zone. A substantial gradient develops in the transfer line and results in an improvement in product distribution compared with that from mixed reactors such as part (a).

TABLE 17.15.—(*continued*)

| Tube | | Formula (D_p and D_t in m) | Range of $N_{Re'}$ or other variable | Remarks |
Diameter, D_t, mm	Length L, m			
100 square	1	$N_{Pe'} = 2.4$ to 6.3	$G \simeq 1000 \, kg/m^2 h$	
100	0.2–0.4	Graphs in paper	Gas velocity: 2500–7200 m/h	Special apparatus at low velocities
50	0.05–0.2	$\dfrac{K_r}{k_g} = 5.0 + 0.061\left(\dfrac{D_p G}{\mu}\right)$	30–100	
50–100		$\dfrac{K_r}{k_g} = 10.0 + 0.267\left(\dfrac{G}{\mu a_v}\right)$; $h_w = 2.07\left(\dfrac{G}{\mu a_v}\right)^{0.47}$	20–500	
127	up to 1	$K_r = 0.27 + 0.00146\dfrac{\sqrt{a_p G}}{\mu}$; $h_w = 8.51 \, G^{0.33}$	G (kg/m²h): 850–6000	
25–100	0.1–0.4	$\dfrac{K_r}{k_g} = \begin{cases} 5.5 + 0.05\left(\dfrac{D_p G}{\mu}\right) \\ 1.72\left(\dfrac{D_p G}{\mu}\right)^{0.41} \\ 0.209\left(\dfrac{D_p G}{\mu}\right)^{0.87} \end{cases}$	0–30 30–100 100–1000	See also Hatta and Maeda (1948 a, b, 1949), Maeda (1950), and Maeda and Kawazoe (1953)
41	0.75	$K_r = 0.36 + 0.00162\left(\dfrac{D_p G}{\mu}\right)$; $h_w = 0.04 \, G$	30–1100 500<G<17000	
65	0.3	$\dfrac{K_r}{k_g} = 10.5 + 0.076 N_{Pr}\left(\dfrac{4G}{\mu a_v}\right)$ $\dfrac{h_w D_p}{k_g} = 0.155 N_{Pr}^{\frac{1}{3}}\left(\dfrac{4G}{\mu a_v}\right)^{0.75}$	10–3500 150–4000	For rings see paper
35–95	0.16–0.32	$\dfrac{K_r}{k_g} = 1.23\left(\dfrac{\sqrt{a_p}\,G}{\mu}\right)^{0.43}$ No correction for h_w	100–3000	The first paper gives a slightly different formula for cooling
50	0.3	See graph in paper. No correction for h_w	400–3500	
30–50	0.2–0.3	$\dfrac{K_r}{k_g} = \dfrac{K_{r,0}}{k_g} + 0.10(a_v D_t)^{0.50}\left(\dfrac{G}{\mu a_v}\right)^{0.69}$	10–1000	No correction for h_w
50		Graph in paper of N'_{Pe} vs. N'_{Re}	5–2400	Diffusion of methylene blue in water

[a] a_p = surface of a particle, a_v = surface/volume in the bed. (Kjaer, 1958).

Hundreds of fluidized bed crackers are in operation. The vessels are large, as much as 10 m or so in diameter and perhaps twice as high. Such high linear velocities of vapors are maintained that the entire catalyst content of the vessels circulates through the cyclone collectors in an hour or so. Electrical precipitators after the cyclone collectors have been found unnecessary.

Two other fluidized bed petroleum reactors are illustrated as Figures 17.31(c) and (d) and several nonpetroleum applications in Figure 17.32.

GAS–LIQUID REACTIONS WITH SOLID CATALYSTS

The number of commercial processes of this type is substantial. A brief list arranged according to the kind of reactor is in Table 17.21. Depending on the circumstances, however, it should be noted that some reactions are conducted industrially in more than one kind of reactor.

Leading characteristics of five main kinds of reactors are described following. Stirred tanks, fixed beds, slurries, and three-phase fluidized beds are used. Catalyst particle sizes are a com-promise between pressure drop, ease of separation from the fluids, and ease of fluidization. For particles above about 0.04 mm dia, diffusion of liquid into the pores and, consequently, accessibility of the internal surface of the catalyst have a minor effect on the overall conversion rate, so that catalysts with small specific surfaces, of the order of $1 \, m^2/g$, are adequate with liquid systems. Except in trickle beds the gas phase is the discontinuous one. In some operations of bubble towers, the catalyst remains in the vessel, although minor amounts of catalyst entrainment may occur.

1. Stirred tanks with suspended catalyst are used both in batch and continuously. Hydrogenation of fats or oils with Raney nickel or of caprolactam usually are in batch. Continuous processes include some hydrogenations of fats, some fermentation processes with cellular enzymes and air and the hydrogenation of nitrogen monoxide to hydroxylamine. The gas is distributed with spargers or introduced at the eye of a high-speed impeller in a draft tube. Internal recirculation of the gas also is practiced. The power input depends on the settling tendency of the particles and the required intimacy of gas–liquid mixing. It is greater than

TABLE 17.16. Data for the Overall Heat Transfer Coefficient, u(kcal/m²h°C), in Packed Beds

Authors	Method of Measurement	Heating or Cooling of Gas	Gas	Particles		
				Material	Shape	Diameter D_p, mm
Campbell and Huntington (1952)	Packed bed heat exchanger	H, C	Air, natural gas (82% CH₄)	Glass, alumina, aluminum	Spheres, cylinders	5–25
Chu and Storrow (1952)	''	H	Air	Glass, steel, lead, Socony-Vacuum catalyst beads	Spheres	1–6
Colburn (1931)	''	H	Air	Porcelain, zinc, etc.	Spheres, granules	5–25
Kling (1938b)	''	H	Air	Steel, glass	Spheres	3–4
Leva (1947)	''	H	Air, CO₂	Glass, clay, porcelain	Spheres	3–13
Leva and Grummer (1948)	''	H	Air	Glass, clay, metals, etc.	Spheres, cylinders, granules, etc.	2–25
Leva, Weintraub, Grummer, and Clark (1948)	''	C	Air, CO₂	Glass, porcelain	Spheres	3–13
Leva (1950)	''	H	Air	Glass, clay, porcelain, metal	Spheres, rings, cylinders	4–18
Maeda (1952)	''	C	Air	Catalyst	Cylinders	3–10
Maeda and Kawazoe (1953)	''	C	Air		Granules, rings, saddles	3–25
Verschoor and Schuit (1950)	''	H	Air, H₂	Lead, glass, etc.	Spheres, cylinders, granules	3–10
Tasker (1946)	Phthalic anhydride synthesis	C	Air	Catalyst on quartz (?)	Granules	1.7–2.0

in the absence of solids; for example, the solid catalyzed hydrogenation of nitrogen monoxide employs a power input of about 10 kW/m³ (51 HP/1000 gal) compared with 5–10 HP/1000 gal for ordinary liquid–liquid mixing.

2. In ebullated (liquid fluidized) beds the particles are much larger (0.2–1 mm) than in gas fluidization (0–0.1 mm). Little expansion of the bed occurs beyond that at minimum fluidization, so that the bed density is essentially the same as that of the fixed bed. Because substantial internal circulation of the liquid is needed to maintain fluidization, the fluids throughout the reactor are substantially uniform. In the hydrodesulfurization and hydrocracking of petroleum fractions and residua at 100 atm and 400°C, a temperature variation of only 2°C or so is obtained in the reactor.

3. Slurry reactors (bubble towers) are fluidized with continuous flow of gas. The particles are smaller (less than 0.1 mm) than in the liquid fluidized systems (0.2–1 mm). In some operations the liquid and solid phases are stationary, but in others they circulate through the vessel. Such equipment has been used in

TABLE 17.16.—(continued**)**

Diameter, D_t, mm	Length L, m	Formula (D_p and D_t in m)	Range of $N_{Re'}$ or other variable	Remarks
50–150		$\dfrac{U}{GC_p} = 0.76\, e^{-0.0225\, a_v D_t}\left(\dfrac{G}{\mu a_v}\right)^{-0.42}$	30–1000	U refers to tube axis temperature
25	0.3–1.2	$\dfrac{UD_t}{k_g} = 0.134\left(\dfrac{D_p}{D_t}\right)^{-1.13}\left(\dfrac{L}{D_t}\right)^{-0.90}\left(\dfrac{D_pG}{\mu}\right)^{1.17}$ $\dfrac{UD_t}{k_g} = 15\left(\dfrac{D_p}{D_t}\right)^{-0.90}\left(\dfrac{L}{D_t}\right)^{-1.82}\left(\dfrac{D_pG}{\mu}\right)^{n}$ $n = 0.55\left(\dfrac{L}{D_t}\right)^{0.165}$	$\dfrac{D_tG}{\mu} < 1600$ $1600 <$ $\dfrac{D_tG}{\mu} < 3500$	
35–80	0.5–1.2	$U = f\left(\dfrac{D_p}{D_t}\right)G^{0.83}$	Range of G(kg/m²h): 4500–45000	Function f given in paper. Maximum 0.045 for $\dfrac{D_p}{D_t} = 0.15$
50	0.3	Graph given in paper	400–3500	
15–52	0.3–0.9	$\dfrac{UD_t}{k_g} = 0.813\, e^{-6\frac{D_p}{D_t}}\left(\dfrac{D_pG}{\mu}\right)^{0.90}$	50–3500	
21–52	0.3–0.9		100–4500	Correction factor used for metallic packings
21–52	0.3–0.9	$\dfrac{UD_t}{k_g} = 3.50\, e^{-4.6\frac{D_p}{D_t}}\left(\dfrac{D_pG}{\mu}\right)^{0.7}$	150–3000	
15–52	0.3–0.9	$\dfrac{UD_p}{k_g} = 0.125\left(\dfrac{D_pG}{\mu}\right)^{0.75}$	500–12000	Correlation valid for high values of $\dfrac{D_p}{D_t}$
25–100	0.1–0.4	$\dfrac{UD_t}{k_g} = 4.9\, e^{-2.2\frac{D_p}{D_t}}\left(\dfrac{D_pG}{\mu}\right)^{0.60}$	100–600	
52–154		See original paper	30–900	Formula varies with shape of material
30–50	0.2–0.3	$\dfrac{UD_t}{k_g} = 5.783\dfrac{K_{r,0}}{k_g} + 0.085\left(\dfrac{D_p}{D_t}\right)^{-0.50}\left(\dfrac{D_pG}{\mu}\right)^{0.69}$ $+ 0.066\left(\dfrac{D_t}{L}\right)\left(\dfrac{D_p}{D_t}\right)^{-1}\left(\dfrac{D_pG}{\mu}\right)$	40–4000	$K_{r,0}$ is thermal conductivity of bed with stagnant gas
38	0.4–0.7	$U^{-1} = 0.00123 + 0.54G^{-0.83}$	Range of G (kg/m²h): 3000–12000	U refers to tube axis temperature and is corrected for radiation

Fischer–Tropsch plants and for hydrogenation of fatty esters to alcohols, furfural to furfuryl alcohol, and of glucose to sorbitol. Hydrogenation of benzene to cyclohexane is done at 50 bar and 220–225°C with Raney nickel of 0.01–0.1 mm dia. The relations between gas velocities, solids concentrations, bubble sizes, and rates of heat transfer are extensively documented in the literature.

4. In trickle bed reactors the gas and liquid both flow downward through a fixed bed of catalyst. The gas phase is continuous, and the liquid also is continuous as a film on the particles. Provided that the initial distribution is good, liquid distribution remains substantially uniform at rates of 10–30 m³/m² hr superficially, but channelling and hot spots may develop at lower rates. Redistributors sometimes are used. The many correlations that have

TABLE 17.17. Heat Transfer Coefficient between Particle and Gas

Authors	Method of Measurement	Heating or Cooling of Gas	Gas	Particles		
				Material	Shape	Diameter D_p, mm
Furnas (1930a, b, c, 1932)	Unsteady heat transfer	H, C	Air, flue gas	Iron ore, limestone, coke, etc.	Granules	4–70
Löf and Hawley (1948)	''	C	Air	Granitic gravel	Granules	8–34
Saunders and Ford (1940)	''	C	Air	Steel, lead, glass	Spheres	1.6–6.4
Tsukhanova and Shapatina (1943) Chukhanov and Shapatina (1946)	''	C	Air	Steel, chamotte, copper	Spheres, cylinders, granules	2–7
Dayton et al. (1952)	Cyclic variations		Air	Glass	Spheres	3–6
Glaser (1955)	''		Air	Stoneware	Raschig rings	5–17
Gamson, Thodos, and Hougen (1943)	Drying		Air	Porous celite	Spheres, cylinders	2–19
Wilke and Hougen (1945)	''		Air	Porous celite	Cylinders	2–19
Taecker and Hougen (1949)	''		Air	Porous claykieselguhr	Raschig rings, Berl saddles	6–50
Eichhorn and White (1952)	Dielectrical heating		Air	Plastic	Spheres	0.1–0.7
Satterfield and Resnick (1954)	Decomposition of H_2O_2		Vapors of H_2O and H_2O_2	Catalyst	Spheres	5

been developed for packed bed mass transfer are applicable to trickle bed operation. Commercial reactors are 1–4 m dia and 10–30 m long. Hydrocracking and hydrodesulfurization of petroleum and hydration of olefins are commonly practiced in trickle beds at superficial liquid velocities of 3–90 m/hr.

5. **Upflow fixed beds.** The liquid phase is continuous and the gas phase dispersed. This mode of operation has the advantages of better mixing, higher rates of mass and heat transfer, better distribution of liquid flow across the cross section, and better scouring of deactivating deposits from the surface of the catalyst. The disadvantages relative to trickle beds are higher pressure drop, the possibility of occurrence of flooding, and the need for mechanical restraint to prevent fluidization and entrainment of the catalyst. The most prominent example of upflow operation is the SYNTHOIL coal liquefaction process, but this mode of operation is competitive in other cases with the trickle bed, depending on the balance of advantages and disadvantages in particular situations.

TABLE 17.17.—(*continued*)

Tube Diameter, D_t, mm	Length L, m	Formula (D_p and D_t in m)	Range of $N_{Re'}$ or other variable	Remarks
150–230	0.5–1	$h_v = A \dfrac{G^{0.7}}{D_p^{0.9}} T^{0.3} 10^{1.68\varepsilon - 3.56\varepsilon^2}$	Range of G (kg/m²h): 2300–9200	A given in paper. Corrections for temperature and voids not very reliable
ca. 300 square	0.9	$h_v = 1.82\left(\dfrac{G}{D_p}\right)^{0.7}$	G: 300–1600	
50–200	0.09–0.34	Graphs in paper	G: 2670–5340	Correlated by Löf and Hawley (1948) as: $h_v = 0.152\dfrac{G}{D_p}$
	0.01–0.25	Graphs and $\dfrac{hD_p}{k_g} = 0.24\left(\dfrac{D_p G}{\mu}\right)^{0.83}$	Gas velocity: 0.7–2 m/sec.	
	0.05	Graphs in paper	100–1000	
350		$\dfrac{hD_p}{k_g} = A\left(\dfrac{D_p G}{\mu}\right)^{0.61}$	130–2000	A varies from 0.590 to 0.713. See also Glaser (1938)
		$j_h = \dfrac{h}{GC_p} N_{Pr}^{\frac{2}{3}} = 1.064\left(\dfrac{D_p G}{\mu}\right)^{-0.41}$	350–4000	
		$j_h = \dfrac{h}{GC_p} N_{Pr}^{\frac{2}{3}} = 1.96\left(\dfrac{D_p G}{\mu}\right)^{-0.51}$ Rings: $j_h = 1.148\left(\dfrac{\sqrt{a_p}\, G}{\mu}\right)^{-0.41}$ Saddles: $j_h = 0.920\left(\dfrac{\sqrt{a_p}\, G}{\mu}\right)^{-0.34}$	50–350 100–20000 70–3000	
38 square		Graphs in paper	1–18	
47–75	0.024	$j_h = 0.992\left(\dfrac{D_p G}{\mu}\right)^{-0.34}$	15–160	

$^a a_p$ = surface of a particle, a_v = surface/volume in the bed. (Kjaer, 1958).

TABLE 17.18. Formulas for the Heat Transfer Coefficient at the Walls of Packed Vessels[a]

Name	Geometry	Formula
1. Beek (1962)	spheres	$Nu = 0.203\,Re^{1/3}\,Pr^{1/3} + 0.220\,Re^{0.8}\,Pr^{0.4}$, $Re < 40$
2. Beek (1962)	cylinders	$Nu = 2.58\,Re^{1/3}\,Pr^{1/3} + 0.094\,Re^{0.8}\,Pr^{0.4}$, $Re < 40$
3. Yagi-Wakao (1959)	spheres	$Nu = 0.186\,Re^{0.8}$
4. Hanratty (1954)	cylinders	$Nu = 0.95\,Re^{0.5}$
5. Hawthorn (1968)		$Nu = 0.28\,Re^{0.77}\,Pr^{0.4}$
6. Doraiswamy and Sharma (1984)	spheres	$Nu = 0.17\,Re^{0.79}$, $L/d_t > 50$, $20 < Re < 7600$, $0.05 < d_p/d_t < 0.30$
7. Doraiswamy and Sharma (1984)	cylinders	$Nu = 0.16\,Re^{0.93}$, $L/d_t > 50$, $20 < Re < 800$, $0.03 < d_p/d_t < 0.2$
8. Gnielinski–Martin, Schlünder (1978)		$Nu/(2.5-1.5\varepsilon) = 0.8[2 + F(Re/\varepsilon)^{1/2}(Pr)^{1/3}]$ $F = 0.664\left\{1 + \left[\dfrac{0.0577(Re/\varepsilon)^{0.3}Pr^{0.67}}{1 + 2.44(Pr^{2/3} - 1)(Re/\varepsilon)^{-0.1}}\right]^2\right\}^{1/2}$
9. Gnielinski–Martin–Schlünder (1978)		$\ln\dfrac{Nu}{2.5-1.5\varepsilon} \simeq 0.750 + 0.1061\ln(Re/\varepsilon) + 0.0281[\ln(Re/\varepsilon)]^2$

[a] Definitions: $Nu = h_w d_p/k_f$, $Pr = (C_p\mu/k)_f$, $h_w =$, wall coefficient, d_p = particle diameter = $6V_p/A_p$, k_f = fluid molecular conductivity, ε = porosity, $Re = d_p G/\mu$, G = superficial mass velocity per unit cross section.

(a)

(b)

(c)
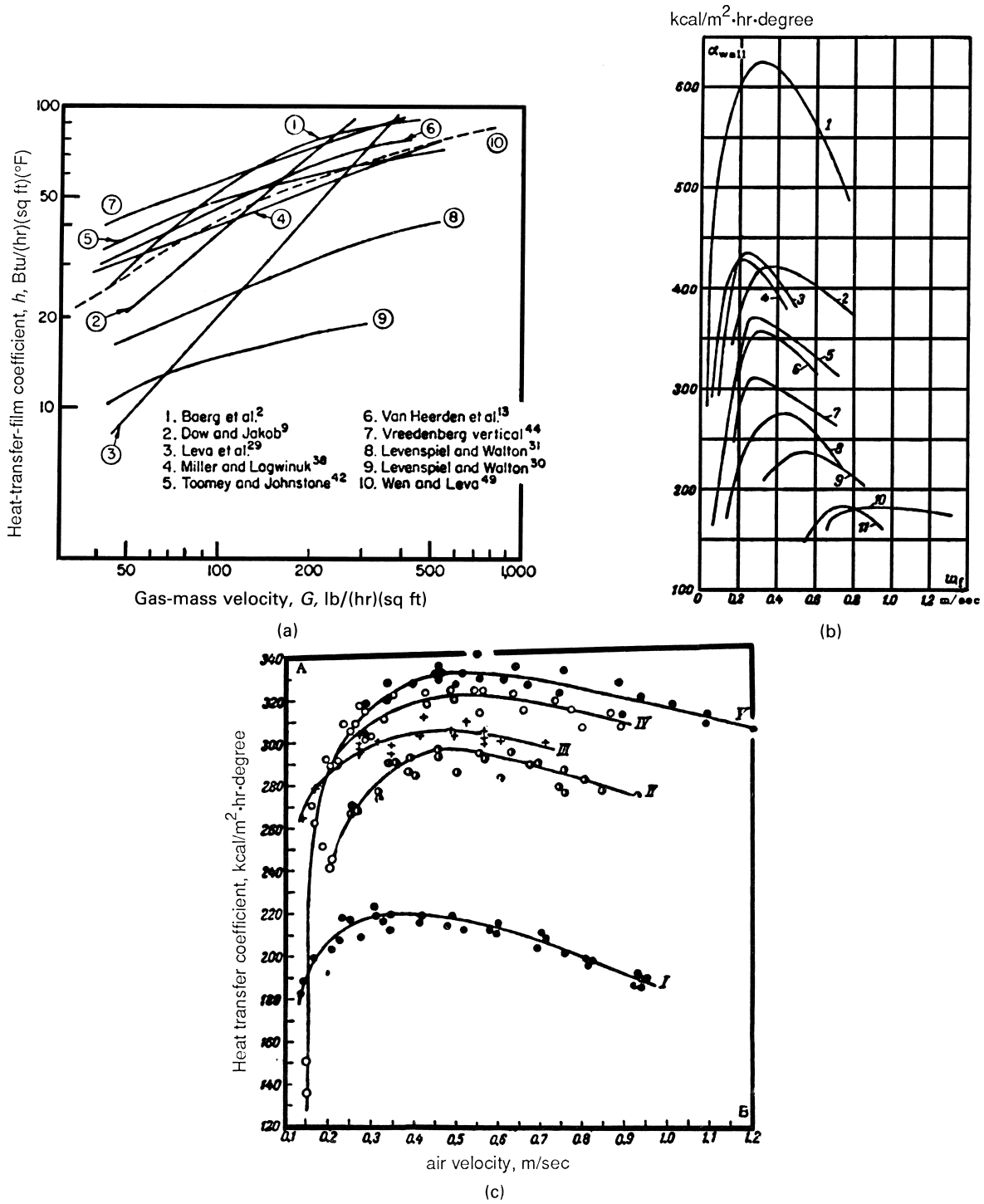
Figure 17.37. Some measured and predicted values of heat transfer coefficients in fluidized beds. 1 Btu/hr(sqft) ($°F$) = 4.88 kcal/(hr)(m^2)($°C$) = 5.678 W/(m^2)($°C$). (a) Comparison of correlations for heat transfer from silica sand with particle size 0.15 mm dia fluidized in air. Conditions are identified in Table 17.19 (*Leva, 1959*). (b) Wall heat transfer coefficients as function of the superficial fluid velocity, data of Varygin and Martyushin. Particle sizes in microns: (1) ferrosilicon, $d = 82.5$; (2) hematite, $d = 173$; (3) carborundum, $d = 137$; (4) quartz sand, $d = 140$; (5) quartz sand, $d = 198$; (6) quartz sand, $d = 216$; (7) quartz sand, $d = 428$; (8) quartz sand, $d = 515$; (9) quartz sand, $d = 650$; (10) quartz sand, $d = 1110$; (11) glass spheres, $d = 1160$. (*Zabrodsky et al., 1976, Fig. 10.17*). (c) Effect of air velocity and particle physical properties on heat transfer between a fluidized bed and a submerged coil. Mean particle diameter 0.38 mm: (I) BAV catalyst; (II) iron-chromium catalyst; (III) silica gel; (IV) quartz; (V) marble (*Zabrodsky et al., 1976, Fig. 10.20*).

Equation of line: $\dfrac{hD_p}{k_g(1-\epsilon)}\left(\dfrac{k_g}{c_g\rho_g}\right)^{0.43}=0.033\ C_R\left(\dfrac{D_pG}{\mu}\right)^{0.23}\left(\dfrac{c_s}{c_g}\right)^{0.80}\left(\dfrac{\rho_p}{\rho_g}\right)^{0.66}$

(for $k_g/c_g\rho_g$ in sq ft/hr)

○ Mickley and Fairbanks
■ Olin and Dean
▽ Toomey and Johnstone
✗ Baerg, Klassen, and Gishler
△ Mickley and Trilling
◉ Commercial Fluid Hydroformer
  Catalyst Regenerator Bed Coolers

(a)

COORDINATES

D_pG/μ	$f\times10^4$
0.04	0.275
0.1	0.83
0.4	3.80
1.0	8.0
4.0	19.9
10.0	28.1
40.0	36.8

○ Bartholomew and Katz
✗ Dow and Jacob
■ Leva, Weintraub, and Grummer
△ Toomey and Johnstone
▽ Mickley and Trilling
  (runs at low $1-\epsilon$ omitted)

(b)

Figure 17.38. Heat transfer coefficient in fluidized beds (*Wender and Cooper*, 1958). (a) Heat transfer at immersed vertical tubes. All groups are dimensionless except $k_g/C_g\rho_g$, which is sqft/hr. The constant C_R is given in terms of the fractional distance from the center of the vessel by $C_R = 1 + 3.175(r/R) - 3.188(r/R)^2$. (b) Heat transfer at the wall of a vessel. L_H is bed depth, D_T is vessel diameter.

TABLE 17.19. Experimental Investigations of Heat Transfer in Fluidized Beds[a]

Reference	Solids	Voidage range	Absolute density, lb per cu ft	Particle-size range, ft	Type of apparatus and operation	Vessel diam., in.	Height of heat-transfer area, in.	Bed height, in.	Fluids	Flow range, lb/(hr) (sq ft)	Temp, °F
1	Sands, graphite, soft brick	Dense phase	83–166	8–14 mesh to 36–72 mesh	Steam-jacketed column	1.5	14.5	. . . .	Air	150–1,200	
2	Iron powder, sands, glass beads catalyst	38.8–75	119–434	0.000198–0.00288	Central electric heat	1.25 in. 5.5	4	10	Air	1.85–605	23.5–65.0
3	Sand, aluminum, calcium carbonate	54–95	160–167	0.000277–0.000822	Wall electric heat	4.0	30	30	Air	96–935	300–450
4	Glass beads	Dilute phase	. . . .	0.00023–0.0036	Electric heat from outside	1.959	12	. . . .	Air	95–3,780	
6	Sand, aluminum, graphite, copper catalyst	Dense phase	24.6–27.2	0.00079–0.0126	Central cooling	2.31	Immersed cooling coil	. . . .	Air	40–100	87–145
9	Aerocat, coke, iron powder	52–69	121–466	0.000363–0.000560	Wall steam heating	2.06 and 3.07	23 and 26.5	2–13	Air	50–300	200–220
13	Carborundum, iron oxide, coke, lead fly ash, alloy	Dense phase	37.5–694	0.000262–0.00213	Wall water cooling	3.4	4	16	Air, CH_4, CO_2, town gas, H_2 and N_2 mixtures	44–779	Approx 10–30°C
17	Glass beads	Dense phase	154	0.00010–0.0011	Internal heating by electric wire	3.0	. . . .	. . . .	Air, CO_2, Freon-12, He, H_2, H_2 and N_2 mixtures		
26, 29	Sand, iron catalyst, silica gel	35–75	80–500	0.000129–0.00149	Wall steam heat	2.0 and 4.0	25 and 26	12–25	Air, CO_2, He, N_2	1.47–1.095	258–413
30	Coal	Dense phase	. . . .	0.000432–0.00386	Wall cooling (air)	4.0	24	. . . .	Air	50–1,100	
31	Glass beads catalyst, coal	41.7–86.2	63.6–180	0.000250–0.0142	Wall electric heating	4.0	3 sections, 2, 5, and 2 in.	10–30	Air	79–4,350	
36	Glass beads, microspheres	Dense phase	138–153	0.00022–0.00027	Small electric heater probe	. . . .	. . . .	Approx 18–20	He, air, CH_4, argon	10–150	
37	Glass beads	Dilute phase	151–177	0.000133–0.00149	Internal and external heating	2.875 and 1.00	. . . .	. . . .	Air	2,700	500
38	Silicon carbide, Al_2O_3, silica gel	Dense phase	70–243	0.000287–0.000817	Center wall cooling	2.0	22	. . . .	Air, He, CO_2	6.4–200	120–414
42	Glass beads	Dense phase	167–179	0.000179–0.00278	Wall water cooling	4.73	7 sections, each 5 in. high	13.2–24.6	Air	23.7–1,542	
43, 44	Sand, iron ore	Dense phase	165–330	0.000766–0.00197	Internal cooling	1.35 in. 22.2	. . . .	47, 68	Air	65–300	Approx 100–400
50	Carborundum sand, aluminum powder, lead powder, glass beads	Dense phase	160–700	0.00020–0.010	Internal heating by small cylindrical element	3.94	. . . .	. . . .	Air, CO_2, H_2		

[a] Another list of 29 sources is given by Zabrodsky (1966). (Leva, 1959).

TABLE 17.20. Heat Transfer Coefficients in Fluidized Beds[a]

1. At vertical tubes (Vreedenburg, 1960):

$$[h(D - d_t)/k_g](d_t/D)^{1/3}(k_g/C_s\mu_g)^{1/2} = C[u(D - d_t)\rho_s/\mu_g]^n$$

Conditions:

$\rho_s d_s u/\mu_g < 2050$,

$\begin{cases} \rho_s u(D - d_t)/\mu_g < 2.4 \times 10^5, \ C = 2.7 \times 10^{-16}, \ n = 3.4 \\ \rho_s u(D - d_t)/\mu_g > 2.4 \times 10^5, C = 2.2, \quad n = 0.44 \end{cases}$

$$[h(D - d_t)/k_g](d_t d_s k_g/[(D - d_t)C_s\mu_g]^{1/3} = C[u(D - d_t)g^{0.5}d_s^{1.5}]^n$$

Conditions:

$\rho_s d_s u/\mu_g > 2550$,

$\begin{cases} u(D - d_t)g^{0.5}d_s^{1.5} < 1070, \ C = 1.05 \times 10^{-4}, \ n = 2.0 \\ u(D - d_t)g^{0.5}d_s^{1.5} > 1070, \ C = 240, \quad n = 0.8 \end{cases}$

For off-center locations, the factor C is multiplied by C_R which is given in terms of the fractional distance from the center by

$$C_R = 1 + 3.175(r/R) - 3.188(r/R)^2$$

2. At vertical tubes, see the correlation of Wender and Cooper on Figure 17.17(a)

3. At horizontal tubes (Vreedenburg, *loc. cit.*; Andeen and Glicksman, ASME Paper 76-HT-67, 1976):

$$(hd_t/k_g)(k_g/C_s\mu_g)^{0.3} = 0.66[\rho_s d_t u(1 - \varepsilon)/\mu_g\varepsilon]^{0.44},$$
$$\rho_s d_s u/\mu_g < 2500$$
$$(hd_t/k_g)(k_g/C_s\mu_g)^{0.3} = 900(1 - \varepsilon)(d_t u\mu_g/d_s^3\rho_s g)^{0.326},$$
$$\rho_s d_s u/\mu_g > 2550$$

4. At vessel walls, see Figure 17.17(b) for the correlation of Wender and Cooper.

[a] Notation: Subscript s for solid, subscript g for gas, d_t = tube diameter, D = vessel diameter, g = acceleration of gravity.

TABLE 17.21. Examples of Industrial Gas–Liquid–Solid Reaction Processes

A. Fixed-bed reactors
1. Trickle beds (downflow)
   a. Catalytic hydrodesulfurization, hydrocracking and hydrogenation
   b. Butynediol from acetylene and aqueous formaldehyde
   c. Sorbitol from glycerol
   d. Oxidation of SO_2 in the presence of activated carbon
   e. Hydrogenation of aniline to cyclohexylaniline
2. Upflow (bubble) reactors
   a. Coal liquefaction by SYNTHOIL process
   b. Fischer–Tropsch process
   c. Selective hydrogenation of phenylacetylene and styrene

B. Suspended solid reactors
1. Stirred tanks
   a. Catalytic hydrogenation of fats and oils
   b. Hydrogenation of acetone and nitrocaprolactam

   c. Aerated fermentation with cellular enzymes
   d. Reaction between methanol and hydrogen chloride with $ZnCl_2$ catalyst
2. Slurry towers
   a. Fischer–Tropsch process
   b. Hydrogenation of methyl styrene and carboxy acids
   c. Oxidation and hydration of olefins
   d. Polymerization of ethylene
   e. Calcium hydrophosphite from white phosphorous and lime slurry
   f. Lime/limestone process for removal of SO_2 from flue gases
3. Fluidized bed of catalyst
   a. Calcium acid sulfite from $CaCO_3 + SO_2 + H_2O$
   b. Coal liquefaction
   c. Hydrocracking and hydrodesulfurization

REFERENCES

General

J. Beek, Design of packed catalytic reactors, *Adv. Chem. Eng.*, **3**, 203–271 (1962).

L.K. Doraiswamy and M.M. Sharma, *Heterogeneous Reactions: Analysis, Examples and Reactor Design*, Wiley, New York, 1984, 2 vols.

E.B. Nauman, and B.A. Buffham, *Mixing in Continuous Flow Systems*, Wiley, New York, 1983.

H.F. Rase, *Chemical Reactor Design in Chemical Plants*, Wiley, New York, 1977, 2 vols.

Rodiguin and Rodiguina, *Consecutive Chemical Reactions*, Van Nostrand, New York, 1964.

Y.T. Shah, *Gas-Liquid-Solid Design*, McGraw-Hill, New York, 1979.

M.O. Tarhan, *Catalytic Reactor Design*, McGraw-Hill, New York, 1983.

S.M. Walas, *Reaction Kinetics for Chemical Engineers*, McGraw-Hill, New York, 1959.

S.M. Walas, Chemical reactor data, *Chem. Eng.*, 79–83 (October 14, 1985).

C.Y. Wen and L.T. Fan, *Models for Flow Systems and Chemical Reactors*, Dekker, Chech New York, 1975.

K.R. Westerterp, W.P.M. Van Swaaij, and A.A.C.M. Beenackers, *Chemical Reactor Design and Operation*, Wiley, New York, 1984.

Types of Reactors

G. Astarita, D.N. Savage, and A. Bisio, *Gas Treating With Chemical Solvents*, Wiley, New York, 1983.

Gillespie and Kenson, *Chemtech*, 625 (October 1971).

A.L. Kohl and R.B. Nielsen, *Gas Purification*, Gulf, Houston, 1979.

Kraft, Ulrich, and O'Conner, in D. Othmer (Ed.), *Fluidization*, Reinhold, New York, 1956.

W.L. Nelson, *Petroleum Refinery Engineering*, McGraw-Hill, New York, 1958.

J.L. Patton et al., *Pet. Ref.*, **37**(11), 180 (1958).

Sukhanov, *Pet. Processing*, Mir, Moscow, 1982.

Ullman, in *Encyclopedia of Chemical Technology*, 3rd ed., Vol. 15, Verlag Chemie, Weinheim, Germany, 1964, p. 456.

Ullman, Reaktionsapparate, in *Encyclopedia of Chemical Technology*, Vol. 3, Verlag Chemie, Weinheim, Germany, 1973, pp. 320–518.

Winnacker-Weingartner, *Chemische Technologie*, Carl Hanser Verlag, Munich, Germany, 1950–1954.

Catalysts and Chemical Processes

J.E. Bailey, and D.F. Ollis, *Biochemical Engineering Fundamentals*, McGraw-Hill, New York, 1986.

C.H. Bamford and C.F.H. Tipper (Eds.), *Complex Catalytic Processes*, Comprehensive Chemical Kinetics, Vol. 20, Elsevier, New York, 1978.

D.E. Dyson and P. Simon, *Ind. Eng. Chem. Fundamentals*, **7**, 605–610 (1968).

B.C. Gates, J.R. Katzer, and O.C.A. Schutt, *Chemistry of Catalytic Processes*, McGraw-Hill, New York, 1979.

P.H. Groggins, *Unit Processes in Organic Synthesis*, 5th ed., McGraw-Hill, New York, 1958.

Kadlec, Pour, and Regner, *Coll. Czech. Chem. Com.*, **33**, 2388, 2526 (1968).

B.E. Leach (Ed.), *Applied Industrial Catalysis*, Academic, New York, 1983–1985, 3 vols.

H. Pines, *Chemistry of Catalytic Conversions of Hydrocarbons*, Academic, New York, 1981.

V.A. Roiter (Ed.), *Handbook of Catalytic Properties of Substances* (in Russian), Academy of Sciences, Ukrainian SSR, Kiev, USSR, 1968–date, 4 vols, to date.

C.N. Satterfield, *Mass Transfer in Heterogeneous Catalysis*, MIT Press, Cambridge, MA, 1970.

C.N. Satterfield, *Heterogeneous Catalysis in Practice*, McGraw-Hill, New York, 1980.

C.N. Satterfield, and P.J. Cadle, *Ind. Eng. Chem. Process Design and Development*, **7**, 256 (1968).

Spes, *Chem. Eng. Tech.*, **38**, 963 (1966).

S. Strelzoff, *Technology and Manufacture of Ammonia*, Wiley, New York, 1981.

C.L. Thomas, *Catalytic Processes and Proven Catalysts*, Academic, New York, 1970.

D.L. Trimm, *Design of Industrial Catalysts*, Elsevier, New York, 1980.

Ujhidy et al., *Chemtech*, **18**, 625 (1966).

Ullmann, *Encyclopedia of Chemical Technology*, Biotechnologie, Vol. 8, 1972, pp. 497–526; Enzyme, Vol. 10, 1975, pp. 47–561; Verlag Chemie, Weinheim, Germany.

C.A. Vancni, *Synthesis of Ammonia*, Macmillan, New York, 1971.

Heat Transfer in Reactors

H.R. Batchelder and H.A. Ingols, U.S. Bureau of Mines Report Invest. No., 4781 (1951).

L. Berg, in Othmer (Ed.), *Fluidization*, Reinhold, New York, 1956

N.P. Cheremisinoff, and P.N. Cheremisinoff, *Hydrodynamics of Gas-Solid Fluidization*, Gulf, Houston, 1984, abstract section.

E.D. Ermanc, Ermani, *Chem. Eng. Prog.*, **52**, 149 (1956).

Froment, *Adv. Chem. Ser.*, **109** (1970).

M.B. Glaser and G. Thodos, Heat and momentum transfer in flow of gases through packed beds, *A.I.Ch.E.J.*, **4**, 63–74 (1958).

J.R. Grace, Fluidized bed heat transfer, in Hetsroni (Ed.), *Handbook of Multiphase Systems*, Hemisphere, New York, 1982.

T.J. Hanratty, *Chem. Eng. Sci.*, **3**, 209 (1954).

R.D. Hawthorn, G.H. AcKermom, and A.C. Nixon *AI.Ch.E.J.*, **14**, 69 (1968).

G. Hetsroni, *Handbook of Multiphase Systems*, McGraw-Hill, New York, 1982.

Kjaer, *Measurement and Calculation of Temperature and Conversion in Fixed-Bed Catalytic Converters*, Haldor Topsoe, Copenhagen, 1958.

L.A. Korotjanskaja, et al., cited by L.K. Doraiswamy and M.M. Sharma, 1984, p. 323.

M. Leva, *Fluidization*, McGraw-Hill, New York, 1959.

R.A. Meyers (Ed.), *Handbook of Synfuels Technology*, McGraw-Hill, New York, 1984.

J.Y. Oldshue, *Fluid Mixing Technology*, McGraw-Hill, New York, 1983.

Paraho, Oil Shale Demonstration, Grand Junction, CO.

H.F. Rase, *Chemical Reactor Design for Process Plants*, Wiley, New York, 1977, 2 vols.

E.U. Schlunder, Transport phenomena in packed bed reactors, in *Chemical Reactor Engineering Reviews-Houston*, ACS Symposium 72, American Chemical Society, Washington, D.C., 1978.

J.W. Smith, in Meyers (Ed.), *Handbook of Synfuels Technology*, McGraw-Hill, New York, 1984.

H.A. Vreedenberg, Heat transfer between a fluidized bed and a horizontal tube, *Chem. Eng. Sci.*, **9**, 52–60 (1958); Vertical tubes, *Chem. Eng. Sci.*, **11**, 274–285 (1960).

L. Wender, and G.T. Cooper, Heat transfer between fludized beds and boundary surfaces-correlation of data, *A.I.Ch.E.J.*, **4**, 15–23 (1958).

T. Yagi-Wakao, *Chem. Eng. Sci.*, **5**, 79 (1959).

S.S. Zabrodsky, *Hydrodynamics and Heat Transfer in Fluidized Beds*, MIT Press, Cambridge, MA, 1966.

S.S. Zabrodsky, N.V. Antonishin, and A.L. Parnas, On fluidized bed to surface heat transfer, *Can. J. Chem. Eng.* **54**, 52–58 (1976).

18

PROCESS VESSELS

Vessels in chemical processing service are of two kinds: those substantially without internals and those with internals. The main functions of the first kinds, called drums or tanks, are intermediate storage or surge of a process stream for a limited or extended period or to provide a phase separation by settling. Their sizes are established by process calculations or by general rules of thumb based on experience. The second category comprises the shells of equipment such as heat exchangers, reactors, mixers, fractionators, and other equipment whose housing can be designed and constructed largely independently of whatever internals are necessary. Their major dimensions are established by process requirements described in other chapters, but considerations of adequate strength of vessels at operating pressures and temperatures will be treated in this chapter.

The distinction between drums and tanks is that of size and is not sharp. Usually they are cylindrical vessels with flat or curved ends, depending on the pressure, and either horizontal or vertical. In a continuous plant, drums have a holdup of a few minutes. They are located between major equipment to supply feed or accumulate product. Surge drums between equipment provide a measure of stability in that fluctuations are not transmitted along a chain of equipment, including those fluctuations that are characteristic of control instruments of normal sensitivity. For example, reflux drums provide surge between a condenser and its tower and downstream equipment; a drum ahead of a compressor will ensure freedom from liquid entrainment and one ahead of a fired heater will protect the tubes from running dry; a drum following a reciprocating compressor will smooth out pressure surges, etc. Tanks are larger vessels, of several hours holdup usually. For instance, the feed tank to a batch distillation may hold a day's supply, and tanks between equipment may provide several hours holdup as protection of the main storage from possible off-specification product or as opportunity for local repair and servicing without disrupting the entire process.

Storage tanks are regarded as outside the process battery limits, on tank farms. Their sizes are measured in units of the capacities of connecting transportation equipment: 34,500 gal tank cars, 8000 gal tank trucks, etc., usually at least 1.5 times these sizes. Time variations in the supply of raw materials and the demand for the products influence the sizes and numbers of storage tanks.

Liquid storage tanks are provided with a certain amount of vapor space or freeboard, commonly 15% below 500 gal and 10% above 500 gal. Common erection practices for liquid storage tanks are:

a. For less than 1000 gal, use vertical tanks mounted on legs.
b. Between 1000 and 10,000 gal, use horizontal tanks mounted on concrete foundation.
c. Beyond 10,000 gal, use vertical tanks mounted on concrete foundations.

Liquids with high vapor pressures and liquified gases are stored in elongated horizontal vessels. Gases under high pressure may be stored in elongated horizontal vessels but often in spherical tanks. Gases at or near atmospheric pressure are stored in gas holders with floating roofs and are sealed with a liquid in a double wall built onto the holder.

Liquefied gases are maintained at subatmospheric temperatures with external refrigeration or autorefrigeration whereby evolved vapors are compressed, condensed, cooled, and returned to storage.

Liquids stored at near atmospheric pressure are subject to breathing losses: As the tank cools during the night, air is drawn in, then vaporization occurs to saturation, and the vapor mixture is expelled as the tank warms up during the day. Volatile liquids such as gasoline consequently suffer a material loss and also a change in composition because of the selective loss of lighter constituents.

In order to minimize such effects, several provisions are made, for example:

1. A floating roof is a pad which floats on the surface of the stored liquid with a diameter of about a foot less than that of the tank. The annular space between the float and the shell may be sealed by one of several available methods.
2. An expansion roof allows thermal expansion of the vapor space. It rides with the changing vapor and is sealed with liquid in a double wall.
3. A bag of vapor resistant fabric is allowed to expand into a housing of much smaller diameter than that of the storage tank. This is a lower cost construction than either of the other two.

Weather resistant solids such as coal or sulfur or ores are stored in uncovered piles from which they are retrieved with power shovels and conveyors. Other solids are stored in silos. For short-time storage for process use, solids are stored in bins that are of rectangular or circular cross section with cone bottoms and hooked up to process with conveyors. All aspects of the design of such equipment are covered by Reisner and Rothe (1971), Stepanoff (1969), and Steve (2000).

18.1. DRUMS

Liquid drums are usually placed horizontally and gas–liquid separators vertically, although reflux drums with gas as an overhead product commonly are horizontal. The length to diameter ratio is in the range of 2.5–5.0, the smaller diameters at higher pressures and for liquid–liquid settling. A rough dimension of L/D dependent on pressure is

P (psig)	0–250	251–500	501+
L/D	3	4	5

The volume of a drum is related to the flow rate through it, but it depends also on the kinds of controls and on how harmful would be the consequences of downstream equipment running dry. Conventionally, the volume often is expressed in terms of the number of minutes of flow on a half-full basis. For many services, 5–10 min half-full is adequate but two notable exceptions are:

1. Fired heater feed surge drum for which the size is 10–30 min half-full.
2. Compressor feed liquid knockout drum which is made large enough to hold 10–20 min of liquid flow, with a minimum volume of 10 min worth of gas flow rate.

Other major services require more detailed consideration, as follows.

18.2. FRACTIONATOR REFLUX DRUMS

Commonly their orientation is horizontal. When a small amount of a second liquid phase (for example, water in an immiscible organic) is present, it is collected in and drawn off a pot at the bottom of the drum. The diameter of the pot is sized on a linear velocity of 0.5 ft/sec is a minimum of 16 in dia in drums of 4–8 ft dia, and 24 in. dia. in larger sizes. The minimum vapor space above the high level is 20% of the drum diameter or 10 in (Sigales, 1975).

A method of sizing reflux drums proposed by Watkins (1967) is based on several factors itemized in Table 18.1. A factor F_3 is applied to the net overhead product going downstream, then instrument factors F_1 and labor factors F_2 which are added together and applied to the weighted overhead stream, and finally a factor F_4 is applied, which depends on the kind and location of level indicators. When L is the reflux flow rate and D the overhead net product rate, both in gpm, the volume of the drum (gal) is given by

TABLE 18.1. Factors for Sizing Reflux Accumulators

a. Factors F_1 and F_2 on the Reflux Flow Rate

	Minutes				
	Instrument Factor F_1		Labor Factor F_2		
Operation	w/Alarm	w/o Alarm	Good	Fair	Poor
FRC	$\frac{1}{2}$	1	1	1.5	2
LRC	1	$1\frac{1}{2}$	1	1.5	2
TRC	$1\frac{1}{2}$	2	1	1.5	2

b. Factor F_3 on the Net Overhead Product Flow to External Equipment

Operating Characteristics	F_3
Under good control	2.0
Under fair control	3.0
Under poor control	4.0
Feed to or from storage	1.25

c. Factor F_4 for Level Control

	F_4
Board-mounted level recorder	1.0
Level indicator on board	1.5
Gage glass at equipment only	2.0

(Watkins, 1967).

$$V_d = 2F_4(F_1 + F_2)(L + F_3D) \text{ gal, full.} \tag{18.1}$$

For example, with $L = 400$ gpm and $D = 200$ gpm, at average conditions $F_1 = 1$, $F_2 = 1.5$, $F_3 = 3$, $F_4 = 1.5$, and

$$V_d = 2(1.5)(1 + 1.5)(400 + 3(200)) = 7500 \text{ gal, full}$$

or, 6.25 min half-full. With the best of everything, $F_1 = 0.5$, $F_2 = 1$, $F_3 = 2$, $F_4 = 1$, and

$$V_d = 2(0.5 + 1)(400 + 2(200)) = 2400 \text{ gal, full}$$

or 2.0 min half-full. The sizes figured this way are overruled when the destination of the net product is to a fired heater or a compressor; then the numbers cited in Section 18.1 are applicable.

Although this method seems to take into account a number of pertinent factors, it is not rigorous. Some practitioners may size drums on the basis of 5 minutes holdup half-full.

18.3. LIQUID–LIQUID SEPARATORS

Vessels for the separation of two immiscible liquids usually are made horizontal and operate full, although some low rate operations are handled conveniently in vertical vessels with an overflow weir for the lighter phase. The latter mode also is used for particularly large flows at near atmospheric pressures, as in the mixer–settler equipment of Figure 3.22. With the usual L/D ratio of three or more, the travel distance of droplets to the separated phase is appreciably shorter in horizontal vessels.

Since the rise or fall of liquid droplets is interfered with by lateral flow of the liquid, the diameter of the drum should be made large enough to minimize this adverse effect. A rule based on the Reynolds number of the phase through which the movement of the liquid drops occurs is proposed by Hooper and Jacobs (1979). The Reynolds number is $D_h u \rho / \mu$, where D_h is the hydraulic diameter and u is the linear velocity of the continuous phase. The rules are:

N_{Re}	Effect
Less than 5000	little problem
5000–20,000	some hindrance
20,000–50,000	major problem may exist
Above 50,000	expect poor separation

The jet effect of an inlet nozzle also may interfere with the phase separation. Ideally the liquid should be introduced uniformly over the cross section, but a baffle at the inlet nozzle may reduce such a disturbance adequately. More elaborate feed diffusers sometimes may be worthwhile. Figure 18.1 shows a perforated baffle.

Fall or rise of droplets of one liquid in another is represented closely by Stokes law,

$$u = g_c(\rho_2 - \rho_1)d^2/18\mu. \tag{18.2}$$

In English units,

$$u = 9.97(10^6)(\rho_2 - \rho_1)d^2/\mu^2, \text{ ft/min,} \tag{18.3}$$

where the ρ_i are specific gravities, d is the droplet diameter (ft), and μ is the viscosity of the continuous phase (cP).

The key property is the droplet diameter, of which many studies have been made under a variety of conditions. In agitated vessels, experience shows that the minimum droplet diameters are in the range of 500–5000 μm. In turbulent pipeline flow, Middleman (1974) found that very few droplets were smaller than 500 μm. Accordingly, for separator design a conservative value is 150 μm,
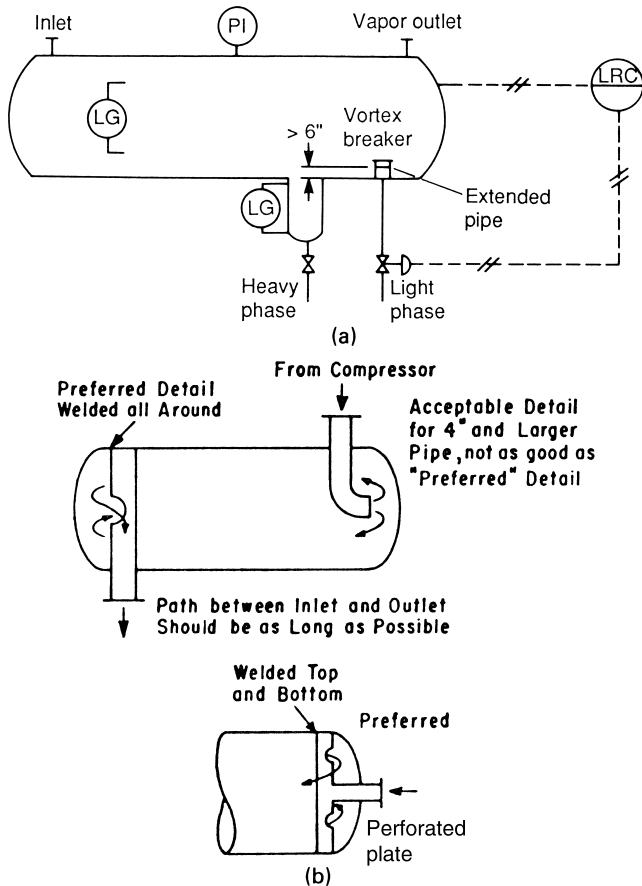
Figure 18.1. Drums for distillation tower reflux and for reciprocating compressor surge. (a) A reflux drum with a pot for accumulation and removal of a heavy phase. The main liquid is removed on level control through a vortex breaker. When the pot is large enough, it can accommodate an interface control for automatic drainage; otherwise the drain valve is hand set and monitored by an operator. (b) Arrangement of a surge drum for eliminating the high frequency response of a reciprocating compressor. Details are given by Ludwig (1995, Vol. 1, p. 258).

which also has been taken as a standard in numerous refinery waste operations. With this diameter,

$$u = 2.415(\rho_2 - \rho_1)/\mu, \text{ ft/min.} \qquad (18.4)$$

Which phase is the dispersed one can be identified with the factor

$$\psi = \frac{Q_L}{Q_H}\left(\frac{\rho_L u_H}{\rho_H u_L}\right)r^{0.3} \qquad (18.5)$$

with the statements of this table (Selker and Schleicher, 1965):

ψ	Result
< 0.3	light phase always dispersed
0.3–0.5	light phase probably dispersed
0.5–2.0	phase inversion probable, design for worst case
2.0–3.3	heavy phase probably dispersed
3.3	heavy phase always dispersed

These relations are utilized in Example 18.1 and the resulting design is represented on Figure 18.2.

COALESCENCE

The rate of separation of liquid phases can be enhanced by shortening the path through which the droplets need rise or fall or by increasing their diameters. Both effects are achieved by forcing the flow between parallel flat or crimped plates or through tower packing or through a mass of packed fibers. The materials should be wetted by the disperse phase and preferably rough. Fine droplets will impinge on the surfaces and will grow by accretion of other droplets. The separator in such cases will consist of a coalescing section and an open section where the now enlarged droplets can separate freely. Figure 18.3(a) is of a separator equipped with a coalescer that is especially suited to the removal of relatively small quantities of dispersed liquid. Figure 18.3(b) is an oil-water separator with corrugated plate coalescers. Cartridge-type coalescers are described by Redmon (1963). Packed separators have been studied by Davies, Jeffrys, and Azfal (1972) and the subject is reviewed by Laddha and Degaleesan (1983). Coalescence also can be induced electrically, a process that is used widely for the precipitation of brine from crude oils. Proprietary equipment is available for this purpose. The subject is discussed by Waterman (1965) and in detail by Fronczak (1983). High performance polymer fiber coalescers to break difficult emulsions and dispersions are discussed by Wines and Brown (1997).

OTHER METHODS

Very fine dispersions can be separated effectively with disk-type centrifuges. Commercial units have capacities of 5–500 gpm and are capable of removing water from hydrocarbons down to the ppm range. A mild centrifugal action is achieved in hydrocyclones. They have been studied for liquid–liquid separation by Sheng, Welker, and Sliepcevich (1974), but their effectiveness was found only modest. The use of hydrocyclones primarily for the recovery of solid particles from liquids is described in the book of Bradley (1965). A symposium on coalescence includes papers by Belk (1965), Jordan (1965), Landis (1965), and Waterman (1965).

18.4. GAS–LIQUID SEPARATORS

Droplets of liquid are removed from a gas phase by three methods:

1. Settling out under the influence of gravity.
2. Settling out under centrifugal action.
3. Impingement and coalescence on solid surfaces followed by settling.

Vapor-liquid separators often perform two functions. Their primary task is to separate the vapor phase from the liquid phase but they may also provide surge capacity. They must be sized to provide a low velocity and thus separate the liquid from the vapor.

Available methods for the design of liquid separators are arbitrary in some respects but can be made safe economically. Figure 18.4 illustrates some of these methods.

DROPLET SIZES

The period of time needed for settling out depends on the droplet size distribution and the required completeness of removal. A few observations of droplet sizes are mentioned by York (1983). Walas (1988) discussed droplet sizes from various types of equipment (e.g., spray nozzles, spray disks, etc.). The droplet sizes varied from 10 μm to 5,000 μm but sprays in process equipment usually range between 10 μm to 20 μm.

The amount of entrainment has been studied with respect to distillation equipment. A typical plot of entrainment from sieve

EXAMPLE 18.1
Separation of Oil and Water

Find the dimensions of a drum for the separation of oil and water at these conditions:

Oil at 180 cfh, sp gr = 0.90, viscosity = 10 cP.
water at 640 cfh, sp gr = 1.00, viscosity = 0.7 cP.

Take a droplet size to be 150 μm (0.0005 ft) and that the holdup in the tank is in the same proportions as in the feed. The geometry of the cross section:
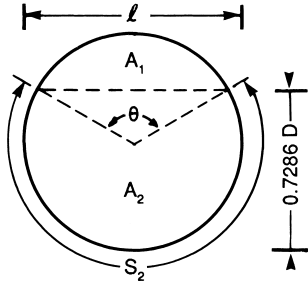
$$A_1 = \frac{180}{120}\frac{\pi}{4}D^2 = \frac{D_2}{8}(\theta - \sin\theta),$$

$$\therefore \theta = 2.192 \text{ rad},$$

$$A_2 = 0.7805\frac{\pi}{4}D^2 = 0.6130D^2,$$

$$L = D\sin(\theta/2) = 0.8894D,$$

$$S_2 = D\left(\pi - \frac{\theta}{2}\right) = 2.0456D.$$

Hydraulic diameter of heavy liquid

$$D_h = (4A_2)/(L + S_2) = \{[(4)(0.6130)D^2]/$$
$$[0.8894D + 2.0456D]\} = 0.8354D$$

The dispersion discriminant is

$$\psi = \frac{Q_L}{Q_H}\left(\frac{\rho_L}{\rho_H}\frac{\mu_H}{\mu_L}\right)^{0.3} = \frac{180}{640}\left(\frac{0.9(0.7)}{10}\right)^{0.3} = 0.123$$
$$< 0.30.$$

Oil is the light or dispersed phase:

$$N_{\text{Re}} = \frac{D_h u\rho}{\mu} = \frac{D_h\rho}{\mu}\frac{Q}{\frac{1}{4}\pi D^2} = \frac{(62.4)640}{42(0.7)\pi}\frac{(0.8354)}{D}$$
$$= \frac{25,076}{D}.$$

Velocity of rise:

$$u_r = \frac{2.415(1.00 - 0.90)}{0.7} = 0.345 \text{ ft/min.} \qquad \text{(Eq.18.4)}$$

Time of rise:

$$t = \frac{0.7286D}{0.345} = 2.1119D \text{ min}.$$

Forward velocity:

$$u_H = \frac{Q_H}{A_2} = \frac{640}{60(0.6130D^2)} = \frac{17.40}{D^2} \text{ ft/min.}$$

Flow distance:

$$L_f = tu_H = 2.1119D\left(\frac{17.40}{D^2}\right) = \frac{36.75}{D} \text{ ft.}$$

The tangent to tangent length of the drum will be approximately 24 in. greater than L_f to accommodate inlet and outlet nozzles and baffles.

The Reynolds number identifies the quality of the separation, for good separation $N_{\text{Re}} < 5,000$.

Some trials are

D (ft)	N_{Re}	t	u_H	L_f(ft)
5	5015	10.23	0.696	7.35
3.5	7165	7.16	1.420	10.50
3	8358	6.14	1.933	12.25

A vessel 5 × 9 ft would give excellent separation; 3 × 15 ft would be acceptable. A sketch of the latter proposed drum is in Figure 18.1(a).

---

trays is shown in Figure 18.5. Example 18.2 is an application of the entrainment data using Figure 18.5. Equation 18.11 incorporates entrainment data indirectly.

In general, practice has shown that about 95% of entrainment can be removed economically in gravity separators and in excess of 99% in separators with wire demisters or other solid surfaces on which impingement and coalescence are forced. In scrubbers and high-speed centrifuges this figure approaches 100%.

RATE OF SETTLING

The terminal or maximum settling velocity of a small droplet or particle in a gas is governed by one of Newton's equations.

$$u = f\sqrt{g_c D(\rho/\rho_g - 1)}. \qquad (18.6)$$

where
   u = terminal or maximum settling velocity
   D = diameter of the droplet
   ρ = density of the droplet, consistent units
   ρ_g = density of gas, consistent units
   f = friction factor

In laminar flow the friction factor becomes a simple function of the Reynolds number,

$$f = 18/(Du\rho_g/\mu_g). \qquad (18.7)$$

When Eq. 18.7 is substituted into Eq. 18.6, the falling velocity becomes

$$u = g_c(\rho - \rho_g)D^2/18\mu, \qquad (18.2')$$
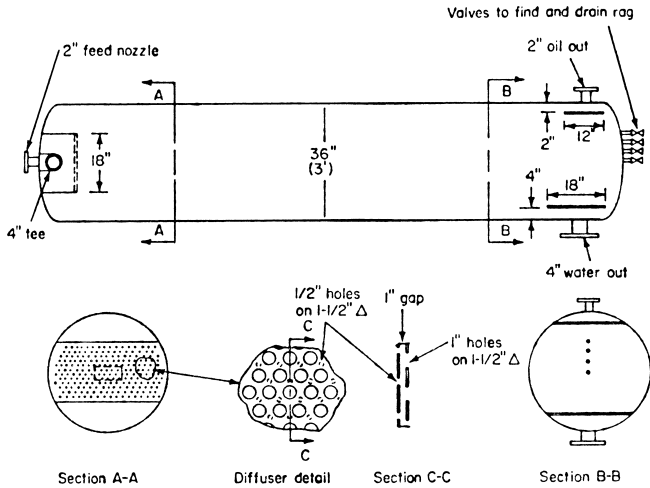
Figure 18.2. A design of an oil-water separator for the conditions of Example 18.1, showing particularly the diffuser at the inlet nozzle and baffles at the outlets. (Jacobs and Penney, 1987).

Figure 18.3. Drums with coalescers for assisting in the separation of small amounts of entrained liquid. (a) A liquid–liquid separating drum equipped with a coalescer for the removal of small amounts of dispersed phase. In water–hydrocarbon systems, the pot may be designed for 0.5 ft/sec. (b) An oil–water separator with corrugated plate coalescers. (Walas, 1988).

which is Stokes' equation. In view of the uncertainties with which droplet sizes are known in practical situations, Stokes equation usually is regarded as sufficiently descriptive of settling behavior. For example it predicts that $100\,\mu$m droplets of water fall at the rate of 1.0 ft/sec in atmospheric air.

Another approximation of Newton's equation is written

$$u = K\sqrt{\rho/\rho_g - 1}, \tag{18.8}$$

where the coefficient K depends on the system. For the $100\,\mu$m droplets of water in air just cited, the coefficient becomes $K = 0.035$, and for other sizes it varies as the square of the diameter.

EMPTY DRUMS

The cross section of a vertical settling drum is found from the vapor rate and the allowable linear velocity with the equation

$$u = 0.14\sqrt{\rho/\rho_g - 1}, \quad \text{ft/sec}, \tag{18.9}$$

in which the coefficient of Eq. (18.8) has been evaluated for $200\,\mu$m. The vertical dimension is more arbitrarily established. The liquid holdup is determined as in Section 18.2 and Table 18.1. For the vapor space, Watkins (1967) proposed the rules illustrated in Figure 18.6. When the calculated length to diameter ratio comes out less than 3, the length is increased arbitrarily to make the ratio 3; when the ratio comes out more than 5, a horizontal drum is preferably employed. Rules for horizontal drums also are shown on Figure 18.6. The vapor space is made a minimum of 20% of the drum volume which corresponds to a minimum height of the vapor space of 25% of the diameter, but with the further restriction that this never is made less than 12 in. When a relatively large amount of liquid must be held up in the drum, it may be advisable to increase the fraction of the cross section open to the vapor.

The diameter again is figured from the volumetric rate of the vapor and the linear velocity from Eq. (18.9). Since the upward drag of the vapor is largely absent in a horizontal drum, however, the coefficient K often is raised by a factor of 1.25. Example 18.3 deals with the design of both kinds of drums.

Evans (1980) proposed a stepwise design procedure for sizing empty vertical and horizontal vapor-liquid separators. The steps are outlined as follows:

For a vertical drum:

The first step is to calculate a vapor-liquid separation factor

$$w_l/w_v = (\rho_v/\rho_l)^{0.5} \tag{18.10}$$

where w_l = liquid flow rate, lb / sec
w_v = vapor flow rate, lb / sec
ρ_v, ρ_l = vapor and liquid densities, respectively, lb/ft^3

Next, enter Figure 18.5(b) to find K_v, the design velocity factor. This plot is for 85% flooding but other plots may be developed similar to Figure 18.5(b) for other percentage flooding.

$$(u_v)_{max} = K_v[(\rho_l - \rho_v)/\rho_v]^{0.5} \text{ in ft/sec} \tag{18.11}$$

Calculate the minimum vessel cross-sectional area:

$$A_{min} = Q_v/(u_v)_{max} \text{ in ft}^2 \tag{18.12}$$

Figure 18.4. Typical installations of mesh pads in equipment (*Metal Textile Corp Bulletin ME-7, from Ludwig, 1995, Vol. I, p. 253*).

Determine the vessel diameter:

$$D_{\min} = (4A_{\min}\pi)^{0.5} \text{ in ft} \tag{18.13}$$

As a practical consideration, set the vessel diameter from $D_{\min}$ to the next largest 6 inches.

To completely design the vessel, the minimum and maximum velocity in the inlet nozzle is obtained by using the empirical criteria:

$$(u_{\max})_{\text{nozzle}} = 100(\rho_{\text{mix}})^{0.5} \text{ in ft/sec} \tag{18.14}$$

$$(u_{\min})_{\text{nozzle}} = 60(\rho_{\text{mix}})^{0.5} \text{ in ft/sec} \tag{18.15}$$

Sketch the vessel as in Figure 18.7.

From Table 18.1, select the appropriate full surge volume in seconds. Calculate the required vessel volume.

$$V = Q_l/(\text{design time to fill}) \text{ in ft}^3 \tag{18.16}$$

where Q_l = liquid flow rate in ft^3/sec

Next, calculate the liquid height:

$$H_1 = V(4/\pi D^2) \tag{18.17}$$

Check the geometry such that $(H_l + H_v)/D$ is between 3 and 5.

(*Note*: Evans suggested that for small liquid volumes, it may be necessary to provide more liquid surge so that L/D is > 3. However, if the liquid surge volume is greater than that possible in a vessel having an L/D < 5, a horizontal drum should be used.)

For a horizontal drum design:

To size a horizontal drum, the following procedure is recommended:

Calculate the vapor-liquid separation factor by Eq. 18.10, as shown earlier:

$$w_l/w_v = (\rho_v/\rho_l)^{0.5} \tag{18.10}$$

In the case of the horizontal drum

$$K_H = 1.25 K_V \tag{18.18}$$

where
K_H = horizontal vapor velocity factor
K_V = vertical vapor velocity factor
Next, calculate the maximum vapor velocity

$$(u_v)_{\max} = K_H \left[(\rho_1 - \rho_v)/\rho_v\right]^{0.5} \text{ in ft/sec} \tag{18.11}$$

Calculate the required vapor flow area by Eq. 18.12:

$$(A_v)_{\min} = Q_v/(u_v)_{\max} \text{ in ft}^2 \tag{18.12}$$

From Table 18.1, select the appropriate design surge time and calculate the full liquid volume. The remainder of the sizing procedure is done by trial and error as follows:

When the vessel is full

$$(A_{\text{total}})_{\min} = (A_v)_{\min}/0.2 \tag{18.19}$$

$$D_{\min} = [4(A_{\text{total}})_{\min}/\pi]^{0.5} \tag{18.13}$$
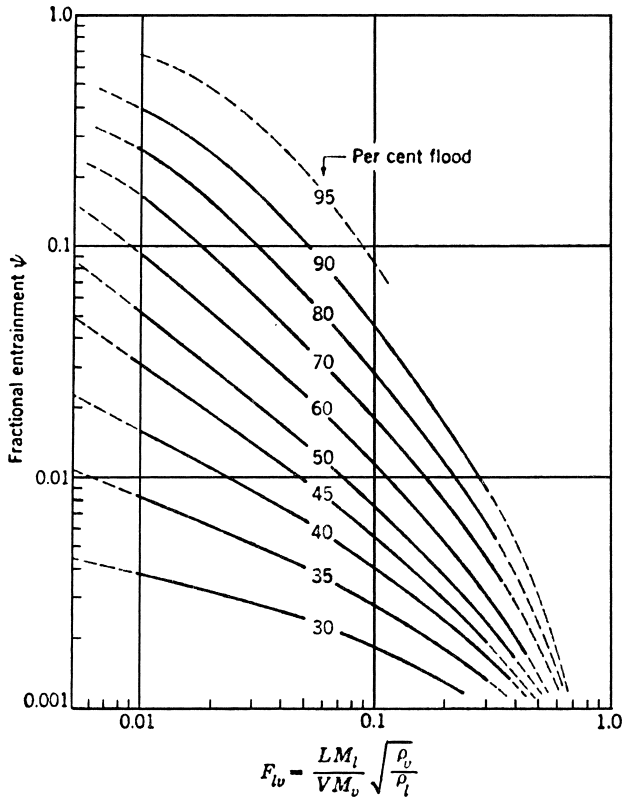
Figure 18.5a. Entrainment from sieve trays in the units mols liquid entrained/mol of liquid downflow; LM_L is the weight rate of flow of liquid and VM_V is the weight rate of flow of vapor. The flooding correlation is Figure 13.32(b). (*Fair and Matthews, 1958*).

Next, calculate the vessel length:

$$L = (\text{Full liquid volume})/(\pi D^2/4) \tag{18.20}$$

Then $D = D_{\min}$ to the next largest 6 in.
If $5 < L/D < 3$, then resize the tank.

Figure 18.5(b) is a plot of the vapor velocity factor k/v for vertical vapor liquid separators.

WIRE MESH PAD DEENTRAINERS

Pads of fine wire mesh induce coalescence of impinging droplets into larger ones, which then separate freely from the gas phase. Tower packings function similarly but are less effective and more difficult to install. The pads are made of metal wires or plastic strands or fiber glass. The data in Table 18.2 apply to stainless steel construction:

TABLE 18.2. Wire Mesh Efficiency as a Function of K Values

Efficiency Type	Efficiency (%)	lbs/cuft	sqft/cuft	Pressure	Vacuum
Low	99.0	5–7	65	0.40	
Standard	99.5	9	85	0.35	
					0.20–0.27
High	99.9	12	115	0.35	
Very high	99.9	13–14	120	0.25	

Because the wire mesh has not been standardized, no standard equations have been developed for pressure drop through the mesh.

A pad thickness of 4 in. is minimum, 6 in. is popular, and up to 12 in. may be required for fine mists.

The values of K in the preceding table are with a standard disengaging height of 10 in. The effect of other heights h is given by the equation

$$K = 0.021 + 0.0325h, \quad 3 \le h \le 12, \tag{18.21}$$

with a maximum value of 0.40. This relation is for standard efficiency pads. Lower values can be expected in aqueous systems where the surface tension has been reduced by surfactants.

When the pad is installed in a vertical or inclined position, practice has shown that K values should be about 2/3 of the value for pads mounted in a horizontal position.
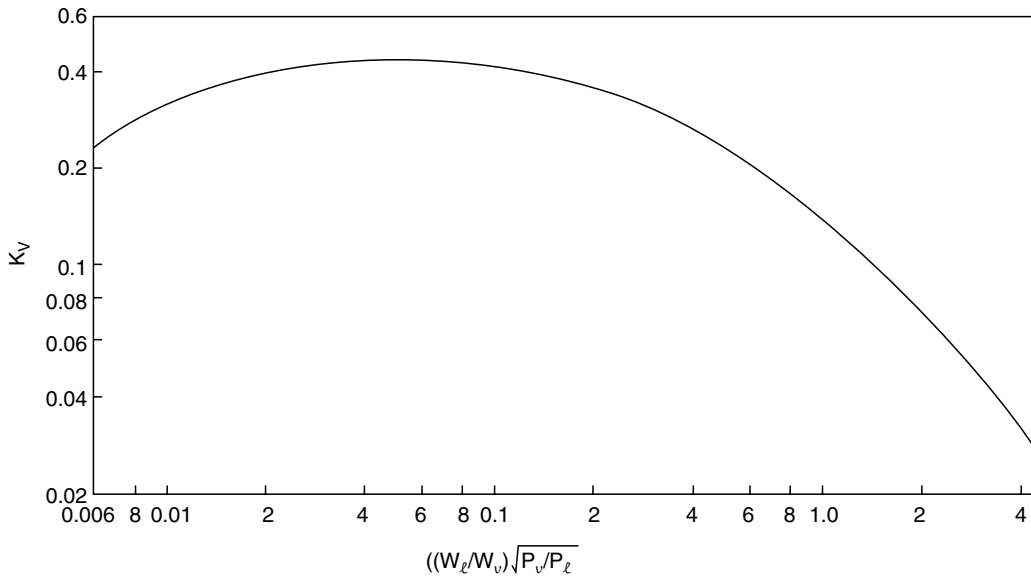
Figure 18.5b. Vapor velocity design factor for vapor liquid separators at 85% of flooding

Quantity of Entrainment on the Basis of Sieve Tray Correlations

A C_3 splitter has a 24-in. sieve tray spacing and will operate at 80% flooding. The following data apply:

$W_l = 259,100$ lb/hr of liquid
$W_v = 271,500$ lb/hr of vapor
$\rho_l = 29.3$ lb/ft^3
$\rho_v = 2.75$ lb/ft^3

In Figure 18.5(a), the flooding factor, the abscissa, is

$$F_{lv} = (LM_l/VM_v)(\rho_v/\rho_l)^{0.5} = (W_l/W_v)(\rho_v/\rho_l)^{0.5}$$

where LM_l = the weight rate of flow of liquid
and VM_v = the weight rate of flow of vapor

Therefore,

$$(W_l/W_v)(\rho_v/\rho_l)^{0.5} = (259, 100/271,500)\,(2.75/29.3)^{0.5} = 0.292$$

From Figure 18.5 at 80% flooding,

$$\psi = 0.008 \text{ mol entrained liquid/mol liquid downflow}$$

Since $W_l/W_v = (259,100 / 271,500) = 0.954$ mol liquid/mol vapor, assuming the same molecular weights, the entrainment expressed with reference to the vapor flow is

$$\psi = (0.008)\,(0.954) = 0.0076 \text{ mol liquid/mol vapor flow}$$

At high liquid rates droplets tend to be reentrained and the pad may become flooded. Some data are cited by York (1983, p. 194). A graphical correlation credited to the Fluor Co. is represented by Branan (1983, p. 67) by the equation

$$K = -0.0073 + \frac{0.263}{x^{1.294} + 0.573}, 0.04 \leq x \leq 6.0, \tag{18.22}$$
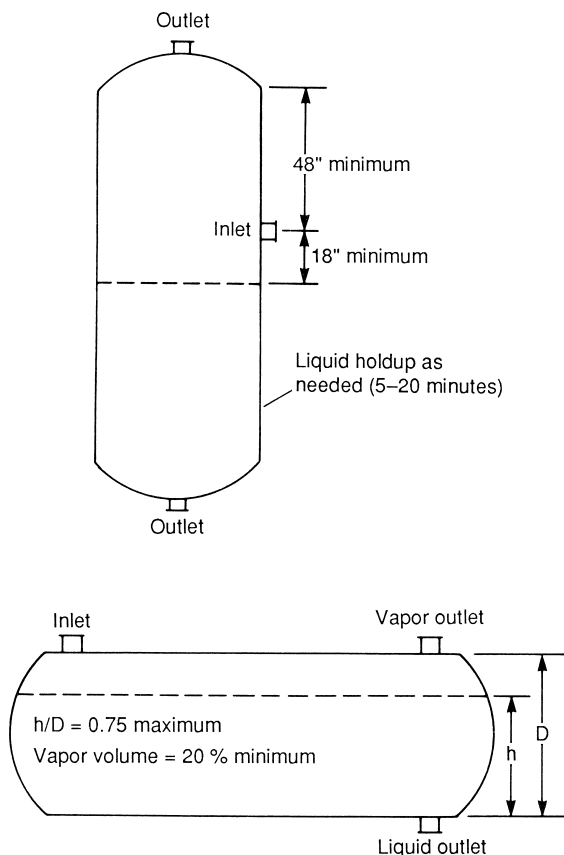
Figure 18.6. Knockout drums. Key dimensions of vertical and horizontal types.

where x is a function of the weight flow rates and densities of the phases

$$x = (W_L/W_V)\sqrt{\rho_v/\rho_L}. \tag{18.23}$$

Good performance can be expected at velocities of 30–100% of those calculated with the given K_s. Flooding velocities are at 120–140% of the design rates. At low velocities the droplets drift through the mesh without coalescing. A popular design velocity is about 75% of the allowable. Some actual data of the harmful effect of low velocities were obtained by Carpenter and Othmer (1955); they found, for example, that 99% of 6 μm droplets were removed at 6.8 ft/sec, but 99% of 8 μm at the lower velocity of 3.5 ft/sec.

Pressure drop in pads usually is small and negligible except at flooding; the topic is discussed by York (1983).

In existing drums or when the drum size is determined primarily by the required amount of liquid holdup, the pad dimensions must conform to the superficial velocities given by the design equation. This may necessitate making the pad smaller than the available cross section of the drum. Figure 18.7 shows typical installations. On the other hand, when the pad size is calculated to be greater than the available cross section and there develops a possibility of reentrainment of large droplets from the exit surface of the pad, a downstream settling drum or a high space above the mesh can be provided.

Good design practice is a disengaging space of 6–18 in., the more the better, ahead of the pad and 12 in. above the pad. Other details are shown on Figure 18.8. A design is provided in Example 18.4.

The most widely used type of equipment of separate a solid-laden gas stream is the cyclone separator. The gas stream enters a cylindrical- or conical-shaped vessel tangentially at a high velocity. The gas stream rotates several times, slinging the particles toward the outside of the vessel, and leaves through a pipe centrally located at the top of the chamber. The solids will drop out of the gas stream to the bottom of the vessel as the gravitational acceleration exceeds the centrifugal acceleration and leave through an opening to a receiver. Such equipment has been studied widely, particularly for the removal of dusts and catalyst fines in fluidized bed systems. The literature has been reviewed extensively by Rietema and Verver (1961), Mass (1979), Zenz (1982), and Pell and Dunston (1999).

EXAMPLE **18.3**
Liquid Knockout Drum (Empty)
Gas at the rate of 3000 cfm and liquid at 25 cfm enter a drum in which entertainment is to be removed. Holdup of liquid in the drum is 10 min. The properties are those of air and water at atmospheric conditions. Find the size of the drum needed to remove droplets greater than 200 μm dia.
Vertical drum, with Eq. (18.9):

$$u = 0.14\sqrt{62.4/0.075 - 1} = 4.04 \, \text{ft/sec},$$

$$D = \sqrt{3000/60(\pi/4)(4.04)} = 3.97 \, \text{ft}, \quad \text{say 4.0 ft.}$$

From Figure 18.6, the vapor space is a minimum of 5.5 ft. The liquid depth is

$$L_{\text{liq}} = \frac{250}{(\pi/4)D^2} = 19.9 \text{ ft for 10 min holdup,}$$

$$L = 19.9 + 5.5 = 25.4 \, \text{ft,}$$

$$L/D = 25.4/4 = 6.35.$$

If the diameter is increased to 4.5 ft, then $L = 15.7 + 5.5 = 21.2$, and $L/D = 4.71$.

Horizontal drum
The allowable vapor velocity is 25% greater:

$$u = 1.25(4.04) = 5.05 \, \text{ft/sec.}$$

Try several fractional vapor cross sections ϕ:

$$D = \sqrt{50/5.05(\pi/4)\phi} = \sqrt{12.61/\phi},$$

$$L = 250/(1 - \phi)(\pi/4)D^2 = 25.24\phi/(1 - \phi),$$

$$h = \text{depth of liquid.}$$

ϕ	h/D	D	L	L/D
0.2	0.75	7.94 (8.0)	6.31 (6.2)	0.78
0.3	0.66	6.48 (6.5)	10.82 (10.8)	1.66
0.4	0.58	5.61 (5.5)	16.83 (17.5)	3.18
0.5	0.50	5.02 (5.0)	25.24 (25.5)	5.10

Accordingly, a horizontal vessel between 5.0 and 5.5 ft dia with a liquid depth between 58 and 50% of the diameter falls in the usual economic range.

There are a variety of commercial and homemade devices that can remove entrainment more or less effectively, as shown in Figure 18.8. Their design is based on the following:

1. A change of direction and impingement on the walls of a drum
2. Impingement on a baffle
3. Tangential entry at high velocity and change of direction
4. Multiple baffles, with or without spray irrigation
5. A pipeline deentrainer

The capacity and effectiveness of proprietary devices such as items Figures 18.8(c) (d) and (e) cannot be estimated from general knowledge; however, manufacturers usually claim that they can be designed to remove 99% of 8 μm droplets or particles. For manufacturers of this equipment, see the *Chemical Engineering Buyers' Guide* (2002).

Typical cyclone dimension ratios are indicated on Figure 18.9.

For liquid knockout the bottom head often is made dished as on Figure 18.10, which also shows standard dimensions. Liquid-solid separators are called hydroclones. Inlet velocities should be in the range 100–150 ft/sec, the higher the better, but may be limited by the occurrence of reentrainment and unacceptable pressure drop. The pressure drop is estimated in terms of velocity heads, a value of four being commonly taken. Accordingly,

$$\Delta P = 4\rho V^2/2g = 4.313\rho(\text{ft/sec}/100)^2, \text{ psi.} \quad (18.24)$$
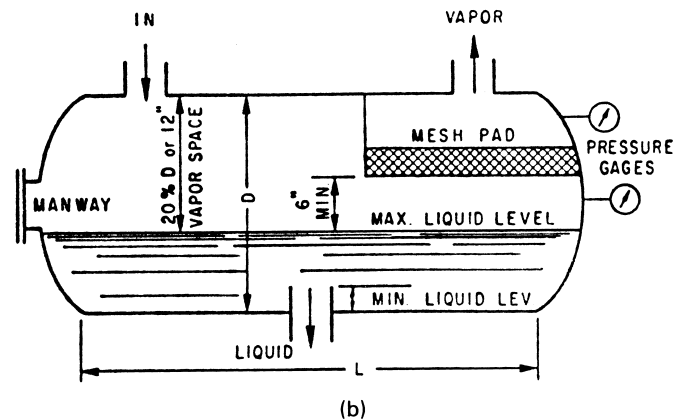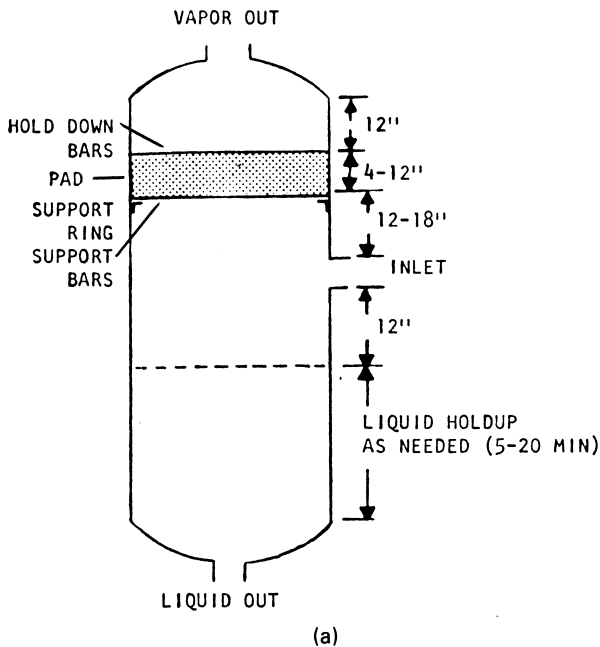
Figure 18.7. Key dimensions of knockout drums equipped with mesh pads. (a) Vertical knockout drum. (b) Horizontal knockout drum.
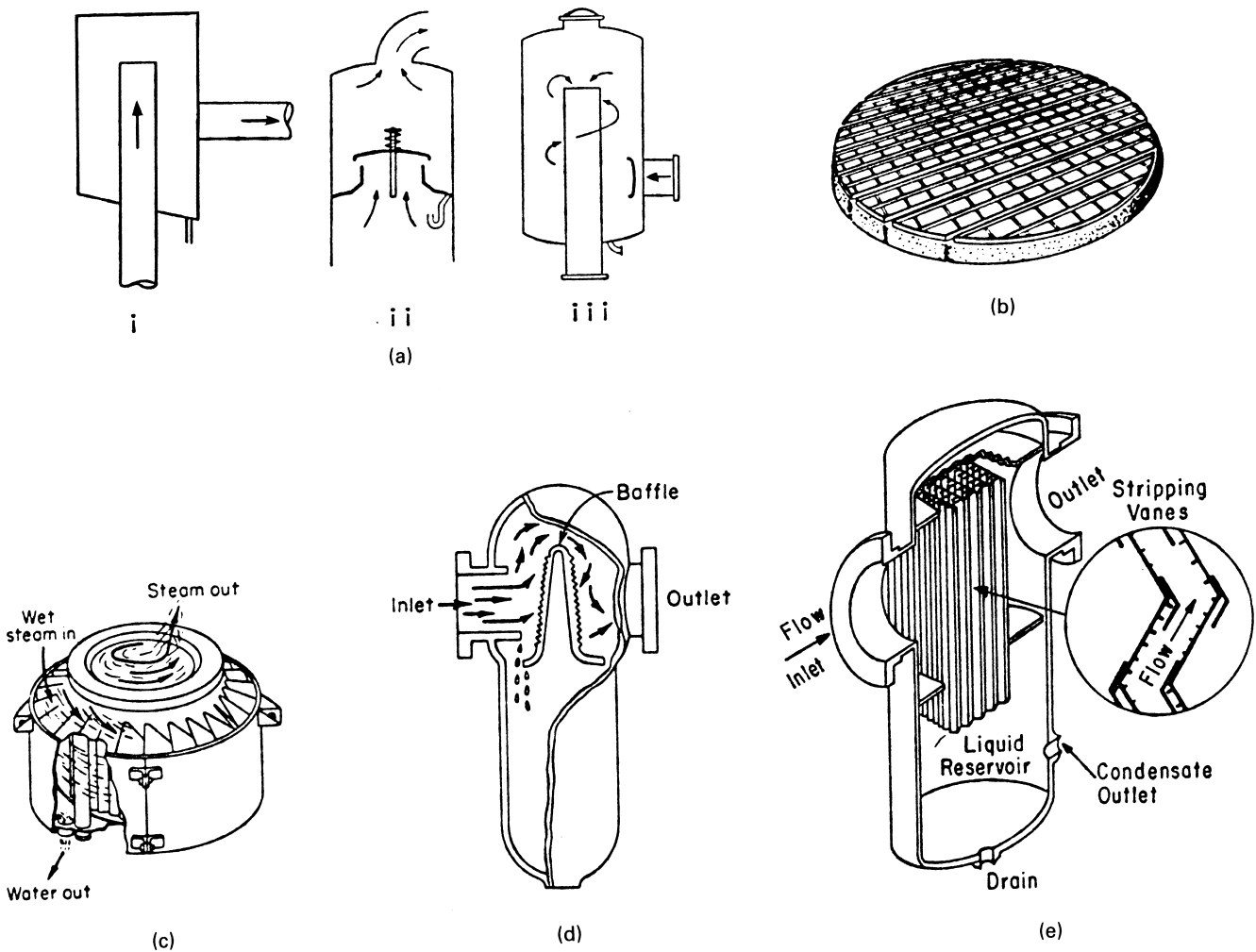
Figure 18.8. Principles of entrainment separation and some commercial types of equipment. (a) Basic principles of entrainment separating equipment: (i) change of direction; (ii) impingement on a baffle; (iii) tangential inlet resulting in centrifugal force. (b) Wire or fiber mesh pad, typical installations as in Figure 18.7. (c) A separator combining impingement and centrifugal force. (d) Equipment with impingement and change of direction. (e) Multiple zig-zag baffle arrangement. (See Walas, 1988).

For atmospheric air, for instance, this becomes

$$\Delta P = 0.323(ft/sec/100)^2, \text{ psi.} \qquad (18.25)$$

For the design of Figure 18.10, the size of the inlet is selected at a specified inlet velocity and required volumetric rate; the other dimensions then are fixed as given for this standard.

Very high velocities tend to skim the liquid film off the vessel wall and off the liquid at the bottom. The liquid also tends to creep up the wall and down the exit pipe where it is picked up by the exit gas. The horizontal plate in Figure 18.9 prevents vortexing of the accumulated liquid and pickup off its surface.

Efficiencies of 95% for collection of 5 μm droplets can be achieved by proper design of cyclone separators. For applications such as knockout drums on the suction of compressors, however, it is sufficient to remove only droplets greater than 40–50 μm.

Capacity and efficiency depend on the inlet velocity and the dimensions of the vessel. Correlated studies have been made chiefly for the design of Figure 18.9 with a rectangular inlet whose width is $D/4$ (one-fourth of the vessel diameter) and whose height is 2–3

times the width. A key concept is a critical particle diameter which is the one that is removed to the extent of 50%. The corresponding % removal of other droplet sizes is correlated by Figure 18.10. The equation for the critical particle diameter is

$$(D_p)_{crit} = \left[\frac{9\mu D}{4\pi N_t V(\rho - \rho_g)} \right]^{0.5}, \qquad (18.26)$$

where D is the diameter of the vessel and V is the inlet linear velocity. The quantity N_t is the number of turns made by the gas in the vessel. A graphical correlation given by Zenz (1982) can be represented by the equation

$$N_t = [0.1079 - 0.00077V + 1.924(10^{-6})V^2]V \qquad (18.27)$$

with V in ft/sec. With a height of opening equal to 2.5 times the width, the volumetric rate is

$$Q = AV = 2.5D^2V/16. \qquad (18.28)$$

EXAMPLE 18.4
Knockout Drum with Wire Mesh Deentrainer
For the flow conditions of Example 18.3, design a vertical drum with a standard efficiency stainless steel wire mesh pad. For this condition, from Table 18.2, $k = 0.35$, so that

$$u = 0.35\sqrt{62.4/0.075 - 1} = 10.09 \, \text{ft/sec},$$

$$D = \sqrt{50/(\pi/4)u} = 2.51 \, \text{ft. (30 in.)}$$

With 2 in. support rings the pad will have a diameter of 34 in.

The size of the drum is set largely by the required liquid holdup, which is 25 cfm times a 10 min holdup on 250 cuft. On the basis of Figure 18.7, the height of vessel above the liquid level is 4 ft. As in Example 18.3, take the diameter to be 4.5 ft. Then

$$L_{\text{liq}} = 25[10/(\pi/4)(4.5)^2] = 15.7 \, \text{ft},$$

$$L = 15.7 + 4.0 = 19.7 \, \text{ft},$$

$$L/D = 19.7/4.5 = 4.38.$$

This ratio is acceptable. As a check, use Eqs. (18.22) and (18.23):

$$x \equiv (W_L/W_u)\sqrt{P_u/P_L} = V_L/V_u\sqrt{P_L/P_u}$$

$$= 25/3000\sqrt{62.4/0.075} = 0.24,$$

$$k = -0.0073 + 0.263/[(0.24)^{1.294} + 0.573]$$

$$= 0.353,$$

which is close to the assumed value, $k = 0.35$.
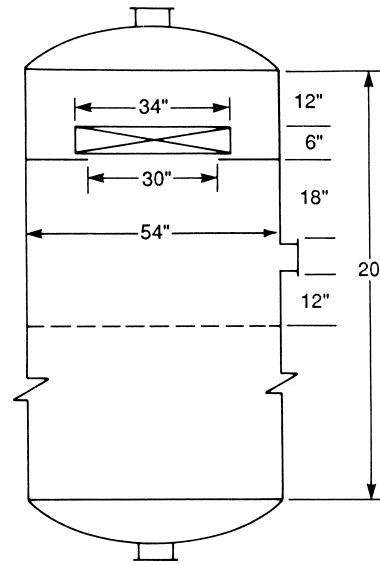
To obtain a high efficiency, the vessel diameter must be small, but in order to accommodate a required volumetric rate, many units in parallel may be needed. These units, called multicyclones, may be incorporated in a single shell at a cost that may be justifiable in view of greater efficiency and lower pressure drop. See Chapter 20.

DIMENSIONS IN INCHES

NUMBER	A	B	C	D	E
1	3	6	38	22	30
2	4	8	38	22	30
3	6	12	38	22	30
4	8	18	42	26	36
5	10	24	54	36	48
6	14	28	68	45	60
7	16	30	76	50	66
8	18	36	80	54	72
9	20	42	94	63	84
10	24	48	108	72	96
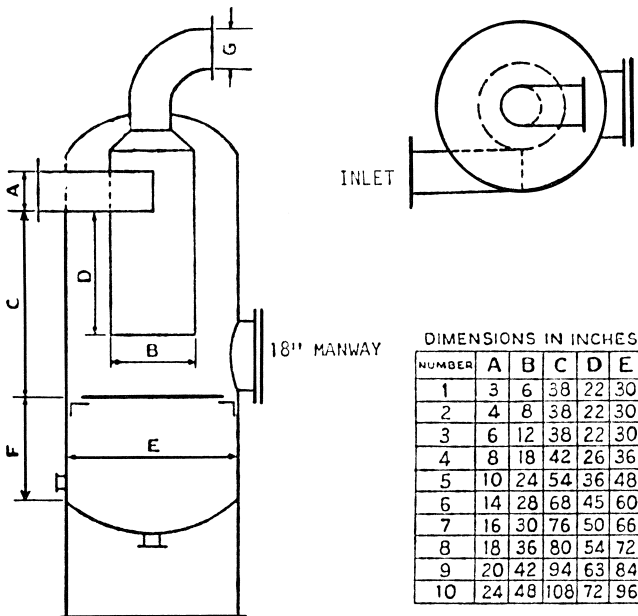
Figure 18.9. Dimensions of standard liquid knockout drums with tangential inlets.
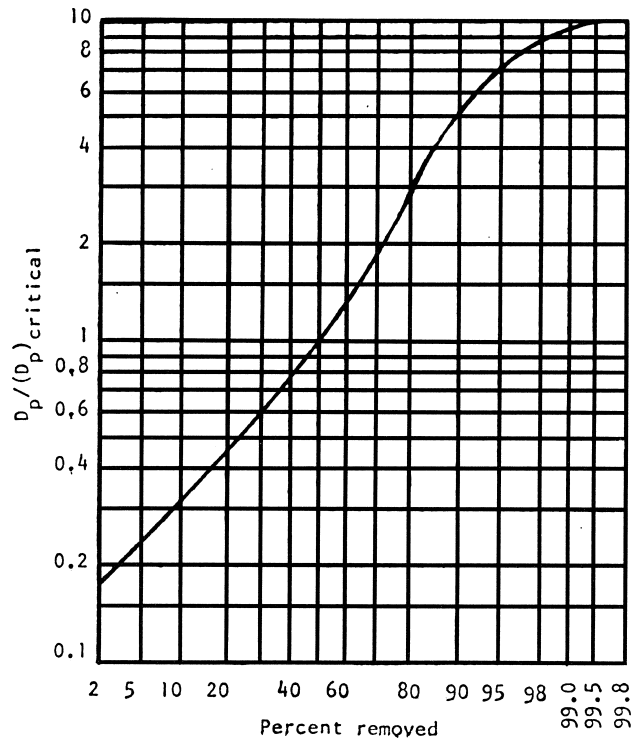
Figure 18.10. Percent removal of particles in a liquid-vapor separator as a function of their diameters relative to the critical diameter given by Eqs. (18.26) and (18.27). (*Zenz, 1982*).

18.5. STORAGE TANKS

Cylindrical storage tanks for inflammable liquids above and underground at or near atmospheric pressure are subject to standards and codes of Underwriter Laboratory (www.ul.com), or the American Petroleum Institute (www.api.org), or regulations of the EPA. The Underwriter Laboratory covers small tanks up to 25,000 gals. Both sets of standards are restricted to steel construction for noncorrosive service. Manufacturers often fabricate and supply Underwriter or API tanks as a matter of course. The latest standards can be obtained by visiting the above web sites.

Of course various materials of construction for corrosive service and for elevated temperatures and/or pressures may be fabricated. Stainless steels and stainless-lined or other corrosion-resistant liners are frequently used. Under certain corrosive conditions, a variety of plastic materials have been employed for storage

tanks. A large body of literature has been published in the last decade that is dedicated to tank design and operation both for above-ground and underground tanks, the most significant are Braune (1996), Grainawe (1996), Geyer (1992, 1996), and Amrouche et al. (2002).

Standard tanks are fabricated in discrete sizes with some latitude in combinations of diameter and length. For example, in Table 18.3, there are a variety of Underwriter and API sizes. Note that in Table 18.3(c) there are several heights for 30 ft diameter API standard tanks; the major difference is in the metal wall thickness. In some smaller tanks, the thickness is determined by the requirements of rigidity rather than strength. Some general statements about metal thickness are given throughout this section.

Horizontal tanks. Above ground they are limited to 35,000 gal. Normally they are supported on steel structures or concrete saddles at elevations of 6 to 10 ft. The minimum thickness of shell and

TABLE 18.3. Storage Tanks, Underwriter or API Standard, Selected Sizes

a. Small Horizontal Underwriter Label

| Capacity Gallons | Dimensions | | | Weight in Pounds |
	Diameter	Length	Thickness	
280	42″	4′ − 0″	$\frac{3}{16}''$	540
550	48″	6′ − 0″	$\frac{3}{16}''$	800
1000	48″	10′ − 8″	$\frac{3}{16}''$	1260
1000	64″	6′ − 0″	$\frac{3}{16}''$	1160
1500	64″	9′ − 0″	$\frac{3}{16}''$	1550
2000	64″	12′ − 0″	$\frac{3}{16}''$	1950
3000	64″	18′ − 0″	$\frac{3}{16}''$	2730
4000	64″	24′ − 0″	$\frac{3}{16}''$	3510

b. Horizontal or Vertical with Underwriter Label

| Nominal Capacity Gallons | Dimensions | | | Weight | No. of Supports |
	Diameter	Approx. Length	Thickness		
5,000	6′ − 0″	23′ − 9″	$\frac{1}{4}''$	5,440	3
5,000	7′ − 0″	17′ − 6″	$\frac{1}{4}''$	5,130	2
6,000	8′ − 0″	16′ − 1″	$\frac{1}{4}''$	5,920	2
6,000	8′ − 0″	16′ − 1″	$\frac{5}{16}''$	6,720	2
8,000	8′ − 0″	21′ − 4″	$\frac{1}{4}''$	7,280	2
8,000	8′ − 0″	21′ − 4″	$\frac{5}{16}''$	8,330	2
10,000	8′ − 0″	26′ − 7″	$\frac{1}{4}''$	8,860	3
10,000	8′ − 0″	26′ − 7″	$\frac{5}{16}''$	10,510	3
10,000	10′ − 0″	17′ − 2″	$\frac{1}{4}''$	8,030	2
10,000	10′ − 0″	17′ − 2″	$\frac{5}{16}''$	9,130	2
10,000	10′ − 6″	15′ − 8″	$\frac{1}{4}''$	8,160	2
10,000	10′ − 6″	15′ − 8″	$\frac{5}{16}''$	9,020	2
15,000	8′ − 0″	39′ − 11″	$\frac{1}{4}''$	13,210	4
15,000	8′ − 0″	39′ − 11″	$\frac{5}{16}''$	14,620	4
20,000	10′ − 0″	34′ − 1″	$\frac{1}{4}''$	14,130	3
20,000	10′ − 0″	34′ − 1″	$\frac{5}{16}''$	16,330	3
25,000	10′ − 6″	38′ − 9″	$\frac{1}{4}''$	17,040	4
25,000	10′ − 6″	38′ − 9″	$\frac{5}{16}''$	19,010	4

TABLE 18.3.—(*continued*)

c. Large Vertical, API Standard

Dimensions		Capacity			Shell Plates (Butt Welded)									
Diameter	Height	42 gal per bbl	U.S. Gal	Bottom Plates	Ring 1	Ring 2	Ring 3	Ring 4	Ring 5	Ring 6	Ring 7	Top Angle	Roof Plates
21'0"	18'0$\frac{3}{4}$"	1,114	46,788	$\frac{1}{4}$"	$\frac{3}{16}$"	$\frac{3}{16}$"	$\frac{3}{16}$"					$3'' \times 3'' \times \frac{1}{4}''$	$\frac{3}{16}$"
24'0"	24'0"	1,933	81,186	$\frac{1}{4}$"	$\frac{3}{16}$"	$\frac{3}{16}$"	$\frac{3}{16}$"	$\frac{3}{16}$"				$3'' \times 3'' \times \frac{1}{4}''$	$\frac{3}{16}$"
30'0"	24'0"	3,024	127,008	$\frac{1}{4}$"	$\frac{3}{16}$"	$\frac{3}{16}$"	$\frac{3}{16}$"	$\frac{3}{16}$"				$3'' \times 3'' \times \frac{1}{4}''$	$\frac{3}{16}$"
30'0"	29'11$\frac{1}{4}$"	3,769	158,300	$\frac{1}{4}$"	$\frac{3}{16}$"	$\frac{3}{16}$"	$\frac{3}{16}$"	$\frac{3}{16}$"	$\frac{3}{16}$"			$3'' \times 3'' \times \frac{1}{4}''$	$\frac{3}{16}$"
30'0"	35'10$\frac{1}{2}$"	4,510	189,420	$\frac{1}{4}$"	$\frac{3}{16}$"	$\frac{3}{16}$"	$\frac{3}{16}$"	$\frac{3}{16}$"	$\frac{3}{16}$"	$\frac{3}{16}$"		$3'' \times 3'' \times \frac{1}{4}''$	$\frac{3}{16}$"
30'0"	37'10$\frac{1}{4}$"	4,766	200,161	$\frac{1}{4}$"	$\frac{1}{4}$"	$\frac{3}{16}$"	$\frac{3}{16}$"	$\frac{3}{16}$"	$\frac{3}{16}$"	$\frac{3}{16}$"		$3'' \times 3'' \times \frac{1}{4}''$	$\frac{3}{16}$"
30'0"	41'9$\frac{3}{4}$"	5,264	221,088	$\frac{1}{4}$"	$\frac{3}{16}$"	$\frac{3}{16}$"	$\frac{3}{16}$"	$\frac{3}{16}$"	$\frac{3}{16}$"	$\frac{3}{16}$"	$\frac{3}{16}$"	$3'' \times 3'' \times \frac{1}{4}''$	$\frac{3}{16}$"
40'0"	33'10$\frac{3}{4}$"	7,586	318,612	$\frac{1}{4}$"	$\frac{1}{4}$"	$\frac{1}{4}$"	$\frac{3}{16}$"	$\frac{3}{16}$"	$\frac{3}{16}$"			$3'' \times 3'' \times \frac{1}{4}''$	$\frac{3}{16}$"
50'0"	47'9"	16,700	701,400	$\frac{1}{4}$"	0.35"	0.29"	0.25"	$\frac{1}{4}$"	$\frac{1}{4}$"	$\frac{1}{4}$"		$3'' \times 3'' \times \frac{1}{4}''$	$\frac{3}{16}$"
60'0"	39'10"	20,054	842,268	$\frac{1}{4}$"	0.34"	0.27"	$\frac{1}{4}$"	$\frac{1}{4}$"	$\frac{1}{4}$"			$3'' \times 3'' \times \frac{1}{4}''$	$\frac{3}{16}$"
70'0"	40'1"	27,472	1,153,824	$\frac{1}{4}$"	0.40"	0.32"	0.25"	$\frac{1}{4}$"	$\frac{1}{4}$"			$3'' \times 3'' \times \frac{3}{8}''$	$\frac{3}{16}$"
100'0"	40'0"	55,960	2,350,320	$\frac{1}{4}$"	0.57"	0.45"	0.33"	$\frac{1}{4}$"	$\frac{1}{4}$"			$3'' \times 3'' \times \frac{3}{8}''$	$\frac{3}{16}$"
150'0"	48'0"	151,076	6,345,192	$\frac{1}{4}$"	1.03"	0.85"	0.68"	0.50"	0.33"	$\frac{1}{4}$"		$3'' \times 3'' \times \frac{3}{8}''$	$\frac{3}{16}$"
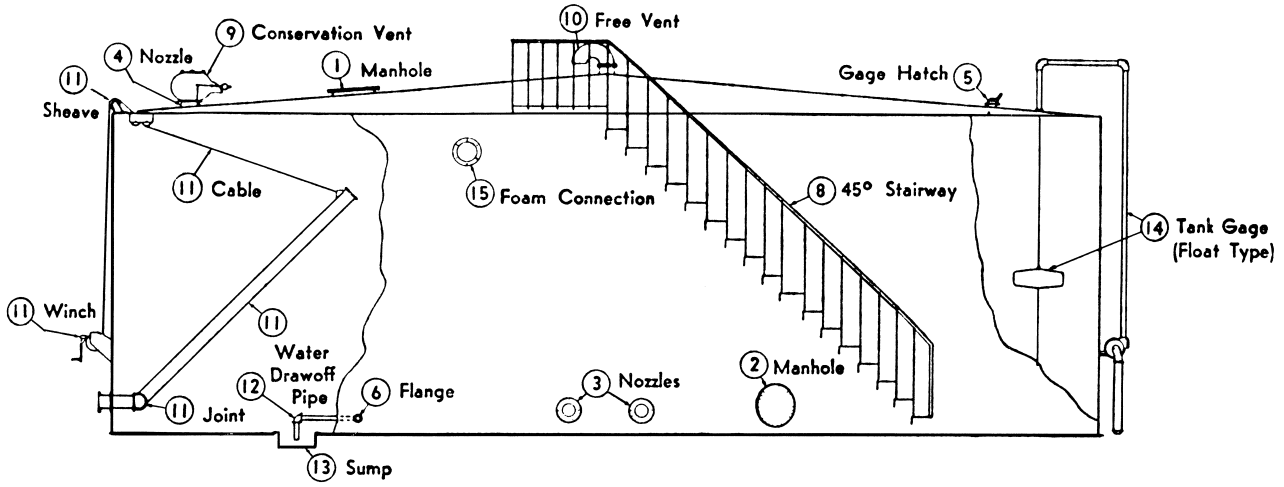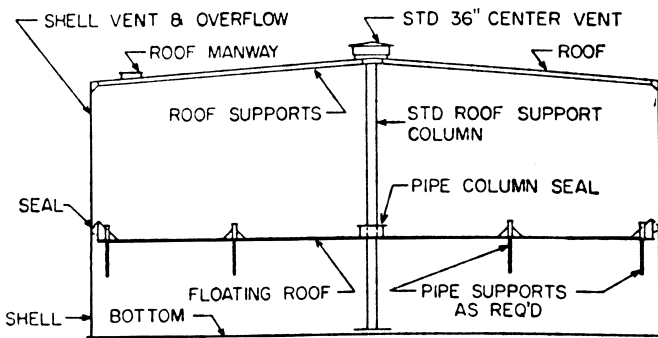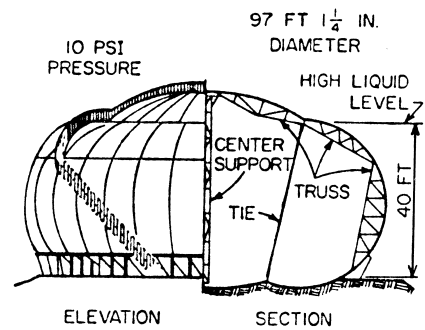
Figure 18.11. Examples of equipment for storage of liquids and gases in large quantities. (a) A large tank and its appurtenances, but with no provision for conservation of breathing losses. (b) Schematic of a covered floating roof tank in which the floating roof rides on the surface of the liquid. They also are made without the fixed roof. (c) Cutaway of a 40,000 Bbl spheroid for operation at 10 psig. (d) Design principles of tanks for storage of gases or liquids subject to breathing losses at atmospheric pressure: water seal, dry seal with flexible curtain, and variable vapor space controlled by a flexible curtain. (Walas, 1988).

(d)

(e)

SPHERE
30–220 psig
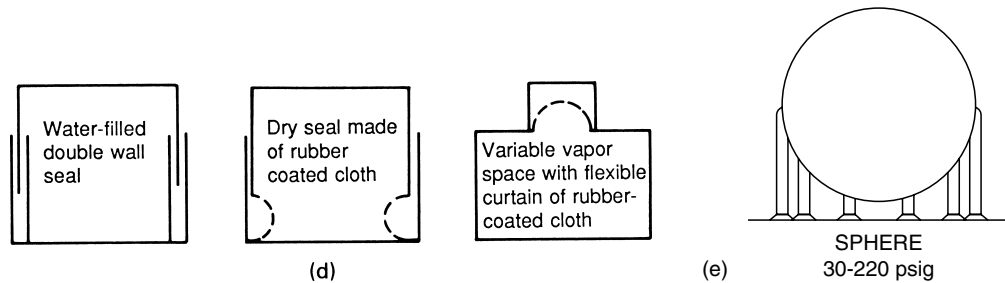
Figure 18.11.—(*continued*)

heads is 3/16 in. in diameters of 48–72 in. and 1/4 in. in diameters of 73–132 in.

Vertical tanks. Those supported above ground are made with dished or conical bottoms. Flat bottomed tanks rest on firm foundations of oiled sand or concrete. Supported flat bottoms usually are 1/4 in. thick. Roof plates are 3/16 in. thick. Special roof constructions that minimize vaporization losses were mentioned earlier in this chapter; they are illustrated by Mead (1964) and in manufacturers catalogs. The curved sides are made of several courses of plate with thicknesses graduated to meet requirements of strength. The data of the selected API tanks of Table 18.3 include this information. Figure 18.11 illustrates the oppurtenances that normally are provided for a large storage tank.

In order to minimize hazards, storage tanks for inflammable or toxic materials may be buried. Then they are provided with an overburden of 1.3 times the weight of water that the tank could hold in order to prevent the tank floating to the surface after heavy rainfalls.

Cylinders with curved heads are used for pressure storage at 5–230 psig. In the range of 5–10 psig, spheroids and other constructions made up with curved surfaces, as in Figure 18.11(c) are being

used in quite large sizes, often with refrigeration to maintain sufficiently low pressures. More illustrations of such equipment appear in manufacturers' catalogs and in Mead (1964).

Mention of vessels for the storage of gases was made at the beginning of this chapter, and Figure 18.11d shows the principles of some suitable designs. Design for storage of granular solids includes provisions for handling and withdrawal, as in the case of Figure 18.12.

18.6. MECHANICAL DESIGN OF PROCESS VESSELS

Process design of vessels establishes the pressure and temperature ratings, the length and diameter of the shell, the sizes and locations of nozzles and other openings, all internals, and possibly the material of construction and corrosion allowances. This information must be supplemented with many mechanical details before fabrication can proceed, notably wall thicknesses.

Large storage tanks are supported on a concrete pad on the ground. Other vessels are supported off the ground by various means, as in Figure 18.13, 18.12.

For safety reasons, the design and construction of pressure vessels are subject to legal and insurance standards. The ASME Codes apply to vessels greater than 6 in. dia operating above 15 psig. Section VIII Division 1 applies to pressures below 3000 psig and is the one most often applicable to process work. Above 3000 psig some further restrictions are imposed. Division 2 is not pressure limited but has other severe restrictions. Some of the many details covered by Division 1 are indicated by the references to parts of the code on Figure 18.14.

DESIGN PRESSURE AND TEMPERATURE

In order to allow for possible surges in operation, it is customary to raise the maximum operating pressure by 10% or 10–25 psi, whichever is greater. The maximum operating pressure in turn may be taken as 25 psi greater than the normal. The design pressure of vessels operating at 0–10 psig and 600–1000°F is 40 psig. Vacuum systems are designed for 15 psig and full vacuum. Between −20 and 650°F, 50°F is added to the operating temperature, but higher margins of safety may be advisable in critical situations. When subzero temperatures have an adverse effect on the materials of construction, the working temperature is reduced appropriately for safety.

Allowable tensile stresses are one-fourth the ultimate tensile strength of the material of construction. Values at different temperatures are given in Table 18.5 for some steels of which shells and heads are made. Welded joint efficiencies vary from 100% for double-welded butt joints that are fully radiographed to 60% for single-welded butt joints without backing strips and without radiographing. The Code has details.
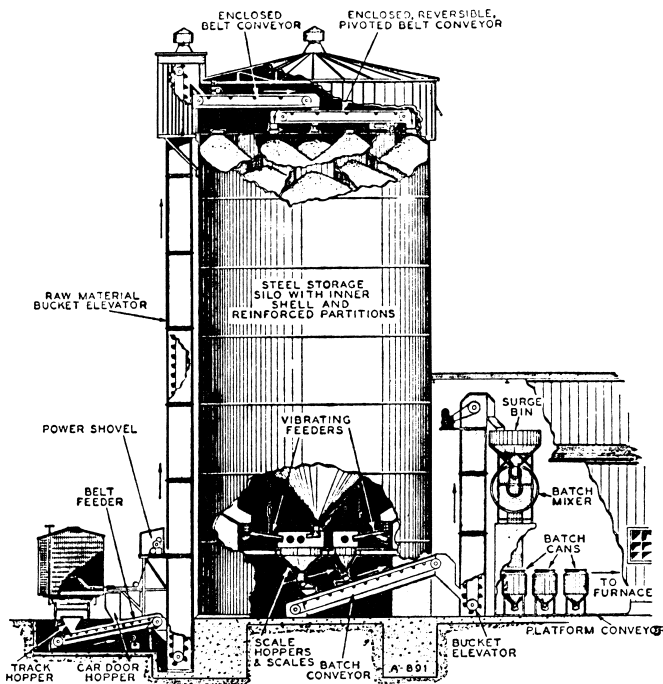
Figure 18.12. Equipment for handling, storing and withdrawing of granular solids in a glass manufacturing plant. (Walas, 1988).
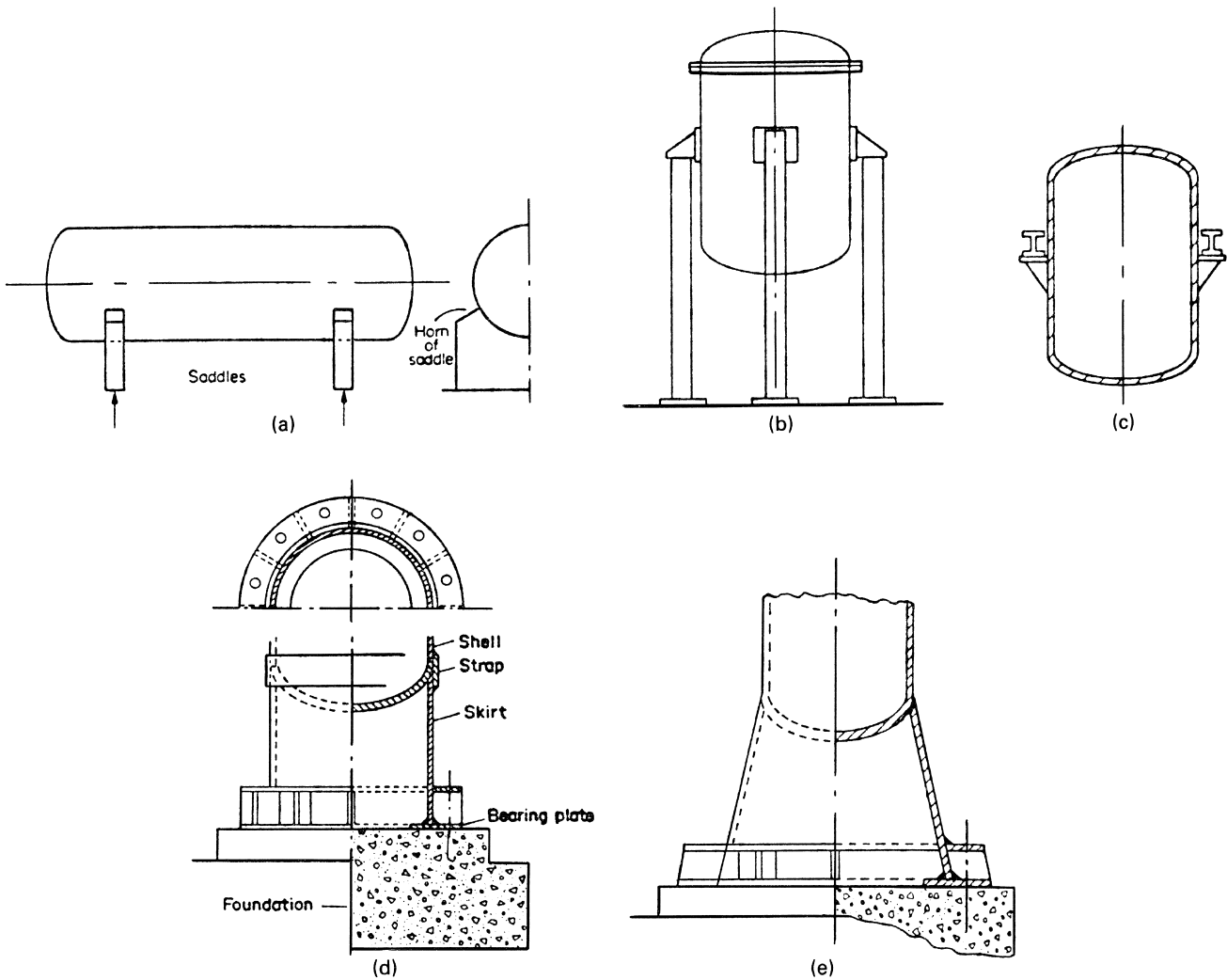
Figure 18.13. Methods of supporting vessels. (a) Saddle supports for horizontal vessels, usually of concrete. (b) Bracket or lug supports resting on legs, for either vertical or horizontal vessels. (c) Bracket or lug supports resting on steel structures, for either vertical or horizontal vessels. (d) Straight skirt support for towers and other tall vessels; the bearing plate is bolted to the foundation. (e) Flared skirt for towers and other tall vessels, used when the required number of bolts is such that the bolt spacing becomes less than the desirable 2 ft.

SHELLS AND HEADS

Although spherical vessels have a limited process application, the majority of pressure vessels are made with cylindrical shells. The heads may be flat if they are suitably buttressed, but preferably they are some curved shape. The more common types of heads are illustrated on Figure 18.16. Formulas for wall thicknesses are in Table 18.4. Other data relating to heads and shells are found in Table 18.6. Included are the full volume V_0 and surface S as well as the volume fraction V/V_0 corresponding to a fractional depth H/D in a horizontal vessel. Figure 18.15 graphs this last relationship. For ellipsoidal and dished heads the formulas for V/V_0 are not exact but are within 2% over the whole range.

Azbel and Cheremisinoff (1982) also presented formulas for the design of shells, vessel bottoms, heads, and appertenances.

FORMULAS FOR STRENGTH CALCULATIONS

The ASME Code provides formulas that relate the wall thickness to the diameter, pressure, allowable stress, and weld efficiency. Since they are theoretically sound only for relatively thin shells, some

restrictions are placed on their application. Table 18.4 lists these relations for cylindrical and spherical shells and for all but the last of the heads of Figure 18.16. For unusual shapes there are no simple methods of design; experience and testing are the only means for designing such shapes.

The formulas are expressed in terms of inside dimensions. Although they are rarely needed, formulas in terms of outside dimensions, say D_o, may be derived from the given ones by substitution of $D_o - 2t$ for D. For the 2:1 ellipsoidal head, for instance,

$$t = \frac{PD}{2SE - 0.2P} = \frac{P(D_o - 2t)}{2SE - 0.2P} = \frac{PD_o}{2SE + 1.8P}. \tag{18.29}$$

Example 18.5 is an illustration of a calculation for the dimensions and weight of a vessel to meet specifications. It is brought out that pressure vessels with large L/D ratios are lighter and presumably cheaper. A drawback may be the greater ground space needed by the slimmer and longer construction.

In addition to the shell and heads, contributions to the weight of a vessel include nozzles, manways, any needed internals, and

Flange types
Fig 2-4,
Fig UW-13.2
App 2,Y,S
Par UG-44

Skirt length
Par UG-32,33
Fig UW-13
Par UHT-19

Fillet welds
Par. UW-18 and 36

Knuckle thickness
Toriconical head
Par UG-32

Inspection opening
Par. UG-46

Conical head
Par. UG-32
App 1-5,L1,L2

Corrosion telltale
holes Par UG-25,
UCL-25,ULW-76

Minus head
pressure on
convex side
Par. UG-33
App. L

Threaded
connections
Par. UG-43,
Table UG-43

Bolts
Par. UG-12
App -Z,2,Y

Flat heads
Par. UG-34

Fullfaced gasket
App 1-6,2,Y

Reinforced openings
Par.UG-37—41,
App L-7

Telltale hole
Par. UW-15

Head attach-
ment overlap
Par. UW-9 and 13
Fig. UW-13

Nozzle thickness
Par. UG-45

Radiography
Par. UW-51,52

Weld joint
efficiencies
Par. UW-12
Table UW-12

Alignment tolerance
longitudinal joint
Par. UW-33

Plus head
pressure on
concave side
Par. UG-32
App 1

Backing strip
Par UW-2,12,
16,35

Corrosion
allowance App. E
Par. UG-25,UCS-25
UHT-25, UCL-25

Stiffening ring
Par. UG-29,30,ULT-29
UCS-29,UHA-29,UHT-28-30
App. L

Alignment
tolerance
Par UW-34
Circumferential
joints

Tapered plate
edges
Par. UW-9,13,32
33,34
UHT-34
Fig. UW-9

Torispherical
head
L = crown radius

Stagger long seams at least 5 X t
unless radiographed at intersec-
tions
Par. UW-9d

Opening in or
adjacent to welds
Par. UW-14, ULT-18

Linings
Par UG-26
Part-UCL
App. F

h — Depth of head

l

h/3
Par.
UG-28

Knuckle
radius
Par.UG-32

Bolted heads
Par UG-35
Fig. 1-6, App 1-6

Casting
Par. UG-7,11,24,35
UCI-35,UCD-35

Hemispherical head
Par. UG-32,16,81
UCS-79, App 1

R = radius
of shell
Par. UG-27

Post weld heat
treatment
Par. UW-40

Ellipsoidal head = $\dfrac{h}{1/4 \text{ inside dia.}}$
Par. UG-32d,UCS-79
App. L

Skirt length
Par. UG-32
UW-13,
UHT-19

Staybolts Par. UW-19
Par UG-14,47-50

Bars & structural
shapes Par. UG-14,
UW-19

Stayed surfaces
Par. UG-27,47

Fusion welded connections
Par. UW-15 and Fig.UW-16

Jacketed vessel
closure ring. App -9

Jacketed vessels
Par. UG-27,28,47
ULW-22, App -9

Max. weld reinforcement
Par. UW-35

Figure 18.14. References to items covered in the ASME Code for Boilers and Unfired Pressure Vessels, Section VIII, 1989.

TABLE 18.4. Formulas for Design of Vessels under Internal Pressure[a]

Item	Thickness t(in.)	Pressure p(psi)	Stress S(psi)	Notes
Cylindrical shell	$\dfrac{PR}{SE - 0.6P}$	$\dfrac{SEt}{R + 0.6t}$	$\dfrac{P(R + 0.6t)}{t}$	$t \le 0.25D, P \le 0.385SE$
Flat flanged head (a)	$D\sqrt{0.3P/S}$	$t^2 S/0.3D^2$	$0.3D^2 P/t^2$	
Torispherical head (b)	$\dfrac{0.885PL}{SE - 0.1P}$	$\dfrac{SEt}{0.885L + 0.1t}$	$\dfrac{P(0.885L + 0.1t)}{t}$	$r/L = 0.06,\ L \le D + 2t$
Torispherical head (b)	$\dfrac{PLM}{2SE - 0.2P}$	$\dfrac{2SEt}{LM + 0.2t}$	$\dfrac{P(LM + 0.2t)}{2t}$	$M = \dfrac{3 + (L/r)^{1/2}}{4}$
Ellipsoidal head (c)	$\dfrac{PD}{2SE - 0.2P}$	$\dfrac{2SEt}{D + 0.2t}$	$\dfrac{P(D + 0.2t)}{2t}$	$h/D = 4$
Ellipsoidal head (c)	$\dfrac{PDK}{2SE - 0.2P}$	$\dfrac{2SEt}{DK + 0.2t}$	$\dfrac{P(DK + 0.2t)}{2Et}$	$K = [2 + (D/2h)^2]/6,\ 2 \le D/h \le 6$
Hemispherical head (d) or shell	$\dfrac{PR}{2SE - 0.2P}$	$\dfrac{2SEt}{R + 0.2t}$	$\dfrac{P(R + 0.2t)}{2t}$	$t \le 0.178D,\ P \le 0.685SE$
Toriconical head (e)	$\dfrac{PD}{2(SE - 0.6P)\cos\alpha}$	$\dfrac{2SEt\cos\alpha}{D + 1.2t\cos\alpha}$	$\dfrac{P(D + 1.2t\cos\alpha)}{2t\cos\alpha}$	$\alpha \le 30°$

[a] Nomenclature: D = diameter (in.), E = joint efficiency (0.6–1.0), L = crown radius (in.), P = pressure (psig), h = inside depth of ellipsoidal head (in.), r = knuckle radius (in.), R = radius (in.), S = allowable stress (psi), t = shell or head thickness (in.).
Note: Letters in parentheses in the first column refer to Figure 18.16.

TABLE 18.5. Maximum Allowable Tensile Stresses (psi) of Plate Steels

(a) Carbon and Low Alloy Steels

A.S.M.E. Specification No.	Grade	Nominal Composition	Spec. Min. Tensile Strength	For Temperatures not Exceeding °F.						
				−20 to 650	700	800	900	1000	1100	1200
Carbon Steel										
SA515	55	C-Si	55,000	13,700	13,200	10,200	6,500	2,500		
SA515	70	C-Si	70,000	17,500	16,600	12,000	6,500	2,500		
SA516	55	C-Si	55,000	13,700	13,200	10,200	6,500	2,500		
SA516	70	C-Si	70,000	17,500	16,600	12,000	6,500	2,500		
SA285	A	...—...	45,000	11,200	11,000	9,000	6,500			
SA285	B	...—...	50,000	12,500	12,100	9,600	6,500			
SA285	C	...—...	55,000	13,700	13,200	10,200	6,500			
Low-Alloy Steel										
SA202	A	Cr-Mn-Si	75,000	18,700	17,700	12,600	6,500	2,500		
SA202	B	Cr-Mn-Si	85,000	21,200	19,800	12,800	6,500	2,500		
SA387	D[*]	$2\frac{1}{4}$ Cr-I Mo	60,000	15,000	15,000	15,000	13,100	2,800	4,200	1,600

(b) High Alloy Steels

A.S.M.E. Specification No.	Grade	Nominal Composition	Specified Minimum Tensile Strength	For Temperatures not Exceeding °F.										
				−20 to 100	200	400	700	900	1000	1100	1200	1300	1400	1500
SA-240	304	18 Cr-8 Ni	75,000	18,700	15,600	12,900	11,000	10,100	9,700	8,800	6,000	3,700	2,300	1,400
SA-240	304L[†]	18 Cr-8 Ni	70,000	15,600	13,300	10,000	9,300							
SA-240	310S	25 Cr-20 Ni	75,000	18,700	16,900	14,900	12,700	11,600	9,800	5,000	2,500	700	300	200
SA-240	316	16 Cr-12 Ni-2 Mo	75,000	18,700	16,100	13,300	11,300	10,800	10,600	10,300	7,400	4,100	2,200	1,700
SA-240	410	13 Cr	65,000	16,200	15,400	14,400	13,100	10,400	6,400	2,900	1,000			

(ASME Publications).

supporting structures such as lugs for horizontal vessels and skirts for vertical ones. Nozzles and manways are standardized for discrete pressure ratings; their dimensions and weights are listed in manufacturers' catalogs. Accounting for these items may contribute 10–20% to the calculated weight of the vessel.

Mechanical design specification sheets (Appendix B) summarize the information that a fabricator needs in addition to the general specifications of the vessel codes. Not all of the data on
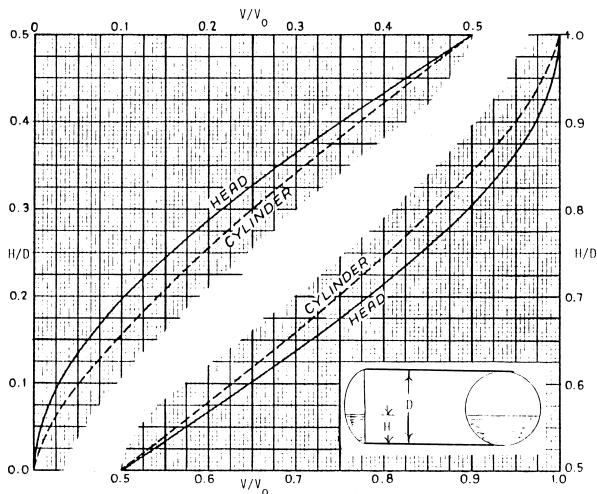
Figure 18.15. Fractional volumes of horizontal cylinders and curved heads at corresponding fractional depths, H/D.

TABLE 18.6. Heads and Horizontal Cylinders: Formulas for Partially Filled Volumes and Other Data

Nomenclature
D = diameter of cylinder
H = depth of liquid
S = surface of head
V_0 = volume of full head
θ = angle subtended by liquid level or angle of cone

Cylinder
$\theta = 2 \arccos(1 - 2H/D)$
$\theta(\text{rad}) = \theta°/57.3$
$V/V_o = (1/2\pi)(\theta - \sin\theta)$

Hemispherical head
$S = 1.571D^2$
$V = (\pi/3)H^2(1.5D - H)$
$V_o = (\pi/12)D^3$
$V/V_0 = 2(H/D)^2(1.5 - H/D)$

Ellipsoidal head ($h = D/4$)
$S = 1.09D^2$
$V_0 = 0.1309D^3$
$V/V_0 = 2(H/D)^2(1.5 - H/D)$

Torispherical ($L = D$)
$S = 0.842D^2$
$V_0 = 0.0778D^3$
$V/V_0 = 2(H/D)^2(1.5 - H/D)$

Conical
$H = [(D - d)/2]\tan\theta$
$= \begin{cases} 0.5(D - d), & \theta = 45° \\ 0.2887(D - d), & \theta = 30° \end{cases}$
$S = 0.785(D + d)\sqrt{4H^2 + (D - d)^2}$, curved surface
$V = 0.262H(D^2 + Dd + d^2)$
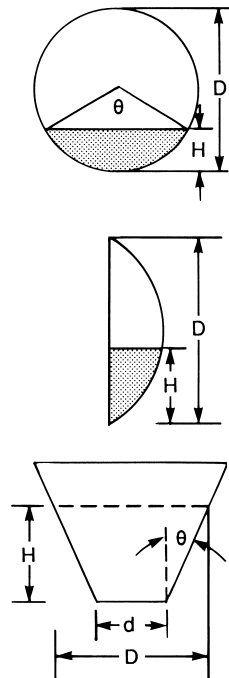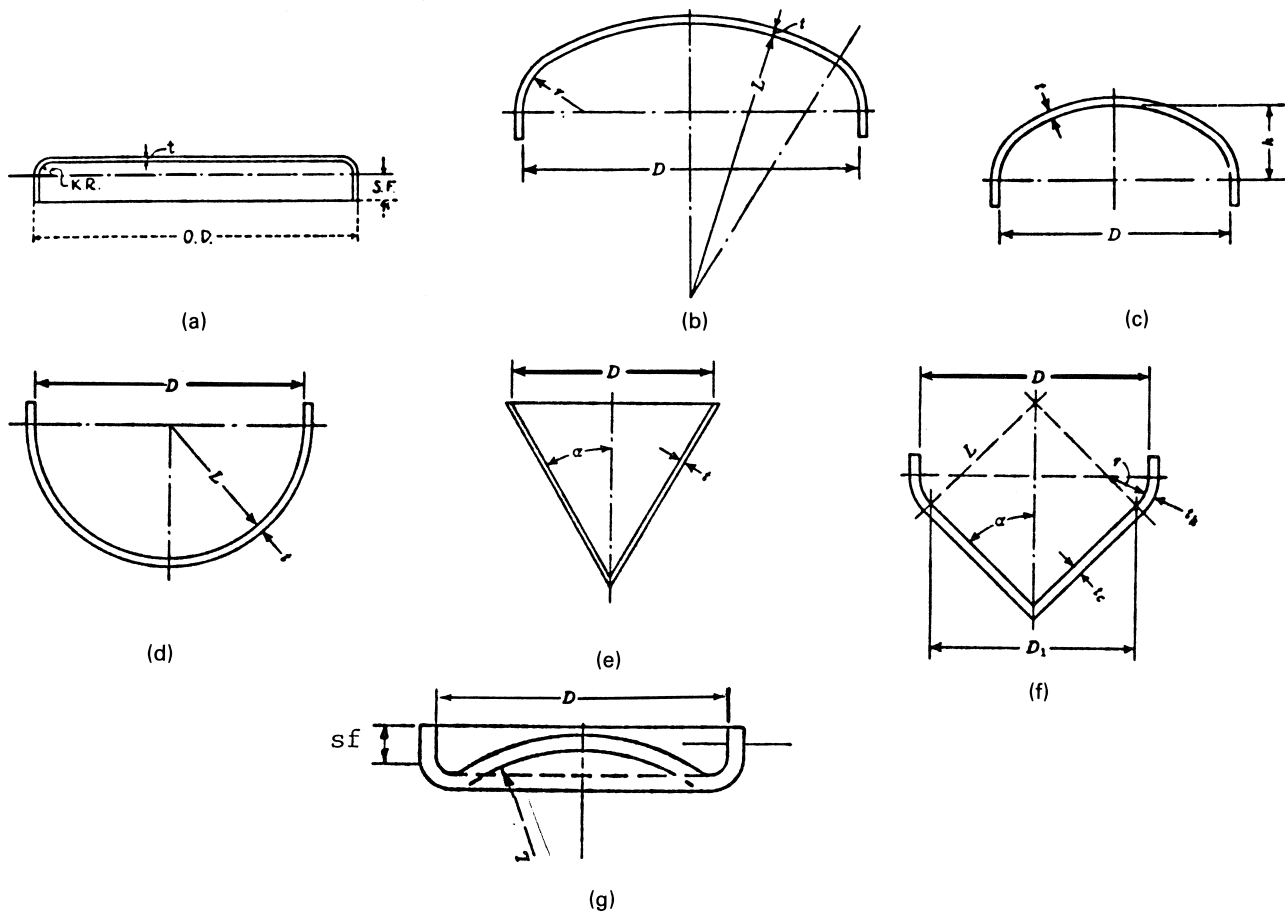
Figure 18.16. Types of heads for cylindrical pressure vessels. (a) Flat flanged: KR = knuckle radius, SF = straight flange. (b) Torispherical (dished). (c) Ellipsoidal. (d) Spherical. (e) Conical, without knuckle. (f) Conical, with knuckle. (g) Nonstandard, one of many possible types in use.

EXAMPLE 18.5
Dimensions and Weight of a Horizontal Pressure Drum

A drum is to operate at 500°F and 350 psig and to hold 5000 gal at a depth $H/D = 0.8$. Torospherical dished heads are to be used. The material is SA285A. Examine the proportions $L/D = 3$ and 5. Formulas are in Table 18.5:

$$V_{\text{tank}} = 5000/7.48 = 668.4 \text{ cuft.}$$

Two heads, capacity with $H/D = 0.8$,

$$V_h = V_0(V/V_0) = 2[0.0778D^3(2)(H/D)^2(1.5 - H/D)]$$
$$= 0.1394D^3$$

Shell capacity with $H/D = 0.8$,

$$\theta = 2 \arccos(1 - 1.6) = 4.4286 \text{ rad},$$
$$V_s = V_0(V/V_0) = (\pi/4)D^2L(1/2\pi)(\theta - \sin\theta)$$
$$= 0.6736D^2L$$
$$V_{\text{liquid}} = 668.4 = 0.1394D^3 + 0.6736D^2L$$

with $L/D = 3$,

$$D = \left(\frac{668.4}{2.1601}\right)^{1/3} = 6.76 \text{ ft, say } 6.5 \text{ ft},$$

$$L = \frac{668.4 - 0.1394D^3}{0.6736D^2} = 22.1 \text{ ft, say } 22.0.$$

Allowable stress $S = 11,200$ psi.
Say joint efficiency is $E = 0.9$:

$$t_{\text{shell}} = \frac{PR}{SE - 0.6P} = \frac{350(39)}{0.9(11,200) - 0.6(350)} = 1.38 \text{ in.}$$

Dished head with $L = D$ and $r/L = 0.06$:

$$t_h = \frac{0.885(350)(78)}{0.9(11,200) - 0.1(350)} = 2.41 \text{ in.}$$

Surfaces:

shell, $S = \pi DL = 449.3$ sqft,

heads, $S = 2(0.842)D^2 = 71.2$ sqft,

$$\text{Weight} = [449.3(1.4) + 71.2(2.4)]491/12$$
$$= 32,730 \text{ lbs.}$$

The results for $L/D = 3$ and 5 are summarized.

Item	L/D = 3	L/D = 5
D (ft)	6.5	5.5
L (ft)	22.0	32.0
t_{shell} (in.)	1.38 (1.4)	0.957 (1.0)
t_{head} (in.)	2.41 (2.4)	1.67 (1.7)
Weight (lb)	32,730	26,170

The completed vessel will include the weights of nozzles, a manway and reinforcing around the openings, which may total another 10–20%. The weights of these auxiliaries are stated in manufacturers' catalogs.
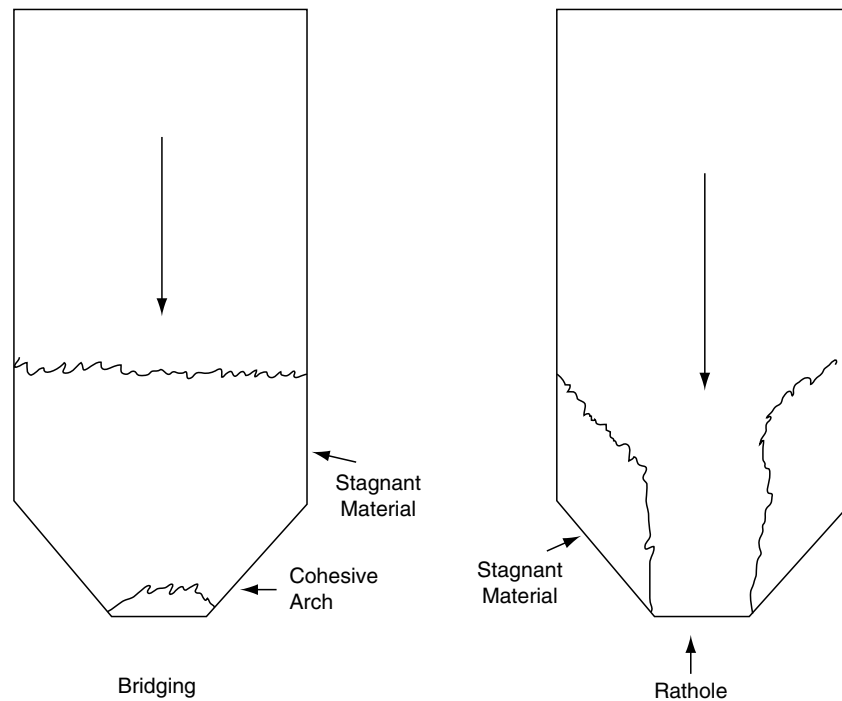
Figure 18.17. Solids Flow Problems

the specification summary are necessarily in the province of the process engineer; it may depend on the stage of the design and on who else in the organization (e.g., a mechanical engineer) is available to do the work.

18.7. BINS AND HOPPERS

These equipment items are used to store feed and, in some cases, process bulk solids. The design of economical hopper systems is dependent on the physical, chemical, and flow properties of the materials being stored. It is essential to provide bin, hopper, and feeder designs to enhance the flow of the material from the hopper and to minimize potential problems.

Two types of problems can result from improper bin design. In arching or bridging, a stable configuration forms at the narrowest cross-section of the bin, the discharge outlet. The bridge supports the contents of the bin, preventing the material from discharging. Another problem, "ratholing," occurs with the formation of a

stable cavity over the outlet and the material in a stagnant zone that remains until some force is applied to cause the material to empty the hopper. If a material gains "cohesive strength," which is related to consolidation pressure, a "bridge" or "rathole" might form, as shown in Figure 18.17.

Two types of bin flow patterns are possible to minimize the occurrence of these two problems. In a "mass" flow bin, all the material is in motion when discharging occurs and there are no stagnant regions. A mass flow bin has a long tapered discharge section. To prevent arching, a mass flow bin has a minimum diameter for a circular cross-section outlet and a minimum slotted width for a slotted or oval outlet. If a material has a critical outlet diameter of 10 in. and a bin is designed with a 6 in. diameter outlet, arching or bridging will occur; however, if the outlet is 12 in. or greater, then arching will not form and the material will flow, according to Carson and Marinelli (1994).

Jenicke (1964) developed techniques to achieve mass flow wherein all the material is moving whenever any material is
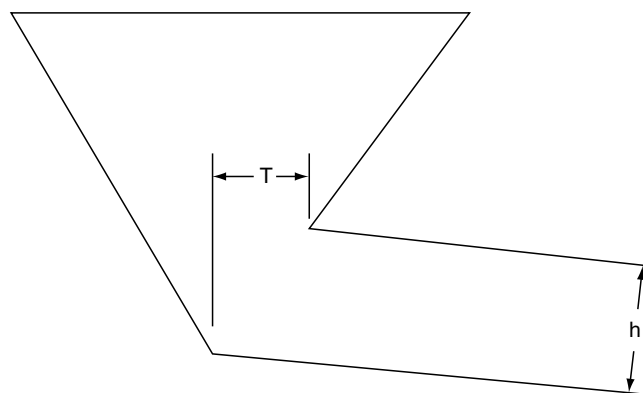
Figure 18.18. Ideal Hopper Design (FMC Technologies, 2000)

discharged. This flow pattern is necessary to reliably handle powders and bulk solids.

The other option is "funnel" flow when designing a hopper. The choice depends on the material being stored. Mass flow occurs when all the material in a bin is in motion, as when any material is withdrawn. Material flows along the steep walls of the vessel and when the walls are smooth enough to overcome friction between the wall surface and the solid material. Stable "ratholes" cannot form in mass flow bins, so mass flow designs are suitable for cohesive solids, fine powders, solids that segregate, or materials that degrade. Funnel flow occurs when some of the material in the vessel moves while the rest remains stationary. Materials that are coarse or free-flowing that do not degrade are often stored in funnel flow bins. If a material has sufficient cohesive strength, it may bridge near the outlet. If the narrow flow channel empties, a "rathole" forms and thus decreases the storage capacity of the bin. According to Marinelli (2002), funnel flow bins are beneficial because they require less headroom and result in lower fabrication costs.

FMC Technologies recommends that to obtain a uniform material flow pattern, the ratio of the throat (T) to the hopper gate height (H) be 0.6 for an "ideal" hopper design. The material at the front and the rear of the hopper will then move at nearly the same velocity. An "acceptable" design may be obtained if the ratio of T/H is between 0.5 and 1.0; however, a ratio outside these limits may distort the material flow patterns and reduce the feed rates (FMC Technologies, 2000). See Figure 18.18.

Johanson (2002) points out that there are four basic flow problems that occur in bins and their associated feeders:

1. Solids hang-ups or arching where some of the solids remain in the bin when the valve at the discharge is opened and the feeder is started.
2. Erratic flow from the outlet such that the feeder is starved.
3. Solids segregation such that the solid mixture leaving the hopper and the feeder is not of the same composition as the material entering the hopper.
4. Excessive the power requirements for the feeder causing the feeder to break shear pins, stop drive motor, and cause low flow to the feeder.

All these problems are the result of the interaction of solids, solids flow properties, and the design of the equipment. Johanson (2002) has identified seven indices that relate to the bulk flow properties of solids.

The choice of bin design—conical or pyramidal—affects in part the problems noted above. Steve (2000) discusses the capacity of a bin as a function of bin geometry and gave equations for the design of bins. In nonconical hoppers (e.g., a wedge-shaped bin with an elongated outlet), a wider range of conditions for a material can occur without flow stoppages. Carson and Marinelli (1994) recommend that the length of the outlet should be three times the width or greater to minimize hopper problems.

BIN DEVICES

Unique designs and appurtenances have been developed by modifying internal changes to the bin geometry.

In years past, rapping devices or blow-back bags were mounted near the bottom of the one or pyramidal bottom of the hopper to overcome bridging, but these devices often were ineffective, compacting the solids within the hopper.

Carson (2002) mentions that inserts have been placed within the hopper to expand the size of the active flow channel and/or to relieve pressure at the discharge. Inverted cones and pyramids have been used with limited success. He suggests a hopper within a hopper so that material flows in the area between the inner and outer hoppers and through the inner hopper if it does not have a cover on it. By proper design of the geometry of the hopper, a uniform velocity profile can be achieved such that there is a minimum amount of particle segregation. Sometimes in-bin blenders have also been used for this purpose.

Hopper walls must be smooth and become so with continual use; however, an alternative is to line the hopper with an ultrahigh molecular weight polyethylene liner. Another alternative might be a thin coat of epoxy paint or plasma coating. In the latter case, a porous substrate is flame-sprayed over base metal and then the substrate is impregnated with a low-friction polymer. Another suggestion made by Carson (2002) was to modify the hopper, employing sloping surfaces with vertical end walls rather than a conical cross section.

REFERENCES

Y. Amrouche, C. Dave, K. Gursahani, R. Lee, and L. Montemayor, General rules for aboveground storage tank design and operation, *Chem. Eng. Progr.,* 54–58 (December 2002).

D. Azbel and N.P. Cheremisinoff, *Chemical and Process Design: Vessel Design and Selection,* Butterworths, London, 1982.

T.E. Belk, Effect of physical and chemical parameters on coalescence, *Chem. Eng. Prog.*, **61**(10), 72–76 (1965).

D. Bradley, *The Hydroclone,* Pergamon, New York, 1965.

C. Branan, *The Process Engineers' Pocket Handbook,* Gulf, Houston, 1976 (Vol.1, pp.101–110), 1983 (Vol. 2, p. 67).

S. Braune, G. Thorpe et al., Aboveground storage tanks, Part II, Field-erected tanks, *Chem. Eng.,* 104–109 (August 1996).

C.L. Carpenter and D.F. Othmer, Entrainment removal by a wire mesh separator, *AIChE J.,* **1**, 549–557 (1955).

J.W. Carson, Equipment modeling and testing: Bulk solids handling, *Chem. Eng.,* 98–100 (August 2002).

J.W. Carson and J. Marinelli, Characterize bulk solids to ensure smooth flow, *Chem. Eng.,* 78–90 (April 1994).

Chemical Engineering Buyers' Guide, Chemical Week, New York, 2002.

R. Chuse and S.M. Eber, *The ASME Code Simplified,* McGraw-Hill, New York, 1984.

D.A. Craig and R.T. Hossfeld, Measuring powder flow properties, *Chem. Eng.*, 41–46 (September 2002).

G.A. Davies, G.V. Jeffrys, and M. Azfal, A new packing for coalescence and separation of dispersions, *Br. Chem. Eng.,* **17**, 709–714 (1972).

F.L. Evans, *Equipment Process Design for Refineries and Chemical Plants*, Gulf, Houston, Vol. 2, 153–165, 1980.

J.R. Fair, and R.L. Mathews, *Pet. Refiner,* **37**(4), 153 (1958).

FMC Technologies, Working with hoppers, Homer City, PA, May 2000.

R.V. Fronczak, Electrical desalting, *Encyclopedia of Chemical Processing and Design,* Dekker, New York, Vol. 17, 223–251, 1983.

W. Geyer, Bringing storage tanks to the surface, *Chem. Eng.,* 94–102 (July 1992).

W. Geyer, How do your tanks measure up? Part I Underground storage, *Chem. Eng.,* 84–92, (July 1996).

L. Grainawe, Aboveground storage, Part I Decoding shop-built tanks, *Chem. Eng.,* 98–103, (August 1996).

W.B. Hooper, and L.J. Jacobs, Decantation, in P.A. Schweitzer (Ed.), *Handbook of Separation Methods for Chemical Engineers,* McGraw-Hill, New York, 1979, pp. 1.343–1.358.

L.J. Jacobs, and W.R. Penney, Phase separation, in R.W. Rousseau (Ed.), *Handbook of Separation Process Technmology,* Wiley, New York, 1987.

A.W. Jenicke, Storage and flow of solids, *Bulletin 123, University of Utah Engineering Experiment Station,* Salt Lake City, UT, November 1964.

J.R. Johanson, Troubleshooting bins, hoppers and feeders, *Chem. Eng. Progr.*, 24–36, (April 2002).

G.V. Jordan, Coalescence with porous materials, *Chem. Eng. Progr.,* **61**(10), 64–71 (1965).

G.S. Laddha, and T.E. Degaleesan, in T.C. Lo, M.H.I. Baird, and C. Hanson (Eds.), *Handbook of Solvent Extraction,* Wiley, New York, 1983, p. 125.

D.M. Landis, Centrifugal coalescers, *Chem. Eng. Progr.,* **61**(10), 58–63 (1965).

E.E. Ludwig, *Applied Process Design for Chemical and Petrochemical Plants,* Gulf, Houston, Vol.1, 1995.

J. Marinelli, A practical approach to bins and feeders, *Chem. Eng.,* 39–42 (July 2002).

W.J. Mead, Hoppers and bins and tanks, *Encyclopedia of Chemical Process Equipment,* Reinhold, New York, 1964, pp. 546–559, 941–957.

Middleman, Ind. Eng. Chem. Proc. Des. Dev., 13(1), 78–83(1974).

M. Pell, and J.B. Dunson, Gas-solid separation-cyclones, *Chemical Engineers' Handbook*, 7th ed., McGraw-Hill, New York, 1999, pp. 17,26–17,32.

Metal Textile Corporation, Bulletin ME-7, Roselle, NJ.

O.C. Redmon, Cartridge type coalescers, *Chem. Eng. Progr.,* **58**(9), 87–89 (1963).

W. Reisner, and M. E. Rothe, Bins and bunkers for handling bulk materials, *Trans. Tech. Publication,* Clausthal, Germany, 1971.

S.S. Safarian, and E.C. Harris, *Design and Construction of Silos and Bunkers,* Van Nostrand Reinhold, New York, 1985.

A.H. Selker, and C.A. Schleicher, Factors affecting which phase will disperse when immiscible liquids are stirred together, *Can. J. Chem. Eng.,* **43**, 298–301 (1965).

H.P. Sheng, J.R. Welker, and C.M. Sliepcevich, Liquid-liquid separations in a conventional hydroclone, *Can. J. Chem. Eng.,* **52**, 487–491 (1974).

B. Sigales, How to design reflux drums, *Chem. Eng.,* 157–160 (March 3, 1975); How to design settling drums, *Chem. Eng.,* 141–143 (June 23, 1975); More on how to design settling drums, *Chem. Eng.,* 87–89 (September 29, 1975).

A.J. Stepanoff, *Gravity Flow of Bulk Solids and Transport of Solids in Suspension*, Wiley, New York, 1969.

Stephens Adamson Manufacturing Company, Catalog.

E.H. Steve, Sizing up the bin storage, *Chem. Eng.,* 84–88 (July 2000).

S.M. Walas, *Chemical Engineering Equipment: Selection and Design*, Butterworth (Elsevier), 1988.

L.C. Waterman, Electrical coalescers, *Chem. Eng. Progr.,* **61**(10), 51–57 (1965).

R.N. Watkins, Sizing separators and accumulators, *Hydrocarbon, Proc.,* **46**(11), 253–256 (1967).

T.H. Wines, and R.L. Brown, Difficult liquid-liquid separations, *Chem. Eng.,* 104–109 (December 1997).

O.H. York, Entrainment separation, *Encyclopedia of Chemical Processing and Design,* Dekker, New York, 1983, Vol. 14, pp. 82–97, and Vol 19, pp. 168–206.

F.A. Zenz, Cyclones, *Encyclopedia of Chemical Processing and Design,* Dekker, New York, Vol. 14, 1982, pp. 82–97.

19

MEMBRANE SEPARATIONS

T he subject of membrane separations can be broadly extended to include not only the separation of gaseous mixtures, but the two-phase separation of liquid-phase components into a gaseous phase, a process called pervaporation, and the separation of liquid phases as such, plus the separation of solutions, or solid-rich concentrates apart from liquids or lean solutions. Variously included are the processes called reverse osmosis, hyperfiltration, and ultrafiltration. What is called the permeate phase may be the desired product, or what is called the reject or raffinate phase may instead be the desired product. At the same time, we may speak of single-stage separations, multistage separations, and differential permeations—and of concurrent and countercurrent flow— all with or without recycle. Concomitantly, we may make the usually necessary simplification of perfect mixing within a phase.

19.1. MEMBRANE PROCESSES

The methods and literature are briefly reviewed for solid-suspension separations, solution-phase separations, liquid-phase separations, and gas-phase separations. In the terminology used, the objective is to separate a feed stream (or streams) into a permeate phase and a reject phase, either of which may contain the component(s) of more interest. For a single membrane, say, the permeate phase remains on the feed side or high-pressure side of the membrane, and is subsequently discharged, whereas the reject or raffinate phase builds up on the opposite or low-pressure side of the membrane, and is then discharged.

For the most part, the membrane is regarded as a solid, albeit liquid membranes may serve if sufficiently immiscible with the feed, reject, and permeate phases—whether gas or liquid. Whenever and wherever applicable, membranes afford some unique benefits in separations technology. Representative directions in which membrane research is headed include that of coal-derived gases and liquids and their further separation and/or conversion. (In this latter regard there is the subject of high-temperature ceramic membranes and the use of membranes as catalytic reactors. Similar remarks could be made for metallic membranes, such as the diffusion of hydrogen through metals). Membrane separation processes in the petroleum and petrochemical industry constitute another direction, and the upgrading of subquality natural gas is in the offing.

With regard to separations emphasizing liquids, some recent developments are presented in *Membrane Separations Technology: Single-Stage, Multistage, and Differential Permeation* (Hoffman, 2003), to which subsequent referrals will be made, especially with regard to gaseous separations, with derivations and calculations provided. Developments in liquid-phase separations by what may be called *hyperfiltration* are also of interest—for example, between ethanol and water, which is examined numerically in Example 19.2. The commercial implementation for this route largely remains to be seen.

The subject of membranes has been dealt with in a number of comprehensive references, a few of which are cited here: *Membrane Handbook* by Ho and Sirkar (1992). There are also the appropriate entries in the *Encyclopedia of Chemical Processing and Design* by McKetta and Cunningham (1988), and *Kirk-Othmer Encyclopedia of Chemical Technology* by Grayson and Eckroth (1981). Evidently, the subject has not yet reached the status of a chemical engineering unit operation, since the necessary process-type calculations are as yet not routinely presented—with the possible exception of Hoffman's (2003) work. For a perspective, consult the section on mem-

brane separations in the seventh edition of *Perry's Chemical Engineers' Handbook* (Perry et al., 1997).

Other monographs of note include *Membrane Separations Technology: Principles and Applications* (Noble and Stern, 1995), *Membrane Processes in Separation and Purification* (Crespo and Böddeker, 1993), *Membrane Separations in Chemical Processing* (Flynn and Way, 1982), and *Membrane Separation Processes* (Meares, 1976). Additional references may be found at the end of the chapter.

In addition to the usual considerations of membrane science and technology, and of membrane materials or membrane cells per se, another item of interest lies in establishing the derivations and process-type calculations involved in predicting the degree of membrane separation that can be attained. It is a matter more complicated than ordinarily thought or expected, and is allied with the unit operations concept as embodied in chemical and process engineering. This aspect has been dealt with at length by Ho and Sirkar (1992), as previously indicated, and will be briefly introduced later in this chapter, as applicable mainly to single-stage separations.

MEMBRANE SEPARATION SYSTEMS

Membrane technology is variously used for separating phases and component—starting, say, with suspensions and colloidal suspensions, and solutions, and moving on to liquids and gases. A brief overview follows.

Suspensions and Solutions. The particle-size range for the separation of suspended solids from fluids is diagrammed in Figure 19.1. As noted, the solid particulate sizes vary from the macro to the ionic, thereby entering the domain of true solutions. The fluid is usually a liquid, but there are of course solid and liquid (or droplet) suspensions occurring in a gaseous phase.

The separation of suspensions is the selective removal of suspended solids, say, by the ordinary processes of filtration. Application can also made to the separation of colloidal suspensions of minute or microscopic solid particles, and even of emulsions, the suspension of minute immiscible liquid droplets within another liquid phase. A distinguishing feature of ordinary filtration is usually that the discharged liquid phase does not form a continuum on the downflow or reject side of the membrane, or filter, and more or less exists at atmospheric pressure. If otherwise, if a continuunum is formed, the process is more that of reverse osmosis, also called hyperfiltration. In common use, notably for the upgrading or desalination of salt water or brackish water, reverse osmosis is a subject for special consideration.
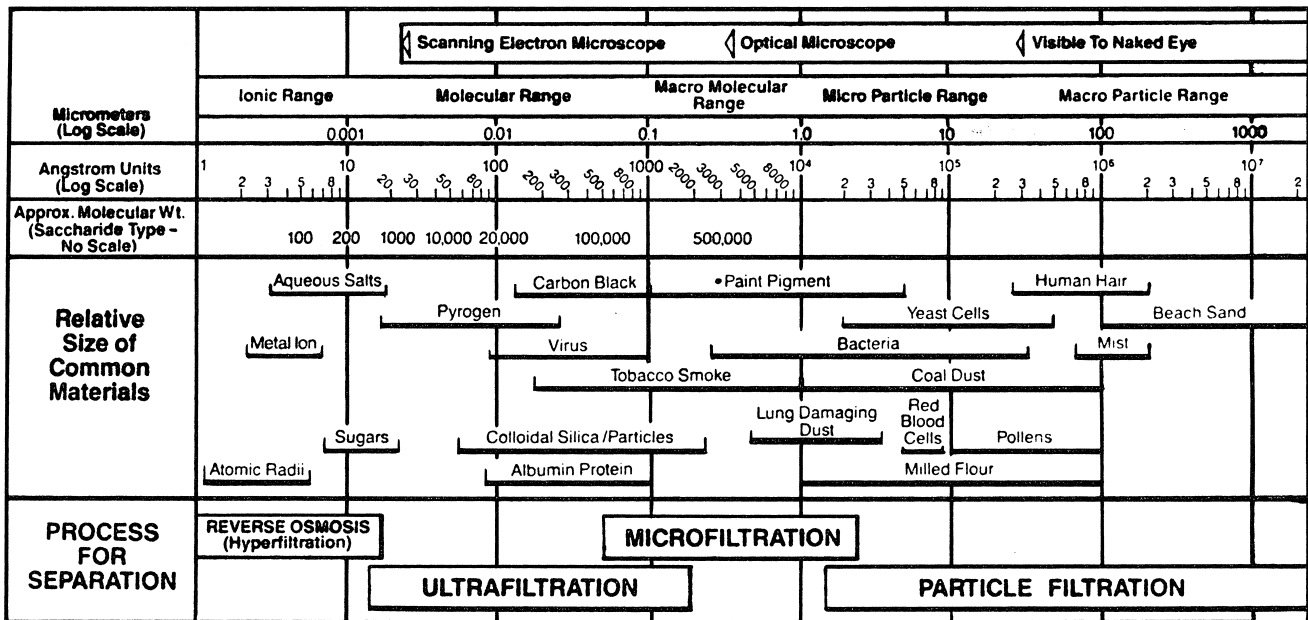
Figure 19.1. Range of molecular weights and particle or droplet sizes of common materials, how they are measured, and the methods employed for their removal from fluids (*Osmonics Inc.*). (Walas, 1988)

Reverse Osmosis. Membranes, usually of organic polymers, can be constructed for separation of liquids from dissolved or suspended substances of a wide range of sizes smaller than those normally processed by the kind of filtration equipment described in Chapter 11. The full range of sizes of molecules and particles is illustrated in Figure 19.1. For small dissolved molecules, a phenomenon known as *osmosis* is the basis for a means of separation. Osmosis becomes manifest when two solutions at the same temperature and pressure, but of different concentrations, are separated by a semipermeable membrane, namely one that allows passage of the solvent but not the solute. Figure 19.2 illustrates this process. One theory of the action is that the solvent dissolves in the membrane at the face of higher concentration or higher partial pressure and is released at the other face where the concentration is lower.

The natural tendency is for the solvent to flow in the direction that will equalize the concentrations. It turns out, however, that if a certain pressure, called the *osmotic pressure*, is imposed on the more concentrated solution, flow of the solvent can be forced in the direction from the more concentrated to the more dilute solution. Example 19.1 illustrates the osmotic pressure relationship, and points out how rapidly the osmotic pressure falls off with increasing molecular weight of the solute.

Size ranges for membrane processing by reverse osmosis are shown in Figure 19.1. Reverse osmosis is effective in removing solvents away from dissolved molecules. Because of limitations in crushing strengths of membranes, pressures are limited to maxima of about 1000 psi (68 atm). Flow rates of 2–200 gal/(sqft)(day) or 0.0001–0.1 kg water/m²-sec are attained in various units. Ultrafiltration operates at 1–10 atm differential pressure and is effective for the molecular weight range or 1000–2,000,000 which includes many proteins, viruses, and bacteria. Ultra and microfiltrations somewhat overlap. Pressures for microfiltration are about 1 atm differential. Since these processes are relatively expensive, their applications are limited largely to analytical purposes and in water treatment for pharmaceutical manufacturing. Some specific applications are listed in Table 19.1.

Membranes for Reverse Osmosis. The first commercially successful membrane was the anisotropic or asymmetric structure invented by Loeb and Sourirajan (1960; cited by Sourirajan, 1970). It is made of cellulose acetate and consists of a dense layer 0.2–0.5 μm diameter. The thin film has the desired solute retention property while offering little resistance to flow, and the porous substructure offers little resistance to flow but provides support for the skin. The characteristics of available membranes for reverse osmosis and ultrafiltration are listed in Tables 19.2 through 19.4.

Hollow fiber membranes are primarily homogeneous. In use, their lower permeability is compensated for by large surface per unit volume of vessel. Fibers are 25–250 μm. The cross section of a vessel for reverse osmosis may have 20–35 million fibers/sqft and a surface of 5500–9000 sqft/cuft of vessel. Recently developed hollow fibers for gas permeation processes have anisotropic structures.

Liquids and Solutions. With respect to the separation of a mixture of what may be called miscible liquids, most often of an organic nature but which may include water, the available information is less pervasive, save for the instance of pervaporation, producing a vaporized permeate. However, the information for aqueous solutions containing inorganic constituents is more voluminous, especially in terms of dialysis and reverse osmosis, the notable application being desalination. Generally speaking, dialysis pertains more to the separation (removal) of ionic constituents per se from solution. (Ion exchange, involving other factors, will be excluded.) Reverse osmosis, however, pertains to the separation and removal of the dissolved salt.

In further comment, the term *osmosis* refers to the movement of the solvent phase itself to regions of solute concentration via a semipermeable membrane—that is, a membrane impervious to the salt but not to the solvent. (The effect is to build up an osmotic pressure difference, which may be estimated by methods presented in most physical chemistry texts, and is illustrated in Example 19.1.) This naturally occurring pressure difference must be overcome or reversed in order that the movement of the solvent be from the more solute concentrated region to the less concentrated region—

(a)

(b)
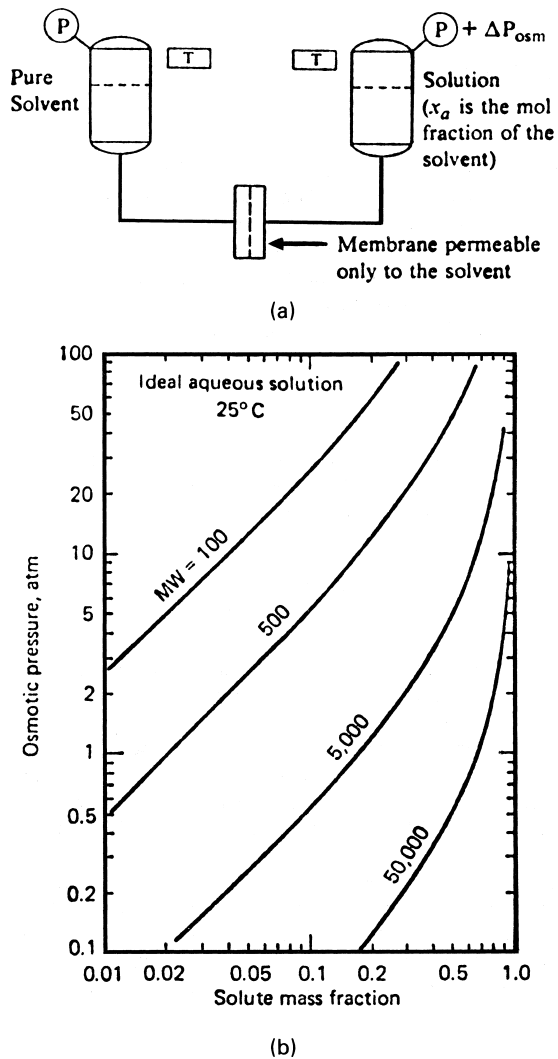
Figure 19.2. Diagram of osmotic behavior and the effect of solute concentration and molecular weight on osmotic pressure. (a) Osmotic-pressure behavior of solutions; ΔP_{osm} is the excess pressure on the solution required to stop flow of solvent through the semipermeable membrane. (b) Effects of solute concentration and molecular weight on osmotic pressure. (Walas, 1988)

hence the term *reverse osmosis*. For most practical purposes, the working pressure drop is overriding, and need not be corrected for the osmotic pressure difference.

(A similar phenomenon, called the *Donnan effect*, pertains to the separation of ions via a semipermeable membrane, being permeable to some ions but not others.)

Miscible Liquid Behavior. Further concerning osmotic behavior, there is the behavior of, say, two miscible liquids, or miscible liquid components, but with each separated from the other by a semipermeable membrane, more permeable to one liquid than the other. Movement of the more permeable liquid phase to the less permeable liquid phase will occur, building up a pressure difference. However, there will likely be membrane "leakage" from the latter phase to the former, in the reverse direction, eventually producing the same equilibrium composition on both sides of the membrane. This brings up the relative permeation of two miscible liquids from a zone of composition on the one side of a membrane

to a zone of different composition on the other side. There would again be the buildup of a pressure difference, but due to leakage in the other direction, this would eventually result in an equilibrium state with both zones having the same composition. These are static phenomena, however, whereas steady-state membrane separation processes are to be rate-determined and unidirectional, and not inclusive of static behavior.

Gases. With respect to gases per se, membrane technology is an accepted means for separating noncondensable gases—that is, gases that condense only under low temperature or cryogenic conditions. The technology might be in wider use if (1) better and more selective membrane materials were available and (2) the necessary mathematical representations and calculations were better spelled out for the separations attainable. In fact, one sometimes depends on the other. Of particular interest are ways in which separations could be enhanced using relatively nonselective membranes, such as by multistage, cascaded membrane-cell juxtapositions.

As a special case there is pervaporation, in which the feed material is a liquid, but the permeate becomes a gas or vapor. That is, the temperature and pressure of the permeate produced are such that the permeate product will exist in the gaseous or vapor phase. Conceivably and conversely, the feed stream could be a gas but the permeate conditions would be such that the components selectively obtained would constitute a liquid phase. In any event, compositional phase changes (e.g., flash vaporizations) can affect the outcome.

The general subject has been explored in a number of reviews, as annotated in Hoffman (2003), and has been a concern in such serial publications as the *Journal of Membrane Science* and *Membrane Separation Processes*. The subject has also been of interest to the Gas Research Institute (now the Institute of Gas Technology) as per workshops that have been held on the subject (Gas Research Institute, 1981, 1982). In fact, the Gas Research Institute jointly sponsored a project with the Dow Corning Corporation and others aimed at correlating and predicting the permeability behavior of membranes from the chemical structure, as noted in Hoffman (1987) and Hoffman et al. (1988).

The American Institute of Chemical Engineers has maintained an active interest through its Symposium Series, as has the American Chemical Society. For continuing developments, there is the Internet, and of course *Chemical Abstracts*, and for book titles, there are Books in Print and WorldCat, services in conjunction with OCLC (Online Computer Library Center). Additionally, there is the U.S. Department of Energy, which keeps up-to-date reviews of the subject, and the National Technical Information Service (NTIS), which keeps a bibliographic database. Generally speaking, the entries for membrane-related research number into the thousands, much of it biomedical, although the entries for membrane gas separation, for example, constitute only a relatively small part.

Membrane Processes in Separation and Purification (Crespo and Böddeker, 1993) contains chapters on pervaporation, facilitated transport membrane processes, membrane gas absorption processes, hollow fiber contactors, membrane reactors, and the preparation and application of inorganic membranes. In addition to an introductory chapter by the editors, *Polymeric Gas Separation Membranes* (Paul and Yampol'skii, 1994) has chapters on the following subject areas: the diffusion of gases in polymers; the relationship between polymer structure and transport properties for aromatic materials; the relationship between polymer structure and transport properties for high free volume materials; the formation of membranes specifically for gas separations; a discussion of facilitated and active transport; nonhomogeneous and moving membranes; membranes for separating organic vapors from gas streams; gas separation practices in Japan; further commercial and

EXAMPLE 19.1
Applications of the Equation for Osmotic Pressure

For the case of pure solvent on the low pressure side of the membrane, the osmotic pressure relationship is

$$\ln \gamma_w x_w = -\frac{1}{RT} \int_0^{P_{osm}} \bar{V}_w dP = -\frac{\bar{V}_w}{RT} P_{osm}$$

where γ is the activity coefficient, x is the mole fraction, and $\bar{V}$ is the partial molal volume; subscript w identifies the solvent. For ideal solutions, the activity coefficient is unity. Since noinideality is of common occurrence, this equation may be used to find activity coefficients from measurements of osmotic pressure.

a. The osmotic pressure of a sucrose solution is 148.5 atm at 20°C. The concentration is 1.43 kg sucrose/kg of water, corresponding to a mol fraction of 0.0700 of sucrose. The partial molal volume of water is approximately 0.018 L/gmol. Accordingly, the activity coefficient is

$$\gamma = \frac{1}{1 - 0.07} \exp\left[-\frac{0.018(148.5)}{0.082(293.2)}\right] = 0.9622$$

The difference from unity appears to be small but is nevertheless significant. At this concentration, if the activity coefficient were unity, the osmotic pressure would be

$$P = -\frac{0.082(293.2)}{0.018}\ln(1 - 0.07) = 97 \text{atm}$$

which is considerably in error.

(Rising osmotic pressures are quite remarkable for increasingly concentrated solutions. Thus, at 2.02 grams of sucrose per liter of solution, the observed osmotic pressure is 0.134 atm; at 45.0 grams per liter, the observed osmotic pressure is 2.97 atm; at 100 grams per liter, 26.8 atm; and at 750 grams per liter, it rises to 134.7 atm.)

b. The effect of molecular weight on ideal osmotic pressures of a variety of solutions containing 0.1 kg solute/kg water is demonstrated in this tabulated comparison:

Mol Weight	Mol Fraction x	Ideal Osmotic P in atm
58.5 (as NaCl)	0.0374	50.9
100	0.0177	23.9
342 (as sucrose)	0.00524	7.0
1000	0.0018	2.4
10,000	$1.8(E-4)$	0.24
100,000 (virus and protein)	$1.8(E-5)$	0.024

Figure 19.1 identifies sizes of common molecules and particles. Clearly, osmotic pressures are essentially negligible for molecular weight above 10,000 or so (and clearly can represent significant pressures to overcome in reverse osmosis).

TABLE 19.1. Examples of Applications for Ultrafiltration

(a) Applications Involving Retained Colloidal Particles

Material	Application
Pigments and dispersed dyes	Concn/purification of organic pigment slurries; sepn of solvents, etc. from pigment/resin in electropaints; concn of pigments in printing effluents
Oil-in-water emulsion globules	Concn of waste oils from metal working/textile scouring; concn of lanolin/dirt from wool scouring
Polymer lattices and dispersions	Concn of emulsion polymers from reactors and washings
Metals/nonmetals/oxides/salts	Concn of silver from photographic wastes; concn of activated carbon slurries; concn of inorganic sludges
Dirt, soils, and clays	Retention of particulates and colloids in turbid water supplies; concn of fines in kaolin processing
Microorganisms	Retention of microbiological solids in activated sludge processing; concn of viral/bacterial cell cultures
Plant/animal cellular materials	Separation of fermentation products from broth; retention of cell debris in fruit juices, etc.; retention of cellular matter in brewery/distillery wastes

(b) Applications Involving Soluble Macromolecules

Material	Application
Proteins and polypeptides	Concn/purification of enzymes; concn/purification of casein and whey proteins; concn/purification of gluten/zein; concn/purification of gelatin; concn/purification of animal blood; retention of haze precursors in clear beverages; retention of antigens in antibiotic solutions; concn/purification of vegetable protein extracts; concn/purification of egg albumen; concn/purification of fish protein; retention of proteins in sugar diffusion juice
Polysaccharides and oligosaccharides	Concn of starch effluents; concn of pectin extracts
Polyphenolics	Concn/purification of lignosulphonates
Synthetic water-soluble polymers	Concn of PVA/CMC desize wastes

TABLE 19.2. Data of Commercial Equipment for Reverse Osmosis and Ultrafiltration

(a) Equipment of Amicon Corp.

Diaflow®	Nominal mol wt cutoff	Apparent pore diam in Å	Water flux in gal/ft³/day at 55 psi
UM 05	500	21	10
UM 2	1,000	24	20
UM 10	10,000	30	60
PM 10	10,000	38	
PM 30	30,000	47	500
XM 50	50,000	66	250
XM 100A	100,000	110	650
XM 300	300,000	480	1300

(b) Equipment of Nucleopore Corp.

Specified Pore Size, μm	Pore-size Range, μm	Nominal pore Density, Pores/cm²	Nominal Thickness, μm	Water, gpm/ft³ $\Delta P=10$ psig, 70°F	N₂ in ft³/min-ft³ $\Delta P=10$psig, 70°F
8.0	6.9–8.0	1×10^5	8.0	144.0	138.0
5.0	4.3–5.0	4×10^5	8.6	148.0	148.0
3.0	2.5–3.0	2×10^6	11.0	121.0	128.0
1.0	0.8–1.0	2×10^7	11.5	67.5	95.0
0.8	0.64–0.80	3×10^7	11.6	48.3	76.0
0.6	0.48–0.60	3×10^7	11.6	16.3	33.0
0.4	0.32–0.40	1×10^8	11.6	17.0	33.0
0.2	0.16–0.20	3×10^8	12.0	3.1	9.9
0.1	0.08–0.10	3×10^8	5.3	1.9	5.3
0.08	0.064–0.080	3×10^8	5.4	0.37	2.6
0.05	0.040–0.050	6×10^8	5.4	1.12	1.3
0.03	0.024–0.030	6×10^8	5.4	0.0006	0.19

(c) Equipment of Koch Membrane Systems (Formerly Abcor)

Membrane Type (1)	Nominal MW Cutoff (2)	Max Temp in °C (3)	pH Range (4)	Max Press in psi (kg/cm²)	Configuration (5)
MSD-324*	1,500	90	1–13	150 (10.5)	S
HFK-132	3,500	90	1–13	150 (10.5)	S
HFK-131	5,000	90	1–13	150 (10.5)	S
HFD-300	8,000	90	2–12	150 (10.5)	T
HFM-100	10,000	90	1–13	150 (10.5)	S,T
HFA-251*	15,000	50	2–8	150 (10.5)	T
HFM-180	18,000	90	1–13	150 (10.5)	S,T
HFM-163	18,000	60	2–12	150 (10.5)	S,T
HFP-276	35,000	90	1–13	150 (10.5)	S,T
MSD-181	200,000	90	1–13	150 (10.5)	S,T
MSD-400*	100,000	90	1–13	150 (10.5)	S,T
MSD-405*	250,000	90	1–13	150 (10.5)	S,T
MMP-406*	0.2 Microns	90	1–13	150 (10.5)	S,T
MMP-404*	0.4 Microns	90	1–13	150 (10.5)	S,T
MMP-516*	2 Microns	90	1–13	150 (10.5)	S,T
MMP-407*	2–3 Microns	90	1–13	50 (3.5)	S,T
MMP-600	1–3 Microns	90	1–13	50 (3.5)	S,T
MMP-602	2–3 Microns	90	1–13	50 (3.5)	S

(1) Membranes beginning with ''H'' designation are stock items. (* = hydrophilic)
(2) The nominal molecular weight (MW) cutoff is prvided as a guide to the relative pore size for these membranes. Since many factors influence the actual MW cutoff, tests must be run to confirm retention for any specific application.
(3) At pH −6.
(4) At 25˚C.
(5) F = Flat sheet; S = Spiral; T = Tubular (Walas, 1988)

practical aspects of gas separation membranes; and a comparison of membrane separations with other gas separation technologies. Neither of these volumes details the process-type calculations involved for determining the degree of separation.

As for a comparison of membrane gas separation technologies, such as pressure swing absorption (PSA) and low-temperature or cryogenic separations, the last chapter in (Paul and Yampol'skii, 1994) must remain somewhat inconclusive, given the

TABLE 19.3. Properties of Membranes for Reverse Osmosis

(a) Cellulose Acetate Membranes

Membrane	Mfr	Volumetric flow rate (1/m²d)	NaCl retention (%)	Pressure (bars or ~atm)	NaCl concentration (%)
CA* (Tubing/flat)	Kalle	500–2500	98.6–60	40	0.5
CA* (Flat)	DDS***	350–220	99–78	42	0.05
CA* (Tubing)	Patterson Candy Int.		97–50	40	0.5
CA* (In situ cast; pipe)	Abcor	450–900	98–90	42	0.5
CA* (Wound module)	Univ Oil Prod (Gulf)	650	98	70	3.5
CA* (Hollow fiber)	Monsanto	130	94	18	3.5
CTA** (Hollow fiber)	Dow Chem Co	50	99.5	70	3.5
CTA** Ultra-thin wound module	Univ Oil Prod (Gulf)	550	99.3	70	3.5

Note: (From A. Walch, *Proceedings Membrane Conference*, Lund Sweden, 1976; *Ullman's Encyclopedia of Chemical Technology*, Verlag Chemie, Weinheim, Vol. 16, pp. 515–535.) (Walas, 1988)
*CA: Cellulose-2,5-acetate; **CTA: Cellulosetriacetate, ***De Danske Sukkerfabriken.

(b) Other kinds of Membranes

Membrane	Type	Mfr	Vol/ΔP in ml/min-cm²-bar	MW range	Conditions
Polyelectrolyte (composite)	UM 05 - UM 10	Amicon	0.005–0.08	500–10,000	4 bar, 50C H 4-10
Polysulfone (hollow fibers)	PM 10 - PM 30	Amicon	0.4–13	10,000–30,000	4 bar, 115C H 0-12
Mod acrylic (hollow fibers)	Xm 50 - XM 300	Amicon	0.6–2.0	50,000–300,000	2 bar, 70C pH 0-12
Polyelectrolyte (composite)	PSAC, PSDM	Millipore	0.18–0.15	1000–40,000	7 bar, 50C pH 4-10
Cellulosetriacetate (60 μm)	PEM	Gelman	0.004	50,000	80C pH 1-10
Regen cellulose (hollow fibers)	BF 50	Dow	-	5000	70C H1-12
Cellulose acetate (hollow fibers)	BF 80	Dow	-	30,000	50C pH 2-8
Regen cellulose (100 μm)	115	Sartorius	0.001–0.1	20,000–160,000	80C pH 1-12
Cellulose acetate (100 μm)	117	Sartorius	0.001–0.1	20,000–160,000	80C pH 2-8
Cellulose nitrate (100 μm)	121	Sartorius	0.005–0.02	10,000–50,000	80C pH 1-10
ZrO₂/Carbon (tube bundle)	Ucarsep	Union Carbide	0.02	30,000 etc	10 bar 100C pH 1-14
Polyamide, -imide (composite/hollow)	BM 10 -	Berghof	0.004–0.7	1000–50,000	100C pH 2-10
Copolyacrylonitrile (sym)		Rhone-Poulenc	0.17	70,000	2 bar pH 2-12
Cellulose acetate (asym)	800–500	DDS***	0.01–0.04	6000–60,000	20-100 bar bar30-50C pH 3-7
Polysulfone (asym)	GR 5, 6, 8	DDS***	-	10,000–20,000	80C pH 0-14
Polyacrylonitrile (asym)	FPB-GPA	DorrOliver	0.1–0.35	1200–100,000	2-4 bar 80C pH 1-13
Cellulose acetate (asym)	T2/A-T5A	PCI*	-	1000–20,000	10-25 bar 30-50C pH 3-7
Cellulose deriv	T6/B	PCI*	-	120,000	10 bar, 60C pH 2-11
Cellulose acetate (asym)	HFA/100-HFA/300	Abcor	0.005–0.3	15,000–50,000	14-100 bar 30-50C pH 3-7
Polyamide (asym)		Abcor	-	50,000	-
Cellulose acetate (asym)	UF 6-UF 100	Kalle	0.01–0.1	6000–100,000	3-10 bar 50C, pH 3-7
Polyamide (asym)	PA 40-PA 100	Kalle	0.06–0.1	40,000–100,000	3-6 bar, 70C pH 1-11

(Walas, 1988)

wide range of variables, parameters, and applications as detailed in a chapter on the comparison of membranes. Moreover, for the most part, the separations compared only that of air and hydrogen-containing systems.

In particular, the entry with the title and subtitle *Membrane Gas Separation* (as per citations from the NTIS Bibliographic Database) is abstracted with a lead-off qualifier, to the effect that "the bibliography contains citations concerning the research and development techniques involving the use of plastic and metal or metallic membranes." A specific example of an additional state-ment of scope is (e.g., June 1993): "Included are such topics as recent advances in membrane science and technology, gas separations using composite hollow fiber membranes, optimal cascade theory for the separation of mixtures on semipermeable membranes and gas separation by a continuous membrane column." Another example is (e.g., August 1993): "Citations review isotope separation, osmotic techniques, reverse osmosis, and preparation of membranes for specific separation processes. The permeability of polymer membranes is discussed in terms of physical properties as well as molecular structure." And in closing,

TABLE 19.4. Properties of Membranes for Ultrafiltration

	Membrane	Mfr	Vol. rate (l/m²d)	NaCl retention (%)	Press (bar)	NaCl conc.	Stability
Polyamide	Aromatic polyamide (asym hollow fiber 89)	DuPont	50	95	28	0.15	35C pH 4-11
	Copolyamide (asym hollow fiber 810)	DuPont	30	98.5	56	3.0	30C pH 5-9
	Polyamide hydrazide (asym wound module	DuPont	500	99	70	3.5	-
	Polypiperazinamide (asym fibers)	Montecatini	600	98	80	1	Chlorresistant
	Arom. polyamide (ultrathin wound modules)	Universal Oil Prod.	1700	98.9	70	3.5	-
Polyurea	Ethyleneimine, toluylene diisocyanate NS 100 (ultrathin wound modules	North Star Res. Inst (UOP)	500	99..6	70	3.5	pH 2-12
Polyfural	Furfuryl alcohol, H_2SO_4; NS 100 (ultrathin)	North Star Res. Inst.	1000	99..6	70	3.5	pH 2-12
Polyether	Polyphenylene oxide sulfone (5 μm on polypropylene tube)	General Electric	1500	84	77	0.1	54C
	Polysulfone	Rhone-Poulenc	90	99	60	3.5	60C
Polyhetroaromatics	Polybenzimidazole (asym tube)	Celanese	800	95	41	0.5	-
	Polybenzimidazole (asym hollow fiber)	Celanese	50	99.4	70	3.5	-
	Polimide, methoxyl (10 μm)	Battelle (BRD)	20	99..7	100	3.5	-
Fluoropolymer	Naflon (sulf, 250 μm)	DuPont	3	85	100	3.5	-
	Permion (pyridine, 25 μm)	RAI-Res. Corp.	1	98..8	100	3.5	-
Inorganic Membranes	Glass hollow fiber	Stanford Res. Inst.	15	83	102	1	-
	Glass hollow fiber	Schott & Gen.	-	98	120	0.5	-
	Graphite, oxidized	Westinghouse (Union Carbide)	50	80	41	0.5	-
Dynamically formed membranes	XrO2/polyacrylic acid	Oak Ridge Natl Lab	5000	90	70	0.3	-
	Polyacrylic acid	Univ Oil Prod. (Gulf)	2000	80	102	0.3	-
Vinyl polymers	Polyfinylpyrrolidone (cross linked 75 μm)	Univ Oil Prod. (Gulf)	0.5	99	34	0.8	-
	Polyvinyl alcohol (cross linked 29 μm)	Princeton Univ.	3	93	42	0.6	-
	Polyvinyl carbonate (94 μm)	Aerojet-Gen. Corp.	3	94	102	3.5	-
	Vinyl copolymer (10 μm)	Battelle (BRD)	70	96	100	0.5	-

(From A. Walch, *Proceedings Membrane Conference*, Lund Sweden, 1976; *Ullman's Encyclopedia of Chemical Technology*, Verlag Chemie, Weinheim, Vol. 16, pp. 515–535.) (Walas, 1988)

"The selectivity of polymeric films for a variety of gases is also included." A subject or terms index and title list are included. As the examples will indicate, the coverage is extensive.

19.2. LIQUID-PHASE SEPARATIONS

The most common sort of embodiment involving a liquid phase is the membrane separation of suspended solids from liquids, denoted variously by the terms *filtration, microfiltration*, and *ultrafiltration*, depending on the particle size, and which may include colloidal suspensions and emulsions. The solid particulates, for the most part, are deposited in the interstices or pores of a membrane barrier, and accordingly will require an intermittent backflushing operation.

As a further case, there is the situation whereby the solids are dissolved to form a true solution, or at least constitute a stable colloidal solution, but nevertheless are retained in the membrane barrier. The objective is to achieve a more concentrated solution, even precipitated solute, at the reject or high-pressure side of the membrane, and essentially solute-free solvent in the on the low-pressure or permeate side. Inasmuch as the applied pressure difference has to counteract the natural osmotic pressure, which acts in the reverse direction, the process is called *reverse osmosis*. Desalination is the ubiquitous example.

In yet another case, called *dialysis*, there is the situation where it is desired to separate two (or more) dissolved substances from the solvent. The dissolved substances have different membrane permeabilities, such that the less-permeable substance(s) will concentrate in the reject stream, and the more permeable substance(s) will concentrate in the permeate stream.

Last, there is the case involving liquids per se. The liquid phases may be entirely miscible, as occurs with many organic liquids, and with water-soluble organics and water. Notable examples of the former are various hydrocarbon mixtures, and the notable example of the latter is the ethanol-water system. The membrane material per se is sometimes described as hydrophilic

or wetting to the one component and hydrophobic to the other, producing relative rates of passage. Although membrane methods are an alternative, distillation methods are the common standard, albeit liquid-liquid extraction methods may also be called for, especially if constant-boiling azeotropes are involved.

As a special case, there may be immiscibility or limited miscibility, resulting in emulsions, but which can be handled by membrane separation. The addition of emulsion-breaking substances may be necessary, and electrostatic methods may also be indicated, as in the separation of oil-water emulsions.

The extrapolation is to what is called *pervaporation*, where the feed mixture is a liquid, but the permeate vaporizes during permeation, induced by the relatively low pressure maintained on the permeate side of the membrane. Accordingly, the reject or retentate remains a liquid, but the permeate is a vapor. Thus, there are features of gas permeation as well as liquid permeation. The process is eminently applicable to the separation of organics and to the separation of organics and water (e.g., ethanol and water). In the latter case, either water vapor may be the permeate, as in dehydration, or the organic vapor may be the permeate. The obvious, potential application is to the separation of azeotropic mixtures and close-boiling mixtures—as an alternative or adjunct to distillation or liquid-liquid extraction methods.

The subject of pervaporation is featured in a chapter in Part III of Ho and Sirkar (1992).

19.3. GAS PERMEATION

Differences in rates of permeation of membranes by various gases are utilized for the separation of mixtures—for instance, of hydrogen from ammonia plant gas, of carbon dioxide from natural gas, and of helium from natural gas. The successful "Prism" process of the Monsanto Company (the Prism process is now owned by Air Products and Chemicals) employs hollow fibers of a porous polysulfone base coated with a thin layer of silicone rubber. The fibers are about $800\,\mu m$ outside diameter and $400\,\mu m$ inside diameter. They are housed in vessels 4–8 in. in diameter and 10–20 ft long, and may contain 10,000–100,000 fibers per bundle. A schematic of such a unit is shown in Figure 19.3(a). Pressures up to 150 atm are allowable. A unit of 4 in. in diameter by 10 ft long was able to upgrade 290,000 SCFD of ammonia plant purge gas, making a product with 90% hydrogen and a waste of 20% hydrogen from a feed with 37% hydrogen.

Because of the long, narrow configuration, the equipment appears to function as if in countercurrent mode. Other data of experiments with gas permeation as continuous columns appear in Figures 19.5(a) and (b); the original paper has data on other binary and some complex mixtures.

Permeability of a membrane is determined partly by gas diffusivity, but adsorption phenomena can also exist at higher pressures, which affects the outcome. Separation factors of two substances are approximately in the ratios of their permeabilities, which can be defined by $\alpha_{AB} = P_{oA}/P_{oB}$, or more simply $\alpha_{AB} = P_A/P_B$, where the symbol P represents the permeability at a stated reference condition. Some data of permeabilites and separation factors are listed in Table 19.7, together with a list of membranes that have been used commercially for particular separations. Similar but not entirely consistent data are tabulated in the *Chemical Engineers' Handbook* (Li and Ho, 1984, pp. 17.16, 17.18). The different units used for permeability will undergo further inspection in a subsequent section.

19.4. MEMBRANE MATERIALS AND APPLICATIONS

A considerable array of membrane materials exist, notably for various gaseous separations, some more effective than others (Hoffman et al., 1988). That is, some are more permeable and more selective than others. It will also depend on the system to be separated. In other words, materials are not yet available for the full array of gaseous mixtures encountered. As to other mixtures, a partial listing is shown in Table 19.3 for reverse osmosis, and in Table 19.4 for ultafiltration, with performance data in Tables 19.5 and 19.6. Table 19.7 pertains to gas permeation, giving permeabilities and selectivities or relative permeabilities. Much more information is furnished in Appendix 1 of Hoffman (2003) as well as in other references.

The oxygen/nitrogen membrane separation for air, perhaps the most obvious, has been one of the most-studied examples and is sort of a baseline reference. The sharp separation between nitrogen and oxygen on a commercial scale remains in the domain of cryogenics, although membrane separations have been used successfully when only a relatively minor increase in the oxygen content of air is sought, as in portable oxygen concentrators for home use.

The separation of refinery gases is also an item of interest, such as gas streams containing hydrogen. In the main, membrane methods pertain to the separation of noncondensable gases—that is, to gases that are not readily liquefiable except by low temperature or cryogenic means.

The interim state and future needs of membrane technology for various binary gaseous separations are shown in the tabulation below, adapted from Appendix 1 of Hoffman (2003):

Of special interest is the separation of nitrogen and methane, or methane plus, as per the upgrading of subquality natural gas. This topic will be further addressed in a subsequent section.

Formerly, membrane materials consisted mainly of barrier types, sometimes called *permeable* and *semi-permeable*, in which the gases flowed into and through the pores and interstices, which

TABLE 19.5. Specifications of Spiral and Tubular Equipment for Reverse Osmosis and Ultrafiltration*

Module	Length	Membrane Area/Module
Tubular UF 1″ (2.5 cm) diam	5 ft (1.5 m)	1.1 sq ft (0.10 m^2)
Tubular UF 1″ (2.5 cm) diam	10 ft (3 m)	2.2 sq ft (0.20 m^2)
ULTRA-COR™ UF Tubes 0.5″ (1.27) diam	10 ft (3 m)	7.4 sq ft (0.68 m^2)
SUPER-COR™ UF Tubes	10 ft (3 m)	24 sq ft (2.2 m^2)
Tubular RO 1/2″ (1.27 cm) diam	12 ft (3.6 m)	48 sq ft (4.4 m^2)
Spiral UF 2″ (5 cm) diam	1.2 ft (0.36 m)	2.5 sq ft (0.23 m^2)
Spiral UF 4″ (10 cm) diam	3 ft (0.9 m)	35-60 sq ft (3.2-5.5 m^2)
Spiral UF 8″ (20 cm) diam	3 ft (0.9 m)	150-250 sq ft (13.9-23 m^2)
Spiral RO 4″ (10 cm) diam	3 ft (0.9 m)	60 sq ft (5.5 m^2)

*The "Ultracor" model has 7 and the "Supercor" has 19 tubes/shell (Koch Membrane Systems, formerly Abcor). (Walas, 1988)

TABLE 19.6. Performance Data of Reverse Osmosis Membrane Modules

(a) Data of Belfort (1984).

Module Design	Packing Density (ft²/ft³)	Water flux at 600 psi (gal/ft²-day)	Salt Rejection	Water Output per unit Volume (gal/ft³-day)	Flow Channel Size (in.)	Ease of Cleaning
Tubular						
Brine flow inside tube	30-50	10	Good	300-500	0.5-1.0	Very good
Brine flow outside tube	140	10	Good	1400	0.0-0.125	Good
Spiral wrap	250	10	Good	2500	0.1	Fair
Fiber						
Brine flow inside fiber	1000	5	Fair	5000	0.254	Fair
Brine flow outside fiber	5000-2500	1-3	Fair	500-7500	0.0002	Poor
Flat plate	35	10	Good	350	0.01-0.02	Good
Dynamic membrane	50	100	Poor	5000	~0.25	Good

(b) Data of Crits [*Ind. Water Eng.*, 20–23 (December 1976–January 1977)].

	Tri-acetate Hollow Fibers	Polyamide Hollow Fibers	Cellulose Acetate Hollow Fibers
Module sizes; flow in gpd at 400 psi	5 × 48″, 4000 gpd; 10 × 48″, 20,000 gpd	4 × 48″, 4200 gpd (1); 8 × 48″, 14,000 gpd (1)	4″ × 21′, 4200 gpd (6); 8″ × 21′, 24,000 gpd (6)
Recommended operating pressure, psi	400	400	400
Flux of permeate, gpd/ft²	1.5	2	15-18
Seals, pressure	2	2	12
Recommended max operating temp, °F	86	95	85
Effluent quality (guaranteed % rejection)	90	90	90
pH range	4-7.5	4-11 0.1 > pH 8.0	4-6.5
Chlorine tolerance	0.5-1.0	0.25 > pH 8.0	0.5-1.0
Influent quality (relative–FI*)	FI<4	FI<3	FI<!5
Recommended influent quality	FI<3	FI<3	FI<3
Permeate back pressure (static), psi	75	75	0
Biological attack resistance	Resistant	Most resistant	Least resistant
Flushing cleaning	Not effective	Not effective	Effective
Module casing	Epoxy-coated steel	FRP	Epoxy-coated steel and FRP
Field membrane replacement	Yes	No (future yes)	Yes

*FI = fouling index.[2] (1) Initial flow. (6) Six modules per 4200 gas/day.

TABLE 19.7. Data of Membranes for Gas Permeation Separation

(a) Permeabilities of Helium, Nitrogen, and Methane in Several Membranes at 20°C (Permeability values are given in the units of 10^{-7} cm²/s bar. To convert from bars to atm. multiply by 0.9869.)

Membrane	He	N_2	CH_4
Silicon rubber	17.25	11.25	44.26
Polycarbonate	5.03	0.35	0.37
Teflon FEP	4.65	0.19	0.11
Natural rubber	2.70	0.79	—
Polystyrene	2.63	0.17	0.17
Ethyl cellulose	2.33	0.21	0.83
Polyvinyl chloride (plasticized)	1.05	—	0.15
Polyethylene	0.75	0.14	—
Polyvinylfluoride	0.14	0.0014	0.00048

(b) Separation Factors $\alpha_{AB} = P_{0A}/P_{0B}$ for Three Mixtures

Membrane	He/CH_4	He/O_2	H_2/CH_4
Polyacrylonitrile	60,000	—	10,000
Polyethylene	264	35.5	162
Polytetrafluoroethylene	166	45	68.5
Regenerated cellulose	400	48	—
Polyamide 66	214	39	—
Polystyrene	14.6	5.5	21.2
Ethylcellulose	48	3.2	6.6

TABLE 19.7.—(*continued***)**

(c) Examples of Commercial Separations and the Kinds of Membranes Used

Separation Process	Membrane
O_2 from air	Ethyl cellulose, silicon rubber
He from natural gas	Teflon FEP, asymmetric cellulose acetate
H_2 from refinery gas	Polyimide, polyethylene-terephthalate, polyamide 6
CO_2 from air	Silicone rubber
NH_3 from synthesis gas	polyethylene-terephthalate
H_2S from natural and refinery gas	Silicon rubber, polyvinylidene fluoride
H_2 purification	Pd/Ag alloys

[Membranen, in *Ullman's Encyclopedia of Chemical Technology*, Verlag Chemie, Weinheim, Vol. 16, p. 515ff. Many more data are collected by Hwang, Choi, and Kammermeyer, *Separation Sci. 9*(6), 461–478 (1974).]

Known Separations	To Be Determined
H_2/C_1+	H_2/CO_2
H_2/CO	H_2S/CO_2
He/Cl	NH_3/H_2
$H_2O(g)/C_1+$	NH_3/C_1+
H_2S/C_1+	NH_3/N_2
CO_2/C_1+	SO_2/C_1+
CO_2/N_2	SO_2/CO_2
CO_2/CO	NO_2/C_1+
NO_2/CO	C_1/C_2
NO_2/N_2	N_2/C_1
CO_2/air	Ar/air
	Organic vapors

were of near-molecular dimensions (e.g., measured in angstroms). (The term *semi-permeable* is used to connote that the membrane was permeable to one component but not the other.) There is the use of materials similar to molecular-sieve adsorbents, and ion-exchange resins, for example. For single-phase liquid systems or solutions, the processes may be referred to by the terms *dialysis* and *osmosis*, the former indicating a separation between dissolved salts or ions (e.g., in water), the latter a separation between a dissolved salt or salts and the solvent (generally water). Whereas for gas-liquid or gas-solid or liquid-solid separations, the terms *micro-* and *ultrafiltration* are more appropriate. The term *hyperfiltration* is sometimes used for the membrane separation of two (or more) miscible liquids.

Some recent developments in membrane processes for the separation of organic liquids have been previously noted, as has the use of hyperfiltration as applied in ethanol recovery. Filtration per se is of relevance in the processing of nonpasteurized beers, for example in the separation of spent yeasts after fermentation.

The more modern embodiment for the membrane separation notably of gases is the diffusion-type mechanism, whereby the gases actually dissolve in the material and pass through by molecular diffusion. Another embodiment is the facilitated transport membrane, which acts as an absorber on the high-pressure side and as an absorbent regenerator on the low-pressure side. Investigations have also been made concerning liquid membranes. Metal or metallic membranes are also under study, as are ceramics, whereas the usual materials are polymeric in nature. Metallic and ceramic membranes can be used at higher temperatures and may also serve as membrane reactors—that is, permit the concurrent removal of reaction products so as to enhance the conversion.

More information about unusual gaseous separations is provided in Gas Research Institute (1982). Furthermore, as previously noted, membranes afford the possibility of catalysis. Consider as

well the subject of membrane reactors, as per Chapter 8 of Hoffman (2003).

As previously mentioned, a study into the structure-permeability relationships for silicone membranes was jointly sponsored by the Gas Research Institute and the Dow Corning Corporation (Hoffman, 1987). The attempt was made toward correlating, understanding, and predicting the permeability behavior of silicone polymers from their chemical structure. This behavior was in terms of the permeability and selectivity to various common gases and their separation. The ultimate objective was to systematize and generalize this behavior so that it could be applied to other kinds of membrane materials and other gases and gaseous mixtures.

19.5. MEMBRANE CELLS AND EQUIPMENT CONFIGURATIONS

Four principal kinds of membrane assemblies are in use:

1. In tubular assemblies the membrane is deposited either on the inside or outside of porous tube, most commonly inside for reverse osmosis and outside for ultrafiltration. Figure 19.3(a) shows a single-tube construction, but units with 7 or 19 tubes in a single shell are made as standard items. Table 19.5 lists some available sizes. "Dynamic membranes" may be deposited on porous stainless steel tubes from a feed solution that consists of polyacrylic acid and hydrous zirconium oxide. Such a membrane can be deposited in 1 hr and replaced as quickly. Fluxes are very high; 100 gal/(sqft)(day) is shown in Table 19.6(a). Some applications are described by Turbak (Vol. II, 1981, pp. 434–453).

2. Plate-and-frame construction is shown in Figures 19.3(b) and (c). It is used more commonly in ultrafiltration. A related kind of equipment is the electrodialysis plate-and-frame equipment of Figure 15.26.

3. Spiral wound assemblies are illustrated in Figure 19.4. They consist of a long envelope of membrane sealed on the edges and enclosing a porous material that serves as a channel for the flow of the permeate. The spacer for the feed solution flow channel is a meshlike material through which the solution is forced under pressure. The modules listed in Table 19.5 are 2–8 in. in diameter, up to 3 ft long, and provide about 250 sqft of membrane surface/cuft of vessel. Dimensions are shown in Figure 19.4(c). According to Table 19.6, reverse osmosis rates of 2500 gas/(sqft)(day) are attained.

4. Hollow fiber assemblies function as one-ended shell-and-tube devices. At one end the fibers are embedded in an epoxy tube-sheet and at the other end they are sealed. Overall flows of feed solution and permeate thus are in counterflow. Flow of permeate is into the tubes, which takes advantage of the great crushing strengths of the small diameter fibers. This also constitutes a
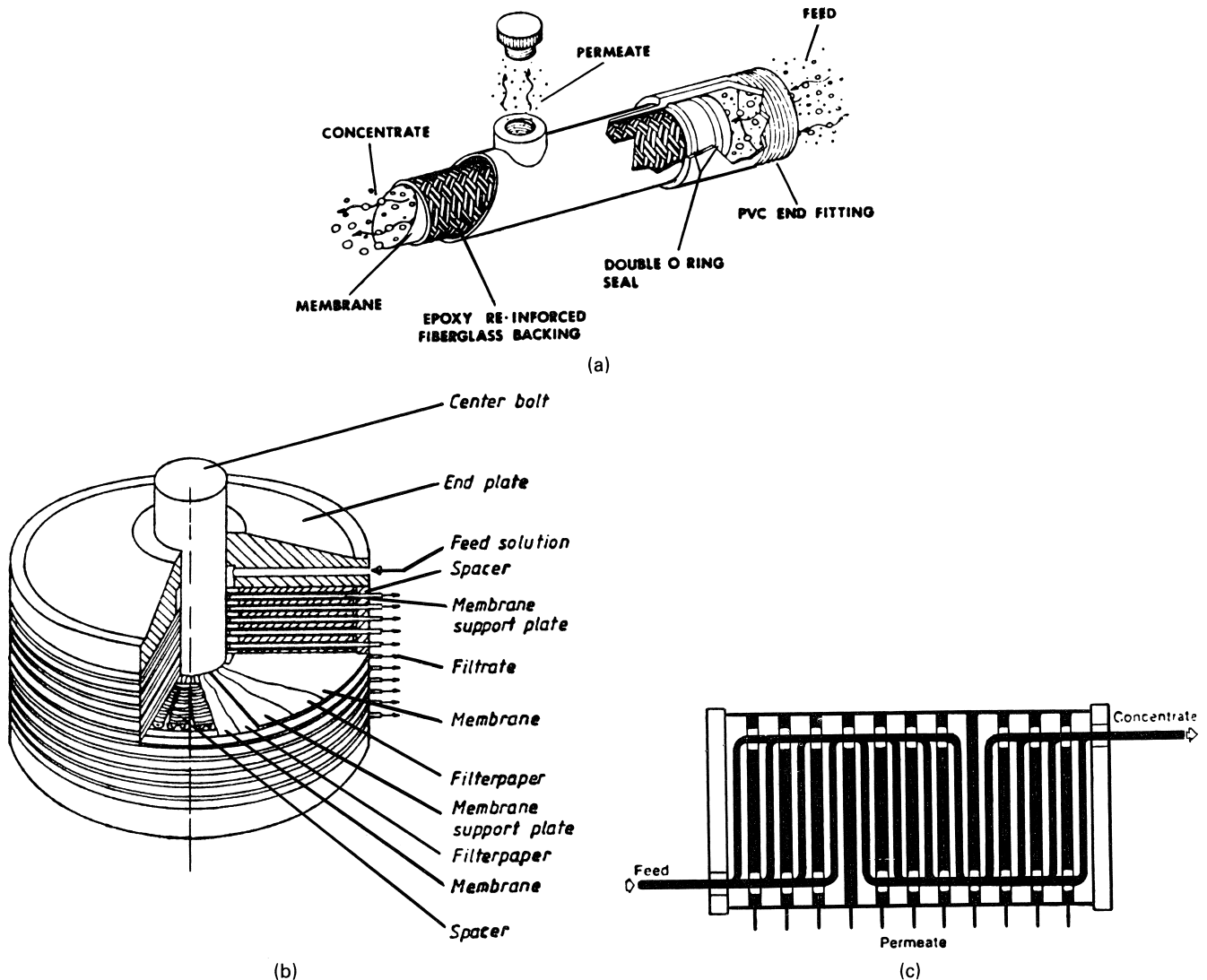
Figure 19.3. Tubular and plate-and-frame membrane modules for reverse osmosis and ultrafiltration. (a) Construction and flow pattern of a single 1 in. dia tube with membrane coating on the inside; in Table 19.4, the "Ultracor" model has seven tubes in a shell and the "Supercor" has 19 [*Koch Membrane Systems* (*Abcor*)]. (b) Assembly of a plate-and-frame ultrafiltration module (*Danish Sugar Co.*). (c) Flow in a plate-and-frame ultrafiltration module.

"fail-safe" operation, since collapse of the fibers results on closure, whereas bursting would result in leakage. The most serious drawback is some difficulty in cleaning. A widely used equipment of this type is illustrated in Figure 19.5.

19.6. INDUSTRIAL APPLICATIONS

The greatest use for membranes is for reverse osmosis desalination of seawater and purification of brackish waters. Spiral wound and hollow fiber equipment primarily are applied to this service. Table 19.6 has some operating data, but the literature is very extensive and reference should be made there for details of performance and economics.

Because of the low energy requirements of separations by reverse osmosis, much attention has been devoted to other separations of aqueous solutions, at least on a laboratory scale, for instance, or ethanol/water. Membranes have been found that are moderately effective, but the main obstacle to the process is the very

high pressure needed to remove water from high concentrations of ethanol against pure water on the low pressure side. A practical method of circumventing this problem is to replace the water on the low-pressure side by a solution of sufficiently high concentration to allow the application of only moderate pressure. The case examined in Example 19.2 utilizes a solution of ethylene glycol of such concentration that a concentration of ethanol above the azeotropic composition can be achieved with a pressure of only 1000 psig. The glycol is easily separated from water by distillation.

19.7. SUBQUALITY NATURAL GAS

A potentially large market for membrane applications is the upgrading of subquality natural gas (Hoffman, 2003, 1988). Subquality natural gas contains significant concentrations of nonhydrocarbons, which must be partially or totally removed in order to market and utilize the gas. The three principal nonhydrocarbons found are nitrogen, carbon dioxide, and hydrogen sulfide,
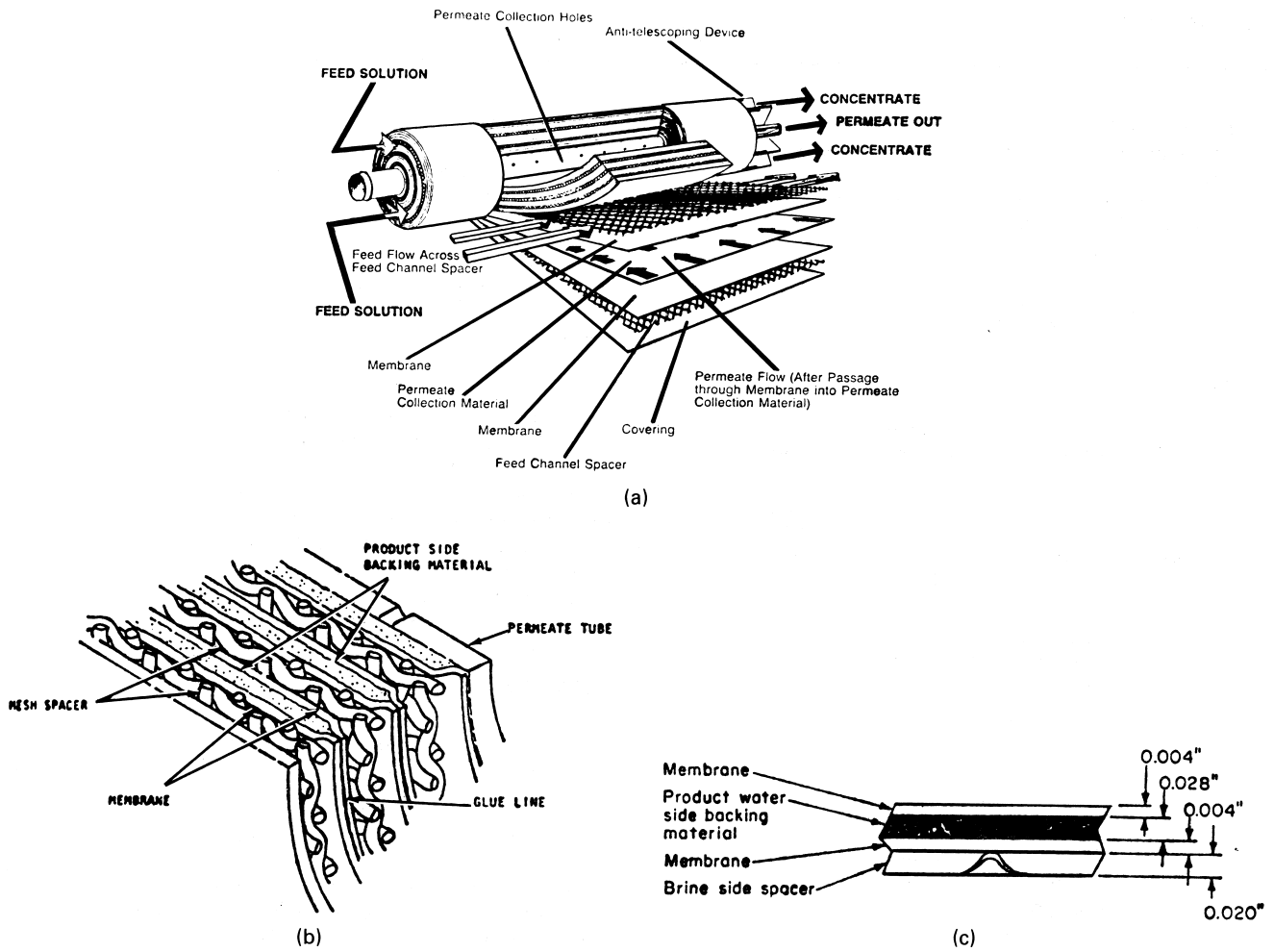
Figure 19.4. The spiral wound membrane module for reverse osmosis. (a) Cutaway view of a spiral wound membrane permeator, consisting of two membranes sealed at the edges and enclosing a porous structure that serves as a passage for the permeate flow, and with mesh spacers outside each membrane for passage of feed solution, then wound into a spiral. A spiral 4 in. dia by 3 ft long has about 60 sqft of membrane surface. (b) Detail, showing particularly the sealing of the permeate flow channel. (c) Thickness of membranes and depths of channels for flows of permeate and feed solutions.
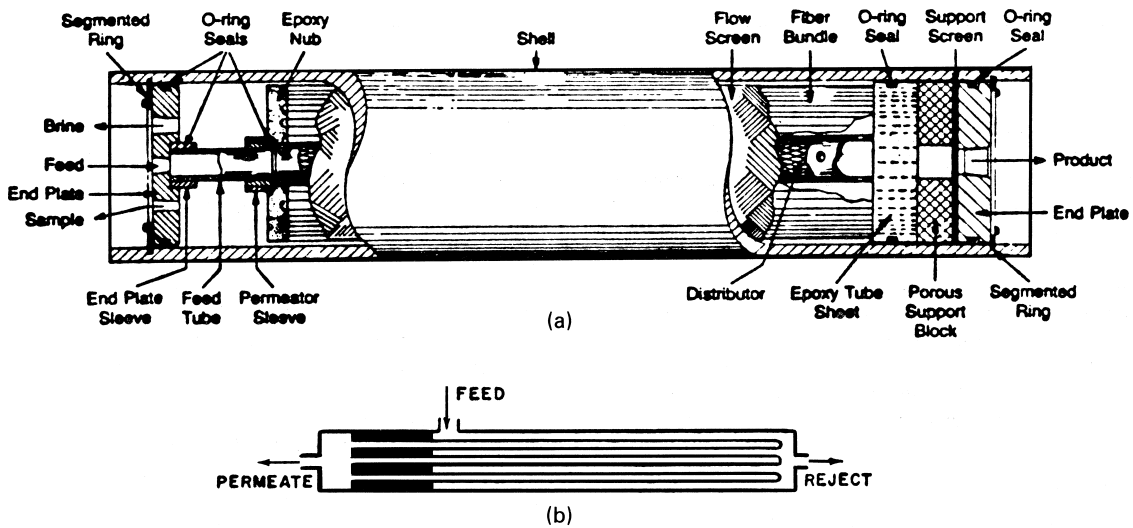
Figure 19.5. The "Permasep" hollow fiber module for reverse osmosis. (a) Cutaway of a DuPont "Permasep" hollow fiber membrane module for reverse osmosis; a unit 1 ft dia and 7 ft active length contains 15–30 million fibers with a surface area of 50,000–80,000 sqft; fibers are 25–250 μm outside dia with wall thickness of 5–50 μm (*DuPont Co.*). (b) The countercurrent flow pattern of a "Permasep" module.

EXAMPLE 19.2
Concentration of a Water/Ethanol Mixture by Reverse Osmosis
The pressure required to drive water out of mixtures of various concentrations of ethyl alcohol against pure water at 30°C is calculated from the osmotic equation

$$1 - x_{\text{alc}} = \exp\left[-\frac{0.018P}{0.082(303.2)}\right]$$

with the results:

Wt % Alcohol	Mol Fr. Alcohol	P (atm)
10	0.0417	59
50	0.281	456
90	0.779	2085
95.5 (azeotrope)	0.8925	3081
96	0.9038	3234
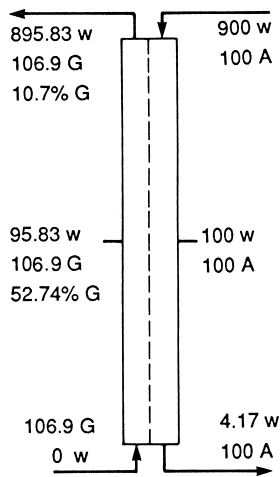
It appears that the pressures needed to make higher than azeotropic composition are beyond the strength of available membranes. A pressure of 1000 psi is feasible. With this pressure, the concentrations of solute on the two sides of the membrane are related by

$$\frac{1 - x_1}{1 - x_2} = \exp\left[-\frac{0.018(68)}{0.082(303.2)}\right] = 0.9520$$

whence

$$x_2 = 1 - (1 - x_1)/0.9520$$

As long as the mol fraction of solute on the low-pressure side is kept above the value given by this equation, water can be driven from the side with mol fraction x_1 across the membrane. The solute on the low-pressure side should be one that is easily separated from water and any alcohol that may bleed through. Ethylene glycol is such a material, and it also has the advantage of a relatively low molecular weight, 62. The required minimum concentrations of glycol corresponding to various alcohol concentrations on the high-pressure side (68 atm) are tabulated as follows:

Wt % Alcohol	Mol Fr. Alcohol	Mol Fr. Glycol	Wt % Glycol
10	0.0417	≥0	≥0
50	0.281	≥0.2447	≥52.74
90	0.779	≥0.7679	≥91.93
96	0.9038	≥0.8989	≥96.84

The flowsketch shows a feed stream consisting of 100 kg/hr alcohol and 900 kg/hr of water, and making a stream with 96% alcohol. If pure glycol is charged countercurrently at the rate of 106.9 kg/hr, the % glycol will be at 52.74%, which is high enough to ensure that water can be driven out by a pressure of 68 atm. Beyond this point, the content of glycol will be high enough to ensure transfer of water out of the alcohol solution. The aqueous glycol will be distilled and recycled. A small increase in its amount will permit some water to be present in the recycle stream.

---

in decreasing order. Carbon dioxide and hydrogen sulfide are selectively removed by well-known and successful technologies. Chief among these are acid gas absorption and adsorption methods, which are well documented in the literature.

It may be added, however, that membrane systems have been used successfully to separate carbon dioxide from natural gas, notably in enhanced oil recovery operations. Here (supercritical) carbon dioxide is injected into a petroleum-bearing formation where the carbon dioxide acts to increase the oil mobility and its subsequent recovery. The carbon dioxide-rich gaseous effluent is recovered, and the carbon dioxide concentrated and re-injected.

With nitrogen, it is another story. The two principal methods in current but limited use are low-temperature or cryogenic separation, or distillation, and selective adsorption. The former is judged too costly, the latter is starting to make inroads. Membrane separations await in the wings. More detail on the general subject of upgrading natural gas follows.

To be adjudged pipeline-quality natural gas, the hydrogen sulfide content must be below 25 grains per SCF (standard cubic foot), which calculates out to about 0.0004 mol %. The hydrogen sulfide removed and recovered may be oxidized to the sulfur oxides,

to be vented or preferably to be converted say in a lime-water wash for disposal as calcium sulfate (gypsum). In sufficient quantities and concentrations, the recovered hydrogen sulfide may be partially oxidized to elemental sulfur via the Claus process or its equivalent.

Permissible carbon dioxide levels in pipeline-quality natural gas are characteristically up to 2–3 mol %. The recovered carbon dioxide is being increasingly touted for enhanced oil recovery operations rather than being vented to the atmosphere.

The allowable nitrogen content is mostly dictated by the required Btu content for the natural gas. Assuming the natural gas per se is at about 1000 Btu/SCF, the nitrogen content could range up to 10 mol %, whereby the Btu content would be no lower than 900 Btu/SCF, the generally accepted cutoff for the Btu rating. However, pipeline requirements are starting to be more stringent for the nitrogen content, and in some instances about 3 mol % is the maximum allowable.

Whereas low-temperature or cryogenic methods can be used to separate the nitrogen, this technology is expensive and is not commonly used. The use of selective adsorbents is emerging, and may prove economically viable. There is the possibility, however, that membrane separations may prove equally viable, an assessment yet

to be determined, and will in large part depend on the further development of suitable membrane materials.

Thus, there are needs, at least on the horizon, for reducing the nitrogen content of natural gases, where in fact perhaps a fourth of the total natural gas reserves can be judged as subquality. Of more than usual interest is a band of high-nitrogen gas running from southwest Arkansas, across north Texas and out into West Texas and the Panhandle, through eastern and northeastern New Mexico and up into eastern Colorado, then back into western Kansas and down into northcentral Oklahoma, virtually completing the circuit. Other notable occurrences are in the Central Valley of California and in West Virginia.

Subquality natural gas is apparently a ready resource, awaiting the need and the necessary upgrading technologies, of which membrane separations is one of the emerging possibilities.

19.8. THE ENHANCEMENT OF SEPARATION

With a membrane showing high selectivity between the gases to be separated, a single-stage operation suffices. For membranes of lower selectivity, more involved juxtapositions become necessary. Examples are shown in Figures 19.6 and 19.7 for multistage taper and cascade arrangements (Hoffman, 2003).

The taper configuration of Figure 19.6 will not produce a sharp separation. In this case, only the less-permeable component tends to be recovered in the pure form as the reject. The permeate product is a mixture, although the proportions will differ from the feed. The effect is similar to the concept of stripping the more permeable component from the reject phase.

The taper configuration can be changed so that the more permeable component will be concentrated in the permeate, whereas the reject product will be a mixture. This would correspond to rectification or absorption, in which the more permeable component is concentrated in the permeate phase. The less permeable component is absorbed from the permeate phase.

The analogy, above, is to distillation practices.

It may be noted that the cascade arrangement of Figure 19.7, if suitably disentangled, will correspond to a multistage operation as encountered in absorption, stripping, and distillation practices.
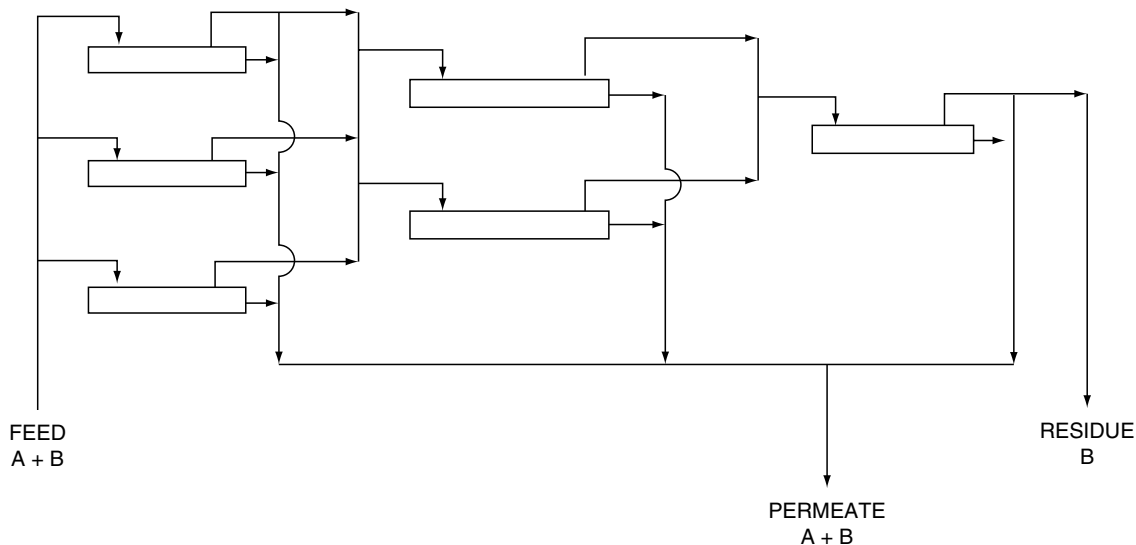
DIFFERENTIAL PERMEATION

Of further interest and concern is the operation of a membrane cell as a continuum, referred to as *differential permeation*.

The permeate may be withdrawn at points along the membrane, as illustrated in Figure 19.8, and may be referred to as crossflow—that is, the feed/reject phase flows along and across the membrane.

Or the cell may be operated in concurrent flow as shown in Figure 19.9, or in countercurrent flow as shown in Figure 19.10.

There is even the possibility of producing two permeate products if two different membrane materials are employed separately in the same unit or module. This is indicated in Figure 19.11.

Another possibility is the use of recycle in a single-stage cell, operating in countercurrent flow, as shown in Figure 19.12 (Hoffman, 2003). More complicated arrangements are shown, for example, in Gas Research Institute (1982). There is the potential here for sharp separations, as will be subsequently derived and explained.

Whereas in single-stage or multistage embodiments perfect mixing may be assumed, the use of concurrent or countercurrent flow can also be assumed in a context corresponding to an absorber, stripper, or distillation column. This is the case with the system in Figure 19.12. More complicated arrangements may be made, as shown in Figures 19.13 and 19.14, and in Figure 19.15, which is entirely analogous to multistage distillation. There is the use of reflux or recycle to enhance the separation, which corresponds to the practices of distillation. Figure 19.16 shows an example of combined multistaged membrane operations.

A difficulty with whatever the juxtaposition or arrangement is the mathematical means for representation and calculation. We will therefore be predominantly concerned with the necessary derivations and their simplifications. Of prime importance is the separation that can be achieved. Also of interest is the necessary sizing of the membrane area.

It may be added that the reject or retentate phase for a membrane cell forms a continuum with the feed—assuming perfect mixing at every point—albeit it will take on a different flow rate and composition as permeation proceeds. Moreover, this

Figure 19.6. Taper configuration.
(Hoffman, 2003)
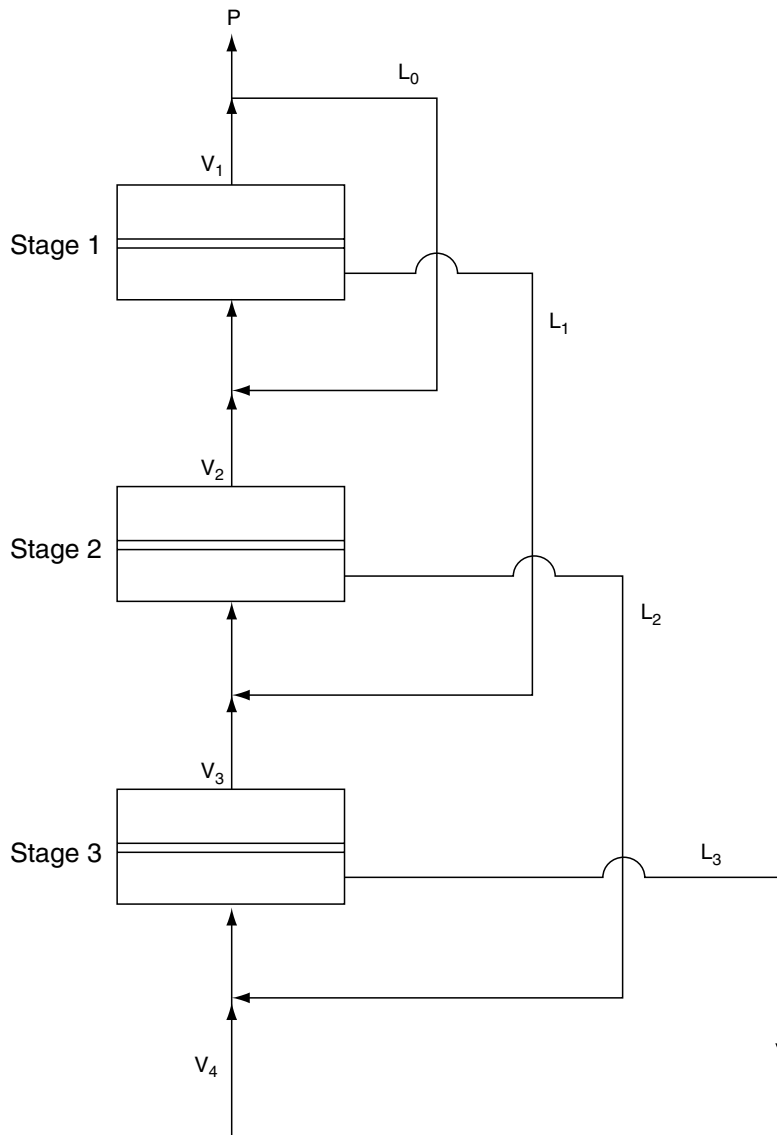
Figure 19.7. Cascade.
(Hoffman, 2003)
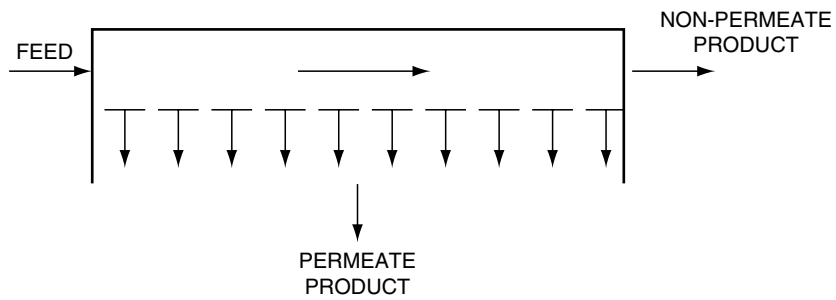
Figure 19.8. Point withdrawal of permeate.
(Hoffman, 2003)
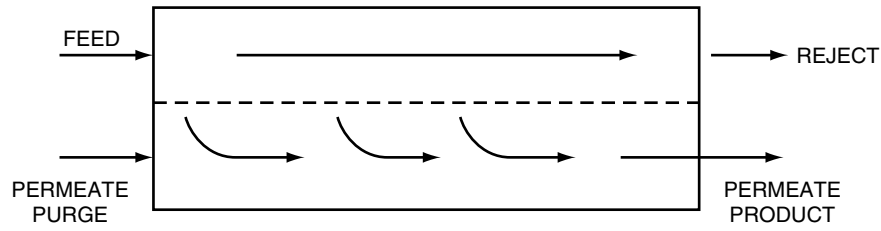
Figure 19.9. Concurrent flow permeation. (Hoffman, 2003)
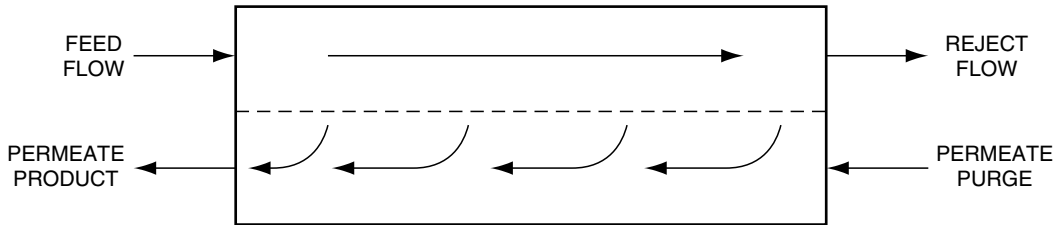
Figure 19.10. Countercurrent flow permeation. (Hoffman, 2003)
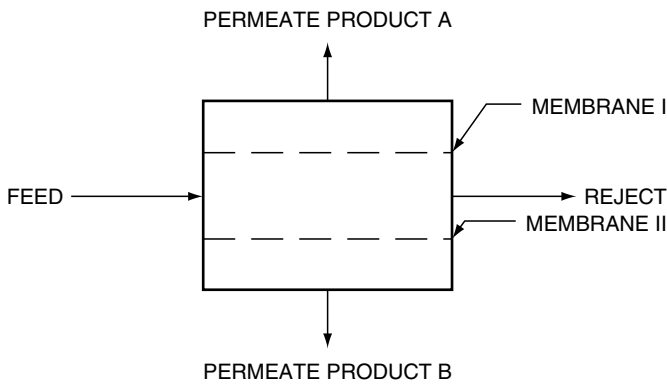
Figure 19.11. Asymmetric permeator configuration. (Hoffman, 2003)

CONVENTIONAL PERMEATOR WITH PRODUCT RECYCLE
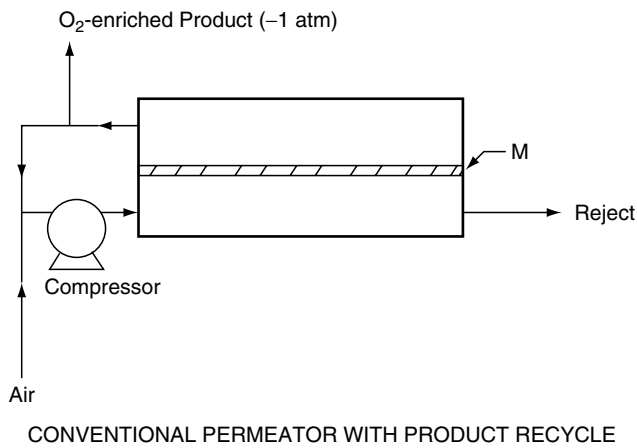
Figure 19.12. Countercurrent permeation with recycle. (Hoffman, 2003)
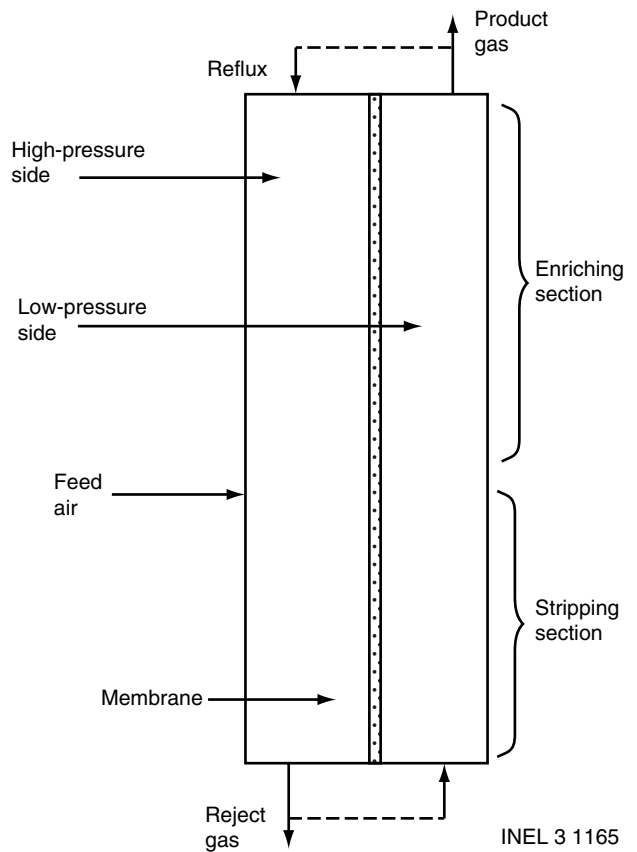
Figure 19.13. Continuous membrane column with reflux from both product streams. (Hoffman, 2003)
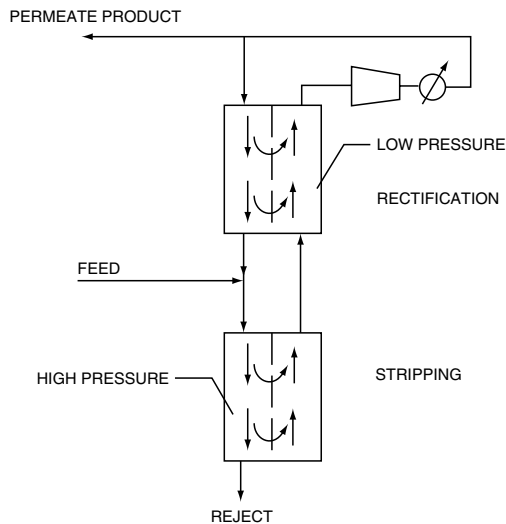
Figure 19.14. Continuous membrane column with reflux from the permeate product.
(Hoffman, 2003)

feed-reject phase is commonly pictured schematically as the ''upper phase,'' and the permeate as the ''lower'' phase—albeit both phases are gaseous or both phases are liquids. As matters proceed, we will choose to adopt the opposite representation, whereby the feed-reject phase is pictured as the lower phase and the permeate is the upper phase. This is for making the representation more closely analogous to that for vapor-liquid separations and distillation calculations. The derived similarity to the representation of vapor-liquid phase behavior is in fact the keystone to systematizing membrane separation calculations. Alternatively, the separation can be viewed in terms of liquid-liquid phase behavior.

19.9. PERMEABILITY UNITS

Permeability may be expressed in different units, usually depending on whether liquids or gases are involved in the permeation, and may be on a pointwise or overall basis.

On an overall basis, we are speaking of a mass, molar, or volumetric flux—that is, the mass, molar, or volumetric flow rate per unit surface area of the membrane normal to flow, per unit pressure difference, for the entirety of the membrane thickness.

(Alternately, a single linear dimension is sometimes used instead of area, signifying that the other linear dimension—say membrane width—is understood to be unity, in whatever dimensions used.)
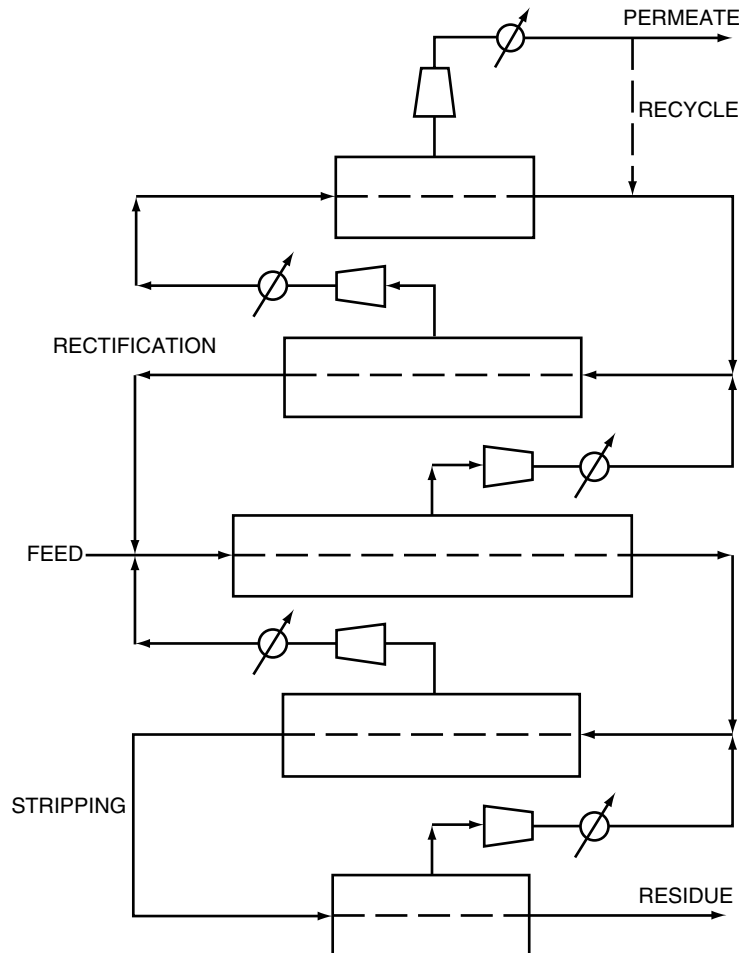
Figure 19.15. Staged permeation cascade with rectification and stripping sections. The individual membrane modules may be operated concurrently or counterconcurrently, or perfect mixing may be assumed to occur.
(Hoffman, 2003)
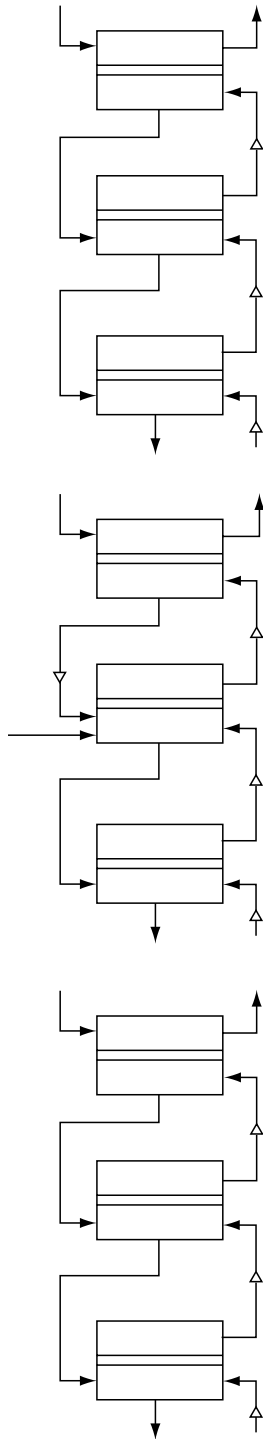
Figure 19.16. Combined multistage membrane operations. (Hoffman, 2003)

Pressure difference may be in pounds per square inch, atmospheres, bars, pascals, centimeters of mercury, inches of water, or whatever chosen. (It may be noted that pressure is ordinarily expressed in mass-distance units, as mass per unit area, rather than as stress in force-distance units, as force per unit area, with the pascal being an example of the latter.) For convenience, a few conversion factors are supplied in Table 19.8.

TABLE 19.8. Conversion Factors for Pressure Units

To convert from	To	Multiply by
(One)	(Two)	(Two)/(One)
Atmospheres	Pounds per sq. in. (psi)	14.696
Atmospheres	Pounds per sq. ft. (psf)	2116.3
Atmospheres	Grams per sq. cm.	3033.3
Atmospheres	Cm. of Hg	76
Atmospheres	In. of Hg	29.9213
Atmospheres	Ft. of water	33.90
Atmospheres	In. of water	406.794
Atmospheres	Bars	1.013250
Atmospheres	kPa (kilopascals)	101.3250
Atmospheres	kgf/cm^2	1.033227
Atmospheres	Dynes/cm^2	1.0133 (10^6)
Bars	Atmospheres	0.9869

Note: If a pointwise permeability value P_i is measured in the units of say 10^{-9}cm^3/cm^2-sec-cm Hg/cm, then multiplying this value of P_i by 76 cm Hg/atm will yield the new value of P_i in 10^{-9}cm^3/cm^2-sec-atm/cm. The new value will be higher since the pressure difference is now measured in the lower value of atm instead of the higher value of cm Hg.

The symbol commonly used for membrane permeability is simply P or P_i, denoting the permeability of (or to) a component i. The particular units of P_i are best defined merely by its usage, and may pertain either to the pointwise value or the overall value. Moreover, this use of the symbol P is to be distinguished from the usage for the fluid flowing pressure P, which may be further distinguished by P_L for the high-pressure side or reject side of the membrane, and P_V for the low-pressure or permeate side, as utilized in Hoffman (2003) and in Section 19.10 of this chapter.

For gases, the pointwise permeability P_i is commonly expressed in the units of 10^{-9} cm^3(STP)/cm^2-sec-cm Hg/cm, although other units may be used. That is, the volumetric gaseous flow is referenced to standard conditions of temperature and pressure (ordinarily at 0°C and 1 atm). The corresponding overall membrane permeability—again designated as P_i—would be in the units of 10^{-9} cm^3(STP)/cm^2-sec-cm Hg/cm, all divided by the membrane thickness Δm in cm to yield P_i in 10^{-9} cm^3(STP)/cm^2-sec-cm Hg. That is, the overall permeability decreases as the membrane thickness increases. In other words, P_i (pointwise)/$\Delta m = P_i$ (overall). Or, if one chooses, the overall permeability could be distinguished by the use of an overbar, say as $\bar{P}_i$.

Other convenient units for pointwise permeability are g-moles/cm^2-sec-atm/cm., applicable to both liquids and gases. The conversion for gaseous pointwise permeability utilizes the value of 22,414 cm^3 (STP) per gram-mole, and a value of 76 cm Hg/atm. Thus

$$P_i(\text{in} \frac{10^{-9} \ cm^3}{cm^2 - sec - cmHg/cm}) \times 76 \frac{cm \ Hg}{atm}$$
$$\times \frac{10^{-9}}{22,414} \frac{g - moles}{cm^3} = P_i(\text{in} \frac{g - moles \ of \ i}{cm^2 - sec - atm/cm})$$

The same sort of conversion can be used for the overall permeability.

For an example of the above conversion, consider a membrane that has a pointwise permeability of 20 in the units of 10^{-9} cm^3(STP)/cm^2-sec-cm Hg/cm. Therefore, the new pointwise permeability value will be

$$P_i = 20(10^{-9}) \frac{76}{22,414} = 20(10^{-9})(0.00339) \frac{g - moles \ of \ i}{cm^2 - sec - atm/cm}$$

For a membrane thickness Δm of 10 microns or $10(10^{-4})$ cm, the result becomes

$$P_i = \frac{20(10^{-9})}{10(10^{-4})} \frac{76}{22,414} = 20(10^{-6})(0.00339) \frac{g - \text{moles of } i}{cm^2 - sec - atm}$$

which is now the overall membrane permeability (albeit, for convenience, the same symbol is used).

As has been mentioned, the selectivity or relative permeability for a membrane to two different substances is given by $\alpha_{i-j} = P_i/P_j$. It may also be noted that the permeability as measured for a pure component will most likely be different for that component in a mixture (Hoffman, 2003, p. 118).

Representative membrane permeabilities and other characteristics for a variety of purposes are supplied in Table 19.9 as taken from Appendix 1 in Hoffman (2003).

It should be emphasized that membrane permeability is different from the permeability for flow through porous media, which is commonly distinguished by the symbol K or K_i, and has the units of volume^3/time^2. In fact, the porous media permeability divided by the viscosity (in the units of mass/distance-time) gives what is called the mobility in area/time-pressure, which turns out to be entirely equivalent to membrane permeability. The various manipulations involved are presented in Example 19.3, as taken from Hoffman (2003).

(It should also be noted that the symbol K_i is utilized for the mol fraction ratio y_i/x_i in comparing the permeate composition to the reject or raffinate composition, as will be developed in Example 19.4. This is the usual symbolism as used in phase equilibria, say that of the K-value or equilibrium vaporization ratio for correlating the behavior of vapor/liquid systems—and, ideally, reflects Raoult's law. The foregoing illustrates the general problem

TABLE 19.9. Excel Spreadsheet Representation of Selected Membrane Permeabilities

Table	Type of Permeation	Component(s)	Concentration (in wt %)	Membrane	Thickness	Pore Size	Temp.	Feed Pressure	Permeate Pressure
A1.1	gas	H		Cu			500°C		
A1.2	gas	CH_4		Silicone			30°C		
A1.3	gas	H_2		Rubber			25–35°C		
A1.5	gas	O_2		Silicone					
A1.9	pervaporation	EtOH-H_2O	0–100% EtOH				25°C		0–04 kPa
A1.10	pervaporation	I-Butanol-H_2O	8.4% H_2O						
A1.11	pervaporation	EtOH-H_2O	87–100% EtOH	GFT memb			60°C		not given
A1.14	liquids	EtOH-H_2O	4.9% EtOH	PTFE					
A1.15	liquids	Benzene		Cellophane	0.075 mm		20°C	35 kg/cm^2	
A1.16	liquids (pervap)	Xylenes		Polyethylene			45°C		
A1.17	reverse osmosis	NaCl-H_2O	50,000 ppm	Cellulose acetate				8 Mpa	
A1.19	Cs transport	$NaNO_3$-HNO_3	162 mg/liter	liquid membrane					
A1.20	microfiltration	Water		polypropylene					
A1.20	ultrafiltration	Water		Cellulosic					
A1.21	microfiltration	Water		Al_2O_3		0.2 microm	20°C		
A1.21	ultrafiltration			Al_2O_3		50 nanom	20°C		
2.1, Ex 2.4	liquids (pervap)	nC7-iC8	75 vol%nC7		1 mil		100°C	15 psig	
2.1, Ex 2.4	liquids (pervap)	nC7-iC8	75 vol%nC7		1 mil		100°C	115 psig	

	Permeability and Units									Flux		
Table	10^{-9}cm^3/ cm^2-sec-cm Hg/cm (pointwise)	10^{-6}cm^2/ sec-atm (pointwise)	ft^2/hr Di in conc units (pointwise)	cm/hr Di in conc units (overall)	cm^3(STP)/ cm^2-sec -cmHg×10^5 (overall)	ml liq/ pressure -hr-cm^2 (overall)	(10^{-10})m^3 /s-m^2-Pa (overall)	liters/hr-m^2-bar (overall)	Kg/m^2-hr	×10^4incm^3/ cm^2-sec (or gal/ft^2-day)	gal/ft^2-hr×10^3
A1.1		3.5									
A1.2	59										
A1.3	0.49										
A1.5	50										
A1.9									0.1–0.5 H_2O		
A1.10											
A1.11									0-1.6 EtOH		
A1.14									8.8		
A1.15						3.9					
A1.16					1.69						
A1.17										9.17(19.4)	
A1.19				1.3 cm/hr							
A1.20							140				
A1.20							9				
A1.21								2000			
A1.21								250			
2.1, Ex 2.4			0.016(10–4)								140
2.1, Ex 2.4			0.016(10–4)								140

(From Hoffman, 2003, Table A1.23).

EXAMPLE 19.3
Conversion between Porous Media and Membrane Permeabilities

The permeability relationship for the forced horizontal flow of fluids through porous media may be derived from a differential energy balance (dE) for steady-state fluid flow, assuming no heat exchange (dq) or work exchange (dw) with the surroundings. Thus, consider the following energy balance, based on unit mass of flowing fluid, in consistent mass-distance units:

$$dE = dq - dw = 0 = \frac{1}{\rho} dP + dlw$$

where dP is the differential pressure change and ρ is the fluid density, and where dlw represents the differential lost work change or intrinsic energy change, otherwise called the irreversibilities, and may be represented in the form for the Fanning friction factor:

$$dlw = f \frac{v^2}{2g_c D} dL$$

where v is the superficial velocity (based on the crossectional area), g_c is the conversion factor between mass-distance units and force-distance units ($g_c = 32.2$ in the English system of units), D is a linear dimension characteristic of the flow system, and dL represents the differential distance in the direction of flow. For laminar or viscous flow, the Fanning friction factor f is inversely proportional to a dimensionless Reynolds number Re, whereby

$$f = \frac{C}{\text{Re}} = \frac{C}{\frac{Dv\rho}{\mu}}$$

where C is a constant characteristic of the flow system geometry and μ is the fluid viscosity in consistent units. Substituting and rearranging, it will turn out that

$$v = -\frac{\left(\frac{g_c D^2}{C}\right)}{\mu} \frac{dP}{dL} = -\frac{K}{\mu} \frac{dP}{dL} = -\frac{K}{\mu} \frac{dP}{dx}$$

where K becomes the permeability coefficient for flow through porous media, and the ratio K/μ is called the mobility—which corresponds to the membrane permeability P_i. If it is agreed that flow occurs in the x-direction, then $dL = dx$.

The units for K will depend on the units prescribed for the other terms. Thus, in the English system of units, if the pressure change is in psf (pounds per square foot), the distance is in feet, and the viscosity value is in Bvu's (British viscosity units of pounds/ft-sec), with the velocity in ft/sec, then the dimensions of K will be ft^3/sec^2. (It may be noted that the viscosity in poises has the dimensions of grams/cm-sec, and the viscosity in centipoises has the dimensions of centigrams/cm-sec. Accordingly, to convert a viscosity value in centipoises, multiply the value by 6.72×10^{-4} to yield the viscosity value in Bvu's.)

If the flow velocity is to be in ft/hr, then the viscosity would be measured in lb/ft-hr. That is, the viscosity in centipoises would be multiplied by $(6.72 \times 10^{-4})(3600) = 2.42$, and the units for K would be ft^3/hr^2.

In the cgs system of units, if the pressure change is in grams per square centimeter), the distance is in cm, and the viscosity value is in poisies (grams/cm-sec), with the velocity in cm/sec, then the dimensions of K will be cm^3/sec^2.

However, the unit of permeability used in the petroleum industry for the flow of fluids through porous media, in oil and gas production, is called the *darcy*. More usually, the permeability of oil and gas producing formations is given in *millidarcies*, a millidarcy being 1/1000 of a darcy. The origins are in the Darcy (d'Arcy) relationship, which is but the previously derived permeability expression relating flow rate to the pressure gradient:

$$v = -\frac{K}{\mu} \frac{dP}{dx}$$

The superficial velocity v is the actual volumetric rate divided by the total crossectional area normal to the direction of flow.

A darcy is defined by the following characteristics for a flow system. Thus, a porous medium having a permeability of 1 darcy will, at standard conditions, permit the flow of a fluid of 1 centipoise viscosity at the superficial rate of 1 cm/sec under a pressure gradient of 1 atm/cm. In the formula above, v is in cm/sec, K is in darcies, μ is in centipoises (centigrams/cm-sec), P is in atm, and x is in cm. The actual equivalent units for K in darcies would be centigram-cm/atm-sec^2. It may be converted to cm^3/sec^2 by multiplying

$$\left(\frac{1}{100} \frac{\text{grams}}{\text{centigram}}\right)\left(\frac{1}{1033.3} \frac{\text{atm}}{\text{grams/cm}^2}\right) = 9.677(10^{-6}) \frac{\text{atm} - \text{cm}^2}{\text{centigram}}$$

The indication is that the porous media permeabilities encountered in oil and gas production are very small.

Conversion may be made to the actual volumetric rate by multiplying by the crossectional area normal to flow. In turn, conversion may be made to the mass flow rate by multiplying the actual volumetric flow rate by the density of the fluid at flow conditions. Dividing by the molecular weight of the fluid will give the molar flow rate.

The conversion between K in say ft^3/hr^2 and K' in darcies (or darcys) is given by

$$K(\text{in ft}^3/\text{hr}^2) = K'(\text{in cg} - \text{cm/atm} - \text{sec}) \times \frac{\left(\frac{1}{100}\right)\left(\frac{1}{453.6}\right)\left(\frac{1}{30.48}\right)}{(14.696)(144)\left(\frac{1}{3600}\right)}$$

$$= K'(\text{in cg} - \text{cm/atm} - \text{sec}) \times 0.00443$$

That is,

$$K(\text{in ft}^3/\text{hr}^2) = K'(\text{in darcies}) \times 0.00443$$

To obtain K in ft^3/sec^2, the conversion is

$$K(\text{in ft}^3/\text{sec}^2) = K'(\text{in darcies}) \times (1/3600)^2 \times 0.00443$$
$$= K'(\text{in darcies}) \times 3.418(10^{-10})$$

As previously noted, the ratio K/μ is called the mobility, and based on the Darcy concept, the mobility will have the dimensions of cm^2/sec-atm. The mobility for porous media is identical in principle to what is called the permeability as used in the relationship for membrane permeation. The conversion of units is therefore of interest. It is as follows:

$$\frac{K}{\mu}(\text{in } \frac{\text{cm}^2}{\text{sec} - \text{atm}}) = P_i(\text{in } \frac{10^{-9} \text{ cm}^3}{\text{cm}^2 - \text{sec} - \text{cmHg/cm}}) \times 76 \times 10^{-9}$$

$$\frac{K}{\mu}(\text{in } \frac{\text{darcies}}{\text{centipoises}}) = P_i(\text{in } \frac{10^{-9} \text{ cm}^3}{\text{cm}^2 - \text{sec} - \text{cm Hg/cm}}) \times 76 \times 10^{-9}$$

The value of K, above, could more properly be subscripted as K_i to denote the permeability to a particular component or mixture i or I. However, the Darcy concept assumes that the

(continued)

EXAMPLE 19.3—(*continued*)

permeability of a porous medium is independent of the fluid, whether gaseous or liquid, and whatever the composition. That is, the consideration is that the viscosity term alone suffices to distinguish the fluid. Accordingly the mobility (K/μ) will be fluid dependent. (It may be noted, moreover, that porous media may be anisotropic, displaying different permeability values in different directions.)

Nevertheless, as an example, if the membrane permeability to a gaseous component were

$$P_i = 20(10^{-9}) \text{ cm}^3/\text{cm}^2\text{-sec-cm Hg/cm}$$

then the mobility would be

$$K/\mu = 20(10^{-9})(76) = 1.520(10^{-6}) \text{ darcies/centipoise}$$

For a gas with a viscosity of 0.01 centipoise, the permeability coefficient K for component i would become

$$K_i = 1.520(10^{-8}) \text{ darcies or } 1.520(10^{-3}) \text{ millidarcies}$$

This is extremely low, since a typical permeable petroleum reservoir formation or rock may have a permeability on the order of as much as 1 darcy or 1000 millidarcies, or as little as, say, 10^{-2} darcies or 10 millidarcies, or conceivably even 10^{-3} darcies or 1 millidarcy, but which is still many orders of magnitude greater than membrane permeabilities or mobilities.

---

of utilizing a common symbolism that is, by custom, applied to each of two or more diverse phenomena.)

The gaseous diffusion coefficient or diffusivity D_i is measured in distance^2/time (commonly cm^2/sec), and can be related to, or made equal to, the permeability when the units are cleared and made consistent (Hoffman, 2003, p. 37). The exercise is included within the derivations of Example 19.4.

19.10. DERIVATIONS AND CALCULATIONS FOR SINGLE-STAGE MEMBRANE SEPARATIONS

The most usual problem encountered is that of determining the degree of separation for a single-stage embodiment, which can certainly be complicated. The extension to multistage and differential permeation operations will only be alluded to, with referral made to Hoffman (2003).

Consider the schematic membrane stream juxtaposition, by analogy with a phase separation, as diagrammed in Figure 19.17. The conditions and compositions for each stream do not change with position, whereby the circumstance is called perfect mixing. Nor do the conditions and compositions change with time, signifying the steady-state.

The mole fraction compositions y_i and x_i are therefore to be uniform on each side of the membrane, where the subscript i denotes components 1, 2, 3, ..., k. The respective steady-state molar stream rates are denoted by F, L, and V. These may designate the total flow rate of the each stream, or may be a flux rate based on the membrane area.

Stream F denotes the feed, stream V the permeate, and stream L the reject. Ordinarily, all phases are gaseous, but alternately
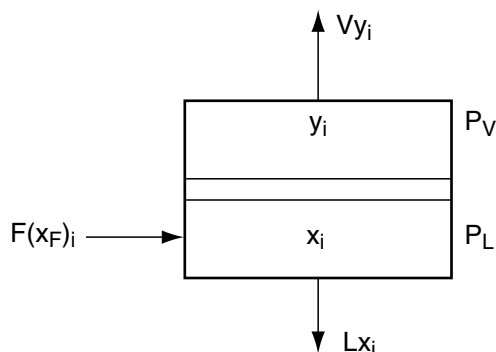
Figure 19.17. Single-stage membrane separation with perfect mixing.

may be all liquids. That is, no phase separations are involved. Furthermore, the system is nonreacting. The kinds of calculations involved are presented in a number of references, as applicable to phase separations, at equilibrium, between liquids and gases or vapors. By a fortuitous circumstance in the representations, the same methodology can be applied to membrane separations.

The material balances are

$$F = L + V$$
$$F(x_F)_i = Lx_i + Vy_i$$

where

$$\sum (x_F)_i = 1 \quad \sum x_i = 1 \quad \sum y_i = 1$$

Furthermore,

$$(L + V)(x_F)_i = Lx_i + Vy_i$$

whereby

$$\frac{L}{V} = \frac{y_i - (x_F)_i}{(x_F)_i - xi}$$

or

$$y_i = -\frac{L}{V}x_i + [\frac{L}{V} + 1](x_F)_i$$

The above will be a straight line in $y_i - x_i$ space with the slope (-L/V) and with the y-intercept at $[L/V + 1](x_F)_i$ for constant parameters of V—but which in general is a variable.

The membrane rate balance is, for each component i,

$$Vy_i = P_i(P_L x_i - P_V y_i)A$$

where
P_i = overall membrane permeability to component i in moles per unit time per unit area per unit pressure difference or partial pressure difference
P_L = system pressure on high-side
P_V = system pressure on low-side
A = membrane area perpendicular to flow; preferably based on permeate side

It is understood that the feed pressure P_F is higher than or approximately equal to P_L, such that flow is sustained.

The foregoing rate equation can alternately be expressed in terms of the permeate flux, designated as $V'' = V/A$ or as $G = V/A$. Thus

$$V''y_i = P_i(P_L x_i - P_V y_i)$$

As a further note, the membrane permeability to a component i is most likely determined experimentally using only pure component i. Whereas in the application to mixtures, the projection is made that the same value for the permeability can be used if the driving force is in terms of the partial pressure of the component i.

It may be further observed that

$$\sum V''y_i = V'' \sum y_i = V'' = P_L \sum P_i x_i - P_v \sum P_i y_i$$

This serves as an expression for the variable $V'' = V/A$ in terms of the y_i and x_i.

Since $F = V + L$ and $F(x_F)_i = V y_i + L x_i$ it follows that either V or the y_i or the x_i can be eliminated as a variable or variables.

Note also that

$$y_i = V y_i/V = V''y_i/V'' = (P_L P_i x_i - P_V P_i y_i)/(P_L \sum P_i x_i - P_V \sum P_i y_i)$$

Thus, the mole fraction can also be expressed in terms of the pressures and permeabilities.

It may be noted that the foregoing is related to an integrated form (across the membrane) of Fick's law of diffusion, which is written in the differential form as

$$G_i = -D_i \frac{dc_i}{dx} = -P_i \frac{dc_i}{dx}$$

where

$G_i = V'' = $ mass or molar flux of a component i
$D_i = $ the diffusion coefficient or diffusivity for component i
$c_i = $ concentration of component i in mass or moles per unit volume
$x = $ linear coordinate in direction opposite to flow

In the above notation, the units of D_i will be distance^2/time, and the permeability P_i may be expressed in the same units. If different units are to be adopted for P_i then the form of the gas law or equation of state may be introduced, whereby $(Py_i)V = z\, n_i\, RT$, where Py_i is the partial pressure (or absolute activity) of component i, n_i is the moles of component i, and z is the compressibility factor (which in general is applicable to single-phase liquids as well as gases). Accordingly,

$$c_i = \frac{n_i}{V} = \frac{Py_i}{zRT}$$

such that

$$G_i = -\frac{D_i}{zRT}\frac{d(Py_i)}{dx} = -\frac{P_i}{zRT}\frac{d(Py_i)}{dx} = -P_i\frac{d(Py_i)}{dx}$$

whereby permeability is now in the units of distance^2/time divided by zRT (here, moles of component i per unit volume per unit partial pressure) will give the permeability in the more usual flux units of moles/distance^2-time-partial pressure/distance (where for convenience the same symbol is used for the permeability in both cases). Which further brings up the subject of terms and units.

TERMS AND UNITS

It is understood that if the membrane permeability is in the units of moles/time, then the flow rate L will be in moles per unit time per unit membrane area. (The other flow rates may also be based on membrane area, if so desired.) In turn, the notation L may be replaced by the flux G_L. That is, flow rate may be placed on an areal basis.

If the units of permeability are in volume per unit time, then the flow rates will be in volume per unit time, although adjustments or accommodations must be made for the pressure (and temperature).

If the total permeate flow rate is given by V, say, the component flow rate can be designated as

$$V_i = V y_i$$

whereas the corresponding flux rate for component i in the permeate phase can be written as $(G_V)_i = (G_V)y_i = V''y_i$. For the flux of component i in any phase in general, the symbol G_i would suffice.

Membrane permeability is customarily based on pressure drop per unit membrane thickness. The overall permeability would then become the permeability as per unit thickness divided by the thickness. Thus, as the membrane thickness increases, the overall permeability decreases.

As has been previously stated, the units commonly used for pointwise gaseous membrane permeability (or mobility) are

$$10^{-9}\, \text{cm}^3/\text{sec} - \text{cm}^2 - \text{cmHg/cm}$$

where the unit term cm Hg/cm represents the partial pressure drop in centimeters of mercury per unit membrane thickness. The volume in cm^3 is at standard conditions.

The relative permeability, one component to another, has also been defined as the relative permeability of selectivity α. Thus

$$\alpha = \alpha_{i-j} = P_i/P_j$$

is the permeability of component i relative to component j. The term α will not be further employed as such.

A relative permeation flux φ or φ_{i-j} may be defined for the permeate phase as

$$\varphi \text{ or } \varphi_{-j} = (G_V)_i/(G_V)_j = V''y_i/V''y_j = V y_i/V y_j$$

The relative permeation flux will in general differ from the selectivity, and will depend upon composition as well as pressure. It is also a term that will not be employed further.

MOLE FRACTION RELATIONSHIPS

It follows from rearranging the rate balance for a component i that

$$y_i = \frac{P_i P_L}{V'' + P_i P_V} x_i$$

or

$$y_i = K_i x_i$$

where K_i is defined by the substitution. This represents a straight line in $y_i - x_i$ space with slope K_i, extending from the origin for constant parameters of the variable V''. It is of the same notation and symbolism as the equilibrium vaporization ratio or K-value encountered in the representation of vapor-liquid equilibria, and

may be called the permeation coefficient or distribution coefficient for component i.

It may be observed that the units for V'' are the same as for both V/A and P_iP_V, whereby its usage P_i refers to the overall permeability rather than the pointwise permeability. That is, strictly speaking, the comparison is as follows, in the conventions adopted for units:

$$\frac{\text{moles}}{\text{time} - \text{area}} \text{ vs } \frac{\text{moles of } i}{\text{time} - \text{area} - pp_i}\text{(total pressure)}$$

$$= \frac{\text{moles of } i}{\text{time} - \text{area} - pp_i}\text{(total pressure)}$$

$$= \frac{\text{moles of } i}{\text{time} - \text{area} - \text{(total pressure)}\frac{\text{moles of } i}{\text{total moles}}}\text{(total pressure)}$$

$$= \frac{\text{total moles}}{\text{time} - \text{area}}$$

where, for convenience, pp_i denotes the partial pressure of component i.

Note in particular that the ratio of the K's as represented above is *not* the selectivity as would be defined by the permeability ratios—that is, by $\alpha_{i-j} = P_i/P_j$. Furthermore, the selectivity as used here is different from the concept of relative volatility, which is the ratio of the K-values, one to another. Furthermore, the ratio of the K's so determined will be lower than would be suspected from the ratio of the permeabilities. *The implication is that the ensuing permeability separations will be much less sharp than would be suspected from the permeability ratios or selectivities.*

Another way of saying it is: The presence of the parameter or variable V'', notably affects the ratio of the K's as defined above. That is,

$$\frac{K_i}{K_j} = \frac{P_iP_L}{P_jP_L}\frac{V'' + P_jP_V}{V'' + P_iP_V} = \frac{P_i}{P_j}\frac{1 + P_j(P_V/V'')}{1 + P_i(P_V'/V'')}$$

Furthermore, the relatively larger the value of V'', the more likely that the K-ratio as designated above will approximate the permeability ratio. The relatively smaller the value of V'' the more likely that the K-ratio will approach unity. Last, however, the K-ratio must be greater than unity for a separation to occur.

The foregoing provides a foremost reason for the fact that single-phase or pure component permeabilities do not necessarily pertain to mixtures, as previously noted (Hoffman, 2003, p. 118). *That is, the effective permeabilities for the components in mixtures tend to be less, or much less, than for the permeabilities of the pure components determined alone.*

The parameter or variable V'' will have the dimensions of permeability times pressure, as previously observed in terms of moles. However, in terms of the total gas volume permeated, and using the pointwise permeability and dealing with volume fractions, then V'' would have the dimensions of

$$\frac{\text{cm}^3}{\text{cm}^2 - \text{sec} - \dfrac{1}{\text{cm}}} = \frac{\text{cm}^2}{\text{sec}}$$

which, interestingly, are the customary units for the diffusion coefficient or diffusivity.

It should be further emphasized, however, that if the permeability is expressed as the overall permeability (by dividing by membrane thickness in cm), then V'' would have the net dimensions of velocity:

$$\frac{\text{cm}^3}{\text{cm}^2 - \text{sec}} = \frac{\text{cm}}{\text{sec}}$$

If the volumetric permeate flow in standard cm^3 is converted to g-moles (by dividing by 22,414 standard cm^3/g-mole), the dimensions would then of course be

$$\frac{\text{g} - \text{moles}}{\text{cm}^2 - \text{sec}}$$

which are the dimensions for molar flux. In this way, the membrane area can be related to or determined from the molar flux. That is, $A = V/V''$ in consistent units, as will be illustrated in Example 19.4.

Bubble-Point Type Determination. Note that when $V/F \rightarrow 0$ it is required that

$$\sum y_i = 1 = \sum K_i x_i = \sum \frac{P_iP_L}{V'' + P_iP_V}x_i$$

This would correspond to the bubble-point calculation as performed for vapor-liquid equilibrium, the object being to determine the temperature at a given pressure, or vice versa, whereby the first "drop" of vapor ensues from the vaporization of the liquid phase. That is, it would correspond to a point or locus of points on the saturated liquid curve.

Here, however, the situation would correspond to the circumstance, where the first "drop" of permeate ensues. Or, if the permeate rate is to be finite, then both the feed and reject must be infinite, or increase without limit. Another way of saying it is: All the feed stream is rejected, albeit an infinitely small amount of permeate phase is produced.

Observe that the composition of the permeate is y_i, whereas the composition of the reject x_i is the same as that of the feed.

Dew-Point Type Determination. Alternately,

$$\sum x_i = 1 = \sum \frac{y_i}{K_i} = \sum \frac{V'' + P_iP_V}{P_iP_L}y_i$$

This would correspond to the dew-point calculation as performed for a vapor-liquid equilibrium condition. That is, it would correspond to a point or locus of points on the saturated vapor curve, as distinguished from the saturated liquid curve. (For a single or pure component, they are one and the same.)

In permeation, however, this corresponds to the case where all the feed stream goes through the membrane, hence the permeate rate equals the feed rate, and the reject rate is nil—albeit the composition x_i pertains to the (infinitesimal) "drop" of reject produced, whereas the composition y_i is the same as that of the feed.

It may be added, however, that the representations and calculations above pertain to non-equilibrium behavior for the membrane permeation of the components of gaseous systems. The same sort of notation may be adapted to liquid systems.

Transient vs. Steady-State Behavior in Permeability Determinations. The foregoing derivations raise some intriguing speculations about the measurement and determination of permeabilities for the respective components in a mixture. Thus, if a true or complete steady-state condition exists during the experiment, whereby *all* of the feed stream passes through the membrane, then the ratio $V/F = 1$ and the ratio $L/F = 0$. That is, it can be said that no reject phase whatsoever is produced.

Furthermore, when $V/F = 1$, *no* finite separation whatsoever occurs, albeit a dew-point type calculation will give a value for the degree or sharpness of separation in terms of mole fraction ratios or K-values. When $V/F \rightarrow 0$, again no finite separation occurs, albeit

EXAMPLE 19.4
Single-Stage Separation Calculations

Various and random membrane information has been tabulated as a matter of course in previous sections and tables. For the calculational purposes here, a representative set of comparative values follows for a membrane of low selectivity between the key components components i and j, with operating pressure levels in the ratio of 3 to 2. The units are unstated inasmuch as the entities calculated will absorb the conversion factors—which are not necessary for calculating the degree of separation and are therefore immaterial except in determining membrane area. The procedure follows that provided in Example 3.1 of Hoffman (2003).

Membrane Data and Operating Data:

$$P_i = 20 \qquad a = P_i P_V = 40$$
$$P_j = 10 \qquad b = P_i P_L = 60$$
$$P_L = 3 \qquad c = P_j P_V = 20$$
$$P_V = 2 \qquad d = P_j P_L = 30$$
$$K_i = 60/(V'' + 40) \qquad \text{where } 10 < V'' < 20$$
$$K_j = 30/(V'' + 20)$$

Feed Composition:

$$(x_F)_i = 0.4$$
$$(x_F)_j = 0.6$$

Substitutions: Equations for two component systems, p.

$$\alpha = \frac{V/F}{1 - V/F}(60) + 40 \quad \text{where } b = 60 \; a = 40$$

$$\beta = \frac{V/F}{1 - V/F}(30) + 20 \quad \text{where } d = 30 \; c = 20$$

$$(\bar{x}_F)_i = \frac{60}{1 - V/F}(0.4) = \frac{24}{1 - V/F}$$

$$(\bar{x}_F)_j = \frac{30}{1 - V/F}(0.6) = \frac{18}{1 - V/F}$$

Furthermore,

$$x_i = \frac{(\bar{x}_F)_i}{\varDelta + V''} \quad x_j = \frac{(\bar{x}_F)_j}{\varDelta + V''}$$

$$K_i = \frac{b}{V'' + a} \quad K_j = \frac{d}{V'' + c}$$

$$y_i = K_i x_i \quad y_j = K_j x_j$$

Calculational Sequence

The calculational sequence is provided in the following tabulations for the range of values of V/F.

(a) Calculation of Constants

V/F	α	β	$(\bar{x}_F)_i$	$(\bar{x}_F)_j$	αβ
0.0	40	20	24	18	800
0.1	46.67	23.333	26.67	20	1,088.81
0.2	55	27.50	30	22.5	1,512.50
0.3	65.714	32.857	34.286	25.714	2,159.16
0.4	80	40	40	30	3,200
0.5	100	50	48	36	5,000
0.6	130	65	60	45	8,450
0.7	180	90	80	60	16,200
0.8	280	140	120	90	39,200
0.9	580	290	240	180	168,200
1.0	—	—	—	—	—

(b) Calculation of Constants (Cont.)

V/F	α+β	$(\bar{x}_F)_i + (\bar{x}_F)_j$	B	$\alpha(\bar{x}_F)_i$	$\beta(\bar{x}_F)_j$	C
0.0	60	42	18	480	720	−400.00
0.1	70	46.67	23.33	622.22	933.34	−466.75
0.2	82.5	52.5	30	825	1237.5	−550
0.3	98.571	60	38.571	1126.54	1689.77	−657.15
0.4	120	70	50	1600	2400	−800
0.5	150	84	66	2400	3600	−1000
0.6	195	105	90	3900	5850	−1300
0.7	270	140	130	7200	10800	−1800
0.8	420	210	210	16800	25200	−2800
0.9	870	420	450	69600	104400	−5800
1.0	—	—				

(c) Calculation of V'' and the K_i

V/F	V''	K_i	K_j	$K_i K_j$
0.0	12.9317	1.133536	0.910977	1.0326
0.1	12.8874	1.134485	0.912203	1.0349
0.2	12.8388	1.135529	0.913553	1.0373
0.3	12.7938	1.136500	0.914807	1.0397
0.4	12.7493	1.137458	0.916053	1.0420
0.5	12.7056	1.138399	0.917274	1.0443
0.6	12.6628	1.139325	0.918476	1.0465
0.7	12.6209	1.140231	0.919656	1.0487
0.8	12.5798	1.141123	0.920816	1.0508
0.9	12.5395	1.141998	0.92196	1.0529
1.0	12.5000	1.142857	0.92308	1.0530

(d) Calculation of Phase Compositions (of Permeate V and Reject L)

V/F	α+ L	y_i	$1/K_i$	x_i	β+ L	y_j	$1/K_j$	x_j
0.0	52.9317	0.4534	0.8829	0.4000	32.9317	0.5466	1.0977	0.6000
0.1	59.5574	0.4478	0.8815	0.3947	36.2207	0.5522	1.0962	0.6053
0.2	67.8388	0.4422	0.8806	0.3894	40.3388	0.5578	1.0946	0.6106
0.3	78.5078	0.4367	0.8799	0.3843	45.6508	0.5633	1.0931	0.6157
0.4	92.7492	0.4313	0.8792	0.3792	52.7492	0.5687	1.0916	0.6208
0.5	112.7056	0.4259	0.8784	0.3741	62.7056	0.5741	1.0902	0.6259
0.6	142.6628	0.4206	0.8777	0.3692	77.6628	0.5794	1.0888	0.6309
0.7	192.6209	0.4153	0.8770	0.3642	102.6209	0.5847	1.0874	0.6358
0.8	292.5798	0.4101	0.8763	0.3594	152.5798	0.5899	1.0860	0.6406
0.9	592.5395	0.4050	0.8757	0.3546	302.5395	0.5950	1.0847	0.6454
1.0	—	0.4000	0.8750	0.3500	—	0.6000	1.0833	0.6500

(e) Separations and Recoveries

V/F	$y_i/x_i = K_i$	$Vy_i/F(x_F)_i$	L/F	$x_j/y_j = 1/K_j$	$Lx_j/F(x_F)_j$
0.0	1.1335	0.0000	1.0	1.0977	1.0000
0.1	1.1345	0.1120	0.9	1.0962	0.9080
0.2	1.1356	0.2211	0.8	1.0946	0.8141
0.3	1.1364	0.3275	0.7	1.0931	0.7183
0.4	1.1374	0.4313	0.6	1.0916	0.6208
0.5	1.1385	0.5324	0.5	1.0902	0.5216
0.6	1.1392	0.6309	0.4	1.0888	0.4206
0.7	1.1403	0.7268	0.3	1.0874	0.3179
0.8	1.1411	0.8202	0.2	1.0860	0.2135
0.9	1.1421	0.9113	0.1	1.0847	0.1083
1.0	1.1429	1.0000	0.0	1.0833	0.0000

Note: When $V/F = 0$, essentially only a "drop" of the feed has permeated through the membrane. The determination corresponds to a bubble-point calculation as practiced in vapor-liquid phase separations (where $V \to 0$). When $V/F = 1$, essentially all the feed material has permeated through the membrane, leaving a "drop" of reject as calculated. The calculation corresponds to that of a

(*continued*)

EXAMPLE 19.4—(*continued*)

dew-point determination in vapor-liquid phase separations (where $L \to 0$). Interestingly, the results correspond to that of differential permeation with permeate flow, as presented in Chapter 6 of Hoffman (2003).

The V/F ratio is a process variable or parameter to be affixed by the operator. Furthermore, it can be assumed that P_L and P_V are set by back-pressure controllers on gas streams L and V. The feed rate F may be increased or reduced by a valve in the line (e.g., by a flow controller), where the upstream feed pressure is sufficiently high. Ordinarily, it would be set at a constant rate, at a fixed reject pressure P_L.

In turn, the rates L and V will adjust to the pressure difference maintained across the membrane, which is also related to the membrane permeability. If a higher permeate rate is desired, then the pressure P_V must be lowered and/or the feed rate F increased. (Alternately, albeit it is not a process control variable, the membrane surface or size can be increased.) It should be emphasized, moreover, that the calculations are process design estimations, prior to fabrication and operation.

CALCULATION OF MEMBRANE AREA

The separation calculations have not required any units for permeability and pressure, or pressure difference, nor for membrane thickness. Accordingly, units will now be assumed with the numbers supplied. Thus, let

$P_i = 20(10^{-9})\,\mathrm{cm}^3/\mathrm{cm}^2\text{-sec-cm Hg/cm}$
$P_j = 10$
$P_L = 30\ \mathrm{atm}$
$P_V = 20\ \mathrm{atm}$
$\Delta m = 10$ microns or $10(10^{-4})\,\mathrm{cm}$, the membrane thickness

Accordingly, to convert from the dimensionless properties supplied, the conversion factor for the dimensionless flux value V''. As previously derived,

$$V'' = \frac{V}{A} = G = P_L \Sigma P_i x_i - P_V \Sigma P_i y_i$$

where the summation is for both components i and j. It will follow that for the units specified above, the corresponding value of V'' as previously calculated must have the following units for a gaseous separation, if pressure is in atmospheres:

$$\frac{(10^{-9})\mathrm{cm}^3}{\mathrm{cm}^2 - \sec - \mathrm{cm\ Hg/cm}}\frac{\mathrm{cm\ Hg}}{\mathrm{atm}}$$

Note that a pointwise permeability is specified, which must be divided by the membrane thickness in order to obtain the overall permeability. The foregoing units may be converted to more convenient units by multiplying V'' as previously calculated, as follows:

$$V'' \times \frac{76\,\mathrm{cm\ Hg}}{\mathrm{atm}}\frac{1}{(\Delta m \text{ in cm})}\frac{(10/1)}{\{(22,414(10^9)\mathrm{in}[(10^{-9})\,\mathrm{cm}^3]/(\mathrm{g-mole})\}}$$
$$= V'' \times \frac{76}{22,414}\frac{10^{-8}}{(\Delta m \text{ in cm})}$$

where the factor $(10/1)$ denotes that the membrane pressures have been converted from a nominal 3 and 2 to 30 and 20 atm, thus differing by a multiple of 10 in this case.

In the term in braces in the denominator above, there would be the number $22,414(10^9)$ measured in the units of $[(10^{-9})\,\mathrm{cm}^3]$ of

gas per g-mole (which of course is identical to 22,414 cm^3 of gas per lb-mole). Significantly, however, the units of $(10^{-9})\,\mathrm{cm}^3$ cancel out with these same units as occurring in P_i.

The foregoing convoluted conversion of units will give a new value for the permeate flux V'' in the following units:

$$\frac{\mathrm{g\text{-}moles}}{\mathrm{cm}^2 - \sec}$$

The value so obtained can be placed on the basis of g-mole/sec of feedstream F.

Thus, the corresponding area requirement for each value of V'' in Table (c) would be

$$A = \frac{V}{F}\frac{10^9}{V''\frac{76}{22,414}\frac{(10/1)}{(\Delta m \text{ in cm})}} = \frac{V}{F}\frac{1}{V''}\frac{1}{0.00339074}\frac{(\Delta m \text{ in cm})(10^9)}{10}$$

For a membrane thickness of 10 microns or $10(10^{-4})\,\mathrm{cm}$, the above transforms to

$$A = \frac{V}{F}\frac{1}{V''}\frac{1}{0.00339074}\frac{(10)(10^{-4})(10^9)}{10} = \frac{V}{F}\frac{1}{V''}\frac{1}{0.00339074(10^{-5})}$$
$$= \frac{V}{F}\frac{1}{V''}\frac{1}{3.39074(10^{-8})}$$

where in this case the number $3.39074(10^{-8})$ can be treated as a conversion factor. The area requirement so obtained is in cm^2 per g-mole of feed per second. It may be noted that 929 cm^2 is 1 ft^2.

For a value say of $V'' \sim 12.7$, where $V/F = 0.5$, and $\Delta m = 10(10^{-4})\,\mathrm{cm}$ as stipulated, the area calculates to $1.16(10^6)\,\mathrm{cm}^2$ or 1,250 ft^2 for a feed rate of 1 g-mole/sec.

For a feed rate of only 1 g-mole per hour, the area in sq ft would be

$$A = \frac{1.16(10^6)}{3600(929)} = 0.35\,\mathrm{ft}^2$$

In any event, the foregoing illustrates the obvious—that low membrane permeabilities can translate to significantly high equipment demands if high feed rates are involved, along with appreciable membrane thicknesses.

The corresponding spreadsheet-type calculations are shown in Appendix 3 of Hoffman (2003), which may be generalized.

THE ENHANCEMENT OF SEPARATION

Multistage or cascade operations may be employed to enhance the sharpness of separation, as set forth in Chapter 4 of Hoffman (2003). (This includes short-cut methods, such as a McCabe-Thiele type of graphical representation for binary mixtures, similar to that used in distillation calculations.) The efficacy will depend on the number of stages and the internal recycle or reflux ratios between the stages utilized, as previously diagrammed in Figures 19.15 and 19.16. As a more or less upper calculated limit, utilizing the same feed mixture, with five stages above and five stages below the feed location, and appreciable recycle or reflux ratios, the overhead and bottoms mole fraction compositions for component i were determined to be 0.756 and 0.097, respectively, and for component j the corresponding values were 0.244 and 0.903. Spreadsheet methodologies are furnished in Appendix 4 of Hoffman (2003).

The use of differential permeation in countercurrent flow with recycle is developed in Chapter 7 and Appendix 7 of Hoffman (2003).

a bubble-point calculation will give a value for the degree or sharpness of separation in terms of mole fraction ratios or K-values.

(It may be added that, for a single pure component, whether or not a reject phase can be said to exist is of no concern, since V/F or L/F does not enter into the determination and calculations.)

However, in actual test measurements, at what point if any can it be said that all the feed passes through the membrane? That is to say, does holdup not occur on the upstream pressure side? For in any kind of short-term or transient test—say in what might be called a batch or semi-continuous laboratory or bench-scale test—does not a reject phase exist? At any point in time, is there not a situation where the feed which has not yet passed through the membrane thereby constitutes a reject phase? Only for a long-term, steady-state test—without any reject side stream—can it truly be said that all the feed passes through the membrane. This sort of long-term test, would then provide the true measure of membrane permeabilities for the components within a mixture. Whether or not discrepancies should therefore exist between the results of short-term tests and long-term tests is an interesting philosophical question.

In any event, the permeability determinations of component for mixtures are apparently at variance with those determined separately for each of the pure components. It is part of the general problem so often encountered of trying to project from pure component behavior to the behavior of mixtures.

Unit Permeation Rate. The expression for the K-value can conveniently be rewritten as

$$K_i = \frac{P_i P_L}{V'' + P_i P_V} = \frac{P_i P_L / P_i P_V}{V^* + 1} = \frac{P_L / P_V}{V^* + 1}$$

where $V^* = V''/P_i P_L$ can be called the dimensionless or reduced permeation flux, or some other designator can be used.

It may be observed that, since K is dimensionless, the units of V are to be in the same units as the feed rate F, and will be in the same units as the combinations $P_i P_V$ or $P_i P_L$. These combined units may be in cc per unit time (at standards conditions), or in moles per unit time, or so on. That is, the areal basis can pertain to the entire membrane or membrane assembly. Accordingly, the permeability P_i can pertain to the entire membrane per se.

Alternately, P_i can of course be placed on a unit area basis (e.g., per square centimeter). In turn, the feed rate F, permeate rate V, and reject rate L would then be on the same common unit area basis.

For the further purposes here, the K-value calculations will utilize V'' rather than V^*, inasmuch as V'' will more directly stand for the permeate flux in multistage operations.

Expected vs. Actual Separations. As has been previously indicated, the permeabilities within mixtures are generally less than those for the pure components. In other words, the degree of separation in mixtures is less sharp than would be expected from the permeabilities of the pure components.

MULTICOMPONENT SEPARATION CALCULATIONS

In general, for any circumstance, since

$$\begin{aligned} F(x_F)_i &= V y_i + L x_i \\ &= V K_i x_i + L x_i \\ &= V y_i + L\, y_i / K_i \end{aligned}$$

then

$$\sum \frac{(x_F)_i}{\frac{V}{F} K_i + \frac{L}{F}} = \sum x_i = 1$$

or

$$\sum \frac{(x_F)_i}{\frac{V}{F} + \frac{L}{F}\frac{1}{K_i}} = \sum y_i = 1$$

where

$$\frac{V}{F} + \frac{L}{F} = 1$$

and

$$K_i = \frac{P_i P_L}{V'' + P_i P_V} = \frac{P_i P_L / P_i P_V}{V^* + 1} = \frac{P_L / P_V}{V^* + 1}$$

Where

$$V^* = \frac{V''}{P_i P_V}$$

Given the $(x_F)_i$, then for each value V/F (and/or L/F) there is a unique solution for V''.

The above is a variation on the single-stage flash calculation for a vapor-liquid separation.

The calculation for a multicomponent system is in general trial-and-error, establishing the x_i and the y_i along with a corresponding value for V''. In turn, given the feed rate F and the specified ratio V/F, the absolute value of the permeate rate V with respect to F will follow. Similarly, this process determines an absolute value for the reject rate L relative to F.

As the limiting conditions, note that if $V/F = 0$ and $L/F = 1$, then

$$\sum K_i (x_F)_i = \sum y_i = 1$$

and if $V/F = 0$ and $L/F = 1$, then

$$\sum (x_F)_i / K_i = \sum x_i = 1$$

Given the $(x_F)_i$, these calculations would establish the respective values of V'' for each of the limiting conditions, along with the respective compositions x_i and y_i. These limiting bubble-point type and dew-point type determinations have been previously described.

Key Components. In the parlance used for distillation calculations, the two key components can be designated as those whose distribution behavior is closest to unity, with the one key component showing a K-value less than 1, and the other greater than 1. The latter would exhibit the greater "volatility" or activity—in this case, the greater value for K.

Thus if

$$K_i = \frac{P_i P_L}{V'' + P_i P_V} > 1$$

and

$$K_j = \frac{P_j P_L}{V'' + P_j P_V} < 1$$

then i would be perceived as the more "volatile" or active component.

Note further that if $K_i > K_j$, then

$$\frac{P_iP_L}{V'' + P_iP_V} - \frac{P_jP_L}{V'' + P_jP_V} > 0$$

or

$$V''P_iP_L + P_iP_jP_LP_V - V''P_jP_L - P_iP_jP_LP_V > 0$$

Collecting terms,

$$V''P_L(P_i - P_j) > 0 \quad \text{or} \quad (P_i - P_j) > 0$$

That is, if $P_i > P_j$, then component i would have the greater permeability, and would also have the higher "volatility" or activity.

TWO-COMPONENT CALCULATIONS

As a special case of multicomponent separation calculations, the double trial-and-error type calculations involved for two components are best done utilizing spreadsheet techniques as set forth in Appendix 3 of Hoffman (2003). However, it is possible to obtain an analytic solution for two components, albeit involved and unwieldy. For the record, this latter procedure is as follows.

A simplification can be made for binary systems, whereby for two components i and j let

$$\frac{(x_F)_i}{V/F + (1 - V/F)[\frac{V''+a}{b}]} + \frac{(x_F)_j}{V/F + (1 - V/F)[\frac{V''+c}{d}]} = 1$$

where

$$a = P_iP_V$$
$$b = P_iP_L$$
$$c = P_jP_V$$
$$d = P_jP_L$$

The above may be further arranged as

$$\frac{\frac{b(x_F)_i}{(1-V/F)}}{[\frac{V/F}{1-V/F}b + a] + V''} + \frac{\frac{d(x_F)_j}{(1-V/F)}}{[\frac{V/F}{1-V/F}d + c] + V''} = 1$$

or

$$\frac{(\bar{x}_F)_i}{\alpha + V''} + \frac{(\bar{x}_F)_j}{\beta + V''} = 1$$

where the introduced quantities are defined by the substitutions.

Accordingly,

$$\beta(\bar{x}_F)_i + V''(\bar{x}_F)_i + \alpha(\bar{x}_F)_j + V''(\bar{x}_F)_j = \alpha\beta + V''(\alpha + \beta) + (V'')^2$$

or

$$0 = (V'')^2 + \{(\alpha + \beta) - [(\bar{x}_F)_i + (\bar{x}_F)_j]\}V''$$
$$+ (-[\beta(\bar{x}_F)_i + \alpha(\bar{x}_F)_j] + \alpha\beta\}$$

and which is representable as

$$0 = A(V'')^2 + BV'' + C$$

Therefore, solving the quadratic for V'',

$$V'' = \frac{-B \pm \sqrt{B^2 - 4AC}}{2A}$$

where the quantities are defined by the substitutions, with $A = 1$, and where

$$\alpha = \frac{V/F}{1 - V/F}b + a$$
$$\beta = \frac{V/F}{1 - V/F}d + c$$
$$(\bar{x}_F)_i = \frac{b}{1 - V/F}(x_F)_i$$
$$(\bar{x}_F)_j = \frac{d}{1 - V/F}(x_F)_j$$

The quantity B in the quadratic will be positive and the $\pm$ sign will be used as its plus value.

The calculation is readily performed for the condition $V/F \to 0$, analogous to the bubble-point type determination. If, however, $V/F \to 1$, then the dew-point type determination must be used, such that

$$1 = \sum x_i = \sum y_i/K_i$$

or

$$1 = \frac{V'' + a}{b}(\bar{x}_F)_i + \frac{V'' + c}{d}(\bar{x}_F)_j$$

whereby

$$bd = V''d (x_F)_i + ad (x_F)_i + V''b (x_F)_j + bc (x_F)_j$$

where the constants a, b, c, and d have been previously identified. Collecting terms and solving for V'',

$$V'' = \frac{bd - [ad(\bar{x}_F)_i + bc(\bar{x}_F)_j]}{d(\bar{x}_F)_i + b(\bar{x}_F)_j}$$

where, as noted, the quantities have previously been defined.

The actual calculations are performed as shown in Example 19.4.

MULTISTAGE AND DIFFERENTIAL PERMEATION DERIVATIONS AND CALCULATIONS FOR TWO KEY COMPONENTS

As can be expected, the derivations and calculations become increasingly complicated for multistage and differential permeation. The subject is detailed in the later pages of Hoffman (2003), with examples provided, including systematic spreadsheet calculations.

REFERENCES

G. Belfort, *Materials Science of Synthetic Membranes: Fundamentals and Water Applications*, Academic Press, New York, 1984.

T.D. Brock, *Membrane Filtration: A User's Guide and Reference Manual*, Science Tech, 1983.

J.G. Crespo and K.W. Böddeker (Eds.), *Membrane Processes in Separation and Purification*, Kluwer Academic Publishers, Dordrecht, The Netherlands, 1993. Published in cooperation with the NATO Scientific Affairs Division.

T. Flynn and J.D. Way, *Membrane Separations in Chemical Processing*, National Bureau of Standards, U.S. Department of Commerce, Boulder, CO, 1982.

Gas Research Institute. Proceedings of the First GRI Gas Separations Workshop, held in Denver, October 22–23, 1981. Chicago: Gas Research Institute.

Gas Research Institute. Proceedings of the Second GRI Gas Separations Workshop, held in Boulder, CO, October 21–21, 1982. Chicago: Gas Research Institute.

M. Grayson and D. Eckroth (Eds.), *Kirk-Othmer Encyclopedia of Chemical Technology*, 3rd ed. Vol. 15, Wiley, New York, 1981.

W.S.W. Ho and K.K. Sirkar (Eds.), *Membrane Handbook*. Van Nostrand, New York, 1992.

E.J. Hoffman, *Membrane Separations Technology: Single-Stage, Multistage, and Differential Permeation*, Gulf Professional Publishing, an Imprint of Elsevier Science, Amsterdam, 2003.

E.J. Hoffman, Subquality natural gas: The resource and its potential, In *Investigation of Structure Permeability Relationships of Silicone Membranes*, Final Report, edited by Chi-long Lee, S.A. Stern, J.E. Mark, and E. Hoffman. Report No. GRI-87/0037. Chicago: Gas Research Institute, 1987. Report available from the National Technical Information Service.

E.J. Hoffman, Subquality natural gas reserves, *Energy Sources*, **10**(4), 239–244 (1988).

E.J. Hoffman, K. Venkataraman, and J.L. Cox, Membrane separations for subquality natural gas, *Energy Progress*, **8**(1), 6–13 (March 1988).

S.-T. Hwang, C.K. Choi, and K. Kammermeyer, Gaseous transfer coefficients in membranes, *Separation Sci.*, **3**, 461–478 (1974).

International Critical Tables, McGraw-Hill, New York, 1926–1930.

N.N. Li and W.S.W. Ho, Membrane processes, in *Chemical Engineers' Handbook*, McGraw-Hill, New York, 1984, pp. 17.14–17.34.

D.R. Lloyd (Ed.), *Materials Science of Synthetic Membranes*, ACS Symposium Series **269**, American Chemical Society, Washington, DC, 1985.

P. Meares, *Membrane Separation Processes*, Elsevier, Amsterdam, 1976.

J.J. McKetta and W.A. Cunningham (Eds.), *Encyclopedia of Chemical Processing and Design*, Vol. 27, Marcel Dekker, New York, 1988.

R.D. Noble and S.A. Stern (Eds.), *Membrane Separations Technology: Principles and Applications*, Membrane Science and Technology Series, Elsevier, Amsterdam, 1995.

D.R. Paul and Y.P. Yampol'skii (Eds.), *Polymeric Gas Separation Membranes*, CRC Press, Boca Raton, FL, 1994.

R.H. Perry (late Ed.), D.W. Green (Ed.) and J.O. Maloney (Assoc. Editor), *Perry's Chemical Engineers' Handbook*, 7th ed., McGraw-Hill, New York, 1997.

M.C. Porter, Membrane filtration, in P.A. Schweitzer (Ed.), *Handbook of Separation Techniques for Chemical Engineers*, McGraw-Hill, New York, 1979, pp. 2.3–2.103.

S. Souritajan, *Reverse Osmosis*, Academic Press, New York, 1970.

A.F. Turbak (Ed.), *Synthetic Membranes: Vol. 1, Desalination*; *Vol. 2, Hyper and Ultrafiltration Uses*, ACS Symposium Series **153** and **154**, American Chemical Society, Washington, DC, 1981.

NTIS Bibliographic Data Base, National Technical Information Service, Washington, DC.

20

GAS-SOLID SEPARATIONS

*T*his chapter consists of two subsections: a section about gas-solid separations and a section in which a variety of other topics of interest in chemical processing are discussed. The subjects in this latter section do not readily fit into categories in other chapters but are nevertheless valuable in applications in the chemical process industries. The objective here is to describe the principles involved, to point out the main applications, and to refer to sources of more information.

Equipment manufacturers mentioned in this chapter can be identified in the Thomas Register and in the Chemical Engineering Buyers' Guide.

20.1. GAS-SOLID SEPARATIONS

The removal of solids from a gas or air stream is of great industrial importance. This is especially true in the last two or three decades with the increased requirements for effective solids removal from solid-laden streams mandated by law. In addition to environmental control requirements, there are health considerations not only in the workplace but also in the environment surrounding the plant site. Companies have an interest in being good corporate citizens by controlling various emissions from the plant.

Dust collection is the process of removal and collection of solids in a gas phase. Its purpose is to

1. Control air pollution from various industrial plants
2. Eliminate safety and health hazards from the workplace in which grinding, milling, and packaging operations take place
3. Recover valuable products from dryers, conveyors, bagging equipment, and so on, for recycling back into a process
4. Reduce equipment maintenance on rotating equipment caused by dusts

Newer, more effective control equipment has led to more efficient designs and simultaneously to lower operating expenses. This section describes various dust collection equipment, ranging from the simple to the more sophisticated. Design equations for this equipment are proprietary; when contacting equipment manufacturers, they will require certain information so that they can design or recommend the proper equipment applications.

There are four broad groups of gas-solid separation equipment:

1. Cyclone and inertial separators for removal of large solid particles
2. Baghouse collectors for removal of intermediate-sized particle
3. Wet scrubbers employing liquid sprays to entrap solid particles.
4. Electrostatic precipitators to collect fine particles

There are subgroups under each of the these four categories and they will be considered where appropriate.

CYCLONE AND INERTIAL SEPARATORS

Cyclone Separators. The most commonly used equipment for the separation of dust particles from an air/gas stream is the cyclone separator. The literature on design and operation of cyclones has been extensively reviewed by Rietemer and Vetver (1961), Maas (1979), Zenz (1982), and Pell and Dunson (1999). A sketch of a cyclone separator and typical dimensional ratios are found in Figure 20.1(b). The dust-laden gas stream enters near the top of the collection chamber tangentially. The force on the larger particles is greater than the force on the smaller ones because the latter particles have less mass and therefore spiral downward into the dust hopper. When the gas velocity is not sufficient to suspend the particles, gravity causes the particles to fall into the dust collection chamber. Further, a small-diameter cyclone generates a greater centrifugal force than a large diameter unit. To obtain the same performance, a design engineer has the choice of either a smaller diameter and a short chamber or a larger diameter with a longer barrel chamber. Because the tapered section of the cone is smaller than the main chamber, higher velocities are encountered, which may reentrain the finer dust particles and these then may be swept to the outlet of the cyclone. Figure 20.1(a) shows the vortex pattern in a cyclone separator.

Vatavuk (1990) pointed out that a key dimension in the sizing of a cyclone is the inlet area. Properly designed cyclones can remove nearly every particle in the 20–30 micron range. Typically, cyclone separators have efficiencies in the range of 70–90%. Because of the low efficiency of these units, they are often used as a first stage of dust collection, or are referred to as primary collectors.

Typical cyclone dimension ratios are indicated in Figure 20.1 (b). Inlet velocities should be in the range of 100–150 ft/sec, but may be limited by the occurrence of reentrainment of dust particles or by and unacceptable pressure drop. The pressure drop is estimated in terms of velocity heads, a value of 4 being commonly used. Equations 18.24 and 18.25 (shown here again) are expressions for the pressure drop.

$$\Delta P = 4\rho V^2/2g = 4.313\ \rho(ft/sec/100)^2 psi \tag{18.24}$$

And for atmospheric air

$$\Delta P = 0.323(ft/sec/100)^2 psi \tag{18.25}$$

The size of the inlet is selected at a specific inlet velocity and required volumetric rate; the other dimensions then are fixed.

Capacity and efficiency of the cyclone depend on the inlet velocity and dimensions of the vessel. Correlated studies have been made with a rectangular inlet whose width is D/4 and whose height is 2–3 times the width. A key concept is the critical particle diameter which is one that is removed to the extent of 50%. As shown in Chapter 18, the critical particle diameter is given by Equation 18.26.

$$(D_p)_{crit} = [9\mu D/4\pi N_t V(\rho - \rho_g)]^{0.5} \tag{18.26}$$

where D = diameter of the vessel, ft
   V = inlet linear velocity, ft/sec
   N_t = number of turns made by the gas in the vessel

Zenz (1982) presented a graphical correlation that can be represented by Equation 18.27.
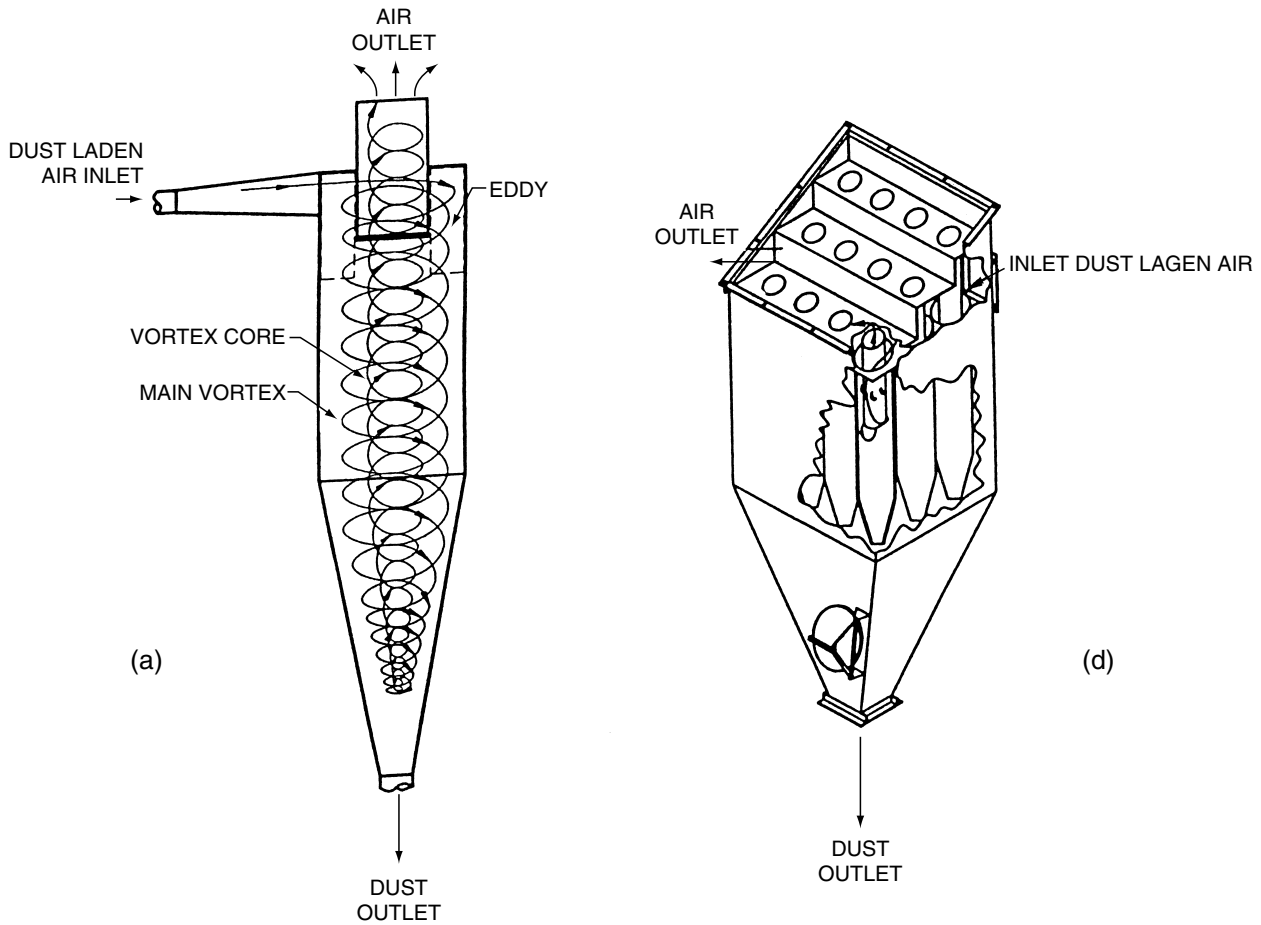
Figure 20.1a. Cyclone separators. (a) Vortex pattern in a cyclone separator. (d) Multiclone separator. (Courtesy of Scientific Dust Collectors 2002).
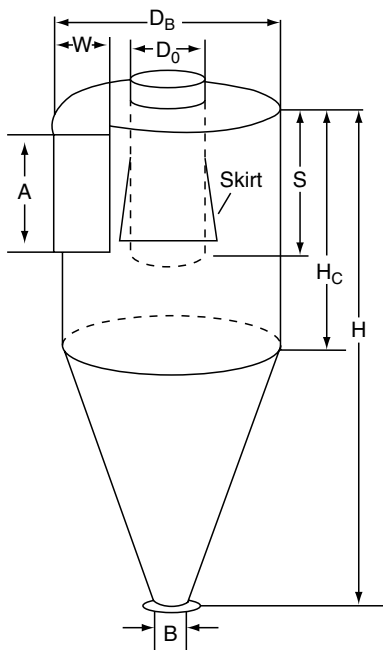
Figure 20.1b. Typical dimension ratios of a cyclone separator.

$$N_t = [0.1079 - 0.00077\ V + 1.924(10^{-6})V^2]\ V \qquad (18.27)$$

with V in ft/sec. With a height opening equal to 2.5 times the width, the volumetric rate is

$$Q = AV = 2.5\ D^2V/16 \qquad (18.28)$$

These relations are used in Example 20.1 to determine the size of a separator corresponding to a specified critical particle diameter. Figure 20.1 (c) is a plot of the percent removal of particles in a cyclone as a function of their diameters relative to the critical particle diameter given by Equations 18.26 and 18.27.

Multiclones. A multiclone separator consists of a number of small cyclones arranged in parallel in a chamber to handle large volumes of dust-laden air. They are capable of having very high

Cyclone dimensional proportions for Figure 21.b are:

$W = D_B/4$	$S = 2D_B + (D_B/8)$
$D_O = D_B/2$	$H = 2D_B + 2D_B = 4D_B$
$A = D_B/2$	$B = $ usually $D_B/4$
$H_C = 2D_B$	

Figure 20.1c. Percent removal of particles in a cyclone as a function of their diameters relative to the critical diameter given by Equations 18.26 and 18.27 (Zenz, 1982).

particle removal efficiencies. Vatavuk (1990) reported that multiclones might have efficiencies up to 80% on 5-micron particles. Figure 20.1(d) is a sketch of a multicone separator.

Inertial Collectors. Inertial separator designs consist of a louver or baffle device mounted in a plenum chamber, as shown in Figure 20.2. Dust-laden air enters beneath the louvers and the flow is diverted, changing direction, therefore slowing the air velocity so that the air stream cannot support the particles. The dust impinges on the louvers, falls into the lower chamber, and is discharged at the bottom of the collector. The "clean" gas leaves at the top of the unit. These collectors are used in applications where the inlet dust loads are small, usually less than 0.5 grain per cubic foot. Heavier loads quickly plug the equipment. As one might expect, this class of air-solid separator is not as efficient and will not perform as well as baghouses, wet scrubbers and the like.

There are other types of inertial separators. One such design consists of a fan-type unit that has specially designed blades and housing for handling what might be abrasive dusts. Due to the design, a fan accelerates the dust entering the unit and throws the particles against the housing of the inertial separator. This type unit is often installed on vents from grinding operations (Scientific Dust Collectors, 2002)

BAGHOUSE COLLECTORS

Industrial processes for which noncleanable filters are not applicable may emit large quantities of dust. The capture of such dusts requires a cleanable filter and this is an application for baghouses. A typical baghouse design is shown in Figure 20.3(a). The baghouse consists of a number of filter bags attached at the top of the bag to a shaker arm enclosed in a rectangular chamber. Most collectors of this type have a device to hold the bags in tension. Dust-laden air enters near the bottom of the chamber and flows inside the bag. The dust is trapped on the inside of the bag and the clean air flows through the bag and exits at the top of the chamber. Periodically, when the pressure drop rises to a predetermined value, a shaker device is activated, loosening the dust that falls into the dust hopper at the bottom of the chamber. The shakers are operated automatically and the frequency of operation is important. The more frequent the shaking operation, the more wear and tear on the bags.

EXAMPLE 20.1
Size and Capacity of Cyclone Separators
Air at 1000 cuft/sec and density of 0.075 lb/cuft contains particles with density 75 lb/cuft. 50% of the 10 μm diameter particles are to be recovered. Find the sizes and numbers of cyclones needed with inlet velocities in the range of 50–150 ft/sec. The inlet is rectangular with width $D/4$ and height $2.5D/4$, where D is the diameter of the vessel.
Equations (18.26) becomes

$$\frac{D}{N_t V} = \frac{4\pi(\rho - \rho_g)D_p^2}{9\mu} = \frac{4\pi(75 - 0.075)}{9(1.285)(10^{-5})}\left(\frac{10}{304,800}\right)^2 = 0.00876,$$

where N_t is given by Eq. (18.16). The number of vessels in parallel is

$$n = \frac{Q'}{AV} = \frac{100}{(2.5/16)D^2 V} = \frac{6400}{D^2 V}.$$

The results at several velocities are summarized.

V (cfs)	N_t	D (ft)	n
50	3.71	1.62	48.8
100	5.01	4.39	3.32
144	5.32	6.71	1.0

From Figure 18.11, the percentage recoveries of other-sized particles are:

$D_p/(D_p)_{\text{crit}}$	% Recovered
0.3	9
0.5	22
0.6	30
1	50
2	70
6	90
9	98.5

When the smallest of these cyclones, 1.62 ft dia, is operated at 150 cuft/sec,

$$N_t = 5.35,$$

$$(D_p)_{\text{crit}} = \left[\frac{9(1.285)(10^{-5})(1.62)}{4\pi(5.35)(150)(75 - 0.075)}\right]^{0.5}$$

$$= 1.574(10^{-5})\text{ft}, \ 4.80\mu\text{m}.$$
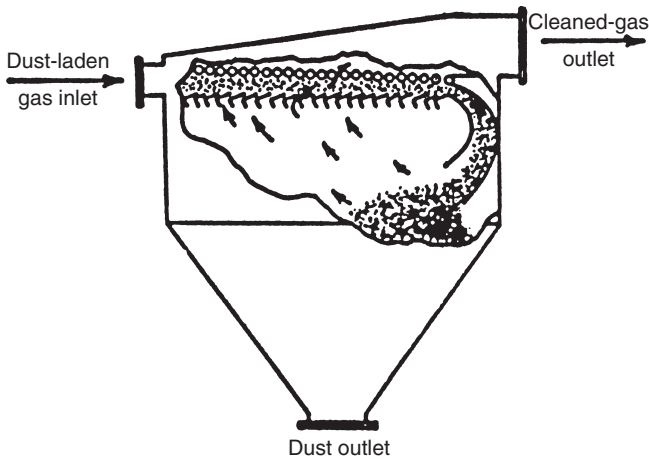
Figure 20.2. Louver dust collector. (Courtesy, Scientific Dust Collectors, 2002)

Another type bag collector is designed so that the dust collects on the outside of an envelope bag. The bags are attached to a shaker device mounted near the bottom of the unit. In this design, the dust-laden air enters near the bottom of the unit; the air passes through the bag and exits at the top of the collector. Figure 20.3(b) is a diagram of the envelope collector.

A typical wire retainer device for holding the bags vertically and preventing them from collapsing under high air pressure is shown in Figure 20.3(c).

When selecting fabric materials for baghouses, the following criteria must be considered:

Temperature of the process air stream
Electrostatic characteristics of the dust
Abrasiveness of the dust
Moisture in the air and collector
Hygroscopic nature of the dust
Acid or alkali chemical resistance
Ease of disengaging the dust from the filter material
Size of the dust particles
Permeability of the fabric so that only air will pass through the filter bag
Cost of the material

The bags are made of the following materials (Scientific Dust Collectors, 2002):

Polyester—the standard and most commonly used material
Polypropylene—for superior chemical resistance
Fiberglass—for high temperatures and in acid and alkaline conditions
Aramid—for high temperature applications
Polytetrafluoroethylene—used to capture fine particles where an artificial dust cake is required

Shaker filters have the drawback that they must be taken off stream to clean the bags. Since continuous on stream operation is required, several baghouse chambers are installed in parallel with dampers, permitting one section to be in the cleaning cycle while the rest of the baghouse is filtering the dust-laden gas stream.

Baghouses are high-maintenance items due to internal movement in a dust-laden stream. They operate at low air-to-cloth ratios and the collectors are large and more costly than some other devices described in this section.

Fan-Pulsed Dust Collector. The next advance in the development of dust collection equipment was to be able to clean the filter bags continuously. The fabric filter tubes are arranged in a radial fashion in a cylindrical housing, as shown in Figure 20.4. A rotating arm has a traveling manifold through which air is supplied by a fan mounted outside of the shell of the chamber. Reverse air is admitted through the arm as it travels over the filter element openings, blocking the airflow to adjacent elements in the cleaning step.

Pulsed Jet Baghouse Collector. Another type of continuous cleaning collector of the pulsed jet type is also known as the *blow ring collector*. The dust-laden air enters the unit in a manifold at the top of the collector and the air flows from inside the cloth tube through the media to the clean air outlet at the bottom of the collector. The dust collects on the inside of the cloth tubes and a blow ring travels up and down on the outside of the bag. Jets of air are emitted by the blow ring and pass through the fabric, dislodging the dust inside the bag that falls to the dust hopper below. Figure 20.5 is a diagram of the pulsed jet baghouse collector with a blow ring.

Although pulsed jet baghouse collectors operate at low pressure and can accommodate a wide range of dust loadings, they are not suitable for high temperatures and in corrosive environments. The main disadvantages are the abrasion of the bags by the traveling jet ring and the high maintenance of the blow rings.

All bag collectors discussed in this section require regular inspection. The bags or filter elements should be inspected for

Coating of dust that cannot be removed by cleaning
Deposit of moist material on one side of the filter element
Hardness of the coating for evidence of condensation

(a)
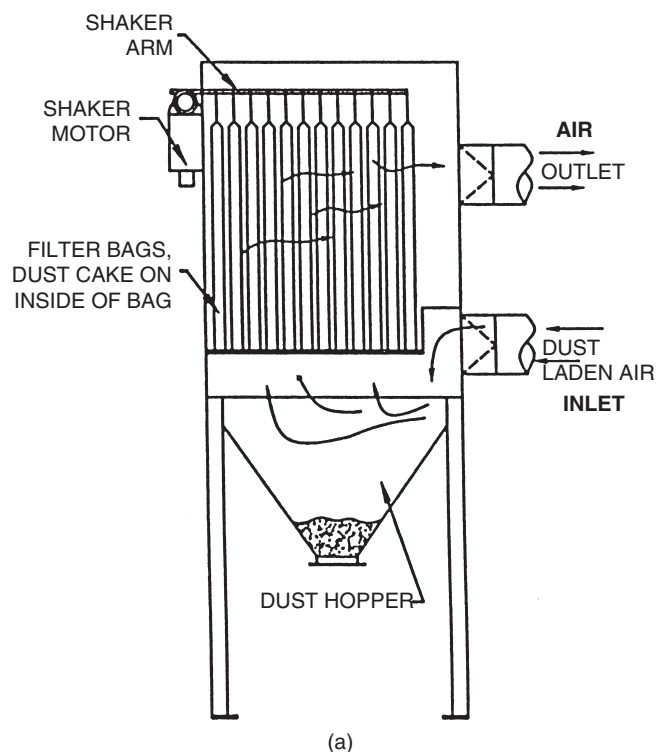
Figure 20.3. Baghouse collectors. (a) Tubular shaker collector. (b) Baghouse collector with envelope filter bags. (Courtesy Scientific Dust Collectors 2002). (c) Bag wire retainers.

(b)

(c)
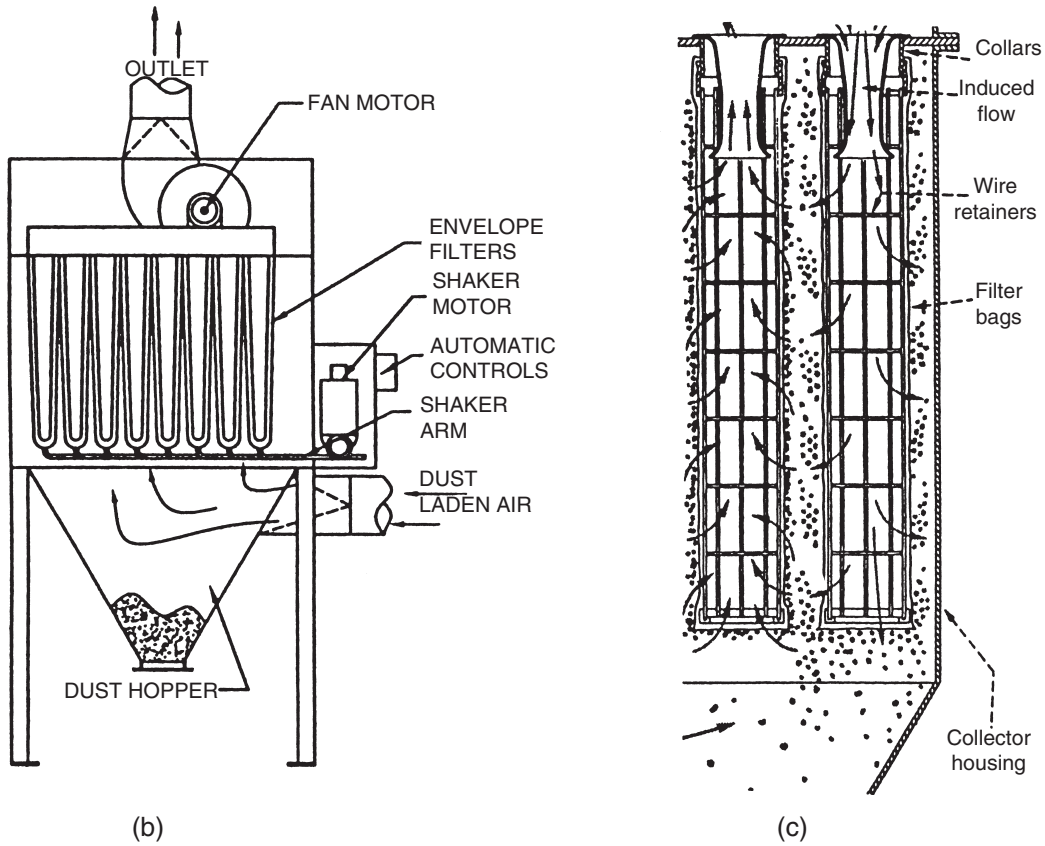
Figure 20.3.—(*continued*)
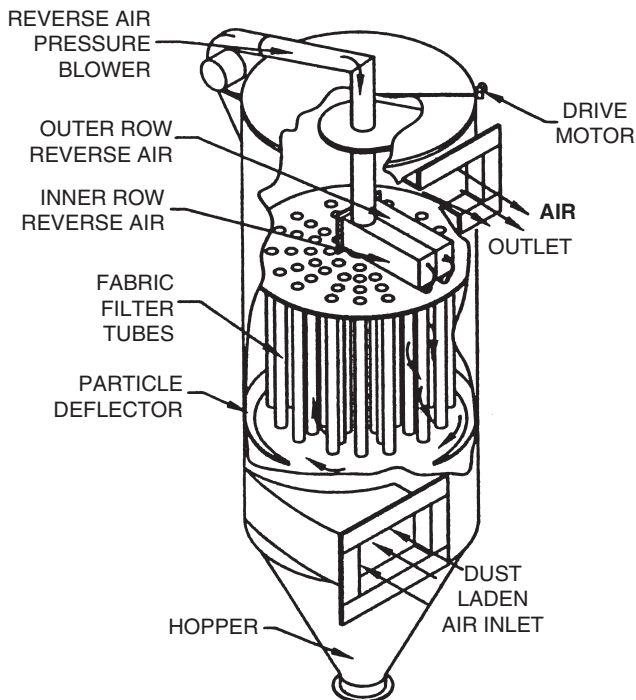
Figure 20.4. Fan-pulsed dust collector. (Courtesy of Scientific Dust Collectors 2002).

Thickness of the coating along the length of the filter element
Color of the coating compared to the color of the dust
Condition of the filter element, openings of the weave, tears, and wear due to flexing of the material

Further, baghouse interiors should be inspected for buildup of powder on the walls of the housing and in the dust hopper.
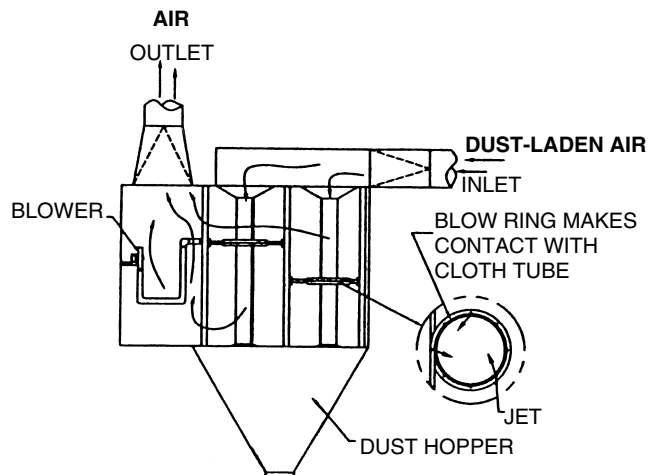
Figure 20.5. Pulsed jet baghouse showing blow ring. (Courtesy of Scientific Dust Collectors 2002).

WET SCRUBBERS

A disadvantage of cyclones and inertial collectors is that dust particles are frequently swept back into the exiting air stream. Wet scrubbers were designed to overcome this disadvantage.

Wet Cyclone Scrubbers. This air washer is a variation on the dry cyclone separator. The wet collector is equipped with spray nozzles that atomize water. Dust-laden air enters tangentially near the bottom of the unit spirally upward into the water spray. Figure 20.6(a) is a sketch of this equipment showing a manifold equipped with spray nozzles. Plugging of the nozzles is a high-maintenance item. In one design, the spray nozzles are mounted in the wall of the collector, spraying water inward into the dust-laden air, making the nozzles more accessible for maintenance.

A baffle or impingement device is often installed in the center of the chamber to break up the swirling air-water-dust stream.

Spray Scrubbers. Spray scrubbers consist of an empty cylindrical chamber in which dust-laden air is contacted with water from spray nozzles, as shown in Figure 20.6(b). The dust-laden air enters the tower near the bottom and passes upward through the water spray. This type of equipment is similar to the spray towers used in mass transfer operations. Proper water distribution can be a problem, so multiple banks of spray nozzles mounted on a manifold produce better air-water contact. The spray knocks down the dust that leaves the bottom of the unit as a dust-water mixture. An entrainment separator is mounted in the upper part of the chamber to reduce the potential spray carryover into the exiting gas stream.

Venturi Scrubbers. Venturi scrubbers are used to separate air streams from solids that are noxious, hazardous, or explosive. The exiting liquid stream, usually a solid-water suspension or a slurry, may be returned to the process for recovery.

This type scrubber operates typically at high air velocities between 15,000 and 20,000 ft/min, causing high shear stresses forming very fine water droplets (Bonn, 1963). Water is added in the range of 5 gallons/1,000 cfm in the venturi throat (Scientific Dust Collectors, 2002). The water droplets cause the collection of fine dust particles that may be recovered as a suspension or slurry. Near the exit of the scrubber, a mist eliminator of the inertial or cyclone type is essential to separate the mist from the exiting air stream by changing direction of the airflow. Figure 20.6(c) is a sketch of a venturi scrubber.

Any surface that was not wet would form a mud, causing frequent cleaning of the collector interior. In order to have a scrubber operating efficiently, the velocity in the scrubber has to be such as to drive the dust particles into the water. Venturi scrubbers have efficiencies in the range of 90–95% compared to dry cyclones in the range of 75–85%.

Orifice Scrubbers. This type scrubber is essentially an inertial trap in which air impinges against a water-wet surface. In the unit, large water droplets are formed using large quantities of water. The collision of the air with the water causes wetting of the dust and the droplets are separated from the air by changing the flow direction, sometimes two or more direction changes, before the air leaves the unit, as in Figure 20.6(d). This design has considerable appeal
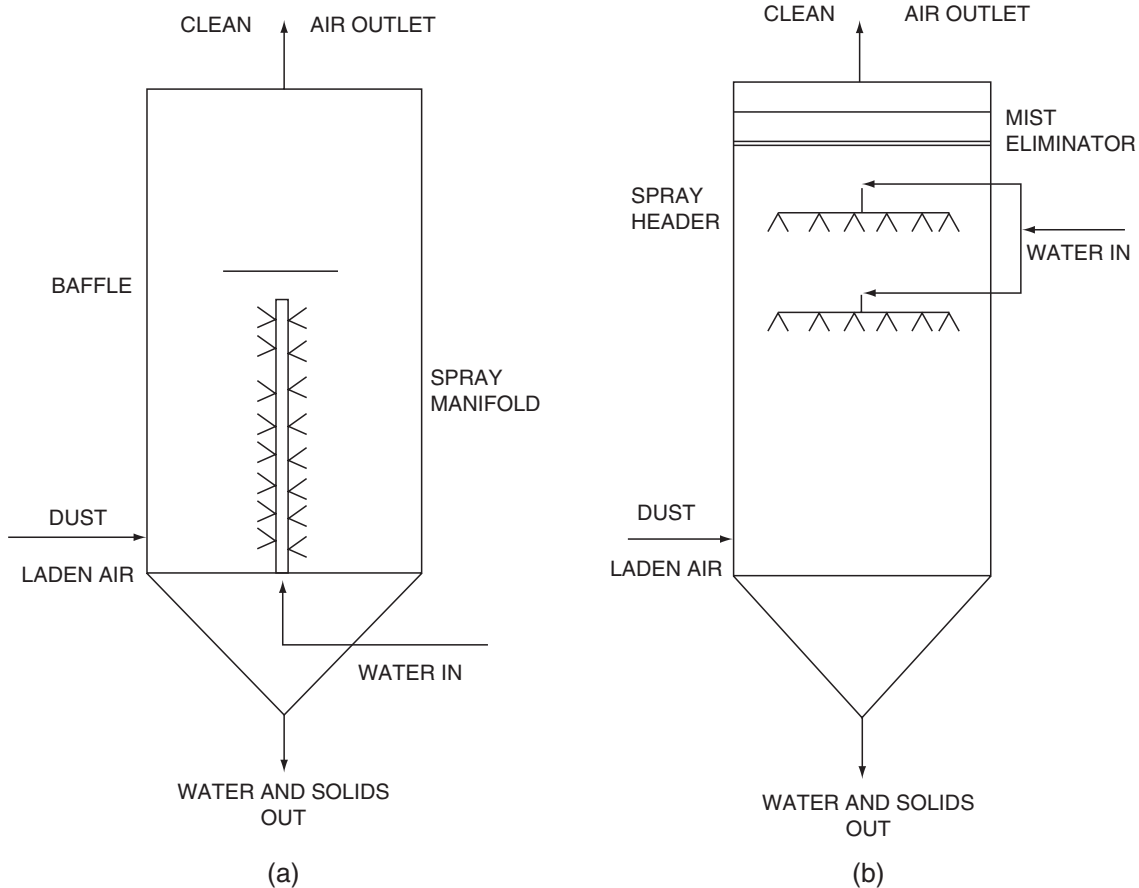
Figure 20.6. Wet scrubbers. (a) Wet cyclone scrubber. (b) Spray scrubber. (c) Venturi scrubber. (d) Orifice scrubber.

CLEAN AIR OUTLET

MIST ELIMINATOR

WATER IN

DUST
LADEN
AIR IN

VENTURI

(c)

WATER AND SOLIDS OUT

CLEAN AIR OUTLET

AIR
OUT

(d)

DUST LADEN
AIR INLET

WATER
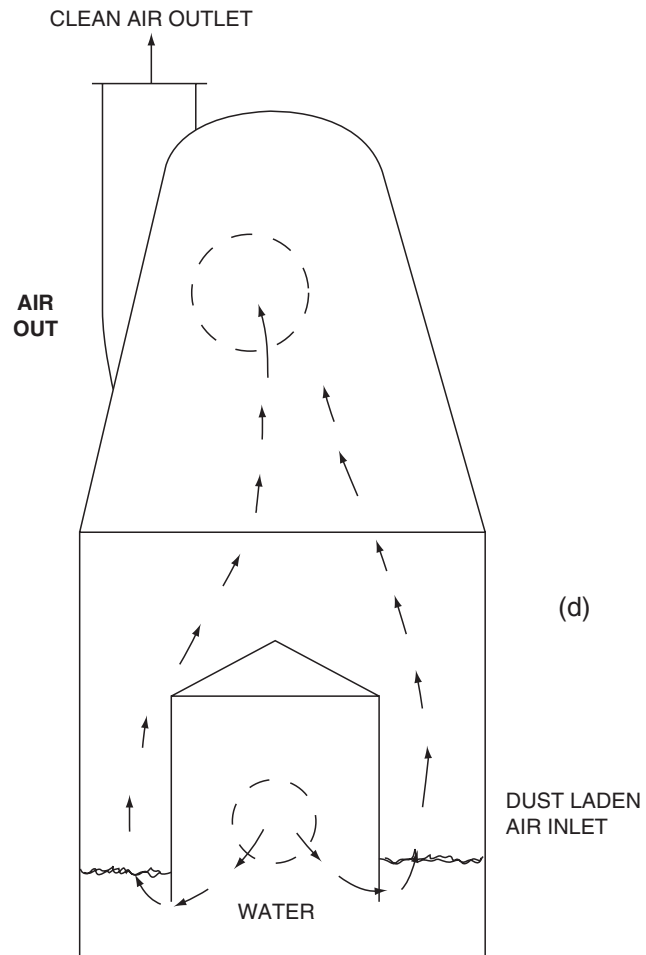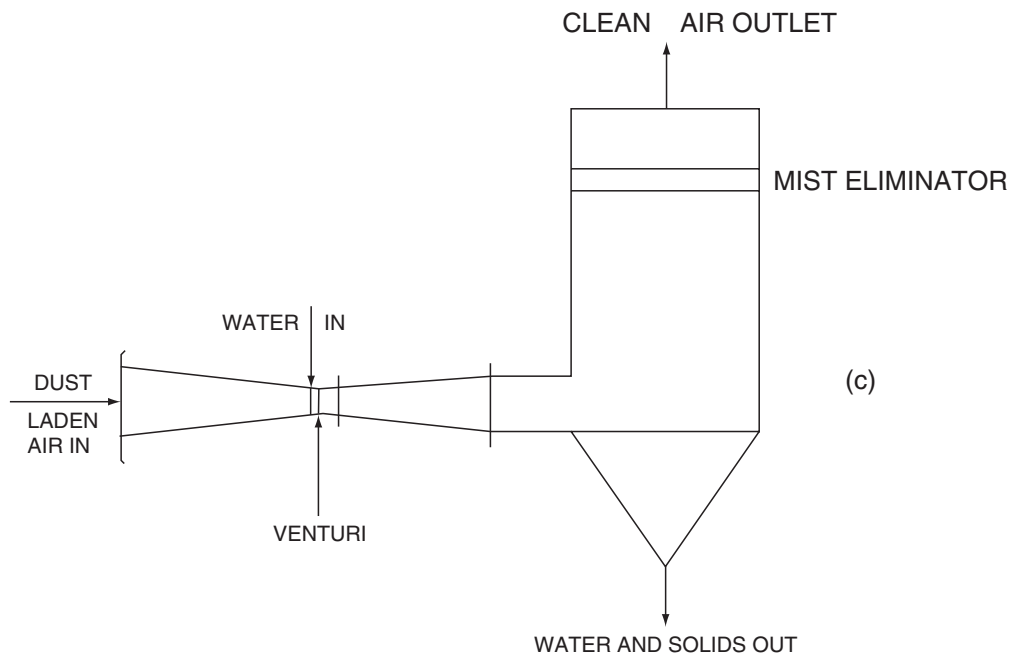
Figure 20.6.—(*continued*)

since there is an absence of ledges, moving parts, and restricted passages, making the unit easier to clean.

Wet Dynamic Scrubbers. These scrubbers are also known as *mechanical scrubbers*, as seen in Figure 20.7. They have a power-driven rotor to produce a spray that is centered in the inlet of the unit such that the blades of the rotor are coated with water. As the dust-laden stream enters, it contacts the water surfaces and the dust-water mixture is thrown outward against the walls.
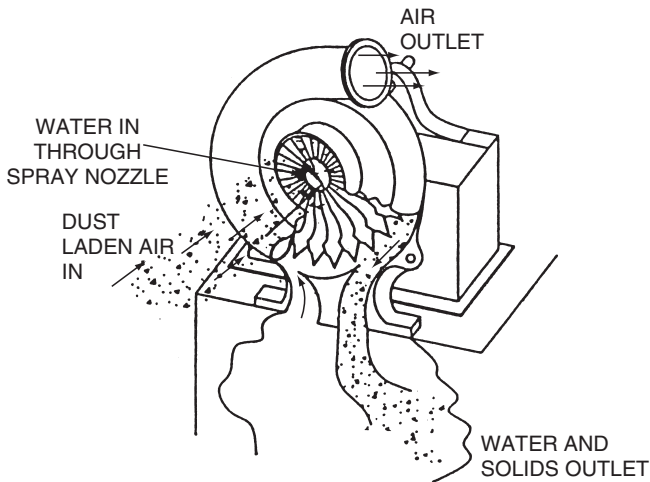
Figure 20.7. Dynamic wet precipitator. (Adapted from Scientific Dust Collectors 2002).

An entrainment separator is attached to the scrubber near the exit to prevent spray carryover. This design is limited in the dust loading because the wear on the rotor blades is high due to the solids.

Other Types of Wet Scrubbers. Plate towers, like sieve, valve, and bubble cap towers, and packed beds have been used in the past for dust collection but these are all subject to plugging.

Comments about Wet Scrubbers. Despite numerous claims "that wetting of dust particles by the scrubbing liquid plays a major role in the collection process, there is no unequivocal evidence that this is the case" (Pell and Dunson, 1999). There have been suggestions that wetting agents in the scrubbing liquid may be beneficial but this is controversial.

ELECTROSTATIC PRECIPITATORS

An electrostatic precipitator is a rectangular chamber enclosing a number of grounded vertical plates that are equally spaced to allow dust-laden air to flow between them, as shown in Figure 20.8. Electrodes at high voltage, between 40,000 and 60,000 volts, are suspended between collector plates. This high voltage causes the gas to ionize and thus dust becomes negatively charged. Some dust particles have a high charge and the forces to attract the particles to the grounded collecting plates will be high. The forces depend on the dielectric characteristics of the dust. The precipitators operate on dust streams of low concentration.

In Figure 20.8, several chambers are included in the rectangular chamber, each consisting of electrodes and collection plates. Generally, electrostatic precipitators are high-efficiency units but
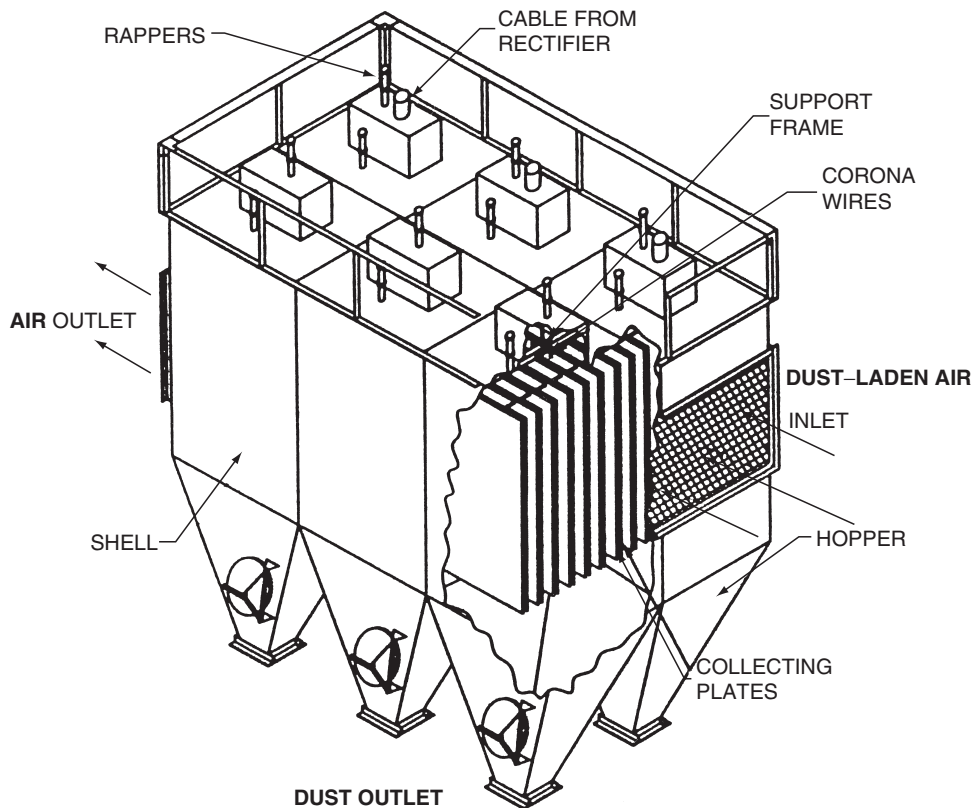
Figure 20.8. Electrostatic precipitator. (Courtesy of Scientific Dust Collectors 2002).

the efficiency depends on the velocity of the gas stream. The lower the gas velocity, the higher the efficiency, which may be 99%, but at high velocity this figure may drop to 50%. The pressure drop through an electrostatic precipitator is low, on the order of 0.5 in water or less, but in order to maintain good collection efficiency, it is necessary to have a uniform velocity distribution through the unit. There are several electrode designs, such as stretched wires and framed electrodes with points jutting out to rods or flat plates. There is also a tubular design that consists of pipes with electrodes in the center of the pipes. There are two-stage precipitators that have a high voltage zone followed by a zone of lower intermediate voltages. The dust passes through both zones and in order to maintain high efficiency, the air distribution must be even. To remove the dust from the collector, plates are wrapped with an air-powered device during which the electric power to the precipitator is shut off and the dust falls into the hopper.

The advantages of an electrostatic precipitator are:

1. Efficiency is very high, often exceeding 99%.
2. The particle size must be very small.
3. Standard precipitators operate up to temperatures of 700°F.
4. Large flow rates are possible.
5. Collectors can tolerate extremely corrosive conditions.
6. The collected dust is dry.
7. Electric power requirements are low.

The disadvantages are:

1. The initial capital investment is high.
2. Due to very high or low resistivity, particles may be difficult to collect.
3. Variable air flow can significantly affect the efficiency adversely.
4. Space requirements are greater than baghouses.
5. A cyclone may be needed upstream from a precipitator to reduce the dust load on the unit.

ARRANGEMENT OF COLLECTION EQUIPMENT

In many cases, more than one collection device may be necessary to control dust problems. For example, a cyclone collector may be followed by a baghouse, and then perhaps by an electrostatic precipitator, or the cyclone may be upstream from a wet scrubber, since a single unit may not do a thorough cleaning job.

20.2. FOAM SEPARATION AND FROTH FLOTATION

Foams are dispersions of gas in a relatively small amount of liquid. When they are still on the surface of the which they were formed, they also are called froths. Bubbles range in size from about 50 μm to several mm. The data of Table 20.1 show densities of water/air foams to range from 0.8 to 24 g/L. Some dissolved or finely divided substances may concentrate on the bubble surfaces. Beer froth, for instance, has been found to contain 73% protein and 10% water. Surface active substances attach themselves to dissolved materials and accumulate in the bubbles whose formation they facilitate and stabilize. Foam separation is most effective for removal of small contents of dissolved impurities. In the treatment of waste waters for instance, impurities may be reduced from a content measured in parts per million to one measured in parts per billion. High contents of suspended solids or liquids are removed selectively from suspension by a process of froth flotation.

FOAM FRACTIONATION

Some dissolved substances are attracted to surfactants and thus are concentrated and removed with a foam. Such operations are performed in batch or continuous stirred tanks, or in continuous towers as in the flowsketch of Figure 20.9. Compressed air may be supplied through a sparger or ambient air may be drawn into a high speed rotating gas disperser. Improved separation is achieved by staged operation, so that a packed tower is desirable. Moreover, packing assists in the formation of a stable foam since that is difficult to do in an empty tower of several feet in diameter. Larger contents of surfactant usually are needed in large towers than in laboratory units. In pilot plant work associated with the laboratory data of Table 20.1, a tower 2 ft square by 8 ft high was able to treat 120 gal/hr of feed. The laboratory unit was 1 in. dia, so that the gas rate of 154 cm^3/min of Table 20.1 corresponds to a superficial gas velocity of 1.1 ft/min.

Most of the work on foam fractionation reported in the literature is exploratory and on a laboratory scale. A selected list of about 150 topics has been prepared with literature references by Okamoto and Chou (1979). They are grouped into separation of metallic ions, anions, colloids, dyes and organic acids, proteins, and others.

Stable foams that leave the fractionator are condensed for further processing or for refluxing. Condensation may be effected by a blast of steam, by contact with a hot surface, by chemical

TABLE 20.1. Data of Foam Separation Experiments Made in a 1 in. Dia Column on a Waste Water Containing Radioactive Components and Utilizing Several Different Surfactants

| Surfactant | Surf. conc. (gm/liter) | Flow rates (cm³/min) | | | Foam density, ρ_t (gm/liter) | Average bubble diameter, $\overline{D}$ (cm) |
		Gas, V	foam, Q	Foam Foam cond., F		
Aerosol AY	6.5	154	176	0.197	1.12	0.06
Alipal CO-436	0.375	154	186	0.950	5.10	0.05
Alipal LO-529	0.4	154	174	0.415	2.40	0.06
Deriphat 170C	0.5	154	60	4.92	74	0.025
Igepon CN-42	0.12	154	72	1.6	24	0.038
Tergitol 7	2.0	154	202	0.763	3.77	0.05
Ultrawet SK	0.08	154	173	0.137	0.79	0.10

(Davis and Haas, 1972, pp. 279–297).
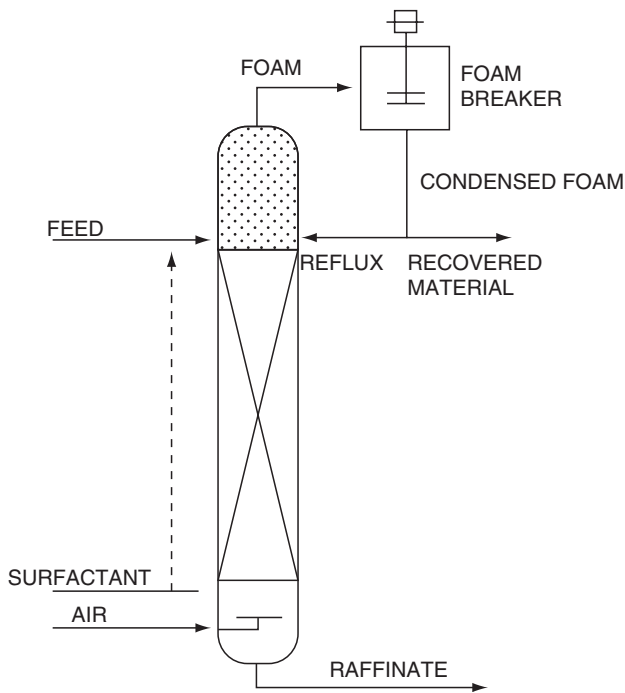
Figure 20.9. Sketch of a foam fractionating column. Surfactants or other foaming agents may be introduced with the feed or separately at a lower feed point. Packing may be employed to minimize axial mixing.

antifoaming agents, sonically or ultrasonically, or by contact with a high speed rotating disk as appears in the flowsketch, Figure 20.9.

FROTH FLOTATION

Finely divided solids or immiscible liquids can be made to adhere to gas bubbles and then can be removed from the main liquid. Affinity of a solid for an air bubble can be enhanced with surfactants which adhere to the surface of the solid and make it nonwetting. The main application of froth flotation is the separation of valuable minerals from gangue. Ores of Cu, Zn, Mo, Pb, and Ni are among those commercially preconcentrated in this way. Reagent requirements of each ore are unique and are established by test. A large amount of experience exists, however, and information is supplied freely by reagent manufacturers. Some recipes are given with descriptions of flotation processes in books on mineral dressing, for example, that of Wills (1985).

Promoters or collectors give the mineral the water-repellent coating that will adhere to an air bubble. Frothers enhance the formation and stability of the air bubbles. Other additives are used to control the pH, to prevent unwanted substances from floating, or to control formation of slimes that may interfere with selectivity.

Air is most commonly dispersed with mechanical agitation. Figure 20.10 illustrates a popular kind of flotation cell in which the gas is dispersed and the pulp is circulated with impellers. Such vessels have capacities of 300–400 cuft. Usually several are connected in series as in Figure 20.10(b). The froth is removed from each cell as it is formed, but the pulp goes through the battery in series. The froth is not highly stable and condenses readily without

(a)

(b)
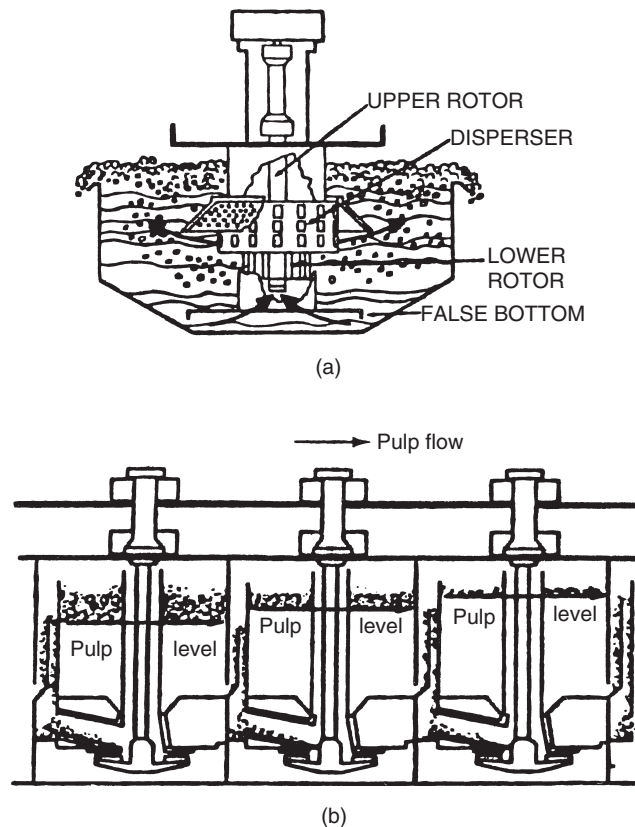
Figure 20.10. The interaction of air and pulp in a froth flotation cell and a series arrangement of such cells: (a) Sectional schematic of flotation cell. Upper portion of rotor draws air down the standpipe for thorough mixing with pulp. Lower portion of rotor draws pulp upward through rotor. Disperser breaks air into minute bubbles. Larger flotation units include false bottom to aid pulp flow. (*WEMCO Division, Envirotech Corp.*). (b) A bank of three flotation cells. The floating concentrate is withdrawn continuously from each stage but the remaining pulp flows in series through the cells.

special provisions as it overflows. Since some entrainment of gangue occurs, usually it is desirable to reprocess the first froth. The flowsketch of Figure 20.11 illustrates such reprocessing. The solids to the first stage are ground here to −65 mesh, which normally is fine enough to release the mineral, and to −200 mesh in the final stage.

Total residence time in a bank of cells may range from 4 to 14 min. A table of approximate capacities of several makes of flotation cells for a pulp with 33% solids of specific gravity = 3 is given in the *Chemical Engineers' Handbook* (1984, p. 21.49); on an average, an 8-cell bank with 4-min holdup has a capacity of about 1.5 tons solid/(hr) (cuft of cell) and a power requirement of about 0.6 HP/(cuft of cell).

The chief nonmineral application of froth flotation is to the removal or oil or grease or fibrous materials from waste waters of refineries or food processing plants. Oil droplets, for instance, attach themselves to air bubbles which rise to the surface and are skimmed off. Coagulant aids and frothers often are desirable. In one kind of system, the water is saturated with air under pressure and then is pumped into a chamber maintained under a partial vacuum. Bubbles form uniformly throughout the mass and carry out the impurities. The unit illustrated in Figure 20.12 operates at 9 in. mercury vacuum and removes both skimmed and settled
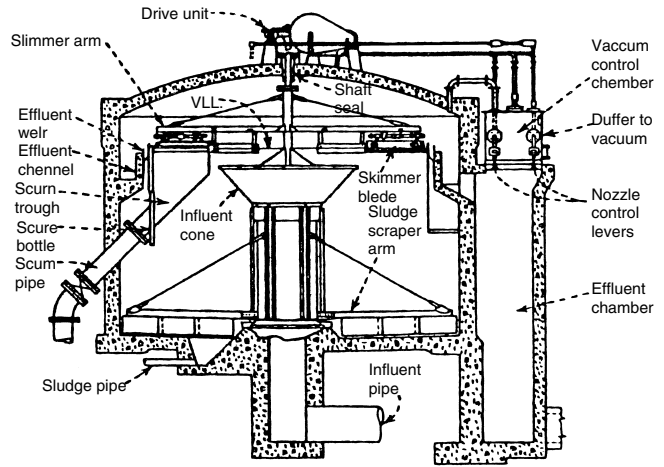
Figure 20.12. Vacuator of the ''constant-level'' type. The cylindrical tank with a dome-shaped cover is under a constant vacuum of about 9 in. of mercury. Sewage enters a central draft tube from which it is distributed by means of a flared-top section. Floating solids, buoyed up by fine air bubbles, are skimmed from the liquid surface and carried to a trough. Settled solids are removed from the bottom with a scraper mechanism. (*Courtesy of* Engineering News-Record).
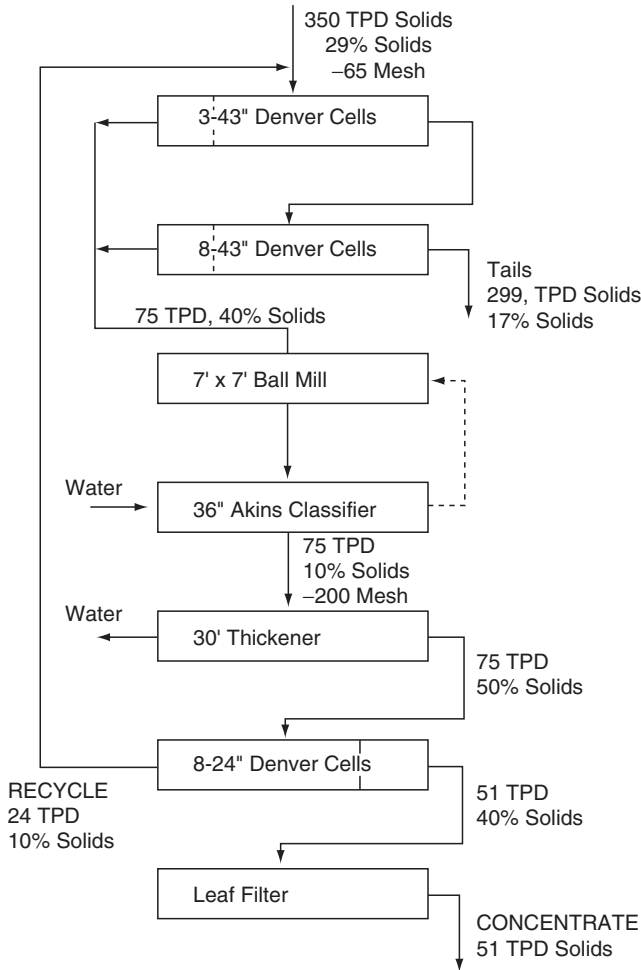
sludges. Because of the flocculation effect it is able to process waste water at an enhanced rate of about 5000 gal/(sqft)(day) instead of the usual rate of 800–1000.

In another application, particles of plastics in waste stream are chopped to diameters of 5 mm or less, passed through flotation cells containing proprietary surfactants, and removed as an air froth.

20.3. SUBLIMATION AND FREEZE DRYING

Sublimation is the transformation of a solid directly into vapor and desublimation is the reverse process of condensing the vapor as a solid. The term pseudosublimation is applied to the recovery of solid condensate from the vaporization of a liquid.

The goal of a commercial sublimation is the separation of a valuable material from nonvolatile ones at temperatures low enough to avoid thermal degradation. The preservation of cell structure (and taste) is a deciding factor in the choice of freeze drying, a special instance of sublimation, foods, pharmaceuticals, and medical products.

Only a few solids have vapor pressures near atmospheric at safe temperatures, among them CO_2, UF_6, $ZrCl_4$, and about 30 organics. Ammonium chloride sublimes at 1 atm and 350°C with decomposition into NH_3 and HCl, but these recombine into pure NH_4Cl upon cooling. Iodine has a triple point 113.5°C and 90.5 Torr; it can be sublimed out of aqueous salt solutions at atmospheric pressure because of the entraining effect of vaporized water.

Sublimation pressures down to 0.001 bar are considered feasible. At lower pressures and in some instances at higher ones, entrainer gas is used, usually air or nitrogen or steam. By such means, for instance, salicyclic acid is purified by sublimation at 150°C with an entrainer of air with sufficient CO_2 to prevent decarboxylation of the acid. At the operating temperature, the vapor pressure is only 0.0144 bar. Operating conditions corresponding to equilibrium in a salicylic acid sublimer appear in Figure 20.13. Equilibrium may be approached in equipment where contact between phases is intimate, as in fluidized beds, but in tray types percent saturation may be as low as 10%.

Figure 20.11. Flotation section of a flowsheet for concentration of 350 tons/day of a copper ore (*data of Pima Mining Co., Tucson, AZ*).
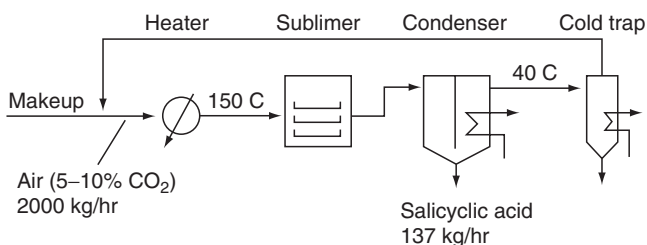
Figure 20.13. Sublimation of salicyclic acid at 1 bar. Vapor pressures are 14.4 mbar at 150°C and 0.023 mbar at 40°C. The air rate shown corresponds to equilibrium in the sublimer, but in some kinds of vessels percent saturation may be as low as 10%. The conditions are those of Mullin [Crystallisation, *Butterworths, London*, **288** (*1972*)].

Among substances that are sublimed under vacuum are anthranilic acid, hydroxyanthraquinone, naphthalene, and β-naphthol. Pyrogallol and *d*-camphor distill from the liquid state but condense as solids. Several metals are purified by sublimation, for instance, magnesium at 600°C and 0.01–0.15 Torr.

The common carrier gases are air or nitrogen or steam. Condensate from a carrier usually is finely divided, snowlike in character, which is sometimes undesirable. Substances which are sublimed in the presence of a carrier gas include anthracene, anthraquinone, benzoic acid, phthalic anhydride, and the formerly mentioned salicylic acid.

A partial list of substances amenable to sublimation is in Table 20.2.

EQUIPMENT

The process of sublimation is analogous to the drying of solids so much the same kind of equipment is usable, including tray dryers (Fig. 9.6), rotary tray dryers (Fig. 9.8), drum dryers [Fig. 9.11], pneumatic conveying dryers (Fig. 9.12), and fluidized beds (Fig. 9.13). The last of these requires the subliming material to be deposited on an inert carrier which is the fluidized material proper.

Condensers usually are large air-cooled chambers whose walls are kept clear with brushes or scrapers or even swinging weights. Scraped or brushed surface crystallizers such as Figure 16.11(a) should have some application as condensers. When a large rate of entrainer gas is employed, a subsequent collecting chamber will be needed. One of the hazards of entrainer sublimation with air is the possibility of explosions even of substances that are considered safe in their normal states.

FREEZE DRYING

Preservation of cell structure, food taste, and avoidance of thermal degradation are reasons for the removal of moisture from such materials by sublimation. The process is preceded by quick freezing which forms small crystals and thus minimum damage to cell walls, and is likely to destroy bacteria. Some of the materials that are being freeze dried commercially are listed in Table 20.2(b).

The most advanced technique of quick freezing is by pouring the material onto a freezing belt. Before drying, the material is granulated or sliced to improve heat and diffusional mass transfer. These operations are conducted in cold rooms at about −46°C.

Sublimation temperatures are in the range of −10 to −40°C and corresponding vapor pressures of water are 2.6–0.13 mbar. Cabinet tray dryers are the most commonly used type. The trays are lifted out of contact with hot surfaces so the heat transfer is entirely by radiation. Loading of 2.5 lb/sqft is usual for foodstuffs.

TABLE 20.2. Materials That May Be Purified by Sublimation or Are Being Freeze-Dried

(a) Substances Amenable to Purification by Sublimation[a]

Aluminium chloride	Naphthalene
Anthracene	β-Naphthol
Anthranilic acid	Phthalic anhydride
Anthraquinone	α-Phthalimide
Benzanthrone	Pyrogallol
Benzoic acid	Salicylic acid
Calcium	Sulphur
Camphor	Terephthalic acid
Chromium chloride	Titanium tetrachloride
Ferric chloride	Thymol
Iodine	Uranium hexafluoride
Magnesium	Zirconium tetrachloride

[a]Some others are mentioned in the text.

(b) Products That Are Being Freeze-Dried Commercially

Foodstuffs	Pharmaceuticals	Animal Tissues and Extracts
Coffee extract	Antibiotics	Arteries
Fish and seafood	Bacterial cultures	Blood
Fruits	Serums	Bones
Fruit juices	Virus solutions	Hormones
Meat		Skin
Milk		Tumors
Tea extract		
Vegetables		

Drying capacity of shelf-type freeze dryers is 0.1–1.0 kg/(hr)(m² exposed surface). Another estimate is 0.5–1.6 lb/(hr)(sqft). The ice surface has been found to recede at the rate of 1 mm/hr. Freeze drying also is carried out to a limited extent in vacuum pans, vibrating conveyors, and fluidized beds. Condensers operate as low as −70°C.

Typical lengths of cycles for food stuffs are 5–10 hr, for bacterial pellets 2–20 hr, and for biological fluids 20–50 hr. A production unit with capacity of 500 L may have 75 kW for refrigeration and 50 kW for heating. Conditions for the preparation of freeze dried coffee are preparation of an extract with 20–25% solids, freezing at −25–−43°C, sublimation at approx. 200 Torr to a final final moisture content of 1–3%, total batch processing time of 6–8 hrs.

20.4. SEPARATIONS BY THERMAL DIFFUSION

Separation of mixtures based on differences in thermal diffusivity at present are feasible only for analytical purposes or for production on a very small scale of substances not otherwise recovered easily. Nevertheless, the topic is of some interest to the process engineer as a technique of last resort.

In a vessel with a temperature gradient between a hot and cold surface, a corresponding concentration gradient of a fluid likewise can develop. The substance with the smaller molecular volume usually concentrates in the high temperature region, but other factors including that of molecular shape also affect the relative migrations of components of mixtures. Thus, the sequence of separation of hydrocarbons from hot to cold regions generally is: light normal paraffins, heavy normal paraffins, naphthenes and mono-

cyclic aromatics, and bicyclic aromatics. Isotopes with small differences in molecular weights were the first substances separated by thermal diffusion, but isomers which have identical molecular weights also are being separated.

The basic construction of a horizontal thermal diffusion cell is sketched in Figure 20.14(a). When gases are to be separated, the distance between the plates can be several mm; for liquids it is a fraction of a mm. The separation effects of thermal diffusion and convection currents are superimposed in the equipment of Figure 20.14(b), which is called a thermogravitational or Clusius–Dickel column after the inventors in 1938. A commercially available

column used for analytical purposes is in Figure 20.14(c). Several such columns in series are needed for a high degree of separation.

Clusius and Dickel used a column 36 m long to make 99+% pure isotopes of chlorine in HCl. The cascade of Figure 20.15 has a total length of 14 m; most of the annular diameter is 25.4 mm, and the annular widths range from 0.18 to 0.3 mm. The cascade is used to recover the heavy isotope of sulfur in carbon disulfide; a production rate of a 90% concentrate of the heavy isotope of 0.3 g/day was achieved.

Separation of the hydrocarbon isomers of Table 20.3(a) was accomplished in 48 hr in the column of Figure 20.14(c) with 50°C
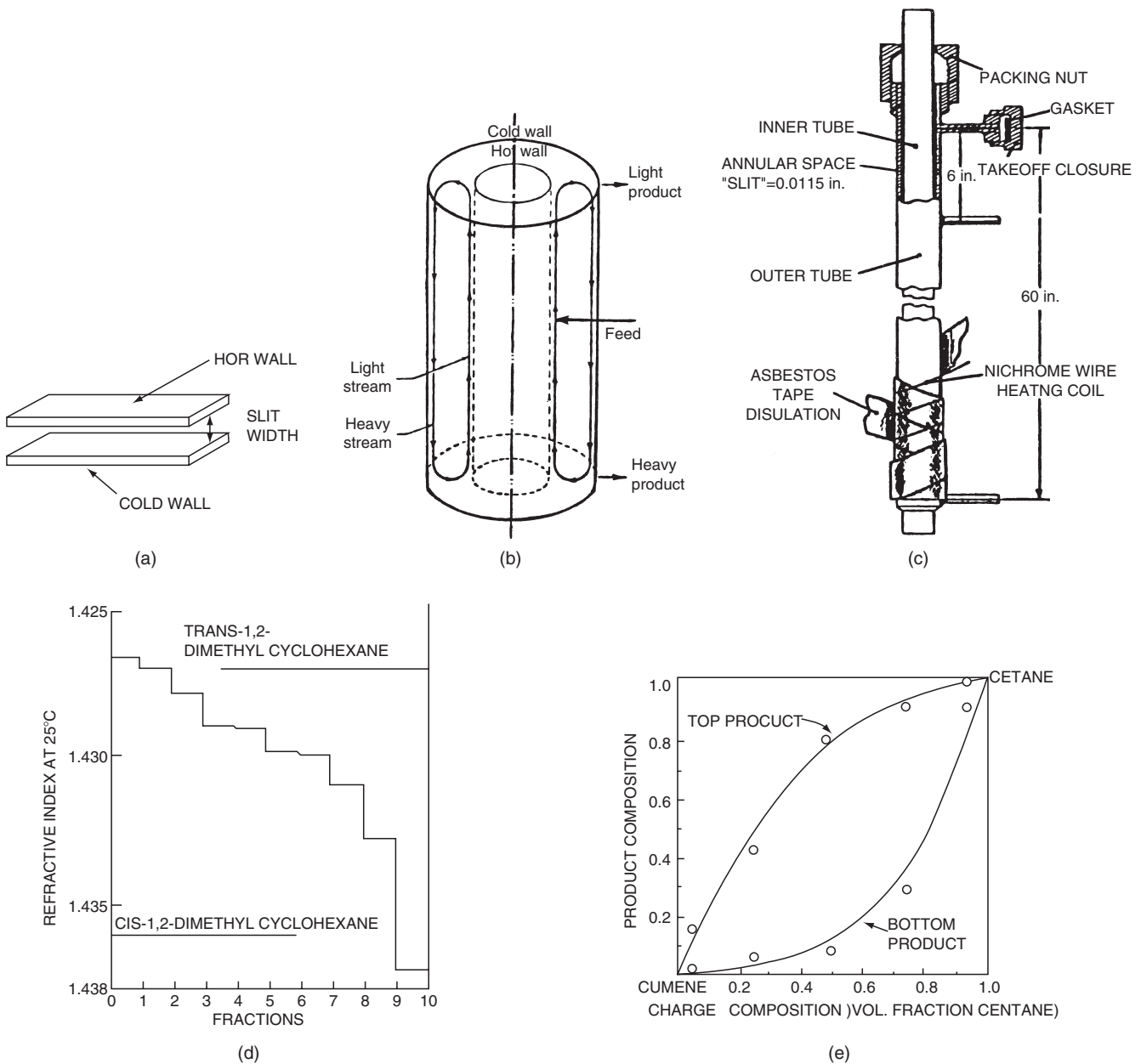
Figure 20.14. Construction and performance of thermal diffusion columns. (a) Basic construction of a thermal diffusion cell. (b) Action in a thermogravitational column. (c) A commercial column with 10 takeoff points at 6 in. intervals; the mean dia of the annulus is 16 mm, width 0.3 mm, volume 22.5 mL (*Jones and Brown, 1960*). (d) Concentration gradients in the separation of cis and trans isomers of 1,2-dimethylcyclohexane (*Jones and Brown, 1960*). (e) Terminal compositions as a function of charge composition of mixtures of cetane and cumene; time 48 hr, 50°C hot wall, 29°C cold wall (*Jones and Brown, 1960*).
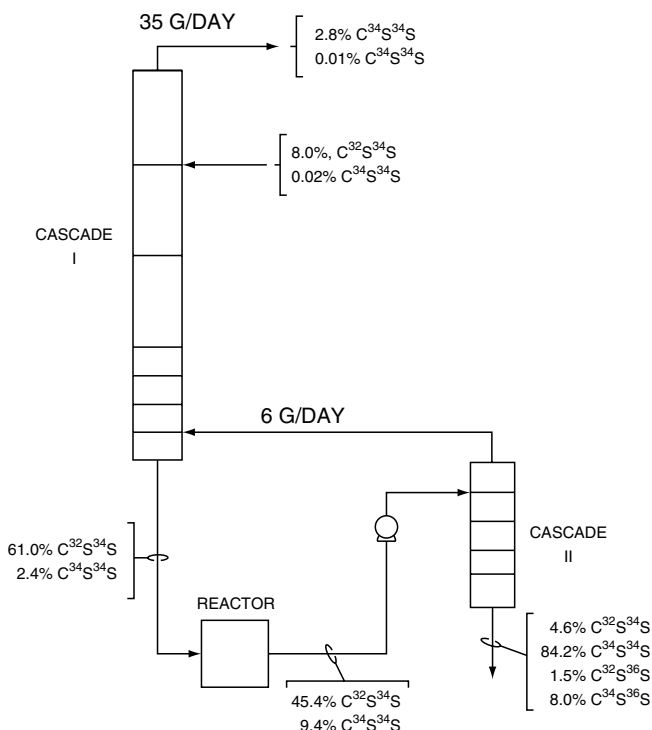
Figure 20.15. The liquid thermal diffusion system for the recovery of heavy sulfur isotope in carbon disulfide. The conditions prevailing at the time after 90% ^{34}S is reached. Each rectangle in the cascades represents a column, each height being proportional to the length of the column. The two cascades have a combined height of 14 m, annular dia 25.4 mm, and annular width 0.18–0.3 mm. Production rate of 90% concentrate of ^{34}S was 0.3 g/day. (Rutherford, 1978).

hot wall and 20°C cold wall. The concentration gradient that develops in such a column is shown in Figure 20.14(d). The equilibrium terminal compositions depend on the overall composition, as indicated in Figure 20.14(e). Other kinds of behaviors also occur.

Thus mixtures of benzene and cyclohexane are not separated, nor can mixtures of benzene and octadecane when the latter is in excess.

Examples of separations of isotopes are in Table 20.3(b). The concentration of U-235 listed there was accomplished in a cascade of 2100 columns, each with an effective height of 14.6 m, inner tube 5 cm dia, gap 0.25 mm, hot surface 87–143°C, and cold surface 63°C, just above the condensation temperature at the operating pressure of 6.7 MPa. Although the process was a technical success, it was abandoned in favor of separation by gaseous diffusion which had only 0.7% of the energy consumption.

For separation of hydrocarbons, thermal requirements are estimated to range from 70,000 to 350,000 Btu/lb, compared with heats of vaporization of 150 Btu/lb.

Although thermal diffusion equipment is simple in construction and operation, the thermal requirements are so high that this method of separation is useful only for laboratory investigations or for recovery of isotopes on a small scale, which is being done currently.

20.5. ELECTROCHEMICAL SYNTHESES

Electrolysis plays a role in the manufacture of some key inorganic chemicals on an industrial scale, but rather a minor one in the manufacture of organic chemicals. Chlorine, alkalis, metals, hydrogen, oxygen, and strong oxidizing agents such as $KMnO_4$, F_2, and Cu_2O are made this way. Electroorganic processes of commercial or potentially commercial scale are listed in Table 20.4, which implies that much research is being done in pilot plants and may pay off in the near future. In the United States, the four large tonnage applications are to the manufacture of adiponitrile, the Nalco process for lead tetraethyl, which is being phased out from the gasoline industry, the Miles process for dialdehyde starch, which is on standby until the demand picks up, and the 3M electro-fluorination process for a variety of products.

Pros and cons of electrochemical processes are not always clear cut. In a few cases, they have lower energy requirements than conventional chemical methods but not usually according to the survey of Table 20.5. The Monsanto process for adiponitrile by electrochemical reduction of acetonitrile is an outstanding example; moreover, comparison of the performances of the original and improved cells [sketched on Figures 20.16(e) and (f)] suggests

TABLE 20.3. Examples of Separations by Thermal Diffusion

(a) Hydrocarbon Isomers

Components	Vol. %	Mol. wt.	Density	Final Composition, Vol. %		Separation, %
				Top	Bottom	
n-Heptane	50	100	0.6837	95	10	75.4
Triptane	50	100	0.6900	5	90	
Isoöctane	50	114	0.6919	58	40	11.4
n-Octane	50	114	0.7029	42	60	
2- Methylnaphthalene	50	142	0.9905	55.5	42.5	13.1
1-Methylnaphthalene	50	142	1.0163	44.5	57.5	
trans-1,2- Dimethylcyclohexane	40	112	0.7756	100	0	100
cis-1,2- Dimethylcyclohexane	60	112	0.7963	0	100	
p-Xylene	50	106	0.8609	92	0	92
o- Xylene[a]	50	106	0.8799	8	100	
m-Xylene	50	106	0.8639	100	19	80
o- Xylene[a]	50	106	0.8799	0	81	
p-Xylene	50	106	0.8609	50	50	0
m-Xylene	50	106	0.8639	50	50	

(Jones and Brown, 1960).
[a] *o*-Xylene contains paraffinic impurity.

TABLE 20.3.—(continued**)**

(b) Isotopes

Working fluid	Isotope separated	mol % product	Phase	Single Column (S) or Cascade (C)	Investigator	Year
HCl	^{35}Cl	99.6	Gas	S	Clusius and Dickel	1939
	^{37}Cl	99.4				
Kr	^{34}Kr	98.2	Gas	S	Clusius and Dickel	1941
	^{86}Kr	99.5				
O_2	^{17}O	0.5	Gas	C	Clusius and Dickel	1944
	^{18}O	99.5				
UF_6	^{235}U	0.86	Liquid	C	Manhattan Dist.	1945
N_2	^{15}N	99.8	Gas	S	Clusius & Dickel	1950
Xe	^{134}Xe	1	Gas	C	Clusius et al.	1956
	^{136}Xe	99				
He	^{3}He	10	Gas	C	Bowring and Davies	1958
A	^{36}A	99.8	Gas	C	ORNL[†]	1961
	^{38}A	23.2				
Ne	^{20}Ne	99.99	Gas	C	ORNL	1961
	^{22}Ne	99.99				
Kr	^{78}Kr	10	Gas	C	ORNL	1961
	^{86}Kr	96.1				
He[§]	^{3}He	99	Gas	C	Mound Lab.[‡]	1962
Ne	^{21}Ne	33.9	Gas	C	ORNL	1963
CH_4	^{13}C	90	Gas	C	Mound Lab.	1963
Xe	^{124}Xe	4.4	Gas	C	ORNL	1964

[†] Oak Ridge National Laboratory, U.S. AEC, Oak Ridge, Tennessee.
[‡] Mound Laboratory, U.S. AEC, Miamisburg, Ohio.
[§] Feed not of normal abundance, contained 1 percent ^{3}He from nuclear reaction.
(Benedict et al., 1981).

the often great leeway in cell design. Small scale electrode processes frequently are handicapped because of the expense of developing efficient components of cells such as electrodes, diaphragms, membranes, and electrolytes which usually can be justified only for large scale operation.

In comparison with chemical oxidations and reductions, however, electrode reactions are nonpolluting and nonhazardous because of low pressure and usually low temperature. Although electricity usually is more expensive than thermal energy, it is clean and easy to use. Electrolytic processes will become more attractive when inexpensive sources of electricity become developed.

ELECTROCHEMICAL REACTIONS

An equilibrium electrical potential is associated with a Gibbs energy of formation by the equation

$$E^0 = -\Delta G^0/23.06n,$$

where n is the number of gram equivalents involved in the stoichiometric equation of the reaction, ΔG^0 is in kcal/g mol, and E^0 is the potential developed by the reaction in volts. Thus, for the reaction $H_2O \rightleftarrows H_2 + \frac{1}{2}O_2$ at 25°C,

$$E^0 = 54.63/(2)(23.06) = 1.18 \text{ V}$$

and for $HCl \rightleftarrows \frac{1}{2}H_2 + \frac{1}{2}Cl_2$ at 25°C,

$$E^0 = 22.78/23.06 = 0.99 \text{ V}.$$

Practically, reactions are not conducted at equilibrium so that amounts greater than equilibrium potentials are needed to drive a reaction. Major contributions to inefficiency are friction in the electrolyte and other elements of a cell and particularly the overvoltages at the electrodes. The latter are due to adsorption or buildup of electrolysis products such as hydrogen at the electrode surfaces. Figure 20.17(a) shows magnitudes of hydrogen overvoltages at several metals and several currents. The several contributions to voltage drops in a cell are identified in Figures 20.17(b) and (c), whereas Figure 20.17(d) indicates schematically the potential gradient in a cell comprised of five pairs of electrodes in series.

Electrochemical cells are used to supply electrical energy to chemical reactions, or for the reverse process of generating electrical energy from chemical reactions. The first of these applications is of current economic importance, and the other has significant promise for the near future.

FUEL CELLS

A few chemical reactions can be conducted and controlled readily in cells for the production of significant amounts of electrical energy at high efficiency, notably the oxidations of hydrogen or carbon monoxide. Some data of such processes are in Figure 20.18. The basic processes that occur in hydrogen/air cells are in Figure 20.18(a). Equilibrium voltage of such a cell is in excess of 1.0 V at moderate temperatures, but under practical conditions this drops off rapidly and efficiency may become less than 40%, as Figure 20.18(b) shows. Theoretical cell potentials for several reactions of fuel cell interest are in Figure 20.18(c), in theory at least, the oxidations of hydrogen and carbon monoxide are competitive. High temperatures may be adopted to speed up the electrode processes, but they have adverse effects on the equilibria of these particular reactions. Figure 20.18(d) shows the characteristics of major electrochemical fuel systems that have been emphasized thus far. Most of the development effort has been for use in artificial satellites where cost has not been a primary consideration, but

TABLE 20.4. Electroorganic Synthesis Processes Now Applied Commercially or Past the Pilot Plant Stage

Product[a]	Raw Material[a]	Company (country)	Scale	Type of Process
Commercialized				
Adiponitrile	Acrylonitrile	Monsanto (US)	10^8 kg/yr	Reductive coupling
		Monsanto (UK)	10^8 kg/yr	
		Asahi (Japan)	2×10^7 kg/yr	
p-Aminophenol	Nitrobenzene	(Japan)	Not available	Reductive rearrangement
		Holliday (UK)	Not available	
Anthraquinone	Anthracene	Holliday (UK)	Not available	Indirect oxidation
2,5-Dimethoxydihydrofuran	Furan	(Japan)	Not available	Oxidative addition
		BASF (West Germany)	Not available	
Fluorinated Organics	Hydrocarbons, aliphatic carboxylic acids, sulfonic acids, amines, etc.	Dia Nippon (Japan) 3M (US)[b] (India)	Not available Not available	Anodic substitution
Gluconic Acid	Glucose		3×10^5 kg/yr	Oxidation of functional group
Glyoxylic Acid	Oxalic acid	(Japan)	Not available	Reduction of functional group
Hexahydrocarbazole	Tetrahydrocarbazole	BASF (West Germany)	Not available	Reduction
Piperidine	Pyridine	Robinson Bros. (UK)	1.2×10^5 kg/yr	Reduction
Succinic Acid	Maleic acid	(India)	6×10^4 kg/yr	Reduction
Hexadecanedioic Acid	Monomethylazelate	Soda Aromatic Co. (Japan)	Not available	Crum Brown-Walker[c]
Tetraethyl Lead	Ethylmagnesium halide	Nalco (US)	Not available	Anodic
Propylene Oxide	Propylene	BASF (West Germany) others in UK and West Germany	Past pilot-plant Past pilot-plant	Paired synthesis
4,4'-bis-Pyridinium Salts	Pyridinium salts	(Japan)	Past pilot-plant	Paired synthesis
Salicylaldehyde	Salicylic acid	(India)	Past pilot- plant	Reduction of functional group
Sebacid Acid Diesters	Adipic acid half esters	BASF (West Germany) (Japan) (USSR)	Past pilot-plant Past pilot-plant Commercial?	Crum Brown-Walker[c]
Benzaldehyde	Toluene	(India)	Past pilot-plant	Indirect oxidation [Mn(III)]
Dihydrophthalic Acid	Phthalic acid	BASF (West Germany)	Commercial?	Reduction
Hydroquinone or Quinone	Benzene	Several	Past pilot-plant	Paired synthesis or anodic oxidation + chemical reduction
Maltol	Furfuryl alcohol	Otsuka (Japan)	Past pilot-plant	Oxidation
Pinacol	Acetone	(Japan) BASF (West Germany)	Past pilot-plant	Reductive coupling

[a]Formulas are given in Appendix A.
[b]Added by author.
[c]Oxidative coupling.
(Baizer, 1980).

TABLE 20.5. Comparative Energy Requirements of Electrochemical and Chemical Processes

		kcal/kg		
Chemical		Electrochemical[a]	Chemical	
Adiponitrile	b	43,177 (10,520)	65,808	c
Aniline				
Nitrobenzene route	b	36,172	13,919	
Phenol route	b	–	16,736	c
Sorbitol		9,649	958	
Terephthalic Acid		17,382	700	
Phenol	b	35,592	12,251	c
Methyl Ethyl Ketone		6,187	6,690	
			3,233	c
Melamine	b	30,159	15,472	
Hydroquinone	b	52,739	30,814	
Dichloroethane				
HCl route	b	17,773	6,131	
Cl$_2$ route	b	–	14,819	c

[a]Electrochemical energy adjusted for generating plant efficiency.
[b]Improved Monsanto process.
[c]Energy charged is for hydrocarbon raw materials (different compounds); other compounds begin with the same raw materials.
[d]Chemical route energy given by Rudd et al.; others estimated by Beck et al.
(Beck et al., 1979).
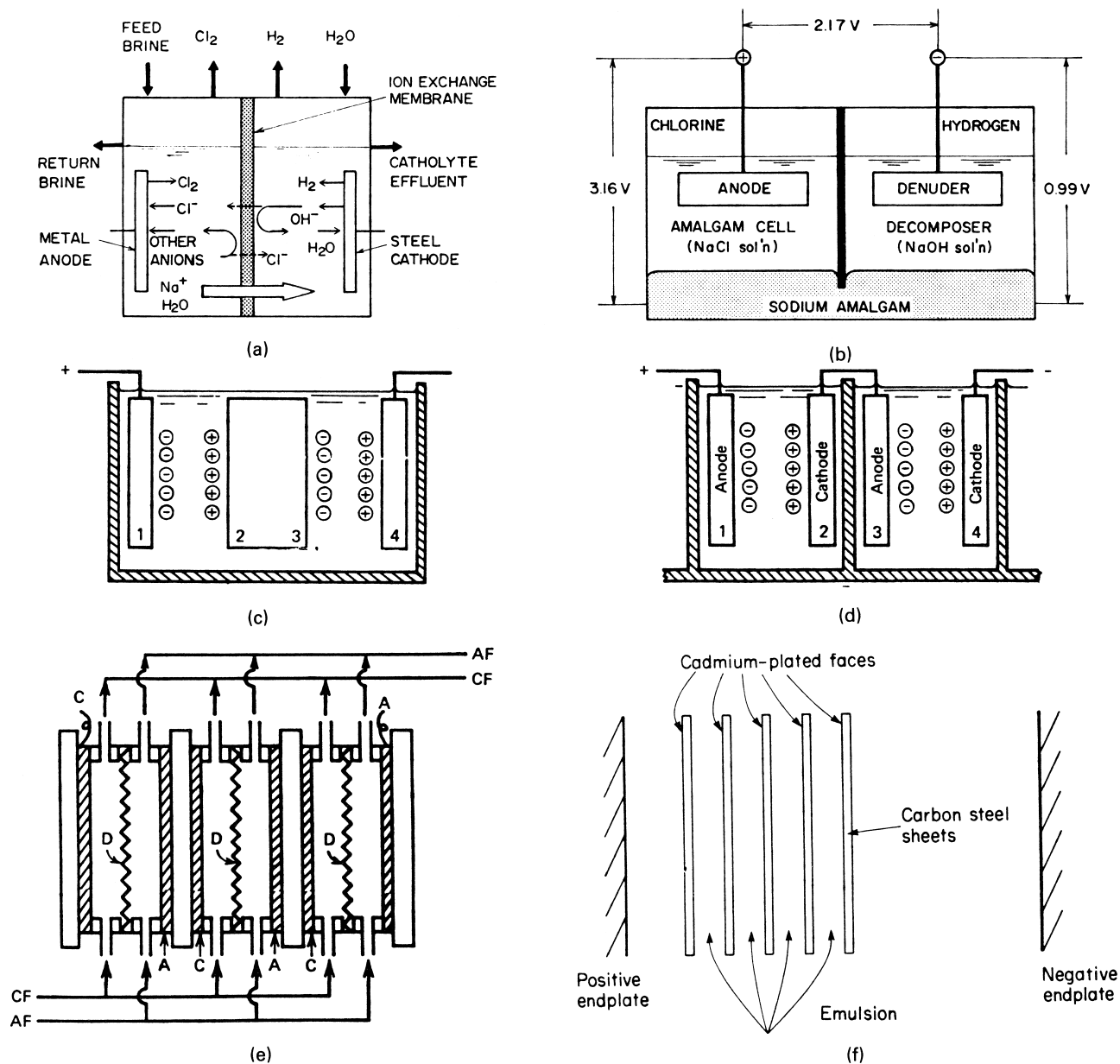
Figure 20.16. Basic designs of electrolytic cells. (a) Basic type of two-compartment cell used when mixing of anolyte and catholyte is to be minimized; the partition may be a porous diaphragm or an ion exchange membrane that allows only selected ions to pass. (b) Mercury cell for brine electrolysis. The released Na dissolves in the Hg and is withdrawn to another zone where it forms salt-free NaOH with water. (c) Monopolar electrical connections; each cell is connected separately to the power supply so they are in parallel at low voltage. (d) Bipolar electrical connections; 50 or more cells may be series and may require supply at several hundred volts. (e) Bipolar-connected cells for the Monsanto adiponitrile process. Spacings between electrodes and membrane are 0.8–3.2 mm. (f) New type of cell for the Monsanto adiponitrile process, without partitions; the stack consists of 50–200 steel plates with 0.0–0.2 mm coating of Cd. Electrolyte velocity of 1–2 m/sec sweeps out generated O_2.

spinoff to industrial applications has some potential for the near future.

CELLS FOR SYNTHESIS OF CHEMICALS

Cells in which desired chemical reactions can be conducted and controlled are assemblages of pairs of anodes and cathodes between which the necessary potential difference is impressed. The regions near the electrodes may be separated by porous diaphragms to minimize convective mixing of the products formed at the individual electrodes. In recent years, semipermeable or ion-exchange membranes have been employed as diaphragms. In Figure 20.16a, the membrane allows only Na^+ ions to pass so that the caustic that is made in the cell is essentially free of NaCl. In the mercury cell of Figure 20.16(b), no partition is necessary because the released Na dissolves in the mercury; the amalgam is

Metal	Current Density (amp cm^{-2})		
	0	0.01	0.10
Platinized Platinum	0.005	0.035	0.055
Gold	0.02	0.56	0.77
Iron	0.08	0.56	0.82
Smooth Platinum	0.09	-- --	0.39
Silver	0.15	0.76	0.90
Nickel	0.21	0.65	0.89
Copper	0.23	0.58	0.82
Lead	0.64	1.09	1.20
Zinc	0.70	0.75	1.06
Mercury	0.78	1.10	1.18

(a)

	Amalgam cell at 100 A/dm^2	Diaphragm cell at 25 A/dm^2
Decomposition voltage	3.16 V	2.17 V
Anode overvoltage, DSA	0.20 V	0.03 V
Cathode overvoltage	0.05 V	0.30 V
Solution IR, including bubble effects	0.44 V	0.35 V
Diaphragm		0.60 V
Metal hardware	0.05 V	0.20 V
(Sum) Terminal voltage	3.91 V	3.65 V

(b)
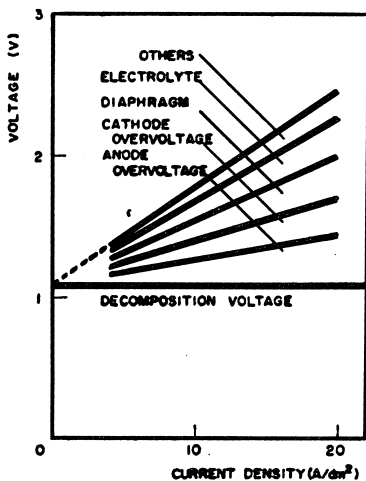
(c)
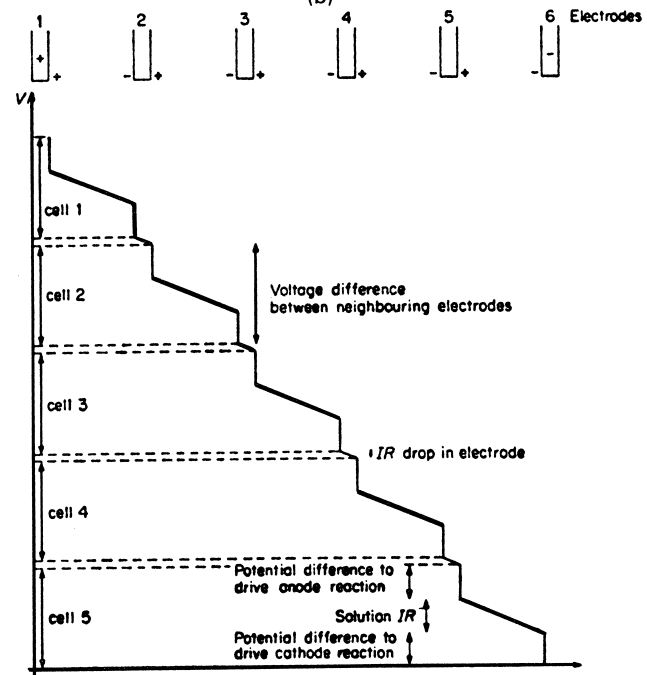
(d)

Figure 20.17. Overvoltage and distribution of voltage drops in cells (*Hine, 1985*). (a) Overvoltage of hydrogen on some metals. (b) Voltage distribution in two kinds of cells for electrolysis of brine. (c) Variation of voltage distribution with current density in the electrolysis of HCl. (d) Schematic of voltage profile in a bipolar cell with five pairs of electrodes.

reacted with water in an electrically neutral zone of the cell to make salt-free caustic. Because of pollution by escaped mercury, such cells have been largely phased out for production of salt-free caustic.

The same process sometimes can be performed efficiently in cells either with or without diaphragms. Figures 20.16(e) and (f) are for making adiponitrile by reduction of acetonitrile. In the newer design, Figure 20.16(f), the flow rate of the electrolyte is high enough to sweep out the generated oxygen quickly enough to prevent reverse oxidation of the product.

Either parallel, called monopolar, or series, called bipolar, electrical connections can be made to the pairs of electrodes in a complete cell. The monopolar types have individual connections to each electrode and thus require only individual pair potential to be applied to the cell assembly. The bipolar mode has electrical connections only to the terminal electrodes. One design such as

Figure 20.16f has 48 pairs of electrodes in series and requires 600 V. The equipment of Figure 20.19(a) also has bipolar connections. The voltage profile in such equipment is indicated schematically in Figure 20.16(c) and Figure 20.17(d). Bipolar equipment is favored because of its compactness and, of course, the simplicity of the electrical connections. No adverse comments appear to be made about the high voltages needed.

Although the basic cell design shown schematically in Figures 20.16(a) and 20.19(d) is effective for many applications when dimensions and materials of construction are properly chosen, many special designs have been developed and used, of which only a few can be described here. For the cracking of heavy hydrocarbons to olefins and acetylenes, for instance, the main electrodes may be immersed in a slurry of finely divided coke; the current discharges from particle to particle generate the unsaturates. Only 100–200 V appears to be sufficient.

(a)

(b)
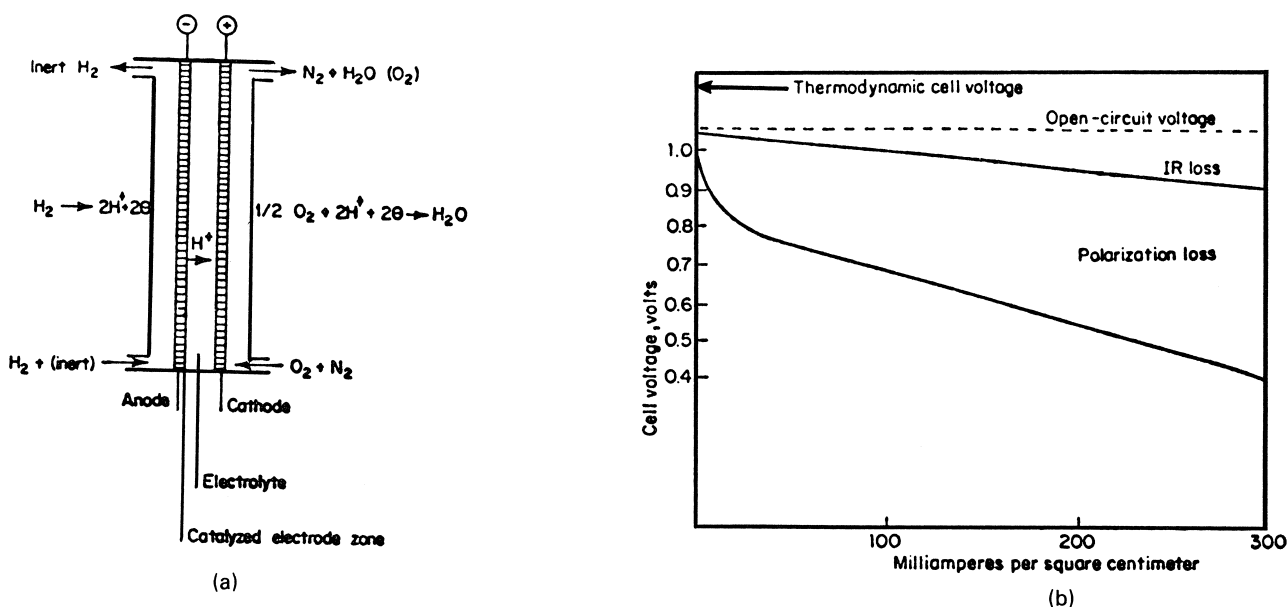
Reaction	Cell potential, volts					
	25°C	100°C	250°C	500°C	750°C	1000°C
$C + O_2 \rightarrow CO_2$	1.02	1.02	1.02	1.02	1.02	1.01
$2C + O_2 \rightarrow 2CO$	0.71	0.75	0.82	0.93	1.04	1.15
$2CO + O_2 \rightarrow 2CO_2$	1.33	1.30	1.23	1.11	1.00	0.88
$2H_2 + O_2 \rightarrow 2H_2O$	1.23	1.18	1.12	1.05	0.97	0.90

(c)

Electrolyte	Current transport	Operating temperature, °C	Electrode catalyst	Reactants		State of development
				Fuel	Oxidant	
Aqueous potassium hydroxide (KOH)	OH⁻	20–90	Nickel, silver, platinum metals	Hydrogen, hydrazine	Oxygen, scrubbed air, H₂O₂	Multikilowatt systems developed by several manufacturers.
Aqueous sulfuric acid (H₂SO₄)	H⁺	20–90	Tungsten carbide, platinum metals, carbon	Impure hydrogen*	Air	Long life demonstrated in laboratory cells.
Concentrated phosphoric acid (H₃PO₄)	H⁺	70–175	Platinum metals	Impure hydrogen*	Air	Multikilowatt system developed and larger systems in development. Long life has been demonstrated.
Fused alkali carbonate	CO₃⁻⁻	600–800	Nickel, silver	Impure hydrogen*	Air	Several months' life for small cells demonstrated.
Stabilized zirconium oxide	O⁻⁻	700–1000	Base metal oxides	Impure hydrogen*	Air	10,000 hours' life demonstrated in single cells. Multikilowatt systems in design.

(d)

Figure 20.18. Data of electrochemical fuel cells. (a) Processes in a fuel cell based on the reaction between hydrogen and oxygen. (b) Voltage-current characteristic of a hydrogen-air fuel cell operating at 125°C with phosphoric acid electrolyte [*Adlhart, in* Energy Technology Handbook (*Considine, Ed.*), *1977, p. 4.61.* (c) Theoretical voltages of fuel cell reactions over a range of temperatures. (d) Major electrochemical systems for fuel cells (*Adlhart, in Considine,* loc. cit., *1977, p. 4.62*).

The most widely used brine electrolytic cells are the Hooker and Diamond Shamrock which are both monopolar, but bipolar designs like that of Figure 20.19(a) also are popular. That figure does not indicate the presence of a diaphragm but one must be used.

Rotating electrodes characterize the BASF cell of Figure 20.19(b), which is used for making adiponitrile. The cell described in the literature has 100 pairs of electrodes 40 cm dia spaced 0.2 mm

apart. The rapid flow rate eliminates the need for diaphragms by sweeping out the oxygen as it is formed.

Lead alkyls are made by the action of Grignard reagents on lead anodes in the equipment of Figure 20.19(c). Lead pellets serve as the anode and are replenished as they are consumed. Several tubes 5 cm dia are housed in a single shell for temperature control and as required for capacity.

(a)

(b)

(c)

(d)
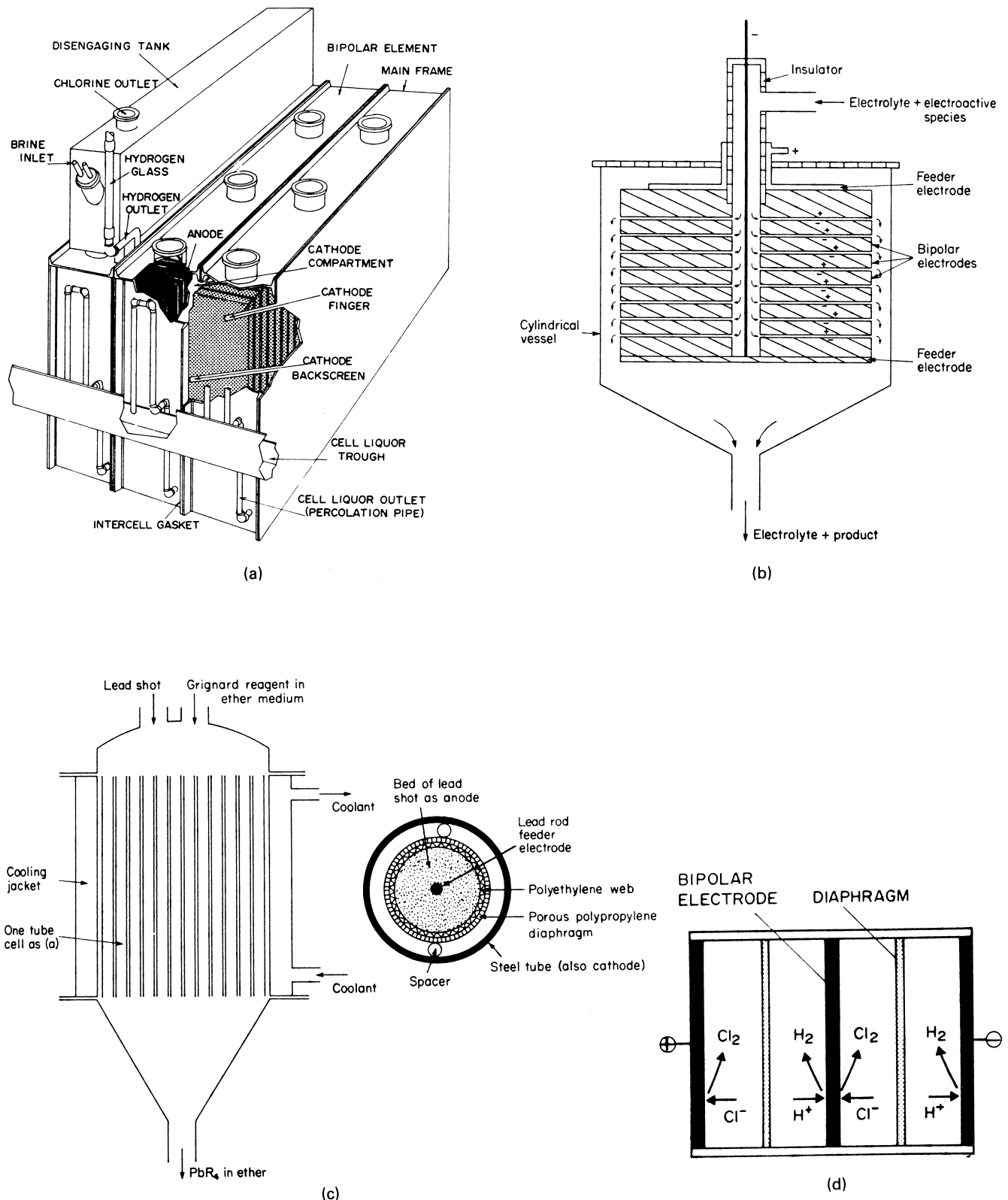
Figure 20.19. Some special designs of electrolytic cells. (a) Glanor bipolar diaphragm-type cell assembly for chlor-alkali production (*PPG Industries*). (b) BASF capillary gap cell has 100 pairs of graphite plates with gaps of 0.2 mm used for adiponitrile synthesis; anodes are electroplated with lead dioxide [*Beck and Guthke*, Chem. Ing. Tech. **41**, 943(*1969*)]. (c) Principle of the shell-and-tube reactor for electrolytic oxidation of Grignard reagents to lead alkyls. Lead shot serves as consumable anode which is replenished continuously. Individual tubes are 5 cm dia by 75 cm long [*Danly*, Encycl. Chem. Technol. **8**, *702* (*1979*)]. (d) Simple cells of the type used for electrolysis of HCl and water; voltage breakdown is shown in Figure 20.16(c).

The simplest kind of cell construction, shown in Figure 20.19(d), suffices for the production of hydrogen by electrolysis of water and for the recovery of chlorine from waste HCl. The term filter-press cell is applied to this kind of equipment because of the layered construction. These two electrolyses are economically feasible under some conditions. Some details are given by Hine (1985).

It has been mentioned already that only a few inorganic and organic electrochemical processes have made it to commercial scale, but the potential may be there and should not be ignored. Recent surveys of the field and of the literature have been made by Hine (1985), Fletcher (1982), and Roberts et al. (1982).

20.6. FERMENTATION PROCESSING

Industrial fermentation is any process involving microorganisms that results in useful products. Among the useful microorganisms are molds, yeasts, algae, and bacteria. They are distinguished from plants and animals by being made of cells of only one kind. Although some kinds are grown as food, yeast or algae, for instance, the main interest here is in chemical manufacture with their assistance. This they accomplish by creating enzymes which catalyze specific reactions. In many respects biochemical processing is like ordinary chemical processing. The recovery and purification of biochemical products, however, often is a more demanding task and offers opportunities for the exercise of ingenuity and the application of techniques that are exotic from the point of view of conventional processing. A distinction also is drawn between processes that involve whole cells and those that utilize their metabolic products, enzymes, as catalysts for further processing. A brief glossary of biochemical terms is in Table 20.6.

Major characteristics of microbial processes are:

a. The reaction medium is aqueous.
b. The products are made in low concentration, rarely more than 5–10% for chemicals and much less for enzyme recovery.
c. Reaction temperatures with microorganisms or isolated enzymes are low, usually in the range of 10–60°C, but the optimum spread in individual cases may be 5°C or less.
d. With only a few exceptions, such as potable ethanol or glucose isomerate, the scale of commercial processes is modest, and for enzymes it is measured only in kilograms per day.

TABLE 20.6. A Biochemical Glossary

Microorganisms (microbes) are living cells, single or in multiples of the same kind, including bacteria, yeasts, fungi, molds, algae and protozoa. Their metabolic products may be of simple or complex structure.

Fermentation is a metabolic process whereby microorganisms grow in the presence of nutrients and oxygen, sometimes in the absence of oxygen. The terms used are aerobic (in the presence of oxygen) and anaerobic (in the absence of oxygen)

Substrate consists of the nutrients on which a microorganism subsists or the chemicals upon which an enzyme acts

Enzymes are made by living cells, and are proteins with molecular weights ranging from about 15,000 to 1,000,000.
They are able to catalyze specific reactions

Enzymes, immobilized, are attached to a solid support by adsorption or chemical binding or mechanical entrapment in the pores of a gel structure, yet retain most of their catalytic powers

-ase is a suffix identifying that the substance is an enzyme. The main part of the name describes the nature of the chemical reaction that can be catalyzed, as in cellulase, an enzyme that catalyzes the decomposition of cellulose

e. Batch processing is used preponderantly, but so many conditions must be regulated carefully that computer control is common.

Because of the small scale of enzyme production, laboratory types of separation and purification operations are often feasible, including: dialysis to remove salts and some low molecular weight substances, ion exchange to remove heavy metals, ultrafiltration with pore sizes under $0.5\,\mu m$ and pressures of 1–10 atm to remove substances with molecular weights in the range of 15,000–1 million, reverse osmosis to remove water and to concentrate low molecular weight products, and gel permeation chromatography to fractionate a range of high molecular weight substances. Conventional processes of filtration and centrifugation, of drying by freezing or vacuum or spraying, and colloid milling also are used for processing enzymes.

PROCESSING

The three main kinds of fermentation processes are:

a. Growth of microorganisms such as bacteria, fungi, yeasts and others as end products.
b. Recovery of enzymes from cell metabolism, either intracellularly or as secretions, mostly the latter.
c. Production of relatively low molecular weight substances by enzyme catalysis, either with isolated enzymes or with the whole cell.

Some industrial products are listed in Table 20.7. Chemical and fermentation syntheses sometimes are competitive, for instance, of ethanol, acetone, and butanol.

Enzymes are proteins with molecular weights in the range of 15,000–1,000,000 or so. In 1968, for instance, about 1300 were known, but only a few are of industrial significance. Today there are many more. They are named after the kinds of reactions that

TABLE 20.7. Industrial Products of Microbial and Related Processes

A. Significant or marginal products
  Acetic acid
  Amino acids
  Butyric acid
  Citric acid
  Ethanol
  Fructose from glucose
  Glucose from starch
  Gluconic acid
  Methane
  Nucleotides (glutamic acid, guanyl acid, xanthyllic acid)
B. Products under development or absolesced from microbial synthesis
  Acids: fumaric, lactic, malic, oxalic and some others
  Acetone
  Butanol
  Butanediol
  Glycerine
  Lipids
  Polyalcohols and other substances
C. Enzymes (extensive lists with properties and industrial suppliers are in the book by Godfrey and Reichelt, 1983).
D. Antibiotics (Lists with major characteristics, sources and manufacturing methods are in, for example, the book of Bailey and Ollis, 1986).

they promote rather than to identify the structure which often is still unknown. Some kinds of enzymes are:

Amylase, which converts polysaccharides (starch or cellulose) to sugars.
Cellulase, which digests cellulose.
Glucose oxidase, which converts glucose to dextrose and levulose.
Isomerase, which converts glucose to fructose.
Lipase, which splits fats to glycerine and fatty acids.
Protease, which breaks down proteins into simpler structures.

Biochemical manufacturing processes consist of the familiar steps of feed preparation, reaction, separation, and purification. The classic mode handles the microorganisms in slurry form in a stirred reactor. Enzyme-catalyzed processes also are performed primarily in stirred tanks, but when the enzymes can be suitably immobilized, that is, attached to solid structures, other kinds of reactor configurations may be preferred. Microbes also are grown in pans or rotating drums under moistened conditions, processes known as solid culture processing. Figure 20.20(a) shows the three modes of microbe culture. Processes that demand extensive handling of moist solids are practiced only on a small scale or when stirred tank action is harmful to cell structures. The process of Figure 20.20(b) consists largely of feed preparation steps.

OPERATING CONDITIONS

The optimum ranges of conditions for microbe growth or enzyme activity are quite narrow and must be controlled closely.

Concentration. A major characteristic of microbial growth and enzymatic conversion processes is low concentrations. The rates of these processes are inhibited by even moderate concentrations of most low molecular weight organic substances, even 1 g/L often being harmful. Nutrients also must be limited, for instance, the following in g/L:

Ammonia	5
Phosphates	10
Nitrates	5
Ethanol	100
Glucose	100

In the fermentation for ethanol, the concentration limit normally is about 8 wt% ethanol, but newer processes have been claimed to function at 10% or so. The search is on for microorganisms, or for creating them, that tolerate high concentrations of reaction products and higher temperatures.

Temperature. Most microbe metabolisms and enzymatic processes function well only in the range of 10–60°C, but in particular cases the active spread of temperatures is only 5–10°C. A classification of microorganisms that is sometimes made is with respect to peak activities near 15°C or near 35°C or near 55°C. The maximum heat effects of metabolic processes can be estimated from heats of formation when the principal chemical participants are known, for instance:

glucose → ethanol, heat of reaction 0.10 kcal/g glucose,
glucose → CO_2 + H_2O, heat of reaction 3.74 kcal/g glucose.
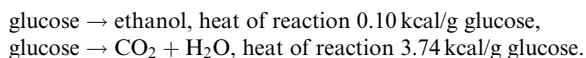
Some of the energy is used to form the cell structure. Reactions catalyzed by enzymes may be either endo- or exothermic depending on the particular stoichiometry. Because of the diluteness of the solutions normally handled, temperature control is achieved read-ily. Stirred fermenters are provided with cooling jackets. Internal cooling oils are undesirable because of the difficulty of cleaning them. Fixed beds of immobilized enzymes do not lend themselves readily to jacket cooling, but in many instances the heat effect is so low that the temperature range can be maintained within the required limits by adjustment of the feed temperature. Multitubular reactors with cooling medium on the shell side are practical with enzymes immobilized on granules.

Sterilization. This is necessary to prevent the growth of foreign microorganisms. Air is sterilized adequately by the heat of compression. Filters at the inlet remove oil and any microbes that may be present, and filters at the air outlet prevent backflow of foreign microorganisms. The inoculum is prepared under sterile conditions in the laboratory. The substrate is sterilized in an external vessel by holding it at 120°C or so for 1 hr or so.

Aeration. Since metabolism of microorganisms is an oxidative process, the substrate should be kept as nearly saturated as possible. At usual fermenter operating conditions the solubility of oxygen is about 0.03 mmol/L. When the content falls to 0.01 mmol/L, the growth rate falls to about one-half the maximum. Compressed air is introduced through spargers. Dispersion with high-speed agitators rarely is feasible because of possible mechanical destruction of cells. In some sensitive systems, all of the necessary agitation may be provided with an adequate air flow.

Agitation. The purpose of agitation is to keep the microorganisms in suspension, to maintain uniformity to eliminate concentration gradients and hot spots, and to improve heat transfer to the cooling jacket. For the design of agitation systems refer to Chapter 10. In vessels of a 1000 gal or more, a power input of about 10 HP/1000 gal and impeller tip speeds of 15–20 ft/sec are adequate, but the standard fermenter described in Table 20.8 is supplied with about four times this power.

pH. Biochemical processes are highly sensitive to hydrogen-ion concentration. Most enzymes function best in the range of pH from 5 to 7, but some extremes are pepsin at pH of 1.5 and araginase at pH of 10. For classes of microorganisms, these ranges are common:

Complex cells	6.5–7.5
Bacteria	4–8
Molds	3–7
Yeasts	3–6

Control of pH is accomplished by additions of dilute acid or alkali.

Ion Concentration. Heavy metals, particularly calcium, inhibit enzyme activity. The only feasible method of removing them is with ion exchange resins.

Foam Control. Fermentations tend to froth because metabolites have surfactant properties. Prevention commonly is by addition of antifoam agents such as oils, heavy alcohols, fatty acids, or silicones. High-speed rotating impellers destroy bubbles by direct impact and by throwing them against the wall of the vessel.

REACTORS

Stirred tanks are the chief kind of reactors for handling microorganisms or dissolved isolated enzymes, either as batch units or as continuous stirred tank batteries. When the enzymes are immobil-
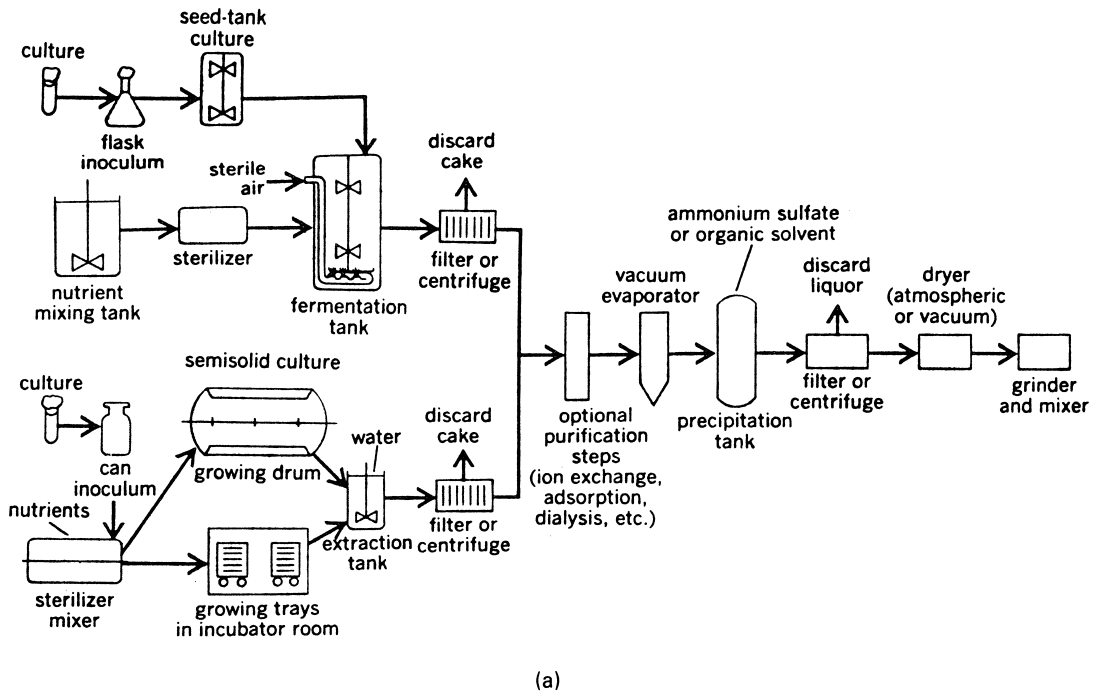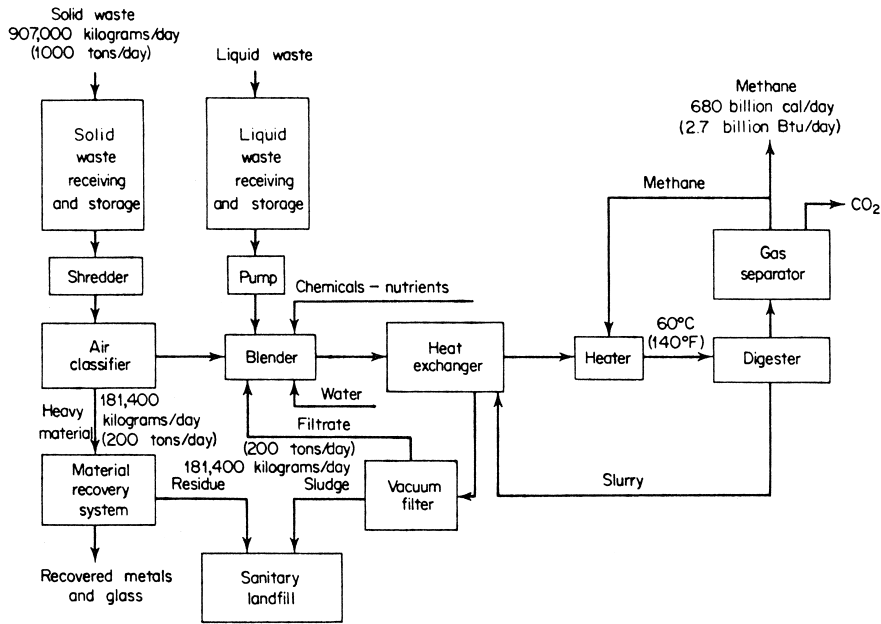
Figure 20.20. Flowsketches of two processes employing fermentation. (a) Process for enzyme production, showing the use of growing trays, growing drums and stirred tank. Purification steps are the same for all three modes of culture growth. (b) Production of methane-rich gas by anaerobic digestion of finely divided waste solids in a 10–20% slurry. Residence time in the digester is five days. (Considine, 1977).

ized, a variety of reactor configurations is possible and continuous operation is easily implemented. The immobilization may be on granules or on sheets, and has the further advantage of making the enzymes reusable since recovery of dissolved enzymes rarely is feasible.

Many aspects of the design of biochemical reactors are like those of ordinary chemical reactors. The information needed for design are the kinetic data and the dependence of enzyme activity on time and temperature. Many such data are available in the literature, but usually a plant design is based on laboratory data

obtained with small fermenters. Standard sizes of such units range from 50 to 1000 L capacity.

A sketch of a plant size fermenter and some of its auxiliaries is in Figure 20.21. Although not shown here, a bottom drive mechanical agitator usually is provided. The standard specification, Table 20.8, of one make of commercial fermenter includes a listing of the many openings that are required, as well as other general information.
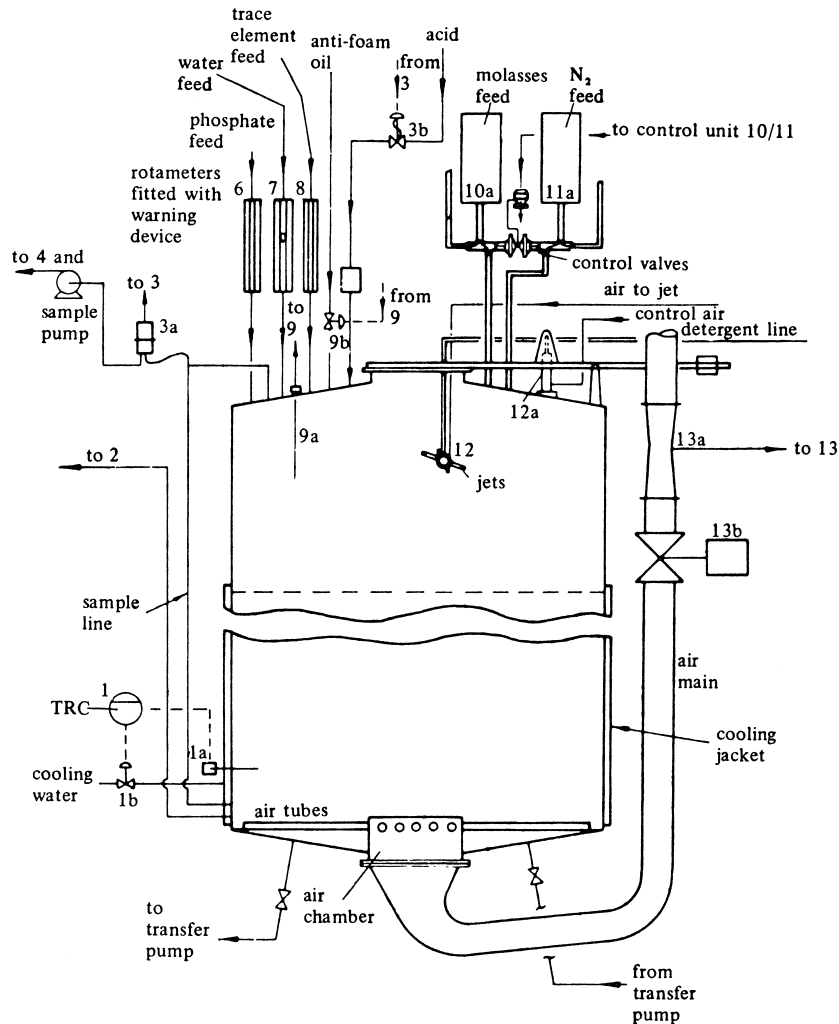
*1	Temperature controller and recorder	*9	Foam controller
1a	Resistance thermometer	9a	Foam detector
1b	Control valve	9b	Control valve
*2	Fermenter level	10/11	Dosage control unit
*3	pH recorder and controller	10a	Molasses feed
3a	pH electrode system	11a	Nitrogen feed
3b	Control valve	12	Rotor jet
*4	Yeast concentration recorder	12a	Power unit
*5	Recorder controller	*13	Air controller recorder
6	Phosphate feed rotameter	13a	Venturi
7	Water feed rotameter	13b	Power operated air control valve
8	Trace element feed rotameter		* Indicates panel-mounted instruments.

Figure 20.21. Sketch of a fermenter with its auxiliary equipment. In most cases supplemental agitation by mechanical stirrers is common. [*A.J.C. Olsen*, Chem. Ind., *416 (1960)*].

TABLE 20.8. Standard Specifications of a Fermenter

1. Surfaces in contact with culture are 316 SS, all others 304 SS; free of crevices, mechanically ground and polished to approx 220 grit
2. Approx proportions: height/diameter = 2, impeller/vessel diameter = 0.35, baffle width/vessel diameter = 0.1
3. Maximum working volume = 75–80%, minimum = 25%
4. Ports and penetrations are 20 in number, namely
   A. Steam-sterilizable inoculation/addition port
   B. Combination viewing window/filling port on headplate
   C. Light entrance window and lamp on headplate
   D. Air inlet line
   E. Air exhaust line
   F. Well for temperature control sensor and temperature recorder sensor
   G. Well for thermometer
   H. Water inlet line to jacket of vessel
   I. Water outlet line from jacket of vessel
   J. Rupture disc on headplate and pressure relief valve on jacket
   K. Diaphragm-type pressure gauge
   L. Steam-sterilizable sample port
   M. Steam-sterilizable bottom drain port, discharge valve is flush-bottom
   N. Side-entry port for pH electrode
   O. Top-entering or side-entering (size-dependent) port for installation of the dissolved oxygen electrode
   P. Top-entering port for foam sensor
   Q. Side-entering ports for acid, base, and antifoam addition (valved and piped as required)
   R. Spare penetrations on headplate for insertion of additional sensors i.e., 1 1/8 in. NPT, 1 3/8 in. NPT, 1 3/4 in. NPT
5. Foam breaking: Injection port provided for chemical breaking; mechanical breaker optional, consists of a double disk rotated at high speed with its own drive
6. Agitation system has three six-bladed turbine impellers adjustable along the shaft, maximum tip speed of 1200 ft/min, standard drive of 40 HP for a 5000-L vessel, bottom drive standard, top drive optional
7. Controls and monitors: liquid level, pH, dissolved oxygen, reduction–oxidation (Redox) potential, air rate, temperature, optional automatic sterilization cycle control, rupture disk on vessel, relief valve on jacket

(New Brunswick Scientific Co.).

REFERENCES

Gas-Solids Separation

Anon. ——, *A Scientific Review of Dust Collection*, Scientific Dust Collectors, Alsip, IL, 2002.

D.E. Bonn, Wet type dust collectors, *Chem. Eng. Prog.*, **59**(10), 69–74 (October 1963).

J.M. Maas, Cyclone separators, in P.A. Schweitzer (Ed.), *Handbook of separation methods for Chemical Engineers*, McGraw-Hill, New York, 1979, p. 6.10–6.17.

M. Pell, and J.B. Dunson, Gas-solid separations and equipment, in *Chemical Engineers' Handbook*, 7th ed., Section 17, McGraw-Hill, New York, 1999.

K. Rietemer, and C.G. Verver *Cyclones in Industry*, Elsevier, New York, 1961.

W.M. Vatavuk, *Estimating Costs of Air Pollution Control*, Lewis Publishers, Chelsea, MI, 1990.

F.A. Zenz, *Cyclones, Encyclopedia of Chemical Processing and Design*, Dekku, New York, Vol. 14, 1982, pp. 82–97.

Foam Separation and Flotation

Chemical Engineers' Handbook, 6th ed., McGraw-Hill, New York, 1984.

J. Davis, and D. Hass, in R. Lemlich (Ed.), *Adsorptive Bubble Separation Techniques*, Academic, New York, 1972.

R. Lemlich, *Adsorptive Bubble Separation Techniques*, Academic, New York, 1972.

Y. Okamoto, and E.J. Chou, Foam separation processes, in P.A. Schweitzer (Ed.), *Handbook of Separation Techniques for Chemical Engineers*, McGraw-Hill, New York, 1979, pp. 2.183–2.197.

P. Somasundaran, Foam separation methods: A review, in Perry and van Oss (Eds.), *Separation and Purification Methods*, Vol. 1, 1972, pp. 117–199.

T. Sorensen, Flotation, in *Chemical Engineers' Handbook*, 6th ed., McGraw-Hill, New York, 1984, pp. 21.46–21.52.

B.A. Wills, *Mineral Processing Technology*, Pergamon, New York, 1985.

Sublimation and Freeze Drying

W. Corder, Sublimation, in *Chemical Engineers' Handbook*, 6th ed., McGraw-Hill, New York, 1984, pp. 17.12–17.14.

N. Ganiaris, Freeze drying, in D.M. Considine (Ed.), *Chemical and Process Technology Encyclopedia*, McGraw-Hill, New York, 1974, pp. 523–527.

C.A. Holden, and H.S. Bryant, Sublimation, *Separation Sci.*, **4**(1), 1 (1969).

C.J. Major, Freeze drying, in *Chemical Engineers' Handbook*, 5th ed., 1973, pp. 17.26–17.28.

G. Matz, Sublimation, in *Uhlmann's Encyclopedia of Chemical Technology*, Vol. 2, Verlag Chemie, Weinheim, 1972, pp. 664–671.

J.W. Mullin, Sublimation, in *Crystallization*, Butterworths, London, 1972, pp. 284–290.

Thermal Diffusion

M. Benedict, T.H. Pigford, and H.W. Levi, *Nuclear Chemical Engineering*, McGraw-Hill, New York, 1981.

A.L. Jones, and G.B. Brown, Liquid thermal diffusion, in McKetta and Kobe (Eds.), *Advances in Petroleum Chemistry and Refining*, Vol. III, Wiley, New York, 1960, pp. 43–76.

W.M. Rutherford, Ind. Eng. Chem. Proc. Des. Dev. 17, 17–81 (1978).

G. Vasaru et al., *The Thermal Diffusion Column*, VEBN Deutscher Verlag der Wissenschaften, Berlin, 1969.

Electrochemical Syntheses

J. Adlhart, in Energy Rheumology Handbook, D.M. Couriclices (Ed.) McGraw-Hill, New York, 1977, p. 4.61.

M.M. Baizer, *J. Appl. Electrochemistry*, **18**, 285 (1980).

T. Beck, and M. Guthke, Chem. Ing. Tech., 41, 943 (1969).

T. Beck et al., *A Survey of Electrolytic Processes*, ANL/OEPM, 79–5, Electrochemical Technology Corporation, 1979.

D.E. Danly, Encycl. Chem. Technolo; 8, 702 (1979).

D. Fletcher, *Industrial Electrochemistry*, Chapman and Hall, London, 1982.

F. Hine, *Electrode Processes and Electrochemical Engineering*, Plenum, New York, 1985.

R. Roberts, R.P. Ouellete, and P.N. Cheremisinoff, *Industrial Applications of Electroorganic Synthesis*, Ann Arbor Science, Ann Arbor, MI, 1982.

Fermentation Processing

B. Atkinson, *Biochemical Reactors*, Pion Ltd., London, 1974.

B. Atkinson, and F. Mativuna, *Biochemical Engineering and Biotechnology Handbook*, Macmillan, Surrey, England, 1983.

J.E. Bailey, and D.F. Ollis, *Biochemical Engineering Fundamentals*, McGraw-Hill, New York, 1986.

D.M. Considine, *Energy Technology Handbook*, McGraw-Hill, New York, 1977.

T. Godfrey, and J. Reichelt, *Industrial Enzymology*, Macmillan, Surrey, England, 1983.

A.J.C. Olsen, Chem. Ind. 416 (1960).

W.M. Rutherford, *Ind. Eng., Proc. Des. Dev.*, **17**, 17–81 (1978).

P.F. Stanbury, and A. Whitaker, *Principles of Fermentation Technology*, Pergamon, New York, 1984.

21

COSTS OF INDIVIDUAL EQUIPMENT

The choice of appropriate equipment often is influenced by considerations of price. A lower efficiency or a shorter life may be compensated for by a lower price. Funds may be low at the time of purchase and expected to be more abundant later, or the economic life of the process is expected to be limited. Alternate kinds of equipment for the same service may need to be considered: water-cooled exchangers vs. air coolers, concrete cooling towers vs. redwood, filters vs. centrifuges, pneumatic conveyors vs. screw or bucket elevators, and so on.

In this chapter, the prices of classes of the most frequently used equipment are collected in the form of correlating equations. The prices are given in terms of appropriate key characteristics of the equipment, such as sqft, gpm, lb/hr, etc. Factors for materials of construction and performance characteristics other than the basic ones also are provided. Although graphs are easily read and can bring out clearly desirable comparisons between related types of equipment, algebraic representation has been adopted here. Equations are capable of consistent reading, particularly in comparison with interpolation on logarithmic scales, and are amenable to incorporation in computer programs.

Unless otherwise indicated, the unit price is $1000, $K. Except where indicated, notably for fired heaters, refrigeration systems, and cooling towers (which are installed prices), the prices are purchase prices, FOB, with delivery charges extra. In the United States delivery charges are of the order of 5% of the purchase price, but, of course, dependent on the unit value, as cost per lb or per cuft. Multipliers have been developed whereby the installed cost of various kinds of equipment may be found. Such multipliers range from 1.2 to 3.0, but details are shown in Table 21.3.

TABLE 21.1. Index of Equipment

1. Agitators
2. Compressors, turbines, fans
   Centrifugal compressors
   Reciprocating compressors
   Screw compressors
   Turbines
     Pressure discharge
     Vacuum discharge
   Fans
3. Conveyors
   Troughed belt
   Flat belt
   Screw, steel
   Screw, stainless
   Bucket elevator
   Pneumatic
4. Cooling towers
   Concrete
   Wooden
5. Crushers and grinders
   Cone crusher
   Gyratory crusher
   Jaw crusher
   Hammer mill
   Ball mill
   Pulverizer
6. Crystallizers
   External forced circulation
   Internal draft tube
   Batch vacuum
7. Distillation and absorption towers
   Distillation tray towers
   Absorption tray towers
   Packed towers
8. Dryers
   Rotary, combustion gas heated
   Rotary, hot air heated
   Rotary, steam tube heated
   Cabinet dryers
   Spray dryers
   Multiple hearth furnace
9. Evaporators
   Forced circulation
   Long tube

   Falling film
10. Fired heaters
    Box types
    Cylindrical types
11. Heat exchangers
    Shell-and-tube
    Double pipe
    Air coolers
12. Mechanical separators
    Centrifuges
    Cyclone separators
      Heavy duty
      Standard duty
      Multiclone
    Disk separators
    Filters
      Rotary vacuum belt discharge
      Rotary vacuum scraper discharge
      Rotary vacuum disk
      Horizontal vacuum belt
      Pressure leaf
      Plate-and-frame
    Vibrating screens
13. Motors and couplings
    Motors
    Belt drive coupling
    Chain drive coupling
    Variable speed drive coupling
14. Pumps
    Centrifugal
    Vertical mixed flow
    Vertical axial flow
    Gear pumps
    Reciprocating pumps
15. Refrigeration
16. Steam ejectors and vacuum pumps
    Ejectors
    Vacuum pumps
17. Vessels
    Horizontal pressure vessels
    Vertical pressure vessels
    Storage tanks, shop fabricated
    Storage tanks, field erected

Cost data were obtained from a number of different sources and are referred to for each algorithm in Table 21.2. All algorithms have been updated to the first quarter of 2003 and the cost data were checked with equipment manufacturers' data. Any cost index may be used but the Chemical Engineering Index found in the magazine *Chemical Engineering* is satisfactory for costing equipment.

Material of construction is a major factor in the price of equipment so that multipliers for prices relative to carbon steel on other standard materials are given for many of the items covered here. Usually only the parts in contact with process substances need be of special construction, so that, in general, the multipliers are not always as great as they are for vessels that are made entirely on special materials. Thus, when the tube side of an exchanger is special and the shell is carbon steel, the multiplier will vary with the amount of tube surface, as shown in that section. For multipliers see information under each type equipment in Table 21.2.

As with most collections of data, the price data correlated here exhibit a certain amount of scatter. This is due in part to the incomplete characterizations in terms of which the correlations are made, but also to variations among manufacturers, qualities of construction, design differences, market situations, and other factors. Accordingly, the accuracy of the correlations cannot be claimed to be better than $\pm 25\%$ or so.

TABLE 21.2. Purchase Prices of Process Equipment Costs 1st Q 2003

1. Agitators

$C = 1.218 \exp [a + b \ln \mathrm{HP} + c(\ln \mathrm{HP})^2]$ K\$, $1 < \mathrm{HP} < 400$

		Single Impeller			Dual Impeller		
		Speed 1	**2**	**3**	**1**	**2**	**3**
Carbon	a	8.57	8.43	8.31	8.80	8.50	8.43
steel	b	0.1195	−0.0880	−0.1368	0.1603	0.0257	−0.1981
	c	0.0819	0.1123	0.1015	0.0659	0.0878	0.1239
Type 316	a	8.82	8.55	8.52	9.25	8.82	8.72
	b	0.2474	0.0308	−0.1802	0.2801	0.1235	−0.1225
	c	0.0654	0.0943	0.1158	0.0542	0.0818	0.1075

Speeds 1: 30, 37, and 45 rpm
    2: 56, 68, 84, and 100 rpm
    3: 125, 155, 190, and 230 rpm

2. Compressors, turbines, and fans (K\$)

Centrifugal compressors, without drivers

$C = 7.90(\mathrm{HP})^{0.62}$ K\$, $200 < \mathrm{HP} < 30{,}000$

Reciprocating compressors without drivers

$C = 7.19(\mathrm{HP})^{0.61}$ K\$, $100 < \mathrm{HP} < 20{,}000$

Screw compressors with drivers

$C = 1.81(\mathrm{HP})^{0.71}$ K\$, $10 < \mathrm{HP} < 800$

Turbines:

Pressure discharge, $C = 0.378(HP)^{0.81}$ K\$, $20 < \mathrm{HP} < 5000$
Vacuum discharge, $C = 1.10(HP)^{0.81}$ K\$, $200 < \mathrm{HP} < 8000$

Fans with motors

$C = 1.218 f_m f_p \exp[a + b \ln Q + c(\ln Q)^2]$ installed cost, K\$, Q in KSCFM

	a	b	c	Q
Radial blades	0.4692	0.1203	0.0931	2–500
Backward curved	0.0400	0.1821	0.0786	2–900
Propeller	−0.4456	0.2211	0.0820	2–300
Propeller, with guide vanes	−1.0181	0.3332	0.0647	2–500

Installation factor, f_m

Carbon steel	2.2
Fibreglass	4.0
Stainless steel	5.5
Nickel alloy	11.0

TABLE 21.2.—(*continued*)

Pressure Factors, F_p

Pressure (kPa[gage])	Centrifugal		Axial	
	Radial	**Backward Curved**	**Prop.**	**Vane**
1	1.0	1.0	1.0	1.00
2	1.15	1.15	—	1.15
4	1.30	1.30	—	1.30
8	1.45	1.45	—	—
16	1.60	—	—	—

3. Conveyors K$

Troughed belt: $C = 1.71L^{0.66}, 10 < L < 1300$ ft
Flat belt: $C = 1.10L^{0.66}, 10 < L < 1300$ ft
Screw (steel): $C = 0.49L^{0.76}, 7 < L < 100$ ft
Screw (stainless steel): $C = 0.85L^{0.78}, 7 < L < 100$ ft
Bucket elevator: $C = 5.14L^{0.63}, 10 < L < 100$ ft
Pneumatic conveyor 600 ft length

$$C = 1.218 \exp[3.5612 - 0.0048 \ln W + 0.0913(\ln W)^2], 10 < W < 100 \, \text{klb/hr}$$

4. Cooling towers, installed K$

Concrete $C = 164fQ^{0.61}, 1 < Q < 60$ K gal/min:

$\Delta t(°C)$	10	12	15
f	1.0	1.5	2.0

Redwood, without basin: $C = 44.3Q^{0.65}, 1.5 < Q < 20 \, Kgal/min$

5. Crushers and grinders K$

Cone crusher: $C = 1.89W^{1.05}$, $20 < W < 300$ tons/hr
Gyratory crusher: $C = 9.7W^{0.60}$, $25 < W < 200$ tons/hr
Jaw crusher: $C = 7.7W^{0.57}$, $10 < W < 200$ tons/hr
Hammer mill: $C = 2.97W^{0.78}$, $2 < W < 200$ tons/hr
Ball mill: $C = 61.0W^{0.69}$, $1 < W < 30$ tons/hr
Pulverizer: $C = 27.5W^{0.39}$, $1 < W < 5$ tons/hr

6. Crystallizers

External forced circulation:
$C = 1.218 \, f \exp \{4.868 + 0.3092 \ln W + 0.0548(\ln W)^2\}$, $10 < W < 100 \, \text{klb/hr of crystals}$

Internal draft tube: $\quad C = 217f \, W^{0.58}$, $15 < W < 100 \, \text{klb/hr of crystals}$
Batch vacuum: $\quad C = 9.94fV^{0.47}$, $50 < V < 1000$ cuft of vessel

Type	Material	f
Forced circulation	Mild steel	1.0
	Stainless type 304	2.5
Vacuum batch	Mild steel	1.0
	Rubber-lined	1.3
	Stainless type 304	2.0

7. Distillation and absorption towers, tray and packed prices in $

Tray towers:
$\quad C_t = 1.218[f_1 C_b + Nf_2 f_3 f_4 C_t + C_{pt}]$
Purchased and installed costs are in 1,000.
Distillation:
$\quad C_b = 1.218 \exp [7.123 + 0.1478(\ln W) + 0.02488(\ln W)^2 + 0.01580(L/D) \ln (T_b/T_D)]$, $9020 < W < 2,470,000$ lbs
$\qquad$ of shell exclusive of nozzles and skirt
$\quad C_t = 457.7 \exp (0.1739 \, D), 2 < D < 16$ ft tray diameter
$\quad N = $ number of trays
$\quad C_{p1} = 249.6 \, D^{0.6332}L^{0.8016}$, $2 < D < 24$, $57 < L < 170$ ft (platforms and ladders)

TABLE 21.2.—(*continued***)**

Material	f_1	f_2
Stainless steel, 304	1.7	$1.189 + 0.0577\,D$
Stainless steel, 316	2.1	$1.401 + 0.0724\,D$
Carpenter 20CB-3	3.2	$1.525 + 0.0788\,D$
Nickel-200	5.4	
Monel-400	3.6	$2.306 + 0.1120\,D$
Inconel-600	3.9	
Incoloy-825	3.7	
Titanium	7.7	

Tray Types	f_3
Valve	1.00
Grid	0.80
Bubble cap	1.59
Sieve (with downcorner)	0.95

$f_4 = 2.25/(1.0414)^N$, when the number of trays **N** is less than 20

T_b is the thickness of the shell at the bottom, T_p is thickness required for the operating pressure, D is the diameter of the shell and tray, L is tangent-to-tangent length of the shell

Absorption:
$C_b = 1.218\exp[6.629 + 0.1826(\ln W) + 0.02297(\ln W)^2]$, $4250 < W < 980,000$ lb shell
$C_{p1} = 300D^{0.7396}L^{0.7068}$, $3 < D < 21$, $27 < L < 40$ ft (platforms and ladders),
f_1, f_2, f_3, and f_4 as for distillation

Packed towers:
$C = 1.218[f_1 C_b + V_p C_p + C_{p1}]$

V_p is volume of packing, C_p is cost of packing \$/cuft

Packing Type	C_p (\$/cuft)
Ceramic Raschig rings, 1 in.	23.9
Metal Raschig rings, 1 in.	39.3
Intalox saddles, 1 in.	23.9
Ceramic Raschig rings, 2 in.	76.6
Metal Raschig rings, 2 in.	28.0
Metal Pall rings, 1 in.	39.3
Intalox saddles, 2 in.	17.4
Metal Pall rings, 2 in.	28.0

8. Dryers

Rotary combustion gas heated: $C = 1.218(1 + f_g + f_m)\exp[4.9504 - 0.5827(\ln A) + 0.0925(\ln A)^2]$, $200 < A < 30,000$ sqft lateral surface
Rotary hot air heated: $C = 2.90(1 + f_g + f_m)A^{0.63}$, $200 < A < 4000$ sqft lateral surface
Rotary steam tube: $C = 2.23FA_t^{0.60}$, $500 < A_t < 18,000$ sqft tube surface, $F = 1$ for carbon steel, $F = 1.75$ for 304 stainless
Cabinet dryer: $C = 1.40f_p A^{0.77}$, $10 < A < 50$ sqft tray surface

Pressure	f_p
Atmospheric pressure	1.0
Vacuum	2.0

Material	f_m
Mild steel	1.0
Stainless type 304	1.4

Drying Gas	f_g
Hot air	0.00
Combustion gas (direct contact)	0.12
Combustion gas (indirect contact)	0.35

TABLE 21.2.—(*continued***)**

Materials	f_m
Mild steel	0.00
Lined with stainless 304–20%	0.25
Lined with stainless 316–20%	0.50

Spray dryers:
   $C = 1.218\,F \exp(0.8403 + 0.8526(\ln x) - 0.0229(\ln x)^2$, $30 < x < 3000\,\text{lb/hr}$ evaporation

Material	F
Carbon steel	0.33
304, 321	1.00
316	1.13
Monel	3.0
Inconel	3.67

Multiple hearth furnaces (Hall, 1984)
   $C = 1.218 \exp(a + 0.88\,N)$, $4 < N < 14$ number of hearths

Diameter (ft)	6.0	10.0	14.25	16.75	18.75	22.25	26.75
Sqft/hearth, approx	12	36	89	119	172	244	342
a	5.071	5.295	5.521	5.719	5.853	6.014	6.094

9. Evaporators (IFP)

Forced circulation: $C = 1.218\,f_m \exp[5.9785 - 0.6056(\ln A) + 0.08514(\ln A)^2]$, $150 < A < 8000\,\text{sqft}$ heat transfer surface
Long tube: $C = 0.44 f_m A^{0.85}$, $300 < A < 20{,}000\,\text{sqft}$
Falling film (316 internals, carbon steel shell)
   $C = 1.218 \exp[3.2362 - 0.0126(\ln A) + 0.0244(\ln A)^2]$, $150 < A < 4000\,\text{sqft}$
   C is in K$

Forced-Circulation Evaporators

Construction Material: Shell/Tube	f_m
Steel/copper	1.00
Monel/cupronickel	1.35
Nickel/nickel	1.80

Long-Tube Evaporators

Construction Material: Shell/Tube	f_m
Steel/copper	1.0
Steel/steel	0.6
Steel/aluminum	0.7
Nickel/nickel	3.3

10. Fired heaters, installed

Box type: $C = 1.218\,k(1 + f_d + f_p)Q^{0.86}$, $20 < Q < 200\,\text{M Btu/hr}$

Tube Material	k
Carbon steel	25.5
CrMo steel	33.8
Stainless	45.0

Design Type	f_d
Process heater	0
Pyrolysis	0.10
Reformer (without catalyst)	0.35

Design Pressure, (psi)	f_p
Up to 500	0
1,000	0.10
1,500	0.15
2,000	0.25
2,500	0.40
3,000	0.60

Cylindrical type: $C = 1.218\,k(1 + f_d + f_p)Q^{0.82}$, $2 < Q < 30\,\text{MBtu/hr}$

TABLE 21.2.—(_continued_**)**

Tube Material	k
Carbon steel	27.3
CrMo steel	40.2
Stainless	42.0

Design Type	f_d
Cylindrical	0
Dowtherm	0.33

Design Pressure (psi)	f_p
Up to 500	0
1,000	0.15
1,500	0.20

11. Heat exchangers

Shell-and-tube: $C = 1.218\, f_d f_m f_p C_b$, price in \$
$C_b = \exp\,[8.821 - 0.30863(\ln\ A) + 0.0681(\ln A)^2]$, $150 < A < 12,000$ sqft

Type	f_d
Fixed-head	$\exp[-1.1156 + 0.0906(\ln A)]$
Kettle reboiler	1.35
U-tube	$\exp[-0.9816 + 0.0830(\ln\ A)]$

Pressure Range (psig)	f_p
100–300	$0.7771 + 0.04981(\ln\ A)$
300–600	$1.0305 + 0.07140(\ln\ A)$
600–900	$1.1400 + 0.12088(\ln\ A)$
	$f_m = g_1 + g_2(\ln\ A)$

Material	g_1	g_2
Stainless steel 316	0.8603	0.23296
Stainless steel 304	0.8193	0.15984
Stainless steel 347	0.6116	0.22186
Nickel 200	1.5092	0.60859
Monel 400	1.2989	0.43377
Inconel 600	1.2040	0.50764
Incoloy 825	1.1854	0.49706
Titanium	1.5420	0.42913
Hastelloy	0.1549	0.51774

Double pipe: $C = 1096 f_m f_p A^{0.18}$, $2 < A < 60$ sqft, price in \$

Material: Shell/Tube	f_m
cs/cs	1.0
cs/304L stainless	1.9
cs/316 stainless	2.2

Pressure (bar)	f_p
≤4	1.00
4–6	1.10
6–7	1.25

Air coolers: $C = 30.0 A^{0\ 40}$, $0.05 < A < 200$ Ksqft, price in K\$

12. Mechanical separators

Centrifuges: solid bowl, screen bowl or pusher types
    $C = 1.218[a + bW]$, K\$

Material	Inorganic Process		Organic Process	
	a	b	a	b
Carbon steel	42	1.63	—	—
316	65	3.50	98	5.06
Monel	70	5.50	114	7.14
Nickel	84.4	6.56	143	9.43
Hastelloy	—	—	300	10.0
	$10 < W < 90$		$5 < W < 40$ tons/hr	

TABLE 21.2.—(continued**)**

Disk separators, 316 stainless:
$C = 9.74\ Q^{0.52}$, $15 < Q < 150$ gpm, K\$
Cyclone separators: K\$
    Heavy duty: $C = 1.69\ Q^{0.96}$, $2 < Q < 40$ K SCFM
    standard duty: $C = 0.79\ Q^{0.91}$, $2 < Q < 40$ K SCFM
    Multiclone: $C = 1.90\ Q^{0.68}$, $9 < Q < 180$ K SCFM
Filters, prices in \$/sqft:
    rotary vacuum belt discharge: $C = 1.218\ \exp[11.20 - 1.2252(\ln\ A) + 0.0587(\ln\ A)^2]$, $10 < A < 800$ sqft
    rotary vacuum drum scraper discharge: $C = 1.218\ \exp[11.27 - 1.3408(\ln\ A) + 0.0709(\ln\ A)^2]\$/sqft$, $10 < A < 1500$ sqft
rotary vacuum disk: $C = 1.218\ \exp[10.50 - 1.008(\ln\ A) + 0.0344(\ln\ A)^2]\$/sqft$, $100 < A < 4000$ sqft
horizontal vacuum belt: $C = 34469/A^{0.5}\$/sqft$, $10 < A < 1200$ sqft
pressure leaf: $C = 847/A^{0.29}\$/sqft$, $30 < A < 2500$ sqft
Plate-and-frame: $C = 560/A^{0.45}\$/sqft$, $10 < A < 1000$ sqft
vibrating screen: $C = 3.8/A^{0.59}$ K\$, $0.5 < A < 35$ sqft

13. Motors and couplings, prices in \$

Motors: $C = 1.46\ \exp[a_1 + a_2(\ln\ HP) + a_3(\ln\ HP)^2]$
Belt drive coupling: $C = 1.46\ \exp[3.689 + 0.8917(\ln\ HP)]$
Chain drive coupling: $C = 1.46\ \exp[5.329 + 0.5048(\ln\ HP)]$
Variable speed drive coupling: $C = 14616/(1.562 + 7.877/HP)$, $HP < 75$

		Coefficients		
Type	a_1	a_2	a_2	**HP limit**
Open, drip-proof				
3600 rpm	4.8314	0.09666	0.10960	1–7.5
	4.1514	0.53470	0.05252	7.5–250
	4.2432	1.03251	−0.03595	250–700
1800 rpm	4.7075	−0.01511	0.22888	1–7.5
	4.5212	0.47242	0.04820	7.5–250
	7.4044	−0.06464	0.05448	250–600
1200 rpm	4.9298	0.30118	0.12630	1–7.5
	5.0999	0.35861	0.06052	7.5–250
	4.6163	0.88531	−0.02188	250–500
Totally enclosed, fan-cooled				
3600 rpm	5.1058	0.03316	0.15374	1–7.5
	3.8544	0.83311	0.02399	7.5–250
	5.3182	1.08470	−0.05695	250–400
1800 rpm	4.9687	−0.00930	0.22616	7.5–250
	4.5347	0.57065	0.04609	250–400
1200 rpm	5.1532	0.28931	0.14357	1–7.5
	5.3858	0.31004	0.07406	7.5–350
Explosion-proof				
3600 rpm	5.3934	−0.00333	0.15475	1–7.5
	4.4442	0.60820	0.05202	7.5–200
1800 rpm	5.2851	0.00048	0.19949	1–7.5
	4.8178	0.51086	0.05293	7.5–250
1200 rpm	5.4166	0.31216	0.10573	1–7.5
	5.5655	0.31284	0.07212	7.5–200

14. Pumps

Centrifugal prices in \$: $C = F_M F_T C_b$, base cast-iron, 3550 rpm VSC
    $C_b = 1.39\ \exp[8.833 - 0.6019(\ln\ Q\sqrt{H}) + 0.0519(\ln\ Q\sqrt{H})^2]$, Q in gpm, H in ft head

Material	Cost Factor F_M
Cast steel	1.35
304 or 316 fittings	1.15
Stainless steel, 304 or 316	2.00
Cast Gould's alloy no. 20	2.00
Nickel	3.50
Monel	3.30
ISO B	4.95
ISO C	4.60
Titanium	9.70
Hastelloy C	2.95
Ductile Iron	1.15
Bronze	1.90

TABLE 21.2.—(continued)

$$F_T = \exp[b_1 + b_2(\ln Q\sqrt{H}) + b_3(\ln Q\sqrt{H})^2]$$

Type	b_1	b_2	b_3
One-stage, 1750 rpm, VSC	5.1029	−1.2217	0.0771
One-stage, 3550 rpm, HSC	0.0632	0.2744	−0.0253
One-stage, 1750 rpm, HSC	2.0290	−0.2371	0.0102
Two-stage, 3550 rpm, HSC	13.7321	−2.8304	0.1542
Multistage, 3550 rpm, HSC	9.8849	−1.6164	0.0834

Type	Flow Range (gpm)	Head Range (ft)	HP (max)
One-stage, 3550 rpm, VSC	50–900	50–400	75
One-stage, 1750 rpm, VSC	50–3500	50–200	200
One-stage, 3550 rpm, HSC	100–1500	100–450	150
One-stage, 1750 rpm, HSC	250–5000	50–500	250
Two-stage, 3550 rpm, HSC	50–1100	300–1100	250
Two-stage, 3550 rpm, HSC	100–1500	650–3200	1450

Vertical mixed flow: $C = 0.044(\text{gpm})^{0.82}$K\$, $500 < \text{gpm} < 130,000$
Vertical axial flow: $C = 0.024(\text{gpm})^{0.78}$K\$, $1000 < \text{gpm} < 130,000$
Gear pumps: $C = 1.218 \exp[-0.0881 + 0.1986(\ln Q) + 0.0291(\ln Q)^2]$K\$, $10 < Q < 900$ gpm

Reciprocating:
Cast iron: $C = 76.9Q^{0.81}$K\$, $15 < Q < 400$ gpm
Others: $C = 795FQ^{0.52}$K\$, $1 < Q < 400$ gpm

316 stainless	$F = 1.00$
Al bronze	1.40
Nickel	1.86
Monel	2.20

15. Refrigeration: $C = 178FQ^{0.65}$K\$, $0.5 < Q < 400$ M Btu/hr, installed prices

Temperature Level (°C)	F
0	1.00
−10	1.55
−20	2.10
−30	2.65
−40	3.20
−50	4.00

16. Steam ejectors and vaccum pumps

Ejectors: $C = 13.3f_1f_2f_3X^{0.41}$K\$, $0.1 < X < 100$
$X = (\text{fb air/hr})/(\text{suction pressure in Torr})$

Type	f_1	No. Stages	f_2	Material	f_3
No condenser	1.0	1	1.0	carbon steel	1.0
1 surface condenser	1.6	2	1.8	stainless steel	2.0
1 barometric condenser	1.7	3	2.1	astelloy	3.0
2 surface condensers	2.3	4	2.6		
2 barometric condensers	1.9	5	4.0		

Vacuum pumps: $C = 9.93X^{1.03}$K\$,
$0.3 < X < 15$ (lbs air/hr)/(suction Torr).

17. Vessels prices in \$

Horizontal pressure vessels: $C = F_M C_b + C_a$
$C_b = 1.218 \exp[8.571 - 0.2330(\ln W) + 0.04333(\ln W)^2]$, $800 < W < 914,000$ lb shell weight
$C_a = 1669D^{0.2029}$, $3 < D < 12$ ft diameter (platforms and ladders)

Vertical vessels: $C = F_M C_b + C_a$

$C_b = 1.218 \exp[9.100 - 0.2889(\ln W) + 0.04576(\ln W)^2]$, $5000 < W < 226,000$ lb
$C_a = 300D^{0.7396}L^{0.7066}$, $6 < D < 10, 12 < L < 20$ ft tangent-to-tangent

Material	Cost Factor F_M
Stainless steel, 304	1.7
Stainless steel, 316	2.1
Carpenter 20CB-3	3.2
Nickel-200	5.4
Monel-400	3.6
Inconel-600	3.9
Incoloy-825	3.7
Titanium	7.7

TABLE 21.2.—(_continued_**)**

Storage tanks, shop fabricated: $C = 1.218 F_M \exp[2.631 + 1.3673(\ln V) - 0.06309(\ln V)^2]$, $1300 < V < 21,000$ gal
Storage tanks, field erected: $C = 1.218 F_M \exp[11.662 - 0.6104(\ln V) + 0.04536(\ln V)^2]$, $21,000 < V < 11,000,000$ gal

Material of Construction	Cost Factor F_M
Stainless steel 316	2.7
Stainless steel 304	2.4
Stainless steel 347	3.0
Nickel	3.5
Monel	3.3
Inconel	3.8
Zirconium	11.0
Titanium	11.0
Brick-and-rubber-or brick-and-polyester-lined steel	2.75
Rubber- or lead-lined steel	1.9
Polyster, fiberglass-reinforced	0.32
Aluminium	2.7
Copper	2.3
Concrete	0.55

EXAMPLE 21.1
Installed Cost of a Distillation Tower
Shell and trays are made of AISI 304 stainless steel. Dimensional data are:

$D = 4$ ft,
$L = 120$ ft,
$N = 58$ sieve trays,
wall thickness $t_p = 0.50$ in. for pressure,
$t_b = 0.75$ in. at the bottom,
flanged and dished heads weigh 325 lb each,
weight $W = (\pi/4)(16)(120(0.5/12)(501) + 2(325) = 32,129$ lb

$$C_b = 1.218 \exp[7.123 + 0.1478(10.38) + 0.02488(10.38)^2$$
$$+ 0.158(120/4)\ln(0.75/0.50)] = 697,532,$$

$f_1 = 1.7$,
$f_2 = 1.189 + 0.0577(4) = 1.420$,

$f_3 = 0.85$,
$f_4 = 1$,
$C_t = 457.7 \exp[0.1739(4)] = 917.6$,
$C_{p1} = 249.6(4)^{0.6332}(120)^{0.8016} = 27,923$
purchase price $C = 1.7(697,532) + 58(1.42)(0.85)(917.6)$
$\qquad\qquad + 27,867 = \$1,266,414 \;\$1,266,470$
From Table 3, the installation factor is 2.1 so that the installed price is

$$C_{\text{installed}} = 2.1(\$1,266,470) = \$2,659,587.$$

A tower packed with 2 in. pall rings instead of trays:
packing volume $V_p = (\pi/4)(4)^2(120) = 1508$ cuft,

$$C_{\text{installed}} = 2.1[1.7(697,532) + 1508(28.0) + 27,923] = 2,637,436$$

EXAMPLE 21.2
Purchased and Installed Prices of Some Equipment
a. A box type fired heater with CrMo tubes for pyrolysis at 1500 psig with a duty of 40 million Btu/hr. From Item No. 10 (Table 21.2), the installed price is $ 1,228,000

$$C_{\text{installed}} = (1218)33.8(1.0 + 0.10 + 0.15)(40)^{0.86} = 1,219,602$$

b. A 225 HP reciprocating compressor with motor drive and belt drive coupling. Items Nos. 2 and 13 (Table 21.2). The installation factor is 1.3.
Compressor $C = 7190(225)^{0.61} = 197,572$,

$$\text{motor}, 1800 \text{ rpm}, \text{TEFC}, C = 1.46 \times \exp[4.5347 + 0.57065(5.42)$$
$$+ 0.04069(5.42)^2] = \$11,858$$

belt drive coupling, $C = 1.46 \exp[3.689 + 0.8917(5.42)]$
$\qquad\qquad = \$8,772$,
total installed cost, $C_{\text{total}} = 1.3(197,572 + 11,858 + 8772)$
$\qquad\qquad = \$283,663$.
c. A two-stage steam ejector with one surface condenser to handle 200 lb/hr of air at 25 Torr, in carbon steel construction. From Table 21.3 the installation factor is 1.7.
$X = 200/25 = 8$,
$f_1 = 1.6, f_2 = 1.8, f_3 = 1.0$
purchase $C_p = 13.3(1.6)(1.8(1.0)(8))^{0.41} = \$90,510$,
installed $C = 1.7C_p = \$153,866$.

TABLE 21.3. Multipliers for Installed Costs of Process Equipment[a]

Equipment	Multiplier	Equipment	Multiplier
Agitators, carbon steel	1.3	Heat exchangers, shell and tube, carbon/steel/aluminum	2.2
stainless steel	1.2	shell and tube, carbon steel/copper	2.0
Air heaters, all types	1.5	shell and tube, carbon steel/Monal	1.8
Beaters	1.4	shell and tube, Monel/Monel	1.6
Blenders	1.3	shell and tube, carbon steel/Hastelloy	1.4
Blowers	1.4	Instruments, all types	2.5
Boilers	1.5	Miscellaneous, carbon steel	2.0
Centrifuges, carbon steel	1.3	stainless steel	1.5
stainless steel	1.2	Pumps, centrifugal, carbon steel	2.8
Chimneys and stacks	1.2	centrifugal, stainless steel	2.0
Columns, distillation, carbon steel	3.0	centrifugal, Hastelloy trim	1.4
distillation, stainless steel	2.1	centrifugal, nickel trim	1.7
Compressors, motor driven	1.3	centrifugal, Monel trim	1.7
steam on gas driven	1.5	centrifugal, titanium trim	1.4
Conveyors and elevators	1.4	all others, stainless steel	1.4
Cooling tower, concrete	1.2	all others, carbon steel	1.6
Crushers, classifiers and mills	1.3	Reactor kettles, carbon steel	1.9
Crystallizers	1.9	kettles, glass lined	2.1
Cyclones	1.4	kettles, carbon steel	1.9
Dryers, spray and air	1.6	Reactors, multitubular, stainless steel	1.6
other	1.4	multitubular, copper	1.8
Ejectors	1.7	multitubular, carbon steel	2.2
Evaporators, calandria	1.5	Refrigeration plant	1.5
thin film, carbon steel	2.5	Steam drums	2.0
thin film, stainless steel	1.9	Sum of equipment costs, stainless steel	1.8
Extruders, compounding	1.5	Sum of equipment costs, carbon steel	2.0
Fans	1.4	Tanks, process, stainless steel	1.8
Filters, all types	1.4	Tanks, process, copper	1.9
Furnaces, direct fired	1.3	process, aluminum	2.0
Gas holders	1.3	storage, stainless steel	1.5
Granulators for plastic	1.5	storage, aluminum	1.7
Heat exchangers, air cooled, carbon steel	2.5	storage, carbon steel	2.3
coil in shell, stainless steel	1.7	field erected, stainless steel	1.2
Glass	2.2	field erected, carbon steel	1.4
Graphite	2.0	Turbines	1.5
plate, stainless steel	1.5	Vessels, pressure, stainless steel	1.7
plate, carbon steel	1.7	pressure, carbon steel	2.8
shell and tube, stainless/stainless steel	1.9		

[a][J. Gran, *Chem. Eng.*, (6 Apr. 1981)].
Installed Cost = (purchase price) (multiplier).
Note: The multipliers have remained essentially the same through late 2002.

Example 21.1 and 21.2 illustrate the use of the algorithms to obtain equipment cost data.

REFERENCES

Chemical Engineering Magazine, Modern Cost Engineering, McGraw-Hill, New York, 1979.

Chemical Engineering Magazine, Modern Cost Engineering II, McGraw-Hill, New York, 1984.

J. Cran, Improved factor method give better preliminary cost estimates, *Chemical Engineering Magazine, Modern Cost Engineering II*, McGraw-Hill, New York, 1984, pp. 76–90.

L.B. Evans, A. Mulet, A.B. Corripio, and K.S. Chretien, Costs of pressure vessels, storage tanks, centrifugal pumps, motors, distillation and absorption towers, in *Chemical Engineering Magazine, Modern Cost Engineering II*, McGraw-Hill, New York, 1984, pp. 140–146, 177–183.

D.W. Green, and J. O. Maloney (Eds.), *Perry's Chemical Engineers' Handbook*, 6th ed., McGraw-Hill, New York, 1984, cost data on pp. 6.7, 6.22, 6.112, 6.113, 6.121, 7.19, 11.19, 11.20, 11.21, 11.29, 11.42, 17.27, 17.33,

18.45, 18.46, 18.47, 19.13, 19.40, 19.45, 19.65, 19.89, 19.101, 19.102, 20.37, 20.38, 21.22, 21.45, 22.134, 22.135, 25.69, 25.73–25.75.

R.S. Hall, J. Matley, and K.J. McNaughton, *Chemical Engineering Magazine, Modern Cost Engineering II*, McGraw-Hill, New York, 1984, pp. 102–137.

Institut Francaise du Petrole (IFP), *Manual of Economic Analysis of Chemical Processes*, Technip 1976, McGraw-Hill, New York, 1981.

B.G. Liptak, Costs of process instruments, in *Chemical Engineering Magazine, Modern Cost Engineering*, McGraw-Hill, New York, pp. 1979, 343–375.

C. Meyers and J. Kime, *Chemical Engineering*, (McGraw-Hill, New York) pp. 109–112 (September 1976).

A. Pikulik and H.E. Diaz, Costs of process equipment and other items, in *Chemical Engineering Magazine, Modern Cost Engineering*, 1979, pp. 302–317.

G.P. Purohit, Costs of shell-and-tube heat exchangers, *Chemical Engineering*, 22 (August 1983, 4 March 1985, 18 March 1985).

G.D. Ulrich, *A Guide to Chemical Engineering Process Design and Economics*, Wiley, New York, 1984.

W.M. Vatavuk, Coasts of baghouses, electrostatic precipitators, venturi scrubbers, carbon adsorbers, flares and incinerators, in *Estimating Costs of Air Pollution Control*, Lewis Publishers, Chelsea, MI, 1990.

Appendix A

UNITS, NOTATION, AND GENERAL DATA

TABLE A1. Units and Conversions

Prefixes for Unit Multiples and Submultiples:

10^{-18} atto	a	10^1	deca	da
10^{-15} femto	f	10^2	hecto	h
10^{-12} pico	p	10^3	kilo	k
10^{-9} nano	n	10^6	mega	M
10^{-6} micro	μ	10^9	giga	G
10^{-3} milli	m	10^{12}	tera	T
10^{-2} centi	c			
10^{-1} deci	d			

Length:

$$1\,\text{ft} = 0.3048\,\text{m} = 30.48\,\text{cm} = 304.8\,\text{mm}$$

Volume:

$$1\,\text{cuft} = 0.0283\,\text{cum} = 7.481\,\text{U.S. gal}$$
$$1\,\text{cum} = 35.34\,\text{cuft} = 1000\,\text{L}$$

Standard gas volume:

22.414 L/g mol at 0°C and 1 atm
359.05 cuft/lb mol at 32°F and 1 atm

Gas constant R:

Energy	Temperature Mole		R
lb ft^2/sec^2	°Rankine	lb	4.969×10^4
ft lbf	°Rankine	lb	1544
cuft atm	°Rankine	lb	0.7302
cuft (lbf/sqin.)	°Rankine	lb	10.73
Btu	°Rankine	lb	1.987
hP hr	°Rankine	lb	7.805×10^{-4}
kW hr	°Rankine	lb	5.819×10^{-4}
J (abs)	Kelvin	g	8.314
kg m^2/sec^2	Kelvin	kg	8.314×10^3
kg fm	Kelvin	kg	8.478×10^2
cucm atm	Kelvin	g	82.0562
calorie	Kelvin	g	1.987

Gravitational constant:

$$g_c = 1\,\text{kg mass/N sec}^2$$
$$= 1\,\text{g cm/dyn sec}^2$$
$$= 9.806\,\text{kg mass/kg force sec}^2$$
$$= 32.174\,\text{lb mass/lb force sec}^2$$

Mass:

$$1\,\text{lb} = 0.4536\,\text{kg}$$
$$1\,\text{kg} = 2.2046\,\text{lb}$$

Density:

1 lb/cuft = 16.018 kg/cum
1 gm/cucm = 62.43 lb/cuft
°API = 141.5/(specific gravity) − 131.5
specific gravity = 141.5/(°API + 131.5)

Force:

1 lb force = 0.4536 kg force = 4.448 Newtons

Pressure:

$$1\,\text{atm} = 760\,\text{Torr} = 760\,\text{mm Hg} = 101,325\,\text{N/sqm}$$
$$= 1.01325\,\text{bar} = 10,330\,\text{kg/sqm} = 14.696\,\text{lbf/sq in}$$
$$= 2,116.2\,\text{lbf/sqft}$$
$$1\,\text{bar} = 100,000\,\text{N/sqm}$$
$$1\,\text{Pa} = 1\,\text{N/sqm}$$

Energy, work, and heat:

$$1\,\text{Btu} = 252.16\,\text{cal} = 1055.06\,\text{J} = 0.2930\,\text{W hrs}$$
$$= 10.41\,\text{L atm}$$
$$1\,\text{HP hr} = 0.7457\,\text{kWh} = 778\,\text{ft lbf} = 2545\,\text{cal}$$
$$1\,\text{cal} = 4.1868\,\text{J}$$
$$1\,\text{J} = 1\,\text{N m} = 1\,\text{W sec} = 0.2388\,\text{cal} = 0.000948\,\text{Btu}$$

Power:

$$1\,\text{ft lbf/sec} = 0.0018182\,\text{HP} = 1.356\,\text{W} = 0.0012856$$
$$\text{Btu/sec} = 0.3238\,\text{cal/sec}$$
$$1\,\text{W} = 1\,\text{J/sec} = 1\,\text{N m/sec}$$

Temperature:

K (Kelvin) = °C (centigrade) + 273.16 = [°F (Fahrenheit) + 459.6]/1.8 = °R (Rankine)/1.8
°R = 1.8 K = °F + 459.6
°C = (°F − 32)/1.8

Temperature difference:

1°C = 1°K = 1.8°R = 1.8°F

Heat capacity and entropy:

1 cal/(g) (°K) = 4.1868 J/(g)(°K) = Btu/(lb)(°R)

TABLE A1.—(continued**)**

Specific energy:

$$1\,\text{cal/g} = 4.1868\,\text{J/g} = 1.8\,\text{Btu/lb}$$

Volumetric flow:

$$1\,\text{cuft/sec} = 0.028316\,\text{cum/sec} = 28.316\,\text{L/sec}$$

Heat flux:

$$1\,\text{Btu/(hr)(ft}^2) = 3.1546\,\text{W/m}^2$$
$$= 2.172\,\text{kcal/(hr)(m}^2)$$

Heat transfer coefficient:

$$1\,\text{Btu/(hr)(ft}^2)(F) = 5.6783\,\text{W/m}^2\text{K}$$

Surface tension:

$$1\,\text{dyn/cm} = 1\,\text{erg/cm}^2$$
$$= 0.001\,\text{N sec/m}^2$$

Viscosity, dynamic:

$$1\,\text{cP} = 0.001\,\text{N sec/m}^2$$
$$= 0.001\,\text{Pa sec}$$
$$= 0.000672\,\text{lb}_\text{m}/\text{ft sec}$$
$$= 2.42\,\text{lb}_\text{m}/\text{ft hr}$$
$$= 0.0752\,\text{lb}_\text{f}\,\text{hr}/\text{ft}^2$$

Viscosity, kinematic:

$$1\,\text{centistoke} = 0.00360\,\text{m}^2/\text{hr}$$
$$= 0.0388\,\text{ft}^2/\text{hr}$$

TABLE A2. Notation[a]

C_p	=	heat capacity at constant pressure
C_V	=	heat capacity at constant volume
g_c	=	gravitational constant (numerical values in Table A1)
h	=	individual heat transfer coefficient
H	=	enthalpy
k	=	thermal conductivity
k	=	C_p/C_v
$K = y/x$	=	vaporization equilibrium ratio, VER
m_i	=	mass fraction of component i of a mixture
M	=	molecular weight
P	=	pressure
Q	=	volumetric flow rate
Q	=	heat transfer rate
R	=	gas constant (numerical values in Table A1)
S	=	entropy
T	=	temperature, usually °R or °K
u	=	linear velocity
U	=	overall heat transfer coefficient
V	=	volume
x_i	=	mol fraction of component i in the liquid phase
y_i	=	mol fraction of component i in the vapor phase
z_i	=	mol fraction of component i in a mixture
z	=	PV/RT, compressibility
μ	=	viscosity
ρ	=	density
σ	=	surface tension

[a]Most symbols are defined near where they are used in equations. Unless defined otherwise locally, certain notations have the meanings in this list.

TABLE A3. Properties of Steam and Water

Temp., °F	Absolute pressure, lb/sq in.	Latent heat of evaporation, Btu/lb	Specific volume of steam, cu ft/lb	Density of liquid water, lb/cu ft	Viscosity of liquid water, centipoises	Thermal conductivity of liquid water, (Btu)(ft)/(°F)(ft²)(hr)
32	0.0885	1075.8	3306	62.42	1.786	0.320
35	0.1000	1074.1	2947	62.42	1.689	0.322
40	0.1217	1071.3	2444	62.42	1.543	0.326
45	0.1475	1068.4	2036.4	62.42	1.417	0.329
50	0.1781	1065.6	1703.2	62.39	1.306	0.333
55	0.2141	1062.7	1430.7	62.39	1.208	0.336
60	0.2563	1059.9	1206.7	62.35	1.121	0.340
65	0.3056	1057.1	1021.4	62.30	1.044	0.343
70	0.3631	1054.3	867.9	62.28	0.975	0.346
75	0.4298	1051.5	740.0	62.23	0.913	0.349
80	0.5069	1048.6	633.1	62.19	0.857	0.352
85	0.5959	1045.8	543.5	62.14	0.807	0.355
90	0.6982	1042.9	468.0	62.12	0.761	0.358
95	0.8153	1040.1	404.3	62.03	0.719	0.360
100	0.9492	1037.2	350.4	62.00	0.681	0.362
105	1.1016	1034.3	304.5	61.92	0.646	0.364
110	1.275	1031.6	265.4	61.85	0.614	0.367
115	1.471	1028.7	231.9	61.80	0.585	0.369
120	1.692	1025.8	203.27	61.73	0.557	0.371
125	1.942	1022.9	178.61	61.66	0.532	0.373
130	2.222	1020.0	157.34	61.55	0.509	0.375
135	2.537	1017.0	138.95	61.46	0.487	0.376
140	2.889	1014.1	123.01	61.39	0.467	0.378
145	3.281	1011.2	109.15	61.28	0.448	0.379
150	3.718	1008.2	97.07	61.21	0.430	0.381
155	4.203	1005.2	86.52	61.10	0.414	0.382
160	4.741	1002.3	77.29	61.01	0.398	0.384
165	5.335	999.3	69.19	60.90	0.384	0.385
170	5.992	996.3	62.06	60.79	0.370	0.386
175	6.715	993.3	55.78	60.68	0.357	0.387
180	7.510	990.2	50.23	60.58	0.345	0.388
185	8.383	987.2	45.31	60.47	0.334	0.389
190	9.339	984.1	40.96	60.36	0.333	0.390
195	10.385	981.0	37.09	60.25	0.312	0.391
200	11.526	977.9	33.64	60.13	0.303	0.392
205	12.777	974.8	30.57	60.02	0.293	0.392
210	14.123	971.6	27.82	59.88	0.284	0.393
212	14.696	970.3	26.80	59.75	0.281	0.393
215	15.595	968.4	25.37	59.70	0.277	0.393
220	17.186	965.2	23.15	59.64	0.270	0.394
225	18.93	962.0	21.17	59.48	0.262	0.394
230	20.78	958.8	19.382	59.39	0.255	0.395
235	22.80	955.5	17.779	59.24	0.248	0.395
240	24.97	952.2	16.323	59.10	0.242	0.396
245	27.31	948.9	15.012	58.93	0.236	0.396
250	29.82	945.5	13.821	58.83	0.229	0.396
260	35.43	938.7	11.763	58.52	0.218	0.396
270	41.86	931.8	10.061	58.24	0.208	0.396
280	49.20	924.7	8.645	57.94	0.199	0.396
290	57.55	917.5	7.461	57.64	0.191	0.396
300	67.01	910.1	6.466	57.31	0.185	0.396
310	77.68	902.6	5.626	56.98		0.396
320	89.66	894.9	4.914	56.55		0.395
330	103.06	887.0	4.307	56.31		0.393
340	118.01	879.0	3.788	55.96		0.392
350	134.62	870.7	3.342	55.59		0.390
360	153.04	862.2	2.957	55.22		0.388
370	173.37	853.5	2.625	54.85		0.387
380	195.77	844.6	2.335	54.46		0.385
390	220.37	835.4	2.0836	54.05		0.383
400	247.31	826.0	1.8633	53.65		0.382

Source: Condensed from Keenan and Keyes, *Thermodynamic Properties of Steam*, Wiley, New York, 1936).

TABLE A4. Properties of Air and Steam at Atmospheric Pressure

T (F)	ρ (lb$_m$/cuft)	c_p (Btu/lb$_m$F)	$\mu \times 10^5$ (lb$_m$/ftsec)	$\nu \times 10^3$ (sqft/sec)	k (Btu/hr ft F)
Air					
0	0.086	0.239	1.110	0.130	0.0133
32	0.081	0.240	1.165	0.145	0.0140
100	0.071	0.240	1.285	0.180	0.0154
200	0.060	0.241	1.440	0.239	0.0174
300	0.052	0.243	1.610	0.306	0.0193
400	0.046	0.245	1.750	0.378	0.0212
500	0.0412	0.247	1.890	0.455	0.0231
600	0.0373	0.250	2.000	0.540	0.0250
700	0.0341	0.253	2.14	0.625	0.0268
800	0.0314	0.256	2.25	0.717	0.0286
900	0.0291	0.259	2.36	0.815	0.0303
1000	0.0271	0.262	2.47	0.917	0.0319
1500	0.0202	0.276	3.00	1.47	0.0400
2000	0.0161	0.286	3.45	2.14	0.0471
2500	0.0133	0.292	3.69	2.80	0.051
3000	0.0114	0.297	3.86	3.39	0.054
Steam					
212	0.0372	0.451	0.870	0.234	0.0145
300	0.0328	0.456	1.000	0.303	0.0171
400	0.0288	0.462	1.130	0.395	0.0200
500	0.0258	0.470	1.265	0.490	0.0228
600	0.0233	0.477	1.420	0.610	0.0257
700	0.0213	0.485	1.555	0.725	0.0288
800	0.0196	0.494	1.700	0.855	0.0321
900	0.0181	0.50	1.810	0.987	0.0355
1000	0.0169	0.51	1.920	1.13	0.0388
1200	0.0149	0.53	2.14	1.44	0.0457
1400	0.0133	0.55	2.36	1.78	0.053
1600	0.0120	0.56	2.58	2.14	0.061
1800	0.0109	0.58	2.81	2.58	0.068
2000	0.0100	0.60	3.03	3.03	0.076
2500	0.0083	0.64	3.58	4.30	0.096
3000	0.0071	0.67	4.00	5.75	0.114

TABLE A5. Properties of Steel Pipe

Nominal pipe size, in.	OD, in.	Schedule No.	ID, in.	Flow area per pipe, in.^{2}	Surface per lin ft, ft^2		Weight per lin ft, lb steel
					Outside	Inside	
1/8	0.405	40†	0.269	0.058	0.106	0.070	0.25
		80‡	0.215	0.036	0.106	0.056	0.32
1/4	0.540	40	0.364	0.104	0.141	0.095	0.43
		80	0.302	0.072	0.141	0.079	0.54
3/8	0.675	40	0.493	0.192	0.177	0.129	0.57
		80	0.423	0.141	0.177	0.111	0.74
1/2	0.840	40	0.622	0.304	0.220	0.163	0.85
		80	0.546	0.235	0.220	0.143	1.09
3/4	1.05	40	0.824	0.534	0.275	0.216	1.13
		80	0.742	0.432	0.275	0.194	1.48
1	1.32	40	1.049	0.864	0.344	0.274	1.68
		80	0.957	0.718	0.344	0.250	2.17
1 1/4	1.66	40	1.380	1.50	0.435	0.362	2.28
		80	1.278	1.28	0.435	0.335	3.00
1 1/2	1.90	40	1.610	2.04	0.498	0.422	2.72
		80	1.500	1.76	0.498	0.393	3.64
2	2.38	40	2.067	3.35	0.622	0.542	3.66
		80	1.939	2.95	0.622	0.508	5.03
2 1/2	2.88	40	2.469	4.79	0.753	0.647	5.80
		80	2.323	4.23	0.753	0.609	7.67
3	3.50	40	3.068	7.38	0.917	0.804	7.58
		80	2.900	6.61	0.917	0.760	10.3
4	4.50	40	4.026	12.7	1.178	1.055	10.8
		80	3.826	11.5	1.178	1.002	15.0
6	6.625	40	6.065	28.9	1.734	1.590	19.0
		80	5.761	26.1	1.734	1.510	28.6
8	8.625	40	7.981	50.0	2.258	2.090	28.6
		80	7.625	45.7	2.258	2.000	43.4
10	10.75	40	10.02	78.8	2.814	2.62	40.5
		60	9.75	74.6	2.814	2.55	54.8
12	12.75	30	12.09	115	3.338	3.17	43.8
16	16.0	30	15.25	183	4.189	4.00	62.6
20	20.0	20	19.25	291	5.236	5.05	78.6
24	24.0	20	23.25	425	6.283	6.09	94.7

†Schedule 40 designates former ''standard'' pipe.
‡Schedule 80 designates former ''extra-strong'' pipe.

TABLE A6. Standard Gauges of Sheets, Plates, and Wires

Sheet mills roll steel sheets to U. S. gauge unless otherwise ordered. Plate mills usually roll heavy plates, $\frac{3}{16}$ and heavier, and light plate No. 8 to No. 12, to Birmingham gauge. In figuring weights of steel plates add to above the allowance for overweight, adopted by Association American Steel Manufacturers. All steel sheets in our stock are rolled to the U. S. Standard Gauge. Brass is rolled to thickness by Brown & Sharpe's American Gauge. Copper is rolled to thickness by Stubs' or Birmingham Gauge.

| No. of Gauge | THICKNESS AND WEIGHT OF SHEETS AND PLATES | | | | | | WIRE |
| | U. S. Standard Gauge Adopted by U. S. Government March 1, 1937 | | Birmingham or Stubs' Gauge | | American or Brown & Sharpe's Gauge | | Washburn & Moen Gauge |
	Thickness Inches	Weight Lbs. per Sq. Ft.	Thickness, Inches	Weight Lbs. per Sq. Ft.	Thickness, Inches	Weight Lbs. per Sq. Ft.	Thickness, Inches
000	$\frac{3}{8}$	......	15.00	.425	17.28	.410	16.71	.363
00	$\frac{11}{32}$	......	13.75	.380	15.45	.365	14.88	.331
0	$\frac{21}{64}$	......	12.50	.340	13.82	.325	13.26	.307
1	$\frac{19}{64}$	......	11.25	.300	12.20	.289	11.80	.283
2	$\frac{9}{32}$	......	10.625	.284	11.55	.258	10.51	.263
3	$\frac{1}{4}$	.239	10.00	.259	10.53	.229	9.36	.244
4	$\frac{15}{64}$	.224	9.375	.238	9.68	.204	8.34	.225
5	$\frac{7}{32}$	.209	8.75	.220	8.95	.182	7.42	.207
6	$\frac{3}{16}$	.194	8.125	.203	8.25	.162	6.61	.192
7	$\frac{11}{64}$	.179	7.50	.180	7.32	.144	5.89	.177
8	$\frac{5}{32}$	.164	6.875	.165	6.71	.128	5.24	.162
9	$\frac{9}{64}$	.149	6.25	.148	6.02	.114	4.67	.148
10	$\frac{1}{8}$	.134	5.625	.134	5.45	.102	4.16	.135
11	$\frac{7}{64}$	.120	5.00	.120	4.88	.091	3.70	.120
12	$\frac{1}{10}$	.105	4.375	.109	4.43	.08	3.30	.105
13	$\frac{3}{32}$	.09	3.75	.095	3.86	.072	2.94	.092
14	$\frac{5}{64}$	.075	3.125	.083	3.37	.064	2.62	.080
15	......	.067	2.813	.072	2.93	.057	2.33	.072
16	$\frac{1}{16}$	.060	2.50	.065	2.64	.05	2.07	.063
17	......	.054	2.25	.058	2.36	.045	1.85	.054
18	$\frac{3}{64}$	.048	2.00	.049	1.99	.04	1.64	.047
19	......	.042	1.75	.042	1.71	.036	1.46	.041
20	......	.036	1.50	.035	1.42	.032	1.31	.035
21	$\frac{1}{32}$	.033	1.375	.032	1.30	.028	1.16	.032
22	......	.030	1.25	.028	1.14	.025	1.03	.027
23	......	.027	1.125	.025	1.02	.023	.922	.026
24	......	.024	1.00	.022	.895	.020	.82	.023
25	......	.021	.875	.020	.813	.018	.73	.020
26	......	.018	.750	.018	.732	.016	.649	.018
27	......	.016	.687	.016	.651	.014	.579	.017
28	......	.015	.625	.014	.569	.012	.514	.016
29	......	.014	.563	.013	....	.011	.461	.015
30	......	.012	.500	.012	....	.01	.408	.014

TABLE A7. Weights and Angles of Slide of Various Materials

***Weights of Materials**—The following list gives weights in pounds per cubic foot. Unless otherwise noted, weights are for material in loose, least compacted form. **In figuring Horse Powers**, weights should be increased in proportion to their compressibility.

†**Angles of Slide**—The angles given are the **minimum** at which the various materials will slide on a steel plate, under **best** condition, for determination of friction. The minimum angle will **increase** as size of particles decrease and with higher moisture content. For definite recommendations refer to S-A Engineers. The inclination of **chutes must be steeper** than minimum angle of slide and S-A Engineers should be consulted for minimum chute slopes.

Friction Factors—The moving-friction factor for any material listed, sliding on steel plate, equals the natural tangent of the "angle of slide" given for that material. See table of natural functions of angles—listed in data section of book. **For example**, the friction factor of cement equals .809 (the natural tangent of 39°, which is the angle of slide for cement).

Specific Gravity—The specific gravity of a material is its weight (in a solid block) compared with that of water at 62° F. Example: As water weighs 62.4 pounds per cubic foot and sulphur weighs 125 pounds, the specific gravity of sulphur is twice that of water or 2.0.

Green Timber—Usually weighs from one-fifth to nearly one-half more than dry. Ordinary building timbers, tolerably seasoned, weigh about one-sixth more.

▲ Solid Cube of material—weights of broken or crushed material decrease, for example, see figures given for coal and for limestone.
** Figures listed are for best conditions (dry, sized and without dust)—The minimum angle will **increase** as size of particles decrease and with higher moisture content. For other conditions refer to S-A Engineers for definite recommendations.

DESCRIPTION	Average Wt. per cu. ft. pounds*	Minimum Angle of Slide†	DESCRIPTION	Average Wt. per cu. ft. pounds*	Minimum Angle of Slide†
Air (Atmospheric at 60°F., Under pressure of one atmosphere, 14.7 lbs. per square in., weighs 1/815 as much as water)	.0765	....	Cellulose Acetate, granular	10	33°
Alabaster (marble) ▲	168	....	Cement, Portland (per Bbl. net 376 lbs.) (per bag 94 lbs.)	90–100	39°
Alabaster (Real, a compact white plaster of Paris) ▲	144	....	" Mortar, Portland, 1:2½	135	....
Alfalfa, Ground	15	31°**	Chalk, ▲	137	....
" Coarse	9	31°	" Precipitated, Powdered	18	45°
Alumina, sized or briquette	65	22°	Charcoal, Bone, (Carbonated), granular	60	27°
Alumina, Fine, Granulated	55	35°**	" Wood Pulp, granular	26.4	35°
Alum, ground	62	35°**	Chips, Wood	15–30	22°
Aluminum Hydrate, Ground	13½	34°*	Chocolate, Powder	40	45°
Aluminum, Sulphate, Granular	54	32°	Chromic Acid, Flake	75	25°
Ammonium, Sulphate, Damp Granulated	40	45°	Cinders, (Coal, Ashes and Clinkers)	40–45	35°**
Argols, Roasted, Pulverized	63	32°	" Blast Furnace	57	35°**
Ash, Black, Ground	105	27°**	Clay, Dry in Lump Loose	40–100	35°
" Fly, Powdered	45	40–45°**	" Blended for Tile 11% Moist, Powdered	45	45°
" Volcanic, Powdered	45	45°**	" Ground	60–100	35°
Ashes of Bituminous Coal	35–45	40°	" Fire, Powdered	25–80	45°
" Damp	40–50	50°	" Gray, Granular	50–95	35°
Asphaltum	81	....	" Pulverized Fire Brick	100	35°
Babassu Nuts, ground	45	40°**	Coal, Anthracite, (Solid) ▲	97	....
Bagasse, Wet Sawdust	4	45°**	" " broken of any Size, Loose	52 to 57	22°
Baking Powder	47	38°	" " " Moderately Shaken	56 to 60	
Barytes, Granular	144	30°**	" " " , one ton, loose, occupies 40 to 43 cu. ft.		
Basalt (Similar to Marble) ▲	184	....	" " Chestnut	46	22°
Bathstone, Oolite ▲	131	....	Coal, Bituminous, (Solid) ▲	84	....
Bauxite, Calcined (Granular without dust)	70	26°	" " minus ¼", slack, dry	40–50	29°
" Ground dried	68	35°	" " " " " moderately wet	45–55	40°
" Mine run	85	31°**	" " " " " very wet	50–60	33°
Bentonite, pulverized	50	42°	" " broken, 1 ton, loose, occupies 43 to 48 cu. ft.		
Bismuth ▲	612.4		" " sized, wet or dry	40–50	27"
Bones, Animal, pulverized	50	50°	" " pulverized	30	40°
Bone Char, ground	40	35°	Cocoanut (see Grains, Seeds and Cereals)		
Borax, Dehydrated, powdered	75	40°	Coke, pulverized	25	34°
Bran	16–26	36°	" Loose, 1 ton occupies 80 to 97 cu. ft.	23 to 32	
Brick, Best Pressed ▲	140	....	" Petroleum, crushed	33–36	27°
" Common ▲	120	....	Concrete, Cinder with Portland Cement ▲	112	....
" Fire ▲	137 to 144	....	" Gravel and Sand with Portland Cement ▲	150	....
" Soft inferior ▲	100	....	" Trap with Portland Cement ▲	155	....
Brickwork, Press Brick, fine joints ▲	128	....	Copper, Oxide, Powdered	190	40°
" Medium Quality	112	....	" Sulphate, Ground	75	31°**
" Coarse, Inferior or Soft ▲	103	....	Cork, ¾" to 0"	6	30°
Calcium Bichromate, Granular	62	25°	Cryolite ½" to 200 mesh, crushed	52	32°
" Carbide ▲	139	....	Cullet (Scrap Glass Sized)	80–120	25°
" Carbide, Spent, Powdered	40	45°	Dolomite, pulverized	46	41°
" Carbonate (See Limestone)			" Solid ▲	181	....
" Oxide, Powdered (See Lime)	27	43°	Dust, flue, Blast Furnace	40	45°
" Phosphate, See Phosphates			" Foundry	55–65	38°
Carbon, ground	50	21°	" Limestone	55–65	38°
" Coke, crushed, sized	30	28°	Earth, Common Loam, Perfectly Dry	72 to 80	....
Casein, granular	38–43	30°	" " " Moist	75–85	....
			" Fullers, Raw	42	35°

▲ * † ** See notes preceding table.

TABLE A7—(continued)

DESCRIPTION	Average Wt. per cu. ft. pounds*	Minimum Angle of Slide†	DESCRIPTION	Average Wt. per cu. ft. pounds*	Minimum Angle of Slide†
Eggs	48	....	Gypsum	142	45°
Feldspar, Pulverized	50–60	40°	" In Irregular Lumps	82	30°
" (Crushed)	100	32°	" Ground, see Plaster of Paris	56	40°
Ferric Sulphate▲	194	....	Hornblende, Solid▲	187	....
Ferrous Sulphate (Copperas)▲	119	....	Humus	30–40	....
Flint▲	162	....	Ice▲	57.4	....
Fuller's Earth (See Earth)	....	38°	Ilmenite, granulated	148	31°
Gelatin, Granulated	38	38°	" Fine Ground	120	40°
Glass, Common and Plate▲	161	....	Iron Oxide Pigment	25	40°
" Batch, Average Mix	100	45°	Ivory▲	114	....
Glue (Pellet)	45	25°	Kalsomine (powder)	32	42°
Gneiss, Solid▲	168	....	Kaolin, Green Crushed	64	35°
" in Loose Piles	90–100	....	" Pulverized	22	45°
Grains, Seeds and Cereals			Kieselguhr, crushed	15	40°
Barley (48 lb. per bushel)	38	....	Lead, #70 Red	230	40°
Beans, Cocoa	37	25°	" Silicate, Granulated	230	30°
" Navy	54	22°	" Sulphate, Basic Pulverized	184	45°**
Beans, Soy—Cake	45	32°	Leather▲	59	....
" " Meal	40	27°	Lime, Briquette	60	26°
" " —Flour	27	40°	" Burned, Pebble (sized)	53	30°
Beans, Soy—Crushed	34	35°	Lime, Burned, Pulverized	27	43°
" " Whole	45–50	22°	" Fine (Spent Dry Carbide)	45	40°
" " Split	44	25°	" Mason	17	40°
Bran	16–26	36°	" Burned or Quick, crushed	50	40°
Brewers Grits	33	24°	" Hydrated	10–25	42°
Buckwheat (46 lbs., per bu.)	34.5	25°	Limestone, solid▲	166	....
Clover Seed (60 lbs., per bu.)	48	28°	" Pulverized	85	42°
Cocoa Nibs	32	26°	" Mixed Sizes	105	35°
Cocoanut Meal	32	38°	" Coarse, Sized	98	25°
" Shredded	25	27°	**Liquids**		
Coffee Beans, Green	42	25°	Alcohol	49.3	....
" Steel Cut	28	23°	Benzine	53.1	....
Corn, Field (on cob)	45	20°	Milk	64.3	....
" Shelled (56 lbs. per bu.)	45	21°	Naptha	53.1	....
Corn Flakes	12	22°	Oils, Vegetable	58.7	....
" Germ	25	25°	Oils, Mineral	57.1	....
" " Flakes	25	36°	Petroleum	54.8	....
" Grits	40	24°	Tallow	58.6	....
Cornmeal (50 lbs. per bu.)	40	35°	Turpentine	54	....
" Muffin Mixture	28	45°	Water Pure Rain Distilled @ 32° F. Bar. 30 in	62.417	....
Cotton Seed	25	29°	" " " " @ 62° F. " "	62.355	....
" " Meal	33	35°	" " " " @ 212° F. " "	59.7	....
Farina	44	29°	Water, Sea	64.08	....
Feed Gluten	31	34°	Wood, Spirit	49.9	....
" Molasses	25	40°	Lithapone, Granulated	70	40°
Flax Seed Ground	28	35°	" Pulverized	73	40°
" " (56 lbs. per bu.)	45	21°	Magnesium Carbonate Powdered	9	36°
Flour (196 lbs. per Barrel)	35 to 40	31°	Masonry of Granite or Limestone, Well Dressed	165	....
" Prepared Biscuit	26	40°	" " Brickwork (See Brickwork)	....	....
Grain, Brewers Spent (Sloppy Wet)	84	....	**Metals**		
Grass, Blue, Seed (14 lbs. per bu.)	11.5	30°	Aluminum▲	165	....
Hay in Bales	20	....	Babbitt▲	500–650	....
Hemp Seed (48 lbs. per bu.)	36	....	Brass (7.8 Copper to 8.4 Zinc)▲	504	....
Hominy	45	21°	" Rolled▲	534	....
Linseed Meal	27	34°	Bronze (8 Copper to 1 Tin) (Gunmetal)▲	552	....
Linseed Rolled	25	34°	Cadmium▲	539	....
Malt, Dry	32	21°	Chromium▲	432	....
" Spent Dry	10	28°	Copper Cast▲	542	....
Malt Sugar (Ground) Hygroscopic	35	31°	Copper Rolled▲	555	....
" " (Unground) "	30	31°	Gold, Cast Pure or 24 Karat▲	1204	....
Oats, 32 Lbs. Per Bushel	26	21°	Iron, Cast▲	446	....
" Rolled	18	28°	Iron Ore, Hematite, Magnetite	135	....
Pablum	9	32°	" " , Taconite	115	....
" Waste	14	38°	Lead, Commercial▲	710	....
Rice	50	20°	Magnesium▲	109	....
Rye (56 Lbs. Per Bu.)	45	23°	Magnesium Sulfate (Epsom Salts) Crystals	55	25°
Timothy Seed, (45 Lbs. Per Bu.)	36	28°	Manganese▲	475	....
Wheat (60 Lbs. Per Bu.)	48	23°	Mercury at 32° F.▲	849	....
" Germ	32	30°	Nickel▲	537	....
" " Ground	32	36°	Silver▲	655	....
Granite Solid▲	159	....	Steel▲	489.6	....
Granite, Gneiss▲	175	....	Tin, Cast▲	459	....
Gravel	120	30°	Zinc or Spelter▲	437.5	....
Green Stone, Trap, Solid▲	187	....	Mica, Solid▲	183	....
" " " Quarried in Loose Piles	107	35°	" Ground	13.5	36°
			Milk, Powdered	40	45°

▲ * † ** See notes preceding table

TABLE A7.—(continued)

DESCRIPTION	Average Wt. per cu. ft. pounds*	Minimum Angle of Slide†	DESCRIPTION	Average Wt. per cu. ft. pounds*	Minimum Angle of Slide†
Molasses, Powdered	21	45°	Starch, (Powdered)	25–45	45°
Molybdenumite Ore, Powdered	107	40°	" (Lump & Pelleted)	30	28°
Mortar, Hardened	103	....	" Tablet, Granular Crystals	40	24°
Mud Wet Fluid	108	....	Straw in Bales	25	....
Nails and Spikes, 106 Lbs. Per Keg	....	....	Stucco (Tubed and Untubed), Powdered	50	36° to 38°
Nitrate of Soda, Pellet Type Granular	68	24°	Sulphur, Pulverized	50	45°
Nuchar, Granular	22	30°	" Coarse	76	32°
Paste, Dried, Flaky	10	36°	Sugar, Brown	40–50	45°
Phosphate, Powdered	60	40°	" Powdered	45	45°
" Dicalcium, Granular	60	30°	" Granulated	50	35°
" Super, Ground	51	45°	" Tailings	57	38°
" Tri-Sodium, Granulated	60	26°	Talc, Solid (Soapstone) ▲	169	....
" Tri-Sodium Pulverized	50	40°	" Micaceous, Granulated	62	36°
" Rock ▲	200	....	Tankage, Ground	49	32°
" Florida #20 Mesh, Air Cleaned	93	27°	Tar ▲	75	....
" Mono Calcium, Powdered	61	40°	Tartaric Acid (Cream of Tartar), Granular	60	35°
Phthalic Anhydride, Flaky	42	24°	Tin, Oxide, Ground	100	35°
Pigment (For Rubber Tires) Powdered	52	45°	Titanium Dioxide (paint pigment), powdered	25	45°
Pitch ▲	70	....	Tobacco Stems, Chopped, Coarse	16	23°
" Flake	42	27°	Trap, Rock ▲	187	....
Plaster of Paris, Powdered	50	40°	" Quarried, in Piles	107	....
Potassium, Chloride ▲	124	....	Tripoli (Powdered)	80	40°
" Sulphate ▲	167	....	**Vegetables and Fruits**		
Powder, Face	36	45°	Apples (56# per Bushel)	45	....
Powder, Pudding	40–45	36–40°	" Dried (22# per Bushel)	17	....
Pumice, Pulverized	40	45°	Beets, Shredded Sugar	7.6	31°
Pyrethrum flowers, coarse ground	20	30°	Onions (60# per Bushel)	48	....
" spent flowers	32	40°	Peas (64 Lbs. Per Bushel)	51	....
Pyro, Powdered	56	33°	Potatoes (60 Lbs. Per Bushel)	48	....
Quartz ▲	165	....	Copra, Medium Sized Pieces	33	20°
Resin, Synthetic (from plant), Crushed	40	30°	" Meal, Ground	40	39°
Resin and Wood Flour, Powdered	19	40°	" Expeller Cake Ground	32	30°
Rock, Phosphate Pulv	60	40°	" Expeller Cake Chopped	29	20°
" " Solid ▲	200	....	Walnut Shells, Ground (320 Mesh)	21	55°
" Florida Phosphate #20 Mesh Air Cleaned	93	27°	Wax, Bees ▲	60	....
Rosin (From Crude Turpentine) ▲	67	....	**Woods**		
Rubber, Scrap (Ground)	23	35°	Cedar	22	....
Rutile, Red Oxide of Lead, Fine Ground	132	32°	Cherry (Perfectly Dry)	44	....
" Powdered	107	40°	Chestnut (Dry)	30	....
Salt, Granulated	81	31°	Chips (Dry)	15–32	22°
" Rock Crushed, sized	75	25°	Cypress	32	....
Sand, Mine run	90–120	35°**	Elm (Perfectly Dry)	35	....
Sand, Coarse sized	90–100	30°	Fir, Eastern	25	....
" Very fine	90–110	32°	Hemlock (Perfectly Dry)	29	....
" Core	65	39°	Hickory (Perfectly Dry)	48	....
" Voids Full of Water	110 to 130	45°**	Lignumvitae, Dry	41 to 83	....
Sandstone, Solid ▲	147	....	Locust, Dry	46	....
" Quarried & Piled	82	....	Mahogany	35–53	....
Serpentine (Talc) ▲	169	....	Maple, Dry	33–40	....
Shales, Slate ▲	172	....	Oak, Live, Perfectly Dry	59	....
Silex	70	44°	" Red, Perfectly Dry	41 to 45	....
Silica, Flour	80	45°	Pine, White Perfectly Dry	27	....
Slag ▲	160 to 180	....	" Yellow Perfectly Dry Short leaf	38	....
" Furnace Granulated	122	25°	" " " " Long leaf	44	....
" Birmingham	82	25°	Poplar, Dry	29	....
Slate, Solid ▲	175	....	Red Wood, California Dry	26 to 30	....
" Fine Ground	82	35°	Sawdust, Dry	10–30	36°
" Granules, Flaky	87	28°	" Ground	20	45°
" Flour	45	45°	Shingles Per 1000, Short 900 Lbs. Long 1400 Lbs.	....	....
Snow (Fresh Fallen)	5 to 12	....	Spruce, Dry, California	25	....
" (Moistened) Compacted By Rain	15 to 50	....	Sycamore (Perfectly Dry)	37	....
Soap Chips	5–15	28–32°	Walnut, Black (Perfectly Dry)	42	....
Soapstone, Talc ▲	169	....	Wool Mineral	10	30°
" Fine Ground	60	40°	Zinc calcines, Powdered	85	54°
Soda Ash, Light	25–35	37°	" Ore, roasted, Granular	110	38°
" " Dense	66	32°	" Oxide	20	45°
" " Briquette	50	22°	" " Leaded, Ground	25–40	50°
" " and Silica Sand (1 to 1.85)	80	29°	" Sulphate, Powdered	72	44°
" Bicarbonate	30–55	42°	Zonolite, Fine, Granular	7	30°
Sodium, Aluminate Ground	72	25–50°			
" Antimonate Crushed	49	31°**			
" Carbonate, Powdered (Soda Ash)	....	....			
" Nitrate, Granular	68	24°			
" Phosphates, See Phosphates					
" Sulfite, Powdered	96	40°			
" Sulfate (fine and lumps)	88	31°			

▲ * † ** See notes preceding table.

Data of Stephens-Adamson Co., Catalog 66, Aurora, IL, 1954. See also Table 5.3.

TABLE A8. Petroleum Products, Typical Compositions

	Summary of Product Types Produced From Petroleum																				
Number of Carbon Atoms	C_1	C_2	C_3	C_4	C_5	C_6	C_7	C_8	C_9	C_{10}	C_{11}	C_{12}	C_{13}	C_{14}	C_{15}	C_{16}	C_{17}	C_{18}	C_{19}	C_{20}	$> C_{20}$
Boiling Point of Normal $\{$ °C	−161	−89	−42	−0.5	+36	69	98	126	151	174	196	216	235	253	270	287	302	316	329	343	
Paraffin at 760 mm $\{$ °F	−259	−127	−44	+31	97	156	209	258	303	345	384	421	456	488	519	548	575	601	625	649	

Liquefied Petroleum Gas
Precipitation Naphtha
VM&P Naphtha
Mineral Spirits
Reformate
Gasoline
Kerosene, Diesel Fuel
Aviation Turbine Fuel
Gas Oil, Fuel Oil
Transformer Oil
Lubricating Oil
Asphalt, Pitch
Wax

Source: Humble Oil Co.

EQUIPMENT SPECIFICATION FORMS

Specification forms make provision for key data of the equipment and its position in the process, including design characteristics and required performance. A major purpose is a basis for price quotations by suppliers of the equipment.

Although a few forms have been prepared by industry-wide organizations such as TEMA, Hydraulic Institute, and API, most have been prepared for their own use by engineering contractors and design divisions of chemical process organizations. Most private firms have their own libraries, but the merits of some forms have been recognized and copied widely so that much uniformity exists.

The selection of forms in this Appendix is made available through the courtesy of individual companies identified on each form, although one major contributor did not wish to be identified. For the most part, only the most often used kind of equipment is represented, except for the few items in category K.

A related kind of information is the suppliers inquiry forms of Appendix C.

Following is a listing of the equipment specification forms, included in this Appendix. The number appearing in italic is the page number on which the form appears.

CATALYTIC CONSTRUCTION CO.
ENGINEERING DIVISION

AGITATOR DATA SHEET

JOB NO. _____ SPEC NO. _____ PAGE ____ OF ____
CLIENT _____ ITEM NO. _____ REQ. NO. _____
LOCATION _____ BY _____ DATE _____
NUMBER REQD. _____ REVISION   DATE   BY

PERFORMANCE DATA

AGITATOR APPLICATION _____
TYPE OF AGITATION _____
FOAMING TENDENCY _____
WORKING CAPACITY-(BATCH OR CONTINUOUS, MIN. & MAX.) _____
MIXING CYCLE _____

MATERIALS TO BE MIXED						MIXING TEMP. _____ °F
COMPONENT	VOLUME %	WEIGHT %	SPECIFIC GRAVITY	VISCOSITY CENTIPOISE	TEMP. °F	ALTITUDE _____
						DUTY _____ HRS/DAY
						INSTALLATION
						INDOOR _____
						OUTDOOR _____
						CORROSION OR EROSION
FINISHED MIX	/////					DUE TO _____
SOLIDS IN FINISHED MIX				SETTLING VELOCITY _____ FT/MIN

PARTICLE SIZE _____
AGITATOR IN OPERATION DURING FILLING _____, DURING DRAW-OFF ___
VERTICAL DISTANCE: VESSEL BOTTOM TO DRAW-OFF _____
ADDITIONAL NOTES & DATA _____

VESSEL DATA

VESSEL _____ ITEM NO. _____ SKETCH OR DWG. NO. _____
CAPACITY _____ GAL., DESIGN PRESSURE _____ PSIG & TEMP. _____ °F, MATERIAL ____
CLEARANCE AVAILABLE FROM MOUNTING FLANGE FOR INSTALLING OR REMOVING AGITATOR ____
DIMENSIONS OF LARGEST OPENING TO PASS IMPELLER _____
NO. & DIMENSIONS OF BAFFLES REQ'D _____

VENDOR'S UNIT CHARACTERISTICS

MANUFACTURER _____	OUTLINE DWG. NO. _____
TYPE OR MODEL _____ B.H.P. _____	SECTIONAL DWG. NO. _____
DRIVE TYPE (DIRECT OR GEARED) _____	**MATERIALS**
_____ RATIO _____	IMPELLER _____
IMPELLER: TYPE _____, QUANTITY ____	SCRAPER BLADE _____
R.P.M. ____ DIA. ____ SPACING ____	STABILIZER RING _____
SHAFT LENGTH BELOW MOUNTING FLANGE ____	IMPELLER SHAFT _____
IMPELLER SHAFT SEAL TYPE ____	MIXER DRIVE HOUSING ____
BEARINGS TYPE _____	MOUNTING FLANGE _____
COUPLING TYPE _____	PACKING _____
LUBRICATION TYPE _____	GLAND _____
MOUNTING TYPE & OPER. ANGLE ____	LANTERN RING _____
NO. & TYPE STEADY BEARINGS ____	COUPLING _____
ELEC. MOTOR: MANUFACTURER ____	GASKET _____
TYPE ____ FRAME NO. ____ B.H.P. ____	MECH SEAL _____
VOLTS, PHASE, CYCLE, R.P.M. ____	STEADY BEARING _____
STARTING CURRENT ____ FULL LOAD CURRENT ____	WEIGHT: AGITATOR _____ LBS.
POWER FACTOR _____	WEIGHT: MOTOR _____ LBS.

REMARKS: _____

AGITATOR
SPECIFICATION SHEET

Page 1 of 2

_____
                                    Project _____

1 Service of Unit _____ Pos. No. _____
2 Number Required _____ Location _____
3 Type _____ Mounting _____ Manufacturer _____
4 Model No. _____

5   PROCESS CONDITIONS

6 Class of Operation _____
7 Type of Agitation _____ Period of Agitation _____
C Cycle: Batch: Smallest _____ gal.   Normal _____ gal.
                     Max. _____ gal.
9 Continuous: Rate of flow _____ GPM

10	Liquid	Liquid	Solids or Gas
11 Material			
12 Quantity			
13 Viscosity	____ cp @ ____ °F	____ cp @ ____ °F	____ Mcp @ ____ °F
14 Specific Gravity	____ @ ____ °F	____ @ ____ °F	____ @ ____ °F
15 Components			

16 Solids Characteristics: Size _____ Description _____
17 Mixture Characteristics: Sp.G. ____ @ ____ °F Viscosity ____ cp @ ____ °F
18 Foaming Tendency _____ Separation Time _____ hr.
19 Operating Conditions: Normal Temp. ____ °F Press. _____ psig
                           Max. Temp. ____ °F Press. _____ psig
20 Vessel Volume: ____ Gals; Diam: _____ ; Str. Shell: _____

21   MECHANICAL DESIGN DATA

22 Vessel Ref. Drawing: _____ (Attached)
23 Impeller Type: _____ ; No. _____ ; Size ____ in; Speed ____ rpm; Spacing ____ in.
24 Shaft Length ____ in.   Diameter ____ in.
25 Bearing Type: Shaft _____ Foot _____
26 Seal Type _____ Seal Flow _____
27 Seal Mfr. _____
28 Lubricator _____ Type Lubricant _____
29 Coupling Type: Motor _____ Reducer _____ Shaft _____
30 Stuffing Box Type _____
31 Stabilizer _____ Baffles: No.: ____ Width: _____
32 Mounting Nozzle; _____ Rating: _____ Facing: _____
33 Size of Nozzle for Impeller Installation: _____

REMARKS | APPRV | DATE SUPRV | CHKD BY | REV BY

PROJ. ENG. | DES SUPRV. | CHECKED BY | DRAWN BY | INITIATOR

TITLE _____

SCALE
ISSUE DATE
BLDG. NO.
DRAWING NO.

E100G1 (4-71)

AGITATOR SPECIFICATION SHEET

Page 2 of 2

34 <u>DRIVE DATA</u>

35 Driver Type: _____ rpm: _____ hp: _____ Manufacturer: _____
36 Current Characteristics: _____ v _____ ph _____ cycles; Type Encl. _____
37 Starting Torque: _____ Full Load Amps: _____ NEMA Code Letter: _____ Frame: _____
38 Speed Reducer Type: _____
39 Expected Noise Level (Measured 3 ft. from Source) _____ dB
40 _____

41 <u>MATERIALS OF CONSTRUCTION</u>

42 Impeller_____ Lantern Ring _____
43 Impeller Shaft_____ Packing Gland _____
44 Impeller Shaft Coupling(s) _____ Packing_____
45 Mounting Flange_____ Seal_____
46 Mounting Flange Facing _____
47 Seal Faces: Rotating _____ Stationary_____
48 Stuffing Box _____

49 <u>REMARKS</u>

50 _____
51 _____
52 _____
53 _____
54 _____
55 _____

Left margin labels (top to bottom): REMARKS | APPRV | DATE | Supv. | CHKD | BY | REV | DES SUPRV. | CHECKED BY | DRAWN BY | INITIATOR

Bottom: TITLE | ISSUE DATE | SCALE | BLDG. NO. | DRAWING NO.

E100G1 (4-71)

741

TANK MIXER TOP ENTERING (TYPICAL)

1 SERVICE: _____ INDOOR/OUTDOOR: ENGLISH/METRIC UNITS
2 FEED TO TANK: COMPOSITION/CONCENTRATION. _____
3 SOLIDS: TYPE/CONCENTRATION. _____
4 OPERATING PARAMETERS: PRESS. _____ TEMP. _____
5 SP. GR. @ OP. TEMP. _____ @MAX. _____ VISCOSITY @ OP. TEMP. _____ @MAX. _____
6 DESIGN PARAMETERS: PRESS. _____ TEMP. _____ DESIGN LEVEL _____
7 TANK-ITEM NO. _____ CAPACITY _____ SIZE _____
8 DESIGN _____ BAFFLES _____
9 TANK MIXER-ITEM NO. _____ QTY. _____
10 MANUF. _____ MODEL NO. _____
11 REDUCT. GEAR EFFIC. _____ SERVICE FACTOR _____ CAL. PRI. PUMPING CAP. _____
12 DESIGN LOADS: TORQUE _____ STATIC MOMENT _____
13 DYNAMIC MOMENT _____ DOWNWARD WEIGHT _____
14 FIRST CRITICAL SHAFT SPEED _____ OP. SPEED _____ STEADY BEARING: YES/NO
15 IMPELLER: SIZE _____ NO. _____ TYPE _____ MAT'L. OF CONST. _____
16 ACTUAL H.P. ABSORBED @ IMPELLER _____ PITCH _____ REMOVE IMP. THRU _____
17 SHAFT: DIAMETER _____ LENGTH _____ MAT'L. OF CONST. _____
18 OUTPUT SHAFT BEARING: TYPE _____ AFBMA L-10 LIFE _____ LUB. TYPE _____
19 OTHER BEARINGS: TYPE _____ AFBMA L-10 LIFE _____ LUB. TYPE _____
20 MOUNTING FLANGE: TYPE _____ SIZE _____ MAT'L. OF CONST. _____
21 SEAL TYPE: _____ MANUF. _____ MODEL NO. _____
22 MAT'L. OF CONST: ROTATING FACES: _____ INTL'S, METALLIC _____ FLEX. _____
23 BALANCED. YES/NO: TANK SHUTOFF. YES/NO. FLUSH FLUID _____
24 SEAL DESIGN: PRESS. _____ TEMP. _____
25 GEAR HOUSING: V-BELT/GEAR. MAT'L. OF CONST. _____ AGMA GEAR CLASS _____
26 TYPE OF SUPPORT _____ GEAR BOX LUB. TYPE _____
27 Motor: Item No. _____ Mtr. _____ Model No. _____ Qty. _____
28 Area Class _____ Gr. _____ Div. _____ /Non-Hazardous: Volts _____ Phase _____ Hertz _____
29 Enclosure _____ Insulation _____ ; Temp. Rise _____ °C above _____ °C By _____ @ _____ S.F.
30 Space Heater: Volts _____ Phase _____ Hertz _____

Item No.	HP KW	Current		Eff.		P.F.		Full Load RPM	Frame No.	Brg. Lub. (1)	Weight LB/KG	Allow-Thrust Up/Down LB/KG	Space Heater Watts	S.F.
		Full Load	Locked Rotor	4/4	3/4	4/4	3/4							
Mixer														

35 WEIGHT: SHIPPING _____ INSTALLED _____
36 PAINT SPECIFICATION _____
37 NOTES: _____
38 _____
39 _____
40 _____

41 VENDOR TO SHOW LOC. AND   TOP VIEW: SHOW LOC. OF
42 ANGLE. DIMENSIONS: MTG. FLG: DIR. OF ROTATION
43 1.
44 2.
45 3.
46 4.
47 5.
48 6.
49 7.
50 8.

KELLOGG

MANAGING OFFICE | ENGINEERING OFFICE

DATA SHEET/SKETCH

CLIENT _____
LOCATION _____ JOB NO. _____
ITEM _____
ITEM NO. _____ SPEC. NO. _____
REQ'N. NO. _____ PAGE _____ OF _____

REVISIONS | NO. | DATE | ENGINEER | CHK/REVIEW | APPROVE

Agitator Specification Sheet—(*continued*)

TANK MIXER SIDE ENTERING (TYPICAL)

1 SERVICE:_____ INDOOR/OUTDOOR: ENGLISH/METRIC UNITS
2 FEED TO TANK: COMPOSITION/CONCENTRATION._____
3 SOLIDS: TYPE/CONCENTRATION._____
4 OPERATING PARAMETERS: PRESS._____ TEMP._____
5 SP.GR.@ OP. TEMP._____@MAX._____ VISCOSITY @ OP. TEMP._____@MAX._____
6 DESIGN PARAMETERS: PRESS._____ TEMP._____ DESIGN LEVEL_____
7 TANK-ITEM NO._____ CAPACITY_____ SIZE_____
8 DESIGN_____ BAFFLES_____
9 TANK MIXER-ITEM NO._____ QTY._____
10 MANUF._____ MODEL NO._____
11 REDUCT. GEAR EFFIC._____ SERVICE FACTOR_____ CAL. PRI. PUMPING CAP._____
12 DESIGN LOADS: TORQUE_____ STATIC MOMENT_____
13   DYNAMIC MOMENT_____ DOWNWARD WEIGHT_____
14 FIRST CRITICAL SHAFT SPEED_____ OPER. SPEED_____
15 PROPELLER: SIZE_____ TYPE_____ MAT'L. OF CONST._____
16 ACTUAL H.P. ABSORBED @ PROPELLER_____ PITCH_____ REMOVE PROP. THRU_____
17 SHAFT: DIAMETER_____ LENGTH_____ MAT'L. OF CONST._____
18 OUTPUT SHAFT BEARING: TYPE_____ AFBMA L-10 LIFE_____ LUB. TYPE_____
19 OTHER BEARINGS: TYPE_____ AFBMA L-10 LIFE_____ LUB. TYPE_____
20 MOUNTING FLANGE: TYPE_____ SIZE_____ MAT'L. OF CONST._____
21 ANGLE-θ_____: RIGHT/LEFT HAND MOUNT: DIR. OF ROTAT._____ FROM MOTOR END
22 SEAL TYPE:_____ MANUF._____ MODEL NO._____
23 MAT'L. OF CONST: ROTATING FACES:_____ INTL'S. METALIC_____ FLEX._____
24 BALANCED. YES/NO: TANK SHUTOFF. YES/NO. FLUSH FLUID_____
25 SEAL DESIGN: PRESS._____ TEMP._____ AGMA GEAR CLASS_____
26 GEAR HOUSING: V-BELT/GEAR. MAT'L. OF CONST._____ AGMA GEAR CLASS_____
27 TYPE OF SUPPORT_____ GEAR BOX LUB. TYPE_____
28 Motor: Item No._____ Mfr._____ Model No._____ Qty.____
29 Area Class_____ Gr._____ Div.____/Non-Hazardous: Volts_____ Phase_____ Hertz_____
30 Enclosure_____ Insulation_____; Temp. Rise____°C above____°C By____@____S.F.
31 Space Heater: Volts_____ Phase_____ Hertz_____

Item No.	HP KW	Current		Eff.	P.F.	Full Load RPM	Frame No.	Brg. Lub. (1)	Weight LB/KG	Allow-Thrust Up/Down LB/KG	Space Heater Watts	S.F.
		Full Load	Locked Rotor	4/4	3/4	4/4	3/4						
Mixer												

36 WEIGHT: SHIPPING_____ INSTALLED_____
37 PAINT SPECIFICATION_____
38 NOTES:_____
39
40
41
42 VENDOR TO SHOW LOCATIONS
43 AND ANGLE.
44 DIMENSION:
45 1.
46 2.
47 3.
48 4.
49 5.
50 6.
    7.

MLL
M GEAR BOX

NO.	DATE	ENGINEER	CHK/REVIEW	APRROVE
6				
5				
4				
3				
2				
1				
0				

REVISIONS

KELLOGG   MANAGING OFFICE   ENGINEERING OFFICE

DATA SHEET/SKETCH

CLIENT_____
LOCATION_____ JOB NO._____
ITEM_____
ITEM NO._____ SPEC. NO._____
REQ'N. NO._____ PAGE____OF____

742

| PROCESS DESIGN SECTION CORPORATE ENGINEERING | SYPHON PUMP (MIXING TEE) DATA SHEET |

EQUIP. POSITION NO.				
SYPHON PUMP NO.				
FLOWSHEET NO.				
PROCESS DATA				
INLET FLUID #1				
DESCRIPTION				
SPECIFIC GRAVITY				
VISCOSITY; CP				
PRESSURE; PSIG				
TEMPERATURE; °F				
FLOW				
INLET FLUID #2				
DESCRIPTION				
SPECIFIC GRAVITY				
VISCOSITY; CP				
PRESSURE; PSIG				
TEMPERATURE; °F				
FLOW				
OUTLET				
TEMPERATURE; °F				
MATERIALS of CONST'N.				
MANUFACTURER				
SIZE NO.				
PIPE CONN'S. · INCHES				
PRESS. INLET				
SUCT. & DELIVERY				

REMARKS
APPRV
DATE
CHKD SUPRV
BY
REV
PROJ. ENG.
DES SUPRV.
CHECKED BY
DRAWN BY
INITIATOR
DATE

NOTES:

JOB NO._____ PLANT LOCATION_____
PROJECT NO._____ REF. DWG. NO._____ SEE ABOVE LIST_____
TITLE_____
POSITION NO. · SEE ABOVE LIST_____ SERIES_____ STEP NO._____

ISSUE DATE   SCALE   BLDG. NO.
DRAWING NO.

E 14089

CENTRIFUGAL COMPRESSOR SPECIFICATION

GENERAL ENGINEERING DIVISION
FORM 66-55 SM 7-54 G.S.

THE FLUOR CORPORATION LTD.

VENDOR MUST FURNISH ALL PERTINENT DATA FOR THIS
SPECIFICATION SHEET BEFORE RETURNING

SHEET NO.	REV.
DATE	
BY	CHK'D.
JOB NO.	

ITEM NO. , SERVICE

NO. REQ'D. , DRIVE   MANUFACTURER:

GAS HANDLED				SIZE & TYPE , STAGES
CORROSION FACTORS				DESCRIPTION

OPERATING CONDITION	1:	2:	3:	COMPRESSOR MATERIALS
CAPACITY				CASE
CFM @ INLET CONDS				DIAPHRAGMS
WT. FLOW, LBS./HR.				GUIDE VANES
(M³SCFD) (SCFM)*				INTER STAGE LABYRINTHS
TEMP., INLET, °F				IMPELLER HUBS & COVERS
DISCH. °F				IMPELLER VANES
PRESS., INLET, PSIA				SHAFT
DISCH. PSIA				SHAFT SLEEVES
DIFFER. PSI				BALANCE DRUM OR DISC
COMP. RATIO				CONSTRUCTION DETAILS
MOLECULAR WT.				CASE: SWP PSIG. MAX. HYDTEST PSIG
SP. GR. (AIR=1)				SPLIT: (HORIZONTAL: VERTICAL: BARREL)
REL. HUMIDITY, %				SUPPORT: (FOOT: PEDESTAL: BRACKET)
"K" VALUE, CP/CV				IMPELLER: TYPE: (OPEN: SEMI-ENCLOSED: ENCLOSED)
COMPRESSIBILITY, "Z"				CONSTR: (CAST: FORGED: RIVETED: WELDED)
ELEV. ABOVE SEA LEVEL				DIAMETER ", VANE THICKNESS "
BHP (INCL. GEAR LOSS)				SHAFT: DIAM. AT IMP ", AT BRGS "
RPM				SPAN: C-C BRGS ", IMP OVERHANG "
IMP. TIP VEL., FPS				CRITICAL SPEED RPM
WATER RATE, #/HP/HR				BRGS: LOCATION (INTERNAL: EXTERNAL)
				RADIAL: TYPE : PROJ. AREA SQ "
MAX. CAP., CFM @ INL. : MAX. BHP				THRUST: TYPE : EFF. AREA SQ "
MIN. CFM, (SURGE POINT)				SEALS:
CONTROL: (SPEED: SUCTION VALVE: INLET VANES)				
SOURCE: (MANUAL: FC: PC: TC)				COUPLING CPLG GRD: YES, NO
STEAM: PRESS. PSIG: TEMP. °F: EXH.				BASE PLATE:
POWER: VOLTS: PH. CYC., COOLING WATER °F				

MFGR SHALL SUPPLY THE FOLLOWING	DRAWING NO.		NOZZLES	SIZE	RATING	FACING	LOCATION
PERFORMANCE CURVE			INLET				
SECTIONAL DRAWING			DISCHARGE				
OUTLINE DRAWING			DRAINS				
ROTATION FACING CPLG: CW: CCW			TURB. INLET				
			TURB. EXHAUST				

LUBRICATION SYSTEM	COMPRESSOR WEIGHTS	
COMBINED WITH DRIVER: YES, NO	WT., TOP HALF	LBS
TWIN OIL COOLERS	WT., ROTOR	LBS
TWIN OIL FILTERS	WT., COMPR. BARE	LBS
MAIN OIL PUMP	WT., BASEPLATE	LBS
AUX. OIL PUMP	WT., ACCESSORIES	LBS
OIL PRESS. SHUT DOWN	SHIPG WT. LESS DRIVE	LBS
OIL TEMP. ALARM	FLOOR SPACE	

TESTS: MECHANICAL RUN IN: YES, NO	
WITNESSED PERFORMANCE: YES, NO	
OVERSPEED IMPELLERS TO	RPM
OVERSPEED ROTOR TO	RPM
HYDROSTATIC TEST PRESS.	PSIG
SHOP INSPECTION: YES, NO	

DRIVER: MAKE				REDUCTION GEAR	
TYPE				MFGR:	
RATED HP				TYPE:	
RPM				ARRANGEMENT: (COUPLED) (INTEGRAL)	
SHIPPING WEIGHT				LOW SPEED SHAFT.	RPM
SHIPPING POINT				RATING	HP
SHIPMENT, MONTHS				SERVICE FACTOR	
REMARKS:				LUBRICATION:	

*"STANDARD" CONDITIONS ARE 60°F & 14.7 PSIA

743

RECIPROCATING COMPRESSOR SPECIFICATION SHEET

THE C.W. NOFSINGER COMPANY
KANSAS CITY, MISSOURI

SHEET NO.	
ITEM NO.	
CWN JOB NO.	

CUSTOMER

LOCATION

SERVICE

MFR.   MODEL NO.

CUST. JOB NO.	
DATE	
NO. REQUIRED BY	
SERIAL NO. REVISED	

OPERATING CONDITIONS

			NORM	RATED
1	VAPOR - GAS	MOL.WT.(INCL H₂O)		
2	ELEVATION, FT.	BAROMETER, PSIA		
3	INDOOR - OUTDOOR	HEATED: YES - NO		
4	CORR/EROS PROPERTIES			
5			NORM	RATED
6	MMSCFD/SCFM (14.7 PSIA-60 °F)			
7	WT.FLOW, LB/HR			
8	SUCTION, PSIA AT °F			
9	DISCHARGE PRESS, PSIA			
10	CP/CV, K (SUCT)			
11	COMPRESSIBILITY, Z (SUCT)			

CONSTRUCTION DETAILS

FRAME RATING: HP	RPM
LUBE: TYPE	RESERVOIR CAP.MIN
FLOW, GPM	TEMP. IN/OUT, °F
WATER: GPM	TEMP. IN/OUT, °F
WEIGHTS: COMPR	DRIVER
FLYWHEEL	SHIPPING
TESTS: SHOP INSPECT	PERFORMANCE
HYDROSTATIC, PSIG	WITNESS
ACCESS: SUCT.VA.UNLOADING, MANUAL-AUTO	
CLEARANCE POCKETS, FIXED-VARIABLE	
OUTLINE DWG.NO.	API 618: YES-NO

PERFORMANCE (EACH STAGE)

		1ST	2ND	3RD	4TH	5TH
12	STAGE - CYLINDERS/STAGE					
13	DISCHARGE PSIA/°F					
14	RPM					
15	BORE & STROKE					
16	CYL.DISPLACEMENT, ACFM					
17	CLEARANCE, %					
18	COMPRESSION RATIO					
19	VOLUMETRIC EFF.					
20	CAPACITY, MMCFD					
21	BHP/STAGE					
22	VALVE: TYPE					
23	LIFT (IN/OUT), MILS					
24	GAS VELOCITY, FPM					
25	TEST PRESS (WORKING P x 1.5), PSIG					
26	ROD LOAD: TENSION, PSI					
27	COMPRESSION, PSI					
28	INTAKE NOZZLE: SIZE-RATING-FACING					
29	DISCH. NOZZLE: SIZE-RATING-FACING					

MATERIALS

30	CYLINDER/LINER
31	PISTON/RINGS
32	RODS
33	VALVES/SPRINGS
34	ROD PACKING

MOTOR DRIVER

35	SUPPLIED BY	MOUNTED BY
36	MFR.	TYPE
37	ENCLOSURE	RPM
38	HP	SF
39	FRAME	INSULATION
40	VOLTS/PH/HZ	TEMP.RISE,°F
41	BEARINGS	LUBE
42	DRIVE TRAIN: BY	MFR.
43	MODEL	RATIO
44	TORSIONAL STUDY: YES-NO	BY
45	SEPARATE SPEC IF: DIESEL, GAS	

TURBINE DRIVER

SUPPLIED BY		MOUNTED BY		
MFR.		TYPE		
HP	RPM	WATER RATE, LB/HP-HR		
INLET STM.PRESS, PSIG: NORM		MAX		
INLET STM.TEMP,°F: NORM		MAX		
EXHAUST STM.PRESS, PSIG: NORM		MAX		
BEARINGS		LUBE		
NOZZLES	SIZE	RATING	FACING	LOCATION
INLET				
EXHAUST				
API-611: YES - NO				

FORM 21-A6, 4-76

VENDOR TO SUPPLY INFORMATION MARKED

FAN OR BLOWER DATA SHEET

PROCESS DESIGN SECTION	FAN OR BLOWER
CORPORATE ENGINEERING	DATA SHEET

OPERATING CONDITIONS

GAS: _____
SP. GR. (AIR = 1.0) _____
POUNDS/HR: _____
STD. CFM: _____
FLOW TEMP: _____ °F

CFM AT FLOW TEMP: _____
REL. HUMIDITY AT FLOW TEMP: _____ %
SUCTION PRESS: _____ PSIA
DISCH. PRESS: _____ PSIA
DIFFERENTIAL PRESS: _____ PSIA

MECHANICAL DATA

MFG: _____
SIZE & TYPE: _____

NOZZLES	SIZE	ASA RATING	FACING	POSITION
SUCTION				
DISCH.				
DRAIN				

IMPELLER DIAM: RATED: _____ MAX: _____
TYPE: _____

BEARINGS – TYPE: _____
TYPE OF CLOSURE: _____
METHOD OF SEALING: _____
LUBRICATION: _____
COOLING: _____
COUPLING MFG: _____
TYPE: _____
SHAFT DIAM: _____

MATERIALS OF CONSTRUCTION

CASE: _____
IMPELLER: _____
SHAFT: _____
SHAFT SLEEVE: _____

WEAR RINGS: _____
COUPLING: _____
GASKETS: _____

PERFORMANCE

PROPOSAL CURVE NO: _____
NO. OF STAGES: _____ RPM _____
RATED EFF: _____ RATED BHP: _____
MAX. BHP-RATED IMP. _____

TIP SPEED: _____
OUTLET VELOCITY: _____
ROTATION FACING COUPLING END:
X CW ☐   CCW ☐

MOTOR DRIVE DATA

ITEM NO. _____ MTD. BY _____
HP _____ RPM _____ FRAME _____
MFG. _____
TYPE: _____ INSUL. _____
ENCLOSURE: CLASS I   GROUP D

VOLTS/PHASE/CYCLE _____ / _____ / _____
BEARINGS: _____ LUBE: _____
FULL LOAD AMPS: _____ S.F. _____
L.R. AMPS: _____

MISCELLANEOUS

OUTLINE DWG. NO. _____
SECTION DWG. NO. _____
FAN OR BLOWER SERIAL NO. _____

ACTUAL IMPELLER DIA. _____
TEST CURVE NO. _____
WEIGHT POUNDS NET. _____

REMARKS

_____

JOB NO. _____
PROJECT NO. _____
TITLE _____
POSITION NO. _____

PLANT LOCATION _____
REF. DWG. NO. _____
SERIES _____ STEP NO. _____

ISSUE DATE

SCALE
BLDG. NO.

DRAWING NO.

E223B39

REMARKS / APPR'V / DATE / CHKD SUPRV / BY / REV / DES SUPRV. / CHECKED BY / DRAWN BY / INITIATOR

VACUUM PUMP DATA SHEET

PROCESS DESIGN SECTION	VACUUM PUMP
CORPORATE ENGINEERING	DATA SHEET

OPERATING CONDITIONS

GAS HANDLED: _____
MOLECULAR WGT: _____
SUCTION PRESS: _____ "Hg VACUUM
DISCHARGE PRESS: _____ PSIA
SUCTION TEMP: _____ °F
DISCHARGE TEMP: _____ °F
CAPACITY: _____ LB./HR.
CAPACITY: _____ SCFM
CAPACITY INTAKE: _____ ACFM
"K" VALUE: _____
RELATIVE HUMIDITY: _____ %
ALTITUDE: _____ FT.

SEAL FLUID:
    COMPOSITION: _____
    TEMPERATURE _____ °F
    DENSITY: _____ LB./CU. FT.
    VISCOSITY: _____ CPS
    VAPOR PRESS: _____ PSIA
HEAT EXCHANGER COOLING WATER:
    INLET TEMP: _____ °F
    OUTLET TEMP: _____ °F
    INLET PRESS: _____ PSIG
    ALLOWABLE PRESS. DROP: _____ PSI

MECHANICAL DATA

MFG. _____
SIZE & TYPE _____

NOZZLES	SIZE	ASA RATING	FACING	POSITION
SUCTION				
DISCH.				
HEAT EXCH. COOLING				
DRAIN				
SEAL LIQUID				

CPLG. MFG. _____
TYPE: _____

RECEIVER
    CAPACITY: _____ GALS.
    SIZE: _____
    DESIGN PRESS: _____ PSIG-TEMP. _____ °F
    CODED: ☐   NON CODED: ☐
HEAT EXCHANGER:
    SURFACE AREA _____ SQ. FT.
    DUTY: _____ BTU./HR.
    SHELL DESIGN: _____ PSIG-TEMP. _____ °F
    TUBE DESIGN: _____ PSIG-TEMP. _____ °F
MAX. CASING PRESS: _____ PSIG.

MATERIALS OF CONSTRUCTION

PUMP:
CASING: _____ IMPELLER: _____
SHAFT: _____
SHAFT SEAL: _____
RECEIVER: _____

HEAT EXCHANGER:
    SHELL: _____
    TUBES: _____
    CHANNEL: _____
    BAFFLES: _____

PERFORMANCE

RATED CAPACITY: _____ CFM @ _____ "Hg. VAC.
PUMP SPEED: _____ RPM
NO. OF STAGES: _____
RATED BHP _____

SEAL FLUID FLOW RATE: _____ GPM
COOLING WATER FLOW RATE: _____ GPM
ROTATION FACING PUMP END:
CLOCKWISE ☐   COUNTERCLOCKWISE ☐

MOTOR DRIVE DATA

ITEM NO. _____ MTD. BY _____
VOLTS/PHASE/CYCLE/ _____ / _____ / _____
HP _____ RPM _____ FRAME _____ BEARINGS: _____ LUBE _____
MFG. _____ FULL LOAD AMPS: _____ SF _____
TYPE: _____ INSUL: _____ LR AMPS: _____
ENCLOSURE: CLASS I GROUP D

ACCESSORIES

SILENCER: _____
CONTROL VALVE: _____
SOLENOID VALVE: _____
SEPARATOR: _____

JOB NO. _____
PROJECT NO. _____
TITLE _____
POSITION NO. _____

PLANT LOCATION _____
REF. DWG. NO. _____
SERIES _____ STEP NO. _____

ISSUE DATE

SCALE
BLDG. NO.

DRAWING NO.

E217B33

REMARKS / APPR'V / DATE / CHKD SUPRV / BY / REV / DES SUPRV. / CHECKED BY / DRAWN BY / INITIATOR

SHEET 1 of 2

| PROCESS DESIGN SECTION | STEAM EJECTOR |
| CORPORATE ENGINEERING | DATA SHEET SHEET 1 of 2 |

Service _____ Manufacturer _____
No. of Units _____ Model No. _____
Type _____

PROCESS CONDITIONS

Non-Condensables _____ lb./hr. M.W. _____
Condensables Vapors (Air etc.) _____ lb./hr. M.W. _____
Steam _____ lb./hr.
Suction Conditions at Ejector: Abs. Press. _____ mmHg. Temp. _____ °F.
Discharge Conditions at Ejector: _____ psig Temp. _____ °F.
Volume of Evacuated System _____ cu.ft. Max. Evacuating Time: _____ Minutes
Expected Air Leakage _____ lb./hr.
Duty _____ hrs./day _____ days/week
Steam Conditions Normal: Press _____ psig Temp. ____ °F. Min: Press. _____ psig Temp. ____ °F.
Consumption at Rated Load _____ lb./hr. at Press. _____ psig Temp. ____ °F.
Water Pressure Normal: _____ psig Min: _____ psig Temp. ____ °F
Consumption at Rated Load: _____ gpm

MECHANICAL DESIGN DATA

EJECTOR	1st Stage	2nd Stage	3rd Stage	4th Stage	5th Stage	6th Stage
Size						
Suction Conn. Size						
Discharge Conn. Size						
Steam Conn. Size						
Design Pressure, psig						
Test Pressure, psig						
MATERIALS:						
Suction Chamber						
Steam Chest						
Steam Nozzle						
Diffuser						

BAROMETRIC CONDENSER			
Location: (Precondenser, Intercondenser etc.)			
Size			
Condenser Water Rate gpm			
Outlet Water Temp. °F.			
Inlet Water Pressure Req'd; psig			
Vapor Inlet Nozzle Size			
Vapor Outlet Nozzle Size			
Water Inlet Nozzle Size			
Water Outlet Nozzle Size			
Design Pressure, psig			
Test Pressure, psig			
MATERIALS:			
Shell			
Baffles			
Spray Nozzle			

JOB NO. _____ PLANT LOCATION _____
PROJECT NO. _____ REF. DWG. NO. _____
TITLE _____
POSITION NO. _____ SERIES _____ STEP NO. _____

ISSUE DATE

SCALE
BLDG. NO.
DRAWING NO.

REMARKS · APPR'V · DATE · SUPV · CHKD · BY · REV
PROJ. ENG. · DES SUPRV. · CHECKED BY · DRAWN BY · INITIATOR · DATE

E 162 B 20

SHEET 2 of 2

| PROCESS DESIGN SECTION | STEAM EJECTOR |
| CORPORATE ENGINEERING | DATA SHEET SHEET 2 of 2 |

MECHANICAL DESIGN CONT'D.

SURFACE CONDENSER

Location Precondenser, Intercondenser, etc.			
Size			
Surface Area; sq.ft.			
Tubes; No. x O.D. x BWG x Length	x x x	x x x	x x x
Water Flow Rate; gpm			
Water Temp; In /Out °F	/	/	/
Water Side ΔP; psig			
Tubeside Nozzle Sizes; In /Out	/	/	/
Shellside Nozzle Sizes; In /Out	/	/	/
Design Press; psig Shell /Tubes	/	/	/
Test Press; psig Shell /Tubes	/	/	/
MATERIALS			
Tubes			
Tube Sheet			
Channel			
Shell			
Shell Baffles			
Impingement Plate			

REMARKS

1 Unit to have complete stability at zero load and to be designed for 25 % overcapacity _____
2 Tail pipes furnished by _____
3 Interconnecting piping by _____

JOB NO. _____ PLANT LOCATION _____
PROJECT NO. _____ REF. DWG. NO. _____
TITLE _____
POSITION NO. _____ SERIES _____ STEP NO. _____

ISSUE DATE

SCALE
BLDG. NO.
DRAWING NO.

REMARKS · APPR'V · DATE · SUPV · CHKD · BY · REV
DES SUPRV. · CHECKED BY · DRAWN BY · INITIATOR

FORM NO. 2829
1M 4-56 MP&S

SOUTHWESTERN ENGINEERING COMPANY
4800 SANTA FE AVENUE   LOS ANGELES 58, CALIFORNIA   SHEET____OF____

SWECO

ELECTRIC MOTOR DATA SHEET

R E V

1	CUSTOMER		EQUIP. NO.	
2	PLANT LOCATION		FILE NO.	
3	SERVICE			
4	MANUFACTURER	TYPE	FRAME NO.	
5	INDUCTION MOTOR		SYNCHRONOUS MOTOR	
6	HORSEPOWER		HORSEPOWER	
7	RPM		RPM	
8	VOLTS		VOLTS	
9	PHASES		PHASES	
10	CYCLES		CYCLES	
11	FULL LOAD AMPERES		REQUIRED TORQUE	
12	LOCKED ROTOR AMPERES		LOAD WR^2	
13	STARTING TORQUE - PERCENT		FULL LOAD AMPERES	
14	BREAKDOWN TORQUE - PERCENT		LOCKED ROTOR AMPERES	
15	FULL LOAD RPM		STARTING TORQUE - PERCENT	
16	EFFICIENCY - PERCENT		PULL-IN TORQUE - PERCENT	
17	FULL LOAD		PULL-OUT TORQUE - PERCENT	
18	¾ LOAD		POWER FACTOR RATING	
19	½ LOAD		FIELD AMPS @ FULL LOAD	
20	POWER FACTOR		EFFICIENCY - PERCENT	
21	FULL LOAD		FULL LOAD	
22	¾ LOAD		¾ LOAD	
23	½ LOAD		½ LOAD	
24	ELEV. ABOVE SEA LEVEL - FT.		POWER FACTOR	
25	SERVICE FACTOR		FULL LOAD	
26	TEMPERATURE RISE		¾ LOAD	
27	ROTATION FACING END OPP. COUP.		½ LOAD	
28	CLASSIFICATION		ELEV. ABOVE SEA LEVEL - FT.	
29	GENERAL PURPOSE		SERVICE FACTOR	
30	SPLASH PROOF		ROTATION FACING END OPP. COUP.	
31	TEFC		ENCLOSURE	
32	TEFC EXPLOSION PROOF		RADIAL BEARINGS	
33	MOUNTING		LUBRICATION	
34	HORIZONTAL		DRIVE CONNECTION	
35	VERTICAL		BASE	
36	SHAFT - SOLID, HOLLOW		WEIGHT	
37	SHAFT DIAMETER		OUTLINE DRAWING	
38	LOAD THRUST - LBS.		SERIAL NUMBER	
39	MAX. ALLOWABLE THRUST		EXCITER - TYPE	
40	TYPE INSULATION		DRIVE	
41	RADIAL BEARINGS - BALL OR SLEEVE		(IF MOTOR, DESCRIBE AT LEFT)	
42	THRUST BEARINGS - BALL OR SLEEVE		RPM	
43	LUBRICATION - OIL OR GREASE		VOLTS, D.C.	
44	DRIVE CONNECTION		AMPS @ FULL LOAD	
45	BASE		SHUNT OR COMPOUND WOUND	
46	WEIGHT		SERVICE FACTOR	
47	OUTLINE DRAWING NUMBER		TEMPERATURE RISE	
48	SERIAL NUMBER		ENCLOSURES	
49	NEMA CODE LETTER		TYPE INSULATION	
50	MISCELLANEOUS		TYPE BEARINGS	
51	OIL COOLER - TYPE		LUBRICATION	
52	COOLING WATER @ °F & GPM		BASE	
53	FORCED FEED LUBRICATION		WEIGHT	
54	PUMP BUILT-IN OR MOTOR DRIVEN		OUTLINE DRAWING	
55	MOTOR HP - VOLTS - PHASE - CYCLES		SERIAL NUMBER	
56	REMARKS:			
57				

(Left margin vertical labels: KW > ᴍ - OZ, DATE, BY, VₐₚₚᵣₒᵥₑD, DATE, BY, CHECKED, ENGINEER, PROJ. ENG.)

746

HIGH VOLTAGE INDUCTION MOTORS (LESS THAN 1500 HP/1119 KW)

1	○ Motor Design Data ○ English ○ Metric Units	○ Shop Inspection and Test
2	Mfr. _____ Model No. _____	Required Witness
3	Serial No. _____ Qty __	Shop Inspection ○ ○
4	Driven Equip. _____	Testing Per NEMA(MG-1) ○ ○
5	Site Data:	Mfr. Std. Shop Test ○ ○
6	Altitude ____ Amb.Temp.Max.___°C Min.__°C	Special Tests Listed Below:
7	Dust/Fumes/Other _____	_____ ○ ○
8	Area Class___ Gr.___ Div.___/Non-hazardous	_____ ○ ○
9	Basic Data:	_____ ○
10	Volts _____ Phase _____ Hertz ____	Couplings Supplied By:
11	Nameplate H.P./KW _____ S.F.__	Mfr. _____ Model No. ____
12	RPM ____	○ Motor Mfr. ○ Driven Equip.Mfr. ○ Purch.
13	Insulation: Class _____ Type _____	to Mount Motor Half.
14	Temp. Rise ____°C above ____°C By ___	Painting: Mfr. Std.____ Spec. No._____
15	NEMA Design ___ Type: ○ Hor. ○ Vert.	Shipment: ○ Domestic ○ Export
16	Starting:	○ Export Boxing Required
17	○ Full Voltage ○ Reduced Voltage _____%	○ Outdoor Storage for Over Three (3) Months
18	○ Loaded ○ Unloaded	☐ Manufacturer's Data
19	○ Voltage Dip _____%	Frame No.: _____ Full Load RPM _____
20	Drive Systems:	Efficiency: F.L.____ 3/4L____ 1/2L____
21	○ Direct Connected ○ Gear	Power Factor: F.L.____ 3/4L____ 1/2L____
22	○ Other _____	Current (Rated Volt). F.L.____ L.R.____
23	Enclosure:	Locked Rotor Power Factor _____
24	○ Open Drip Proof ○ Weather Protected __	Lock.Rtr. W/Stnd.Time (Cold Start)___ Sec.
25	○ Totally Enclosed Fan Cooled	Lock.Rtr. W/Stnd.Time (Hot Start) ___ Sec.
26	○ Other _____	Torques: Full Load _____
27	Driven Equipment Inertia _____	Locked Rotor _____
28	Bearing Type _____ Lub. _____	Pull-Up _____
29	No. Starts:___/hr,Motor @ Amb.Temp. ___°C	Breakdown _____
30	No. Starts:___/hr,Motor @ Rated Temp. ___°C	Acceleration Time (Motor & Load @ 100%/80%
31	Rotation Facing Coupling End: _____	Rated Voltage) _____ Sec./____ Sec.
32	Vibration:○ NEMA Std. ○	Rotor WK^2 _____
33	Noise:○ NEMA Std. ○	Allow. WK^2 @ Motor Shaft _____
34	Space Heaters:○ Yes ○ No	Min. Allowable Acceleration Volt._____
35	Volts _____ Phase _____ Hertz ___	Total Shaft End Float _____
36	Maximum Sheath Temp. _____ °C	Limit End Float To _____
37	Accessories:	Space Heater KW _____
38	○ Baseplates ○ Soleplates	Max. Stator Winding Temp.: ____°C Alarm
39	○ Mfr. Std. Fans ○ Non-Sparking Fans	____°C for Shutdown.
40	Winding Temp. Detector: No./Phase _____	Thrust Brg.Cap.(Vert.): Up____ Down____
41	Type_____	Dimensions:
42	Selector Switch & Ind. By:○ Purch. ○ Mfr.	Length_____ Width____ Height____
43	Winding Temp. Detector & Space Htr. Leads:	Weight:
44	○ Separate Conduit Box ○ Same Conduit Box	Net____ Rotor____ Shipping____
45	Specifications:	Note:_____
46		_____
47		_____
48		_____
49		_____
50	Note: ○ Indicates information to be completed by Purchaser; ☐ By Manufacturer	

REVISIONS					
6				**KELLOGG**	MANAGING OFFICE	ENGINEERING OFFICE
5					
4				**EQUIPMENT DATA SHEET**	
3				CLIENT _____	
2				LOCATION_____ JOB NO.____	
1				ITEM_____	
0				ITEM NO _____ SPEC. NO.____	
NO	DATE	ENGINEER	CHK/REVIEW	APPROVE	REQ'N. NO. _____ PAGE__ OF__

ENG EQUIP 38 (3-78) | KELLOGG | **The M.W. Kellogg Company**

JOB NO. _____ ITEM NO. _____
REQ. NO. _____
PAGE NO. _____ OF _____ BY : _____
DATE : _____ REV. NO. _____

GAS ENGINE DATA

RATED HP _____ RATED RPM _____
MODEL _____ BMEP _____ PSI
[ ] INTEGRAL [ ] SEPARATE
BORE _____ IN. STROKE _____ IN.
NO. POWER CYLINDERS _____ ENGINE CYCLES _____
FUEL RATE _____ BTU / BHP HR. @ RATED LOAD
RPM MAXIMUM _____ MINIMUM _____
POWER CYLINDERS [ ] WET   [ ] DRY
                [ ] LINED   [ ] UNLINED
[ ] TURBOCHARGED   [ ] SUPERCHARGED
[ ] LOW FIRE HAZARD IGNATION [ ] STANDARD IGNITION

GOVERNOR

[ ] CONSTANT SPEED   [ ] VARIABLE SPEED
RESET BY: [ ] PNEUMATIC SIGNAL
          [ ] ELECTRONIC SIGNAL
          [ ] MANUAL
SPEED RANGE: RPM _____ MAX. _____ MIN.
SIGNAL RANGE: RPM _____ MAX. _____ MIN.
ON SIGNAL FAILURE VALVE TO: [ ] OPEN [ ] CLOSE
GOVERNOR MFR. _____ TYPE: _____
REGULATION: NEMA CLASS _____

WEIGHTS AND DIMENSIONS

NET WEIGHT: _____
MAX. ERECTION WEIGHT _____ MAX. MAINT. WT. _____
APPROX. FLOOR SPACE LENGTH _____
                    WIDTH _____
                    HEIGHT _____
ADDITIONAL DISTANCE TO REMOVE POWER RODS _____

ACCESSORIES

AIR INLET FILTER [ ] DRY [ ] OIL BATH [ ] MFR. STD.
MANUFACTURER _____ MODEL _____
EXHAUST SILENCER
MANUFACTURER _____ MODEL _____
STYLE _____
EXHAUST MANIFOLD [ ] WATERCOOLED [ ] INSULATED
TACHOMETER
[ ] ELECT. _____ ENCL. [ ] MECH. [ ] VIBR. REED
TACHOMETER RANGE _____
FLYWHEEL TURNING BAR AND STAND
[ ] MANUAL [ ] AIR JACK AIR _____ PSIG
LUBE OIL FILTER [ ] FULL FLOW [ ] SLIPSTREAM
_____
_____
_____
FUEL GAS SURGE DRUM BY: [ ] PURCHASER [ ] ENG MFR
RECOMMENDED VOLUME _____ FT 3
STARTING AIR COMPR. BY: [ ] PURCHASER [ ] ENG MFR
DRIVER: [ ] MOTOR [ ] GAS [ ] GASOLINE
NO. REQUIRED _____ CAPACITY _____ CFM
MANUFACTURER _____ MODEL _____
[ ] AUTOMATIC START / STOP CONTROL
STARTING AIR RECEIVER BY: [ ] PURCHASER [ ] ENG MFR.
NO. RECEIVER [ ] HORIZ. [ ] VERT.
RECEIVER CAPACITY _____ FT PRESSURE _____ PSIG
NO. CONSECUTIVE STARTS _____ STARTS / HR. _____
CU. FT. / START _____
_____
_____
_____
_____

AUXILIARY SYSTEMS

[ ] ENGINE MANUFACTURER SHALL FURNISH POWER CYLINDER COOLING WATER PIPING FROM A SINGLE INLET FLANGE TO A SINGLE DISCHARGE FLANGE.
SURGE TANK, ENGINE JACKET COOLER, CIRCULATING PUMP BY [ ] PURCHASER [ ] ENGINE MANUFACTURER
[ ] CIRCULATING WATER PUMP DRIVEN BY ENGINE SHAFT.
[ ] SEPARATELY MOUNTED PUMP AND DRIVER BY [ ] PURCHASER [ ] ENGINE MANUFACTURER
LUBE OIL INTERCONNECTING PIPING AND FITTINGS BY [ ] PURCHASER [ ] ENGINE MANUFACTURER

REMARKS: _____
_____
_____
_____
_____
_____
_____

REVISION	NO.	0	1	2	3	4	5	6	7	8	9	10	11	12
	DATE													
	BY													
	CHK.													

GENERAL PURPOSE STEAM TURBINE SPECIFICATION

1	CONSTRUCTION FEATURES				hp
2	[ ] Potential Max. Horsepower at Normal Steam Conditions				
3	[ ] Outline Dwg. No.	[ ] Sectional Dwg. No.			
4	Turbine Mounting	( ) Vertical		( ) Horizontal	
5	Support	[ ] Centerline		[ ] Foot	
6	Case Split	( ) Radial		( ) Axial	
7	[ ] No. of Stages	[ ] Wheel Diam.			
8	[ ] Single Stage	[ ] 2 Row [ ] 3 Row		[ ] Reentry	
9	Interstage Gland Seal	( ) Carbon		( ) Labyrinth	
10	End Gland Seal	( ) Carbon		( ) Labyrinth	
11	[ ] No. of Rings/Box				
12	Bearing Type	[ ] Radial		[ ] Thrust	
13	[ ] rpm Max. Cont.	Trip			
14	[ ] rpm Max. Allowable		1st Critical		
15	[ ] Case Max. Allow. Working Press.	Inlet	psig Exhaust		psig
16	Max. Inlet Temp. °F Max. Exhaust Temp.	°F			
17	Min. Allowable Exhaust Pressure		psig		
18	[ ] R.V. Set Press. Exh.		psig	Capacity	lb/hr
19	[ ] Hydrotest Press.	Inlet	psig	Exhaust	psig
20	( ) Lube System	( ) Ring Oil	( ) Purchasers	( ) Other	
21	( ) Corrosion Resistant Drain Lines				
22	[ ] Oil Required			gpm	psig
23	MATERIALS				
24	[ ] High Press. Casing		[ ] Exhaust Casing		
25	[ ] Nozzles		[ ] Blades		
26	[ ] Shaft		[ ] Wheels		
27	[ ] Under Packing				
28	[ ] Trip Valve Body		[ ] Gov. Valve Trim		
29	CONNECTIONS				

		SIZE	ANSI RATING	FACING	POSITION
30					
31	Inlet				
32	Exhaust				
33	Drain				
34	Cooling Water				
35	[ ] Manufacturer to give allowable piping forces & moments on nozzles on separate sheet.				

36	TESTS					
37		REQ'D.	WITN.		REQ'D	WITN.
38	Hydrostatic	⊗	( )	Aux. Equipment	( )	( )
39	No Load Run	⊗	( )	Disassembly After Test	( )	( )
40	Performance	( )	( )	Test Data Sheets	( )	
41	Gov. Response to Contr. Signal	( )	( )	Inspection ( ) Surface ( ) Parts		
42						
43	WEIGHTS					
44	[ ] Turbine lb [ ] Cooler lb [ ] Mounted lb.					
45	APPLICABLE SPECIFICATIONS					
46	( ) API 611 Gen. Purpose Steam Turbines ( ) - R-1 Painting					
47	( ) - GN-1 Noise ( )					
48						
49	REMARKS:					
50						
51						
52						
53						
54						
55						
56						

BE-UE-P-5-2 (Rev. 5/83)

BADGER ENGINEERS, INC. [A Raytheon Company]

ISSUE	DATE	SHEET	OF

SOUTHWESTERN ENGINEERING COMPANY

FORM NO. 2868
IM 4-56 MP&S

SWECO

4800 SANTA FE AVENUE   LOS ANGELES 58, CALIFORNIA   SHEET___OF___

GEAR DRIVE DATA SHEET

REV

#				
1	CUSTOMER		EQUIP. NO.	
2	PLANT LOCATION		FILE NO.	
3	SERVICE			
4	MANUFACTURER	TYPE	SIZE	
5	OPERATION		BEARINGS	
6	CONTINUOUS OR INTERMITTENT		H.S. SHAFT - OUTBOARD	
7	GEAR RATING - BHP		H.S. SHAFT - INBOARD	
8	THERMAL RATING - HP		INTERMEDIATE SHAFT - OUTBOARD	
9	SERVICE RATING - HP		INTERMEDIATE SHAFT - INBOARD	
10	MECHANICAL HP RATING		L.S. SHAFT - OUTBOARD	
11	AGMA SERVICE FACTOR		L.S. SHAFT - INBOARD	
12	AGMA CLASS GEARS			
13	GEAR RATIO		COUPLINGS	
14	EFFICIENCY @ BHP RATING		H.S. SHAFT COUPLING - TYPE	
15	NO. OF REDUCTIONS OR INCREASES		SIZE	
16	HIGH SPEED SHAFT RPM		MFG.	
17	LOW SPEED SHAFT RPM		L.S. SHAFT COUPLING - TYPE	
18	ACTUAL DRIVEN MACHINE RPM		SIZE	
19	ROTATION H.S. SHAFT FACING DRIVER		MFG.	
20	ROTATION L.S. SHAFT FACING DRIVER		COUPLING GUARDS	
21				
22	CONSTRUCTION & MATERIAL		TESTING	
23	CASE TYPE		WITNESS PERFORMANCE TEST	
24	CASE MATERIAL		INSPECTION	
25	H. S. PINION OR WORM			
26	H.S. GEAR		MISCELLANEOUS	
27	H.S. SHAFT		WEIGHT	
28	INTERMEDIATE PINION OR WORM		OUTLINE DWG. NO.	
29	INTERMEDIATE GEAR		CROSS SECTION DWG. NO.	
30	INTERMEDIATE SHAFT		SERIAL NO.	
31	L.S. PINION OR WORM			
32	L. S. GEAR		PRIME MOVER	
33	L.S. SHAFT		TYPE - MOTOR, TURBINE, OTHER	
34	H.S. SHAFT - SINGLE OR DB'L. EXT.		RATED HP	
35	L.S. SHAFT - SINGLE OR DB'L. EXT.		DRIVER RPM /FULL LOAD RPM	/
36	H.S. SHAFT O.D. AT CLPG.		ROTATION FACING END OPP. CLPG.	
37	L.S. SHAFT O.D. AT CLPG.		MANUFACTURER	
38	CASE GASKETS		TYPE /SIZE	/
39	CASE BOLTS		WEIGHT	
40	BEDPLATE		NOM. SHAFT O.D. AT CLPG.	
41			DRAWING NO.	
42				
43	LUBRICATION		DRIVEN MACHINERY	
44	TYPE LUBRICATION - GEARS		MACHINE DRIVEN	
45	TYPE LUBRICATION - BEARINGS		BHP REQUIRED	
46	OIL PUMP TYPE		REQUIRED DRIVEN RPM	
47	OIL PUMP DRIVE		ROTATION FACING SHAFT END	
48	VISIBLE LUBRICATOR SIGHT GLASS		MANUFACTURER	
49	OIL FILTER OR STRAINER		TYPE /SIZE	/
50	OIL COOLER REQUIRED		WEIGHT	
51	TYE OIL COOLER		NOM. SHAFT O.D. AT CLPG.	
52	COOLING WATER @ °F & GPM		DRAWING NO.	
53	SIZE COOLING WATER CONN.			
54				
55				
56	REMARKS:			
57				

Side labels: No. REVISIONS, DATE, BY, APPROVED

DATE
BY
CHECKED
ENGINEER
PROJ. ENG.

STANDARDS OF TUBULAR EXCHANGER MANUFACTURERS ASSOCIATION

EXCHANGER SPECIFICATION SHEET

#				
1			JOB NO.	
2	CUSTOMER		REFERENCE NO.	
3	ADDRESS		INQUIRY NO.	
4	PLANT LOCATION		DATE	
5	SERVICE OF UNIT		ITEM NO.	
6	SIZE	TYPE	CONNECTED IN	
7	GROSS SURFACE PER UNIT	SHELLS PER UNIT	SURFACE PER SHELL	
8	PERFORMANCE OF ONE UNIT			
9		SHELL SIDE		TUBE SIDE
10	FLUID CIRCULATED			
11	TOTAL FLUID ENTERING			
12	VAPOR			
13	LIQUID			
14	STEAM			
15	NON-CONDENSABLES			
16	FLUID VAPORIZED OR CONDENSED			
17	STEAM CONDENSED			
18	GRAVITY—LIQUID			
19	VISCOSITY—LIQUID			
20	MOLECULAR WEIGHT—VAPORS			
21	SPECIFIC HEAT—LIQUIDS		BTU/LB/°F	BTU/LB/°F
22	LATENT HEAT—VAPORS		BTU/LB/°F	BTU/LB/°F
23	TEMPERATURE IN		°F	°F
24	TEMPERATURE OUT		°F	°F
25	OPERATING PRESSURE		PSI	PSI
26	NUMBER OF PASSES PER SHELL			
27	VELOCITY		FT./SEC.	FT./SEC.
28	PRESSURE DROP		PSI	PSI
29	FOULING RESISTANCE			
30				
31	HEAT EXCHANGED—BTU/HR.		M.T.D. (Corrected)	
32	TRANSFER RATE—SERVICE	EFF. SURFACE PER UNIT		

CONSTRUCTION

#				
34	DESIGN PRESSURE		PSI	PSI
35	TEST PRESSURE		PSI	PSI
36	DESIGN TEMPERATURE		°F	°F
37	TUBES NO. O.D. BWG. LENGTH PITCH			
38	SHELL I.D. O.D.			
39	SHELL COVER		FLOATING HEAD COVER	
40	CHANNEL		CHANNEL COVER	
41	TUBE SHEETS—STATIONARY		FLOATING	
42	BAFFLES—CROSS	TYPE		
43	BAFFLE—LONG	TYPE		
44	TUBE SUPPORTS			
45	GASKETS			
46	CONNECTIONS—SHELL—IN	OUT	RATING	PSI
47	CHANNEL—IN	OUT	RATING	PSI
48	CORROSION ALLOWANCE—SHELL SIDE		TUBE SIDE	
49	CODE REQUIREMENTS		TEMA CLASS	
50	WEIGHTS—EACH SHELL	BUNDLE	FULL OF WATER	
51	NOTE: INDICATE AFTER EACH PART WHETHER STRESS RELIEVED (S. R.) AND WHETHER RADIOGRAPHED (X-R)			
52	REMARKS:			

AIR COOLED EXCHANGER SPECIFICATION SHEET

N Northern Natural Gas Company

LOCATION _____ FILE NO. _____
ITEM NO. _____ JOB NO. _____ W. O. NO. _____
PREPARED BY _____ DATE _____
CHECKED BY _____ DATE _____
APPROVED BY _____ DATE _____
△ INDICATES REVISION

SERVICE OF UNIT		NO. OF BAYS	
SIZE	TYPE		
SURFACE ITEM--EXTERNAL	BARE TUBE		SQ FT
HEAT EXCHANGED--BTU/HR	EFFECTIVE MTD		°F
TRANSFER RATE--EXT SURF.	BARE TUBE SURF.		BTU/HR SQ FT°F

PERFORMANCE DATA

TUBE SIDE

FLUID CIRCULATED		TEMPERATURE IN	°F
TOTAL FLUID ENTERING	LBS/HR	TEMPERATURE OUT	°F
VAPOR		INLET PRESSURE	PSIG
LIQUID		GRAVITY—LIQUID	
STEAM		VISCOSITY CPS@°F	
NON-CONDENSABLES		VISCOSITY CPS@°F	
VAPOR CONDENSED		MOLECULAR WEIGHT	
STEAM CONDENSED		SPECIFIC HEAT	BTU/LB°F
DENSITY: VAPOR-LIQUID MIXTURE	LBS/CU FT	LATENT HEAT	BTU/LB
CONDUCTIVITY	BTU FT/HR SQ FT°F	ALLOW. PRESS. DROP	PSI
FOULING RESISTANCE I.S.	HR SQ FT °F/BTU	DESIGN PRESS. DROP	PSI

AIR SIDE

AIR QTY	LBS/HR SCFM	TEMP IN	°F	ALTITUDE	FT
AIR QTY/FAN	ACFM	TEMP OUT	°F		

CONSTRUCTION

DESIGN PRESSURE	PSI	TEST PRESSURE	PSI	DESIGN TEMP	°F

SECTION		HEADER		TUBE	
SIZE	ROWS	TYPE		MATERIAL	☐ SEAMLESS ☐ WELDED
NO./BAY		MATERIAL			
ARRANGEMENT:		NO. PASSES		OD IN. BWG AVG MIN WALL	
SECTIONS IN PARALLEL		PLUG-DESIGN		NO./SECTION	
IN SERIES		MATERIAL		LENGTH	FT
BAYS IN PARALLEL		GASKET MATERIAL		PITCH IN.△☐◇	
IN SERIES		CORROSION ALLOWANCE	IN.	FIN	
		SIZE INLET NOZZLE	IN.	MATERIAL	
MISC.		SIZE OUTLET NOZZLE	IN.	OD	
STRUCTURE		RATING		NO./IN.	
		CODE		TYPE	
		VENT DRAIN			

MECHANICAL EQUIPMENT

FAN		DRIVER		SPEED REDUCER	
TYPE		MFR		MFR	
NO./BAY		TYPE		TYPE	
TIP SPEED	FT/MIN	NO./BAY		NO./BAY	
DIAM FT RPM		HP/DRIVER	RPM	MODEL	
HP/FAN PITCH ☐ADJUST.		ENCLOSURE		AGMA HP RATING	
NO. BLADES ☐AUTO.VAR				RATIO /1	
BLADE MATL					
HUB MATL					

NOTES:

DIMENSIONS: LENGTH   WIDTH   HEIGHT   SHIP. WT   LBS

749

SPECIFICATIONS FOR FIN FAN HEAT EXCHANGERS FLUOR-GRISCOM RUSSELL
INTEROFFICE

#		INSIDE TUBES		AIR DATA	
1	Customer			Proposal No.	
2	Address			Date	
3	Plant				
4	Fin Fan Model				
5					
6					
7	Service				
8		**INSIDE TUBES**		**AIR DATA**	
9	Class of Fluid			Altitude	Feet
10	Specific Gravity @ 60 F			Inlet Air Temp.	°F.
11	Specific Heat @ Ave. Temp.			Air	#/Hr.
12	Latent Heat @ Ave. Temp.		B.T.U./#	Outlet Air Temp.	°F.
13	Density @ Ave. Conditions		#/Cu. Ft.	Static Pressure	"H₂O
14	Molecular Weight			**MECHANICAL EQUIPMENT**	
15	Conductivity			Fans: Model	
16	Viscosity	Centipoises at	°F.	Number	
17		Centipoises at	°F.	Diameter	
18	Quantity—Liquid		#/Hr.	No. of Blades	
19	Vapor or Gas	Cu. Ft./24 Hr. @ 14.7# Abs. & 60°F.		R.P.M.	
20	Vapor		#/Hr.	Horsepower per Fan	
21	Steam		#/Hr.		
22	N. C. Gas		#/Hr.	Gears: Model	
23	Fluid Vap. or Condsd.		#/Hr.	Make	
24	Steam Condensed		#/Hr.		
25	Operating Temperature	In °F. : Out	°F.	Drive Shaft:	
26	Operating Pressure		#/☐"		
27	Pressure Drop		#/☐"	Motors: Type	
28	Design Pressure		#/☐"	Make	
29	Test Pressure		#/☐"	Number	
30	Design Temperature		°F.	H.P.	
31				R.P.M.	
32				Volts	
33	Heat Exchanged		B.T.U./Hr.	Phase	
34	Surface per Section		Sq. Ft.	Cycle	
35	Total Surface		Sq. Ft.	Turbines:.Model	
36	**MATERIALS AND CONSTRUCTION**			Turbines:.Model	
37	Headers			Make	
38	Thrust Members			Number	
39	Tubes			H.P.	
40	Fins			R.P.M.	
41	Tube Plugs			Steam In.	#/☐"
42	Retarders			Steam Ex.	#/☐"
43	Connections	In		Water Rate	#/H.P. Hr.
44		Out			
45	Number of Passes			Gas Engines: Model	
46				Make	
47				Number	
48				H.P.	
49				R.P.M.	

Price: F.O.B. Shipping Point, not erected . . . . $ _____
Freight . . . . $ _____
TOTAL PRICE $ _____

Estimated Erection Labor . . . . $ _____
Shipping Weight . . . . _____ lbs.

THE GRISCOM-RUSSELL CO.
G-FIN TANK HEATER SPECIFICATIONS

1	Customer		Item No.	
2	Address		Inq. No.	
3	Plant		Date	
4	Unit Required			
5				
6	Service		Type Internal External	
7		SHELLS	TUBES	
8	Class of Fluid			
9	Specific Gravity @ 60°F.			
10	Specific Heat @ Ave. Temp.			
11	Latent Heat @ Ave. Temp.	B.T.U. /#	B.T.U. /#	
12	Viscosity	S.S.U. at °F.		
13	Viscosity	Centipoises at °F.	Centipoises at °F.	
14	Viscosity	Centipoises at °F.	Centipoises at °F.	
15	Quantity	GPM #/Hr.	#/Hr.	
16	Operating Temperature	In °F. : Out °F.	In °F. : Out °F.	
17	Operating Pressure	#/□"	#/□"	
18	No. Passes per Shell	1	2	
19	Design Pressure	#/□"	#/□"	
20	Test Pressure	#/□"	#/□"	
21	Design Temperature (Max. Metal Temp.)	°F.	°F.	
22	Heat Exchanged	BTU/Hr. Surface Per Unit	Sq. Ft.	
23	Corrected M.T.D. Design Rate	Surface Per Shell	Sq. Ft.	
24		MATERIALS AND CONSTRUCTION		
25	SHELL: Steel	CHANNEL: Steel	Baffles: Steel Standard Spacing	
26	INLET CONN. SIZE	INLET CONN. SIZE:	Tie Rods and Spacers: Steel	
27	Drilling: 150#	Drilling: 150# P.T.	Gaskets: Durabla	
28	OUTLET CONN. SIZE	OUTLET CONN. SIZE	Saddles: Steel (Type HSU-CSU only)	
29	Drilling: 150#	Drilling: 150# P.T.	Structural Codes	
30	Tank Manhole Flange Size : O.D.	Tubes—¾" IPS Seamless Steel	Inspection by:	
31	Bolt Circle No. Dia.	Fins—Steel. Nom. Length:	OVERALL LENGTH	
32	Tube Sheet—Steel with Cone Seat Tube Joints and Lock Nuts		OUTSIDE SHELL DIAMETER	
33	Support Plate on Open Shell Unit Steel 1" Thick		Reference Print	
34	GUARANTEE: This unit will give full capacity with tank liquid level 2 Ft. or more above unit.			

SUGGESTIONS:
1. Steam trace all oil lines.
2. Use steam trap large enough to handle indicated steam condensate.
3. Vent steam side of unit.
4. Provide drains for steam side to take care of shut down during cold weather.
5. This is an instantaneous heater; steam required only when pumping oil.

750

KELLOGG

COMPRESSOR COOLER DATA SHEET

JOB NO. _____ ITEM NO. _____
REQ. NO. _____
PAGE NO. _____ OF _____

ENG EQUIP 37 (6-77)

INTERCOOLERS AND AFTERCOOLERS

ITEM NUMBER OR LOCATION   _____ _____ _____ _____ _____

BETWEEN STAGE NUMBER   _____ _____ _____ _____ _____

COOLER FURNISHED BY:
□ COMPRESSOR MANUFACTURER   □ PURCHASER   _____ _____ _____ _____ _____

COOLER MANUFACTURER   _____ _____ _____ _____ _____
COOLER MODEL OR TYPE

SPECIFICATIONS —	MANUFACTURERS STANDARDS	_____	_____	_____	_____	_____
	OTHER	_____	_____	_____	_____	_____
TYPE	SHELL AND TUBE	_____	_____	_____	_____	_____
	CONCENTRIC PIPE	_____	_____	_____	_____	_____
	PIPE LINE	_____	_____	_____	_____	_____
	FINTUBE	_____	_____	_____	_____	_____
MATERIALS	SHELL OR OUTER PIPE	_____	_____	_____	_____	_____
	TUBES OR INNER PIPE	_____	_____	_____	_____	_____
	TUBE SHEETS	_____	_____	_____	_____	_____
	TUBE SIZE. O.D., INCHES AND BWG.					
COOLING WATER—	GPM	_____	_____	_____	_____	_____
	TEMPERATURE IN °F	_____	_____	_____	_____	_____
	TEMPERATURE OUT °F	_____	_____	_____	_____	_____
	PRESSURE DROP PSI	_____	_____	_____	_____	_____
	MAXIMUM WORKING PRESSURE, PSIG					
GAS SIDE	FLOW RATE AT INTAKE, LBS./HR	_____	_____	_____	_____	_____
	TEMPERATURE AT INTAKE °F	_____	_____	_____	_____	_____
	TEMPERATURE AT OUTLET °F	_____	_____	_____	_____	_____
	INLET PRESSURE, PSIG	_____	_____	_____	_____	_____
	PRESSURE DROP, PSIG	_____	_____	_____	_____	_____
DESIGN	DESIGN PRESSURE, PSIG	_____	_____	_____	_____	_____
	DESIGN TEMPERATURE °F	_____	_____	_____	_____	_____
	EFFECTURE SURFACE, SQUARE FEET	_____	_____	_____	_____	_____
	RECOMMENDED RELIEF VALVE SETING, PSIG	_____	_____	_____	_____	_____
	HYDROSTATIC TEST PRESSURE PSIG					

MOISTURE SEPARATORS

FURNISHED BY: □ COMPRESSOR MANUFACTURER □ PURCHASER □ SEPARATE □ INTEGRAL WITH COOLERS

MANUFACTURER   _____ _____ _____ _____ _____
TYPE AND MODEL   _____ _____ _____ _____ _____
SHELL MATERIAL   _____ _____ _____ _____ _____
TRAPS OR LIQUID COLLECTION DRUMS, GAUGE GLASS, DRAIN OUT VALUE, HIGH LIQUID LEVEL ALARM CONTACTS
TO BE FURNISHED BY: □ COMPRESSOR MANUFACTURER   □ PURCHASER

AIR RECEIVER

FURNISHED BY: □ COMPRESSOR MANUFACTURER   □ PURCHASER
CAPACITY _____ CUBIC FEET
RATED PRESSURE _____ PSIG
□ RECEIVER TO COMPLY WITH _____ PRESSURE VESSEL CODE
□ RECEIVER TO FURNISHED WITH SUPPORTING STAND FOR FLOOR MOUNTING
□ RECEIVER COMPLETE WITH SAFETY VALVE, PRESSURE GAUGE, AND DRAIN VALVE.

REVISIONS	NO.	0	1	2	3	4	5	6	7	8	9	10
	DATE											
	BY											
	CHECK											
	APPRVD.											

PLATE & FRAME EXCHANGER SPECIFICATION SHEET

	ENG'R	DATE
REP'D BY		
CHKD BY		
APPR'D BY		

REV.	BY	CHKD	DATE

PROJECT	POS. NO.
PROJ. NO.	F. S. REF.
BLDG. NO.	NO. REQ'D.
SERVICE OF UNIT	MODEL
SIZE	NO. OF PLATES
SURFACE PER UNIT	SURFACE PER PLATE

PERFORMANCE OF ONE UNIT

		HOT SIDE		COLD SIDE	
		IN	OUT	IN	OUT
FLUID CIRCULATED					
TOTAL FLUID ENTERING	LB/HR				
LIQUID					
STEAM					
STEAM CONDENSED					
GRAVITY-LIQUID					
VISCOSITY-LIQUID	CENTIPOISE				
SPECIFIC HEAT	BTU/LB. °F				
THERMAL CONDUCTIVITY	BTU/HR., FT², °F/FT				
LATENT HEAT-VAPORS	BTU/LB.				
TEMPERATURE	°F				
OPERATING PRESSURE	PSIG				
NUMBER OF PASSES					
VELOCITY	FT/SEC.				
PRESSURE DROP - ALLOWABLE/CALC.	PSI				
FOULING RESISTANCE (MIN.)					
HEAT EXCHANGED-BTU/HR.			M.T.D. (CORRECTED). °F - THEORETICAL		
TRANSFER RATE-SERVICE		CLEAN			

CONSTRUCTION

DESIGN PRESSURE	PSI		
TEST PRESSURE	PSI		
DESIGN TEMPERATURE	°F		

MATERIALS OF CONSTRUCTION	PRESSURE PLATE	CONNECTING PLATE	
ENDS PLATES	THERMAL PLATES	FRAME	
EXTERNAL BOLTING	INTERNAL BOLTING	HOT SIDE GASKET	
PROTECTION SHROUD	PAINT	COLD SIDE GASKET	

CONNECTIONS - HOT SIDE	IN	OUT	SERIES
COLD SIDE	IN	OUT	SERIES
FABRICATION SPEC			
INSPECTION & TEST		TEST PRESSURE, PSIG	
WEIGHT: LBS.-EMPTY	FULL OF WATER	OPERATING	

REMARKS: _____

KELLOGG

STEAM SURFACE CONDENSER DATA SHEET

CUSTOMER _____ EST. NO. _____

LOCATION _____ JOB NO. _____

  PAGE NO. _____

SERVICE OF UNIT _____ ITEM NO. _____

  DATE _____

A. Condenser

1. Manufacturer
   a. Name: _____
   b. Location: _____
2. Condenser surface (total effective): _____ sq ft
3. Number of water passes: _____
4. Design basis — operating conditions and performance
   a. Nature and source of circulating water: _____
   b. Duty (net heat rejected to circulating water): _____ Btu per hr
   c. Circulating water quantity: _____ gpm
   d. Circulating water inlet temperature: _____ F
   e. Cleanliness factor: _____ %
   f. Average circulating water velocity in tubes: _____ fps
   g. Absolute pressure (to be measured at point specified in the Heat Exchange Institute Standards): _____ in. Hg
   h. Deaeration — maximum free oxygen in condensate (42) (14) (7) — (Indicate): _____ ppb
   i. Circulating water friction loss through clean tubes and waterboxes: _____ ft
   j. Supplementary (expected) performance on curve sheets: _____
5. Tubes
   a. Main Condensing Sections:
      (1) No.: _____ Size: _____ in. OD Gauge: _____ BWG
      (2) Length, effective: _____ Overall: _____ ft
      (3) Material: _____
   b. Gas Removal Sections:
      (1) No.: _____ Size: _____ in. OD Gauge: _____ BWG
      (2) Length, effective: _____ Overall: _____ ft
      (3) Material: _____
   c. Impingement Sections:
      (1) No.: _____ Size: _____ in. OD Gauge: _____ BWG
      (2) Length, effective: _____ Overall: _____ ft
      (3) Material: _____
   d. Method of connection — Inlet end: _____ Outlet end: _____
   e. Furnished by: _____
   f. Installed by: _____
6. Waterboxes — Covers (if required)
   a. Material (Waterbox): _____
   b. Material (Covers): _____
   c. Divided or non-divided: _____
   d. Design pressure: _____ psig Test pressure: _____ psig
   e. Number and size — Inlet nozzles: _____ Outlet nozzles: _____

KELLOGG

STEAM SURFACE CONDENSER DATA SHEET (con't.)

CUSTOMER _____

LOCATION _____

SERVICE OF UNIT _____

EST. NO. _____

JOB NO. _____

PAGE NO. _____

ITEM NO. _____

DATE _____

7. Shell

   a. Material:_____

   b. Thickness:_____ Number of sections:_____

   c. Method of connecting sections:_____

   d. Provision for tube expansion:_____

   e. Number and size of venting connections:_____

8. Hotwell

   a. Type:_____Capacity:_____gals

   b. Material: _____

   c. Thickness:_____ Number of sections:_____

9. Tube sheets

   a. Number and size: _____Thickness:_____

   b. Material: _____

10. Tube support plates

   a. Number:_____Thickness:_____

   b. Material:_____

11. Steam inlet neck and exhaust connection

   a. Material: _____

   b. Thickness: _____ Number of sections:_____

   c. Connection to shell — (flanged) or (welded) : _____ To turbine — (flanged) or (welded) :_____

   d. Height — top of waterbox flange to turbine exhaust including expansion joint (if any) :_____

   e. Provision for vertical expansion (condenser hung) (spring supports) (expansion joint).

   f. Spring supports (if used). Type: _____

   g. Expansion joint (if used). Type:_____

     Material: _____

     Height:_____ Ends — (flanged) or (welded) :_____

12. Approximate weights, condenser with tubes

   a. Dry:_____lbs In service:_____lbs

   b. Steam space only filled with water:_____lbs

13. Preliminary drawing(s) :_____

14. Descriptive bulletin(s) (or specifications) :_____

752

KELLOGG

STEAM SURFACE CONDENSER DATA SHEET (con't.)

CUSTOMER _____

LOCATION _____

SERVICE OF UNIT _____

EST. NO. _____

JOB NO. _____

PAGE NO. _____

ITEM NO. _____

DATE _____

B. Steam Jet Air Ejector(s)

1. Manufacturer

   a. Name: _____

   b. Location: _____

2. Total number of Ejector Units:_____

3. Size and type:_____ No. of elements:_____ No. of stages:_____

   mounted on: _____ surface inter- and after-condensers

4. Operating Conditions and Performance

   a. Design capacity — 100 per cent —

     Suction pressure:_____in. Hg abs

     Suction temperature:_____F

     Dry air leakage:_____SCFM corresponding to:_____lbs per hr

     Non-condensible gases other than air leakage:_____(_____)_____lbs per hr

     _____(_____)_____lbs per hr

     _____(_____)_____lbs per hr

     _____(_____)_____lbs per hr

     Associated saturated water vapor:_____lbs per hr

     Total gas-vapor mixture:_____lbs per hr

     Design capacity each element:_____per cent

     Number of elements operating for 100% capacity:_____

     Curve(s) of approximate capacity vs. suction pressure:_____

   b. Steam conditions —

     Maximum initial pressure:_____psig Total temp :_____F

     Minimum operating pressure (at nozzles) :_____psig Total temp :_____F

   c. Steam Consumption (100 per cent design capacity) : _____lbs per hr

5. Condenser Data

   a. Surface sq ft:_____Inter-condenser_____After-condenser

   b. Surface:_____per cent design capacity

   c. Tube size:_____in. OD:_____BWG:_____Length (effective-overall)

   d. Method of fastening tubes:_____

   e. Cooling Water (condensate) (raw water) :_____

     Minimum flow required at:_____per cent design capacity:_____gpm

     Maximum design flow:_____gpm

     Friction loss at maximum design flow:_____feet of water

   f. Waterboxes — Maximum design pressure:_____psig

6. Materials

   a. Suction chambers: _____

   b. Diffusers:_____

   c. Steam nozzles: _____

   d. Steam chests (nozzle heads) :_____

   e. Condenser shells:_____

KELLOGG

STEAM SURFACE CONDENSER DATA SHEET (con't.)

EST. NO. _____

CUSTOMER _____ JOB NO. _____

LOCATION _____ PAGE NO. _____

ITEM NO. _____

SERVICE OF UNIT _____ DATE _____

    f. Water chambers: _____

    g. Tube sheets: _____

    h. Tubes: _____

7. Fittings and Accessories included

    a. Air leakage meter: _____

    b. Other: _____

8. Approximate weight, each ejector unit: _____ lbs

9. Preliminary drawing(s): _____

10. Descriptive bulletin(s) (or specifications): _____

C. Hogging Ejectors

1. Manufacturer

    a. Name: _____

    b. Location: _____

2. (Steam) (Air) (Water) Operated. Number per condenser: _____ Size: _____

3. Operating Conditions and Performance

    a. Capacity: _____ lb per hr dry air at _____ in. Hg abs Suction Pressure

    b. Steam consumption: _____ lb per hr at _____ psig _____ F

    c. Maximum design steam conditions: _____ psig _____ F

    d. Air consumption: _____ SCFM at _____ psig

    e. Water consumption: _____ gpm at _____ psig

4. Approximate weight, each: _____ lbs

5. Preliminary drawing(s): _____

6. Fittings and accessories included: _____

7. Descriptive bulletin(s) (or specifications): _____

D. Remarks: _____

_____

_____

_____

_____

_____

_____

_____

_____

_____

_____

_____

_____

Steam Surface Condenser—(*continued*)

753

SWECO

SOUTHWESTERN ENGINEERING COMPANY
4800 SANTA FE AVENUE   LOS ANGELES 58, CALIFORNIA   SHEET___ OF___

FIRED HEATER SPECIFICATION SHEET   REV

#				
1	CUSTOMER		EQUIP. NO.	
2	PLANT LOCATION		FILE NO.	
3	SERVICE			
4	MANUFACTURER	TYPE	SIZE	
5				
6	**THERMAL DESIGN**			
7	FLUID CIRCULATED			
8	TOTAL FLUID ENTERING	#/HR		
9			INLET	OUTLET
10	TOTAL VAPOR	#/HR		
11	TOTAL LIQUID			
12	GRAVITY LIQUID	°API		
13	DENSITY VAPOR	#/CU. FT.		
14	VISCOSITY LIQUID	CP		
15	VISCOSITY VAPOR	CP		
16	SPECIFIC HEAT	BTU/#		
17	LATENT HEAT	BTU/#		
18	TEMPERATURE	°F		
19	OPERATING PRESSURE	PSIG		
20	MOLECULAR WEIGHT OF VAPOR			
21				
22				
23	ALLOWABLE PRESSURE DROP	PSI	CALCULATED PRESSURE DROP	PSI
24	TYPE OF FLOW		SERIES	PARALLEL
25	EFFECTIVE SURFACE	SQ. FT.	RADIANT	CONVECTION
26	HEAT ABSORPTION	BTU/HR.	RADIANT	CONVECTION
27	HEAT ABSORPTION	BTU/HR.	TOTAL	
28	LIQUID TEMPERATURE	°F		
29				
30	RADIANT TRANS. RATE	BTU/SQ. FT./HR.	AVERAGE	MAXIMUM
31	CONVECTION TRANS. RATE	BTU/SQ. FT./HR.	AVERAGE	MAXIMUM
32	EFFICIENCY	% - LHV/HHV		
33	FLUE GAS TEMP. (APPROX.)	°F		
34	TYPE OF FUEL			
35	LHV OF FUEL	BTU/		
36				
37	PRESSURE AVAILABLE AT BURNER - PSIG	FOR GAS	NORMAL	MAXIMUM
38		FOR FUEL OIL	NORMAL	MAXIMUM
39		FOR STEAM	NORMAL	MAXIMUM
40				
41	**MECHANICAL DESIGN**			
42				
43	NO. OF TUBES	RADIANT	CONVECTION	
44	EFFECTIVE TUBE LENGTH	RADIANT	CONVECTION	
45	RADIANT TUBES	INCHES O.D.	TUBEWALL	INCHES MATERIAL
46	CONVECTION TUBES	INCHES O.D.	TUBEWALL	INCHES MATERIAL
47	RETURN BENDS	TYPE	MATERIAL	
48	NOZZLES	INLET	OUTLET	
49	DESIGN RADIANT	PRESSURE PSIG	TEMPERATURE °F	
50	CONVECTION	PRESSURE PSIG	TEMPERATURE °F	
51	CODE	CUSTOMERS SPECIFICATION		
52	BURNERS - NO. TYPE	MFG.	PILOTS REQ'D.	
53	HEATER TYPE	HEATER WEIGHT		
54	TYPE SHELL CONSTRUCTION	TYPE ASSEMBLY		
55				
56	REMARKS:			
57				

REVISIONS

DATE

BY

APPROVED

DATE

BY

CHECKED

ENGINEER

PROJ. ENG.

SCOPE: _____

_____
_____
_____
_____
_____
_____

PERFORMANCE REQUIREMENTS

	FEED	DISTILLATE	CONCENTRATE
IDENTIFICATION			
QUANTITY: LBS/HR.			
NORMAL OPERATING			
DESIGN			
COMPOSITION:			
PHYSICAL PROPERTIES			
MOLECULAR WEIGHT			
SPECIFIC GRAVITY			
VISCOSITY; CP			
SPECIFIC HEAT: BTU/#°F			
LATENT HEAT: BTU/#			
THERMAL CONDUCTIVITY –			
BTU/#°F FT.			
VAPOR PRESS. MMH_G			
MELTING POINT – °C			

Sidebar labels: REMARKS | APPR'V | DATE | CHKD SUPRV | BY | REV | DES SUPRV. | CHECKED BY | DRAWN BY | INITIATOR

754

JOB NO.   PLANT LOCATION   SCALE
PROJECT NO.   REF. DWG. NO.
TITLE   ISSUE
                                                            DATE   BLDG. NO.
POSITION NO.   SERIES   STEP NO.

DRAWING NO.

OPERATING CONDITIONS

	PROCESS	JACKET	CONDENSER
FLUID DESCRIPTION			
TEMPERATURE	FEED _____ °C	INLET _____ °C	
	DISTILLATE _____ °C	OUTLET _____ °C	
	CONCENT. _____ °C		
VAPORIZATION TEMP.	_____ °C	_____ °C	_____ °C
DESIGN TEMP.	_____ °C	_____ °C	_____ °C
MAX. ALLOW. TEMP.	_____ °C	_____ °C	_____ °C
OPERATING PRESS.	_____ PSIG	_____ PSIG	_____ PSIG
DESIGN PRESS.	_____ PSIG	_____ PSIG	_____ PSIG
NORMAL FLOW RATE			
MAX. FLOW RATE			
PRESSURE DROP			
MAX. ALLOW. PRESS DROP			
MAX. AIR LEAKAGE RATE			
HEAT DUTIES:			
PRE-HEAT			
VAPORIZATION			
CONDENSING			
SURFACE REQUIRED			
VAPORIZATION			
CONDENSATION			

MATERIALS

MAIN VESSEL _____   MECH. SEAL
JACKET _____   ROTATING FACE _____
SHAFT _____   STATIONARY FACE _____
WIPER BLADES _____   SEAL RING _____
BEARINGS _____   "O" RINGS _____
INTERNAL COND. TUBES _____   MAIN GASKETS _____
INTERNAL COND. TUBESHEET _____

MOTOR DRIVE DATA

ITEM NO. _____ MTD BY. _____   VOLTS/PHASE/HZ: _____ / __ / __
HP _____ RPM _____ FRAME _____   BEARINGS _____ LUBE _____
MFR. _____   FULL LOAD AMPS: _____ S.F. _____
TYPE _____ INSUL. _____   L.R. AMPS _____
ENCLOSURE: CLASS 1   GROUP D-DIV.

Sidebar labels: REMARKS | APPR'V | DATE | CHKD SUPRV | BY | REV | DES SUPRV. | CHECKED BY | DRAWN BY | INITIATOR

JOB NO.   PLANT LOCATION   SCALE
PROJECT NO.   REF. DWG. NO.
TITLE   ISSUE
                                                            DATE   BLDG. NO.
POSITION NO.   SERIES   STEP NO.

DRAWING NO.

VENDOR DATA (RETURNED BY VENDOR)

HEATING SURFACE _____ SQ. FT.

UNIT SIZE & TYPE: _____

CONDENSING SURFACE: _____ SQ. FT.

NOZZLES	SIZE	RATING	FACING	POSITION
FEED				
VAPOR (VAC)				
RESIDUE				
DISTILLATE				
JACKET-IN				
JACKET-OUT				

PACKING: TYPE _____
SIZE _____ NO. RINGS _____
PRESS. ON PACKING BOX. _____ PSIG
MECH. SEAL: TYPE _____
MFR. _____
SEAL FLUID _____
_____

MOTOR: SIZE & TYPE _____ MFG: _____
RPM _____ PERIPHERAL SPEED _____ FT./SEC.
DRIVE TYPE _____
VENDOR TO SUPPLY DIMENSIONAL PRINTS OF ALL UNITS.
WEIGHT OF UNIT: EMPTY _____ FULL OF WATER _____

UTILITIES AVAILABLE

STEAM	_____ #/HR @ _____	PSIG @ _____	°F
COOLING WATER	_____ GPM @ _____	PSIG @ _____	°F
HOT OIL	_____ GPM @ _____	PSIG @ _____	°F
ELECTRICITY	_____ VOLTS _____	PHASE _____	CYCLES

MISCELLANEOUS REQUIREMENTS

QUOTATIONS:
VENDOR QUOTATION SHOULD INCLUDE THE FOLLOWING:
1 - EQUIPMENT DESCRIPTION WITH DEFINITIVE SPECIFICATIONS INCLUDING SIZE, OPERATING AND DESIGN PRESSURES, AND MATERIALS OF CONSTRUCTION ON ALL PARTS.
2 - VENDOR SHALL STATE THE REQUIRED FLOWS, PRESSURE DROPS AND DESIGN DUTIES FOR EACH JACKET, STILL CONDENSER, AND FREEZEOUT TRAP.
3 - SUMMARY OF UTILITY REQUIREMENTS.
4 - RECOMMENDED INSTRUMENTATION.
5 - RECOMMENDED LAYOUTS AND REQUIRED STRUCTURES.
6 - RECOMMENDED SPARE PARTS LIST AND COST OF EACH ITEM

TESTS
ALL EQUIPMENT AND MANIFOLDS DESCRIBED IN THIS SPECIFICATION SHALL BE ASSEMBLED AND TESTED UNDER DESIGN VACUUMS AT THE VENDORS SHOPS TO ASSURE PROPER FIT, VACUUM TIGHTNESS AND THE GENERAL OPERABILITY OF THE DESIGN. ROCHE INSPECTION AND APPROVAL OF THE RUN-IN TESTS IS REQUIRED PRIOR TO SHIPMENT.

GUARANTEES:
THE VENDOR SHALL GUARANTEE THE MECHANICAL OPERATION OF THE EQUIPMENT AND SYSTEM PROVIDED FOR A MINIMUM OF ONE YEAR AFTER START-UP. HLR EXPECTS PROCESS GUARANTEES ON THE SPECIFIED DISTILLATION RATES, CONDENSER PERFORMANCE, AND MAXIMUM PRESSURE DROPS. ENTRAINMENT, AIR LEAKAGE RATES AND UTILITY CONSUMPTIONS SHALL BE SPECIFIED. ALL PRODUCT AND PROCESS SPECIFICATIONS WHICH THE VENDOR CANNOT GUARANTEE SHALL BE ENUMERATED.

JOB NO.	PLANT LOCATION		SCALE
PROJECT NO.	REF. DWG. NO.	ISSUE DATE	
TITLE			BLDG. NO.
POSITION NO.	SERIES	STEP NO.	
		DRAWING NO.	

E230B46 SHEET 3

REMARKS / APP'R'V / DATE / CHKD SUPV / BY / REV
DES SUPRV / CHECKED BY / DRAWN BY / INITIATOR

GENERAL NOTES

1 - VESSEL FABRICATION TO BE IN ACCORDANCE WITH THE FOLLOWING:

☐ _____ ASME CODE, SECTION VIII.   STAMP REQ'D. ☐   NOT REQ'D. ☐
☐   SPEC.   UNFIRED PRESSURE VESSELS.

2 -   SPECIFICATIONS TO BE COMPLETED BY VENDOR AND RETURNED WITH PROPOSAL.

JOB NO.	PLANT LOCATION		SCALE
PROJECT NO.	REF. DWG. NO.	ISSUE DATE	
TITLE			BLDG. NO.
POSITION NO.	SERIES	STEP NO.	
		DRAWING NO.	

E230B46 SHEET 4

REMARKS / APP'R'V / DATE / CHKD SUPV / BY / REV
DES SUPRV / CHECKED BY / DRAWN BY / INITIATOR

Wiped Film Evaporator—(*continued*)

REMARKS

OPERATING CONDITIONS

MAT'L. TO BE DRIED: _____
CHARACTERISTICS: _____
_____
BULK DENSITY: AVG. _____ LB./CU. FT.
      MIN. _____ LB./CU. FT.
MOISTURE: _____
INITIAL MOISTURE CONTENT: _____ WT. %
FINAL MOISTURE CONTENT: _____ WT. %
AMT. OF MAT'L PER BATCH _____ LBS.
WORKING CAPACITY REQ'D. _____ CU. FT.
MAX. TEMP: WET _____ °F DRY _____ °F
DRYING RATE: _____ LB./HR.
EST. DRYING TIME/BATCH _____ HRS.
MOISTURE RECOVERY: REQ'D. ☐ NOT REQ'D. ☐

OPERATING PRESS. _____ PSIA
DESIGN PRESS. _____ PSIG
JACKET DESIGN PRESS. _____ PSIG
HEAT TRANSFER RATE: _____ BTU/HR.
UTILITIES AVAILABLE:
ELECTRICITY: VOLTS/PHASE/CYCLE/- _____
WATER: TEMP. MIN. _____ °F MAX. _____ °F
      PRESS. _____ PSIG
STEAM: PRESS. _____ PSIG
      TEMP. _____ °F
BRINE: PRESS. _____ PSIG
      TEMP. _____ °F
OTHER: _____

MECHANICAL DATA

MFR. _____
SIZE & TYPE _____
TOP OPENING: SIZE _____ TYPE _____
BOT. OUTLET: SIZE _____ TYPE _____
DRYER RPM: _____
DRIVE: MFR. _____
     TYPE _____

VACUUM SEAL: TYPE _____
PACKING: TYPE _____
      SIZE _____ NO. RINGS _____
MECH. SEAL: MFR. _____
      TYPE _____
COUPLING: MFR. _____
      TYPE _____

MATERIALS

SHELL: _____
INTERNAL FINISH #: _____
JACKET: _____
VACUUM TUBE: _____
FILTER: _____
PACKING: _____

MECH. SEAL: ROTATING FACE: _____
      STATIONARY FACE: _____
BOT. OUTLET VALVE: _____
VACUUM PIPING: _____
JACKET PIPING: _____
GASKETS: _____

MOTOR DRIVE DATA

	DRYER	VAC. PUMP	
ITEM NO./MTD. BY	/	/	/
HP/RPM/FRAME	/ /	/ /	/ /
MFR.			
TYPE/INSUL.	/	/	/
ENCLOSURE			
VOLTS/PHASE/CYCLE	/ /	/ /	/ /
BEARINGS/LUBE.	/	/	/
FULL LOAD AMPS/SF	/	/	/
L.R. AMPS			

JOB NO.
PROJECT NO.
TITLE
POSITION NO.   SERIES   STEP NO.
PLANT LOCATION
REF. DWG. NO.
ISSUE DATE
SCALE
BLDG. NO.
DRAWING NO.

E219B35

756

REMARKS

MISCELLANEOUS DATA

LIST OF ACCESSORIES TO BE FURNISHED BY VENDOR:
☐ COMPLETE VACUUM SYSTEM INCL. PUMP, CONDENSER, RECEIVER AND PIPING
☐ COMPLETE HEATING SYSTEM INCL. PUMP, EXCHANGER AND PIPING
☐ VACUUM CONTROL SYSTEM
☐ HEATING CONTROL SYSTEM
☐ AUTOMATIC JOGGING AND POSITIONING SYSTEM FOR DRYER
☐ INSTRUMENT SPECIFICATIONS FOR PURCHASE BY H.L.R.
☐ BOTTOM OUTLET VALVE
☐ THERMOWELL
☐ VIBRATOR
☐ UNMOUNTED EXPANDABLE SLEEVES

REMARKS

_____
_____
_____
_____
_____
_____
_____
_____
_____
_____
_____
_____
_____
_____
_____
_____
_____
_____
_____

JOB NO.
PROJECT NO.
TITLE
POSITION NO.   SERIES   STEP NO.
PLANT LOCATION
REF. DWG. NO.
ISSUE DATE
SCALE
BLDG. NO.
DRAWING NO.

E219B35

BOILER DATA SHEET
BOILER SHALL BE FURNISHED IN ACCORDANCE WITH THE M. W. KELLOGG COMPANY SPEC.

1. OPERATING CONDITIONS

RATED CAPACITY: _____ PPH CONTINUOUS PER UNIT

STEAM PRESSURE: _____ PSIG AT S.H. OUTLET

STEAM TEMP.: _____ F AT S.H. OUTLET

_____ ON _____ FIRED OPERATION

FEED WATER TEMP. _____ F, BLOWDOWN _____ %

FUEL

A.P.I GRAVITY

% BY

ASH

HYDROGEN

CARBON

SULPHUR

H.H.V. BTU/

L.H.V. BTU/

PSIG @ BURNER

TEMP. @ BURNER F.

TYPE OF INSTALLATION: _____

CASING: _____

AMBIENT TEMP: _____ F

ALTITUDE: _____ FT. ABOVE SEA LEVEL

DESIGN WIND LOADING: _____ LB/SQ. FT.

EARTH QUAKE LOADING: _____ ZONE.

INSTRUMENT AIR: _____ PSIG

START-UP

11. EXPECTED PERFORMANCE

STEAM ACTUAL M. LB/HR				
BLOWDOWN %				
FUEL				
LOAD DURATION				
FURNACE LIBERATION				
M.B.T.U./CU. FT./HR.				
FURNACE HEAT RATE				
M.B.T.U./SQ. FT./HR.				
EXCESS AIR LEAVING BLR. %				

QUANT. M LB/HR					
	FUEL (GAS CFM)				
	FLUE GAS ENT. A.H.				
	FLUE GAS LEAVING A.H.				
	AIR LEAVING A.H.				

STEAM AT S.H. OUTLET – PSIG

TEMP. F					
	SUPER HEATED STEAM				
	FLUE GAS LEAVING BLR				
	FLUE GAS LEAVING				
	WATER ENT. ECON.				
	WATER ENT. BLR.				
	AIR ENT. A.H.				
	AIR LEAVING A.H.				

DRAFT LOSS IN. OF WATER					
	FURNACE				
	BOILER AND S.H.				
	ECONOMIZER				
	AIR HEATER				
	FLUES				
	NET DRAFT LOSS				
	ACROSS INST. CONNECT				

AIR RESISTANCE IN. OF WATER					
	BURNERS WINDBOX				
	DUCTS				
	AIR HEATER				
	NET RESISTANCE				

EFFICIENCY %

		LB/HR	IN. H2O	F
F.D. FAN	NET RATING			
	TEST RATING			
F.D. FAN	NET RATING			
	TEST RATING			

REVISIONS					
6					
5					
4					
3					
2					
1					
0					
NO.	DATE	ENGINEER	CHK/REVIEW	APPROVE	

KELLOGG

MANAGING OFFICE	ENGINEERING OFFICE

EQUIPMENT DATA SHEET

CLIENT _____

LOCATION _____

ITEM _____

ITEM NO. _____ SPEC. NO. _____

REQ'N. NO. _____ PAGE _____ OF _____

757

PACKAGE BOILER DATA SHEET

III EQUIPMENT

BOILER

TYPE _____

DESIGN PRESSURE, PSIG _____

FURNACE TYPE _____

FURNACE VOLUME, CU. FT. _____

HEATING SURFACE
(RADIANT SURFACE: FLAT PROJECTED BASIS.
CONVENTION SURFACE: CIRCUMFERNTIAL BASIS)

FURNACE, SQ. FT. _____

BOILER, SQ. FT. _____

TOTAL, SQ. FT. _____

DRUMS: _____

NO. REQUIRED _____

UPPER DIMENSION _____

LOWER DIMENSION _____

VERT. HT. (C.L. TO C.L.) _____

SUPER-HEATER

TYPE _____

TEMP. CONTROL _____

SURFACE AREA, SQ. FT. _____

ECONO-MISER

TYPE _____

SURFACE AREA, SQ. FT. _____

AIR HTR.

TYPE _____

SURFACE AREA, SQ. FT. _____

BURNERS

		NO. REQ.	TYPE MAKE	LOAD RANGE	PRESS RANGE
OIL					
GAS					

COMBUSTION CONTROLS

FURNISHED BY _____

STACKS

IN ACCORDANCE WITH KELLOGG SPEC. _____

TYPE _____

HEIGHT, FT. _____ DIAMETER _____

ARRANGEMENT _____

DUCT FLUES

FURNISHED BY _____

PLAT FORM LOADERS

FURNISHED BY _____

IN ACCORDANCE WITH KELLOGG SPEC. _____

SOOT BLOWERS

BOILER _____

SUPERHEATER _____

AIR HEATER _____

DIMEN SIONS

SETTING (OVERALL) _____

UNIT (OVERALL) _____

CONNEC-TIONS

STEAM _____

WATER FEED _____

CHEMICAL FEED _____

BLOW-DOWN _____

WEIGHT

SHIPPING _____ LBS

OPERATING _____ LBS

MAX. ERECTION _____ LBS

IV GUARANTEE CONDITIONS

FUEL _____

CAPACITY, P.P.H. _____

STEAM TEMP. DEG. F. _____

(@ S.H. OUTLET) _____

THERMAL EFFIC. % _____

MAX. NET DRAFT LOSS _____

MAX. NET AIR RESISTANCE _____

SOLIDS CARRY OVER P.P.M. _____

BLOW-DOWN _____

FEED WATER TEMP. DEG. F. _____

MAX ALLOWABLE BOILER _____

CONCENTRATION P.P.M. _____

REVISIONS					
6					
5					
4					
3					
2					
1					
0					
NO	DATE	ENGINEER	CHK/REVIEW	APPROVE	

KELLOGG

MANAGING OFFICE	ENGINEERING OFFICE

EQUIPMENT DATA SHEET

CLIENT _____

LOCATION _____ JOB NO. _____

ITEM _____

ITEM NO. _____ SPEC. NO. _____

REQ'N. NO. _____ PAGE _____ OF _____

COOLING TOWER SPECIFICATIONS

Job No._____

B/M No._____

Page of Pages	
Unit Price	
No. Units	
Item No.	

PERFORMANCE

Water Circulating Rese: _____ Spm. Temp. Fn: _____ °F Temp. Out: _____ °F

Cooling Duly _____ Stu/Hrs Perform, Test Cose _____

*As Option of Owner _____

SELECTION

Manufacturer: _____ Models _____

Type: _____ No. of Calls: _____

DESIGN

Wet Bulb Temp: _____ *Fx Static Pumping Ht. _____ Ft. Elf. Cool. Vol. _____ Cu. Ft.

Fill Wetted Surf. _____ Sq.Fts. Total Wetted Surf. _____ Sq. Fts. EN. Splash Surf. _____ Cu. Ft.

No. of Fens Req'd. _____ Clm/Fen _____ ; SteNc Press _____ In. H2O;Normal BHP/Fen _____

Evaporation Less. Max, % _____ Saray Less. Max. % _____

MATERIALS OF CONSTRUCTION

Frame work _____ Casing _____ Fill _____

Fen Cylinder _____ Steirway _____

Salts Nutes, Mise, Hardware _____ Nails _____

Water Inlet Hdrs. _____ Mexxles _____ Basin _____

Fen Blade _____ Fen Hub _____ Fan Sheft. _____

Code for Lumber Grades _____ Code for Lumbar Strech Design _____

**Exceptions B1 and Lending, See Inquiry or P.O. _____

AUXILIARY EQUIPMENT

Fen

Manufacturer _____ Type _____

Diameter _____ Fts. Speed _____ RPM: Tip Speed _____ Spm.

Geer

Manufacturer _____ Type _____ Size _____

ReducNon Restle _____ Reted Cop. _____ BHP: Mechanical EN. _____ %

Driver

Manufacuerer _____ Type _____ Speed _____ RPM

Electric Power _____ BHP _____ Service Factor _____ Frame _____

REMARKS

By	Chk.d.	App.	Rev.	Rev.	Rev.
Date					

P.O.Tet _____

S & W FORM C-1407

STONE & WEBSTER ENGINEERING CORPORATION

INSTRUMENT SPECIFICATION

Item _____
Page _____
Preliminary _____
Final _____

1. Client _____ J. O. No. _____
2. Apparatus _____ Project No. _____
3. Service _____ Date _____ By _____
4. Based on _____ Process Page _____ Dated _____

#	INSTRUMENT CASE		BULBS OR THERMOCOUPLES	
5				
6	Location		Location	
7	Type		Bulb Type	
8	Case Finish		Thermocouple Matl	
9	Connections	Back — Bottom	Socket Material	
10	Mounting	Flush — Projecting	Socket Length	
11	Chart or Dial	No Size	Ext Neck Length	
12	Range	Flow Static Press.	Standard Pipe Thread	
13		Temp. Diff. Press.	Bulb Distance From Instr	Above Below / Above Below
14	Control Point	No of pens	Tubing or Lead	
15	Chart Volume	Measured on °F lb. Abs Basis	RESPONSES	
16	Clock	Electric — Spring Wound, 7 Day 24 Hour	Throttling Band	
17	Current	Volts AC DC Cycles	Reset	Automatic Manual
18	Accessories	Ink, 100 Charts etc to be included	Rate Response	Yes — No
19			Pneumatic Set	

#	INSTRUMENT		CONTROLLED VALVE — Item No.	
20				
21	Location		Service	
22	Type			
23	Float Body	Case Flanged Matl Trim	Valve	Size in. Drilling
24	Float Flange Conn.	Size Drilling	Plug Type Valve	Balanced Parabolic V-Port or Equal
25	Float	Size in. Matl	Type	Spring Diaphragm Weight Loaded
26	Stuffing Box	With Grease Seal	Body	Matl Trim
27	Orifice Flanges	Matl Drilling	Stem	Sliding — Rotary
28	Orifice Plate	Matl	Stuffing Box	With Grease Seal
29	Instr Body Diff Range	0 — in. Water Column	Operating Medium	Gas Comp Air @ lb ga Corrosive Yes No
30	Instr Body Located	above liquid level ft below orifice plate	Valve Action	Open Close with Fall of
31	Instr Body Distance	liquid level ft from orifice plate		Open Close with Failure of
32	Mercury Included		Valve Positioner	Yes - No with Bypass
33	Sealing Medium		Radiating Fins	Yes - No

#	CONDITIONS AND REQUIREMENTS				
34					
35		In	Control Valve	In	Control Valve
36	Fluid			Nor Quantity @	°F P
37	Sp Gr @ 60° F Air = 1 Water = 1			Max Quantity @	°F P
38	Sp Gr @ Nor T & P Air = 1 Water = 1			Min Quantity @	°F P
39	Viscosity	cp @ °F	cp @ °F	Nor Pressure (Up Stream)	lb ga / lb ga
40	Corrosion Present	Yes — No	Yes — No	Max Pressure (Up Stream)	lb ga / lb ga
41	Line Size	in.	in.	Down Stream Pressure	lb ga / lb ga
42	Normal Temperature	°F	°F	Pressure Drop	lb / lb
43	Max Temperature	°F	°F	Amount of Superheat	°F / °F
44	Supply Metal Tag, securely wired, marked with Item Number				

REMARKS

46 _____
47 _____
48 _____
49 _____
50 _____
51 _____
52 _____
53 _____
54 _____
55 _____

56 For Typical Installation Details See

57 General Specifications for Instrument, Page _____ ; for Valve, Page _____

Copy to	Date	Checked	Date	Approved	Date
Revised:					

DIFFERENTIAL PRESSURE TYPE FLOW INSTRUMENT

SERVICE DATA	PRESENT	NEW
ITEM NO.		
LOCATION		
SERVICE		
LINE SIZE		
ORIFICE SIZE (Bevel)		
MANOMETER (Range & Mfg.)		
MANOMETER TYPE (Mercury, Aneroid)		
CONNECTIONS (Flange & Series)		
FLOWING FLUID		
SP. GR. AT 60F		
FLOWING TEMP.		
FLOWING PRESSURE		
SEAL MATERIAL		
SEAL TEMP.		
SEAL GRAVITY AT 60F		
MAX. FLOW		
CHART NO.		

INSTRUMENT

PRIMARY METER
TYPE - Recording, Indicating, Blind, Transmitting
MFR. MODEL
MANOMETER - 1500 psi - Carbon Steel

RECEIVER
TYPE - Conventional, Miniature, None
MFR. MODEL
MOUNTING - Control Board, Local
CHART TYPE - Circular 24 Hour, Strip
CHART DRIVE - Spring, Pneumatic

CONTROLLER
TYPE - Conventional, Force Balance, Pneumatic
MFR. MODEL
MOUNTING - Control Board, Field
MANUAL CONTROL BYPASS - Yes, No
PNEUMATIC SET - Adjustable, Fixed, None
CONTROL FEATURES - Prop. Band, Reset, Rate
INCREASE IN FLOW, OUTPUT TO - Increase, Decrease
REQUISITION OR REQUEST -
REF. SPEC. SHEET-
REF. DRAWING -
INST. TAG DATA

REMARKS

By
App'd.
Date

HUMBLE OIL & REFINING CO.
BAYTOWN ENGINEERING DIVISION
INSTRUMENT SPECIFICATION

Appr'n.
Sub _____ Zone
NO.

REV. 2

REV. 1

By App'd. Date

By App'd. Date

E-172

MATERIAL REQUISITION
FOSTER WHEELER CORPORATION
165 BROADWAY
NEW YORK, U. S. A.

TEMP.-PRESS.
INSTRUMENTS

CUSTOMER'S NAME
CONTRACT No.
ITEM
SERVICE

REQUISITION No.

DATE
PAGE No.
CHANGE No.

INSTRUMENT

No. Req'd ____ Type	—— TEMPERATURE BULBS ——
	Location
	Type
Location ____ Case	No. Req'd ____ Bulb Mat'l
Mounting	Bulb. Elev. ____ Instrument
Range ____ Scale	Type Socket ____ Mat'l
Chart	Length Below Threads
Thermal System	Ext. Above Threads
Press. Element	S. P. T. Size
Control Point ____ No. Pens	Tubing Mat'l
Control	Tubing Length
	Special
Clock	
Current ____ Volts ____ Cycle ____ Phase	
Connections	
Accessories: ____ type air reducing valve,	
air filter ____ charts, ink set and air gauges	
Special	

CONTROLLED VALVE

Type	Operating Medium ____ @ ____ Lbs. Ga.
Location	Valve to ____ With Increase in
No. Req'd ____ Size ____ Diaphragm Control Valve	Valve to ____ With Failure of Air
Body Material ____ Ends	Air-Cooled Bonnet Required
Faced and Drilled	Valve Positioner Required
Trim	Extra Reducing Valve and Filter Required
Valve Plug	Special
Stuffing Box ____ Sealed, Isolating Valve	

SERVICE CONDITIONS AND REQUIREMENTS

		VALVE				VALVE
Fluid				Nor. Quan. @ ____ ° F.		
Sp. Gr. @ 60° F. Air =1 Water=1				Max. Quan. @ ____ ° F.		
Sp. Gr. @ Nor. Con. (T & P)				Nor. Press. (Upstream) Lb. Ga.		
Viscosity @ ____ ° F.				Max. Press. (Upstream) Lb. Ga.		
Line Size				Downstream Press.		
Normal Temp., ° F				Pressure Drop		
Max. Temp., ° F						

REMARKS:

Form D41-A

FORM NO. 2788

N Northern Natural Gas Company

LEVEL INSTRUMENTS SPECIFICATION SHEET

LOCATION _____ FILE NO. _____
ITEM NO. _____ JOB NO. _____ W.O. NO. _____
PREPARED BY _____ DATE _____
CHECKED BY _____ DATE _____
APPROVED BY _____ DATE _____

△INDICATES REVISION

	GENERAL				
1	TYPE				
2					
3	TAG NO.				
4	VESSEL OR EQUIPMENT NO.				
	BODY				
5	MATERIAL				
6	TOP CONN LOCATION				
7	BTM CONN LOCATION				
8	CONN-SIZE				
9	CONN SCREWED OR FLANGED				
10	CASE MOUNTING				
11	FLANGE ORIENTATION				
12	ROTATABLE HEAD				
13					
	FLOAT OR DISPLACER				
14	DIAMETER OR LENGTH				
15	EXTENSION				
16	MATERIAL				
17	TORQUE TUBE MATERIAL				
18	AIR FIN				
19					
	TRANSMITTER				
20	TYPE				
21	OUTPUT				
22	RECEIVERS ON SHEET NO.				
	CONTROL				
23	TYPE				
24	PROPORTIONAL-% RESET				
25	OUTPUT				
26	ON LEVEL INCREASE; OUTPUT				
27					
	ACCESSORIES				
28	FILTER AND REGULATOR				
29	GAGE GLASS CONNECTIONS				
30	GAGE GLASS				
31	PURGE CONNECTION				
32	ELECTRIC SWITCH				
33					
34					
	SERVICE CONDITIONS				
35	UPPER LIQUID				
36	LOWER LIQUID				
37	SP GR UPPER LOWER				
38	PRESS MAX. NORM				
39	TEMP MAX. NORM				
40					
41					

REMARKS:

REPRODUCTION OF STANDARD NO. 53.02-1

EDD FORM 2792 1-64

N Northern Natural Gas Company

GAUGE GLASSES AND COCKS SPECIFICATION SHEET

LOCATION _____ FILE NO. _____
ITEM NO. _____ JOB NO. _____ W.O. NO. _____
PREPARED BY _____ DATE _____
CHECKED BY _____ DATE _____
APPROVED BY _____ DATE _____

△INDICATES REVISION

GAUGE GLASSES

1 SUPPLY ☐ GAUGES ONLY ☐ GAUGES & COCKS
NO NIPPLES REQUIRED
2 TYPE ☐ TRANSPARENT ☐ TUBULAR ☐ REFLEX
3 CONNECTIONS ☐ 1/2" ☐ 3/4" ☐ "
☐ TOP & BOTTOM ☐ SIDE ☐ BACK
☐ WELDING PAD OTHER _____
4 MATERIAL ☐ STEEL OTHER _____
5 MINIMUM RATING _____ PSIG @ _____ °F

ACCESSORIES

6 ILLUMINATORS: _____
7 SHIELDS: _____
8 HEATING-COOLING ⎱ INTERNAL _____
9 CHAMBERS ⎰ EXTERNAL _____
10 NON-FROSTING TYPE: _____
11 CALIBRATED SCALE _____
12 SUPPORT PLATES: _____
13 GUARD RODS: _____
14 OTHER _____

NOTES:

GAUGE COCKS

15 SUPPLY ☐ COCKS ONLY
16 TYPE ☐ OFFSET ☐ ANGLE
17 CONNECTIONS-NPT VESSEL GAUGE DRAIN
MALE FEMALE FEMALE
☐ 1/2" ☐ 1/2" ☐ 1/2"
☐ 3/4" ☐ 3/4" ☐ 3/4"
☐ OTHER ☐ ☐

		BODY	TRIM
18	MAT'L		

19 MINIMUM RATING _____ PSIG @ _____ °F

20 CONST. ☐ PLAIN CLOSING ☐ QUICK CLOSING
☐ HANDWHEEL ☐ LEVER HANDLE
21 VESSEL ☐ PLAIN UNION ☐ SOLID SHANK
CONN. ☐ SPHERICAL UNION _____ OTHER
22 GAUGE ☐ PLAIN UNION ☐ PLAIN
CONN. ☐ SPHERICAL UNION _____ OTHER
23 BONNET ☐ SCREWED ☐ UNION ☐ BOLTED
24 SCREW ☐ INSIDE ☐ OUTSIDE
25 RENEWABLE SEAT ☐ YES ☐ NO
26 BALL CHECKS ☐ YES ☐ NO
27 PACKING ☐ MFR STD _____ OTHER

28 MFR MODEL NO. _____
NOTES:

REV.	QUAN.	TAG NO.	NO. OF SECT.	VISIBLE LENGTH	₵ CPLGS	MFR. MOD. NO.	OPER. PRESS	OPER. TEMP.	SERVICE	ACCES-SORIES	NOTES

REPRODUCTION OF STANDARD NO. 53.02-2

CONTROL VALVE SPECIFICATION SHEET

SPECIFICATION No._____

B/M NUMBER			
ITEM NUMBER			
TAG NUMBER			
INSTRUMENT OR CONTROL SERVICE			

PROCESS CONDITIONS

FLUID THROUGH VALVE			
CORROSIVE DUE TO			
INLET OP. TEMP., °F NORMAL			
MAXIMUM			
INLET OP. PRESS., PSIG, NORMAL			
MAXIMUM			
PRESSURE DROP, PSI, NORMAL			
MAXIMUM			
NORM. FLOW AT NORM. OP. TEMP., VAPOR			
LIQUID			
TOTAL			
MAX. FLOW AT NORM. OP. TEMP., VAPOR			
LIQUID			
TOTAL			
M.W. OF VAPOR			
SP. GR. OF LIQ. REL. TO WATER AT 60°F			
AT NORM. OP. TEMP.			
VIS. OF LIQUID, CPS @ °F			
CPS @ °F			

CONSTRUCTION

CATALOG OR TYPE NO.			
NOMINAL SIZE, INCHES			
REDUCED AREA PORTS			
BODY CONNECTIONS & RATING			
FLANGE FACING			
LUBRICATOR REQUIRED			
MATERIALS: BODY			
PLUG			
SEAT			
TYPE OF PLUG			
TYPE OF STUFFING BOX			
ACCESSORIES: VALVE POSITIONER			
PILOT RANGE			
FINS REQUIRED			
ACTUATING FLUID			
VALVE TO: OPEN WITH INCREASE OF			
CLOSE WITH INCREASE OF			
ON ACTUATING FLUID FAILURE, VALVE TO:			

REMARKS: _____

REVISION	1	2	3	4	5	6	7	8	9	10	11
BY											
DATE											

MADE BY:	CHECKED BY:	W.N. NO.	PAGE
DATE:	DATE:	CONT. NO.	OF

ARTHUR G. McKEE & COMPANY   **CLEVELAND, OHIO**
FORM 459

761

DD FORM 2834 5-64   PAGE 1 OF ___

VALVE OPERATOR SPECIFICATION SHEET

N Northern Natural Gas Company

LOCATION _____ FILE NO. _____
ITEM NO. _____ JOB NO. _____ W. O. NO. _____
PREPARED BY _____ DATE _____
CHECKED BY _____ DATE _____
APPROVED BY _____ DATE _____
△ INDICATES REVISION _____

GENERAL INFORMATION

1 NUMBER OF UNITS REQUIRED _____

OPERATOR

2 ☐ ELECTRIC   ☐ PNEUMATIC   ☐ HYDRAULIC
☐ PNEUMATIC HYDRAULIC
3 MODEL NO._____
4 TIME: FULL OPEN   MIN_____   MAX _____
FULL CLOSE   MIN_____   MAX _____
5 MINIMUM TORQUE OUTPUT W/FULL POWER GAS PRESSURE _____

VALVE

6 MANUFACTURE: _____
7 FIGURE NO. _____ SIZE _____ LOT _____
8 DESIGN PRESSURE _____ PSI
9 MAX DIFFERENTIAL _____ PSI
10 VALVE STEM POSITION: ☐ HORIZONTAL ☐ VERTICAL
11 GEAR RATIO _____
12 TORQUE REQUIREMENT_____

OPERATOR

ELECTRIC

13 POWER SUPPLY: VOLTAGE _____ PHASE _____ FREQ._____
14 MOTOR ENCLOSURE:
☐ CLASS I GP.D ☐ GENERAL PURPOSE
☐ OTHER _____
☐ BREATHER AND DRAIN
15 DUTY RATING: ☐ 5 MIN. ☐ 15 MIN. ☐ CONTINUOUS
16 BEARINGS TYPE _____

PNEUMATIC OR HYDRAULIC

17 POWER GAS: ☐ AIR   ☐ GAS
18 PRESSURE _____ PSI
19 DRIVER MOTOR: ☐ TURBINE ☐ VANE ☐ PISTON
☐ VANE MOTOR W/GEARING

CONTROL

PILOT VALVE

20 ELECTRIC:
☐ CLASS I GP.D ☐ GENERAL PURPOSE
☐ OTHER _____
21 VALVE ACTUATION: PILOT VALVE
☐ ACTUATES ☐ DEACTUATES
22 VOLTAGE _____
23 PNEUMATIC: PILOT PRESSURE FOR VALVE ACTUATION
☐ INCREASES ☐ DECREASES
24 CONTROL SYSTEM: ☐ ONE VALVE ☐ TWO VALVES

25 ☐ EMERGENCY SHUT DOWN SYSTEM
26 ESD OPERATION WHEN PILOT:
☐ PRESSURIZED ☐ DE-PRESSURIZED
27 SYSTEM PRESSURE _____
28 VALVE ON SHUTDOWN: ☐ TO OPEN ☐ TO CLOSE
29 ESD TO OVER-RIDE: ☐ REMOTE OPERATION ☐ LOCAL

MANUAL OPERATION

30 OVER-RIDE: ☐ MANUAL ☐ AUTOMATIC

PUSHBUTTON

31 CONTACT: ☐ MOMENTARY ☐ MAINTAINED
32 MOUNTED: ☐ REMOTE ☐ INTEGRALLY

ELECTRIC CONTACTER

33 MOUNTING: ☐ INTEGRAL
34 ENCLOSURE: ☐ CLASS 1 GROUP D ☐ GENERAL PURPOSE ☐ OTHER _____
35 HEATERS: ☐ OVERLOAD HEATERS ☐ SPACE HEATERS ☐ WITH THERMOSTAT

ACCESSORIES

36 LIMIT LIGHTS: ☐ LOCAL ☐ INTG. MTD.
37 ☐ REMOTE SLIDE WIRE TRANSMITTER
38 ☐ REMOTE POSITIVE INDICATOR W/PWR. SUP.
39 ☐ INTEGRALLY MOUNTED REVERSING STARTER
40 ☐ MANUAL HAND VALVE:
41 ___NO. OF RELAYS ☐ TIME DELAY ☐ AUXILIARY
42 LIMIT SWITCHES: ☐ ELECTRIC ☐ PNEUMATIC ☐ ADJUSTABLE POSITION ☐ GEAR DRIVE

_____ TYPE OF ELECT. SWITCH
_____NORMALLY OPEN IN EA. DIR. OF TRAVEL
_____NORMALLY CLOSED IN EA. DIR. OF TRAVEL
43 ADJ. TORQUE SW: ☐ OPENED END ☐ CLOSED END
44 ENCLOSURE: ☐ EXPLOSION PROOF ☐ GENERAL PURPOSE
45 ☐ MANUAL HAND PUMP
46 ☐ GAS HYDRAULIC TANKS
47 ☐ ALL NECESSARY ADAPTERS TO FIT UNIT TO VALVE
48 ☐ POWER STORAGE TANKS

MISCELLANEOUS

49 ☐ ALL WIRING BROUGHT TO EXPLOSION PROOF JUNCTION BOX
50 ☐ ALL TUBING BROUGHT TO BULKHEAD FITTINGS

REPRODUCTION OF STANDARD NO 53.02-3

ARTHUR G. McKEE & COMPANY
RELIEF VALVES

REVISION DATE			
ITEM No.			
TAG No.			
VALVE SERVICE			
MANUFACTURER & TYPE No.			
NUMBER VALVES REQ'D.			
NORMAL SYSTEM PRESS., PSIG.			
NORMAL SYSTEM TEMP., °F.			
GOVERNING UPSET CONDITION			
ACCUMULATION, PERCENT			
FLOWING FLUID			
FLOW QUANTITY, GPM, SCFM, #/HR.			
FLOW SP. GR. OR MW.			
FLOW TEMP. °F.			
FLOW VISCOSITY			
SET PRESSURE, PSIG.			
ACCUM. INLET PRESSURE, PSI. ABS.			
BACK PRESS., PSIG. (STATIC-VALVE CL.)			
REQ'D. ORIFICE AREA, SQ. IN.			
NOMINAL SIZE, INS.			
ORIFICE AREA, SQ. IN./VALVE			
TOTAL ACTUAL AREA, SQ. IN.			
BODY CONN. & RATING—INLET			
—OUTLET			
BODY & BONNET			
TRIM			
SPRING			
RADIATING BONNET			
STYLE TOP			
LIFTING GEAR—REG./PACKED			
TEST ROD			

Left margin labels: MADE BY / DATE / APP. BY / DATE; MADE BY / DATE / APP. BY / DATE; VALVE SIZING CONDITIONS; CONSTRUCTION; ACCESSORIES; MAT'L; SIZE/RATING

REMARKS:

WN No.	PAGE OF	CONT. No.	B/M No.

FORM 495 500 3-56

CENTRIFUGAL PUMP DATA SHEET

FOR		JOB NO.	
PLANT		PUMP NO.	
LOCATION		NO. UNITS	
SERVICE		MOTOR DRIVE	
VENDOR - SIZE & MODEL		TURBINE DRIVE	
TYPE		SERIAL NO	

OPERATING CONDITIONS

FLUID		NORMAL GPM @ PT		NPSH AVAIL	FT. FLUID
PUMP TEMP. °F		DESIGN GPM @ PT		NPSH REQ'D.	FT. WATER
SP. GR. @ P.T.		DISCHARGE PRESS.-PSIG		NPSH REQ'D.	FT. FLUID
VAP. PR @ PT-PSIA		SUCTION PRESS- PSIG			
VISC @ PT- SSU		Δ P PSI FT.			

DESIGN

CASE SPLIT		RADIAL BRG TYPE		SHAFT- MAX .DIAM. "AT CPLG "
SUPPORT		THRUST BRG TYPE		WEAR RING CLEARANCE
IMPELLER TYPE		BRG LUBE		STUFFING BOX ID "DEPTH "
CORROSSION ALLOW.		VISIBLE LUBRICATOR		BASE PLATE
CW PIPING FURNISH BY				CPLG GUARD

COOLING WATER	°F. @	PSIG	NOZZLES	POSITION	SIZE	RATING			
C.W.JACKETS	REQ'D.	GPM	SUCT				TESTS	REQ'D.	WITNESSED
RAD BRG			DISCH.				SHOP INSPECTION		
THRUST BRG			VENT				HYDROSTATIC		
PACKING			DRAIN				PERFORMANCE		
PEDESTAL			SEAL				NPSH		

MATERIALS

CASE		PACKING		THROAT BUSHING
IMPELLER		N° & SIZE RING		CASING GASKET
CASE WRG RING		MECH. SEAL		GLAND
IMP WRG RING		ROTATING FACE		BASE PLATE
SHAFT		STATIONARY FACE		COUPLING
SHAFT SLEEVE		SEAL RING		
LANTERN RING		AUX. GLAND		

PERFORMANCE

NO. STAGES		ROTATION FACING PUMP CPLG			WEIGHTS :	
MAX. IMPELLER - INCHES		SHUTOFF HD W/DESIGN IMP		PSI	PUMP & CPLG.	#
BID IMPELLER - INCHES		MAX. W.P.	PSIG @	°F	BASE	#
MIN. IMPELLER - INCHES		HYDRO TEST PRESSURE		PSIG	TOTAL	#
EYE AREA - SQ.INCHES		FURNISHED BY	VENDOR	R.M.PARSONS	SPACE REQUIREMENTS : WITH DRIVER	
SPEED RPM		PUMP			OVERALL LENGTH	INCHES
DESIGN EFF %		BASE			OVERALL WIDTH	INCHES
DESIGN BHP		COUPLING			OUTLINE DRG #	
MAX. BHP, BID IMP.		CPLG GUARD			CROSS-SECTION #	
MAX. BHP, MAX IMP.		MOTOR			PERFORMANCE CURVE #	
		TURBINE			GFP #	

DRIVER

MOTOR	HP	RPM	TURBINE	HP	RPM	
VOLTS	PHASE	CYCLE	STEAM	PSIG	°F SUPER HT.	
ENCL.			EXHAUST	PSIG	WR#/HP-HR	
FRAME N°	WT.	#	TOTAL STEAM #/HR.		WT. #	
SPEC. N°			SPEC. N°			

THE RALPH M. PARSONS
COMPANY
LOS ANGELES

N°	DATE	REVISIONS	BY	CH'K	APP'D.	APP'D.

ED-525-1 PRINTED IN USA.

CENTRIFUGAL PUMP

SERVICE		DRIVE	QTY	SERIAL		ITEM
	OPER					
	SPARE					

GENERAL SPEC
PUMP CLASS   MFR
    SIZE AND TYPE

PROCESS-DATA

LIQUID	GPM HOT	SUBMERGENCE AVAIL FT
PUMP-TEMP F	DISCH PRESS PSIG	SUBMERGENCE REQD FT
SP GR @ PT	SUCT PRESS PSIG	TOTAL SUCT LIFT FT
VAP PR @ PT PSIA	DIFF HEAD PSI	NPSH AVAIL FT
VIS @ PT SSU	DIFF HEAD FT	NPSH REQD FT WATER
CORR DUE TO	MAX SUCT-PRESS PSIG	NPSH REQD FT OIL
SOLIDS	IF CRITICAL, MIN GPM	

REQUIREMENTS

AXIS	MIN CASE CORR-ALLOW	CPLG GUARD		
SPLIT	SUPPORT	BASEPLATE		
IMPELLER	BRG LUBE	DRIVERS BY		
COOLING WATER F@ PSIG	FLUSH REQD FLUID GPM	DRIVERS MTD BY		
C-W JACKETS REQD GPM	CAGE RING	TESTS	REQD	WITNESS
RADIAL BEARING	WEAR RING	SHOP INSPECTION		
THRUST BEARING	GLAND	HYDROSTATIC		
PACKING BOX	THROAT BUSH	RUNNING		
PEDESTAL	SEAL	NPSH		

MATERIALS

CASE	PACKING BOX	DIFFUSERS
INNER CASE	THROAT-BUSH OR -RING	BAL DRUM
IMPELLER	PACKING	BAL SLEEVE
CASE WRG-RING	CAGE RING	BASEPLATE
IMP WRG-RING	GLAND AND BUSH	CASE STUDS
SHAFT	MECHANICAL SEAL	GLAND STUDS
SHAFT SLEEVE	ROTATING FACE	CASE GASKET
SPACER SLEEVE	STATIONARY FACE	DISCH COLUMN
CASE BUSH	O-RING	SURFACE HEAD
DIAPHRAGMS	AUX GLAND	SUCT BELL

DESIGN

NO STAGES	ROTATION FACING CPLG	CPLG
MAX IMPELLER	SEAL	CPLG SIZE
BID IMPELLER	PACKING SIZE	RADIAL BRG
MIN IMPELLER	NO OF PACKING RINGS	THRUST BRG
EYE-AREA SQ IN	SHUTOFF HD, IMP, PSI	COLUMN BRG
SPEED RPM	MAX WP PSIG @ F	DESIGN THRUST, LB
DESIGN EFF	HYDRO TEST-PRESS PSIG	MAX THRUST, LB
DESIGN BHP	NOZZLE ORIENT SIZE RATING	THRUST DIRECTION
MAX BHP, BID IMPELLER	SUCT	WT W/O DRIVER, LB
MAX BHP, MAX IMPELLER	DISCH	OUTLINE
MOTOR HP	VENT	CROSS SECTION
TURBINE BHP	DRAIN	PERFORMANCE

REMARKS   SUPPLIER FILLS IN ALL DATA MARKED X

763

RECIPROCATING PUMP
SPECIFICATION SHEET

SHEET NO. _____
ITEM NO. _____
CWN JOB NO. _____
CUST. JOB NO. _____

CUSTOMER _____ DATE _____
LOCATION _____ BY _____
SERVICE _____ NO. REQUIRED _____ REVISED _____
MFR. _____ MODEL NO. _____ SERIAL NO. _____

OPERATING CONDITIONS   **PERFORMANCE**

	OPERATING CONDITIONS			PERFORMANCE
1	LIQUID	GPM AT PT: NORM	41	CURVE NO.
2	PT. °F	RATED	42	OUTLINE DWG. NO.
3	SP GR AT PT.	DISCH PRESS, PSIG	43	PUMP SPEED, RPM
4	VAP PRESS AT PT	SUCT PRESS, PSIG	44	PISTON: STROKES/MIN FPS
5	VIS AT PT: SSU - CP	DIFF PRESS, PSI	45	EFF AT DESIGN
6	CORR/EROS PROPERTIES	DIFF HEAD, FT	46	BHP: DES MAX
7		NPSHA, FT	47	SHUT-OFF HEAD, FT
			48	RELIEF VA: INT - EXT
	CONSTRUCTION		49	SETTING, PSIG
8	ARRANGEMENT: HORIZ - VERT		50	CLG WATER, GPM
9	DIRECT - SINGLE - DOUBLE ACTING		51	BEARINGS JACKET
10	SIMPLEX - DUPLEX - TRIPLEX POW.FRAME: PISTON - PLUNGER		52	PEDESTAL
11	CASE DES PRESS, PSIG SWP, PSIG		53	PRESS, PSIG T.°F
12	TAPPED CONNECTIONS: VENT - DRAIN - GAUGE		54	FLUSH
13	NOZZLES SIZE RATING FACE LOCATION		55	JACKETED: YES - NO
14	SUCTION		56	STM PRESS.PSIG T.°F
15	DISCHARGE		57	
16				
17	PUMP SIZE, IN: BORE STROKE			**SHOP TESTS**
18	CYLINDER LINER		58	SHOP INSPECTION
19	VALVES(LIQ) TYPE NUMBER AREA,SQ.IN.		59	PERFORMANCE
20	SUCTION		60	HYDROSTATIC, PSIG/°F
21	DISCHARGE		61	WITNESS
22	BEARINGS: RADIAL THRUST		62	
23	LUBE: OIL - GREASE OILER: YES - NO		63	WEIGHTS:
24	CPLG: MFR MODEL GUARD: YES - NO		64	PUMP DRIVER
25	PACKING BASE: MFR.STD.- OTHER		65	REDUCER SHPG

LIQUID CYLINDER MATERIALS   **DRIVER CYLINDER MATERIALS**

	LIQUID CYLINDER MATERIALS		DRIVER CYLINDER MATERIALS	
26	CYLINDER	VALVES	CYLINDER	VALVES
27	CYL LINER	PISTON ROD	PISTON	GASKETS
28	LANTERN RINGS	GASKETS	PISTON RINGS	
29	PISTON - PLUNGER		PISTON ROD	

MOTOR DRIVER   **TURBINE/PISTON DRIVER**

	MOTOR DRIVER		TURBINE/PISTON DRIVER	
30	SUPPLIED BY	MOUNTED BY	SUPPLIED BY	MOUNTED BY
31	MFR	TYPE	MFR	TYPE
32	ENCLOSURE	RPM	HP RPM	WATER RATE,LB/HP-HR
33	HP	SF	INLET STM PRESS, PSIG: NORM MAX	
34	FRAME	INSULATION	INLET STM TEMP, °F: NORM MAX	
35	VOLTS/PH/HZ	TEMP RISE.°F	EXHAUST STM PRESS, PSIG:NORM OTHER	
36	BEARINGS	LUBE	BEARINGS	LUBE
37			NOZZLES SIZE RATING FACE LOCATION	
38	SPEED REDUCER: INTEGRAL - SEPARATE		INLET	
39	MFR	MODEL	EXHAUST	
40	RATIO	CLASS	API 611: YES - NO SEPARATE DRIVER SPEC: YES - NO	

VENDOR TO SUPPLY INFORMATION MARKED _____

FORM 21-A3. 4-76

ENG EQUIP 46 (5-77)   KELLOGG

ROTARY PUMP DATA SHEET

FOR _____
LOCATION _____
ITEM NO _____
SERVICE _____
NO. REQUIRED _____ MOTOR DRIVE _____ TURBINE DRIVE _____

JOB NO _____
SHEET NO. _____
PAGE _____ OF _____

OPERATING CONDITIONS

PRODUCT HANDLED _____
CORROSIVE DUE TO _____
PUMPING TEMPERATURE _____ DEG F VAPOR PRESS _____ PSIA
GRAVITY AT 60 DEG F SP GR _____ API GR. _____
SP GR AT SUC COND _____ SP GR AT DIS. COND. _____
VISCOSITY _____ AT _____ DEG F.
CAPACITY – G P D AT 60 DEG F NORMAL _____
DESIGN _____
G P M AT PUMP TEMP NORMAL _____
DESIGN _____

DISCHARGE PRESSURE _____ PSIG
SUCTION PRESSURE _____ PSIG
DIFFERENTIAL PRESSURE _____ PSI
DESIGN HEAD _____
NPSH* AVAIL _____ FT. NPSH REQUIRED _____ FT.
NPSH INCLUDES _____ FT.FT. STATIC HEAD — LIFT _____
STEAM PRESSURE _____ PSIG
% SATUR OR TOTAL TEMP. _____
EXHAUST STEAM PRESSURE _____
MOTOR CHARACTERISTICS _____ VOLTS _____ PHASE _____ CYCLE

SPECIFICATIONS

PUMP SHALL BE FURNISHED IN ACCORDANCE WITH _____

MANUFACTURER _____
TYPE _____
SIZE _____
RATED CAPACITY _____ G P M AT _____ RPM
ROTATION—COUNTER—CLOCKWISE FACING COUPLING END
SUC. FLANGE SIZE _____
DIS. FLANGE SIZE _____
CASE DESIGN PRESS. _____
RELIEF VALVE TO BE FURN. BY _____
MAX. REL. VALVE SET TO PREVENT MOTOR OVERLOAD _____ PSIG

HYD. H.P. —NORMAL _____ DESIGN _____
PUMP. EFF. %—NORMAL _____ DESIGN _____
BRAKE H.P. —NORMAL _____ DESIGN _____
B.H.P. AT RATED CAPACITY _____
MOTOR H.P. _____ TURBINE H.P. _____
DRIVER (S) TO BE FURNISHED BY _____
PUMP BASE _____
DRIVER BASE _____
COUPLING _____ WITH GUARD

MATERIALS AND DETAILS

CASE _____ MIN THICK _____
END COVERS _____
FLANGES _____
SHAFT _____
SHAFT SLEEVES _____
ROTORS _____
DRIVE GEARS _____
RADIAL BEARING _____
THRUST BEARING _____

LUBRICATION _____
PACKING BOX—TYPE _____ NO. _____
SIZE—I D _____ O.D. _____ LENGTH _____
PACKING ARRANGEMENT _____
SPARE PACKING _____
PACKING GLAND—TYPE _____
GLAND STUDS _____
LANTERN RING _____

GENERAL INFORMATION

COOLING WATER _____ DEG. F _____ G P M
PACKING BOXES _____ G P M
COOLING OIL LANTERN RINGS _____ DEG. F _____ G P M
FLUSHING OIL TO THROAT BUSHING _____ G P M
COOLING WATER PIPING _____ SYSTEM BY _____
GLAND OIL PIPING BY _____
FLUSHING OIL PIPING BY _____
BYPASS CONTROL—TO BE FURNISHED BY KELLOGG

INSULATION BY _____
INSPECTION—HYDRO TEST _____
PERFORM TEST _____
SPECIAL TESTS _____
DIMEN. PRINT NO. _____ SERIAL NO. _____
NET WEIGHT—PUMP AND BASE _____ LB.
FOUNDATION BOLTS—TO BE FURNISHED BY KELLOGG
FLANGE STUDS—TO BE FURNISHED BY PUMP MFR.

* NPSH AVAILABLE MEASURED TO TOP OF PUMP FOUNDATION
REMARKS _____

NO.	0	1	2	3	4	5	6	7	8	9	10	11	12
DATE													
BY													
CHECK													
APPRVD													

REVISION

764

CHEMICAL PROCESS PLANTS DEPARTMENT
CORPORATE ENGINEERING

ROTARY PUMP
DATA SHEET   Sheet 1 of 2

OPERATING CONDITIONS

FLUID PUMPED _____ CAPACITY NORMAL _____ GPM
FLUID CHARACTERISTICS _____ CAPACITY DESIGN _____ GPM
TEMP. MAX _____ °F MIN _____ °F NORMAL _____ °F   TDH DESIGN _____ FT. FLUID
VISCOSITY AT MIN. P.T. _____ SUCTION PRESS. _____ DISCH. PRESS. _____
SPECIFIC GRAVITY AT MIN. P.T. _____ NPSH AVAILABLE _____ FT. FLUID
VAPOR PRESS. AT MAX. P.T. _____ HYDRAULIC HP _____

TYPE OF OPERATION: ☐ CONTINUOUS ☐ INTERMITTENT HRS./DAY _____
LOCATION: ☐ INDOORS ☐ OUTDOORS

MATERIALS

BODY _____ MECH. SEAL: _____
HEADS _____ ROTATING FACE _____
ROTORS _____ STATIONARY FACE _____
SHAFT _____ METAL PARTS _____
PACKING GLAND _____ RELIEF VALVE _____
LANTERN RING _____ CASING GASKET _____

CONSTRUCTION DATA

PUMP TYPE: _____
PACKING: TYPE _____ MFR. _____
MECH. SEAL: TYPE _____ MFR. _____ CODE _____
NOTES: _____
SEAL FLUID: _____
RELIEF VALVE: BUILT-IN _____ SEPARATE _____

MOTOR DRIVE DATA

ITEM NO. _____ MTD. BY _____
H.P. _____ RPM _____ FRAME _____
MFR. _____ CPLG. GUARD _____
TYPE _____ INSUL. _____
ENC'L: CLASS I-GROUP _____ DIVISION 1
OTHER _____
VOLTS/PHASE/Hz: _____
BEARINGS _____ LUBE _____
FULL LOAD AMPS _____ SF _____
LR AMPS _____

TESTS

	SHOP TESTS	NOT WITNESSED	WITNESSED	CERT. DATA
Running Perf.				
NPSH				

HYDROSTATIC _____ PSIG

MANUFACTURER'S DATA

MFR. _____ PUMP BEARINGS _____
MODEL NO. _____ RPM _____ PUMP LUBRICATION _____

NOZZLES	SIZE	ASA RATING	FACING	POSITION
SUCTION				
DISCH.				

PRESS. IN SEALING CHAMBER _____ PSIG
SHAFT DIA. IN SEALING CHAMBER _____ INCHES
WATER COOLING AVAIL. AT _____ PSIG _____ °F
MAX. ALLOW. W.P. _____ PSIG   TEMP. _____ °F   BEARINGS _____ GPM
NPSH REQ'D. (WATER) FT. _____ STUFF. BOX _____ GPM
DESIGN EFF. _____ DESIGN BHP _____ PEDESTAL _____ GPM
SHUT-OFF HEAD FT. _____ TOTAL WATER REQ'D. _____ GPM
ROTATION FACING CP'LG. END _____ PACKING LUBRICATION _____
CP'LG. MFR. _____ SEAL LUBRICATION _____
TYPE _____

JOB NO. _____ PLANT LOCATION _____
PROJECT NO. _____ REF. DWG. NO. _____
TITLE _____
POSITION NO. _____ SERIES _____ STEP NO. _____

SCALE
ISSUE DATE
BLDG. NO.
DRAWING NO.

REMARKS / APP'R.V / DATE / SUPRV / CHKD BY / REV.
PROJ. ENG. / DES SUPRV. / CHECKED BY / DRAWN BY / INITIATOR / DATE

E 142B10* (REV. 4/83)

Left Form

CHEMICAL PROCESS PLANTS DEPARTMENT
CORPORATE ENGINEERING

ROTARY PUMP
DATA SHEET Sheet 2 of 2

MANUFACTURER'S DATA CONT'D.

REMARKS

WEIGHTS: PUMP _____ BASE _____ DRIVE _____
SEAL FLUSH _____
SEAL QUENCH & DRAIN _____
SPEED REDUCER: MFR. _____
                     TYPE _____
BASEPLATE _____

SPECIAL REQUIREMENTS & NOTES

1. VENDOR IS TO QUOTE MOST ENERGY-EFFICIENT PUMP-DRIVE COMBINATION AS ALTERNATE IF DIFFERENT THAN UNIT(S) OFFERED.
2. GROUNDING LUG TO BE PROVIDED IN MOTOR CONDUIT BOX.
3. MOTOR SHALL BE IN CONFORMANCE WITH FOLLOWING STANDARD PROCUREMENT SPECIFICATION:
   ☐ E16 - 150P, PROCESS ELECTRICAL EQUIPMENT - LOW VOLTAGE MOTORS, ALTERNATING CURRENT.
   ☐ E16 - 151P, PROCESS ELECTRICAL EQUIPMENT - MEDIUM VOLTAGE MOTORS, ALTERNATING CURRENT.
   ☐ E16 - 160P, PROCESS ELECTRICAL EQUIPMENT - VARIABLE FREQUENCY AC MOTORS
4. MOTOR SHALL BE PROVIDED IN ACCORDANCE WITH DATA GIVEN ON STANDARD DATA SHEET FORM E242P1 ELECTRICAL ALTERNATING CURRENT MOTORS.

REV. BY CHKD SUPRV. DATE APP'R'V

PROJ. ENG. DES SUPRV.
CHECKED BY
DRAWN BY
INITIATOR
DATE

765

JOB NO. _____ PLANT LOCATION _____
PROJECT NO. _____ REF. DWG. NO. _____
TITLE _____
POSITION NO. _____ SERIES _____ STEP NO. _____

ISSUE DATE

SCALE
BLDG. NO.
DRAWING NO.

E 142B10* (REV. 4/83)

Rotary Pump—(*continued*)

Right Form

KELLOGG **MOTOR DRIVEN PROPORTIONING & RECIPROCATING PUMP DATA SHEET**

FOR: _____ JOB NO. _____
LOCATION: _____ ITEM NO _____
SERVICE: _____ PAGE: _____ OF _____
NO. REQUIRED: _____ SPARES: _____

KG 0977 (4 81)

SERVICE CONDITIONS

FLUID PUMPED _____	DISCHARGE PRESSURE _____ PSIG
CORROSIVE DUE TO _____	INLET PRESSURE _____ PSIG
INLET TEMPERATURE _____	DIFFERENTIAL PRESSURE _____ PSI
SPECIFIC GRAVITY AT INLET TEMP. _____	VAPOR PRESSURE AT INLET TEMP. _____ PSIA
CAPACITY AT INLET TEMP NORMAL _____	NPSH* AVAILABLE AT TOP OF PUMP FOUNDATION _____ FT
CAPACITY AT INLET TEMP. DESIGN	NPSH REQUIRED AT TOP OF PUMP FOUNDATION _____ FT

MECHANICAL DATA (PUMPS TO BE FURNISHED IN ACCORDANCE WITH KELLOGG SPEC _____ DATED _____

MANUFACTURER _____	BRAKE KW NORMAL _____ DESIGN _____
SIZE AND TYPE _____	INLET SIZE AND RATING _____
NO. CYLINDERS _____ SPM _____	DISCH—SIZE AND RATING _____
LIQUID END DESIGN PRESSURE _____ PSIG	STEAM IN SIZE _____
STALLING PRESSURE _____ PSIG	EXHAUST SIZE _____

PROPORTIONING PUMP DATA	RECIPROCATING PUMP DATA
CAPACITY CYL. A MAX _____ MIN _____	STEAM PRESSURE _____
CAPACITY CYL. B MAX _____ MIN _____	% SATURATION OR TOTAL TEMP _____
TYPE CAPACITY ADJ _____	EXHAUST STEAM PRESSURE _____
RANGE OF ADJ _____	TOTAL STEAM LB/HR NORMAL _____ DESIGN _____
BORE CYL. A _____ CYL. B _____	VALVE TYPE _____
STROKE CYL. A _____ CYL. B _____	STEAM END PACKING _____

MATERIALS

CYLINDER _____	CASE _____
PLUNGER _____	LINER _____
VALVE _____	PISTON _____
VALVE SEAT _____	PISTON ROD _____
VALVE SPRINGS _____	PISTON RING _____

MECHANICAL DETAILS

COMMON BASE FOR PUMP AND MOTOR BY _____	PACKING BOX TYPE _____ NO. OF BOXES _____
COUPLING WITH GUARD BY _____	PACKING BOX SIZE _____ O.D. _____ LENGTH
LUBRICATOR _____	PACKING TYPE _____
REVOLUTION COUNTER _____	☐ 100% ☐ 200% SPARE PACKING (BY MFGR.)
INSULATION: STM END BY _____ LIQ END BY _____	☐ LANTERN RING IN CENTER WITH CONN. PLUGGED
☐ HYDROSTATIC TEST WITNESSED _____	☐ GLAND OIL _____ GPM
☐ PERFORMANCE TEST WITNESSED _____	☐ FLUSHING OIL _____ GPM
☐	☐ COOLING WATER _____ GPM

MOTOR DATA (MOTOR TO BE FURNISHED IN ACCORDANCE WITH KELLOGG SPEC _____ DATED _____

MANUFACTURER _____	FRAME _____
KILOWATTS _____ RPM _____	RATED LOAD CURRENT _____
VOLTS _____ PHASE _____ CYCLE _____	LOCKED ROTOR CURRENT _____
ENCLOSURE _____	EFFICIENCY 4/4 _____ 3/4 _____ 1/2 _____
SERVICE FACTOR _____	POWER FACTOR 4/4 _____ 3/4 _____ 1/2 _____
TEMPERATURE RISE _____ C	SPEED REDUCER TYPE _____ RATIO _____

GENERAL

APPROX. BASE SIZE _____ TOTAL WEIGHT _____ KG
EQUIPMENT TO BE SUITABLE FOR OUTDOOR INSTALLATION   SERIAL NO _____
* NPSH — NET POSITIVE SUCTION HEAD TO TOP OF PUMP FOUNDATION
MANUFACTURER SHALL SUBMIT THIS SHEET FULLY COMPLETED WITH HIS QUOTATION
REMARKS _____

REVISION	NO.	0	1	2	3	4	5	6	7	8	9	10	11	12
	DATE													
	BY													
	CHECK													
	APPRVD													

PACKAGED REFRIGERATION SYSTEM

1 Refrigerant: _____ Indoor/Outdoor; English/Metric Units
2 Mfr: _____ Model No. _____ Qty. ____
3 Design: ASME Code Section VIII, Division 1, _____ Edition and all Mandatory Addenda.
4 Stamped: Yes/No, TEMA _____ Edition _____
5 Dry Bulb Temp. _____ Wet Bulb Temp. _____ Altitude _____ Barometric Press. _____
6 Item No.   Service   Refrig. Temp. (In/Out)   Refrig. Press.(In/Out)   Duty
7 _____ Condenser _____ / _____ _____ / _____ _____
8 _____ Evaporator _____ / _____ _____ / _____ _____
9 _____ Oil Cooler _____ / _____ _____ / _____ _____
10 _____ / _____ / _____
11 Cooling Water: Supply Press. _____ Maximum △Pressure _____
12 Temp. In/Out _____ Total Flowrate _____
13 Compressor: Item No. _____ Type _____ Qty. _____
14 Maximum Capacity _____ @ _____ RPM _____ BHP
15 Condenser (TEMA ____): Item No. _____ Type _____ Size _____ Qty. ____
16 Design Press. Shell _____ Tubes _____ Mat'l.: Shell _____ Tubes _____
17 Cooling Medium: Flow Inlet _____ Outlet _____ Mat'l. _____ △Press. _____
18 Receiver: Item No. _____ Type _____ Size _____ Mat'l. _____ Qty. ____
19 Design Press./Temp. _____ / _____ Oper. Press./Temp. _____ / _____
20 Knock-Out Drum: Item No. _____ Type _____ Size _____ Mat'l. _____ Qty. ____
21 Design Press./Temp. _____ / _____ Oper. Press./Temp. _____ / _____
22 Sub-Cooler: Yes/No Item No. _____ Type _____ Size _____ Mat'l. _____ Qty. ____
23 Design Press/Temp. _____ / _____ Oper. Press./Temp. _____ / _____
24 Oil Separator: Item No. _____ Type _____ Size _____ Mat'l. _____ Qty. ____
25 Design Press./Temp. _____ / _____ Oper. Press./Temp. _____ / _____
26 Oil Heater: Qty. _____ Volts _____ Phase _____ Hertz _____ Watts _____
27 Oil Cooler (TEMA ____):Item No. _____ Type _____ Size _____ Qty. ____
28 Design Press.: Shell _____ Tube _____ Mat'l.: Shell _____ Tube _____
29 Cooling Medium _____ Flow _____ Maximum △Press. _____
30 Oil Filters: Item No. _____ Type _____ Size _____ Micron Size _____ Qty. ____
31 Design Press. _____ Oper. Press./Temp. _____ / _____ Mat'l. _____
32 Flow Rate: Normal _____ Maximum △Press. _____
33 Oil Pump: Mfr. _____ Model No. _____ Type _____ Qty. ____
34 Press.: Discharge _____ Flow Max. Cap. _____ @ _____ BHP; Mat'l: _____
35 Purger: Mfr. _____ Model No. _____ Type _____ Qty. ____
36 Size _____ Mat'l. _____
37 Motor: Compressor (less than 200 HP)   Oil Pump
38 Mfr./Mod. No./Qty. _____ / _____ / _____ _____ / _____ / _____
39 Volts/Phase/Hertz _____ / _____ / _____ _____ / _____ / _____
40 Enclosure/Insulation _____ / _____ _____ / _____
41 Area Class. Class _____ Group _____ by _____ Division _____ /Non-Hazardous.
42 Temp. Rise _____ °C above _____ °C by _____ @ _____ S.F.; Temp. Code _____
43 Space Heater Required: Yes/No: Heater; Volts _____ Phase _____ Ø _____ Hertz _____

Item No.	HP KW	Current Full Load	Current Locked Rotor	Effy. 4/4	Effy. 3/4	P.F. 4/4	P.F. 3/4	Full Load RPM	Frame No.	Brg. Lub.	Weight LB/KG	Mtg. H/V	Allow-Thrust Up/Down LB/KG	Space Htr. Watts	S.F.
44															
45															
46															

47
48
49 Remarks: _____
50

NO.	DATE	ENGINEER	CHK/REVIEW	APPROVE	
6					
5					
4					
3					
2					
1					
0					

KELLOGG   MANAGING OFFICE   ENGINEERING OFFICE

EQUIPMENT DATA SHEET

CLIENT _____
LOCATION _____ JOB NO. _____
ITEM _____
ITEM NO. _____ SPEC. NO. _____
REQ'N. NO. _____   PAGE ____ OF ____

PACKAGED REFRIGERATION SYSTEM

1 Oper. Parameters   L O W   S T A G E   H I G H   S T A G E   Units
2 Capacity % _____ _____
3 Inlet Flow _____ _____
4 Inlet Temp. _____ _____
5 Inlet Press. _____ _____
6 Outlet Temp. _____ _____
7 Outlet Press. _____ _____
8 BHP _____ _____
9 Pockets/Valve Open _____ _____
10   RECIPROCATING COMPRESSOR
11 Mfr. _____ Model No. _____ Qty. _____
12 Cylinder Data: Low Stg.   High Stg.   Low Stg.   High Stg.
13 Cylinder Per Stg. _____ _____   Type of Valves _____ _____
14 Cylinder Type _____ _____   Piston Speed Norm/Max. _____ _____
15 Cyl. Liner Yes/No _____ _____   Rod Diameter _____ _____
16 Cyl. Liner Wet/Dry _____ _____   Rod Load. Tension Norm/Max. _____ _____
17 Bore/Stroke (In.) _____ / _____ / _____   Rod Load. Comp. Norm/Max. _____ _____
18 Piston Displ. _____ _____   Cyl. Press/Temp. Max. _____ _____
19 Vol. Eff. % _____ _____   Recommended R.V. Press. _____ _____
20 No. In/Out _____ / _____ / _____   Hydro. Test Pressure _____ _____
21 Mat'l of Const: Low Stg.   High Stg.   Low Stg.   High Stg.
22 Cylinders _____ _____   Valve Seats _____ _____
23 Cylinder Liners _____ _____   Valve Springs _____ _____
24 Pistons _____ _____   Valve Stops _____ _____
25 Piston Rings _____ _____   Valve Plates _____ _____
26 Piston Rods _____ _____
27 Cooling Water: Comp.   Cyl.   Comp.   Cyl.
28 Flow Rate _____ _____   Press. Drop _____ _____
29 Temp. In/Out: _____ / _____   Max. Press. _____ _____
30 Packing: Cooling Water; Yes/No.   Vented to _____
31 Capacity Control: Variable Speed _____ % to _____ %. Mfr. Std. Control: Yes/No;
32 Start/Stop; Yes/No, 2/3/5 Step Control. Suction Valve Lifters: Manual/Automatic
33 Air/Power Failure, Compressor shall Load/Unload.
34 Accessories: Gear   Low Speed CPLG   Belt Drive
35 Mfr. _____ Mfr. _____ _____
36 Model No. Size _____ Model No. _____ _____
37 H.P. Rating/AGMA S.F. _____ / _____ Type _____ _____
38 Ratio/Efficiency _____ / _____ No. Required _____ _____
39 Separate Moisture Separators with Traps: By Compressor Mfr. _____
40 Frame Lubrication: Splash System/Pressure System w/Comp. Shaft Driven Oil Pump/Elect.
41 Driven Oil Pump/Hand Operated Pump for Starting.
42 System Oil Capacity _____
43 Electric Heater w/Thermostat: Setting _____ No. Heaters _____ Watts _____
44 Cylinder Lubrication: Lubricator to be driven by Comp. Shaft/Electric Motor
45 System Oil Capacity _____ No. of Compartments _____
46 Electric Heater w/Thermostat: Setting _____ No. Heaters _____ Watts _____
47 Remarks: _____
48
49
50

NO.	DATE	ENGINEER	CHK/REVIEW	APPROVE	
6					
5					
4					
3					
2					
1					
0					

KELLOGG   MANAGING OFFICE   ENGINEERING OFFICE

EQUIPMENT DATA SHEET

CLIENT _____
LOCATION _____ JOB NO. _____
ITEM _____
ITEM NO. _____ SPEC. NO. _____
REQ'N. NO. _____   PAGE ____ OF ____

POSITIVE DISPLACEMENT ROTARY COMPRESSOR

1. Mfr.: _____ Model No. _____
2. Speed: Max. Allow. RPM _____ Critical RPM 1st _____ 2nd _____
3. Casing: Casing split: _____ Thickness _____ Corr. Allow. _____
4. Max. Working Press. _____. Max. Rated Press. _____ Temp.: Max. Work ___ Min. Oper. ___
5. Test Pressure Hydro. _____
6. Rotor: Diameter _____ Type _____ Material _____
7. Type Fabrication: _____ No. of Lobes: Male _____ Female _____
8. Rotor Length to Dia. Ratio (L/D) _____ Rotor Clearance _____ Max. Deflection _____
9. Shaft: Dia. @ Rotor _____ Dia. @ Coupling _____ Shaft End: Tapered/Cylindrical
10. Sleeves at Shaft Seals _____ Shaft Seal Type _____ Seal Sys. Type _____
11. Inter Oil Leakage Guarantee (Vol./Day/Seal) _____ Type Buffer Gas _____
12. Buffer Gas Flow (Per Seal) _____
13. Normal _____ #/Minimum _____ Press. _____
14. Maximum _____ #/Minimum _____ Press. _____
15. Bearings: Housing Type (Separate/Integral) _____ Split _____
16. Radial Bearing Type _____ Span _____ Area _____ Loading: Act. _____ Allow. _____
17. Thrust Bearing Type _____ Area _____ Loading: Act. _____ Allow. _____
18. Gas Loading _____ CPLG. Slip Load _____ CPLG. Coeff. Frict. _____
19. CPLG. Gear Pitch Dia. _____ Balance Piston Compensating Load _____
20. Timing Gears: Size _____ Type _____
21. Couplings: Driver-Comp./Gear Gear/Comp. _____ Driver-Comp./Gear Gear/Comp.
22. Make _____ Limited End Float Req'd. _____
23. Model _____ Idling Adaptor Req'd. _____
24. Lubrication _____ CPLG. Rating (HP/100 RPM) _____
25. Mt. CPLG. Halves _____ Keyed (1) or (2) or Hydr. CPLG _____
26. Spacers Required _____
27. Material of Construction: Casing _____ Rotor _____ Shaft _____
28. Shaft Sleeves _____ Timing Gear _____ Bearings _____

INSPECTION AND TEST

29. Mfr. Standard Shop Test/Running Test with Shop Driver/Lube and Seal System/Hydrostatic/
30. Mechanical Run/Vibration-Axial Displacement/Noise Level/Consoles/Other: _____
31.
32. Purchaser will Witness: _____

ACCESSORIES

33. Relief Valves/Pulsation Dampeners (Volume Bottles)/Inter-Connecting Piping/Initial
34. Charges (Oil, Refrigerant, Etc.) _____
35. Remarks: _____

(Line numbers 1–50 run down the left margin)

767

					KELLOGG	MANAGING OFFICE	ENGINEERING OFFICE
6							
5					EQUIPMENT DATA SHEET		
4					CLIENT		
3					LOCATION	JOB NO.	
2					ITEM		
1					ITEM NO.	SPEC. NO.	
0					REQ'N. NO.		PAGE OF
NO.	DATE	ENGINEER	CHK/REVIEW	APPROVE			

Packaged Refrigeration System—(continued)

The vendor shall furnish as a minimum the equipment and components shown in the sketch and as called for on the data sheets.

Controls shown outside Skid Limit are by the Purchaser.

Sym◊	Size	Rating	Facing				Weights	LBS/KG
a				Dimensions	Length	Width Height	Erection	
b				Skid No. 1			Maintenance	
c							Operating	
d							Shipping	

					KELLOGG	MANAGING OFFICE	ENGINEERING OFFICE
6							
5					EQUIPMENT DATA SHEET		
4					CLIENT		
3					LOCATION	JOB NO.	
2					ITEM		
1					ITEM NO.	SPEC. NO.	
0					REQ'N. NO.		PAGE OF
NO.	DATE	ENGINEER	CHK/REVIEW	APPROVE			

PACKAGED REFRIGERATION SYSTEM (CONT'D)

INSTRUMENTATION AND CONTROLS

Line		
1		
2	Panel: Freestanding/Other	Covered/Uncovered
3	Electrical Instruments: NEMA	Enclosures
4	Panel: Vibration Isolators/Strip Heaters/Purge/Other	
5	Panels Required: Local/Lube Oil/Other	

MINIMUM DISPLAY ON LOCAL PANEL	MINIMUM NO. ALARMS AND SHUTDOWN	ALARM	SHUTDOWN
Lube Oil Pressure Gauge	Lube Oil Low Pressure	*	*
Lube Oil Temperature Gauge	Lube Oil High Pressure		
Compressor Suction Pressure Gauge	Compressor Low Suction Press.		
Compressor Suction Temperature Gauge	Compressor High Suction Press.	*	
Compressor Discharge Pressure Gauge	Compressor High Disch. Press.	*	
Compressor Discharge Temperature Gauge	System High Discharge Temp.	*	
	K.O. Drum High Level	*	
	K.O. Drum High-High Level		*
	Sub-Cooler High Level	*	
	Sub-Cooler High-High Level		*
	High Water Temperature	*	
	Receiver High Level	*	

Remarks:
1) Shutdown switches shall incorporate time delay relays, where required, to permit starting-up the system.
2) Packaged refrigeration system shall operate completely automatic after start-up.
3) Manual/automatic selector switch shall be provided, by the vendor, for manual start/stop of each refrigeration unit.
4) Condenser cooling water valve shall "fail open" and provide no less than minimum rated flow.
5) Liquid sub-cooler level control valve shall "fail open" on instrument air failure.
6) All control valves, furnished by the vendor, shall have blocks and by-passes.
7) A pair of "N.O." contacts shall be provided, by vendor, for purchasers shutdown alarm to be activated only when the system malfunctions.
8) A horn shall be mounted on the unit and wired to the shutdown circuit.
9) Copper, brass, bronze, aluminum and aluminum alloys shall not be used where exposed to ammonia, ammonia vapors, ammonia solutions or the general plant atmosphere, without the specific approval of M.W. Kellogg Engineering.
10) Vendor shall supply a completely piped and wired skid mounted packaged refrigeration system, which shall include but not be limited to the following: all components, piping, valves, instruments, alarms, shutdowns, control, control panels, special tools and equipment necessary to operate the unit at its rated capacity.
11) All relief valves shall be routed to the common manifold header, (if required).
12) All required utilities shall be piped to the skid limit for purchaser connections.

REVISIONS						
6					MANAGING OFFICE	ENGINEERING OFFICE
5				KELLOGG		
4					EQUIPMENT DATA SHEET	
3				CLIENT		
2				LOCATION	JOB NO.	
1				ITEM		
0				ITEM NO.	SPEC. NO.	
NO.	DATE	ENGINEER	CHK/REVIEW	APPROVE	REQ'N. NO.	PAGE OF

Packaged Refrigeration System—(*continued*)

PROCESS DESIGN SECTION	VIBRATING FEEDER
CORPORATE ENGINEERING	DATA SHEET

FEED MATERIAL CHARACTERISTICS

FEED MATERIAL: _____   WEIGHT % MOISTURE: _____
BULK DENSITY: _____ LBS./CU. FT.   TEMPERATURE _____ °F
PARTICLE SIZE: AVERAGE: _____   ABRASIVENESS: _____
MAXIMUM: _____   TENDENCY TO PACK: _____
PRODUCT DESCRIPTION: _____   DESCRIPTION: _____

OPERATING CONDITIONS

FEED RATE – LBS/HR. NORMAL _____   LOCATION: INDOOR ☐   OUTDOOR ☐
MAX. _____   MAX. ROOM TEMP: _____ °F
REQ'D. WIDTH OF FEED _____   INLET TO OUTLET LENGTH: _____
REQ'D. DEPTH OF FEED _____   ATMOSPHERIC CONDITIONS: DUSTY ☐
MODE OF OPERATION _____   CORROSIVE ☐   EXPLOSIVE ☐
_____   OTHER _____

DESIGN DATA

TROUGH TYPE: _____   COVER CLAMPS: _____
LENGTH/WIDTH/DEPTH _____   FREQUENCY – CPM: _____
THICKNESS: _____   SPEED OF MAT'L. CONVEYED–FPM: _____
COVER: REQ'D. _____   NATURAL FREQUENCY: REQ'D. _____
TYPE _____   SPRINGS: _____
MOUNTING: FLOOR ___ SUSPENSION ___   AMPLIFICATION _____
INCLINE ___ DECLINE ___   ISOLATION _____
CONTROL _____   HANGERS– TYPE: _____
BASE _____   NO. _____

MATERIALS OF CONSTRUCTION

TROUGH _____   SPRINGS – AMPLIFICATION _____
COVER _____   ISOLATION _____
BASE _____   DRIVE COVER _____
GASKETS _____

MOTOR DRIVE DATA

ITEM NO. _____ MTD. BY _____   BEARINGS _____ LUBE _____
MFG. _____   FULL LOAD AMPS _____ SF _____
TYPE _____ FRAME _____   L.R. AMPS _____
HP _____ RPM _____
VOLTS/PHASE/CYCLE ___ / ___ / ___   MOUNTING: BOTTOM ☐   OVERHEAD ☐

MISCELLANEOUS

TOTAL WEIGHT _____   VENDOR DWG. NO. _____
PAINTING _____   FEEDER SERIAL NO. _____
GALVANIZING _____
FINISH REQ'D. _____

JOB NO.	PLANT LOCATION		SCALE
PROJECT NO.	REF. DWG. NO.		
TITLE		ISSUE DATE	BLDG. NO.
POSITION NO.	SERIES	STEP NO.	
		DRAWING NO.	

E227B43

FEED MATERIAL CHARACTERISTICS

FEED MATERIAL _____   ABRASIVENESS _____

BULK DENSITY: _____ _____ LBS./CU. FT.   STICKINESS _____

PARTICLE SIZE _____   DUSTINESS _____

MAXIMUM SIZE _____   CHEMICAL ACTION _____

ANGLE OF REPOSE _____   TEMPERATURE _____ °F

PRODUCT DESCRIPTION _____

_____

OPERATING CONDITIONS

CAPACITY: LBS./HR.   NORMAL _____   LOADING CLASSIFICATION _____

MAX. _____   LOCATION: INDOOR ☐   OUTDOOR ☐

RPM OF SCREW _____

CONSTRUCTION AND MATERIALS

TROUGH: TYPE _____   SHAFT DIAM.. _____

MAT'L. _____   TROUGH END _____

THICKNESS _____   TYPE HANGERS _____

COVER: TYPE _____   SADDLES _____

MAT'L. _____   DUST SEALS _____

THICKNESS _____   BEARINGS: TYPE – HARD IRON _____

FLIGHT: PITCH _____   BABBITED _____

MAT'L. _____   BRONZE _____

THICKNESS _____   ANTI-FRICTION _____

FLAT VALVE PLATE GATE _____   JACKETED TROUGH _____

RACK & PINION GATE – FLAT VALVE PLATE _____

CURVED VALVE PLATE _____

DRIVE DATA   MOTOR DATA

CHAIN-ASA NO. _____   ITEM NO. _____ MTD. BY _____

SPROKETS – DRIVER NO. TEETH _____   MFG. _____

DRIVEN NO. TEETH _____   TYPE _____ FRAME _____

V-BELT NO. & SIZE _____   HP _____ RPM _____

SHEAVES – DRIVER-PITCH DIA. _____   VOLTS/PHASE/CYCLE _____ / _____ / _____

DRIVEN-PITCH DIA. _____   BEARINGS _____ LUBE _____

REDUCER – MFGR. _____   FULL LOAD AMPS _____ SF _____

MODEL NO. _____   LR AMPS _____

SERVICE FACTOR _____

INPUT RPM _____   RANGE _____

OUTPUT RPM _____   _____

COUPLING – MFG'R. _____   _____

TYPE _____   _____

_____   _____

JOB NO. _____   PLANT LOCATION _____   SCALE

PROJECT NO. _____   REF. DWG. NO. _____   ISSUE DATE

TITLE _____   BLDG. NO.

POSITION NO. _____   SERIES _____ STEP NO. _____

DRAWING NO.

E228B44

REMARKS · APP'R'V · DATE · CHKD SUPRV · BY · REV · DES SUPRV. · CHECKED BY · DRAWN BY · INITIATOR

769

MISCELLANEOUS

PAINTING: _____

GALVANIZING _____

TOTAL WEIGHT _____

MFG. _____

TYPE & MODEL NO. _____

VENDOR DWG. NO. _____

CONVEYOR SERIAL NO. _____

FINISH OF INTERNAL PARTS: _____

_____

REMARKS

_____

_____

_____

_____

_____

_____

_____

_____

_____

_____

_____

_____

_____

_____

_____

_____

_____

_____

_____

_____

_____

_____

_____

_____

_____

_____

_____

_____

_____

_____

_____

_____

JOB NO. _____   PLANT LOCATION _____   SCALE

PROJECT NO. _____   REF. DWG. NO. _____   ISSUE DATE

TITLE _____   BLDG. NO.

POSITION NO. _____   SERIES _____ STEP NO. _____

DRAWING NO.

E228B44
SHEET 2

REMARKS · APP'R'V · DATE · CHKD SUPRV · BY · REV · DES SUPRV. · CHECKED BY · DRAWN BY · INITIATOR

Left Sheet

PROCESS DESIGN SECTION CORPORATE ENGINEERING	BUCKET ELEVATOR DATA SHEET

OPERATING CONDITIONS

MATERIAL CONVEYED: _____
PRODUCT DESCRIPTION: _____
_____
BULK DENSITY: _____ LBS./CU. FT.
SCREEN ANALYSIS: _____ %
PRODUCT TEMP: _____ °F

MOISTURE CONTENT: _____ WGT. %
CAPACITY: TONS/HR. NORMAL _____ MAX. _____
MODE OF OPERATION: _____
BUCKET SPEED: _____ FPM
ANGLE OF INCLINE: _____
INSTALLATION: INDOOR ☐   OUTDOOR ☐

MECHANICAL DATA

TYPE: CENTRIFUGAL ☐   CONTINUOUS ☐
DISTANCE BETWEEN HEAD & TAIL SHAFTS: _____
CASING – CROSS SECTION DIMENSION: _____
CASING GAUGE _____
CASING HD. SECT. – GAUGE DISCH. OPENING: _____
BOOT – TYPE: _____
    GAUGE: _____
    LOADING OPENINGS _____
CHAIN CARRIER FOR BUCKETS
    TYPE: _____
    HEAD SHAFT SPROCKET P.D: _____
    TAIL SHAFT P.D: _____
SIZE OF BUCKETS: _____ INCHES
BUCKET SPACING: _____ INCHES
BUCKET BOLTS–TYPE: _____
    NO. PER BUCKET: _____

BELT CARRIER FOR BUCKETS:
    WIDTH: _____ NO. OF PLIES: _____
    WT. OF DUCK: _____ COVER THICKNESS: _____
    TYPE OF BELT SPLICE: _____
    HEAD PULLEY DIA: _____ FACE WIDTH: _____
    TAIL PULLEY DIA: _____ FACE WIDTH: _____
    HEAD SHAFT DIA: _____ TAIL SHAFT DIA: _____
    TYPE OF BEARINGS: _____
    HEAD SHAFT SPEED: _____ RPM
    TYPE OF TAKE-UP: _____
        LOCATIONS: _____
    INLET CHUTE ANGLE: _____
    DISCH. CHUTE ANGLE: _____
    INLET OPENING W/LOADING LEG: _____
    FEED HOPPER _____

MATERIALS OF CONSTRUCTION

CASING: _____
HEAD SECTION: _____
BOOT: _____
BUCKETS: _____
HEAD & TAIL SHAFTS: _____
HEAD & TAIL SHAFT BEARINGS: _____
BELT & COVERS: _____
HEAD & TAIL PULLEYS: _____

CHAIN: _____
HEAD & TAIL SPROCKETS: _____
TAKE-UP DEVICE: _____
BUCKET BOLTS: _____
BUCKET FILLER PIECES: _____
GASKETS: _____
JOINTS: _____
DOORS & MANWAYS: _____

MOTOR DRIVE DATA

ITEM NO. _____ MTD. BY. _____
HP _____ RPM _____ FRAME _____
MFG. _____
TYPE _____ INSUL. _____
ENCLOSURE: CLASS I GROUP D
VOLTS/PHASE/CYCLE _____ / _____ / _____
BEARINGS _____ LUBE _____
FULL LOAD AMPS. _____ S.F. _____

LR AMPS _____
REDUCTION UNIT:
    TYPE _____ RATIO _____
    MFG. _____
TYPE DRIVE: CHAIN ☐   BELT ☐
MOTOR COUPLING: TYPE _____
MFG. _____

JOB NO. PROJECT NO.	PLANT LOCATION REF. DWG. NO.
TITLE	
POSITION NO. SERIES STEP NO.	

ISSUE DATE   SCALE   BLDG. NO.

DRAWING NO.

E225B41

Side labels (left column, top to bottom): REMARKS, APP'R'V, DATE, CHKD SUPRV, BY, REV, DES SUPRV, CHECKED BY, DRAWN BY, INITIATOR

Right Sheet

PROCESS DESIGN SECTION CORPORATE ENGINEERING	PRESSURE LEAF FILTER DATA SHEET

OPERATING CONDITIONS

FLUID: _____
CHARACTERISTICS: _____
_____
SPECIFIC GRAVITY: _____
pH: _____
TEMPERATURE: _____ °F
VISCOSITY: _____ CP
SOLIDS CONTENT: _____ WT. %
FLOW RATE: _____ GPM

WORKING PRESS. _____ PSIG
ALLOWABLE ΔP-MAX. _____ PSIG
FILTER MEDIA: _____
FILTER AID: _____
WASH MEDIA: _____
TYPE OPERATION: _____
TIME ON STREAM: _____
CLEANING FREQUENCY: _____
_____

MECHANICAL DATA

MFR. _____
SIZE & TYPE _____
FILTRATION AREA: _____ SQ. FT.
NO. OF LEAVES _____ SPACING _____
BUBBLE RING _____
LAKE CAPACITY _____
LAKE THICKNESS _____
SLUICER _____ DRIVE _____
JACKET _____ FOR _____ PSIG

TANK: VERTICAL ☐   HORIZONTAL ☐
    DIAM. _____ VOLUME _____
COVER LIFT _____
CARRIAGE DRIVE _____
COVER CLOSURE _____
LEAF SPACERS _____ VIBRATOR _____
FILTRATE MANIFOLD _____
CONNECTIONS-TYPE _____
CODE STAMP: REQ'D. ☐   NOT REQ'D. ☐

MATERIALS

TANK: _____
LINING: _____
LEAVES: _____
SURFACE MEMBER _____
INTERMED. MEMBER _____

O-RING LEAF GASKETS _____
COVER GASKETS _____
MANIFOLD PIPING _____
JACKET _____
FINISH _____ INTERIOR _____ EXTERIOR

ACCESSORIES

☐ PRE-COAT OR SLURRY TANK:
    VERTICAL ☐   HORIZONTAL ☐
    DIAM. _____ VOLUME _____
    MATERIAL _____
    FINISH _____
    LINING _____
    COVER TYPE _____
    LEVEL INDICATOR: YES ☐   NO ☐
☐ AGITATOR
    RPM _____
    MFR _____
    SIZE & TYPE _____
    MOTOR: H.P. _____ RPM _____
    VOLTS/PHASE/CYCLE _____ / _____ / _____

☐ PRECOAT OR FILTER FEED PUMP:
    CAPACITY: _____ GPM @ _____ TDH
    MATERIAL: _____
    MFR: _____
    SIZE & TYPE: _____
    MOTOR: H.P. _____ RPM _____
    VOLTS/PHASE/CYCLE _____
☐ FILTERAID INJECTION PUMP:
    CAPACITY: _____ GPM @ _____ TDH
    MATERIAL: _____
    MFR: _____
    SIZE & TYPE _____
    MOTOR H.P. _____ RPM _____
    VOLTS/PHASE/CYCLE _____ / _____ / _____

NOTE: ALL MOTORS TO BE CLASS-1-GROUP-D EXP. PROOF

JOB NO. PROJECT NO.	PLANT LOCATION REF. DWG. NO.
TITLE	
POSITION NO. SERIES STEP NO.	

ISSUE DATE   SCALE   BLDG. NO.

DRAWING NO.

E221B37

Side labels (right column, top to bottom): REMARKS, APP'R'V, DATE, CHKD SUPRV, BY, REV, DES SUPRV, CHECKED BY, DRAWN BY, INITIATOR

INTAKE AIR FILTER

1	Service _____ Indoor/Outdoor; English/Metric Units
2	Mfr. _____ Model No. _____ Qty. _____
3	Site: Alt. _____ Amb. Temp.: Max. _____ Min. _____ ; Wind Velocity: Max. _____
4	Unusual Conditions: Dust/Fumes/Sand/Snow/Other _____
5	Air Flow: Normal _____ Rated _____ @ Temp. _____ Press. _____
6	AFI Dust Spot Efficiency (Atmospheric Dust): _____ %.
7	Unit Shall Remove _____ / _____ of all Particles ____ / ____ Microns & Larger.
8	Rated Data: Stage No. 1 Stage No. 2
9	Filter Type
10	Model No.
11	Max. Possible Air Capacity
12	Pressure Drop (Clean Filter)
13	Max. Press. Drop (Dirty Filter)
14	No. of Elements
15	Size of each Element
16	Filtration Area
17	Filtration Material
18	Face Velocity
19	Dust Holding Capacity
20	Weight of Element
21	Element Retention Method in Frame
22	Louvers @ Filter Inlet: Size _____ Type _____ Material _____
23	Inlet Trash Screen: Size _____ Wire Gauge _____ Material _____
24	Filter Housing: Material _____ Internal/External Paint
25	Access Doors: Qty. ___. Blow in Doors: Qty. ___. Filter Outlet: Side/Bottom/Back Conn.
26	Motor: Mfr. _____ Model No. _____. Qty. _____
27	Area Class ____ Gr. ____ Div. ____ /Non-Hazardous; Volts ____ Phase ____ Hertz ____
28	Enclosure _____ Insulation _____ ; Temp. Rise ____ °C above ____ by ____ @ ____ S.F.

Service	PWR	Current		Effy.	P.F.	Full	Frame	Brg.	Weight	Mtg.	Allow. Thrust	Space	S.F.
	HP	Full Load	Locked Rotor	4/4	3/4	4/4	3/4	Load RPM	No.	Lub.	LB/KG	H/V	Up/Down LB/KG	Heater Watts	
	KW													

33	Diff. Press. Switch: Range _____ Set Press. _____ Qty. ____
34	Diff. Press. Ind. Type _____ Range _____ Qty. ____
35	Specifications: Paint _____ Wind _____ M.W.K. _____
36	Earthquake _____
37	Notes: 1) The structure, consisting of the plenum chamber & filter, shall be of such
38	design that it can be supported by means of four (4) steel columns, one (1) at each
39	corner. 2) Plenum chamber shall be of sufficient strength & bracing to prevent wall,
40	floor or ceiling from pulsating or oscillating. 3) For ammonia/urea plants or other
41	installations with ammonia in the atmosphere, no copper, aluminum or their alloys
42	shall be used for parts exposed to the air. 4) Seals & filter material shall be
43	resistant to vapors present in the inlet air (ammonia, hydrocarbons, etc.). 5) Unit
44	shall be completely assembled and shipped as one unit. 6) Instruments & controls to
45	be completely piped and wired. 7) Outlet connection screen (0.25 in.) (6 mm) wire
46	mesh, with back up bars to withstand seven (7) psi/0.5 kg/cm^2 $\triangle$ Press. across the
47	screen. _____

REVISIONS

NO	DATE	ENGINEER	CHK/REVIEW	APPROVE		
6					MANAGING OFFICE	ENGINEERING OFFICE
5						
4					**EQUIPMENT DATA SHEET**	
3					CLIENT _____	
2					LOCATION _____ JOB NO. ____	
1					ITEM _____	
0					ITEM NO _____ SPEC. NO. ____	

KELLOGG

REQ'N. NO. _____   PAGE ____ OF ____

| PROCESS DESIGN SECTION | LINE FILTER |
| CORPORATE ENGINEERING | SPECIFICATION SHEET 1 OF 2 |

REMARKS · APPRV · DATE · CHKD SUPRV · BY · REV

PROJ. ENG. · DES SUPRV · CHECKED BY · DRAWN BY · INITIATOR · DATE

1. **FUNCTION:** _____
   _____
   _____
   _____
   _____
   _____
   _____
   _____
   _____
   _____

2. **SERVICE CONDITIONS**

   FLUID FLOWING: _____

   FLOW RATE: NORMAL _____ GPM

   MAX. _____ GPM

   PRESSURE: _____ PSIG

   TEMPERATURE: _____ °F

   FLUID VISCOSITY: _____ CP

   FLUID SPECIFIC GRAVITY: _____

   PARTICLE SIZE ANALYSIS: _____
   _____
   _____

   SOLIDS LOADING: _____

   FILTER PRESSURE DROP: _____ PSIG

   FILTER RATING: _____

3. **TYPE AND DESCRIPTION:** _____
   _____
   _____
   _____
   _____
   _____

JOB NO. _____	PLANT LOCATION _____	SCALE
PROJECT NO. _____	REF. DWG. NO. _____	ISSUE DATE
TITLE _____		BLDG. NO.
POSITION NO. _____	SERIES ____ STEP NO. ____	
		DRAWING NO.

E 121 85°

630E0

Line Filter Specification (Sheet 2 of 2)

PROCESS DESIGN SECTION   LINE FILTER

CORPORATE ENGINEERING   SPECIFICATION   SHEET 2 OF 2

Left margin (top to bottom): REMARKS | APP'R'V | DATE | SUPRV. | CHKD BY | REV | DES SUPRV. | CHECKED BY | DRAWN BY | INITIATOR

4. MECHANICAL

MATERIALS OF CONSTRUCTION

HOUSING: _____

FILTER ELEMENT: _____

GASKETS: _____

CONNECTIONS:

   INLET: _____

   OUTLET: _____

DESIGN PRESSURE: _____PSIG

DESIGN TEMPERATURE: _____ °F

ACCESSORIES: _____
_____
_____
_____
_____
_____

NO. OF UNITS REQUIRED: _____

A.S.ME CODE: REQUIRED WHEN FILTER IS LARGER THAN 6'' IN DIAMETER OR HOLDS MORE THAN 5 CU. FT. IN VOLUME, OR IF DESIGN PRESSURE IS GREATER THAN 15 P.S.I.G.

JOB NO. _____ PLANT LOCATION _____

PROJECT NO. _____ REF. DWG. NO. _____

TITLE _____

POSITION NO. _____ SERIES _____ STEP NO. _____

ISSUE DATE | SCALE | BLDG. NO.

DRAWING NO.

E 121 85·

Centrifuge Data Sheet (Sheet 1 of 2)

PROCESS DESIGN SECTION   CENTRIFUGE

CORPORATE ENGINEERING   DATA SHEET   SHEET 1 OF 2

Left margin (top to bottom): REMARKS | APP'R'V | DATE | SUPRV. | CHKD BY | REV | DES SUPRV. | CHECKED BY | DRAWN BY | INITIATOR

OPERATING CONDITIONS

FEED MATERIAL: _____   CAKE CAPACITY: _____ CU. FT.

CHARACTERISTICS: _____   CAKE DENSITY: _____ LB./CU. FT.

_____   CAKE MOISTURE: _____ %

DENSITY OF SLURRY: _____ LB./CU. FT.   SOLIDS PARTICLE SIZE: _____ MESH

PERCENT SOLIDS: _____   WASH REQUIRED: _____

VISCOSITY OF SLURRY: _____ CP   MAT'L _____

TEMPERATURE OF SLURRY: _____ °F   RATE _____ GAL./LB. CAKE

FEED RATE: NORM. _____ MAX. _____   DESIGN PRESS. _____ PSIG

SG. SOLIDS _____ SG. LIQUID _____   REQ'D. CAPACITY: _____ LB/HR

MECHANICAL DATA

	CONNECTIONS	SIZE	TYPE
MFR. _____	FEED PIPE		
SIZE & TYPE _____	SPRAY PIPE		
BASKET DIAM. _____	M.L. DRAIN		
TYPE: PERFORATE ☐ INPERFORATE ☐	CAKE DISCH.		
BASKET DEPTH: _____	LIGHT GLASS		
BASKET RING OPENING DIAM. _____	SIGHT GLASS		
CAKE THICKNESS _____	VENT		
CAPACITY UNDER TOP RING _____ CU. FT.	PURGE		
BASKET RPM _____			

DRIVE TYPE: ELECTRIC ☐
          HYDRAULIC ☐   UNLOADING PLOW: REQ'D. ☐ NOT REQ'D. ☐

COVER TYPE: FULL ☐ HALF ☐   SKIMMING TUBE: REQ'D. ☐ NOT REQ'D. ☐

   FUME TIGHT ☐ NON-FUME TIGHT ☐   INTERLOCK REQ'D. ☐

MATERIALS

CASE _____	FEED PIPE _____
LINING _____	SPRAY PIPE _____
CASE RING _____	DRAIN NOZZLE _____
SCREENS _____	DISCH. NOZZLE _____
RETAINING RING _____	VENT NOZZLE _____
BASKET _____	PURGE NOZZLE _____
FEED CONE _____	UNLOADING PLOW _____
COVER _____	SKIMMING TUBE _____
SPINDLE _____	FILTER CLOTH _____
BEARINGS _____	GASKETS _____

ACCESSORIES

☐ AUTOMATIC CENTRIFUGING CYCLE CONTROLS
   (SEE REMARKS COLUMN FOR PROPOSED CYCLE)
☐ CONTROL PANEL

JOB NO. _____ PLANT LOCATION _____

PROJECT NO. _____ REF. DWG. NO. _____

TITLE _____

POSITION NO. _____ SERIES _____ STEP NO. _____

ISSUE DATE | SCALE | BLDG. NO.

DRAWING NO.

E222B38

Line Filter Specification—*(continued)*

Left Form (Centrifuge Data Sheet — Sheet 2 of 2)

PROCESS DESIGN SECTION	CENTRIFUGE
CORPORATE ENGINEERING	DATA SHEET SHEET 2 OF 2

DRIVE DATA

MOTOR
ITEM NO. _____ MTD BY _____
MFR. _____
TYPE _____ FRAME _____
H.P. _____ RPM _____
VOLTS/PHASE/CYCLE _____ / _____ / _____

ENCLOSURE: CLASS 1 GROUP D
BEARINGS. _____ LUBE _____
FULL LOAD AMPS _____ SF _____
L.R. AMPS _____

HYDRAULIC
MFR. _____
SIZE & TYPE _____

OIL COOLER
MFR _____
SIZE & TYPE _____

REMARKS

1 - INTERIOR BASKET FINISH TO BE _____

(ruled blank lines)

JOB NO.	PLANT LOCATION		SCALE
PROJECT NO.	REF. DWG. NO.	ISSUE DATE	
TITLE			BLDG. NO.
POSITION NO.	SERIES	STEP NO.	
		DRAWING NO.	

E222B38 SHEET 2

Side labels: REMARKS · APP'R'V · DATE · CHK'D SUPR'V · REV BY · DES SUPRV. · CHECKED BY · DRAWN BY · INITIATOR · DATE · PROJ. ENG.

Right Form (Vibrating Screen Data Sheet — Sheet 1 of 2)

PROCESS DESIGN SECTION	VIBRATING SCREEN
CORPORATE ENGINEERING	DATA SHEET SHEET 1 OF 2

FEED MATERIAL CHARACTERISTICS

FEED MATERIAL: _____
BULK DENSITY _____ LBS./CU. FT.
ANGLE OF REPOSE _____
WEIGHT % MOISTURE _____
PRODUCT DESCRIPTION _____

ABRASIVENESS _____
STICKINESS _____
CHEMICAL ACTION _____
DUSTINESS _____
TEMPERATURE _____ °F

MATERIAL TO BE SCREENED OUT _____
PART. SIZE ON 1ST SCREEN/% RETAINED _____
PART. SIZE ON 2ND SCREEN/% RETAINED _____
PART. SIZE ON 3RD SCREEN/% RETAINED _____

OPERATING CONDITIONS

FEED RATE – TONS/HR: _____ NORMAL/MAX. _____
% OF SOLIDS _____
FEED LINE SIZE _____
METHOD OF FEED _____

SUCTION IN DISCH. LINE _____
PRESS. IN DISCH. LINE _____
LOCATION: INDOOR ☐ OUTDOOR ☐
MODE OF OPERATION: _____

DESIGN DATA

NO. OF SCREENS REQ'D. _____
SCREEN TYPE/SIZE _____
1ST SCREEN MESH _____
2ND SCREEN MESH _____
3RD SCREEN MESH _____
1ST SCREEN DISCH. SIZE _____
2ND SCREEN DISCH. SIZE _____
3RD SCREEN DISCH. SIZE _____
SCREEN AREA FREE/GROSS 1ST SCREEN SQ. FT. ____
SCREEN AREA FREE/GROSS 2ND SCREEN SQ. FT. ____
SCREEN AREA FREE/GROSS 3RD SCREEN SQ. FT. ____
SCREEN BACKING REQ'D./TYPE 1ST SCREEN _____
SCREEN BACKING REQ'D./TYPE 2ND SCREEN _____
SCREEN BACKING REQ'D./TYPE 3RD SCREEN _____

DISCH. SIZE TABLE _____
FEED DISTRIBUTOR REQ'D. _____
SCREEN ANGLE: DESIGN _____
                       MAX. _____
COVER REQ'D. _____
MOUNTING: FLOOR ☐ SUSPENSION ☐
TYPE OF SCREEN CLEANER _____
INLET DIAM. _____

MATERIALS OF CONSTRUCTION

SCREEN DECKS _____
SCREENS _____
SCREEN SUPPORT RINGS _____
BASE _____
TABLE ASSY. (IN CONTACT WITH PRODUCT) _____
TABLE ASSY. (NOT IN CONTACT WITH PRODUCT) ___
MISC. _____

HOUSING _____
FEED DISTRIBUTOR _____
SPRINGS _____
COLLECTING PANS _____

JOB NO.	PLANT LOCATION		SCALE
PROJECT NO.	REF. DWG. NO.	ISSUE DATE	
TITLE			BLDG. NO.
POSITION NO.	SERIES	STEP NO.	
		DRAWING NO.	

E226B42

Side labels: REMARKS · APP'R'V · DATE · CHK'D SUPR'V · REV BY · DES SUPRV · CHECKED BY · DRAWN BY · INITIATOR

Centrifuge Data Sheet—(*continued*)

PROCESS DESIGN SECTION
CORPORATE ENGINEERING

VIBRATING SCREEN
DATA SHEET

SHEET 2 OF 2

REMARKS

MOTOR DRIVE DATA

ITEM NO. _____ MTD. BY_____ BEARINGS _____ LUBE _____

MFG. _____ FULL LOAD AMPS _____ SF. _____

TYPE _____ FRAME _____ L.R. AMPS _____

HP _____ RPM _____

VOLTS/PHASE/CYCLES _____/_____/_____ V BELT DRIVE _____

GEAR REDUCER _____

MISCELLANEOUS

PAINTING _____

GALVANIZING _____

TOTAL WEIGHT_____

VENDORS DWG. NO. _____

SIFTER SERIAL NO. _____

INLET & OUTLET FLEX. CONNECTIONS _____

VENDORS MODEL NO. _____

REMARKS

APP'RV

DATE

CHKD SUPRV

BY

REV

PROJ. ENG.

DES SUPRV.

CHECKED BY

DRAWN BY

INITIATOR

DATE

E226B42
SHEET 2

JOB NO. _____

PROJECT NO. _____

TITLE _____

POSITION NO. _____

PLANT LOCATION _____

REF. DWG. NO. _____

SERIES _____ STEP NO. _____

SCALE

ISSUE DATE

BLDG. NO.

DRAWING NO.

Vibrating Screen—(*continued*)

COLUMN SPECIFICATIONS

ITEM NO.	NO. REQ'D	DESCRIPTION

PERFORMANCE DATA

FLUIDS PROCESSED:

_____

_____

_____

PRESSURE:

OPERATING:_____

DESIGN:_____

TEST:_____

TEMPERATURE:

OPERATING:_____

DESIGN:_____

CONSTRUCTION DATA

☐ CODE:_____

☐ MANHOLES:

SIZE_____ SHAPE_____ NO._____

LOCATION_____

☐ HANDHOLES:

SIZE_____ SHAPE_____ NO._____

LOCATION:_____

INSULATION:

REMARKS: FOR INTERIOR CONSTRUCTION AND SUPPORT DATA SEE ATTACHED SHEETS.

DESCRIPTION OF FUNCTION OF VESSEL AND REMARKS

_____

_____

_____

_____

NOTE:
DATA FOR ITEMS MARKED THUS ☐ ARE NORMALLY SUPPLIED BY ENG'R'G DEPT. DATA ENTRIES FOR THESE ITEMS MADE BY OTHER THAN ENG'R'G DEPT. INDICATE MANDATORY REQUIREMENTS DICTATED BY PROCESS, PROPOSAL, CONTRACT, OR CUSTOMER.

SHELL DATA

TANGENT LINE — ☐ CONICAL HEAD

TANGENT LINE — ☐ DISHED HEAD

TYPE_____

☐ BLIND FLANGE COVER

☐ FLANGED TOP CLOSURE

TANGENT LINE

☐ STRAIGHT SHELL

DIAMETER_____ I. D.

_____ O. D.

LENGTH_____

TO TANG. LINE OR FACE OF FLANGE OR FLANGES.

NOTE:
WHERE INTERMEDIATE FLANGES OR OTHER SHELL DETAILS ARE RE-QUIRED, INDICATE BY SKETCH ON ADJACENT DRAWING AND LOCATE BY DIMENSIONS.

TANGENT LINE

TANGENT LINE

TANGENT LINE

☐ MATERIAL OF CONSTRUCTION:_____

REMARKS:_____

_____

APPR.				CHKD.	MADE	DATE	NO.
APPR.							
APPR.			REFERENCES				
APPR.					REVISIONS		
CHKD.			CHEMICAL PLANTS DIVISION				
MADE			BLAW-KNOX CONSTRUCTION COMPANY PITTSBURGH, PENNA.				

PAGE _____ OF _____

774

STONE & WEBSTER ENGINEERING CORPORATION
BUBBLE TOWER SPECIFICATION

Item _____
Page _____
Rev. 1 _____
Rev. 2 _____

Client	Location	J. O. No.
Apparatus		Project No.
		Date _____ By _____
Based on		Rating Page _____ Dated _____

DESIGN CONDITIONS

Oper Pr	lb/sq in ga	Oper Temp	°F	Hammer Test	Yes	No
Des Pr	lb/sq in ga	Des Temp	°F	Field Hyd Test	Yes	No
Wind - Proj Area	lb/sq ft	Self Supporting	Yes No	Other Tests		
Max. Horizontal Deflection at Top Tray		in				
Earthquake 0.2 Operating Weight applied at c.g.			Yes No			

MECHANICAL DATA

Code		Stress Relieve Yes No	Shell & Heads ASTM Spec
		Radiograph Yes No	Type of Heads

THICKNESS:	Calculated	Corrosion	Total Thick	Liner Mat	Liner Thick
Shell	in	in	in		in
	in	in	in		in
	in	in	in		in
Top Head	in	in	in		in
Intermediate Head	in	in	in		in
	in	in	in		in
Bottom Head	in	in	in		in
Cone Section	in	in	in		in
Skirt	in	in	in		in
Insulation			in		
Stiffener Rings	Number Req'd	Size	in ×	in	

NOZZLES:	Number	Type	Series	Size	Mark No.
Feed				in	
O H Vapor				in	
Reflux In				in	
Reflux Out				in	
Bottoms				in	
Drains				in	
Reboiler Vapor				in	
Reboiler Liquid				in	
				in	
				in	
Safety Valve				in	
Manholes				in	
Thermocouples				in	
				in	
				in	
Gage Glass				in	
Pr Gage				in	
Level Control				in	
				in	
Vent				in	
Steam out				in	

TRAYS:					CAPS:		
Tray No.	Diameter	Spacing	Type	Materials	Size	Type	Materials
	' "	"					
	' "	"					
	' "	"					
Baffles, etc.							

Insulation Supports: Yes No: Number Req'd _____ Size _____ in × _____ in: Shop _____ Field _____

Platform Clips: Yes No: Number Req'd _____ Shop _____ Field _____ Ladder Clips: Yes No: Number Req'd _____ Shop _____ Field _____

Manhole Davits Required For All Covers Weighing Over 75 Lb

For Further Details Refer To: _____

Remarks: _____

Copy To	Date _____	Checked _____ Date _____	Approved _____ Date _____

Estimated Weight _____ lb

775

TANGENT LINE

TANGENT LINE

BY _____
DATE _____
CHK'D _____
APP'D _____

ST-L1-094

DESIGN DATA

CODE STAMP			
OTHER SPECS.: ST-L4-496			
DESIGN PRESS. @ TEMP.	PSI @		°F
OPER. PRESS. @ TEMP.	PSI @		°F
STRESS RELIEVING			
WELD EXAMINATION			
JOINT EFFICIENCY SHELL	%	HEADS	%
CORR. ALLOWANCE SHELL		HEADS	
LINING			
MAX.ALL.PRESS.(NEW & COLD)			PSI
HYDROSTATIC TEST			PSI
HAMMER TEST			PSI

MATERIALS	
SHELL	
HEADS	
SUPPORT	
INTERNALS	
TRAYS	

FIREPROOFING	
INSULATION	
INS. SUPP. RINGS	
PAINT	
NET FAB. WEIGHT (LESS CAPS)	LBS.
FAB. WEIGHT WITH CAPS	LBS.

FOUNDATION DATA		
EMPTY WEIGHT		LBS.
OPERATING WEIGHT		LBS.
TEST WEIGHT		LBS.
WIND	M_B =	FT. LBS.
EARTHQUAKE	M_B =	FT. LBS.

MANHOLE (HINGED OR DAVITED)

NOTES & REF. DRGS. ST-L4-496

MK.	RTG.	FCG.	SIZE	MK.	RTG.	FCG.	SIZE

NOZZLE SCHEDULE

VESSEL FABRICATOR TO SUPPLY CLIPS ONLY FOR

PLATFORMS			NO. PIPE SUPPORT CLIPS		
NO.					TYPE I
SIZE					TYPE II
WIDTH					TYPE III
PLATFORM WEIGHT				VESSEL DAVIT	
LADDER	CAGE		WT.		
PIPE GUIDES 1/2 CPLGS.	3000#				
CONTRACT NO.			DRG. NO.		

DESIGN DATA

CODE STAMP	
OTHER SPECS.: ST-L4-496	
DESIGN PRESS. @ TEMP.	PSI @ °F
OPER. PRESS. @ TEMP.	PSI @ °F
STRESS RELIEVING	
WELD EXAMINATION	
JOINT EFFICIENCY SHELL % HEADS %	
CORR. ALLOWANCE SHELL HEADS	
LINING	
MAX. ALL. PRESS. (NEW & COLD)	PSI
HYDROSTATIC TEST	PSI
HAMMER TEST	PSI

MATERIALS:
- SHELL
- HEADS
- SUPPORT
- INTERNALS

FIREPROOFING	
INSULATION	
PAINT	
NET FAB WEIGHT	LBS.
EMPTY WEIGHT	LBS.
OPERATING WEIGHT	LBS.
TEST WEIGHT	LBS.
MANHOLE ("HINGED OR DAVITED)	
BY DATE CHK'D APP'D	

ST-L1-097

NOTES & REF. DRGS. ST-L4-496

MK.	RTG.	FCG.	SIZE	MK.	RTG.	FCG.	SIZE

NOZZLE SCHEDULE

VESSEL FABRICATOR TO SUPPLY CLIPS ONLY FOR
PLATFORM WT.
LADDER CAGE WT.

CONTRACT NO. DRG. NO.

THE FLUOR CORPORATION LTD.

PROCESS DESIGN SECTION
CORPORATE ENGINEERING

DATA SHEET Sheet 1 of 2

GENERAL VESSEL DATA

Reactor ☐ ; Tank ☐ ; Other _____ .
Vertical ☐ ; Horizontal ☐ ; Jacketed ☐ ; Unjacked ☐ .
Rated capacity, gals. _____ ; Flanged head ☐ ; One piece construction ☐ .
Standard Head Openings ☐ ; Non standard head required. ☐
Specification Based on Pfaudler Series _____ or equal.

VESSEL OPENINGS

TOP HEAD

Manhole ☐ or Handhole ☐ with 4" sightglass ☐ ; Agitator Opening ☐ .
Size _____ " for 4" light glass   Size _____ " for _____
Size _____ " for _____   Size _____ " for _____
Size _____ " for _____   Size _____ " for _____
Size _____ " for _____   Size _____ " for _____

BOTTOM HEAD   Opening _____ " .

JACKET

Shell Openings, Standard ☐ ; Special _____
Jacket Head Openings, Standard ☐ ; Special _____

ORIENTATION

Orientation of Process openings: – By vendor ☐ ; HLR approval of Vendors dwg. req'd ☐
Other _____
Orientation of Jacket Openings: By Vendor ☐ ; HLR approval of Vendors dwg. req'd. ☐
Other _____

JACKET

Working Conditions: Water ☐ ; Steam ☐ ; Brine ☐ ; Hot Oil ☐ ;
Other _____
Working temperature: _____ °F to _____ °F
Working Pressure: Atmospheric ☐ ; _____ psig; Vacuum ☐

VESSEL SUPPORT

Leg Couplings: – Size _____ " ; Number _____ .
Vendor to supply: – Adjusting Nuts and Pedistals ☐ ; Legs ☐
Distance from face of bottom outlet to floor _____
Lugs: – Four required ☐ ; size _____ "
Position: – On ℄ of manhole ☐ ; 45° off ℄ Manhole ☐ ; _____ " below face of flange;
_____ " above face of bottom outlet.
Vessel weight if special _____ lbs.

GLASS-LINED ACCESSORIES

_____ " x _____ " glass–lined flush bottom valve ☐
Reducing flanges: ☐ _____ " x _____ " ; ☐ _____ " x _____ " x ☐ _____ " x _____ " .
Others: _____
_____
_____

REMARKS

APPR'V | DATE | CHKD Suprv. | BY | REV

PROJ. ENG. | DES SUPRV.
CHECKED BY
DRAWN BY
DATE | INITIATOR

JOB NO. _____	PLANT LOCATION _____	SCALE
PROJECT NO. _____	REF. DWG. NO. _____	
TITLE		ISSUE DATE
POSITION NO. _____ SERIES _____ STEP NO. _____		BLDG. NO.
	DRAWING NO.	

Left Sheet

PROCESS DESIGN SECTION
CORPORATE ENGINEERING

GLASS LINED VESSEL

DATA SHEET   Sheet 2 of 2

REMARKS

GENERAL NOTES

Insulation Thickness _____ ". By Hoffmann–La Roche.

Matching flanges to be supplied by HLR ☐ ;   Piping contractor ☐ .

Material:_s/s ☐ ;   Other _____

Vendor to supply: _Approval drawing ☐ ;   Certified drawing ☐ .

Vendor to fill in all missing information on: _Approval drawing ☐ ; Certified drawing ☐

AGITATION

DUTY

For: _Simple mixing ☐ ; Extraction ☐ ; Reaction ☐ ;   Heat transfer ☐ .

Gas incorporation ☐ ; Solids incorporation ☐ .

1 Phase liquid ☐ ; d_4 ____ ; Viscosity Cp/____°C _____

Bottom layer, d_4 ____ ; Viscosity Cp/____ °C _____

Liquid_gas ☐ ; Liquid d_4 ____ ; Viscosity Cp/____ C ____ ; Gas _____

Liquid_solid ☐ ; Liquid d_4 _____ ; Viscosity Cp/____ ° C ____ ; Solid _____

Change during process: _____

TYPE

Anchor ☐ ; Impeller ☐ ; Other ____ ; rpm ____ .

Agitation quality: _Mild ☐ ; Good ☐ ; Vigorous ☐ ; Violent ☐ .

BAFFLES

None ☐ ; Thermowell ☐ ; Flat ☐ ; Std. up ☐ .

Std. down ☐ ; Long ☐ ; To be used for thermowell ☐ ;

G.L. restricted tip ☐ ; Tantalum tip ☐ ; Hastelloy tip ☐ .

Dimensions by _____ instrument eng. I.D. _____ "; Length _____".

MOTOR

HP ____ ; 3 phase, 60 cycle, 220/440 volts, rpm _____ .

Enclosure; Class 1 Group D ☐ Other _____ .

WORKING CONDITIONS

Level at start: _gals, _____ ; Straight shell _____ ".

Level at end: _gals, _____ ; Straight shell _____".

Pressure: _Atmospheric ☐ ; _____ psig; Vacuum ☐

Temperature range _____ °F to _____ °F

Chemicals: _____

Plugs permitted:_ Tantalum ☐ ; Hastelloy ☐ ; Other _____ .

PROCESS DESCRIPTION

_____
_____
_____
_____
_____
_____
_____

REMARKS | APPR'V | DATE | CHKD SUPV. | BY | REV

PROJ. ENG. | DES SUPRV. | CHECKED BY | DRAWN BY | INITIATOR | DATE

JOB NO. _____   PLANT LOCATION _____
PROJECT NO. _____   REF. DWG. NO. _____
TITLE _____
POSITION NO. _____ SERIES _____ STEP NO. _____

ISSUE DATE

SCALE

BLDG. NO.

DRAWING NO.

Right Sheet

PROCESS DESIGN SECTION
CORPORATE ENGINEERING

FRACTIONATOR TRAY DESIGN
DATA SHEET

REMARKS

REBOILER TYPE (KETTLE OR THERMOSYPHON) _____ SERVICE _____

TRAYS NUMBERED FROM TOP OR BOTTOM

TRAY NUMBER _____				
TOWER INSIDE DIAM. (SEE NOTE 1)				
TOTAL TRAYS IN SECTION				
TRAY SPACING (INCHES) (SEE NOTE 1)				
NO. OF LIQUID PASSES (SEE NOTE 1)				
MAX. ΔP ( ) /TRAY				
TRAY EFFICIENCY (SEE NOTE 1)				
ENTRAINMENT (SEE NOTE 1)				
INTERNAL CONDITIONS				
VAPOR TO TRAY MAX.				
RATE (#/HR.) MIN.				
DENSITY (# FT.³)				
PRESSURE (PSIA)				
TEMPERATURE (°F)				
LIQUID FROM TRAY MAX.				
RATE (# /HR) MIN.				
DENSITY (# FT.³)				
TEMPERATURE (°F)				
VISCOSITY, CP				
SURFACE TENSION (DYNES/CM)				
FOAMING TENDENCY				

MECHANICAL DATA

TOWER MANHOLE _____ I.D. (INCHES) (NOTE 2)
MATERIAL
   DECK _____
   CAP _____
   HOLDOWN _____
   NUTS & BOLTS _____
   SUPPORT RING _____
DECK THICKNESS (GAGE). (NOTE 1) _____
SUPPORT RING WIDTH & THK. (INCHES) (NOTE 1) _____
DOWNCOMER BOLT BAR THK. (INCHES) (NOTE 1) _____
CORROSION ALLOWANCE _____
   TRAYS (INCHES) _____
   TOWER ATTACHMENTS (INCHES) _____
TRAYS INSTALLED FROM TOP OR BOTTOM _____

TYPE OF TRAY INSTALLATION:
REMOVABLE ☐ ,   WELDED ☐ ,
BOLTED ☐
HATCHWAY _____

NOTES: 1. VENDOR SHALL FILL IN ALL BLANKS AND RETURN WITH QUOTATION.
        2. SMALLEST I.D. THROUGH WHICH TRAY PARTS MUST PASS.
        3. WEIR ADJUSTABILITY OF ± 1/2" REQUIRED.
        4. VENDORS GUARANTEE: THE VENDOR SHALL BE EXPECTED TO GUARANTEE HIS DESIGN:
           IF HE CANNOT DO THIS WITHIN THE LIMITS SPECIFIED FOR DIAMETER, TRAY SPACING OR
           DOWNCOMER AREA, HE SHOULD SUBMIT A DESIGN WHICH HE CAN GUARANTEE FOR THE
           SPECIFIED SERVICE.

REMARKS | APPR'V | DATE | CHKD SUPV. | BY | REV

PROJ. ENG. | DES SUPRV. | CHECKED BY | DRAWN BY | INITIATOR | DATE

E 144B12·

JOB NO. _____ PLANT LOCATION _____
PROJECT NO. _____ REF. DWG. NO. _____
TITLE _____
POSITION NO. _____ SERIES _____ STEP NO. _____

ISSUE DATE

SCALE

BLDG. NO.

DRAWING NO.

Glass Lined Vessel—(*continued*)

CATALYTIC CONSTRUCTION COMPANY
PHILADELPHIA 2, PA.

TRAY SPECIFICATION

1	I.D. VESSEL	
2	ITEM NO.	
3	DESIGN TEMP. °F *	
4	I.D. VESSEL MANHOLE	
5	NO. & TYPE TRAYS	
6	TRAY MATERIAL	
7	TRAY CORROSION ALLOW.(Total)	
8	D'CH'R AREA-TOP % Tower Area Sq. Inches	
9	D'CH'R AREA-BOT. % Tower Area Sq. Inches	
10	OUTLET WEIR PERIPHERY	
11	OUTLET WEIR HEIGHT	
12	OUTLET WEIR ADJUSTMENT	
13	OUTLET WEIR NOTCH	
14	INLET WEIR HEIGHT	
15	TRAY MANWAY **	
16	TRAY SPACING	
17	D'CH'R CLEARANCE	
18	SUMP & DRAWOFF REQUIREMENTS	
19	NO. CAPS PER TRAY	
20	CAP & RISER MATERIAL	
21	CAP & RISER ASSY. TYPE	
22	SIZE OF CAPS	
23	CAP SPACING	
24	CAP SKIRT CLEARANCE	
25	CAP SLOT SPEC.	
26	TOP OF SLOT ABOVE TRAY	
27	TYPE OF SLOT IN CAP	
28	I.D. & HEIGHT OF RISERS	
29	SIZE OF TRAY SUPPORT BAR	
30	TRAY SUPPORT - MATERIAL	

REMARKS:

REVISIONS

* - Trays to be designed for 1/8" Max. Deflection at Design Temp.
** - Tray Manways to be removable from top and bottom

FORM CC-220

APPROVAL: DATE: DWG. NO.   REV.

PROCESS DESIGN SECTION
CORPORATE ENGINEERING

TOWER INTERNALS
DATA SHEET

REMARKS APPR'V DATE CHKD SUPRV. BY REV

DISTRIBUTOR
TOWER INSIDE DIA. _____
MATERIAL _____
CORROSION ALLOWANCE _____
LIQUID FLOW—NORMAL _____
    MAX. _____ MIN. _____
LIQUID DENSITY _____
DESIGN TEMP. _____°F or _____°C
MIN. DIA. OF ACCESS _____
SPECIAL REQUESTS _____

SUPPORT PLATE
TOWER INSIDE DIA. _____
MATERIAL _____
CORROSION ALLOWANCE _____
DESIGN LOAD (LIQUID) _____ LB/SQ. FT/HR
DESIGN LOAD (VAPOR) _____ LB/SQ. FT/HR
DESIGN TEMP. _____°F or _____°C
MIN. DIA. OF ACCESS _____
PACKING SIZE & TYPE _____
PACKING DEPTH _____
SPECIAL REQUESTS _____

HOLD—DOWN PLATE
TOWER INSIDE DIA. _____
MATERIAL _____
CORROSION ALLOWANCE _____
DESIGN TEMP. _____°F or _____°C
MIN. DIA. OF ACCESS _____
PACKING SIZE & TYPE _____
SPECIAL REQUESTS _____

BED LIMITER
TOWER INSIDE DIA. _____
MATERIAL _____
CORROSION ALLOWANCE _____
DESIGN TEMP. _____°F or _____°C
MIN. DIA. OF ACCESS _____
PACKING SIZE & TYPE _____
SPECIAL REQUESTS _____

COLLECTOR PLATE
TOWER INSIDE DIA. _____
MATERIAL _____
CORROSION ALLOWANCE _____
DESIGN TEMP. _____°F or _____°C
LIQUID FLOW—NORMAL _____
    MAX. _____ MIN. _____
MIN. DIA. OF ACCESS _____
SUPPORT LEDGE _____ WIDE x _____ THK.
MAX. % LEAKAGE _____
NO. OF SUMPS _____
GAS FLOW _____
SPECIAL REQUESTS _____

REDISTRIBUTOR
TOWER INSIDE DIA. _____
MATERIAL _____
CORROSION ALLOWANCE _____
LIQUID FLOW—NORMAL _____
    MAX. _____ MIN. _____
LIQUID DENSITY _____
SUPPORT LEDGE _____ WIDE x _____ THK.
DESIGN TEMP. _____°F or _____°C
GAS FLOW _____
MIN. DIA. OF ACCESS _____
SPECIAL REQUESTS _____

PROJ. ENG. DES SUPRV. CHECKED BY DRAWN BY INITIATOR DATE

JOB NO. _____ PLANT LOCATION _____
PROJECT NO. _____ REF. DWG. NO. _____
TITLE _____
POSITION NO. _____ SERIES _____ STEP NO. _____

ISSUE DATE

SCALE
BLDG. NO.
DRAWING NO.

E 162818

CHLORINATION SYSTEM

1. Service: _____ Indoor/Outdoor; English/Metric Unit
2. Type of Water to be Chlorinated: _____
3. Chlorine: Liquid/Gas; Dosage: Rate/Schedule _____ / _____
4. Reg. Chlorine In. Pressure _____ Chlorinator/Ejector Distance _____
5. Chlorinator: Item No. _____ Qty. _____ Capacity _____
6. Mfr. _____ Model No. _____
7. Min./Max./Shock Flow _____ / _____ / _____ Material _____
8. Evaporator: Item No. _____ Qty. _____ Water In. Press./Temp. _____ / _____
9. Mfr. _____ Model No. _____
10. Min./Max./Shock Flow _____ / _____ / _____ Material _____
11. Ejector: Item No. _____ Qty. _____ Material _____
12. Mfr. _____ Model No. _____
13. Press.: Water In. _____ Chlor./Inj. _____ Chlor./Water Out _____
14. Chlorine Residual Analyzer: Item No. _____ Qty. _____ Mat'l. _____
15. Mfr. _____ Model No. _____
16. Electrical: Area Class _____ Gr. _____ Div. _____ Volts _____ PH _____ HZ _____ Power _____ KW
17. Chlorinator House: Item No. _____ Qty. _____ Mat'l. of Const. _____
18. Ventilation System, Type: _____
19. Accessories: Control _____
20.
21. Water Test Kit: Mfr. _____ Model No. _____ Range _____
22. Specifications: Painting
23. The Vendor shall furnish as a minimum the equipment and components shown on this sheet.

Sym ◊	Size	Rating	Facing
a			
b			
c			
d			
e			
f			
g			

	Dimensions	Length	Width	Height	Weight		LBS/KG
	Analyzer				Anal. (Inst)		
	Chlorinator				Chlor.(Inst)		
	Ejector				Evap. (Inst)		
	Evaporator				Shipping		

KELLOGG — EQUIPMENT DATA SHEET
MANAGING OFFICE ENGINEERING OFFICE
CLIENT _____
LOCATION _____ JOB NO. _____
ITEM _____
ITEM NO. _____ SPEC. NO. _____
REQ'N. NO. _____ PAGE ___ OF ___

REVISIONS | NO. | DATE | ENGINEER | CHK/REVIEW | APPROVE

COALESCERS

1. Service: _____ Indoor/Outdoor; English/Metric Units
2. Mfr. _____ Model No. _____ Qty. ___
3. Unit: Type _____ Size _____ Support (Type) _____
4. Design: ASME Code Section VIII, Div. 1. _____ Edition and all Mandatory Addendas.
5. Mech. Design Press. _____ Temperature _____ Corr. Allow. _____ Stamped Yes/No
6. Des. Vel.: Acid Serv. -15 FPM/Caustic or Water Serv.-10 FPM/Hydrocarbon-Vendor Std.
7. Material Handled: _____ Corr. Mat'l. _____ Mol. % _____
8. Rated Capacity: _____ Oper. Press. _____ Temp. _____
9. Vapor Capacity: _____ Mol. Wt. _____ Mol. % _____
10. Liquid Capacity: _____ Mol. Wt. _____ Mol. % _____
11. Liquid Removal %: _____ Vendors Guaranteed Removal % _____
12. Sp. Gr. @ Oper. Temp: _____ Visc. @ Oper. Temp. _____ Allow Press.Drop _____
13. Contaminants: Liq.% _____; Solids % _____; Part. Size (Range) _____ Micron
14. Inhibitors: Type _____ Concentration _____ pH of Liq. _____
15. Gas Coalescing Media: _____
16. Liquid Coalescing Media: Excelsior/Comb. Pack/Other _____
17. Materials of Construction: Heads _____ Shell _____
18. Nozzles _____ Headgasket _____ Support (Int.) _____
19. Sump _____ Media _____
20. Coalescer: Head.Flanged/Quick Opening/Hinged/Davit; Supports: Saddles/Legs.
21. Instruments: By Purchaser/Vendors; Diff. Press. Gauge, Level Gauge, Press. Gauge,
22. Relief Valve, Temp. Indicator with Thermowell.
23. Specifications: Wind _____ Earthquake _____ Paint _____
24.
25. Notes: 1) Elastomer O-rings are not permitted in hydrocarbon service. 2) Slip-on flgs.
26. Require Purch. Approval. 3) Combination pack shall consist of four (4) demister
27. pads separated from each other by glass wool mats (three required) and held together
28. by end support grids to form a removable cartridge. Demister pads shall be four (4)
29. inch thick herringbone knitted stainless steel (AISI Type 316) wire mesh. Glass wool
30. mats shall consist of a four (4) inch thickness, compressed to two (2) inch of 15 lb
31. per cu. ft., standard glass wool batting combined with an inert binder suitable for
32. the service conditions. _____

The vendor shall furnish as a minimum the equipment and components shown on this sheet.

Sym	Size	Rating	Facing
a	3/4"		
b			
c			
d			
e	1"		

	Dimensions	Length	Width	Height	Weight	LBS/KG
					Shipping	
					Operating	

KELLOGG — EQUIPMENT DATA SHEET
MANAGING OFFICE ENGINEERING OFFICE
CLIENT _____
LOCATION _____ JOB NO. _____
ITEM _____
ITEM NO. _____ SPEC. NO. _____
REQ'N. NO. _____ PAGE ___ OF ___

REVISIONS | NO. | DATE | ENGINEER | CHK/REVIEW | APPROVE

1	MANUFACTURER_____ MODEL _____ QTY. ____ ENGLISH/METRIC UNITS	
2	WATER STORAGE CAPACITY_____ HEATER: +HORIZONTAL/VERTICAL	
3	DESIGN PRESSURE: ASME BPV CODE SECT. VIII DIV. I PRESS._____ AND FULL VACUUM	
4	OPERATING DATA	
5	[1] RATED WATER INLET QTY/PRESS/TEMP _____ / ____ / ____	
6	[2] RATED 2 PH. Cond. Ret. QTY/PRESS/TEMP _____ / ____ / ____	
7	[3] RATED STEAM INLET QTY/PRESS/TEMP _____ / ____ / ____	
8	[4] RATED VENT QTY/PRESS/TEMP _____ / ____ / ____	
9	[5] RATED WATER OUTLET QTY/PRESS/TEMP _____ / ____ / ____	
10	LIMITING INLET COND. AT NOZZLES: (COND. SHOWN WILL NOT OCCUR SIMULTANEOUSLY)	
11	CONDENSATE AND MAKE-UP 2 PH. CONDENSATE RETURN	
12	MAX. QTY/PRESS/TEMP: _____ / ____ / ____ _____ / ____ / ____	
13	MIN. QTY/PRESS/TEMP: _____ / ____ / ____ _____ / ____ / ____	
14	STEAM	
15	MAX. QTY/PRESS/TEMP: _____ / ____ / ____	
16	MIN. QTY/PRESS/TEMP: _____ / ____ / ____	
17	MECHANICAL DATA	
18	DEAERATOR UNIT:	
19	DEAERATOR AND STORAGE MATERIAL: ASME ▶ SA _____ ◀	
20	HEATER AND STORAGE/CORROSION ALLOWANCE: _____ / ____	
21	HEATER INTERNAL MATERIALS: _____	
22	TRAY MATERIAL: _____	
23	SPRAY VALVE MATERIAL: _____	
24	MANWAYS SIZE HEATER/STORAGE: _____ / ____	
25	VORTEX BREAKERS: _____	
26	[1] WATER AND I PH. CONDENSATE NOZZLE: SIZE _____	
27	[2] 2PH. Condensate Nozzle: Size _____	
28	[3] LOW PRESSURE STEAM NOZZLE: SIZE _____	
29	[5] DEAERATOR WATER Outlet Nozzle: Size _____	
30	PUMP BALANCE LINE NOZZLE: SIZE/QTY. _____ / ____	
31	DEAERATOR DRAIN NOZZLE: SIZE _____	
32	PUMP KICKBACK/Sparger Nozzle: Size _____ / ____	
33	ACCESSORIES:	
34	RELIEF VALVE/VAC. BRKR: SIZE/SET. PRESS. _____ / ____ / ____	
35	[4] VENT VALVE: SIZE _____	
36	INLET CONTROL:	BY: VENDOR/KELLOGG
37	LEVEL CONTROL MANUF./MODEL NO.	_____ / ____
38	OVERFLOW CONTROL:	BY: VENDOR/KELLOGG
39	CONTROL VALVE: SIZE/MFR/MOD. NO.	_____ / ____ / ____
40	CONTROL VALVE MATERIALS: ▶	_____ / ____ ◀
41	LEVEL CONTROL MANUF./MODEL NO.	_____ / ____
42	INSTRUMENT AIR PRESSURE/AREA CLASSIFICATION	_____ / ____
43	INSTRUMENTS:	BY: VENDOR/KELLOGG
44	LEVEL SWITCHES/LEVEL GAUGE MFR/MOD. NO.	_____ / ____ / ____
45	PRESS. GAUGE/THERMOMETERS MFR/MOD. NO.	_____ / ____ / ____
46	NOTES: 1. LADDER/PLATFORM SPEC. _____	REMARKS:
47	2. PAINTING SPEC. _____	
48	3. INSULATION CLIPS SPEC. _____	
49	4. WIND/EARTHQUAKE SPEC. _____	
50	+VENDORS OPTION	

REVISIONS

NO.	DATE	ENGINEER	CHK/REVIEW	APPROVE	
6					
5					
4					
3					
2					
1					
0					

KELLOGG

MANAGING OFFICE | ENGINEERING OFFICE

EQUIPMENT DATA SHEET

CLIENT _____
LOCATION _____ JOB NO. _____
ITEM _____
ITEM NO. _____ SPEC. NO. _____
REQ'N. NO. _____ PAGE ___ OF ___

The vendor shall furnish as a minimum the equipment and components shown on the sketch and as called for on the data sheets.

Flow Balance

$$\boxed{1} + \boxed{2} + \boxed{3} = \boxed{4} + \boxed{5}$$

Sym ◊	Size	Rating	Facing	Dimensions		Weight	LBS/KG
a	3/4"	6000#	Threaded			Shipping	
b	1"	6000#	Threaded	A		Deaerator	
c	2"	150#	R.F.	B		Storage	
d		150#	R.F.	C		Operating	
e		150#	R.F.	D		Flooded	
Size by Vendor				E			

REVISIONS

NO.	DATE	ENGINEER	CHK/REVIEW	APPROVE	
6					
5					
4					
3					
2					
1					
0					

KELLOGG

MANAGING OFFICE | ENGINEERING OFFICE

EQUIPMENT DATA SHEET

CLIENT _____
LOCATION _____ JOB NO. _____
ITEM _____
ITEM NO. _____ SPEC. NO. _____
REQ'N. NO. _____ PAGE ___ OF ___

PROPOSAL DATA SHEET

1	NO. & TYPE VESSELS	
2	SIZE: DIAM. X STR. SIDE	
3	DESIGN PRESSURE/CONSTRUCTION	
4	LINING: TYPE & THICKNESS	
5	INTERNALS: TYPE AND MATERIAL	
6	UPPER DISTRIBUTOR	
7	REGENERANT DISTRIBUTOR	
8	INTERFACIAL COLLECTOR	
9	UNDERDRAIN	
10	MAIN PIPING : SIZE/MATERIAL/LINING	
11	CONTROL VALVES: TYPE	
12	MATERIAL: BODY/LINING	
13	RESIN: VOLUME PER VESSEL	
14	CATION/ANION	
15	MANUFACTURER & I.D. NUMBER	
16	RATING: KGR/FT3	
17	BED DEPTH/FREE BOARD	
18	ACID DOSAGE: LBS/FT3 & LBS/REGEN.	
19	CAUSTIC DOSAGE: LBS/FT3 & LBS/REGEN.	
20	GALLONS PER REGEN. : GROSS/NET	
21	FLOW: GPM/SQ.FT. AT MAX. FLOW	
22	PRESSURE DROP AT MAX. FLOW	
23	SKID MOUNTED AND PREASSEMBLED	
24	PIPING PER SPECIFICATION	
25	INSTR. PER SPECIFICATION	
26		
27		
28		
29		
30	EXCEPTIONS TO SPECIFICATION	
31		
32		
33		
34		
35		
36		
37		
38		
39		
40		

ALL BLANKS ON THIS FORM TO BE FILLED IN BY THE BIDDER AND THE FORM ATTACHED TO THE BIDDERS PROPOSAL. PROPOSALS SUBMITTED WITHOUT THIS COMPLETED FORM WILL BE CONSIDERED NON-RESPONSIVE.

781

REVISIONS	6					KELLOGG	MANAGING OFFICE	ENGINEERING OFFICE
	5							
	4						DATA SHEET	
	3					CLIENT		
	2					LOCATION		
	1					ITEM DEMINERALIZER		
	0					ITEM NO.	SPEC. NO.	
	NO	DATE	ENGINEER	CHK. REVIEW	APPROVE	REQ'N. NO.		PAGE OF

CATION OR ANION (TYPICAL)

— — — SKID LIMITS

CATION OR ANION UNIT TO BE PREASSEMBLED ON A STRUCTURAL STEEL SKID, WITH EQUIPMENT TUBED AND/OR WIRED TO THE SOLENOID VALVE BOX. SUBJECT TO SHIPPING CLEARANCES, MORE THAN ONE VESSEL CAN BE MOUNTED ON A COMMON SKID.

CONDUCTIVITY INSTRUMENT AND CELL USUALLY NOT FURNISHED FOR CATION UNITS. (REFER TO DATA SHEETS).

INTERCONNECTING HEADERS BY VENDOR, FOR FIELD INSTALLATION BY M.W. KELLOGG. WHERE ITEMS ARE MARKED (OPTIONAL), SEE DATA SHEETS.

PANEL MOUNTED INSTRUMENTS SHOWN OUTSIDE THE SKID LIMITS SHALL BE PROVIDED BY THE VENDOR.

REVISIONS	6					KELLOGG	MANAGING OFFICE	ENGINEERING OFFICE
	5							
	4						EQUIPMENT SKETCH	
	3					CLIENT		
	2					LOCATION	JOB NO.	
	1					ITEM		
	0					ITEM NO.	SPEC. NO.	
	NO.	DATE	ENGINEER	CHK/REVIEW	APPROVE	REQ'N. NO.		PAGE OF

AIR DRIERS (HEATLESS)

1 Service: _____ Indoor/Outdoor; English/Metric Units
2 Mfr.: _____ Model No.: _____ Qty.: _____
3 Design: ASME Code Section VIII, Div. 1 Latest Edition and all Mandatory Addendas.
4 Pressure _____ Temp. _____ Stamped Yes/No
5 Drier Inlet: Flow _____ Press. _____ Temp. _____ Moisture Content _____
6 DrierOutlet Dewpoint _____ ; @ Line Press.
7 Drier: Desiccant Type _____ Wt. per TWR. _____
8 Reg. Time Cycle ____ Min.; Purge Fl. ____ Guar. Fl. ____ ; Drying Time Cycle ____ Min.
9 Press. Drop Across Drier _____ Mat'l. of Const. _____ Corr. Allow ½
10 Oil Separator: Yes/No; Mfr. _____ Model No. _____ Qty. ____
11 Material of Construction _____
12 Prefilter: Mfr. _____ Model No. _____ Qty. ____
13 Mat'l. of Const. _____ △Clean _____ Micron Size ____
14 After Filter: Mfr. _____ Model No. _____ Qty. ____
15 Mat'l. of Const. _____ △Clean _____ Micron Size ____
16 △Across Entire Skid @ Max. Cap. (Allowed Max./Calc.) ____
17 Area Class: Class ____ Group ____ Div. ____ ; Volts ____ Phase ____ Hertz ____ Watts ____
18 Inst. & Controls: Pneu./Elect./Automatic/Other _____
19 Specifications _____
20 Accessories: Alarms,By-passes (for filters only), Control Panel, Diff. Press. Ind.,
21 Flow Ind., Ind. Lights, Moisture Ind., Piping, Pressure Gauges, Relief Valves,
22 Switching Valves, Temp. Ind., Timer, Transformer and Valves.
23 Notes: 1) Provide Dry Contacts (Isolated) to Transmit C.T.A. Signal to Purch. Ann.
24
25
26
27 The Vendor shall furnish as a minimum the equipment & components shown on this sheet.

Sym◇	Size	Rating	Facing
a			
b			
c			
d			

			Dimensions	Length	Width	Height	Weight	LBS/KG
							Shipping	
							Operating	

KELLOGG

				MANAGING OFFICE	ENGINEERING OFFICE

EQUIPMENT DATA SHEET

CLIENT _____
LOCATION _____ JOB NO. _____
ITEM _____
ITEM NO. _____ SPEC. NO. _____
REQ'N. NO. _____ PAGE ____ OF ____

NO	DATE	ENGINEER	CHK/REVIEW	APPROVE	

REVISIONS: 0,1,2,3,4,5,6

782

PROCESS DESIGN SECTION, CORPORATE ENGINEERING — MECHANICAL SCALE DATA SHEET

SERVICE	LOCATION
NO. REQUIRED	MANUFACTURER
DUTY	MODEL NO.
TYPE	

PROCESS CONDITIONS

CHARACTERISTICS OF MATERIAL

MATERIAL			
STATE OF MATERIAL			
ANGLE OF REPOSE			
TEMP. °F			
BULK DENSITY-LB./FT.³			
AMOUNT/BATCH			

TOTAL VOLUME OF MATERIAL	
AVERAGE DENSITY	
TOTAL WEIGHT OF MATERIAL	
ACCURACY	SENSITIVITY
ATMOSPHERE	

MECHANICAL DESIGN DATA

DESIGN CAPACITY NET WEIGHT	
WEIGHT OF CONTAINER EMPTY	
SIZE OF CONTAINER	
LOCATION OF DIAL WITH RESPECT TO SCALE (HEIGHT)	
LOCATION OF SUPPORTING LEVEL WITH RESPECT TO SCALE (HEIGHT)	
TOTAL SCALE CAPACITY	
MAXIMUM MOVEMENT WHEN FULLY LOADED	
DIAL GRADUATIONS (MINIMUM)	
ADJUSTABLE MARKERS REQUIRED	
TARE BEAM	CAPACITY BEAM
DUNNAGE	
DIAL DIAMETER	SCALE PLATFORM SIZE

REMARKS

(Left margin labels: REMARKS, APP'R'V, DATE, SUPRV, CHKD, REV BY, REV, DES SUPRV, CHECKED BY, DRAWN BY, INITIATOR)

JOB NO. _____ PLANT LOCATION _____
PROJECT NO. _____ REF. DWG. NO. _____
TITLE _____
POSITION NO. _____ SERIES _____ STEP NO. _____

SCALE
ISSUE DATE
BLDG. NO.
DRAWING NO.

E218B34

PROCESS DESIGN SECTION
CORPORATE ENGINEERING

ROTARY VALVE
DATA SHEET

OPERATING DATA

THROUGHPUT: _____ LBS/HR.
PARTICLE SIZE: _____
BULK DENSITY: _____ LBS./HR.
SOLIDS ARE: CRYSTALLINE ☐   STICKY OR GUMMY ☐   LIGHT OR FLUFFY ☐
SOLIDS: WET ☐   DRY ☐ _____ % MOISTURE
OPERATING PRESS: UPSTREAM _____ PSIG – DOWNSTREAM _____ PSIG
OPERATING TEMP: _____ °F
PRODUCT DESCRIPTION: _____

MECHANICAL DATA

MFGR: _____
SIZE & TYPE: _____
ROTOR TYPE: _____
VALVE TO HAVE OUTBOARD BEARING AND STUFFING BOX.

MATERIALS OF CONSTRUCTION

CASING: _____
ROTOR: _____
SHAFT: _____
PACKING: TYPE _____ SIZE _____ NO. OF RINGS _____
PACKING GLAND _____
GASKETS: _____

MOTOR DRIVE DATA

ITEM NO: _____ MTD. BY: _____
HP: _____ RPM: _____ FRAME: _____
MFG'R: _____
TYPE: _____ INSUL. _____
ENCLOSURE: CLASS I   GROUP D
VOLTS/PHASE/CYCLE _____ / _____ / _____
BEARINGS: _____ LUBE: _____
FULL LOAD AMPS: _____ S.F. _____
L.R. AMPS: _____

SPEED REDUCER: MFG'R. _____
                 TYPE: _____ RATIO _____

MISCELLANEOUS

TOTAL WEIGHT: _____
VENDOR DWG. NO: _____
VALVE SERIAL NO: _____
_____
_____
_____

JOB NO.	PLANT LOCATION		SCALE
PROJECT NO.	REF. DWG. NO.	ISSUE	
TITLE		DATE	BLDG. NO.
POSITION NO.	SERIES STEP NO.		

DRAWING NO.

REMARKS
APPRV
DATE
SUPRV CHKD BY REV

DES SUPRV. CHECKED BY DRAWN BY INITIATOR

E224B40

QUESTIONNAIRES OF EQUIPMENT SUPPLIERS

Equipment is supplied on the basis of information about the needs provided by the ultimate purchaser and user. Although the more information, within limits, the better, suppliers do require a certain minimum amount before they can make recommendations of equipment and price. Some kinds of equipment are sufficiently standardized to allow their specification by standard forms like those of Appendix B. The questionnaires of individual Suppliers sampled in Appendix C are mostly of specialized equipment that requires custom designing to a greater extent. This is a random selection and other suppliers of each type are available to provide service. Following is a listing of questionnaires contained in this Appendix C. The number appearing in italic is the page number on which the form appears.

STURTEVANT
MILL COMPANY

103 Clayton Street
Boston, MA 02122
617·825·6500
Cable EMERYSTONE
Telex 94·0677

Request for Information

To allow us to better assist you in solving dry processing problems,
please use this form when requesting information on Sturtevant equipment.

1. Material to be Processed: _____

2. Processing Method(s) Required (Number in order needed):

   a. Crushing _____   f. Mixing _____

   b. Grinding _____   g. Screening _____

   c. Air Separating _____   h. Conveying _____

   d. Micronizing _____   i. Elevating _____

   e. Blending _____   j. Other (specify) _____

3. Characteristics of Material being Processed:

   a. Specific Gravity _____   d. Moisture Content _____ %

   b. Hardness _____   e. Handling Hazards _____

   c. Feed Size _____   f. Temperature Limits _____°F. or _____°C.

4. Production Requirements:

   a. Product Size Required _____   c. Contamination Tolerance _____

   b. Capacity Required _____

5. If Air Separating is required:

   a. Amount of product
      entrained in feed _____ %   d. Is heating or cooling
                                              required in separation _____

   b. Grinding media pre-
      ceding separation _____   e. Product size
                                                    tolerance, if any _____

   c. Preferred load if
      in closed circuit _____

6. Any comments which would help our engineers evaluate your requirements:

Name _____ Title _____

Company _____ Address _____

City _____ State _____ Zip Code _____

786

WILLIAMS

Williams Patent Crusher & Pulverizer Company
2701 N. Broadway • St. Louis, Missouri 63102 • 314/621-3348

Thank you for your interest in Williams size reduction equipment and/or systems.
As a first step toward giving you a highly personalized answer to your need, we
would appreciate your supplying the following information.

Company Name_____

Address_____ Zip_____

Your Name_____ Title_____

Type of Feed_____ Nominal Size_____

Compressive Strength or Work Index_____

Abrasiveness (contains quartz, silica, etc.)_____

Moisture Content_____% Oil, Fat, etc. Content_____%

Temperature Limitations: Softens_____°F. Melts_____°F. Decomposes_____°F.

Chilling Permissible_____ Heating Permissible_____

Special Characteristics (volatile, toxic, hygroscopic, corrosive, etc.)_____

_____

Volume of Feed in Tons Per Hour, U.S. (Metric)_____ (_____)

Product Size Desired_____ Moisture Desired_____

Fines Desired (Min. - Max.)_____% Bulk Density Desired_____

Air Classification of Product Desired? Yes_____ No_____

Additional Comments on Product_____

_____

Thank you for your help. We will be back to you soon.

Form No. 943

SYSTEMS DATA

DUCON CONVEYING TECHNOLOGY
A DIVISION OF THE DUCON COMPANY INCORPORATED

HAPMAN Hapman Conveyor Co.
6002 E. Kilgore Road
Kalamazoo, Michigan 49003
(616) 343-1675
Telex: 224468

data sheet
(Fill out completely)

DATE _____

CUSTOMER: _____ REPRESENTATIVE: _____

_____

_____

PRODUCT CHARACTERISTICS

Name _____

Particle size _____ % minus _____ U.S. mesh   _____ % minus _____ U.S. mesh
_____ % minus _____ U.S. mesh   _____ % minus _____ U.S. mesh

	GIVEN	ASSUMED			GIVEN	ASSUMED
Bulk density lbs/cu. ft.			Hygroscopic			
Angle of repose			Corrosive			
% Silica			Moh's hardness number			
Particle shape			Temp of product °F			
Surface texture			Specific heat			
Change of state temp °F			Is breakage objectionable?			
Hazardous (explos., toxic, etc)			If so, what % permissible?			
Tendency to bridge						
Moisture content % free						

SYSTEM REQUIREMENTS

	1	2	3	4
Capacity - lbs/min (instantaneous/avg)				
Horizontal Distance - feet				
Vertical lift - feet				
45° Elbows				
90° Elbows				
Ambient temp at blower inlet °F				
Material of construction in contact with product				

787

DESCRIPTION (Use back for simple system sketch)

_____

_____

_____

_____

_____

GENERAL

Starters: furnished _____ ; not furnished _____
Available current _____ v _____ phase _____ Hz
Available water _____ gpm _____ psig _____ °F
Available air _____ scfm _____ psig
Available steam _____ #/hr @ _____ psig

Motor enclosure
Open drip proof _____
Totally enclosed _____
Explosion proof _____

840 FIRST AVENUE • KING OF PRUSSIA, PA. 19406 • PHONE (215) 337-3770 • TELEX 84-6325

CUSTOMER _____ DATE _____
ADDRESS _____ ZIP _____
ATTN: _____ TITLE _____ PHONE (___) _____

LOCATION OF INSTALLATION _____
( ) TUBULAR CONVEYOR
( ) BUCKET CONVEYOR
( ) OSCILLATING CONVEYOR
( ) OTHER _____

DESCRIPTION OF MATERIAL TO BE HANDLED

1. Material _____

_____

2. Particle Size (Mesh or Fraction of Inch) _____

_____ Max. _____ Min. _____

Proportions _____

3. Actual Weight per Cubic Foot _____

4. Percentage and Type of Liquid Present _____

_____

5. Temperature of Material at Conveyor Receiving

Point _____

6. Temperature Present at Conveyor Discharge

Point _____

7. Flowability: Very Free _____ Free _____

Sluggish _____

8. Abrasiveness: No _____ Mild _____ Very

9. Special Characteristics: Corrosive _____

Explosive _____ Light and Fluffy _____

Aerates and becomes Fluid _____ Packs under

Pressure _____

Describe any possible contamination problems

_____

_____

Pressure Zones _____

IMPORTANT: FURNISH SKETCH ON BACK OF THIS SHEET OR ON SEPARATE SHEET. Show plan, end elevation and/or side elevation properly indicated as such with all pertinent dimensions. Show your idea of preferred conveyor path together with possible alternates. Also indicate all clearances and obstructions to allow us *to select the most practical circuit should this differ from your sketches.*

SERVICE REQUIREMENTS

Required Capacity (in cubic feet/hour or min.)

_____

Operation: Continuous _____

Intermittent _____

Operating Period: Hours _____

Frequency _____

MOTOR CHARACTERISTICS

Voltage _____ AC/DC _____

Phase: _____ Cycles _____

( ) Totally Enclosed — Fan Cooled

( ) Explosion Proof: Class _____ Group _____

CONSTRUCTION SPECIFICATIONS

1. Casing — Mild Steel _____

#304 S.S. _____ #316 S.S. _____

2. Chain — Sealed Pins _____

Mild St'l. _____ #304 S.S. _____ #316 S.S. _____

Open Pin Construction _____

3. Flight Material — Factory Spec. _____

Other _____

_____

Miscellaneous _____

_____

SALES REPRESENTATIVE:

_____

Note: When sending in Sample, attach label showing Kind of Material, Company Name, Representative, and Date. Three to four cubic feet of material are required for complete testing.

OVER

Form H-100

MEYER
MACHINE COMPANY

P.O. BOX 5460, SAN ANTONIO, TEXAS 78201
512/736-1811

DESIGNERS AND MANUFACTURERS
OF CONVEYING AND PROCESSING EQUIPMENT

Gentlemen:

Please quote us on a SIMPLEX CONVEYING ELEVATOR to meet the specifications and approximate dimensions as indicated below and on the reverse side of this sheet.

PRODUCT TO BE HANDLED _____

APPROXIMATE WEIGHT OF PRODUCT PER CUBIC FOOT _____

DESIRED MAXIMUM CAPACITY, pounds per hour _____

IS PRODUCT CORROSIVE? _____ DUSTY? _____ FINE POWDER? _____ GRANULES? _____

STICKY? _____ ABRASIVE? _____ PIECES? _____ AVERAGE SIZE OF PIECES _____

TYPE OF BUCKETS PREFERRED: Fabricated Stainless Steel _____ Mild Steel _____ Plastic _____

Cast Aluminum Alloy _____ Other _____

IS DUST-TIGHT/WEATHER-TIGHT ENCLOSURE REQ'D? _____

END DISCHARGE ONLY _____ WITH SIDE DISCHARGES _____ NUMBER OF SIDE DISCHARGES _____

(Indicate on drawing (Fig. 3) on reverse side if discharges are to be Left Hand or Right Hand when viewed from intake end of SIMPLEX. Also indicate approximate location of discharges).

SIDE DISCHARGES TO BE MANUALLY CONTROLLED _____ or SOLENOID CONTROLLED for remote

operation _____ .

TYPE OF FEEDER/HOPPER PREFERRED: STANDARD INTAKE HOPPER only _____ BUILT-IN FEEDER,

less hopper (for feeding from bin) _____ VIBRA-FLEX FEEDER with LARGE HOPPER built separately from

SIMPLEX, (for manual feeding) _____ with ECCENTRIC DRIVE _____ with ELECTRO-MAGNETIC

DRIVE _____ Feed Trough and Hopper to be Stainless Steel _____ Mild Steel _____

or Galvanized _____ .

If head room is restricted, state ceiling height _____

Per _____

Title _____

Company _____

Address _____

Date _____

Phone No. _____

788

QUESTIONNAIRE DRYING SYSTEMS

BOWEN

The information below is required to enable us to prepare a design and quotation. All information given will be treated in strict confidence. We appreciate that some data may not be available or relevant. Please circle chosen alternates. Please return to:

BOWEN ENGINEERING INC., P.O. Box 898, Somerville, New Jersey 08876, U.S.A.
Telephone: (201) 725 3232   Telex: 4754087 (ΠΤ)

COMPANY

Company Name: ....
Address: ....
....
....
Telephone: ....
Telex: ....

Ref./Project No: ....
Personnel: ....
....
....
....
Plant Location: ....

MATERIAL/PROCESS

Name/Composition: ....
Chemical formulae: ....
Process: dry/cool/heat/agglomerate/react/absorb/congeal/calcine/ ....
Type of dryer envisaged: spray ....
Process gas flow: once through/partial recycle/closed cycle/self-inertized/inert/ ....
Heat source: direct/indirect: gas/LPG/oil/steam/electricity/HT oil. ....
Has material been dried before: yes/no. If so, how .... Temperatures ....

CAPACITY DATA

	Feed rate lb/h	at Feed conc. % solids	Evap. rate lb/h
For minimum evaporation rate :	....	....	....
For design evaporation rate :	....	....	....
For maximum evaporation rate:	....	....	....

Product rate: lb/h :   min ...., normal ...., max ...., design ....
Feed rate   :   lb/h :   min ...., max ....

FEED DATA

Type: solution/suspension/emulsion   .... Corrosive: yes/no
From: tank/filter   .... Toxic   : yes/no
Feed rheology (liquid): Newtonian/pseudoplastic/dilatant/Bingham plastic/thixotropic/rheopectic/viscoelastic.............
Feed rheology (solid): free flowing/friable/cohesive/sticky/paste/ ....
Does rheology change markedly with feed concentration? yes/no. If so, add notes overleaf.
Feed concentration: % solids: min ...., normal ...., max.............................
Moisture: water/other (see solvent data overleaf). Impurities in feed: ....
If feed is suspension, what concentration of solubles in liquid...
Does feed form stable foam? yes/no. Material of construction in contact with feed: ....
Feed temperature: ....°F   Viscosity:...................cp at ....°F   pH range:.........................
Density/bulk density : .... lb/ft³ at ....°F

Please turn over.

PRODUCT DATA

Moisture content: .... % normal, ... % design, ... % maximum.

Is product heat sensitive: yes/no. If yes, what maximum temperature for dry solids .... °F

Material of construction in contact with dry solid: ....

Required particle size: min......................... micron, av ....micron, max..............................micron .

Required bulk density range: ....to .... lb/ft³ . Required final discharge temperature:...................................... °F

Melting point: .... °F Specific heat: .... BTU/lb. °F Heat of crystallisation: .... BTU/lb.

Other special properties:..

Toxic: yes/no. Flammable: yes/no. Explosive: yes/no. Abrasive: yes/no. Hygroscopic: yes/no.

Thermoplastic: yes/no. If yes, at what temperature: .... °F

SOLVENT DATA

Name: .... Toxic: yes/no. Corrosive: yes/no.

Impurities: ....

Flammable: yes/no. If yes, explosive limits: .... Flash point ....

Boiling point: .... °F Latent heat of vaporisation:...BTU/lb.

Specific heat liquid .... BTU/lb. °F Specific heat vapour:...BTU/lb. °F.

Other data: ....

ANALYTICAL METHODS

Moisture content: ....

Other: ....

....

ENVIRONMENT/SAFETY

Permissable emmission in exhaust air: .... grn/ft³ Effluent water limits..

Maximum noise level: In plant .... dBA at 3 ft. Community .... dBA at .... ft.

If area classified hazardous, give division, group, etc.

Is dust flammable: yes/no. Ignition temperature, cloud .... °F layer .... °F at .... inch thick

Is dust explosive: yes/no. Dust class .... Max.explosive pressure .... Max.rate press. rise....................

LOCAL CONDITIONS

Plant location: indoors/outdoors. Existing building: yes/no. If yes, submit drawings.

Altitude: .... ft. above sea level. Max. wind velocity .... Earthquake: Richter ....

Ambient temperature: Minimum .... °F Average .... °F Maximum....................................... °F.

Range ambient conditions for design evaporation rate: Winter .... °F at .... %RH, Summer .... °F at .... %RH max.

Special conditions: high dust loading/freezing fog/ ....

UTILITIES

Steam pressure at plant: .... psig. Towns water: .... °F at .... psig. at grade.

Compressed air:... psig. Instrument air: .... psig. at .... °F dew point.

Electricity: Power ....V, ... ph, ... Hz; Control .... V AC/DC.

Fuel gas: Name ...., Gross calorific value .... BTU/scf. Pressure .... psig./inch WG.

Fuel oil: Grade.. viscosity ...., Gross calorific value................................... BTU/lb.

Cooling water: Supply .... °F Return .... °F max, Available pressure differential ....

Other: ....

REMARKS

GOSLIN-BIRMINGHAM, INC.
EVAPORATOR INFORMATION SHEET

COMPANY _____

NAME OF INDIVIDUAL _____

POSITION _____

MAILING ADDRESS _____

PLANT ADDRESS OR JOBSITE _____

FEED SOLUTION _____ PPH _____ % Dissolved Solids _____

Temperature _____ Specific Gravity _____ Specific Heat _____

Analysis _____

% Suspended Solids _____ Viscosity _____ pH _____

Temperature Limit _____ Thermal Conductivity _____

PRODUCT _____ % Dissolved _____ % Suspended Solids _____

Viscosity _____ at Temperature _____ Specific Gravity _____

Scaling? _____ Foamy? _____ Specific Heat _____

Thermal Conductivity _____

OTHER DATA Available Steam _____

Low Pressure _____ Psig _____ Temp. _____ Cost _____

High Pressure _____ Psig _____ Temp. _____ Cost _____

Cooling Water _____ High Temp. _____ Low Temp. _____

Power _____ AC _____ DC _____ Cost/KWH

_____ Volts _____ Hertz _____ Phase

Material of Construction

    Liquid _____

    Vapors _____

REMARKS _____

_____

_____

_____

_____

Signed .... Date ....

DRYER QUESTIONNAIRE

KRAUSSMAFFEI CORPORATION

COMPANY	KMC PROJECT NO.

CONTACT PERSON	KMC CONTACT PERSON

1. **PRODUCT:** formula, trade name

2. **DRYER CAPACITY:**
2.1 Wet product feed _____ lb/h @ _____% moisture
2.2 Dry prod.discharge _____ lb/h @ _____% moisture
2.3 Evaporated liquid _____ lb/h
2.4 Bone dry product _____ lb/h

3. **WET PRODUCT FEED**
3.1 Originates from: filter centrifuge other _____
3.2 Feed: continuous batch other _____
3.3 Volume/batch _____ gal.
3.4 Batch cycle _____ min.
3.5 Consistency: liquid sticky pasty friable thixotropic other _____
3.6 What conveyors worked satisfactorily?
3.7 Particle size analysis

3.8 Wet product temperature _____ °F
3.9 Composition of product _____ % _____
moisture (vapor pressure _____ % _____
curves?) _____ % _____
3.10 Moisture determination:
- Drying chamber _____ °F
_____ min.
constant weight _____
under vacuum _____ in Hg
- other _____
3.11 Wet bulk density (loose) _____ lbs/ft³
3.12 Dry bulk density (loose) _____ lbs/ft³
3.13 True product bulk density _____ lbs/ft³
way of measuring the bulk density?
3.14 Melting Point _____ °F
3.15 Spec. heat wet product _____ BTU/lb
3.16 Spec. heat solids _____ BTU/lb
3.17 Spec. heat moisture _____ BTU/lb
3.18 ph value _____
3.19 Max. admissible wet product temp. _____ °F
3.20 Dryer atmosphere: air, inert, vacuum

4. **DRY PRODUCT:**
4.1 Requested form of dry product
4.2 Admissible dry product temp. _____ °F
4.3 Dry product to be cooled ____ yes ____ no to ____ °F
4.4 Is there some isothermal absorption known of the dry product? (Please enclose) _____ yes _____ no
4.5 Electrostatic charging _____ yes _____ no
4.6 Risk of oxidation _____ yes _____ no
4.7 Is the product hygroscopic? _____ yes _____ no
4.8 Melting point _____ °F
4.9 Conveyability?

5. Do you dry the product in your plant now? What dryer type? With what results?

6. If moisture is a solvent, is recovery required?

7. Which materials of construction should be used or must not be used?
For contact w/wet product _____
For contact w/dry product _____
For contact w/fresh gas _____
For contact w/exhaust gas _____

8. **SPECIAL REFERENCES, REQUESTS, SUGGESTIONS**
PLEASE ENCLOSE SAFETY DATA SHEETS RELATING TO HAZARDOUS PROPERTIES
(TOXIC, IGNITABLE, INFLAMMABLE, ETC.)

9. **AMBIENT AIR CONDITIONS**
9.1 Temperature ____ °F
9.2 Humidity ____% or ____ Lbs. H₂O/lb. Dry Air

10. **UTILITIES**
10.1 Electrical characteristics
_____ V, _____ PH, _____ Cycles
10.2 Heating Media:
Steam _____ @ _____ PSIG
OIL _____ @ _____ BTU/lb
GAS _____ @ _____ BTU/ft³

WOOTEN-WICHITA

SELAS

DEHYDRATOR DATA SHEET

Date_____

Selas Corporation of America
Dresher, Pa.
Attn: General Industry Division

Gentlemen:

I am interested in a Selas Dehydrator to meet the following specifications. Please send proposal, with the understanding that I am under no obligation:

GAS AS SUPPLIED TO DEHYDRATOR FOR DRYING
Type of gas:. . . . .
Volume at standard atmospheric conditions. . . . . cfm or at working pressure:. . . . . cfm
Gas temperature entering Dehydrator:. . . . . °F
Working pressure:. . . . . psig
Moisture content: saturated at entering temperature ☐ or what % of saturation. . . . .
Specific gravity:. . . . .
Specific heat:. . . . .

GAS LEAVING DEHYDRATOR
Final moisture content: dewpoint. . . . . °F
or. . . . . grains per cubic foot at. . . . . psig
Final temperature . . . . °F

DEHYDRATOR OPERATING SCHEDULE
Continuous ☐, or, if intermittent, _____ hours on, _____ hours off.

TYPE OF OPERATION
☐ Manual ☐ Semi-automatic ☐ Fully Automatic

TYPE OF ELECTRICAL CONSTRUCTION
☐ Standard open ☐ Weatherproof ☐ Explosion proof
☐ Other . . . .

UTILITIES AVAILABLE AT OPERATING POINT
Electricity: Control ☐ AC ☐ DC _____ Volts _____ Phase _____ Cycle
Power ☐ AC ☐ DC _____ Volts _____ Phase _____ Cycle
Steam Pressure: . . . . psig
Cooling water temperature: Summer _____ °F, Winter _____ °F.
Cooling water pressure: _____ psig, minimum.
Preferred heat source for desiccant reactivation . . . .

MECHANICAL CONSTRUCTION
☐ ASME Code ☐ Non-Code ☐ Other. . . . .

REMARKS: _____
_____
_____
_____

FIRM NAME _____
PLANT ADDRESS: _____
SUBMITTED BY: _____
TITLE: _____

M 318

ROTARY EQUIPMENT INQUIRY

Date . . . .

TO: VULCAN IRON WORKS, INC.
Miners National Bank Bldg., Rm. 1050
Wilkes-Barre, Pennsylvania 18701

We are interested in equipment for the following process:
drying . . . . . . , cooling . . . . . . , calcining . . . . . . (other) . . . .

Our interest is related to our:
preliminary design . . . . . .   economic evaluation . . . .
budget estimate . . . . .   final analysis & purchasing . . . .

Process data available includes:
type of material . . . .
material wt./cu. ft.;   wet . . . . ,   dry . . . .
material specific heat . . . .
material particle size . . . . (screen analysis desirable)
capacity—feed rate . . . . or discharge rate . . . .
moisture content, initial . . . . % and final . . . . %.
material temperature, initial . . . . and final . . . .
maximum temperature of material without injury . . . .
duty cycle . . . . hours per day and . . . . days per week.
final product temperature desired . . . .
type of fuel to be used:
Oil @ . . . . . . btu/gal., ... psig and . . . . . . SSU.
Gas @ . . . . . . btu/cu. ft., and . . . . . . psig.
Other . . . .

Burner is to be automatically . . . . or manually . . . . controlled.
Material can . . . . . . , cannot . . . . . . be processed in contact with gases of combustion.
The . . . . sticky, ... abrasive, ... corrosive nature of the material requires
special consideration.

Motors: . . . . TEFC . . . . Open . . . . Phase . . . . Cycle . . . . Volts
Installation is to be indoor, ... outdoor . . . .
Elevation of installation, ... feet above sea level.
Dust collection equipment to be included . . . . (yes or no).
Exhaust fan to be included . . . . (yes or no).

Your response on or before . . . . is desired.
(Date)

Please reply to: (Company) . . . .
(Address) . . . .
(Attention) . . . .
(Telephone) . . . .

GLITSCH, INC.

PLANT & HOME OFFICE LOCATION: 4900 SINGLETON BLVD. ● DALLAS, TEXAS ● 214/631-3841 ● TELEX 73-329

MIST ELIMINATION AND LIQUID DROPLET COALESCING EQUIPMENT APPLICATION DATA

General Information:
Operating: Pressure_____ Temperature _____
Allowable Pressure drop_____
Vapor (Gas) Phase:
Composition _____ wt. % or mol. %
_____ (state which)
_____
_____
Rate _____
Liquid Phase:
Composition _____ wt. % or mol. %
_____ (state which)
_____
_____
Rate _____
Viscosity _____ @ operating temp.
Droplet size range _____
Source of droplets (condensation, spray, etc.)_____

_____
Does liquid present a fouling problem when collected?
Yes ☐   No ☐
If yes, what type_____
Please describe any problems encountered_____

_____
Does the vapor or liquid phase have any insoluble solids in
it?   Yes☐   No ☐ If yes, describe their nature.

_____
Does the liquid phase have any dissolved solids in it?
Yes ☐   No ☐ If yes, describe their nature._____

_____
If the potential application involves a number of units, please
state the anticipated annual requirement._____

MIST ELIMINATORS
Is the mist eliminator to go into an existing vessel?
Yes ☐   No ☐
If yes, please provide a detailed sketch or blueprint of the
vessel to be used._____
Do you wish to have Glitsch quote on a suitable vessel?
Yes ☐   No ☐
LIQUID DROPLET COALESCERS
Note: The coalescers are generally sold only as a complete
unit with vessel.
SPACE LIMITATION
Are there any physical limitations due to vessel size?
Yes ☐   No ☐   If yes, please describe _____

_____
SUITABLE MATERIALS OF CONSTRUCTION
(See list below.)
Shell:_____ ●
Mist eliminator and/or coalescer_____ ●
Support grids _____ ●

304 Stainless	Inconel	Copper
316 Stainless	Carpenter 20	Carbon Steel
317 Stainless	Incoloy	Bethanized Steel
430 Stainless	Hastelloy C	Kynar ®
434A Stainless	Titanium	Polypropylene
Monel	Tantalum	Teflon ®
Nickel	Aluminum	
Other (specify)_____		

*A corrosion allowance is acceptable for the shell and support grids.
Other wetted parts should have the ability to withstand corrosion.

Inquiry data sheet

Raymond® Jet-Stream™ Classifiers

C-E Raymond's experience in the classification of powdered materials and the success of the *Jet-Stream*™ classifier in providing consistently sharp cut-points at full production capacities can be put to work for you to help provide the kind of quality product you demand. For a no-cost evaluation of your application, simply remove this sheet, answer the questions below, fold and mail. If you need assistance, call us at [312] 236-4044.

(please print)

Your name _____ Company _____

Address _____ City _____ State _____ Zip _____

Telephone (_____) _____ Best time to call: _____ am pm

Material to be classified: _____ Bulk density (lbs/cu ft) _____

Specific gravity _____ Feed temperature (°F) _____

Moisture in feed (% by weight) _____ Feed capacity (lbs/hr) _____

Elevation above sea level (ft) _____ .

Fineness Requirements

Micron Size	Cumulative percent of product smaller than micron size shown		
	Feed to Classifier	Fine Product	Coarse Product

Method of analysis (*Ro-Tap*® sieve shaker, *SediGraph*® particle size analyzer, or other equipment)*

_____

_____

Electric power available: Phase _____ Hz _____ Volts _____

Type of final dust collection equipment _____

Special materials of construction required _____

_____

_____

Remarks _____

_____

Krebs Cyclone problem questionnaire

Company		
Address		
City	State	Zip
Your name		
Telephone	Date	

General description of the cyclone application:

_____

_____

_____

(Please complete flow diagram below.)

Feed slurry characteristics

	lbs/hour		Specific Gravity
SOLIDS			
LIQUID	lbs/hour		Specific Gravity
SLURRY	lbs/hour		Specific Gravity
Liquid Viscosity, CPS		pH	Temp. (°F,°C)
System Pressure, psi			
Flowrate (USGPM)			
Other feed information (corrosive, abrasive, etc.)			

Feed Size Analysis

Mesh/Micron/mm	Ind. Wt.%	Cum. Wt.%

Overflow slurry characteristics (fine fraction)

* Desired mesh of separation
• Desired weight percent solids

Underflow slurry characteristics (coarse fraction)

Desired weight percent solids

Special requirements

_____

_____

_____

Flow diagram

FEED FROM:
- ☐ Evaporator
- ☐ Crystallizer
- ☐ Reaction Vessel
- ☐ Leach Agitator
- ☐ Other

CYCLONE

PUMP

OVERFLOW TO:
- ☐ Thickener (Settler)
- ☐ Centrifuge
- ☐ Filter
- ☐ Evaporator
- ☐ Screen
- ☐ Other

UNDERFLOW TO:
- ☐ Centrifuge
- ☐ Filter
- ☐ Classifier
- ☐ Screen
- ☐ Other
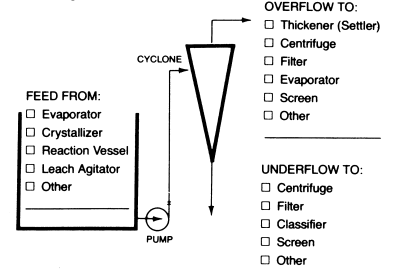
*Mesh of separation—Particle size that equals 1-3% plus by weight of overflow solids.

D. R. SPERRY & CO.
112 N. Grant Street
North Aurora, Illinois 60542

Date_____

Company _____

Address _____

Telephone No._____

Name of Individual Reporting _____

Title _____

Type of Operation (Chemical, Tannery, Brewery, etc. _____
_____Location _____
_____

(Please answer as many questions as possible)

Description of Material to be Filtered _____

Liquid _____

Solids _____

Specific Gravity of Slurry_____@_____°F

Emulsion_____? Solution_____?

Viscosity_____ _____ pH _____
                          (Units)

Avg. Particle Size of Solids _____

Concentration of Solids _____(ppm, lbs., %, etc.)

Physical Nature of Solids _____
                         (Sticky, granular, flocculent, etc.)

Specific Gravity of Solids_____gms/cc

Chemical Composition of Solids _____
_____

Nature of Filtrate_____
                  (Water, alcohol, varnish, mixture, etc.)

Specific Gravity of Filtrate_____gms/cc @_____°F

Vapor Pressure of Filtrate _____mmHg

Dissolved Salts _____

Solubility: @ 32°F _____ Units _____

         @ 68°F _____ Units_____

         @   °F _____ Units

Conditions and Recommendations

General Comments _____

Filtration Temperature_____°F Max. Permissible_____°F.

Min. Permissible_____°F.

Size of Batch _____gals. _____

Closed or Open Discharge Desired _____

Filtration Pressure _____psig

Filter Cycle Desired _____hrs.

Is Product_____Cake_____Filtrate_____Both_____

Cake Washing Necessary (Yes, No) _____ Name of Wash Liquid _____

Temperature of Wash Liquid_____°F.

Desirable Dryness of Cake: % Solids_____

Physical Condition of Cake _____
                           (pastry, sticky, dry, cracks)

Thickness of Cake_____in.

Quality of Filtrate - Desire or Allowed _____Brilliant _____Clear_____

                    Turbid _____Decolorized _____

If Turbid - Max. Allowable particle size of solids _____microns

If Filtrate is the Product

Filter aid to be used   Yes _____   No _____

If Yes: Precoat_____ Quantity _____

        Body Feed_____ % _____

        Both_____

Type, Brand, Grade _____%_____

Activated Carbon
or Bleaching Earth used   Yes _____   No _____%_____
or
Flocculation Agent_____Type_____Brand_____%_____

Recommended Materials of Construction_____
_____

Materials of Construction not Permitted _____
_____

Filter Media: Cloth _____   Paper _____

               Type _____   Grade _____

Filter Area _____ft.²

Filter Cake Volume _____ft.³

Laboratory Filter Tests

Filter Type _____

Area of Filter _____

Cake Volume of Filter_____

Media _____

Test Conditions _____

RESULTS _____
_____

793

BIRD Application Data Sheet
SOLIDS/LIQUIDS SEPARATION

PRODUCT DATA

Company _____

Address _____

City _____ State _____

Plant address _____

City _____ State _____

Project References _____

Bid date _____

Completion date _____

Project Status: □ R&D Laboratory
     □ Pilot Plant
     □ Semi-works
     □ In production

Customer Contacts

R&D _____

Engineering _____

Process _____

Purchasing _____

PROCESS DATA

Present problems _____

_____

Present results _____

_____

Feed

% Susp. solids (ss) _____

Sp. gr. ____ Viscosity ____ (cp) at ____ (°F)

Process

Temp. _____ (°F) Pressure _____ (PSIG)

Rate _____ (GPM) _____ (lbs/hr ss)

Valuable Component(s) _____

BOD or COD (for waste) _____

Type (origin) of waste _____

Solids

Composition _____

_____

□ Slimy   □ Soft   □ Crystalline

□ Fibrous   □ Abrasive   □ Amorphous

Size Distribution

_____ Sieve ____ % On ____ Cumul. %

+ _____ M _____ _____

+ _____ M _____ _____

+ _____ M _____ _____

− _____ M _____ _____

Sp. gr. _____ Shape _____

Ash content _____

Grease content _____

Permissable Flocculants _____

Bulk density _____

Mother Liquor

Composition _____

_____

Dissolved: Solids ____ % Impurities ____ %

Sp. gr. _____ at _____ (°F) pH _____

[continued next page]

PROCESSING REQUIREMENTS

Max. liquid content in solids _____

Max. impurities in solids _____

Max. ss in clarified ML _____

Material of const. _____

Vaportight/pressure const. _____

Wash separation from ML _____

Wash Requirements

Temp. _____ °F   □ Spray □ Drip pipe

□ Countercurrent □ Other _____

_____

Composition _____

Ratio _____

Rate _____ lbs/hr. wet cake

Disposition of wash _____

_____

Disposition of cake product _____

Disposition of Mother Liquor (ML) _____

_____

Testing Information

□ Large scale   □ Preliminary   □ Field

Equipment preference _____

Size of sample available _____

Precautions necessary _____

_____

To be witnessed: □ Yes □ No

By: _____

Disposal: of testing residue _____

_____

of test samples _____

FLOW SHEET

Comments _____

_____

_____

ROBATEL INC.

Centrifuge
Application Information

CENTRIFUGE APPLICATION
INFORMATION
PAGE 2

795

1. Company_____

2. Address_____

3. Submitted by_____Telephone_____Date_____

. . . .

A. PROCESS REQUIREMENTS

4. Name of Product_____

5. Production rate desired_____lbs/hr., bone dry basis, or other_____

6. Purpose (circle those which apply): recover solids, dewater solids, wash solids, classify solids, recover liquor, clarify liquor, separate 2 liquids, other_____

B. MATERIAL TO BE CENTRIFUGED

7. Name of solids in the feed_____Amount of solids_____% by wt.

Amount of solids_____% by vol.

8. Feed. Temp____°F min,____°F max,____°F normal. Pressure_____psig. Viscosity_____Cps at_____°F. Bulk density_____lbs/cu ft. pH_____ Solids variation by wt_____% max,_____% min.

9. Is feed produced continuously or by batch. For_____hrs/24 hrs.

10. Solids characteristics (circle those which apply)

explosive	amorphous	fragile	mineral	granular
inflammable	colloidal	free draining	natural	hygroscopic
toxic	crystalline	slow draining	synthetic	slimy
abrasive	fibrous	gelatinous	organic	

Other_____

11. Solid particle size distribution. Apparatus used: Tyler, other____Tested wet,dry.
retained on___mesh___% by wt.   retained on___mesh___% by wt.
"   ____ " ____   "   ____ " ____ "
"   ____ " ____   "   ____ " ____ "
"   ____ " ____   passing   ____ " ____ "

12. Solids specific gravity. Real_____Apparent_____

13. Liquor in feed Name % by vol. Vic. (Cps) Sp. gr. pH

_____ _____ _____ _____ _____

_____ _____ _____ _____ _____

14. Liquor characteristics (circle those which apply): explosive, inflammable, toxic, foamy, heat sensitive, dermal sensitive, corrosive, other_____

C. OPERATING CONDITIONS

15. Feed Rate_____gpm min,_____gpm max_____gpm normal.

16. Solids discharge requirements___lbs/hr., bone dry basis, Residual moisture by wt_____% min,_____% max,_____% normal, how determined_____Bulk density_____lbs/cu ft. Allowable crystal breakage_____%

17. Liquor discharge requirements_____gpm. Allowable solids_____% by wt.

18. Is washing of solids required_____Name of wash liquor_____ Allowable wash temp____to____°F. Amount____lbs wash liquor/lb solids.

19. Must wash liquor be kept separate from mother liquor_____

20. Are additives permitted_____type and amount_____

21. For liquid-liquid separation_____% of liquid (name)_____ is allowable in liquid (name)____Density____% solids in either phase_____

22. Type of operation (circle one): Batch manual, batch automatic, continuous.

23. Operating requirements (circle those which apply): vapor tight, venting, inert atmosphere, pressurized. Other_____

D. CENTRIFUGE MACHINE SPECIFICATIONS & MISC.

24. Materials of construction for parts in contact with process material_____ _____

25. Motor enclosure (circle one): drip proof, TEFC, explosion proof, other_____

26. Available power: 1 phase,____volts____hertz____
3 phase,____volts____hertz____

27. What handling precautions are necessary_____ _____

28. Is product now being separated_____Machine type_____ Diameter & length of bowl or basket____x____" Cake Thickness_____ Bowl Capacity per cycle in lbs____or Feed Rate in lbs/hr or GPM____ RPM Feed____; RPM Spin____; RPM Discharge____; Feed Time____; Spin Time____; Wash Time____; Spin Time____ Discharge Time____; Automatic, Semi-Automatic, Manual (circle one) What problems exist (circle those which apply): erosion, corrosion, capacity, efficiency, blinding, crystal breakage, cake moisture, other_____

29. Attach Flow or Process Diagram.

))PAUL O. ABBE ⅛((

QUESTIONNAIRE FOR MIXING OR BLENDING EQUIPMENT

In order to help our Engineering staff recommend the correct type and size mixer to satisy your individual needs, it is essential that you supply us with as much information as possible. The answers to the questions listed here will greatly assist us in making a prompt, intelligent reply to your inquiry. All information received will be held in strict confidence.

Company_____ Department _____

Address_____ Location of Plant_____

Inquiry initiated by_____ Title_____ Date_____

1. Name (if possible) material to be mixed or give names of similar well-know materials - also bulk density _____

_____

2. Is this material currently being mixed by you?_____ If so, what type and size mixer is being used and

what HP is required?_____

3. Will the material be mixed in dry, liquid or paste form? _____

4. Should this operation be batch or continuous?_____

5. What size batch do you wish to mix at one time, or how much production is required per hour, or per day of_____

hours?_____

6. What is the approximate weight per cu. ft. or gallon of the combined ingredients?_____

_____

7. Describe the consistency or viscosity of the material _____

8. Is the material abrasive? _____

9. Will it be necessary to heat or cool the material during the mixing process?_____

_____ If so, what temperature is required?_____

10. If steam heat is to be used, what pressure will be used in the Jacket?_____

11. Is the mixing to be done under pressure or vacuum? If so, to what extent?_____

_____

12. Is special dust tight construction required? _____

13. What clearance is desired under the discharge?_____

14. Should parts coming in contact with your material be made of special materials such as stainless steel, bronze, aluminum,

Monel, etc?_____ If so, what material is preferred?_____

_____

15. Should motor be standard open, totally enclosed or explosion proof?_____

Give voltage, phase, and cycles of your electric current _____

16. Outline any specific problems which may be involved in mixing this material and let us have any other information which

you feel would be helpful to us in providing the best recommendations _____

_____

_____

_____

796

bepex corporation

MIXING TEST INQUIRY DATA

Name: _____ Title: _____

Company: _____ Division: _____

Street: _____

City: _____ State: _____ Zip: _____ Telephone: (___) ___ - _____

Name of Material: _____ Amount: _____ Value: _____

Shipped Prepaid from: _____ Via: _____ Date: _____
                      (Name of Company)

Sample of Finished Product being sent: Yes: _____ No: _____ Via: _____ Date: _____

Return Tested Material to: _____ Attn: _____
                           (Name of Company)

Address: _____ Amount: _____

Other Disposition Instructions: _____

_____

_____

TECHNICAL DATA

Statement of Mixing Application (Include Proportions of Ingredients): _____

_____

_____

_____

_____

_____

_____

_____

_____

_____

Blending or Dispersion Required: _____

Capacity Per Hour Wanted — Min. and Max.: _____

Caution If Explosive, Inflammable, Poisonous, Noxious: _____

Characteristics Unusual as Hygroscopic, Volatile, Corrosive: _____

Temperature Limitations: Softens: _____ Melts: _____ Decomposes: _____

Chilling Permissible: _____ Heating Permissible: _____

Normal Moisture Content: _____ %. Oil, Fat, Etc., Content: _____ %

Drying Permissible to: _____ %. Addition of Water Permissible to: _____ %

Abrasive As Containing Silica, Quartz, etc.: _____

Bulk Density: _____ lbs./cu. ft.; Product: _____ ; Ingredients: _____

Method of Packing and Preserving Perishable Materials: _____

Solubility, and Fluids Recommended for Cleaning Equipment: _____

Power Available: Volts: _____ Phase: _____ Cycles: _____

Information Request Form

MAIL TO ONE OF THE ADDRESSES SHOWN BELOW

For Internal use:

P.P. _____

date _____

I would like a preliminary estimate of the cost and performance of Prism® separators for the application described below.

Note: If more than one stream is to be considered, please machine copy this form and complete the information requested for each stream.

1. Feed stream data
   a. Source _____
   b. Temperature _____ c. Pressure _____

	Maximum _____
d. Flowrate	Expected _____
	Minimum _____

Component	Vol. %	Component	Vol. %

   e. Feed gas composition

2. Desired Results:

	Recovery	Purity	Pressure
permeate			
non-permeate			

3. If a tradeoff between purity and recovery is necessary, which is more important?
   ☐ Purity
   ☐ Recovery

4. Use/Special Requirements for the non-permeate gas
   _____
   _____

NAME: _____
TITLE: _____
COMPANY: _____
ADDRESS: _____
CITY: _____ STATE: _____ ZIP: _____
COUNTRY: _____
TELEPHONE: ( ) _____
TELEX: _____
PLANT LOCATION: _____

FRITZ W. GLITSCH & SONS, INC.

P. O. Box 6227 • Dallas, Texas 75222

D I S T I L L A T I O N
Process Design Data Sheet

Item No. or Service				
Tower diameter, I.D.				
Tray spacing, inches				
Total trays in section				
Max. △ P, mm Hg				
Conditions at Tray No.				
Vapor to tray, °F				
Pressure, ...				
Compressibility				
*Density, lb./cu. ft.				
*Rate, lb./hr.				
cu. ft./sec. (cfs)				
cfs $\sqrt{D_V/(D_L-D_V)}$				
Liquid from tray, °F				
Surface tension				
Viscosity, cp				
*Density, lb./cu. ft.				
*Rate, lb./hr.				
GPM hot liquid				

Foaming tendency . . . . None _____ Moderate _____ High _____ Severe _____

*These values are required in this form for direct computer input.

NOTES:

1. This form may be used for several sections of trays in one tower, for several towers, or for various loading cases. Use additional sheets if necessary.
2. Is maximum capacity at constant vapor-liquid ratio desired? _____
3. Minimum rate as % of design rate: _____ %
4. Allowable downcomer velocity (if specified): _____ ft/sec
5. Number of flow paths or passes: _____ FWG Choice; _____
   Bottom tray downcomer: Total draw _____ ; Other _____
6. Trays numbered: top to bottom _____ ; bottom to top _____
7. Enclose tray and tower drawings for existing columns.
8. Manhole size, I.D., _____ inches.
9. Manways removable: top _____ ; bottom _____ ; top & bottom _____
10. Corrosion allowance: c.s. _____ ; other _____
11. Adjustable weirs required: yes _____ no _____
12. Packing material if required _____ ; not required _____
13. Tray material and thickness _____
14. Valve material _____
15. Ultimate user _____
16. Plant location _____
17. Other _____

Form No. PE-8

1. NATURE OF THE OPERATION

    .

_____

2. PHASE TO EXTRACT

    . Nature of diluent
    . Nature of solution to extract
    . Concentration in solution
    . Density
    . Output

_____

3. SOLVENT

    . Nature of solvent
    . Density
    . Output

_____

4. REQUIRED CHARACTERISTICS OF EXTRACT IMPOVERISHED IN SOLUTION

    . Concentration in solution
    . Approximate density

_____

5. REQUIRED CHARACTERISTICS OF EXTRACT ENRICHED IN SOLUTION

    . Concentration in solution
    . Approximate density

_____

6. NUMBER OF THEORETIC STAGES CORRESPONDING TO THE REQUIRED EXTRACTION AMOUNT

    (if possible, enclose a diagram of balance or the maximum information concerning the miscibility of the solvent and of the diluent).

_____

7. OPTIMUM TEMPERATURE OF EXTRACTION

_____

8. SOLIDS IN SUSPENSION

    Does one of the 2 phases comprise any solid in suspension before extraction?

    Which one?

798

Are these particles soluble in the other phase?

Can these particles be eliminated before introduction into the extractor?

. by filtration

. by centrifugal decantation

If particles can be eliminated by centrifugal decantation state:

. time of decantation

. Decanter bowl diameter

. Speed of rotation

With the two initial phases having no particles in suspension, do any precipitates appear during the process of extraction? In this case, after centrifugation are these precipitates situated:

. within one of the phases

. on the surface of the light phase

. at the bottom of the heavy phase

. in the zone of separation between the 2 phases

_____

9. SPECIAL CHARACTERISTICS

    Does an emulsion appear when the two phases are vigorously stirred?

    In case of emulsion:

    . If the phases separate themselves by static decantation state:

    - time required

    . If the phases separate themselves by centrifugal decantation state:

    - time required

    - decanter bowl diameter

    - speed of rotation

After decantation is the surface of separation between the 2 phases very distinct?

Does one of the 2 phases stay cloudy?

Which one?

_____

10. DIVERSE INFORMATION

    Materials of construction

    Electricity supply available

    Explosion and flameproofing requirements

    Type of supporting base or structure

_____

SWENSON®CRYSTALLIZER CHECKLIST
CHECKLIST OF DATA REQUESTED ON CRYSTALLIZER INQUIRIES
Fill in or attach as much information as is available so the most economic design can be prepared.

1. Product being crystallized _____ Production Rate _____

2. Liquid Properties   Feed   Mother Liquor   Purge

    Rate

    Temperature

    Composition _____

    Density

    Viscosity

    K (thermal conductivity)

    Cp (specific heat)

    Boiling point elevation

3. Evaporation Rate _____

    For organic vapors only give latent heat of evaporation/specific volume/vapor viscosity _____

4. Solubility of Solute in solvent at various temperatures (solubility curve) or phase diagram if several solutes are present.

5. Product   Heat of Crystallization   Specific Gravity   Heat of Reaction if Reaction in Crystallizer Produces Crystals   Specific Heat

6. Crystal shape if known _____

7. Product size required _____

8. Suitable materials of construction for operating temperature range:

    Bodies _____ Tubes _____ Pumps _____ Vacuum Equipment _____

9. Type of seals required in agitators or pumps and their materials of construction _____

10. Gasket material required if known _____

11. Utilities Available   Steam Pressure   Cooling Water Temperature   Current Characteristics

12. Describe flowsheet required or used and whether one or several bodies are required (or the economic factors which are to be used in determining the number of stages or effects. These factors include steam cost, water cost, electricity cost, amortization period, etc.)

13. Any other data which the customer feels would be of help such as heat transfer data; present conditions under which the product is produced and type of equipment used; present crystal size; and effects of agitation, additives and/or temperature on crystal size, shape, recovery, or purity.

14. If the solution is organic and test work is desired, give the flash point of the solution _____

VULCAN IRON WORKS, INC.
1050 UNITED PENN BANK BUILDING
WILKES-BARRE, PENNSYLVANIA 18701
(717) 822-2161   TELEX: 831-831

Questionnaire
INQUIRY DATA

A.   PROCESS REQUIREMENTS   (PLEASE FURNISH ALL RELATED INFORMATION THAT IS READILY AVAILABLE)

B.   INCINERATION (THERMAL OXIDATION) WITH OR WITHOUT HEAT RECOVERY. (PLEASE FURNISH ALL INFORMATION THAT IS READILY AVAILABLE.)
    TYPE OF PLANT AND PROCESS _____

WASTES

SOLIDS _____ QUANTITY LBS./HR.
SOLIDS _____ SOLIDS WASTE TYPE
SOLIDS _____ HEAT VALUE BTU/LB
SOLIDS _____ ASH CONTENT %
SOLIDS _____ MOISTURE CONTENT %
SOLIDS _____ QUANTITY LBS./HR.
SLUDGES _____ TYPE OF SLUDGE
SLUDGES _____ ASH CONTENT %
SLUDGES _____ WATER CONTENT %
SLUDGES _____ COMBUSTIBLES CONTENT %
SLUDGES _____ HEAT CONTENT OF COMBUSTIBLES CONTENT %
SLUDGES _____ HEAT CONTENT OF COMBUSTIBLES BTU/HR.
LIQUIDS _____ QUANTITY GAL./HR.
LIQUIDS _____ WASTE LIQUID TYPE
LIQUIDS _____ HEAT VALUE BTU/GAL
LIQUIDS _____ VISCOSITY
LIQUIDS _____ SPECIFIC GRAVITY
FUMES _____ QUANTITY SCFM
FUMES _____ TEMP.
FUMES _____ EFFLUENT TYPE
FUMES _____ EFFLUENT QUANTITY

TYPE OF HEAT RECOVERY THAT CAN BE UTILIZED
STEAM GENERATION:
_____ LBS./HR. REQUIRED
_____ PSI OPERATING PRESSURE
_____ °F. OPERATING TEMP.

THERMAL LIQUID
_____ HEAT LOAD BTU/HR.
_____ HEATING STATIONS
_____ °F. TEMP. AT STATIONS

FUME PRE-HEATER
(GAS TO GAS HEAT EXCHANGER):
_____ HEAT RECOVERY EFFICIENCY
_____ °F. GAS INLET TEMP.
_____ °F. HOT GAS OUTLET TEMP.

HOT WATER HEATING
_____ GAL./MIN.
_____ TEMP. RISE

ASPHALT HEATING
_____ GAL./MIN.
_____ °F. TEMP. RISE

INDICATE ADDITIONAL INFORMATION AND COMMENTS ON REVERSE SIDE

COMPANY _____ TELEPHONE _____

ADDRESS _____ ZIP _____

LOCATION OF PROJECT _____

INDIVIDUAL _____ TITLE _____ DATE _____

MAIL TO: VULCAN IRON WORKS, INC.
     1050 UNITED PENN BANK BLDG. ● WILKES-BARRE, PA. 18701   U.S.A.
     TELEX: 831-831

bēpex corporation

CENTRAL LABORATORY
TEST INQUIRY DATA
THERMAL PROCESSING

Project No.:_____

Date:_____

Company:_____

Address:_____

Contact:_____

MATERIAL SHIPMENT AND RETURN

Test Material:_____ Lbs Of Dry Material,_____ Lbs Wet Feed Is Being Shipped Prepaid

From:_____ Via:_____ Date:_____ Container:_____

Samples Of Feed ☐   Desired Product ☐   Shipped Via:_____ Date:_____

Test Material Return Instructions: **MATERIALS NOT DISPOSABLE IN SANITARY LANDFILL MUST BE RETURNED**

_____

_____

PURPOSE OF TEST

_____

_____

MATERIAL DATA

Dry Material Name:_____   Final Moisture (Wet Basis):_____

Liquid Name:_____   Chemically Free:_____ % Combined:_____%

Spec. Gravity, Solids:_____   Feed Consistency:_____

Loose Bulk Density, Lb/Ft^3:_____Wet_____Dry   Melting:_____^oF, Softening:_____^oF, Sticking:_____^oF

Angle Of Repose:_____Wet_____Dry   Abrasive:_____Hygroscopic:_____

Spec. Heat:_____Solids:_____Liquid   Soluble:_____
(If Soluble In Liquid, Attach Solubility Curve)

Heat, Fusion:_____Hydration:_____Crystalliz._____   Particle Size | Feed | Prod. Req'd. | Prod. Allowed

Latent Heat, Liquid:_____Boiling Point_____   %—On_____ _____ _____ _____

Molecular Weight Of Liquid:_____   %—On_____ _____ _____ _____

Initial Moisture (Wet Basis):_____   %—On_____ _____ _____ _____

Chemically Free:_____ % Combined:_____   %—On_____ _____ _____ _____

ANALYTICAL PROCEDURES

Partical Size:_____   Other:_____

Volatiles:_____   _____

PROCESS DATA

Production Rate:_____Lbs/Year At:_____Hrs/Year = _____Lbs/Hr

Temperature In:_____^oF

Inert Gas Required:_____. Contact With Combustion Products OK ?_____

Quality Criteria:_____

From What Equipment Is Feed Delivered ?_____

Ultimate Product Use:_____Construction Materials:_____

Present Process And Equipment:_____

Equipment Cleaning Method:_____

UTILITIES

Electricity:_____Steam At_____Psig_____^oF, Dowtherm At_____Psig_____^oF

Hot Oil At_____Psig_____^oF, Molten Salt At_____Psig_____^oF

Fuel Gas At_____Btu/Cu Ft,_____Fuel Oil At_____Btu/Lbs, Cooling Water At_____Psig_____^oF

ENVIRONMENT

Plant At_____Ft Above Sea Level,_____To_____^oF. Design For_____% Relative Humidity

800

FEECO INTERNATIONAL, INC.
3913 ALGOMA RD.
GREEN BAY, WISCONSIN 54301
U. S. A.
PHONE 414—468-1000
TELEX 263456

Company _____

Address _____

Commercial Name of Material to be pelletized _____

Chemical Formula _____ Specific Heat _____

CAPACITY

Capacity Required _____ lbs./hr. Feed Rate ☐ or Discharge rate ☐

Agglomerator will operate____hrs. per day;____days per week;____weeks per year

is feed uniform in quantity _____ moisture _____ temperature _____

MATERIAL

Moisture Content _____ % before pelletizing _____ % product

LBS./CU. FT. _____

Particle Size   Average _____ Smallest _____ Largest _____ Hygroscopic _____

Furnish screen analysis if possible	Mesh				
	Passing %				

Material is sticky _____ Abrasive _____ Corrosive _____ Plastic _____ Brittle _____ Dusty _____ Hazardous _____

Special additive (binder) required?

Describe the process before and after pelletizing.

POWER   110 volt   phase _____ cycle _____ AC _____ DC _____

220 volt   phase _____ cycle _____ AC _____ DC _____

440 volt   phase _____ cycle _____ AC _____ DC _____

AGGLOMERATION EXPERIENCE

We have been Agglomeration _____ material. Size of disc _____. Operating conditions _____

Capacity _____

Agglomerator to be made of carbon steel ☐ stainless steel ☐ other ☐ _____

DELIVERY

Drawings required _____ Proposal required _____

Quotation Date _____ Equipment delivery date _____

Information furnished by _____

Return to _____

FEECO
INTERNATIONAL
AGGLOMERATION
DATA
SHEET

3913 ALGOMA ROAD   FEECO INTERNATIONAL   GREEN BAY, WISCONSIN 54301

bepex corporation

10225 Higgins Road · Rosemont, Illinois 60018 · (312) 825-8010 · Telex: 25-3279

A P P L I C A T I O N   D A T A

BRIQUETTING/COMPACTING – GRANULATING MACHINERY & SYSTEMS

Please provide as much information as is presently available, so that we may determine your application requirements. This information, which we will consider confidential, is essential to determine equipment that would be necessary for laboratory tests, budget estimates, and occasionally, to allow us to supply a firm quotation.

1 - We are interested in:

( ) Briquetting for a definite shape and size

( ) Compaction/granulation for a granular material

( ) Agglomerating systems in general

2 - Our immediate need is for:

( ) Costs for laboratory evaluation

( ) Budget estimate for economic evaluation

( ) A detailed proposal and quotation, if obtainable from this information

3 - Material to be processed _____

Bulk density (lbs./cu. ft.) _____

Specific gravity _____

Screen analysis _____% + ____mesh   _____% + ____mesh

_____% + ____mesh   _____% + ____mesh

Moisture _____% Free _____% Combined

( ) Water   ( ) Other _____

Temperature required for removal _____

Maximum temperature the material can withstand without damage _____

Estimated feed temperature to the machine _____

Estimated maximum temperature of the feed material from the previous processing step that could be considered for machine feed _____

Physical nature of the material:

( ) Sticky   ( ) Abrasive   ( ) Corrosive

( ) Hygroscopic   ( ) Thixotropic   ( ) Toxic

( ) Aerated   ( ) Irritant

If corrosive or abrasive, state some typical materials of construction you consider acceptable with this application.

_____

If toxic or irritating, give safety precautions and the LD_{50} value, if known _____

_____

4 - The material ( ) can ( ) cannot be processed in contact with the gases of combustion

( ) A special atmosphere is required for processing

Specify _____

( ) The material contains combustible matter which could be considered as a source of heat if the material is heated to processing temperature by direct flame.

Combustible matter _____

Percentage by weight _____

Estimate BTU/lb. _____

5 - What operation(s) will be performed immediately preceeding the agglomeration step _____

6 - Estimated production rate required _____ ( ) tons ( ) pounds per hour. Operation will be ( ) continuous ( ) intermittent

Estimated _____hrs./day _____days/week _____days/yr.

7 - Final product desired:

( ) Briquets or pellets _____" x _____" x _____"

( ) Granular material - _____mesh + _____mesh

( ) Other _____

Moisture (solvent) _____that may remain _____%

8 - Most materials are briquetted or compacted by pressure alone.
However, in some cases, a binder must be utilized to supple-
ment the mechanical forces required for agglomeration. The
binder has to be inert and non-contaminating to the material.
Please state whether this approach would be permissible with
your material.

    ( ) Yes   ( ) No   Why? _____

_____

9 - Electrical power available:

    _____ Volts _____Cycles _____Hz.

All motors over _____ H.P. are to be for _____ volt service.

All motors are to be ( ) TEFC   ( ) Explosion proof,

Class _____   ( ) Open ( ) Industrial standard

( ) Other _____

10 - How is the agglomeration equipment to be used.

    ( ) Completely new product proposed for production

    ( ) Installation in a current process to improve or change
        the material's properties

    ( ) Expansion of a current process using agglomeration equip-
        ment

    ( ) Improvement of a current agglomeration process

11 - Why is agglomeration being considered at this time?

    ( ) Improve product properties

    ( ) Reduce dusting

    ( ) Improve efficiency in a current process

    ( ) To produce a specific size and shape

    ( ) Meet a competitive condition

    ( ) Reduce process costs

Briquetting—(*continued*)

MATERIAL SAFETY DATA SHEET

Required under USDL Safety and Health Regulations for Ship Repairing,
Shipbuilding, and Shipbreaking (29 CFR 1915, 1916, 1917)

SECTION I

MANUFACTURER'S NAME	EMERGENCY TELEPHONE NO.
ADDRESS *(Number, Street, City, State, and ZIP Code)*	

CHEMICAL NAME AND SYNONYMS	TRADE NAME AND SYNONYMS
CHEMICAL FAMILY	FORMULA

SECTION II - HAZARDOUS INGREDIENTS

PAINTS, PRESERVATIVES, & SOLVENTS	%	TLV (Units)	ALLOYS AND METALLIC COATINGS	%	TLV (Units)
PIGMENTS			BASE METAL		
CATALYST			ALLOYS		
VEHICLE			METALLIC COATINGS		
SOLVENTS			FILLER METAL PLUS COATING OR CORE FLUX		
ADDITIVES			OTHERS		
OTHERS					

HAZARDOUS MIXTURES OF OTHER LIQUIDS, SOLIDS, OR GASES	%	TLV (Units)

SECTION III - PHYSICAL DATA

BOILING POINT (°F.)		SPECIFIC GRAVITY (H$_2$O=1)	
VAPOR PRESSURE (mm Hg.)		PERCENT, VOLATILE BY VOLUME (%)	
VAPOR DENSITY (AIR=1)		EVAPORATION RATE (_____ =1)	
SOLUBILITY IN WATER			
APPEARANCE AND ODOR			

SECTION IV - FIRE AND EXPLOSION HAZARD DATA

FLASH POINT (Method used)	FLAMMABLE LIMITS	Lel	Uel
EXTINGUISHING MEDIA			
SPECIAL FIRE FIGHTING PROCEDURES			
UNUSUAL FIRE AND EXPLOSION HAZARDS			

PAGE (1)   (Continued on reverse side)   Form OSHA-20
Rev. May 72

SECTION V - HEALTH HAZARD DATA

THRESHOLD LIMIT VALUE

EFFECTS OF OVEREXPOSURE

EMERGENCY AND FIRST AID PROCEDURES

SECTION VI - REACTIVITY DATA

STABILITY	UNSTABLE		CONDITIONS TO AVOID
	STABLE		

INCOMPATABILITY *(Materials to avoid)*

HAZARDOUS DECOMPOSITION PRODUCTS

HAZARDOUS POLYMERIZATION	MAY OCCUR		CONDITIONS TO AVOID
	WILL NOT OCCUR		

SECTION VII - SPILL OR LEAK PROCEDURES

STEPS TO BE TAKEN IN CASE MATERIAL IS RELEASED OR SPILLED

WASTE DISPOSAL METHOD

SECTION VIII - SPECIAL PROTECTION INFORMATION

RESPIRATORY PROTECTION *(Specify type)*

VENTILATION	LOCAL EXHAUST	SPECIAL
	MECHANICAL *(General)*	OTHER

PROTECTIVE GLOVES	EYE PROTECTION

OTHER PROTECTIVE EQUIPMENT

SECTION IX - SPECIAL PRECAUTIONS

PRECAUTIONS TO BE TAKEN IN HANDLING AND STORING

OTHER PRECAUTIONS

GPO 934-110

PAGE (2)

Form OSHA-20
Rev. May 72

Material Safety Data Sheet—(*continued*)

Index